NAS1.9/4:33/9

TECHNOLOGY & SCIENCE
DETROIT PUBLIC LIBRARY

RED
SEAL

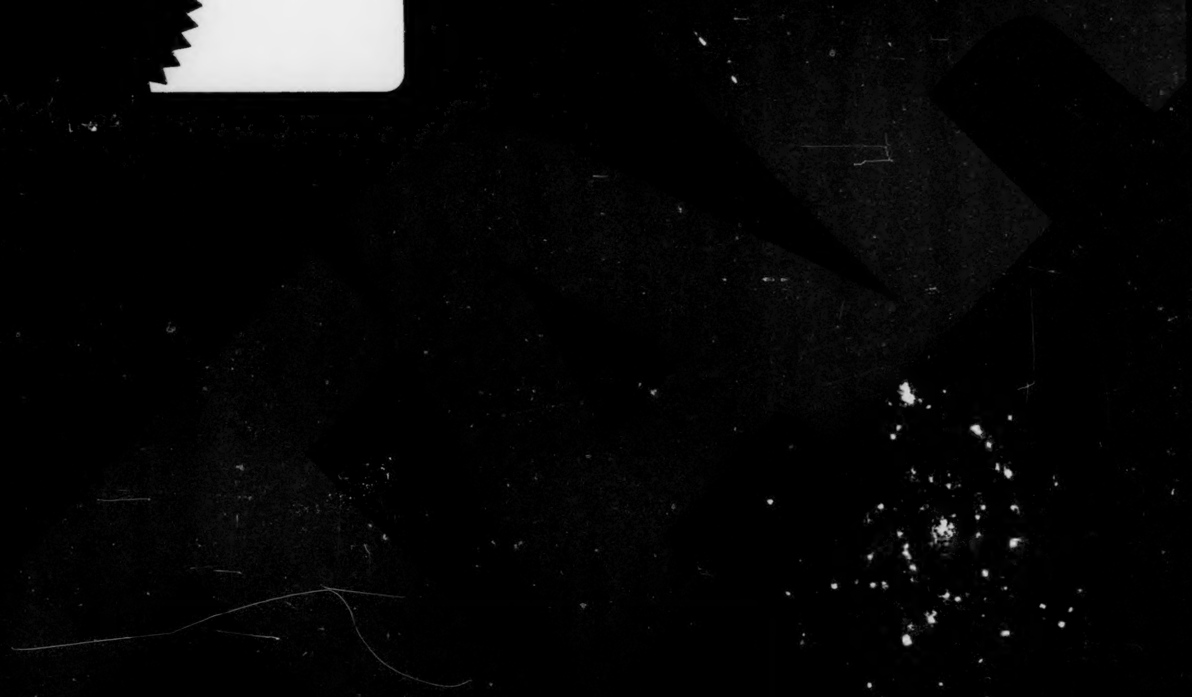

An Abstract Journal

NASA

Volume 33, Number 9
September 1995
N95-26342 to N95-28677

The NASA STI Office ... in Profile

Since its founding, NASA has been dedicated to the advancement of aeronautics and space science. The NASA Scientific and Technical Information (STI) Office plays a key part in helping NASA maintain this important role.

The NASA STI Office provides access to the NASA STI Database, the largest collection of aeronautical and space science STI in the world. The Office is also NASA's institutional mechanism for disseminating the results of its research and development activities.

Specialized services that help round out the Office's diverse offerings include creating custom thesauri, translating material to or from 34 foreign languages, building customized databases, organizing and publishing research results ... even providing videos.

For more information about the NASA STI Office, you can:

- **Phone** the NASA Access Help Desk at (301) 621-0390
- **Fax** your question to the NASA Access Help Desk at (301) 621-0134
- **E-mail** your question via the **Internet** to help@sti.nasa.gov
- **Write** to:

NASA Access Help Desk
NASA Center for AeroSpace Information
800 Elkridge Landing Road
Linthicum Heights, MD 21090-2934

DETROIT PUBLIC LIBRARY
3 5674 02477635 4

Scientific and Technical Aerospace Reports

STAR

Scientific and Technical Aerospace Reports (STAR), is published each month as a major product of the NASA Scientific and Technical Information (STI) Office.

Inside this issue you will find:

- **Front Matter** containing a typical citation and abstract sample explaining the standard format, including codes for ordering reports
- **An Abstract Section** containing citations and abstracts of reports and publications that provide comprehensive coverage of worldwide aerospace-related topics including aeronautics and space science technology. *STAR* lists published and publicly available reports entered into the NASA STI Database during the four weeks preceding publication of this issue. These citations and abstracts are listed by subject categories.
- **An Index Section**
    - Subject
    - Personal author
    - Corporate source
    - Contract number
    - Report number
- **An Appendix** containing a guide for ordering cited reports, registering with the NASA STI Office, and using the available products and services. Additionally, price schedules, phone numbers, and addresses are included in this information packed section.

NASA also sponsors the companion journal, *NASA Open Volumes on Aerospace (NOVA)*, which lists abstracts of the open literature on aerospace subjects available worldwide. *NOVA* is for internal NASA use only, available from the NASA Center for AeroSpace Information (CASI).

Entries found in *STAR* are available through the NASA online retrieval service, RECON.

The NASA STI Office gathers information through national and international agreements and exchanges and makes this information available to the NASA community and to the public in many forms through various outlets.

For additional information on the NASA STI Office, call the NASA Access Help Desk at (301) 621-0390, or write to:

NASA Center for AeroSpace Information
800 Elkridge Landing Road
Linthicum Heights, Maryland 21090-2934

US ISSN 0036-8741

Detroit Public Library
AUG 31 1995
Depository Document

The New NASA Video Catalog is Here

Free!

To order your free copy call
the NASA Access Help Desk at
(301) 621-0390 or
fax to (301) 621-0134 or
e-mail to helpdesk@sti.nasa.gov

EXPLORE THE UNIVERSE

This publication was prepared by the NASA Center for AeroSpace Information,
800 Elkridge Landing Road, Linthicum Heights, MD 21090-2934, (301) 621-0390.

Volume 33 Number 9 / September 1995

TABLE OF CONTENTS

AERONAUTICS For related information see also *Astronautics.*

01 AERONAUTICS (GENERAL) **2117**

02 AERODYNAMICS **2120**
Includes aerodynamics of bodies, combinations, wings, rotors, and control surfaces; and internal flow in ducts and turbomachinery. For related information see also *34 Fluid Mechanics and Heat Transfer.*

03 AIR TRANSPORTATION AND SAFETY **2125**
Includes passenger and cargo air transport operations; and aircraft accidents. For related information see also *16 Space Transportation* and *85 Urban Technology and Transportation.*

04 AIRCRAFT COMMUNICATIONS AND NAVIGATION **2126**
Includes digital and voice communication with aircraft; air navigation systems (satellite and ground based); and air traffic control. For related information see also *17 Space Communications, Spacecraft Communications, Command and Tracking* and *32 Communications and Radar.*

05 AIRCRAFT DESIGN, TESTING AND PERFORMANCE **2128**
Includes aircraft simulation technology. For related information see also *18 Spacecraft Design, Testing and Performance* and *39 Structural Mechanics.* For land transportation vehicles see *85 Urban Technology and Transportation.*

06 AIRCRAFT INSTRUMENTATION **2138**
Includes cockpit and cabin display devices; and flight instruments. For related information see also *19 Spacecraft Instrumentation* and *35 Instrumentation and Photography.*

07 AIRCRAFT PROPULSION AND POWER **2139**
Includes prime propulsion systems and systems components, e.g., gas turbine engines and compressors; and onboard auxiliary power plants for aircraft. For related information see also *20 Spacecraft Propulsion and Power, 28 Propellants and Fuels,* and *44 Energy Production and Conversion.*

08 AIRCRAFT STABILITY AND CONTROL **2141**
Includes aircraft handling qualities; piloting; flight controls; and autopilots. For related information see also *05 Aircraft Design, Testing and Performance.*

09 RESEARCH AND SUPPORT FACILITIES (AIR) **2142**
Includes airports, hangars and runways; aircraft repair and overhaul facilities; wind tunnels; shock tubes; and aircraft engine test stands. For related information see also *14 Ground Support Systems and Facilities (Space).*

ASTRONAUTICS For related information see also *Aeronautics.*

12 ASTRONAUTICS (GENERAL) **2144**
For extraterrestrial exploration see *91 Lunar and Planetary Exploration.*

13 ASTRODYNAMICS **2146**
Includes powered and free-flight trajectories; and orbital and launching dynamics.

14 GROUND SUPPORT SYSTEMS AND FACILITIES (SPACE) **2154**
Includes launch complexes, research and production facilities; ground support equipment, e.g., mobile transporters; and simulators. For related information see also *09 Research and Support Facilities (Air).*

15 LAUNCH VEHICLES AND SPACE VEHICLES **2154**
Includes boosters; operating problems of launch/space vehicle systems; and reusable vehicles. For related information see also *20 Spacecraft Propulsion and Power.*

16 SPACE TRANSPORTATION **2159**
Includes passenger and cargo space transportation, e.g., shuttle operations; and space rescue techniques. For related information see also *03 Air Transportation and Safety* and *18 Spacecraft Design, Testing and Performance.* For space suits see *54 Man/System Technology and Life Support.*

17 SPACE COMMUNICATIONS, SPACECRAFT COMMUNICATIONS, COMMAND AND TRACKING **2161**
Includes telemetry; space communications networks; astronavigation and guidance; and radio blackout. For related information see also *04 Aircraft Communications and Navigation* and *32 Communications and Radar.*

N.A.—No abstracts were assigned to this category for this issue.

18 SPACECRAFT DESIGN, TESTING AND PERFORMANCE 2161
Includes satellites; space platforms; space stations; spacecraft systems and components such as thermal and environmental controls; and attitude controls. For life support systems see *54 Man/System Technology and Life Support.* For related information see also *05 Aircraft Design, Testing and Performance, 39 Structural Mechanics,* and *16 Space Transportation.*

19 SPACECRAFT INSTRUMENTATION .... N.A.
For related information see also *06 Aircraft Instrumentation* and *35 Instrumentation and Photography.*

20 SPACECRAFT PROPULSION AND POWER 2166
Includes main propulsion systems and components, e.g., rocket engines; and spacecraft auxiliary power sources. For related information see also *07 Aircraft Propulsion and Power, 28 Propellants and Fuels, 44 Energy Production and Conversion,* and *15 Launch Vehicles and Space Vehicles.*

CHEMISTRY AND MATERIALS

23 CHEMISTRY AND MATERIALS (GENERAL) 2177

24 COMPOSITE MATERIALS 2179
Includes physical, chemical, and mechanical properties of laminates and other composite materials. For ceramic materials see *27 Nonmetallic Materials.*

25 INORGANIC AND PHYSICAL CHEMISTRY 2199
Includes chemical analysis, e.g., chromatography; combustion theory; electrochemistry; and photochemistry. For related information see also *77 Thermodynamics and Statistical Physics.*

26 METALLIC MATERIALS 2211
Includes physical, chemical, and mechanical properties of metals, e.g., corrosion; and metallurgy.

27 NONMETALLIC MATERIALS 2224
Includes physical, chemical, and mechanical properties of plastics, elastomers, lubricants, polymers, textiles, adhesives, and ceramic materials. For composite materials see *24 Composite Materials.*

28 PROPELLANTS AND FUELS 2242
Includes rocket propellants, igniters and oxidizers; their storage and handling procedures; and aircraft fuels. For related information see also *07 Aircraft Propulsion and Power, 20 Spacecraft Propulsion and Power,* and *44 Energy Production and Conversion.*

29 MATERIALS PROCESSING 2244
Includes space-based development of products and processes for commercial application. For biological materials see *55 Space Biology:*

ENGINEERING For related information see also *Physics.*

31 ENGINEERING (GENERAL) 2245
Includes vacuum technology; control engineering; display engineering; cryogenics; and fire prevention.

32 COMMUNICATIONS AND RADAR 2247
Includes radar; land and global communications; communications theory; and optical communications. For related information see also *04 Aircraft Communications and Navigation* and *17 Space Communications, Spacecraft Communications, Command and Tracking.* For search and rescue see *03 Air Transportation and Safety,* and *16 Space Transportation.*

33 ELECTRONICS AND ELECTRICAL ENGINEERING 2259
Includes test equipment and maintainability; components, e.g., tunnel diodes and transistors; microminiaturization; and integrated circuitry. For related information see also *60 Computer Operations and Hardware* and *76 Solid-State Physics.*

34 FLUID MECHANICS AND HEAT TRANSFER 2273
Includes boundary layers; hydrodynamics; fluidics; mass transfer and ablation cooling. For related information see also *02 Aerodynamics* and *77 Thermodynamics and Statistical Physics.*

35 INSTRUMENTATION AND PHOTOGRAPHY 2289
Includes remote sensors; measuring instruments and gauges; detectors; cameras and photographic supplies; and holography. For aerial photography see *43 Earth Resources and Remote Sensing.* For related information see also *06 Aircraft Instrumentation* and *19 Spacecraft Instrumentation.*

36 LASERS AND MASERS 2294
Includes parametric amplifiers. For related information see also *76 Solid-State Physics.*

37 MECHANICAL ENGINEERING 2300
Includes auxiliary systems (nonpower); machine elements and processes; and mechanical equipment.

38 QUALITY ASSURANCE AND RELIABILITY 2306
Includes product sampling procedures and techniques; and quality control.

39 STRUCTURAL MECHANICS 2307
Includes structural element design and weight analysis; fatigue; and thermal stress. For applications see *05 Aircraft Design, Testing and Performance* and *18 Spacecraft Design, Testing and Performance.*

GEOSCIENCES For related information see also *Space Sciences.*

42 GEOSCIENCES (GENERAL) 2313

43 EARTH RESOURCES AND REMOTE SENSING 2313
Includes remote sensing of earth resources by aircraft and spacecraft; photogrammetry; and aerial photography. For instrumentation see *35 Instrumentation and Photography.*

44 ENERGY PRODUCTION AND CONVERSION 2316
Includes specific energy conversion systems, e.g., fuel cells; global sources of energy; geophysical conversion; and windpower. For related information see also *07 Aircraft Propulsion and Power, 20 Spacecraft Propulsion and Power,* and *28 Propellants and Fuels.*

45 ENVIRONMENT POLLUTION 2326
Includes atmospheric, noise, thermal, and water pollution.

46 GEOPHYSICS 2334
Includes aeronomy; upper and lower atmosphere studies; ionospheric and magnetospheric physics; and geomagnetism. For space radiation see *93 Space Radiation.*

47 METEOROLOGY AND CLIMATOLOGY 2340
Includes weather forecasting and modification.

48 OCEANOGRAPHY 2345
Includes biological, dynamic, and physical oceanography; and marine resources. For related information see also *43 Earth Resources and Remote Sensing.*

LIFE SCIENCES

51 LIFE SCIENCES (GENERAL) 2348

52 AEROSPACE MEDICINE 2352
Includes physiological factors; biological effects of radiation; and effects of weightlessness on man and animals.

53 BEHAVIORAL SCIENCES 2355
Includes psychological factors; individual and group behavior; crew training and evaluation; and psychiatric research.

54 MAN/SYSTEM TECHNOLOGY AND LIFE SUPPORT 2358
Includes human engineering; biotechnology; and space suits and protective clothing. For related information see also *16 Space Transportation.*

55 SPACE BIOLOGY .... N.A.
Includes exobiology; planetary biology; and extraterrestrial life.

MATHEMATICAL AND COMPUTER SCIENCES

59 MATHEMATICAL AND COMPUTER SCIENCES (GENERAL) .... N.A.

60 COMPUTER OPERATIONS AND HARDWARE 2361
Includes hardware for computer graphics, firmware, and data processing. For components see *33 Electronics and Electrical Engineering.*

61 COMPUTER PROGRAMMING AND SOFTWARE 2362
Includes computer programs, routines, algorithms, and specific applications, e.g., CAD/CAM.

62 COMPUTER SYSTEMS 2376
Includes computer networks and special application computer systems.

63 CYBERNETICS 2379
Includes feedback and control theory, artificial intelligence, robotics and expert systems. For related information see also *54 Man/System Technology and Life Support.*

64 NUMERICAL ANALYSIS 2388
Includes iteration, difference equations, and numerical approximation.

65 STATISTICS AND PROBABILITY 2393
Includes data sampling and smoothing; Monte Carlo method; and stochastic processes.

66 SYSTEMS ANALYSIS 2396
Includes mathematical modeling; network analysis; and operations research.

67 THEORETICAL MATHEMATICS 2396
Includes topology and number theory.

PHYSICS For related information see also *Engineering.*

70 PHYSICS (GENERAL) 2398
For precision time and time interval (PTTI) see *35 Instrumentation and Photography*; for geophysics, astrophysics or solar physics see *46 Geophysics, 90 Astrophysics*, or *92 Solar Physics.*

71 ACOUSTICS 2400
Includes sound generation, transmission, and attenuation. For noise pollution see *45 Environment Pollution.*

72 ATOMIC AND MOLECULAR PHYSICS 2403
Includes atomic structure, electron properties, and molecular spectra.

73 NUCLEAR AND HIGH-ENERGY PHYSICS 2419
Includes elementary and nuclear particles; and reactor theory. For space radiation see *93 Space Radiation.*

74 OPTICS 2423
Includes light phenomena and optical devices. For lasers see *36 Lasers and Masers.*

75 PLASMA PHYSICS 2429
Includes magnetohydrodynamics and plasma fusion. For ionospheric plasmas see *46 Geophysics.* For space plasmas see *90 Astrophysics.*

76 SOLID-STATE PHYSICS 2436
Includes superconductivity. For related information see also *33 Electronics and Electrical Engineering* and *36 Lasers and Masers.*

77 THERMODYNAMICS AND STATISTICAL PHYSICS 2447
Includes quantum mechanics; theoretical physics; and Bose and Fermi statistics. For related information see also *25 Inorganic and Physical Chemistry* and *34 Fluid Mechanics and Heat Transfer.*

SOCIAL SCIENCES

80 SOCIAL SCIENCES (GENERAL) 2450
Includes educational matters.

81 ADMINISTRATION AND MANAGEMENT 2450
Includes management planning and research.

82 DOCUMENTATION AND INFORMATION SCIENCE 2452
Includes information management; information storage and retrieval technology; technical writing; graphic arts; and micrography. For computer documentation see *61 Computer Programming and Software.*

83 ECONOMICS AND COST ANALYSIS .... N.A.
Includes cost effectiveness studies.

84 LAW, POLITICAL SCIENCE AND SPACE POLICY .... N.A.
Includes NASA appropriation hearings; aviation law; space law and policy; international law; international cooperation; and patent policy.

85 URBAN TECHNOLOGY AND TRANSPORTATION 2458
Includes applications of space technology to urban problems; technology transfer; technology assessment; and surface and mass transportation. For related information see *03 Air Transportation and Safety, 16 Space Transportation,* and *44 Energy Production and Conversion.*

SPACE SCIENCES For related information see also *Geosciences.*

88 SPACE SCIENCES (GENERAL) .... N.A.

89 ASTRONOMY 2458
Includes radio, gamma-ray, and infrared astronomy; and astrometry.

90 ASTROPHYSICS 2461
Includes cosmology; celestial mechanics; space plasmas; and interstellar and interplanetary gases and dust. For related information see also *75 Plasma Physics.*

91 LUNAR AND PLANETARY EXPLORATION 2463
Includes planetology; and manned and unmanned flights. For spacecraft design or space stations see *18 Spacecraft Design, Testing and Performance.*

92 SOLAR PHYSICS 2464
Includes solar activity, solar flares, solar radiation and sunspots. For related information see also *93 Space Radiation.*

93 SPACE RADIATION 2465
Includes cosmic radiation; and inner and outer earth's radiation belts. For biological effects of radiation see *52 Aerospace Medicine.* For theory see *73 Nuclear and High-Energy Physics.*

GENERAL

Includes aeronautical, astronautical, and space science related histories, biographies, and pertinent reports too broad for categorization; histories or broad overviews of NASA programs.

99 GENERAL 2466

SUBJECT INDEX I-1

PERSONAL AUTHOR INDEX I-165

CORPORATE SOURCE INDEX I-183

CONTRACT NUMBER INDEX I-207

REPORT NUMBER INDEX I-213

APPENDIX A-1

TYPICAL CITATION AND ABSTRACT

NASA SPONSORED ↓ ↓ **ON MICROFICHE**

ACCESSION NUMBER → **N95-10148*#** National Aeronautics and Space Administration. Lewis ← **CORPORATE SOURCE**
Research Center, Cleveland, OH.
TITLE → **EFFECTS OF A FORWARD-SWEPT FRONT ROTOR ON THE FLOWFIELD OF A COUNTERROTATION PROPELLER**
AUTHORS → M. Nallasamy (NYMA, Inc., Brook Park, OH.) and Gary G. Podboy Aug. ← **PUBLICATION DATE**
1994 19 p Presented at the 30th Joint Propulsion Conference, Indianapolis, IN, 27-29 Jun. 1994; sponsored by AIAA, ASME, SAE, and ASEE
CONTRACT OR GRANT → (Contract NAS3-27186; RTOP 538-03-11)
REPORT NUMBERS → (NASA-TM-106671; E-8994; NAS 1.15:106671; AIAA Paper 94-2694) Avail: ← **AVAILABILITY SOURCE AND PRICE CODE**
CASI HC A03/MF A01; 6 functional color pages

The effects of a forward-swept front rotor on the flowfield of a counterrotation model propeller at takeoff conditions at zero degree angle of attack are studied by solving the unsteady three-dimensional Euler equations. The configuration considered is an uneven blade count counterrotation model with twelve forward-swept blades on the fore rotor and ten aft-swept blades on the aft rotor. The flowfield is compared with that of a reference aft-swept counterrotation geometry and Laser Doppler Velocimeter (LDV) measurements. At the operating conditions considered, the forward-swept blade experiences a higher tip loading and produces a stronger tip vortex compared to the aft-swept blade, consistent with the LDV and acoustic measurements. Neither the solution nor the LDV data indicated the formation of a leading edge vortex. The predicted radial distribution of the circumferentially averaged axial velocity at the measurement station agreed very closely with LDV data, while crossflow velocities showed poor agreement. The discrepancy between prediction and LDV data of tangential and radial velocities is due in part to the insufficient mesh resolution in the region between the rotors and in the tip region to track the tip vortex. The vortex is diffused by the time it arrives at the measurement station. The uneven blade count configuration requires the solution to be carried out for six blade passages of the fore rotor and five passages of the aft rotor, thus making grid refinement prohibitive.

Author

VOLUME 33 NUMBER 9 / September 1995

Scientific and Technical Aerospace Reports

A Monthly Publication of the National Aeronautics and Space Administration

01 AERONAUTICS (GENERAL)

N95-26363*# Purdue Univ., West Lafayette, IN.
WINCLR: A COMPUTER CODE FOR HEAT TRANSFER AND CLEARANCE CALCULATION IN A COMPRESSOR
T. K. Bose and S. N. B. Murthy Jun. 1994 170 p
(Contract NAG3-481; RTOP 505-62-52; DTFA03-83-A-00328)
(NASA-CR-195436; E-9461; NAS 1.26:195436; DOT/FAA/CT-TN94-61; M/NAFA/94-1) Avail: CASI HC A08/MF A02

One of the concerns during inclement weather operation of aircraft in rain and hail storm conditions is the nature and extent of changes in compressor casing clearance. An increase in clearance affects efficiency while a decrease may cause blade rubbing with the casing. The change in clearance is the result of geometrical dimensional changes in the blades, the casing and the rotor due to heat transfer between those parts and the two-phase working fluid. The heat transfer interacts nonlinearly with the performance of the compressor, and, therefore, the determination of clearance changes necessitates a simultaneous determination of change in performance of the compressor. A computer code the WINCLR has been designed for the determination of casing clearance, that is operated interactively with the PURDU-WINCOF I code designed previously for determining the performance of a compressor. A detailed description of the WINCLR code is provided in a companion report. The current report provides details of the code with an illustrative example of application to the case of a multistage compressor. It is found in the example case that under given ingestion and operational conditions, it is possible for a compressor to undergo changes in performance in the front stages and rubbing in the back stages. Author

N95-26381*# National Aeronautics and Space Administration. Langley Research Center, Hampton, VA.
FLUTTER CLEARANCE FLIGHT TESTS OF AN OV-10A AIRPLANE MODIFIED FOR WAKE VORTEX FLIGHT EXPERIMENTS
Robert V. Doggett, Jr., Jose A. Rivera, Jr., and Eric C. Stewart Apr. 1995 14 p
(RTOP 505-63-50-13)
(NASA-TM-109168; NAS 1.15:109168) Avail: CASI HC A03/MF A01

The envelope expansion, flight flutter tests of a modified OV-10A aircraft are described. For the wake vortex research program, the airplane was modified to incorporate three forward-extending instrumentation booms, one extending forward from each wing tip and one from the right side of the fuselage. The booms were instrumented with sensors to measure the velocity and direction of local air flow. The flutter test results show that the modified OV-10A aircraft is free from flutter at speeds up to 330 KEAS at 5000 feet altitude. Author

N95-26409 Industrial Coll. of the Armed Forces, Washington, DC.
STRATEGY IN THE COMMERCIAL AIRCRAFT INDUSTRY IN THE UNITED STATES: A COMPARISON OF DECISIONMAKING BY MCDONNELL-DOUGLAS AND BOEING AIRCRAFT COMPANIES FROM 1977-1983 Research Report, Aug. 1993 - Apr. 1994
Dave Gillett Apr. 1994 38 p Limited Reproducibility: More than 20% of this document may be affected by microfiche quality
(AD-A288289; NDU-ICAF-94-F2) Avail: Issuing Activity (Defense Technical Information Center (DTIC))

This paper studies strategic decision making in the commercial aircraft manufacturing market. It compares the decisions made by McDonnell-Douglas Corporation with those of Boeing Aircraft Company in the late 70s and early 80s. The study concludes that strategic decisions were made based on each companies vision of its core business. McDonnell-Douglas refused to risk its capital on a new commercial aircraft because its core business was defense. Boeing on the other hand was willing to risk the company on new aircraft development because its core business was the commercial aircraft market. DTIC

N95-26455 Industrial Coll. of the Armed Forces, Washington, DC.
SURVIVING THE PEACE. LESSONS LEARNED FROM THE AIRCRAFT INDUSTRY IN THE 1920S AND 1930S Research Report, Aug. 1993 - Apr. 1994
Ellen M. Pawlikowski Apr. 1994 39 p Limited Reproducibility: More than 20% of this document may be affected by microfiche quality
(AD-A288284; NDU-ICAF-94-F56) Avail: Issuing Activity (Defense Technical Information Center (DTIC))

Many of America's defense industries are struggling to survive in today's peacetime environment. As they prepare for the future, US business and government leaders can learn from defense industries that survived the last extended peace. This paper examines the American aircraft industry during the peace from 1920 to 1939. During that time, the industry retained core capability for future defense needs while establishing alternative markets for its products. They succeeded because they placed a strong emphasis on broad based R&D and conducted a concerted effort to establish alternative markets. Industry and national leaders used those alternative markets to strengthen the industry and the national economy. The federal government supported industry efforts by funding research and development, establishing a national aviation infrastructure, and opening foreign markets. The Congress also funded military aircraft production that helped the industry weather market downturns. Although commercial markets existed, aircraft manufacturers failed to achieve independence from government contracts. This failure was due to government procurement practices, poor business management by aviation pioneers, the high cost of technology development, and the small size of commercial markets. Today's defense industries should study the lessons of the aircraft manufacturers as they determine business strategy for the 1990s. The federal government can also apply these lessons as it makes decisions regarding research investments, military-commercial integration, acquisition reform, and export policies. We can never repeat history, but we can learn from it. By studying the lessons of the last extended peace, perhaps we can avoid the mistakes and duplicate the successes. DTIC

N95-26629 Battelle Memorial Inst., Columbus, OH.
DEVELOPMENT OF REPAIR PROCESSES AND SOURCES FOR C/KC-135 AIRCRAFT WINDOWS/WINDSHIELDS Final Technical Report, 1 Sep. 1991 - 31 Jan. 1994
Richard J. Olson Sep. 1994 521 p Limited Reproducibility: More than 20% of this document may be affected by microfiche quality
(Contract F09603-90-D-2217)
(AD-A288348) Avail: Issuing Activity (Defense Technical Information Center (DTIC))

The U.S. Air Force has historically rejected the notion of using repaired windows/windshields (W/WS). With increasing pressure to reduce fleet operating costs and based on the favorable experience that commercial fleets have had, interest in using repaired W/WS is receiving greater attention. To ensure that repaired W/WS are safe and that they provide similar benefits for the Air Force, a program of evaluation and testing was undertaken to compare new and repaired C/KC-135 W/WS. Optical and electrical properties, pressure integrity, and bird impact resistance of repaired and new W/WS have been evaluated. The bird impact test results are the first data that the Air Force have collected for C/KC-135 W/WS. The functional testing indicated that repaired W/WS are not equal to new W/WS; the new W/WS outperform the repaired W/WS. However, in terms of removal for cause criteria and absolute performance requirements, the repaired W/WS appear to be good enough. Concerning costs, the direct costs for repair of the W/WS in this program ranged from 65-75% of new W/WS cost, suggesting that money can be saved. DTIC

N95-26710*# Army Aviation Systems Command, Hampton, VA.
DEVELOPMENT AND VALIDATION OF A BLADE-ELEMENT MATHEMATICAL MODEL FOR THE AH-64A APACHE HELICOPTER
M. Hossein Mansur Apr. 1995 98 p
(RTOP 505-59-36)
(NASA-TM-108863; A-95034; NAS 1.15:108863; USAATCOM-TR-94-A-022)
Avail: CASI HC A05/MF A02

A high-fidelity blade-element mathematical model for the AH-64A Apache Advanced Attack Helicopter has been developed by the Aeroflightdynamics Directorate of the U.S. Army's Aviation and Troop Command (ATCOM) at Ames Research Center. The model is based on the McDonnell Douglas Helicopter Systems' (MDHS) Fly Real Time (FLYRT) model of the AH-64A (acquired under contract) which was modified in-house and augmented with a blade-element-type main-rotor module. This report describes, in detail, the development of the rotor module, and presents some results of an extensive validation effort. Author

N95-26817# General Accounting Office, Washington, DC. National Security and International Affairs Div.
ASIAN AERONAUTICS: TECHNOLOGY ACQUISITION DRIVES INDUSTRY DEVELOPMENT. REPORT TO CONGRESSIONAL REQUESTERS
4 May 1994 19 p
(GAO/NSIAD-94-140; B-256707) Avail: CASI HC A03/MF A01; GAO, PO Box 6015, Gaithersburg, MD 20884-6015 HC

This report responds to a request to review the aeronautics research and development (R&D) activities of Asian countries. More specifically, we are providing information on (1) the approaches these Asian nations use to develop their aeronautics industries, (2) the level of aeronautics development each country has achieved, and (3) the implications of this development for the U.S. aeronautics industry. This report represents an amalgamation of many pieces of data obtained from dozens of U.S. and foreign sources. However, because of the nature of much of the data, we were unable to verify its accuracy or make an independent assessment of the extent and progress of each country's R&D efforts. Derived from text

N95-26941# Wichita State Univ., Wichita, KS. National Inst. for Aviation Research.
AIAA TECHFEST 20 PROCEEDINGS
William H. Wentz, ed. 1994 275 p Techfest held in Wichita, KS, 12-13 Nov. 1993
(NIAR-94-1) Avail: CASI HC A12/MF A03

A wide range of topics concerned with aerodynamics and design considerations is addressed. Also addressed are structures-related topics and the manufacturing considerations associated with the designing of a high altitude long endurance aircraft. The airspace database is discussed, as well as the results and capabilities of a new jet facility at the University of Kansas. As part of miscellaneous topics, prevention and control of inlet unstart using an SR-71 simulation is presented, along with an easy way to analyze longitudinal and lateral-directional trim problems with AEO or OEI. For individual titles, see N95-26942 through N95-26956.

N95-26942# Kansas Univ., Lawrence, KS.
PRELIMINARY DESIGN PROBLEMS AND SOLUTIONS FOR A SUPERSONIC OBLIQUE ALL-WING TRANSPORT AIRCRAFT Abstract only c05
Troy Downen *In* Wichita State Univ., AIAA Techfest 20 Proceedings 1994 2 p (For primary document see N95-26941 09-01)
Avail: CASI HC A01/MF A03

Although the oblique all-wing transport (OAWT) has been studied in some detail for the last twenty years, some of the most basic design features of such aircraft have not received much attention. Due to the unique configuration of the OAWT, passenger ingress/egress and cargo loading will present problems, as will the internal cabin arrangement, engine placement and take-off attitude. This presentation examines the nature of these preliminary design problems and proposes one or more viable solutions for each. Author

N95-26943# Wichita State Univ., Wichita, KS.
AN EXPLORATORY APPLICATION OF NEURAL NETWORKS FOR AIRFOIL DESIGN Abstract Only c63
Steve Huang, L. S. Miller, and J. E. Steck *In its* AIAA Techfest 20 Proceedings 1994 26 p (For primary document see N95-26941 09-01)
Avail: CASI HC A03/MF A03

This document reports the use of artificial neural networks (A.N.N.) for airfoil design, and it focuses on the following sections: (1) Investigative goals -- to develop an inverse airfoil design method using A.N.N. for single element airfoils and using experience to determine the possibility of using A.N.N. for multi-element airfoil design; (2) Airfoil design methods -- iterative method and inverse method; (3) Artificial neural network -- method to solve complex non-linear problems (image processing, speech recognition, adaptive control, and airfoil performance analysis), highly parallel computational devices, can be trained to learn a set of input/output patterns, able to generalize outside its training domain, and usually implemented using a software package which simulates the parallel architecture; (4) Training data -- utilize eppler code to generate training data, symmetric airfoil sections, reynolds number, thickness to chord ratios, and pressure recovery points; and (5) Results, Conclusions, and Recommendations. CASI

N95-26944# Lear Jet Industries, Inc., Wichita, KS.
AIRCRAFT NOSEWHEEL STEERING SIMULATION Abstract Only c09
Wayne Stout *In* Wichita State Univ., AIAA Techfest 20 Proceedings 1994 48 p (For primary document see N95-26941 09-01)
Avail: CASI HC A03/MF A03

This paper reports the simulation of aircraft nosewheel steering and it has the following objectives: demonstrate power and effectiveness of simulation tools, highlight modular (subsystem) buildup of complex simulation model, show complexity of suspension/steering dynamics, and highlight characteristics of pilot when performing nosewheel steering task. CASI

N95-26945*# National Aeronautics and Space Administration. Lewis Research Center, Cleveland, OH.
THE HIGH SPEED CIVIL TRANSPORT AND NASA'S HIGH SPEED RESEARCH (HSR) PROGRAM Abstract only c05
Robert J. Shaw *In* Wichita State Univ., AIAA Techfest 20 Proceedings 1994 2 p (For primary document see N95-26941 09-01)
Avail: CASI HC A01/MF A03

Ongoing studies being conducted not only in this country but in Europe and Asia suggest that a second generation supersonic transport, or High-Speed Civil Transport (HSCT), could become an important part of the 21st century international air transportation system. However, major environmental compatibility and economic viability issues must be resolved if the HSCT is to become a reality. This talk will overview the NASA High-Speed Research (HSR) program which is aimed at providing the U.S. industry with a technology base to allow them to consider launching an HSCT program early in the next century. The talk will also discuss some of the comparable activities going on within Europe and Japan. Author

N95-26946# Wichita State Univ., Wichita, KS.
CREATING AN ALTERNATIVE PARAMETER OPTIMIZATION METHOD (APO) Abstract Only c02
William C. Forrest *In its* AIAA Techfest 20 Proceedings 1994 8 p (For primary document see N95-26941 09-01)
Avail: CASI HC A02/MF A03

Current project goals are (1) to couple a numerical optimization scheme to an existing airfoil design code to enable multiple-objective optimization, targeted optimization, and alternative airfoil definition; and (2) to demonstrate validation/application of the enhanced design method. This viewgraph presentation gives a background on optimization processes in general and earlier applications to airfoils; implementation of the goals in the codes EPPLER, KS-OPT, and APO; and the resulting airfoils generated. CASI

N95-26947# Kansas Univ., Lawrence, KS.
DESIGN OF A HIGH ALTITUDE LONG ENDURANCE AIRCRAFT WITH MANUFACTURING CONSIDERATIONS Abstract Only **c05**
Catherine Grant, Richard Hazlewood, Howard Sacks, and Troy Downen *In* Wichita State Univ., AIAA Techfest 20 Proceedings 1994 2 p (For primary document see N95-26941 09-01)
Avail: CASI HC A01/MF A03

There is a current need for a low cost, low maintenance, unmanned High Altitude Long Endurance (HALE) aircraft to conduct high altitude atmospheric studies. Future military applications are possible. The preliminary design of a HALE vehicle is presented with special attention to low cost (low maintenance, low support requirements) and manufacturability. Emphasis is also placed on the propulsion system design, using an advanced ducted engine for low noise and improved propulsive efficiency. Author

N95-26948# Kansas Univ., Lawrence, KS.
PREVENTION AND CONTROL OF INLET UNSTART USING AN SR-71 SIMULATION Abstract Only
Troy Downen *In* Wichita State Univ., AIAA Techfest 20 Proceedings 1994 1 p (For primary document see N95-26941 09-01)
Avail: CASI HC A01/MF A03

The effect of inlet unstart -- a major concern in the development of a next generation high speed civil transport, -- is addressed. The University of Kansas' presentation pertaining to the problems associated with the inlet unstart is outlined. Derived from text

N95-26949# Kansas Univ., Lawrence, KS.
AN EASY WAY TO ANALYZE LONGITUDINAL AND LATERAL-DIRECTIONAL TRIM PROBLEMS WITH AEO OR OEI **c08**
Jan Roskam and William Anemaat (Design, Analysis and Research Corp., Lawrence, KS.) *In* Wichita State Univ., AIAA Techfest 20 Proceedings 1994 22 p (For primary document see N95-26941 09-01)
Avail: CASI HC A03/MF A03

Analyzing longitudinal and lateral-directional trim problems of airplanes with all-engines-operating (AEO) and with one-engine-inoperative (OEI) requires the solution of two sets of simultaneous equations. For longitudinal trim the set includes drag, lift, pitching moment, and elevator wheel force equations. For lateral-directional trim the set includes side-force, rolling moment, yawing moment, rudder pedal force, and aileron wheel force equations. Both sets of equations are non-linear; the process of finding a solution is therefore an iterative process. Solutions are very much dependent on the detailed aerodynamic design of the airplane, on the center of gravity location, and on various characteristics of the flight control system. The equations have been programmed as part of the user-friendly Advanced Aircraft Analysis (AAA) program. The purpose of the paper is to discuss several examples of how the stability and control engineer can use this aspect of the AAA program to rapidly resolve issues of control force levels, control force gradients, and flight path stability with AEO and OEI. Derived from text

N95-26950# Wichita State Univ., Wichita, KS.
THE AEROSPACE DATABASE: AN INTRODUCTION TO AIAA'S COMPUTERIZED SOURCE FOR IDENTIFYING SCIENTIFIC AND TECHNICAL INFORMATION Abstract Only **c82**
Thomas G. DePetro *In its* AIAA Techfest 20 Proceedings 1994 2 p (For primary document see N95-26941 09-01)
Avail: CASI HC A01/MF A03

The AIAA Technical Information Service in New York in conjunction with DIALOG Information Services, Inc. in Palo Alto, California provides online and CD-ROM computer access to AIAA's Aerospace Database. This database references scientific and technical literature and information including such sources as NASA documents, reports, and publications, AIAA books, journals papers, and conferences and other relevant items that record the results of aerospace research and development. Beginning with the year 1962 and continuing to the present, the database electronically combines two printed indexes: NASA's 'Scientific and Technical Aerospace Reports' (STAR) and AIAA's 'International Aerospace Abstracts' (IAA). Items written by AIAA members and others can be quickly identified by title, subject descriptors for the 'NASA Thesaurus', keywords, conference, etc. using DIALOG commands and Boolean logic to combine sets of terms in the database. These items are then accessed in libraries, or photocopies can be ordered from the AIAA Quality Express Document delivery service. This session will include a demonstration of the database to show how it can be used in the process of aerospace research and development and technology transfer. Author

N95-26951# Kansas Univ., Lawrence, KS.
PRELIMINARY RESULTS AND RESEARCH CAPABILITIES OF A NEW JET FACILITY AT THE UNIVERSITY OF KANSAS **c09**
Jason Frank, Tom Sherwood, and Ray Taghavi *In* Wichita State Univ., AIAA Techfest 20 Proceedings 1994 16 p (For primary document see N95-26941 09-01)
Avail: CASI HC A03/MF A03

The recently completed free jet facility at the University of Kansas was designed to be versatile in research capabilities. The free-shear flow testing apparatus operates in both subsonic and supersonic regimes to test jet exhaust nozzles, diffusers, and combustor geometries with and without swirl. Currently proposed areas of research have application in engine exhaust design, jet diffusion, and supersonic jet noise research. The equipment is comprised of a plenum tank, flow conditioners, bellmouth, and adapter and various subsonic and supersonic nozzle attachments. A jet engine starting unit provides enough flow to choke a 3.5 inch diameter nozzle. Flow field variables can be measured with pitot tubes and hot-wire anemometry, as well as with laser Doppler velocimetry. Preliminary data indicate a top hat exit velocity profile with less than 1% core turbulence intensity. Author

N95-26952*# National Aeronautics and Space Administration. Lewis Research Center, Cleveland, OH. Sverdrup Technology.
VISUALIZATION OF THE MULTIPLE SUPERSONIC JET OSCILLATIONS BY SWEPT FOCUSED STROBED SCHLIEREN TECHNIQUE
Ganesh Raman and Ray Taghavi (Kansas Univ., Lawrence, KS.) *In* Wichita State Univ., AIAA Techfest 20 Proceedings 1994 8 p (For primary document see N95-26941 09-01)
Avail: CASI HC A02/MF A03

The natural flapping mode oscillations of a multiple rectangular supersonic jet is visualized by the newly developed strobed focusing schlieren technique. Four parallel underexpanded, converging rectangular jets, exhausting into ambient air at a fully expanded Mach number of 1.61 are visualized in this study. This technique clearly shows the oscillations at the natural screech frequency and offers tremendous flexibility in the study of these flow fields. Author

N95-26953# Wichita State Univ., Wichita, KS. Dept. of Aerospace Engineering.
THE NEAR-WAKE FLOW BEHAVIOR OF AN OSCILLATING AIRFOIL WITH MODIFIED TRAILING EDGE **c02**
Roy Y. Myose and Jiro Iwata *In its* AIAA Techfest 20 Proceedings 1994 12 p (For primary document see N95-26941 09-01)
Avail: CASI HC A03/MF A03

This report covers work which produced the following conclusions: (1) complex three-dimensional vortices were shed as a result of oscillating an airfoil with saw-tooth trailing edge; (2) results from the turbulent boundary layer simulation experiment were consistent with envisioned vortical system; and (3) flow conditions at trailing edge have significant influence on performance of airfoil. No work was done on oscillating airfoils with modified trailing edge. CASI

N95-26954# Wichita State Univ., Wichita, KS. Dept. of Aerospace Engineering.
FULL SPAN FLAPERONS FOR A BIPLANE **c05**
Bonnie L. Johnson *In its* AIAA Techfest 20 Proceedings 1994 16 p (For primary document see N95-26941 09-01)
Avail: CASI HC A03/MF A03

The work on this project produced the following conclusions: (1) full span flaperons involved the use of stabilator power for maneuvering flight not trim and reduced the pilot workload in approach to landing phase; (2) aerodynamically balanced ailerons work for flap deflections up to 12 deg, reduce the hinge moments for actuator design and produce roll authority up to flaps 12; and (3) full span flaps are a poor man's variable camber wing for maneuvering flight. CASI

N95-26955# Wichita State Univ., Wichita, KS.
AN EXPERIMENTAL INVESTIGATION OF HELICOPTER DOWNWASH AND TAILBOOM INTERACTION AT THE WICHITA STATE UNIVERSITY 7X10 FOOT WIND TUNNEL c02
Scot Kruse, James E. Leigh, Kevin A. Moore, and Scott Randle *In its* AIAA Techfest 20 Proceedings 1994 12 p (For primary document see N95-26941 09-01)
Avail: CASI HC A03/MF A03

The two goals of this experiment were: (1) to study the unsteady aerodynamics of a helicopter main rotor in hovering flight; and (2) test the wind tunnel's instrumentation speed for velocity and pressure measurement. Derived from text

N95-26956*# National Aeronautics and Space Administration. Langley Research Center, Hampton, VA.
INCORPORATING BIPLANE WING THEORY INTO A LARGE, SUBSONIC, ALL-CARGO TRANSPORT c05
Michael K. Zyskowski *In* Wichita State Univ., AIAA Techfest 20 Proceedings 1994 p 1-15 (For primary document see N95-26941 09-01)
Avail: CASI HC A03/MF A03

If the air-cargo market increases at the pace predicted, a new conceptual aircraft will be demanded to meet the needs of the air-cargo industry. Furthermore, it has been found that not only should this aircraft be optimized to carry the intermodal containers used by the current shipping industry, but it should also be be able to operate at existing airports. The best solution to these problems is a configuration incorporating a bi-wing planform, which has resulted in significant improvements over the monoplane in lift/drag, weight reduction, and span reduction. The future of the air-cargo market, biplane theory, wind tunnel tests, and a comparison of the aerodynamic characteristics of the biplane and monoplane are discussed. The factors pertaining to a biplane cargo transport are then examined, resulting in biplane geometric parameters. Author

N95-27543* National Aeronautics and Space Administration, Washington, DC.
AERONAUTICAL ENGINEERING: A CONTINUING BIBLIOGRAPHY WITH INDEXES (SUPPLEMENT 318)
Jun. 1995 93 p
(NASA-SP-7037(318); NAS 1.21:7037(318)) Avail: CASI HC A05

This bibliography lists 217 reports, articles, and other documents introduced into the NASA scientific and technical information system in June 1995. Subject coverage includes: design, construction and testing of aircraft and aircraft engines; aircraft components, equipment, and systems; ground support systems; and theoretical and applied aspects of aerodynamics and general fluid dynamics. Author

N95-28610 American Inst. of Aeronautics and Astronautics, Washington, DC.
PROCEEDINGS OF THE AIAA/FAA JOINT SYMPOSIUM ON GENERAL AVIATION SYSTEMS Final Report
Gus Ferrara and Roberto DiMichele Sep. 1994 627 p Symposium held in Starkville, MS, 24-25 May 1994 Limited Reproducibility: More than 20% of this document may be affected by microfiche quality
(AD-A289830; DOT/FAA/CT-94/63) Avail: Issuing Activity (Defense Technical Information Center (DTIC))

The 1994 AIAA/FAA Joint Symposium on General Aviation Systems was the result of the combined efforts of the AIAA General Aviation Systems Technical Committee and the Federal Aviation Administration Technical Center. This symposium offered the opportunity to present and review the current state of the art in research that is being conducted in support of general aviation. All told, the papers presented covered the entire spectrum of research, and the participants had the opportunity to hear presentations on everything from alternate fuels to developments in air traffic control. DTIC

02 AERODYNAMICS

Includes aerodynamics of bodies, combinations, wings, rotors, and control surfaces; and internal flow in ducts and turbomachinery.

For related information see also *34 Fluid Mechanics and Heat Transfer.*

N95-26382*# National Aeronautics and Space Administration. Langley Research Center, Hampton, VA.
AIRFOIL MODIFICATION EFFECTS ON SUBSONIC AND TRANSONIC PRESSURE DISTRIBUTIONS AND PERFORMANCE FOR THE EA-6B AIRPLANE
Dennis O. Allison and William G. Sewall May 1995 86 p
(RTOP 505-59-10-30)
(NASA-TP-3516; L-17360; NAS 1.60:3516) Avail: CASI HC A05/MF A01

Longitudinal characteristics and wing-section pressure distributions are compared for the EA-6B airplane with and without airfoil modifications. The airfoil modifications were designed to increase low-speed maximum lift for maneuvering, while having a minimal effect on transonic performance. Section contour changes were confined to the leading-edge slat and trailing-edge flap regions of the wing. Experimental data are analyzed from tests in the Langley 16-Foot Transonic Tunnel on the baseline and two modified wing-fuselage configurations with the slats and flaps in their retracted positions. Wing modification effects on subsonic and transonic performance are seen in wing-section pressure distributions of the various configurations at similar lift coefficients. The modified-wing configurations produced maximum lift coefficients which exceeded those of the baseline configuration at low-speed Mach numbers (0.300 and 0.400). This benefit was related to the behavior of the wing upper surface leading-edge suction peak and the behavior of the trailing-edge pressure. At transonic Mach numbers (0.725 to 0.900), the wing modifications produced a somewhat stronger nose-down pitching moment, a slightly higher drag at low-lift levels, and a lower drag at higher lift levels. Author

N95-26649*# MCAT Inst., San Jose, CA.
CFD RESEARCH, PARALLEL COMPUTATION AND AERODYNAMIC OPTIMIZATION Final Report, Jul. 1989 - Jan. 1995
James S. Ryan Jan. 1995 7 p Original contains color illustrations
(Contracts NCC2-505; NCC2-796)
(NASA-CR-197748; NAS 1.26:197748; MCAT-95-18) Avail: CASI HC A02/MF A01; 1 functional color page

Over five years of research in Computational Fluid Dynamics and its applications are covered in this report. Using CFD as an established tool, aerodynamic optimization on parallel architectures is explored. The objective of this work is to provide better tools to vehicle designers. Submarine design requires accurate force and moment calculations in flow with thick boundary layers and large separated vortices. Low noise production is critical, so flow into the propulsor region must be predicted accurately. The High Speed Civil Transport (HSCT) has been the subject of recent work. This vehicle is to be a passenger vehicle with the capability of cutting overseas flight times by more than half. A successful design must surpass the performance of comparable planes. Fuel economy, other operational costs, environmental impact, and range must all be improved substantially. For all these reasons, improved design tools are required, and these tools must eventually integrate optimization, external aerodynamics, propulsion, structures, heat transfer and other disciplines. Derived from text

N95-26713 Air Force Systems Command, Wright-Patterson AFB, OH. National Air Intelligence Center.
NUMERICAL INVESTIGATION TO S-INLET FLOWS (NUMERICAL SIMULATION STUDY OF S-INLET FLOWS)
Zhang Shucheng and Huang Xijun 17 Nov. 1994 20 p Transl. into ENGLISH from unidentified Chinese language periodical, p 169-174 Limited Reproducibility: More than 20% of this document may be affected by microfiche quality
(AD-A289590; NAIC-ID(RS)T-0922-92) Avail: Issuing Activity (Defense Technical Information Center (DTIC))

This work improves Denton's finite volume time marching methods. It takes this type of method, in which there is 1st order accuracy in time and 2d order accuracy in space, and improves it to be a calculation method in which there is 2d degree accuracy in time and 2d degree accuracy in space. In conjunction with this, application is made to numerical simulations of inlet flow fields associated with the interior flows of S type inlets as well as exterior flows which inlets possess. Calculations are carried out for actual cases, and we obtained reasonable calculation results. DTIC

N95-26719 Air Force Systems Command, Wright-Patterson AFB, OH. National Air Intelligence Center.
PLATE MANIPULATORS
Shi Shengxi and Zhou Mingde 17 Nov. 1994 16 p Transl. into ENGLISH from Kongqidonglixue Xuebao, (China), v. 9, no. 3, Sep. 1991 p 367-371 Limited Reproducibility: More than 20% of this document may be affected by microfiche quality
(AD-A289601; NAIC-ID(RS)T-0918-92) Avail: Issuing Activity (Defense Technical Information Center (DTIC))

This article reviews the course of the development of research relating to flat plate type turbulence control devices or plate manipulators. It sets up, on the foundation of our own flow visualizations or displays, a proposal for a new drag reduction mechanism. It refines designs, and, in conjunction with that, achieves relatively good drag reduction results. DTIC

N95-26735*# MCAT Inst., San Jose, CA.
NUMERICAL SIMULATION OF THE FLOW ABOUT THE F-18 HARV AT HIGH ANGLE OF ATTACK Final Report
Scott M. Murman Feb. 1995 36 p Original contains color illustrations
(Contract NCC2-729)
(NASA-CR-197755; NAS 1.26:197755; MCAT-95-13) Avail: CASI HC A03/MF A01; 2 functional color pages

This research has been aimed at validating numerical methods for computing the flow about the complete F-18 HARV at alpha = 30 deg and alpha = 45 deg. At 30 deg angle of attack, the flow about the F-18 is dominated by the formation, and subsequent breakdown, of strong vortices over the wing leading-edge extensions (LEX). As the angle of attack is increased to alpha = 45 deg, the fuselage forebody of the F-18 contains significant laminar and transitional regions which are not present at alpha = 30 deg. Further, the flow over the LEX at alpha = 45 deg is dominated by an unsteady shedding in time, rather than strong coherent vortices. This complex physics, combined with the complex geometry of a full-aircraft configuration, provides a challenge for current computational fluid dynamics (CFD) techniques. The following sections present the numerical method and grid generation scheme that was used, a review of prior research done to numerically model the F-18 HARV, and a discussion of the current research. The current research is broken into three main topics; the effect of engine-inlet mass-flow rate on the F-18 vortex breakdown position, the results using a refined F-18 computational model to compute the flow at alpha = 30 deg and alpha = 45 deg, and research done using the simplified geometry of an ogive-cylinder configuration to investigate the physics of unsteady shear-layer shedding. The last section briefly summarizes the discussion. Derived from text

N95-26740# Tokyo Univ., Sagamihara (Japan). Inst. of Space and Astronautical Science.
WIND TUNNEL EXPERIMENTS ON WAKE FLOW FIELD BEHIND A REENTRY CAPSULE FROM A VIEWPOINT OF PARACHUTE DEPLOYMENT AT SUPERSONIC SPEEDS
Kojiro Suzuki and Takashi Abe Dec. 1994 27 p Repr. from Institute of Space and Astronautical Science Report No. 655 (Sagamihara, Japan, Tokyo Univ.), Dec. 1994 p 1-24
(ISSN 0285-6808)
(ISAS-R-655) Avail: CASI HC A03/MF A01

The wake flow field behind the EXPRESS capsule at supersonic speeds is studied experimentally in the wind tunnel. The schlieren photographs and the measurements of the Pitot pressure and the static pressure in the wake clarify the structure of the wake flow field and the effects of the freestream Mach number on it. The wake structure is classified into two types, that is, the subsonic wake neck type and the supersonic wake neck type. The flow characteristics of each wake neck type are discussed. From a viewpoint of the parachute deployment, the effects of the freestream Mach number on the dynamic pressure in the wake are investigated. The recovery ratio of the dynamic pressure in the wake increases with the decrease in the Mach number. At lower Mach number, however, the recovery is delayed due to the extension of the recirculating region behind the capsule bottom. The numerical simulations of the wake flow field are carried out by solving the laminar Navier-Stokes equations and it is pointed out that the recovery of the flow velocity and the dynamic pressure may be enhanced significantly by the turbulent transition on the wake trail. Author

N95-26757 Notre Dame Univ., IN. Dept. of Aerospace and Mechanical Engineering.
EFFECTS OF THREE-DIMENSIONAL IMPOSED 3-D DISTURBANCES ON BLUFF-BODY NEAR WAKE FLOWS Final Report
Albin A. Szewczyk and Peter W. Bearman 1994 6 p Limited Reproducibility: More than 20% of this document may be affected by microfiche quality
(Contract N00014-90-J-4083)
(AD-A289553) Avail: Issuing Activity (Defense Technical Information Center (DTIC))

This experimental research effort focuses on the underlying three-dimensional flow structure in the near wake of a bluff body when subjected to imposed geometrical disturbances. To understand the effects of three dimensionality that are characterized by vortex splitting and looping and how they are related to other wake parameters such as base pressure shedding frequency, wake width and wake formation length. DTIC

N95-26760*# MCAT Inst., San Jose, CA.
DEVELOPMENT OF AN UPWIND, FINITE-VOLUME CODE WITH FINITE-RATE CHEMISTRY Final Report, 1 Aug. 1994 - 31 Jan. 1995
Gregory A. Molvik Jan. 1995 19 p Original contains color illustrations
(Contract NCC2-498)
(NASA-CR-197747; NAS 1.26:197747; MCAT-95-01) Avail: CASI HC A03/MF A01; 5 functional color pages

Under this grant, two numerical algorithms were developed to predict the flow of viscous, hypersonic, chemically reacting gases over three-dimensional bodies. Both algorithms take advantage of the benefits of upwind differencing, total variation diminishing techniques and of a finite-volume framework, but obtain their solution in two separate manners. The first algorithm is a zonal, time-marching scheme, and is generally used to obtain solutions in the subsonic portions of the flow field. The second algorithm is a much less expensive, space-marching scheme and can be used for the computation of the larger, supersonic portion of the flow field. Both codes compute their interface fluxes with a temporal Riemann solver and the resulting schemes are made fully implicit including the chemical source terms and boundary conditions. Strong coupling is used between the fluid dynamic, chemical and turbulence equations. These codes have been validated on numerous hypersonic test cases and have provided excellent comparison with existing data. This report summarizes the research that took place from August 1,1994 to January 1, 1995. Author

N95-26854 Aeronautical Systems Div., Eglin AFB, FL.
USER DOCUMENTATION OF THE CTA PROGRAM Final Report, Sep. - Nov. 1994
Greg Wilder Nov. 1994 50 p Limited Reproducibility: More than 20% of this document may be affected by microfiche quality
(AD-A289508; ASC-TR-94-1022) Avail: Issuing Activity (Defense Technical Information Center (DTIC))

This report is a user's manual for the CTA program. CTA is a FORTRAN program which converts Cartesian aero-angle aerodynamic coefficients, as generated by the Missile DATCOM aerodynamic prediction code, to polar aeroballistic angle coefficients. The output format of the aeroballistic coefficients matches the format used in the CADAC 6 DOF flyout simulation. DTIC

N95-26859 Air Force Systems Command, Wright-Patterson AFB, OH. National Air Intelligence Center.
A NUMERICAL METHOD FOR UNSTEADY TRANSONIC FLOW ABOUT WINGS WITH CONTROL SURFACES
Tao Yu and Jianbai Zhang 15 Dec. 1994 17 p Transl. into ENGLISH from Kongqidonglixue Xuebao (China), v. 9, no. 3, Sep. 1991 p 338-343 Limited Reproducibility: More than 20% of this document may be affected by microfiche quality
(AD-A289631; NAIC-ID(RS)T-0920-92) Avail: Issuing Activity (Defense Technical Information Center (DTIC))

This article introduces a type of finite difference calculation method for unsteady transonic speed flows associated with wings having control surfaces. The equations which are chosen for use are modified three dimensional nonsteady transonic speed small perturbation geopotential equations. Use is made of time integration methods. Solution forms are approximate factor type resolutions of alternating direction implicit (ADI) type forms. Use is made of this type of method to calculate the unsteady aerodynamic forces associated with F-5 wings in oncoming flows with Mach numbers of 0.9 and 0.925 as well as the unsteady aerodynamic forces associated with control surface oscillations. Comparisons were carried out of calculation results with NLR test results from outside of China and calculation results from XTRAN3S methods. This clearly showed that calculations were successful. DTIC

N95-26875 Air Force Inst. of Tech., Wright-Patterson AFB, OH.

A NEW DRAG MEASUREMENT SYSTEM FOR WIND TUNNEL TESTING OF THE RACING BICYCLE AND RIDER TO DETERMINE A LOW DRAG CONFIGURATION M.S. Thesis

Brian A. Parker Dec. 1994 92 p Limited Reproducibility: More than 20% of this document may be affected by microfiche quality
(AD-A289375; AFIT/GAE/ENY/94D-17) Avail: Issuing Activity (Defense Technical Information Center (DTIC))

This study investigated the application of splitter plate effects to reduce the aerodynamic drag of the racing bicycle and rider system. A sensitive, low-force, beam-type, single-component balance was developed to provide drag measurements accurate to within 0.053 N (0.012 lbf). The performance of the new system was verified by comparing the measured drag on a three-dimensioaal, right-circular cylinder model, 0.127 m (5.0 in) in diameter and 0.610 m (24 in) long, with the results from a commercial balance and a other similar data. The bicycle and rider model consisted of a full-scale mannequin comprising only the hips, legs and feet, mounted on a regulation 0.48 m (19 in) size bicycle. Rotation of the wheels and a stationary ground plane were also simulated. Two frame configurations in conjunction with a disk type wheel were tested to determined the lowest drag configuration for narrow and wide spacing of the rider's legs. The results show that for the standard tube construction frame, the conventional wisdom to streamline as much as possible prevails. When an aerodynamic frame was tested, the overall drag was reduced. Although the standard spacing still provided the lowest drag configuration, any further streamlining showed an increase in drag. DTIC

N95-26901 Air Force Inst. of Tech., Wright-Patterson AFB, OH. School of Engineering.

PERFORMANCE CHARACTERIZATION OF A HIGHLY-OFFSET DIFFUSER WITH AND WITHOUT BLOWING VORTEX GENERATOR JETS M.S. Thesis

Michael B. Senseney Dec. 1994 191 p Limited Reproducibility: More than 20% of this document may be affected by microfiche quality
(AD-A289334; AFIT/GAE/ENY/94D-14) Avail: Issuing Activity (Defense Technical Information Center (DTIC))

The effect of blowing vortex generator jets (VGJ's) on the performance of a highly-offset (s-duct) diffuser was investigated experimentally. VGJ's are pitched, skewed jets which generate streamwise vortices as well as injecting high-momentum fluid into the boundary layer. Diffuser performance with and without VGJ's was measured for an inlet Mach number of 0.6 (Re/x = l.27e7 per cm). Pitot static and hot-film instrumentation was used to measure flow properties at the diffuser inlet and exit planes. Without blowing, the flow on the lower surface of the diffuser was massively separated. Blowing at 0.48% mass flow ratio through three lower-surface VGJ's reduced the size of the separated flow region, reduced the thickness of the boundary layer at the exit plane, increased pressure recovery by 1.3%, and increased the static pressure rise achieved in the diffuser by over 50%. Turbulence intensity, turbulent shear stress, and turbulent kinetic energy were reduced as well. Distortion of the exit plane flowfield increased with blowing. DTIC

N95-27248*# Overset Methods, Inc., Los Altos, CA.

GLOBAL FLOWFIELD ABOUT THE V-22 TILTROTOR AIRCRAFT Progress Report

Robert L. Meakin 23 Mar. 1995 18 p Submitted for publication
(Contract NCC2-747)
(NASA-CR-198603; NAS 1.26:198603; OMI-01-92) Avail: CASI HC A03/MF A01

The Chimera overset grid method is reviewed and discussed in the context of a method of solution and analysis of unsteady three-dimensional viscous flows. The state of maturity of the various pieces of support software required to use the approach is discussed. A variety of recent applications of the method is presented. Current limitations of the approach are identified. Author

N95-27258*# National Aeronautics and Space Administration. Ames Research Center, Moffett Field, CA.

CALCULATION OF THREE-DIMENSIONAL (3-D) INTERNAL FLOW BY MEANS OF THE VELOCITY-VORTICITY FORMULATION ON A STAGGERED GRID

Paul M. Stremel May 1995 35 p
(RTOP 505-59-36)
(NASA-TM-110352; A-950063; NAS 1.15:110352) Avail: CASI HC A03/MF A01

A method has been developed to accurately compute the viscous flow in three-dimensional (3-D) enclosures. This method is the 3-D extension of a two-dimensional (2-D) method developed for the calculation of flow over airfoils. The 2-D method has been tested extensively and has been shown to accurately reproduce experimental results. As in the 2-D method, the 3-D method provides for the non-iterative solution of the incompressible Navier-Stokes equations by means of a fully coupled implicit technique. The solution is calculated on a body fitted computational mesh incorporating a staggered grid methodology. In the staggered grid method, the three components of vorticity are defined at the centers of the computational cell sides, while the velocity components are defined as normal vectors at the centers of the computational cell faces. The staggered grid orientation provides for the accurate definition of the vorticity components at the vorticity locations, the divergence of vorticity at the mesh cell nodes and the conservation of mass at the mesh cell centers. The solution is obtained by utilizing a fractional step solution technique in the three coordinate directions. The boundary conditions for the vorticity and velocity are calculated implicitly as part of the solution. The method provides for the non-iterative solution of the flow field and satisfies the conservation of mass and divergence of vorticity to machine zero at each time step. To test the method, the calculation of simple driven cavity flows have been computed. The driven cavity flow is defined as the flow in an enclosure driven by a moving upper plate at the top of the enclosure. To demonstrate the ability of the method to predict the flow in arbitrary cavities, results will he shown for both cubic and curved cavities. Author

N95-27541# National Renewable Energy Lab., Golden, CO.

WIND-TUNNEL TEST OF THE S814 THICK ROOT AIRFOIL

D. M. Somers (Airfoils, Inc., State College, PA.) and J. L. Tangler Jan. 1995 7 p Presented at the 1995 American Society of Mechanical Engineers (ASME) Energy Sources Technology Conference and Exhibition, Houston, TX, 29 Jan. - 1 Feb. 1995
(Contract DE-AC36-83CH-10093)
(DE95-000268; NREL/TP-442-7388; CONF-950116-7) Avail: CASI HC A02/MF A01

The objective of this wind-tunnel test was to verify the predictions of the Eppler Airfoil Design and Analysis Code for a very thick airfoil having a high maximum lift coefficient c(sub L,max) designed to be largely insensitive to leading edge roughness effects. The 24-percent-thick S814 airfoil was designed with these characteristics to accommodate aerodynamic and structural considerations for the root region of a wind-turbine blade. In addition, the airfoil's maximum lift-to-drag ratio was designed to occur it a high lift coefficient. To accomplish the objective, a two-dimensional wind-tunnel test of the S814 thick root airfoil was conducted in January 1994 in the low-turbulence wind tunnel of the Delft University of Technology Low Speed Laboratory. Data were obtained for transition-free and transition-fixed conditions at Reynolds numbers of 0.7, 1.0, 1.5, 2.0, and 3.0 x 10(exp 6). For the design Reynolds numbers of 1.5 x 10(exp 6), the transition-free c(sub L,max) is 1.3 which satisfies the design specification. However, this value is significantly lower than the predicted c(sub L,max) of almost 1.6. With transition-fixed at the is 1.2. The difference in c(sub L,max) between the transition-free and transition-fixed conditions demonstrates the airfoil's minimal sensitivity to roughness effects. The

S814 root airfoil was designed to complement existing NREL low c(sub L,max) tip-region airfoils for rotor blades 10 to 15 meters in length. DOE

N95-28003*# Clemson Univ., SC. Dept. of Mechanical Engineering.
A GENERAL THEORY OF TWO- AND THREE-DIMENSIONAL ROTATIONAL FLOW IN SUBSONIC AND TRANSONIC TURBOMACHINES Final Report
Chung-Hua Wu May 1993 241 p
(Grant NAG3-1072; RTOP 505-90-21; RTOP 335-05-01)
(NASA-CR-4496; E-7267; NAS 1.26:4496) Avail: CASI HC A11/MF A03

This report represents a general theory applicable to axial, radial, and mixed flow turbomachines operating at subsonic and supersonic speeds with a finite number of blades of finite thickness. References reflect the evolution of computational methods used, from the inception of the theory in the 50's to the high-speed computer era of the 90's. Two kinds of relative stream surfaces, S(sub 1) and S(sub 2), are introduced for the purpose of obtaining a three-dimensional flow solution through the combination of two-dimensional flow solutions. Nonorthogonal curvilinear coordinates are used for the governing equations. Methods of computing transonic flow along S(sub 1) and S(sub 2) stream surfaces are given for special cases as well as for fully three-dimensional transonic flows. Procedures pertaining to the direct solutions and inverse solutions are presented. Information on shock wave locations and shapes needed for computations are discussed. Experimental data from a Deutsche Forschungs- und Versuchsanstalt fur Luft- und Raumfahrt e.V. (DFVLR) rotor and from a Chinese Academy of Sciences (CAS) transonic compressor rotor are compared with the computed flow properties. Author (revised)

N95-28193*# Virginia Polytechnic Inst., Blacksburg, VA. Dept. of Aerospace and Ocean Engineering.
FLOW STRUCTURE GENERATED BY PERPENDICULAR BLADE VORTEX INTERACTION AND IMPLICATIONS FOR HELICOPTER NOISE PREDICTIONS Semiannual Report
William J. Devenport and Stewart A. L. Glegg (Florida Atlantic Univ., Boca Raton, FL.) Apr. 1995 53 p Original contains color illustrations
(Grant NAG1-1539)
(NASA-CR-198590; NAS 1.26:198590) Avail: CASI HC A04/MF A01; 15 functional color pages

This report summarizes accomplishments and progress for the period ending April 1995. Much of the work during this period has concentrated on preparation for an analysis of data produced by an extensive wind tunnel test. Time has also been spent further developing an empirical theory to account for the effects of blade-vortex interaction upon the circulation distribution of the vortex and on preliminary measurements aimed at controlling the vortex core size. Derived from text

N95-28230*# Boeing Military Airplane Development, Seattle, WA.
TranAir: A FULL-POTENTIAL, SOLUTION-ADAPTIVE, RECTANGULAR GRID CODE FOR PREDICTING SUBSONIC, TRANSONIC, AND SUPERSONIC FLOWS ABOUT ARBITRARY CONFIGURATIONS. USER'S MANUAL
F. T. Johnson, S. S. Samant, M. B. Bieterman, R. G. Melvin, D. P. Young, J. E. Bussoletti, and C. L. Hilmes Dec. 1992 198 p
(Contract NAS2-12513; RTOP 505-61-21)
(NASA-CR-4349; A-90092; NAS 1.26:4349) Avail: CASI HC A09/MF A03

The TranAir computer program calculates transonic flow about arbitrary configurations at subsonic, transonic, and supersonic freestream Mach numbers. TranAir solves the nonlinear full potential equations subject to a variety of boundary conditions modeling wakes, inlets, exhausts, porous walls, and impermeable surfaces. Regions with different total temperature and pressure can be represented. The user's manual describes how to run the TranAir program and its graphical support programs. Author

N95-28241*# National Aeronautics and Space Administration. Langley Research Center, Hampton, VA.
MEASUREMENTS OF STORE FORCES AND MOMENTS AND CAVITY PRESSURES FOR A GENERIC STORE IN AND NEAR A BOX CAVITY AT SUBSONIC AND TRANSONIC SPEEDS
Robert L. Stallings, Jr. (Lockheed Engineering and Sciences Co., Hampton, VA.), E. B. Plentovich, M. B. Tracy, and Michael J. Hemsch (Lockheed Engineering and Sciences Co., Hampton, VA.) May 1995 178 p
(RTOP 505-68-70-09)
(NASA-TM-4611; L-17388; NAS 1.15:4611) Avail: CASI HC A09/MF A02

An experimental force and moment study was conducted in the Langley 8-Foot Transonic Pressure Tunnel for a generic store in and near rectangular box cavities contained in a flat-plate configuration at subsonic and transonic speeds. Surface pressures were measured inside the cavities and on the flat plate. The length-to-height ratios were 5.42, 6.25, 10.83, and 12.50. The corresponding width-to-height ratios were 2.00, 2.00, 4.00, and 4.00. The free-stream Mach number range was from 0.20 to 0.95. Surface pressure measurements inside the cavities indicated that the flow fields for the shallow cavities were either closed or transitional near the transitional/closed boundary. For the deep cavities, the flow fields were either open or near the open/transitional boundary. The presence of the store did not change the type of flow field and had only small effects on the pressure distributions. For transitional or open transitional flow fields, increasing the free-stream Mach number resulted in large reductions in pitching-moment coefficient. Values of pitching-moment coefficient were always much greater for closed flow fields than for open flow fields. Author

N95-28265*# Boeing Military Airplane Development, Seattle, WA.
TranAir: A FULL-POTENTIAL, SOLUTION-ADAPTIVE, RECTANGULAR GRID CODE FOR PREDICTING SUBSONIC, TRANSONIC, AND SUPERSONIC FLOWS ABOUT ARBITRARY CONFIGURATIONS. THEORY DOCUMENT
F. T. Johnson, S. S. Samant, M. B. Bieterman, R. G. Melvin, D. P. Young, J. E. Bussoletti, and C. L. Hilmes Dec. 1992 252 p
(Contract NAS2-12513; RTOP 505-61-21)
(NASA-CR-4348; A-90093; NAS 1.26:4348) Avail: CASI HC A12/MF A03

A new computer program, called TranAir, for analyzing complex configurations in transonic flow (with subsonic or supersonic freestream) was developed. This program provides accurate and efficient simulations of nonlinear aerodynamic flows about arbitrary geometries with the ease and flexibility of a typical panel method program. The numerical method implemented in TranAir is described. The method solves the full potential equation subject to a set of general boundary conditions and can handle regions with differing total pressure and temperature. The boundary value problem is discretized using the finite element method on a locally refined rectangular grid. The grid is automatically constructed by the code and is superimposed on the boundary described by networks of panels; thus no surface fitted grid generation is required. The nonlinear discrete system arising from the finite element method is solved using a preconditioned Krylov subspace method embedded in an inexact Newton method. The solution is obtained on a sequence of successively refined grids which are either constructed adaptively based on estimated solution errors or are predetermined based on user inputs. Many results obtained by using TranAir to analyze aerodynamic configurations are presented. Author

N95-28331 Naval Postgraduate School, Monterey, CA.
CONSTRUCTION AND WIND TUNNEL TEST OF A 1/12TH SCALE HELICOPTER MODEL Master's Thesis
Michael A. Capasso Sep. 1994 82 p Limited Reproducibility: More than 20% of this document may be affected by microfiche quality
(AD-A288487) Avail: Issuing Activity (Defense Technical Information Center (DTIC))

This thesis reports on the construction of a 1/12th scale model of the award winning Arapaho attack helicopter design and wind tunnel test to determine both the model and full scale equivalent flat plate area. Tests were conducted for lg level flight and included yawed flight conditions up to 10 degrees. The significance of equivalent flat plate area for helicopters is that it is the principal parameter that establishes rotor propulsive force requirements. The Model was constructed from the original design submitted by the 1993 NPS Helicopter Design Team and is 47.5 inches long with a 48-inch main rotor diameter. The model was tested in the NPS Low Speed Wind Tunnel to measure the drag force on the main body of the model at wind tunnel velocities up to 72 knots. Drag force on the model was also measured with the rotor head and longbow radome installed, and at various yaw angles up to 10 degrees. The equivalent flat plate area was then calculated from these measurements and compared to other helicopters. Recommendations for further wind tunnel testing were made. DTIC

N95-28669*# National Aeronautics and Space Administration. Langley Research Center, Hampton, VA.
STUDY OF POTENTIAL AERODYNAMIC BENEFITS FROM SPANWISE BLOWING AT WINGTIP Ph.D. Thesis - George Washington Univ., 1992
Raymond E. Mineck Jun. 1995 102 p
(RTOP 505-59-10-30)
(NASA-TP-3515; L-17368; NAS 1.60:3515) Avail: CASI HC A06/MF A02

Comprehensive experimental and analytical studies have been conducted to assess the potential aerodynamic benefits from spanwise blowing at the tip of a moderate-aspect-ratio swept wing. Previous studies on low-aspect-ratio wings indicated that blowing from the wingtip can diffuse the tip vortex and displace it outward. The diffused and displaced vortex will induce a smaller downwash at the wing, and consequently the wing will have increased lift and decreased induced drag at a given angle of attack. Results from the present investigation indicated that blowing from jets with a short chord had little effect on lift or drag, but blowing from jets with a longer chord increased lift near the tip and reduced drag at low Mach numbers. A Navier-Stokes solver with modified boundary conditions at the tip was used to extrapolate the results to a Mach number of 0.72. Calculations indicated that lift and drag increase with increasing jet momentum coefficient. Because the momentum of the jet is typically greater than the reduction in the wing drag and the increase in the wing lift due to spanwise blowing is small, spanwise blowing at the wingtip does not appear to be a practical means of improving the aerodynamic efficiency of moderate-aspectratio swept wings at high subsonic Mach numbers.
Author

N95-28674*# National Aeronautics and Space Administration. Langley Research Center, Hampton, VA.
NUMERICAL STUDY TO ASSESS SULFUR HEXAFLUORIDE AS A MEDIUM FOR TESTING MULTIELEMENT AIRFOILS
Daryl L. Bonhaus, W. Kyle Anderson, and Dimitri J. Mavriplis (Institute for Computer Applications in Science and Engineering, Hampton, VA.) Jun. 1995 31 p
(RTOP 505-59-53-01)
(NASA-TP-3496; L-17401; NAS 1.60:3496) Avail: CASI HC A03/MF A01

A methodology is described for computing viscous flows of air and sulfur hexafluoride (SF6). The basis is an existing flow solver that calculates turbulent flows in two dimensions on unstructured triangular meshes. The solver has been modified to incorporate the thermodynamic model for SF6 and used to calculate the viscous flow over two multielement airfoils that have been tested in a wind tunnel with air as the test medium. Flows of both air and SF6 at a free-stream Mach number of 0.2 and a Reynolds number of 9 x 10(exp 6) are computed for a range of angles of attack corresponding to the wind-tunnel test. The computations are used to investigate the suitability of SF6 as a test medium in wind tunnels and are a follow-on to previous computations for single-element airfoils. Surface-pressure, lift, and drag coefficients are compared with experimental data. The effects of heavy gas on the details of the flow are investigated based on computed boundary-layer and skin-friction data. In general, the predictions in SF6 vary little from those in air. Within the limitations of the computational method, the results presented are sufficiently encouraging to warrant further experiments. Author

N95-26946# Wichita State Univ., Wichita, KS.
CREATING AN ALTERNATIVE PARAMETER OPTIMIZATION METHOD (APO) Abstract Only
William C. Forrest *In its* AIAA Techfest 20 Proceedings 1994 8 p (For primary document see N95-26941 09-01)
Avail: CASI HC A02/MF A03

N95-26953# Wichita State Univ., Wichita, KS. Dept. of Aerospace Engineering.
THE NEAR-WAKE FLOW BEHAVIOR OF AN OSCILLATING AIRFOIL WITH MODIFIED TRAILING EDGE
Roy Y. Myose and Jiro Iwata *In its* AIAA Techfest 20 Proceedings 1994 12 p (For primary document see N95-26941 09-01)
Avail: CASI HC A03/MF A03

N95-26955# Wichita State Univ., Wichita, KS.
AN EXPERIMENTAL INVESTIGATION OF HELICOPTER DOWNWASH AND TAILBOOM INTERACTION AT THE WICHITA STATE UNIVERSITY 7X10 FOOT WIND TUNNEL
Scot Kruse, James E. Leigh, Kevin A. Moore, and Scott Randle *In its* AIAA Techfest 20 Proceedings 1994 12 p (For primary document see N95-26941 09-01)
Avail: CASI HC A03/MF A03

N95-27974*# Rockwell International Corp., Golden, CO. Wind Energy Research Center.
HORIZONTAL AXIS WIND TURBINE POST STALL AIRFOIL CHARACTERISTICS SYNTHESIZATION
James L. Tangler and Cyrus Ostowari (Texas A&M Univ., College Station, TX.) *In* DASCON Engineering, Collected Papers on Wind Turbine Technology May 1995 p 35-39 (For primary document see N95-27970 09-44)
(Contract DE-AC04-76DP-03533)
Avail: CASI HC A01/MF A03

N95-27975*# Oregon State Univ., Corvallis, OR.
PRELIMINARY ANALYSIS OF DYNAMIC STALL EFFECTS ON A 91-METER WIND TURBINE ROTOR
Robert E. Wilson *In* DASCON Engineering, Collected Papers on Wind Turbine Technology May 1995 p 41-46 (For primary document see N95-27970 09-44)
Avail: CASI HC A02/MF A03

N95-27976*# Wichita State Univ., Wichita, KS.
COMPARATIVE WIND TUNNEL TESTS OF NACA 23024 AIRFOILS WITH SEVERAL AILERON AND SPOILER CONFIGURATIONS
W. H. Wentz, Jr. and M. H. Snyder *In* DASCON Engineering, Collected Papers on Wind Turbine Technology May 1995 p 47-52 Presented at the DOE/NASA Workshop on Horizontal Axis Wind Turbine Technology, Cleveland, OH, 8-10 May 1994 (For primary document see N95-27970 09-44)
(Grant NsG-3277)
Avail: CASI HC A02/MF A03

N95-27977*# Ohio State Univ., Columbus, OH.
COMPARATIVE WIND TUNNEL TEST AT HIGH REYNOLDS NUMBERS OF NACA 64 621 AIRFOILS WITH TWO AILERON CONFIGURATIONS
G. M. Gregorek *In* DASCON Engineering, Collected Papers on Wind Turbine Technology May 1995 p 53-66 Presented at the DOE/NASA Workshop on Horizontal Axis Wind Turbine Technology, Cleveland, OH, 8-10 May 1984 (For primary document see N95-27970 09-44)
(Grant NAG3-330)
Avail: CASI HC A03/MF A03

N95-27978*# Boeing Aerospace Co., Seattle, WA.
COMPARATIVE PERFORMANCE TESTS ON THE Mod-2, 2.5-mW WIND TURBINE WITH AND WITHOUT VORTEX GENERATORS
G. E. Miller *In* DASCON Engineering, Collected Papers on Wind Turbine Technology May 1995 p 67-77 Presented at the DOE/NASA Workshop on Horizontal Axis Wind Turbine Technology, Cleveland, OH, 8-10 May 1984 (For primary document see N95-27970 09-44)
Avail: CASI HC A03/MF A03

N95-27981*# General Electric Co., Philadelphia, PA.
AEROELASTIC STABILITY OF WIND TURBINE BLADE/AILERON SYSTEMS
J. C. Strain and L. Mirandy (General Electric Co., Schenectady, NY.) *In* DASCON Engineering, Collected Papers on Wind Turbine Technology May 1995 p 99-114 (For primary document see N95-27970 09-44)
(Contract DEN3-153)
Avail: CASI HC A03/MF A03

03 AIR TRANSPORTATION AND SAFETY

Includes passenger and cargo air transport operations; and aircraft accidents.

For related information see also *16 Space Transportation* and *85 Urban Technology and Transportation.*

N95-26485 Federal Aviation Administration, Atlanta, GA. Technical Center.

THE 1994 UPDATED NATIONAL AIRSPACE SYSTEM PERFORMANCE ASSESSMENT FOR YEAR 2005

Douglas Baart and Anny Cheung Oct. 1994 31 p Limited Reproducibility: More than 20% of this document may be affected by microfiche quality

(AD-A288652; DOT/FAA/CT-TN94/41; FAA-AOR-100-94-009) Avail: Issuing Activity (Defense Technical Information Center (DTIC))

This report documents the evaluation of the National Airspace System (NAS) performance for year 2005. The National Airspace System Performance Analysis Capability (NASPAC) Simulation Modeling System (SMS) was used to simulate the future air traffic control (ATC) system. Airport airfield and technological improvements expected to be completed by year 2005 were included in this analysis. Future air traffic demand was based on the 1993 Terminal Area Forecasts (TAF). The study results indicate that most of the delay in the system for year 2005 is caused by airfield capacity limitations. Three-fourths of the delay is related to ground operations or ground manifestation of airspace congestion. About 45 percent of the total delay is related to ground operations or ground manifestation of airspace congestion. About 45 percent of the total delay is attributed to adverse weather. Airports that have no future airfield improvements planned show the highest delay estimates. DTIC

N95-26497 Lightning Technologies, Inc., Pittsfield, MA.

AIRCRAFT FUEL SYSTEM LIGHTNING PROTECTION DESIGN AND QUALIFICATION TEST PROCEDURES DEVELOPMENT Final Report

Keith E. Crouch Sep. 1994 193 p Limited Reproducibility: More than 20% of this document may be affected by microfiche quality

(Contract DTFA03-92-C-00003)

(AD-A288401; LT-94-1067; DOT/FAA/CT-94/74) Avail: Issuing Activity (Defense Technical Information Center (DTIC))

The Navy and the Air Force recognized the need for improved test procedures for evaluating the lightning protection design of aircraft fuel systems. Under their sponsorship, a program to develop adjustable, standard ignition sources which could be used to calibrate techniques for detecting ignition sources during lightning testing was established. The minimum ignition levels of voltage sparks and hot spots were established under the program before it was terminated due to funding problems. The present program under FAA sponsorship, is a continuation of the original program. The Standard Voltage Spark Ignition Source and the Standard Hot Spot Ignition Source were completed and documented. The most promising approach for developing a Standard Thermal Spark Ignition Source was determined and is presented. Photographic detection techniques were investigated and the limitations determined. The presence of light on a photographic film indicated the possibility of an ignition source but can not confirm the ignition probability (if any). Hydrogen mixtures appear to provide the ability to have adjustable ignition probabilities and low energy (low over-pressure) ignitions. DTIC

N95-26498# National Transportation Safety Board, Washington, DC.

AIRCRAFT ACCIDENT REPORT: CONTROLLED COLLISION WITH TERRAIN TRANSPORTES AEREOS EJECUTIVOS, S.A. (TAESA) LEARJET 25D, XA-BBA DULLES INTERNATIONAL AIRPORT CHANTILLY, VIRGINIA, JUNE 18, 1994

7 Mar. 1995 69 p

(NTSB/AAR-95/02; PB95-910402) Avail: CASI HC A04/MF A01

This report explains the accident involving the TAESA Learjet 25D that crashed near the threshold of runway 1R at Dulles International Airport, Chantilly, Virginia, on June 18, 1994. Safety issues in the report focused on weather at the airport, flightcrew training, qualifications, and performance, flightcrew fatigue, operations specifications, passenger seating, and the ground proximity warning system. Safety recommendations concerning some of these issues were made to the Federal Aviation Administration. Author

N95-26527 Diffracto Ltd., Windsor (Ontario).

CHARACTERIZATION OF CORROSION AND DEVELOPMENT OF A BREADBOARD OF A D SIGHT AIRCRAFT INSPECTION SYSTEM, PHASE 1 Final Report

F. Karpala and O. L. Hageniers Aug. 1994 369 p Sponsored by FAA Limited Reproducibility: More than 20% of this document may be affected by microfiche quality

(AD-A288347; DOT/FAA/CT-94/56) Avail: Issuing Activity (Defense Technical Information Center (DTIC))

This report presents Phase 1 results of a joint Project Arrangement between the FAA and Transport Canada Aviation for the development and testing of a nondestructive inspection (NDI) system for aircraft corrosion detection in fuselage lap joints. The process is based on D Sight, an optical technique developed by Diffracto Limited. This research project had the following major components: (1) identification of corrosion areas of concern; (2) collection of corrosion samples; (3) acceleration of specimen corrosion in the laboratory; (4) construction and testing of a breadboard inspection device; and (5) laboratory and field trials of the breadboard device. The outcome can be summarized as follows: (1) a library of aircraft corrosion samples has been established; (2) a corrosion process has been developed that matches in-service corrosion well, (3) a breadboard D Sight NDI system has been built and tested; and (4) a proposal for follow-on work has been completed. DTIC

N95-27186 DACCO SCI, Inc., Columbia, MD.

THE USE OF ELECTROCHEMISTRY AND ELLIPSOMETRY FOR IDENTIFYING AND EVALUATING CORROSION ON AIRCRAFT Monthly Report, 15 Sep. - 14 Oct. 1994

Chester M. Dacres 14 Oct. 1994 2 p Limited Reproducibility: More than 20% of this document may be affected by microfiche quality

(Contract F49620-94-C-0042)

(AD-A288536; AFOSR-94-0687TR) Avail: Issuing Activity (Defense Technical Information Center (DTIC))

The reporting for this period and the data from the feasibility study show that the signature from the corroding aircraft is repeatable. The first template design for the paint application was abandoned due to the conductive paint consistency. A more practical approach, using adhesive tape to lay the grid pattern, proved a better technique for paint application. Silver paint was added to the test, because it is lower than gold paint in cost and has better electrical conductivity than carbon paint. The conductivity of gold paint increases with cure temperature, which could adversely alter the coating integrity. A cure temperature of 50 C was established for all paints to maintain coating integrity. Last, using the AC Impedance technique, it was found that the two-electrode approach is ideally suited for in-situ real-time analysis of metal/coating systems. CASI

N95-27762*# National Aeronautics and Space Administration. Lewis Research Center, Cleveland, OH.

FURTHER INVESTIGATIONS OF ICING EFFECTS ON AN ADVANCED HIGH-LIFT MULTI-ELEMENT AIRFOIL

Dean Miller, Jaiwon Shin, David Sheldon, Abdollah Khodadoust (McDonnell-Douglas Aerospace, Long Beach, CA.), Peter Wilcox (McDonnell-Douglas Aerospace, Long Beach, CA.), and Tammy Langhals (NYMA, Inc., Brook Park, OH.) May 1995 19 p Presented at the Applied Aerodynamics Conference, San Diego, CA, 19-22 Jun. 1995; sponsored by AIAA

(Contract NAS3-27186; RTOP 505-68-10)

(NASA-TM-106947; E-9683; NAS 1.15:106947; AIAA Paper 95-1880)

Avail: CASI HC A03/MF A01

In 1993 an experimental effort was initiated to investigate the effect of ice accretions on an advanced high-lift, multi-element airfoil. This airfoil is representative of an advanced transport wing, and has a state-of-the-art three element high lift system. This experimental effort is part of a cooperative program between McDonnell Douglas Aerospace and the NASA Lewis Research Center. The goal of this program is to improve the current understanding of ice accretion characteristics on multi-element airfoils. One key objective of this program is to establish an experimental database of multi-element ice accretions using the NASA-Lewis Icing Research Tunnel (IRT). The first multi-element icing test in this cooperative effort was conducted in 1993. A second 'follow on' icing test was conducted in 1994, for the purpose of augmenting the multi-element ice accretion database obtained in 1993, and also for studying the effect of flap gap setting on ice accretions. This paper presents selected results from the 1994 multi-element icing test, and will emphasize the effect of angle-of-attack, and flap gap setting on multi-element ice accretions. Author

N95-27859*# National Aeronautics and Space Administration. John F. Kennedy Space Center, Cocoa Beach, FL.

A REVIEW OF FALCONRY AS A BIRD CONTROL TECHNIQUE WITH RECOMMENDATIONS FOR USE AT THE SHUTTLE LANDING FACILITY, JOHN F. KENNEDY SPACE CENTER, FLORIDA, USA

Vickie L. Larson (Bionetics Corp., Cocoa Beach, FL.), Sean P. Rowe (Bionetics Corp., Cocoa Beach, FL.), David R. Breininger (Bionetics Corp., Cocoa Beach, FL.), and Reuven Yosef (Archbold Biological Station, Lake Placid, FL.) Jun. 1994 47 p
(Contract NAS10-11624)
(NASA-TM-110142; NAS 1.15:110142) Avail: CASI HC A03/MF A01

Falconry has been proposed as a method of reducing the bird/aircraftstrike hazard, in addition to current bird control techniques, at the Shuttle Landing Facility (SLF), John F. Kennedy Space Center (KSC), Florida, U.S. Bird control programs using falconry have been employed at a number of military and commercial airfields in the U.S., Canada, and Europe. Most falconry programs have been discontinued. In most situations, falconry did not prove cost effective when compared to alternative bird control techniques. Available literature and documents, as well as several raptor specialists and military personnel, suggest that falconry may be useful only against certain problem species and when other bird control methods have been proven inadequate. Because many of the most commonly used falcons are protected species, acquisition of falcons will complicate their use in bird control programs. Many avian species found at the SLF are federally and state protected or of conservation concern, therefore, environmental impacts may also result from the use of falcons. Author

N95-27907# National Academy of Sciences - National Research Council, Washington, DC.

HIGH-STAKES AVIATION: US-JAPAN TECHNOLOGY LINKAGES IN TRANSPORT AIRCRAFT

National Academy Press 1994 152 p
(LC-94-65759; ISBN-0-309-05045-6) Copyright Avail: CASI HC A08/MF A02

The context, current status, and implications of U.S.-Japan relationship in the area of development and transfer of aircraft technology are examined. Future trends are evaluated. Policy recommendations to U.S. aircraft manufacturers, the Department of Defense, and NASA concerning the maintaining of U.S. leadership in aircraft manufacturing and aviation are formulated. CASI

N95-28454 Army Natick Research and Development Command, MA.

THE PERFORMANCE OF CARGO AIRDROP SYSTEMS USING G-12E PARACHUTES: STATISTICAL DETERMINATION OF MINIMUM ALTITUDE Final Report, Mar. 1993 - Nov. 1994

Steven E. Kunz Feb. 1995 42 p Limited Reproducibility: More than 20% of this document may be affected by microfiche quality
(AD-A291666; NATICK/TR-95/017) Avail: Issuing Activity (Defense Technical Information Center (DTIC))

In order to reduce the exposure of aircraft to hostile fire, the U.S. Air Force is interested in dropping cargo from the lowest possible altitude above ground level. Using trajectory data from previous airdrop system testing, this report statistically determines the minimum altitude above ground level (AOL) from which airdrop systems (comprising clusters of two to three G-12E parachutes) may safely deliver cargoes up to 5000 pounds. The methods used to compute variables of interest, such as system tension and system orientation, are presented. To support this statistical analysis, intervals were defined based upon clearly discernible events. This led to a reexamination of so-called functional phases, used by the airdrop community. Some phases were found unsuitable for statistical purposes. To resolve this problem, process intervals were defined based upon clearly discernible process states or events. Based upon the limited data available, it was found that G-12E airdrop systems can safely deliver cargoes of up to 5000 pounds when released from aircraft at an altitude of approximately 300 feet AGL. DTIC

N95-28630 Simula, Inc., Phoenix, AZ.

ROTORCRAFT CRASHWORTHY AIRFRAME AND FUEL SYSTEM TECHNOLOGY DEVELOPMENT PROGRAM Final Report

Joseph W. Coltman Oct. 1994 175 p Limited Reproducibility: More than 20% of this document may be affected by microfiche quality
(Contract DTFA03-84-R-40032)
(AD-A289986; TR-90425; DOT/FAA/CT-91/7) Avail: Issuing Activity (Defense Technical Information Center (DTIC))

A research program was initiated by the Federal Aviation Administration (FAA) Technical Center to investigate crash resistance design technology applicable to U.S. civil rotorcraft. The purpose of the program was to identify crash resistance design technology consistent with rotorcraft type, primary use, and the expected crash environments for civil helicopters. The program examined crash resistance technology for landing gear, fuselage structure, seating systems, and fuel systems. A trade-off study was conducted to identify an optimum level of crash resistance for three weight classes of civil rotorcraft. The results of the research program were a series of crash impact design and test criteria for civil rotorcraft, as well as an assessment of the weight penalties that would be incurred in meeting these criteria. The program was conducted by Simula Inc. with assistance from Bell Helicopter Textron Inc. and Sikorsky Aircraft. DTIC

04 AIRCRAFT COMMUNICATIONS AND NAVIGATION

Includes digital and voice communication with aircraft; air navigation systems (satellite and ground based); and air traffic control.

For related information see also *17 Space Communications, Spacecraft Communications, Command and Tracking* and *Communications and Radar.*

N95-26454 Mitre Corp., McLean, VA. Center for Advanced Aviation System Development.

AIR TRAFFIC OPERATIONAL INVENTORY CY 1994 Final Report

S. L. Rother Aug. 1994 248 p Supersedes MTR-90W00179 Limited Reproducibility: More than 20% of this document may be affected by microfiche quality
(Contract DTFA01-93-C-00001)
(AD-A288281; MTR-94W0000110; DOT/FAA/AT-94/1; MTR-90W00179)
Avail: Issuing Activity (Defense Technical Information Center (DTIC))

The Federal Aviation Administration's (FAA) air traffic control (ATC) services are provided by Air Route Control Centers (ARTCC's), Combined Center Radar Approach Controls (CERAP's), Terminal Radar Approach Control (TRACON) facilities, and Air Traffic Control Towers (ATCT's). TRACON's are subdivided into Metroplex Control Facilities (MCF's) and standalone facilities. The modernization of these facilities will be based upon operational and economic considerations. This report serves as an inventory reference document for high level operational facility planning and requirements' development. The report presents a current and projected pictorial description of ATC facilities arranged by ARTCC geographic boundaries. All FAA and Department of Defense (DOD) radar facilities and their associated control towers are included. Included is information on radar connectivities, automation equipment, tower display systems, radar operational positions, and air traffic staffing. DTIC

N95-26585# National Aerospace Lab., Tokyo (Japan). Flight Research Div.

FLIGHT EVALUATION OF GPS/DGPS SENSOR SYSTEMS INSTALLED IN NAL Do228

Kazutoshi Ishikawa, Takatsugu Ono, Masaaki Murata, Toshiaki Tsujii, Hitoshi Mineno (National Space Development Agency, Tokyo, Japan.), and Shuichi Matsumoto (National Space Development Agency, Tokyo, Japan.) Mar. 1994 87 p In JAPANESE
(ISSN 0389-4010)
(NAL-TR-1230) Avail: CASI HC A05/MF A01

Navigation systems have been tested with a Dornier 228-200 (Do228), experimental research airplane of the National Aerospace Laboratory (NAL) at Sendai airport, Japan. A C/A code single channel Global Positioning System (GPS) receiver (Rockwell/Collins Navcore 1) was installed in the Do228. The receiver can operate in real-time differential GPS (DGPS) during differential corrections coming from a GPS base station operated at a known position. The base station will track up to four visible satellites and measure the error in pseduo-range to each tracked satellite, based on broadcast emphemeris data and known position. A laser tracker was used to determine a reference trajectory of the airplane. Navigation accuracy of the onboard receiver is evaluated by direct comparison between reference trajectories and sensor outputs. Position accuracies of the GPS receiver are determined by pseudo-range errors between satellites and receiver. These ranging errors include common errors and receiver's specific residual errors. For all GPS receivers located within 200 kilometers of each other, common errors include satellite clock error, ephemeris error, refraction (ionospheric/tropospheric delay) and selective availability (SA) error. This paper describes GPS/DGPS accuracies during approach and landing of the aircraft. All data in which GDOP is less than five are divided into three cases: (1) stand-alone navigation with SA, (2) differential navigation with SA and (3) stand alone navigation without SA tested on January 1991. Stand-alone navigation accuracy under no SA is 20 meters, that is because the receiver's specific errors are more than common errors. The effectiveness of DGPS under SA was demonstrated by flight experiments. Author

N95-26587*# National Aeronautics and Space Administration. Ames Research Center, Moffett Field, CA.
FLIGHTPATH SYNTHESIS AND HUD SCALING FOR V/STOL TERMINAL AREA OPERATIONS (Diskette)
Vernon K. Merrick and James A. Jeske Apr. 1995 46 p Diskette: 3.5-inch Mac diskette
(RTOP 505-59-36)
(NASA-TM-110348; A-950052; NAS 1.15:110348; NONP-NASA-DK-95-48301) Avail: CASI SET A05 (HC,DK)

A two circle horizontal flightpath synthesis algorithm for Vertical/Short Takeoff and Landing (V/STOL) terminal area operations is presented. This algorithm provides a flightpath that is tangential to the aircraft's velocity vector at the instant of flightpath select and has continuous curvature. The algorithm corrects deficiencies noted in tests conducted with the V/STOL Systems Research Aircraft (VSRA) using a single circle algorithm described in NASA TM 104027. In addition, a more general vertical flightpath synthesis algorithm is presented, aimed primarily at minimizing the rapid increase of pilot workload during the final phase of decelerating transition just prior to acquiring the station-keeping point. Finally, a new technique for lateral scaling of a V/STOL Head Up Display (HUD) is presented, aimed at minimizing the inevitable anomalies that such scaling produces. All the above named items have been tested in flight with the VSVR, and all have produced improvements. Author

N95-26898 Air Force Inst. of Tech., Wright-Patterson AFB, OH. School of Engineering.
ANALYSIS AND SIMULATION OF NARROWBAND GPS JAMMING USING DIGITAL EXCISION TEMPORAL FILTERING M.S. Thesis
Gerald L. Falen Dec. 1994 187 p Limited Reproducibility: More than 20% of this document may be affected by microfiche quality
(AD-A289328; AFIT/GE/ENG/94D-09) Avail: Issuing Activity (Defense Technical Information Center (DTIC))

The purpose of this thesis is to investigate the performance of the Digital Excision Temporal Filter (DETF) to reject narrowband jammers used against the Global Positioning System (GPS). The DETF takes the Fast Fourier Transform (FFT) of the GPS signal and excises any FFT bins that are above a preselected threshold level. Then the excised signal is Inverse Fourier Transformed and fed to the GPS receiver. Several jammer types are simulated including Continuous Wave (CW), Pulse CW, Swept CW, Narrowband Spot Noise, and Wideband Barrage Noise jammers. Cases are also simulated using all but the Wideband Barrage Noise jammer at one time. The DETF can effectively reject all of the types of jammers simulated except for the Wideband Barrage Noise jammer. The DETF degrades the GPS system performance in the presence of the Wideband Barrage Noise jammer. In an actual DETF implementation, the excision threshold should be set from six to nine dB above the excision cutoff level, where the excision cutoff level is equal to the GPS signal strength plus receiver thermal noise level. DTIC

N95-26978 Federal Aviation Administration, Atlantic City, NJ.
THE CONTROLLER MEMORY GUIDE. CONCEPTS FROM THE FIELD
Earl S. Stein and Jim Bailey Sep. 1994 44 p Limited Reproducibility: More than 20% of this document may be affected by microfiche quality
(AD-A289263; DOT/FAA/CT-TN94/28) Avail: Issuing Activity (Defense Technical Information Center (DTIC))

Memory is an elusive human ability which both helps and hinders air traffic controllers' performance. This document was developed based on the ideas of controllers themselves when they were asked what they did to manage their memory resources. The guide is a job aide meant to help controllers think about what they do and about the little things they could use to help them reduce the possibilities for errors based on memory lapses. The material is presented in graphical cartoon format along with a very direct and minimalized text narrative. The goal was to provide the concepts in a readable format that controllers could review when they had the time. The issues covered in the guide all relate to memory in one way or another, but in many cases transcend memory issues alone, and look at the more basic issue of any person-machine system performance. Human and system performance are the bottom line in any complex command and control system such as air traffic control. DTIC

N95-26985 Air Force Inst. of Tech., Wright-Patterson AFB, OH. School of Engineering.
AN INTEGRATED GPS/INS/BARO AND RADAR ALTIMETER SYSTEM FOR AIRCRAFT PRECISION APPROACH LANDINGS M.S. Thesis
Robert A. Gray Dec. 1994 265 p Limited Reproducibility: More than 20% of this document may be affected by microfiche quality
(AD-A289280; AFIT/GE/ENG/94D-13) Avail: Issuing Activity (Defense Technical Information Center (DTIC))

Currently, the Department of Defense (DOD) and the commercial airline industry are utilizing the Instrument Landing System (ILS) during aircraft landings for precision approaches. The replacement system for the aging ILS was thought to he the Microwave Landing System (MLS). Instead, use of the Global Positioning System (GPS) is now thought to be a viable replacement for ILS precision approaches. The majority of current precision landing research has exploited 'stand-alone' GPS receiver techniques. This thesis instead explores the possibilities of using an extended Kalman filter (EKF) that integrates an Inertial Navigation System (INS), GPS, Barometric Altimeter, Pseudolite and Radar Altimeter for aircraft precision approaches. This thesis shows that integrating the INS, GPS, Barometric Altimeter and Radar Altimeter meets Federal Aviation Administration (FAA) requirements for a Category I precision approach and integrating the INS, GPS, Barometric Altimeter, Radar Altimeter and a single Pseudolite meets FAA requirements for a Category 2 precision approach. DTIC

N95-27903 Federal Aviation Administration, Atlanta, GA.
PRECISION LANDING SYSTEM MATHEMATICAL MODELING STUDY REPORT FOR ANDREWS AIR FORCE BASE, RUNWAY 19L, CAMP SPRINGS, MD Technical Note, Jun. - Jul. 1993
Jesse Jones, Elliott Rushton, and Ronald Lockhart Nov. 1994 129 p Limited Reproducibility: More than 20% of this document may be affected by microfiche quality
(AD-A289015; DOT/FAA/CT-TN93/35) Avail: Issuing Activity (Defense Technical Information Center (DTIC))

This technical note describes Microwave Landing System (MLS) and Precision Distance Equipment (DME/P) mathematical modeling performed for runway 19L, Andrews Air Force Base (ADW), Camp Springs, Maryland. This study evaluates the effects of scattering and shadowing from selected buildings, hangars, aircraft, and terrain. Results are provided as plots illustrating the predicted multipath levels, separation angles, and the resulting error plots from the worst case contributors. Scenarios were modeled to determine the effects of the multipath sources in the modeled environment. These resulting errors were analyzed and compared to error tolerance (FAA-STD-022d) to determine if the errors are acceptable. The effects of the ADW environment were analyzed and evaluated. It was determined that the proposed site will perform satisfactorily with no changes. DTIC

N95-28188*# Technion Research and Development Foundation Ltd., Haifa (Israel). Dept. of Projects Promotion and R and D Administration.
ADVANCED INTERACTIVE DISPLAY FORMATS FOR TERMINAL AREA TRAFFIC CONTROL Semiannual Progress Report, 1 Oct. 1994 - 31 Mar. 1995
Arthur J. Grunwald May 1995 38 p

(Contract NCCw-0045)
(NASA-CR-198576; NAS 1.26:198576) Avail: CASI HC A03/MF A01

The basic design considerations for perspective Air Traffic Control displays are described. A software framework has been developed for manual viewing parameter setting (MVPS) in preparation for continued, ongoing developments on automated viewing parameter setting (AVPS) schemes. The MVPS system is based on indirect manipulation of the viewing parameters. Requests for changes in viewing parameter setting are entered manually by the operator by moving viewing parameter manipulation pointers on the screen. The motion of these pointers, which are an integral part of the 3-D scene, is limited to the boundaries of screen. This arrangement has been chosen, in order to preserve the correspondence between the new and the old viewing parameter setting, a feature which contributes to preventing spatial disorientation of the operator. For all viewing operations, e.g. rotation, translation and ranging, the actual change is executed automatically by the system, through gradual transitions with an exponentially damped, sinusoidal velocity profile, in this work referred to as 'slewing' motions. The slewing functions, which eliminate discontinuities in the viewing parameter changes, are designed primarily for enhancing the operator's impression that he, or she, is dealing with an actually existing physical system, rather than an abstract computer generated scene. Current, ongoing efforts deal with the development of automated viewing parameter setting schemes. These schemes employ an optimization strategy, aimed at identifying the best possible vantage point, from which the Air Traffic Control scene can be viewed, for a given traffic situation. Author

N95-28540# Federal Aviation Administration, Washington, DC. Office of Aviation Medicine.

DEVELOPMENT OF A CODING FORM FOR APPROACH CONTROL/PILOT VOICE COMMUNICATIONS Final Report

O. V. Prinzo, T. W. Britton, and A. M. Hendrix (Hendrix, Alfred M., Carrizozo, NM.) May 1995 31 p
(Contract DTFA02-91-C-91089)
(DOT/FAA/AM-95/15) Avail: CASI HC A03/MF A01

The Aviation Topics Speech Acts Taxonomy (ATSAT) is a tool for categorizing pilot/controller communications according to their purpose and for classifying communication errors. Air traffic controller communications that deviate from FAA Air Traffic Control Order 7110.65, and pilot communications that depart from the suggested communication in the Airman's Information Manual can be identified and labeled using the error codes provided in the ATSAT. By using the same procedures and tool to analyze communications, direct comparisons can be made between controller phraseology usage in the field and during simulation. Results of a preliminary study to measure inter-coder agreement revealed that novice coders were more dependent on the surface characteristics of the verbatim transcripts and experts relied more on domain specific background knowledge and experience with ATC phraseology to code ATC communications. If a researcher elects to use the ATSAT, we recommend that all coders receive the same orientation and instruction sessions prior to using it. Author

N95-27791*# Lockheed Martin Corp., Denver, CO. Management and Data Systems.

DETERMINING GPS AVERAGE PERFORMANCE METRICS Abstract Only

G. V. Moore *In* NASA. Goddard Space Flight Center, Flight Mechanics/Estimation Theory Symposium 1995 May 1995 p 307 (For primary document see N95-27763 09-13)
Avail: CASI HC A01/MF A04

05 AIRCRAFT DESIGN, TESTING AND PERFORMANCE

Includes aircraft simulation technology.

For related information see also *18 Spacecraft Design, Testing and Performance* and *39 Structural Mechanics.*For land transportation vehicles see *85 Urban Technology and Transportation.*

N95-26389 Defence Science and Technology Organisation, Melbourne (Australia). Aeronautical and Maritime Research Lab.

F/A-18 IFOSTP FATIGUE TEST AIRBAG LOAD DETERMINATION ON THE VERTICAL AND HORIZONTAL TAILS

M. F. Lee Jan. 1995 54 p
(DSTO-TR-0135; AR-009-193) Copyright Avail: Issuing Activity (DSTO, Melbourne Victoria, Australia)

A simplistic method for determining discrete loads to approximate a distributed load is shown to have a number of deficiencies, both theoretically and in its practical results. A new method which utilizes Lagrange multipliers is derived and applied to an aerodynamic pressure distribution with improved results. The concept of weighting functions is introduced as a means of comparing the different methods in absolute terms. Weighting functions are also used to assess the effect of removing a load actuator from the standard configuration. Author

N95-26481 Air Force Inst. of Tech., Wright-Patterson AFB, OH.

DEVELOPMENT OF A NONLINEAR SIMULATION FOR THE MCDONNELL DOUGLAS F-15 EAGLE WITH A LONGITUDINAL TECS CONTROL-LAW M.S. Thesis - Washington Univ.

James P. Dutton, Jr. Sep. 1994 158 p Limited Reproducibility: More than 20% of this document may be affected by microfiche quality
(AD-A288610; AFIT/CI/CIA/94-136) Avail: Issuing Activity (Defense Technical Information Center (DTIC))

The purpose of this report is to develop using SIMULINK an aircraft simulation that couples the nonlinear equations of motion with the nonlinear aerodynamic and engine performance data. The simulation has been designed using data from actual flight testing of the McDonnell Douglas E-15 Eagle. The ultimate objective is to provide a generic framework for the development of nonlinear simulations of other aircraft with minimal required changes. Design of a longitudinal autopilot using the Total Energy Control System (TECS) concept is accomplished using the linearized model and later validated with the nonlinear model. The model characteristics and the relevant support modules for the F-15 described in are summarized. The numerical data were provided in the format of a Genesis simulation used at Wright-Patterson and the coding was subsequently converted from FORTRAN to MATLAB. A detailed description of the model is in Chapter 2. The evaluation of the open-loop nonlinear model and the design of the TECS control law will be accomplished at the two flight points. Other flight conditions throughout the flight envelope will also be investigated. DTIC

N95-26507 Department of the Navy, Washington, DC.

SUPPRESSOR OF OSCILLATIONS IN AIRFRAME CAVITIES Patent

Robert A. Smith, inventor (to Navy), Ephraim Gutmark, inventor (to Navy), Klaus C. Schadow, inventor (to Navy), and Kenneth J. Wilson, inventor (to Navy) 23 Aug. 1994 8 p Filed 14 Feb. 1992
(AD-D017265; US-Patent-5,340,054; US-Patent-Appl-SN-839721; US-Patent-Class-244-1) Avail: US Patent and Trademark Office

The oscillations found to occur in the cavities of a structural frame moving through a fluid are substantially eliminated by the adoption of perturbation elements located at the leading edge of the cavity and reflecting any remaining oscillations out of the cavity at the trailing edge. The perturbation elements may take the form of multiple pins of various shape and geometrical arrangement which prevents the generation and growth of vortices causing acoustic oscillations. The reflection of remaining oscillations out of the cavity may be accomplished by ramping the trailing edge of the cavity. DTIC

N95-26525# National Aerospace Lab., Tokyo (Japan). Advanced Aircraft Research Group.

EXPERIMENTAL INVESTIGATION OF STATIC AND DYNAMIC GROUND EFFECT ON HOPE ALFLEX VEHICLE

Masashi Shigemi, Akihito Iwasaki, Kenichi Rinoie, Toshimi Fujita, Takeshi Ohnuki, Hidehiko Nakayasu (National Space Development Agency, Tokyo,

Japan.), and Masakazu Sagisaka (National Space Development Agency, Tokyo, Japan.) May 1994 59 p In JAPANESE
(ISSN 0389-4010)
(NAL-TR-1236) Avail: CASI HC A04/MF A01

A wind tunnel test was conducted to investigate the ground effect on an 8.9% model of the ALFLEX vehicle. The objectives of this experiment were: (1) to make a preliminary inspection of the influence of the new model supporting system on the main flow; (2) to collect data of the static ground effect; and (3) to collect data of the dynamic ground effect. A robot designed for general industrial use was employed as a tool for model support. The model equipped at the tip of the robot arm could be controlled to change its position as well as its pitch, roll and yaw angles. The merits of utilizing the robot in our experiment was not only to raise the efficiency of the static measurements but also to make it possible to collect the dynamic data in the ground effect test. Comparison between results from static and dynamic tests showed that the amount of the dynamic ground effect is no more than the static effect. Author

N95-26537 Department of the Navy, Washington, DC.
BALANCED ON AIR AIRCRAFT Patent Application
John Reeves, inventor (to Navy) 21 Jul. 1994 8 p Limited Reproducibility: More than 20% of this document may be affected by microfiche quality
(AD-D017251; US-Patent-Appl-SN-010986) Avail: Issuing Activity (Defense Technical Information Center (DTIC))

This patent application concerns the development of a new design for a Balance on Air Aircraft. CASI

N95-26590*# MCAT Inst., San Jose, CA.
AEROELASTICITY OF WING AND WING-BODY CONFIGURATIONS ON PARALLEL COMPUTERS Final Report, Feb. 1992 - Jan. 1995
Chansup Byun Jan. 1995 24 p Original contains color illustrations
(Contract NCC2-740)
(NASA-CR-197756; NAS 1.26:197756; MCAT-95-14) Avail: CASI HC A03/MF A01; 7 functional color pages

The objective of this research is to develop computationally efficient methods for solving aeroelasticity problems on parallel computers. Both uncoupled and coupled methods are studied in this research. For the uncoupled approach, the conventional U-g method is used to determine the flutter boundary. The generalized aerodynamic forces required are obtained by the pulse transfer-function analysis method. For the coupled approach, the fluid-structure interaction is obtained by directly coupling finite difference Euler/Navier-Stokes equations for fluids and finite element dynamics equations for structures. This capability will significantly impact many aerospace projects of national importance such as Advanced Subsonic Civil Transport (ASCT), where the structural stability margin becomes very critical at the transonic region. This research effort will have direct impact on the High Performance Computing and Communication (HPCC) Program of NASA in the area of parallel computing. Derived from text

N95-26591*# MCAT Inst., San Jose, CA.
COMPUTATIONAL ANALYSIS OF FOREBODY TANGENTIAL SLOT BLOWING ON THE HIGH ALPHA RESEARCH VEHICLE Final Report
Ken Gee Jan. 1995 57 p Original contains color illustrations
(Contract NCC2-657)
(NASA-CR-197754; NAS 1.26:197754; MCAT-95-11) Avail: CASI HC A04/MF A01; 1 functional color page

A numerical analysis of forebody tangential slot blowing as a means of generating side force and yawing moment is conducted using an aircraft geometry. The Reynolds-averaged, thin-layer, Navier-Stokes equations are solved using a partially flux-split, approximately-factored algorithm. An algebraic turbulence model is used to determine the turbulent eddy viscosity values. Solutions are obtained using both patched and overset grid systems. In the patched grid model, and actuator plane is used to introduce jet variables into the flow field. The overset grid model is used to model the physical slot geometry and facilitate modeling of the full aircraft configuration. A slot optimization study indicates that a short slot located close to the nose of the aircraft provided the most side force and yawing moment per unit blowing coefficient. Comparison of computed surface pressure with that obtained in full-scale wind tunnel tests produce good agreement, indicating the numerical method and grid system used in the study are valid. Full aircraft computations resolve the changes in vortex burst point due to blowing. A time-accurate full-aircraft solution shows the effect of blowing on the changes in the frequency of the aerodynamic loads over the vertical tails. A study of the effects of freestream Mach number and various jet parameters indicates blowing remains effective through the transonic Mach range. An investigation of the force onset time lag associated with forebody blowing shows the lag to be minimal. The knowledge obtained in this study may be applied to the design of a forebody tangential slot blowing system for use on flight aircraft. Author

N95-26651*# MCAT Inst., San Jose, CA.
DESIGN AND TESTING OF LOW SONIC BOOM CONFIGURATIONS AND AN OBLIQUE ALL-WING SUPERSONIC TRANSPORT Final Report, Dec. 1991 - Jan. 1995
Christopher A. Lee Feb. 1995 7 p Original contains color illustrations
(Contract NCC2-617)
(NASA-CR-197744; NAS 1.26:197744; MCAT-95-07) Avail: CASI HC A02/MF A01; 1 functional color page

From December 1991 to June 1992, applied aerodynamic research support was given to the team working on Low Sonic Boom configurations in the RAC branch at NASA Ames Research Center. This team developed two different configurations: a conventional wing-tail and a canard wing, in an effort to reduce the overpressure of shock waves and the accompanying noise which are projected to the ground from supersonic civil transport aircraft. A generic description of this sensitive technology is given. Derived from text

N95-26652 Naval Postgraduate School, Monterey, CA.
COMPARISON OF FIXED WING AIRCRAFT ALGORITHMS FOR JANUS M.S. Thesis
Charles L. Daniels, II Sep. 1994 85 p Limited Reproducibility: More than 20% of this document may be affected by microfiche quality
(AD-A288503) Avail: Issuing Activity (Defense Technical Information Center (DTIC))

This research compares the fixed wing altitude algorithms utilized in the United States and the Australian versions of the combat modeling tool, JANUS(A). The Australian Army Battle Simulation Group has recently developed a new algorithm that more realistically models aircraft flight profiles within JANUS(A). A Low-High-Low strike profile was simulated, using both algorithms, against low level, littoral anti-aircraft weaponry. The simulated aircraft were flown in a weapons hold environment and number of detections were recorded over the entire strike route as the principal MOE. The simulated aircraft were then subjected to a weapons free environment where engagement data was compiled. The Australian algorithm enabled the operator to alter aircraft altitude and speed during the simulation on command. The ability to alter altitude and speed are essential to accurately modelling tactical evasive maneuvers. These alterations are not features incorporated in the present U.S. version of JANUS(A). Analysis indicates this controllability not only reduced the number of detections significantly, but also increased aircraft survivability within the strike environment. Both of these phenomenon are expected outcomes of such evasive actions. This work also provided the basis for future work that could incorporate virtual simulation with JANUS(A). DTIC

N95-26684 Veda, Inc., Dayton, OH.
INTEGRATED MISSION PRECISION ATTACK COCKPIT TECHNOLOGY (IMPACT). PHASE 1: IDENTIFYING TECHNOLOGIES FOR AIR-TO-GROUND FIGHTER INTEGRATION Final Report, 1 Apr. 1993 - 11 May 1994
Anthony J. Montecalvo, Mark C. Redden, Evan P. Rolek, Horace A. Orr, and Gregory J. Barbato 31 Oct. 1994 126 p Limited Reproducibility: More than 20% of this document may be affected by microfiche quality
(Contract F33615-93-D-3800)
(AD-A289562; WL-TR-94-3143) Avail: Issuing Activity (Defense Technical Information Center (DTIC))

The Integrated Mission Precision Attack Cockpit Technology (IMPACT) Program focuses on the analysis, design, and test of cockpit control and display concepts for a single seat, multirole fighter performing precision strike missions against mobile and fixed targets, at night and in adverse weather. This report details the results of the first 'role playing' exercise. This was an exploratory evaluation assessing: (1) pilot workload associated with an air interdiction mission in a single seat fighter; and (2) advanced technologies having the potential to reduce workload and increase mission effectiveness. Subjective workload measures were collected for a baseline

F-15E, conceptual single-seat F-15E, and an Advanced Technology Cockpit (ATC) using the Subjective Workload Assessment Technique (SWAT) and Subjective Workload Dominance (SWORD) technique. Advanced technologies, assumed to be in use in the year 2005, and their possible mechanizations, were rated using questionnaires and interviews. This report describes the role playing methodology and the test results. DTIC

N95-26813*# MCAT Inst., San Jose, CA.
SUPERSONIC CIVIL AIRPLANE STUDY AND DESIGN: PERFORMANCE AND SONIC BOOM Final Report, Jul. 1989 - Jan. 1995
Samson Cheung Jan. 1995 117 p Original contains color illustrations
(Contract NCC2-617)
(NASA-CR-197745; NAS 1.26:197745; MCAT-95-7) Avail: CASI HC A06/MF A02; 11 functional color pages

Since aircraft configuration plays an important role in aerodynamic performance and sonic boom shape, the configuration of the next generation supersonic civil transport has to be tailored to meet high aerodynamic performance and low sonic boom requirements. Computational fluid dynamics (CFD) can be used to design airplanes to meet these dual objectives. The work and results in this report are used to support NASA's High Speed Research Program (HSRP). CFD tools and techniques have been developed for general usages of sonic boom propagation study and aerodynamic design. Parallel to the research effort on sonic boom extrapolation, CFD flow solvers have been coupled with a numeric optimization tool to form a design package for aircraft configuration. This CFD optimization package has been applied to configuration design on a low-boom concept and an oblique all-wing concept. A nonlinear unconstrained optimizer for Parallel Virtual Machine has been developed for aerodynamic design and study. Derived from text

N95-26844 Air Force Inst. of Tech., Wright-Patterson AFB, OH. School of Engineering.
A COMPARISON OF THE NEAL-SMITH AND OMEGA TAU FUNCTION, ZETA FUNCTION AND TAU FUNCTION FLYING QUALITIES CRITERIA M.S. Thesis
Brian A. Kish Dec. 1994 145 p Limited Reproducibility: More than 20% of this document may be affected by microfiche quality
(AD-A289503; AFIT/GAE/ENY/94D-11) Avail: Issuing Activity (Defense Technical Information Center (DTIC))

Aircraft pitch response is a vital element of piloted vehicle flying qualities. There has been controversy over both the form and the substance of the requirements for short-term pitch response. Currently, MIL-STD-1797A offers six different methods for evaluating short-term pitch response. These six methods often give conflicting results. Two methods are analyzed in this thesis - the Neal-Smith criteria and the omega(sub sp) Tau(sub theta 2), zeta(sub sp), tau(sub theta) criteria. Domains from both criteria are mapped into each other identifying regions of conflict and regions of agreement. Parametric studies are performed and evaluated for trends. Further, a real-time analysis tool for evaluating these methods is developed. DTIC

N95-26873 Air Force Inst. of Tech., Wright-Patterson AFB, OH. School of Engineering.
AN ANALYSIS OF THE KC-135 THREE-PERSON COCKPIT M.S. Thesis
Robert A. Deivert Dec. 1994 66 p Limited Reproducibility: More than 20% of this document may be affected by microfiche quality
(AD-A289540; AFIT/GSO/ENS/94D-06) Avail: Issuing Activity (Defense Technical Information Center (DTIC))

In an effort to quantitatively determine the utility of mission effectiveness of the KC-135, this research used value-focused thinking to measure the impact of replacing the KC-135 navigator with upgraded avionics. A value model was developed as a hierarchy with fundamental objectives at the highest level and attributes at the lowest level. Weights were assigned to show the contribution each level had to the one above it. The attributes were given a score and an additive model was used to determine utility with and without a navigator. Break-even analysis and net present value calculations were done to show the costs associated with each alternative. This study reveals that the cockpit with the navigator has a higher utility than the cockpit with the upgraded avionics. Value-focused thinking identified additional equipment that would increase the utility of the upgraded avionics. This approach can be used to identify equipment alternatives in the future that add the most utility. This methodology can be used by the Air National Guard to determine whether they should keep navigators as part of the KC-135 crew. DTIC

N95-26876 Air Force Inst. of Tech., Wright-Patterson AFB, OH.
THE PHOTO-REALISTIC AFIT VIRTUAL COCKPIT M.S. Thesis
Milton E. Diaz Dec. 1994 115 p Limited Reproducibility: More than 20% of this document may be affected by microfiche quality
(AD-A289376; AFIT/GCS/ENG/94D-02) Avail: Issuing Activity (Defense Technical Information Center (DTIC))

The Air Force Institute of Technology (AFIT) has pursued research in virtual environments since 1988. This research expands the current capabilities of the AFIT Virtual Cockpit (VC) by increasing the realism of the cockpit environment and improving the pilot's command interface. Realism is improved creating console elements from texture maps and polygonal models; these elements include working dials, switches and circuit breakers. The pilot command interface is improved in part by adapting the AFIT Information Pod using a two-dimensional mouse input to the virtual three-dimensional environment. This immersive virtual environment is also improved by modifications to the Head Mounted Display (HMD) reducing jitter and allowing the simulation pilot to adjust his/her position within the cockpit. DTIC

N95-26993 Army Aeromedical Research Lab., Fort Rucker, AL.
THE EFFECTS OF UH-1 EXPERIENCE ON UH-60 SIMULATOR PERFORMANCE: A PRELIMINARY STUDY Final Report
Charles A. Salter, John A. Caldwell, Jr., John S. Crowley, and Ronald L. Smith Nov. 1994 35 p Limited Reproducibility: More than 20% of this document may be affected by microfiche quality
(DA Proj. 3M1-62787-A-879)
(AD-A289457; USAARL-95-4) Avail: Issuing Activity (Defense Technical Information Center (DTIC))

Efforts to expand the pool of volunteers for research in the UH-60 simulator prompted USAARL to determine whether UH-1 pilots could be used as an alternative to UH-60 subjects. In this quasi-experimental preliminary study, eight UH-1 pilots were provided with training in the UH-60 simulator. Afterwards, they were required to fly a standardized profile, parts of which had been used in an earlier investigation with UH-60 pilots. The performance accuracy of the groups (UN-1 versus UH-60) were compared on equivalent maneuvers. Results showed that the UH-1 pilots used in this initial study actually performed better on most maneuvers than did the UH-60 pilots who were used in an earlier investigation. Thus, it appears that UH-1 pilots, who are easier to recruit than rated UH-60 pilots, may be suitable as subjects in future simulator studies involving basic instrument pilotage skills. However, before drawing definitive conclusions, these results should be replicated in a controlled study where the pilots are randomly assigned to training and testing conditions during a more limited time frame. DTIC

N95-26994 Army Aviation Technical Test Center, Fort Rucker, AL.
TEST OPERATIONS PROCEDURE (TOP) 7-3-534 AIRWORTHINESS TESTING OF FIXED WING AIRCRAFT: ASYMMETRIC POWER TESTING
23 Dec. 1994 17 p Limited Reproducibility: More than 20% of this document may be affected by microfiche quality
(AD-A289458; TOP-7-3-534) Avail: Issuing Activity (Defense Technical Information Center (DTIC))

This TOP establishes procedures and methods for evaluating the asymmetric power handling qualities of multi-engine fixed-wing aircraft during developmental testing. This TOP is limited to handling qualities only and does not address aircraft performance. DTIC

N95-27018 AEPCO, Inc., Rockville, MD.
AH-1F COBRA REWIRE PROGRAM MANPRINT ANALYSIS
Robert A. Clarke and William J. Boltralik 31 Aug. 1994 12 p Limited Reproducibility: More than 20% of this document may be affected by microfiche quality
(Contract DABT60-90-D-0010)
(AD-A289190) Avail: Issuing Activity (Defense Technical Information Center (DTIC))

The purpose of this analysis was to review and analyze the AH-1F Cobra Rewire Program from a MANPRINT perspective. This was accomplished through examination of the AH-1F Cobra Rewire Program documentation and its technical publication, the Cobra Helicopter Rewire

Manual (CHRM). Review of this program's documentation was conducted to identify MANPRINT deficiencies and develop corrective recommendations that ensure the CHRM would mitigate these shortcomings. The scope of this effort was primarily confined to the AH-1F Cobra Rewire Programs CHRM. Inputs to the CHRM were received from the AH-1 Cobra Project Management office (PMO), Army aviation maintenance facilities, fielded AH-1F Cobra units, and Korean Air Lines (KAL). Government furnished information (GFI) and contractor furnished information (CFI) from KAL were received in a fairly timely manner. Total integration of all AH-1F Cobra Rewire Program acquisitions efforts was beyond the scope of the delivery order. DTIC

N95-27042 Air Force Inst. of Tech., Wright-Patterson AFB, OH. School of Engineering.
IMPLEMENTATION AND DEMONSTRATION OF A MULTIPLE MODEL ADAPTIVE ESTIMATION FAILURE DETECTION SYSTEM FOR THE F-16 M.S. Thesis
Peter K. Eide Dec. 1994 215 p Limited Reproducibility: More than 20% of this document may be affected by microfiche quality
(AD-A289301; AFIT/GE/ENG/94D-06) Avail: Issuing Activity (Defense Technical Information Center (DTIC))

A Multiple Model Adaptive Estimation (MMAE) algorithm is implemented with the fully nonlinear six-degree-of-motion, Simulation Rapid-Prototyping Facility (SRF) VISTA F-16 software simulation tool. The algorithm is demonstrated to be capable of identifying flight critical aircraft actuator and sensor failures at a low dynamic pressure (20,000 ft, .4 Mach). Research included single and dual complete failures. Tuning methods for accommodating model mismatch, including addition of discrete dynamics pseudonoise and continuous measurement pseudonoise, are discussed and demonstrated. Scalar residuals within each filter are also examined and characterized for possible use as an additional failure declaration voter. Robustness to sensor failures provided by MMAE-based control is also demonstrated. An investigation of algorithm performance off the nominal design conditions is accomplished as a first step towards full flight envelope coverage. The algorithm is composed of a bank of Kalman filters modeled to match particular hypotheses of the real world. Each presumes a single failure in one of the flight critical actuators (left/right stabilators, left/right flaperon, rudder), or sensors (forward velocity, angle of attack, pitch rate, normal acceleration, roll rate, yaw rate, and lateral acceleration), and one presumes no failure. For dual failures, a hierarchical structure is used to keep the number of on-line filters to a minimum. This research advances the technology by testing algorithm performance against the most complete simulation model currently available. DTIC

N95-27143*# National Aeronautics and Space Administration. Ames Research Center, Moffett Field, CA.
THE LIFT-FAN AIRCRAFT: LESSONS LEARNED
Wallace H. Deckert Mar. 1995 64 p
(Contract NAS2-5364)
(NASA-CR-196694; A-95041; NAS 1.26:196694) Avail: CASI HC A04/MF A01

This report summarizes the highlights and results of a workshop held at NASA Ames Research Center in October 1992. The objective of the workshop was a thorough review of the lessons learned from past research on lift fans, and lift-fan aircraft, models, designs, and components. The scope included conceptual design studies, wind tunnel investigations, propulsion systems components, piloted simulation, flight of aircraft such as the SV-5A and SV-5B and a recent lift-fan aircraft development project. The report includes a brief summary of five technical presentations that addressed the subject The Lift-Fan Aircraft: Lessons Learned. Author

N95-27180*# Texas A&M Univ., College Station, TX.
SAILPLANE GLIDE PERFORMANCE AND CONTROL USING FIXED AND ARTICULATING WINGLETS M.S. Thesis
James David Colling May 1995 100 p
(Grant NAG1-1522)
(NASA-CR-198579; NAS 1.26:198579) Avail: CASI HC A05/MF A02

An experimental study was conducted to investigate the effects of controllable articulating winglets on glide performance and yawing moments of high performance sailplanes. Testing was conducted in the Texas A&M University 7 x 10 foot Low Speed Wind Tunnel using a full-scale model of the outboard 5.6 feet of a 15 meter class high performance sailplane wing. Different wing tip configurations could be easily mounted to the wing model. A winglet was designed in which the cant and toe angles as well as a rudder on the winglet could be adjusted to a range of positions. Cant angles used in the investigation consisted of 5, 25, and 40 degrees measured from the vertical axis. Toe-out angles ranged from 0 to 22.5 degrees. A rudder on the winglet was used to study the effects of changing the camber of the winglet airfoil on wing performance and wing yawing moments. Rudder deflections consisted of-10, 0, and 10 degrees. Test results for a fixed geometry winglet and a standard wing tip are presented to show the general behavior of winglets on sailplane wings, and the effects of boundary-layer turbulators on the winglets are also presented. By tripping the laminar boundary-layer to turbulent before laminar separation occurs, the wing performance was increased at low Reynolds numbers. The effects on the lift and drag, yawing moment, pitching moment, and wing root bending moment of the model are presented. Oil flows were used on the wing model with the fixed geometry winglet and the standard wing tip to visualize flow directions and areas of boundary layer transition. A cant angle of 25 degrees and a toe-out angle of 2.5 degrees provided an optimal increase in wing performance for the cant and toe angles tested. Maximum performance was obtained when the winglet rudder remained in the neutral position of zero degrees. By varying the cant, toe, and rudder angles from their optimized positions, wing performance decreases. Although the winglet rudder proved to be more effective in increasing the yawing moment compared to varying the cant and toe angles, the amount of increased yawing moment was insignificant when compared to that produced by the vertical tail. A rudder on the winglet was determined to be ineffective for providing additional yaw control. Author

N95-27371*# Lockheed Engineering and Sciences Co., Hampton, VA.
A VERIFICATION PROCEDURE FOR MSC/NASTRAN FINITE ELEMENT MODELS
Alan E. Stockwell Jun. 1995 24 p
(Contract NAS1-19000; RTOP 233-01-01-03)
(NASA-CR-4675; NAS 1.26:4675) Avail: CASI HC A03/MF A01

Finite Element Models (FEM's) are used in the design and analysis of aircraft to mathematically describe the airframe structure for such diverse tasks as flutter analysis and actively controlled landing gear design. FEM's are used to model the entire airplane as well as airframe components. The purpose of this document is to describe recommended methods for verifying the quality of the FEM's and to specify a step-by-step procedure for implementing the methods. Author

N95-27440# Geophex Ltd., Raleigh, NC.
GEOPHEX AIRBORNE UNMANNED SURVEY SYSTEM
I. J. Won and D. W. A. Taylor 1995 13 p Presented at the Opportunity 95: Environmental Technology Through Small Business, Morgantown, WV, 16-17 Nov. 1994
(Contract DE-AR21-93MC-30358)
(DE95-007566; DOE/MC-30358/95/C0432; CONF-9411149-4) Avail: CASI HC A03/MF A01

The purpose of this effort is to design, construct, and evaluate a portable, remotely-piloted, airborne, geophysical survey system. This nonintrusive system will provide 'stand-off' capability to conduct surveys and detect buried objects, structures, and conditions of interest at hazardous locations. This system permits two operators to rapidly conduct geophysical characterization of hazardous environmental sites. During a survey, the operators remain remote from, but within visual distance, of, the site. The sensor system never contacts the Earth, but can be positioned near the ground so that weak anomalies can be detected. DOE

N95-27504# Advisory Group for Aerospace Research and Development, Neuilly-Sur-Seine (France). Structures and Materials Panel.
COMPOSITE REPAIR OF MILITARY AIRCRAFT STRUCTURES [LA REPARATION COMPOSITE DES STRUCTURES D'AVIONS MILITAIRES]
Jan. 1995 290 p In ENGLISH and FRENCH The 79th meeting was held in Seville, Spain, 3-5 Oct. 1994 Original contains color illustrations
(AGARD-CP-550; ISBN-92-836-0010-X) Copyright Avail: CASI HC A13/MF A03

The AGARD Structures and Materials Panel held a specialists' Meeting to address composite repair of military aircraft. The meeting focused on two main areas, repair of metal structures using composite patches and repair of composite structures using composite or metal patches. The work presented had direct application to the maintenance and support of military aircraft. Repair of military aircraft provides both a means to extend the useful life of the airframe beyond the original design life and a method to maintain military readiness by returning damaged aircraft to service. For individual titles, see N95-27505 through N95-27528.

N95-27505# Defence Science and Technology Organisation, Melbourne (Australia). Aeronautical and Maritime Research Lab.

BONDED COMPOSITE REPAIR OF METALLIC AIRCRAFT COMPONENTS: OVERVIEW OF AUSTRALIAN ACTIVITIES

A. A. Baker *In* AGARD, Composite Repair of Military Aircraft Structures Jan. 1995 14 p (For primary document see N95-27504 09-05)
Copyright Avail: CASI HC A03/MF A03

After first providing an overview of the status of Australian applications of bonded composite repairs to metallic aircraft structure (mainly based on boron/epoxy composites) the problems in certifying composite repairs to critical cracks in primary metallic structure are discussed. The development of acceptable generic certification procedures is essential if the use of this efficient cost-effective repair technology is to be widely employed in military and civil aircraft. One requirement for certification is the ability to predict the fatigue-crack growth behavior in patched components. An approach to developing this capability is described, based on Rose's model to estimate stress intensity in patched panels. The model is extended to allow for disbonding damage in the patch system. Experimental results are presented to demonstrate the validity of this approach for boron/epoxy-FM73 repairs to aluminum alloy 2024T3. Author

N95-27506# Textron Specialty Materials, Lowell, MA.

STATUS OF BONDED BORON/EPOXY DOUBLERS FOR MILITARY AND COMMERCIAL AIRCRAFT STRUCTURES

E. B. Belason *In* AGARD, Composite Repair of Military Aircraft Structures Jan. 1995 12 p (For primary document see N95-27504 09-05)
Copyright Avail: CASI HC A03/MF A03

Bonded boron/epoxy doublers are an alternative method vs. riveted doublers for repair and reinforcement of metallic aircraft structures. The boron/epoxy doublers provide cost and/or performance advantages for many applications. Today over 4,500 are flying on military aircraft, mostly in Australia and the U.S.A., and the use is increasing. Commercial aircraft, which are also aging, are beginning to use this technology, with about 50 boron doublers flying for flight evaluation since 1989 (plus about another 100 since the mid 1970s in France). This paper summarizes the major uses of boron/epoxy doublers, focusing on recent and current U.S. applications (other papers at this Meeting describe activities in Australia, Canada, and France). These include a 1993 report summarizing the successful use on the wing pivot of over 400 F-111s for 20 years (no disbonds have been noted); fleetwide installations on the B-1 and C-141 (over 1800 doublers); and flight testing on F-16, T-38, C-130 and KC-135 aircraft. Commercially there have been successful flight evaluations on 2 Fed Ex 747s and the Lycoming ALF 502 engine cowl on 2 BAE 146s. A Service Bulletin has been issued for retrofit of over 1200 cowls for the latter. This paper also summarizes the installation process (which is very viable), and describes two recent technical advances in chemically preparing aluminum surfaces for bonding of boron/epoxy doublers. This paper also presents the results of an extensive test program sponsored by Textron at Boeing of 110 ultimate tensile strength and 143 fatigue tests of boron/epoxy doublers bonded to 7075-T6 aluminum with simulated cracks. Author

N95-27507# Defence Research Agency, Farnborough, Hampshire (England). Structural Materials Centre.

ADHESIVELY BONDED COMPOSITE PATCH REPAIR OF CRACKED ALUMINUM ALLOY STRUCTURES

P. Poole, A. Young, and A. S. Ball (British Aerospace Defence Ltd., Farnborough, England.) *In* AGARD, Composite Repair of Military Aircraft Structures Jan. 1995 12 p (For primary document see N95-27504 09-05)
Copyright Avail: CASI HC A03/MF A03

Research at the Defence Research Agency (DRA) on adhesively bonded composite patch repair of fatigue cracked aluminum alloy structures is reviewed briefly. Theoretical and experimental results are reported which indicate the effectiveness of such repairs in terms of the reductions in stress intensity factor due to patching. The influence of warm-moist environments on the long-term performance of bonded patches is considered, and the advantages and disadvantages of using carbon fiber reinforced plastic (CFRP) patches, rather than boron fiber reinforced plastic (BFRP) patches, are discussed. An investigation by British Aerospace of the feasibility of using bonded composite patches to repair cracked primary aircraft structures is summarized. For the range of applications investigated, bonded composite patch repairs are shown to offer potential savings of 60-75 percent, compared to conventional repair methods. The current position regarding in-service trials is summarized, with no evidence of crack growth after 990 flying hours. Author

N95-27508# Dassault Aviation, Saint-Cloud (France).

COMPOSITE REPAIR OF METALLIC AIRFRAME: TWENTY YEARS OF EXPERIENCE [REPARATIONS COMPOSITES DE STRUCTURES METALLIQUES: VINGT ANS D'EXPERIENCE]

Micheline Druet *In* AGARD, Composite Repair of Military Aircraft Structures Jan. 1995 8 p In FRENCH (For primary document see N95-27504 09-05)
Copyright Avail: CASI HC A02/MF A03

During the 70's, the availability of unidirectional boron fiber fabric at Dassault Aviation did allow reinforcement of metallic structures by direct ply lay up on the metal. To be able to apply these reinforcement on airplanes, it was necessary to define a resin system inducing low thermal stresses in the metal during its cure, and with acceptable mechanical properties after aging. Validation was done by simple tests on samples, by complex test with simultaneous thermal and mechanical cycling, and application of test repairs on the major fatigue test of the Mercure airplane. Reinforcements of that type are in service for almost 20 years on the Mercure airliner. Author

N95-27509# National Research Council of Canada, Ottawa (Ontario). Structures, Materials and Propulsion Lab.

BONDED COMPOSITE REPAIR OF THIN METALLIC MATERIALS: VARIABLE LOAD AMPLITUDE AND TEMPERATURE CYCLING EFFECTS

M. D. Raizenne, T. J. Benak, J. B. R. Heath, D. L. Simpson, and A. A. Baker (Defence Science and Technology Organisation, Melbourne, Australia.) *In* AGARD, Composite Repair of Military Aircraft Structures Jan. 1995 12 p Original contains color illustrations (For primary document see N95-27504 09-05)
Copyright Avail: CASI HC A03/MF A03

An investigation into the effectiveness of bonded boron/epoxy composite patch repairs on edge notched Al 2024-T3 sheets has been completed. Testing was carried out under variable amplitude load and temperature cycling. Nine sandwich type specimens were precracked of which eight were repaired using bonded precured unidirectional boron fiber reinforced epoxy patches. Three structural adhesive systems were evaluated, two thermally activated epoxies, FM73 and FM300, and a room temperature cure acrylic, Versilok 201. The variable amplitude load sequence used was FALSTAFF, a typical fighter aircraft loading spectrum. The temperature profile was derived from F/A-18 usage data. Temperatures varied between -35 C and +80 C with a one in eight temperature cycle occurrence of +108 C. The effect of moisture absorption in the adhesive and the matrix was also investigated. Bonded patches on three specimens were preconditioned to a moisture weight gain of 1.5 percent prior to testing. The data generated compares specimen fatigue crack growth rates between the three adhesives for three environments: room temperature, temperature cycled and temperature cycled with moisture preconditioning. Author

N95-27510# Bombardier, Inc., Montreal (Quebec). Defence Systems Div.

DESIGN AND STRUCTURAL VALIDATION OF CF116 UPPER WING SKIN BORON DOUBLER

J. Smith *In* AGARD, Composite Repair of Military Aircraft Structures Jan. 1995 11 p (For primary document see N95-27504 09-05)
Copyright Avail: CASI HC A03/MF A03

Cracks were found around fastener holes in the critical area known as the 'Golden Triangle' on the upper wing skin of several CF116 aircraft. To restore the structural integrity of the wing, cracks around these fastener holes are removed and interference fit steel bushings are installed. A boron-epoxy doubler is then bonded over the reworked area to reduce stress levels. The doubler is viewed as a fatigue enhancement device and not as a repair to a cracked skin. An analytical methodology is used to assess the bond line integrity and the load transfer in the doubler. A 49% reduction of stress level is predicted by the bonded joint analytical approach. A finite element analysis reveals that a 47% stress reduction is expected in the exterior surface of the wing skin, while a 37% reduction in the interior surface is predicted. Based on a strain survey performed following the installation of a doubler on the CF116 full scale fatigue test, it is shown that analytical predictions agree with experimental results. Author

N95-27511# Georgia Inst. of Tech., Atlanta, GA. Computational Modeling Center.

A FEAM BASED METHODOLOGY FOR ANALYZING COMPOSITE PATCH REPAIRS OF METALLIC STRUCTURES

D. S. Pipkins and S. N. Atluri *In* AGARD, Composite Repair of Military Aircraft Structures Jan. 1995 16 p (For primary document see N95-27504 09-05)

Copyright Avail: CASI HC A03/MF A03

A Finite Element Alternating Method based methodology applicable to the analysis of composite patch repairs of metallic structures is presented. The method is completely general and may be used to efficiently analyze factors affecting repair design such as: global stiffening of the aircraft structure due to the high stiffness of the composite patch; the effect of size, shape, thickness and material properties of the composite patch on the crack-tip stress intensity factors; the effect of the material properties of the adhesive on the crack-tip stress intensity factors; the effect of thermal cycling on the composite repair; and the effect of disbonds on the effectiveness of the composite repair. Author

N95-27512# Lockheed Aeronautical Systems Co., Marietta, GA.

STRUCTURAL MODIFICATION AND REPAIR OF C-130 WING STRUCTURE USING BONDED COMPOSITES

J. Grosko *In* AGARD, Composite Repair of Military Aircraft Structures Jan. 1995 9 p (For primary document see N95-27504 09-05)

Copyright Avail: CASI HC A02/MF A03

Lockheed Aeronautical Systems Company (LASC) -- in a program sponsored by the United States Air Force, Warner Robins Air Logistics Center, C-130 Directorate -- has developed concepts wherein bonded high-modulus composite materials can be applied to structurally repair or enhance the wing box of C-130 aircraft. Two separate approaches are taken. In the first, boron/epoxy reinforcing strips are applied to wing box lower surface structure to relieve high stress at a particular location in the wing surface panel. This modification is ideally used on undamaged structure to prevent wing surface cracking. In the second approach, graphite reinforced patches are applied in the same vicinity to arrest crack growth. Both concepts were successfully demonstrated on opposite sides of a full-scale wing test article. Design details, the materials and processes, the methods of installation and the measured effectiveness of both the boron/epoxy strips and the graphite/epoxy patches are discussed. Author (revised)

N95-27513# Lehigh Univ., Bethlehem, PA. Inst. of Fracture and Solid Mechanics.

EVALUATION OF PATCH EFFECTIVENESS IN REPAIRING AIRCRAFT COMPONENTS

G. C. Sih and E. E. Gdoutos (Thrace Univ., Xanthe, Greece.) *In* AGARD, Composite Repair of Military Aircraft Structures Jan. 1995 8 p (For primary document see N95-27504 09-05)

Copyright Avail: CASI HC A02/MF A03

Reinforcement of aircraft components by patching is never completely effective because of improper bonding or damage of the reinforcement in service. There is always the uncertainty for evaluating the remaining strength or life of a repaired structure. Developed in this work is a methodology for evaluating the reinforcement effectiveness by considering two basic types of partially damaged patches; they are referred to as collinear and transverse debonding with respect to the crack plane. The former refers to debonding over a region ahead of only one of the crack tips where the load and geometry are symmetric across the crack plane, while the latter is concerned with debonding over a region to the side of the crack where symmetry is no longer preserved across the crack plane. Finite elements are employed to obtain the stresses and strains from which the strain energy densities can be determined for analyzing the failure behavior of the patched panels. The local and global maximum of the minimum strain energy density function, designated by((dW/dV)(sup max, sub min))(sub L) at L and ((dW/DV)(sup max, sub min)(sub G) at G, are found and applied to define failure instability. The distance ell between L and G serves as a measure of crack instability; it increases with the debonded area. That is, debonding tends to enhance failure instability by fracture initiating from the existing crack. For approximately the same area of debonding, crack initiation for collinear debonding would be more unstable as compared with transverse debonding for loads directed normal to the crack. Introduced also is a Patch Effectiveness Index (PEI) that serves as a measure of the load carrying capacity of the damaged patch. In this case, transverse debonding is more detrimental than collinear debonding because a more significant reduction in the load transfer path occurs in the former case. In general, both ell and PEI would have to be considered for assessing the integrity of the damaged patch. Author

N95-27514# Naval Air Warfare Center, Warminster, PA. Aircraft Div.

FIELD REPAIR MATERIALS FOR NAVAL AIRCRAFT

R. Cochran, R. Trabocco, P. Mehrkam, and M. DiBerardino *In* AGARD, Composite Repair of Military Aircraft Structures Jan. 1995 7 p (For primary document see N95-27504 09-05)

Copyright Avail: CASI HC A02/MF A03

The Navy is unique in that a portion of the maintenance actions performed on operational aircraft must be accomplished on board ship or in remote field locations. Historically, Navy driven composite repair programs have addressed materials and concepts specifically directed at accomplishing repairs in the fleet operating environment. This paper discusses recent developments in the area of composite repair materials for the application of bonded patches to honeycomb and complex shaped monolithic composite structure. A two part adhesive that meets the storage and processing requirements for field repair applications was evaluated for use in repair of honeycomb structure. Low temperature adhesive processing and honeycomb compatibility tests were investigated. In another effort, wet lay-up repair resins and processes were characterized for repair of highly curved composite structure. The materials and equipment used in the study are fully compatible with field repair requirements. Composite repair materials for application of bonded patches to honeycomb and complex shaped monolithic composite structure are described. Low temperature adhesive processing development for bonding composite patches to moisturized structure is described. Cure temperatures as low as 90 C were used for curing a two part ambient storable adhesive. Mechanical properties and thermal stability of the cured adhesive is reported using a number of cycles. In another effort wet lay-up repair resins and processes were characterized which allow for the fabrication of fully inspectable wet lay-up patches. The materials and equipment are fully compatible with field repair requirements. Laminate mechanical properties and resin storage stability were characterized and reported. Author

N95-27515# Deutsche Aerospace A.G., Munich (Germany). Military Aircraft Div.

ON AIRCRAFT REPAIR VERIFICATION OF A FIGHTER A/C INTEGRALLY STIFFENED FUSELAGE SKIN

J. Bauer and A. Maier *In* AGARD, Composite Repair of Military Aircraft Structures Jan. 1995 14 p (For primary document see N95-27504 09-05)

Copyright Avail: CASI HC A03/MF A03

A considerably large four point bending test box was available simulating the curved integrally stiffened CFC fuselage skin of a fighter aircraft. This box was used for a skin repair trial with subsequent testing. The repair was performed in the environment of an external test laboratory, i.e. abroad of the original shop or maintenance facilities. 'On Aircraft' conditions have been simulated with all the referring access, tooling and quality assurance difficulties. The repaired test box demonstrated during static testing, loading the repair in tension, compression and shear, that the applied repair procedure is feasible to be applied on CFC structures. The repair procedure and the subsequent testing will be presented and the results will be discussed. Author

N95-27516# Lockheed-Fort Worth Co., Fort Worth, TX.

RAPID REPAIR OF LARGE AREA DAMAGE TO CONTOURED AIRCRAFT STRUCTURES

James A. Frailey and Douglas W. Carter (Wright Lab., Wright-Patterson AFB, OH.) *In* AGARD, Composite Repair of Military Aircraft Structures Jan. 1995 9 p (For primary document see N95-27504 09-05)

Copyright Avail: CASI HC A02/MF A03

In a program sponsored by Air Force Wright Laboratory (WL/FIVST), Lockheed Fort Worth Company has developed field-level procedures for repair of large area damage to highly contoured aircraft structures. The combination of aircraft structures designed with enhanced survivability and the utilization of larger and more powerful ballistic threats have resulted in the requirement to develop new, creative approaches for rapid repair of large area structural damage. Furthermore, current aircraft design employing advanced composite materials on highly contoured surfaces increases the challenge of implementing workable battle damage repairs. This paper details the development of an advanced battle damage repair concept designed to repair damage up to approximately 15 inches in diameter on highly contoured surfaces. It employs a quick, reusable tooling mold that replicates the contour of the damaged aircraft for the purpose of processing a composite patch. Several one year room temperature storable, thermoset, composite systems were examined for processability, handleability and mechanical performance to determine their suitability as repair patch materials. The most promising were further tested and demonstrated in a large scale validation test. Author

N95-27517# Deutsche Aerospace A.G., Munich (Germany). Military Aircraft Div.

COMPOSITE REPAIR OF A CF18: VERTICAL STABILIZER LEADING EDGE

A. E. Maier and G. Guenther *In* AGARD, Composite Repair of Military Aircraft Structures Jan. 1995 16 p (For primary document see N95-27504 09-05)

Copyright Avail: CASI HC A03/MF A03

This paper describes the engineering and manufacturing procedures that were applied in a repair task of a CF18 Vertical Stabilizer Leading Edge, made out of CFC honeycomb structure with multiple in-service impact damages in an aerodynamic sensitive area of the fin. 'On-aircraft' damage assessment, manufacturing of a relatively thin contoured CFC doubler, replacement of metal honeycomb core and finally quality assurance and strength verification procedures of the repair are described to restore full design strength of the component and the operational aircraft capability. Author

N95-27518# Defence Research Establishment Pacific, Victoria (British Columbia).

COMPOSITE REPAIR ISSUES ON THE CF-18 AIRCRAFT

A. J. Russell and J. S. Ferguson *In* AGARD, Composite Repair of Military Aircraft Structures Jan. 1995 8 p (For primary document see N95-27504 09-05)

Copyright Avail: CASI HC A02/MF A03

This paper addresses three separate composite repair issues currently being investigated at the Defence Research Establishment Pacific (DREP) in support of Canada's CF-18 aircraft. First, the problem of skin/core debonding that can occur during elevated temperature bonded repairs of honeycomb sandwich structure is discussed and the results of tests which help to quantify the role played by bondline degradation are presented. Next, the final development phase of an on-going effort to establish a reliable and effective means of repairing delamination damage is reported. In particular, the design of a resin injection device and a series of tests to evaluate its performance are described. Finally, a battle damage repair issue, namely the advantages and disadvantages of cleaning up the damaged composite material found around entry and exit holes created by live fire, is discussed. Test data is presented which compares the different consequences under tensile and compression loading. Author

N95-27519# Northrop Grumman Corp., Hawthorne, CA. Aircraft Div.

REPAIR TECHNOLOGY FOR THERMOPLASTIC AIRCRAFT STRUCTURES

M. W. Heimerdinger et al *In* AGARD, Composite Repair of Military Aircraft Structures Jan. 1995 12 p (For primary document see N95-27504 09-05)

Copyright Avail: CASI HC A03/MF A03

The Flight Dynamics and Materials Directorates of the U.S. Air Force Wright Aeronautical Laboratories jointly sponsored a program for 'Repair Technology for Thermoplastic Aircraft Structures' (REPTAS) performed by Northrop Corporation, Aircraft Division. In the program Northrop developed, validated and demonstrated on-aircraft repair design concepts and processes for field repair of advanced thermoplastic structures. The REPTAS program was accomplished through the performance of a 48-month effort comprising three phases. Phase 1 assessed field level repair facilities and technology that are currently available and identified their applicability to repair thermoplastic (TP) structures. A baseline aircraft structure was selected to validate the selected repair process. Currently available thermoplastic materials were reviewed and materials selected for evaluation. In the selection process the objective was to select one semicrystalline, one amorphous, and one pseudo-thermoplastic material. APC-2 was evaluated as the baseline material for the process development efforts. Novel processing techniques were investigated for the repair procedures. Phase 2 developed the selected technologies for the on-aircraft repair of TP structures at a coupon and subelement level. Design concepts were developed that are compatible with field level capabilities and restore structural integrity to the aircraft. In the process of developing a bonding procedure using polyetheretherketone (PEEK) as the bonding film, it became apparent that the required bonding temperature of 385 C (725 F) created internal thermal stresses in the base structure and resulted in unacceptable delaminations. As an alternative, an investigation of amorphous bonding was included which demonstrated its feasibility for TP repair. In Phase 3 a full-scale advanced thermoplastic composite structural component was selected and used as a demonstration article for the selected design concept. Derived from text

N95-27520# Vought Corp., Dallas, TX. Aircraft Div.

REPAIR OF HIGH TEMPERATURE COMPOSITE AIRCRAFT STRUCTURE

Jerome J. Connolly *In* AGARD, Composite Repair of Military Aircraft Structures Jan. 1995 12 p (For primary document see N95-27504 09-05)

Copyright Avail: CASI HC A03/MF A03

This paper describes the final portion of a high temperature composite repair development program sponsored by Wright Patterson Materials Directorate. Initially, BMI adhesives and prepregs were selected based on their compatibility with in-service repair cure scenarios. These typically involve curing in a non-autoclave environment using vacuum consolidation only. The selected material systems were then used to develop a comprehensive repair procedure for highly curved aircraft structure. Once developed, the procedure was then applied to a curved structure representative of a flight surface leading edge. Baseline and repair specimens were fabricated and tested in compression at both room temperature dry and elevated temperature dry conditions. The results of these test validated the repair procedure. Author

N95-27521# British Aerospace Defence Ltd., Preston (England). Military Aircraft Div.

COMPOSITE REPAIR OF COMPOSITE STRUCTURES

C. S. Frame *In* AGARD, Composite Repair of Military Aircraft Structures Jan. 1995 11 p (For primary document see N95-27504 09-05)

Copyright Avail: CASI HC A03/MF A03

Composite repair results from previous Phases of the Ministry of Defence/British Aerospace funded 'Defect, Damage and Repair' (DDR) program are used to illustrate the ability to perform adequate strength repairs to composite structures using composite materials. Problems inhibiting the wider use of composite repairs are discussed and work in progress in the current Phase of the DDR program aimed at overcoming these problems, is presented. Author

N95-27522# Eurocopter Deutschland G.m.b.H., Munich (Germany).

EXTERNAL PATCH REPAIR OF CFRP/HONEYCOMB SANDWICH

K. Wolf and R. Schindler *In* AGARD, Composite Repair of Military Aircraft Structures Jan. 1995 11 p (For primary document see N95-27504 09-05)

Copyright Avail: CASI HC A03/MF A03

This paper addresses the repair of impact-damaged honeycomb sandwich structures with thin skins made of carbon fiber reinforced plastic (CFRP). An experimental study concerned with evaluating several types of bonded external patch repairs is presented. The evaluation included cocured as well as precured patch techniques utilizing advanced repair materials. Three repair schemes were applied to honeycomb sandwich manufactured from 125 C as well as 175 C curing carbon fiber reinforced fabric prepregs. The effectiveness of the repairs was examined through a series of static and fatigue compression tests. Based on the mechanical test results and a comparison of the repair procedures it was found that the bonded precured patch concept is the most suitable approach for repairing impact-damaged sandwich structures under field-level maintenance limitations. Author

N95-27523# Defence Science and Technology Organisation, Melbourne (Australia). Aeronautical and Maritime Research Lab.

SCARF REPAIRS TO GRAPHITE/EPOXY COMPONENTS

A. A. Baker, R. J. Chester, G. R. Hugo, and T. C. Radtke *In* AGARD, Composite Repair of Military Aircraft Structures Jan. 1995 12 p (For primary document see N95-27504 09-05)

Copyright Avail: CASI HC A03/MF A03

Significant damage to graphite/epoxy laminates up to 16 plies in thickness is often repaired with a bonded external patch. This type of repair is well suited to honeycomb panels and is relatively easy to apply even under field conditions. Thicker laminates generally carry too much load for external patch repairs and so either bolted patches or scarf repairs are generally used. Scarf repairs exhibit a nominally uniform shear stress distribution within the joint and have the advantage of low peel stress due to the lack of eccentricity in the load path. Scarf repairs are, however, difficult to produce, may involve the removal of a significant amount of parent material, and the uniform shear stresses may make the joint susceptible to creep failure. An experimental program was undertaken to determine the strain capacity of a scarf repair to a 21 ply laminate. The aim of the program is to demonstrate a strain capability in the repair of at least 5200 microstrain when tested under hot/wet conditions. Although some of the specimens tested have achieved this strain level, the performance of the current scarf joint is marginal under these conditions. Detailed analysis of this joint shows that high stresses arise from ply drop-offs within the repair doubler and at the ends of the scarf taper. Good correlation has been observed between the results from the Finite-Element models and those from experimental specimens, indicating that the models are a useful tool to assist in the design of joints of this type. Author

N95-27524# Turkish Land Forces Command, Ankara (Turkey).

SCARF JOINT TECHNIQUE WITH COCURED AND PRECURED PATCHES FOR COMPOSITE REPAIR

F. Elaldi, S. Lee (Institute for Aerospace Research, Ottawa, Ontario.), and R. F. Scott (Institute for Aerospace Research, Ottawa, Ontario.) *In* AGARD, Composite Repair of Military Aircraft Structures Jan. 1995 12 p (For primary document see N95-27504 09-05)

Copyright Avail: CASI HC A03/MF A03

The scarf joint technique is one of the latest techniques used for repairing composite aircraft structures. This paper describes scarf joints comprised of vacuum and autoclave precured and cocured fiber glass epoxy patches bonded to autoclave and vacuum precured parent fiber glass epoxy laminates. Autoclave and vacuum cured parent laminates and the scarf joints were prepared and exposed to the same temperature and moisture environment for comparison. All specimens were loaded in tension at three temperatures. Interlaminar shear strength (ILSS) tests were also carried out for the parent materials. As expected, the tensile strength and ILSS decrease when the material has been exposed to moisture and tested at elevated temperature. No significant difference was reported for either tensile strength or ILSS between autoclave and vacuum cured materials. The room temperature repair efficiencies are reported for single scarf repairs comprised of vacuum cocured and precured patches. These repair efficiencies were found to be similar to the efficiency of the autoclave precured patch repair. This result supports the feasibility of scarf joint repairs in base level facilities. Author

N95-27525# Aerospatiale, Toulouse (France). Composite Structures Div.

COMPOSITE OR METALLIC BOLTED REPAIRS ON SELF-STIFFENED CARBON WING PANEL OF THE COMMUTER ATR72 DESIGN CRITERIA, ANALYSIS, VERIFICATION BY TEST

A. Tropis *In* AGARD, Composite Repair of Military Aircraft Structures Jan. 1995 21 p (For primary document see N95-27504 09-05)

Copyright Avail: CASI HC A03/MF A03

The introduction into service, in 1989, of ATR72 with an outer wing in carbon led Aerospatiale to develop primary structure repair processes which fulfill Airworthiness requirements and which could be performed by the airlines in typical maintenance conditions. This paper describes the two types of bolted repairs developed within the scope of the wing certification: composite doubler or metallic doubler. An analytical microcomputer calculation program allows the critical area and the strength capability of the repaired panel to be determined. This program is validated by tests. Author

N95-27526# Deutsche Airbus G.m.b.H., Hamburg (Germany).

DAMAGE OCCURRENCE ON COMPOSITES DURING TESTING AND FLEET SERVICE: REPAIR OF AIRBUS AIRCRAFT

G. Stemmer *In* AGARD, Composite Repair of Military Aircraft Structures Jan. 1995 8 p (For primary document see N95-27504 09-05)

Copyright Avail: CASI HC A02/MF A03

The application of composite materials to civil aircraft structure was growing during the past 25 years with every new aircraft which went into service. With these materials in commercial use it became necessary to define repairs in the case the component becomes damaged. During fatigue testing at component level the limits for allowable damage and maximum repair sizes were determined for standard damage events and manufacturing defects. The values are depending on structural design, material behavior and local strains or stresses. For simple damages on regular structures necessary repair actions are defined in the Structural Repair Manual. With an approved inspection philosophy the structure is under observation during airline service. It will be presented how the repair philosophy within Airbus Industrie partner companies is defined and which damages were reported on aircraft already in service. Some examples should explain the lessons we have learned from those failures occurred during component testing and airline service. Author

N95-27527# Construcciones Aeronauticas S.A., Madrid (Spain).

REPAIRS OF CFC PRIMARY STRUCTURES

H. GarciaNunez, A. BarrioCardaba, and A. Franganillo *In* AGARD, Composite Repair of Military Aircraft Structures Jan. 1995 10 p (For primary document see N95-27504 09-05)

Copyright Avail: CASI HC A02/MF A03

The use of composites in the last decades has been mainly restricted to secondary structures, with repair methods well known to the airlines. In today's aircraft, a significant amount of primary structure is designed and built in high strength composite materials. Repairs for these elements must take into consideration the restoration of structural strength and stiffness, still being easy to be applied by aircraft operators, with a minimum of special facilities, and requiring a minimum of aircraft-on-ground time. A large number of important structural elements in CFC now in service have been designed and manufactured by CASA. This paper describes how composite repairs are dealt with at CASA, starting from the design board, and the analyses and tests carried out to demonstrate compliance with certification requirements. Author

N95-27528# Royal Australian Air Force, Amberley (Australia). Aero-Mechanical Technologies and Standards.

THE DEVELOPMENT OF AN ENGINEERING STANDARD FOR COMPOSITE REPAIRS

M. J. Davis *In* AGARD, Composite Repair of Military Aircraft Structures Jan. 1995 11 p (For primary document see N95-27504 09-05)

Copyright Avail: CASI HC A03/MF A03

The RAAF has used bonded composite patches for structural repairs to aircraft for nearly twenty years, and they are now seen as a reliable alternative to mechanically fastened repairs. To control the implementation of the repair technology, RAAF propose to adopt Engineering Standard C5033 on Composite Materials and Adhesive Bonded Repairs. The Standard addresses repair authorization and design, as well as repair methodology and quality control. This paper will describe the philosophy of repair design contained in the standard, and outline the materials and process controls necessary for performance of repairs which comply with ISO 9001. Author

N95-27910# General Accounting Office, Washington, DC. National Security and International Affairs Div.

REPORT TO CONGRESSIONAL COMMITTEES. COMANCHE HELICOPTER: TESTING NEEDS TO BE COMPLETED PRIOR TO PRODUCTION DECISIONS

May 1995 30 p

(GAO/NSIAD-95-112; B-259389) Avail: CASI HC A03/MF A01; GAO, PO Box 6015, Gaithersburg, MD 20884-6015 HC

Cost and technical issues associated with the Department of the Army's Comanche helicopter program are reported. CASI

N95-27918 Defence Science and Technology Organisation, Melbourne (Australia). Aeronautical and Maritime Research Lab.

A REVIEW OF AUSTRALIAN AND NEW ZEALAND INVESTIGATIONS ON AERONAUTICAL FATIGUE DURING THE PERIOD APR. 1993 - MAR. 1995

J. M. Grandage and G. S. Jost Mar. 1995 34 p Presented at the 24th Conference of the International Committee on Aeronautical Fatigue, Melbourne, Australia, 1-2 May 1995

(AR-009-202; DSTO-TN-0002) Copyright Avail: Issuing Activity (Defence Science and Technology Organisation, Melbourne, Australia)

This document was prepared for presentation to the 24th Conference of the International Committee on Aeronautical Fatigue scheduled to be held in Melbourne, Australia on 1-2 May 1995. A review is given of the aircraft fatigue research and associated activities which form part of the programs of the Aeronautical and Maritime Research Laboratory, Universities, the Civil Aviation Authority and the Defence Scientific Establishment, New Zealand. The review summarizes fatigue-related research programs as well as fatigue investigations on specific military and civil aircraft. Author

N95-28262*# California Univ., Los Angeles, CA.

AEROELASTICITY AND STRUCTURAL OPTIMIZATION OF COMPOSITE HELICOPTER ROTOR BLADES WITH SWEPT TIPS

K. A. Yuan and P. P. Friedmann Hampton, VA NASA May 1995 433 p

(Grant NAG1-833; RTOP 505-63-36-06)

(NASA-CR-4665; NAS 1.26:4665) Avail: CASI HC A19/MF A04

This report describes the development of an aeroelastic analysis capability for composite helicopter rotor blades with straight and swept tips, and its application to the simulation of helicopter vibration reduction through structural optimization. A new aeroelastic model is developed in this study which is suitable for composite rotor blades with swept tips in hover and in forward flight. The hingeless blade is modeled by beam type finite elements. A single finite element is used to model the swept tip. Arbitrary cross-sectional shape, generally anisotropic material behavior, transverse shears and out-of-plane warping are included in the blade model. The nonlinear equations of motion, derived using Hamilton's principle, are based on a moderate deflection theory. Composite blade cross-sectbnal properties are calculated by a separate linear, two-dimensional cross section analysis. The aerodynamic loads are obtained from quasi-steady, incompressible aerodynamics, based on an implicit formulation. The trim and steady state blade aeroelastic response are solved in a fully coupled manner. In forward flight, where the blade equations of motion are periodic, the coupled trim-aeroelastic response solution is obtained from the harmonic balance method. Subsequently, the periodic system is linearized about the steady state response, and its stability is determined from Floquet theory. Author

N95-28409 Israel Inst. of Metals, Haifa (Israel).

PREDICTION OF FATIGUE CRACK GROWTH UNDER CONSTANT AMPLITUDE AND RANDOM LOADING USING SPECIMENS WITH MULTIPLE CRACKS Final Report, 1 Oct. 1993 - 30 Sep. 1994

Sh. Ustilovsky, R. Arone, J. Oshrat, E. Sterin, and G. Nesviszsky Dec. 1994 78 p Limited Reproducibility: More than 20% of this document may be affected by microfiche quality

(Contract F49620-93-1-0579)

(AD-A291614; TR-524727; EOARD-TR-95-06) Avail: Issuing Activity (Defense Technical Information Center (DTIC))

Fatigue crack growth under stationary Gaussian random loading is considered. A specially developed computerized testing system and software are used for generation of the random loading and investigation of crack growth. The sliding summation numerical method was used for generation of a random loading history characterized by a given autocorrelation function. As far as the loading history of a sufficient length is generated a sequence of maxima and minima is extracted and arranged with the predetermined frequency. The next Operation is elimination of the small amplitude cycles in accordance with the predetermined threshold value and. determination of the minima and maxima two-dimensional distribution of the edited process. A specially built transition matrix derived from this distribution was used for the real-time generation of the random loading during the test. Experimental investigation of the developed random loading generation procedure and crack growth process was performed using aluminium alloy multicrack panel type specimens providing possibility of observation of an array of simultaneously growing cracks. Dependence of fatigue crack life time on random loading parameters as well as stochastic characteristics of crack growth were studied. DTIC

N95-28411 Department of Defense, Washington, DC.

UNMANNED AERIAL VEHICLES, 1994 MASTER PLAN

1995 131 p Limited Reproducibility: More than 20% of this document may be affected by microfiche quality

(AD-A291628) Avail: Issuing Activity (Defense Technical Information Center (DTIC))

The Unmanned Aerial Vehicles (UAV) Joint Project Office was officially established in response to Congressional direction by a charter signed by the Director of Defense Research and Engineering on 16 October 1989. This 1994 UAV Master Plan is the sixth submission to Congress. It provides the acquisition and technology strategies, management, and program plans for nonlethal UAV's. Lethal UAV's are addressed in the classified Department of Defense Standoff Weapons Master Plan. This Master Plan is structured into three parts: an Executive Summary, a main body of 10 sections providing extensive detail, and an appendix of supporting material including discussions of dual uses of UAV's and UAV civil airspace management issues. DTIC

N95-28504 Duke Univ., Durham, NC. Dept. of Mechanical Engineering and Materials Science.

NONLINEAR DYNAMICS AND AEROELASTICITY OF ROTORCRAFT IN FORWARD FLIGHT Final Report, 1 Aug. 1991 - 31 Jul. 1994

Earl H. Dowell Feb. 1995 4 p Limited Reproducibility: More than 20% of this document may be affected by microfiche quality

(Contract DAAL03-91-G-0308)

(AD-A291714; ARO-28493.1-EG) Avail: Issuing Activity (Defense Technical Information Center (DTIC))

Large amplitude (nonlinear) oscillations of rotor blades due to self-excitation (flutter) or external excitation (mechanical or aerodynamic) frequently occur and are often design critical for rotorcraft. The present work is a combined theoretical-experimental study to develop improved understanding and mathematical models for enhanced design and performance. DTIC

N95-28567 Defence Science and Technology Organisation, Melbourne (Australia). Aeronautical and Maritime Research Lab.

TIE-DOWN TRIALS INVOLVING A SIKORSKY S-70B-2 HELICOPTER

Jeremy Blackwell Jan. 1995 40 p Original contains color illustrations

(DSTO-TR-0132; AR-008-418) Copyright Avail: Issuing Activity

Two tie-down trials involving a Sikorsky S-70B-2 helicopter are outlined. The first was land-based and utilized a hydraulic tilt table. The second took place on board an FFG-7 frigate. The trials are part of a DSTO (Defense Science and Technology Organization) investigation aimed at improving the tie-down procedures of S-70 B-2 helicopters when operating from ships. A preliminary analysis of the data is presented and indicates that the type of lashing used to secure the helicopter can have a significant effect on the loads transmitted to the fuselage as well as affecting the relative motion of the aircraft. The effect of aircraft brakes on or off was examined and found to result in noticeable differences to the aircraft behavior. During the ship trial, one type of tie-down lashing was observed to suffer from significant slippage through its locking mechanism. Author

N95-28626 Naval Postgraduate School, Monterey, CA.

MODELING HELICOPTER BLADE DYNAMICS USING A MODIFIED MYKLESTAD-PROHL TRANSFER MATRIX METHOD M.S. Thesis

Juan D. Cuesta Dec. 1994 74 p Limited Reproducibility: More than 20% of this document may be affected by microfiche quality

(AD-A289891) Avail: Issuing Activity (Defense Technical Information Center (DTIC))

Rotor Blade vibratory stresses are of utmost importance in helicopter design. A modified Myklestad-Prohl method for rotating beams has been coded to assist in preliminary helicopter rotor blade design. The rotor blade dynamics program is part of the Joint Army/Navy Rotorcraft Analysis and Design (JANRAD) program which was developed to aid in the preliminary design and analysis of helicopter rotor performance, stability and control, and rotor dynamics. JANRAD is an interactive, user friendly program written in MATLAB version 4.0 programming language and has been used extensively in the Naval Postgraduate School's capstone helicopter design course (AA 4306). A sample case is run and results are discussed. DTIC

N95-28636# Technische Univ., Delft (Netherlands).
NUMERICAL SIMULATION OF CRACK GROWTH IN PRESSURIZED FUSELAGES Ph.D. Thesis
H. A. J. Knops 26 Sep. 1994 208 p
(PB95-192415; ISBN-90-9007413-9) Avail: CASI HC A10/MF A03

The main objective of the present research is to develop a number of tools for the numerical simulation of crack behavior in pressurized fuselages. In these calculations the geometrically nonlinear effects described above and the influence of stiffening components on the crack behavior will be taken into account. Since the flapping phenomenon that is observed in experiments on pressurized aircraft fuselages with initially longitudinal cracks is not yet well understood, a major goal of the present research is to simulate crack flapping numerically and to predict whether a crack will flap and at what crack length. In real structures there will always be a plastic zone around the crack tip. However, the behavior of such 'real' cracks is still believed to be dictated by a number of linear elastic crack tip parameters. Therefore in our research we will assume that linear-elastic fracture mechanics conditions hold and that the state of stress around the crack tip is characterized by these linear-elastic crack tip parameters. NTIS

N95-26942# Kansas Univ., Lawrence, KS.
PRELIMINARY DESIGN PROBLEMS AND SOLUTIONS FOR A SUPERSONIC OBLIQUE ALL-WING TRANSPORT AIRCRAFT Abstract only
Troy Downen *In* Wichita State Univ., AIAA Techfest 20 Proceedings 1994 2 p (For primary document see N95-26941 09-01)
Avail: CASI HC A01/MF A03

N95-26945*# National Aeronautics and Space Administration. Lewis Research Center, Cleveland, OH.
THE HIGH SPEED CIVIL TRANSPORT AND NASA'S HIGH SPEED RESEARCH (HSR) PROGRAM Abstract only
Robert J. Shaw *In* Wichita State Univ., AIAA Techfest 20 Proceedings 1994 2 p (For primary document see N95-26941 09-01)
Avail: CASI HC A01/MF A03

N95-26947# Kansas Univ., Lawrence, KS.
DESIGN OF A HIGH ALTITUDE LONG ENDURANCE AIRCRAFT WITH MANUFACTURING CONSIDERATIONS Abstract Only
Catherine Grant, Richard Hazlewood, Howard Sacks, and Troy Downen *In* Wichita State Univ., AIAA Techfest 20 Proceedings 1994 2 p (For primary document see N95-26941 09-01)
Avail: CASI HC A01/MF A03

N95-26954# Wichita State Univ., Wichita, KS. Dept. of Aerospace Engineering.
FULL SPAN FLAPERONS FOR A BIPLANE
Bonnie L. Johnson *In its* AIAA Techfest 20 Proceedings 1994 16 p (For primary document see N95-26941 09-01)
Avail: CASI HC A03/MF A03

N95-26956*# National Aeronautics and Space Administration. Langley Research Center, Hampton, VA.
INCORPORATING BIPLANE WING THEORY INTO A LARGE, SUBSONIC, ALL-CARGO TRANSPORT
Michael K. Zyskowski *In* Wichita State Univ., AIAA Techfest 20 Proceedings 1994 p 1-15 (For primary document see N95-26941 09-01)
Avail: CASI HC A03/MF A03

N95-28278*# Martin Marietta Corp., Baltimore, MD. Aero and Naval Systems.
APPLICATION OF FIBER-REINFORCED BISMALEIMIDE MATERIALS TO AIRCRAFT NACELLE STRUCTURES
Vasilios Peros, John Ruth, and David Trawinski *In* FAA, Ninth DOD/NASA/FAA Conference on Fibrous Composites in Structural Design, Volume 3 Sep. 1992 p 1333-1347 (For primary document see N95-28266 09-24)
Copyright Avail: CASI HC A03/MF A04

N95-28440*# Wright Lab., Wright-Patterson AFB, OH. Flight Dynamics Directorate.
STRUCTURAL DESIGN OPTIMIZATION WITH SURVIVABILITY DEPENDENT CONSTRAINTS APPLICATION: PRIMARY WING BOX OF A MULTI-ROLE FIGHTER
Douglas J. Dolvin *In* FAA, Ninth DOD/NASA/FAA Conference on Fibrous Composites in Structural Design, Volume 1 Sep. 1992 p 465-48 (For primary document see N95-28420 09-24)
Avail: CASI HC A03/MF A04

N95-28444*# National Aeronautics and Space Administration. Lewis Research Center, Cleveland, OH.
PROBABILISTIC EVALUATION OF FUSELAGE-TYPE COMPOSITE STRUCTURES
Michael C. Shiao (Sverdrup Technology, Inc., Brook Park, OH.) and Christos C. Chamis *In* FAA, Ninth DOD/NASA/FAA Conference on Fibrous Composites in Structural Design, Volume 1 Sep. 1992 p 535-54 Previously announced as N93-12735 (For primary document see N95-28420 09-24)
Avail: CASI HC A03/MF A04

N95-28470*# National Aeronautics and Space Administration. Langley Research Center, Hampton, VA.
TEST AND ANALYSIS RESULTS FOR COMPOSITE TRANSPORT FUSELAGE AND WING STRUCTURES
Jerry W. Deaton, Susan M. Kullerd (Lockheed Engineering and Sciences Co., Hampton, VA.), Ram C. Madan (Douglas Aircraft Co., Inc., Long Beach, CA.), and Victor L. Chen (Douglas Aircraft Co., Inc., Long Beach, CA.) *In* FAA, Ninth DOD/NASA/FAA Conference on Fibrous Composites in Structural Design, Volume 2 Sep. 1992 p 719-74 Previously announced as X92-10413 (For primary document see N95-28462 09-24)
Avail: CASI HC A03/MF A04

N95-28471*# National Aeronautics and Space Administration. Langley Research Center, Hampton, VA.
TENSION FRACTURE OF LAMINATES FOR TRANSPORT FUSELAGE. PART 1: MATERIAL SCREENING
T. H. Walker (Boeing Commercial Airplane Co., Seattle, WA.), W. B. Avery (Boeing Commercial Airplane Co., Seattle, WA.), L. B. Ilcewicz (Boeing Commercial Airplane Co., Seattle, WA.), C. C. Poe, Jr., and C. E. Harris *In* FAA, Ninth DOD/NASA/FAA Conference on Fibrous Composites in Structural Design, Volume 2 Sep. 1992 p 747-78 Previously announced as X92-10414 (For primary document see N95-28462 09-24)
(Contract NAS1-18889)
Avail: CASI HC A03/MF A04

N95-28473*# Boeing Commercial Airplane Co., Seattle, WA.
LOCAL DESIGN OPTIMIZATION FOR COMPOSITE TRANSPORT FUSELAGE CROWN PANELS
G. D. Swanson, L. B. Ilcewicz, T. H. Walker, D. Graesser (Washington Univ., Seattle, WA.), M. Tuttle (Washington Univ., Seattle, WA.), and Z. Zabinsky (Washington Univ., Seattle, WA.) *In* FAA, Ninth DOD/NASA/FAA Conference on Fibrous Composites in Structural Design, Volume 2 Sep. 1992 p 795-81 Previously announced as X92-10416 (For primary document see N95-28462 09-24)
(Contract NAS1-18889)
Avail: CASI HC A03/MF A04

N95-28474*# Boeing Commercial Airplane Co., Seattle, WA.
COMPOSITE FUSELAGE CROWN PANEL MANUFACTURING TECHNOLOGY
Kurtis Willden, S. Metschan, C. Grant (Hercules Aerospace Co., Magna, UT.), and T. Brown (Hercules Aerospace Co., Magna, UT.) *In* FAA, Ninth DOD/NASA/FAA Conference on Fibrous Composites in Structural Design, Volume 2 Sep. 1992 p 815-84 Previously announced as X92-10417 (For primary document see N95-28462 09-24)

(Contract NAS1-18889)
Avail: CASI HC A03/MF A04

N95-28476*# Lockheed Aeronautical Systems Co., Marietta, GA.
ADVANCED TEXTILE APPLICATIONS FOR PRIMARY AIRCRAFT STRUCTURES
Anthony C. Jackson, Ronald E. Barrie, Bharat M. Shah, and Jay G. Shukla *In* FAA, Ninth DOD/NASA/FAA Conference on Fibrous Composites in Structural Design, Volume 2 Sep. 1992 p 875-90 Previously announced as X92-10419 (For primary document see N95-28462 09-24)
(Contract NAS1-18888)
Avail: CASI HC A03/MF A04

N95-28480*# Dow-United Technologies Composite Products, Inc., Wallingford, CT.
APPLICATION OF DAMAGE TOLERANCE METHODOLOGY IN CERTIFICATION OF THE PIAGGIO P-180 AVANTI
Jerry Johnson *In* FAA, Ninth DOD/NASA/FAA Conference on Fibrous Composites in Structural Design, Volume 2 Sep. 1992 p 999-1012 (For primary document see N95-28462 09-24)
Avail: CASI HC A03/MF A04

N95-28482*# Boeing Commercial Airplane Co., Seattle, WA.
IMPACT DAMAGE RESISTANCE OF COMPOSITE FUSELAGE STRUCTURE, PART 1
E. F. Dost, W. B. Avery, L. B. Ilcewicz, D. H. Grande, and B. R. Coxon (Integrated Technologies, Inc., Bothell, WA.) *In* FAA, Ninth DOD/NASA/FAA Conference on Fibrous Composites in Structural Design, Volume 2 Sep. 1992 p 1037-1069 (For primary document see N95-28462 09-24)
(Contract NAS1-18889)
Avail: CASI HC A03/MF A04

N95-28487*# National Aeronautics and Space Administration. Langley Research Center, Hampton, VA.
DAMAGE TOLERANCE OF A GEODESICALLY STIFFENED ADVANCED COMPOSITE STRUCTURAL CONCEPT FOR AIRCRAFT STRUCTURAL APPLICATIONS
Marshall Rouse and Damodar R. Ambur *In* FAA, Ninth DOD/NASA/FAA Conference on Fibrous Composites in Structural Design, Volume 2 Sep. 1992 p 1111-1121 (For primary document see N95-28462 09-24)
Avail: CASI HC A03/MF A04

N95-28488*# Grumman Aerospace Corp., Bethpage, NY. Aircraft Systems.
ADVANCED WING DESIGN SURVIVABILITY TESTING AND RESULTS
J. Bruno and M. Tobias (Naval Air Development Center, Warminster, PA.) *In* FAA, Ninth DOD/NASA/FAA Conference on Fibrous Composites in Structural Design, Volume 2 Sep. 1992 p 1123-1137 (For primary document see N95-28462 09-24)
Avail: CASI HC A03/MF A04

N95-28489*# Boeing Commercial Airplane Co., Seattle, WA. 777 Empennage Structures.
NASA-ACEE/BOEING 737 GRAPHITE-EPOXY HORIZONTAL STABILIZER SERVICE
J. T. Quinlivan, J. A. Kent, and D. R. Wilson *In* FAA, Ninth DOD/NASA/FAA Conference on Fibrous Composites in Structural Design, Volume 2 Sep. 1992 p 1139-1150 (For primary document see N95-28462 09-24)
Avail: CASI HC A03/MF A04

06 AIRCRAFT INSTRUMENTATION

Includes cockpit and cabin display devices; and flight instruments.

For related information see also *19 Spacecraft Instrumentation* and *35 Instrumentation and Photography.*

N95-27003 Wright Lab., Wright-Patterson AFB, OH.
PARTIAL DISCHARGE TESTING OF HIGH VOLTAGE WIRING HARNESS FOR AIRBORNE DISPLAYS Final Report, 15 Dec. 1993 - 15 Feb. 1994
Gregory L. Rhoads, John Horwath, and Daniel Schweickart Oct. 1994 18 p Limited Reproducibility: More than 20% of this document may be affected by microfiche quality
(AD-A289150; WL-TR-94-2099) Avail: Issuing Activity (Defense Technical Information Center (DTIC))

The pilots of advanced tactical airplanes must evaluate increasingly more information. Innovations such as the heads-up display were designed to decrease the visual workload. More flexible helmet-mounted CRT's are now being developed, presenting new design challenges. For example, high voltage leads for helmet-mounted displays must incorporate a quick release, load-break mechanism into the wiring harness to accommodate pilot ejection. The potential presence of flammable vapors resulted in an arc-suppressing, quick-disconnect connector design which opens the high voltage via hermetically sealed contacts. The sealed contacts contain any arcing and break the circuit before the connector separates. The prototype harness routes two 13.5 kilovolt rated direct current leads along with other wiring via the quick-disconnect connector. The high voltage and compact design motivate concerns about partial discharge degradation of the insulation, particularly at sub-atmospheric pressures. The harness has been tested for partial discharges at simulated altitudes up to 70,000 feet in the Aerospace Power Division's High Power Laboratory. DTIC

N95-28203*# Georgia Inst. of Tech., Atlanta, GA. Center of Human-Machine Systems Research.
OPERATOR MODELING IN COMMERICAL AVIATION: COGNITIVE MODELS, INTELLIGENT DISPLAYS, AND PILOT'S ASSISTANTS Final Report, 1 Jul. 1990 - 30 Apr. 1994
T. Govindaraj and C. M. Mitchell 30 Apr. 1994 22 p
(Contract NCC2-675)
(NASA-CR-198609; NAS 1.26:198609) Avail: CASI HC A03/MF A01

One of the goals of the National Aviation Safety/Automation program is to address the issue of human-centered automation in the cockpit. Human-centered automation is automation that, in the cockpit, enhances or assists the crew rather than replacing them. The Georgia Tech research program focused on this general theme, with emphasis on designing a computer-based pilot's assistant, intelligent (i.e, context-sensitive) displays, and an intelligent tutoring system for understanding and operating the autoflight system. In particular, the aids and displays were designed to enhance the crew's situational awareness of the current state of the automated flight systems and to assist the crew's situational awareness of the current state of the automated flight systems and to assist the crew in coordinating the autoflight system resources. The activities of this grant included: (1) an OFMspert to understand pilot navigation activities in a 727 class aircraft; (2) an extension of OFMspert to understand mode control in a glass cockpit, Georgia Tech Crew Activity Tracking System (GT-CATS); (3) the design of a training system to teach pilots about the vertical navigation portion of the flight management system -VNAV Tutor; and (4) a proof-of-concept display, using existing display technology, to facilitate mode awareness, particularly in situations in which controlled flight into terrain (CFIT) is a potential. Derived from text

N95-28586 Air Force Inst. of Tech., Wright-Patterson AFB, OH. School of Logistics and Acquisition Management.
LIFE CYCLE COSTS OF ALTERNATIVES FOR F-16 PRINTED CIRCUIT BOARD DIAGNOSIS EQUIPMENT M.S. Thesis
Kent R. Montgomery and Clifford B. Thorstenson Dec. 1994 53 p Limited Reproducibility: More than 20% of this document may be affected by microfiche quality
(AD-A288744; AFIT/GSS/LAR/94D-3) Avail: Issuing Activity (Defense Technical Information Center (DTIC))

This study analyzes two alternatives for printed circuit board (PCB) diagnosis for the F-16 depot PCB repair shop from a life cycle cost (LCC) perspective. Alternative 1 assumes the use of the current F-16 automatic test equipment (ATE) while Alternative 2 augments the current ATE with infrared imaging test equipment. Infrared imaging is a developed technology that is currently available to the Air Force in a commercial-off-the-shelf (COTS) form. Using the Cost Analysis and Strategy Assessment (CASA) Life Cycle Cost (LCC) Model and data from the DL41 database on F-16 PCB's this study determined that over the current expected life of the F-16, the next twenty-five years, a savings of approximately $1.1 million (1994 dollars) can be realized by augmenting the current F-16 ATE with infrared imaging test equipment 15% of the F-16 printed circuit boards (PCB's) are single card PCB's which can be tested using infrared imaging test. This study assumes that the total number of PCB's and the percentage of single card PCB's does not change over the F-16's lifetime. Sensitivity analyses are performed varying the percentage of single card PCB's, the total number of PCB's and the F-16 lifetime to determine the effects these changes might have on the total life cycle cost of Alternative 2. DTIC

07 AIRCRAFT PROPULSION AND POWER

Includes prime propulsion systems and systems components, e.g., gas turbine engines and compressors; and onboard auxilliary power plants for aircraft.

For related information see also *20 Spacecraft Propulsion and Power, 28 Propellants and Fuels,* and *44 Energy Production and Conversion.*

N95-26412*# National Aeronautics and Space Administration. Ames Research Center, Moffett Field, CA.

SIMULATION MODEL OF THE INTEGRATED FLIGHT/PROPULSION CONTROL SYSTEM, DISPLAYS, AND PROPULSION SYSTEM FOR ASTOVL LIFT-FAN AIRCRAFT

W. Y. William Chung, Paul F. Borchers, and James A. Franklin Apr. 1995 50 p
(RTOP 505-68-32)
(NASA-TM-108866; A-950048; NAS 1.15:108866) Avail: CASI HC A03/MF A01

A simulation model has been developed for use in piloted evaluations of takeoff, transition, hover, and landing characteristics of an advanced, short takeoff, vertical landing lift fan fighter aircraft. The flight/propulsion control system includes modes for several response types which are coupled to the aircraft's aerodynamic and propulsion system effectors through a control selector tailored to the lift fan propulsion system. Head-up display modes for approach and hover, tailored to their corresponding control modes are provided in the simulation. Propulsion system components modeled include a remote lift and a lift/cruise engine. Their static performance and dynamic response are represented by the model. A separate report describes the subsonic, power-off aerodynamics and jet induced aerodynamics in hover and forward flight, including ground effects. Author

N95-26424 Defence Science and Technology Organisation, Melbourne (Australia). Aeronautical and Maritime Research Lab.

CHARACTERISTICS OF THE TURBINE INLET TEMPERATURE SENSING CIRCUIT FOR THE T56 TURBO-PROP ENGINE

K. F. Fraser Nov. 1994 57 p
(DSTO-TR-0095; AR-008-374) Copyright Avail: Issuing Activity (DSTO, Melbourne Victoria, Australia)

The temperature to voltage transfer characteristics of the standard turbine inlet temperature averaging sensor for the T56 turbo-prop engine are derived using measured resistance parameters for the 18-thermocouple network. The transfer characteristics of an add-on individual thermocouple temperature sensing circuit are also derived and some of the requirements of the associated signal conditioning circuit are briefly reviewed. Author

N95-26600# National Aerospace Lab., Tokyo (Japan). Remjet Propulsion Research Div.

EXPERIMENT ON A RECTANGULAR CROSS SECTION SCRAMJET COMBUSTOR. 2: EFFECTS OF FUEL INJECTOR GEOMETRY

Atsuo Murakami, Tomoyuki Komuro, and Kenji Kudou Dec. 1993 27 p In JAPANESE
(ISSN 0389-4010)
(NAL-TR-1220) Avail: CASI HC A03/MF A01

An experimental study of a rectangular cross section scramjet combustor was carried out. The effects on mixing and combustion performances of the rearward-facing steps, fuel injection orifice arrangements and the length of the constant height section downstream of the step were examined. The peak wall pressure, namely the strength of the precombustion shock, increased as the length of the constant height section downstream of the injection orifices increased. The injected fuel jets coalesced if the precombustion shock was too strong, while they stratified if it was too weak. Hence the mixing and combustion efficiencies of these two cases were low. To achieve better fuel mixing, the length of the constant height section must be selected so that it gives the most suitable strength of the precombustion shock. Sweep of the rearward-facing steps and the orifice arrangements had little effect on the mixing and combustion efficiencies. Author

N95-26706# National Aerospace Lab., Tokyo (Japan). Ramjet Propulsion Research Div.

EFFECTS OF DUST FROM STORAGE HEATERS ON IGNITION IN SCRAMJETS

Apr. 1994 20 p In JAPANESE
(ISSN 0389-4010)
(NAL-TR-1234) Avail: CASI HC A03/MF A01

The effect of dust on ignition delay in ground-testing of scramjet engines was investigated analytically. Incandescent particles issued from a storage air heater cause premature ignition of H2 - fuel injected into the combustor. In order to prevent erroneous experimental results, the concentration of particles greater than about 40 microns in size must be restricted to less than 10(exp 3) particles/m(exp 3). The thermal and chemical inhibition effects due to fine particles can be neglected in engine testing, if the mass fraction of dust in the heated air is less than 10(exp -1) in the wind tunnel. This analysis is applicable to the mechanism of powdered flame suppressants. Author

N95-26777*# MCAT Inst., San Jose, CA.

TURBOMACHINERY DESIGN AND TONAL ACOUSTICS COMPUTATIONS Final Report, Jun. 1993 - Jan. 1995

Akil A. Rangwalla Jan. 1995 53 p Original contains color illustrations
(Contract NCC2-767)
(NASA-CR-197749; NAS 1.26:197749; MCAT-95-17) Avail: CASI HC A04/MF A01; 2 functional color pages

The objective of this research was two-fold. The first objective was to complete the three-dimensional unsteady calculations of the flow through a new transonic turbine and study the effects of secondary flows due to the hub and casing, tip clearance vortices, and the inherent three-dimensional mixing of the flow. It should be noted that this turbine was and is still in the design phase and the results of the calculations have formed an integral part of the design process. The second objective of this proposal was to evaluate the capability of rotor-stator interaction codes to calculate tonal acoustics. Derived from text

N95-26878 Air Force Inst. of Tech., Wright-Patterson AFB, OH. School of Engineering.

STALL PRECURSOR STUDY OF HIGH FREQUENCY DATA FOR THREE HIGH SPEED, SWEPT COMPRESSOR ROTORS M.S. Thesis

James F. Anderton Dec. 1994 165 p Limited Reproducibility: More than 20% of this document may be affected by microfiche quality
(AD-A289379; AFIT/GAE/ENY/94D-13) Avail: Issuing Activity (Defense Technical Information Center (DTIC))

The frequency spectra of three single stage, high speed compressor rotors were derived and analyzed from experimental data. The compressor rotors included straight, backward-swept, and forward-swept blade designs. Data was acquired from four pressure transducers located on the compressor casing and arranged axially between locations 40% of blade chord upstream of the rotor face to just over the leading edge of the blades. Each rotor was throttled to stall at two constant speeds between 90% and 100% of design speed. Data digitization at 20 kHz revealed multiples of the rotor frequency up to and beyond a dominant blade passing frequency. Further analyses for characteristics of impending stall included examination of integrated signal power and cross-correlations of transducer signals from the upstream and downstream-most pressure transducers. Results of the integrated signal power approach showed promise as a potential pre-stall warning. This technique detected differences in the signal power at the two transducers in the immediate pre-stall time frame. Pre-stall warning times varied from several seconds to less than 0.5 second, with higher rotor speeds giving less warning time. Results for the forward-swept rotor, however, showed that integrated signal power did not warn of impending stall, and that surge energies played an important role in this rotor's stalling characteristics. An hypothesis for the behavior of the forward swept rotor, based on the possibility of stall development beginning in the near-hub radial region of this compressor, was developed. DTIC

N95-27860*# National Aeronautics and Space Administration. Lewis Research Center, Cleveland, OH.
OPTIMIZATION OF WAVE ROTORS FOR USE AS GAS TURBINE ENGINE TOPPING CYCLES
Jack Wilson (NYMA, Inc., Brook Park, OH.) and Daniel E. Paxson Jun. 1995 11 p Presented at the 1995 Aerospace Atlantic Conference and Exposition, Dayton, OH, 23-25 May 1995; sponsored by SAE
(Contract NAS3-27186; RTOP 505-90-58)
(NASA-TM-106951; E-9689; NAS 1.15:106951) Avail: CASI HC A03/MF A01

Use of a wave rotor as a topping cycle for a gas turbine engine can improve specific power and reduce specific fuel consumption. Maximum improvement requires the wave rotor to be optimized for best performance at the mass flow of the engine. The optimization is a trade-off between losses due to friction and passage opening time, and rotational effects. An experimentally validated, one-dimensional CFD code, which includes these effects, has been used to calculate wave rotor performance, and find the optimum configuration. The technique is described, and results given for wave rotors sized for engines with sea level mass flows of 4, 26, and 400 lb/sec. Author

N95-27866*# Allison Engine Co., Indianapolis, IN.
PROPULSION SYSTEM ASSESSMENT FOR VERY HIGH UAV UNDER ERAST Final Report
James L. Bettner, Craig S. Blandford, and Bernie J. Rezy Cleveland, OH NASA May 1995 156 p
(Contract NAS3-25950; RTOP 537-10-20)
(NASA-CR-195469; E-9653; NAS 1.26:195469; EDR-17199) Avail: CASI HC A08/MF A02

A series of propulsion systems were configured to power a sensor platform to very high altitudes under the Experimental Research Advanced Sensor Technology (ERAST) program. The unmanned aircraft was required to carry a 100 kg instrument package to 90,000 ft altitude, collect samples and make scientific measurements for 4 hr, and then return to base. A performance screening evaluation of 11 propulsion systems for this high altitude mission was conducted. Engine configurations ranged from turboprop, spark ignition, two- and four-stroke diesel, rotary, and fuel cell concepts. Turbo and non-turbo-compounded, recuperated and nonrecuperated arrangements, along with regular JP and hydrogen fuels were interrogated. Each configuration was carried through a preliminary design where all turbomachinery, heat exchangers, and engine core concepts were sized and weighed for near-optimum design point performance. Mission analysis, which sized the aircraft for each of the propulsion systems investigated, was conducted. From the array of configurations investigated, the propulsion system for each of three different technology levels (i.e., state of the art, near term, and far term) that was best suited for this very high altitude mission was identified and recommended for further study. Author

N95-28227*# McDonnell-Douglas Corp., Saint Louis, MO.
PERFORMANCE STUDY FOR INLET INSTALLATIONS
Donald C. Bingaman Nov. 1992 94 p
(Contract NAS1-19462; RTOP 505-68-70-06)
(NASA-CR-189714; NAS 1.26:189714) Avail: CASI HC A05/MF A01

A conceptual design trade study was conducted by McDonnell Aircraft Company (MCAIR) and NASA LARC PAB to determine the impact of inlet design features incorporated for reduced detectability on inlet performance, weight, and cost, for both fighter and attack-type aircraft. Quality Function Deployment (QFD) techniques were used to prioritize trade study issues, and select 'best' air induction system configurations for each of two notional aircraft, the Multi-Role Fighter (MRF) and the Advanced Medium Attack (AMA) bomber. Database deficiencies discovered in the trade study process were identified, and technology roadmaps were developed to address these deficiencies. Finally, two high speed inlet wind tunnel model concepts were developed for follow-on wind tunnel investigations. Author

N95-28343*# National Aeronautics and Space Administration. Langley Research Center, Hampton, VA.
EXPERIMENTAL INVESTIGATION OF INLET-COMBUSTOR ISOLATORS FOR A DUAL-MODE SCRAMJET AT A MACH NUMBER OF 4
Saied Emami (Lockheed Engineering and Sciences Co., Hampton, VA.), Carl A. Trexler, Aaron H. Auslender (Lockheed Engineering and Sciences Co., Hampton, VA.), and John P. Weidner May 1995 93 p
(RTOP 505-70-62-01)
(NASA-TP-3502; L-17422; NAS 1.60:3502) Avail: CASI HC A05/MF A01

This report details experimentally derived operational characteristics of numerous two-dimensional planar inlet-combustor isolator configurations at a Mach number of 4. Variations in geometry included (1) inlet cowl length; (2) inlet cowl rotation angle; (3) isolator length; and (4) utilization of a rearward-facing isolator step. To obtain inlet-isolator maximum pressure-rise data relevant to ramjet-engine combustion operation, configurations were mechanically back pressured. Results demonstrated that the combined inlet-isolator maximum back-pressure capability increases as a function of isolator length and contraction ratio, and that the initiation of unstart is nearly independent of inlet cowl length, inlet cowl contraction ratio, and mass capture. Additionally, data are presented quantifying the initiation of inlet unstarts and the corresponding unstart pressure levels. Author

N95-28344*# National Aeronautics and Space Administration. Lewis Research Center, Cleveland, OH.
NUMERICAL ANALYSIS OF INTRA-CAVITY AND POWER-STREAM FLOW INTERACTION IN MULTIPLE GAS-TURBINE DISK-CAVITIES
M. M. Athavale (CFD Research Corp., Huntsville, AL.), A. J. Przekwas (CFD Research Corp., Huntsville, AL.), R. C. Hendricks, and B. M. Steinetz May 1995 19 p Presented at the Turbo Expo 1995, Houston, TX, 5-8 Jun. 1995; sponsored by ASME
(RTOP 242-50-01)
(NASA-TM-106886; E-9523; NAS 1.15:106886) Avail: CASI HC A03/MF A01

A numerical analysis methodology and solutions of the interaction between the power stream and multiply-connected multi-cavity sealed secondary flow fields are presented. Flow solutions for a multi-cavity experimental rig were computed and compared with experimental data of Daniels and Johnson. The flow solutions illustrate the complex coupling between the main-path and the cavity flows as well as outline the flow thread that exists throughout the subplatform multiple cavities and seals. The analysis also shows that the de-coupled solutions on single cavities is inadequate. The present results show trends similar to the T-700 engine data that suggests the changes in the CDP seal altered the flow fields throughout the engine and affected the engine performance. Author

N95-28646 Ceramic Composites, Inc., Millersville, MD.
CERAMIC COMPOSITE COMBUSTOR CANS FOR EXPENDABLE TURBINE ENGINES Final Report, 29 Apr. 1993 - 15 Feb. 1994
Larry L. Fehrenbacher and John A. Hanigofsky Mar. 1994 35 p Limited Reproducibility: More than 20% of this document may be affected by microfiche quality
(Contract F33615-93-C-2321)
(AD-A289551; WL-TR-95-2001) Avail: Issuing Activity (Defense Technical Information Center (DTIC))

Ceramic matrix composite fabrication by microwave assisted chemical vapor infiltration (MWCVI) has been demonstrated as a feasible, faster, and more economical technique as compared to conventional CVI. Two deposition systems, carbon and silicon carbide, were investigated using this processing technique. Densification rates over an order of magnitude higher have been achieved on small cylindrical Nicalon fiber preforms. Economic forecasts based on previous SiC deposition and this Phase 1 work shows a significant improvement in part cost as compared to conventional CVI work. A reduction in cost of a factor of 20 has been calculated. A larger, commercial microwave system has been designed for scaled up prototype part fabrication. DTIC

N95-28275*# Pratt and Whitney Aircraft Group, West Palm Beach, FL.
COMPOSITE INTERMEDIATE CASE MANUFACTURING SCALE-UP FOR ADVANCED ENGINES
Rowena H. Ecklund *In* FAA, Ninth DOD/NASA/FAA Conference on Fibrous Composites in Structural Design, Volume 3 Sep. 1992 p 1289-1302 (For primary document see N95-28266 09-24)
(Contract F33615-85-C-5152)
Copyright Avail: CASI HC A03/MF A04

N95-28277*# National Aeronautics and Space Administration. Lewis Research Center, Cleveland, OH.
ANALYSIS OF AIRCRAFT ENGINE BLADE SUBJECT TO ICE IMPACT
E. S. Reddy (Sverdrup Technology, Inc., Brook Park, OH.), G. H. Abumeri (Sverdrup Technology, Inc., Brook Park, OH.), C. C. Chamis, and P. L. N. Murthy *In* FAA, Ninth DOD/NASA/FAA Conference on Fibrous Composites in Structural Design, Volume 3 Sep. 1992 p 1319-1331 Previously announced as N92-15402 (For primary document see N95-28266 09-24)
Copyright Avail: CASI HC A03/MF A04

08 AIRCRAFT STABILITY AND CONTROL

Includes aircraft handling qualities; piloting; flight controls; and autopilots.

For related information see also *05 Aircraft Design, Testing and Performance.*

N95-26487 Technical Univ. of Lublin, Lublin (Poland). Dept. of Fundamental Electrical Engineering.
ELECTROMAGNETIC DEVICES AND PROCESSES IN ENVIRONMENT PROTECTION
9 Sep. 1994 336 p Presented at the International Conference ELMECO 1994, Lublin, Poland, 8-9 Sep. 1994 Sponsored by Army; and Trans-European Mobility Scheme for Univ. Studies Limited Reproducibility: More than 20% of this document may be affected by microfiche quality
(Contract N68171-94-M-6201)
(AD-A288656; R/D-7463-CH-02; ISBN-83-86333-60-X) Avail: Issuing Activity (Defense Technical Information Center (DTIC))

In the late twentieth century, ecological problems have become essential to the development of civilization on Earth and affect not only ecologists but everyone. The electrical power industry has made a substantial contribution to the destruction of the natural environment and therefore electrical engineers are particularly obliged to repair the damage and to make the least amount of harm as possible. For a long time some electromagnetic devices and processes have been known and applied to clean the air and water and to replace those more noxious to the environment. Recently, low temperature plasma has been especially used as developed applications to treat water, sewage, air and toxic gases. Ozone synthesis and toxic gas neutralization are carried out by means of electric methods in electromagnetic devices. DTIC

N95-26555 Naval Postgraduate School, Monterey, CA.
DESIGN AND SYNTHESIS OF A REAL-TIME CONTROLLER FOR AN UNMANNED AIR VEHICLE M.S. Thesis
Peter M. Hoffman Sep. 1994 121 p Limited Reproducibility: More than 20% of this document may be affected by microfiche quality
(AD-A289134) Avail: Issuing Activity (Defense Technical Information Center (DTIC))

The Naval Postgraduate School is developing a vertical take-off and landing (VTOL) unmanned air vehicle (UAV) that can transition to horizontal flight, once airborne, in order to take advantage of the improvements in speed, range, and loiter time that horizontal, fixed-wing flight provides. This research investigates the design requirements of the central controlling device for that UAV, including the specific problems of defining the necessary hardware components and developing software for executive control. First, hardware requirements needed to be determined. By exploring the general operational requirements of the UAV and taking into account space and weight limitations, a hardware suite was selected which could provide adequate functionality to replace the human traits of a pilot. In order to provide 'awareness' of the operational environment, motion sensors, navigation equipment, and communication equipment was required. Controllable servo-motors were necessary to move control surfaces appropriately. Computer hardware, necessary to provide system intelligence, was selected in order to inter-operate with the other hardware. Next, a Real-Time Executive (RTE) software program was designed to provide the functionality and coordination of all hardware components. Device drivers for each component were developed, and overall coordination was planned using a Yourdon style essential model. Periodic interrupts were used to control execution time. Last, the specifications and configuration of all hardware components were completely documented, and the operation of the RTE program fully explained. From this understanding of the overall control system, future development can continue, resulting in a more effective and efficient UAV design. DTIC

N95-26773*# Army Aviation Systems Command, Moffett Field, CA. Aeroflightdynamics Directorate.
AN INVESTIGATION OF THE EFFECTS OF PITCH-ROLL (DE)COUPLING ON HELICOPTER HANDLING QUALITIES
C. L. Blanken (National Aeronautics and Space Administration. Ames Research Center, Moffett Field, CA.), H. J. Pausder (Deutsche Forschungs- und Versuchsanstalt fuer Luft- und Raumfahrt, Brunswick, Germany.), and C. J. Ockier (Deutsche Forschungs- und Versuchsanstalt fuer Luft- und Raumfahrt, Brunswick, Germany.) May 1995 120 p
(RTOP 505-59-36)
(NASA-TM-110349; A-950055; NAS 1.15:110349; USAATCOM-TR-95-A-003) Avail: CASI HC A06/MF A02

An extensive investigation of the effects of pitch-roll coupling on helicopter handling qualities was performed by the U.S. Army and Deutsche Forschungsanstalt fur Luft- und Raumfahrt (DLR), using a NASA ground-based and a DLR in-flight simulator. Over 90 different coupling configurations were evaluated using a high gain roll-axis tracking task. The results show that although the current ADS-33C coupling criterion discriminates against those types of coupling typical of conventionally controlled helicopters, it is not always suited for the prediction of handling qualities of helicopters with modern control systems. Based on the observation that high frequency inputs during tracking are used to alleviate coupling, a frequency domain pitch-roll coupling criterion that uses the average coupling ratio between the bandwidth and neutral stability frequency is formulated. This criterion provides a more comprehensive coverage with respect to the different types of coupling, shows excellent consistency, and has the additional benefit that compliance testing data are obtained from the bandwidth/phase delay tests, so that no additional flight testing is needed. Author

N95-26957 Air Force Inst. of Tech., Wright-Patterson AFB, OH. School of Engineering.
ELECTRO-HYDROSTATIC ACTUATOR CONTROLLER DESIGN USING QUANTITATIVE FEEDBACK THEORY M.S. Thesis
Ki Ho Kang Dec. 1994 111 p Limited Reproducibility: More than 20% of this document may be affected by microfiche quality
(AD-A289220; AFIT/GE/ENG/94D-18) Avail: Issuing Activity (Defense Technical Information Center (DTIC))

The Electro-Hydrostatic Actuator (EHA) technology offers a higher degree of combat survivability and easier maintainability of the aircraft flight control system, because all the components necessary to operate the actuator are collocated with the actuator. Quantitative Feedback Theory (QFT) is used to design a control system for the EHA. The impact of parameter variations, sensor noise, and flight conditions are explicitly considered in the design process. The solution utilizes a two loop QFT feedback structure. The inner loop structure stabilizes the motor's angular velocity and decreases the outer loop's uncertainty. The outer loop structure controls the RAM piston's position to track the input command. The resulting design is not only robust with respect to plant parameter variations, but is also insensitive to the effects of sensor noise. The actuator's phase lag is reduced by incorporating phase constraints in the QFT design paradigm. QFT is shown to be a viable tool in solving a real-world problem. DTIC

N95-26958 Air Force Inst. of Tech., Wright-Patterson AFB, OH.
A QUANTITATIVE FEEDBACK THEORY FCS DESIGN FOR THE SUBSONIC ENVELOPE OF THE VISTA F-16 INCLUDING CONFIGURATION VARIATION M.S. Thesis
Scott N. Phillips Dec. 1994 170 p Limited Reproducibility: More than

20% of this document may be affected by microfiche quality
(AD-A289221; AFIT/GE/ENG/94D-24) Avail: Issuing Activity (Defense Technical Information Center (DTIC))

An aircraft's response to control inputs varies widely throughout its flight envelope. The aircraft configuration also impacts control response through variations in center of gravity and moments of inertia. Designing a flight control system (FCS) to accommodate the full flight envelope and configuration set of an aircraft is clearly a complex undertaking. Quantitative feedback theory (QFT) is a design tool which enables the engineer to attack this task in an efficient way. Although QFT is a robust control design technique, it is an interactive algorithm allowing the engineer full control over compensator order and gain. In this research effort, a full subsonic flight envelope FCS is designed for the VISTA F-16 aircraft using QFT. Four aircraft configurations are considered. The strict control of the compensator order and gain allowed by QFT facilitates the attainment of desired performance while avoiding physical saturations. In addition, flying qualities are imbedded in the longitudinal design through the use of a control parameter which varies with the aircraft's energy state. This parameter is synthesized to closely reflect the actual control desires of the pilot throughout the aircraft flight envelope. Linear simulations with realistically large control inputs are used to validate the design. DTIC

N95-26981 Air Force Inst. of Tech., Wright-Patterson AFB, OH. School of Engineering.

ADVANCED FORMATION FLIGHT CONTROL M.S. Thesis

Michael J. Veth Dec. 1994 145 p Limited Reproducibility: More than 20% of this document may be affected by microfiche quality
(AD-A289271; AFIT/GE/ENG/94D-30) Avail: Issuing Activity (Defense Technical Information Center (DTIC))

In this thesis, the formation flight control problem is continued from four previous theses. Automatic formation flight involves controlling multiple aircraft equipped with standard Mach-hold, altitude hold, and heading-hold autopilots to maintain a desired distance from a lead aircraft or 'rabbit'. Changes in the rabbit's states are treated as disturbances to the system and rejected. Previous research is advanced in the following areas: Higher-order aircraft/autopilot models are included into the design and a new feedback control law is employed, resulting in more accurate simulations. An energy tracking scheme is developed and is shown to reduce wing aircraft energy excursions. Finally, the formation hold autopilot is modified to allow the wing aircraft to orbit a stationary reference point on the earth at a desired range, airspeed, and altitude. The importance of the disturbance rejection capability of the controller is demonstrated through comparisons of linearized model predictions with nonlinear simulations. The design tradeoffs between performance and robustness are emphasized. DTIC

N95-27036 Air Force Inst. of Tech., Wright-Patterson AFB, OH.

FLIGHT CONTROL DESIGN USING MIXED H2/MICRON OPTIMIZATION M.S. Thesis

Douglas D. Decker Dec. 1994 159 p Limited Reproducibility: More than 20% of this document may be affected by microfiche quality
(AD-A289288; AFIT/GA/ENY/94D-8) Avail: Issuing Activity (Defense Technical Information Center (DTIC))

This thesis examines the use of the mixed H2/Microns optimal control synthesis method in the design of a flight control system for the lateral/directional axes of the F-16 Variable Stability In-Flight Simulator Test Aircraft (VISTA). The method is designed to minimize the H2 norm (two-norm) for a given value of microns. This should provide adequate noise and disturbance rejection while maintaining robustness against several types of uncertainties in the system. This thesis finds that, for this problem, the two-norm is not an accurate representation of the outputs of interest. When the two-norm is broken up into its constituent parts an appropriate solution can be found. This thesis also finds that it is possible to use an H2 controller which is destabilizing to the evaluation model as the starting point in the mixed H2/IL curve and still get an acceptable answer. A numerical approach was used, utilizing a recently improved computer algorithm. DTIC

N95-27839*# National Aeronautics and Space Administration. Langley Research Center, Hampton, VA.

MODELING OF AIRCRAFT UNSTEADY AERODYNAMIC CHARACTERISTICS. PART 2: PARAMETERS ESTIMATED FROM WIND TUNNEL DATA

Vladislav Klein (Joint Inst. for Advancement of Flight Sciences, Hampton, VA.) and Keith D. Noderer (Joint Inst. for Advancement of Flight Sciences, Hampton, VA.) Apr. 1995 43 p
(RTOP 505-64-52-01)
(NASA-TM-110161; NAS 1.15:110161) Avail: CASI HC A03/MF A01

Aerodynamic equations with unsteady effects were formulated for an aircraft in one-degree-of-freedom, small-amplitude, harmonic motion. These equations were used as a model for aerodynamic parameter estimation from wind tunnel oscillatory data. The estimation algorithm was based on nonlinear least squares and was applied in three examples to the oscillatory data in pitch and roll of 70 deg triangular wing and an X-31 model, and in-sideslip oscillatory data of the High Incidence Research Model 2 (HIRM 2). All three examples indicated that a model using a simple indicial function can explain unsteady effects observed in measured data. The accuracy of the estimated parameters and model verification were strongly influenced by the number of data points with respect to the number of unknown parameters. Author

N95-28598 Air Force Inst. of Tech., Wright-Patterson AFB, OH.

DEVELOPMENT OF A TECS CONTROL-LAW FOR THE LATERAL DIRECTIONAL AXIS OF THE MCDONNELL DOUGLAS F-15 EAGLE M.S. Thesis

Michael A. Bruzzini Dec. 1994 114 p Limited Reproducibility: More than 20% of this document may be affected by microfiche quality
(AD-A289771; AFIT/CI/CIA/94-159) Avail: Issuing Activity (Defense Technical Information Center (DTIC))

The purpose of this report is to develop automatic aircraft flight control systems using the concept of Total Energy Control System (TECS) in the lateral directional axis for the McDonnell Douglas F-15 Eagle. Nonlinear simulation was originally developed from actual flight tests conducted by the U.S. Air Force and generated into a Fortran code. Lt James P. Dutton then took the flight data code and generated a SIMULINK file 10. Using the SIMULINK file a control law developed on the linearized model can then be tested on the nonlinear model. DTIC

N95-26949# Kansas Univ., Lawrence, KS.

AN EASY WAY TO ANALYZE LONGITUDINAL AND LATERAL-DIRECTIONAL TRIM PROBLEMS WITH AEO OR OEI

Jan Roskam and William Anemaat (Design, Analysis and Research Corp., Lawrence, KS.) *In* Wichita State Univ., AIAA Techfest 20 Proceedings 1994 22 p (For primary document see N95-26941 09-01)
Avail: CASI HC A03/MF A03

N95-28281*# Naval Weapons Center, China Lake, CA.

COMPOSITE FLIGHT-CONTROL ACTUATOR DEVELOPMENT

Richard Bott and Fred Ching (Textron, Inc., Valencia, CA.) *In* FAA, Ninth DOD/NASA/FAA Conference on Fibrous Composites in Structural Design, Volume 3 Sep. 1992 p 1389-1404 (For primary document see N95-28266 09-24)
(Contract N60530-88-C-0260)
Copyright Avail: CASI HC A03/MF A04

09 RESEARCH AND SUPPORT FACILITIES (AIR)

Includes airports, hangars and runways; aircraft repair and overhaul facilities; wind tunnels; shock tubes; and aircraft engine test stands.

For related information see also *14 Ground Support Systems and Facilities (Space).*

N95-26378 Defence Science and Technology Organisation, Melbourne (Australia). Aeronautical and Maritime Research Lab.

DESIGN AND DEVELOPMENT OF A TEST RIG FOR THE HIGH FREQUENCY TESTING OF ROLLING SLEEVE AIRSPRINGS

G. Swanton Feb. 1995 32 p Original contains color illustrations
(DSTO-TN-0001; AR-009-201) Copyright Avail: Issuing Activity

AMRL's F/A-18 IFOSTP fatigue test has introduced several new concepts in the field of aircraft structural testing. One of the innovations has been the development of the pneumatic actuator or 'rolling sleeve' airspring for the application of aircraft maneuver loads. These airsprings have been subjected to several preliminary acceptance test phases, one of which simulated the effects of high frequency buffet loads. This report details the design and implementation of the test rig developed to conduct this type of testing. Author

N95-26556 Institute for Defense Analyses, Alexandria, VA.

THE VALUE OF SIMULATION FOR TRAINING Final Report, Sep. 1993 - Apr. 1994

Jesse Orlansky, Carl J. Dahlman, Colin P. Hammon, John Metzko, Henry L. Taylor, and Christine Youngblut Sep. 1994 173 p Limited Reproducibility: More than 20% of this document may be affected by microfiche quality

(AD-A289174; IDA-P-2982; IDA/HQ-94-45529; SBI-AD-E501-856) Avail: Issuing Activity (Defense Technical Information Center (DTIC))

All types of simulation are considered: (1) stand-alone; (2) networked interactive simulation; (3) live exercises; and (4) combat models. The utility of simulation is examined for individual and collective training conducted at institutions and in operational units. Cost data are reported on individual training at schools, training technology, collective training in units, operating tempo, and procurement of simulation. Simulators used for flight training and maintenance training are cost-effective, compared to the use of actual equipment; the same is true for computer-based instruction. The acceptance and use of simulators depends heavily on the existence of adequate training programs, adequate performance feed-back, ability to replicate actual operating conditions, and user acceptance by unit commanders. Distributed interactive simulation is expected to make a major improvement in collective and joint training but it is too early to assess its utility. Suggestions are made with regard to the development of cost data needed for establishing policy on the use of simulation for training as well as for the support of technology needed to improve collective and joint training and joint readiness. DTIC

N95-26768*# Old Dominion Univ., Norfolk, VA. Dept. of Aerospace Engineering.

EXTENSION TO THE DYNAMIC MODELING OF THE LARGE ANGLE MAGNETIC SUSPENSION TEST FIXTURE M.S. Thesis - Old Dominion Univ., May 1995 Progress Report, 1 Nov. 1994 - 30 Apr. 1995

Lucas E. Foster and Colin P. Britcher May 1995 133 p

(Grant NAG1-1056)

(NASA-CR-197801; NAS 1.26:197801) Avail: CASI HC A07/MF A02

The Large Angle Magnetic Suspension Test Fixture (LAMSTF) is a laboratory scale proof-of-concept system. The configuration is unique in that the electromagnets are mounted in a circular planar array. A mathematical model of the system had previously been developed, but was shown to have inaccuracies. These inaccuracies showed up in the step responses. Eddy currents were found to be the major cause of the modeling errors. In the original system, eddy currents existed in the aluminum baseplate, iron cores, and the sensor support frame. An attempt to include the eddy current dynamics in the system model is presented. The dynamics of a dummy sensor ring were added to the system. Adding the eddy current dynamics to the simulation improves the way it compares to the actual experiment. Also presented is a new method of determining the yaw angle of the suspended element. From the coil currents the yaw angle can be determined and the controller can be updated to suspend at the new current. This method has been used to demonstrate a 360 degree yaw angle rotation. Author

N95-26775*# MCAT Inst., San Jose, CA.

COMPUTATIONAL SUPPORT OF THE LAMINAR FLOW SUPERSONIC WIND TUNNEL, CNSFV CODE DEVELOPMENT, MAGLEV, AND GRID GENERATION Final Report, 1 Jun. 1989 - 31 Jan. 1995

Goetz H. Klopfer 31 Jan. 1995 84 p Original contains color illustrations

(Contract NCC2-616)

(NASA-CR-197750; NAS 1.26:197750; MCAT-05-06) Avail: CASI HC A05/MF A01; 10 functional color pages

This final report covers the work done on corporate agreement NCC2-616 over a period of 5 1/2 years. It is broken into three segments of approximately 1 1/2 to 2 years each. The report is a summary report and is not intended to be comprehensive of all the work done under this corporate agreement. A more complete coverage of the work done is obtained from the papers and reports listed in the 'Papers' section. Additional reporting of significant work was done through 'Technical Highlights' and 'Research and Technical Summaries'. A listing of copies are given in the 'Technical Highlights and R and T' section. The work was also reported in a series of seminars, conference meetings, branch reviews, workshops, and project reviews. A list of these talks is given in the 'Presentation' section. Also during this time three students ranging from high school to graduate level were supervised. A list of the students and the type of work accomplished is given in the 'Mentoring' section. The report concludes with the 'Appendices' sections which include the three papers produced during the last 1 1/2 years of this corporate agreement. Author

N95-26837 Polish Academy of Sciences, Warsaw (Poland). Acoustic Metrology Lab.

PHOTOACOUSTIC CHAMBERS FOR STUDYING SOLIDS AND GASES: THEORY AND PRACTICAL EXAMPLES [KOMORY FOTOAKUSTYCZNE DO BADANIA CIAL STALYCH I GAZOW: TEORIA I PROZYKLADY ROZWIAZAN]

Jerzy Motylewski and Tomasz Zmierczak 1994 34 p In POLISH

(ISSN 0208-5658)

(IFTR-39/1994) Avail: Issuing Activity (Polish Academy of Sciences, Warsaw, Poland)

In this article the authors describe examples of theoretical models of the operation of photoacoustic chambers designed to operate in photoacoustic spectroscopic systems used to analyze the physical and chemical properties of solids and gases by means of photoacoustic spectroscopy (PAS). In particular, the theoretical analysis covers the effect of the chamber's dimensions, the analyzed sample, and the modulation of the exciting light on the amplitude of the photoacoustic signal and the ways in which energy losses in the photoacoustic detector are accounted for. The authors note the possibility of reducing the effect of penetrating acoustic noise in chambers used to analyze the properties of gases by using acoustic filters. The authors describe examples of photoacoustic chambers designed to analyze solids and gases. Transl. by SCITRAN

N95-26966 Air Force Inst. of Tech., Wright-Patterson AFB, OH.

AN INVESTIGATION OF THE AFIT 2-INCH SHOCK TUBE AS A FLOW SOURCE FOR SUPERSONIC TESTING M.S. Thesis

Kevin M. Vlcek Dec. 1994 52 p Limited Reproducibility: More than 20% of this document may be affected by microfiche quality

(AD-A289246; AFIT/GA/ENY/94D-1) Avail: Issuing Activity (Defense Technical Information Center (DTIC))

An investigation of the AFIT high pressure shock tube was conducted to determine how closely it followed ideal shock tube theory and to determine the available test times for an attached Mach 3 nozzle. The driver section was five feet (1.52 m) long and the driven section was 25 feet (7.62 m) long. The driver gas used for this study was helium while the driven gas was atmospheric air. The pressure rise measured behind the incident shock wave was, on average, 30% lower than predicted by the ideal shock tube relations. Behind the reflected shock, the pressure rise was 65% lower than predictions based on initial driver gas pressure. Due to supply pressure limits and lower than predicted pressures behind the shock waves, fully expanded flow in the Mach 3 nozzle was not attained. However, steady overexpanded flows of Mach 2.74-2.96 were observed for periods of 4-12 milliseconds. DTIC

N95-27176*# National Aeronautics and Space Administration. Lewis Research Center, Cleveland, OH.

NASA LEWIS RESEARCH CENTER'S COMBUSTOR TEST FACILITIES AND CAPABILITIES

Jean Bianco May 1995 13 p Presented at the 31st Joint Propulsion Conference and Exhibit, San Diego, CA, 10-12 Jul. 1995; cosponsored by AIAA, ASME, SAE, and ASEE

(RTOP 505-62-82)

(NASA-TM-106903; E-9599; NAS 1.15:106903; AIAA Paper 95-2681)

Avail: CASI HC A03/MF A01

NASA Lewis Research Center (LeRC) presently accommodates a total of six combustor test facilities with unique capabilities. The facilities are used to evaluate combustor and afterburner concepts for future engine applications, and also to test the survivability and performance of innovative high temperature materials, new instrumentation, and engine components in a realistic jet engine environment. The facilities provide a variety of test section interfaces and lengths to allow for flametube, sector and component testing. The facilities can accommodate a wide range of operating conditions due to differing capabilities in the following areas: inlet air pressure, temperature, and flow; fuel flow rate, pressure, and fuel storage capacity; maximum combustion zone temperature; cooling water flow rate and pressure; types of exhaust - atmospheric or altitude; air heater supply pressure; and types of air heaters - vitiated or nonvitiated. All of the facilities have provisions for standard gas (emissions) analysis, and a few of the facilities are equipped with specialized gas analysis equipment, smoke and particle size measurement devices, and a variety of laser systems. This report will present some of the unique features of each of the high temperature/high pressure combustor test facilities at NASA LeRC. Author

N95-27297 Army Cold Regions Research and Engineering Lab., Hanover, NH.
SUBSURFACE RADAR INVESTIGATIONS AT THE PEGASUS GLACIAL-ICE RUNWAY AND WILLIAMS FIELD, MCMURDO STATION, ANTARCTICA
Steven A. Arcone, Allan J. Delaney, and Wayne Tobiasson Nov. 1994 29 p Limited Reproducibility: More than 20% of this document may be affected by microfiche quality
(Grant NSF DPP-87-20063; DA Proj. 4A1-61102-AT-24)
(AD-A289323; CRREL-94-12) Avail: Issuing Activity (Defense Technical Information Center (DTIC))

Subsurface radar was used to profile ice and snow conditions on the Ross Ice Shelf at McMurdo Station, Antarctica, during mid-January 1993. Deconvolution and migration were often used to improve vertical resolution and spatial imaging. Profiles at a pulse center frequency of 400 MHz along the 3.2-km-long Pegasus ice runway show many low-density horizons above 9 m depth that are up to 30 m long. They are associated with air bubbles included during refreezing of meltwater and are interpreted as layers between a few and tens of centimeters thick. There is a strong reflecting horizon at about 9 m depth that is probably from brine intrusion as it is continuous with the intrusion into the snow to the east. Diffraction asymptotes give a dielectric constant near 3.2 for material above the brine level, a value that implies near-solid ice. Profiles at 100 MHz along the road between Pegasus runway and Williams Field in the accumulation zone show snow features such as layer deformation and intrusive brine layers that both abruptly and gradually change in depth. A single profile at a relic solid waste dump at Williams Field detected buried debris and ice within the upper 7 m. A survey of a suspected fuel spill shows some local disturbances near the center, but no excavation was done to verify the findings. Profiles traversing the sewage sumps at Williams Field outline the extent of the sewage deposition, and give depths to contaminated snow that closely agree with observation. Despite variability in dielectric properties, single-layer migration effectively improves the resolution of subsurface conditions. Recommendations are made for future surveys. DTIC

N95-28151 Federal Aviation Administration, Washington, DC. Office of Airport Planning and Programming.
ENPLANEMENT AND ALL CARGO ACTIVITY
Apr. 1994 153 p Limited Reproducibility: More than 20% of this document may be affected by microfiche quality
(AD-A280074; DOT/FAA/PP-94-1) Avail: Issuing Activity (Defense Technical Information Center (DTIC))

The Enplanement and All-Cargo Activity publication is a summary of enplanement data extracted from the Air Carrier Activity Information System (ACAIS). The ACAIS is a database which contains revenue passenger enplanement data and all-cargo landing data. The database supports the Federal Aviation Administration's Airport Inprovement Program (AIP) entitlement activities. Derived from text

N95-26944# Lear Jet Industries, Inc., Wichita, KS.
AIRCRAFT NOSEWHEEL STEERING SIMULATION Abstract Only
Wayne Stout *In* Wichita State Univ., AIAA Techfest 20 Proceedings 1994 48 p (For primary document see N95-26941 09-01)
Avail: CASI HC A03/MF A03

N95-26951# Kansas Univ. Lawrence, KS.
PRELIMINARY RESULTS AND RESEARCH CAPABILITIES OF A NEW JET FACILITY AT THE UNIVERSITY OF KANSAS
Jason Frank, Tom Sherwood, and Ray Taghavi *In* Wichita State Univ., AIAA Techfest 20 Proceedings 1994 16 p (For primary document see N95-26941 09-01)
Avail: CASI HC A03/MF A03

12 ASTRONAUTICS (GENERAL)

For extraterrestrial exploration see *91 Lunar and Planetary Exploration.*

N95-26426*# Colorado Univ., Boulder, CO. Dept. of Aerospace Engineering Sciences.
MICRON ACCURACY DEPLOYMENT EXPERIMENT (MADE), PHASE A. VOLUME 1 Final Report
Lee D. Peterson and Mark S. Lake 31 Mar. 1995 35 p Original contains color illustrations
(Contract NASw-4873)
(NASA-CR-197792; NAS 1.26:197792) Avail: CASI HC A03/MF A01; 6 functional color pages

This report documents a Phase A In-STEP flight experiment development effort. The objective of the experiment is to deploy a portion of a segmented reflector on the Shuttle and study its micron-level mechanics. Ground test data are presented which projects that the on-orbit precision of the test article should be approximately 5 microns. Extensive hardware configuration development information is also provided. Author

N95-26583*# United States Space Foundation, Colorado Springs, CO.
SPACE COMMERCE 1994 FORUM: THE 10TH NATIONAL SPACE SYMPOSIUM. PROCEEDINGS REPORT
Beth Ann Lipskin, ed., Sara Patterson, ed., Larry Aragon, ed., David A. Brescia, ed., Jack Flannery, ed., Roberty Mossey, ed., Christopher Regan, ed., Kurt Steeby, ed., Stacy Suhr, ed., and Chuck Zimkas, ed. 5 Apr. 1994 242 p Symposium held in Colorado Springs, CO, 5-8 Apr. 1995; sponsored in cooperation with Business Week, Aviation Week and Space Technology, and KPMG Peat Marwick Sponsored by NASA Original contains color illustrations
(NASA-CR-198031; NAS 1.26:198031; ISBN-0-9616962-8-1) Avail: CASI HC A11/MF A03; 3 functional color pages

The theme of the 10th National Space Symposium was 'New Windows of Opportunity'. These proceedings cover the following: Business Trends in High Tech Commercialization; How to Succeed in Space Technology Business -- Making Dollars and Sense; Obstacles and Opportunities to Success in Technology Commercialization NASA's Commercial Technology Mission -- a New Way of Doing Business: Policy and Practices; Field Center Practices; Practices in Action -- A New Way: Implementation and Business Opportunities; Space Commerce Review; Windows of Opportunity; the International Space Station; Space Support Forum; Spacelift Update; Competitive Launch Capabilities; Supporting Life on Planet Earth; National Security Space Issues; NASA in the Balance; Earth and Space Observations -- Did We Have Cousins on Mars?; NASA: A New Vision for Science; and Space Technology Hall of Fame. CASI

N95-27133 Air Force Inst. of Tech., Wright-Patterson AFB, OH. School of Engineering.
A METHODOLOGY TO ASSESS THE UTILITY OF FUTURE SPACE SYSTEMS M.S. Thesis
Bruce Rayno Dec. 1994 89 p Limited Reproducibility: More than 20% of this document may be affected by microfiche quality
(AD-A289414; AFIT/GSO/ENS/94D-14) Avail: Issuing Activity (Defense Technical Information Center (DTIC))

This research identifies the assumptions and simplifications in the SPACECAST 2020 value model and assesses modifications. The model determines and prioritizes future space systems' utility toward controlling and exploiting space. This study shows that the assumption of using an additive utility function is valid. This research shows that the mission areas are mutually utility independent allowing the use of the multiplicative utility function. This research also uses the multilinear function, which requires utility independence implied in mutual utility independence. This study makes modifications to the 98 SPACECAST 2020 measure of merit scoring functions. These scoring functions all used the same scoring scale and they do not allow for the determination of the overall current capability toward controlling and exploiting space. Most of these functions are replaced with either a concave, convex, linear, or 'S' scoring function, which has an expanded capability range to include current and future capabilities. The modified scoring functions and alternate utility functions do not alter the SPACECAST 2020 results but do improve upon the model. This study also presents a flexible but formalized method of space system concept identification, which explicitly considers space operational requirements. DTIC

N95-27171# Joint Publications Research Service, Arlington, VA.
JPRS REPORT: SCIENCE AND TECHNOLOGY. CENTRAL EURASIA
29 Mar. 1995 80 p Transl. into ENGLISH from various Eurasian articles
(JPRS-UST-95-014) Avail: CASI HC A05/MF A01

Translated articles cover the following topics: schedule of Russian spaceflights in 1993-1994 detailed; and shock-wave compression of aluminum under 1.7 TPa pressure. Author

N95-27856# General Accounting Office, Washington, DC. National Security and International Affairs Div.
BRIEFING REPORT TO THE RANKING MINORITY MEMBER, SUBCOMMITTEE ON SPACE AND AERONAUTICS, COMMITTEE ON SCIENCE, HOUSE OF REPRESENTATIVES. CASSINI MISSION: ESTIMATED LAUNCH COSTS FOR NASA'S MISSION TO SATURN Report, Aug. 1994 - Mar. 1995
Frank Degnan, Raymond H. Denmark, and Sandra D. Gove May 1995 33 p
(GAO/NSIAD-95-141BR; B-260888) Avail: CASI HC A03/MF A01; GAO, PO Box 6015, Gaithersburg, MD 20884-6015 HC

This report is a result of an investigation into NASA's April 1994 estimated cost of $475 million for a Titan 4-Centaur launch of the Cassini spacecraft. The goal of the investigation was to determine the extent to which cost saving opportunities exist. The Air Force agreement to provide NASA with an expendable launch vehicle for this project prompted the analyses of Air Force as well as NASA documents, including memoranda of agreement, estimated and negotiated costs, funding and budget data, the mission integration contract, and launch and production schedules. Since the initial call to investigate, the cost estimate has been reduced by NASA to $452 million, principally because a reduction of the estimate of mission integration costs. The investigation determined a further reduction in overall cost may be possible because NASA completed its negotiation of the mission integration contract for $15 million less than estimated. However, cost savings in other areas of the Cassini launch are unlikely, and some of NASA's costs could increase. A briefing section details these findings. CASI

N95-27919*# National Aeronautics and Space Administration, Washington, DC.
MISSION TO PLANET EARTH. STRATEGIC ENTERPRISE PLAN, 1995-2000
May 1995 52 p
(NASA-TM-110620; NAS 1.15:110620) Avail: CASI HC A04/MF A01

Mission to Planet Earth (MTPE) provides long-term understanding of the earth system needed to protect and improve our environment, now and for future generations. This MTPE Strategic Enterprise Plan states how NASA intends to meet its responsibility to the Nation for developing a long-term, integrated program of environmental observation in support of informed decision-making. This plan implements the NASA Strategic Plan for the MTPE Enterprise; it is the first version of a rolling 5-year plan that will be updated annually. It is consistent with the interagency program developed by the Committee on Environment and Natural Resources of the National Science and Technology Council and implemented in large part through the U.S. Global Change Research Program. This report consists of the following sections: (1) introduction; (2) scientific foundation; (3) mission (destination and purposes); (4) principle of operation (ethical and quality assurance standards); (5) customer base (to ensure that the right products and services are delivered); (6) internal and external assessments; (7) assumptions; (8) goals, objectives, and strategies; (9) linkages to other strategic enterprises; and (10) summary. Derived from text

N95-28257# Joint Publications Research Service, Arlington, VA.
JPRS REPORT: SCIENCE AND TECHNOLOGY. CENTRAL EURASIA
11 May 1995 61 p Transl. into ENGLISH from various Eurasian articles
(JPRS-UST-95-020) Avail: CASI HC A04/MF A01

Translated articles cover the following topics: Increasing the speed associated with accurate computation of satellite orbits with large eccentricities; Comparison of optimal and locally optimal geocentric boosts of a solar-sail-equipped spacecraft; Use of a laser altimeter in satellite remote sensing of the Earth's surface; Method of determining optical state of the atmosphere and surface Albedo from multiangle convergent observations; Effect of number of gradations of brightness levels on textural features of radar images; Displaying sea state with Synthetic-Aperture Radars (Comparative analysis of data obtained by Almaz-1 and ERS-1 Satellites); Problems with Russian Elektro Weather Satellite described; and Threats to Russian space program. CASI

N95-28261*# Lockheed Martin Corp., Denver, CO.
MARS SAMPLE RETURN MISSION UTILIZING IN-SITU PROPELLANT PRODUCTION Final Report
Robert Zubrin and Steve Price 31 Mar. 1995 69 p Original contains color illustrations
(Contract NAS9-19359)
(NASA-CR-188371; NAS 1.26:1988371; MCR-95-557) Avail: CASI HC A04/MF A01; 7 functional color pages

This report presents the results of a study examining the potential of in-situ propellant production (ISPP) on Mars to aid in achieving a low cost Mars Sample Return (MSR) mission. Two versions of such a mission were examined: a baseline version employing a dual string spacecraft, and a light weight version employing single string architecture with selective redundancy. Both systems employed light weight avionics currently being developed by Lockheed Martin, Jet Propulsion Lab and elsewhere in the aerospace community, both used a new concept for a simple, light weight parachuteless sample return capsule, both used a slightly modified version of the Mars Surveyor lander currently under development at Lockheed Martin for flight in 1998, and both used a combination of the Sabatier-electrolysis and reverse water gas shift ISPP systems to produce methane/oxygen propellant on Mars by combining a small quantity of imported hydrogen with the Martian CO2 atmosphere. It was found that the baseline mission could be launched on a Delta 7925 and return a 0.5 kg sample with 82 percent mission launch margin;over and beyond subsystem allocated contingency masses . The lightweight version could be launched on a Mid-Lite vehicle and return a 0.25 kg sample with 11 percent launch margin, over and above subsystem contingency mass allocations. Author

N95-27394*# California Univ., Davis, CA. Computer Science Dept.
COMPREHENSION AND RETRIEVAL OF FAILURE CASES IN AIRBORNE OBSERVATORIES
Sergio J. Alvarado and Kenrick J. Mock *In* NASA. Goddard Space Flight Center, The 1995 Goddard Conference on Space Applications of Artificial Intelligence and Emerging Information Technologies May 1995 p 237-251 (For primary document see N95-27375 09-63)
(Contract NCA2-721)
Avail: CASI HC A03/MF A03

N95-27657*# National Aeronautics and Space Administration. Langley Research Center, Hampton, VA.
FROM LDEF TO A NATIONAL SPACE ENVIRONMENT AND EFFECTS (SEE) PROGRAM: A NATURAL PROGRESSION Abstract Only
David E. Bowles, Robert L. Calloway, Joan G. Funk, William H. Kinard, and Arlene S. Levine *In its* LDEF: 69 Months in Space. Third Post-Retrieval Symposium, Part 3 Feb. 1995 p 1247-1248 (For primary document see N95-27629 09-99)
Avail: CASI HC A01/MF A04

N95-27667*# Ishikawajima-Harima Heavy Industries Co. Ltd., Tokyo (Japan).
ELEMENT MATERIAL EXPERIMENT BY EFFU
Yoshihiro Hashimoto, Masaaki Ichikawa, Mitsuru Takei (National Space Development Agency, Tsukuba, Japan.), Yoshihiro Torii (National Space Development Agency, Tsukuba, Japan.), and Kazuo Ota (National Space Development Agency, Tsukuba, Japan.) *In* NASA. Langley Research Center, LDEF: 69 Months in Space. Third Post-Retrieval Symposium, Part

3 Feb. 1995 p 1321-1329 (For primary document see N95-27629 09-99)
Avail: CASI HC A02/MF A04

13 ASTRODYNAMICS

Includes powered and free-flight trajectories; and orbital and launching dynamics.

N95-27033 Air Force Inst. of Tech., Wright-Patterson AFB, OH.
COMPUTING NORAD MEAN ORBITAL ELEMENTS FROM A STATE VECTOR M.S. Thesis
Dwight E. Andersen Dec. 1994 63 p Limited Reproducibility: More than 20% of this document may be affected by microfiche quality
(AD-A289281; AFIT/GSO/ENS/94D-01) Avail: Issuing Activity (Defense Technical Information Center (DTIC))

NORAD maintains and disseminates mean orbital elements on Earth-orbiting satellites in the form of Two-Line Element Sets (TLE). Five mathematical propagator models were developed for NORAD's use to predict the position and velocity using TLE's. This study investigated two approaches, Newton's method and direct iteration, to inverting this process by iterating to obtain NORAD-compatible mean orbital elements from a position and velocity state vector and the drag term. The Newton's iteration method was developed but not tested. The less computationally intensive direct iteration method was developed, coded in FORTRAN, and tested. The initial guess and subsequent corrections in the iterative process used the osculating elements computed from the state. The results showed the computation of the osculating elements to be unstable for low-Earth orbits with low eccentricity and moderate inclination, never converging to a solution for those cases. The scope of this research was limited to using two of the five propagators: Simplified General Perturbation Version 4 (SGP4) for low Earth orbits and SDP4 for deep space orbits. DTIC

N95-27035 Air Force Inst. of Tech., Wright-Patterson AFB, OH.
WEIGHTING SCHEME FOR THE SPACE SURVEILLANCE NETWORK AUTOMATED TASKER M.S. Thesis
Beth L. Petrick Dec. 1994 96 p Limited Reproducibility: More than 20% of this document may be affected by microfiche quality
(AD-A289285; AFIT/GSO/ENS/94D-13) Avail: Issuing Activity (Defense Technical Information Center (DTIC))

The purpose of this research is to find the best weighting scheme in the SPADOC 4C Sensor Tasking Prototype. This software, known as the Prototype Tasker, assigns a tasking to each sensor of the Space Surveillance Network. A tasking is a list of objects in which the sensor needs to gather positional data, called observations. One of the inputs to the Prototype Tasker is a user-definable weighting scheme. The goal is to find the weighting scheme that produces the most efficient taskings. This problem was solved using a Simulated Annealing algorithm. The values in the weighting scheme were the variables of the problem. The objective function was a measure of the goodness of each tasking produced. The Simulated Annealing algorithm was set to vary the weighting scheme and find the one that produces the tasking with the highest objective function. There were four successful executions of the simulated annealing algorithm. Each one produced a different weighting scheme. However, there were noticeable trends in the relative magnitudes of the weights. Also, it was noticed that a slight decrease in the number of observations on the taskings will increase the expected amount of information gathered by the Space Surveillance Network. DTIC

N95-27763*# National Aeronautics and Space Administration. Goddard Space Flight Center, Greenbelt, MD.
FLIGHT MECHANICS/ESTIMATION THEORY SYMPOSIUM 1995
Kathy R. Hartman, ed. May 1995 424 p Symposium held in Greenbelt, MD, 16-18 May 1995
(RTOP 550-00-00)
(NASA-CP-3299; Rept-95B00075; NAS 1.55:3299) Avail: CASI HC A18/MF A04

This conference publication includes 41 papers and abstracts presented at the Flight Mechanics/ Estimation Theory Symposium on May 16-18, 1995. Sponsored by the Flight Dynamics Division of Goddard Space Flight Center, this symposium featured technical papers on a wide range of issues related to orbit-attitude prediction, determination, and control; attitude sensor calibration; attitude determination error analysis; attitude dynamics; and orbit decay and maneuver strategy. Government, industry, and the academic community participated in the preparation and presentation of these papers. For individual titles, see N95-27764 through N95-27804.

N95-27764*# Computer Sciences Corp., Lanham, MD.
ANALYSIS OF FILTER TUNING TECHNIQUES FOR SEQUENTIAL ORBIT DETERMINATION
T. Lee, C. Yee, and D. Oza *In* NASA. Goddard Space Flight Center, Flight Mechanics/Estimation Theory Symposium 1995 May 1995 p 3-15 (For primary document see N95-27763 09-13)
(Contract NAS5-31500)
Avail: CASI HC A03/MF A04

This paper examines filter tuning techniques for a sequential orbit determination (OD) covariance analysis. Recently, there has been a renewed interest in sequential OD, primarily due to the successful flight qualification of the Tracking and Data Relay Satellite System (TDRSS) Onboard Navigation System (TONS) using Doppler data extracted onboard the Extreme Ultraviolet Explorer (EUVE) spacecraft. TONS computes highly accurate orbit solutions onboard the spacecraft in realtime using a sequential filter. As the result of the successful TONS-EUVE flight qualification experiment, the Earth Observing System (EOS) AM-1 Project has selected TONS as the prime navigation system. In addition, sequential OD methods can be used successfully for ground OD. Whether data are processed onboard or on the ground, a sequential OD procedure is generally favored over a batch technique when a realtime automated OD system is desired. Recently, OD covariance analyses were performed for the TONS-EUVE and TONS-EOS missions using the sequential processing options of the Orbit Determination Error Analysis System (ODEAS). ODEAS is the primary covariance analysis system used by the Goddard Space Flight Center (GSFC) Flight Dynamics Division (FDD). The results of these analyses revealed a high sensitivity of the OD solutions to the state process noise filter tuning parameters. The covariance analysis results show that the state estimate error contributions from measurement-related error sources, especially those due to the random noise and satellite-to-satellite ionospheric refraction correction errors, increase rapidly as the state process noise increases. These results prompted an in-depth investigation of the role of the filter tuning parameters in sequential OD covariance analysis. This paper analyzes how the spacecraft state estimate errors due to dynamic and measurement-related error sources are affected by the process noise level used. This information is then used to establish guidelines for determining optimal filter tuning parameters in a given sequential OD scenario for both covariance analysis and actual OD. Comparisons are also made with corresponding definitive OD results available from the TONS-EUVE analysis. Author

N95-27765*# National Aeronautics and Space Administration. Goddard Space Flight Center, Greenbelt, MD.
EVALUATION AND MODELING OF AUTONOMOUS ATTITUDE THRUST CONTROL FOR THE GEOSTATION OPERATIONAL ENVIRONMENTAL SATELLITE (GOES)-8 ORBIT DETERMINATION
W. Forcey (Computer Sciences Corp., Lanham, MD.), C. R. Minnie (Computer Sciences Corp., Lanham, MD.), and R. L. DeFazio *In its* Flight Mechanics/Estimation Theory Symposium 1995 May 1995 p 17-29 (For primary document see N95-27763 09-13)
(Contract NAS5-31500)
Avail: CASI HC A03/MF A04

The Geostationary Operational Environmental Satellite (GOES)-8 experienced a series of orbital perturbations from autonomous attitude control thrusting before perigee raising maneuvers. These perturbations influenced differential correction orbital state solutions determined by the Goddard Space Flight Center (GSFC) Goddard Trajectory Determination System (GTDS). The maneuvers induced significant variations in the converged state vector for solutions using increasingly longer tracking data spans. These solutions were used for planning perigee maneuvers as well as initial estimates for orbit solutions used to evaluate the effectiveness of the perigee raising maneuvers. This paper discusses models for the incorporation of attitude thrust effects into the orbit determination process. Results from definitive attitude solutions are modeled as impulsive thrusts in orbit determination solutions created for GOES-8 mission support. Due to the attitude orientation of GOES-8, analysis results are presented that attempt to absorb the effects of attitude thrusting by including a solution for the coefficient of reflectivity, C(R). Models to represent the attitude maneuvers are tested against orbit determination solutions generated during real-time support of the GOES-8 mission. The modeling techniques discussed in this investigation offer benefits to the remaining missions in the GOES NEXT series. Similar missions with large autonomous attitude control thrusting, such as the Solar and Heliospheric Observatory (SOHO) spacecraft and the INTELSAT series, may also benefit from these results. Author

N95-27766*# National Aeronautics and Space Administration. Goddard Space Flight Center, Greenbelt, MD.

DIFFERENCED RANGE VERSUS INTEGRATED DOPPLER (DRVID) IONOSPHERIC ANALYSIS OF METRIC TRACKING IN THE TRACKING AND DATA RELAY SATELLITE SYSTEM (TDRSS)

M. S. Radomski (Computer Sciences Corp., Lanham, MD.) and C. E. Doll *In its* Flight Mechanics/Estimation Theory Symposium 1995 May 1995 p 31-45 (For primary document see N95-27763 09-13)
(Contract NAS5-31500)
Avail: CASI HC A03/MF A04

The Differenced Range (DR) Versus Integrated Doppler (ID) (DRVID) method exploits the opposition of high-frequency signal versus phase retardation by plasma media to obtain information about the plasma's corruption of simultaneous range and Doppler spacecraft tracking measurements. Thus, DR Plus ID (DRPID) is an observable independent of plasma refraction, while actual DRVID (DR minus ID) measures the time variation of the path electron content independently of spacecraft motion. The DRVID principle has been known since 1961. It has been used to observe interplanetary plasmas, is implemented in Deep Space Network tracking hardware, and has recently been applied to single-frequency Global Positioning System user navigation This paper discusses exploration at the Goddard Space Flight Center (GSFC) Flight Dynamics Division (FDD) of DRVID synthesized from simultaneous two-way range and Doppler tracking for low Earth-orbiting missions supported by the Tracking and Data Relay Satellite System (TDRSS) The paper presents comparisons of actual DR and ID residuals and relates those comparisons to predictions of the Bent model. The complications due to the pilot tone influence on relayed Doppler measurements are considered. Further use of DRVID to evaluate ionospheric models is discussed, as is use of DRPID in reducing dependence on ionospheric modeling in orbit determination. Author

N95-27767*# National Aeronautics and Space Administration. Goddard Space Flight Center, Greenbelt, MD.

KEPLER EQUATION SOLVER

F. Landis Markley *In its* Flight Mechanics/Estimation Theory Symposium 1995 May 1995 p 47-57 (For primary document see N95-27763 09-13)
Avail: CASI HC A03/MF A04

Kepler's Equation is solved over the entire range of elliptic motion by a fifth-order refinement of the solution of a cubic equation. This method is not iterative, and requires only four transcendental function evaluations: a square root, a cube root, and two trigonometric functions. The maximum relative error of the algorithm is less than one part in 10(exp 18), exceeding the capability of double-precision computer arithmetic. Roundoff errors in double-precision implementation of the algorithm are addressed, and procedures to avoid them are developed. Author

N95-27768*# National Aeronautics and Space Administration. Goddard Space Flight Center, Greenbelt, MD.

ACCURATE ORBIT DETERMINATION STRATEGIES FOR THE TRACKING AND DATA RELAY SATELLITES

D. H. Oza (Computer Sciences Corp., Lanham, MD.), D. T. Bolvin (Computer Sciences Corp., Lanham, MD.), J. M. Lorah (Computer Sciences Corp., Lanham, MD.), T. Lee (Computer Sciences Corp., Lanham, MD.), and C. E. Doll *In its* Flight Mechanics/Estimation Theory Symposium 1995 May 1995 p 59-72 (For primary document see N95-27763 09-13)
(Contract NAS5-31500)
Avail: CASI HC A03/MF A04

The National Aeronautics and Space Administration (NASA) has developed the Tracking and Data Relay Satellite (TDRS) System (TDRSS) for tracking and communications support of low Earth-orbiting satellites. TDRSS has the operational capability of providing 85% coverage for TDRSS-user spacecraft. TDRSS currently consists of five geosynchronous spacecraft and the White Sands Complex (WSC) at White Sands, New Mexico. The Bilateration Ranging Transponder System (BRTS) provides range and Doppler measurements for each TDRS. The ground-based BRTS transponders are tracked as if they were TDRSS-user spacecraft. Since the positions of the BRTS transponders are known, their radiometric tracking measurements can be used to provide a well-determined ephemeris for the TDRS spacecraft. For high-accuracy orbit determination of a TDRSS user, such as the Ocean Topography Experiment (TOPEX)/Poseidon spacecraft, high-accuracy TDRS orbits are required. This paper reports on successive refinements in improved techniques and procedures leading to more accurate TDRS orbit determination strategies using the Goddard Trajectory Determination System (GTDS). These strategies range from the standard operational solution using only the BRTS tracking measurements to a sophisticated iterative process involving several successive simultaneous solutions for multiple TDRSs and a TDRSS-user spacecraft. Results are presented for GTDS-generated TDRS ephemerides produced in simultaneous solutions with the TOPEX/Poseidon spacecraft. Strategies with different user spacecraft, as well as schemes for recovering accurate TDRS orbits following a TDRS maneuver, are also presented. In addition, a comprehensive assessment and evaluation of alternative strategies for TDRS orbit determination, excluding BRTS tracking measurements, are presented.
Author

N95-27769*# National Aeronautics and Space Administration. Goddard Space Flight Center, Greenbelt, MD.

OPERATIONAL IMPROVEMENTS OF LONG-TERM PREDICTED EPHEMERIDES OF THE TRACKING AND DATA RELAY SATELLITES (TDRSs)

J. L. Kostoff (Computer Sciences Corp., Lanham, MD.), D. T. Ward (Computer Sciences Corp., Lanham, MD.), O. O. Cuevas, and R. M. Beckman *In its* Flight Mechanics/Estimation Theory Symposium 1995 May 1995 p 73-79 (For primary document see N95-27763 09-13)
(Contract NAS5-31500)
Avail: CASI HC A02/MF A04

Tracking and Data Relay Satellite (TDRS) orbit determination and prediction are supported by the Flight Dynamics Facility (FDF) of the Goddard Space Flight Center (GSFC) Flight Dynamics Division (FDD). TDRS System (TDRSS)-user satellites require predicted TDRS ephemerides that are up to 10 weeks in length. Previously, long-term ephemerides generated by the FDF included predictions from the White Sands Complex (WSC), which plans and executes TDRS maneuvers. TDRSs typically have monthly stationkeeping maneuvers, and predicted postmaneuver state vectors are received from WSC up to a month in advance. This paper presents the results of an analysis performed in the FDF to investigate more accurate and economical long-term ephemerides for the TDRSs. As a result of this analysis, two new methods for generating long-term TDRS ephemeris predictions have been implemented by the FDF. The Center-of-Box (COB) method models a TDRS as fixed at the center of its stationkeeping box. Using this method, long-term ephemeris updates are made semiannually instead of weekly. The impulse method is used to model more maneuvers. The impulse method yields better short-term accuracy than the COB method, especially for larger stationkeeping boxes. The accuracy of the impulse method depends primarily on the accuracy of maneuver date forecasting.
Author

N95-27770*# National Aeronautics and Space Administration. Goddard Space Flight Center, Greenbelt, MD.

A PC-BASED MAGNETOMETER-ONLY ATTITUDE AND RATE DETERMINATION SYSTEM FOR GYROLESS SPACECRAFT

M. Challa (Computer Sciences Corp., Lanham, MD.), G. Natanson (Computer Sciences Corp., Lanham, MD.), J. Deutschmann, and K. Galal *In its* Flight Mechanics/Estimation Theory Symposium 1995 May 1995 p 83-96 (For primary document see N95-27763 09-13)
(Contract NAS5-31500)
Avail: CASI HC A03/MF A04

This paper describes a prototype PC-based system that uses measurements from a three-axis magnetometer (TAM) to estimate the state (three-axis attitude and rates) of a spacecraft given no a priori information other than the mass properties. The system uses two algorithms that estimate the spacecraft's state - a deterministic magnetic-field only algorithm and a Kalman filter for gyroless spacecraft. The algorithms are combined by invoking the deterministic algorithm to generate the spacecraft state at epoch using a small batch of data and then using this deterministic epoch solution as the initial condition for the Kalman filter during the production run. System input comprises processed data that includes TAM and reference magnetic field data. Additional information, such as control system data and measurements from line-of-sight sensors, can be input to the system if available. Test results are presented using in-flight data from two three-axis stabilized spacecraft: Solar, Anomalous, and Magnetospheric Particle Explorer (SAMPEX) (gyroless, Sun-pointing) and Earth Radiation Budget Satellite (ERBS) (gyro-based, Earth-pointing). The results show that, using as little as 700 s of data, the system is capable of accuracies of 1.5 deg in attitude and 0.01 deg/s in rates; i.e., within SAMPEX mission requirements. Author

N95-27771*# National Aeronautics and Space Administration. Goddard Space Flight Center, Greenbelt, MD.

DEVELOPMENT OF A DIRECT MATCH TECHNIQUE FOR STAR IDENTIFICATION ON THE SWAS MISSION

Walter K. Daniel (ITHACO Technical Services, Lanham, MD.), Thomas E. Correll, and Mark O. Anderson *In its* Flight Mechanics/Estimation Theory Symposium 1995 May 1995 p 97 (For primary document see N95-27763 09-13)

Avail: CASI HC A03/MF A04

A direct match technique for star identification was developed for use with the star tracker on the SWAS (Submillimeter Wave Astronomy Satellite) spacecraft. In this technique, tracker searches are used in a two-step process for an implicit direct match star identification. A simulation of the star acquisition process was created and used in the preparation of guide star selection requirements. Flight software implementing this star acquisition technique has been developed and tested. Derived from text

N95-27772*# Software Corp. of America, Lanham, MD.

ATTITUDE DETERMINATION USING AN ADAPTIVE MULTIPLE MODEL FILTERING SCHEME

Quang Lam and Surendra N. Ray *In* NASA. Goddard Space Flight Center, Flight Mechanics/Estimation Theory Symposium 1995 May 1995 p 113-114 (For primary document see N95-27763 09-13)

Avail: CASI HC A01/MF A04

Attitude determination has been considered as a permanent topic of active research and perhaps remaining as a forever-lasting interest for spacecraft system designers. Its role is to provide a reference for controls such as pointing the directional antennas or solar panels, stabilizing the spacecraft or maneuvering the spacecraft to a new orbit. Least Square Estimation (LSE) technique was utilized to provide attitude determination for the Nimbus 6 and G. Despite its poor performance (estimation accuracy consideration), LSE was considered as an effective and practical approach to meet the urgent need and requirement back in the 70's. One reason for this poor performance associated with the LSE scheme is the lack of dynamic filtering or 'compensation'. In other words, the scheme is based totally on the measurements and no attempts were made to model the dynamic equations of motion of the spacecraft. We propose an adaptive filtering approach which employs a bank of Kalman filters to perform robust attitude estimation. The proposed approach, whose architecture is depicted, is essentially based on the latest proof on the interactive multiple model design framework to handle the unknown of the system noise characteristics or statistics. The concept fundamentally employs a bank of Kalman filter or submodel, instead of using fixed values for the system noise statistics for each submodel (per operating condition) as the traditional multiple model approach does, we use an on-line dynamic system noise identifier to 'identify' the system noise level (statistics) and update the filter noise statistics using 'live' information from the sensor model. The advanced noise identifier, whose architecture is also shown, is implemented using an advanced system identifier. To insure the robust performance for the proposed advanced system identifier, it is also further reinforced by a learning system which is implemented (in the outer loop) using neural networks to identify other unknown quantities such as spacecraft dynamics parameters, gyro biases, dynamic disturbances, or environment variations. Derived from text

N95-27773*# Allied-Signal Corp., Morristown, NJ. Technical Services Div.

OBSERVATIONAL MAGNETOMETER CALIBRATION WITH THE HUBBLE SPACE TELESCOPE'S NEW MAGNETOMETERS

Sidney M. Broude *In* NASA. Goddard Space Flight Center, Flight Mechanics/Estimation Theory Symposium 1995 May 1995 p 115-126 (For primary document see N95-27763 09-13)

(Contract NAS5-31000)

Avail: CASI HC A03/MF A04

The two magnetometers recently replaced on the Hubble Space Telescope during the STS-61 Servicing Mission are now being used successfully for Coarse Attitude Determination during spacecraft vehicle safemode recovery operation. The magnetometer alignments relative to the spacecraft's vehicle's reference frame and the magnetic coupling of the sensors to the four magnetic torquer bars were determined. Coarse Attitude determination errors are now reduced to an average of 0.6 deg. Magnetometer Sensing System calibration and Coarse Attitude determination testing with the new calibration parameters is a geometrical problem. Telemetered earth magnetic field data was collected at twenty-six different vehicle attitudes. The spacecraft attitudes selected were distributed as widely apart as possible throughout the Geocentric Inertial Coordinate reference frame. It is also desirable to sample the Earth's magnetic field over as many different locations of the spacecraft's passage over the Earth as possible, within the limitation of the +/- 28.5 deg orbital inclination. A full range of magnetic moment outputs from the torquer bars needs to be sampled, +/- 3600 ampmeters squared, as well as data when the torquer bars have zero current. Graphic utilities were also developed to visually aid in optimizing the data collection process. Finally, a brief discussion of a method for collecting data for future calibrations is suggested. Author

N95-27774*# State Univ. of New York, Buffalo, NY.

AN AUTOMATED METHOD OF TUNING AN ATTITUDE ESTIMATOR

Paul A. C. Mason and D. Joseph Mook *In* NASA. Goddard Space Flight Center, Flight Mechanics/Estimation Theory Symposium 1995 May 1995 p 127-135 (For primary document see N95-27763 09-13)

Avail: CASI HC A02/MF A04

Attitude determination is a major element of the operation and maintenance of a spacecraft. There are several existing methods of determining the attitude of a spacecraft. One of the most commonly used methods utilizes the Kalman filter to estimate the attitude of the spacecraft. Given an accurate model of a system and adequate observations, a Kalman filter can produce accurate estimates of the attitude. If the system model, filter parameters, or observations are inaccurate, the attitude estimates may be degraded. Therefore, it is advantageous to develop a method of automatically tuning the Kalman filter to produce the accurate estimates. In this paper, a three-axis attitude determination Kalman filter, which uses only magnetometer measurements, is developed and tested using real data. The appropriate filter parameters are found via the Process Noise Covariance Estimator (PNCE). The PNCE provides an optimal criterion for determining the best filter parameters. Author

N95-27775*# National Aeronautics and Space Administration. Goddard Space Flight Center, Greenbelt, MD.

AN MME-BASED ATTITUDE ESTIMATOR USING VECTOR OBSERVATIONS

John L. Crassidis and F. Landis Markley *In its* Flight Mechanics/Estimation Theory Symposium 1995 May 1995 p 137-151 (For primary document see N95-27763 09-13)

Avail: CASI HC A03/MF A04

In this paper, an optimal batch estimator and filter based on the Minimum Model Error (MME) approach is developed for three-axis stabilized spacecraft. Three different MME algorithms are developed. The first algorithm estimates the attitude of a spacecraft using rate measurements. The second algorithm estimates the attitude without using rate measurements. The absence of rate data may be a result of intentional design or from unexpected failure of existing gyros. The third algorithm determines input-torque modeling error trajectories. All of the algorithms developed in this paper use attitude sensors (e.g., three-axis magnetometers, sun sensors, star trackers, etc.). Results using these new algorithms indicate that an MME-based approach accurately estimates the attitude, rate, and input torque trajectories of an actual spacecraft. Author

N95-27776*# Analytical Engineering Corp., Boulder, CO.

POST KALMAN PROGRESS

David Sonnabend *In* NASA. Goddard Space Flight Center, Flight

Mechanics/Estimation Theory Symposium 1995 May 1995 p 153-164 (For primary document see N95-27763 09-13)
Avail: CASI HC A03/MF A04

In a paper here last year, an idea was put forward that much greater performance could be obtained from an observer, relative to a Kalman filter if more general performance indices were adopted, and the full power spectra of all the noises were employed. The considerable progress since then is reported here. Included are an extension of the theory to regulators, direct calculation of the theory's fundamental quantities - the noise effect integrals - for several theoretical spectra, and direct derivations of the Riccati equations of LQG (Linear-Quadratic-Gaussian) and Kalman theory yielding new insights. Author

N95-27777*# National Aeronautics and Space Administration. Goddard Space Flight Center, Greenbelt, MD.

DEVELOPMENT OF A ROBUST STAR IDENTIFICATION TECHNIQUE FOR USE IN ATTITUDE DETERMINATION OF THE ACE SPACECRAFT

Mark Woodard and Dave Rohrbaugh (Computer Sciences Corp., Lanham, MD.) *In its* Flight Mechanics/Estimation Theory Symposium 1995 May 1995 p 167-172 (For primary document see N95-27763 09-13)
Avail: CASI HC A02/MF A04

The Advanced Composition Explorer (ACE) spacecraft is designed to fly in a spin-stabilized attitude. The spacecraft will carry two attitude sensors - a digital fine Sun sensor and a charge coupled device (CCD) star tracker - to allow ground-based determination of the spacecraft attitude and spin rate. Part of the processing that must be performed on the CCD star tracker data is the star identification. Star data received from the spacecraft must be matched with star information in the SKYMAP catalog to determine exactly which stars the sensor is tracking. This information, along with the Sun vector measured by the Sun sensor, is used to determine the spacecraft attitude. Several existing star identification (star ID) systems were examined to determine whether they could be modified for use on the ACE mission. Star ID systems which exist for three-axis stabilized spacecraft tend to be complex in nature and many require fairly good knowledge of the spacecraft attitude, making their use for ACE excessive. Star ID systems used for spinners carrying traditional slit star sensors would have to be modified to model the CCD star tracker. The ACE star ID algorithm must also be robust, in that it will be able to correctly identify stars even though the attitude is not known to a high degree of accuracy, and must be very efficient to allow real-time star identification. The paper presents the star ID algorithm that was developed for ACE. Results from prototype testing are also presented to demonstrate the efficiency, accuracy, and robustness of the algorithm. Author

N95-27778*# National Aeronautics and Space Administration. Goddard Space Flight Center, Greenbelt, MD.

OPTIMAL ATTITUDE MANEUVER EXECUTION FOR THE ADVANCED COMPOSITION EXPLORER (ACE) MISSION

Mark A. Woodard and David Baker *In its* Flight Mechanics/Estimation Theory Symposium 1995 May 1995 p 173-183 (For primary document see N95-27763 09-13)
Avail: CASI HC A03/MF A04

The Advanced Composition Explorer (ACE) spacecraft will require frequent attitude reorientations in order to maintain the spacecraft high gain antenna (HGA) within 3 deg of earth-pointing. These attitude maneuvers will be accomplished by employing a series of ground-commanded thruster pulses, computed by ground operations personnel, to achieve the desired change in the spacecraft angular momentum vector. With each maneuver, attitude nutation will be excited. Large nutation angles are undesirable from a science standpoint. It is important that the thruster firings be phased properly in order to minimize the nutation angle at the end of the maneuver so that science collection time is maximized. The analysis presented derives a simple approximation for the nutation contribution resulting from a series of short thruster burns. Analytic equations are derived which give the induced nutation angle as a function of the number of small thruster burns used to execute the attitude maneuver and the phasing of the burns. The results show that by properly subdividing the attitude burns, the induced nutation can be kept low. The analytic equations are also verified through attitude dynamics simulation and simulation results are presented. Finally, techniques for quantifying the post-maneuver nutation are discussed. Author

N95-27779*# National Aeronautics and Space Administration. Goddard Space Flight Center, Greenbelt, MD.

EXPERIENCE FROM THE IN-FLIGHT CALIBRATION OF THE EXTREME ULTRAVIOLET EXPLORER (EUVE) AND UPPER ATMOSPHERE RESEARCH SATELLITE (UARS) FIXED HEAD STAR TRACKERS (FHSTs)

Michael Lee *In its* Flight Mechanics/Estimation Theory Symposium 1995 May 1995 p 185-199 (For primary document see N95-27763 09-13)
Avail: CASI HC A03/MF A04

Since the original post-launch calibration of the FHSTs (Fixed Head Star Trackers) on EUVE (Extreme Ultraviolet Explorer) and UARS (Upper Atmosphere Research Satellite), the Flight Dynamics task has continued to analyze the FHST performance. The algorithm used for inflight alignment of spacecraft sensors is described and the equations for the errors in the relative alignment for the simple 2 star tracker case are shown. Simulated data and real data are used to compute the covariance of the relative alignment errors. Several methods for correcting the alignment are compared and results analyzed. The specific problems seen on orbit with UARS and EUVE are then discussed. UARS has experienced anomalous tracker performance on an FHST resulting in continuous variation in apparent tracker alignment. On EUVE, the FHST residuals from the attitude determination algorithm showed a dependence on the direction of roll during survey mode. This dependence is traced back to time tagging errors and the original post launch alignment is found to be in error due to the impact of the time tagging errors on the alignment algorithm. The methods used by the FDF (Flight Dynamics Facility) to correct for these problems is described. Author

N95-27780*# National Aeronautics and Space Administration. Goddard Space Flight Center, Greenbelt, MD.

SAMPEX SPECIAL POINTING MODE

F. Landis Markley, Thomas W. Flatley, and Theodore Leoutsakos (Allied-Signal Technical Services Corp., Lanham, MD.) *In its* Flight Mechanics/Estimation Theory Symposium 1995 May 1995 p 201-215 (For primary document see N95-27763 09-13)
Avail: CASI HC A03/MF A04

A new pointing mode has been developed for the Solar, Anomalous, and Magnetospheric Particle Explorer (SAMPEX) spacecraft. This pointing mode orients the instrument boresights perpendicular to the field lines of the Earth's magnetic field in regions of low field strength and parallel to the field lines in regions of high field strength, to allow better characterization of heavy ions trapped by the field. The new mode uses magnetometer signals and is algorithmically simpler than the previous control mode, but it requires increased momentum wheel activity. It was conceived, designed, tested, coded, uplinked to the spacecraft, and activated in less than seven months. Author

N95-27781*# State Univ. of New York, Buffalo, NY. Dept. of Mechanical and Aerospace Engineering.

USE OF NONLINEAR IDENTIFICATION IN ROBUST ATTITUDE AND ATTITUDE RATE ESTIMATION FOR SAMPEX Abstract Only

D. Joseph Mook, Juan DePena, Kelly Trost, Jung Wen, and Michael McPartland *In* NASA. Goddard Space Flight Center, Flight Mechanics/Estimation Theory Symposium 1995 May 1995 p 217 (For primary document see N95-27763 09-13)
Avail: CASI HC A01/MF A04

A method is described for obtaining optimal attitude estimation/identification algorithms for spacecraft lacking attitude rate measurement devices (rate gyros), and then demonstrated using actual flight data from the Solar, Anomalous, and Magnetospheric Particle Explorer (SAMPEX) spacecraft. SAMPEX does not have on-board rate sensing, and relies on sun sensors and a three-axis magnetometer for attitude determination. The absence of rate data normally reduces both the total amount of data available and the sampling density (in time) by a substantial fraction. In addition, attitude data is occasionally unavailable (for example, during sun occultation). As a result, the sensitivity of the estimates to model uncertainty and to measurement noise increases. In order to maintain accuracy in the attitude estimates, there is an increased need for accurate models of the rotational dynamics. The Minimum Model Error(MME)/Least Square Correlation(LSC) algorithm accurately identifies an improved model for SAMPEX to be used during periods of complete data loss or extreme noise. The model correction is determined by estimating only one orbit(the identification pass) just prior to the assumed data loss(the prediction pass). The MME estimator correctly predicted the states during the identification phase, but more importantly determines the necessary model correction trajectory, d(t). The LSC algorithm is then used to find this trajectory's functional form, H(x(t)). The results show significant improvement of the new corrected model's attitude estimates as compared to the original uncorrected model's estimates. The possible functional form of the correction term is limited at this point in the study to functions strictly of the estimated states. The results, however, strongly suggest that functions based on the relative position of the satellite may also be possible candidates for future consideration. Author

N95-27782*# National Aeronautics and Space Administration. Goddard Space Flight Center, Greenbelt, MD.

A SIMPLE METHOD FOR VERIFYING THE DEPLOYMENT OF THE TOMS-EP SOLAR ARRAYS c19

James R. Koppersmith and Eleanor Ketchum *In its* Flight Mechanics/Estimation Theory Symposium 1995 May 1995 p 219-227
(For primary document see N95-27763 09-13)
Avail: CASI HC A02/MF A04

The Total Ozone Mapping Spectrometer-Earth Probe (TOMS-EP) mission relies upon a successful deployment of the spacecraft's solar arrays. Several methods of verification are being employed to ascertain the solar array deployment status, with each requiring differing amounts of data. This paper describes a robust attitude-independent verification method that utilizes telemetry from the coarse Sun sensors (CSS's) and the three-axis magnetometers (TAM's) to determine the solar array deployment status - and it can do so with only a few, not necessarily contiguous, points of data. The method developed assumes that the solar arrays are deployed. Telemetry data from the CSS and TAM are converted to the Sun and magnetic field vectors in spacecraft body coordinates, and the angle between them is calculated. Deployment is indicated if this angle is within a certain error tolerance of the angle between the reference Sun and magnetic field vectors. Although several other methods can indicate a non-deployed state, with this method there is a 70% confidence level in confirming deployment as well as a nearly 100% certainty in confirming a non-deployed state. In addition, the spacecraft attitude (which is not known during the first orbit after launch) is not needed for this algorithm because the angle between the Sun and magnetic field vectors is independent of the spacecraft attitude. This technique can be applied to any spacecraft with a TAM and with CSS's mounted on the solar array(s). Author

N95-27783*# National Aeronautics and Space Administration. Goddard Space Flight Center, Greenbelt, MD.

EARTH HORIZON MODELING AND APPLICATION TO STATIC EARTH SENSORS ON TRMM SPACECRAFT

J. Keat (Computer Sciences Corp., Lanham, MD.), M. Challa (Computer Sciences Corp., Lanham, MD.), D. Tracewell, and K. Galal *In its* Flight Mechanics/Estimation Theory Symposium 1995 May 1995 p 229-239
(For primary document see N95-27763 09-13)
(Contract NAS5-31500)
Avail: CASI HC A03/MF A04

Data from Earth sensor assemblies (ESA's) often are used in the attitude determination (AD) for both spinning and Earth-pointing spacecraft. The ESA's on previous such spacecraft for which the ground-based AD operation was performed by the Flight Dynamics Division (FDD) used the Earth scanning method. AD on such spacecraft requires a model of the shape of the Earth disk as seen from the spacecraft. AD accuracy requirements often are too severe to permit Earth oblateness to be ignored when modeling disk shape. Section 2 of this paper reexamines and extends the methods for Earth disk shape modeling employed in AD work at FDD for the past decade. A new formulation, based on a more convenient Earth flatness parameter, is introduced, and the geometric concepts are examined in detail. It is shown that the Earth disk can be approximated as an ellipse in AD computations. Algorithms for introducing Earth oblateness into the AD process for spacecraft carrying scanning ESA's have been developed at FDD and implemented into the support systems. The Tropical Rainfall Measurement Mission (TRMM) will be the first spacecraft with AD operation performed at FDD that uses a different type of ESA - namely, a static one - containing four fixed detectors D(sub i) (i = 1 to 4). Section 3 of this paper considers the effect of Earth oblateness on AD accuracy for TRMM. This effect ideally will not induce AD errors on TRMM when data from all four D(sub i) are present. When data from only two or three D(sub i) are available, however, a spherical Earth approximation can introduce errors of 0.05 to 0.30 deg on TRMM. These oblateness-induced errors are eliminated by a new algorithm that uses the results of Section 2 to model the Earth disk as an ellipse. Author

N95-27784*# Florida Univ., Gainesville, FL. Dept. of Aerospace Engineering, Mechanics and Engineering Science.

A MODIFIED PROPORTIONAL NAVIGATION SCHEME FOR RENDEZVOUS AND DOCKING WITH TUMBLING TARGETS: THE PLANAR CASE c17

Norman Fitz-Coy and Ming-Cheng Liu *In* NASA. Goddard Space Flight Center, Flight Mechanics/Estimation Theory Symposium 1995 May 1995 p 243-252 (For primary document see N95-27763 09-13)
(Grant NAG8-280)
Avail: CASI HC A02/MF A04

A two-phase proportional navigation scheme is developed for the case of two rigid bodies engaged in a rendezvous/docking maneuver. The target vehicle is nonmaneuvering, but does have constant nonzero angular and linear velocities. Under these conditions, it is shown that previously obtained solutions are not applicable. Analytical solutions are obtained leading to relationships between the transverse and LOS navigation constants. It is shown that the transverse navigation constant for the second phase of the maneuver must be 2. Also, initial conditions necessary for rendezvous are presented. Author

N95-27785*# Allied-Signal Technical Services Corp., Columbia, MD.

TELEMETRY DOWN-LINK DOPPLER AS AN ATTITUDE SENSOR FOR SPIN STABILIZED SPACECRAFT c17

S. D. Hendry *In* NASA. Goddard Space Flight Center, Flight Mechanics/Estimation Theory Symposium 1995 May 1995 p 253-266
(For primary document see N95-27763 09-13)
(Contract NAS5-31000)
Avail: CASI HC A03/MF A04

The communications antenna on a spin stabilized spacecraft is seldom located on the spin axis, hence, the antenna is in motion relative to the center of mass of the spacecraft. The Doppler shift observed at the ground or space relay communications receivers will include oscillations whose frequency and amplitude are functions of the motion of the antenna and the attitude of the spacecraft relative to the line of sight (LOS). This functional dependence creates the possibility of estimating attitude parameters from Doppler measurements. This paper presents mathematical models of Doppler oscillations from spinning spacecraft, including the effects of nutation. Algorithms for estimating spin rate, attitude and nutation angle are described. Results of analysis of Doppler tracking of GOES-8 and WIND are also discussed. Author

N95-27786*# Jet Propulsion Lab., California Inst. of Tech., Pasadena, CA.

MULTI-SPACECRAFT COHERENT DOPPLER AND RANGING FOR INTERPLANETARY-NAVIGATION c17

Vincent M. Pollmeier *In* NASA. Goddard Space Flight Center, Flight Mechanics/Estimation Theory Symposium 1995 May 1995 p 267-276
(For primary document see N95-27763 09-13)
Avail: CASI HC A02/MF A04

Future plans for planetary exploration currently include using multiple spacecraft to simultaneously explore one planet. This never before encountered situation places new demands on tracking systems used to support navigation. One possible solution to the problem of heavy ground resource conflicts is the use of multispacecraft coherent radio metric data, also known as, bent-pipe data. Analysis of the information content of these data types show that the information content of multi-spacecraft Doppler is dependent only on the frequency of the final downlink leg and is independent of the frequencies used on other legs. Numerical analysis shows that coherent bent-pipe data can provide significantly better capability to estimate the location of a lander on the surface of Mars than can direct lander to Earth radio metric data. However, this is complicated by difficulties in separating the effect of a lander position error from that of an orbiter position error for single passes of data. Author

N95-27787*# Jet Propulsion Lab., California Inst. of Tech., Pasadena, CA.

ULYSSES ORBIT DETERMINATION AT HIGH DECLINATIONS

Timothy P. McElrath and George D. Lewis *In* NASA. Goddard Space Flight Center, Flight Mechanics/Estimation Theory Symposium 1995 May 1995 p 277-287 (For primary document see N95-27763 09-13)
Avail: CASI HC A03/MF A04

The trajectory of the Ulysses spacecraft caused its geocentric declination to exceed 60 deg South for over two months during the Fall of 1994, permitting continuous tracking from a single site. During this time, spacecraft operations constraints allowed only Doppler tracking data to be collected, and imposed a high radial acceleration uncertainty on the orbit determination process. The unusual aspects of this situation have motivated a re-examination of the Hamilton-Melbourne results, which have been used before to estimate the information content of Doppler tracking for trajectories closer to the ecliptic. The addition of an acceleration term to this equation is found to significantly increase the declination uncertainty for symmetric passes. In addition, a simple means is described to transform the symmetric results when the tracking pass is non-symmetric. The analytical results are then compared against numerical studies of this tracking geometry and found to be in good agreement for the angular uncertainties. The results of this analysis are applicable to the Near Earth Asteroid Rendezvous (NEAR) mission and to any other missions with high declination trajectories, as well as to missions using short tracking passes and/or one-way Doppler data. Author

N95-27788*# Jet Propulsion Lab., California Inst. of Tech., Pasadena, CA.

APPLICATION OF NON-COHERENT DOPPLER DATA TYPES FOR DEEP SPACE NAVIGATION **c17**

Shyam Bhaskaran *In* NASA. Goddard Space Flight Center, Flight Mechanics/Estimation Theory Symposium 1995 May 1995 p 289-299 (For primary document see N95-27763 09-13)
Avail: CASI HC A03/MF A04

Recent improvements in computational capability and Deep Space Network technology have renewed interest in examining the possibility of using one-way Doppler data alone to navigate interplanetary spacecraft. The one-way data can be formulated as the standard differenced-count Doppler or as phase measurements, and the data can be received at a single station or differenced if obtained simultaneously at two stations. A covariance analysis is performed which analyzes the accuracy obtainable by combinations of one-way Doppler data and compared with similar results using standard two-way Doppler and range. The sample interplanetary trajectory used was that of the Mars Pathfinder mission to Mars. It is shown that differenced one-way data is capable of determining the angular position of the spacecraft to fairly high accuracy, but has relatively poor sensitivity to the range. When combined with single station data, the position dispersions are roughly an order of magnitude larger in range and comparable in angular position as compared to dispersions obtained with standard data two-way types. It was also found that the phase formulation is less sensitive to data weight variations and data coverage than the differenced-count Doppler formulation. Author

N95-27789*# Draper (Charles Stark) Lab., Inc., Cambridge, MA.

THE TRANSITION OF GTDS TO THE UNIX WORKSTATION ENVIRONMENT **c60**

D. Carter, R. Metzinger, R. Proulx, and P. Cefola *In* NASA. Goddard Space Flight Center, Flight Mechanics/Estimation Theory Symposium 1995 May 1995 p 301-302 (For primary document see N95-27763 09-13)
Avail: CASI HC A01/MF A04

Future Flight Dynamics systems should take advantage of the possibilities provided by current and future generations of low-cost, high performance workstation computing environments with Graphical User Interface. The port of the existing mainframe Flight Dynamics systems to the workstation environment offers an economic approach for combining the tremendous engineering heritage that has been encapsulated in these systems with the advantages of the new computing environments. This paper will describe the successful transition of the Draper Laboratory R&D version of GTDS (Goddard Trajectory Determination System) from the IBM Mainframe to the Unix workstation environment. The approach will be a mix of historical timeline notes, descriptions of the technical problems overcome, and descriptions of associated SQA (software quality assurance) issues. Author (revised)

N95-27790*# National Aeronautics and Space Administration. Goddard Space Flight Center, Greenbelt, MD.

FLIGHT DYNAMICS SOFTWARE IN A DISTRIBUTED NETWORK ENVIRONMENT **c61**

J. Jeletic, D. Weidow, and D. Boland (Computer Sciences Corp., Lanham, MD.) *In its* Flight Mechanics/Estimation Theory Symposium 1995 May 1995 p 303-304 (For primary document see N95-27763 09-13)
Avail: CASI HC A01/MF A04

As with all NASA facilities, the announcement of reduced budgets, reduced staffing, and the desire to implement smaller/quicker/cheaper missions has required the Agency's organizations to become more efficient in what they do. To accomplish these objectives, the FDD has initiated the development of the Flight Dynamics Distributed System (FDDS). The underlying philosophy of FDDS is to build an integrated system that breaks down the traditional barriers of attitude, mission planning, and navigation support software to provide a uniform approach to flight dynamics applications. Through the application of open systems concepts and state-of-the-art technologies, including object-oriented specification concepts, object-oriented software, and common user interface, communications, data management, and executive services, the FDD will reengineer most of its six million lines of code. Author (revised)

N95-27791*# Lockheed Martin Corp., Denver, CO. Management and Data Systems.

DETERMINING GPS AVERAGE PERFORMANCE METRICS Abstract Only **c04**

G. V. Moore *In* NASA. Goddard Space Flight Center, Flight Mechanics/Estimation Theory Symposium 1995 May 1995 p 307 (For primary document see N95-27763 09-13)
Avail: CASI HC A01/MF A04

Analytic and semi-analytic methods are used to show that users of the GPS constellation can expect performance variations based on their location. Specifically, performance is shown to be a function of both altitude and latitude. These results stem from the fact that the GPS constellation is itself non-uniform. For example, GPS satellites are over four times as likely to be directly over Tierra del Fuego than over Hawaii or Singapore. Inevitable performance variations due to user location occur for ground, sea, air and space GPS users. These performance variations can be studied in an average relative sense. A semi-analytic tool which symmetrically allocates GPS satellite latitude belt dwell times among longitude points is used to compute average performance metrics. These metrics include average number of GPS vehicles visible, relative average accuracies in the radial, intrack and crosstrack (or radial, north/south, east/west) directions, and relative average PDOP or GDOP. The tool can be quickly changed to incorporate various user antenna obscuration models and various GPS constellation designs. Among other applications, tool results can be used in studies to: predict locations and geometries of best/worst case performance, design GPS constellations, determine optimal user antenna location and understand performance trends among various users. Author

N95-27792*# Jet Propulsion Lab., California Inst. of Tech., Pasadena, CA.

A DEMONSTRATION OF UNIFIED TDRS/GPS TRACKING AND ORBIT DETERMINATION

B. Haines, S. Lichten, J. Srinivasan, and L. Young *In* NASA. Goddard Space Flight Center, Flight Mechanics/Estimation Theory Symposium 1995 May 1995 p 309-320 (For primary document see N95-27763 09-13)
Avail: CASI HC A03/MF A04

We describe results from an experiment in which TDRS and GPS satellites were tracked simultaneously from a small (3 station) ground network in the western United States. We refer to this technique as 'GPS-like tracking' (GLT) since the user satellite - in this case TDRS - is essentially treated as a participant in the GPS constellation. In the experiment, the TDRS K(sub space-to-ground link (SGL) was tracked together with GPS L-band signals in enhanced geodetic-quality GPS receivers (TurboRogue). The enhanced receivers simultaneously measured and recorded both the TDRS SGL and the GPS carrier phases with sub-mm precision, enabling subsequent precise TDRS orbit determination with differential GPS techniques. A small number of calibrated ranging points from routine operations at the TDRS ground station (White Sands, NM) were used to supplement the GLT measurements in order to improve determination of the TDRS longitude. Various tests performed on TDRS ephemerides derived from data collected during this demonstration - including comparisons with the operational precise orbit generated by NASA Goddard Space Flight Center - provide evidence that the TDRS orbits have been determined to better than 25 m with the GLT technique. Author (revised)

N95-27793*# Lockheed Technical Operations Co., Crofton, MD.
GPS AS AN ORBIT DETERMINATION SUBSYSTEMS
Richard Fennessey, Pat Roberts, Robin Knight, and Bart VanVolkinburg *In* NASA. Goddard Space Flight Center, Flight Mechanics/Estimation Theory Symposium 1995 May 1995 p 321-331 (For primary document see N95-27763 09-13)
(Contract F04690-92-C-0529)
Avail: CASI HC A03/MF A04

This paper evaluates the use of Global Positioning System (GPS) receivers as a primary source of tracking data for low-Earth orbit satellites. GPS data is an alternative to using range, azimuth, elevation, and range-rate (RAER) data from the Air Force Satellite Control Network antennas, the Space Ground Link System (SGLS). This evaluation is applicable to missions such as Skipper, a joint U.S. and Russian atmosphere research mission, that will rely on a GPS receiver as a primary tracking data source. The Detachment 2, Space and Missile Systems Center's Test Support Complex (TSC) conducted the evaluation based on receiver data from the Space Test Experiment Platform Mission O (STEP-O) and Advanced Photovoltaic and Electronics Experiments (APEX) satellites. The TSC performed orbit reconstruction and prediction on the STEP-0 and APEX vehicles using GPS receiver navigation solution data, SGLS RAER data, and SGLS anglesonly (azimuth and elevation) data. For the STEP-O case, the navigation solution based orbits proved to be more accurate than SGLS RAER based orbits. For the APEX case, navigation solution based orbits proved to be less accurate than SGLS RAER based orbits for orbit prediction, and results for orbit reconstruction were inconclusive due to the lack of a precise truth orbit. After evaluating several different GPS data processing methods, the TSC concluded that using GPS navigation solution data is a viable alternative to using SGLS RAER data. Author

N95-27794*# National Aeronautics and Space Administration. Goddard Space Flight Center, Greenbelt, MD.
OPERATIONAL CONSIDERATIONS OF USING GPS FOR SPACECRAFT NAVIGATION c17
Roger C. Hart and Kathy R. Hartman *In its* Flight Mechanics/Estimation Theory Symposium 1995 May 1995 p 333-339 (For primary document see N95-27763 09-13)
Avail: CASI HC A02/MF A04

The Flight Dynamics Facility (FDF) at the NASA Goddard Space Flight Center (GSFC) has provided operational spacecraft orbit support for many years, currently generating orbit products for about 20 satellites. To date, operational orbit determination in the FDF has been performed on the ground using data from ground-based or space-based tracking systems. Current development of spaceborne Global Positioning System (GPS) receivers is projected to have a significant effect on the support needed for operational satellite navigation. This paper identifies the functions performed in spacecraft navigation and examines and quantifies how the functions and support levels will be affected as onboard GPS receivers are implemented on spacecraft. Cases are considered spacecraft using or not using NASA ground and space networks resources. Author

N95-27795*# National Aeronautics and Space Administration. Goddard Space Flight Center, Greenbelt, MD.
THE GLOBAL POSITIONING SYSTEM (GPS) AND ATTITUDE DETERMINATION: APPLICATIONS AND ACTIVITIES IN THE FLIGHT DYNAMICS DIVISION
Eleanor Ketchum and Joe Garrick *In its* Flight Mechanics/Estimation Theory Symposium 1995 May 1995 p 341-349 (For primary document see N95-27763 09-13)
Avail: CASI HC A02/MF A04

The application of GPS to spacecraft attitude determination is a new and growing field. Although the theoretical literature is extensive, space flight testing is currently sparse and inadequate. As an operations organization, the Flight Dynamics Division (FDD) has the responsibility to investigate this new technology, and determine how best to implement the innovation to provide adequate support for future missions. This paper presents some of the current efforts within FDD with regard to GPS attitude determination. This effort specifically addresses institutional capabilities to accommodate a new type of sensor, critically evaluating the literature for recent advancements, and in examining some available -albeit crude- flight data. Author

N95-27796*# National Aeronautics and Space Administration. Goddard Space Flight Center, Greenbelt, MD.
CONTINGENCY MANEUVER STRATEGIES FOR THE TOTAL OZONE MAPPING SPECTROMETER-EARTH PROBE (TOMS-EP)
James Kestler (Computer Sciences Corp., Lanham, MD.) and Donna Walls *In its* Flight Mechanics/Estimation Theory Symposium 1995 May 1995 p 351-363 (For primary document see N95-27763 09-13)
(Contract NAS5-31500)
Avail: CASI HC A03/MF A04

The Total Ozone Mapping Spectrometer-Earth Probe (TOMS-EP) is a polar-orbiting spacecraft designed to measure total ozone levels in the Earth's atmosphere. The nominal mission orbit is a 955-kilometer circular Sun-synchronous orbit with an ascending node mean local crossing time (MLT) between 11:02 a.m. and 11:25 a.m. These two mean local ascending node times constitute the boundaries of the MLT box for this mission. The MLT boundaries were chosen to maintain the Sun-to-Earth-to-vehicle orbit-normal (SVN) angle within a preselected set of seasonally independent boundaries. Because the SVN angle is seasonally dependent, but the MLT is not, contingency options for correcting the MLT of orbital states that fall outside of the required MLT range become time dependent. This paper focuses on contingency orbit adjustment strategies developed at the Goddard Space Flight Center (GSFC) Flight Dynamics Division (FDD) during the mission planning phase of TOMS-EP. Time-dependent delta-V strategies are presented for correcting mission orbit states lying outside of the MLT range. Typically, passive control of the MLT drift rate can be used to restore the orbit state to the required MLT before a seasonal violation of SVN angle constraints can occur. Passive control of the MLT drift rate is obtained through adjustment of the semimajor axis and/or the inclination. The time between initial arrival on orbit at an 'out-of-the box' MLT state and violation of the SVN angle constraints is always less than or equal to 1 year. The choice of which parameter(s) to adjust is dictated by the duration of this time period, the desired mission lifetime, the delta-V cost, and operational constraints. Author

N95-27797*# National Aeronautics and Space Administration. Goddard Space Flight Center, Greenbelt, MD.
SUMMARY OF EOS FLIGHT DYNAMICS ANALYSIS
Lauri Kraft Newman and David C. Folta *In its* Flight Mechanics/Estimation Theory Symposium 1995 May 1995 p 365-366 (For primary document see N95-27763 09-13)
Avail: CASI HC A01/MF A04

From a flight dynamics perspective, the Earth Observing System (EOS) spacecraft present a number of challenges to mission designers. The Flight Dynamics Support Branch of NASA GSFC has examined a number of these challenges, including managing the EOS constellation, disposing of the spacecraft at the end-of-life (EOL), and achieving the appropriate mission orbit given launch vehicle and ascent propulsion constraints. The EOS program consists of a number of spacecraft including EOS-AM, an ascending node spacecraft, EOS-PM, a descending node spacecraft, the EOS Chemistry mission (EOS-CHEM), the EOS Altimetry Laser (EOS-LALT), and the EOS-Altimetry Radar (EOS-RALT). The orbit characteristics of these missions are presented. In order to assure that downlinking data from each spacecraft will be possible without interference between any two spacecraft, a careful examination of the relationships between spacecraft and how to maintain the spacecraft in a configuration which would minimize these communications problems must be made. The FDSB has performed various analyses to determine whether the spacecraft will be in a position to interfere with each other, how the orbit dynamics will change the relative positioning of the spacecraft over their lifetimes, and how maintenance maneuvers could be performed, if needed, to minimize communications problems. Prompted by an activity at NASA HQ to set guidelines for spacecraft regarding their end-of-life dispositions, much analysis has also been performed to determine the spacecraft lifetime of EOS-AM1 under various conditions, and to make suggestions regarding the spacecraft disposal. In performing this analysis, some general trends have been observed in lifetime calculations. The paper will present the EOS-AM1 lifetime results, comment on general reentry conclusions, and discuss how these analyses reflect on the HQ NMI. Placing the EOS spacecraft into their respective mission orbits involves some intricate maneuver planning to assure that all mission orbit requirements are met, given the initial conditions supplied by the launch vehicle at injection. The FDSB has developed an ascent scenario to meet the mission requirements. This paper presents results of the ascent analysis. Author

N95-27798*# National Aeronautics and Space Administration. Goddard Space Flight Center, Greenbelt, MD.

GEOSTATIONARY OPERATIONAL ENVIRONMENTAL SATELLITE (GOES)-8 MISSION FLIGHT EXPERIENCE c18

C. H. Noonan (Computer Sciences Corp., Lanham, MD.), R. J. McIntosh (Computer Sciences Corp., Lanham, MD.), J. N. Rowe (Computer Sciences Corp., Lanham, MD.), R. L. DeFazio, and K. F. Galal *In its* Flight Mechanics/Estimation Theory Symposium 1995 May 1995 p 369-378
(For primary document see N95-27763 09-13)
(Contract NAS5-31500)
Avail: CASI HC A02/MF A04

The Geostationary Operational Environmental Satellite (GOES)-8 spacecraft was launched on April 13, 1994, at 06:04:02 coordinated universal time (UTC), with separation from the Atlas-Centaur launch vehicle occurring at 06:33:05 UTC. The launch was followed by a series of complex, intense operations to maneuver the spacecraft into its geosynchronous mission orbit. The Flight Dynamics Facility (FDF) of the Goddard Space Flight Center (GSFC) Flight Dynamics Division (FDD) was responsible for GOES-8 attitude, orbit maneuver, orbit determination, and station acquisition support during the ascent phase. This paper summarizes the efforts of the FDF support teams and highlights some of the unique challenges the launch team faced during critical GOES-8 mission support. FDF operations experience discussed includes: (1) The abort of apogee maneuver firing-1 (AMF-1), cancellation of AMF-3, and the subsequent replans of the maneuver profile; (2) The unexpectedly large temperature dependence of the digital integrating rate assembly (DIRA) and its effect on GOES-8 attitude targeting in support of perigee raising maneuvers; (3) The significant effect of attitude control thrusting on GOES-8 orbit determination solutions; (4) Adjustment of the trim tab to minimize torque due to solar radiation pressure; and (5) Postlaunch analysis performed to estimate the GOES-8 separation attitude. The paper also discusses some key FDF GOES-8 lessons learned to be considered for the GOES-J launch which is currently scheduled for May 19, 1995. Author

N95-27799*# Computer Sciences Corp., Lanham, MD.

ESTIMATION OF ATTITUDE SENSOR TIMETAG BIASES

J. Sedlak *In* NASA. Goddard Space Flight Center, Flight Mechanics/Estimation Theory Symposium 1995 May 1995 p 379-403
(For primary document see N95-27763 09-13)
(Contract NAS5-31500)
Avail: CASI HC A03/MF A04

This paper presents an extended Kalman filter for estimating attitude sensor timing errors. Spacecraft attitude is determined by finding the mean rotation from a set of reference vectors in inertial space to the corresponding observed vectors in the body frame. Any timing errors in the observations can lead to attitude errors if either the spacecraft is rotating or the reference vectors themselves vary with time. The state vector here consists of the attitude quaternion, timetag biases, and, optionally, gyro drift rate biases. The filter models the timetags as random walk processes: their expectation values propagate as constants and white noise contributes to their covariance. Thus, this filter is applicable to cases where the true timing errors are constant or slowly varying. The observability of the state vector is studied first through an examination of the algebraic observability condition and then through several examples with simulated star tracker timing errors. The examples use both simulated and actual flight data from the Extreme Ultraviolet Explorer (EUVE). The flight data come from times when EUVE had a constant rotation rate, while the simulated data feature large angle attitude maneuvers. The tests include cases with timetag errors on one or two sensors, both constant and time-varying, and with and without gyro bias errors. Due to EUVE's sensor geometry, the observability of the state vector is severely limited when the spacecraft rotation rate is constant. In the absence of attitude maneuvers, the state elements are highly correlated, and the state estimate is unreliable. The estimates are particularly sensitive to filter mistuning in this case. The EUVE geometry, though, is a degenerate case having coplanar sensors and rotation vector. Observability is much improved and the filter performs well when the rate is either varying or noncoplanar with the sensors, as during a slew. Even with bad geometry and constant rates, if gyro biases are independently known, the timetag error for a single sensor can be accurately estimated as long as its boresight is not too close to the spacecraft rotation axis. Author

N95-27800*# National Aeronautics and Space Administration. Goddard Space Flight Center, Greenbelt, MD.

A NEW ANGLE ON THE EULER ANGLES c64

F. Landis Markley and Malcolm D. Shuster (Florida Univ., Gainesville, FL.) *In its* Flight Mechanics/Estimation Theory Symposium 1995 May 1995 p 395-403 (For primary document see N95-27763 09-13)
Avail: CASI HC A02/MF A04

We present a generalization of the Euler angles to axes beyond the twelve conventional sets. The generalized Euler axes must satisfy the constraint that the first and the third are orthogonal to the second; but the angle between the first and third is arbitrary, rather than being restricted to the values 0 and pi/2, as in the conventional sets. This is the broadest generalization of the Euler angles that provides a representation of an arbitrary rotation matrix. The kinematics of the generalized Euler angles and their relation to the attitude matrix are presented. As a side benefit, the equations for the generalized Euler angles are universal in that they incorporate the equations for the twelve conventional sets of Euler angles in a natural way. Author

N95-27801*# National Aeronautics and Space Administration. Goddard Space Flight Center, Greenbelt, MD.

A MAGNETIC HYSTERESIS MODEL c70

Thomas W. Flatley and Debra A. Henretty *In its* Flight Mechanics/Estimation Theory Symposium 1995 May 1995 p 405-415
(For primary document see N95-27763 09-13)
Avail: CASI HC A03/MF A04

The Passive Aerodynamically Stabilized Magnetically Damped Satellite (PAMS) will be deployed from the Space Shuttle and used as a target for a Shuttle-mounted laser. It will be a cylindrical satellite with several corner cube reflectors on the ends. The center of mass of the cylinder will be near one end, and aerodynamic torques will tend to align the axis of the cylinder with the spacecraft velocity vector. Magnetic hysteresis rods will be used to provide passive despin and oscillation-damping torques on the cylinder. The behavior of the hysteresis rods depends critically on the 'B/H' curves for the combination of materials and rod length-to-diameter ratio ('l-over-d'). These curves are qualitatively described in most Physics textbooks in terms of major and minor 'hysteresis loops'. Mathematical modeling of the functional relationship between B and H is very difficult. In this paper, the physics involved is not addressed, but an algorithm is developed which provides a close approximation to empirically determined data with a few simple equations suitable for use in computer simulations. Author

N95-27802*# CTA Space Systems, McLean, VA.

AUTONOMOUS CONTROL SYSTEM RECONFIGURATION FOR SPACECRAFT WITH NON-REDUNDANT ACTUATORS Abstract Only c18

Walter Grossman *In* NASA. Goddard Space Flight Center, Flight Mechanics/Estimation Theory Symposium 1995 May 1995 p 417 (For primary document see N95-27763 09-13)
Avail: CASI HC A01/MF A04

The Small Satellite Technology Initiative (SSTI) 'CLARK' spacecraft is required to be single-failure tolerant, i.e., no failure of any single component or subsystem shall result in complete mission loss. Fault tolerance is usually achieved by implementing redundant subsystems. Fault tolerant systems are therefore heavier and cost more to build and launch than non-redundent, non fault-tolerant spacecraft. The SSTI CLARK satellite Attitude Determination and Control System (ADACS) achieves single-fault tolerance without redundancy. The attitude determination system system uses a Kalman Filter which is inherently robust to loss of any single attitude sensor. The attitude control system uses three orthogonal reaction wheels for attitude control and three magnetic dipoles for momentum control. The nominal six-actuator control system functions by projecting the attitude correction torque onto the reaction wheels while a slower momentum management outer loop removes the excess momentum in the direction normal to the local B field. The actuators are not redundant so the nominal control law cannot be implemented in the event of a loss of a single actuator (dipole or reaction wheel). The spacecraft dynamical state (attitude, angular rate, and momentum) is controllable from any five-element subset of the six actuators. With loss of an actuator the instantaneous control authority may not span R(3) but the controllability gramian integral(limits between t,0) Phi(t, tau)B(tau)B(prime)(tau) Phi(prime)(t, tau)d tau retains full rank. Upon detection of an actuator failure the control torque is decomposed onto the remaining active axes. The attitude control torque is effected and the over-orbit momentum is controlled. The resulting control system performance approaches that of the nominal system. Author

N95-27803*# National Aeronautics and Space Administration. Goddard Space Flight Center, Greenbelt, MD.

CONTINGENCY DESIGNS FOR ATTITUDE DETERMINATION OF TRMM

John L. Crassidis, Stephen F. Andrews, F. Landis Markley, and Kong Ha (Orbital Sciences Corp., Greenbelt, MD.) *In its* Flight Mechanics/Estimation Theory Symposium 1995 May 1995 p 419-433 Sponsored by National Research Council Postdoctoral Fellowship (For primary document see N95-27763 09-13)
Avail: CASI HC A03/MF A04

In this paper, several attitude estimation designs are developed for the Tropical Rainfall Measurement Mission (TRMM) spacecraft. A contingency attitude determination mode is required in the event of a primary sensor failure. The final design utilizes a full sixth-order Kalman filter. However, due to initial software concerns, the need to investigate simpler designs was required. The algorithms presented in this paper can be utilized in place of a full Kalman filter, and require less computational burden. These algorithms are based on filtered deterministic approaches and simplified Kalman filter approaches. Comparative performances of all designs are shown by simulating the TRMM spacecraft in mission mode. Comparisons of the simulation results indicate that comparable accuracy with respect to a full Kalman filter design is possible. Author

N95-27804*# MATRA Marconi Space Systems, Stevenage (England).

ORION: A SUPERSYNCHRONOUS TRANSFER ORBIT MISSION

I. M. Walters, J. F. Baker, and I. M. Shurmer *In* NASA. Goddard Space Flight Center, Flight Mechanics/Estimation Theory Symposium 1995 May 1995 p 435-447 (For primary document see N95-27763 09-13)
Avail: CASI HC A03/MF A04

ORION F1 was launched on 29th November 1994 on an Atlas IIA launch vehicle. It was designed, built and delivered in-orbit by Matra Marconi Space Systems Plc and was handed over to ORION Satellite Corporation on 20th January 1995 at its on-station longitude of 37.5 deg W. The mission differed significantly from that of any other geostationary communications satellite in that the Transfer Orbit apogee altitude of 123,507 km was over three times geosynchronous (GEO) altitude and one third of the way to the moon. The SuperSynchronous Transfer Orbit (SSTO) mission is significantly different from the standard Geostationary Transfer Orbit (GTO)mission in a number of ways. This paper discusses the essential features of the mission design through its evolution since 1987 and the details of the highly successful mission itself including a detailed account of the attitude determination achieved using the Galileo Earth and Sun Sensor (ESS). Derived from text

14 GROUND SUPPORT SYSTEMS AND FACILITIES (SPACE)

Includes launch complexes, research and production facilities; ground support equipment, e.g., mobile transporters; and simulators.

For related information see also *09 Research and Support Facilities (Air).*

N95-27264*# Jet Propulsion Lab., California Inst. of Tech., Pasadena, CA.

PERFORMANCE OF THE SATELLITE TEST ASSISTANT ROBOT IN JPL'S SPACE SIMULATION FACILITY

Douglas McAffee, Mark Long, Ken Johnson, and Georg Siebes (California Inst. of Tech., Pasadena, CA.) *In* NASA. Johnson Space Center, The 29th Aerospace Mechanisms Symposium May 1995 p 45-57 (For primary document see N95-27260 09-15)
Avail: CASI HC A03/MF A04

N95-27671*# Phillips Lab., Kirtland AFB, NM.

A NEW TECHNIQUE FOR GROUND SIMULATION OF HYPERVELOCITY DEBRIS

R. Roybal, J. Shively, C. Stein, C. Miglionico, and R. Robertson *In* NASA. Langley Research Center, LDEF: 69 Months in Space. Third Post-Retrieval Symposium, Part 3 Feb. 1995 p 1379-1388 (For primary document see N95-27629 09-99)
Avail: CASI HC A02/MF A04

15 LAUNCH VEHICLES AND SPACE VEHICLES

Includes boosters; operating problems of launch/space vehicle systems; and reusable vehicles.

For related information see also *20 Spacecraft Propulsion and Power.*

N95-26524 Department of the Navy, Washington, DC.

A HIGH VELOCITY ELECTROMAGNETIC MASS LAUNCHER HAVING AN ABLATION RESISTANT INSULATOR Patent Application

Robert A. Meger, inventor (to Navy) 1 Jun. 1994 24 p Limited Reproducibility: More than 20% of this document may be affected by microfiche quality
(AD-A288231; US-Patent-Appl-SN-252474) Avail: Issuing Activity (Defense Technical Information Center (DTIC))

A railgun having a composite insulator of laminated materials positioned between the rails is described in this document. The composite insulator is comprised of a series of conducting layers oriented with the edges toward the bore, or barrel, of the railgun and the wide edges away from the bore. The laminate is lain lengthwise along the rails and comprised of conducting layers of a high heat conductivity metal interleaved with an insulator material. The insulator material allows the composite insulator to stand off the voltages in a plasma armature even under high radiation flux conditions. Below the conducting material's ablation threshold the amount of ablation produced by the composite insulator is reduced by the reduction of insulator surface area exposed to the radiation. This allows better control of armature growth, mass acceleration by the plasma armature, secondary formation, and other factors normally found to retard projectile acceleration. DTIC

N95-27245*# GPS Solutions, Inc., Carson City, NV.

REUSABLE LAUNCH VEHICLE DEVELOPMENT RESEARCH Final Report

16 Jan. 1995 47 p
(Contract NAS8-40257)
(NASA-CR-196614; NAS 1.26:196614) Avail: CASI HC A03/MF A01

NASA has generated a program approach for a SSTO reusable launch vehicle technology (RLV) development which includes a follow-on to the Ballistic Missile Defense Organization's (BMDO) successful DC-X program, the DC-XA (Advanced). Also, a separate sub-scale flight demonstrator, designated the X-33, will be built and flight tested along with numerous ground based technologies programs. For this to be a successful effort, a balance between technical, schedule, and budgetary risks must be attained. The adoption of BMDO's 'fast track' management practices will be a key element in the eventual success of NASA's effort. Derived from text

N95-27260*# National Aeronautics and Space Administration. Lyndon B. Johnson Space Center, Houston, TX.

THE 29TH AEROSPACE MECHANISMS SYMPOSIUM

William C. Schneider, ed. May 1995 397 p Symposium held in League City, TX, 17-19 May 1995; sponsored by LMSC
(NASA-CP-3293; S-794; NAS 1.55:3293) Avail: CASI HC A17/MF A04

The proceedings of the 29th Aerospace Mechanisms Symposium, which was hosted by NASA Johnson Space Center and held at the South Shore Harbour Conference Facility on May 17-19, 1995, are reported. Technological areas covered include actuators, aerospace mechanism applications for ground support equipment, lubricants, pointing mechanisms joints, bearings, release devices, booms, robotic mechanisms, and other mechanisms for spacecraft. For individual titles, see N95-27261 through N95-27292.

N95-27261*# Spar Aerospace Ltd., Brampton (Ontario). Space Systems Div.

DESIGN, TESTING AND EVALUATION OF LATCHING END EFFECTOR **c37**

B. Walker and R. Vandersluis *In* NASA. Lyndon B. Johnson Space Center, The 29th Aerospace Mechanisms Symposium May 1995 p 1-16 (For primary document see N95-27260 09-15)

Avail: CASI HC A03/MF A04

The Latching End Effector (LEE) forms part of the Space Station Remote Manipulator System (SSRMS) for which Spar Aerospace Ltd, Space Systems Division is the prime contractor. The design, testing and performance evaluation of the Latching End Effector mechanisms is the subject of this paper focusing on: (1) ambient, thermal and vibration testing; (2) snare/rigidize performance testing and interaction during payload acquisition; and (3) latch/umbilical test results and performance. Author

N95-27262*# Fokker Space and Systems, Leiden (Netherlands).

SOME MECHANICAL DESIGN ASPECTS OF THE EUROPEAN ROBOTIC ARM **c37**

Peter J. Lambooy, Wart M. Mandersloot, and Richard H. Bentall (European Space Agency. European Space Research and Technology Center, ESTEC, Noordwijk, Netherlands.) *In* NASA. Johnson Space Center, The 29th Aerospace Mechanisms Symposium May 1995 p 17-29 (For primary document see N95-27260 09-15)

Avail: CASI HC A03/MF A04

The European Robotic Arm (ERA) is a contribution to the Russian Segment of the International Space Station Alpha. It will start operating on the Russian Segment during the assembly phase. ERA is designed and produced by a large industrial consortium spread over Europe with Fokker Space & Systems as prime contractor. In this paper, we will describe some of the overall design aspects and focus on the development of several mechanisms within ERA. The operation of ERA during the approach of its end effector towards the grapple interface and the grapple operation is discussed, with a focus on mechanisms. This includes the geometry of the end effector leading edge, which is carefully designed to provide the correct and complete tactile information to a torque-force sensor (TFS). The data from this TFS are used to steer the arm such that forces and moments are kept below 20 N and 20 N.m respectively during the grappling operation. Two hardware models of the end effector are built. The problems encountered are described as well as their solutions. The joints in the wrists and the elbow initially used a harmonic drive lubricated by MoS2. During development testing, this combination showed an insufficient lifetime in air to survive the acceptance test program. The switch-over to a system comprising planetary gearboxes with grease lubrication is described. From these development efforts, conclusions are drawn and recommendations are given for the design of complex space mechanisms. Author

N95-27263*# National Aeronautics and Space Administration. Lyndon B. Johnson Space Center, Houston, TX.

ADVANCED DEVELOPMENT FOR SPACE ROBOTICS WITH EMPHASIS ON FAULT TOLERANCE **c37**

D. Tesar (Texas Univ., Austin, TX.), J. Chladek, R. Hooper (Texas Univ., Austin, TX.), D. Sreevijayan (Texas Univ., Austin, TX.), C. Kapoor (Texas Univ., Austin, TX.), J. Geisinger (Texas Univ., Austin, TX.), M. Meaney (Texas Univ., Austin, TX.), G. Browning (Texas Univ., Austin, TX.), and K. Rackers (Texas Univ., Austin, TX.) *In its* 29th Aerospace Mechanisms Symposium May 1995 p 30-4 (For primary document see N95-27260 09-15)

Avail: CASI HC A03/MF A04

This paper describes the ongoing work in fault tolerance at the University of Texas at Austin. The paper describes the technical goals the group is striving to achieve and includes a brief description of the individual projects focusing on fault tolerance. The ultimate goal is to develop and test technology applicable to all future missions of NASA (lunar base, Mars exploration, planetary surveillance, space station, etc.). Author

N95-27264*# Jet Propulsion Lab., California Inst. of Tech., Pasadena, CA.

PERFORMANCE OF THE SATELLITE TEST ASSISTANT ROBOT IN JPL'S SPACE SIMULATION FACILITY **c14**

Douglas McAffee, Mark Long, Ken Johnson, and Georg Siebes (California Inst. of Tech., Pasadena, CA.) *In* NASA. Johnson Space Center, The 29th Aerospace Mechanisms Symposium May 1995 p 45-57 (For primary document see N95-27260 09-15)

Avail: CASI HC A03/MF A04

An innovative new telerobotic inspection system called STAR (the Satellite Test Assistant Robot) has been developed to assist engineers as they test new spacecraft designs in simulated space environments. STAR operates inside the ultra-cold, high-vacuum, test chambers and provides engineers seated at a remote Operator Control Station (OCS) with high resolution video and infrared (IR) images of the flight articles under test. STAR was successfully proof tested in JPL's 25-ft (7.6-m) Space Simulation Chamber where temperatures ranged from +85 C to -190 C and vacuum levels reached 5.1 x 10(exp -6) torr. STAR's IR Camera was used to thermally map the entire interior of the chamber for the first time. STAR also made several unexpected and important discoveries about the thermal processes occurring within the chamber. Using a calibrated test fixture arrayed with ten sample spacecraft materials, the IR camera was shown to produce highly accurate surface temperature data. This paper outlines STAR's design and reports on significant results from the thermal vacuum chamber test. Author

N95-27265*# Jet Propulsion Lab., California Inst. of Tech., Pasadena, CA.

THE ALPHA-PROTON-X-RAY SPECTROMETER DEPLOYMENT MECHANISM: AN ANTHROPOMORPHIC APPROACH TO SENSOR PLACEMENT ON MARTIAN ROCKS AND SOIL **c91**

Richard S. Blomquist *In* NASA. Johnson Space Center, The 29th Aerospace Mechanisms Symposium May 1995 p 61-78 (For primary document see N95-27260 09-15)

Avail: CASI HC A03/MF A04

On July 4,1997, the Mars Pathfinder spacecraft lands on Mars and starts conducting technological and scientific experiments. One experiment, the Alpha-Proton-X-ray Spectrometer, uses a sensor head placed against rocks and soil to determine their composition. To guarantee proper placement, a deployment mechanism mounted on the Mars Rover aligns the sensor head to within 20 deg of the rock and soil surfaces. In carrying out its task, the mechanism mimics the action of a human hand and arm. Consisting of a flexible wrist, a parallel link arm, a brush dc motor actuator, and a revolutionary non-pyrotechnic fail-safe release device, the mechanism correctly positions the sensor head on rocks as high as 0.29 m and on targets whose surfaces are tilted as much as 45 deg from the nominal orientation of the sensor head face. The mechanism weighs less than 0.5 kg, can withstand 100 g's, and requires less than 2.8 N x m of actuation torque. The fail-safe coupler utilizes Cerrobend, a metal alloy that melts at 60 C, to fuse the actuator and the rest of the mechanism together. A film heater wrapped around the coupler melts the metal, and Negator springs drive the mechanism into its stowed position. The fail-safe actuates using 6.75 Watts for 5 minutes in the event of an actuator failure. Author

N95-27266*# Lockheed Missiles and Space Co., Sunnyvale, CA.

SOLAR ARRAY DEPLOYMENT MECHANISM **c37**

Mark C. Calassa and Russell Kackley *In* NASA. Johnson Space Center, The 29th Aerospace Mechanisms Symposium May 1995 p 79-93 (For primary document see N95-27260 09-15)

Avail: CASI HC A03/MF A04

This paper describes a Solar Array Deployment Mechanism (SADM) used to deploy a rigid solar array panel on a commercial spacecraft. The application required a deployment mechanism design that was not only lightweight, but also could be produced and installed at the lowest possible cost. This paper covers design, test, and analysis of a mechanism that meets these requirements. Author

N95-27267*# Starsys Research Corp., Boulder, CO.

CHANGING PARADIGMS: MANUFACTURING VS. FABRICATING A HIGH VOLUME HOLD DOWN AND RELEASE MECHANISM **c37**

Daryl Maus and Doug Monick *In* NASA. Johnson Space Center, The

29th Aerospace Mechanisms Symposium May 1995 p 94-108 (For primary document see N95-27260 09-15)
Avail: CASI HC A05/MF A04

A detailed description of the Hold Down and Release Mechanisms designed for a 70+ constellation of spacecraft is presented. The design is reviewed to understand the practical implications of severely constraining cost. Strategies for adapting the traditional aerospace design paradigm to a more commercial, cost driven paradigm are discussed and practical examples are cited. Author

N95-27268*# Naval Research Lab., Washington, DC.
THE CLEMENTINE MECHANISMS **c18**
William Purdy and Michael Hurley *In* NASA. Johnson Space Center, The 29th Aerospace Mechanisms Symposium May 1995 p 109-127 (For primary document see N95-27260 09-15)
Avail: CASI HC A03/MF A04

The Clementine spacecraft was developed under the 'faster, better, cheaper' theme. The constraints of a low budget coupled with an unusually tight schedule forced many departures from the normal spacecraft development methods. This paper discusses technical lessons learned about several of the mechanisms on the Clementine spacecraft as well as managerial lessons learned for the entire mechanisms subsystem. A quick overview of the Clementine mission is included; the mission schedule and environment during the mechanisms releases and deployment are highlighted. This paper then describes the entire mechanisms subsystem. The design and test approach and key philosophies for a fast-track program are discussed during the description of the mechanisms subsystem. The mechanism subsystem included a marman clamp separation system, a separation nut separation system, a solar panel deployment and pointing system, a high gain antenna feed deployment system, and two separate sensor cover systems. Each mechanism is briefly discussed. Additional technical discussion is given on the marman clamp design, the sensor cover designs, and the design and testing practices for systems driven by heated actuators (specifically paraffin actuators and frangibolts). All of the other mechanisms were of conventional designs and will receive less emphasis. Lessons learned are discussed throughout the paper as they applied to the systems being discussed. Since there is information on many different systems, this paper is organized so that information on a particular topic can be quickly referenced. Author

N95-27269*# ACE-Able Engineering Co., Inc., Goleta, CA.
LOW-COST TUBULAR ANTENNA DEPLOYER FOR WISP-2 **c37**
Robert M. Warden *In* NASA. Johnson Space Center, The 29th Aerospace Mechanisms Symposium May 1995 p 131-135 (For primary document see N95-27260 09-15)
Avail: CASI HC A01/MF A04

A new tubular boom deployment mechanism has been designed, built, and flown as part of the second Waves In Space Program (WISP-2) through Cornell University. For this program, two booms were needed to form a dipole antenna but existing units were found to be too complicated and costly. A low-cost alternative was developed which combined flight-proven tubular boom technology with a new support and deployment mechanism. The simplicity of this new design was a major factor in providing a highly reliable and cost-effective system. Author

N95-27270*# SSG, Inc., Waltham, MA.
ULTRA-HIGH, RESOLUTION, MODULAR OPTICAL ANGLE ENCODER FOR SPACE-BASED OPTO-MECHANICAL APPLICATIONS **c74**
Holger Luther, Paul Beard, Donald Mitchell (BEI Sensors and Systems Co., Needham, MA.), and William Thorburn (BEI Sensors and Systems Co., Needham, MA.) *In* NASA. Johnson Space Center, The 29th Aerospace Mechanisms Symposium May 1995 p 136-146 (For primary document see N95-27260 09-15)
Avail: CASI HC A01/MF A04

A 27-bit optical encoder using a novel patent pending technology has been developed by the MicroE Development Center of BEI Sensors & Systems Company and tested by the Sensor Systems Group (SSG) Inc., in a positioning and stabilization mirror assembly (PSMA) designed and constructed under a grant from the Marshall Space Flight Center. Test results verified performance within the specifications of the PSMA. Author

N95-27271*# Societe d'Applications Generales d'Electricite et de Mecanique, Paris (France).
HIGH PERFORMANCE STEPPER MOTORS FOR SPACE MECHANISMS **c33**
Patrick Sega and Christine Estevenon *In* NASA. Johnson Space Center, The 29th Aerospace Mechanisms Symposium May 1995 p 141-146 Sponsored by CNES (For primary document see N95-27260 09-15)
Avail: CASI HC A02/MF A04

Hybrid stepper motors are very well adapted to high performance space mechanisms. They are very simple to operate and are often used for accurate positioning and for smooth rotations. In order to fulfill these requirements, the motor torque, its harmonic content, and the magnetic parasitic torque have to be properly designed. Only finite element computations can provide enough accuracy to determine the toothed structures' magnetic permeance, whose derivative function leads to the torque. It is then possible to design motors with a maximum torque capability or with the most reduced torque harmonic content (less than 3 percent of fundamental). These later motors are dedicated to applications where a microstep or a synchronous mode is selected for minimal dynamic disturbances. In every case, the capability to convert electrical power into torque is much higher than on DC brushless motors. Author

N95-27272*# Schaeffer Magnetics, Inc., Chatsworth, CA.
DEVELOPMENT OF A MINIATURE ACTUATOR/CONTROLLER SYSTEM **c33**
Scott P. Stanley *In* NASA. Johnson Space Center, The 29th Aerospace Mechanisms Symposium May 1995 p 147-151 (For primary document see N95-27260 09-15)
Avail: CASI HC A01/MF A04

Development of new products is often hampered or prevented by the cost and resource commitments required by a traditional engineering approach. Schaeffer Magnetics, Inc. identified the potential need for a miniature incremental actuator with an integrated controller but did not want the development to be subject to the obstacles inherent in the traditional approach. In response a new approach - the Pathfinder Engineering Program (PEP) - was developed to streamline new product generation and improve product quality. The actuator/controller system resulting from implementation of this new procedure is an exceptionally compact and self-contained device with many applications. Author

N95-27273*# National Aeronautics and Space Administration. Goddard Space Flight Center, Greenbelt, MD.
BASIC SPACE PAYLOAD FASTENER **c37**
J. M. Vranish and Stephen Gorevan (Honeybee Robotics Ltd., New York, NY.) *In* NASA. Johnson Space Center, The 29th Aerospace Mechanisms Symposium May 1995 p 152-157 (For primary document see N95-27260 09-15)
Avail: CASI HC A02/MF A04

A new basic space fastener has been developed and tested by the GSFC. The purposes of this fastener are to permit assembly and servicing in space by astronauts and/or robots and to facilitate qualification of payloads on Earth prior to launch by saving time and money during the systems integration and component testing and qualification processes. The space fastener is a rework of the basic machine screw such that crossthreading is impossible; it is self-locking and will not work its way out during launch (vibration proof); it will not wear out despite repeated use; it occupies a small foot print which is comparable to its machine screw equivalent, and it provides force and exhibits strength comparable to its machine screw equivalent. Construction is ultra-simple and cost effective and the principle is applicable across the full range of screw sizes ranging from a #10 screw to 2.5 cm (1 in) or more. In this paper, the fastener principles of operation will be discussed along with test results and construction details. The new fastener also has considerable potential in the commercial sector. A few promising applications will be presented. Author

N95-27274*# Orbital Sciences Corp., Dulles, VA.
NON-EXPLOSIVE ACTUATION FOR THE ORBCOMM (TM) SATELLITE **c37**
Anthony Robinson, Craig Courtney (G and H Technology, Inc., Camarillo, CA.), and Tom Moran (G and H Technology, Inc., Camarillo, CA.) *In* NASA. Johnson Space Center, The 29th Aerospace Mechanisms

Symposium May 1995 p 158-161 (For primary document see N95-27260 09-15)
Avail: CASI HC A01/MF A04

Spool-based non-explosive actuator (NEA) devices are used for three important holddown and release functions during the establishment of the ORBCOMM (TM) constellation. Non-explosive separation nuts are used to restrain and release the 26 individual satellites into low earth orbit. Cable release mechanisms based on the same technology are used to release the solar arrays and antenna boom. Author

N95-27275*# Martin Marietta Astronautics, Denver, CO.
DEVELOPMENT OF A HIGH FORCE THERMAL LATCH c37
William D. Nygren *In* NASA. Johnson Space Center, The 29th Aerospace Mechanisms Symposium May 1995 p 162-166 (For primary document see N95-27260 09-15)
Avail: CASI HC A01/MF A04

This paper describes the preliminary development of a high force thermal latch (HFTL). The HFTL has one moving part which is restrained in the latched position by a low melting temperature or fusible metal alloy. When heated the fusible alloy flows to a receiving chamber and in so doing at first releases the tension load in the latch bolt and later releases the bolt itself. The HFTL can be used in place of pyrotechnically activated spacecraft release devices in those instances where the elimination of both pyrotechnic shock-loading and rapid strain-energy release take precedence over the near instantaneous release offered by ordnance initiated devices. Author

N95-27276*# NYMA, Inc., Cleveland, OH.
A ROTATING ARM USING SHAPE-MEMORY ALLOY c37
Phillip P. Jenkins and Geoffrey A. Landis *In* NASA. Johnson Space Center, The 29th Aerospace Mechanisms Symposium May 1995 p 167-171 (For primary document see N95-27260 09-15)
Avail: CASI HC A01/MF A04

NASA's Mars Pathfinder mission, to be launched in 1996, reflects a new philosophy of exploiting new technologies to reduce mission cost and accelerate the pace of space exploration. One of the experiments on board Pathfinder will demonstrate the first use in space of a multi-cycle, electrically-activated, shape-memory alloy (SMA) actuator. SMA's are metal alloys which, when heated, undergo a crystalline phase change. This change in phase alters the alloy lattice-constant, resulting in a change of dimension. Upon cooling, the alloy returns to its original lattice formation. Wire drawn from an SMA contracts in length when heated. The reversible change in length is 3 percent to 5 percent. The wire used in this actuator is a nickel-titanium alloy known as nitinol. Author

N95-27277*# Sandia National Labs., Albuquerque, NM. Intelligent Systems and Robotics Center.
RETROFITTING A FINE-POINTING SYSTEM TO SATELLITE OPTICS c74
Robert O. Woods *In* NASA. Johnson Space Center, The 29th Aerospace Mechanisms Symposium May 1995 p 175-182 (For primary document see N95-27260 09-15)
(Contract DE-AC04-94AL-85000)
Avail: CASI HC A02/MF A04

This paper describes a system added to an existing satellite-borne telescope design for the purpose of compensating the boresight errors that had been observed in earlier flights of similar instruments. Those errors had been found to be caused by thermal distortion of the spaceframe. This retrofit design was subjected to severe volume restrictions because it was fitted into an already tightly-packaged instrument envelope. It was found practical to improve the basic design by converting a redundant structure into a statically-determinate one. It was also possible to use portions of the mechanical actuation system to facilitate the position encoding needed for computer interfacing. Author

N95-27278*# Honeywell, Inc., Durham, NC. Electro Components.
ELECTROMECHANICAL ROTARY ACTUATOR c33
S. P. Smith and W. J. McMahon *In* NASA. Johnson Space Center, The 29th Aerospace Mechanisms Symposium May 1995 p 183-192 (For primary document see N95-27260 09-15)
Avail: CASI HC A02/MF A04

An electromechanical rotary actuator has been developed as the prime mover for a liquid oxygen modulation valve on the Centaur Vehicle Rocket Engine. The rotary actuator requirements, design, test, and associated problems and their solutions are discussed in this paper. Author

N95-27279*# National Aeronautics and Space Administration. Goddard Space Flight Center, Greenbelt, MD.
DESIGN, DEVELOPMENT AND TESTING OF THE X-RAY TIMING EXPLORER HIGH GAIN ANTENNA SYSTEM c32
Javier Lecha, Claudia Woods, and Minh Phan *In* NASA. Johnson Space Center, The 29th Aerospace Mechanisms Symposium May 1995 p 193-207 (For primary document see N95-27260 09-15)
Avail: CASI HC A03/MF A04

The High Gain Antenna System (HGAS), consisting of two High Gain Antenna Deployment Systems (HGADS) and two Antenna Pointing Systems (APS), is used to position two High Gain Antennas (HGA) on the X-Ray Timing Explorer (XTE). A similar APS will be used on the upcoming Tropical Rainfall Measuring Mission (TRMM). Both XTE and TRMM are NASA in-house satellites. The salient features of the system include the two-axis gimbal and control electronics of the APS and the spring deployment and latch/release mechanisms of the HGADS. This paper describes some of the challenges faced in the design and testing of this system and their resolutions. Author

N95-27280*# National Aeronautics and Space Administration. Marshall Space Flight Center, Huntsville, AL.
THE SOLAR X-RAY IMAGER VACUUM DOOR ASSEMBLY c18
Donald H. McQueen, Jr. *In* NASA. Johnson Space Center, The 29th Aerospace Mechanisms Symposium May 1995 p 208-217 (For primary document see N95-27260 09-15)
Avail: CASI HC A02/MF A04

This paper discusses the design and development of the Solar X-ray Imager (SXI) vacuum door assembly (VDA). Rationale for the type of mechanism, seal, and prime mover is covered. An overview of the testing performed is included. Author

N95-27281*# European Space Agency. European Space Research and Technology Center, ESTEC, Noordwijk (Netherlands).
SPECIAL FEATURES OF THE CLUSTER ANTENNA AND RADIAL BOOMS DESIGN, DEVELOPMENT AND VERIFICATION c18
G. Gianfiglio, M. Yorck, and H. J. Luhmann *In* NASA. Johnson Space Center, The 29th Aerospace Mechanisms Symposium May 1995 p 221-237 (For primary document see N95-27260 09-15)
Avail: CASI HC A03/MF A04

CLUSTER is a scientific space mission to in-situ investigate the Earth's plasma environment by means of four identical spin-stabilized spacecraft. Each spacecraft is provided with a set of four rigid booms: two Antenna Booms and two Radial Booms. This paper presents a summary of the boom development and verification phases addressing the key aspects of the Radial Boom design. In particular, it concentrates on the difficulties encountered in fulfilling simultaneously the requirements of minimum torque ratio and maximum allowed shock loads at boom latching for this two degree of freedom boom. The paper also provides an overview of the analysis campaign and testing program performed to achieve sufficient confidence in the boom performance and operation. Author

N95-27282*# Astro Aerospace Corp., Carpinteria, CA.
FORTE ANTENNA ELEMENT AND RELEASE MECHANISM DESIGN c37
David J. Rohweller and Thomas A. Butler (Los Alamos National Lab., NM.) *In* NASA. Johnson Space Center, The 29th Aerospace Mechanisms Symposium May 1995 p 238-252 (For primary document see N95-27260 09-15)
Avail: CASI HC A03/MF A04

The Fast On-Orbit Recording of Transient Events (FORTE) satellite being built by Los Alamos National Laboratory (LANL) and Sandia National Laboratories (SNL) has as its most prominent feature a large deployable (11 m by 5 m) log periodic antenna to monitor emissions from electrical storms on the Earth. This paper describes the antenna and the design for the long elements and explains the dynamics of their deployment and the damping system employed. It also describes the unique paraffin-actuated reusable tie-down and release mechanism employed in the system. Author

N95-27283*# Cambridge Univ., Cambridge (England). Dept. of Engineering.

DEPLOYMENT AND RETRACTION OF A CABLE-DRIVEN SOLAR ARRAY: TESTING AND SIMULATION c37

P. Kumar and S. Pellegrino *In* NASA. Johnson Space Center, The 29th Aerospace Mechanisms Symposium May 1995 p 253-267 Sponsored by Cambridge Commonwealth Trust (For primary document see N95-27260 09-15)

Avail: CASI HC A03/MF A04

The paper investigates three critical areas in cable-driven rigid-panel solar arrays: First, the variation of deployment and retraction cable tensions due to friction at the hinges; Second, the change in deployment dynamics associated with different deployment histories; Third, the relationship between the level of pre-tension in the closed contact loops and the synchronization of deployment. A small scale model array has been made and tested, and its behavior has been compared to numerical simulations. Author

N95-27284*# National Aeronautics and Space Administration. Goddard Space Flight Center, Greenbelt, MD.

DEVELOPMENT OF THE SOLAR ARRAY DEPLOYMENT AND DRIVE SYSTEM FOR THE XTE SPACECRAFT c37

Rodger Farley and Son Ngo *In* NASA. Johnson Space Center, The 29th Aerospace Mechanisms Symposium May 1995 p 268-282 (For primary document see N95-27260 09-15)

Avail: CASI HC A03/MF A04

The X-ray Timing Explorer (XTE) spacecraft is a NASA science low-earth orbit explorer-class satellite to be launched in 1995, and is an in-house Goddard Space Flight Center (GSFC) project. It has two deployable aluminum honeycomb solar array wings with each wing being articulated by a single axis solar array drive assembly. This paper will address the design, the qualification testing, and the development problems as they surfaced of the Solar Array Deployment and Drive System. Author

N95-27285*# MPB Corp., Keene, NH.

EFFECTS OF BEARING CLEANING AND LUBE ENVIRONMENT ON BEARING PERFORMANCE c37

Peter C. Ward *In* NASA. Johnson Space Center, The 29th Aerospace Mechanisms Symposium May 1995 p 285-300 Sponsored by Hamilton Standard; and United Technologies (For primary document see N95-27260 09-15)

Avail: CASI HC A03/MF A04

Running torque data of SR6 ball bearings are presented for different temperatures and speeds. The data are discussed in contrast to generally used torque prediction models and point out the need to obtain empirical data in critical applications. Also, the effects of changing bearing washing techniques from old, universally used CFC-based systems to CFC-free aqueous/alkaline solutions are discussed. Data on wettability, torque and lubricant life using SR3 ball bearings are presented. In general, performance is improved using the new aqueous washing techniques. Author

N95-27286*# Honeywell, Inc., Glendale, AZ. Satellite Systems Operations.

BALL BEARING VIBRATIONS AMPLITUDE MODELING AND TEST COMPARISONS c37

Richard A. Hightower, III and Dave Bailey *In* NASA. Johnson Space Center, The 29th Aerospace Mechanisms Symposium May 1995 p 301-315 (For primary document see N95-27260 09-15)

Avail: CASI HC A03/MF A04

Bearings generate disturbances that, when combined with structural gains of a momentum wheel, contribute to induced vibration in the wheel. The frequencies generated by a ball bearing are defined by the bearing's geometry and defects. The amplitudes at these frequencies are dependent upon the actual geometry variations from perfection; therefore, a geometrically perfect bearing will produce no amplitudes at the kinematic frequencies that the design generates. Because perfect geometry can only be approached, emitted vibrations do occur. The most significant vibration is at the spin frequency and can be balanced out in the build process. Other frequencies' amplitudes, however, cannot be balanced out. Momentum wheels are usually the single largest source of vibrations in a spacecraft and can contribute to pointing inaccuracies if emitted vibrations ring the structure or are in the high-gain bandwidth of a sensitive pointing control loop. It is therefore important to be able to provide an a priori knowledge of possible amplitudes that are singular in source or are a result of interacting defects that do not reveal themselves in normal frequency prediction equations. This paper will describe the computer model that provides for the incorporation of bearing geometry errors and then develops an estimation of actual amplitudes and frequencies. Test results were correlated with the model. A momentum wheel was producing an unacceptable 74 Hz amplitude. The model was used to simulate geometry errors and proved successful in identifying a cause that was verified when the parts were inspected. Author

N95-27287*# National Aeronautics and Space Administration. Goddard Space Flight Center, Greenbelt, MD.

A CRYOGENIC SCAN MECHANISM FOR USE IN FOURIER TRANSFORM SPECTROMETERS c35

Claef F. Hakun and Kenneth A. Blumenstock *In* NASA. Johnson Space Center, The 29th Aerospace Mechanisms Symposium May 1995 p 316-333 (For primary document see N95-27260 09-15)

Avail: CASI HC A03/MF A04

This paper describes the requirements, design, assembly and testing of the linear Scan Mechanism (SM) of the Composite Infrared Spectrometer (CIRS) Instrument. The mechanism consists of an over constrained flexible structure, an innovative moving magnet actuator, passive eddy current dampers, a Differential Eddy Current (DEC) sensor, Optical Limit Sensors (OLS), and a launch lock. Although all the components of the mechanism are discussed, the flexible structure and the magnetic components are the primary focus. Several problems encountered and solutions implemented during the development of the scan mechanism are also described. Author

N95-27288*# Ball Corp., Boulder, CO. Aerospace Systems Div.

HIGH-PERFORMANCE REACTIONLESS SCAN MECHANISM c74

Ellen I. Williams, Richard T. Summers, and Miroslaw A. Ostaszewski *In* NASA. Johnson Space Center, The 29th Aerospace Mechanisms Symposium May 1995 p 334-349 Sponsored by Dick Maxwell (For primary document see N95-27260 09-15)

Avail: CASI HC A03/MF A04

A high-performance reactionless scan mirror mechanism was developed for space applications to provide thermal images of the Earth. The design incorporates a unique mechanical means of providing reactionless operation that also minimizes weight, mechanical resonance operation to minimize power, combined use of a single optical encoder to sense coarse and fine angular position, and a new kinematic mount of the mirror. A flex pivot hardware failure and current project status are discussed. Author

N95-27289*# McDonnell-Douglas Space and Defense Systems, Cocoa Beach, FL.

DEVELOPMENT AND TESTING OF THE RACK INSERTION DEVICE c37

G. Scott Strickland *In* NASA. Johnson Space Center, The 29th Aerospace Mechanisms Symposium May 1995 p 353-367 (For primary document see N95-27260 09-15)

Avail: CASI HC A03/MF A04

Installing and removing experiment racks in a Space Station Logistics Module will become a repetitive operation at Kennedy Space Center (KSC) in the near future. A Rack Insertion Device (RID) consisting of an Extendible Boom, End Effector, and Positioning Base is being developed for the task. This paper discusses the key elements of the RID's function and design. Prototype test results for the RID's Extendible Boom and End Effector are presented. Also discussed are future end effectors that will further enhance the RID's Space Station processing capability. Author

N95-27290*# National Aeronautics and Space Administration. Langley Research Center, Hampton, VA.

LINEAR PROOF MASS ACTUATOR c37

S. E. Holloway, III *In* NASA. Johnson Space Center, The 29th Aerospace Mechanisms Symposium May 1995 p 368-380 (For primary document see N95-27260 09-15)

Avail: CASI HC A03/MF A04

This paper describes the mechanical design, analysis, fabrication, testing, and lessons learned by developing a uniquely designed spaceflight-like actuator. The Linear Proof Mass Actuator (LPMA) was designed to attach to both a large space structure and a ground test model without modification.

Previous designs lacked the power to perform in a terrestrial environment while other designs failed to produce the desired accelerations or frequency range for spaceflight applications. Thus, the design for a unique actuator was conceived and developed at NASA Langley Research Center. The basic design consists of four large mechanical parts (Mass, Upper Housing, Lower Housing, and Center Support) and numerous smaller supporting components including an accelerometer, encoder, and four drive motors. Fabrication personnel were included early in the design phase of the LPMA as part of an integrated manufacturing process to alleviate potential difficulties in machining an already challenging design. Operational testing of the LPMA demonstrated that the actuator is capable of various types of load functions. Author

N95-27291*# Lockheed Engineering and Sciences Co., Houston, TX. Mechanical Systems Lab.

LOAD MEASUREMENT SYSTEM WITH LOAD CELL LOCK-OUT MECHANISM **c37**

Thang Le, Monty Carroll, and Jonathan Liu *In* NASA. Johnson Space Center, The 29th Aerospace Mechanisms Symposium May 1995 p 381-392 (For primary document see N95-27260 09-15)
Avail: CASI HC A03/MF A04

In the frame work of the project Shuttle Plume Impingement Flight Experiment (SPIFEX), a Load Measurement System was developed and fabricated to measure the impingement force of Shuttle Reaction Control System (RCS) jets. The Load Measurement System is a force sensing system that measures any combination of normal and shear forces up to 40 N (9 lbf) in the normal direction and 22 N (5 lbf) in the shear direction with an accuracy of +/- 0.04 N (+/- 0.01 lbf) Since high resolution is required for the force measurement, the Load Measurement System is built with highly sensitive load cells. To protect these fragile load cells in the non-operational mode from being damaged due to flight loads such as launch and landing loads of the Shuttle vehicle, a motor driven device known as the Load Cell Lock-Out Mechanism was built. This Lock-Out Mechanism isolates the load cells from flight loads and re-engages the load cells for the force measurement experiment once in space. With this highly effective protection system, the SPIFEX load measurement experiment was successfully conducted on STS-44 in September 1994 with all load cells operating properly and reading impingement forces as expected. Author

N95-27292*# Societe Anonyme d'Etudes et Realisations Nucleaires, Limeil-Brevannes (France).

MICROMECHANISMS FOR OPTIMISM SEISMOMETER **c37**

Nicolas Paulin, Pierre Dumas, and Marc Pochard *In* NASA. Johnson Space Center, The 29th Aerospace Mechanisms Symposium May 1995 p 393-400 (For primary document see N95-27260 09-15)
Avail: CASI HC A02/MF A04

Within the framework of the Mars 94 mission, it was decided to design and build a new vertical axis seismometer in order to continuously record the seismic events occurring on the Mars planet. The mission requirements lead to very stringent constraints on power, volume, mass and shock resistance at the landing. The seismometer must be capable of automatic leveling and automatic fitting to the local gravity. This paper deals with the mechanisms designed for this seismometer. Due to the short allotted time for its development and low cost, the baseline was to apply the rules of spatial tribology and, when it was possible, to customize existing components for space applications. Author

16 SPACE TRANSPORTATION

Includes passenger and cargo space transportation, e.g., shuttle operations; and space rescue techniques.

For related information see also *03 Air Transportation and Safety* and *18 Spacecraft Design, Testing and Performance.* For space suits see *54 Man/System Technology and Life Support.*

N95-26379*# National Aeronautics and Space Administration. Lyndon B. Johnson Space Center, Houston, TX.

ORBITAL IMPACTS AND THE SPACE SHUTTLE WINDSHIELD

Karen S. Edelstein 1 Mar. 1995 10 p Presented at Aerospace/Defense Sensing and Dual-Use Photonics, Orlando, FL, 17-21 Apr. 1995
(NASA-TM-110594; NAS 1.15:110594) Avail: CASI HC A02/MF A01

The Space Transportation System (STS) fleet has flown more than sixty missions over the fourteen years since its first flight. As a result of encounters with on-orbit particulates (space debris and micrometeoroids), 177 impact features (chips) have been found on the STS outer windows (through STS-65). Forty-five of the damages were large enough to warrant replacement of the window. NASA's orbital operations and vehicle inspection procedures have changes over the history of the shuttle program, in response to concerns about the orbital environment and the cost of maintaining the space shuttle. These programmatic issues will be discussed, including safety concerns, maintenance issues, inspection procedures and flight rule changes. Examples of orbital debris impacts to the shuttle windows will be provided. There will also be a brief discussion of the impact properties of glass and what design changes have been considered to improve the impact properties of the windows. Author

N95-26398*# Science Applications International Corp., New York, NY. Advanced Technology Div.

PROBABILISTIC RISK ASSESSMENT OF THE SPACE SHUTTLE. PHASE 3: A STUDY OF THE POTENTIAL OF LOSING THE VEHICLE DURING NOMINAL OPERATION, VOLUME 1 Final Report

Joseph R. Fragola, Gaspare Maggio, Michael V. Frank (Safety Factors Associates, Inc., Encinitas, CA.), Luis Gerez (Empresarios Agrupados, Madrid, Spain.), Richard H. McFadden, Erin P. Collins, Jorge Ballesio, Peter L. Appignani, and James J. Karns 28 Feb. 1995 159 p
(Contract NASw-4911)
(NASA-CR-197808; NAS 1.26:197808; SAICNY95-02-25-Vol-1) Avail: CASI HC A08/MF A02

This document is the Executive Summary of a technical report on a probabilistic risk assessment (PRA) of the Space Shuttle vehicle performed under the sponsorship of the Office of Space Flight of the US National Aeronautics and Space Administration. It briefly summarizes the methodology and results of the Shuttle PRA. The primary objective of this project was to support management and engineering decision-making with respect to the Shuttle program by producing (1) a quantitative probabilistic risk model of the Space Shuttle during flight, (2) a quantitative assessment of in-flight safety risk, (3) an identification and prioritization of the design and operations that principally contribute to in-flight safety risk, and (4) a mechanism for risk-based evaluation proposed modifications to the Shuttle System. Secondary objectives were to provide a vehicle for introducing and transferring PRA technology to the NASA community, and to demonstrate the value of PRA by applying it beneficially to a real program of great international importance. Derived from text

N95-26399*# Science Applications International Corp., New York, NY. Advanced Technology Div.

PROBABILISTIC RISK ASSESSMENT OF THE SPACE SHUTTLE. PHASE 3: A STUDY OF THE POTENTIAL OF LOSING THE VEHICLE DURING NOMINAL OPERATION. VOLUME 2: INTEGRATED LOSS OF VEHICLE MODEL

Joseph R. Fragola, Gaspare Maggio, Michael V. Frank (Safety Factors Associates, Inc., Encinitas, CA.), Luis Gerez (Empresarios Agrupados, Madrid, Spain.), Richard H. McFadden, Erin P. Collins, Jorge Ballesio, Peter L. Appignani, and James J. Karns 28 Feb. 1995 581 p
(Contract NASw-4911)
(NASA-CR-197809; NAS 1.26:197809; SAICNY95-02-25-Vol-2) Avail: CASI HC A25/MF A06

The application of the probabilistic risk assessment methodology to a Space Shuttle environment, particularly to the potential of losing the Shuttle during nominal operation is addressed. The different related concerns are identified and combined to determine overall program risks. A fault tree model is used to allocate system probabilities to the subsystem level. The loss of the vehicle due to failure to contain energetic gas and debris, to maintain proper propulsion and configuration is analyzed, along with the loss due to Orbiter, external tank failure, and landing failure or error. CASI

N95-26400*# Science Applications International Corp., New York, NY. Advanced Technology Div.

PROBABILISTIC RISK ASSESSMENT OF THE SPACE SHUTTLE. PHASE 3: A STUDY OF THE POTENTIAL OF LOSING THE VEHICLE DURING NOMINAL OPERATION. VOLUME 3: BASIC EVENTS AND MINIMAL CUTSETS

Joseph R. Fragola, Gaspare Maggio, Michael V. Frank (Safety Factors Associates, Inc., Encinitas, CA.), Luis Gerez (Empresarios Agrupados, Madrid, Spain.), Richard H. McFadden, Erin P. Collins, Jorge Ballesio, Peter L. Appignani, and James J. Karns 28 Feb. 1995 357 p
(Contract NASw-4911)
(NASA-CR-197810; NAS 1.26:197810; SAICNY95-02-25-Vol-3) Avail: CASI HC A16/MF A03

In Volume 3 of Phase 3 of the Space Shuttle Probabilistic Risk Assessment, the basic events database and minimal cutsets are presented, along with their predicted probability in tabular form. CASI

N95-26401*# Science Applications International Corp., New York, NY. Advanced Technology Div.

PROBABILISTIC RISK ASSESSMENT OF THE SPACE SHUTTLE. PHASE 3: A STUDY OF THE POTENTIAL OF LOSING THE VEHICLE DURING NOMINAL OPERATION. VOLUME 4: SYSTEM MODELS AND DATA ANALYSIS

Joseph R. Fragola, Gaspare Maggio, Michael V. Frank (Safety Factors Associates, Inc., Encinitas, CA.), Luis Gerez (Empresarios Agrupados, Madrid, Spain.), Richard H. McFadden, Erin P. Collins, Jorge Ballesio, Peter L. Appignani, and James J. Karns 28 Feb. 1995 435 p
(Contract NASw-4911)
(NASA-CR-197811; NAS 1.26:197811; SAICNY95-02-25-Vol-4) Avail: CASI HC A19/MF A04

In this volume, volume 4 (of five volumes), the discussion is focussed on the system models and related data references and has the following subsections: space shuttle main engine, integrated solid rocket booster, orbiter auxiliary power units/hydraulics, and electrical power system. CASI

N95-26403*# Science Applications International Corp., New York, NY. Advanced Technology Div.

PROBABILISTIC RISK ASSESSMENT OF THE SPACE SHUTTLE. PHASE 3: A STUDY OF THE POTENTIAL OF LOSING THE VEHICLE DURING NOMINAL OPERATION. VOLUME 5: AUXILIARY SHUTTLE RISK ANALYSES

Joseph R. Fragola, Gaspare Maggio, Michael V. Frank (Safety Factors Associates, Inc., Encinitas, CA.), Luis Gerez (Empresarios Agrupados, Madrid, Spain.), Richard H. McFadden, Erin P. Collins, Jorge Ballesio, Peter L. Appignani, and James J. Karns 28 Feb. 1995 1036 p
(Contract NASw-4911)
(NASA-CR-197812; NAS 1.26:197812; SAICNY95-02-25-Vol-5) Avail: CASI HC A99/MF A10

Volume 5 is Appendix C, Auxiliary Shuttle Risk Analyses, and contains the following reports: Probabilistic Risk Assessment of Space Shuttle Phase 1 - Space Shuttle Catastrophic Failure Frequency Final Report; Risk Analysis Applied to the Space Shuttle Main Engine - Demonstration Project for the Main Combustion Chamber Risk Assessment; An Investigation of the Risk Implications of Space Shuttle Solid Rocket Booster Chamber Pressure Excursions; Safety of the Thermal Protection System of the Space Shuttle Orbiter - Quantitative Analysis and Organizational Factors; Space Shuttle Main Propulsion Pressurization System Probabilistic Risk Assessment, Final Report; and Space Shuttle Probabilistic Risk Assessment Proof-of-Concept Study - Auxiliary Power Unit and Hydraulic Power Unit Analysis Report. CASI

N95-26634 Naval Postgraduate School, Monterey, CA.

THE DESIGN AND IMPLEMENTATION OF THE MILITARY APPLICATIONS OF SHIPTRACKS EXPERIMENT ON SPACE TRANSPORTATION SYSTEM - 65 M.S. Thesis

Andrew R. Kirschbaum Sep. 1994 61 p Limited Reproducibility: More than 20% of this document may be affected by microfiche quality
(AD-A288488) Avail: Issuing Activity (Defense Technical Information Center (DTIC))

A detailed discussion is presented on the design, documentation participants, mission conduct, and payload support involved in the MAST (Military Applications of Shiptracks) experiment onboard the STS-65 mission. A comparison is shown between the high resolution imagery obtained from the MAST experiment and current weather imagery from NOAA satellites. Recommendations are made for further MAST payloads on future Space Shuttle flights. DTIC

N95-27154*# MCAT Inst., San Jose, CA.

DEVELOPMENT OF NUMERICAL METHODS FOR OVERSET GRIDS WITH APPLICATIONS FOR THE INTEGRATED SPACE SHUTTLE VEHICLE Final Report

William M. Chan Jan. 1995 77 p Original contains color illustrations
(Contract NCC2-654)
(NASA-CR-197759; NAS 1.26:197759) Avail: CASI HC A05/MF A01; 1 functional color page

Algorithms and computer code developments were performed for the overset grid approach to solving computational fluid dynamics problems. The techniques developed are applicable to compressible Navier-Stokes flow for any general complex configurations. The computer codes developed were tested on different complex configurations with the Space Shuttle launch vehicle configuration as the primary test bed. General, efficient and user-friendly codes were produced for grid generation, flow solution and force and moment computation. Author

N95-27238*# National Aeronautics and Space Administration. John F. Kennedy Space Center, Cocoa Beach, FL.

DEBRIS/ICE/TPS ASSESSMENT AND INTEGRATED PHOTOGRAPHIC ANALYSIS OF SHUTTLE MISSION STS-67 Final Report, 1-20 Mar. 1995

Gregory N. Katnik, Barry C. Bowen, and J. Bradley Davis Apr. 1995 101 p Original contains color illustrations
(NASA-TM-110651; NAS 1.15:110651) Avail: CASI HC A06/MF A02; 48 functional color pages

A debris/ice/thermal protection system assessment and integrated photographic analysis was conducted for Shuttle mission STS-67. Debris inspections of the flight elements and launch pad were performed before and after launch. Icing conditions on the External Tank were assessed by the use of computer programs and infrared scanner data during cryogenic loading of the vehicle, followed by on-pad visual inspection. High speed photography of the launch was analyzed to identify ice/debris sources and evaluate potential vehicle damage and/or in flight anomalies. This report documents the ice/debris/thermal protection (TPS) conditions and integrated photographic analysis of Shuttle mission STS-67, and the resulting effect on the Space Shuttle Program. Author

N95-28258*# Rockwell International Corp., Downey, CA. Space Systems Div.

TASK 4 SUPPORTING TECHNOLOGY. PART 1: DETAILED TEST PLAN FOR LEADING EDGE TILE DEVELOPMENT. LEADING EDGE MATERIAL DEVELOPMENT AND TESTING

P. A. Hogenson, Paul Staszak, and Karrie Hinkle 30 May 1995 39 p
(Contract NCC8-79)
(NASA-CR-198633; NAS 1.26:198633; SSD95D0239-Pt-1) Avail: CASI HC A03/MF A01

This task develops two alternative candidate tile materials for leading edge applications: coated alumina enhanced thermal barrier (AETB) tile and silicone impregnated reusable ceramic ablator (SIRCA) tile. Upon reentry of the X-33/RLV space vehicle, the leading edges experience the highest heating rates and temperatures. The wing leading edge and nose cap experience peak temperatures in the range 2000 to 2700 F. Replacing reinforced carbon-carbon (RCC) with tile-based thermal protection system (TPS) materials is the primary objective. Weight, complexity, coating impact damage, and repairability are among the problems that this tile technology development addresses. The following subtasks will be performed in this development effort: tile coating development; SIRCA tile development; robustness testing of tiles; tile repair development; tile operations/processing; tile leading edge configuration; and life cycle testing. CASI

17 SPACE COMM., SPACECRAFT COMM., COMMAND & TRACKING

Includes telemetry; space communications networks; astronavigation and guidance; and radio blackout.

For related information see also *04 Aircraft Communications and Navigation* and *32 Communications and Radar.*

N95-26458 Naval Postgraduate School, Monterey, CA.
AN ANALYSIS OF ORBITAL PROPAGATORS FOR LOW EARTH ORBIT RENDEZVOUS M.S. Thesis
Kenneth R. Pollock Sep. 1994 57 p Limited Reproducibility: More than 20% of this document may be affected by microfiche quality
(AD-A288883) Avail: Issuing Activity (Defense Technical Information Center (DTIC))

This thesis examines the performance of three different orbital propagators to determine which provide the best performance for use in Low Earth Orbit Rendezvous. The performance evaluation is based upon the propagator's accuracy and the amount of time required to produce a solution. A Cowell high-fidelity propagator is used as a base line for comparison with an Encke and Clohessy-Wiltshire propagator. To further enhance the examination a Jacchia-70 atmospheric model and a GEM-9 Geopotential model are used to provide perturbing acceleration inputs to the propagators. All comparisons are performed in a Local Vertical, Local Horizontal Reference Frame with the target spacecraft at the coordinate center. Tainting of the input data set by a prior processor make the findings suspect. Findings support the prediction that while the Cowell propagator is the most accurate it also takes the most time to achieve results. Also, the Clohessy-Wiltshire, while taking the least time is the most inaccurate. The Encke propagator deliveries the most balanced result. DTIC

N95-28581 Office of Naval Research, Arlington, VA.
RADIO TELEMETRY BUOY FOR LONG-RANGE COMMUNICATION Patent Application
James D. Hagerty, inventor (to Navy) 11 Oct. 1994 18 p Filed 11 Oct. 1994 Limited Reproducibility: More than 20% of this document may be affected by microfiche quality
(AD-D017269; Navy-Case-75668; US-Patent-Appl-SN-322656) Avail: Issuing Activity (Defense Technical Information Center (DTIC))

A remotely controlled radio telemetry buoy serves as a communication link between an underwater acoustic interrogation/receiving transponder system and a remotely located surface platform. The buoy houses a transmission device, a transceiver device and a controller. The transmission device transmits data received from the transponder system as electromagnetic energy in a frequency range of 162-173 MHz. The transceiver device exchanges digital control signals between the surface platform and the buoy in the frequency range of 2-16 MHz. The controller transfers the control signals between the transceiver device and the transmission device and the transponder system. DTIC

N95-27784*# Florida Univ., Gainesville, FL. Dept. of Aerospace Engineering, Mechanics and Engineering Science.
A MODIFIED PROPORTIONAL NAVIGATION SCHEME FOR RENDEZVOUS AND DOCKING WITH TUMBLING TARGETS: THE PLANAR CASE
Norman Fitz-Coy and Ming-Cheng Liu *In* NASA. Goddard Space Flight Center, Flight Mechanics/Estimation Theory Symposium 1995 May 1995 p 243-252 (For primary document see N95-27763 09-13)
(Grant NAG8-280)
Avail: CASI HC A02/MF A04

N95-27785*# Allied-Signal Technical Services Corp., Columbia, MD.
TELEMETRY DOWN-LINK DOPPLER AS AN ATTITUDE SENSOR FOR SPIN STABILIZED SPACECRAFT
S. D. Hendry *In* NASA. Goddard Space Flight Center, Flight Mechanics/Estimation Theory Symposium 1995 May 1995 p 253-266 (For primary document see N95-27763 09-13)
(Contract NAS5-31000)
Avail: CASI HC A03/MF A04

N95-27786*# Jet Propulsion Lab., California Inst. of Tech., Pasadena, CA.
MULTI-SPACECRAFT COHERENT DOPPLER AND RANGING FOR INTERPLANETARY-NAVIGATION
Vincent M. Pollmeier *In* NASA. Goddard Space Flight Center, Flight Mechanics/Estimation Theory Symposium 1995 May 1995 p 267-276 (For primary document see N95-27763 09-13)
Avail: CASI HC A02/MF A04

N95-27788*# Jet Propulsion Lab., California Inst. of Tech., Pasadena, CA.
APPLICATION OF NON-COHERENT DOPPLER DATA TYPES FOR DEEP SPACE NAVIGATION
Shyam Bhaskaran *In* NASA. Goddard Space Flight Center, Flight Mechanics/Estimation Theory Symposium 1995 May 1995 p 289-299 (For primary document see N95-27763 09-13)
Avail: CASI HC A03/MF A04

N95-27794*# National Aeronautics and Space Administration. Goddard Space Flight Center, Greenbelt, MD.
OPERATIONAL CONSIDERATIONS OF USING GPS FOR SPACECRAFT NAVIGATION
Roger C. Hart and Kathy R. Hartman *In its* Flight Mechanics/Estimation Theory Symposium 1995 May 1995 p 333-339 (For primary document see N95-27763 09-13)
Avail: CASI HC A02/MF A04

18 SPACECRAFT DESIGN, TESTING AND PERFORMANCE

Includes satellites; space platforms; space stations; spacecraft systems and components such as thermal and environmental controls; and attitude controls.

For life support systems see *54 Man/System Technology and Life Support.* For related information see also *05 Aircraft Design, Testing and Performance, 39 Structural Mechanics,* and *16 Space Transportation.*

N95-26428*# National Aeronautics and Space Administration. Langley Research Center, Hampton, VA.
A CLASS OF STABILIZING CONTROLLERS FOR FLEXIBLE MULTIBODY SYSTEMS
Suresh M. Joshi, Atul G. Kelkar, and Peiman G. Maghami May 1995 46 p
(RTOP 233-01-01-05)
(NASA-TP-3494; L-17413; NAS 1.60:3494) Avail: CASI HC A03/MF A01

The problem of controlling a class of nonlinear multibody flexible space systems consisting of a flexible central body to which a number of articulated appendages are attached is considered. Collocated actuators and sensors are assumed, and global asymptotic stability of such systems is established under a nonlinear dissipative control law. The stability is shown to be robust to unmodeled dynamics and parametric uncertainties. For a special case in which the attitude motion of the central body is small, the system, although still nonlinear, is shown to be stabilized by linear dissipative control laws. Two types of linear controllers are considered: static dissipative (constant gain) and dynamic dissipative. The static dissipative control law is also shown to provide robust stability in the presence of certain classes of actuator and sensor nonlinearities and actuator dynamics. The results obtained for this special case can also be readily applied for controlling single-body linear flexible space structures. For this case, a synthesis technique for the design of a suboptimal dynamic dissipative controller is also presented. The results obtained in this paper are applicable to a broad class of multibody and single-body systems such as flexible multilink manipulators, multipayload space platforms, and space antennas. The stability proofs use the Lyapunov approach and exploit the inherent passivity of such systems. Author

N95-26586*# National Aeronautics and Space Administration. Lyndon B. Johnson Space Center, Houston, TX. Structures and Mechanics Div.

A PERSPECTIVE ON THE HUMAN-RATING PROCESS OF US SPACECRAFT: BOTH PAST AND PRESENT

George Zupp, ed. Apr. 1995 14 p Prepared in cooperation with NASA. Marshall Space Flight Center, Huntsville, AL; NASA. John F. Kennedy Space Center, Cocoa Beach, FL; NASA. John C. Stennis Space Center, Bay Saint Louis, MS

(NASA-SP-6104; S-798; NAS 1.21:6104) Avail: CASI HC A03/MF A01

The purpose of this report is to characterize the process of Human-Rating as employed by NASA for human spaceflight. An Agency-wide committee was formed in November 1992 to develop a Human-Rating Requirements Definition for Launch Vehicles based on conventional (historical) methods. The committee members were from NASA Headquarters, Marshall Space Flight Center, Kennedy Space Center, Stennis Space Center, and Johnson Space Center. After considerable discussion and analysis, committee members concluded that Human-Rating is the process of satisfying the mutual constraints of cost, schedule, mission performance, and risk while addressing the requirements for human safety, human performance, and human health management and care. Author

N95-26715 Air Force Systems Command, Wright-Patterson AFB, OH. National Air Intelligence Center.

ENGINEERING CALCULATIONS ASSOCIATED WITH THE ABLATIVE THERMAL PROTECTIVE STRUCTURES OF RETURNABLE SATELLITES

Lianqun Xing 17 Nov. 1994 24 p Transl. into ENGLISH from Zhongguo Kongjian Kexue Jishu (China), no. 2, 1991 p 26-34 Limited Reproducibility: More than 20% of this document may be affected by microfiche quality

(AD-A289593; NAIC-ID(RS)T-0004-93) Avail: Issuing Activity (Defense Technical Information Center (DTIC))

The paper describes one type of ablative thermal protective structure form associated with returnable satellites. It carries out discussions of ablation mechanisms and calculation methods associated with FL composite materials and silicone rubber. In conjunction with this, it carries out comparisons with flight tests and gives concluding opinions. DTIC

N95-26850 Phillips Lab., Kirtland AFB, NM.

SPACE DEBRIS RESEARCH PHASE ONE PROGRAM: ABSTRACTS FROM PUBLISHED PAPERS (1990-1993) Final Report, Sep. 1993 - May 1994

Scott R. Maethner Jun. 1994 41 p Limited Reproducibility: More than 20% of this document may be affected by microfiche quality

(AF Proj. AFOT)

(AD-A289504; PL-TR-94-1005) Avail: Issuing Activity (Defense Technical Information Center (DTIC))

This document contains the abstracts from 63 papers published in support of the U.S. Air Force Phillips Laboratory Phase One Space Debris Research Program. This program, which was completed on 31 Dec 93, focused on characterizing the low earth orbit space debris environment and establishing the current and projected hazards to U.S. Air Force and Department of Defense space assets. The program emphasized both the measurement and modeling efforts needed to characterize the current debris environment for debris sizes down to 1 mm. In addition to the paper abstracts, this document lists paper titles, authors, and the paper publication sources. DTIC

N95-26887 Air Force Inst. of Tech., Wright-Patterson AFB, OH. School of Engineering.

OPTIMIZATION OF A NUTATION DAMPER ATTACHED TO A SPIN-STABILIZED SATELLITE M.S. Thesis

Brady P. Hauboldt Dec. 1994 67 p Limited Reproducibility: More than 20% of this document may be affected by microfiche quality

(AD-A289424; AFIT/GSO/ENY/94D-2) Avail: Issuing Activity (Defense Technical Information Center (DTIC))

This study uses linearized equations of motion for a rigid body with an attached spring-mass-damper to maximize the decay rate of a satellite's coning motion. An analysis of the numerical eigenvalues is presented which leads to an optimal relationship between relevant parameters: damper placement, spring constant, damping coefficient, system moments of inertia, and damper mass fraction. The coupled system's eigenvalues do not provide true critical damping, thus the real eigenvalue parts are minimized in order to achieve damping which requires the minimum amount of time. A comparison between this optimal design method and a classical method concludes with a noticeable improvement in damping performance for the optimized systems. DTIC

N95-26902 Aerospace Corp., El Segundo, CA. Technology Operations.

LONG-TERM VARIABILITY OF ELECTRON RADIATION DOSE IN GEOSYNCHRONOUS ORBIT Technical Report

H. C. Koons, D. J. Gorney, and J. B. Blake 30 Nov. 1994 10 p Limited Reproducibility: More than 20% of this document may be affected by microfiche quality

(Contract F04701-93-C-0094)

(AD-A289335; TR-93(3940)-13; SMC-TR-95-49) Avail: Issuing Activity (Defense Technical Information Center (DTIC))

A neural network that was developed to model the temporal variations of relativistic (greater than 3 MeV) electrons at geosynchronous orbit has been used to estimate the long-term variability of the radiation dose to geosynchronous spacecraft. The input to the neural network consists of 10 consecutive days of the daily sum of the planetary magnetic index Epsilon Kp. The output is an estimate of the daily-averaged electron flux for the tenth day. The model was used to compute the daily-averaged electron flux for energies greater than 3 MeV for each day from January 1933 through December 1988. Assuming that the average energy spectrum is independent of time, the annual radiation dose of electrons greater than 300 keV is obtained by scaling the model output to 300 keV and summing the daily-averaged flux for each year. The annual dose is found to vary from 0.25 to 0.4 times its average value. The dose is found to correlate only weakly with the annual mean sunspot number. The results are also applicable to studies of the effect on the middle atmosphere of the long-term variability of the precipitation of these electrons into the atmosphere. DTIC

N95-26916 Air Force Inst. of Tech., Wright-Patterson AFB, OH. School of Engineering.

CONTROL OF A LARGE SPACE STRUCTURE USING MULTIPLE MODEL ADAPTIVE ESTIMATION AND CONTROL TECHNIQUES M.S. Thesis

Gordon C. Griffin, Jr. Dec. 1994 249 p Limited Reproducibility: More than 20% of this document may be affected by microfiche quality

(AD-A289309; AFIT/GE/ENG/94D-14) Avail: Issuing Activity (Defense Technical Information Center (DTIC))

A moving bank multiple model adaptive estimator/controller (MMAE/MMAC), based on linear system, quadratic cost, and Gaussian noise (LQG) assumptions, is used to quell unwanted vibrations in a large flexible space structure. The structure, known as the SPace Integrated Controls Experiment, or SPICE, exists at Phillips Laboratory, Kirtland AFB, NM. The structure consists of a large platform and a smaller platform connected by a tripod of flexible legs. The purpose of the control system is to maintain a very precise line-of-sight vector through the center of the spacecraft. Kalman filtering, used to estimate the position and velocity of the bending modes of the structure, and LQG control techniques are the primary design tools used in the MMAE/MMAC algorithms. Implementing a parallel bank of filters increases robustness when uncertainties exist in the system model, here specifically allowing adaptation to uncertain and changing undamped natural frequencies of the bending modes of the structure. A moving bank is used to reduce computational loading. The MMAE/MMAC design method provides an excellent method of estimating undamped natural frequency variations and quelling vibrations in the structure. The MMAE/MMAC was able to track numerous parameter changes and jumps while providing adequate control for the structure. DTIC

N95-26918 Air Force Inst. of Tech., Wright-Patterson AFB, OH. School of Engineering.

ANALYSIS OF MODAL BEHAVIOR AT FREQUENCY CROSS-OVER Final Report

Robert N. Costa, Jr. 28 Nov. 1994 250 p Limited Reproducibility: More than 20% of this document may be affected by microfiche quality

(AD-A289304; AFIT/GA/ENY/94D-6) Avail: Issuing Activity (Defense Technical Information Center (DTIC))

The existence of the mode crossing condition is detected and analyzed in the Active Control of Space Structures Model 4 (ACOSS4). The condition is studied for its contribution to the inability of previous algorithms to successfully optimize the structure and converge to a feasible solution. A new algorithm is developed to detect and correct for mode crossings. The existence of the mode crossing condition is verified in ACOSS4 and found not to have appreciably affected the solution. The structure is then successfully optimized using new analytic methods based on modal expansion. An unrelated error in the optimization algorithm previously used is verified and corrected, thereby equipping the optimization algorithm with a second analytic method for eigenvector differentiation based on Nelson's Method. The second structure is the Control of Flexible Structures (COFS). The COFS structure is successfully reproduced and an initial eigenanalysis completed. DTIC

N95-26963 Air Force Inst. of Tech., Wright-Patterson AFB, OH. School of Engineering.

SATELLITE SURFACE MATERIAL COMPOSITION FROM SYNTHETIC SPECTRA M.S. Thesis

Eugene L. Caudill Dec. 1994 118 p Limited Reproducibility: More than 20% of this document may be affected by microfiche quality
(AD-A289236; AFIT/GEO/ENP/94D-02) Avail: Issuing Activity (Defense Technical Information Center (DTIC))

The objective of this research was to determine if measurements from a Sagnac interferometer could provide reliable estimates of satellite material composition. The Sagnac interferometer yields a spatial interferogram that can be sampled by a linear detector array. The interferogram is related to the spectrum of the source through a Fourier transform. Here, spectral reflectivities of nine common satellite materials were used to simulate the spectrum on obtains from an ideal Sagnac interferometer in the beam-train of a ground-based telescope whose mission is to view satellites. The signal-to-noise ratio of the spectrum was varied to simulate the effect of range variation between the sensor and the satellite. The simulated spectra consisted of a linear mixture of spectra from two of the nine materials. Three different architectures were developed and their performances compared. One of the three architectures consisted of nine artificial neural networks (ANN's), one for each material, and a linear estimator that estimated the satellite surface area attributable to each material. This method estimates the material composition by using a classifier to identify the materials contributing to the mixture, then eliminating unlikely contributors to the mixture before performing a constrained linear estimate. It is shown that due to high classification errors, the system using solely a linear estimator provides the estimate with the lowest errors. DTIC

N95-26970 Air Force Inst. of Tech., Wright-Patterson AFB, OH. School of Engineering.

A STATE-SPACE MODEL OF A LARGE, LIGHTLY DAMPED SPACE STRUCTURE USING THE EIGENSYSTEM REALIZATION ALGORITHM M.S. Thesis

Robert D. Woods Dec. 1994 166 p Limited Reproducibility: More than 20% of this document may be affected by microfiche quality
(AD-A289251; AFIT/GA/ENY/94D-2) Avail: Issuing Activity (Defense Technical Information Center (DTIC))

Large, lightweight space structures of the future will require state-of-the-art vibration suppression systems. To design such a system, it is necessary to have a mathematical model that adequately describes the motion of the system. Coulomb damping compensation was utilized to remove a known nonlinearity from the frequency response functions obtained from the Passive and Active Control of Space Structures (PACOSS) Dynamic Test Article (DTA). Via the Eigensystem Realization algorithm (ERA), the frequency response functions were then used to generate a mathematical representation of the structure's dynamics. Two models were obtained. The first model, without friction compensation, acted as a baseline. The second was obtained using friction compensation. Comparing the models, it was determined that active friction compensation was worthwhile and resulted in a more accurate mathematical description of the system. DTIC

N95-26980 Air Force Inst. of Tech., Wright-Patterson AFB, OH.

TELEPRESENT SPACECRAFT DOCKING WITH OBJECT-BASED BILATERAL CONTROL (OBBC) M.S. Thesis

Paul Woznick Dec. 1994 125 p Limited Reproducibility: More than 20% of this document may be affected by microfiche quality
(AD-A289268; AFIT/GA/ENY/94D-9) Avail: Issuing Activity (Defense Technical Information Center (DTIC))

The concept of object-based control is extended to the field of teleoperation, specifically to accomplish the task of spacecraft docking via a bilateral manual controller. An object-based controller with bilateral feedback controls the motion of the grasped object, not the trajectory of the manipulator. For this reason it can be designed with feedback that is intricately linked with the task kinematics. The benefits derived from anthropomorphicity and force feedback are possible without kinematically/geometrically similar master-slave systems, complex calibration and joint mapping schemes, or expensive, high degree-of-freedom force reflection. Object-based control is ideal for low-level telerobotic interfaces. A hand controller and a spacecraft docking simulation are designed and constructed to demonstrate object-based bilateral control. The dominant task objective in spacecraft docking is the approach to a target vehicle along a single axis of motion. Several methods of bilateral feedback linked with this dominant objective are proposed in addition to simple force reflection. One method involves virtual forces and another utilizes velocity reflection. Each method, practical only with object-based control, enhance the man-machine interface by providing a heuristic method of control. DTIC

N95-26987 Air Force Inst. of Tech., Wright-Patterson AFB, OH.

GENERIC SATELLITE MONITORING EXPERT SYSTEM M.S. Thesis

Loretta A. Kelemen Dec. 1994 133 p Limited Reproducibility: More than 20% of this document may be affected by microfiche quality
(AD-A289209; AFIT/GSO/ENG/94D-02) Avail: Issuing Activity (Defense Technical Information Center (DTIC))

Air Force Satellite Operations is undergoing major changes. Operators no longer receive detailed satellite training, instead they are taught basic fundamentals of satellite operations and expected to control multiple multimillion dollar satellites. The need is clear. An efficient and economical automated system is necessary to assist the satellite operator in the daily tasks of maintaining these DOD priority resources. Satellite intelligent controllers have been under R&D since the early 1980's to meet this need. These systems, however, have focused on the control of one constellation of satellites. In a military striving for efficiency and lower costs, developing a unique intelligent controller for each satellite constellation is unaffordable. This research provided support for the concept of a generic satellite intelligent controller, through the development of a prototype expert system. This capability would allow a generic rule-base to operate and maintain multiple satellite systems. The initial prototype detected anomalies on one subsystem of two different satellites. After the third satellite prototype was created, a third satellite was analyzed to show support for the viability of the satellite prototype. More research is necessary, but this thesis has created support for the concept of generic satellite controller and has laid the foundation for future extensions. DTIC

N95-27026*# Lockheed Missiles and Space Co., Sunnyvale, CA.

STRUCTURES AND MATERIALS TECHNOLOGY NEEDS FOR COMMUNICATIONS AND REMOTE SENSING SPACECRAFT Final Report, May 1994 - Mar. 1995

M. J. Gronet, G. A. Jensen, and J. W. Hoskins Apr. 1995 105 p
(Contract NAS1-19241; RTOP 233-01-01-02)
(NASA-CR-198166; NAS 1.26:198166) Avail: CASI HC A06/MF A02

This report documents trade studies conducted from the perspective of a small spacecraft developer to determine and quantify the structures and structural materials technology development needs for future commercial and NASA small spacecraft to be launched in the period 1999 to 2005. Emphasis is placed on small satellites weighing less than 1800 pounds for two focus low-Earth orbit missions: commercial communications and remote sensing. The focus missions are characterized in terms of orbit, spacecraft size, performance, and design drivers. Small spacecraft program personnel were interviewed to determine their technology needs, and the results are summarized. A systems-analysis approach for quantifying the benefits of inserting advanced state-of-the-art technologies into a current reference, state-of-the-practice small spacecraft design is developed and presented. This approach is employed in a set of abbreviated trade studies to quantify the payoffs of using a subset of 11 advanced technologies selected from the interview results The 11 technology development opportunities are then ranked based on their relative payoff. Based on the strong potential for significant benefits, recommendations are made to pursue development of 8 and the 11 technologies. Other important technology development areas identified are recommended for further study. Author

N95-27093*# Remtech, Inc., Huntsville, AL.
RAREFIED GAS EFFECTS ON AEROBRAKING/REENTRY VEHICLES WITH WAKES Final Report
Amolak C. Jain 28 Feb. 1995 93 p
(Contract NAS8-39368; SBIR-02.04-8581)
(NASA-CR-196586; NAS 1.26:196586; RTR-249-01) Avail: CASI HC A05/MF A01

The purpose of the present investigation is to understand the basic nature of the wake flow behind an Aeroassisted Space Transfer Vehicle (ASTV) or Aeroassisted Flight Experiment Vehicle (AFE). The astronauts were supposed to fly in the bay of an ASTV or AFE. This problem of thermal environment on the bay of the vehicle becomes important to ensure the safety of the astronauts. A computer code based on the full Navier-Stokes equations with surface slip and temperature jump boundary conditions is developed. The governing equations are expressed in spherical-cylindrical coordinates and a third order accurate upwind-biased scheme with provision to use a second order accurate central-difference scheme of numerical integration, is used. To ensure a high order of accuracy, complete flowfield from the stagnation line to the wake flow is computed. For this purpose, the computer code is divided into three parts, viz., stagnation part, forepart and aftpart and has the provision to converge each part to provide boundary conditions to the next part or we can compute the entire flow in each iteration. Extensive numerical computations have been carried out for a number of prescribed conditions, but for the sake of brevity, the results of computations for SR3 tunnel conditions of CNRS, France, are reported here. Computations have been carried out on a cylindrical body with a spherical nose (also called sphere-cylinder body) and on a hemisphere with a cylindrical bay with radius equal to a quarter of the radius of the base of hemisphere, to simulate a generic AFE configuration. Comparison of the results on sphere-cylinder and on the generic AFE body helps us to understand the rarefaction effects and the effect of wake flow on the main flowfield. Comparison with the DSMC data from NASA LaRC indicates general agreement about the nature of wake, but our results differ quantitatively with the DSMC results. At the present moment, the results from the CNRS tunnel are not available. As such, a quantitative comparison of the present results with the experimental data is not possible. In general, it is found that the wake on a generic AFE is a slow moving, high temperature, low density and, consequently, low pressure fluid. Author

N95-27144 Air Force Inst. of Tech., Wright-Patterson AFB, OH.
A MULTI-ATTRIBUTE-UTILITY-THEORY MODEL THAT MINIMIZES INTERVIEW-DATA REQUIREMENTS: A CONSOLIDATION OF SPACE LAUNCH DECISIONS M.S. Thesis
Raymond W. Staats Dec. 1994 123 p Limited Reproducibility: More than 20% of this document may be affected by microfiche quality
(AD-A289421; AFIT/GSO/ENS/94D-15) Avail: Issuing Activity (Defense Technical Information Center (DTIC))

This research uses multi-attribute utility theory (MAUT) to define a mathematical representation of a decision maker's utility associated with a satellite system. While developing the survey instrument, we focused on making it simpler to administer, primarily by eliminating the use of lottery questions. These simplifications enabled us to shorten our interview with the decision maker to under two hours for a rather complex model. The MAUT model gives National Air Intelligence Center (NAIC) analysts the ability to rank order satellite systems using the common measurement scale of 'utiles.' This tool allows a meaningful comparison of vastly different satellites. Properly prioritized launch of space assets will be key to maintaining our capabilities in the long term. The ordering methodology of this model was extended to a multi-criterion optimization (MCO) problem to demonstrate its potential use in prioritizing and scheduling limited launch resources. The results of these two case studies and the MCO application are combined to develop some characterizations of a theoretical group utility function. Most complex decisions are made by groups rather than by an individual. This research concludes with some insights on the impact of an individual's preferences on a decision that is ultimately made by the group. DTIC

N95-27730*# National Aeronautics and Space Administration. Lewis Research Center, Cleveland, OH.
STATIC STABILITY OF A THREE-DIMENSIONAL SPACE TRUSS M.S. Thesis - Case Western Reserve Univ., 1994
John F. Shaker May 1995 114 p
(RTOP 478-42-10)
(NASA-TM-106944; E-9679; NAS 1.15:106944) Avail: CASI HC A06/MF A02

In order to deploy large flexible space structures it is necessary to develop support systems that are strong and lightweight. The most recent example of this aerospace design need is vividly evident in the space station solar array assembly. In order to accommodate both weight limitations and strength performance criteria, ABLE Engineering has developed the Folding Articulating Square Truss (FASTMast) support structure. The FASTMast is a space truss/mechanism hybrid that can provide system support while adhering to stringent packaging demands. However, due to its slender nature and anticipated loading, stability characterization is a critical part of the design process. Furthermore, the dire consequences surely to result from a catastrophic instability quickly provide the motivation for careful examination of this problem. The fundamental components of the space station solar array system are the (1) solar array blanket system, (2) FASTMast support structure, and (3) mast canister assembly. The FASTMast once fully deployed from the canister will provide support to the solar array blankets. A unique feature of this structure is that the system responds linearly within a certain range of operating loads and nonlinearly when that range is exceeded. The source of nonlinear behavior in this case is due to a changing stiffness state resulting from an inability of diagonal members to resist applied loads. The principal objective of this study was to establish the failure modes involving instability of the FASTMast structure. Also of great interest during this effort was to establish a reliable analytical approach capable of effectively predicting critical values at which the mast becomes unstable. Due to the dual nature of structural response inherent to this problem, both linear and nonlinear analyses are required to characterize the mast in terms of stability. The approach employed herein is one that can be considered systematic in nature. The analysis begins with one and two-dimensional failure models of the system and its important components. From knowledge gained through preliminary analyses a foundation is developed for three-dimensional analyses of the FASTMast structure. The three-dimensional finite element (FE) analysis presented here involves a FASTMast system one-tenth the size of the actual flight unit. Although this study does not yield failure analysis results that apply directly to the flight article, it does establish a method by which the full-scale mast can be evaluated. Author

N95-27761*# National Aeronautics and Space Administration. Lewis Research Center, Cleveland, OH.
DESIGN OF A UNIDIRECTIONAL COMPOSITE MOMENTUM WHEEL RIM
Bradley Shogrin (Case Western Reserve Univ., Cleveland, OH.), William R. Jones, Jr., and Joseph M. Prahl (Case Western Reserve Univ., Cleveland, OH.) May 1995 28 p
(RTOP 274-00-00)
(NASA-TM-106911; E-9613; NAS 1.15:106911) Avail: CASI HC A03/MF A01

A preliminary study comparing twelve unidirectional-fiber composite systems to five metal materials conventionally used in momentum wheels is presented. Six different fibers are considered in the study: E-Glass, S-Glass, Boron, AS, T300, and Kevlar. Because of the possibility of high momentum requirements, and thus high stresses, only two matrix materials are considered: a high-modulus (HM) and a intermediate-modulus-high-strength (IMHS) matrix. Each of the six fibers are coupled with each of the two matrix materials. In an effort to optimize the composite system, each composite is considered while varying the fiber volume ratio from 0.0 to 0.7 in increments of 0.1. For fiber volume ratios above 0.2, all twelve unidirectional-fiber composite systems meet the study's requirements with higher factors of safety and less mass than the five conventional isotropic (metal) materials. For example, at a fiber volume ratio of 0.6, the Kevlar/IMHS composite system has a safety factor 4.5 times greater than that of a steel (maraging) system and an approximately 10 percent reduction in weight. Author

N95-27836*# Smithsonian Institution, Cambridge, MA. Astrophysical Observatory.
DYNAMICS AND CONTROL OF SEDSAT TETHERED MULTI-PROBE FOR THERMOSPHERIC RESEARCH FLIGHT DATA ANALYSIS OF SEDS-2 SATELLITE: TETHERED SYSTEMS DYNAMICS AND FLIGHT DATA ANALYSIS Final Report, 22 Feb. 1994 - 21 Feb. 1995
Enrico C. Lorenzini, Gordon E. Gullahorn, Mario L. Cosmo, and Mario D. Grossi May 1995 107 p
(Grant NAG8-1046)
(NASA-CR-198653; NAS 1.26:198653) Avail: CASI HC A06/MF A02

The three topics are summarized as follows: (1) dynamics and control of the satellite SEDSAT; (2) tethered multi-probe for thermospheric research; and (3) analysis of SEDS-2 flight data. CASI

N95-27842*# National Aeronautics and Space Administration. Lyndon B. Johnson Space Center, Houston, TX.
PRE-INTEGRATED TRUSS SPACE STATION AND METHOD OF ASSEMBLY Patent
Timothy E. Pelischek, inventor (to NASA), Edgar O. Castro, inventor (to NASA), Gregg A. Edeen, inventor (to NASA), David A. Hamilton, inventor (to NASA), Jon B. Kahn, inventor (to NASA), James B. McDede, inventor (to NASA), Kornel Nagy, inventor (to NASA), John V. Rivers, inventor (to NASA), Irene E. Verinder, inventor (to NASA), and Donald C. Wade, inventor (to NASA) et al 18 Apr. 1995 9 p Filed 24 Dec. 1992 Supersedes N93-20042 (31 - 7, p 1823)
(NASA-Case-MSC-22015-1; US-Patent-5,407,152;
US-Patent-Appl-SN-996763; US-Patent-Class-244-159;
US-Patent-Class-244-161; Int-Patent-Class-B64G-1/10) Avail: US Patent and Trademark Office

The present invention is directed to methods and apparatus relating to design, construction, integration and assembly of a space station. The present invention uses pre-integrated open (unpressurized) truss segments for modular construction of the space station. Each segment includes a truss structure and utility subsystem which may be fully assembled and tested on Earth. The segments may be latched together on orbit using a remote latching system. Utility subsystems, such as solar panels and radiators, are pre-integrated into the appropriate truss segment, and are deployable from the respective truss segment on orbit. Rails run lengthwise along the assembled truss. The rails may be used with a mobile transporter for translating truss segments with respect to the spacecraft as part of the space station assembly process. The rails may also be used with a mobile transporter for carrying crew personnel, a robotic arm, and other equipment. With the present invention, the EVA time required for assembly as Space Station Freedom is markedly reduced.
Official Gazette of the U.S. Patent and Trademark Office

N95-28150 Naval Postgraduate School, Monterey, CA.
PRELIMINARY FLIGHT SOFTWARE SPECIFICATION FOR THE PETITE AMATEUR NAVY SATELLITE (PANSAT) M.S. Thesis
Teresa O. Ford Mar. 1994 210 p Limited Reproducibility: More than 20% of this document may be affected by microfiche quality
(AD-A280068) Avail: Issuing Activity (Defense Technical Information Center (DTIC))

PANSAT is a small, spread-spectrum, communications satellite under design at the Naval Postgraduate School. It will support a store and forward bulletin board system for use by the amateur radio community. The flight software is responsible for the autonomous telemetry collection and hardware control operations of the satellite, communications and file transfer protocols allowing access to the bulletin board system, and command interpretation and response to ground control commands. in this thesis, the complete flight software architecture and module interfaces are specified using the Estelle Format Description Technique. The module bodies dealing with communications and file transfer protocols are specified in detail in Estelle. The current design goat for the remainder of the flight software modules are discussed. Appendices include the preliminary flight software specification itself, a data flow diagram interpretation of the specification, and a summary of the Estelle syntax used. DTIC

N95-28342# Committee on Science, Space and Technology (U.S. House), Washington, DC.
GLOBAL TRADE IN SATELLITES AND LAUNCH SERVICES
Washington GPO 1994 140 p Hearing before the Committee on Science, Space, and Technology, 103d Congress, 2d Session, No. 153, 29 Sep. 1994
(GPO-84-811; ISBN-0-16-046489-7) Avail: CASI HC A07/MF A02; Subcommittee on Space, House of Representatives, Washington, DC 20515; SOD HC

Hearing before the Subcommittee on Space of the Committee on Science, Space, and Technology of the House of Representatives is presented. Written testimony, submittals for the record, and responses to written questions are included. Topics concerning the global trade in satellites and launch services include foreign competition, the China and Russia trade agreements, Commerce licensing on international sales and export, trade control, technology transfer, satellite communications and the economy, satellites and the global information infrastructure, commercial space revenues, and enforcement of trade policies. CASI

N95-28578 Boston Coll., Chestnut Hill, MA. Inst. for Space Research.
THE COMBINED RELEASE AND RADIATION EFFECTS SATELLITE TIME HISTORY DATA BASE SYSTEM Final Report, 26 Apr. 1990 - 30 Nov. 1994
Dennis E. Deforey and Paul N. Pruneau 30 Nov. 1994 159 p Limited Reproducibility: More than 20% of this document may be affected by microfiche quality
(Contract F19628-90-K-0028)
(AD-A289835; BC-ISR-95-01; PL-TR-94-2273) Avail: Issuing Activity (Defense Technical Information Center (DTIC))

A Time History Data Base (THDB) and Analysis System was developed for the Combined Release and Radiation Effects Satellite (CRRES). This data base contains data from all sensors associated with the Geosynchronous Transfer Orbit (GTO) portion of the mission. All associated data has been structured in the generic THDB form. This data base serves as a prime input for event as well as long term statistical studies. DTIC

N95-27104 Martin Marietta Corp., Denver, CO. Astronautics Group.
CLEANLINESS VERIFICATION PROCESS AT MARTIN MARIETTA ASTRONAUTICS
Elizabeth A. King and Thomas J. Giordano *In* Johns Hopkins Univ., Environmentally Benign Cleaning and Degreasing Technology: JANNAF Safety and Protection Subcommittee and Propellant Development and Characterization Subcommittee Joint Workshop Jun. 1994 p 17-26
(For primary document see N95-27101 09-27)
(Contract F04701-85-C-0019)
Avail: CPIA, 10630 Little Patuxent Pkwy., Suite 202, Columbia, MD 21044-3200 HC

N95-27124* Thiokol Corp., Huntsville, AL.
SCEENING, DOWN SELECTION, AND IMPLEMENTATION OF ENVIRONMENTALLY COMPLIANT CLEANING AND INSULATION BONDING FOR MNASA
Jill M. Keen, D. E. Hutchens, G. M. Smith, and T. W. Dillard *In* Johns Hopkins Univ., Environmentally Benign Cleaning and Degreasing Technology: JANNAF Safety and Protection Subcommittee and Propellant Development and Characterization Subcommittee Joint Workshop Jun. 1994 p 225-233 (For primary document see N95-27101 09-27)
(Contract NAS8-38100)
Avail: CPIA, 10630 Little Patuxent Pkwy., Suite 202, Columbia, MD 21044-3200 HC

N95-27268*# Naval Research Lab., Washington, DC.
THE CLEMENTINE MECHANISMS
William Purdy and Michael Hurley *In* NASA. Johnson Space Center, The 29th Aerospace Mechanisms Symposium May 1995 p 109-127
(For primary document see N95-27260 09-15)
Avail: CASI HC A03/MF A04

N95-27280*# National Aeronautics and Space Administration. Marshall Space Flight Center, Huntsville, AL.
THE SOLAR X-RAY IMAGER VACUUM DOOR ASSEMBLY
Donald H. McQueen, Jr. *In* NASA. Johnson Space Center, The 29th Aerospace Mechanisms Symposium May 1995 p 208-217 (For primary document see N95-27260 09-15)
Avail: CASI HC A02/MF A04

N95-27281*# European Space Agency. European Space Research and Technology Center, ESTEC, Noordwijk (Netherlands).
SPECIAL FEATURES OF THE CLUSTER ANTENNA AND RADIAL BOOMS DESIGN, DEVELOPMENT AND VERIFICATION
G. Gianfiglio, M. Yorck, and H. J. Luhmann *In* NASA. Johnson Space Center, The 29th Aerospace Mechanisms Symposium May 1995 p 221-237 (For primary document see N95-27260 09-15)
Avail: CASI HC A03/MF A04

N95-27377*# Commonwealth Scientific and Industrial Research Organization, Ryde (Australia). Div. of Information Technology.
AN ARCHITECTURE AND PROTOCOL FOR COMMUNICATIONS SATELLITE CONSTELLATIONS REGARDED AS MULTI-AGENT SYSTEMS
Craig A. Lindley *In* NASA. Goddard Space Flight Center, The 1995 Goddard Conference on Space Applications of Artificial Intelligence and Emerging Information Technologies May 1995 p 15-28 (For primary document see N95-27375 09-63)
Avail: CASI HC A03/MF A03

N95-27662*# National Aeronautics and Space Administration. Lyndon B. Johnson Space Center, Houston, TX.
SPACE STATION PROGRAM STATUS AND RESEARCH CAPABILITIES
Alan C. Holt *In* NASA. Langley Research Center, LDEF: 69 Months in Space. Third Post-Retrieval Symposium, Part 3 Feb. 1995 p 1285-1288 (For primary document see N95-27629 09-99)
Avail: CASI HC A01/MF A04

N95-27663*# McDonnell-Douglas Space Systems Co., Huntington Beach, CA. Space Station Div.
SPACE STATION AS A LONG DURATION EXPOSURE FACILITY
Adrienne Folley and Jim Scheib *In* NASA. Langley Research Center, LDEF: 69 Months in Space. Third Post-Retrieval Symposium, Part 3 Feb. 1995 p 1289-1300 (For primary document see N95-27629 09-99)
Avail: CASI HC A03/MF A04

N95-27664*# National Aeronautics and Space Administration. Langley Research Center, Hampton, VA.
A MATERIALS EXPOSURE FACILITY
Wayne S. Slemp and Don E. Avery *In its* LDEF: 69 Months in Space. Third Post-Retrieval Symposium, Part 3 Feb. 1995 p 1301-1304 (For primary document see N95-27629 09-99)
Avail: CASI HC A01/MF A04

N95-27665*# National Aeronautics and Space Administration. Marshall Space Flight Center, Huntsville, AL.
AN LDEF FOLLOW-ON SPACECRAFT CONCEPT Abstract Only
Vernon Keller, Larry Breazeale, Don Perkinson, and William H. Kinard (National Aeronautics and Space Administration. Langley Research Center, Hampton, VA.) *In* NASA. Langley Research Center, LDEF: 69 Months in Space. Third Post-Retrieval Symposium, Part 3 Feb. 1995 p 1307 (For primary document see N95-27629 09-99)
Avail: CASI HC A01/MF A04

N95-27798*# National Aeronautics and Space Administration. Goddard Space Flight Center, Greenbelt, MD.
GEOSTATIONARY OPERATIONAL ENVIRONMENTAL SATELLITE (GOES)-8 MISSION FLIGHT EXPERIENCE
C. H. Noonan (Computer Sciences Corp., Lanham, MD.), R. J. McIntosh (Computer Sciences Corp., Lanham, MD.), J. N. Rowe (Computer Sciences Corp., Lanham, MD.), R. L. DeFazio, and K. F. Galal *In its* Flight Mechanics/Estimation Theory Symposium 1995 May 1995 p 369-378 (For primary document see N95-27763 09-13)
(Contract NAS5-31500)
Avail: CASI HC A02/MF A04

N95-27802*# CTA Space Systems, McLean, VA.
AUTONOMOUS CONTROL SYSTEM RECONFIGURATION FOR SPACECRAFT WITH NON-REDUNDANT ACTUATORS Abstract Only
Walter Grossman *In* NASA. Goddard Space Flight Center, Flight Mechanics/Estimation Theory Symposium 1995 May 1995 p 417 (For primary document see N95-27763 09-13)
Avail: CASI HC A01/MF A04

N95-28292*# National Aeronautics and Space Administration. Langley Research Center, Hampton, VA.
DESIGNING FOR TIME-DEPENDENT MATERIAL RESPONSE IN SPACECRAFT STRUCTURES
M. W. Hyer (Virginia Polytechnic Inst. and State Univ., Blacksburg, VA.), Lynda L. S. Oleksuk (Virginia Polytechnic Inst. and State Univ., Blacksburg, VA.), and D. E. Bowles *In* FAA, Ninth DOD/NASA/FAA Conference on Fibrous Composites in Structural Design, Volume 3 Sep. 1992 p 1617-1630 (For primary document see N95-28266 09-24)
(Grant NAG1-343)
Copyright Avail: CASI HC A03/MF A04

N95-28293*# National Aeronautics and Space Administration. Ames Research Center, Moffett Field, CA.
COMPOSITE FLEXIBLE INSULATION FOR THERMAL PROTECTION OF SPACE VEHICLES
Demetrius A. Kourtides, Huy K. Tran, and S. Amanda Chiu (Sterling Software, Inc., Palo Alto, CA.) *In* FAA, Ninth DOD/NASA/FAA Conference on Fibrous Composites in Structural Design, Volume 3 Sep. 1992 p 1631-1646 (For primary document see N95-28266 09-24)
Copyright Avail: CASI HC A03/MF A04

19 SPACECRAFT INSTRUMENTATION

For related information see also *06 Aircraft Instrumentation* and *35 Instrumentation and Photography.*

N95-27390*# Organisatie voor Toegepast Natuurwetenschappelijk Onderzoek, Delft (Netherlands). Instrumentation Dept.
MODEL-BASED MONITORING AND DIAGNOSIS OF A SATELLITE-BASED INSTRUMENT
Andre Bos, Jorg Callies (European Space Agency. European Space Research and Technology Center, ESTEC, Noordwijk, Netherlands.), and Alain Lefebvre (European Space Agency. European Space Research and Technology Center, ESTEC, Noordwijk, Netherlands.) *In* NASA. Goddard Space Flight Center, The 1995 Goddard Conference on Space Applications of Artificial Intelligence and Emerging Information Technologies May 1995 p 195-207 (For primary document see N95-27375 09-63)
Avail: CASI HC A03/MF A03

N95-27782*# National Aeronautics and Space Administration. Goddard Space Flight Center, Greenbelt, MD.
A SIMPLE METHOD FOR VERIFYING THE DEPLOYMENT OF THE TOMS-EP SOLAR ARRAYS
James R. Koppersmith and Eleanor Ketchum *In its* Flight Mechanics/Estimation Theory Symposium 1995 May 1995 p 219-227 (For primary document see N95-27763 09-13)
Avail: CASI HC A02/MF A04

20 SPACECRAFT PROPULSION AND POWER

Includes main propulsion systems and components, e.g., rocket engines; and spacecraft auxilliary power sources.

For related information see also *07 Aircraft Propulsion and Power, 28 Propellants and Fuels, 44 Energy Production and Conversion,* and *15 Launch Vehicles and Space Vehicles.*

N95-26390*# TRW Systems and Energy, Redondo Beach, CA.
HIGH PRESSURE EARTH STORABLE ROCKET TECHNOLOGY PROGRAM: BASIC PROGRAM Final Contractor Report
M. L. Chazen, D. Sicher, D. Huang, and T. Mueller Mar. 1995 78 p
(Contract NAS3-27002; RTOP 242-70-02)
(NASA-CR-195449; E-9514; NAS 1.26:195449) Avail: CASI HC A05/MF A01

The HIPES Program was conducted for NASA-LeRC by TRW. The Basic Program consisted of system studies, design of testbed engine, fabrication and testing of engine. Studies of both pressure-fed and pump-fed systems were investigated for N2O4 and both MMH and N2H4 fuels with the result that N2H4 provides the maximum payload for all satellites over MMH. The higher pressure engine offers improved performance with smaller envelope and associated weight savings. Pump-fed systems offer maximum payload for large and medium weight satellites while pressure-fed systems offer maximum payload for small light weight satellites. The major benefits of HIPES are high performance within a confined length maximizing payload for lightsats which are length (volume) constrained. Three types of thrust chambers were evaluated -- Copper heatsink at 400, 500 and 600 psia chamber pressures for performance/thermal; water cooled to determine heat absorbed to predict rhenium engine operation; and rhenium to validate the concept. The HIPES engine demonstrated very high performance at 50 lbf thrust (epsilon = 150) and Pc = 500 psia with both fuels: Isp = 337 sec using N2O4-N2H4 and ISP = 327.5 sec using N2O4-MMH indicating combustion efficiencies greater than 98%. A powder metallurgy rhenium engine demonstrated operation with high performance at Pc = 500 psia which indicated the viability of the concept. Author (revised)

N95-26489 Aerospace Corp., El Segundo, CA. Technology Operations.
PLUME MEASUREMENTS WITH THE T5 XENON ION THRUSTER
James E. Pollard 30 Sep. 1994 17 p Limited Reproducibility: More than 20% of this document may be affected by microfiche quality
(Contracts F04701-93-C-0094; F04701-88-C-0089)
(AD-A288697; TR-94(4507)-2; SMC-TR-94-44) Avail: Issuing Activity (Defense Technical Information Center (DTIC))

Two measurement techniques for investigating performance and life-limiting characteristics of ion engines are applied to a 10 cm T5 xenon thruster: (1) Thrust vector stability is evaluated with four double-wire Langmuir probes, aligned in the form of a cross, which are placed in the exhaust plume and are translated by a motorized positioning system to balance the currents collected along two orthogonal axes. The thrust vector position is thereby tracked with an angular resolution of less than 0.01 deg and a response time of less than 5 s. (2) A plume-sampling mass spectrometer has been developed for measuring the xenon charge state distribution and the flux of erosion products from the discharge chamber as a function of operating point. To demonstrate the capability for real-time erosion monitoring, plume spectra that reveal trace amounts of metal ions are presented. DTIC

N95-26799# National Aerospace Lab., Tokyo (Japan). Rocket Propulsion Research Div.
DEVELOPMENT TEST OF A LIQUID APOGEE ENGINE FOR THE ETS-6
Oct. 1994 25 p In JAPANESE
(ISSN 0389-4010)
(NAL-TR-1250) Avail: CASI HC A03/MF A01

A pressure-fed, full-blowdown, nitrogen tetroxide (NTO)/hydrazine (N2H4) bipropellant liquid apogee propulsion system was selected for engineering test satellite - VI (ETS-VI), a 2000-kg Japanese engineering test satellite. This 2000-kg mass geostationary satellite is scheduled to be launched by an H-II rocket in 1994. The apogee engine required a high reliability and relatively high performance for a pressure fed system. In the preliminary development phase of the apogee engine, a peak vacuum specific impulse Ispv of 325 s was set as the initial development target. This performance requirement of the apogee engine is greater than that of the bipropellant engine using NTO/monomethyl hydrazine (MMH). To meet such high performance requirements, the authors employed a NTO/N2H4 propellant system instead of NTO/MMH propellant and used a very large area ratio nozzle (nozzle area ratio is 200 to 300). To enhance the reliability of the apogee propulsion system, we selected a pressure-fed, full-blowdown system. Fundamental studies including hard-start, pop and thermal problems were also conducted during the development series of apogee engine started in 1983. Performance characteristics of apogee engine developed in 1990 were as follows: chamber pressure Pc = 0.97 approximately 0.63 MPa, mixture ratio MR = 0.85 approximately 1.05, vacuum thrust = 1980 approximately 1280 N, mean vacuum specific impulse Ispv = 320.0 +- 2.7 s, and total burn time = 2900 s. Delivered peak Ispv was less than the initial development target, however, the engine performance was higher than that of the engine for NTO/MMH propellant. This paper describes mainly the development studies of the injectors used in the apogee engine. Author

N95-26880 Air Force Inst. of Tech., Wright-Patterson AFB, OH. School of Engineering.
INVESTIGATION OF BOUNDARY LAYER AND PERFORMANCE EFFECTS OF TRANSPIRATION COOLING THROUGH A POROUS PLATE IN A ROCKET NOZZLE M.S. Thesis
David N. Keener Dec. 1994 116 p Limited Reproducibility: More than 20% of this document may be affected by microfiche quality
(AD-A289393; AFIT/GA/ENY/94D-3) Avail: Issuing Activity (Defense Technical Information Center (DTIC))

This study used a range of low blowing ratios with air through an area of porous material in a Mach 2.0 nozzle to quantity the change in boundary layer thickness as a function of blowing ratio. Also, exit and wall Mach number profiles at each blowing ratio were collected to characterize performance losses as a result of blowing. Performance in terms of specific impulse was also studied. As expected, the boundary layer thickness increased and nozzle performance in terms of exit Mach number decreased with increasing blowing ratio. DTIC

N95-27153 Air Force Inst. of Tech., Wright-Patterson AFB, OH. School of Engineering.
EFFECTS OF BLOWING RATIO ON HEAT TRANSFER TO THE THROAT REGION OF A POROUS-WALLED NOZZLE Final Report
Joseph L. Lenertz Dec. 1994 108 p Limited Reproducibility: More than 20% of this document may be affected by microfiche quality
(AD-A289459; AFIT/GA/ENY/94D-7) Avail: Issuing Activity (Defense Technical Information Center (DTIC))

This experiment analyzed the effects of blowing ratio on heat transfer to the throat region of a porous-walled nozzle, using the AFIT low speed shock tube. Heat flux data were taken from both sides of a two-dimensional Mach 2.0 (Re/m = 5.2 x 10(exp 7) nozzle using thin film resistance thermometers. One side was transpiration-cooled by secondary air injection through a sintered wall, while the other side served as a control. Control results were validated using empirical relations, and cooled side results showed up to a 14% reduction in heat transfer coefficient at blowing ratios of only 0.51%. The linear nature of cooling effectiveness at these low blowing ratios allowed a modification of nozzle heat transfer equations to include a blowing ratio parameter. Disturbance of primary flow was also minimized, causing no measurable reduction of nozzle performance. DTIC

N95-27177*# National Aeronautics and Space Administration. Lewis Research Center, Cleveland, OH.
A REVIEW OF NICKEL HYDROGEN BATTERY TECHNOLOGY
John J. Smithrick and Patricia M. ODonnell May 1995 10 p Presented at the 30th Intersociety Energy Conversion Engineering Conference, Orlando, FL, 31 Jul. - 4 Aug. 1995; cosponsored by ASME, IEEE, AIChE, ANS, ACS and AIAA
(RTOP 233-01-0B)
(NASA-TM-106918; E-9626; NAS 1.26:106918; ASME-95-367) Avail: CASI HC A02/MF A01

This paper on nickel hydrogen batteries is an overview of the various nickel hydrogen battery design options, technical accomplishments, validation test results and trends. There is more than one nickel hydrogen battery design, each having its advantage for specific applications. The major battery designs are individual pressure vessel (IPV), common pressure vessel (CPV), bipolar and low pressure metal hydride. State-of-the-art (SOA) nickel hydrogen batteries are replacing nickel cadmium batteries in almost all geosynchronous orbit (GEO) applications requiring power above 1 kW. However, for the more severe low earth orbit (LEO) applications (greater than 30,000 cycles), the current cycle life of 4000 to 10,000 cycles at 60 percent DOD should be improved. A NASA Lewis Research Center innovative advanced design IPV nickel hydrogen cell led to a breakthrough in cycle life enabling LEO applications at deep depths of discharge (DOD). A trend for some future satellites is to increase the power level to greater than 6 kW. Another trend is to decrease the power to less than 1 kW for small low cost satellites. Hence, the challenge is to reduce battery mass, volume and cost. A key is to develop a light weight nickel electrode and alternate battery designs. A common pressure vessel (CPV) nickel hydrogen battery is emerging as a viable alternative to the IPV design. It has the advantage of reduced mass, volume and manufacturing costs. A 10 Ah CPV battery has successfully provided power on the relatively short lived Clementine Spacecraft. A bipolar nickel hydrogen battery design has been demonstrated (15,000 LEO cycles, 40 percent DOD). The advantage is also a significant reduction in volume, a modest reduction in mass, and like most bipolar designs, features a high pulse power capability. A low pressure aerospace nickel metal hydride battery cell has been developed and is on the market. It is a prismatic design which has the advantage of a significant reduction in volume and a reduction in manufacturing cost. Author

N95-27424*# Alabama Univ., Huntsville, AL. Dept. of Mechanical Engineering.
ADVANCED EARTH-TO-ORBIT PROPULSION TECHNOLOGY INFORMATION, DISSEMINATION AND RESEARCH Final Report, 28 Jul. 1993 - 28 Mar. 1995
S. T. Wu 28 Mar. 1995 161 p
(Contract NAS8-38609)
(NASA-CR-196582; NAS 1.26:196582) Avail: CASI HC A08/MF A02

In this period of performance a conference (The 1994 Conference on Advanced Earth-to-Orbit Propulsion Technology) was organized and implemented by the University of Alabama in Huntsville and held May 15-17 to assemble and disseminate the current information on Advanced Earth-to-Orbit Propulsion Technology. The results were assembled for publication as NASA-CP-3282, Volume 1 and 2 and NASA-CP-3287. Author

N95-27434*# National Aeronautics and Space Administration. Lewis Research Center, Cleveland, OH.
COMPARISON OF NUMERICAL RESULTS AND MULTICAVITY PURGE AND RIM SEAL DATA WITH EXTENSIONS TO DYNAMICS
Mahesh Athavale (CFD Research Corp., Huntsville, AL.), Andrzej J. Przekwas (CFD Research Corp., Huntsville, AL.), Robert C. Hendricks, and Bruce M. Steinetz May 1995 26 p Presented at the Third Northern Ohio Technical Symposium, Aerospace Today, Cleveland, OH, 16 May 1994; sponsored by the AIAA Original contains color illustrations
(RTOP 232-01-02)
(NASA-TM-106685; E-9039; NAS 1.15:106685) Avail: CASI HC A03/MF A01; 6 functional color pages

The computation of flows within interconnected, multiple-disk cavities shows strong interaction between the cavities and the power stream. For this reason, simulations of single cavities in such cases are not realistic; the complete, linked configuration must be considered. Unsteady flow fields affect engine stability and can engender power-stream-driven secondary flows that produce local hot spotting or general cavity heating. Further, a concentric whirling rotor produces a circumferential pressure wave, but a statically eccentric whirling rotor produces a radial wave; both waves affect cavity ingestion and the stability of the entire engine. It is strongly suggested that seals be used to enhance turbojet engine stability. Simple devices, such as swirl brakes, honeycomb inserts, and new seal configurations, should be considered. The cost effectiveness of the NASA Lewis Research Center seals program can be expressed in terms of program goals (e.g., the Integrated High-pressure/Temperature Engine Technology (IHPTET) cannot be achieved without such a program), cost (savings to $250 million/1-percent decrease in specific fuel consumption), and indirect benefits (reduction of atmospheric NO(x) and CO2 and reduction of powerplant downtime). Author

N95-27727*# National Aeronautics and Space Administration. Lewis Research Center, Cleveland, OH.
ELECTRIC PROPULSION FOR GEOSTATIONARY ORBIT INSERTION
Steven R. Oleson (NYMA, Inc., Brook Park, OH.), Francis M. Curran, and Roger M. Myers (NYMA, Inc., Brook Park, OH.) May 1995 8 p Presented at the 30th Intersociety Energy Conversion Engineering Conference, Orlando, FL, 31 Jul. - 4 Aug. 1995; cosponsored by ASME, IEEE, AIChE, ANS, ACS, and AIAA
(Contract NAS3-27186; RTOP 564-09-20)
(NASA-TM-106942; E-9671; NAS 1.15:106942) Avail: CASI HC A02/MF A01

Solar electric propulsion (SEP) technology is already being used for geostationary satellite stationkeeping to increase payload mass. By using this same technology to perform part of the orbit transfer additional increases in payload mass can be achieved. Advanced chemical and N2H4 arcjet systems are used to increase the payload mass by performing stationkeeping and part of the orbit transfer. Four mission options are analyzed which show the impact of either sharing the orbit transfer between chemical and SEP systems or having either complete the transfer alone. Results show that for an Atlas 2AS payload increases in net mass (geostationary satellite mass less wet propulsion system mass) of up to 100 kg can be achieved using advanced chemical for the transfer and advanced N2H4 arcjets for stationkeeping. An additional 100 kg can be added using advanced N2H4 arcjets for part of a 40 day orbit transfer. Author

N95-27861*# National Aeronautics and Space Administration. Lewis Research Center, Cleveland, OH.
DIRECT DRIVE OPTIONS FOR ELECTRIC PROPULSION SYSTEMS
John A. Hamley May 1995 8 p Presented at the 30th Intersociety Energy Conversion Engineering Conference, Orlando, FL, 31 Jul. - 4 Aug. 1995; cosponsored by ASME, IEEE, AIChE, ANS, ACS, and AIAA
(RTOP 242-70-02)
(NASA-TM-106576; E-9618; NAS 1.15:106576; AIAA Paper 95-364) Avail: CASI HC A02/MF A01

Power processing units (PPU's) in an electric propulsion system provide many challenging integration issues. The PPU must provide power to the electric thruster while maintaining compatibility with all of the spacecraft power and data systems. Inefficiencies in the power processor produce heat, which must be radiated to the environment in order to ensure reliable operation. Although PPU efficiencies are generally greater than 0.9, heat loads are often substantial. This heat must be rejected by thermal control systems which generally have specific masses of 15-30 kg/kW. PPU's also represent a large fraction of the electric propulsion system dry mass. Simplification or elimination of power processing in a propulsion system would reduce the electric propulsion system specific mass and improve the overall reliability and performance. A direct drive system would eliminate all or some of the power supplies required to operate a thruster by directly connecting the various thruster loads to the solar array. The development of concentrator solar arrays has enabled power bus voltages in excess of 300 V which is high enough for direct drive applications for Hall thrusters such as the Stationary Plasma Thruster (SPT). The option of solar array direct drive for SPT's is explored to provide a comparison between conventional and direct drive system mass. Author

N95-27862*# National Aeronautics and Space Administration. Lewis Research Center, Cleveland, OH.
DISCHARGE IGNITION BEHAVIOR OF THE SPACE STATION PLASMA CONTACTOR
Timothy R. Sarver-Verhey (NYMA, Inc., Brook Park, OH.) and John A. Hamley May 1995 15 p Presented at the 30th Joint Propulsion Conference, Indianapolis, IN, 27-29 Jun. 1994; sponsored by AIAA, ASME, SAE, and ASEE
(RTOP 478-43-00)
(NASA-TM-106925; E-9643; NAS 1.15:106925; AIAA Paper 94-3311)
Avail: CASI HC A03/MF A01

Ignition testing of hollow cathode assemblies being developed for the Space Station plasma contactor system has been initiated to validate reliable multiple restart capability. An ignition approach was implemented that was derived from an earlier arcjet program that successfully demonstrated over 11,600 ignitions. For this, a test profile was developed to allow accelerated cyclic testing at expected operating conditions. To date, one hollow cathode assembly has been used to demonstrate multiple ignitions. A prototype hollow cathode assembly has achieved 3,615 successful ignitions at a nominal anode voltage of 18.0 V. During the ignition testing several parameters were investigated, of which the heater power and pre-heat time were the only parameters found to significantly impact ignition rate. Author

N95-28000*# Electric Propulsion Lab., Inc., Tehachapi, CA.
MICRO ELECTRIC PROPULSION FEASIBILITY Final Report
Graeme Aston and Martha Aston Nov. 1992 74 p
(Contract NAS3-26062; RTOP 506-42-31)
(NASA-CR-189139; E-7428; NAS 1.26:189139) Avail: CASI HC A04/MF A01

Miniature, 50 kg class, strategic satellites intended for extended deployment in space require an on-board propulsion capability to perform needed attitude control adjustments and drag compensation maneuvers. Even on such very small spacecraft, these orbit maintenance functions can be significant and result in a substantial propellant mass requirement. Development of advanced propulsion technology could reduce this propellant mass significantly, and thereby maximize the payload capability of these spacecraft. In addition, spacecraft maneuverability could be enhanced and/or multi-year mission lifetimes realized. These benefits cut spacecraft replacement costs, and reduce services needed to maintain the launch vehicles. For SDIO brilliant pebble spacecraft, a miniaturized hydrazine propulsion system provides both boost and divert thrust control. This type of propulsion system is highly integrated and is capable of delivering large thrust levels for short time periods. However, orbit maintenance functions such as drag make-up require only very small velocity corrections. Using the boost and/or divert thrusters for these small corrections exposes this highly integrated propulsion system to continuous on/off cycling and thereby increases the risk of system failure. Furthermore, since drag compensation velocity corrections would be orders of magnitude less than these thrusters were designed to deliver, their effective specific impulse would be expected to be lower when operated at very short pulse lengths. The net result of these effects would be a significant depletion of the on-board hydrazine propellant supply throughout the mission, and a reduced propulsion system reliability, both of which would degrade the interceptors usefulness. In addition to SDIO brilliant pebble spacecraft, comparably small spacecraft can be anticipated for other future strategic defense applications such as surveillance and communication. For such spacecraft, high capability and reliability, minimal detectability and low cost are requirements. All these miniature spacecraft share a common characteristic: because of their on-board electronic equipment they have, by design, solar order 50-100 W. In a relative sense, such spacecraft are power rich when compared to other larger spacecraft. This power rich situation is offset by very tight mass budgets, which make reductions in propellant mass requirements a key issue in meeting overall spacecraft minimum mass goals. In principle, power rich and propellant poor brilliant pebbles class spacecraft can benefit from using high specific impulse electric propulsion to reduce chemical propellant mass requirements. However, at power levels of order 50 W, arcjets cannot be made to function, ion thrusters are too complex and heavy and resistojets have too low a specific impulse. Recognizing these capability limitations in existing electric propulsion technology, the SDIO/IST sponsored the Phase I SBIR Micro Electric Propulsion (MEP) thruster study described in this report. The objective of this study was to examine the feasibility of developing a very simple, low mass and small volume, electric thruster for operation on hydrazine at less than 100 W of input power. The feasibility of developing such a MEP thruster was successfully demonstrated by EPL by the discovery of a novel plasma acceleration process. The sections in this report summarize the approach, test results and major accomplishments of this proof-of-concept program. Author

N95-28036*# National Aeronautics and Space Administration. Lewis Research Center, Cleveland, OH.

ANALYSIS OF SOLAR RECEIVER FLUX DISTRIBUTIONS FOR US/RUSSION SOLAR DYNAMIC SYSTEM DEMONSTRATION ON THE MIR SPACE STATION

Thomas W. Kerslake and James Fincannon Jun. 1995 8 p Presented at the 30th Intersociety Energy Conversion Engineering Conference, Orlando, FL, 31 Jul. - 1 Aug. 1995
(RTOP 547-10-11)
(NASA-TM-106933; E-9660; NAS 1.15:106933; IECEC-95-136) Avail: CASI HC A02/MF A01

The United States and Russia have agreed to jointly develop a solar dynamic (SD) system for flight demonstration on the Russian MIR space station starting in late 1997. Two important components of this SD system are the solar concentrator and heat receiver provided by Russia and the U.S., respectively. This paper describes optical analysis of the concentrator and solar flux predictions on target receiver surfaces. The optical analysis is performed using the code CIRCE2. These analyses account for finite sun size with limb darkening, concentrator surface slope and position errors, concentrator petal thermal deformation, gaps between petals, and the shading effect of the receiver support struts. The receiver spatial flux distributions are then combined with concentrator shadowing predictions. Geometric shadowing patterns are traced from the concentrator to the target receiver surfaces. These patterns vary with time depending on the chosen MIR flight attitude and orbital mechanics of the MIR spacecraft. The resulting predictions provide spatial and temporal receiver flux distributions for any specified mission profile. The impact these flux distributions have on receiver design and control of the Brayton engine are discussed. Author

N95-28213*# National Aeronautics and Space Administration. Lewis Research Center, Cleveland, OH.

ANALYSIS OF SHADOWING EFFECTS ON MIR PHOTOVOLTAIC AND SOLAR DYNAMIC POWER SYSTEMS

James Fincannon May 1995 8 p Presented at the 30th Intersociety Energy Conversion Engineering Conference, Orlando, FL, 31 Jul. - 4 Aug. 1995; sponsored by ASME, IEEE, AICHE, ANS, ACS, and AIAA
(RTOP 478-12-10)
(NASA-TM-106940; E-9668; NAS 1.15:106940) Avail: CASI HC A02/MF A01

The NASA Lewis Research Center is currently working with RSC-Energia, the Russian Space Agency, and Allied Signal in developing a flight demonstration solar dynamic power system. This type of power system is dependent upon solar flux that is reflected and concentrated into a thermal storage system to provide the thermal energy input to a closed-cycle Brayton heat engine. The solar dynamic unit will be flown on the Russian Mir space station in anticipation of use on the International Space Station Alpha. By the time the power system is launched, the Mir will be a spatially complex configuration which will have, in addition to the three-gimbaled solar dynamic unit, eleven solar array wings that are either fixed or track the Sun along one axis and a variety or repositionable habitation and experiment modules. The proximity of arrays to modules creates a situation which makes it highly probable that there will be varying solar flux due to shadowing on the solar dynamic unit and some of the arrays throughout the orbit. Shadowing causes fluctuations in the power output from the arrays and the solar dynamic power system, thus reducing the energy capabilities of the spacecraft. An assessment of the capabilities of the power system under these conditions is an important part in influencing the design and operations of the spacecraft and predicting its energy performance. This paper describes the results obtained from using the Orbiting Spacecraft Shadowing Analysis Station program that was integrated into the Station Power Analysis for Capability Evaluation (SPACE) electrical power system computer program. OSSA allows one to consider the numerous complex factors for analyzing the shadowing effects on the electrical power system including the variety of spacecraft hardware geometric configurations, yearly and daily orbital variations in the vehicle attitude and orbital maneuvers (for communications coverage, payload pointing requirements and rendezvous/docking with other vehicles). The geometric models of the MIR with a solar dynamic power unit that were used in performing shadowing analyses are described. Also presented in this paper are results for individual orbits for several flight attitude cases which include assessments of the shadowing impacts upon the solar dynamic unit and the solar arrays. These cases depict typical MIR flight attitudes likely to have shadowing impact. Because of the time varying nature of the Mir orientation with respect to the Sun and the lack of knowledge of the precise timing of the attitude changes, strategies must be devised to assess and depict the shadowing impacts on power generation throughout the year. To address this, the best, nominal and worst impacts of shadowing considering a wide possible range of parameter changes for typical mission operation period are shown. Author

N95-28263*# National Aeronautics and Space Administration. Marshall Space Flight Center, Huntsville, AL.

DEVELOPMENTAL PROBLEMS AND THEIR SOLUTION FOR THE SPACE SHUTTLE MAIN ENGINE ALTERNATE LIQUID OXYGEN HIGH-PRESSURE TURBOPUMP: ANOMALY OR FAILURE INVESTIGATION THE KEY

R. Ryan and L. A. Gross Washington May 1995 79 p
(NASA-TP-3553; M-780; NAS 1.60:3553) Avail: CASI HC A05/MF A01

The Space Shuttle main engine (SSME) alternate high-pressure liquid oxygen pump experienced synchronous vibration and ball bearing life problems that were program threatening. The success of the program hinged on the ability to solve these development problems. The design and solutions to these problems are engirded in the lessons learned and experiences from prior programs, technology programs, and the ability to properly conduct failure or anomaly investigations. The failure investigation determines the problem cause and is the basis for recommending design solutions. For a complex problem, a comprehensive solution requires that formal investigation procedures be used, including fault trees, resolution logic, and action items worked through a concurrent engineering-multidiscipline team. The normal tendency to use an intuitive, cut-and-try approach will usually prove to be costly, both in money and time and will reach a less than optimum, poorly understood answer. The SSME alternate high-pressure oxidizer turbopump development has had two complex problems critical to program success: (1) high synchronous vibrations and (2) excessive ball bearing wear. This paper will use these two problems as examples of this formal failure investigation approach. The results of the team's investigation provides insight into the complexity of the turbomachinery technical discipline interacting/sensitivities and the fine balance of competing investigations required to solve problems and guarantee program success. It is very important to the solution process that maximum use be made of the resources that both the contractor and Government can bring to the problem in a supporting and noncompeting way. There is no place for the not-invented-here attitude. The resources include, but are not limited to: (1) specially skilled professionals; (2) supporting technologies; (3) computational codes and capabilities; and (4) test and manufacturing facilities. Author

N95-28294 Johns Hopkins Univ., Columbia, MD. Chemical Propulsion Information Agency.
THE 1994 JANNAF SAFETY AND ENVIRONMENTAL PROTECTION SUBCOMMITTEE MEETING, VOLUME 1
Lorri A. Pickett, ed. Aug. 1994 442 p Meeting held in San Diego, CA, 1-4 Aug. 1994
(Contract N00014-91-C-0001)
(CPIA-Publ-614-Vol-1) Avail: CPIA, 10630 Little Patuxent Pkwy., Suite 202, Columbia, MD 21044-3200 HC

This publication contains thirty-nine technical papers and progress reports presented at the 1994 Joint Army-Navy-NASA-Air Force (JANNAF) Safety and Environmental Protection Subcommittee (S&EPS) Meeting held 1-4 August 1994 at the Town & Country Hotel, San Diego, California. Topics covered include: toxic vapor detection methods; hazardous waste management and waste minimization techniques; occupational safety and industrial hygiene issues; explosives safety; reclamation, disposal, and demilitarization methods; and environmental impacts associated with propulsion and ordnance related operations. The proceedings are published in two volumes. Volume 2 contains four papers limited in distribution. For individual titles, see N95-28295 through N95-28326.

N95-28295 Environmental Protection Agency, Washington, DC. Stratospheric Ozone Protection Div.
THE IMPORTANCE OF PROPULSION ENGINEERS IN PROTECTING THE GLOBAL ENVIRONMENT **c45**
Stephen O. Andersen *In* Johns Hopkins Univ., The 1994 JANNAF Safety and Environmental Protection Subcommittee Meeting, Volume 1 Aug. 1994 p 1-8 (For primary document see N95-28294 09-20)
Avail: CPIA, 10630 Little Patuxent Pkwy., Suite 202, Columbia, MD 21044-3200 HC

This paper describes how industry was persuaded to protect the ozone layer and how engineers contributed to the success. It describes the voluntary and cooperative efforts of industry to speed protection of the ozone layer and it explains the U.S. EPA strategy for technical cooperation with developing countries which involves government/industry partnerships and project leadership companies. Some of most critical remaining uses of ozone-depleting solvents are for rocket motor manufacturing, operation, and refurbishment. Propulsion systems engineers are key to developing and implementing alternatives and substitutes to these uses. Author (revised)

N95-28296 Radian Corp., Oak Ridge, TN.
OB/OD TREATMENT: THE EFFECTIVE USE OF MEASURED FIELD DATA AND AIR MODELING TO SUPPORT AN ENVIRONMENTAL ASSESSMENT **c45**
T. J. Tope, H. C. Simmons, and W. F. Howell *In* Johns Hopkins Univ., The 1994 JANNAF Safety and Environmental Protection Subcommittee Meeting, Volume 1 Aug. 1994 p 13-22 (For primary document see N95-28294 09-20)
(Contract DACW05-92-D-0016)
Avail: CPIA, 10630 Little Patuxent Pkwy., Suite 202, Columbia, MD 21044-3200 HC

The most commonly used treatment and disposal method for managing unserviceable conventional munition wastes generated by Department of Defense (DOD) installations is open burning/open detonation (OB/OD). Regulatory constraints over the past decade, however, have reduced and limited the accessibility and frequency of OB/OD activities. Impeding the acceptance of OB/OD by regulators and the public is the lack of credible and valid data that may be used in an environmental assessment to support OB/OD as a treatment and disposal method that does not impact human health and the environment. This paper presents the technical approach and results for the air environmental assessments performed to support permitting of OB/OD facilities at three Air Force installations. In general these assessments include calculating the worst case airborne concentrations from OB/OD treatment at the nearest off-site receptor and demonstrating these concentrations pose no adverse human health risk. This is accomplished through the use of emission factors developed through BangBox testing, air dispersion modeling, and comparison of worst-case modeling results with federal and state limitations on criteria and non-criteria air pollutant emissions. The results of the assessment demonstrate that no adverse impacts to human health would occur as result of the OB/OD activities performed at these Air Force installations. Author

N95-28297 Dugway Proving Ground, UT.
EVALUATING THE ENVIRONMENTAL VIABILITY OF OPEN BURNING/OPEN DETONATION OPERATIONS **c45**
MacDonald B. Johnson and Douglass P. Bacon (Energy Conversion Corp., Salt Lake City, UT.) *In* Johns Hopkins Univ., The 1994 JANNAF Safety and Environmental Protection Subcommittee Meeting, Volume 1 Aug. 1994 p 23-31 (For primary document see N95-28294 09-20)
Avail: CPIA, 10630 Little Patuxent Pkwy., Suite 202, Columbia, MD 21044-3200 HC

Despite their historical record of safety and efficiency, open burning/open detonation (OB/OD) operations now face serious questions about their suitability for destroying propellants, energetic munitions, and energetic wastes. Environmental regulators are demanding emissions data to support applications for OB/OD permits submitted under provisions of the Resource Conservation and Recovery Act (RCRA) subpart X. Until recent development of the BangBox testing system, no means existed for obtaining these data. This paper describes the evolution of the integrated testing system (consisting of personnel, instrument and equipment, procedures, and facilities), successful audits conducted by the U.S. Environmental Agency (USEPA), and application of results. The system's development and its technologies are significant because there is no other method which can accurately and credibly characterize OB/OD combustion products. Of particular interest is that volatile and semivolatile organic compounds resulting from OB/OD of propellants, explosives, and energetic munitions are proving to be far below levels of environmental concern and do not pose a threat to health or the environment. Author

N95-28298 Radian Corp., Austin, TX.
USE OF MUSSELS IN BIOMONITORING OF ENVIRONMENTAL IMPACTS OF PROPELLANTS, PROJECTILES, EXPLOSIVES, AND PYROTECHNICS **c51**
J. Hixson, R. Jennings, and C. H. Stagg (Joint Readiness Training Center, Fort Polk, LA.) *In* Johns Hopkins Univ., The 1994 JANNAF Safety and Environmental Protection Subcommittee Meeting, Volume 1 Aug. 1994 p 33-42 (For primary document see N95-28294 09-20)
Avail: CPIA, 10630 Little Patuxent Pkwy., Suite 202, Columbia, MD 21044-3200 HC

The primary mission of the Ft. Polk Military Reservation is to provide a base of operations for the Joint Readiness Training Center (JRTC). Army and Air Force contingency forces conduct joint training operations at the JRTC which replicate, as closely as possible, those of real low- and mid-intensity conflicts. The reservation operates an open burning/open detonation (OB/OD) unit primarily to treat unserviceable ammunition and explosives generated as a result of routine training operations. The unit is located in a national forest, and consequently there has been concern regarding potential impacts of OB/OD activities on wildlife. The U.S. Forest Service (the site owner) requested that an environmental assessment be performed for the unit to evaluate these potential impacts. The entire military reservation, including the OB/OD unit, is located in an area with numerous wetlands and streams. Based on a prior investigation of limited scope, there was some concern that activities at the reservation may have adversely impacted aquatic invertebrates. It was decided that a biomonitoring study should be conducted to clarify the results of the previous investigation and to determine the contribution of the activities on the reservation to downstream population effects. The biomonitoring study was designed to be performed in two stages. The first stage, discussed in this paper, was a screening analysis to determine whether specific chemicals were present in mussels within and downstream of the reservation. This stage will be followed with a more detailed analysis including population studies as well as chemical analyses of biota collected from multiple locations. Author

N95-28299 Naval Surface Weapons Center, Indian Head, MD. Indian Head Div.

BIODEGRADATION OF NITRATE ESTERS **c25**

Johnathan R. Stacy, M. K. Speedie (Maryland Univ., Baltimore, MD.), L. Geelhaar (Maryland Univ., Baltimore, MD.), Min Meng (Maryland Univ., Baltimore, MD.), Gregory Payne (Maryland Univ. Baltimore County, Catonsville, MD.), W. Q. Sun (Maryland Univ. Baltimore County, Catonsville, MD.), Anemi Patal (Maryland Univ. Baltimore County, Catonsville, MD.), and Rakesh Govind (Cincinnati Univ., OH.) *In* Johns Hopkins Univ., The 1994 JANNAF Safety and Environmental Protection Subcommittee Meeting, Volume 1 Aug. 1994 p 43-50 (For primary document see N95-28294 09-20)

Avail: CPIA, 10630 Little Patuxent Pkwy., Suite 202, Columbia, MD 21044-3200 HC

The development of biological treatment methods for nitrate ester contaminated soil and water will be discussed. The approach is to develop existing biological treatment methods for use with nitrate ester contaminated soil and water. These methods would be applied using existing and commonly used engineering methods. The advantage to the multi-technique approach is that it would address sites with different problems and characteristics. Technologies for water treatment address ground water contamination, wastewater from soil washing techniques, and leachate from contaminated soils. Soil techniques will address in situ as well as active land farming techniques. Whole cell and enzymatic approaches are being investigated. The nitrate esters used in this investigation are nitroglycerin (NG), propyleneglycol dinitrate (PGDN), trimethylolethane trinitrate (TMETN), and triethyleneglycol dinitrate (TEGDN). Working with the University of Maryland at Baltimore, we are isolating the enzymes used by bacteria to denitrify the nitrate esters. This technique can be used for both contaminated soils and wastewaters. For the whole cell approach we are working with the University of Cincinnati on the study of the kinetics for the biodegradation of nitrate esters in soil. Two organisms have been isolated that are capable of denitrifying nitrate esters; Bacillus thuringiensis/cerus (N) and Enterobactor agglomerans (AT25). We will present the results of C-14 NG and C-14 PGDN studies that show complete denitrification to glycerol and propylene glycol respectively by enzyme extracts from the Bacillus organism. The status of the work on isolating and identifying this enzyme will be reported. The results of kinetic study of the biodegradation of nitrate esters in soil performed at the University of Cincinnati will be presented. Author

N95-28300 Florida Solar Energy Center, Cape Canaveral, FL.

RADIANT EXCHANGE CONSIDERATIONS IN DESIGN AND SCALEUP OF PHOTOCATALYTIC REACTORS FOR PURIFICATION OF NITROGLYCERINE-CONTAMINATED AIR **c45**

Nazim Z. Muradov, Ali T-Raissi, and Charles R. Painter (Naval Surface Weapons Center, Indian Head, MD.) *In* Johns Hopkins Univ., The 1994 JANNAF Safety and Environmental Protection Subcommittee Meeting, Volume 1 Aug. 1994 p 51-61 (For primary document see N95-28294 09-20)

Avail: CPIA, 10630 Little Patuxent Pkwy., Suite 202, Columbia, MD 21044-3200 HC

This paper describes the progress made to date toward the design of a 5-SCFM photocatalytic detoxification unit that employs a mercury vapor lamp and immobilized titania for purification of NG-contaminated air streams. Author

N95-28301 Army Armament Research, Development and Engineering Center, Picatinny Arsenal, NJ.

DESTRUCTION OF PYROTECHNICS MANUFACTURE WASTEWATER TREATMENT SLUDGE BY PLASMA ARC PYROLYSIS **c25**

Donald J. Freeman, Hany H. Zaghloul (Army Construction Engineering Research Lab., Champaign, IL.), and Robert E. Haun (Retech, Inc., Ukiah, CA.) *In* Johns Hopkins Univ., The 1994 JANNAF Safety and Environmental Protection Subcommittee Meeting, Volume 1 Aug. 1994 p 63-79 (For primary document see N95-28294 09-20)

Avail: CPIA, 10630 Little Patuxent Pkwy., Suite 202, Columbia, MD 21044-3200 HC

The wastewater sludge generated by the manufacture of military pyrotechnics at Longhorn Army Ammunition Plant (LHAAP) is a listed hazardous waste (KO44) that also contains several toxicity characteristic leachate procedure (TCLP) metals - barium, chromium and lead - as well as various toxic organics. Currently, this hazardous waste is disposed of in a controlled landfill, which is expensive and leaves the government with a potential liability in case of a future accidental release to the environment. Plasma arc pyrolysis is an ultra-high temperature process that destroys all organics and renders TCLP metals non-leachable by sealing them into a fused vitreous slag, resulting in a non-hazardous material that can be placed in an uncontrolled landfill or used as a construction material. This paper evaluates the use of an improved small-scale plasma arc centrifugal treatment (PACT) unit with a secondary combustion chamber (SCC) and a high-efficiency off-gas treatment baghouse to treat the LHAAP sludge. To underscore the ability of plasma arc pyrolysis to render TCLP metals nonleachable, 1-2% each of barium, chromium and lead compounds were added to one batch of sludge. In addition, 2% hexachlorobenzene, a semi-volatile TCLP organic used in pyrotechnic manufacture, was added in order to perform a modified DRE (destruction and removal efficiency) test to confirm organics destruction. Partitioning of the volatile metals, lead and chromium, between the slag and the off-gas particulate were also investigated as part of process development. This test has demonstrated that plasma arc pyrolysis can be used for the destruction of listed military pyrotechnics manufacture wastewater treatment sludges containing TCLP metals and toxic organics. However, unexpected problems with the analyses and mass balances led to a number of 'lessons learned' that will be applied to a planned new test. Author

N95-28302 Rockwell International Corp., Canoga Park, CA.

RECOVERY, EVALUATION, AND DECONTAMINATION OF LANDFILLED PENTABORANE CYLINDERS, FORMER LIQUID PROPELLANT ROCKET ENGINE TEST FACILITY, WASHOE COUNTY, NEVADA **c45**

S. L. Shestag, C. J. Rozas, R. Gnat (Hydro-Search, Denver, CO.), and J. Gold (Integrated Environmental Services, Atlanta, GA.) *In* Johns Hopkins Univ., The 1994 JANNAF Safety and Environmental Protection Subcommittee Meeting, Volume 1 Aug. 1994 p 81-91 (For primary document see N95-28294 09-20)

Avail: CPIA, 10630 Little Patuxent Pkwy., Suite 202, Columbia, MD 21044-3200 HC

During excavation of a landfill associated with a former liquid propellant test facility, forty eight pentaborane cylinders were discovered. The test facility was part of a 126,000 acre property used for liquid propellant rocket engine and solid propellant testing in the 1960's. Operations at the test facility ceased in 1970 and the area was later developed into a rural residential community. Because of the extreme toxicity of pentaborane and the proximity of the cylinders to adjacent residents, minimizing the potential for a release of pentaborane to the atmosphere was critical. Upon encountering the initial cylinder, preparation of a work plan for the safe handling, decontamination and disposal of cylinders was developed. Review of available information and knowledgeable sources indicated that no procedure for handling pentaborane cylinders of unknown integrity had been previously developed. Development of the work plan included air dispersion modeling to evaluate potential area of impact in the event of a release and evaluation of treatment and disposal options. Two onsite treatment methods were identified for decontaminating the cylinders. They included pyrolytic incineration if the cylinders contained pentaborane and chemical treatment for decontaminating the empty cylinders. Upon excavating and inspecting the cylinders, all were found to contain only residual quantities of pentaborane, if any. The chemical treatment process was used to decontaminate the cylinders. After controlled venting of any hydrogen gas which may have accumulated in the cylinders, residual pentaborane was dissolved with dilute caustic solution. Methanol was used to rinse the cylinders and then they were flushed with large quantities of water. The caustic rinse solution was neutralized in a reaction vessel using sulfuric acid. The process resulted in generation of non-hazardous waste products including boric acid, alcohol/water mixture and neutralized solid residue. Stored and landfilled pentaborane cylinders are known to exist at other similar installations. The procedures presented herein provide a reference

method for the safe handling and decontamination of potentially toxic pentaborane cylinders. The handling and treatment process developed resulted in the safe decontamination and disposal of the cylinders.
Author

N95-28303 Yamada Science and Art Corp., Los Alamos, NM.
THREE-DIMENSIONAL FORECAST MODELS FOR EMERGENCY RESPONSE MANAGEMENT c45
Ted Yamada *In* Johns Hopkins Univ., The 1994 JANNAF Safety and Environmental Protection Subcommittee Meeting, Volume 1 Aug. 1994 p 93-100 (For primary document see N95-28294 09-20)
(Contract F08637-94-C-6013)
Avail: CPIA, 10630 Little Patuxent Pkwy., Suite 202, Columbia, MD 21044-3200 HC

An innovative scheme was developed to interactively operate HOTMAC, a three-dimensional mesoscale forecast model, and RAPTAD, a three-dimensional Lagrangian statistical diffusion model. HOTMAC runs continuously and always maintains a 24-hour forecast of meteorological data. The interactive scheme dictates that as soon as RAPTAD starts computation, HOTMAC halts its forecasting so that all computational power is used for RAPTAD. RAPTAD displays an hourly surface-concentration distribution plot on the screen as soon as one hourly computation is completed. The RAPTAD computation is fast compared with the HOTMAC computation, typically taking less than 20 sec. for a one hour simulation on a SPARC10 workstation. The HOTMAC/RAPTAD modeling system is operational on a desk-top or lap-top workstation. Thus, the HOTMAC/RAPTAD modeling system can be used for emergency response management to predict concentration distributions of toxic materials over complex terrain.
Author

N95-28304 Martin Marietta Aerospace, Denver, CO.
CHEMICAL REACTIONS IDENTIFIED IN THE TITAN 2, TITAN 4, AND DELTA 2 PROPELLANT SYSTEMS AND THEIR APPLICATION TO SOURCE MODELING
S. P. Prince, D. W. Banning, and F. L. Wiseman (Air Force Systems Command, Tyndall AFB, FL.) *In* Johns Hopkins Univ., The 1994 JANNAF Safety and Environmental Protection Subcommittee Meeting, Volume 1 Aug. 1994 p 101-112 (For primary document see N95-28294 09-20)
(Contract F08635-92-C-0056)
Avail: CPIA, 10630 Little Patuxent Pkwy., Suite 202, Columbia, MD 21044-3200 HC

A series of tests involving the combustion of solid and liquid propellants used to fuel the Titan 2, Titan 4, and Delta 2 launch vehicles was performed. The purpose of these tests was to evaluate the nature and amounts of combustion gases from reacting these propellants in various proportions, and to apply the derived data to predicting toxic chemical emissions arising from a launch vehicle explosion. Propellants tested in this study included Aerozine-50 and nitrogen tetroxide (liquid propellants used in the Titan 2 and Titan 4 launch vehicles), PBAN solid propellant (used on the Titan 4 solid rocket motor), RP-1 and liquid oxygen (liquid propellants used to fuel the Delta 2 launch vehicle), and the Castor IVA solid rocket propellant used on the Delta 2 first stage engine. Tests were conducted in a 150-liter stainless steel combustion chamber in air at nominal pressure (0.8 atmospheres at Denver barometric conditions). Measurements of the chamber gas temperature and internal pressure were taken and gas samples were withdrawn and analyzed for expected combustion gases, unreacted propellants, organic vapors, and oxygen reacted from the air. A stainless steel witness plate was used to collect condensates which formed during the course of the propellant combustion tests. Results of this study suggest significantly different chemical fates for some of the rocket propellants than those predicted by chemical theory only. A description of the test parameters, results, and application to source predictions is presented.
Author

N95-28305 Aerospace Corp., Los Angeles, CA. Mechanics and Materials Technology Center.
USE OF SURFACE CHEMKIN TO MODEL MULTIPHASE ATMOSPHERIC CHEMISTRY: APPLICATION TO NITROGEN TETROXIDE SPILLS c45
Brian B. Brady and L. Robbin Martin *In* Johns Hopkins Univ., The 1994 JANNAF Safety and Environmental Protection Subcommittee Meeting, Volume 1 Aug. 1994 p 113-122 (For primary document see N95-28294 09-20)
Avail: CPIA, 10630 Little Patuxent Pkwy., Suite 202, Columbia, MD 21044-3200 HC

SURFACE CHEMKIN is a widely available computer program developed for kinetic modeling of chemical vapor deposition. We show that it may be adapted for kinetic modeling of multiphase chemistry in the atmosphere, with broad capability to deal with complex chemistry and physics. It can deal with multiple phases having different reaction manifolds in each phase, it deals with gas, surface, and bulk reactions and mass transfer rates, it keeps track of the phase equilibria with realistic activities, and it can operate in an adiabatic mode to include the effect of heat release on the system. The adapted model is applied here to the problem of a nitrogen tetroxide spill in the troposphere. The model is able to predict the formation of a nitric acid/water aerosol and to follow the chemistry taking place in both the gas and liquid phases as the spill dilutes in the surrounding atmosphere. The model predicts that in such a spill, most (70 - 90%) of the nitrogen oxides released are converted to nitric acid over a wide range of relative humidity.
Author

N95-28306 Naval Surface Weapons Center, Indian Head, MD.
UPGRADE OF THE COMPUTER MODELING PROGRAMS POLU10 AND POLU13A FOR OPEN BURNING AND OPEN DETONATION OF ENERGETIC MATERIALS c45
Edward E. Baroody *In* Johns Hopkins Univ., The 1994 JANNAF Safety and Environmental Protection Subcommittee Meeting, Volume 1 Aug. 1994 p 123-131 (For primary document see N95-28294 09-20)
Avail: CPIA, 10630 Little Patuxent Pkwy., Suite 202, Columbia, MD 21044-3200 HC

Two popular ways to dispose of explosives and propellants (energetic materials) are by burning or detonating in the open air(OB/OD). Both methods have been used at disposal sites for many years as the safest, most cost effective means of treatment of reactive wastes associated with the production, use, maintenance an demilitarization of munitions and ordnance. To protect the environment, the disposal employing OB/OD sites are carefully controlled and must be issued an OB/OD permit by the State Environmental Protection Agency (EPA). This permit comes under the Resource Conservation and Recovery Act (RCRA) Part B permits, and the OB/OD sites are regulated by the EPA final hazardous waste management regulations under 40 CFR subpart X. A screening technique is required to provide a rapid and inexpensive approach to determine if the disposal site has the potential to cause adverse health impacts due to air emissions. This involves the use of computer models to estimate air emissions and the resultant ambient downwind concentrations of pollutants of concern. A computer program, POLU10, was developed to predict the pollution product caused by the OB/OD of energetic materials. The data from the POLU10 program have been used extensively by military sites to obtain OB/OD permits for the disposal of energetic materials. The program is referred to several times in the AEHA manual for application of OB/OD permits. As a result, copies of the POLU10 computer program have been sent to numerous military sites and their subcontractors. Author (revised)

N95-28307 Weather Squadron (45th), Patrick AFB, FL.
WEATHER HAZARDS TO A TITAN 4 ON-PAD DESTACK-RESTACK OPERATION c47
W. P. Roeder, J. B. Lorens, J. W. Weems, and B. F. Boyd *In* Johns Hopkins Univ., The 1994 JANNAF Safety and Environmental Protection Subcommittee Meeting, Volume 1 Aug. 1994 p 133-141 (For primary document see N95-28294 09-20)
Avail: CPIA, 10630 Little Patuxent Pkwy., Suite 202, Columbia, MD 21044-3200 HC

From December 1993 through February 1994 the 45th Space Wing completed the first ever on the launch pad Titan 4 Solid Rocket Motors (SRM's) total destack-restack. This weather sensitive operation required specialized weather support. Weather impacted the operation 29 of 58 days (50%). Specialized weather support proved invaluable throughout the entire operation.
Author

N95-28308 Edgerton, Germeshausen and Grier, Inc., Cocoa Beach, FL.
CAPE CANAVERAL AIR STATION LAUNCH EMERGENCY RESPONSE FORCES AND TOXIC MATERIALS RELEASE CONTINGENCY PLANS c81
S. W. Brown *In* Johns Hopkins Univ., The 1994 JANNAF Safety and

Environmental Protection Subcommittee Meeting, Volume 1 Aug. 1994 p 143-148 (For primary document see N95-28294 09-20)
Avail: CPIA, 10630 Little Patuxent Pkwy., Suite 202, Columbia, MD 21044-3200 HC

Toxic materials release contingency plans and launch emergency response plans have been developed/revised for the Cape Canaveral Air Station (CCAS). This paper will describe the various emergency response plans utilized at CCAS to process and launch Expendable Launch Vehicles (ELV). The plans define the roles and responsibilities of the various disaster response elements, the chain of command for a given hazardous material release, post accident procedures for propellant spills, and catastrophic launch accident preparations. The Launch Emergency Response Force (LERF) plan and the Major Accident Response Exercises (MARE) performed at the CCAS are described. The use of real time toxic plume dispersion models during the implementation of the CCAS emergency response plans is also explained. Author

N95-28309* National Aeronautics and Space Administration. John F. Kennedy Space Center, Cocoa Beach, FL.
EVALUATION OF A CONDUCTIVE POLYMER-BASED SENSOR FOR DETECTION OF HYDRAZINES AT THE PART-PER-BILLION LEVEL **c25**
Dale Lueck, Dan Curran (I-NET, Inc., Cocoa Beach, FL.), and Mitch Zakin (Spectral Sciences, Inc., Burlington, MA.) *In* Johns Hopkins Univ., The 1994 JANNAF Safety and Environmental Protection Subcommittee Meeting, Volume 1 Aug. 1994 p 149-156 (For primary document see N95-28294 09-20)
(Contract NAS10-11943)
Avail: CPIA, 10630 Little Patuxent Pkwy., Suite 202, Columbia, MD 21044-3200 HC

A conductive polymer-based hydrazine sensor (CPHS) was developed by Spectral Sciences, Inc., and Spire Corp. under an Small Business Innovative Research (SBIR) contract for the United States Air Force (USAF). During preliminary testing, the sensor showed promise as a dosimeter with the ability to detect hydrazine (N2H4) and unsymmetrical dimethylhydrazine (UDMH) at levels well below the proposed threshold limit value (TLV) of 10 part per billion (ppb). The original sensor developed and tested by Spectral Sciences and Spire Corp. demonstrated a minimum detectable dose of approximately 1 part per billion-hour (ppb-hr) and a saturation dose of approximately 250 ppb-hr in dry conditions, offering adequate coverage of the proposed TLV limit of 80 ppb-hr (8 hours at the proposed TLV level of 10 ppb). However, initial testing in a more realistic humidified environment (relative humidities (RH) to over 60%) indicated an increased sensor reactivity, yielding a saturation dose of only approximately 30 ppb-hr at humidities greater than 60%. A second version of the sensor (CPHS2) was fabricated utilizing a thicker polymer film in an attempt to increase the saturation dose back up to a level that would provide a better dynamic range. Initial tests of the CPHS2 by Spectral Sciences at the NASA Toxic Vapor Detection Laboratory (TVDL) in November 1993 exhibited a minimum detectable dose in the range of 1 to 2 ppb-hr, an increase in the saturation dose to approximately 150 ppb-hr in humid conditions and a measurement accuracy of +/-20%. The CPHS2 sensors are currently undergoing tests at the TVDL. The TVDL has the unique ability to generate calibrated sample vapor streams of N2H4 and UDMH over a range from less than 10 ppb to thousands of parts per million (ppm) with full environmental control of humidity (0 to 90%) and temperature (0 to 50 C). The polymer-based sensors will be subjected to extensive testing over a wide range of humidities at N2H4 and UDMH concentrations of 12.7 an 10.6 ppb respectively. Author

N95-28310* National Aeronautics and Space Administration. John F. Kennedy Space Center, Cocoa Beach, FL.
PROTOTYPE DEVELOPMENT AND TEST RESULTS OF A CONTINUOUS AMBIENT AIR MONITORING SYSTEM FOR HYDRAZINE AT THE 110 ppb LEVEL **c45**
Dale E. Lueck, Barry Meneghelli (I-NET, Inc., Cocoa Beach, FL.), Clyde Parrish (I-NET, Inc., Cocoa Beach, FL.), and Ron Barile (I-NET, Inc., Cocoa Beach, FL.) *In* Johns Hopkins Univ., The 1994 JANNAF Safety and Environmental Protection Subcommittee Meeting, Volume 1 Aug. 1994 p 157-166 (For primary document see N95-28294 09-20)
(Contract NAS10-11943)
Avail: CPIA, 10630 Little Patuxent Pkwy., Suite 202, Columbia, MD 21044-3200 HC

A Hydrazine Vapor Area Monitor (HVAM) system is currently being field tested as a detector for the presence of hydrazine in ambient air. The MDA/Polymetron Hydrazine Analyzer has been incorporated within the HVAM system as the core detector. This analyzer is a three-electrode liquid analyzer typically used in boiler feed water applications. The HVAM system incorporates a dual-phase sample collection/transport method which simultaneously pulls ambient air samples containing hydrazine and a very dilute sulfuric acid solution (0.0001 M) down a length of 1/4 inch outside diameter (OD) tubing from a remote site to the analyzer. The hydrazine-laden dilute acid stream is separated from the air and the pH is adjusted by addition of a dilute caustic solution to a pH greater than 10.2 prior to analysis. Both the dilute acid and caustic used by the HVAM are continuously generated during system operation on an 'as needed' basis by mixing a metered amount of concentrated acid/base with dilution water. All of the waste water generated by the analyzer is purified for reuse by Barnstead ion-exchange cartridges so that the entire system minimizes the generation of waste materials. The pumping of all liquid streams and mixing of the caustic solution and dilution water with the incoming sample are done by a single pump motor fitted with the appropriate mix of peristaltic pump heads. The signal to noise (S/N) ratio of the analyzer has been enhanced by adding a stirrer in the MDA liquid cell to provide mixing normally generated by the high liquid flow rate designed by the manufacturer. An onboard microprocessor continuously monitors liquid levels, sample vacuum, and liquid leak sensors, as well as handles communications and other system functions (such as shut down should system malfunctions or errors occur). The overall system response of the HVAM can be automatically checked at regular intervals by measuring the analyzer response to a metered amount of calibration standard injected into the dilute acid stream. Author (revised)

N95-28311* Naval Research Lab., Washington, DC.
THE SENSITIVE DETECTION OF HYDRAZINE USING CHEMILUMINESCENCE **c25**
G. E. Collins and S. L. Rose-Pehrsson *In* Johns Hopkins Univ., The 1994 JANNAF Safety and Environmental Protection Subcommittee Meeting, Volume 1 Aug. 1994 p 167-176 (For primary document see N95-28294 09-20)
(NASA Order CC-82360-A)
Avail: CPIA, 10630 Little Patuxent Pkwy., Suite 202, Columbia, MD 21044-3200 HC

A novel, chemiluminescent detector for hydrazine vapor, N2H4, is described, capable of monitoring subparts-per-billion levels of hydrazine in air. The catalytic oxidation of hydrazine by colloidal platinum forms an intermediate, oxidizing agent (e.g. OH or O2) which subsequently oxidizes luminol, generating a chemiluminescence signal that is proportional to the hydrazine concentration. The major components of the instrument itself are a photomultiplier tube (PMT), a short length of glass tubing coiled directly in front of the PMT surface, a vacuum pump for sampling the air, and a peristaltic pump for circulating the liquid reagent. The liquid reagent is comprised of a basic solution (pH = 13) of luminol and colloidal platinum which is continuously recycled in front of the PMT. The chemiluminescent reaction is initiated by pumping the hydrazine vapor down a short length of teflon tubing that is concurrently transporting the liquid reagent. The liquid is collected in a modified glass bubbler and quickly sent to the PMT for detection. Studies have included the effect of pH, luminol and platinum concentrations, and air and liquid flow rates on the analytical characteristics of this system. A linear dynamic range for hydrazine has been obtained from 10 to 2000 ppb in air, with a response that is fully reversible and achieves plateau response in less than 2 minutes. Investigations have included the incorporation of these chemiluminescent reagents within thin, polymeric films in order to further simplify the instrumentation requirements for a hydrazine detection system. A solid phase, chemiluminescent detector operates by placing the solid film directly in front of the PMT surface, and using a vacuum pump to draw the hydrazine vapor across the surface of the film. Polymers exhibiting different chemical character have been utilized as an additional parameter for defining the selectivity of these devices. Author

N95-28312* National Aeronautics and Space Administration. John F. Kennedy Space Center, Cocoa Beach, FL.
A NEW METHOD FOR MEASURING HYPERGOL SCRUBBER EMISSIONS **c25**
Dale E. Lueck, Rebecca C. Young, Ron Barile (I-NET, Inc., Cocoa Beach, FL.), Clyde Parrish (I-NET, Inc., Cocoa Beach, FL.), and Dan Curran (I-NET, Inc., Cocoa Beach, FL.) *In* Johns Hopkins Univ., The 1994 JANNAF Safety and Environmental Protection Subcommittee Meeting, Volume 1 Aug. 1994 p 177-186 (For primary document see N95-28294 09-20)
(Contract NAS10-11943)
Avail: CPIA, 10630 Little Patuxent Pkwy., Suite 202, Columbia, MD 21044-3200 HC

Hypergolic propellants are used in spacecraft such as Space Shuttle, Titan, and others launched at Kennedy Space Center (KSC) and Cape Canaveral Air Force Station (CCAFS). Fueling and deservicing spacecraft constitute the bulk of operations in which environmental emissions occur. Monomethylhydrazine (MMH), nitrogen tetroxide (N2O4), and hydrazine (N2H4) are the main propellants of concern Federal and State regulations require that KSC and CCAFS measure the amount of hypergols released to the environment. However, existing stack monitoring procedures are not applicable to hypergol operations that are intermittent and forced through the scrubber by inert gases, either nitrogen or helium. NASA and I-NET Space Services developed and validated a method to measure the emissions of toxic vapors under conditions where measurement of the total flow rate through a scrubber is difficult if not impossible to determine. This method is based on: (1) accurate measurements of the scrubber efficiency (EFF) for each type of operation; (2) an estimate of the number of operations and their contributions to the total annual flow through the scrubber; and (3) a measure of the concentration change of toxic vapors trapped by or reacted with reagents in the scrubber liquor. The concentration change of the component of interest in the scrubber liquor before and after an operation can be used to calculate the emissions. For example, the increase of hypergol in the scrubber solution was used to calculate the amount of hypergol that passed through the scrubber: Emissions (wt.) = ((1/EFF) - 1) x change in (wt. of hypergol). Emissions based on the scrubber liquor compared closely with emissions measured under controlled conditions where gas concentrations and total flow rate were known. A special sample system was constructed at the Toxic Vapor Detection Laboratory (TVDL) of KSC to measure hypergolic fuel or oxidizer in sample gas entering and exiting the test scrubber. The sample system was enclosed in a purged cart, except for tubing and valve electrical service leading to the sample ports and for sample valves positioned at the sample ports. This permitted operation of the sampling system during hazardous operations. This system and the data collected to validate the system are presented. Author

N95-28313 Naval Air Warfare Center, China Lake, CA. Weapons Div.
A CONTINUOUS EMISSIONS MONITOR FOR AIRBORNE METALS **c45**
Michael D. Seltzer *In* Johns Hopkins Univ., The 1994 JANNAF Safety and Environmental Protection Subcommittee Meeting, Volume 1 Aug. 1994 p 187-194 (For primary document see N95-28294 09-20)
Avail: CPIA, 10630 Little Patuxent Pkwy., Suite 202, Columbia, MD 21044-3200 HC

Instrumentation, capable of continuous emissions monitoring of airborne metals, was recently tested in conjunction with the evaluation of an experimental incinerator used for the demilitarization of pyrotechnic materials. A sample air stream was continuously transported from the incinerator stack to a computer-controlled inductively coupled plasma spectrometer to allow real-time detection of entrained airborne metals by atomic emission spectrometry. Realtime detection of hazardous air pollutants offers several advantages over slower, more conventional techniques including the potential for active process control efforts aimed at ensuring environmental compliance. Details of instrument design, calibration, sample transport, and results of preliminary field testing are presented. Author

N95-28314 Army Research Lab., Aberdeen Proving Ground, MD.
A NOVEL SENSITIVE DETECTOR OF ATMOSPHERIC NITROCOMPOUNDS BASED ON LASER PHOTOFRAGMENTATION/IONIZATION SPECTROMETRY **c25**
Rosario C. Sausa, Josef B. Simeonsson, and George W. Lemire *In* Johns Hopkins Univ., The 1994 JANNAF Safety and Environmental Protection Subcommittee Meeting, Volume 1 Aug. 1994 p 205-214 (For primary document see N95-28294 09-20)
Avail: CPIA, 10630 Little Patuxent Pkwy., Suite 202, Columbia, MD 21044-3200 HC

The sensitive detection and monitoring of trace atmospheric vapors of energetic materials presents an important technical challenge for the defense of our troops as well as for aviation security, forensics, and demilitarization safety applications. In this paper, we report a new method for detecting trace atmospheric vapors of NO2-containing compounds using one color laser photofragmentation/fragment ionization spectrometry. An ArF laser is employed to both photolytically fragment the target molecules and ionize the characteristic NO fragments. The production of NO is hypothesized to result from a combination of two NO2 unimolecular fragmentation pathways, one yielding NO in its (Chi(2)2) electronic ground state and the other in its Alpha(2)Sigma(+) excited state. Ionization of ground state NO molecules is accomplished by resonance-enhanced multiphoton ionization processes via their Alpha(2)Sigma(+) from Chi(2)2 (3,0), Beta(2)2 from Chi(2)2 (7,0) and/or Delta(2)Sigma(+) from Chi(2)2 (0,1) bands at 193 nm. The analytical utility of this method is demonstrated in a molecular beam time-of-flight apparatus. Limits of detection range from the parts-per-million (ppm) to parts-per-billion (ppb) level for NO, NO2, CH3NO2, dimethylnitramine (DMNA), ortho- and meta-nitrotoluene, nitrobenzene, and trinitrotoluene (TNT). Under effusive beam experimental conditions, discrimination between structural isomers, ortho-nitrotoluene and meta-nitrotoluene, has been demonstrated with the use of their characteristic photofragmentation/photoionization mass spectra. This technique is also useful for the detection and monitoring of environmental NO(x) pollutants for pollution prevention, compliance, and cleanup. Author

N95-28315 Hercules Aerospace Co., Magna, UT.
HAZARDS ANALYSIS OF AN INTEGRAL CLASS 1.1/1.3 ROCKET MOTOR DEMILITARIZATION AND INGREDIENT RECOVERY SYSTEM USING AMMONIA **c28**
Philip M. Stevens, M. H. Reed, L. A. Losee, K. A. Hendrickson, and D. H. Mitchell *In* Johns Hopkins Univ., The 1994 JANNAF Safety and Environmental Protection Subcommittee Meeting, Volume 1 Aug. 1994 p 227-238 (For primary document see N95-28294 09-20)
Avail: CPIA, 10630 Little Patuxent Pkwy., Suite 202, Columbia, MD 21044-3200 HC

The Department of Defense has a technical requirement to develop alternative technologies to dispose of large numbers of solid propellant rocket motors while minimizing environmental impact. Research efforts conducted at the bench-scale have demonstrated the U.S. Army Missile Command (MICOM) near-critical fluid technology as a viable method of demilitarizing solid rocket motors. This method has been successfully used to recover valuable ingredients, such as cyclotetramethylene tetranitramine (HMX), cyclotrimethylene trinitramine (RDX), ammonium perchlorate (AP), and aluminum (Al)/binder crumb from tactical and strategic Class 1.1 and 1.3 solid propellants. This process utilizes liquid anhydrous ammonia for ingredient extraction and recovery. Under an Army-sponsored effort, Hercules Aerospace Company and Rust International have been awarded a contract to design and construct a pilot plant demilitarization test facility and to demonstrate this technology on Class 1.1 and 1.3 solid propellant tactical rocket motors. This report describes the hazards analysis efforts which have been ongoing since the start of the program. Hazards testing has characterized the sensitivity of propellants, process streams, and extracted materials. Hazards analysis techniques, such as logic diagrams, and failure modes and effects analysis (FMEA), have identified credible hazards in the equipment design and pilot plant operations. These potential hazards have been tracked by a closed loop system and have been mitigated by design features or operating controls. Major hazards identified will be discussed along with methods for mitigation. Also feedback from initial pilot plant operations will be reported to the extent that information is available. Author

N95-28316 Martin Marietta Corp., San Diego, CA.
DEVELOPMENT AND IMPLEMENTATION OF A SYSTEM SAFETY PROGRAM FOR THE SPACE LAUNCH COMPLEX 3 EAST (SLC-3E) GROUND SUPPORT SYSTEM PROJECT TO SUPPORT ATLAS 2 FAMILY OF SPACE LAUNCH VEHICLES **c81**
S. Iyengar and M. McCombs (Air Force Systems Command, Vandenberg AFB, CA.) *In* Johns Hopkins Univ., The 1994 JANNAF Safety and Environmental Protection Subcommittee Meeting, Volume 1 Aug. 1994

p 239-249 (For primary document see N95-28294 09-20)
(Contract F04701-92-C-0019)
Avail: CPIA, 10630 Little Patuxent Pkwy., Suite 202, Columbia, MD 21044-3200 HC

This paper describes the development and implementation of a system safety program for the design, construction, test and validation of ground support systems for Atlas 2 rocket launching capability at Vandenberg Air Force Base. The SLC-3E project System Safety Program is based on MIL-STD-882B, specifically tailored for the upgrade. The program has tasks to cover the management and technical aspects of a System Safety Program. Management tasks include assurance of a good organization with qualified personnel and periodic reviews, and technical tasks include hazard analyses at both system and subsystem levels. One key aspect to the program was providing specific system safety training to system design engineers. As a result, with system safety engineers actively participating in product development teams, many safety issues were recognized by design engineers and resolved in the concept and preliminary design phases. In summary, this paper describes the management and technical tasks involved, several examples of building safety into design, examples of hazard mitigation by a disciplined analysis approach and risk acceptance process to assure safety consideration in all aspects of the project, and minimization of residual hazards in a complex construction project of this nature. Author

N95-28317 GPS Technologies, Inc., Tampa, FL.

PRESSURE VESSEL BURST TEST STUDY Progress Report **c39**

Maurice R. Cain and Robert J. Hall *In* Johns Hopkins Univ., The 1994 JANNAF Safety and Environmental Protection Subcommittee Meeting, Volume 1 Aug. 1994 p 267-283 (For primary document see N95-28294 09-20)
(Contract F08650-93-C-0066)
Avail: CPIA, 10630 Little Patuxent Pkwy., Suite 202, Columbia, MD 21044-3200 HC

A progress report is provided on a program developed to study through test and analysis, the characteristics of blast waves and fragmentation generated by ruptured gas filled pressure vessels. Prior papers on this USAF/NASA program have been presented to AIAA, to JANNAF, to the NASA Pressure Systems Seminar and to a DOD Explosives Safety Board subcommittee meeting. One Vessel has been burst with water pressure and eighteen with pneumatic pressure. All of the planned testing has been completed with the last test series having been completed in November 1993. The tests were designed to have a predetermined burst geometry and pressure level to study burst characteristics in an instrumented arena. Data trends for experiments are presented. The paper presents results from the last test series which were not available earlier and compares all the pneumatic burst test results. Author

N95-28318 Aerospace Medical Research Labs., Wright-Patterson AFB, OH. Toxicology Div.

ACUTE AND SUBACUTE TOXICITY OF AMMONIUM DINITRAMIDE (ADN) **c52**

D. R. Tocco, S. A. Salins (ManTech Environmental Technology, Inc., Wright-Patterson AFB, OH.), R. E. Wolfe (ManTech Environmental Technology, Inc., Wright-Patterson AFB, OH.), and E. R. Kinkead (ManTech Environmental Technology, Inc., Wright-Patterson AFB, OH.) *In* Johns Hopkins Univ., The 1994 JANNAF Safety and Environmental Protection Subcommittee Meeting, Volume 1 Aug. 1994 p 331-334 (For primary document see N95-28294 09-20)
(Contract F33615-90-C-0532)
Avail: CPIA, 10630 Little Patuxent Pkwy., Suite 202, Columbia, MD 21044-3200 HC

Ammonium Dinitramide (ADN) is currently being considered to replace ammonium perchlorate by the Department of Defense. The chemical will be used in solid rocket engine propellant mixtures as well as a high explosive. No acute or chronic toxicity data is currently available for ADN, however field reports from exposed personnel indicate that the chemical is readily absorbed by the skin, resulting in numbness of the fingers. Because the most significant exposure route expected for ADN would be dermal exposure or possibly accidental ingestion, acute oral and dermal toxicity tests were conducted. In preparation for a reproductive screen on ADN, stability and palatability studies were also conducted. Oral administration of ADN at 5g/kg body weight (EPA limit dose) produced convulsions and rapid death in all treated rats. Subsequent studies indicated an acute LD(sub 50) in F-344 rats of 823 mg/kg. Dermal application of 2g/kg (EPA limit dose) produced no toxic signs in rabbits. Administration of either 12, 25, 50, or 100 mg ADN/ml drinking water on a continuous basis for 2 weeks to male and females SD rats produced no apparent effect on body weight gains, water consumption, organ weights, hemoglobin concentration, or methemoglobin formation. A reproductive toxicity screen of ADN in drinking water is currently in progress. Author

N95-28319 Walter Reed Army Inst. of Research, Wright-Patterson AFB, OH.

TOXICITY ASSESSMENT OF LIQUID PROPELLANT XM46 **c52**

Daniel J. Caldwell *In* Johns Hopkins Univ., The 1994 JANNAF Safety and Environmental Protection Subcommittee Meeting, Volume 1 Aug. 1994 p 335-342 (For primary document see N95-28294 09-20)
Avail: CPIA, 10630 Little Patuxent Pkwy., Suite 202, Columbia, MD 21044-3200 HC

Liquid propellant XM46 is a developmental propellant that will be used with the regenerative injection gun in the Advanced Field Artillery System. The components of XM46 are both strongly reducing and oxidizing agents, are corrosive, and possess strong nitrating characteristics. XM46 is moderately toxic; the primary systemic effects are the production of methemoglobin, altered liver function, and enlargement of the spleen and liver. XM46 also produces skin irritation, is a strong eye irritant, and causes skin sensitization in guinea pigs but not humans. Aerosolized XM46 produces respiratory irritation. Genotoxicity evaluations of XM46 were negative. Since the Army recently opened to women many previously male-only occupational specialties, women now face potential accidental exposure to XM46 during both operational and maintenance procedures. XM46 was evaluated to determine its potential to produce reproductive toxicity, such as alterations in paternal fertility, maternal pregnancy and lactation, and growth and development of offspring. Sprague-Dawley rats were dosed with 200, 1000, or 2000 mg XM46 per liter of drinking water (target dose of 12, 60, and 120 mg of XM46 per kg body weight per day, i.e., mg/kg/day) for 14 days prior to mating, during gestation, postpartum (21 days), and for four weeks postweaning for a total of 90 days. Pups were maintained on treated water for four weeks postweaning. Although there were dose related effects in parental animals, there were no treatment related adverse reproductive effects (mating, fertility index, length of gestation, sex ratio, gestation index, or mean number of offspring per litter) compared to control (i.e., non-treated) animals. Mean pup weights showed no statistically significant differences between treated and control groups. In a mouse dominant lethal assay, XM46 was shown not to have dominant lethal effects on fertility or reproduction at doses of 100, 200, and 400 mg/kg/day compared to control animals. A teratology study was undertaken to determine if XM46 causes birth defects in the developing fetus. Animals were treated with XM46 at doses of 162.5, 325, and 650 mg/kg/day during the major period of organogenesis to determine if developmental variations and malformations were produced in offspring. The incidence of fetal death (number of dead fetuses plus the number of resorptions) was not significantly different between dose groups. The number of live fetuses per litter was not significantly different between dose groups. No evidence of fetal toxicity related to XM46 exposure was noted in any of the dose groups. Based on these data it is concluded that XM46 is not a reproductive toxicant or teratogen in the rat. Author

N95-28320 Wulfman (D. S.) and Associates, Inc., Rolla, MO.

COMMERCIAL REFORMULATION: AN ECONOMIC AND ENVIRONMENTALLY NEUTRAL MEANS OF MANAGING EXPLOSIVES AND SOLID PROPELLANTS **c28**

David S. Wulfman, Oliver C. Sitton (Technology Development, Inc., Rolla, MO.), Paul Worsey (Missouri Univ., Rolla, MO.), Mike Johnson (Naval Surface Warfare Center, Crane, IN.), and Dan Burch (Naval Surface Warfare Center, Crane, IN.) *In* Johns Hopkins Univ., The 1994 JANNAF Safety and Environmental Protection Subcommittee Meeting, Volume 1 Aug. 1994 p 343-349 (For primary document see N95-28294 09-20)
Avail: CPIA, 10630 Little Patuxent Pkwy., Suite 202, Columbia, MD 21044-3200 HC

The reformulation of military explosives and solid propellants into commercial explosives offers a unique solution to the problem of disposing of high energy materials with essentially zero environmental impact at a low cost and with a salable product. Studies using the insensitive PBX, PBXN-4 have been completed through the pilot plant stage and have been successfully tested as a mining explosive. A number of other military explosives have been examined and their VOD's (velocity on detonation) and heats of explosions determined and in some instances tested in 'field' operations. The equipment and unit operations required for reformulation are simple and inexpensive. The total market potential is far larger than the available supply of PBX's and other military explosives. The extension of the reformulation approach to 1.1 solid rocket propellants is in progress. Initial studies indicate that the method is viable. The quantities involved have the potential of impacting less than 1% of the very large US explosives market. The products available from reformulation are in part a function of the means of removal of the 1.1 propellants from the cases. With dry methods, a range of products from 'super' blasting gelatins to materials comparable to ANFO are available in the form of dry or slurried explosives. With wet methods, the range is narrower with VOD's of approximately 4 km/sec and heats of explosion of approximately 1000 cal/g at a density of 1.25 g/cc being easily attainable in the form of slurries. With both HE and 1.1 propellant streams it is possible to tailor the power of the resultant explosives to reach a desired set of properties. This permits the handling of a variable stream of redundant materials and the furnishing of a 'constant' product to the customer. The technology involved has essentially no waste stream and very closely meets the goals of the US Resource Conservation and Recovery Act (RCRA). Author

N95-28321 Universal Tech Corp., Riverton, KS.

ALTERNATE USE OF ROCKET PROPELLANTS AS INGREDIENTS IN COMMERCIAL WATERGEL EXPLOSIVES c28

J. Brent Gilion, Gary Eck, O. Machacek (Universal Tech Corp., Dallas, TX.), R. Perry (United Technologies Corp., San Jose, CA.), A. McKenzie (United Technologies Corp., San Jose, CA.), and L. Morgan (United Technologies Corp., San Jose, CA.) *In* Johns Hopkins Univ., The 1994 JANNAF Safety and Environmental Protection Subcommittee Meeting, Volume 1 Aug. 1994 p 351-360 (For primary document see N95-28294 09-20)

Avail: CPIA, 10630 Little Patuxent Pkwy., Suite 202, Columbia, MD 21044-3200 HC

The research presented herein is the result of efforts under subcontract to United Technologies Chemical Systems Division San Jose, California. The efforts were focused on investigating the feasibility of using excess rocket propellants from both production processes and demilitarization processes as ingredients in commercial explosives. Both Class 1.3 and Class 1.1 propellants were evaluated. As a result of the tests presented herein, a Propellant Evaluation Model (PEM) was developed which will provide guidelines for future work in the same area. According to the United States Department of the Interior, Bureau of Mines, the United States uses over 2 million metric tons (4 billion pounds) of commercial explosives per year. Of this quantity, approximately 600 million pounds are used which would provide the most feasible avenue for the inclusion/incorporation of solid rocket propellants. The possibility of using these rocket propellants in even a small portion of the commercial explosives which are used presents a significant outlet. This paper discusses the findings of research in which several Large Rocket Motor Propellants were evaluated for use as ingredients in commercial explosive formulations. Aspects such as chemical compatibility, processing safety, and final product performance were investigated. Explosive characteristics such as detonation velocity, critical diameter, and energy release were also measured. It was concluded that the use of each of the propellants which were evaluated would be beneficial in several areas. The propellant/commercial explosive blended products exhibited significantly enhanced explosive characteristics over those of the standard formulations. The alternate use of the propellants would give them a 'useful product' status and remove them from a 'hazardous material' status. Finally, this alternate use could be accomplished in an economical method which would allow for significant cost avoidance over less desirable methods of disposal of these materials. The alternate use approach discussed should not be seen as a disposal technology. It is a resource recycling approach which can be done economically, safely, and in an environmentally sound manner. Author

N95-28322 Missouri Univ., Rolla, MO. Toxicology Div.

THE DEMILITARIZATION OF CLASS 1.1 ROCKET MOTORS USING HIGH PRESSURE WATERJETS c28

Oliver Sitton, Paul N. Worsey, David Summers, Karla Bier, Dan Burch (Naval Surface Warfare Center, Crane, IN.), and Mike Johnson (Naval Surface Warfare Center, Crane, IN.) *In* Johns Hopkins Univ., The 1994 JANNAF Safety and Environmental Protection Subcommittee Meeting, Volume 1 Aug. 1994 p 371-379 (For primary document see N95-28294 09-20)

Avail: CPIA, 10630 Little Patuxent Pkwy., Suite 202, Columbia, MD 21044-3200 HC

The Naval Surface Warfare Center, Crane Division (NAVSURFWARCENDIV) has been tasked by the Joint Service Large Rocket Motor Disposal Program to develop high pressure waterjet technology to remove Class 1.1 propellant from large rocket motors. A contract was awarded to the Rock Mechanics and Explosives Research Center (RMERC) at the University of Missouri-Rolla (UMR) to validate the safety of the washout operation and demonstrate the capability to effectively washout the propellant and treat the process streams. The ultimate goal of the project is to recover the propellant for use as commercial blasting agents. RMERC, in support of the Navy, had demonstrated in the past the applicability of using high pressure waterjets to demilitarize PBX warheads. The washout of Class 1.1 propellants containing nitroglycerine (NG) and ammonium perchlorate (AP) has raised safety concerns regarding the sensitivity of the propellant to washout impact pressures and the treatment of the process streams. A systematic approach was developed by NAVSURFWARCENDIV Crane and RMERC to demonstrate the viability of the high pressure waterjet technology: the determination of waterjet impact sensitivity, cutting parameterization, process streams characterization, NG safety assessment, subscale motor washout and process streams treatment. Testing conducted to date on samples of five different Class 1.1 propellants from Navy, Air Force and Army missiles showed that all of the propellants can be effectively removed at a waterjet pressure of 69 MPa (10,000 psi) with a minimum safety factor of 16. The analysis of liquid samples from parameterization show that the water is not saturated in NG for each of the propellants. AP, Resorcinol and NG showed the highest solubilization into the water phase. Work is on-going in assessing potential technologies for the treatment of the NG/AP containing streams. RMERC is currently washing out subscale motors utilizing their Waterjet Ordnance and Munition Blastcleaner with Automated Tellurometry (WOMBAT) which is located in an underground facility and remotely operated by computer control. Author

N95-28323 TPL, Inc., Albuquerque, NM.

A COMPREHENSIVE ENERGETIC MATERIALS RESOURCE RECOVERY AND RECYCLING PROGRAM c28

H. M. Stoller, T. J. Schilling, and Dan Burch (Naval Surface Warfare Center, Crane, IN.) *In* Johns Hopkins Univ., The 1994 JANNAF Safety and Environmental Protection Subcommittee Meeting, Volume 1 Aug. 1994 p 381-387 (For primary document see N95-28294 09-20)

Avail: CPIA, 10630 Little Patuxent Pkwy., Suite 202, Columbia, MD 21044-3200 HC

TPL is conducting a comprehensive program in energetic materials resource recovery and recycling (R3), developing environmentally acceptable reprocessing methods, and formulating the recycled materials into high valued commercial products. Energetic materials investigated include: plastic-bonded and conventional explosives, nitrocellulose (NC)-based propellants, Hazard Class 1.1 an 1.3 propellants, pyrotechnics, and primers. The majority of this work has been conducted as part of the Ordnance Reclamation Program of the Naval Sea Systems Command. Implementation of aspects of the developed technologies into operational status has been achieved through participation in the AMCCOM Conventional Ammunition (Small Arms) Resource Recovery Program and technology development support has also been provided through the U.S. Army's Demilitarization R&D Program as well as IRAD funds. TPL's experiences in the R3 of three classes of energetic materials are summarized. Author (revised)

N95-28324 General Atomics Co., San Diego, CA.

CRYOGENIC WASHOUT OF SOLID ROCKET PROPELLANTS c28

J. P. Elliott, W. P. Creedon, M. H. Spritzer, J. A. Hurley (Air Force Systems Command, Tyndall AFB, FL.), and S. A. Rising (Air Force Systems Command, Tyndall AFB, FL.) *In* Johns Hopkins Univ., The 1994 JANNAF Safety and Environmental Protection Subcommittee Meeting, Volume 1 Aug. 1994 p 397-406 (For primary document see N95-28294 09-20)
(Contracts F08635-91-C-0179; F08635-92-C-0075)

Avail: CPIA, 10630 Little Patuxent Pkwy., Suite 202, Columbia, MD 21044-3200 HC

Cryogenic washout (U.S. Patent No. 5025632) is a process using liquid nitrogen (LN2) as a washout medium to remove the propellant from within solid rocket motors. The process produces dry, size reduced particles which are well suited for disposal or for reuse in applications such as commercial explosives. A prototype cryogenic washout facility is being readied for testing on Minuteman II Stage III motors, under contract to the U.S. Air Force. Design support testing for the facility has been completed, and an overview of test results is presented. Design support testing included laboratory and bench-scale testing on Hazard Class 1.1 and 1.3 propellants. The laboratory tests established that essentially no change in the sensitivity of the test propellants occurred between ambient and cryogenic temperatures. Recent bench scale testing utilized LN2 pressures of up to 117 MPa (17,000 psi) and flow rates up to 6.4 X 10(exp -4) cu m/s (12 gpm) to demonstrate cryogenic washout rates of up to 0.1 kg/s (765 lb/hr) for Class 1.1 propellant. This represents a 'removal efficiency' of 0.17 kg propellant per kg LN2. Further improvements in propellant removal rate and efficiency are expected during prototype testing in 1994. The prototype equipment design is described with emphasis on engineered safeguards. Challenging operating environments include cryogenic temperatures and high pressures. Author

N95-28325 General Atomics Co., San Diego, CA.
HYDROTHERMAL OXIDATION OF SOLID ROCKET PROPELLANT AND OTHER DEPARTMENT OF DEFENSE HAZARDOUS WASTES c28
D. A. Hazlebeck, K. W. Downey, D. D. Jensen, M. H. Spritzer, J. P. Elliott, J. A. Hurley (Air Force Systems Command, Tyndall AFB, FL.), and S. A. Rising (Air Force Systems Command, Tyndall AFB, FL.) *In* Johns Hopkins Univ., The 1994 JANNAF Safety and Environmental Protection Subcommittee Meeting, Volume 1 Aug. 1994 p 407-414 (For primary document see N95-28294 09-20)
Avail: CPIA, 10630 Little Patuxent Pkwy., Suite 202, Columbia, MD 21044-3200 HC

Hydrothermal oxidation (HTO), also referred to as supercritical water oxidation, is an emerging technology for the destruction of hazardous and nonhazardous wastes. HTO destroys combustible materials using an oxidation in water process at temperatures in the range of 350 C (662 F) to 600 C (1112 F) and pressures of 17 MPa (2500 psi) or greater. Relative to incineration, HTO offers the advantages of lower temperature oxidation, compact reactor design, enhanced process stability, low NO(x) and SO(x) production, and complete containment of all effluents. Oxidation is accomplished under near-homogenous, single-phase conditions which provide excellent mixing and high mass and heat transfer rates. High destruction efficiencies are achieved in relatively small reactor volumes. Oxidation is performed in a completely enclosed system, permitting full containment of all process effluents prior to subsequent analysis and release. Relative to other non-incineration technologies (e.g., wet air oxidation), HTO offers the advantage of conversion of hazardous waste to environmentally benign products in a single process without the need for follow-on treatment or processing. The results of two ongoing research and demonstration programs conducted by General Atomics (GA) and its subcontractors for the application of HTO to DOD waste problems are updated. Both programs call for design, construction, and testing of prototype plants with throughputs of 0.026 l/s to 0.066 l/s (600 to 1500 gal/day). The first program, performed for the U.S. Air Force involves the treatment of a Hazard Class 1.1 solid propellant removed from rocket motor casings. The second program, performed for the Advanced Research Projects Agency (ARPA), involves the treatment of solid propellants as well as chemical agents and other DOD wastes. Author

N95-28326 Army Missile Research and Development Command, Redstone Arsenal, AL. Propulsion Directorate.
RECOVERY AND REUSE OF ROCKET MOTOR PROPELLANT INGREDIENTS c28
William S. Melvin and Jeffery S. Wright *In* Johns Hopkins Univ., The 1994 JANNAF Safety and Environmental Protection Subcommittee Meeting, Volume 1 Aug. 1994 p 427-435 (For primary document see N95-28294 09-20)
Avail: CPIA, 10630 Little Patuxent Pkwy., Suite 202, Columbia, MD 21044-3200 HC

The Department of Defense (DOD) has a technical requirement to develop alternative, rocket motor demilitarization technologies which are environmentally safe and affordable. Environmental regulations now require industry and government agencies to conserve resources, when technically feasible, through the reclamation and reuse of commodities that otherwise would be incinerated or destroyed. The technical capability to recover and reclaim valuable ingredients and hardware components from both class 1.1 and 1.3 solid rocket motors has been demonstrated. This Army developed technology is being scaled for demonstration in an integrated, rocket motor demilitarization pilot plant that is nearing construction completion. Reclaimed RDX is being evaluated for potential commercial and military reuse. The U.S. Army TOW-2 flight motor was used for demonstrating the recovery of RDX for reuse/recycle in a commercial mining cast booster. Standard one pound cast boosters were manufactured by Austin Powder Company using the reclaimed RDX and compared to a standard 'Orange Cap' Composition-B, commercial mining booster. Booster tests were conducted by Austin Powder Company and the U.S. Bureau of Mines. Detonation velocity, borehole field validation, and hazards characterization testing were performed. Test results confirm that the reclaimed/recycled RDX cast booster was virtually identical to the commercial product. Author

N95-27355*# Manhattan Coll., New York, NY. Dept. of Mechanical Engineering.
RTE: A COMPUTER CODE FOR ROCKET THERMAL EVALUATION
Mohammad H. N. Naraghi *In* NASA. Lewis Research Center, The Sixth Annual Thermal and Fluids Analysis Workshop Jan. 1995 p 141-162 (For primary document see N95-27345 09-34)
Avail: CASI HC A03/MF A03

23 CHEMISTRY AND MATERIALS (GENERAL)

N95-26391*# Boeing Defense and Space Group, Seattle, WA.
LONG DURATION EXPOSURE FACILITY MINI-DATA BASE USER'S GUIDE: MACINTOSH VERSION (Diskette)
Gail Bohnhoff-Hlavacek, H. Gary Pippin, and Harry W. Dursch Hampton, VA NASA Apr. 1995 29 p Diskette: 3.5-inch Mac diskette
(Contracts NAS1-18224; NAS1-19247; RTOP 506-43-61-01; RTOP 233-03-02-04)
(NASA-CR-4656; NAS 1.26:4656; NONP-NASA-DK-95-48683) Avail: CASI SET A09 (HC,DK)

One of the objectives of the LDEF Special Investigation Group (SIG) was to develop a LDEF data base that identifies the experiment objectives and hardware flown, summarizes results and conclusions, and provides a system analysis overview, including spacecraft design guidelines and space environmental effects. Compiling the information into an easily accessible data base format, and making it available to the space community was a major task accomplished by the System and Materials SIG effort beginning in 1891. Included in this document is a short user's manual for the LDEF Mini-Data Bases. The user's manual contains pertinent examples from the data base on specifically how to access and work with the LDEF information. Accompanying this document are the mini-data bases on disk. Author

N95-26434 Logicon R and D Associates, Albuquerque, NM.
EXTENDED EQUATION-OF-STATE FOR DICHLORODIFLUOROMETHANE (CCl2F2) Technical Report, 10 Feb. 1992 - 21 May 1993
Alan I. Lampson, Peter G. Crowell, and Gary P. Ganong 1 Dec. 1994 66 p Limited Reproducibility: More than 20% of this document may be affected by microfiche quality
(Contract DNA001-93-C-0138)
(AD-A288885; DNA-TR-94-25) Avail: Issuing Activity (Defense Technical Information Center (DTIC))

A new equation-of-state for decomposed CCl2F2 (dichlorodifluoromethane) has been developed. This new equation-of-state is based upon equilibrium composition calculations of the components and possible products of CCl2F2 and utilizes tables of thermochemical properties for each of the gas species. Since the thermochemical property tables had an upper temperature limit of 6000 K, these tables first had to be extended to cover the temperature range of interest. The new equation-of-state covers the pressure range of 0.1 to 100,000 bar and the temperature range from 200 to 30,000 K, and with certain limitations, up to 500,000 K. The methods used to extend the thermochemical tables and to determine the equilibrium gas composition are described. DTIC

N95-26567 PD-LD, Inc., Princeton, NJ.
A NEW GROWTH TECHNOLOGY FOR HIGHLY NON-LINEAR, OPTICAL QUALITY ORGANIC FILMS: ORGANIC VAPOR PHASE DEPOSITION Interim Report, 1 Nov. - 1 Dec. 1994
V. S. Ban 12 Dec. 1994 3 p Limited Reproducibility: More than 20% of this document may be affected by microfiche quality
(Contract N00014-94-C-0168)
(AD-A289006; Rept-0004) Avail: Issuing Activity (Defense Technical Information Center (DTIC))

NMR spectroscopy identified the main impurity in DAST films grown by OVPD method. The impurity is a trimethilated compound described previously. Thus our films consist of over 90% DAST and some 5 to 10% of the above impurity. An apparatus for measuring second harmonic generation properties of OVPD DAST films has been constructed and described. The optimization of growth conditions of the OVPD method is described. DTIC

N95-26569 Minnesota Univ., Minneapolis, MN. Dept. of Chemical Engineering and Materials Science.
ELECTROCRYSTALLIZATION OF AN ORDERED ORGANIC MONOLAYER: SELECTIVE EPITAXIAL GROWTH OF BETA(ET)2I3 ONGRAPHITE Technical Report, 1 May 1994 - 30 Jun. 1995
Andrew C. Miller, Jeffrey B. Maxson, and Michael D. Ward 8 Dec. 1994 20 p Submitted for publication Sponsored by NSF Limited Reproducibility: More than 20% of this document may be affected by microfiche quality
(Contract N00014-93-1-0563)
(AD-A288942; TR-6) Avail: Issuing Activity (Defense Technical Information Center (DTIC))

We report electrochemical and in situ atomic force microscopy observations of the formation of a new class of crystalline organic monolayer, which consists of a conductive organic salt containing bis(ethylenedithiolo)-tetrathiafulvalene (ET), on highly oriented pyrolytic graphite (HOPG). Growth of this monolayer accompanies the electrochemical oxidation of ET in the presence of the I3 (iodine 3) anion at a freshly cleaved HOPG electrode. The monolayer covers large areas of the graphite substrate (greater than 100 square micrometers) and can be removed at potentials cathodic of the ET/ET+ couple. High resolution AFM imaging of the monolayer and a 15.5 angstrom monolayer thickness are consistent with the formation of a single (001) layer of beta-(ET)2I3, with the long axes of the ET molecules oriented nearly perpendicular to the graphite basal plane. The preferential formation of beta(ET)2I3 over other polymorphs is a consequence of favorable epitaxial interactions between the overlayer lattice and that of the graphite substrate, and is manifest in selective growth of bulk beta(ET)2I3 crystals on this electrode surface. These results demonstrate that controlled deposition of conducting mono- and multi-layer films can be achieved in the presence of strong interfacial interactions during nucleation, suggesting a route to the fabrication of electronic devices based upon molecular design principles. DTIC

N95-26570 University of Central Florida, Orlando, FL. Dept. of Electro-Optics and Laser.
NEAR-RESONANT PROPERTIES OF NONLINEAR ORGANIC MATERIALS FOR OPTICAL DEVICES Annual Report, 15 Sep. 1991 - 14 Sep. 1994
George I. Stegeman 14 Sep. 1994 6 p Limited Reproducibility: More than 20% of this document may be affected by microfiche quality
(Grant AF-AFOSR-0331-91)
(AD-A288339; AFOSR-94-0683TR) Avail: Issuing Activity (Defense Technical Information Center (DTIC))

The nonlinear optics of sublimated films of 2-dimensional conjugated planar molecules has been investigated by third harmonic generation. Two were planar phthalocyanines, metal-free and copper substituted, and the third was an asymmetric (non-planar) phthalocyanine (subphthalocyanine), employed as a precursor in the synthesis of certain phtalocyanines. A very rich spectrum has been observed in each case and the analysis is currently underway. In the future this work will be expanded to include other materials. DTIC

N95-26712 Titan Corp., Chatsworth, CA.
MATERIAL MODELING IN THE CRALE CODE. USERS' MANUAL Technical Report, 12 Mar. - 12 Dec. 1993
Shel Schuster 1 Dec. 1994 103 p Limited Reproducibility: More than 20% of this document may be affected by microfiche quality
(Contract DNA001-93-C-0055)
(AD-A288988; TRT-3336-TR-1) Avail: Issuing Activity (Defense Technical Information Center (DTIC))

Finite difference for continuum mechanics codes are capable of providing solutions for the behavior of a wide range of materials under a variety of boundary and initial conditions. The key to obtaining accurate solutions lies in the fidelity of models used to describe the material's response to the strains imposed, i.e., its Equation of State (EOS). This report presents both the general EOS algorithms used in the CRALE 1- and 2D codes and several specific EOS models currently in use. A driver routine that exercises these models over specific load/unload paths is available to assist in developing and checking the parameters needed for materials of interest. A discussion of this driver and a users manual to assist in its use are also presented. In the course of developing EOS models of interest to DNA and as part of the TRT participation in the DNA HYDROPLUS program, a number of data bases have been developed. These include files containing; experimental shock Hugoniots and release paths, parameters for EOS models used in the HYDROPLUS program, and the nuclear shot experimental and calculational data bases developed for HYDROPLUS. A description of the various data bases with instructions for their access is included in this report. DTIC

N95-28154 Pennsylvania Univ., Philadelphia, PA.
COMPUTATIONAL AND MATRIX ISOLATION STUDIES OF (2- AND 3-FURYL)METHYLENE M.S. Thesis
Vincent A. McDermott 1994 126 p Limited Reproducibility: More than 20% of this document may be affected by microfiche quality
(AD-A280085) Avail: Issuing Activity (Defense Technical Information Center (DTIC))

(2- and 3-Furyl)methylene were investigated using both ab initio molecular orbital calculations and matrix isolation spectroscopy. Initial approaches to 2-furylmethylene were via the diazirine precursor. However, its synthesis was never realized. We therefore formed the diazo precursor for both compounds and purified them in preparation for matrix isolation. Ab initio calculations on 2-furylmethylene predict that the o = 0 deg conformer 2.2 to be more stable than the o = 180 deg conformer 2.1 in both the singlet and triplet states. Additionally, the energy barrier for ring fragmentation of the singlet carbene is predicted to be - 2.5 Kcal/mol. For 3-furylmethylene, two different levels of theory predict the opposite ground state multiplicity. DTIC

N95-28334 Minnesota Univ., Minneapolis, MN. Dept. of Chemical Engineering and Materials Science.
SELF-ASSEMBLY OF LOW-DIMENSIONAL MOLECULAR NANOCLUSTERS ON Au(111) SURFACES Technical Report
Joachim Hossick Schott, Christopher M. Yip, and Michael D. Ward 8 Dec. 1994 34 p Revised Submitted for publication Limited Reproducibility: More than 20% of this document may be affected by microfiche quality
(Contract N00014-93-1-0563)
(AD-A288936; TR-7-Rev) Avail: Issuing Activity (Defense Technical Information Center (DTIC))

Two-dimensional nanoclusters of (TTF)(TCNQ) (TTF = tetrathiafulvalene, TCNQ = tetracyanoquinodimethane) and Li(+)TCNQ(-), formed on Au(111) surfaces by vapor phase sublimation under ambient conditions prior to growth of bulk crystals of these low-dimensional organic conductors, have been observed with scanning tunneling microscopy (STM) and scanning electron microscopy (SEM). The molecular planes of the constituents in individual nanoclusters are oriented perpendicular to the Au(111) substrate, while the clusters exhibit azimuthal orientations conforming to the threefold Au(110) directions. The nanocluster morphology and structure suggest that self-assembly of the nanoclusters is governed by specific interactions between the molecular species and the substrate and molecular diffusion along (110) troughs on the Au(111) substrate surface. In the case of the (TTF)(TCNQ) nanoclusters, TTF and TCNQ molecules assemble into molecular rows normal to the stacking direction, with intermolecular distances along the stacking direction which are nearly identical to those observed in bulk (TTF)(TCNQ). In contrast, the intermolecular spacings between TCNQ molecules along the molecular stacking axis in Li + TCNQ nanoclusters are substantially larger than that observed in bulk M+TCNQ.salts. The large intermolecular spacing in Li + TCNQ.nanoclusters is consistent with Coulomb repulsion between fully reduced p = 1 TCNQ(dot) anion sites in the Li+TCNQ.nanoclusters (p = formal charge). DTIC

N95-28360* National Aeronautics and Space Administration. Langley Research Center, Hampton, VA.

POLY(N-ARYLENBENZIMIDAZOLES) VIA AROMATIC NUCLEOPHILIC DISPLACEMENT Patent

John W. Connell, inventor (to NASA), Paul M. Hergenrother, inventor (to NASA), and Joseph G. Smith, Jr., inventor (to NASA) 25 Apr. 1995 13 p Filed 5 Mar. 1993
(NASA-Case-LAR-14939-1; US-Patent-5,410,012;
US-Patent-Appl-SN-045339; US-Patent-Class-528-125;
US-Patent-Class-528-128; US-Patent-Class-528-171;
US-Patent-Class-528-172; US-Patent-Class-528-174;
US-Patent-Class-528-183; Int-Patent-Class-C08G-73/18) Avail: US Patent and Trademark Office

Novel poly(N-arylenebenzimidazole)s (PNABIs) are prepared by the aromatic nucleophilic displacement reaction of novel di(hydroxyphenyl-N-arylene benzimidazole) monomers with activated aromatic dihalides or activated aromatic dinitro compounds. The polymerizations are carried out in polar aprotic solvents such as N-methyl-2-pyrrolidinone or N,N-dimethylacetamide using alkali metal bases such as potassium carbonate at elevated temperatures under nitrogen. The di(hydroxyphenyl N-arylenebenzimidazole) monomers are synthesized by reacting phenyl 4-hydroxybenzoate with bis(2-aminoanilino) arylenes in diphenylsulfone. Moderate molecular weight PNABIs of new chemical structures were prepared that exhibit a favorable combination of physical and mechanical properties. The use of the novel di(hydroxyphenyl N-arylenebenzimidazole)s permits a more economical and easier way to prepare PNABIs than previous routes. Official Gazette of the U.S. Patent and Trademark Office

N95-28361* National Aeronautics and Space Administration. Langley Research Center, Hampton, VA.

POLYBENZIMIDAZOLES VIA AROMATIC NUCLEOPHILIC DISPLACEMENT Patent

John W. Connell, inventor (to NASA), Paul M. Hergenrother, inventor (to NASA), and Joseph G. Smith, Jr., inventor (to NASA) 2 May 1995 18 p Filed 5 Apr. 1993
(NASA-Case-LAR-14924-1-CU; US-Patent-5,412,059;
US-Patent-Appl-SN-045335; US-Patent-Class-528-183;
US-Patent-Class-528-125; US-Patent-Class-528-126;
US-Patent-Class-528-128; US-Patent-Class-528-172;
US-Patent-Class-528-174; US-Patent-Class-528-210) Avail: US Patent and Trademark Office

Novel molecular weight controlled and endcapped polybenzimidazoles (PBI) are prepared by the aromatic nucleophilic displacement reaction of di(hydroxyphenyl benzimidazole) monomers with activated aromatic dihalides or activated aromatic dinitro compounds. The PBI are endcapped with mono(hydroxyphenyl) benzimidazoles. The polymerizations are carried out in polar aprotic solvents such as N-methyl-2-pyrrolidinone or N,N-dimethylacetamide using alkali metal bases such as potassium carbonate at elevated temperatures under nitrogen. Mono(hydroxyphenyl) benzimidazoles are synthesizedby reacting phenyl-4-hydroxybenzoate with aromatic (o-diamine)s in diphenylsulfone. Molecular weight controlled and endcapped PBI of new chemical structures are prepared that exhibit a favorable combination of physical and mechanical properties.
Official Gazette of the U.S. Patent and Trademark Office

N95-27117 Envirogen, Inc., Lawrenceville, NJ.

BIOREMEDIATION OF CHLORINATED ORGANICS: PCBs, TCE, HCFCs

Ronald Unterman *In* Johns Hopkins Univ., Environmentally Benign Cleaning and Degreasing Technology: JANNAF Safety and Protection Subcommittee and Propellant Development and Characterization Subcommittee Joint Workshop Jun. 1994 p 165-167 (For primary document see N95-27101 09-27)
Avail: CPIA, 10630 Little Patuxent Pkwy., Suite 202, Columbia, MD 21044-3200 HC

N95-27119 UMEI, Baltimore, MD.

MICROBIAL TREATMENT FOR SHIPBOARD COLLECTION, HOLD ING, AND TRANSFER SYSTEM TANKS

William R. Jones (Naval Surface Weapons Center, Silver Spring, MD.), John S. Hind (Naval Surface Weapons Center, Silver Spring, MD.), Joan Jones-Meehan (Naval Surface Weapons Center, Silver Spring, MD.), and M. Walch (Naval Surface Weapons Center, Silver Spring, MD.) *In* Johns Hopkins Univ., Environmentally Benign Cleaning and Degreasing Technology: JANNAF Safety and Protection Subcommittee and Propellant Development and Characterization Subcommittee Joint Workshop Jun. 1994 p 175-183 Sponsored by NAVSEADET (For primary document see N95-27101 09-27)
Avail: CPIA, 10630 Little Patuxent Pkwy., Suite 202, Columbia, MD 21044-3200 HC

N95-27120 UMBI, Baltimore, MD.

APPLICATION OF BACTERIAL BIOEMUSIFIERS TO IN SITU MAINTENANCE OF OIL/WATER SEPARATORS

John S. Hind (Naval Surface Weapons Center, Silver Spring, MD.), M. Beard (Naval Surface Weapons Center, Silver Spring, MD.), Joan Jones-Meehan (Naval Surface Weapons Center, Silver Spring, MD.), and M. Walch (Naval Surface Weapons Center, Silver Spring, MD.) *In* Johns Hopkins Univ., Environmentally Benign Cleaning and Degreasing Technology: JANNAF Safety and Protection Subcommittee and Propellant Development and Characterization Subcommittee Joint Workshop Jun. 1994 p 185-194 Sponsored by David Taylor Research Center (For primary document see N95-27101 09-27)
Avail: CPIA, 10630 Little Patuxent Pkwy., Suite 202, Columbia, MD 21044-3200 HC

24 COMPOSITE MATERIALS

Includes physical, chemical, and mechanical properties of laminates and other composite materials.

For ceramic materials see *27 Nonmetallic Materials.*

N95-26484 Rockwell International Science Center, Thousand Oaks, CA.

A STUDY OF THE USE BETA-ALUMINA AS A WEAK INTERFACE IN ALUMINA FIBER COMPOSITES Final Report, 1 Sep. 1991 - 31 Aug. 1994

Peter E. Morgan and David B. Marshall Nov. 1994 95 p Limited Reproducibility: More than 20% of this document may be affected by microfiche quality
(Contract N00014-91-C-0157)
(AD-A288629; SC71056.FR) Avail: Issuing Activity (Defense Technical Information Center (DTIC))

Results are presented from a three-year study aimed at identifying and developing suitable inter-phase materials for oxide-oxide composites that are stable in high temperature oxidizing environments, yet sufficiently weak to allow debonding as required for toughening. Most of the effort was devoted to two systems: LaPO4 (monazite) and beta-aluminas. Monazite satisfied all of the requirements for an interphase in alumina-alumina composites (and most likely many other ceramic matrix-fiber combinations). It has a high melting point (2074 C); it is stable with alumina at high temperature in both oxidizing and slightly reducing environments and it forms a sufficiently weak bond with alumina. Beta-alumina materials, which possess weak mica-like planes in their crystal structures, are phase compatible with alumina, and their debonding characteristics are adequate. However, their use and fabrication temperatures are limited by morphological instability of the fiber/matrix interface (grain growth of the beta-alumina platelets into the fibers). DTIC

N95-26565 Army Research Lab., Aberdeen Proving Ground, MD.

A FAST NUMERICAL METHOD FOR ISOTHERMAL RESIN TRANSFER MOLD FILLING Final Report, Dec. 1993 - Apr. 1994

R. S. Maier, T. F. Rohaly, S. G. Advani, and K. D. Fickie Nov. 1994 34 p Limited Reproducibility: More than 20% of this document may be affected by microfiche quality
(DA Proj. 1L1-62618-AH-80)
(AD-A288944; ARL-TR-610) Avail: Issuing Activity (Defense Technical Information Center (DTIC))

An efficient numerical scheme is presented for simulating the isothermal flow in resin transfer molding (RTM). The problem involves transient, free surface flow of an incompressible fluid into a nondeforming porous medium. A new variant of the control volume finite element (CVFE) algorithm is explained in detail. It is shown how the pressure solutions at each time step can be obtained by adding a single row and column to the Cholesky factorization of the stiffness matrix derived from a finite-element formulation for the pressure field. This approach reduces the computation of a new pressure solution at each time step to essentially just two sparse matrix back-substitutions. The resulting performance improvement facilitates interactive simulation and the solution of inverse problems which require many simulations of the filling problem. The computational complexity of the calculation is bounded by O(n sup 2.5), where n is the number of nodes in the finite element mesh. A 100-fold speedup over a conventional CVFE implementation was obtained for a 2213-node problem. DTIC

N95-26571 Wright Lab., Wright-Patterson AFB, OH. Materials Directorate.
LIFE PREDICTION METHODOLOGY FOR COMPOSITE LAMINATES. PART 1: CONSTANT AMPLITUDE AND TWO-STRESS LEVEL FATIGUE Interim Report, 15 Jan. 1993 - 30 Aug. 1994
Jeffery R. Schaff and Barry D. Davidson (Syracuse Univ., NY.) Sep. 1994 45 p Limited Reproducibility: More than 20% of this document may be affected by microfiche quality
(AF Proj. 2419)
(AD-A288343; WL-TR-94-4046) Avail: Issuing Activity (Defense Technical Information Center (DTIC))

A strength-based wearout model is presented for predicting the residual strength and life of composite laminates subjected to constant amplitude or two-stress level fatigue loadings. It is assumed that the laminate undergoes proportional loading, that its residual strength is a monotonically decreasing function of the number of loading cycles, and that the probability of failure after an arbitrary number of cycles may be represented by a two parameter Weibull function. The model also incorporates a 'cycle mix factor' to account for the degradation of strength and life that may be associated with frequent changes in the stress amplitude of the loading. Experimental results from two-stress level loadings are used to evaluate the model's predictive capability for sequencing effects, as in a low-high or high-low test, and for cycle mix effects, as in a low-high-low-high repeating test. Good correlation between theory and experiment is obtained for all loadings and laminates studied. DTIC

N95-26572 Missouri Univ., Rolla, MO. Dept. of Chemistry.
INTERFACIAL MOBILITY AND ITS EFFECT ON FLEXURAL STRENGTH AND FRACTURE TOUGHNESS IN GLASS-FIBER FABRIC REINFORCED EPOXY LAMINATES Technical Report, 1 Jan. - 19 Nov. 1994
Timothy W. Wang and Frank D. Blum 21 Nov. 1994 8 p Sponsored by ONR Limited Reproducibility: More than 20% of this document may be affected by microfiche quality
(AD-A288344; UMR-FDB-44) Avail: Issuing Activity (Defense Technical Information Center (DTIC))

Constant-strain-rate mechanical testing was used, to study the fracture mechanical characterization of E-glass fiber fabric reinforced epoxy composites. Testing was performed as a function of the silane coupling agent used with compact tension (CT) specimens for fracture toughness and rectangular specimens for flexural strength. Two silane coupling agents, y-aminopropyltriethoxysilane (APS) and y-aminobutyltrithoxy-silane (ABS) were used for this purpose. The fracture toughness, K1c, of ABS treated composites was shown to be lower than that for APS treated composites. Treatment with either is better than using bare glass. A three point bend test showed the flexural strength and modulus were increased in order of untreated<ABS<APS treated composites in both dry and wet conditions. Since these silanes have similar chemistry, we believe that the difference is due to the interfacial mobility of the coupling agent layer. DTIC

N95-26626 City Coll. of the City Univ. of New York, NY. Dept. of Mechanical Engineering.
MICROMECHANICAL PREDICTION OF TENSILE DAMAGE FOR CERAMIC MATRIX COMPOSITES UNDER HIGH TEMPERATURE Final Report, 15 Aug. 1990 - 15 Feb. 1994
F. Delale and B. M. Liaw 15 Feb. 1994 142 p Limited Reproducibility: More than 20% of this document may be affected by microfiche quality
(Grant AF-AFOSR-0341-90)
(AD-A288238; AFOSR-94-0701TR) Avail: Issuing Activity (Defense Technical Information Center (DTIC))

This report documents the experimental and theoretical results obtained in studying the tensile damage behavior of ceramic matrix composites (namely Nicalon/CAS II composites) at room and elevated temperature. First the composite specimens were machined into dog-bone shape and polished to increase efficacy of observation in the SEM. Then the specimens were placed inside the chamber of a scanning electron microscope (SEM) and subject to tensile loading at room and higher temperatures up to 700 C. At each temperature, the load was increased until failure of the specimen and the progression of damage was observed and recorded from first crack to total failure. Damage usually started with matrix cracking, followed by debonding along fiber-matrix interface, fiber pullout and finally fiber breakage. At each load level, the displacement was measured, resulting in a stress-strain curve with linear and non-linear portions.Similar behavior was observed at higher temperatures. Theoretical models to predict and simulate the observed behavior were also developed. A singular integral formulation with periodic matrix cracking and interface debonding explains well the fact that embedded matrix cracks almost always propagate to the interface and are arrested by the fibers. The results obtained from finite element model with multiple rows of matrix cracks and debonding at the fiber/matrix interface, compare extremely well with the experimental data. DTIC

N95-26667# National Aerospace Lab., Tokyo (Japan). Airframe Div.
STATISTICAL ANALYSIS OF TENSILE MECHANICAL PROPERTY DATA OF CARBON/POLYIMIDE COMPOSITES
Toshiyuki Shimokawa, Yasumasa Hamaguchi, Yoshiaki Kakuta, Shigeo Sanbongi, Yoshiki Morino (National Space Development Agency, Tokyo, Japan.), and Masataka Yamamoto (National Space Development Agency, Tokyo, Japan.) Jun. 1994 17 p In JAPANESE
(ISSN 0389-4010)
(NAL-TR-1238) Avail: CASI HC A03/MF A01

The objective of this study is to statistically evaluate the tensile mechanical properties of two kinds of carbon/polyimide composites, i.e., Celion 6K/PMR-15 and T800H/PMR-15 with a quasi-isotropic stacking sequence. Tensile tests were conducted under room temperature using about thirty smooth specimens. Mechanical properties measured are ultimate strength, failure strain, elastic modulus, and Poisson's ratio. Statistical analyses use four kinds of distribution models such as the normal, log-normal, type-1 extreme-value, and two-parameter Weibull distributions. These analyses derive the estimates of central tendencies and scatter parameters, and B allowables. The modified Kolmogorov-Smirnov goodness-of-fit of each mechanical property data for the four kinds of distribution models. Correlation between mutual mechanical properties is examined, and a multiple regression analysis is applied to predict the ultimate strength. Moreover, a simple equation to predict the ultimate strength is derived using the product of the failure strain and elastic modulus. Author

N95-26686 Naval Surface Warfare Center, Bethesda, MD.
MICROENGINEERED CONDUCTING COMPOSITES FROM NANOCHANNEL TEMPLATES Technical Report
Carmen A. Huber, Mostafa Sadoqi, Tito E. Huber, and Daborah Chacko Jan. 1995 15 p Limited Reproducibility: More than 20% of this document may be affected by microfiche quality
(AD-A289573; CARDIVNSWC-TR-1) Avail: Issuing Activity (Defense Technical Information Center (DTIC))

Metallic nanostructures can be prepared from nanochannel dielectric hosts by injection of the conducting melt. Nanowire arrays and random networks have been fabricated in this way. The role of the microstructure in the bulk electronic properties of the composites as well as applications of these materials are discussed. DTIC

N95-26764*# National Aeronautics and Space Administration. Langley Research Center, Hampton, VA.
COMPOSITE SANDWICH STRUCTURE AND METHOD FOR MAKING SAME Patent Application
Charles J. Magurany, inventor (to NASA) (Lockheed Engineering and Sciences Co., Hampton, VA.) 30 Mar. 1995 32 p
(NASA-Case-LAR-14898-1; NAS 1.71:LAR-14898-1; US-Patent-Appl-SN-413301) Avail: CASI HC A03/MF A01

A core for a sandwich structure which has multi-ply laminate ribs separated by voids is made as an integral unit in one single curing step. Tooling blocks corresponding to the voids are first wrapped by strips of prepreg layup equal to one half of each rib laminate so a continuous wall of prepreg material is formed around the tooling blocks. The wrapped tooling blocks are next pressed together laterally, like tiles, so adjoining walls from two tooling blocks are joined. The assembly is then cured by conventional methods, and afterwards the tooling blocks are removed so voids are formed. The ribs can be provided with integral tabs forming bonding areas for face sheets, and face sheets may be co-cured with the core ribs. The new core design is suitable for discrete ribcores used in space telescopes and reflector panels, where quasiisotropic properties and zero coefficient of thermal expansion are required. NASA

N95-26847 California Univ., Santa Barbara, CA.

MECHANICAL PERFORMANCE OF FIBER REINFORCED METAL MATRIX COMPOSITES AND MICROSTRUCTURAL DEVELOPMENT OF POLYCRYSTALLINE ALUMINA FIBERS SYNTHESIZED FROM LIQUID PRECURSORS Final Report, 1 Jul. 1992 - 28 Feb. 1994

A. G. Evans, F. Zok, C. G. Levi, and F. F. Lange 31 Dec. 1994 8 p Limited Reproducibility: More than 20% of this document may be affected by microfiche quality
(Contract N00014-92-J-1991)
(AD-A289518) Avail: Issuing Activity (Defense Technical Information Center (DTIC))

The research of the Office of Naval Research grant at UCSB focused on the research concerns of mechanical properties of fiber reinforced metal matrix composites as well as the understanding of microstructural development in polycrystalline Al2O3 fibers synthesized from liquid precursors. It has been closely coordinated with the DARPA/ONR URI program dealing with the design of high performance composites. DTIC

N95-26848 Nuclear Metals, Inc., Concord, MA.

DUCTILE - DUCTILE BERYLLIUM ALUMINUM METAL MATRIX COMPOSITE MANUFACTURED BY EXTRUSION Interim Report, 1 Dec. 1994 - 1 Jan. 1995

Nancy F. Levoy 1 Jan. 1995 8 p Limited Reproducibility: More than 20% of this document may be affected by microfiche quality
(Contract N00014-94-C-0135)
(AD-A289519) Avail: Issuing Activity (Defense Technical Information Center (DTIC))

The current program is designed to develop a method for extruding a cast beryllium-aluminum composite, establish a basis for estimating the properties that can ultimately be achieved with an optimized process, and produce an extruded structural shape of moderate complexity. Specific technical objectives are as follows: (1) Develop an extrusion process suitable for beryllium-aluminum composites that maximizes product yield, minimizes processing steps, gives good surface finish, and is suited for producing complex shapes; (2) Determine mechanical and physical properties to demonstrate potential; and (3) Define potential for property enhancements and cost reductions that could be achieved through continued development of this technology. DTIC

N95-26865 Air Force Inst. of Tech., Wright-Patterson AFB, OH. School of Engineering.

FATIGUE BEHAVIOR OF A CROSS-PLY METAL MATRIX COMPOSITE AT ELEVATED TEMPERATURE UNDER STRAIN CONTROLLED MODE M.S. Thesis

Leon B. Dennis Dec. 1994 127 p Limited Reproducibility: More than 20% of this document may be affected by microfiche quality
(AD-A289425; AFIT/GAE/ENY/94D-7) Avail: Issuing Activity (Defense Technical Information Center (DTIC))

This research extends the existing knowledge of cross-ply metal matrix composites (MMC) to include fatigue behavior under strain-controlled fully reversed loading. This study investigated fatigue life, failure modes and damage mechanisms of the SCS-6/Ti-15-3, (0/90)2's, MMC. The laminate was subjected to fully reversed fatigue at elevated temperature (427 C) at various strain levels. Stress, strain and modulus data were analyzed to characterize the macro-mechanical behavior of the composite. Microscopy and fractography were accomplished to identify and characterize the damage mechanisms at the microscopic level. Failure modes varied according to the maximum applied strain level showing either mixed mode (i.e. combination of both fiber and matrix dominated modes) or matrix dominated fatigue failures. As expected, higher strain loadings resulted in more ductility of the matrix at failure, evidenced by fracture surface features. For testing of the same composite laminate, the fatigue life under strain controlled mode slightly increased, compared to its load-controlled mode counterpart, using the effective strain range comparison basis. However, the respective fatigue life curves converged in the high cycle region, suggesting that the matrix dominated failure mode produces equivalent predicted fatigue lives for both control modes. DTIC

N95-26868 Air Force Inst. of Tech., Wright-Patterson AFB, OH.

VISCOPLASTIC CHARACTERIZATION AND FATIGUE MODELING OF TITANIUM BASED METAL MATRIX COMPOSITES M.S. Thesis

Mark A. Foringer Dec. 1994 105 p Limited Reproducibility: More than 20% of this document may be affected by microfiche quality
(AD-A289430; AFIT/GAE/ENY/94D-5) Avail: Issuing Activity (Defense Technical Information Center (DTIC))

Viscoplastic characterization and fatigue modeling of titanium-based metal matrix composites was accomplished by combining a unified viscoplastic theory, a nonlinear micromechanics model, and a linear damage accumulation model. Ti 15-3 was characterized using the Bodner-Partom viscoplastic theory. A micromechanics model was then employed in a linear damage accumulation fatigue model to predict the fatigue behavior of titanium based composites. The viscoplastic behavior predictions of the micromechanics model were used to eliminate separately defined time dependent terms in the fatigue model. Also, a new linear damage accumulation model was developed from the fatigue behavior of the composite constituents. Finally, it was found that the microstresses in the 0 degree ply could be used to accurately predict the fatigue behavior of a laminate containing these plies. DTIC

N95-26886 Air Force Inst. of Tech., Wright-Patterson AFB, OH. School of Engineering.

CHARACTERIZATION OF FATIGUE BEHAVIOR OF 2-D WOVEN FABRIC REINFORCED CERAMIC MATRIX COMPOSITE AT ELEVATED TEMPERATURE Final Report M.S. Thesis

Daniel J. Groner Dec. 1994 128 p Limited Reproducibility: More than 20% of this document may be affected by microfiche quality
(AD-A289423; AFIT/GAE/ENY/94D-15) Avail: Issuing Activity (Defense Technical Information Center (DTIC))

This study investigated the fatigue behavior and associated damage mechanisms in notched and unnotched enhanced SiC/SiC ceramic matrix composite specimens at 1100 C. Stiffness degradation, strain variation, and hysteresis were evaluated to characterize material behavior. Microscopic examination was performed to characterize damage mechanisms. During high cycle/low stress fatigue tests, far less fiber/matrix interface debond was evident than in low cycle/high stress fatigue tests. Notched specimens exhibited minimal stress concentration during monotonic tensile testing and minimal notch sensitivity during fatigue testing. Damage mechanisms were also similar to unnotched. DTIC

N95-26967 Dayton Univ., OH. Research Inst.

EVALUATION OF COMPOSITE JOINTS Interim Report, Nov. 1993 - Apr. 1994

Seng C. Tan Apr. 1994 34 p Prepared in cooperation with Wright Materials Research Co. Limited Reproducibility: More than 20% of this document may be affected by microfiche quality
(Contract F33615-89-C-5643)
(AD-A289247; WL-TR-94-4077) Avail: Issuing Activity (Defense Technical Information Center (DTIC))

A study of bolted, bonded, and bolted-bonded composite single lap joints was conducted. Graphite thermoplastic composite material (AS4/APC2) and two stacking sequences, (0,90,45 ,135)2s and (0,0,45,135)2s, were used. Five joint designs were tested: (1) bonded (FM400); (2) bolted-bonded with two bolts; (3) bolted bonded with four bolts; (4) bolted with six bolts; and (5) bolted with eight bolts. Load deflection measurements were made and joint efficiencies computed. Failure mechanisms were determined. Peak joint efficiencies were in the 55% vicinity and occurred for the six-bolt configuration and the (0,90,45,135)2s laminate. For the tests in this study, the adhesive bond failed interfacially at relatively low load levels. DTIC

N95-26969 Air Force Inst. of Tech., Wright-Patterson AFB, OH. School of Engineering.
FATIGUE BEHAVIOR OF A CROSS-PLY CERAMIC MATRIX COMPOSITE AT ELEVATED TEMPERATURE UNDER TENSION-TENSION LOADING M.S. Thesis
Craig D. Steiner Dec. 1994 149 p Limited Reproducibility: More than 20% of this document may be affected by microfiche quality
(AD-A289250; AFIT/GAE/ENY/94D-9) Avail: Issuing Activity (Defense Technical Information Center (DTIC))

This study investigated the fatigue behavior and damage mechanisms of a (0/90)4s SiC/MAS ceramic matrix composite under tension-tension loading at two elevated temperatures and two frequencies. Stress and strain hystereses, maximum and minimum strain, and modulus of elasticity were evaluated to characterize the material behavior. Microscopy and fractography were used to evaluate damage progression and mechanisms. Fatigue life was independent of frequency at both temperatures. DTIC

N95-27080# Los Alamos National Lab., NM.
A STUDY OF INTERNAL DAMAGE OF METAL MATRIX COMPOSITES BY NEUTRON DIFFRACTION
N. Shi, M. A. M. Bourke, and J. A. Goldstone 1994 7 p Presented at the 1994 Fall Meeting of the Materials Research Society (MRS), Boston, MA, 28 Nov. - 2 Dec. 1994
(Contract W-7405-eng-36)
(DE95-005157; LA-UR-94-4246; CONF-941144-44) Avail: CASI HC A02/MF A01

Using neutron diffraction, we have measured the elastic phase strains of Al/TiC and Al/SiC composites under uniaxial tensile loading. The phase strains were used to reconstruct the global elastic strain. It has been found that, above macroscopic yield, the global elastic strain response is not linear. A theoretical model shows that the nonlinearity is dictated by changes in the ratio of longitudinal phase stresses. Furthermore, the changes in this ratio resulting from matrix plasticity and reinforcement fracture are different which leads to distinct slope changes in the global elastic strain response that can be used to distinguish the onset of these two processes on the global elastic strain loading curve. DOE

N95-27134 Air Force Inst. of Tech., Wright-Patterson AFB, OH. School of Engineering.
FATIGUE BEHAVIOR OF A CROSS-PLY CERAMIC MATRIX COMPOSITE SUBJECTED TO TENSION-TENSION CYCLING WITH HOLD TIME M.S. Thesis
Scott A. Grant Dec. 1994 138 p Limited Reproducibility: More than 20% of this document may be affected by microfiche quality
(AD-A289418; AFIT/GAE/ENY/94D-16) Avail: Issuing Activity (Defense Technical Information Center (DTIC))

This study was carried out to investigate the elevated temperature behavior of the SiC-MAS5 cross-ply (O/9O)4S ceramic matrix composite manufactured by Corning Inc. to fatigue with loading waveforms that combine the characteristics of stress rupture and high cycle fatigue. The test results were compiled in the form of S-N (cycles to failure), S-T (exposure time versus cycles to failure), S-S (energy exposure versus cycles to failure), normalized modulus degradation, strain progression, and hysteresis loop progression. From the mechanical behavior demonstrated by these curves, relationships between the effect of the environment and loading waveform were developed. In addition, a post-mortem SEM analysis of the fracture surface was conducted and the results compared to the mechanical behavior. DTIC

N95-27142 Army Research Lab., Watertown, MA. Materials Directorate.
MODELING CONSIDERATIONS IN THE PREDICTION OF RESIDUAL STRENGTH IN COMPOSITE LAMINATES
Eric Saether Nov. 1994 62 p Limited Reproducibility: More than 20% of this document may be affected by microfiche quality
(AD-A289128; ARL-MR-211) Avail: Issuing Activity (Defense Technical Information Center (DTIC))

The prediction of residual strength in damaged composite structures is complicated by the need to accurately characterize internal damage states and to mathematically simulate the material behavior which displays a variety of damage mechanisms and failure modes. Numerous analyses have been developed which, in general, have been restricted to specific damage modes and idealized geometric configurations. Modeling issues include micromechanical fiber/matrix failure phenomena, delamination growth, buckling of laminate sublayers, and nonlinear material and geometric response to applied loads. For the reliable design of composite components, the modeling approaches utilized in various specialized analyses need to be synthesized into a combined, robust methodology. The purpose of the present investigation is to identify the various salient failure phenomena involved in damaged composite laminates and to discuss mathematical modeling approaches to represent such damage. The identification of analytic approaches provides a basis for further extension to overcome existing limitations in the prediction of residual strength. DTIC

N95-27188 California Univ., Santa Barbara, CA.
BIMATERIAL INTERLACES AND THEIR ROLE IN THE MECHANICAL PERFORMANCE OF THE IN-SITU COMPOSITES Annual Report, 1 Jan. - 31 Dec. 1994
Anthony G. Evans 31 Dec. 1994 384 p Limited Reproducibility: More than 20% of this document may be affected by microfiche quality
(Contract N00014-93-I-0213)
(AD-A288973) Avail: Issuing Activity (Defense Technical Information Center (DTIC))

The annual report of the Office of Naval Research grant at UCSB on Bimaterial Interfaces and their role in the Mechanical Performance is concerned basically with the mechanical properties of ceramic/metal bonded systems and with establishing criteria for interface decohesion for sliding and for cracking across interlaces. Please refer to the executive summary for further details. DTIC

N95-27192*# National Aeronautics and Space Administration. Langley Research Center, Hampton, VA.
COMPOSITE PREPREG APPLICATION DEVICE Patent Application
Donald A. Sandusky, inventor (to NASA) (College of William and Mary, Williamsburg, VA.) and Joseph M. Marchello, inventor (to NASA) (Old Dominion Univ., Hampton, VA.) 21 Mar. 1995 14 p
(NASA-Case-LAR-15259-1; NAS 1.71:LAR-15259-1; US-Patent-Appl-SN-411231) Avail: CASI HC A03/MF A01

A heated shoe and cooled pressure roller assembly for composite prepreg application is provided. The shoe assembly includes a heated forward contact surface having a curved pressure surface. The following cooled roller provides a continuous pressure to the thermoplastic while reducing the temperature to approximately 5 C below glass transition temperature. Electric heating coils inside the forward portion of the shoe heat a thermoplastic workpiece to approximately 100 C above the glass transition. Immediately following the heated contact surface, a cooled roller cools the work. The end sharpened shape of the heated shoe trailing edge tends to prevent slag buildup and maintain a uniform, relaxed stress fabrication. NASA

N95-27421# Los Alamos National Lab., NM.
MICROMECHANICAL MODELING OF DAMAGE AND INELASTICITY OF COMPOSITE MATERIALS IN MACROSCOPIC STRUCTURAL ANALYSIS
R. W. Macek, J. P. Gardner, and R. M. Hackett (Mississippi State Univ., Mississippi State, MS.) 1994 4 p Presented at the ASCE Engineering Mechanics Conference, Boulder, CO, 21-24 May 1995
(Contract W-7405-eng-36)
(DE95-003666; LA-UR-94-3960; CONF-9505115-1) Avail: CASI HC A01/MF A01

The method of cells has been extended to include damage or debonding between all adjacent subcells using a finite element formulation for the original cells assembly. Damage is implemented by placing a nonlinear three-dimensional spring between adjacent subcells. With this arrangement the damage is inherently anisotropic. The 'nonlinear substructure' cells finite element model is incorporated as a user defined material routine in a general purpose finite element code. The primary motivation for casting the method of cells as a finite element assemblage is to provide a composite constitutive model that facilitates the incorporation of various constituent material models, as well as any level of detail desired in the microstructure geometry. At present, the constituent material models may be anisotropic elastic or isotropic viscoelastic-plastic, while damage evolution is based on the macroscopic strain. The capability of the model is demonstrated through analyses of some simple structures loaded to failure. DOE

N95-27428# Los Alamos National Lab., NM.
VARIATION OF SOLVENT SCATTERING-LENGTH DENSITY SMALL-ANGLE NEUTRON SCATTERING AS A MEANS OF DETERMINING STRUCTURE OF COMPOSITE MATERIALS
R. P. Hjelm, W. Wampler (Sid Richardson Carbon Co., Forth Worth, TX.), and M. Gerspacher (Sid Richardson Carbon Co., Forth Worth, TX.) 1994 6 p Presented at the 1994 Fall Meeting of the Materials Research Society (MRS), Boston, MA, 28 Nov. - 2 Dec. 1994
(Contract W-7405-eng-36)
(DE95-005394; LA-UR-94-4220; CONF-941144-40) Avail: CASI HC A02/MF A01

As part of our work on the structure of composite materials we have been exploring the use of small-angle neutron scattering using the method of contrast variation to dissect the component form, structure and distribution. This approach has resulted in a new look at a very old problem of reinforcement of elastomers by carbon black. Using this approach we studied an experimental high surface area (HSA) carbon black and a gel of 'HSA-bound' rubber in cyclohexane/deuterocyclohexane mixtures. HSA in cyclohexane is found to be short rodlike particle aggregates. The aggregates have a shell-core structure with a high density graphitic outer shell and an inner core of lower density amorphous carbon. The core is continuous throughout the carbon black aggregate, making the aggregate a stiff, integral unit. Contrast variation of swollen composite gels shows that there are two length scales in the gel structure. Above 10 (Angstrom), scattering from carbon black predominates, and below 10 (Angstrom) the scattering is from both carbon black and the elastomer. The HSA in the composite is completely embedded in polyisoprene. An estimate of the carbon black structure factor shows strong exclusion of neighboring aggregates, probably from excluded volume effects. The surface structure of the carbon black is unaltered by the interactions with elastomer and appears smooth over length scales above about 10 (Angstrom). These results show that contrast variation can provide information on composite structure that is not available by other means. This information relates to the reinforcement mechanism of elastomers by carbon blacks. DOE

N95-27717*# National Aeronautics and Space Administration. Lewis Research Center, Cleveland, OH.
CERAMIC FIBER-REINFORCED MONOCLINIC CELSIAN PHASE GLASS-CERAMIC MATRIX COMPOSITE MATERIAL Patent Application
Narottam P. Bansal, inventor (to NASA) and James A. DiCarlo, inventor (to NASA) 31 Mar. 1994 14 p Continuation-in-part of US-Patent-Appl-SN-986399, filed 7 Dec. 1992
(NASA-Case-LEW-15714-1; NAS 1.71:LEW-15714-1; US-Patent-Appl-SN-221128; US-Patent-Appl-SN-986399) Avail: CASI HC A03/MF A01

A hyridopolysilazane-derived ceramic fiber reinforced monoclinic celsian phase barium aluminum silicate glass-ceramic matrix composite material is prepared by ball-milling an aqueous slurry of BAS glass powder and fine monoclinic celsian seeds. The fibers improve the mechanical strength and fracture toughness and with the matrix provide superior dielectric properties. NASA

N95-27955# Oak Ridge National Lab., TN.
THERMAL SHOCK BEHAVIOR OF FIBER-REINFORCED COMPOSITES
H. Wang, R. N. Singh, S. C. Beecher, and R. B. Dinwiddie 1995 12 p Presented at the 96th Annual Meeting and Exposition of the American Ceramic Society (ACerS), Indianapolis, IN, 24-28 Apr. 1995
(Contract DE-AC05-84OR-21400)
(DE95-006746; CONF-9504124-1) Avail: CASI HC A03/MF A01

The thermal shock behavior of three types of continuous fiber-reinforced ceramic composites (Nextel(trademark) or Nicalon(trademark) fiber-reinforced chemical vapor infiltrated or polymer-derived SiC matrix composites) was studied using the water quench technique. The thermal shock induced damage was characterized by both destructive and nondestructive techniques. As compared with monolithic ceramics, the continuous fiber-reinforced ceramic composites were capable of preventing catastrophic failure caused by thermal shock and were able to retain a significant portion of their original strength at Delta T = 1000 C. The nondestructive techniques involved measuring the thermal diffusivity by the flash technique and determining the Young's modulus by the dynamic resonance method. It has been demonstrated that these nondestructive techniques can detect damage induced by thermal shock and are more sensitive in detecting damage in the early stage than the conventional destructive technique of measuring the retained strength. DOE

N95-28043# Oak Ridge National Lab., TN.
STRESS TRANSFER FROM AXIALLY LOADED FIBER TO MATRIX IN A MICROCOMPOSITE
Chun-Hway Hsueh 1995 11 p Presented at the 1994 Fall Meeting of the Materials Research Society (MRS), Boston, MA, 28 Nov. - 2 Dec. 1994
(Contract DE-AC05-84OR-21400)
(DE95-007366; CONF-941144-69) Avail: CASI HC A03/MF A01

The shear lag model has been used extensively to analyze the stress transfer in a single fiber-reinforced composite (i.e., a microcomposite). To achieve analytical solutions, various simplifications have been adopted in the stress analysis. Questions regarding the adequacy of those simplifications are discussed in the present study for the following two cases: bonded interfaces and frictional interfaces. Specifically, simplifications regarding: (1) the radial dependences of axial stresses in the fiber and the matrix, and (2) Poisson's effect are addressed. For bonded interfaces, the latter can be ignored, and the former can generally be ignored. However, when the volume fraction of the fiber is high, the radial dependence of the axial stress in the fiber should be considered. For frictional interfaces, the former can be ignored, but the latter should be considered; however, it can be considered in an average sense to simplify the analysis. Comparisons among results obtained from analyses with various simplifications are made. DOE

N95-28068# Argonne National Lab., IL.
EFFECTS OF HIGH-TEMPERATURE ENVIRONMENTS ON FLAW GENERATION AND FRACTURE BEHAVIOR OF SIC/SIC COMPOSITES
J. P. Singh and D. Singh Feb. 1995 8 p Presented at the 5th International Conference on the Science of Hard Materials, Maui, HI, 20-24 Feb. 1995
(Contract W-31-109-eng-38)
(DE95-008270; ANL/ET/CP-83155; CONF-950245-1) Avail: CASI HC A02/MF A01

Flaw generation and fracture behavior of Nicalon-fiber-reinforced SiC matrix composites are influenced by high temperatures. Therefore, the authors evaluated the effects of temperature by measuring the strength of these composites at several temperatures ranging from 800 to 1,300 C, and by characterizing their microstructure. While composite strength increased from approximately 400 MPa at room temperature to approximately 532 MPa at 800 C, it decreased to approximately 270 MPa at 1,300 C. Such degradation of composite strength at high temperature is believed to be partly due to fiber degradation. In-situ fiber strength of composites tested at room and elevated temperatures was estimated by fractographic techniques. The in-situ strength of fibers in composites was significantly lower than that of as-received fibers. This decrease is believed to be related to flaws that develop during processing and to exposure to elevated-temperature service environments. DOE

N95-28069# Argonne National Lab., IL.
HIGH-TEMPERATURE DEFORMATION OF ZrO2-Al2O3/SiC WHISKER COMPOSITES FABRICATED BY TWO TECHNIQUES
J. M. CalderonMoreno (Seville Univ., Spain.), A. R. DeArellano-Lopez (Seville Univ., Spain.), A. Dominguez-Rodriguez (Seville Univ., Spain.), and J. L. Routbort 1995 17 p Presented at the 5th International Conference on the Science of Hard Materials, Maui, HI, 20-24 Feb. 1995
(Contract W-31-109-eng-38)
(DE95-008273; ANL/ET/CP-85762; CONF-950245-2) Avail: CASI HC A03/MF A01

ZrO2-Al2O3/SiC whisker-reinforced composites, with whisker volume fractions of 0 to 28%, fabricated both by powder and precursor processing, have been deformed at temperatures of 1300-1500 C under constant compression rates of 1.7 x 10(exp -5) to 6.8 x 10(exp -5) s(exp -1). Above 1400 C, a stress at which the work-hardening rate became zero could be measured and correlated with whisker content. On the other hand, at 1300 C all samples broke within the elastic regime. At 1350 C, increased whisker content appeared to inhibit fracture, so plastic behavior was obtained for samples containing 28% SiC. In the range of temperatures and compression rates, noted above, stress exponents were determined and tentatively correlated with microstructural features and their evolution during plastic deformation. DOE

N95-28145# Sandia National Labs., Albuquerque, NM.
TEM CHARACTERIZATION OF Al/Al2O3 COMPOSITE FABRICATED BY REACTIVE METAL INFILTRATION
Y. Gao, J. Jia, R. E. Loehman, and K. G. Ewsuk 1994 6 p Presented at the 1994 Fall Meeting of the Materials Research Society (MRS), Boston, MA, 28 Nov. - 2 Dec. 1994
(Contracts DE-AC04-94AL-85000; DE-AC04-76DP-00789)
(DE95-008508; SAND-95-0468C; CONF-941144-85) Avail: CASI HC A02/MF A01

The microstructure of Al/(alpha)-Al2O3 composites made by infiltrating Al into dense mullite preforms has been characterized using transmission electron microscopy. Observations revealed that the formation of the Al/Al2O3 composites involves three stages. Initially, Al infiltrates into a dense mullite preform through grain boundary diffusion, and reacts with mullite at grain boundaries to form a partial reaction zone. Then, a complete reaction takes place in the reaction region between the partial reaction zone and the full reaction zone to convert the dense mullite preform to a composite of (alpha)-Al2O3 (matrix) and an Al-Si phase (thin channels). Finally, the reduced Si from the reaction diffuses out of the Al/Al2O3 composite through the metal channels, whereas Al from the molten Al pool is continuously drawn to the reaction region until the mullite preform is consumed or the sample is removed from the molten Al pool. Based on the observed microstructure, infiltration mechanisms have been discussed, and a growth model of the composites is proposed in which the process involves repeated nucleation of Al2O3 grains and grain growth. DOE

N95-28207# Oak Ridge National Lab., TN. Engineering Technology Div.
FRACTURE TESTING AND ANALYSIS OF ADHESIVELY BONDED JOINTS FOR AUTOMOTIVE APPLICATIONS
Raymond G. Boeman and C. David Warren 1994 10 p Presented at the 10th Annual ASM/ESD Advanced Composites Conference, Dearborn, MI, 7-10 Nov. 1994
(Contract DE-AC05-84OR-21400)
(DE95-007024; CONF-941195-1) Avail: CASI HC A02/MF A01

In 1992, the Oak Ridge National Laboratory (ORNL) began a cooperative effort with the Automotive Composites Consortium (ACC) to conduct research and development that would overcome technological hurdles to the adhesive bonding of current and future automotive materials. This effort is part of a larger Department of Energy (DOE) program to promote the use of lighter weight materials in automotive structures for the purpose of increasing fuel efficiency and reducing environmental pollutant emissions. In accomplishing this mission, the bonding of similar and dissimilar materials was identified as being of primary importance to the automotive industry since this enabling technology would give designers the freedom to choose from an expanded menu of low mass materials for component weight reduction. This paper concentrates on the details of developing accurate fracture test methods for adhesively bonded joints in the automotive industry. The test methods being developed are highly standardized and automated so that industry suppliers will be able to pass on reliable data to automotive designers in a timely manner. Mode I fracture tests have been developed that are user friendly and automated for easy data acquisition, data analysis, test control and test repeatability. The development of this test is discussed. In addition, materials and manufacturing issues are addressed which are of particular importance when designing adhesive and composite material systems. DOE

N95-28266*# Federal Aviation Administration, Washington, DC.
NINTH DOD/NASA/FAA CONFERENCE ON FIBROUS COMPOSITES IN STRUCTURAL DESIGN, VOLUME 3
Joseph R. Soderquist, comp., Lawrence M. Neri, comp. (Federal Aviation Administration, Atlantic City, NJ.), and Herman L. Bohon, comp. (Galaxy Scientific Corp., Hampton, VA.) Sep. 1992 483 p Conference held in Lake Tahoe, NV, 4-7 Nov. 1991; sponsored by NASA, AF, Army, and Navy Sponsored by NASA
(NASA-CR-198718; NAS 1.26:198718; DOT/FAA/CT-92-25-Vol-3)
Copyright Avail: CASI HC A21/MF A04

This publication contains the proceedings of the Ninth DOD/NASA/FAA Conference on Fibrous Composites in Structural Design held at Lake Tahoe, Nevada, during 4-7 Nov. 1991. Presentations were made in the following areas of composite structural design: perspectives in composites, design methodology, design applications, design criteria, supporting technology, damage tolerance, and manufacturing. For individual titles, see N95-28267 through N95-28293.

N95-28267*# Lockheed Aeronautical Systems Co., Burbank, CA. Composites Development Center.
PROCESS AND CONTROL SYSTEMS FOR COMPOSITES MANUFACTURING
T. H. Tsiang and John L. Wanamaker (Lockheed Aeronautical Systems Co., Marietta, GA.) *In* FAA, Ninth DOD/NASA/FAA Conference on Fibrous Composites in Structural Design, Volume 3 Sep. 1992 p 1153-1162 (For primary document see N95-28266 09-24)
Copyright Avail: CASI HC A02/MF A04

A precise control of composite material processing would not only improve part quality, but it would also directly reduce the overall manufacturing cost. The development and incorporation of sensors will help to generate real-time information for material processing relationships and equipment characteristics. In the present work, the thermocouple, pressure transducer, and dielectrometer technologies were investigated. The monitoring sensors were integrated with the computerized control system in three non-autoclave fabrication techniques: hot-press, self contained tool (self heating and pressurizing), and pressure vessel). The sensors were implemented in the parts and tools. Author

N95-28268*# General Dynamics/Convair, San Diego, CA.
DEVELOPMENT OF A LOW-COST, MODIFIED RESIN TRANSFER MOLDING PROCESS USING ELASTOMERIC TOOLING AND AUTOMATED PREFORM FABRICATION
William J. Doane and Ronald G. Hall *In* FAA, Ninth DOD/NASA/FAA Conference on Fibrous Composites in Structural Design, Volume 3 Sep. 1992 p 1163-1173 (For primary document see N95-28266 09-24)
Copyright Avail: CASI HC A03/MF A04

This paper describes the design and process development of low-cost structural parts made by a modified resin transfer molding process. Innovative application of elastomeric tooling to increase laminate fiber volume and automated forming of fiber preforms are discussed, as applied to fabrication of a representative section of a cruise missile fuselage. Author

N95-28269*# Draper (Charles Stark) Lab., Inc., Cambridge, MA.
DESIGN OF FABRIC PREFORMS FOR DOUBLE DIAPHRAGM FORMING
Steven Luby and Edward Bernardon *In* FAA, Ninth DOD/NASA/FAA Conference on Fibrous Composites in Structural Design, Volume 3 Sep. 1992 p 1175-1184 Sponsored by Dow-United Technologies Composite Products, Inc. (For primary document see N95-28266 09-24)
Copyright Avail: CASI HC A02/MF A04

Resin Transfer Molding (RTM) has the potential of becoming one of the most cost effective ways of producing composite structures since the raw materials used, resin and dry fabric, are less costly than prepregs. Unfortunately these low material costs are offset by the high labor costs incurred to layup the dry fabric into 3D shapes. To reduce the layup costs, double diaphragm forming is being investigated as a potential technique for creating a complex 3D preform from a simple flat layup. As part of our effort to develop double diaphragm forming into a production capable process, we have undertaken a series of experiments to investigate the interactions between process parameters, mold geometry, fabric weave, tow size, and the quality of the formed part. The results of these tests will be used to determine the forming geometry limitations of double diaphragm forming and to characterize the formability of fabric configurations. An important part of this work was the development of methods to measure and analyze fiber orientations, deformation angles, tow spreading, and shape conformation of the formed parts. This paper will describe the methods used to mark plies, the double diaphragm forming process, the techniques used to measure the formed parts, and the calculation of the parameters of interest. The results can be displayed as 3D contour plots. These experimental results have also been used to verify and improve a computer model which simulates the draping of fabrics over 3D mold shapes. Author

N95-28270*# Sikorsky Aircraft, Stratford, CT.
STATIC AND FATIGUE TESTING OF FULL-SCALE FUSELAGE PANELS FABRICATED USING A Therm-X(R) PROCESS
Albert J. DiNicola, Christos Kassapoglou, and Jack C. Chou *In* FAA, Ninth DOD/NASA/FAA Conference on Fibrous Composites in Structural Design, Volume 3 Sep. 1992 p 1185-1210 (For primary document see N95-28266 09-24)
(Contract NAS1-18799)
Copyright Avail: CASI HC A03/MF A04

Large, curved, integrally stiffened composite panels representative of an aircraft fuselage structure were fabricated using a Therm-X process, an alternative concept to conventional two-sided hard tooling and contour vacuum bagging. Panels subsequently were tested under pure shear loading in both static and fatigue regimes to assess the adequacy of the manufacturing process, the effectiveness of damage tolerant design features co-cured with the structure, and the accuracy of finite element and closed-form predictions of postbuckling capability and failure load. Test results indicated the process yielded panels of high quality and increased damage tolerance through suppression of common failure modes such as skin-stiffener separation and frame-stiffener corner failure. Finite element analyses generally produced good predictions of postbuckled shape, and a global-local modelling technique yielded failure load predictions that were within 7% of the experimental mean. Author

N95-28271*# Hercules Aerospace Co., Magna, UT. Composite Structures Group.
ADVANCED TOW PLACEMENT OF COMPOSITE FUSELAGE STRUCTURE
Robert L. Anderson and Carroll G. Grant *In* FAA, Ninth DOD/NASA/FAA Conference on Fibrous Composites in Structural Design, Volume 3 Sep. 1992 p 1211-1222 (For primary document see N95-28266 09-24)
Copyright Avail: CASI HC A03/MF A04

The Hercules NASA ACT program was established to demonstrate and validate the low cost potential of the automated tow placement process for fabrication of aircraft primary structures. The program is currently being conducted as a cooperative program in collaboration with the Boeing ATCAS Program. The Hercules advanced tow placement process has been in development since 1982 and was developed specifically for composite aircraft structures. The second generation machine, now in operation at Hercules, is a production-ready machine that uses a low cost prepreg tow material form to produce structures with laminate properties equivalent to prepreg tape layup. Current program activities are focused on demonstration of the automated tow placement process for fabrication of subsonic transport aircraft fuselage crown quadrants. We are working with Boeing Commercial Aircraft and Douglas Aircraft during this phase of the program. The Douglas demonstration panels has co-cured skin/stringers, and the Boeing demonstration panel is an intricately bonded part with co-cured skin/stringers and co-bonded frames. Other aircraft structures that were evaluated for the automated tow placement process include engine nacelle components, fuselage pressure bulkheads, and fuselage tail cones. Because of the cylindrical shape of these structures, multiple parts can be fabricated on one two placement tool, thus reducing the cost per pound of the finished part. Author

N95-28272*# Foster-Miller Associates, Inc., Waltham, MA.
SERVICE TOUGH COMPOSITE STRUCTURES USING THE Z-DIRECTION REINFORCEMENT PROCESS
Glenn Freitas, Constance Magee, Joseph Boyce, and Richard Bott (Naval Weapons Center, China Lake, CA.) *In* FAA, Ninth DOD/NASA/FAA Conference on Fibrous Composites in Structural Design, Volume 3 Sep. 1992 p 1223-1229 (For primary document see N95-28266 09-24)
(Contract N60530-88-C-0370)
Copyright Avail: CASI HC A02/MF A04

Foster-Miller has developed a new process to provide through thickness reinforcement of composite structures. The process reinforces laminates locally or globally on-tool during standard autoclave processing cycles. Initial test results indicate that the method has the potential to significantly reduce delamination in carbon-epoxy. Laminates reinforced with the z-fiber process have demonstrated significant improvements in mode 1 fracture toughness and compression strength after impact. Unlike alternative methods, in-plane properties are not adversely affected. Author

N95-28273*# Atlantic Research Corp., Alexandria, VA.
THROUGH-THE THICKNESS(R) BRAIDED COMPOSITES FOR AIRCRAFT APPLICATIONS
Richard T. Brown *In* FAA, Ninth DOD/NASA/FAA Conference on Fibrous Composites in Structural Design, Volume 3 Sep. 1992 p 1231-1247 (For primary document see N95-28266 09-24)
Copyright Avail: CASI HC A03/MF A04

Material and structural specimens of Through-the-Thickness(R) braided textile composites were tested in a variety of experiments. The results have demonstrated that the preform architecture provides significant payoffs in damage tolerance, delamination resistance, and attachment strength. This paper describes the braiding process, surveys the experimental data base, and illustrates the application of three dimensional braiding in aircraft structures. Author

N95-28274*# McDonnell Aircraft Co., Saint Louis, MO.
ACT/ICAPS: THERMOPLASTIC COMPOSITE ACTIVITIES
M. P. Renieri, S. J. Burpo, L. M. Roundy, and S. M. Todd *In* FAA, Ninth DOD/NASA/FAA Conference on Fibrous Composites in Structural Design, Volume 3 Sep. 1992 p 1253-1288 (For primary document see N95-28266 09-24)
Copyright Avail: CASI HC A03/MF A04

McDonnell Aircraft Company (MCAIR) is teamed with Douglas Aircraft Company (DAC) under NASA's Advanced Composite Technology (ACT) initiative in a program entitled Innovative Composite Aircraft Primary Structures (ICAPS). Efforts at MCAIR have focused on the use of thermoplastic composite materials in the development of structural details associated with an advanced fighter fuselage section with applicability to transport design. Based on innovative design/manufacturing concepts for the fuselage section primary structure, elements were designed, fabricated, and structurally tested. These elements focused on key issues such as thick composite lugs and low cost forming of fastenerless, stiffener/moldline concepts. Manufacturing techniques included autoclave consideration, single diaphragm co-consolidation (SDCC), and roll-forming. Author

N95-28275*# Pratt and Whitney Aircraft Group, West Palm Beach, FL.
COMPOSITE INTERMEDIATE CASE MANUFACTURING SCALE-UP FOR ADVANCED ENGINES c07
Rowena H. Ecklund *In* FAA, Ninth DOD/NASA/FAA Conference on Fibrous Composites in Structural Design, Volume 3 Sep. 1992 p 1289-1302 (For primary document see N95-28266 09-24)
(Contract F33615-85-C-5152)
Copyright Avail: CASI HC A03/MF A04

This Manufacturing Technology for Propulsion Program developed a process to produce a composite intermediate case for advanced gas turbine engines. The method selected to manufacture this large, complex part uses hard tooling for surfaces in the airflow path and trapped rubber to force the composite against the mold. Subelements were manufactured and tested to verify the selected design, tools, and processes. The most significant subelement produced was a half-scale version of a composite intermediate case. The half-scale subelement maintained the geometry and key dimensions of the full-scale case, allowing relevant process development and structural verification testing to be performed on the subelement before manufacturing the first full-scale case. Author

N95-28276*# National Aeronautics and Space Administration. Langley Research Center, Hampton, VA.
RESIN TRANSFER MOLDING OF TEXTILE PREFORMS FOR AIRCRAFT STRUCTURAL APPLICATIONS
Gregory H. Hasko (Lockheed Engineering and Sciences Co., Hampton, VA.), H. Benson Dexter, and Mark H. Weideman (Virginia Polytechnic Inst. and State Univ., Blacksburg, VA.) *In* FAA, Ninth DOD/NASA/FAA Conference on Fibrous Composites in Structural Design, Volume 3 Sep. 1992 p 1303-1315 (For primary document see N95-28266 09-24)
Copyright Avail: CASI HC A03/MF A04

The NASA LaRC is conducting and supporting research to develop cost-effective fabrication methods that are applicable to primary composite aircraft structures. One of the most promising fabrication methods that has evolved is resin transfer molding (RTM) of dry textile material forms. RTM has been used for many years for secondary structures, but has received increased emphasis because it is an excellent method for applying resin to damage-tolerant textile preforms at low cost. Textile preforms based on processes such as weaving, braiding, knitting, stitching, and combinations of these have been shown to offer significant improvements in damage tolerance compared to laminated tape composites. The use of low-cost resins combined with textile preforms could provide a major breakthrough in achieving cost-effective composite aircraft structures. RTM uses resin in its lowest cost form, and storage and spoilage costs are minimal. Near net shape textile preforms are expected to be cost-effective because automated machines can be used to produce the preforms, post-cure operations such as machining and fastening are minimized, and material scrap rate may be reduced in comparison with traditional prepreg molding. The purpose of this paper is to discuss experimental and analytical techniques that are under development at NASA Langley to aid the engineer in developing RTM processes for airframe structural elements. Included are experimental techniques to characterize preform and resin behavior and analytical methods that were developed to predict resin flow and cure kinetics. Author

N95-28277*# National Aeronautics and Space Administration. Lewis Research Center, Cleveland, OH.
ANALYSIS OF AIRCRAFT ENGINE BLADE SUBJECT TO ICE IMPACT c07
E. S. Reddy (Sverdrup Technology, Inc., Brook Park, OH.), G. H. Abumeri (Sverdrup Technology, Inc., Brook Park, OH.), C. C. Chamis, and P. L. N. Murthy *In* FAA, Ninth DOD/NASA/FAA Conference on Fibrous Composites in Structural Design, Volume 3 Sep. 1992 p 1319-1331 Previously announced as N92-15402 (For primary document see N95-28266 09-24)
Copyright Avail: CASI HC A03/MF A04

The ice impact problem on an engine blade made of layered composite is simulated. The ice piece is modeled as an equivalent spherical object and has the velocity opposite to that of the aircraft with direction parallel to the engine axis. Near the impact region and along the leading edge, the blade is assumed to be fully stressed and undergoes large deflection. A specified portion of the blade around the impact region is modeled. The effect of ice size and velocity on the average leading edge strain are investigated for a modified SR-2 model unswept composite propfan blade. Parametric studies are performed to study the response due to ice impact at various locations along the span. Also, the effects of engine speed on the strain and impact displacements are discussed. It is found that for a given engine speed, a critical ice speed exists that corresponds to the maximum strain and this critical speed increases with increase in the engine speed. Author

N95-28278*# Martin Marietta Corp., Baltimore, MD. Aero and Naval Systems.
APPLICATION OF FIBER-REINFORCED BISMALEIMIDE MATERIALS TO AIRCRAFT NACELLE STRUCTURES c05
Vasilios Peros, John Ruth, and David Trawinski *In* FAA, Ninth DOD/NASA/FAA Conference on Fibrous Composites in Structural Design, Volume 3 Sep. 1992 p 1333-1347 (For primary document see N95-28266 09-24)
Copyright Avail: CASI HC A03/MF A04

Existing aircraft engine nacelle structures employ advanced composite materials to reduce weight and thereby increase overall performance. Use of advanced composite materials on existing aircraft nacelle structures includes fiber-reinforced epoxy structures and has typically been limited to regions furthest away from the hot engine core. Portions of the nacelle structure that are closer to the engine require materials with a higher temperature capability. In these portions, existing nacelle structures employ aluminum sandwich construction and skin/stringer construction. The aluminum structure is composed of many detail parts and assemblies and is usually protected by some form of ablative, insulator, or metallic thermal shield. A one-piece composite inner cowl for a new-generation engine nacelle structure has been designed using fiber-reinforced bismaleimide (BMI) materials and honeycomb core in a sandwich construction. The new composite design has many advantages over the existing aluminum structure. Multiple details were integrated into the one-piece composite design, thereby significantly reducing the number of detail parts and fasteners. The use of lightweight materials and the reduction of the number of joints result in a significant weight reduction over the aluminum design; manufacturing labor and the overall number of tools required have also been reduced. Several significant technical issues were addressed in the development of a BMI composite design. Technical evaluation of the available BMI systems led to the selection of a toughened BMI material which was resistant to microcracking under thermal cyclic loading and enhanced the damage tolerance of the structure. Technical evaluation of the degradation of BMI materials in contact with aluminum and other metals validated methods for isolation of the various materials. Graphite-reinforced BMI in contact with aluminum and some steels was found to degrade in salt spray testing. Isolation techniques such as those used for graphite-reinforced epoxy structures were shown to provide adequate protection. The springback and producibility of large BMI structures were evaluated by manufacturing prototype hardware which had the full-scale cross section of the one-piece composite structure. Author

N95-28279*# McDonnell Aircraft Co., Saint Louis, MO.
ASSEMBLY INDUCED DELAMINATIONS IN COMPOSITE STRUCTURES
J. Goering, R. Bohlmann, S. Wanthal, E. Kautz (Naval Air Development Center, Warminster, PA.), and Lawrence M. Neri (Federal Aviation Administration, Atlantic City, NJ.) *In* FAA, Ninth DOD/NASA/FAA Conference on Fibrous Composites in Structural Design, Volume 3 Sep. 1992 p 1353-1377 (For primary document see N95-28266 09-24)
(Contract N62269-90-C-0281)
Copyright Avail: CASI HC A03/MF A04

Experimental and analytical studies of the development of delaminations around fastener holes in composite structures are presented. This type of delamination is known to occur in composite skins that are mechanically fastened to a poorly mating substructure. Results of an experimental study to determine the resistance of laminates to the initiation of assembly induced delaminations and the residual strength of assembly damaged coupons are presented for AS4/3501-6, IM7/8551-7A, and AS4/PEEK material systems. A survey of existing analytical models for predicting the residual strength and stability of delaminations is presented, and the development of a new model for predicting the initiation of delaminations around a fastener hole is outlined. The fastener hole damage initiation model utilizes a finite element based Fourier series solution, and is validated through comparisons of analytical and experimental results. Author

N95-28280*# Army Armament Research, Development and Engineering Center, Watervliet, NY. Close Combat Armaments Center.
STRESS ANALYSIS AND FAILURE OF AN INTERNALLY PRESSURIZED COMPOSITE-JACKETED STEEL CYLINDER c39
Peter C. T. Chen *In* FAA, Ninth DOD/NASA/FAA Conference on Fibrous Composites in Structural Design, Volume 3 Sep. 1992 p 1379-1388 (For primary document see N95-28266 09-24)
Copyright Avail: CASI HC A02/MF A04

This paper presents a nonlinear stress analysis of a thick-walled compound tube subjected to internal pressure. The compound tube is constructed of a steel liner and a graphite-bismaleimide outer shell. Analytical expressions for the stresses, strains, and displacements are derived for all loading ranges up to failure. Numerical results for the stresses and the maximum value that the compound tube can contain without failure are presented. Author

N95-28281*# Naval Weapons Center, China Lake, CA.
COMPOSITE FLIGHT-CONTROL ACTUATOR DEVELOPMENT c08
Richard Bott and Fred Ching (Textron, Inc., Valencia, CA.) *In* FAA, Ninth DOD/NASA/FAA Conference on Fibrous Composites in Structural Design, Volume 3 Sep. 1992 p 1389-1404 (For primary document see N95-28266 09-24)
(Contract N60530-88-C-0260)
Copyright Avail: CASI HC A03/MF A04

The composite actuator is 'jam resistant', satisfying a survivability requirement for the Navy. Typically, the push-pull force needed to drive through the wound area of the composite actuator is 73 percent less than that of an all-metal actuator. In addition to improving the aircraft's combat survivability, significant weight savings were realized. The current design of the survivable, composite actuator cylinder is 36 percent lighter than that of the production steel cylinder, which equates to a 15 percent overall actuator weight savings. Author

N95-28282*# McDonnell Aircraft Co., Saint Louis, MO.
HIGHER ORDER FINITE ELEMENT ANALYSIS OF THICK COMPOSITE LAMINATES
J. Goering and H. J. Kim *In* FAA, Ninth DOD/NASA/FAA Conference

on Fibrous Composites in Structural Design, Volume 3 Sep. 1992 p 1407-1415 (For primary document see N95-28266 09-24)
(Contract NAS1-18862)
Copyright Avail: CASI HC A02/MF A04

A higher order, sub-parametric, laminated, 3D solid finite element was used for the analysis of very thick laminated composite plates. The geometry of this element is defined by four nodes in the X-Y plane which define a prism of material through the thickness of the laminate. There are twenty-four degrees of freedom at each node; translations at the upper and lower surfaces of the laminate in each of the three coordinate directions, and the derivatives of these translations with respect to each coordinate. This choice of degrees of freedom leads to displacement and strain compatibility at the corners. Stacking sequence effects are accounted for by explicitly integrating the strain energy density through the thickness of the element. The laminated solid element was combined with a gap-contact element to analyze thick laminated composite lugs loaded through flexible pins. The resulting model accounts for pin bending effects that produce non-uniform bearing stresses through the thickness of the lug. A thick composite lug experimental test program was performed, and provided data that was used to validate the analytical model. Two lug geometries and three stacking sequences were tested. Author

N95-28283*# Army Materials Technology Lab., Watertown, MA. Mechanics and Structures Branch.
AN IMPROVED PLATE THEORY OF ORDER (1,2) FOR THICK COMPOSITE LAMINATES
A. Tessler *In* FAA, Ninth DOD/NASA/FAA Conference on Fibrous Composites in Structural Design, Volume 3 Sep. 1992 p 1417-1430 (For primary document see N95-28266 09-24)
Copyright Avail: CASI HC A03/MF A04

A new (1,2)-order theory is proposed for the linear elasto-static analysis of laminated composite plates. The basic assumptions are those concerning the distribution through the laminate thickness of the displacements, transverse shear strains and the transverse normal stress, with these quantities regarded as some weighted averages of their exact elasticity theory representations. The displacement expansions are linear for the inplane components and quadratic for the transverse component, whereas the transverse shear strains and transverse normal stress are respectively quadratic and cubic through the thickness. The main distinguishing feature of the theory is that all strain and stress components are expressed in terms of the assumed displacements prior to the application of a variational principle. This is accomplished by an a priori least-square compatibility requirement for the transverse strains and by requiring exact stress boundary conditions at the top and bottom plate surfaces. Equations of equilibrium and associated Poisson boundary conditions are derived from the virtual work principle. It is shown that the theory is particularly suited for finite element discretization as it requires simple C(sup 0)- and C(sup -1)-continuous displacement interpolation fields. Analytic solutions for the problem of cylindrical bending are derived and compared with the exact elasticity solutions and those of our earlier (1,2)-order theory based on the assumed displacements and transverse strains. Author

N95-28284*# Materials Sciences Corp., Blue Bell, PA.
FAILURE ANALYSIS OF THICK COMPOSITE CYLINDERS UNDER EXTERNAL PRESSURE c39
A. Caiazzo and B. W. Rosen *In* FAA, Ninth DOD/NASA/FAA Conference on Fibrous Composites in Structural Design, Volume 3 Sep. 1992 p 1431-1446 Prepared for ORNL, TN; and Martin Marietta Energy Systems, Inc., Oak Ridge, TN (For primary document see N95-28266 09-24)
Copyright Avail: CASI HC A03/MF A04

Failure of thick section composites due to local compression strength and overall structural instability is treated. Effects of material nonlinearity, imperfect fiber architecture, and structural imperfections upon anticipated failure stresses are determined. Comparisons with experimental data for a series of test cylinders are described. Predicting the failure strength of composite structures requires consideration of stability and material strength modes of failure using linear and nonlinear analysis techniques. Material strength prediction requires the accurate definition of the local multiaxial stress state in the material. An elasticity solution for the linear static analysis of thick anisotropic cylinders and rings is used herein to predict the axisymmetric stress state in the cylinders. Asymmetric nonlinear behavior due to initial cylinder out of roundness and the effects of end closure structure are treated using finite element methods. It is assumed that local fiber or ply waviness is an important factor in the initiation of material failure. An analytical model for the prediction of compression failure of fiber composites, which includes the effects of fiber misalignments, matrix inelasticity, and multiaxial applied stresses is used for material strength calculations. Analytical results are compared to experimental data for a series of glass and carbon fiber reinforced epoxy cylinders subjected to external pressure. Recommendations for pretest characterization and other experimental issues are presented. Implications for material and structural design are discussed. Author

N95-28285*# Utah Univ., Salt Lake City, UT. Dept. of Materials Science and Engineering.
ON THE THERMALLY-INDUCED RESIDUAL STRESSES IN THICK FIBER-THERMOPLASTIC MATRIX (PEEK) CROSS-PLY LAMINATED PLATES c39
Shoufeng Hu and John A. Nairn *In* FAA, Ninth DOD/NASA/FAA Conference on Fibrous Composites in Structural Design, Volume 3 Sep. 1992 p 1447-1454 (For primary document see N95-28266 09-24)
(Contract NAS1-18833)
Copyright Avail: CASI HC A02/MF A04

An analytical method for calculating thermally-induced residual stresses in laminated plates is applied to cross-ply PEEK laminates. We considered three cooling procedures: slow cooling (uniform temperature distribution); convective and radiative cooling; and rapid cooling by quenching (constant surface temperature). Some of the calculated stresses are of sufficient magnitude to effect failure properties such as matrix microcracking. Author

N95-28286*# National Aeronautics and Space Administration. Langley Research Center, Hampton, VA.
ANALYSIS OF STRESSES IN FINITE ANISOTROPIC PANELS WITH CENTRALLY LOCATED CUTOUTS c39
Vicki O. Britt *In* FAA, Ninth DOD/NASA/FAA Conference on Fibrous Composites in Structural Design, Volume 3 Sep. 1992 p 1485-1505 (For primary document see N95-28266 09-24)
Copyright Avail: CASI HC A03/MF A04

A method for analyzing biaxial- and shear-loaded anisotropic rectangular panels with centrally located circular and elliptical cutouts is presented in the present paper. The method is based on Lekhnitskii's complex variable equations of plane elastostatics combined with a boundary collocation method and a Laurent series approximation. Results are presented for anisotropic panels with elliptical cutouts and subjected to combined shear and compression loading. The effects on the stress field of panel aspect ratio, anisotropy, cutout size, and cutout orientation are addressed. Angle-ply laminates, unidirectional off-axis laminates, and ((+ or - 45/0/90)(sub 3))s, ((+ or - 45/0(sub 2))(sub 3))s, and ((+ or - 45/90(sub 2))(sub 3))s laminates are examined. Author

N95-28287*# Douglas Aircraft Co., Inc., Long Beach, CA.
THE ROLE OF BIAXIAL STRESSES IN DISCRIMINATING BETWEEN MEANINGFUL AND ILLUSORY COMPOSITE FAILURE THEORIES c39
L. J. Hart-Smith *In* FAA, Ninth DOD/NASA/FAA Conference on Fibrous Composites in Structural Design, Volume 3 Sep. 1992 p 1507-1528 (For primary document see N95-28266 09-24)
Copyright Avail: CASI HC A03/MF A04

The irrelevance of most composite failure criteria to conventional fiber-polymer composites is claimed to have remained undetected primarily because the experiments that can either validate or disprove them are difficult to perform. Uniaxial tests are considered inherently incapable of validating or refuting any composite failure theory because so much of the total load is carried by the fibers aligned in the direction of the load. The Ten-Percent Rule, a simple rule-of-mixtures analysis method, is said to work well only because of this phenomenon. It is stated that failure criteria can be verified for fibrous composites only by biaxial tests, with orthogonal in-plane stresses of the same as well as different signs, because these particular states of combined stress reveal substantial differences between the predictions of laminate strength made by various theories. Three scientifically plausible failure models for fibrous composites are compared, and it is shown that only the in-plane shear test (orthogonal tension and compression) is capable of distinguishing between them. This is because most theories are 'calibrated' against the measured uniaxial tension and compression tests and any cross-plied laminate tests dominated by those same states of stress must inevitably 'confirm' the theory. Author

N95-28288*# Hercules, Inc., Magna, UT. Advanced Materials and Systems Co.
STATIC AND DYNAMIC STRAIN ENERGY RELEASE RATES IN TOUGHENED THERMOSETTING COMPOSITE LAMINATES **c39**
Douglas S. Cairns *In* FAA, Ninth DOD/NASA/FAA Conference on Fibrous Composites in Structural Design, Volume 3 Sep. 1992 p 1529-1538 Previously announced in IAA as A92-37000 (For primary document see N95-28266 09-24)
Copyright Avail: CASI HC A02/MF A04

In this work, the static and dynamic fracture properties of several thermosetting resin based composite laminates are presented. Two classes of materials are explored. These are homogeneous, thermosetting resins and toughened, multi-phase, thermosetting resin systems. Multi-phase resin materials have shown enhancement over homogenous materials with respect to damage resistance. The development of new dynamic tests are presented for composite laminates based on Width Tapered Double Cantilevered Beam (WTDCB) for Mode 1 fracture and the End Notched Flexure (ENF) specimen. The WTDCB sample was loaded via a low inertia, pneumatic cylinder to produce rapid cross-head displacements. A high rate, piezo-electric load cell and an accelerometer were mounted on the specimen. A digital oscilloscope was used for data acquisition. Typical static and dynamic load versus displacement plots are presented. The ENF specimen was impacted in three point bending with an instrumented impact tower. Fracture initiation and propagation energies under static and dynamic conditions were determined analytically and experimentally. The test results for Mode 1 fracture are relatively insensitive to strain rate effects for the laminates tested in this study. The test results from Mode 2 fracture indicate that the toughened systems provide superior fracture initiation and higher resistance to propagation under dynamic conditions. While the static fracture properties of the homogeneous systems may be relatively high, the apparent Mode 2 dynamic critical strain energy release rate drops significantly. The results indicate that static Mode 2 fracture testing is inadequate for determining the fracture performance of composite structures subjected to conditions such as low velocity impact. A good correlation between the basic Mode 2 dynamic fracture properties and the performance is a combined material/structural Compression After Impact (CAI) test is found. These results underscore the importance of examining rate-dependent behavior for determining the longevity of structures manufactured from composite materials. Author

N95-28289*# McDonnell Aircraft Co., Saint Louis, MO.
ANALYSIS TECHNIQUES FOR THE PREDICTION OF SPRINGBACK IN FORMED AND BONDED COMPOSITE COMPONENTS
Michael F. Gasick and Gary D. Renieri *In* FAA, Ninth DOD/NASA/FAA Conference on Fibrous Composites in Structural Design, Volume 3 Sep. 1992 p 1539-1558 (For primary document see N95-28266 09-24)
Copyright Avail: CASI HC A03/MF A04

Two finite element analysis codes are used to model the effects of cooling on the dimensional stability of formed and bonded composite parts. The two analysis routines, one h-version and one p-version, are compared for modeling time, analysis execution time, and exactness of solution as compared to actual test results. A recommended procedure for predicting temperature effects on composite parts is presented, based on the results of this study. Author

N95-28290*# National Aeronautics and Space Administration. Langley Research Center, Hampton, VA.
STIFFNESS AND STRENGTH TAILORING IN UNIFORM SPACE-FILLING TRUSS STRUCTURES **c39**
Mark S. Lake *In* FAA, Ninth DOD/NASA/FAA Conference on Fibrous Composites in Structural Design, Volume 3 Sep. 1992 p 1561-1587 Previously announced as N92-24546 (For primary document see N95-28266 09-24)
Copyright Avail: CASI HC A03/MF A04

This paper presents a deterministic procedure for tailoring the continuum stiffness and strength of uniform space-filling truss structures through the appropriate selection of truss geometry and member sizes (i.e., flexural and axial stiffnesses and length). The trusses considered herein are generated by replication of a characteristic truss cell uniformly through space. The repeating cells are categorized by one of a set of possible geometric symmetry groups derived using the techniques of crystallography. The elastic symmetry associated with each geometric symmetry group is identified to aid in the selection of an appropriate truss geometry for a given application. Stiffness and strength tailoring of a given truss geometry is enabled through explicit expressions relating the continuum stiffnesses and failure stresses of the truss to the stiffnesses and failure loads of its members. These expressions are derived using an existing equivalent continuum analysis technique and a newly developed analytical failure theory for trusses. Several examples are presented to illustrate the application of these techniques, and to demonstrate the usefulness of the information gained from this analysis. Author

N95-28291*# Aerospace Corp., El Segundo, CA. Mechanics and Materials Technology Center.
DESIGN PREDICTION FOR LONG TERM STRESS RUPTURE SERVICE OF COMPOSITE PRESSURE VESSELS **c39**
Ernest Y. Robinson *In* FAA, Ninth DOD/NASA/FAA Conference on Fibrous Composites in Structural Design, Volume 3 Sep. 1992 p 1589-1616 (For primary document see N95-28266 09-24)
(Contract F04701-88-C-0089)
Copyright Avail: CASI HC A03/MF A04

Extensive stress rupture studies on glass composites and Kevlar composites were conducted by the Lawrence Radiation Laboratory beginning in the late 1960's and extending to about 8 years in some cases. Some of the data from these studies published over the years were incomplete or were tainted by spurious failures, such as grip slippage. Updated data sets were defined for both fiberglass and Kevlar composite stand test specimens. These updated data are analyzed in this report by a convenient form of the bivariate Weibull distribution, to establish a consistent set of design prediction charts that may be used as a conservative basis for predicting the stress rupture life of composite pressure vessels. The updated glass composite data exhibit an invariant Weibull modulus with lifetime. The data are analyzed in terms of homologous service load (referenced to the observed median strength). The equations relating life, homologous load, and probability are given, and corresponding design prediction charts are presented. A similar approach is taken for Kevlar composites, where the updated stand data do show a turndown tendency at long life accompanied by a corresponding change (increase) of the Weibull modulus. The turndown characteristic is not present in stress rupture test data of Kevlar pressure vessels. A modification of the stress rupture equations is presented to incorporate a latent, but limited, strength drop, and design prediction charts are presented that incorporate such behavior. The methods presented utilize Cartesian plots of the probability distributions (which are a more natural display for the design engineer), based on median normalized data that are independent of statistical parameters and are readily defined for any set of test data. Author

N95-28292*# National Aeronautics and Space Administration. Langley Research Center, Hampton, VA.
DESIGNING FOR TIME-DEPENDENT MATERIAL RESPONSE IN SPACECRAFT STRUCTURES **c18**
M. W. Hyer (Virginia Polytechnic Inst. and State Univ., Blacksburg, VA.), Lynda L. S. Oleksuk (Virginia Polytechnic Inst. and State Univ., Blacksburg, VA.), and D. E. Bowles *In* FAA, Ninth DOD/NASA/FAA Conference on Fibrous Composites in Structural Design, Volume 3 Sep. 1992 p 1617-1630 (For primary document see N95-28266 09-24)
(Grant NAG1-343)
Copyright Avail: CASI HC A03/MF A04

To study the influence on overall deformations of the time-dependent constitutive properties of fiber-reinforced polymeric matrix composite materials being considered for use in orbiting precision segmented reflectors, simple sandwich beam models are developed. The beam models include layers representing the face sheets, the core, and the adhesive bonding of the face sheets to the core. A three-layer model lumps the adhesive layers with the face sheets or core, while a five-layer model considers the adhesive layers explicitly. The deformation response of the three-layer and five-layer sandwich beam models to a midspan point load is studied. This elementary loading leads to a simple analysis, and it is easy to create this loading in the laboratory. Using the correspondence principle of viscoelasticity, the models representing the elastic behavior of the two beams are transformed into time-dependent models. Representative cases of time-dependent material behavior for the facesheet material, the core material, and the adhesive are used to evaluate the influence of these constituents being time-dependent on the deformations of the beam. As an example of the results presented, if it assumed that, as a worst case, the polymer-dominated shear properties of the core behave as a Maxwell fluid such that under constant shear stress the shear strain increases by a factor of 10 in 20 years, then it is shown that the beam deflection increases by a factor of 1.4 during that time. In addition to quantitative conclusions, several assumptions are discussed which simplify the analyses for use with more complicated material models. Finally, it is shown that the simpler three-layer model suffices in many situations. Author

N95-28293*# National Aeronautics and Space Administration. Ames Research Center, Moffett Field, CA.
COMPOSITE FLEXIBLE INSULATION FOR THERMAL PROTECTION OF SPACE VEHICLES **c18**
Demetrius A. Kourtides, Huy K. Tran, and S. Amanda Chiu (Sterling Software, Inc., Palo Alto, CA.) *In* FAA, Ninth DOD/NASA/FAA Conference on Fibrous Composites in Structural Design, Volume 3 Sep. 1992 p 1631-1646 (For primary document see N95-28266 09-24)
Copyright Avail: CASI HC A03/MF A04

A composite flexible blanket insulation (CFBI) system considered for use as a thermal protection system for space vehicles is described. This flexible composite insulation system consists of an outer layer of silicon carbide fabric, followed by alumina mat insulation, and alternating layers of aluminized polyimide film and aluminoborosilicate scrim fabric. A potential application of this composite insulation would be as a thermal protection system for the aerobrake of the Aeroassist Space Transfer Vehicle (ASTV). It would also apply to other space vehicles subject to high convective and radiative heating during atmospheric entry. The thermal performance of this composite insulation as exposed to a simulated atmospheric entry environment in a plasma arc test facility is described. Other thermophysical properties which affect the thermal response of this system are also described. Analytical modeling describing the thermal performance of this composite insulation is included. It shows that this composite insulation is effective as a thermal protection system at total heating rates up to 30.6 W/sq cm. Author

N95-28420*# Galaxy Scientific Corp., Hampton, VA.
NINTH DOD/NASA/FAA CONFERENCE ON FIBROUS COMPOSITES IN STRUCTURAL DESIGN, VOLUME 1
Joseph R. Soderquist, comp., Lawrence M. Neri, comp. (Federal Aviation Administration, Atlantic City, NJ.), and Herman L. Bohon, comp. (Galaxy Scientific Corp., Hampton, VA.) Sep. 1992 548 p Conference held in Lake Tahoe, NV, 4-7 Nov. 1991; sponsored by NASA, AF, Army, and Navy Sponsored by NASA
(NASA-CR-198723; NAS 1.26:198723; DOT/FAA/CT-92-25-Vol-1) Avail: CASI HC A23/MF A04

This publication contains the proceedings of the Ninth DOD/NASA/FAA conference on Fibrous Composites in structural Design. Presentations were made in the following areas of composite structural design: perspectives in composites; design methodology; design applications; design criteria; supporting technology; damage tolerance; and manufacturing. For individual titles, see N95-28421 through N95-28446.

N95-28421*# Army Materiel Command, Aberdeen Proving Ground, MD.
UTILIZATION OF COMPOSITE MATERIALS BY THE US ARMY: A LOOK AHEAD
Richard Chait *In* FAA, Ninth DOD/NASA/FAA Conference on Fibrous Composites in Structural Design, Volume 1 Sep. 1992 p 7-34 (For primary document see N95-28420 09-24)
Avail: CASI HC A03/MF A04

An overview of the use of composite materials in the Army is given. Important efforts to document design information, supporting research, and some national applications for composite materials are given. The use of Kevlar fiber in both vests and helmets for the soldier is outlined. The advantages of using fiberglass in the hull of the Bradley fighting ground vehicle is given. The full potential of composite materials is realized in the recently awarded LH Comanche RAH-66 program. The use of composites for application to rocket motor uses, wings, fins, and casings is under development. Because of the uncertain funding profile, it is more important than ever that technology planning provide the basis for effective prioritization and leveraging of the tech base efforts involving advanced materials. CASI

N95-28422*# Naval Air Development Center, Warminster, PA.
BENEFITS AND LIMITATIONS OF COMPOSITES IN CARRIER-BASED AIRCRAFT
Donald P. McErlean *In* FAA, Ninth DOD/NASA/FAA Conference on Fibrous Composites in Structural Design, Volume 1 Sep. 1992 p 35-92 (For primary document see N95-28420 09-24)
Avail: CASI HC A04/MF A04

There are many unique aspects of Navy air missions that lead to the differentiation between the design and performance of ship and shore-based aircraft. The major aspects are discussed from which essentially all Navy aircraft design requirements derive. (1) Navy aircraft operate from carriers at sea imposes a broad spectrum of physical conditions, constraints, and requirements ranging from the harsh sea environment, the space limitations of a carrier, takeoff and landing requirements as well as for endurance at long distances from the carrier. (2) Because the carrier and its airwing are intended to be capable of responding to a broad range of contingencies, mission flexibility is essential (maximum weapon carriage, rapid reconfiguration, multiple mission capability). (3) The embarked aircraft provides the long range defense of the battle group against air, surface and subsurface launched antiship missiles. (4) The carrier and its aircraft must operate independently and outside of normal supply lines. Taking into account these aspects, the use of composite materials in the design and performance of naval aircraft is outlined, also listing advantages and disadvantages. Author

N95-28423*# Lockheed Engineering and Sciences Co., Hampton, VA.
MECHANICAL PROPERTIES OF TRIAXIALLY BRAIDED COMPOSITES: EXPERIMENTAL AND ANALYTICAL RESULTS
John E. Masters, Raymond L. Foye (North Carolina Agricultural and Technical State Univ., Greensboro, NC.), Christopher M. Pastore (North Carolina Univ., Raleigh, NC.), and Yasser A. Gowayed (North Carolina Univ., Raleigh, NC.) *In* FAA, Ninth DOD/NASA/FAA Conference on Fibrous Composites in Structural Design, Volume 1 Sep. 1992 p 99-124 Previously announced as N92-19725 (For primary document see N95-28420 09-24)
Avail: CASI HC A03/MF A04

The unnotched tensile properties of 2-D triaxial braid reinforced composites from both an experimental and an analytical viewpoint are studied. The materials are graphite fibers in an epoxy matrix. Three different reinforcing fiber architectures were considered. Specimens were cut from resin transfer molded (RTM) composite panels made from each braid. There were considerable differences in the observed elastic constants from different size strain gage and extensometer reading. Larger strain gages gave more consistent results and correlated better with the extensometer reading. Experimental strains correlated reasonably well with analytical predictions in the longitudinal, 0 degrees, fiber direction but not in the transverse direction. Tensile strength results were not always predictable even in reinforcing directions. Minor changes in braid geometry led to disproportionate strength variations. The unit cell structure of the triaxial braid was discussed with the assistance of computer analysis of the microgeometry. Photomicrographs of braid geometry were used to improve upon the computer graphics representations of unit cells. These unit cells were used to predict the elastic moduli with various degrees of sophistication. The simple and the complex analyses were generally in agreement but none adequately matched the experimental results for all the braids. Author

N95-28424*# Rockwell International Science Center, Thousand Oaks, CA.
MECHANISMS OF COMPRESSIVE FAILURE IN WOVEN COMPOSITES AND STITCHED LAMINATES
B. N. Cox, M. S. Dadkhah, R. V. Inman, W. L. Morris, and S. Schroeder *In* FAA, Ninth DOD/NASA/FAA Conference on Fibrous Composites in Structural Design, Volume 1 Sep. 1992 p 125-13 (For primary document see N95-28420 09-24)
(Contract NAS1-18840)
Avail: CASI HC A03/MF A04

Stitched laminates and angle interlock woven composites have been studied in uniaxial, in-plane, monotonic compression. Failure mechanisms have been found to depend strongly on both the reinforcement architecture and the degree of constraint imposed by the loading grips. Stitched laminates show higher compressive strength, but are brittle, possessing no load bearing capacity beyond the strain for peak load. Post-mortem inspection shows a localized shear band of buckled and broken fibers, which is evidently the product of an unstably propagating kink band. Similar shear bands are found in the woven composites if the constraint of lateral displacements is weak; but, under strong constraint, damage is not localized but distributed throughout the gauge section. While the woven composites tested are weaker than the stitched laminates, they continue to bear significant loads to compressive strains of approx. 15 percent, even when most damage is confined to a shear band. Author

N95-28425*# Naval Air Development Center, Warminster, PA.

EFFECT OF THE FIBER-MATRIX INTERPHASE ON THE TRANSVERSE TENSILE STRENGTH OF THE UNIDIRECTIONAL COMPOSITE MATERIAL

H. C. Tsai and A. M. Arocho *In* FAA, Ninth DOD/NASA/FAA Conference on Fibrous Composites in Structural Design, Volume 1 Sep. 1992 p 139-15 (For primary document see N95-28420 09-24)

Avail: CASI HC A03/MF A04

A simple one-dimensional fiber-matrix interphase model has been developed and analytical results obtained correlated well with available experimental data. It was found that by including the interphase between the fiber and matrix in the model, much better local stress results were obtained than with the model without the interphase. A more sophisticated two-dimensional micromechanical model, which included the interphase properties was also developed. Both one-dimensional and two-dimensional models were used to study the effect of the interphase properties on the local stresses at the fiber, interphase and matrix. From this study, it was found that interphase modulus and thickness have significant influence on the transverse tensile strength and mode of failure in fiber reinforced composites. Author

N95-28426*# Delaware Univ., Newark, DE. Dept. of Mechanical Engineering.

THE EFFECT OF MATERIAL HETEROGENEITY IN CURVED COMPOSITE BEAMS FOR USE IN AIRCRAFT STRUCTURES

Brendan J. OToole and Michael H. Santare *In* FAA, Ninth DOD/NASA/FAA Conference on Fibrous Composites in Structural Design, Volume 1 Sep. 1992 p 157-16 (For primary document see N95-28420 09-24)

(Contract NAS1-18758)

Avail: CASI HC A02/MF A04

A design tool is presented for predicting the effect of material heterogeneity on the performance of curved composite beams for use in aircraft fuselage structures. Material heterogeneity can be induced during processes such as sheet forming and stretch forming of thermoplastic composites. This heterogeneity can be introduced in the form of fiber realignment and spreading during the manufacturing process causing a gradient in material properties in both the radial and tangential directions. The analysis procedure uses a separate two-dimensional elasticity solution for the stresses in the flanges and web sections of the beam. The separate solutions are coupled by requiring the forces and displacements match at the section boundaries. Analysis is performed for curved beams loaded in pure bending and uniform pressure. The beams can be of any general cross-section such as a hat, T-, I-, or J-beam. Preliminary results show that geometry of the beam dictates the effect of heterogeneity on performance. Heterogeneity plays a much larger role in beams with a small average radius to depth ratio, R/t, where R is the average radius of the beam and t is the difference between the inside and outside radius. Results of the analysis are in the form of stresses and displacements, and they are compared to both mechanics of materials and numerical solutions obtained using finite element analysis. Author

N95-28427*# Boeing Defense and Space Group, Seattle, WA. Military Airplane Div.

INVESTIGATION OF STATIC AND CYCLIC BEARING FAILURE MECHANISMS FOR GR/EP LAMINATES

R. W. Walter and M. M. Tuttle *In* FAA, Ninth DOD/NASA/FAA Conference on Fibrous Composites in Structural Design, Volume 1 Sep. 1992 p 167-18 (For primary document see N95-28420 09-24)

Avail: CASI HC A03/MF A04

Static, cyclic load (fatigue), and residual strength testing of graphite-epoxy (GR/EP) and aluminum pin bearing joints was completed to study bearing failure mechanisms. Parameters investigated included static strength, failure mode, fatigue life, hole growth, joint stiffness, and residual strength. Comparative evaluation of these results show that the MIL-HDBK-5 convention for the definition of bearing strength can be used for GR/EP materials while maintaining the same, or improved, level of structural integrity shown for metal joints. Author

N95-28428*# National Aeronautics and Space Administration. Langley Research Center, Hampton, VA.

COMPRESSION FAILURE OF ANGLE-PLY LAMINATES

L. D. Peel (Mirage Carriage Works, West Valley, UT.), M. W. Hyer (Virginia Polytechnic Inst. and State Univ., Blacksburg, VA.), and M. J. Shuart *In* FAA, Ninth DOD/NASA/FAA Conference on Fibrous Composites in Structural Design, Volume 1 Sep. 1992 p 185-19 (For primary document see N95-28420 09-24)

(Grant NAG1-343)

Avail: CASI HC A03/MF A04

Test results from the compression loading of (+ or - Theta/ - or + Theta)(sub 6s) angle-ply IM7-8551-7a specimens, 0 less than or = Theta less than or = 90 degs, are presented. The observed failure strengths and modes are discussed, and typical stress-strain relations shown. Using classical lamination theory and the maximum stress criterion, an attempt is made to predict failure stress as a function of Theta. This attempt results in poor correlation with test results and thus a more advanced model is used. The model, which is based on a geometrically nonlinear theory, and which was taken from previous work, includes the influence of observed layer waviness. The waviness is described by the wave length and the wave amplitude. The theory is briefly described and results from the theory are correlated with test results. It is shown that by using levels of waviness observed in the specimens, the correlation between predictions and observations is good. Author

N95-28429*# Northrop Corp., Hawthorne, CA. Aircraft Div.

ANALYSIS OF COMPOSITE STRUCTURES WITH DELAMINATIONS UNDER COMBINED BENDING AND COMPRESSION

Han-Pin Kan, Edward Kautz (Naval Air Development Center, Warminster, PA.), and Larry Neri (Federal Aviation Administration, Atlantic City, NJ.) *In* FAA, Ninth DOD/NASA/FAA Conference on Fibrous Composites in Structural Design, Volume 1 Sep. 1992 p 197-21 (For primary document see N95-28420 09-24)

(Contract N62269-90-C-0282)

Avail: CASI HC A03/MF A04

A methodology had been developed for strength prediction of composite structures with delaminations under combined bending and compression loads. The methodology is an extension of the delamination analysis method developed under the USAF/Boeing/Northrop 'Damage Tolerance of Composites' program. Delamination buckling and strain energy release rate analyses are used as basic tools in the strength prediction. In addition, failure mode interaction and structural configuration effects are considered. The influence of fasteners on the strength of a delaminated structure is incorporated to evaluate assembly-caused delaminations. The capabilities and limitations of the analysis method are shown by correlating the analytical results with the existing experimental data. The failure load, failure mode and failure sequence of a structure containing delaminations are predicted and the analytical results are compared with test data. Author

N95-28430*# National Aeronautics and Space Administration. Langley Research Center, Hampton, VA.

BUCKLING BEHAVIOR OF LONG SYMMETRICALLY LAMINATED PLATES SUBJECTED TO COMBINED LOADS

Michael P. Nemeth *In* FAA, Ninth DOD/NASA/FAA Conference on Fibrous Composites in Structural Design, Volume 1 Sep. 1992 p 227-25 Previously announced as N92-25160 (For primary document see N95-28420 09-24)

Avail: CASI HC A03/MF A04

A parametric study of the buckling behavior of infinitely long symmetrically laminated anisotropic plates subjected to combined loadings is presented. The loading conditions considered are axial tension and compression, transverse tension and compression, and shear. Results obtained using a special purpose analysis, well suited for parametric studies are presented for clamped and simply supported plates. Moreover, results are presented for some common laminate constructions, and generic buckling design charts are presented for a wide range of parameters. The generic design charts are presented in terms of useful nondimensional parameters, and dependence of the nondimensional parameters on laminate fiber orientation, stacking sequence, and material properties is discussed. An important finding of the study is that the effects of anisotropy are much more pronounced in shear-loaded plates than in compression loaded plates. In addition, the effects of anisotropy on plates subjected to combined loadings are generally manifested as a phase shift of self-similar buckling interaction curves. A practical application of this phase shift is the buckling resistance of long plates can be improved by applying a shear loading with a specific orientation. In all cases considered, it is found that the buckling coefficients of infinitely long plates are independent of the bending stiffness ratio (D sub 11/D sub 22) sup 1/4. Author

N95-28431*# Massachusetts Inst. of Tech., Cambridge, MA. Technology Lab. for Advanced Composites.

COMPRESSIVE RESIDUAL STRENGTH OF GRAPHITE/EPOXY LAMINATES AFTER IMPACT

Teresa A. Guy and Paul A. Lagace *In* FAA, Ninth DOD/NASA/FAA Conference on Fibrous Composites in Structural Design, Volume 1 Sep. 1992 p 253-27 (For primary document see N95-28420 09-24)

Avail: CASI HC A03/MF A04

The issue of damage tolerance after impact, in terms of the compressive residual strength, was experimentally examined in graphite/epoxy laminates using Hercules AS4/3501-6 in a (+ or - 45/0)(sub 2S) configuration. Three different impactor masses were used at various velocities and the resultant damage measured via a number of nondestructive and destructive techniques. Specimens were then tested to failure under uniaxial compression. The results clearly show that a minimum compressive residual strength exists which is below the open hole strength for a hole of the same diameter as the impactor. Increases in velocity beyond the point of minimum strength cause a difference in the damage produced and cause a resultant increase in the compressive residual strength which asymptotes to the open hole strength value. Furthermore, the results show that this minimum compressive residual strength value is independent of the impactor mass used and is only dependent upon the damage present in the impacted specimen which is the same for the three impactor mass cases. A full 3-D representation of the damage is obtained through the various techniques. Only this 3-D representation can properly characterize the damage state that causes the resultant residual strength. Assessment of the state-of-the-art in predictive analysis capabilities shows a need to further develop techniques based on the 3-D damage state that exists. In addition, the need for damage 'metrics' is clearly indicated. Author

N95-28432*# Boeing Defense and Space Group, Philadelphia, PA. Helicopters Div.

APPLICATION OF ADVANCED MATERIAL SYSTEMS TO COMPOSITE FRAME ELEMENTS

Steven Llorente, Pierre Minguet, Russell Fay, and Steven Medwin (Du Pont de Nemours, E. I. and Co., Wilmington, DE.) *In* FAA, Ninth DOD/NASA/FAA Conference on Fibrous Composites in Structural Design, Volume 1 Sep. 1992 p 277-29 (For primary document see N95-28420 09-24)

Avail: CASI HC A03/MF A04

A three phase program has been conducted to investigate DuPont's Long Discontinuous Fiber (LDF) composites. Additional tests were conducted to compare LDF composites against toughened thermosets and a baseline thermoset system. Results have shown that the LDF AS4/PEKK offers improved interlaminar (flange bending) strength with little reduction in mechanical properties due to the discontinuous nature of the fibers. In the third phase, a series of AS4/PEKK LDF C-section curved frames (representing a typical rotorcraft light frame) were designed, manufactured and tested. Specimen reconsolidation after 'stretch forming' and frame thickness were found to be key factors in this light frame's performance. A finite element model was constructed to correlate frame test results with expected strain levels determined from material property tests. Adequately reconsolidated frames performed well and failed at strain levels at or above baseline thermoset material test strains. Finally a cost study was conducted which has shown that the use of LDF for this frame would result in a significant cost savings, for moderate to large lot sizes compared with the hand lay-up of a thermoset frame. Author

N95-28433*# National Aeronautics and Space Administration, Washington, DC.

DESIGN, ANALYSIS, AND TESTING OF A METAL MATRIX COMPOSITE WEB/FLANGE INTERSECTION

S. B. Biggers (Clemson Univ., SC.), N. F. Knight, Jr. (Clemson Univ., SC.), S. G. Moran, and R. Olliffe (Lockheed Aeronautical Systems Co., Marietta, GA.) *In* FAA, Ninth DOD/NASA/FAA Conference on Fibrous Composites in Structural Design, Volume 1 Sep. 1992 p 297-32 (For primary document see N95-28420 09-24)

Avail: CASI HC A03/MF A04

An experimental and analytical program to study the local design details of a typical T-shaped web/flange intersection made from a metal matrix composite is described. Loads creating flange bending were applied to specimens having different designs and boundary conditions. Finite element analyses were conducted on models of the test specimens to predict the structural response. The analyses correctly predict failure load, mode, and location in the fillet material in the intersection region of the web and the flange when specimen quality is good. The test program shows the importance of fabrication quality in the intersection region. The full-scale test program that led to the investigation of this local detail is also described. Author

N95-28434*# Purdue Univ., West Lafayette, IN. School of Aeronautics and Astronautics.

CHARACTERISTICS OF LAMINATES WITH DELAMINATION CONTROL STRIPS

C. T. Sun, J. C. Goering (McDonnell Aircraft Co., Saint Louis, MO.), J. M. Alper (Naval Air Development Center, Warminster, PA.), and L. W. Gause (Naval Air Development Center, Warminster, PA.) *In* FAA, Ninth DOD/NASA/FAA Conference on Fibrous Composites in Structural Design, Volume 1 Sep. 1992 p 329-35 Sponsored by ONR and McDonnell Aircraft Co. (For primary document see N95-28420 09-24)

Avail: CASI HC A03/MF A04

Tough resin is needed to resist delamination crack propagation. However, modulus often has to be compromised because it is difficult to retain both high modulus and toughness in a matrix material. A potential solution is to use a hybrid system in which tough resin strips are included within a conventional matrix composite. By adjusting the spacing of the tough resin strips, maximum delamination size can be controlled. Experimental results for impact damage and subsequent damage propagation in laminates containing tough resin strips are reported. Plain adhesive strips and fiber-reinforced tough resin composite strips were used in constructing the hybrid laminates. Test results indicated that size of delamination inflicted by impact was confined between the tough resin strips. As a result, significantly increased residual compressive strength was obtained. Impacted laminates containing tough resin strips were also fatigue tested. It was found that these strips reduced the growth of the impact damage area relative to the growth seen in coupons with no tough resin strips. Damage growth from an open hole under tension fatigue was evaluated using both tough resin strips and glass fiber reinforced tough resin strips. Unreinforced tough resin strips retarded delamination growth from the open hole, but did not stop matrix cracks growing in the fiber direction. Fiber reinforced tough resin strips did not contain axial delamination growth from the open hole. However, they did act as crack arresters, stopping the through-the-thickness tension crack originating from the hole. Author

N95-28435*# Virginia Polytechnic Inst. and State Univ., Blacksburg, VA. Dept. of Engineering Science and Mechanics.

VIBRATIONAL BEHAVIOR OF ADAPTIVE AIRCRAFT WING STRUCTURES MODELLED AS COMPOSITE THIN-WALLED BEAMS

O. Song, L. Librescu, and C. A. Rogers *In* FAA, Ninth DOD/NASA/FAA Conference on Fibrous Composites in Structural Design, Volume 1 Sep. 1992 p 361-38 (For primary document see N95-28420 09-24)

(Contract N00014-88-C-0721)

Avail: CASI HC A03/MF A04

The vibrational behavior of cantilevered aircraft wings modeled as thin-walled beams and incorporating piezoelectric effects is studied. Based on the converse piezoelectric effect, the system of piezoelectric actuators conveniently located on the wing yield the control of its associated vertical and lateral bending eigenfrequencies. The possibility revealed by this study enabling one to increase adaptively the eigenfrequencies of thin-walled cantilevered beams could play a significant role in the control of the dynamic response and flutter of wing and rotor blade structures. Author

N95-28436*# California Univ., Davis, CA.
UNIQUE CONSIDERATIONS IN THE DESIGN AND EXPERIMENTAL EVALUATION OF TAILORED WINGS WITH ELASTICALLY PRODUCED CHORDWISE CAMBER
Lawrence W. Rehfield, Peter J. Zischka, Michael L. Fentress, and Stephen Chang *In* FAA, Ninth DOD/NASA/FAA Conference on Fibrous Composites in Structural Design, Volume 1 Sep. 1992 p 383-40 (For primary document see N95-28420 09-24)
(Contract NAS1-18754)
Avail: CASI HC A03/MF A04

Some of the unique considerations that are associated with the design and experimental evaluation of chordwise deformable wing structures are addressed. Since chordwise elastic camber deformations are desired and must be free to develop, traditional rib concepts and experimental methodology cannot be used. New rib design concepts are presented and discussed. An experimental methodology based upon the use of a flexible sling support and load application system has been created and utilized to evaluate a model box beam experimentally. Experimental data correlate extremely well with design analysis predictions based upon a beam model for the global properties of camber compliance and spanwise bending compliance. Local strain measurements exhibit trends in agreement with intuition and theory but depart slightly from theoretical perfection based upon beam-like behavior alone. It is conjectured that some additional refinement of experimental technique is needed to explain or eliminate these (minor) departures from asymmetric behavior of upper and lower box cover strains. Overall, a solid basis for the design of box structures based upon the bending method of elastic camber production has been confirmed by the experiments. Author

N95-28437*# Northrop Corp., Hawthorne, CA.
C-130 ADVANCED TECHNOLOGY CENTER WING BOX CONCEPTUAL DESIGN/COST STUDY
R. S. Whitehead, C. R. Foreman (LTV Aerospace Corp., Dallas, TX.), and K. Silva (Wright Lab., Wright-Patterson AFB, OH.) *In* FAA, Ninth DOD/NASA/FAA Conference on Fibrous Composites in Structural Design, Volume 1 Sep. 1992 p 401-41 (For primary document see N95-28420 09-24)
(Contract F33657-90-D-0027)
Avail: CASI HC A03/MF A04

A conceptual design was developed by Northrop/LTV for an advanced C-130 Center Wing Box (CWB) which could meet the severe mission requirements of the SOF C-130 aircraft. The goals for the advanced technology CWB relative to the current C-130H CWB were: (1) the same acquisition cost; (2) lower operating support costs; (3) equal or lower weight; (4) a 30,000 hour service life for the SOF mission; and (5) minimum impact on the current maintenance concept. Initially, the structural arrangement, weight, external and internal loads, fatigue spectrum, flutter envelope and design criteria for the SOF C-130 aircraft CWB were developed. An advanced materials assessment was then conducted to determine the suitability of advanced materials for a 1994 production availability and detailed trade studies were performed on candidate CWB conceptual designs. Finally, a life-cycle cost analysis was performed on the advanced CWB. The study results showed that a hybrid composite/metallic CWB could meet the severe SOF design requirements, reduce the CWB weight by 14 pct., and was cost effective relative to an all metal beefed up C-130H CWB. Author

N95-28438*# McDonnell Aircraft Co., Saint Louis, MO.
DEVELOPMENT OF COMPOSITE CARRYTHROUGH BULKHEAD
R. J. Ehlen and M. Libeskind (Naval Air Development Center, Warminster, PA.) *In* FAA, Ninth DOD/NASA/FAA Conference on Fibrous Composites in Structural Design, Volume 1 Sep. 1992 p 421-44 (For primary document see N95-28420 09-24)
(Contract N62269-87-C-0216)
Avail: CASI HC A03/MF A04

A structural development program was recently completed in which the weight and fatigue advantages of an all composite major load carrying bulkhead was successfully demonstrated. Fabrication of a full scale article, including static and fatigue testing of the carry-through beam portion verified the producibility, strength and durability of this design, thereby presenting the opportunity for use on aircraft upgrades and new aircraft. A 15% weight saving is achievable and, more importantly, the fatigue problems that normally plague metal bulkheads are virtually eliminated. Derived from text

N95-28439*# National Aeronautics and Space Administration. Langley Research Center, Hampton, VA.
EFFECTS OF FLOOR LOCATION ON RESPONSE OF COMPOSITE FUSELAGE FRAMES
Huey D. Carden, Lisa E. Jones, and Edwin L. Fasanella (Lockheed Engineering and Sciences Co., Hampton, VA.) *In* FAA, Ninth DOD/NASA/FAA Conference on Fibrous Composites in Structural Design, Volume 1 Sep. 1992 p 443-45 (For primary document see N95-28420 09-24)
Avail: CASI HC A03/MF A04

Experimental and analytical results are presented which show the effect of floor placement on the structural response and strength of circular fuselage frames constructed of graphite-epoxy composite material. The research was conducted to study the behavior of conventionally designed advanced composite aircraft components. To achieve desired new designs which incorporate improved energy absorption capabilities requires an understanding of how these conventional designs behave under crash type loadings. Data are presented on the static behavior of the composite structure through photographs of the frame specimen, experimental strain distributions, and through analytical data from composite structural models. An understanding of this behavior can aid the dynamist in predicting the crash behavior of these structures and may assist the designer in achieving improved designs for energy absorption and crash behavior of future structures. Derived from text

N95-28440*# Wright Lab., Wright-Patterson AFB, OH. Flight Dynamics Directorate.
STRUCTURAL DESIGN OPTIMIZATION WITH SURVIVABILITY DEPENDENT CONSTRAINTS APPLICATION: PRIMARY WING BOX OF A MULTI-ROLE FIGHTER **c05**
Douglas J. Dolvin *In* FAA, Ninth DOD/NASA/FAA Conference on Fibrous Composites in Structural Design, Volume 1 Sep. 1992 p 465-48 (For primary document see N95-28420 09-24)
Avail: CASI HC A03/MF A04

The superior survivability of a multirole fighter is dependent upon balanced integration of technologies for reduced vulnerability and susceptability. The objective is to develop a methodology for structural design optimization with survivability dependent constraints. The design criteria for optimization will be survivability in a tactical laser environment. The following analyses are studied to establish a dependent design relationship between structural weight and survivability: (1) develop a physically linked global design model of survivability variables; and (2) apply conventional constraints to quantify survivability dependent design. It was not possible to develop an exact approach which would include all aspects of survivability dependent design, therefore guidelines are offered for solving similar problems. Derived from text

N95-28441*# Northrop Corp., Hawthorne, CA. Aircraft Div.
RELIABILITY ANALYSIS OF COMPOSITE STRUCTURES
Han-Pin Kan *In* FAA, Ninth DOD/NASA/FAA Conference on Fibrous Composites in Structural Design, Volume 1 Sep. 1992 p 489-50 (For primary document see N95-28420 09-24)
(IRAD Proj. R-1056)
Avail: CASI HC A03/MF A04

A probabilistic static stress analysis methodology has been developed to estimate the reliability of a composite structure. Closed form stress analysis methods are the primary analytical tools used in this methodology. These structural mechanics methods are used to identify independent variables whose variations significantly affect the performance of the structure. Once these variables are identified, scatter in their values is evaluated and statistically characterized. The scatter in applied loads and the structural parameters are then fitted to appropriate probabilistic distribution functions. Numerical integration techniques are applied to compute the structural reliability. The predicted reliability accounts for scatter due to variability in material strength, applied load, fabrication and assembly processes. The influence of structural geometry and mode of failure are also considerations in the evaluation. Example problems are given to illustrate various levels of analytical complexity. Author

N95-28442*# Army Materials Technology Lab., Watertown, MA.
UNCERTAINTIES IN OBTAINING HIGH RELIABILITY FROM STRESS-STRENGTH MODELS **c38**
Donald M. Neal, William T. Matthews, and Mark G. Vangel *In* FAA, Ninth DOD/NASA/FAA Conference on Fibrous Composites in Structural Design, Volume 1 Sep. 1992 p 503-52 (For primary document see N95-28420 09-24)
Avail: CASI HC A03/MF A04

There has been a recent interest in determining high statistical reliability in risk assessment of aircraft components. The potential consequences are identified of incorrectly assuming a particular statistical distribution for stress or strength data used in obtaining the high reliability values. The computation of the reliability is defined as the probability of the strength being greater than the stress over the range of stress values. This method is often referred to as the stress-strength model. A sensitivity analysis was performed involving a comparison of reliability results in order to evaluate the effects of assuming specific statistical distributions. Both known population distributions, and those that differed slightly from the known, were considered. Results showed substantial differences in reliability estimates even for almost nondetectable differences in the assumed distributions. These differences represent a potential problem in using the stress-strength model for high reliability computations, since in practice it is impossible to ever know the exact (population) distribution. An alternative reliability computation procedure is examined involving determination of a lower bound on the reliability values using extreme value distributions. This procedure reduces the possibility of obtaining nonconservative reliability estimates. Results indicated the method can provide conservative bounds when computing high reliability. An alternative reliability computation procedure is examined involving determination of a lower bound on the reliability values using extreme value distributions. This procedure reduces the possibility of obtaining nonconservative reliability estimates. Results indicated the method can provide conservative bounds when computing high reliability. Author

N95-28443*# LTV Aerospace and Defense Co., Dallas, TX. Aircraft Div.
PROBABILISTIC DESIGN OF ADVANCED COMPOSITE STRUCTURE
P. M. Gray and M. G. Riskalla *In* FAA, Ninth DOD/NASA/FAA Conference on Fibrous Composites in Structural Design, Volume 1 Sep. 1992 p 523-53 (For primary document see N95-28420 09-24)
Avail: CASI HC A03/MF A04

Advanced composite technology offers potentials for sizable improvements in many areas: weight savings, maintainability, durability, and reliability. However, there are a number of inhibitors to these improvements. One of the biggest inhibitors is the imposition of traditional metallic approaches to design of composite structure. This is especially detrimental in composites because new materials technology demands new design approaches. Of particular importance are the decisions made regarding structural criteria. Significant changes cannot be implemented without careful consideration and exploration. This new approach is to implement changes on a controlled, verifiable basis. Probabilistic design is the methodology and the process to accomplish this. Its foundation is to base design criteria and objectives on reliability targets instead of arbitrary factors carried over from metallic structural history. The background is discussed of probabilistic design and the results are presented of a side-by-side comparison to generic aircraft structure designed the 'old' way and the 'new'. Activities are also defined that need to be undertaken to evolve available approaches to probabilistic design followed by summary and recommendations. Author

N95-28444*# National Aeronautics and Space Administration. Lewis Research Center, Cleveland, OH.
PROBABILISTIC EVALUATION OF FUSELAGE-TYPE COMPOSITE STRUCTURES **c05**
Michael C. Shiao (Sverdrup Technology, Inc., Brook Park, OH.) and Christos C. Chamis *In* FAA, Ninth DOD/NASA/FAA Conference on Fibrous Composites in Structural Design, Volume 1 Sep. 1992 p 535-54 Previously announced as N93-12735 (For primary document see N95-28420 09-24)
Avail: CASI HC A03/MF A04

A methodology is developed to computationally simulate the uncertain behavior of composite structures. The uncertain behavior includes buckling loads, natural frequencies, displacements, stress/strain etc., which are the consequences of the random variation (scatter) of the primitive (independent random) variables in the constituent, ply, laminate and structural levels. This methodology is implemented in the IPACS (Integrated Probabilistic Assessment of Composite Structures) computer code. A fuselage-type composite structure is analyzed to demonstrate the code's capability. The probability distribution functions of the buckling loads, natural frequency, displacement, strain and stress are computed. The sensitivity of each primitive (independent random) variable to a given structural response is also identified from the analyses. Derived from text

N95-28445*# Naval Postgraduate School, Monterey, CA.
PROOF TEST METHODOLOGY FOR COMPOSITES
Edward M. Wu and David K. Bell *In* FAA, Ninth DOD/NASA/FAA Conference on Fibrous Composites in Structural Design, Volume 1 Sep. 1992 p 549-56 Sponsored in part by DARPA (For primary document see N95-28420 09-24)
Avail: CASI HC A03/MF A04

The special requirements for proof test of composites are identified based on the underlying failure process of composites. Two proof test methods are developed to eliminate the inevitable weak fiber sites without also causing flaw clustering which weakens the post-proof-test composite. Significant reliability enhancement by these proof test methods has been experimentally demonstrated for composite strength and composite life in tension. This basic proof test methodology is relevant to the certification and acceptance of critical composite structures. It can also be applied to the manufacturing process development to achieve zero-reject for very large composite structures. Derived from text

N95-28446*# Naval Air Development Center, Warminster, PA.
NAVY COMPOSITE MAINTENANCE AND REPAIR EXPERIENCE
T. M. Donnellan, R. C. Cochran, E. L. Rosenzweig, and R. E. Trabocco *In* FAA, Ninth DOD/NASA/FAA Conference on Fibrous Composites in Structural Design, Volume 1 Sep. 1992 p 565-57 (For primary document see N95-28420 09-24)
Avail: CASI HC A02/MF A04

The Navy has been a strong proponent of composites for aircraft structure. Fleet use of composites started with the F-14 in the early 1970's and has steadily increased. This experience base provides sufficient information to allow an evaluation of the maintenance performance of polymer composites in service. A summary is presented of the Navy's experience with maintenance of composite structure. The general types of damage experienced in the fleet as well as specific examples of composite damage to aircraft is described. The impact of future designs on supportability is also discussed. Author

N95-28462*# Federal Aviation Administration, Washington, DC.
NINTH DOD/NASA/FAA CONFERENCE ON FIBROUS COMPOSITES IN STRUCTURAL DESIGN, VOLUME 2
Joseph R. Soderquist, comp., Lawrence M. Neri, comp. (Federal Aviation Administration, Atlantic City, NJ.), and Herman L. Bohon, comp. (Galaxy Scientific Corp., Hampton, VA.) Sep. 1992 565 p Conference held in Lake Tahoe, NV, 4-7 Nov. 1991; sponsored by NASA, AF, Army, and Navy Sponsored by NASA
(NASA-CR-198722; NAS 1.26:198722; DOT/FAA/CT-92-25-Vol-2) Avail: CASI HC A24/MF A04

This publication contains the proceedings of the Ninth DOD/NASA/FAA Conference on Fibrous Composites in Structural Design held at Lake Tahoe, Nevada, during 4-7 Nov. 1991. Presentations were made in the following areas of composite structural design: perspectives in composites, design methodology, design applications, design criteria, supporting technology, damage tolerance, and manufacturing. For individual titles, see N95-28463 through N95-28489.

N95-28463*# National Aeronautics and Space Administration. Langley Research Center, Hampton, VA.
OVERVIEW OF THE ACT PROGRAM

John G. Davis, Jr. *In* FAA, Ninth DOD/NASA/FAA Conference on Fibrous Composites in Structural Design, Volume 2 Sep. 1992 p 577-59 (For primary document see N95-28462 09-24)
Avail: CASI HC A03/MF A04

NASA's Advanced Composites Program (ACT) was initiated in 1988. A National Research Announcement was issued to solicit innovative ideas that could significantly contribute to development and demonstration of an integrated technology data base and confidence level that permits cost-effective use of composite primary structures in transport aircraft. Fifteen contracts were awarded by the Spring of 1989 and the participants include commercial and military airframe manufacturers, materials developers and suppliers, universities, and government laboratories. The program approach is to develop materials, structural mechanics methodology, design concepts, and fabrication procedures that offer the potential to make composite structures cost-effective compared to aluminum structure. Goals for the ACT program included 30-50 percent weight reduction, 20-25 percent acquisition cost reduction, and provided the scientific basis for predicting materials and structures performance. This paper provides an overview of the ACT program status, plans, and selected technical accomplishments. Sixteen additional papers, which provide more detailed information on the research and development accomplishments, are contained in this publication. Author

N95-28464*# National Aeronautics and Space Administration. Langley Research Center, Hampton, VA.

DESIGNERS' UNIFIED COST MODEL

W. Freeman, L. Ilcewicz (Boeing Commercial Airplane Co., Seattle, WA.), G. Swanson (Boeing Commercial Airplane Co., Seattle, WA.), and T. Gutowski (Massachusetts Inst. of Tech., Cambridge, MA.) *In* FAA, Ninth DOD/NASA/FAA Conference on Fibrous Composites in Structural Design, Volume 2 Sep. 1992 p 601-61 Previously announced as X92-10406 (For primary document see N95-28462 09-24)
Avail: CASI HC A03/MF A04

The Structures Technology Program Office (STPO) at NASA LaRC has initiated development of a conceptual and preliminary designers' cost prediction model. The model will provide a technically sound method for evaluating the relative cost of different composite structural designs, fabrication processes, and assembly methods that can be compared to equivalent metallic parts or assemblies. The feasibility of developing cost prediction software in a modular form for interfacing with state-of-the-art preliminary design tools and computer aided design programs is being evaluated. The goal of this task is to establish theoretical cost functions that relate geometric design features to summed material cost and labor content in terms of process mechanics and physics. The output of the designers' present analytical tools will be input for the designers' cost prediction model to provide the designer with a database and deterministic cost methodology that allows one to trade and synthesize designs with both cost and weight as objective functions for optimization. This paper presents the team members, approach, goals, plans, and progress to date for development of COSTADE (Cost Optimization Software for Transport Aircraft Design Evaluation). Author

N95-28465*# Analytical Services and Materials, Inc., Hampton, VA.

COINS: A COMPOSITES INFORMATION DATABASE SYSTEM c82

Shahid Siddiqi, Louis F. Vosteen, Ralph Edlow, and Teck-Seng Kwa *In* FAA, Ninth DOD/NASA/FAA Conference on Fibrous Composites in Structural Design, Volume 2 Sep. 1992 p 621-62 Previously announced as X92-10407 (For primary document see N95-28462 09-24)
Avail: CASI HC A02/MF A04

An automated data abstraction form (ADAF) was developed to collect information on advanced fabrication processes and their related costs. The information will be collected for all components being fabricated as part of the ACT program and include in a COmposites INformation System (COINS) database. The aim of the COINS development effort is to provide future airframe preliminary design and fabrication teams with a tool through which production cost can become a deterministic variable in the design optimization process. The effort was initiated by the Structures Technology Program Office (STPO) of the NASA LaRC to implement the recommendations of a working group comprised of representatives from the commercial airframe companies. The principal working group recommendation was to re-institute collection of composite part fabrication data in a format similar to the DOD/NASA Structural Composites Fabrication Guide. The fabrication information collection form was automated with current user friendly computer technology. This work in progress paper describes the new automated form and features that make the form easy to use by an aircraft structural design-manufacturing team. Author

N95-28466*# National Aeronautics and Space Administration. Langley Research Center, Hampton, VA.

COMPOSITE FUSELAGE SHELL STRUCTURES RESEARCH AT NASA LANGLEY RESEARCH CENTER

James H. Starnes, Jr. and Mark J. Shuart *In* FAA, Ninth DOD/NASA/FAA Conference on Fibrous Composites in Structural Design, Volume 2 Sep. 1992 p 631-65 Previously announced as X92-10408 (For primary document see N95-28462 09-24)
Avail: CASI HC A03/MF A04

Fuselage structures for transport aircraft represent a significant percentage of both the weight and the cost of these aircraft primary structures. Composite materials offer the potential for reducing both the weight and the cost of transport fuselage structures, but only limited studies of the response and failure of composite fuselage structures have been conducted for transport aircraft. The behavior of these important primary structures must be understood, and the structural mechanics methodology for analyzing and designing these complex stiffened shell structures must be validated in the laboratory. The effects of local gradients and discontinuities on fuselage shell behavior and the effects of local damage on pressure containment must be thoroughly understood before composite fuselage structures can be used for commercial aircraft. This paper describes the research being conducted and planned at NASA LaRC to help understand the critical behavior or composite fuselage structures and to validate the structural mechanics methodology being developed for stiffened composite fuselage shell structure subjected to combined internal pressure and mechanical loads. Stiffened shell and curved stiffened panel designs are currently being developed and analyzed, and these designs will be fabricated and then tested at Langley to study critical fuselage shell behavior and to validate structural analysis and design methodology. The research includes studies of the effects of combined internal pressure and mechanical loads on nonlinear stiffened panel and shell behavior, the effects of cutouts and other gradient-producing discontinuities on composite shell response, and the effects of local damage on pressure containment and residual strength. Scaling laws are being developed that relate full-scale and subscale behavior of composite fuselage shells. Failure mechanisms are being identified and advanced designs will be developed based on what is learned from early results from the LaRC research activities. Results from combined load tests will be used to validate analytical models of critical nonlinear response mechanisms as well as shell scaling laws. Author

N95-28467*# Lockheed Aeronautical Systems Co., Marietta, GA.

STRUCTURAL TESTING OF THE TECHNOLOGY INTEGRATION BOX BEAM c39

C. F. Griffin *In* FAA, Ninth DOD/NASA/FAA Conference on Fibrous Composites in Structural Design, Volume 2 Sep. 1992 p 659-67 Previously announced as X92-10409 (For primary document see N95-28462 09-24)
Avail: CASI HC A03/MF A04

A full-scale section of a transport aircraft wing box was designed, analyzed, fabricated, and tested. The wing box section, which was called the technology integration box beam, contained blade stiffened covers and T-stiffened channel spars constructed using graphite/epoxy materials. Covers, spars, and the aluminum ribs were assembled using mechanical fasteners. The box beam was statically tested for several loading conditions to verify the stiffness and strength characteristics of the composite wing design. Failure of the box beam occurred at 125 percent of design limit load during the combined upbending and torsion ultimate design load test. It appears that the failure initiated at a stiffener runout location in the upper cover which resulted in rupture of the upper cover and portions of both spars. Author

N95-28468*# National Aeronautics and Space Administration. Langley Research Center, Hampton, VA.

TECHNOLOGY INTEGRATION BOX BEAM FAILURE STUDY Status Report c39

Mark J. Shuart, Damodar R. Ambur (Lockheed Aeronautical Systems Co., Marietta, GA.), D. D. Davis, Jr. (Lockheed Aeronautical Systems Co., Marietta,

GA.), R. C. Davis (Lockheed Aeronautical Systems Co., Marietta, GA.), G. L. Farley (Lockheed Aeronautical Systems Co., Marietta, GA.), C. G. Lotts (Lockheed Aeronautical Systems Co., Marietta, GA.), and J. T. Wang (Lockheed Aeronautical Systems Co., Marietta, GA.) *In* FAA, Ninth DOD/NASA/FAA Conference on Fibrous Composites in Structural Design, Volume 2 Sep. 1992 p 673-68 Previously announced as X92-10410 (For primary document see N95-28462 09-24)
Avail: CASI HC A03/MF A04

The objective of this paper is to describe current results from an on-going study of the mechanisms that led to the failure of the TIBB. Experimental and analytical results are presented. Experimental results include load, strain, and deflection data for the TIBB (Technology Integration Box Beam). An analytical investigation was conducted to compliment the experimental investigation and to gain additional insight into the TIBB structural response. Analytical results include strain and deflection results from a global analysis of the TIBB. A local analysis of the failure region is being completed. These analytical results are validated through comparisons with the experimental results from the TIBB tests. The experimental and analytical results from the TIBB tests are used to determine a sequence of events that may have resulted in failure of the TIBB. A potential cause of failure is high stresses in a stiffener runout region. Typical analytical results are presented for a stiffener runout specimen that is being defined to simulate the TIBB failure mechanisms. The results of this study are anticipated to provide better understanding of potential failure mechanisms in composite aircraft structures, to lead to future design improvements, and to identify needed analytical tools for design and analysis.
Derived from text

N95-28469*# National Aeronautics and Space Administration. Langley Research Center, Hampton, VA.
DEVELOPMENT OF STITCHED/RTM COMPOSITE PRIMARY STRUCTURES
Susan M. Kullerd (Lockheed Engineering and Sciences Co., Hampton, VA.) and Marvin B. Dow *In* FAA, Ninth DOD/NASA/FAA Conference on Fibrous Composites in Structural Design, Volume 2 Sep. 1992 p 689-71 Previously announced as X92-10411 (For primary document see N95-28462 09-24)
Avail: CASI HC A03/MF A04

The goal of the NASA Advanced Composites Technology (ACT) Program is to provide the technology required to gain the full benefit of weight savings and performance offered by composite primary structures. Achieving the goal is dependent on developing composite materials and structures which are damage tolerant and economical to manufacture. Researchers at NASA LaRC and Douglas Aircraft Company are investigating stitching reinforcement combined with resin transfer molding (RTM) to create structures meeting the ACT program goals. The Douglas work is being performed under a NASA contract entitled Innovative Composites Aircraft Primary Structures (ICAPS). The research is aimed at materials, processes and structural concepts for application in both transport wings and fuselages. Empirical guidelines are being established for stitching reinforcement in primary structures. New data are presented in this paper for evaluation tests of thick (90-ply) and thin (16-ply) stitched laminates, and from selection tests of RTM composite resins. Tension strength, compression strength and post-impact compression strength data are reported. Elements of a NASA LaRC program to expand the science base for stitched/RTM composites are discussed.
Author (revised)

N95-28470*# National Aeronautics and Space Administration. Langley Research Center, Hampton, VA.
TEST AND ANALYSIS RESULTS FOR COMPOSITE TRANSPORT FUSELAGE AND WING STRUCTURES c05
Jerry W. Deaton, Susan M. Kullerd (Lockheed Engineering and Sciences Co., Hampton, VA.), Ram C. Madan (Douglas Aircraft Co., Inc., Long Beach, CA.), and Victor L. Chen (Douglas Aircraft Co., Inc., Long Beach, CA.) *In* FAA, Ninth DOD/NASA/FAA Conference on Fibrous Composites in Structural Design, Volume 2 Sep. 1992 p 719-74 Previously announced as X92-10413 (For primary document see N95-28462 09-24)
Avail: CASI HC A03/MF A04

Automated tow placement (ATP) and stitching of dry textile composite preforms followed by resin transfer molding (RTM) are being investigated by researchers at NASA LaRC and Douglas Aircraft Company as cost-effective manufacturing processes for obtaining damage tolerant fuselage and wing structures for transport aircraft. The Douglas work is being performed under a NASA contract entitled 'Innovative Composites Aircraft Primary Structures (ICAPS)'. Data are presented in this paper to assess the damage tolerance of ATP and RTM fuselage elements with stitched-on stiffeners from compression tests of impacted three-J-stiffened panels and from stiffener pull-off tests. Data are also presented to assess the damage tolerance of RTM wing elements which had stitched skin and stiffeners from impacted single stiffener and three blade-stiffened compression tests and stiffener pull-off tests.
Author

N95-28471*# National Aeronautics and Space Administration. Langley Research Center, Hampton, VA.
TENSION FRACTURE OF LAMINATES FOR TRANSPORT FUSELAGE. PART 1: MATERIAL SCREENING c05
T. H. Walker (Boeing Commercial Airplane Co., Seattle, WA.), W. B. Avery (Boeing Commercial Airplane Co., Seattle, WA.), L. B. Ilcewicz (Boeing Commercial Airplane Co., Seattle, WA.), C. C. Poe, Jr., and C. E. Harris *In* FAA, Ninth DOD/NASA/FAA Conference on Fibrous Composites in Structural Design, Volume 2 Sep. 1992 p 747-78 Previously announced as X92-10414 (For primary document see N95-28462 09-24)
(Contract NAS1-18889)
Avail: CASI HC A03/MF A04

Transport fuselage structures are designed to contain pressure following a large penetrating damage event. Applications of composites to fuselage structures require a database and supporting analysis on tension damage tolerance. Tests with 430 fracture specimens were used to accomplish the following: (1) identify critical material and laminate variables affecting notch sensitivity; (2) evaluate composite failure criteria; and (3) recommend a screening test method. Variables studied included fiber type, matrix toughness, lamination manufacturing process, and intraply hybridization. The laminates found to have the lowest notch sensitivity were manufactured using automated tow placement. This suggests a possible relationship between the stress distribution and repeatable levels of material inhomogeneity that are larger than found in traditional tape laminates. Laminates with the highest notch sensitivity consisted of toughened matrix materials that were resistant to a splitting phenomena that reduces stress concentrations in major load bearing plies. Parameters for conventional fracture criteria were found to increase with crack length for the smallest notch sizes studied. Most material and laminate combinations followed less than a square root singularity for the largest crack sizes studied. Specimen geometry, notch type, and notch size were evaluated in developing a screening test procedure. Traitional methods of correcting for specimen finite width were found to be lacking. Results indicate that a range of notch sizes must be tested to determine notch sensitivity. Data for a single small notch size (0.25 in. diameter) was found to give no indication of the sensitivity of a particular material and laminate layup to larger notch sizes.
Author

N95-28472*# Iowa Univ., Iowa City, IA. Dept. of Biomedical Engineering.
INDENTABILITY OF CONVENTIONAL AND NEGATIVE POISSON'S RATIO FOAMS
R. S. Lakes and K. Elms *In* FAA, Ninth DOD/NASA/FAA Conference on Fibrous Composites in Structural Design, Volume 2 Sep. 1992 p 789-79 Previously announced as X92-10415 (For primary document see N95-28462 09-24)
Avail: CASI HC A01/MF A04

The indentation resistance of foams, both of conventional structure and of re-entrant structure giving rise to negative Poisson's ratio, is studied using holographic interferometry. In holographic indentation tests, re-entrant foams had higher yield strengths sigma(sub y) and lower stiffness E than conventional foams of the same original relative density. Calculated energy absorption for dynamic impact is considerably higher for re-entrant foam than conventional foam.
Author

N95-28473*# Boeing Commercial Airplane Co., Seattle, WA.
LOCAL DESIGN OPTIMIZATION FOR COMPOSITE TRANSPORT FUSELAGE CROWN PANELS c05
G. D. Swanson, L. B. Ilcewicz, T. H. Walker, D. Graesser (Washington Univ., Seattle, WA.), M. Tuttle (Washington Univ., Seattle, WA.), and Z. Zabinsky (Washington Univ., Seattle, WA.) *In* FAA, Ninth DOD/NASA/FAA Conference on Fibrous Composites in Structural Design, Volume 2 Sep.

1992 p 795-81 Previously announced as X92-10416 (For primary document see N95-28462 09-24)
(Contract NAS1-18889)
Avail: CASI HC A03/MF A04

Composite transport fuselage crown panel design and manufacturing plans were optimized to have projected cost and weight savings of 18 percent and 45 percent, respectively. These savings are close to those quoted as overall NASA ACT program goals. Three local optimization tasks were found to influence the cost and weight of fuselage crown panels. This paper summarizes the effect of each task and describes in detail the task associated with a design cost model. Studies were performed to evaluate the relationship between manufacturing cost and design details. A design tool was developed to aid in these investigations. The development of the design tool included combining cost and performance constraints with a random search optimization algorithm. The resulting software was used in a series of optimization studies that evaluated the sensitivity of design variables, guidelines, criteria, and material selection on cost. The effect of blending adjacent design points in a full scale panel subjected to changing load distributions and local variations was shown to be important. Technical issues and directions for future work were identified. Author

N95-28474*# Boeing Commercial Airplane Co., Seattle, WA.
COMPOSITE FUSELAGE CROWN PANEL MANUFACTURING TECHNOLOGY **c05**
Kurtis Willden, S. Metschan, C. Grant (Hercules Aerospace Co., Magna, UT.), and T. Brown (Hercules Aerospace Co., Magna, UT.) *In* FAA, Ninth DOD/NASA/FAA Conference on Fibrous Composites in Structural Design, Volume 2 Sep. 1992 p 815-84 Previously announced as X92-10417 (For primary document see N95-28462 09-24)
(Contract NAS1-18889)
Avail: CASI HC A03/MF A04

Commercial fuselage structures contain significant challenges in attempting to save manufacturing costs with advanced composite technology. Assembly issues, material costs, and fabrication of elements with complex geometry are each expected to drive the cost of composite fuselage structures. Boeing's efforts under the NASA ACT program have pursued key technologies for low-cost, large crown panel fabrication. An intricate bond panel design and manufacturing concepts were selected based on the efforts of the Design Build Team (DBT). The manufacturing processes selected for the intricate bond design include multiple large panel fabrication with the Advanced Tow Placement (ATP) process, innovative cure tooling concepts, resin transfer molding of long fuselage frames, and utilization of low-cost material forms. The process optimization for final design/manufacturing configuration included factory simulations and hardware demonstrations. These efforts and other optimization tasks were instrumental in reducing cost by 18 percent and weight by 45 percent relative to an aluminum baseline. The qualitative and quantitative results of the manufacturing demonstrations were used to assess manufacturing risks and technology readiness. Author

N95-28475*# National Aeronautics and Space Administration. Langley Research Center, Hampton, VA.
RECENT PROGRESS IN NASA LANGLEY TEXTILE REINFORCED COMPOSITES PROGRAM
H. Benson Dexter, Charles E. Harris, and Norman J. Johnston *In* FAA, Ninth DOD/NASA/FAA Conference on Fibrous Composites in Structural Design, Volume 2 Sep. 1992 p 845-87 Previously announced as X92-10418 (For primary document see N95-28462 09-24)
Avail: CASI HC A03/MF A04

The NASA LaRC is conducting and sponsoring research to explore the benefits of textile reinforced composites for civil transport aircraft primary structures. The objective of this program is to develop and demonstrate the potential of affordable textile reinforced composite materials to meet design properties and damage tolerance requirements of advanced aircraft structural concepts. In addition to in-house research, the program was recently expanded to include major participation by the aircraft industry and aerospace textile companies. The major program elements include development of textile preforms, processing science, mechanics of materials, experimental characterization of materials, and development and evaluation of textile reinforced composite structural elements and subcomponents. The NASA Langley in-house focus is as follows: development of a science-based understanding of resin transfer molding (RTM), development of powder-coated towpreg processes, analysis methodology, and development of a performance database on textile reinforced composites. The focus of the textile industry participation is on development of multidirectional, damage-tolerant preforms, and the aircraft industry participation is in the areas of design, fabrication and testing of textile reinforced composite structural elements and subcomponents. Textile processes such as 3D weaving, 2D and 3D braiding, and knitting/stitching are being compared with conventional laminated tape processes for improved damage tolerance. Through-the-thickness reinforcements offer significant damage tolerance improvements. However, these gains must be weighed against potential loss in in-plane properties such as strength and stiffness. Analytical trade studies are underway to establish design guidelines for the application of textile material forms to meet specific loading requirements. Fabrication and testing of large structural components are required to establish the full potential of textile reinforced composite materials. Author

N95-28476*# Lockheed Aeronautical Systems Co., Marietta, GA.
ADVANCED TEXTILE APPLICATIONS FOR PRIMARY AIRCRAFT STRUCTURES **c05**
Anthony C. Jackson, Ronald E. Barrie, Bharat M. Shah, and Jay G. Shukla *In* FAA, Ninth DOD/NASA/FAA Conference on Fibrous Composites in Structural Design, Volume 2 Sep. 1992 p 875-90 Previously announced as X92-10419 (For primary document see N95-28462 09-24)
(Contract NAS1-18888)
Avail: CASI HC A03/MF A04

Advanced composite primary structural concepts have been evaluated for low cost, damage tolerant structures. Development of advanced textile preforms for fuselage structural applications with resin transfer molding and powder epoxy material is now under development. Author

N95-28477*# Grumman Aerospace Corp., Bethpage, NY. Aircraft Systems.
COMPARISON OF RESIN FILM INFUSION, RESIN TRANSFER MOLDING, AND CONSOLIDATION OF TEXTILE PREFORMS FOR PRIMARY AIRCRAFT STRUCTURE
J. Suarez and S. Dastin *In* FAA, Ninth DOD/NASA/FAA Conference on Fibrous Composites in Structural Design, Volume 2 Sep. 1992 p 903-93 Previously announced as X92-10420 Sponsored by NASA. Langley Research Center (For primary document see N95-28462 09-24)
Avail: CASI HC A03/MF A04

Under NASA's Novel Composites for Wing and Fuselage Applications (NCWFA) Program, Grumman is developing innovative design concepts and cost-effective fabrication processes for damage-tolerant primary structures that can perform at a design ultimate strain level of 6000 micro-inch/inch. Attention has focused on the use of textile high-performance fiber-reinforcement concepts that provide improved damage tolerance and out-of-plane load capability, low-cost resin film infusion (RFI) and resin transfer molding (RTM) processes, and thermoplastic forming concepts. The fabrication of wing 'Y' spars by four different materials/processes methods is described: 'Y' spars fabricated using IM7 angle interlock 0/90 deg woven preforms with +/- 45 deg plies stitched with Toray high-strength graphite thread and processed using RFI and 3501-6 epoxy; 'Y' spars fabricated using G40-800 knitted/stitched preforms and processed using RFI and 3501-6 epoxy; 'Y' spars fabricated using G40-800 knitted/stitched preforms and processed using RTM and Tactix 123/H41 epoxy; and 'Y' spars fabricated using AS4(6k)/PEEK 150-g commingled angle interlock 0/90 deg woven preforms with +/- 45 deg commingled plies stitched using high-strength graphite thread and processed by consolidation. A comparison of the structural efficiency, processability, and projected acquisition cost of these representative spars is presented. Author

N95-28478*# Boeing Defense and Space Group, Philadelphia, PA.
CHARACTERIZATION AND MANUFACTURE OF BRAIDED COMPOSITES FOR LARGE COMMERCIAL AIRCRAFT STRUCTURES
Mark J. Fedro and Kurtis Willden (Boeing Commercial Airplane Co., Seattle, WA.) *In* FAA, Ninth DOD/NASA/FAA Conference on Fibrous Composites in Structural Design, Volume 2 Sep. 1992 p 935-97 Previously announced as X92-10421 (For primary document see N95-28462 09-24)
(Contract NAS1-18889)
Avail: CASI HC A03/MF A04

Braided composite materials, one of the advanced material forms which is under investigation in Boeing's ATCAS program, have been recognized as a potential cost-effective material form for fuselage structural elements. Consequently, there is a strong need for more knowledge in the design, manufacture, test, and analysis of textile structural composites. The overall objective of this work is to advance braided composite technology towards applications to a large commercial transport fuselage. This paper summarizes the mechanics of materials and manufacturing demonstration results which have been obtained in order to acquire an understanding of how braided composites can be applied to a commercial fuselage. Textile composites consisting of 1D, 2D triaxial, and 3D braid patterns with thermoplastic and two RTM resin systems were investigated. The structural performance of braided composites was evaluated through an extensive mechanical test program. Analytical methods were also developed and applied to predict the following: internal fiber architectures, stiffnesses, fiber stresses, failure mechanisms, notch effects, and the entire history of failure of the braided composites specimens. The applicability of braided composites to a commercial transport fuselage was further assessed through a manufacturing demonstration. Three foot fuselage circumferential hoop frames were manufactured to demonstrate the feasibility of consistently producing high quality braided/RTM composite primary structures. The manufacturing issues (tooling requirements, processing requirements, and process/quality control) addressed during the demonstration are summarized. The manufacturing demonstration in conjunction with the mechanical test results and developed analytical methods increased the confidence in the ATCAS approach to the design, manufacture, test, and analysis of braided composites. Author

N95-28479*# National Aeronautics and Space Administration. Langley Research Center, Hampton, VA.

THE USE OF IMPACT FORCE AS A SCALE PARAMETER FOR THE IMPACT RESPONSE OF COMPOSITE LAMINATES

Wade C. Jackson (Army Aerostructures Directorate, Hampton, VA.) and C. C. Poe, Jr. *In* FAA, Ninth DOD/NASA/FAA Conference on Fibrous Composites in Structural Design, Volume 2 Sep. 1992 p 981-99
Previously announced as N92-17007 (For primary document see N95-28462 09-24)
Avail: CASI HC A03/MF A04

The building block approach is currently used to design composite structures. With this approach, the data from coupon tests are scaled up to determine the design of a structure. Current standard impact tests and methods of relating test data to other structures are not generally understood and are often used improperly. A methodology is outlined for using impact force as a scale parameter for delamination damage for impacts of simple plates. Dynamic analyses were used to define ranges of plate parameters and impact parameters where quasi-static analyses are valid. These ranges include most low-velocity impacts where the mass of the impacter is large, and the size of the specimen is small. For large-mass impacts of moderately thick (0.35-0.70 cm) laminates, the maximum extent of delamination damage increased with increasing impact force and decreasing specimen thickness. For large-mass impact tests at a given kinetic energy, impact force and hence delamination size depends on specimen size, specimen thickness, boundary conditions, and indenter size and shape. If damage is reported in terms of impact force instead of kinetic energy, large-mass test results can be applied directly to other plates of the same thickness. Author

N95-28480*# Dow-United Technologies Composite Products, Inc., Wallingford, CT.

APPLICATION OF DAMAGE TOLERANCE METHODOLOGY IN CERTIFICATION OF THE PIAGGIO P-180 AVANTI c05

Jerry Johnson *In* FAA, Ninth DOD/NASA/FAA Conference on Fibrous Composites in Structural Design, Volume 2 Sep. 1992 p 999-1012
(For primary document see N95-28462 09-24)
Avail: CASI HC A03/MF A04

The Piaggio P-180 Avanti, a twin pusher-prop engine nine-passenger business aircraft was certified in 1990, to the requirements of FAR Part 23 and Associated Special Conditions for Composite Structure. Certification included the application of a damage tolerant methodology to the design of the composite forward wing and empennage (vertical fin, horizontal stabilizer, tailcone, and rudder) structure. This methodology included an extensive analytical evaluation coupled with sub-component and full-scale testing of the structure. The work from the Damage Tolerance Analysis Assessment was incorporated into the full-scale testing. Damage representing hazards such as dropped tools, ground equipment, handling, and runway debris, was applied to the test articles. Additional substantiation included allowing manufacturing discrepancies to exist unrepaired on the full-scale articles and simulated bondline failures in critical elements. The importance of full-scale testing in the critical environmental conditions and the application of critical damage are addressed. The implication of damage tolerance on static and fatigue testing is discussed. Good correlation between finite element solutions and experimental test data was observed. Author

N95-28481*# National Aeronautics and Space Administration. Langley Research Center, Hampton, VA.

EFFECT OF LOW-SPEED IMPACT DAMAGE AND DAMAGE LOCATION ON BEHAVIOR OF COMPOSITE PANELS

Dawn Jegley *In* FAA, Ninth DOD/NASA/FAA Conference on Fibrous Composites in Structural Design, Volume 2 Sep. 1992 p 1013-1036
Previously announced as N92-23981 (For primary document see N95-28462 09-24)
Avail: CASI HC A03/MF A04

An investigation of the effects of low-speed impact damage on the compression and tension strength of thin (less than .05 inches thick) and moderately thick (between .12 and .17 inches thick) composite specimens was conducted. Impact speeds ranged from 50 to 550 ft/sec (impact energies from .25 to 30.7 ft-lb) and impact locations were near or away from a lateral unloaded edge. In this study, thin tension-loaded or compression-loaded specimens with only 90 deg and +/- 40 deg plies which were impacted away from the unloaded edge suffered less reduction in maximum load-carrying capability due to impact damage than the same specimens impacted near the unloaded edge. Unlike the thin laminates, failure loads of thicker compression-loaded specimens with a similar stacking sequence were independent of impact location. Failure loads of thin tension-loaded specimens with 0 deg plies were independent of impact location while failure loads of thicker compression-loaded specimens with 0 deg plies were dependent upon impact location. A finite-element analysis of strain distributions across the panel width indicated that high axial strains occur near the unloaded edges of postbuckled panels, indicating that impacts near the unloaded edge would significantly effect the behavior of postbuckled panels. Author

N95-28482*# Boeing Commercial Airplane Co., Seattle, WA.

IMPACT DAMAGE RESISTANCE OF COMPOSITE FUSELAGE STRUCTURE, PART 1 c05

E. F. Dost, W. B. Avery, L. B. Ilcewicz, D. H. Grande, and B. R. Coxon (Integrated Technologies, Inc., Bothell, WA.) *In* FAA, Ninth DOD/NASA/FAA Conference on Fibrous Composites in Structural Design, Volume 2 Sep. 1992 p 1037-1069 (For primary document see N95-28462 09-24)
(Contract NAS1-18889)
Avail: CASI HC A03/MF A04

The impact damage resistance of laminated composite transport aircraft fuselage structures was studied experimentally. A statistically based designed experiment was used to examine numerous material, laminate, structural, and extrinsic (e.g., impactor type) variables. The relative importance and quantitative measure of the effect of each variable and variable interactions on responses including impactor dynamic response, visibility, and internal damage state were determined. The study utilized 32 three-stiffener panels, each with a unique combination of material type, material forms, and structural geometry. Two manufacturing techniques, tow placement and tape lamination, were used to build panels representative of potential fuselage crown, keel, and lower side-panel designs. Various combinations of impactor variables representing various foreign-object-impact threats to the aircraft were examined. Impacts performed at different structural locations within each panel (e.g., skin midbay, stiffener attaching flange, etc.) were considered separate parallel experiments. The relationship between input variables, measured damage states, and structural response to this damage are presented including recommendations for materials and impact test methods for fuselage structure. Author

N95-28483*# General Dynamics Corp., Fort Worth, TX.

APPLICATIONS OF A DAMAGE TOLERANCE ANALYSIS METHODOLOGY IN AIRCRAFT DESIGN AND PRODUCTION

M. R. Woodward, S. D. Owens, G. E. Law, and L. A. Mignery *In* FAA, Ninth DOD/NASA/FAA Conference on Fibrous Composites in Structural

Design, Volume 2 Sep. 1992 p 1071-1081 (For primary document see N95-28462 09-24)
Copyright Avail: CASI HC A03/MF A04

Objectives of customer mandated aircraft structural integrity initiatives in design are to guide material selection, to incorporate fracture resistant concepts in the design, to utilize damage tolerance based allowables and planned inspection procedures necessary to enhance the safety and reliability of manned flight vehicles. However, validated fracture analysis tools for composite structures are needed to accomplish these objectives in a timely and economical manner. This paper briefly describes the development, validation, and application of a damage tolerance methodology for composite airframe structures. A closed-form analysis code, entitled SUBLAM was developed to predict the critical biaxial strain state necessary to cause sublaminate buckling-induced delamination extension in an impact damaged composite laminate. An embedded elliptical delamination separating a thin sublaminate from a thick parent laminate is modelled. Predicted failure strains were correlated against a variety of experimental data that included results from compression after impact coupon and element tests. An integrated analysis package was developed to predict damage tolerance based margin-of-safety (MS) using NASTRAN generated loads and element information. Damage tolerance aspects of new concepts are quickly and cost-effectively determined without the need for excessive testing. Author

N95-28484*# Stanford Univ., CA. Dept. of Aeronautics and Astronautics.

COMPRESSIVE STRENGTH OF DAMAGED AND REPAIRED COMPOSITE PLATES

c39

Scott R. Finn and George S. Springer *In* FAA, Ninth DOD/NASA/FAA Conference on Fibrous Composites in Structural Design, Volume 2 Sep. 1992 p 1083-1095 (For primary document see N95-28462 09-24)
(Contract NAS1-18778)
Avail: CASI HC A03/MF A04

Tests were performed assessing the effectiveness of repair in restoring the mechanical properties of damaged, solid composite plates made of Fiberite T300/976 graphite-epoxy. Some (75%) or all (100%) of the damaged zone was cut out, and the plate was repaired by plugging and patching the hole. The effectiveness of the repair was evaluated by measuring the compressive strengths of undamaged plates, damaged plates with no cutout, damaged plates with a cutout, and plates that had been repaired. Author

N95-28485*# Wright Lab., Wright-Patterson AFB, OH. Flight Dynamics Directorate.

POST IMPACT COMPRESSIVE STRENGTH IN COMPOSITES

c39

Edvins Demuts, Raghbir S. Sandhu, and John A. Daniels *In* FAA, Ninth DOD/NASA/FAA Conference on Fibrous Composites in Structural Design, Volume 2 Sep. 1992 p 1097-1104 (For primary document see N95-28462 09-24)
Avail: CASI HC A02/MF A04

Presented in this paper are the plan, equipment, procedures, and findings of an experimental investigation of the tolerance to low velocity impact of a graphite epoxy (AS4/3501-6) and graphite bismaleimide (M6/CYCOM3100) advanced composites. The applied impacts were governed by the Air Force Guide Specification 87221. Specimens of each material system having a common nominal layup (10% 0 deg; 80% +/-45 deg; 10% 90 deg), a common 7 inch (17.78 cm) by 10 inch (25.40 cm) size, five different thicknesses (9, 26, 48, 74, and 96 plies), and ambient moisture content were impacted and strength tested at room temperature. Damaged areas and post impact compression strengths (PICS) were among the most significant findings obtained. While the undamaged per ply compression strength of both materials is a strong function of laminate thickness, the per ply PICS is not. The average difference in per ply PICS between the two material systems is about seven percent. Although a smaller percentage of the applied kinetic energy was absorbed by the Gr/BMI than by the Gr/Epoxy composites, larger damaged areas were produced in the Gr/BMI than in Gr/Epoxy. Within the limitations of this investigation, the Gr/BMI system seems to offer no advantage in damage tolerance over the Gr/Epoxy system examined. Derived from text

N95-28486*# Rockwell International Science Center, Thousand Oaks, CA.

FUNDAMENTAL CONCEPTS IN THE SUPPRESSION OF DELAMINATION BUCKLING BY STITCHING

B. N. Cox *In* FAA, Ninth DOD/NASA/FAA Conference on Fibrous Composites in Structural Design, Volume 2 Sep. 1992 p 1105-1110 (For primary document see N95-28462 09-24)
Avail: CASI HC A02/MF A04

Elementary results are presented for the buckling of stitched, laminated composites containing delamination cracks. The stitching fibers are assumed to provide continuous, linear restoring tractions opposing the deflection of the delaminated layer adjacent to the crack. It is shown that there exists a characteristic length a(0) for buckling: if the length, 2a, of the delamination crack exceeds 2a(0), then, when buckling occurs, it will consist of waves of period 2a(0) and will usually not span the whole delamination. Simple expressions are derived for the critical buckling load and the minimum stitching density required to suppress buckling of the delaminated layer. Author

N95-28487*# National Aeronautics and Space Administration. Langley Research Center, Hampton, VA.

DAMAGE TOLERANCE OF A GEODESICALLY STIFFENED ADVANCED COMPOSITE STRUCTURAL CONCEPT FOR AIRCRAFT STRUCTURAL APPLICATIONS

c05

Marshall Rouse and Damodar R. Ambur *In* FAA, Ninth DOD/NASA/FAA Conference on Fibrous Composites in Structural Design, Volume 2 Sep. 1992 p 1111-1121 (For primary document see N95-28462 09-24)
Avail: CASI HC A03/MF A04

This paper describes the features of a geodesically stiffened panel concept that was designed for a fuselage application with a combined axial compression loading of 3,000 lb/in. and a shear loading of 600 lb/in. Specimens representative of this panel concept were tested in uniaxial compression both with and without low-speed impact damage to study the buckling and postbuckling response of the structure. Experimental results that describe the stiffness and failure characteristics of undamaged and impacted damage specimens are presented. A finite element analysis model that captures the principal details of the specimens was developed and used to predict the panel response. Analytical results on panel end-shortening are compared with the experimental results. Analytical results that describe panel end-shortening, out-of-plane displacement and stress resultants are presented. Derived from text

N95-28488*# Grumman Aerospace Corp., Bethpage, NY. Aircraft Systems.

ADVANCED WING DESIGN SURVIVABILITY TESTING AND RESULTS

c05

J. Bruno and M. Tobias (Naval Air Development Center, Warminster, PA.) *In* FAA, Ninth DOD/NASA/FAA Conference on Fibro us Composites in Structural Design, Volume 2 Sep. 1992 p 1123-1137 (For primary document see N95-28462 09-24)
Avail: CASI HC A03/MF A04

Composite wings on current operational aircraft are conservatively designed to account for stress/strain concentrations, and to assure specified damage tolerance. The technology that can lead to improved composite wing structures and associated structural efficiency is to increase design ultimate strain levels beyond their current limit of 3500 to 4000 micro-in/in to 6000 micro-in/in without sacrificing structural integrity, durability, damage tolerance, or survivability. Grumman, under the sponsorship of the Naval Air Development Center (NADC), has developed a high-strain composite wing design for a subsonic aircraft wing using novel and innovative design concepts and manufacturing methods, while maintaining a state-of-the-art fiber/resin system. The current advanced wing design effort addressed a tactical subsonic aircraft wing using previously developed, high-strain wing design concepts in conjunction with newer/emerging fiber and polymer matrix composite (PMC) materials to achieve the same goals, while reducing complexity. Two categories of advanced PMC materials were evaluated: toughened thermosets; and engineered thermoplastics. Advanced PMC materials offer the technological opportunity to take maximum advantage of improved material properties, physical characteristics, and tailorability to increase performance and survivability over current composite structure. Damage tolerance and survivability to various threats, in addition to structural integrity and durability, were key technical issues addressed during this study, and evaluated through test. This paper focuses on the live-fire testing, and the results performed to experimentally evaluate the survivability of the advanced wing design. Derived from text

N95-28489*# Boeing Commercial Airplane Co., Seattle, WA. 777 Empennage Structures.

NASA-ACEE/BOEING 737 GRAPHITE-EPOXY HORIZONTAL STABILIZER SERVICE **c05**

J. T. Quinlivan, J. A. Kent, and D. R. Wilson *In* FAA, Ninth DOD/NASA/FAA Conference on Fibrous Composites in Structural Design, Volume 2 Sep. 1992 p 1139-1150 (For primary document see N95-28462 09-24)
Avail: CASI HC A03/MF A04

The 737 graphite-epoxy horizontal stabilizer was developed by Boeing as part of the NASA-ACEE (Aircraft Energy Efficiency) Advanced Composite Structures Program. NASA-ACEE programs challenged large-transport manufacturers to use graphite material in redesigning existing aircraft components. The goal of the program was to develop the necessary data and technology to achieve production commitments to advanced composites. Boeing designed, fabricated, and certified five shipsets of horizontal stabilizers for the 737-200 airframe. The program was initiated in July 1977 and certification was achieved in August 1982. Schedule highlights are shown. The work performed on this program is reported in NASA technical summaries and final reports. Boeing introduced the stabilizer into commercial operation in 1984, and has maintained surveillance for seven years of in-service evaluation. Outstanding performance was demonstrated with no service incidents attributed to the graphite-epoxy structure. Boeing will continue to monitor and support these aircraft, adding to the database of commercial composite experience. Derived from text

N95-28639 Rutherford Appleton Lab., Oxford (England).

NON-LINEAR VISCOELASTIC BEHAVIOUR

A. D. Irving, S. J. Watson, L. J. J. Speet, N. Cunliffe, and T. Dewson Dec. 1994 27 p Prepared in cooperation with Technische Univ.
(PB95-192811; RAL-94-123) Avail: Issuing Activity (National Technical Information Service (NTIS))

This paper is concerned with the development of a quantitative analysis method that can extract the mixed linear and non-linear dynamical response of a viscoelastic process in composite materials. A tractable set of simultaneous equations with well behaved coefficients can be generated by taking time series moments of a suitably truncated Volterra series expansion. This moment hierarchy is a set of inhomogeneous non-linear integral equations, based on a vector multidimensional convolution form of the Volterra functional series expansion. The hierarchy developed is used to analyze the time dependent viscoelastic properties of fiber reinforced composite materials. Estimates of the temporal response of the measured stress to the measured mechanical force were then used to predict the out of sample stress field values. It is demonstrated that the response functions provided a good representation of the viscoelastic process. Generally speaking, the response functions estimated from the data are used to determine the dynamic and steady state transport coefficients, which can be used to develop either an empirical field theory of the phenomena or alternatively be used in the design process. NTIS

N95-27636*# Nebraska Univ., Lincoln, NE. Dept. of Electrical Engineering.

LEO DEGRADATION OF GRAPHITE AND CARBON-BASED COMPOSITES ABOARD SPACE SHUTTLE FLIGHT STS-46

Blaine R. Spady, R. A. Synowicki, Jeffrey S. Hale, M. J. DeVries, John A. Woollam, Arthur W. Moore (Union Carbide Corp., Parma, OH.), and Max Lake (Applied Sciences, Inc., Cedarville, OH.) *In* NASA. Langley Research Center, LDEF: 69 Months in Space. Third Post-Retrieval Symposium, Part 3 Feb. 1995 p 989-997 (For primary document see N95-27629 09-99)
(Grant NAG3-95)
Avail: CASI HC A02/MF A04

25 INORGANIC AND PHYSICAL CHEMISTRY

Includes chemical analysis, e.g., chromatography; combustion theory; electrochemistry; and photochemistry.

For related information see also *77 Thermodynamics and Statistical Physics.*.

N95-26350 University of Northern Illinois, De Kalb, IL. Dept. of Chemistry.

INVESTIGATION OF THE INTERFACE BETWEEN IMMISCIBLE ELECTROLYTES APPLIED TO MEMBRANE ELECTROCHEMISTRY Final Report, 16 Apr. 1991 - 15 Oct. 1994

Petr Vanysek 14 Dec. 1994 11 p Limited Reproducibility: More than 20% of this document may be affected by microfiche quality
(Contract N00014-91-J-1058)
(AD-A288887) Avail: Issuing Activity (Defense Technical Information Center (DTIC))

The report summarizes achievements during the contract performance. It gives the list of personnel, publications, presentations and complete list of technical reports filed. The main achievements highlighted are: Use of ultramicrointerface, slow scan cyclic voltammetry on porous materials, impedance of conducting polymers, zinc ion transport through Nafion films, anomalous conductivity through narrow pores, and interfacial tension measurements using quartz oscillator. DTIC

N95-26352 Surrey Univ., Guildford (England). Thermochemistry Lab.

THERMODYNAMICS OF ELECTROLYTE SOLUTIONS FOR USE IN HIGH ENERGY LITHIUM BATTERIES

Angela F. DanildeMamor 1994 4 p Limited Reproducibility: More than 20% of this document may be affected by microfiche quality
(Contract N68171-94-C-9121)
(AD-A288897; R/D-7475-CH-01) Avail: Issuing Activity (Defense Technical Information Center (DTIC))

This report contains information regarding: (1) Thermodynamic parameters for the complexation of 15-crown-5 and lithium salts at 288.15 K in order to assess the temperature effect on these processes; and (2) Gibbs energies, enthalpies and entropies for the binding of lithium with 4'-nitrobenzo-15-crown-5 in acetonitrile at the standard temperature. This part of research aims to investigate the effect of substituents on the complexing abilities of 15-crown-5 and lithium cations. DTIC

N95-26416 Georgia Univ., Athens, GA. Center for Computational Quantum Chemistry.

ENVIRONMENTAL EFFECTS ON HIGH ENERGY DENSITY MATERIALS Annual Technical Report, 1 Sep. 1993 - 31 Aug. 1994

Henry F. Schaefer, III 13 Oct. 1994 5 p Limited Reproducibility: More than 20% of this document may be affected by microfiche quality
(Contract F49620-93-J-0529)
(AD-A288296; AFOSR-94-0678TR) Avail: Issuing Activity (Defense Technical Information Center (DTIC))

The object of this research is to characterize, using ab initio quantum mechanical methods, the stabilizing or destabilizing effects of hydrogen and/or oxygen matrices on proposed high energy density molecular (HEDM) systems. In addition, the unimolecular fragmentation reactions of large HEDM species such as N20 will be studied via density functional methods. DTIC

N95-26417 Yale Univ., New Haven, CT. High Temperature Chemical Reaction Engineering Lab.

TRANSPORT PHENOMENA AND INTERFACIAL KINETICS IN MULTIPHASE COMBUSTION SYSTEMS Final Report, 15 Feb. 1991 - 14 Feb. 1994

Daniel E. Rosner Mar. 1994 45 p Limited Reproducibility: More than 20% of this document may be affected by microfiche quality
(Grant AF-AFOSR-0170-91; AF Proj. 2308)
(AD-A288297; AFOSR-94-0691TR) Avail: Issuing Activity (Defense Technical Information Center (DTIC))

The performance of ramjets burning slurry fuels (leading to condensed oxide aerosols and liquid film deposits), gas turbine engines in dusty or marine atmospheres, or when using fuels from non-traditional sources, depends upon the formation and transport of small particles across non-isothermal combustion gas boundary layers (BLs). Even airbreathing engines burning 'clean' hydrocarbon fuels can experience soot formation/deposition problems (e.g., combustor liner burnout, accelerated turbine blade erosion and 'hot' corrosion). Moreover, particle formation and transport are important in many chemical reactors used to synthesize or process aerospace materials (turbine blade coatings, optical waveguides, ceramic precursor powders, fibers for composites,...) Accordingly, our research is directed toward providing chemical propulsion systems engineers and materials- oriented engineers with new techniques and quantitative information on important particle- and vapor-mass transport mechanisms and rates. The purpose of this report is to summarize our research methods accomplishments. DTIC

N95-26422 Dartmouth Coll., Hanover, NH. School of Engineering.
A BOOK AND SERIES OF MONOGRAPHS ON ICE PHYSICS Final Report, 1 Jun. 1991 - 31 May 1994
Victor F. Petrenko 22 Aug. 1994 6 p Limited Reproducibility: More than 20% of this document may be affected by microfiche quality
(Contract DAAL03-91-G-0164)
(AD-A288319; ARO-28599.4-GS) Avail: Issuing Activity (Defense Technical Information Center (DTIC))

During the period June 1, 1991, through May 31, 1994 five monographs on the physics of ice were written and printed: (1) the structure of ordinary ice. part 1: ideal structure of ice; (2) defects in ice. part 1: point defects; (3) defects in ice. part 2: dislocations and plane defects; (4) electrical properties of ice: part 1. conductivity and dielectric permittivity of ice. part 2. advanced topics and new physical phenomena; and (5) the surface of ice. These monograph number 456 pages including 145 figures and 510 references. The lists of the monographs in contents is in the Appendix. The first five monographs of the series passed through intensive review and were very well accepted by scientists and engineers working on ice. The sixth monograph entitled electromechanical effects in ice is written and is being reviewed. DTIC

N95-26432 Army Cold Regions Research and Engineering Lab., Hanover, NH.
FREZCHEM: A CHEMICAL-THERMODYNAMIC MODEL FOR AQUEOUS SOLUTIONS AT SUBZERO TEMPERATURES
Giles M. Marion and Steven A. Grant Jul. 1994 40 p Limited Reproducibility: More than 20% of this document may be affected by microfiche quality
(AD-A288456; CRREL-SR-94-18) Avail: Issuing Activity (Defense Technical Information Center (DTIC))

This report documents a FORTRAN version of the Spencer-Moller-Weare chemical thermodynamic model for aqueous electrolyte solutions at sub-zero temperatures (FREZCHEM). FREZCHEM is structured to predict the chemical composition and unfrozen water of aqueous solutions between -60 and +25 C at atmospheric pressure (0.101325 MPa). FREZCHEM includes two reaction pathways: freezing at variable temperature and fixed total water and evaporation at variable water and fixed temperature. Activity coefficients and the activity of water are calculated using the Pitzer equations, which are valid to high solution ionic strengths (approximately 20 mol/kg). Fifteen chloride and sulfate salts of sodium, potassium, calcium, and magnesium are included in the model. Predicted and experimental measurements of solute molalities and the unfrozen water fraction during sea water freezing are in good agreement. At -50 C, 0.3% of sea water remains unfrozen with 99.7% of Na and 95.5% of Cl having precipitated into one of four salts. FREZCHEM should find many applications in physicochemical studies of aqueous solutions and freezing. DTIC

N95-26451 Massachusetts Inst. of Tech., Cambridge, MA.
CONTINUUM MECHANICAL MODELING OF SOLIDS UNDERGOING A PHASE TRANSFORMATION Final Report, 1 Jan. 1991 - 30 Jun. 1994
Rohan Abeyaratne 25 Aug. 1994 11 p Limited Reproducibility: More than 20% of this document may be affected by microfiche quality
(Contract DAAL03-91-G-0011)
(AD-A288274; ARO-227538.12-EG) Avail: Issuing Activity (Defense Technical Information Center (DTIC))

This report summarizes our research on the continuum mechanical modeling of materials that undergo stress and temperature induced phase transitions. It contains a problem statement, a summary of results, a list of publications, and names of personnel. The results pertain to the construction of the model, the study of the model in both quasi-static and inertial settings, a study of coupled thermomechanical effects, a study of cyclic effects and comparison with experiments. DTIC

N95-26452 Dartmouth Coll., Hanover, NH.
STRUCTURE OF ORDINARY ICE Ih. PART 2: DEFECTS IN ICE. VOLUME 1: POINT DEFECTS
Victor F. Petrenko and Robert W. Whitworth (Birmingham Univ., England.) Apr. 1994 46 p Limited Reproducibility: More than 20% of this document may be affected by microfiche quality
(Contract DAAL03-91-G-0164)
(AD-A288279; CRREL-SR-94-4; ARO-28599.3-GS) Avail: Issuing Activity (Defense Technical Information Center (DTIC))

This report examines point defects in ice: molecular defects (vacancies and interstitials), protonic point defects (ions and Bjerrum defects) and electronic point defects (solvated electrons and radicals). Experimental results and theoretical models of the defects' atomic and electronic structures, energies and mobilities are reviewed. Special attention is given to the results of studies from the last two decades. Among the experimental techniques under consideration are nuclear magnetic resonance, X-rays topography, electron spin resonance, measurements of ice conductivity and dielectric permittivity, spectra of optical absorption and photoluminescence, and measurements of diffusion coefficients of the oxygen and hydrogen isotopes in ice. Ab initio calculations, computer simulations, Jaccard's theory and soliton models are used to discuss the defects' structures and their properties. DTIC

N95-26523# National Aerospace Lab., Tokyo (Japan). Aeroengine Div.
NUMERICAL SIMULATION OF COMBUSTION FLOW AROUND A FLAME HOLDER WITH HYDROGEN INJECTION
Takeshi Yamamoto and Takashi Tamaru Apr. 1994 17 p In JAPANESE Original contains color illustrations
(ISSN 0389-4010)
(NAL-TR-1233) Avail: CASI HC A03/MF A01

In the National Aerospace Laboratory, research work on a hydrogen-fueled ramjet engine for the spaceplane is being carried out. As a part of their research, a bluff-body type flame holder with fuel injection was tested at atmospheric conditions and prospective results were obtained for the engine. However, the capability of the experimental facility was limited, and it was difficult to investigate the engine performance over a wide operating range. so a two-dimensional CFD (Computational Fluid Dynamics) code was developed to simulate engine performance over a wide operating range. The code is based on the SIMPLER algorithm, and the power law scheme is used for the discretization of the governing equations. Turbulence is simulated by Myong-Kasagi's low Reynolds number type k-epsilon model. Magnussen's eddy-dissipation concept is used to simulate the combustion. In this report, details of the CFD code and some typical results of the numerical simulation are described. Author

N95-26528 Pittsburgh Univ., Pittsburgh, PA. Dept. of Chemistry.
PHOTO AND THERMAL EXCITATION OF SURFACE CHEMISTRY ON MODEL CATALYST SURFACES Final Report, 1 Sep. 1991 - 31 Aug. 1994
John T. Yates, Jr. 28 Jun. 1994 34 p Limited Reproducibility: More than 20% of this document may be affected by microfiche quality
(Contract DAAL03-91-G-0323)
(AD-A288541; ARO-29227.16-CH) Avail: Issuing Activity (Defense Technical Information Center (DTIC))

This is an overview of 16 publications written in the 36 month period of a contract from ARO. The work falls into three main categories: (1) Oxidation of phosphorus on Mo catalyst surfaces, probing the rate limiting step in the oxidative destruction of organophosphonate compounds. (2) Carbon monoxide and oxygen dissociative chemistry on Mo(110) surfaces, probing the fate of CO and oxygen. CO is an important oxidation product in the catalytic oxidative destruction of organic compounds. (3) Photodesorption and photocatalysis on oxide surfaces. DTIC

N95-26540# Helsinki Univ. of Technology, Espoo (Finland). Polymer Science Center.
FRACTIONATION STUDIES OF POLYETHYLENE USING DSC-TECHNIQUE
P. Starck 18 Oct. 1994 45 p *Its* Polymer Technology Publ. No. 21

(ISSN 0785-7144)
(PB95-185252; ISBN-951-22-2347-3) Avail: CASI HC A03/MF A01

This review will discuss work done on both well characterized LDPE, LLDPE and VLLDPE resins as well as on commercially available 'metallocene' type polyethylenes and corresponding test grades produced at Helsinki University of Technology (HUT) and at Borealis, respectively. The technique applied in this work is a segregation fractionation technique (SFT) by differential scanning calorimetry (DSC). In this technique the polymers studied have been annealed in stages at decreasing temperatures starting from a temperature just above the melting temperature. The results obtained will be compared to earlier obtained Temperature Rising Elution Fractionation (TREF)-data and discussed together with most recent literature in this area. NTIS

N95-26544 Columbia Univ., New York, NY. Dept. of Chemistry.
APPLICATIONS OF SECOND HARMONIC AND SUM FREQUENCY GENERATION TO GRAPHITE AND SILICA TYPE INTERFACES Final Technical Report, Apr. 1991 - Aug. 1994
E. Borguet, A. N. Tarmovsky, X. Wang, D. Zhang, and K. B. Eisenthal
Aug. 1994 17 p Limited Reproducibility: More than 20% of this document may be affected by microfiche quality
(Grant AF-AFOSR-0190-91)
(AD-A288228; AFOSR-94-0695TR) Avail: Issuing Activity (Defense Technical Information Center (DTIC))

Second Harmonic (SHG) and Sum-Frequency Generation (SFG) have enabled the investigation of the physical and chemical properties of aqueous interfaces, yielding new information and considerable insight into the structure and dynamics at a molecular level. Novel behavior has been observed and valuable new methodologies have been developed. IR-Visible SFG has enabled the behavior of distinct chromophores within a molecular species at an aqueous interface to be monitored for the first time. An unexpected phase transition was observed at the liquid/vapor interface of aqueous solutions of acetonitrile. The structural change is manifested by shifts in the vibrational frequency and in the polarization of the SFG signal of the interfacial acetonitrile. This transition is analogous to those observed for monolayers of long chain amphiphilic species, also monitored for the first time with chromophore sensitivity. These results provide direct evidence that head and tail groups of amphiphilic molecules can orient independently, and a challenging picture of the nature of phase transitions in two dimensional molecular assemblies. Electric Field Induced Second Harmonic Generation (EFISHG), a novel probe of charged interfaces, has been developed and applied to the study of the silica/aqueous interface and charged amphiphilic monolayers. Fundamental chemical quantities, such as the pKa of interfacial molecules, have been measured. In general, the interfacial acid-base equilibrium is shifted, with respect to the bulk, in a direction that favors the neutral species. Studies of the acid-base equilibrium of the silica/aqueous interface revealed two silanol sites whose acidity and thermodynamic parameters were determined. DTIC

N95-26606 Columbia Univ., New York, NY. Dept. of Chemistry.
STABILIZATION AND CONTROL OF HIGH ENERGY INTERMEDIATES THROUGH ADSORPTION OF RESTRICTED SPACES Final Technical Report, 1 Sep. 1991 - 31 Aug. 1994
Nicholas J. Turro 16 Sep. 1994 12 p Limited Reproducibility: More than 20% of this document may be affected by microfiche quality
(Grant AF-AFOSR-0340-91; AF Proj. 2303)
(AD-A288552; AFOSR-94-0679TR) Avail: Issuing Activity (Defense Technical Information Center (DTIC))

The research supported by this AFOSR grant has involved a multi-technique (NMR, ESR, laser flash photolysis, single photon counting, photoluminescence, tailor-made syntheses, computer simulation) approach to address problems concerning the structure and dynamics of transient high energy intermediates. These techniques have been employed to investigate the behavior of these intermediates when the latter are confined to the interfacial regions of restricted reaction spaces such as micelles, zeolites, cyclodextrins, water soluble polymers, and silica. Unique information has been obtained concerning the nature of interactions between the transients as substrates bound to receptors by non-covalent bonding. This information, in turn, has been exploited to investigate situations for which the transients display extraordinary dynamic properties such as reactivity which is controlled by the application of very weak applied magnetic fields. DTIC

N95-26678 Army Research Lab., Aberdeen Proving Ground, MD.
RAM ACCELERATOR PERFORMANCE CALCULATIONS USING A MODIFIED VERSION OF THE NASA CET89 EQUILIBRIUM CHEMISTRY CODE Final Report, Sep. 1993 - Mar. 1994
Federico Liberatore Dec. 1994 54 p Limited Reproducibility: More than 20% of this document may be affected by microfiche quality
(AD-A289554; ARL-TR-687) Avail: Issuing Activity (Defense Technical Information Center (DTIC))

The equilibrium chemistry code, CET89, is modified to calculate the performance of ram projectiles using 1-D control volume derived governing equations. The modified program is capable of calculating the projectile thrust and chemical energy release as functions of projectile velocity. This information is then used to calculate the distance versus time trace of a projectile traveling through an accelerator barrel. The modified program retains the full use of the thermodynamic database of the original code thus permitting performance calculations for a wide range of reactant mixtures. DTIC

N95-26707 Air Force Systems Command, Wright-Patterson AFB, OH. National Air Intelligence Center.
ROOM-TEMPERATURE PHOTOCURRENT SPECTROSCOPY OF GaAs/GaAlAs MULTIPLE QUANTUM WELLS
Hailong Duan and Qiuning Wang 15 Nov. 1994 16 p Transl. into ENGLISH from Bandaoti Xuebao (China), v. 12, no. 7, Jul. 1991 p 399-404 Limited Reproducibility: More than 20% of this document may be affected by microfiche quality
(AD-A289607; NAIC-ID(RS)T-0385-94) Avail: Issuing Activity (Defense Technical Information Center (DTIC))

By means of room temperature photocurrent spectroscopy, we have studied the effect of electric fields on exciton absorption in GaAs/GaAlAs multiple quantum wells (MQW) and discuss in this paper the effect of an electric field on the photocurrent spectra for some kinds of MWQ structures. The material requirement for related optoelectric devices MQW is also discussed. DTIC

N95-26750 National Physical Lab., Teddington (England). Div. of Materials Metrology.
MEASUREMENT OF VISCOSITY BY CAPILLARY RHEOMETRY: DWELL TIME EFFECTS
C. S. Brown and C. R. G. Allen May 1994 16 p
(PB95-190203; NPL-DMM-(A)-140) Copyright Avail: Issuing Activity (National Technical Information Service (NTIS))

Reliable viscosity data are needed by industry for a number of reasons, as a guide to designing products and choosing appropriate grades of material, to predict how a polymer will flow in commercial processing situations and to provide feedback during processing operations. Capillary rheometry is often used by industry to measure the viscosity of polymers. However, there is uncertainty over how long to leave a sample in the rheometer prior to measuring its viscosity. This has become more of a problem as processing temperatures have been pushed to the limit. The effect of different dwell times on viscosity measurement was examined in the context of the ISO Standard 11443. It was concluded that dwell times of five minutes were insufficient to achieve reliable viscosity measurements, whereas dwell times of thirty minutes were found to be sufficient. No evidence of degradation was observed for dwell times of two hours or less where the testing temperature was within the recommended processing temperature range, however, at higher temperatures a slight (less than 10%) reduction in viscosity was recorded. The unusual behavior of filled polypropylene increasing in viscosity, seen previously in rotational rheometry, was not observed in capillary rheometry. This is in agreement with the explanation proposed previously. This work should enable industry to use capillary rheometry to measure viscosity with more confidence in the future. NTIS

N95-26870 Washington Univ., Seattle, WA.
DETERMINING NANOSCALE PHYSICAL PROPERTIES OF MATERIALS BY MICROSCOPY AND SPECTROSCOPY
Mehmet Sarikaya, H. K. Wickramasinghe, and Michael Isaacson 1994 610 p Prepared in cooperation with IBM T. J. Watson Research Center, and Cornell Univ. Limited Reproducibility: More than 20% of this document may be affected by microfiche quality

(Contract N00014-94-1-0076)
(AD-A289532) Avail: Issuing Activity (Defense Technical Information Center (DTIC))

As the capabilities of microscopy techniques to investigate materials at smaller dimensions improve, processing techniques advance in parallel. In fact, materials synthesis with better-controlled spatial variations at a smaller scale has been demonstrated in many areas of materials and biological sciences. The major purpose of this symposium was not only to use microscopy and spectroscopy techniques for imaging, and compositional and chemical analysis of bulk and surface structures, but also to show that these newly emerging techniques are now capable of directly measuring physical and chemical properties of nanostructured biological and synthetic materials at a local scale. The concept of determining nanoscale properties of materials by microscopy and spectroscopy, therefore, can be expected to open up new avenues for science and engineering of materials, as firmly demonstrated by this symposium. Microscopy techniques included those that use photons, x-rays, electrons, and scanning probe techniques at their highest resolutions, all less than 1000 A down to nanometer and molecular levels, and in some cases 1 A and smaller. Similarly, spectroscopy techniques included local measurements of bonding, electronic, optical, and magnetic properties, again using probes at the nanometer scale. All of the invited presentations, and many of the extraordinary contributed papers, represented the latest applications of the techniques at the highest resolution levels. DTIC

N95-26896 Air Force Inst. of Tech., Wright-Patterson AFB, OH. School of Engineering.
PHOTOLUMINESCENCE SPECTROSCOPY OF 4H- AND 6H-SIC M.S. Thesis
William A. Davis Dec. 1994 81 p Limited Reproducibility: More than 20% of this document may be affected by microfiche quality
(AD-A289326; AFIT/GAP/ENP/94D-02) Avail: Issuing Activity (Defense Technical Information Center (DTIC))

Typical undoped bulk grown SiC shows n- or p-type conductivity due to residual impurities such as nitrogen, boron, or aluminum. In order to produce high resistivity material, vanadium can be used as a compensating dopant. Since vanadium is an amphoteric dopant in SiC, it produces either a donor state, V(sub Si)(4+) (3d sup 1) yields V(sub Si)(5+) (3d sup 0), or an acceptor state, V(sub Si)(4+) (3d sup 1) yields V(sub Si)(3+)(3d sup 2). Thus, vanadium doping can compensate both n- and p-type conductivity. In this work, vanadium doped and undoped 4H- and 6H-SiC grown by the sublimation method have been studied using low temperature photoluminescence (PL). It was found that the luminescence observed between 0.85 to 0.95 eV of the intra-3d-shell transition of V(sub Si)(4+) (3d sup 1) increased by an order of magnitude in samples intentionally doped with vanadium compared to samples unintentionally doped. In addition, the dominant visible-region luminescence was attributed to titanium which is an isoelectronic trap in SiC. The presence of a broad peak centered at approx. 1.90 eV in some samples is believed to be attributed to donor-acceptor pair recombination between a Ti sub Si-N(sub c) complexdonor and the boron defect complex acting as an acceptor. Finally, the Ti sub Si-N(sub c) complex donor location in the bandgap of 6H-SiC is estimated to be E sub c-0.54 eV. DTIC

N95-27136# Sandia National Labs., Albuquerque, NM.
OPTICAL FEATURES OF NANOSIZE IRON AND MOLYBDENUM SULFIDE CLUSTERS
J. P. Wilcoxon, G. Samara, and P. Newcomer 1995 4 p Presented at the 1994 Fall Meeting of the Materials Research Society (MRS), Boston, MA, 28 Nov. - 2 Dec. 1994
(Contract DE-AC04-94AL-85000)
(DE95-005417; SAND-94-3001C; CONF-941144-49) Avail: CASI HC A01/MF A01

In the bulk state FeS2 and MoS2 are optically opaque, narrow bandgap semiconductors with no optical applications. We demonstrate that nanosize FeS2 and MoS2 have bandgaps that can be adjusted to the visible and even UV region of the spectrum by control of the cluster size. This opens up a host of applications of these materials as inexpensive solar photocatalysts. We demonstrate that the band-gap of both materials shifts to the blue with decreasing size but ceases shifting when a size of approximately 3 nm (in the case of MoS2) is attained. We interpret this observation as a change from bulk quantum confinement of the hole-electron pair of a tiny semiconductor to a set of discrete molecular-like transitions more characteristic of a whopper molecule. Room temperature photoemission studies of these clusters demonstrate that, while photoemission shifts to the blue with increasing bandgap for large clusters, small clusters have photoemission exclusively from trapped sub-bandgap surface states. Chemical modification of the surface to introduce hole or electron traps can result in either an enhancement or a decrease in the photoluminescence. In addition, we report our results concerning chemical purification and preliminary surface characterization of MoS2 clusters by chromatography. DOE

N95-27137# Sandia National Labs., Albuquerque, NM.
MOLECULAR APPROACH TO MESOPOROUS METAL SULFIDES
M. T. Anderson and P. Newcomer 1995 6 p Presented at the 1994 Fall Meeting of the Materials Research Society (MRS), Boston, MA, 28 Nov. - 2 Dec. 1994
(Contract DE-AC04-94AL-85000)
(DE95-005418; SAND-94-1770C; CONF-941144-48) Avail: CASI HC A02/MF A01

We have synthesized metal-sulfide/surfactant nanocomposite materials by cooperative assembly of molecular precursors in a aqueous medium. The template-mediated synthetic approach is applicable to metals sulfides that exhibit aqueous thiometallate chemistry. The products are lamellar and have a bilayers or interdigitated layers of surfactant molecules sandwiched between metal sulfide layers. The layers of anionic metal sulfide molecules are not completely condensed in the nanocomposites, which results in a negative charge on the metal sulfide layers. The materials are stable at room temperature in water, methanol, 1 M HCl, 30 wt% NH3, and 1 M NaOH. The materials do not dissolve at 80 C in water and are stable to at least 180 C in air. The nanocomposites exhibit ion exchange of smaller surfactants, alkali-metal ions, and divalent metal ions. DOE

N95-27155# Joint Publications Research Service, Arlington, VA.
JPRS REPORT: SCIENCE AND TECHNOLOGY. CENTRAL EURASIA
12 May 1995 82 p Transl. into ENGLISH from various Central Eurasian articles
(JPRS-UST-95-021) Avail: CASI HC A05/MF A01

Translated articles cover the following topics: possibility of implementing solid-phase chemical reactions in an ultrasound field; frequency dependence of the conductivity of TlGaSe2 single crystals; photoinduced absorption in Fe- and Cu-doped Bi12TiO20 single crystals; producing motor fuel from plant biomass gasification gases; thermoplus - data base manager for database on thermodynamic properties of substances in a condensed state; suspension fuels with high energy content; and mass losses of materials in vacuum. Mathematical model. Author

N95-27168*# Eril Research, Inc., San Rafael, CA.
IONIZING RADIATION MEASUREMENTS ON LDEF: A0015 FREE FLYER BIOSTACK EXPERIMENT Final Report, Sep. 1991 - Mar. 1995
E. V. Benton, A. L. Frank, E. R. Benton, I. Csige, and L. A. Frigo 30 Mar. 1995 127 p
(Contract NAS8-38610)
(NASA-CR-196603; NAS 1.26:196603) Avail: CASI HC A07/MF A02

This report covers the analysis of passive radiation detectors flown as part of the A0015 Free Flyer Biostack on LDEF (Long Duration Exposure Facility). LET (linear energy transfer) spectra and track density measurements were made with CR-39 and Polycarbonate plastic nuclear track detectors. Measurements of total absorbed dose were carried out using Thermoluminescent Detectors. Thermal and resonance neutron dose equivalents were measured with LiF/CR-39 detectors. High energy neutron and proton dose equivalents were measured with fission foil/CR-39 detectors. Author

N95-27199# Universidad Nacional Autonoma de Mexico, Mexico City (Mexico).
IRON OXIDES CHARACTERIZATION BY MOESSBAUER SPECTROSCOPY Ph.D. Thesis [CARACTERIZACION DE OXIDOS DE HIERRO POR ESPECTROSCOPIA MOSSBAUER]
R. BasurtoSanchez 1993 58 p In SPANISH
(DE95-607869; INIS-mf-14397) Avail: CASI HC A04/MF A01 (US Sales Only)

In this work rust development on low carbon wire surface after the conformation process at different temperatures was studied by Moessbauer spectroscopy. The characterization was made by determining the following spectral parameters; Quadrupole splitting, Isomer shift, and Magnetic splitting. The area quantification determined the percentage amount of three different iron oxides. These iron oxides were: Wustite (FeO), Hematite (Fe2O3), and Magnetite (Fe3O4) which were present in the rust studied. With the results it was possible to establish the best temperature to favor the development of each of these iron oxides. DOE

N95-27200# Bhabha Atomic Research Centre, Bombay (India).
[ANALYTICAL SPECTROSCOPY] Progress Report, Jul. 1992 - Jun. 1993
Mahavir Singh, ed. 1994 126 p
(DE95-607896; BARC-1994/P/003) Avail: CASI HC A07/MF A02 (US Sales Only)

The research and development activities of the Spectroscopy Division during the year July 1992-June 1993 are reported in the form of individual summaries. These are arranged under the headings: analytical spectroscopy; infrared and Raman spectroscopy; atomic spectra; electronic spectra; laser spectroscopy; synchrotron beam foil and plasma spectroscopy; optics; electronics and instrumentation; and design, fabrication and workshop etc. The list of publications and papers presented at the various conferences, symposia, workshops etc. by the staff members of the Division during the report period is also given. DOE

N95-27204 National Inst. of Standards and Technology, Gaithersburg, MD.
CHEMICAL ENGINEERING: MEASUREMENTS FOR A COMPETITIVE AGE (Videotape)
1986 Videotape: 19 min. playing time, in color, with sound
(NONP-NASA-VT-95-49098) Avail: CASI VHS A02/BETA A22

The NIST (National Institute of Standards and Technology) activities supporting chemical research, environmental research, combustion and fuel research, and related industries are described in this video. Highlights include private sector involvement in the research and associated and guest scientist programs, the calibration of customers' instruments, and the direct funding for the NIST research projects by outside industries. CASI

N95-27295 Air Force Inst. of Tech., Wright-Patterson AFB, OH. School of Engineering.
HIGH RESOLUTION FOURIER TRANSFORM SPECTROSCOPY OF THE FIRST OVERTONE OF THE N-O STRETCH IN NITROSYL BROMIDE M.S. Thesis
Todd E. Wiest Sep. 1994 117 p Limited Reproducibility: More than 20% of this document may be affected by microfiche quality
(AD-A289318; AFIT/GAP/ENP/94D-11) Avail: Issuing Activity (Defense Technical Information Center (DTIC))

Infrared Fourier transform spectroscopy of the first overtone of the nitric oxide (NO) bond stretch in nitrosyl bromide (ONBr) has been performed at a resolution of 0.02 cm(exp -1) to obtain the rotational parameters of the v(sub 1) = 2 energy level. Roughly 1000 transitions have been observed for rotational levels up to J = 80 and K(sub a) = 7. The calculation of the complete set of rotational energy levels of this asymmetric molecule requires the numerical diagonalization of four tridiagonal matrices for each J. From a nonlinear least squares fit of observed transitions with J less than or equal to 40 using an approximation for the energy levels, the maximum J value accurately approximated was determined to be twenty-four. The fit was reaccomplished for J less than or equal to 24. Monte Carlo analysis suggests the need to use higher J levels to determine the distortion constants. DTIC

N95-27401# Pacific Northwest Lab., Richland, WA.
THE INFLUENCE OF SURFACE STRUCTURE ON THE INTERACTION OF WATER WITH TIO2(100)
M. A. Henderson Nov. 1994 6 p Presented at the 1994 Fall Meeting of the Materials Research Society (MRS), Boston, MA, 28 Nov. - 2 Dec. 1994
(Contract DE-AC06-76RL-01830)
(DE95-004927; PNL-SA-25472; CONF-941144-30) Avail: CASI HC A02/MF A01

The influence of surface structure on the interaction of water with TiO2(100) (rutile) was investigated. Two unique surface structures of the (100) crystal face can be prepared by oxidation (the bulk-terminated surface) and by vacuum reduction (the (110)- microfaceted surface). Thermal desorption profiles, which measure the strength of the adsorbate-surface interaction, indicate that submonolayer coverages of water are more stable on the bulk-terminated surface than on the (110)-microfaceted surface. Also, subtle differences exist in the way water interacts with 2-coordinate O(sup 2-) sites on these two surfaces. The implications of these results for chemistry on microcrystallines particle are considered. DOE

N95-27420# Pittsburgh Univ., Pittsburgh, PA.
PROBE MOLECULE STUDIES: ACTIVE SPECIES IN ALCOHOL SYNTHESIS Final Report, Jul. 1993 - 1994
D. G. Blackmond, I. Wender, R. Oukaci, and Jian Wang Jul. 1994 158 p
(Contract DE-FG22-90PC-90305)
(DE95-003514; DOE/PC-90305/T13) Avail: CASI HC A08/MF A02

The objectives of this project are to investigate the role(s) of cobalt and copper in constructing the active sites for the formation of higher alcohols from CO/H2 over the Co-Cu based catalysts by using different reduction treatments and applying selected characterization tools such as TPR, TPD, XRD and XPS as well as to generate mechanistic information on the reaction pathway(s) and key intermediate(s) of higher alcohol synthesis from CO/H2 over Co-Cu/ZnO catalysts by the approach of in-situ addition of a probe molecule (nitromethane). DOE

N95-27423# Sandia National Labs., Albuquerque, NM.
COMPARISON OF THE ACTIVITIES OF FINE-PARTICLE SIZE CATALYSTS
F. V. Stohl, K. V. Diegert, and D. C. Goodnow 1994 7 p Presented at the 209th American Chemical Society National Meeting, Anaheim, CA, 2-7 Apr. 1995
(Contract DE-AC04-94AL-85000)
(DE95-004773; SAND-94-2917C; CONF-950402-1) Avail: CASI HC A02/MF A01

The objectives of Sandia's fine-particle size catalyst testing project are to evaluate and compare the activities of the fine-particle size catalysts being developed in DOE/PETC's Advanced Research Coal Liquefaction Program by using standard coal liquefaction test procedures. The standard procedures use Blind Canyon coal, phenanthrene as the reaction solvent, and a factorial experimental design with temperatures from 350 C to 400 C, reaction times from 20 to 60 minutes, and catalyst loadings up to 1 wt%. Catalytic activity is measured in terms of tetrahydrofuran conversion, heptane conversion, the amount of 9, 10-dihydrophenanthrene in the product, and the gas yield. Several catalysts have been evaluated including a commercially available pyrite, a sulfated iron oxide from the University of Pittsburgh, and several preparations of 6-line ferrihydrites from Pacific Northwest Laboratories. Results have demonstrated that significant differences in activity can be detected among these catalysts. DOE

N95-27437# Los Alamos National Lab., NM.
THREE-DIMENSIONAL COMPUTER MODELING OF HYDROGEN INJECTION AND COMBUSTION
Norman L. Johnson, Anthony A. Amsden, Jeff D. Naber (Sandia Labs., Livermore, CA.), and Dennis L. Siebers (Sandia Labs., Livermore, CA.) 1995 10 p Presented at the SMS Simulation Multiconference: Simulation As A Critical Technology, Phoenix, AZ, 9-13 Apr. 1995 Sponsored by the Department of Energy Hydrogen Program
(Contract W-7405-eng-36)
(DE95-006261; LA-UR-95-210; CONF-950439-7) Avail: CASI HC A02/MF A01

The hydrodynamics of hydrogen gas injection into a fixed-volume combustion chamber is analyzed and simulated using KIVA-3, a three-dimensional, reactive flow computer code. Comparisons of the simulation results are made to data obtained at the Combustion Research Facility at Sandia National Laboratory-California (SNL-CA). Simulation of the gas injection problem is found to be of comparable difficulty as the liquid fuel injection in diesel engines. The primary challenge is the large change of length scale from the flow of gas in the orifice to the penetration in the combustion chamber. In the current experiments, the change of length scale is about 4,000. A reduction of the full problem is developed that reduces the change in length scale in the simulation to about 400, with a comparable improvement in computational times. Comparisons of the simulation to the experimental data shows good agreement in the penetration history and pressure rise in the combustion chamber. At late times the comparison is sensitive to the method of determination of the penetration in the simulations. In a comparison of the combustion modeling of methane and hydrogen, hydrogen combustion is more difficult to model, and currently available kinetic models fail to predict the observed autoignition delay at these conditions. DOE

N95-27438# National Renewable Energy Lab., Golden, CO.
BIOMASS PYROLYSIS OIL PROPERTIES AND COMBUSTION MEETING
1995 398 p Meeting held in Estes Park, CO, 26-28 Sep. 1994; cosponsored by the US DOE; NREL; Natural Resources Canada; and VJJ Energy, Finland
(Contract DE-AC36-83CH-10093)
(DE95-004017; NREL-CP-430-7215; CONF-9409224) Avail: CASI HC A17/MF A04

These proceedings contain extended abstracts from the Biomass Pyrolysis Oil Properties and Combustion Meeting held September 26-28, 1994. This meeting is cosponsored by the DOE, NREL, NRCan, and VTT Energy (Finland) for the discussion of developments in the application of biomass-derived pyrolysis oil. DOE

N95-27451# Oak Ridge National Lab., TN.
MEASUREMENTS OF THE VOLATILITIES OF ELECTROLYTES: APPLICATION TO WATER/STEAM CYCLES
D. A. Palmer, J. M. Simonson, and J. P. Jensen (Technical Univ. of Denmark, Lyngby, Denmark.) 1995 13 p Presented at the 4th International Conference on Fossil Plant Cycle Chemistry, Atlanta, GA, 7-9 Sep. 1994
(Contract DE-AC05-84OR-21400)
(DE95-007103; CONF-940982-1) Avail: CASI HC A03/MF A01

This article describes recent results of a laboratory-scale research project aimed at measuring partitioning constants for a range of electrolytes that are known to be present in commercial power-plant boilers and/or are a potential hazard in terms of chemical carry-over of corrosive species to the LP turbines. Particular emphasis has been placed on measurements of NaOH, H2SO4 and the intermediate salts NaHSO4 and Na2SO4. These results indicate that a rapid chemical equilibrium exists with the formation of minor accounts of 'sulfites' at the elevated temperatures investigated, viz. to 350 C 662 F, or ca. 165 bar, or 2400 psi. A computerized model is under development incorporating the partitioning constants of HCl, NH4Cl, NaCl, NaOH, H2SO4, NaHSO4, and NH3, as well as the related hydrolysis constants and the ion product of water with the goal of providing a tool for predicting the composition of steam and condensate formed in the water/steam cycle of power plants with drum boilers. These calculations are by necessity based on equilibrium conditions, but demonstrate the impact of the ratio of amount of condensate formed to steam generated, particularly with respect to the pH of the condensate and the build-up of high concentrations of solutes. Moreover, the most recent calculations indicate the importance of the Na(sup +):anion ratio in the boiler water with regard to the pH of the first condensate. A number of examples of various boiler water compositions have been tested using this program, STEAMCYC, and some typical results are given. DOE

N95-27458# Purdue Univ., West Lafayette, IN. Dept. of Chemistry.
PRECONVERSION CATALYTIC DEOXYGENATION OF PHENOLIC FUNCTIONAL GROUPS Quarterly Technical Progress Report, 1 Jun. 1994 - - 31 Aug. 1994
C. P. Kubiak 1995 10 p
(Contract DE-FG22-93PC-93208)
(DE95-007556; DOE/PC-93208/T4) Avail: CASI HC A02/MF A01

Recent research in this laboratory has established the viability of the catalytic deoxygenation of phenols by carbon monoxide. The initial phases of the author's work focus on identifying catalyst requirements essential for low temperature deoxygenation using potential mono(aryloxide) catalysts Rh(triphos)(O-Ph) and Pt(triphos)(O-Ph)(sup +) triphos = bis(2 diphenylphosphinoethyl)phenylphosphine. DOE

N95-27467# Los Alamos National Lab., NM.
PHOTON BURST MASS SPECTROMETRY--ULTRASENSITIVE DETECTION OF RARE ISOTOPES
C. S. Hansen (Colorado State Univ., Fort Collins, CO.), X. J. Pan (Colorado State Univ., Fort Collins, CO.), W. M. Fairbank, Jr. (Colorado State Univ., Fort Collins, CO.), H. Oona, E. P. Chamberlin, N. S. Nogar, and B. L. Fearey 1995 5 p Presented at the SPIE '95: SPIE Conference on Optics, Electro-optics, and Laser Application in Science, Engineering and Medicine, San Jose, CA, 5-10 Feb. 1995
(Contract W-7405-eng-36)
(DE95-006403; LA-UR-95-49; CONF-950226-11) Avail: CASI HC A01/MF A01

Progress is reported on the development of a new technique for measurement of trace levels of radioisotopes which is based on fluorescence detection of output from a mass spectrometer. Significant achievements include the observation of fluorescence and burst signals from Kr isotopes, including enriched samples of Kr-85 with a 4-collector system. An abundance sensitivity is demonstrated with Kr-83 and Kr-85. DOE

N95-27496# Lawrence Livermore National Lab., Livermore, CA.
PXAMS: PROJECTILE X RAY AMS: X RAY YIELDS AND APPLICATIONS
J. E. McAninch, G. S. Bench, S. P. H. T. Freeman, M. L. Roberts, J. R. Southon, J. S. Vogel, and I. D. Proctor Oct. 1994 14 p Presented at the 13th International Conference on the Application of Accelerators in Research and Industry, Denton, TX, 7-10 Nov. 1994
(Contract W-7405-eng-48)
(DE95-006438; UCRL-JC-118859; CONF-941129-13) Avail: CASI HC A03/MF A01

Characteristic X rays have recently been explored as a method for the detection and identification of ions in accelerator mass spectrometry (AMS). After analysis in the AMS spectrometer, the ions stop in an appropriately chosen target and the induced X rays identify the ions by atomic number. For the application of AMS to higher mass isotopes, characteristic X rays allow significantly better discrimination of competing atomic isobars than is possible using energy loss detectors. Characteristic X rays also show promise as a convenient component in hybrid detection systems. Measurements of X ray yields are presented for Si, Fe, Ni, Se, Mo, and Pd ions of 0.5-2 MeV/AMU. The yields rise by more than a factor of 10 over this energy range, and approach 1 X-ray per incident ion at 2 MeV/AMU for the lighter ions. Preliminary work on the application of PXAMS to the detection of Se-79 is described. DOE

N95-27549# Surface/Interface, Inc., Mountain View, CA.
CHARGE DISTRIBUTION ANALYSIS OF CATALYSTS UNDER SIMULATED REACTION CONDITIONS Quarterly Technical Progress Report No. 7, 1 Apr. - 30 Jun. 1994
F. Freund 1995 8 p
(Contract DE-AC22-92PC-92106)
(DE95-006943; DOE/PC-92106/T7) Avail: CASI HC A02/MF A01

The charge distribution of heterogeneous catalysts (such as iron oxides) has been measured under reaction conditions. During this period, various problems with the analysis equipment were rectified. DOE

N95-27556# Los Alamos National Lab., NM. Technology and Safety Assessment and Earth and Environmental Science Div.
MODELING PRECIPITATION FROM CONCENTRATED SOLUTIONS WITH THE EQ3/6 CHEMICAL SPECIATION CODES
Lee F. Brown and Michael H. Ebinger 13 Jan. 1995 12 p Presented at the Waste Management '95 Conference, Tucson, AZ, 26 Feb. - 2 Mar. 1995
(Contract W-7405-eng-36)
(DE95-006264; LA-UR-95-201; CONF-950216-46) Avail: CASI HC A03/MF A01

One of the more important uncertainties of using chemical speciation codes to study dissolution and precipitation of compounds is the results of modeling which depends on the particular thermodynamic database being used. The authors goal is to investigate the effects of different thermodynamic databases on modeling precipitation from concentrated solutions. They used the EQ3/6 codes and the supplied databases to model precipitation in this paper. One aspect of this goal is to compare predictions of precipitation from ideal solutions to similar predictions from nonideal solutions. The largest thermodynamic databases available for use by EQ3/6 assume that solutions behave ideally. However, two databases exist that allow modeling nonideal solutions. The two databases are much less extensive than the ideal solution data, and they investigated the comparability of modeling ideal solutions and nonideal solutions. They defined four fundamental problems to test the EQ3/6 codes in concentrated solutions. Two problems precipitate Ca(OH)(sub 2) from solutions concentrated in Ca(++). One problem tests the precipitation of Ca(OH)(sub 2) from high ionic strength (high concentration) solutions that are low in the concentrations of precipitating species (Ca(++) in this case). The fourth problem evaporates the supernatant of the problem with low concentrations of precipitating species. The specific problems are discussed. DOE

N95-27680# Grambling State Univ., LA.
NQR-NMR STUDIES OF HIGHER ALCOHOL SYNTHESIS Cu-Co CATALYSTS Quarterly Technical Progress Report, 15 Jun. 1994 - 15 Sep. 1994
U. A. Donatto, T. L. Hoard, and A. N. Murty 1995 10 p
(Contract DE-FG22-89PC-89761)
(DE95-007926; DOE/PC-89761/T10) Avail: CASI HC A02/MF A01

The selectivity and conversion efficiency of the catalyst are reported to be governed by inter-metallic ratios of the three elements. High yields of methanol in copper-rich field, hydrocarbons in cobalt-rich field and mixed alcohols in the intermediate range were observed. The basic mechanism, the extent and effect of inter-metallic interactions, or the role and function of chromium still remain unclear. To examine the correspondence between the catalytic and magnetic behavior of the catalyst, the author has investigated the Zero-field Nuclear Magnetic Resonance spectra and Hysteresis character of a series of Cu/Co/Cr trimetallics with Cu/Co ratio varying from 0.2 to 8.0. The magnetic moment of the catalyst system is very low for Cu/Co less than 1.5, dramatically increases when 1.5 less than Cu/Co less than 5.0 and drops for Cu/Co greater than 5.0. The NMR results indicate that chromium serves as a support and inhibits any strong intermetallic interaction between copper and cobalt. DOE

N95-27681# Sandia National Labs., Albuquerque, NM.
MATERIAL ANALYSIS USING COMBINED ELASTIC RECOIL DETECTION AND RUTHERFORD/ENHANCED RUTHERFORD BACKSCATTERING SPECTROMETRY
J. H. Burkhart (Idaho State Univ., Pocatello, ID.) and J. C. Barbour 1994 12 p Presented at the 13th International Conference on the Application of Accelerators in Research and Industry, Denton, TX, 7-10 Nov. 1994
(Contract DE-AC04-94AL-85000)
(DE95-005415; SAND-94-1885C; CONF-941129-12) Avail: CASI HC A03/MF A01

Three complimentary ion beam techniques will be combined in the analysis of oxide and nitride based materials, in particular BN/SiC and La(0.85)Sr(0.15)CoO(3). These materials can be synthesized over composition ranges which vary the physical and electrical properties, and therefore an accurate measure of the composition profiles is critical for controlling these properties. Elastic Recoil Detection (ERD) revealed the composition of light elements from H to O, and Rutherford Backscattering Spectrometry (RBS) gave the composition of heavier elements (e.g., Si, Sr, Co and La). Enhanced Rutherford Backscattering Spectrometry (FRBS) complimented these techniques by utilizing enhanced cross-sections, greater than Rutherford, to increase the signal-to-noise ratio for analysis of mid-range elements O, C, and N. ERD with 24 MeV Si ions gave profiles for H, B, and N in thin films, and 30 MeV Si was able to profile O in the top portion of heavier samples. Although 2.8 MeV He RBS worked well for heavier elements, ERBS utilized He ions at 3.5 MeV for N analysis and 8.7 MeV for O analysis, because at these energies the cross sections are 2 and 22 times Rutherford, respectively. Also, the depth of analysis was greater with ERBS because of the increased incident energy. DOE

N95-27683# Sandia National Labs., Albuquerque, NM.
NUMERICAL METHODS FOR DETERMINING INTERSTITIAL OXYGEN IN SILICON
J. O. Stevenson and J. W. Medernach Jan. 1995 39 p
(Contract DE-AC04-94AL-85000)
(DE95-007710; SAND-93-0349) Avail: CASI HC A03/MF A01

The interstitial oxygen (O(i)) concentration in Czochralski silicon and the subsequent SiO(x) precipitation are important parameters for integrated circuit fabrication. Uncontrolled SiO(x) precipitation during processing can create detrimental mechanical and electrical effects that contribute to poor performance. An inability to consistently and accurately measure the initial O(i) concentration in heavily doped silicon has led to contradictory results regarding the effects of dopant type and concentration on SiO(x) precipitation. The authors have developed a software package for reliably determining and comparing O(i) in heavily doped silicon. The SiFTIR(copyright) code implements three independent oxygen analysis methods in a single integrated package. Routine oxygen measurements are desirable over a wide range of silicon resistivities, but there has been confusion concerning which of the three numerical methods is most suitable for the low resistivity portion of the continuum. A major strength of the software is an ability to rapidly produce results for all three methods using only a single Fourier Transform Infrared Spectroscopy (FTIR) spectrum as input. This ability to perform three analyses on a single data set allows a detailed comparison of the three methods across the entire range of resistivities in question. Integrated circuit manufacturers could use the enabling technology provided by SiFTIR(copyright) to monitor O(i) content. Early detection of O(i) using this diagnostic could be beneficial in controlling SiO(x) precipitation during integrated circuit processing. DOE

N95-27690# Lehigh Univ., Bethlehem, PA. Dept. of Chemistry.
NO DECOMPOSITION IN NON-REDUCING ATMOSPHERES Technical Progress Report, Sep. 1994 - Nov. 1994
K. Klier, R. G. Herman, and I. Jirka Jan. 1995 9 p
(Contract DE-FG22-93PC-93222)
(DE95-007895; DOE/PC-93222/5) Avail: CASI HC A02/MF A01

Two new samples of Co(2)/Ce(3) ion exchanged A zeolites were prepared by a solid ion exchange technique. A new continuous flow NO decomposition reactor system was built and tested. This system can be evacuated, operated under reduced pressure, or operated at ambient pressure. Reactants and product are analyzed by an online quadrupole mass spectrometer. Analyses of Na A zeolite, Co(2) A zeolite s, and Co(2)/Ce(3) A zeolites, as well as Na X zeolite, Na Y zeolite, and Na mordenite for comparison purposes, have been carried out by X ray photoelectron spectroscopy and Auger spectroscopy methods. Interesting variations in Auger parameters have been observed, and interpretation of these results are in progress. DOE

N95-27691# State Univ. of New York, Stony Brook, NY.
SUPERIOR CATALYSTS FOR SELECTIVE CATALYTIC REDUCTION OF NITRIC OXIDE Annual Technical Report, 30 Sep. 1993 - 29 Sep. 1994
J. P. Chen, M. C. Hausladen, and R. T. Yang 1995 37 p
(Contract DE-FG22-93PC-93217)
(DE95-007903; DOE/PC-93217/T4) Avail: CASI HC A03/MF A01

A delaminated Fe2O3-pillared clay catalyst was prepared for the selective catalytic reduction (SCR) of NO by NH3 at above 300 C. The delaminated pillard clay was characterized by ICP-AES (Inductively Coupled Plasma-Atomic Emission Spectroscopy) chemical analysis, XRD (X ray diffraction) structure and line broadening analyses, micropore size probing, and Moessbauer analysis. These analyses showed that the catalyst contained fragmented Fe2O3- pillared clay forming (open 'house-of-cards' structure with dispersed Fe2O3 particles approximately 170 (angstrom) in size. The SCR activity of the delaminated pillard clay was higher than the commercial-type V2O5) + WO3/TiO2 catalyst, and also higher than the undelaminated pillard clay and supported Fe2O3 catalysts, under conditions with SO2. Infrared measurements of adsorbed NH3 showed strong Bronsted acidity which was caused possibly by interactions between Fe2O3 and clay. DOE

N95-27692# Notre Dame Univ., IN. Dept. of Chemical Engineering.
TRANSIENT STUDIES OF LOW TEMPERATURE CATALYST FOR METHANE CONVERSION Quarterly Technical Progress Report, 1 Oct. 1994 - 31 Dec. 1994
E. E. Wolf 1995 4 p
(Contract DE-FG22-92PC-92529)
(DE95-007913; DOE/PC-92529/T9) Avail: CASI HC A01/MF A01

This report summarizes results obtained with a new approach to the production of synthesis gas from methane. The LaRhO3 perovskite catalyst previously studied, as well as other Rh supported catalysts have been studied using fast flows or millisecond residence times. DOE

N95-27695*# Toledo Univ., OH. Dept. of Chemical Engineering.
HIGH TEMPERATURE KINETIC STUDY OF THE REACTIONS H + O2 = OH + O AND O + H2 = OH + H IN H2/O2 SYSTEM BY SHOCK TUBE-LASER ABSORPTION SPECTROSCOPY Final Contractor Report
Si-Ok Ryu, Soon Muk Hwang, and Kenneth J. DeWitt Cleveland, OH NASA May 1995 123 p
(Grant NAG3-1307; RTOP 505-62-52)
(NASA-CR-195473; E-9670; NAS 1.26:195473) Avail: CASI HC A06/MF A02

The reactions: (1) H + O2 = OH + O; and (2) O + H2 = OH + H are the most important elementary reactions in gas phase combustion. They are the main chain-branching reaction in the oxidation of H2 and hydrocarbon fuels. In this study, rate coefficients of the reactions and have been measured over a wide range of composition, pressure, density and temperature behind the reflected shock waves. The experiments were performed using the shock tube - laser absorption spectroscopic technique to monitor OH radicals formed in the shock-heated H2/O2/Ar mixtures. The OH radicals were detected using the P(1)(5) line of (0,0) band of the A(exp 2) Sigma(+) from X(exp 2) Pi transition of OH at 310.023 nm (air). The data were analyzed with the aid of computer modeling. In the experiments great care was exercised to obtain high time resolution, linearity and signal-to-noise. The results are well represented by the Arrhenius expressions. The rate coefficient expression for reaction (1) obtained in this study is k(1) = (7.13 +/- 0.31) x 10(exp 13) exp(-6957+/- 30 K/T) cu cm/mol/s (1050 K less than or equal to T less than or equal to 2500 K) and a consensus expression for k(1) from a critical review of the most recent evaluations of k(1) (including our own) is k(1) = 7.82 x 10(exp 13) exp(-7105 K/T) cu cm/mol/s (960 K less than or equal to T less than or equal to 5300 K). The rate coefficient expression of k(2) is given by k(2) = (1.88 +/- 0.07) x 10(exp 14) exp(-6897 +/- 53 K/T) cu cm/mol/s (1424 K less than or equal to T less than or equal to 2427 K). For k(1), the temperature dependent A-factor and the correlation between the values of k(1) and the inverse reactant densities were not found. In the temperature range of this study, non-Arrhenius expression of k(2) which shows the upward curvature was not supported. Author

N95-27707# Lawrence Livermore National Lab., Livermore, CA.
ABSORPTION OF SPARINGLY SOLUBLE GASES BY REACTIVE MEDIA IN SELF-AERATED GAS-LIQUID CONTACTORS: A SCALE-UP PROCEDURE
Yury Zundelevich Jan. 1995 18 p
(Contract W-7405-eng-48)
(DE95-006429; UCRL-ID-119563) Avail: CASI HC A03/MF A01

Absorption of sparingly soluble gases, such as NO or O2, is greatly enhanced if the latter react with the media. Among a dozen of reactive solvents for NO(x) abatement, aqueous acidic urea appears the most economically and environmentally attractive because urea is a cheap reagent and because products of reaction of urea with nitrous acid, formed in the liquid phase via absorption of NO and NO2, are carbon dioxide and nitrogen, which can be directly released into the atmosphere. That makes urea process unique among other wet scrubbing processes that routinely produce secondary waste. Its full potential has never been realized, perhaps due to the lack of an efficient gas-liquid contactor to overcome low solubility of NO in aqueous solutions. LLNL has recently designed and built a bench scale gas-liquid contactor for nitric acid regeneration with oxygen. The contactor proved very effective in overcoming the problem of low solubility of oxygen converting back to nitric acid approximately 99% of nitrous acid formed at the cathode (which would otherwise convert to NO(x). The bench scale contactor consists of a 12 inch diameter tank with self-inducting impeller/aerator of very high gas capacity. The aerator represents a 3.5 inch turbine mounted on a vertical shaft inside the draft tube equipped with a stator. During operation the lower half of the turbine induces liquid and the upper half induces gas from the draft tube. The new contactor offers two approaches to solving the NO(x) pollution problem. Where full recovery of nitric acid is desired, oxygen can be fed into the contactor to convert nitrous acid into nitric. This approach was demonstrated at LLNL. Alternately, in the proposed acidic urea process nitrous acid, as it forms from NO(x), would be converted to nitrogen, water and carbon dioxide. DOE

N95-27750# Sandia National Labs., Albuquerque, NM.
A COMPATIBILITY STUDY OF CONTAINMENT MATERIALS IN FEFO, BIS-(2-FLUORO-2,2-DINITROETHYL) FORMAL
T. J. Shepodd, S. H. Goods, W. E. Moddeman (Mason and Hanger-Silas Mason Co., Inc., Amarillo, TX.), and P. Foster (Mason and Hanger-Silas Mason Co., Inc., Amarillo, TX.) Feb. 1995 20 p
(Contract DE-AC04-94AL-85000)
(DE95-007548; SAND-94-8508) Avail: CASI HC A03/MF A01

We report on a program to evaluate the compatibility of energetic fluids with candidate containment materials. The energetic fluids are constituents of various extrudable explosives developed by Lawrence Livermore National Laboratory. These paste-like explosives consist of explosive particulates (HMX, TATB for example) suspended in mixtures of energetic liquids and are designed to remain extrudable over a wide temperature range for many years. It is important to preclude or minimize interactions between the constituents of the paste and the containment materials since such interactions could result in decreased reliability or failure of the containment vessel as well as intrinsic changes in the flow or explosive characteristics of the paste. In this report we focus on one specific paste formulation: RX-52-AE (Transferable Insensitive Explosive, TIE), composed principally of the solid explosive TATB and the energetic liquid, FEFO. Compatibility between a number of organic and metallic materials with neat FEFO has been evaluated. The 300 series stainless steels, Al 6061-T6, and Monel 400 showed evidence of surface attack (oxidation or pitting). Polished gold coupons became discolored and XPS analysis revealed the formation gold cyanide. Platinum, iridium, titanium, tantalum and Ta-10% W showed little evidence of reaction. Among the organic materials, the per-fluorinated materials showed only slight interaction with the FEFO while the polyethylene, polyester and Aclar(r) materials were attacked by the liquid. These interactions were manifested in changes in color, net weight gain and mechanical properties. The changes were exaggerated by higher temperatures. DOE

N95-27755# Argonne National Lab., IL.
MAGNETIC AND STRUCTURAL PROPERTIES OF Fe/Pd MULTILAYERS STUDIED BY MAGNETIC X-RAY DICHROISM AND X-RAY ABSORPTION SPECTROSCOPY
S. M. Mini (Paris-Sud Univ., Orsay, France.), E. E. Fullerton, and C. H. Sowers Dec. 1994 8 p Presented at the 1994 Fall Meeting of the Materials Research Society (MRS), Boston, MA, 28 Nov. - 2 Dec. 1994
(Contract W-31-109-eng-38)
(DE95-007095; ANL/MSD/CP-85324; CONF-941144-63) Avail: CASI HC A02/MF A01

The results of magnetic circular x-ray dichroism (MCXD) measurements and extended x-ray absorption fine structure measurements (EXAFS) of the Fe K-edges of textured Fe(110)/Pd(111) multilayers are reported. The EXAFS results indicate that the iron in the system goes from bcc to a more densely packed system as the thickness of the iron layer is decreased. The magnetic properties were measured by SQUID magnetometry from 5-350 K. For all the samples, the saturation magnetization was significantly enhanced over the bulk values indicating the interface Pd atoms are polarized by the Fe layer. The enhancement corresponds to a moment of approximately 2.5 mu(sub B) per interface Pd atom. DOE

N95-27838# Michigan Univ., Ann Arbor, MI.
HYDROGEN INDUCED C-C, C-N, AND C-S BOND ACTIVITIES ON Pt AND Ni SURFACES
J. L. Gland 1994 11 p
(Contract DE-FG02-91ER-14190)
(DE95-006251; DOE/ER-14190/T1) Avail: CASI HC A03/MF A01

This document summarizes research applied to chemical bond activation studies. Topics summarized include: Carbon nitrogen bonds experimentation with aniline on Ni(111), Ni(100), and Pt(111) surfaces; carbon sulfur bonds experimentation with methanethiol, phenylthiol, and dimethyl disulfide on Pt(111) and Ni(111) surfaces; carbon-carbon bonds experimentation on Ni(100), Ni(111), and Pt(111) surfaces; and in-situ fluorescence yield near edge spectroscopy. DOE

N95-27851# Los Alamos National Lab., NM.
A LABORATORY SCALE SUPERSONIC COMBUSTIVE FLOW SYSTEM
E. C. Sams, D. K. Zerkle, H. A. Fry, and P. J. Wantuck 1995 16 p Presented at the 33rd American Institute of Aeronautics and Astronautics

(AIAA) Aerospace Sciences Meeting, Reno, NV, 9-12 Jan. 1995
(Contract W-7405-eng-36)
(DE95-006347; LA-UR-95-42; CONF-950130-7) Avail: CASI HC A03/MF A01

A laboratory scale supersonic flow system (Combustive Flow System (CFS)) which utilizes the gaseous products of methane-air and/or liquid fuel-air combustion has been assembled to provide a propulsion type exhaust flow field for various applications. Such applications include providing a testbed for the study of planar two-dimensional nozzle flow fields with chemistry, three-dimensional flow field mixing near the exit of rectangular nozzles, benchmarking the predictive capability of various computational fluid dynamic codes, and the development and testing of advanced diagnostic techniques. This paper provides a detailed description of the flow system and data related to its operation. DOE

N95-27880# International Centre for Theoretical Physics, Trieste (Italy).
THE SURFACE OF LIQUID He-4 AT NONZERO TEMPERATURES
K. A. Gernoth, J. W. Clark (Washington Univ., Saint Louis, MO.), and M. L. Ristig (Cologne Univ., Germany.) Jul. 1994 8 p
(DE95-607841; IC-94/160) Avail: CASI HC A02/MF A01 (US Sales Only)

We outline a general approach to microscopic evaluation of the properties of strongly interacting, spatially inhomogeneous Bose systems at finite temperature. A minimum principle for the Helmholtz free energy is used together with an appropriate trial density matrix to generalize the correlated variational wave function theory that has proven so successful in the treatment of the ground states and elementary excitations of quantum fluids at zero temperature. Euler-Lagrange equations are obtained that determine the optimal structure through the one-and two-body densities and the optimal density fluctuation operators and energies characterizing the elementary excitations. Some results of an application of this correlated density matrix theory to the He-4 liquid-vapor interface are presented, with particular focus on the characterization of resonant vapor modes. DOE

N95-27904 Pittsburgh Univ., Pittsburgh, PA. Surface Science Center.
FTIR STUDIES OF CH3OH ON POROUS SILICON
John A. Glass, Jr., Edward A. Wovchko, and John T. Yates, Jr. Nov. 1994 9 p Limited Reproducibility: More than 20% of this document may be affected by microfiche quality
(Contract N00014-91-J-1641)
(AD-A289038) Avail: Issuing Activity (Defense Technical Information Center (DTIC))

Fourier transform infrared spectroscopy (FTIR) was used to investigate the reaction of methanol with porous silicon and hydrogen passivated porous silicon. At 300 K methanol adsorbs onto hydrogen free porous silicon by cleavage of the O-H bond. Both of the resulting surface species, Si-H and Si-OCH3, were determined to be stable up to approx. 500 K. Above 500 K the Si-OCH3 moiety decomposes by breakage of the C-O and C-H bonds. The resulting carbon and oxygen were incorporated into the porous layer and additional Si-H surface species were detected. Further heating to 900 K removed the Si-H surface species. Adsorption of methanol onto hydrogen-passivated porous silicon did not occur until 600 K. At temperatures beyond 600 K, oxygen and carbon incorporation into the porous layer and Si-OCH3, Si-CH3, and Si-H surface species were seen. The previously unseen Si-CH3 surface species is believed to be stabilized by oxygen incorporation. DTIC

N95-27921# Dartmouth Coll., Hanover, NH.
PHOTOINDUCED DIPOLES AND CHARGE PAIRS IN CONDENSED PHASE Progress Report, 14 Nov. 1993 - 15 Nov. 1994
1994 4 p
(Contract DE-FG02-86ER-13592)
(DE95-007071; DOE/ER-13592/9) Avail: CASI HC A01/MF A01

Efforts during the past year centered on expanding the understanding of the photocurrent transients produced by photoinduced dipoles in solution. In addition to exploring intramolecular charge transfer in a molecule which exhibits a giant dipole, the authors began an intensive look at intermolecular electron transfer between photoexcited electron donors and acceptors. The three projects which are farthest along are described in abstract form in the paragraphs which follow. The first makes use of the generous gift from Dr. Michael Wasielewski (Argonne National Laboratory) of a carefully constructed molecular triad which exemplifies artificial photosynthesis. Measurements reveal that the triad possesses a substantial ground state dipole moment as well as the long-lived charge separation which was expected for the excited state. The second and third abstracts describe the quantification of fractional charge transfer in excited state complexes (exciplexes). All exciplexes are not the same and the authors found that the fractional electron transfer increases with reaction exoergicity. The first and second abstracts describe work which is nearly ready to be submitted. The third outlines the mechanistically fascinating story of how one donor replaces another in an excited state complex. Their tentative conclusion is that the mechanism depends on reaction exoergicity. DOE

N95-27929# International Centre for Theoretical Physics, Trieste (Italy).
ULTRASONIC STUDY ON TERNARY LIQUID SYSTEMS BY LASER-SOUND INTERACTION
Mehdi Behboudnia (Ostad Berzeger, Urumiye, Iran.), F. NecatiEcevit (Middle East Technical Univ., Ankara, Turkey.), and Ramazan Aydin Sep. 1994 10 p
(DE95-608783; LAMP-94/7) Avail: CASI HC A02/MF A01 (US Sales Only)

To investigate the ultrasound velocity in liquid mixtures an interferometer based on Raman-Nath diffraction of laser light by sound waves is described. Ultrasonic velocity measurements in water in dependence of temperature and in carboxylic acids with triethylamine in benzene of different mole fractions are presented. DOE

N95-27951# Ohio State Univ., Columbus, OH. Research Foundation.
PHOTOCHEMISTRY IN CONSTRAINED SPACES: ZEOLITES AND LAYERED DOUBLE METAL HYDROXIDES Progress Report, 15 Sep. 1993 - 15 Sep. 1994
P. K. Dutta 1995 3 p
(Contract DE-FG02-90ER-14105)
(DE95-006417; DOE/ER-14105/5) Avail: CASI HC A01/MF A01

The authors have continued their research in the area of assembly and reactivity of photochemical systems in zeolites and double layered metal hydroxides. Over the last year, the authors have focused on two issues, increasing the photochemical efficiency of charge separation in a triad system and the chemistry of Ru(bpy)(sup 3+)(sub 3) in zeolites. DOE

N95-27952# Massachusetts Univ., Amherst, MA. Dept. of Chemical Engineering.
KINETICS AND DYNAMICS OF OXIDATION REACTIONS INVOLVING ADSORBED CO SPECIES ON BULK SUPPORTED Pt AND COPPER OXIDES Final Project Report, 1 Jan. 1991 - 31 Dec. 1993
Wm. C. Conner and M. Harold 1995 6 p
(Contract DE-FG02-87ER-13772)
(DE95-006420; DOE/ER-13772/T2) Avail: CASI HC A02/MF A01

This research was an integrated experimental and modeling study of oxidation reactions involving CO as a key player - be it a reactant, adsorbed intermediate, and/or partial oxidation product - in the catalytic sequence and chemistry. The reaction systems of interest in the project include CO, formaldehyde, and methanol oxidation by O2, and CO oxidation by NO, on both Pt and copper oxide catalysts. These reactions are of importance in automobile exhaust catalysis. There is a paucity of rate data in the literature for these important environmental control reactions. A complicating factor is the propensity of these reactions to exhibit complex steady state and dynamic behavior, including multiple rate controlling steps, steady state multiplicity, and oscillatory phenomena. Such phenomena are rooted in some of the central issues of catalysis, including edsorbate interactions, and catalyst structural instabilities, such as surface reconstruction and surface chemical changes by oxidation-reduction. The goal of this research is to better understand the catalytic chemistry and kinetics of oxidation reactions involving CO as an adsorbed intermediate. Successfully meeting this goal requires an integration of basic kinetic measurements, in situ catalyst surface monitoring, kinetic modeling, and nonlinear mathematical tools. While the kinetics experiments have standard microreactor design, the potential for multiple and periodic rate states demands detailed procedures to pinpoint the bifurcation (ignition, extinction, Hopf) points. Kinetic models are constructed from rational mechanistic sequences and sound surface chemistry. DOE

N95-27956# Oak Ridge National Lab., TN.

ELECTRICAL CONDUCTIVITY MEASUREMENTS OF AQUEOUS ELECTROLYTE SOLUTIONS AT HIGH TEMPERATURES AND HIGH PRESSURES

P. C. Ho and D. A. Palmer 1995 16 p Presented at the Conference on Properties of Water and Steam, Orlando, FL, 12 Sep. 1994
(Contract DE-AC05-84OR-21400)
(DE95-006748; CONF-9409219-5) Avail: CASI HC A03/MF A01

In aqueous solutions all electrolytes tend to associate at high temperatures (low dielectric constants). Ion association results in the formation of uncharged substrates, which are substantially more volatile than their precursor ions. Thus knowledge of the association constants is important in interpreting the thermodynamics of the partitioning of electrolytes to the vapor phase in a fully speciated approach. Electrical conductance measurements provide a unique window into ionic interactions of solutions at high temperatures and pressures. In this study, the electrical conductivities of dilute (less than 0.1 molal) aqueous solutions of NaCl (100-600 C to 300 MPa) and sodium and potassium hydroxides (0-600 and 100-600 C, respectively, and to 300 MPa) were measured. The results show that the extent of association of Na(+) and Cl(-) is similar to those for Na(+) and K(+) with OH(-) in solution from subcritical to supercritical conditions. DOE

N95-27960# Oak Ridge National Lab., TN.

AQUEOUS ELECTROLYTE MODELING IN ASPEN PLUS(TRADEMARK)

G. F. Bloomingburg, J. M. Simonson, R. C. Moore, R. E. Mesmer, and H. D. Cochran 1995 24 p Presented at the Conference on Properties of Water and Steam, Orlando, FL, 12 Sep. 1994
(Contract DE-AC05-84OR-21400)
(DE95-007008; CONF-9409219-7) Avail: CASI HC A03/MF A01

The presence of electrolytes in aqueous solutions has long been recognized as contributing to significant departures from thermodynamic ideality. The presence of ions in process streams can greatly add to the difficulty of predicting process behavior. The difficulties are increased as temperatures and pressures within a process are elevated. Because many chemical companies now model their processes with chemical process simulators it is important that such codes be able to accurately model electrolyte behavior under a variety of conditions. Here the authors examine the electrolyte modeling capability of ASPEN PLUS(trademark), a widely used simulator. Specifically, efforts to model alkali metal halide and sulfate systems are presented. The authors show conditions for which the models within the code work adequately and how they might be improved for conditions where the simulator models fail. DOE

N95-27961# Oak Ridge National Lab., TN.

D/H AND O-18/O-16 PARTITIONING BETWEEN WATER LIQUID AND VAPOR IN THE SYSTEM H2O-Na-K-Mg-Ca-Cl-SO4 FROM 0 TO 350 C

J. Horita, D. J. Wesolowski, and D. R. Cole 1995 9 p Presented at the Conference on Properties of Water and Steam, Orlando, FL, 12 Sep. 1994
(Contract DE-AC05-84OR-21400)
(DE95-007013; CONF-9409219-6) Avail: CASI HC A02/MF A01

Oxygen and hydrogen isotope partitioning between liquid water and water vapor has been precisely determined by means of direct mass-spectrometric measurements of isotopic abundances of the two phases from room temperature to 350 C. Measurable changes in the liquid-vapor partitioning were observed upon the addition of salts (NaCl, KCl, MgCl2, CaCl2, Na2SO4, and MgSO4) to the system. The results of isotope partitioning for the isotopic mixtures and the literature data of vapor pressure measurements of separate isotopic waters agree well for pure water, but show notable discrepancy for salt solutions. DOE

N95-27965# Argonne National Lab., IL.

ANALYSIS OF THE DIMERIZED Sb/Si(001)-(2x1) SURFACE BY X-RAY STANDING WAVES

P. F. Lyman (Northwestern Univ., Evanston, IL.), Y. Qian, and M. J. Bedzyk (Northwestern Univ., Evanston, IL.) Dec. 1994 7 p Presented at the 1994 Fall Meeting of the Materials Research Society (MRS), Boston, MA, 28 Nov. - 2 Dec. 1994
(Contract W-31-109-eng-38)
(DE95-007097; ANL/MSD/CP-85241; CONF-941144-61) Avail: CASI HC A02/MF A01

X-ray standing wave measurements were undertaken to study the bonding position of Sb adatoms on the Sb-saturated Si(001)-(2 x 1) surface. Using the (004) and (022) Bragg reflections, the authors find that the Sb atoms form dimers, and that the center of the Sb ad-dimers lies 1.64 A above the bulk-like Si(004) surface atomic plane. These in-plane results are compared to two structural models consisting of dimers whose bonds are parallel to the surface plane and whose centers are either shifted or unshifted (parallel to the dimer bond direction) relative to the underlying substrate planes. The authors thus find two special cases consistent with these data: one with symmetric (unshifted) dimers having a dimer bond length of 2.81 A, and the other with midpoint-shifted dimers, having a bond length of 2.88 A and a lateral shift of 0.21 A. DOE

N95-28006 Gas Research Inst., Chicago, IL.

RESEARCH ON COMBUSTION PROCESSES RELEVANT TO BURNERS IN HVAC SYSTEMS Final Report, 1 Jul. 1991 - 31 Jul. 1994

S. R. Gollahalli Dec. 1994 200 p Sponsored by Gas Research Inst. Limited Reproducibility: More than 20% of this document may be affected by microfiche quality
(Contract GRI-5091-260-2178)
(PB95-179735; GRI-94/0420) Avail: CASI HC A09

An experimental investigation of the effects of using noncircular geometries for the fuel nozzles, primary-air venturi inlets, and burner exit ports in the inshot burners of residential natural gas heating systems is presented. These burners generally produce partially-premixed laminar flames. For global characterization, primary-air entrainment and exhaust emission indices of NO, NOx, and CO were measured. For detailed flame structure, radial profiles of temperature and major species concentration were recorded. Shadowgraphy was used for flow visualization. Most of the experiments were performed in lab-scale combustion chambers. Some verification tests were conducted in a full-scale furnace. The results show that, generally, primary-air premixing and secondary-air entrainment increase, and the NOx emission decreases for noncircular cross-sections. However, CO emission can increase in some of these cases. Deeper examination of the flow and chemistry coupling mediated by noncircular shapes is warranted before clear design paths of applying noncircular shapes are recommended. NTIS

N95-28042# Oak Ridge K-25 Site, TN.

VAPOR PRESSURES OF MIXTURES OF CFC-114 WITH THE POTENTIAL REPLACEMENT COOLANTS C4F(10) ANDc-C4F 8

L. D. Trowbridge and M. G. Otey (Paducah Gaseous Diffusion Plant, KY.) Sep. 1994 34 p Sponsored by United States Enrichment Corp.
(Contract DE-AC05-84OT-21400)
(DE95-003444; K/TCD-1118) Avail: CASI HC A03/MF A01

The U.S. Enrichment Corporation's production of isotopically enriched uranium depends solely on two plants which utilize the gaseous diffusion process. This process uses large quantities of CFC-114 as an evaporative coolant. CFC-114, however, will be phased out of production at the end of 1995 due to its potential to deplete stratospheric ozone. A search has been underway for substitutes for a number of years. The initial search (1988-89) for an ozone-friendly, commercially available, chemically compatible substitute yielded two candidates, FC-c318 (c-C4F8) and FC-3110 (C4F10). The intended mode of replacing coolant was to stage the new coolant into independent subsystems of the plants, so that some systems would continue to operate on CFC-114, and an increasing number would operate on the new coolant. During that changeover process, the possibility of coolant mixing arises in variety of scenarios. This work was intended to generate sufficient experimental information to be able to predict the vapor pressure of coolant mixtures over the range of operating conditions likely to be found in the diffusion plants. Specifically, vapor pressures were measured over the temperature range 322 to 355 K (120 F to 180 F) and over the full range of mole fractions for binary mixtures of CFC-114 with FC-3110, and of CFC-114 with FC-c318. DOE

N95-28086# California Univ., Berkeley. Lawrence Berkeley Lab, CA.

BEYOND TRANSITION STATE THEORY: RIGOROUS QUANTUM APPROACHES FOR DETERMINING CHEMICAL REACTION RATES

W. H. Miller Jan. 1995 42 p
(Contract DE-AC03-76SF-00098)
(DE95-008483; LBL-36751) Avail: CASI HC A03/MF A01

Transition state theory (TST) has historically been the most important and widely used theoretical approach for describing the rates of chemical reactions, and for qualitative pictures and order-of-magnitude estimates one does not expect this situation to change. However a rigorous, quantitative treatment of chemical reaction rates must go beyond TST. A rigorous description, for example, must be based on a quantum mechanical description of the molecular system, but the fundamental assumption on which TST is based - namely that the molecular dynamics is 'direct,' i.e., that no trajectories recross a dividing surface which separates reactants and products (vide infra) - is couched inherently in the language of classical mechanics. There is no unambiguous way to quantize TST, for the various ways of trying to do so invariably require one to introduce additional assumptions about the reaction dynamics. As one tries to eliminate these 'additional assumptions' one is driven ultimately to an exact quantum treatment of the reaction dynamics which is then no longer a transition state theory (i.e., approximation) but simply an exact formulation. It is such exact approaches, those without inherent approximations, that are the subject of this chapter. DOE

N95-28088# Los Alamos National Lab., NM.
BUBBLE CHAMBER SPECTROSCOPY FOR CHEMICAL ANALYSIS: A NEW CONCEPT
Jerry H. Atencio, Xin Luo, E. Iain McCreary, Andrew W. McCown, and Robert K. Sander 1995 8 p Presented at the SPIE 1995: SPIE Conference on Optics, Electro-optics, and Laser Application in Science, Engineering and Medicine, San Jose, CA, 5-10 Feb. 1995
(Contract W-7405-eng-36)
(DE95-006350; LA-UR-95-57; CONF-950226-19) Avail: CASI HC A02/MF A01

A new technique for the detection of trace concentrations of molecules in solution has been developed. This system utilizes the amplification characteristics of a bubble chamber in which energy deposition from laser absorption is monitored. In the experimental set-up, a trace quantity of solute is introduced into liquid propane that is contained in a small (10 ml) stainless steel cell at 120 psi. The propane is superheated by sudden reduction of the cell pressure. Before wall nucleated boiling occurs, target solute molecules are energized by a laser pulse. Absorption of pump laser energy results in the formation of nucleation centers which develop into bubbles and which in turn are detected by CCD camera. Preliminary experiments with crystal violet used as a test absorber have demonstrated detection sensitivity of 10 parts per trillion (ppt). DOE

N95-28164# Princeton Univ., NJ. Dept. of Chemistry.
ANALYSIS OF FORWARD AND INVERSE PROBLEMS IN CHEMICAL DYNAMICS AND SPECTROSCOPY Progress Report, 1 Feb. 1993 - 31 Jul. 1994
Herschel Rabitz 30 Aug. 1994 38 p
(Contract DE-FG02-86ER-13480)
(DE95-009309; DOE/ER-13480/5) Avail: CASI HC A03/MF A01

Three primary topics were pursued: (1) inverse algorithm development for extracting potential surfaces from laboratory data (Ar + OH A(sup 2) Sigma(sup +)) and extracting diabatic coupling potentials from inelastic scattering data); (2) model reduction of complex kinetic mechanisms (nonlinear transformations of chemical species, nonlinear lumping in chemical kinetics, and perturbation theory); and (3) identification of key variables and their interrelationships in dynamics and kinetics phenomena (effect of shape of potential surfaces on collision cross sections, F + H2 reaction probability, Ne excitation by He(+), Na + I collision, excitation of O(D-1) atoms, H(+) + F((sup 2)P(sub 1/2)), Na((sup 2)P(sub 1/2)) + He or Ar, He(+) + Ne(2p(sup 6)), Li + I, thermal runaway, combustion kinetics of CO + H2 + O2, and energy eigenvalues). DOE

N95-28182*# National Aeronautics and Space Administration. Lewis Research Center, Cleveland, OH.
TRANSPORT COEFFICIENTS FOR THE NASA LEWIS CHEMICAL EQUILIBRIUM PROGRAM
Roger A. Svehla Apr. 1995 29 p
(RTOP 505-62-52)
(NASA-TM-4647; E-9173; NAS 1.15:4647) Avail: CASI HC A03/MF A01

The new transport property data that will be used in the NASA Lewis Research Center's Chemical Equilibrium and Applications Program (CEA) is presented. It complements a previous publication that documented the thermodynamic and transport property data then in use. Sources of the data and a brief description of the method by which the data were obtained are given. Coefficients to calculate the viscosity, thermal conductivity, and binary interactions are given for either one, or usually, two temperature intervals, typically 300 to 1000 K and 1000 to 5000 K. The form of the transport equation is the same as used previously. The number of species was reduced from the previous database. Many species for which the data were estimated were eliminated from the database. Some ionneutral interactions were added. Author

N95-28218# California Univ., Berkeley. Lawrence Berkeley Lab, CA.
VIBRATIONAL SPECTROSCOPY OF WATER INTERFACES Ph.D. Thesis
Q. Du Dec. 1994 133 p
(Contract DE-AC03-76SF-00098)
(DE95-006592; LBL-36546) Avail: CASI HC A07/MF A02

The second order nonlinear optical processes of second harmonic generation and sum frequency generation are powerful and versatile tools for studying all kinds of surfaces. They possess unusual surface sensitivity due to the symmetry properties of the second order nonlinear susceptibility. The technique of infrared-visible sum frequency generation (SFG) is particularly attractive because it offers a viable way to do vibrational spectroscopy on any surfaces accessible to light with submonolayer sensitivity. In this thesis, the author applies SFG to study a number of important water interfaces. At the air/water interface, hydrophobic solid/water and liquid/water interfaces, it was found that approximately 25% of surface water molecules have one of their hydrogen pointing away from the liquid water. The large number of unsatisfied hydrogen bonds contributes significantly to the large interfacial energy of the hydrophobic surfaces. At the hydrophilic fused quartz/water interface and a fatty acid monolayer covered water surface, the structure and orientation of surface water molecules are controlled by the hydrogen bonding of water molecules with the surface OH groups and the electrostatic interaction with the surface field from the ionization of surface groups. A change of pH value in the bulk water can significantly change the relative importance of the two interactions and cause a drastic change in orientation of the surface water molecules. SFG has also been applied to study the tribological response of some model lubricant films. Monolayers of Langmuir-Blodgett films were found to disorder orientationally under mildly high pressure and recover promptly upon removal of the applied pressure. DOE

N95-28229# California Univ., Berkeley. Lawrence Berkeley Lab, CA.
HYDROGEN-ION TITRATIONS OF AMINO ACIDS AND PROTEINS IN SOLUTIONS CONTAINING CONCENTRATED ELECTROLYTE
F. Fergg, D. E. Kuehner, H. W. Blanch, and J. M. Prausnitz Dec. 1994 64 p
(Contract DE-AC03-76SF-00098)
(DE95-008356; LBL-36511) Avail: CASI HC A04/MF A01

This report describes a first attempt to quantify the net charge as a function of solution pH for lysozyme and (alpha)-chymotrypsin at 0.1 M, 1.0 M and 3.0 M ionic strength, (IS). The calculations are based on the residue (titratable group) pK(sub a)'s in the amino-acid sequence of the protein. To determine these pK(sub a)'s, a simple theory was used which assumes that the pK(sub a)'s are independent from each other in the protein and are equal to their pK(sub a) values in free amino-acid solution (Independent-Site Theory, IST). Residue pK(sub a)'s were obtained from amino-acid hydrogen-ion titrations at three different KCl concentrations corresponding to 0.1M, 1.0M and 3.0M ionic strength. After construction of a suitable apparatus, the experimental procedure and data reduction were computerized to perform a large number of titrations. Most measured pK(sub a)'s showed high reproducibility (the difference of pK(sub a) values observed between two experiments was less than 0.05). For IS = 0.1M, observed pK(sub a)'s agreed with literature values to within a few hundredths of a pH unit. Furthermore, the ionic-strength dependence of the pK(sub a)'s followed the trends reported in the literature, viz. pK(sub a) values decrease with increasing ionic strength until they reach a minimum at about IS = 0.5M. At still higher IS, pK(sub a)'s increase as the ionic strength rises to 3M. The known pK(sub a)'s of all titratable groups in a protein were used with the IST to give a first approximation of how the protein net charge varies with pH at high ionic strength. A comparison of the titration curves based on the IST with experimental lysozyme and (alpha)-chymotrypsin titration data indicates acceptable agreement at IS = 0.1M. However, comparison of measured and calculated titration curves at IS = 1M and IS = 3M indicates only quantitative agreement. DOE

N95-28584 Department of the Navy, Washington, DC.
MATERIAL CHARACTERIZATION SYSTEM Patent
Gilbert F. Lee, inventor (to Navy) and Bruce Hartmann, inventor (to Navy) 15 Nov. 1994 10 p Filed 14 Apr. 1994
(AD-D017385; US-Patent-5,363,701; US-Patent-Appl-SN-227771; US-Patent-Class-73-574) Avail: US Patent and Trademark Office

A plurality of elongated test specimens undergo vibrations induced by random noise within an acoustical frequency range establishing standing waves therein having resonant frequencies at which the collection of measurement data through accelerometers mounted at the ends of the specimens provides for calculation of physical material properties. The processing of the data during collection, analysis and calculation is automated by programmed computer control. DTIC

N95-28585 Department of the Navy, Washington, DC.
IN SITU DYNAMIC MATERIAL PROPERTY MEASUREMENT SYSTEM Patent
Walter Madigosky, inventor (to Navy) 15 Nov. 1994 6 p Filed 19 Oct. 1992
(AD-D017387; US-Patent-5-365,457; US-Patent-Appl-SN-963177; US-Patent-Class-364-506) Avail: US Patent and Trademark Office

Material is periodically indented by a probe driven at an oscillation frequency by a shaker regulated by an analyzer to which input measurement data is fed from a sensing head connecting the shaker to the probe for in Situ measurement of material resistance to indentation to which such input data relates. A computer connected to the analyzer is programmed to calculate steady-state data on dynamic material properties as a time dependent function, from outputs of the analyzer restricted to limits determined from the input measurement data. DTIC

N95-28621 Southwest Research Inst., San Antonio, TX. Belvoir Fuels and Lubricants Research Facility.
MECHANISM OF DEPOSIT FORMATION ON FUEL-WETTED HOT METAL SURFACES Interim Report, May 1989 - Dec. 1992
Leo L. Stavinoha, Steven R. Westbrook, and Lona A. McInnis Jan. 1995 91 p Limited Reproducibility: More than 20% of this document may be affected by microfiche quality
(Contracts DAAK70-87-C-0043; DAAK70-92-C-0059)
(AD-A289847; BFLRF-290) Avail: Issuing Activity (Defense Technical Information Center (DTIC))

Experiments were performed in a Single-Tube Heat Exchanger (STHE) apparatus and a Hot Liquid process meet Jet Fuel Thermal Oxidation Tester (JFTOT) ASTM D 3241 requirements. The HLPS-JFTOT heater tubes used were 1018 mild steel, 316 stainless steel (SS) 304 SS, and 304 SS tubes coated with aluminum, magnesium, gold, and copper. A low-sulfur was used to create deposits on the heater tubes at temperatures of 300 C, 340 C, and 380 C. Deposit thickness was measured by dielectric breakdown voltage and Auger ion milling. Pronounced differences between the deposit thickness measuring techniques suggested that both Auger milling rate and the dielectric strength of the deposit may be affected by deposit morphology/composition (such as metal ions that have become included in the bulk of the deposit). Carbon burnoff data were obtained as a means of judging the validity of DMD-derive deposit evaluations. ESCA data suggest that the thinnest deposit was the magnesium-coated test tube. The scanning Electron Microscope (SEM) photographs showed marked variations in the deposit morphology and the results suggested composition has a significant effect on the mechanism of deposition. DTIC

N95-28652 Selskapet for Industriell og Teknisk Forskning, Trondheim (Norway).
PHOTOEMISSION STUDY OF SOLID STATE REACTION AND INITIAL OXIDATION OF THE Ce/Al(100) SYSTEM Journal Article
C. Berg, S. Raaen, and A. Borg 19 May 1994 11 p Prepared in cooperation with Trondheim Univ.
(PB95-195368; STF19-S94003) Copyright Avail: Issuing Activity (National Technical Information Service (NTIS))

High resolution photoemission spectroscopy has been used to study interface formation and initial oxidation of the Ce/Al(111) system at room temperature and at approximately 100 K. Both the evolution of the interface layer and the initial oxide growth have been investigated in detail. Evaporated Ce overlayers in the range 1-8 Angstroms were found to interdiffuse with Al(111) to form a mixed interface with at least three different Ce-Al coordinations. At room temperature, one of the Ce-Al coordinations predominates as the mixed layer grows. At 100 K a wide variation of Ce-Al coordination is observed, but none of these is preferred during growth. NTIS

N95-27630*# National Aeronautics and Space Administration. Lyndon B. Johnson Space Center, Houston, TX.
AN OVERVIEW OF THE EVALUATION OF OXYGEN INTERACTIONS WITH MATERIALS 3 EXPERIMENT: SPACE SHUTTLE MISSION 46, JULY-AUGUST 1992
Steven L. Koontz, Lubert J. Leger, James T. Visentine, Don E. Hunton (Phillips Lab., Hanscom AFB, MA.), Jon B. Cross (Los Alamos National Lab., NM.), and Charles L. Hakes (Lockheed Engineering and Sciences Co., Houston, TX.) *In* NASA. Langley Research Center, LDEF: 69 Months in Space. Third Post-Retrieval Symposium, Part 3 Feb. 1995 p 869-902 (For primary document see N95-27629 09-99)
Avail: CASI HC A03/MF A04

N95-27631*# National Aeronautics and Space Administration. Lyndon B. Johnson Space Center, Houston, TX.
EVALUATION OF OXYGEN INTERACTIONS WITH MATERIALS 3: MISSION AND INDUCED ENVIRONMENTS
Steven L. Koontz, Lubert J. Leger, Steven L. Rickman, Charles L. Hakes (Los Alamos National Lab., NM.), David T. Bui (Los Alamos National Lab., NM.), Donald Hunton (Phillips Lab., Hanscom AFB, MA.), and Jon B. Cross (Lockheed Engineering and Sciences Co., Houston, TX.) *In* NASA. Langley Research Center, LDEF: 69 Months in Space. Third Post-Retrieval Symposium, Part 3 Feb. 1995 p 903-916 (For primary document see N95-27629 09-99)
Avail: CASI HC A03/MF A04

N95-27632*# Aerospace Corp., El Segundo, CA. Mechanics and Materials Technology Center.
SPACECRAFT MATERIALS STUDIES ON THE AEROSPACE CORPORATION TRAY ON EOIM-3
Wayne K. Stuckey, Carol S. Hemminger, Gary L. Steckel, Malina M. Hills, and Michael R. Hilton *In* NASA. Langley Research Center, LDEF: 69 Months in Space. Third Post-Retrieval Symposium, Part 3 Feb. 1995 p 917-930 (For primary document see N95-27629 09-99)
(Contract F04701-93-C-0094)
Avail: CASI HC A03/MF A04

N95-27633*# Aerospace Corp., El Segundo, CA. Mechanics and Materials Technology Center.
EXPOSURE OF LDEF MATERIALS TO ATOMIC OXYGEN: RESULTS OF EOIM 3
C. H. Jaggers and M. J. Meshishnek *In* NASA. Langley Research Center, LDEF: 69 Months in Space. Third Post-Retrieval Symposium, Part 3 Feb. 1995 p 931-955 (For primary document see N95-27629 09-99)
Avail: CASI HC A03/MF A04

N95-27641*# National Aeronautics and Space Administration. Marshall Space Flight Center, Huntsville, AL.
EVALUATION OF SPACE ENVIRONMENTAL EFFECTS ON METALS AND OPTICAL THIN FILMS ON EOIM-3
Jason A. Vaughn, Roger C. Linton, Miria M. Finckenor, and Rachel R. Kamenetzky *In* NASA. Langley Research Center, LDEF: 69 Months in Space. Third Post-Retrieval Symposium, Part 3 Feb. 1995 p 1053-1065 (For primary document see N95-27629 09-99)
Avail: CASI HC A03/MF A04

N95-27642*# Boeing Defense and Space Group, Seattle, WA.
ANALYSIS OF SELECTED SPECIMENS FROM THE STS-46 ENERGETIC OXYGEN INTERACTION WITH MATERIALS-3 EXPERIMENT
Johnny L. Golden, Roger J. Bourassa, Harry W. Dursch, and H. Gary Pippin *In* NASA. Langley Research Center, LDEF: 69 Months in Space. Third Post-Retrieval Symposium, Part 3 Feb. 1995 p 1067-1094 (For

primary document see N95-27629 09-99)
Avail: CASI HC A03/MF A04

N95-27644*# Jet Propulsion Lab., California Inst. of Tech., Pasadena, CA.
BMDO MATERIALS TESTING IN THE EOIM-3 EXPERIMENT
Shirley Y. Chung, David E. Brinza, Timothy K. Minton, and Ranty H. Liang *In* NASA. Langley Research Center, LDEF: 69 Months in Space. Third Post-Retrieval Symposium, Part 3 Feb. 1995 p 1115-1128 (For primary document see N95-27629 09-99)
Avail: CASI HC A03/MF A04

N95-27645*# National Aeronautics and Space Administration. Lyndon B. Johnson Space Center, Houston, TX.
STS-46 PLASMA COMPOSITION MEASUREMENTS USING THE EOIM-3 MASS SPECTROMETER Abstract Only
Donald E. Hunton, Edmund Trzcinski, Roger Gosselin, Steven Koontz, Lubert Leger, and James T. Visentine *In* NASA. Langley Research Center, LDEF: 69 Months in Space. Third Post-Retrieval Symposium, Part 3 Feb. 1995 p 1129 (For primary document see N95-27629 09-99)
Avail: CASI HC A01/MF A04

N95-27648*# Centre National d'Etudes Spatiales, Toulouse (France).
SYSTEM RESULTS FROM FRECOPA
Christian Durin, Lucinda Berthoud, and Jean-Claude Mandeville *In* NASA. Langley Research Center, LDEF: 69 Months in Space. Third Post-Retrieval Symposium, Part 3 Feb. 1995 p 1153-1165 (For primary document see N95-27629 09-99)
Avail: CASI HC A03/MF A04

N95-27656*# National Aeronautics and Space Administration. Langley Research Center, Hampton, VA.
HARDWARE CLEANLINESS METHODOLOGY AND CERTIFICATION
Gale A. Harvey, Thomas J. Lash, and J. Richard Rawls *In its* LDEF: 69 Months in Space. Third Post-Retrieval Symposium, Part 3 Feb. 1995 p 1237-1243 (For primary document see N95-27629 09-99)
Avail: CASI HC A02/MF A04

N95-28299 Naval Surface Weapons Center, Indian Head, MD. Indian Head Div.
BIODEGRADATION OF NITRATE ESTERS
Johnathan R. Stacy, M. K. Speedie (Maryland Univ., Baltimore, MD.), L. Geelhaar (Maryland Univ., Baltimore, MD.), Min Meng (Maryland Univ., Baltimore, MD.), Gregory Payne (Maryland Univ. Baltimore County, Catonsville, MD.), W. Q. Sun (Maryland Univ. Baltimore County, Catonsville, MD.), Anemi Patal (Maryland Univ. Baltimore County, Catonsville, MD.), and Rakesh Govind (Cincinnati Univ., OH.) *In* Johns Hopkins Univ., The 1994 JANNAF Safety and Environmental Protection Subcommittee Meeting, Volume 1 Aug. 1994 p 43-50 (For primary document see N95-28294 09-20)
Avail: CPIA, 10630 Little Patuxent Pkwy., Suite 202, Columbia, MD 21044-3200 HC

N95-28301 Army Armament Research, Development and Engineering Center, Picatinny Arsenal, NJ.
DESTRUCTION OF PYROTECHNICS MANUFACTURE WASTEWATER TREATMENT SLUDGE BY PLASMA ARC PYROLYSIS
Donald J. Freeman, Hany H. Zaghloul (Army Construction Engineering Research Lab., Champaign, IL.), and Robert E. Haun (Retech, Inc., Ukiah, CA.) *In* Johns Hopkins Univ., The 1994 JANNAF Safety and Environmental Protection Subcommittee Meeting, Volume 1 Aug. 1994 p 63-79 (For primary document see N95-28294 09-20)
Avail: CPIA, 10630 Little Patuxent Pkwy., Suite 202, Columbia, MD 21044-3200 HC

N95-28309* National Aeronautics and Space Administration. John F. Kennedy Space Center, Cocoa Beach, FL.
EVALUATION OF A CONDUCTIVE POLYMER-BASED SENSOR FOR DETECTION OF HYDRAZINES AT THE PART-PER-BILLION LEVEL
Dale Lueck, Dan Curran (I-NET, Inc., Cocoa Beach, FL.), and Mitch Zakin (Spectral Sciences, Inc., Burlington, MA.) *In* Johns Hopkins Univ., The 1994 JANNAF Safety and Environmental Protection Subcommittee Meeting, Volume 1 Aug. 1994 p 149-156 (For primary document see N95-28294 09-20)
(Contract NAS10-11943)
Avail: CPIA, 10630 Little Patuxent Pkwy., Suite 202, Columbia, MD 21044-3200 HC

N95-28311* Naval Research Lab., Washington, DC.
THE SENSITIVE DETECTION OF HYDRAZINE USING CHEMILUMINESCENCE
G. E. Collins and S. L. Rose-Pehrsson *In* Johns Hopkins Univ., The 1994 JANNAF Safety and Environmental Protection Subcommittee Meeting, Volume 1 Aug. 1994 p 167-176 (For primary document see N95-28294 09-20)
(NASA Order CC-82360-A)
Avail: CPIA, 10630 Little Patuxent Pkwy., Suite 202, Columbia, MD 21044-3200 HC

N95-28312* National Aeronautics and Space Administration. John F. Kennedy Space Center, Cocoa Beach, FL.
A NEW METHOD FOR MEASURING HYPERGOL SCRUBBER EMISSIONS
Dale E. Lueck, Rebecca C. Young, Ron Barile (I-NET, Inc., Cocoa Beach, FL.), Clyde Parrish (I-NET, Inc., Cocoa Beach, FL.), and Dan Curran (I-NET, Inc., Cocoa Beach, FL.) *In* Johns Hopkins Univ., The 1994 JANNAF Safety and Environmental Protection Subcommittee Meeting, Volume 1 Aug. 1994 p 177-186 (For primary document see N95-28294 09-20)
(Contract NAS10-11943)
Avail: CPIA, 10630 Little Patuxent Pkwy., Suite 202, Columbia, MD 21044-3200 HC

N95-28314 Army Research Lab., Aberdeen Proving Ground, MD.
A NOVEL SENSITIVE DETECTOR OF ATMOSPHERIC NITROCOMPOUNDS BASED ON LASER PHOTOFRAGMENTATION/IONIZATION SPECTROMETRY
Rosario C. Sausa, Josef B. Simeonsson, and George W. Lemire *In* Johns Hopkins Univ., The 1994 JANNAF Safety and Environmental Protection Subcommittee Meeting, Volume 1 Aug. 1994 p 205-214 (For primary document see N95-28294 09-20)
Avail: CPIA, 10630 Little Patuxent Pkwy., Suite 202, Columbia, MD 21044-3200 HC

26 METALLIC MATERIALS

Includes physical, chemical, and mechanical properties of metals, e.g., corrosion; and metallurgy.

N95-26359 Polish Academy of Sciences, Warsaw (Poland). Dept. of the Strength of Materials.
DETERMINATION OF THE CYCLICAL PROPERTIES OF 18G2A STEEL ON THE BASIS OF SKELETON CURVES FOR A PLANAR STRESS STATE [OKRESLANIE CYKLICZNYCH WLASCIWOSCI STALI 18G2A NA PODSTAWIE KRZYWYCH SZKIELETOWYCH DLA PLASKIEGO STANU NAPREZENIA]
Zbigniew L. Kowalewski, Marek Sliwowski, and Grzegorz Socha Cooperative Publishing House Ltd. Oct. 1994 54 p In POLISH
(ISSN 0208-5658)
(IFTR-32/1994) Avail: Issuing Activity (Polish Academy of Sciences, Warsaw, Poland)

The purpose of this study was to evaluate the properties of the low-alloy structural steel known as 18G2A steel after a program of cyclical loading on the basis of skeleton curves. Tests were conducted using thin-walled tubular specimens in a planar stress state produced by different combinations of axial force and torque. The properties of the material as supplied were estimated on the basis of plasticity surface determined by testing a large number of samples and served as a reference point for comparing the changes in the properties of the material caused by intentional cyclical deformation. The authors propose a new concept for evaluating the properties of a material subjected to cyclical deformation based on the determination of the so-called cyclical plasticity surface. The cycling loading program used by the authors, which included constant loads and loads of diminishing amplitude, caused the steel to weaken in the range of plastic deformations studied, with the most weakening occurring in the directions in which the cyclical loading was applied. The authors' tests revealed that the material in question, which as supplied had anisotropic plastic properties, exhibited the same degree of weakening for each direction analyzed under the impact of the cyclical loading program.

Transl. by Schreiber Translations Inc.

N95-26411 Naval Postgraduate School, Monterey, CA.

CHARACTERIZATION OF ULTRA-LOW CARBON BAINTIC STEELS FOR USE AS WELD WIRE CONSUMABLES M.S. Thesis

Michael L. Beno Sep. 1994 97 p Limited Reproducibility: More than 20% of this document may be affected by microfiche quality
(Contracts N00167-94-WR-40321; N00014-94-WX-35069)
(AD-A288292) Avail: Issuing Activity (Defense Technical Information Center (DTIC))

The use of Ultra-Low Carbon Bainitic (ULCB) steels for weld wire applications is an area of current interest to the U. S. Navy and is being jointly studied by the Naval Postgraduate School and the Naval Surface Warfare Center, Annapolis, MD. The focus of the present work is to determine the effect of macrostructure, microstructure, and the size, distribution and chemical composition of the non-metallic inclusions on the strength and impact toughness of multipass Gas Metal Arc (GMA) and Gas Tungsten Arc (GTA) welds. Eight sample multipass GMA and GTA weldments using ULCB weld wire were studied by optical, scanning electron and transmission electron microscopy (SEM and TEM). The microstructures of the weld metals were dominantly bainitic except for the recrystallized regions of the GTA welds which had become ferritic. The macrostructure of the GMA weldments was dominated by columnar grains. SEM and optical fractography suggested that this macrostructure is responsible for the corresponding poor toughness in these weldments. In all weldments the non-metallic inclusions were found to be very small (on average % 0.5 microns) with a somewhat higher volume fraction in the GMA vice GTA weldments. Based on previous work, the small average size of these inclusions are surmised to have had very little effect on toughness. DTIC

N95-26490 Arizona Univ., Tucson, AZ. Research Labs.

ELASTIC PROPERTIES OF METALLIC SUPERLATTICES Final Report

Charles M. Falco and George I. Stegeman 30 Nov. 1994 8 p Revised Limited Reproducibility: More than 20% of this document may be affected by microfiche quality
(Contracts N00014-88-K-0298; N00014-91-J-1104)
(AD-A288699) Avail: Issuing Activity (Defense Technical Information Center (DTIC))

This Final Report describes some of the significant results from our research program on the elastic properties of metallic multilayers and superlattices. The elastic properties of composition-modulated metallic superlattice films have received considerable attention over the past fifteen years following the initial reports of anomalous enhancements of some elastic moduli as measured by the bulge tester method. For example, it was reported that the Ag/Pd system exhibited an increase of the biaxial modulus of up to 500%. However, more recent measurements failed to reproduce such large enhancements of elastic moduli in the systems for which the elastic anomaly was originally measured. The elastic anomalies observed in subsequent experiments were considerably smaller, although they showed a functional dependence on lambda with either stiffening or softening taking place in different material systems for lambda in the range of approximately 25-40 A. In apparent contrast, some Brillouin light scattering (BLS) measurements have shown a softening of the shear elastic constant C(sub 44) in some bcc/fcc systems, although a stiffening was found in Au/Cr. Because of these apparent contradictions, coupled with the importance of this problem, we initiated a program with ONR funding to investigate these effects. In this report, we review some of our significant results obtained with ONR funding, on the structural and elastic properties observed metallic superlattice films. DTIC

N95-26512 Polish Academy of Sciences, Warsaw (Poland). Dept. of the Strength of Materials.

IDENTIFICATION OF THE PLASTIC ANISOTROPY OF AN ALUMINUM ALLOY [IDENTYFIKACJA PLASTYCZNEJ ANIZOTROPII STOPU ALUMINIUM]

Lech Dietrich, Romuald Kiryk, Grzegorz Socha, and Marek Sliwowski 1994 50 p In POLISH
(ISSN 0208-5658)
(IFTR-26/1994) Avail: Issuing Activity (Polish Academy of Sciences, Warsaw, Poland)

This article contains the results of experimental studies in complex stress states produced on thin-walled tubular specimens subjected to different combinations of simultaneously operating axial force (tensile or compressive) and bi-directional torque. The specimens were prepared from complete extruded rods of PA6 aluminum alloy. The basic purpose of this study was to identify the type of plastic anisotropy and calculate its coefficients on the basis of tests in complex stress states using a large number of specimens, each of which was subjected to loading along different proportional paths in the stress pace under consideration. The author used Mises' (1928) anisotropic condition of plasticity in an updated version which accounts for the Bauschinger effect to approximate the experimental points which describe the shape and location of the materials' plasticity surface. The authors also compared the plasticity surface determined in this way with surfaces obtained in the basis of a frequently used streamlined test procedure in which only a single specimen is successively subjected to different stress states.

Transl. by Schreiber Translations Inc.

N95-26517 Polish Academy of Sciences, Warsaw (Poland). Inst. of the Strength of Materials.

THE DEVELOPMENT OF THE ANISOTROPIC PROPERTIES OF COPPER UNDER PLASTIC DEFORMATION INDUCED BY CREEP AND MONOTONIC LOADING [ROZWOJ ANIZOTROPOWYCH WLASNOSCI MIEDZI POD WPLYWEM DEFORMACJI PLASTYCZNEJ PRZY PELZANIU I MONOTONICZNYM OBCIAZANIU]

Lech Dietrich and Zbnigniew L. Kowalewski 1994 43 p In POLISH
(ISSN 0208-5658)
(IFTR-23/1994) Avail: Issuing Activity (Polish Academy of Sciences, Warsaw, Poland)

An experimental analysis of the plastic properties of electrolytic copper in its original condition and subjected to different types of initial deformation is presented. The analysis was based on the location and dimensions of plasticity surfaces determined. In the first phase of the study, the authors determined the original surface by a method involving alternating and identical holes in the same specimen, which served as a starting point for comparisons of plastic surfaces determined for the same material after intentional deformation. In subsequent phases of the study, the authors applied the same initial deformations under creep at a constant elevated temperature and a constant stress level and under monotonic loading at room temperature. After the specimens were deformed to the extent specified in advance, the authors determined their plasticity surfaces using the same method of alternating holes as they did in determining the original surface. The experimental results were then approximated under the assumption of an anisotropic plasticity condition. Transl. by Schreiber Translations Inc.

N95-26666 Polish Academy of Sciences, Warsaw (Poland). Dept. of the Strength of Materials.

CHANGES IN THE ANISOTROPY PARAMETERS OF AN ALUMINUM ALLOY CAUSED BY CYCLICAL DEFORMATION [ZMIANY PARAMETROW ANIZOTROPII STOPU ALUMINIUM POD WPLYWEM DEFORMACJI CYKLICZNEJ]

Lech Dietrich, Zbigniew L. Kowalewski, and Marek Sliwowski 1994 49 p In POLISH
(ISSN 0208-5658)
(IFTR-27/1994) Avail: Issuing Activity (Polish Academy of Sciences, Warsaw, Poland)

This article contains the results of experiments concerning the effect of multi-axial cyclical plastic deformation on the changes in the anisotropy constants of PA6 aluminum alloy in a planar stress state. The experiments were performed on thin-walled tubular specimens subjected to simultaneous loading with a combination of axial force and reversible torque. The specimens were prepared from rods as supplied by the mill and studies of their original plasticity surface confirmed the high anisotropy of the alloy, which it had acquired in the manufacturing process. The primary purpose of this study was to determine the vulnerability of the material with its original texture to multi-directional cyclical plastic deformation in plastic working. The authors' tests revealed that the plastic behavior of the alloy is highly dependent on the direction of the initial cyclical loading relative to the axis of anisotropy associated with the axis of the rod. The authors found that complex multi-directional cyclical loading does not cause any change in the main axis of anisotropy associated with the axis of the specimen. The authors also discovered that there was no rotation of the plasticity surfaces corresponding to all the directions of initial deformation. The only effect that the direction of initial cyclical loading had was on the size of the axis of the plasticity surface aligned with the axis of the rod, while the changes in the axis of the plasticity surface perpendicular to the main axis of anisotropy were negligible. For purposes of comparison, the authors indicate that cyclical plastic deformation results in greater changes in the dimensions of the plasticity surface than the equivalent monotonic plastic deformation. Author

N95-26675# Sains Malaysia Univ., Perak Darul Ridzuan (Malaysia).

FATIGUE FRACTURE ANALYSIS IN MEDIUM CARBON STRUCTURAL STEEL AND AUSTENITIC STAINLESS STEEL BY X-RAY FRACTOGRAPHY

N. N. Rao and Azmi binRahmat 1994 26 p Presented at the National Seminar on the Assessment of IRPA Research Achievement in 5th Malaysian Plan, Kedah, Malaysia, 20-24 Dec. 1991

(DE95-601504; INIS-MF-13965; CONF-9112185) Avail: CASI HC A03/MF A01 (US Sales Only)

Apart from the residual stresses present in the bulk material, a growing fatigue crack may develop its own stress field ahead of the crack tip which in turn could influence the crack propagation behaviour. A fracture surface analysis through measurement of the residual stress of a failed component may provide some additional useful information to that obtained through conventional metallurgical and fracture mechanics investigations. This method of fracture surface analysis using x-ray diffraction technique is known as 'X-ray Fractography'. Residual stress ((rho) sub (gamma)) and the full width at half maximum (FWHM) of the x-ray diffraction profile of any reflection are determined at different crack lengths on the fracture surface. These are then correlated to the fracture toughness parameters such as fracture toughness K(sub IC), the maximum stress intensity factor K(sub max) and the stress intensity factor range (delta)K. The present investigation aims at detailed x-ray analysis of the fatigue fractured surfaces of the compact tension specimens prepared from ferritic and austenitic stainless steels. The ferritic steel has been subjected to various heat treatments to obtain different microstructures and mechanical properties. The overall observations are analyzed through fatigue (cumulative) damage and material science concepts. DOE

N95-26681 Naval Postgraduate School, Monterey, CA. Dept. of Mechanical Engineering.

LATTICE PARAMETERS AND DEBYE-WALLER FACTORS OF GAMMA-TIAI ALLOYS

Sarath K. Menon and Alan G. Fox Dec. 1994 16 p Limited Reproducibility: More than 20% of this document may be affected by microfiche quality

(Contract FY1457-94-N5026)

(AD-A288843; NPS-ME-94-009) Avail: Issuing Activity (Defense Technical Information Center (DTIC))

Accurate lattice parameters of the tetragonal gamma-TiAl phase with the L1(0) structure have been determined by X-ray diffraction. The results showed that in binary alloys, the A parameter decreases while the C parameter increases with increasing Al content. Integrated X-ray intensities were determined from annealed powder samples with powder size less than 5 microns in order to estimate the temperature factors. Difficulties associated with such evaluations due to the effects of extinction are also discussed. In addition, the 110, 111, and 200 structure factor amplitudes of gamma-phase Ti-56 at.% Al alloy were accurately determined from critical-voltage electron diffraction measurements. The Debye-Waller factors determined from X-ray experiments and the critical voltage experiments are compared and the results discussed. DTIC

N95-26838 Polish Academy of Sciences, Warsaw (Poland). Dept. of the Strength of Materials.

ANNEALING-INDUCED CHANGES IN THE ANISOTROPY OF AN ALUMINUM ALLOY [ZMIANY ANIZOTROPII STOPU ALUMINIUM POD WPLYWEM WYZARZANIA]

Lech Dietrich, Romuald Kiryk, and Karol Turski 1994 41 p In POLISH (ISSN 0208-5658)

(IFTR-24/1994) Avail: Issuing Activity (Polish Academy of Sciences, Warsaw, Poland)

Tubular specimens of PA6 alloy annealed at two different temperatures were tested under loading consisting of axial force and torque. The authors observed uneven changes in plastic anisotropy after annealing at different temperatures. The authors plotted the plasticity surfaces and ranges of variation of their parameters as functions of the annealing temperature. Plasticity surfaces may be described as an ellipse with an axis ratio which changes between 2 to 1.95 with an increase in annealing temperature.

Transl. by Schreiber Translations Inc.

N95-26862*# National Aeronautics and Space Administration. Pasadena Office, CA.

ULTRA HIGH PURITY, DIMENSIONALLY STABLE INVAR 36 Patent Application

Witold M. Sokolowski, inventor (to NASA) (Jet Propulsion Lab., California Inst. of Tech., Pasadena, CA.), Marc S. Lane, inventor (to NASA) (Jet Propulsion Lab., California Inst. of Tech., Pasadena, CA.), Timothy P. ODonnell, inventor (to NASA) (Jet Propulsion Lab., California Inst. of Tech., Pasadena, CA.), and Cheng H. Hsieh, inventor (to NASA) (Jet Propulsion Lab., California Inst. of Tech., Pasadena, CA.) 23 Jun. 1994 23 p

(NASA-Case-NPO-19358-1-CU; NAS 1.71:NPO-19358-1-CU; US-Patent-Appl-SN-273511) Avail: CASI HC A03/MF A01

An INVAR 36 material having long-term dimensional stability is produced by sintering a blend of powders of nickel and iron under pressure in an inert atmosphere to form an alloy containing less than 0.01 parts of carbon and less than 0.1 part aggregate and preferably 0.01 part individually of Mn, Si, P, S and Al impurities. The sintered alloy is heat treated and slowly and uniformly cooled to form a material having a coefficient of thermal expansion of less than 1 ppm/C and a temporal stability of less than 1 ppm/year. NASA

N95-27032 Virginia Univ., Charlottesville, VA. School of Engineering and Applied Science.

ENVIRONMENTALLY ASSISTED CRACKING OF HIGH STRENGTH BETA TITANIUM ALLOYS Final Report, 15 Sep. 1991 - 15 Sep. 1994

R. P. Ganglogg, J. R. Scully, and R. G. Kelly Nov. 1994 264 p Limited Reproducibility: More than 20% of this document may be affected by microfiche quality

(Contract N00014-91-J-4164)

(AD-A289156; UVA//525461/MSE95/102) Avail: Issuing Activity (Defense Technical Information Center (DTIC))

The objective of this integrated research program is to define the conditions under which high strength Beta-titanium alloys resist environmentally assisted cracking (EAC) in marine environments. Specific goals are to: (1) characterize EAC for metallurgical, chemical, and mechanical conditions that could destabilize crack tip passive films to promote local dissolution and hydrogen uptake, (2) test the hydrogen embrittlement mechanism for EAC, and (3) develop a mechanism-based model of EAC by integrating crack chemistry, surface dissolution and repassivation kinetics, hydrogen uptake to trap sites, and crack tip process zone micromechanics and damage. This final report presents a summary of the results and includes papers published during the period of this grant from Sep. 1991 to Sep. 1994. DTIC

N95-27082# Los Alamos National Lab., NM.

FIRST-PRINCIPLES STUDY OF INTERMETALLIC PHASE STABILITY IN THE TERNARY Ti-Al-Nb ALLOY SYSTEM

M. Asta, A. Ormeci, J. M. Wills, and R. C. Albers 1995 7 p Presented at the 1994 Fall Meeting of the Materials Research Society (MRS), Boston, MA, 28 Nov. - 2 Dec. 1994

(Contract W-7405-eng-36)

(DE95-005259; LA-UR-94-4079; CONF-941144-46) Avail: CASI HC A02/MF A01

The stability of bcc-based phases in the Ti-Al-Nb alloy system has been studied from first-principles using a combination of ab-initio total energy and cluster variation method (CVM) calculations. Total energies have been computed for 18 binary and ternary bcc superstructures in order to determine low temperature ordering tendencies. From the results of these calculations a set of effective cluster interaction parameters have been derived. These interaction parameters are required input for CVM computations of alloy thermodynamic properties. The CVM has been used to study the effect of composition on finite-temperature ordering tendencies and site preferences for bcc-based phases. Strong ordering tendencies are observed for binary Nb-Al and Ti-Al bcc phases as well as for ternary alloys with compositions near Ti2AlNb. For selected superstructures we have also analyzed structural stabilities with respect to tetragonal distortions which transform the bcc into an fcc lattice. Instabilities with respect to such distortions are found to exist for binary but not ternary bcc compounds. DOE

N95-27086# Pacific Northwest Lab., Richland, WA.
EFFECTS OF HELIUM PRE-IMPLANTATION ON THE MICROSTRUCTURE AND MECHANICAL PROPERTIES OF IRRADIATED 316 STAINLESS STEEL
M. B. Toloczko, G. R. Tedeski, G. E. Lucas, G. R. Odette, R. E. Stoller, and M. L. Hamilton Nov. 1994 8 p Presented at the 1994 Fall Meeting of the Materials Research Society (MRS), Boston, MA, 28 Nov. - 2 Dec. 1994
(Contracts DE-AC06-76RL-01830; DE-FG03-87ER-52143; DE-AC05-84OR-21400)
(DE95-007162; PNL-SA-25670; CONF-941144-60) Avail: CASI HC A02/MF A01

Transmission electron microscopy (TEM) specimens of a First Core heat of 316 stainless steel, in both the solution annealed and 20% cold worked condition, were irradiated to 46 dpa at 420 C, to 49 dpa at 520 C, and to 34 dpa at 600 C in FFTF/MOTA. Prior to irradiation, about half of the specimens were pre-implanted with approximately 100 appm of helium, and of these, several of the solution annealed and pre-implanted specimens were aged at 800 C for 2 hr. Post-irradiation density measurements showed little difference in density between the unimplanted alloys and their helium implanted counterparts. Microstructural observations on specimens irradiated at 420 C and 520 C showed relatively minor differences in defect distributions between the unimplanted and the helium implanted materials; in all cases the defect sizes and number densities were consistent with data in the literature. Where possible, irradiation hardening of the alloys was experimentally evaluated by microhardness and shear punch; experimentally obtained values were compared to values calculated using a computer model based on barrier hardening and the microstructural data. All methods indicated relatively small effects of helium implantation, and both measured and calculated values were in agreement with the range of values reported in the literature. DOE

N95-27088# Pacific Northwest Lab., Richland, WA.
SIMULATING THE PRODUCTION OF FREE DEFECTS IN IRRADIATED METALS
H. L. Heinisch Jul. 1994 14 p Presented at the 2nd International Conference on Computer Simulation of Radiation Effects, Santa Barbara, CA, 24-29 Jul. 1994
(Contract DE-AC06-76RL-01830)
(DE95-007165; PNL-SA-24441; CONF-940731-4) Avail: CASI HC A03/MF A01

Under cascade-producing irradiation by high energy neutrons or charged particles, only a small fraction of the initially displaced atoms contribute to the population of free defects, i.e. those that are available to migrate throughout the metal and cause microstructural changes. Although, in principle, computer simulations of free defect production could best be done using molecular dynamics, in practice, the wide ranges of time and distance scales involved can be done only by a combination of atomistic models that employ various levels of approximation. An atomic-scale, multimodel approach has been developed that combines molecular dynamics, binary collision models and stochastic annealing simulation. The annealing simulation is utilized in calibrating binary collision simulations to the results of molecular dynamics calculations, as well as to model the subsequent migration of the defects on more macroscopic time and size scales. The annealing simulation and the method of calibrating the multimodel approach are discussed, and the results of simulations of cascades in copper are presented. The temperature dependence of free defect production following simulated annealing of isolated cascades in copper shows a differential in the fractions of free vacancies and interstitial defects escaping from the cascade above Stage V. This differential, a consequence of the direct formation of interstitial clusters in cascades and the relative thermal stability of vacancy and interstitial clusters du ring subsequent annealing, is the basis for the production bias mechanism of void swelling. DOE

N95-27167*# Texas Univ., San Antonio, TX. Engineering Div.
PROBABILISTIC MATERIAL STRENGTH DEGRADATION MODEL FOR INCONEL 718 COMPONENTS SUBJECTED TO HIGH TEMPERATURE, HIGH-CYCLE AND LOW-CYCLE MECHANICAL FATIGUE, CREEP AND THERMAL FATIGUE EFFECTS Final Technical Report, Jun. 1992 - Jan. 1995
Callie C. Bast and Lola Boyce Jan. 1995 86 p
(Grant NAG3-867)
(NASA-CR-197832; NAS 1.26:197832) Avail: CASI HC A05/MF A01

This report presents the results of both the fifth and sixth year effort of a research program conducted for NASA-LeRC by The University of Texas at San Antonio (UTSA). The research included on-going development of methodology for a probabilistic material strength degradation model. The probabilistic model, in the form of a postulated randomized multifactor equation, provides for quantification of uncertainty in the lifetime material strength of aerospace propulsion system components subjected to a number of diverse random effects. This model is embodied in the computer program entitled PROMISS, which can include up to eighteen different effects. Presently, the model includes five effects that typically reduce lifetime strength: high temperature, high-cycle mechanical fatigue, low-cycle mechanical fatigue, creep and thermal fatigue. Statistical analysis was conducted on experimental Inconel 718 data obtained from the open literature. This analysis provided regression parameters for use as the model's empirical material constants, thus calibrating the model specifically for Inconel 718. Model calibration was carried out for five variables, namely, high temperature, high-cycle and low-cycle mechanical fatigue, creep and thermal fatigue. Methodology to estimate standard deviations of these material constants for input into the probabilistic material strength model was developed. Using an updated version of PROMISS, entitled PROMISS93, a sensitivity study for the combined effects of high-cycle mechanical fatigue, creep and thermal fatigue was performed. Then using the current version of PROMISS, entitled PROMISS94, a second sensitivity study including the effect of low-cycle mechanical fatigue, as well as, the three previous effects was performed. Results, in the form of cumulative distribution functions, illustrated the sensitivity of lifetime strength to any current value of an effect. In addition, verification studies comparing a combination of high-cycle mechanical fatigue and high temperature effects by model to the combination by experiment were conducted. Thus, for Inconel 718, the basic model assumption of independence between effects was evaluated. Results from this limited verification study strongly supported this assumption. Author

N95-27255# Bhabha Atomic Research Centre, Bombay (India).
CURRENT PROGRAMMES ON PHYSICAL METALLURGY AND RELATED AREAS IN BARC
1994 152 p
(DE95-607939; BARC-1994/E/007) Avail: CASI HC A08/MF A02 (US Sales Only)

Current research and development programmes on physical metallurgy and related areas from the following Divisions of Bhabha Atomic Research Centre are included in this report: Atomic Fuels Division, High Pressure Physics Division, Metallurgy Division, Radio Metallurgy Division, Solid State Physics Division. Important publications corresponding to each activity have also been listed. DOE

N95-27256# Universidad Nacional Autonoma de Mexico, Mexico City (Mexico).
STRESS CORROSION CRACKING SUSCEPTIBILITY OF THE EARTHQUAKE RESISTANT NOM B457 MEXICAN STEEL Ph.D. Thesis
Carlos Rosendo ArganisJuarez 1994 215 p
(DE95-607956; INIS-mf-14408) Avail: CASI HC A10/MF A03 (US Sales Only)

The Mexican construction code was modified after the Mexico city 1985 earthquake, substituted the medium carbon reinforced steel NOM B6 by the new micro alloyed steel NOM B457 in 42 Kg/sq mm grade. The present study reports the evaluation of the NOM B457 steel behavior in mortar with and without 2% wt. in chlorides and in Ca(OH)2 saturated solutions. The results are compared with the NOM B6 steel behavior in the same conditions. The Stress Corrosion Cracking (SCC) is not present in all the conditions used in this study and there are not susceptibility potential range to SCC when the material is evaluated by electrochemical Tests, Constant Extension Rate Tests (CERT) and Constant Load Test at

80% of yield stress. A susceptibility potential range to Hydrogen Induced Cracking (HIC) is detected, below -900 mV. vs Standard Calomel Electrode (SCE) by CERT at constant potential. DOE

N95-27319# Oak Ridge National Lab., TN.
NON-METALLIC OXIDE INCLUSION FORMATION IN C-MnLOW ALLOY STEEL WELDS
S. S. Babu (Pennsylvania State Univ., University Park, PA.), K. Mundra (Pennsylvania State Univ., University Park, PA.), T. DebRoy (Pennsylvania State Univ., University Park, PA.), S. A. David, and J. M. Vitek 1995 3 p Presented at the 76th American Welding Society Convention, Cleveland, OH, 2-7 Apr. 1995
(Contract DE-AC05-84OR-21400)
(DE94-019160; CONF-950443-1) Avail: CASI HC A01/MF A01

Inclusion characteristics influence weld metal microstructure development, especially the formation of high toughness acicular ferrite phase. Important inclusion characteristics are: size distribution, number density, volume fraction, and composition. Previous work considered a sequential formation of various oxides and compounds to estimate the inclusion characteristics; however, effects of weld metal composition, nucleation, and growth conditions on inclusion formation were ignored. In this work, the principles of ladle deoxidization and transformation kinetics involving nucleation and growth are used to estimate the inclusion characteristics as a function of weld metal composition and cooling conditions. DOE

N95-27328# Westinghouse Savannah River Co., Aiken, SC.
RECYCLE OF RADIOLOGICALLY CONTAMINATED AUSTENITIC STAINLESS STEELS
K. J. Imrich, D. R. Leader, N. C. Iyer, and M. R. Louthan, Jr. 1995 14 p
(Contract DE-AC09-89SR-18035)
(DE95-006464; WSRC-MS-94-0612) Avail: CASI HC A03/MF A01

The United States Department of Energy owns large quantities of radiologically contaminated austenitic stainless steel which could by recycled for reuse if appropriate release standards were in place. Unfortunately, current policy places the formulation of a release standard for USA industry years, if not decades, away. The Westinghouse Savannah River Company, Idaho National Engineering Laboratory and various university and industrial partners are participating in initiative to recycle previously contaminated austenitic stainless steels into containers for the storage and disposal of radioactive wastes. This paper describes laboratory scale experiments which demonstrated the decontamination and remelt of stainless steel which had been contaminated with radionuclides. DOE

N95-27446# Los Alamos National Lab., NM.
ATOMISTIC STUDY OF ENERGY AND STRUCTURE OF SURFACES IN NIO
M. Yan, S. P. Chen, A. F. Voter, and T. E. Mitchell 1994 8 p
Presented at the 1994 Fall Meeting of the Materials Research Society (MRS), Boston, MA, 28 Nov. - 2 Dec. 1994
(Contract W-7405-eng-36)
(DE95-005207; LA-UR-94-4219; CONF-941144-41) Avail: CASI HC A02/MF A01

The structure and energy of surfaces in NiO have been studied by atomistic calculations employing short range Buckingham potentials fitted to properties of NiO. The polarizability of lattice anions is included by using the shell model. The results show that the surface energy depends strongly on surface orientation, and the 100 surface has the lowest energy. Surfaces with higher energy prefer to reconstruct into 100 facets to lower their energy and to stabilize their structure. DOE

N95-27450 Oak Ridge National Lab., TN.
TENSILE PROPERTIES OF Fe-16 AT. % Al ALLOYS
V. K. Sikka 1995 19 p Presented at the 8th Annual Conference on Fossil Energy Materials, Oak Ridge, TN, 10-12 May 1994 Limited Reproducibility: More than 20% of this document may be affected by microfiche quality
(Contract DE-AC05-84OR-21400)
(DE95-007102; CONF-9405143-9) Avail: CASI HC A03

A newly developed melting method for Fe-16 at. % Al alloy (FAPY) is described. Tensile data on the air-induction-melted (AIM) and vacuum-induction-melted (VIM) heats of FAPY after identical processing are presented. Optical, scanning electron micrographs (SEM), and microprobe analysis were carried out to explain the lower room-temperature ductility and more scatter in the data for the AIM material as opposed to the VIM material. DOE

N95-27462# Brookhaven National Lab., Upton, NY.
SPIN-DENSITY-WAVE MAGNETISM IN DILUTE COPPER-MANGANESE ALLOYS
F. J. Lamelas (Marquette Univ., Milwaukee, WI.), S. A. Werner (Missouri Univ., Columbia, MO.), S. M. Shapiro, and J. Mydosh 1995 11 p Presented at the 1994 Fall Meeting of the Materials Research Society (MRS), Boston, MA, 28 Nov. - 2 Dec. 1994
(Contract DE-AC02-76CH-00016)
(DE95-005121; BNL-61260; CONF-941144-97) Avail: CASI HC A03/MF A01

Elastic neutron-scattering measurements on two samples of Cu alloyed with 1.3% Mn and 0.55% Mn show that the spin-density-wave (SDW) features found in more concentrated alloys persist in the limit of very dilute alloys. These features consist of temperature-dependent incommensurate peaks in magnetic neutron scattering, with positions and strengths which are fully consistent with those in the concentrated alloys. The implications of these measurements are twofold. First, it is clear from this data that SDW magnetic ordering occurs across the entire range of CuMn alloys which have typically been interpreted as spin glasses. Second, the more fundamental significance of this work is the suggestion via extrapolation that a peak in the magnetic susceptibility x(q) occurs in pure copper, at a value of q given by the Fermi-surface diameter 2k(sub F). DOE

N95-27463# Los Alamos National Lab., NM.
C15 INTERMETALLIC COMPOUNDS HfV2+Nb
F. Chu, S. P. Chen, T. E. Mitchell, D. P. Pope (Pennsylvania Univ., Philadelphia, PA.), and C. T. Liu (Oak Ridge National Lab., TN.) 1994 7 p Presented at the IUMRS International Conference in Asia, Hsinchu, HI, 14-18 Dec. 1994
(Contract W-7405-eng-36)
(DE95-005264; LA-UR-94-4288; CONF-941252-1) Avail: CASI HC A02/MF A01

Phase fields and equilibria in the Hf-V-Nb system were determined using a combination-of SEM, EDS and x ray diffraction. The structural stability of the C15 HfV2(+)Nb was studied by x ray diffraction and specific heat measurements. The elastic constants of C15 HfV2(+)Nb were measured by the resonant ultrasound spectroscopy technique. First-principle quantum mechanical calculations based on the local-density-functional theory have been employed to study the total energy and electronic structure of C15 HfV2, which can be used to understand the physical and metallurgical properties of the C15 intermetallics HfV2(+)Nb. DOE

N95-27464# Oak Ridge National Lab., TN.
ADVANCED NEUTRON SOURCE MATERIALS SURVEILLANCE PROGRAM
S. M. Heavilin (Purdue Univ., West Lafayette, IN.) Jan. 1995 37 p
(Contract DE-AC05-84OR-21400)
(DE95-005700; ORNL/M-3733) Avail: CASI HC A03/MF A01

The Advanced Neutron Source (ANS) will be composed of several different materials, one of which is 6061-T6 aluminum. Among other components, the reflector vessel and the core pressure boundary tube (CPBT), are to be made of 6061-T6 aluminum. These components will be subjected to high thermal neutron fluences and will require a surveillance program to monitor the strength and fracture toughness of the 6061-T6 aluminum over their lifetimes. The purpose of this paper is to explain the steps that were taken in the summer of 1994 toward developing the surveillance program. The first goal was to decide upon standard specimens to use in the fracture toughness and tensile testing. Second, facilities had to be chosen for specimens representing the CPBT and the reflector vessel base, weld, and heat-affected-zone (HAZ) metals. Third, a timetable had to be defined to determine when to remove the specimens for testing. DOE

N95-27473# Oak Ridge National Lab., TN.
AEM INVESTIGATION OF TETRAHEDRALLY COORDINATED Ti(4+) IN NICKEL-TITANATE SPINEL

I. M. Anderson, J. Bentley, and C. B. Carter (Minnesota Univ., Minneapolis, MN.) 1994 7 p Presented at the Fall Meeting of the Materials Research Society (MRS), Boston, MA, 29 Nov. - 3 Dec. 1993
(Contract DE-AC05-84OR-21400)
(DE95-006624; CONF-931108-113) Avail: CASI HC A02/MF A01

Stoichiometry and site distribution of metastable nickel-titanate spinel was studied with AEM. Results of EDXS and EELS agree that the metastable spinel is nonstoichiometric and titanium-deficient relative to its hypothetical endmember composition, 'Ni2TiO4'. The titanium deficiency ha s been determined by EELS to be (Delta) = 0.025 +/- 0.005. Channeling-enhanced microanalysis and ELNES studies indicate that the Ti(4+) and Ni(2+) cations are in tetrahedral and octahedral coordination, respectively, so that the metastable spinel has the normal cat on distribution: Ti(sub I-(Delta))(Ni2(1+(Delta))) O(sub 4). This is consistent with neutron powder-diffraction studies and SiO2-solubility measurements of similar equilibrated and quenched spinel-containing specimens. Metastable nickel-titanate spinel therefore contrasts with stable stoichiometric spinels which tend to the inverse cation distribution, Me(MeTi)O4). DOE

N95-27477# Edgerton, Germeshausen and Grier, Inc., Idaho Falls, ID. Idaho National Engineering Lab.

LASER ULTRASONIC GENERATION AT THE SURFACE OF A LIQUID METAL

J. B. Walter, K. L. Telschow, and R. J. Conant (Montana State Univ., Bozeman, MT.) 1995 6 p Presented at the Review of Progress in Quantitative Nondestructive Examination, Snowmass, CO, 1-5 Aug. 1994
(Contract DE-AC07-76ID-01570)
(DE95-004999; EGG-M-94170; CONF-9408208-1) Avail: CASI HC A02/MF A01

The noncontacting nature of laser-based ultrasonic measurement has made it attractive in many applications. While most applications thus far involve solid samples, molten metals encountered in some stages of metal processing appear well suited to this technique. Possible applications for liquid metals include locating and characterizing the liquid/solid interface; characterizing a surface layer, contaminant, or alloying constituent; and measuring the temperature of the sample surface or bulk. This work aimed to characterize laser generation of ultrasound in liquid metals to facilitate the development of techniques for these applications. This paper describes measurements of the angular distribution and energy dependence of laser-generated ultrasound in mercury at ambient temperature. Mercury was chosen as the model liquid metal because it is liquid at room temperature, and so should have negligible temperature gradients beyond those produced in the laser generation process, and because it exhibits a very shallow optical penetration depth. Brief descriptions about the theory of laser generation by thermoelastic and ablation sources at the surface of a liquid metal are included. Both thermoelastic expansion and ablation cause similar ultrasound generation in liquid metals when laser generated ultrasonic pulses are directed perpendicular to the surface of liquid metals. The ultrasonic pulse amplitude is proportional to the absorbed laser pulse energy for both mechanisms. The simple threshold model presented for ablation describes the transition from thermoelastic generation with the model's two parameters being material dependent. For mercury, ablation produces about 100 times larger ultrasonic pulse amplitudes than thermoelastic expansion and has a threshold of about 6 MW/square cm. Molten metals offer a good medium for studying ablation, since the surface is always refreshed and ablation, at least for mercury, dominates ultrasonic generation above the threshold. DOE

N95-27479# Pacific Northwest Lab., Richland, WA.

EFFECT OF INTERNAL HYDROGEN ON THE MIXED-MODE 1/3 FRACTURE TOUGHNESS OF A FERRIFIC/MARTENSITIC STAINLESS STEEL

Huaxin Li (Associated Western Universities, Inc., Richland, WA.), R. H. Jones, D. S. Gelles, and J. P. Hirth (Washington State Univ., Pullman, WA.) Sep. 1994 10 p Presented at the 5th International Conference on Hydrogen Effects on Material Behavior, Moran, WY, 11-15 Sep. 1994
(Contract DE-AC06-76RL-01830)
(DE95-005722; PNL-SA-24007; CONF-940945-6) Avail: CASI HC A02/MF A01

The effects of H on the mixed-mode 1/3 critical J-integrals (J(sub TC)) and tearing moduli (dJ/da) were examined for a martensitic stainless steel at ambient temperature. A H content of 4 ppm(wt) was attained after charging in a H2 gas chamber (138 MPa) at 300 C for 2 weeks. Results showed that H decreased J(sub TC) and dJ/da values compared to steel tested without H. However, the presence of H did not change the dependence of J(sub TC) and dJ/da values on the crack angles. Both J(sub IC) and dJ(sub 1)/da exhibited the highest relative values. The minimum values of both J(sub TC) and dJ/da occurred at a crack angle between 35 and 55 deg P(sub iii) /(P(sub iii) + P(sub i)) = 0.4 and 0.6. A mechanism of the combined effect of H and mixed-mode on J(sub TC) and dJ/da is discussed. DOE

N95-27488# Los Alamos National Lab., NM.

ENGINEERED MATERIALS FOR APPLIATION IN SEVERE METALLURGICAL ENVIRONMENTS: TANTALUM-CARBON ALLOY DEVELOPMENT

K. M. Axler Feb. 1995 154 p
(Contract W-7405-eng-36)
(DE95-006838; LA-12876-T) Avail: CASI HC A08/MF A02

A suite of investigations has been completed to develop and demonstrate a construction material for use in severely corrosive metallurgical processing environments. The material is a tantalum-base alloy with inclusions of Ta2C. Alloy development work involved multi-step thermal processing to invoke specific microstructural features. The kinetics of carbide formation from supersaturated solid solutions of carbon in tantalum were established. Performance evaluation of the alloy was conducted and the alloy has been demonstrated to outperform any previously studied metallic construction material used in pyrometallurgical processing of plutonium. Specific microstructural features of the alloy have been identified which provide the extreme corrosion resistance. Grain boundary occupancy by the Ta2C phase is associated with the corrosion resistance to liquid metal. Precipitation from the supersaturated condition invokes a microstructure with the most significant grain boundary delineation by carbide inclusions and hence provides the most corrosion resistant attributes. It has been experimentally proven that the precipitate growth rate is not dictated solely by the diffusion rate of the interstitial species and is more complex. The observed growth rate of carbide precipitates involves several competing effects. DOE

N95-27492# Pacific Northwest Lab., Richland, WA.

RADIATION-INDUCED SEGREGATION: A MICROCHEMICAL GAUGE TO QUANTIFY FUNDAMENTAL DEFECT PARAMETERS

E. P. Simonen and S. M. Bruemmer Dec. 1994 8 p Presented at the 1994 Fall Meeting of the Materials Research Society (MRS), Boston, MA, 28 Nov. - 2 Dec. 1994
(Contract DE-AC06-76RL-01830)
(DE95-005720; PNL-SA-24864; CONF-941144-50) Avail: CASI HC A02/MF A01

Defect Kinetic parameters are evaluated for austenitic stainless alloys by comparing model predictions to measured responses for radiation-induced grain boundary segregation. Heavy-ions, neutrons and proton irradiations having substantial statistical bases are examined. The combined modeling and measurement approach is shown to be useful for quantifying fundamental defect parameters. The mechanism evaluation indicates vacancy migration energies of 1.15 eV or less and a vacancy formation energy at grain boundaries of 1.5 eV. Damage efficiencies of about 0.03 were established for heavy-ions and for light-water reactor neutrons. Inferred proton damage efficiencies were about 0.15. Segregation measured in an advanced gas-cooled reactor component was much greater than expected using the above parameters. DOE

N95-27493# Pacific Northwest Lab., Richland, WA.

RADIATION-INDUCED GRAIN BOUNDARY SEGREGATION IN AUSTENITIC STAINLESS STEELS

S. M. Bruemmer, L. A. Charlot, J. S. Vetrano, and E. P. Simonen Nov. 1994 12 p Presented at the 1994 Fall Meeting of the Materials Research Society (MRS), Boston, MA, 28 Nov. - 2 Dec. 1994
(Contract DE-AC06-76RL-01830)
(DE95-005721; PNL-SA-25507; CONF-941144-51) Avail: CASI HC A03/MF A01

Radiation-induced segregation (RIS) to grain boundaries in Fe-Ni-Cr-Si stainless alloys has been measured as a function of irradiation temperature and dose. Heavy-ion irradiation was used to produce damage levels from 1 to 20 displacements per atom (dpa) at temperatures from 175 to 550 C. Measured Fe, Ni, and Cr segregation increased sharply with irradiation

dose (from 0 to 5 dpa) and temperature (from 175 to about 350 C). However, grain boundary concentrations did not change significantly as dose or temperatures were further increased. Although interfacial compositions were similar, the width of radiation-induced enrichment or depletion profiles increased consistently with increasing dose or temperature. Impurity segregation (Si and P) was also measured, but only Si enrichment appeared to be radiation-induced. Grain boundary Si peaked at levels approaching 10 at% after irradiation doses to 10 dpa at an intermediate temperature of 325 C. No evidence of grain boundary silicide precipitation was detected after irradiation at any temperature. Equilibrium segregation of P was measured in the high-P alloys, but interfacial concentration did not increase with irradiation exposure. Comparisons to reported RIS in neutron-irradiated stainless steels revealed similar grain boundary compositional changes for both major alloying and impurity elements.
DOE

N95-27544# Oak Ridge National Lab., TN.
MATERIALS CONSIDERATIONS FOR MOLTEN SALT ACCELERATOR-BASED PLUTONIUM CONVERSION SYSTEMS
J. H. DeVan, J. R. DiStefano, W. P. Eatherly, J. R. Keiser, and R. L. Klueh 1994 13 p Presented at the International Conference on Accelerator-driven Transmutation Technologies and Applications, Las Vegas, NV, 25-28 Jul 1994
(Contract DE-AC05-84OR-21400)
(DE95-006743; CONF-9407103-34) Avail: CASI HC A03/MF A01

A Molten-Salt Reactor Program for power applications was initiated at the Oak Ridge National Laboratory in 1956. In 1965 the Molten Salt Reactor Experiment (MSRE) went critical and was successfully operated for several years. Operation of the MSRE revealed two deficiencies in the Hastelloy N alloy that had been developed specifically for molten-salt systems. The alloy embrittled at elevated temperatures as a result of exposure to thermal neutrons (radiation damage) and grain boundary embrittlement occurred in materials to fuel salt. Intergranular cracking was found to be associated with fission products, viz. tellurium. An improved Hastelloy N composition was subsequently developed that had better resistance to both of these problems. However, the discovery that fission product cracking could be significantly decreased by making the salt sufficiently reducing offers the prospect of improved compatibility with molten salts containing fission products and resistance to radiation damage in ABC applications. Recommendations are made regarding the types of corrosion tests and mechanistic studies needed to qualify materials for operation with PuF_3-containing molten salts. DOE

N95-27553# Brookhaven National Lab., Upton, NY.
CHARACTERIZATION OF DEFECTS IN DEUTERIUM-IMPLANTED BERYLLIUM
R. A. Anderl (Idaho National Engineering Lab., Idaho Falls, ID.), A. B. Denison (Idaho National Engineering Lab., Idaho Falls, ID.), S. Szpala, P. Asoka-Kumar, K. G. Lynn, and B. Nielsen 1994 11 p Presented at the 5th International Conference on Hydrogen Effects on Material Behavior, Moran, WY, 11-15 Sep. 1994
(Contracts DE-AC02-76CH-00016; DE-AC07-94ID-13223)
(DE95-005688; BNL-61143; CONF-940945-5) Avail: CASI HC A03/MF A01

This work investigated surface material modifications in high-purity beryllium foils resulting from 1-keV deuterium ion implantation into specimens for which the anneal temperatures and implantation temperatures were varied. Defects in unimplanted and in deuterium-implanted beryllium were characterized principally by positron-beam depth-profile analyses. Depth-profiles of the defect distributions in the specimens were made by stepping the energy of the positron beam from 0.055 keV to 40 keV, accompanied by measurements of the Doppler-broadened annihilation radiation line shape at each positron energy. These analyses identified a varying defect structure in beryllium, dependent on the previous anneal history of the material and on the temperature of the material during implantation with energetic deuterium ions. For specimens implanted at room temperature with 1-keV/D ions, the beam-induced defect structure had a profile that was peaked near the mean. range of the implanting deuterium and that extended beyond the implantation zone. Isochronal step-thermal anneal experiments revealed that deuterium was released from these defects at a temperature of about 400 k, indicative of shallow traps, and that the defect structure annealed at temperatures above 623 K. The beam-induced vacancy-defect complexes were estimated to be 1-nm voids for 1-keV/D implantation into Be at room temperature. For beryllium implanted at temperatures of 723 K with 1-keV/D ions, these measurements revealed that the beam-induced defect structure was much broader and extended far beyond the implantation zone. Isochronal stepthermal anneal experiments for these specimens revealed a more stable defect structure, with the onset of defect annealing at 775 K. There was no evidence of deuterium release at lower temperatures, indicating that for beryllium implanted at elevated temperatures, deuterium is retained in deep traps.
DOE

N95-27555# Los Alamos National Lab., NM.
SYSTEMATIC STUDY OF THE ION BEAM MIXING OF OXIDE MARKERS INTO ALUMINA
Elizabeth A. Cooper, Harriet Kung, and Michael Nastasi 1995 19 p Presented at the 9th International Conference on Ion Beam Modification of Materials, Canberra, Australia, 5-10 Feb. 1995
(Contract W-7405-eng-36)
(DE95-006262; LA-UR-95-208; CONF-950220-2) Avail: CASI HC A03/MF A01

The study of ion beam mixing of layered compositions is important in two regards: first, there is the potential of alloying the layers into a new functionally different composition and, secondly, from a fundamental aspect, it is important be able to anticipate the potential damage due to degradation of the layer structure that could be caused in these materials due to a radiation environment. The authors have completed a systematic study of ion beam mixing of thin marker layers into amorphous alumina. The degree of mixing was found to be controlled by thermodynamic factors, the nature of the marker (oxidation state), and matrix crystallinity. Ballistic mixing was observed for all markers, but the mixing of some oxide markers exhibits a thermally activated regime at higher temperatures. The experiments were conducted from a low temperature of -170 C to a maximum temperature of 75O C. 210 keV Ar was used to ion beam mix the marker layer at the various temperatures. The marker spreading was analyzed using RBS. The mixing of one marker (Fe_2O_3) into crystalline alumina (sapphire) was compared to that of the amorphous alumina. It was found that the marker mixed asymmetrically into the two matrix materials, with a higher degree of mixing into the amorphous matrix. TEM cross-section results verify that there is a preference for the marker to mix into the amorphous alumina layer preferentially to the crystalline layer. The interest in ion beam mixing of marker layers in ceramic systems is motivated by the fact that layered oxides are technologically important materials for fusion reactor applications. DOE

N95-27713# Israel Atomic Energy Commission, Beersheba (Israel).
STUDY OF THE PHASE TRANSFORMATIONS AND MICROSTRUCTURES OF URANIUM RICH ALLOYS OF THE BINARY URANIUM-GALLIUM SYSTEM Ph.D. Thesis
David Dayan Jul. 1994 146 p
(DE95-609624; NRCN-605) Avail: CASI HC A07/MF A02 (US Sales Only)

Little data was found on the properties of the binary alloy system of uranium-gallium. Therefore, an extensive investigation of the crystal-phase transformations, crystallography and metallography of this alloy system was carried out. Various experimental techniques were employed. The investigation provided information on the morphology of dilute U(Ga) alloys, on the kinetics and on the mechanism of the crystallography of the martensitic transformation beta-alpha. The main results are: (1) Gallium is soluble in the allotropic tau and beta-uranium phases. (2) The delta-phase corresponds to the stoichiometric U_3Ga_5 compound. (3) Gallium is a beta-stabilizing element similar to chromium. (4) The beta-phase is unstable at room temperature and undergoes ultimately a shear-like transformation into the alpha-U, which itself is a metastable variant of the alpha-U structure. (5) Ultrasonic sound velocity measurements were used to determine the elastic constants, Young, shear and bulk moduli of the polycrystalline beta-stabilized uranium 1.6 at.% Ga and uranium 2.3 at.% Ga alloys between 77 and 300 deg K. (6) Transmission electron microscopy was used to study the crystallography of the martensitic transformation taking place in an U-1.6 at.% Ga alloy. (7) The atomistic model proposed for the beta-alpha transformation in U(Ga) alloy is based on the crystallographic results and the observed low activation energy. (h) The correspondence which describes mathematically the way in which the parent beta-U and the daughter alpha-U phase are related was calculated by the means of an axis transformation using the known lattice parameters and the orientation relationships between the two structures. DOE

N95-27722# Sandia National Labs., Albuquerque, NM.
PROCESSING AND PROPERTIES OF CHROMATE-FREE CONVERSION COATINGS ON ALUMINUM
R. G. Buchheit, C. A. Drewien, M. A. Martinez, and G. E. Stoner (Virginia Univ., Charlottesville, VA.) 1994 14 p Presented at the Corrosion '95: National Association of Corrosion Engineers (NACE) International Annual Conference and Corrosion Show, Orlando, FL, 26-31 Mar. 1995
(Contract DE-AC04-94AL-85000)
(DE95-004768; SAND-94-3141C; CONF-950304-8) Avail: CASI HC A03/MF A01

A conversion coating method has been developed based on precipitation of Li2(Al2(OH)6)2 center-dot CO3 center-dot 3H2O from alkaline lithium salt solutions. The process is procedurally similar to chromate conversion coating but does not use or produce hazardous chemicals. The coating that forms is polycrystalline, continuous, and conformal. The coating meets the MIL-C-5541E corrosion resistance, electrical contact resistance, and paint adhesion requirements for certain aluminum alloys, but does not match the levels of performance exhibited by chromate conversion coatings. Methods for producing the coating are described. Corrosion resistance has been characterized using electrochemical impedance spectroscopy and salt spray exposure. The structural, compositional, and property changes attending post-coating thermal exposure are discussed. Performance in standardized corrosion, electrical, and paint adhesion tests is also presented. DOE

N95-27728*# National Aeronautics and Space Administration. Lewis Research Center, Cleveland, OH.
A NEW Cu-8 Cr-4 Nb ALLOY FOR HIGH TEMPERATURE APPLICATIONS
D. L. Ellis (Case Western Reserve Univ., Cleveland, OH.), G. M. Michal (Case Western Reserve Univ., Cleveland, OH.), and R. L. Dreshfield Jun. 1995 6 p
(Contract NCC3-94; RTOP 242-20-06)
(NASA-TM-106910; E-9612; NAS 1.15:106910) Avail: CASI HC A02/MF A01

Various applications exist where a high conductivity alloy with good strength and creep resistance are required. NASA LeRC has developed a Cu-8 at. percent Cr-4 at. percent Nb (Cu-8 Cr-4 Nb) alloy for these applications. The alloy is designed for use up to 700 C and shows exceptional strength, low cycle fatigue (LCF) resistance, and creep resistance. Cu-8 Cr-4 Nb also has a thermal conductivity of at least 72 percent that of pure Cu. Furthermore, the microstructure and mechanical properties of the alloy are very stable. In addition to the original application in combustion chambers, Cu-8 Cr-4 Nb shows promise for welding electrodes, brazing fixtures, and other applications requiring high conductivity and strength at elevated temperatures. Author

N95-27748# Johns Hopkins Univ., Baltimore, MD.
SIMULATIONS OF METAL DISSOLUTION AND CORROSION Final Report, Jan. 1993 - Jun. 1994
P. C. Searson 1995 14 p
(Contract DE-FG02-89ER-45388)
(DE95-007486; DOE/ER-45388/T3) Avail: CASI HC A03/MF A01

There has been considerable interest in microscopic aspects of material removal processes in fields such as corrosion, erosion, evaporation, battery technology, electropolishing, and semiconductor etching. Reports of theoretical work related to many of these problems can be found in the literature although metal dissolution is a noticeable exception. Critical issues common to all dissolution reactions include the relationship between the surface morphology and the driving term (e.g. potential, concentration, temperature); the role of surface active sites, dislocations, and other heterogeneities to the dissolution kinetics; and the influence of surface diffusion. We have shown that microscopic analysis of electrochemically dissolving metal surfaces via computer simulations can lead to a fundamental understanding of the relationship between surface morphology and dissolution kinetics. Microscopic information on surface processes is not contained in phenomenological equations such as the Butler-Volmer equation, which is commonly used to describe electrode dissolution. In particular, we find that the surface roughness and, consequently, the number of surface active sites, are determined by thermodynamic parameters such as the applied electrode potential. The morphology of surfaces has been shown to be an essential aspect of kinetic processes such as crystal growth and mineral dissolution. Electrochemical processes, however, are fundamentally different in that they feature the presence of very high electrical fields at the interface, which directly affect the surface reactions. To date, treatments of the kinetics of electrochemically dissolving metal surfaces have ignored surface morphology. Over the next few years, results from theoretical modeling of dissolution processes, in conjunction with new experimental techniques such as STM, are expected to provide a new insight into the processes controlling metal dissolution and corrosion. DOE

N95-27752# Argonne National Lab., IL.
PARTICLE-LIKE ABSORPTION SPECTRA IN SMALL TRANSITION METAL CLUSTERS
M. B. Knickelbein 1995 5 p
(Contract W-31-109-eng-38)
(DE95-007082; ANL/CHM/PP-80412) Avail: CASI HC A01/MF A01

Research at Argonne has found that small clusters of certain transition metal atoms display optical absorption spectra that are fundamentally different from those typically observed for other small molecules. A new laser technique known as photodissociation spectroscopy was used to record the absorption spectra of nickel clusters containing three to seven atoms and of niobium clusters containing between seven and twenty atoms. Instead of displaying spectra with distinct and separate absorption 'bands' as is usually seen for small molecules, these metal clusters possess absorption spectra that are continuous and smooth throughout the visible and near ultraviolet regions, indicating that they absorb light at every wavelength. This behavior is in fact more like that displayed by much larger metal particles containing hundreds or thousands of atoms. This surprising result may indicate that the electronic structures of these small clusters are much closer to those of a corresponding macroscopic piece of nickel or niobium metal than was previously thought. These studies are aimed at understanding the electronic structure of the active metal cluster sites in catalysts, and may in addition provide valuable insights into the design and properties of new cluster assembled materials. DOE

N95-27756# International Centre for Theoretical Physics, Trieste (Italy).
A FIRST PRINCIPLES APPROACH TO PHASE STABILITY AND ORDER-DISORDER TRANSFORMATION: APPLICATION TO LI-AI ALLOYS
Ashok Arya, Srikumar Banerjee (Bhabha Atomic Research Centre, Bombay, India.), and Gour P. Das Aug. 1994 36 p
(DE95-609152; IC-94/242) Avail: CASI HC A03/MF A01 (US Sales Only)

Starting from TB-LMTO electronic structure total energy calculations of ordered binary alloys, we have determined the configurationally averaged effective (multisite) cluster interactions (ECI's) using the Connolly-Williams inversion method. The configurational entropy has been calculated in the mean field approximation of the Ising model using the cluster variation method (CVM). The resulting configurational free energy (or equivalently the grand potential) has been minimized and order-disordered transformation behavior in Li-Al alloys has been discussed. DOE

N95-27757# International Centre for Theoretical Physics, Trieste (Italy).
CROSSOVER INTEGRAL EQUATION THEORY FOR THE LIQUID STRUCTURE STUDY
S. K. Lai and H. C. Chen (National Central Univ., Chung-Li, Taiwan.) Aug. 1994 13 p
(DE95-609155; IC-94/252) Avail: CASI HC A03/MF A01 (US Sales Only)

The main purpose is to report on a calculation that describes the role of the long-range bridge function as applied to the study of structure of simple liquid metals. It was found here that this bridge function accounts pretty well for the major part of long-range interactions but is physically inadequate for describing the short-range part of liquid structure. To improve on the theory we have drawn attention to the crossover integral equation method which, in essence, amounts to adding to the above bridge function a short-range correction of bridge diagrams. The suggested crossover procedure has been tested for the case of liquid metal Cs. Remarkably good agreement with experiment was obtained confirming our conjecture that the crossover integral equation approach as stressed in this work is potentially an appropriate theory for an accurate study of liquid structure possibly for the supercooled liquid regime. DOE

N95-27758# International Centre for Theoretical Physics, Trieste (Italy).
ELECTRONIC STRUCTURE OF DISORDERED Cu-Ag ALLOYS
S. S. A. Razee Aug. 1994 11 p
(DE95-609156; IC-94/258) Avail: CASI HC A03/MF A01 (US Sales Only)

We present a self-consistent-field Korringa-Kohn-Rostoker coherent potential approximation study of the electronic structure of disordered Cu(x)Ag(1-x) alloys for x = 0.0, 0.25, 0.50, 0.75, and 1.0. In particular, we focus on the Fermi surface, density of states, and Bloch spectral density, and study how they evolve as a function of x. We find that Fermi surface dimensions have a nonlinear composition dependence. The disorder-induced smearing of the Fermi surface, as expected, is very high along the zone axes (111) direction; both the Cu and Ag Fermi surfaces have a neck in this direction. Whenever possible we have compared our results with the available experimental data. DOE

N95-27759# International Centre for Theoretical Physics, Trieste (Italy).
THE ROLE OF EDGE DISLOCATIONS IN THE DEFORMATION OF BCC METALS
C. W. Lung Aug. 1994 7 p
(DE95-609157; IC-94/263) Avail: CASI HC A02/MF A01 (US Sales Only)

It was widely accepted that the screw dislocation is responsible for the strong temperature dependence of the yield stresses observed in bcc metals. We show the role of edge dislocations in the deformation of bcc metals and point out that in some cases, its main contribution to the yield stress cannot be ignored. DOE

N95-27934 Selskapet for Industriell og Teknisk Forskning, Trondheim (Norway). Dept. of Materials Technology.
FORMING METALLURGY: SUPERVISED DRAWING COURSE, NTH
T. Iveland 1994 104 p Prepared in cooperation with Technical Univ. of Norway, Trondheim
(PB95-196507; STF24-A94510) Avail: Issuing Activity (National Technical Information Service (NTIS))

A short introduction of texture and deformation models of polycrystalline metals is given. Work hardening based on dislocation theory and the effect of factors such as strain rate and temperature are also discussed. Some useful empirical relations between stress and strain are presented, and the size and shape of the yield surface during plastic deformation is described by continuum mechanics equations. Some of the most common test methods used to determine the formability of metallic materials are presented. Examples of such methods are the tension, the compression, and the torsion test. A brief presentation of common plastic forming processes along with some approximate methods to decide the necessary deformation force and the flow pattern during the forming operations are given. Finally, simplified analysis methods are applied on forming processes by using some of these simplified methods and a brief view of the possibilities using finite element methods in bending operations is presented. NTIS

N95-27958# Sandia National Labs., Albuquerque, NM.
FIRST-PRINCIPLES CALCULATIONS FOR AlN, GaN, AND InN: BULK AND ALLOY PROPERTIES
A. F. Wright and J. S. Nelson 1995 17 p
(Contract DE-AC04-94AL-85000)
(DE95-006822; SAND-95-0144C) Avail: CASI HC A03/MF A01

First-principles density-functional calculations utilizing ab initio pseudopotentials and plane-wave expansions are used to determine lattice parameters, bulk moduli, and band structures for AlN, GaN, and InN. It is found that large numbers of plane waves are necessary to resolve the nitrogen 2p wave functions and that explicit treatment of the gallium 3d and indium 4d electrons is important for an accurate description of GaN and InN. Several properties of ternary zinc-blende alloys are determined including their bond-length and bond-angle relaxation and their energy-gap bowing parameters. The similarity of the calculated zinc-blende and wurtzite direct gaps also allows estimates to be made of the energy gap versus composition for wurtzite alloys. DOE

N95-27966# Argonne National Lab., IL.
THE OXIDATION STATE AND MAGNETIC BEHAVIOUR OF Tb IN HIGH-(Tc) RELATED MATERIALS
L. Soderholm, U. Staub, S. Skanthakumar, and M. R. Antonio 1995 7 p Presented at the 1994 Fall Meeting of the Materials Research Society (MRS), Boston, MA, 28 Nov. - 2 Dec. 1994
(Contract W-31-109-eng-38)
(DE95-007129; ANL/CHM/CP-85152; CONF-941144-59) Avail: CASI HC A02/MF A01

L(3)-X-ray absorption spectroscopy is used together with inelastic neutron scattering and magnetic susceptibility measurements to characterize the Tb oxidation state and bonding in the high-(T(c)) related materials Y(1 - x)Tb(x)Ba2Cu3O7 and Pb2Sr2TbCu3O8. The Tb is found to be essentially trivalent in both compounds with no indications of significant hybridization. However, there is evidence of significant Tb-Tb magnetic interactions in Pb2Sr2TbCu3O8 that persist to temperatures much higher than the Tb long-range ordering temperature. DOE

N95-27968# Sandia National Labs., Albuquerque, NM.
A NEW TECHNIQUE FOR MEASURING THE SEPARATION OF CLOSELY SPACED DISLOCATIONS USING RESIDUAL CONTRAST CONDITIONS
J. E. Angelo and M. J. Mills 1995 3 p Presented at the Microscopy Society of America and Microbeam Analysis Society Joint Meeting, New Orleans, LA, 31 Jul. - 5 Aug. 1994
(Contract DE-AC04-94AL-85000)
(DE95-007147; SAND-94-8596C; CONF-940753-25) Avail: CASI HC A01/MF A01

In order to measure the spacing of closely spaced dislocations, a method with sufficient spatial resolution must be used. The author presents a method for measuring such spatial resolution. Applications of this method to copper, NiAl, and Ni3Al will be discussed. DOE

N95-28005# Westinghouse Hanford Co., Richland, WA.
EFFECTS OF HYDROGEN ON CARBON STEELS AT THE MULTI-FUNCTION WASTE TANK FACILITY
W. C. Carlos Feb. 1995 29 p
(Contract DE-AC06-87RL-10930)
(DE95-007194; WHC-SD-W236A-ES-004) Avail: CASI HC A03/MF A01

Concern has been expressed that hydrogen produced by corrosion, radiolysis, and decomposition of the waste could cause embrittlement of the carbon steel waste tanks at Hanford. The concern centers on the supposition that the hydrogen evolved in many of the existing tanks might penetrate the steel wall of the tank and cause embrittlement that might lead to catastrophic failure. This document reviews literature on the effects of hydrogen on the carbon steel proposed for use in the Multi-Function Waste Tank Facility for the time periods before and during construction as well as for the operational life of the tanks. The document draws several conclusions about these effects. Molecular hydrogen is not a concern because it is not capable of entering the steel tank wall. Nascent hydrogen produced by corrosion reactions will not embrittle the steel because the mild steel used in tank construction is not hard enough to be susceptible to hydrogen stress cracking and the corrosion product hydrogen is not produced at a rate sufficient to cause either loss in tensile ductility or blistering. If the steel intended for use in the tanks is produced to current technology, fabricated in accordance with good construction practice, postweld heat treated, and operated within the operating limits defined, hydrogen will not adversely affect the carbon steel tanks during their 50-year design life. DOE

N95-28026# Los Alamos National Lab., NM.
PHASE STABILITY AND ELASTICITY OF C15 TRANSITION-METAL INTERMETALLIC COMPOUNDS
F. Chu, T. E. Mitchell, S. P. Chen, M. Sob (Pennsylvania Univ., Philadelphia, PA.), R. Siegl (Pennsylvania Univ., Philadelphia, PA.), and D. P. Pope (Pennsylvania Univ., Philadelphia, PA.) 1995 12 p Presented at the Annual Meeting and Exhibition of the Minerals, Metals and Materials Society, Las Vegas, NV, 12-16 Feb. 1995
(Contract W-7405-eng-36)
(DE95-007876; LA-UR-95-473; CONF-950201-6) Avail: CASI HC A03/MF A01

First-principle quantum mechanical calculations based on the local-density-functional theory have been performed to study the electronic, physical and metallurgical properties of C15 intermetallics MV2 (M = Zr, Hf, or Ta). The elastic constants of C15 HfV2 + Nb were measured by the resonant ultrasound spectroscopy technique. The phase stability of C15 HfV2 + Nb was studied by specific heat measurements and by transmission electron microscopy in a low temperature specimen holder. The total energies and their lattice volume dependence were used to obtain the equilibrium lattice constants and bulk modulus. The band structures at the X-point near the Fermi level were employed to understand the anomalous temperature dependence of shear modulus of the C15 intermetallics. It was found that the double degeneracy with a linear dispersion relation of electronic levels at the X-point near the Fermi surface is mainly responsible for the C15 anomalous elasticity. The density of states at the Fermi level, N(E(sub F)), and the Fermi surface geometry were obtained to understand the low temperature phase instability of C15 HfV2 and ZrV2 and the stability of C15 TaV2. It was proposed that the large N(E(sub F)) and Fermi surface nesting are the physical reasons for the structural instability of the C15 HfV2 and ZrV2 at low temperatures. The relation between anomalous elasticity and structural instability of C15 HfV2 and ZrV2 is also discussed. DOE

N95-28039# International Centre for Theoretical Physics, Trieste (Italy).
BETA-DYNAMICS IN SIMPLE LIQUID METAL
S. K. Lai Aug. 1994 24 p
(DE95-609154; IC-94/247) Avail: CASI HC A03/MF A01 (US Sales Only)

The modified hypernetted chain theory is applied to calculate the static liquid structure factor for simple liquid metals at rapid cooling. With a proper choice of bridge function, it is found that this integral equation theory is capable of yielding reasonably accurate liquid structure factor in the supercooled liquid region. To exploit the usefulness of the calculated liquid structure, we combine these structure data with the mode-coupling theory to investigate the dynamics of the (beta)-process. It is demonstrated in this work that the critical temperature for an ideal glass transition predicted here for liquid metals Na and K are slightly lower than those determined previously using computer simulated structure factors. In particular, we show that the material-dependent exponent parameter (lambda) which is used widely in the literature as a fitting parameter in the analysis of light scattering experiments can be given more physical significance if one correlates the change of (lambda) with the microscopic interaction or particles specifically for the liquid metal, Lennard-Jones fluid and hard-sphere system. The implication of the present results and the possibility to extract useful information for more complicated systems will be discussed in the text. DOE

N95-28044# Oak Ridge National Lab., TN.
EFFECTS OF INTERLAYERS ON THE SCRATCH ADHESION PERFORMANCE OF ULTRA-THIN FILMS OF COPPER AND GOLD ON SILICON SUBSTRATES
S. D. McAdams, T. Y. Tsui, G. M. Pharr (Rice Univ., Houston, TX.), and W. C. Oliver (Nano Instruments, Inc., Knoxville, TN.) 1995 7 p Presented at the 1994 Fall Meeting of the Materials Research Society (MRS), Boston, MA, 28 Nov. - 2 Dec. 1994
(Contracts DE-AC05-84OR-21400; DE-AC05-76OR-00033)
(DE95-007367; CONF-941144-68) Avail: CASI HC A02/MF A01

Scratch testing has long been used to assess the adhesion of a film to its substrate. As film thicknesses have decreased, the need for greater precision and sensitivity in the scratch testing apparatus has increased. To this end, a nanoindenter was modified to make finely controlled, low-load scratches. Scratches at various loads and two orientations of a Berkovich scratching diamond were made in films of 100 nm of gold and 200 nm of copper, each on single crystal silicon. For each film type, samples with no interlayer, with an SiO2 interlayer, and with a TiW on SiO2 interlayer were tested. The scratch morphology was found to vary in a regular way with load, diamond orientation and interlayer material. DOE

N95-28046# Oak Ridge National Lab., TN.
TRACE ELEMENTS AND THE MECHANICAL PROPERTIES OF INTERMETALLIC COMPOUNDS
Hui Lin (Pennsylvania Univ., Philadelphia, PA.), D. P. Pope (Pennsylvania Univ., Philadelphia, PA.), and E. P. George 1995 41 p Presented at the International Conference on Ultrahigh Purity Metals, Sendai, Japan, 23-27 May 1994
(Contract DE-AC05-84OR-21400)
(DE95-007378; CONF-9405290-1) Avail: CASI HC A03/MF A01

In this paper the brittleness of grain boundaries in Ni3Al is discussed with special emphasis on the effects of B. The effects of alloy stoichiometry, environment (hydrogen), grain boundary character and B levels are described and interpreted in terms of current theories. It is shown that the grain boundaries in Ni3Al are intrinsically weaker than the bulk (the weakness is not an impurity effect), the weakness is exacerbated by atmospheric moisture, and that B in the boundaries both increases the intrinsic strength of the boundaries and reduces the deleterious effects of atmospheric moisture. Only low angle boundaries and twin boundaries are intrinsically strong in Ni3Al, even in the absence of B. DOE

N95-28049# Missouri Univ., Rolla, MO.
DEFECT CHARACTERIZATION OF ELECTRONIC CONDUCTING PSEUDO-PEROVSKITE SYSTEMS Final Report
H. U. Anderson, M. Nasrallah, D. M. Sparlin, and P. E. Parris 1994 19 p
(Contract DE-FG02-85ER-45219)
(DE95-007487; DOE/ER-45219/T3) Avail: CASI HC A03/MF A01

The goal of the program has been to study the interrelationships between electrical conductivity, oxidation-reduction kinetics, defect structure, and composition of n- and p-type binary and ternary transition metal oxides. The stimulus for making these studies was the observation that both conducting n- and p-type oxides displayed a dependence on oxygen activity that was not predicted by the defect chemistry of their majority defects. The project has focused primarily on the understanding of electronic and ionic conduction in the REBO3 oxides, where RE is a rare earth ion and B is a transition metal ion. This is being done by studying the interrelationships between the electronic and ionic conductivity, the electronic structure of the B site transition metal ion, and the acceptor concentration. The dependence of these characteristics on the oxygen activity, the temperature, and the defect chemistry of the oxide system is being determined. Theoretical mechanisms and models are being developed from the body of experimental results to provide a predictive tool. The effect of dopants and impurities, processing, electrical and thermal stability as a function of oxygen activity and temperature and their relationship to defect chemistry of the perovskite type oxides have been studied extensively by this research team. As a result of the difference in mobility between electronic and ionic defects, the electrical conductivity changes as the concentration of electronic defects changes. Thus, electrodes or resistors consisting of such oxides are susceptible to instabilities in resistance as they are cycled into temperature regimes where thermodynamic equilibrium may be attained. Many of the new energy conversion systems which use such oxides are encountering difficulties as a result of this instability in resistivity. DOE

N95-28072# Argonne National Lab., IL.
GAMMA RAY-INDUCED EMBRITTLEMENT OF PRESSURE VESSEL ALLOYS
D. E. Alexander, L. E. Rehn, K. Farrell (Oak Ridge National Lab., TN.), and R. E. Stoller (Oak Ridge National Lab., TN.) Nov. 1994 9 p Presented at the 1994 Fall Meeting of the Materials Research Society (MRS), Boston, MA, 28 Nov. - 2 Dec. 1994
(Contract W-31-109-eng-38)
(DE95-007133; ANL/MSD/CP-83383; CONF-941144-72) Avail: CASI HC A02/MF A01

High-energy gamma rays emitted from the core of a nuclear reactor produce displacement damage in the reactor pressure vessel (RPV). The contribution of gamma damage to RPV embrittlement has in the past been largely ignored. However, in certain reactor designs the gamma flux at the RPV is sufficiently large that its contribution to displacement damage can be substantial. For example, gamma rays have been implicated in the accelerated RPV embrittlement observed in the High Flux Isotope Reactor (HFIR) at Oak Ridge National Laboratory. In the present study, mechanical property changes induced by 10-MeV electron irradiation of a model Fe alloy and an RPV alloy of interest to the HFIR were examined. Mini-tensile specimens were irradiated with high-energy electrons to reproduce damage characteristic of the Compton recoil-electrons induced by gamma bombardment. Substantial increases in yield and ultimate stress were observed in the alloys after irradiation to doses up to 5.3x10(exp -3) dpa at temperatures (approximately 50 C) characteristic of the HFIR pressure vessel. These measured increases were similar to those previously obtained following neutron irradiation, despite the highly disparate nature of the damage generated during electron and neutron irradiation. DOE

N95-28075# Oak Ridge National Lab., TN.
HIGH TEMPERATURE HEXOLOY(TRADEMARK) SX SILICON CARBIDE Final Report
G. V. Srinivasan, S. K. Lau, and R. S. Storm Sep. 1994 98 p Prepared in cooperation with Carborundum Co., Nia gara Falls, NY Sponsored by Martin Marietta Energy Systems, Inc.
(Contract DE-AC05-84OR-21400)
(DE95-007290; ORNL/Sub-91-SG341/1) Avail: CASI HC A05/MF A02

HEXOLOY(reg sign) SX-SiC, fabricated with Y and Al containing compounds as sintering aids, has been shown to possess significantly improved strength and toughness over HEXOLOY(reg sign)SA-SiC. This study was undertaken to establish and benchmark the complete mechanical property database of a first generation material, followed by a process optimization task to further improve the properties. Mechanical characterization on the first generation material indicated that silicon-rich pools, presumably formed as a reaction product during sintering, controlled the strength from room temperature to 1,232 C. At 1,370 C in air, the material was failing due to a glass-phase formation at the surface. This glass-phase formation was attributed to the reaction of yttrium aluminates, which exist as a second phase in the material, with the ambient. This process was determined to be a time-dependent one that leads to slow crack growth. Fatigue experiments clearly indicated that the slow crack growth driven by the reaction occurred only at temperatures greater than 1,300 C, above the melting point of the glass phase. Process optimization tasks conducted included the selection of the best SiC powder source, studies on mixing/milling conditions for SiC powder with the sintering aids, and a designed experiment involving a range of sintering and post-treatment conditions. The optimization study conducted on the densification variables indicated that lower sintering temperatures and higher post-treatment pressures reduce the Si-rich pool formation, thereby improving the room-temperature strength. In addition, it was also determined that furnacing configuration and atmosphere were critical in controlling the Si-rich formation. DOE

N95-28082# Oak Ridge National Lab., TN. Materials and Ceramics Div.
THE EFFECTS OF PROCESSING VARIABLES ON REACTION SYNTHESIS OF Fe-Al ALLOYS
D. L. Joslin, D. S. Easton, C. T. Liu, and S. A. David 1994 7 p Presented at the 1994 Fall Meeting of the Materials Research Society, Boston, MA, 28 Nov. - 2 Dec. 1994
(Contract DE-AC05-84OR-21400)
(DE95-007405; CONF-941144-75) Avail: CASI HC A02/MF A01

The effects of alloy composition and reaction atmosphere on reaction synthesis of binary FeAl alloys were studied. Reactions were observed in an open (air) furnace, under static vacuum (in an evacuated quartz tube) and in a dynamic vacuum furnace. High-speed videotapes of reaction syntheses of compacts formed from 45 micrometer Fe and 10 micrometer Al powders reacted in air and under static vacuum revealed that an unusual 'two-stage' reaction exists in this system under these conditions. The first stage of the two-stage reaction lasts several seconds and starts at around 650 C. The second stage begins at about 900 C, reaching temperatures between 1,250 and 1,350 C. The progress of the reaction to the second stage is sensitive to the alloy composition and reaction environment. The reaction behavior is explained in terms of thermodynamics and heat transfer, which control the delicate balance between beat accumulation and heat loss during reaction synthesis. DOE

N95-28102 General Dynamics Corp., Warren, MI. Land Systems Div.
IMPROVED HARDNESS RHA WELDABILITY AND MATERIAL PROPERTY TESTING Final Technical Report, Aug. 1991 - Jun. 1994
Michael L. Foos Dec. 1994 126 p Limited Reproducibility: More than 20% of this document may be affected by microfiche quality
(Contract DAAL04-91-C-0040)
(AD-A289127) Avail: Issuing Activity (Defense Technical Information Center (DTIC))

The M1-PMO, in conjunction with the US Army Research Laboratory (ARL) would like to potentially up-armor the M1 family of vehicles by increasing the hardness of rolled homogeneous armor (RHA) MIL-A-12560 steel. The basic thrust of the program is to utilize lower tempering temperatures and chemistries of slightly more hardenability to produce a RHA armor with a Rockwell 'C' hardness of 39-48 without altering the current specification MIL-A-12560 steel. It is believed that the increased hardness levels will provide increased ballistic protection against large caliber kinetic energy threats. Weldability and material property tests were performed on the improved hardness RHA steel supply by the US ARL. The program involves basic material characterization, weldability, machinability and plate cutting studies. The material characterization was performed on two thicknesses (1.25' and 1.50'). The weldability study included Y-groove preheat testing, stud welding and maximum heat input testing. The machinability testing involved machining parts including drilling, tapping, reaming, boring and milling. Plasma and Oxy-fuel thermal cutting were studied to gauge processing of the steel by present armor vehicle fabrication. The ballistic testing was performed by US Combat Systems Test Activity (CSTA) at Aberdeen, MD. The results show the candidate steel can processed typical to RHA steel with minor impact to welding and machining. DTIC

N95-28116# Sandia National Labs., Albuquerque, NM.
PULSED ION BEAM SURFACE TREATMENT FOR PREPARING RAPIDLY SOLIDIFIED CORROSION RESISTANT STEEL AND ALUMINUM SURFACES
R. G. Buchheit, L. M. Maestas, D. C. McIntyre, R. W. Stinnett, and J. B. Greenly (Cornell Univ., Ithaca, NY.) 1995 10 p Presented at the Annual Meeting and Exhibition of the Minerals, Metals and Materials Society, Las Vegas, NV, 12-16 Feb. 1995
(Contract DE-AC04-94AL-85000)
(DE95-007741; SAND-95-0281C; CONF-950201-5) Avail: CASI HC A02/MF A01

Intense, pulsed ion beams were used to melt and rapidly resolidify Types 316F, 316L, and sensitized 304 stainless steel surfaces to eliminate the negative effects of microstructural heterogeneity on localized corrosion resistance. Anodic polarization curves determined for 316F and 316L showed that passive current densities were reduced and pitting potentials were increased due to ion beam treatment. Type 304 samples sensitized at 600 C for 100 h showed no evidence of grain boundary attack when surfaces were ion beam treated. Equivalent ion beam treatments were conducted with a 6061-T6 aluminum alloy. Electrochemical impedance experiments conducted with this alloy exposed to an aerated chloride solution showed that the onset of pitting was delayed compared to untreated control samples. DOE

N95-28120# Oak Ridge National Lab., TN.
TOWARD A MECHANISTIC UNDERSTANDING OF RADIATION EFFECTS IN MATERIALS
J. E. Pawel, E. E. Bloom, L. K. Mansur, A. F. Rowcliffe, S. J. Zinkle, R. E. Stoller, and P. J. Maziasz 1995 3 p Presented at the Ishino Conference, Tokyo, Japan, 15-16 Dec. 1994
(Contract DE-AC05-84OR-21400)
(DE95-006530; CONF-941258-1) Avail: CASI HC A01/MF A01

Substantial progress has been made to understanding radiation effects in materials, and in formulating and testing a metallurgical approach for developing radiation-resistant alloys. This understanding is a combination of theoretical modeling with experiments using mixed spectrum fission reactors, fast reactors and ion irradiations. The development of materials with properties to meet the challenges of advanced reactors has four major steps: (1) the development of a mechanistic understanding of the behavior of materials during irradiation in appropriate environments; (2) selection of candidate materials based on physical, chemical, and mechanical properties; (3) development of these candidate materials through compositional and microstructural control to achieve the necessary properties and radiation damage resistance; and (4) the development of a database sufficient to support engineering design, performance analysis, and safety assessment. This paper will present a brief overview of the present understanding of radiation effects in materials, with emphasis on work performed at Oak Ridge National Laboratory as part of the U.S. fusion materials and basic energy sciences programs. Progress in fundamental understanding of void swelling, phase formation and stability, irradiation creep, and post-irradiation mechanical properties has been gained through comparison of experimental data with the predictions of theoretical models.

Applications of the understanding of radiation effects in materials have led to the development of candidate structural materials for use in aggressive radiation environments such as fast breeder reactors and proposed fusion energy systems. Because of the successes associated with the development of radiation resistant austenitic stainless steels, it is believed that these principles will provide the basis for addressing radiation issues in a variety of materials systems. DOE

N95-28129# Pacific Northwest Lab., Richland, WA.
BASES FOR EXTRAPOLATING MATERIALS DURABILITY IN FUEL STORAGE POOLS
A. B. Johnson, Jr. Dec. 1994 7 p Presented at the Spent Nuclear Fuel Meeting: Challenges and Initiatives, Salt Lake City, UT, 14-16 Dec. 1994
(Contract DE-AC06-76RL-01830)
(DE95-007746; PNL-SA-24126; CONF-941207-25) Avail: CASI HC A02/MF A01

A major body of evidence indicates that zirconium alloys have the most consistent and reliable durability in wet storage, justifying projections of safe wet storage greater than 50 y. Aluminum alloys have the widest range of durabilities in wet storage; systematic control and monitoring of water chemistry have resulted in low corrosion rates for more than two decades on some fuels and components. However, cladding failures have occurred in a few months when important parameters were not controlled. Stainless steel is extremely durable when stress, metallurgical and water chemistry factors are controlled. LWR SS cladding has survived for 25 y in wet storage. However, sensitized, stressed SS fuels and components have seriously degraded in fuel storage pools (FSP's) at approximately 30 C. Satisfactory durability of fuel assembly and FSP component materials in extended wet storage requires investments in water quality management and surveillance, including chemical and biological factors. The key aspect of the study is to provide storage facility operators and other decision makers a basis to judge the durability of a given fuel type in wet storage as a prelude to basing other fuel management plans (e.g. dry storage) if wet storage will not be satisfactory through the expected period of interim storage. DOE

N95-28130# Pacific Northwest Lab., Richland, WA.
SOLID-STATE SINTERING OF TUNGSTEN HEAVY ALLOYS
W. E. Gurwell Oct. 1994 11 p Presented at the 1994 International Conference on Tungsten and Refractory Metals, McLean, VA, 17-19 Oct. 1994
(Contract DE-AC06-76RL-01830)
(DE95-007749; PNL-SA-24841; CONF-9410213-5) Avail: CASI HC A03/MF A01

Solid-state sintering is a technologically important step in the fabrication of tungsten heavy alloys. This work addresses practical variables affecting the sinterability: powder particle size, powder mixing, and sintering temperature and time. Compositions containing 1 to 10 micrometer ((mu)M) tungsten (W) powders can be fully densified at temperatures near the matrix solidus. Blending with an intensifier bar provided good dispersion of elemental powders and good as-sintered mechanical properties under adequate sintering conditions. Additional ball milling increases powder bulk density which primarily benefits mold and die filling. Although fine, 1 (mu)m W powder blends have high sinterability, higher as-sintered ductilities are reached in shorter sintering times with coarser, 5 (mu)m W powder blends; 10(mu)m W powder blends promise the highest as-sintered ductilities due to their coarse microstructural W. DOE

N95-28134# Michigan Univ., Ann Arbor, MI.
THE ROLE OF HYDROGEN IN THE HYDROGENATION AND HYDROGENOLYSIS OF ANILINE ON THE NICKEL SINGLE CRYSTAL SURFACES: ITS IMPLICATION ON THE MECHANISMS OF HDN REACTIONS
S. X. Huang, J. L. Gland, and D. A. Fischer (National Inst. of Standards and Technology, Gaithersburg, MD.) 1995 13 p Presented at the 2nd International Symposium on Advances in Hydrotreating Catalysts, Washington, DC, 22-26 Aug. 1994
(Contract DE-FG02-91ER-14190)
(DE95-006687; CONF-9408210-1) Avail: CASI HC A03/MF A01

The selectivity of hydrogenation and hydrogenolysis reactions for organonitrogen compounds on transition metal surfaces depends heavily on the availability of surface hydrogen under reaction conditions. The surface hydrogen produced during dehydrogenation of adsorbed aniline upon thermal activation does not significantly modify hydrogenolysis reactions because it desorbs below the reaction temperatures. A series of experiments which use external hydrogen to control the concentration of surface hydrogen at reaction temperatures are reported here. In situ kinetic measurements in the presence of reactive hydrogen environments have been used to probe the details of the adsorbed species and reaction mechanisms. Nickel single crystals have been used as well defined model catalysts for hydrodenitrogenation (HDN) reactions. Previously, the effect of external hydrogen on aniline hydrogenolysis on the Pt(111) surface has been reported. On Pt(111), C-N bond activation is substantially enhanced in the presence of hydrogen. The increased C-N bond cleavage is facilitated by hydrogen which maintains a parallel adsorption of the aromatic derivative of aniline. In the absence of surface hydrogen, the adsorbed intermediate tilts away from surface because of partial dehydrogenation with increasing temperature at about 400 K. This paper will discuss a recent study of aniline reactions on the Ni(100) and Ni(111) surfaces both in the presence and absence of hydrogen. Reactivity comparisons will also be made for these two nickel surfaces towards adsorbed aniline. DOE

N95-28163# Pacific Northwest Lab., Richland, WA.
ACCURACY ISSUES IN MODELING SUPERPLASTIC METAL FORMING
K. I. Johnson, M. A. Khaleel, C. A. Lavender, and M. T. Smith Feb. 1995 17 p Presented at the Annual Meeting and Exhibition of the Minerals, Metals and Materials Society, Las Vegas, NV, 12-16 Feb. 1995
(Contract DE-AC06-76RL-01830)
(DE95-008934; PNL-SA-24828; CONF-950201-8) Avail: CASI HC A03/MF A01

The utility of finite element modeling in optimizing superplastic metal forming is dependent on accurate representation of the material constitutive behavior and the frictional response of the sheet against the die surface. This paper presents work conducted to estimate the level of precision that is necessary in constitutive relations for finite element analysis to accurately predict the deformation history of actual SPF components. Previous work identified errors in SPF testing methods that use short tensile specimens with gauge length-to-width ratios of 2:1 or less. The analysis of the present paper was performed to estimate the error in predicted stress that results from using the short specimens. Stress correction factors were developed and an improved constitutive relation was implemented in the MARC finite element code to simulate the forming of a long, rectangular tray. The coefficient of friction in a Coulomb friction model was adjusted to reproduce the amount of material draw-in observed in the forming experiments. Comparisons between the finite element predictions and the forming experiments are presented. DOE

N95-28166# Brookhaven National Lab., Upton, NY.
PRECURSOR PHENOMENON OF MARTENSITIC TRANSFORMATION IN Au-49.5AT%Cd ALLOY
Takuya Ohba (Teikyo Univ., Utsunomiya, Japan.), S. M. Shapiro, Shingo Aoki (Tsukuba Univ., Ibaraki, Japan.), and Kazuhiro Otsuka (Tsukuba Univ., Ibaraki, Japan.) 1994 6 p Presented at the 1994 Fall Meeting of the Materials Research Society (MRS), Boston, MA, 28 Nov. - 2 Dec. 1994
(Contract DE-AC02-76CH-00016)
(DE95-007698; BNL-61391; CONF-941144-66) Avail: CASI HC A02/MF A01

Phonon softening was observed in the parent phase of a AuCd alloy which transforms from the beta(sub 2)(B2) parent to zeta'(sub 2) (trigonal) martensitic. Since Cd strongly absorbs neutrons, the isotope Cd-114 was used in preparing the single crystal for the measurements. The (zeta zeta 0)TA(sub 2) phonon branch was measured and found to be anomalously low. A minimum is present at zeta = 0.35 which softens with decreasing temperature towards Ms. The results are consistent with the model proposed by Ohba et al. based upon a crystallographic study of the zeta'(sub 2) phase. DOE

N95-28167# Lawrence Livermore National Lab., Livermore, CA.
FENIX EXPERIMENTAL RESULTS OF LARGE-SCALE CICC MADE OF BRONZE-PROCESSED Nb3Sn STRANDS
S. S. Shen, B. Felker, J. M. Moller, J. M. Parker, T. Isono (Japan Atomic Energy Research Inst., Naka, Japan.), Y. Yasukawa (Japan Atomic Energy Research Inst., Naka, Japan.), F. Hosono (Japan Atomic Energy Research

Inst., Naka, Japan.), and M. Nishi (Japan Atomic Energy Research Inst., Naka, Japan.) 13 Oct. 1994 6 p Presented at the Applied Superconductivity Conference, Boston, MA, 16-21 Oct. 1994
(Contract W-7405-eng-48)
(DE95-007965; UCRL-JC-116967; CONF-941013-27) Avail: CASI HC A02/MF A01

The Fusion ENgineering International eXperiments (FENIX) Test Facility recently has successfully completed the testing of a pair of Nb3Sn cable-in-conduit conductors developed by the Japan Atomic Energy Research Institute. These conductors, made of bronze-processed strands, were designed to operate stably with 40-kA transport current at a magnetic field of 13 T. In addition to the measurements of major design parameters such as current-sharing temperature, FENIX provided several experiments specifically designed to provide results urgently needed by magnet designers. Performed experiments include measurements of ramp-rate limit, current-distribution, stability, and joint performance. This paper presents the design and results of these special experiments. DOE

N95-28189 Army Research Lab., Aberdeen Proving Ground, MD.
THE HIGH STRAIN RATE DEFORMATION OF TUNGSTEN SINGLE CRYSTALS Final Report, Aug. 1992 - Apr. 1994
Edward J. Horwath Nov. 1994 66 p Limited Reproducibility: More than 20% of this document may be affected by microfiche quality
(DA Proj. 1L1-62618-AH-80)
(AD-A288874; ARL-TR-620) Avail: Issuing Activity (Defense Technical Information Center (DTIC))

Samples of single-crystal tungsten, in three orientations (100, 110, 111), were compressively deformed at high strain rates (1,000-2,000 /s) using a Kolsky (split-Hopkinson) type pressure bar apparatus. Samples of the single-crystal tungsten were also deformed at low strain rate (0.0001/s) using a conventional load frame. The 110 orientation exhibited constraint of flow consistent with twofold crystal symmetry about this axis, resulting in skewed flow and noncylindrical specimens after the Kolsky bar test. Both the 111 and 110 orientations exhibited a yield or load drop phenomenon. This load drop may have been associated with either: (1) lack of screw dislocation cross slip at high strain rate; (2) twinning of the crystal lattice; or (3) interstitial solute atoms such as nitrogen or carbon pinning dislocations. As a result of this load drop for the lower symmetry 111 and 110 orientations, the quasi-static (0.0001/s) test had higher flow stress for a given strain than the higher strain rate tests with the Kolsky bar. The 100 orientation crystals exhibited uniform deformation and high rate of work-hardening at both low and high strain rates. The unique behavior of these crystals is postulated in terms of the crystal symmetry, structural evolution at various strain rates, and dislocation flow mechanisms. DTIC

N95-28208# Oak Ridge National Lab., TN.
REACTOR PRESSURE VESSEL STRUCTURAL INTEGRITY RESEARCH
W. E. Pennell and W. R. Corwin 1994 17 p Presented at the 22nd Transactions of the Water Reactor Safety Information Meeting, Bethesda, MD, 24-26 Oct. 1994 Sponsored in part by Martin Marietta Energy Systems, Inc.
(Contracts DE-AC05-84OR-21400; NRC-1886-8011-9B; NRC-1886-8109-8L)
(DE95-007034; CONF-9410216-10) Avail: CASI HC A03/MF A01

Development continues on the technology used to assess the safety of irradiation-embrittled nuclear reactor pressure vessels (RPV's) containing flaws. Fracture mechanics tests on RPV steel, coupled with detailed elastic-plastic finite-element analyses of the crack-tip stress fields, have shown that (1) constraint relaxation at the crack tip of shallow surface flaws results in increased data scatter but no increase in the lower-bound fracture toughness; (2) the nil ductility temperature (NDT) performs better than the reference temperature for nil ductility transition (RT(sub NDT)) as a normalizing parameter for shallow-flaw fracture toughness data; (3) biaxial loading can reduce the shallow-flaw fracture toughness; (4) stress-based dual-parameter fracture toughness correlations cannot predict the effect of biaxial loading on shallow-flaw fracture toughness because in-plane stresses at the crack tip are not influenced by biaxial loading; and (5) an implicit strain-based dual-parameter fracture toughness correlation can predict the effect of biaxial loading on shallow-flaw fracture toughness. Experimental irradiation investigations have shown that (1) the irradiation-induced shift in Charpy V-notch vs temperature behavior may not be adequate to conservatively assess fracture toughness shifts due to embrittlement, and (2) the wide global variations of initial chemistry and fracture properties of a nominally uniform material within a pressure vessel may confound accurate integrity assessments that require baseline properties. DOE

N95-28250# International Centre for Theoretical Physics, Trieste (Italy).
ELECTRONIC STRUCTURE OF ORDERED AND DISORDERED TRANSITION METAL ALUMINIDES
I. Dasgupta, T. Saha, A. Mookerjee, and G. P. Das Aug. 1994 17 p
(DE95-609034; IC-94/241) Avail: CASI HC A03/MF A01 (US Sales Only)

We have studied the density of states of the series of alloys: FeAl, CoAl and NiAl both in the ordered and disordered states, using the Augmented Space Recursion technique with the Tight-Binding Muffin-tin Orbitals method. We have estimated the local moments in these alloys using the spin-polarized version of the TB-LMTO. DOE

N95-28332 Duke Univ., Durham, NC. Dept. of Chemistry.
ON THE SYNTHESIS OF MIXED-METAL AND MIXED-PNICOGEN13-15 RING-SYSTEMS
Richard L. Wells, Andrew T. McPhail, Peter S. White (North Carolina Univ., Chapel Hill, NC.), Michael S. Lube, and Leonidas J. Jones 7 Dec. 1994 7 p Submitted for publication Limited Reproducibility: More than 20% of this document may be affected by microfiche quality
(Contract N00014-89-J-1545; ONR Proj. 4135-008)
(AD-A288869; DU/DC/TR-45) Avail: Issuing Activity (Defense Technical Information Center (DTIC))

Several pathways toward the synthesis of mixed-metal and mixed-pnicogen 13-15 ring systems have been explored. Equilibration reactions have proven successful toward the preparation of the latter compounds while most attempts to prepare mixed-metal compounds have resulted in unexpected and novel 13-15 species. These reactions and their products are discussed. DTIC

N95-28534# Lawrence Livermore National Lab., Livermore, CA.
THE ELEVATED TEMPERATURE TENSILE PROPERTIES OF S-200E COMMERCIALLY PURE BERYLLIUM
G. A. Henshall, S. G. Torres, and J. E. Hanafee 1 Mar. 1995 23 p
(Contract W-7405-eng-48)
(DE95-009331; UCRL-ID-120258) Avail: CASI HC A03/MF A01

Experiments were performed at 300-100 C in longitudinal and transverse orientations at quasi-static strain rate 5.5 x 10(exp -4)/s. Results show that the stress-strain curve is smooth, without yield points or serrations. Yield stress and ultimate tensile stress decrease monotonically with temperature. Similar strengths were measured for both orientations. Failure elongation vs temperature is complex. DOE

N95-28543# Argonne National Lab., IL.
RESIDUAL STRESS, STRAIN, AND FAULTS IN NANOCRYSTALLINE PALLADIUM AND COPPER
P. G. Sanders (Northwestern Univ., Evanston, IL.), A. B. Witney (Northwestern Univ., Evanston, IL.), J. R. Weertman (Northwestern Univ., Evanston, IL.), R. Z. Valiev (Academy of Sciences, Ufa, Russia.), and R. W. Siegel Feb. 1995 9 p Presented at the 1994 Fall Meeting of the Materials Research Society, Boston, MA, 28 Nov. - 2 Dec. 1994 Sponsored in part by the Office of Naval Reseach and COBASE
(Contracts W-31-109-eng-38; DE-FG02-86ER-45229)
(DE95-008294; ANL/MSD/CP-83453; CONF-941144-83) Avail: CASI HC A02/MF A01

Nanocrystalline Pd and Cu, prepared by inert gas condensation and warm compaction, were studied using x-ray diffraction techniques. A sample of Cu with sub-micrometer grain size produced by severe plastic deformation was also examined. The Warren-Averbach technique was used to separate the line broadening due to grain size, root-mean-squared strain, and faults. Peak shifts and asymmetry were used to determine the long range surface stresses, stacking fault probability, and twin probability. The Young's modulus of a Pd sample was determined by an ultrasonic technique, and compared with the coarse-grained, fully-dense value. DOE

N95-28593# Sandia National Labs., Albuquerque, NM.
THE UNUSUAL PROPERTIES OF BERYLLIUM SURFACES
R. Stumpf (Tennessee Univ., Knoxville, TN.) and J. B. Hannon 1994 20 p Presented at the Workshop on Electronic Surfaces and Interface

States on Metallic Systems, Bad Honnef, Germany, 17-20 Oct. 1994
(Contract DE-AC04-94AL-85000)
(DE95-006471; SAND-94-3025C; CONF-9410293-1) Avail: CASI HC A03/MF A01

Be is a 'marginal metal'. The stable phase, hcp-Be, has a low Fermi-level density of states and very anisotropic structural and elastic properties, similar to a semiconductor's. At the Be(0001) surface, surface states drastically increase the Fermi-level density of states. The different nature of bonding in bulk-Be and at the Be(0001) surface explains the large outward relaxation. The presence of surface states causes large surface core-level shifts by inducing a higher electrostatic potential in the surface layers and by improving the screening at the surface. The authors experimental and theoretical investigations of atomic vibrations at the Be(0001) surface demonstrate clearly that Be screening of atomic motion by the surface states makes the surface phonon dispersion fundamentally different from that of the bulk. Properties of Be(0001) are so different from those of the bulk that the surface can be considered a new 'phase' of beryllium with unique electronic and structural characteristics. For comparison they also study Be(11'20), a very open surface without important surface states. Be(11'20) is the only clean s-p metal surface known to reconstruct (1 x 3 missing row reconstruction). DOE

N95-28644 Helsinki Univ. of Technology, Espoo (Finland).
HIGH TEMPERATURE OXIDATION OF NICKEL CONCENTRATES
P. Nurmi, A. Jokilaakso, and S. Stroemberg 1994 33 p Limited Reproducibility: More than 20% of this document may be affected by microfiche quality
(PB95-195566; TKK-V-B97) Avail: CASI HC A03

Only a limited number of studies have been published on the oxidation behavior of Ni-concentrate. In the report a brief literature review of both suspension and ignition temperature experiments is presented. In the experimental part of the study, the behavior of a nickel concentrate was investigated in a laminar flow furnace under simulated flash smelting conditions. Sulfur removal from the Ni-concentrate was found to accelerate with increasing gas preheating temperature and/or oxygen content of the reaction gas. Particle size had a noticeable effect on the sulfur removal only at low experimental temperatures and O2-contents. NTIS

N95-28660 Selskapet for Industriell og Teknisk Forskning, Trondheim (Norway).
FATIGUE PROPERTIES OF AN A356 (AlSi7Mg) ALUMINUM ALLOY FOR AUTOMOTIVE APPLICATIONS: FATIGUE LIFE PREDICTION
J. A. Oedegard and K. Pedersen 1994 10 p See also PB92-151299
(PB95-196424) Avail: Issuing Activity (National Technical Information Service (NTIS))

In the present paper a thorough study of the fatigue crack initiation mechanisms of a defect-free and a commercially cast A356 aluminum alloy are presented. Further, fatigue crack growth has been investigated in these materials. Finally an attempt to describe the fatigue behavior by using a fracture mechanic based fatigue life-time model have been accomplished. NTIS

N95-27113 Sandia National Labs., Albuquerque, NM.
CORROSIVE EFFECTS OF SUPERCRITICAL CARBON DIOXIDE AND COSOLVENTS ON METALS
E. M. Russick, G. A. Poulter, Carol L. J. Adkins, and N. R. Sorensen *In* Johns Hopkins Univ., Environmentally Benign Cleaning and Degreasing Technology: JANNAF Safety and Protection Subcommittee and Propellant Development and Characterization Subcommittee Joint Workshop Jun. 1994 p 125-135 See also N95-11360 (For primary document see N95-27101 09-27)
(Contract DE-ACO4-94AL-85000)
Avail: CPIA, 10630 Little Patuxent Pkwy., Suite 202, Columbia, MD 21044-3200 HC

27 NONMETALLIC MATERIALS

Includes physical, chemical, and mechanical properties of plastics, elastomers, lubricants, polymers, textiles, adhesives, and ceramic materials.

For composite materials see *24 Composite Materials.*

N95-26351 Pittsburgh Univ., Pittsburgh, PA. Dept. of Chemistry.
SURFACE CHEMISTRY OF SILICON
Hanne N. Waltenburg and John T. Yates, Jr 11 Nov. 1994 241 p Submitted for publication Sponsored by DanishResearch Academy, and Office of Naval Research Limited Reproducibility: More than 20% of this document may be affected by microfiche quality
(Contract N00014-91-J-1641)
(AD-A288893; TR-63) Avail: Issuing Activity (Defense Technical Information Center (DTIC))

The chemistry of silicon single crystal surfaces is reviewed along with the surface reconstruction processes which occur on clean silicon single crystal surfaces. Examples of surface reactivity with elements and compounds from each group of the periodic table are included. In addition, a table of current references to adsorption systems involving over 1000 recent papers is included, and this information is arranged for easy access. DTIC

N95-26448 National Physical Lab., Teddington (England). Div. of Materials Metrology.
CREEP RECOVERY OF PVC AND POLYPROPYLENE
B. E. Read and P. E. Tomlins Dec. 1994 33 p See also PB94-105079
(PB95-185112; NPL-DMM(A)-151) Copyright Avail: Issuing Activity (National Technical Information Service (NTIS))

Tensile creep and recovery data have been obtained for PVC and polypropylene at 23 C for different age states, creep durations and stress levels. The recovery behavior has been analyzed by a superposition procedure involving an extension to our model for nonlinear creep and different assumptions regarding possible variations in retardation time during the recovery. Accurate predictions have been made of the recovery following long-term, low-stress creep in polypropylene by allowing for the physical aging (increase in retardation time) which occurs during the creep. Attempts to predict the recovery after creep at elevated stresses have been partially successful, and suggest further studies of an apparent deaging at the unloading stage and subsequent reactivation of aging. NTIS

N95-26456 Colorado Univ., Boulder, CO. Dept. of Chemistry and Biochemistry.
SILOXANE-BASED FERROELECTRIC LIQUID CRYSTAL ELASTOMERS AND SELF-ASSEMBLED MONO- AND MULTILAYERS Final Report
David M. Walba and Noel A. Clark 23 Jun. 1994 3 p Limited Reproducibility: More than 20% of this document may be affected by microfiche quality
(Contract N00014-91-J-2005)
(AD-A288285; Rept-153-4147) Avail: Issuing Activity (Defense Technical Information Center (DTIC))

A convenient new method for synthesis of self-assembled monolayers on float glass substrates has been developed. This method allows the synthesis of SAM's composed of ferroelectric liquid crystal mesogens. Using the ferroelectric liquid crystal SAM's or simple alkane SAM's, a unique type of liqiud crystal alignment is demonstrated where the surface, which is smooth to a few angstroms by atomic force microscopy, provides a uniform tilt in the direction of rubbing when rubbed SAM's are used as substrates for the liquid crystal sample. DTIC

N95-26470 Colorado State Univ., Fort Collins, CO. Dept. of Chemistry.
HIGH PRESSURE CONDUCTIVITY STUDY OF TEMPLATE SYNTHESIZED POLYPYRROLE: OBSERVATION OF A CROSSOVER FROM THREE TO ONE DIMENSIONAL VARIABLE RANGE HOPPING Technical Interim Report
B. Lorenz, J. P. Spatz, H. D. Hochheimer, V. Menon, and R. Parthasarathy Nov. 1994 18 p Limited Reproducibility: More than 20% of this document may be affected by microfiche quality
(Contract N00014-82-K-0612)

(AD-A288367; TR-99) Avail: Issuing Activity (Defense Technical Information Center (DTIC))

We have studied thin films composed of thin and thick wall template synthesized polypyrrole microtubules. We observe a crossover from three to one dimensional variable range hopping in our samples at low temperatures. Our results clearly indicate that the geometry of the microtubules has an influence on the conductivity. The transition temperature from 3 to 1 dimensional variable range hopping shifts to lower temperatures when high pressure is applied. The results are discussed on the basis of the geometry of the microtubules. DTIC

N95-26472 Colorado State Univ., Fort Collins, CO. Dept. of Chemistry.
TEMPLATE SYNTHESIS OF ELECTRONICALLY CONDUCTIVE POLYMER NANOSTRUCTURES
Charles R. Martin Nov. 1994 39 p Limited Reproducibility: More than 20% of this document may be affected by microfiche quality
(Contract N00014-82-K-0612)
(AD-A288373; TR-98) Avail: Issuing Activity (Defense Technical Information Center (DTIC))

Nanochemistry is an emerging subdiscipline in the chemical and materials sciences that deals with the development of methods for synthesizing nanoscopic bits of a desired material and with chemical and other investigations of the nanomaterial obtained. My research group has been exploring a general method, called 'template-synthesis,' for preparing nanomaterials. This method entails synthesizing the desired material within the pores of a nanoporous membrane. The membranes employed have cylindrical pores of uniform diameter. In essence, we view each of these pores as a 'nanobeaker' in which a piece of the desired material is synthesized. We have used this method to prepare nanostructures composed of electronically conductive polymers, metals, semiconductors, and other materials. In this Accounts article, I discuss my work on template synthesis of electronically conductive polymer nanostructures. I will show that these conductive polymer nanostructures have interesting and unusual electronic properties and that these nanostructures provide an opportunity for exploring how molecular and supermolecular structure affect conductivity in conductive polymers. DTIC

N95-26482 Geo-Centers, Inc., Newton, MA.
SYNTHESIS AND CHARACTERIZATION OF POLYMERIC MATERIALS Final Annual Report No. 3, 28 Sep. 1990 - 15 Aug. 1994
J. Nagode, E. Greenwald, H. Hu, J. Prince, and J. Wegand 14 Oct. 1994 44 p Limited Reproducibility: More than 20% of this document may be affected by microfiche quality
(Contract N00014-90-C-2269)
(AD-A288613; GC-TR-94-2303) Avail: Issuing Activity (Defense Technical Information Center (DTIC))

Partial contents include the following: Evaluation of Sonar Dome Damage: Radiographic Inspection, Inspection Results, Improved Nondestructive Evaluation (NDE) Methods, X-ray Backscatter Tomography (XBT), Image Processing of Radiographic Data, and Database Management; SDRW/SRD Corrective Action Programs, Failure Analysis, Cord Load Measurements, SRD; Acoustic Deflection Project, New Materials/Design - Testing and Analysis, Polymer Synthesis and Evaluation; Fluorinated Polymers, L-Proline Modified Nylons, Elastomers and Blend Characterization, Conductive Polymers, and Phthalonitrile Resins. DTIC

N95-26499 Naval Research Lab., Washington, DC.
ADVANCED SOLID LUBRICANT FILMS BY ION-BEAM ASSISTED DEPOSITION
Irwin L. Singer, Robert N. Bolster, Larry E. Seitzman, Kathryn J. Wahl, Marshall B. Peterson (Wear Sciences, Inc., Arnold, MD.), and Robert L. Mowery 28 Nov. 1994 12 p Sponsored in part by ONR and SDIO Limited Reproducibility: More than 20% of this document may be affected by microfiche quality
(AD-A288866; NRL/MR/6170-94-7633) Avail: Issuing Activity (Defense Technical Information Center (DTIC))

NRL is developing advanced solid lubricating films for bearing assemblies. The films are deposited by ion-beam assisted deposition (IBAD) to thickness that can be controlled from 0.02 micrometers (1 micro inch) to greater than or equal to 1 micrometer (40 micro inches). Unlike evaporated or sputter-deposited films, IBAD films are dense and adhere well to virtually all solid surfaces. Durable films have been deposited on bearing steels, Ti alloys and many ceramic substrates, including Si3N4, alumina, SiC, TiN and CVD diamond. IBAD's multibeam capabilities have also been exploited to produce binary and ternary alloys over a wide range of stoichiometries. Studies of two solid lubricating films, MoS2 and ternary metal oxides, will be highlighted. IBAD MoS2 films exhibit reduced susceptibility to moisture degradation during storage. Alloyed MoS2 films show increased durability in sliding and rolling contact without sacrificing the ultra-low friction behavior of MoS2. For high temperatures, a class of binary metal oxide films are being investigated. Candidate lubricants have been chosen based on tribological behavior of oxide and predictions from thermodynamic phase diagrams. A recent study of the Cu-Mo-O system will be presented. DTIC

N95-26526 Department of the Navy, Washington, DC.
NON-COVALENT IMMOBILIZATION OF PROTEINS AND ENZYMES ON POLYMERIZED LIPID ASSEMBLIES Patent Application
Alok Singh, inventor (to Navy) 30 Mar. 1994 56 p Limited Reproducibility: More than 20% of this document may be affected by microfiche quality
(AD-A288234; US-Patent-Appl-SN-220124) Avail: Issuing Activity (Defense Technical Information Center (DTIC))

It is therefore an object of the present invention to form polymerizable metal chelating lipids that can be polymerized and interspersed into polymerizable non-chelating lipids to form lipid microstructures. It is therefore another object of the present invention to form lipid microstructures such as liposomes or bilayers from the polymerization of polymerizable metal chelating lipids and polymerizable non-chelating lipids. It is therefore yet another object of the present invention to form lipids capable of forming microstructures such as liposomes or bilayers, capable of non-covalently immobilizing proteins and enzymes and also capable of being polymerized so that the microstructures formed (e.g. liposomes or bilayers) do not break apart upon, for example, mild sonication or under working conditions, for example, of pH between about 2 to about 11 and temperature of between about 0 C to about 80 C. It is a further object of the present invention to form liposomes that are formed from polymerizable lipids and which lipids are interspersed with polymerizable metal chelating lipids capable of chelating with metal ions, which metal ions are further capable of chelating with proteins and/or enzymes in order to non-covalently immobilize the proteins and/or enzymes. DTIC

N95-26561 Southwest Research Inst., San Antonio, TX.
SCALE MODEL EXPERIMENTS WITH CERAMIC LAMINATE TARGETS Final Report, 25 Mar. 1992 - 1 Aug. 1994
Charles E. Anderson, Jr., Scott A. Mullin, Andrew J. Piekutowski (Dayton Univ. Research Inst., OH.), Neil W. Blaylock, and Kevin L. Poorman (Dayton Univ. Research Inst., OH.) Jun. 1994 41 p Limited Reproducibility: More than 20% of this document may be affected by microfiche quality
(Contracts DAAL03-91-C-0021; DE-AC04-90AI-58770)
(AD-A288322; ARO-29647.3-MS; SwRI-3593/004) Avail: Issuing Activity (Defense Technical Information Center (DTIC))

Ballistic impact experiments were performed on ceramic laminate targets at three scale sizes, nominally 1/3, 1/6, and 1/12, to quantify the effects of scale on various responses, in particular, the ballistics limit velocity. The experiments were carefully designed and controlled so that the different scale sizes were high fidelity replicas of each other. A variety of responses, such as residual projectile quantities, hole size, and the extent of bulging, were measured. Some of the measured quantities showed little or no dependence on scale size, whereas other quantities, particularly the ballistic limit velocity, were found to vary with scale size. The percentage difference was quantified, and the results extrapolated to estimate full scale response from the subscale tests. DTIC

N95-26599# Santo Tomas Univ. Hospital, Manila (Phillippines).
THE EFFECT OF PROTEINS ON THE AGING PROPERTIES OF RADIATION VULCANIZED NATURAL RUBBER LATEX Master's Thesis
Lucille V. Abad 18 Mar. 1993 172 p Sponsored by the Philippine Nuclear Research Inst.Philippines; and the Takasaki Radiation Chemistry Research Establishment of the Japan Atomic Energy Research Inst. Japan
(DE95-603357; INIS-MF-14365) Avail: CASI HC A08/MF A02 (US Sales Only)

The effect of natural rubber latex (NRL) proteins on the aging properties of NRL films was investigated. SDS-PAGE electrophoresis of the rubber proteins in NRL (Sri-Lanka) indicated a total of 18 proteins. A sharp decrease in tensile strength was observed after aging when NRL films were leached in 1% NH4OH. However, when these films were soaked in ethanol prior to leaching, the aging properties approximated those of the unleached samples. Electrophoretic analysis of the proteins present in the NH3 extracts of leached RVNRL films showed a high concentration of the protein herein. This protein was not found in the NH3 extracts of ethanol soaked films. NRL proteins were shown to decelerate the aging process of Radiation Vulcanized Natural Rubber Latex (RVNRL) films. Among the proteins, herein exhibited good anti-aging properties. The hydrolyzates from NR proteins also enhanced considerably the aging properties of RVNRL. DOE

N95-26623 Washington Univ., Seattle, WA. Dept. of Materials Science.
MATERIALS DESIGN AND PROCESSING BY BIOMIMICKING. SECTION 1: RESEARCH PROGRESS Final 3rd Year Report, 1 Jun. 1991 - 31 May 1994
Mehmet Sarikaya and James T. Staley 31 May 1994 89 p Limited Reproducibility: More than 20% of this document may be affected by microfiche quality
(Grant AF-AFOSR-0281-91)
(AD-A288229; AFOSR-94-0694TR) Avail: Issuing Activity (Defense Technical Information Center (DTIC))

The goal of this research has been to find dispersants for ceramic processing applications. The polyelectrolytes currently in use in the industry are synthesized from toxic precursors which present health hazards to workers. We have investigated polyelectrolytes produced from natural sources such as bacteria and kelp, as well as some polymers which have been produced synthetically. The polyelectrolytes which we have investigated include polysaccharides (alginate and dextran) and polypeptides (polyglutamic acid and polyaspartic acid). Some have been obtained from cultures of bacteria grown in our laboratories, others have been obtained from chemical supply houses. In addition, we have investigated the feasibility of using an in situ process by which we incubate the polymer-producing bacteria in the presence of ceramic powders. In this system, polymer adsorbs to the powder in a high affinity state, allowing subsequent washing to remove the bacterial cells, while retaining the adsorbed polymer. DTIC

N95-26624 Washington Univ., Seattle, WA.
DESIGN AND PROCESSING OF MATERIALS BY BIOMIMICKING. SECTION 2. PUBLICATIONS Final 3rd Year Report, Jun. 1991 - 31 May 1994
Mehmet Sarikaya and James T. Staley Sep. 1994 301 p Limited Reproducibility: More than 20% of this document may be affected by microfiche quality
(Grant AF-AFOSR-0281-91)
(AD-A288230; AFOSR-94-0694TR) Avail: Issuing Activity (Defense Technical Information Center (DTIC))

The goal of this research has been to find dispersants for ceramic processing applications. The polyelectrolytes currently in use in the industry are synthesized from toxic precursors which present health hazards to workers. We have investigated polyelectrolytes produced from natural sources such as bacteria and kelp, as well as some polymers which have been produced synthetically. The polyelectrolytes which we have investigated include polysaccharides (alginate and dextran) and polypeptides (polyglutamic acid and polyaspartic acid). Some have been obtained from cultures of bacteria grown in our laboratories, others have been obtained from chemical supply houses. In addition, we have investigated the feasibility of using an in situ process by which we incubate the polymer-producing bacteria in the presence of ceramic powders. In this system, polymer adsorbs to the powder in a high affinity state, allowing subsequest washing to remove the bacterial cells, while retaining the adsorbed polymer. DTIC

N95-26627 Illinois Univ., Urbana, IL. Dept. of Materials Science and Engineering.
MATERIALS WITH SELF ORGANIZED SURFACES: 2D POLYMER ASSEMBLIES Technical Report, 1 May 1993 - 30 Apr. 1994
Samuel I. Stupp, Vassou LeBonheur, and Kenneth A. Walker 1 Dec. 1994 4 p Presented at the American Chemical Society Meeting, Anaheim, CA, 2-7 Apr. 1995 Limited Reproducibility: More than 20% of this document may be affected by microfiche quality
(Contract N00014-93-1-0534)
(AD-A288928; TR-1) Avail: Issuing Activity (Defense Technical Information Center (DTIC))

Our laboratory has developed the concept of 'bulk' synthesized 2D polymers through self assembly of reactive oligomers into layered structures. The products from these supermolecular reaction schemes are high molar mass flat macromolecules which in fusible systems retain their shape during solid to liquid phase transitions. We describe here a new system based on nanophase separated rodcoils functionalized at one terminus with the objective of producing 2D polymers with two chemically different surfaces. One surface of the macromolecule contains closely packed methyl groups and it is therefore highly hydrophobic, whereas the other is hydrophilic being composed of phenolic or carboxyl functions. Interestingly, solvent cast 'macroscopic' films of the layered assemblies develop spontaneously one hydrophobic surface and a very sticky one which is readily wet by water. This of a bulk material with self organized surfaces, an important objective for the exploitation of self assembly in manufacturing. Such materials would open the door to concepts such as self organized interfaces for composite materials, self organized tapes and membranes with chemically defined surfaces, as well as tubes with chemically defined lumina. DTIC

N95-26637 Nuclear Energy Unit, Bangi (Malaysia).
RADIATION VULCANIZATION OF NATURAL RUBBER LATEX
Wan Manshol binWanZin and Norjanah bintiMohid 1994 25 p Presented at the National Seminar on the Assessment of IRPA Research Achievement in 5th Malaysian Plan: Industrial Sector, Kedah, Malaysia, 20-24 Dec. 1991 Limited Reproducibility: More than 20% of this document may be affected by poor print
(DE95-600026; INIS-MF-14332; CONF-9112185) Avail: Issuing Activity (Department of Energy (DOE)) (US Sales Only)

This paper describes the experimental techniques and the results of radiation vulcanization of natural rubber latex carried out on several high ammonia latices available in the country. The efficiency of various sensitizers and stabilizers used were evaluated in terms of the gamma radiation dose required to produce the maximum tensile strengths. The extent of crosslinking of RVNRL sample films were estimated by equilibrium swelling ratio measurements. The stability of pre-irradiated and post-irradiated samples were monitored using viscosity measurements as the parameter. DOE

N95-26744 National Physical Lab., Teddington (England).
RHEOLOGICAL MEASUREMENT METHODS FOR FIBRE FILLED PLASTICS
M. Rides Sep. 1994 34 p
(PB95-190088; NPL-DMM(A)-149) Copyright Avail: Issuing Activity (National Technical Information Service (NTIS))

A review is presented of various rheological measurement methods that are suitable for characterizing the flow behavior of fiber filled plastics. The advantages and disadvantages of the various methods are discussed. Variation in the fiber content of a material has the greatest effect on its extensional flow behavior rather than on its shear flow behavior. Methods for characterizing extensional flow behavior of fiber filled plastics are also examined. Applications for rheological data include the simulation of injection and compression molding, resin transfer molding and for cure monitoring. NTIS

N95-26745 National Physical Lab., Teddington (England). Div. of Materials Metrology.
STABILITY OF REFERENCE MASSES 4: GROWTH OF CARBONACEOUS CONTAMINATION ON PLATINUM-IRIDIUM MASS STANDARD SURFACES, AND ITS CLEANING BY UV/OZONE TREATMENT
P. J. Cumpson and M. P. Seah Sep. 1994 82 p
(PB95-190096; NPL-DMM(A)126) Copyright Avail: Issuing Activity (National Technical Information Service (NTIS))

The SI unit of mass is the kilogram, defined as the mass of the 'international prototype', a cylinder of platinum-10% iridium alloy kept at the Bureau International des Poids et Mesures (BIPM) at Sevres, near Paris. This is the only remaining SI unit to be defined in terms of a physical artifact. Comparisons of mass can now be performed with great precision, but the accuracy with which the SI kilogram can be disseminated is limited by the stability of the artifacts themselves. Three main types of contamination are thought to occur at the surface; sorption of water vapor, carbonaceous contamination, and mercury. In this work we examine the contribution of the carbonaceous contamination, and how it can be reproducibly removed. We propose that the carbonaceous contamination consists of two distinct components, one from adsorbed hydrocarbons from the atmosphere, which form an adsorbed layer in dynamic equilibrium with the environment, and a more strongly bonded, cross-linked layer, similar to the dehydrogenated layers often observed on industrial platinum catalysts. This second form of carbonaceous contamination is more important because it grows monotonically and is typically in the range of tens of micrograms for a prototype in service; the latter part of the present work deals with the removal of carbonaceous contamination using UV radiation and ozone. NTIS

N95-26746 National Physical Lab., Teddington (England).
SURVEY OF SUB-MICROMETRE POWDER SIZE MEASUREMENT FOR CERAMIC AND CERMET POWDERS
M. Stewart Oct. 1994 10 p
(PB95-190104; NPL-DMM(A)-152) Copyright Avail: Issuing Activity (National Technical Information Service (NTIS))

This report is the result of a survey carried out to discover the measurement needs for submicrometer sizing in the ceramic and cermet industry. NTIS

N95-26747 National Physical Lab., Teddington (England).
OVERVIEW OF THROUGH-THICKNESS TEST METHODS FOR POLYMER MATRIX COMPOSITES
W. R. Broughton and G. D. Sims Oct. 1994 57 p
(PB95-190112; NPL-DMM(A)-148) Copyright Avail: Issuing Activity (National Technical Information Service (NTIS))

One of the initial objectives of the project is to evaluate critically the test methods available for the determination of all the out-of-plane or through-thickness (T-T) tensile, compressive and shear properties. A decision analysis technique was applied to quantitatively evaluate each method in terms of 14 criteria, encompassing a number of key issues. These included data producibility, cost of fabrication, cost of testing, availability of a standard test method, ease of data reduction and accuracy of test data. The relative importance of the criteria was based on an assessment by industry. NTIS

N95-26897 Air Force Inst. of Tech., Wright-Patterson AFB, OH. School of Engineering.
DESIGN, FABRICATION, MODELING, AND OPTICAL CHARACTERIZATION OF ORGANIC POLYMER NONLINEAR DIRECTIONAL COUPLERS M.S. Thesis
John N. Berry Dec. 1994 136 p Limited Reproducibility: More than 20% of this document may be affected by microfiche quality
(AD-A289327; AFIT/GEO/ENP/94D-01) Avail: Issuing Activity (Defense Technical Information Center (DTIC))

This research was an investigation into the suitability of a recently developed polymer, polyphenylene, as a material for integrated optical circuits (IOC's). Polymers show great promise in the area of IOC's because of material processing advantages, compatibility with most existing integrated circuit technology, and relatively strong nonlinear optical characteristics. This thesis contains an overview of: dielectric waveguides, linear and nonlinear directional coupler theory; various models useful in the design and analysis of optical waveguides; the fabrication of three different waveguide designs; the experimental apparatus and procedure used to optically characterize the waveguides; and the experimental results of the characterization. Waveguiding of near infrared light through polyphenylene, in both a slab waveguide and strip-loaded guides, was observed for the first time in this polymer. Coupling of light between guides of a multi-channel directional coupler was also observed. No definitive conclusions concerning nonlinear effects are possible due to the non-identical, multi-channel nature of the fabricated waveguides. The results of this research indicate that polyphenylene is a candidate for use in IOC's and that the polymer should be the topic of further research. DTIC

N95-26973 Colorado Univ., Boulder, CO. Dept. of Electrical and Computer Engineering.
CHARACTERIZATION OF OPTICAL POLYMERS FOR MULTI-LAYERED ELECTRO-OPTIC DEVICES Ph.D. Thesis
Lori E. Rohlev Oct. 1994 166 p Limited Reproducibility: More than 20% of this document may be affected by microfiche quality
(Contract N00014-92-J-1190)
(AD-A289255; ECE/GWOL/60) Avail: Issuing Activity (Defense Technical Information Center (DTIC))

Nonlinear optical (NLO) polymers could potentially replace standard inorganic electrooptic materials, such as LiNbO3 and GaAs, in integrated optoelectronic devices and systems. The large electrooptic coefficients and the low dielectric constants of poled polymers make them ideal for high-speed electrooptic applications. Electrooptic devices can be easily fabricated by spin coating the polymer onto a substrate, forming optical channels by bleaching and making material electrooptic by poling the channels. This simple fabrication procedure makes polymers ideal for multilayered applications. As new materials are developed and used in new configurations and applications, they must be characterized for optimum device design and performance. DTIC

N95-27101 Johns Hopkins Univ., Columbia, MD. Chemical Propulsion Information Agency.
ENVIRONMENTALLY BENIGN CLEANING AND DEGREASING TECHNOLOGY: JANNAF SAFETY AND PROTECTION SUBCOMMITTEE AND PROPELLANT DEVELOPMENT AND CHARACTERIZATION SUBCOMMITTEE JOINT WORKSHOP
Lori A. Pickett, ed. Jun. 1994 272 p Workshop held at Naval Surface Warfare Center, Indian Head, MD, 14-15 Jun. 1994
(Contract N00014-91-C-0001)
(CPIA-Publ-611) Avail: CPIA, 10630 Little Patuxent Pkwy., Suite 202, Columbia, MD 21044-3200 HC

This document contains the proceedings of a workshop entitled 'Environmentally Benign Cleaning and Degreasing Technology', sponsored by the Joint Army-Navy-NASA-Air Force (JANNAF) Safety & Environmental Protection Subcommittee (S&EPS) and the Propellant Development & Characterization Subcommittee (PDCS) on June 14-15, 1994, at the Naval Surface Warfare Center, Indian Head, MD. Mr. George Nauflett and Mr. John Dow, Naval Surface Warfare Center, Indian Head, MD, served as the workshop chairmen. These proceedings are a compilation of papers and viewgraphs presented at the workshop. For individual titles, see N95-27102 through N95-27130.

N95-27102 American Univ., Washington, DC.
JUNKYARD CHEMISTRY **c45**
Paul F. Waters *In* Johns Hopkins Univ., Environmentally Benign Cleaning and Degreasing Technology: JANNAF Safety and Protection Subcommittee and Propellant Development and Characterization Subcommittee Joint Workshop Jun. 1994 p 1-8 (For primary document see N95-27101 09-27)
Avail: CPIA, 10630 Littlo Patuxent Pkwy., Suite 202, Columbia, MD 21044-3200 HC

The technologies that are available for confronting the environmental problems inherent in waste disposal, transport, industrial and agricultural waste spilloffs, radioactive waste production and disposal, sewage sludge disposal, and toxic waste disposal violations are addressed in this document. These technologies are available now or can feasibly be developed through the use of already established scientific approaches. Several of the problems addressed are categorized and addressed and two areas of technological solutions to the related problems, viscoelasticity and reduction pyrolysis, are discussed. CASI

N95-27103 Litton Industries, Blacksburg, VA.
THE EVALUATION OF A FLUOROCHEMICAL DRYING PROCESS FOR AN ELECTRICAL CONTACT **c35**
Charles William Reed *In* Johns Hopkins Univ., Environmentally Benign Cleaning and Degreasing Technology: JANNAF Safety and Protection Subcommittee and Propellant Development and Characterization Subcommittee Joint Workshop Jun. 1994 p 9-16 (For primary document see N95-27101 09-27)
Avail: CPIA, 10630 Little Patuxent Pkwy., Suite 202, Columbia, MD 21044-3200 HC

Litton Poly-Scientific Security Products manufactures a 'shocking' sensor used to detect intrusion. The sensor functions as a make/break contact assembly with the movable contact being a gold plated brass disk (or 'slug'). Debris, drying stains, and other soils or contaminants able to interrupt the current flow through the contact assembly can create a false alarm. Therefore, a very high level of contact cleanliness is required. The drying process following electroplating was a six step process using CFC-113. A two step process using a perfluorocarbon was evaluated. Using ESCA, the new process was determined to be at least as good as the old six step process using CFC-113. Author

N95-27104 Martin Marietta Corp., Denver, CO. Astronautics Group.
CLEANLINESS VERIFICATION PROCESS AT MARTIN MARIETTA ASTRONAUTICS **c18**
Elizabeth A. King and Thomas J. Giordano *In* Johns Hopkins Univ., Environmentally Benign Cleaning and Degreasing Technology: JANNAF Safety and Protection Subcommittee and Propellant Development and Characterization Subcommittee Joint Workshop Jun. 1994 p 17-26 (For primary document see N95-27101 09-27)
(Contract F04701-85-C-0019)
Avail: CPIA, 10630 Little Patuxent Pkwy., Suite 202, Columbia, MD 21044-3200 HC

The Montreal Protocol and the 1990 Clean Air Act Amendments mandate CFC-113, other chlorinated fluorocarbons (CFC's) and 1,1,1-Trichloroethane (TCA) be banned from production after December 31, 1995. In response to increasing pressures, the Air Force has formulated policy that prohibits purchase of these solvents for Air Force use after April 1, 1994. In response to the Air Force policy, Martin Marietta Astronautics is in the process of eliminating all CFC's and TCA from use at the Engineering Propulsion Laboratory (EPL), located on Air Force property PJKS. Gross and precision cleaning operations are currently performed on spacecraft components at EPL. The final step of the operation is a rinse with a solvent, typically CFC-113. This solvent is then analyzed for nonvolatile residue (NVR), particle count and total filterable solids (TFS) to determine cleanliness of the parts. The CFC-113 used in this process must be replaced in response to the above policies. Martin Marietta Astronautics, under contract to the Air Force, is currently evaluating and testing alternatives for a cleanliness verification solvent. Completion of test is scheduled for May, 1994. Evaluation of the alternative solvents follows a three step approach. This first is initial testing of solvents picked from literature searches and analysis. The second step is detailed testing of the top candidates from the initial test phase. The final step is implementation and validation of the chosen alternative(s). Testing will include contaminant removal, nonvolatile residue, material compatibility and propellant compatibility. Typical materials and contaminants will be tested with a wide range of solvents. Final results of the three steps will be presented as well as the implementation plan for solvent replacement. Author

N95-27105 Litton Industries, Blacksburg, VA.
A SUMMARY OF ODS REPLACEMENT TECHNOLOGIES AT LITTON POLY-SCIENTIFIC
Charles William Reed *In* Johns Hopkins Univ., Environmentally Benign Cleaning and Degreasing Technology: JANNAF Safety and Protection Subcommittee and Propellant Development and Characterization Subcommittee Joint Workshop Jun. 1994 p 27-31 (For primary document see N95-27101 09-27)
Avail: CPIA, 10630 Little Patuxent Pkwy., Suite 202, Columbia, MD 21044-3200 HC

Litton Poly-Scientific (LPS) has successfully determined CFC-113 and 1,1,1-trichloroethane replacement technologies for all its processes. More than 45,000 Kg/year (100,000 lbs/year) of each of these ozone depleting chemicals was being used in 1989. Replacement technologies include aqueous cleaning, organic solvents, solvent/surfactant systems, and perfluorocarbons. The ODS elimination has been realized with a significant net savings on yearly solvent expenditures. An active team involvement has been critical to the success of the endeavor. Technologies which were evaluated, but not used for various reasons, include the following: CO2 snow, supercritical CO2 extraction, perfluorocarbon drying, semi-aqueous cleaning (citrus based terpenes), volatile siloxanes, NMP, and hydrocarbon blends. Not all the replacement processes are optimized, however. In addition, new technologies are continuing to be evaluated as replacements for those presently being used. Most promising, at present, is solvent cleaning using ethyl lactate. Author

N95-27106 Virginia Polytechnic Inst. and State Univ., Blacksburg, VA. Dept. of Chemistry.
OBSERVATIONS ON THE SOLVATING POWER OF SUPERCRITICAL FLUIDS
Larry T. Taylor *In* Johns Hopkins Univ., Environmentally Benign Cleaning and Degreasing Technology: JANNAF Safety and Protection Subcommittee and Propellant Development and Characterization Subcommittee Joint Workshop Jun. 1994 p 33-52 (For primary document see N95-27101 09-27)
Avail: CPIA, 10630 Little Patuxent Pkwy., Suite 202, Columbia, MD 21044-3200 HC

The solvating power of supercritical fluids and their potential for use in cleaning applications are reviewed. Solubility data for numerous compounds are presented. The implications of using polar liquids to modify the solvating power of CO2 are discussed. Enhanced solvating power can be achieved for most analytes when a modifier of similar polarity is employed. Author

N95-27107 Ogden Air Logistics Center, Hill AFB, UT.
WIPE SOLVENT SUBSTITUTIONS FOR 1,1,1-TRICHLOROETHANE (TCA) AND METHYL ETHYL KETONE (MEK) AT HILL AIR FORCE BASE
S. Barney, J. Vidic, D. Frederick, S. Rasmussen, J. Jusko, and S. Edwards *In* Johns Hopkins Univ., Environmentally Benign Cleaning and Degreasing Technology: JANNAF Safety and Protection Subcommittee and Propellant Development and Characterization Subcommittee Joint Workshop Jun. 1994 p 53-59 (For primary document see N95-27101 09-27)
Avail: CPIA, 10630 Little Patuxent Pkwy., Suite 202, Columbia, MD 21044-3200 HC

The purpose of this paper is to present the challenges faced by Hill Air Force Base in meeting the obligations in the Montreal Protocol and the Clean Air Act. Focus is on selecting substitute cleaners for the hand-wipe cleaning processes which use TCA and MEK. Candidate cleaners were subjected to laboratory testing to determine cleanability, corrosion potential, polysulfide sealant compatibility, evaporation rate, and effect on polyimide wiring. The top-ranking cleaners were categorized by their characteristic material properties. A low vapor pressure solvent blend (LVSB), an aliphatic hydrocarbon and an aqueous cleaner were selected to replace TCA and MEK in hand-wipe applications. Existing processes were modified and pilot testing was performed. The objectionable odor of the LVSB and the poor cleaning efficiency of the aqueous cleaner has limited implementation. The aliphatic hydrocarbon, on the other hand, has been well received and is currently being implemented. Methods of decreasing the solvent dry time and minimizing vapor emissions are in place. Surface analysis techniques will be used the future to determine the non-volatile residue and corrosion products left from the replacement cleaners. Author

N95-27108 Martin Marietta Corp., Denver, CO.
ALTERNATIVE CLEANING SOLVENTS AND LUBRICANTS AT THE AIR FORCE PJKS FACILITY
S. P. Prince, B. L. Worthington, M. W. Ireland, and William E. McGuire *In* Johns Hopkins Univ., Environmentally Benign Cleaning and Degreasing Technology: JANNAF Safety and Protection Subcommittee and Propellant Development and Characterization Subcommittee Joint Workshop Jun. 1994 p 61-72 (For primary document see N95-27101 09-27)
(Contract F04701-85-C-0019)
Avail: CPIA, 10630 Little Patuxent Pkwy., Suite 202, Columbia, MD 21044-3200 HC

In accordance with required eliminations of chlorofluorocarbon 113 (CFC-113) and 1,1,1- trichloroethane (TCA), Martin Marietta has evaluated non-ozone depleting chemicals for implementation at the Air Force PJKS facility. These replacements are intended for all operations in which CFC-113 and TCA were previously used, and are targeted at mechanical cleaning operations, electrical cleaning operations, and the replacement of an anti-seize lubricant. Selection criteria for mechanical cleaners include the cleaning power of the solvent, the compatibility with materials being cleaned, the cleaning ability after loading with dissolved contaminants, the toxicity and relative safety of using the cleaner, and the waste disposal requirements. In addition, because the PJKS facility conducts tests on propulsion systems for missiles and satellites, the cleaner must be compatible with liquid rocket propellants (Aerozine-50 fuel and nitrogen tetroxide oxidizer). Electrical processes involved the cleaning of rotary contacts used in amplifier modules. Replacement of an anti-seize compound used to lubricate bolt threads was also required. This material is used as a shop aid in protecting threaded fasteners from exposure to high stress, high temperature, or corrosive atmospheres. After conducting screening, demonstration, and validation tests, replacement candidates for these materials were selected. These candidates met or exceeded all technical requirements identified for their intended applications. Author

N95-27109 Cold Jet, Inc., Loveland, OH.

CO2 PELLET BLAST CLEANING AND DEGREASING: THE TRUE ENVIRONMENTALLY BENIGN TECHNOLOGY

Michael W. Lewis *In* Johns Hopkins Univ., Environmentally Benign Cleaning and Degreasing Technology: JANNAF Safety and Protection Subcommittee and Propellant Development and Characterization Subcommitee Joint Workshop Jun. 1994 p 79-94 (For primary document see N95-27101 09-27)

Avail: CPIA, 10630 Little Patuxent Pkwy., Suite 202, Columbia, MD 21044-3200 HC

Frozen carbon dioxide (CO2) or dry-ice blast cleaning and degreasing technology utilizes a naturally occurring gas that's converted to a solid and is used as a projectile cleaning medium. The liquid CO2 used in this process is a recycled waste product from multiple industrial processes and therefore has no net effect on CO2 gas emissions. This process can be somewhat compared to grit blasting. However, dry-ice blasting leaves absolutely no residue and doesn't generate any waste whatsoever because it sublimates (reverts directly back to a gas) instantly upon impacting the object or surface being cleaned because dry-ice has no molecular density. This allows the process to clean machined surfaces without abrasion. The process also works well on non-metallic surfaces as long as well defined operating parameters are closely followed. What's left over is a surface cleanliness that cannot be attained by virtually any other single step cleaning process. Even Methylethylketone (MEK) surface preparation processes cannot duplicate this level of cleanliness according to Optically stimulated Electron Emission (OSEE) tests conducted in Europe. Derived from text

N95-27110 Sandia National Labs., Albuquerque, NM.

THE USE OF SUPERCRITICAL CARBON DIOXIDE FOR CONTAMINANT REMOVAL FROM SOLID WASTE **c45**

Carol L. J. Adkins, Edward M. Russick, H. Mike Smith (Allied-Signal Corp., Kansas City, MO.), and Ron B. Olson (Allied-Signal Corp., Kansas City, MO.) *In* Johns Hopkins Univ., Environmentally Benign Cleaning and Degreasing Technology: JANNAF Safety and Protection Subcommittee and Propellant Development and Characterization Subcommittee Joint Workshop Jun. 1994 p 95-103 (For primary document see N95-27101 09-27)

(Contracts DE-AC04-76DP-00613; DE-AC04-94AL-85000)

Avail: CPIA, 10630 Little Patuxent Pkwy., Suite 202, Columbia, MD 21044-3200 HC

Supercritical carbon dioxide is being explored as a waste minimization technique for separating oils, greases and solvents from solid waste. The contaminants are dissolved into the supercritical fluid and precipitated out upon depressurization. The carbon dioxide solvent can then be recycled for continued use. Definitions of the temperature, pressure, flowrate and potential co-solvents are required to establish the optimum conditions for hazardous contaminant removal. Excellent extractive capability for common manufacturing oils, greases, and solvents has been observed in both supercritical and liquid carbon dioxide. Solubility measurements are being used to better understand the extraction process, and to determine if the minimum solubility required by federal regulations is met. Author

N95-27111 Phasex Corp., Lawrence, MA.

PRECISION PARTS CLEANING WITH SUPERCRITICAL CO2: PRACTICAL APPLICATIONS AND SOLUTIONS

Paula Gallagher-Wetmore, E. Moy, and V. Krukonis *In* Johns Hopkins Univ., Environmentally Benign Cleaning and Degreasing Technology: JANNAF Safety and Protection Subcommittee and Propellant Development and Characterization Subcommittee Joint Workshop Jun. 1994 p 105-114 (For primary document see N95-27101 09-27)

(Contract F04704-92-C-0017)

Avail: CPIA, 10630 Little Patuxent Pkwy., Suite 202, Columbia, MD 21044-3200 HC

Supercritical fluids (SCF's) have long been known to display interesting dissolving capabilities. But the ramifications of utilizing SCF's as processing tools was not fully realized until 1955 when Todd and Elgin first suggested their use as extractive solvents. Over the past two decades supercritical fluids have been utilized as solvents for carrying out separations of materials in such diverse areas as foods, polymers, pharmaceuticals, petrochemicals and specialty chemicals, natural products, and explosives. More recently they have been used for non-extractive applications, such as recrystallization, deposition, reactions, and surface modification. The ability to tailor the solubility characteristics of supercritical fluids to suit a particular application forms the basis for processing with these unique solvents. Proper manipulation of operating temperature and pressure can result in selective extraction of a component from a mixture. As industrial and consumer awareness regarding the environmental and health hazards of traditional solvent use increases, it is anticipated that the utilization and acceptance of supercritical fluids as alternative solvents will become widespread. Derived from text

N95-27112 Research Triangle Inst., Research Triangle Park, NC.

ETHYL LACTATE AS A SOLVENT ALTERNATIVE FOR CLEANING METAL PARTS

Elizabeth A. Hill and K. David Carter, Jr. *In* Johns Hopkins Univ., Environmentally Benign Cleaning and Degreasing Technology: JANNAF Safety and Protection Subcommittee and Propellant Development and Characterization Subcommittee Joint Workshop Jun. 1994 p 115-123 Sponsored by PURAC America, Inc. (For primary document see N95-27101 09-27)

Avail: CPIA, 10630 Little Patuxent Pkwy., Suite 202, Columbia, MD 21044-3200 HC

Cleaning tests and solvent analyses were performed with ethyl lactate to determine its effectiveness for cleaning metal parts. Nine contaminants were removed from stainless steel substrates using the solvent and ultrasonic agitation. The cleaning efficiencies were calculated from gravimetric measurements obtained with an electronic microbalance. All nine contaminants were removed with efficiencies better than 99.94%, using only ethyl lactate cleaning and rinsing. Further testing on two contaminants with Electron Scanning for Chemical Analysis (ESCA) showed that less than a monolayer of contaminant remained on the surfaces after the cleaning steps. The nonvolatile residue and metal ion content were also measured and determined to be acceptable for most precision metal cleaning applications. Preliminary compatibility tests were run on three metal alloys. Author

N95-27113 Sandia National Labs., Albuquerque, NM.

CORROSIVE EFFECTS OF SUPERCRITICAL CARBON DIOXIDE AND COSOLVENTS ON METALS **c26**

E. M. Russick, G. A. Poulter, Carol L. J. Adkins, and N. R. Sorensen *In* Johns Hopkins Univ., Environmentally Benign Cleaning and Degreasing Technology: JANNAF Safety and Protection Subcommittee and Propellant Development and Characterization Subcommittee Joint Workshop Jun. 1994 p 125-135 See also N95-11360 (For primary document see N95-27101 09-27)

(Contract DE-ACO4-94AL-85000)

Avail: CPIA, 10630 Little Patuxent Pkwy., Suite 202, Columbia, MD 21044-3200 HC

With the eventual phase-out of chlorofluorocarbons, and restrictive regulations concerning the use of cleaning solvents such as hydrochlorofluorocarbons, and other volatile organic compounds, it is essential to seek new, environmentally acceptable cleaning processes. In the DOE Complex and in industry, an environmentally sound process for precision cleaning of machined metal parts is one of the issues that needs to be addressed. At Sandia, we are investigating the use of supercritical carbon dioxide (CO2) as an alternative cleaning solvent for this application. Carbon dioxide is nontoxic, recyclable, and relatively inexpensive. Supercritical CO2 has been demonstrated as a solvent for many nonpolar organic compounds, including hydrocarbon-based machining and lubricating oils. The focus of this work is to investigate any corrosive effects of supercritical CO2 cleaning on metals. Sample coupons of several common metals were statically exposed to pure supercritical CO2, water saturated supercritical CO2, and 10% wt. methanol/CO2 cosolvent at 24,138 kPa (3500 psi) and 323 K (50 C) for 24 hours. Gravimetric analysis and magnified visual inspection of the coupons were performed before and after the exposure tests. Electron microprobe, x-ray photoelectron spectroscopy (XPS), and Auger electron surface analyses were done as needed where visual and gravimetric changes in the samples were evident. The results of these experiments will be reported. Author

N95-27114 CF Technologies, Inc., Boston, MA.

PRECISION PARTS CLEANING WITH SUPERCRITICAL CARBON DIOXIDE

William E. McGovern, J. M. Moses, and D. C. Weber *In* Johns Hopkins

Univ., Environmentally Benign Cleaning and Degreasing Technology: JANNAF Safety and Protection Subcommittee and Propellant Development and Characterization Subcommittee Joint Workshop Jun. 1994 p 137-142 (For primary document see N95-27101 09-27)
Avail: CPIA, 10630 Little Patuxent Pkwy., Suite 202, Columbia, MD 21044-3200 HC

Chlorofluorocarbon (CFC) solvents have been used effectively for parts cleaning within a number of diverse industries, including the electronics, aerospace, metal finishing, and medical industries. The phaseout of CFC production has resulted in the evaluation of supercritical carbon dioxide (CO2) as an environmentally acceptable, cost effective replacement solvent for a number of these parts cleaning applications. In addition to being non-toxic, non-flammable and non-hazardous, CO2 has a near ambient critical temperature of 31 C and a moderate critical pressure of 1070 psi. Solvent properties, such as density and viscosity, can be adjusted by relatively small changes in temperature and pressure, allowing CO2 to dissolve a wide range of organic compounds. This paper will report on the projected use of supercritical CO2 as a replacement solvent for military and industrial cleaning operations; the technical barriers to integration into the workplace; specific applications for CO2-based cleaning systems, and commercial manufacturing activity at CF TECH. Author

N95-27115 Polymer Solutions, Inc., Blacksburg, VA.
EVALUATIONS OF THE EFFECTIVENESS OF ENVIRONMENTALLY BENIGN CLEANING METHODOLOGIES **c38**
James D. Rancourt *In* Johns Hopkins Univ., Environmentally Benign Cleaning and Degreasing Technology: JANNAF Safety and Protection Subcommittee and Propellant Development and Characterization Subcommittee Joint Workshop Jun. 1994 p 143-145 (For primary document see N95-27101 09-27)
Avail: CPIA, 10630 Little Patuxent Pkwy., Suite 202, Columbia, MD 21044-3200 HC

Due to environmental concerns many very effective cleaning methodologies and materials must be replaced. Systems were developed in the past for which the performance had been verified. Now, old but environmentally benign cleaning methodologies, and new cleaning systems are being applied. It is necessary that the performance of these systems be documented. Analytical methods that can be used for materials inspection and quality assurance purposes will be presented. Author

N95-27116 Naval Command, Control and Ocean Surveillance Center, San Diego, CA. Remediation Research Lab.
THE BIODEGRADATION OF FUELS IN SOILS AND SEDIMENTS: DIFFERENCES AS A FUNCTION OF MINERALOGY **c45**
Sabine E. Apitz and Kathleen J. Meyers-Schulte (Computer Sciences Corp., San Diego, CA.) *In* Johns Hopkins Univ., Environmentally Benign Cleaning and Degreasing Technology: JANNAF Safety and Protection Subcommittee and Propellant Development and Characterization Subcommittee Joint Workshop Jun. 1994 p 155-163 Sponsored by Office of Naval Technology, SERDP, DERA, and the Aircraft Environmental Support Office (For primary document see N95-27101 09-27)
Avail: CPIA, 10630 Little Patuxent Pkwy., Suite 202, Columbia, MD 21044-3200 HC

Experiments were carried out to determine the effects of substrate mineralogy on the biodegradability of fuel components. Samples of quartz sand (Fischer Sea Sand) and illite clay (API#35) were spiked with DFM (diesel fuel marine), aged, slurried and inoculated with DFM-acclimated soil microorganisms. Then, the concentrations of fuel components were monitored over time. While there was clear chromatographic and biomarker evidence of TPH (total petroleum hydrocarbon) biodegradation on the sands, illite samples showed no evidence of biogenic loss of aliphatic components. PAHs (polycyclic aromatic hydrocarbons) on the other hand, degraded equally well on both substrates, and in both cases, degraded to a much greater extent than did TPH. Author

N95-27117 Envirogen, Inc., Lawrenceville, NJ.
BIOREMEDIATION OF CHLORINATED ORGANICS: PCBs, TCE, HCFCs **c23**
Ronald Unterman *In* Johns Hopkins Univ., Environmentally Benign Cleaning and Degreasing Technology: JANNAF Safety and Protection Subcommittee and Propellant Development and Characterization Subcommittee Joint Workshop Jun. 1994 p 165-167 (For primary document see N95-27101 09-27)
Avail: CPIA, 10630 Little Patuxent Pkwy., Suite 202, Columbia, MD 21044-3200 HC

Halogenated organic compounds have been widely used industrially because of their combination of chemical properties and thermal stability. For example: the use of PCB's as a fire retardent fluid in heat exchangers, electrical equipment, and high temperature hydraulic fluids; TCE and other chlorinated solvents as nonflammable industrial solvents; and CFC's as nonreactive refrigerants and degreasing agents. However, the same chemical properties that confer upon these compounds their thermal and chemical stability, also confer upon them a general recalcitrance for biodegradation. Although these chemicals have been shown to be biochemically stable, research has shown that PCB's, TCE, and HCFC's are biodegradable, this work having been performed over the past twenty, ten, and two years, respectively. Different areas of bioremediation technologies and applications are addressed in this document. Derived from text

N95-27118 SPB Technologies, Inc., Gulf Breeze, FL.
COMBINED USE OF GROUND WATER CIRCULATION (UVB) TECHNOLOGY AND IN SITU BIOREACTORS FOR ENHANCED BIOREMEDIATION OF SUBSURFACE CONTAMINATION **c45**
Jim G. Muller and E. J. Klingel (IEG Technologies, Inc., Gulf Breeze, FL.) *In* Johns Hopkins Univ., Environmentally Benign Cleaning and Degreasing Technology: JANNAF Safety and Protection Subcommittee and Propellant Development and Characterization Subcommittee Joint Workshop Jun. 1994 p 169-174 (For primary document see N95-27101 09-27)
Avail: CPIA, 10630 Little Patuxent Pkwy., Suite 202, Columbia, MD 21044-3200 HC

Contamination of soil and ground water by trichloroethylene (TCE), a conventional degreasing agent, is recognized by the U.S. EPA as one of the more critical environmental problems facing the Nation today. Thus, from an end-user's perspective, conventional remedial technologies (such as pump-and-treat) are often unacceptable from a regulatory perspective, prohibitively expensive to implement, and technically inadequate. In an effort to overcome several factors known to limit the biodegradation of TCE (trichloroethylene) in the subsurface, we are focusing on the development of combined ground water circulation and contaminant vaporization technology coupled with an immobilized-cell bioreactor. The ground water circulation system is based on patented Vacuum-Vaporized Well (German: Unterdruck-Verdampfer-Brunnen; abbreviation UVB) technology (U.S. Patents 4,892,688; 4,943,305; 5,143,607; 5,095,975; 5,143,606; 5,171,103) for in situ treatment of the capillary fringe, phreatic and vadose zones contaminated with volatile organic compounds (VOCs), including NAPLs. The UVB system represents a promising technology for simultaneous in situ remediation of contaiminated soil and ground water, especially those contaminated with volatile and semi-volatile organics. Derived from text

N95-27119 UMBI, Baltimore, MD.
MICROBIAL TREATMENT FOR SHIPBOARD COLLECTION, HOLD ING, AND TRANSFER SYSTEM TANKS **c23**
William R. Jones (Naval Surface Weapons Center, Silver Spring, MD.), John S. Hind (Naval Surface Weapons Center, Silver Spring, MD.), Joan Jones-Meehan (Naval Surface Weapons Center, Silver Spring, MD.), and M. Walch (Naval Surface Weapons Center, Silver Spring, MD.) *In* Johns Hopkins Univ., Environmentally Benign Cleaning and Degreasing Technology: JANNAF Safety and Protection Subcommittee and Propellant Development and Characterization Subcommittee Joint Workshop Jun. 1994 p 175-183 Sponsored by NAVSEADET (For primary document see N95-27101 09-27)
Avail: CPIA, 10630 Little Patuxent Pkwy., Suite 202, Columbia, MD 21044-3200 HC

Cleaning and maintenance of pipes, grease traps and organic waste tanks conventionally involves manual or chemical methods. These involve many limitations, in that they are labor intensive, expensive and pose waste disposal problems. Alternatively, microbial cleaners have the potential to clean more effectively while eliminating the use of acids, bases and solvents and reducing costs significantly. We are analyzing enzymatic and/or bacterial products available commercially, biosurfactants that are approved by the FDA and EPA, and microbes obtained from collection, holding and transfer (CHT) tanks, as well as bioemulsifier-producing microbes we have previously used for heavy hydrocarbon and lipase biodegradation. The objectives are to establish methods for evaluating the performance of microbial degreasing products, identify the best microbial products available, determine the best methods for the use of the products, and test them in shipboard CHT tanks. Microbial components have been screened for lipase activity and tested in functional assays for their ability to remove animal fat in benchtop models constructed of glass tubing. We have quantitated degreasing activity for correlation with lipase and esterase activity and established parameters for the use of some of the products. Author

N95-27120 UMBI, Baltimore, MD.

APPLICATION OF BACTERIAL BIOEMUSIFIERS TO IN SITU MAINTENANCE OF OIL/WATER SEPARATORS c23

John S. Hind (Naval Surface Weapons Center, Silver Spring, MD.), M. Beard (Naval Surface Weapons Center, Silver Spring, MD.), Joan Jones-Meehan (Naval Surface Weapons Center, Silver Spring, MD.), and M. Walch (Naval Surface Weapons Center, Silver Spring, MD.) *In* Johns Hopkins Univ., Environmentally Benign Cleaning and Degreasing Technology: JANNAF Safety and Protection Subcommittee and Propellant Development and Characterization Subcommittee Joint Workshop Jun. 1994 p 185-194 Sponsored by David Taylor Research Center (For primary document see N95-27101 09-27)

Avail: CPIA, 10630 Little Patuxent Pkwy., Suite 202, Columbia, MD 21044-3200 HC

Parallel plate oil/water separators (OWS) remove petroleum products (e.g. lubricating oils and hydraulic fluids) from shipboard oily bilge water. The oily waste is retained aboard and water meeting oily waste discharge limits is discharged. Separation of oil and water is dependent on laminar flow of oily bilge water through parallel corrugated polypropylene plates. During operation, oily sludge builds-up on the plates, disrupting the laminar flow and reducing the efficiency of the separator. To restore normal operating efficiency the separator must be dismantled and cleaned by hand. This is a labor intensive and costly task that may expose personnel to toxic and hazardous material. We have developed an in situ process that utilizes bacterial bioemulsifiers to remove oily sludge from the plates of the OWS and restore normal operating efficiency without need to dismantle the OWS. A laboratory system was developed for comparing the effectiveness of bacterial bioemulsifiers and biosurfactants in removal of oily sludge from polypropylene plates. We used this system to determine the optimum conditions required for emulsifier activity and selected bacterial bioemulsifiers and commercial products for testing in a model OWS system. The model 1 gallon/min OWS system was used to test selected bioemulsifiers and to optimize conditions for cleaning of the OWS system. Author

N95-27121* National Aeronautics and Space Administration. John F. Kennedy Space Center, Cocoa Beach, FL.

AQUEOUS DEGREASING, PRECISION CLEANING, AND CLEANLINESS VERIFICATION

Marcia D. Littlefield, G. S. Melton, P. J. Welch, and R. J. Werlink *In* Johns Hopkins Univ., Environmentally Benign Cleaning and Degreasing Technology: JANNAF Safety and Protection Subcommittee and Propellant Development and Characterization Subcommittee Joint Workshop Jun. 1994 p 205-210 (For primary document see N95-27101 09-27)

Avail: CPIA, 10630 Little Patuxent Pkwy., Suite 202, Columbia, MD 21044-3200 HC

The NASA Materials Science Laboratory at the John F. Kennedy Space Center (KSC) has been working with the base cleaning contractor, Wiltech, Inc.; the Development Testing Laboratory; and the Mechanical Engineering Design Division to develop and implement aqueous processes at the Base Cleaning Facility before 1995, when the use of chlorofluorocarbon 113 (CFC-113) will be banned. The Base Cleaning Facility (BCF) operates to the KSC specification KSC-C-123, 'Surface Cleanliness of Fluid Systems'. Ground support equipment (GSE) and some flight hardware for the Space Shuttle program and other military or civilian programs at KSC and the Cape Canaveral Air Force Station (CCAFS) are processed through the cleaning facility. Developmental work in these field cleaning areas will be discussed in this paper. Author

N95-27122 Polymer Solutions, Inc., Blacksburg, VA.

SURVEY OF ENVIRONMENTALLY BENIGN CLEANING METHODOLOGIES AND MATERIALS

Dale C. Messer and James D. Rancourt *In* Johns Hopkins Univ., Environmentally Benign Cleaning and Degreasing Technology: JANNAF Safety and Protection Subcommittee and Propellant Development and Characterization Subcommittee Joint Workshop Jun. 1994 p 211-213 (For primary document see N95-27101 09-27)

Avail: CPIA, 10630 Little Patuxent Pkwy., Suite 202, Columbia, MD 21044-3200 HC

A great deal of effort is being devoted to the identification, implementation and evaluation of new environmentally benign cleaning systems. This presentation will provide a survey of environmentally benign systems that are available to consumers and industries. Older technologies that are being revisited and the newer technologies will be presented. Author

N95-27123 MART Corp., Saint Louis, MO.

CLEANING OF PARTS FOR NEW MANUFACTURING AND PARTS REBUILDING c31

Jeff Doherty *In* Johns Hopkins Univ., Environmentally Benign Cleaning and Degreasing Technology: JANNAF Safety and Protection Subcommittee and Propellant Development and Characterization Subcommittee Joint Workshop Jun. 1994 p 215-223 (For primary document see N95-27101 09-27)

Avail: CPIA, 10630 Little Patuxent Pkwy., Suite 202, Columbia, MD 21044-3200 HC

Parts cleaning is the largest single expense, and the most time consuming activity, in rebuilding and new manufacturing. On average, 25% to 40% of the total labor and overhead burden is spent on cleaning. EPA and OSHA pressures add to the burden by making some methods and chemicals obsolete. Some of the processes and chemicals in current use will be curtailed and or outlawed in the future. How can a shops and industries make long term decisions or capital investments in cleaning and process improvements when the government keeps changing its rules? At the MART Corporation in Saint Louis, Missouri, we manufacture a line of cabinet-style batch cleaning machines known as Power Washers. Twenty years ago MART invented and patented the Power Washer process, a cleaning method that recycles wash solution and blasts contaminates as they are washed off the more heavily contaminated parts. Since the initial invention MART has continued to R&D the washing process and develop ancillary systems that comply with EPA and OSHA regulations. For applications involving new industrial parts or items requiring specification cleaned surfaces. MART provides filtration and solution conditioning systems, part drying operations, and triple rinsing. Units are available in stainless steel or higher alloys. We are not alone in the washer manufacturing business. You have many choices of cleaning solutions (no pun intended) which will perform in your operations and yield good results. As a manufacturer, we are interested in your success with our equipment. We have all heard the horror stories of companies having selected inappropriate cleaning systems and or processes which then brought the company to its knees, production wise. Assembly, appearance, warranty, and performance shortcomings of finished products can often be directly related to the cleaning process and its shortcomings. Author

N95-27124* Thiokol Corp., Huntsville, AL.

SCEENING, DOWN SELECTION, AND IMPLEMENTATION OF ENVIRONMENTALLY COMPLIANT CLEANING AND INSULATION BONDING FOR MNASA c18

Jill M. Keen, D. E. Hutchens, G. M. Smith, and T. W. Dillard *In* Johns Hopkins Univ., Environmentally Benign Cleaning and Degreasing Technology: JANNAF Safety and Protection Subcommittee and Propellant Development and Characterization Subcommittee Joint Workshop Jun. 1994 p 225-233 (For primary document see N95-27101 09-27)
(Contract NAS8-38100)

Avail: CPIA, 10630 Little Patuxent Pkwy., Suite 202, Columbia, MD 21044-3200 HC

MNASA, a quarter-scale space shuttle solid rocket motor, has historically been processed using environmentally and physiologically harmful chemicals. This program draws from previous testing done in support of full-scale manufacturing and examines the synergy and interdependency between environmentally acceptable materials for Solid Rocket Motor insulation applications, bonding, corrosion inhibiting, painting, priming and cleaning; and then implements new materials and processes in sub-scale motors. Tests have been conducted to eliminate or minimize hazardous chemicals used in the manufacture of MNASA components and identify alternate materials and/or processes following NASA Operational Environment Team (NOET) priorities. This presentation describes implementation of high pressure water refurbishment cleaning, aqueous precision cleaning using both Brulin 815 GD and Jettacin and insulation case bonding using ODC compliant primers and adhesives. Author

N95-27125 American Univ., Washington, DC.

A PRACTICAL APPROACH TO SOIL REMEDIATION **c45**

Paul F. Waters *In* Johns Hopkins Univ., Environmentally Benign Cleaning and Degreasing Technology: JANNAF Safety and Protection Subcommittee and Propellant Development and Characterization Subcommittee Joint Workshop Jun. 1994 p 235-239 (For primary document see N95-27101 09-27)

Avail: CPIA, 10630 Little Patuxent Pkwy., Suite 202, Columbia, MD 21044-3200 HC

As a consequence of the rapid expansion of manufacturing and testing facilities, ignorance of the long-term harmful effects of exposure to many chemicals, and the improvident storage and disposal of harmful chemicals, scores of thousands of contaminated sites exist throughout the nation today. Several technologies have been advanced and applied in efforts to decontaminate the affected soils. Among the approaches are aeration, solvent extraction, incineration, steam distillation, electroosmosis, and the plasma arc. The technology discussed in this presentation is both feasible and economical because it is founded in the ancient art of reduction pyrolysis carried out in the reduction pyrolysis furnace (RPF). Derived from text

N95-27126 THAR Designs, Inc., Pittsburgh, PA

DESIGN CONSIDERATIONS IN SUPERCRITICAL FLUID TECHNOLOGY

Abstract Only

M. Lalith Kumar *In* Johns Hopkins Univ., Environmentally Benign Cleaning and Degreasing Technology: JANNAF Safety and Protection Subcommittee and Propellant Development and Characterization Subcommittee Joint Workshop Jun. 1994 p 241 (For primary document see N95-27101 09-27)

Avail: CPIA, 10630 Little Patuxent Pkwy., Suite 202, Columbia, MD 21044-3200 HC

Considerable interest has been exhibited in Supercritical Fluid Technology for extraction and cleaning. Supercritical fluid technology employs a mobile phase (or solvent) that is a highly compressed gas near or above its critical temperature and critical pressure points. Carbon dioxide is the most widely used supercritical fluid. Supercritical carbon dioxide is a superior solvent over conventional hydrocarbons, such as hexane or methylene chloride, for extraction because it is chemically inert, non-toxic, non-flammable non-corrosive and relatively inexpensive. The critical temperature of carbon dioxide is 31 C and the critical pressure is 73 atm. At the critical temperature of a substance, the vapor and liquid phases have identical densities. A gas cannot be liquefied when it is above its critical temperature, irrespective of the pressure. Above the critical temperature, the substance exists as a supercritical fluid. Supercritical fluid extraction (SFE) is becoming more widely accepted for the extraction of compounds due to the ability to achieve rapid, sensitive and reproducible extractions from many different types of matrices. The benefits are: (1) SF is rapid - a supercritical fluid has diffusion coefficients 1 - 2 orders of magnitude higher than comparable liquid solvents; (2) SF is selective - by varying pressure and temperature, SF can selectively extract compounds of interest from complex matrices or perform class fractionations; and (3) SFE eliminates hazardous solvents - carbon dioxide is an inexpensive non-toxic and nonflammable solvent. Thus, there is no-need to purchase and then dispose of liters and drums of organic solvents. Thar Designs has redesigned the various major products that are part of a supercritical fluid system. These redesigned products are not only superior in performance but also are relatively inexpensive to manufacture. Some of the features are use of ceramics for increased seal life, long term stability, temperature control and 'finger tight' closures. Author

N95-27127 Petroferm, Inc., Fernandina Beach, FL.

RETROFITTING CONVENTIONAL VAPOR DEGREASERS TO USE A SOLVENT WASH/FLUOROCHEMICAL RINSE PROCESS

Kevin R. Hrebenar, Michael E. Hayes, Christine S. Fouts, and Robert D. Sell *In* Johns Hopkins Univ., Environmentally Benign Cleaning and Degreasing Technology: JANNAF Safety and Protection Subcommittee and Propellant Development and Characterization Subcommittee Joint Workshop Jun. 1994 p 243-249 (For primary document see N95-27101 09-27)

Avail: CPIA, 10630 Little Patuxent Pkwy., Suite 202, Columbia, MD 21044-3200 HC

Solvent wash/fluorochemical rinse processes offer a high-performance vapor degreasing method of cleaning which is economical, easy, fast, and efficient. They use no ozone-depleting solvents, toxic chemicals or water. Among the solvent wash/fluorochemical rinse processes, the Advanced Vapor Degreasing (AVD(TM*)) process avoids the use of flammables, as well. It works in virtually all vapor degreasing applications in the electronics, electrical, precision, and metalworking industries, providing highly effective degreasing of complex, delicate and difficult-to-clean parts. It is ideal for manufacturers who need to produce clean, dry parts without using water. The cleaning performance of the AVD process is as good as, or better than, conventional degreasing systems that use conventional vapor degreasing solvents. Laboratory and on-site tests in customers' factories have demonstrated that it is possible to effectively retrofit conventional vapor degreasers to be able to run the AVD process. Smaller systems like the Baron-Blakeslee Model MSR 120 or the Branson B-400 can be retrofitted, usually for costs between $15,000 and $20,000. AVD retrofitted equipment is conventional vapor degreasing equipment which has been modified to standards that enable it to use the AVD process satisfactorily, that is, it can produce clean, dry parts. The modifications to existing equipment include providing, as a minimum, the following: (1) 150% freeboard; (2) a rinse sump sparger; (3) filtration system in the boil sump; (4) ultrasonics in the boil sump; (5) chiller coil(s) above the primary condensing coils; and (6) ultrasonics in the rinse sump A detailed AVD process description will be provided. AVD process advantages and disadvantages relative to existing CFC solvent alternatives will be discussed. Cleaning results realized by several customers will also be provided. Author

N95-27128 CF Technologies, Inc., Boston, MA.

THE EXPERIENCE OF CF TECHNOLOGIES, INC. (CF TECH) IN CRITICAL FLUID PROCESSING

William E. McGovern, J. M. Moses, and D. C. Weber *In* Johns Hopkins Univ., Environmentally Benign Cleaning and Degreasing Technology: JANNAF Safety and Protection Subcommittee and Propellant Development and Characterization Subcommittee Joint Workshop Jun. 1994 p 253-257 (For primary document see N95-27101 09-27)

Avail: CPIA, 10630 Little Patuxent Pkwy., Suite 202, Columbia, MD 21044-3200 HC

Founded in 1989, CF Technologies, Inc. (CF TECH) is dedicated to the development and commercialization of critical fluid processes for government and industrial applications. The company is currently involved in several different application areas related to critical fluid processing, including critical fluid extraction, supercritical fluid drying for aerogel manufacturing, reactions in supercritical fluid media, and the design and manufacturing of high pressure vessels and processing equipment. This paper will report on research and engineering developments at CF TECH and critical fluid processing equipment designed and built for a variety of commercial applications, including precision parts cleaning, conventional weapons demilitarization, and aerogel manufacturing. Author

N95-27129 Pacific Northwest Lab., Richland, WA.

FLUID DYNAMIC EFFECTS ON PRECISION CLEANING WITH SUPERCRITICAL FLUIDS **c34**

Max R. Phelps, M. O. Hogan, and L. J. Silva *In* Johns Hopkins Univ., Environmentally Benign Cleaning and Degreasing Technology: JANNAF Safety and Protection Subcommittee and Propellant Development and Characterization Subcommittee Joint Workshop Jun. 1994 p 259-268 See also N95-14663 (For primary document see N95-27101 09-27) (Contract DE-AC06-76RL-01830)

Avail: CPIA, 10630 Little Patuxent Pkwy., Suite 202, Columbia, MD 21044-3200 HC

Pacific Northwest Laboratory staff have assembled a small supercritical fluids parts cleaning test stand to characterize how system dynamics affects the efficacy of precision cleaning with supercritical carbon dioxide. A soiled stainless steel coupon, loaded into a 'Berty' autoclave, was used to investigate how changes in system turbulence and solvent temperature influenced the removal of test dopants. A pulsed laser beam through a fiber optic was used to investigate real-time contaminant removal. Test data show that cleaning efficiency is a function of system agitation, solvent density, and temperature. These data also show that high levels of cleaning efficiency can generally be achieved with high levels of system agitation at relatively low solvent densities and temperatures. Agitation levels, temperatures, and densities needed for optimal cleaning are largely contaminant-dependent. Using proper system conditions, the levels of cleanliness achieved with supercritical carbon dioxide compare favorably with conventional precision cleaning methods. Additional research is currently being conducted to generalize the relationship between cleaning performance and parameters such as contaminant solubilities, mass transfer rates, and solvent agitation. These correlations can be used to optimize cleaning performance, system design, and time and energy consumption for particular parts-cleaning applications. Author

N95-27130 Missouri Univ., Rolla, MO. High Pressure Waterjet Lab.

THE APPLICATION OF WATERJETS FOR CLEANING c34

D. A. Summers and Robert Fossey *In* Johns Hopkins Univ., Environmentally Benign Cleaning and Degreasing Technology: JANNAF Safety and Protection Subcommittee and Propellant Development and Characterization Subcommittee Joint Workshop Jun. 1994 p 269-277 (For primary document see N95-27101 09-27)

Avail: CPIA, 10630 Little Patuxent Pkwy., Suite 202, Columbia, MD 21044-3200 HC

The last 25 years has seen a dramatic growth in the use of high pressure waterjets for cleaning purposes. Throughout recorded history and no doubt for a long time before that, the dual role of water as both a solvent and a lubricant has been one of the major ways of washing surfaces down regardless of what the surface was. Also, the power built into a waterjet stream has allowed it to be used in moving material. In ancient Egypt rivers were commonly diverted to erode valuable mineral deposits and it was not until 1852 that the modern innovation of hydraulic mining got its start in the hills around Sacramento. The power of the waterjets used in those mining operations were such that most of the gold in California and later in Idaho and many of the other western states was mined hydraulically. Subsequently, the technology has advanced considerably by the use of increasingly high pressures and smaller jets to the point where today abrasive laden waterjets at pressures above 35,000 psi are becoming the tool of choice for cutting glass, titanium, and composite materials. Applications of high pressure waterjets to cutting are usually however, governed by a different set of requirements to those of the cleaning operation. Specifically, while in a cutting or mining operation one is seeking to remove the most volume of material with the least amount of energy looking for deep cuts and applying a highly focused jet energy to the surface. Frequent cleaning requires the ability to remove only one or two surface coatings which may be very shallow. It is generally important that the underlying material or substrate is not damaged by the cleaning process, and thus, the energy of the jet must often be more diffuse. In contrast also with conventional cutting where the depth of the cut has great importance in cleaning it is the area which can be covered in a given time which better optimizes the process. An example of the types of requirement needed can be illustrated by the failure of paint. Where an overcoat of paint fails, that layer must be removed from the surface before a fresh protective coating can be applied. By the early 1980's the cost of this operation in the UK alone exceeded 600 million dollars. Derived from text

N95-27163# Joint Inst. for Nuclear Research, Dubna (USSR).

NEW RADIATION STABLE AND LONG-LIVED PLASTIC SCINTILLATORS

V. Senchishin, V. Koba, and O. Korneeva 1994 18 p

(DE95-608622; JINR-E-13-94-159) Avail: CASI HC A03/MF A01 (US Sales Only)

A study of the influence of the concentration of secondary addition, high concentrations of primary dopant, diffusion enhancer and stabilizer on radiation hardness is presented. It is concluded that the diffusion enhancing technique is the most powerful method for improving radiation hardness. A new polystyrene scintillator which contains 2% pT, 0.02% POPOP, 20% diffusion enhancer and 0.02% stabilizer gave 91% of initial light output immediately after 3 Mrad irradiation in air. Data are presented that show that scintillator prepared from commercial polymer is more radiation-hard and has greater light output than scintillator prepared from monomer. It is assumed that this difference is due to different molecular weight distributions. Some protocols for acceleration of aging (yellowing and crazing) are presented. It is shown that one of the main reasons for aging of plastic scintillators is residual monomer. DOE

N95-27187 Oregon Graduate Inst. of Science and Technology, Beaverton, OR. Dept. of Electrical Engineering and Applied Physics.

LOW TEMPERATURE MATERIALS GROWTH AND PROCESSING DEVELOPMENT FOR FLAT PANEL DISPLAY TECHNOLOGY APPLICATIONS Quarterly Technical Report, 15 Aug. - 14 Nov. 1994

C. N. Berglund 14 Nov. 1994 11 p Limited Reproducibility: More than 20% of this document may be affected by microfiche quality

(Contract N00014-93-1-0312)

(AD-A288970) Avail: Issuing Activity (Defense Technical Information Center (DTIC))

The goal of this phase of the project is to make DC, AC, transient measurements on the thin-film transistors (TFT's), fabricated by Professor Sigmon and his group at Arizona State University using low temperature processing techniques. From these measurements, SPICE parameters will be extracted and these results will be used for process monitoring and device and process optimization for display applications. This work was started by Rao Gudimetla on 10/1/94 and this technical report covers the period 10/1/94 to 12/1/94. The devices from ASU are expected to be ready in early 1995. Meanwhile, previously obtained measurements on TFT's fabricated at Tektronix Inc. are being used to establish a reliable extraction methodology. Both n- and p-channel TFT's, obtained from Tektronix Inc., were fabricated in silicon-implanted polysilicon, followed by a long time anneal without any grain boundary hydrogenation. The gate lengths are 12.5 and 5 microns with 100 micron width. S-parameter measurements (which were converted to Y-parameters) were made at several bias points over the frequency range of 300 kHz to 20 MHz. The following are the key accomplishments. (1) An often suggested AC equivalent circuit for TFT's was used to extract the parameters such as transconductance, gate to source capacitance, gate to drain capacitance, and drain to source capacitance as functions of frequency at different bias points. (2) A detailed analysis for the AC performance of TFT's, developed in the past by the author in the linear and triode regions of I-V data, is being compared with the extracted parameters of the devices and equivalent circuit. DTIC

N95-27324 Army Tank-Automotive Research and Development Command, Warren, MI.

EVALUATION OF HIGH ESTER CONTENT PAO BASED SINGLE HYDRAULIC FLUID IN HIGH HUMIDITY CONDITIONS Final Report, 1 Jun. 1993 - 31 Jul. 1993

Ellen M. Purdy Nov. 1994 19 p Limited Reproducibility: More than 20% of this document may be affected by microfiche quality

(AD-A289374; TARDEC-TR-13609) Avail: Issuing Activity (Defense Technical Information Center (DTIC))

A Polyalphaolefin/Ester based Fire Resistant Hydraulic Fluid was subjected to high humidity conditions to determine water absorbance tendencies of the fluid. Fluid was subjected to 300 hours of humidification in an environment of 85% Relative Humidity. Four distinct fluid formulations containing ester contents of 34%-40% by weight were found to absorb no more than 0.25% water after the 300 hour period. A performance evaluation of the humidified fluid revealed no loss in performance regardless of the absorbed water present in the fluid. Because satisfactory performance was obtained, the hydraulic fluid formulations can contain up to 40% ester with no loss of performance. The increased ester content in the fluid formulations will provide sufficient seal swell for Army hydraulic systems that use the PAO based hydraulic fluid. DTIC

N95-27325 Army Tank-Automotive Research and Development Command, Warren, MI.

USE OF CTFE AS AN ADDITIVE TO ENHANCE FIRE RESISTANCE OF SINGLE HYDRAULIC FLUID Final Report, 2 Feb. - 30 Sep. 1993

Ellen M. Purdy Nov. 1994 21 p Limited Reproducibility: More than 20% of this document may be affected by microfiche quality

(AD-A289377; TARDEC-TR-13610) Avail: Issuing Activity (Defense Technical Information Center (DTIC))

A Polyalphaolefin/ester base fire resistant hydraulic fluid was reformulated to include chlorotrifluoroethylene (CTFE) as an additive to enhance fire resistance. CTFE was added to the formulation at 2%-10% by weight. Each of the formulations were evaluated for performance and flammability. Addition of the CTFE was found to promote excess foaming when tested for foaming characteristics. The formulations were adjusted to include an anti-foam additive to counteract this effect. The new formulations were found to provide satisfactory performance and improvement in fire resistance. Addition of CTFE increased the flash and fire points of the fluid. In addition, the autoignition temperature, hot manifold spray ignition temperature were both increased above what is available from MIL-HA6147O, the current military specification fire resistant hydraulic fluid. DTIC

N95-27455# Argonne National Lab., IL.
MAGNETIC RESONANCE IMAGING OF SOLVENT TRANSPORT IN POLYMER NETWORKS
R. E. Botto and G. D. Cody 1995 6 p
(Contract W-31-109-eng-38)
(DE95-007142; ANL/CHM/PP-80411) Avail: CASI HC A02/MF A01

The spectroscopic technique of magnetic resonance imaging (MRI) has recently provided a new window into transport of solvents in polymer networks. Diffusion of solvent as a rate-controlling phenomenon is paramount to understanding transport in many important industrial and biological processes, such as upgrading fossil fuels, film casting and coating, development of photoresists, design of drug-delivery systems, development of solvent resistant polymers, etc. By MRI mapping the migration of solvent molecules through various polymer specimens, researchers Robert Botto and George Cody of Argonne National Laboratory, with support from the Division of Chemical Sciences at DOE, were able to characterize and distinguish between different modes of transport behavior associated with fundamentally different types of polymer systems. The method was applied to rubbers, glassy polymers, and coals. In polymers shown to undergo a glass transition from a rigid to rubbery state, a sharply defined solvent front was observed that propagated through specimens in the manner of a constant velocity shock wave. This behavior was contrasted with a smooth solvent concentration gradient found in polymer systems where no glass transition was observed. The results of this analysis have formed the basis of a new model of anomalous transport in polymeric solids and are helping to ascertain fundamental information on the molecular architectures of these materials. DOE

N95-27460# Sandia National Labs., Albuquerque, NM.
THE RESPONSE OF HYDROTALCITE COATED ALUMINUM TO SEALING WITH TRANSITION METAL SALT SOLUTIONS
R. G. Buchheit and M. A. Martinez 1994 2 p Presented at the 187th Meeting of the Electrochemical Society, Reno, NV, 21-26 May 1995
(Contract DE-AC04-94AL-85000)
(DE95-004767; SAND-94-3046C; CONF-950518-1) Avail: CASI HC A01/MF A01

Objective was to determine if the protective coating could be enhanced by filling intercrystalline spaces or by reinforcing the coating at intermetallic particles by exposure to aqueous transition metal salt solutions. Two oxy-anion analogs to chromate were used: permanganate and molybdate. Ce(3)(as Ce(NO3(sub 3)) was also studied. (Al alloys 2024-T3 and 6061-T6 were used as substrates.) Results are summarized. DOE

N95-27468# Los Alamos National Lab., NM.
REVIEW OF ACTIVITIES IN USA ON HTS MATERIALS
D. E. Peterson 1995 5 p Presented at the 7th Conference on Superconductivity and Applications, Buffalo, NY, 7-9 Sep. 1994
(Contract W-7405-eng-36)
(DE95-006404; LA-UR-95-48; CONF-940926-6) Avail: CASI HC A01/MF A01

Rapid progress in attaining practical applications of High Temperature Superconductors (HTS) has been made since the discovery of these new materials. Many critical parameters influencing HTS powder synthesis and wire processing have been identified through a combination of fundamental exploration and applied research. The complexity of these novel materials with regard to phase behavior and physical properties has become evident as a result of these careful studies. Achieving optimal mechanical and superconducting properties in wires and tapes will require further understanding and synergy among several different technical disciplines. Highlights of efforts towards producing practical superconductors for electric power applications based on rare earth-, bismuth-, and thallium-based systems are reviewed. DOE

N95-27472# California Univ., Berkeley. Lawrence Berkeley Lab, CA.
GROWTH OF HYDROGENATED AMORPHOUS SILICON (a-Si:H) ON PATTERNED SUBSTRATES FOR INCREASED MECHANICAL STABILITY
W. S. Hong, J. C. D. Nieto, O. Ruiz, and V. Perez-Mendez Dec. 1994 11 p Presented at the 1994 Fall Meeting of the Materials Research Society (MRS), Boston, MA, 28 Nov. - 2 Dec. 1994
(Contract DE-AC03-76SF-00098)
(DE95-006589; LBL-36398; CONF-941144-64) Avail: CASI HC A03/MF A01

Residual stress in hydrogenated amorphous silicon (a-Si:H) film, which causes substrate bending and delamination, is studied. The internal stress can be reduced by controlling deposition parameters, but it is known to produce a trade-off between stress and electronic quality. Selective area deposition, in which the deposition area is reduced by making islands, reduced the stress when the lateral dimension of the islands becomes comparable to the film thickness. The overall stress is reduced by approximately 40% when the lateral dimension is decreased to 40 (mu)m, but the adhesion was not improved much. However, substrates having a 2-dimensional array of inversed pyramids of 200 (mu)m in lateral dimension produced overall stress 3 to approximately 4 times lower than that on the normal substrates. Such substrates were prepared by anisotropic etching of silicon wafers. The inversed pyramid structure also has other advantages including minimized delamination and increased effective thickness. Computer simulation confirmed that the overall stress can be reduced by deposition on the pyramidal structure. DOE

N95-27476# Pacific Northwest Lab., Richland, WA.
THE DEVELOPMENT OF MECHANICAL STRENGTH IN A CERAMIC MATERIAL DURING FIRING
L. R. Bunnell and S. W. Piippo (Richland School District, WA.) Nov. 1994 8 p Presented at the National Educators' Workshop Update '94 Conference, Gaithersburg, MD, 7-9 Nov. 1994
(Contract DE-AC06-76RL-01830)
(DE95-004925; PNL-SA-25035; CONF-9411179-1) Avail: CASI HC A02/MF A01

This experiment was designed for high school students who have a very limited background in ceramic materials, but the experiments could also be used at the college level. The objective of the experiment is to teach students about the development of mechanical strength in a ceramic material as a result of the firing process and about testing methods used for brittle materials. In the experiment, clay-based ceramic bars of uniform circular cross section are prepared by extrusion. The bars are then fired at temperatures high enough to achieve high strength by development of a glassy bonding phase. Finally, the bars will be stressed to failure in a simple testing machine. This will quantify the increase in strength as a function of firing temperature. DOE

N95-27481# New Mexico Univ., Albuquerque, NM.
METHODS DEVELOPMENT FOR MEASURING AND CLASSIFYING FLAMMABILITY/COMBUSTIBILITY OF REFRIGERANTS. TASK 2: TEST PLAN Interim Report
E. W. Heinonen and R. E. Tapscott Jul. 1994 62 p Prepared for the Air-Conditioning and Refrigeration Technology Inst., Inc., Arlington, VA
(Contract DE-FG02-91CE-23810)
(DE95-007066; DOE/CE-23810/42H; NMERI-OC-94-32) Avail: CASI HC A04/MF A01

Regulations on alternative refrigerants and concerns for the environment are forcing the refrigeration industry to consider the use of potentially flammable fluids to replace CFC fluids currently in use. The objectives of this program are to establish the conditions under which refrigerants and refrigerant blends exhibit flammability and to develop appropriate methods to measure flammability. DOE

N95-27486# Oak Ridge National Lab., TN.
SMALL ANGLE NEUTRON SCATTERING STUDY OF THE MICELLE STRUCTURE OF AMPHIPHILIC BLOCK COPOLYMERS
H. Yamaoka (Kyoto Univ., Japan.), H. Matsuoka (Kyoto Univ., Japan.), K. Sumaru (Kyoto Univ., Japan.), S. Hanada (Kyoto Univ., Japan.), M. Imai (Tokyo Univ., Japan.), and G. D. Wignall 31 Jul. 1994 13 p Presented at the Neutron Scattering, Sendai, Japan, 11-14 Oct. 1994

(Contract DE-AC05-84OR-21400)
(DE95-006625; CONF-9410165-12) Avail: CASI HC A03/MF A01

The amphiphilic block copolymers of vinyl ether were prepared by living cationic polymerization. The partially deuterated copolymers for SANS experiments were especially synthesized by introducing deuterated phenyl units in the hydrophobic chain. SANS measurements were performed for aqueous solutions of these copolymers by changing H2O/D2O ratios. The SANS profiles indicate that the micelles in the present system exhibit a core-shell structure and that the size and shape of micelles are largely dependent on the length of hydrophobic chain. The micelle of shorter hydrophobic chain was found to be nearly spherical, whereas the micelle of longer hydrophobic chain was confirmed to have an ellipsoidal shape. DOE

N95-27499# Oak Ridge National Lab., TN.
STRUCTURAL CERAMICS INCORPORATING WHISKERS, PLATELETS, AND PARTICULATE PHASES
P. F. Becher, C. H. Hsueh, K. B. Alexander, H. T. Lin, W. H. Warwick, C. G. Westmoreland, and S. B. Waters 1995 22 p Presented at the 3rd Conference on Ceramic-Ceramic Composites, Mons, Belgium, 18-20 Oct. 1994
(Contract DE-AC05-84OR-21400)
(DE95-007048; CONF-941059-2) Avail: CASI HC A03/MF A01

Advances in the development of ceramics toughened with whiskers, particles, or platelets are reviewed with emphasis on the development of both fracture strength and toughness. In the systems described here, the primary focus is on toughening attained by crack bridging processes (e.g., frictional bridging and pullout) in the wake of the crack tip. Examples of the influence of resultant improvements in other mechanical properties (e.g., strength, fatigue, and thermal shock resistance) are also given for whisker-reinforced aluminas. It is shown that similar increases in fracture toughness may also be brought about by the incorporation of platelet phases in ceramics, either by their addition or by their formation during densification. In addition, the development of ceramic matrix composites containing transformable tetragonal zirconia grains is discussed. Here, it is shown that both the zirconia grain size and content, combined with thermal expansion mismatch stresses, influence the transformability of the zirconia and the resultant transformation toughening effects. Examples reveal that by addressing the microstructural characteristics, as well as the reinforcement and matrix properties, high strength toughened ceramics with exceptional damage resistance can be developed. DOE

N95-27503*# National Aeronautics and Space Administration. Lewis Research Center, Cleveland, OH.
PREFERENTIALLY ETCHED EPITAXIAL LIFTOFF OF InP MATERIAL Patent Application
Sheila G. Bailey, inventor (to NASA), David M. Wilt, inventor (to NASA), and Frank L. DeAngelo, inventor (to NASA) 27 Mar. 1995 11 p
(NASA-Case-LEW-15760-1; NAS 1.71:LEW-15760-1;
US-Patent-Appl-SN-411357) Avail: CASI HC A03/MF A01

The present invention is directed toward a method of removing epitaxial substrates from host substrates. A sacrificial release layer of ternary material is placed on the substrate. A layer of InP is then placed on the ternary material. Afterward a layer of wax is applied to the InP layer to apply compressive force and an etchant material is used to remove the sacrificial release layer. NASA

N95-27687# Sandia National Labs., Albuquerque, NM.
ECR PLASMA-ASSISTED DEPOSITION OF Al2O3 AND DISPERSION-STRENGTHENED AlO2
J. C. Barbour, D. M. Follstaedt, and S. M. Myers 1995 25 p Presented at the 9th International Conference on Ion Beam Modification of Materials, Canberra, Australia, 5-10 Feb. 1995
(Contract DE-AC04-94AL-85000)
(DE95-007743; SAND-94-2417C; CONF-950220-3) Avail: CASI HC A03/MF A01

Electron cyclotron resonance (ECR) O2 plasmas, in conjunction with electron-beam evaporation of Al, were used to grow thick AlO(x) films were varying but controlled composition and microstructure. The ion energy was varied from 30 to 190 eV, and growth temperatures varied from 35 C to 400 C. The ECR-film compositions were varied from AlO(0.1) to Al2O3 by controlling the plasma parameters and Al deposition rate. The Al-rich alloys exhibited a fine-grain (10-100 nm) fcc Al microstructure with (gamma)-Al2O3 precipitates approximately 1 nm, similar to that found in the gigapascal-strength O-implanted Al. The measured hardness of the ECR Al-O alloys approximately 3 GPa was also similar to the ion-implanted alloys which implies that the yield strength of the ECR material is approximately 1 GPa. Moreover, the Al-O alloys retain much of the elasticity of the Al metal matrix. As-deposited stoichiometric Al2O3 samples grown with an applied bias of -140 to -160 V at 400 C were fine-grain polycrystalline (gamma)-Al2O3. The amorphous films crystallized into the (gamma)-Al2O3 phase upon vacuum annealing to 800 C. DOE

N95-27694*# Loyola Coll., Baltimore, MD. Japanese Technology Evaluation Center.
JTEC MONOGRAPH ON BIODEGRADABLE POLYMERS AND PLASTICS IN JAPAN: RESEARCH, DEVELOPMENT, AND APPLICATIONS
Robert W. Lenz (Massachusetts Univ., Amherst, MA.) Mar. 1995 44 p
Sponsored by NASA, Washington; DOE; Dept. of Commerce; DOD; Eastman Chemical Co.; Ecochem; Cargill; International Specialty Products; Johnson and Johnson; Kimberly Clark Corp.; Rohm and Haas Co.; 3M; Tambrands, Inc.; United States Surgial Corp.; and Zeneca BioProducts
(Grants NSF ENG-93-14162; NSF ENG-92-17849)
(NASA-CR-198562; NAS 1.26:198562; ISBN-1-883712-38-6) Avail: CASI HC A03/MF A01

A fact-finding team of American scientists and engineers visited Japan to assess the status of research and development and applications in biodegradable polymers. The visit was sponsored by the National Science Foundation and industry. In Japan, the team met with representatives of 31 universities, government ministries and institutes, companies, and associations. Japan's national program on biodegradable polymers and plastics evaluates new technologies, testing methods, and potential markets for biodegradables. The program is coordinated by the Biodegradable Plastics Society of Japan, which seeks to achieve world leadership in biodegradable polymer technology and identify commercial opportunities for exploiting this technology. The team saw no major new technology breakthroughs. Japanese scientists and engineers are focusing on natural polymers from renewable resources, synthetic polymers, and bacterially-produced polymers such as polyhydroxyalkanoates, poly(amino acids), and polysaccharides. The major polymers receiving attention are the Zeneca PHBV copolymers, Biopol(registered trademark), poly(lactic acid) from several sources, polycaprolactone, and the new synthetic polyester, Bionolle(registered trademark), from Showa High Polymer. In their present state of development, these polymers all have major deficiencies that inhibit their acceptance for large-scale applications. Author

N95-27702*# National Aeronautics and Space Administration. Lewis Research Center, Cleveland, OH.
PROCESS FOR NON-CONTACT REMOVAL OF ORGANIC COATINGS FROM THE SURFACE OF PAINTINGS Patent Application
Bruce A. Banks, inventor (to NASA) and Sharon K. Rutledge, inventor (to NASA) 11 May 1995 12 p
(NASA-Case-LEW-15896-1; NAS 1.71:LEW-15896-1;
US-Patent-Appl-SN-439544) Avail: CASI HC A03/MF A01

The present invention discloses a method of removing organic protective coatings from a painting. In the present invention degraded protective coatings such as lacquers, acrylics, natural resins, carbons, soot, and polyurethane are safely removed from the surface of a painting without contact to the surface of the painting. This method can be used for restoration of paintings when they have been damaged, through age, fire, etc. NASA

N95-27732* National Aeronautics and Space Administration. Langley Research Center, Hampton, VA.
PHENYLETHYNYL TERMINATED IMIDE OLIGOMERS Patent
Paul M. Hergenrother, inventor (to NASA), Robert G. Bryant, inventor (to NASA), Brian J. Jensen, inventor (to NASA), and Stephen J. Havens, inventor (to NASA) 5 Feb. 1995 14 p Filed 3 Mar. 1994 Supersedes N95-14185 (33 - 3, p 450)
(NASA-Case-LAR-15175-1; US-Patent-5,412,066;
US-Patent-Appl-SN-209512; US-Patent-Class-528-353;
US-Patent-Class-528-128; US-Patent-Class-528-172;
US-Patent-Class-528-173; US-Patent-Class-528-174;

US-Patent-Class-528-176; US-Patent-Class-528-183) Avail: US Patent and Trademark Office

Four phenylethynyl amine compounds - 3 and 4-aminophenoxy-4'-phenylethynylbenzophenone, and 3 and 4-amino-4'-phenylethynylbenzophenone - were readily prepared and were used to endcap imide oligomers. Phenylethynyl-terminated amide acid oligomers and phenylethynyl-terminated imide oligomers with various molecular weights and compositions were prepared and characterized. These oligomers were cured at 300 to 400 C to provide crosslinked polyimides with excellent solvent resistance, high strength and modulus, and good high temperature properties. Adhesive panels, composites, films, and moldings from these phenylethynyl terminated imide oligomers gave excellent mechanical performance.

Official Gazette of the U.S. Patent and Trademark Office

N95-27733# Pacific Northwest Lab., Richland, WA.

AMORPHIZATION OF COMPLEX CERAMICS BY HEAVY-PARTICLE IRRADIATIONS

R. C. Ewing (New Mexico Univ., Albuquerque, NM.), L. M. Wang (New Mexico Univ., Albuquerque, NM.), and W. J. Weber Nov. 1994 13 p Presented at the 1994 Fall Meeting of the Materials Research Society (MRS), Boston, MA, 28 Nov. - 2 Dec. 1994
(Contract DE-AC06-76RL-01830)
(DE95-005725; PNL-SA-25579; CONF-941144-56) Avail: CASI HC A03/MF A01

Complex ceramics, for the purpose of this paper, include materials that are generally strongly bonded (mixed ionic and covalent), refractory, and frequently good insulators. They are distinguished from simple, compact ceramics (e.g., MgO and UO2) by structural features which include: (1) open network structures, best characterized by a consideration of the shape, size, and connectivity of coordination polyhedra; (2) complex compositions which characteristically lead to multiple cation sites and lower symmetry; (3) directional bonding; and (4) bond-type variations within the structure. The heavy particle irradiations include ion-beam irradiations and recoil-nucleus damage resulting from alpha-decay events from constituent actinides. The latter effects are responsible for the radiation-induced transformation to the metamict state in minerals. The responses of these materials to irradiation are complex, as energy may be dissipated ballistically by transfer of kinetic energy from an incident projectile or radiolytically by conversion of radiation-induced electronic excitations into atomic motion. This results in isolated Frenkel defect pairs, defect aggregates, isolated collision cascades, or bulk amorphization. Thus, the amorphization process is heterogeneous. Only recently have there been systematic studies of heavy particle irradiations of complex ceramics on a wide variety of structure-types and compositions as a function of dose and temperature. In this paper, we review the conditions for amorphization for the tetragonal orthosilicate, zircon (ZrSiO4); the hexagonal orthosilicate/phosphate apatite structure-type (X10(ZO4)6(F,Cl,O)2); the isometric pyrochlores (A(sub 1-2)B2O6(O,OH,F)(sub 0-1p)H2O) and its monoclinic derivative zirconotite (CaZrTi2O7); the olivine (derivative - hcp) structure types, alpha-(sup VI)A2(sup IV)BO4, and spinel (ccp), gamma-(sup VI)A2(sup IV)BO4. DOE

N95-27857*# Old Dominion Univ., Norfolk, VA. Dept. of Civil Engineering.

POLYMER INFILTRATION STUDIES Final Report, 1 Oct. 1993 - 30 Apr. 1995

Joseph M. Marchello May 1995 16 p
(Grant NAG1-1067)
(NASA-CR-198601; NAS 1.26:198601) Avail: CASI HC A03/MF A01

Polymer infiltration investigations were directed toward development of methods by which to produce advanced composite material for automated part fabrication utilizing textile and robotic technology in the manufacture of subsonic and supersonic aircraft. Significant progress was made during the project on the preparation of carbon fiber composites using advanced polymer resins. The findings and results of the project are summarized in the attached paper entitled 'Powder-Coated Towpreg: Avenues to Near Net Shape Fabrication of High Performance Composite.' Also attached to this report is the second of two patent applications submitted as a result of these studies. Derived from text

N95-27879# Sandia National Labs., Albuquerque, NM.

TUNGSTEN CARBIDE FRAGMENTATION: EXPERIMENTAL CHARACTERIZATION AND NUMERICAL MODELLING

E. S. Hertel, Jr. and D. E. Grady 1995 9 p Presented at the 15th International Symposium on Ballistics, Haifa, Israel, 21-24 May 1995
(Contract DE-AC04-94AL-85000)
(DE95-008521; SAND-94-2344C; CONF-950537-1) Avail: CASI HC A02/MF A01

Tungsten Carbide is a high density ceramic (generally found in ceramic/metal mixtures) with attractive shear and tensile strength properties in certain ballistic applications. We have determined a Hugoniot elastic limit of approximately 4 GPa, followed by strong hardening behavior, with spall strengths of 2.7-3.6 GPa. In addition, a series of experiments where Tungsten Carbide spheres impacted PMMA indicates that a sharp transition to fine-grained fragmentation occurred at impact velocities between 2.4 and 2.9 km/s. The well-characterized experiments described above were used to assess the effectiveness of CTH in predicting the axial and radial dispersion of the projectile after break-up. CTH has a fracture model that relies on a P(sub min) criteria to allow computational void to relieve a tensile condition. Comparisons with the experimental data were made using the P(sub min) model and an additional model based on an energy-based theory of Grady and Kipp. We found that the simple models are not capable of predicting the complex fragmentation behavior seen in the experiments. DOE

N95-27943# Los Alamos National Lab., NM.

PREDICTION OF MATERIAL STRENGTH AND FRACTURE OF GLASS USING THE SPHINX SMOOTH PARTICLE HYDRODYNAMICS CODE

D. A. Mandell and C. A. Wingate Aug. 1994 31 p
(Contract W-7405-eng-36)
(DE95-004869; LA-12830) Avail: CASI HC A03/MF A01

The design of many military devices involves numerical predictions of the material strength and fracture of brittle materials. The materials of interest include ceramics, that are used in armor packages; glass that is used in truck and jeep windshields and in helicopters; and rock and concrete that are used in underground bunkers. As part of a program to develop advanced hydrocode design tools, the authors have implemented a brittle fracture model for glass into the SPHINX smooth particle hydrodynamics code. The authors have evaluated this model and the code by predicting data from one-dimensional flyer plate impacts into glass, and data from tungsten rods impacting glass. Since fractured glass properties, which are needed in the model, are not available, the authors did sensitivity studies of these properties, as well as sensitivity studies to determine the number of particles needed in the calculations. The numerical results are in good agreement with the data. DOE

N95-27946# Oak Ridge National Lab., TN.

THE DEVELOPMENT AND TESTING OF CERAMIC COMPONENTS IN PISTON ENGINES Final Report

B. J. McEntire, R. W. Willis (TRW, Inc., Cleveland, OH.), and R. E. Southam (TRW, Inc., Cleveland, OH.) Oct. 1994 56 p
(Contract DE-AC05-84OR-21400)
(DE95-005759; ORNL/Sub-90-SG151/1) Avail: CASI HC A04/MF A01

Within the past 10-15 years, ceramic hardware has been fabricated and tested in a number of piston engine applications including valves, piston pins, roller followers, tappet shims, and other wear components. It has been shown that, with proper design and installation, ceramics improve performance, fuel economy, and wear and corrosion resistance. These results have been obtained using rig and road tests on both stock and race engines. Selected summaries of these tests are presented in this review paper. DOE

N95-27962# Oak Ridge National Lab., TN.

ASSAY OF WEATHERING EFFECTS ON PROTECTIVE POLYMER COATINGS USING POSITRON ANNIHILATION SPECTROSCOPY

L. D. Hulett, Jr., S. Wallace, Jun Xu, B. Nielsen (Brookhaven National Lab., Upton, NY.), Cs. Szeles (Brookhaven National Lab., Upton, NY.), K. G. Lynn (Brookhaven National Lab., Upton, NY.), J. Pfau, and A. Schaub 1995 15 p Presented at the 6th International Workshop on Slow-positron Beam Techniques for Solids and Surfaces (SLOPOS6), Makuhari, Japan, 18-22 May 1994

(Contracts DE-AC05-84OR-21400; DE-AC02-76CH-00016)
(DE95-007040; CONF-9405198-4) Avail: CASI HC A03/MF A01

Polymer coatings, both with and without pigments, have been subjected to solar radiation and water spray weathering. The degrees of penetration of the weathering effects have been measured by injecting positrons of varying energy, i.e. to variable depths, into the films and observing the Doppler broadening of the annihilation radiation. The method is capable of detecting changes due to weathering effects at very early stages, long before visual examination reveals degradation. As little as one week of exposure caused measurable changes in the polymer structure, which were reflected in the Doppler broadening. Given further development, positron spectroscopy could possibly become a useful complement to the other methods of determining weatherabilities of protective polymer coatings. DOE

N95-27967 Argonne National Lab., IL.
THE STRUCTURE OF LEAD-INDIUM PHOSPHATE GLASS
K. Suzuya, D. L. Price, C. K. Loong, B. C. Sales, and L. A. Boatner Dec. 1994 6 p Presented at the 1994 Fall Meeting of the Materials Research Society (MRS), Boston, MA, 28 Nov. - 2 Dec. 1994 Limited Reproducibility: More than 20% of this document may be affected by microfiche quality
(Contract W-31-109-eng-38)
(DE95-007130; ANL/IPNS/CP-85110; CONF-941144-58) Avail: CASI HC A02

Lead-indium phosphate-lasses exhibit a number of useful properties such as a high index-of-refraction, low preparation temperature and melt viscosity, and good chemical durability. The structure of such a glass (composition in wt.%: 65 PbO, 29 P2O5, 6 In2O3) has been investigated by total neutron scattering using the GLAD diffractometer at Argonne's spallation neutron source IPNS. Peaks corresponding to the P-0, Pb-O/In-O, and O-O pairs were observed in the radial distribution function. The short-range structure in the -lass, in terms of average coordination numbers and bond distances, is compared with those of a pure P2O5 glass and with the crystal structure of lead pyrophosphate, Pb2P2O7. Unlike silicate glasses in which the SiO4 tetrahedra form a 3-dimensional network, the PO4 tetrahedra in phosphate glasses form a chain-like structure. The structural modification by the lead cations in phosphate glasses appears to occur mainly in the medium range-affecting, the lengths and connectivity of the chain-like structure. DOE

N95-27993# Sandia National Labs., Albuquerque, NM.
MANUFACTURING TAILORED PROPERTY CERAMIC COMPOSITES
Kevin G. Ewsuk and Larry W. Harrison 14 Nov. 1994 23 p Presented at the 96th Annual Meeting of the Ameri can Ceramic Society, Indianapolis, IN, 25-28 Apr. 1994 Prepared in cooperation with Du Pont de Nemours (E. I.) and Co., Wilmington, DE
(Contract DE-AC04-94AL-85000)
(DE95-006303; SAND-93-1875C; CONF-940416-32) Avail: CASI HC A03/MF A01

Composite materials are desirable for many advanced engineering applications where the properties of a single phase material cannot meet all of the service requirements; however, existing process technology has limited the development and commercialization of composites. Lack of reproducible sintering to high density is one of the major obstacles to commercializing ceramic composites. Final-stage, non-reactive liquid phase sintering (NLPS) theory provides metrics for sinterability that can be used as guidelines to design and manufacture dense ceramic-filled-glass (CFG) composites. Additionally, within the constraints defined by the NLPS theory, sum-property models can be used to predict CFG composite properties, and to design composites with properties tailored to specific applications. By integrating composite process models with composite property models, processable, application-tailored CFG composites for microelectronics packaging have been designed and fabricated. DOE

N95-28080# Oak Ridge National Lab., TN. Solid State Div.
MODIFICATION OF THE OPTICAL PROPERTIES OF GLASS BY SEQUENTIAL ION IMPLANTATION
R. H. Magruder, III, D. H. Osborne, Jr. (Vanderbilt Univ., Nashville, TN.), and R. A. Zuhr 1994 13 p Presented at the 13th International Conference on the Application of Accelerators in Research and Industry, Denton, TX, 7-10 Nov. 1994 Sponsored by Martin Marietta Energy Systems, Inc.
(Contracts DE-AC05-84OR-21400; DAAH04-93-G-0123)
(DE95-007401; CONF-941129-15) Avail: CASI HC A03/MF A01

The linear and nonlinear optical properties of a series of samples formed by the sequential implantation of Ti, O and Au are examined. Energies of implantation for each ion were chosen using TRIM calculations to insure overlap of the ion distributions. The Ti was implanted with nominal doses of 1.2 and 2 x 10(exp 17) ions/sq cm. The samples were implanted with oxygen to the same nominal dose as the Ti. Au was then implanted with a nominal dose of 6 x 10(exp 16) ions/sq cm. The samples were subsequently annealed in oxygen at 900 C for two hours. The Ti and O are incorporated into the host network, while the Au forms nanosize colloids. The presence of the Ti in the substrate causes a shift in the surface plasmon resonance frequency of the Au metal colloids as well as an increase in the nonlinear response of the composites. The results are interpreted in terms of effective medium theory. DOE

N95-28089# Sandia National Labs., Albuquerque, NM.
COPPER CVD USING LIQUID COINJECTION OF (hfac)Cu(TMVS) AND TMVS
J. S. Custer, G. A. Petersen, P. M. Smith, J. E. Parmeter, C. A. Apblett, J. A. T. Norman, A. K. Hochberg, and D. A. Roberts 1994 5 p Presented at the Advanced Metallizaion for ULSI Applications in 1994, Austin, TX, 4-6 Oct. 1994
(Contract DE-AC04-94AL-85000)
(DE95-008155; SAND-94-2544C; CONF-9410178-1) Avail: CASI HC A01/MF A01

Copper chemical vapor deposition using liquid coinjection of the Cu(I) precursor (hfac)Cu(TMVS) along with TMVS has been demonstrated. The coinjection of TMVS with (hfac)Cu(TMVS) stabilizes the Cu precursor until it enters the reaction chamber, allowing for better control of the deposition and faster deposition rates. Using this technique, we have grown films with as-deposited resistivities of 1.86 +/- 0.04 (mu)(Omega)-cm, independent of film thickness. Deposition rates of well over 100 nm/min are possible. Good step coverage and gap fill down to 0.6 micrometer lines is demonstrated, with gap fill being limited by the large Cu grain sizes in these films. DOE

N95-28090# Stanford Linear Accelerator Center, Stanford, CA.
AMBIENT-PRESSURE SILICA AEROGEL FILMS
S. S. Prakash (New Mexico Univ., Albuquerque, NM.), C. J. Brinker (New Mexico Univ., Albuquerque, NM.), and A. J. Hurd 1994 7 p Presented at the 1994 Fall Meeting of the Materials Research Society (MRS), Boston, MA, 28 Nov. - 2 Dec. 1994
(Contract DE-AC04-94AL-85000)
(DE95-008161; SAND-95-0350C; CONF-941144-87) Avail: CASI HC A02/MF A01

Very highly porous (aerogel) silica films with refractive index in the range 1.006-1.05 (equivalent porosity 98.5-88%) were prepared by an ambient-pressure process. It was shown earlier using in situ ellipsometric imaging that the high porosity of these films was mainly attributable to the dilation or 'springback' of the film during the final stage of drying. This finding was irrefutably reconfirmed by visually observing a 'springback' of great er than 500% using environmental scanning electron microscopy (ESEM). Ellipsometry and ESEM also established the near cent per cent reversibility of aerogel film deformation during solvent intake and drying. Film thickness profile measurements (near the drying line) for the aerogel, xerogel and pure solvent cases are presented from imaging ellipsometry. The thickness of these films (crack-free) were controlled in the range 0.1-3.5 micrometers independent of refractive index. DOE

N95-28097 North Carolina State Univ., Raleigh, NC.
LOW TEMPERATURE DEPOSITION AND CHARACTERIZATION OF N- AND P-TYPE SILICON CARBIDE THIN FILMS AND ASSOCIATED OHMIC AND SCHOTTKY CONTACTS Semiannual Technical Report, 1 Jul. - 31 Dec. 1994
Robert F. Davis and Robert J. Nemanich Dec. 1994 39 p Limited Reproducibility: More than 20% of this document may be affected by microfiche quality
(Contract N00014-92-J-1500)
(AD-A289107) Avail: Issuing Activity (Defense Technical Information Center (DTIC))

Exposure of heated 6H-SiC wafers to SiH4 contained both in a gas stream and an activated plasma was investigated for low temperature SiC cleaning and oxygen removal prior to thin film deposition. UPS revealed the first observation of surface states on the cleaned 6H-SiC surface. Monocrystalline epitaxial films of Beta(3C)-SiC(111) and alpha(6H)-SiC(0001) were grown on vicinal (approximately 3.50 deg off (0001) towards) alpha(6H)-SiC(0001) substrates via gas-source MBE from 1050 to 1250 C using Si2H6 and C2H4. Undoped films were n-type; p-type films were achieved using Al evaporation during growth. The undoped 3C-SiC films grown on thin AlN buffer layers had carrier concentrations as low as 3 x 10(exp 15)/cu cm. Extremely efficient activation of n-type (Al) dopants has been achieved. Initial attempts at n-type doping using NH3 are also described. Surfaces of 6H-SiC(0001) homoepitaxial layers deposited on vicinal and on-axis 6H-SiC wafers by CVD have also been investigated using ultra-high vacuum scanning tunneling microscopy (UHV STM). The vicinal surface showed strongly undulating step configurations. The on-axis surface possessed much wider terraces and much smoother step undulations. Step heights on both surfaces were 2.5 A corresponding to a single bilayer containing one Si and one C layer. After annealing at T greater than 110 C for 3-5 min. in UHV. selected terraces contained honeycomb-like regions most likely caused by the transformation to graphite as a result of Si sublimation. DTIC

N95-28117# Sandia National Labs., Albuquerque, NM.
CHROMATE-FREE CORROSION RESISTANT CONVERSION COATINGS FOR ALUMINUM ALLOYS
R. G. Buchheit, C. A. Drewien, M. A. Martinez, and G. E. Stoner (Virginia Univ., Charlottesville, VA.) 1995 10 p Presented at the Annual Meeting and Exhibition of the Minerals, Metals and Materials Society, Las Vegas, NV, 12-16 Feb. 1995
(Contract DE-AC04-94DP-85000)
(DE95-007742; SAND-95-0280C; CONF-950201-2) Avail: CASI HC A02/MF A01

Inorganic polycrystalline hydrotalcite, Li2(Al2(OH)6)2 center-dot CO3 center-dot 3H2O, coatings can be formed on aluminum and aluminum alloys by exposure to alkaline lithium carbonate solutions. This process is conducted using methods similar to traditional chromate conversion coating procedures, but does not use or produce toxic chemicals. The coating provides anodic protection and delays the onset of pitting during anodic polarization. Cathodic reactions are also inhibited which may also contribute to corrosion protection. Recent studies have shown that corrosion resistance can be increased by sealing hydrotalcite coated surfaces to transition metal salt solutions including Ce(NO3)3, KMnO4, and Na2MoO4. Results from these studies are also reported. DOE

N95-28133# New Mexico Univ., Albuquerque, NM.
METHODS DEVELOPMENT FOR MEASURING AND CLASSIFYING FLAMMABILITY/COMBUSTIBILITY OF REFRIGERANTS. TASK 1: ANNOTATED BIBLIOGRAPHY Interim Summary Report
E. W. Heinonen and R. E. Tapscott Jun. 1994 118 p
(Contract DE-FG02-91CE-23810)
(DE95-007232; DOE/CE-23810/42G; NMERI-OC-94/31) Avail: CASI HC A06/MF A02

For Task 1 of the flammable refrigerant methods development contract, NMERI performed a literature search to identify references on the flammability of refrigerants. A database to store a bibliographic record of the literature search was then developed. This database is contained in the Microsoft Access(reg sign) relational database management system for Windows(trademark). Searches for applicable sources were made on-line using the STN(reg sign) scientific and technical network; off-line using the National Technical Information Service (NTIS) database; WorldCat CD-rom database; the University of New Mexico library search; the Air-Conditioning and Refrigeration Institute (ARI) Refrigerant Database; and personal contacts. Three specific areas were searched: refrigerant properties, flammability test methods, and ignition technology. Many of the articles retrieved fall into multiple categories. Ignition technology was included as a separate category because of the importance of the ignition process to flammability and the vast amount of information available on ignition of gaseous fuels, especially hydrocarbons. Over 90 separate references have been entered into the database. Two separate report formats have been developed to display the results of the literature search. Appendix B is the short report format--without abstract, while Appendix C is the long format-with abstract. DOE

N95-28212* National Aeronautics and Space Administration. Ames Research Center, Moffett Field, CA.
BORON-CARBON-SILICON POLYMERS AND THE CERAMIC THEREOF Patent
Salvatore R. Riccitiello, inventor (to NASA), Ming-ta S. Hsu, inventor (to NASA), and Timothy S. Chen, inventor (to NASA) 22 Jan. 1991 8 p Filed 5 Jun. 1989
(NASA-Case-ARC-11891-1-SB; US-Patent-4,987,201; US-Patent-Appl-SN-361471; US-Patent-Class-528-4; US-Patent-Class-528-5; US-Patent-Class-528-7; US-Patent-Class-556-402; US-Patent-Class-556-403; Int-Patent-Class-C08G-79/08) Avail: US Patent and Trademark Office

The present invention relates to a process for the production of an organoborosilicon preceramic polymer. The prepolymer is pyrolyzed to produce a ceramic article useful in high temperature (e.g., aerospace) or extreme environmental applications.
Official Gazette of the U.S. Patent and Trademark Office

N95-28226# California Univ., Berkeley. Lawrence Berkeley Lab, CA.
FEASIBILITY STUDIES FOR SEPARATION PROCESSES USING ENVIRONMENTALLY SENSITIVE HYDROGELS
A. P. Sassi, H. W. Blanch, and J. M. Prausnitz Dec. 1994 18 p
(Contract DE-AC03-76SF-00098)
(DE95-008355; LBL-36405) Avail: CASI HC A03/MF A01

Temperature- and pH-sensitive hydrogels can be used to separate or concentrate proteins from dilute solution. Two possible separation processes are discussed here. Experimental partitioning data are used to compare the efficiencies of neutral, weakly acidic, weakly basic, and polyampholytic poly-N-isopropylacrylamide copolymer gels for separating cytochrome c from ovalbumin. For each process, attention is given to the influence of the solute partition coefficient and swelling equilibria on process efficiency. DOE

N95-28235# Argonne National Lab., IL. Chemistry Div.
SYNTHESIS AND PROPERTIES OF LANTHANIDE-EXCHANGED PREYSSLER'S HETEROPOLYANIONS
Mark R. Antonio, J. Malinsky, and L. Soderholm 1994 6 p Presented at the 1994 Fall Meeting of the Materials Research Society, Boston, MA, 28 Nov. - 2 Dec. 1994
(Contract W-31-109-eng-38)
(DE95-007136; ANL/CHM/CP-83289; CONF-941144-78) Avail: CASI HC A02/MF A01

Na(+) in the Preyssler heteropolytungstate anion (NaP5W30O110)(sup 14-) can be exchanged for a trivalent lanthanide ion. The potential significance of this new class of lanthanide heteropolyanions relates to their applications in catalysis science. This view follows from the fact that Keggin heteropolyanions and their free acids are used as heterogeneous solid catalysts and homogeneous solution catalysts. The authors describe synthetic conditions that lead to the incorporation of Ce(3+) and Pr(3+) within the Preyssler anion, and the coprecipitation of Ce(3+) and the Preyssler anion. Initial studies indicate that the latter, coprecipitated, material deserves study for bifunctional catalytic activity. DOE

N95-28358# Sandia Labs., Albuquerque, NM.
CESIUM/OXIDE INTERACTIONS FOR ULTRATHIN FILMS ON (ALPHA)-Al2O3(001) AND (ALPHA)-Al2O3(1(BAR 1)O2)
K. R. Zavadil and J. L. Ing (AEA Technology, Albuquerque, NM.) 1995 7 p Presented at the 1994 Fall Meeting of the Materials Research Society (MRS), Boston, MA, 28 Nov. - 2 Dec. 1994
(Contract DE-AC04-94AL-85000)
(DE95-008159; SAND-95-0309C; CONF-941144-84) Avail: CASI HC A02/MF A01

The interaction of cesium at the (0001) and (1(bar 1)O2) surfaces of sapphire has been investigated using a variety of surface analytical techniques. Reflection mass spectrometric measurements yield initial Cs adsorption probabilities of 0.9 and 0.85 for the unreconstructed (0001) and (1(bar 1)O2) surfaces, respectively. The adsorption probability decreases dramatically for these surfaces at critical Cs coverages of 2.0 x 10(exp 14) and 3.4 x 10(exp 14) atoms/sq cm, respectively. Thermally induced reconstruction of the (0001) surface to form an oxygen deficient surface results in a decrease in the initial probability and capacity for Cs adsorption. Low energy electron diffraction (LEED) demonstrates that an intermediate, mixed domain surface yields an initial adsorption probability of 0.5 while a ((radical)31 x (radical)31) R (+/-) 9 deg reconstructed surface yields a value of 0.27. Thermal desorption mass spectrometry (TDMS) shows that surface reconstruction eliminates the high binding energy states of Cs (2.7 eV/atom), consistent with the observed changes in adsorption probability. In contrast, reconstruction of the (1(bar 1)O2) surface produces only minor changes in Cs adsorption. X-ray photoelectron spectroscopy (XPS) indicates that no formal reductive/oxidative chemistry takes place at the interface. We interpret the facile adsorption and strong binding of Cs on sapphire to result from Cs interacting with coordinatively unsaturated oxygen. DOE

N95-28385*# KTA-Tator, Inc., Humble, TX.
WEIGHTLESS ENVIRONMENT TRAINING FACILITY (WETF) MATERIALS COATING EVALUATION, VOLUME 1 Final Report
1995 103 p
(Contract NAS9-18973)
(NASA-CR-188366-Vol-1; NAS 1.26:188366-Vol-1) Avail: CASI HC A06/MF A02

The Weightless Environment Training Facility Material Coating Evaluation project has included preparing, coating, testing, and evaluating 800 test panels of three differing substrates. Ten selected coating systems were evaluated in six separate exposure environments and subject to three tests for physical properties. Substrate materials were identified, the manner of surface preparation described, and exposure environments defined. Exposure environments included immersion exposure, cyclic exposure, and field exposure. Cyclic exposures, specifically QUV-Weatherometer and the KTA Envirotest were found to be the most agressive of the environments included in the study when all three evaluation criteria are considered. This was found to result primarily from chalking of the coatings under ultraviolet (UV) light exposure. Volumes 2 and 3 hold the 5 appendices to this report. Derived from text

N95-28386*# KTA-Tator, Inc., Humble, TX.
WEIGHTLESS ENVIRONMENT TRAINING FACILITY (WETF) MATERIALS COATING EVALUATION, VOLUME 2 Final Report
1995 311 p
(Contract NAS9-18973)
(NASA-CR-188366-Vol-2; NAS 1.26:188366-Vol-2) Avail: CASI HC A14/MF A03

This volume consists of Appendices A and B to the report on the Weightless Environment Training Facility Materials Coating Evaluation project. The project selected 10 coating systems to be evaluated in six separate exposure environments, and subject to three tests for physical properties. Appendix A holds the coating system, surface preparation, and application data. Appendix B holds the coating material infrared spectra. CASI

N95-28387*# KTA-Tator, Inc., Humble, TX.
WEIGHTLESS ENVIRONMENT TRAINING FACILITY (WETF) MATERIALS COATING EVALUATION, VOLUME 3 Final Report
1995 279 p
(Contract NAS9-18973)
(NASA-CR-188366-Vol-3; NAS 1.26:188366-Vol-3) Avail: CASI HC A13/MF A03

This volume consists of Appendices C, D, E, and F to the report on the Weightless Environment Training Facility Materials Coating Evaluation project. The project selected 10 coating systems to be evaluated in six separate exposure environments, and subject to three tests for physical properties. Appendix C is the photographic appendix of the test panels. Appendix D details methods and procedures. Appendix E lists application equipment costs. Appendix F is a compilation of the solicitation of the candidate coating systems. CASI

N95-28397# Oak Ridge National Lab., TN.
DEVELOPMENT OF LOW-EXPANSION CERAMICS WITH STRENGTH RETENTION TO ELEVATED TEMPERATURES Final Report
D. A. Hirschfeld and J. J. Brown, Jr. (Virginia Polytechnic Inst., Blacksburg, VA.) Sep. 1994 140 p
(Contract DE-AC05-84OR-21400)
(DE95-005760; ORNL/Sub-86-22049/2) Avail: CASI HC A07/MF A02

The development of advanced engines has resulted in the need for new ceramic compositions which exhibit thermo-mechanical properties suitable for the engine environment, e.g., low thermal expansion, stability to 1,200 C, and thermal shock resistance. To meet these goals, a two phase research program was instituted. In the first phase, new oxide ceramics were identified in the AlPO4-(beta)-eucryptite, (beta)-cristobalite, mullite and zircon systems. This research focused on screening and property characterization of ceramics in the four systems. The most promising compositions in the AlPO4-(beta)-eucryptite and zircon systems were then further evaluated and developed in the second phase with the goal of being ready for prototype testing in actual engines. Of the compositions, calcium magnesium zirconium phosphate (zircon system) exhibits the most desirable properties and is presently being developed for commercialization. DOE

N95-28400# Sandia National Labs., Albuquerque, NM.
FUNCTIONALIZED BLOCK COPOLYMERS AS ADHESION PROMOTERS
M. S. Kent and R. Saunders 1995 4 p Presented at the 18th Annual Meeting of the Adhesion Society, Hilton Head, SC, 19-22 Feb. 1995
(Contracts DE-AC04-94AL-85000; W-31-109-eng-38)
(DE95-008158; SAND-95-0378C; CONF-950273-1) Avail: CASI HC A01/MF A01

The goal of this work is to develop novel functionalized block copolymers to promote adhesion at inorganic substrate/polymer interfaces. We envision several potential advantages of functionalized block copolymers over small molecule coupling agents. Greater control over the structure of the interphase region should result through careful design of the backbone of the copolymer. The number of chains per area, the degree of entanglement between the copolymer and the polymer matrix, the number of sites per chain able to attach to the substrate, and the hydrophobicity of the interphase region can all be strongly affected by the choice of block lengths and the monomer sequence. In addition, entanglement between the copolymer and the polymer matrix, if achieved, should contribute significantly to adhesive strength. Our program involves four key elements: the synthesis of suitable functionalized block copolymers, characterization of the conformation of the copolymers at the interface by neutron reflectivity and atomic force microscopy, characterization of the degree of bonding by spectroscopy, and measurement of the mechanical properties of the interface. In this paper we discuss block copolymers designed as adhesion promoters for the copper/epoxy interface. We have synthesized a diblock with one block containing imidazole groups to bond to copper and a second block containing secondary amines to react with the epoxy matrix. We have also prepared a triblock copolymer containing a hydrophobic middle block. Below we describe the synthesis of the block copolymers by living, ring-opening metathesis polymerization (ROMP) and the first characterization data obtained by neutron reflectivity. DOE

N95-28401# Sandia National Labs., Albuquerque, NM.
THE MINIMUM PORE SIZE OBTAINABLE IN A SILICA GEL DURING DRYING
S. Wallace, C. J. Brinker, and D. M. Smith (New Mexico Univ., Albuquerque, NM.) 1994 7 p Presented at the 1994 Fall Meeting of the Materials Research Society (MRS), Boston, MA, 28 Nov. - 2 Dec. 1994
(Contract DE-AC04-94AL-85000)
(DE95-008162; SAND-95-0391C; CONF-941144-86) Avail: CASI HC A02/MF A01

The pore size r(sub p) in a gel is determined by the extent of shrinkage of the gel network during drying. Shrinkage is driven by the collapse of the gel network in response to the capillary pressure P(sub c) exerted by the pore fluid. The extent of shrinkage depends on the balance between the capillary pressure P(sub c) in the pore fluid and the bulk modulus K(sub p) of the gel. The hydraulic pore radius, r(sub H) = 2V(sub p)/S(sub a), where V(sub p) is the pore volume and S(sub a) is the apparent N2 BET surface area, is often used to characterize the pore size of a gel. A series of acid catalyzed silica gels dried in pore fluids with different (gamma)(sub lv), showed that there is a limit to the minimum apparent r(sub H) obtainable in a gel, and when the volume fraction of porosity (phi) less than or equal to 0.37, r(sub H) becomes constant and approximately 0.8 nm. In contrast, experimental data show that the true pore size r(sub p) of gels continues to decrease when (phi) less than or equal to 0.37. Analysis of their adsorption isotherms show that while r(sub H) apparently stays constant: (1) the BET C constant continues to increase; (2) the width and average of their pore size distributions continue to decrease;

and (3) as shrinkage continues the gels eventually become non-porous to N2 at 77 K but are still porous to CO2 at 273 K. This paper reviews these results and addresses micropore formation in silica gels with the goal of determining how P(sub c) influences the final r(sub p), and why r(sub p) and r(sub H) diverge when (phi) less than or equal to 0.37. DOE

N95-28404# Sandia National Labs., Albuquerque, NM.
NEW DEVELOPMENTS FOR SOL-GEL FILM AND FIBER PROCESSING
A. J. Hurd 1995 8 p Presented at the International Conference on Novel Techniques in Synthesis and Processing, Rosemont, IL, 2 Oct. 1994
(Contract DE-AC04-94AL-85000)
(DE95-008175; SAND-95-0343C; CONF-9410319-1) Avail: CASI HC A02/MF A01

New insights into the development of microstructure in sol-gel films have recently been revealed by several diagnostic techniques, including imaging ellipsometry, 'chemical imaging' by fluorescent tracers, light scattering from capillary waves, and finite-element modeling. The evolution of porosity during the continuous transition from dilute sol to porous solid in restricted geometries such as films and fibers is becoming clearer through fundamental understanding of evaporation dynamics and capillarity. DOE

N95-28405# Sandia National Labs., Albuquerque, NM.
MECHANICAL PROPERTIES OF HYSOL EA-9394 STRUCTURAL ADHESIVE
T. R. Guess, E. D. Reedy, and M. E. Stavig Feb. 1995 29 p
(Contract DE-AC04-94AL-85000)
(DE95-008187; SAND-95-0229) Avail: CASI HC A03/MF A01

Dextor's Hysol EA-9394 is a room temperature curable paste adhesive representative of the adhesives used in wind turbine blade joints. A mechanical testing program has been performed to characterize this adhesive. Tension, compression stress relaxation, flexural, butt tensile, and fracture toughness test results are reported. DOE

N95-28457 Connecticut Univ., Storrs, CT.
MOLECULAR ENGINEERING OF THIN POLYMER FILMS PREPARED FROM FUNCTIONALLY-TERMINATED OLIGOMERS Final Report, 1 Aug. 1991 - 31 Jul. 1994
Jeffrey T. Koberstein 19 Feb. 1995 6 p Limited Reproducibility: More than 20% of this document may be affected by microfiche quality
(Contract DAAL03-91-G-0139)
(AD-A291681; ARO-27863.14-MS) Avail: Issuing Activity (Defense Technical Information Center (DTIC))

The research performed under this contract focused on the molecular engineering of thin polymer films prepared from functionally terminated oligomers by application of Langmuir Blodgett monolayer and multilayer film transfer techniques. The goals of the work were to: (1) Fabricate ultrathin films (i.e. 1-10 nm thickness) with controlled thickness, orientation, and surface chemistry; (2) Use these films to develop boundary lubricants that are stable at high temperatures; (3) Apply these films to stabilize the aging characteristics of bulk acoustic wave oscillators. DTIC

N95-28508 Case Western Reserve Univ., Cleveland, OH.
THE 18TH ASILOMAR CONFERENCE ON POLYMERIC MATERIALS Final Report, 1 Sep. 1994 - 31 Aug. 1995
Eric Baer Feb. 1995 26 p Conference held at Pacific Grove, CA, 12-15 Feb. 1995 Limited Reproducibility: More than 20% of this document may be affected by microfiche quality
(Contract DAAH04-94-G-0390)
(AD-A291721; ARO-33469.1-MS-CF) Avail: Issuing Activity (Defense Technical Information Center (DTIC))

Partial contents include the following: cooperative effects in fiber microbuckling; processing, structure, and properties of PBO fibers - a lyotropic system; high performance synthetic fibers for composites; polymer adhesion to surfaces in composite materials; novel adsorption systems based on high surface area fibers; grafting of microparticles onto fiber surfaces; delamination failure mechanisms of PC/SAN microlayers; liquid crystalline polymer fibers - the next generation; processing, structure and properties of extended chain polyethylene fibers; new structural polymers after natural materials; interfaces in multiphase blends; novel methods of fiber production land use; crystallization of thermoplastic composites: poly(ethylene terephthalate) polycarbonate blends; nanoscopic supermolecules - controlled three dimensional dendritic polymers; and oscillating catalysts for block polymer synthesis. DTIC

N95-28531 Sandia National Labs., Albuquerque, NM.
POROSITY IN HEXYLENE-BRIDGED POLYSILSESQUIOXANES: EFFECTS OF MONOMER CONCENTRATION
Brigitta Baugher, Douglas A. Loy, Roger A. Assink, S. Prabakar (Advanced Materials Lab., Albuquerque, NM.), Kenneth J. Shea (California Univ., Irvine, CA.), and Henry Oviatt (California Univ., Irvine, CA.) 1994 7 p Presented at the 1994 Fall Meeting of the Materials Research Society, Boston, MA, 28 Nov. - 2 Dec. 1994 Limited Reproducibility: More than 20% of this document may be affected by microfiche quality
(Contract DE-AC04-94AL-85000)
(DE95-005421; SAND-94-3197C; CONF-941144-28) Avail: CASI HC A02

Hexylene-bridged polysilsesquioxanes can be prepared as mesoporous or non-porous xerogels simply by switching from basic to acidic polymerization conditions. In this study, we looked at the effect of monomer concentration on porosity of hexylene-bridged xerogels prepared under acidic and basic conditions. 1, 6-Hexylene-bridged polysilsesquioxanes were prepared by sol-gel polymerizations of 1, 6-bis(triethoxysilyl)hexane 1 with concentrations between 0.1 to 1.2 M in ethanol. Gelation times ranged from seconds for 1.2 M concentration to months for 0.2 M. The gels were processed into xerogels by an aqueous work-up and the dry gels characterized by scanning electron microscopy (SEM), solid state C-13 and Si-29 CP MAS NMR spectroscopy, and gas sorption porosimetry. DOE

N95-28532# Sandia National Labs., Albuquerque, NM.
COMPARISON OF BRIDGED POLYSILSESQUIOXANE XEROGELS PREPARED FROM METHOXY- AND ETHOXY-SILYL MONOMERS
Douglas A. Loy, Brigitta Baugher, Roger A. Assink, S. Prabakar (Advanced Materials Lab., Albuquerque, NM.), and Kenneth J. Shea (California Univ., Irvine, CA.) 1994 7 p Presented at the 1994 Fall Meeting of the Materials Research Society, Boston, MA, 28 Nov. - 2 Dec. 1994
(Contract DE-AC04-94AL-85000)
(DE95-005422; SAND-94-3196C; CONF-941144-29) Avail: CASI HC A02/MF A01

Hydrocarbon-bridged polysilsesquioxanes are prepared by the sol-gel polymerization of monomers with more than one trialkoxysilyl group attached directly to the bridging group by Si-C bonds. While the effects of varying the identity of the bridging group (length, rigidity, etc.), monomer concentration, and type of catalyst have been studied, the effect of different alkoxy ligands on the silicon atoms has not been investigated. For this study, 1, 6-bis(triethoxysilyl)hexane 1 and 1, 6-bis(trimethoxysilyl)hexane 2 were polymerized under acidic and basic conditions in ethanol and methanol, respectively, and in tetrahydrofuran (THF). The resulting gels were processed to afford xerogels that were characterized by SEM, solid state C-13 and Si-29 Cross Polarization Magic Angle Spinning (CP MAS) NMR spectroscopy, and nitrogen sorption porosimetry. DOE

N95-28547# Brookhaven National Lab., Upton, NY.
SURFACE SCANNING TECHNIQUES TO LOCATE AND STUDY DEFECTS IN PAINTED ZINC AND ZINC ALLOY COATED STEELS
H. S. Isaacs (Korrosionsinstitutet, Stockholm, Sweden.), A. J. Aldykiewicz, Jr. (Korrosionsinstitutet, Stockholm, Sweden.), D. Thierry (Korrosionsinstitutet, Stockholm, Sweden.), and T. C. Simpson 1995 10 p Presented at the Corrosion 1995: National Association of Corrosion Engineers (NACE) International Annual Conference and Corrosion Show, Orlando, FL, 26-31 Mar. 1995
(Contract DE-AC02-76CH-00016)
(DE95-006099; BNL-61239; CONF-950304-13) Avail: CASI HC A02/MF A01

Current density and impedance mapping measurements have been used to locate and monitor corrosion and defects on painted surfaces in solution. Measurements are reported for painted zinc and aluminum-zinc alloy coated steel surfaces. When scratched, current density mapping showed corrosion of the metal coating started at localized sites in both dilute chloride and sulfate solutions. Different scribing techniques were tested exposing only the metal coating and both the coating and the underlying steel. Effect of roll forming was investigated. Current density mapping located corrosion susceptible defects on painted roll formed materials that were not readily discernible optically. Scanning ac mapping showed that artificially formed defects were readily observed. Local impedance variations with frequency were measured for simulated defects and defect free areas of painted surfaces. Variations in paint thickness and the presence of defects were detected using the ac techniques. DOE

N95-28560# Oak Ridge National Lab., TN.
[AN OVERVIEW OF ACTIVITIES AND ACCOMPLISHMENTS OF THE METALS AND CERAMICS DIVISION] Progress Report, 31 Dec. 1993
D. F. Craig, R. A. Bradley, and J. R. Weir, Jr. Jul. 1994 245 p
(Contract DE-AC05-84OR-21400)
(DE95-007020; ORNL-6780) Avail: CASI HC A11/MF A03

This report provides an overview of activities and accomplishments of the division from October 1992 through December 1993; the division is organized to provide technical support, mainly in the area of high-temperature materials, for technologies being developed by DOE. Activities span the range from basic research to industrial interactions (cooperative research and technology transfer). Sections 1-5 describe the different functional groups (engineering materials, high-temperature materials, materials science, ceramics, nuclear fuel materials). Sect. 6 provides an alternative view of the division in terms of the major programs, most of which cross group lines. Sect. 7 summarizes external interactions including cooperative R and D programs and technology transfer functions. Finally, Sect. 8 briefly describes the division's involvement in educational activities. Several organizational changes were effected during this period. DOE

N95-28574 Naval Undersea Warfare Center, New London, CT.
MOLECULAR MODELING: AN APPROACH FOR THE STUDY OF PIEZOELECTRIC POLYMERS Final Report
George J. Kavarnos 12 Dec. 1994 61 p Limited Reproducibility: More than 20% of this document may be affected by microfiche quality
(AD-A289821; NUWC-NPT-TR-10771) Avail: Issuing Activity (Defense Technical Information Center (DTIC))

This report describes the use of molecular modeling and computational chemistry techniques to investigate and tailor the piezoelectric properties of polyvinylidene fluoride (PVDF) and its copolymer with trifluoroethylene (PVDF-TrFE) for underwater hydrophone and acoustic projector applications. The effect of changing the ratios of vinylidene fluoride and trifluoroethylene monomers was studied using a combination of semiempirical molecular orbital theory, molecular mechanics, and crystal packing approaches. Molecular mechanics calculations on model end-capped polymer chains show that the tgtg'conformation of PVDF is 0.5 to 0.7 kcal/mol more stable than the all-trans formation but that for copolymer compositions less than 90 mol% vinylidene fluoride (VDF), the all-trans conformation is favored. Crystal packing calculations confirm the stability of the tgtg' for PVDF and the all-trans for the copolymers. To calculate the elastic compliances of PVDF and copolymer unit cell crystals along the poling direction, the b-axes were deformed in small increments and the crystal packing energies of each deformed structure were calculated. This procedure was used to determine the elastic compliances, which were calculated to be 2.59 x 10(exp -11)sq m/N for PVDF, 3.97 x 10(exp -11)sq m/N for 75 mol% VDF copolymer, and 5.38 x 10(exp -11)sq m/N for 50 mol% VDF copolymer. The d33c constants of the unit cells were calculated to be -3.3 pC/N for PVDF, -4.0 pC/N for 75 mol% VDF copolymer, and -4.3 pC/N for 50 mol% VDF copolymer. Although these values are much lower than the experimental d33 constants of semicrystalline polymer, a procedure used to calculate the d33 constants of semicrystalline polymer yields d33 constants much more in agreement with the experimental values. DTIC

N95-28582 Office of Naval Research, Arlington, VA.
ASH-BASED CERAMIC MATERIALS Patent Application
Inna G. Talmy, inventor (to Navy), Deborah A. Haught, inventor (to Navy), and Curtis A. Martin, inventor (to Navy) 1 Sep. 1994 26 p Filed 1 Sep. 1994 Limited Reproducibility: More than 20% of this document may be affected by microfiche quality
(AD-D017272; Navy-Case-76174; US-Patent-Appl-SN-299388) Avail: Issuing Activity (Defense Technical Information Center (DTIC))

A ceramic material made from raw coal fly ash or raw municipal solid waste fly ash and sodium tetraborate or a mixture of sodium tetraborate and a calcium containing material that is triple superphosphate, lime, dolomitic lime, or mixtures thereof. DTIC

N95-28592 Georgia Inst. of Tech., Atlanta, GA. School of Mechanical Engineering.
DEFORMATION BEHAVIOR OF THIN LUBRICANT FILMS AT ELEVATED PRESSURE
Scott Bair, F. Qureshi, Y. K. Lee, and W. O. Winer Dec. 1994 99 p Sponsored by ONR Limited Reproducibility: More than 20% of this document may be affected by microfiche quality
(AD-A288906) Avail: Issuing Activity (Defense Technical Information Center (DTIC))

The elastohydrodynamic (EHD) regime of lubrication is responsible for the generation of a protective film and the transfer of shear across concentrated contacts in many machine elements including bearings, cams and gears. It is now understood that small scale EHD plays a major role in the boundary lubrication of rough surfaces. Many high pressure metal working operations share the pressure and kinematics of elastohydrodynamics. A complete solution of the EHD problem, however, requires a thorough knowledge of the lubricant constitutive behavior and the attending properties as functions of temperature and pressure. The Newtonian assumption alone is inadequate. DTIC

N95-28604# Virginia Polytechnic Inst. and State Univ., Blacksburg, VA.
COATINGS OF NON-OXIDE CERAMICS FOR IMPROVED CORROSION RESISTANCE IN HIGH TEMPERATURE COAL COMBUSTION Quarterly Progress Report No. 2, 1 Sep. - 31 Dec. 1994
S. Yang and J. J. Brown 31 Dec. 1994 12 p
(Contract DE-FG22-94PC-94224)
(DE95-006932; DOE/PC-94224/T2) Avail: CASI HC A03/MF A01

High temperature alkali corrosion has caused premature failure of SiC and Si3N4 components used in advanced high temperature coal combustion systems. The objective of this research is to develop and characterize CMZP (((Ca(0.6), Mg(0.4))Zr4Po4)6) and Mg-doped Al2TiO5 coatings on dense SiC and Si3N4 heat exchanger materials and to strive to expand the existing knowledge of the mechanism of coal combustion corrosion of SiC and Si3N4 in the temperature range 1,000 to 1,400 C. DOE

N95-28609# International Centre for Theoretical Physics, Trieste (Italy).
SUPERCOOLED LIQUID DYNAMICS FOR THE CHARGED HARD-SPHERE MODEL
S. K. Lai and S. Y. Chang (National Central Univ., Chung-Li, Taiwan.) Aug. 1994 15 p
(DE95-609158; IC-94/267) Avail: CASI HC A03/MF A01 (US Sales Only)

We study the dynamics of supercooled liquid and the liquid-glass transition by applying the mode coupling theory to the charged hard-sphere model. By exploiting the two independent parameters inherent in the charged hard-sphere system we examine structurally the subtle and competitive role played by the short-range hard-core correlation and the long-range Coulomb tail. It is found in this work that the long-range Coulombic charge factor effect is generally a less effective contribution to structure when the plasma parameter is less than 500 and becomes dominant when it is greater thereof. To extend our understanding of the supercooled liquid and the liquid-glass transition, an attempt is made to calculate and to give physical relevance to the mode-coupling parameters which are frequently used as mere fitting parameters in analysis of experiments on supercooled liquid systems. This latter information enables us to discuss the possible application of the model to a realistic system. DOE

N95-28620 Air Force Civil Engineering Center, Tyndall AFB, FL.
SILICONE JOINT SEALANTS FOR PAVEMENTS
14 Dec. 1994 11 p Limited Reproducibility: More than 20% of this document may be affected by microfiche quality
(AD-A289843; AFCESA-ETL-94-9) Avail: Issuing Activity (Defense Technical Information Center (DTIC))

This ETL provides a specification for silicone sealants used to seal joints in Air Force pavements. DTIC

N95-28661 Duke Univ., Durham, NC. Dept. of Chemistry.
ISOLATION AND X-RAY CRYSTAL STRUCTURES OF (Li(mu2-As(SiMe3)2) (mu3-As(SiMe3)2)(THF))2 AND ((Me3Si)2AsLi(THF)2)2
L. T. Jones, A. T. McPhail, and R. L. Wells 7 Dec. 1994 20 p Submitted for publication Limited Reproducibility: More than 20% of this

document may be affected by microfiche quality
(Contract N00014-89-J-1545; ONR Proj. 4135-008)
(AD-A288870; DU/DC/TR-46) Avail: Issuing Activity (Defense Technical Information Center (DTIC))

The lithium arsenides (Li2(mu2-As(SiMe3)2)(mu3-As(SiMe3)2)(THF))2 (I) THF = tetrahydrofuran) and (Me3Si)2AsLi(THF)22 (II) were isolated and their solid-state structuresdetermined by X-ray methods. Compound I crystallizes in the monoclinic system, space group P2(sub 1)/c, with a = 10.147(1) A, b = 19.665(2) A, c = 16.768(2) A, p = 107.78(1) and Z = 2. The core structure consists of an LiAs4 ladder-like framework with four antiparallel adjacent As-Li rungs. The two lithium atoms of the central ring each bridge three arsenic centers while the two lithium atoms belonging solely to the outer rings each span two arsenic atoms and are coordinated to one THF molecule. Monoclinic crystals of compound II belong to space group C2/c, with a = 17.877(4) A, b = 14.077(3) A, c = 19.006(4) A, p = 109.16(2) and Z = 4. The structure consists of a centrosymmetric dimer containing a four-membered As-Li-As-Li ring wherein each lithium atom is coordinated to two molecules of THF. DTIC

N95-27638*# National Aeronautics and Space Administration. Marshall Space Flight Center, Huntsville, AL.
EFFECTS OF ATOMIC OXYGEN ON POLYMERIC MATERIALS FLOWN ON EOIM-3
Rachel R. Kamenetzky, Roger C. Linton, Miria M. Finckenor, and Jason A. Vaughn *In* NASA. Langley Research Center, LDEF: 69 Months in Space. Third Post-Retrieval Symposium, Part 3 Feb. 1995 p 1011-1023 (For primary document see N95-27629 09-99)
Avail: CASI HC A03/MF A04

N95-27639*# National Aeronautics and Space Administration. Marshall Space Flight Center, Huntsville, AL.
THERMAL CONTROL MATERIALS ON EOIM-3
Miria M. Finckenor, Roger C. Linton, Rachel R. Kamenetzky, and Jason A. Vaughn *In* NASA. Langley Research Center, LDEF: 69 Months in Space. Third Post-Retrieval Symposium, Part 3 Feb. 1995 p 1025-1035 (For primary document see N95-27629 09-99)
Avail: CASI HC A03/MF A04

N95-27640*# McDonnell-Douglas Aerospace, Huntington Beach, CA. Materials and Processes.
SOLID FILM LUBRICANTS AND THERMAL CONTROL COATINGS FLOWN ABOARD THE EOIM-3 MDA SUB-EXPERIMENT
Taylor J. Murphy, Kaia E. David, and Hank W. Babel *In* NASA. Langley Research Center, LDEF: 69 Months in Space. Third Post-Retrieval Symposium, Part 3 Feb. 1995 p 1037-1052 (For primary document see N95-27629 09-99)
Avail: CASI HC A03/MF A04

N95-27655*# National Aeronautics and Space Administration. Goddard Space Flight Center, Greenbelt, MD.
SPACE ENVIRONMENTAL EFFECTS OBSERVED ON THE HUBBLE SPACE TELESCOPE
Joel E. Edelman (Long Duration Exposure Facility Newsletter, Silver Spring, MD.) and James B. Mason *In* NASA. Langley Research Center, LDEF: 69 Months in Space. Third Post-Retrieval Symposium, Part 3 Feb. 1995 p 1231-1236 (For primary document see N95-27629 09-99)
Avail: CASI HC A02/MF A04

N95-27661*# McDonnell-Douglas Space Systems Co., Huntington Beach, CA. Space Station Program.
LDEF'S CONTRIBUTION TO THE SELECTION OF THERMAL CONTROL COATINGS FOR THE SPACE STATION
Henry W. Babel *In* NASA. Langley Research Center, LDEF: 69 Months in Space. Third Post-Retrieval Symposium, Part 3 Feb. 1995 p 1273-1283 (For primary document see N95-27629 09-99)
Avail: CASI HC A03/MF A04

N95-27669*# Canadian Space Agency, Saint Hubert (Quebec). Strategic Technologies for Automation and Robotics Program.
THE STRATEGIC TECHNOLOGIES FOR AUTOMATION AND ROBOTICS (STEAR) PROGRAM: PROTECTION OF MATERIALS IN THE SPACE ENVIRONMENT SUBPROGRAM
Lorne R. Schmidt, J. Francoeur, Alina Aguero (Cametoid Advanced Technologies, Inc., Whitby, Ontario.), Michael R. Wertheimer (Ecole Polytechnique, Montreal, Quebec.), J. E. Klemberg-Sapieha (Ecole Polytechnique, Montreal, Quebec.), L. Martinu (Ecole Polytechnique, Montreal, Quebec.), J. W. Blezius (MPB Technologies, Inc., Pointe Claire, Quebec.), M. Oliver (MPB Technologies, Inc., Pointe Claire, Quebec.), and A. Singh (National Optics Inst., Ste-Foy, Quebec.) *In* NASA. Langley Research Center, LDEF: 69 Months in Space. Third Post-Retrieval Symposium, Part 3 Feb. 1995 p 1341-1359 (For primary document see N95-27629 09-99)
Avail: CASI HC A03/MF A04

28 PROPELLANTS AND FUELS

Includes rocket propellants, igniters, and oxidizers; their storage and handling procedures; and aircraft fuels.

For related information see also *07 Aircraft Propulsion and Power, 20 Spacecraft Propulsion and Power,* and *44 Energy Production and Conversion.*

N95-26781*# GenCorp Aerojet, Sacramento, CA.
PROPELLANT INJECTION SYSTEMS AND PROCESSES
Jackson I. Ito 1995 23 p Presented at the 2nd International Symposium on Liquid Rocket Propulsion, Paris, France, 19-21 Jun. 1995
(NASA-TM-110632; NAS 1.15:110632) Avail: CASI HC A03/MF A01

The previous 'Art of Injector Design' is maturing and merging with the more systematic 'Science of Combustion Device Analysis.' This technology can be based upon observation, correlation, experimentation and ultimately analytical modeling based upon basic engineering principles. This methodology is more systematic and far superior to the historical injector design process of 'Trial and Error' or blindly 'Copying Past Successes.' The benefit of such an approach is to be able to rank candidate design concepts for relative probability of success or technical risk in all the important combustion device design requirements and combustion process development risk categories before committing to an engine development program. Even if a single analytical design concept cannot be developed to predict satisfying all requirements simultaneously, a series of risk mitigation key enabling technologies can be identified for early resolution. Lower cost subscale or laboratory experimentation to demonstrate proof of principle, critical instrumentation requirements, and design discriminating test plans can be developed based on the physical insight provided by these analyses. Derived from text

N95-26842 Air Force Inst. of Tech., Wright-Patterson AFB, OH. School of Engineering.
A NUMERICAL MODEL TO PREDICT THE FATE OF JETTISONED AVIATION FUEL M.S. Thesis
Karl Durant Pfeiffer Dec. 1994 107 p Limited Reproducibility: More than 20% of this document may be affected by microfiche quality
(AD-A289336; AFIT/GCS/ENC/94D-01) Avail: Issuing Activity (Defense Technical Information Center (DTIC))

While airborne, military and civilian aircraft must occasionally jettison unburned aviation fuel into the atmosphere. This research investigates the fate of a jettisoned fuel (e.g. JP-4, JP-8, etc.) from initial release to final ground fall by numerically modeling the physical phenomena governing the fate of this fuel: evaporation, advection, and dispersion. Using previous work in evaporation and free fall of fuel droplets as a foundation, this thesis presents an integrated evaporation advection and dispersion model designed to run under the resources of a typical personal computer. This integrated model is capable of using near real-time meteorological data (i.e. vertical profiles of temperature, pressure and wind) in all model calculations. Physical assumptions in the numerical model are presented, along with sample model calculations supporting these assumptions. Model calculations performed for two jettison scenarios show good agreement with previously published results. DTIC

N95-27415# National Renewable Energy Lab., Golden, CO.
HYDROGEN PROGRAM
Feb. 1995 28 p
(DE94-011827; DOE/GO-10095-088) Avail: CASI HC A03/MF A01

Hydrogen is an energy carrier with the potential to join electricity as a key component of a sustainable energy system. As an energy carrier and fuel, its future integration into the energy economy will help make renewable energy sources viable and practical. Primary sources are used directly to provide energy for services, but often they are used to create an energy carrier, such as electricity, to move the energy from the place of production to where it is needed to provide goods and services for society. Hydrogen has the potential to be a more versatile energy carrier than electricity. In the future, it may be produced cost effectively from renewable energy sources, then stored and transported for use in home and office heating, generating electricity, industrial processes, and surface and air transportation. It can accomplish this while also preventing pollution by substituting for and reducing the use of fossil fuels. The benefits of hydrogen make it the ideal component of a renewable, sustainable energy system of the future. It can be produced from water -- an abundant supply sources -- using direct sunlight, renewable electricity, and some biological organisms. When burned directly as a fuel, or converted to electricity, its principal by-product is water, which can be safely returned to the environment or reused to produce more hydrogen. The versatility of hydrogen will enable the more rapid expansion of the use of domestic renewable energy sources than might occur with electricity alone, resulting in reduced energy imports. Hydrogen energy has the potential for substantially contributing to the reduction of climate-changing emissions and other atmospheric pollutants. Unfortunately, the widespread use of hydrogen energy is not currently feasible because of economic and technological barriers. Hydrogen is presently used in a variety of industrial applications and, from this base, research and development will move hydrogen into widespread energy applications. DOE

N95-27944# Oak Ridge National Lab., TN.
ALTERNATIVE FUELS AND VEHICLES CHOICE MODEL
D. L. Greene Oct. 1994 80 p
(Contract DE-AC05-84OR-21400)
(DE95-005695; ORNL/TM-12738) Avail: CASI HC A05/MF A01

This report describes the theory and implementation of a model of alternative fuel and vehicle choice (AFVC), designed for use with the US Department of Energy's Alternative Fuels Trade Model (AFTM). The AFTM is a static equilibrium model of the world supply and demand for liquid fuels, encompassing resource production, conversion processes, transportation, and consumption. The AFTM also includes fuel-switching behavior by incorporating multinomial logit-type equations for choice of alternative fuel vehicles and alternative fuels. This allows the model to solve for market shares of vehicles and fuels, as well as for fuel prices and quantities. The AFVC model includes fuel-flexible, bi-fuel, and dedicated fuel vehicles. For multi-fuel vehicles, the choice of fuel is subsumed within the vehicle choice framework, resulting in a nested multinomial logit design. The nesting is shown to be required by the different price elasticities of fuel and vehicle choice. A unique feature of the AFVC is that its parameters are derived directly from the characteristics of alternative fuels and vehicle technologies, together with a few key assumptions about consumer behavior. This not only establishes a direct link between assumptions and model predictions, but facilitates sensitivity testing, as well. The implementation of the AFVC model as a spreadsheet is also described. DOE

N95-28001*# Boeing Defense and Space Group, Seattle, WA.
TANK PRESSURE CONTROL IN LOW GRAVITY BY JET MIXING Final Report
Michael D. Bentz Mar. 1993 201 p A videocassette supplement Lewis Video 93-219 is available through NASA. Lewis Research Center Video Dept.
(Contract NAS3-25363; RTOP 589-01-2C)
(NASA-CR-191012; NAS 1.26:191012) Avail: CASI HC A10/MF A03

The Tank Pressure Control Experiment (TPCE) is a space experiment developed to help meet the need for a critical aspect of cryogenic fluid management technology: control of storage tank pressures in the absence of gravity by forced convective mixing. The experiment used a 13.7-liter tank filled to a constant 83 percent level with refrigerant 113 at near saturation conditions to simulate the fluid dynamics and thermodynamics of cryogenic fluids in space applications. The objectives of TPCE were to characterize the fluid dynamics of axial jet-induced mixing in low gravity, to evaluate the validity of empirical mixing models, and to provide data for use in developing and validating computational fluid dynamic models of mixing processes. TPCE accomplished all of its objectives in flight on Space Shuttle Mission STS-3 in August of 1991. The range of flow patterns photographed generally confirmed a prior correlation based on drop tower tests. A closed-form equation derived from a simple thermodynamic model was found to provide a first-order prediction of the pressure reduction time as a function of mixer parameters, tank size, and fluid thermophysical properties. Low energy mixing jets were found to be effective and reliable at reducing thermal non-uniformities, promoting heat and mass transfer between the phases, and reducing tank pressure. Author

N95-28064# Lawrence Livermore National Lab., Livermore, CA.
LLNL INPUT TO FY94 HYDROGEN ANNUAL REPORT
R. N. Schock, J. R. Smith, G. Rambach, R. W. Pekala, C. K. Westbrook, and J. H. Richardson 16 Dec. 1994 23 p
(Contract W-7405-eng-48)
(DE95-007950; UCRL-ID-119322) Avail: CASI HC A03/MF A01

This report summarizes the FY 1994 progress made in hydrogen research at the Lawrence Livermore National Laboratory. Research programs covered include: Technical and Economic Assessment of the Transport and Storage of Hydrogen; Research and Development of an Optimized Hydrogen-Fueled Internal Combustion Engine; Hydrogen Storage in Engineered Microspheres; Synthesis, Characterization and Modeling of Carbon Aerogels for Hydrogen Storage; Chemical Kinetic Modeling of H2 Applications; and Municipal Solid Waste to Hydrogen. DOE

N95-28152 Coordinating Research Council, Inc., Atlanta, GA.
THE EFFECT OF AVIATION FUELS CONTAINING LOW AMOUNTS OF STATIC DISSIPATER ADDITIVE ON ELECTROSTATIC CHARGE GENERATION
May 1994 132 p Limited Reproducibility: More than 20% of this document may be affected by microfiche quality
(AD-A280075) Avail: Issuing Activity (Defense Technical Information Center (DTIC))

The purpose of the CRC program was to determine whether commingled fuels containing low levels of static dissipater additive pose any additional electrostatic hazard over unadditized fuel. Specifically, the program conducted the necessary experiments to determine electrostatic effects of commingled fuels containing static dissipater additive with a conductivity less than 50 pico-Siemens/meter (pS/m). It was also a goal of this program to survey existing systems and make an assessment whether future fueling systems could cause additional electrostatic hazards during the fueling operation. In order to achieve these goals, it was the scope of this program: to assess the range of conductivities present in Jet A at various locations; to assess the charging tendency of Jet A presently being used in the United States; to perform laboratory scale tests to further study the charging tendency of ASA-3 and Stadis 450 in both commingled Jet A and clay treated Jet A as needed to verify the results of the other tests; and to develop a database of the residence times typical of existing fueling systems. DTIC

N95-28634 MACH 1, Inc., King of Prussia, PA.
SURFACTANTS AND DESENSITIZING WAX SUBSTITUTES FOR TNT-BASED SYSTEMS Final Report, 2 Jul. 1992 - 1 Jul. 1994
Gary Statton and Robert C. Taylor Oct. 1994 263 p Limited Reproducibility: More than 20% of this document may be affected by microfiche quality
(Contract F08630-92-C-0058)
(AD-A289652; WL-TR-94-7058) Avail: Issuing Activity (Defense Technical Information Center (DTIC))

MACH I, Inc. developed three polyvinylpyrrolidones (Ganex resins) that are effective emulsifiers for microcrystalline or selected substitute desensitizing waxes in AFX-644 TNT melt cast bomb explosive. Ganex resins also are excellent dispersants for TNT melt casting and PBX in which they provide important benefits: wetting, coating, dispersion, lubrication, thinning, void filling, desensitization, and increased production rate. Ganex resins are expected to be effective emulsifiers and dispersants with microcrystalline desensitizing waxes or the recommended substitutes in any melt cast system such as Compositions B, HBX-1, D-2, and H-6. Furthermore, by reducing viscosity Ganex resins are expected to facilitate processing of PBX compositions such as AFX-931 in batch mixers as well as continuous mixers (e.g., twin-screw extruders). The Ganex surfactants appear promising for use in most munitions mixing processes for production of: ammunition, bombs, missiles, projectiles, demolition charges and special purpose devices. MACH I, Inc. also developed promising polar wax substitutes, having different desensitizing mechanisms, to enhance the benefits cited above. These substitutes offer greater formulation flexibility than conventional waxes to mitigate possible fuzing insensitivity or loss of explosive power. In contrast to conventional desensitizing wax, they are easier to emulsify and are dependably available in ample quantity and consistent quality. DTIC

N95-28315 Hercules Aerospace Co., Magna, UT.
HAZARDS ANALYSIS OF AN INTEGRAL CLASS 1.1/1.3 ROCKET MOTOR DEMILITARIZATION AND INGREDIENT RECOVERY SYSTEM USING AMMONIA
Philip M. Stevens, M. H. Reed, L. A. Losee, K. A. Hendrickson, and D. H. Mitchell *In* Johns Hopkins Univ., The 1994 JANNAF Safety and Environmental Protection Subcommittee Meeting, Volume 1 Aug. 1994 p 227-238 (For primary document see N95-28294 09-20)
Avail: CPIA, 10630 Little Patuxent Pkwy., Suite 202, Columbia, MD 21044-3200 HC

N95-28320 Wulfman (D. S.) and Associates, Inc., Rolla, MO.
COMMERCIAL REFORMULATION: AN ECONOMIC AND ENVIRONMENTALLY NEUTRAL MEANS OF MANAGING EXPLOSIVES AND SOLID PROPELLANTS
David S. Wulfman, Oliver C. Sitton (Technology Development, Inc., Rolla, MO.), Paul Worsey (Missouri Univ., Rolla, MO.), Mike Johnson (Naval Surface Warfare Center, Crane, IN.), and Dan Burch (Naval Surface Warfare Center, Crane, IN.) *In* Johns Hopkins Univ., The 1994 JANNAF Safety and Environmental Protection Subcommittee Meeting, Volume 1 Aug. 1994 p 343-349 (For primary document see N95-28294 09-20)
Avail: CPIA, 10630 Little Patuxent Pkwy., Suite 202, Columbia, MD 21044-3200 HC

N95-28321 Universal Tech Corp., Riverton, KS.
ALTERNATE USE OF ROCKET PROPELLANTS AS INGREDIENTS IN COMMERCIAL WATERGEL EXPLOSIVES
J. Brent Gilion, Gary Eck, O. Machacek (Universal Tech Corp., Dallas, TX.), R. Perry (United Technologies Corp., San Jose, CA.), A. McKenzie (United Technologies Corp., San Jose, CA.), and L. Morgan (United Technologies Corp., San Jose, CA.) *In* Johns Hopkins Univ., The 1994 JANNAF Safety and Environmental Protection Subcommittee Meeting, Volume 1 Aug. 1994 p 351-360 (For primary document see N95-28294 09-20)
Avail: CPIA, 10630 Little Patuxent Pkwy., Suite 202, Columbia, MD 21044-3200 HC

N95-28322 Missouri Univ., Rolla, MO. Toxicology Div.
THE DEMILITARIZATION OF CLASS 1.1 ROCKET MOTORS USING HIGH PRESSURE WATERJETS
Oliver Sitton, Paul N. Worsey, David Summers, Karla Bier, Dan Burch (Naval Surface Warfare Center, Crane, IN.), and Mike Johnson (Naval Surface Warfare Center, Crane, IN.) *In* Johns Hopkins Univ., The 1994 JANNAF Safety and Environmental Protection Subcommittee Meeting, Volume 1 Aug. 1994 p 371-379 (For primary document see N95-28294 09-20)
Avail: CPIA, 10630 Little Patuxent Pkwy., Suite 202, Columbia, MD 21044-3200 HC

N95-28323 TPL, Inc., Albuquerque, NM.
A COMPREHENSIVE ENERGETIC MATERIALS RESOURCE RECOVERY AND RECYCLING PROGRAM
H. M. Stoller, T. J. Schilling, and Dan Burch (Naval Surface Warfare Center, Crane, IN.) *In* Johns Hopkins Univ., The 1994 JANNAF Safety and Environmental Protection Subcommittee Meeting, Volume 1 Aug. 1994 p 381-387 (For primary document see N95-28294 09-20)
Avail: CPIA, 10630 Little Patuxent Pkwy., Suite 202, Columbia, MD 21044-3200 HC

N95-28324 General Atomics Co., San Diego, CA.
CRYOGENIC WASHOUT OF SOLID ROCKET PROPELLANTS
J. P. Elliott, W. P. Creedon, M. H. Spritzer, J. A. Hurley (Air Force Systems Command, Tyndall AFB, FL.), and S. A. Rising (Air Force Systems Command, Tyndall AFB, FL.) *In* Johns Hopkins Univ., The 1994 JANNAF Safety and Environmental Protection Subcommittee Meeting, Volume 1 Aug. 1994 p 397-406 (For primary document see N95-28294 09-20)
(Contracts F08635-91-C-0179; F08635-92-C-0075)
Avail: CPIA, 10630 Little Patuxent Pkwy., Suite 202, Columbia, MD 21044-3200 HC

N95-28325 General Atomics Co., San Diego, CA.
HYDROTHERMAL OXIDATION OF SOLID ROCKET PROPELLANT AND OTHER DEPARTMENT OF DEFENSE HAZARDOUS WASTES
D. A. Hazlebeck, K. W. Downey, D. D. Jensen, M. H. Spritzer, J. P. Elliott, J. A. Hurley (Air Force Systems Command, Tyndall AFB, FL.), and S. A. Rising (Air Force Systems Command, Tyndall AFB, FL.) *In* Johns Hopkins Univ., The 1994 JANNAF Safety and Environmental Protection Subcommittee Meeting, Volume 1 Aug. 1994 p 407-414 (For primary document see N95-28294 09-20)
Avail: CPIA, 10630 Little Patuxent Pkwy., Suite 202, Columbia, MD 21044-3200 HC

N95-28326 Army Missile Research and Development Command, Redstone Arsenal, AL. Propulsion Directorate.
RECOVERY AND REUSE OF ROCKET MOTOR PROPELLANT INGREDIENTS
William S. Melvin and Jeffery S. Wright *In* Johns Hopkins Univ., The 1994 JANNAF Safety and Environmental Protection Subcommittee Meeting, Volume 1 Aug. 1994 p 427-435 (For primary document see N95-28294 09-20)
Avail: CPIA, 10630 Little Patuxent Pkwy., Suite 202, Columbia, MD 21044-3200 HC

29 MATERIALS PROCESSING

Includes space-based development of products and processes for commercial applications.

For biological materials see *55 Space Biology.*

N95-26709*# Worcester Polytechnic Inst., MA. Mechanical Engineering Dept.
DESIGN AND DEVELOPMENT OF EXPERIMENTAL FACILITIES FOR SHORT DURATION, LOW-GRAVITY COMBUSTION AND FIRE EXPERIMENTS Final Report, 25 May 1993 - 5 May 1994
Jun. 1994 198 p
(Contract NCC3-312; RTOP 656-61-23)
(NASA-CR-195458; E-9579; NAS 1.26:195458) Avail: CASI HC A09/MF A03

This report contains the results of three projects conducted by undergraduate students from Worcester Polytechnical Institute at the NASA's Lewis Research Center under a NASA Award NCC3-312. The students involved in these projects spent part of the summer of 1993 at the Lewis Research Center (LeRC). The Principal Investigator at Worcester Polytechnic Institute was Professor Vahid Motevalli. Professor Motevalli served as the principal project advisor for two of the three projects which were in Mechanical Engineering. The third project was advised by Professor Duckworth of Electrical and Computer Engineering, while Professor Motevalli acted as the co-advisor. These projects provided an excellent opportunity for the students to participate in the cutting edge research and engineering design, interact with NASA engineers and gain valuable exposure to a real working environment. This report has been divided to three sections, representing the outcome of each of the separate projects. The three reports which have been written by the students under the supervision of their advisors have been compiled into a combined report by Dr. Motevalli. Each project report is presented here as a section which is essentially self-contained. Each section contains chapters introducing the problem, solution approach, description of the experiments, results and analysis, conclusions and appendixes as appropriate. Author (revised)

N95-26769*# National Aeronautics and Space Administration. Marshall Space Flight Center, Huntsville, AL.
EFFECT OF PROCESSING PARAMETERS ON SURFACE FINISH FOR FUSED DEPOSITION MACHINABLE WAX PATTERNS
F. E. Roberts, III Washington Mar. 1995 256 p
(NASA-TP-3550; M-777; NAS 1.60:3550) Avail: CASI HC A12/MF A03

This report presents a study on the effect of material processing parameters used in layer-by-layer material construction on the surface finish of a model to be used as an investment casting pattern. The data presented relate specifically to fused deposition modeling using a machinable wax. Author

N95-26888*# National Aeronautics and Space Administration. Marshall Space Flight Center, Huntsville, AL.
DEVICE AND METHOD FOR SCREENING CRYSTALLIZATION CONDITIONS IN SOLUTION CRYSTAL GROWTH Patent Application
Daniel C. Carter, inventor (to NASA) 17 Apr. 1995 43 p
(NASA-Case-MFS-28985-1; NAS 1.71:MFS-28985-1;
US-Patent-Appl-SN-422963) Avail: CASI HC A03/MF A01

A device and method for detecting optimum protein crystallization conditions and for growing protein crystals in either 1g or microgravity environments comprising a housing, defining at least one pair of chambers for containing crystallization solutions is presented. The housing further defines an orifice therein for providing fluid communication between the chambers. The orifice is adapted to receive a tube which contains a gelling substance for limiting the rate of diffusive mixing of the crystallization solutions. The solutions are diffusively mixed over a period of time defined by the quantity of gelling substance sufficient to achieve equilibration and to substantially reduce density driven convection disturbances therein. The device further includes endcaps to seal the first and second chambers. One of the endcaps includes a dialysis chamber which contains protein solution in which protein crystals are grown. Once the endcaps are in place, the protein solution is exposed to the crystallization solutions wherein the solubility of the protein solution is reduced at a rate responsive to the rate of diffusive mixing of the crystallization solutions. This allows for a controlled approach to supersaturation and allows for screening of crystal growth conditions at preselected intervals. NASA

N95-27500*# National Aeronautics and Space Administration. Marshall Space Flight Center, Huntsville, AL.
APPARATUS FOR DIFFUSION CONTROLLED DIALYSIS UNDER MICROGRAVITY CONDITIONS Patent Application
Daniel C. Carter, inventor (to NASA) 27 Feb. 1995 14 p
(NASA-Case-MFS-28986-1; NAS 1.71:MFS-28986-1;
US-Patent-Appl-SN-394862) Avail: CASI HC A03/MF A01

Apparatus for implementing crystal growth by allowing mixing of solutions under microgravity conditions includes a housing within which a number of pairs of chambers are formed. The chambers of each pair are aligned and a rotary valve is positioned between the chambers of each pair. When the valve is in a first position one chamber of each pair may communicate with the other chamber. A separate valve is provided for each pair of chambers so that each pair of chambers may be activated independently of the others and sequentially at selected intervals. Protein solution may be located within a small cavity in a cap which closes one of the chambers of a pair, and the cavity in the cap is closed by a dialysis membrane. The length of certain pairs of chambers may differ from the length of other pairs of chambers to optimize conditions for various dialysis productions, and wicking material may be incorporated into selected chambers for controlling the critical approach to supersaturation. Author

N95-28460*# National Aeronautics and Space Administration, Washington, DC.
MICROGRAVITY SCIENCE AND APPLICATIONS. PROGRAM TASKS AND BIBLIOGRAPHY FOR FY 1994
Mar. 1995 761 p
(NASA-TM-4677; NAS 1.15:4677) Avail: CASI HC A99/MF A06

This annual report includes research projects funded by the Office of Life and Microgravity Sciences and Applications, Microgravity Science and Applications Division, during FY 1994. It is a compilation of program tasks (objective, description, significance, progress, students funded under research, and bibliographic citations) for flight research and ground-based research in five major scientific disciplines: benchmark science, biotechnology, combustion science, fluid physics, and materials science. ATD (Advanced Technology Development) program task descriptions are also included. The bibliography cites the related PI (Principal Investigator) publications and presentations for these program tasks in FY 1994. Three appendices include Table of Acronyms, Guest Investigator Index, and Principal Investigator Index. Derived from text

31 ENGINEERING (GENERAL)

Includes vacuum technology; control engineering; display engineering; cryogenics; and fire prevention.

N95-26410 Wright State Univ., Dayton, OH.
PROCESS CONTROL OF MICROSTRUCTURE IN MANUFACTURING Final Report, 1 Sep. 1990 - 1 Dec. 1993
Ramana V. Grandhi Jun. 1994 252 p Limited Reproducibility: More than 20% of this document may be affected by microfiche quality
(Contract F33615-90-C-5950; AF Proj. 2306)
(AD-A288291; WL-TR-94-4109) Avail: Issuing Activity (Defense Technical Information Center (DTIC))

This report presents a systematic methodology for the design of optimal process parameters for forging processes. The procedure for construction of a state space model utilizing nonlinear rigid-viscoplastic finite element formulation is developed. A coupled state space model is built to represent the deformation and thermal behavior of the material, with nodal velocities and nodal temperatures as the state variables, and die velocity as input to the system. The output variables of the state space system are the effective strain rate and critical nodal temperature. The linear quadratic regulator (LQR) theory with finite time control is used in designing the ram velocity and initial die temperature. Model reduction schemes are adopted in generating reduced order analytical models from the full size state space representation. The methodology developed is demonstrated on axisymmetric and plane strain forging cases. The performance of the procedure is evaluated using measures such as temperature and strain rate variation within the billet, load requirement, and total process time. DTIC

N95-26500 Department of the Navy, Washington, DC.
SPLIT PIPE TESTING DEVICE FOR THE MEASUREMENT OF BOND OF REINFORCEMENT UNDER CONTROLLED CONFINEMENT Patent
Javier Malvar, inventor (to Navy) 5 Jul. 1994 10 p Filed 14 Aug. 1992
(AD-D017258; US-Patent-5,325,722; US-Patent-Appl-SN-931464;
US-Patent-Class-73-789) Avail: US Patent and Trademark Office

This patent discloses a method and apparatus for determining the stress-slip relationship of specimens in concrete including a pipe with a plurality of longitudinal slots evenly spaced around the circumference of the pipe, a specimen and concrete block located in one end of the pipe, a confining device for applying a constant force to the circumference of the concrete block before, during and after a test, a device for measuring the displacement of the specimen relative to the concrete block, and a device for measuring the radial displacement of the concrete block. DTIC

N95-26508 Department of the Navy, Washington, DC.
NONDESTRUCTIVE TESTING APPARATUS FOR DETERMINING THE ORIENTATION OF REINFORCING BARS WITHIN A CONCRETE STRUCTURE Patent
Roman Kruchowy, inventor (to Navy), Dan Goff, inventor (to Navy), and Anthony Smith, inventor (to Navy) 16 Aug. 1994 14 p Filed 17 Dec. 1992
(AD-D017267; US-Patent-5,339,023; US-Patent-Appl-SN-991939;
US-Patent-Class-324-67) Avail: US Patent and Trademark Office

A measuring apparatus which accurately locates reinforcing bars in underwater concrete structures (such as piers, retaining walls, easements and the like) and measures the amount of concrete covering each reinforcing bar. The measuring apparatus comprises a probe which generates a magnetic field and which is moved over the surface of the underwater concrete structure under test When the poles of the magnetic field are in parallel alignment with and directly over a reinforcing bar within the structure a disturbance occurs in the magnetic field with the magnitude of the disturbance being indicative of the depth of concrete covering the reinforcing bar. An electronics module electrically coupled to the probe provides an analog output signal which is indicative of the distance between a reinforcing bar within the concrete structure under test and the probe. This analog signal is supplied to a meter which provides a visual indication of the location of the reinforcing bar and a microprocessor which then calculates the depth of the reinforcing bar within the concrete structure. DTIC

N95-26548 Army Cold Regions Research and Engineering Lab., Hanover, NH.
LAYER COEFFICIENTS FOR NHDOT PAVEMENT MATERIALS
Vincent C. Janoo Sep. 1994 52 p Limited Reproducibility: More than 20% of this document may be affected by poor print and microfiche quality
(AD-A288262; CRREL-SP-94-30) Avail: Issuing Activity (Defense Technical Information Center (DTIC))

In 1992, the New Hampshire Department of Transportation (NHDOT) experimented with the use of reclaimed asphalt concrete as a base course material, identified by NHDOT as reclaimed stabilized base (RSB). The RSB and a control test section were placed on Interstate 93 between exits 18 and 19. The RSB test section was designed to the same structural number (SN) as the control. To evaluate the structural capacity of these test sections, the U.S. Army Cold Regions Research and Engineering Laboratory (CRREL) conducted deflection tests using a Dynatest 8000 falling weight deflectometer (FWD). Preliminary analysis of the results by NHDOT personnel showed higher deflection in the reclaimed asphalt concrete test sections. The explanation was that the layer coefficient used for the RSB layer in the design was probably incorrect. A total of 10 test sections constituting the base course materials used by NHDOT were built near Bow, New Hampshire. CRREL evaluated and estimated the layer coefficients of the base course materials. The test program was developed to characterize the material in more than one way. Tests were conducted with the heavy weight deflectometer (HWD), dynamic cone penetrometer (DCP) and the Clegg hammer. In situ California bearing ratio (CBR) tests were also conducted. The deflection from the HWD were used with the WESDEF back calculation program to determine the layer moduli. The moduli were than used with the AASHTO Design Guide to calculate the layer coefficients. The layer coefficients were also determined with the method proposed by Rohde. The CBR values from the Clegg hammer, in situ CBR and DCP tests were also used in the relationships in the HDM model to determine the layer coefficients. DTIC

N95-26566 Air Force Civil Engineering Center, Tyndall AFB, FL.
ENGINEERING TECHNICAL LETTER (ETL) 94-5: FIRE PROTECTION ENGINEERING CRITERIA AND TECHNICAL GUIDANCE. EMERGENCY LIGHTING AND MARKING OF EXITS
8 Nov. 1994 16 p Limited Reproducibility: More than 20% of this document may be affected by microfiche quality
(AD-A288953) Avail: Issuing Activity (Defense Technical Information Center (DTIC))

This engineering technical letter (ETL) provides criteria for emergency lighting and the marking methods for means of egress. DTIC

N95-26722 Naval Postgraduate School, Monterey, CA.
AIR CUSHIONED LANDING CRAFT (LCAC) BASED SHIP TO SHORE MOVEMENT SIMULATION: A DECISION AID FOR THE AMPHIBIOUS COMMANDER. A (SMMAT) APPLICATION M.S. Thesis
Edward P. Kearns, III Sep. 1994 44 p Limited Reproducibility: More than 20% of this document may be affected by microfiche quality
(AD-A289635) Avail: Issuing Activity (Defense Technical Information Center (DTIC))

Amphibious forces are the enabling force of choice to globally project rapid and sustainable combat power in the littoral. Whether delivering supplies and equipment for military operations or for humanitarian or disaster relief, the air cushioned landing craft (LCAC) is the primary surface ship-to-shore movement craft. The time needed to transfer the forces ashore may be critical to operational success and is an important planning consideration. Many factors complicate accurate prediction of this time. Even so, various commanders must use the best available information, given mission priorities and resource and capability limitations, to make numerous tradeoff decisions in planning and executing the movement of forces. A simulation toolbox, the simulated mobility modeling and analysis toolbox (SMMAT), is introduced, and a robust LCAC ship-to-shore simulation model is developed as an extension to SMMAT. This model provides the commander a prediction and tradeoff analysis tool for planning and executing the projection of power ashore. DTIC

N95-27048# Helsinki Univ. of Technology, Espoo (Finland). Faculty of Civil Engineering and Surveying.
SUMMARIES OF THESES FOR THE DEGREE OF DIPLOMA ENGINEER 1992-1993 M.S. Thesis
J. Kiiras 31 Aug. 1994 136 p See also PB93-111821
(PB95-184867; ISBN-951-22-2220-5) Avail: CASI HC A07/MF A02

This publication contains the summaries of the diploma theses made in the Department of Structural Engineering during the years 1992-1993 in Helsinki University of Technology, Faculty of Civil Engineering and Surveying. NTIS

N95-27203 National Inst. of Standards and Technology, Gaithersburg, MD.
NIST AUTOMATED MANUFACTURING RESEARCH FACILITY (AMRF): MARCH 1987 (Videotape)
Judith E. Herbert, ed. and Richard Kane, ed. Mar. 1987 Videotape: 19 min. playing time, in color, with sound
(NONP-NASA-VT-95-49097) Avail: CASI VHS A02/BETA A22

The completion and advances to the NIST Automated Manufacturing Research Facility (AMRF) is described in this video. The six work stations: (1) horizontal machining; (2) vertical machining; (3) turning machinery; (4) cleaning and deburring; (5) materials handling; and (6) inspection are shown and uses for each workstation are cited. Visiting researchers and scientists within NIST describe the advantages of each of the workstations, what the facility is used for, future applications for the technological advancements from the AMRF, including examples of how AMRF technology is being transferred to the U.S. Navy industry and discuss future technological goals for the facility. CASI

N95-27213# Joint Publications Research Service, Washington, DC.
JPRS REPORT: SCIENCE AND TECHNOLOGY. CENTRAL EURASIA
6 Apr. 1995 82 p Transl. into ENGLISH from various Central Eurasian articles
(JPRS-UST-95-015) Avail: CASI HC A05/MF A01

Translated articles cover the following topics: thermochemical energy storage using carbide-acetylene technology; and laser-stimulated thermochemical synthesis and grafting of polymers in solid phase. Author

N95-27404# Edgerton, Germeshausen and Grier, Inc., Idaho Falls, ID.
SPRAY-FORMED TOOLING
K. M. McHugh and J. F. Key 1994 6 p Presented at the Society of Automotive Engineers' Convergence '94, Detroit, MI, 18-27 Oct. 1994
(Contracts DE-AC07-76ID-01570; DE-AC07-94ID-13223)
(DE95-005031; EGG-M-94370; CONF-9410256-3) Avail: CASI HC A02/MF A01

The United States Council for Automotive Research (USCAR) has formed a partnership with the Idaho National Engineering Laboratory (INEL) to develop a process for the rapid production of low-cost tooling based on spray forming technology developed at the INEL. Phase 1 of the program will involve bench-scale system development, materials characterization, and process optimization. In Phase 2, prototype systems will be designed, constructed, evaluated, and optimized. Process control and other issues that influence commercialization will be addressed during this phase of the project. Technology transfer to USCAR, or a tooling vendor selected by USCAR, will be accomplished during Phase 3. The approach INEL is using to produce tooling, such as plastic injection molds and stamping dies, combines rapid solidification processing and net-shape materials processing into a single step. A bulk liquid metal is pressure-fed into a de Laval spray nozzle transporting a high velocity, high temperature inert gas. The gas jet disintegrates the metal into fine droplets and deposits them onto a tool pattern made from materials such as plastic, wax, clay, ceramics, and metals. The approach is compatible with solid freeform fabrication techniques such as stereolithography, selective laser sintering, and laminated object manufacturing. Heat is extracted rapidly, in-flight, by convection as the spray jet entrains cool inert gas to produce undercooled and semi-solid droplets. At the pattern, the droplets weld together while replicating the shape and surface features of the pattern. Tool formation is rapid; deposition rates in excess of 1 ton/h have been demonstrated for bench-scale nozzles. DOE

N95-27699# Joint Publications Research Service, Arlington, VA.
JPRS REPORT: SCIENCE AND TECHNOLOGY. CENTRAL EURASIA
17 May 1995 48 p Transl. into ENGLISH from various Russian articles
(JPRS-UST-94-022) Avail: CASI HC A03/MF A01

Some of the latest achievements in science & technology in Russia and Ukraine are compiled and reported. Brief summaries of publications relating to materials science, engineering and equipment, and life sciences are presented. Among the topics are those concerned with flight control of aerospace vehicles; the flow separation characteristics of turbomachinery; the hydrodynamics of bodies intersecting the free surface of liquids; and protective coatings for friction joints. CASI

N95-27909*# Loyola Coll., Baltimore, MD. World Technology Evaluation Center.
WTEC PANEL REPORT ON RESEARCH SUBMERSIBLES AND UNDERSEA TECHNOLOGIES Final Report
Richard J. Seymore, D. Richard Blidberg, Claude P. Brancart, Larry L. Gentry, Algis N. Kalvaitis, Michael J. Lee, Brad Mooney, and Don Walsh Jun. 1994 342 p Sponsored by NASA, Washington; ARPA; DOE; Dept. of Commerce; DOD; Texas A and M Univ.; Northeastern Univ.; Draper Labs.; Lockheed Missiles and Space Co., Inc.; NOAA; Monterey Bay Aquarium Research Inst.; John B. Mooney, Jr.; and International Maritime, Inc.
(Grant NSF ENG-92-17849)
(NASA-CR-198565; NAS 1.26:198565; ISBN-1-883712-33-5; PB94-184843)
Avail: CASI HC A15/MF A03

This report covers research submersibles and related subsea technologies in Finland, France, Russia, Ukraine and the United Kingdom. Manned, teleoperated, and autonomous submersibles were of interest. The panel found that, in contrast to the United States, Europe is making substantial progress in cooperative and coordinated research in subsea technology, including the development of standards. France is a leader in autonomous vehicle technology. Because much less was known a priori about the technologies in Russia and Ukraine, there were more new findings in those countries than in those Western European nations visited. However, Russia and Ukraine have a sizeable (and currently underutilized) infrastructure in this field, including a highly educated and experienced manpower pool, impressive (in some cases unique) facilities for physical testing, extensive fleets of seagoing research vessels capable of long voyages, and state-of-the-art facilities for conducting oceanographic investigations. The panel visited newly-formed commercial companies associated with long-standing submersible R&D and production centers in Russia and Ukraine. So far, these new efforts are undercapitalized, and as such represent opportunities at very low cost for Western nations, as detailed in the site reports. Author

N95-28008 National Inst. of Standards and Technology, Gaithersburg, MD.
ALGORITHM TO DESCRIBE THE SPREAD OF A WALL FIRE UNDER A CEILING
H. E. Mitler Nov. 1994 62 p Limited Reproducibility: More than 20% of this document may be affected by microfiche quality
(PB95-182259; NISTIR-5547) Avail: CASI HC A04

After some discussion of wall fires, the effects that a ceiling has on a wall fire are analyzed and discussed qualitatively. There are two kinds of effects: first, when the upper sill of the ventilating opening lies below the ceiling (as is usual), a layer of hot gas is trapped, which heats the walls by convection and radiation; the heated ceiling also radiates to the walls. A calculation which uses the wall-fire computer model SPREAD is carried out to demonstrate how these effects can be calculated now. Second, when the flame impinges on the ceiling, it bifurcates and spreads horizontally, rather than vertically. A simple algorithm is presented which calculates the spread rate of these horizontal flame extensions, as well as the modified pyrolysis rate, due to the modified radiation feedbacks. NTIS

N95-28187 California Univ., Santa Barbara, CA. Dept. of Materials.
A KNOWLEDGE HIGHWAY FOR INTEGRATED MODELLING FROM MANUFACTURING TO DESIGN Final Report, 13 Jan. - 31 Sep. 1994
A. G. Evans 30 Nov. 1994 44 p Prepared in cooperation with Harvard Univ., Cambridge, MA Limited Reproducibility: More than 20% of this document may be affected by microfiche quality
(Contract N00014-94-1-0224)
(AD-A288872) Avail: Issuing Activity (Defense Technical Information Center (DTIC))

A workshop was held to discuss a new paradigm for choosing the preferred materials and processes needed for manufacturing a component, based on an analysis of the targeted attributes, performance and cost. This paradigm was developed around the idea of a 'knowledge highway'--a disciplined process for generating, storing and using the information most relevant to the manufacturing and design engineers. Model systems were used to develop this idea, which combined many of the technical aspects of greatest concern in manufacturing and design-processing, microstructural evolution, property profiles, fail-safe design, and costing. The concept integrated experimental studies, simulation and analysis. The final result would be software designed to be used by manufacturing and design engineers in selecting materials and processes to meet specific technical/commercial objectives. DTIC

N95-28419*# Precision Castparts Corp., Portland, OR.
AMCC CASTING DEVELOPMENT. VOLUME 1: EXECUTIVE SUMMARY Final Report
28 Mar. 1995 8 p
(Contract NAS8-39027)
(NASA-CR-196597; NAS 1.26:196597) Avail: CASI HC A02/MF A01

The Advanced Combustion Chamber Casting (AMCC) has been a technically challenging part due to its size, configuration, and alloy type. The height and weight of the wax pattern assembly necessitated the development of a hollow gating system to ensure structural integrity of the shell throughout the investment process. The complexity in the jacket area of the casting required the development of an innovative casting technology that PCC has termed 'TGC' or Thermal Gradient Control. This method, of setting up thermal gradients in the casting during solidification, represents a significant process improvement for PCC and has been successfully implemented on other programs. Metallurgical integrity of the final four castings was very good. Only the areas of the parts that utilized 'TGC Shape & Location System #2' showed any significant areas of microshrinkage when evaluated by non-destructive tests. Alumina oxides detected by FPI on the 'float' surfaces (top sid surfaces of the casting during solidification) of the part were almost entirely less than the acceptance criteria of .032 inches in diameter. Destructive chem mill of the castings was required to determine the effect of the process variables used during the processing of these last four parts (with the exception of the 'Shape & Location of TGC' variable). Derived from text

N95-27123 MART Corp., Saint Louis, MO.
CLEANING OF PARTS FOR NEW MANUFACTURING AND PARTS REBUILDING
Jeff Doherty *In* Johns Hopkins Univ., Environmentally Benign Cleaning and Degreasing Technology: JANNAF Safety and Protection Subcommittee and Propellant Development and Characterization Subcommittee Joint Workshop Jun. 1994 p 215-223 (For primary document see N95-27101 09-27)
Avail: CPIA, 10630 Little Patuxent Pkwy., Suite 202, Columbia, MD 21044-3200 HC

32 COMMUNICATIONS AND RADAR

Includes radar; land and global communications; communications theory; and optical communications.

For related information see also *04 Aircraft Communications and Navigation* and *17 Space Communications, Spacecraft Communications, Command and Tracking.* For search and rescue see *03 Air Transportation and Safety,* and *16 Space Transportation.*

N95-26344 Organisatie voor Toegepast Natuurwetenschappelijk Onderzoek, Delft (Netherlands).
ASSESSMENT OF LONG-DISTANCE HF RADIO AND SATELLITE COMMUNICATION ASSETS FOR RNLAF OUT-OF-AREA OPERATIONS
R. VanAken, P. J. VanVliet, and P. Ch. Hoefsloot Sep. 1994 78 p Limited Reproducibility: More than 20% of this document may be affected by microfiche quality

(AD-A288633; TNO-FEL-94-A200; TDCK-94-0887) Avail: Issuing Activity (Defense Technical Information Center (DTIC))

This report presents the relative assessment of various long-haul communication systems in order to fulfill the need for communications between the rear area and Royal Netherlands Airforce (RNLAF) units deployed in out-of-area operations. Four different communication systems are compared with respect to the operational aspects: High Frequency (HF) radio communication systems; Military satellite communication (SATCOM) systems; Public access SATCOM systems (such as the INMARSAT system); Private SATCOM networks (based on the use of very small aperture terminals (VSATs)). The comparison is based on the current available communications assets. Future technical developments and their consequences for the system comparison are also discussed. DTIC

N95-26349 Naval Research Lab., Washington, DC.

SPEECH ANALYSIS AND SYNTHESIS BASED ON PITCH-SYNCHRONOUS SEGMENTATION OF THE SPEECH WAVEFORM Report, 1 Oct. 1992 - 30 Sep. 1993

George S. Kang and Lawrence J. Fransen 9 Nov. 1994 55 p Limited Reproducibility: More than 20% of this document may be affected by microfiche quality

(AD-A288824; NRL/FR/5550-94-9743) Avail: Issuing Activity (Defense Technical Information Center (DTIC))

This report describes a new speech analysis/synthesis method. This new technique does not attempt to model the human speech production mechanism. Instead, we represent the speech waveform directly in terms of the speech waveform defined in a pitch period. A significant merit of this approach is the complete elimination of pitch interference because each pitch-synchronously segmented waveform does not include a waveform discontinuity. One application of this new speech analysis/synthesis method is the alteration of speech characteristics directly on raw speech. With the increased use of man-made speech in tactical voice message systems and virtual reality environments, such a speech generation tool is highly desirable. Another application is speech encoding operation at low data rates (2400 b/s or less). According to speech intelligibility tests, our new 2400 b/s encoder outperforms the current 2400-b/s LPC. This is also true in noisy environments. Because most tactical platforms are noisy (e.g., helicopter, high-performance aircraft, tank, destroyer), our 2400-b/s speech encoding technique will make tactical voice communication more effective; it will become an indispensable capability for future C4I. DTIC

N95-26356 Naval Air Warfare Center, Warminster, PA.

MODIFIED GAUSSIAN ELIMINATION FOR ADAPTIVE BEAMFORMING USING RNS ARITHMETIC Final Report, 6 Jul. - 11 Sep. 1992

Barry J. Kirsch and Peter R. Turner (Naval Academy, Annapolis, MD.) 1 Sep. 1994 38 p Limited Reproducibility: More than 20% of this document may be affected by microfiche quality

(AD-A288809; NAWCADWAR-94112-50) Avail: Issuing Activity (Defense Technical Information Center (DTIC))

This paper is concerned with the development of a solution to the adaptive beamforming problem. The proposed solution consists of an algorithm-architecture-arithmetic combination which has the potential for very fast solution of the problem on a physically small platform which might be suitable for use on aircraft or sonobuoys. The arithmetic system used in the proposed solution is the RNS system implemented on an array of RNS processors which can be reassigned as the algorithm proceeds. The underlying algorithm is a modification of Gaussian elimination. The (non-RNS) division operations are eliminated in favor of some scaling and the adaptive use of the processor array to accommodate the growth in dynamic range which is implicit in this divisionless implementation. DTIC

N95-26407 Defence Research Establishment Ottawa, Ottawa (Ontario). Electronic Support Measures Section.

BALANCED DATA FOCUSING: DIRECTION OF ARRIVAL ESTIMATION WITH MAXIMUM LIKELIHOOD PERFORMANCE

William J. L. Read Nov. 1994 55 p Limited Reproducibility: More than 20% of this document may be affected by microfiche quality

(AD-A288252; DREO-1233) Avail: Issuing Activity (Defense Technical Information Center (DTIC))

The performance of a direction of arrival estimation procedure at low signal-to-noise ratios and limited data samples is an important characteristic. The approach based on maximum likelihood (ML) estimation is considered to be among the best for this problem as long as the underlying signal model is properly chosen. Unfortunately, in most cases, there is no closed-form solution so fast search procedures are employed. Given to a priori knowledge, selecting the initial parameter values for these search procedures can be a difficult problem, especially under low signal-to-noise conditions. In this paper, a new method for uniform linear sensor arrays which overcomes the initial value problem is introduced. This method is called Balanced Data Focusing (BDF). Simulation results are included comparing the performance of this new method to that of the ML approach using the Alternating Projection Maximization search procedure and another popular estimation approach, the root-MUSIC method. DTIC

N95-26450# Helsinki Univ. of Technology, Espoo (Finland). Electromagnetics Lab.

ANALYSIS OF ELECTROMAGNETIC PROBLEMS INVOLVING CHIRAL, BI-ISOTROPIC, AND UNIAXIAL BIANISOTROPIC MEDIA Ph.D. Thesis

Paeivi K Koivisto Nov. 1994 31 p

(ISSN 0784-848X)

(PB95-185096; ISBN-951-22-2361-9) Avail: CASI HC A03/MF A01

The following topics are included: introduction to the subject; constitutive relations; electromagnetic fields; bi-isotropic waveguides; uniaxial bianisotropic medium; image methods; and a summary of 8 papers in which the author of this thesis (P. Koivisto) was the author, or a co-author. NTIS

N95-26465 Department of the Navy, Washington, DC.

METHOD OF PHASED MAGNITUDE CORRELATION USING BINARY SEQUENCES Patent

Michael Pender, inventor (to Navy) 19 Jul. 1994 28 p Filed 15 Nov. 1993

(AD-D017257; US-Patent-5,331,328; US-Patent-Appl-SN-153864; US-Patent-Class-342-189) Avail: US Patent and Trademark Office

This patent discloses a method for allowing a correlation function to be applied to binary codes of length 3 to length 128. A user may specify the desired length of the binary codes for correlation processing; whether the binary code is to use a phase sidelobe level as the threshold or a sidelobe amplitude as the threshold. The user will also be asked to specify the threshold as well as an in phase coefficient referred to as alpha and an out of phase coefficient referred to as a beta. The user may also specify that the codes be expanded which results in correlated compounds having a length twice that of the specified length being displayed to the user. When the user has specified the parameters for correlation processing of the binary code length selected by the user, the program of the present invention will process the binary codes eliminating allomorphic and symmetrical forms of the codes from correlation and then display the results to the user. DTIC

N95-26493 British Broadcasting Corp., Tadworth (England). Research and Development Dept.

RESEARCH AND DEVELOPMENT REPORT. DIGITAL AUDIO BROADCASTING: COMPARISON OF COVERAGE AT BAND 2 AND BAND 3

I. R. Pullen, P. J. Doherty, and M. C. D. Maddocks 1994 21 p Original contains color illustrations

(BBC-RD-1994/16) Copyright Avail: Issuing Activity (BBC, Kingswood Warren, Tadworth, Surrey, England)

A Digital Audio Broadcasting (DAB) system capable of reliable reception in vehicles and portables has been developed by the EUREKA 147 project. This report describes a set of experiments performed to compare the coverage area when radiating a DAB signal of equal power in Band 2 and Band 3. Author

N95-26505 Department of the Navy, Washington, DC.

MULTIPURPOSE BUS INTERFACE UTILIZING A DIGITAL SIGNAL PROCESSOR Patent

Christian L. Houlberg, inventor (to Navy) 20 Sep. 1994 72 p Filed 5 May 1992

(AD-D017264; US-Patent-5,349,685; US-Patent-Appl-SN-878713; US-Patent-Class-395-800) Avail: US Patent and Trademark Office

A multi-purpose bus interface comprising a digital signal processor which receives a clock signal and control signals from a Manchester type encoder/decoder and then processes the clock and control signals allowing for the serial transfer of data to and from the 1553 multiplex data bus, the encoder/decoder and the digital signal processor into an IC memory card for storage in or retrieval from the IC memory card. Software stored in an electrically erasable programmable read only memory controls how the data is transferred and interpreted making it easier to modify the digital signal processor's operation to accommodate its use with different bus standards and data protocols/formats. The encoder/decoder of the present invention formats and protocols data transferred from the electrically erasable programmable read only memory to the 1553 multiplex data bus as well data transferred from the 1553 multiplex data bus to the memory, as appropriate. The multipurpose bus interface of the present invention also includes an RS-232 interface and an RS-422 interface controlled by the digital signal processor which provides for data transfer to and from a host computer or the like into the IC memory card. DTIC

N95-26509 Department of the Navy, Washington, DC.
TARGET DETECTION FOR VISION SYSTEMS Patent
Michael W. Pullen, inventor (to Navy) 2 Aug. 1994 13 p Filed 3 May 1993
(AD-D017271; US-Patent-5,335,297; US-Patent-Appl-SN-055455; US-Patent-Class-395-800) Avail: US Patent and Trademark Office

An autonomous real-time adaptive video target detection and position location apparatus and method. Adaptive low pass filters produce horizontal leading and trailing edge and vertical thresholds from each frame of input target and a background or clutter video signal. A user selectable input is used with the three adaptive thresholds, input video, and horizontal synchronization signal to produce a signal representing valid target detection and position information. DTIC

N95-26545 Defence Research Establishment Ottawa, Ottawa (Ontario). Surface Radar Section.
EVALUATION OF THE FMICW WAVEFORM IN HF SURFACE RADAR APPLICATIONS
Hing C. Chan Jan. 1994 62 p Limited Reproducibility: More than 20% of this document may be affected by microfiche quality
(AD-A288245; DREO-1219) Avail: Issuing Activity (Defense Technical Information Center (DTIC))

The operation and performance of the Frequency Modulated Interrupted Continuous Wave (FMICW) waveform in ship and aircraft detection using high frequency surface wave radar are analyzed. A modified processing scheme for the FMICW waveform which circumvents the problem of ambiguous range response is presented. The increase in hardware complexity for the modified processing scheme is moderate. The signal-to-clutter ratio and the signal-to-noise ratio are used to evaluate the performance of the FMICW. It is concluded that the FMICW is superior to the simple pulsed waveform in ship-detection application. For aircraft detection, the advantage of the FMICW is marginal. Parameters optimized for ship-detection application will not be optimal for aircraft-detection application because of their much higher velocity which exacerbates the range- walk problem. DTIC

N95-26562 Army Research Lab., White Sands Missle Range, NM. Battlefield Environment Directorate.
THE ATTENUATION OF MICROWAVE RADIATION BY FOG AND RAIN Final Report
J. D. Pendleton and Stanley Niles Aug. 1994 65 p Limited Reproducibility: More than 20% of this document may be affected by microfiche quality
(AD-A288326; ARL-TR-527) Avail: Issuing Activity (Defense Technical Information Center (DTIC))

In this report, the equations which describe the attenuation of long-wavelength electromagnetic radiation by water fogs and rain are briefly reviewed and explained under the assumption that the aerosol droplets are spherical and that the irradiance of the beam is in the 'linear' regime. Calculations of water fog attenuation coefficients are made using the Rayleigh approximation, and an approximate error analysis of this approximation is made by comparing Rayleigh approximation calculations of absorption efficiency with exact Mie theory calculations of extinction efficiency. Numerical integration of the Mie extinction efficiency is used to compute the attenuation coefficient for rain with a Marshall-Palmer drop size distribution for various rain rates and temperatures. These results are compared with those given by a power law relationship with coefficients given by Olsen, Rogers, and Hodge which was used in the Near Milimeter Wave (NMMW) Module of the Electro- Optical Systems Atmospheric Effects Library (EOSAEL). DTIC

N95-26564 Naval Research Lab., Washington, DC.
ELECTROMAGNETIC SPECTRUM OCCUPANCY STUDY OF A POTENTIAL TRANSMITTER SITE FOR THE HF ACTIVE AURORAL RESEARCH PROGRAM (HAARP) Interim Report, May - Jun. 1993
Joseph A. Goldstein, Edward J. Kennedy, and Monroe Y. McGown 30 Sep. 1994 50 p Limited Reproducibility: More than 20% of this document may be affected by microfiche quality
(AD-A288909; NRL/MR/5554-7622) Avail: Issuing Activity (Defense Technical Information Center (DTIC))

The results of measurements conducted by the Naval Research Laboratory in May and June 1993 are presented. The purpose of the measurements was to ascertain the radio frequency occupancy in the immediate vicinity of the proposed High Frequency Active Auroral Research Program (HAARP) facility to be constructed in the Gakona, Alaska area. The HAARP facility will consist of a large planar array of antennas excited by phased high power transmitters operating in the lower portion of the HF band (2.8 to 8 MHz). The existing electromagnetic spectrum usage in the vicinity of Gakona was measured in order to assess the potential for electromagnetic interference problems arising from the HAARP facility. The measurements covered the frequency spectrum from 2 MHz to 1000 MHz. Data was collected for a period of 17 days in May and early June 1993. There are a large number of users in the HF band and data shows a normal diurnal pattern of energy increase in the lower portion of the band in the nighttime hours. The number of users decreases with increasing frequency because the propagation path at higher frequencies is dependent upon line-of-sight signal paths. Gakona is a very rural area and is separated by hilly terrain from surrounding residential and commercial activities. Above the HF bend, the most prominent signal identified is a 152 MHz transient signal that saturates the signal path of our measurement apparatus. The signal is so strong that it produces harmonics throughout the measurement band and distorts the display of the data. Another strong feature that is sometimes observed is a 450 MHz signal. DTIC

N95-26670 British Broadcasting Corp., Tadworth (England). Research and Development Dept.
COM(SUP 3): A COMPOSITE-COMPATIBLE COMPONENT CODING SYSTEM
G. A. Thomas 1994 34 p Original contains color illustrations
(BBC-RD-1994/17) Copyright Avail: Issuing Activity

This Report describes a method for conveying a component video signal on a single cable in such a way that it may be passed through any existing composite studio equipment that has a bandwidth of approximately 9 MHz. Author

N95-26696 British Broadcasting Corp., Tadworth (England). Research and Development Dept.
RESEARCH AND DEVELOPMENT REPORT. EUREKA 147: TESTS OF THE ERROR PERFORMANCE OF THE DAB SYSTEM
N. H. C. Gilchrist 1994 13 p
(BBC-RD-1994/18) Copyright Avail: Issuing Activity

This Report describes tests carried out by the BBC and other members of Eureka 147 Working Group 2-A, to assess the performance of the DAB (Digital Audio Broadcasting) system with a low carrier-to-noise ratio at the receiver. The tests were conducted using a number of listeners to judge the audio quality, making collaborative decisions with the knowledge of the conditions under which the system was operating at all times. The primary purpose of the work described in this Report was to inform the Eureka 147 project about the failure characteristics of the DAB system as the carrier-to-noise ratio is reduced. Author

N95-26708*# Georgia Tech Research Inst., Atlanta, GA. Contracting Support Div.
AN ACOUSTIC CHARGE TRANSPORT IMAGER FOR HIGH DEFINITION TELEVISION APPLICATIONS Semiannual Status Report, 1 Jan. 1994 - 31 Mar. 1995
W. D. Hunt and Kevin F. Brennan Oct. 1994 162 p Sponsored in part by NSF and ARPA

(Contract NAGw-2753; E21-H36)
(NASA-CR-197841; NAS 1.26:197841) Avail: CASI HC A08/MF A02

The primary goal of this research is to develop a solid-state high definition television (HDTV) imager chip operating at a frame rate of about 170 frames/sec at 2 Megapixels per frame. This imager offers an order of magnitude improvement in speed over CCD designs and will allow for monolithic imagers operating from the IR to the UV. The technical approach of the project focuses on the development of the three basic components of the imager and their integration. The imager chip can be divided into three distinct components: (1) image capture via an array of avalanche photodiodes (APD's), (2) charge collection, storage and overflow control via a charge transfer transistor device (CTD), and (3) charge readout via an array of acoustic charge transport (ACT) channels. The use of APD's allows for front end gain at low noise and low operating voltages while the ACT readout enables concomitant high speed and high charge transfer efficiency. Currently work is progressing towards the development of manufacturable designs for each of these component devices. In addition to the development of each of the three distinct components, work towards their integration is also progressing. The component designs are considered not only to meet individual specifications but to provide overall system level performance suitable for HDTV operation upon integration. The ultimate manufacturability and reliability of the chip constrains the design as well. The progress made during this period is described in detail in Sections 2-4. Derived from text

N95-26717 Air Force Systems Command, Wright-Patterson AFB, OH. National Air Intelligence Center.
SIGNALS PROCESSING USING ACOUSTO-OPTICAL TECHNOLOGY
Ning Li 14 Nov. 1994 14 p Transl. into ENGLISH from Guangxue Xuebao (China), v. 8, no. 5, May 1988 p 429-434 Limited Reproducibility: More than 20% of this document may be affected by microfiche quality
(AD-A289597; NAIC/ID(RS)T-0369-94) Avail: Issuing Activity (Defense Technical Information Center (DTIC))

An experimental system for simulative signals processing using high frequency wideband acousto-optical device is proposed herein and the mathematical expressions of system output are derived. The experimental results of both space and time integrating convolution (correlation) for the simulative signals composed of root impulses conform on the whole with calculations. DTIC

N95-26725 Naval Postgraduate School, Monterey, CA.
SPACE TETHER-RADAR DATA PROCESSING M.S. Thesis
Wayne A. Brewster Sep. 1994 81 p Limited Reproducibility: More than 20% of this document may be affected by microfiche quality
(AD-A289654) Avail: Issuing Activity (Defense Technical Information Center (DTIC))

NASA conducted the Delta-PMG tethered satellite mission. It was conducted to verify the hollow cathode plasma source's ability to couple electric currents from each end of a long wire tether traversing the ambient low earth orbit ionosphere plasma. Observations were obtained through a suite of sensors which included large ground based VHF radars. The goal of this thesis was to process the radar data received at the radar based in Hawaii to study disturbances in the earth's ionosphere caused by the tether. After extensive analysis, unique radar returns were identified that were associated with the passage of the tether system through magnetic field lines threading the radar's field of view. These returns were interpreted as a plasma cloud propagating along a magnetic field line and reflecting back along another. This phenomenon produced dual returns with inverted Doppler frequency content. DTIC

N95-26738 Air Force Inst. of Tech., Wright-Patterson AFB, OH. School of Engineering.
REDUCTION OF OFF-BORESIGHT FIELDS FOR A TEM HORN ANTENNA M.S. Thesis
Dennis J. Wolstenholme Dec. 1994 173 p Limited Reproducibility: More than 20% of this document may be affected by microfiche quality
(AD-A289708; AFIT/GE/ENG/94D-33) Avail: Issuing Activity (Defense Technical Information Center (DTIC))

This research involves the design, modeling, and testing of both tapered periodic surfaces (TPS) and transverse electromagnetic (TEM) horns. The goal is to reduce the off-boresight fields for a TEM horn and increase the peak-to-peak field levels on boresight. This is accomplished by applying a TPS to the free space end. Two tapers are designed - one that approximates an exponential impedance function and one that approximates a triangular impedance function. Both reduce the off-boresight fields of the TEM horn. In most cases the exponential taper reduces the field levels further than the triangular taper. This research shows that a TPS is an effective method of reducing diffraction. A procedure for designing a TPS to approximate a specific impedance function is presented. A two-dimensional finite difference time domain (FDTD) model predicts the tapers will reduce the diffraction. Experimental results verify the TPS's ability to reduce the peak off-boresight fields for a TEM horn antenna. DTIC

N95-26759 Edgewood Research Development and Engineering Center, Aberdeen Proving Ground, MD.
COMPUTATION OF ELECTROMAGNETIC SCATTERING PARAMETERS FOR LOGNORMAL DISTRIBUTIONS OF MAGNETIC SPHERES: THEORY AND ALGORITHMS Final Report, Jan. 1991 - Jan. 1994
Merrill E. Milham Oct. 1994 34 p Limited Reproducibility: More than 20% of this document may be affected by microfiche quality
(DA Proj. 1O1-62622-A-552)
(AD-A289672; ERDEC-TR-212) Avail: Issuing Activity (Defense Technical Information Center (DTIC))

In this report, relevant parts of the scattering theory for magnetic spheres are presented. Mass extinction coefficients, and the lognormal size distribution are defined. The theory and algorithms for integrating scattering parameters over size distributions are developed. The integrations are carried out in terms of dimensionless scattering, and size distribution parameters, which are simply related to the usual mass scattering coefficients. Fortran codes, which implement the algorithmic design, are presented, and examples of code use are given. Code listings are included. DTIC

N95-26835 Polish Academy of Sciences, Warsaw (Poland). Inst. of Acoustic Phonetics.
THE AUTOMATIC EXTRACTION OF SELECTED SPEECH SPECTRAL CHARACTERISTICS [AUTOMATYCZNA EKSTRAKCJA WYBRANYCH CECH WIDMOWYCH MOWY]
Henryk Kubzdela 1994 20 p In POLISH
(ISSN 0208-5658)
(IFTR-2/1994) Avail: Issuing Activity (Polish Academy of Sciences, Warsaw, Poland)

The operation of automatic segmentation of a speech signal into basic phones is an especially difficult aspect of modelling the process of decoding the information contained in speech. Spectral characteristics which characterize the spectrographic patterns of different speech sounds should be used as the basis for this segmentation. Unfortunately, speech signals have properties which make it difficult to extract these characteristics. The imperfection of digital acoustic signal analysis also causes problems. The author assumed that the distinctive spectral characteristics of a sound are primarily contained in the level and frequency of the strongest component and the components occurring in the vicinity of points of the amplitude spectrum indicated by the positions of the extrema of a function (FMOW) which models the envelope of the spectrum. A discrete pattern of this function can be obtained by two-step equalizing transformation of the peaks of the amplitude spectrum. The author uses examples to illustrate the results of procedures for determining the intervals of convexities, concavities, and extrema of the FMOW function. The author also provides examples which illustrate the segmentation values of the information contained in time curves of the level of the spectrum at the points indicated by the peaks of the FMOW function. Transl. by Schreiber Translations Inc.

N95-26836 Polish Academy of Sciences, Warsaw (Poland). Inst. of Acoustic Phonetics.
AN EXPERIMENTAL VERSION OF THE MZT (SPEECH-FROM-TEXT) SYSTEM WITH EXTERNAL F(SUB 0) CONTROL [WERSJA EKSPERYMENTALNA SYSTEMU MZT (MOWY Z TEKSTU) Z ZEWNETRZNYM STEROWANIEM FO]
Ignacy Nowak Cooperative Publishing House Ltd. 1994 29 p In POLISH
(ISSN 0208-5658)
(IFTR-14/1994) Avail: Issuing Activity

The version of a Polish speech from text system described in this article was developed using the speech-from-text system. The new system has additional functions which make it possible to enter commands in edited orthographic text to control the phrase component and accentuation parameters. This makes it possible to generate a series of modified intonation contours in the texts spoken by the system. The effects obtained are made easier to control by a graphic illustration of the base frequency pattern in phrases that were last 'spoken' by the system. This version of the system was designed as a test prototype which will help us expand and refine our set of rules for automatic generation of intonation contours, which in turn will enable the fully automated speech-from-text system to generate speech with a more varied and precisely formed fundamental frequency pattern. Transl. by Schreiber Translations Inc.

N95-26851 Army Combat Systems Test Activity (Provisional), Aberdeen Proving Ground, MD.

TEST OPERATIONS PROCEDURE (TOP) 2-2-613, ELECTROMAGNETIC INTERFERENCE TESTING AND ELECTRICAL SUBSYSTEM - NON-COMMUNICATION

16 Dec. 1994 23 p Limited Reproducibility: More than 20% of this document may be affected by microfiche quality
(AD-A289521; TOP-2-2-613) Avail: Issuing Activity (Defense Technical Information Center (DTIC))

This TOP describes procedures for conducting electromagnetic interference (EMI) tests of non-communication electronic equipment (NCEE) and mobile equipment power (MEP) sources. DTIC

N95-26867 Air Force Inst. of Tech., Wright-Patterson AFB, OH. School of Engineering.

PERCEPTUAL BASED IMAGE FUSION WITH APPLICATIONS TO HYPERSPECTRAL IMAGE DATA M.S. Thesis

Terry A. Wilson Dec. 1994 213 p Limited Reproducibility: More than 20% of this document may be affected by microfiche quality
(AD-A289429; AFIT/GE/ENG/94D-32) Avail: Issuing Activity (Defense Technical Information Center (DTIC))

Development of new imaging sensors has created a need for image processing techniques that can fuse images from different sensors or multiple images produced by the same sensor. The methods presented here focus on combining image data from the Airborne Visual and Infrared Imaging Spectrometer (AVIRIS) hyperspectral sensor into a single or smaller subset of images while maintaining the visual information necessary for human analysis. Three hierarchical multi-resolution image fusion techniques are implemented and tested using the AVIRIS image data and test images that contain various levels of correlated or uncorrelated noise. Two of the algorithms are published fusion methods that combine images from multiple sensors. The third method was developed to fuse any co-registered image data. This new method uses the spatial frequency response (contrast sensitivity) of the human visual system to determine which parts of the input images contain the salient features that need to be preserved in the composite image(s). After analyzing the signal-to-noise ratios and visual aesthetics of the fused images, contrast sensitivity based fusion is shown to provide excellent fusion results and, in every case, clearly outperformed the other two methods. Finally, as an illustrative example of how the fusion techniques are independent of the hyperspectral application, they are applied to fusing multiple polarimetric images from a Synthetic Aperture Radar to enhance automated targeting techniques. DTIC

N95-26869 Air Force Inst. of Tech., Wright-Patterson AFB, OH. School of Engineering.

A 3-D FINITE DIFFERENCE TIME DOMAIN INVESTIGATION OF MICROWAVE PROPAGATION THROUGH INHOMOGENEOUS BIOLOGICAL MATERIALS M.S. Thesis

David B. Dunn, Jr. Dec. 1994 158 p Limited Reproducibility: More than 20% of this document may be affected by microfiche quality
(AD-A289431; AFIT/GE/ENG/94D-05) Avail: Issuing Activity (Defense Technical Information Center (DTIC))

This paper extends past analysis of an optimal source distribution around a homogeneous sphere of muscle tissue by using a 3-D finite difference time domain (FDTD) scenario in which an anatomically correct human head model is irradiated. It first duplicates the analytical solution within an FDTD space using an FDTD computer code developed at Penn State University. This duplication uses a 9.45 cm radius sphere represented in an FDTD space of 2.35 mm cubic cells. FDTD simulations are then performed on four, three, and two layer laminated spheres, designed to provide simple models of a head. Finally, four simulations were performed in FDTD on the human head model developed at Penn State from an MRI scan of an actual human head. The comparison of analytic simulations to the FDTD simulations on a homogeneous sphere showed a pixel by pixel average of 5.34% error between the two with a standard deviation of 7.84%. The layered sphere models showed considerable spiking at the two poles along with a small amount of spiking due to the stair-step approximation of the spheres. None of these spikes increased the power beyond that at the surface and hence were not critical. The simulations on a true human head showed improvement in depth due to the low-loss of the bone tissue. This study demonstrates that microwave hyperthermia with good resolution is possible in an anatomically correct head model. DTIC

N95-26871 Naval Postgraduate School, Monterey, CA.

THE AMBIGUITY FUNCTION OF THE STEPPED FREQUENCY RADAR Final Report

Jen-Chih Huang Sep. 1994 97 p Limited Reproducibility: More than 20% of this document may be affected by microfiche quality
(AD-A289533) Avail: Issuing Activity (Defense Technical Information Center (DTIC))

High range resolution radar systems have many advantages such as target classification, resolution of multiple target, accurate range profile, and detection of low radar cross section (RCS) targets in clutter. High range resolution requires large bandwidths. Stepped frequency waveforms can achieve high range resolution by increasing the effective bandwidth without increasing the instantaneous bandwidth which would increase the hardware requirements including higher analog to digital (A/D) sampling rates which are limited by existing technology. Under today's hardware limitations, the stepped frequency waveform becomes very important. This thesis briefly discusses the stepped frequency radar and associated signal processing; it investigates the ambiguity function of the stepped frequency waveform and the stepped frequency radar system. Mathematical expressions of ambiguity functions are derived and the improvement of clutter suppression capability for the stepped frequency radar by rejecting initial pulses is also discussed. DTIC

N95-26877 Air Force Inst. of Tech., Wright-Patterson AFB, OH.

CLASSIFICATION OF ULTRA HIGH RANGE RESOLUTION RADAR USING DECISION BOUNDARY ANALYSIS M.S. Thesis

Christopher L. Eisenbies Dec. 1994 122 p Limited Reproducibility: More than 20% of this document may be affected by microfiche quality
(AD-A289378; AFIT/GE/ENG/94D-07) Avail: Issuing Activity (Defense Technical Information Center (DTIC))

This thesis examines the discrimination of targets with Ultra High Range Resolution (UHRR) radar data. Using these measured signals from frontal aspect angles of four aircraft classes, the baseline performance of the Adaptive Gaussian Classifier (AGC) is tested with respect to aligning exemplars to templates. Alignment plays a crucial role in the AGC's classification performance which can degrade by 11% for a target class. The AGC is compared to non-parametric classifiers, but no statistically significant degradation of performance is found. Data separability is analyzed by hounding the Bayes error. The data is well separated in a statistical sense. A feature selection algorithm based on analysis of the decision boundary, is applied to find a reduced feature set, which are linear combinations of the original features. These features are optimized with respect to classification error rather than reconstruction error. This technique is extended to deduce the relevant features in the original feature space. Fewer than 5% of the features in the original feature space may be used to attain an improved classification rate. This new method is a true reduction of features and shows improvement up to 15%. Discrimination of UHRR radar signatures using a multiresolution analysis is proposed. The decision boundary analysis chooses relevant wavelet scales with respect to classification. Some improved performance against an entropy based measure is observed for limited feature sets. The technique developed here successfully chooses the scale that causes classification performance to peak within 5% of the performance in the full-dimensional or reduced-dimensional UHRR radar signature space. DTIC

N95-26893 Air Force Inst. of Tech., Wright-Patterson AFB, OH.

IMPROVING THE PERFORMANCE OF SPIRAL ANTENNAS BY USING PASSIVE SCATTERERS Final Report

Joseph S. Zaren Dec. 1994 349 p Limited Reproducibility: More than

20% of this document may be affected by microfiche quality
(AD-A289324; AFIT/GE/ENG/94D-34) Avail: Issuing Activity (Defense Technical Information Center (DTIC))

The purpose of this study was to explore the viability of improving the performance of cavity-backed antennas. Traditionally antenna cavities are filled with electromagnetic absorber to mitigate interference effects that would otherwise cause the antenna radiation pattern to vary widely at different frequencies. The approach used in this research was to replace the absorber with dielectric slabs, some of which contained arrays of dipoles. These dipole arrays were modeled as frequency selective surfaces using two periodic moment method based - computer programs and one transmission line program. A systematic study was performed that identified the effect of changing the dipole array parameters on prospective cavity designs. Seven different cavity configurations were tested using a log periodic trapezoid wire antenna system designed to support 2.3-12.4 0Hz. Cavity configurations using one, two, and three layers of dipole arrays were tested and compared to both absorber-filled and dielectric-filled cavity configurations. The results were inconclusive because even though some two layer designs and one three layer design had better gain almost entirely throughout the 2-12 GHz region, the gain of the baseline absorber-filled and dielectric-filled cavities varied widely over this bandwidth. No cavity condition provided an extended 3 dB bandwidth. Additional research is recommended. DTIC

N95-26908 Helsinki Univ. of Technology, Espoo (Finland). Radio Lab.

PREDICTION OF RAIN ATTENUATION AND TOTAL ATMOSPHERIC ATTENUATION FOR LOW-AVAILABILITY SATELLITE COMMUNICATIONS IN EUROPE

S. Karhu and E. Salonen Aug. 1994 58 p Limited Reproducibility: More than 20% of this document may be affected by microfiche quality
(PB95-184925; ISBN-951-22-2144-6) Avail: CASI HC A04

Attenuation models for oxygen, water vapor, clouds, and rainfall, as well as the meteorological data from the ECMWF (the European Centre for Medium-Range Weather Forecasts), are outlined in order to predict the average annual distributions of the total atmospheric attenuation at 10-50 GHz for Europe. The distributions are intended for the design of low-availability satellite communication systems operating at the outage time greater than 0.1% of the year. The fair weather attenuation due to oxygen, water vapor, and clouds is calculated for a specified frequency, site, and elevation angle from the distributions at 12, 20, 30, 40, and 50 GHz, determined in the zenith direction from the time series of the ECMWF grid data. The methods are introduced for the scaling of the frequency and the altitude, for the interpolation in the horizontal direction, and for the scaling of the elevation angle. The distribution of the total atmospheric attenuation is determined on the equiprobability basis from the distributions of the fair weather attenuation and rain attenuation. The models and data are tested in three ways at the annual outage percentage range of 0.1-10% by comparing 23 predicted and measured attenuation distributions of 11.4-30 GHz from eight European sites. NTIS

N95-26914 Helsinki Univ. of Technology, Espoo (Finland). Electromagnetics Lab.

CONDITIONS FOR THE PARAMETER DYADICS OF LOSSLESS BI-ANISOTROPIC MEDIA

I. V. Lindell, A. H. Sihvola, P. Puska, and L. H. Ruotanen Oct. 1994 13 p Limited Reproducibility: More than 20% of this document may be affected by microfiche quality
(PB95-185104; ISBN-951-22-2341-4) Avail: CASI HC A03

Dyadic parameters of lossless bi-anisotropic media are considered and conditions based on the positive definite energy function are derived. As examples of the conditions, inequalities limiting the magnitude of the magnetoelectric parameters are considered for various nondispersive bi-anisotropic media treated in the literature. NTIS

N95-26923 General Accounting Office, Washington, DC. Resources Community and Economic Development Div.

INFORMATION SUPERHIGHWAY: ISSUES AFFECTING DEVELOPMENT

Sep. 1994 77 p Limited Reproducibility: More than 20% of this document may be affected by microfiche quality
(AD-A289434; GAO/RCED-94-285) Avail: Issuing Activity (Defense Technical Information Center (DTIC))

Technological advances in the transmission of voice, video, and data are fostering fundamental changes in the telecommunications industry. For example, large local telephone companies plan to offer video services in competition with cable and broadcast television, while cable television companies plan to offer local telephone service over their wires in competition with the local telephone companies. The administration believes that these technological changes provide the opportunity to develop an 'Information Superhighway' that could provide every element of society with ready access to data, voice, and video communications. Concurrently, the Congress is considering sweeping changes to telecommunications regulations to keep pace with this dynamic industry. GAO prepared this report to serve as an overview of three key issues that decisionmakers may face as they deliberate telecommunications legislation; it focuses on three pivotal issues they face in formulating new telecommunications legislation: (1) managing the transition to a more competitive local telecommunications marketplace; (2) ensuring that all consumers have access to affordable telecommunications as competition develops; and (3) ensuring that the Information Superhighway provides adequate security, privacy, reliability, and interoperability. DTIC

N95-26924 Colorado Univ., Boulder, CO. Guided Wave Optics Lab.

ACTIVE ANTENNAS WITH PERIODIC STRUCTURES Ph.D. Thesis

Kuang Y. Chen Oct. 1994 145 p Limited Reproducibility: More than 20% of this document may be affected by microfiche quality
(Contract N00014-92-J-1190)
(AD-A289437; ECE/GWOL/61) Avail: Issuing Activity (Defense Technical Information Center (DTIC))

Integration of a solid-state transistor oscillator with a radiative element has many advantages: it eliminates the feed network; replaces the expensive waveguide transition; reduces the size of the antenna system; and provides active impedance matching. Active devices also offer promise for optical control of beam steering antenna arrays. The objective of this thesis is to determine the physical characteristics of an active antenna and understand its operational principles. DTIC

N95-26929 Helsinki Univ. of Technology, Espoo (Finland). Lab. of Telecommunications Technology.

MILESTONES IN TELECOMMUNICATIONS IN SOME SELECTED COUNTRIES

K. Kivinen Oct. 1994 64 p Limited Reproducibility: More than 20% of this document may be affected by microfiche quality
(PB95-184826; ISBN-951-22-2291-4) Avail: CASI HC A04

The publication presents an overall picture of the development of telecommunications in the United States, the United Kingdom, Sweden, and Finland. Modern telecommunications, as we see it today, is a result of work done and decisions made in several fields such as basic research, component technology, the needs of business and households, general attitudes towards telecommunications during periods of peace and during wars, questions of 'natural monopoly' and market economy. The book acknowledges this fact and thus deals with more than the development of the technology. It follows as strict as possible a chronological order, so that chains of events can be followed up. The book is a compilation of facts found in different sources. NTIS

N95-26972 Air Force Inst. of Tech., Wright-Patterson AFB, OH. School of Engineering.

POLARIZATION SENSITIVITY OF MONOPULSE RADAR BORESIGHT ERROR INDUCED BY LARGE, OGIVE RADOMES M.S. Thesis

Kelce S. Wilson Dec. 1994 91 p Limited Reproducibility: More than 20% of this document may be affected by microfiche quality
(AD-A289254; AFIT/GE/ENG/94D-31) Avail: Issuing Activity (Defense Technical Information Center (DTIC))

The dependence of Boresight Error (BSE) on incident Electric Field (E-Field) polarization tilt angle is investigated. BSE, defined as the angular difference between a target's actual and radar-indicated position, is influenced by the radome used to protect the antenna. A reliable computer model for predicting the BSE of electrically large radar-radome systems has been demonstrated and used to investigate the dependence of radome-induced BSE for various combinations of scan angle, element polarization, and incident E-Field polarization. The analysis includes a development of a transmission/depolarization model to justify the results of the computer model. Results compare very well with empirical, published, and experimentally measured data for specific scan angle and polarization cases considered. Generally, BSE exhibits a noticeable dependence on E-Field polarization, except under limited scanning conditions for specific linearly polarized antenna apertures. DTIC

N95-26976 Air Force Inst. of Tech., Wright-Patterson AFB, OH. School of Engineering.

PROCESSING OF WIDE-ANGLE SYNTHETIC APERTURE RADAR SIGNALS FOR DETECTION OF OBSCURED GROUND TARGETS M.S. Thesis

Richard J. Sumner Dec. 1994 79 p Limited Reproducibility: More than 20% of this document may be affected by microfiche quality
(AD-A289243; AFIT/GE/ENG/94D-28) Avail: Issuing Activity (Defense Technical Information Center (DTIC))

This thesis investigates advanced processing techniques for the detection of radar targets in the presence of clutter. It is assumed that the radar data available consist of multi-aspect angle, fully polarimetric Synthetic Aperture Radar (SAR) images. Various techniques are introduced and tested on available SAR data. These techniques attempt to exploit the multi-aspect angles in order to extract target characteristics not available in any single image. SAR images are manipulated in such a way to decrease the probability of false alarms in the target detection process. Target detection performance of the techniques is presented and compared. The techniques are shown to give superior results than that of regular SAR. DTIC

N95-26977 Colorado Univ., Boulder, CO. Dept. of Electrical and Computer Engineering.

ON-AXIS POLARIZATION COUPLING IN y-CUT TITANIUM IN-DIFFUSED LITHIUM NIOBATE SLAB WAVEGUIDES Technical Report

Stephen L. Kwiatkowski, Alan R. Mickelson, and Dag R. Hjelme Oct. 1994 42 p Limited Reproducibility: More than 20% of this document may be affected by microfiche quality
(Contract N00014-92-J-1190)
(AD-A289260; ECE/GWOL/65) Avail: Issuing Activity (Defense Technical Information Center (DTIC))

We report on polarization coupling from x-propagating TE-polarized waveguide modes to TM-polarized radiation modes in y-cut titanium in-diffused lithium niobate slab waveguides. The polarization coupling is linear with respect to the TE-polarized input power and depends on the titanium diffusion time. Furthermore, the polarization coupling was not affected by white light flooding the waveguide. The maximum conversion from a TE-polarized waveguide mode to a TM-polarized radiation mode is 3.2%/cm using a conservative estimate for the power initially in the TE waveguide mode. We observe no turn-on delay greater than 1 s between the excitation of the TE waveguide mode and the observation of the TM radiation. In addition, intentional amplitude modulations of the TE-polarized waveguide mode were registered as equivalent amplitude modulations by the TM-polarized radiation modes. We did not observe polarization coupling from x-propagating TM-polarized waveguide modes to TE-polarized radiation modes. DTIC

N95-26983 Phillips Lab., Hanscom AFB, MA.

NOTES ON THE CALIBRATION OF THE JHU-APL SOLAR VECTOR MAGNETOGRAPH AT NSO-Sec PEAK

Gianna Cauzzi 21 Dec. 1994 56 p Limited Reproducibility: More than 20% of this document may be affected by microfiche quality
(AF Proj. 2311)
(AD-A289277; PL-TR-94-2308) Avail: Issuing Activity (Defense Technical Information Center (DTIC))

We discuss two different techniques for the comparison of polarization signal in magnetic fields, the calibration curves and derivative methods, for the case of an imaging magnetograph. The advantages and typical errors of both techniques are analyzed in respect to the instrumental characteristics, particularly the spectral response. Both methods present high degree of errors, but the calibration curves method is probably more suitable for the present instrumental configuration of the SVMG. DTIC

N95-26988 Air Force Inst. of Tech., Wright-Patterson AFB, OH. School of Engineering.

MULTIPOINT MULTIRATE SIGNAL PROCESSING M.S. Thesis

Roger L. Claypoole, Jr. Dec. 1994 93 p Limited Reproducibility: More than 20% of this document may be affected by microfiche quality
(AD-A289211; AFIT/GE/ENG/94D-02) Avail: Issuing Activity (Defense Technical Information Center (DTIC))

This thesis provides a fundamentally new, systematic study of multipoint multirate signal processing systems. The multipoint multirate operators are analyzed via equivalent circuits comprised entirely of conventional multirate operators. Interconnections of the operators are demonstrated, and the multipoint noble identities are derived. The multipoint polyphase representation is presented, and the M channel multipoint multirate system with vector length N is presented as an MN channel multipoint polyphase system. The conditions sufficient for perfect reconstruction in the multipoint multirate system are derived. These conditions constrain the multipoint filter banks to be composed of comb filters generated from paraunitary sets of conventional filters. The perfect reconstruction multipoint multirate system is then combined with the multiresolution wavelet decomposition to form the generalized wavelet decomposition with varying vector decimation length at each level. The generalized wavelet decomposition is used as an algorithm to redistribute the energy of a signal throughout the levels of the decomposition. It is shown that, for band pass and high pass signals, significant improvements can be made in the energy distribution. It is recommended that this algorithm be studied as a front end to a vector quantizer for data compression applications. DTIC

N95-27005 Radex, Inc., Bedford, MA.

AUTO-PROCESSING OF OTH RADAR AMPLITUDE/RANGE/DOPPLER DATA

D. S. Reynolds and G. S. Sales 20 Jul. 1994 37 p Limited Reproducibility: More than 20% of this document may be affected by microfiche quality
(Contract F19628-93-C-0023)
(AD-A289152; RXR-94071; Scientific-5; PL-TR-94-2202) Avail: Issuing Activity (Defense Technical Information Center (DTIC))

A synoptic data collection effort was begun using the East Coast Radar System (ECRS), as part of Air Force investigations of equatorial ionospheric clutter. Due to the volume of data, an automatic processing scheme has been developed to characterize radar Doppler frequency spectra in terms of a small number of parameters. These parameters allow reconstruction of reasonable facsimiles of the original spectra, and facilitate a comprehensive statistical analysis. A data compression algorithm has also been implemented to provide smoothing and further data reduction. This report describes the compression and processing algorithms, and presents some results from the January, 1992 data campaign. DTIC

N95-27006 Naval Command, Control and Ocean Surveillance Center, San Diego, CA.

VOCAR: AN EXPERIMENT IN VARIABILITY OF COASTAL ATMOSPHERIC REFRACTIVITY

Richard A. Paulus Oct. 1994 5 p Limited Reproducibility: More than 20% of this document may be affected by microfiche quality
(AD-A289202) Avail: Issuing Activity (Defense Technical Information Center (DTIC))

A previous radio-meteorological experiment conducted along the coast of southern California showed a high correlation between UHF signals and the base of the elevated temperature inversion. A reanalysis of this experimental data with a recently developed hybrid propagation model confirmed this correlation and a method to remotely sense the refractive structure was proposed. An experiment called Variability of Coastal Atmospheric Refractivity (VOCAR) was designed under a larger program called Coastal Variability Analysis, Measurements, and Prediction. VOCAR is a multi-year experimental effort to investigate the variability of atmospheric refractivity with emphasis on the coastal zone. The experiment is being conducted by the Naval Command, Control and Ocean Surveillance Center RDT&E Division jointly with the Naval Air Warfare Center Weapons Division, Point Mugu, CA, the Naval Research Laboratory (Washington, DC and Monterey), and the Naval Postgraduate School. In addition, the National Oceanic and Atmospheric Administration Environmental Technology Laboratory, Penn State University Applied Research Laboratory and Johns Hopkins University Applied Physics Laboratory participated in the intensive measurement phase of VOCAR. The objectives of VOCAR are to provide an assessment capability for horizontally varying refractivity conditions in a coastal environment and to develop a remote sensing capability. The propagation measurements being made during VOCAR consist of monitoring signal strength variations of VHF/UHF transmitters in the southern California coastal region. Corresponding meteorological measurements are made during routine, special, and intensive observation periods. Measurements began in May 1993 and will be conducted periodically through 1994. DTIC

N95-27008 Air Force Inst. of Tech., Wright-Patterson AFB, OH.
VOICE ANALYSIS USING THE BISPECTRUM M.S. Thesis
Deborah A. Douglass Dec. 1994 73 p Limited Reproducibility: More than 20% of this document may be affected by microfiche quality
(AD-A289204; AFIT/GSO/ENG/94D-01) Avail: Issuing Activity (Defense Technical Information Center (DTIC))

The theory of the bispectrum has been studied, though very few practical applications have yet been considered in any depth. One application mentioned in the literature is the use of the bispectrum for voice signal processing. The aim of this thesis was to research the bispectrum towards the particular application of speech enhancement. The technique is based on the fact that the bispectrum is zero for a Gaussian white noise signal, and the bispectrum of two signals added together is the sum of the two signal bispectra. Theoretically, processing signals in the bispectra domain should increase the signal-to-noise ratio of the speech signal. The signal can then be reconstructed from the bispectrum. Though the theory of the estimation techniques were proven, the applicability of the bispectrum to voice processing was questionable. Since any additive white noise is a random process, it will only be the expected value that is zero. With speech signal, the signal is considered stationary for only approximately 20 milliseconds. This does not allow a significant amount of the noise energy to be removed through the averaging process. Classical methods are just as effective. DTIC

N95-27009 Air Force Inst. of Tech., Wright-Patterson AFB, OH.
ADAPTIVE BEAMFORMING IN FREQUENCY-DISPERSIVE MULTIPATH ENVIRONMENTS M.S. Thesis
David A. Murray Dec. 1994 70 p Limited Reproducibility: More than 20% of this document may be affected by microfiche quality
(AD-A289206; AFIT/GE/ENG/94D-22) Avail: Issuing Activity (Defense Technical Information Center (DTIC))

It is well known that an antenna array with N degrees of freedom (DOF) can cancel N - 1 interferers if they approach the array from directions other than that of the desired signal. It has been shown that there are cases in which it is possible for an array with N DOF to effectively cancel more than N - 1 interferers. Specifically, we show how this can be done when there is incident upon an N-element array not only the desired signal and a jammer signal, but more than N - 1 Doppler-shifted multipath copies of the jammer signal as well. In this situation the received signal is nonstationary; therefore, updates of the weight vector must use only as many samples as those which correspond to the time interval over which the signal can be considered locally stationary. In this frequency-dispersive environment, it is desirable to recalculate the weight vector often; in some cases, we would like to do so with every sample. However, recalculating the weight vector involves estimating and inverting the covariance matrix of the received signal. Using traditional methods, this is an O(N sup 3) process, where N represents the degrees of freedom in the array. For large N this becomes time-prohibitive. In this paper, the authors examine the application of eigenvalue decomposition and rank-one updating of the covariance matrix to reduce the computation required. By exploiting the structure of the matrix they find that they are able to decrease the time required for its estimation and inversion. Using these techniques, they can update the weight vector every sample, enabling them to operate effectively in a frequency-dispersive environment. DTIC

N95-27021 Naval Command, Control and Ocean Surveillance Center, San Diego, CA. Research, Development, Technology and Evaluation Div.
MODELING SURFACE EFFECTS WITH THE PARABOLIC EQUATION METHOD
Herbert V. Hitney Oct. 1994 6 p Limited Reproducibility: More than 20% of this document may be affected by microfiche quality
(AD-A289199) Avail: Issuing Activity (Defense Technical Information Center (DTIC))

An approximate but efficient technique is presented that accounts for vertical polarization and rough surface effects over the sea for ducting conditions using the split-step, parabolic equation method. The primary justification for this semi-empirical technique is that in most cases propagation loss predictions match results from a waveguide model that is believed to account for these effects properly. The technique and comparisons of modeled results versus waveguide results and measured data are examined. DTIC

N95-27049# Helsinki Univ. of Technology, Espoo (Finland). Electromagnetics Lab.
SIMPLE EQUIVALENT DIPOLE DISTRIBUTIONS FOR DIELECTRIC SPHEROIDAL SCATTERERS
J. C. E. Sten Oct. 1994 14 p
(PB95-184883; ISBN-951-22-2322-8) Avail: CASI HC A03/MF A01

Equivalent source distributions are identified for dielectric spheroids when immersed in a homogeneous electrostatic field. It is shown that for a prolate spheroid, the volume polarization shrinks into a line dipole distribution lying between the foci of the spheroid. The equivalent charge distributions responsible for the field scattered by an oblate spheroid arise on the circular disk of focal radius. The solutions give rise to an alternative way of calculating electromagnetic fields near spheroidal particles in the regime of the quasi-static approximation. NTIS

N95-27060 Off World Labs., Inc., Austin, TX.
A FOVEATED SYSTEM TO REDUCE TRANSMISSION BANDWIDTH OF VIDEO IMAGES FROM REMOTE CAMERA SYSTEMS Annual Report, 30 Sep. - 30 Oct. 1994
Bill Geisler Oct. 1994 7 p Limited Reproducibility: More than 20% of this document may be affected by microfiche quality
(Contract F49620-94-C-0090)
(AD-A288516; AFOSR-94-0755TR) Avail: Issuing Activity (Defense Technical Information Center (DTIC))

Three design meetings were held at the University of Texas Vision Labs with Dr Bill Geisler's staff, this month to define the communication protocol and the specifications for the initial screen. (1) A preliminary protocol design has been completed and approved by both UT design team and OWL design team. (2) A specification for the operational parameters of the initial system has been designed. (3) OWL completed a preliminary design of the screen driver. DTIC

N95-27062 Air Force Inst. of Tech., Wright-Patterson AFB, OH.
ISOLATED DIGIT RECOGNITION WITHOUT TIME ALIGNMENT M.S. Thesis
Jeffrey Mark Gay Dec. 1994 148 p Limited Reproducibility: More than 20% of this document may be affected by microfiche quality
(AD-A289344; AFIT/GE/ENG/94D-12) Avail: Issuing Activity (Defense Technical Information Center (DTIC))

This thesis examines methods for isolated digit recognition without using time alignment. Resource requirements for isolated word recognizers that use time alignment can become prohibitively large as the vocabulary to be classified grows. Thus, methods capable of achieving recognition rates comparable to those obtained with current methods using these techniques are needed. The goals of this research are to find feature sets for speech recognition that perform well without using time alignment, and to identify classifiers that provide good performance with these features. Using the digits from the TI46 database, baseline speaker-independent recognition rates of 95.2% for the complete speaker set and 98.1% for the male speaker set are established using dynamic time warping (DTW). This work begins with features derived from spectrograms of each digit. Based on a critical band frequency scale covering the telephone bandwidth (300-3000 Hz), these critical band energy features are classified alone and in combination with several other feature sets, with several different classifiers. With this method, there is one 'short' feature vector per word. For speaker-independent recognition using the complete speaker set and a multi-layer perceptron (MLP) classifier, a recognition rate of 92.4% is achieved. For the same classifier with the male speaker set, a recognition rate of 97.1% is achieved. For the male speaker set, there is no statistical difference between results using DTW, and those using the MLP and no time alignment. This shows that there are feature sets that may provide high recognition rates for isolated word recognition without the need for time alignment. DTIC

N95-27079 Air Force Inst. of Tech., Wright-Patterson AFB, OH.
MULTICLASSIFIER FUSION OF AN ULTRASONIC LIP READER IN AUTOMATIC SPEECH RECOGNITION M.S. Thesis
David L. Jennnings Dec. 1994 100 p Limited Reproducibility: More

than 20% of this document may be affected by microfiche quality
(AD-A289207; AFIT/GE/ENG/94D-16) Avail: Issuing Activity (Defense Technical Information Center (DTIC))

This thesis investigates the use of two active ultrasonic devices in collecting lip information for performing and enhancing automatic speech recognition. The two devices explored are called the 'Ultrasonic Mike' and the 'Lip Lock Loop.' The devices are tested in a speaker dependent isolated word recognition task with a vocabulary consisting of the spoken digits from zero to nine. Two automatic lip readers are designed and tested based on the output of the ultrasonic devices. The automatic lip readers use template matching and dynamic time warping to determine the best candidate for a given test utterance. The automatic lip readers alone achieve accuracies of 65-89%, depending on the number of reference templates used. Next the automatic lip reader is combined with a conventional automatic speech recognizer. Both classifier level fusion and feature level fusion are investigated. Feature fusion is based on combining the feature vectors prior to dynamic time warping. Classifier fusion is based on a pseudo probability mass function derived from the dynamic time warping distances. The combined systems are tested with various levels of acoustic noise added. In one typical test, at a signal to noise ratio of 0dB, the acoustic recognizer's accuracy alone was 78%, the automatic lip reader's accuracy was 69%, but the combined accuracy was 93%. This experiment demonstrates that a simple ultrasonic lip motion detector, that has an output data rate 12,500 times less than a typical video camera, can significantly improve the accuracy of automatic speech recognition in noise. DTIC

N95-27149 Air Force Inst. of Tech., Wright-Patterson AFB, OH.

A DEMONSTRATION OF CLIENT-SERVER TECHNOLOGY USING REMOTE PROCEDURE CALLS WITH AN APPLICATION IN FILE MIGRATION USING HEURISTICS

Eric DeLange Dec. 1994 69 p Limited Reproducibility: More than 20% of this document may be affected by microfiche quality
(AD-A289467; AFIT/CI/CIA/94-144) Avail: Issuing Activity (Defense Technical Information Center (DTIC))

Client/Server technology is one of the fastest growing areas of interest and research in the computer field. Remote Procedure Calling (RPC) is a popular framework for programming in a distributed client/server environment since it facilitates communication between machines operating on different platforms and resembles traditional programming methodologies. This paper first explores the fundamental concepts behind the implementation of RPC programming. Once a basic explanation of the RPC concept is given, a small example program is illustrated in order to highlight essential elements in any RPC program. A discussion of RPC's applicability in the area of file migration ensues. Specifically, the utility of RPC in automatically migrating files according to specific rules is examined, such as when a file has been accessed a predetermined number of times from a remote source. An explanation of some of the features of a program developed by the author (in conjunction with others named in the Preface) then follows. Finally, a way to provide a front end in the HP-UX workspace environment is presented after which the author reviews the lessons learned from and possible amplifications to the project. A bibliography and appendices containing code to the RPC applications are also provided. DTIC

N95-27185 Drexel Univ., Philadelphia, PA. Dept. of Electrical and Computer Engineering.

NONLINEAR SIGNAL PROCESSING SCHEMES FOR ROBUST TARGET DETECTION IN RADAR Final Technical Report, 1 Jul. 1992 - 30 Sep. 1994

Nihat M. Bilgutay and Jafar Saniie (Illinois Inst. of Tech., Chicago, IL.) 28 Nov. 1994 7 p Limited Reproducibility: More than 20% of this document may be affected by microfiche quality
(Contract N00014-92-J-1735)
(AD-A288449) Avail: Issuing Activity (Defense Technical Information Center (DTIC))

In detection, the interference due to clutter or jamming can severely deteriorate the quality of the received signal to the point of concealing the target. The objective of this investigation is to improve detection in high density clutter or jamming by using nonlinear signal processing in conjunction with frequency diverse techniques. In particular, analysis and experimental studies have been concerned with the application of Order Statistic (OS) processing and Split Spectrum Processing (SSP) to detect target signals corrupted by strong clutter. The study of OS processing is also extended to morphological processors to improve signal-to-noise ratio (SNR) and feature extraction for recognition and classification. These studies have applications in radar, ultrasound, sonar, and imaging where clutter is the primary limiting factor. DTIC

N95-27249 Institute for Defense Analyses, Alexandria, VA.

THE EVOLUTION AND IMPACT OF PCS TECHNOLOGY Final Report

John R. Lawson Sep. 1994 49 p Limited Reproducibility: More than 20% of this document may be affected by microfiche quality
(AD-A288606; IDA-D-1595) Avail: Issuing Activity (Defense Technical Information Center (DTIC))

In today's mobile society, communications services that focus on location (wired) are increasingly inadequate. But services that center around the individual (wireless) are being developed to serve society in a way that only recently could consumers have imagined. People-oriented communications tools will make life simpler and more productive. The essence of this concept is captured in a family of wireless services and devices that allow the user to communicate independent of location--Personal Communications Services, known as PCS. First generation PCS devices such a pagers and cellular phones were the instruments of the first wireless revolution, but they will soon be forced to relinquish the spotlight to the new generation of PCS and what should be a dazzling variety of individualized advanced telecommunications services and devices. Within the next two years, these new PCS models, recently described as 'the most exciting development in telecommunications since the breakup of AT&T,' should hit the marketplace, changing the way we communicate and, in turn, the way we live. This paper explores the status and likely development of PCS generally, including 'new PCS.' DTIC

N95-27313# International Centre for Theoretical Physics, Trieste (Italy).

A MODEL OF THE EXTENDED ELECTRON AND ITS NONLOCAL ELECTROMAGNETIC INTERACTION: GAUGE INVARIANCE OF THE NONLOCAL THEORY

Kh. Namsrai (Academy of Sciences, Ulan Bator, Mongolia.) and N. Nyamtseren Sep. 1994 7 p
(DE95-608803; IC-94/271) Avail: CASI HC A02/MF A01 (US Sales Only)

A model of the extended electron is constructed by using definition of the d-operation. Gauge invariance of the nonlocal theory is proved. We use the Efimov approach to describe the nonlocal interaction of quantized fields. DOE

N95-27335# Joint Inst. for Nuclear Research, Dubna (USSR). Lab. of High Energy.

RADIATION OF A UNIFORMLY MOVING CHARGE

V. N. Streltsov 1994 3 p
(DE95-608757; JINR-D-2-94-177) Avail: CASI HC A01/MF A01 (US Sales Only)

A preliminary analysis of the experiments, in which the radiation of uniformly moving charges below Cherenkov radiation threshold has been observed, is conducted. The main peculiarities of this radiation are defined by the Poynting vector of the 'velocity part' of the field. The corresponding expressions for retarded field strengths follow from the Lienard-Wiechert potentials. DOE

N95-27435*# National Aeronautics and Space Administration. Wallops Flight Facility, Wallops Island, VA.

PULSE CODE MODULATION (PCM) ENCODER HANDBOOK FOR AYDIN VECTOR MMP-900 SERIES SYSTEM

David Raphael Jun. 1995 131 p
(RTOP 822-00-00)
(NASA-RP-1365; Rept-95B00088; NAS 1.61:1365) Avail: CASI HC A07/MF A02

This handbook explicates the hardware and software properties of a time division multiplex system. This system is used to sample analog and digital data. The data is then merged with frame synchronization information to produce a serial pulse coded modulation (PCM) bit stream. Information in this handbook is required by users to design congruous interface and attest effective utilization of this encoder system. Aydin Vector provides all of the components for these systems to Goddard Space Flight Center/Wallops Flight Facility. Author

N95-27716# Joint Inst. for Nuclear Research, Dubna (USSR).

LANDAU QUASI-ENERGY SPECTRUM DESTRUCTION FOR AN ELECTRON IN BOTH A STATIC MAGNETIC FIELD AND A RESONANT ELECTROMAGNETIC WAVE

A. A. Skoblin 1994 6 p
(DE95-610176; JINR-E-4-94-176) Avail: CASI HC A02/MF A01 (US Sales Only)

Free. nonrelativistic electrons in both a static magnetic field and an electromagnetic wave are considered. A plane-polarized wave propagates along a magnetic field; its frequency is close to the electron rotation frequency in a magnetic field. Electron spin is taken into account. An electron quasi energy spectrum and steady states (quasi energy states) are constructed. DOE

N95-27840 Los Alamos National Lab., NM.

CLASSIFICATION OF RF TRANSIENTS IN SPACE USING DIGITAL SIGNAL PROCESSING AND NEURAL NETWORK TECHNIQUES

K. R. Moore, P. C. Blain, S. D. Briles, and R. G. Jones 1995 11 p Presented at the SPIE International Symposium on Aerospace/Defense Sensing and Dual-Use Photonics, Orlando, FL, 17-21 Apr. 1995 Limited Reproducibility: More than 20% of this document may be affected by microfiche quality
(Contract W-7405-eng-36)
(DE95-006287; LA-UR-95-413; CONF-950472-1) Avail: CASI HC A03

The FORTE' (Fast On-Orbit Recording of Transient Events) small satellite experiment scheduled for launch in October, 1995, will attempt to measure and classify electromagnetic transients as sensed from space. The FORTE' payload will employ an event classifier to perform onboard classification of radio frequency transients from terrestrial sources such as lightning. These transients are often dominated by a constantly changing assortment of man-made 'clutter' such as TV, FM, and radar signals. The FORTE' event classifier, or EC, uses specialized hardware to implement various signal processing and neural network algorithms. The resulting system can process and classify digitized records of several thousand samples onboard the spacecraft at rates of about a second per record. In addition to reducing downlink rates, the EC minimizes command uplink data by normally using uploaded algorithm sequences rather than full code modules (although it is possible for full code modules to be uploaded from the ground). The FORTE' event classifier experiment combines science and engineering in an evolutionary step toward useful and robust adaptive processing systems in space. DOE

N95-28095 California Inst. of Tech., Pasadena, CA.

AN INTRODUCTION TO WAVELET TRANSFORMS

P. P. Vaidyanathan and Igor Djokovic Aug. 1994 121 p Limited Reproducibility: More than 20% of this document may be affected by microfiche quality
(Contract N00014-93-1-0231)
(AD-A289083) Avail: Issuing Activity (Defense Technical Information Center (DTIC))

These notes are meant to provide an introduction to wavelet transforms. The first five sections can be accessed by readers with some exposure to signal processing tools. While maintaining a mathematically rigorous presentation level, we have attempted to make the presentation accessible to signal processors, and engineers in general. To make this possible, we have included three review sections on mathematics, especially L(1) and L(2) Fourier transforms. Derived from text

N95-28231# Lawrence Livermore National Lab., Livermore, CA.

THE CONCENTRATION-ESTIMATION PROBLEM FOR MULTIPLE-WAVELENGTH DIFFERENTIAL ABSORPTION LIDAR

A. N. Payne Jul. 1994 5 p Presented at the 1994 CALIOPE ITR Conference, Livermore, CA, 26-28 Apr. 1994
(Contract W-7405-eng-48)
(DE95-008375; UCRL-JC-118312; CONF-9404162-17) Avail: CASI HC A01/MF A01

We are seeking to develop a reliable methodology for multi-chemical detection and discrimination based upon multi-wavelength differential absorption lidar measurements. In this paper, we summarize some preliminary results of our efforts to devise suitable concentration-estimation algorithms for use in detection and discrimination schemes. DOE

N95-28254# Australian National Univ., Canberra (Australia). Research School of Physical Sciences.

SHEAR ALFVEN WAVE EXCITATION BY DIRECT ANTENNA COUPLING AND FAST WAVE RESONANT MODE CONVERSION

G. G. Borg 1994 26 p
(DE95-609109; ANU-PRL-TR-94/1) Avail: CASI HC A03/MF A01 (US Sales Only)

Antenna coupling to the shear Alfven wave by both direct excitation and fast wave resonant mode conversion is modelled analytically for a plasma with a one dimensional linear density gradient. We demonstrate the existence of a shear Alfven mode excited directly by the antenna. For localized antennas, this mode propagates as a guided beam along the steady magnetic field lines intersecting the antenna. Shear Alfven wave excitation by resonant mode conversion of a fast wave near the Alfven resonance layer is also demonstrated and we prove that energy is conserved in this process. We compare the efficiency of these two mechanisms of shear Alfven wave excitation and present a simple analytical formula giving the ratio of the coupled powers. Finally, we discuss the interpretation of some experimental results. DOE

N95-28354# Helsinki Univ. of Technology, Espoo (Finland). Electromagnetics Lab.

SCATTERING BY A SMALL OBJECT CLOSE TO AN INTERFACE. 3. BURIED OBJECT

M. E. Ermutlu, K. Muinonen, K. A. Lumme, I. V. Lindell, and A. H. Sihvola Oct. 1994 20 p See also PB90-249806 and PB90-249814
(PB95-184909; ISBN-951-22-2297-3) Avail: CASI HC A03/MF A01

Exact Image Theory (EIT) is applied to the problem of electromagnetic wave scattering from a small object below the interface separating two isotropic and homogeneous media. The object is assumed to be electrically small so that it can be approximated by an electric dipole with known dyadic polarizability. Scattering from a buried small dielectric sphere is considered as an example of the theory. The present work might help us to understand light scattering by solar system dust particles in planetary regoliths, for which the so-called opposition effect and negative linear polarization have been observed; that is, nonlinear brightening and reversal of linear polarization near the backscattering direction. NTIS

N95-28391 Rhode Island Univ., Kingston, RI. Dept. of Electrical and Computer Engineering.

FAULT TOLERANT FEATURES AND EXPERIMENTS OF ANTS DISTRIBUTED REAL-TIME SYSTEM Semiannual Report, 16 Jul. 1994 - 15 Jan. 1995

Patrick Dominic-Savio, Jien-Chung Lo, and Donald W. Tufts 15 Jan. 1995 41 p Limited Reproducibility: More than 20% of this document may be affected by microfiche quality
(Contract N00014-94-1-0479)
(AD-A290133) Avail: Issuing Activity (Defense Technical Information Center (DTIC))

The ANTS project at the University of Rhode Island introduces the concept of Active Nodal Task Seeking (ANTS) as a way to efficiently design and implement dependable, high-performance, distributed computing. This paper presents the fault tolerant design features that have been incorporated in the ANTS experimental system implementation. The results of performance evaluations and fault injection experiments are reported. The fault-tolerant version of ANTS categorizes all computing nodes into three groups. They are: the up-and-running green group, the self-diagnosing yellow group and the failed red group. Each available computing node will be placed in the yellow group periodically for a routine diagnosis. In addition, for long-life missions, ANTS uses a monitoring scheme to identify faulty computing nodes. In this monitoring scheme, the communication pattern of each computing node is monitored by two other nodes. DTIC

N95-28407# Argonne National Lab., IL.

THE ELF CONTROVERSY

G. Myers 1995 21 p Presented at the Midwest Chapter of Health Physics Society Meeting, Lombard, IL, 1 Feb. 1995
(Contract W-31-109-eng-38)
(DE95-008283; ANL/ESH/VU-85484; CONF-950275-1-Vugraphs) Avail: CASI HC A03/MF A01

This document contains the principal points in a presentation about the

Electromagnetic field controversy, including introduction to EMF's, possible health problems, explanations, and exposure doses. DOE

N95-28449# Helsinki Univ. of Technology, Espoo (Finland).
INTERNAL ELECTRIC FIELD OF ANISOTROPIC AND BI-ANISOTROPIC SPHERES
A. Cherepanov and A. Sihvola Nov. 1994 17 p
(PB95-195491; ISBN-951-22-2371-6) Avail: CASI HC A03/MF A01

This paper discusses the problem of a spherical anisotropic scatterer exposed to a homogeneous electrostatic field. It has been common in the literature to treat this problem analogously to the case of an isotropic sphere for which it is known that the internal field is constant. In this paper, a proof is given for the uniformity of the field inside the anisotropic sphere, which--to the authors' knowledge--has not been proven before. This result puts those analyses on solid foundation in which the polarizability matrices of anisotropic inclusions are determined and the effective material parameters of anisotropic mixtures are calculated. In the present article, the proof is also generalized for bi-anisotropic spheres within an electromagnetostatic field. NTIS

N95-28450# Helsinki Univ. of Technology, Espoo (Finland).
CRUSHING THE DELAY: TOOLS FOR FRACTIONAL DELAY FILTER DESIGN
T. I. Laakso, V. Vaelimaeki, M. Karjalainen, and U. K. Laine 25 Oct. 1994 81 p Prepared in cooperation with Westminster Univ.
(PB95-195509; ISBN-951-22-2345-7) Avail: CASI HC A05/MF A01

A comprehensive review of FIR (Finite Impulse Response) and allpass filter design techniques for bandlimited approximation of a fractional digital delay is presented. Emphasis is on simple and efficient methods that are well suited for fast coefficient update or continuous control of the delay value. Several new approaches are proposed and numerous examples are provided that illustrate the performance of the methods. NTIS

N95-28451# Helsinki Univ. of Technology, Espoo (Finland).
METHOD OF IMAGES APPLIED TO ELECTROMAGNETIC PROBLEMS INVOLVING SPHERICAL, SPHEROIDAL AND PLANAR GEOMETRIES Ph.D. Thesis
J. C. E. Sten 19 Dec. 1994 136 p
(PB95-195517; ISBN-951-22-2384-8) Avail: CASI HC A07/MF A02

The present thesis consists of a survey and the following ten publications: Electrostatic image theory for the dielectric sphere with an internal source; Image theory for a point charge inside a layered dielectric sphere; Electrostatic image method for the interaction of two dielectric spheres; Image polarization and dipole moment of a cluster of two similar conducting spheres; Low frequency image theory for the dielectric sphere; Low frequency image theory for a current dipole in front of a permeable sphere; Static field solutions and image theory for a conducting sphere with radial anisotropy; An electrostatic image solution for the conducting prolate spheroid; Static image method for the interaction of two co-axial conducting prolate spheroids; and Quasi-static image method applied to bi-isotropic microstrip geometry. NTIS

N95-28453 California Univ., Los Angeles, CA.
NEW TRENDS AND IDEAS IN THE FIELDS OF MICROWAVE TECHNOLOGY
T. Itoh 30 Sep. 1994 5 p Limited Reproducibility: More than 20% of this document may be affected by microfiche quality
(Contract DAAH04-93-G-0068)
(AD-A291663; ARO-30921.21-EL) Avail: Issuing Activity (Defense Technical Information Center (DTIC))

This paper presents a subjective view toward new directions and some examples for changing microwave research. The paper is written primarily from the point of view of how the electromagnetic research must change and what kind of impact such a change can give rise to stimulation for the device and circuit research for microwave technology. it is emphasized that interdisciplinary treatment of electromagnetic research is vital for the future of microwave technology. DTIC

N95-28455 MathSoft, Inc., Seattle, WA. Statistical Sciences Div.
DENOISING AND ROBUST NON-LINEAR WAVELET ANALYSIS
Andrew G. Bruce, David L. Donoho, Hong-Ye Gao, and R. D. Martin Apr. 1994 12 p Prepared in cooperation with Standford University, Stanford, CA Limited Reproducibility: More than 20% of this document may be affected by microfiche quality
(AD-A291668) Avail: Issuing Activity (Defense Technical Information Center (DTIC))

In a series of papers, Donoho and Johnstone develop a powerful theory based on wavelets for extracting non-smooth signals from noisy data. Several nonlinear smoothing algorithms are presented which provide high performance for removing Gaussian noise from a wide range of spatially inhomogeneous signals. However, like other methods based on the linear wavelet transform, these algorithms are very sensitive to certain types of non-Gaussian noise, such as outliers. In this paper, we develop outlier resistance wavelet transforms. In these transforms, outliers and outlier patches are localized to just a few scales: By using the outlier resistant wavelet transforms, we improve upon the Donoho and Johnstone nonlinear signal extraction methods. The outlier resistant wavelet algorithms are included with the S+Wavelets object-oriented toolkit for wavelet analysis. DTIC

N95-28456 Oklahoma Univ., Norman, OK.
DIMENSIONALLY SELF REGULATING MATERIALS Final Report, 1 May 1991 - 31 Oct. 1994
John E. Furneaux 15 Dec. 1994 8 p Limited Reproducibility: More than 20% of this document may be affected by microfiche quality
(Contract DAAL03-91-G-0049)
(AD-A291671; ARO-28746.4-MS-SM) Avail: Issuing Activity (Defense Technical Information Center (DTIC))

This is a collaborative project between the - University of Oklahoma (OU) and Boston University (BU) studying the possibility of producing an infrared detector which integrates the function of a spectrometer. The successful implementation of these ideas could lead to a smart infrared detector. The system we are studying as a prototype is the two-dimensional electron system (2DES) GaAs-AlGaAs modulation-doped heterostructure system patterned with very narrow gates. This leads to a transition to an one-dimensional electron system (1 DES). We expect this system to be particularly sensitive to infrared radiation just at the crossover from a 2DES to a IDES. DTIC

N95-28513 Michigan Univ., Ann Arbor, MI.
THEORETICAL AND EXPERIMENTAL STUDY OF LOW-LOSS, HIGH-EFFICIENCY MONOLITHIC ANTENNA STRUCTURES AT 94 GHz Final Report, 1 Jun. 1991 - 30 Jun. 1994
Linda Katehi and Gabriel M. Rebeiz 1 Feb. 1995 13 p Limited Reproducibility: More than 20% of this document may be affected by microfiche quality
(Contract DAAL03-91-G-0116)
(AD-A291785; ARO-28483.28-EL) Avail: Issuing Activity (Defense Technical Information Center (DTIC))

Work was studied on power combining applications using coplanar waveguide (cpw)-fed slot antenna oscillators. In this work, a large amount of oscillators are combined together to result in a high power source. The problems encountered with such systems is the non-linear interaction in the coupled-oscillators. As a single oscillator, we use a slot-antenna with a single microwave transistor designed to oscillate at 20 GHz. We have successfully combined a 2x2 array of these slot-antenna oscillators at 20 GHz to generate a total radiated power of 70 mW with a dc-RF efficiency of 15%. The power combining efficiency was 100%. Since the antennas are placed on a dielectric lens and therefore result in a high-gain pattern, the effective radiated power is around 4.5w. This configuration does not suffer from substrate mode problems and therefore can be easily extended to 94 GHz power combining systems. DTIC

N95-28528 Washington Univ., Seattle, WA. Applied Physics Lab.
NUMERICAL AND THEORETICAL STUDIES OF ROUGH SURFACE SCATTERING Final Report, 1 Apr. 1992 - 30 Sep. 1994
Eric I. Thorsos 28 Dec. 1994 34 p Limited Reproducibility: More than 20% of this document may be affected by microfiche quality
(Contract DAAL03-92-G-0102)
(AD-A291748; ARO-29404.1-GS) Avail: Issuing Activity (Defense Technical Information Center (DTIC))

The goal of this project was to improve our understanding of electromagnetic scattering from conducting rough surfaces when the roughness is small in comparison with the radiation wavelength. Research was conducted in two related areas for p-polarized scattering from conducting surfaces: the generation of surface waves, and the development of renormalized perturbation theory for scattering from perfectly conducting surfaces. To understand the excitation of surface waves better, a numerical method was developed for displaying the field near the surface; surface waves can then be shown explicitly. The method is based on integral equation solutions, and no fundamental approximations are required. The existence of surface waves for p-polarized scattering leads to difficulties in theoretical treatments of scattering from conductors. This work is specialized to the case of scattering from perfect conductors, for which the theoretical problems are most evident. A renormalized perturbation theory is implemented that is free from the deficiencies inherent in standard perturbation theory. The renormalized perturbation theory is extended beyond lowest order, and comparisons with exact integral equation results show that this approach yields predictions for the bistatic scattering cross section that are accurate over a broad range of surface parameters. DTIC

N95-28559# Instituto de Pesquisas Espaciais, Sao Jose dos Campos (Brazil).

BINARY SEGMENTATION OF SAR IMAGES BY THE ICM ALGORITHM [SEGMENTACAO BINARIA DE IMAGENS SAR PELO ALGORITMO ICM]

Alejandro C. Frery and Nelson D. A. Mascarenhas 1993 12 p In PORTUGUESE

(INPE-5464-PRE/1772) Avail: CASI HC A03/MF A01

We present a derivation and an implementation of the ICM (Iterated Conditional Modes) algorithm for the binary segmentation of Synthetic Aperture Radar (SAR) images contaminated by a signal dependent noise called 'speckle'. The ICM algorithm is based on the modelling of the 'a priori' distribution under the Markov Random Fields framework. The obtained results with real SAR images display a significant improvement with respect to the pixel-by-pixel maximum likelihood classification, at a reasonable computational cost, with the incorporation of the spatial context. Author

N95-28568 Defence Science and Technology Organisation, Melbourne (Australia). Aeronautical and Maritime Research Lab.

THE PROTECTION OF ELECTRO-EXPLOSIVE DEVICES (EEDS) AND ELECTRONICS FROM ELECTROSTATIC DISCHARGE (ESD) HAZARDS

Horace Billon Dec. 1994 42 p

(DSTO-TR-0100; AR-008-973) Copyright Avail: Issuing Activity

This report is a review of the various electrostatic discharge (ESD) threats to EED's and electronics. Methods of overcoming these hazards are outlined. A description is also presented of the methods and standards used for vulnerability testing. Author

N95-28569# Instituto de Pesquisas Espaciais, Sao Jose dos Campos (Brazil). Ministry of Science and Technology.

SAR NOISE REDUCTION THROUGH THE UTILIZATION OF ROBUST FILTERS [REDUCAO DE RUIDO EM IMAGENS SAR PELO USO DE FILTROS ROBUSTOS]

A. C. Frery and S. J. S. Santanna 1993 14 p In PORTUGUESE Study presented at the Brazilian Symposium on Remote Sensing, 7, Curitiba, 10-14 May 1993

(INPE-5504-PRE/1787) Avail: CASI HC A03/MF A01

After briefly reviewing some classical filters for speckle removal, we derive and implement three filters with characteristics of robustness suitable for speckle noise reduction: one based on the median; one based on the inter-quartile range; and one based on the median al absolute deviation. Assuming that observations within a synthetic aperture radar image are outcomes of independent Rayleigh random variables, these filters exhibit a good performance from both the signal-to-noise reduction and from the edge preserving criteria. The problem of filtering in an image is posed as an estimation problem. Author

N95-28573 Defence Research Establishment Ottawa, Ottawa (Ontario).

DATA ACQUISITION SOFTWARE FOR DREO'S NEAR-FIELD ANTENNA MEASUREMENT FACILITY

Claude J. Brochu and Gilbert A. Morin Dec. 1994 61 p Limited Reproducibility: More than 20% of this document may be affected by microfiche quality

(AD-A289819; DREO-1253) Avail: Issuing Activity (Defense Technical Information Center (DTIC))

HREO has built an antenna anechoic facility for microwave and millimetre-wave measurement. The facility includes a spherical near-field antenna measurement system that allows far-field measurement of small antennas and near-field measurement of larger antennas (up to one meter) within the chamber. This report describes the facility including the equipment, the instrumentation, and the DREO Antenna Measurement Acquisition (DAMAS) software that was developed. The purpose of DAMAS is to control the measurement and acquisition process in real-time, and to present the data to the operator. The major objectives of this software development project were the streamlining of the process so that an antenna could be accurately characterized in the minimum amount of time, and the improvement of the reliability of the software. DTIC

N95-28576 Naval Command, Control and Ocean Surveillance Center, Kailua, HI.

VOCODED KING DATA BASE Final Report, Feb. - Aug. 1994

P. C. Grossnickle Oct. 1994 43 p Limited Reproducibility: More than 20% of this document may be affected by microfiche quality

(AD-A289827; NCCOSC/RDT/E-TD-2721) Avail: Issuing Activity (Defense Technical Information Center (DTIC))

This document reports the development of a data base of vocoded speech that has been passed through several popular voice coders and their corresponding decoders. The KING data base consists of samples from 26 male speakers recorded sequentially on DAT tape. Two products were produced: five DAT tapes. each consisting of the original KING data base on one channel and the vocoded version on the other; and raw binary files, one for each vocoded and speaker combination. DTIC

N95-28580 Defence Research Establishment Ottawa, Ottawa (Ontario).

LOW-ANGLE TRACKING IN THE PRESENCE OF DUCTING, COHERENT AND INCOHERENT MULTIPATH

Eloi Bosse, Ross M. Turner, and Denis Dion Nov. 1994 53 p Limited Reproducibility: More than 20% of this document may be affected by microfiche quality

(AD-A289838; DREO-1240) Avail: Issuing Activity (Defense Technical Information Center (DTIC))

This report presents results on recent improvements to the low-angle tracking algorithm based on the Refined Maximum Likelihood (RML) method. Specifically the report describes results obtained for three different models: (1) the RML model; (2) a model which accounts for radar fluctuation of the specular return; (3) a third model which accounts for the effect of ducting. The results indicate that the simple RML model produces better results than obtained by using a model that attempts to account for the incoherent fluctuation in the specular direction. In the case of ducting, under moderate sea state conditions, the parabolic approximation of the Helmholtz wave equation gives accurate tracking while a simple two-ray multipath model (Kerr) is used for standard propagation conditions. For very high sea states, phase monopulse with averaging over a number of estimates at different frequencies gives sufficient accuracy for most applications. DTIC

N95-28601# Los Alamos National Lab., NM.

HIGH PERFORMANCE GROUND PENETRATING RADAR SURVEY OF TA-49/AREA 2 Final Report

R. F. Hoeberling and M. J. Rangel, III (Analysis Programming Processing Instrumentation, Santa Barbara, CA.) Sep. 1994 31 p

(Contract W-7405-eng-36)

(DE95-006856; LA-12821-MS) Avail: CASI HC A03/MF A01

The results of high performance ground penetrating radar study of Area 2 at Technical Area 49 are presented. The survey was commissioned as part of Los Alamos Laboratory's continuing Environmental Remediation program and was completed and analyzed before borehole studies in Area 2 were started. Based upon the ground penetrating radar results, the location of one of the planned boreholes was moved to assure the drilling area was as safe as possible. While earlier attempts to use commercial radar devices at this facility had not been successful, the radar and digital processing system developed at Los Alamos were able to significantly improve the buried physical detail of the site. DOE

N95-28615 Department of the Navy, Washington, DC.

METHOD AND APPARATUS FOR MAINTAINING LINEARITY AND FREQUENCY ACCURACY OF AN FM CHIRP WAVEFORM Patent

Roger I. Martinez, inventor (to Navy), Michael L. Sanders, inventor (to

Navy), and John H. Ashton, inventor (to Navy) 27 Dec. 1994 13 p Filed 4 Apr. 1994
(AD-D017398; US-Patent-5,376,938; US-Patent-Appl-SN-224611; US-Patent-Class-342-128) Avail: US Patent and Trademark Office

A homodyne radar apparatus and method for performing radar cross-section measurement by maintaining the linearity and compensating for frequency drift of an FM (frequency modulation) chirp waveform produced by a YIG (yttrium-indium-garnet) tuned oscillator. A digital computer uses a predetermined data look-up table of each YIG oscillator frequency characteristic in conjunction with a digital to analog converter to provide a compensating sweep signal to linearize the frequency output of the oscillator. The computer uses an analog to digital converter in conjunction with a reference circuit output to compare the actual YIG signal nulls resulting from the reference circuit to the nulls in a signal produced by a lab standard oscillator in the reference circuit to adjust start sample delay of the ADC (analog-to-digital converter) and to correct any frequency drift evidenced by the difference in the null of the signal. DTIC

N95-28624 Rochester Univ., NY. Dept. of Computer Science.
TRAINS: DIALOGUE TRANSCRIPTION TOOLS
Peter A. Heeman and James F. Allen Aug. 1994 61 p Limited Reproducibility: More than 20% of this document may be affected by microfiche quality
(Contract N00014-92-J-1512; NSF IRI-90-13160)
(AD-A289869; TRAINS-TN-94-1) Avail: Issuing Activity (Defense Technical Information Center (DTIC))

This document describes a toolkit and guidelines for the transcription of dialogues. The premise of these tools is that a dialogue between two people can be broken down into a series of utterance files, each spoken by one participant. This allows the transcription tools and standards already designed for single speaker speech to be used. DTIC

N95-27279*# National Aeronautics and Space Administration. Goddard Space Flight Center, Greenbelt, MD.
DESIGN, DEVELOPMENT AND TESTING OF THE X-RAY TIMING EXPLORER HIGH GAIN ANTENNA SYSTEM
Javier Lecha, Claudia Woods, and Minh Phan *In* NASA. Johnson Space Center, The 29th Aerospace Mechanisms Symposium May 1995 p 193-207 (For primary document see N95-27260 09-15)
Avail: CASI HC A03/MF A04

33 ELECTRONICS AND ELECTRICAL ENGINEERING

Includes test equipment and maintainability; components, e.g., tunnel diodes and transistors; microminiaturization; and integrated circuitry.

For related information see also *60 Computer Operations and Hardware* and *76 Solid-State Physics.*

N95-26425 Defence Science and Technology Organisation, Melbourne (Australia). Aeronautical and Maritime Research Lab.
ELECTRICAL PERFORMANCE CHARACTERISATION OF SINGLE-SHOT SWITCHES IN HIGH SPEED, HIGH VOLTAGE AND HIGH CURRENT APPLICATIONS
Michael Podlesak Aug. 1994 48 p
(DSTO-RR-0010; AR-008-582) Copyright Avail: Issuing Activity (DSTO, Melbourne Victoria, Austrailia)

The electrical performance characteristics of single-shot closing switches for slapper detonator applications were measured via the discharge of a low impedance transmission line. The switch performance, characterized by its time-dependent resistance behavior, could not be assessed via the more conventional methods of measurement because of high bandwidth requirements at comparatively high levels of voltage and current. Hence, an alternative technique based on a transmission line discharge was devised in which the time-dependent resistance of the switch can be determined from the measured current waveform of the switch, the initial open circuit voltage and the transmission line parameters only. Under certain conditions a simple lossless transmission line formula is sufficient for the calculation of the switch resistance waveform. However, if the transmission line losses cannot be neglected, a correction can be readily implemented through numerical signal processing. The bandwidth of this technique is limited to the bandwidth of the switch current measurement only, which proved to be particularly useful for the measurement of switches for slapper detonator applications where inductive pick-up noise in the switch voltage waveform is large and where high voltage probes of sufficiently high bandwidth are not readily available. In this report, both numerically simulated and experimental examples are given, together with the method of calculation of switch resistance which takes into account practical transmission line losses. It was found that best results are obtained if the magnitude of the switch resistance is of a similar order as the characteristic impedance of the transmission line, or higher. Author

N95-26433 Department of the Navy, Washington, DC. Office of Naval Research.
HIGH POWER, BROADBAND FOLDED WAVEGUIDE GYROTRON-TRAVELING-WAVE-AMPLIFIER Patent Application
Carter M. Armstrong, inventor (to Navy), Jin J. Choi, inventor (to Navy), and Achintya K. Ganguly, inventor (to Navy) 30 Jun. 1994 35 p Filed 30 June 1994 Limited Reproducibility: More than 20% of this document may be affected by microfiche quality
(AD-A288847; US-Patent-Appl-SN-269278; Navy-Case-76320) Avail: Issuing Activity (Defense Technical Information Center (DTIC))

A folded waveguide gyrotron-traveling-wave-amplifier comprises: an electron gun for transmitting an axis-encircling beam of electrons with large transverse energy along a first path having an axis; an RF source for producing and applying in a second path an RF input millimeter wave signal having a bandwidth in a preselected frequency domain and having a transverse electric field; a source for generating a solenoid magnetic field parallel to the axis along the first path; a beam collector; and an interaction circuit such as an H-plane bend serpentine waveguide positioned within the solenoid magnetic field and having a narrow wall containing a beam tunnel hole for passing the axis-encircling beam of electrons there through to the beam collector, an output end, and an input end for receiving and passing the RF input millimeter wave signal through the H-plane bend serpentine waveguide to the output end to modulate the axis-encircling electron beam, the modulated axis-encircling electron beam amplifying the RF input signal and also broadening the instantaneous bandwidth of the amplified RF input signal through the negative mass instability in the fundamental forward space harmonic of both fast and slow wave regions in the preselected frequency domain. In a second embodiment, a double-ridged TE folded waveguide is used in place of the H-plane bend serpentine waveguide. In a third embodiment, there is no RF input signal and the interaction circuit generates an RF signal which is outputted from one of the input and output ends. DTIC

N95-26496# Helsinki Univ. of Technology, Espoo (Finland). Circuit Theory Lab.
MICROWAVE CIRCUIT SIMULATION USING HIGHER-ORDER DYNAMIC ELEMENTS
Martti Valtonen Oct. 1994 41 p
(ISSN 0784-5979)
(PB95-185088; ISBN-951-22-2301-5) Avail: CASI HC A03/MF A01

Realizations of a memristor, R-, L-, C-, and M-dynamic elements, as well as mixed and higher-order dynamic elements, are given with the aid of static and dynamic voltage-controlled current sources. The dynamic elements are treated with several state variables and ports. The memristor as well as R-, L-, C-, and M-dynamic elements with arbitrary number of state variables, are implemented in circuit design tool APLAC. As an application, a circuit model for the MESFET trapping and abrupt doping effects is presented that describes the small-signal output conductance and susceptance of a sample MESFET as a function of frequency and drain voltage in the range of f = 20 Hz,..., 1 MHz and V(D) = 0.5 V,..., 3 V. The model simulates the measured properties of the sample MESFET in a qualitative manner. NTIS

N95-26550 Massachusetts Univ., Amherst, MA. Dept. of Mechanical Engineering.
INTELLIGENT COMPUTER BASED RELIABILITY ASSESSMENT OF MULTICHIP MODULES Final Technical Report, 7 Apr. 1993 - 6 Apr. 1994
Ian R. Grosse, Prasanna Katragadda, Sandeepan Bhattacharya, and Sarang

Kulkarni 6 Apr. 1994 63 p Limited Reproducibility: More than 20% of this document may be affected by microfiche quality
(Contract F30602-93-C-0084)
(AD-A288833) Avail: Issuing Activity (Defense Technical Information Center (DTIC))

To deliver reliable Multichip (MCM's) in the face of rapidly changing technology, computer-based tools are needed for predicting the thermal mechanical behavior of various MCM package designs and selecting the most promising design in terms of performance, robustness, and reliability. The design tool must be able to address new design technologies manufacturing processes, novel materials, application criteria, and thermal environmental conditions. Reliability is one of the most important factors for determining design quality and hence must be a central condition in the design of Multichip Module packages. Clearly, design engineers need computer based simulation tools for rapid and efficient electrical, thermal, and mechanical modeling and optimization of advanced devices. For three dimensional thermal and mechanical simulation of advanced devices, the finite element method (FEM) is increasingly becoming the numerical method of choice. FEM is a versatile and sophisticated numerical techniques for solving the partial differential equations that describe the physical behavior of complex designs. AUTOTHERM(TM) is a MCM design tool developed by Mentor Graphics for Motorola, Inc. This tool performs thermal analysis of MCM packages using finite element analysis techniques. The tools used the philosophy of object oriented representation of components and simplified specification of boundary conditions for the thermal analysis so that the user need not be an expert in using finite element techniques. Different package types can be assessed and environmental conditions can be modeled. It also includes a detailed reliability module which allows the user to choose a desired failure mechanism (model). All the current tools perform thermal and/or stress analysis and do not address the issues of robustness and optimality of the MCM designs and the reliability prediction techniques are based on closed form analytical models and can often fail to predict the cycles of failure (N(f)) by order of magnitude, although they can be used to compare the different designs. Candidate MCM designs are evaluated in terms of the reliability performance parameters (maximum temperature/stress/strain) rather than the absolute reliability of the device. In this regard we propose a methodology and associated computer based design tool for multichip modules which embodies these ideas and addresses the issues of optimum and robust MCM package design. An object oriented approach and design of experiments methodology is adopted and integrated into the already existing Intelligent Multichip Module Analyzer (IMCMA) system. Derived from text

N95-26646# Helsinki Univ. of Technology, Espoo (Finland). Radio Lab.
SURVEY ON STEP RECOVERY DIODE AND ITS APPLICATIONS
Zhang Jian and Antti Raeisaenen Sep. 1994 30 p
(ISSN 1237-4938)
(PB95-184974; S-208; ISBN-951-22-2270-1) Avail: CASI HC A03/MF A01

The state of the art of the step recovery diode (SRD) and its applications are reviewed from the very beginning up to now. Used as a charge controlled switch, the SRD has found extensive applications in frequency comb generation, frequency multiplication, and pulse shaping and waveform generating circuits. The designs of SRD circuits are based on the idealized nonlinear capacitance model of the SRD. The frequency-domain analyses of SRD circuits have been developed and the circuits simulated with computers. With the development of the SRD device itself, the SRD has the great prospect of being used at millimeter and even at submillimeter wavelengths. More accurate analyses and designs should, therefore, be studied correspondingly. A list of the publications concerning the SRD is furnished at the end of this report. NTIS

N95-26690 Army Research Lab., Adelphi, MD.
AN OPTOELECTRONIC ATTENUATOR FOR THE HIGH-SPEED CONTROL OF MICROWAVE INTEGRATED CIRCUITS Final Report, Nov. 1990 - Dec. 1993
Stephen E. Saddow and Chi H. Lee Nov. 1994 83 p Limited Reproducibility: More than 20% of this document may be affected by microfiche quality
(AD-A289579; ARL-TR-387) Avail: Issuing Activity (Defense Technical Information Center (DTIC))

An optoelectronic attenuator suitable for the optical control of microwave integrated circuits is presented. High-speed photoconductive switches are embedded in planar microwave transmission lines, and semiconductor laser diodes (LD's) are used to control the microwave signal level on these high-speed lines. With a silicon coplanar waveguide-photoconductive switch (Si:CPW-PCS), up to 45 dB of microwave attenuation has been achieved with a fiber-pigtailed laser diode having 144 mW of optical power. Measurements made using a vector network analyzer show that the attenuator performance can be explained by a classical plasma absorption argument, whereby the microwave signal is attenuated by the optically induced solid-state plasma. Edge-coupled Fabry-Perot aluminum-gallium-arsenide/gallium-arsenide (AlGaAs/GaAs) semiconductor LD's, as well as both silicon and gallium-arsenide (GaAs) CPW-PCS's, were developed for the optoelectronic attenuator. When conventional gain-switching techniques are used, LD peak output powers greater than 1 W have been demonstrated, and when an optical Q-switching scheme is used, 6 W of peak power has been achieved in tens of picoseconds. DTIC

N95-26716 Ohio State Univ., Columbus, OH. Electroscience Lab.
JOINT SERVICES ELECTRONICS PROGRAM Annual Report No. 17, Sep. 1993 - Sep. 1994
Nov. 1994 75 p Limited Reproducibility: More than 20% of this document may be affected by microfiche quality
(Contract N00014-89-J-1007)
(AD-A289594; ESL-721563-7-APP) Avail: Issuing Activity (Defense Technical Information Center (DTIC))

This Appendix contains the reprints published under JSEP in the time September 1993 to September 1994. In addition to the 8 reprints contained herein, there are 10 papers already accepted for publication during the next contract period, 12 papers submitted and 10 papers in preparation. DTIC

N95-26767 Air Force Inst. of Tech., Wright-Patterson AFB, OH. School of Engineering.
SILICON BASED MICROACTUATORS FOR TELEROBOTIC TACTILE STIMULATION Master's Thesis
Britton C. Read, III Dec. 1994 194 p Limited Reproducibility: More than 20% of this document may be affected by microfiche quality
(AD-A289340; AFIT/GE/ENG-94D-25) Avail: Issuing Activity (Defense Technical Information Center (DTIC))

Silicon based microelectromechanical (MEM) devices using both surface and bulk micromachining have been realized to provide tactile stimulation. The bulk MEM devices utilize the bimorph principle and are fabricated in a complementary metal oxide semiconductor (CMOS) process through MOS implementation system (MOSIS). The surface MEM devices utilize the electrostatic principle and are fabricated in the multi-user MEM process (MUMPS) through MCNC. Eleven major designs are presented and tested to determine if they are suitable to provide tactile stimulation. The bimorph and electrostatic designs were tested using a probe station, a laser interferometer, and a force tester. Measurements were taken on the deflections, cutoff frequencies, and loaded operation of the devices. The bimorph designs fabricated in the CMOS process showed the most potential. The tests results indicate that the cantilever beam designs deflect over 30 microns. They operate at frequencies below 130 Hz. The devices operate under a load of approximately 5 microN. An endurance test was performed by actuating a device over 2.5 million times. DTIC

N95-26816*# Nebraska Univ., Lincoln, NE. Dept. of Electrical Engineering.
MATERIALS, STRUCTURES, AND DEVICES FOR HIGH-SPEED ELECTRONICS Final Report, 1 Jan. 1981 - 31 Dec. 1992
John A. Woollam and Paul G. Snyder 31 Dec. 1992 29 p
(Grant NAG3-154)
(NASA-CR-197815; NAS 1.26:197815) Avail: CASI HC A03/MF A01

Advances in materials, devices, and instrumentation made under this grant began with ex-situ null ellipsometric measurements of simple dielectric films on bulk substrates. Today highly automated and rapid spectroscopic ellipsometers are used for ex-situ characterization of very complex multilayer epitaxial structures. Even more impressive is the in-situ capability, not only for characterization but also for the actual control of the growth and etching of epitaxial layers. Spectroscopic ellipsometry has expanded from the research lab to become an integral part of the production of materials and structures for state of the art high speed devices. Along the way, it has contributed much to our understanding of the growth characteristics and material properties. The following areas of research are summarized: Si3N4 on GaAs, null ellipsometry; diamondlike carbon films; variable angle spectroscopic ellipsometry (VASE) development; GaAs-AlGaAs heterostructures; Ta-Cu diffusion barrier films on GaAs; GaAs-AlGaAs superlattices and multiple quantum wells; superconductivity; in situ elevated temperature measurements of III-V's; optical constants of thermodynamically stable InGaAs; doping dependence of optical constants of GaAs; in situ ellipsometric studies of III-V epitaxial growth; photothermal spectroscopy; microellipsometry; and Si passivation and Si/SiGe strained-layer superlattices. Derived from text

N95-26890*# National Aeronautics and Space Administration. Marshall Space Flight Center, Huntsville, AL.
DYNAMICALLY TIMED ELECTRIC MOTOR Patent Application
Ann M. Casper, inventor (to NASA) (United Technologies Corp., Huntsville, AL.) 29 Dec. 1994 12 p
(Contract NAS8-50000)
(NASA-Case-MFS-28958-1; NAS 1.71:MFS-28958-1;
US-Patent-Appl-SN-365880) Avail: CASI HC A03/MF A01

The invention disclosed in this document is a brushless DC motor including a housing having an end cap secured thereto. The housing encloses a rotor, a stator and a rotationally displaceable commutation board having 5 sensors secured thereon and spaced around the periphery of the rotor. An external rotational force is applied to the commutation board for displacement of the sensors to various positions whereby varying feedback signals are generated by the positioning of the sensors relative to the rotating rotor. The commutation board is secured in a fixed position in response to feedback signals indicative of optimum sensor position being determined. The rotation of the commutation board and the securing of the sensors in the desired fixed position is accomplished without requiring the removal of the 5 end cap and with the DC motor operating. NASA

N95-26921 Air Force Inst. of Tech., Wright-Patterson AFB, OH. School of Engineering.
DESIGN AND CHARACTERIZATION OF RESONANT CAVITY LIGHT-EMITTING DIODES M.S. Thesis
Thomas M. Fitzgerald Dec. 1994 135 p Limited Reproducibility: More than 20% of this document may be affected by microfiche quality
(AD-A289307; AFIT/GEO/ENP/94D-02) Avail: Issuing Activity (Defense Technical Information Center (DTIC))

This thesis describes an investigation into the emission properties of Resonant Cavity Light Emitting Diodes (RCLED). RCLED's are a new photonic device that promise laser-like properties of narrow output frequency spread and high output power, without the usual laser disadvantages of shorter lifetime and increased maintenance and lifetime costs. Specifically, this thesis examines the functional dependence between emitted wavelength and the RCLED microcavity, and attempts to correlate theory with experimental data. This thesis introduces a classical wave interference model that calculates the Spontaneous Emission Enhancement Factor (Z-) with angular dependence. DTIC

N95-26964 California Inst. of Tech., Pasadena, CA. Dept. of Electrical Engineering.
STRUCTURES FOR TIME-REVERSED INVERSION IN FILTER BANKS
P. P. Vaidyanathan and Tsuhan Chen 1994 4 p Prepared in cooperation with AT and T Bell Lab Limited Reproducibility: More than 20% of this document may be affected by microfiche quality
(Contract N00014-93-1-0231)
(AD-A289238) Avail: Issuing Activity (Defense Technical Information Center (DTIC))

Anticausal inversion of IIR transfer functions has gained importance in recent years, in the efficient implementation of IIR digital filter banks. In this paper we first introduce the idea of a causal dual, as an intermediate step in the implementation of anticausal IIR inverses. With time reversal operators at the input and output of the causal dual, we get the anticausal inverse of the original structure. The causal dual eliminates the need for similarity transformations, during a key step called blockwise state transfer, in implementing anticausal inverses. In the paper we identify efficient structures for causal duals of standard structures like the direct-form, cascade-form, coupled form, and IIR lattice structures, including the tapped lattice. DTIC

N95-27002 North Carolina Agricultural and Technical State Univ., Greensboro, NC. Dept. of Electrical Engineering.
SELF-CHECKING STATE MACHINE REALIZATION IN CMOS Progress Report, 1 Jul. - 31 Dec. 1994
P. K. Lala and A. Walker 31 Dec. 1994 20 p Limited Reproducibility: More than 20% of this document may be affected by microfiche quality
(Contract N00014-94-1-0462)
(AD-A289149) Avail: Issuing Activity (Defense Technical Information Center (DTIC))

In this reporting period we have accomplished the following: (1) developed a procedure for totally self-checking (TSC) checker design for m-out-of-2m codes at the transistor level and (2) derived a technique for designing TSC fault-tolerant systems. DTIC

N95-27015 Colorado Univ., Boulder, CO. Dept. of Electrical and Computer Engineering.
CHARACTERIZATION OF MICROWAVE MESFET CIRCUITS UNDER LASER ILLUMINATION. APPLICATIONS TO PHASED ARRAY RADAR, MICROWAVE COMMUNICATIONS, AND DIGITAL CLOCK CONTROL Ph.D. Thesis
Sheryl M. Genco Oct. 1994 411 p Limited Reproducibility: More than 20% of this document may be affected by microfiche quality
(Contract N00014-92-J-1190)
(AD-A289181; ECE/GWOL/62) Avail: Issuing Activity (Defense Technical Information Center (DTIC))

Optical injection of MESFET's directly affects the operating characteristics of the devices. The MESFET properties, induced by optical injection, can stabilize oscillator operating frequency, control amplifier gain, and open the door for feasible integrated microwave-optical devices. The optical injection of DC MESFET's, oscillators, and amplifiers is explored. Systems applications, including phased array radar, wave division multiplexing (WDM), and computer clock control, are provided. The main contributions of this research are analyzing the modulation properties of the locked laser subsystem, using the locked laser system to inject MESFET devices and characterizing the photo-effects in MESFET circuits, reducing the phase noise in a microwave oscillator via optical injection, and developing a theoretical description of the injection properties of oscillators that can be used to describe an injection locked laser and a microwave oscillator with a change of constants. DTIC

N95-27023# Joint Inst. for Nuclear Research, Dubna (USSR).
COMPARISON OF THE RESISTANCE OF THE MOS INTEGRATED CIRCUITS WITH VARIOUS TYPES OF NUCLEAR RADIATION
A. Yu. Didyk, G. G. Gulbekyan, and W. Wronski 1994 10 p
(DE95-608623; JINR-E-14-94-217) Avail: CASI HC A02/MF A01 (US Sales Only)

Principal conceptions on simulation of radiation effects in semiconductor devices caused by fast neutrons with the use of accelerated heavy ions with the energies exceeding 1 MeV/n are presented. Models explaining radiation effects on semiconductors and devices thereof under radiation ionization are described. Experimental results on parameter degradation of shift registers at irradiation by heavy ions, electrons, gamma-quanta, and fast neutrons are obtained. On the basis of data obtained the efficiency coefficients and terminal threshold fluences for different types of radiation ionization are determined. DOE

N95-27024# Joint Inst. for Nuclear Research, Dubna (USSR).
INVESTIGATION OF RADIATION RESISTANCE OF TRANSISTORS AND INTEGRATED CIRCUITS USING THE HEAVY IONS BEAM OF ENERGY HIGHER THAN 1 MeV/amu AND FAST NEUTRONS
A. Yu. Didyk, V. N. Nazarov, G. G. Gulbekyan, and W. Wronski 1994 11 p
(DE95-608624; JINR-E-14-94-218) Avail: CASI HC A03/MF A01 (US Sales Only)

Planar transistors and logical gates NAND were irradiated at ion beam of Ne-22 and C-12 of the energy 27.9 MeV and 91 MeV, respectively. The degradation of the direct current gain (h(sub 21E)) and the output voltage of the logical level '1' have been recorded. The exposition dose limits (EDL), which are measure of the radiation resistance of the investigated devices for ions as well as for fast neutrons, have been determined. On the basis of the EDL values the efficiency coefficients of the heavy ions in relation to fast neutrons have also been determined. DOE

N95-27050 Helsinki Univ. of Technology, Espoo (Finland). Circuit Theory Lab.

MODELING OF TRAPPING AND ABRUPT DOPING EFFECTS IN MESFET'S USING R-DYNAMIC ELEMENT

J. Ladvanszky and M. Valtonen Oct. 1994 19 p Limited Reproducibility: More than 20% of this document may be affected by microfiche quality
(PB95-184891; ISBN-951-22-2302-3) Avail: CASI HC A03

A circuit model for the metal semiconductor field effect transistor (MESFET) trapping and abrupt doping effects is presented that describes the small-signal output conductance and susceptance as a function of frequency and drain voltage. The frequency dependence is created using R-dynamic element. It is shown that the model simulates the measured properties of a sample MESFET in a qualitative manner. NTIS

N95-27067 Army Construction Engineering Research Lab., Champaign, IL.

TESTING OF UNINTERRUPTIBLE POWER SUPPLIES WITH NONLINEAR LOADS Final Report

Gerald Heydt, Steve Briggs, Franklin Holcomb, and Daiva Edgar Sep. 1994 88 p Prepared in cooperation with Purdue University Limited Reproducibility: More than 20% of this document may be affected by microfiche quality
(DA Proj. 4A1-62784-AT-45)
(AD-A289353; CERL-FE-94/23) Avail: Issuing Activity (Defense Technical Information Center (DTIC))

Uninterruptible power supplies (UPS's) are used to provide power to sensitive and critical loads when the commercial supply has been interrupted. These loads may be nonlinear, which in the military often includes communications equipment, adjustable speed drives, fluorescent lighting, and mainframe and small computers. Most electrical characteristics of UPS's are not currently subject to codes and standards, and there are no military specifications for UPS's. Existing standards assume that UPS's will be operated with linear loads. Since most UPS systems are operated with nonlinear loads, there is concern that UPSs will suffer degraded performance or failure when operated with these loads. This work developed a test methodology by which UPS systems can be tested and their susceptibility to nonlinear loads quantified. The tests measure load transfer, efficiency, heating, load support, voltage regulation, and isolation. Several commercially available UPS systems are recommended for testing. DTIC

N95-27083# Oak Ridge National Lab., TN.

THE EFFECT ON STABILITY AND THERMAL HYDRAULIC QUENCHBACK OF PERFORATING THE JACKET OF A CABLE-IN-CONDUIT CONDUCTOR

L. Dresner 1994 4 p Presented at the Applied Superconductivity Conference, Boston, MA, 16-21 Oct. 1994
(Contract DE-AC05-84OR-21400)
(DE95-005392; CONF-941013-29) Avail: CASI HC A01/MF A01

This paper continues earlier work on the reduction of the quench pressure in a doubler cable-in-conduit conductor achieved by perforating the inner jacket. The present study examines the effect of the perforations on the stability margin and on the onset of thermal hydraulic quenchback. DOE

N95-27096 Advanced Device Technologies, Inc., Charlottesville, VA.

NOVEL FIELD EFFECT TRANSISTORS FOR LOW POWER ELECTRONICS Progress Report No. 2

28 Nov. 1994 9 p Limited Reproducibility: More than 20% of this document may be affected by microfiche quality
(Contract N00014-94-C-0260)
(AD-A288650) Avail: Issuing Activity (Defense Technical Information Center (DTIC))

The primary objective of this Phase 1 project is to determine the extent of the significant reduction in power consumption of integrated circuits which may be achieved by utilizing a novel sidegate FET technology. The new FET technology promises to eliminate the Narrow Channel Effect (NCE) which is one of the primary factors limiting the minimum power consumption of integrated circuits. By eliminating the NCE, we will be able to scale the device size dramatically and reduce the power consumption by an order of magnitude. The project will assess the power, speed, circuit design, processing, and manufacturability of the new FET technology for both digital and analog circuit applications. In particular, we will extract device parameters from the new ultra-low power FETs fabricated at UVa, develop device models, incorporate these models into a new SPICE package (AIM-Spice), simulate different logic families including DCFL and SCFL, and compare the predicted performance with the standard DCFL and SCFL logic. We will also analyze the gate current leakage and subthreshold slope as the primary factors limiting the noise margins at low power supplies, establish the minimum required bias voltage for reliable operation, and analyze the factors determining the threshold voltage changes from device to device as well as other factors which may limit the yield and integration scale. DTIC

N95-27152 Rome Lab., Griffiss AFB, NY.

A FINITE ELEMENT BASED TECHNIQUE FOR SIMULATION HELIX TWT INTERACTION CIRCUIT THERMAL BEHAVIOR Report, Jan. 1993 - Apr. 1994

Peter J. Rocci Oct. 1994 30 p Limited Reproducibility: More than 20% of this document may be affected by microfiche quality
(AF Proj. 2338)
(AD-A289552; RL-TR-94-166) Avail: Issuing Activity (Defense Technical Information Center (DTIC))

A technique was developed to assess the thermal performance of a helix Traveling Wave Tube (TWT) interaction circuit accounting for the thermal contact resistance between the circuit's components. This method employed iterative finite element analyses techniques and an analytical expression that related contact pressure to thermal contact resistance. Temperature gradients across the interfaces between the helix and support rods and between the support rods and barrel increase operating temperatures, which can lead to a decline in the tube's performance. Since the circuit analyzed contained no brazes or epoxy at the component interfaces, these thermal drops become more significant. parametric runs were made using this methodology for different assembly loads as well as for both beryllia and boron nitride (APBN) support rods. Results showed that the thermal contact resistance effect was more pronounced at lower assembly loads and higher thermal loads. That is, as the thermal loading to the circuit increases, the percent increase of the maximum helix temperature over the helix temperature when the resistance is not accounted for, increases. This effect was also more pronounced when APBN support rods were modeled. The helix temperature increased a greater amount when accounting for the thermal contact resistance for APBN support rods than for BeO support rods. DTIC

N95-27170# Joint Publications Research Service, Arlington, VA.

JPRS REPORT: SCIENCE AND TECHNOLOGY. CENTRAL EURASIA

10 Apr. 1995 94 p Transl. into ENGLISH from various Central Eurasian articles
(JPRS-UST-95-016) Avail: CASI HC A05/MF A01

Translated articles cover the following topics: sections technology in parallel computer tomography; deep interference fading of millimetric waves with back reflection along direct visibility path; radiation emission from conformal aperture of antenna mounted on cylinder of finite length; method of signal reconstruction from modulus of amplitude spectrum; estimating coherence intervals in highly stable oscillations of millimetric-wave sources; using high-frequency and ultrahigh-frequency plasma discharges in production of optical quartz fibers; and pseudodeep hologram with real physical recording depth. Author

N95-27196 Keystone Engineering Ltd., Blacksburg, VA.

IMAGE QUALITY METRICS FOR COLOR CRT DISPLAYS Interim Report, Jan. - Jul. 1993

Robert J. Beaton and Willard W. Farley Aug. 1994 91 p Limited Reproducibility: More than 20% of this document may be affected by microfiche quality
(Contract F33615-89-C-0532; AF Proj. 7184)
(AD-A288934; AL/CF-TR-1994-0115) Avail: Issuing Activity (Defense Technical Information Center (DTIC))

This study explores several different image quality metrics currently employed by the visual display community in the context of color CRT display technology. The specific techniques included in the study are the Modulation Transfer Function, the Contrast Threshold/Sensitivity Function, the Modulation Transfer Function Area, the Integrated Contrast Sensitivity metric, and the Square-Root Integral metric. These metrics include and are based on visual psychometric data and suggest that operator performance may be predicted from the objective, image quality data. DTIC

N95-27226*# Loyola Coll., Baltimore, MD. Japanese Technology Evaluation Center.
JTEC PANEL REPORT ON ELECTRONIC MANUFACTURING AND PACKAGING IN JAPAN Final Report
Michael J. Kelly (Georgia Inst. of Tech., Atlanta, GA.), William R. Boulton, ed. (Auburn Univ., AL.), John Kukowski (Rochester Inst. of Tech., NY.), Gene Meieran (INTEL Corp., Chandler, AZ.), Michael Pecht (Maryland Univ., College Park, MD.), John Peeples (American Telephone and Telegraph Co., West Columbia, SC.), Rao Tummala (Georgia Inst. of Tech., Atlanta, GA.), Michael J. DeHaemer, Geoff Holdridge, ed., and George Gamota (Mitre Corp., Bedford, MA.) Feb. 1995 260 p
(Grant NSF ENG-92-17849)
(NASA-CR-197830; NAS 1.26:197830; PB95-188116; ISBN-1-88712-37-8)
Avail: CASI HC A12/MF A03

This report summarizes the status of electronic manufacturing and packaging technology in Japan in comparison to that in the United States, and its impact on competition in electronic manufacturing in general. In addition to electronic manufacturing technologies, the report covers technology and manufacturing infrastructure, electronics manufacturing and assembly, quality assurance and reliability in the Japanese electronics industry, and successful product realization strategies. The panel found that Japan leads the United States in almost every electronics packaging technology. Japan clearly has achieved a strategic advantage in electronics production and process technologies. Panel members believe that Japanese competitors could be leading U.S. firms by as much as a decade in some electronics process technologies. For individual titles, see N95-27227 through N95-27233.

N95-27227*# Loyola Coll., Baltimore, MD.
MICROELECTRONICS IN JAPAN
William R. Boulton (Auburn Univ., AL.) *In its* JTEC Panel Report on Electronic Manufacturing and Packaging in Japan Feb. 1995 p 1-20 (For primary document see N95-27226 09-33)
Avail: CASI HC A03/MF A03

The purpose of this JTEC study is to evaluate Japan's electronic manufacturing and packaging capabilities within the context of global economic competition. To carry out this study, the JTEC panel evaluated the framework of the Japanese consumer electronics industry and various technological and organizational factors that are likely to determine who will win and lose in the marketplace. This study begins with a brief overview of the electronics industry, especially as it operates in Japan today. Succeeding chapters examine the electronics infrastructure in Japan and take an in-depth look at the central issues of product development in order to identify those parameters that will determine future directions for electronic packaging technologies. Author

N95-27228*# Loyola Coll., Baltimore, MD.
BUILDING THE ELECTRONIC INDUSTRY'S ROADMAPS
William R. Boulton (Auburn Univ., AL.) *In its* JTEC Panel Report on Electronic Manufacturing and Packaging in Japan Feb. 1995 p 21-34 (For primary document see N95-27226 09-33)
Avail: CASI HC A03/MF A03

JTEC panelists found a strong consistency among the electronics firms they visited: all the firms had clear visions or roadmaps for their research and development activities and had committed resources to ensure that they achieve targeted results. The overarching vision driving Japan's electronics industry is that of achieving market success through developing appealing, high-quality, low-cost consumer goods - ahead of the competition. Specifics of the vision include improving performance, quality, and portability of consumer electronics products. Such visions help Japanese companies define in detail the roadmaps they will follow to develop new and improved electronic packaging technologies. Author

N95-27229*# Loyola Coll., Baltimore, MD.
JAPAN'S TECHNOLOGY AND MANUFACTURING INFRASTRUCTURE
William R. Boulton (Auburn Univ., AL.), Eugene S. Meieran (INTEL Corp., Chandler, AZ.), and Rao R. Tummala (Georgia Inst. of Tech., Atlanta, GA.) *In its* JTEC Panel Report on Electronic Manufacturing and Packaging in Japan Feb. 1995 p 35-58 (For primary document see N95-27226 09-33)
Avail: CASI HC A03/MF A03

The JTEC panel found that, after four decades of development in electronics and manufacturing technologies, Japanese electronics companies are leaders in the development, support, and management of complex, low-cost packaging and assembly technologies used in the production of a broad range of consumer electronics products. The electronics industry's suppliers provide basic materials and equipment required for electronic packaging applications. Panelists concluded that some Japanese firms could be leading U.S. competitors by as much as a decade in these areas. Japan's technology and manufacturing infrastructure is an integral part of its microelectronics industry's success. Author

N95-27230*# Loyola Coll., Baltimore, MD.
JAPAN'S ELECTRONIC PACKAGING TECHNOLOGIES
Rao R. Tummala (Georgia Inst. of Tech., Atlanta, GA.) and Michael Pecht (Maryland Univ., College Park, MD.) *In its* JTEC Panel Report on Electronic Manufacturing and Packaging in Japan Feb. 1995 p 59-96 (For primary document see N95-27226 09-33)
Avail: CASI HC A03/MF A03

The JTEC panel found Japan to have significant leadership over the United States in the strategic area of electronic packaging. Many technologies and products once considered the 'heart and soul' of U.S. industry have been lost over the past decades to Japan and other Asian countries. The loss of consumer electronics technologies and products is the most notable of these losses, because electronics is the United States' largest employment sector and is critical for growth businesses in consumer products, computers, automobiles, aerospace, and telecommunications. In the past there was a distinction between consumer and industrial product technologies. While Japan concentrated on the consumer market, the United States dominated the industrial sector. No such distinction is anticipated in the future; the consumer-oriented technologies Japan has dominated are expected to characterize both domains. The future of U.S. competitiveness will, therefore, depend on the ability of the United States to rebuild its technological capabilities in the area of portable electronic packaging. Author

N95-27231*# Loyola Coll., Baltimore, MD.
ELECTRONICS MANUFACTURING AND ASSEMBLY IN JAPAN
John A. Kukowski (Rochester Inst. of Tech., NY.) and William R. Boulton (Auburn Univ., AL.) *In its* JTEC Panel Report on Electronic Manufacturing and Packaging in Japan Feb. 1995 p 97-114 (For primary document see N95-27226 09-33)
Avail: CASI HC A03/MF A03

In the consumer electronics industry, precision processing technology is the basis for enhancing product functions and for minimizing components and end products. Throughout Japan, manufacturing technology is seen as critical to the production and assembly of advanced products. While its population has increased less than 30 percent over twenty-five years, Japan's gross national product has increase thirtyfold; this growth has resulted in large part from rapid replacement of manual operations with innovative, high-speed, large-scale, continuously running, complex machines that process a growing number of miniaturized components. The JTEC panel found that introduction of next-generation electronics products in Japan goes hand-in-hand with introduction of new and improved production equipment. In the panel's judgment, Japan's advanced process technologies and equipment development and its highly automated factories are crucial elements of its domination of the consumer electronics marketplace - and Japan's expertise in manufacturing consumer electronics products gives it potentially unapproachable process expertise in all electronics markets. Author

N95-27232*# Loyola Coll., Baltimore, MD.
QUALITY ASSURANCE AND RELIABILITY IN THE JAPANESE ELECTRONICS INDUSTRY
Michael Pecht (Maryland Univ., College Park, MD.) and William R. Boulton (Auburn Univ., AL.) *In its* JTEC Panel Report on Electronic Manufacturing and Packaging in Japan Feb. 1995 p 115-126 (For primary document see N95-27226 09-33)
Avail: CASI HC A03/MF A03

Quality and reliability are two attributes required for all Japanese products, although the JTEC panel found these attributes to be secondary to customer cost requirements. While our Japanese hosts gave presentations on the challenges of technology, cost, and miniaturization, quality and reliability were infrequently the focus of our discussions. Quality and reliability were assumed to be sufficient to meet customer needs. Fujitsu's slogan, 'quality built-in, with cost and performance as prime consideration,' illustrates this point. Sony's definition of a next-generation product is 'one that is going to be half the size and half the price at the same performance of the existing one'. Quality and reliability are so integral to Japan's electronics industry that they need no new emphasis. Author

N95-27233*# Loyola Coll., Baltimore, MD.
SUCCESSFUL PRODUCT REALIZATION STRATEGIES
John Peeples (American Telephone and Telegraph Co., West Columbia, SC.) and William R. Boulton (Auburn Univ., AL.) *In its* JTEC Panel Report on Electronic Manufacturing and Packaging in Japan Feb. 1995 p 127-154 (For primary document see N95-27226 09-33)
Avail: CASI HC A03/MF A03

Product realization is the process of defining, designing, developing, and delivering products to the market. While the main thrust of this JTEC panel was to conduct a complete investigation of the state of Japanese low-cost electronic packaging technologies, it is very difficult to totally separate the development of technology and products from the product realization process. Japan's electronics firms adhere to a product realization strategy based on a strong customer focus, a consistent commitment to excellence in design, and a cost-effective approach to technology commercialization. The Japanese product-pull strategy has been a successful driver and influencing factor in every aspect of the product development cycle. Author

N95-27294 Air Force Inst. of Tech., Wright-Patterson AFB, OH. School of Engineering.
ACCELERATING CONSERVATIVE PARALLEL SIMULATION OF VHDL CIRCUITS M.S. Thesis
Joel F. Hurford Dec. 1994 96 p Limited Reproducibility: More than 20% of this document may be affected by microfiche quality
(AD-A289317; AFIT/GCS/ENG/94D-10) Avail: Issuing Activity (Defense Technical Information Center (DTIC))

This research effort considers heuristic and cost model based techniques for the optimal partitioning of VHDL circuits for parallel simulation. Correlation statistics are gathered on a wide variety of graph-based a priori parameters. Linear regression is used to identify significant parameters for inclusion in a representative cost model. Driving a greedy search, this cost model is used to improve upon initial heuristic partitions. The influence of feedback dominated previous research so a no-feedback algorithm is used to create the initial partition. The circuits studied range from 1050 to 4243 gates. DTIC

N95-27296 Air Force Inst. of Tech., Wright-Patterson AFB, OH.
MODEL OF A SINGLE IMPURITY IN A WIDE BANDGAP SEMICONDUCTOR DESCRIBING ELECTRIC FIELD SCREENING M.S. Thesis
Anthony N. Dills Dec. 1994 77 p Limited Reproducibility: More than 20% of this document may be affected by microfiche quality
(AD-A289322; AFIT/GAP/ENP/94D-3) Avail: Issuing Activity (Defense Technical Information Center (DTIC))

A mathematical model of the influence on electric field screening arising from a single impurity in a wide bandgap semiconductor has been numerically investigated and compared with analytically derived solutions. The parameter set chosen to perform the comparison of analytical solution and numerical solution is based upon a bismuth silicate crystal. Both the analytical calculations and the numerical calculations are an attempt to mathematically model the internal electric field within a semiconductor. Two types of impurities were looked at: a single donor level and a single trap impurity level. In general, after an abrupt application of a voltage across the semiconductor, net charge regions begin to redistribute and create internal electric fields that screen the applied field. A trap impurity is found to be more self-consistent with the analytical solutions than a donor impurity, the former satisfying the assumption of a constant free electron lifetime. The analytical solutions are valid for observation times much less than the Maxwellian relaxation time tau sub M: t much less than tau sub M. The analytical solution properly predicts stratification conditions when the observation time is prior to tau sub M; however, oscillatory behavior, characteristic of stratification, of the internal electric field occurs for times much greater than tau sub M. During this regime the analytical solutions are invalid. DTIC

N95-27374*# National Aeronautics and Space Administration. Lewis Research Center, Cleveland, OH.
THE 77 K OPERATION OF A MULTI-RESONANT POWER CONVERTER
Biswajit Ray (National Academy of Sciences - National Research Council, Cleveland, OH.), Scott S. Gerber (NYMA, Inc., Brook Park, OH.), Richard L. Patterson, and Ira T. Myers May 1995 8 p Presented at the Power Engineering Society Conference, Atlanta, GA, 18-22 Jun. 1995; sponsored by IEEE
(Contract NAS3-27186; RTOP 233-02-0C)
(NASA-TM-106941; E-9669; NAS 1.15:106941) Avail: CASI HC A02/MF A01

The liquid-nitrogen temperature (77 K) operation of a 55 W, 200 kHz, 48/28 V zero-voltage switching multi-resonant dc/dc converter designed with commercially available components is reported. Upon dipping the complete converter (power and control circuits) into liquid-nitrogen, the converter performance improved as compared to the room-temperature operation. The switching frequency, resonant frequency, and the characteristic impedance did not change significantly. Accordingly, the zero-voltage switching was maintained from no-load to full-load for the specified line variations. Cryoelectronics can provide high density power converters, especially for high power applications. Author

N95-27403# Edgerton, Germeshausen and Grier, Inc., Idaho Falls, ID.
ELECTROMAGNETIC HYSTERETIC RESPONSE CALCULATION FOR SUPERCONDUCTORS IN DEMAGNETIZING GEOMETRIES
L. S. Koo and K. L. Telschow 1994 6 p Presented at the 1994 Review of Progress in Quantitative Nondestructive Evaluation Conference, Snowmass, CO, 31 Jul. - 5 Aug. 1994
(Contract DE-AC07-76ID-01570)
(DE95-005028; EGG-M-94113; CONF-9407123-5) Avail: CASI HC A02/MF A01

A method has been outlined for calculating the flux front profile for a superconducting sample in either a uniform or nonuniform applied magnetic field possessing azimuthal symmetry. This technique relies upon finding a surface with zero vector potential. This surface is determined by simple integration of its derivative with respect to the external field, found by resolving a linear integral equation of the first kind. Measurement induced voltages and the entire hysteresis loop response can be found by extension of the ZFC magnetization response with increasing external field. Other experimentally measured quantities relating to the critical state can be calculated directly from the hysteresis loop if the time dependence of the external field is known. The technique shown in this report for solving the critical state model in the Bean approximation can be extended to field-dependent critical currents and other azimuthally symmetrical external fields. This work is presently in progress. DOE

N95-27405# International Centre for Theoretical Physics, Trieste (Italy).
THE EFFECTS OF TEMPERATURE ON SCHOTTKY DIODE BARRIER HEIGHT AND EVIDENCE OF MULTIPLE BARRIER
K. V. O. Rabah Jul. 1994 27 p
(DE95-609147; IC-94/181) Avail: CASI HC A03/MF A01 (US Sales Only)

Experimental study of Capacitance-Voltage-Temperature (C-V-T) plots, Current-Voltage-Temperature (I-V-T) characteristics have been undertaken in order to determine the height of the Schottky barrier. The results of the barrier height obtained by the above two methods were found to differ as well as vary with temperature change. In view of this discrepancy in barrier height values, two further experiments were performed: one on activation energy (I-T) plots and the other on pulsed (I-V-T) characteristics, and the results were found to show a similar trend. The Schottky diode studied was a 30CP040. DOE

N95-27474# Sandia National Labs., Albuquerque, NM. Battery Development Dept.
ELECTROLYTE EFFECTS IN LI(SI)/FeS2 THERMAL BATTERIES
Ronald A. Guidotti and Frederick W. Reinhardt 1994 17 p Presented

at the 19th International Power Sources Symposium, Brighton, England, 24-26 Apr. 1995
(Contract DE-AC04-94AL-85000)
(DE95-001614; SAND-94-1870C; CONF-950461-1) Avail: CASI HC A03/MF A01

The most common electrochemical couple for thermally activated ('thermal') batteries is the Li-alloy/FeS2 system. The most common Li-alloys used for anodes are 20% Li-80% Al and 44% Li-56% Si (by weight); liquid Li immobilized with iron powder has also been used. The standard electrolyte that has been used in thermal batteries over the years is the LiCl-KCl eutectic that melts at 352 C. The LiCl-LiBr-LiF eutectic had the best rate and power characteristics. This electrolyte melts at 436(degrees)C and shows very low polarization because of the absence of Li(+) gradients common with the LiCl-KCl eutectic. The low-melting electrolytes examined included a KBr-LiBr-LiCl eutectic (melting at 321 C), a LiBr-KBr-LiF eutectic (melting at 313 C), and a CsBr-LiBr-KBr eutectic (melting at 238 C). The CsBr-based salt had poor conductivity and was not studied further. The LiBr-KBr-LiF eutectic outperformed the KBr-LiBr-LiCl eutectic and was selected for more extensive testing. Because of their lower melting points and larger liquidi relative to the LiCl-KCl eutectic, the low-melting electrolytes are prime candidates for long-life applications (i.e., for activated lives of one hour or more). This paper will detail the relative performance of the Li(Si)/FeS2 couple using primarily the LiCl-KCl (standard) eutectic, the LiCl-LiBr-LiF (all-Li) eutectic, and the LiBr-KBr-LiF (low-melting) eutectic electrolytes. Most of the tests were conducted with 5-cell batteries; validation tests were also carried out with appropriate full-sized batteries. DOE

N95-27554# Brookhaven National Lab., Upton, NY.
INDUCED AXIAL OSCILLATIONS IN SUPERCONDUCTING DIPOLE WINDINGS
W. B. Sampson and A. K. Ghosh 1994 4 p Presented at the Applied Superconductivity Conference, Boston, MA, 16-21 Oct. 1994
(Contract DE-AC02-76CH-00016)
(DE95-005690; BNL-60349; CONF-941013-23) Avail: CASI HC A01/MF A01

When superconducting accelerator magnets wound from multi-stranded conductor are energized a periodic variation appears in the magnetic field along the axis. This oscillation is present in al components of the field and has a period that is equal to the transposition pitch of the superconducting cable. Such axial variations have been observed even in windings which are not carrying any transport current. A magnetic field was applied to a portion of a dipole winding using a second magnet. Axial oscillations were induced along the total length of the windings including the portion not in the applied field. The amplitude of these oscillations varied with the amount of inert winding inside the energizing magnet and with t;he angle of the applied field. These field variations could be completely applied field. These field variations could be completely eliminated in the external portion of the coil by heating a small section of the winding above the transition temperature. DOE

N95-27678# California Univ., Berkeley. Lawrence Berkeley Lab, CA. Physics Div.
AMORPHOUS SILICON PIXEL RADIATION DETECTORS AND ASSOCIATED THIN FILM TRANSISTOR ELECTRONICS READOUT
V. Perez-Mendez, J. Drewery, W. S. Hong, T. Jing, S. N. Kaplan, H. Lee, and A. Mireshghi Oct. 1994 21 p Presented at the Electrochemical Society Thin Film Technology Symposium, Miami, FL, 10-14 Oct. 1994
(Contract DE-AC03-76SF-00098)
(DE95-006568; LBL-36025; CONF-941063-12) Avail: CASI HC A03/MF A01

We describe the characteristics of thin (1 micrometer) and thick (greater than 30 micrometers) hydrogenated amorphous silicon p-i-n diodes which are optimized for detecting and recording the spatial distribution of charged particles, x rays and (gamma) rays. For x ray, (gamma) ray, and charged particle detection we can use thin p-i-n photosensitive diode arrays coupled to evaporated layers of suitable scintillators. For direct detection of charged particles with high resistance to radiation damage, we use the thick p-i-n diode arrays. Deposition techniques using helium dilution, which produce samples with low stress are described. Pixel arrays for flux exposures can be readout by transistor, single diode or two diode switches. Polysilicon charge sensitive pixel amplifiers for single event detection are described. Various applications in nuclear, particle physics, x ray medical imaging, neutron crystallography, and radionuclide chromatography are discussed. DOE

N95-27693# Lawrence Livermore National Lab., Livermore, CA.
COMPARISON OF THE CALCULATED AND MEASURED STABILITY OF A NbTi CABLE-IN-CONDUIT CONDUCTOR
R. L. Wong and C. T. Yeaw (Wisconsin Univ., Madison, WI.) 13 Oct. 1994 6 p Presented at the Applied Superconductivity Conference, Boston, MA, 16-21 Oct. 1994
(Contract W-7405-eng-48)
(DE95-007964; UCRL-JC-116965; CONF-941013-26) Avail: CASI HC A02/MF A01

Calculated curves of cable-in-conduit conductor energy stability margins vs. current are compared to experimental curves obtained at Oak Ridge National Laboratory for NbTi single triplex conductors. The conductors ranged in length from 1.8 m to 4.8 m, and had no imposed helium flow. The initiating heat pulse was applied for 16.7 ms over the entire conductor length. The calculated stability curves display the large decrease in energy margin from the low current and high energy margin 'well-cooled' stability region, to the high current and low energy margin 'ill-cooled' region that was determined experimentally. The calculated 'limiting current' of 250 A (boundary between the ill-cooled and well-cooled regions) also agrees with experiment. The multi-valued stability margins measured for lengths of 3.1 and 3.8 m could not be obtained by the computer model. Excluding the multiple stabilities, the calculated margins are generally 30% lower than the experimental values. The decrease in energy margin in the ill-cooled region was found to be due to the low critical to operating temperature difference (2.2 K at 250 A). This prevents an initiating pulse in the ill-cooled region from being able to generate significant Joule heating without quenching, limiting the energy margin. DOE

N95-27706# Sandia National Labs., Albuquerque, NM.
FLAT PANEL DISPLAY DEVELOPMENT ACTIVITIES AT SANDIA NATIONAL LABORATORIES
Edward G. DiBello, Walter Worobey, Steven Burchett, Willard Hareland, Tom Felter, and Bob Mays 1994 5 p Presented at the SID '95: Society for Information Display, Orlando, FL, 21-26 May 1995 Sponsored in part by the Advanced Research Projects Agency
(Contract DE-AC04-94AL-85000)
(DE95-005442; SAND-94-3109C; CONF-9505157-1) Avail: CASI HC A01/MF A01

The flat panel display development activities underway at Sandia National Laboratories are described. Research is being conducted in the areas of glass substrates, phosphors, large area processes, and electron emissions. Projects are focused on improving process yield, developing large area processes, and using modeling techniques to predict design performance. DOE

N95-27719# National Renewable Energy Lab., Golden, CO.
CURRENT STATUS OF ENVIRONMENTAL, HEALTH, AND SAFETY ISSUES OF LITHIUM POLYMER ELECTRIC VEHICLE BATTERIES
D. Corbus and C. J. Hammel Feb. 1995 76 p
(Contract DE-AC36-83CH-10093)
(DE95-004005; NREL/TP-463-7540) Avail: CASI HC A05/MF A01

Lithium solid polymer electrolyte (SPE) batteries are being investigated by researchers worldwide as a possible energy source for future electric vehicles (EV's). One of the main reasons for interest in lithium SPE battery systems is the potential safety features they offer as compared to lithium battery systems using inorganic and organic liquid electrolytes. However, the development of lithium SPE batteries is still in its infancy, and the technology is not envisioned to be ready for commercialization for several years. Because the research and development (R&D) of lithium SPE battery technology is of a highly competitive nature, with many companies both in the United States and abroad pursuing R&D efforts, much of the information concerning specific developments of lithium SPE battery technology is proprietary. This report is based on information available only through the open literature (i.e., information available through library searches). Furthermore, whereas R&D activities for lithium SPE cells have focused on a number of different chemistries, for both electrodes and electrolytes, this report examines the general environmental, health, and safety (EH&S) issues common to many lithium SPE chemistries. However, EH&S issues for specific lithium SPE cell chemistries are discussed when sufficient information exists. Although lithium batteries that do not have a SPE are also being considered for EV applications, this report focuses only on those lithium battery technologies that utilize the SPE technology. The lithium SPE battery technologies considered in this report may contain metallic lithium or nonmetallic lithium compounds (e.g., lithium intercalated carbons) in the negative electrode. DOE

N95-27724 Sandia National Labs., Albuquerque, NM.
TIME-OPTIMAL CONTROL OF THE MAGNETICALLY LEVITATED PHOTOLITHOGRAPHY PLATEN
Jim Redmond and Susan Tucker Jan. 1995 39 p Limited Reproducibility: More than 20% of this document may be affected by microfiche quality
(Contract DE-AC04-94AL-85000)
(DE95-005493; SAND-94-2423) Avail: CASI HC A03

This report summarizes two approaches to time-optimal control of a nonlinear magnetically levitated platen. The system of interest is a candidate technology for next-generation photolithography machines used in the manufacture of integrated circuits. The dynamics and the variable peak control force of the electro-magnetic actuators preclude the direct application of classical time-optimal control methodologies for determining optimal rest-to-rest maneuver strategies. Therefore, this study explores alternate approaches using a previously developed computer simulation. In the first approach, conservative estimates of the available control forces are used to generate suboptimal switching curves. In the second approach, exact solutions are determined iteratively and used as a training set for an artificial neural network. The trained network provides optimal actuator switching times that incorporate the full nonlinearities of the magnetic levitation actuators. Sample problems illustrate the effectiveness of these techniques as compared to traditional proportional-derivative control. DOE

N95-27754# Los Alamos National Lab., NM.
AFC GENERATOR DEVELOPMENT
B. L. Freeman, C. M. Fowler, M. G. Sheppard, and K. D. Sowder Feb. 1995 17 p
(Contract W-7405-eng-36)
(DE95-007094; LA-12860-MS) Avail: CASI HC A03/MF A01

By adapting the disk generator tested by Fowler, Hoeberling, and Marsh, the advanced flux compression (AFC) generator is able to produce a maximum dI/dt that is greater than 3 MA/microsecond. This current rise characteristic results in an inductive voltage across a 0.5-nH load of greater than or equal to 1.5 kV. This has been achieved with high gain, low loss, and a compact size. The AFC generator has been tested in four shots, and is performing beyond initial goals. DOE

N95-27853*# National Aeronautics and Space Administration. Lewis Research Center, Cleveland, OH.
LINEARLY TAPERED SLOT ANTENNA IMPEDANCE CHARACTERISTICS
Rainee N. Simons (NYMA, Inc., Brook Park, OH.) and Richard Q. Lee May 1995 6 p Presented at the IEEE/AP-S International Symposium and USNC/URSI Radio Science Meeting, Newport Beach, CA, 18-23 Jun. 1995; sponsored by the IEEE Antennas and Propagation Society and International Union of Radio Science
(RTOP 506-44-2C)
(NASA-TM-106912; E-9614; NAS 1.15:106912) Avail: CASI HC A02/MF A01

The paper presents for the first time an experimental technique to de-embed the input impedance of a LTSA from the measured reflection coefficient. The results show that the input impedance is dependent on the semi-flare angle and the length of the LTSA. The Re(Z(sub in)) is large when the electrical length of the LTSA is small and is on the order of few thousand ohms. However for an electrically large LTSA the Re(Z(sub in)) is in the range of 55 to 130 ohms. These results have potential applications in the design of broad band impedance matching networks for LTSA. Author

N95-27926# Kansas State Univ., Manhattan, KS.
DOE/KEURP SITE OPERATOR PROGRAM Second Quarter Report, 1 Oct. - 31 Dec. 1994
1994 22 p
(Contract DE-FC07-91ID-13074)
(DE95-007116; DOE/ID-13074/T14) Avail: CASI HC A03/MF A01

This is the 2nd quarter report of year four of the Kansas State University electric vehicle research program. Kansas State University (K-State), in support of the Department of Energy's and the Kansas Electric Utilities Research Program's subject contract, continues to demonstrate and develop electric vehicle and infrastructure technology. K-State is operating two Soleq's EVcort vehicles. During this reporting period both vehicles were returned to Chicago for warranty service. These vehicles have continued to operate and 'show' in a functional manner; however, one vehicle failed while being driven and the other vehicle's charger failed. It is expected that both vehicles will be returned to operational status within the early part of the next quarter. K-State continues to remain appraised of the issues surrounding the purchase of new technology S-10 electric pickup trucks, along with other Site Operator Program membership. K-State remains concerned that these vehicles may not ever arrive on site due to problems being discussed at this time. DOE

N95-27999*# Douglas Aircraft Co., Inc., Long Beach, CA. Advanced Aircraft Systems Dept.
EVALUATION OF ALL-ELECTRIC SECONDARY POWER FOR TRANSPORT AIRCRAFT Final Report
W. E. Murray, L. J. Feiner, and R. R. Flores 24 Jan. 1992 311 p
(Contract NAS3-25965)
(NASA-CR-189077; NAS 1.26:189077; MDC-91K0418) Avail: CASI HC A14/MF A03

This report covers a study by Douglas Aircraft Company (DAC) of electrical power systems for advanced transport aircraft based upon an all-electric design concept. The concept would eliminate distributed hydraulic and pneumatic secondary power systems, and feature an expanded secondary electrical power system redesigned to supply power to the loads customarily supplied by hydraulic or pneumatic power. The initial study was based on an advanced 20-kHz electrical power transmission and distribution system, using a system architecture supplied by NASA-Lewis Research Center for twin-engine aircraft with many advanced power conversion concepts. NASA-LeRC later requested DAC to refocus the study on 400-Hz secondary power distribution. Subsequent work was based on a three-engine MD-11 aircraft, selected by DAC as a baseline system design that would provide data for the comparative cost/benefit analysis. The study concluded that the 20-kHz concept produced many expected benefits, and that the all-electric trijet weight savings on hardware redesign would be 2,304 pounds plus a 2.1-percent fuel reduction and resized for a total weight reduction of 11,000 pounds. Cost reductions for a fleet of 800 aircraft in a 15-year production program were estimated at $76.71 million for RDT&E; $2.74 million per aircrat for production; $9.84 million for nonrecurring expenses; $120,000 per aircraft for product support; and $300,000 per aircraft per year for operating and maintenance costs, giving a present value of $1.914 billion saved or a future value of $10.496 billion saved. Author

N95-28015# Lawrence Livermore National Lab., Livermore, CA.
A NUMERICAL STUDY OF ULTRA-SHORT-PULSE REFLECTOMETRY
B. I. Cohen, B. B. Afeyan, and A. E. Chou (California Univ., Los Angeles, CA.) May 1994 16 p Presented at the 10th Topical Conference on High-temperature Plasma Diagnostics, Rochester, NY, 8-12 May 1994
(Contracts W-7405-eng-48; DE-FG03-86ER-53225)
(DE95-008070; UCRL-JC-117939; CONF-940552-43) Avail: CASI HC A03/MF A01

Ultra-short-pulse reflectometry is studied by means of the numerical integration of a one-dimensional full-wave equation for ordinary modes propagating in a plasma. The numerical calculations illustrate the potential of using the reflection of ultra-short-pulse, microwaves as an effective probe of the density profile even in the presence of significant density fluctuations. The difference in time delays of differing frequency components of the microwaves can be used to deduce the density profile. The modification of the reflected pulses in the presence of density fluctuations is examined and can be understood based on considerations of Bragg resonance. A simple and effective profile-reconstruction algorithm using the zero-crossings of the reflected pulse and subsequent Abel inversion is demonstrated. The robustness of the profile reconstruction algorithm in the presence of a sufficiently small amplitude density perturbation is assessed. DOE

N95-28048# Oak Ridge National Lab., TN.
STABILITY MEASUREMENTS ON A 1-T HIGH TEMPERATURE SUPERCONDUCTING MAGNET
J. W. Lue, L. Dresner, S. W. Schwenterly, D. Aized (American Superconductor Corp., Westborough, MA.), J. M. Campbell (American Superconductor Corp., Westborough, MA.), and R. E. Schwall (American Superconductor Corp., Westborough, MA.) 1995 5 p Presented at the Applied Superconductivity Conference, Boston, MA, 16-21 Oct. 1994
(Contract DE-AC05-84OR-21400)
(DE95-007411; CONF-941013-24) Avail: CASI HC A01/MF A01

A high temperature superconducting magnet based on Bi-2223 conductor was built at the American Superconductor Corporation. The magnet was constructed by a react and wind technique using conductors made from a metallic precursor process. It was a winding ID of 25.4 mm, OD of 87.6 mm, and height of 107.3 mm. A heater, two thermometers, and several voltage taps were built into the high field region of the magnet for stability measurements. The magnet generates 1.1 T central field at 4.2 K when operating at 1 micro V/cm over the entire conductor length, including all the joints. Stability measurements were performed in background fields up to 2.5 T from 4.2 K to 77 K. Stability margins more than 2 orders of magnitude higher than a low temperature superconductor were observed. DOE

N95-28105# Public Service Electric and Gas Co., Newark, NJ.
ELECTRIC VEHICLE ACTIVITIES Final Report, Sep. 1991 - Oct. 1994
J. L. DelMonaco and D. A. Pandya Feb. 1995 26 p
(Contract DE-FC07-91ID-13073)
(DE95-006648; DOE/ID-13073/1) Avail: CASI HC A03/MF A01

The data and information collected for the Public Service Electric and Gas Company's (PSE&G) electric vehicle demonstration program were intended to support and enhance DOE's Electric and Hybrid Vehicle Site Operator Program. The DOE Site Operator Program is focused on the life cycle and reliability of Electric Vehicles (EV's). Of particular interest are vehicles currently available with features that are likely to be put into production or demonstrate new technology. PSE&G acquired eight GMC Electric G-Vans in 1991, and three TEVans in 1993, and conducted a program plan to test and assess the overall performance of these electric vehicles. To accomplish the objectives of DOE's Site Operator's test program, a manual data collection system was implemented. The manual data collection system has provided energy use and mileage data. From September 1991 to October 1994 PSE&G logged 69,368 miles on eleven test vehicles. PSE&G also demonstrated the EVs to diverse groups and associations at fifty seven various events. Included in the report are lessons learned concerning maintenance, operation, public reactions, and driver's acceptance of the electric vehicles. DOE

N95-28131# Pacific Northwest Lab., Richland, WA.
STABILITY OF CHROMITE INTERCONNECTIONS IN DUAL ENVIRONMENTS
T. R. Armstrong, J. W. Stevenson, P. Raney, and L. R. Pederson Nov. 1994 5 p Presented at the Fuel Cell Seminar, San Diego, CA,28 Nov. - 1 Dec. 1994
(Contract DE-AC06-76RL-01830)
(DE95-007755; PNL-SA-25014; CONF-941109-1) Avail: CASI HC A01/MF A01

One of the most critical technical concerns in high-temperature SOFC's is the physical, chemical, and electrical stability of the interconnect (typically a doped lanthanum chromite) in the dual (oxidizing and reducing atmosphere) SOFC environment. The reducing or fuel side may experience oxygen partial pressures (P(O2)) from 10(exp -18) to 10(exp -6) atmospheres, while the oxidizing side may have P(O2) from 10(exp -6) to greater than 1 atm. These conditions limit the possible candidate materials to lanthanum or yttrium chromites. In the past decade, much work has centered on development of air-sinterable chromites and understanding their physical properties; little work, however, has focused on the stability of these chromites in dual environments. Chromite powders were synthesized using the glycine-nitrate process. The powders were calcined at 1,000 C for 1 hour and then uniaxially pressed into bars (46mm x 16mm x 3mm) at 55 MPa and isostatically pressed at 138 MPa. Samples were sintered in air. The dependence of the physical properties of sintered lanthanum chromites upon ambient P(O2) and temperature (using dilatometry, thermogravimetric analysis, and oxygen permeation measurements) were studied. La(1-x)A(x)CrO3 and Y(1-x)Ca(x)CrO3, where A is Ca or Sr and x was varied from 0.1 to 0.4 were evaluated in this study. The P(O2) was varied using a buffered CO2/Ar-4%H2 gas system, enabling expansion measurements to be made over a partial pressure range from 10(exp -5) to 10(exp -18) atmosphere at 800, 900, and 1,000 C. DOE

N95-28143# Stanford Linear Accelerator Center, Stanford, CA.
DEVELOPMENTS IN THE ELECTRON GUN SIMULATION PROGRAM, EGUN
W. B. Herrmannsfeldt Nov. 1994 6 p Presented at the Pulsed Radio Frequency Sources for Linear Colliders, Long Island, NY, 2-7 Oct. 1994
(Contract DE-AC03-76SF-00515)
(DE95-008137; SU-SLAC-PUB-6726; CONF-9410218-7) Avail: CASI HC A02/MF A01

This paper discusses the developments in the electron gun simulation programs that are based on EGUN with its derivatives and supporting programs. Much of the code development has been inspired by technology changes in computer hardware; the implications of this evolution on EGN2 are discussed. Some examples and a review of the capabilities of the EGUN family are described. DOE

N95-28146# Sandia National Labs., Albuquerque, NM.
NON-DESTRUCTIVE INTER-LEVEL DIELECTRIC VIA IN-LINE PROCESS MONITORING BY ATOMIC FORCE MICROSCOPY
A. J. Howard, A. G. Baca, and R. J. Shul 1994 5 p Presented at the 1995 GaAs Manufacturing Technology Conference, New Orleans, LA, 7-11 May 1995
(Contract DE-AC04-94AL-85000)
(DE95-008516; SAND-94-2823C; CONF-9505189-1) Avail: CASI HC A01/MF A01

A new application using atomic force microscopy (AFM) for in-line process control monitoring (PCM) of an interlevel dielectric via etching step is reported. The AFM with its near atomic-level resolution is capable of nondestructively measuring whether micron-sized vias have been etched to completion. Etch completion is determined by comparing the AFM measured etch depth of adjacent via holes through approximately 4000 (Angstrom) thick Si3N4 over Au-based ohmic and W gate metallizations. Due to etch selectivity, of the SF6/O2 reactive ion etch (RIIE) generated plasma, the ohmic metal acts as an etch stop whereas the W-based refractory gate continues to etch. For etch times beyond endpoint in the range of 20 to 50%, the AFM measured via etch depth differences is 250 to 400 (Angstrom) when comparing via depths over ohmic metal and W gate metal. This etch depth difference is a specific marker for etch completion and it is measured nondestructively at a point in the process where rework is still a feasible option. DOE

N95-28147# Sandia National Labs., Albuquerque, NM.
LOW-POWER, PARALLEL PHOTONIC INTERCONNECTIONS FOR MULTI-CHIP MODULE APPLICATIONS
R. F. Carson, M. L. Lovejoy, and K. L. Lear 1994 7 p Presented at the 45th Electronic Components and Technology Conference, Las Vegas, NV, 22-26 May 1995
(Contract DE-AC04-94AL-85000)
(DE95-008518; SAND-94-2878C; CONF-9505121-1) Avail: CASI HC A02/MF A01

New applications of photonic interconnects will involve the insertion of parallel-channel links into Multi-Chip Modules (MCM's). Such applications will drive photonic link components into more compact forms that consume far less power than traditional telecommunication data links. MCM-based applications will also require simplified drive circuitry, lower cost, and higher reliability than has been demonstrated currently in photonic and optoelectronic technologies. The work described is a parallel link array, designed for vertical (Z-Axis) interconnection of the layers in a MCM-based signal processor stack, operating at a data rate of 100 Mb/s. This interconnect is based upon high-efficiency VCSEL's, HBT photoreceivers, integrated micro-optics, and MCM-compatible packaging techniques. DOE

N95-28148# Sandia National Labs., Albuquerque, NM.
MULTIVARIATE CLASSIFICATION OF BPSG THIN FILMS USING MAHALANOBIS DISTANCES
S. Zhang (New Mexico Univ., Albuquerque, NM.), J. E. Franke (New Mexico Univ., Albuquerque, NM.), T. M. Niemczyk (New Mexico Univ., Albuquerque,

NM.), D. M. Haaland, J. N. Cox, I. Banerjee, J. Gee, T. Dang, and M. Puich 1995 7 p Presented at the 4th International Symposium on Diamond Materials, Reno, NV, 21-26 May 1995
(Contract DE-AC04-94AL-85000)
(DE95-008519; SAND-95-0394C; CONF-9505192-1) Avail: CASI HC A02/MF A01

Infrared absorption spectra of borophosphosilicate glass (BPSG) thin films were collected to develop a rapid classification method for determining if the films are within the desired specifications. Classification of samples into good and bad categories was performed using principal component analysis applied to the spectra. Mahalanobis distances were used as the classification metric. The highest overall percentage of correct classification of samples based upon their spectra was 91.6%. DOE

N95-28156# Oak Ridge National Lab., TN.
POLARIZATION RELAXATION IN ZINC OXIDE VARISTORS FROM 77 K TO 450 K
R. W. Major, A. E. Werner, C. B. Wilson, and F. A. Modine Oct. 1994 13 p Presented at the 96th Annual Meeting of the American Ceramic Society (ACS), Indianapolis, IN, 25-28 Apr. 1994
(Contract DE-AC05-84OR-21400)
(DE95-007761; CONF-940416-33) Avail: CASI HC A03/MF A01

The time and temperature dependences of polarization currents are investigated to higher temperatures and with greater temperature resolution than has been reported previously for zinc oxide varistors. Arrhenius plots yield thermal activation energies near 140 and 8 MeV, which are in reasonable agreement with values reported recently, as well as an additional thermally activated level at 0.66 eV, which emerges in the extension of the measurements to T greater than 300 K. Conductance data in this higher temperature range for the same samples yield the nearly identical energy of 0.68 eV for the intergranular (Schottky) barrier height. The temperature dependence of the exponent m in the power-law expression for the current-time dependence I = I(sub o)t(sup -m) was carefully examined and found to change twice from 0.5 to 1.0. The non-monotonic behavior of m with temperature is interpreted as due to resolution of the polarization currents from two different traps each of which makes the transition from diffusive to dispersive transport as temperature is lowered rather than, for example, a complicated distribution of relaxation times. DOE

N95-28181*# Lawrence Livermore National Lab., Livermore, CA.
THE DETERMINATION OF THE CONSTITUTIVE PARAMETERS OF A MEDIUM WITH APPLICATION TO A REINFORCED CONCRETE PAD
A. J. Poggio, G. L. Burke, and S. T. Pennock Jun. 1995 58 p
(NASA Order L-79902-C; RTOP 538-01-13-01)
(NASA-CR-4674; NAS 1.26:4674; UCRL-CR-120519) Avail: CASI HC A04/MF A01

This report describes the experimental and analytical efforts performed to determine the constitutive parameters of a reinforced concrete pad on which an aircraft (the NASA Boeing 757) was parked while its internal electromagnetic environment was measured. This concrete pad is part of the Large Electromagnetic System-Level Illuminator (LESLI) test facility at the Phillips Laboratory, Kirtland Air Force Base, New Mexico. The relative dielectric constant, conductivity, index of refraction, and reflection coefficient have been determined over the frequency range of 0 to 300 MHz and are presented. Author

N95-28198# Ohio State Univ., Columbus, OH.
THEORY OF EXOTIC SUPERCONDUCTIVITY AND NORMAL STATES OF HEAVY ELECTRON AND HIGH TEMPERATURE SUPERCONDUCTIVITY MATERIALS Progress Report, 15 Feb. 1994 - - 14 Feb. 1995
D. L. Cox 1995 6 p
(Contract DE-FG02-87ER-45326)
(DE95-006637; DOE/ER-45326/T5) Avail: CASI HC A02/MF A01

This is a progress report for the DOE project covering the period 2/15/94 to 2/14/95. The PI had a fruitful sabbatical during this period, and had some important new results, particularly in the area of new phenomenology for heavy fermion superconductivity. Significant new research accomplishments are in the area of odd-in-time-reversal pairing states/staggered superconductivity, the two-channel Kondo lattice, and a general model for Ce impurities which admits one-, two-, and three-channel Kondo effects. Papers submitted touch on these areas: staggered superconductivity - a new phenomenology for UPt(sub 3); theory of the two-channel Kondo lattice in infinite dimensions; general model of a Ce(3+) impurity. Other work was done in the areas: Knight shift in heavy fermion alloys and compounds; symmetry analysis of singular pairing correlations for the two-channel Kondo impurity model. DOE

THE PAPER AND INK USED IN THE ORIGINAL PUBLICATION MAY AFFECT THE QUALITY OF THE MICROFORM EDITION.

N95-28200# Sandia National Labs., Albuquerque, NM.
LITHIUM ION RECHARGEABLE SYSTEMS STUDIES
Samuel C. Levy, Robert R. Lasasse, Randall T. Cygan, and James A. Voigt 1995 6 p Presented at the 12th International Seminar on Primary and Secondary Battery Technology and Application, Deerfield Beach, FL, 6-8 Mar. 1995
(Contract DE-AC04-94AL-85000)
(DE95-006810; SAND-95-0157C; CONF-950312-1) Avail: CASI HC A02/MF A01

Lithium ion systems, although relatively new, have attracted much interest worldwide. Their high energy density, long cycle life and relative safety, compared with metallic lithium rechargeable systems, make them prime candidates for powering portable electronic equipment. Although lithium ion cells are presently used in a few consumer devices, e.g., portable phones, camcorders, and laptop computers, there is room for considerable improvement in their performance. Specific areas that need to be addressed include: (1) carbon anode-increase reversible capacity, and minimize passivation; (2) cathode-extend cycle life, improve rate capability, and increase capacity. There are several programs ongoing at Sandia National Laboratories which are investigating means of achieving the stated objectives in these specific areas. This paper will review these programs. DOE

N95-28201# Sandia National Labs., Albuquerque, NM.
OBIC ANALYSIS OF STRESSED, THERMALLY-ISOLATED POLYSILICON RESISTORS
Edward I. Cole, Jr., Kenneth A. Peterson, Ann N. Campbell, Eric S. Snyder, Donald G. Pierce, John S. Suehle (National Inst. of Standards and Technology, Gaithersburg, MD.), and Prasad Chaparala (Maryland Univ., College Park, MD.) 1994 10 p Presented at the International Reliability Physics Symposium, Las Vegas, NV, 3-6 Apr. 1995
(Contract DE-AC04-94AL-85000)
(DE95-008511; SAND-94-2464C; CONF-950432-1) Avail: CASI HC A02/MF A01

High gain Optical Beam Induced Current (OBIC) imaging has been used for the first time to examine the internal structural effects of electrical stress on thermally-isolated polysilicon resistors. The resistors are examined over a wide range of current densities, producing Joule heating up to (approximately) 1200 C. Throughout this current density range, the OBIC images indicate a clustering of dopant under dc stress and a more uniform distribution under ac conditions. The OBIC images also reveal areas that are precursors to catastrophic resistor failure. In addition to OBIC imaging, conventional electrical measurements were performed, examining the polysilicon resistance degradation and time-to-failure as a function of electrical stress. The electrical measurements show a monotonic increase in polysilicon resistor lifetime with frequency (up to 2 kHz) when subjected to a bipolar ac stress. The enhanced lifetime was observed even under high temperature (from Joule heating) stress conditions previously reported to be electromigration-free. The dopant redistribution indicated by the OBIC images is consistent with an electromigration stress experienced by the polysilicon resistors. The implications for thermally-isolated polysilicon resistor reliability are examined briefly. DOE

N95-28239*# Loyola Coll., Baltimore, MD. Japanese Technology Evaluation Center.
JTEC PANEL REPORT ON MICROELECTROMECHANICAL SYSTEMS IN JAPAN Final Report
Kensall D. Wise (Michigan Univ., Ann Arbor, MI.), Richard S. Muller (California Univ., Berkeley, CA.), Henry Guckel (Wisconsin Univ., Madison, WI.), Joseph M. Giachino (Ford Motor Co., Dearborn, MI.), G. Benjamin Hocker (Honeywell, Inc., Bloomington, MN.), and Stephen C. Jacobsen (Utah Univ., Salt Lake City, UT.) Sep. 1994 311 p
(Grant NSF ENG-92-17849)
(NASA-CR-197831; NAS 1.26:197831; PB95-100244; ISBN-1-883-712-35-1) Avail: CASI HC A14/MF A03

This report summarizes recent activities in the development of microelectromechanical systems (MEMS) in Japan. For the purposes of this study, 'MEMS' means batch-fabricated miniature devices that convert physical parameters to or from electrical signals and that depend on mechanical structures or parameters in important ways for their operation. The report covers advanced materials and process technology; sensors and sensing microstructures; microactuators and actuation mechanisms; sensor-circuit integration and system partitioning; advanced packaging, microassembly, and testing technologies; and MEMS design techniques, applications, and infrastructure. The panel found that Japanese industry is emphasizing approaches to MEMS that are similar to those taken by U.S. industry (i.e., approaches based on silicon integrated-circuit technology); these efforts are comparable in their level of development to those in the United States. However, the ten-year, $250 million, MITI-sponsored program in micromachines emphasizes the miniaturization of more traditional (nonlithographic) machining processes, an area in which there is no comparable U.S. effort. Packaging technology and applications for batch-fabricated MEMS devices is considered a major challenge in both countries. The panel concluded that these and other issues will require global leadership and international cooperation to realize the benefits of MEMS in a timely way. Author

N95-28244# Brookhaven National Lab., Upton, NY.
LOW NOISE MONOLITHIC SI JFETS FOR OPERATION IN THE 90-300K RANGE AND IN HIGH RADIATION ENVIRONMENTS
V. Radeka, M. Citterio, S. Rescia, P. F. Manfredi (Pavia Univ., Italy.), and V. Speziali (Pavia Univ., Italy.) Dec. 1994 3 p Presented at the Low Temperature Electronics and High Temperature Superconductivity Conference, Reno, NV, 21-26 May 1995
(Contract DE-AC02-76CH-00016)
(DE95-007303; BNL-61328; CONF-9505163-1) Avail: CASI HC A01/MF A01

Development of low noise preamplifiers for large ionization chambers with liquid argon (LAr) and liquid krypton (LKr) used in high energy physics experiments for measurement of energy of charged particles and photons requires die choice of a technology able to withstand the environment: a temperature of 90-120 K; an ionizing radiation dose of 1-2 Mrad; a neutron fluence of 0.5-1.10(exp 14)n/sq cm. Silicon JFET's (junction field effect transistors) by virtue of their reliable noise behavior and their intrinsic radiation hardness appear to be very suitable devices for applications both at room and cryogenic temperatures. We describe the noise properties of JFET devices and a monolithic preamplifier suitable for amplification of charge and current signals. DOE

N95-28339# Brookhaven National Lab., Upton, NY.
FIELD QUALITY IMPROVEMENTS IN SUPERCONDUCTING MAGNETS FOR RHIC
R. Gupta, A. Jain, S. Kahn, G. Morgan, P. Thompson, P. Wanderer, and E. Willen 1994 3 p Presented at the 4th European Particle Accelerator Conference, London, England, 27 Jun. - 1 Jul. 1994
(Contract DE-AC02-76CH-00016)
(DE95-006096; BNL-60352; CONF-940618-117) Avail: CASI HC A01/MF A01

A number of techniques have been developed and tested to improve the field quality in the superconducting dipole and quadrupole magnets to be used in the Relativistic Heavy Ion Collider (RHIC). These include adjustments in the coil midplane gap to compensate for the allowed and non-allowed harmonics, inclusion of holes and cutouts in the iron yoke to reduce the so harmonics, and magnetic tuning shims to correct for the residual errors. We compare the measurements with the calculations to test the validity of these concepts. DOE

N95-28341* National Aeronautics and Space Administration. Goddard Space Flight Center, Greenbelt, MD.
FORBACK DC-TO-DC CONVERTER Patent
Alan T. Lukemire, inventor (to NASA) 23 May 1995 33 p Filed 24 Mar. 1993
(NASA-Case-GSC-13404-1; US-Patent-5,418,709;
US-Patent-Appl-SN-038746; US-Patent-Class-323-222;
US-Patent-Class-323-282; US-Patent-Class-323-285;
US-Patent-Class-363-21; US-Patent-Class-363-97;
Int-Patent-Class-G05F-1/613; Int-Patent-Class-H02M-3/335) Avail: US Patent and Trademark Office

A pulse-width modulated DC-to-DC power converter including a first inductor, i.e. a transformer or an equivalent fixed inductor equal to the inductance of the secondary winding of the transformer, coupled across a source of DC input voltage via a transistor switch which is rendered alternately conductive (ON) and nonconductive (OFF) in accordance with a signal from a feedback control circuit is described. A first capacitor capacitively couples one side of the first inductor to a second inductor which is connected to a second capacitor which is coupled to the other side of the first inductor. A circuit load shunts the second capacitor. A semiconductor diode is additionally coupled from a common circuit connection between the first capacitor and the second inductor to the other side of the first inductor. A current sense transformer generating a current feedback signal for the switch control circuit is directly coupled in series with the other side of the first inductor so that the first capacitor, the second inductor and the current sense transformer are connected in series through the first inductor. The inductance values of the first and second inductors, moreover, are made identical. Such a converter topology results in a simultaneous voltsecond balance in the first inductance and ampere-second balance in the current sense transformer.
Official Gazette of the U.S. Patent and Trademark Office

N95-28349 Electrofuels Mfg. Co., Toronto (Ontario).
DEVELOPMENT OF AN ULTRA-SAFE RECHARGEABLE LITHIUM-ION BATTERY Status Report, 15 Aug. - 15 Nov. 1994
J. K. Jacobs 15 Nov. 1994 4 p Limited Reproducibility: More than 20% of this document may be affected by microfiche quality
(Contract N00014-94-C-0141)
(AD-A288959) Avail: Issuing Activity (Defense Technical Information Center (DTIC))

The project activities had an official start on August 15. Based on previous work, a statement of the basic design framework to be used was an important first step. The basic cell is to be a bonded flat-pack containing all active cell components in a sealed envelope. Cell integrity is to be provided by internal bonding, and not through external support. This design approach is fundamentally different from that commonly used in wound and hard-case cells, and has the advantage of ease of scaling for a variety of different form factors. An innovative variant on the fan-fold geometry has been chosen for its manufacturability advantages. Equipment capable of handling the semi-continuous requirements of the fan-fold structure had already been outlined. There are specific advantages in at least three areas: (1) Control of dimensional tolerances; (2) Production rate; (3) Connection of power lead-outs and final assembly. Cell chemistry is viewed to be of less fundamental importance than structural considerations within the bounds of the lithium-ion concept. DTIC

N95-28388 Naval Postgraduate School, Monterey, CA.
THERMAL ANALYSIS OF PANSAT BATTERIES AND ELECTRICAL POWER SUBSYSTEM M.S. Thesis
Sheila A. Patterson Sep. 1994 203 p Limited Reproducibility: More than 20% of this document may be affected by microfiche quality
(AD-A290013) Avail: Issuing Activity (Defense Technical Information Center (DTIC))

The thermal design of a spacecraft ensures proper heat transfer so all components and subsystems remain within prescribed temperature limits during all aspects of the spacecraft's mission. This thesis develops a point to-point heat flow model of the Electrical Power Subsystem (EPS) and its associated housing for the Petite Amateur Navy Satellite (PANSAT). This analysis was performed to identify physical locations in the EPS where temperatures may exceed the limits established to protect sensitive electronic components, and to define the expected environment of the batteries. The Integrated Thermal Analysis System (ITAS) and a Steady State Thermal Analyzer and Model Builder were used to perform steady state and transient analyses on the EPS: analysis of the batteries was performed using ITAS only. The simulated transient temperatures within the EPS housing remained within limits, but the batteries exceeded specifications. It is suggested that a passive thermal control technique be adapted for the batteries and its design be experimentally validated before flight. DTIC

N95-28448 Helsinki Univ. of Technology, Espoo (Finland).
MEASUREMENT-BASED MESFET MODEL IN APLAC
M. Laehepelto and M. Valtonen Oct. 1994 25 p Limited Reproducibility: More than 20% of this document may be affected by microfiche quality
(PB95-195483; ISBN-951-22-2348-1) Avail: CASI HC A03

A measurement-based MESFET model is presented where the large-signal model is constructed from measured small-signal S parameters and DC currents. The S parameters are measured at various frequencies and converted to Y parameters using nth order Chebyshev power series expansion. The nonlinear static, dynamic, and higher-order components in the model are created with the aid of line integration over the voltage waveforms. The nonlinear large-signal model proposed is valid for a very wide bias range, and may also be used in the time domain. The model as well as the model extractor are implemented in Analysis Program for Linear Active Circuits (APLAC). NTIS

N95-28512 Massachusetts Inst. of Tech., Cambridge, MA.
BASIC AND APPLIED RESEARCH IN THE FIELD OF ELECTRONICS AND COMMUNICATIONS Final Report, 1 Nov. 1991 - 31 Oct. 1994
Jonathan Allen 21 Feb. 1995 24 p Limited Reproducibility: More than 20% of this document may be affected by microfiche quality
(Contract DAAL03-92-C-0001)
(AD-A291727; ARO-28925.166-ELJSEP) Avail: Issuing Activity (Defense Technical Information Center (DTIC))

The MIT research Laboratory of Electronics Joint Services Program comprises seventeen work units that span a broad array of topics in high-speed optics, surface and phase transitions, submicron structures and atomic-effect devices, the electrical behavior of interconnect structures, and atomic and molecular physics. The work units include InGaAlAs Quantum Heterostructures for High-Performance Devices: InAlAs/InGaAs Heterostructure Field-Effect Transistors for Telecommunications: Chemical Beam Epitaxy of II-VI/III-V Quantum Wells; Sub-100nm Structures: Technology and Electronics; Single-Electron Transistors; Quantum Transport in Low-Dimensional Disordered Systems; Statistical Mechanics of Quantum Dot; Femtosecond Quantum Optics; Ultrafast Optical and Electronic Processes; Excitations, Ground State Properties, end Phase Transitions of Surfaces; Synchrotron X-ray Studies of Surface Disordering; Statistical Mechanics of Surface Systems and Quantum-Correlated System; Step Structures and Epitaxy; Molecular Beam Etching of and Deposition on Silicon; Optical Frequency Metrology; Precision Instrumentation; and Electromagnetic Waves in Multilayer Media. DTIC

N95-28515# Brookhaven National Lab., Upton, NY.
MANUFACTURE AND TESTING OF THE SUPERCONDUCTING WIRE AND CABLE FOR THE RHIC DIPOLES AND QUADRUPOLES
A. F. Greene, M. G. Garber, A. K. Ghosh, D. McChesney, A. Morgillo, R. Shah, S. DelRe (Oxford Superconducting Technology, Carteret, NJ.), G. Epstein (Oxford Superconducting Technology, Carteret, NJ.), S. Hong (Oxford Superconducting Technology, Carteret, NJ.), and J. Lichtenwalner (Oxford Superconducting Technology, Carteret, NJ.) et al 1994 3 p Presented at the Applied Superconductivity Conference, Boston, MA, 16-21 Oct. 1994
(Contract DE-AC02-76CH-00016)
(DE95-006000; BNL-60350; CONF-941013-30) Avail: CASI HC A01/MF A01

Production of superconducting wire and cable for Relativistic Heavy Ion Collider (RHIC) dipoles and quadrupoles is now complete. This report presents final statistics generated during the manufacture and testing of this cable. DOE

N95-28529 Georgia Inst. of Tech., Atlanta, GA.
QUASI-OPTICAL MILLIMETER WAVE POWER COMBINING Final Report, 20 May 1991 - 31 Dec. 1994
C. J. Summers, J. C. Wiltse, H. M. Harris, R. W. McMillan, and A. Torabi Feb. 1995 9 p Limited Reproducibility: More than 20% of this document may be affected by microfiche quality
(Contract DAAL03-91-G-0160)
(AD-A291767; ARO-28339.9-EL) Avail: Issuing Activity (Defense Technical Information Center (DTIC))

The research described in this report was based on concepts advanced earlier by Dr. James W. Mink, then of the Army Research Office. His analyses for quasi-optical power combining from solid-state source arrays have formed a strong basis for a number of investigations in this field in recent years. Previous studies dealt with microwave arrays, while the present one was the first to deal with millimeter-wave arrays of FET's and HEMT's. Dr. Mink served as the A.R.O. technical monitor for the majority of this project, and the authors would like to express appreciation for his advice and contributions. DTIC

N95-28544 Colorado Univ., Boulder, CO. Dept. of Electrical and Computer Engineering.
EVALUATION OF DEFECT-RELATED DIFFUSION IN SEMICONDUCTORS BY ELECTROOPTICAL SAMPLING
Paul Biernacki, Henry Lee, and Alan R. Mickelson 15 Feb. 1995 48 p Limited Reproducibility: More than 20% of this document may be affected by microfiche quality
(Contracts N00014-92-J-1190; DAAL03-92-G-0289)
(AD-A291630; ECE/CWOL/67) Avail: Issuing Activity (Defense Technical Information Center (DTIC))

The electrooptical sampling technique is used to assess the electrical behavior of ohmic contact regions in GaAs. For purpose, unique ohmic contact coplanar waveguides were fabricated and tested. A reduced electrooptical sampling signal is detected in certain ohmic contact regions. Since the electrical fields present in this device are known a priori, the deviation of the electrooptical signal from its nominal value is attributed to a deviation in the electrooptical coefficient. Defects introduced during the annealing step of the ohmic contact accelerated by existing dislocations are discussed as a mechanism capable of disrupting the electrooptic coefficient. A simple phenomenological diffusion model is presented to explain the mechanism responsible for the nulling of the electrooptical coefficient. DTIC

N95-28565# Joint Publications Research Service, Arlington, VA.
JPRS REPORT: SCIENCE AND TECHNOLOGY. CENTRAL EURASIA
10 May 1995 66 p Transl. into ENGLISH from various Russian articles
(JPRS-UST-95-019) Avail: CASI HC A04/MF A01

Translated articles cover the following topics: neural networks in thin magnetic films for associative memory; combination method of calculating scattering fields of intricate cylindrical objects; methods of approximately calculating probability of correct ambiguity removal from phase-lock direction finders with plane antenna arrays; two-dimensional arrays of antenna-coupled Schottky-barrier diodes for formation of millimetric-wave images; welding PTZV titanium alloy examined; and mechanism, kinetics of active, active-passive dissolution of titanium in acidic media. Author

N95-28570*# Illinois Univ., Urbana-Champaign, IL. Electromagnetic Communication Lab.
EFFICIENT MODELING OF INTERCONNECTS AND CAPACITIVE DISCONTINUITIES IN HIGH-SPEED DIGITAL CIRCUITS Thesis
K. S. Oh and J. Schutt-Aine Jun. 1995 139 p
(Grant NAG2-823)
(NASA-CR-198728; NAS 1.26:198728; UILU-ENG-95-2544; Rept-95-1)
Avail: CASI HC A07/MF A02

Modeling of interconnects and associated discontinuities with the recent advances high-speed digital circuits has gained a considerable interest over the last decade although the theoretical bases for analyzing these structures were well-established as early as the 1960s. Ongoing research at the present time is focused on devising methods which can be applied to more general geometries than the ones considered in earlier days and, at the same time, improving the computational efficiency and accuracy of these methods. In this thesis, numerically efficient methods to compute the transmission line parameters of a multiconductor system and the equivalent capacitances of various strip discontinuities are presented based on the quasi-static approximation. The presented techniques are applicable to conductors embedded in an arbitrary number of dielectric layers with two possible locations of ground planes at the top and bottom of the dielectric layers. The cross-sections of conductors can be arbitrary as long as they can be described with polygons. An integral equation approach in conjunction with the collocation method is used in the presented methods. A closed-form Green's function is derived based on weighted real images thus avoiding nested infinite summations in the exact Green's function; therefore, this closed-form Green's function is numerically more efficient than the exact Green's function. All elements associated with the moment matrix are computed using the closed-form formulas. Various numerical examples are considered to verify the presented methods, and a comparison of the computed results with other published results showed good agreement. Author

N95-28597# Sandia National Labs., Albuquerque, NM.
CHARACTERIZATION OF A FUSED SILICA CAPACITANCE STANDARD

M. G. Daniel Jan. 1995 21 p
(Contract DE-AC04-94AL-85000)
(DE95-006457; SAND-94-3146) Avail: CASI HC A03/MF A01

An ovenized 10 pF standard capacitor was constructed by the National Institute of Standards and Technology (NIST). The dielectric material used as Suprasil II grade fused silica. This report discusses a temperature coefficient analysis of the capacitor performed at the Primary Standards Laboratory (PSL) of Sandia National Laboratories (SNL). The effects of temperature change on dielectric loss will also be discussed. DOE

N95-28599* National Aeronautics and Space Administration. Pasadena Office, CA.
LEAK DETECTION UTILIZING ANALOG BINAURAL (VLSI) TECHNIQUES Patent
Frank T. Hartley, inventor (to NASA) (Jet Propulsion Lab., California Inst. of Tech., Pasadena, CA.) 23 Jun. 1995 23 p Filed 18 Aug. 1993 Prepared in cooperation with Jet Propulsion Lab., California Inst. of Tech., Pasadena, CA
(Contract NAS7-918)
(NASA-Case-NPO-18399-1-CU; US-Patent-5,417,113; US-Patent-Appl-SN-111317; US-Patent-Class-73-587; US-Patent-Class-73-592; US-Patent-Class-381-68.2; US-Patent-Class-367-125; Int-Patent-Class-G01M-3/24) Avail: US Patent and Trademark Office

A detection method and system utilizing silicon models of the traveling wave structure of the human cochlea to spatially and temporally locate a specific sound source in the presence of high noise pandemonium. The detection system combines two-dimensional stereausis representations, which are output by at least three VLSI binaural hearing chips, to generate a three-dimensional stereausis representation including both binaural and spectral information which is then used to locate the sound source.
Official Gazette of the U.S. Patent and Trademark Office

N95-28613 Department of the Navy, Washington, DC.
ENERGY-MEASURING RESISTOR BANK Patent
Anthony M. Marques, inventor (to Navy), Paul R. Kelley, inventor (to Navy), William K. Jones, inventor (to Navy), and Masatoshi Fuk, inventor (to Navy) 16 Aug. 1994 5 p Filed 30 Mar. 1993
(AD-D017392; US-Patent-5-339,066; US-Patent-Appl-SN-045340; US-Patent-Class-338-306) Avail: US Patent and Trademark Office

A resistor bank consisting of a group of resistors formed on the surface of a die, all electrically connected together in parallel. All of the resistors have identical individual resistances, but each has a unique energy dissipating capacity. When an event subjects the resistor bank to a surge of current, some of the resistors blow out, thereby changing the resistance of the bank. By measuring the resistance of the bank before and after an event the energy of the surge can be determined. DTIC

N95-28614 Department of the Navy, Washington, DC.
NON-LINEAR RESISTIVE GRID KERNEL ESTIMATOR USEFUL IN SINGLE FEATURE, TWO-CLASS PATTERN CLASSIFICATION Patent
Jeffrey L. Solka, inventor (to Navy), George W. Rogers, inventor (to Navy), Carey E. Priebe, inventor (to Navy), Wendy L. Poston, inventor (to Navy), and Harold Szu, inventor (to Navy) 15 Nov. 1994 6 p Filed 26 Nov. 1993
(AD-D017394; US-Patent-5-365,472; US-Patent-Appl-SN-157553; US-Patent-Class-364-807) Avail: US Patent and Trademark Office

A discrete non-linear estimator is provided to establish a probability density function useful in classification of a feature as belonging to one of two classes. A first and second known feature space associated with respective first and second classes are each converted to a plurality of voltages reflecting corresponding first and second feature space bins. A first and second one-dimensional, non-linear resistive grid has input nodes that continuously receive the voltages reflecting the respective first and second known feature space. Each resistive grid produces an output voltage at each of a corresponding plurality of first and second output nodes. Each of a plurality of voltage comparators are used to compare voltages at corresponding first and second output nodes to output a discrete probability density function that considers corresponding ones of the first and second feature space bins. A display may be used to visually or otherwise provide each probability density function from each voltage comparator. DTIC

N95-28629 Advanced Device Technologies, Inc., Charlottesville, VA.
NOVEL FIELD EFFECT TRANSISTORS FOR LOW POWER ELECTRONICS Progress Report No. 3
16 Jan. 1995 10 p Limited Reproducibility: More than 20% of this document may be affected by microfiche quality
(Contract N00014-94-C-0260)
(AD-A289929) Avail: Issuing Activity (Defense Technical Information Center (DTIC))

The primary objective of this Phase 1 project is to determine the extent of the significant reduction in power consumption of integrated circuits which may be achieved by utilizing a novel sidegate FET technology. The new FET technology promises to eliminate the Narrow Channel Effect (NCE) which is one of the primary factors limiting the minimum power consumption of integrated circuits. Bv eliminating the NCE, we will be able to scale the device size dramatically and reduce the power consumption by an order of magnitude. The project will assess the power, speed, circuit design, processing, and manufacturability of the new FET technology for both digital and analog circuit applications. In particular, we will extract device parameters from the new ultra-low power FET's fabricated at UVA to develop device models, incorporate these models into a new SPICE package (AIM-SPICE), simulate different logic families including DCFL and SCFL, and compare the predicted performance with the standard DCFL and SCFL logic. We will also analyze the gate current leakage and subthreshold slope as the primary factors limiting the noise margins at low power supplies, establish the minimum required bias voltage for reliable operation, and analyze the factors determining the threshold voltage changes from device to device as well as other factors which may limit the yield and integration scale. DTIC

N95-28655# Helsinki Univ. of Technology, Espoo (Finland).
STRUCTURAL OPTIMISATION OF CAGE INDUCTION MOTORS USING FINITE ELEMENT ANALYSIS Thesis
S. Palko 1994 61 p
(PB95-195434; ISBN-951-22-2392-9) Avail: CASI HC A04/MF A01

The current trend in motor design is to have highly efficient, low noise, low cost, and modular motors with a high power factor. High torque motors are useful in applications like servo motors, lifts, cranes, and rolling mills. This report contains a detailed review of different optimization methods applicable in various design problems. Special attention is given to the performance of different methods, when they are used with finite element analysis (FEA) as an objective function, and accuracy problems arising from the numerical simulations. Also an effective method for designing high starting torque and high efficiency motors is presented. The method described in this work utilizes FEA combined with algorithms for the optimization of the slot geometry. The optimization algorithm modifies the position of the nodal points in the element mesh. The number of independent variables ranges from 14 to 140 in this work. NTIS

N95-28663 Rutherford Appleton Lab., Oxford (England).
CHARACTERISTICS OF THE STANDARD CURRENT TRIP CIRCUIT
R. M. Cutler and M. Allenby Oct. 1994 15 p
(PB95-192886; RAL-94-111) Avail: Issuing Activity (National Technical Information Service (NTIS))

This report sets out to characterize the standard trip circuit commonly used to prevent latchup on spacecraft circuits. In addition, a negative rail version, and a higher voltage version, are examined. The sensitivity of the circuit to Hfe, supply voltage, and temperature were also measured. NTIS

N95-28666 California Univ., Berkeley, CA.
CHUA'S CIRCUITS: PHENOMENA AND APPLICATIONS Final Report, 1 Dec. 1993 - 30 Nov. 1994
Leon O. Chua 10 Jan. 1995 104 p Presented at the International Symposium on Nonlinear Theory and Its Applications, Waikiki, HI, 5-10 Dec. 1993 Limited Reproducibility: More than 20% of this document may be affected by microfiche quality
(Contract N00014-94-1-0308)
(AD-A291638) Avail: Issuing Activity (Defense Technical Information Center (DTIC))

A workshop on Chua's Circuit: Chaotic Phenomena and Applications was held December 7, 1993 in conjunction with the 1993 International Symposium on Nonlinear Theory and its Applications (NOLTA 93), Honolulu, Hawaii. DTIC

N95-26786*# Aerospace Corp., El Segundo, CA. Electronics Technology Center.
PROGRESS TOWARDS COMPUTER SIMULATION OF NIH2 BATTERY PERFORMANCE OVER LIFE
Albert H. Zimmerman and M. V. Quinzio *In* NASA. Marshall Space Flight Center, The 1994 27th Annual NASA Aerospace Battery Workshop Feb. 1995 p 177-183 (For primary document see N95-26785 09-44)
Avail: CASI HC A02/MF A06

N95-26787*# Lockheed Missiles and Space Co., Sunnyvale, CA.
LONG LIFE 80Ah STANDARD IPV NIH2 BATTERY CELL
Jon D. Armantrout and J. S. Waller *In* NASA. Marshall Space Flight Center, The 1994 27th Annual NASA Aerospace Battery Workshop Feb. 1995 p 185-207 (For primary document see N95-26785 09-44)
Avail: CASI HC A03/MF A06

N95-26788*# Eagle-Picher Industries, Inc., Joplin, MO.
HIGH-RATE/HIGH-TEMPERATURE CAPABILITY OF A SINGLE-LAYER ZICAR-SEPARATOR NICKEL-HYDROGEN CELL
James R. Wheeler *In* NASA. Marshall Space Flight Center, The 1994 27th Annual NASA Aerospace Battery Workshop Feb. 1995 p 243-246 (For primary document see N95-26785 09-44)
Avail: CASI HC A01/MF A06

N95-26789*# Naval Surface Warfare Center, Crane, IN.
AIR FORCE NI-H2 CELL TEST PROGRAM: STATE OF CHARGE TEST
Bruce Moore and Douglas Smellie (Phillips Lab., Kirtland AFB, NM.) *In* NASA. Marshall Space Flight Center, The 1994 27th Annual NASA Aerospace Battery Workshop Feb. 1995 p 247-258 (For primary document see N95-26785 09-44)
Avail: CASI HC A03/MF A06

N95-26790*# National Aeronautics and Space Administration. Lyndon B. Johnson Space Center, Houston, TX.
CALORIMETRIC EVALUATION OF COMMERCIAL NI-MH CELLS AND CHARGES
Eric C. Darcy and Brent M. Hughes (Lockheed Engineering and Sciences Co., Houston, TX.) *In* NASA. Marshall Space Flight Center, The 1994 27th Annual NASA Aerospace Battery Workshop Feb. 1995 p 345-400 (For primary document see N95-26785 09-44)
Avail: CASI HC A04/MF A06

N95-26791*# National Aeronautics and Space Administration. Marshall Space Flight Center, Huntsville, AL.
NICKEL METAL HYDRIDE LEO CYCLE TESTING
Eric Lowery *In its* The 1994 27th Annual NASA Aerospace Battery Workshop Feb. 1995 p 445-460 (For primary document see N95-26785 09-44)
Avail: CASI HC A03/MF A06

N95-26792*# Naval Research Lab., Washington, DC.
THE 50 Ah NIH2 CPV QUALIFICATION TESTS
J. C. Garner, Wilbert L. Barnes, and Gary L. Hickman *In* NASA. Marshall Space Flight Center, The 1994 27th Annual NASA Aerospace Battery Workshop Feb. 1995 p 475-487 (For primary document see N95-26785 09-44)
Avail: CASI HC A03/MF A06

N95-26793*# Eagle-Picher Industries, Inc., Joplin, MO.
UNIQUE FEATURES OF A NEW NICKEL-HYDROGEN 2-CELL CPV
James R. Wheeler *In* NASA. Marshall Space Flight Center, The 1994 27th Annual NASA Aerospace Battery Workshop Feb. 1995 p 489-491 (For primary document see N95-26785 09-44)
Avail: CASI HC A01/MF A06

N95-26794*# National Aeronautics and Space Administration. Marshall Space Flight Center, Huntsville, AL.
HUBBLE SPACE TELESCOPE NICKEL-HYDROGEN BATTERY TESTING: AN UPDATE
Thomas H. Whitt and Jeffrey C. Brewer *In its* The 1994 27th Annual NASA Aerospace Battery Workshop Feb. 1995 p 565-580 (For primary document see N95-26785 09-44)
Avail: CASI HC A03/MF A06

N95-26795*# National Aeronautics and Space Administration. Marshall Space Flight Center, Huntsville, AL.
ADIABATIC CHARGING OF NICKEL-HYDROGEN BATTERIES
Chuck Lurie (TRW, Inc., Redondo Beach, CA.), S. Foroozan (TRW, Inc., Redondo Beach, CA.), Jeff Brewer, and Lorna Jackson *In its* The 1994 27th Annual NASA Aerospace Battery Workshop Feb. 1995 p 581-598 (For primary document see N95-26785 09-44)
Avail: CASI HC A03/MF A06

N95-26796*# National Aeronautics and Space Administration. Goddard Space Flight Center, Greenbelt, MD.
ALTERNATE CHARGING PROFILES FOR THE ONBOARD NICKEL CADMIUM BATTERIES OF THE EXPLORER PLATFORM/EXTREME ULTRAVIOLET EXPLORER
Gopalakrishna M. Rao and Jill S. Prettyman-Lukoschek *In* NASA. Marshall Space Flight Center, The 1994 27th Annual NASA Aerospace Battery Workshop Feb. 1995 p 599-607 (For primary document see N95-26785 09-44)
Avail: CASI HC A02/MF A06

N95-27271*# Societe d'Applications Generales d'Electricite et de Mecanique, Paris (France).
HIGH PERFORMANCE STEPPER MOTORS FOR SPACE MECHANISMS
Patrick Sega and Christine Estevenon *In* NASA. Johnson Space Center, The 29th Aerospace Mechanisms Symposium May 1995 p 141-146 Sponsored by CNES (For primary document see N95-27260 09-15)
Avail: CASI HC A02/MF A04

N95-27272*# Schaeffer Magnetics, Inc., Chatsworth, CA.
DEVELOPMENT OF A MINIATURE ACTUATOR/CONTROLLER SYSTEM
Scott P. Stanley *In* NASA. Johnson Space Center, The 29th Aerospace Mechanisms Symposium May 1995 p 147-151 (For primary document see N95-27260 09-15)
Avail: CASI HC A01/MF A04

N95-27278*# Honeywell, Inc., Durham, NC. Electro Components.
ELECTROMECHANICAL ROTARY ACTUATOR
S. P. Smith and W. J. McMahon *In* NASA. Johnson Space Center, The 29th Aerospace Mechanisms Symposium May 1995 p 183-192 (For primary document see N95-27260 09-15)
Avail: CASI HC A02/MF A04

N95-27354*# Dynamic Soft Analysis, Inc., Pittsburgh, PA.
CAE FOR THERMAL MANAGEMENT OF AEROSPACE ELECTRONIC BOARDS USING THE BETASOFT PROGRAM
Kimberly Bobish *In* NASA. Lewis Research Center, The Sixth Annual Thermal and Fluids Analysis Workshop Jan. 1995 p 133-140 (For primary document see N95-27345 09-34)
Avail: CASI HC A02/MF A03

N95-27635*# National Aeronautics and Space Administration. Marshall Space Flight Center, Huntsville, AL.
INFLIGHT RESISTANCE MEASUREMENT ON HIGH-T(SUB c) SUPERCONDUCTING THIN FILMS EXPOSED TO ORBITAL ATOMIC OXYGEN ON CONCAP-2 (STS-46)
J. C. Gregory (Alabama Univ., Huntsville, AL.), G. N. Raiker (Alabama Univ., Huntsville, AL.), J. A. Bijvoet (Alabama Univ., Huntsville, AL.), P. D. Nerren (Alabama Univ., Huntsville, AL.), W. T. Sutherland, A. Mogro-Camperso (General Electric Co., Schenectady, NY.), L. G. Turner (General Electric Co., Schenectady, NY.), Hoi Kwok (State Univ. of New York, Buffalo, NY.), I. D. Raistrick (Lockheed Engineering and Sciences Co., Houston, TX.), and J. B. Cross (Lockheed Engineering and Sciences Co., Houston, TX.) et al *In* NASA. Langley Research Center, LDEF: 69 Months in Space. Third Post-Retrieval Symposium, Part 3 Feb. 1995 p 971-988 (For primary document see N95-27629 09-99)
Avail: CASI HC A03/MF A04

N95-27984*# Power Technologies, Inc., Schenectady, NY.
ANALYSIS METHODS FOR WIND TURBINE CONTROL AND ELECTRICAL SYSTEM DYNAMICS
E. N. Hinrichsen *In* DASCON Engineering, Collected Papers on Wind Turbine Technology May 1995 p 153-156 (For primary document see N95-27970 09-44)
Avail: CASI HC A01/MF A03

N95-27987*# Electrotek Concepts, Inc., Knoxville, TN.
A CONCEPTUAL FRAMEWORK FOR EVALUATING VARIABLE SPEED GENERATOR OPTIONS FOR WIND ENERGY APPLICATIONS
T. W. Reddoch, T. A. Lipo (Wisconsin Univ., Madison, WI.), E. N. Hinrichsen (Power Technologies, Inc., Schenectady, NY.), T. L. Hudson (Oak Ridge National Lab., TN.), and R. J. Thomas (Cornell Univ., Ithaca, NY.) *In* DASCON Engineering, Collected Papers on Wind Turbine Technology May 1995 p 185-190 Sponsored by DOE (For primary document see N95-27970 09-44)
Avail: CASI HC A02/MF A03

N95-27988*# Wisconsin Univ., Madison, WI. Dept. of Electrical and Computer Engineering.
VARIABLE SPEED GENERATOR TECHNOLOGY OPTIONS FOR WIND TURBINE GENERATORS
T. A. Lipo *In* DASCON Engineering, Collected Papers on Wind Turbine Technology May 1995 p 191-197 (For primary document see N95-27970 09-44)
Avail: CASI HC A02/MF A03

N95-27989*# General Electric Co., Philadelphia, PA.
VARIABLE SPEED GENERATOR APPLICATION ON THE MOD-5A 7.3 mW WIND TURBINE GENERATOR
Robert S. Barton *In* DASCON Engineering, Collected Papers on Wind Turbine Technology May 1995 p 199-210 Presented at the DOE/NASA Workshop on Horizontal Axis Wind Turbine Technology, Cleveland, OH, 8-10 May 1984 (For primary document see N95-27970 09-44)
Avail: CASI HC A03/MF A03

34 FLUID MECHANICS AND HEAT TRANSFER

Includes boundary layers; hydrodynamics; fluidics; mass transfer; and ablation cooling.

For related information see also *02 Aerodynamics* and *77 Thermodynamics and Statistical Physics.*

N95-26380*# National Aeronautics and Space Administration. Lewis Research Center, Cleveland, OH.
A FULLY IMPLICIT TIME ACCURATE METHOD FOR HYPERSONIC COMBUSTION: APPLICATION TO SHOCK-INDUCED COMBUSTION INSTABILITY
Shaye Yungster and Krishnan Radhakrishnan (NYMA, Inc., Brook Park, OH.) Aug. 1994 16 p Presented at the 30th Joint Propulsion Conference, Indianapolis, IN, 27-29 Jun. 1994; cosponsored by AIAA, ASME, SAE, and ASEE
(Contracts NAS3-27186; NCC3-233; RTOP 505-90-5K)
(NASA-TM-106707; ICOMP-94-18; E-9069; NAS 1.15:106707; AIAA Paper 94-2965) Avail: CASI HC A03/MF A01

A new fully implicit, time accurate algorithm suitable for chemically reacting, viscous flows in the transonic-to-hypersonic regime is described. The method is based on a class of Total Variation Diminishing (TVD) schemes and uses successive Gauss-Siedel relaxation sweeps. The inversion of large matrices is avoided by partitioning the system into reacting and nonreacting parts, but still maintaining a fully coupled interaction. As a result, the matrices that have to be inverted are of the same size as those obtained with the commonly used point implicit methods. In this paper we illustrate the applicability of the new algorithm to hypervelocity unsteady combustion applications. We present a series of numerical simulations of the periodic combustion instabilities observed in ballistic-range experiments of blunt projectiles flying at subdetonative speeds through hydrogen-air mixtures. The computed frequencies of oscillation are in excellent agreement with experimental data. Author

N95-26405 New York Univ., New York, NY. Inst. of Mathematical Sciences.
COMPUTATIONAL FLUID DYNAMICS AND TRANSONIC FLOW Final Technical Report, 1 Oct. 1990 - 30 Sep. 1994
Paul R. Garabedian 31 Oct. 1994 6 p Limited Reproducibility: More than 20% of this document may be affected by microfiche quality
(Grant AF-AFOSR-0042-91)
(AD-A288962; AFOSR-94-0760TR) Avail: Issuing Activity (Defense Technical Information Center (DTIC))

The project was concerned with the development of high performance computer codes for problems in transonic aerodynamics. A practical rule to calculate the wave drag for solutions of the Euler equations was developed from an entropy equality. Symmetric shockless airfoils were analyzed for which uniqueness fails in the transonic case not just for potential flow, but also for the Euler equations. DTIC

N95-26418 Wright Lab., Wright-Patterson AFB, OH.
A NON-ITERATIVE GRID DEFORMATION ALGORITHM FOR COMPUTATIONAL FLUID DYNAMICS FOR AEROELASTICITY Interim Report, Jun. - Jul. 1994
Richard D. Synder Sep. 1994 25 p Limited Reproducibility: More than 20% of this document may be affected by microfiche quality
(AF Proj. 2401)
(AD-A288298; WL-TM-94-3130) Avail: Issuing Activity (Defense Technical Information Center (DTIC))

This Technical Memorandum presents an algorithm for deforming a two- or three-dimensional aerodynamic grid given deflections on a physical boundary. This algorithm is to be used in coupling a computational fluid dynamics code with a computational structural mechanics code. The deformation algorithm was tested successfully on both two- and three-dimensional grids. The method sufficiently maintains grid quality for smooth deflections of realistic orders of magnitude. The method is computationally efficient: the time required to deform the grid is small compared to the time required to solve the fluid dynamics. DTIC

N95-26445# Iowa State Univ. of Science and Technology, Ames, IA.
A FIXED TIME PERFORMANCE EVALUATION OF PARALLEL CFD APPLICATIONS
A. M. Baker and S. X. Ying (Ames Lab., IA.) 1994 14 p Presented at the Supercomputing '94 Meeting, Washington, DC, 14-18 Nov. 1994
(Contract W-7405-eng-82)
(DE94-014240; IS-M-790; CONF-941118-3) Avail: CASI HC A03/MF A01

The inviscid gas dynamics equations have been solved on the nCUBE 2s computer to better understand the challenges and opportunities that parallel processing presents. Two basic computational fluid dynamics applications problems representing different flow physics are used as test cases. The first problem involves a supersonic flow inside a channel with a ramp surface. This internal flow problem is dominated by large gradients due to shock waves reflected between channel walls. The equations solved are coupled nonlinear hyperbolic partial differential equations. The second problem is an external flow over airfoil. The flow is subsonic, resulting in a set of elliptic pdes. Analysis of the parallel performance for these applications is presented following a fixed time measurement approach. The results from this study demonstrate that even though these flow simulation problems are communication intensive, they are scalable. This is true even if subdomain communication includes non-nearest neighbors. Parallel computing is shown to be an effective tool for future CFD challenges. DOE

N95-26576*# Institute for Computer Applications in Science and Engineering, Hampton, VA.
WAVENUMBER SELECTION FOR SMALL-WAVELENGTH GOERTLER VORTICES IN CURVED CHANNEL FLOWS Final Report
Andrew Dando (Manchester Univ., England.) and Philip Hall (Manchester Univ., England.) Apr. 1995 29 p Submitted for publication
(Contract NAS1-19480; RTOP 505-90-52-01)
(NASA-CR-195063; NAS 1.26:195063; ICASE-95-21) Avail: CASI HC A03/MF A01

The problem of wavenumber selection for fully nonlinear, small-wavelength Goertler vortices in a curved channel flow is considered. These types of Goertler vortices were first considered by Hall & Lakin

(1988) for an external boundary layer flow. They proved particularly amenable to asymptotic description, it was possible to consider vortices large enough so that the mean flow correction driven by them is as large as the basic state, and this prompted the authors to consider them in a curved channel flow as an initial application of the phase-equation approach to Goertler vortices. This involves the assumption that the phase variable of these Goertler vortices varies on slow spanwise and time scales, then an analysis of both inside and outside the core region, to which vortex activity is restricted, leads to a system of partial differential equations which can be solved numerically for the wavenumber. The authors consider in particular the effect on the wavenumber of the outer channel wall varying on the same slow spanwise scale as the phase variable. Author

N95-26588*# MCAT Inst., San Jose, CA.
ALGORITHMS FOR PARALLEL FLOW SOLVERS ON MESSAGE PASSING ARCHITECTURES Final Report
Rob F. VanderWijngaart Jan. 1995 32 p Original contains color illustrations
(Contract NCC2-752)
(NASA-CR-197758; NAS 1.26:197758; MCAT-95-15) Avail: CASI HC A03/MF A01; 1 functional color page

The purpose of this project has been to identify and test suitable technologies for implementation of fluid flow solvers -- possibly coupled with structures and heat equation solvers -- on MIMD parallel computers. In the course of this investigation much attention has been paid to efficient domain decomposition strategies for ADI-type algorithms. Multi-partitioning derives its efficiency from the assignment of several blocks of grid points to each processor in the parallel computer. A coarse-grain parallelism is obtained, and a near-perfect load balance results. In uni-partitioning every processor receives responsibility for exactly one block of grid points instead of several. This necessitates fine-grain pipelined program execution in order to obtain a reasonable load balance. Although fine-grain parallelism is less desirable on many systems, especially high-latency networks of workstations, uni-partition methods are still in wide use in production codes for flow problems. Consequently, it remains important to achieve good efficiency with this technique that has essentially been superseded by multi-partitioning for parallel ADI-type algorithms. Another reason for the concentration on improving the performance of pipeline methods is their applicability in other types of flow solver kernels with stronger implied data dependence. Analytical expressions can be derived for the size of the dynamic load imbalance incurred in traditional pipelines. From these it can be determined what is the optimal first-processor retardation that leads to the shortest total completion time for the pipeline process. Theoretical predictions of pipeline performance with and without optimization match experimental observations on the iPSC/860 very well. Analysis of pipeline performance also highlights the effect of uncareful grid partitioning in flow solvers that employ pipeline algorithms. If grid blocks at boundaries are not at least as large in the wall-normal direction as those immediately adjacent to them, then the first processor in the pipeline will receive a computational load that is less than that of subsequent processors, magnifying the pipeline slowdown effect. Extra compensation is needed for grid boundary effects, even if all grid blocks are equally sized. Derived from text

N95-26589*# MCAT Inst., San Jose, CA.
NUMERICAL SIMULATION OF THE SOFIA FLOW FIELD Final Report
Stephen P. Klotz Jan. 1995 99 p
(Contract NCC2-636)
(NASA-CR-197757; NAS 1.26:197757; MCAT-95-08) Avail: CASI HC A05/MF A02

This report provides a concise summary of the contribution of computational fluid dynamics (CFD) to the SOFIA (Stratospheric Observatory for Infrared Astronomy) project at NASA Ames and presents results obtained from closed- and open-cavity SOFIA simulations. The aircraft platform is a Boeing 747SP and these are the first SOFIA simulations run with the aircraft empennage included in the geometry database. In the open-cavity runs the telescope is mounted behind the wings. Results suggest that the cavity markedly influences the mean pressure distribution on empennage surfaces and that 110-140 decibel (db) sound pressure levels are typical in the cavity and on the horizontal and vertical stabilizers. A strong source of sound was found to exist on the rim of the open telescope cavity. The presence of this source suggests that additional design work needs to be performed in order to minimize the sound emanating from that location. A fluid dynamic analysis of the engine plumes is also contained in this report. The analysis was part of an effort to quantify the degradation of telescope performance resulting from the proximity of the port engine exhaust plumes to the open telescope bay. Author

N95-26665*# MCAT Inst., San Jose, CA.
TURBULENCE MODELING Final Annual Report
Jorge E. Bardina Feb. 1995 74 p Original contains color illustrations
(Contract NCC2-585)
(NASA-CR-197751; NAS 1.26:197751; MCAT-95-04) Avail: CASI HC A04/MF A01; 1 functional color page

The objective of this work is to develop, verify, and incorporate the baseline two-equation turbulence models which account for the effects of compressibility into the three-dimensional Reynolds averaged Navier-Stokes (RANS) code and to provide documented descriptions of the models and their numerical procedures so that they can be implemented into 3-D CFD codes for engineering applications. Derived from text

N95-26718 Air Force Systems Command, Wright-Patterson AFB, OH. National Air Intelligence Center.
SUPG FINITE NUMERICAL ELEMENT SOLUTIONS FOR NON-COMPRESSIBLE NAVIER-STOKES EQUATION SETS
Guoqun Xu and Guofu Zhang 15 Nov. 1994 17 p Transl. into ENGLISH from Kongqidonglixue Xuebao (China), v. 9, no. 3, Sep. 1991 p 372-378 Limited Reproducibility: More than 20% of this document may be affected by microfiche quality
(AD-A289600; NAIC-ID(RS)T-0917-92) Avail: Issuing Activity (Defense Technical Information Center (DTIC))

This article sets out from steady state non-compressible Navier-Stokes equation sets and constructs weighted residual SUPG formulations. In order to guarantee the precision of numerical value solutions, this article -- with regard to speeds -- selects eight points for the interpolation of values and maintains the second order derivative quantities in perturbation terms. Looking from the point of view of calculation instances made using the methods of this article, the calculated results have proved very satisfying. DTIC

N95-26739# Tokyo Univ., Sagamihara (Japan). Inst. of Space and Astronautical Science.
VISCOUS SHOCK-LAYER ANALYSIS ON HYPERSONIC FLOW OVER REENTRY CAPSULE WITH NONEQUILIBRIUM CHEMISTRY
Kojiro Suzuki and Takashi Abe Dec. 1994 20 p Repr. from Institute of Space and Astronautical Science Report No. 656 (Sagamihara, Japan, Tokyo Univ.), Dec. 1994 p 1-17
(ISSN 0285-6808)
(ISAS-R-656) Avail: CASI HC A03/MF A01

The aerothermodynamic environment around a 'EXPRESS' reentry capsule at hypersonic speed is studied in the flight regime of the severe wall heating rate with emphasis on the effects of the wall catalycity and temperature by using the axisymmetric viscous shock-layer equations with the seven-air-species nonequilibrium chemistry. The wall heating rate and the electron number density in the shock-layer over the capsule are predicted at various altitudes on its flight trajectory. In order to evaluate the wall catalycity, the finite catalytic wall model is introduced. The sensitivity of the wall heating rate to the uncertainties in the chemical reaction model and the wall condition model is investigated parametrically. The extent of the influences of the wall conditions on the shock-layer flow properties strongly depends on the extent of flow nonequilibrium. Author

N95-26741# Tokyo Univ., Sagamihara (Japan). Inst. of Space and Astronautical Science.
STATISTICAL MODEL FOR MOLECULAR INTERNAL ENERGY EXCHANGE IN DSMC METHOD FOR RAREFIED FLOW ANALYSIS
Takashi Abe Nov. 1994 12 p Repr. from Institute of Space and Astronautical Science Report No. 654 (Sagamihara, Japan, Tokyo Univ.), Nov. 1994 p 1-9
(ISSN 0285-6808)
(ISAS-R-654) Avail: CASI HC A03/MF A01

New statistical direct simulation Monte Carlo model for internal energy exchange for molecules is proposed. The derivation of the model is based on the inelastic collision cross section which ensures the relation of detailed balance at equilibrium between microscopic states. It is shown that the present derivation method gives us a general frame-work to generate various models for the inelastic collision. The present derivation method can generate not only the present internal energy exchange model but also the Koura's inelastic cross-section model. The present internal energy exchange model was applied to an adiabatic thermal relaxation problem in a stationary reservoir and was compared with Koura's statistical inelastic cross-section model. Author

N95-26742# Tokyo Univ., Sagamihara (Japan). Inst. of Space and Astronautical Science.
ANOMALOUS COLLISION RATE IN THE TIME COUNTER SCHEME OF THE DIRECT SIMULATION MONTE CARLO METHOD FOR RAREFIED GAS FLOW ANALYSIS
Takashi Abe Nov. 1994 17 p Repr. from Institute of Space and Astronautical Science Report No. 653 (Sagamihara, Japan, Tokyo Univ.), Nov. 1994 p 1-14
(ISSN 0285-6808)
(ISAS-R-653) Avail: CASI HC A03/MF A01

In the direct simulation Monte Carlo method (DSMC), it is shown that a widely used time counter (TC) scheme proposed by Bird gives inaccurate results for certain non-equilibrium distribution functions. The functions are defined in the text and include as an extreme case the distribution function of the cold counter-streaming flow. When the TC scheme is applied to these distribution functions it results in counting a rate of collision too largely, and there is consequently a corresponding error in advancing the simulation time. This effect appears in functions which differ from the equilibrium one by more than a certain threshold amount. The threshold is shown to depend on the number of particles being simulated, and increases with their number. That is, the applicability of the TC scheme increases with particle numbers. A new scheme based on the collision rate is proposed to overcome the difficulty with the TC scheme. The CPU time of the new scheme is proportional to the particle numbers and is comparable to both the TC scheme and the no-time counter scheme in computation efficiency. Author

N95-26751 New Mexico State Univ., Las Cruces, NM. Dept. of Mechanical Engineering.
DEMONSTRATION STUDY OF HIERARCHICAL CONTROL OF FLUID-DYNAMIC PHENOMENA Final Report
Gregory A. Reynolds and Edward Hensel 20 Dec. 1994 25 p Limited Reproducibility: More than 20% of this document may be affected by microfiche quality
(Contract N00014-89-J-3018)
(AD-A289341) Avail: Issuing Activity (Defense Technical Information Center (DTIC))

This document is a final report for ONR grant N00014-89-J-3018, 'Demonstration Study of Hierarchical Control of Fluid-Dynamic Phenomena.' Our overall objective was to develop a laboratory experiment wherein the performance of a fluid dynamic process would be effectively controlled using a model-based system controller. We considered, as a sample fluid-dynamic process, the flow over a high-lift circulation-control wing. The essence of our model-based approach was a progression of fluid-dynamic models corresponding to the expected range of complexity in the attached and separated flow of the experiment. Development of the demonstration involved both fabrication and testing of the high-lift wing model and test apparatus, as well as coding and evaluation of the control algorithms and fluid-dynamic models. preparatory to this development, a flow facility in which to conduct the experiments had to be designed and constructed. Unfortunately, due to delays in completion of this facility, the demonstration experiments could not be carried out within the budget of the grant. Our overall objective was therefore not met, however, we will report here on the substantial progress we did make to establish the capabilities cited above. DTIC

N95-26766*# MCAT Inst., San Jose, CA.
PROGRESS IN INCOMPRESSIBLE NAVIER-STOKES COMPUTATIONS FOR PROPULSION FLOWS AND ITS DUAL-USE APPLICATIONS Final Report
Cetin Kiris Jan. 1995 37 p Original contains color illustrations
(Contract NCC2-500)
(NASA-CR-197746; NAS 1.26:197746; MCAT-95-02) Avail: CASI HC A03/MF A01; 7 functional color pages

Development of an incompressible Navier-Stokes solution procedure was performed for the analysis of a liquid rocket engine pump components and for the mechanical heart assist devices. The solution procedure for the propulsion systems is applicable to incompressible Navier-Stokes flows in a steadily rotating frame of reference for any general complex configurations. The computer codes were tested on different complex configurations such as liquid rocket engine inducer and impellers. As a spin-off technology from the turbopump component simulations, the flow analysis for an axial heart pump was conducted. The baseline Left Ventricular Assist Device (LVAD) design was improved by adding an inducer geometry by adapting from the liquid rocket engine pump. The time-accurate mode of the incompressible Navier-Stokes code was validated with flapping foil experiment by using different domain decomposition methods. In the flapping foil experiment, two upstream NACA 0025 foils perform high-frequency synchronized motion and generate unsteady flow conditions for a downstream larger stationary foil. Fairly good agreement was obtained between unsteady experimental data and numerical results from two different moving boundary procedures. Incompressible Navier-Stokes code (INS3D) has been extended for heat transfer applications. The temperature equation was written for both forced and natural convection phenomena. Flow in a square duct case was used for the validation of the code in both natural and forced convection. Author

N95-26776*# MCAT Inst., San Jose, CA.
DIRECT NUMERICAL SIMULATION OF TRANSITIONAL AND TURBULENT FLOW OVER A HEATED FLAT PLATE USING FINITE-DIFFERENCE SCHEMES Final Report, Aug. 1993 - Jan. 1995
Nateri K. Madavan Jan. 1995 30 p Original contains color illustrations
(Contract NCC2-755)
(NASA-CR-197753; NAS 1.26:197753; MCAT-95-16) Avail: CASI HC A03/MF A01; 2 functional color pages

This report deals with the direct numerical simulation of transitional and turbulent flow at low Mach numbers using high-order-accurate finite-difference techniques. A computation of transition to turbulence of the spatially-evolving boundary layer on a heated flat plate in the presence of relatively high freestream turbulence was performed. The geometry and flow conditions were chosen to match earlier experiments. The development of the momentum and thermal boundary layers was documented. Velocity and temperature profiles, as well as distributions of skin friction, surface heat transfer rate, Reynolds shear stress, and turbulent heat flux, were shown to compare well with experiment. The results indicate that the essential features of the transition process have been captured. The numerical method used here can be applied to complex geometries in a straightforward manner. Author (revised)

N95-26809# Cambridge Univ., Cambridge (England). Dept. of Engineering.
THE STABILITY OF THE FLOW IN A LAMINAR SEPARATION BUBBLE Thesis
Tai Ran Niew Sep. 1993 204 p Sponsored by St. John's College and Rolls Royce plc.
(ISSN 0309-7293)
(CUED/A-AERO/TR-22) Avail: CASI HC A10/MF A03

This dissertation reports a study into the underlying concepts used to analyze incompressible laminar separation bubbles. The suggestion that absolute instability could play a role in bubble flows was further developed, and was the focal point of this project. From a review of previous work and preliminary experiments on a backward faxing step, it was suggested that for some bubbles the reattachment region of the flow field could be absolutely unstable. A cornerstone of this view is that the completion of transition is not a prerequisite for the start of reattachment; and that a more fundamental mechanism involves significant interaction between the two processes. This concept was first tested by solving the eigenvalue problem of the Orr-Sommerfeld equation for a family of reverse flow profiles. The results indicated that with sufficient reverse flow, wall-bounded separated shear-layers that are similar to experimentally measured profiles can be absolutely unstable. This is consistent with the hypothesis outlined above. The numerical study also showed that for convectively unstable profiles, the predominant parameter that determines the spatial growth rate of instability waves is the distance of the separated shear layer from the wall. Furthermore, viscosity only has a weak effect on the stability characteristics of both absolutely and convectively unstable profiles at generic bubble Reynolds numbers. Experiments were then carried out on the flow behind a backward facing step using artificially excited instability waves, and the key issues in formulating a conceptually robust experimental method to test the above hypothesis was discussed. If the forcing was carried out with a non-acoustic source, it was shown that the use of impulse excitation could provide a rigorous procedure. Two qualitatively different transition mechanisms, 'wave' and 'spot' type, were also observed in these experiments. A new perspective of bubble behavior was then developed that considered the interaction of turbulent breakdown, reattachment and inducing of reverse flow. The concept of the absolutely unstable reattachment region is an integral part of this view, and the analysis was used to account for the different breakdown processes detected. Based on this alternative framework for analyzing bubble flows, a comprehensive list of fresh areas for future research was also suggested. Derived from text

N95-26819 Air Force Inst. of Tech., Wright-Patterson AFB, OH. School of Engineering.

ANALYSIS OF HYPERSONIC BOUNDARY LAYER SECOND MODE INSTABILITY OVER A 7 DEG CONE M.S. Thesis

Richard A. Dennery Dec. 1994 93 p Limited Reproducibility: More than 20% of this document may be affected by microfiche quality
(AD-A289471; AFIT/GA/ENY/94D-20) Avail: Issuing Activity (Defense Technical Information Center (DTIC))

This paper presents the results of the analysis of Mach 8.0 flow over a seven degree half-angle cone. The purpose of this analysis was to develop techniques to examine boundary layer transition at hypersonic velocities. The specific objectives were to look for second mode instability waves characteristic of the transition process and to quantify the percentage of turbulent flow. Two sets of data were used in this analysis. The first set of data was taken at several axial positions at a freestream Reynolds number 4.265 million per meter. This data was used to develop the analysis techniques. The second set of data was taken at station 35 for Reynolds numbers of 3.28, 3.94, 4.92, and 6.56 million per meter. Spectral analysis was used to identify second mode disturbances, if they existed. The energy associated with the disturbances was then removed from the data signal to produce a new signal. The new signal was then evaluated using conditional sampling techniques. Additional methods used to assess turbulent intermittency were histogram analysis and examination of the power spectrum of the data signal. It was determined that removal of the disturbances from the raw data signal produced a cleaner signal. However, the new signals were not amenable to conditional sampling techniques. The histogram analysis proved to be inconclusive. Examination of the power spectrum showed that a laminar flow could be identified by the presence of a strong peak corresponding to the second mode disturbances, but could not be used to identify a flow as being turbulent by the absence of this peak. DTIC

N95-26821 Air Force Inst. of Tech., Wright-Patterson AFB, OH. School of Engineering.

COMPRESSIBLE TURBULENCE MEASUREMENTS IN A SUPERSONIC BOUNDARY LAYER INCLUDING FAVORABLE PRESSURE GRADIENT EFFECTS M.S. Thesis

Raymond S. Miller 13 Dec. 1994 115 p Limited Reproducibility: More than 20% of this document may be affected by microfiche quality
(AD-A289475; AFIT/GAE/ENY/94D-19) Avail: Issuing Activity (Defense Technical Information Center (DTIC))

The effect of a favorable pressure gradient on the turbulent flow structure in a Mach 2.9 boundary layer (Re/m approximately equal to 1.5 x 10(exp 7)) is investigated experimentally. Conventional flow and hot film measurements of turbulent fluctuation properties have been made upstream of and along an expansion ramp. Upstream measurements were taken in a zero pressure gradient boundary layer 44 cm from the nozzle throat in a 6.35 cm square test section. Measurements are obtained in the boundary layer, above the expansion ramp, 71.5 cm from the nozzle throat. Mean flow and turbulent flow characteristics are measured in all three dimensions. Comparisons are made between data obtained using single and multiple-overheat cross-wire anemometry as well as conventional mean flow probes. Conventional flow measurements were taken using a Pitot probe and a 10 degree cone static probe. Flow visualization was conducted via imaging techniques (Schlieren and shadowgraph photographs). Results suggest that compressibility effects, as seen through the density fluctuations in the Reynolds shear stress, are roughly 10% relative to the mean velocity and are large relative to the velocity fluctuations. This is also observed in the total Reynolds shear stress; compressibility accounts for 50-75% of the total shear. This is particularly true in the favorable pressure gradient region, where though the peak fluctuation intensities are diminished, the streamwise component of the mean flow is larger, hence the contribution of the compressibility term is significant in the Reynolds shear. DTIC

N95-26822 Air Force Inst. of Tech., Wright-Patterson AFB, OH. School of Engineering.

COMPRESSIBLE TURBULENCE MEASUREMENTS IN A SUPERSONIC FLOW WITH ADVERSE PRESSURE GRADIENT M.S. Thesis

Jon W. Dotter Dec. 1994 121 p Limited Reproducibility: More than 20% of this document may be affected by microfiche quality
(AD-A289477; AFIT/GAE/ENY/94D-10) Avail: Issuing Activity (Defense Technical Information Center (DTIC))

Mean flow and compressible turbulence measurements have been obtained upstream and in the vicinity of a compression ramp in Mach 3 flow. Compressible turbulence models have met with little success in the accurate prediction of high-speed flows involving complicated shock boundary interactions and adverse pressure gradients because of a crucial lack of experimental data. Data were collected using conventional Pitot and cone static probes, single overheat cross-wire anemometry, multiple overheat cross-wire anemometry, and flow visualization techniques. Direct measurements of the total Reynolds shear stress were obtained using a turbulence transformation. Results indicate that compressibility effects, as evidenced by the density fluctuations, are large relative to the velocity fluctuations and should be accounted for rigorously in new turbulence models. DTIC

N95-26827 Notre Dame Univ., IN. Dept. of Aerospace and Mechanical Engineering.

UNSTEADY BASE PRESSURE MEASUREMENTS IN THE NEAR WAKE OF A CYLINDER WITH IMPOSED THREE-DIMENSIONAL DISTURBANCES

J. P. Borg and A. A. Szewczyk 1995 2 p Limited Reproducibility: More than 20% of this document may be affected by microfiche quality
(Contract N00014-90-J-4083)
(AD-A289498) Avail: Issuing Activity (Defense Technical Information Center (DTIC))

The effects of geometrically imposed three-dimensional disturbances that were introduced by a spanwise-periodic trailing-edge splitter plate on the instantaneous base pressure of a circular cylinder were investigated. Measurements indicate a direct coupling to the shedding frequency between the stagnation-line and base-pressure signals. A low frequency component in the base pressure power spectra was found and was directly related to the irregular shedding observed in the wake. DTIC

N95-26852 Naval Research Lab., Washington, DC.

ADDRESSING TENSION INSTABILITY IN SPH METHODS Interim Report

C. T. Dyka and R. P. Ingel 30 Dec. 1994 23 p Limited Reproducibility: More than 20% of this document may be affected by microfiche quality
(AD-A289531; NRL/MR/6384-94-7641) Avail: Issuing Activity (Defense Technical Information Center (DTIC))

Smoothed particle hydrodynamics (SPH) has the potential to be an important method for structural analysis. However, the SPH method is currently plagued by tension instability. A new unconventional approach is introduced, in which the stresses are calculated at points other than the SPH nodes, to address this difficulty. This algorithm is implemented into a one dimensional (1D) program called SPH1D. In addition, objective stress rate calculations are discussed and specialized to 1D applications. The results from applying the unconventional approach to a simple bar are very encouraging. The bar holds together in tension and compares quite well to a finite element analysis. DTIC

N95-26928# Helsinki Univ. of Technology, Espoo (Finland). Inst. of Mathematics.

CONSTRUCTION OF ARBITRARY ORDER SCHEMES FOR MANY DIMENSIONAL WAVE EQUATION

J. Tuomela Sep. 1994 34 p
(PB95-184818; RR-A336) Avail: CASI HC A03/MF A01

The authors show that it is possible to construct arbitrary order stable schemes for the homogeneous and heterogeneous wave equation in any dimension. The construction is elementary and uses formal power series techniques. We shall also calculate exact stability limits in various cases, and apparently this limit depends only on the dimension of the space. NTIS

N95-26968 Air Force Inst. of Tech., Wright-Patterson AFB, OH. School of Engineering.
EXPERIMENTAL INVESTIGATION OF THE EFFECTS OF RELATIVE PHYSICAL ORIENTATION BETWEEN EVAPORATOR AND CONDENSER FOR A LOOP HEAT PIPE M.S. Thesis
Brad R. Thompson Dec. 1994 83 p Limited Reproducibility: More than 20% of this document may be affected by microfiche quality
(AD-A289248; AFIT/GA/ENY/94D-10) Avail: Issuing Activity (Defense Technical Information Center (DTIC))

This research examined the effects on performance of varying angular orientation and height differences between evaporator and condenser for a loop heat pipe. Performance was defined as the difference in temperature between evaporator and condenser (DELTA T). The pipe was evaluated at varying input power (Qin) for: varying evaporator and condenser angles, different coolant temperatures, and varying relative height differences. All analysis included only steady state operation. The performance was influenced by condenser angles, with an optimal condenser angle for best performance being +45 degrees from horizontal. Additionally, the evaporator angles were found to influence performance only at low Qin and low coolant temperatures. For high Qin' performance was independent of evaporator angle. For small Qin the DELTA T increased (poorer performance) with decreasing coolant temperature. However, for high Qin the DELTA T was independent of coolant temperature. For small Qin the DELTA T increased with increasing heights of evaporator over condenser. However, for high Qin the DELTA T was independent of the height difference. Additionally, pipe operation was sensitive to the rate of decrease of Qin. Finally, an unexplained anomaly shows the pipe to operate at two different DELTA T values for a given heat input. DTIC

N95-26986 Air Force Inst. of Tech., Wright-Patterson AFB, OH.
FLOW VISUALIZATION OF A TURBULENT SHEAR FLOW USING AN OPTICAL WAVEFRONT SENSOR M.S. Thesis
Daniel W. Jewell Dec. 1994 70 p Limited Reproducibility: More than 20% of this document may be affected by microfiche quality
(AD-A289208; AFIT/GEO/ENG/94D-04) Avail: Issuing Activity (Defense Technical Information Center (DTIC))

The research reported here investigated the use of a shearing interferometer (SI) wavefront sensor to determine the effects of shear-layer turbulence on an optical wavefront. A collimated helium-neon laser beam was propagated through a plane shear-layer produced by mixing helium and nitrogen at different velocities. Since the gases have different indices of refraction, the optical wavefront was distorted by different amounts by each gas. The SI measured the wavefront slope across the sampled area of the wavefront. The shear-layer was viewed from two orthogonal directions. This document contains shadow graphs, interference patterns imaged by each of the SI's six cameras, interferograms containing fringes with separation proportional to the wavefront slope, and phase maps showing the shape of the perturbed optical wavefronts. The side view showed an area of steep slope along the mixing area of the two gases. The slope gradually changed as the distance from the mixing layer region increased. For the top view, the peaks and valleys grew as they propagated away from the shear-layer turbulence generator. The results also indicated that the interference patterns recorded by the SI cameras provide a simple way to visualize turbulence in a manner that provides phase information about the wavefront. DTIC

N95-26995*# Syracuse Univ., NY. Dept. of Mechanical, Aerospace and Manufacturing Engineering.
THE NOISE REDUCTION POTENTIAL OF DUAL-STREAM COAXIAL RECTANGULAR IMPROPERLY EXPANDED JET FLOWS Final Report, Mar. 1991 - 1993
Darshan Dosanjh and Eric F. Spina Apr. 1995 10 p
(Grant NAG1-1240)
(NASA-CR-197820; NAS 1.26:197820) Avail: CASI HC A02/MF A01

The research performed began during Spring 1991 as a project to assess the noise reduction potential of rectangular coaxial nozzle configurations for improperly expanded jets. The research plan consisted of: (1) design of coaxial rectangular nozzle configuration by Syracuse graduate research assistant; (2) construction of nozzles by NASA Langley machinists; and (3) acquisition of preliminary acoustic and optical data for a variety of inner and outer jet pressure ratios. Author

N95-26998 Houston Univ., TX. Dept. of Mechanical Engineering.
BASIC STUDIES IN TURBULENT SHEAR FLOWS Summary Report, Fiscal Year 1994
Fazle Hussain 1994 33 p Limited Reproducibility: More than 20% of this document may be affected by microfiche quality
(Contract N00014-89-J-1361)
(AD-A289145) Avail: Issuing Activity (Defense Technical Information Center (DTIC))

The goal of this research is to understand the underlying physics of turbulence phenomena through coherent structures (CS). The aim is not only to understand the flow physics but also to devise methods for turbulence prediction and control. Our approach utilizes experiment, numerics, and theory to understand both CS dynamics and structure. CS are studied in two ways: (1) long-time, global dynamics using experimental data and dynamical systems theory and (2) crucial, localized CS interactions understood via vorticity dynamics. Below, we have summarized results in several key areas: (1) global dynamics in a forced plane mixing layer (2) ODE models for spatially developing free shear flows, (3) core dynamics and transition in a plane mixing layer, (4) vorticity and helicity statistics in a circular jet, (5) new approaches to identifying sources of jet noise, and (6) the kinematic separation of homogeneous mixtures. DTIC

N95-26999 Colorado Univ., Boulder, CO.
NONLINEAR PROBLEMS IN FLUID DYNAMICS AND INVERSE SCATTERING: PROPAGATION AND CAPTURING OF SINGULARITIES IN PROBLEMS OF FLUID DYNAMICS AND INVERSE SCATTERING Final Report, 1 Sep. 1991 - 31 Dec. 1994
Gregory Beylkin 21 Dec. 1994 5 p Limited Reproducibility: More than 20% of this document may be affected by microfiche quality
(Contract N00014-91-J-4037)
(AD-A289146) Avail: Issuing Activity (Defense Technical Information Center (DTIC))

Research investigations addressed problems of solving PDE's using orthonormal bases with controlled localization in the time-frequency domain (e.g. wavelets). We have developed a number of fast algorithms and started investigations in several new areas. Among the results is the unequally spaced fast Fourier transform (USFFT) algorithm and a new approach to numerical homogenization. Derived from text

N95-27000 Stanford Univ., CA. Center for Materials Research.
GROWTH AND EVALUATION OF NONLINEAR OPTICAL CRYSTALS FOR LASER APPLICATIONS: LITHIUM BORATE, BARIUM BORATE AND SILVER GALLIUM SELENIDE Final Technical Report, 1 Aug. 1990 - 30 Jun. 1994
Robert S. Feigelson and Roger K. Route 8 Dec. 1994 96 p Limited Reproducibility: More than 20% of this document may be affected by microfiche quality
(Contract N00014-90-J-4092)
(AD-A289147) Avail: Issuing Activity (Defense Technical Information Center (DTIC))

This report summarizes a four year program on the development of high efficiency nonlinear optical materials. Major achievements were the development of effective top-seeded solution growth techniques for beta-barium borate (BBO) and lithium triborate (LBO). BBO crystals were also grown for the first time in the US by the direct melt growth technique, a metastable method that leads to significantly higher growth rates than the commercial solution-growth technique. High quality crystals were made available for optical property determinations and nonlinear optical device development at government and commercial laboratories. Additional accomplishments involved development of an optimum heat-treatment technology for eliminating optical scattering centers from as-grown crystals of silver gallium selenide. Cooperative programs were carried out with NRL to quantify the effects of intrinsic and extrinsic defects on residual absorption. It was discovered that silver gallium selenide and silver gallium sulfide crystals grown from silver-rich solutions are free of anomolous absorption in the 2 micron waveband which is currently the major problem limiting generation of high intensity, tunable 3-5 micron radiation by OPO methods using these materials. A new nonlinear optical material, (La,Gd)Sc3(BO3)4 has been identified for future study. DTIC

N95-27001 Colorado Superconductor, Inc., Fort Collins, CO.
NONLINEAR PROBLEMS IN FLUID DYNAMICS AND INVERSE SCATTERING: NONLINEAR WAVES AND INVERSE SCATTERING Final Report, 1 Sep. 1991 - 31 Dec. 1994
Mark J. Ablowitz 14 Dec. 1994 5 p Limited Reproducibility: More than 20% of this document may be affected by microfiche quality
(Contract N00014-91-J-4037)
(AD-A289148) Avail: Issuing Activity (Defense Technical Information Center (DTIC))

Research investigations involving the fundamental understanding and applications of nonlinear wave motion and related studies of inverse scattering and numerical computation have been carried out and a number of significant results have been obtained. A class of nonlinear wave equations which can be solved by the inverse scattering transform (IST) have been studied, including the Kadaomtsev-Petviashvili (KP) equation, the Davey-Stewartson equation, and the 2+1 Toda system. The solutions obtained by IST correspond to the Cauchy initial value problem with decaying initial data. We have also solved two important systems via the IST method: a 'Volterra' system in 2+1 dimensions and a new one dimensional nonlinear equation which we refer to as the Toda differential-delay equation. Research in computational chaos in moderate to long time numerical simulations continues. CASI

N95-27019 Colorado Univ., Boulder, CO.
NONLINEAR PROBLEMS IN FLUID DYNAMICS AND INVERSE SCATTERING: LANGMUIR CIRCULATIONS AND SPIRAL FLOWS Final Report, 1 Sep. 1991 - 30 Nov. 1994
Duane P. Sather 30 Nov. 1994 4 p Limited Reproducibility: More than 20% of this document may be affected by microfiche quality
(Contract N00014-91-J-4037)
(AD-A289194; CU-1534648) Avail: Issuing Activity (Defense Technical Information Center (DTIC))

Research investigations on the interaction of surface waves, wind, and currents in stratified ocean layers have been carried out. The research program involves the development of appropriate models for general physical situations (e.g., systems of coupled nonlinear partial differential equations) as well as the analysis of these models for certain specific problems such as Langmuir circulations and double-diffusive convection. During the period of the report, six papers were published and two papers were accepted for publication. Some of the results obtained and the methods used in these papers are outlined in this report. DTIC

N95-27027*# Institute for Computer Applications in Science and Engineering, Hampton, VA.
UNSTRUCTURED MESH GENERATION AND ADAPTIVITY Final Report
D. J. Mavriplis Apr. 1995 48 p
(Contract NAS1-19480; RTOP 505-90-52-01)
(NASA-CR-195069; NAS 1.26:195069; ICASE-95-26) Avail: CASI HC A03/MF A01

An overview of current unstructured mesh generation and adaptivity techniques is given. Basic building blocks taken from the field of computational geometry are first described. Various practical mesh generation techniques based on these algorithms are then constructed and illustrated with examples. Issues of adaptive meshing and stretched mesh generation for anisotropic problems are treated in subsequent sections. The presentation is organized in an education manner, for readers familiar with computational fluid dynamics, wishing to learn more about current unstructured mesh techniques. Author

N95-27028*# Institute for Computer Applications in Science and Engineering, Hampton, VA.
ON THE NONLINEAR STABILITY OF THE UNSTEADY, VISCOUS FLOW OF AN INCOMPRESSIBLE FLUID IN A CURVED PIPE Final Report
Trudi A. Shortis (Manchester Univ., England.) and Philip Hall (Manchester Univ., England.) Apr. 1995 24 p
(Contract NAS1-19480; RTOP 505-90-52-01)
(NASA-CR-195065; NAS 1.26:195065; ICASE-95-23) Avail: CASI HC A03/MF A01

The stability of the flow of an incompressible, viscous fluid through a pipe of circular cross-section curved about a central axis is investigated in a weakly nonlinear regime. A sinusoidal pressure gradient with zero mean is imposed, acting along the pipe. A WKBJ perturbation solution is constructed, taking into account the need for an inner solution in the vicinity of the outer bend, which is obtained by identifying the saddle point of the Taylor number in the complex plane of the cross-sectional angle co-ordinate. The equation governing the nonlinear evolution of the leading order vortex amplitude is thus determined. The stability analysis of this flow to periodic disturbances leads to a partial differential system dependent on three variables, and since the differential operators in this system are periodic in time, Floquet theory may be applied to reduce this system to a coupled infinite system of ordinary differential equations, together with homogeneous uncoupled boundary conditions. The eigenvalues of this system are calculated numerically to predict a critical Taylor number consistent with the analysis of Papageorgiou. A discussion of how nonlinear effects alter the linear stability analysis is also given, and the nature of the instability determined. Author

N95-27047 Virginia Polytechnic Inst. and State Univ., Blacksburg, VA.
[TWO-LAYER OR FREE SURFACE SHEAR FLOWS AND VISCOELASTIC SHEAR FLOWS AND THE RELATIONSHIP BETWEEN STABILITY AND EIGENVALUES]
1995 5 p Limited Reproducibility: More than 20% of this document may be affected by microfiche quality
(Contract N00014-92-J-1664)
(AD-A289510) Avail: Issuing Activity (Defense Technical Information Center (DTIC))

Work on the following topics is summarized: two-layer or free surface shear flows; viscoelastic shear flows and the relationship between stability and eigenvalues; convection flows; problems with open boundaries; viscoelastic flow near corners; breakup of viscoelastic jets; and spreading of surfactants. CASI

N95-27065 Air Force Inst. of Tech., Wright-Patterson AFB, OH. School of Engineering.
THE EFFECTS OF TRANSVERSE VIBRATION ON THE PERFORMANCE OF AN AXIAL GROOVE WICK HEAT PIPE M.S. Thesis
Kenneth A. Carpenter Dec. 1994 110 p Limited Reproducibility: More than 20% of this document may be affected by microfiche quality
(AD-A289349; AFIT/GA/ENY/94D-5) Avail: Issuing Activity (Defense Technical Information Center (DTIC))

An experimental investigation was performed to determine the effects of transverse vibrations on the performance of an ammonia/aluminum axial groove wick heat pipe. Theoretical calculations predicted a performance degradation due to the working fluid being shaken out of the upper capillary grooves. A benchtop shaker was used to apply transverse, sinusoidal vibrations of 30, 35, and 40 Hertz, corresponding to peak acceleration amplitudes of 1.84g, 2.50g, and 3.27g, respectively. Maximum heat throughput, Q(sub max), of the vibrating heat pipe was measured. A comparison of these values and static Q(sub max) values indicated a degradation in heat pipe performance. A mean performance deterioration of 27.6 Watts was measured for the 1.84g case, an average degradation of 12.9 percent from static heat pipe performance. At 2.50g peak acceleration the degradation rose to 37.3 watts, an average decrease of 14.8 percent from static performance. An average deterioration in performance of 28.1 percent was recorded for the 3.27g case. This amounted to a mean performance degradation of 69.3 watts. The results of this investigation revealed that transverse, sinusoidal vibrations have a detrimental impact on the performance of an ammonia/axial groove wick heat pipe. Further, the performance degradation increases with increasing vibrational peak acceleration amplitude. DTIC

N95-27165*# California State Univ., Long Beach, CA.
THE CALCULATION OF THE MASS MOMENT OF INERTIA OF A FLUID IN A ROTATING RECTANGULAR TANK Final Report
[1977] 46 p

(Grant NAG2-510)
(NASA-CR-197777; NAS 1.26:197777) Avail: CASI HC A03/MF A01

This analysis calculated the mass moment of inertia of a nonviscous fluid in a slowly rotating rectangular tank. Given the dimensions of the tank in the x, y, and z coordinates, the axis of rotation, the percentage of the tank occupied by the fluid, and angle of rotation, an algorithm was written that could calculate the mass moment of inertia of the fluid. While not included in this paper, the change in the mass moment of inertia of the fluid could then be used to calculate the force exerted by the fluid on the container wall. Derived from text

N95-27175*# National Aeronautics and Space Administration. Lewis Research Center, Cleveland, OH.
AN OUTFLOW BOUNDARY CONDITION FOR AEROACOUSTIC COMPUTATIONS
M. Ehtesham Hayder and Thomas Hagstrom (New Mexico Univ., Albuquerque, NM.) May 1995 8 p Presented at the ASME Fluids Engineering Division Summer Meeting, Hilton Head Island, SC, 13-18 Aug. 1995; cosponsored by ASME, JSME, and EALA
(Contract NCC3-370; RTOP 505-90-5K)
(NASA-TM-106930; E-9651; NAS 1.15:106930; ICOMP-95-10) Avail: CASI HC A02/MF A01

A formulation of boundary condition for flows with small disturbances is presented. The authors test their methodology in an axisymmetric jet flow calculation, using both the Navier-Stokes and Euler equations. Solutions in the far field are assumed to be oscillatory. If the oscillatory disturbances are small, the growth of the solution variables can be predicted by linear theory. Eigenfunctions of the linear theory are used explicitly in the formulation of the boundary conditions. This guarantees correct solutions at the boundary in the limit where the predictions of linear theory are valid. Author

N95-27179*# Institute for Computer Applications in Science and Engineering, Hampton, VA.
ACOUSTIC FIELD IN UNSTEADY MOVING MEDIA Final Report
F. Bauer (New York Univ., New York, NY.), L. Maestrello, and L. Ting (New York Univ., New York, NY.) May 1995 48 p
(Contract NAS1-19480; RTOP 505-90-52-01)
(NASA-CR-198162; NAS 1.26:198162; ICASE-95-39) Avail: CASI HC A03/MF A01

In the interaction of an acoustic field with a moving airframe the authors encounter a canonical initial value problem for an acoustic field induced by an unsteady source distribution, q(t,x) with q equivalent to 0 for t less than or equal to 0, in a medium moving with a uniform unsteady velocity U(t)i in the coordinate system x fixed on the airframe. Signals issued from a source point S in the domain of dependence D of an observation point P at time t will arrive at point P more than once corresponding to different retarded times, Tau in the interval (0, t). The number of arrivals is called the multiplicity of the point S. The multiplicity equals 1 if the velocity U remains subsonic and can be greater when U becomes supersonic. For an unsteady uniform flow U(t)i, rules are formulated for defining the smallest number of I subdomains V(sub i) of D with the union of V(sub i) equal to D. Each subdomain has multiplicity 1 and a formula for the corresponding retarded time. The number of subdomains V(sub i) with nonempty intersection is the multiplicity m of the intersection. The multiplicity is at most I. Examples demonstrating these rules are presented for media at accelerating and/or decelerating supersonic speed. Author

N95-27197 Minnesota Univ., Minneapolis, MN. Inst. for Mathematics and Its Applications.
FLOW CONTROL Final Technical Report, 1 Oct. 1992 - 21 Dec. 1994
Avner Friedman 21 Dec. 1994 13 p Limited Reproducibility: More than 20% of this document may be affected by microfiche quality
(Contract N00014-93-1-0027)
(AD-A289262) Avail: Issuing Activity (Defense Technical Information Center (DTIC))

The objective of the workshop on Flow Control was to bring together the ever growing community of mathematicians who are addressing these problems by sophisticated numerical and analytical techniques. They used a variety of mathematical tools and the workshop provided them an opportunity for an exchange and comparison of the different approaches. The second objective met by the workshop was to identify some of the important problems, from the point of view of applications, that need to be addressed by mathematicians, including specific flow control and optimization problems of interest to engineers. Derived from text

N95-27240*# Nevada Univ., Reno, NV. Engineering Research and Development Center.
APPLICATION OF CFD TO THE ANALYSIS AND DESIGN OF HIGH-SPEED INLETS Final Report, 1 Jan. - 31 Dec. 1994
William C. Rose 25 May 1995 75 p Original contains color illustrations
(Contract NCC2-507)
(NASA-CR-198574; NAS 1.26:198574) Avail: CASI HC A04/MF A01; 15 functional color pages

Over the past seven years, efforts under the present Grant have been aimed at being able to apply modern Computational Fluid Dynamics to the design of high-speed engine inlets. In this report, a review of previous design capabilities (prior to the advent of functioning CFD) was presented and the example of the NASA 'Mach 5 inlet' design was given as the premier example of the historical approach to inlet design. The philosophy used in the Mach 5 inlet design was carried forward in the present study, in which CFD was used to design a new Mach 10 inlet. An example of an inlet redesign was also shown. These latter efforts were carried out using today's state-of-the-art, full computational fluid dynamics codes applied in an iterative man-in-the-loop technique. The potential usefulness of an automated machine design capability using an optimizer code was also discussed. Derived from text

N95-27242*# Manchester Univ. (England). Dept. of Mathematics.
NONLINEAR STABILITY OF NON-STATIONARY CROSS-FLOW VORTICES IN COMPRESSIBLE BOUNDARY LAYERS
J. S. B. Gajjar Cleveland, OH NASA May 1995 34 p
(Contract NCC3-370; RTOP 505-90-5K)
(NASA-CR-189184; E-9608; NAS 1.26:189184; ICOMP-95-7) Avail: CASI HC A03/MF A01

The nonlinear evolution of long wavelength non-stationary cross-flow vortices in a compressible boundary layer is investigated and the work extends that of Gajjar (1994) to flows involving multiple critical layers. The basic flow profile considered in this paper is that appropriate for a fully three-dimensional boundary layer with O(1) Mach number and with wall heating or cooling. The governing equations for the evolution of the cross-flow vortex are obtained and some special cases are discussed. One special case includes linear theory where exact analytic expressions for the growth rate of the vortices are obtained. Another special case is a generalization of the Bassom & Gajjar (1988) results for neutral waves to compressible flows. The viscous correction to the growth rate is derived and it is shown how the unsteady nonlinear critical layer structure merges with that for a Haberman type of viscous critical layer. Author

N95-27247*# Institute for Computer Applications in Science and Engineering, Hampton, VA.
SPECTRAL METHODS ON ARBITRARY GRIDS Final Report
Mark H. Carpenter and David Gottlieb (Brown Univ., Providence, RI.) May 1995 30 p
(Contracts NAS1-19480; RTOP 505-90-52-01; AF-AFOSR-0090-93; N00014-91-J-4016; NSF DMS-92-11820)
(NASA-CR-198158; NAS 1.26:198158; ICASE-95-37) Avail: CASI HC A03/MF A01

Stable and spectrally accurate numerical methods are constructed on arbitrary grids for partial differential equations. These new methods are equivalent to conventional spectral methods but do not rely on specific grid distributions. Specifically, we show how to implement Legendre Galerkin, Legendre collocation, and Laguerre Galerkin methodology on arbitrary grids. Author

N95-27257*# Vigyan Research Associates, Inc., Hampton, VA.
COMPUTER PROGRAM BL2D FOR SOLVING TWO-DIMENSIONAL AND AXISYMMETRIC BOUNDARY LAYERS
Venkit Iyer NASA May 1995 98 p
(Contract NAS1-19672; RTOP 537-03-23-03)
(NASA-CR-4668; NAS 1.26:4668) Avail: CASI HC A05/MF A02

This report presents the formulation, validation, and user's manual for the computer program BL2D. The program is a fourth-order-accurate solution scheme for solving two-dimensional or axisymmetric boundary layers in speed regimes that range from low subsonic to hypersonic Mach numbers. A basic implementation of the transition zone and turbulence modeling is also included. The code is a result of many improvements made to the program VGBLP, which is described in NASA TM-83207 (February 1982), and can effectively supersede it. The code BL2D is designed to be modular, user-friendly, and portable to any machine with a standard fortran77 compiler. The report contains the new formulation adopted and the details of its implementation. Five validation cases are presented. A detailed user's manual with the input format description and instructions for running the code is included. Adequate information is presented in the report to enable the user to modify or customize the code for specific applications. Author

N95-27338# Joint Inst. for Nuclear Research, Dubna (USSR). Lab. of Nuclear Problems.

DIAGNOSTIC SYSTEM CRYO-D FOR THE DETERMINATION OF PARAMETERS OF VAPOR-LIQUID CURRENTS OF THE COOLANT [DIAGNOSTICHESKAYA SISTEMA KRIO-D OPREDELENIYA PARAMETROV PAROZHIDKOSTNYKH POTOKOV KHLADOAGENTA]

Yu. G. Alenitskij, A. L. Belyaev, A. P. Buzdavin, N. L. Zaplatin, A. V. Novikov, V. I. Pryanichnikov, V. A. Saenko, and V. I. Sukhanov 1994 7 p In RUSSIAN

(DE95-608775; JINR-R-8-94-184) Avail: CASI HC A02/MF A01 (US Sales Only)

The diagnostic system 'Cryo-D' which provides measurement and control of the most important data of the two-phase coolant flow in the channels of the cryogenic circulating system, the temperature, pressure, consumption and vapor consistence, has been created and investigated. A bench test and software are prepared. The diagnostic system 'Cryo-D' is recommended for control of the two-phase helium flow in the superconducting magnetic system of the deuteron cyclotron DC-1 prototype. DOE

N95-27339# International Centre for Theoretical Physics, Trieste (Italy).

ON PERMANENT CAPILLAR-HEAVY WAVES IN CIRCULAR SHAPED CHANNELS

N. Moussa Aug. 1994 11 p

(DE95-608779; IC-94/233) Avail: CASI HC A03/MF A01 (US Sales Only)

E. Zeidler gave an existence and uniqueness proof for permanent heavy and capillar-heavy waves in circular shaped channels. Based on this proof and on a general computational method for constructing the solutions numerically given by the author, the case of permanent heavy waves in circular shaped channels was recently computed by the author. In this work the case of permanent capillar-heavy waves in circular shaped channels will be considered. DOE

N95-27345*# National Aeronautics and Space Administration. Lewis Research Center, Cleveland, OH.

THE SIXTH ANNUAL THERMAL AND FLUIDS ANALYSIS WORKSHOP

Jan. 1995 314 p Workshop held in Brook Park, OH, 15-19 Aug. 1994 rk, OH, 15-19 Aug. 1994

(NASA-CP-10161; E-9214; NAS 1.55:10161) Avail: CASI HC A14/MF A03

The Sixth Annual Thermal and Fluids Analysis Workshop consisted of classes, vendor demonstrations, and paper sessions. The classes and vendor demonstrations provided participants with the information on widely used tools for thermal and fluids analysis. The paper sessions provided a forum for the exchange of information and ideas among thermal and fluids analysis. Paper topics included advances an uses of established thermal and fluids computer codes (such as SINDA and TRASYS) as well as unique modeling techniques and applications. For individual titles, see N95-27346 through N95-27365.

N95-27346*# Missouri Univ., Rolla, MO.

EXTENSIONAL FLOW CONVECTING A REACTANT UNDERGOING A FIRST ORDER HOMOGENEOUS REACTION AND DIFFUSIONAL MASS TRANSFER FROM A SPHERE AT LOW TO INTERMEDIATE PECLET AND DAMKOHLER NUMBERS

N. Y. Shah and X. B. Reed, Jr. *In* NASA. Lewis Research Center, The Sixth Annual Thermal and Fluids Analysis Workshop Jan. 1995 p 1-23 (For primary document see N95-27345 09-34)

Avail: CASI HC A03/MF A03

Forced convective diffusion-reaction is considered for viscous axisymmetric extensional convecting velocity in the neighborhood of a sphere. For Peclet numbers in the range 0.1 less than or equal to Pe less than or equal to 500 and for Damkohler numbers increasing with increasing Pe but in the overall range 0.02 less than or equal to Da less than or equal to 10, average and local Sherwood numbers have been computed. By introducing the eigenfunction expansion c(r, Theta) = Sum of c(n)(r)P(n)(cos Theta) into the forced convective diffusion equation for the concentration of a chemical species undergoing a first order homogeneous reaction and by using properties of the Legendre functions Pn(cos Theta), the variable coefficient PDE can be reduced to a system of N + 1 second order ODEs for the radial functions c(sub n)(r), n = 0, 1, 2,..., N. The adaptive grid algorithm of Pereyra and Lentini can be used to solve the corresponding 2(N + 1) first order differential equations as a two-point boundary value problem on 1 less than or equal to r less than or equal to r(sub infinity). Convergence of the expansion for a specific value of N can thus be established and provides 'spectral' behavior as well as the full concentration field c(r, Theta). Author

N95-27347*# University of South Florida, Tampa, FL. Dept. of Mechanical Engineering.

COMPUTATION OF THREE-DIMENSIONAL MIXED CONVECTIVE BOUNDARY LAYER FLOW

Prashandt Gadepalli and Muhammad M. Rahman *In* NASA. Lewis Research Center, The Sixth Annual Thermal and Fluids Analysis Workshop Jan. 1995 p 25-36 (For primary document see N95-27345 09-34)

Avail: CASI HC A03/MF A03

The paper presents the numerical solution of heat and mass transfer during cross-flow (orthogonal) mixed convection. In this class of flow, a buoyancy-driven transport in the vertical direction and a forced convective flow in the horizontal direction results in a three-dimensional boundary layer structure adjacent to the plate. The rates of heat and mass transfer are determined by a combined influence of the two transport processes. The equations for the conservation of mass, momentum, energy, and species concentration were solved along with appropriate boundary conditions to determine the distributions of velocity components, temperature, and concentration across the thickness of the boundary layer at different locations on the plate. Results were expressed in dimensionless form using Reynolds number, Richardson number for heat transfer, Richardson number for mass transfer, Prandtl number, and Schmidt number as parameters. It was found that the transport is dominated by buoyancy at smaller vertical locations and at larger distances away from the forced convection leading edge. Effects of forced convection appeared to be very strong at smaller horizontal distances from the leading edge. The cross stream forced convection enhanced the rate of heat and mass transfer by a very significant amount. Author

N95-27348*# University of South Florida, Tampa, FL. Dept. of Mechanical Engineering.

ANALYSIS OF GAS ABSORPTION TO A THIN LIQUID FILM IN THE PRESENCE OF A ZERO-ORDER CHEMICAL REACTION

S. Rajagopalan and M. M. Rahman *In* NASA. Lewis Research Center, The Sixth Annual Thermal and Fluids Analysis Workshop Jan. 1995 p 37-52 (For primary document see N95-27345 09-34)

Avail: CASI HC A03/MF A03

The paper presents a detailed theoretical analysis of the process of gas absorption to a thin liquid film adjacent to a horizontal rotating disk. The film is formed by the impingement of a controlled liquid jet at the center of the disk and subsequent radial spreading of liquid along the disk. The chemical reaction between the gas and the liquid film can be expressed as a zero-order homogeneous reaction. The process was modeled by establishing equations for the conservation of mass, momentum, and species concentration and solving them analytically. A scaling analysis was used to determine dominant transport processes. Appropriate boundary conditions were used to solve these equations to develop expressions for the local concentration of gas across the thickness of the film and distributions of film height, bulk concentration, and Sherwood number along the radius of the disk. The partial differential equation for species concentration was solved using the separation of variables technique along with the Duhamel's theorem and the final analytical solution was expressed using confluent hypergeometric functions. Tables for eigenvalues and eigenfunctions are presented for a number of reaction rate constants. A parametric study was performed using Reynolds number, Ekman number, and dimensionless reaction rate as parameters. At all radial locations, Sherwood number increased with Reynolds number (flow rate) as well as Ekman number (rate of rotation). The enhancement of mass transfer due to chemical reaction was found to be small when compared to the case of no reaction (pure absorption), but the enhancement factor was very significant when compared to pure absorption in a stagnant liquid film. The zero-order reaction processes considered in the present investigation included the absorption of oxygen in aqueous alkaline solutions of sodiumdithionite and rhodium complex catalyzed carbonylation of methanol. Present analytical results were compared to previous theoretical results for limiting conditions, and were found to have very good agreement. Author

N95-27349*# National Aeronautics and Space Administration. Goddard Space Flight Center, Greenbelt, MD.

FEATURES AND APPLICATIONS OF THE GROOVE ANALYSIS PROGRAM (GAP)

Jentung Ku, Tu M. Nguyen (OAO Corp., Greenbelt, MD.), and Patrick J. Brennan (OAO Corp., Greenbelt, MD.) *In* NASA. Lewis Research Center, The Sixth Annual Thermal and Fluids Analysis Workshop Jan. 1995 p 53-68 (For primary document see N95-27345 09-34)
Avail: CASI HC A03/MF A03

An IBM Personal Computer (PC) version of the Groove Analysis program (GAP) was developed to predict the steady state heat transport capability of an axially grooved heat pipe for a specified groove geometry and working fluid. In the model, the capillary limit is determined by the numerical solution of the differential equation for momentum conservation with the appropriate boundary conditions. This governing equation accounts for the hydrodynamic losses due to friction in liquid and vapor flows and due to liquid/vapor shear interaction. Back-pumping in both 0-g and 1-g is accounted for in the boundary condition at the condenser end. Slug formation in 0-g and puddle flow in 1-g are also considered in the model. At the user's discretion, the code will perform the analysis for various fluid inventories (undercharge, nominal charge, overcharge, or a fixed fluid charge) and heat pipe elevations. GAP will also calculate the minimum required heat pipe wall thickness for pressure containment at design temperatures that are greater than or lower than the critical temperature of the working fluid. This paper discusses the theory behind the development of the GAP model. It also presents the many useful and powerful capabilities of the model. Furthermore, a correlation of flight test performance data and the predictions using GAP are presented and discussed. Author

N95-27350*# Lockheed Engineering and Sciences Co., Houston, TX.

VALIDATION OF THE SINDA/FLUINT CODE USING SEVERAL ANALYTICAL SOLUTIONS

John R. Keller *In* NASA. Lewis Research Center, The Sixth Annual Thermal and Fluids Analysis Workshop Jan. 1995 p 69-84 (For primary document see N95-27345 09-34)
Avail: CASI HC A03/MF A03

The Systems Improved Numerical Differencing Analyzer and Fluid Integrator (SINDA/FLUINT) code has often been used to determine the transient and steady-state response of various thermal and fluid flow networks. While this code is an often used design and analysis tool, the validation of this program has been limited to a few simple studies. For the current study, the SINDA/FLUINT code was compared to four different analytical solutions. The thermal analyzer portion of the code (conduction and radiative heat transfer, SINDA portion) was first compared to two separate solutions. The first comparison examined a semi-infinite slab with a periodic surface temperature boundary condition. Next, a small, uniform temperature object (lumped capacitance) was allowed to radiate to a fixed temperature sink. The fluid portion of the code (FLUINT) was also compared to two different analytical solutions. The first study examined a tank filling process by an ideal gas in which there is both control volume work and heat transfer. The final comparison considered the flow in a pipe joining two infinite reservoirs of pressure. The results of all these studies showed that for the situations examined here, the SINDA/FLUINT code was able to match the results of the analytical solutions. Author

N95-27351*# Air Force Inst. of Aviation Medicine, Manching (Germany).

TRANSIENT STUDIES OF G-INDUCED CAPILLARY DRYOUT AND REWET

M. K. Reagan and W. J. Bowman *In* NASA. Lewis Research Center, The Sixth Annual Thermal and Fluids Analysis Workshop Jan. 1995 p 85-105 (For primary document see N95-27345 09-34)
Avail: CASI HC A03/MF A03

A transient, one-dimensional numerical code is developed to model the liquid motion in an axial groove with square cross section. Axial variation in liquid level, shear stress and heat transfer between the groove wall and the liquid, evaporation and transient body forces are accounted for in the model. Dryout and rewet of the groove are allowed; the front location is determined numerically using conservation of mass and linear extrapolation. Several numerical test results are presented and discussed. Author

N95-27352*# National Aeronautics and Space Administration. Lewis Research Center, Cleveland, OH.

ANALYSIS OF DEVELOPING LAMINAR FLOWS IN CIRCULAR PIPES USING A HIGHER-ORDER FINITE-DIFFERENCE TECHNIQUE

Herbert J. Gladden, Ching L. Ko (Oakland Univ., Rochester, MI.), and Douglas E. Boddy (Oakland Univ., Rochester, MI.) *In its* The Sixth Annual Thermal and Fluids Analysis Workshop Jan. 1995 p 107-114 (For primary document see N95-27345 09-34)
Avail: CASI HC A02/MF A03

A higher-order finite-difference technique is developed to calculate the developing-flow field of steady incompressible laminar flows in the entrance regions of circular pipes. Navier-Stokes equations governing the motion of such a flow field are solved by using this new finite-difference scheme. This new technique can increase the accuracy of the finite-difference approximation, while also providing the option of using unevenly spaced clustered nodes for computation such that relatively fine grids can be adopted for regions with large velocity gradients. The velocity profile at the entrance of the pipe is assumed to be uniform for the computation. The velocity distribution and the surface pressure drop of the developing flow then are calculated and compared to existing experimental measurements reported in the literature. Computational results obtained are found to be in good agreement with existing experimental correlations and therefore, the reliability of the new technique has been successfully tested. Author

N95-27353*# Mississippi State Univ., Mississippi State, MS. Dept. of Mechanical Engineering.

A CASE STUDY OF VIEW-FACTOR RECTIFICATION PROCEDURES FOR DIFFUSE-GRAY RADIATION ENCLOSURE COMPUTATIONS

Robert P. Taylor and Rogelio Luck *In* NASA. Lewis Research Center, The Sixth Annual Thermal and Fluids Analysis Workshop Jan. 1995 p 115-131 (For primary document see N95-27345 09-34)
Avail: CASI HC A03/MF A03

The view factors which are used in diffuse-gray radiation enclosure calculations are often computed by approximate numerical integrations. These approximately calculated view factors will usually not satisfy the important physical constraints of reciprocity and closure. In this paper several view-factor rectification algorithms are reviewed and a rectification algorithm based on a least-squares numerical filtering scheme is proposed with both weighted and unweighted classes. A Monte-Carlo investigation is undertaken to study the propagation of view-factor and surface-area uncertainties into the heat transfer results of the diffuse-gray enclosure calculations. It is found that the weighted least-squares algorithm is vastly superior to the other rectification schemes for the reduction of the heat-flux sensitivities to view-factor uncertainties. In a sample problem, which has proven to be very sensitive to uncertainties in view factor, the heat transfer calculations with weighted least-squares rectified view factors are very good with an original view-factor matrix computed to only one-digit accuracy. All of the algorithms had roughly equivalent effects on the reduction in sensitivity to area uncertainty in this case study. Author

N95-27354*# Dynamic Soft Analysis, Inc., Pittsburgh, PA.

CAE FOR THERMAL MANAGEMENT OF AEROSPACE ELECTRONIC BOARDS USING THE BETASOFT PROGRAM c33

Kimberly Bobish *In* NASA. Lewis Research Center, The Sixth Annual Thermal and Fluids Analysis Workshop Jan. 1995 p 133-140 (For primary document see N95-27345 09-34)
Avail: CASI HC A02/MF A03

Aerospace electronic boards require special attention to thermal management due to constraints such as their need to be light, small, and maintain high power densities. Also, cooling is mainly through conductive and radiative modes with minor or negligible convective cooling. Due to these particular requirements, thermal design has become an integrated part of the electronic design process in order to avoid expensive repeat prototyping and to ensure high reliability. To achieve high speed simulations, the BETAsoft code uses semi-empirical formulations and an advanced finite difference scheme that incorporates local adaptive grids. Detailed conduction, convection and radiation heat transfer is considered. Various benchmark verifications of the software simulation compared to infrared images typically prove to be within 10% of each other. The thermal analysis of a sample avionic card in a natural convection environment is shown. Then, the individual effects of attaching metal screws to the casing, increasing radiative emissivities of the casing, increasing the conductance of the wedge lock, adding an aluminum core to the board, adding metal strips in board layers, inserting conduction pads under components, and adding heat sinks to components are demonstrated. Author

N95-27355*# Manhattan Coll., New York, NY. Dept. of Mechanical Engineering.

RTE: A COMPUTER CODE FOR ROCKET THERMAL EVALUATION

c20

Mohammad H. N. Naraghi *In* NASA. Lewis Research Center, The Sixth Annual Thermal and Fluids Analysis Workshop Jan. 1995 p 141-162 (For primary document see N95-27345 09-34)

Avail: CASI HC A03/MF A03

The numerical model for a rocket thermal analysis code (RTE) is discussed. RTE is a comprehensive thermal analysis code for thermal analysis of regeneratively cooled rocket engines. The input to the code consists of the composition of fuel/oxidant mixture and flow rates, chamber pressure, coolant temperature and pressure. dimensions of the engine, materials and the number of nodes in different parts of the engine. The code allows for temperature variation in axial, radial and circumferential directions. By implementing an iterative scheme, it provides nodal temperature distribution, rates of heat transfer, hot gas and coolant thermal and transport properties. The fuel/oxidant mixture ratio can be varied along the thrust chamber. This feature allows the user to incorporate a non-equilibrium model or an energy release model for the hot-gas-side. The user has the option of bypassing the hot-gas-side calculations and directly inputting the gas-side fluxes. This feature is used to link RTE to a boundary layer module for the hot-gas-side heat flux calculations. Author

N95-27356*# National Aeronautics and Space Administration. Langley Research Center, Hampton, VA.

EFFECT OF TURBULENCE MODELS ON CRITICALITY CONDITIONS IN SWIRLING FLOWS

Thomas B. Gatski and Robert E. Spall (University of South Alabama, Mobile, AL.) *In* NASA. Lewis Research Center, The Sixth Annual Thermal and Fluids Analysis Workshop Jan. 1995 p 163-173 (For primary document see N95-27345 09-34)

Avail: CASI HC A03/MF A03

The critical state of vortex cores downstream of vortex breakdown has been studied. Base vortical flows were computed using the Reynolds-averaged, axisymmetric Navier-Stokes equations. Standard K - epsilon, RNG and second-order Reynolds stress models were employed. Results indicate that the return to supercriticality is highly dependent on the turbulence model. The K - epsilon model predicted a rapid return of the vortex to supercritical conditions, the location of which showed little sensitivity to changes in the swirl ratio. The Reynolds stress model predicted that the vortex remains subcritical to the end of the domain for each of the swirl ratios employed, and provided results in qualitative agreement with experimental work. The RNG model produced intermediate results, with a downstream movement in the critical location with increasing swirl. Calculations for which area reductions were introduced at the exit in a subcritical flow were also performed using the Reynolds stress model. The structure of the resulting recirculation zone was altered significantly. However, when area reductions were employed within supercritical flows as predicted using the two-equation models, no significant influence on the recirculation zone was noted. Author

N95-27357*# Engineering Mechanics Research, Inc., Troy, MI.

NUMERICAL SOLUTION OF FLUID FLOW AND HEAT TRANFER PROBLEMS WITH SURFACE RADIATION

S. Ahuja and K. Bhatia *In* NASA. Lewis Research Center, The Sixth Annual Thermal and Fluids Analysis Workshop Jan. 1995 p 175-188 (For primary document see N95-27345 09-34)

Avail: CASI HC A03/MF A03

This paper presents a numerical scheme, based on the finite element method, to solve strongly coupled fluid flow and heat transfer problems. The surface radiation effect for gray, diffuse and isothermal surfaces is considered. A procedure for obtaining the view factors between the radiating surfaces is discussed. The overall solution strategy is verified by comparing the available results with those obtained using this approach. An analysis of a thermosyphon is undertaken and the effect of considering the surface radiation is clearly explained. Author

N95-27358*# Missouri Univ., Rolla, MO.

SINGLE-DROP REACTIVE EXTRACTION/EXTRACTIVE REACTION WITH FORCED CONVECTIVE DIFFUSION AND INTERPHASE MASS TRANSFER

Leonid S. Kleinman and X. B. Reed, Jr. *In* NASA. Lewis Research Center, The Sixth Annual Thermal and Fluids Analysis Workshop Jan. 1995 p 189-213 (For primary document see N95-27345 09-34)

Avail: CASI HC A03/MF A03

An algorithm has been developed for the forced convective diffusion-reaction problem for convection inside and outside a droplet by a recirculating flow field hydrodynamically coupled at the droplet interface with an external flow field that at infinity becomes a uniform streaming flow. The concentration field inside the droplet is likewise coupled with that outside by boundary conditions at the interface. A chemical reaction can take place either inside or outside the droplet or reactions can take place in both phases. The algorithm has been implemented and results are shown here for the case of no reaction and for the case of an external first order reaction, both for unsteady behavior. For pure interphase mass transfer, concentration isocontours, local and average Sherwood numbers, and average droplet concentrations have been obtained as a function of the physical properties and external flow field. For mass transfer enhanced by an external reaction, in addition to the above forms of results, we present the enhancement factor, with the results now also depending upon the (dimensionless) rate of reaction. Author

N95-27359*# University of Southern Illinois, Carbondale, IL. Dept. of Mechanical Engineering and Energy Processes

A PROBABILISTIC MODEL OF A POROUS HEAT EXCHANGER

O. P. Agrawal and X. A. Lin *In* NASA. Lewis Research Center, The Sixth Annual Thermal and Fluids Analysis Workshop Jan. 1995 p 215-226 (For primary document see N95-27345 09-34)

Avail: CASI HC A03/MF A03

This paper presents a probabilistic one-dimensional finite element model for heat transfer processes in porous heat exchangers. The Galerkin approach is used to develop the finite element matrices. Some of the submatrices are asymmetric due to the presence of the flow term. The Neumann expansion is used to write the temperature distribution as a series of random variables, and the expectation operator is applied to obtain the mean and deviation statistics. To demonstrate the feasibility of the formulation, a one-dimensional model of heat transfer phenomenon in superfluid flow through a porous media is considered. Results of this formulation agree well with the Monte-Carlo simulations and the analytical solutions. Although the numerical experiments are confined to parametric random variables, a formulation is presented to account for the random spatial variations. Author

N95-27360*# NYMA, Inc., Brook Park, OH.

TRANSITIONAL FLOW IN THIN TUBES FOR SPACE STATION FREEDOM RADIATOR

Patrick Loney and Mounir Ibrahim (Cleveland State Univ., OH.) *In* NASA. Lewis Research Center, The Sixth Annual Thermal and Fluids Analysis Workshop Jan. 1995 p 227-232 (For primary document see N95-27345 09-34)

Avail: CASI HC A02/MF A03

A two dimensional finite volume method is used to predict the film coefficients in the transitional flow region (laminar or turbulent) for the radiator panel tubes. The code used to perform this analysis is CAST (Computer Aided Simulation of Turbulent Flows). The information gathered from this code is then used to augment a Sinda85 model that predicts overall performance of the radiator. A final comparison is drawn between the results generated with a Sinda85 model using the Sinda85 provided transition region heat transfer correlations and the Sinda85 model using the CAST generated data. Author

N95-27361*# National Aeronautics and Space Administration. Lewis Research Center, Cleveland, OH. Internal Fluid Mechanics Div.

A NAVIER-STOKES BOUNDARY ELEMENT SOLVER

D. R. Reddy, O. Lafe (OLTech Corp., Chesterland, OH.), and A. H-D. Cheng (Delaware Univ., Newark, DE.) *In its* The Sixth Annual Thermal and Fluids Analysis Workshop Jan. 1995 p 233-246 (For primary document see N95-27345 09-34)

Avail: CASI HC A03/MF A03

Using global interpolation functions (GIF's) boundary element solutions are obtained for two-dimensional laminar flows. Two schemes are proposed for handling the convective terms. The first treats convection as a forcing function, and converts the flow equations to pseudo-Poisson equations. In the second scheme, some convective effect is incorporated into the fundamental solution used in constructing the pertinent integral equations. The lid-driven cavity flow is selected as the benchmark problem. Author

N95-27362*# National Aeronautics and Space Administration. Lewis Research Center, Cleveland, OH.

TURBULANCE BOUNDARY CONDITIONS FOR SHEAR FLOW ANALYSIS, USING THE DTNS FLOW SOLVER

M. Mizukami *In its* The Sixth Annual Thermal and Fluids Analysis Workshop Jan. 1995 p 247-262 (For primary document see N95-27345 09-34)

Avail: CASI HC A03/MF A03

The effects of different turbulence boundary conditions were examined for two classical flows: a turbulent plane free shear layer and a flat plate turbulent boundary layer with zero pressure gradient. The flow solver used was DTNS, an incompressible Reynolds averaged Navier-Stokes solver with k-epsilon turbulence modeling, developed at the U.S. Navy David Taylor Research Center. Six different combinations of turbulence boundary conditions at the inflow boundary were investigated: In case 1, 'exact' k and epsilon profiles were used; in case 2, the 'exact' k profile was used, and epsilon was extrapolated upstream; in case 3, both k and epsilon were extrapolated; in case 4, the turbulence intensity (I) was 1 percent, and the turbulent viscosity (mu(sub t)) was equal to the laminar viscosity; in case 5, the 'exact' k profile was used and mu(sub t) was equal to the laminar viscosity; in case 6, the I was 1 percent, and epsilon was extrapolated. Comparisons were made with experimental data, direct numerical simulation results, or theoretical predictions as applicable. Results obtained with DTNS showed that turbulence boundary conditions can have significant impacts on the solutions, especially for the free shear layer. Author

N95-27363*# European Space Agency. European Space Research and Technology Center, ESTEC, Noordwijk (Netherlands). Thermal Control and Life Support Div.

THERMAL NEUTRAL FORMAT BASED ON THE STEP TECHNOLOGY

P. Planas Almazan and J. L. LeGal (Centre National d'Etudes Spatiales, Toulouse, France.) *In* NASA. Lewis Research Center, The Sixth Annual Thermal and Fluids Analysis Workshop Jan. 1995 p 263-273 (For primary document see N95-27345 09-34)

Avail: CASI HC A03/MF A03

The exchange of models is one of the most serious problems currently encountered in the practice of spacecraft thermal analysis. Essentially, the problem originates in the diversity of computing environments that are used across different sites, and the consequent proliferation of native tool formats. Furthermore, increasing pressure to reduce the development's life cycle time has originated a growing interest in the so-called spacecraft concurrent engineering. In this context, the realization of the interdependencies between different disciplines and the proper communication between them become critical issues. The use of a neutral format represents a step forward in addressing these problems. Such a means of communication is adopted by consensus. A neutral format is not directly tied to any specific tool and it is kept under stringent change control. Currently, most of the groups promoting exchange formats are contributing with their experience to STEP, the Standard for Exchange of Product Model Data, which is being developed under the auspices of the International Standards Organization (ISO 10303). This paper presents the different efforts made in Europe to provide the spacecraft thermal analysis community with a Thermal Neutral Format (TNF) based on STEP. Following an introduction with some background information, the paper presents the characteristics of the STEP standard. Later, the first efforts to produce a STEP Spacecraft Thermal Application Protocol are described. Finally, the paper presents the currently harmonized European activities that follow up and extend earlier work on the area. Author

N95-27364*# National Aeronautics and Space Administration. Lewis Research Center, Cleveland, OH.

THE BENARD PROBLEM: A COMPARISON OF FINITE DIFFERENCE AND SPECTRAL COLLOCATION EIGEN VALUE SOLUTIONS

J. Raymond Lee Skarda, Frances E. McCaughan (Case Western Reserve Univ., Cleveland, OH.), and Nessan Fitzmaurice (Case Western Reserve Univ., Cleveland, OH.) *In its* The Sixth Annual Thermal and Fluids Analysis Workshop Jan. 1995 p 275-290 (For primary document see N95-27345 09-34)

Avail: CASI HC A03/MF A03

The application of spectral methods, using a Chebyshev collocation scheme, to solve hydrodynamic stability problems is demonstrated on the Benard problem. Implementation of the Chebyshev collocation formulation is described. The performance of the spectral scheme is compared with that of a 2nd order finite difference scheme. An exact solution to the Marangoni-Benard problem is used to evaluate the performance of both schemes. The error of the spectral scheme is at least seven orders of magnitude smaller than finite difference error for a grid resolution of N = 15 (number of points used). The performance of the spectral formulation far exceeded the performance of the finite difference formulation for this problem. The spectral scheme required only slightly more effort to set up than the 2nd order finite difference scheme. This suggests that the spectral scheme may actually be faster to implement than higher order finite difference schemes. Author

N95-27365*# Missouri Univ., Rolla, MO.

SINGLE-DROP REACTIVE EXTRACTION/EXTRACTIVE REACTION WITH FORCED CONVECTIVE DIFFUSION AND INTERPHASE MASS TRANSFER

Leonid S. Kleinman and X. B. Red, Jr. *In* NASA. Lewis Research Center, The Sixth Annual Thermal and Fluids Analysis Workshop Jan. 1995 p 291-315 (For primary document see N95-27345 09-34)

Avail: CASI HC A03/MF A03

An algorithm has been developed for time-dependent forced convective diffusion-reaction having convection by a recirculating flow field within the drop that is hydrodynamically coupled at the interface with a convective external flow field that at infinity becomes a uniform free-streaming flow. The concentration field inside the droplet is likewise coupled with that outside by boundary conditions at the interface. A chemical reaction can take place either inside or outside the droplet, or reactions can take place in both phases. The algorithm has been implemented, and for comparison results are shown here for the case of no reaction in either phase and for the case of an external first order reaction, both for unsteady behavior. For pure interphase mass transfer, concentration isocontours, local and average Sherwood numbers, and average droplet concentrations have been obtained as a function of the physical properties and external flow field. For mass transfer enhanced by an external reaction, in addition to the above forms of results, we present the enhancement factor, with the results now also depending upon the (dimensionless) rate of reaction. Author

N95-27369*# National Aeronautics and Space Administration. Lewis Research Center, Cleveland, OH.

COMPOSITE HEAT PIPE DEVELOPMENT STATUS: DEVELOPMENT OF LIGHTWEIGHT PROTOTYPE CARBON-CARBON HEAT PIPE WITH INTEGRAL FINS AND METAL FOIL LINER

Albert J. Juhasz and Richard D. Rovang (Rockwell International Corp., Canoga Park, CA.) May 1995 12 p Presented at the 9th International Heat Pipe Conference, Albuquerque, NM, 1-5 May 1995; sponsored by LANL

(RTOP 233-02-0B)
(NASA-TM-106909; E-9611; NAS 1.15:106909) Avail: CASI HC A03/MF A01

This report discusses development and proof-of-concept testing of a new lightweight carbon-carbon (C-C) space radiator heat pipe, carried out under the NASA Civil Space Technology Initiative (CSTI) High Capacity Power Program. The prototype heat pipe, equipped with a niobium-zirconium foil liner, was filled with potassium working fluid and tested for 11 hours, including startup from ambient temperature with the working fluid initially in the frozen state to near 700 K condenser temperature. Steady-state heat pipe input power during testing was facility limited to about 300 watts. Post test inspection showed the heat pipe to be in excellent condition after eight thermal cycles from ambient to steady-state operating temperature. Utilization of other liner materials and working fluids would greatly extend the spectrum of service temperatures for this technology, with potential applications ranging from small spacecraft heat rejection to aircraft and terrestrial uses. Author

N95-27454# Argonne National Lab., IL.
A NEW FINITE ELEMENT FORMULATION FOR INCOMPRESSIBLE FLOW
L. V. Curfman 1995 27 p
(Contract W-31-109-eng-38)
(DE95-007141; ANL/MCS/PP-80304) Avail: CASI HC A03/MF A01

A basic objective in computational fluid dynamics is the efficient solution of nonlinear systems of equations that arise in finite element modeling of convective-diffusive flow. The use of implicit Newton-like schemes to solve the coupled system of Navier-Stokes and continuity equations enables rapid convergence, although the well-known difficulty of indirect pressure linkage requires attention when forming the Jacobian matrices. Traditional approaches for overcoming this obstacle include reordering strategies, modification of diagonal terms, and changes of variables. In contrast, the author develops a primitive variable finite element formulation which employs an auxiliary pressure equation derived from the Navier-Stokes and continuity equations. This formulation extends the work of Rice and Schnipke, where a similar equation was developed in the context of a segregated solution method. Approximate Newton methods using the new finite element formulation are evaluated in terms of accuracy, convergence rate, and overall efficiency for flow problems with varying degrees of nonlinearity. DOE

N95-27721# California Univ., Berkeley. Lawrence Berkeley Lab, CA.
THE USE OF WAVELET TRANSFORMS IN THE SOLUTION OF TWO-PHASE FLOW PROBLEMS
G. J. Moridis, M. Nikolaou (Texas A&M Univ., College Station, TX.), and Yong You (Texas A&M Univ., College Station, TX.) Oct. 1994 10 p Presented at the Symposium on Reservoir Simulation, San Antonio, TX, 12-15 Feb. 1995
(Contract DE-AC03-76SF-00098)
(DE95-004688; LBL-36328; CONF-950206-1) Avail: CASI HC A02/MF A01

We present the use of wavelets to solve the nonlinear partial differential equation (PDE) of two-phase flow in one dimension. The wavelet transforms allow a drastically different approach in the discretization of space. In contrast to the traditional trigonometric basis functions, wavelets approximate a function not by cancellation but by placement of wavelets at appropriate locations. When an abrupt change, such as a shock wave or a spike, occurs in a function, only local coefficients in a wavelet approximation will be affected. The unique feature of wavelets is their multi-resolution analysis (MRA) property, which allows seamless investigation at any spatial resolution. The use of wavelets is tested in the solution of the one-dimensional Buckley-Leverett problem against analytical solutions and solutions obtained from standard numerical models. Two classes of wavelet bases (Daubechies and Chui-Wang) and two methods (Galerkin and collocation) are investigated. We determine that the Chui-Wang wavelets and a collocation method provide the optimum wavelet solution for this type of problem. Increasing the resolution level improves the accuracy of the solution, but the order of the basis function seems to be far less important. Our results indicate that wavelet transforms are an effective and accurate method which does not suffer from oscillations or numerical smearing in the presence of steep fronts. DOE

N95-27760*# Institute for Computer Applications in Science and Engineering, Hampton, VA.
ON THE MODULATIONAL INSTABILITY OF LARGE AMPLITUDE WAVES IN SUPERSONIC BOUNDARY LAYERS Final Report
Philip Hall (Manchester Univ., England.) and Demetrios T. Papageorgiou (New Jersey Inst. of Tech., Newark, NJ.) Apr. 1995 44 p Submitted for publication
(Contracts NAS1-19480; RTOP 505-90-52-01; F49620-94-1-0242)
(NASA-CR-195072; NAS 1.26:195072; ICASE-95-29) Avail: CASI HC A03/MF A01

The evolution of large amplitude Tollmien-Schlichting waves in a supersonic boundary layer is investigated. Disturbances which have their wavenumber and frequency slowly varying in time and space are described using a phase equation type of approach. Unlike the incompressible case we find that the initial bifurcation to a finite amplitude Tollmien-Schlichting wave is subcritical for most Mach numbers. In fact the bifurcation is only supercritical for a small range of Mach numbers and even then for only a finite range of wave propagation angles. The modulational instability of large amplitude wavetrains is considered and is shown to be governed by an equation similar to Burgers equation but with the viscous term replaced by a fractional derivative. A numerical investigation of the solution of this equation is described. It is shown that uniform wavetrains are unstable. Author

N95-27845# Los Alamos National Lab., NM.
THREE-DIMENSIONAL VISUALIZATION OF REACTIVE FLOWS IN COMPLEX GEOMETRIES
M. S. Fairfield 1995 7 p Presented at the SMS Simulation Multiconference: Simulation as a Critical Technology, Phoenix, AZ, 9-13 Apr. 1995
(Contract W-7405-eng-36)
(DE95-006332; LA-UR-95-251; CONF-950439-5) Avail: CASI HC A02/MF A01

The visualization of fluid flows has become more challenging, as recent advancements in computational methods have increased the complexity and size of simulations. Our objective is to develop a flexible flow visualization tool for fluid simulations that include the full physics and geometrical complexities found in modeling practical combustion systems, such as internal combustion engines. The challenges to flow visualization come from: (1) the large simulation output, especially when using massively parallel computers; (2) the increasingly complex geometries that include moving surfaces such as pistons and valves; (3) the complex physical phenomena in realistic problems of fuel injection, combustion fronts, boundary flows, and large scale turbulence; and (4) the numerical complexity of indirect addressing of computational elements, variable mesh connectivity, distorted elements, and moving meshes. We have developed a visualization program that addresses these complexities. The program was developed as a post-processor to the KIVA family of codes for reactive flow simulations. Because of the complexity of the KIVA codes, the visualization program is very versatile and applicable to any code with meshes of arbitrary hexahedrons. No comparable commercial visualization package could be found. To visualize the fluid flow, we use massless tracer particles that follow the movement of the fluid as determined from output files from the simulation. The movement of the tracer particles is based on a second-order spatial and temporal interpolation of the fluid velocities from successive simulation output files. The visualization program runs on a Silicon Graphics IRIS GTX workstation. DOE

N95-27854*# National Aeronautics and Space Administration. Lewis Research Center, Cleveland, OH.
TWO-PHASE FLOW RESEARCH USING THE LEARJET APPARATUS
John B. McQuillen and Eric S. Neumann May 1995 16 p
(RTOP 963-20-0C)
(NASA-TM-106814; E-9340; NAS 1.15:106814) Avail: CASI HC A03/MF A01

Low-gravity, gas-liquid flow research can be conducted aboard the NASA Lewis Learjet, the Lewis DC-9, or the Johnson Space Center KC-135. Air and water solutions serve as the test liquids in cylindrical test sections with an inner diameter of 1.27 cm and lengths up to 1.5 m. Superficial velocities range from 0.1 to 1.1 m/sec for liquids and from 0.1 to 25 m/sec for air. Flow rate, differential pressure, void fraction, film thickness, wall-shear stress, and acceleration data are measured and recorded throughout the 20 sec duration of the experiment. Flow is visualized by photographing at 400 frames with a high-speed, 16-mm camera. Author

N95-27882*# National Aeronautics and Space Administration. Lewis Research Center, Cleveland, OH.

INDUSTRY-WIDE WORKSHOP ON COMPUTATIONAL TURBULENCE MODELING

Aamir Shabbir, comp. Mar. 1995 271 p Workshop held in Cleveland, OH, 6-7 Oct. 1994; sponsored by Institute for Computational Mechanics inPropulsion; Center for Modeling of Turbulence and Transition; and Ohio Aerospace Inst.
(Contract NCC3-233; RTOP 505-90-5K)
(NASA-CP-10165; ICOMP-94-30; E-9295; NAS 1.55:10165; CMOTT-94-9)
Avail: CASI HC A12/MF A03

This publication contains the presentations made at the Industry-Wide Workshop on Computational Turbulence Modeling which took place on October 6-7, 1994. The purpose of the workshop was to initiate the transfer of technology developed at Lewis Research Center to industry and to discuss the current status and the future needs of turbulence models in industrial CFD. For individual titles, see N95-27883 through N95-27902.

N95-27883*# National Aeronautics and Space Administration. Lewis Research Center, Cleveland, OH.

TURBULENCE PROGRAM FOR PROPULSION SYSTEMS

Tsan-Hsing Shih *In its* Industry-Wide Workshop on Computational Turbulence Modeling Mar. 1995 p 1-27 (For primary document see N95-27882 09-34)
Avail: CASI HC A03/MF A03

Program goals at the Center for Modeling of Turbulence and Transition (CMOTT), NASA Lewis Research Center, are (1) to develop reliable turbulence (including bypass transition) and combustion models for complex flows in propulsion systems and (2) to integrate developed models into deliverable CFD tools for propulsion systems in collaboration with industry. This viewgraph presentation covers the following topics: development of turbulence and combustion models; collaboration with industry and technology transfer; isotropic eddy viscosity models; algebraic Reynolds stress models; scalar turbulence models; second order closure models; multiple scale k-epsilon models; and PDF modeling of turbulent reacting flows. CASI

N95-27884*# Lockheed-Fort Worth Co., Fort Worth, TX. CFD Group.

TURBULENCE MODEL DEVELOPMENT AND APPLICATION AT LOCKHEED FORT WORTH COMPANY

Brian R. Smith *In* NASA. Lewis Research Center, Industry-Wide Workshop on Computational Turbulence Modeling Mar. 1995 p 29-37 (For primary document see N95-27882 09-34)
Avail: CASI HC A02/MF A03

This viewgraph presentation demonstrates that computationally efficient k-l and k-kl turbulence models have been developed and implemented at Lockheed Fort Worth Company. Many years of experience have been gained applying two equation turbulence models to complex three-dimensional flows for design and analysis. CASI

N95-27885*# General Electric Co., Cincinnati, OH. Aircraft Engines.

A SUMMARY OF COMPUTATIONAL EXPERIENCE AT GE AIRCRAFT ENGINES FOR COMPLEX TURBULENT FLOWS IN GAS TURBINES

Ronald D. Zerkle and Chander Prakash *In* NASA. Lewis Research Center, Industry-Wide Workshop on Computational Turbulence Modeling Mar. 1995 p 39-46 (For primary document see N95-27882 09-34)
Avail: CASI HC A02/MF A03

This viewgraph presentation summarizes some CFD experience at GE Aircraft Engines for flows in the primary gaspath of a gas turbine engine and in turbine blade cooling passages. It is concluded that application of the standard k-epsilon turbulence model with wall functions is not adequate for accurate CFD simulation of aerodynamic performance and heat transfer in the primary gas path of a gas turbine engine. New models are required in the near-wall region which include more physics than wall functions. The two-layer modeling approach appears attractive because of its computational complexity. In addition, improved CFD simulation of film cooling and turbine blade internal cooling passages will require anisotropic turbulence models. New turbulence models must be practical in order to have a significant impact on the engine design process. A coordinated turbulence modeling effort between NASA centers would be beneficial to the gas turbine industry. Derived from text

N95-27886*# McDonnell-Douglas Aerospace, Saint Louis, MO.

THE APPLICABILITY OF TURBULENCE MODELS TO AERODYNAMIC AND PROPULSION FLOWFIELDS AT MCDONNELL-DOUGLAS AEROSPACE

Linda D. Kral, John A. Ladd, and Mori Mani *In* NASA. Lewis Research Center, Industry-Wide Workshop on Computational Turbulence Modeling Mar. 1995 p 47-63 (For primary document see N95-27882 09-34)
Avail: CASI HC A03/MF A03

The objective of this viewgraph presentation is to evaluate turbulence models for integrated aircraft components such as the forebody, wing, inlet, diffuser, nozzle, and afterbody. The one-equation models have replaced the algebraic models as the baseline turbulence models. The Spalart-Allmaras one-equation model consistently performs better than the Baldwin-Barth model, particularly in the log-layer and free shear layers. Also, the Sparlart-Allmaras model is not grid dependent like the Baldwin-Barth model. No general turbulence model exists for all engineering applications. The Spalart-Allmaras one-equation model and the Chien k-epsilon models are the preferred turbulence models. Although the two-equation models often better predict the flow field, they may take from two to five times the CPU time. Future directions are in further benchmarking the Menter blended k-w/k-epsilon and algorithmic improvements to reduce CPU time of the two-equation model. Derived from text

N95-27887*# General Electric Co., Schenectady, NY. Research and Development.

EXPERIENCE WITH k-EPSILON TURBULENCE MODELS FOR HEAT TRANSFER COMPUTATIONS IN ROTATING

Prabbat Tekriwal *In* NASA. Lewis Research Center, Industry-Wide Workshop on Computational Turbulence Modeling Mar. 1995 p 65-77 (For primary document see N95-27882 09-34)
Avail: CASI HC A03/MF A03

This viewgraph presentation discusses geometry and flow configuration, effect of y+ on heat transfer computations, standard and extended k-epsilon turbulence model results with wall function, low-Re model results (the Lam-Bremhorst model without wall function), a criterion for flow reversal in a radially rotating square duct, and a summary. Derived from text

N95-27888*# Pratt and Whitney Aircraft, West Palm Beach, FL. CFD Group.

TURBULENCE MODELS FOR GAS TURBINE COMBUSTORS

Andreja Brankovic *In* NASA. Lewis Research Center, Industry-Wide Workshop on Computational Turbulence Modeling Mar. 1995 p 79-85 (For primary document see N95-27882 09-34)
Avail: CASI HC A02/MF A03

This viewgraph presentation covers gas turbine combustor flow physics, turbulence model investigations, turbulent combustion modeling, and present status and future needs. Derived from text

N95-27889*# General Electric Co., Cincinnati, OH. Aircraft Engines.

COMBUSTION SYSTEM CFD MODELING AT GE AIRCRAFT ENGINES

D. Burrus, H. Mongia, Anil K. Tolpadi (General Electric Co., Schenectady, NY.), S. Correa (General Electric Co., Schenectady, NY.), and M. Braaten (General Electric Co., Schenectady, NY.) *In* NASA. Lewis Research Center, Industry-Wide Workshop on Computational Turbulence Modeling Mar. 1995 p 87-97 (For primary document see N95-27882 09-34)
Avail: CASI HC A03/MF A03

This viewgraph presentation discusses key features of current combustion system CFD modeling capabilities at GE Aircraft Engines provided by the CONCERT code; CONCERT development history; modeling applied for designing engine combustion systems; modeling applied to improve fundamental understanding; CONCERT3D results for current production combustors; CONCERT3D model of NASA/GE E3 combustor; HYBRID CONCERT CFD/Monte-Carlo modeling approach; and future modeling directions. CASI

N95-27890*# Allison Engine Co., Indianapolis, IN.

RECENT PROGRESS IN THE JOINT VELOCITY-SCALAR PDF METHOD

M. S. Anand *In* NASA. Lewis Research Center, Industry-Wide Workshop

on Computational Turbulence Modeling Mar. 1995 p 99-10 (For primary document see N95-27882 09-34)
Avail: CASI HC A02/MF A03

This viewgraph presentation discusses joint velocity-scalar PDF method; turbulent combustion modeling issues for gas turbine combustors; PDF calculations for a recirculating flow; stochastic dissipation model; joint PDF calculations for swirling flows; spray calculations; reduced kinetics/manifold methods; parallel processing; and joint PDF focus areas. CASI

N95-27891*# Rockwell International Corp., Canoga Park, CA. Rocketdyne Div.
OVERVIEW OF TURBULENCE MODEL DEVELOPMENT AND APPLICATIONS AT ROCKETDYNE
A. H. Hadid, E. D. Lynch, and Munir M. Sindir *In* NASA. Lewis Research Center, Industry-Wide Workshop on Computational Turbulence Modeling Mar. 1995 p 107-117 (For primary document see N95-27882 09-34)
Avail: CASI HC A03/MF A03

This viewgraph presentation discusses turbulence modeling requirements, development philosophy, and approach; two major areas of concentration (high speed and low speed turbulence modeling); high speed turbulence modeling; compressibility effects; turbulence models adapted to USA code; M = 9.2 flat plate flow; Mach 7.05 flow over axisymmetric flare; Mach 8.6 flow over cold wall edge; low speed turbulence modeling; turbulence models being assessed; turbulence model deck structure and integration with Navier-Stokes solver; nonlinear algebraic-stress model; rotation modified k-epsilon model; and Reynolds stress model. CASI

N95-27892*# CFD Research Corp., Huntsville, AL.
RECENT ADVANCES IN PDF MODELING OF TURBULENT REACTING FLOWS
Andrew D. Leonard and F. Dai *In* NASA. Lewis Research Center, Industry-Wide Workshop on Computational Turbulence Modeling Mar. 1995 p 119-129 (For primary document see N95-27882 09-34)
Avail: CASI HC A03/MF A03

This viewgraph presentation concludes that a Monte Carlo probability density function (PDF) solution successfully couples with an existing finite volume code; PDF solution method applied to turbulent reacting flows shows good agreement with data; and PDF methods must be run on parallel machines for practical use. Derived from text

N95-27893*# Fluent, Inc., Lebanon, NH.
EXPERIENCE WITH TURBULENCE INTERACTION AND TURBULENCE-CHEMISTRY MODELS AT FLUENT INC.
D. Choudhury, S. E. Kim, D. P. Tselepidakis, and M. Missaghi *In* NASA. Lewis Research Center, Industry-Wide Workshop on Computational Turbulence Modeling Mar. 1995 p 131-142 (For primary document see N95-27882 09-34)
Avail: CASI HC A03/MF A03

This viewgraph presentation discusses (1) turbulence modeling: challenges in turbulence modeling, desirable attributes of turbulence models, turbulence models in FLUENT, and examples using FLUENT; and (2) combustion modeling: turbulence-chemistry interaction and FLUENT equilibrium model. As of now, three turbulence models are provided: the conventional k-epsilon model, the renormalization group model, and the Reynolds-stress model. The renormalization group k-epsilon model has broadened the range of applicability of two-equation turbulence models. The Reynolds-stress model has proved useful for strongly anisotropic flows such as those encountered in cyclones, swirlers, and combustors. Issues remain, such as near-wall closure, with all classes of models.
Derived from text

N95-27894*# CFD Research Corp., Huntsville, AL.
EXPERIENCES WITH TWO-EQUATION TURBULENCE MODELS
Ashok K. Singhal, Yong G. Lai, and Ram K. Avva *In* NASA. Lewis Research Center, Industry-Wide Workshop on Computational Turbulence Modeling Mar. 1995 p 143-153 (For primary document see N95-27882 09-34)
Avail: CASI HC A03/MF A03

This viewgraph presentation discusses the following: introduction to CFD Research Corporation; experiences with two-equation models - models used, numerical difficulties, validation and applications, and strengths and weaknesses; and answers to three questions posed by the workshop organizing committee - what are your customers telling you, what are you doing in-house, and how can NASA-CMOTT (Center for Modeling of Turbulence and Transition) help. Derived from text

N95-27895*# Fluid Dynamics International, Inc., Evanston, IL.
PROGRESS IN SIMULATING INDUSTRIAL FLOWS USING TWO-EQUATION MODELS: CAN MORE BE ACHIEVED WITH FURTHER RESEARCH?
Vahe Haroutunian *In* NASA. Lewis Research Center, Industry-Wide Workshop on Computational Turbulence Modeling Mar. 1995 p 155-169 (For primary document see N95-27882 09-34)
Avail: CASI HC A03/MF A03

This viewgraph presentation provides a brief review of two-equation eddy-viscosity models (TEM's) from the perspective of applied CFD. It provides objective assessment of both well-known and newer models, compares model predictions from various TEM's with experiments, identifies sources of modeling error and gives historical perspective of their effects on model performance and assessment, and recommends directions for future research on TEM's. Derived from text

N95-27896*# Analysis and Design Application Co. Ltd., Melville, NY.
TURBULENCE MODELING NEEDS OF COMMERCIAL CFD CODES: COMPLEX FLOWS IN THE AEROSPACE AND AUTOMOTIVE INDUSTRIES
Bizhan A. Befrui *In* NASA. Lewis Research Center, Industry-Wide Workshop on Computational Turbulence Modeling Mar. 1995 p 171-192 (For primary document see N95-27882 09-34)
Avail: CASI HC A03/MF A03

This viewgraph presentation discusses the following: STAR-CD computational features; STAR-CD turbulence models; common features of industrial complex flows; industry-specific CFD development requirements; applications and experiences of industrial complex flows, including flow in rotating disc cavities, diffusion hole film cooling, internal blade cooling, and external car aerodynamics; and conclusions on turbulence modeling needs.
Derived from text

N95-27897*# Advanced Scientific Computing Ltd., Waterloo (Ontario).
TURBULENCE REQUIREMENTS OF A COMMERICAL CFD CODE
J. P. VanDoormaal, C. M. Mueller, and M. J. Raw *In* NASA. Lewis Research Center, Industry-Wide Workshop on Computational Turbulence Modeling Mar. 1995 p 193-202 (For primary document see N95-27882 09-34)
Avail: CASI HC A02/MF A03

This viewgraph presentation gives a profile of Advanced Scientific Computing (ASC) Ltd., applications, clients and clients' needs, ASC's directions, and how the Center for Modeling of Turbulence and Transition (CMOTT) can help. CASI

N95-27898*# Cornell Univ., Ithaca, NY. Dept. of Mechanical and Aerospace Engineering.
SECOND-ORDER CLOSURES FOR COMPRESSIBLE TURBULENCE
J. L. Lumley, S. Savarese, and C. C. Volte *In* NASA. Lewis Research Center, Industry-Wide Workshop on Computational Turbulence Modeling Mar. 1995 p 203-217 (For primary document see N95-27882 09-34)
Avail: CASI HC A03/MF A03

This viewgraph presentation discusses project description, turbulence models, and computational engine and results for second-order closures for compressible turbulence. Derived from text

N95-27899*# California Univ., Berkeley, CA. Dept. of Mechanical Engineering.
MODELING OF TURBULENT CHEMICAL REACTION
J.-Y. Chen *In* NASA. Lewis Research Center, Industry-Wide Workshop on Computational Turbulence Modeling Mar. 1995 p 219-230 (For primary document see N95-27882 09-34)
Avail: CASI HC A03/MF A03

Viewgraphs are presented on modeling turbulent reacting flows, regimes of turbulent combustion, regimes of premixed and regimes of non-premixed turbulent combustion, chemical closure models, flamelet model, conditional moment closure (CMC), NO(x) emissions from turbulent H2 jet flames, probability density function (PDF), departures from chemical equilibrium, mixing models for PDF methods, comparison of predicted and measured

H_2O mass fractions in turbulent nonpremixed jet flames, experimental evidence of preferential diffusion in turbulent jet flames, and computation of turbulent reacting flows. CASI

N95-27900*# NYMA, Inc., Brook Park, OH.
PDF METHODS FOR TURBULENT REACTIVE FLOWS
Andrew T. Hsu *In* NASA. Lewis Research Center, Industry-Wide Workshop on Computational Turbulence Modeling Mar. 1995 p 247-257 (For primary document see N95-27882 09-34)
Avail: CASI HC A03/MF A03

Viewgraphs are presented on computation of turbulent combustion, governing equations, closure problem, PDF modeling of turbulent reactive flows, validation cases, current projects, and collaboration with industry and technology transfer. CASI

N95-27901*# NYMA, Inc., Cleveland, OH.
A COMPOSITION JOINT PDF METHOD FOR THE MODELING OF SPRAY FLAMES
M. S. Raju *In* NASA. Lewis Research Center, Industry-Wide Workshop on Computational Turbulence Modeling Mar. 1995 p 259-268 (For primary document see N95-27882 09-34)
Avail: CASI HC A02/MF A03

This viewgraph presentation discusses an extension of the probability density function (PDF) method to the modeling of spray flames to evaluate the limitations and capabilities of this method in the modeling of gas-turbine combustor flows. The comparisons show that the general features of the flowfield are correctly predicted by the present solution procedure. The present solution appears to provide a better representation of the temperature field, particularly, in the reverse-velocity zone. The overpredictions in the centerline velocity could be attributed to the following reasons: (1) the use of k-epsilon turbulence model is known to be less precise in highly swirling flows and (2) the swirl number used here is reported to be estimated rather than measured. Derived from text

N95-27902*# National Aeronautics and Space Administration. Lewis Research Center, Cleveland, OH.
IMPROVEMENTS AND NEW FEATURES IN THE PDF MODULE
Andrew T. Norris *In its* Industry-Wide Workshop on Computational Turbulence Modeling Mar. 1995 p 269-275 (For primary document see N95-27882 09-34)
Avail: CASI HC A02/MF A03

This viewgraph presentation discusses what models are used in this package and what their advantages and disadvantages are, how the probability density function (PDF) model is implemented and the features of the program, and what can be expected in the future from the NASA Lewis PDF code. Derived from text

N95-27917*# Institute for Computer Applications in Science and Engineering, Hampton, VA.
A NUMERICAL METHOD FOR SOLVING THE THREE-DIMENSIONAL PARABOLIZED NAVIER-STOKES EQUATIONS Final Report
Domenic DAmbrosio and Robert Marsilio May 1995 24 p
(Contract NAS1-19480; RTOP 505-90-52-01)
(NASA-CR-198159; NAS 1.26:198159; ICASE-95-38) Avail: CASI HC A03/MF A01

A numerical technique that solves the parabolized form of the Navier-Stokes equations is presented. Such a method makes it possible to obtain very detailed descriptions of the flowfield in a relatively modest CPU time. The present approach is based on a space-marching technique, uses a finite volume discretization and an upwind flux-difference splitting scheme for the evaluation of the inviscid fluxes. Second order accuracy is achieved following the guidelines of the the ENO schemes. The methodology is used to investigate three-dimensional supersonic viscous flows over symmetric corners. Primary and secondary streamwise vortical structures embedded in the boundary layer and originated by the interaction with shock waves are detected and studied. For purpose of validation, results are compared with experimental data extracted from literature. The agreement is found to be satisfactory. In conclusion, the numerical method proposed seems to be promising as it permits, at a reasonable computational expense, investigation of complex three-dimensional flowfields in great detail. Author

N95-28021# Pacific Northwest Lab., Richland, WA.
SMALL ANGLE X RAY SCATTERING STUDIES OF REVERSE MICELLES IN SUPERCRITICAL FLUIDS
D. M. Pfund and J. L. Fulton Oct. 1994 10 p Presented at the 3rd International Symposium on Supercritical Fluids, Strasbourg, France, 17-19 Oct. 1994
(Contract DE-AC06-76RL-01830)
(DE95-007803; PNL-SA-25782; CONF-9410114-6) Avail: CASI HC A02/MF A01

The nature of aggregates formed in a supercritical fluid determines its solvent power and selectivity. Small angle X ray scattering (SAXS) is a powerful tool for studying the properties of aggregates with sizes in the 10(angstrom) to 200(angstrom) range. It is also useful in studying those interparticle interactions which operate over a similar distance. The authors have used SAXS to examine the aggregates formed in pure fluids, in mixtures and in fluid/surfactant/water systems. The scattered intensity as a function of angle depends on the geometry, polydispersity, X ray contrast, and interaction strength of the particles as well as on the phase behavior of the system. In this paper the authors present the results of modeling the X-ray scattering from AOT/water reverse micelles in supercritical propane and in propane/carbon dioxide mixtures. They examine the effect of dilution with CO_2 anti-solvent on the phase behavior of the system and on the strength of intermicellar attractions. A better understanding of these systems must be obtained before the applications of supercritical reverse micelle systems to extractions, reactions, and enhanced oil recovery can be fully developed. DOE

N95-28055# Texas Univ., Austin, TX.
NORMAL MODES AND CONTINUOUS SPECTRA
N. J. Balmforth and P. J. Morrison Dec. 1994 26 p
(Contract DE-FG05-80ET-53088)
(DE95-006166; DOE/ET-53088/686; IFSR-686) Avail: CASI HC A03/MF A01

The authors consider stability problems arising in fluids, plasmas and stellar systems that contain singularities resulting from wave-mean flow or wave-particle resonances. Such resonances lead to singularities in the differential equations determining the normal modes at the so-called critical points or layers. The locations of the singularities are determined by the eigenvalue of the problem, and as a result, the spectrum of eigenvalues forms a continuum. They outline a method to construct the singular eigenfunctions comprising the continuum for a variety of problems. DOE

N95-28155 State Univ. of New York at Buffalo, Amherst, NY. Dept. of Mechanical and Aerospace Engineering.
DNS, LES AND STOCHASTIC MODELING OF TURBULENT REACTING FLOWS Final Report, 1 Jun. 1990 - 30 Apr. 1994
Peyman Givi Mar. 1994 338 p Limited Reproducibility: More than 20% of this document may be affected by microfiche quality
(Contract N00014-90-J-4013)
(AD-A280099) Avail: CASI HC A15

This is a Final Report providing a summary of accomplishments in our research sponsored by the Office of Naval Research (ON-R), Grant N00014-90-J-4013 (Young In Program - FY 1990) under the management of Dr. Gabriel D. Roy, Mechanics Division, Code 1132P. The contributions made in each part of this investigation are described, followed by a highlight of our important findings. A few of the technical papers written in conjunction with this work are attached as appendices for those who are interested in reviewing our work in a greater detail. DTIC

N95-28225# California Univ., Berkeley. Lawrence Berkeley Lab, CA.
NUMERICAL SIMULATION OF COUPLED FLOW AND TRANSPORT WITH TOUGH2: A VERIFICATION STUDY
C. M. Oldenburg and K. Pruess Oct. 1994 23 p
(Contract DE-AC03-76SF-00098)
(DE95-008351; LBL-35273) Avail: CASI HC A03/MF A01

We have tested T2DM, the dispersion module of TOUGH2, on two classic flow problems: (1) the seawater intrusion problem of Henry (1964); and (2) the pure solutal free convection problem of Elder (1967). T2DM produces results in agreement with prior work for similar spatial discretizations. In the Henry problem, finer spatial discretization allows the seawater tongue to penetrate slightly farther without affecting the overall flow dynamics. In the strongly coupled pure solutal free convection problem of Elder, results produced by T2DM using high-resolution grids differ markedly from lower-resolution results. These high-resolution simulations agree closely with laboratory experiments. DOE

N95-28228*# Institute for Computer Applications in Science and Engineering, Hampton, VA.
A PHENOMENOLOGICAL TREATMENT OF ROTATING TURBULENCE Final Report
Ye Zhou May 1995 14 p Submitted for publication
(Contract NAS1-19480; RTOP 505-90-52-01)
(NASA-CR-198168; NAS 1.26:198168; ICASE-95-43) Avail: CASI HC A03/MF A01

The strong similarity between the magnetohydrodynamic (MHD) turbulence and initially isotropic turbulence subject to rotation is noted. We then apply the MHD phenomenologies of Kraichnan and Matthaeus & Zhou to rotating turbulence. When the turbulence is subject to a strong rotation, the energy spectrum is found to scale as E(k) = C(sub Omega)(Omega(sub epsilon))(sup 1/2)k(sup -2), where Omega is the rotation rate, k is the wavenumber, and epsilon is the dissipation rate. This spectral form is consistent with a recent letter by Zeman. However, here the constant C(sub Omega) is found to be related to the Kolmogorov constant and is estimated in the range 1.22 - 1.87 for the typical values of the latter constant. A 'rule' that relates spectral transfer times to the eddy turnover time and the time scale for decay of the triple correlations is deduced. A hypothesis for the triple correlation decay rate leads to the spectral law which varies between the '-5/3' (without rotation) and '-2' laws (with strong rotation). For intermediate rotation rates, the spectrum varies according to the value of a dimensionless parameter that measures the strength of the rotation wavenumber k(sub Omega) = (Omega(sup 3)/epsiolon)(sup 1/2) relative to the wavenumber k. An eddy viscosity is derived with an explicit dependence on the rotation rate. Author

N95-28351 Georgia Inst. of Tech., Atlanta, GA. School of Mechanical Engineering.
[MODELING THE SHOCK RESPONSE OF SUBMERGED STRUCTURES] Final Report
Jerry H. Ginsburg 15 Dec. 1994 24 p Limited Reproducibility: More than 20% of this document may be affected by microfiche quality
(Contract N00014-94-1-0834)
(AD-A289082) Avail: Issuing Activity (Defense Technical Information Center (DTIC))

The task of modelling the shock response of submerged structures has always been implemented in the time domain, in constrast to the frequency domain approch used for structural acoustic modeling of radiation and scattering. One approach used to create time domain representations of the interaction of the structure and the surrounding fluid is to develop a finite element simulation in which a large domain of the fluid is included in the mesh. Because this procedure leads to a very large model that strains avaiable computer resources, it limits the fidelity with which the structure may be modeled. For this reason approximate procedures that replace the fluid with an impedance-type conditions have been derived. Of these, the most widely implemented is the doubly-asymptotic approximation (DAA), which has been developed in a variety of versions. This paper discusses a method for testing the accuracy of DAA in modeling fluid-structure interaction for realistically shape submerged structure. The approach uses the frequency-domain equivalent of the time-domain DAA differential equations, and then compares it to the results obtained from a standard structural acoustics approach of known accuracy. Derived from text

N95-28523 Princeton Univ., NJ. Dept. of Mechanical and Aerospace Engineering.
STRUCTURE OF HIGH-SPEED SPRAYS Final Technical Report, 15 Dec. 1984 - 14 Feb. 1989
Frediano V. Bracco Jan. 1995 119 p Limited Reproducibility: More than 20% of this document may be affected by microfiche quality
(Contract DAAG29-85-K-0028)
(AD-A291696; ARO-21781.10-EG) Avail: Issuing Activity (Defense Technical Information Center (DTIC))

This work covered both measurements and computations and its results are documented in eight appendices. Measurements were made of drop velocity in vaporizing, steady, full-cone sprays and of drop velocity and drop size in non-vaporizing steady full-cone sprays. In similar conditions, measurements had previously been made of the intact core and of the size of the drops in the immediate vicinity of the injector, thus generating an extensive set of data which were particularly useful for the assessment and the development of multidimensional models of engine sprays. On the computational side, a line source technique was introduced to simulate the intact-core in engine sprays and two extensive numerical studies were carried out to explain the strong anisotropy of the drop velocity fluctuations that had been found in the measurements. In another interesting and timely study, the accuracy of the stochastic method of computing drop collisions and coalescence (which is the one universally used) was assessed by corresponding deterministic computations (more accurate but much more time consuming). It was concluded that the accuracy of the stochastic method in practical computations can be wanting. Finally, a numerical study of the structure of hollow-cone sprays was initiated that has since been followed by significant experimental and computational work on liquid-only and air-assisted hollow-cone injectors and sprays. DTIC

N95-28533# Oak Ridge National Lab., TN.
THIRD-ORDER-ACCURATE NUMERICAL METHODS FOR EFFICIENT, LARGE TIME-STEP SOLUTIONS OF MIXED LINEAR AND NONLINEAR PROBLEMS
J. W. Cobb Feb. 1995 52 p
(Contract DE-AC05-84OR-21400)
(DE95-009184; ORNL/TM-12891) Avail: CASI HC A04/MF A01

There is an increasing need for more accurate numerical methods for large-scale nonlinear magneto-fluid turbulence calculations. These methods should not only increase the current state of the art in terms of accuracy, but should also continue to optimize other desired properties such as simplicity, minimized computation, minimized memory requirements, and robust stability. This includes the ability to stably solve stiff problems with long time-steps. This work discusses a general methodology for deriving higher-order numerical methods. It also discusses how the selection of various choices can affect the desired properties. The explicit discussion focuses on third-order Runge-Kutta methods, including general solutions and five examples. The study investigates the linear numerical analysis of these methods, including their accuracy, general stability, and stiff stability. Additional appendices discuss linear multistep methods, discuss directions for further work, and exhibit numerical analysis results for some other commonly used lower-order methods. DOE

N95-28571* Institute for Computer Applications in Science and Engineering, Hampton, VA.
A GENUINELY MULTIDIMENSIONAL UPWIND SCHEME AND EFFICIENT MULTIGRID SOLVER FOR THE COMPRESSIBLE EULER EQUATIONS
David Sidilkover Nov. 1994 37 p Limited Reproducibility: More than 20% of this document may be affected by microfiche quality
(Contract NAS1-19480)
(NASA-CR-195000; NAS 1.26:195000; AD-A289712; ICASE-94-84) Avail: Issuing Activity (Defense Technical Information Center (DTIC))

We present a new approach towards the construction of a genuinely multidimensional high-resolution scheme for computing steady-state solutions of the Euler equations of gas dynamics. The unique advantage of this approach is that the Gauss-Seidel relaxation is stable when applied directly to the high-resolution discrete equations, thus allowing us to construct a very efficient and simple multigrid steady-state solver. This is the only high-resolution scheme known to us that has this property. The two-dimensional scheme is presented in detail. It is formulated on triangular (structured and unstructured) meshes and can be interpreted as a genuinely two-dimensional extension of the Roe scheme. The quality of the solutions obtained using this scheme and the performance of the multigrid algorithm are illustrated by the numerical experiments. Construction of the three dimensional scheme is outlined briefly as well. DTIC

N95-28603# Los Alamos National Lab., NM.
COMPUTATIONAL AND EXPERIMENTAL STUDIES OF HYDRODYNAMIC INSTABILITIES AND TURBULENT MIXING
V. A. Andronov, I. G. Zhidov, E. E. Meskov, N. V. Nevmerzhitskii, V. V. Nikiforov, A. N. Razin, V. G. Rogatchev, A. I. Tolshmyakov, and Yu. V. Yanilkin Feb. 1995 214 p
(Contract W-7405-eng-36)
(DE95-006837; LA-12896) Avail: CASI HC A10/MF A03

This report describes an extensive program of investigations conducted at Arzamas-16 in Russia over the past several decades. The focus of the work is on material interface instability and the mixing of two materials. Part 1 of the report discusses analytical and computational studies of hydrodynamic instabilities and turbulent mixing. The EGAK codes are described and results are illustrated for several types of unstable flow. Semiempirical turbulence transport equations are derived for the mixing of two materials, and their capabilities are illustrated for several examples. Part 2 discusses the experimental studies that have been performed to investigate instabilities and turbulent mixing. Shock-tube and jelly techniques are described in considerable detail. Results are presented for many circumstances and configurations. DOE

N95-28619 Arizona State Univ., Tempe, AZ. National Air Intelligence Center.
MONTE-CARLO SIMULATION METHODS FOR FINITE FLAT PLATE WINDING FLOWS
Yuzhong Shi, Qifen Wu, and Bing Ren 15 Nov. 1994 18 p Transl. into ENGLISH from Kongqidonglixue Xuebao, China, v. 9, no. 3, Sep. 1991 p 324-329 Limited Reproducibility: More than 20% of this document may be affected by microfiche quality
(AD-A289842; NAIC-ID(RS)T-0919-92) Avail: Issuing Activity (Defense Technical Information Center (DTIC))

This article opts for the use of direct simulation Monte-Carlo methods to solve such problems as those associated with winding flows around flat plates of finite length. The methods in question are ones which go through tracking the movements of simulated molecules by computer in order to realize numerical value simulations. Collision calculations between simulated molecules are determined from statistical samplings. As far as collision models are concerned, respective selections were made for the use of hard sphere molecule models and inverse power law models. As far as simulation molecule and solid wall effects are concerned, option was made for the use of models which are made up from mixtures on the basis of ratios of fully diffused reflection and specular or mirror surface reflection. For the sake of the reliability of empirical test methods, calculations were also done of the one dimensional flow movements associated with such questions and Rayleigh problems and shock wave structures. Two dimensional calculations opted for the use of synchronous parallel programs. Numerical value results clearly showed that direct simulation Monte-Carlo methods were capable of relatively good simulations of a number of problems in rarefied gas mechanics. As far as two dimensional calculations are concerned, the machine time expended and the necessary content are both within ranges permitted by domestic machines. DTIC

N95-28637 Technische Univ., Delft (Netherlands).
EXPERIMENTAL STUDY ON TRANSITION CHARACTERISTICS OF NATURAL-CONVECTION FLOW Ph.D. Thesis
I. J. Opstelten 17 Oct. 1994 150 p
(PB95-192423; ISBN-90-9007545-3) Copyright Avail: Issuing Activity (National Technical Information Service (NTIS))

In this thesis, an experimental study on transition characteristics of natural-convection flow in cubical cavities is described. Natural convection is spoken of when the flow arises from the force of gravity working on density differences in the fluid, as opposed to forced convection, where the flow arises from pressure differences. The density differences can be due to different processes, such as concentration differences of chemical elements, a mixture of various fluids, or multiphase flows. Another common source for density differences is temperature differences in a fluid. Such temperature differences can occur in various technical applications, such as cooling of electronic equipment, heat transfer in solar collectors, insulation by double-glazed windows and climate control in buildings and greenhouses. The natural-convection flow investigated in this work is a result from temperature differences too. NTIS

N95-28673*# Institute for Computer Applications in Science and Engineering, Hampton, VA.
RESPONSE OF MULTI-PANEL ASSEMBLY TO NOISE FROM A JET IN FORWARD MOTION Final Report
A. Bayliss (Northwestern Univ., Evanston, IL.), L. Maestrello (National Aeronautics and Space Administration. Langley Research Center, Hampton, VA.), J. L. McGreevy (Philadelphia Coll. of Pharmacy and Science, PA.), and C. C. Fenno, Jr. (National Academy of Sciences - National Research Council, Hampton, VA.) May 1995 30 p Submitted for publication
(Contract NAS1-19480; RTOP 505-90-52-01)
(NASA-CR-198164; NAS 1.26:198164; ICASE-95-41) Avail: CASI HC A03/MF A01

A model of the interaction of the noise from a spreading subsonic jet with a 4 panel assembly is studied numerically in two dimensions. The effect of forward motion of the jet is accounted for by considering a uniform flow field superimposed on a mean jet exit profile. The jet is initially excited by a pulse-like source inserted into the flow field. The pulse triggers instabilities associated with the inviscid instability of the jet shear layer. These instabilities generate sound which in turn serves to excite the panels. We compare the sound from the jet, the responses of the panels and the resulting acoustic radiation for the static jet and the jet in forward motion. The far field acoustic radiation, the panel response and sound radiated from the panels are all computed and compared to computations of a static jet. The results demonstrate that for a jet in forward motion there is a reduction in sound in downstream directions and an increase in sound in upstream directions in agreement with experiments. Furthermore, the panel response and radiation for a jet in forward motion exhibits a downstream attenuation as compared with the static case. Author

N95-27129 Pacific Northwest Lab., Richland, WA.
FLUID DYNAMIC EFFECTS ON PRECISION CLEANING WITH SUPERCRITICAL FLUIDS
Max R. Phelps, M. O. Hogan, and L. J. Silva *In* Johns Hopkins Univ., Environmentally Benign Cleaning and Degreasing Technology: JANNAF Safety and Protection Subcommittee and Propellant Development and Characterization Subcommittee Joint Workshop Jun. 1994 p 259-268 See also N95-14663 (For primary document see N95-27101 09-27)
(Contract DE-AC06-76RL-01830)
Avail: CPIA, 10630 Little Patuxent Pkwy., Suite 202, Columbia, MD 21044-3200 HC

N95-27130 Missouri Univ., Rolla, MO. High Pressure Waterjet Lab.
THE APPLICATION OF WATERJETS FOR CLEANING
D. A. Summers and Robert Fossey *In* Johns Hopkins Univ., Environmentally Benign Cleaning and Degreasing Technology: JANNAF Safety and Protection Subcommittee and Propellant Development and Characterization Subcommittee Joint Workshop Jun. 1994 p 269-277 (For primary document see N95-27101 09-27)
Avail: CPIA, 10630 Little Patuxent Pkwy., Suite 202, Columbia, MD 21044-3200 HC

N95-27973*# Pacific Northwest Lab., Richland, WA.
LARGE HAWT WAKE MEASUREMENT AND ANALYSIS
A. H. Miller, H. L. Wegley, and J. W. Buck *In* DASCON Engineering, Collected Papers on Wind Turbine Technology May 1995 p 27-33
(For primary document see N95-27970 09-44)
(Contract DE-AC06-76RL-01830)
Avail: CASI HC A02/MF A03

35 INSTRUMENTATION AND PHOTOGRAPHY

Includes remote sensors; measuring instruments and gages; detectors; cameras and photographic supplies; and holography.

For aerial photography see *43 Earth Resources and Remote Sensing*. For related information see also *06 Aircraft Instrumentation*, and *19 Spacecraft Instrumentation.*

N95-26461 Arizona Univ., Tucson, AZ. Dept. of Electrical and Computer Engineering.
PERFORMANCE MODELING OF HYPERSPECTRAL IMAGING SENSORS FOR ATMOSPHERIC STUDIES Final Technical Report
Yudi Adityawarman and R. A. Schowengerdt Sep. 1994 25 p Limited Reproducibility: More than 20% of this document may be affected by microfiche quality
(Contract N00014-94-1-G004)
(AD-A289017) Avail: Issuing Activity (Defense Technical Information Center (DTIC))

In this research project, we have developed a sensor model for the

Navy's HYDICE system, using current engineering specifications and data from Hughes Danbury Optical Systems, the manufacturer. This sensor imaging model has been integrated into an end-to-end simulation system, Multispectral Image Simulator (MIS). Using MIS with the HYDICE model we have investigated Signal to Noise Ratios (SNR's) that might be expected from HYDICE under low radiance conditions, such as images of coastal water areas. The results are presented in Section 4.1. We also used the Cuprite, Nevada, AVIRIS database developed earlier, for simulation of natural HYDICE imagery. This is presented in Section 4.2. Finally, we have also initiated investigation of large view angle effects on image contrast, using the Advanced Very High Resolution Radiometer (AVHRR) module in MIS since it allows a range of +55 deg in view angle cross-track. These simulation results are presented in Section 4.3. DTIC

N95-26541 Wales Univ., Bangor (United Kingdom). School of Electronic Engineering and Computer Systems.

LARGE AREA SMART PIEZOELECTRIC AND PYROELECTRIC SENSORS Interim Report, No. 6

D. K. Das-Gupta and M. P. Wenger Nov. 1994 10 p Limited Reproducibility: More than 20% of this document may be affected by microfiche quality

(Contract DAJA45-93-C-0017)

(AD-A288565; R/D-6980-EE-01) Avail: Issuing Activity (Defense Technical Information Center (DTIC))

The nature of the pyroelectric properties of the composite %Ca/Epikote 828 with 50/50 and 60/40 percent volume was reported in the fifth interim report. The present report provides an account of the preparation of pure lead titanate (H) and calcium modified lead titanate (%Ca) by the Sol-Gel process. X-ray Spectroscopic Structural Analysis and Differential Scanning Calorimetric (DSC) studies of the ceramic grains produced by this technique were made and the results are given in this report. The Sol-Gel method for preparation of ferroelectric ceramics can offer many advantages over conventional processing techniques. Ceramics produced via the Sol-Gel method show high degrees of purity and homogeneity, can produce fine powders as well as being able to be formed into a variety of structures and they possess the ability to be processed at lower temperatures. DTIC

N95-26702*# Cornell Univ., Ithaca, NY. Center for Radiophysics and Space Research.

THE DEVELOPMENT OF INFRARED DETECTORS AND MECHANISMS FOR USE IN FUTURE INFRARED SPACE MISSIONS Final Report

James R. Houck 27 Apr. 1995 15 p

(Grant NAGw-2870)

(NASA-CR-197819; NAS 1.26:197819) Avail: CASI HC A03/MF A01

The environment above earth's atmosphere offers significant advantages in sensitivity and wavelength coverage in infrared astronomy over ground-based observatories. In support of future infrared space missions, technology development efforts were undertaken to develop detectors sensitive to radiation between 2.5 micron and 200 micron. Additionally, work was undertaken to develop mechanisms supporting the imaging and spectroscopy requirements of infrared space missions. Arsenic-doped-Silicon and Antimony-doped-Silicon Blocked Impurity Band detectors, responsive to radiation between 4 micron and 45 micron, were produced in 128x128 picture element arrays with the low noise, high sensitivity performance needed for space environments. Technology development continued on Gallium-doped-Germanium detectors (for use between 80 micron and 200 micron), but were hampered by contamination during manufacture. Antimony-doped-Indium detectors (for use between 2.5 micron and 5 micron) were developed in a 256x256 pixel format with high responsive quantum efficiency and low dark current. Work began on adapting an existing cryogenic mechanism design for space-based missions; then was redirected towards an all-fixed optical design to improve reliability and lower projected mission costs. Author

N95-26714 Naval Postgraduate School, Monterey, CA.

EVALUATION OF A NEW LABORATORY ACOUSTIC DOPPLER VELOCIMETER M.S. Thesis

Gary N. Underwood Dec. 1994 63 p Limited Reproducibility: More than 20% of this document may be affected by microfiche quality

(AD-A289592) Avail: Issuing Activity (Defense Technical Information Center (DTIC))

A small, rugged and relatively inexpensive velocity meter has been developed to measure uniform and oscillatory water flows in laboratory facilities. The Acoustic Doppler Velocimeter (ADV-1) is capable of measuring three-dimensional velocities. The ADV-1 measures velocities from 0 to 2.5 m/s at a sampling rate of up to 25 Hz. The measurements are made in a sampling volume located 5 cm in front of the probe. Since this instrument is new, the objective is to compare the ADV-1 with other laboratory current meters and prepare operational guidelines for the ADV-1 system. Three-dimensional velocities are measured in a wave tank with the ADV-1 horizontal velocity average 0.9 cm/s higher than the laser Doppler anemometer (LDA) and the ADV-1 vertical velocity average 0.93 cm/s lower than the LDA. A horizontal velocity profile is measured in a wave flume by the ADV-1 and a pitot tube, and the instruments differ by 3.5%. Measuring velocity profiles around a stationary cylinder with the ADV-1 in the wave flume was highly successful, showing the ability of this instrument to measure velocities near structures in future laboratory research. The ADV-1 is portable and can be used for extended periods without recalibration. DTIC

N95-26765*# National Aeronautics and Space Administration. Pasadena Office, CA.

METHOD AND APPARATUS FOR POLARADIOMETRIC PYROMETER Patent Application

Ali A. Abtahi, inventor (to NASA) (Jet Propulsion Lab., California Inst. of Tech., Pasadena, CA.) 22 Jun. 1994 20 p

(NASA-Case-NPO-19064-1-CU; NAS 1.71:NPO-19064-1-CU; US-Patent-Appl-SN-273542) Avail: CASI HC A03/MF A01

A radiation pyrometer for measuring the true temperature of a body is provided by detecting and measuring thermal radiation from the body based on the principle that the effects of angular emission I(sub 1) and reflection I(sub 2) on the polarization states p and s of radiation are complementary such that upon detecting the combined partial polarization state components I(sub p) = I(sub 1p) + I(sub 2p) and I(sub s) = I(sub 1s) + I(sub 2s) and adjusting the intensity of the variable radiation source of the reflected radiation I(sub 2) until the combined partial radiation components I(sub p) and I(sub s) are equal, the effects of emissivity as well as diffusivity of the surface of the body are eliminated, thus obviating the need for any post processing of brightness temperature data. NASA

N95-26982 Wisconsin Univ., Madison, WI. Dept. of Chemistry.

BORON-INDUCED MORPHOLOGY CHANGES IN SILICON CVD GROWTH: A SCANNING TUNNELING MICROSCOPY STUDY Interim Report

Robert J. Hamers and Yajun Wang 20 Dec. 1994 10 p Limited Reproducibility: More than 20% of this document may be affected by microfiche quality

(Contract N00014-91-J-1629)

(AD-A289275; TR-24) Avail: Issuing Activity (Defense Technical Information Center (DTIC))

Scanning tunneling microscopy has been used to investigate the influence of surface boron on silicon growth via chemical vapor deposition (CVD). The presence of boron-induced reconstructions on the Si(001) surface dramatically changes the surface morphology during subsequent CVD growth of silicon using disilane at 815 Kelvin. Boron-induced reconstructions inhibit the lateral diffusion of silicon atoms from terraces to step edges, leading to greatly enhanced island nucleation, and also reduce the local surface reactivity toward disilane. Strong segregation of boron to the growth surface allows the enhanced island nucleation to persist to subsequent terraces during multilayer CVD growth of silicon, producing a rough but epitaxial surface. DTIC

N95-26989 Air Force Inst. of Tech., Wright-Patterson AFB, OH. School of Engineering.

DISTRIBUTED INTERACTIVE SIMULATION VIRTUAL CASSETTE RECORDER (DIS VCR); A DATALOGGER WITH VARIABLE SPEED REPLAY M.S. Thesis

Jonathan L. Fortner Dec. 1994 106 p Limited Reproducibility: More than 20% of this document may be affected by microfiche quality

(AD-A289212; AFIT/GE/ENG/94D-10) Avail: Issuing Activity (Defense Technical Information Center (DTIC))

The overall objective of the Distributed Interactive Simulation Virtual Cassette Recorder (DIS VCR) is to add a flexible replay capability to any

DIS environment and specifically to the Remote Debriefing Tool (RDT). The DIS VCR's abilities include selective filtering of incoming DIS Protocol Data Units (PDUs), variable-speed replays, ability to pause, fast-forward, rewind, efficient data storage and retrieval, and an interface that simplifies the execution of those functions. The thesis includes a DIS VCR-compatible design for concurrent replay of audio extracted from signal PDUs and an extension to the replay design that supports unmodifiable rendering or receiving applications. For variable-speed replays, the authors created a scalable simulation clock and a new PDU (the Replay PDU). Applications modified for replays use the simulation clock to govern their dead reckoning algorithms while the DIS VCR uses it to control the timed release of stored PDUs. The Replay PDU communicates mode and speed changes between the DIS VCR and replay-modified applications. The DIS VCR's full functionality was successfully demonstrated at the 1994 AFA convention. DTIC

N95-27030*# National Aeronautics and Space Administration. Lewis Research Center, Cleveland, OH.

CRYOGENIC AND SIMULATED FUEL JET BREAKUP IN ARGON, HELIUM AND NITROGEN GAS FLOWS

Robert D. Ingebo May 1995 15 p Presented at the 31st Joint Propulsion Conference, San Diego, CA, 10-12 Jul. 1995; sponsored by AIAA, ASME, SAE, AND ASEE
(RTOP 505-62-52)
(NASA-TM-106923; E-9636; NAS 1.15:106923; AIAA Paper 95-2554)
Avail: CASI HC A03/MF A01

Two-phase flow atomization of liquid nitrogen jets was experimentally investigated. They were co-axially injected into high-velocity gas flows of helium, nitrogen and argon, respectively, and atomized internally inside a two-fluid fuel nozzle. Cryogenic sprays with relatively high specific surface areas were produced, i.e., ratios of surface area to volume were fairly high. This was indicated by values of reciprocal Sauter mean diameters, RSMD's, as measured with a scattered- light scanning instrument developed at NASA Lewis Research Center. Correlating expressions were derived for the three atomizing gases over a gas temperature range of 111 to 422 K. Also, the correlation was extended to include waterjet breakup data that had been previously obtained in simulating fuel jet breakup in sonic velocity gas flow. The final correlating expression included a new dimensionless molecular-scale acceleration group. It was needed to correlate RSMD data, for LN2 and H2O sprays, with the fluid properties of the liquid jets and atomizing gases used in this investigation. Author

N95-27138*# National Aeronautics and Space Administration. Langley Research Center, Hampton, VA.

MULTI-CHANNEL ELECTRONICALLY SCANNED CRYOGENIC PRESSURE SENSOR Patent Application

John J. Chapman, inventor (to NASA) (Chapman, John J., Wareneck, VA.), Purnell Hopson, Jr., inventor (to NASA) (Hopson, Purnell, Jr., Seaford, VA.), and Nancy M. H. Kruse, inventor (to NASA) (Kruse, Nancy M. H., Hayes, VA.) 4 Apr. 1995 27 p
(NASA-Case-LAR-15062-1; NAS 1.71:LAR-15062-1;
US-Patent-Appl-SN-416596) Avail: CASI HC A03/MF A01

A miniature, multi-channel, electronically scanned pressure measuring device uses electrostatically bonded silicon dies in a multielement array. These dies are bonded at specific sites on a glass, prepatterned substrate. Thermal data is multiplexed and recorded on each individual pressure measuring diaphragm. The device functions in a cryogenic environment without the need of heaters to keep the sensor at constant temperatures. NASA

N95-27173*# National Aeronautics and Space Administration. Lewis Research Center, Cleveland, OH.

FUZZY INFERENCE ENHANCED INFORMATION RECOVERY FROM DIGITAL PIV USING CROSS-CORRELATION COMBINED WITH PARTICLE TRACKING

Mark P. Wernet May 1995 17 p Presented at Conference on Optical Techniques in Fluid, Thermal and Combusting Flows, San Diego, CA, 9-14 Jul. 1995; sponsored by the Society for Photo-Optical Instrumentation Engineers Original contains color illustrations
(RTOP 505-62-50)
(NASA-TM-106896; E-9544; NAS 1.15:106896) Avail: CASI HC A03/MF A01; 3 functional color pages

Particle Image Velocimetry provides a means of measuring the instantaneous 2-component velocity field across a planar region of a seeded flowfield. In this work only two camera, single exposure images are considered where both cameras have the same view of the illumination plane. Two competing techniques which yield unambiguous velocity vector direction information have been widely used for reducing the single exposure, multiple image data: cross-correlation and particle tracking. Correlation techniques yield averaged velocity estimates over subregions of the flow, whereas particle tracking techniques give individual particle velocity estimates. The correlation technique requires identification of the correlation peak on the correlation plane corresponding to the average displacement of particles across the subregion. Noise on the images and particle dropout contribute to spurious peaks on the correlation plane, leading to misidentification of the true correlation peak. The subsequent velocity vector maps contain spurious vectors where the displacement peaks have been improperly identified. Typically these spurious vectors are replaced by a weighted average of the neighboring vectors, thereby decreasing the independence of the measurements. In this work fuzzy logic techniques are used to determine the true correlation displacement peak even when it is not the maximum peak on the correlation plane, hence maximizing the information recovery from the correlation operation, maintaining the number of independent measurements and minimizing the number of spurious velocity vectors. Correlation peaks are correctly identified in both high and low seed density cases. The correlation velocity vector map can then be used as a guide for the particle tracking operation. Again fuzzy logic techniques are used, this time to identify the correct particle image pairings between exposures to determine particle displacements, and thus velocity. The advantage of this technique is the improved spatial resolution which is available from the particle tracking operation. Particle tracking alone may not be possible in the high seed density images typically required for achieving good results from the correlation technique. This two staged approach offers a velocimetric technique capable of measuring particle velocities with high spatial resolution over a broad range of seeding densities. Author

N95-27191*# National Aeronautics and Space Administration. Langley Research Center, Hampton, VA.

SCHLIEREN SYSTEM AND METHOD FOR MOVING OBJECTS Patent Application

Leonard M. Weinstein, inventor (to NASA) 14 Feb. 1995 14 p
(NASA-Case-LAR-15053-1; NAS 1.71:LAR-15053-1;
US-Patent-Appl-SN-388652) Avail: CASI HC A03/MF A01

A system and method are provided for recording density changes in a flow field surrounding a moving object. A mask having an aperture for regulating the passage of images is placed in front of an image recording medium. An optical system is placed in front of the mask. A transition having a light field-of-view and a dark field-of-view is located beyond the test object. The optical system focuses an image of the transition at the mask such that the aperture causes a band of light to be defined on the image recording medium. The optical system further focuses an image of the object through the aperture of the mask so that the image of the object appears on the image recording medium. Relative motion is minimized between the mask and the transition. Relative motion is also minimized between the image recording medium and the image of the object. In this way, the image of the object and density changes in a flow field surrounding the object are recorded on the image recording medium when the object crosses the transition in front of the optical system. NASA

N95-27259*# National Aeronautics and Space Administration. Langley Research Center, Hampton, VA.

HIGH-PRECISION BUFFER CIRCUIT FOR SUPPRESSION OF REGENERATIVE OSCILLATION

John S. Tripp, David A. Hare, and Ping Tcheng May 1995 18 p
(RTOP 505-59-54-02)
(NASA-TM-4658; L-17453; NAS 1.15:4658) Avail: CASI HC A03/MF A01

Precision analog signal conditioning electronics have been developed for wind tunnel model attitude inertial sensors. This application requires low-noise, stable, microvolt-level DC performance and a high-precision buffered output. Capacitive loading of the operational amplifier output stages due to the wind tunnel analog signal distribution facilities caused regenerative oscillation and consequent rectification bias errors. Oscillation suppression techniques commonly used in audio applications were inadequate to maintain the performance requirements for the measurement of attitude for wind tunnel models. Feedback control theory is applied to develop a suppression technique based on a known compensation (snubber) circuit, which provides superior oscillation suppression with high output isolation and preserves the low-noise low-offset performance of the signal conditioning electronics. A practical design technique is developed to select the parameters for the compensation circuit to suppress regenerative oscillation occurring when typical shielded cable loads are driven. Author

N95-27368*# Southern Univ., Baton Rouge, LA. College of Engineering.
STUDY OF DEVELOPMENT AND UTILIZATION OF A MULTIPURPOSE ATMOSPHERIC CORROSION SENSOR Annual Research Technical Report
Ravinder M. Diwan, A. Raman, and P. K. Bhattacharya Dec. 1994 55 p
(Grant NAG10-0127)
(NASA-CR-198595; NAS 1.26:198595) Avail: CASI HC A04/MF A01

There has been a critical need for analyzing various aspects of atmospheric corrosion and for the development of atmospheric corrosion microsensors. The project work has involved the following activities: (1) making of multielectrode corrosion monitors on dielectric substrates; (2) testing them in the laboratory for functional characteristics; (3) preparing a report on the state of the art of atmospheric corrosion sensor development around the world; and (4) corrosion testing of electrochemical changes of sensor specimens and related fog testing. The study included work on the subject of development and utilization of a multipurpose atmospheric corrosion sensor and this report is the annual report on work carried out on this research project. This has included studies on the development of sensors of two designs, stage 1 and stage 2, and with glass and alumina substrate, experimentation and development and characterization of the coating uniformity, aspects of corrosion monitoring, literature search on the corrosion sensors and their development. A state of the art report on atmospheric corrosion sensor development was prepared and submitted. Derived from text

N95-27465# Mississippi State Univ., Mississippi State, MS.
INTRUSIVE MULTI-PROBE SYSTEM
R. A. Green, L. R. Hester, and C. W. Bouchillon 1995 30 p
(Contract DE-AC02-80ET-15601)
(DE95-006258; DOE/ET-15601/T63) Avail: CASI HC A03/MF A01

The Diagnostic Instrumentation and Analysis Laboratory (DIAL) in the College of Engineering at Mississippi State University is the result of the efforts of several faculty members in the Aerospace and Chemical Engineering Departments obtaining funding in 1976. At that time, an initial research project was begun which was funded by the US Department of Energy as part of the national magnetohydrodynamic (MHD) program. Initial research efforts concentrated in heat recovery and seed recovery (HRSR) from the MHD combustion process as well as some materials investigations. Over the years, efforts at DIAL were shifted from HRSR studies to the development of optical based, microprocessor controlled instrumentation for use in the harsh MHD environment. DOE

N95-27677# Brookhaven National Lab., Upton, NY.
PRECISION ELECTROMAGNETIC CALORIMETRY WITH LIQUID KRYPTON
H. Takai 1995 7 p Presented at the 4th International Conference on Advanced Technology and Particle Physics, Como, Italy, 3-7 Oct. 1994
(Contract DE-AC02-76CH-00016)
(DE95-006685; BNL-61316; CONF-941060-3) Avail: CASI HC A02/MF A01

Test beam results of a liquid krypton electromagnetic calorimeter with projective accordion electrode are presented. The electrode design includes a fine segmentation section to enhance the pi(sup 0) rejection and pointing. The test was carried out at the H4 beam line at the CERN SPS with electron beams of energy from 20 to 200 GeV. Preliminary results of energy resolution, linearity, mu response are presented. The author also presents the dependence of the energy resolution on the amount of inactive material in front of the calorimeter. DOE

N95-27711# International Centre for Theoretical Physics, Trieste (Italy).
VISUALIZATION AND DIRECT COMPARISON OF LARGE DISPLACEMENTS USING DIFFERENCE HOLOGRAPHIC INTERFEROMETRY
F. NecatiEcevit (Middle East Technical Univ., Ankara, Turkey.) and R. Aydin Sep. 1994 11 p
(DE95-608782; LAMP-94/6) Avail: CASI HC A03/MF A01 (US Sales Only)

The difference holographic interferometry provides the possibility of direct comparison of large displacements and deformations of two similar but different objects by application of a special kind of illumination. In this work, the principles of the difference holographic interferometry and the experimental results obtained by applying the single beam technique to large displacements is presented. DOE

N95-27738# Brookhaven National Lab., Upton, NY.
PERFORMANCE OF AN ACCORDION ELECTROMAGNETIC CALORIMETER WITH LIQUID KRYPTON
David Lissauer 1994 9 p Presented at the 5th International Conference on Calorimetry in High Energy Physics, Upton, NY, 25 Sep. - 1 Oct. 1994
(Contract DE-AC02-76CH-00016)
(DE95-006693; BNL-61315; CONF-9409268-4) Avail: CASI HC A02/MF A01

Beam test results of the liquid krypton electromagnetic calorimeter with a projective accordion type electrode structure are presented. The electrode had a fine segmentation in the front to enhance pi(sup 0) rejection and pointing. The test was carried out at the H4 line at the CERN SPS with e(-) beams between 20 and 200 GeV. Preliminary results of energy resolution, linearity, mu response and the dependence of the energy resolution on the amount of inactive material in front of the calorimeter are presented. DOE

N95-27751# Fermi National Accelerator Lab., Batavia, IL.
THE KTeV PURE CsI CALORIMETER
Ronald E. Ray Dec. 1994 8 p Presented at the 5th International Conference on Calorimetry in High Energy Physics, Upton, NY, 25 Sep. - 1 Oct. 1994; sponsored by Brookhaven National Lab.
(Contract DE-AC02-76CH-03000)
(DE95-005747; FNAL/C-94/418; CONF-9409268-7) Avail: CASI HC A02/MF A01

KTeV is currently building a state-of-the-art pure CsI electromagnetic calorimeter with a sophisticated digital readout. The CsI array is expected to have better than 1% resolution over a dynamic range of 2-64 GeV. The design of the CsI array is driven by the difficult physics goal of attempting to measure the CP violation parameter Re(epsilon'/epsilon) to 1 part in 10000 in a high-rate neutral beam environment. The physics requirements and their impact on the final design will be discussed. DOE

N95-27863*# Loyola Coll., Baltimore, MD. Japanese Technology Evaluation Center.
JTEC PANEL ON DISPLAY TECHNOLOGIES IN JAPAN Final Report
Lawrence E. Tannas, Jr., William E. Glenn, Thomas Credelle, J. William Doane, Arthur H. Firester, and Malcolm Thompson Jun. 1992 295 p
Sponsored by NASA, Washington; NSF; Dept. of Commerce; DOE; ONR; DARPA; and AF
(NASA-CR-198564; NAS 1.26:198564) Avail: CASI HC A13/MF A03

This report is one in a series of reports that describes research and development efforts in Japan in the area of display technologies. The following are included in this report: flat panel displays (technical findings, liquid crystal display development and production, large flat panel displays (FPD's), electroluminescent displays and plasma panels, infrastructure in Japan's FPD industry, market and projected sales, and new a-Si active matrix liquid crystal display (AMLCD) factory); materials for flat panel displays (liquid crystal materials, and light-emissive display materials); manufacturing and infrastructure of active matrix liquid crystal displays (manufacturing logistics and equipment); passive matrix liquid crystal displays (LCD basics, twisted nematics LCD's, supertwisted nematic LCD's, ferroelectric LCD's, and a comparison of passive matrix LCD technology); active matrix technology (basic active matrix technology, investment environment, amorphous silicon, polysilicon, and commercial products and prototypes); and projection displays (comparison of Japanese and U.S. display research, and technical evaluation of work). Derived from text

N95-27915*# National Aeronautics and Space Administration. Langley Research Center, Hampton, VA.

OPTIMIZATION OF MEASUREMENTS WITH PRESSURE SENSITIVE PAINTS

Donald M. Oglesby (Old Dominion Univ., Norfolk, VA.), Chith K. Puram (Vigyan Research Associates, Inc., Hampton, VA.), and Billy T. Upchurch Jun. 1995 9 p
(RTOP 505-59-54-02)
(NASA-TM-4695; L-17474; NAS 1.15:4695) Avail: CASI HC A02/MF A01

Use of luminescent paints for the measurement of global pressures on wind tunnel model surfaces requires a full understanding of the inherent accuracy of the technique. Theoretical emission of the paint luminophor follows the well known Stern-Volmer relation. Inherent in this relation are fundamental limits to achievable sensitivity and accuracy. Equations for relative error in pressure as a function of relative signal intensity (emittance), relative error in pressure as a function of pressure, and the relationship between sensitivity and pressure are derived and represented graphically.
Author

N95-28037*# National Aeronautics and Space Administration. Lewis Research Center, Cleveland, OH.

A PHASE-STEPPED POINT DIFFRACTION INTERFEROMETER USING LIQUID CRYSTALS

Carolyn R. Mercer, Katherine Creath (Arizona Univ., Tucson, AZ.), and Nasser Rashidnia (NYMA, Inc., Brook Park, OH.) May 1995 9 p Presented at the International Symposium on Optical Science, Engineering, and Instrumentation, San Diego, CA, 9-14 Jul. 1995; sponsored by Society of Photo-Optical Instrumentation Engineers
(Contract NAS3-27186; RTOP 505-62-50)
(NASA-TM-106922; E-9634; NAS 1.15:106922) Avail: CASI HC A02/MF A01

A new instrument, the liquid crystal point diffraction interferometer (LCPDI), has been developed for the measurement of phase objects. This instrument maintains the compact, robust design of Linnik's point diffraction interferometer (PDI) and adds to it phase stepping capability for quantitative interferogram analysis. The result is a compact, simple to align, environmentally insensitive interferometer capable of accurately measuring optical wavefronts with high data density and with automated data reduction. The design of the LCPDI is briefly discussed. An algorithm is presented for eliminating phase measurement error caused by object beam intensity variation from frame-to-frame. The LCPDI is demonstrated by measuring the temperature distribution across a heated chamber filled with silicone oil. The measured results are compared to independently measured results and show excellent agreement with them. It is expected that this instrument will have application in the fluid sciences as a diagnostic tool, particularly in space based applications where autonomy, robustness, and compactness are desirable qualities. It should also be useful for the testing of optical elements, provided a master is available for comparison. Author

N95-28178# Stanford Linear Accelerator Center, Stanford, CA.

CAN TMAE PHOTOCATHODE BE USED FOR HIGH RATE APPLICATIONS?

J. Vavra 1995 6 p Presented at the 7th Vienna Wire Chamber Conference, Vienna, Austria, 13-17 Feb. 1995
(Contract DE-AC03-76SF-00515)
(DE95-008594; SU-SLAC-PUB-95-6759; CONF-950276-1) Avail: CASI HC A02/MF A01

The paper explores the problems associated with wire aging, charging effects, and self-sustaining cathode currents in the TMAE (Tetrakis dimethylamino ethylene) based photodetectors. It is generally believed that anode wire aging is the most serious problem encountered in TMAE-based Cherenkov ring imaging detectors. Although charging effects and self-sustaining cathode currents have not been studied systematically, there is concern that they too could become significant over a long period of time. DOE

N95-28345* National Aeronautics and Space Administration. Ames Research Center, Moffett Field, CA.

METHOD AND APPARATUS FOR MEASURING TEMPERATURES IN FABRICS AND FLEXIBLE THERMAL INSULATIONS Patent

Demetrius A. Kourtides, inventor (to NASA) 21 Mar. 1995 4 p Filed 26 Jul. 1993
(NASA-Case-ARC-11984-1; US-Patent-5,399,019;
US-Patent-Appl-SN-096540; US-Patent-Class-374-208;
US-Patent-Class-374-179; US-Patent-Class-136-230;
US-Patent-Class-136-233; Int-Patent-Class-G01K-1/14;
Int-Patent-Class-G01K-1/10; Int-Patent-Class-G01K-1/12) Avail: US Patent and Trademark Office

A temperature sensor uses a type R thermocouple wire element in a ceramic sheath to sense temperatures up to 3,200 deg F., and is particularly suitable for flexible insulations. The sensor includes a thermocouple wire embedded in a sheath having two sections disposed at right angles to each other. The junction of the thermocouple is located at one end of one of the sections and the lead wires extend from the other section. The section which includes the junction is secured to a flexible surface with ceramic cement.
Official Gazette of the U.S. Patent and Trademark Office

N95-28362* National Aeronautics and Space Administration. John F. Kennedy Space Center, Cocoa Beach, FL.

PARTICLE FALLOUT/ACTIVITY SENSOR Patent

Ihlefeld M. Curtis, inventor (to NASA), Robert C. Youngquist, inventor (to NASA), John S. Moerk, inventor (to NASA), and Kenneth A. Rose, III, inventor (to NASA) 2 May 1995 11 p Filed 26 Apr. 1994
(NASA-Case-KSC-11687-1; US-Patent-5,412,221;
US-Patent-Appl-SN-233584; US-Patent-Class-250-573;
US-Patent-Class-356-338; Int-Patent-Class-G01N-15/06) Avail: US Patent and Trademark Office

A particle fallout/activity sensor measures relative amounts of dust or other particles which collect on a mirror in an area to be monitored. The sensor includes a sensor module and a data acquisition module, both of which can be operated independently of one another or in combination with one another. The sensor module includes a housing containing the mirror, an LED assembly for illuminating the mirror and an optical detector assembly for detecting light scattered off of the mirror by dust or other particles collected thereon. A microprocessor controls operation of the sensor module's components and displays results of a measurement on an LCD display mounted on the housing. A push button switch is also mounted on the housing which permits manual initiation of a measurement. The housing is constructed of light absorbing material, such as black delrin, which minimizes detection of light by the optical detector assembly other than that scattered by dust or particles on the mirror. The data acquisition module can be connected to the sensor module and includes its own microprocessor, a timekeeper and other digital circuitry for causing the sensor module to make a measurement periodically and send the measurement data to the data acquisition module for display and storage in memory for later retrieval and transfer to a separate computer. The time tagged measurement data can also be used to determine the relative level of activity in the monitored area since this level is directly related to the amount of dust or particle fallout in the area.
Official Gazette of the U.S. Patent and Trademark Office

N95-28389 Massachusetts Inst. of Tech., Lexington, MA. Lincoln Lab.

DESIGN, CONSTRUCTION, TEST AND EVALUATION OF A FREQUENCY SCANNING RADIOMETER FOR MEASURING OIL SLICK THICKNESSES Final Report, Oct. 1992 - Jun. 1994

G. L. Hover, J. Murphy, E. R. Brown, G. G. Hogan, and O. B. McMahon Jun. 1994 141 p Limited Reproducibility: More than 20% of this document may be affected by microfiche quality
(Contract F19628-90-C-0002)
(AD-A290040; USCG-D-29-24) Avail: Issuing Activity (Defense Technical Information Center (DTIC))

Single frequency microwave radiometry has been used to detect and estimate oil slick thicknesses. Because only a single sampling point is used, estimates of oil thickness can become ambiguous. MIT Lincoln Laboratory proposed the concept of using a frequency scanning radiometer to sample multiple points across a frequency band, thus resolving the problem of ambiguities in oil thickness estimation. A laboratory-prototype FSR capable of scanning over Ka-band (26 -40GHz) was designed, built, and tested. The FSR was used in laboratory proof-of-principle testing to (1) measure uniform thickness oil layers under various ambient weather conditions (day, night, clear, cloudy, drizzle, and snow) and different oil types, and (2) measure the phenomenology of non-uniform thickness oil layers and emulsions. Comparisons of measured data sets with theoretical predictions demonstrated that the expected response of oil is consistent regardless of oil type or ambient weather condition. Comparisons of uniform oil layer measurements and non-uniform measurements with theoretical predictions indicate that the radiometric brightness temperature (TB) of the oil above that of water is a function of the percentage of that thickness of oil within the antenna field-of-view. Water/oil emulsions were measured and have a higher TB than a uniform layer of pure oil at the same thickness. Recommendations for FSR modifications and improvements, as well as future collection work are included. DTIC

N95-28410 Army Aeromedical Research Lab., Fort Rucker, AL.
THREE-DIMENSIONAL PHOTOGRAMMETRY FOR LABORATORY APPLICATIONS Final Report
Nabih M. Alem Dec. 1994 31 p Limited Reproducibility: More than 20% of this document may be affected by microfiche quality
(DA Proj. 301-62787-A-878)
(AD-A291624; USAARL-95-6) Avail: Issuing Activity (Defense Technical Information Center (DTIC))

The direct linear transformation (DLT) is a method that simplifies measurements of the three-dimensional coordinates of a point target in the laboratory using photographic two-dimensional imagery. This report describes a procedure to implement the DLT equations and gives the Fortran code of computer programs for the DLT calibration of multicamera system and 3-D reconstruction of a single point from several images. DTIC

N95-28612 Department of the Navy, Washington, DC.
CRYOGENIC TEMPERATURE CONTROL AND TENSION/COMPRESSION ATTACHMENT STAGE FOR AN ELECTRON MICROSCOPE Patent
Dale E. Taylor, inventor (to Navy) 18 Oct. 1994 5 p Filed 14 Dec. 1993
(AD-D017390; US-Patent-5,355,683; US-Patent-Appl-SN-169922; US-Patent-Class-62-51) Avail: US Patent and Trademark Office

A tension-compression attachment stage for an electron microscope having a cryogenic heat exchanger is provided. The attachment stage has a support assembly for mounting brackets to support a pair of load screws and a load screw drive assembly and for mounting a fixed jaw. A moveable jaw is supported and moved by the pair of load screws. A cryogenic heat exchanger is soldered to the fixed jaw and slideably engages the moveable jaw through heat conducting slider blocks. The combination allows control of test specimen test within 1 deg-4 deg F. DTIC

N95-28651 Selskapet for Industriell og Teknisk Forskning, Trondheim (Norway).
TV-HOLOGRAPHY AT HIGH TEMPERATURES: IN SITU OBSERVATIONS OF THE OXIDATION OF ADVANCED MATERIALS
J. T. Malmo and O. J. Loekberg 22 Sep. 1994 14 p Prepared in cooperation with Norges Tekniske Hoegskole
(PB95-195343; STF19-S94005) Avail: Issuing Activity (National Technical Information Service (NTIS))

TV-holography provides real-time mapping of the deformations and vibrations of surfaces, and is relatively immune towards object instability due to the combination of short exposure and high framing rate. By use of image processing, the fringe pattern can be converted into absolute values of displacement or vibration amplitude and phase. The study of oxidation represents a new interesting application of the technique. NTIS

N95-27103 Litton Industries, Blacksburg, VA.
THE EVALUATION OF A FLUOROCHEMICAL DRYING PROCESS FOR AN ELECTRICAL CONTACT
Charles William Reed *In* Johns Hopkins Univ., Environmentally Benign Cleaning and Degreasing Technology: JANNAF Safety and Protection Subcommittee and Propellant Development and Characterization Subcommittee Joint Workshop Jun. 1994 p 9-16 (For primary document see N95-27101 09-27)
Avail: CPIA, 10630 Little Patuxent Pkwy., Suite 202, Columbia, MD 21044-3200 HC

N95-27287*# National Aeronautics and Space Administration. Goddard Space Flight Center, Greenbelt, MD.
A CRYOGENIC SCAN MECHANISM FOR USE IN FOURIER TRANSFORM SPECTROMETERS
Claef F. Hakun and Kenneth A. Blumenstock *In* NASA. Johnson Space Center, The 29th Aerospace Mechanisms Symposium May 1995 p 316-333 (For primary document see N95-27260 09-15)
Avail: CASI HC A03/MF A04

N95-27670*# Institute for Space Science and Technology, Inc., Gainesville, FL.
THE ORBITAL DEBRIS DETECTOR CONSORTIUM: SUPPLIERS OF INSTRUMENTS FOR IN-SITU MEASUREMENTS OF SMALL-PARTICLES IN THE SPACE ENVIRONMENT
C. G. Simon, R. Muenzenmeyer (Technical Univ. of Munich, Muchen, Germany.), W. G. Tanner, Jr. (Baylor Univ., Waco, TX.), O. M. Uy (Johns Hopkins Univ., Laurel, MD.), R. A. Skrivanek (Visidyne, Inc., Burlington, MA.), A. J. Tuzzolino (Chicago Univ., Chicago, IL.), C. Maag (T and M Engineering, Glendora, CA.), and J. J. Wortman (North Carolina State Univ., Raleigh, NC.) *In* NASA. Langley Research Center, LDEF: 69 Months in Space. Third Post-Retrieval Symposium, Part 3 Feb. 1995 p 1361-1377 (For primary document see N95-27629 09-99)
Avail: CASI HC A03/MF A04

36 LASERS AND MASERS

Includes parametric amplifiers.
For related information see also *76 Solid-State Physics.*

N95-26503 Department of the Navy, Washington, DC.
SILICATE GEL DYE LASER Patent
Ilzoo Lee, inventor (to Navy) and Josephine Covino-Hrbacek, inventor (to Navy) 12 Jul. 1994 4 p Filed 31 Mar. 1993
(AD-D017262; US-Patent-5,329,540; US-Patent-Appl-SN-051106; US-Patent-Class-372-53) Avail: US Patent and Trademark Office

A dye laser comprising a solid state laser medium and a pumping energy source, the laser medium comprising a lasing concentration of a water or alcohol soluble organic dye which is incorporated into a hydrolyzed silicon organometallic solution, and forming a gel which is dried to form a transparent silicate glass which is doped with the organic dye. DTIC

N95-26568 Arizona Univ., Tucson, AZ.
AN ORGANIC THIN FILM LASER DIODE: A NOVEL LIGHT SOURCE
N. Peyghambarian, N. R. Armstrong, H. Hall, A. Padias, and S. Mazumdar 28 Nov. 1994 13 p Limited Reproducibility: More than 20% of this document may be affected by microfiche quality
(Contract N00014-94-1-0322)
(AD-A289007; TR-1) Avail: Issuing Activity (Defense Technical Information Center (DTIC))

The development of an entirely new diode laser based upon electroluminescent organic thin films is discussed. The authors proposed to develop new polymers for this important application. As shown below, significant progress was made during the ten first months of this project toward the realization of these challenging objectives. The authors have successfully fabricated a promising LED based on a new aluminum quinolate derivative that emits in the blue-green and that can be dissolved in a polymer matrix and spin-cast. DTIC

N95-26874 Air Force Systems Command, Wright-Patterson AFB, OH. National Air Intelligence Center.
CHARACTERISTICS OF THERMAL LENS IN A COPPER-VAPOR LASER
Hua Renzhong and Liang Peihui 15 Dec. 1994 16 p Transl. into ENGLISH from Zhongguo Jiguang (China), vol. 21, no. 3, Mar. 1994 p 172-177 Limited Reproducibility: More than 20% of this document may be affected by microfiche quality
(AD-A289545; NAIC-ID(RS)T-0704-94) Avail: Issuing Activity (Defense Technical Information Center (DTIC))

The thermal lenses in operating copper vapor lasers and in the fused silica windows were measured by use of the deflection method and the interferometer method respectively. Experimental results show that the overall thermal lens is composed of a negative lens in the discharge gas and two positive lenses in two pieces of laser windows. Theoretical analysis agrees well with experimental results. DTIC

N95-26906 David Sarnoff Research Center, Princeton, NJ.
HIGH-SPEED COHERENT LASER ARRAYS Final Report, Jul. 1992 - 1993
Marc K. Felisky, Richard DeFreez, Joseph H. Abeles, Daniel W. Bechtle, and S. Y. Naravan Nov. 1994 54 p Limited Reproducibility: More than 20% of this document may be affected by microfiche quality
(Contract F30602-92-C-0111; ARPA Order 8799)
(AD-A289373; RL-TR-94-195) Avail: Issuing Activity (Defense Technical Information Center (DTIC))

This research describes a novel approach to semiconductor lasers capable of ultra-high speed modulation. This approach uses the interaction between elements in a coherent diode laser array that results in lateral mode locking. This method potentially allows narrow-band modulation at rates above the relaxation oscillation frequency of the lasers, thus removing a major impediment to ultra-high speed modulation. Linearized analysis of coupled laser rate equations shows that the array can be asymptotically stable for values of the coupling attainable with index-guided lasers. The small-signal responsivity for a two-element array, for 180 deg out-of-phase/modulation, extends far beyond the relaxation oscillation frequency when examining the optical output from a single element. Large-signal analysis using full rate equations were used to demonstrate schemes for utilizing these microwave frequency resonances for high-speed optical signal transmissions. It was shown that digital signals with bit rates many times the relaxation oscillation frequency could be transmitted. Using lasers with a 4-GHz relaxation oscillation frequency, it is theoretically shown that rates greater than 25 Gb/s can be achieved. This scheme can also be used for encoding analog information using narrow band amplitude modulation. It was demonstrated that a 44 GHz carrier with a 1-GHz amplitude modulated envelope signal could be successfully implemented (same device parameters as used for the digital example). DTIC

N95-26961 Air Force Inst. of Tech., Wright-Patterson AFB, OH. School of Engineering.
GENERATION OF A SINGLE-LOBE, FAR-FIELD INTENSITY PATTERN FROM A LASER DIODE ARRAY USING AN OPTICAL DELAY LINE M.S. Thesis
Thomas A. Summers Dec. 1994 97 p Limited Reproducibility: More than 20% of this document may be affected by microfiche quality
(AD-A289226; AFIT/GAP/ENP/94D-10) Avail: Issuing Activity (Defense Technical Information Center (DTIC))

A simple and practical technique is demonstrated to generate a stable, single-lobe, far-field intensity pattern from a one-dimensional, antiphased, laser diode array with gain-guided elements. The two far-field lobes of the array are combined after introducing an optical delay line into the path of one of the lobes to make the lobes mutually incoherent. The incoherent superposition of intensities produces a near-diffraction-limited, single-lobe, far-field intensity pattern containing 84% of the power, exceeding any previous (known) phase control experiments. This technique compares favorably with more elaborate schemes advanced previously using integrated phase plates, etc. The method is directly applicable to one-dimensional laser diode arrays and could be adapted for use with two-dimensional arrays as well. DTIC

N95-26974 Air Force Inst. of Tech., Wright-Patterson AFB, OH. School of Engineering.
LASER BEAM PROPAGATION IN NON-KOLMOGOROV ATMOSPHERIC TURBULENCE M.S. Thesis
Bruce E. Stribling 13 Dec. 1994 91 p Limited Reproducibility: More than 20% of this document may be affected by microfiche quality
(AD-A289256; AFIT/GEO/ENG/94D-04) Avail: Issuing Activity (Defense Technical Information Center (DTIC))

Several observations of atmospheric turbulence statistics have been reported which do not obey Kolmogorov's power spectral density model. These observations have prompted the study of optical propagation through turbulence described by non-classical power spectra. This thesis presents an analysis of optical propagation through turbulence which causes index of refraction fluctuations to have spatial power spectra that obey arbitrary power laws. The spherical and plane wave structure functions are derived using Mellin transform techniques and are applied to the field mutual coherence function (MCF) using the extended Huygens-Fresnel principle. The MCF is used to compute the Strehl ratio of a focused, constant amplitude beam propagating in non-Kolmogorov turbulence as the power law for the spectrum of the index of refraction fluctuations is varied from -3 to -4. The relative contributions of the log amplitude and phase structure functions to the wave structure function are computed. If inner and outer scale effects are neglected, no turbulence exists when the power law equals -3. At power laws close to -3, the magnitude of the log amplitude and phase perturbations are determined by the system Fresnel ratio. At power laws approaching -4, phase effects dominate in the form of random tilts. DTIC

N95-26996 Naval Research Lab., Washington, DC.
SURFACE DAMAGE EFFECTS GENERATED BY A FAST-PULSE LASER BEAM
P. G. Burkhalter, J. H. Konnert, and E. F. Gabl 6 Dec. 1994 15 p Limited Reproducibility: More than 20% of this document may be affected by microfiche quality
(AD-A289131; NRL/MR/6680-94-7634) Avail: Issuing Activity (Defense Technical Information Center (DTIC))

A fast-pulse laser was used to induce damage on the surface of a polished silicon wafer. Effects of focused-laser heating at threshold for damage were examined with high-resolution imaging microscopes. The extent and characteristics of various ripple structures were measured with an atomic force microscope. DTIC

N95-27022 Phillips Lab., Hanscom AFB, MA.
A BRIEF HISTORY OF LASER GUIDED LIGHTNING DISCHARGE MODELS AND EXPERIMENTS Final Report, 23 May - 27 Jun. 1994
Matthew A. Kozma 5 Jul. 1994 25 p Limited Reproducibility: More than 20% of this document may be affected by microfiche quality
(AD-A289448; PL-TR-94-2193; ERP-1153) Avail: Issuing Activity (Defense Technical Information Center (DTIC))

Laser guided lightning discharge uses lasers instead of rockets to trigger lightning. Artificially triggered lightning has several important applications including aerospace vehicle launch protection and electrical power line transmission protection, among others. A brief history of the theoretical models used to predict triggered lightning, the experimentation completed with rocket triggered lightning, and the work completed on laser guided lightning discharge is presented. A bibliography of work related to lightning modeling, rocket-triggered lightning, and laser-triggered lightning is also included. DTIC

N95-27132 Air Force Inst. of Tech., Wright-Patterson AFB, OH.
TOWARD COHERENT EXCITATION: DEVELOPMENT OF A SINGLE-SOURCE PUMP FOR THE RUBIDIUM HYPERFINE GROUND STATE DOUBLET M.S. Thesis
Edward B. Tomme Dec. 1994 63 p Limited Reproducibility: More than 20% of this document may be affected by microfiche quality
(AD-A289413; AFIT/CI/CIA/94-152) Avail: Issuing Activity (Defense Technical Information Center (DTIC))

Coherent excitation is a phenomenon which, if achieved, could provide a new tool for the investigation of many fundamental questions in atomic physics and quantum optics. A design which could produce such coherences could lead to applications as varied as lasing without inversion and electromagnetically induced transparency. In this thesis, the basic theory concerning the generation of coherent superpositions of the ground states of atomic rubidium is reviewed. Next, the design, construction, and testing of a Littrow-style grating-tuned laser and a standing wave electro-optic modulator used in generating sidebands at the frequency matching the rubidium hyperfine ground state doublet are described. An experiment demonstrating simultaneous absorption by the Rb-85 F = 2 and Rb-85 F = 3 using a single laser as the pump is chronicled. An experiment to test coherences generated by this method of single-source pumping of the ground state doublet is proposed. DTIC

N95-27172 Air Force Inst. of Tech., Wright-Patterson AFB, OH.
COLLISIONAL DYNAMICS AND SPECTROSCOPIC STUDIES OF HIGHLY EXCITED ROVIBRATIONAL LEVELS OF I2(X)(0(+)(SUB g)) VIA STIMULATED EMISSION PUMPING Ph.D. Thesis
Melvin L. Nowlin Nov. 1994 309 p Limited Reproducibility: More than

20% of this document may be affected by microfiche quality
(AD-A289447; AFIT/CI/CIA/94-039D) Avail: Issuing Activity (Defense Technical Information Center (DTIC))

Highly excited vibrational levels of I2(X) are thought to play an important role in the mechanism of iodine dissociation in the chemical oxygen iodine laser. It has been proposed that I2 is dissociated in the laser with processes such as: (1) I2(X;v(double prime) = 0) + M(*) yields I2(X;v(double prime) greater than 20) + M; (2) I2(X;v(double prime) greater than 20) + M(*) yields I2(A(sub 1u)) + M; and (3) I2(X;v(double prime) greater than 20) + M(*) yields 2I + M, where M(*) is I(2 P(1/2)) or O2(1 delta) and M is O2(3 Sigma) or I(2 P(3/2)). In the chain branching mechanism, initiation would involve near-resonant E-V transfer populating vibrational levels around v(double prime) = 40. Consequently, the relaxation dynamics of these levels are of interest as they may control the efficiency of the laser. The author examined the nascent state distribution of the I2(X) product using pulsed laser photolysis and probe techniques. In these experiments, I(2 P(1/2)) was generated by 496 nm photolysis of I2. Within several microseconds after the photolysis laser, I2(X;23 less than v(double prime) less than 47) is detected by laser excitation of the D-X transition at wavelengths in the 280-300 nm range. Rotationally-resolved spectra under single collision conditions were recorded for the D-X transitions 4 less than v(prime) less than 12 from 23 less than v(double prime) less than 47. Analysis of the data indicated that the molecular constants for the D state did not extrapolate to the v(prime) less than 30 levels reliably. In order to improve the characterization of the D state, a least-squares analysis generated improved spectroscopic constants. DTIC

N95-27550# Oak Ridge National Lab., TN.
LASER IONIZATION OF MOLECULAR CLUSTERS
S. Desai (Tennessee Univ., Knoxville, TN.), C. S. Feigerle (Tennessee Univ., Knoxville, TN.), and J. C. Miller 1995 5 p Presented at the 7th International Symposium on Resonance Ionization Spectroscopy and its Applications, Bernkastel-Kues, Germany, 3-8 Jul. 1994
(Contract DE-AC05-84OR-21400)
(DE95-007011; CONF-940706-2) Avail: CASI HC A01/MF A01

Multiphoton ionization coupled with mass spectrometry was used to investigate molecular cluster distributions. Three examples will be discussed in this presentation. First, in studies of neat nitric oxide clusters, (NO)(sub m), an interesting odd-even intensity alternation was observed and will be discussed in terms of electron-pairing considerations. In a separate study, the binary clusters comprising nitric oxide and methane preferentially form a stoichiometric cluster made up of repeating units of NO2CH4. These presumably represent a particularly strongly bound 'van der Waals' subunit. Finally, in similar studies of neat carbon disulfide clusters, (CS2)(sub m), additional photon absorption after the two-photon ionization step stimulates a series of intracluster ion-molecular reactions leading to formation of S(sub m)(sup +) and (CS)(sub m)(sup +) polymers, as well as intermediate species such as S(sub m)(sup +) (CS(sub 2)). This molecular cluster analogue of 'laser snow' will be described in detail. DOE

N95-27557# Los Alamos National Lab., NM.
FREE ELECTRON LASER PHYSICAL PROCESS CODE (FELPPC)
L. E. Thode, K. C. D. Chan, and M. J. Schmitt 1995 12 p Presented at the SPIE '95: SPIE Conference on Optics, Electro-optics, and Laser Application in Science, Engineering and Medicine, San Jose, CA, 5-10 Feb. 1995
(Contract W-7405-eng-36)
(DE95-006276; LA-UR-95-339; CONF-950226-10) Avail: CASI HC A03/MF A01

Even at the conceptual level, the strong coupling between subsystem elements complicates the understanding and design of a free electron laser (FEL). Given the requirements for high-performance FELS, the coupling between subsystems must be included to obtain a realistic picture of the potential operational capability. The concept of an Integrated Numerical Experiment (INEX) was implemented to accurately calculate the coupling between the FEL subsystems. During the late 1980's, the INEX approach was successfully applied to a large number of accelerator and FEL experiments. Unfortunately, because of significant manpower and computational requirements, the integrated approach is difficult to apply to trade-off and initial design studies. However, the INEX codes provided a base from which realistic accelerator, wiggler, optics, and control models could be developed. The Free Electron Laser Physical Process Code (FELPPC) includes models developed from the INEX codes, provides coupling between the subsystem models, and incorporates application models relevant to a specific study. In other words, FELPPC solves the complete physical process model using realistic physics and technology constraints. FELPPC can calculate complex FEL configurations including multiple accelerator and wiggler combinations. When compared with the INEX codes, the subsystem models have been found to be quite accurate over many orders-of-magnitude. As a result, FELPPC has been used for the initial design studies of a large number of FEL applications: high-average-power ground, space, plane, and ship based FELS; beacon and illuminator FELS; medical and compact FELS; and XUV FELS. DOE

N95-27672# Los Alamos National Lab., NM. Chemical Science and Technology Div.
CONTINUOUSLY-TUNABLE, NARROW-LINEWIDTH, Q-SWITCHED Cr:LISAF LASER FOR LIDAR APPLICATIONS
James W. Early, Charles S. Lester, C. Robert Quick, Joe J. Tiee, Tsutomu Shimada, and Nigel J. Cockroft 1995 5 p Presented at the Advanced Solid-state Laser Conference, Memphis, TN, 29 Jan. - 1 Feb. 1995
(Contract W-7405-eng-36)
(DE95-006285; LA-UR-95-406; CONF-950101-3) Avail: CASI HC A01/MF A01

A continuously-tunable, narrow-linewidth, flashlamp-pumped, Q-switched Cr:LiSAF laser has been developed (energy: 30 mJ, pulsewidth: 40 ns, linewidth:<2 GHz) and was used successfully for the DIAL(differential absorption lidar) measurements of atmospheric water vapor and LIF lidar for the remote detection of metal oxide fluorescence. DOE

N95-27674# California Univ., Berkeley. Lawrence Berkeley Lab, CA.
FEMTOSECOND X-RAY GENERATION THROUGH 90 DEGREES T HOMSON SCATTERING: STATUS OF THE LBL EXPERIMENT
W. Leemans, R. Schoenlein, A. Chin, E. Glover, M. Conde, S. Chattopadhyay, K. J. Kim, and C. V. Shank Nov. 1994 15 p Presented at the 6th Workshop on Advanced Accelerator Concepts, Lake Geneva, WI, 12-18 Jun. 1994
(Contract DE-AC03-76SF-00098)
(DE95-006560; LBL-36369; CBP-107; CONF-940681-9) Avail: CASI HC A03/MF A01

Scattering of femotosecond laser pulses off a low energy relativistic electron beam at 90 deg offers the possibility to generate ultrashort X ray pulses. Experiments are under preparation in the Beam Test Facility of the Center for Beam Physics at LBL to demonstrate the generation and detection of such pulses. The experiments involve a relativistic electron beam (tunable from 25-50 MeV) with a bunch length of 10 ps containing 1-2 nC, and an ultra short pulse (50-200 fs), high peak power (greater than 2 TW) 0.8 micrometers Ti:Al2O3 laser system. The electron beam, focused down to about a 50 micrometers waist size intersects the focused laser beam at 90 deg. The laser field acts as an electromagnetic undulator with strength K (quiver velocity of an electron normalized to the speed of light) for the relativistic electron beam, generating radiation up-shifted by 2(gamma)(sup 2)/(1+K(sup 2)/2) and a pulse length given by the overlapped interaction length in time of the laser beam and the electron beam. Here (gamma) is the usual Lorentz factor. Wavelength tuning will be accomplished in the experiment by generating wiggler strengths on the order of one as well as by electron beam energy tuning. For a 50 MeV electron beam and a laser beam focused to an intensity on the order of 10(exp 16) W/sq cm, the authors expect 10(exp 5) photons at 0.4 (angstrom) (10% bandwidth) in a cone angle of 6 mrad in a 170 fs pulse. DOE

N95-27705# Los Alamos National Lab., NM.
IMPROVED PERFORMANCE 1590 nm Er:YLF LASER
R. D. Marchbanks, R. R. Petrin, and N. J. Cockroft 1994 9 p Presented at the 15th Conference on Lasers and Electro-optics and 5th Quantum Electronics and Laser Science Conference, Baltimore, MD, 21-26 May 1995
(Contract W-7405-eng-36)
(DE95-003691; LA-UR-94-3823; CONF-950540-1) Avail: CASI HC A02/MF A01

We present an improvement in the performance of a 1590 nm ER:YLF laser through simultaneous laser operation at 2717 nm. A slope efficiency of 7.0% with an output of 13.2 mW has been achieved with 971 nm pumping. DOE

N95-27718# Los Alamos National Lab., NM.
SPECTRAL BROADENING OF KrF LASER RADIATION BY SELF-SEEDED RAMAN AMPLIFICATION IN LONG AIR PATHS
N. A. Kurnit, D. C. Thompson, S. J. Thomas, and H. S. Steele 1994 8 p Presented at the 15th Conference on Lasers and Electro-optics and 5th Quantum Electronics and Laser Science Conference, Baltimore, MD, 21-26 May 1995
(Contract W-7405-eng-36)
(DE95-003697; LA-UR-94-3834; CONF-950540-2) Avail: CASI HC A02/MF A01

Broadening of the spectral content with little loss of focusability has been demonstrated in nearly-collimated propagation of KrF laser pulses having spectral components that overlap the rotational Raman lines in air. DOE

N95-27731* National Aeronautics and Space Administration. Pasadena Office, CA.
LASER WITH OPTICALLY DRIVEN Q-SWITCH Patent
Hamid Hemmati, inventor (to NASA) (Jet Propulsion Lab., California Inst. of Tech., Pasadena, CA.) 18 Apr. 1995 5 p Filed 15 Jul. 1993 Supersedes N94-15932 (32 - 3, p 1038)
(Contract NAS7-918)
(NASA-Case-NPO-18470-1-CU; US-Patent-5,408,480; US-Patent-Appl-SN-094332; US-Patent-Class-372-10; US-Patent-Class-372-11; Int-Patent-Class-H01S-3/11) Avail: US Patent and Trademark Office

An optically driven interactive Q-switch, i.e., a Q-switch that responds to a short pulse of light, for example, from external light-emitting diodes (LED's) or diode lasers, is provided for producing an output laser pulse from electronic energy stored in a laser medium. Q-switching is thus achieved on demand by electrically pulsing the light source to produce a pulse of light directed onto a Q-switch medium in the laser cavity. Electronic control of the light pulse from the external source will thus provide not only efficient Q-switching frequency but also independent control of output laser pulse width with a fast rise time for each output laser pulse.
Official Gazette of the U.S. Patent and Trademark Office

N95-27736 Los Alamos National Lab., NM.
APPLICATION OF CONVENTIONAL LASER TECHNOLOGY TO GAMMA-GAMMA COLLIDERS
Christopher E. Clayton (California Univ., Los Angeles, CA.), Norman A. Kurnit, and David D. Meyerhofer (Rochester Univ., NY.) 1995 27 p Presented at the Workshop on Gamma-gamma Colliders, Berkeley, CA, 28-31 Mar. 1994 Limited Reproducibility: More than 20% of this document may be affected by microfiche quality
(Contract W-7405-eng-36)
(DE95-006341; LA-UR-95-34; CONF-940351-5) Avail: CASI HC A03

A future e(-)e(+) (electron-positron) linear collider can be configured with perhaps minimal modification to serve as a gamma-gamma or a e(-)-gamma collider. This is accomplished by Compton-backscattering low energy photons (from a laser source) off of the high-energy electron beams prior to the crossing of the electron beams. However, to be competitive with the e(-)e(+) configuration, the luminosity cannot be compromised in the process. This requires that the laser source deliver a sufficient number of photons per pulse with a pulse format and rate matching that of the electron beams. As it turns out, this requires an average optical power of 5 to 15 kW from the laser which is beyond the current state of the art. In this paper, the authors address how to generate the required pulse format and how the high average power requirement can be met with conventional laser technology. They also address concerns about the survivability of mirrors located near the interaction point. Finally, they list a program of research and development which addresses some of the unknowns in such a system. DOE

N95-27737# California Univ., Berkeley. Lawrence Berkeley Lab, CA. Accelerator and Fusion Research Div.
TIME-DEPENDENT MULTI-DIMENSIONAL SIMULATION STUDIES OF THE ELECTRON OUTPUT SCHEME FOR HIGH POWER FELS
S. J. Hahn, W. M. Fawley, K. J. Kim, and J. A. Edighoffer Dec. 1994 4 p Presented at the 16th International Free Electron Laser Conference, Stanford, CA, 21-26 Aug. 1994
(Contract DE-AC03-76SF-00098)
(DE95-006593; LBL-35534; CONF-9408146-18) Avail: CASI HC A01/MF A01

The authors examine the performance of the so-called electron output scheme recently proposed by the Novosibirsk group. In this scheme, the key role of the FEL oscillator is to induce bunching, while an external undulator, called the radiator, then outcouples the bunched electron beam to optical energy via coherent emission. The level of the intracavity power in the oscillator is kept low by employing a transverse optical klystron (TOK) configuration, thus avoiding excessive thermal loading on the cavity mirrors. Time-dependent effects are important in the operation of the electron output scheme because high gain in the TOK oscillator leads to sideband instabilities and chaotic behavior. The authors have carried out an extensive simulation study by using 1D and 2D time-dependent codes and find that proper control of the oscillator cavity detuning and cavity loss results in high output bunching with a narrow spectral bandwidth. Large cavity detuning in the oscillator and tapering of the radiator undulator is necessary for the optimum output power. DOE

N95-27841# Los Alamos National Lab., NM.
ANALYSIS OF SURFACES, FILMS AND MULTILAYERS BY RESONANT LASER ABLATION
T. M. Allen, C. H. Smith, P. B. Kelly, J. E. Anderson, G. C. Eiden, A. W. Garrett, C. G. Gill, P. H. Hemberger, and N. S. Nogar 1995 13 p Presented at the SPIE '95: SPIE Conference on Optics, Electro-optics, and Laser Application in Science, Engineering and Medicine, San Jose, CA, 5-10 Feb. 1995
(Contract W-7405-eng-36)
(DE95-006295; LA-UR-95-116; CONF-950226-9) Avail: CASI HC A03/MF A01

We review briefly the history of resonant laser ablation (RLA), and discuss some current ideas regarding sample preparation, laser parameters, and mechanisms. We also discuss current applications including spectral analysis of trace components, depth profiling of thin films and multilayer structures, and the use of RLA with the Ion Trap Mass Spectrometer (ITMS). DOE

N95-27850# Los Alamos National Lab., NM.
TRIDENT AS AN ULTRAHIGH IRRADIANCE LASER
R. P. Johnson, N. K. Moncur, J. A. Cobble, R. G. Watt, and R. B. Gibson 1995 10 p Presented at the SPIE '95: SPIE Conference on Optics, Electro-optics, and Laser Application in Science, Engineering and Medicine, San Jose, CA, 5-10 Feb. 1995
(Contract W-7405-eng-36)
(DE95-006345; LA-UR-95-41; CONF-950226-8) Avail: CASI HC A02/MF A01

The Trident Nd:glass ICF laser at Los Alamos may be operated in a mode that produces high ultrashort pulses by the chirp/compression method. The 125-ps pulses from a standard moderated, Nd:YLF oscillator are first frequency-broadened to 3-nm bandwidth, chirped in a quartz fiber, and then compressed with a grating pair to 1.5 ps. A second quartz fiber then provides nonlinear polarization rotation for background and satellite suppression and to further broaden the spectrum to greater than 7 nm. Pulses are chirped again to 1 ns width with a second grating pair and amplified in a ND:YAG pumped Ti:sapphire regenerative amplifier. Millijoule-level output is then amplified through the existing phosphate glass Trident amplifier chain before compression to less than 400 fs. Energy greater than or equal to 1 J with excellent beam quality and contrast ratio is routinely produced by compressing after three rod amplifier stages. Higher energies are possible by compression further along the amplifier chain. Simultaneous use of long (approximately 1 ns) pulses for plasma formation is also possible. DOE

N95-27868# Nagoya Univ., Nagoya (Japan). Plasma Science Center.
FAR-INFRARED LASER INTERFEROMETRY MEASUREMENTS ON THE STP-3(M) REVERSED-FIELD PINCH
Shigeyuki Kubota, Masaaki Nagatsu, Takashige Tsukishima (Aichi Inst. of Tech., Toyota, Japan.), Hideki Arimoto, Koichi Sato, and Akio Matsuoka (Gunma Univ., Kiryu, Japan.) Sep. 1993 23 p
(DE94-765440; PSC-30) Avail: CASI HC A03/MF A01 (US Sales Only)

Far-infrared laser interferometry at 432 micro m was carried out on the STP-3(M) reversed-field pinch. Measurements along two vertical chords showed a change from a parabolic-like to a flat-like electron density profile after field reversal. A density profile inversion and a correlated toroidal magnetic flux perturbation were also observed during the transition from the current rising to the current decay phase. Measurements of electron density fluctuations indicated relative fluctuation levels of approx. 10% for both chords during the current rising phase and approx. 5% and approx. 15% during the current decay phase for the central and outer chords, respectively. Spectral analysis showed a approx. 30 kHz mode consistent with poloidal mode number m = 0 magnetic fluctuations, and a approx. 90 kHz mode localized to the outer region of the plasma, which was strongly excited during the current decay phase and may be connected to particle and energy transport in STP-3(M). DOE

N95-27876# Lawrence Livermore National Lab., Livermore, CA.
PORTABLE LASER LABORATORY
J. T. Weir Jul. 1994 2 p Presented at the 1994 CALIOPE ITR, Livermore, CA, 26-28 Apr. 1994
(Contract W-7405-eng-48)
(DE95-008376; UCRL-JC-118288; CONF-9404162-16) Avail: CASI HC A01/MF A01

A Portable Laser Laboratory (PLL) is being designed and built for the CALIOPE Program tests which will begin in October of 1994. The PLL is designed to give maximum flexibility for evolving laser experiments and can be readily moved by loading it onto a standard truck trailer. The internal configuration for the October experiments will support a two line DIAL system running in the mid-IR. Brief descriptions of the laser and detection systems are included. DOE

N95-27969# Sandia National Labs., Albuquerque, NM.
EFFECT OF NOISE ON FREQUENCY-RESOLVED OPTICAL GATING MEASUREMENTS OF ULTRASHORT PULSES
D. N. Fittinghoff, K. W. DeLong, C. L. Ladera, and R. Trebino 1995 8 p Presented at the 15th Conference on Lasers and Electro-Optics and 5th Quantum Electronics and Laser Science Conference, Baltimore, MD, 21-26 May 1995
(Contract DE-AC04-94AL-85000)
(DE95-007149; SAND-95-8467C; CONF-950540-3) Avail: CASI HC A02/MF A01

We study the effects of noise in Frequency-Resolved Optical Gating measurements of ultrashort pulses. We quantify the measurement accuracy in the presence of additive, multiplictive, and quantization noise, and discuss filtering and pre-processing of the data. DOE

N95-28027# Los Alamos National Lab., NM.
TIME-DEPENDENT MODEL FOR VERTICAL-CAVITY SURFACE-EMITTING LASER
L. Thode, G. Csanak, R. Hotchkiss, and C. Snell 1995 13 p Presented at the SPIE 1995: SPIE Conference on Optics, Electro-optics, and Laser Application in Science, Engineering and Medicine, San Jose, CA, 5-10 Feb. 1995
(Contract W-7405-eng-36)
(DE95-007880; LA-UR-95-534; CONF-950226-23) Avail: CASI HC A03/MF A01

Two models have been developed to simulate a vertical-cavity surface-emitting laser (VCSEL). The first model is a two-dimensional time-dependent solution of Maxwell's equations, with frequency-independent bulk dielectric and absorption coefficients. These bulk coefficients depend upon the material, lattice temperature, and carrier concentration. This field model is coupled with a frequency-dependent gain model that describes the quantum well regions in the time domain. Treatment of frequency-dependent media in a finite-difference time-domain code is computationally intensive. On the other hand, because the volume of the active region is small relative to the volume of the distributed laser cavity, the computational overhead is reasonable. A semi-empirical transport model is used to describe the bulk transport, which drives the quantum well transport. In addition, the semi-empirical model provides a spatial distribution for the lattice temperature and carrier concentrations. The second model is a three-dimensional solution of Maxwell's equations. The three-dimensional model can be used for cold-cavity calculations. The two-dimensional code generates the dielectric and absorption coefficients assuming azimuthal symmetry, providing the initial conditions for the three-dimensional calculation. DOE

N95-28059# Los Alamos National Lab., NM.
HIGH POWER FREE-ELECTRON LASER CONCEPTS AND PROBLEMS
J. C. Goldstein 1995 14 p Presented at the SPIE '95: SPIE Conference on Optics, Electro-optics, and Laser Application in Science, Engineering and Medicine, San Jose, CA, 5-10 Feb. 1995
(Contract W-7405-eng-36)
(DE95-007841; LA-UR-95-830; CONF-950226-17) Avail: CASI HC A03/MF A01

Free-electron lasers (FEL's) have long been thought to offer the potential of high average power operation. That potential exists because of several unique properties of FEL's, such as the removal of 'waste heat' at the velocity of light, the 'laser medium' (the electron beam) is impervious to damage by very high optical intensitites, and the technology of generating very high average power relativistic electron beams. In particular, if one can build a laser with a power extraction efficiency 11 which is driven by an electron beam of average Power P(sub EB), one expects a laser output power of P(sub L) = eta P(sub EB). One approach to FEL devices with large values of eta (in excess of 10%) is to use a 'tapered' (or nonuniform) wiggler. This approach was followed at several laboratories during the FEL development Program for the Strategic Defense Initiative (SDI) project. In this paper, we review some concepts and technical requirements for high-power tapered-wiggler FELs driven by radio-frequency linear accelerators (RF-linacs) which were developed during the SDI project. Contributions from three quite different technologies - RF-accelerators, optics, and magnets - are needed to construct and operate an FEL oscillator. The particular requirements on these technologies for a high-power FEL were far beyond the state of the art in those areas when the SDI project started, so significant advances had to be made before a working device could be constructed. Many of those requirements were not clearly understood when the project started, but were developed during the course of the experimental and theoretical research for the project. This information can be useful in planning future high-power FEL projects. DOE

N95-28104# California Univ., Berkeley. Lawrence Berkeley Lab, CA.
FINITE PULSE EFFECTS IN SELF-AMPLIFIED-SPONTANEOUS EMISSION
Kwang-Je Kim and Sang June Hahn Sep. 1994 10 p Presented at the 16th International Free Electron Laser Conference, Stanford, CA, 21-26 Aug. 1994
(Contract DE-AC03-76SF-00098)
(DE95-006585; LBL-36582; CONF-9408146-15) Avail: CASI HC A02/MF A01

The authors study the effects of the electron density profile on self amplified spontaneous emission (SASE). A general formalism in the linear regime is developed by deriving the coupled Maxwell-Klimontovich equations for an arbitrary density profile and including the effects of the energy spread, diffraction, and the betatron oscillation. An explicit solution is obtained for the one-dimensional (1-D) case. The temporal and the spectral intensity profiles of SASE depend linearly on the initial electron correlation function. The correlation function consists of two terms, a term giving rise to the usual spontaneous radiation and its amplification to SASE, and a term representing the coherent bunched beam effect. The latter term has been neglected so far in the treatments of SASE, but it could be significant when there is a variation in the electron density at a length scale comparable to the wavelength. The theory reproduces the well-known results when the electron density is uniform. It also reproduces a recent theory for a finite top-hat density profile and a vanishing energy spread. DOE

N95-28124# Los Alamos National Lab., NM.
PULSED LASER DEPOSITION OF ZEOLITIC MEMBRANES
N. M. Peachey, R. C. Dye, and P. D. Ries (Dow Chemical Co., Midland, MI.) 1995 8 p Presented at the 17th International Conference on Lasers and Applicators, Qubec, Canada, 12-14 Dec. 1994
(Contract W-7405-eng-36)
(DE95-006274; LA-UR-95-342; CONF-941259-1) Avail: CASI HC A02/MF A01

The pulsed laser deposition of zeolites to form zeolitic thin films is described. Films were grown using both mordenite and faujasite targets and were deposited on various substrates. The optimal films were obtained when the target and substrate were separated by 5 cm. These films are comprised of small crystallites embedded in an amorphous matrix. Transmission electron microscopy reveals that the amorphous material is largely porous and that the pores appear to be close to the same size as the parent zeolite. Zeolotic thin films are of interest for sensor, gas separation, and catalytic applications. DOE

N95-28128# Sandia National Labs., Albuquerque, NM.
SURFACE-EMITTING SEMICONDUCTOR LASER FOR INTRACAVITY SPECTROSCOPY AND MICROSCOPY
K. E. Meissner, P. L. Gourley, T. M. Brennan, B. E. Hammons, and A. E. McDonald 1995 10 p Presented at the SPIE 1995: SPIE Conference on Optics, Electro-optics, and Laser Application in Science, Engineering and Medicine, San Jose, CA, 5-10 Feb. 1995
(Contract DE-AC04-94AL-85000)
(DE95-007745; SAND-95-0162C; CONF-950226-13) Avail: CASI HC A02/MF A01

The authors demonstrate lasing action in a novel microcavity laser which can be utilized for intracavity spectroscopy as well as high contrast imaging of small (approximately 10(mu)m) structures. The system can be easily visualized as a Fabry-Perot cavity containing a gain media and an object for study. Since the primary constraint on the object is transparency at the lasing wavelength, investigation of lasing in objects such as microspheres, liquid droplets, and biological cells is possible. The resonator consists of an epitaxial NME grown mirror and gain region on a GaAs wafer. This is essentially an open-cavity vertical cavity surface emitting laser (VCSEL). The object to be studied is placed on the wafer and covered with a glass dielectric mirror which acts as the output coupler. When the semiconductor gain region is photo-pumped, the object within the cavity provides lateral optical confinement through its index difference with the surrounding media, increases the cavity Q, and thus encourages lasing action. The emitted laser light can be spectrally and spatially resolved. The narrow lasing lines can provide information about the lasing modes supported and the size of the object. The spatially resolved laser light provides high contrast microscopic images of the electromagnetic modes oscillating in the resonator. The authors present an investigation of stable lasing modes in polystyrene spheres. This device could prove useful in biomedical diagnostics. It covers the correct spatial dimensions as well as wavelength region. In fact, an integrated system of these devices may provide a high speed, compact method of performing cell diagnostics. DOE

N95-28132# Sandia National Labs., Albuquerque, NM.
COMPREHENSIVE NUMERICAL MODEL FOR CW VERTICAL-CAVITY SURFACE-EMITTING LASERS
G. R. Hadley, K. L. Lear, M. E. Warren, K. D. Choquette, J. W. Scott (Optical Concepts, Inc., Lompoc, CA.), and S. W. Corzine (California Univ., Santa Barbara, CA.) 1995 12 p Presented at the SPIE 1995: SPIE Conference on Optics, Electro-optics, and Laser Application in Science, Engineering and Medicine, San Jose, CA, 5-10 Feb. 1995
(Contract DE-AC04-94AL-85000)
(DE95-007758; SAND-95-0274C; CONF-950226-14) Avail: CASI HC A03/MF A01

The authors present a comprehensive numerical model for vertical-cavity surface-emitting lasers that includes all major processes effecting CW operation of axisymmetric devices. In particular, the model includes a description of the 2D transport of electrons and holes through the cladding layers to the quantum well(s), diffusion and recombination processes of these carriers within the wells, the 2D transport of heat throughout the device, and a multi-lateral-mode effective index optical model. The optical gain acquired by photons traversing the quantum wells is computed including the effects of strained band structure and quantum confinement. They employ the model to predict the behavior of higher-order lateral modes in proton-implanted devices, and to provide an understanding of index-guiding in devices fabricated using selective oxidation. DOE

N95-28219# Sandia National Labs., Albuquerque, NM.
LOW POWER LIMITS IN ULTRASHORT PULSE MEASUREMENT USING FREQUENCY-RESOLVED OPTICAL GATING
D. N. Fittinghoff, K. W. DeLong, R. Jennings, C. L. Ladera, and R. Trebino 1995 4 p Presented at the 15th Conference on Lasers and Electro-Optics and 5th Quantum Electronics and Laser Science Conference, Baltimore, MD, 21-26 May 1995
(Contract DE-AC04-94AL-85000)
(DE95-007150; SAND-95-8465C; CONF-950540-4) Avail: CASI HC A01/MF A01

We quantify the low power limits in SHG and PG FROG, in both single- and multi-shot configurations, for pulses as weak as 30 peccadilloes. We anticipate that femtojoule operation may be possible. DOE

N95-28220# Sandia National Labs., Albuquerque, NM.
ULTRASHORT PULSE RETRIEVAL USING FROG TRACE IRRADIANCE MOMENTS AND THE ADAPTIVE NEURAL NETWORKS BACKPROPAGATION ALGORITHM
C. L. Ladera, K. W. DeLong, R. Trebino, and D. N. Fittinghoff 1995 5 p Presented at the 15th Conference on Lasers and Electro-optics and 5th Quantum Electronics and Laser Science Conference, Baltimore, MD, 21-26 May 1995
(Contract DE-AC04-94AL-85000)
(DE95-007153; SAND-95-8485C; CONF-950540-5) Avail: CASI HC A01/MF A01

We use the irradiance moments of traces obtained in Frequency Resolved Optical Gating and the Feed-forward Backpropagation Algorithm of Adaptive Neural Networks for recovering the phase and the intensity of ultrashort laser pulses. DOE

N95-28223# Sandia National Labs., Albuquerque, NM.
SWORDS TO PLOWSHARES: SHOCK WAVE APPLICATIONS TO ADVANCED LITHOGRAPHY
T. G. Trucano, D. E. Grady, G. D. Kubiak, M. E. Kipp, R. E. Olson, and A. Farnsworth 1995 18 p Presented at the 1994 Hypervelocity Impact Symposium, Santa Fe, NM, 16-20 Oct. 1994
(Contract DE-AC04-94AL-85000)
(DE95-008154; SAND-95-0307C; CONF-9410131-12) Avail: CASI HC A03/MF A01

Extreme UltraViolet Lithography (EUVL) seeks to apply radiation in a wavelength region centered near 13 nm to produce microcircuits having features sizes 0.1 micron or less. A critical requirement for the commercial application of this technology is the development of an economical, compact source of this radiation which is suitable for lithographic applications. A good candidate is a laser-plasma source, which is generated by the interaction of an intermediate intensity laser pulse (up to 10(exp 12) W/sq cm) with a metallic target. While such a source has radiative characteristics which satisfy the needs of an EUVL source, the debris generated during the laser-target interaction strikes at the economy of the source. Here, the authors review the use of concepts and computer modeling, originally developed for hypervelocity impact analysis, to study this problem. DOE

N95-28330# Malaya Univ., Kuala-Lumpur (Malaysia).
APPLICATIONS OF LASERS AND ELECTRO-OPTICS
B. C. Tan, K. S. Low, Y. H. Chen, Harith Ahmad, and T. Y. Tou 1994 16 p Presented at the National Seminar on the Assessment of IRPA Research Achievement in 5th Malaysian Plan: Industrial Sector, Kedah, Malaysia, 20-24 Dec. 1991
(DE95-600841; INIS-mf-14339; CONF-9112185) Avail: CASI HC A03/MF A01 (US Sales Only)

Supported by the IRPA Programme on Laser Technology and Applications, many types of lasers have been designed, constructed and applied in various areas of science, medicine and industries. Amongst these lasers constructed were high power carbon dioxide lasers, rare gas halide excimer lasers, solid state Neodymium-YAG lasers, nitrogen lasers, flashlamp pumped dye lasers and nitrogen and excimer laser pumped dye lasers. These lasers and the associated electro-optics system, some with computer controlled, are designed and developed for the following areas of applications: (1) industrial applications of high power carbon dioxide lasers for making of i.c. components and other materials processing purposes -- prototype operational systems have been developed; (2) Medical applications of lasers for cancer treatment using the technique of photodynamic therapy -- a new and more effective treatment protocol has been proposed; (3) agricultural applications of lasers in palm oil and palm fruit-fluorescence diagnostic studies -- fruit ripeness signature has been developed and palm oil oxidation level were investigated; (4) development of atmospheric pollution monitoring systems using laser lidar techniques -- laboratory scale systems were developed; and (5) other applications of lasers including laser holographic and interferometric methods for the non destructive testing of materials. DOE

N95-28333 University of Central Florida, Orlando, FL. Center for Research in Electro-Optics and Lasers.
PASSIVE SPATIAL BEAM CONTROL, APPENDIX Final Report
Eric W. VanStryland 29 Sep. 1994 434 p Limited Reproducibility: More than 20% of this document may be affected by microfiche quality
(Contract DAAB07-88-6-F405)
(AD-A288913; NV-95-C01) Avail: Issuing Activity (Defense Technical Information Center (DTIC))

This document discussed the following sections: Eclipsing Z-scan measurement of lambda/10(exp 4)wave-front distortion; Time-resolved Z-scan measurements of optical nonlinearities; Nondegenerate optical Kerr effect in semiconductors; Characterization of nonlinear optical absorption and referaction; High dynamic range passive optical limiters; Characterization of nonlinear absorption and refraction in advanced materials; Nonlinear optical materials at 10 micro m: from picoseconds to nanoseconds; Laser-induced acoustic photon grating in semiconductor thin films; and Characterization of nonlinear optical materials. Author

N95-28398# Colorado Univ., Boulder, CO.
TIME-RESOLVED FTIR EMISSION STUDIES OF LASER PHOTOFRAGMENTATION AND RADICAL REACTIONS
1994 6 p
(Contract DE-FG02-88ER-13860)
(DE95-008125; DOE/ER-13860/T1) Avail: CASI HC A02/MF A01

Fourier transform infrared emission experiments were used to study photofragmentation processes, single collision reactions, energy transfer events, and laser-initiated radical-radical reactions: CH3 + O, Cl + C2H5, CF3CH2 + D, H + H2O, H + HF, and H + NH2. DOE

N95-28458 Oklahoma State Univ., Stillwater, OK.
CHARACTERIZATION OF SOLID STATE LASER AND NONLINEAR OPTICAL MATERIALS Final Report, 12 Apr. 1991 - 30 Jun. 1994
Jin-Joo Song 2 Feb. 1995 288 p Limited Reproducibility: More than 20% of this document may be affected by microfiche quality
(Contract DAAL03-91-G-0099)
(AD-A291684; ARO-28472.11-PH) Avail: Issuing Activity (Defense Technical Information Center (DTIC))

Optical properties of materials having applications in solid state laser systems were investigated. The work was divided into two areas based on the materials useful in the different methods for obtaining frequency agility: narrow line emitters with multiple lasing channels and nonlinear optical materials. In the first category the spectral dynamics and lasing properties of a variety of materials such as fluoride and oxide crystals and glasses codoped with two or more rare-earth ions were studied and computers models developed to explain their spectral dynamics. The nonlinear optical materials investigated included rare-earth doped glasses, photorefractive crystals, and semiconductors. Laser spectroscopy techniques used to characterize these materials included four-wave mixing, two photon absorption and fluorescence line narrowing. The results were related to laser device parameters in order to determine the basic physical processes in the operational device parameters. DTIC

N95-28509 New Mexico State Univ., Las Cruces, NM. Physics Dept.
LASER BEAM AEROSOL INTERACTIONS Final Report, 1 Oct. 1990 - 28 Feb. 1995
Robert L. Armstrong 28 Feb. 1995 9 p Limited Reproducibility: More than 20% of this document may be affected by microfiche quality
(Contract DAAL03-90-G-0176)
(AD-A291723; NMSU-PHYS-01-95; ARO-28052.1-GS) Avail: Issuing Activity (Defense Technical Information Center (DTIC))

This report details experimental investigations undertaken to understand the interactions of aerosol particles with laser beams. Both optical and thermal interactions were examined, including elastic scattering and fluorescence, as well as a variety of nonlinear interactions. A number of new and significant experimental findings we made which are detailed in this report. These findings provide the experimental basis for potential applications in the fields of atmospheric probing, remote sensing, and photonics. DTIC

N95-28549# Sandia National Labs., Livermore, CA.
PHASE RETRIEVAL AND TIME-FREQUENCY METHODS IN THE MEASUREMENT OF ULTRASHORT LASER PULSES
K. W. DeLong, D. N. Fittinghoff, C. L. Ladera, and R. Trebino 1995 4 p Presented at the Signal Recovery and Synthesis Conference, Salt Lake City, UT, 12 Mar. 1995
(Contract DE-AC04-94AL-85000)
(DE95-006499; SAND-95-8458C; CONF-950396-2) Avail: CASI HC A01/MF A01

Recently several techniques have become available to measure the time- (or frequency-) dependent intensity and phase of ultrashort laser pulses. One of these, Frequency-Resolved Optical Gating (FROG), is rigorous and has achieved single-laser-shot operation. FROG combines the concepts of time-frequency analysis in the form of spectrogram generation (in order to create a two-dimensional problem), and uses a phase-retrieval-based algorithm to invert the experimental data to yield the intensity and phase of the laboratory laser pulse. In FROG it is easy to generate a spectrogram of the unknown signal, and inversion of the spectrogram to recover the signal is the main goal. Because the temporal width of a femtosecond laser pulse is much shorter than anything achievable by electronics, FROG uses the pulse to measure itself. In FROG, the laser pulse is split into two replicas of itself by a partially reflecting beamsplitter, and the two replicas interact with each other in a medium with an instantaneous nonlinear-optical response. This interaction generates a signal field that is then frequency-resolved using a spectrometer. The spectrum of the signal field is measured for all relevant values of the temporal delay between the two pulses. Here, the authors employ FROG and FROG related techniques to measure the time-dependent intensity and phase of an ultrashort laser pulse. DOE

N95-28633 Air Force Systems Command, Wright-Patterson AFB, OH. National Air Intelligence Center.
INFLUENCES OF FILM STRUCTURES ON LASER DAMAGE THRESHOLDS
Wu Zhouling and Fan Zhengxiu 15 Dec. 1994 14 p Transl. into ENGLISH from Guangxue Xuebao, China, v. 9, no. 9, Sep. 1989 p 830-834 Limited Reproducibility: More than 20% of this document may be affected by microfiche quality
(AD-A289647; NAIC-ID(RS)T-0639-93) Avail: Issuing Activity (Defense Technical Information Center (DTIC))

This article takes TiO2/SiO2 and ZrO2/SiO2 film systems as examples and studies the influences of different film structures. It combines studies on measurements of optical losses and the effects of protective film thicknesses, making a preliminary probe into laser damage mechanisms as associated with optical thin films. DTIC

N95-28650 Air Force Systems Command, Wright-Patterson AFB, OH. National Air Intelligence Center.
THERMALLY-INDUCED UNSYMMETRIC OPTICAL DISTORTION OF OUTPUT WINDOW OF HIGH-POWER CO2 LASER
Chen Peifeng and Qiu Junlin 16 Dec. 1994 11 p Transl. into ENGLISH from Jiguang Zazhi, China, v. 15, no. 3, 1994 p 113-116 Limited Reproducibility: More than 20% of this document may be affected by microfiche quality
(AD-A289604; NAIC-ID(RS)T-0702-94) Avail: Issuing Activity (Defense Technical Information Center (DTIC))

Thermally-induced unsymmetric optical distortion of the output window of high-power CO2 lasers has been investigated theoretically and experimentally. This kind of distortion could lead to resonator misalignment. DTIC

37 MECHANICAL ENGINEERING

Includes auxiliary systems (nonpower); machine elements and processes; and mechanical equipment.

N95-26504 Department of the Navy, Washington, DC.
VALVE MECHANISM FOR AN ACOUSTIC MODULATOR Patent
James L. Sullivan, inventor (to Navy) and Gary S. Borgen, inventor (to Navy) 27 Sep. 1994 12 p Filed 23 Aug. 1993
(AD-D017263; US-Patent-5,349,986; US-Patent-Appl-SN-112814) Avail: US Patent and Trademark Office

A valve mechanism for an acoustic modulator which modulates air flowing through the acoustic modulator. The valve mechanism comprises a pair of cylindrical shaped members with each member having a plurality of elongated ports. The first cylindrical shaped member is held in a fixed position, while the second cylindrical shaped member is movable with respect to the first member. There is located at the lower end of the second cylindrical shaped member a drive coil which is positioned in a magnetic field such that when the coil is excited by an electrical sinusoidal input signal, movement of the second member occurs, partially aligning the ports of the second member with the ports of the first member which opens the valve mechanism. The sinusoidal input signal causes a frequency 'doubling' to occur, that is the valve mechanism of the present invention completes an open-close-open-close cycle during each cycle of the sinusoidal input signal. This frequency 'doubling' modulation of air flow through the acoustic modulator is accomplished by exposing the same open port area for both the positive going portion and the negative going portion of the sinusoidal input signal. The valve mechanism 'closes' when the sinusoidal input signal is at zero volts. DTIC

N95-26688 Army Test and Evaluation Command, Aberdeen Proving Ground, MD.

POWER TRAIN TORQUE MEASUREMENT Test Operations Procedure

30 Dec. 1994 11 p Supersedes report dated 25 Aug. 1981, AD-A103787 Limited Reproducibility: More than 20% of this document may be affected by microfiche quality

(AD-A289577; TOP-2-2-806) Avail: Issuing Activity (Defense Technical Information Center (DTIC))

This test operations procedure (TOP) describes methods for measuring torque in tracked and wheeled vehicle power trains. DTIC

N95-26774*# National Aeronautics and Space Administration. Lewis Research Center, Cleveland, OH.

COMPARISON OF LIFE THEORIES FOR ROLLING-ELEMENT BEARINGS

Erwin V. Zaretsky, Joseph V. Poplawski (Poplawski, J. V. and Associates, Bethlehem, PA.), and Steven M. Peters (Poplawski, J. V. and Associates, Bethlehem, PA.) Apr. 1995 28 p Presented at Annual Meeting, Chicago, IL, 14-19 May 1995; sponsored by Society of Tribologists and Lubrication Engineers

(RTOP 505-63-5B)

(NASA-TM-106585; E-9473; NAS 1.15:106585) Avail: CASI HC A03/MF A01

Nearly five decades have passed since G. Lundberg and A. Palmgren published their life theory in 1947 and 1952 and it was adopted as an ANSI/ABMA and ISO standard in 1950 and 1953. Subsequently, many variations and deviations from their life theory have been proposed, the most recent being that of E. Ioannides and T.A. Harris in 1985. This paper presents a critical analysis comparing the results of different life theories and discussing their implications in the design and analysis of rolling-element bearings. Variations in the stress-life relation and in the critical stress related to bearing life are discussed using stress fields obtained from three-dimensional, finite-element analysis of a ball in a nonconforming race under varying load. The results showed that for a ninth power stress-life exponent the Lundberg-Palmgren theory best predicts life as exhibited by most air-melted bearing steels. For a 12th power relation reflected by modern bearing steels, a Zaretsky-modified Weibull equation is superior. The assumption of a fatigue-limiting stress distorts the stress-life exponent and overpredicts life. Author

N95-26926 Carnegie-Mellon Univ., Pittsburgh, PA. Robotics Inst.

A SYSTEMS ENGINEERING APPROACH TO ELECTRO-MECHANICAL RECONFIGURATION FOR MOBILITY AUTONOMY

R. C. Coulter 15 Aug. 1994 48 p Limited Reproducibility: More than 20% of this document may be affected by microfiche quality

(Contracts DAAE07-90-C-R059; DACA76-89-C-0014)

(AD-A289479; CMU-RI-TR-94-27) Avail: Issuing Activity (Defense Technical Information Center (DTIC))

The performance of a system is a function of the performance of each of its individual components. This work explores the relationship between system performance and subcomponent performance in the electro-mechanical configuration of a mobile robot under the premise that the performance of the mobile robot can be greatly improved through the systematic analysis and design of an efficient electro-mechanical configuration. This work further presumes that the concept of mobility adequately encompasses the metrics by which complete mobile robotic systems may be measured; the purpose of building a mobile robot is assumed to be the creation of a maximally mobile autonomous machine. The performance cost of converting an existing machine into an autonomous machine is then measured by its mobility degradation. DTIC

N95-27098 Carnegie-Mellon Univ., Pittsburgh, PA. Robotics Inst.

DYNAMIC COUPLING OF UNDERACTUATED MANIPULATORS Research Report

Marcel Bergerman, Christopher Lee, and Yangsheng Xu Aug. 1994 36 p Limited Reproducibility: More than 20% of this document may be affected by microfiche quality

(AD-A289404; CMU-RI-TR-94-25) Avail: Issuing Activity (Defense Technical Information Center (DTIC))

In recent years, researchers have been turning their attention to so called underactuated systems, where the term underactuated refers to the fact that the system has more joints than control actuators. Some examples of underactuated systems are robot manipulators with failed actuators; free-floating space robots, where the base can be considered as a virtual passive linkage in inertia space; legged robots with passive joints; hyper-redundant (snake-like) robots with passive joints, etc. From the examples above, it is possible to justify the importance of the study of underactuated systems. For example, if some actuators of a conventional manipulator fail, the loss of one or more degrees of freedom may compromise an entire operation. In free-floating space systems, the base (satellite) can be considered as a 6-DOF device without positioning actuators. Finally, manipulators with passive joints and hyper-redundant robots with few actuators are important from the viewpoint of energy saving, lightweight design and compactness. DTIC

N95-27178*# National Aeronautics and Space Administration. Lewis Research Center, Cleveland, OH.

EFFECT OF HOOP STRESS ON BALL BEARING LIFE PREDICTION

Erwin V. Zaretsky, Richard August (NYMA, Inc., Brook Park, OH.), and Harold H. Coe May 1995 21 p Presented for Annual Meeting, Chicago, IL, 14-19 May 1995; sponsored by the Society of Tribologists and Lubrication Engineers

(RTOP 505-63-5B)

(NASA-TM-106874; E-9497; NAS 1.15:106874) Avail: CASI HC A03/MF A01

A finite-element analysis (FEA) of a generic, dimensionally normalized inner race of an angular-contact ball bearing was performed under varying conditions of speed and the press (or interference) fit of the inner-race bore on a journal. The FEA results at the ball-race contact were used to derive an equation from which was obtained the radius of an equivalent cylindrical bearing race with the same or similar hoop stress. The radius of the equivalent cylinder was used to obtain a generalized closed-form approximation of the hoop stresses at the ball-inner-race contact in an angular-contact ball bearing. A life analysis was performed on both a 45- and a 120-mm-bore, angular-contact ball bearing. The predicted lives with and without hoop stress were compared with experimental endurance results obtained at 12000 and 25000 rpm with the 120-mm-bore ball bearing. A life factor equation based on hoop stress is presented. Author

N95-27244*# Alabama Univ., Huntsville, AL. Center for Applied Optics.

SXI PROTOTYPE MIRROR MOUNT Final Report

Apr. 1995 81 p

(Contract NAS8-38609)

(NASA-CR-196613; NAS 1.26:196613) Avail: CASI HC A05/MF A01

This final report describes the work performed from June 1993 to January 1995. The purpose of this contract was to provide optomechanical engineering and fabrication support to the Solar X-ray Imager (SXI) program in the areas of mirror, optical bench and camera assemblies of the telescope. The Center for Applied Optics (CAO) worked closely with the Optics and S&E technical staff of MSFC to develop and investigate the most viable and economical options for the design and fabrication of a number of parts for the various telescope assemblies. All the tasks under this delivery order have been successfully completed within budget and schedule. Author (revised)

N95-27373*# National Aeronautics and Space Administration. Lewis Research Center, Cleveland, OH.
DIAGNOSIS OF HELICOPTER GEARBOXES USING STRUCTURE-BASED NETWORKS
Vinay B. Jammu (Massachusetts Univ., Amherst, MA.), Kourosh Danai (Massachusetts Univ., Amherst, MA.), and David G. Lewicki (Army Research Lab., Cleveland, OH.) Jun. 1995 7 p Presented at the Symposium on Applied Monitoring and Diagnositics, Seattle, WA, 21-23 Jul. 1995; sponsored by American Automatic Control Council
(RTOP 505-62-36; DA Proj. 1L1-62211-A-47-A)
(NASA-TM-106932; E-9659; NAS 1.15:106932; ARL-TR-761) Avail: CASI HC A02/MF A01

A connectionist network is introduced for fault diagnosis of helicopter gearboxes that incorporates knowledge of the gearbox structure and characteristics of the vibration features as its fuzzy weights. Diagnosis is performed by propagating the abnormal features of vibration measurements through this Structure-Based Connectionist Network (SBCN), the outputs of which represent the fault possibility values for individual components of the gearbox. The performance of this network is evaluated by applying it to experimental vibration data from an OH-58A helicopter gearbox. The diagnostic results indicate that the network performance is comparable to those obtained from supervised pattern classification. Author

N95-27545# Oak Ridge National Lab., TN.
ADVANCES IN WELDING SCIENCE: A PERSPECTIVE
S. A. David, J. M. Vitek, S. S. Babu (Pennsylvania State Univ., University Park, PA.), and T. DebRoy (Pennsylvania State Univ., University Park, PA.) 1995 23 p Presented at the Welding Technology Institute of Australia (WTIA) Annual Conference, Melbourne, Australia, 24-27 Oct. 1994
(Contract DE-AC05-84OR-21400)
(DE95-006745; CONF-9410296-1) Avail: CASI HC A03/MF A01

The ultimate goal of welding technology is to improve the joint integrity and increase productivity. Over the years, welding has been more of an art than a science, but in the last few decades major advances have taken place in welding science and technology. With the development of new methodologies at the crossroads of basic and applied sciences, enormous opportunities and potential exist to develop a science-based tailoring of composition, structure, and properties of welds with intelligent control and automation of the welding processes. DOE

N95-27698*# National Aeronautics and Space Administration. Lewis Research Center, Cleveland, OH.
USING HOB OFFSET TO BALANCE DYNAMIC STRENGTH IN SPUR GEARS
Chuen-Huei Liou (Memphis Univ., Memphis, TN.), Hsi Hsiang Lin (Memphis Univ., Memphis, TN.), Fred B. Oswald, and Dennis P. Townsend May 1995 11 p Presented at the 31st Joint Propulsion Conference and Exhibit, San Diego, CA, 10-12 Jul. 1995; sponsored by AIAA, ASME, SAE, and ASEE
(RTOP 505-62-36; DA Proj. 1L1-62211-A-47-A)
(NASA-TM-106934; E-9661; NAS 1.15:106934; ARL-TR-764; AIAA Paper 95-3046) Avail: CASI HC A03/MF A01

This paper presents an analytical study on the effect of hob offset on the dynamic tooth strength of spur gears. The study was limited to equal and opposite offset values applied to the pinion and gear to maintain the standard operating center distance. The analysis presented in this paper was performed using a new version of the NASA gear dynamics code DANST. The operating speed of the transmission has a significant influence on the amount of hob offset required to equalize the dynamic stresses in the pinion and gear. In the transmission studied, at low speeds, the optimum hob offset value was found to fluctuate. At higher speeds, the optimum value was constrained by the minimum allowed thickness at the tip of the pinion tooth. For gears that must operate over a range of speeds, an average offset value may be used. Spur gears designed with the procedure presented here can have significant improvements in load capacity. Author

N95-27844 Southampton Univ. (England). Inst. of Sound and Vibration Research.
THE VIBRATION TRANSMISSION OF LIFT TRUCK SUSPENSION SEATS
Xuting Wu, Michael J. Griffin, and Christopher H. Lewis Apr. 1995 41 p
(ISVR-TR-245) Copyright Avail: Issuing Activity (Southampton Univ., Southampton, England)

The vibration isolation efficiencies of three suspension seats have been measured according to a draft standard for the vibration transmitted by the seats of lift trucks. The vertical vibration transmission ratios were measured with spectra corresponding to the z-axis motions of two classes of lift truck. The results of the measurements on each seat are presented in appendices. The effect of subject weight is discussed and the 50th percentile subject weight is suggested to replace the 55 (+0 to -3) kg and 98 (+5 to -0) kg subject weight recommended in the draft. End-stop impacts may be an important problem with real vehicle motion. It is suggested that a method of testing for end-stop impacts should be included in the standard. Author

N95-27855*# Army Research Lab., Cleveland, OH.
VIBRATION ANALYSIS OF A SPLIT PATH GEARBOX
Timothy L. Krantz and Majid Rashidi (Cleveland State Univ., OH.) May 1995 15 p Presented at the 31st Joint Propulsion Conference, San Diego, CA, 10-12 Jul. 1995; cosponsored by AIAA, SAE, and ASME
(RTOP 505-62-36; DA Proj. 1L1-62211-A-47-A)
(NASA-TM-106875; E-9498; NAS 1.15:106875; ARL-TR-723; AIAA Paper 95-3048) Avail: CASI HC A03/MF A01

Split path gearboxes can be attractive alternatives to the common planetary designs for rotorcraft, but because they have seen little use, they are relatively high risk designs. To help reduce the risk of fielding a rotorcraft with a split path gearbox, the vibration and dynamic characteristics of such a gearbox were studied. A mathematical model was developed by using the Lagrangian method, and it was applied to study the effect of three design variables on the natural frequencies and vibration energy of the gearbox. The first design variable, shaft angle, had little influence on the natural frequencies. The second variable, mesh phasing, had a strong effect on the levels of vibration energy, with phase angles of 0 deg and 180 deg producing low vibration levels. The third design variable, the stiffness of the shafts connecting the spur gears to the helical pinions, strongly influenced the natural frequencies of some of the vibration modes, including two of the dominant modes. We found that, to achieve the lowest level of vibration energy, the natural frequencies of these two dominant modes should be less than those of the main excitation sources. Author

N95-27875# Oak Ridge National Lab., TN.
PUMPING CHARACTERISTICS OF A CRYOPUMP WITH Ar SORBENT IN He AND IN D2/He MIXTURE
M. M. Menon, M. R. Wade, R. Maingi, D. L. Hillis, G. J. Laughon (General Atomics Co., San Diego, CA.), and M. A. Mahdavi (General Atomics Co., San Diego, CA.) 1995 14 p Presented at the 41st Annual American Vacuum Society Symposium, Denver, CO, 24-28 Oct. 1994, and at the 3rd International Conference on Nanometer-Scaled Science and Technology, Denver, CO, 24-28 Oct. 1994
(Contracts DE-AC05-84OR-21400; DE-AC03-89ER-51114)
(DE95-007049; CONF-941001-11; CONF-9410295-1) Avail: CASI HC A03/MF A01

The He ash generated as a result of D/T burn in a fusion reactor must be exhausted from the plasma to avoid fuel dilution effects. In view of this, transport and exhaust studies of He in fusion plasmas are getting increasing attention in recent years. In fusion plasmas, the exhaust gas will be a combination of D2 and He, with He forming only a small fraction (about 10%). The authors have investigated the cryosorption pumping characteristics of pure He and a mixture of D2 and He (90% D2) using a cryosorption pump with condensed layers of Ar as sorbent. A cryocondensation pump cooled by liquid He at 4.3 K, and located in the outboard divertor region of the DIII-D tokamak, was used for the experiment. The investigation was conducted in a pressure regime that is relevant for particle exhaust from fusion plasmas. The experiment revealed that: (1) cryosorption pumping speed of pure He drops precipitously if the Ar/He ratio falls below about 20; (2) the pumping speed for He in a D2/He mixture decreases in an exponential manner with the amount of D2 pumped; (3) increasing the thickness of Ar in the range of 1 - 12 micro m had little effect on the pumping speed for He in a D2/He mixture; and (4) for a pumping surface coated with a thick (greater than 2 micro m)layer of Ar, surrounded by a radiation shield having a transparency factor of about 6, a He pumping speed in the range of 15-25 cu m/s sq m, in the millitorr pressure range for pulse duration of about 5 s can be obtained after pumping about 80 torr 1 of D2. DOE

N95-27911*# National Aeronautics and Space Administration. Lewis Research Center, Cleveland, OH.
SYSTEM IDENTIFICATION OF DAMPED TRUSS-LIKE SPACE STRUCTURES Ph.D. Thesis - Cleveland State Univ., Mar. 1994
Sasan Armand May 1995 281 p
(RTOP 505-69-50)
(NASA-TM-106638; E-8941; NAS 1.15:106638) Avail: CASI HC A13/MF A03

A spacecraft payload flown on a launch vehicle experiences dynamic loads. The dynamic loads are caused by various phenomena ranging from the start-up of the launch vehicle engine to wind gusts. A spacecraft payload should be designed to meet launch vehicle dynamic loads. One of the major steps taken towards determining the dynamic loads is to correlate the finite element model of the spacecraft with the test results of a modal survey test. A test-verified finite element model of the spacecraft should possess the same spatial properties (stiffness, mass, and damping) and modal properties (frequencies and mode shapes) as the test hardware representing the spacecraft. The test-verified and correlated finite element model of the spacecraft is then coupled with the finite element model of the launch vehicle for analysis of loads and stress. Modal survey testing, verification of a finite element model, and modification of the finite element model to match the modal survey test results can easily be accomplished if the spacecraft structure is simple. However, this is rarely the case. A simple structure here is defined as a structure where the influence of nonlinearity between force and displacement (uncertainty in a test, for example, with errors in input and output), and the influence of damping (structural, coulomb, and viscous) are not pronounced. The objective of this study is to develop system identification and correlation methods with the focus on the structural systems that possess nonproportional damping. Two approaches to correct the nonproportional damping matrix of a truss structure were studied, and have been implemented on truss-like structures such as the National Aeronautics and Space Administration's space station truss. The results of this study showed nearly 100 percent improvement of the correlated eigensystem over the analytical eigensystem. The first method showed excellent results with up to three modes used in the system identification process. The second method could handle more modes, but required more computer usage time, and the results were less accurate than those of the first method. Author

N95-27947# Oak Ridge National Lab., TN.
ANALYTICAL AND EXPERIMENTAL EVALUATION OF JOINING SILICON CARBIDE TO SILICON CARBIDE AND SILICON NITRIDE TO SILICON NITRIDE FOR ADVANCED HEAT ENGINE APPLICATIONS, PHASE 2 Final Report
G. J. Sundberg, A. M. Vartabedian, J. A. Wade, and C. S. White Oct. 1994 122 p
(Contract DE-AC05-84OR-21400)
(DE95-005761; ORNL/Sub-87-SB045/2) Avail: CASI HC A06/MF A02

The purpose of joining, Phase 2 was to develop joining technologies for HIP'ed Si3N4 with 4wt% Y2O3 (NCX-5101) and for a siliconized SiC (NT230) for various geometries including: butt joins, curved joins and shaft to disk joins. In addition, more extensive mechanical characterization of silicon nitride joins to enhance the predictive capabilities of the analytical/numerical models for structural components in advanced heat engines was provided. Mechanical evaluation were performed by: flexure strength at 22 C and 1,370 C, stress rupture at 1,370 C, high temperature creep, 22 C tensile testing and spin tests. While the silicon nitride joins were produced with sufficient integrity for many applications, the lower join strength would limit its use in the more severe structural applications. Thus, the silicon carbide join quality was deemed unsatisfactory to advance to more complex, curved geometries. The silicon carbide joining methods covered within this contract, although not entirely successful, have emphasized the need to focus future efforts upon ways to obtain a homogeneous, well sintered parent/join interface prior to siliconization. In conclusion, the improved definition of the silicon carbide joining problem obtained by efforts during this contract have provided avenues for future work that could successfully obtain heat engine quality joins. DOE

N95-28029# Lawrence Livermore National Lab., Livermore, CA.
A HYBRID VEHICLE EVALUATION CODE AND ITS APPLICATION TO VEHICLE DESIGN. REVISION 1
S. M. Aceves and J. R. Smith 15 Sep. 1994 26 p Presented at the Society of Automotive Engineers International Congress and Exposition, Detroit, MI, 27 Feb. - 2 Mar. 1995
(Contract W-7405-eng-48)
(DE95-008053; UCRL-JC-117918-Rev-1; CONF-950256-1) Avail: CASI HC A03/MF A01

This paper describes a hybrid vehicle simulation model which can be applied to many of the vehicles currently being considered for low pollution and high fuel economy. The code operates in batch mode with all the vehicle information stored in data files. The code calculates fuel economy for three driving schedules, time for 0-96 km/h at maximum acceleration, hill climbing performance, power train dimensions, and pollution generation rates. This paper also documents the application of the code to a hybrid vehicle that utilizes a hydrogen internal combustion engine. The simulation model is used for parametric studies of the vehicle. The results show the fuel economy of the vehicle as a function of vehicle mass, aerodynamic drag, engine efficiency, accessory load, and flywheel efficiency. The code also calculates the minimum flywheel energy and power to obtain a desired performance. The hydrogen hybrid vehicle analyzed in the paper has a predicted range of 480 km (300 miles), with a gasoline equivalent fuel efficiency of 34.2 km/liter (80.9 mpg). DOE

N95-28070# Argonne National Lab., IL.
TRANSPORTATION R AND D INCLUDED IN THERMAL AND MECHANICAL SCIENCES PROGRAM
1995 30 p
(Contract W-31-109-eng-38)
(DE95-008275; ANL/ITD/CP-85767) Avail: CASI HC A03/MF A01

Argonne National Laboratory is a multiprogram research and development laboratory operated by The University of Chicago for the US Department of Energy. At Argonne, applied research in thermal and mechanical sciences is performed within the Thermal and Mechanical Sciences Section of the Energy Technology Division. Current program areas include compact evaporators and condensers for the process and transportation industries, ice slurries for district cooling, advanced fluids for improved heat transfer and reduced pressure drop, flow-induced vibration and flow distribution in shell-and-tube heat exchangers, and dynamics and control of maglev systems. In general, the objective of the research is to extend the technology base in each of these areas and to facilitate its application in solving problems of importance to US industries and utilities. This is accomplished by developing validated design correlations and predictive methods. The staff of the Thermal and Mechanical Sciences Section have extensive experimental and analytical experience in heat transfer, multiphase flow, structural dynamics and control, fluid-structure interaction, transient flow and mixing, thermally driven flows, and flow visualization using ultra-high-speed video. Large, general-purpose test facilities and smaller, single-purpose test apparatuses are available for experiments and component design evaluation. A world-class capability in the study of flow-induced vibrations exists within the section. Individual fact sheets, describing currently active research program areas and related facilities and listing, as a contact, the principal investigator, are included. DOE

N95-28139# Lawrence Livermore National Lab., Livermore, CA.
A HYBRID VEHICLE EVALUATION CODE AND ITS APPLICATION TO VEHICLE DESIGN, REVISION 2
S. M. Aceves and J. R. Smith 13 Dec. 1994 26 p Presented at the Society of Automotive Engineers International Congress and Exposition, Detroit, MI, 27 Feb. - 2 Mar. 1995
(Contract W-7405-eng-48)
(DE95-008060; UCRL-JC-117918-Rev-2; CONF-950256-1-Rev-2) Avail: CASI HC A03/MF A01

This paper describes a hybrid vehicle simulation model which can be applied to many of the vehicles currently being considered for low pollution and high fuel economy. The code operates in batch mode with all the vehicle information stored in data files. The code calculates power train dimensions, fuel economy for three driving schedules, time for 0-96 km/h at maximum acceleration, hill climbing performance, and pollution generation rates. This paper also documents the application of the code to a hybrid vehicle that utilizes a hydrogen internal combustion engine. The simulation model is used for parametric studies of the vehicle. The results show the fuel economy of the vehicle as a function of vehicle mass, aerodynamic drag, engine efficiency, accessory load, and flywheel efficiency. The code also calculates the minimum flywheel energy and power to obtain a desired performance. The hydrogen hybrid vehicle analyzed in the paper has a range of 480 km (300 miles), with a predicted gasoline equivalent fuel efficiency of 33.7 km/liter (79.3 mpg). DOE

N95-28256* National Aeronautics and Space Administration. Ames Research Center, Moffett Field, CA.
COOLING APPARATUS AND COUPLINGS THEREFOR Patent
Curtis Lomax, inventor (to NASA) and Bruce Webbon, inventor (to NASA) 16 Nov. 1993 11 p Filed 21 May 1991
(NASA-Case-ARC-11921-1; US-Patent-5,261,482;
US-Patent-Appl-SN-703649; US-Patent-Class-165-10;
US-Patent-Class-165-104.17; US-Patent-Class-165-78;
US-Patent-Class-62-59; US-Patent-Class-62-259.3; US-Patent-Class-62-299;
Int-Patent-Class-F28D-20/00) Avail: US Patent and Trademark Office

A cooling apparatus includes a container filled with a quantity of coolant fluid initially cooled to a solid phase, a cooling loop disposed between a heat load and the container. A pump for circulating a quantity of the same type of coolant fluid in a liquid phase through the cooling loop, a pair of couplings for communicating the liquid phase coolant fluid into the container in a direct interface with the solid phase coolant fluid.
Official Gazette of the U.S. Patent and Trademark Office

N95-28259*# Rockwell International Corp., Downey, CA. Space Systems Div.
TASK 4 SUPPORTING TECHNOLOGY. PART 2: DETAILED TEST PLAN FOR THERMAL SEALS. THERMAL SEALS EVALUATION, IMPROVEMENT AND TEST. CAN8-1, REUSABLE LAUNCH VEHICLE (RLV), ADVANCED TECHNOLOGY DEMONSTRATOR: X-33. LEADING EDGE AND SEALS THERMAL PROTECTION SYSTEM TECHNOLOGY DEMONSTRATION
P. A. Hogenson and Tina Lu 30 May 1995 24 p
(Contract NCC8-79)
(NASA-CR-198628; NAS 1.26:198628; SSD95D0240-Pt-2) Avail: CASI HC A03/MF A01

The objective is to develop the advanced thermal seals to a technology readiness level (TRL) of 6 to support the rapid turnaround time and low maintenance requirements of the X-33 and the future reusable launch vehicle (RLV). This program is divided into three subtasks: (1) orbiter thermal seals operation history review; (2) material, process, and design improvement; and (3) fabrication and evaluation of the advanced thermal seals. CASI

N95-28347* National Aeronautics and Space Administration. Marshall Space Flight Center, Huntsville, AL.
APPARATUS FOR TESTING HIGH PRESSURE INJECTOR ELEMENTS Patent
William Neill Myers, inventor (to NASA), Ewell M. Scott, inventor (to NASA), John C. Forbes, inventor (to NASA), and Michael D. Shadoan, inventor (to NASA) 9 May 1995 19 p Filed 7 Sep. 1993
(NASA-Case-MFS-28773-1; US-Patent-5,412,981;
US-Patent-Appl-SN-117587; US-Patent-Class-73-119;
US-Patent-Class-359-509; Int-Patent-Class-G01M-15/00;
Int-Patent-Class-F02M-65/00) Avail: US Patent and Trademark Office

An apparatus for testing and evaluating the spray pattern of high pressure fuel injector elements for use in supplying fuel to combustion engines is presented. Prior art fuel injector elements were normally tested by use of low pressure apparatuses which did not provide a purge to prevent mist from obscuring the injector element or to prevent frosting of the view windows; could utilize only one fluid during each test; and had their viewing ports positioned one hundred eighty (180 deg) apart, thus preventing optimum use of laser diagnostics. The high pressure fluid injector test apparatus includes an upper hub, an upper weldment or housing, a first clamp and stud/nut assembly for securing the upper hub to the upper weldment, a standoff assembly within the upper weldment, a pair of window housings having view glasses within the upper weldment, an injector block assembly and purge plate within the upper weldment for holding an injector element to be tested and evaluated, a lower weldment or housing, a second clamp and stud/nut assembly for securing the lower weldment to the upper hub, a third clamp and stud/nut assembly for securing the lower hub to the lower weldment, mechanisms for introducing fluid under high pressure for testing an injector element, and mechanisms for purging the apparatus to prevent frosting of view glasses within the window housings and to permit unobstructed viewing of the injector element.
Official Gazette of the U.S. Patent and Trademark Office

N95-28359* National Aeronautics and Space Administration. John F. Kennedy Space Center, Cocoa Beach, FL.
WATER DRIVEN TURBINE/BRUSH PIPE CLEANER Patent
Rudy J. Werlink, inventor (to NASA) 18 Apr. 1995 8 p Filed 7 Mar. 1994
(NASA-Case-KSC-11669-1; US-Patent-5,406,666;
US-Patent-Appl-SN-207313; US-Patent-Class-15-104.12;
US-Patent-Class-15-104.31; Int-Patent-Class-B08B-9/02) Avail: US Patent and Trademark Office

Assemblies are disclosed for cleaning the inside walls of pipes and tubes. A first embodiment includes a small turbine with angled blades axially mounted on one end of a standoff support. An O-ring for stabilizing the assembly within the pipe is mounted in a groove within the outer ring. A replaceable circular brush is fixedly mounted on the opposite end of the standoff support and can be used for cleaning tubes and pipes of various diameters, lengths and configurations. The turbine, standoff support, and brush spin in unison relative to a hub bearing that is fixedly attached to a wire upstream of the assembly. The nonrotating wire is for retaining the assembly in tension and enabling return of the assembly to the pipe entrance. The assembly is initially placed in the pipe or tube to be cleaned. A pressurized water or solution source is provided at a required flow-rate to propel the assembly through the pipe or tube. The upstream water pressure propels and spins the turbine, standoff support and brush. The rotating brush combined with the solution cleans the inside of the pipe. The solution flows out of the other end of the pipe with the brush rotation controlled by the flow-rate. A second embodiment is similar to the first embodiment but instead includes a circular shaped brush with ring backing mounted in the groove of the exterior ring of the turbine, and also reduces the size of the standoff support or eliminates the standoff support.
Official Gazette of the U.S. Patent and Trademark Office

N95-28364*# National Aeronautics and Space Administration. Marshall Space Flight Center, Huntsville, AL.
BEARING DEFECT SIGNATURE ANALYSIS USING ADVANCED NONLINEAR SIGNAL ANALYSIS IN A CONTROLLED ENVIRONMENT Final Report
T. Zoladz, E. Earhart, and T. Fiorucci Washington May 1995 48 p
(CDDF Proj. 93-10)
(NASA-TM-108491; NAS 1.15:108491) Avail: CASI HC A03/MF A01

Utilizing high-frequency data from a highly instrumented rotor assembly, seeded bearing defect signatures are characterized using both conventional linear approaches, such as power spectral density analysis, and recently developed nonlinear techniques such as bicoherence analysis. Traditional low-frequency (less than 20 kHz) analysis and high-frequency envelope analysis of both accelerometer and acoustic emission data are used to recover characteristic bearing distress information buried deeply in acquired data. The successful coupling of newly developed nonlinear signal analysis with recovered wideband envelope data from accelerometers and acoustic emission sensors is the innovative focus of this research. Author

N95-27261*# Spar Aerospace Ltd., Brampton (Ontario). Space Systems Div.
DESIGN, TESTING AND EVALUATION OF LATCHING END EFFECTOR
B. Walker and R. Vandersluis *In* NASA. Lyndon B. Johnson Space Center, The 29th Aerospace Mechanisms Symposium May 1995 p 1-16 (For primary document see N95-27260 09-15)
Avail: CASI HC A03/MF A04

N95-27262*# Fokker Space and Systems, Leiden (Netherlands).
SOME MECHANICAL DESIGN ASPECTS OF THE EUROPEAN ROBOTIC ARM
Peter J. Lambooy, Wart M. Mandersloot, and Richard H. Bentall (European Space Agency. European Space Research and Technology Center, ESTEC, Noordwijk, Netherlands.) *In* NASA. Johnson Space Center, The 29th

Aerospace Mechanisms Symposium May 1995 p 17-29 (For primary document see N95-27260 09-15)
Avail: CASI HC A03/MF A04

N95-27263*# National Aeronautics and Space Administration. Lyndon B. Johnson Space Center, Houston, TX.
ADVANCED DEVELOPMENT FOR SPACE ROBOTICS WITH EMPHASIS ON FAULT TOLERANCE
D. Tesar (Texas Univ., Austin, TX.), J. Chladek, R. Hooper (Texas Univ., Austin, TX.), D. Sreevijayan (Texas Univ., Austin, TX.), C. Kapoor (Texas Univ., Austin, TX.), J. Geisinger (Texas Univ., Austin, TX.), M. Meaney (Texas Univ., Austin, TX.), G. Browning (Texas Univ., Austin, TX.), and K. Rackers (Texas Univ., Austin, TX.) *In its* 29th Aerospace Mechanisms Symposium May 1995 p 30-4 (For primary document see N95-27260 09-15)
Avail: CASI HC A03/MF A04

N95-27266*# Lockheed Missiles and Space Co., Sunnyvale, CA.
SOLAR ARRAY DEPLOYMENT MECHANISM
Mark C. Calassa and Russell Kackley *In* NASA. Johnson Space Center, The 29th Aerospace Mechanisms Symposium May 1995 p 79-93 (For primary document see N95-27260 09-15)
Avail: CASI HC A03/MF A04

N95-27267*# Starsys Research Corp., Boulder, CO.
CHANGING PARADIGMS: MANUFACTURING VS. FABRICATING A HIGH VOLUME HOLD DOWN AND RELEASE MECHANISM
Daryl Maus and Doug Monick *In* NASA. Johnson Space Center, The 29th Aerospace Mechanisms Symposium May 1995 p 94-108 (For primary document see N95-27260 09-15)
Avail: CASI HC A05/MF A04

N95-27269*# ACE-Able Engineering Co., Inc., Goleta, CA.
LOW-COST TUBULAR ANTENNA DEPLOYER FOR WISP-2
Robert M. Warden *In* NASA. Johnson Space Center, The 29th Aerospace Mechanisms Symposium May 1995 p 131-135 (For primary document see N95-27260 09-15)
Avail: CASI HC A01/MF A04

N95-27273*# National Aeronautics and Space Administration. Goddard Space Flight Center, Greenbelt, MD.
BASIC SPACE PAYLOAD FASTENER
J. M. Vranish and Stephen Gorevan (Honeybee Robotics Ltd., New York, NY.) *In* NASA. Johnson Space Center, The 29th Aerospace Mechanisms Symposium May 1995 p 152-157 (For primary document see N95-27260 09-15)
Avail: CASI HC A02/MF A04

N95-27274*# Orbital Sciences Corp., Dulles, VA.
NON-EXPLOSIVE ACTUATION FOR THE ORBCOMM (TM) SATELLITE
Anthony Robinson, Craig Courtney (G and H Technology, Inc., Camarillo, CA.), and Tom Moran (G and H Technology, Inc., Camarillo, CA.) *In* NASA. Johnson Space Center, The 29th Aerospace Mechanisms Symposium May 1995 p 158-161 (For primary document see N95-27260 09-15)
Avail: CASI HC A01/MF A04

N95-27275*# Martin Marietta Astronautics, Denver, CO.
DEVELOPMENT OF A HIGH FORCE THERMAL LATCH
William D. Nygren *In* NASA. Johnson Space Center, The 29th Aerospace Mechanisms Symposium May 1995 p 162-166 (For primary document see N95-27260 09-15)
Avail: CASI HC A01/MF A04

N95-27276*# NYMA, Inc., Cleveland, OH.
A ROTATING ARM USING SHAPE-MEMORY ALLOY
Phillip P. Jenkins and Geoffrey A. Landis *In* NASA. Johnson Space Center, The 29th Aerospace Mechanisms Symposium May 1995 p 167-171 (For primary document see N95-27260 09-15)
Avail: CASI HC A01/MF A04

N95-27282*# Astro Aerospace Corp., Carpinteria, CA.
FORTE ANTENNA ELEMENT AND RELEASE MECHANISM DESIGN
David J. Rohweller and Thomas A. Butler (Los Alamos National Lab., NM.) *In* NASA. Johnson Space Center, The 29th Aerospace Mechanisms Symposium May 1995 p 238-252 (For primary document see N95-27260 09-15)
Avail: CASI HC A03/MF A04

N95-27283*# Cambridge Univ., Cambridge (England). Dept. of Engineering.
DEPLOYMENT AND RETRACTION OF A CABLE-DRIVEN SOLAR ARRAY: TESTING AND SIMULATION
P. Kumar and S. Pellegrino *In* NASA. Johnson Space Center, The 29th Aerospace Mechanisms Symposium May 1995 p 253-267 Sponsored by Cambridge Commonwealth Trust (For primary document see N95-27260 09-15)
Avail: CASI HC A03/MF A04

N95-27284*# National Aeronautics and Space Administration. Goddard Space Flight Center, Greenbelt, MD.
DEVELOPMENT OF THE SOLAR ARRAY DEPLOYMENT AND DRIVE SYSTEM FOR THE XTE SPACECRAFT
Rodger Farley and Son Ngo *In* NASA. Johnson Space Center, The 29th Aerospace Mechanisms Symposium May 1995 p 268-282 (For primary document see N95-27260 09-15)
Avail: CASI HC A03/MF A04

N95-27285*# MPB Corp., Keene, NH.
EFFECTS OF BEARING CLEANING AND LUBE ENVIRONMENT ON BEARING PERFORMANCE
Peter C. Ward *In* NASA. Johnson Space Center, The 29th Aerospace Mechanisms Symposium May 1995 p 285-300 Sponsored by Hamilton Standard; and United Technologies (For primary document see N95-27260 09-15)
Avail: CASI HC A03/MF A04

N95-27286*# Honeywell, Inc., Glendale, AZ. Satellite Systems Operations.
BALL BEARING VIBRATIONS AMPLITUDE MODELING AND TEST COMPARISONS
Richard A. Hightower, III and Dave Bailey *In* NASA. Johnson Space Center, The 29th Aerospace Mechanisms Symposium May 1995 p 301-315 (For primary document see N95-27260 09-15)
Avail: CASI HC A03/MF A04

N95-27289*# McDonnell-Douglas Space and Defense Systems, Cocoa Beach, FL.
DEVELOPMENT AND TESTING OF THE RACK INSERTION DEVICE
G. Scott Strickland *In* NASA. Johnson Space Center, The 29th Aerospace Mechanisms Symposium May 1995 p 353-367 (For primary document see N95-27260 09-15)
Avail: CASI HC A03/MF A04

N95-27290*# National Aeronautics and Space Administration. Langley Research Center, Hampton, VA.
LINEAR PROOF MASS ACTUATOR
S. E. Holloway, III *In* NASA. Johnson Space Center, The 29th Aerospace Mechanisms Symposium May 1995 p 368-380 (For primary document see N95-27260 09-15)
Avail: CASI HC A03/MF A04

N95-27291*# Lockheed Engineering and Sciences Co., Houston, TX. Mechanical Systems Lab.
LOAD MEASUREMENT SYSTEM WITH LOAD CELL LOCK-OUT MECHANISM
Thang Le, Monty Carroll, and Jonathan Liu *In* NASA. Johnson Space Center, The 29th Aerospace Mechanisms Symposium May 1995 p 381-392 (For primary document see N95-27260 09-15)
Avail: CASI HC A03/MF A04

N95-27292*# Societe Anonyme d'Etudes et Realisations Nucleaires, Limeil-Brevannes (France).
MICROMECHANISMS FOR OPTIMISM SEISMOMETER
Nicolas Paulin, Pierre Dumas, and Marc Pochard *In* NASA. Johnson Space Center, The 29th Aerospace Mechanisms Symposium May 1995 p 393-400 (For primary document see N95-27260 09-15)
Avail: CASI HC A02/MF A04

N95-27985*# General Electric Co., Philadelphia, PA.
CONTROL SYSTEM DESIGN FOR THE MOD-5A 7.3 mW WIND TURBINE GENERATOR
Robert S. Barton, Theodore J. Hosp, and George P. Schanzenbach *In* DASCON Engineering, Collected Papers on Wind Turbine Technology May 1995 p 157-174 Presented at the DOE/NASA Workshop on Horizontal Axis Wind Turbine Technology, Cleveland, OH, 8-10 May 1984 (For primary document see N95-27970 09-44)
(Contract DEN3-153)
Avail: CASI HC A03/MF A03

N95-27986*# Boeing Aerospace Co., Seattle, WA.
USE OF BLADE PITCH CONTROL TO PROVIDE POWER TRAIN DAMPING FOR THE Mod-2, 2.5-mW WIND TURBINE
W. A. Blissell, Jr. *In* DASCON Engineering, Collected Papers on Wind Turbine Technology May 1995 p 175-1190 Presented at the DOE/NASA Workshop on Horizontal Axis Wind Turbine Technology, Cleveland, OH, 8-10 May 1984 Sponsored by DOE (For primary document see N95-27970 09-44)
(Contract DEN3-153)
Avail: CASI HC A02/MF A03

38 QUALITY ASSURANCE AND RELIABILITY

Includes product sampling procedures and techniques; and quality control.

N95-26778*# National Aeronautics and Space Administration. Langley Research Center, Hampton, VA.
COMBINED INVESTIGATION OF EDDY CURRENT AND ULTRASONIC TECHNIQUES FOR COMPOSITE MATERIALS NDE
C. W. Davis (Army Aviation Systems Command, Hampton, VA.), S. Nath (Analytic Services and Materials, Inc., Hampton, VA.), J. P. Fulton (Analytic Services and Materials, Inc., Hampton, VA.), and M. Namkung [1993] 7 p
(NASA-TM-110599; NAS 1.15:110599) Avail: CASI HC A02/MF A01

Advanced composites are not without trade-offs. Their increased designability brings an increase in the complexity of their internal geometry and, as a result, an increase in the number of failure modes associated with a defect. When two or more isotropic materials are combined in a composite, the isotropic material failure modes may also combine. In a laminate, matrix delamination, cracking and crazing, and voids and porosity, will often combine with fiber breakage, shattering, waviness, and separation to bring about ultimate structural failure. This combining of failure modes can result in defect boundaries of different sizes, corresponding to the failure of each structural component. This paper discusses a dual-technology NDE (Non Destructive Evaluation) (eddy current (EC) and ultrasonics (UT)) study of graphite/epoxy (gr/ep) laminate samples. Eddy current and ultrasonic raster (Cscan) imaging were used together to characterize the effects of mechanical impact damage, high temperature thermal damage and various types of inserts in gr/ep laminate samples of various stacking sequences. Derived from text

N95-26927 Educational Testing Service, Princeton, NJ.
CAN THERE BE RELIABILITY WITHOUT RELIABILITY? Final Report
Robert J. Mislevy Oct. 1994 24 p Limited Reproducibility: More than 20% of this document may be affected by microfiche quality
(Contract N00014-91-J-4101; RR04204)
(AD-A289480; RM-94-18-ONR) Avail: Issuing Activity (Defense Technical Information Center (DTIC))

A recent article by Pamela Moss asks the title question, 'Can there be validity without reliability?' If by reliability we mean only KR-2O coefficients or inter-rater correlations, the answer is yes. Sometimes these particular indices for evaluating evidence suit the problem we encounter; sometimes they don't. If by reliability we mean credibility of evidence, where credibility is defined as 'appropriate to the intended inference, the answer is no, we cannot have validity without reliability. Because 'validity' encompasses the process of reasoning as well as the data, uncritically accepting observations as strong evidence, when they may be incorrect, misleading, unrepresentative, or fraudulent, may lead coincidentally to correct conclusions but not to valid ones. This paper discusses and illustrates a broader conception of 'reliability' in educational assessment, to ground a deeper understanding of the issues raised by Professor Moss's question. DTIC

N95-27253*# Illinois Univ., Urbana, IL. Coordinated Science Lab.
MEASURING FAULT TOLERANCE WITH THE FTAPE FAULT INJECTION TOOL
Timothy K. Tsai and Ravishankar K. Iyer [1995] 16 p Submitted for publication
(Contract NAG1-613; DABT63-94-C-0045)
(NASA-CR-197773; NAS 1.26:197773) Avail: CASI HC A03/MF A01

This paper describes FTAPE (Fault Tolerance And Performance Evaluator), a tool that can be used to compare fault-tolerant computers. The major parts of the tool include a system-wide fault-injector, a workload generator, and a workload activity measurement tool. The workload creates high stress conditions on the machine. Using stress-based injection, the fault injector is able to utilize knowledge of the workload activity to ensure a high level of fault propagation. The errors/fault ratio, performance degradation, and number of system crashes are presented as measures of fault tolerance. Author

N95-27723# Sandia National Labs., Albuquerque, NM. Failure Analysis Dept.
I(SUB DDQ) TESTING AND DEFECT CLASSES: A TUTORIAL
Jerry M. Soden and Charles F. Hawkins (New Mexico Univ., Albuquerque, NM.) 1994 10 p Presented at the Custom Integrated Circuits Conference, Santa Clara, CA, 1-4 May 1995
(Contract DE-AC04-94AL-85000)
(DE95-005467; SAND-94-3257C; CONF-9505154-1) Avail: CASI HC A02/MF A01

I(sub DDQ) testing of CMOS IC's is a technique for production quality and reliability improvement, design validation, and failure analysis. The origin and basic concepts of I(sub DDQ) testing are reviewed. The relationship of I(sub DDQ) testing to other test methods is considered in the context of the whole IC life cycle from design, fabrication, and test through end use. A comprehensive test strategy is described that uses defect classes based on defect electrical properties rather than traditional fault models. DOE

N95-28034*# Washington Univ., Saint Louis, MO. Dept. of Physics.
PHYSICAL INTERPRETATION AND DEVELOPMENT OF ULTRASONIC NONDESTRUCTIVE EVALUATION TECHNIQUES APPLIED TO THE QUANTITATIVE CHARACTERIZATION OF TEXTILE COMPOSITE MATERIALS Semiannual Progress Report, 15 Sep. 1994 - 14 Mar. 1995
James G. Miller 14 Mar. 1995 16 p Original contains color illustrations
(Grant NsG-1601)
(NASA-CR-198591; NAS 1.26:198591) Avail: CASI HC A03/MF A01;2 functional color pages

In this Progress Report, the author describes the continuing research to explore the feasibility of implementing medical linear array imaging technology as a viable ultrasonic-based nondestructive evaluation method to inspect and characterize complex materials. Images obtained using an unmodified medical ultrasonic imaging system of a bonded aluminum plate sample with a simulated disbond region are presented. The disbond region was produced by adhering a piece of plain white paper to a piece of cellophane tape and applying the paper-tape combination to one of the aluminum plates. Because the area under the paper was not adhesively bonded to the aluminum plate, this arrangement more closely simulates a disbond. Images are also presented for an aluminum plate sample with an epoxy strip adhered to one side to help provide information for the interpretation of the images of the bonded aluminum plate sample containing the disbond region. These images are compared with corresponding conventional ultrasonic contact transducer measurements in order to provide information regarding the nature of the disbonded region. The results of this on-going investigation may provide a step toward the development of a rapid, real-time, and portable method of ultrasonic inspection and characterization based on linear array technology. In Section 2 of this Progress Report, the preparation of the aluminum plate specimens is described. Section 3 describes the method of linear array imaging. Sections 4 and 5 present the linear array images and results from contact transducer measurements, respectively. A discussion of the results are presented in Section 6. Derived from text

N95-27115 Polymer Solutions, Inc., Blacksburg, VA.
EVALUATIONS OF THE EFFECTIVENESS OF ENVIRONMENTALLY BENIGN CLEANING METHODOLOGIES
James D. Rancourt *In* Johns Hopkins Univ., Environmentally Benign Cleaning and Degreasing Technology: JANNAF Safety and Protection Subcommittee and Propellant Development and Characterization Subcommittee Joint Workshop Jun. 1994 p 143-145 (For primary document see N95-27101 09-27)
Avail: CPIA, 10630 Little Patuxent Pkwy., Suite 202, Columbia, MD 21044-3200 HC

N95-28442*# Army Materials Technology Lab., Watertown, MA.
UNCERTAINTIES IN OBTAINING HIGH RELIABILITY FROM STRESS-STRENGTH MODELS
Donald M. Neal, William T. Matthews, and Mark G. Vangel *In* FAA, Ninth DOD/NASA/FAA Conference on Fibrous Composites in Structural Design, Volume 1 Sep. 1992 p 503-52 (For primary document see N95-28420 09-24)
Avail: CASI HC A03/MF A04

39 STRUCTURAL MECHANICS

Includes structural element design and weight analysis; fatigue; and thermal stress.

For applications see *05 Aircraft Design, Testing and Performance* and *18 Spacecraft Design, Testing and Performance.*

N95-26342 Organisatie voor Toegepast Natuurwetenschappelijk Onderzoek, Delft (Netherlands).
MANUAL FOR SHOCK3D, VERSION 2.0. COMPUTER PROGRAM FOR NON-LINEAR SHOCK RESPONSE
B. Q. Westgeest and R. Regoord 26 Aug. 1994 93 p Sponsored by Ministry of Defence Limited Reproducibility: More than 20% of this document may be affected by microfiche quality
(AD-A288631; TNO/R-94-CMC-R0539; TDCK-TD-94-2019) Avail: Issuing Activity (Defense Technical Information Center (DTIC))

The program SHOCK3D deals with the shock response of a 3D structure, being composed from elastic parts, rigid bodies and non-linear mountings. Shock loading is in the form of prescribed shock motions as they are defined by several Navies in Equipment Shock Specifications (UNDEX shock) or in the form of prescribed forces. Mass- and stiffness matrices for the elastic parts are assembled within a separate f.e.m. program. A transient response analysis leads to time histories which can be plotted. Test problems have been added. A pc version may be used in case there is no need to include elastic parts. DTIC

N95-26387*# Texas Univ., Austin, TX. Dept. of Aerospace Engineering and Engineering Mechanics.
ANALYSIS AND DEVELOPMENT OF FINITE ELEMENT METHODS FOR THE STUDY OF NONLINEAR THERMOMECHANICAL BEHAVIOR OF STRUCTURAL COMPONENTS Final Contractor Report
J. Tinsley Oden Cleveland, OH NASA May 1995 152 p
(Grant NAG3-329; RTOP 505-63-5B)
(NASA-CR-195354; E-9005; NAS 1.26:195354) Avail: CASI HC A08/MF A02

Underintegrated methods are investigated with respect to their stability and convergence properties. The focus was on identifying regions where they work and regions where techniques such as hourglass viscosity and hourglass control can be used. Results obtained show that underintegrated methods typically lead to finite element stiffness with spurious modes in the solution. However, problems exist (scalar elliptic boundary value problems) where underintegrated with hourglass control yield convergent solutions. Also, stress averaging in underintegrated stiffness calculations does not necessarily lead to stable or convergent stress states. Author

N95-26464 Oklahoma State Univ., Stillwater, OK.
USER'S GUIDE: COMPUTER PROGRAM FOR ANALYSIS OF BEAM-COLUMN STRUCTURES WITH NONLINEAR SUPPORTS (CBEAMC) Final Report
William P. Dawkins Nov. 1994 113 p Sponsored by Army Corps. of Engineers Limited Reproducibility: More than 20% of this document may be affected by microfiche quality
(AD-A289031; WES/IR/ITL-94-6; ITL-94-6) Avail: Issuing Activity (Defense Technical Information Center (DTIC))

This report documents a computer program--CBEAMC--for analysis of general beam-column structures supported and/or loaded by components which interact with displacements of the beam and/or column. Chapter 2 describes the general beam-column system considered and the mathematical model used for analysis; Chapter 3 presents the force-displacement relationships for the mathematical model and describes the computational procedure used for solution; and Chapter 4 provides example solution obtained with the program. The computer program described in this report has been checked to ensure that the results are accurate within the limitations of the procedures employed. However, there may be unusual situations which were not anticipated, and these situations may cause the program to produce questionable results. It is the responsibility of the user to judge the validity of the results. No responsibility is assumed by the author for the design or behavior of any structure based on results obtained with the program. DTIC

N95-26521# National Aerospace Lab., Tokyo (Japan). Airframe Div.
ANALYSIS OF FATIGUE FRACTOGRAPHIC DATA OF A ROD END HOUSING USING A MONTE CARLO SIMULATION
Toshiyuki Shgimokawa and Yoshiaki Kakuta Feb. 1994 15 p In JAPANESE
(ISSN 0389-4010)
(NAL-TR-1225) Avail: CASI HC A03/MF A01

This paper presents a new method using a Monte Carlo simulation to estimate a life distribution of fatigue crack propagation on the basis of crack length versus striation spacing data. This simulation is based on the distributions of two parameter estimates of a regression line and the reasonable correlation of the two parameter estimates. One cycle of the Monte Carlo scheme generates a set of parameter estimates which give a life of fatigue crack propagation. The analyzed data were obtained by scanning electron microscope (SEM) observation of a fatigue fracture surface of the rod end housing of a hydraulic actuator, which was used for a main landing gear in transport aircraft. A conventional regression analysis provides a set of two deterministic-parameter estimates, a life estimate of fatigue crack propagation, and the statistical properties of striation spacing. Stochastic-process modes of crack growth and practical probabilistic methods including the proposed method are used to estimate the life distributions of fatigue crack propagation on the basis of the results of the regression analysis. The obtained results are discussed and compared. The proposed method approximates the fatigue life of the rod end housing as the B-allowable life when the initial crack length is assumed to be 0 mm. Author

N95-26547 Stanford Univ., CA.
MODIFIED EIGENVALUE PROBLEMS WITH APPLICATIONS TO STRUCTURAL DYNAMIC RE-ANALYSIS ON PARALLEL COMPUTERS Final Report, 1 Feb. 1991 - 31 Mar. 1994
Gene H. Golub and Kinncho H. Law Aug. 1994 4 p Limited Reproducibility: More than 20% of this document may be affected by microfiche quality
(Contract DAAL03-91-G-0038)
(AD-A288257; ARO-28377.11-MA) Avail: Issuing Activity (Defense Technical Information Center (DTIC))

In this project, researchers have developed and implemented a number of parallel algorithms related to matrix factorization and generalized eigenvalue problems. Furthermore, a Lanczos based method for the modified eigenvalue problem has been developed. Results are summarized in the final report. DTIC

N95-26625 Naval Postgraduate School, Monterey, CA. Dept. of Mechanical Engineering.
EFFECT OF SURFACE COATING ON ONE-DIMENSIONAL SYSTEM SUBJECTED TO UNIT STEP PRESSURE WAVE Progress Report, 1 Oct. 1993 - 30 Sep. 1994
T. P. Brasek, Y. W. Kwon, and Y. S. Shin 30 Sep. 1994 51 p Limited Reproducibility: More than 20% of this document may be affected by microfiche quality
(Contract MIPR-94-573)
(AD-A288237; NPS-ME-94-006) Avail: Issuing Activity (Defense Technical Information Center (DTIC))

The response of a one-dimensional, coated, aluminum structure subjected to a unit step pressure wave is studied. The coating is either an elastic material or a viscoelastic tread stock rubber of variable stiffness; it separates the structure from an air or a water medium. The stress and nodal velocity of the structure coated with different materials is compared to a system without a coating (homogeneous system). Both the stress and nodal velocity of the structure increase with a decreasing coating stiffness regardless of the coating type or bounding medium. This phenomenon indicates that the coating stiffness governs the degree of strain energy release from the structure to the medium. A softer coating appears to trap this excess energy increasing the stress in the structure. In all cases studied, the stiffer coating reduced the dynamic response of the structure when compared to the homogeneous system. A rubber shear modulus of approximately 6000 psi and greater ensured a favorable dynamic response for a coated aluminum structure enacted upon by a step pressure wave travelling in either air or water. The threshold value may vary depending upon the geometry and material properties of both the coating and the structure. DTIC

N95-26743 National Inst. of Standards and Technology, Gaithersburg, MD. Fire Science Div.
PROCEEDINGS: WORKSHOP ON RESEARCH NEEDS IN WIND ENGINEERING
R. D. Marshall Feb. 1995 78 p Workshop held in Gaithersburg, MD, 12-13 Sep. 1994
(PB95-189528; NISTIR-5597) Avail: Issuing Activity (National Technical Information Service (NTIS))

This report presents findings and recommendations developed at a workshop on research needs in wind engineering. Representatives from universities, the private sector, and Federal agencies presented program overviews and participated in working group sessions addressing various aspects of wind engineering research and wind disaster mitigation. Research needs and topics for technology transfer were identified and prioritized. It was concluded that current funding of wind engineering research in the United States falls far short of what is needed to effectively address the problem of spiraling losses due to wind damage. There is, however, considerable wind engineering knowledge now available for implementation by the model building codes and by the building industry in general. NTIS

N95-26749 National Physical Lab., Teddington (England).
ANALYSIS OF PLATE-TWIST TEST FOR IN-PLANE SHEAR MODULUS OF COMPOSITE MATERIALS (REVISED)
G. D. Sims, W. Nimmo, A. F. Johnson, and D. H. Ferriss Jan. 1994 16 p
(PB95-190195; NPL-DMM(A)-54-Rev) Copyright Avail: Issuing Activity (National Technical Information Service (NTIS))

In this report an improved analysis of the plate-twist test for the measurement of in-plane shear modulus of composite materials and the shear modulus of isotropic materials is described and experimentally validated. The analysis removes errors connected with the position of the loading points and allows greater freedom in their positioning. In particular it is no longer necessary to position the loading points exactly on the corners of the plate. An error of 1.0 mm in the positioning of the loading points on a 150 mm square plate results in an error of 3.4% in the measured shear modulus. A draft standard has been produced for this test method, which will be used in a round-robin exercise to obtain precision data. The existing standards for the use of this method to measure the shear modulus of wood products will be checked, as they may have similar sources of error to those evaluated in this report. NTIS

N95-26839 Naval Postgraduate School, Monterey, CA.
STUDY OF DAMAGE EVOLUTIONS IN COMPOSITE PLATES SUBJECTED TO BENDING LOADS USING MICRO-MACRO ANALYSIS M.S. Thesis
Bruce Howard Hamilton Sep. 1994 62 p Limited Reproducibility: More than 20% of this document may be affected by microfiche quality
(AD-A288523) Avail: Issuing Activity (Defense Technical Information Center (DTIC))

The purpose of this study is to develop a computer program that will predict the damage progression in composite plates subjected to bending loads. Kwon's micromechanical model is used to compute the smeared effective moduli from the material properties of fiber and matrix as well as to determine stresses at the constituent level. Failure criteria based on micro-stresses are then applied to determine the extent and type of damage that occur in the composite under various loading conditions. The progression of damage throughout the composite until complete failure of the composite can then be simulated using the current computer program. The numerical prediction for a laminated composite plate containing a hole and subjected to a bending load agrees well with the experimental data. DTIC

N95-26905 Air Force Inst. of Tech., Wright-Patterson AFB, OH. School of Engineering.
THE COLLAPSE OF COMPOSITE CYLINDRICAL PANELS WITH VARIOUS THICKNESS USING FINITE ELEMENT ANALYSIS M.S. Thesis
Christopher P. Chaplin Dec. 1994 149 p Limited Reproducibility: More than 20% of this document may be affected by microfiche quality
(AD-A289370; AFIT/GA/ENY/94D-4) Avail: Issuing Activity (Defense Technical Information Center (DTIC))

This study compared numerical collapse results of graphite/epoxy cylindrical panels with free vertical edges undergoing axial compression for three different shell theories. Symmetric quasi-isotropic laminates were investigated using solid panels and panels with five different centralized cutouts with three thicknesses. The theories compared in the study were the Simplified Large displacement moderate Rotation (SLR) theory, the Donnell Cylindrical Shell (Modified Donnell) theory, and the Classical Donnell theory. The purpose of the study was to determine when large rotations and through-the-thickness shear become important in the numerical collapse analysis of cylindrical composite shells. By observing cases where the numerical collapse results for each of the three theories differed noticeably (greater than 3%), it could be determined when large rotations and through-the-thickness shear were important. The effects of large rotations were noticed in nearly all of the panels with large cutouts (greater than 3% panel area). Large rotations were also found to be important for thicker panels with either no cutout or a small cutout. The effects of through-the-thickness shear were only noticed in the thickest panels with large cutouts. DTIC

N95-26911 Helsinki Univ. of Technology, Espoo (Finland). Systems Analysis Lab.
CHARACTERIZATION OF THE MEMBRANE THEORY OF A CLAMPED SHELL. THE HYPERBOLIC CASE
J. Piila Oct. 1994 29 p Limited Reproducibility: More than 20% of this document may be affected by microfiche quality
(PB95-185021; RR-A337) Avail: CASI HC A03

We study the membrane-dominated deformation state of a thin shell, the midsurface of which is located on a hyperbolic surface of revolution. The lateral shape of the shell is assumed to be that of a curvilinear polygon. The shell is loaded by a surface traction and rigidly supported throughout its edge. Proceeding from the classical shell model of Koiter-Sanders-Novozhilov, an asymptotic membrane-theory model is constructed to describe the limit behavior of the shell as the thickness tends to zero. Mathematical characteristics of the membrane theory are analyzed and the convergence rate estimate between the two models is proven. NTIS

N95-26975 Air Force Inst. of Tech., Wright-Patterson AFB, OH. School of Engineering.
INVESTIGATION INTO THE BEHAVIOR OF GEOMETRICALLY NONLINEAR COMPOSITE ARCHES M.S. Thesis
John C. Bailey Dec. 1994 110 p Limited Reproducibility: More than 20% of this document may be affected by microfiche quality

(AD-A289258; AFIT/GAE/ENY/94D-02) Avail: Issuing Activity (Defense Technical Information Center (DTIC))

This research modifies the existing finite element formulation of a potential energy based large deformation and moderate rotation theory. Hermitian shape functions replace the existing linear bending angle interpolations. Negligible differences between the two formulations indicate the underlying kinematics limit the accuracy, not the finite element interpolations. Using the new program, numerous nonlinear arch geometries are modeled to investigate the effects of arc length and thickness variations. Local and global snapping phenomena are captured as well as through the thickness shear driven nonlinearities. DTIC

N95-27135 Air Force Inst. of Tech., Wright-Patterson AFB, OH. School of Engineering.

AN EXPERIMENTAL INVESTIGATION OF SANDWICH FLAT PANELS UNDER LOW VELOCITY IMPACT M.S. Thesis

Timberlyn M. Harrington Dec. 1994 274 p Limited Reproducibility: More than 20% of this document may be affected by microfiche quality

(AD-A289420; AFIT/GAE/ENY/94D-22) Avail: Issuing Activity (Defense Technical Information Center (DTIC))

This study evaluated the failure modes and mechanisms associated with increasing face sheet thickness of flat sandwich panels under low velocity impact. The sandwich panels were fabricated using 1.27 cm thick, 145 kg/cu m (9 lb/cu ft), 3.175 mm (1/8 in.) cell size Nomex honeycomb core, FM 300-2 film adhesive and AS4/3501-6 graphite/epoxy face sheets. The thickness of the core remained 1.27 cm, and the thickness of the adhesive remained 0.25 mm. The thickness of the face sheets varied using the following stacking sequences: (O/90)s, (O/90)2s, (O/90)4s, (O/90)8s, and (O/90)12s. The sandwich panels were subjected to various low velocity impacts using the Dynatup Impact Test Machine. Pulse-Echo C-scans and optical microscopy of panel cross-sections were performed to characterize the damage. The cross-sections indicated that delamination and transverse cracking contribute to internal damage of the face sheets, while crushing, buckling, and crippling contribute to damage of the core. Cracks in the adhesive also contribute to damage in some cases. DTIC

N95-27174*# National Aeronautics and Space Administration. Lewis Research Center, Cleveland, OH.

PROBABILISTIC SIMULATION OF LONG TERM BEHAVIOR IN POLYMER MATRIX COMPOSITES

A. R. Shah (NYMA, Inc., Brook Park, OH.), S. N. Singhal (NYMA, Inc., Brook Park, OH.), P. L. N. Murthy, and C. C. Chamis Apr. 1995 21 p Presented at the 35th Structures, Structural Dynamics and Materials Conference, Hilton Head, SC, 18-21 Apr. 1994; sponsored by AIAA, ASME, AHS, and ASCE

(Contract NAS3-27186; RTOP 505-62-10)

(NASA-TM-106893; E-9537; NAS 1.15:106893; AIAA Paper 94-1445) Avail: CASI HC A03/MF A01

A methodology to compute cumulative probability distribution functions (CDF) of fatigue life for different ratios, r of applied stress to the laminate strength based on first ply failure criteria has been developed and demonstrated. Degradation effects due to long term environmental exposure and mechanical cyclic loads are considered in the simulation process. A unified time-stress dependent multi-factor interaction equation model developed at NASA Lewis Research Center has been used to account for the degradation/aging of material properties due to cyclic loads. Fast probability integration method is used to perform probabilistic simulation of uncertainties. Sensitivity of fatigue life reliability to uncertainties in the primitive random variables are computed and their significance in the reliability based design for maximum life is discussed. The results show that the graphite/epoxy (0/+45/90) deg laminate with ply thickness 0.125 in. has 500,000 cycles life for applied stress to laminate strength ratio of 0.6 and a reliability of 0.999. Also, the fatigue life reliability has been found to be most sensitive to the ply thickness and matrix tensile strength. Tighter quality controls must therefore be enforced on ply thickness and matrix strength in order to achieve high reliability of the structure. Author

N95-27305# Sandia National Labs., Albuquerque, NM.

THE EFFECTS OF FINITE ELEMENT GRID DENSITY ON MODEL CORRELATION AND DAMAGE DETECTION OF A BRIDGE

Todd Simmermacher, R. L. Mayes, G. M. Reese, G. H. James, and David Zimmerman (Houston Univ., TX.) 1995 16 p Presented at the AIAA Adaptive Structures Conference, New Orleans, LA, 13-14 Apr. 1995

(Contract DE-AC04-94AL-85000)

(DE94-018895; SAND-94-2082C; CONF-950444-1) Avail: CASI HC A03/MF A01

Variation of model size as determined by grid density is studied for both model refinement and damage detection. In model refinement, it is found that a large model with a fine grid is preferable in order to achieve a reasonable correlation between the experimental response and the finite element model. A smaller model falls victim to the inaccuracies of the finite element (FE) method. As the grid become increasing finer, the FE method approaches an accurate representation. In damage detection the FE method is only a starting point. The model is refined with a matrix method which doesn't retain the FE approximation; therefore a smaller model that captures most of the dynamics of the structure can be used and is preferable. DOE

N95-27745# Sandia National Labs., Albuquerque, NM. Experimental Impact Physics Dept.

SCALING ISSUES IN DYNAMIC FRAGMENTATION

Dennis Grady 1995 13 p Presented at the Defense Nuclear Agency Workshop on Scaling Aspects of Hardened Structures, Albuquerque, NM, 24-26 Jan. 1995 Prepared in cooperation with AT and T Technologies, Inc., Albuquerque, NM

(Contracts DE-AC04-94AL-85000; DE-AC04-76DP-00789)

(DE95-008509; SAND-94-3187C; CONF-950169-1) Avail: CASI HC A03/MF A01

A set of relations which would allow the experimental results of impact fragmentation experiments conducted under the controlled environment of a testing laboratory to be confidently scaled to realistic system dimensions would be an effective tool in the developments toward a predictive capability in full scale applications involving fragmentation. Here some of the issues governing scaling relations in dynamic fragmentation are discussed. Dimensional arguments are pursued. Some of the consequences indicate that fragmentation scaling relations are dependent on the specific material properties and mechanisms governing the fragmentation process. Transitions in functional forms of the scaling relations can be expected under conditions in which fragmentation mechanism transitions occur in complex engineering materials. Some computational simulations and experimental impact fragmentation results are examined. DOE

N95-27837# Sandia National Labs., Albuquerque, NM.

A MICROSTRUCTURALLY BASED MODEL OF SOLDER JOINTS UNDER CONDITIONS OF THERMOMECHANICAL FATIGUE

D. R. Frear, S. N. Burchett, and M. M. Rashid (California Univ., Davis, CA.) 1994 14 p Presented at the InterPack '95: International Electronic Packaging Conference, Maui, HI, 26-30 Mar. 1995

(Contract DE-AC04-94AL-85000)

(DE95-006226; SAND-94-0951C; CONF-950344-5) Avail: CASI HC A03/MF A01

The thermomechanical fatigue failure of solder joints is increasingly becoming an important reliability issue. We present two computational methodologies that have been developed to predict the behavior of near eutectic Sn-Pb solder joints under fatigue conditions that are based on metallurgical tests as fundamental input for constitutive relations. The two-phase model mathematically predicts the heterogeneous coarsening behavior of near eutectic Sn-Pb solder. The finite element simulations from this model agree well with experimental thermomechanical fatigue tests. The simulations show that the presence of an initial heterogeneity in the solder microstructure could significantly degrade the fatigue lifetime. The single phase model is a computational technique that was developed to predict solder joint behavior using materials data for constitutive relation constants that could be determined through straightforward metallurgical experiments. A shear/torsion test sample was developed to impose strain in two different orientations. Materials constants were derived from these tests and the results showed an adequate fit to experimental results. The single-phase model could be very useful for conditions where microstructural evolution is not a dominant factor in fatigue. DOE

N95-27846 Southampton Univ. (England). Inst. of Sound and Vibration Research.

EXPERIMENTAL STUDIES TO TEST SIMPLE FLEXURAL NEUTRALIZERS FITTED TO BEAMS

P. Clark and R. G. White Oct. 1994 53 p Sponsored by the Marine Technology Directorate Ltd, the Science and Engineering Research Council, and the Procurement Executive, Ministry of Defence
(ISVR-TR-239) Copyright Avail: Issuing Activity (Southampton Univ., Southampton, England)

The control of vibration in one-dimensional structures is of considerable interest in practical engineering. With the majority of industrial machinery installations, it is this type of structure, for example, beams, pipework vibrating at low frequencies and other mechanical linkages, which forms one of the main vibration paths that bypass isolator systems. It is of interest to consider discontinuities that may be incorporated into these types of structure since they significantly affect the vibration characteristics of the complete installation. One such discontinuity that may be employed in vibration control is the vibration neutralizer. Previous work in this area of research has developed theoretical models of the neutralizer performance as a vibration control technique with particular reference to the effect of incorporating alternative mounting methods. In this work, complementary experimental studies are presented with a view to validating those theoretical studies previously undertaken. Author

N95-27865*# Virginia Polytechnic Inst. and State Univ., Blacksburg, VA. Center for Composite Materials and Structures
LOAD TRANSFER IN THE STIFFENER-TO-SKIN JOINTS OF A PRESSURIZED FUSELAGE Report, 1 Nov. 1991 - 30 Apr. 1995
Eric R. Johnson and Naveen Rastogi May 1995 222 p
(Grant NAG1-537)
(NASA-CR-198610; NAS 1.26:198610; CCMS-95-04; VPI-E-95-01) Avail: CASI HC A10/MF A03

Structural analyses are developed to determine the linear elastic and the geometrically nonlinear elastic response of an internally pressurized, orthogonally stiffened, composite material cylindrical shell. The configuration is a long circular cylindrical shell stiffened on the inside by a regular arrangement of identical stringers and identical rings. Periodicity permits the analysis of a unit cell model consisting of a portion of the shell wall centered over one stringer-ring joint. The stringer-ring-shell joint is modeled in an idealized manner; the stiffeners are mathematically permitted to pass through one another without contact, but do interact indirectly through their mutual contact with the shell at the joint. Discrete beams models of the stiffeners include a stringer with a symmetrical cross section and a ring with either a symmetrical or an asymmetrical open section. Mathematical formulations presented for the linear response include the effect of transverse shear deformations and the effect of warping of the ring's cross section due to torsion. These effects are important when the ring has an asymmetrical cross section because the loss of symmetry in the problem results in torsion and out-of-plane bending of the ring, and a concomitant rotation of the joint at the stiffener intersection about the circumferential axis. Data from a composite material crown panel typical of a large transport fuselage structure are used for two numerical examples. Although the inclusion of geometric nonlinearity reduces the 'pillowing' of the shell, it is found that bending is localized to a narrow region near the stiffener. Including warping deformation of the ring into the analysis changes the sense of the joint rotation. Transverse shear deformation models result in increased joint flexibility. Author

N95-28031*# Akron Univ., Akron, OH. Dept. of Civil Engineering.
ROBUST INTEGRATION SCHEMES FOR GENERALIZED VISCOPLASTICITY WITH INTERNAL-STATE VARIABLES. PART 1: THEORETICAL DEVELOPMENTS AND APPLICATIONS Final Report
Atef F. Saleeb and Wei Li May 1995 79 p Original contains color illustrations
(Grant NAG3-1493; RTOP 505-63-5B)
(NASA-CR-195452-Pt-1; E-9534-Pt-1) Avail: CASI HC A05/MF A01; 5 functional color pages

This two-part report is concerned with the development of a general framework for the implicit time-stepping integrators for the flow and evolution equations in generalized viscoplastic models. The primary goal is to present a complete theoretical formulation, and to address in detail the algorithmic and numerical analysis aspects involved in its finite element implementation, as well as to critically assess the numerical performance of the developed schemes in a comprehensive set of test cases. On the theoretical side, the general framework is developed on the basis of the unconditionally-stable, backward-Euler difference scheme as a starting point. Its mathematical structure is of sufficient generality to allow a unified treatment of different classes of viscoplastic models with internal variables. In particular, two specific models of this type, which are representative of the present start-of-art in metal viscoplasticity, are considered in applications reported here; i.e., fully associative (GVIPS) and non-associative (NAV) models. The matrix forms developed for both these models are directly applicable for both initially isotropic and anisotropic materials, in general (three-dimensional) situations as well as subspace applications (i.e., plane stress/strain, axisymmetric, generalized plane stress in shells). On the computational side, issues related to efficiency and robustness are emphasized in developing the (local) interative algorithm. In particular, closed-form expressions for residual vectors and (consistent) material tangent stiffness arrays are given explicitly for both GVIPS and NAV models, with their maximum sizes 'optimized' to depend only on the number of independent stress components (but independent of the number of viscoplastic internal state parameters). Significant robustness of the local iterative solution is provided by complementing the basic Newton-Raphson scheme with a line-search strategy for convergence. In the present first part of the report, we focus on the theoretical developments, and discussions of the results of numerical-performance studies using the integration schemes for GVIPS and NAV models. Author

N95-28032*# Akron Univ., Akron, OH. Dept. of Civil Engineering.
ROBUST INTEGRATION SCHEMES FOR GENERALIZED VISCOPLASTICITY WITH INTERNAL-STATE VARIABLES. PART 2: ALGORITHMIC DEVELOPMENTS AND IMPLEMENTATION Final Report
Wei Li and Atef F. Saleeb May 1995 36 p
(Grant NAG3-1493; RTOP 505-63-5B)
(NASA-CR-195453-Pt-2; E-9535-Pt-2; NAS 1.26:195453-Pt-2) Avail: CASI HC A03/MF A01

This two-part report is concerned with the development of a general framework for the implicit time-stepping integrators for the flow and evolution equations in generalized viscoplastic models. The primary goal is to present a complete theoretical formulation, and to address in detail the algorithmic and numerical analysis aspects involved in its finite element implementation, as well as to critically assess the numerical performance of the developed schemes in a comprehensive set of test cases. On the theoretical side, the general framework is developed on the basis of the unconditionally-stable, backward-Euler difference scheme as a starting point. Its mathematical structure is of sufficient generality to allow a unified treatment of different classes of viscoplastic models with internal variables. In particular, two specific models of this type, which are representative of the present start-of-art in metal viscoplasticity, are considered in applications reported here; i.e., fully associative (GVIPS) and non-associative (NAV) models. The matrix forms developed for both these models are directly applicable for both initially isotropic and anisotropic materials, in general (three-dimensional) situations as well as subspace applications (i.e., plane stress/strain, axisymmetric, generalized plane stress in shells). On the computational side, issues related to efficiency and robustness are emphasized in developing the (local) interative algorithm. In particular, closed-form expressions for residual vectors and (consistent) material tangent stiffness arrays are given explicitly for both GVIPS and NAV models, with their maximum sizes 'optimized' to depend only on the number of independent stress components (but independent of the number of viscoplastic internal state parameters). Significant robustness of the local iterative solution is provided by complementing the basic Newton-Raphson scheme with a line-search strategy for convergence. In the present second part of the report, we focus on the specific details of the numerical schemes, and associated computer algorithms, for the finite-element implementation of GVIPS and NAV models. Author

N95-28098 Texas A&M Univ., College Station, TX. Dept. of Mechanical Engineering.
DEFORMATION LIMITS ON TWO-PARAMETER FRACTURE MECHANICS IN TERMS OF HIGHER ORDER ASYMPTOTICS Final Report, Jan. 1992 - Sep. 1994
D. L. Crane and T. L. Anderson Sep. 1994 226 p Limited Reproducibility: More than 20% of this document may be affected by microfiche quality
(Contract N61533-92-K-0030)
(AD-A289113) Avail: Issuing Activity (Defense Technical Information Center (DTIC))

This report addresses the limitations of two-parameter fracture mechanics. We performed an asymptotic analysis of the general power series representation of the crack tip stress potential in an elastic plastic material that obeys a Ramberg-Osgood constitutive law. Expansion of the power series over a substantial number of terms yields. only three independent coefficients for low. and medium-hardening materials. The first independent The second and third independent coefficients, K2 and K4 are a function of geometry and loading level. A two-parameter theory implies that the crack tip stress fields have two degrees of freedom, but the asymptotic analysis implies that three parameters are required to characterize near-tip conditions. Thus two-parameter fracture theory is a valid engineering model only when there is an approximately unique relationship between K2 and K4. We performed elastic-plastic finite element analyses on several geometries and evaluated K2 and K4 as a function of deformation level. A reference,two-parameter solution (which gives a unique relation between K2 and K4) was provided by the modified boundary layer (MBL) geometry. Results indicate that the near tip stresses in all but the deeply cracked SENT (a/W-.5.O.9) and SENT (a/W-0.9) lend themselves to a two-parameter characterization. However, the deeply cracked SENT and SENT specimens maintain a high level of constraint to relatively large deformation levels. Thus single-parameter fracture mechanics is fairly robust for these high constraint geometries, but two-parameter theory is of little value when constraint loss eventually occurs. DTIC

N95-28100 Texas A&M Univ., College Station, TX.

AN EXPERIMENTAL AND NUMERICAL INVESTIGATION OF SPECIMEN SIZE REQUIREMENTS FOR CLEAVAGE FRACTURE TOUGHNESS Final Report, Jan. 1992 - Sep. 1994

T. L. Anderson and R. H. Dodds, Jr. (Illinois Univ., Urbana, IL.) Sep. 1994 53 p Limited Reproducibility: More than 20% of this document may be affected by microfiche quality

(Contract N61533-92-K-0030)

(AD-A289120; NUREG-CR-6272; CARDIVNSWC-TR-61-CR-94/05) Avail: Issuing Activity (Defense Technical Information Center (DTIC))

Cleavage fracture toughness can be influenced by specimen dimensions. Crack tip constraint can relax in small specimens, resulting in higher apparent toughness. Moreover, there is a statistical sampling effect, where thicker specimens tend to have lower toughness than thin specimens due to an increased sample volume. In deeply notched bend and compact specimens, theoretical modeling, finite element analysis, and experimental data indicate that the results will not be significantly influenced by crack tip constraint as long as the following specimen size requirements are met: a/W greater than 0.5, B greater than or equal to MJ(c)/sigma(y), B/b greater than or equal to 1 where a is the crack length, W is the specimen width, B is the specimen thickness, b is the uncracked ligament, J(c) is the critical 3 value, sigma(y) is the effective yield strength and M is a dimensionless constant. These size requirements are conservative if M is set equal to 100; M- 50 appears to be adequate for many materials, but the authors recommend the stricter requirement until fracture validation is performed. When specimens meet the above requirements, fracture toughness should not be influenced by size, provided statistical thickness effects are taken into account. DTIC

N95-28214*# National Aeronautics and Space Administration. Marshall Space Flight Center, Huntsville, AL.

THE SOLAR ARRAY-INDUCED DISTURBANCE OF THE HUBBLE SPACE TELESCOPE POINTING SYSTEM

C. L. Foster, M. L. Tinker, G. S. Nurre, and W. A. Till Washington May 1995 34 p

(NASA-TP-3556; M-782; NAS 1.60:3556) Avail: CASI HC A03/MF A01

The investigation of the vibrational disturbances of the Hubble Space Telescope that were discovered soon after deployment in orbit is described in detail. It was found that the disturbances were particularly evident during orbital day-night crossings, and that the magnitudes of the disturbances were considerably larger than the design jitter requirements. This paper describes the process by which the vibrations were characterized and isolated to a particular mechanism. The analysis of the flight data and comparisons with computer simulation results showed that the source of the disturbances was the thermally driven deformation of the solar arrays in conjunction with frictional effects in the array mechanisms. The control system was successfully modified to attenuate the disturbances to tolerable levels pending mechanical and thermal redesign of the solar arrays. The new arrays were installed during the first space telescope servicing mission and, in combination with the enhanced control system algorithm, reduced the disturbances to satisfactory levels. Author

N95-28337# Lawrence Livermore National Lab., Livermore, CA.

COMPUTATIONAL STUDIES OF PROJECTILE MELT IN IMPACT WITH TYPICAL WHIPPLE SHIELDS

C. E. Rhoades, Jr. and M. L. Alme (Alme and Associates, Columbia, MD.) Dec. 1994 9 p Presented at the Nuclear Explosives Code Developers Conference (NECDC), Las Vegas, NV, 27 Oct. 1994

(Contract W-7405-eng-48)

(DE95-005916; UCRL-JC-118566; CONF-9410254-4) Avail: CASI HC A02/MF A01

Protecting space-based structures against the impact of orbital debris is an important problem of current interest. This paper presents scaling results based on simulations with the CALE computer program of aluminum projectile impacting typical aluminum Whipple shields at speeds of 6 to 14 km/sec. The objective was to determine the extent of projectile and shield material melting. The approach was to perform a matrix of computer simulations varying the impact speed from 6 to 14 km/sec and varying the areal density of the shield from 5 percent to 80 percent of the centerline areal density of the projectile. The projectile radius was fixed at 9.5 mm (mass = 1.27 grams). The melt state of the projectile material and the shield material was assessed after release of the initial shock. The post-release specific energy in the projectile and in the shield was compared with the enthalpy of incipient melt and the enthalpy of complete melt provided in the Hultgren Tables. Material with specific energy greater than the enthalpy of complete melt was assumed to be fully melted. Material with specific energy greater than the enthalpy of incipient melt but less than that of complete melt was assumed to be partially solid and partially melted mixed phase material with no strength. Material with specific energy less than the enthalpy of incipient melt was assumed to be in a solid state with strength. It is likely that this solid material is in a highly fragmented state as a result of the initial shock. DOE

N95-28539# Los Alamos National Lab., NM.

INVESTIGATION OF HE DRIVEN CYLINDRICAL LINER

Tai-Ho Tan 1995 9 p Presented at the 4th International Symposium on Behavior and Dense Media Under High Dynamic Pressure, Tours, France, 5-9 Jun. 1995

(Contract W-7405-eng-36)

(DE95-007866; LA-UR-95-686; CONF-9506142-1) Avail: CASI HC A02/MF A01

We developed a technique that can compress most materials to densities much higher than their original values and shock them hard enough to undergo phase changes to various partially ionized states. The process involves using high explosives to drive a thin cylindrical liner so that it will progressively implode and converge along the axis at very high velocity. The device is simple yet versatile. Its configuration is ideally suited as a compact laboratory for the investigation of the behavior of dense media under extreme conditions. Code simulations show that liners made from most metals can be successfully imploded to converge on axis, producing over 10 MB pressure. For example, a 2D hydrocode calculation predicts that in a simple configuration where a hollow core PBX-9501 explosive cylinder is corner initiated to drive a thin seamless 304 SS tubing, the final convergence velocity can exceed 1 cm/(mu)s to produce a 15 MB pressure at impact as the density increases to 19.5 g/cc. The temperature from shock heating rises rapidly above 8 eV, and the result is a combination of radiation and plasma emissions. We have carried out several experiments with a wide array of diagnostics to investigate the implosion dynamics and final state interaction phenomena, and the results are compared with the code predictions. Radiographs of the liner implosion strongly indicate that the hydrodynamic processes are well behaved and calculable. Temperature measurement from the optical radiation is generally consistent with the code prediction. The velocity of the plasma front is measured by using optical pins and fast framing photography, and is found to lie between 11-17 cm/(mu)s. Fast framing photographs were taken with the aid of self luminous light to observe the evacuated chamber inside the imploding liner. The experimental results and their comparison with the calculation are discussed. DOE

N95-28616 California Univ., Berkeley, CA. Dept. of Engineering.
INSPECTION METHODS FOR UNDERWATER CABLES M.S. Thesis
Robin Y. Noyes 14 Dec. 1994 140 p Limited Reproducibility: More than 20% of this document may be affected by microfiche quality
(AD-A289610) Avail: Issuing Activity (Defense Technical Information Center (DTIC))

Underwater cables serve many purposes, both military and commercial. The most common use of underwater cables is for telecommunications, where voice is transformed into either electrical current or pulses of laser light which are transmitted across the world's oceans via underwater cables. The military uses underwater cables in several ways in support of national defense. Hydrophone arrays deployed from underwater cables form an extensive integrated undersea surveillance system (RYSS) which is used to monitor the activities of submannes. The military also uses underwater cables for training, testing, and evaluation ranges in the ocean. These ranges use transponder units to track air, surface, and submerged targets for purposes such as measuring surface ship radiated noise or evaluating weapons systems accuracy. The underwater cables provide the means to transmit communications and data to control facilities. DTIC

N95-28649 Strathclyde Univ., Glasgow (Scotland).
SMART MATERIALS: SURFACES, TRANSFORMS AND INTERFACES. THE COMMENSURATE ENGINEERING DIMENSION
Alaster McDonach, Peter T. Gardiner, Ron S. McEwen, and Brian Culshaw 18 Nov. 1994 391 p Presented at the Second European Conference on Smart Structures and Materials, Glasgow, England, 1994 Limited Reproducibility: More than 20% of this document may be affected by microfiche quality
(Contract N0014-94-J-9030)
(AD-A289598) Avail: Issuing Activity (Defense Technical Information Center (DTIC))

The future of molecularly based smart materials hinges on the development of integrated technologies addressing synthesis, assembly, shaping, etc. and some of these are now becoming clear. Even in the bolt on era new technologies will allow issues of commensurate engineering to be addressed. DTIC

N95-27972*# DASCON Engineering, Bay Village, OH.
A MODEL OF ROTATIONALLY-SAMPLED WIND TURBULENCE FOR PREDICTING FATIGUE LOADS IN WIND TURBINES
David A. Spera *In its* Collected Papers on Wind Turbine Technology May 1995 p 17-26 (For primary document see N95-27970 09-44)
Avail: CASI HC A02/MF A03

N95-27980*# Sandia National Labs., Albuquerque, NM.
A NASTRAN-BASED COMPUTER PROGRAM FOR STRUCTURAL DYNAMIC ANALYSIS OF HORIZONTAL AXIS WIND TURBINES
Don W. Lobitz *In* DASCON Engineering, Collected Papers on Wind Turbine Technology May 1995 p 89-97 Sponsored by DOE (For primary document see N95-27970 09-44)
(Contract DE-AC04-76DP-00789)
Avail: CASI HC A02/MF A03

N95-27982*# General Electric Co., Schenectady, NY.
CALCULATION OF DESIGN LOAD FOR THE MOD-5A 7.3 mW WIND TURBINE SYSTEM
L. Mirandy and J. C. Strain *In* DASCON Engineering, Collected Papers on Wind Turbine Technology May 1995 p 115-138a (For primary document see N95-27970 09-44)
(Contract DEN3-153)
Avail: CASI HC A03/MF A03

N95-27983*# Boeing Aerospace Co., Seattle, WA.
COMPARISON OF MEASURED AND CALCULATED DYNAMIC LOADS FOR THE Mod-2 2.5 mW WIND TURBINE SYSTEM
D. K. Zimmerman, S. A. Shipley, and R. D. Miller *In* DASCON Engineering, Collected Papers on Wind Turbine Technology May 1995 p 139-152 (For primary document see N95-27970 09-44)
Avail: CASI HC A03/MF A03

N95-28280*# Army Armament Research, Development and Engineering Center, Watervliet, NY. Close Combat Armaments Center.
STRESS ANALYSIS AND FAILURE OF AN INTERNALLY PRESSURIZED COMPOSITE-JACKETED STEEL CYLINDER
Peter C. T. Chen *In* FAA, Ninth DOD/NASA/FAA Conference on Fibrous Composites in Structural Design, Volume 3 Sep. 1992 p 1379-1388 (For primary document see N95-28266 09-24)
Copyright Avail: CASI HC A02/MF A04

N95-28284*# Materials Sciences Corp., Blue Bell, PA.
FAILURE ANALYSIS OF THICK COMPOSITE CYLINDERS UNDER EXTERNAL PRESSURE
A. Caiazzo and B. W. Rosen *In* FAA, Ninth DOD/NASA/FAA Conference on Fibrous Composites in Structural Design, Volume 3 Sep. 1992 p 1431-1446 Prepared for ORNL, TN; and Martin Marietta Energy Systems, Inc., Oak Ridge, TN (For primary document see N95-28266 09-24)
Copyright Avail: CASI HC A03/MF A04

N95-28285*# Utah Univ., Salt Lake City, UT. Dept. of Materials Science and Engineering.
ON THE THERMALLY-INDUCED RESIDUAL STRESSES IN THICK FIBER-THERMOPLASTIC MATRIX (PEEK) CROSS-PLY LAMINATED PLATES
Shoufeng Hu and John A. Nairn *In* FAA, Ninth DOD/NASA/FAA Conference on Fibrous Composites in Structural Design, Volume 3 Sep. 1992 p 1447-1454 (For primary document see N95-28266 09-24)
(Contract NAS1-18833)
Copyright Avail: CASI HC A02/MF A04

N95-28286*# National Aeronautics and Space Administration. Langley Research Center, Hampton, VA.
ANALYSIS OF STRESSES IN FINITE ANISOTROPIC PANELS WITH CENTRALLY LOCATED CUTOUTS
Vicki O. Britt *In* FAA, Ninth DOD/NASA/FAA Conference on Fibrous Composites in Structural Design, Volume 3 Sep. 1992 p 1485-1505 (For primary document see N95-28266 09-24)
Copyright Avail: CASI HC A03/MF A04

N95-28287*# Douglas Aircraft Co., Inc., Long Beach, CA.
THE ROLE OF BIAXIAL STRESSES IN DISCRIMINATING BETWEEN MEANINGFUL AND ILLUSORY COMPOSITE FAILURE THEORIES
L. J. Hart-Smith *In* FAA, Ninth DOD/NASA/FAA Conference on Fibrous Composites in Structural Design, Volume 3 Sep. 1992 p 1507-1528 (For primary document see N95-28266 09-24)
Copyright Avail: CASI HC A03/MF A04

N95-28288*# Hercules, Inc., Magna, UT. Advanced Materials and Systems Co.
STATIC AND DYNAMIC STRAIN ENERGY RELEASE RATES IN TOUGHENED THERMOSETTING COMPOSITE LAMINATES
Douglas S. Cairns *In* FAA, Ninth DOD/NASA/FAA Conference on Fibrous Composites in Structural Design, Volume 3 Sep. 1992 p 1529-1538 Previously announced in IAA as A92-37000 (For primary document see N95-28266 09-24)
Copyright Avail: CASI HC A02/MF A04

N95-28290*# National Aeronautics and Space Administration. Langley Research Center, Hampton, VA.
STIFFNESS AND STRENGTH TAILORING IN UNIFORM SPACE-FILLING TRUSS STRUCTURES
Mark S. Lake *In* FAA, Ninth DOD/NASA/FAA Conference on Fibrous Composites in Structural Design, Volume 3 Sep. 1992 p 1561-1587 Previously announced as N92-24546 (For primary document see N95-28266 09-24)
Copyright Avail: CASI HC A03/MF A04

N95-28291*# Aerospace Corp., El Segundo, CA. Mechanics and Materials Technology Center.
DESIGN PREDICTION FOR LONG TERM STRESS RUPTURE SERVICE OF COMPOSITE PRESSURE VESSELS
Ernest Y. Robinson *In* FAA, Ninth DOD/NASA/FAA Conference on Fibrous Composites in Structural Design, Volume 3 Sep. 1992

p 1589-1616 (For primary document see N95-28266 09-24)
(Contract F04701-88-C-0089)
Copyright Avail: CASI HC A03/MF A04

N95-28317 GPS Technologies, Inc., Tampa, FL.
PRESSURE VESSEL BURST TEST STUDY Progress Report
Maurice R. Cain and Robert J. Hall *In* Johns Hopkins Univ., The 1994 JANNAF Safety and Environmental Protection Subcommittee Meeting, Volume 1 Aug. 1994 p 267-283 (For primary document see N95-28294 09-20)
(Contract F08650-93-C-0066)
Avail: CPIA, 10630 Little Patuxent Pkwy., Suite 202, Columbia, MD 21044-3200 HC

N95-28467*# Lockheed Aeronautical Systems Co., Marietta, GA.
STRUCTURAL TESTING OF THE TECHNOLOGY INTEGRATION BOX BEAM
C. F. Griffin *In* FAA, Ninth DOD/NASA/FAA Conference on Fibrous Composites in Structural Design, Volume 2 Sep. 1992 p 659-67 Previously announced as X92-10409 (For primary document see N95-28462 09-24)
Avail: CASI HC A03/MF A04

N95-28468*# National Aeronautics and Space Administration. Langley Research Center, Hampton, VA.
TECHNOLOGY INTEGRATION BOX BEAM FAILURE STUDY Status Report
Mark J. Shuart, Damodar R. Ambur (Lockheed Aeronautical Systems Co., Marietta, GA.), D. D. Davis, Jr. (Lockheed Aeronautical Systems Co., Marietta, GA.), R. C. Davis (Lockheed Aeronautical Systems Co., Marietta, GA.), G. L. Farley (Lockheed Aeronautical Systems Co., Marietta, GA.), C. G. Lotts (Lockheed Aeronautical Systems Co., Marietta, GA.), and J. T. Wang (Lockheed Aeronautical Systems Co., Marietta, GA.) *In* FAA, Ninth DOD/NASA/FAA Conference on Fibrous Composites in Structural Design, Volume 2 Sep. 1992 p 673-68 Previously announced as X92-10410 (For primary document see N95-28462 09-24)
Avail: CASI HC A03/MF A04

N95-28484*# Stanford Univ., CA. Dept. of Aeronautics and Astronautics.
COMPRESSIVE STRENGTH OF DAMAGED AND REPAIRED COMPOSITE PLATES
Scott R. Finn and George S. Springer *In* FAA, Ninth DOD/NASA/FAA Conference on Fibrous Composites in Structural Design, Volume 2 Sep. 1992 p 1083-1095 (For primary document see N95-28462 09-24)
(Contract NAS1-18778)
Avail: CASI HC A03/MF A04

N95-28485*# Wright Lab., Wright-Patterson AFB, OH. Flight Dynamics Directorate.
POST IMPACT COMPRESSIVE STRENGTH IN COMPOSITES
Edvins Demuts, Raghbir S. Sandhu, and John A. Daniels *In* FAA, Ninth DOD/NASA/FAA Conference on Fibrous Composites in Structural Design, Volume 2 Sep. 1992 p 1097-1104 (For primary document see N95-28462 09-24)
Avail: CASI HC A02/MF A04

42 GEOSCIENCES (GENERAL)

N95-28099 Minnesota Univ., Minneapolis, MN. Inst. for Matematics and its applications
EMERGING APPLICATIONS OF PROBABILITY (STOCHASTIC MODELS IN GEOSYSTEMS) Final Report, 1 Jan. - 31 Jul. 1994
Avner Friedman 16 Dec. 1994 21 p Limited Reproducibility: More than 20% of this document may be affected by microfiche quality
(Contract N00014-94-1-0301)
(AD-A289117) Avail: Issuing Activity (Defense Technical Information Center (DTIC))

The workshop was devoted to several of the most active topics in this area and, in particular, covered: Probabilistic models in geophysics including hierarchical models for geophysical structures, homogenization of random elastic media, propagation of seismic waves, statistical methods for estimation of parameters of seismic waves, prediction problems for seismic phenomena and other geophysical fields. Modern probabilistic and statistical methods in oceanography and atmospheric sciences including: probabilistic and statistical mechanical models of large scale ocean circulation; random fields and stochastic partial differential equations techniques; waves in the ocean in presence of random topography and random forcing, random field modeling of salinity, temperature and other physical fields; weak turbulence; prediction problems; distribution functions for vorticity, velocity and dissipation rates; intermittency and structure functions; singularities in Euler equations and their relation to turbulence; and turbulent cascades and martingales. DTIC

43 EARTH RESOURCES AND REMOTE SENSING

Includes remote sensing of earth resources by aircraft and spacecraft; photogrammetry; and aerial photography.
For instrumentation see *35 Instrumentation and Photography.*

N95-26476 Naval Research Lab., Bay Saint Louis, MS. Marine Geosciences Div.
DIGITAL MAPPING, CHARTING, AND GEODESY ANALYSIS PROGRAM: INITIAL TECHNICAL REVIEW OF RASTER PRODUCT FORMAT Final Report
Kevin B. Shaw, John Breckenridge, S. D. Coughlan, Tom Fetterer, Ruth Guldry, Jerry Landrum, Greg Terrie, Susan V. Carter, Steve Kuder, and H. Vincent Miller (Mississippi State Univ., Bay Saint Louis, MS.) 31 Oct. 1994 18 p Sponsored by Oceanographer of the Navy Limited Reproducibility: More than 20% of this document may be affected by microfiche quality
(AD-A289039; NRL/MR/7441-94-7546) Avail: Issuing Activity (Defense Technical Information Center (DTIC))

Rounding out the Defense Mapping Agency's (DMA) effort for a raster standard to complement the existing Vector Product Format and proposed Text Product Standard, the Raster Product Format (RPF), is the proposed format for accommodating raster data. The Naval Research Laboratory's Digital Mapping, Charting, and Analysis Program (DMAP) has been requested by DMA (via NO96) to establish the usefulness of such a standard for naval purposes. In its technical review, DMAP discusses the overall view of a raster standard and how the development of such a standard should proceed. The RPF, for example, should be modified to be compatible with already-existing standards. The suitability of RPF as it currently exists is also discussed by DMAP. DTIC

N95-26645# Helsinki Univ. of Technology, Espoo (Finland). Space Technology Lab.
RADIOMETER MEASUREMENTS OF SNOW IN SODANKYLAE, 1991-1993
Lauri Kurvonen Sep. 1994 104 p
(ISSN 0786-8154)
(PB95-184966; Rept-16; ISBN-951-22-2274-4) Avail: CASI HC A06/MF A02

A helicopter-borne multifrequency radiometer (24, 34, 48 and 94 GHz vertical polarization) was used to investigate the behavior of the brightness temperature of snow in Sodankyla. Several measurements were made in dry, wet and no snow conditions. The angle of incidence was 45 deg in all measurements. The radiometer measurements and their analyses are presented. The analyses have focused on the effect of vegetation and land type on the brightness temperature of snow. The aim of the study is to determine: (1) the general behavior of the brightness temperature of snow in different land types; (2) the effect of forest vegetation on the brightness temperature of snow; (3) the capability of the radiometer system to discriminate refrozen snow patches in forests during the melting period; and (4) the brightness temperature of dry snow versus the water equivalent of snow. NTIS

N95-26682 Naval Research Lab., Bay Saint Louis, MS. Marine Geosciences Div.

DIGITAL MAPPING, CHARTING, AND GEODESY ANALYSIS PROGRAM TECHNICAL REVIEW OF VECTOR QUANTIZATION (VQ) DECOMPRESSION FOR THE NATIONAL IMAGERY TRANSMISSION FORMAT STANDARD (NITFS) Final Report

H. Vincent Miller (Mississippi State Univ., Bay Saint Louis, MS.), S. Danette Coughlan, Thomas A. Fetterer, Ruth A. Guidry, Maura C. Lohrenz, Mike E. Trenchard, Perry B. Wischow, Kevin B. Shaw, and Susan V. Carter 30 Nov. 1994 16 p Limited Reproducibility: More than 20% of this document may be affected by microfiche quality
(AD-A288998; NRL-MR/7441-94-7541) Avail: Issuing Activity (Defense Technical Information Center (DTIC))

The Draft Military Standard Vector Quantization (VQ) Decompression for the National Imagery Transmission Format Standard, providing a format for images compressed via a VQ scheme, has been reviewed by the Naval Research Laboratory's Digital Mapping, Charting, and Geodesy Analysis Program (DMAP) at the request of the Oceanographer of the Navy. The written standard itself is practically complete; DMAP provides exact details on essential modifications to the document. In addition, suggested modifications and editorial comments are supplied in an effort to enhance the document. DMAP's main issue, however, is the lack of information on the relationship of this standard to the already-under-development Raster Product Format (RPF), which also provides for the compressed images and is not confined to a single compression scheme. DMAP contends that once the VQ file structure is demonstrated not to conflict with the RPF, the VQ standard will provide an acceptable format, compatible with the more comprehensive RPF, for VQ compressed images. DTIC

N95-26815*# Purdue Univ., West Lafayette, IN. School of Electrical Engineering.

CONVERSION OF SUNFLOWER MULTIBAND RADIOMETER POLARIZATION MEASUREMENTS TO POLARIZATION PARAMETERS Final Report

Larry L. Biehl 13 Apr. 1995 61 p
(Contract NCC2-5038)
(NASA-CR-197774; NAS 1.26:197774) Avail: CASI HC A04/MF A01

The data processing analysis and conversion of polarization measurements to polarization parameters from the Sunflower multiband radiometer is presented in this final report. Included is: (1) the actual data analysis; (2) the comparison of the averaging techniques and the percent polarization derived from the original and averaged I, Q, U parameters; (3) the polarizer angles used in conversion; (4) the Matlab files; (5) the relative ground size, field of view location, and view zenith angles, and (6) the summary of all the sky data for all dates. CASI

N95-26841 Naval Air Systems Command, Arlington, VA.

NAVAL AVIATION SYSTEM TEAM MAPPING, CHARTING, AND GEODESY HANDBOOK Final Report

John H. Harden, Jr. and Zdenka S. Willis 15 Jul. 1994 70 p Limited Reproducibility: More than 20% of this document may be affected by microfiche quality
(AD-A288590) Avail: Issuing Activity (Defense Technical Information Center (DTIC))

This handbook is specifically tailored for Naval Aviation Systems Team (TEAM) weapon systems developers. It is a primary reference for information about Mapping, Charting, and Geodesy (MC&G) support from the Defense Mapping Agency (DMA). Handbook objectives are: (1) to clarify MC&G relevance to TEAM systems development and the developer's job; (2) to guide developers in acquiring a necessary basic competence in MC&G; (3) to explain the process for getting DMA MC&G data and services; and (4) to point developers towards helping on MC&G issues within the TEAM, DMA, and elsewhere. The Handbook has the following features: (1) it is organized for browsing; (2) the Executive Gouge summarizes everything on one page; (3) details to access topical sources are located in the Where To Find It box at the end of each section; and (4) useful appendices include product statistics and list key individuals. After initial hard copy distribution, this handbook will be maintained in soft copy on the Naval Air Systems Command (NAVAIR) Head quarters Network (NHN). DTIC

N95-27156 National Academy of Sciences - National Research Council, Washington, DC. Committee on Geodesy.

AIRBORNE GEOPHYSICS AND PRECISE POSITIONING: SCIENTIFIC ISSUES AND FUTURE DIRECTIONS

1995 119 p
(LC-94-68678; ISBN-0-309-05183-5) Copyright Avail: Issuing Activity (NAS-NRC)

Since the Challenger circumnavigated the globe on its oceanographic survey in the mid-1870's, scientists have mounted extensive interdisciplinary expeditions to study large regions of the Earth. The ability to probe the Earth from remote platforms has resulted in numerous scientific advances, such as the revolutionary images of previously uncharted ocean floor that were produced by marine geophysical technology in the 1960s. These images eventually helped to trigger a major paradigm shift in the earth sciences with the development of a fundamental theory of modern geophysics, plate tectonics. The purpose of this report is to highlight the advances, both potential and realized, that airborne geophysics and precise positioning have made or can make possible to the solid earth sciences. The report first discusses the state of the art in airborne geophysics as integrated with new precise positioning systems, focusing first on the new technology to map topography and the gravity field and then on recent advances in precise positioning. The scientific goals of a focused effort in airborne geophysics, including advances in our understanding of solid earth science, global climate change, the environment, and resources are outlined. The technological advances in measurement, positioning, and aircraft design that will be required to aggressively pursue the scientific goals discussed previously are identified. The recommendations of the Committee on Geodesy for achieving the goals and directions outlined in the report are presented. Derived from text

N95-27998*# Hydex Corp., Vienna, VA.

REMOTE SENSING OF HYDROLOGIC VARIABLES IN BOREAL AREAS, PHASE 2 Final Report, Apr. 1994 - Apr. 1995

Eugene L. Peck and Thomas R. Carroll (National Weather Service, Chanhassen, MN.) May 1995 28 p
(Contract NAS5-32336)
(NASA-CR-198717; NAS 1.26:198717) Avail: CASI HC A03/MF A01

During Phase 2 airborne Gamma Radiation measurements were conducted over 48 BOREAS (boreal ecosystem atmosphere study) flight lines. Ground measurements of the soil moisture (SM) of the mineral soil and the depth and water content (WC) of the moss/humus layer were collected for calibration of the flight lines. Special attention has been given to the flight lines over, and near, the primary tower sites in the southern study area (SSA); Old Black Spruce (OBS), Old Jack Pine, Old Aspen, and Young Aspen. Multiple ground surveys (September 1993, July, August, and September 1994) show the variation of the water content of the moss/humus layers and changes in the amount of standing water near the SSA OBS tower during the period September 1993 to September 1994. All ground data, airborne estimates and locations of flight lines and ground sampling points have been submitted to BORIS (BOREAS Information System). On 8-10 September 1994 exceptionally high values of cosmic radiation were observed by the airborne gamma radiation system over the SSA. Follow up investigation has not determined the source of, or what caused, the high cosmic count rates. Author

N95-28053# Lawrence Livermore National Lab., Livermore, CA.

REMOTE MEASUREMENT OF GROUND TEMPERATURE AND EMISSIVITY

J. R. Henderson Jun. 1994 12 p Presented at the Annual Meeting of the Society of Photo-Optical Instrumentation Engineers, San Diego, CA, 24-29 Jul. 1994
(Contract W-7405-eng-48)
(DE95-008055; UCRL-JC-117673; CONF-940723-35) Avail: CASI HC A03/MF A01

TAISIR, Temperature and Imaging System InfraRed, is a nominally satellite based platform for remote sensing of the earth. One of its design features is to acquire atmospheric data simultaneous with ground data, resulting in minimal dependence on external atmospheric models for data correction. Extensive modeling of the rms error of determining a ground temperature and emissivity for a gray body has been performed as a function of integration time, spectroscopic resolution of the system, ground emissivity, atmospheric variables, and atmospheric data accuracy. We find that increased resolution improves measurement accuracy by emphasizing those regions where the atmospheric transmission is highest and atmospheric emission/absorption lowest. We find rms temperature errors (le)1K and rms emissivity errors less than 0.01 are obtainable for reasonable seeing and with sufficient information about the atmosphere. A new method is developed for modeling the dependence of the band-averaged transmission and emission. Monte Carlo simulations of satellite data taken using a multi-angle technique are used to derive signal-to-noise requirements. The applicability of those results to the TAISIR system requirements are discussed. DOE

N95-28180# Selskapet for Industriell og Teknisk Forskning, Trondheim (Norway). Div. of Industrial Mathematics.
SPECKLE SPECTRUM OF THE ERS-1 WAVEMODE PRODUCT
Jul. 1994 43 p
(PB95-196564; STF10-A94008) Avail: Issuing Activity (National Technical Information Service (NTIS))

The present report contains a brief discussion of the speckle spectrum of the ERS-1 (UWA) Wavemode product. The speckle spectrum has been determined by a simple fit to directly computed spectra from a set of imagettes. The spectrum turns out to be Gaussian in azimuth direction, whereas the functional form in the range direction is significantly different with a rather flat region up to .05/m. It is also demonstrated that the origin of the low wavenumber noise in many of the UWA spectra may simply be a lack of spectral smoothing before the spectrum is encoded into the UWA format. NTIS

N95-28209*# City Univ. of New York, NY. Remote Sensing Lab.
STUDIES OF RADAR BACKSCATTER AS A FUNCTION OF WAVE PROPERTIES AND THE WINDS IN THE TURBULENT MARINE ATMOSPHERE Final Report
Willard J. Pierson, Jr. and Winfield B. Sylvester May 1995 50 p
(Grant NAGw-690)
(NASA-CR-198608; NAS 1.26:198608) Avail: CASI HC A03/MF A01

The research on model functions for ADEOS and ERS-1 are summarized and an analysis of the differences between the three kinds of models is provided in this final report. The success of the AMI on ERS-1 obtained at GSFC and NMC is highlighted. The problem of wind stress description is reviewed within and the scatterometer model being developed for high winds monitoring for the AMI on ERS-1 and ERS-2 is described.
Derived from text

N95-28211* National Aeronautics and Space Administration. Goddard Space Flight Center, Greenbelt, MD.
METHOD FOR DETERMINING SURFACE COVERAGE BY MATERIALS EXHIBITING DIFFERENT FLUORESCENT PROPERTIES Patent
Emmett W. Chappelle, inventor (to NASA), Craig S. T. Daughtry, inventor (to NASA), and James E. McMurtrey, III, inventor (to NASA) 2 May 1995 9 p Filed 22 Nov. 1993
(NASA-Case-GSC-13539-1; US-Patent-5,412,219; US-Patent-Appl-SN-155605; US-Patent-Class-250-461.1; US-Patent-Class-250-253; Int-Patent-Class-G01N-21/64) Avail: US Patent and Trademark Office

An improved method for detecting, measuring, and distinguishing crop residue, live vegetation, and mineral soil is presented. By measuring fluorescence in multiple bands, live and dead vegetation are distinguished. The surface of the ground is illuminated with ultraviolet radiation, inducing fluorescence in certain molecules. The emitted fluorescent emission induced by the ultraviolet radiation is measured by means of a fluorescence detector, consisting of a photodetector or video camera and filters. The spectral content of the emitted fluorescent emission is characterized at each point sampled, and the proportion of the sampled area covered by residue or vegetation is calculated.
Official Gazette of the U.S. Patent and Trademark Office

N95-28392 Woods Hole Oceanographic Inst., MA.
ALTIMETER ANALYSIS OF OCEAN CURRENTS Technical Report
Sandipa Singh, Michael J. Caruso, and Kathryn A. Kelly Jul. 1994 25 p Limited Reproducibility: More than 20% of this document may be affected by microfiche quality
(Contract N00014-92-J-1486)
(AD-A290167; WHOI-94-16) Avail: Issuing Activity (Defense Technical Information Center (DTIC))

Altimeter data from satellites are being used in an ongoing effort to obtain data sets with temporal as well as global coverage. This report describes the algorithms formulated and the programs written for the use of altimeter data from the European Space Agency (ESA) European Remote Sensing Satellite, ERS-1, for a repeat track analysis of ocean currents. It also presents some results from the California Current region. DTIC

N95-28520# Brookhaven National Lab., Upton, NY.
REMOTE SENSING OF THE ATMOSPHERE BY RESONANCE RAMAN LIDAR
A. J. Sedlacek, D. Harder, K. P. Leung, P. B. Zuhoski, Jr., D. Burr, and C. L. Chen Dec. 1994 4 p Presented at the 6th Optical Society of America (OSA) Meeting on Remote Sensing of the Atmosphere, Salt Lake City, UT, 6-9 Feb. 1995
(Contract DE-AC02-76CH-00016)
(DE95-007312; BNL-61283; CONF-950277-1) Avail: CASI HC A01/MF A01

When in resonance, Raman scattering exhibits strong enhancement ranging from four to six orders of magnitude. This physical phenomenon has been applied to remote sensing of the Earth's atmosphere. With a 16 inch Cassegrain telescope and spectrometer/ CCD-detector system, 70-150 ppm-m of SO2 in the atmosphere has been detected at a distance of 0.5 kilometer. This system can be used to detect/monitor chemical effluence in the atmosphere by their unique Raman fingerprints. Experimental result together with detailed resonance Raman and atmospheric laser propagation effects will be discussed. DOE

N95-28554# Instituto de Pesquisas Espaciais, Sao Jose dos Campos (Brazil). Ministry of Science and Technology.
MODELS USED TO FORECAST AGRICULTURAL CORN CROPS IN THE MICRO-REGION OF RIBEIRAO PRETO-SP [MODELOS DE PREVISAO DE SAFRA AGRICOLA PARA A CULTURA DE MILHO NA MICRORREGIAO DE RIBEIRAO PRETO-SP]
Sherry ChouChen Jun. 1993 18 p In PORTUGUESE
(INPE-5513-NTC/309) Avail: CASI HC A03/MF A01

To forecast production of a specific crop, its area and yield have to be estimated in advance. In this study a comparison was made using three different approaches to estimate corn yield of the micro-region Ribeirao Preto in Sao Paulo State. The first two approaches were based on yield-weather modelling using monthly meteorological data while the third used a growth simulation model (CERES-MAIZE). Results show that the first yield-weather model is better due to its simplicity of modelling in addition to the low yield estimation errors of the independent test data set. Author

N95-28643# Helsinki Univ. of Technology, Espoo (Finland).
RADON TRANSFORM AND ITS APPLICATIONS IN GRIDDING AIRBORNE GEOPHYSICAL SURVEY DATA Research Report
Z. Chen and M. Peltoniemi 1995 46 p See also PB93-197283
(PB95-195533; TKK-IGE-A16) Avail: CASI HC A03/MF A01

The Radon transform method has been studied as a means of presentation of geophysical data, and in an attempt to develop a better gridding technique for line-based airborne geophysical data. The observed line-based data are usually spatially aliased because the line spacing is too large compared with the wavelength of features in the cross-track direction. Another problem for conventional gridding methods is that they tend to destroy the continuity of elongated anomalies whose strike direction is not perpendicular to the grid-line direction. The radon transform gridding method transforms the observed parallel profiles into the strike-wavenumber domain. The Fourier spectrum of the desired grid is constructed from the strike-wavenumber domain using projection-slice theorem, and the final square grid is obtained by performing an inverse Fourier transform of the spectrum. Hence, two interpolations must be made in the application of the method to line-survey geophysical data: the first one is during transforming the observed parallel profiles into the strike-wavenumber domain, and the second one during the inverse process. NTIS

N95-28656 Helsinki Univ. of Technology, Espoo (Finland).
MODELING AND RETRIEVAL OF SNOW AND SEA ICE CHARACTERISTICS IN THE FREQUENCY RANGE 6 TO 90 GHz Final Report
J. Grandell and M. Hallikainen Mar. 1994 65 p Limited Reproducibility: More than 20% of this document may be affected by microfiche quality
(PB95-195467; ISBN-951-22-2364-3) Avail: Issuing Activity (National Technical Information Service (NTIS))

The aim of the study is to provide tools for the analysis of multi-frequency multi-polarization spaceborne radiometer data in the retrieval of snow and sea ice characteristics. The emphasis is laid on studying the possible advantages of using higher frequency channels (up to 90 GHz). The most advanced spaceborne radiometers currently in operation (Special Sensor Microwave Imager SSM/I) or under consideration (Multi-Frequency Imaging Microwave Radiometer MIMR), operate in a frequency range up to 90 GHz. Chapter headings include: Data Acquisition; Retrieval of Snow Parameters from SSM/I Data; Retrieval of Sea Ice Parameters from SSM/I Data; Verification of Emission Algorithms Using SSM/I Data; Measurements With The HUT (Helsinki University of Technology) Radiometer System; Measurements With The HUTSCAT Scatterometer; Software Developed During the Study. NTIS

N95-28672# Instituto de Pesquisas Espaciais, Sao Jose dos Campos (Brazil). Dept. of Science and Technology.
NEURAL NETWORKS IN THE CLASSIFICATION OF USES OF THE SOIL IN SATELLITE IMAGES [REDES NEURAIS NA CLASSIFICACAO DE USOS DO SOLO EM IMAGENS DE SATELITES]
Maria SuelenaSantiagoBarros 1993 10 p In PORTUGUESE Presented at the Brazilian Symposium of Operational Research (SOBRAPO), Salvador, Bahia, Nov. 1992
(INPE-5478-PRE/1777) Avail: CASI HC A02/MF A01

This work analyses the potential of Backpropagation Networks' use as a powerful approach, although not completely understood, to land-cover classification in satellite images when there are many not well separated classes to be identified. Some classification results are shown and the importance of the training sites, the number of classes and learning cycles in the training phase are discussed. Author

44 ENERGY PRODUCTION AND CONVERSION

Includes specific energy conversion systems, e.g., fuel cells; global sources of energy; geophysical conversion; and windpower.

For related information see also *07 Aircraft Propulsion and Power, 20 Spacecraft Propulsion and Power,* and *28 Propellants and Fuels.*

N95-26393*# Rockwell International Corp., Canoga Park, CA. Rocketdyne Div.
FEASIBILITY OF FLYWHEEL ENERGY STORAGE SYSTEMS FOR APPLICATIONS IN FUTURE SPACE MISSIONS Final Contractor Report
G. Espiritu Santo, S. P. Gill, J. F. Kotas, and R. Paschall Jan. 1995 152 p
(Contract NAS3-25808; RTOP 476-14-10)
(NASA-CR-195422; E-9367; NAS 1.26:195422) Avail: CASI HC A08/MF A02

The objective of this study was to examine the overall feasibility of deploying electromechanical flywheel systems in space used for excess energy storage. Results of previous Rocketdyne studies have shown that the flywheel concept has a number of advantages over the NiH2 battery, including higher specific energy, longer life and high roundtrip efficiency. Based on this prior work, this current study was broken into four subtasks. The first subtask investigated the feasibility of replacing the NiH2 battery orbital replacement unit (ORU) on the international space station (ISSA) with a flywheel ORU. In addition, a conceptual design of a generic flywheel demonstrator experiment implemented on the ISSA was completed. An assessment of the life cycle cost benefits of replacing the station battery energy storage ORU's with flywheel ORU's was performed. A fourth task generated a top-level development plan for critical flywheel technologies, the flywheel demonstrator experiments and its evolution into the production unit flywheel replacement ORU. Author

N95-26543# Fuel Cell Engineering Corp., Danbury, CT.
MOLTEN CARBONATE FUEL CELL (MCFC) PRODUCT DEVELOPMENT TEST Second Annual Report
15 Dec. 1994 29 p
(Contract DE-FC21-92MC-29237)
(DE95-007345; DOE/MC-29237/3983) Avail: CASI HC A03/MF A01

This is the second annual report covering progress made under DOE cooperative agreement DE-FC21-92MC29237, Molten Carbonate Fuel Cell Product Development Test. The project is for the design, construction, and testing of a 2MW carbonate fuel cell power plant in the City of Santa Clara, California. The report is divided into sections which describe the progress in various program activities, and provides an overview of the program, including the project objectives, site location, and schedule. DOE

N95-26734*# DASCON Engineering, Bay Village, OH.
BIBLIOGRAPHY OF NASA-RELATED PUBLICATIONS ON WIND TURBINE TECHNOLOGY 1973-1995 Final Contractor Report
David A. Spera Apr. 1995 128 p
(Contract NAS3-25776; RTOP 776-33-41)
(NASA-CR-195462; E-9597; NAS 1.26:195462; DOE/NASA/5776-3)
Avail: CASI HC A07/MF A02

A major program of research and development projects on wind turbines for generating electricity was conducted at the NASA Lewis Research Center from 1973 to 1988. Most of these projects were sponsored by the U.S. Department of Energy (DOE), as a major element of its Federal Wind Energy Program. One other large-scale wind turbine project was sponsored by the Bureau of Reclamation of the Department of Interior (DOI). The peak years for wind energy work at Lewis were 1979-80, when almost 100 engineers, technicians, and administrative personnel were involved. From 1988 their conclusion in 1995, NASA wind energy activities have been directed toward the transfer of technology to commercial and academic organizations. Wind energy activities at NASA can be divided into two broad categories which are closely related and often overlapping: (1) Designing, building, and testing a series of 12 large-scale, experimental, horizontal-axis wind turbines (HAWT's); and (2) conducting supporting research and technology (SR&T) projects. The purpose of this bibliography is to assist those active in the field of wind energy in locating the technical information they need on wind power planning, wind loads, turbine design and analysis, fabrication and installation, laboratory and field testing, and operations and maintenance. This bibliography contains approximately 620 citations of publications by over 520 authors and co-authors. Sources are: (1) NASA reports authored by government grantee, and contractor personnel, (2) papers presented by attendees at NASA-sponsored workshops and conferences, (3) papers presented by NASA personnel at outside workshops and conferences, and (4) outside publications related to research performed at NASA/ DOE wind turbine sites. Author

N95-26762 Naval Postgraduate School, Monterey, CA.
ANNEALING OF RADIATION DAMAGED GALLIUM ARSENIDE SOLAR CELLS BY LASER ILLUMINATION M.S. Thesis
Richard D. Kramer Sep. 1994 91 p Limited Reproducibility: More than 20% of this document may be affected by microfiche quality
(AD-A289683) Avail: Issuing Activity (Defense Technical Information Center (DTIC))

In this research, preliminary results of a new approach for annealing previously irradiated Gallium Arsenide solar cells is reported. This technique examines the use of laser illumination to induce Forward-Biased current annealing. Five GaAs solar cells were irradiated with 65 MeV electrons at varying fluence levels. Visible laser light produced a 0.5 A/sq cm forward-biased current density and raised the solar cell temperature by 30 C. Ten to fifteen percent recovery of degraded parameters was achieved in four of the five tested cells. The results show that a laser can produce some annealing in radiation damaged GaAs solar cells. Further investigation into the results also indicate that the 65 MeV energy level of the electron irradiation could have caused unrecoverable permanent damage to the solar cells. Follow up research of this annealing technique should be conducted on GaAs cells that are being irradiated at a lower energy level as well as lower fluence level. Repetitive annealing of lightly damaged cells in previous research has provided appreciative recovery using forward bias current techniques. One can expect similar results using the laser induced annealing technique proposed in this research. DTIC

N95-26785*# National Aeronautics and Space Administration. Marshall Space Flight Center, Huntsville, AL.
THE 1994 27TH ANNUAL NASA AEROSPACE BATTERY WORKSHOP
Jeffrey C. Brewer, comp. Washington Feb. 1995 638 p Workshop held in Huntsville, AL, 15-17 Nov. 1994
(NASA-CP-3292; M-772; NAS 1.55:3292) Avail: CASI HC A99/MF A06

The proceedings of the 27th Annual NASA Aerospace Battery Workshop, hosted by the Marshall Space Flight Center on November 15-17, 1994 are presented. The workshop was attended by representatives from various government agencies, as well as contractors and manufacturers, both U.S. and abroad. The subjects covered included: (1) nickel-cadium; (2) nickel-hydrogen, (3) nickel-metal hydride, and (4) lithium based technologies, as well as flight and ground test data. For individual titles, see N95-26786 through N95-26796.

N95-26786*# Aerospace Corp., El Segundo, CA. Electronics Technology Center.
PROGRESS TOWARDS COMPUTER SIMULATION OF NIH2 BATTERY PERFORMANCE OVER LIFE c33
Albert H. Zimmerman and M. V. Quinzio *In* NASA. Marshall Space Flight Center, The 1994 27th Annual NASA Aerospace Battery Workshop Feb. 1995 p 177-183 (For primary document see N95-26785 09-44)
Avail: CASI HC A02/MF A06

The long-term performance of rechargeable battery cells has traditionally been verified through life-testing, a procedure that generally requires significant commitments of funding and test resources. In the situation of nickel hydrogen battery cells, which have the capability of providing extremely long cycle life, the time and cost required to conduct even accelerated testing has become a serious impediment to transitioning technology improvements into spacecraft applications. The utilization of computer simulations to indicate the changes in performance to be expected in response to design or operating changes in nickel hydrogen cells is therefore a particularly attractive tool in advanced battery development, as well as for verifying performance in different applications. Computer-based simulations of the long-term performance of rechargeable battery cells have typically had very limited success in the past. There are a number of reasons for the lack in progress in this area. First, and probably most important, all battery cells are relatively complex electrochemical systems, in which performance is dictated by a large number of interacting physical and chemical processes. While the complexity alone is a significant part of the problem, in many instances the fundamental chemical and physical processes underlying long-term degradation and its effects on performance have not even been understood. Second, while specific chemical and physical changes within cell components have been associated with degradation, there has been no generalized simulation architecture that enables the chemical and physical structure (and changes therein) to be translated into cell performance. For the nickel hydrogen battery cell, our knowledge of the underlying reactions that control the performance of this cell has progressed to where it clearly is possible to model them. The recent development of a relative generalized cell modelling approach provides the framework for translating the chemical and physical structure of the components inside a cell into its performance characteristics over its entire cycle life. This report describes our approach to this task in terms of defining those processes deemed critical in controlling performance over life, and the model architecture required to translate the fundamental cell processes into performance profiles. Derived from text

N95-26787*# Lockheed Missiles and Space Co., Sunnyvale, CA.
LONG LIFE 80Ah STANDARD IPV NIH2 BATTERY CELL c33
Jon D. Armantrout and J. S. Waller *In* NASA. Marshall Space Flight Center, The 1994 27th Annual NASA Aerospace Battery Workshop Feb. 1995 p 185-207 (For primary document see N95-26785 09-44)
Avail: CASI HC A03/MF A06

A standard Nickel-Hydrogen (NiH2) Individual Pressure Vessel (IPV) battery cell is needed to meet future low cost, high performance mission requirements for NASA, military, and civil space programs. A common or standard cell design has evolved from the heritage of HST, Milstar, and other Air Force Mantech cell designs with substantial flight experience, while incorporating some of the historical COMSAT cell design features described in a previous NASA publication. Key features include slurry process nickel electrodes having high strength, long life and high yield (lower cost), and dual layer zircar separators for improved KOH retention, uniformality, and longer life. The cell design will have a zirconium oxide wall wick inside the pressure vessel to redistribute electrolyte and extend life. The slurry electrode will be 35 mils thick to take advantage of qualified cell mechanical configurations and proven assembly and activation techniques developed by Eagle Picher Industries (EPI) for the Hubble Space Telescope (HST) RNH-90-3 and 'Generic HST' RNH-90-5 cell designs with back-to-back nickel electrodes produced by the dry sinter process. The 80Ah common cell design can be scaled to meet capacity requirements from 60Ah to 100Ah. Producibility, commonality, and long life performance will be enhanced with the robust cell design described herein. Derived from text

N95-26788*# Eagle-Picher Industries, Inc., Joplin, MO.
HIGH-RATE/HIGH-TEMPERATURE CAPABILITY OF A SINGLE-LAYER ZICAR-SEPARATOR NICKEL-HYDROGEN CELL c33
James R. Wheeler *In* NASA. Marshall Space Flight Center, The 1994 27th Annual NASA Aerospace Battery Workshop Feb. 1995 p 243-246 (For primary document see N95-26785 09-44)
Avail: CASI HC A01/MF A06

A 50 Ampere-hour nickel-hydrogen cell with a single-layer Zircar separator stack design was fully charged and then discharged at a 2C current rate to an end voltage of 1 volt. This extreme test resulted in high temperatures which were recorded at three locations on the cell, i.e., the cell wall, the boss (barrel of the compression seal), and a terminal. The results provide new information about the high-temperature and high-discharge-rate capabilities of nickel-hydrogen cells. This information also adds to the growing data base for single-layer zirconium-oxide-cloth (Zircar) separator cell designs. Author

N95-26789*# Naval Surface Warfare Center, Crane, IN.
AIR FORCE NI-H2 CELL TEST PROGRAM: STATE OF CHARGE TEST c33
Bruce Moore and Douglas Smellie (Phillips Lab., Kirtland AFB, NM.) *In* NASA. Marshall Space Flight Center, The 1994 27th Annual NASA Aerospace Battery Workshop Feb. 1995 p 247-258 (For primary document see N95-26785 09-44)
Avail: CASI HC A03/MF A06

Nickel-Hydrogen cells are being cycled under a LEO (low earth orbit) test regime to examine the benefits of operating the cells at lower States of Charge (SOC) than typically used. A group of four cells are cycled using a voltage limiting charge regime that limits the State of Charge that the cells are allowed to reach. The test cells are then compared to identical cells being cycled at or near 100% State of Charge using a constant current charge regime. Derived from text

N95-26790*# National Aeronautics and Space Administration. Lyndon B. Johnson Space Center, Houston, TX.
CALORIMETRIC EVALUATION OF COMMERCIAL NI-MH CELLS AND CHARGES c33
Eric C. Darcy and Brent M. Hughes (Lockheed Engineering and Sciences Co., Houston, TX.) *In* NASA. Marshall Space Flight Center, The 1994 27th Annual NASA Aerospace Battery Workshop Feb. 1995 p 345-400 (For primary document see N95-26785 09-44)
Avail: CASI HC A04/MF A06

The test objectives are to evaluate the electrical and thermal performance of commercial Ni-MH cells and to evaluate the effectiveness of commercial charge control circuits. The ultimate design objectives are to determine which cell designs are most suitable for scale-up and to guide the design of future Shuttle and Station based battery chargers. Derived from text

N95-26791*# National Aeronautics and Space Administration. Marshall Space Flight Center, Huntsville, AL.
NICKEL METAL HYDRIDE LEO CYCLE TESTING c33
Eric Lowery *In its* The 1994 27th Annual NASA Aerospace Battery Workshop Feb. 1995 p 445-460 (For primary document see N95-26785 09-44)
Avail: CASI HC A03/MF A06

The George C. Marshall Space Flight Center is working to characterize aerospace AB5 Nickel Metal Hydride (NiMH) cells. The cells are being evaluated in terms of storage, low earth orbit (LEO) cycling, and response to parametric testing (high rate charge and discharge, charge retention, pulse current ability, etc.). Cells manufactured by Eagle Picher are the

subjects of the evaluation. There is speculation that NiMH cells may become direct replacements for current Nickel Cadmium cells in the near future.
Derived from text

N95-26792*# Naval Research Lab., Washington, DC.
THE 50 Ah NIH2 CPV QUALIFICATION TESTS c33
J. C. Garner, Wilbert L. Barnes, and Gary L. Hickman *In* NASA. Marshall Space Flight Center, The 1994 27th Annual NASA Aerospace Battery Workshop Feb. 1995 p 475-487 (For primary document see N95-26785 09-44)
Avail: CASI HC A03/MF A06

In 1992, the Naval Research Laboratory (NRL) started a program to qualify a large diameter common pressure vessel (CPV) nickel-hydrogen (NiH2) batteries for use on future Navy/NRL spacecraft electrical power subsystems. NRL's involvement with the qualification of CPV NiH2 batteries dates back to 1988 when COMSAT and Johnson Controls, Inc. initiated a joint effort to fly the first ever NiH2 CPV in space. A later NRL-JCI cooperative research and development agreement led to the launch of a space experiment in 1993 and to the use of a single NiH2 CPV battery on the BMDO Clementine spacecraft in 1994. NRL initiated procurement of two, 50 Ah CPV NiH2 batteries in the Fall of 1992. The two batteries were delivered to NRL in June 1994. NiH2 CPV batteries have almost 2x the specific energy (Wh/kg) of nickel cadium batteries and 2x the energy density (Wh/l) of individual pressure vessel NiH2 CPV's. This presentation discusses the results of electrical and mechanical qualification tests conducted at NRL. The tests included electrical characterization, standard capacity, random vibration, peak load, and thermal vacuum. The last slides of the presentation show initial results from the life cycle tests of the second NiH2 CPV battery at 40% depth of discharge and a temperature of 10 C. Derived from text

N95-26793*# Eagle-Picher Industries, Inc., Joplin, MO.
UNIQUE FEATURES OF A NEW NICKEL-HYDROGEN 2-CELL CPV c33
James R. Wheeler *In* NASA. Marshall Space Flight Center, The 1994 27th Annual NASA Aerospace Battery Workshop Feb. 1995 p 489-491 (For primary document see N95-26785 09-44)
Avail: CASI HC A01/MF A06

Two-cell nickel-hydrogen common pressure vessel (CPV) units with some unusual design features have been successfully built and tested. The features of interest are half-normal platinum loading for the negative electrodes, the use of rabbit-ear terminals for a CPV unit, and the incorporation of a wall wick. The units have a nominal capacity of 20 Ah and are 3.5 inches in diameter. Electric performance data are provided. The data support the growing viability of the two-cell CPV design concept. Author

N95-26794*# National Aeronautics and Space Administration. Marshall Space Flight Center, Huntsville, AL.
HUBBLE SPACE TELESCOPE NICKEL-HYDROGEN BATTERY TESTING: AN UPDATE c33
Thomas H. Whitt and Jeffrey C. Brewer *In its* The 1994 27th Annual NASA Aerospace Battery Workshop Feb. 1995 p 565-580 (For primary document see N95-26785 09-44)
Avail: CASI HC A03/MF A06

The Marshall Space Flight Center (MSFC) began testing the HST Ni-H2 Six Battery Test and the 'Flight Spare Battery' Tests approximately one year before the launch of the HST. These tests are operated and reported on by the MSFC, but are managed and funded by Goddard Space Flight Center in direct support of the HST program. The HST Ni-H2 batteries are built from Eagle Picher RNH-90-3 cells. The HST EPS (electrical power system) is a direct energy transfer power system. The HST Ni-H2 Six Battery Test is a breadboard of the HST EPS. The batteries in the test are composed of test module cells and packaged into three battery modules identical to the flight modules. This test is the HST EPS testbed. The 'Flight Spare Battery' Test is a simulation of one of the six battery channels on the HST. The cells in the test are from the flight spare lot of cells, which are the same lot of cells that three of the six HST flight batteries are made from. This test is the battery life test for the HST program.
Derived from text

N95-26795*# National Aeronautics and Space Administration. Marshall Space Flight Center, Huntsville, AL.
ADIABATIC CHARGING OF NICKEL-HYDROGEN BATTERIES c33
Chuck Lurie (TRW, Inc., Redondo Beach, CA.), S. Foroozan (TRW, Inc., Redondo Beach, CA.), Jeff Brewer, and Lorna Jackson *In its* The 1994 27th Annual NASA Aerospace Battery Workshop Feb. 1995 p 581-598 (For primary document see N95-26785 09-44)
Avail: CASI HC A03/MF A06

Battery management during prelaunch activities has always required special attention and careful planning. The transition from nickel-cadium to nickel-hydrogen batteries, with their high self discharge rate and lower charge efficiency, as well as longer prelaunch scenarios, has made this aspect of spacecraft battery management even more challenging. The AXAF-I Program requires high battery state of charge at launch. The use of active cooling, to ensure efficient charging, was considered and proved to be difficult and expensive. Alternative approaches were evaluated. Optimized charging, in the absence of cooling, appeared promising and was investigated. Initial testing was conducted to demonstrate the feasibility of the 'Adiabatic Charging' approach. Feasibility was demonstrated and additional testing performed to provide a quantitative, parametric data base. The assumption that the battery is in an adiabatic environment during prelaunch charging is a conservative approximation because the battery will transfer some heat to its surroundings by convective air cooling. The amount is small compared to the heat dissipated during battery overcharge. Because the battery has a large thermal mass, substantial overcharge can occur before the cells get too hot to charge efficiently. The testing presented here simulates a true adiabatic environment. Accordingly the data base may be slightly conservative. The adiabatic charge methodology used in this investigation begins with stabilizing the cell at a given starting temperature. The cell is then fully insulated on all sides. Battery temperature is carefully monitored and the charge terminated when the cell temperature reaches 85 F. Charging has been evaluated with starting temperatures from 55 to 75 F. Derived from text

N95-26796*# National Aeronautics and Space Administration. Goddard Space Flight Center, Greenbelt, MD.
ALTERNATE CHARGING PROFILES FOR THE ONBOARD NICKEL CADMIUM BATTERIES OF THE EXPLORER PLATFORM/EXTREME ULTRAVIOLET EXPLORER c33
Gopalakrishna M. Rao and Jill S. Prettyman-Lukoschek *In* NASA. Marshall Space Flight Center, The 1994 27th Annual NASA Aerospace Battery Workshop Feb. 1995 p 599-607 (For primary document see N95-26785 09-44)
Avail: CASI HC A02/MF A06

The Explorer Platform/Extreme Ultraviolet Explorer (EP/EUVE) spacecraft power is provided by the Modular Power Subsystems (MPS) which contains three 50 ampere-hour Nickel Cadmium (NiCd) batteries. The batteries were fabricated by McDonnell Douglas Electronics Systems Company, with the cells fabricated by Gates Aerospace Batteries (GAB), Gainesville, Florida. Shortly following launch, the battery performance characteristics showed similar signatures as the anomalous performance observed on both the Upper Atmosphere Research Satellite (UARS) and the Compton Gamma Ray Observatory (CGRO). This prompted the development and implementation of alternate charging profiles to optimize the spacecraft battery performance. The Flight Operations Team (FOT), under the direction of Goddard Space Flight Center's (GSFC) EP/EUVE Project and Space Power Applications Branch have monitored and managed battery performance through control of the battery Charge to Discharge (C/D) ratio and implementation of a Solar Array (SA) offset. This paper provides a brief overview of the EP/EUVE mission, the MPS, the FOT's battery management for achieving the alternate charging profile, and the observed spacecraft battery performance. Author

N95-26846 Aerospace Corp., El Segundo, CA. Technology Operations.
DEVELOPMENT OF WELDED SOLAR ARRAYS FOR DMSP AND GPS SATELLITES Technical Report
P. C. Brennan 15 Sep. 1994 38 p Limited Reproducibility: More than 20% of this document may be affected by microfiche quality
(Contract F04701-93-C-0094)
(AD-A289512; TR-94(4478)-3; SMC-TR-94-48) Avail: Issuing Activity (Defense Technical Information Center (DTIC))

The integrity of welds used to join solar cells to interconnect materials was investigated in two development programs, one for DMSP and the second for GPS. Previous solar arrays for these programs utilized soldering to join the interconnect to the cells. It is critical to both programs to demonstrate the ability of the welded interconnects to withstand the thermal cycling expected on orbit. Initial test boards for DMSP indicated that additional development was necessary to generate a weld process capable of meeting mission requirements. The Aerospace Corporation was successful in improving the weld survival rates for DMSP, but ultimately recommended that the process be abandoned in favor of an alternate weld design or solder approach. The GPS design was much more successful. Weld evaluations before and after thermal cycling indicated that the GPS design was capable of surpassing mission requirements. An SEM evaluation technique, mechanical fatigue tester, and a rapid thermal-cycle tester were designed in support of these programs. This report relates the findings generated during the two development programs and discusses the reasons behind the failure of the DMSP weld program and the success of the GPS program. DTIC

N95-26891 Air Force Inst. of Tech., Wright-Patterson AFB, OH. School of Engineering.

ANALYSIS OF INSTABILITY GROWTH AND COLLISIONLESS RELAXATION IN THERMIONIC CONVERTERS USING 1-D PIC SIMULATIONS M.S. Thesis

Bret B. Kreh Dec. 1994 70 p Limited Reproducibility: More than 20% of this document may be affected by microfiche quality
(AD-A289310; AFIT/GAP/ENP/94D-06) Avail: Issuing Activity (Defense Technical Information Center (DTIC))

This work investigates the role that the beam-plasma instability may play in a thermionic converter. The traditional assumption of collisionally dominated relaxation is questioned, and the beam-plasma instability is proposed as a possible dominant relaxation mechanism. Theory is developed to describe the beam-plasma instability in the cold-plasma approximation, and the theory is tested with two common Particle-in-Cell (PIC) simulation codes. The theory is first confirmed using an unbounded plasma PIC simulation employing periodic boundary conditions, ES1. The theoretically predicted growth rates are on the order of the plasma frequencies, and ESI simulations verity these predictions within the order of 1%. For typical conditions encountered in thermionic converters, the resulting growth period is on the order of 7x10(exp -11) seconds. The bounded plasma simulation PDP was used to evaluate the influence of finite geometry and the electrode boundaries. For this bounded plasma, a two-stream interaction was supported and resulted in nearly complete thermalization in approximately 5x10(exp -10) seconds. Since the electron-electron collision rate of 109 Hz and the electron atom collision rate of 107 Hz are significantly slower than the rate of development of these instabilities, the instabilities appear to be an important relaxation mechanism. DTIC

N95-27193*# Cleveland State Univ., OH. Advanced Manufacturing Center.

SOLAR CONCENTRATOR TECHNOLOGY DEVELOPMENT FOR SPACE BASED APPLICATIONS, VOLUME 1 Final Report

A. Pintz, C. H. Castle, and R. R. Reimer 31 Dec. 1992 168 p
(Contract NCC3-77)
(NASA-CR-197723; NAS 1.26:197723; CSU-ER-1001) Avail: CASI HC A08/MF A02

Thermoelectric conversion using a radio-isotope heat source has been used where outer planetary space craft are too far away for absorbing significant solar energy. Solar dynamic power (SDP) conversion is one technology that offers advantages for applications within the inner planet region. Since SDP conversion efficiency can be 2 to 3 times higher than photovoltaic, the collecting surfaces are much reduced in area and therefore lighter. This becomes an advantage in allocating more weight to launched payloads. A second advantage results for low earth orbit applications. The reduced area results in lower drag forces on the spacecraft and requires less reboost propellant to maintain orbit. A third advantage occurs because of the sun-to-shade cycling while in earth orbit. Photovoltaic systems require batteries to store energy for use when in the shade, and battery life for periods of 10 to 15 years is not presently achievable. For these reasons the Solar Dynamics and Thermal Systems Branch at NASA LeRC has funded work in developing SDP systems. The generic SDP system uses a large parabolic solar concentrator to focus solar energy onto a power conversion device. The concentrators are large areas and must therefore be efficient and have low specific weights. Yet these surfaces must be precise and capable of being stowed in a launch vehicle and then deployed and sometimes unfurled in space. There are significant technical challenges in engineering such structures, and considerable investigation has been made to date. This is the first of two volumes reporting on the research done by the Advanced Manufacturing Center at Cleveland State University to assist NASA LeRC in evaluating this technology. The objective of the grant was to restore the solar concentrator development technology of the 1960s while improving it with advances that have occurred since then. This report summarizes the work done from January 1989 through December 1991. Derived from text

N95-27194*# Cleveland State Univ., OH. Advanced Manufacturing Center.

SOLAR CONCENTRATOR TECHNOLOGY DEVELOPMENT FOR SPACE BASED APPLICATIONS, VOLUME 2 Final Report

A. Pintz, C. H. Castle, and R. R. Reimer 31 Dec. 1992 298 p
(Contract NCC3-77)
(NASA-CR-197724; NAS 1.26:197724; CSU-ER-1001) Avail: CASI HC A13/MF A03

Thermoelectric conversion using a radio-isotope heat source has been used where outer planetary space craft are too far away for absorbing significant solar energy. Solar dynamic power (SDP) conversion is one technology that offers advantages for applications within the inner planet region. Since SDP conversion efficiency can be 2 to 3 times higher than photovoltaic, the collecting surfaces are much reduced in area and therefore lighter. This becomes an advantage in allocating more weight to launched payloads. A second advantage results for low earth orbit applications. The reduced area results in lower drag forces on the spacecraft and requires less reboost propellant to maintain orbit. A third advantage occurs because of the sun-to-shade cycling while in earth orbit. Photovoltaic systems require batteries to store energy for use when in the shade, and battery life for periods of 10 to 15 years is not presently achievable. For these reasons the Solar Dynamics and Thermal Systems Branch at NASA LeRC has funded work in developing SDP systems. The generic SDP system uses a large parabolic solar concentrator to focus solar energy onto a power conversion device. The concentrators are large areas and must therefore be efficient and have low specific weights. Yet these surfaces must be precise and capable of being stowed in a launch vehicle and then deployed and sometimes unfurled in space. There are significant technical challenges in engineering such structures, and considerable investigation has been made to date. This is the second of two volumes reporting on the research done by the Advanced Manufacturing Center at Cleveland State University to assist NASA LeRC in evaluating this technology. This volume includes the appendices of selected data sets, drawings, and procedures. The objective of the grant was to restore the solar concentrator development technology of the 1960s while improving it with advances that have occurred since then. This report summarizes the work done from January 1989 through December 1991. Derived from text

N95-27236# Oregon Inst. of Tech., Klamath Falls, OR.

GEOTHERMAL DIRECT-HEAT UTILIZATION ASSISTANCE Quarterly Progress Report, Oct. - Dec. 1994

1994 19 p
(Contract DE-FG07-90ID-13040)
(DE95-007247; DOE/ID-13040/T26) Avail: CASI HC A03/MF A01

The report summarizes activities of the Geo-Heat Center (GHC) at Oregon Institute of Technology for the first quarter of Fiscal Year 1995. It describes contacts with parties during this period related to assistance with geothermal direct heat projects. Areas dealt with include geothermal heat pumps, space heating, greenhouses, aquaculture, resources and equipment. Research is also being conducted on geothermal energy cost evaluation, low-temperature geothermal resource assessment, use of silica waste from the Cerro Prieto geothermal field as construction materials and geothermal heat pumps. Outreach activities include the publication of a quarterly bulletin on direct heat applications and dissemination of information on low-temperature geothermal resources and utilization. DOE

N95-27459# National Renewable Energy Lab., Golden, CO.

A COMPARISON OF MEASURED WIND PARK LOAD HISTORIES WITH THE WISPER AND WISPERX LOAD SPECTRA

N. D. Kelley Jan. 1995 8 p Presented at the 1995 American Society of Mechanical Engineers (ASME) Energy Sources Technology Conference and Exhibition, Houston, TX, 29 Jan. - 1 Feb. 1995

(Contract DE-AC36-83CH-10093)
(DE95-000295; NREL/TP-442-7226; CONF-950116-6) Avail: CASI HC A02/MF A01

The blade-loading histories from two adjacent Micon 65/13 wind turbines are compared with the variable-amplitude test-loading histories known as the WISPER and WISPERX spectra. These standardized loading sequences were developed from blade flapwise load histories taken from nine different horizontal-axis wind turbines operating under a wide range of conditions in Europe. The subject turbines covered a broad spectrum of rotor diameters, materials, and operating environments. The final loading sequences were developed as a joint effort of thirteen different European organizations. The goal was to develop a meaningful loading standard for horizontal-axis wind turbine blades that represents common interaction effects seen in service. In 1990, NREL made extensive load measurements on two adjacent Micon 65/13 wind turbines in simultaneous operation in the very turbulent environment of a large wind park. Further, before and during the collection of the loads data, comprehensive measurements of the statistics of the turbulent environment were obtained at both the turbines under test and at two other locations within the park. The trend to larger but lighter wind turbine structures has made an understanding of the expected lifetime loading history of paramount importance. Experience in the US has shown that the turbulence-induced loads associated with multi-row wind parks in general are much more severe than for turbines operating individually or within widely spaced environments. Multi-row wind parks are much more common in the US than in Europe. In this paper we report on our results in applying the methodology utilized to develop the WISPER and WISPERX standardized loading sequences using the available data from the Micon turbines. While the intended purpose of the WISPER sequences were not to represent a specific operating environment, we believe the exercise is useful, especially when a turbine design is likely to be installed in a multi-row wind park. DOE

N95-27475# National Renewable Energy Lab., Golden, CO.
PERFORMANCE OF A STAND-ALONE WIND-ELECTRIC ICE MAKER FOR REMOTE VILLAGES
Holly C. Davis, Michael J. Brandemuehl (Colorado Univ., Boulder, CO.), and Michael L. S. Bergey (Bergey Windpower Co., Inc., Norman, OK.) Jan. 1995 10 p Presented at the 14th American Society of Mechanical Engineers-Energy Sources Technology Conferenceand Exhibition Wind Energy Symposium Houston, TX, 29 Jan. - 1 Feb. 1995
(Contract DE-AC36-83CH-10093)
(DE95-004006; NREL/TP-441-7223; CONF-950116-5) Avail: CASI HC A02/MF A01

Two ice makers in the 1.1 metric tons per 24 hours (1.2 tons per day) size range were tested to determine their performance when directly coupled to a variable-frequency wind turbine generator. Initial tests were conducted using a dynamometer to simulate to wind to evaluate whether previously determined potential problems were significant and to define basic performance parameters. Field testing in Norman, Oklahoma, was completed to determine the performance of one of the ice makers under real wind conditions. As expected, the ice makers produced more ice at a higher speed than rated, and less ice at a lower speed. Due to the large start-up torque requirement of reciprocating compressors, the ice making system experienced a large start-up current and corresponding voltage drop which required a larger wind turbine that expected to provide the necessary current and voltage. Performance curves for ice production and power consumption are presented. A spreadsheet model was constructed to predict ice production at a user-defined site given the wind conditions for that location. Future work should include long-term performance tests and research on reducing the large start-up currents the system experiences when first coming on line. DOE

N95-27682# Brookhaven National Lab., Upton, NY.
HEALTH AND ENVIRONMENTAL HAZARDS OF CdTe PHOTOVOLTAIC MODULE PRODUCTION, USE AND DECOMMISSIONING
P. D. Moskowitz, H. Steinberger, and W. Thumm 1995 4 p Presented at the 1st World Conference on Photovoltaic Energy Conversion, Waikoloa, HI, 5-9 Dec. 1994
(Contract DE-AC02-76CH-00016)
(DE95-006688; BNL-61324; CONF-941203-21) Avail: CASI HC A01/MF A01

Health and environmental (H&E) risks presented by CdTe photovoltaic module production, use and decommissioning have been reviewed and discussed by several authors. Several H&E concerns exist. The estimated risks are based on extrapolations of toxicity, environmental mobility, and bioavailability data for other inorganic cadmium compounds. Little information, however, is available about CdTe itself. In response to the increased interest in CdTe, Brookhaven National Laboratory (BNL) has been engaged in a cooperative research program with the National Institute of Environmental Health Sciences (NIEHS), the Fraunhofer Institute for Solid State Technology (IFT), and the GSF Institute of Chemical Ecology to develop fundamental toxicological and environmental data for CdTe. This paper describes the results of these studies, and their potential implications with respect to the H&E hazards presented by CdTe module production, use and decommissioning. DOE

N95-27704# National Renewable Energy Lab., Golden, CO.
RECENT PROGRESS IN THE PHOTOVOLTAIC MANUFACTURING TECHNOLOGY PROJECT (PVMaT)
C. Edwin Witt, Richard L. Mitchell, Holly Thomas, Lloyd O. Herwig (Department of Energy, Washington, DC.), Douglas S. Ruby (Sandia National Labs., Albuquerque, NM.), and Rick Sellers Dec. 1994 11 p Presented at the 1st World Conference on Photovoltaic Energy Conversion, Waikoloa, HI, 5-9 Dec. 1994 Prepared in cooperation with Sandia National Labs., Albuquerque, NM
(Contract DE-AC36-83CH-10093)
(DE95-000279; NREL/TP-411-7416; CONF-941203-14; SAND-94-3078C) Avail: CASI HC A03/MF A01

The Photovoltaic Manufacturing Technology (PVMaT) Project was initiated in 1990 to help the US photovoltaic (PV) industry extend its world leadership role in manufacturing and commercially developing PV modules and systems. It is being conducted in several phases, staggered to support industry progress. The four most recently awarded subcontracts (Phase 2B) are now completing their first year of research. They include two subcontracts on CdTe, one on Spheral Solar(trademark) Cells, and one on cast polysilicon. These subcontracts represent new technology additions to the PVMaT Project. Subcontracts initiated in earlier phases are nearing completion, and their progress is summarized. An additional phase of PVMaT, Phase 4A, is being initiated which will emphasize product-driven manufacturing research and development. The intention of Phase 4A is to emphasize improvement and cost reduction in the manufacture of full-system PV products. The work areas may include, but are not limited to, issues such as improvement of module manufacturing processes; system and system component packaging, integration, manufacturing, and assembly; product manufacturing flexibility; and balance-of-system development with the goal of product manufacturing improvements. DOE

N95-27746# Morgantown Technology Center, WV.
THE US MOLTEN CARBONATE FUEL-CELL DEVELOPMENT AND COMMERCIALIZATION EFFORT
Mark C. Williams, Edward L. Parsons, Jr., and M. J. Mayfield 1995 5 p Presented at the Fuel Cell Seminar, San Diego, CA,28 Nov. - 1 Dec. 1994; sponsored by the Electric Power Research Inst.; the Gas Research Inst.; and the US Department of Energy
(DE95-008580; DOE/METC-C/95/7171; CONF-941109-2) Avail: CASI HC A01/MF A01

The authors discuss the status of molten carbonate fuel-cell (MCFC) development in the US, including the role of the US Department of Energy (DOE) in commercializing MCFC power-plant products for use by gas utility and electric power industries. The authors describe major fundamental stack research issues, as well as MCFC power-plant network and system issues, that need to be resolved before MCFC technology can be commercialized. A significant initiative in MCFC research is the spatial configuration of MCFC stacks into networks in a fuel-cell power plant. DOE

N95-27936# New Energy and Industrial Technology Development Organization, Tokyo (Japan).
INVESTIGATION OF HIGH-TEMPERATURE SUPERCONDUCTING FLYWHEEL ENERGY STORAGE DEVICES
Mar. 1994 201 p In JAPANESE
(DE95-759242; NEDO-P-9310) Avail: CASI HC A10/MF A03

The paper studies a possibility of the technology of a high-temperature superconducting flywheel energy storage system and extracts its technical subjects. As a result of investigating the present status of technology and development of the flywheel for the electric energy storage system, it is found that it is a promising technology which has basically a wide applicability to multipurposes. A combination of the technology only with the existing element technology is fully feasible, and the system shows excellent performance in energy storage for medium-scale capacity for a relatively short period. However, there have been seen few application examples. For application to power systems and industrial systems, it is necessary to reduce operational loss of the system and to realize flywheels which can store much larger capacities of energy. It is proposed that a combination of high-temperature superconducting bulk and permanent magnet is used for magnetic supporting of the flywheel. Technical problems are also extracted of the high temperature superconducting flywheel system as an energy storage system for load leveling. DOE

N95-27940 New Energy and Industrial Technology Development Organization, Tokyo (Japan).
INVESTIGATION ON ENERGY CONVERSION TECHNOLOGY USING BIOCHEMICAL REACTION ELEMENTS, 2
Mar. 1994 252 p In JAPANESE Limited Reproducibility: More than 20% of this document may be affected by microfiche quality
(DE95-759250; NEDO-GET-9302-2) Avail: CASI HC A12

For measures taken for resource/energy and environmental issues, a study is made on utilization of microbial biochemical reaction. As a reaction system using chemical energy, cited is production of petroleum substitution substances and food/feed by CO2 fixation using hydrogen energy and hydrogen bacteria. As to photo energy utilization, regarded as promising are CO2 fixation using photo energy and microalgae, and production of hydrogen and useful carbon compound using photosynthetic organisms. As living organism/electric energy interconversion, cited is the culture of chemoautotrophic bacteria which fix CO2 using electric energy. For enhancing its conversion efficiency, it is important to develop a technology of gene manipulation of the bacteria and a system to use functional biochemical elements adaptable to the electrode reaction. With regard to utilization of the microorganism metabolic function, the paper presents emission of soluble nitrogen in the hydrosphere into the atmosphere using denitrifying bacteria, removal of phosphorus, reduction in environmental pollution caused by heavy metal dilute solutions, and recovery as resources, etc. DOE

N95-27970*# DASCON Engineering, Bay Village, OH.
COLLECTED PAPERS ON WIND TURBINE TECHNOLOGY
David A. Spera, ed. May 1995 236 p
(Contracts NAS3-25776; RTOP 776-33-41; DE-AI01-76ET-20320)
(NASA-CR-195432; E-9439; NAS 1.26:195432; DOE/NASA/5776-2)
Avail: CASI HC A11/MF A03

R and D projects on electricity generating wind turbines were conducted at the NASA Lewis Research Center from 1973 to 1988. Most projects were sponsored by the U.S. Department of Energy (DOE), a major element of its Federal Wind Energy Program. Another large wind turbine project was by the Bureau of Reclamation of the U.S. Department of Interior (DOI). From 1988 to 1995, NASA wind energy activities have been directed toward the transfer of technology to commercial and academic organizations. As part of these technology transfer activities, previously unpublished manuscripts have been assembled and presented here to share the wind turbine research results with the wind energy community. A variety of wind turbine technology topics are discussed: Wind and wake models; Airfoil properties; Structural analysis and testing; Control systems; Variable speed generators; and acoustic noise. Experimental and theoretical results are discussed. For individual titles, see N95-27971 through N95-27992.

N95-27971*# Pacific Northwest Lab., Richland, WA.
BASIC PRINCIPLES AND RECENT OBSERVATIONS OF ROTATIONALLY SAMPLED WIND c47
James R. Connell *In* DASCON Engineering, Collected Papers on Wind Turbine Technology May 1995 p 1-15 (For primary document see N95-27970 09-44)
(Contract DE-AC06-76LR-01830)
Avail: CASI HC A03/MF A03

The concept of rotationally sampled wind speed is described. The unusual wind characteristics that result from rotationally sampling the wind are shown first for early measurements made using an 8-point ring of anemometers on a vertical plane array of meteorological towers. Quantitative characterization of the rotationally sampled wind is made in terms of the power spectral density function of the wind speed. Verification of the importance of the new concept is demonstrated with spectral analyses of the response of the MOD-OA blade flapwise root bending moment and the corresponding rotational analysis of the wind measured immediately upwind of the MOD-OA using a 12-point ring of anemometers on a 7-tower vertical plane array. The Pacific Northwest Laboratory (PNL) theory of the rotationally sampled wind speed power spectral density function is tested successfully against the wind spectrum measured at the MOD-OA vertical plane array. A single-tower empirical model of the rotationally sampled wind speed is also successfully tested against the measurements from the full vertical plane array. Rotational measurements of the wind velocity with hotfilm anemometers attached to rotating blades are shown to be accurate and practical for research on winds at the blades of wind turbines. Some measurements at the rotor blade of a MOD-2 turbine using the hotfilm technique in a pilot research program are shown. They are compared and contrasted to the expectations based upon application of the PNL theory of rotationally sampled wind to the MOD-2 size and rotation rate but without teeter, blade bending, or rotor induction accounted for. Finally, the importance of temperature layering and of wind modifications due to flow over complex terrain is demonstrated by the use of hotfilm anemometer data, and meteorological tower and acoustic doppler sounder data from the MOD-2 site at Goodnoe Hills, Washington. Author

N95-27972*# DASCON Engineering, Bay Village, OH.
A MODEL OF ROTATIONALLY-SAMPLED WIND TURBULENCE FOR PREDICTING FATIGUE LOADS IN WIND TURBINES c39
David A. Spera *In its* Collected Papers on Wind Turbine Technology May 1995 p 17-26 (For primary document see N95-27970 09-44)
Avail: CASI HC A02/MF A03

Empirical equations are presented with which to model rotationally-sampled (R-S) turbulence for input to structural-dynamic computer codes and the calculation of wind turbine fatigue loads. These equations are derived from R-S turbulence data which were measured at the vertical-plane array in Clayton, New Mexico. For validation, the equations are applied to the calculation of cyclic flapwise blade loads for the NASA/DOE Mod-2 2.5-MW experimental HAWT's (horizontal-axis wind turbines), and the results compared to measured cyclic loads. Good correlation is achieved, indicating that the R-S turbulence model developed in this study contains the characteristics of the wind which produce many of the fatigue loads sustained by wind turbines. Empirical factors are included which permit the prediction of load levels at specified percentiles of occurrence, which is required for the generation of fatigue load spectra and the prediction of the fatigue lifetime of structures. Author

N95-27973*# Pacific Northwest Lab., Richland, WA.
LARGE HAWT WAKE MEASUREMENT AND ANALYSIS c34
A. H. Miller, H. L. Wegley, and J. W. Buck *In* DASCON Engineering, Collected Papers on Wind Turbine Technology May 1995 p 27-33
(For primary document see N95-27970 09-44)
(Contract DE-AC06-76RL-01830)
Avail: CASI HC A02/MF A03

From the theoretical fluid dynamics point of view, the wake region of a large horizontal-axis wind turbine has been defined and described, and numerical models of wake behavior have been developed. Wind tunnel studies of single turbine wakes and turbine array wakes have been used to verify the theory and further refine the numerical models. However, the effects of scaling, rotor solidity, and topography on wake behavior are questions that remain unanswered. In the wind tunnel studies, turbines were represented by anything from scaled models to tea strainers or wire mesh disks whose solidity was equivalent to that of a typical wind turbine. The scale factor compensation for the difference in Reynolds number between the scale model and an actual turbine is complex, and not typically accounted for. Though it is wise to study the simpler case of wakes in flat topography, which can be easily duplicated in the wind tunnel, current indications are that wind turbine farm development is actually occurring in somewhat more complex terrain. Empirical wake studies using large horizontal-axis wind turbines have not been thoroughly composited, and, therefore, the results have not been applied to the well-developed theory of wake structure. The measurement programs have made use of both in situ sensor systems, such as instrumented towers, and remote sensors, such as kites and tethered, balloonborne anemometers. We present a concise overview of the work that has been performed, including our own, which is based on the philosophy that the MOD-2 turbines are probably their own best detector of both the momentum deficit and the induced turbulence effect downwind. Only the momentum deficit aspects of the wake/machine interactions have been addressed. Both turbine power output deficits and wind energy deficits as measured by the onsite meteorological towers have been analyzed from a composite data set. The analysis has also evidenced certain topographic influences on the operation of spatially diverse wind turbines. Author

N95-27974*# Rockwell International Corp., Golden, CO. Wind Energy Research Center.

HORIZONTAL AXIS WIND TURBINE POST STALL AIRFOIL CHARACTERISTICS SYNTHESIZATION c02

James L. Tangler and Cyrus Ostowari (Texas A&M Univ., College Station, TX.) *In* DASCON Engineering, Collected Papers on Wind Turbine Technology May 1995 p 35-39 (For primary document see N95-27970 09-44)

(Contract DE-AC04-76DP-03533)

Avail: CASI HC A01/MF A03

Blade-element/momentum performance prediction codes are routinely used for wind turbine design and analysis. A weakness of these codes is their inability to consistently predict peak power upon which the machine structural design and cost are strongly dependent. The purpose of this study was to compare post-stall airfoil characteristics synthesization theory to a systematically acquired wind tunnel data set in which the effects of aspect ratio, airfoil thickness, and Reynolds number were investigated. The results of this comparison identified discrepancies between current theory and the wind tunnel data which could not be resolved. Other factors not previously investigated may account for these discrepancies and have a significant effect on peak power prediction. Author

N95-27975*# Oregon State Univ., Corvallis, OR.

PRELIMINARY ANALYSIS OF DYNAMIC STALL EFFECTS ON A 91-METER WIND TURBINE ROTOR c02

Robert E. Wilson *In* DASCON Engineering, Collected Papers on Wind Turbine Technology May 1995 p 41-46 (For primary document see N95-27970 09-44)

Avail: CASI HC A02/MF A03

Analytical investigation of dynamic stall on HAWT (horizontal-axis wind turbines) rotor loads was conducted. Dynamic stall was modeled using the Gormont approach on the MOD-2 rotor, treating the blade as a rigid body teetering about a fixed axis. Blade flapwise bending moments at station 370 were determined with and without dynamic stall for spatial variations in local wind speed due to wind shear and yaw. The predicted mean flapwise bending moments were found to be in good agreement with test results. Results obtained with and without dynamic stall showed no significant difference for the mean flapwise bending moment. The cyclic bending moments calculated with and without dynamic stall effects were substantially the same. None of the calculated cyclic loads reached the level of the cyclic loads measured on the MOD-2 using the Boeing five-minute-average technique. Author

N95-27976*# Wichita State Univ., Wichita, KS.

COMPARATIVE WIND TUNNEL TESTS OF NACA 23024 AIRFOILS WITH SEVERAL AILERON AND SPOILER CONFIGURATIONS c02

W. H. Wentz, Jr. and M. H. Snyder *In* DASCON Engineering, Collected Papers on Wind Turbine Technology May 1995 p 47-52 Presented at the DOE/NASA Workshop on Horizontal Axis Wind Turbine Technology, Cleveland, OH, 8-10 May 1994 (For primary document see N95-27970 09-44)

(Grant NsG-3277)

Avail: CASI HC A02/MF A03

This paper reviews research efforts at Wichita State University sponsored by NASA Lewis Research Center to design and evaluate aerodynamic braking devices which will be smaller and lighter than full-chord blade pitch control. Devices evaluated include a variety of aileron configurations, and spoilers located at both trailing edge and near the leading edge. The paper discusses analytical modeling, wind tunnel tests, and for some configurations, full-scale rotor tests. Current designs have not provided adequate control power at high angles of attack (low tip-speed-ratios). The reasons for these limitations are discussed. Analysis and wind tunnel test data indicate that several options are available to the designer to provide aerodynamic slowdown without full-chord pitch control. Three options are suggested; adding venting in front of the control surface hingeline, using spoilers located near the leading edge, and using a two-piece control combining downward deflection inboard with upward deflection outboard. Author

N95-27977*# Ohio State Univ., Columbus, OH.

COMPARATIVE WIND TUNNEL TEST AT HIGH REYNOLDS NUMBERS OF NACA 64 621 AIRFOILS WITH TWO AILERON CONFIGURATIONS c02

G. M. Gregorek *In* DASCON Engineering, Collected Papers on Wind Turbine Technology May 1995 p 53-66 Presented at the DOE/NASA Workshop on Horizontal Axis Wind Turbine Technology, Cleveland, OH, 8-10 May 1984 (For primary document see N95-27970 09-44)

(Grant NAG3-330)

Avail: CASI HC A03/MF A03

An experimental program to measure the aerodynamic characteristics of the NACA 64-621 airfoil when equipped with plain ailerons of 0.38 chord and 0.30 chord and with 0.38 chord balanced aileron has been conducted in the pressurized O.S.U. 6 x 12 ft High Reynolds Number Wind Tunnel. Surface pressures were measured and integrated to yield lift and pressure drag coefficients for angles of attack from -3 to +42 deg and for selected aileron deflections from 0 to -90 deg at nominal Mach and Reynolds numbers of 0.25 and 5 x 10(exp 6). When resolved into thrust coefficient for wind turbine aerodynamic control applications, the data indicated the anticipated decrease in thrust coefficient with negative aileron deflection at low angles of attack; however, as angle of attack increased, thrust coefficients eventually became positive. All aileron configurations, even at -90 deg deflections showed this trend. Hinge moments for each configuration complete the data set. Author

N95-27978*# Boeing Aerospace Co., Seattle, WA.

COMPARATIVE PERFORMANCE TESTS ON THE Mod-2, 2.5-mW WIND TURBINE WITH AND WITHOUT VORTEX GENERATORS c02

G. E. Miller *In* DASCON Engineering, Collected Papers on Wind Turbine Technology May 1995 p 67-77 Presented at the DOE/NASA Workshop on Horizontal Axis Wind Turbine Technology, Cleveland, OH, 8-10 May 1984 (For primary document see N95-27970 09-44)

Avail: CASI HC A03/MF A03

A test program was conducted on the third Mod-2 unit at Goldendale, Washington, to systematically study the effect of vortex generators (VG's) on power performance. The subject unit was first tested without VG's to obtain baseline data. Vortex generators were then installed on the mid-blade assemblies, and the resulting 70% VG configuration was tested. Finally, vortex generators were mounted on the tip assemblies, and data was recorded for the 100% VG configuration. This test program and its results are discussed in this paper. The development of vortex generators is also presented. Author

N95-27979*# Paragon Pacific, Inc., El Segundo, CA.

DESIGN OF A REAL-TIME WIND TURBINE SIMULATOR USING A CUSTOM PARALLEL ARCHITECTURE c61

John A. Hoffman, R. Gluck (TRW Space Technology Labs., Redondo Beach, CA.), and S. Sridhar (TRW Space Technology Labs., Redondo Beach, CA.) *In* DASCON Engineering, Collected Papers on Wind Turbine Technology May 1995 p 79-87 Sponsored by DOE (For primary document see N95-27970 09-44)

Avail: CASI HC A02/MF A03

The design of a new parallel-processing digital simulator is described. The new simulator has been developed specifically for analysis of wind energy systems in real time. The new processor has been named: the Wind Energy System Time-domain simulator, version 3 (WEST-3). Like previous WEST versions, WEST-3 performs many computations in parallel. The modules in WEST-3 are pure digital processors, however. These digital processors can be programmed individually and operated in concert to achieve real-time simulation of wind turbine systems. Because of this programmability, WEST-3 is very much more flexible and general than its two predecessors. The design features of WEST-3 are described to show how the system produces high-speed solutions of nonlinear time-domain equations. WEST-3 has two very fast Computational Units (CU's) that use

minicomputer technology plus special architectural features that make them many times faster than a microcomputer. These CU's are needed to perform the complex computations associated with the wind turbine rotor system in real time. The parallel architecture of the CU causes several tasks to be done in each cycle, including an IO operation and the combination of a multiply, add, and store. The WEST-3 simulator can be expanded at any time for additional computational power. This is possible because the CU's interfaced to each other and to other portions of the simulation using special serial buses. These buses can be 'patched' together in essentially any configuration (in a manner very similar to the programming methods used in analog computation) to balance the input/ output requirements. CU's can be added in any number to share a given computational load. This flexible bus feature is very different from many other parallel processors which usually have a throughput limit because of rigid bus architecture.
Author

N95-27980*# Sandia National Labs., Albuquerque, NM.
A NASTRAN-BASED COMPUTER PROGRAM FOR STRUCTURAL DYNAMIC ANALYSIS OF HORIZONTAL AXIS WIND TURBINES **c39**
Don W. Lobitz *In* DASCON Engineering, Collected Papers on Wind Turbine Technology May 1995 p 89-97 Sponsored by DOE (For primary document see N95-27970 09-44)
(Contract DE-AC04-76DP-00789)
Avail: CASI HC A02/MF A03

This paper describes a computer program developed for structural dynamic analysis of horizontal axis wind turbines (HAWT's). It is based on the finite element method through its reliance on NASTRAN for the development of mass, stiffness, and damping matrices of the tower end rotor, which are treated in NASTRAN as separate structures. The tower is modeled in a stationary frame and the rotor in one rotating at a constant angular velocity. The two structures are subsequently joined together (external to NASTRAN) using a time-dependent transformation consistent with the hub configuration. Aerodynamic loads are computed with an established flow model based on strip theory. Aeroelastic effects are included by incorporating the local velocity and twisting deformation of the blade in the load computation. The turbulent nature of the wind, both in space and time, is modeled by adding in stochastic wind increments. The resulting equations of motion are solved in the time domain using the implicit Newmark-Beta integrator. Preliminary comparisons with data from the Boeing/NASA MOD2 HAWT indicate that the code is capable of accurately and efficiently predicting the response of HAWT's driven by turbulent winds.
Author

N95-27981*# General Electric Co., Philadelphia, PA.
AEROELASTIC STABILITY OF WIND TURBINE BLADE/AILERON SYSTEMS **c02**
J. C. Strain and L. Mirandy (General Electric Co., Schenectady, NY.) *In* DASCON Engineering, Collected Papers on Wind Turbine Technology May 1995 p 99-114 (For primary document see N95-27970 09-44)
(Contract DEN3-153)
Avail: CASI HC A03/MF A03

Aeroelastic stability analyses have been performed for the MOD-5A blade/aileron system. Various configurations having different aileron torsional stiffness, mass unbalance, and control system damping have been investigated. The analysis was conducted using a code recently developed by the General Electric Company - AILSTAB. The code extracts eigenvalues for a three degree of freedom system, consisting of: (1) a blade flapwise mode; (2) a blade torsional mode; and (3) an aileron torsional mode. Mode shapes are supplied as input and the aileron can be specified over an arbitrary length of the blade span. Quasi-steady aerodynamic strip theory is used to compute aerodynamic derivatives of the wing-aileron combination as a function of spanwise position. Equations of motion are summarized herein. The program provides rotating blade stability boundaries for torsional divergence, classical flutter (bending/torsion) and wing/aileron flutter. It has been checked out against fixed-wing results published by Theodorsen and Garrick. The MOD-5A system is stable with respect to divergence and classical flutter for all practical rotor speeds. Aileron torsional stiffness must exceed a minimum critical value to prevent aileron flutter. The nominal control system stiffness greatly exceeds this minimum during normal operation. The basic system, however, is unstable for the case of a free (or floating) aileron. The instability can be removed either by the addition of torsional damping or mass-balancing the ailerons. The MOD-5A design was performed by the General Electric Company, Advanced Energy Program Department under Contract DEN3-153 with NASA Lewis Research Center and sponsored by the Department of Energy.
Author

N95-27982*# General Electric Co., Schenectady, NY.
CALCULATION OF DESIGN LOAD FOR THE MOD-5A 7.3 mW WIND TURBINE SYSTEM **c39**
L. Mirandy and J. C. Strain *In* DASCON Engineering, Collected Papers on Wind Turbine Technology May 1995 p 115-138a (For primary document see N95-27970 09-44)
(Contract DEN3-153)
Avail: CASI HC A03/MF A03

Design loads are presented for the General Electric MOD-SA wind turbine. The MOD-SA system consists of a 400 ft. diameter, upwind, two-bladed, teetered rotor connected to a 7.3 mW variable-speed generator. Fatigue loads are specified in the form of histograms for the 30 year life of the machine, while limit (or maximum) loads have been derived from transient dynamic analysis at critical operating conditions. Loads prediction was accomplished using state of the art aeroelastic analyses developed at General Electric. Features of the primary predictive tool - the Transient Rotor Analysis Code (TRAC) are described in the paper. Key to the load predictions are the following wind models: (1) yearly mean wind distribution; (2) mean wind variations during operation; (3) number of start/shutdown cycles; (4) spatially large gusts; and (5) spatially small gusts (local turbulence). The methods used to develop statistical distributions from load calculations represent an extension of procedures used in past wind programs and are believed to be a significant contribution to Wind Turbine Generator analysis. Test/theory correlations are presented to demonstrate code load predictive capability and to support the wind models used in the analysis. In addition MOD-5A loads are compared with those of existing machines. The MOD-5A design was performed by the General Electric Company, Advanced Energy Program Department, under Contract DEN3-153 with NASA Lewis Research Center and sponsored by the Department of Energy.
Author

N95-27983*# Boeing Aerospace Co., Seattle, WA.
COMPARISON OF MEASURED AND CALCULATED DYNAMIC LOADS FOR THE Mod-2 2.5 mW WIND TURBINE SYSTEM **c39**
D. K. Zimmerman, S. A. Shipley, and R. D. Miller *In* DASCON Engineering, Collected Papers on Wind Turbine Technology May 1995 p 139-152 (For primary document see N95-27970 09-44)
Avail: CASI HC A03/MF A03

The Boeing Company, under contract to the Electric Power Research Institute (EPRI), has completed a test program on the Mod-2 wind turbines at Goodnoe Hills, Washington. The objectives were to update fatigue load spectra, discern site and machine differences, measure vortex generator effects, and to evaluate rotational sampling techniques. This paper shows the test setup and loads instrumentation, loads data comparisons and test/analysis correlations. Test data are correlated with DYLOSAT predictions using both the NASA interim turbulence model and rotationally sampled winds as inputs. The latter is demonstrated to have the potential to improve the test/analysis correlations. The paper concludes with an assessment of the importance of vortex generators, site dependence, and machine differences on fatigue loads. The adequacy of prediction techniques used are evaluated and recommendations are made for improvements to the methodology.
Author

N95-27984*# Power Technologies, Inc., Schenectady, NY.
ANALYSIS METHODS FOR WIND TURBINE CONTROL AND ELECTRICAL SYSTEM DYNAMICS **c33**
E. N. Hinrichsen *In* DASCON Engineering, Collected Papers on Wind Turbine Technology May 1995 p 153-156 (For primary document see N95-27970 09-44)
Avail: CASI HC A01/MF A03

The integration of new energy technologies into electric power systems requires methods which recognize the full range of dynamic events in both the new generating unit and the power system. Since new energy technologies are initially perceived as small contributors to large systems, little attention is generally paid to system integration, i.e. dynamic events in the power system are ignored. As a result, most new energy sources are only capable of base-load operation, i.e. they have no load following or cycling capability. Wind turbines are no exception. Greater awareness of this implicit (and often unnecessary) limitation is needed. Analysis methods are recommended which include very low penetration (infinite bus) as well as very high penetration (stand-alone) scenarios. Author

N95-27985*# General Electric Co., Philadelphia, PA.

CONTROL SYSTEM DESIGN FOR THE MOD-5A 7.3 mW WIND TURBINE GENERATOR **c37**

Robert S. Barton, Theodore J. Hosp, and George P. Schanzenbach *In* DASCON Engineering, Collected Papers on Wind Turbine Technology May 1995 p 157-174 Presented at the DOE/NASA Workshop on Horizontal Axis Wind Turbine Technology, Cleveland, OH, 8-10 May 1984 (For primary document see N95-27970 09-44)
(Contract DEN3-153)
Avail: CASI HC A03/MF A03

This paper provides descriptions of the requirements analysis, hardware development and software development phases of the Control System design for the MOD-5A 7.3 mW Wind Turbine Generator. The system, designed by General Electric Company, Advanced Energy Programs Department, under contract DEN 3-153 with NASA Lewis Research Center and DOE, provides real time regulation of rotor speed by control of both generator torque and rotor torque. A variable speed generator system is used to provide both airgap torque control and reactive power control. The wind rotor is designed with segmented ailerons which are positioned to control blade torque. The central component of the control system, selected early in the design process, is a programmable controller used for sequencing, alarm monitoring, communication, and real time control. Development of requirements for use of aileron controlled blades and a variable speed generator required an analytical simulation that combined drivetrain, tower and blade elastic modes with wind disturbances and control behavior. An orderly two phase plan was used for controller software development. A microcomputer based turbine simulator was used to facilitate hardware and software integration and test. Author

N95-27986*# Boeing Aerospace Co., Seattle, WA.

USE OF BLADE PITCH CONTROL TO PROVIDE POWER TRAIN DAMPING FOR THE Mod-2, 2.5-mW WIND TURBINE **c37**

W. A. Blissell, Jr. *In* DASCON Engineering, Collected Papers on Wind Turbine Technology May 1995 p 175-1190 Presented at the DOE/NASA Workshop on Horizontal Axis Wind Turbine Technology, Cleveland, OH, 8-10 May 1984 Sponsored by DOE (For primary document see N95-27970 09-44)
(Contract DEN3-153)
Avail: CASI HC A02/MF A03

The Control System for the Mod-2 wind turbine system is required to provide not only for startup, RPM regulation, maximizing or regulating power, and stopping the rotor, but also for load limiting, especially in the power train. Early operations with above-rated winds revealed an instability which was caused primarily by coupling between the quill shaft and the rotor air loads. This instability caused the first of several major Mod-2 Control System changes which are reviewed in the paper. Author

N95-27987*# Electrotek Concepts, Inc., Knoxville, TN.

A CONCEPTUAL FRAMEWORK FOR EVALUATING VARIABLE SPEED GENERATOR OPTIONS FOR WIND ENERGY APPLICATIONS **c33**

T. W. Reddoch, T. A. Lipo (Wisconsin Univ., Madison, WI.), E. N. Hinrichsen (Power Technologies, Inc., Schenectady, NY.), T. L. Hudson (Oak Ridge National Lab., TN.), and R. J. Thomas (Cornell Univ., Ithaca, NY.) *In* DASCON Engineering, Collected Papers on Wind Turbine Technology May 1995 p 185-190 Sponsored by DOE (For primary document see N95-27970 09-44)
Avail: CASI HC A02/MF A03

Interest in variable speed generating technology has accelerated as greater emphasis on overall efficiency and superior dynamic and control properties in wind-electric generating systems are sought. This paper reviews variable speed technology options providing advantages and disadvantages of each. Furthermore, the dynamic properties of variable speed systems are contrasted with synchronous operation. Finally, control properties of variable speed systems are examined. Author

N95-27988*# Wisconsin Univ., Madison, WI. Dept. of Electrical and Computer Engineering.

VARIABLE SPEED GENERATOR TECHNOLOGY OPTIONS FOR WIND TURBINE GENERATORS **c33**

T. A. Lipo *In* DASCON Engineering, Collected Papers on Wind Turbine Technology May 1995 p 191-197 (For primary document see N95-27970 09-44)
Avail: CASI HC A02/MF A03

The electrical system options for variable speed operation of a wind turbine generator are treated in this paper. The key operating characteristics of each system are discussed and the major advantages and disadvantages of each are identified Author

N95-27989*# General Electric Co., Philadelphia, PA.

VARIABLE SPEED GENERATOR APPLICATION ON THE MOD-5A 7.3 mW WIND TURBINE GENERATOR **c33**

Robert S. Barton *In* DASCON Engineering, Collected Papers on Wind Turbine Technology May 1995 p 199-210 Presented at the DOE/NASA Workshop on Horizontal Axis Wind Turbine Technology, Cleveland, OH, 8-10 May 1984 (For primary document see N95-27970 09-44)
Avail: CASI HC A03/MF A03

This paper describes the application of a Scherbiustat type variable speed subsystem in the MOD-5A Wind Turbine Generator. As designed by General Electric Company, Advanced Energy Programs Department, under contract DEN3-153 with NASA Lewis Research Center and DOE, the MOD-5A utilizes the subsystem for both starting assistance in a motoring mode and generation in a controlled airgap torque mode. Reactive power control is also provided. The Scherbiustat type arrangement of a wound rotor machine with a cycloconverter in the rotor circuit was selected after an evaluation of variable speed technologies that followed a system evaluation of drivetrain cost and risk. The paper describes the evaluation factors considered, the results of the evaluations and summarizes operating strategy and performance simulations. Author

N95-27990*# Bionetics Corp., Hampton, VA.

MEASUREMENT AND PREDICTION OF BROADBAND NOISE FROM LARGE HORIZONTAL AXIS WIND TURBINE GENERATORS **c71**

F. W. Grosveld, K. P. Shepherd, and H. H. Hubbard (College of William and Mary, Williamsburg, VA.) *In* DASCON Engineering, Collected Papers on Wind Turbine Technology May 1995 p 211-220 (For primary document see N95-27970 09-44)
Avail: CASI HC A02/MF A03

A method is presented for predicting the broadband noise spectra of large wind turbine generators. It includes contributions from such noise sources as the inflow turbulence to the rotor, the interactions between the turbulent boundary layers on the blade surfaces with their trailing edges and the wake due to a blunt trailing edge. The method is partly empirical and is based on acoustic measurements of large wind turbines and airfoil models. Spectra are predicted for several large machines including the proposed MOD-5B. Measured data are presented for the MOD-2, the WTS-4, the MOD-OA, and the U.S. Windpower Inc. machines. Good agreement is shown between the predicted and measured far field noise spectra. Author

N95-27991*# Midwest Research Inst., Golden, CO.

OBSERVED ACOUSTIC AND AEROELASTIC SPECTRAL RESPONSES OF A MOD-2 TURBINE BLADE TO TURBULENCE EXCITATION **c71**

N. D. Kelley, H. E. McKenna, and E. W. Jacobs *In* DASCON Engineering, Collected Papers on Wind Turbine Technology May 1995 p 221-227 (For primary document see N95-27970 09-44)
(Contracts DE-AC02-83CH-10093; EG-77-C-01-4042)
Avail: CASI HC A02/MF A03

Early results from a recent experiment designed to directly evaluate the aeroacoustic/elastic spectral responses of a MOD-2 turbine blade to turbulence-induced unsteady blade loads are discussed. The experimental procedure consisted of flying a hot-film anemometer from a tethered balloon in the turbine inflow and simultaneously measuring the fluctuating airload and aeroelastic response at two blade span stations (65% and 87% spans) using surface-mounted, subminiature pressure transducers and standard strain gage instrumentation. The radiated acoustic pressure field was measured with a triad of very-low-frequency microphones placed at ground level, 1.5 rotor diameters upwind of the disk. Initial transfer function estimates for acoustic radiation, blade normal forces, flapwise acceleration/displacement, and chord/flapwise moments are presented. Author

N95-27992*# Massachusetts Inst. of Tech., Cambridge, MA.
ANECHOIC WIND TUNNEL STUDY OF TURBULENCE EFFECTS ON WIND TURBINE BROADBAND NOISE **c71**
B. Loyd and W. L. Harris *In* DASCON Engineering, Collected Papers on Wind Turbine Technology May 1995 p 229-236 Presented at the DOE/NASA Workshop on Horizontal Axis Wind Turbine Technology, Cleveland, OH, 8-10 May 1984 (For primary document see N95-27970 09-44)
(Grant NAG3-378)
Avail: CASI HC A02/MF A03

This paper describes recent results obtained at MIT on the experimental and theoretical modelling of aerodynamic broadband noise generated by a downwind rotor horizontal axis wind turbine. The aerodynamic broadband noise generated by the wind turbine rotor is attributed to the interaction of ingested turbulence with the rotor blades. The turbulence was generated in the MIT anechoic wind tunnel facility with the aid of biplanar grids of various sizes. The spectra and the intensity of the aerodynamic broadband noise have been studied as a function of parameters which characterize the turbulence and of wind turbine performance parameters. Specifically, the longitudinal integral scale of turbulence, the size scale of turbulence, the number of turbine blades, and free stream velocity were varied. Simultaneous measurements of acoustic and turbulence signals were made. The sound pressure level was found to vary directly with the integral scale of the ingested turbulence but not with its intensity level. A theoretical model based on unsteady aerodynamics is proposed. Author

N95-28058# Los Alamos National Lab., NM.
GEOTHERMAL DEVELOPMENT IN AUSTRALIA
K. L. Burns, R. A. Creelman, N. W. Buckingham, and H. J. Harrington 1995 8 p Presented at the World Geothermal Congress: Worldwide Utilization of Geothermal Energy, Florence, Italy, 18-31 May 1995
(Contract W-7405-eng-36)
(DE95-007837; LA-UR-95-775; CONF-950514-9) Avail: CASI HC A02/MF A01

In Australia, natural hot springs and hot artesian bores have been developed for recreational and therapeutic purposes. A district heating system at Portland, in the Otway Basin of western Victoria, has provided uninterrupted service for 12 Sears without significant problems, is servicing a building area of 18 990 sq m, and has prospects of expansion to manufacturing uses. A geothermal well has provided hot water for paper manufacture at Traralgon, in the Gippsland Basin of eastern Victoria. Power production from hot water aquifers was tested at Mulka in South Australia, and is undergoing a four-year production trial at Birdsville in Queensland. An important Hot Dry Rock resource has been confirmed in the Cooper Basin. It has been proposed to build an HDR experimental facility to test power production from deep conductive resources in the Sydney Basin near Muswellbrook. DOE

N95-28394# National Renewable Energy Lab., Golden, CO.
REVIEW AND ANALYSIS OF THE 1980-1989 BIOMASS THERMOCHEMICAL CONVERSION PROGRAM
D. J. Stevens Sep. 1994 274 p
(Contract DE-AC36-83CH-10093)
(DE95-000287; NREL/TP-421-7501) Avail: CASI HC A12/MF A03

In the period between 1980 and 1989, the U.S. Department of Energy (DOE) sponsored research and development projects through its Biomass Thermochemical Conversion (BTC) Program. Thermochemical conversion technologies use elevated temperatures to convert biomass into more useful forms of energy such as fuel gases or transportation fuels. The BTC Program included a wide range of biomass conversion projects in the areas of gasification, pyrolysis, liquefaction, and combustion. This work formed the basis of the present DOE research and development efforts on advanced liquid fuel and power generation systems. At the beginning of Fiscal Year 1989, the management of the BTC Program was transferred from Pacific Northwest Laboratory (PNL) to National Renewable Energy Laboratory (NREL, formerly Solar Energy Research Institute). This document presents a summary of the research which was performed under the BTC Program during the 1981-1989 time frame. The document consists of an analysis of the research projects which were funded by the BTC Program and a bibliography of published documents. This work will help ensure that information from PNL's BTC Program is available to those interested in biomass conversion technologies. The background of the BTC Program is discussed in the first chapter of this report. In addition, a brief summary of other related biomass research and development programs funded by the U.S. Department of Energy and others is presented with references where additional information can be found. The remaining chapters of the report present a detailed summary of the research projects which were funded by the BTC Program. The progress which was made on each project is summarized, the overall impact on biomass conversion is discussed, and selected references are provided. DOE

N95-28395# National Renewable Energy Lab., Golden, CO.
THE U.S. DEPARTMENT OF ENERGY WIND TURBINE DEVELOPMENT PROGRAM
H. Link, A. Laxson, B. Smith, and P. Goldman (Department of Energy, Washington, DC.) Mar. 1995 9 p Presented at the American Society of Mechanical Engineers/Japanese Society of Mechanical Engineers/Japan Solar Energy Society International Solar Energy Conference, Lahaina, HI, 19-24 Mar. 1995
(Contract DE-AC36-83CH-10093)
(DE95-000292; NREL/TP-441-7390; CONF-950336-20) Avail: CASI HC A02/MF A01

The development of technologically-advanced wind turbines continues to be a high priority of the US wind industry. The United States Department of Energy (DOE) is sponsoring a range of projects that assist the wind industry to design, develop, and test new wind turbines. The overall goal is to develop turbines that can compete with conventional electric generation with a cost of energy (COE) of 5 cents/kWh at 5.8 m/s (13 mph sites) by the mid-1990s and with a cost of energy of 4 cents/kWh or less at 5.8 m/s sites by the year 2000. These goals will be supported through the DOE Turbine Development Program. The Turbine Development Program uses a two-path approach. The first path assists US industry to develop and integrate innovative technologies into utility-grade wind turbines for the near-term (mid-1990s). The second path assists industry to develop a new generation of turbines for the year 2000. This paper describes present and planned projects under the Turbine Development Program. DOE

N95-28396# National Renewable Energy Lab., Golden, CO.
BUILDING-INTEGRATED PHOTOVOLTAICS: A CASE STUDY
G. Kiss, J. Kinkead, and M. Raman Mar. 1995 139 p
(Contract DE-AC36-83CH-10093)
(DE95-004032; NREL/TP-472-7574) Avail: CASI HC A07/MF A02

In 1992, Kiss Cathcart Anders Architects performed a study for NREL on Building-Integrated Photovoltaics (BIPV) issues as seen from the perspective of the building community. In general, the purpose of the study was to list major issues and potential applications; by it's nature it asked more questions than it answered. This second phase study was to produce quantitative data on the performance of specific BIPV systems. Only roof systems are evaluated. The energy performance, construction cost and simple payback for five different BIPV roof options are evaluated in six different locations: Oakland, New York, Miami, Phoenix, Chicago, and Cincinnati. The roof options evaluated include the following: single-glazed PV roof using glass-substrate PVs; double-glazed PV roof with insulating PV modules; ballasted roof-mounted system; sawtooth light monitor roof with indirect north daylighting; sawtooth roof with north light and active heat recovery. DOE

N95-28517# Brookhaven National Lab., Upton, NY.
STRATEGIES FOR RECYCLING CdTe PHOTOVOLTAIC MODULES
Chris Eberspacher (UNISUN, Newbury Park, CA.), Charles F. Gay (UNISUN, Newbury Park, CA.), and Paul D. Moskowitz 1994 5 p Presented at the 1st World Conference on Photovoltaic Energy Conversion, Waikoloa, HI, 5-9 Dec. 1994
(Contract DE-AC02-76CH-00016)
(DE95-006776; BNL-61321; CONF-941203-22) Avail: CASI HC A01/MF A01

Recycling end-of-life cadmium telluride (CdTe) photovoltaic (PV) modules may enhance the competitive advantage of CdTe PV in the marketplace, but the experiences of industries with comparable Environmental, Health and Safety (EH&S) challenges suggest that collection and recycling costs can impose significant economic burdens. Customer cooperation and pending changes to US Federal law may improve recycling economics. DOE

N95-27649*# Boeing Defense and Space Group, Seattle, WA.
SPACE ENVIRONMENTAL EFFECT ON SOLAR CELLS: LDEF AND OTHER FLIGHT TESTS
Peter Gruenbaum and Harry Dursch *In* NASA. Langley Research Center, LDEF: 69 Months in Space. Third Post-Retrieval Symposium, Part 3 Feb. 1995 p 1167-1177 (For primary document see N95-27629 09-99)
(Contract NAS1-19247)
Avail: CASI HC A03/MF A04

45 ENVIRONMENT POLLUTION

Includes atmospheric, noise, thermal, and water pollution.

N95-26362*# National Academy of Sciences - National Research Council, Washington, DC.
FINDING THE FOREST IN THE TREES. THE CHALLENGE OF COMBINING DIVERSE ENVIRONMENTAL DATA
1995 143 p
(Contracts NASA Order W-88958; DE-FG02-92ER-61514; EPA-68-D-10096; NIST-50SBNB3C7500; NASA-INT-91-18880)
(NASA-CR-197798; B-345; NAS 1.26:197798; LC-95-67403; ISBN-0-309-05082-0) Copyright Avail: CASI HC A07/MF A02

Development of analytical and functional guidelines to help researchers and technicians engaged in interdisciplinary research to better plan and implement their supporting data management activities is addressed. An emphasis is on the projects that involve both geophysical and ecological issues. Six case studies were used to identify and to understand problems associated with collecting, integrating, and analyzing environmental data from local to global spatial scales and over a range of temporal scales. These case studies were also used to elaborate the common barriers to interfacing data of disparate sources and types. A number of lessons derived from the case studies are summarized and analyzed.
Derived from text

N95-26429*# Yale Univ., New Haven, CT. Dept. of Geology and Geophysics.
NONLINEAR DYNAMICS OF GLOBAL ATMOSPHERIC AND EARTH SYSTEM PROCESSES Final Report, 15 Jul. 1993 - 15 Jan. 1995
Taiping Zhang (Yale Univ., New Haven, CT.), Mikhail Verbitsky (Yale Univ., New Haven, CT.), Barry Saltzman (Yale Univ., New Haven, CT.), Michael E. Mann (Yale Univ., New Haven, CT.), Jeffrey Park (Yale Univ., New Haven, CT.), and Upmanu Lall (Utah State Univ., Logan, UT.) 15 Jan. 1995 8 p
(Grant NAG5-2316)
(NASA-CR-197926; NAS 1.26:197926) Avail: CASI HC A02/MF A01

During the grant period, the authors continued ongoing studies aimed at enhancing their understanding of the operation of the atmosphere as a complex nonlinear system interacting with the hydrosphere, biosphere, and cryosphere in response to external radiative forcing. Five papers were completed with support from the grant, representing contributions in three main areas of study: (1) theoretical studies of the interactive atmospheric response to changed biospheric boundary conditions measurable from satellites; (2) statistical-observational studies of global-scale temperature variability on interannual to century time scales; and (3) dynamics of long-term earth system changes associated with ice sheet surges. Author (revised)

N95-26431 Naval Postgraduate School, Monterey, CA. Dept. of Operations Research.
QUANTITATIVE MODELING AND ANALYSIS IN ENVIRONMENTAL STUDIES
Donald P. Gaver Oct. 1994 59 p Limited Reproducibility: More than 20% of this document may be affected by microfiche quality
(AD-A288451; NPS-OR-94-0113) Avail: Issuing Activity (Defense Technical Information Center (DTIC))

This paper reviews some of the many mathematical modeling and statistical data analysis problems that arise in environmental studies. It makes no claim to be comprehensive nor truly up-to-date. It will appear as a chapter in a book on ecotoxicology to be published by CRC Press, probably in 1995. DTIC

N95-26610 Norwegian Radium Hospital, Oslo (Norway). Inst. for Cancer Research.
[FLOW CYTOMETRY AS A MEANS OF DETECTING, ENUMERATING AND CHARACTERIZING BACTERIA FOR MONITORING OF THE ENVIRONMENT] Quarterly Report, 8 Jan. - 11 Mar. 1994
1994 5 p Limited Reproducibility: More than 20% of this document may be affected by microfiche quality
(Contract N68171-94-C-9101)
(AD-A288997; R/D-7186-CN-01) Avail: Issuing Activity (Defense Technical Information Center (DTIC))

The general purpose of the present project is to evaluate flow cytometry as a means of detecting, enumerate and characterize bacteria harvested from air and water samples as part of a system for continuous monitoring of the environment with regard to potentially harmful organisms. In this initial phase of the project we have, in accordance with the project proposal, concentrated on the aspect of detection and enumeration of bacteria, using as a model a variety of species grown in culture. When bacteria are measured for monitoring purposes it is preferable to work with vital unfixed cells, partly to save time and partly because fixation of cells may cause aggregation, and also mask phenomena associated with vital functions, including the very aspect of vital versus dead. Thus, much of our effort has been directed towards development of staining procedures for unfixed samples. In order to establish such procedures, screening experiments with different fluorescent dyes were necessary. The emphasis has been primarily on the effects of different buffers and temperature as means of permeabilizing the cell wall sufficiently to admit the dyes used, but not enough to facilitate efflux of macromolecules. Flow cytometry (FCM) is a technique for measuring the fluorescence and the light scattering of individual cells in large numbers. The cells are measured as they flow in a fluid stream one by one through the focus of an intense light source. The fluorescence intensity (FL) is (usually) proportional to the cellular content of the fluorescent substance(s). Most FCM's can measure two or more fluorescence wavelength components simultaneously, thus facilitating the staining of cells with two or more different dyes. DTIC

N95-26639# Sains Malaysia Univ., Penang (Malaysia). School of Housing Building and Planning.
ENVIRONMENTAL POLLUTION-EFFECTS ON NATIONAL DEVELOPMENT
Mahyuddin binRamli and Mohammed Fazil binMohammedIdris 1994 20 p Presented at the 5th Asia Pacific Physics Conference, Kaula Lampur (Malaysia), 10-15 Aug. 1992
(DE95-600439; INIS-mf-14335; CONF-9208131) Avail: CASI HC A03/MF A01 (US Sales Only)

Environmental pollution is among the major issues highlighted in many discussion between the Government and Non-Government officials whether in the developed or developing countries. The problems becoming worsen when not many people are concerned on its detrimental effects on the future generations. The increasing number of forest activities without proper replanting will also expose to flood problems, soil erosion, landslides and many more as results of environmental impacts. The urbanization process, couple with the rapid industrial development, without having proper planning and inadequate pollutions control, may also create a long term disasters. Penang island territory has been experiencing the most highly physical development growth in this country. Hence, environmental problems are becoming the major issues. This paper will discuss on the various environmental problem, particularly in Penang and possible remedials to be taken by the state and federal authority to overcome the problems. The type of pollutions such as air and water pollutions, acid rain and of course the reduction of ozone layer. Besides that the increase of heat in our climate will also be of our concern in the process of urbanization.
DOE

N95-26808*# University of Central Florida, Orlando, FL. Sponsored Research Div.
ANALYSIS OF MAGNETIC FIELD LEVELS AT KSC Final Report
Christos G. Christodoulou 5 Aug. 1994 156 p

(Grant NAG10-0126)
(NASA-CR-197678; NAS 1.26:197678; KSC-DF-3772) Avail: CASI HC A08/MF A02

The scope of this work is to evaluate the magnetic field levels of distribution systems and other equipment at Kennedy Space Center (KSC). Magnetic fields levels in several operational areas and various facilities are investigated. Three dimensional mappings and contour are provided along with the measured data. Furthermore, the portion of magnetic fields generated by the 60 Hz fundamental frequency and the portion generated by harmonics are examined. Finally, possible mitigation techniques for attenuating fields from electric panels are discussed. Derived from text

N95-27198# Universidad Nacional Autonoma de Mexico, Mexico City (Mexico).

COMPARATIVE EXPERIMENTAL STUDY OF PIXE AND X-RAY FLUORESCENCE ANALYSIS Ph.D. Thesis [ESTUDIO EXPERIMENTAL COMPARATIVO DE LAS TECNICAS PIXE Y XRF]

Luis Ricardo delaVegaBallesteros 1994 92 p In SPANISH
(DE95-607868; INIS-mf-14394) Avail: CASI HC A05/MF A01 (US Sales Only)

PIXE and X RF techniques are powerful analysis instruments in the determination of traces of elements. Although the physical processes characteristic X-rays production (ionization-emission) are similar in both methods, the representative background of each technique, responsible of its sensitivity, are different. This is because the interaction between exciter agents and the matter produces different effects. In PIXE, the background is caused by the radiation produced by the braking of the secondary electrons: Bremsstrahlung. In X RF, the background is due to the elastic and inelastic scattering of photons: Rayleigh and Compton effects. In this work, we have compared the results of the analysis of environmental samples using both methods, in order to know the scope of each one and develop them as complementary techniques. DOE

N95-27234# Radian Corp., Austin, TX.

COMMUNITY RELATIONS PLAN: GALENA AIRPORT AND CAMP ION AIR FORCE STATION, ALASKA Final Report

11 Nov. 1994 55 p
(Contract F33615-90-D-4013)
(AD-A286722; RAD-93-269-107-12-01) Avail: CASI HC A04/MF A01

The U.S. Air Force has been designated as the lead government agency in cleanup efforts at Gelena Airport and Campion Air Force Station, Alaska. This community relations plan (CRP) is consistent with federal guidance for community relations efforts and satisfies the policies established for Superfund remedial activities by the EPA, under direction of the Comprehensive Environmental Response, Compensation, and Liability Act (CERCLA) of 1980, as amended by the Superfund Amendments and Reauthorization Act (SARA) of 1986. The objectives of the CRP are to: Assess community concerns regarding planned and ongoing studies, and determine how and when the public would like to be involved in the decision-making process; Establish procedures for accurate and timely release of information to potentially affected and interested citizen groups, elected officials, public interest groups, agency officials, and the media; Establish methods to facilitate communication between the Air Force and the community at large; Articulate and clarify key issues for the public; Be responsive to the needs and concerns of public interest groups, agency officials, and the media; Receive and understand all the information that the various interest groups have to communicate; and Search for a consensus of the decisions that are being developed throughout the process. DTIC

N95-27457# Oak Ridge National Lab., TN.

PARALLEL ALGORITHMS FOR SEMI-LAGRANGIAN TRANSPORT IN GLOBAL ATMOSPHERIC CIRCULATION MODELS

J. B. Drake, P. H. Worley, J. Michalakes (Argonne National Lab., IL.), and I. T. Foster (Argonne National Lab., IL.) 1995 6 p Presented at the 7th Society for Industrial and Applied Mathematics (SIAM) Conference on Parallel Processing for Scientific Computing, San Francisco, CA, 15-17 Feb. 1995
(Contracts DE-AC05-84OR-21400; W-31-109-eng-38)
(DE95-007385; CONF-950212-6) Avail: CASI HC A02/MF A01

Global atmospheric circulation models (GCM) typically have three primary algorithmic components: columnar physics, spectral transform, and semi-Lagrangian transport. In developing parallel implementations, these three components are equally important and can be examined somewhat independently. A two-dimensional horizontal data decomposition of the three-dimensional computational grid leaves all physics computations on processor, and the only efficiency issues arise in load balancing. A recently completed study by the authors of different approaches to parallelizing the spectral transform showed several viable algorithms. Preliminary results of an analogous study of algorithmic alternatives for parallel semi-Lagrangian transport are described here. DOE

N95-27469# Oak Ridge National Lab., TN.

INTEGRATED ASSESSMENT AND THE RELATION BETWEEN LAND-USE CHANGE AND CLIMATE CHANGE

V. H. Dale Oct. 1994 3 p Presented at the 2nd US/Japan Workshop on Global Change Modeling and Assessment: Improving Methodologies and Strategies, Honolulu, HI, 24-27 Oct. 1994
(Contract DE-AC05-84OR-21400)
(DE95-006533; CONF-9410306-1) Avail: CASI HC A01/MF A01

Integrated assessment is an approach that is useful in evaluating the consequences of global climate change. Understanding the consequences requires knowledge of the relationship between land-use change and climate change. Methodologies for assessing the contribution of land-use change to atmospheric CO2 concentrations are considered with reference to a particular case study area: south and southeast Asia. The use of models to evaluate the consequences of climate change on forests must also consider an assessment approach. Each of these points is discussed in the following four sections. DOE

N95-27532# Lawrence Livermore National Lab., Livermore, CA.

COUPLED CHEMISTRY/CLIMATE ISSUES

D. A. Rotman and D. J. Wuebbles (Illinois Univ., Urbana, IL.) Sep. 1994 6 p
(Contract W-7405-eng-48)
(DE95-006443; UCRL-ID-118434) Avail: CASI HC A02/MF A01

Driven by both natural and anthropogenic causes, the distributions of trace chemical species in the atmosphere has altered the natural state of the chemical distribution and, the authors believe, the climate system. A clear example of this change and its effect on climate is through tropospheric ozone. Evidence shows that over the last decade tropospheric ozone has increased, probably caused by increasing concentrations and emissions of CH4, CO, NO(x), and NMHC's (nonmethane hydrocarbons). Tropospheric ozone is photochemically produced when nitrogen oxides react in the presence of carbon monoxide, methane, non-methane hydrocarbons and sunlight. The chemistry of ozone and NO(x) isalso closely associated with the hydroxyl radical (OH), which governs the atmospheric lifetime of a number of species, including CH4 and chlorofluorocarbons (CFC's), which are major greenhouse gases and which affect the chemical balance of the stratosphere. Increases in the concentrations of CO and CH4 can lead to decreased concentrations of OH and a positive feedback on the atmospheric lifetimes of CO and methane. The same would occur for other greenhouse gases and for some of the important reactions which form aerosols in the troposphere. This would further enhance the concentrations of the gases and accelerate the radiative effects from these greenhouse species, strongly affecting climate and the accurate prediction of climate. It is believed that warmer climates will also increase the amount of water in the atmosphere, thereby providing another chemistry feedback on OH. DOE

N95-27540# National Renewable Energy Lab., Golden, CO.

REDUCING COLD-START EMISSIONS BY CATALYTIC CONVERTER THERMAL MANAGEMENT

S. D. Burch, T. F. Potter, M. A. Keyser, M. J. Brady (Chrysler Corp., Detroit, MI.), and K. F. Michaels (Chrysler Corp., Detroit, MI.) Jan. 1995 6 p Presented at the Society of Automotive Engineers International Congress and Exposition, Detroit, MI, 27 Feb. - 2 Mar. 1995
(Contract DE-AC36-83CH-10093)
(DE95-000256; NREL/TP-473-7025; CONF-950256-3) Avail: CASI HC A02/MF A01

Vacuum insulation and phase-change thermal storage have been used to enhance the heat retention of a prototype catalytic converter. Storing heat in the converter between trips allows exhaust gases to be converted more quickly, significantly reducing cold-start emissions. Using a small metal hydride, the thermal conductance of the vacuum insulation can be varied continuously between 0.49 and 27 W/sq m.k (R-12 to R-0.2 insulation) to prevent overheating of the catalyst. A prototype was installed in a Dodge Neon with a 2.0-liter engine. Following a standard preconditioning and a 23-hour cold soak, an FTP (Federal Test Procedure) emissions test was performed. Although exhaust temperatures during the preconditioning were not hot enough to melt the phase-change material, the vacuum insulation performed well, resulting in a converter temperature of 146 C after the 23-hour cold soak at 27 C. Compared to the same converter at ambient conditions, overall emissions of CO and HC were reduced by 52% and 29%, to 0.27 and 0.037 g/mile, respectively. The maximum converter temperature during the FTP cycle was 720 C. This limited testing was performed with a nearly-fresh palladium-only catalyst, but demonstrates the potential of this vacuum insulation approach for emissions reduction and thermal control. Further testing is ongoing. An initial assessment of several production issues is made, including high-volume fabrication challenges, durability, and cost. DOE

N95-27558# Lawrence Livermore National Lab., Livermore, CA. Program for Climate Model Diagnosis and Intercomparison.

THE PCMDI VISUALIZATION AND COMPUTATION SYSTEM (VCS): A WORKBENCH FOR CLIMATE DATA DISPLAY AND ANALYSIS

Dean N. Williams and Robert L. Mobley Mar. 1994 107 p
(Contract W-7405-eng-48)
(DE95-008586; UCRL-ID-116890) Avail: CASI HC A06/MF A02

This software was developed by the Program for Climate Model Diagnosis and Intercomparison (PCMDI) at the Lawrence Livermore National Laboratory in Livermore, California. It was designed to provide some of the basic capabilities needed for validating, comparing, and diagnosing climate model behavior. It can be controlled either interactively, or from a script file, or control can alternate between these modes during a session. A script can be saved during an interactive session and merely replayed, or it can be edited and replayed. The state-of-the-system can be dumped, as a script, at any instant, and that script can be used later to restore that instant of the session. Attributes for data can describe variables existing in a file or variables to be computed as a function of previously selected variables. The dimensions of variables can be subset, reversed, transposed, wrapped-around, and thinned by selecting either a stride of nodes or by randomly selecting individual nodes. Grid transformations are supported by allowing a different set of dimension vectors to be specified in the dimension descriptors. A display page can be output as either Adobe PostScript for hardcopy, or as a raster image for hardcopy or animation. DOE

N95-27686# Los Alamos National Lab., NM.

ENGINEERING PHOTOCHEMICAL SMOG THROUGH CONVECTION TOWERS

S. Elliott, M. L. Prueitt, J. E. Bossert, E. J. Mroz, R. A. Krakowski, R. L. Miller, M. Z. Jacobson, and R. P. Turco Feb. 1995 35 p
(Contract W-7405-eng-36)
(DE95-007727; LA-12762-MS) Avail: CASI HC A03/MF A01

Reverse convection towers have attracted attention as a medium for cleansing modern cities. Evaporation of an aqueous mist injected at the tower opening could generate electrical power by creating descent, and simultaneously scavenge unsightly and unhealthful particulates. The study offered here assesses the influence to tower water droplets on the photochemical component of Los Angeles type smog. The primary radical chain initiator OH is likely removed into aqueous phases well within the residence time of air in the tower, and then reacts away rapidly. Organics do not dissolve, but nighttime hydrolysis of N2O5 depletes the nitrogen oxides. A lack of HOx would slow hydrocarbon oxidation and so also ozone production. Lowering of NOx would also alter ozone production rates, but the direction is uncertain. SO2 is available in sufficient quantities in some urban areas to react with stable oxidants, and if seawater were the source of the mist, the high pH would lead to fast sulfur oxidation kinetics. With an accommodation coefficient of 10(exp -3), however, ozone may not enter the aqueous phase efficiently. Even if ozone is destroyed or its production suppressed, photochemical recovery times are on the order of hours, so that tower processing must be centered on a narrow midday time window. The cost of building the number of structures necessary for this brief turnover could be prohibitive. The increase in humidity accompanying mist evaporation could be controlled with condensers, but might otherwise counteract visibility enhancements by recreating aqueous aerosols. Quantification of the divergent forcings convection towers must exert upon the cityscape would call for coupled three dimensional modeling of transport, microphysics, and photochemistry. DOE

N95-27708# Lawrence Livermore National Lab., Livermore, CA. Global Climate Research Div.

CALCULATIONS OF DOWNWARD IR SURFACE FLUXES IN THE 500-3,000 cm(EXP -1) WAVENUMBER RANGE FOR THE 1994 ICRCCM MODEL INTERCOMPARISON STUDY

Allen S. Grossman, Keith E. Grant, and Ted Bakowsky Sep. 1994 16 p Sponsored in part by the DOE's Domestic and International Energy Policy Office of Environmental Analysis, Office of Health and Environmental Research, Environmental Sciences Div.
(Contract W-7405-eng-48)
(DE95-006430; UCRL-ID-119123) Avail: CASI HC A03/MF A01

As part of the intercomparison of radiation codes in climate models (ICRCCM) process of comparing radiative transfer parameterizations used in climate models, several data sets were made available to the radiative modeling community. While a comprehensive report will be issued following a meeting of all participating groups, this report documents the LLNL input to this study. Calculations of the downward infrared (IR) surface radiances have been made in the 500-3,000 cm(exp -1) wavenumber range in accordance with the set of ICRCCM test cases provided to all interested modeling groups. The atmospheric test cases were obtained from clear sky observations of the temperature, pressure, and major trace gas distributions at altitudes from the surface to about 30 km. A set of high resolution observations of the downward radiances, plus a set of line by line radiance calculations in the 500-3,000 cm(exp -1) wavenumber range, for each of the test cases was also supplied. Comparison of the Lawrence Livermore National Laboratory (LLNL) theoretical calculations of the integrated radiances over 25 cm(exp -1) subintervals with the observations and the line by line results shows good agreement over most of the wavenumber range. DOE

N95-27743# Boston Coll., Chestnut Hill, MA. Dept. of Chemistry.

MEASUREMENT OF HETEROGENEOUS CHEMICAL PROCESSES RELEVANT TO AEROSOL SURFACES AND TRACE GASES ACTIVE IN THE MARINE ENVIRONMENT Progress Report, Feb. 1994 - Jan. 1995

P. Davidovits, D. R. Worsnop (Aerodyne Research, Inc., Billerica, MA.), M. S. Zahniser (Aerodyne Research, Inc., Billerica, MA.), J. T. Jayne (Aerodyne Research, Inc., Billerica, MA.), and C. E. Kolb (Aerodyne Research, Inc., Billerica, MA.) Feb. 1995 19 p
(Contract DE-FG02-91ER-61208)
(DE95-008337; DOE/ER-61208/4) Avail: CASI HC A03/MF A01

Biogenically produced reduced sulfur compounds from the marine environment, deliver a sulfur burden to the atmosphere which is about half as large as that due to sulfur oxides produced by fossil fuel combustion. The multiphase chemical processes for these species must be understood in order to evaluate the relative roles of biogenic and combustion produced sulfur oxides over the oceans. The aim of the studies funded by the subject DOE grant is to measure parameters governing the heterogeneous chemistry of the species occurring in the marine environment. During the past year, uptake studies for the sulfur species MSA, DMSO, DMSO2, DMS, OCS, CS2, H2S, and CH3SH have been finalized. Studies of the reactive uptake of Cl2 and Br2 by Br(-) and I(-) solutions as a function of temperature have been completed. The uptake of O3 by aqueous NaI solutions has also been studied for the purpose of comparison. We have begun co-deposition studies and have obtained some preliminary results for the codeposition with ozone of DMS, DMSO, DMSO2 and MSA. For the next phase of the work, a new horizontal bubbler apparatus was designed and built and construction to improve the detection sensitivity of the apparatuses was begun. Altogether during 1994, 8 articles have been accepted for publication and 2 Ph.D. dissertations have been submitted and approved. DOE

N95-27749# Pacific Northwest Lab., Richland, WA.

MULTIMEDIA ENVIRONMENTAL POLLUTANT ASSESSMENT SYSTEM (MEPAS) APPLICATION GUIDANCE. GUIDELINES FOR EVALUATING MEPAS INPUT PARAMETERS FOR VERSION 3.1

J. W. Buck, G. Whelan, J. G. Droppo, Jr., D. L. Strenge, K. J. Castleton, J. P. McDonald, C. Sato, and G. P. Streile Feb. 1995 205 p

(Contract DE-AC06-76RL-01830)
(DE95-007525; PNL-10395) Avail: CASI HC A10/MF A03

The Multimedia Environmental Pollutant Assessment System (MEPAS) was developed by Pacific Northwest Laboratory (PNL) for the U.S. Department of Energy (DOE) Office of Environment, Safety and Health and Office of Environmental Management and Environmental Restoration. MEPAS is a set of computer codes developed to provide decision makers with risk information integrated for hazardous, radioactive, and mixed-waste sites based on their potential hazard to public health. It is applicable to a wide range of environmental management and regulatory conditions, including inactive sites covered under the Comprehensive Environmental Response, Compensation, and Liability Act (CERCLA) and active air and water releases covered under the Clean Air Act, the Clean Water Act, and the Resource Conservation and Recovery Act. MEPAS integrates contaminant release, transport, and exposure models into a single system. An interactive user interface assists the investigator in defining problems, assembling data and entering input, and developing reports. PNL has compiled two documents that explain the methodology behind the MEPAS model and instruct the user in how to input, retrieve, and evaluate data. This report contains detailed guidelines for defining the input data required to conduct an analysis with MEPAS. Entries for each variable have a short definition, units, and text explaining what a variable is and how it can be quantified. As appropriate, ranges and typical values are given. This report also contains listings of the input screens (worksheets) that are used in the MEPAS user interface for these variables. DOE

N95-27864*# District of Columbia Univ., Washington, DC.
A STUDY OF SURFACE TEMPERATURES, CLOUDS AND NET RADIATION Semiannual Report
Harbans Dhuria 1 Mar. 1994 29 p
(Grant NAG5-2345)
(NASA-CR-198589; NAS 1.26:198589) Avail: CASI HC A03/MF A01

The study is continuing and it is focused on examining seasonal relationships between climate parameters such as the surface temperatures, the net radiation and cloud types and amount on a global basis for the period February 1985 to January 1987. The study consists of an analysis of the combined Earth Radiation Budget Experiment (ERBE) and International Satellite Cloud Climatology Program (ISCCP) products. The main emphasis is on obtaining the information about the interactions and relationships of Earth Radiation Budget parameters, cloud and temperature information. The purpose is to gain additional qualitative and quantitative insight into the cloud climate relationship. Author

N95-27878# Sandia National Labs., Albuquerque, NM.
EVALUATION AND QUALIFICATION OF ENVIRONMENTALLY CONSCIOUS MANUFACTURING PROCESSES FOR COMMERCIAL AND MILITARY APPLICATIONS
D. J. Anderson, R. M. Cranwell, R. Iman, and P. D. VanBuren 1995 5 p Presented at the IEEE International Symposium on Electronics and the Environment, Orlando, FL, 1-3 May 1995
(Contract DE-AC04-94AL-85000)
(DE95-008520; SAND-95-0315C; CONF-950591-1) Avail: CASI HC A01/MF A01

Environmental regulations are encouraging the development of new environmentally conscious manufacturing (ECNP) processes. However, the quality and reliability of these processes and hardware produced must be understood prior to implementing these new technologies in factories. Furthermore, military hardware fabrication is governed by standards and specifications that frequently mandate the use of older, less environmentally friendly processes or materials, or prohibit the use of new ECM processes without advance military approval. Sandia National Laboratories, with industrial and military partners, have developed methodologies for evaluating and qualifying new ECM processes for military and commercial applications, and have piloted these methodologies in qualifying new, low-residue soldering technologies and materials. DOE

N95-27935# New Energy and Industrial Technology Development Organization, Tokyo (Japan).
INVESTIGATION ON COMPREHENSIVE FOSSIL FUEL CYCLE ANALYSIS AND ASSESSMENT APPROACH AS VIEWED FROM THE GLOBAL ENVIRONMENT
Mar. 1994 280 p In JAPANESE
(DE95-759241; NEDO-P-9330) Avail: CASI HC A13/MF A03

Investigations are conducted with the aim of establishing the comprehensive fuel cycle analysis and assessment method for the power generation cycle which is provided with CO2 recovery and treatment facilities. Power plants (600MW each) of oxygen-blown IGCC and LNG GTCC are chosen for the model study. A base case where the power plant has no CO2 recovery facilities and a case where it has them are studied for each plant. As CO2 recovery technology, the physical absorption/SELEXOL method is adopted to IGCC and the chemical absorption/MEA method to GTCC. Methods to process the recovered CO2 are deep sea water injection, making it clathrate/injection into the sea bottom, and injection into the underground and the oil well. The energy output is approximately 1.03-1.96 times larger in IGCC than in the base case, and approximately 1.02-1.39 times larger in GTCC. The energy balance is calculated by a ratio of sending-end output to energy output. The energy balance in CO2 recovery is approximately 7.7-3.9 and 6.2-4.6 in IGCC and GTCC, respectively, with decreases of about 24-61% in IGCC and 16-38% in GTCC. DOE

N95-27938# New Energy and Industrial Technology Development Organization, Tokyo (Japan).
INVESTIGATION ON WORKING OUT THE GLOBAL REGENERATION PLAN
Mar. 1994 139 p In JAPANESE
(DE95-759246; NEDO-GET-9309) Avail: CASI HC A07/MF A02

Measures to reduce the CO2 emission which mainly causes the global warming were tabulated for their technological evaluation with objective indexes. The measures were evaluated in technology, economy and subsidiary influence at four stage levels, which were the theoretical level, experimental level based on the present technology, demonstration level and future level to presume the future technological progress. The evaluation was itemized into CO2 production rate, energy efficiency and net reducible quantity of CO2. Those items were related to the problem extraction of technological development. In the subsidiary influence evaluation, the technology in question is assessed in its influence on the global environment and ecological system when it is widely propagated. In the economic evaluation, the investment initial cost and operation running cost are separately and clearly studied for the introduction of technology. Though test application was made to the fuel conversion, energy saving manufacturing and CO2 fixation, the investigation to establish the quantitative and reliable evaluation is left as a future problem. DOE

N95-27939# New Energy and Industrial Technology Development Organization, Tokyo (Japan).
SURVEY ON RESEARCHES RELATED TO OCEAN DISPOSAL OF CARBON DIOXIDE
Mar. 1994 147 p In JAPANESE
(DE95-759247; NEDO-GET-9307) Avail: CASI HC A07/MF A02

Pertaining to the CO2 ocean disposal, surveys were made on the equilibrium and transport properties of CO2-water system, mass transfer models of CO2 in the ocean, behavior of deepsea organisms and ecosystem, economical efficiency of CO2 ocean storage, and overseas technical trend of CO2 ocean disposal. For the equilibrium properties, the data with CO2 hydrate are not sufficiently obtainable with very few examples particularly of measuring the diffusivity at high pressures, so that the conventional methods of estimation can possibly not be applied. For the mass transfer models, the simulation is still at a basic stage. For the deepsea organisms, it is necessary to research into the adaptability and adaption speed of ecosystem to the change in pH due to CO2, vertical food chains between the sea surface and bottom, and oceanic ecosystem simulation model on the global level. To evaluate the economical efficiency of CO2 ocean storage, it was known that, though properly applicable in Japan, the liquid CO2 deepsea storage is still difficult in economy. DOE

N95-27941# New Energy and Industrial Technology Development Organization, Tokyo (Japan).
INVESTIGATION ON TECHNOLOGY FOR INCREASING THE BIOLOGICAL CO2 SINK AND TECHNOLOGY FOR CO2 FIXATION AND REUTILIZATION
Mar. 1994 227 p In JAPANESE
(DE95-759251; NEDO-GET-9301) Avail: CASI HC A11/MF A03

An investigational study is conducted on chemical measures to reduce

CO2 environmental loads. For artificial increasing of the CO2 sink, desert planting and afforestation are important. Besides, anticipated are utilization of solar energy and application of biotechnology such as genetic manipulation. Prevention of deforestation is also important. CO2 fixation in the weathering process of silicate rocks is worth studying. There is a method in which phytoplankton is increased by applying fertilizer into the surface layer of the ocean to promote CO2 absorption/fixation into the ocean. CO2 absorption reactors using microalgae are also proposed. For CO2 fixation and reutilization, the paper studies a photochemical/electrochemical method in which the solar cell power generation and chemical reaction are directly combined, and a photocatalytic method. In the former method, the solar cell power generation is combined with water electrolysis or electrolytic reduction of CO2. In the latter, hydrogen is directly produced and CO2 reduction product is obtained. Also investigated is CO2 fixation/reutilization using various kinds of synthesis by CO2, hydrogen and organic matters. DOE

N95-27942# New Energy and Industrial Technology Development Organization, Tokyo (Japan).
INVESTIGATION ON LCA (LIFE CYCLE ANALYSIS/ASSESSMENT)
Mar. 1994 141 p In JAPANESE
(DE95-759260; NEDO-GET-9304) Avail: CASI HC A07/MF A02

Importance is attached to the life cycle analysis/assessment (LCA) which is a method to analyze and assess the load of products on the environment for the enterprises to concretely take environment protecting actions. To initiate the LCA research, a survey was conducted which covered the collection of information, at home and abroad, about the LCA R and D, development of LCA quantification, and case study related to the power generation/distribution, steel making and chemical process. For the selective assessment of element materials, the LCA was developed mainly around the chemical process, and its framework structured by the EPA and SETAC is worldwidely recognized to be basically used. That framework is composed of target setting and general aspect, inventory analysis, influence assessment, and improvement assessment. As an example of research, surveyed was the present status of the above four items of framework. In case of survey by international organizations, it is absolutely necessary that the data to be compared are identical in quality and definition. Conditions to apply the LCA and problems were also pointed out. DOE

N95-27954# Lawrence Livermore National Lab., Livermore, CA.
ISSUES RELEVANT TO THE DEVELOPMENT OF COUPLED CHEMISTRY/CLIMATE MODELS
J. E. Penner, J. Austin (Meteorological Office, Bracknell, England.), D. Cariolle (Centre National de Recherches Meteorologiques, Toulouse, France.), H. Kelder (Royal Netherlands Meteorological Inst., De Bilt, Netherlands.), A. Kylling (Tromsoe Univ., Norway.), M. J. Prather (California Univ., Irvine, CA.), B. Steil (Max-Planck-Inst. fuer Chemie, Mainz, Germany.), and J. K. Sundet (Oslo Univ., Norway.) Sep. 1994 19 p Presented at the North American Treaty Organization (NATO) Advanced Research Workshop on Atmospheric Ozone As A Climate Gas, Lillehammer, Norway, 19-23 Jun. 1994
(Contract W-7405-eng-48)
(DE95-006441; UCRL-JC-118555; CONF-9406301-1) Avail: CASI HC A03/MF A01

Our belief that climate will inexorably change is driven by the very clear evidence of chemical abundance changes in the atmosphere during the last four decades. In the past, this belief has led to the development of two separate efforts: to understand and build models describing the physical climate system and to understand and build models of the chemical climate system. But how will these two systems interact? Are there important chemical changes that result from climate change that need to be understood and properly accounted for in order to predict the evolution of the climate system? Are there important climate changes that may affect chemical abundances that must be addressed? Large strides have been made in our capability to predict both the physical climate system and the chemical climate system during the past few years. In spite of extant uncertainties in both general circulation models (GCM's) and chemical transport models (CTM's), we should begin the process of understanding how and to what extent these errors might propagate in the coupled system. We have outlined a strategy for quantifying the effective uncertainties and have defined a few initial steps in the process. Systematic study of the importance of uncertainties and their impact in the coupled system is a prerequisite to progress in coupling the chemical and climate systems. Such coupling is necessary if we are to predict the evolution of climate in the future. DOE

N95-28084# State Univ. of New York, Stony Brook, NY.
RESEARCH PROJECT ON CO2-INDUCED CLIMATE CHANGE Annual Progress Report, 1 Mar. 1994 - 28 Feb. 1995
R. D. Cess and S. Hameed 1995 8 p
(Contract DE-FG02-85ER-60314)
(DE95-008339; DOE/ER-60314/6) Avail: CASI HC A02/MF A01

This summarizes current progress in the research project at SUNY Stony Brook on CO2-induced climate change. Three tasks are described, corresponding to the task categories in the US DOE/PRC CAS cooperative project on climate change. Task 1 concerns the intercomparison of CO2 related climatic warming in contemporary general circulation models. Task 2 looks at understanding the natural variability in climatic data and comparing its significant features between observations and model simulations. Task 3 focuses on analysis of historical climate data developed at the Institute of Geography of the Chinese Academy of Sciences. DOE

N95-28118# Lawrence Livermore National Lab., Livermore, CA.
CARBONACEOUS AEROSOLS INFLUENCING ATMOSPHERIC RADIATION: BLACK AND ORGANIC CARBON
J. E. Penner Sep. 1994 35 p Presented at the Dahlem Workshop, Berlin, Germany, 24 Apr. 1994
(Contract W-7405-eng-48)
(DE95-006437; UCRL-JC-118866; CONF-9404123-2) Avail: CASI HC A03/MF A01

Carbonaceous particles in the atmosphere may both scatter and absorb solar radiation. The fraction associated with the absorbing component is generally referred to as black carbon (BC) and is mainly produced from incomplete combustion processes. The fraction associated with condensed organic compounds is generally referred to as organic carbon (OC) or organic matter and is mainly scattering. Absorption of solar radiation by carbonaceous aerosols may heat the atmosphere, thereby altering the vertical temperature profile, while scattering of solar radiation may lead to a net cooling of the atmosphere/ocean system. Carbonaceous aerosols may also enhance the concentrations of cloud condensation nuclei. This paper summarizes observed concentrations of aerosols in remote continental and marine locations and provides estimates for the fine particle (D less than 2.5 microns) source rates of both OC and BC. The source rates for anthropogenic organic aerosols may be as large as the source rates for anthropogenic sulfate aerosols, suggesting a similar magnitude of direct forcing of climate. The role of BC in decreasing the amount of reflected solar radiation by OC and sulfates is discussed. The total estimated forcing depends on the source estimates for organic and black carbon aerosols which are highly uncertain. The role of organic aerosols acting as cloud condensation nuclei (CCN) is also described. DOE

N95-28119# Mississippi State Univ., Mississippi State, MS. Diagnostic Instrumentation and Analysis Lab.
APPLICATION OF MODERN DIAGNOSTIC METHODS TO ENVIRONMENTAL IMPROVEMENT Annual Progress Report, Jan. - Oct. 1994
W. S. Shepard Dec. 1994 193 p
(Contract DE-FG02-93CH-10575)
(DE95-005797; DOE/CH-10575/T2) Avail: CASI HC A09/MF A03

The Diagnostic Instrumentation and Analysis Laboratory (DIAL), a research department in the College of Engineering at Mississippi State University (MSU), is under contract with the US Department of Energy (DOE) to develop and apply advanced diagnostic instrumentation and analysis techniques to real world processes; measurements are made in hot, highly corrosive atmospheres in which conventional measurement devices are ineffective. Task 1 of this agreement is concerned with the development and application of various diagnostic methods to characterize the plasma properties, the melt properties and the downstream emissions from a plasma torch facility designed to vitrify mixed waste. Correlation of the measured properties with the operating parameters of the torch will be sought to improve, optimize and control the overall operation of the plasma treatment process. As part of this program, diagnostic methods will be developed and evaluated for characterization, monitoring and control purposes of treatment processes in general. Task 2 of this agreement is concerned with the development of a system to monitor and control the combustion stoichiometry in real time in order to minimize environmental impact and maximize process efficiency. Staged fuel injection is also being studied to minimize NO(x) formation. DOE

N95-28121# Brookhaven National Lab., Upton, NY.
ANOMALOUS CLOUD ABSORPTION? A CRITIQUE OF THE PAPER ENTITLED ABSORPTION OF SOLAR RADIATION BY CLOUDS: OBSERVATIONS VERSUS MODELS
D. G. Imre and E. Abramson Feb. 1995 33 p
(Contract DE-AC02-76CH-00016)
(DE95-007703; BNL-61427) Avail: CASI HC A03/MF A01

In a recent paper R. Cess and co-authors attempt to prove that general-circulation-models of the atmosphere do not correctly calculate short-wave absorption by cloudy sides. Co-located satellite and surface measurements are used to assess the relative effects of clouds on short-wave fluxes at both the top of the atmosphere and at the surface. The differences, expressed as average, Cloud-Radiative-Forcing (CRF) ratios, am evaluated both directly from measured fluxes and indirectly from plots of the Top-Of-Atmosphere (TOA) albedo against transmission. The two different analyses are then connected via their equation 1. Our study of the paper raised the serious concern that, due to unexamined uncertainties in their analyses, their final conclusions are not well founded. Herein, we give critiques of their two basic methods of analysis, referred to as 'the slope' and 'the direct CRF' methods. DOE

N95-28149# Idaho National Engineering Lab., Idaho Falls, ID.
FY 1994 AMBIENT AIR MONITORING REPORT FOR MCMURDO STATION, ANTARCTICA
R. M. Lugar Dec. 1994 69 p
(Contract DE-AC07-94ID-13223)
(DE95-008565; INEL-94/0114) Avail: CASI HC A04/MF A01

This report presents the results of ambient air monitoring performed during the 1994 fiscal year (FY 1994) in the vicinity of McMurdo Station, Antarctica. Routine monitoring was performed during the 1993-1994 austral summer at three locations for airborne particulate matter less than 10 micrometers (PM-10) and at two locations for carbon monoxide (CO), sulfur dioxide (SO2), and nitrogen oxides (NO, (NO2), and (NO(x)). Selected PM-10 filters were analyzed for arsenic, beryllium, cadmium, chromium, lead, mercury, and nickel. Additional air samples were collected at three McMurdo area locations and at Black Island for determination of the airborne concentration of polychlorinated dibenzo-p-dioxins (PCDD's) and polychlorinated dibenzofurans (PCDF's). Sampling site selection, sampling procedures, and quality assurance procedures used were consistent with US Environmental Protection Agency guidance for local ambient air quality networks. DOE

N95-28153 Edgewood Research Development and Engineering Center, Aberdeen Proving Ground, MD.
PROCEEDINGS OF THE 1993 SCIENTIFIC CONFERENCE ON OBSCURATION AND AEROSOL RESEARCH Final Report
Janice E. Rhodes and Sarah J. Wall Mar. 1994 485 p Conference held in Aberdeen, MD, 22-24 Jun. 1993 Limited Reproducibility: More than 20% of this document may be affected by microfiche quality
(AD-A280084; ERDEC-SP-019) Avail: CASI HC A21

In this report, 26 papers presented at the 1993 Scientific Conference on Obscuration and Aerosol Research are included under the headings of Aerosol Dynamics, Aerosol Characterization Methods, and Optical Properties of Aerosols. DTIC

N95-28157# Lawrence Livermore National Lab., Livermore, CA.
TOWARDS THE DETECTION AND ATTRIBUTION OF AN ANTHROPOGENIC EFFECT ON CLIMATE
B. D. Santer, K. E. Taylor, J. E. Penner, T. M. L. Wigley, and P. D. Jones Jan. 1995 84 p
(Contract W-7405-eng-48)
(DE95-008589; UCRL-ID-119098; PCMDI-21) Avail: CASI HC A05/MF A01

It has been hypothesized recently that cooling caused by anthropogenic sulfate aerosols may be obscuring a warming signal associated with changes in greenhouse gas concentrations. Here the authors use results from model experiments in which sulfate and carbon dioxide have been varied individually and in combination in order to determine whether the simulated surface temperature change patterns are increasingly evident in observed records of temperature change. They use centered (R(t)) and uncentered (C(t)) pattern correlation statistics in order to compare observed time-evolving surface temperature change patterns with the model-predicted equilibrium signal patterns. They show that in the case of temperature signals from the 'CO2-only' and 'sulfate-only' experiments, the C(t) statistic essentially reduces to a measure of observed global-mean temperature changes, and cannot be used to uniquely attribute observed climate changes to a specific causal mechanism. For the signal from the experiment with combined CO2/sulfate aerosol forcing, C(t) provides information on pattern congruence, but trends in C(t) are difficult to interpret without decomposing the statistic into pattern similarity and global-mean change components. They therefore focus on R(t), which is a more useful statistic for discriminating between forcing mechanisms with different pattern signatures but similar rates of global mean change. DOE

N95-28202# Technical Research Centre of Finland, Espoo (Finland).
SIHTI 2: ENERGY AND ENVIRONMENTAL TECHNOLOGY. YEARBOOK 1993 OF THE RESEARCH PROGRAMME
M. Korhonen, ed. and K. Saviharju, ed. 1994 250 p
(DE95-755135; VTT-SYMP-144) Avail: CASI HC A11/MF A03

The SIHTI 2 research programme on energy and environmental technology, established by the Finnish Ministry of Trade and Industry, is concentrating on areas of environmental technology that are vital to Finland or in which Finns can engage in pioneering research. The promotion of product development within the environmental technology industry produces solutions for reducing the emissions of the energy sector. It is also a way of boosting Finland's share of the world market for such technology. The objectives of the programme are to cut down harmful emissions, recycle raw materials, reduce the amount of byproducts and wastes and achieve a greater utilization of wastes. In addition, an objective is to create basic information about the effects of environmental protection technology for the other research programmes financed by the Ministry of Trade and Industry. The development of internationally comparable research, monitoring and measurement methods creates a basis for wide-ranging international cooperation. The programme, to be carried out in 1993 - 1998, is in part a continuation of the previous SIHTI programme. New areas of research are environmental problems connected with energy in the forest and base metal industries as well as the systematic development of life-cycle analyses. This publication is yearbook 1993 of the programme. It contains the project reports of the research and joint development projects and information about the participating institutions. DOE

N95-28535# New Energy and Industrial Technology Development Organization, Tokyo (Japan).
SURVEY ON BIO-CHEMICAL COMPLEX HARMONIZED WITH GLOBAL ENVIRONMENT
Mar. 1994 258 p
(DE95-759252; NEDO-GET-9303) Avail: CASI HC A12/MF A03

In order to develop the process and product harmonized with the global environment, a bio-chemical complex was structured which was focused on the biological technology. The substitution of biological technology for the conventional system of a large energy consumption type was engineered to be maximized by using the unutilized biomass as recyclable resources. A field survey was made and reported on the actual state of biomass resources, agriculture and forestry in the Philippines and Thailand. Then, mention was made of their problems of effective utilization. As a biological technology, selected were the hydrogen production, methane fermentation, CO2 fixation, biodegradation plastics and synthesized single cell protein. As a bioreactive or other selective refining technology, study was made of the film, chromatography, solvent extraction, adsorption, electrophoresis, distillation and crystallization. Besides the concentration as a petrochemical complex, it is also effective to take the local properties into consideration and distribute the production bases on a worldwide scale. DOE

N95-28548# Sandia National Labs., Livermore, CA.
EVALUATION OF MICROPOROUS CARBON FILTERS AS CATALYSTS FOR OZONE DECOMPOSITION
L. Whinnery, D. Coutts, C. Shen, R. Adams, C. Quintana (Sandia National Labs., Albuquerque, NM.), and S. Showalter (Sandia National Labs., Albuquerque, NM.) 1994 7 p Presented at the 1994 Fall Meeting of

the Materials Research Society (MRS), Boston, MA, 28 Nov. - 2 Dec. 1994
(Contract DE-AC04-94AL-85000)
(DE95-006498; SAND-95-8451C; CONF-941144-73) Avail: CASI HC A02/MF A01

Ozone is produced in small quantities in photocopiers and laser printers in the workplace and large quantities in industrial waste water treatment facilities. Carbon filters are commonly used to decompose this unwanted ozone. The three most important factors in producing a filter for this purpose are flow properties, efficiency, and cost. Most ozone decomposition applications require very low back-pressure at modest flow rates. The tradeoff between the number of pores and the size of the pores will be discussed. Typical unfiltered emissions in the workplace are approximately 1 ppm. The maximum permissible exposure limit, PEL, for worker exposure to ozone is 0.1 ppm over 8 hours. Several methods have been examined to increase the efficiency of ozone decomposition. Carbon surfaces were modified with catalysts, the surface activated, and the surface area was increased, in attempts to decompose ozone more effectively. Methods to reduce both the processing and raw material costs were investigated. Several sources of microporous carbon were investigated as ozone decomposition catalysts. Cheaper processing routes including macropore templating, faster drying and extracting methods were also studied. DOE

N95-28550# Lawrence Livermore National Lab., Livermore, CA.

THE NORTHERN WINTERTIME DIVERGENCE EXTREMA AT 200 hPa AND SURFACE CYCLONES AS SIMULATED IN THE INTEGRATION OF THE ECMWF GENERAL CIRCULATION MODEL

J. S. Boyle Nov. 1994 30 p
(Contract W-7405-eng-48)
(DE95-007946; UCRL-ID-114037) Avail: CASI HC A03/MF A01

Divergence and convergence centers at 200 hPa and mean sea level pressure (MSLP) cyclones were located every 6 hr for a 10-yr general circulation model (GCM) simulation with the ECMWF (Cycle 36) for the boreal winters from 1980 to 1988. The simulation used the observed monthly mean sea surface temperature (SST) for the decade. Analysis of the frequency, location, and strength of these centers and cyclones gives insight into the dynamical response of the model to the varying SST. The results indicate that: (1) the model produces reasonable climatologies of upper-level divergence and MSLP cyclones; (2) the model distribution of anomalies of divergence and convergence centers and MSLP cyclones is consistent with observations for the 1982-83 and 1986-87 El Nifio events; (3) the tropical Indian Ocean is the region of greatest divergence activity and interannual variability in the model; (4) the variability of the divergence centers is greater than that of the convergence centers; (5) strong divergence centers occur chiefly over the ocean in the midlatitudes but are more land-based in the tropics, except in the Indian Ocean; and (6) locations of divergence and convergence centers can be a useful tool for the intercomparison of global atmospheric simulations. DOE

N95-28602# Spectral Sciences, Inc., Burlington, MA.

A COMPARISON OF NH3 POINT MONITORING AND DIODE LASER BASED PATH INTEGRATED MEASUREMENTS

N. Goldstein, S. C. Richtsmeier, J. Lee, F. Bien, G. J. Fetzer (Monitor Labs, Inc., Englewood, CO.), and K. W. Groff (Monitor Labs, Inc., Englewood, CO.) 1994 17 p Presented at the Optical Sensing for Environmental and Process Monitoring, McLean, VA, 7-10 Nov. 1994
(Contract DE-FG02-91ER-81196)
(DE95-006892; CONF-9411144-4) Avail: CASI HC A03/MF A01

Measurements made using two different types of ammonia monitors during a two-month field study in the summer of 1994 are discussed. The first was a diode-laser based open path monitor designed for automated operation in an industrial environment. The second is a monitoring analyzer based on thermal decomposition of ammonia to NO and subsequent analysis by O3 - NO chemiluminescence. The two monitors provided consistent measurements of ammonia concentration during weeks of continuous unattended operation. DOE

N95-28605# Oak Ridge National Lab., TN.

THE GLOBAL HISTORICAL CLIMATOLOGY NETWORK: A PREVIEW OF VERSION 2

R. S. Vose, R. L. Schmoyer, T. C. Peterson, and J. K. Eischeid 1995 6 p Presented at the 75th Annual Meeting of the American Meteorological Society: Diamond Anniversary, Dallas, TX, 15-20 Jan. 1995
(Contract DE-AC05-84OR-21400)
(DE95-007003; CONF-950124-6) Avail: CASI HC A02/MF A01

Instruments that could reliably measure temperature, precipitation, and pressure were developed by the late 17th and early 18th centuries. It has been estimated that weather records have been collected at one to two hundred thousand locations since those first instruments were placed in the field. Numerous applications, from global change studies to climate impact assessments to general circulation models, make use of such historical records. Given their importance, it is unfortunate that one cannot approach a single researcher or data center to acquire all of the records for all of the stations, or even a large portion of them. In 1990, the Carbon Dioxide Information Analysis Center (CDIAC), the National Climatic Data Center (NCDC), and the World Meteorological Organization (WMO) undertook a collaborative effort aimed at solving this problem. The initiative completed its first data product, known as the Global Historical Climatology Network (GHCN) version 1.0, in 1992. This data base contains quality-controlled monthly climatic time series from 6,039 temperature, 7,533 precipitation, 1,883 sea level pressure, and 1,873 station pressure stations located on global land areas. This paper describes the data and methods being used to compile GHCN version 2.0, an expanded and improved version of its predecessor. Planned for distribution in early 1995, its enhancements will include: (1) data for additional stations--perhaps three times as many as in version 1.0, plus maximum/minimum temperature measurements; (2) detailed assessments of data quality, including nearest-neighbor checks; and (3) adjustments for nonclimatic inhomogeneities, such as station relocations and land use changes. DOE

N95-28623 Aerospace Corp., El Segundo, CA. Technology Operations.

STRATOSPHERIC OZONE REACTIVE CHEMICALS GENERATED BY SPACE LAUNCHES WORLDWIDE

B. B. Brady, E. W. Fournier, L. R. Martin, and R. B. Cohen 1 Nov. 1994 34 p Limited Reproducibility: More than 20% of this document may be affected by microfiche quality
(Contract F04710-88-C-0089)
(AD-A289852; TR-94(4231)-6) Avail: Issuing Activity (Defense Technical Information Center (DTIC))

We report quantities of inorganic chlorine compounds and aluminum oxide particles (Al2O3) deposited in the stratosphere and troposphere by solid rocket propelled launch vehicles. Totals are presented by launch vehicle type, summarized on an annual basis, and projected to the year 2010 using standard mission models. Data are given for Air Force, NASA (shuttle and expendable vehicles), the European Space Agency (ESA) (Ariane 5), and the Japanese Space Agency (H-1 and H-2). Whereas inorganic chlorine compounds released by solid rockets are directly related to stratospheric ozone depletion, much uncertainty surrounds reactivity of aluminum oxide particles. We also compare current and future effects of space launch on stratospheric ozone depletion with those of Ozone Depleting Chemicals (ODC's). As a baseline, we use projections of future ODC use by SMC, Air Force Materiel Command (AFMC), and the world. Relevant stratospheric chemistry is considered to make a legitimate comparison of ODC and solid rocket exhaust. DTIC

N95-28662# Lawrence Livermore National Lab., Livermore, CA.

A BLACK CARBON EMISSION DATA BASE FOR ATMOSPHERIC CHEMISTRY AND CLIMATE STUDIES

J. Dignon, H. E. Eddleman, and J. E. Penner Oct. 1994 3 p
(Contract W-7405-eng-48)
(DE95-006436; UCRL-ID-119104) Avail: CASI HC A01/MF A01

A global data base of black carbon emissions to the atmosphere from fossil fuel combustion has been compiled for the use in atmospheric chemistry and climate studies. The resolution provided is at 1(degree) latitude by 1(degree) longitude based on previous work by Matthews, Lemer et al., and Dignon. A more extensive description of the assumptions made and emission factors used in this data base can be found in Penner et al. The original work of Penner et al. provides the emissions inventory data on a 5(degree) by 5(degree) resolution. The units of emission for this updated version of the inventory yield a global total of 12.6 TgC/y and are given as the mass in metric tons of carbon for each 1(degree) x 1(degree) grid. It is important to note that this is not equivalent to a flux, in that the area of the grid boxes vary latitudinally. The emissions are expected to represent the emissions for a typical mid-1980s year. The distribution of emission is based on national totals and then mapped on to the 1(degree) x 1(degree) grid according to the updated population mapping of Logan. A description of this mapping procedure can be found in Dignon. DOE

N95-27102 American Univ., Washington, DC.
JUNKYARD CHEMISTRY
Paul F. Waters *In* Johns Hopkins Univ., Environmentally Benign Cleaning and Degreasing Technology: JANNAF Safety and Protection Subcommittee and Propellant Development and Characterization Subcommittee Joint Workshop Jun. 1994 p 1-8 (For primary document see N95-27101 09-27)
Avail: CPIA, 10630 Little Patuxent Pkwy., Suite 202, Columbia, MD 21044-3200 HC

N95-27110 Sandia National Labs., Albuquerque, NM.
THE USE OF SUPERCRITICAL CARBON DIOXIDE FOR CONTAMINANT REMOVAL FROM SOLID WASTE
Carol L. J. Adkins, Edward M. Russick, H. Mike Smith (Allied-Signal Corp., Kansas City, MO.), and Ron B. Olson (Allied-Signal Corp., Kansas City, MO.) *In* Johns Hopkins Univ., Environmentally Benign Cleaning and Degreasing Technology: JANNAF Safety and Protection Subcommittee and Propellant Development and Characterization Subcommittee Joint Workshop Jun. 1994 p 95-103 (For primary document see N95-27101 09-27)
(Contracts DE-AC04-76DP-00613; DE-AC04-94AL-85000)
Avail: CPIA, 10630 Little Patuxent Pkwy., Suite 202, Columbia, MD 21044-3200 HC

N95-27116 Naval Command, Control and Ocean Surveillance Center, San Diego, CA. Remediation Research Lab.
THE BIODEGRADATION OF FUELS IN SOILS AND SEDIMENTS: DIFFERENCES AS A FUNCTION OF MINERALOGY
Sabine E. Apitz and Kathleen J. Meyers-Schulte (Computer Sciences Corp., San Diego, CA.) *In* Johns Hopkins Univ., Environmentally Benign Cleaning and Degreasing Technology: JANNAF Safety and Protection Subcommittee and Propellant Development and Characterization Subcommittee Joint Workshop Jun. 1994 p 155-163 Sponsored by Office of Naval Technology, SERDP, DERA, and the Aircraft Environmental Support Office (For primary document see N95-27101 09-27)
Avail: CPIA, 10630 Little Patuxent Pkwy., Suite 202, Columbia, MD 21044-3200 HC

N95-27118 SPB Technologies, Inc., Gulf Breeze, FL.
COMBINED USE OF GROUND WATER CIRCULATION (UVB) TECHNOLOGY AND IN SITU BIOREACTORS FOR ENHANCED BIOREMEDIATION OF SUBSURFACE CONTAMINATION
Jim G. Muller and E. J. Klingel (IEG Technologies, Inc., Gulf Breeze, FL.) *In* Johns Hopkins Univ., Environmentally Benign Cleaning and Degreasing Technology: JANNAF Safety and Protection Subcommittee and Propellant Development and Characterization Subcommittee Joint Workshop Jun. 1994 p 169-174 (For primary document see N95-27101 09-27)
Avail: CPIA, 10630 Little Patuxent Pkwy., Suite 202, Columbia, MD 21044-3200 HC

N95-27125 American Univ., Washington, DC.
A PRACTICAL APPROACH TO SOIL REMEDIATION
Paul F. Waters *In* Johns Hopkins Univ., Environmentally Benign Cleaning and Degreasing Technology: JANNAF Safety and Protection Subcommittee and Propellant Development and Characterization Subcommittee Joint Workshop Jun. 1994 p 235-239 (For primary document see N95-27101 09-27)
Avail: CPIA, 10630 Little Patuxent Pkwy., Suite 202, Columbia, MD 21044-3200 HC

N95-28295 Environmental Protection Agency, Washington, DC. Stratospheric Ozone Protection Div.
THE IMPORTANCE OF PROPULSION ENGINEERS IN PROTECTING THE GLOBAL ENVIRONMENT
Stephen O. Andersen *In* Johns Hopkins Univ., The 1994 JANNAF Safety and Environmental Protection Subcommittee Meeting, Volume 1 Aug. 1994 p 1-8 (For primary document see N95-28294 09-20)
Avail: CPIA, 10630 Little Patuxent Pkwy., Suite 202, Columbia, MD 21044-3200 HC

N95-28296 Radian Corp., Oak Ridge, TN.
OB/OD TREATMENT: THE EFFECTIVE USE OF MEASURED FIELD DATA AND AIR MODELING TO SUPPORT AN ENVIRONMENTAL ASSESSMENT
T. J. Tope, H. C. Simmons, and W. F. Howell *In* Johns Hopkins Univ., The 1994 JANNAF Safety and Environmental Protection Subcommittee Meeting, Volume 1 Aug. 1994 p 13-22 (For primary document see N95-28294 09-20)
(Contract DACW05-92-D-0016)
Avail: CPIA, 10630 Little Patuxent Pkwy., Suite 202, Columbia, MD 21044-3200 HC

N95-28297 Dugway Proving Ground, UT.
EVALUATING THE ENVIRONMENTAL VIABILITY OF OPEN BURNING/OPEN DETONATION OPERATIONS
MacDonald B. Johnson and Douglass P. Bacon (Energy Conversion Corp., Salt Lake City, UT.) *In* Johns Hopkins Univ., The 1994 JANNAF Safety and Environmental Protection Subcommittee Meeting, Volume 1 Aug. 1994 p 23-31 (For primary document see N95-28294 09-20)
Avail: CPIA, 10630 Little Patuxent Pkwy., Suite 202, Columbia, MD 21044-3200 HC

N95-28300 Florida Solar Energy Center, Cape Canaveral, FL.
RADIANT EXCHANGE CONSIDERATIONS IN DESIGN AND SCALEUP OF PHOTOCATALYTIC REACTORS FOR PURIFICATION OF NITROGLYCERINE-CONTAMINATED AIR
Nazim Z. Muradov, Ali T-Raissi, and Charles R. Painter (Naval Surface Weapons Center, Indian Head, MD.) *In* Johns Hopkins Univ., The 1994 JANNAF Safety and Environmental Protection Subcommittee Meeting, Volume 1 Aug. 1994 p 51-61 (For primary document see N95-28294 09-20)
Avail: CPIA, 10630 Little Patuxent Pkwy., Suite 202, Columbia, MD 21044-3200 HC

N95-28302 Rockwell International Corp., Canoga Park, CA.
RECOVERY, EVALUATION, AND DECONTAMINATION OF LANDFILLED PENTABORANE CYLINDERS, FORMER LIQUID PROPELLANT ROCKET ENGINE TEST FACILITY, WASHOE COUNTY, NEVADA
S. L. Shestag, C. J. Rozas, R. Gnat (Hydro-Search, Denver, CO.), and J. Gold (Integrated Environmental Services, Atlanta, GA.) *In* Johns Hopkins Univ., The 1994 JANNAF Safety and Environmental Protection Subcommittee Meeting, Volume 1 Aug. 1994 p 81-91 (For primary document see N95-28294 09-20)
Avail: CPIA, 10630 Little Patuxent Pkwy., Suite 202, Columbia, MD 21044-3200 HC

N95-28303 Yamada Science and Art Corp., Los Alamos, NM.
THREE-DIMENSIONAL FORECAST MODELS FOR EMERGENCY RESPONSE MANAGEMENT
Ted Yamada *In* Johns Hopkins Univ., The 1994 JANNAF Safety and Environmental Protection Subcommittee Meeting, Volume 1 Aug. 1994 p 93-100 (For primary document see N95-28294 09-20)
(Contract F08637-94-C-6013)
Avail: CPIA, 10630 Little Patuxent Pkwy., Suite 202, Columbia, MD 21044-3200 HC

N95-28305 Aerospace Corp., Los Angeles, CA. Mechanics and Materials Technology Center.
USE OF SURFACE CHEMKIN TO MODEL MULTIPHASE ATMOSPHERIC CHEMISTRY: APPLICATION TO NITROGEN TETROXIDE SPILLS
Brian B. Brady and L. Robbin Martin *In* Johns Hopkins Univ., The 1994 JANNAF Safety and Environmental Protection Subcommittee Meeting, Volume 1 Aug. 1994 p 113-122 (For primary document see N95-28294 09-20)
Avail: CPIA, 10630 Little Patuxent Pkwy., Suite 202, Columbia, MD 21044-3200 HC

N95-28306 Naval Surface Weapons Center, Indian Head, MD.
UPGRADE OF THE COMPUTER MODELING PROGRAMS POLU10 AND POLU13A FOR OPEN BURNING AND OPEN DETONATION OF ENERGETIC MATERIALS
Edward E. Baroody *In* Johns Hopkins Univ., The 1994 JANNAF Safety and Environmental Protection Subcommittee Meeting, Volume 1 Aug. 1994 p 123-131 (For primary document see N95-28294 09-20)
Avail: CPIA, 10630 Little Patuxent Pkwy., Suite 202, Columbia, MD 21044-3200 HC

N95-28310* National Aeronautics and Space Administration. John F. Kennedy Space Center, Cocoa Beach, FL.
PROTOTYPE DEVELOPMENT AND TEST RESULTS OF A CONTINUOUS AMBIENT AIR MONITORING SYSTEM FOR HYDRAZINE AT THE 110 ppb LEVEL
Dale E. Lueck, Barry Meneghelli (I-NET, Inc., Cocoa Beach, FL.), Clyde Parrish (I-NET, Inc., Cocoa Beach, FL.), and Ron Barile (I-NET, Inc., Cocoa Beach, FL.) *In* Johns Hopkins Univ., The 1994 JANNAF Safety and Environmental Protection Subcommittee Meeting, Volume 1 Aug. 1994 p 157-166 (For primary document see N95-28294 09-20)
(Contract NAS10-11943)
Avail: CPIA, 10630 Little Patuxent Pkwy., Suite 202, Columbia, MD 21044-3200 HC

N95-28313 Naval Air Warfare Center, China Lake, CA. Weapons Div.
A CONTINUOUS EMISSIONS MONITOR FOR AIRBORNE METALS
Michael D. Seltzer *In* Johns Hopkins Univ., The 1994 JANNAF Safety and Environmental Protection Subcommittee Meeting, Volume 1 Aug. 1994 p 187-194 (For primary document see N95-28294 09-20)
Avail: CPIA, 10630 Little Patuxent Pkwy., Suite 202, Columbia, MD 21044-3200 HC

46 GEOPHYSICS

Includes aeronomy; upper and lower atmosphere studies; ionospheric and magnetospheric physics; and geomagnetism.
For space radiation see *93 Space Radiation.*

N95-26423*# National Aeronautics and Space Administration. Goddard Space Flight Center, Greenbelt, MD.
TECHNICAL REPORT SERIES ON GLOBAL MODELING AND DATA ASSIMILATION. VOLUME 6: A MULTIYEAR ASSIMILATION WITH THE GEOS-1 SYSTEM: OVERVIEW AND RESULTS
Max J. Suarez, ed., Siegfried Schubert, Richard Rood, Chung-Kyu Park (Maryland Univ., College Park, MD.), Chung-Yu Wu (General Sciences Corp., Laurel, MD.), Yelena Kondratyeva (General Sciences Corp., Laurel, MD.), Andrea Molod (General Sciences Corp., Laurel, MD.), Lawrence Takacs (General Sciences Corp., Laurel, MD.), Michael Seablom (General Sciences Corp., Laurel, MD.), and Wayne Higgins (Climate Analysis Center, Washington, DC.) Apr. 1995 201 p
(Contract NAS5-32332)
(NASA-TM-104606-Vol-6; Rept-95B00079-Vol-6; NAS 1.15:104606-Vol-6)
Avail: CASI HC A10/MF A03

The Data Assimilation Office (DAO) at Goddard Space Flight Center has produced a multiyear global assimilated data set with version 1 of the Goddard Earth Observing System Data Assimilation System (GEOS-1 DAS). One of the main goals of this project, in addition to benchmarking the GEOS-1 system, was to produce a research quality data set suitable for the study of short-term climate variability. The output, which is global and gridded, includes all prognostic fields and a large number of diagnostic quantities such as precipitation, latent heating, and surface fluxes. Output is provided four times daily with selected quantities available eight times per day. Information about the observations input to the GEOS-1 DAS is provided in terms of maps of spatial coverage, bar graphs of data counts, and tables of all time periods with significant data gaps. The purpose of this document is to serve as a users' guide to NASA's first multiyear assimilated data set and to provide an early look at the quality of the output. Documentation is provided on all the data archives, including sample read programs and methods of data access. Extensive comparisons are made with the corresponding operational European Center for Medium-Range Weather Forecasts analyses, as well as various in situ and satellite observations. This document is also intended to alert users of the data about potential limitations of assimilated data, in general, and the GEOS-1 data, in particular. Results are presented for the period March 1985-February 1990. Author

N95-26436# Lawrence Livermore National Lab., Livermore, CA.
FTIR MEASUREMENTS OF THERMAL INFRARED SKY RADIANCE AND TRANSMISSION
C. L. Bennett Jul. 1994 13 p Presented at the Annual Meeting of the Society of Photo-Optical Instrumentation Engineers, San Diego, CA, 24-29 Jul. 1994
(Contract W-7405-eng-48)
(DE95-003642; UCRL-JC-117864; CONF-940723-33) Avail: CASI HC A03/MF A01

Precise relative measurements of sky continuum and line emission and absorption have been made using Fourier transform infrared (FTIR) spectroscopy. During conditions of horizontally uniform air composition, measurements of the variation of the spectral radiance with elevation angle sample an air column that varies simply as the cosecant of the elevation angle. In spectral regions that are optically thin, an extrapolation to zero air mass can be used to accurately determine instrumental background. An ambient temperature black body reference furnishes an accurate measurement of the instrumental spectral response. The excess sky emission above instrumental background relative to the local black body reference spectrum thus provides a calibrated sky radiance spectrum. This spectrum can be used to calculate the atmospheric transmission. As a test, transmission spectra have been directly obtained with the full moon as a backlighting source, and are in excellent agreement with the sky radiance derived transmission spectra. For spectral regions dominated by water, the continuum emission has been measured for paths involving the entire atmospheric column. Reasonable agreement with previous laboratory measurement of the continuum strength is obtained. DOE

N95-26488 Air Force Inst. of Tech., Wright-Patterson AFB, OH.
A STUDY OF MAGNETIC ACTIVITY EFFECTS ON THE THERMOSPHERIC WINDS IN THE LOW IONOSPHERE M.S. Thesis - Utah State Univ.
Ricardo Cruz Davila Sep. 1994 196 p Limited Reproducibility: More than 20% of this document may be affected by microfiche quality
(AD-A288677; AFIT/CI/CIA/94-138) Avail: Issuing Activity (Defense Technical Information Center (DTIC))

The purpose of this thesis is to examine the effects of magnetic activity on the low latitude F-region thermospheric winds. The F-region (120-1600 km) is a partially ionized medium where O+ and O are the major ion and neutral species, respectively. The thermospheric winds at these altitudes are driven primarily by pressure gradient forces resulting from the solar heating during the day and cooling at night. For this study, we use measured Fabry-Perot Interferometer (FPI) winds at Arequipa (16.5 deg S, 71.5 deg W) and measured FPI and incoherent Scatter Radar (ISR) winds at Arecibo (18.6 deg N, 66.8 deg W). DTIC

N95-26520 Northwest Research Associates, Inc., Bellevue, WA.
AN IMPROVED MODEL OF HIGH-LATITUDE F-REGION SCINTILLATION (WBMOD VERSION 13) Final Report, 1 Sep. 1993 - 31 Aug. 1994
James A. Secan and Robert M. Bussey 31 Aug. 1994 93 p Limited Reproducibility: More than 20% of this document may be affected by microfiche quality
(Contract F19628-91-C-0152)
(AD-A288558; NWRA-CR-94-R120; PL-TR-94-2254) Avail: Issuing Activity (Defense Technical Information Center (DTIC))

Many modern military systems used for communications, command and control, navigation, and surveillance depend on reliable and relatively noise-free transmission of radiowave signals through the earth's ionosphere. Small-scale irregularities in the ionospheric density can cause severe distortion, known as radiowave scintillation, of both the amplitude and phase of these signals. The WBMOD computer program can he used to estimate these effects on a wide range of systems. The objective of this study is to investigate improvements to the WBMOD model based on extensive data sets covering both the equatorial and high-latitude regimes. This report summarizes the work completed during the third year of this project, which includes completion of the new model for the high-latitude (auroral and polar cap) region of the WBMOD model. DTIC

N95-26531 Naval Postgraduate School, Monterey, CA.
A PROBABILISTIC TARGET CLASSIFICATION AND DESCRIPTION MODEL FOR SEISMIC SENSORS M.S. Thesis
Mark David vanKan Sep. 1994 104 p Limited Reproducibility: More than 20% of this document may be affected by microfiche quality
(AD-A288548) Avail: Issuing Activity (Defense Technical Information Center (DTIC))

Unattended ground sensors have a tremendous potential for providing information about battlefield targets, but for the most part this potential has been unrealized. The Marine Corps has recently fielded the Phase V seismic sensors of the Tactical Remote Sensor System (TRSS). These sensors are more sensitive than any of the previous versions, and their potential to provide more detailed target information is also greater than that of previous sensors. The current target classification and description model used by TRSS was developed for sensors which were placed in use in the early 1960's. The model is simple and deterministic in nature, and does not take into account the variance in the sensor system or the variance in sensor performance due to target type, target velocity, soil composition, or other potential factors. This thesis examines the sensor system variance and the effect of target type on sensor performance through field testing and develops an improved model for target description that accounts for these effects. The revised model takes advantage of the measured sensor characteristics to better describe the target, and provides the user with bounds that describe the credibility of the model's estimate. DTIC

N95-26592*# North Carolina State Univ., Raleigh, NC. Dept. of Marine, Earth, and Atmospheric Sciences.
MESO-BETA SCALE NUMERICAL SIMULATION STUDIES OF TERRAIN-INDUCED JET STREAK MASS/MOMENTUM PERTURBATIONS Final Report
Yuh-Lang Lin and Michael L. Kaplan May 1995 177 p Sponsored by NASA Headquarters
(Grant NAG5-1790)
(NASA-CR-197804; NAS 1.26:197804) Avail: CASI HC A09/MF A02

Mesoscale model simulations provide insight into the complex jet streak adjustments on 11-12 July 1981 that preceded the first of two significant gravity wave events to have been generated over the Rocky Mountains in Montana. Simulations employing a variety of terrain treatments indicate that prior to wave formation, geostrophic adjustment processes modified the structure of the mid-upper tropospheric jet streak by creating secondary jetlets to the southeast of the polar jet streak in proximity to the gravity wave generation region. This simulated restructuring of the mid-upper tropospheric jet streak is the result of a four stage process. During stage 1, the wind adjusts to the mass field as the jet streak exit region propagates into the inflection point between the upstream trough and downstream ridge in the height field. Stage 2 is initiated as the mass field is forced to adjust to the new ageostrophic wind field created during stage 1. Stage 3 is defined by a second geostrophic adjustment process occurring in a similar manner but to the south and east of the adjustment which occurs during stage 1. A low-level mesoscale jetlet is formed during stage 4 in response to the low-level pressure falls that are established during stage 3. The perturbation of this jetlet, caused by orographically-induced adiabatic and diabatic physical processes, is the likely mechanism responsible for the generation of the first and second episode of observed gravity waves. The dynamics responsible for this wave episode are discussed as differential surface sensible heating inducing an orographically-forced mountain-plains solenoid, resulting in the formation of additional mesoscale jetlets and internal gravity waves. Also discussed is how convective latent heating modifies the numerically simulated terrain-induced internal gravity waves, especially their amplitude and phase velocities, which provide better agreement with those wave characteristics observed in nature. Finally, the three-dimensional linear response of a zonally uniform barotropic flow in a vertically unbounded, continuously stratified, Boussinesq atmosphere which is perturbed from geostrophic equilibrium is investigated.
Derived from text

N95-26594* Maryland Public Television, Owings Mills, MD.
LIVE FROM ANTARCTICA: THEN AND NOW (Videotape)
[1994] Sponsored by NASA; NSF; PBS K-12 Learning Services; DOE; Amoco; and Duracell Its Passport to Knowledge Special Series Videotape: 54 min. playing time, in color, with sound
(NASA-CR-197829; NONP-NASA-VT-95-42903) Avail: CASI VHS A02/BETA A22

This real-time educational video series, featuring Camille Jennings from Maryland Public Television, includes information from Antarctic scientists and interactive discussion between the scientists and school children from both Maryland and Hawaii. This is part of a 'Passport to Knowledge Special' series. In this part of the four part Antarctic series, the history of Antarctica from its founding to the present, its mammals, plants, and other life forms are shown and discussed. The importance of Antarctica as a research facility is explained, along with different experiments and research that the facilities there perform. CASI

N95-26595* Maryland Public Television, Owings Mills, MD.
LIVE FROM ANTARCTICA: THE COLDEST, WINDIEST PLACE ON EARTH (Videotape)
[1994] Sponsored by NASA; NSF; PBS K-12 Learning Services; DOE; Amoco; and Duracell Its Passport to Knowledge Special Series Videotape: 1 hr. playing time, in color, with sound
(NASA-CR-197737; NONP-NASA-VT-95-42904) Avail: CASI VHS A02/BETA A22

In this first part of a four part 'Passport to Knowledge Special', hosted by Camille Jennings from Maryland Public Television, children from Maryland and Texas schools had the opportunity to directly interact with and ask questions of scientists and researchers in Antarctica live. The physical characteristics of Antarctica are featured, along with their effects on the human and microbiological organisms living in the region. The reasons behind the clothing worn in the Antarctic and the importance of the meteorological station are featured. Interviews with Professor Ian Dolziel (U of Texas) and Lt. commander John Joseph, NSFA (the head of the Navy Meteorology Center) occur with the school children, along with actual video footage of the surrounding geological features and geography. The 'Weatherops' is located at McMurdo Station, Antarctica. CASI

N95-26596* Maryland Public Television, Owings Mills, MD.
LIVE FROM ANTARCTICA, VOLUME 4 (Videotape)
[1994] Sponsored by NASA; NSF; PBS K-12 Learning Services; DOE; Amoco; and Duracell Its Passport to Knowledge Special Series Videotape: 57 min. playing time. in color, with sound
(NASA-CR-197828; NONP-NASA-VT-95-42905) Avail: CASI VHS A02/BETA A22

In this fourth video of a four part 'Passport to Knowledge Special', hosted by Camille Moody Jennings from Maryland Public Television, children from Maryland and Alaska public schools had the opportunity to directly interact with and ask questions of scientists and researchers from the Antarctic, and learn about the different geological and meteorological research going on in the Antarctic and McMurdo Base at McMurdo Sound. The scientists questioned included: Donal Manahan (biologist from Un. of So. California), who described some of the geological features from Hut Point, the historic hut built by Capt. Scott in 1902; Sridar Anandakrishnan (Penn State Un.) whose research includes ice plate movement of the central ice sheet and earthquakes and how they affect the sheet; and Lt. j.g. Kate McNitt, who spends her winters investigating the trace gases, aerosols, CFC's and ozone levels over the Antarctic area that are affecting the seasonal ozone hole that appears in that region. Historical film footage of Capt. Scott's exploration of the Antarctic is included. CASI

N95-26622# Lawrence Livermore National Lab., Livermore, CA. Climate System Modeling Group, L-256.
A PARALLEL COUPLED OCEANIC-ATMOSPHERIC GENERAL CIRCULATION MODEL
Michael F. Wehner, Al J. Bourgeois, Peter G. Eltgroth, Phillip B. Duffy, and William P. Dannevik Dec. 1994 14 p Presented at the 6th Workshop on Use of Parallel Processors in Meterology, Reading, England, 24 Nov. 1994 Submitted for publication
(Contract W-7405-eng-48)
(DE95-005918; UCRL-JC-119457; CONF-9411178-1) Avail: CASI HC A03/MF A01

The Climate Systems Modeling group at Lawrence Liwermore National Laboratory (LLNL) has developed a portable coupled oceanic-atmospheric general circulation model suitable for use on a variety of massively parallel (MPP) computers of the multiple instruction, multiple data (MIMD) class.

The model is composed of parallel versions of the UCLA atmospheric general circulation model, the GFDL modular ocean model (MOM) and a dynamic sea ice model based on the Hiber formulation extracted from the OPYC ocean model. The strategy to achieve parallelism is twofold. One level of parallelism is accomplished by applying two dimensional domain decomposition techniques to each of the three constituent submodels. A second level of parallelism is attained by a concurrent execution of AGCM and OGCM/sea ice components on separate sets of processors. For this functional decomposition scheme, a flux coupling module has been written to calculate the heat, moisture and momentum fluxes independent of either the AGCM or the OGCM modules. The flux coupler's other roles are to facilitate the transfer of data between subsystem components and processors via message passing techniques and to interpolate and aggregate between the possibly incommensurate meshes. DOE

N95-26699*# Southwest Research Inst., San Antonio, TX. Instrumentation and Space Research Div.

ENERGIZATION AND TRANSPORT OF IONS OF IONOSPHERIC ORIGIN IN THE TERRESTRIAL MAGNETOSPHERE Final Report, 30 Apr. 1995

J. Hunter Jr. Waite 30 Apr. 1995 57 p

(Grant NAG5-1554)

(NASA-CR-197813; NAS 1.26:197813) Avail: CASI HC A04/MF A01

The work of this grant has been predominantly focused on ion outflows from two data sets: Prognoz 7 and Dynamics Explorer. The Prognoz analysis studied ion densities, temperatures, and flow velocities in the magnetotail. The work performed under this contract consisted of developing a program to load the raw data, computing the background subtraction of a strong sun pulse, and using the net count to calculate the low order moments of the distribution function. The study confirms the results of ISEE with regard to the supply of plasma from the cusp as a major source of plasmasheet plasma and goes beyond this to discuss the use of ion velocities as a way to examine the motions of the magnetotail. The abstract of the work to be reported is included as an appendix. The work on the DE/Retarding Ion Mass Spectrometer is separated into two categories: (1) classification of low-energy ion flows from high-latitudes, and (2) studies of the polar wind. Major publications resulting from this work are also included as an appendix to this report. The polar wind is in a category by itself as a result of the thermal escape of hydrogen and helium because of ambipolar diffusion through the heavier, oxygen-dominated topside ionosphere. The analysis of the polar wind reports the flux variability as a function of season, magnetic activity, etc. Much effort has been expended under this grant to complete a follow on study of the thermal structure of the polar wind. Extensive display tools and analysis software have been developed and used in an attempt to carry out this thermal analysis. The present work uses a constrained fit scheme that combines the ion densities and flow velocities derived from Chandler et al. and a spacecraft potential derived from an empirical relation to the total ion density to determine the remaining fit parameter, the ion temperature, via a least squares fit to the RIMS data. Derived from text

N95-26753 Army Cold Regions Research and Engineering Lab., Hanover, NH.

SOIL MOISTURE PREDICTION DURING FREEZE AND THAW USING A COUPLED HEAT AND MOISTURE FLOW MODEL

Susan R. Bigl and Sally A. Shoop Nov. 1994 25 p Limited Reproducibility: More than 20% of this document may be affected by microfiche quality

(DA Proj. 4A1-62373-DT-08)

(AD-A289343; CRREL-94-11) Avail: Issuing Activity (Defense Technical Information Center (DTIC))

A coupled heat flow and moisture flow model (FROSTB) was used to simulate large scale freeze-thaw experiments to assess its ability to predict soil moisture conditions during freeze and thaw. The experimental data consists of temperature and soil moisture profiles through freeze-thaw cycles of a 1-m layer of frost-susceptible silty sand over roughly 2 m of gravely sand. Two experimental conditions were modeled: (1) where the soil moisture was lower than specific retention (less than 12% by weight) and no water table was present (dry case); and (2) where the soil was fairly wet and the water table was approximately in deep (wet case). During freezing, FROSTB tends to predict ice contents higher than those observed, which causes the simulated soil column to thaw slower. During thawing the predicted moisture contents in the thawed soil were close to the measured values for the wet case but were always higher than the measured moisture contents for the dry case. Possible reasons for the discrepancy are discussed. DTIC

N95-26824 Air Force Inst. of Tech., Wright-Patterson AFB, OH. School of Engineering.

COMPENSATED DECONVOLUTION FROM WAVEFRONT SENSING M.S. Thesis

Lori A. Thorson Dec. 1994 89 p Limited Reproducibility: More than 20% of this document may be affected by microfiche quality

(AD-A289490; AFIT/GE/ENG/94D-29) Avail: Issuing Activity (Defense Technical Information Center (DTIC))

The U.S. Air Force has a continuing mission to obtain imagery of earth-orbiting objects. One of the means for obtaining this imagery is through the use of ground-based observatories. A fundamental problem associated with imaging objects through the atmosphere is that atmospheric turbulence inflicts a large, random aberration on the telescope which effectively limits the realizable resolution to that of a much smaller telescope. Several approaches have been taken to overcome these effects including pure post processing, pure adaptive optics, and hybrid techniques involving both adaptive optics and image post processing. One key result from past approaches is that partially compensated systems can be used in conjunction with image processing to overcome most of the optical effects of atmospheric turbulence while retaining nearly the performance of a fully compensated system. One hybrid approach is compensated deconvolution from wavefront sensing (CDWFS). This method uses wavefront sensor measurements in conjunction with short exposure images to improve the effective optical performance. This thesis formulates and executes a plan which allows fundamental questions regarding partially compensated adaptive optics performance to be answered. Specifically, imaging of extended objects using the CDWFS technique is investigated, through simulation. The simulation results demonstrate that the CDWFS technique can be used to reduce the required closed-loop bandwidth of an imaging system, permitting longer integration times in the wavefront sensor, and thus allowing dimmer objects to be imaged without the use of an artificial guidestar. DTIC

N95-26858 Naval Postgraduate School, Monterey, CA.

A MATHEMATICAL ANALYSIS OF THE JANUS COMBAT SIMULATION WEATHER EFFECTS MODELS AND SENSITIVITY ANALYSIS OF SKY-TO-GROUND BRIGHTNESS RATIO ON TARGET DETECTION M.S. Thesis

Vincent F. Shorts Sep. 1994 80 p Limited Reproducibility: More than 20% of this document may be affected by microfiche quality

(AD-A289629) Avail: Issuing Activity (Defense Technical Information Center (DTIC))

The Janus combat simulation offers the user a wide variety of weather effects options to employ during the execution of any simulation run, which can directly influence detection of opposing forces. Realistic weather effects are required if the simulation is to accurately reproduce 'real world' results. This thesis examines the mathematics of the Janus weather effects models. A weather effect option in Janus is the sky-to-ground brightness ratio (SGR). SGR affects an optical sensor's ability to detect targets. It is a measure of the sun angle in relation to the horizon. A review of the derivation of SGR is performed and an analysis of SGR's affect on the number of optical detections and detection ranges is performed using an unmanned aerial vehicle (UAV) search scenario. For comparison, the UAV's are equipped with a combination of optical and thermal sensors. DTIC

N95-26922*# Lockheed Missiles and Space Co., Palo Alto, CA. Research Lab.

A BATSE INVESTIGATION OF RADIATION BELT ELECTRONS PRECIPITATED BY VLF WAVES Final Report

Dayton W. Datlowe 25 Apr. 1995 18 p

(Contract NAS5-32608)

(NASA-CR-197780; NAS 1.26:197780; LMSC-F254281) Avail: CASI HC A03/MF A01

The Compton Observatory commonly encounters fluxes of energetic electrons which have been scattered from the inner radiation belt to the path of the satellite by resonant interactions with VLF waves from powerful man-made transmitters. The present investigation was motivated by the fact that in the Fall of 1993, the Gamma Ray Observatory was boosted from a 650 km altitude circular orbit to a 750 km altitude circular orbit.

This was an opportunity, for the first time, to make observations at two different altitudes using the same instrument. We have examined DISCLA data from the Burst & Transient Source Experiment (BATSE) experiment from 1 Sep. 1993 to 29 Jan. 1994. During the period of study we identified 48 instances of the satellite encountering a cloud of energetic electrons which had been scattered by VLF transmitters. We find that boosting the altitude of the circular orbit from 650 km to 750 km increased the intensity of cyclotron resonance scattered electrons by a factor of two. To search for long term changes in the cyclotron resonance precipitation, we have compared the approx. 750 km altitude data from 106 days at the end of 1993 with data at the same altitudes and time of year in 1991. The cyclotron resonance events in 1991 were three times more frequent and 25% of those cases were more intense than any seen in the 1993 data. We attribute this difference to increased level of geomagnetic activity in 1991 near the Solar Maximum. Author

N95-27146 Phillips Lab., Hanscom AFB, MA.
ASSESSMENT OF THE AN/FPS-118 IONOSPHERIC MODEL AND PROPOSED IMPROVEMENTS Interim Report
B. S. Dandekar 1 Mar. 1994 66 p Limited Reproducibility: More than 20% of this document may be affected by microfiche quality
(AD-A289439; PL-TR-94-2084; ERP-1148) Avail: Issuing Activity (Defense Technical Information Center (DTIC))

The AN/FPS-118 analytical model for the Over the Horizon Backscatter (OTH-B) radar, developed by General Electric Company for the frequency management and the coordinate registration of the radar operation, was installed at the PL computer center and was tested for accuracy. The errors in the computer logic as well as in documentation were identified and appropriate corrections for improving the performance of the model were carried out and tested at PL; they are recommended for implementation at the radar sites in this report. DTIC

N95-27147 Rome Lab., Hanscom AFB, MA.
MEASUREMENTS OF HF AURORAL CLUTTER USING THE VERONA AVA LINEAR ARRAY RADAR (VALAR) Report, Jun. 1990 - Jun. 1991
David S. Choi, Bertus Weijers, and Neil B. Myers Mar. 1994 25 p Limited Reproducibility: More than 20% of this document may be affected by microfiche quality
(AD-A289442; RL-TR-94-43) Avail: Issuing Activity (Defense Technical Information Center (DTIC))

Measurements of high frequency (HF) auroral clutter using the Verona Ava Linear Array Radar (VALAR) system are presented. VALAR is an experimental HF backscatter system capable of obtaining high resolution synoptic mapping of HF auroral clutter. The receiver system includes a 700 meter long linear array, providing the high azimuthal resolution required for determining the spatial distribution of HF auroral clutter. Since the completion of the system at the end of 1989, data acquisition campaigns have been carried out on a near-monthly basis. In this report, we provide a brief description of VALAR and present preliminary measurements of three types of phenomena: ground backscatter, slant-F, and auroral backscatter. DTIC

N95-27157# International Centre for Theoretical Physics, Trieste (Italy).
VARIABILITY STUDY OF foF2 FOR AN EQUATORIAL STATION
J. O. Adeniyi, S. M. Radicella, and I. A. Adimula (Ilorin Univ., Nigeria.) Aug. 1994 10 p
(DE95-608080; IC-94/194) Avail: CASI HC A02/MF A01 (US Sales Only)

The deviation of hourly values of foF2 from the monthly median values was used to study the variability of foF2. The study was done for th e period of high and low solar activity. Generally the range of variation of the deviation is not dependent on solar activity. There is a tendency for positive deviation to occur on magnetically disturbed days and for negative deviation to occur on quiet days. The magnitude of the deviation does not depend on whether the day is disturbed or quiet. The correlation between Ap index and deviation of foF2 from the median value is generally poor . THe range of deviation at night is usually higher than that of the daytime for the period of high solar activity. Some seasonal effects were also observed on the deviation. DOE

N95-27442# Colorado School of Mines, Golden, CO.
DEPTH MIGRATION IN TRANSVERSELY ISOTROPIC MEDIA WITH EXPLICIT OPERATORS Ph.D. Thesis
O. Uzcategui Dec. 1994 140 p
(Contract DE-FG02-89ER-14079)
(DE95-007670; DOE/ER-14079/37; CWP-163) Avail: CASI HC A07/MF A02

The author presents and analyzes three approaches to calculating explicit two-dimensional (2D) depth-extrapolation filters for all propagation modes (P, SV, and SH) in transversely isotropic media with vertical and tilted axis of symmetry. These extrapolation filters are used to do 2D poststack depth migration, and also, just as for isotropic media, these 2D filters are used in the McClellan transformation to do poststack 3D depth migration. Furthermore, the same explicit filters can also be used to do depth-extrapolation of prestack data. The explicit filters are derived by generalizations of three different approaches: the modified Taylor series, least-squares, and minimax methods initially developed for isotropic media. The examples here show that the least-squares and minimax methods produce filters with accurate extrapolation (measured in the ability to position steep reflectors) for a wider range of propagation angles than that obtained using the modified Taylor series method. However, for low propagation angles, the modified Taylor series method has smaller amplitude and phase errors than those produced by the least-squares and minimax methods. These results suggest that to get accurate amplitude estimation, modified Taylor series filters would be somewhat preferred in areas with low dips. In areas with larger dips, the least-squares and minimax methods would give a distinctly better delineation of the subsurface structures. DOE

N95-27703 Computational Physics, Inc., Newton, MA.
PRISM VALIDATION Technical Report
Robert E. Daniell, William G. Whartenby, and Lincoln D. Brown 13 Jun. 1994 45 p Limited Reproducibility: More than 20% of this document may be affected by microfiche quality
(Contract F19628-92-C-0044)
(AD-A288476; PL-TR-94-2198; SR-1) Avail: Issuing Activity (Defense Technical Information Center (DTIC))

This report describes the validation of PRISM, a parameterized, real-time ionospheric specification model, which was described in PL-TR-91-2299. Data were obtained from both analog and digital ionosondes, polarimeters measuring TEC, incoherent scatter radar (ISR), and in situ measurements of electron density, ion velocity, and auroral particle precipitation. Some of the data was used to drive the model while the remainder of the data was held in reserve for comparison with model output. We found that near ionospheric measurements (i.e., within the decorrelation length of the ionosphere), PRISM provides better than 50% improvement in f sub 0(F sub 2), N sub m(F sub 2), and TEC over the ICED, the currently operational ionospheric model at AFSFC. At distances beyond the decorrelation length, PRISM performs as well as ICED and other climatological models. We conclude that PRISM will significantly enhance the ionospheric specification capability of AFSFC. DTIC

N95-27848# Los Alamos National Lab., NM.
LOW ENERGY NEUTRAL ATOM IMAGING: REMOTE OBSERVATIONS OF THE MAGNETOSPHERE
H. O. Funsten, D. J. McComas, E. E. Scime, and K. R. Moore 1995 19 p Presented at the 33rd American Institute of Aeronautics and Astronautics (AIAA) Aerospace Sciences Meeting, Reno, NV, 9-12 Jan. 1995
(Contract W-7405-eng-36)
(DE95-006342; LA-UR-95-32; CONF-950130-8) Avail: CASI HC A03/MF A01

Recent developments in detection of neutral atom imaging should enable imaging the global structure and dynamics of the terrestrial magnetosphere. The inherent technical challenge of imaging low energy neutral atoms (LENA's) with energy less than 30 keV is their separation from the tremendous UV background, to which LENA detectors are sensitive, without loss of information of LENA trajectory and energy. Three instrument concepts for separating LENA's from the background UV are presented: LENA charge conversion via transmission through an ultrathin carbon foil and subsequent electrostatic deflection, EUV grating polarizers and attenuators, and high frequency shutters. Each of these concepts can be mated to a detector section that provides both LENA imaging capability and coincidence/time-of-flight. DOE

N95-27931# Lawrence Livermore National Lab., Livermore, CA.
A SUMMARY DOCUMENTATION OF THE AMIP MODELS
T. J. Phillips Apr. 1994 354 p
(Contract W-7405-eng-48)
(DE95-008343; UCRL-ID-116384; PCMDI-18) Avail: CASI HC A16/MF A03

This report summarizes essential features of the global atmospheric models of 30 groups that are participating in the Atmospheric Model Intercomparison Project (AMIP), an international effort to simulate the climate of the period 1979-1988 with common ocean boundary conditions and radiative forcings. Salient features of the AMIP models are summarized in tabular form, and the principal numerical, dynamical, and physical properties of each model are described in greater detail as well. An extensive bibliography of references on the algorithms and parameterizations used in the AMIP models is also provided. DOE

N95-27995# Finnish Geodetic Inst., Helsinki (Finland).
THE INSTALLATION OF AND FIRST RESULTS FROM THE SUPERCONDUCTING GRAVIMETER GWR20 AT THE METSAHOVI STATION, FINLAND
Heikki Virtanen and Jussi Kaariainen 1995 18 p
(ISSN 0355-1962)
(Rept-95:1; ISBN-951-711-182-7) Avail: CASI HC A03/MF A01

The superconducting gravimeter of the Finnish Geodetic Institute was installed in the new gravity laboratory building of the Metsahovi Geodetic Observatory in August 1994. This laboratory building was completed at the end of 1994. This report gives a general technical description of the Finnish system, discusses experiences since installation of the gravimeter and reviews the first 113 days of registration. Author (revised)

N95-28035*# Southwest Research Inst., San Antonio, TX. Instrumentation and Space Research Div.
ENERGIZATION AND TRANSPORT OF IONS OF IONOSPHERIC ORIGIN IN THE TERRESTRIAL MAGNETOSPHERE Final Report
J. H. Waite, Jr. 30 Apr. 1995 67 p Revised
(Grant NAG5-1554; SwRI Proj. 15-4258)
(NASA-CR-198618-Rev; NAS 1.26:198618-Rev) Avail: CASI HC A04/MF A01

This serves as a final report entitled Energization and Transport of Ions of Ionospheric Origin in the Terrestrial Magnetosphere. The work has been predominantly focused on ion outflows identified in two data sets: (1) Prognoz 7; and (2) Dynamics Explorer. The study analyzed ion densities, temperatures, and flow velocities in the magnetotail. The work performed under this contract consisted of developing a program to load the raw data, compute the background subtraction of a strong sun pulse, and use the net counts to calculate the low order moments of the distribution function. The study confirms the results of ISEE that the the cusp is a major source of plasmasheet plasma and goes beyond this to discuss the use of ion velocities as a way to examine the motions of the magnetotail. Derived from text

N95-28061# Los Alamos National Lab., NM.
RELATIVISTIC ELECTRONS IN THE OUTER-ZONE: AN 11 YEAR CYCLE, THEIR RELATION TO THE SOLAR WIND
R. D. Belian, T. E. Cayton, R. A. Christensen, J. C. Ingraham, M. M. Meier, G. D. Reeves, and A. J. Lazarus 1994 15 p Presented at the 10th Taos Workshop on the Earth's Trapped Particle Environment, Taos, NM, Aug. 1994
(Contract W-7405-eng-36)
(DE95-007882; LA-UR-95-553; CONF-9408182-4) Avail: CASI HC A03/MF A01

We examine Los Alamos energetic electron data from 1979 through the present to show long term trends in the trapped relativistic electron populations at geosynchronous-earth-orbit (GEO). Data is examined from several CPA and SOPA instruments to cover the interval from 1979 through June 1994. It is shown that the higher energy electrons fluxes (E greater than 300 keV) displayed a cycle of approx. 11 years. In agreement with other investigators, we also show that the relativistic electron cycle is out of phase with the sunspot cycle. We compare the occurrences of relativistic electrons and solar wind high speed streams and determine that on the time scale of 15 years the two do not correlate well. The long-term data set we provide here shows a systematic change of the electron energy spectrum during the course of the solar cycle. This information should be useful to magnetospheric scientists, model designers and space flight planners. DOE

N95-28083# Wisconsin Univ., Madison, WI. Dept. of Geology and Geophysics.
TESTING THE CORRELATION BETWEEN SEISMIC STRATIGRAPHY, DIAGENESIS AND PHYSICAL ROCK PROPERTIES: EVALUATION OF FLUID FLOW DURING EARLY AND LATE DIAGENESIS Progress Report, 15 Apr. 1994 - 14 Apr. 1995
J. M. Bahr 1995 5 p
(Contract DE-FG02-94ER-14439)
(DE95-008338; DOE/ER-14439/1) Avail: CASI HC A01/MF A01

This project is designed to test conceptual models of diagenesis with numerical modeling of fluid flow through the Great Bahama Bank. The finite difference code HST3D is being used to simulate fluid flow, heat transport, and solute transport through the Great Bahama Bank. Initial simulations are focussed on a 2-D profile for which the major hydrologic units and properties were chosen based on available seismic and core data. The model is being used to assess the sensitivity of flow patterns and flow rates to variations in hydraulic, thermal, and density gradients and boundary conditions. The numerical model will also be used to study the effects of sea level fluctuations and changes in permeability due to diagenesis. This will involve modification of the boundary conditions and permeability distribution to reflect conditions that are inferred to have existed during earlier diagenetic periods or as a result of sea level change. DOE

N95-28094 Woods Hole Oceanographic Inst., MA. Dept. of Geology and Geophysics.
SEISMIC CONSTRAINTS ON SHALLOW CRUSTAL PROCESSES AT THE EAST PACIFIC RISE Ph.D. Thesis - MIT
Gail L. Christeson Feb. 1994 185 p Limited Reproducibility: More than 20% of this document may be affected by microfiche quality
(Contract N00014-89-J-1015; NSF OCE-89-17750)
(AD-A289055; WHOI-94-02) Avail: Issuing Activity (Defense Technical Information Center (DTIC))

This thesis is concerned with understanding bow oceanic crust is emplaced at mid-ocean ridges. Nine on-bottom seismic refraction experiments are analyzed in an effort to resolve the structure of the emplacement zone of lavas and dikes at the fast-spreading East Pacific Rise. The results suggest that the volcanic section doubles in thickness within approx. 1 km of the axial summit caldera (ASC) due to the emplacement of lava that either overflows the ASC or is emplaced through eruptions outside of the ASC, and the depth to the top of the sheeted dike complex increases from approximately 130-180 m within the ASC to approximately 300-350 m a kilometer away on the flank. It is suggested that the process of dike subsidence is controlled by the axial magma chamber, which is defined as the melt lens and underlying mush zone. In addition, the results of MCS (multi-channel seismic) and wide-angle experiments over plausible velocity structures are predicted quantitatively. It is concluded that the accuracy of correlating the prominent shallow reflector observed in MCS and wide-angle data with the layer 2A/2B boundary is strongly dependent on the structure within layer 2A. DTIC

N95-28114# Illinois State Water Survey, Champaign, IL.
MEASUREMENT AND ANALYSIS OF THE SURFACE ENERGY BUDGET FOR ARM FIELD EXPERIMENTS Final Report
Kenneth E. Kunkel (Illinois State Water Survey, Champaign, IL.) 1995 44 p Prepared in cooperation with Los Alamos National Lab., NM
(Contract W-7405-eng-36)
(DE95-007646; LA-SUB-95-33) Avail: CASI HC A03/MF A01

The objective is to conduct experiments to investigate the scaling properties of surface-atmosphere interactions and feedbacks as they relate to regional fluxes of heat and water vapor. This is part of the US Department of Energy's Atmospheric Radiation Measurement program. To achieve this objective, two field campaigns were conducted in northeastern Oregon during June 1991 and June 1992. Analysis of the data collected during these campaigns revealed the following: (1) Fluxes over a dry, semi-arid grass/brush area show only small spatial heterogeneity. (2) Fluxes over an irrigated farm were dependent on crop type and stage of development. In particular, fluxes over row crops such as potatoes and corn were very similar to each other, but somewhat different than fluxes over wheat and alfalfa. In general, higher latent and lower sensible heat fluxes were experienced over wheat and alfalfa compared to corn and potatoes. (3) Meteorological factors had a major influence on fluxes. In particular, significantly higher latent heat fluxes were experienced on days with moderate winds compared to days with light winds over the irrigated farm. This was presumably due to the advection of sensible heat from the surrounding dry rangeland. DOE

N95-28126# Los Alamos National Lab., NM.

INVESTIGATION OF RIFTING PROCESSES IN THE RIO GRANDE RIFT USING DATA FROM AN UNUSUALLY LARGE EARTHQUAKE SWARM

Final Report, 1 Oct. 1992 - 30 Sep. 1993

Allan Sanford (New Mexico Inst. of Mining and Technology, Socorro, NM.), Robert Balch (New Mexico Inst. of Mining and Technology, Socorro, NM.), Hans Hartse, and Leigh House 1995 12 p
(Contract W-7405-eng-36)
(DE95-007623; LA-SUB-95-16) Avail: CASI HC A03/MF A01

Because the Rio Grande Rift is one of the best seismically instrumented rift zones in the world, studying its seismicity provides an exceptional opportunity to elucidate the active tectonic processes within continental rifts. Beginning on 29 November 1989, a 15 square km region near Bernardo, NM, produced the strongest and longest lasting sequence of earthquakes in the rift in 54 years. Our research focuses on the Bernardo swarm which occurred 40 km north of Socorro, New Mexico in the axial region of the central Rio Grande rift. Important characteristics concerning hypocenters, fault mechanisms, and seismogenic zones are discussed. DOE

N95-28190# Colorado School of Mines, Golden, CO.

DIP-MOVEOUT PROCESSING BY FOURIER TRANSFORM IN ANISOTROPIC MEDIA

J. Anderson (Mobil Oil Corp., Dallas, TX.) and I. Tsvankin Dec. 1994 39 p Presented at the 64th SEG Annual Meeting, Los Angeles, CA, 1994
(Contract DE-FG02-89ER-14079)
(DE95-007668; DOE/ER-14079/35; CWP-146P; CONF-940004-1) Avail: CASI HC A03/MF A01

Conventional dip-moveout (DMO) processing is designed for isotropic media and cannot handle angle-dependent velocity. The authors show that Hale's isotropic DMO algorithm remains valid for elliptical anisotropy but may lead to serious errors for non-elliptical transversely isotropic models, even if velocity anisotropy is moderate. Here, they present an extension of Hale's constant-velocity DMO method to anisotropic media. The DMO operator, to be applied to normal-moveout (NMO) corrected data, is based on the analytic expression for NMO velocity for dipping reflectors given by Tsvankin (1995a). Since the anisotropic DMO depends on the elastic parameters of the medium, it should be preceded by an inversion procedure designed to obtain the NMO velocity as a function of ray parameter. Another complication introduced by anisotropy is the influence of nonhyperbolic moveout not accounted for in the DMO operator. However, for spreads typical in conventional acquisition design, deviations from hyperbolic moveout for P-waves are not significant. Impulse responses and synthetic examples for typical transversely isotropic models with a vertical symmetry axis (VTI) demonstrate the accuracy and efficiency of this DMO technique. Once the inversion step has been completed, the NMO-DMO sequence does not take any more computing time than that for the generic Hale's method in isotropic media. Their anisotropic DMO operator is not limited to VTI media; it can be applied in the same fashion in symmetry planes of more complicated models such as orthorhombic. DOE

N95-28192# Colorado School of Mines, Golden, CO.

TRANSFORMATION TO ZERO OFFSET IN TRANSVERSELY ISOTROPIC MEDIA

T. Alkhalifah Feb. 1995 32 p
(Contract DE-FG02-89ER-14079)
(DE95-007669; DOE/ER-14079/36; CWP-162) Avail: CASI HC A03/MF A01

Nearly all dip moveout correction (DMO) implementations to date assume isotropic homogeneous media. Usually, this has been acceptable considering the tremendous cost savings of homogeneous isotropic DMO and considering the difficulty of obtaining the anisotropy parameters required for effective implementation. In the presence of typical anisotropy, however, ignoring the anisotropy can yield inadequate results. Since anisotropy may introduce large deviations from hyperbolic moveout, accurate transformation to zero-offset in anisotropic media should address such nonhyperbolic moveout behavior of reflections. Artley and Hale's (1994) v(z) ray tracing-based DMO, developed for isotropic media, provides an attractive approach to treating such problems. By using a ray-tracing procedure crafted for anisotropic media, the author modifies some aspects of Artley and Hale's DMO so that it can work for v(z) anisotropic media. Application of this anisotropic DMO to data from offshore Africa resulted in a considerably better alignment of reflections from horizontal and dipping reflectors in common-midpoint gather than that obtained using an isotropic DMO. Even the presence of vertical inhomogeneity in this medium could not eliminate the importance of considering the shale induced anisotropy. DOE

N95-28194# Colorado School of Mines, Golden, CO.

FOWLER DMO AND TIME MIGRATION FOR TRANSVERSELY ISOTROPIC MEDIA WITH EXPLICIT OPERATORS

J. Anderson (Mobil Oil Corp., Dallas, TX.), T. Alkhalifah, and I. Tsvankin Dec. 1994 26 p Presented at the 64th SEG Annual Meeting, Los Angeles, CA, 1994
(Contract DE-FG02-89ER-14079)
(DE95-007671; DOE/ER-14079/38; CWP-164P; CONF-940004-2) Avail: CASI HC A03/MF A01

In this report, the authors devise a Fowler-type DMO algorithm for transversely isotropic media using the analytic expression for normal-moveout velocity given by Tsvankin (1995a). Alkhalifah and Tsvankin (1995) have shown that in transversely isotropic media with a vertical axis of symmetry (VTI) the P-wave normal-moveout (NMO) velocity as a function of ray parameter can be fully described by just two parameters: the zero-dip NMO velocity V(sub nmo)(O) and the anisotropic parameter eta. In the authors extension of Fowler DMO, resampling in the frequency-wavenumber domain makes it possible to obtain the values of V(sub nmo)(O) and eta by inspecting zero-offset (stacked) panels for different pairs of the two parameters. The simplest way to reduce the range of solutions in this two-dimensional search is to obtain V(sub nmo)(O) from conventional NMO velocity analysis. Since most of the computing time is spent on generating constant-velocity stacks, the added computational effort due to the presence of anisotropy is relatively minor. Synthetic and field-data examples demonstrate that the isotropic Fowler DMO technique fails to generate an accurate zero-offset section and obtain the zero-dip NMO velocity for non-elliptical VTI models. In contrast, their anisotropic algorithm allows one to find the values of the parameters V(sub nmo)(O) and eta, and correct for the influence of transverse isotropy in the DMO processing. Combined with poststack F-K Stolt migration, this method represents a complete inversion-processing sequence capable of recovering the effective parameters of transversely isotropic media and producing migrated images for the best-fit homogeneous anisotropic model. Although the current implementation is limited to transversely isotropic media with a vertical axis of symmetry (VTI), it can be generalized for more complicated anisotropic models. DOE

N95-28575 Radex, Inc., Bedford, MA.

A MODEL OF THE DIURNAL VARIATION IN MAGNESIUM ION DENSITY AND RADIANCE IN THE THERMOSPHERE

W. J. McNeil 6 Oct. 1994 86 p Limited Reproducibility: More than 20% of this document may be affected by microfiche quality
(Contract F19628-93-C-0023)
(AD-A289824; RXR-94101; PL-TR-94-2266; SR-6) Avail: Issuing Activity (Defense Technical Information Center (DTIC))

A model has been developed to investigate the behavior of magnesium ions in the thermosphere. The model includes deposition of the atomic metal, diffusion, kinetic creation and destruction of ions, and ultimate removal of the atomic Mg. Transport of the Mg+ by electric fields is also included. A strong diurnal variation in the Mg+ profiles is observed. These profiles are transformed to radiance for conditions mimicking the GLO experiment, to which the results are compared. Key features of the GLO observations are reproduced well by the model. DTIC

N95-28583# California Univ., Berkeley. Lawrence Berkeley Lab, CA.
CONTACT MICROMECHANICS IN GRANULAR MEDIA WITH CLAY Ph.D. Thesis
S. L. Ita Aug. 1994 194 p
(Contract DE-AC03-76SF-00098)
(DE95-006566; LBL-36515) Avail: CASI HC A09/MF A03

Many granular materials, including sedimentary rocks and soils, contain clay particles in the pores, grain contacts, or matrix. The amount and location of the clays and fluids can influence the mechanical and hydraulic properties of the granular material. This research investigated the mechanical effects of clay at grain-to-grain contacts in the presence of different fluids. Laboratory seismic wave propagation tests were conducted at ultrasonic frequencies using spherical glass beads coated with Montmorillonite clay (SWy-1) onto which different fluids were adsorbed. For all bead samples, seismic velocity increased and attenuation decreased as the contact stiffnesses increased with increasing stress demonstrating that grain contacts control seismic transmission in poorly consolidated and unconsolidated granular material. Coating the beads with clay added stiffness and introduced viscosity to the mechanical contact properties that increased the velocity and attenuation of the propagating seismic wave. Clay-fluid interactions were studied by allowing the clay coating to absorb water, ethyl alcohol, and hexadecane. Increasing water amounts initially increased seismic attenuation due to clay swelling at the contacts. Attenuation decreased for higher water amounts where the clay exceeded the plastic limit and was forced from the contact areas into the surrounding open pore space during sample consolidation. This work investigates how clay located at grain contacts affects the micromechanical, particularly seismic, behavior of granular materials. The need for this work is shown by a review of the effects of clays on seismic wave propagation, laboratory measurements of attenuation in granular media, and proposed mechanisms for attenuation in granular media. DOE

47 METEOROLOGY AND CLIMATOLOGY

Includes weather forecasting and modification.

N95-26343 Organisatie voor Toegepast Natuurwetenschappelijk Onderzoek, Delft (Netherlands).
LONGTERM INFRARED CLOUD CLUTTER RESEARCH
A. C. Kruseman Oct. 1994 108 p Limited Reproducibility: More than 20% of this document may be affected by microfiche quality
(AD-A288632; TNO-FEL-94-A094; TDCK-94-0886) Avail: Issuing Activity (Defense Technical Information Center (DTIC))

An infrared all-sky mapper Scorpio has been developed at TNO-FEL. The system has been used to obtain 10 um sky and cloud backgrounds for about one year. The data cover an area of - 18 up to + 72 in elevation and 340 in azimuth with a spatial resolution of 0.8 mrad. The system has an absolute calibration. Data recording with 12 bit resolution, and image analysis are done with a MASSCOMP computer. The image processing is done in several steps. Non-sky areas in the images are blanked. Clutter calculations are performed in cells of 4 x 12 pixels, with local RMS as a basis. The use of a moving average in the RMS calculations diminishes the content of high clutter values. Clutter and radiance distributions are studied with elevation. Lowtran 7 calculations are performed with a model based cloud structure. These are compared with real Scorpio measurements and show good agreement. The results are discussed for a measured atmospheric height profile as well as for assumed model height profiles, based on ground level data. Scorpio images of a single day have been analysed in much detail. Clutter slope calculations show that it is an important measure for the clutter content of the sky images. An algorithm for cloudiness calculations is discussed. The detection of point targets is discussed. DTIC

N95-26453 Federal Aviation Administration, Atlanta, GA. Technical Center.
WEATHER AND RADAR PROCESSOR (WARP) TEST AND EVALUATION MASTER PLAN (TEMP)
William Benner, Christopher Malitsky, William Hall, and Matthew Printy Oct. 1994 129 p Limited Reproducibility: More than 20% of this document may be affected by microfiche quality
(AD-A288280; DOT/FAA/CT-TN94/36) Avail: Issuing Activity (Defense Technical Information Center (DTIC))

This Test and Evaluation Master Plan (TEMP) describes the Test and Evaluation (T&E) processes which will be used to ensure the Weather and Radar Processor (WARP) system meets the requirements allocated to the project in the NAS-SS-1000, volumes 1, 2, and 5, the NAS-SR-1000, and the WARP System Specification, FAA-E-To Be Determined (TBD). This TEMP defines test strategy, test requirements, and organizational roles and responsibilities and is developed in accordance with Federal Aviation Administration (FAA) Order 1810.4B and FAA-STD-O24a. This version of the TEMP addresses the testing requirements for the first two stages of WARP. This TEMP will be updated with additional detail when the WARP program Stage 1, 2, and 3 NAS Change Proposals (NCP) are developed and as the program progresses through the KDP 3 and KDP 4 phases. The original TEMP and its revisions will be submitted for approval by the Test Policy Rules Committee (TPRC). A WARP system will be deployed in all Air Route Traffic Control Centers (ARTCC) and at the Air Traffic Control System Command Center (ATCSCC). It is an Non-developmental Item (NDI)-based automated interactive meteorological data and information processing service that will serve as the primary source of real-time tactical and strategic weather data for air traffic controllers, traffic management unit (TMU) coordinators and area supervisors, meteorologists, and pilots. The WARP system will provide real-time mosaicked WSR-88D products to the air traffic controllers. DTIC

N95-26463 Army Research Lab., White Sands Missle Range, NM. Battlefield Environment Directorate.
NATURAL AEROSOL EXTINCTION MODULE: XSCALE 1992 USER'S GUIDE Final Report
Robert P. Fiegel, Patti L. Gillepie, ed., and Alan E. Wetmore, ed. Nov. 1994 154 p Limited Reproducibility: More than 20% of this document may be affected by microfiche quality
(AD-A289029; ARL-TR-273) Avail: Issuing Activity (Defense Technical Information Center (DTIC))

XSCALE is an empirical and semi-empirical model based on measurements and theoretical calculations of extinction due to naturally occurring aerosols. This model can be used to calculate transmission along horizontal and slant paths near the surface of the earth. This description of XSCALE is an enhancement of descriptions previously released. DTIC

N95-26479 Phillips Lab., Hanscom AFB, MA.
SYNTHETIC 3-D ATMOSPHERIC TEMPERATURE STRUCTURE: A MODEL FOR KNOWN GEOPHYSICAL POWER SPECTRA USING A HYBRID AUTOREGRESSION AND FOURIER TECHNIQUE Interim Report, 1 Oct. 1992 - 31 May 1994
25 May 1994 53 p Limited Reproducibility: More than 20% of this document may be affected by microfiche quality
(ONR Proj. S311; ONR Proj. 3054)
(AD-A289058; PL-TR-94-2150; ERP-1150) Avail: Issuing Activity (Defense Technical Information Center (DTIC))

Geophysical phenomena are often characterized by smooth continuous power spectra having a domain of negative slope power law dependence. Frequently. Fourier transform analysis has been employed to synthesize scenes from pseudorandom arrays by passing the random samples through a Fourier filter having a desired correlation structure and power spectral dependency. This report approaches synthesis of three-dimensional synthetic structure by invoking autoregression analysis in conjunction with the Fourier method. Since computations that apply multidimensional fast Fourier transforms to large data arrays consume enormous resources, the goal of this study is to seek an alternative method to reduce the computational burden. Future releases of the Phillips Laboratory Strategic High Altitude Atmospheric Radiance Code (SHARC) will feature an ability to calculate structured radiance. The methods explored here provide a process that can complement or sometimes supplement methods presently being used. The three-dimensional temperature structure realizations generated by these methods were used to produce two-dimensional integrated temperature structure scenes that showed compliance with the input specifications. DTIC

N95-26546 Titan Systems, Inc., Princeton, NJ. Research and Technology Div.
THE SMALL-SCALE STRUCTURE OF DISPERSING CLOUDS IN THE ATMOSPHERE Final Report, 1 Jun. 1992 - 31 May 1994
R. Ian Sykes, Robert S. Gabruk, and Douglas S. Henn Jul. 1994 91 p Limited Reproducibility: More than 20% of this document may be affected by microfiche quality
(Contract DAAL03-92-C-0020)
(AD-A288256; ARAP-710; ARO-29369.5-GS) Avail: Issuing Activity (Defense Technical Information Center (DTIC))

The fractal properties of a plume dispersing in a turbulent velocity field have been examined using Large-Eddy Simulation results for neutral and convective boundary layers. A fractal generation technique has been developed that correctly matches a specified mean and variance distribution for the plume. The spatial correlation scale of the fractal realizations can also be specified, and the one-point probability density function can be chosen as clipped normal or lognormal. Realizations generated with the fractal technique show reasonably close resemblance to the LES results. The small-scale structure of the plume is further analyzed using multifractal techniques, and a the generation methodology is extended to incorporate unequal partitioning of the random variance during the refinement process. This procedure corresponds to the localization of small-scale energy in the turbulent cascade process which leads to an intermittent dissipation field. The multifractal spectrum of the dissipation field can be adjusted to match observations and the LES calculation results. The visual appearance of the dissipation field from the fractal/multifractal model is much more intermittent than the fractal realization, and the concentration field shows more localized small-scale fluctuations. These features give better correspondence to the LES realizations. DTIC

N95-26650 Army Research Lab., White Sands Missle Range, NM. Battlefield Environment Directorate.
INDEXING MESO-BETA SURFACE WIND SITE REPRESENTATIVE Final Report
Martin E. Lee and Teizi Henmi Sep. 1994 38 p Limited Reproducibility: More than 20% of this document may be affected by microfiche quality
(AD-A288501; ARL-TR-284) Avail: Issuing Activity (Defense Technical Information Center (DTIC))

Multiple meso-beta surface wind site data representativeness is examined in a comparison of corresponding sets of surface mesoscale model windfield predictions - with and without periodic surface data assimilation. A version of the Higher Order Turbulence Model for atmospheric Circulation (HOTMAC) is used in this study to obtain selected surface gridded windfields. Six different radiosonde initialization data sets are used to generate seven hour HOTMAC surface windfield predictions. Two series of HOTMAC simulations are executed: a control case with sparse radiosonde initialization data (less than 6 observations); and an experimental case, in which supplementary hourly surface wind observations, obtained from a consistent set of fifteen automated surface observation stations over a meso-beta scale complex terrain area, are also periodically assimilated into HOTMAC windfields by locally adjusting predicted windfield solutions toward observed conditions and correcting for mass conservation imbalances in the adjusted fields. After observation site data are interpolated from both gridded HOTMAC control and experimental surface windfield predictions, factor separation and statistical tests are used to characterize the representativeness of available surface observation stations in the modeled meso-beta scale regime. Conclusions and the implications of presented results are summarized. DTIC

N95-26653 Naval Postgraduate School, Monterey, CA.
FLUXES ACROSS THE WEST COAST RESOLVED BY PICKET FENCE OBSERVATIONS DURING STORMFEST M.S. Thesis
Steven J. Bolduc Sep. 1994 161 p Limited Reproducibility: More than 20% of this document may be affected by microfiche quality
(AD-A288511) Avail: Issuing Activity (Defense Technical Information Center (DTIC))

Meteorological features that force mesoscale weather systems developed in the central U.S. often form far upstream over the data-sparse Pacific Ocean. It is hypothesized that the temporal and spatial resolution of the current rawinsonde network along the west coast may not be sufficient to detect and measure flow features moving inland. During the STORMFEST experiment in February-March 1992, a 'Picket Fence' of seven rawinsonde stations were interspersed among the seven regular rawinsonde sites from Port Hardy, British Columbia to San Diego, CA. All sites obtained observations every 3 hours rather than the normal 12 hours. The objective was to examine the feasibility of utilizing extra observations in time and space to improve upstream boundary conditions forecasting of mesoscale weather events in the central U.S. Fluxes of mass, heat, momentum, moisture, kinetic energy, and potential energy across the west coast resolved with various spatial and temporal combinations of 'Picket Fence' data were compared with the 12 hour regular site sondes as the standard. In the best case in which a wave system creased the middle of the 'Picket Fence', significantly different fluxes were calculated with the full spatial and 3 hour 'Picket Fence' observations. For other systems that crossed near the ends of the axis, only small changes were detected by the additional observations. DTIC

N95-26669*# Desert Research Inst., Reno, NV. Atmospheric Sciences Center.
REPLICATOR FOR CHARACTERIZATION OF CIRRUS AND POLAR STRATOSPHERIC CLOUD PARTICLES Final Report
John Hallett and Richard G. Purcell Mar. 1995 17 p
(Grant NAG2-663)
(NASA-CR-197785; NAS 1.26:197785) Avail: CASI HC A03/MF A01

A formvar replicator for installation in an aircraft pod has been designed, built, and flight tested on the NASA DC-8. The system incorporates a deicing capability (which can be pressure activated) to enable climb out through icing situations prior to deployment. The system can be operated at preselected speeds such that data can be recorded over a period of 1 to ten hours on 200 ft of 16mm film. A x2 speed control can be used during flight. Capability exists for detection of chemical constituents by appropriate doping of formvar solution. Author

N95-26689*# National Aeronautics and Space Administration. Goddard Space Flight Center, Greenbelt, MD.
SPECTRAL ANALYSES, CLIMATOLOGY, AND INTERANNUAL VARIABILITY OF NIMBUS-7 TOMS VERSION 6 TOTAL COLUMN OZONE
J. L. Stanford (Iowa State Univ. of Science and Technology, Ames, IA.), J. R. Ziemke, R. D. McPeters, A. J. Krueger, and P. K. Bhartia Apr. 1995 84 p
(Grant NAG5-1519)
(NASA-RP-1360; Rept-95B00045; NAS 1.61:1360) Avail: CASI HC A05/MF A01

This reference publication presents selected results from space-time spectral analyses of 13 years of version 6 daily global ozone fields from the Total Ozone Mapping Spectrometer (TOMS). One purpose is to illustrate more quantitatively the well-known richness of structure and variation in total ozone. A second purpose is to provide, for use by modelers and for comparison with other analysts' work, quantitative measures of zonal waves 1, 2, 3, and medium-scale waves 4-7 in total ozone. Their variations throughout the year and at a variety of latitudes are presented, from equatorial to polar regions. The 13-year averages are given, along with selected individual years which illustrate year-to-year variability. The largest long wave amplitudes occur in the polar winters and early springs of each hemisphere, and are related to strong wave amplification during major warning events. In low attitudes total ozone wave amplitudes are an order of magnitude smaller than at high latitudes. However, TOMS fields contain a number of equatorial dynamical features, including Rossby-gravity and Kelvin waves. Author

N95-26723 Air Force Systems Command, Wright-Patterson AFB, OH. National Air Intelligence Center.
AN OBSERVATIONAL STUDY ON THE ONSET OF THE SUMMER MONSOON OVER EASTERN ASIA IN 1979
Tao Shiyan, He Shixiu, and Yang Zufang 15 Dec. 1994 28 p Limited Reproducibility: More than 20% of this document may be affected by microfiche quality
(AD-A289637; NAIC-ID(RS)T-0093-93) Avail: Issuing Activity (Defense Technical Information Center (DTIC))

This article analyzes the process of seasonal transition from spring to summer during the monsoon test period of May-July 1979. In the area of southern Asia and the northwestern Pacific, ten days before the outbreak of large scale summer monsoons, there was a strengthening process in upper atmosphere jet stream westerlies for the area of the southern hemisphere between 40 deg - 160 deg E in the middle latitudes. As far as the development of longitudinal circulation associated with the middle troposphere of the Southern Hemisphere as well as strengthening of cross-equatorial southerly air flows associated with lower layers of the troposphere are concerned, at this time, there was an increase in wind speed in southwesterly winds of the lower atmosphere in the tropical zones of southern Asia and the northwest Pacific. In conjunction with this, there was an expansion of ranges toward the north and an increase in tropical easterlies in the upper troposphere of the southern Asia area. Monsoon circulation patterns were strengthened, and the rainbelts of eastern China showed the appearance of seasonal northward shifts. It seems that changes in atmospheric circulation in the Southern Hemisphere have a triggering effect on the establishment of summer monsoons in the east Asian area as well as on the initiation of the pushing of them toward the north. DTIC

N95-26724 Air Force Systems Command, Wright-Patterson AFB, OH. National Air Intelligence Center.

SYNOPTIC FEATURES OF THE YUNAN RAINY SEASON BEFORE THE ONSET OF THE TROPICAL MONSOONS

Chen Yuxiang and Zhu Baozhen 15 Dec. 1994 19 p Transl. into ENGLISH from unknown Chinese periodical p 101-106 Limited Reproducibility: More than 20% of this document may be affected by microfiche quality

(AD-A289641; NAIC-ID(RS)T-0095-93) Avail: Issuing Activity (Defense Technical Information Center (DTIC))

This article studies a special type of weather phenomenon associated with the leeward slope of the Qinghai-Tibet Plateau - the Yunnan early rainy season. It discusses weather systems which directly create continuous precipitation as well as the special characteristics of their seasonal development. Diagnostic analysis of static energies clearly show that there are areas of difference between the Yunnan early rainy season and the arrival of the subsequent Indian monsoon with the beginning of its rainy season. It was discovered that there is a correlation between the period of the beginning of the early rainy season each year and the period of the appearance of the first storms in the Bay of Bengal. Finally, it discusses the relationships between this and seasonal changes in East Asian atmospheric circulation. DTIC

N95-26826 Woods Hole Oceanographic Inst., MA.

METEOROLOGICAL AND OCEANOGRAPHIC DATA COLLECTED DURING THE ASREX 91 FIELD EXPERIMENT Technical Report

Nancy R. Galbraith, Anand Gnanadesikan, George H. Tupper, Bryan S. Way, and Eugene A. Terray Aug. 1994 123 p Limited Reproducibility: More than 20% of this document may be affected by microfiche quality

(Contract N00014-91-J-1891)

(AD-A289492; WH01-94-18) Avail: Issuing Activity (Defense Technical Information Center (DTIC))

The 1991 Acoustic Surface Reverberation Experiment (ASREX 91) took place in November and December off the coast of British Columbia. As part of this experiment, three moorings were deployed to characterize the environmental background. The moorings consisted of a meteorological/oceanographic mooring designed to measure surface meteorology, current and temperature in the upper 120 meters, and nondirectional wave parameters and two wave moorings which were instrumented with pitch-roll buoys to characterize the directional wave spectrum. This report presents results from these three moorings. The conditions seen during the experiment were extremely rough, with wind speeds at 3.4 m above the water surface reaching a maximum of 22 m/s and wave heights reaching a maximum of over 10 meters. The air-sea flux of heat was strongly cooling, and the mixed layer deepened over the course of the experiment from approximately 40 to approximately 70 meters. Spectra of the temperature showed a strong semidiurnal tidal signal associated with temperature excursions of several degrees C. The velocity signal showed strong inertial oscillations with amplitudes of 30-50 cm/s. Weaker low-frequency and semidiurnal tidal signals were also seen. The waves were very strong with significant wave heights of 5-6 meters persisting for up to 2 weeks at a time. Waves were generally out of the south or the west. DTIC

N95-26899 Aerospace Corp., El Segundo, CA. Technology Operations.

SUBVISUAL CIRRUS: WHAT IT IS AND WHERE YOU FIND IT Technical Report

David K. Lynch 1 Nov. 1994 15 p Limited Reproducibility: More than 20% of this document may be affected by microfiche quality

(Contract F04701-88-C-0089)

(AD-A289329; TR-93(3308)-1; SMC-TR-94-46) Avail: Issuing Activity (Defense Technical Information Center (DTIC))

Extremely low column density ice clouds (subvisual cirrus) have significant impacts on passive IR remote sensing of both the atmosphere and the Earth. In this report I review the physical properties of subvisual cirrus and discuss their detection and global distribution. DTIC

N95-27148 Air Force Environmental Technical Applications Center, Scott AFB, IL.

SOUTHERN AFRICA: A CLIMATOLOGICAL STUDY

Kathleen M. Traxler, Richard D. Arnold, John W. Louer, III, Michael T. Gilford, Joy L. Harding, Richard C. Bonam, Kenneth R. Walters, Sr., and Christopher A. Donahue Dec. 1994 216 p Limited Reproducibility: More than 20% of this document may be affected by microfiche quality

(USAFETAC Proj. 901033)

(AD-A289466; USAFETAC/TN-94/005) Avail: Issuing Activity (Defense Technical Information Center (DTIC))

This report is a climatological study of Southern Africa, a region that comprises The Republic of South Africa, Zimbabwe, Namibia, Lesotho, Swaziland, Botswana, Madagascar and the southern parts of Mozambique, Angola, Zaire, and Zambia. After describing the geography and major meteorological features of the entire study area, the study discusses the major climatic controls of each of Southern Africa's six climatic 'commonality' regions in detail. Each 'season' is defined and discussed in considerable detail, to include typical weather, clouds, visibility, winds, precipitation, and temperature. DTIC

N95-27366 Royal Netherlands Meteorological Inst., De Bilt (Netherlands).

THREE OBJECTIVE INDICES FOR CLEAR-AIR TURBULENCE RECONSIDERED [DRIE OBJECTIEVE INDICES VOOR CLEAR-AIR TURBULENCE NADER BEKEKEN]

Harry Bakker Dec. 1993 33 p In DUTCH

(ISSN 0169-1708)

(KNMI-TR-160; ISBN-90-369-2047-7) Copyright Avail: Issuing Activity (Royal Netherlands Meteorological Inst., Postbus 201, 3730 AE De Bilt, Wilhelminalaan 10, Netherlands)

This technical report considers three objective forecast methods for Clean-Air Turbulence (CAT). They are the Diagnostic Richardson Tendency (DRT) and two CAT-indices such as those used in Bracknell or the NMC in Washington, respectively. The DRT-method fixes the current Richardson number on the grid points of the model and the deviation therefrom. Then a calculation is made as to how long it will take before the Richardson number exceeds the critical value 1. The Bracknell CAT-index is given by a function wherein horizontal and vertical windshear are the two variables. It provides an opportunity for 'moderate or heavy turbulence'. The NMC-index is the product of horizontal deformation and vertical windshear. This index distinguishes between 'moderate turbulence' and 'moderate or heavy turbulence'. By means of a number of case studies, we consider which method is preferable for application in the Vertical Information Model (VIM). This model is currently within the department of Scientific R & D and should be supported by meteorologists of the Aviation Meteorological Service. The case-studies make clear that the result of the DRT method should be left alone. The two other indices achieve nearly equally good results. The CAT-index of the NMC is slightly preferable for implementation in the VIM, since verification carried out at the Canadian Newfoundland Weather Center indicated that the NMC-index scores somewhat better than the Bracknell CAT-index. Author

N95-27912# General Accounting Office, Washington, DC. Accounting and Information Management Div.

REPORT TO THE CHAIRMAN AND RANKING MINORITY MEMBER, COMMITTEE ON SCIENCE, HOUSE OF REPRESENTATIVES. WEATHER FORECASTING: RADAR AVAILABILITY REQUIREMENT NOT BEING MET

May 1995 49 p

(GAO/AIMD-95-132; B-258872) Avail: CASI HC A03/MF A01; GAO, PO Box 6015, Gaithersburg, MD 20884-6015 HC

The status of the Next Generation Weather Radar (NEXRAD) project is reported. The reasons why some of the NEXRAD units were dropped from the original deployment plan are investigated, along with the feasibility and estimated cost of extending the NEXRAD contract. The Air Force NEXRAD's contribution to the national NEXRAD network is assessed, and the accessibility of the Air Force NEXRAD data to civilian forecastors is examined. In addition, the availability of Air Force and the National Weather Service NEXRAD's is also reported. CASI

N95-27920# Oak Ridge National Lab., TN.

THE DISTRIBUTION OF CLOUD COVER OVER THE FORMER USSR AS DERIVED FROM THE RIHMI 223-STATION 3-HOURLY METEOROLOGICAL DATABASE

D. P. Kaiser, R. S. Vose, T. R. Karl (National Climatic Data Center, Asheville, NC.), and V. N. Razuvaev (Research Inst. of Hydrometeorological Information, Dbninsk, Russia. Obninsk, Russia.) 1995 6 p Presented at the 75th Annual Meeting of the American Meteorological Society: Diamond Anniversary, Dallas, TX, 15-20 Jan. 1995
(Contract DE-AC05-84OR-21400)
(DE95-007046; CONF-950124-5) Avail: CASI HC A02/MF A01

In recent years a great deal of meteorological and climatological data has been exchanged between the two principal climate data centers of the United States and the former Soviet Union: the National Climatic Data Center (NCDC), in Asheville, North Carolina, and the Research Institute of Hydrometeorological Information (RIHMI) in Obninsk, Russia. This was accomplished via Working Group VIB (Influence of Environmental Changes on Climate) of the bilateral initiative known as the Agreement on Protection of the Environment, established on May 23, 1972 by the United States and the USSR. One of the key datasets compiled by RIHMI includes 3-hourly meteorological observations from 223 USSR stations for the period 1966-83. RIHMI has chosen to use daily and hourly data from these stations as the basis for considerable climate research efforts. These data (hereafter referred to as the RIHMI database) will soon be made available by both NCDC and the Department of Energy's Carbon Dioxide Information Analysis Center (CDIAC) in Oak Ridge, Tennessee. The data have undergone extensive quality assurance checks at RIHMI, NCDC, and CDIAC. The data contain observations of some 22 meteorological variables, including near-surface air temperature, sea level pressure, precipitation amount, weather type, and total cloud cover. This study uses the RIHMI database to examine the spatial distribution of total cloud cover over the former USSR (hereafter referred to as the USSR). In this initial assessment, we focus on comparing our results with total cloud cover data presented in the atlas: Global Distribution of Total Cloud Cover and Cloud Type Amounts Over Land for the common data period 1971-81. DOE

N95-27997*# Futuretech Corp., Gaithersburg, MD.

MILLIMETER-WAVE IMAGING RADIOMETER DATA PROCESSING AND DEVELOPMENT OF WATER VAPOR RETRIEVAL ALGORITHMS Semiannual Report, 1 Oct. 1994 - 31 Mar. 1995

L. Aron Chang Apr. 1995 17 p
(Contract NAS5-32705)
(NASA-CR-198593; Rept-95FTC001; NAS 1.26:198593) Avail: CASI HC A03/MF A01

This document describes the current status of Millimeter-wave Imaging Radiometer (MIR) data processing and the technical development of the first version of a water vapor retrieval algorithm. The algorithm is being used by NASA/GSFC Microwave Sensors Branch, Laboratory for Hydrospheric Processes. It is capable of a three dimensional mapping of moisture fields using microwave data from airborne sensor of MIR and spaceborne instrument of Special Sensor Microwave/T-2 (SSM/T-2). Author

N95-28014# Lawrence Livermore National Lab., Livermore, CA.

ADVANCES IN SCIENTIFIC VISUALIZATION

N. Max and R. Crawfis 11 Jan. 1995 6 p Presented at the SPIE '95: SPIE Conference on Optics, Electro-optics, and Laser Application in Science, Engineering and Medicine, San Jose, CA, 5-10 Feb. 1995
(Contract W-7405-eng-48)
(DE95-008065; UCRL-JC-119460; CONF-950226-24) Avail: CASI HC A02/MF A01

This paper discusses scientific visualization of scalar and vector fields, particularly relating to clouds and climate modeling. One cloud rendering method applies a 3-D texture to cloudiness contour surfaces, to simulate a view from outer space. The texture is advected by the wind flow, so that it follows the cloud motion. Another technique simulates multiple scattering of incident light from the sun and sky. This paper also presents a simulation of the microscopic cross-bridge motion which powers muscle contraction. It was rendered by ray-tracing contour surfaces of summed Gaussian ellipsoids approximating the actin and myosin protein shapes. DOE

N95-28191*# New Mexico Tech, Socorro, NM. Langmuir Lab. for Atmospheric Research.

A STUDY OF LIGHTNING IN WINTER THUNDERSTORMS AND THE ANALYSIS OF THUNDERSTORM OVERFLIGHT DATA Final Report, Oct. 1987 - Oct. 1994

Marx Brook 20 May 1995 13 p
(Grant NAG8-066)
(NASA-CR-198577; NAS 1.26:198577) Avail: CASI HC A03/MF A01

Thunderstorms and the activities associated with them was the emphasis of this final report. The primary goal of the investigation of the dynamics, microphysics, and the electrical properties of tropical thunderstorms, was to understand the process or processes which initiate the precipitation in various convective clouds. A concept that the degree of atmospheric instability that determines the updraft velocity is different between those storms that generate electrical activity and those that do not. This is apparent in temperate latitudes, but in tropical regions, little knowledge of these interactions is available. Several ground monitoring stations have been set up and, along with a waveform recorder at one of the stations, the data collected from these stations will be analyzed in conjunction with other data collected from ship and airborne radars and airborne in situ measurements of electrical activity in coordination with the TOGA-COARE program. CASI

N95-28236 Royal Netherlands Meteorological Inst., De Bilt (Netherlands).

NEURAL NETWORKS VERSUS LINEAR REGRESSION: RESEARCH INTO THE VALUE OF NEURAL NETWORKS IN METEOROLOGICAL PRACTICE [NEURALE NETWERKEN VERSUS LINEAIRE REGRESSIE: EEN ONDERZOEK NAAR DE WAARDE VAN NEURALE NETWERKEN IN DE METEOROLGISCHE PRAKTIJK]

R. M. Meuleman 1994 60 p In DUTCH
(ISSN 0169-1708)
(KNMI-TR-165; ISBN-90-369-2057-4) Copyright Avail: Issuing Activity (Royal Netherlands Meteorological Inst., Postbus 201, 3730 AE De Bilt, Wilhelminalaan 10, Netherlands)

Two neural networks and their theoretical backgrounds are described. In the first part of this report the neural networks are applied to an artificial linear regression problem, where the underlying regression is precisely known and where study and test data can be generated. In the second part these neural networks are applied to practical data from meteorological practice with a preponderant linear connection and a weak interaction between tow predictors. In the third part of the report the learning capability is investigated. This investigation concentrates especially on the characteristics of neural networks in comparison with classical statistics. Derived from text

N95-28237 Royal Netherlands Meteorological Inst., De Bilt (Netherlands).

THE PROGRAM FOR CALCULATING SUNSHINE DURATION FROM GLOBAL RADIATION [HET PROGRAMMA VOOR BEREKENING VAN ZONNESCHIJNDUUR UIT GLOBALE STRALING]

U. Bergman 1993 25 p In DUTCH
(ISSN 0169-1708)
(KNMI-TR-158; ISBN-90-369-2045-0) Copyright Avail: Issuing Activity (Royal Netherlands Metheorological Inst., Postbus 201, 3730 AE De Bilt, Wilhelminalaan 10, Netherlands)

For years the KNMI (Koninklijk Nederlands Meteorologisch Instituut) has entered hourly values of sunshine duration for a large number of Netherlands observation stations into a climatological database. These values serve as the basis for all kinds of climatological products. In particular these products involve overviews with daily, monthly, or yearly totals of sunshine duration for the stations. Until recently the Campbell-Stokes autograph served as the operational measuring instrument. The need for automatization arose with respect to the measurement of sunshine duration.

This need was prompted in large measure by the finding of the World Meteorological Organization (WMO) in 1989, when discussing the case of direct radiation of an area on a surface perpendicular to the sun's radiation exceeding a value of 120 W/sq m. Measurements using a Campbell-Stokes instrument in this connection were characterized as obsolete and not objective. It was obvious that a direct radiation meter was needed for the measurement of sunshine duration. It was decided to allow the calculation of sunshine duration from global radiation values. The Campbell-Stokes measurement net has been reduced to 11 locations. The Campbell-Stokes measurements will be continued for the present, with an eye to the comparison of the new method with the old. The data will be stored at the Climatological Service. Derived from text

N95-28340# Argonne National Lab., IL.

SITE SCIENTIFIC MISSION PLAN FOR THE SOUTHERN GREAT PLAINS CART SITE, JANUARY-JUNE 1995

J. M. Schneider (Oklahoma Univ., Norman, OK.), P. J. Lamb (Oklahoma Univ., Norman, OK.), and D. L. Sisterson Dec. 1994 62 p
(Contract W-31-109-eng-38)
(DE95-008393; ARM-95-001) Avail: CASI HC A04/MF A01

The Southern Great Plains (SGP) Cloud and Radiation Testbed (CART) site is designed to help satisfy the data needs of the Atmospheric Measurement (ARM) Program Science Team. This document defines the scientific priorities for site activities during the six months beginning on January 1, 1995, and also looks forward in lesser detail to subsequent six-month periods. The primary purpose of this Site Scientific Mission Plan is to provide guidance for the development of plans for site operations. It also provides information on current plans to the ARM functional teams (Management Team, Experiment Support Team (EST), Operations Team, Data Management Team (DMT), Instrument Team (IT), and Campaign Team) and serves to disseminate the plans more generally within the ARM Program and among the members of the Science Team. This document includes a description of the operational status of the site and the primary envisaged site activities, together with information concerning approved and proposed Intensive Observation Periods (IOPs). Amendments will be prepared and distributed whenever the content changes by more than 30% within a six-month period. The primary users of this document are the site operator, the site scientist, the Science Team through the ARM Program Science Director, the ARM Program Experiment Center, and the aforementioned ARM Program functional teams. This plan is a living document that will be updated and reissued every six months as the observational facilities are developed, tested, and augmented and as priorities are adjusted in response to developments in scientific planning and understanding. DOE

N95-28459 Naval Postgraduate School, Monterey, CA. Dept. of Meteorology.

SYSTEMATIC AND INTEGRATED APPROACH TO TROPICAL CYCLONE TRACK FORECASTING. PART 1: APPROACH OVERVIEW AND DESCRIPTION OF METEOROLOGICAL BASIS Interim Report, Jan. - Dec. 1994

Lester E. Carr, III and Russell L. Elsberry Jan. 1995 285 p Sponsored by the Office of Naval Research Marine Meteorology Program Limited Reproducibility: More than 20% of this document may be affected by microfiche quality
(AD-A291775; NPS-MR-94-002) Avail: Issuing Activity (Defense Technical Information Center (DTIC))

A systematic and integrated approach to tropical cyclone (TC) track forecasting is proposed. The approach is based on the premise that TC forecasters can improve upon dynamical track forecasts generated by numerical models and other objective guidance, if the forecasters are equipped with: (1) a meteorological knowledge base of conceptual models that organizes a wide array of scenarios into a relatively few recurring, dynamically-related situations; and (2) a knowledge base of numerical model TC forecast traits and objective aid traits that is organized around the meteorological knowledge base. The approach is systematic because it includes a methodology for consistently applying the two knowledge bases to generate the official track forecast. The approach is also integrated because the meteorological knowledge base includes motion-relevant characterizations of environment structure, characterizations of TC structure (intensity and size), and motion-affecting alterations of the environment structure caused by various interactions between the TC and the environment. DTIC

N95-28538# Sandia Labs., Albuquerque, NM.

MEASUREMENTS OF DAYTIME AND UPPER TROPOSPHERIC WATER VAPOR PROFILES BY RAMAN LIDAR

S. E. Bisson and J. E. M. Goldsmith 1995 4 p Presented at the 6th Optical Society of America (OSA) Meeting on Remote Sensing of the Atmosphere, Salt Lake City, UT, 6-9 Feb. 1995
(Contract DE-AC04-94AL-85000)
(DE95-007640; SAND-95-8503C; CONF-950277-2) Avail: CASI HC A01/MF A01

One of the most important atmospheric constituents needed for climate and meteorological studies is water vapor. Water vapor plays an important role in driving atmospheric circulations through latent heat release and in determining the earth's radiation budget, both through its radiative effects (water vapor is the major greenhouse gas) and cloud formation. The vertical distribution of water vapor is particularly important because it not only determines convective stability but radiative effects are also strongly altitude dependent. At present, considerable controversy exists over the nature of the vertical redistribution of water vapor in a changing climate, and particularly the distribution of water vapor in the upper troposphere. Understanding upper tropospheric moistening processes such as deep convection are therefore of prime importance in addressing the water vapor feedback question. A powerful, proven technique for the continuous measurement of nighttime water vapor profiles (in clear skies or up to the lowest cloud level) with high spatial and temporal resolution is Raman lidar. As part of the U.S. Department of Energy's (DOE) Atmospheric Radiation Measurement (ARM) program, a high performance dual field-of-view (fov), narrowband Raman lidar system capable of both daytime and nighttime operation has been developed. In this paper, the Sandia Raman lidar system is discussed along with its application to two problems of current interest: daytime tropospheric water vapor profile measurements and upper tropospheric water vapor. We present recent measurements of upper tropospheric moisture made at the DOE Cloud and Radiation Testbed site (CART) in Oklahoma. Recent daytime measurements are also presented. DOE

N95-28556# Sandia National Labs., Albuquerque, NM.

CLOUD CLASSIFICATION USING WHOLE-SKY IMAGER DATA

K. A. Buch, Jr. and Chen-Hui Sun 1995 7 p Presented at the 9th Symposium on Meterological Observations and Instrumentation, Charlotte, NC, 27-31 Mar. 1995
(Contract DE-AC04-94AL-85000)
(DE95-006501; SAND-95-8475C; CONF-9503104-1) Avail: CASI HC A02/MF A01

Clouds are one of the most important moderators of the earth radiation budget and one of the least understood. The effect that clouds have on the reflection and absorption of solar and terrestrial radiation is strongly influenced by their shape, size, and composition. Physically accurate parameterization of clouds is necessary for any general circulation model (GCM) to yield meaningful results. The work presented here is part of a larger project that is aimed at producing realistic three-dimensional (3D) volume renderings of cloud scenes, thereby providing the important shape information for parameterizing GCMs. The specific goal of the current study is to develop an algorithm that automatically classifies (by cloud type) the clouds observed in the scene. This information will assist the volume rendering program in determining the shape of the cloud. Much work has been done on cloud classification using multispectral satellite images. Most of these references use some kind of texture measure to distinguish the different cloud types and some also use topological features (such as cloud/sky connectivity or total number of clouds). A wide variety of classification methods has been used, including neural networks, various types of clustering, and thresholding. The work presented here utilizes binary decision trees to distinguish the different cloud types based on cloud feature vectors. DOE

N95-28577 Naval Research Lab., Monterey, CA.

SEVERE WEATHER GUIDE MEDITERRANEAN Final Report

Dennis C. Perryman, Richard D. Gilmore, and Ronald E. Englebretson Sep. 1994 45 p Limited Reproducibility: More than 20% of this document may be affected by microfiche quality
(AD-A289829; NRL/PU/7541-94-0016) Avail: Issuing Activity (Defense Technical Information Center (DTIC))

This handbook for the port of Istanbul, one in a series of severe weather guides for Mediterranean ports, provides decision-making guidance for ship captains whose vessels are threatened by actual or forecast strong winds, high seas, restricted visibility or thunderstorms in the port vicinity. Causes and effects of such hazardous conditions are discussed. Precautionary or evasive actions are suggested for various vessel situations. The handbook is organized in four sections for ready reference: general guidance on handbook content and use; a quick-look captain's summary; a more detailed review of general information on environmental conditions; and an appendix that provides oceanographic information. DTIC

N95-27389*# Science Applications International Corp., McLean, VA.
RECONSTRUCTION OF AN INFRARED BAND OF METEOROLOGICAL SATELLITE IMAGERY WITH ABDUCTIVE NETWORKS
Harvey A. Singer, John E. Cockayne, and Peter L. Versteegen *In* NASA. Goddard Space Flight Center, The 1995 Goddard Conference on Space Applications of Artificial Intelligence and Emerging Information Technologies May 1995 p 179-191 (For primary document see N95-27375 09-63)
(SAIC-94/1062) Avail: CASI HC A03/MF A03

N95-27666*# National Aeronautics and Space Administration. Goddard Space Flight Center, Greenbelt, MD.
LONG DURATION EXPOSURE FACILITY POST-FLIGHT DATA AS IT INFLUENCES THE TROPICAL RAINFALL MEASURING MISSION
Sharon A. Straka *In* NASA. Langley Research Center, LDEF: 69 Months in Space. Third Post-Retrieval Symposium, Part 3 Feb. 1995 p 1309-1318 (For primary document see N95-27629 09-99)
Avail: CASI HC A02/MF A04

N95-27971*# Pacific Northwest Lab., Richland, WA.
BASIC PRINCIPLES AND RECENT OBSERVATIONS OF ROTATIONALLY SAMPLED WIND
James R. Connell *In* DASCON Engineering, Collected Papers on Wind Turbine Technology May 1995 p 1-15 (For primary document see N95-27970 09-44)
(Contract DE-AC06-76LR-01830)
Avail: CASI HC A03/MF A03

N95-28307 Weather Squadron (45th), Patrick AFB, FL.
WEATHER HAZARDS TO A TITAN 4 ON-PAD DESTACK-RESTACK OPERATION
W. P. Roeder, J. B. Lorens, J. W. Weems, and B. F. Boyd *In* Johns Hopkins Univ., The 1994 JANNAF Safety and Environmental Protection Subcommittee Meeting, Volume 1 Aug. 1994 p 133-141 (For primary document see N95-28294 09-20)
Avail: CPIA, 10630 Little Patuxent Pkwy., Suite 202, Columbia, MD 21044-3200 HC

48 OCEANOGRAPHY

Includes biological, dynamic, and physical oceanography; and marine resources.

For related information see also *43 Earth Resources and Remote Sensing.*

N95-26406 Naval Research Lab., Bay Saint Louis, MS. Oceanography Div.
HINDCASTING WIND-DRIVEN ANOMALIES USING REDUCED-GRAVITY GLOBAL OCEAN MODELS WITH 1/2 DEG AND 1/4 DEG RESOLUTION Final Report
E. Joseph Metzger, Harley E. Hurlburt, Gregg A. Jacobs, and John C. Kindle 30 Sep. 1994 24 p Limited Reproducibility: More than 20% of this document may be affected by microfiche quality
(RM35G93)
(AD-A289060; NRL/FR/7323-93-9444) Avail: Issuing Activity (Defense Technical Information Center (DTIC))

Global versions of the Navy Layered Ocean Model are used to hindcast wind-driven oceanic anomalies. These versions are reduced-gravity with the lowest layer infinitely deep and at rest. Grid resolutions of 0.5 (1/2 deg) and 0.25 (1/4 deg) are used. Winds at the 1000-mbar level from the European Centre for Medium-Range Weather Forecasts are used as forcing functions for the models over the 1981-1990 time frame. The models' ability to reproduce wind-forced anomalies on intraseasonal to interannual time scales is studied by comparing the model solutions with various observational data sets. These include satellite altimetry, drifting buoys, and island/coastal sea-level stations. The effects of varying horizontal and vertical resolution are also investigated. The models are able to hindcast many of the wind-driven anomalies. The best correlation is found in the tropical regions where the oceanic response to atmospheric forcing is the most rapid. At midlatitudes, mesoscale flow instabilities are a major source of oceanic anomalies. However, the resolution of the global models used here is not adequate for these instabilities. In addition, the reduced gravity models lack the barotropic mode and the realistic bottom topography, both of which can play an important role in the flow instabilities. A technique that gives maps showing the fraction of variability in the hindcast that is deterministic (in response to atmospheric forcing) and the fraction that is not deterministic (due to flow instabilities) is also demonstrated. DTIC

N95-26419 Stanford Univ., CA. Solid State Electronics Lab.
JOINT SERVICES ELECTRONICS PROGRAM (JSEP) Final Report, 11 Jan. 1991 - 10 Jan. 1994
J. B. Harris 30 Jun. 1994 28 p Limited Reproducibility: More than 20% of this document may be affected by microfiche quality
(Contract DAAL03-91-C-0010)
(AD-A288299; ARO-28326.30-EL-JSEP) Avail: Issuing Activity (Defense Technical Information Center (DTIC))

This is the final report of the research conducted at Stanford Electronics Laboratories under the sponsorship of the Joint Services Electronics Program from January 11, 1991 through January 10, 1994. This report summarizes the area of publications and presentations. DTIC

N95-26420 Defence Research Establishment Atlantic, Dartmouth (Nova Scotia).
A GEO-ACOUSTIC AND OCEANOGRAPHIC DESCRIPTION OF SEVERAL SHALLOW WATER EXPERIMENTAL SITES ON THE SCOTIAN SHELF
John C. Osler Nov. 1994 49 p Limited Reproducibility: More than 20% of this document may be affected by microfiche quality
(AD-A288300; DREA-TM-94/216) Avail: Issuing Activity (Defense Technical Information Center (DTIC))

This technical memorandum provides a general description of the geo-acoustics and oceanography of the Scotian Shelf. Detailed descriptions are provided for three sites on the Scotian Shelf where the environment can be characterized on the basis of existing geophysical and oceanographic data.These sites will serve as archetypes for much broader regions of the Scotian Shelf with similar geo-acoustic settings. DTIC

N95-26430*# National Aeronautics and Space Administration. Goddard Space Flight Center, Greenbelt, MD.
SeaWIFS TECHNICAL REPORT SERIES. VOLUME 26: RESULTS OF THE SeaWIFS DATA ANALYSIS ROUND-ROBIN, JULY 1994 (DARR-1994)
Stanford B. Hooker, ed., Elaine R. Firestone, ed., David A. Siegel (California Univ., Santa Barbara, CA.), Margaret C. OBrien (California Univ., Santa Barbara, CA.), Jen C. Sorensen (California Univ., Santa Barbara, CA.), Daniel A. Konnoff (California Univ., Santa Barbara, CA.), Eric A. Brody (California Univ., Santa Barbara, CA.), James L. Mueller (San Diego State Univ., San Diego, CA.), Curtiss O. Davis (Naval Research Advisory Committee, Washington, DC.), and W. Joseph Rhea (Naval Research Advisory Committee, Washington, DC.) et al Feb. 1995 63 p
(NASA-TM-104566-Vol-26; Rept-95B00081-Vol-26; NAS 1.15:104566-Vol-26) Avail: CASI HC A04/MF A01

The accurate determination of upper ocean apparent optical properties (AOP's) is essential for the vicarious calibration of the sea-viewing wide field-of-view sensor (SeaWiFS) instrument and the validation of the derived data products. To evaluate the role that data analysis methods have upon values of derived AOP's, the first Data Analysis Round-Robin (DARR-94) workshop was sponsored by the SeaWiFS Project during 21-23 July, 1994. The focus of this intercomparison study was the estimation of the downwelling irradiance spectrum just beneath the sea surface, E(sub d)(0(sup -), lambda); the upwelling nadir radiance just beneath the sea surface, L(sub u)(0(sup -), lambda); and the vertical profile of the diffuse attenuation coefficient spectrum, K(sub d)(z, lambda). In the results reported here, different methodologies from four research groups were applied to an identical set of 10 spectroradiometry casts in order to evaluate the degree to which data analysis methods influence AOP estimation, and whether any general improvements can be made. The overall results of DARR-94 are presented in Chapter 1 and the individual methods of the four groups are presented in Chapters 2-5. The DARR-94 results do not show a clear winner among data analysis methods evaluated. It is apparent, however, that some degree of outlier rejection is required in order to accurately estimate L(sub u)(0(sup -), lambda) or E(sub d)(0(sup -), lambda). Furthermore, the calculation, evaluation and exploitation of confidence intervals for the AOP determinations needs to be explored. That is, the SeaWiFS calibration and validation problem should be recast in statistical terms where the in situ AOP values are statistical estimates with known confidence intervals. Author

N95-26477 Naval Postgraduate School, Monterey, CA. Dept. of Meteorology.

THE EFFECT OF INFRARED SEA SURFACE TEMPERATURE MEASUREMENTS ON EVAPORATION DUCT HEIGHT ESTIMATION

P. A. Frederickson, K. L. Davidson, and F. K. Jones 30 Nov. 1994 21 p Sponsored by Naval Oceanographic Office Limited Reproducibility: More than 20% of this document may be affected by microfiche quality (AD-A289045; NPS-MR-94-003) Avail: Issuing Activity (Defense Technical Information Center (DTIC))

In September 1994 personnel from the Naval postgraduate School (NPS) and the Naval Oceanographic Office (NavO) conducted an experiment off the coast of Mississippi to determine the accuracy of infrared sea surface temperature (SST) measurements made from a small boat1 and the effect of these measurements on estimating the evaporation duct height (z*). It was found that infrared SST measurements are highly accurate, agreeing closely with SST measurements made by other methods, and that a small relative error in the SST measurements can lead to large errors in z* estimates. However, it is difficult to predict the effect a given error in SST will have on the resulting z* estimate, due to the complex relationship between SST and z*. DTIC

N95-26483 Naval Postgraduate School, Monterey, CA.

TEMPORAL AND SPATIAL DECORRELATION SCALES OF THE YELLOW SEA THERMAL FIELDS M.S. Thesis

Susan K. Wells Sep. 1994 116 p Sponsored by Naval Oceanographic Office Limited Reproducibility: More than 20% of this document may be affected by microfiche quality
(AD-A288617) Avail: Issuing Activity (Defense Technical Information Center (DTIC))

Historically, studies on decorrelation scales have been conducted in the deep ocean waters. As the Navy shifts its interest toward the less understood shallow water regions, decorrelation scales need to be computed in order to use formerly deep water models such as the Optimum Thermal Interpolation System (OTIS) for shallow water regions such as the Yellow Sea. A data set containing over 35,000 temperature profiles from 1929 to 1991 was obtained from the Naval Oceanographic Office's MOODS data set. The winter and summer seasons provide realistic results. Winter has the smallest decorrelation scales of all the seasons, approximately 15 days and 165 km. Summer shows that there are different decorrelation scales between the surface and at depth. The surface has scales of 12.3 days and 251 km while at depth the scales are approximately 16.5 days and 163 km. An observational sampling network design is suggested for future sampling of the region. Spring and fall provide mixed results which may be due to the irregularities in time and space of the data set or to the very complex forcing mechanisms found in the region. Overall, this study gives a ground work for better refinement of decorrelation scales and thus, the ability to assess the conversion of deep water models to shallow water regions. DTIC

N95-26533* Washington Univ., Seattle, WA. Applied Physics Lab.

INFRARED FIELD MEASUREMENTS OF SEA SURFACE TEMPERATURE: ANALYSIS OF WAKE SIGNATURES AND COMPARISON OF SKIN LAYER MODELS

Christopher J. Zappa Aug. 1994 276 p Limited Reproducibility: More than 20% of this document may be affected by microfiche quality
(Contracts NAGw-2888; N00014-91-J-1951; N00014-93-1-1326)
(NASA-CR-197849; NAS 1.26:197849; AD-A288579; APL-UW-TR-9412)
Avail: Issuing Activity (Defense Technical Information Center (DTIC))

Infrared field measurements of ocean skin temperature made aboard the R/P FLIP in January of 1992 approximately 400 nautical miles off the coast of San Diego are presented. An extensive literature review accompanies these measurements probing the fundamentals of air-sea interaction, electromagnetics, and free-surface flows. A thin layer at the air-sea interface, known as the ocean skin layer, transfers heat by molecular conduction. The skin layer is on the order of a mm and typically 0.1 to 0.5 C cooler than the water just below for conditions of net heat flux from the ocean to the atmosphere. Two surface-piercing cables hanging from FLIP's port boom, each 1 cm in diameter, provided a disturbance of the skin layer mixing the warmer water from below up to the surface. Employing an infrared imager, we detected the temperature variations, tracked the signatures and quantified the spatial and thermal changes in time of these artificial disturbances, which were on the order of a meter. This unique method of visualizing turbulence at an air-water interface provides a direct measurement of the bulk-skin temperature difference. The recovery rate of the skin layer was found to be directly related to the level, or strength, of the disruption under low wind speed conditions (approximately 2 m/s). At moderate wind speeds (approximately 7 m/s), both the natural (breaking waves) and artificial (wakes) disturbances recovered within 2 s compared to an extrapolated recovery time of up to approximately 120 s under low wind speeds for the wake signatures. The difference is primarily a function of the net heat flux and sublayer thickness, which relate directly to the existing environmental conditions (e.g., turbulence intensity, sea state, wind speed). DTIC

N95-26647 Naval Postgraduate School, Monterey, CA.

DEEP CONVECTION IN THE MEDITERRANEAN SEA M.S. Thesis

Bernard H. Arata Sep. 1994 85 p Limited Reproducibility: More than 20% of this document may be affected by microfiche quality
(AD-A288497) Avail: Issuing Activity (Defense Technical Information Center (DTIC))

It is now understood that deep convection in the ocean plays a dominant role in determining the climate of the world's oceans. Recent theoretical advances in explaining oceanic convection need to be tested by real observations. Satellite observations of deep convection regions may be a promising new tool in studying this phenomenon. This thesis examines deep convection events in two ways: To assess the characteristic elements of a deep convection event using two different prediction models based upon the turbulent kinetic energy budget. To attempt to observe deep convection phenomena signals in altimeter data. In 1987, a deep convection event was observed in the northwestern Mediterranean Sea (Schott and Leaman 1991). These data, combined with GEOSAT altimeter data, were used to verify the Kraus and Turner and the Naval Postgraduate School mixed layer model predictions of the time evolution of temperature, salinity and mixed layer depth. Both models predicted final values similar to the observations, but model tuning was required to reproduce the observed rapid mixed-layer deepening. The interpolated altimeter field does not allow identification with confidence of the Mediterranean convection area. However, a locally persistent feature and the mean winter sea surface topography field agree with in-situ observations and do provide some indication about where and when the convection process occurs. DTIC

N95-26904 Massachusetts Inst. of Tech., Cambridge, MA.

CALCULATION OF SUSPENDED SEDIMENT TRANSPORT BY COMBINED WAVE-CURRENT FLOWS Final Report

Palitha N. Wikramanayake and Ole S. Madsen Nov. 1994 219 p Limited Reproducibility: More than 20% of this document may be affected by microfiche quality
(AD-A289368; WES/CR/DRP-94-7) Avail: Issuing Activity (Defense Technical Information Center (DTIC))

The objective of this study was to investigate the application of simple eddy viscosity models, developed for wave-current interaction, to the problem of sediment suspension and transport. A review of existing models is given; however, it is pointed out that all models compute suspended sediment transport by interacting the product of mean concentration and mean velocity. Because recent field experiments indicate that time-varying quantities may dominate the sediment flux due to mean components, the model described in this report calculates time-varying components of the concentration along with the mean flow component. The report describes the governing equations and boundary conditions, the process used to select an eddy viscosity model for hydrodynamics of wave-current interaction, and the determination of a resuspension coefficient. Detailed summaries of model development and the solution scheme are provided, as well as example calculations using the computer program WCSTRANS. A source listing of the computer model is included. DTIC

N95-27011 Woods Hole Oceanographic Inst., MA.
VERY LOW FREQUENCY SEISMO-ACOUSTIC NOISE BELOW THE SEA FLOOR (0.2-10 Hz) Ph.D. Thesis - MIT
Christopher Robert Bradley Feb. 1994 249 p Limited Reproducibility: More than 20% of this document may be affected by microfiche quality
(Contracts N00014-89-C-0018; N00014-89-J-1012; N00014-90-C-0098; N00014-90-J-1493; N00014-93-1-1352)
(AD-A289164; WHOI-94-09) Avail: Issuing Activity (Defense Technical Information Center (DTIC))

The sources and propagation of sub-seafloor microseismic noise between 0.2 and 10 Hz are investigated. There are two fundamental interface wave modes for noise propagation in the crust: the Stoneley and pseudo-Rayleigh wave. In soft bottoms only the Stoneley interface wave can exist. Longer wavelength noise propagates as Rayleigh and Stoneley modes of the ocean + crust waveguide. During the Low Frequency Acoustic Seismic Experiment (LFASE) a borehole array (SEABASS) was deployed in the Blake Bahama Basin in DSDP Hole 534B. The 0.3 Hz microseism peak is nearly invariant with depth at a level of 65 and 75 dB rel 1 (nm/s(exp 2))(exp 2)/Hz for the vertical and horizontal components respectively. At 100 m depth, the mean microseismic noise levels above 0.7 Hz are 10 dB and 15-20 dB quieter for the vertical and horizontal components respectively. Higher modes in the spectra show narrow bandwidth depth variability in the noise field. Particle motion analysis further verifies that noise propagates through the array as Rayleigh/Stoneley waves. Numerical modeling for hard and soft bottom environments shows that heterogeneities on the order of a seismic wavelength radiate energy into the water column and convert acoustic waves in the water into small wavelength Stoneley waves observed at the borehole. DTIC

N95-27043 Woods Hole Oceanographic Inst., MA.
OBSERVATIONS OF NEAR-BOTTOM FLOW IN A WAVE-DOMINATED NEARSHORE ENVIRONMENT Technical Report
J. J. Fredericks, John H. Trowbridge, and Yogesh C. Agrawal Feb. 1994 168 p Limited Reproducibility: More than 20% of this document may be affected by microfiche quality
(Contract N00014-92-J-12300)
(AD-A289331; WHOI-94-04) Avail: Issuing Activity (Defense Technical Information Center (DTIC))

To provide observational data for analysis of near-bottom, wave-induced flows, a downward-looking laser Doppler velocimeter (LDV) was deployed to profile the near-bed velocity structure of a six meter water column at a site just outside the surfzone off the coast of North Carolina. Ninety second 'snap-shots' of the velocity at six elevations below 20 cm above bottom were measured at 25 Hz while pressure was concurrently measured at 126 cm above bottom. The near-bottom data were supplemented with a benthic acoustic stress sensor (BASS) at approximately 20 cm above bottom which concurrently measured velocity components at 10 Hz. The purposes of this report are to document the collection, processing and archival of these data and to present the profiles for evaluation. DTIC

N95-27151 Woods Hole Oceanographic Inst., MA.
BIOLOGICAL/PHYSICAL MODELING OF UPPER OCEAN PROCESSES
Cabell S. Davis and John H. Steele Sep. 1994 72 p Limited Reproducibility: More than 20% of this document may be affected by microfiche quality
(Contract N00014-92-J-1527)
(AD-A289468; WHOI-94-32) Avail: Issuing Activity (Defense Technical Information Center (DTIC))

To enhance collaboration between researchers who model upper ocean biological/physical processes, a workshop was held at WHOI on June 7-12, 1993. The workshop was part of our on-going URIP project entitled 'Modeling Biological-Physical Interactions: A Population Biological Approach' sponsored by ONR (Grant N00014-92-J-1527). The two principal goals of the workshop were to: (1) identify critical Problems related to mixed-layer biological-physical models; and (2) develop approaches for solving these problems. The workshop was organized into two parts to address these goals. The first part, held over the first day and a half, included three overview presentations given in plenary followed by working groups, organized along disciplinary lines, to identify critical issues. The second part of the workshop consisted of working groups, organized across disciplines, using 'hands-on' modeling to address critical aspects of coupled biological-physical models. Several coupled models were presented and/or developed at the workshop addressing specific aspects of both the biological and physical dynamics. These aspects included the different mixed-layer formulations, a structured grazer population model, and an allometric food-web model including microbial-loop dynamics. DTIC

N95-27189 Naval Research Lab., Bay Saint Louis, MS. Oceanography Div.
STUDY OF THE RESPONSE OF A THREE-DIMENSIONAL COUPLED ICE-OCEAN MODEL TO DAILY VARYING ATMOSPHERIC FORCING Final Report
Shelley K. Riedlinger and Ruth H. Preller 28 Oct. 1994 31 p Sponsored by Naval Ocean Modeling and Prediction Program Limited Reproducibility: More than 20% of this document may be affected by microfiche quality
(ONR Proj. X05-13)
(AD-A289050; NRL/FR/7322-94-9601) Avail: Issuing Activity (Defense Technical Information Center (DTIC))

The Naval Research Laboratory developed a coupled ice-ocean model that simulates ice-ocean interactions in response to atmospheric forcing. This model couples the U.S. Navy's Polar Ice Prediction System ice model, which is based on the Hibler ice model, to a diagnostic version of the Bryan-Cox three-dimensional ocean circulation model. A 6-yr simulation was performed using daily atmospheric data from the Fleet Numerical Meteorology and Oceanography Center's Naval Operational Global Atmospheric Prediction System (NOGAPS) for the years 1986 through 1991. Interannual variability in most NOGAPS fields was large. Ice thickness and ice concentration changes responded directly to fluctuations in surface forcing fields. The thinnest ice of the simulation occurred in 1989, 1990, and 1991. In 1990 and 1991, the surface air temperatures were warm compared to the other years, but in 1989 the net longwave radiation from NOGAPS was anomalously large in the summer. In the summer, solar and sensible heat fluxes are the strongest forcing fields, and they add heat into the ice-ocean system causing ice to melt. In the fall, solar heating diminished and the combination of sensible plus latent fluxes, along with longwave radiation, caused a dramatic cooling that resulted in ice growth. In the winter, the sensible heat flux added heat into the system, but the combination of latent heat flux and longwave cooling dominated; the result was further ice growth. Winds have a pronounced effect on ice growth/melt by directly altering the sensible and latent heat fluxes and by indirectly affecting all heat fluxes by altering the distribution of ice cover and open water. Ice advection may account for more than half of the change in ice thickness in any given month when the winds are strong. DTIC

N95-27805*# Lamont-Doherty Geological Observatory, Palisades, NY.
[AN IN SITU EVALUATION OF TOPEX/POSEIDON ALTIMETRIC MEASUREMENTS VERSUS MEAUREMENTS MADE BY MOORINGS AND INVERTED ECHO SOUNDERS FOR SEA SURFACE HEIGHT] Final Report
[1994] 25 p
(Grants NAG5-2058; JPL-958123)
(NASA-CR-198621; NAS 1.26:198621) Avail: CASI HC A03/MF A01

The classical method of observing the sea surface height has been to make shipboard measurements of the vertical - density profile, and then calculating the surface height relative to a deeper reference surface. Two methods (a moored vertical string of instruments and an inverted echo sounder) were subsequently developed to obtain longer time in situ measurements. The first of these can be thought of as an extension of the discrete bottle hydrocast while the second integrates acoustically over the water column. One purpose of this note is to compare the result when coincidental observations are made by these two methods. This was done at two sites in the western tropical Pacific. Two inverted echo sounders were deployed alongside two enhanced TOGA-COARE moorings to be used in an in situ evaluation of TOPEX/Poseidon altimetric measurements of sea surface height. The mooring and inverted echo sounder data reproduced one another, at low frequency, with a correlation of 0.93 and 0.95 and the altimeter correlated with each of the above values ranging from 0.84 to 0.94. It is concluded that the altimetric measurements are

statistically equivalent to the in situ measurements in the area of study.
Derived from text

N95-27996# Finnish Geodetic Inst., Helsinki (Finland).
ON THE PERSISTENCE OF THE OCEANIC BACKGROUND OF APPARENT SEA LEVEL CHANGES IN THE BALTIC SEA
V. I. Bogdanov (Academy of Sciences, USSR, Moscow, USSR.), M. Yu. Medvedev (Academy of Sciences, USSR, Saint Petersburg, USSR.), and K. A. Taybatorov (Academy of Sciences, USSR, Moscow, USSR.) 1994 23 p
(ISSN 0355-1962)
(Rept-94:5; ISBN-951-711-181-9) Avail: CASI HC A03/MF A01

Evidence of the persistence of a time series representing the noise background of apparent (land uplift-caused) sea level changes in the Baltic Sea has been revealed. The results were obtained by analyzing tide-gauge data of the Stockholm and Kronstadt sea level stations provided by historical series for a 1.5-century period. The physical nature of this phenomenon and its significance were discussed in connection with geodetic studies. The necessity of performing similar calculations for all the sea level stations included in the observational network of the geodetic and geodynamic International 'Baltic Sea Level' Project as well as for coastal stations in the Danish Straits and North Sea was emphasized. Author

N95-28030*# National Aeronautics and Space Administration. Goddard Space Flight Center, Greenbelt, MD. Lab. for Hydrospheric Processes.
SeaWIFS TECHNICAL REPORT SERIES. VOLUME 27: CASE STUDIES FOR SeaWIFS CALIBRATION AND VALIDATION, PART 3
Stanford B. Hooker, ed., Elaine R. Firestone, ed. (General Sciences Corp., Laurel, MD.), James G. Acker, ed. (Hughes STX, Inc., Lanham, MD.), J. L. Mueller (San Diego State Univ., San Diego, CA.), R. S. Fraser, S. F. Biggar (Arizona Univ., Tucson, AZ.), K. J. Thome (Arizona Univ., Tucson, AZ.), P. N. Slater (Arizona Univ., Tucson, AZ.), A. W. Holmes (Santa Barbara Research Center, Goleta, CA.), and R. A. Barnes (ManTech, Inc., Wallops Island, VA.) et al May 1995 51 p
(NASA-TM-104566-Vol-27; 95B00084-Vol-27; NAS 1.15:104566-Vol-27)
Avail: CASI HC A04/MF A01

This document provides brief reports, or case studies, on a number of investigations sponsored by the Calibration and Validation Team (CVT) within the Sea-viewing Wide Field-of-view Sensor (SeaWiFS) Project. Chapter I describes a comparison of the irradiance immersion coefficients determined for several different marine environmental radiometers (MERs). Chapter 2 presents an analysis of how light absorption by atmospheric oxygen will influence the radiance measurements in band 7 of the SeaWiFS instrument. Chapter 3 gives the results of the second ground-based solar calibration of the instrument, which was undertaken after the sensor was modified to reduce the effects of internal stray light. (The first ground-based solar calibration of SeaWiFS is described in Volume 19 in the SeaWiFS Technical Report Series.) Chapter 4 evaluates the effects of ship shadow on subsurface irradiance and radiance measurements deployed from the deck of the R/V Weatherbird 11 in the Atlantic Ocean near Bermuda. Chapter 5 illustrates the various ways in which a single data day of SeaWiFS observations can be defined, and why the spatial definition is superior to the temporal definition for operational usage. Author

N95-28096 Woods Hole Oceanographic Inst., MA.
TOMOGRAPHIC OBSERVATIONS OF DEEP CONVECTION AND THE THERMAL EVOLUTION OF THE GREENLAND SEA GYRE 1988-1989 Ph.D. Thesis - MIT
Ryszard A. Pawlowicz Feb. 1994 175 p Limited Reproducibility: More than 20% of this document may be affected by microfiche quality
(Contracts N00014-92-J-1291; N00014-91-J-1246)
(AD-A289104; WHOI-94-08) Avail: Issuing Activity (Defense Technical Information Center (DTIC))

The Greenland Sea Gyre is studied using results from the 1988-89 Greenland Sea Tomography Experiment. Thermal evolution of the gyre center divides into three periods: a preconditioning phase, a deep mixing phase, and a restratification phase. During preconditioning, ice forms and rejects brine into the surface waters, enabling destabilization of the water column. The onset of the deep mixing phase occurs after ice formation in the gyre center stops, resulting in an area of open water where large heat fluxes can occur. In surrounding regions, including the odden region to the south, ice is still being formed, and the mixed layer does not deepen significantly. The effects of advection are deduced from heat and salt budgets, and appear to be important only during the restratification phase for intermediate depths, and only during the summer for the surface waters. Dynamical processes for bringing the Arctic Intermediate Water (AIW) to the surface in order to form deep water are not needed in this scenario, rather the surface waters are modified until they match the density of the AIW after which surface cooling drives convection. DTIC

51 LIFE SCIENCES (GENERAL)

N95-26360 Tennessee Univ., Memphis, TN. Dept. of Anatomy and Neurobiology.
[RESEARCH ACTIVITIES ON SOMATOSENSORY (SI) CORTICAL NEURONS] Annual Report, 1 Jul. 1993 - 30 Jun. 1994
Randall J. Nelson 21 Nov. 1994 84 p Limited Reproducibility: More than 20% of this document may be affected by microfiche quality
(Grant AF-AFOSR-0333-91)
(AD-A288794; AF-AFOSR-0763-94-TR) Avail: Issuing Activity (Defense Technical Information Center (DTIC))

Three research goals were accomplished during this third year. (1) Analysis of data indicated that the responsiveness of primary somatosensory (SI) cortical neurons is 'unattended' if when behavioral conditions become unpredictable. This observation fits with the hypothesis that during stereotyped behavior, neuronal responsiveness is gated so that the CNS may partially engage in other activities. (2) SI cortical neurons that respond to vibratory go-cues for wrist movement with the greatest fidelity have their activity modulated just prior to movement onset. This observation fits with the hypothesis that prior to active movement, sensory inputs that are no longer behaviorally relevant are gated so as not to interfere with monitoring movement parameters by the primate CNS. (3) SI cortical neurons that may bind together other SI neurons with their rhythmic activity have this activity disrupted at go-cue onset and just prior to movement onset. This observation fits with the hypothesis that prior to behaviorally significant events, the activity of these neurons that may tonically gate other SI neurons is suppressed to allow the monitoring sensory events and the initiation of movements. DTIC

N95-26435 Kansas State Univ., Manhattan, KS. Dept. of Pathology and Microbiology.
ANTI-IDIOTYPE PROBES FOR TOXIN DETECTION Final Report, 15 Sep. 1989 - 14 Oct. 1994
John J. Iandolo and S. K. Chapes 8 Nov. 1994 373 p Limited Reproducibility: More than 20% of this document may be affected by microfiche quality
(Contract DAMD17-89-Z-9039)
(AD-A288955) Avail: Issuing Activity (Defense Technical Information Center (DTIC))

This study was designed to investigate the interaction of staphylococcal enterotoxins and exfoliative toxins with leukocytes and to establish baseline information on the consequences of those interactions. Receptor-ligand interactions were characterized and a new non-major histocompatibility complex (MHC) class 2 receptor on the surface of macrophages was discovered. Once these data were at hand, we also prepared an anti-idiotype antibody to class 2 MHC and have used it to inhibit interaction of toxins with their cognate receptor on macrophage surfaces. These studies have resulted in the publication of 31 manuscripts and 7 published abstracts.
DTIC

N95-26573 North Carolina State Univ., Raleigh, NC.
BIOCHEMICALLY VULNERABLE SITES FOR ANTIFUNGAL INTERCESSION IN THE CONTROL OF FUNGAL GROWTH Final Report, 1 May 1991 - 30 Apr. 1994
L. W. Parks 26 Aug. 1994 4 p Limited Reproducibility: More than 20% of this document may be affected by microfiche quality
(Contract DAAL03-89-D-0003)
(AD-A288345; ARO-29097.3-LS) Avail: Issuing Activity (Defense Technical Information Center (DTIC))

Virtually every antifungal agent in use intercedes some aspect of sterol synthesis or function. Ergosterol is the principal sterol in fungi, while cholesterol is the most abundant sterol in vertebrates. Research in our laboratory has shown that the structural differences in ergosterol, in comparison to cholesterol, have distinctive biochemical and physiological effects in fungi. Under the completed contract we have shown that as the sterol composition of sterol auxotrophic strains of Saccharomyces cerevisiae is altered there is disturbance of the mating efficiency of the strains. The normal sterol, ergosterol, mediates a 30-fold higher productive mating efficiency in the auxotrophs than when the cells are supplied with stigmasterol. Using electron and visible microscopy, we have shown that the mated pairs in stigmasterol remained adherent but prezygotic even after 12 hours incubation. Ergosterol rescued the cells and permitted zygote formation. Based on those experiments it was clear that membrane fusion was perturbed by sterol alterations. Continuing work with the renewal grant is focusing on membrane fusion in various normal cell biological processes. DTIC

N95-26597# Swedish Radiation Protection Inst., Stockholm (Sweden).
RADIATION IN EVERYDAY LIFE
Jack Valentin 1993 9 p Presented at the Regional Seminar on Nuclear Energy, A New Energy for Development, Shanghai, China, 1-3 Nov. 1993
(DE95-604111; INIS-MF-14307; CONF-9311250) Avail: CASI HC A02/MF A01 (US Sales Only)

The presentation attempts to provide brief answers to the following questions: what is the cause of radiation? How much radiation are we exposed to? How dangerous is radiation? DOE

N95-26608 Scripps Research Inst., La Jolla, CA.
COFACTOR-ASSISTED ANTIBODY CATALYSIS Final Report, 1 Sep. 1991 - 31 Aug. 1994
Donald Hilvert 31 Aug. 1994 47 p Limited Reproducibility: More than 20% of this document may be affected by microfiche quality
(Contract N00014-93-MP-24023)
(AD-A288929) Avail: Issuing Activity (Defense Technical Information Center (DTIC))

This report describes progress made toward the development of cofactor-assisted catalytic antibodies. The development of facile immunoassays for screening large numbers of potential catalysts directly for catalytic activity and their application to libraries of RNA receptors are also discussed. DTIC

N95-26727*# Legacy Good Samaritan Hospital, Portland, OR. Neurological Sciences Inst.
COMPARATIVE TRANSDUCTION MECHANISMS OF VESTIBULAR OTOLITH HAIR CELLS Annual Report, 1 Jan. - 31 Dec. 1994
Richard A. Baird 31 Dec. 1994 90 p
(Contract NCC2-651)
(NASA-CR-197980; NAS 1.26:197980) Copyright Avail: CASI HC A05/MF A01

Hair cells in the bullfrog vestibular otolith organs regenerate following aminoglycoside ototoxicity. Hair cells in these organs are differentially sensitive to gentamicin, with saccular hair cells and hair cells in the utricular striola being damaged at lower gentamicin concentrations than hair cells in the utricular extrastriola. Regenerating hair cells in these organs have short hair bundles and can be classified into a number of phenotypes using the same morphological criteria used to identify their mature counterparts. Our studies suggest that some supporting cells can convert, or transdifferentiate,into hair cells without an intervening cell division. By stimulating these processes in humans, clinicians may be able to alleviate human deafness and peripheral vestibular disorders by regenerating and replacing lost hair cells. In vivo and in vitro studies were done on cell proliferation and hair cell regeneration. For individual titles, see N95-26728 through N95-26732.

N95-26728*# Legacy Good Samaritan Hospital, Portland, OR. Neurological Sciences Inst.
REGIONAL DIFFERENCES IN LECTIN BINDING PATTERNS OF VESTIBULAR HAIR CELLS
Richard A. Baird, N. R. Schuff, and J. Bancroft *In its* Comparative Transduction Mechanisms of Vestibular Otolith Hair Cells 31 Dec. 1994 13 p Repr. from Hearing Research (New York, NY, Elsevier Science Publishers B.V.), v. 65, 1993 p 151-163 Sponsored by National Inst. of Deafness and Communicative Disorders, and Oregon Lions Sight and Hearing Foundation (For primary document see N95-26727 09-51)
(ISSN 0378-5955)
Avail: CASI HC A03/MF A01

Surface glycoconjugates of hair cells and supporting cells in the vestibular endorgans of the bullfrog were identified using biotinylated lectins with different carbohydrate specificities. Lectin binding in hair cells was consistent with the presence of glucose and mannose (CON A), galactose (RCA-I), N-acetylgalactosamine (VVA), but not fucose (UEA-I) residues. Hair cells in the bullfrog sacculus, unlike those in the utriculus and semicircular canals, did not stain for N-acetylglucosamine (WGA) or N-acetylgalactosamine (VVA). By contrast, WGA and, to a lesser extent, VVA, differentially stained utricular and semicircular canal hair cells, labeling hair cells located in peripheral, but not central, regions. In mammals, WGA uniformly labeled Type 1 hair cells while labeling, as in the bullfrog, Type 2 hair cells only in peripheral regions. These regional variations were retained after enzymatic digestion. We conclude that vestibular hair cells differ in their surface glycoconjugates and that differences in lectin binding patterns can be used to identify hair cell types and to infer the epithelial origin of isolated vestibular hair cells. Author

N95-26729*# Legacy Good Samaritan Hospital, Portland, OR. Neurological Sciences Inst.
HAIR CELL REGENERATION IN THE BULLFROG VESTIBULAR OTOLITH ORGANS FOLLOWING AMINOGLYCOSIDE TOXICITY
Richard A. Baird, M. A. Torres, and N. R. Schuff *In its* Comparative Transduction Mechanisms of Vestibular Otolith Hair Cells 31 Dec. 1994 11 p Repr. from Hearing Research (New York, NY, Elsevier Science Publishers B.V.), v. 65, 1993 p 164-174 Sponsored by National Inst. of Deafness and communicative Disorders, and Oregon Lions Sight and Hearing Foundation (For primary document see N95-26727 09-51)
Avail: CASI HC A01/MF A01

Adult bullfrogs were given single intraotic injections of the aminoglycoside antibiotic gentamicin sulfate and sacrificed at postinjection times ranging from 0.5 to 9 days. The saccular and utricular maculae of normal and injected animals were examined in wholemount and cross-section. Intraotic 200 (mu) M gentamicin concentrations resulted in the uniform destruction of the hair bundles and, at later times, the cell bodies of saccular hair cells. In the utriculus, striolar hair cells were selectively damaged while extrastriolar hair cells were relatively unaffected. Regenerating hair cells, identified in sectioned material by their small cell bodies and short, well-formed hair bundles, were seen in the saccular and utricular maculae as early as 24-48 h postinjection. Immature versions of mature hair cell types in both otolith organs were recognized by the presence of absence of a bulbed kinocilia and the relative lengths of their kinocilia and longest sterocilia. Utricular hair cell types with kinocilia longer than their longest stereocilia were observed at earlier times than hair cell types with shorter kinocilia. In the same sacculus, the hair bundles of gentamicin-treated animals, even at 9 days postinjection, were significantly smaller than those of normal animals. The hair bundles of utricular hair cells, on the other hand, reached full maturity within the same time period. Author

N95-26730*# Legacy Good Samaritan Hospital, Portland, OR. Dept. of Neuro-otology.
PERIPHERAL INNERVATION PATTERNS OF VESTIBULAR NERVE AFFERENTS IN THE BULLFROG UTRICULUS
Richard A. Baird and N. R. Schuff *In its* Comparative Transduction Mechanisms of Vestibular Otolith Hair Cells 31 Dec. 1994 20 p Repr. from The Journal of Comparative Neurology (New York, NY, Wiley-Liss, Inc.), v. 342, 1994 p 279-298 Sponsored by National Inst. of Deafness and Communicative Disorders, and Oregon Lions Sight and Hearing Foundation (For primary document see N95-26727 09-51)
Avail: CASI HC A03/MF A01

Vestibular nerve afferents innervating the bullfrog utriculus differ in their response dynamics and sensitivity to natural stimulation. They also supply hair cells that differ markedly in hair bundle morphology. To examine the peripheral innervation patterns of individual utricular afferents more closely, afferent fibers were labeled by the extracellular injection of horseradish peroxidase (HRP) into the vestibular nerve after sectioning the vestibular nerve medial to Scarpa's ganglion to allow the degeneration of sympathetic and efferent fibers. The peripheral arborizations of individual afferents were then correlated with the diameters of their parent axons, the regions of the macula they innervate, and the number and type of hair cells they supply. The utriculus is divided by the striola, a narrow zone of distinctive morphology, into media and lateral parts. Utricular afferents were classified as striolar or extrastriolar according to the epithelial entrance of their parent axons and the location of their terminal fields. In general, striolar afferents had thicker parent axons, fewer subepithelial bifurcations, larger terminal fields, and more synaptic endings than afferents in extrstriolar regions. Afferents in a juxtastriolar zone, immediately adjacent to the medial striola, had innervation patterns transitional between those in the striola and more peripheral parts of the medial extrastriola. moast afferents innervated only a single macular zone. The terminal fields of striolar afferents, with the notable exception of a few afferents with thin parent axons, were generally confined to one side of the striola. Hair cells in the bullfrog utriculus have perviously been classified into four types based on hair bundle morphology. Afferents in the extrastriolar and juxtastriolar zones largely or exclusively innervated Type B hair cells, the predominant hair cell type in the utricular macula. Striolar afferents supplied a mixture of four hair cell types, but largely contacted Type B and Type C hair cells, particularly on the outer rows of the medial striola. Afferents supplying more central striolar regions innervated fewer Type B and larger numbers of Type E and Type F hair cells. Striolar afferents with thin parent axons largely supplied Type E hair cells with bulbed kniocilia in the innermost striolar rows. Author

N95-26731*# Legacy Good Samaritan Hospital, Portland, OR. Dept. of Neuro-otology.

COMPARATIVE TRANSDUCTION MECHANISMS OF HAIR CELLS IN THE BULLFROG UTRICULUS. 1: RESPONSES TO INTRACELLULAR CURRENT

Richard A. Baird *In its* Comparative Transduction Mechanisms of Vestibular Otolith Hair Cells 31 Dec. 1994 19 p Repr. from Journal of Neurophysiology (Bethesda, MD, The American Physiological Society), v. 71, no. 2, Feb. 1994 p 666-683 Sponsored by National Inst. of Deafness and Communicative Disorders, and Oregon Lions Sight and Hearing Foundation (For primary document see N95-26727 09-51)
Avail: CASI HC A03/MF A01

Hair cells in the bullfrog sacculus are specifically adapted to sense small-amplitude, high-frequency linear accelerations. These hair cells display many properties that are undesirable or inappropriate for hair cells that must provide static gravity sensitivity. This study resulted in part due to an interest in seeing how the transduction mechanisms of hair cells in a gravity-sensing otolith endorgan would differ from those in the bullfrog sacculus. The bullfrog utriculus is an appropriate model for these studies, because its structure is representative of higher vertebrates in general and its function as a sensor of static gravity and dynamic linear acceleration is well known. Hair cells in the bullfrog utriculus, classifiable as Type 2 by cell body and synapse morphology, differ markedly in hair bundle morphology from those in the bullfrog sacculus. Moreover, the hair bundle morphologies of utricular hair cells, unlike those in the sacculus, differ in different membrane regions. Derived from text

N95-26732*# Legacy Good Samaritan Hospital, Portland, OR. Dept. of Neuro-otology.

COMPARATIVE TRANSDUCTION MECHANISMS OF HAIR CELLS IN THE BULLFROG UTICULUS. 2: SENSITIVITY AND RESPONSE DYNAMICS TO HAIR BUNDLE DISPLACEMENT

Richard A. Baird *In its* Comparative Transduction Mechanisms of Vestibular Otolith Hair Cells 31 Dec. 1994 21 p Repr. from Journal of Neurophysiology (Bethesda, MD, The American Physiological Society), v. 71, no. 2, Feb. 1994 p 685-705 Sponsored by National Inst. of Deafness and Communicative Disorders, and Oregon Lions Sight and Hearing Foundation (For primary document see N95-26727 09-51)
Avail: CASI HC A03/MF A01

The present study was motivated by an interest in seeing whether hair cell types in the bullfrog utriculus might differ in their voltage responses to hair bundle displacement. Particular interest was in assessing the contributions of two factors to the responses of utricular hair cells. First, interest in examining the effect of hair bundle morphology on the sensitivity of hair cells to natural stimulation was motivated by the observation that vestibular hair cells, unlike many auditory hair cells, are not free-standing but rather linked to an accessory cupular or otolithic membrane via the tip of their kinocilium. Interest also laid in examining the contribution, if any, of adaptation to the response properties of utricular hair cells. Hair cells in auditory and vibratory inner ear endorgans adapt to maintained displacements of their hair bundles, sharply limiting their low frequency sensitivity. This adaptation is mediated by a shift in the displacement-response curve (DRC) of the hair cell along the displacement axis. Observations suggest that the adaptation process occurs within the hair bundle and precedes mechanoelectric transduction. Recent observations of time-dependent changes in hair bundle stiffness are consistent with this conclusion. Adaptation would be expected to be most useful in inner ear endorgans in which hair cells are subject to large static displacements that could potentially saturate their instantaneous response and compromise their sensitivity to high frequency stimulation. The adaptation process also permits hair cells to maintain their sensory hair bundle in the most sensitive portion of their DRC. In vestibular otolith organs in which static sensitivity is desirable, any adaptation process in the hair cells may be undesirable. The rate and extent of the decline of the voltage responses was measured of utricular hair cells to step and sinusoidal hair bundle displacements. Then for similar resting potentials and response amplitudes, the voltage responses of individual hair cells were compared to both hair bundle displacement and intracellular current. Derived from text

N95-26761 Arizona Univ., Tucson, AZ.

A MODEL OF THE NEURAL BASIS OF THE RAT'S SENSE OF DIRECTION

William E. Skaggs, James J. Knierim, and Hemant S. Kudrimoti 1994 8 p Limited Reproducibility: More than 20% of this document may be affected by microfiche quality
(AD-A289678) Avail: Issuing Activity (Defense Technical Information Center (DTIC))

In the last decade the outlines of the neural structures subserving the sense of direction have begun to emerge. Several investigations have shed light on the effects of vestibular input and visual input on the head direction representation. In this paper, a model is formulated of the neural mechanisms underlying the head direction system. The model is built out of simple ingredients, depending on nothing more complicated than connectional specificity, attractor dynamics, Hebbian learning and sigmoidal nonlinearities, but it behaves in a sophisticated way and is consistent with most of the observed properties of real head direction cells. In addition it makes a number of predictions that ought to be testable by reasonably straightforward experiments. DTIC

N95-27097 Seattle City Light, WA.

DIAGNOSTIC ANTIGENS OF LEISHMANIA Final Report

Steven G. Reed 31 Jan. 1994 20 p Limited Reproducibility: More than 20% of this document may be affected by microfiche quality
(Contract DAMD17-92-C-2082)
(AD-A288805) Avail: Issuing Activity (Defense Technical Information Center (DTIC))

We report herein the cloning, expression, and seroreactivity of three Leishmania tropica antigens. By ELISA analysis, the majority of confirmed and suspected viscerotropic leishmaniasis patients had significantly higher levels of specific antibody against two of the three recombinant antigens and the repeat portion of one of the antigens, named Lt-Ir, when compared to sera from normal controls. The molecular characterization of these two antigens demonstrated that these are adjacent portions of the same gene and that the repeat portion contains one of the immunodominant epitopes. In addition, this gene was shown to be conserved in all strains of L. tropica parasites recovered from Gulf War participants. The gene does not appear to be highly conserved among all species of Leishmania. Collectively, the data indicate the potential for these antigens to assist in the diagnosis of individuals with viscerotropic leishmamasis. DTIC

N95-27100 Arizona Univ., Tucson, AZ. Research Lab.

HIPPOCAMPAL PLACE FIELDS, THE INTERNAL COMPASS, AND THE LEARNING OF LANDMARK STABILITY

James J. Knierim, Hemant S. Kudrimoti, and Bruce L. McNaughton 16 May 1994 48 p Limited Reproducibility: More than 20% of this document may be affected by microfiche quality
(Contract N00014-90-J-1869)
(AD-A289406) Avail: Issuing Activity (Defense Technical Information Center (DTIC))

Previous studies have shown that hippocampal place fields are controlled by the salient sensory cues in the environment, in that rotation of the cues causes an equal rotation of the place fields. We trained rats to forage for food pellets in a gray cylinder with a single salient directional cue, a white card covering 900 of the wall. Half of the rats were disoriented before being placed in the cylinder, in order to disrupt their internal sense of direction. The other half were not disoriented before being placed in the cylinder; for these rats, there was presumably a consistent relationship between the cue card and their internal direction sense. We subsequently recorded hippocampal place cells and thalamic head direction cells from both groups of rats as they moved in the cylinder, between some sessions the cylinder and cue card were rotated to a new direction. All rats were disoriented before recording. Under these conditions, the cue card had much weaker control over the place fields and head direction cells in the rats that had been disoriented during training than in the rats that had not been disoriented. For the former group, the place fields often rotated relative to the cue card or completely changed their firing properties between sessions. In all recording sessions, the head direction cells and place cells were strongly coupled. It appears that the strength of cue control over place cells and head direction cells depends on the rat's learned perception of the stability of the cues. DTIC

N95-27254# International Centre for Theoretical Physics, Trieste (Italy).
THE ELECTRICAL BEHAVIOUR OF AN EXCITABLE CELL AT DIFFERENT CONDITIONS
M. El-Sayed and A. M. Mohammed Aug. 1994 23 p
(DE95-607911; IC-94/232) Avail: CASI HC A03/MF A01

The Hodgkin-Huxley, H-H, model has been modified, in this work, to study the electrical behaviour of an excitable cell due to changes in the permeability of K and Na ions (g(sub k) and g(sub Na)), the simultaneous stochastic variations of g(sub k) and g(sub Na), the current stimulus (Jstim) and the non-inactivation of Na-channel (NI - NaC). The amplitude and duration of the generated action potential (AP) was found to increase as g(sub k) increases, with the appearance of repetitive AP spikes in the range of 21.5 (greater than or equal to) g(sub k) (greater than or equal to) 3.5 while the K- and Na-currents (J(sub k) and J(sub Na)) showed a pronounced decrease. On the other hand, the increase of g(sub Na) was accompanied by an increase in AP amplitudes and durations and also in J(sub k) and J(sub Na) with the appearance of a repetitive AP at 1400 (greater than or equal to) g(sub Na) (greater than or equal to) 189 ms/sq cm whose frequency increases with the increase of g(sub Na). Moreover, the stochastic variations in g(sub k) and g(sub Na) could generate a repetitive AP whose frequency could be changed either by changing the values of g(sub k) or g(sub Na) or both, and may represent an information carried by the sensory cells for example. The electrical behaviour of the simulated cell can also be affected by Jstim at different values of g(sub k) except at the range of 21.5 (greater than or equal to) g(sub k) (greater than or equal to) 3.5 ms/sq cm and also depended on NI - NaC fraction. DOE

N95-27329*# Benson (Robert H.), Springfield, VA.
MICROGRAVITY SCIENCES BIOTECHNOLOGY FACILITY ASSESSMENT Final Report, 15 Feb. - 29 Mar. 1995
Robert H. Benson 29 Mar. 1995 48 p
(NASA Order H-24601-D)
(NASA-CR-196602; NAS 1.26:196602; MSFC-2) Avail: CASI HC A03/MF A01

This report provides an assessment of the risks of the Biotechnology Facility being developed at the Johnson Space Center for flight on the International Space Station. The assessment includes technical status, schedules, budgets, project management, performance of facility relative to science requirements, and identifies risks and issues that need to be considered in future development activities. Author

N95-27725# Lawrence Livermore National Lab., Livermore, CA.
AUTOMATED INTEGRATION OF GENOMIC PHYSICAL MAPPING DATA VIA PARALLEL SIMULATED ANNEALING
T. Slezak Jun. 1994 19 p Presented at the 3d International Conference on Bioinformatics and Genome Research, Tallahassee, FL, 1-4 Jun. 1994
(Contract W-7405-eng-48)
(DE95-008057; UCRL-JC-117666; CONF-9406311-1) Avail: CASI HC A03/MF A01

The Human Genome Center at the Lawrence Livermore National Laboratory (LLNL) is nearing closure on a high-resolution physical map of human chromosome 19. We have build automated tools to assemble 15,000 fingerprinted cosmid clones into 800 contigs with minimal spanning paths identified. These islands are being ordered, oriented, and spanned by a variety of other techniques including: Fluorescence Insitu Hybridization (FISH) at 3 levels of resolution, ECO restriction fragment mapping across all contigs, and a multitude of different hybridization and PCR techniques to link cosmid, YAC, AC, PAC, and PI clones. The FISH data provide us with partial order and distance data as well as orientation. We made the observation that map builders need a much rougher presentation of data than do map readers; the former wish to see raw data since these can expose errors or interesting biology. We further noted that by ignoring our length and distance data we could simplify our problem into one that could be readily attacked with optimization techniques. The data integration problem could then be seen as an M x N ordering of our N cosmid clones which 'intersect' M larger objects by defining ' intersection' to mean either contig/map membership or hybridization results. Clearly, the goal of making an integrated map is now to rearrange the N cosmid clone 'columns' such that the number of gaps on the object 'rows' are minimized. Our FISH partially-ordered cosmid clones provide us with a set of constraints that cannot be violated by the rearrangement process. We solved the optimization problem via simulated annealing performed on a network of 40+ Unix machines in parallel, using a server/client model built on explicit socket calls. For current maps we can create a map in about 4 hours on the parallel net versus 4+ days on a single workstation. Our biologists are now using this software on a daily basis to guide their efforts toward final closure. DOE

N95-27948# Argonne National Lab., IL.
ENERGY TRANSFER IN REAL AND ARTIFICIAL PHOTOSYNTHETIC SYSTEMS
J. C. Hindman, J. E. Hunt, and J. J. Katz 1995 23 p
(Contract W-31-109-eng-38)
(DE95-005824; ANL/CHM/PP-80864) Avail: CASI HC A03/MF A01

Fluorescence emission from the photosynthetic organisms Tribonema aequale, Anacystis nidulau, and Chlorella vulgais and from some chlorophyll model systems have been recorded as a function of excitation wavelength and temperature. Considerable similarity was observed in the effects of excitation wavelength and temperature on the fluorescence from intact photosynthetic organisms and the model systems. The parallelism in behavior suggest that self-assembly processes may occur in both the in vivo and in vitro systems that give rise to chlorophyll species at low temperature that may differ significantly from those present at ambient temperatures. DOE

N95-28177*# California Univ., Berkeley. Lawrence Berkeley Lab, CA.
MUTAGENESIS IN HUMAN CELLS WITH ACCELERATED H AND Fe IONS Final Report, May 1991 - Apr. 1994
Amy Kronenberg Apr. 1994 12 p
(NASA Order T-9309-R)
(NASA-CR-198599; NAS 1.26:198599) Avail: CASI HC A03/MF A01

The overall goals of this research were to determine the risks of mutation induction and the spectra of mutations induced by energetic protons and iron ions at two loci in human lymphoid cells. During the three year grant period the research has focused in three major areas: (1) the acquisition of sufficient statistics for human TK6 cell mutation experiments using Fe ions (400 MeV/amu), Fe ions (600 MeV/amu) and protons (250 MeV/amu); (2) collection of thymidine kinase- deficient (tk) mutants or hypoxanthine phosphoribosyltransferase deficient (hprt) mutants induced by either Fe 400 MeV/amu, Fe 600 MeV/amu, or H 250 MeV/amu for subsequent molecular analysis; and (3) molecular characterization of mutants isolated after exposure to Fe ions (600 MeV/amu). As a result of the shutdown of the BEVALAC heavy ion accelerator in December 1992, efforts were rearranged somewhat in time to complete our dose-response studies and to complete mutant collections in particular for the Fe ion beams prior to the shutdown. These goals have been achieved. A major effort was placed on collection, re-screening, and archiving of 3 different series of mutants for the various particle beam exposures: tk-ng mutants, tk-sg mutants, and hprt-deficient mutants. Where possible, groups of mutants were isolated for several particle fluences. Comparative analysis of mutation spectra has occured with characterization of the mutation spectrum for hprt-deficient mutants obtained after exposure of TK6 cells to Fe ions (600 MeV/amu) and a series of spontaneous mutants. Author

N95-28496# International Society for Photogrammetry, London (England).

THIRD INTERNATIONAL CONGRESS OF PLANT MOLECULAR BIOLOGY: MOLECULAR BIOLOGY OF PLANT GROWTH AND DEVELOPMENT

Richard B. Hallick, ed. 1995 421 p Congress held in Tucson, AZ, 6-11 Oct. 1991
(Contract DE-FG09-90ER-20012)
(DE95-006482; CONF-9110552-Absts) Avail: CASI HC A18/MF A04

The Congress was held 6-11 Oct. 1991 in Tucson with approximately 3000 scientists attending and over 300 oral presentations and 1800 posters. Plant molecular biology is one of the most rapidly developing areas of the biological sciences. Recent advances in the ability to isolate genes, to study their expression, and to create transgenic plants have had a major impact on our understanding of the many fundamental plant processes. In addition, new approaches have been created to improve plants for agricultural purposes. This is a book of presentation and posters from the conference. DOE

N95-28519 Naval Postgraduate School, Monterey, CA. Dept. of Operations Research.

MODELING AND STATISTICAL ANALYSIS OF BIOASSAY DATA: MEDAKA CELL PROLIFERATION UNDER DEN AND TCE Technical Report

Donald P. Gaver and Patricia A. Jacobs Oct. 1994 48 p Limited Reproducibility: More than 20% of this document may be affected by microfiche quality
(AD-A289998; NPS-OR-94-014) Avail: Issuing Activity (Defense Technical Information Center (DTIC))

The response of medaka liver to the chemicals DEN and TCE is analyzed statistically. The analysis illustrates the application of methods useful in environmetrics, i.e. environmental statistics. It suggests an overall dose-response effect but not an easily-interpreted dose-response functional relationship. DTIC

N95-28525 Virginia Univ., Charlottesville, VA.

DEVELOPMENT AND APPLICATION OF LOW-TEMPERATURE AFM Final Report, 1 Nov. 1991 - 31 Oct. 1994

Jie Yang and Zhifeng Shao 30 Jan. 1995 19 p Limited Reproducibility: More than 20% of this document may be affected by microfiche quality
(Contract DAAL03-92-G-0002)
(AD-A291704; ARO-29194.9-LS) Avail: Issuing Activity (Defense Technical Information Center (DTIC))

With the support from the US Army Research Office, we have established the basis of using state-of-the-art atomic force microscope (AFM) to image biological specimens at sub-nm resolution at cryogenic temperatures under ambient pressure. Our instrumentation demonstrated convincingly that a contamination environment can be obtained as we proposed originally, and the performance of our prototype AFM at cryogenic temperatures was at least comparable to, if not better than, any atomic force microscope available today. We have also developed various methods to facilitate atomic force microscopy of biological specimens at room temperature. Modification of the Kleinschmidt methods enabled us to image DNA specimens in air at a resolution of 4-6 nm. Reliable preparation of supported bilayers enabled us to study the structure of lipid bilayers in situ, leading to the elucidation of interesting phenomena which are impossible to reveal by other available methods, and the imaging of membrane proteins in physiological conditions at a resolution of 1 nm. We also developed methods to image soluble proteins in solution at a resolution of 1 nm. These suggest strongly the usefulness of AFM in biology that it can be used to solve problems which are difficult to tackle with other methods. DTIC

N95-28546 Florida Univ., Gainesville, FL.

INTERNATIONAL JOURNAL OF QUANTUM CHEMISTRY Final Report, 1 Jan. - 31 Dec. 1994

Rodney J. Bartlett Feb. 1995 253 p Presented at the 21st Quantum Biology Symposium, Ponte Verda Beach, FL, 12-19 Feb. 1994 Limited Reproducibility: More than 20% of this document may be affected by microfiche quality
(Contract DAAH04-94-G-0015)
(AD-A291633; ARO-32557.1-PH-CF) Avail: Issuing Activity (Defense Technical Information Center (DTIC))

The 34th Annual Sanibel Symposium, organized by the faculty and staff of the Quantum Theory Project of the University of Florida, was held on February 12-19, 1994, at the Marriott, Sawgrass Resort, Ponte Vedra Beach, Florida. Over 300 participants gathered for 8 days of lectures and informal discussions. The format of the symposium adopted for the past few years was followed again this year with a compact 8-day schedule with an integrated program of quantum biology, quantum chemistry, and condensed matter physics. The topics of the sessions covered by these proceedings include Quantum Chemistry of Biological Molecules, Spectroscopic Signatures of Biological Molecules, Protein Folding, and Photosynthesis. DTIC

N95-28298 Radian Corp., Austin, TX.

USE OF MUSSELS IN BIOMONITORING OF ENVIRONMENTAL IMPACTS OF PROPELLANTS, PROJECTILES, EXPLOSIVES, AND PYROTECHNICS

J. Hixson, R. Jennings, and C. H. Stagg (Joint Readiness Training Center, Fort Polk, LA.) *In* Johns Hopkins Univ., The 1994 JANNAF Safety and Environmental Protection Subcommittee Meeting, Volume 1 Aug. 1994 p 33-42 (For primary document see N95-28294 09-20)
Avail: CPIA, 10630 Little Patuxent Pkwy., Suite 202, Columbia, MD 21044-3200 HC

52 AEROSPACE MEDICINE

Includes physiological factors; biological effects of radiation; and effects of weightlessness on man and animals.

N95-26494 Army Medical Dept. Center and School, Fort Sam Houston, TX. Center for Healthcare Education and Studies.

DEVELOPMENT OF AN ACUITY-BASED NURSE STAFFING SYSTEM FOR THE POST ANESTHESIA CARE UNIT Final Report, 1992 - 1993

Julie K. Zadinsky Nov. 1994 143 p Limited Reproducibility: More than 20% of this document may be affected by microfiche quality
(AD-A288831; HR95-001) Avail: Issuing Activity (Defense Technical Information Center (DTIC))

The purposes of the study were (1) to provide an acuity-based method of determining nurse staffing needs for post anesthesia care units (PACU's) in the Army Medical Department (AMEDD) and (2) to provide a method of analyzing PACU workload variation. This method of determining staffing needs and analyzing workload variation is known as the Post Anesthesia Care Staffing System (PACS). Data were collected using (1) the PACU acuity worksheet at six study sites for a 16-week period, (2) records of nursing hours worked when the acuity information was being collected, and (3) a survey of PACU characteristics sent to 39 Army PACU's in the U.S. Army Health Services Command (HSC, now the U.S. Army Medical Command or MEDCOM). The strong positive correlation (r greater than .90) between daily direct nursing care hours and patient volume supported the development of a general regression model that was used to estimate daily direct nursing care hours from patient volume information. DTIC

N95-26680 Mayo Foundation, Rochester, MN.

MECHANISMS OF HYPERTENSION AFTER CROSS-LINKED HEMOGLOBIN BLOOD-SUBSTITUTE TRANSFUSION Midterm Report

Michael J. Joyner 1 Dec. 1994 19 p Limited Reproducibility: More than 20% of this document may be affected by microfiche quality
(Contract DAMD17-93-C-3116)
(AD-A289558) Avail: Issuing Activity (Defense Technical Information Center (DTIC))

The USAMRDC has developed a 'blood substitute' containing cross-linked human hemoglobin (XL-Hgb) in a physiologic saline solution. In animal models, this material can sustain life in the absence of red blood cells and is effective in resuscitating experimental animals from hypovolemic hemorrhagic shock. A persistent side-effect of XL-Hgb administration in animals has been marked arterial and pulmonary hypertension. The mechanism of this hypertension is unknown, but it is hypothesized that the XL-Hgb scavenges the endogenous vasodilating substance nitric oxide (NO). In experiments to date, our group has demonstrated that XL-Hgb administration (1) appears to blunt NO-mediated vasodilation in isolated blood vessels; (2) disrupts the normal metabolism of catecholamines from the adrenal medulla and sympathetic nerve endings;

(3) blunts NO-mediated vasodilation in vivo; and (4) causes acute volume expansion and hypertension without the normally observed diuresis and natriuresis in vivo. Studies to date generally confirm the hypothesis that XL-Hgb interferes with NO function in isolated tissues and whole animals. Additionally, other poorly understood physiologic mechanisms may also contribute to the hypertension. DTIC

N95-26763 Air Force Occupational Measurement Center, Randolph AFB, TX.

AEROSPACE MEDICINE Occupational Survey Report

Todd W. Kustra, Harold Huguley, III, and Becky Hernandez Nov. 1994 69 p Limited Reproducibility: More than 20% of this document may be affected by microfiche quality

(AD-A289691; AFPT-90-901-961) Avail: Issuing Activity (Defense Technical Information Center (DTIC))

This report summarizes the occupational survey results of the Aerospace Medicine Physician utilization field (935X) and the Aerospace Medicine career field (901X0). USAFSAM/ED requested the survey to analyze the effectiveness of the current training program for Aerospace Medicine utilization field (AFSC 93 5X). The analysis incorporates an assessment of the tasks trained in the Aerospace Medicine Primary course and the Aeromedical Specialist course; there is an evaluation of tasks listed in the Course Training Standard (CTS), Specialty Training Standard (STS), and the Career Development Course (CDC); and a comparison of tasks required versus actual tasks performed by incumbents. In addition, several other issues will be analyzed, such as the emergency skills needed for Squadron Medical Element personnel versus those needed for non-Squadron Medical Element personnel, the amount of time spent on patient care versus time spent performing administrative duties, and the scope of job satisfaction for both officers and enlisted personnel. DTIC

N95-26779 Chicago Univ., Chicago, IL. Dept. of Medicine.

BASIC MECHANISMS AND IMPLICATIONS OF NON-PHOTIC ENTRAINMENT OF CIRCADIAN RHYTHMICITY Annual Report, 1 Sep. 1993 - 31 Aug. 1994

Eve VanCauter 31 Aug. 1994 7 p Limited Reproducibility: More than 20% of this document may be affected by microfiche quality

(Contract F49620-92-J-0347)

(AD-A288433; AFOSR-94-0752TR) Avail: Issuing Activity (Defense Technical Information Center (DTIC))

The overall objectives of AFOSR-sponsored studies in Dr Van Cauter's laboratory are to delineate the synchronizing effects of physical exercise and exposure to darkness on the human circadian system and to test the hypothesis that additive effects of adequately timed exposure to pulses of bright light, darkness and exercise may result in large, immediate phase-shifts of human rhythms. Mr. Buxton performed a series of studies related to the first specific aim of the project, namely, to define the role of exercise intensity and duration in causing phase-shifts. The major rationale for examining the role of exercise intensity and duration in causing phase-shifts is to determine whether exercise sessions that can more readily be achieved in real life conditions than a 3-hour period of arm and leg exercise (which was the exercise period used in our previous studies), will have similar zeitgeber potency. Additionally, the use of a shorter duration, higher intensity stimulus would result in more clear-cut neuroendocrine correlates correlates of exercise and may provide important insights regarding the phase-dependence of exercise-induced neuroendocrine activation. DTIC

N95-26885 Naval Medical Research Inst., Bethesda, MD.

A MODEL OF BUBBLE EVOLUTION DURING DECOMPRESSION BASED ON A MONTE CARLO SIMULATION OF INERT GAS DIFFUSION Technical Report, Jun. 1992 - 1993

R. Ball, J. Himm, L. D. Homer, and E. D. Thalmann Aug. 1994 139 p Limited Reproducibility: More than 20% of this document may be affected by microfiche quality

(DA Proj. MM3-3-P-30)

(AD-A289400; NMRI-94-36) Avail: Issuing Activity (Defense Technical Information Center (DTIC))

Previously, a Monte Carlo simulation of inert gas diffusion in a capillary bed had been developed at this laboratory to explore the effect of tissue heterogeneity and microvascular architecture on gas exchange under normobaric conditions. Because we needed a method of looking at gas phase dynamics during decompression in this environment, the Monte Carlo method was extended to simulate bubble growth and dissolution during decompression. The essence of our approach involves the placement of inert gas particles in a bubble-liquid module and simulating diffusion with random displacements within the module for a short, fixed time period. At the end of the time period the distribution of the particles is used to calculate the number of moles of gas inside the bubble. The new bubble volume is then calculated from the ideal gas law. We developed methods to speed up the simulation by computing distributions of displacements following many random steps so that the simulation of many steps might be made with a simple calculation. In addition, we can calculate the amount of time a particle will stay inside the bubble based on the solubility of the inert gas. We demonstrate that a bubble evolves to the expected equilibrium size and the time course of the evolution compares favorably with that predicted by a partial differential equation model. A Monte Carlo approach is successful in simulating bubble evolution during decompression and is potentially suitable for studying the influence of tissue micro-architecture on gas phase dynamics. DTIC

N95-26889*# National Aeronautics and Space Administration. Langley Research Center, Hampton, VA.

NON-INVASIVE METHOD AND APPARATUS FOR MONITORING INTRACRANIAL PRESSURE AND PRESSURE VOLUME INDEX IN HUMANS Patent Application

John H. Cantrell, inventor (to NASA) and William T. Yost, inventor (to NASA) 24 Aug. 1994 30 p

(NASA-Case-LAR-13894-1; NAS 1.71:LAR-13894-1; US-Patent-Appl-SN-297474) Avail: CASI HC A03/MF A01

Non-invasive measuring devices responsive to changes in a patient's intracranial pressure (ICP) can be accurately calibrated for monitoring purposes by providing known changes in ICP by non-invasive methods, such as placing the patient on a tilting bed and calculating a change in ICP from the tilt angle and the length of the patient's cerebrospinal column, or by placing a pressurized skull cap on the patient and measuring the inflation pressure. Absolute values for the patient's pressure-volume index (PVI) and the steady state ICP can then be determined by inducing two known changes in the volume of cerebrospinal fluid while recording the corresponding changes in ICP by means of the calibrated measuring device. The two pairs of data for pressure change and volume change are entered into an equation developed from an equation describing the relationship between ICP and cerebrospinal fluid volume. PVI and steady state ICP are then determined by solving the equation. Methods for inducing known changes in cerebrospinal fluid volume are described. NASA

N95-26917 Air Force Inst. of Tech., Wright-Patterson AFB, OH. School of Engineering.

IMAGE PERCEPTION WAVELET SIMULATION AND ENHANCEMENT FOR THE VISUALLY IMPAIRED M.S. Thesis

Lemuel R. Myers, Jr. Dec. 1994 96 p Limited Reproducibility: More than 20% of this document may be affected by microfiche quality

(AD-A289303; AFIT/GEO/ENG/94D-03) Avail: Issuing Activity (Defense Technical Information Center (DTIC))

This research delves into the area of image enhancement for the visually impaired. Binocular macular degeneration a visual impairment, affects many Americans; since this condition could not be corrected with conventional glasses the literature suggested using an enhancement system which used a pre-emphasis algorithm to enhance the input image for output to the observer. The work of Dr. Eli Peli, a pioneer in the field of image enhancement, is examined and reproduced. Since his work concentrated mainly on frequency analysis of images, the bulk of this research involves using discrete wavelet analysis to augment that work. A biorthogonal wavelet set is used to enhance images. That same wavelet set is used to provide a simulation of a person's perception of an image based upon that person contrast sensitivity function. The wavelet enhancement follows Dr. Peli's method of enhancement using a modified pre-emphasis filter. The wavelet enhancement results are similar to that technique, with the most notable difference being that wavelet enhancements tend to accentuate the horizontal and vertical details of the image more than the spatial frequency concentric filter techniques outlined by Peli and others. The perception simulations use wavelet analysis and are based on the work accomplished by Peli concerning 'local band-limited contrast,' with the frequency analysis of that work giving way to a wavelet analysis;

the results here are significantly different than those result seen in the Peli simulation. DTIC

N95-26991 Air Force Inst. of Tech., Wright-Patterson AFB, OH. School of Engineering.

EXPERIMENTAL DEFINITION FOR IMPLANTATION OF THE AFIT CORTICAL MULTIELECTRODE ARRAY M.S. Thesis

Adam G. Spenik Dec. 1994 94 p Limited Reproducibility: More than 20% of this document may be affected by microfiche quality
(AD-A289216; AFIT/GE/ENG/94D-27) Avail: Issuing Activity (Defense Technical Information Center (DTIC))

A two-dimensional multiplexed array of 256 electrodes (16 x 16) has been fabricated using conventional CMOS fabrication techniques. The size and spacing of the electrodes (160 x 160 micrometer squares with center-to-center spacing of 250 micrometer) approximate that of the cortical columns. The device is mounted on a small biocompatible package and a protocol to implant this package on the visual cortex of a ferret and a Rhesus monkey was developed and approved. An instrumentation setup to record the data from the device is described as well as the methods used to demultiplex the data. Testing of the device in a simulated cortical environment indicates that the device is capable of recording signals with amplitudes as low as 20 micro volts. This capability is significant as the level of the cortical signal ranges from 20-500 micro volts. An experiment is envisioned in which the primary and secondary visual areas of a mammal are monitored simultaneously in an attempt to gather data while the brain is actually performing perception. This type of study will provide insight to the nature of the organization of the cortico-cortical connectivity matrix and its relation to the function of the cortical column system. DTIC

N95-27039 Air Force Inst. of Tech., Wright-Patterson AFB, OH. School of Engineering.

CHARACTERIZATION AND REDESIGN OF THE AFIT MULTIELECTRODE ARRAY M.S. Thesis

Richard G. Darenberg Dec. 1994 120 p Limited Reproducibility: More than 20% of this document may be affected by microfiche quality
(AD-A289295; AFIT/GE/ENG/94D-03) Avail: Issuing Activity (Defense Technical Information Center (DTIC))

Since 1978, faculty and graduate students from the Air Force Institute of Technology (AFIT) have been working on an implantable circuit array that can record visual signals from the brain or stimulate the brain. In the current design the circuit is a 16 x 16 array of pads, each pad being 160 x 160 micrometers with 250 micrometers spacing with an 'L' shaped reference pad used as a ground reference. The array is multiplexed so that only one I/O line is required to access all 256 pads. This research was twofold: first to analyze the existing circuit and identify sources for noise and then to redesign the circuit with the intent of reducing noise and power consumption. As a result of the research, a new 16 x 17 array has been developed. The new design incorporates new demultiplexing and synchronizing circuitry. The new circuitry exhibits lower noise and consumes much less power. The 'L' shaped reference pad has been removed-instead each pad and the pad to its right are sampled concurrent1y-one as the sample and one as a reference. DTIC

N95-27059 Department of the Air Force, Brooks AFB, TX. Armstrong Lab.

TO DEVELOP AN AEROSOLING IMMUNOMAGNETIC DEVICE FOR RAPID MEDICAL DIAGNOSIS FROM CLINICAL SAMPLES Midterm Report, 26 Jul. 1993 - 30 Sep. 1994

John G. Bruno, John P. Kilian, Arnott S. Moore, Johnathan L. Kiel, and Robert Reyes 15 Oct. 1994 15 p Limited Reproducibility: More than 20% of this document may be affected by microfiche quality
(AD-A288504) Avail: Issuing Activity (Defense Technical Information Center (DTIC))

A system for immunomagnetic capture, fluorescent staining, purification and diagnosis of at least bacterial (if not viral) septicemias is described. The system consists of a semi-automated computer-controlled immunomagnetic column collector and washing device as well as a semi-automated fluorescence microscope which will assist physicians in rapid diagnosis. This system will be used to investigate the efficiency of capture of nonpathogenic (Sterne) Anthrax vegetative cells and spores and possibly other agents of septicemia and body fluid infection. DTIC

N95-27426# Los Alamos National Lab., NM.

MATRIX KERNELS FOR MEG AND EEG SOURCE LOCALIZATION AND IMAGING

J. C. Mosher, P. S. Lewis, and R. M. Leahy (University of Southern California, Los Angeles, CA.) 1994 4 p Presented at the IEEE Conference on Acoustics, Speech and Signal Processing, Detroit, MI, 8-12 May 1995
(Contract W-7405-eng-36)
(DE95-005238; LA-UR-94-4387; CONF-9505158-2) Avail: CASI HC A01/MF A01

The most widely used model for electroencephalography (EEG) and magnetoencephalography (MEG) assumes a quasi-static approximation of Maxwell's equations and a piecewise homogeneous conductor model. Both models contain an incremental field element that linearly relates an incremental source element (current dipole) to the field or voltage at a distant point. The explicit form of the field element is dependent on the head modeling assumptions and sensor configuration. Proper characterization of this incremental element is crucial to the inverse problem. The field element can be partitioned into the product of a vector dependent on sensor characteristics and a matrix kernel dependent only on head modeling assumptions. We present here the matrix kernels for the general boundary element model (BEM) and for MEG spherical models. We show how these kernels are easily interchanged in a linear algebraic framework that includes sensor specifics such as orientation and gradiometer configuration. We then describe how this kernel is easily applied to 'gain' or 'transfer' matrices used in multiple dipole and source imaging models. DOE

N95-27502* National Aeronautics and Space Administration, Washington, DC.

AEROSPACE MEDICINE AND BIOLOGY: A CONTINUING BIBLIOGRAPHY WITH INDEXES (SUPPLEMENT 402)

Jun. 1995 103 p
(NASA-SP-7011(402); NAS 1.21:7011(402)) Avail: CASI HC A06

This bibliography lists 244 reports, articles and other documents introduced into the NASA Scientific and Technical Information System during Nov. 1992. Subject coverage includes: aerospace medicine and physiology, life support systems and man/system technology, protective clothing, exobiology and extraterrestrial life, planetary biology, and flight crew behavior and performance. Author

N95-28136# Senes Oak Ridge, Inc., Oak Ridge, TN.

AN INTRODUCTORY GUIDE TO UNCERTAINTY ANALYSIS IN ENVIRONMENTAL AND HEALTH RISK ASSESSMENT. ENVIRONMENTAL RESTORATION PROGRAM

J. S. Hammonds, F. O. Hoffman, and S. M. Bartell Dec. 1994 39 p
(Contract DE-AC05-84OR-21400)
(DE95-008097; ES/ER/TM-35/R1) Avail: CASI HC A03/MF A01

This report presents guidelines for evaluating uncertainty in mathematical equations and computer models applied to assess human health and environmental risk. Uncertainty analyses involve the propagation of uncertainty in model parameters and model structure to obtain confidence statements for the estimate of risk and identify the model components of dominant importance. Uncertainty analyses are required when there is no a priori knowledge about uncertainty in the risk estimate and when there is a chance that the failure to assess uncertainty may affect the selection of wrong options for risk reduction. Uncertainty analyses are effective when they are conducted in an iterative mode. When the uncertainty in the risk estimate is intolerable for decision-making, additional data are acquired for the dominant model components that contribute most to uncertainty. This process is repeated until the level of residual uncertainty can be tolerated. A analytical and numerical methods for error propagation are presented along with methods for identifying the most important contributors to uncertainty. Monte Carlo simulation with either Simple Random Sampling (SRS) or Latin Hypercube Sampling (LHS) is proposed as the most robust method for propagating uncertainty through either simple or complex models. A distinction is made between simulating a stochastically varying assessment endpoint (i.e., the distribution of individual risks in an exposed population) and quantifying uncertainty due to lack of knowledge about a fixed but unknown quantity (e.g., a specific individual, the maximally exposed individual, or the mean, median, or 95%-tile of the distribution of exposed individuals). Emphasis is placed on the need for subjective judgement to quantify uncertainty when relevant data are absent or incomplete. DOE

N95-28561 Krug Life Sciences, Inc., San Antonio, TX. San Antonio Div.
A STUDY OF HEART RATE AND HEART RATE VARIABILITY DURING RAPID DECOMPRESSION TO 50,000 FT Final Report, 11 May 1989 - 8 Nov. 1992
C. S. Chopp, John B. Bomar, Jr., and John A. Dellinger Sep. 1994 27 p Limited Reproducibility: More than 20% of this document may be affected by microfiche quality
(Contract F33615-89-C-0603)
(AD-A291598; AL/CF-TR-1994-0043) Avail: Issuing Activity (Defense Technical Information Center (DTIC))

A previous study of the heart rate (HR) response to positive pressure breathing (PPB), anxiety and hypoxia during rapid decompression (RD) revealed a consistent pattern in the beat-to-beat or interbeat interval variability of HR, known in the literature as heart rate variability (HRV). One method of analyzing HRV is a noninvasive measure of the respiratory-cardiac neural reflex known as vagal tone monitoring. This method is based on the amplitude of respiratory sinus arrhythmia (RSA) as a manifestation of vagal cardioinhibitory influence on the heart. The RD/HR data were interpreted by two HRV analysis methods, vagal tone monitoring (VTM) and a method developed in-house based on maximum entropy method (MEM) (spectral analysis), as a means of studying the heart rate regulating mechanisms during RD. A significant drop in vagal tone in both HRV measures was shown during the PPB and hypoxia profiles. Conflicting results regarding the anxiety profile during RD leave room for questions as to the use of these HRV measures as a tool for assessing anxiety or emotional stress. However, these measures only examined a subset of the HRV frequency spectrum (the respiratory frequency range) which provides information only on the parasympathetic autonomic contributions. Investigation of other frequency bands may provide more complete data on the autonomic regulation of the cardiovascular system. DTIC

N95-28318 Aerospace Medical Research Labs., Wright-Patterson AFB, OH. Toxicology Div.
ACUTE AND SUBACUTE TOXICITY OF AMMONIUM DINITRAMIDE (ADN)
D. R. Tocco, S. A. Salins (ManTech Environmental Technology, Inc., Wright-Patterson AFB, OH.), R. E. Wolfe (ManTech Environmental Technology, Inc., Wright-Patterson AFB, OH.), and E. R. Kinkead (ManTech Environmental Technology, Inc., Wright-Patterson AFB, OH.) *In* Johns Hopkins Univ., The 1994 JANNAF Safety and Environmental Protection Subcommittee Meeting, Volume 1 Aug. 1994 p 331-334 (For primary document see N95-28294 09-20)
(Contract F33615-90-C-0532)
Avail: CPIA, 10630 Little Patuxent Pkwy., Suite 202, Columbia, MD 21044-3200 HC

N95-28319 Walter Reed Army Inst. of Research, Wright-Patterson AFB, OH.
TOXICITY ASSESSMENT OF LIQUID PROPELLANT XM46
Daniel J. Caldwell *In* Johns Hopkins Univ., The 1994 JANNAF Safety and Environmental Protection Subcommittee Meeting, Volume 1 Aug. 1994 p 335-342 (For primary document see N95-28294 09-20)
Avail: CPIA, 10630 Little Patuxent Pkwy., Suite 202, Columbia, MD 21044-3200 HC

53 BEHAVIORAL SCIENCES

Includes psychological factors; individual and group behavior; crew training and evaluation; and psychiatric research.

N95-26361# Civil Aeromedical Inst., Oklahoma City, OK.
ENHANCING THE EFFECTS OF DIVERSITY AWARENESS TRAINING: A REVIEW OF THE RESEARCH LITERATURE Final Report
Jennifer G. Meyers Mar. 1995 28 p
(DOT/FAA/AM-95/10) Avail: CASI HC A03/MF A01

The projected changes in the demographic makeup of the workforce were primary influences in the spread of diversity awareness training in the private and public sector. One approach to training aims at changing personal attitudes and values to effect positive changes in treatment of others different from oneself (especially protected groups) in the workplace. The effectiveness of training or other interventions that focus on changes in attitudes to change behavior has not been clearly demonstrated. Training interventions need to use a combination of methods or strategies before, during, and after training to enhance the measurable benefits received from diversity awareness training and avoid the potential for 'white male backlash' and psychological risk among participants. Implementation of a training evaluation plan and a research program for identifying characteristics of effective training are also necessary to enhance training effectiveness in the longer term. Author

N95-26683 Air Force Inst. of Tech., Wright-Patterson AFB, OH.
ANALYSIS OF GROUP PERFORMANCE IN VISUAL SIGNAL DETECTION M.S. Thesis
Christopher J. Hays Jan. 1995 119 p Limited Reproducibility: More than 20% of this document may be affected by microfiche quality
(AD-A289561; AFIT/CI/CIA/94-145) Avail: Issuing Activity (Defense Technical Information Center (DTIC))

This study analyzed how a group's decision making performance compared to the predicted performance of a statistically 'optimal' group on a visual signal detection task. The task was to decide, either individually or as a group, whether a stimulus display screen (composed of nine independent information sources) was representative of one of two possible normal distributions (signal or noise). Eight subjects were tested individually and as members of different sized groups. Sorkin and Dai's 1994 model of the Ideal Group was used to analyze the accuracy of group performance (d'(sub grp)). Consistent with the model of the Ideal Group, d'(sub grp) increased with the number of group members, but decreased with intermember correlation and task difficulty. The group decision process was assumed to be based on the group assigning different weights (emphasis) to each group members' input. Overall efficiency, a relative measure of actual performance compared to ideal performance, was relatively high for two-member groups but decreased as the group grew larger. Group weighting strategies appeared to be somewhat variable for the condition in which all sources of information presented to the members were equally valid. However, when the sources of information were unequal, the group appropriately assigned more weight to the group members with the more reliable information. Some interesting social interaction phenomena were theorized to take place during the group decision process. Social loafing, coordination loss, and outgoingness were examined as possible reasons for changes in group performance. Interestingly, the subjects received more weight when they acted as the spokesperson for the group compared to when they did not respond for the group. DTIC

N95-26691 Wright State Univ., Dayton, OH.
CODES OF PROCESSING AND MULTIPLE RESOURCES: MODEL AND METHODOLOGY
Michael A. Stadler 1994 40 p Limited Reproducibility: More than 20% of this document may be affected by microfiche quality
(AD-A289583) Avail: Issuing Activity (Defense Technical Information Center (DTIC))

The current multiple resources methodology was employed to test the spatial-verbal distinction in the Wickens multiple resources model. Twelve subjects participated in a timesharing experiment in which a verbal memory search task was paired with another verbal and a spatial task. Reaction time and error data were examined and revealed that the verbal-verbal combination was generally performed at greater cost and with more interference than the spatial-verbal one. The results were interpreted as general support for the multiple resources distinction between the two codes of processing. DTIC

N95-26692 Aerospace Medical Research Labs., Wright-Patterson AFB, OH.
HANDBOOK OF PERCEPTION AND HUMAN PERFORMANCE, VOLUME 2. COGNITIVE PROCESSES AND PERFORMANCE
Kenneth R. Boff, Lloyd Kaufman, and James P. Thomas 1994 49 p Limited Reproducibility: More than 20% of this document may be affected by microfiche quality
(AD-A289587) Avail: Issuing Activity (Defense Technical Information Center (DTIC))

This chapter has attempted to bring together the laboratory and field-based techniques currently in use to assess workload. No doubt, many specific procedures of interest to particular applications have been left out of this survey. In no sense is this meant to summarily exclude these from any list of valid workload assessment techniques. In fact, several of these are acknowledged to show considerable promise (e.g., occlusion techniques and respiratory rhythms). They are not discussed here partly because of space limitations and partly because a judgment had to be made concerning the practicality and general applicability of each measure. It is hoped that the inclusion of general references will serve to point the interested reader to the individual techniques not included here. Similarly, a class of techniques frequently used to assess workload was deliberately excluded from this chapter. Task analytic methods, particularly as they are used with computer models of whole missions or operations, constitute an important tool for workload investigations during design and other stages of aircraft and systems development. These techniques, however, are primarily off-line analyses that utilize the kind of laboratory and field data gathered with the techniques such as those described in this chapter. They provide an overall systems answer to the workload question and as such deserve separate treatment from highly specific workload measures. DTIC

N95-26825 Wright State Univ., Dayton, OH.
SUBJECTIVE WORKLOAD ASSESSMENT IN A SPATIAL MEMORY TASK
F. T. Eggemeier and Michael A. Stadler Oct. 1994 5 p Prepared in cooperation with Systems Research Lab. Inc. Limited Reproducibility: More than 20% of this document may be affected by microfiche quality
(AD-A289491) Avail: Issuing Activity (Defense Technical Information Center (DTIC))

Twelve subjects performed a spatial short-term memory task under several levels of difficulty and rated the workload associated with each using the Subjective Workload Assessment Technique (SWAT). SWAT ratings proved sensitive to two of the three difficulty manipulations in the memory task, and demonstrated greater sensitivity in this respect than either of two primary task measures that were employed. The results extend the applicability of SWAT to the type of spatial memory task used and, therefore, provide further support for the general applicability of SWAT as a workload measurement technique. DTIC

N95-26843 Maryland Univ., College Park, MD.
LEARNING HAND/EYE COORDINATION BY AN ACTIVE OBSERVER. PART 1: ORGANIZING CENTERS Technical Report
Jean-Yves Herve Jul. 1994 74 p Limited Reproducibility: More than 20% of this document may be affected by microfiche quality
(Contracts DACA76-92-C-0009; N00014-93-1-0257)
(AD-A289502; CAR-TR-725; CS-TR-3319) Avail: Issuing Activity (Defense Technical Information Center (DTIC))

This report, the first of a three-part series, presents preliminary results in a study on the role of the active observer in the hand/eye coordination problem. It was shown elsewhere that the hand/eye coordination problem can be represented, for a given pose of the observer, by the singularities of a surface, the perceptual control surface (PCS). Small changes in the pose of the observer generally produce smooth deformations of the PCS. There are configurations, however, from which arbitrarily small modifications of the point of view result in profound changes in the topological nature of the PCS. This paper studies these bifurcation configurations and, furthermore, investigates the possibility of determining a priori displacements of the observer that can achieve a desired effect on the PCS such as simplifying its topology or reducing the number of singularities separating the current configuration from a goal to be reached. The result of this analysis takes the form of the 'family portrait' of all possible aspects of the PCS, indexed by the geometry of the manipulator and the pose of the observer relative to it. A hand/eye system is then completely coordinated - has 'learned its PCS' - when a 'portrait' has been matched with the experimental data gathered by the low-level controller. DTIC

N95-26909 Helsinki Univ. of Technology, Espoo (Finland). Lab. of Industrial Psychology.
CHANGE, LEARNING AND MENTAL WORK IN ORGANIZATIONS: WORKING PAPERS OF THE 3RD OTANIEMI-DRESDEN WORKSHOP
Matti Vartiainen, ed. and Veikko Teikari, ed. 1994 142 p Workshop was held in Helsinki, Finland, Dec. 1994 Limited Reproducibility: More than 20% of this document may be affected by microfiche quality
(ISSN 0784-3623)
(PB95-184941; ISBN-951-22-2231-0) Avail: CASI HC A07

Contents are as follows: Managing change: Structured Implementation of a Process of Change in an Insurance Company; Job Content and Myocardial Health Risks - Consequences for Occupational Prevention; Analyzing the Implementation of Business Strategy in a Service Organization Critically; What is Organizational Learning; Participative Development and Organizational Learning with Work Flow Game; Mental Work Requirements: Some Issues of Analysis and Evaluation; Research on Leadership and Managerial Behavior - A State of the Art; From Fragmented to Complete Expert Work; The Modeling of Activity Requirements in an Employment Service Agency; and Finnish Experiences in Using TBS-GA. NTIS

N95-26992 Phillips Lab., Hanscom AFB, MA.
DIAGNOSING CLOUDINESS FROM GLOBAL NUMERICAL WEATHER PREDICTION MODEL FORECASTS Final Report, Oct. 1991 - Sep. 1993
Donald C. Norquist, H. S. Muench, Donald L. Aiken, and Douglas C. Hahn 5 Jul. 1994 150 p Limited Reproducibility: More than 20% of this document may be affected by microfiche quality
(AF Proj. 6670)
(AD-A289456; PL-TR-94-2211; ERP-1156) Avail: Issuing Activity (Defense Technical Information Center (DTIC))

We investigated the utility of any information derivable from noncloud numerical weather prediction (NWP) model forecasts in inferring layer cloud amount distributions. This effort involved identifying and preparing a suitable source of the predictand (cloud amount), generating and preparing a suitable source of the predictors (NWP variables and geographic information), and combining them to form diagnostic relationships in a model output statistics approach. Both AFGWC RTNEPH cloud analyses and Phillips Laboratory Global Spectral Model (PL GSM) NWP forecasts were rendered on a 125 km equal-area grid in three cloud deck regimes (high, middle, low). Two statistical methods CLOUD CURVE ALGORITHM (CCA), a univariate method, and multiple linear regression (MLR) were used to relate the cloud amount to relative humidity (CCA) and to relative humidity and a large number of other NWP variables (MLR). The authors found that the CCA method preserves the sharpness of the cloud distribution while sacrificing skill, while MLR produced cloud diagnoses that were more skillful but less sharp. The methods fall short of the error level standards established by Air Force requirements, but show potential for useful cloud forecast skill upon further refinement. DTIC

N95-27012 Aeronautical Systems Div., Wright-Patterson AFB, OH.
VISUAL SYSTEM OPERATIONAL EVALUATION Final Report, 19 Feb. 1993 - 31 Jul. 1994
James E. Brown, Timothy J. Lincourt, Melissa J. Leos, Don R. Poe, and Gary S. Allard 31 Jul. 1994 113 p Limited Reproducibility: More than 20% of this document may be affected by microfiche quality
(AD-A289173; ASC-TR-94-5030) Avail: Issuing Activity (Defense Technical Information Center (DTIC))

This evaluation was undertaken to identify the capability and limitations of current visual simulation to support low altitude flight training. Purpose was: (1) determine trainability of low altitude tasks on available visual display technology; (2) demonstrate current visual requirements; and (3) provide information and data to support future simulation acquisition decisions. Three visual simulation display technologies located at three different sites were evaluated: (1) dome display with head tracked area-of-interest, (2) rear-projection display, and (3) helmet mounted display. Highly experienced F-16C and F-15E instructor pilots evaluated each display technology. A standard list of evaluation tasks was used to evaluate each system in a mission context. Extensive questionnaires were completed and debriefings conducted to rate the training capability of the simulator to provide mission readiness (MR) and continuation training (CT) for operational aircrews (both wingman and flight leads). Major conclusions are (1) single ship air-to-ground tasks are trainable now with the right combination of database, image generator, and matched visual display system; and (2) current systems do not provide adequate resolution, contrast, and brightness to allow for dynamic air model assessment. DTIC

N95-27013 Carnegie-Mellon Univ., Pittsburgh, PA. Robotics Inst.
USING VIRTUAL ACTIVE VISION TOOLS TO IMPROVE AUTONOMOUS DRIVING TASKS
Todd M. Jochem Oct. 1994 23 p Limited Reproducibility: More than 20% of this document may be affected by microfiche quality

(Contracts DACA76-89-C-0014; DAAE07-90-C-R059)
(AD-A289175; CMU-RI-TR-94-39) Avail: Issuing Activity (Defense Technical Information Center (DTIC))

ALVINN is a simulated neural network for road following. In its most basic form, it is trained to take a subsampled, preprocessed video image as input, and produce a steering wheel position as output. ALVINN has demonstrated robust performance in a wide variety of situations, but is limited due to its lack of geometric models. Grafting geometric reasoning onto a nongeometric base would be difficult and would create a system with diluted capabilities. A much better approach is to leave the basic neural network intact, preserving its real-time performance and generalization capabilities, and to apply geometric transformations to the input image and the output steering vector. These transformations form a new set of tools and techniques called virtual active vision. The thesis for this work is: virtual active vision tools will improve the capabilities of neural network based autonomous driving systems. DTIC

N95-27181 Industrial Coll. of the Armed Forces, Washington, DC.
MYERS-BRIGGS TYPE INDICATORS AND KIRTON ADAPTION-INNOVATION INVENTORY CORRELATIONS Research Report, Aug. 1993 - Apr. 1994
Melanie A. Hughes Apr. 1994 38 p Limited Reproducibility: More than 20% of this document may be affected by microfiche quality
(AD-A288435; NDU-ICAF-94-F28) Avail: Issuing Activity (Defense Technical Information Center (DTIC))

This research report focuses upon the results and the raw data of the Myers-Briggs Type Inventory, and the Kirton Adaption Innovation Inventory administered to the Industrial College of the Armed Forces Class of 1994. DTIC

N95-27323# Civil Aeromedical Inst., Oklahoma City, OK.
PRACTICAL COLOR VISION TESTS FOR AIR TRAFFIC CONTROL APPLICANTS: EN ROUTE CENTER AND TERMINAL FACILITIES Final Report
Henry W. Mertens, Nelda J. Milburn, and William E. Collins Apr. 1995 15 p
(DOT/FAA/AM-95/13) Avail: CASI HC A03/MF A01

Two practical color vision tests were developed and validated for use in screening Air Traffic Control Specialist (ATCS) applicants for work at en route center or terminal facilities. The development of the tests involved careful reproduction/simulation of color-coded materials from the most demanding, safety critical color task performed in each type of facility. The tests were evaluated using 106 subjects with normal color vision and 85 with color vision deficiency. The en route center test, named the Flight Progress Strips Test (FPST), required the identification of critical red/black coding in computer printing and handwriting on flight progress strips. The terminal option test, named the Aviation Lights Test (ALT), simulated red/green/white aircraft lights that must be identified in night ATC tower operations. Color coding is a non-redundant source of safety-critical information in both tasks. The FPST was validated by direct comparison of responses to strip reproductions with responses to the original flight progress strips. Validity was high; Kappa = .91. The light point stimuli of the ALT were validated physically with a spectroradiometer. The test lights met the FAA and ICAO standards for colors of aircraft and aviation signal lights. The reliabilities of the FPST and ALT were estimated with Chronbach's alpha and were .93 and .98, respectively. The high job-relevance, validity, and reliability of these tests increases the effectiveness and fairness of ATCS color vision testing. Author

N95-27697*# Legacy Good Samaritan Hospital, Portland, OR. Clinical Vestibular Lab.
ROLE OF SOMATOSENSORY AND VESTIBULAR CUES IN ATTENUATING VISUALLY INDUCED HUMAN POSTURAL SWAY
Robert J. Peterka and Martha S. Benolken [1993] 32 p
(Grants NAG9-117; NAGw-3782; P60-DC-0207-02)
(NASA-CR-197845; NAS 1.26:197845) Avail: CASI HC A03/MF A01

The purpose was to determine the contribution of visual, vestibular, and somatosensory cues to the maintenance of stance in humans. Postural sway was induced by full field, sinusoidal visual surround rotations about an axis at the level of the ankle joints. The influences of vestibular and somatosensory cues were characterized by comparing postural sway in normal and bilateral vestibular absent subjects in conditions that provided either accurate or inaccurate somatosensory orientation information. In normal subjects, the amplitude of visually induced sway reached a saturation level as stimulus amplitude increased. The saturation amplitude decreased with increasing stimulus frequency. No saturation phenomena was observed in subjects with vestibular loss, implying that vestibular cues were responsible for the saturation phenomenon. For visually induced sways below the saturation level, the stimulus-response curves for both normal and vestibular loss subjects were nearly identical implying that (1) normal subjects were not using vestibular information to attenuate their visually induced sway, possibly because sway was below a vestibular-related threshold level, and (2) vestibular loss subjects did not utilize visual cues to a greater extent than normal subjects; that is, a fundamental change in visual system 'gain' was not used to compensate for a vestibular deficit. An unexpected finding was that the amplitude of body sway induced by visual surround motion could be almost three times greater than the amplitude of the visual stimulus in normals and vestibular loss subjects. This occurred in conditions where somatosensory cues were inaccurate and at low stimulus amplitudes. A control system model of visually induced postural sway was developed to explain this finding. For both subject groups, the amplitude of visually induced sway was smaller by a factor of about four in tests where somatosensory cues provided accurate versus inaccurate orientation information. This implied that (1) the vestibular loss subjects did not utilize somatosensory cues to a greater extent than normal subjects; that is, changes in somatosensory system 'gain' were not used to compensate for a vestibular deficit, and (2) the threshold for the use of vestibular cues in normals was apparently lower in test conditions where somatosensory cues were providing accurate orientation information. Author

N95-28176# Lawrence Livermore National Lab., Livermore, CA. The Intelligent Mechatronics and Machine Vision Lab.
LONG-RANGE EYE TRACKING: A FEASIBILITY STUDY
Surya K. Jayaweera and Shin-yee Lu 24 Aug. 1994 48 p Sponsored by the Small Business Program
(Contract W-7405-eng-48)
(DE95-008587; UCRL-ID-118340) Avail: CASI HC A03/MF A01

The design considerations for a long-range Purkinje effects based video tracking system using current technology is presented. Past work, current experiments, and future directions are thoroughly discussed, with an emphasis on digital signal processing techniques and obstacles. It has been determined that while a robust, efficient, long-range, and noninvasive eye tracking system will be difficult to develop, such as a project is indeed feasible. DOE

N95-28253*# BBN Systems and Technologies Corp., Cambridge, MA.
PILOT OPINIONS ON HIGH LEVEL FLIGHT DECK AUTOMATION ISSUES: TOWARD THE DEVELOPMENT OF A DESIGN PHILOSOPHY
Yvette J. Tenney, William H. Rogers, and Richard W. Pew May 1995 111 p
(Contract NAS1-18788; RTOP 505-64-13-21)
(NASA-CR-4669; NAS 1.26:4669) Avail: CASI HC A06/MF A02

There has been much concern in recent years about the rapid increase in automation on commercial flight decks. The survey was composed of three major sections. The first section asked pilots to rate different automation components that exist on the latest commercial aircraft regarding their obtrusiveness and the attention and effort required in using them. The second section addressed general 'automation philosophy' issues. The third section focused on issues related to levels and amount of automation. The results indicate that pilots of advanced aircraft like their automation, use it, and would welcome more automation. However, they also believe that automation has many disadvantages, especially fully autonomous automation. They want their automation to be simple and reliable and to produce predictable results. The biggest needs for higher levels of automation were in pre-flight, communication, systems management, and task management functions, planning as well as response tasks, and high workload situations. There is an irony and a challenge in the implications of these findings. On the one hand pilots would like new automation to be simple and reliable, but they need it to support the most complex part of the job--managing and planning tasks in high workload situations. Author

N95-28676*# University of Southern California, Los Angeles, CA. Inst. of Safety and Systems Management.
THE EFFECTS OF CREW RESOURCE MANAGEMENT (CRM) TRAINING IN AIRLINE MAINTENANCE: RESULTS FOLLOWING THREE YEAR'S EXPERIENCE
J. C. Taylor and M. M. Robertson Jun. 1995 74 p
(Contract NCC2-812)
(NASA-CR-196696; A-950067; NAS 1.26:196696) Avail: CASI HC A04/MF A01

An airline maintenance department undertook a CRM training program to change its safety and operating culture. In 2 1/2 years this airline trained 2200 management staff and salaried professionals. Participants completed attitude surveys immediately before and after the training, as well as two months, six months, and one year afterward. On-site interviews were conducted to test and confirm the survey results. Comparing managers' attitudes immediately after their training with their pretraining attitudes showed significant improvement for three attitudes. A fourth attitude, assertiveness, improved significantly above the pretraining levels two months after training. The expected effect of the training on all four attitude scales did not change significantly thereafter. Participants' self-reported behaviors and interview comments confirmed their shift from passive to more active behaviors over time. Safety, efficiency, and dependability performance were measured before the onset of the training and for some 30 months afterward. Associations with subsequent performance were strongest with positive attitudes about sharing command (participation), assertiveness, and stress management when those attitudes were measured 2 and 12 months after the training. The two month follow-up survey results were especially strong and indicate that active behaviors learned from the CRM training consolidate and strengthen in the months immediately following training. Author

54 MAN/SYSTEM TECHNOLOGY AND LIFE SUPPORT

Includes human engineering; biotechnology; and space suits and protective clothing.

For related information see also *16 Space Transportation.*

N95-26364*# National Aeronautics and Space Administration. Marshall Space Flight Center, Huntsville, AL.
INTERNATIONAL SPACE STATION ALPHA TRACE CONTAMINANT CONTROL SUBASSEMBLY LIFE TEST REPORT Final Report
J. D. Tatara (ION Electronics, Hunsville, AL.) and J. L. Perry Washington Mar. 1995 73 p
(NASA-TM-108488; NAS 1.15:108488) Avail: CASI HC A04/MF A01

The Environmental Control and Life Support System (ECLSS) Life Test Program (ELTP) began with Trace Contaminant Control Subassembly (TCCS) Life Testing on November 9, 1992, at 0745. The purpose of the test, as stated in the NASA document 'Requirements for Trace Contaminant Control Subassembly High Temperature Catalytic Oxidizer Life Testing (Revision A)' was to 'provide for the long duration operation of the ECLSS TCCS HTCO (High Temperature Catalytic Oxidizer) at normal operating conditions... (and thus)... to determine the useful life of ECLSS hardware for use on long duration manned space missions.' Specifically, the test was designed to demonstrate thermal stability of the HTCO catalyst. The report details TCCS stability throughout the test. Graphs are included to aid in evaluating trends and subsystem anomalies. The report summarizes activities through the final day of testing, January 17, 1995 (test day 762). Author

N95-26552 Institute for Defense Analyses, Alexandria, VA.
A MATHEMATICAL FRAMEWORK FOR AN IMPROVED SEARCH MODEL Final Report, Sep. 1993 - Apr. 1994
Jeffrey Nicoll Oct. 1994 103 p Limited Reproducibility: More than 20% of this document may be affected by microfiche quality
(Contract DASW01-94-C-0054)
(AD-A288858; IDA-P-2901; IDA/HQ-93-44557) Avail: Issuing Activity (Defense Technical Information Center (DTIC))

Search is currently modeled for DOD applications by a single exponential function. The two adjustable parameters are the time constant, t, characterizing the exponential; and the long time detection probability, P. Deficiencies of the classical model are: (1) human performance data cannot typically be fit with a single exponent model; (2) the probability of detection for short times is less than that predicted by the classical model; and (3) the effects of multiple targets and clutter can only be included by adjusting the two-model parameters, which is performed in an ad hoc manner and over-constrains the model. This paper introduces a neoclassical model that includes three processes: (1) attending to the target; (2) random wandering around the scene; and (3) attending to other targets/clutter. An expression involving three exponents associated with the three processes is derived and special cases are described. The new model provides uniform treatment of multiple targets and false detections and allows for the separate descriptions of multiple times scales within the search process. Searches can be separated into single region, field-of-view search, and multiple region, field-of-regard search. Field-of-view search can be further subdivided into long searches during which the observer may examine many targets and short searches which are completed after a few target examinations. DTIC

N95-26558 Army Research Inst. of Environmental Medicine, Natick, MA.
PERFORMANCE ENHANCING RATION COMPONENTS PROGRAM: SUPPLEMENTAL CARBOHYDRATE TEST
T. C. Murphy, R. W. Hoyt, T. E. Jones, C. L. Gabaree, E. W. Askew, T. A. Skibinski, and M. L. Barkate (Louisiana State Univ., Baton Rouge, LA.) 28 Jun. 1994 44 p Limited Reproducibility: More than 20% of this document may be affected by microfiche quality
(AD-A288560; USARIEM-T-2/95) Avail: Issuing Activity (Defense Technical Information Center (DTIC))

The Performance Enhancing Ration Components (PERC) project supports the Army Science and Technology Objective 'Nutritional Strategies to Enhance Soldier Performance.' The focus of the PERC project is to demonstrate, through nutrition intervention, enhancement of physical and/or mental performance in extreme environmental conditions or during sustained high-intensity work. In this PERC study, we examined the effects of a liquid carbohydrate (CR0) supplement on exercise endurance of Special Operations Forces (SOF) soldiers. The results of this study have encouraging implications in that they demonstrate that the sustainability and survivability of our combat forces can be enhanced through nutrition intervention. By tailoring the nutrient composition of the diet, environmental and battlefield stress may be attenuated and decrements in performance may be prevented. DTIC

N95-26612 OGDEN/ERC Government Systems, Fairfax, VA.
US COAST GUARD HUMAN SYSTEMS INTEGRATION (HSI) PROCESS MODEL Final Report
Wayne Wright and Richard Hall Apr. 1994 222 p Limited Reproducibility: More than 20% of this document may be affected by microfiche quality
(Contract MIPR-Z51100-2-E00416)
(AD-A289172; CGR/DC-11/94; CG-D-26-94) Avail: Issuing Activity (Defense Technical Information Center (DTIC))

The Coast Guard has identified a need to improve Human System Integration (HSI) in the planning, design, and development of new system acquisitions. A previous effort, 'U.S. Coast Guard Human Systems Integration Program Requirements Document,' revealed that HSI principles are not consistently applied throughout the acquisition process, and that a formal HSI program would ensure that human related issues are addressed during new system acquisitions. This report provides a recommended 'Process Model' for integrating the various elements of HSI (i.e., Manpower, Personnel, Training, Human Factors Engineering, and Safety/Health Hazards) into all new Coast Guard hardware acquisitions, including ships, aircraft, and all equipment / systems / subsystems fielded through the acquisition program. An evaluation was conducted to assess the strengths and weaknesses of existing HSI programs and determine whether elements of existing programs could be used in the Coast Guard environment. Based on this review, a process model was developed to integrate HSI into the Coast Guard acquisition process. DTIC

N95-26736 Navy Clothing and Textile Research Facility, Natick, MA.
LIGHTWEIGHT COLD WEATHER UNDERWEAR INVESTIGATION Final Report, Aug. - Dec. 1992
Tina M. Phaneuf Oct. 1994 22 p Limited Reproducibility: More than 20% of this document may be affected by microfiche quality
(AD-A288506; NCTRF-204) Avail: Issuing Activity (Defense Technical Information Center (DTIC))

The Navy Clothing and Textile Research Facility was tasked by the Marine Corps Systems Command to conduct testing of various types of lightweight cold weather underwear materials for physical and thermal characteristics. These tests were conducted in order to develop a Marine Corps standard for future product development. Based on test results, two fabrics were recommended as good candidates for use in lightweight cold weather underwear. DTIC

N95-26737 Air Force Inst. of Tech., Wright-Patterson AFB, OH. School of Engineering.
ENHANCED VISUAL USER INTERFACE SUPPORT FOR DOMAIN-ORIENTED APPLICATION COMPOSITION SYSTEMS Master's Thesis
Richard A. Guinto Dec. 1994 122 p Limited Reproducibility: More than 20% of this document may be affected by microfiche quality
(AD-A289337; AFIT/GCS/ENG/94D-06) Avail: Issuing Activity (Defense Technical Information Center (DTIC))

This research refined the functionality and usability of a previously developed visual interface for a domain-oriented application composition system. The refinements incorporated more sophisticated user interface design concepts to reduce user workload. User workload was reduced through window reordering, menu redesign, and Human Computer Interaction techniques such as; combining repetitive procedures into single commands, reusing composition information whenever possible and deriving new information from existing information. The Software Refinery environment, including its visual interface tool INTERVISTA, was used to develop techniques for visualizing and manipulating objects contained in a formal knowledge base of objects. The interface was formally validated with digital logic-circuits, digital signal processing, event-driven logic-circuits, and cruise-missile domains. A comparative analysis of the application composition process with the previous visual interface was conducted to quantify the workload reduction realized by the new interface. Level of effort was measured as the number of user interactions (mouse or keyboard) required to compose an application. On average, application composition effort was reduced 34.0% for the test cases. DTIC

N95-26755 Conrad Technologies, Inc., King of Prussia, PA.
DEVELOPMENT OF INJURY PREVENTING HELMET SERVO-SUPPORT SYSTEM FOR HIGH PERFORMANCE AIRCRAFT Progress Report
Donald F. DeCleene 30 Dec. 1994 22 p Limited Reproducibility: More than 20% of this document may be affected by microfiche quality
(Contract N00014-94-C-0179)
(AD-A289547) Avail: Issuing Activity (Defense Technical Information Center (DTIC))

The technical objective of this program is the development of a support system for the aviator's helmet wherein the load created by the helmet and helmet mounted equipment is removed from the aviator's head and is transferred directly to the aviator's seat and airframe. The Support system, while supporting the helmet load, shall be powered and controlled to move with the aviator's head such that the helmet is retained on the aviator's head in a normal manner. The support system shall provide freedom of head movement and allow the aviator to easily control the movement of his/her head, his/her helmet and the helmet mounted equipment. The technical objective of this program is being undertaken in the form of a multi-task program as outlined in the proposal. The objectives of the individual tasks are presented below. DTIC

N95-26863 Aerospace Medical Research Labs., Wright-Patterson AFB, OH. Human Resources Directorate.
DESIGN CONSIDERATIONS FOR FRANKTALK: A DISTRIBUTED GROUP SUPPORT SYSTEM Interim Report, Jan. 1992 - Jun. 1993
Kennon J. Moen, Michael Wolfe, and Alan R. Heminger Oct. 1994 25 p Limited Reproducibility: More than 20% of this document may be affected by microfiche quality
(AD-A289386; AL/HR-TP-1994-0023) Avail: Issuing Activity (Defense Technical Information Center (DTIC))

This paper discusses design considerations for a prototype distributed group support system as well as an initial assessment of its demonstrated functionality. The system created enabled participants in a group process to interact with each other across time and distance. Pilot studies were performed to measure user acceptance and system effectiveness and usability. DTIC

N95-26883 Air Force Inst. of Tech., Wright-Patterson AFB, OH.
AN IMAGE QUALITY ANALYSIS OF ANVIS-6 NIGHT VISION GOGGLES M.S. Thesis
Derek H. Abel Dec. 1994 76 p Limited Reproducibility: More than 20% of this document may be affected by microfiche quality
(AD-A289398; AFIT/CI/CIA/94-146) Avail: Issuing Activity (Defense Technical Information Center (DTIC))

This study was undertaken in an effort to relate ANVIS-6 Night Vision Goggle image quality to user performance. The purpose was to determine which of five image quality metrics best related to performance tasks. The image quality metrics examined Modulation Transfer Function Area (MTFA), Integrated Contrast Sensitivity (ICS), Square Root Integral (SQRI), Resolution, and Signal-to-Noise Ratio (SNR). The performance tasks were detection and recognition of targets under various levels of moon illumination. The metric that best related to target detection was SNR. The SNR results are consistent with visual psychophysics and SNR effects. The metric that best related to target recognition was Resolution. The resolution results are consistent with the position that recognition performance improves for suprathreshold targets as resolving power increases. DTIC

N95-26884* Carnegie-Mellon Univ., Pittsburgh, PA. Robotics Inst.
MULTI-AGENT PERCEPTION FOR HUMAN/ROBOT INTERACTION: A FRAMEWORK FOR INTUITIVE TRAJECTORY MODIFICATION Technical Report
Richard M. Voyles, Jr. and Pradeep K. Khosla 15 Sep. 1994 25 p Limited Reproducibility: More than 20% of this document may be affected by microfiche quality
(Grant NAG1-1075)
(AD-A289399; CMU-RI-TR-94-33) Avail: Issuing Activity (Defense Technical Information Center (DTIC))

An application of distributed perception to a novel human/computer interface is presented. A multi-agent network has been applied to the task of modifying a robotic trajectory based on very sparse physical inputs from the user. The user conveys intentions by nudging the end effector, instrumented with a wrist force/torque sensor, in an intuitive manner. In response, each agent interprets these sparse inputs with the aid of a local, fuzzified, heuristic model of a particular parameter or trajectory shape. The agents then independently determine the confidence of their respective findings and distributed arbitration resolves the interpretation through voting. DTIC

N95-27046 Air Force Inst. of Tech., Wright-Patterson AFB, OH. School of Engineering.
MULTIPLE MODEL ADAPTIVE ESTIMATION AND HEAD MOTION TRACKING IN A VIRTUAL ENVIRONMENT: AN ENGINEERING APPROACH M.S. Thesis
James E. Russell Dec. 1994 195 p Limited Reproducibility: More than 20% of this document may be affected by microfiche quality
(AD-A289299; AFIT/GCS/ENG/94D-21) Avail: Issuing Activity (Defense Technical Information Center (DTIC))

Software engineering tools and techniques were applied to design and implement an application that reduces lag typically present in virtual environment displays. The application was a Multiple Model Adaptive Estimator (MMAE), composed of three Kalman filters, that predicted head orientation one sample period into the future. The environment rendering software used these predictions to generate the environment display. Each of the filters in the MMAE was designed for a different assumed head motion type (benign, moderate, or heavy), which allowed the MMAE to adapt to changes in head movement characteristics. The use of Ada 9X as an implementation language for a virtual environment applications was also investigated. Ada 9X provides object-oriented features for design and development, and it also offers software engineering support that makes it preferable to C or C++ for the application developed. Two significant results were produced. The first is a performance baseline for the MMAE that can be used as a benchmark for future research in this area. The other is a performance-based comparison of equivalent Ada 9X and C++ graphics applications in which Ada 9X performance was practically identical to C++. This second result is somewhat surprising, and should be investigated further. DTIC

N95-27058 Coast Guard, Washington, DC. Research and Development Center.
CREW ADAPTATION EVALUATION OF THE NORWEGIAN CREW CONCEPT (NOROREW) Final Report
Donald I. Tepas (Work Systems Research, Mansfield Center, CT.) and Antonio B. Carvalhais Sep. 1994 69 p Prepared in cooperation with Work Systems Research, Mansfield Center, CT Limited Reproducibility: More than 20% of this document may be affected by microfiche quality
(AD-A288478; USCG-R/DC-27/94; USCG-D-23-94) Avail: Issuing Activity (Defense Technical Information Center (DTIC))

This report documents an Operational Test and Evaluation (OT&E) effort conducted to assess the feasibility of replacing select traditional small boat station shore-side facilities with live-aboard vessels. The success of such a concept is dependent on the crews' ability to adapt and cope with around-the-clock operations from a restricted work and living environment. Survey and log forms were used to collect continuous data on human factors variables, at both a traditional small boat station and an experimental live-aboard concept station, to assess the impact of the live-aboard concept on crew safety and well-being. Results of this evaluation indicate that all human factors variables were well within acceptable limits. The evaluation did not reveal any significant adverse effects on crew members which would prevent the use of the live-aboard concept in Coast Guard small boat stations which are similar to the one in the study. However, it was emphasized that although the results are positive, they may not reflect the reactions of crews in other Coast Guard small boat station environments. DTIC

N95-27099 Army Research Lab., Aberdeen Proving Ground, MD.
GLOVED OPERATOR PERFORMANCE STUDY. THE EFFECTS OF HAND WEAR AND ELASTIC RESISTANCE OF A CONTROL DURING TRACKING PERFORMANCE Final Report
Glen Anderson, Jan Berkhout, Michael Granaas, and Sri Canakapalli May 1994 64 p Limited Reproducibility: More than 20% of this document may be affected by microfiche quality
(DA Proj. 1L1-62716-AH-70)
(AD-A289405; ARL-CR-143) Avail: Issuing Activity (Defense Technical Information Center (DTIC))

This study was to test the effects of wearing gloves during tracking performance at different levels of elastic resistance in a control. Forty-eight undergraduate students served as subjects. Each group contained 16 subjects, one group for each level of control resistance. The control was a spring-centered displacement joystick with resistance settings of 0.12 and 1702. All subjects performed a compensatory tracking task both bare-handed and while wearing a leather and wool glove assembly. Results indicated that: (1) wearing gloves is detrimental to tracking performance for female subjects; (2) female subjects do not benefit from additional exposure to the task before performing the task with gloves as do male subjects; (3) high control resistance may have been beneficial for female subjects during the gloved condition; and (4) small handed female subjects do not perform as well as medium and large handed female subjects, nor as well as male subjects. DTIC

N95-27164*# Alabama Univ., Huntsville, AL. The K. E. Johnson Research Center.
MARSHALL SPACE FLIGHT CENTER SOLID WASTE CHARACTERIZATION AND RECYCLING IMPROVEMENT STUDY Final Report
Michael H. Eley, Lavonne Crews, Ben Johnston, David Lee, and James Colebaugh Apr. 1995 192 p Original contains color illustrations
(Contract NAS8-38609)
(NASA-CR-196594; NAS 1.26:196594; JRC-95-02) Avail: CASI HC A09/MF A02; 7 functional color pages

The MSFC Facilities Office, which is responsible for disposing of all waste generated by MSFC, issued a delivery order to the University of Alabama in Huntsville (UAH) to characterize current MSFC waste streams and to evaluate their existing recycling program. The purpose of the study was to define the nature, quantity, and types of waste produced and to generate ideas for improving the present recycling program. Specifically, the following tasks were to be performed: Identify various surplus and waste materials--as identified by the Contracting Officer's Technical Representative (COTR)--by source, location, and type; Analyze MSFC's current methods for handling, storage, transport, and disposition of waste and surplussed materials; Determine the composition of various surplus and waste materials as to type and quantities from various sources and locations; Analyze different methods for the disposition of various surplus and waste materials, including quality, quantity, preparation, transport cost, and value; Study possible alternatives to current methods of handling, storage, transport, and disposition of surplus and waste materials to improve the quality and quantities recycled or sold and to reduce and minimize the quantities of surplus and waste material currently being disposed of or stored; Provide recommendations for source and centralized segregation and aggregation of materials for recycling and/or disposition; and The analysis could include identification and laboratory level evaluation of methods and/or equipment, including capital costs, operating costs, maintenance requirements, life cycle and return on investment for systems to support the waste reduction program mission. Derived from text

N95-27195 Air Force Inst. of Tech., Wright-Patterson AFB, OH. School of Logistics and Acquisition Management.
FACTORS IN HUMAN-COMPUTER INTERFACE DESIGN (A PILOT STUDY) M.S. Thesis
Susan Stewart Dec. 1994 205 p Limited Reproducibility: More than 20% of this document may be affected by microfiche quality
(AD-A288908; AFIT/GIR/LAR/94D-6) Avail: Issuing Activity (Defense Technical Information Center (DTIC))

The DOD has budgeted over $9.8 billion for 1995 for information technology, yet many government office workers let their existing systems sit idle. This thesis explores why these computers are sitting idle. This researcher's initial hypothesis was that certain features of the human-computer interface can positively or negatively affect efficiency, retention, and satisfaction level of workers. Although some research is being done in this area, interfaces continue to be of poor quality, especially in the DOD, where long procurement cycles, forced purchases, and limited budgets result in out-of-date software. Intuitively most programmers know the human-computer interface impacts on a person's ability to learn, but to what degree? This study is designed to test four basic human-computer interface features: color, white space, verb tense, and parallelism. In addition, it is designed to test the interaction between visual and linguistic features, color and verb tense, as well as between white space and parallelism. DTIC

N95-27501*# National Aeronautics and Space Administration. Marshall Space Flight Center, Huntsville, AL.
AUTOMATIC LOCKING KNEE BRACE JOINT Patent Application
Bruce Weddendorf, inventor (to NASA) 17 Apr. 1995 17 p
(NASA-Case-MFS-28997-1; NAS 1.71:MFS-28997-1; US-Patent-Appl-SN-422961) Avail: CASI HC A03/MF A01

This invention is an apparatus for controlling the pivotal movement of a knee brace comprising a tang-and-clevis joint that has been uniquely modified. Both the tang and the clevis have a set of teeth that, when engaged, can lock the tang and the clevis together. In addition, the tang is biased away from the clevis. Consequently, when there is no axial force (i.e., body weight) on the tang, the tang is free to pivot within the clevis. However, when an axial force is exerted on the tang, the tang is pushed into the clevis, both sets of teeth engage, and the tang and the clevis lock together. NASA

N95-27696# Federal Aviation Administration, Washington, DC. Office of Aviation Medicine
HUMAN FACTORS IN AVIATION MAINTENANCE, PHASE 4 Progress Report, Apr. 1993 - Apr. 1994
William T. Shepherd May 1995 176 p Prepared in cooperation with Galaxy Scientific Corp., Atlanta, GA
(Contract DTFA01-94-C-01013)
(DOT/FAA/AM-95/14) Avail: CASI HC A09/MF A02

The fourth phase of research on human factors in aviation maintenance continued to look at the human's role in the aviation maintenance system via investigations, demonstrations, and evaluations of the research program outputs. This report describes the field evaluation plan for the Performance Enhancement System, a computer-based tool designed to aid Aviation Safety Inspectors in performing their oversight duties (Chapter 2). Chapter 3 describes the design of a computer-based workcard system. The report also discusses the development of an ergonomic audit program for visual inspection, which contains a method of choosing tasks to be audited, an audit checklist, and a computer program to evaluate check-list response against national and international standards (Chapter 4). Chapter 5 reports on an investigation of ergonomic factors that may cause increased inspector stress, fatigue, and workload, particularly in restrictive spaces that cause extreme postures. The continued development and expansion of the hypermedia information system is reported on in Chapter 6. Chapter 7 describes an investigation of individual differences in nondestructive inspection performance. Chapter 8 describes an investigation to determine the effect of an Intelligent Help Agent on the effectiveness of computer-based training. Chapter 9 reports on a joint CAA/FAA investigation of reliability in aircraft inspection in the United Kingdom and United States. Chapter 10 is a bibliographic overview of selected issues in designing computer-based training systems. Author

N95-28390 Army Natick Research and Development Command, MA.
EVALUATION OF LASER-PROTECTIVE EYEWEAR DYES IN UVEX LENSES Final Report, Mar. - Jun. 1992
Leonard A. Levasseur, Joseph F. Roach, and Kathryne B. Brubaker Nov. 1994 20 p Limited Reproducibility: More than 20% of this document may be affected by microfiche quality
(AD-A290076; NATICK/TR-95/006) Avail: Issuing Activity (Defense Technical Information Center (DTIC))

Twenty-seven lenses of various dye combinations were received for testing from Uvex Corp. A previous contract from Uvex for Natick had failed the 240-hour Weatherometer test and this study was to determine which dye or which combination of dyes was responsible for this degradation. Dyes from different suppliers were incorporated into Uvex polycarbonate lenses. These dyes were laser blocking dyes obtained from Gentex, Polaroid, Barnes, Steadfast and Epolin (a Uvex dye) and used in various combinations within the lenses. These lenses were evaluated for optical density, visual transmittance, laser saturation, and solarization. Some of the lenses were tested in the weatherometer only. DTIC

N95-28659 Selskapet for Industriell og Teknisk Forskning, Trondheim (Norway).
PLANNING, DESIGN AND CONSTRUCTION OF THE CAVERN ARENA: HEATING, VENTILATION AND AIR CONDITIONING
H. M. Mathisen and D. W. Lee 29 Apr. 1994 8 p Prepared in cooperation with Hyundai Engineering and Construction
(PB95-196382; STF15-S94002) Avail: Issuing Activity (National Technical Information Service (NTIS))

This paper deals with problems connected with heating and ventilation of underground premises for public use. Some properties of rock and special problems connected with designing ventilation systems for underground spaces are first briefly discussed. The rest of the paper deals with design of ventilation and heating systems. The conclusion is that there are no large problems with heating and ventilation of underground premises, but there are still problems connected with, for instance, thermal properties of rock when water flows in the cracks. An optimum design demands better knowledge of these properties. NTIS

N95-28667 Army Aeromedical Research Lab., Fort Rucker, AL.
MANIKIN INTEGRATED DATA ACQUISITION SYSTEM (MIDAS) INITIAL MODIFICATIONS Final Report
Nabih M. Alem, James A. Lewis, and Robert M. Dillard Dec. 1994 36 p Limited Reproducibility: More than 20% of this document may be affected by microfiche quality
(DA Proj. 301-62787-A-878)
(AD-A291662; USAARL-95-11) Avail: Issuing Activity (Defense Technical Information Center (DTIC))

A prototype manikin with internal data acquisition system (MIDAS) has been developed and received by the US Army Aeromedical Research Laboratory. In addition to a novel design of the spinal column and pelvis of the Hybrid III automotive manikin, the new MIDAS includes a built-in signal conditioning and acquisition electronics. This report documents the initial modifications to the manikin and includes a description of the external software (MIDAS 3.0) for control, communication, and posttest downloading and analysis of the data. DTIC

55 SPACE BIOLOGY

Includes exobiology; planetary biology; and extraterrestrial life.

No abstracts in this category.

59 MATHEMATICAL AND COMPUTER SCIENCES (GENERAL)

No abstracts in this category.

60 COMPUTER OPERATIONS AND HARDWARE

Includes hardware for computer graphics, firmware, and data processing.

For components see *33 Electronics and Electrical Engineering.*

N95-26697*# Institute for Computer Applications in Science and Engineering, Hampton, VA.
PERFORMANCE PREDICTION: A CASE STUDY USING A MULTI-RING KSR-1 MACHINE Final Report
Xian-He Sun (Louisiana State Univ., Baton Rouge, LA.) and Jianping Zhu (Mississippi State Univ., Mississippi State, MS.) Apr. 1995 22 p Presented at the 28th Hawaii International Conference on System Sciences, Jan. 1995 Submitted for publication
(Contract NAS1-19480; RTOP 505-90-52-01)
(NASA-CR-195066; NAS 1.26:195066; ICASE-95-24) Avail: CASI HC A03/MF A01

While computers with tens of thousands of processors have successfully delivered high performance power for solving some of the so-called 'grand-challenge' applications, the notion of scalability is becoming an important metric in the evaluation of parallel machine architectures and algorithms. In this study, the prediction of scalability and its application are carefully investigated. A simple formula is presented to show the relation between scalability, single processor computing power, and degradation of parallelism. A case study is conducted on a multi-ring KSR1 shared virtual memory machine. Experimental and theoretical results show that the influence of topology variation of an architecture is predictable. Therefore, the performance of an algorithm on a sophisticated, heirarchical architecture can be predicted and the best algorithm-machine combination can be selected for a given application. Author

N95-26845 Honeywell, Inc., Minneapolis, MN. Systems and Research Div.
MICRO-TIME STRESS MEASUREMENT DEVICE DEVELOPMENT Final Report, Aug. 1989 - Jan. 1992
Gary Harvey, Steven Louis, and Steven Buska Nov. 1994 88 p Limited Reproducibility: More than 20% of this document may be affected by microfiche quality
(Contract F30602-89-D-0100)
(AD-A289511; RL-TR-94-196) Avail: Issuing Activity (Defense Technical Information Center (DTIC))

This report describes the Micro-Time Stress Measurement Device (TSMD) developed and delivered under this contract. The Micro-TSMD is a microprocessor controlled device to read the installed environmental sensors and record their results in a nonvolatile memory. It is contained in a hybrid package about 1 x 1.8 x 0.2 (inches), weighing less than an ounce. The TSMD contains sensors for temperature, mechanical vibration/shock, and DC voltage monitoring, including transients, and may be connected to external sensors. It requires external power. DTIC

N95-27162# Joint Inst. for Nuclear Research, Dubna (USSR).
MAGNETIC FIELD MEASUREMENT FOR THE SPECTROMETRIC MAGNET OF THE ISTRA-M SETUP [IZMERENIE MAGNITNOGO POLYA SPEKTROMETRICHESKOGO EHLKTROMAGNITA USTANOVKI ISTRA-M]
A. D. Volkov, A. V. Voskanyan, and B. Zh. Zalikhanov et al 1994 10 p
In RUSSIAN
(DE95-608560; JINR-R-1-94-180) Avail: CASI HC A02/MF A01 (US Sales Only)

The results of magnetic field measurement for the spectrometric magnet of the ISTRA-M setup are reported. The automated system of measurements on the basis of PC is described. Designs of the magnet and mechanics of the measuring system on the basis of a three component Hall data unit are shown. A method of division of the whole measured volume into smaller ones was applied during the measurement processing. The average error of the basic component representation within the central part of the working volume is less than 0.1%. DOE

N95-27241*# National Aeronautics and Space Administration. Langley Research Center, Hampton, VA.
A STUDY OF WORKSTATION COMPUTATIONAL PERFORMANCE FOR REAL-TIME FLIGHT SIMULATION
Jeffrey M. Maddalon and Jeff I. Cleveland, II Feb. 1995 10 p
(RTOP 505-90-53-02)
(NASA-TM-109184; NAS 1.15:109184) Avail: CASI HC A02/MF A01

With recent advances in microprocessor technology, some have suggested that modern workstations provide enough computational power to properly operate a real-time simulation. This paper presents the results of a computational benchmark, based on actual real-time flight simulation code used at Langley Research Center, which was executed on various workstation-class machines. The benchmark was executed on different machines from several companies including: CONVEX Computer Corporation, Cray Research, Digital Equipment Corporation, Hewlett-Packard, Intel, International Business Machines, Silicon Graphics, and Sun Microsystems. The machines are compared by their execution speed, computational accuracy, and porting effort. The results of this study show that the raw computational power needed for real-time simulation is now offered by workstations. Author

N95-27914*# National Aeronautics and Space Administration. Flight Research Center, Edwards, CA.
NASA DRYDEN FLOW VISUALIZATION FACILITY
John H. DelFrate Washington May 1995 29 p Original contains color illustrations
(RTOP 505-59-53)
(NASA-TM-4631; H-1972; NAS 1.15:4631) Avail: CASI HC A03/MF A01; 4 functional color pages

This report describes the Flow Visualization Facility at NASA Dryden Flight Research Center, Edwards, California. This water tunnel facility is used primarily for visualizing and analyzing vortical flows on aircraft models and other shapes at high-incidence angles. The tunnel is used extensively as a low-cost, diagnostic tool to help engineers understand complex flows over aircraft and other full-scale vehicles. The facility consists primarily of a closed-circuit water tunnel with a 16- x 24-in. vertical test section. Velocity of the flow through the test section can be varied from 0 to 10 in/sec; however, 3 in/sec provides optimum velocity for the majority of flow visualization applications. This velocity corresponds to a unit Reynolds number of 23,000/ft and a turbulence level over the majority of the test section below 0.5 percent. Flow visualization techniques described here include the dye tracer, laser light sheet, and shadowgraph. Limited correlation to full-scale flight data is shown. Author

N95-27789*# Draper (Charles Stark) Lab., Inc., Cambridge, MA.
THE TRANSITION OF GTDS TO THE UNIX WORKSTATION ENVIRONMENT
D. Carter, R. Metzinger, R. Proulx, and P. Cefola *In* NASA. Goddard Space Flight Center, Flight Mechanics/Estimation Theory Symposium 1995 May 1995 p 301-302 (For primary document see N95-27763 09-13)
Avail: CASI HC A01/MF A04

61 COMPUTER PROGRAMMING AND SOFTWARE

Includes computer programs, routines, alogorithms, and specific applications, e.g., CAD/CAM.

N95-26346 Naval Postgraduate School, Monterey, CA.
VIRTUAL PROTOTYPING AS AN AID FOR CONTROL SYSTEM ANALYSIS M.S. Thesis
Arnold P. Selnick Sep. 1994 49 p Limited Reproducibility: More than 20% of this document may be affected by microfiche quality
(AD-A288819) Avail: Issuing Activity (Defense Technical Information Center (DTIC))

Virtual Prototyping provides an opportunity for control engineers to observe and evaluate their designs in a 'real world' setting without the costs or risks associated with flight test. Designers Workbench is a computer aided design tool that allows a user to create, view, modify and animate three-dimensional databases. These may include instruments, avionics displays and any out-the-window applications such as runways or terrain. The dynamic behavior of specific elements can be observed by linking data to the desired element. In this way a realtime animation of the simulation can be generated. The animation provides another analysis tool for the designer, by representing data in a more intuitive environment. Data files from two separate controller simulations was used. Cockpit instrumentation was modelled and used for each animation to monitor the aircraft states. In addition, each animation had an out-the-window perspective to view the aircraft model as it flew the prescribed trajectory. DTIC

N95-26348 Naval Air Warfare Center, Warminster, PA. Aircraft Div.
AN EVALUATION OF THE SOFTWARE THROUGH PICTURES/T TOOL (StP/T) FOR THE SOFTWARE SUPPORT ACTIVITY (SSA) Final Report
Virgil Banowetz 28 Nov. 1994 135 p Limited Reproducibility: More than 20% of this document may be affected by microfiche quality
(Contract N62269-90-C-0412)
(AD-A288822) Avail: Issuing Activity (Defense Technical Information Center (DTIC))

This study was conducted by the Naval Air Warfare Center Aircraft Division (NAWCADWAR) to evaluate the Interactive Development Environments (IDE) software product known as the T tool. The evaluation was initiated at the request of NAVAIRSYSCOM AIR-54661 to determine the applicability of these tools to the SSA environment. The conduct of the evaluation spanned the time period from March 1994 through September 1994. A 'Plan for Testing the T tool for SSA' was presented to and approved by AIR-54661 in April, 1994. The T tool is a specification based test case generation tool. This means that a specification which describes the inputs and outputs of a process or module is the only basis for producing the test cases. T was previously evaluated by Christine Youngblut of the Institute for Defense Analysis (item h in Applicable Documents) who reported that StP/T is currently being used by various government organizations including the Naval Avionics Center, the Jet Propulsion Laboratories, Naval Coastal Systems Center and US. Army Forts Monmouth and Sill. DTIC

N95-26386*# West Virginia Univ., Morgantown, VA. Software Research Lab.
CONCURRENT ENGINEERING RESEARCH CENTER Annual Report, 1993 - 1994
John R. Callahan Fairmont, WV Jan. 1995 41 p
(Contract NCCw-40)
(NASA-CR-197726; NASA-IVV-94-011; NAS 1.26:197726; WVU-SRL-94-011; CERC-IA-95-001) Avail: CASI HC A03/MF A01

The projects undertaken by The Concurrent Engineering Research Center (CERC) at West Virginia University are reported and summarized. CERC's participation in the Department of Defense's Defense Advanced Research Project relating to technology needed to improve the product development process is described, particularly in the area of advanced weapon systems. The efforts committed to improving collaboration among the diverse and distributed health care providers are reported, along with the research activities for NASA in Independent Software Verification and Validation. CERC also takes part in the electronic respirator certification initiated by The National Institute for Occupational Safety and Health, as well as in the efforts to find a solution to the problem of producing environment-friendly end-products for product developers worldwide. The 3M Fiber Metal Matrix Composite Model Factory Program is discussed. CERC technologies, facilities,and personnel-related issues are described, along with its library and technical services and recent publications. CASI

N95-26388*# West Virginia Univ., Fairmont, WV. Software Research Lab.

THE RELIABLE MULTICAST PROTOCOL APPLICATION PROGRAMMING INTERFACE

Todd Montgomery and Brian Whetten [1995] 20 p
(Contract NCCw-40)
(NASA-CR-197762; NASA-IVV-94-007; NAS 1.26:197762; WVU-SRL-94-007; WVU-SCS-TR-95-7; CERC-TR-RN-94-014) Avail: CASI HC A03/MF A01

The Application Programming Interface for the Berkeley/WVU implementation of the Reliable Multicast Protocol is described. This transport layer protocol is implemented as a user library that applications and software buses link against. Derived from text

N95-26408 Air Force Inst. of Tech., Wright-Patterson AFB, OH.

USING MACHINE LEARNING TO DERIVE EFFICIENT COST AND PERFORMANCE ESTIMATES IN VLSI CAD DESIGNS Ph.D. Thesis - Pittsburgh Univ.

Donald S. Gelosh Sep. 1994 194 p Limited Reproducibility: More than 20% of this document may be affected by microfiche quality
(AD-A288254; AFIT/CI/CIA/94-038D) Avail: Issuing Activity (Defense Technical Information Center (DTIC))

Area and delay estimates facilitate effective decision-making ability in high level synthesis. Current estimation techniques focus on modeling the layout result and fail to deliver timely or accurate estimates. This thesis presents a novel approach to deriving these area and delay estimates by modeling the actions and activities of the layout tool, rather than the layout result. This approach uses machine learning techniques to analyze the input-to-output relationships that result from applying the target layout tool to an input design description and producing a layout as an output. This thesis describes a solution architecture using these machine learning techniques that captures the relationships between general design features and layout concepts. This solution architecture has the following characteristics. First, a set of several training designs captures the general design features. The target layout tool is run on the training designs and produces a set of actual layouts. The general design features and relative placement concepts from the actual layouts makes up a training set. The formulation of this training set is important to adequately describe the set of general design features and the associated layout concepts. Second, a machine learning system analyzes the training set looking for relationships between the design features and layout concepts. This analysis produces a model of the operation of the layout tool. Third, this model is applied to real designs to formulate area and delay estimates. This approach is found to produce accurate area and delay estimates very quickly, even for designs with several thousand gates. DTIC

N95-26446 Carnegie-Mellon Univ., Pittsburgh, PA. Software Engineering Inst.

AN INTRODUCTION TO SOFTWARE ARCHITECTURE Final Report

David Garlan and Mary Shaw Jan. 1994 51 p Submitted for publication Limited Reproducibility: More than 20% of this document may be affected by microfiche quality
(Contracts F33615-93-1-1330; NSF CCR-91-09469)
(AD-A288963; CMU/SEI-94-TR-21; ESC-TR-94-21) Avail: Issuing Activity (Defense Technical Information Center (DTIC))

As the size of software systems increases, the algorithms and data structures of the computation no longer constitute the major design problems. When systems are constructed from many components, the organization of the overall system-the software architecture-presents a new set of design problems. This level of design has been addressed in a number of ways, including informal diagrams and descriptive terms, module interconnection languages, templates, and frameworks for systems that serve the needs of specific domains, and formal models of component integration mechanisms. DTIC

N95-26447 Naval Command, Control and Ocean Surveillance Center, San Diego, CA. RDT and E Div.

ANALYSIS OF HISTORICAL OCEANOGRAPHIC DATA ON A PERSONAL COMPUTER. PROGRAM MDS Final Report

Alvan Fisher, Jr. Oct. 1994 34 p Limited Reproducibility: More than 20% of this document may be affected by microfiche quality
(AD-A288965; NRAD-TD-2703) Avail: Issuing Activity (Defense Technical Information Center (DTIC))

Program MDS uses an IBM-compatible personal computer to process and analyze temperature, salinity, and sound speed data in three formats: two-dimensional plots, histograms, and statistical computation and/or correlations. The data, extracted from the master oceanographic observation data set (MOODS) files maintained by the Naval Oceanographic Office, require prior reformatting to regional files for meaningful analysis. Graphic and printer output of these analyses provides valuable input needed to determine oceanic and acoustic properties of a desired area. DTIC

N95-26467 Carnegie-Mellon Univ., Pittsburgh, PA. School of Computer Science.

AN INTRODUCTION TO SOFTWARE ARCHITECTURE

David Garlan and Mary Shaw Jan. 1994 49 p Limited Reproducibility: More than 20% of this document may be affected by microfiche quality
(Contract F33615-93-1-1330)
(AD-A288356; CMU-CS-94-166) Avail: Issuing Activity (Defense Technical Information Center (DTIC))

As the size of software systems increases, the algorithms and data structures of the computation no longer constitute the major design problems. When systems are constructed from many components, the organization of the overall system - the software architecture - presents a new set of design problems. This level of design has been addressed in a number of ways including informal diagrams and descriptive terms, module interconnection languages, templates and frameworks for systems that serve the needs of specific domains, and formal models of component integration mechanisms. In this paper we provide an introduction to the emerging field of software architecture. We begin by considering a number of common architectural styles upon which many systems are currently based and show how different styles can be combined in a single design. Then we present six case studies to illustrate how architectural representations can improve our understanding of complex software systems. Finally, we survey some of the outstanding problems in the field, and consider a few of the promising research directions. DTIC

N95-26469 Carnegie-Mellon Univ., Pittsburgh, PA. Dept. of Computer Science.

APPLICATION-AWARE ADAPTATION FOR MOBILE COMPUTING

M. Satyanarayanan, Brian Noble, Puneet Kumar, and Morgan Price 28 Jul. 1994 9 p Limited Reproducibility: More than 20% of this document may be affected by microfiche quality
(Contract F19628-93-C-0193)
(AD-A288366; CMU-CS-94-183) Avail: Issuing Activity (Defense Technical Information Center (DTIC))

This paper identifies application-aware adaptation as an essential capability of mobile clients, and provides an overview of Odyssey, an architecture that supports this capability. Functionality that has hitherto been implemented monolithically must now be split between the operating system and individual applications. The role of the operating system is to sense external events, and to monitor and allocate scarce resources. In contrast, the role of individual applications is to adapt to changing conditions by using the information and resources provided by the operating system. DTIC

N95-26474 Rome Lab., Griffiss AFB, NY.

ACT ADAPTIVE FILTERS Report, Aug. 1989 - Jul. 1994

Siemak S. Tabrizi Sep. 1994 32 p Limited Reproducibility: More than 20% of this document may be affected by microfiche quality
(AD-A288385; RL-TR-94-149) Avail: Issuing Activity (Defense Technical Information Center (DTIC))

This report investigates the Acoustic Charge Transport (ACT) Programmable Transversal Filter (PTF) with 128 taps each having a 5-bit tap precision. ACT devices can be used for Finite Impulse Response (FIR) adaptive filtering. The objective of this report is to document the implementation of an adaptive filter with ACT device using a Linear Random

Search (LRS) adaptive algorithm, and its performance. The LRS algorithm was evaluated for a single Continuous-Wave (CW) tone interferer, and its performance (null depth) was compared to theoretical predictions. Specifically, the rate of convergence and filter response after adaptation was simulated using MATLAB and the results were compared to that obtained experimentally. DTIC

N95-26486*# West Virginia Univ., Fairmont, WV. Software Research Lab.

SOFTWARE RISK MANAGEMENT THROUGH INDEPENDENT VERIFICATION AND VALIDATION

John R. Callahan, Tong C. Zhou, and Ralph Wood [1995] 9 p Presented in the Proceedings of the 4th International Conference on Software Quality, American Society for Quality Control, Washington, D.C., 3-5 Oct. 1994

(Contracts NCCw-40; NAG5-2129; MDA972-91-J-102)

(NASA-CR-197767; NASA-IVV-94-002; NAS 1.26:197767; WVU-SRL-94-002; WVU-SCS-TR-94-11; CERC-TR-TM-94-007) Avail: CASI HC A02/MF A01

Software project managers need tools to estimate and track project goals in a continuous fashion before, during, and after development of a system. In addition, they need an ability to compare the current project status with past project profiles to validate management intuition, identify problems, and then direct appropriate resources to the sources of problems. This paper describes a measurement-based approach to calculating the risk inherent in meeting project goals that leverages past project metrics and existing estimation and tracking models. We introduce the IV&V Goal/Questions/Metrics model, explain its use in the software development life cycle, and describe our attempts to validate the model through the reverse engineering of existing projects. Author

N95-26511 Polish Academy of Sciences, Warsaw (Poland). Inst. of Basic Problems of Technology.

BEGINNER'S GUIDE TO UNIX [JAK ZACZAC Z UNIXEM]

Jerzy Supel, A. 1994 79 p In POLISH

(ISSN 0208-5658)

(IFTR-17/1994) Avail: Issuing Activity (Polish Academy of Sciences, Warsaw, Poland)

A compilation of different operating instructions and descriptions of functions of the UNIX application is presented. Some examples of the author's experiences with the SUN computer network at the Institute of Basic Problems of Technology are illustrated. These examples were chosen from the author's observations of users of the network.

Transl. by Schreiber Translations Inc.

N95-26534 Carnegie-Mellon Univ., Pittsburgh, PA. School of Computer Science.

OPERATING SYSTEM SUPPORT FOR COEXISTENCE OF REAL-TIME AND CONVENTIONAL SCHEDULING

David B. Golub 3 Nov. 1994 14 p Limited Reproducibility: More than 20% of this document may be affected by microfiche quality

(Contract DABT63-93-C-0054)

(AD-A288584; CMU-CS-94-212) Avail: Issuing Activity (Defense Technical Information Center (DTIC))

The advent of multimedia calls for new scheduling paradigms to handle the combination of time-critical and conventional applications present on many multimedia systems. The scheduler of the Mach 3.0 Microkernel has been rewritten to allow a wide spectrum of scheduling policies, from real-time through time-sharing to background, to be selected simultaneously for different tasks executing on the same processor. Scheduling policies can be set for a task or for individual threads within the task. The set of scheduling policies allowed on a processor or set of processors may be dynamically altered. Scheduling parameters can be set individually for each thread, task, or scheduling policy enabled on a processor. Each scheduling policy may have its own format for parameters; they are not limited to integer priorities. New scheduling policies may be configured into a kernel and may be ordered in any way desired. The resulting system provides enough flexibility for experimentation with new scheduling regimes, yet is efficient enough to allow a reasonable number of scheduling policies to coexist. When configured with both real-time and time-sharing schedulers, the system smoothly supports both conventional and time-critical applications. DTIC

N95-26536 Carnegie-Mellon Univ., Pittsburgh, PA. School of Computer Science.

SPECIFYING WEAK SETS

Jeannette M. Wing and David C. Steere Sep. 1994 21 p Sponsored by Digital Equipment Corp.; and IBM Limited Reproducibility: More than 20% of this document may be affected by microfiche quality

(Contracts F33615-90-C-1465; F19628-93-C-0193; F33615-93-1-1330; ARPA Order 7597; ARPA Order A700)

(AD-A288587; CMU-94-194) Avail: Issuing Activity (Defense Technical Information Center (DTIC))

We present formal specifications of a new abstraction, weak sets, which can be used to alleviate high latencies when retrieving data from a wide-area information system like the World Wide Web. In the presence of failures, concurrency, and distribution, clients performing queries may observe behavior that is inconsistent with the stringent semantic requirements of mathematical sets. For example, an element retrieved and returned to the client may be subsequently deleted before the query terminates. We chose to specify formally the behavior of weak sets because we wanted to understand the varying degrees of inconsistency clients might be willing to tolerate and to understand the tradeoff between providing strong consistency guarantees and implementing weak sets efficiently. Our specification assertion language uses a novel construct that lets us model reachability explicitly; with it, we can distinguish between the existence of an object and its accessibility. The specifications were instrumental in understanding the design space, and we are currently implementing the most permissive of the specifications in several types of Unix systems. DTIC

N95-26554 Naval Postgraduate School, Monterey, CA.

A SYSTEM DYNAMICS BASED STUDY OF SOFTWARE REUSE AND ITS DETERMINANTS M.S. Thesis

Wayne Lee Aiken Sep. 1994 87 p Limited Reproducibility: More than 20% of this document may be affected by microfiche quality

(AD-A288578) Avail: Issuing Activity (Defense Technical Information Center (DTIC))

Software cost for DOD is a critical issue. Software reuse promises significant cost savings by using previously developed components thus increasing productivity. Quality is improved because these components are well designed, well documented, and well tested. This thesis studies the determinants of software reuse using a system dynamics computer model, the Dynamica Reuse Model, which simulates the activities of a software development organization engaged in organization-wide, systematic software reuse. Results indicate that setting goals of consumption and production of components too low will lead to a decreased reuse rate of turnover of personnel. In the area of consumption and production costs of reusable components, production costs are more critical. Regarding employee turnover, reuse is enhanced by a low rate of turnover of personnel. In establishing a successful reuse program, creating repository is an important factor and the study indicates there is a structurally stable repository value. Concerning the software development rate of components, a steady development rate leads to a more consistent reuse rate. DOD managers can now use these results in formulating policies concerning their systematic reuse program. DTIC

N95-26557 Florida International Univ., Miami, FL.

THE DEVELOPMENT OF A FEATURE-BASED CONCURRENT ENGINEERING SYSTEM Final Report, 1 Jan. 1992 - 31 Aug. 1994

Chin-Sheng Chen and Fred W. Swift 10 Oct. 1994 299 p Limited Reproducibility: More than 20% of this document may be affected by microfiche quality

(Contract MDA972-92-J-1008)

(AD-A288424) Avail: Issuing Activity (Defense Technical Information Center (DTIC))

This research project is aimed at development of a concurrent engineering system for integrated product and process development of machined component designs. Its main purpose is to evaluate the feasibility of implementation of a concurrent engineering system which provides both horizontal and vertical integration of CAD/CAM systems. The research and development of this project has been founded on concepts of form features and object-oriented computer techniques. The R&D tasks identified in the research project are: (1) feature definition and classification; (2) product data representation; (3) product information modeling; (4) manufacturing resources modeling; (5) producibility evaluation; (6) manufacturing process planning; and (7) NC program modeling. Throughout the entire project period, industrial practice and standards have been closely observed and incorporated in the development, when applicable. DTIC

N95-26575*# West Virginia Univ., Morgantown, VA. Dept. of Statistics and Computer Science.

A SOFTWARE BUS FOR THREAD OBJECTS

John R. Callahan and Dehuai Li Fairmont, WV [1995] 19 p
(Contracts NCCw-40; NAG5-2129; N01-LM-3-3525; MDA972-91-J-1022)
(NASA-CR-197764; NASA-IVV-95-005; NAS 1.26:197764; WVU-SRL-94-005; WVU-SCS-TR-95-5; CERC-TR-RN-94-001) Avail: CASI HC A03/MF A01

The authors have implemented a software bus for lightweight threads in an object-oriented programming environment that allows for rapid reconfiguration and reuse of thread objects in discrete-event simulation experiments. While previous research in object-oriented, parallel programming environments has focused on direct communication between threads, our lightweight software bus, called the MiniBus, provides a means to isolate threads from their contexts of execution by restricting communications between threads to message-passing via their local ports only. The software bus maintains a topology of connections between these ports. It routes, queues, and delivers messages according to this topology. This approach allows for rapid reconfiguration and reuse of thread objects in other systems without making changes to the specifications or source code. A layered approach that provides the needed transparency to developers is presented. Examples of using the MiniBus are given, and the value of bus architectures in building and conducting simulations of discrete-event systems is discussed. Author

N95-26605 Carnegie-Mellon Univ., Pittsburgh, PA. Dept. of Computer Science.

MODAL EVENT CALCULUS IN LOLLI Research Report

Iliano Cervesato, Luca Chittaro (Udine Univ., Italy.), and Angelo Montanari (Udine Univ., Italy.) Oct. 1994 24 p Limited Reproducibility: More than 20% of this document may be affected by microfiche quality
(Grant NSF CCR-93-03383)
(AD-A288544; CMU-CS-94-198) Avail: Issuing Activity (Defense Technical Information Center (DTIC))

This paper introduces two variants of the Event Calculus (EC) with relative timing of events: the Credulous and the Skeptical Event Calculus (CREC and SKEC respectively). A model that takes into account the dynamics of event ordering updates is constructed for EC. In this model, that appears to be a restriction of the usual model for the modal logic S4, CREC and SKEC are proved to be the modal counterparts of EC. It is then shown how a full propositional modal logic based on these calculi can be conveniently and elegantly coded by means of the linear logic programming language Lolli. DTIC

N95-26611 ParaSoft Corp., Monrovia, CA.

AUTOMATIC TEST DATA GENERATION TOOL FOR LARGE-SCALE SOFTWARE SYSTEMS Final Report

A. Kolawa, B. Strickland, and A. Hicken 26 May 1994 51 p Sponsored by BMDO Limited Reproducibility: More than 20% of this document may be affected by microfiche quality
(Contract DASG60-94-C-0051)
(AD-A289081) Avail: Issuing Activity (Defense Technical Information Center (DTIC))

The main Phase 1 goals were to: (1) Build a prototype of a TGS System which works with programs written in C. The prototype should have skeletons of the major algorithms which the tool will be using. (2) Assess if the approach which we proposed has a chance to become a real TGS tool, by running the prototype on chosen C programs. The goals of the Phase 1 were achieved. We produced a working prototype of the TgS tool. We implemented the major algorithms: symbolic execution, dynamic data-flow analysis, function minimization methods, heuristics random input generation. DTIC

N95-26628* Illinois Univ., Urbana, IL. Center for Reliable and High-Performance Computing.

COMPILER-ASSISTED DEBUGGING AND MULTIPLE INSTRUCTION RETRY Ph.D. Thesis

Shyh-Kweh Chen Nov. 1994 86 p Limited Reproducibility: More than 20% of this document may be affected by microfiche quality
(Contract NAG1-613; N00014-90-J-1270)
(NASA-CR-197729; NAS 1.26:197729; AD-A288995; UILU-ENG-94-2241; CRHC-94-24) Avail: Issuing Activity (Defense Technical Information Center (DTIC))

Backward execution requires the saving of historic information concurrently with the normal execution in order for a program to roll back. There are several applications for which backward execution is useful. In an environment where reliability is a concern, it may be necessary to roll back the program to a previously executed state in case of system faults. Multiple instruction retry is an alternative to checkpointing for recovery from a transient processor failure, especially when the error detection latency is only a few cycles. Speculative execution can achieve significant speed up for superscalar architectures by utilizing instruction retry to roll back the computation above mispredicted branches. Debugging is another field that can benefit from backward execution. Allowing the user to undo several instructions at specific positions may facilitate program debugging. This thesis describes schemes that have been implemented for multiple instruction retry for both RISC- type scalar processors, and very long instruction word (VLIW) architectures. The thesis also presents approaches that incorporate backward execution into a debugger, at both the compiler and the debugger levels. DTIC

N95-26648*# MCAT Inst., San Jose, CA.

SUPERSONIC TRANSPORT GRID GENERATION, VALIDATION, AND OPTIMIZATION Final Report, 1993 - 31 Jan. 1995

Philip G. Aaronson Jan. 1995 15 p Original contains color illustrations
(Contract NCC2-522)
(NASA-CR-197752; NAS 1.26:197752; MCAT-95-03) Avail: CASI HC A03/MF A01; 1 functional color page

The ever present demand for reduced flight times has renewed interest in High Speed Civil Transports (HSCT). The need for an HSCT becomes especially apparent when the long distance, over-sea, high growth Pacific rim routes are considered. Crucial to any successful HSCT design are minimal environmental impact and economic viability. Vital is the transport's aerodynamic efficiency, ultimately effecting both the environmental impact and the operating cost. Optimization, including numerical optimization, coupled with the use of computational fluid dynamics (CFD) technology, has and will offer a significant improvement beyond traditional methods. Derived from text

N95-26656 Carnegie-Mellon Univ., Pittsburgh, PA. School of Computer Science.

A PARALLEL COMPLEXITY MODEL FOR FUNCTIONAL LANGUAGES

Guy Belloch and John Greiner 20 Oct. 1994 28 p Sponsored by NSF Limited Reproducibility: More than 20% of this document may be affected by microfiche quality
(Contracts F33615-93-1-1330; F19628-91-C-0168)
(AD-A288589; CMU-CS-94-196) Avail: Issuing Activity (Defense Technical Information Center (DTIC))

A complexity model based on the A-calculus with an appropriate operational semantics in presented and related to various parallel machine models, including the PRAM and hypercube models. The model is used to study parallel algorithms in the context of sequential' functional languages and to relate these results to algorithms designed directly for parallel machine models. For example, the paper shows that equally good upper bounds can be achieved for merging two sorted sequences in the pure A-calculus with some arithmetic constants as in the EREW PRAM, when they are both mapped onto a more realistic machine such as a hypercube or butterfly network. In particular for n keys and p processors, they both result in an O(n/p + sq log p) time algorithm. These results argue that it is possible to get good parallelism in functional languages without adding explicitly parallel constructs. In fact, the lack of random access seems to be a bigger problem than the lack of parallelism. DTIC

N95-26668*# West Virginia Univ., Fairmont, WV. Software Research Lab.

USING SCR METHODS TO ANALYZE REQUIREMENTS DOCUMENTATION

John Callahan and Jeffery Morrison [1995] 5 p Presented at 4th International Naval Research Laboratory Software Cost Reduction Workshop,

Washington, DC, 29-30 Nov. 1994
(Contract NCCw-40)
(NASA-CR-197760; NASA-IVV-94-009; NAS 1.26:197760;
WVU-SRL-94-009; WVU-SCS-TR-95-9; CERC-TR-TM-94-009) Avail: CASI
HC A01/MF A01

Software Cost Reduction (SCR) methods are being utilized to analyze and verify selected parts of NASA's EOS-DIS Core System (ECS) requirements documentation. SCR is being used as a spot-inspection tool. Through this formal and systematic approach of the SCR requirements methods, insights as to whether the requirements are internally inconsistent or incomplete as the scenarios of intended usage evolve in the OC (Operations Concept) documentation. Thus, by modelling the scenarios and requirements as mode charts using the SCR methods, we have been able to identify problems within and between the documents.
Derived from text

N95-26685*# National Aeronautics and Space Administration. Langley Research Center, Hampton, VA.

DESIGN TOOL FOR MULTIPROCESSOR SCHEDULING AND EVALUATION OF ITERATIVE DATAFLOW ALGORITHMS

Robert L. Jones, III Apr. 1995 43 p
(RTOP 233-01-03)
(NASA-TP-3491; L-17408; NAS 1.60:3491) Avail: CASI HC A03/MF A01

A graph-theoretic design process and software tool is defined for selecting a multiprocessing scheduling solution for a class of computational problems. The problems of interest are those that can be described with a dataflow graph and are intended to be executed repetitively on a set of identical processors. Typical applications include signal processing and control law problems. Graph-search algorithms and analysis techniques are introduced and shown to effectively determine performance bounds, scheduling constraints, and resource requirements. The software tool applies the design process to a given problem and includes performance optimization through the inclusion of additional precedence constraints among the schedulable tasks.
Author

N95-26693*# West Virginia Univ., Fairmont, WV. Software Research Lab.

SOFTWARE PACKAGER USER'S GUIDE

John R. Callahan [1995] 15 p
(Contracts NCCw-40; NAG5-2129; MDA972-91-J-1022)
(NASA-CR-197763; NASA-IVV-94-006; NAS 1.26:197763;
WVU-SRL-94-006; WVU-SCS-TR-95-6; CERC-TR-RN-94-012) Avail: CASI
HC A03/MF A01

Software integration is a growing area of concern for many programmers and software managers because the need to build new programs quickly from existing components is greater than ever. This includes building versions of software products for multiple hardware platforms and operating systems, building programs from components written in different languages, and building systems from components that must execute on different machines in a distributed network. The goal of software integration is to make building new programs from existing components more seamless -- programmers should pay minimal attention to the underlying configuration issues involved. Libraries of reusable components and classes are important tools but only partial solutions to software development problems. Even though software components may have compatible interfaces, there may be other reasons, such as differences between execution environments, why they cannot be integrated. Often, components must be adapted or reimplemented to fit into another application because of implementation differences -- they are implemented in different programming languages, dependent on different operating system resources, or must execute on different physical machines. The software packager is a tool that allows programmers to deal with interfaces between software components and ignore complex integration details. The packager takes modular descriptions of the structure of a software system written in the package specification language and produces an integration program in the form of a makefile. If complex integration tools are needed to integrate a set of components, such as remote procedure call stubs, their use is implied by the packager automatically and stub generation tools are invoked in the corresponding makefile. The programmer deals only with the components themselves and not the details of how to build the system on any given platform.
Author

N95-26694*# Michigan Univ., Ann Arbor, MI. Radiation Lab.

USER'S AND TEST CASE MANUAL FOR FEMATS

Arindam Chatterjee, John Volakis, Mike Nurnberger, and John Natzke 26 Apr. 1995 65 p Revised
(Grant NAG2-866)
(NASA-CR-197803; NAS 1.26:197803; UMICH-031155-3-T) Avail: CASI
HC A04/MF A01

The FEMATS program incorporates first-order edge-based finite elements and vector absorbing boundary conditions into the scattered field formulation for computation of the scattering from three-dimensional geometries. The code has been validated extensively for a large class of geometries containing inhomogeneities and satisfying transition conditions. For geometries that are too large for the workstation environment, the FEMATS code has been optimized to run on various supercomputers. Currently, FEMATS has been configured to run on the HP 9000 workstation, vectorized for the Cray Y-MP, and parallelized to run on the Kendall Square Research (KSR) architecture and the Intel Paragon.
Author

N95-26695*# West Virginia Univ., Fairmont, WV. Software Research Lab.

A DECENTRALIZED SOFTWARE BUS BASED ON IP MULTICAS TING

John R. Callahan and Todd Montgomery Jan. 1995 15 p
(Contracts NCCw-40; NAG5-2129; MDA972-91-J-0102)
(NASA-CR-197768; NASA-IVV-94-001; NAS 1.26:197768;
WVU-SRL-94-001; WVU-SCS-TR-95-2; CERC-TR-TM-012) Avail: CASI
HC A03/MF A01

We describe decentralized reconfigurable implementation of a conference management system based on the low-level Internet Protocol (IP) multicasting protocol. IP multicasting allows low-cost, world-wide, two-way transmission of data between large numbers of conferencing participants through the Multicasting Backbone (MBone). Each conference is structured as a software bus -- a messaging system that provides a run-time interconnection model that acts as a separate agent (i.e., the bus) for routing, queuing, and delivering messages between distributed programs. Unlike the client-server interconnection model, the software bus model provides a level of indirection that enhances the flexibility and reconfigurability of a distributed system. Current software bus implementations like POLYLITH, however, rely on a centralized bus process and point-to-point protocols (i.e., TCP/IP) to route, queue, and deliver messages. We implement a software bus called the MULTIBUS that relies on a separate process only for routing and uses a reliable IP multicasting protocol for delivery of messages. The use of multicasting means that interconnections are independent of IP machine addresses. This approach allows reconfiguration of bus participants during system execution without notifying other participants of new IP addresses. The use of IP multicasting also permits an economy of scale in the number of participants. We describe the MULITIBUS protocol elements and show how our implementation performs better than centralized bus implementations.
Author

N95-26711*# West Virginia Univ., Fairmont, WV. Software Research Lab.

USING AN ARCHITECTURAL APPROACH TO INTEGRATE HETEROGENEOUS, DISTRIBUTED SOFTWARE COMPONENTS

John R. Callahan and James M. Purtilo (Maryland Univ., College Park, MD.) [1995] 36 p Sponsored in part by National Library of Medicine, ARPA and Domain-Specific Software Architectures
(Contracts NCCw-40; NAG5-2129; MDA972-91-J-0102)
(NASA-CR-197766; NASA-IVV-94-003; NAS 1.26:197766;
WVU-SRL-94-003; WVU-SCS-TR-95-3; CERC-TR-RN-94-009) Avail: CASI
HC A03/MF A01

Many computer programs cannot be easily integrated because their components are distributed and heterogeneous, i.e., they are implemented in diverse programming languages, use different data representation formats, or their runtime environments are incompatible. In many cases, programs are integrated by modifying their components or interposing mechanisms that handle communication and conversion tasks. For example, remote procedure call (RPC) helps integrate heterogeneous, distributed programs. When configuring such programs, however, mechanisms like RPC must be used explicitly by software developers in order to integrate collections of diverse components. Each collection may require a unique integration solution. This paper describes improvements to the concepts of software packaging and some of our experiences in constructing complex software systems from a wide variety of components in different execution environments. Software packaging is a process that automatically determines how to integrate a diverse collection of computer programs based on the types of components involved and the capabilities of available translators and adapters in an environment. Software packaging provides a context that relates such mechanisms to software integration processes and reduces the cost of configuring applications whose components are distributed or implemented in different programming languages. Our software packaging tool subsumes traditional integration tools like UNIX make by providing a rule-based approach to software integration that is independent of execution environments. Author

N95-26726*# National Aeronautics and Space Administration. Ames Research Center, Moffett Field, CA.

THE MULTIDIMENSIONAL SELF-ADAPTIVE GRID CODE, SAGE, VERSION 2

Carol B. Davies (Sterling Software, Inc., Palo Alto, CA.) and Ethiraj Venkatapathy (Thermoscience Inst., Moffett Field, CA.) Apr. 1995 74 p
(RTOP 242-10-01)
(NASA-TM-110350; A-950056; NAS 1.15:110350) Avail: CASI HC A04/MF A01

This new report on Version 2 of the SAGE code includes all the information in the original publication plus all upgrades and changes to the SAGE code since that time. The two most significant upgrades are the inclusion of a finite-volume option and the ability to adapt and manipulate zonal-matching multiple-grid files. In addition, the original SAGE code has been upgraded to Version 1.1 and includes all options mentioned in this report, with the exception of the multiple grid option and its associated features. Since Version 2 is a larger and more complex code, it is suggested (but not required) that Version 1.1 be used for single-grid applications. This document contains all the information required to run both versions of SAGE. The formulation of the adaption method is described in the first section of this document. The second section is presented in the form of a user guide that explains the input and execution of the code. The third section provides many examples. Successful application of the SAGE code in both two and three dimensions for the solution of various flow problems has proven the code to be robust, portable, and simple to use. Although the basic formulation follows the method of Nakahashi and Deiwert, many modifications have been made to facilitate the use of the self-adaptive grid method for complex grid structures. Modifications to the method and the simple but extensive input options make this a flexible and user-friendly code. The SAGE code can accommodate two-dimensional and three-dimensional, finite-difference and finite-volume, single grid, and zonal-matching multiple grid flow problems. Author (revised)

N95-26754 Carnegie-Mellon Univ., Pittsburgh, PA. Robotics Inst.

THE D* ALGORITHM FOR REAL-TIME PLANNING OF OPTIMAL TRAVERSES

Anthony Stentz Sep. 1994 31 p Limited Reproducibility: More than 20% of this document may be affected by microfiche quality
(Contracts DACA76-89-C-0014; DAAE07-90-C-R059)
(AD-A289361; CMU-RI-TR-94-37) Avail: Issuing Activity (Defense Technical Information Center (DTIC))

Finding the lowest-cost path through a graph of states is central to many problems, including route planning for a mobile robot. If arc costs change during the traverse, then the remainder of the path may need to be replanned. Such is the case for a sensor-equipped mobile robot with incomplete or inaccurate information about its environment. As the robot acquires additional information via its sensors, it has the opportunity to revise its plan to reduce the total cost of the traverse. If the prior information is grossly incomplete or inaccurate, the robot may discover useful information in nearly every piece of sensor data. During the replanning process, the robot must either stop and wait for the new path to be computed or continue to move in the wrong direction; therefore, rapid replanning is essential. This paper describes a new algorithm, D*, capable of planning optimal traverses in real-time through focussed state expansion. D* repairs plans quickly by taking advantage of the fact that most arc cost corrections occur in the vicinity of the robot and the path needs only to be replanned out to the robot's current state. D* can be used not only for route planning but for any graph-based cost optimization problem for which arc costs change during the traverse of the solution path. DTIC

N95-26770*# Delaware Univ., Newark, DE. Dept. of Electrical Engineering.

PERFORMANCE AND POLICY DIMENSIONS IN INTERNET ROUTING

David L. Mills, Charles G. Boncelet, John G. Elias, Paul A. Schragger, Alden W. Jackson, and Ajit Thyagarajan Apr. 1995 33 p
(Contract NAG2-638; NSF NCR-93-01002; A30327-93)
(NASA-CR-197772; NAS 1.26:197772; TR-95-4-1) Avail: CASI HC A03/MF A01

The Internet Routing Project, referred to in this report as the 'Highball Project', has been investigating architectures suitable for networks spanning large geographic areas and capable of very high data rates. The Highball network architecture is based on a high speed crossbar switch and an adaptive, distributed, TDMA scheduling algorithm. The scheduling algorithm controls the instantaneous configuration and swell time of the switch, one of which is attached to each node. In order to send a single burst or a multi-burst packet, a reservation request is sent to all nodes. The scheduling algorithm then configures the switches immediately prior to the arrival of each burst, so it can be relayed immediately without requiring local storage. Reservations and housekeeping information are sent using a special broadcast-spanning-tree schedule. Progress to date in the Highball Project includes the design and testing of a suite of scheduling algorithms, construction of software reservation/scheduling simulators, and construction of a strawman hardware and software implementation. A prototype switch controller and timestamp generator have been completed and are in test. Detailed documentation on the algorithms, protocols and experiments conducted are given in various reports and papers published. Abstracts of this literature are included in the bibliography at the end of this report, which serves as an extended executive summary. Author

N95-26802*# West Virginia Univ., Fairmont, WV. Software Research Lab.

DEVELOPMENT AND ANALYSIS OF SCR REQUIREMENTS TABLES FOR SYSTEM SCENARIOS

John R. Callahan and Jeffery L. Morrison [1995] 17 p
(Contract NCCw-40; NAG5-2129)
(NASA-CR-197769; NASA-IVV-94-010; NAS 1.26:197769; WVU-SRL-94-010; WVU-SCS-TR-95-10; CERC-TR-RN-94-013) Avail: CASI HC A03/MF A01

We describe the use of scenarios to develop and refine requirement tables for parts of the Earth Observing System Data and Information System (EOSDIS). The National Aeronautics and Space Administration (NASA) is developing EOSDIS as part of its Mission-To-Planet-Earth (MTPE) project to accept instrument/platform observation requests from end-user scientists, schedule and perform requested observations of the Earth from space, collect and process the observed data, and distribute data to scientists and archives. Current requirements for the system are managed with tools that allow developers to trace the relationships between requirements and other development artifacts, including other requirements. In addition, the user community (e.g., earth and atmospheric scientists), in conjunction with NASA, has generated scenarios describing the actions of EOSDIS subsystems in response to user requests and other system activities. As part of a research effort in verification and validation techniques, this paper describes our efforts to develop requirements tables from these scenarios for the EOSDIS Core System (ECS). The tables specify event-driven mode transitions based on techniques developed by the Naval Research Lab's (NRL) Software Cost Reduction (SCR) project. The SCR approach has proven effective in specifying requirements for large systems in an unambiguous, terse format that enhance identification of incomplete and inconsistent requirements. We describe development of SCR tables from user scenarios and identify the strengths and weaknesses of our approach in contrast to the requirements tracing approach. We also evaluate the capabilities of both approach to respond to the volatility of requirements in large, complex systems. Author

N95-26814*# West Virginia Univ., Fairmont, WV. Software Research Lab.

A PROCESS IMPROVEMENT MODEL FOR SOFTWARE VERIFICATION AND VALIDATION

John Callahan and George Sabolish 1994 11 p Presented at the 19th Annual Software Engineering Workshop, Greenbelt, MD, 30 Nov. - 1 Dec. 1994
(Contract NCCw-40)

(NASA-CR-197761; NASA-IVV-94-008; NAS 1.26:197761; WVU-SRL-94-008; WVU-SCS-TR-95-8; CERC-TR-TM-94-008) Avail: CASI HC A03/MF A01

We describe ongoing work at the NASA Independent Verification and Validation (IV&V) Facility to establish a process improvement model for software verification and validation (V&V) organizations. This model, similar to those used by some software development organizations, uses measurement-based techniques to identify problem areas and introduce incremental improvements. We seek to replicate this model for organizations involved in V&V on large-scale software development projects such as EOS and Space Station. At the IV&V Facility, a university research group and V&V contractors are working together to collect metrics across projects in order to determine the effectiveness of V&V and improve its application. Since V&V processes are intimately tied to development processes, this paper also examines the repercussions for development organizations in large-scale efforts. Author

N95-26820 Academy of Sciences (USSR), Krasnoyarsk (USSR). Computing Center.

SECOND INTERNATIONAL CONFERENCE ON SOFTWARE FOR MULTIPROCESSORS AND SUPERCOMPUTERS THEORY, PRACTICE, EXPERIENCE

23 Sep. 1994 532 p Conference held in Moscow, Russia, 19-23 Sep. 1994 Limited Reproducibility: More than 20% of this document may be affected by microfiche quality
(AD-A289474) Avail: Issuing Activity (Defense Technical Information Center (DTIC))

Papers presented at this conference on parallel software design are grouped under the following sessions: languages, compilers, and programming systems; neural networks; applications; architectures; environments, debugging, and monitoring; parallelization techniques, scheduling, and load balancing; numerical algorithms; and selected SMS-TPE 1993 papers. CASI

N95-26853 Martin Marietta Corp., Denver, CO. Astronautics Group.

NEXT GENERATION CONTROLLER SPECIFICATION FOR AN OPEN SYSTEMS ARCHITECTURE STANDARD - OVERVIEW Final Report, Mar. 1989 - Aug. 1994

28 Sep. 1994 40 p Limited Reproducibility: More than 20% of this document may be affected by microfiche quality
(Contract F33615-89-C-5706)
(AD-A289507; WL-TR-94-8032) Avail: Issuing Activity (Defense Technical Information Center (DTIC))

This report describes an open architecture framework for advanced manufacturing controllers including machine tools, robotics, process control, and coordinate measurement. The methodology described is applicable to both system design as well as system retrofit applications. A component-based approach is used that allows system architectures to be developed from generic building blocks that address system requirements and resulting functionality requirements. Initial architectures are used to produce an 'application architecture' that addresses specific system messaging requirements. An 'application system' is then synthesized using off-the-shelf, reusable 'implementation components' for the application software. Hardware/software specific platform issues are addressed through the use of system 'profiles,' a convention adopted from the IEEE Portable Operating System Interface (POSIX) standard that is now gaining wide acceptance. A number of examples are provided demonstrating use of all aspects of the methodology on a typical machine tool controller application. Appendices provide details with respect to specific components, requirements, and domain models. DTIC

N95-26855 California Univ., Berkeley, CA. Dept. of Mathematics.

DO WE FULLY UNDERSTAND THE SYMMETRIC LANCZOS ALGORITHM YET?

Beresford N. Parlett 9 Jan. 1995 15 p Limited Reproducibility: More than 20% of this document may be affected by microfiche quality
(Contract N00014-90-J-1372)
(AD-A289614) Avail: Issuing Activity (Defense Technical Information Center (DTIC))

Imagine that one has computed the real n-vectors b, Ab, A(exp 2)b,..., A(exp m-1)b where A is a real symmetric n x n matrix. Lanczos showed us in 1950 how to construct a much better basis for the (Krylov) space spanned by these power vectors and for little extra cost. The new basis (q(sub 1), q(sub 2), ..., q(sub m)) now called the Lanczos basis, has two nice properties: (1) it is orthonormal and (2) the representation of A's projection is a symmetric tridiagonal matrix T(sub m). Property (2) is synonymous with the three term recurrence governing the Lanczos vectors. Moreover, some of T(sub m)'s eigenvalues, called Ritz values hereafter, are excellent approximations to some of A's eigenvalues even when m is much less than n. In addition we can tell, with little expense, which Ritz values are also eigenvalues. One surprising implication of these properties is that it is easier to find the largest few eigenvalues of A than to solve Ax=b! When the Lanczos algorithm is implemented in a computer the user discovers an unpleasant fact. Property (1) fails completely for m as small as 20 or 30 and consequently the computed T(sub m)'s relation to A is unclear. Lanczos was aware of this blemish and proposed the obvious remedy: keep applying the Gram-Schmidt process to each new Lanczos vector as it is computed. The catch here is that all the (q(sub i)) must be kept handy whereas in exact arithmetic only the three latest Lanczos vectors are needed and earlier q's may be discarded. The arithmetic cost of this full reorthogonalization grows quadratically with m. So the hope of computing T(sub n) efficiently and accurately by the Lanczos algorithm was dashed and other methods prevailed. In exact arithmetic T(sub n) is similar to A and the algorithm stops. DTIC

N95-26881 Alabama Agricultural and Mechanical Coll., Normal, AL. Dept. of Physics.

DIGITAL OPTICAL COMPUTING Final Report

S. Kupiec and H. J. Caulfield Oct. 1994 47 p Limited Reproducibility: More than 20% of this document may be affected by microfiche quality
(Contract F30602-92-C-0075)
(AD-A289395; RL-TR-94-194) Avail: Issuing Activity (Defense Technical Information Center (DTIC))

Within our previous report, we have described a digital computer architecture, the HOPLA, and algorithms that effectively exploit that architecture. Within the present report, we shall examine the theoretical performance of the HOPLA, implementing various configurations of the multi-read function. The present report consists of the following. The first section consists of a review of the semi-quantitative analysis of the N4 interconnect. In the next section, we apply this analysis to the case of the proposed HOPLA implementation. Proceeding with the results from this section, we then consider the required thresholds and reliability levels of the system under various operating conditions. Finally, we consider the effects of operation at very low power levels with an emphasis on the effects of shot noise. DTIC

N95-26895 Air Force Inst. of Tech., Wright-Patterson AFB, OH. School of Engineering.

EASY-SIM: A VISUAL SIMULATION SYSTEM SOFTWARE ARCHITECTURE WITH AN Ada 9X APPLICATION FRAMEWORK M.S. Thesis

Jordan R. Kayloe Dec. 1994 162 p Limited Reproducibility: More than 20% of this document may be affected by microfiche quality
(AD-A289325; AFIT/GCS/ENG/94D-11) Avail: Issuing Activity (Defense Technical Information Center (DTIC))

Software architectures increase productivity when used as the basis for developing applications in a problem domain. This thesis describes the creation of Easy-Sim, an object-oriented software architecture for visual simulation systems, and its corresponding implementation as an application framework in Ada 9X. The research built upon ObjectSim, an existing object-oriented simulation architecture implemented as a application framework. Both ObjectSim and Easy-Sim operate on Silicon Graphics platforms and use the IRIS Performer graphics programming library. Easy-Sim is implemented using version 1.83 of the GNAT compiler. The investigation for this thesis involved honing ObjectSim's design, implementing the improved result in both C++ and Ada 9X, and developing applications to compare the two versions. The study achieved two main objectives: producing Easy-Sim as an improved visual simulation system architecture by building on ObjectSim's experience, and producing a visual simulation system application from Easy-Sim in Ada 9X that performs at a level comparable to the same application built in C++. DTIC

N95-26903 Software Productivity Consortium, Herndon, VA.

USER-CENTRIC DEVELOPMENT. VERSION 01.00.04 Technical Report

Christine Haapala and James Kirby, Jr. Dec. 1994 55 p Limited Reproducibility: More than 20% of this document may be affected by microfiche quality
(Contract MDA972-92-J-1018)
(AD-A289363; SPC-94061-CMC) Avail: Issuing Activity (Defense Technical Information Center (DTIC))

This technical report describes a case study of at least three software development projects that have employed user-centric software development (UCD). Characteristics of UCD are: (1) The software development team includes some of those who will use the software. (2) The user is an equal participant with the developers in making development decisions. The software development team develops the software using an iterative enhancement approach. A series of versions of the software is developed and delivered with feedback from users of earlier versions of the software driving development of later versions. Results of the case study were obtained by posing a set of questions to those participating in UCD as developers, users, or managers. The questions, captured as a set of assertions, were used to test a theory of UCD. The results describe how a particular software development paradigm was practiced, the advantages and disadvantages of using the paradigm, technology transfer issues, and opportunities for research and technology advancements. The intended audience for this technical report consists of: Technologists interested in evaluating, comparing, improving, and supporting software development methods and processes; and Practitioners responsible for selecting the software development methods and processes that software development projects will employ. DTIC

N95-26907# Helsinki Univ. of Technology, Espoo (Finland). Dept. of Computer Science.
REFERENCE MANUAL: NAIVE PHYSICS SIMULATOR
M. Fraunberg, P. Lampio, T. Raety, P. Salonen, and J. Tuomas 1994 93 p See also PB93-187276
(PB95-184917; TKO-C70) Avail: CASI HC A05/MF A01

The Naive Physics Simulator simulates physical systems, of which state can be described with a fixed set of quantities at each moment of time. The physical system is defined using variables, which represent different properties of the system. The dependencies between the variables are represented using physical laws. These laws are formalized using first-order predicate logic which is augmented with two new constructs increasing the expressive power of the language. The simulator is implemented using Prolog 3 language for logic programming. The Naive Physics Simulator can be used to analyze electric circuits, static or dynamic spring systems and block systems, for example. The circuits may contain diodes, resistors, coils, capacitors, and current or voltage sources. The block system consists of regular blocks lying on an inclined plane. The simulator tries to find out if the system collapses. The spring system consists of balls (mass centers), which are connected to each other using elastic springs. The balls may vibrate (dynamic system) or we may calculate only the elongations of the springs (static system). NTIS

N95-26919 Air Force Inst. of Tech., Wright-Patterson AFB, OH. School of Engineering.
PREDICTING PROTEIN STRUCTURE USING PARALLEL GENETIC ALGORITHMS M.S. Thesis
George H. Gates, Jr. Dec. 1994 122 p Limited Reproducibility: More than 20% of this document may be affected by microfiche quality
(AD-A289305; AFIT/GCS/ENG/94D-03) Avail: Issuing Activity (Defense Technical Information Center (DTIC))

The protein folding problem is a biochemistry Grand Challenge problem. The challenge is to reliably predict natural three-dimensional structures of polypeptides. Genetic algorithms (GA's) are robust, semi-optimal search techniques modeling natural evolutionary processes. Fast messy GA's (fmGA's) are variants of messy GA's that reduce the exponential time complexity to polynomial. This investigation evaluates the merits of parallel SGA's and fmGA's for minimizing the potential energy of a pentapeptide, (Met)-enkephalin. AFIT's energy model is compared to a similar model in a commercial package called QUANTA. Differences between the two models are identified and resolved to enhance GA's abilities to correctly fold molecules. The steps required to unify the behavior of the two implementations is presented. The effectiveness of SGA' while minimizing the potential energy of (Met)-enkephalin is shown to be highly dependent on the choice of population size and mutation rate. It is also demonstrated that choosing parameters from the Schaffer's proposed guidelines cause SGA' to realize near-optimal performance on this particular application. Parallel SGA's are capable of finding near-optimal conformations of (Met)-enkephalin. Parallel fmGA's should ultimately find better solutions in less time. The experiments performed in this investigation determine limitations of parallel SGA's and fmGA's applied to polypeptide energy minimization. DTIC

N95-26930*# Stanford Univ., CA. Space, Telecommunications and Radioscience Lab.
GRAYSCALE/RESOLUTION TRADE-OFF FOR TEXT: MODEL PREDICTIONS AND PSYCHOPHYSICAL RESULTS FOR LETTER CONFUSION AND LETTER DISCRIMINATION Final Report, Oct. 1992 - Mar. 1995
Jennifer Gille (Western Aerospace Labs., Inc., Moffett Field, CA.), Russel Martin (Xerox Palo Alto Research Center, CA.), Jeffrey Lubin (David Sarnoff Research Center, Princeton, NJ.), and James Larimer (National Aeronautics and Space Administration. Ames Research Center, Moffett Field, CA.) 30 Mar. 1995 10 p
(Contract NCC2-777)
(NASA-CR-197784; NAS 1.26:197784) Avail: CASI HC A02/MF A01

In a series of papers presented in 1994, we examined the grayscale/resolution trade-off for natural images displayed on devices with discrete pixellation, such as AMLCD's. In the present paper we extend this study by examining the grayscale/resolution trade-off for text images on discrete-pixel displays. Halftoning in printing is an example of the grayscale/resolution trade-off. In printing, spatial resolution is sacrificed to produce grayscale. Another example of this trade-off is the inherent low-pass spatial filter of a CRT, caused by the point-spread function of the electron beam in the phosphor layer. On a CRT, sharp image edges are blurred by this inherent low-pass filtering, and the block noise created by spatial quantization is greatly reduced. A third example of this trade-off is text anti-aliasing, where grayscale is used to improve letter shape, size and location when rendered at a low spatial resolution. There are additional implications for display system design from the grayscale/resolution trade-off. For example, reduced grayscale can reduce system costs by requiring less complexity in the framestore, allowing the use of lower cost drivers, potentially increasing data transfer rates in the image subsystem, and simplifying the manufacturing processes that are used to construct the active matrix for AMLCD (active-matrix liquid-crystal display) or AMTFEL (active-matrix thin-film electroluminescent) devices. Therefore, the study of these trade-offs is important for display designers and manufacturing and systems engineers who wish to create the highest performance, lowest cost device possible. Our strategy for investigating this trade-off is to generate a set of simple test images, manipulate grayscale and resolution, predict discrimination performance using the ViDEOS(Sarnoff) Human Vision Model, conduct an empirical study of discrimination using psychophysical procedures, and verify the computational results using the psychophysical results. Derived from text

N95-26962 Air Force Inst. of Tech., Wright-Patterson AFB, OH. School of Engineering.
UNIFICATION OF LARCH AND Z-BASED OBJECT MODELS TO SUPPORT ALGEBRAICALLY-BASED DESIGN REFINEMENT: THE Z PERSPECTIVE M.S. Thesis
Kathleen M. Wabiszewski Dec. 1994 215 p Limited Reproducibility: More than 20% of this document may be affected by microfiche quality
(AD-A289234; AFIT/GCS/ENG/94D-24) Avail: Issuing Activity (Defense Technical Information Center (DTIC))

This research established a foundation for formalizing the evolution of based object models to theories, part of a dual approach for formally extending object-oriented analysis models using the Z and LARCH languages. For the initial phase, a comprehensive, consistent, and correct Z language parser was implemented within the SOFTWARE REFINERY(TM) Programming Environment. The Z parser produced abstract syntax trees (AST's) of objects, thereby forming the basis for analyzing the similarities and differences between the based and LARCH-based object representations. The second phase used the analysis of the two languages to identify fundamental core constructs that consisted of similar syntactic and semantic notions of signatures and axioms for describing a problem domain, thereby forming a canonical framework for formal object representations. This canonical framework provides a front-end for producing design refinement artifacts such as synthesis diagrams, theorem proving sentences and interface languages. The final phase of the process demonstrated the feasibility of interface language generation by establishing an executable framework that mapped Z into the SOFTWARE REFINERY(TM) Environment to rapidly prototype object-oriented Z specifications. DTIC

N95-27031 Adaptive Solutions, Inc., Beaverton, OR.
HIGH PERFORMANCE HARDWARE AND SOFTWARE FOR PATTERN RECOGNITION AND IMAGE PROCESSING Research and Development Status Report, 1 Sep. - 30 Nov. 1994
Wendell A. Henry 19 Dec. 1994 5 p Limited Reproducibility: More than 20% of this document may be affected by microfiche quality
(Contract N00014-93-C-0234)
(AD-A289153) Avail: Issuing Activity (Defense Technical Information Center (DTIC))

The CNAPS Development Environment consists of several software tools required by the software developer. These are: CNAPS application program interface; CNAPS-C compiler; CNAPS assembler; CNAPS source-level debugger (command-line interface); and CNAPS source-level debugger (graphical interface). Initial porting of the first three tools was completed in Phase 1. Phase 2 tasks include the porting of the remaining two tools as well as enhancing the first three tools to integrate them with the source-level debugger. Effort on the Phase 2 tasks has commenced and good progress has been made during this reporting period. The CNAPS compiler, assembler, and application program interface have been enhanced to integrate with the source-level debugger. The source-level debugger with a command-line interface has been ported to the Windows 3.x environment and is undergoing testing and bug fixing. DTIC

N95-27037 Air Force Inst. of Tech., Wright-Patterson AFB, OH. School of Engineering.
A GENERAL OBJECT MODEL TRANSFORMATION SYSTEM M.S. Thesis
John P. Mullaney Dec. 1994 85 p Limited Reproducibility: More than 20% of this document may be affected by microfiche quality
(AD-A289289; AFIT/GCS/ENG/94D-18) Avail: Issuing Activity (Defense Technical Information Center (DTIC))

Cecil and Fullenkamp developed a program that transforms knowledge captured in an object-model in one environment into a different object-model in a different environment. This program worked well for the intended purpose, but if one of the object-models is replaced by a different object-model then this transformation program has to be re-engineered. As the object-modeling paradigm becomes more prevalent, many systems are experiencing this problem. The primary goal of this research was to determine what reusable knowledge could be extracted from these types of program and used to build a general object-model transformer that generalizes such transformation programs. Toward this end, we analyzed several cases of object-model transformations, designed a generic version of an object-model transformer, and implemented and tested a prototype transformer. The research results provide an approach to analyzing the problem, designing a solution, and transformation templates for various aspects of a solution strategy. These results should be extremely beneficial to software engineers designing object-model transformation systems. DTIC

N95-27095 Carnegie-Mellon Univ., Pittsburgh, PA. School of Computer Science.
EFFICIENT GENERATION OF COUNTEREXAMPLES AND WITNESSES IN SYMBOLIC MODEL CHECKING
E. Clarke, O. Grumberg (Technion - Israel Inst. of Tech., Haifa, Israel.), K. McMillan (Cadence Berkeley Labs., Berkeley, CA.), and X. Zhao Oct. 1994 20 p Limited Reproducibility: More than 20% of this document may be affected by microfiche quality
(Contract F33615-93-1-1330)
(AD-A288583; CMU-CS-94-204) Avail: Issuing Activity (Defense Technical Information Center (DTIC))

Model checking is an automatic technique for verifying sequential circuit designs and protocols. An efficient search procedure is used to determine whether or not the specification is satisfied. If it is not satisfied, our technique will produce a counterexample execution trace that shows the cause of the problem. Although finding counterexamples is extremely important, there is no description of how to do this in the literature on model checking. We describe an efficient algorithm to produce counterexamples and witnesses for symbolic model checking algorithms. This algorithm is used in the SMV model checker and works quite well in practice. We also discuss how to extend our technique to more complicated specifications. This extension makes it possible to find counterexamples for verification procedures based on showing language containment between various types of w-automata. DTIC

N95-27150 Naval Postgraduate School, Monterey, CA.
DESIGN AND IMPLEMENTATION OF A SOFTWARE COMMUNICATION ARCHITECTURE FOR THE JANUS-3D VISUALIZER M.S. Thesis
Christopher S. Upson Sep. 1994 77 p Limited Reproducibility: More than 20% of this document may be affected by microfiche quality
(AD-A288509) Avail: Issuing Activity (Defense Technical Information Center (DTIC))

During the National Guard's mobilization for Desert Shield/Desert Storm, deficiencies were noted in the command and control skills of battalion and brigade level units. The major problem addressed by this research was to improve these skills by developing a software communication architecture that would allow events occurring in two dimensions in the Janus Combat Modeler to be seen in three dimensions on a visualization tool called the Janus-3D Visualizer over both local ethernet and wide area telephonic networks. The challenge was to minimize network latency along with providing accurate data in order to maintain the time and space coherence of the simulation. The approach taken was to first determine where the needed information resided in the Janus modeler. Next, a protocol was developed to extract the information and send it to the Janus-3D Visualizer over the local network for viewing. Finally, a protocol was developed to transmit this information over a telephonic network upon request in order for it to be viewed 010 a remote Janus-3D Visualizer. As a result of this work, Janus battles can be viewed in three dimensions and in real time by brigade and battalion commanders and their staffs without having to spend valuable training funds to move everyone to a single location. National Guard units can now use the Janus modeler more often and more realistically in order to improve command, control, and communication skills. DTIC

N95-27210 Aerospace Corp., El Segundo, CA. Engineering and Technology Group.
COMPUTER SYSTEMS DIVISION SOFTWARE SYSTEM METRICS APPROACH
S. K. Hoting and R. J. Costello Jul. 1994 13 p Limited Reproducibility: More than 20% of this document may be affected by microfiche quality
(Contract F04701-93-C-0094)
(AD-A288837; TR-94(4904)-3; SMC-TR-94-43) Avail: Issuing Activity (Defense Technical Information Center (DTIC))

Over the decades, the increasing use of software has enabled construction and deployment of ever more capable space systems for SMC. However, managing, controlling, and participating in software development for such software-intensive systems is a difficult and error-prone task that is exacerbated by the lack of meaningful data on key products and processes. Such data should provide visibility into the health and status of the evolving software system, assist in early identification of current and potential problem areas, and aid in predicting such software system characteristics as reliability, maintainability, cost, and schedule. Until recently, comprehensive data collection analysis methods which treat software as an integral part of a larger system have not been available. This report introduces a software system metrics approach that has been developed for this purpose. The report discusses the utility of the approach, key concepts for applying metrics to software-intensive systems, and basic metrics planning guidelines. It also introduces a set of recommended metrics that cover both the system and the software throughout the life cycle. A complete description of the metrics approach, associated contractual guidelines, and detailed descriptions of several of the recommended metrics are the subject of a forthcoming TOR. DTIC

N95-27235# Virginia Commonwealth Univ., Richmond, VA.
OVERVIEW OF MEGAPROGRAMMING COURSE: LECTURES AND EEXERCISES. VERSION 02.00.03 Final Technical Report
Steve Wartik Feb. 1994 113 p
(Contract MDA972-92-J-1018)
(AD-A286723; SPC-93028-CMC) Avail: CASI HC A06/MF A02

This is a short course that introduces megaprogramming concepts. The Teacher Notes for the Overview of Megaprogramming Course complement the lecture and exercise material (ADA 276169). They explain concepts from the lectures in more depth than is possible in the lectures' slide-oriented format. They also discuss the relevance of megaprogramming in today's and tomorrow's industry. They can help teachers understand the importance of the course. The Teacher Notes are tied closely to the rest of the material. They draw heavily on the examples from the lectures and laboratory, giving references to specific slides. An appendix relates each slide to sections in the Teacher Notes. This helps instructors understand the slides as they prepare their lectures. DTIC

N95-27246*# Loral Federal Systems, Manassa, VA.

ADVANCED FLIGHT COMPUTER. SPECIAL STUDY Final Report, Apr. 1994 - Feb. 1995

Dennis Coo Mar. 1995 54 p
(Contract NASA Order L-40679-D; RTOP 233-01-03-23; F29601-89-C-0089)
(NASA-CR-198165; NAS 1.26:198165) Avail: CASI HC A04/MF A01

This report documents a special study to define a 32-bit radiation hardened, SEU tolerant flight computer architecture, and to investigate current or near-term technologies and development efforts that contribute to the Advanced Flight Computer (AFC) design and development. An AFC processing node architecture is defined. Each node may consist of a multi-chip processor as needed. The modular, building block approach uses VLSI technology and packaging methods that demonstrate a feasible AFC module in 1998 that meets that AFC goals. The defined architecture and approach demonstrate a clear low-risk, low-cost path to the 1998 production goal, with intermediate prototypes in 1996. Author

N95-27251 Air Force Inst. of Tech., Wright-Patterson AFB, OH. School of Logistics and Acquisition Management.

A COMPARISON OF ERROR CATEGORIZATION SCHEMES FOR USE IN SOFTWARE SYSTEM SAFETY PROGRAMS M.S. Thesis

Richard Escobedo and Jim Thomas Dec. 1994 93 p Limited Reproducibility: More than 20% of this document may be affected by microfiche quality
(AD-A288741; AFIT/GSS/LAR/94D-1) Avail: Issuing Activity (Defense Technical Information Center (DTIC))

Software safety is becoming increasingly important in the development of DOD advanced weapon systems. To make software safer, hazard conditions must be avoided along with the errors that accompany them. The first step in identifying errors is classifying error data. The area of software error classification is not as advanced as other software development areas. The technical literature lacks examples of comprehensive taxonomies that can be applied to various computer software domains and applications. The predominant approach is to organize errors into categories particular to the program currently in work. The typical error scheme is made of narrow categories that are not interrelated. Errors have been classified by symptom, by cause, by life cycle phase, by severity, and by software control. The focus of this research was to determine the best way to classify errors in order to aid system safety in software development. The research identified common areas used in industry that aid in error classification. A telephone survey of experts in safety and software was used to obtain input on the most effective classification schemes. The research also proposed a taxonomy that will be ideal for DOD software development. Since software is becoming a larger part of advanced weapon systems, development of error-free and safe software to operate and support these weapon systems is increasingly important. DTIC

N95-27252*# West Virginia Univ., Morgantown, VA. Software Research Lab.

A HIGH PERFORMANCE TOTALLY ORDERED MULTICAST PROTOCOL

Todd Montgomery, Brian Whetten (California Univ., Berkeley, CA.), and Simon Kaplan (Illinois Univ., Champaign, IL.) [1995] 32 p
(Contract NCCw-40)
(NASA-CR-197765; NASA-IVV-94-004; NAS 1.26:197765; WVU-SRL-94-004; WVU-SCS-TR-95-4; CERC-TR-RN-94-010) Avail: CASI HC A03/MF A01

This paper presents the Reliable Multicast Protocol (RMP). RMP provides a totally ordered, reliable, atomic multicast service on top of an unreliable multicast datagram service such as IP Multicasting. RMP is fully and symmetrically distributed so that no site bears un undue portion of the communication load. RMP provides a wide range of guarantees, from unreliable delivery to totally ordered delivery, to K-resilient, majority resilient, and totally resilient atomic delivery. These QoS guarantees are selectable on a per packet basis. RMP provides many communication options, including virtual synchrony, a publisher/subscriber model of message delivery, an implicit naming service, mutually exclusive handlers for messages, and mutually exclusive locks. It has commonly been held that a large performance penalty must be paid in order to implement total ordering -- RMP discounts this. On SparcStation 10's on a 1250 KB/sec Ethernet, RMP provides totally ordered packet delivery to one destination at 842 KB/sec throughput and with 3.1 ms packet latency. The performance stays roughly constant independent of the number of destinations. For two or more destinations on a LAN, RMP provides higher throughput than any protocol that does not use multicast or broadcast. Author

N95-27370*# National Aeronautics and Space Administration. Lewis Research Center, Cleveland, OH.

RING-PLANE TRAVELING-WAVE TUBE SLOW-WAVE CIRCUIT DESIGN SIMULATIONS AT V-BAND FREQUENCIES

Carol L. Kory (Analex Corp., Brook Park, OH.) and Jeffrey D. Wilson Jun. 1995 12 p Presented at the 1995 International Conference on Plasma Science, Madison, Wisconsin, 5-8 Jun. 1995 ; sponsored by IEEE Original contains color illustrations
(RTOP 235-01-0A)
(NASA-TM-106949; E-9687; NAS 1.15:106949) Avail: CASI HC A03/MF A01; 2 functional color pages

The V-Band frequency range of 59-64 GHz is a region of the millimeter-wave spectrum that has been designated for intersatellite communications. As a first effort to develop a high-efficiency V-band TWT, variations on a ring-plane slow-wave circuit were computationally investigated to develop an alternative to the more conventional ferruled coupled-cavity circuit. The ring-plane circuit was chosen because of its high interaction impedance, large beam aperture, and excellent thermal dissipation properties. Despite the high-power capabilities of the ring-plane TWT, disadvantages of low bandwidth and high voltage requirements have until now prevented its acceptance outside the laboratory. In this paper, we use the three-dimensional electromagnetic simulation code MAFIA to investigate methods of increasing the bandwidth and lowering the operating voltage. Dispersion, impedance, and attenuation calculations for various geometric variations and loading distributions were performed. Based on the results of the variations, a circuit termed the finned-ladder TWT slowwave circuit was designed and is compared here to the scaled ring-plane prototype and the conventional ferruled coupled-cavity TWT circuit over the V-band frequency range. Author

N95-27418 Carnegie-Mellon Univ., Pittsburgh, PA. Dept. of Computer Science.

SOLVING RECURSIVE DOMAIN EQUATIONS WITH ENRICHED CATEGORIES Ph.D. Thesis

Kim Ritter Wagner Jul. 1994 107 p Limited Reproducibility: More than 20% of this document may be affected by microfiche quality
(AD-A289358; CMU-CS-94-159) Avail: Issuing Activity (Defense Technical Information Center (DTIC))

Both pre-orders and metric spaces have been used at various times as a foundation for the solution of recursive domain equations in the area of denotational semantics. In both cases the central theorem states that a 'converging' sequence of 'complete' domains/spaces with 'continuous' retraction pairs between them has a limit in the category of complete domains/spaces with retraction pairs as morphisms. The pre-order version was discovered first by Scott in 1969, and is referred to as Scott's inverse limit theorem. The metric version was mainly developed by de Bakker and Zucker and refined and generalized by America and Rutten. The theorem in both its versions provides the main tool for solving recursive domain equations. The proofs of the two versions of the theorem look astonishingly similar, but until now the preconditions for the pre-order and the metric versions have seemed to be fundamentally different. In this thesis the authors establish a more general theory of domains based on the notions of enriched categories, and prove Scott's inverse limit theorem in this theory. The metric and pre-order versions are special cases, obtained just by using different logics as parameter to the general theory. DTIC

N95-27436# Sandia National Labs., Albuquerque, NM.
A SPECTRAL ALGORITHM FOR THE SERIATION PROBLEM
J. E. Atkins, E. G. Boman, and B. Hendrickson Nov. 1994 16 p
Presented at the Symposium on Theory of Computing, Las Vegas, NV, 29 May - 1 Jun. 1995
(Contract DE-AC04-94AL-85000)
(DE95-004775; SAND-94-3082C; CONF-9505145-1) Avail: CASI HC A03/MF A01

Given a set of objects and a correlation function f reflecting the desire for two items to be near each other, find all sequences (pi) of the items so that correlation preferences are preserved; that is if (pi)(i) less than (pi)(j) less than (pi)(k) then f(i,j) greater than or equal to f(i,k) and f(j,k) greater than or equal to f(i,k). This seriation problem has numerous applications, for instance, solving it yields a solution to the consecutive ones problem. We present a spectral algorithm for this problem that has a number of interesting features. Whereas most previous applications of spectral techniques provided bounds or heuristics, our result is an algorithm for a nontrivial combinatorial problem. Our analysis introduces powerful tools from matrix theory to the theoretical computer science community. Also, spectral methods are being applied as heuristics for a variety of sequencing problems and our result helps explain and justify these applications. Although the worst case running time for our approach is not competitive with that of existing methods for well posed problem instances, unlike combinatorial approaches our algorithm remains a credible heuristic for the important cases where there are errors in the data. DOE

N95-27495# Oak Ridge National Lab., TN.
A VIDEO STRIP CHART PROGRAM
N. L. Jones 1994 2 p Presented at the 1994 Symposium of the North Eastern Accelerator Personnel (SNEAP-94), Kalamazoo, MI, 12-15 Oct. 1994
(Contract DE-AC05-84OR-21400)
(DE95-006389; CONF-9410294-2) Avail: CASI HC A01/MF A01

A strip chart recorder has been utilized for trend analysis of the Oak Ridge National Laboratory EN tandem since 1987. At the EN, the author could not afford the nice eight channel thermal pen recorder that was used at the 25 URC. He had to suffice with two channel fiber tip or capillary pen type recorders retrieved from salvage and maintained with parts from other salvaged recorders. After cycling through several machines that eventually became completely unserviceable, a search for a new thermal recorder was begun. As much as he hates to write computer code, he decided to try his hand at getting an old data acquisition unit, that had been retrieved several years ago from salvage, to meet his needs. A BASIC language compiler was used because time was not available to learn a more advanced language. While attempting to increase acquisition and scroll speed on the 6 MHz 80286 that the code was first developed on, it became apparent that scrolling only the first small portion of the screen at high speed and then averaging that region and histogramming the average provided both the speed necessary for capturing fairly short duration events, and a trend record without use of back scrolling and disk storage routines. This turned out to be quite sufficient. DOE

N95-27533# Lawrence Livermore National Lab., Livermore, CA.
SCIENTIFIC STATISTICS AND GRAPHICS ON THE MACINTOSH
S. L. Grotch Sep. 1994 14 p Presented at the American Geophysical Union/Paclim Workshop, Asilomar, CA, 19-22 Apr. 1994
(Contract W-7405-eng-48)
(DE95-006445; UCRL-JC-116492; CONF-9404237-1) Avail: CASI HC A03/MF A01

In many organizations scientists have ready access to more than one computer, often both a workstation (e.g., SUN, HIP, SGI) as well as a Macintosh or other PC. The scientist commonly uses the work station for 'number-crunching' and data analysis whereas the Macintosh is relegated to either word processing or serves as a 'dumb terminal' to a larger mainframe computer. In an informal poll of the author's colleagues, very few of them used their Macintoshes for either statistical analysis or for graphical data display. The author believes that this state of affairs is particularly unfortunate because over the last few years both the computational capability, and even more so, the software availability for the Macintosh have become quite formidable. In some instances, very powerful tools are now available on the Macintosh that may not exist (or be far too costly) on the so-called 'high end' workstations. Many scientists are simply unaware of the wealth of extremely useful, 'off-the-shelf' software that already exists on the Macintosh for scientific graphical and statistical analysis. This paper is a very personal view illustrating several such software packages that have proved valuable in the author's own work in the analysis and display of climatic datasets. It is not meant to be either an all-inclusive enumeration, nor is it to be taken as an endorsement of these products as the 'best' of their class. Rather, it has been found, through extensive use that these few packages were generally capable of satisfying his particular needs for both statistical analysis and graphical data display. In the limited space available, the focus will be on some of the more novel features found to be of value. DOE

N95-27729*# Analex Corp., Brook Park, OH.
FDTD-ANT USER MANUAL Final Report
Martin L. Zimmerman Cleveland, OH NASA May 1995 18 p
(Contract NAS3-25776; RTOP 235-01-0C)
(NASA-CR-195444; E-9492; NAS 1.26:195444) Avail: CASI HC A03/MF A01

This manual explains the theory and operation of the finite-difference time domain code FDTD-ANT developed by Analex Corporation at the NASA Lewis Research Center in Cleveland, Ohio. This code can be used for solving electromagnetic problems that are electrically small or medium (on the order of 1 to 50 cubic wavelengths). Calculated parameters include transmission line impedance, relative effective permittivity, antenna input impedance, and far-field patterns in both the time and frequency domains. The maximum problem size may be adjusted according to the computer used. This code has been run on the DEC VAX and 486 PC's and on workstations such as the Sun Sparc and the IBM RS/6000. Author

N95-27849# Los Alamos National Lab., NM.
GENERALIZED CNF SATISFIABILITY, LOCAL REDUCTIONS AND COMPLEXITY OF SUCCINCTLY SPECIFIED PROBLEMS
M. V. Marathe, H. B. Hunt, III, R. E. Stearns, and V. Radhakrishnan 1995 20 p Presented at the 10th IEEE Annual Conference on Structures in Complexity Theory, Las Vegas, NV, May 1995
(Contract W-7405-eng-36)
(DE95-006343; LA-UR-95-22; CONF-9505175-1) Avail: CASI HC A03/MF A01

We study the complexity and efficient approximability of various decision, counting, and optimization problems when instances are specified using (1) the one-dimensional finite periodic narrow specifications of Wanke, (2) the two-way infinite one-dimensional narrow periodic (sometimes called dynamic) specifications of Karp and Orlin et al., and (3) the hierarchical specification language of Lengauer et al. We outline how generalized CNF satisfiability problems and local reductions can be used to obtain both hardness and easiness results for a number of decision, counting, optimization, and approximate optimization problems when instances are specified as in (1), (2), or (3). As corollaries we obtain a number of new PSPACE-hardness and #PSPACE-hardness results and a number of new polynomial time approximation algorithms for natural PSPACE-hard optimization problems. In particular assuming P not equal to PSPACE, we characterize completely the complexities of the generalized CNF satisfiability problems SAT(S) of Schaefer, when instances are specified as in (1), (2), or (3). DOE

N95-27905*# National Aeronautics and Space Administration. Lewis Research Center, Cleveland, OH.
PC SOFTWARE GRAPHICS TOOL FOR CONCEPTUAL DESIGN OF SPACE/PLANETARY ELECTRICAL POWER SYSTEMS
Long V. Truong Apr. 1995 9 p Presented at the 30th Intersociety Energy Conversion Engineering Conference, Orlando, FL, 31 Jul. - 4 Aug. 1995; sponsored by ASME, IEEE, AIChE, ANS, SAE, ACS, and AIAA
(RTOP 323-12-07)
(NASA-TM-106908; E-9610; NAS 1.15:106908; IECEC-95-387) Avail: CASI HC A02/MF A01

This paper describes the Decision Support System (DSS), a personal computer software graphics tool for designing conceptual space and/or planetary electrical power systems. By using the DSS, users can obtain desirable system design and operating parameters, such as system weight, electrical distribution efficiency, and bus power. With this tool, a large-scale specific power system was designed in a matter of days. It is an excellent tool to help designers make tradeoffs between system components, hardware architectures, and operation parameters in the early stages of the design cycle. The DSS is a user-friendly, menu-driven tool with online help and a custom graphical user interface. An example design and results are illustrated for a typical space power system with multiple types of power sources, frequencies, energy storage systems, and loads. Author

N95-28047# Oak Ridge National Lab., TN.

A NEW ALGORITHM FOR GENERATING HIGHLY ACCURATE BENCHMARK SOLUTIONS TO TRANSPORT TEST PROBLEMS

Y. Y. Azmy 1995 10 p Presented at the International Conference on Mathematics and Computations, Reactor Physics, and Environmental Analyses, Portland, OR, 30 Apr. - 4 May 1995
(Contract DE-AC05-84OR-21400)
(DE95-007397; CONF-950420-20) Avail: CASI HC A02/MF A01

We present a new algorithm for solving the neutron transport equation in its discrete-variable form. The new algorithm is based on computing the full matrix relating the scalar flux spatial moments in all cells to the fixed neutron source spatial moments, foregoing the need to compute the angular flux spatial moments, and thereby eliminating the need for sweeping the spatial mesh in each discrete-angular direction. The matrix equation is solved exactly in test cases, producing a solution vector that is free from iteration convergence error, and subject only to truncation and roundoff errors. Our algorithm is designed to provide method developers with a quick and simple solution scheme to test their new methods on difficult test problems without the need to develop sophisticated solution, e.g. acceleration, algorithms before establishing the worthiness of their innovation. We demonstrate the utility of the new algorithm by applying it to the Arbitrarily High Order Transport Nodal (AHOT-N) method, and using it to solve Burre's Test Problem, a suite of benchmark problems that covers a large region in parameter space. Our results provide highly accurate benchmark solutions, that can be distributed electronically and used to verify the pointwise accuracy of other solution methods and algorithms. DOE

N95-28168# Lawrence Livermore National Lab., Livermore, CA.

EDGE DETECTION BY NONLINEAR DYNAMICS

Yiu-Fai Wong Jul. 1994 9 p Presented at the VCIP 1994: Visual Communications and Image Processing, Chicago, IL, 25-28 Sep. 1994
(Contract W-7405-eng-48)
(DE95-008076; UCRL-JC-116696; CONF-9409311-1) Avail: CASI HC A02/MF A01

We demonstrate how the formulation of a nonlinear scale-space filter can be used for edge detection and junction analysis. By casting edge-preserving filtering in terms of maximizing information content subject to an average cost function, the computed cost at each pixel location becomes a local measure of edgeness. This computation depends on a single scale parameter and the given image data. Unlike previous approaches which require careful tuning of the filter kernels for various types of edges, our scheme is general enough to be able to handle different edges, such as lines, step-edges, corners and junctions. Anisotropy in the data is handled automatically by the nonlinear dynamics. DOE

N95-28243# Pacific Northwest Lab., Richland, WA.

AUTOMATED REMEDIAL ASSESSMENT METHODOLOGY SOFTWARE SYSTEM

M. Whiting, M. Wilkins, and D. Stiles Nov. 1994 10 p Presented at the Conference on Development and Application of Computer Techniques To Environmental Studies: Envirosoft '94, San Francisco, CA, 16-18 Nov. 1994
(Contract DE-AC06-76RL-01830)
(DE95-007287; PNL-SA-24754; CONF-941113-2) Avail: CASI HC A02/MF A01

The Automated Remedial Analysis Methodology (ARAM) software system has been developed by the Pacific Northwest Laboratory to assist the U.S. Department of Energy (DOE) in evaluating cleanup options for over 10,000 contaminated sites across the DOE complex. The automated methodology comprises modules for decision logic diagrams, technology applicability and effectiveness rules, mass balance equations, cost and labor estimating factors and equations, and contaminant stream routing. ARAM is used to select technologies for meeting cleanup targets; to determine the effectiveness of the technologies in destroying, removing, or immobilizing contaminants; to decide the nature and amount of secondary waste requiring further treatment; and to estimate the cost and labor involved when applying technologies. DOE

N95-28498# Oak Ridge National Lab., TN.

TEACHING INTERDISCIPLINARY COMPUTATIONAL SCIENCE FROM AN ELECTRONIC BOOK ON THE INTERNET

C. E. Oliver, M. R. Strayer, and V. M. Umar (Vanderbilt Univ., Nashville, TN.) 1994 5 p Presented at the Frontiers in Education Conference, San Jose, CA, 3-6 Nov. 1994
(Contract DE-AC05-84OR-21400)
(DE95-006525; CONF-9411137-2) Avail: CASI HC A01/MF A01

The advances in high performance computing technology have led to great changes in the way applied and pure sciences are being carried out. These advances have left curricula at the graduate level in many disciplines omitting a whole body of essential research tools that students have to seek out on their own to carry out their research. In many cases the skills are not difficult to assimilate and the student develops the required knowledge during the process of carrying out research. Usually this is not a systematic approach, and it often leaves the student with a fragmented knowledge of some of the increasingly important concepts and areas relating to computing. By offering a general introduction and overview to networks, computer architectures, scientific visualization, programming languages, a variety of operating systems and hypertext authoring tools students get a broad comprehensive view of modern high performance computing methodologies. Students from all disciplines benefit from such a course. The survey of such tools is ideally suited for an interdisciplinary curriculum. As high performance computing becomes an essential component of the University curriculum, instructors need to be prepared to incorporate these concepts and methods in their own research and curricula. At this point in time educators are uncertain as to how to proceed, and there appears to be a lack of consensus on the curriculum for computational science. The Computational Science Education Project was initiated in Sep. 1991, by the Department of Energy to develop a syllabus for teaching interdisciplinary computational science. The interdisciplinary nature of the project is intended to contribute to national technological competitiveness by producing a body of graduates with the necessary skills to operate effectively in high performance computing environments. DOE

N95-28521# Lawrence Livermore National Lab., Livermore, CA.

WEIGHTING THE RECURSIVE SPECTRAL BISECTION ALGORITHM FOR UNSTRUCTURED GRIDS

D. Allen, E. Dube, and G. Rodrigue (California Univ., Davis, CA.) Sep. 1994 2 p Presented at the 7th Society for Industrial and Applied Mathematics (SIAM) Conference on Parallel Processing for Scientific Computing, San Francisco, CA, 15-17 Feb. 1995
(Contract W-7405-eng-48)
(DE95-008080; UCRL-JC-118624; CONF-950212-7) Avail: CASI HC A01/MF A01

When solving partial differential equations numerically on parallel computers it is desirable to decompose the domain on which we are solving the equations in such a way as to equalize the workload among the processors while minimizing the communications between them. This is equivalent to finding a partition of the graph representing the calculation into equal subgraphs cutting as few edges as possible. One such algorithm in use is the recursive spectral bisection algorithm (RSB). This algorithm can be shown to arise from rounding to feasibility the solution to relaxation of the following problem: Minimize f(x) = x(sup t)Lx, subject to x(sup t)e = 0, x(sub i) is a member of the set (-1,1) where L is the Laplacian matrix of the graph. The objective function counts the number of edges cut by the partition by a vector x. It can be the case however that the partition generated by the RSB does not have some desired feature. We extend the RSB algorithm to handle those cases. One extension is to modify the RSB algorithm to provide for the weighting of edges. This minimizes the total cost of edges cut by a partition rather than minimizing the number of edges as done in the RSB algorithm. Derived from text

N95-28566# Polish Academy of Sciences, Warsaw (Poland). Inst. of Basic Problems of Technology.
THE DETECTION AND TRACKING OF MOTION BY MEANS OF TIME-SPACE PATTERN MODELLING USING RANDOM FIELDS Ph.D. Thesis [DETEKCJA I SLEDZENIE RUCHU PRZY UZYCIU CZASOWO-PRZESTRZENNEGO MODELOWANIA OBRAZOW ZA POMOCA POL LOSOWYCH]
Adam Kurianski Cooperative Publishing House Ltd. 7 Dec. 1994 90 p In POLISH
(ISSN 0208-5658)
(IFTR-37/1994) Avail: Issuing Activity (Polish Academy of Sciences, Warsaw, Poland)

The dissertation presented deals with issues of motion detection and tracking, by means of a computer vision system, using statistical models called Markov fields. From a formal point of view, the above subjects belong to computer image analysis sometimes also called computer vision. The fast-paced technical advances in the field of computer hardware in recent years, associated with a significant increase in information processing capacities, made the time required for computer motion analysis cease to be an unsurpassable obstacle. The number of potential applications is very large, from traffic monitoring to microbe motion analysis to designing vehicles or objects moving without human supervision. Each of the above-mentioned applications is associated with an overwhelming number of particular problems that must be resolved. This is actually the reason for the extent of the broadly comprehended computer motion analysis. Detection and tracking are only two of the many particular issues.
Transl. by Schreiber Translations Inc.

N95-28588 Air Force Inst. of Tech., Wright-Patterson AFB, OH. School of Logistics and Acquisition Management.
AN AUTOMATED COST UNCERTAINTY PROGRAM M.S. Thesis
Dale N. Fletcher Sep. 1994 115 p Limited Reproducibility: More than 20% of this document may be affected by microfiche quality
(AD-A288747; AFIT/GCA/LAS/94S-4) Avail: Issuing Activity (Defense Technical Information Center (DTIC))

The purpose of this research was to develop a menu driven, computer program that implemented methodologies for cost uncertainty analysis. Cost uncertainties have been quantified using either simulation techniques or through heuristic means. Simulation techniques require time to run the required number of iterations. Current computer based heuristic methods do not check correlation matrices for consistency nor do they enable the analyst to perform queries. This research resulted in the development of an automated heuristic cost uncertainty program which alleviates the limitations of current computer programs. The program contains a file editor for creating and modifying data files, a cost uncertainty module for computing decile level total system cost probabilities and a query function. The FORTRAN computer program is completely menu driven for ease of use.
DTIC

N95-28590 Air Force Inst. of Tech., Wright-Patterson AFB, OH. School of Logistics and Acquisition Management.
ADVANCED EDUCATIONAL METHODS IN THE DEPARTMENT OF DEFENSE: APPLICATION OF CASE THEORY AND COMPUTER-ASSISTED INSTRUCTION TO BUSINESS PROCESS REENGINEERING M.S. Thesis
Brian A. Brown, Susan M. Brown, and Karen L. Cook Dec. 1994 100 p Limited Reproducibility: More than 20% of this document may be affected by microfiche quality
(AD-A288881; AFIT/GIR/LAR/94D-2) Avail: Issuing Activity (Defense Technical Information Center (DTIC))

The goal of this research was to create a computer-assisted instruction (CAI) prototype tutorial to teach the fundamental principles of integrated, computer-aided manufacturing definition activity modeling (IDEFO), a component of business process reengineering within the Department of Defense. To accomplish this, the authors evaluated current instructional material related to IDEFO, then adapted the material to a computerized learning environment using the Authorware Professional(TM) authoring software and a hybrid methodology which incorporated elements both of instructional design and software development. One of the most notable characteristics of this hybrid model was a series of iterations at each phase of development, which eliminated the need for retroactive modifications at successive development phases. The objectives for this study were accomplished by completing a literature review, identifying learning objectives and testing strategies, creating a prototype tutorial using authoring software, incorporating a case study, and then operationally testing the prototype. Analysis of this research is limited to a discussion of the results of a qualitative survey provided to evaluators of the prototype. In general, the results of the survey indicated acceptance of CAI as a method of instruction and provided recommendations for improving the tutorial.
DTIC

N95-28591 Air Force Inst. of Tech., Wright-Patterson AFB, OH.
A CORRELATIONAL STUDY OF THE SEI'S CAPABILITY MATURITY MODEL AND SOFTWARE DEVELOPMENT PERFORMANCE IN DOD CONTRACTS
Robert M. Flowe and James B. Thordahl Dec. 1994 301 p Limited Reproducibility: More than 20% of this document may be affected by microfiche quality
(AD-A288890; AFIT/GSS/LAR/94D-2) Avail: Issuing Activity (Defense Technical Information Center (DTIC))

The Software Engineering Institute's (SEI's) Capability Maturity Model (CMM) is to measure an organization's software development process maturity. The Department of Defense (DOD) has adopted this model with the belief that a more mature software development process will result in a more successful software subject. Although there is a growing body of anecdotal evidence supporting this presumed correlation, there is empirical evidence. Thus, the goal of our research was to determine the nature of the correlation, if any, between software process maturity and software project success, where process maturity is based on a CMM rating and success based on the parameters of cost and schedule. To investigate this correlation we identified software unique aimed CMM rating information on the contractor, collected cost and schedule data from a time frame and schedule of the rating, and interviewed project personnel to collect project context information. Using plots of cost performance versus rating level and nonparametric statistical techniques we found that, within our dataset, a correlation does exist between software development process maturity and project performance. The nature of this appears to be improved cost and schedule performance with higher software process maturity.
DTIC

N95-28625 Army Research Lab., Aberdeen Proving Ground, MD.
EXPLOITING PARALLELISM IN A MONTE CARLO IMAGE-MATCHING ALGORITHM Final Report, Mar. - Jun. 1994
Dale Shires Jan. 1995 60 p Limited Reproducibility: More than 20% of this document may be affected by microfiche quality
(DA Proj. 1L1-62618-AH-80)
(AD-A289872; ARL-TR-667) Avail: Issuing Activity (Defense Technical Information Center (DTIC))

Recovering three-dimensional information from a visual scene requires producing the disparity map of matched stereo images. The matching approach discussed in this paper involves the Metropolis algorithm, a simulated annealing technique. Although simple in principle, this stochastic optimization technique requires immense computational resources. Adapting the algorithm for parallel computing is discussed and demonstrated for several computer architectures. DTIC

N95-28627* Carnegie-Mellon Univ., Pittsburgh, PA. Software Engineering Inst.
SOFTWARE PROCESS IMPROVEMENT IN THE NASA SOFTWARE ENGINEERING LABORATORY Final Technical Report
Frank McGarry (National Aeronautics and Space Administration. Goddard Space Flight Center, Greenbelt, MD.), Rose Pajerski (National Aeronautics and Space Administration. Goddard Space Flight Center, Greenbelt, MD.), Gerald Page (Computer Sciences Corp., Greenbelt, MD.), Sharon Waligora (Computer Sciences Corp., Greenbelt, MD.), Victor Basili (Maryland Univ., College Park, MD.), and Marvin Zelkowitz (Maryland Univ., College Park, MD.) Dec. 1994 79 p Limited Reproducibility: More than 20% of this document may be affected by microfiche quality
(Contract F19628-90-C-0003)
(AD-A289912; CMU/SEI-94-TR-22; ESC-TR-94-022) Avail: Issuing Activity (Defense Technical Information Center (DTIC))

The Software Engineering Laboratory (SEL) was established in 1976 for the purpose of studying and measuring software processes with the intent of identifying improvements that could be applied to the production of ground support software within the Flight Dynamics Division (FDD) at the National Aeronautics and Space Administration (NASA)/Goddard Space Flight Center (GSFC). The SEL has three member organizations: NASA/GSFC, the University of Maryland, and Computer Sciences Corporation (CSC). The concept of process improvement within the SEL focuses on the continual understanding of both process and product as well as goal-driven experimentation and analysis of process change within a production environment. DTIC

N95-28628 Carnegie-Mellon Univ., Pittsburgh, PA. Software Engineering Inst.

REPLACING THE MESSAGE SERVICE COMPONENT IN AN INTEGRATION FRAMEWORK Final Report

Paul F. Zarrella and Alan W. Brown Oct. 1994 40 p Limited Reproducibility: More than 20% of this document may be affected by microfiche quality
(Contract F19628-90-C-0003)
(AD-A289928; CMU/SEI-94-TR-17; ESC-TR-94-017) Avail: Issuing Activity (Defense Technical Information Center (DTIC))

In an on-going set of commercial off-the-shelf (COTS) tool integration experiments being conducted by the CASE Environments Project, we have integrated a set of CASE tools using a combination of data integration mechanisms (PCTE Object Management System (OMS) and UNIX file system) and control integration mechanisms (Broadcast Message Server (BMS) of HP SoftBench). One of the key issues addressed in our work is the extent to which the integration of CASE tools can be independent of particular integration framework technology products. This report describes a task to examine interoperability aspects of the control integration component of the integration framework. The major conclusion from our work is that it is possible to integrate CASE tools using a message-passing approach that is independent of the integration framework product used. This report describes the activities an organization must undertake to integrate CASE tools in order to ensure the interoperation of message-passing integration products. The report also includes a set of lessons learned concerning the experiments we carried out. DTIC

N95-28632# Oak Ridge National Lab., TN.

BUILDING AN ELECTRONIC BOOK ON THE INTERNET. CSEP:AN INTERDISCIPLINARY SYLLABUS FOR TEACHING COMPUTATIONAL SCIENCE AT THE GRADUATE LEVEL

C. E. Oliver, M. R. Strayer, and V. M. Umar (Vanderbilt Univ., Nashville, TN.) 1994 5 p Presented at the Frontiers in Education Conference, San Jose, CA, 3-6 Nov. 1994
(Contract DE-AC05-84OR-21400)
(DE95-006526; CONF-9411137-3) Avail: CASI HC A01/MF A01

The Computational Science Education Project was initiated in Sep. 1991, by the Department of Energy to develop a syllabus for teaching interdisciplinary computational science. CSEP has two major activities. The writing and maintenance of an electronic book (e-book) and educational outreach to the computational science communities through presentations at professional society meetings, journal articles, and by training educators. The interdisciplinary nature of the project is intended to contribute to national technological competitiveness by producing a body of graduates with the necessary skills to operate effectively in high performance computing environments. The educational outreach guides and supports instructors in developing computational science courses and curricula at their institutions. The CSEP e-book provides valuable teaching material around which educators have built. The outreach not only introduces new educators to CSEP, but also establishes a synergistic relationship between CSEP authors, reviewers and users. DOE

N95-28635 Unisys Corp., Reston, VA. Reston Technology Center.

SOFTWARE TECHNOLOGY FOR ADAPTABLE, RELIABLE SYSTEMS (STARS). AdaWise USER'S MANUAL Technical Report

C. A. Barbasch 2 Sep. 1994 44 p Limited Reproducibility: More than 20% of this document may be affected by microfiche quality
(Contract F19628-93-C-0130)
(AD-A289655; STARS-AC-C006/001/01) Avail: Issuing Activity (Defense Technical Information Center (DTIC))

Ada is a high-level language with features to support program reliability and maintenance. An Ada compiler will detect many potential programming errors or non-portabilities that other languages would require a separate analysis tool to detect. However, the Ada language definition includes rules that Ada programs are required to obey, but that compilers are not required to enforce, either at compile-time or at execution-time. An Ada program that violates one or more of these rules can have unpredictable behavior, or can have different effects with different compilers or in different execution environments. DTIC

N95-28645 Newcastle-upon-Tyne Univ., Newcastle (England).

TWO IMPLEMENTATION RELATIONS AND THE CORRECTNESS OF COMMUNICATING REPLICATED PROCESSES Technical Report Series

M. Koutny, L. V. Mancini, and G. Pappalardo Oct. 1994 54 p See also PB92-192350 Prepared in cooperation with Universita di Reggio and Genoa Univ.
(PB95-195640; TRS-491) Copyright Avail: Issuing Activity (National Technical Information Service (NTIS))

This paper studies the correctness of distributed systems made up of replicated processes that communicate by message passing. Processes are described within the divergence model of Communicating Sequential Processes (CSP). The notion of correctness introduced is based on a relation that formally expresses the conformance of an implementation process with the target process it is intended to implement. A weak and strong case of such relations are introduced, aimed at treating acyclic and cyclic process networks respectively. Both allow the study of partial as well as total correctness of implementations, and may cope with non-deterministic targets and implementations. We then show how a target process may be implemented (in the formal sense introduced) by replicating it in a set of copies, a majority of which is non-faulty. NTIS

N95-28647 Martin Marietta Astronautics, Denver, CO.

NEXT GENERATION CONTROLLER SPECIFICATION FOR AN OPEN SYSTEMS ARCHITECTURE STANDARD Final Report, Mar. 1989 - Aug. 1994

28 Sep. 1994 315 p Limited Reproducibility: More than 20% of this document may be affected by microfiche quality
(Contract F33615-89-C-5706)
(AD-A289567; WL-TR-94-8033) Avail: Issuing Activity (Defense Technical Information Center (DTIC))

This report describes an open architecture framework for advanced manufacturing controllers including machine tools, robotics, process control, and coordinate measurement. The methodology described is applicable to both system design as well as system retrofit applications. A component-based approach is used that allows system architectures to the developed from generic building blocks that address system requirements and resulting functionality requirements. Initial architectures are used to produce an application architecture that addresses specific system messaging requirement. An application system is then synthesized using off-the-shelf, reusable implementation components for the application software. Hardware-software specific platform issues are addressed through the use of system profiles, a convention adopted form the IEEE Portable Operating System Interface (POSIX) standard that is now gaining wide acceptance. A number of examples are provided demonstrating use of all aspects of the methodology on a typical machine tool controller application. Appendices provide details with respect to specific components, requirements, and domain models. DTIC

N95-28658 Rutherford Appleton Lab., Oxford (England).

USING COLETTE. (A SIMPLE GUIDE)

S. M. King and R. K. Heenan Jan. 1995 22 p See also PB90-209453
(PB95-195806; RAL-95-005) Avail: Issuing Activity (National Technical Information Service (NTIS))

COLETTE is the name of the data reduction computer program for the LOQ Small-Angle Neutron Scattering (SANS) instrument at the ISIS Spallation Neutron Source. The ISIS data display and manipulation program, GENIE(c), was not designed to handle two-dimensional datasets, an essential operation in the processing of SANS data. COLETTE runs on top of, and thereby incorporates, GENIE(c). Data 'workspaces' are shared between COLETTE and GENIE(c). This means that a COLETTE user can 'shell' into GENIE(c) and use all of its functionality and then return to the COLETTE session without any loss of data. However, for reasons of speed and ease of use COLETTE effectively functions independently of GENIE(c): it has its own command set and its own data input and output routines. COLETTE is designed to run on the Digital Equipment Corporation (DEC) VAX family of computers under Digital's VMS (Version 5.x or higher) or Open VMS (Version 6.1 or higher) operating systems. COLETTE also requires DEC GKS (Graphical Kernel System) Version 4.2 or higher. (Note: DEC GKS Version 5.0 is incompatible with GENIE(c). The next compatible version is GKS 5.2). At the time of writing COLETTE does not run on DEC Alpha computers (even those running Open VMS). NTIS

N95-27383*# Aerospace Corp., Los Angeles, CA.
A SUSTAINABLE GENETIC ALGORITHM FOR SATELLITE RESOURCE ALLOCATION
R. J. Abbott (California State Univ., Los Angeles, CA.), M. L. Campbell, and W. C. Krenz *In* NASA. Goddard Space Flight Center, The 1995 Goddard Conference on Space Applications of Artificial Intelligence and Emerging Information Technologies May 1995 p 103-117 (For primary document see N95-27375 09-63)
Avail: CASI HC A03/MF A03

N95-27388*# Aerospace Corp., Los Angeles, CA.
IMPROVED REDUCED-RESOLUTION SATELLITE IMAGERY
James Ellison and Jaime Milstein *In* NASA. Goddard Space Flight Center, The 1995 Goddard Conference on Space Applications of Artificial Intelligence and Emerging Information Technologies May 1995 p 163-178 (For primary document see N95-27375 09-63)
Avail: CASI HC A03/MF A03

N95-27790*# National Aeronautics and Space Administration. Goddard Space Flight Center, Greenbelt, MD.
FLIGHT DYNAMICS SOFTWARE IN A DISTRIBUTED NETWORK ENVIRONMENT
J. Jeletic, D. Weidow, and D. Boland (Computer Sciences Corp., Lanham, MD.) *In its* Flight Mechanics/Estimation Theory Symposium 1995 May 1995 p 303-304 (For primary document see N95-27763 09-13)
Avail: CASI HC A01/MF A04

N95-27979*# Paragon Pacific, Inc., El Segundo, CA.
DESIGN OF A REAL-TIME WIND TURBINE SIMULATOR USING A CUSTOM PARALLEL ARCHITECTURE
John A. Hoffman, R. Gluck (TRW Space Technology Labs., Redondo Beach, CA.), and S. Sridhar (TRW Space Technology Labs., Redondo Beach, CA.) *In* DASCON Engineering, Collected Papers on Wind Turbine Technology May 1995 p 79-87 Sponsored by DOE (For primary document see N95-27970 09-44)
Avail: CASI HC A02/MF A03

62 COMPUTER SYSTEMS

Includes computer networks and special application computer systems.

N95-26441# Argonne National Lab., IL. Mathematics and Computer Science Div.
MASSIVELY PARALLEL SELF-CONSISTENT-FIELD CALCULATIONS
Jeffrey L. Tilson 29 Oct. 1994 14 p Presented at the Annual Meeting of the American Institute of Chemical Engineers, San Francisco, CA, 13-18 Nov. 1994
(Contract W-31-109-eng-38)
(DE95-004128; ANL/MCS/CP-84764; CONF-941128-3) Avail: CASI HC A03/MF A01

The advent of supercomputers with many computational nodes each with its own independent memory makes possible extremely fast computations. The author's work, as part of the US High Performance Computing and Communications Program (HPCCP), is focused on the development of electronic structure techniques for the solution of Grand Challenge-size molecules containing hundreds of atoms. Their efforts have resulted in a fully scalable Direct- self-consistent field (SCF) program that is portable and efficient. This code, named NWCHEM, is built around a distributed-data model. This distributed data is managed by a software package called Global Arrays developed within the HPCCP. They present performance results for Direct-SCF calculations of interest to the consortium. DOE

N95-26460 Army Research Lab., Aberdeen Proving Ground, MD.
PARALLEL COMPUTING ON VARIOUS PLATFORMS: A CASE STUDY Interim Report, Feb. - Oct. 1994
B. N. Srivastava Nov. 1994 50 p Limited Reproducibility: More than 20% of this document may be affected by microfiche quality
(Contract DAAA15-91-C-0082)
(AD-A289008; ARL-TR-633) Avail: Issuing Activity (Defense Technical Information Center (DTIC))

Parallel computing offers an attractive means for high-performance computing to alleviate the current bottleneck in speedup potential of large application codes for practical problem solving. The challenge of actual implementation, however, can be significant. The objective of this report is to address the issue of porting and parallelizing a Computational Fluid Dynamics (CFD) application code on several supercomputing platforms such as Cray C-90, Cray Y-MP, KSRl, CM-S and Intel PARAGON. This overall objective is achieved through first emulating the application code by conducting a model test code, in an effort to understand the influence of data structure on the code performance. The conclusions derived from this are then utilized to restructure the 2-D/3-D CFD code such that the final version is transportable to a wider class of platforms. DTIC

N95-26471 North Carolina State Univ., Raleigh, NC.
PARALLELISM DETECTION AND SCHEDULING STRATEGIES FOR RELIABLE AND EFFICIENT EXECUTION ON MULTICOMPUTERS Final Report, 8 Feb. 1991 - 16 May 1994
Dharma P. Agrawal 31 Jul. 1994 7 p Limited Reproducibility: More than 20% of this document may be affected by microfiche quality
(Contract DAAL03-91-G-0031)
(AD-A288370; ARO-28192.22-MA) Avail: Issuing Activity (Defense Technical Information Center (DTIC))

Introduced a new concurrent object-oriented language called CORE which solves the inheritance anomaly problem. By separating and localizing the synchronization schemes from the main bodies of the program components, CORE allows a high degree of encapsulation and re-use for the synchronization code and the program modules. DTIC

N95-26529 Carnegie-Mellon Univ., Pittsburgh, PA. Dept. of Computer Science.
PERFORMANCE EVALUATION OF A NEW PARALLEL PRECONDITIONER
Keith D. Gremban, Gary L. Miller, and Marco Zagha Oct. 1994 34 p Limited Reproducibility: More than 20% of this document may be affected by microfiche quality
(Contract F33615-93-1-1330; NSFCCR-90-16641)
(AD-A288563; CMU-CS-94-205) Avail: Issuing Activity (Defense Technical Information Center (DTIC))

Solution of partial differential equations by either the finite element or the finite difference methods often requires the solution of large, sparse linear systems. When the coefficient matrices associated with these linear systems are symmetric and positive definite, the systems are often solved iteratively using the preconditioned conjugate gradient method. We have developed a new class of preconditioners, which we call support tree preconditioners, that are based on the connectivity of the graphs corresponding to the coefficient matrices of the linear systems. These new preconditioners have the advantage of being well-structured for parallel implementation, both in construction and in evaluation. In this paper, we evaluate the performance of support tree preconditioners by comparing them against two common types of preconditioners: those arising from diagonal scaling, and from the incomplete Cholesky decomposition. We solved linear systems corresponding to both regular and irregular meshes on the Cray C-90 using all three preconditioners and monitored the number of iterations required to converge, and the total time taken by the iterative processes. We show empirically that the convergence properties of support tree preconditioners are similar, and superior in many cases, to those of incomplete Cholesky preconditioners, which in turn are superior to those of diagonal scaling. Support tree preconditioners require less overall storage, less work per iteration, and yield better parallel performance than incomplete Cholesky preconditioners. In terms of total execution time, support tree preconditioners outperform both diagonal scaling and incomplete Cholesky preconditioners. Hence, support tree preconditioners provide a powerful, practical tool for the solution of large sparse systems of equations on vector and parallel machines. DTIC

N95-26551 Naval Postgraduate School, Monterey, CA.
GRAIN SIZE MANAGEMENT IN REPETITIVE TASK GRAPHS FOR MULTIPROCESSOR COMPUTER SCHEDULING M.S. Thesis
Greg L. Negelspach Sep. 1994 56 p Limited Reproducibility: More than 20% of this document may be affected by microfiche quality
(AD-A288575) Avail: Issuing Activity (Defense Technical Information Center (DTIC))

Optimal scheduling of parallel programs onto multiprocessor computers is an exponentially hard problem. Because of this, most scheduling algorithms in use today rely on heuristics to determine the best balance of computation and communication costs. However, because of the NP-hard nature of the problem, these heuristics have become very complex. We are concerned with a specific instance of the problem, throughput scheduling, which aims to optimize the completion rate of repetitive programs, expressed as task graphs, for which the computational and communication needs of the tasks are known in advance. We propose a simpler approach for finding better schedules, which involves testing different grain size modified versions of the task graph to find the one that results in the highest throughput for the given scheduling algorithm. Our heuristic works by alternately fusing or fissioning selected tasks of the graph then evaluating the modified task graph by measuring the expected throughput of its resultant schedule. Because of the generality of this approach, it can be applied to any scheduling algorithm that does not already include grain size modification. We test the new heuristic using a simulation of the Navy's new standard digital signal processor, the AN/UYS-2, and using various task graphs and scheduling algorithms. We show that this practical approach to scheduling can increase throughput of the Largest Process Time first algorithm by at least 16 percent for our model computer configured with four, eight, or sixteen processors. DTIC

N95-26840 Carnegie-Mellon Univ., Pittsburgh, PA. Dept. of Computer Science.
AN ARCHITECTURE FOR OPTIMAL ALL-TO-ALL PERSONALIZED COMMUNICATION
Susan Hinrichs, Corey Kosak, David R. OHallaron, Thomas M. Stricker, and Riichiro Take Sep. 1994 33 p Limited Reproducibility: More than 20% of this document may be affected by microfiche quality
(Contracts N00039-93-C-0152; F49620-92-J-0131)
(AD-A288532; CMU-CS-94-140) Avail: Issuing Activity (Defense Technical Information Center (DTIC))

In all-to-all personalized communication (AAPC), every node of a parallel system sends a potentially unique packet to every other node. AAPC is an important primitive operation for modem parallel compilers, since it is used to redistribute data structures during parallel computations. As an extremely dense communication pattern, AAPC causes congestion in many types of networks and therefore executes very poorly on general purpose, asynchronous message passing routers. We present and evaluate a network architecture that executes all-to-all communication optimally on a two-dimensional torus. The router combines optimal partitions of the AAPC step with a self-synchronizing switching mechanism integrated into a conventional wormhole router. Optimality is achieved by routing along shortest paths while fully utilizing all links. A simple hardware addition for synchronized message switching can guarantee optimal AAPC routing in many existing network architectures. The flexible communication agent of the iWarp VLSI component allowed us to implement an efficient prototype for the evaluation of the hardware complexity as well as possible software overheads. The measured performance on an 8 x 8 torus exceeded 2 GigaBytes/sec or 80% of the limit set by the raw speed of the interconnects. We make a quantitative comparison of the AAPC router with a conventional message passing system. The potential gain of such a router for larger parallel programs is illustrated with the example of a two-dimensional Fast Fourier Transform. DTIC

N95-26984 Air Force Inst. of Tech., Wright-Patterson AFB, OH. School of Engineering.
MINIMIZING THE IMPACT OF SYNCHRONIZATION OVERHEAD IN PARALLEL DISCRETE EVENT SIMULATIONS M.S. Thesis
Andrew C. Walton 14 Dec. 1994 145 p Limited Reproducibility: More than 20% of this document may be affected by microfiche quality
(AD-A289278; AFIT/GCS/ENG/94D-25) Avail: Issuing Activity (Defense Technical Information Center (DTIC))

A Parallel Discrete Event Simulation Coprocessor was designed for conservative synchronization protocols and was implemented in software using some of a parallel computer's nodes to act as coprocessors. The coprocessor was designed to offload synchronization overhead and next event queue management from the nodes running the simulation. The coprocessor was designed to accelerate simulations based on the Simulation Protocol Evaluation on a Concurrent Testbed with ReUsable Modules (SPECTRUM) environment. The research was conducted in three steps: (1) the SPECTRUM environment was ported from an Intel iPSC/2 to an Intel Paragon XP/S; (2) the coprocessor was designed; and (3) the simulations were timed, with and without the coprocessor. In some cases, the coprocessor provided up to a 2.5 times speedup. DTIC

N95-27182 California Univ., Berkeley, CA.
CONSTRUCTION OF A CONNECTIONIST NETWORK SUPERCOMPUTER Technical Progress Report, 1 Aug. - 31 Oct. 1994
1 Nov. 1994 4 p Limited Reproducibility: More than 20% of this document may be affected by microfiche quality
(Contract N00014-92-J-1617)
(AD-A288439) Avail: Issuing Activity (Defense Technical Information Center (DTIC))

We have made progress in several areas this quarter. Highlights include: high-level software: public release of Sather 1.0, and major progress on pSather; low-level software - design of 'bare die' test software to be used for actual chip testing; applications - a complete speech recognition application running with the Torrent instruction simulator; network hardware - a new network interface test chip running at 300 Mbits/second; system hardware - completion of the SPERT circuit board design and layout; analog very large scale integration (VLSI) - a new communications protocol for connecting multiple chips efficiently. In addition to the scientific and technical work, we had the occasion to present a summary of our work at two events. At the dedication day for the new U.C. Berkeley Computer Science building, Soda Hall, over 50 visitors from academia, industry and government stopped by our four exhibits showing highlights of the CNS-1 project. DTIC

N95-27183 George Mason Univ., Fairfax, VA. Center for Computational Statistics.
SIMULATING A MULTI-TARGET ACOUSTIC ARRAY ON THE INTEL PARAGON M.S. Thesis
Charles A. Jones Oct. 1994 84 p Limited Reproducibility: More than 20% of this document may be affected by microfiche quality
(Contracts DAAH04-94-G-0267; DAAL03-91-G-0039)
(AD-A288443; TR-108) Avail: Issuing Activity (Defense Technical Information Center (DTIC))

This thesis is built around a parallel programming project which simulates the recordings of a linear array of hydrophones in the presence of several sources of acoustic signals (targets). Simulation of multi-target data with appropriate modeling of multipath, path refraction, and local and distant noise sources is a useful and relatively sophisticated modeling chore. The signal suites include multiple frequency narrow band signals, broad-band flow noise, and randomly generated transient signals. The noise suites include coherent and incoherent Gaussian noise, impulsive noise, and continental shelf reverberation. This project is of interest from a parallel programming viewpoint because it uses the Paragon as a true Multiple Instruction Multiple Data (MIMD) machine with three types of nodes: (1) a manager node, (2) target nodes, and (3) hydrophone nodes. The target nodes are responsible for generating the signal suites, transient noise, and the coherent noise. The hydrophone nodes are responsible for calculation of multipath, refraction and time delay as well as adding the local incoherent noise suite. While this simulation can be used as a stand-alone application, it also will form the foundation for a much larger, more sophisticated simulation, namely producing a virtual Command Information Center (CIC). DTIC

N95-27250 Carnegie-Mellon Univ., Pittsburgh, PA. Software Engineering Inst.
SPINNING A WEB: PUBLISHING THE SEI SOFTWARE CONFIGURATION MANAGEMENT RESEARCH ON THE WORLD WIDE WEB Final Report
Clifford C. Huff Nov. 1994 72 p Limited Reproducibility: More than 20% of this document may be affected by microfiche quality

(Contract F19628-90-C-0003)
(AD-A288708; CMU/SEI-94-TR-18; ESC-TR-94-018) Avail: Issuing Activity (Defense Technical Information Center (DTIC))

Configuration Management research has been performed by members of the CASE Environments Project over the course of the past five years. This report describes the contents of the configuration management research materials that have been published on the SEI World Wide Web (WWW) Server. Primary Web Structures and methods for accessing information on the Web are described. A summary of the problems and challenges encountered and the Web publishing techniques employed in this process are discussed. DTIC

N95-27402# Sandia National Labs., Albuquerque, NM.
XTP AS A TRANSPORT PROTOCOL FOR DISTRIBUTED PARALLEL PROCESSING
W. T. Strayer, M. J. Lewis, and R. E. Cline, Jr. 1994 11 p Presented at the 1994 USENIX Conference, Oakland, CA, 1-2 Aug. 1994
(Contracts DE-AC04-76DP-00789; DE-AC04-94AL-85000)
(DE95-004992; SAND-94-8628C; CONF-9408119-2) Avail: CASI HC A03/MF A01

The Xpress Transfer Protocol (XTP) is a flexible transport layer protocol designed to provide efficient service without dictating the communication paradigm or the delivery characteristics that qualify the paradigm. XTP provides the tools to build communication services appropriate to the application. Current data delivery solutions for many popular cluster computing environments use TCP and UDP. We examine TCP, UDP, and XTP with respect to the communication characteristics typical of parallel applications. We perform measurements of end-to-end latency for several paradigms important to cluster computing. An implementation of XTP is shown to be comparable to TCP in end-to-end latency on preestablished connections, and does better for paradigms where connections must be constructed on the fly. DOE

N95-27422# Los Alamos National Lab., NM.
GIGABIT LAN ISSUES: HIPPI, FIBRE CHANNEL, OR ATM?
D. E. Tolmie 1994 6 p Presented at the International Conference and Exhibition on High-performance Computing and Networking, Milan, Italy, 3-5 May 1995
(Contract W-7405-eng-36)
(DE95-003673; LA-UR-94-3994; CONF-9505116-1) Avail: CASI HC A02/MF A01

Computer networks that operate in the gigabit per second speed range are becoming very important for interconnecting supercomputers, clusters of workstations, and other high end equipment. HIPPI is the current interface of choice, while Fibre Channel and ATM are emerging standards. These systems are examined as to their backgrounds, advantages, and shortcomings. DOE

N95-27709# Oak Ridge National Lab., TN. Informatics Group.
SEQUENCE COMPARISON ON A CLUSTER OF WORKSTATIONS USING THE PVM SYSTEM
X. Guan, R. J. Mural, and E. C. Uberbacher 1995 9 p Presented at the IPPS 95: Parallel Processing Symposium, Santa Barbara, CA, 25-28 Apr. 1995 Sponsored in part by Martin Marietta Energy Systems, Inc.
(Contract DE-AC05-84OR-21400)
(DE95-006527; CONF-950484-2) Avail: CASI HC A02/MF A01

We have implemented a distributed sequence comparison algorithm on a cluster of workstations using the parallel virtual machine (PVM) paradigm. This implementation has achieved similar performance to the intel iPSC/860 Hypercube, a massively parallel computer. The distributed sequence comparison algorithm serves as a search tool for two Internet servers GRAIL and GENQUEST. This paper describes the implementation and the performance of the algorithm. DOE

N95-27741# Argonne National Lab., IL. Mathematics and Computer Science Div.
LANGUAGE CONSTRUCTS AND RUNTIME SYSTEMS FOR COMPOSITIONAL PARALLEL PROGRAMMING
Ian Foster and Carl Kesselman (California Inst. of Tech., Pasadena, CA.) 1995 12 p Presented at the CONPAR Conference, Linz, Austria,15-18 Aug. 1994
(Contract W-31-109-eng-38)
(DE95-008298; ANL/MCS/CP-85720; CONF-9408222-1) Avail: CASI HC A03/MF A01

In task-parallel programs, diverse activities can take place concurrently, and communication and synchronization patterns are complex and not easily predictable. Previous work has identified compositionality as an important design principle for task-parallel programs. In this paper, we discuss alternative approaches to the realization of this principle. We first provide a review and critical analysis of Strand, an early compositional programming language. We examine the strengths of the Strand approach and also its weaknesses, which we attribute primarily to the use of a specialized language. Then, we present an alternative programming language framework that overcomes these weaknesses. This framework uses simple extensions to existing sequential languages (C++ and Fortran) and a common runtime system to provide a basis for the construction of large, task-parallel programs. We also discuss the runtime system techniques required to support these languages on parallel and distributed computer systems. DOE

N95-28019# Oak Ridge National Lab., TN. Mathematical Sciences Section.
A NEW SHARED-MEMORY PROGRAMMING PARADIGM FOR MOLECULAR DYNAMICS SIMULATIONS ON THE INTEL PARAGON
E. F. DAzevedo and C. H. Romine Dec. 1994 62 p
(Contract DE-AC05-84OR-21400)
(DE95-007289; ORNL/TM-12890) Avail: CASI HC A04/MF A01

This report describes the use of shared memory emulation with DOLIB (Distributed Object Library) to simplify parallel programming on the Intel Paragon. A molecular dynamics application is used as an example to illustrate the use of the DOLIB shared memory library. SOTON-PAR, a parallel molecular dynamics code with explicit message-passing using a Lennard-Jones 6-12 potential, is rewritten using DOLIB primitives. The resulting code has no explicit message primitives and resembles a serial code. The new code can perform dynamic load balancing and achieves better performance than the original parallel code with explicit message-passing. DOE

N95-28071# Argonne National Lab., IL.
USING THE SCALABLE NONLINEAR EQUATIONS SOLVERS PACKAGE
W. D. Gropp, L. C. McInnes, and B. F. Smith Feb. 1995 56 p
(Contract W-31-109-eng-38)
(DE95-008323; ANL/MCS-TM-193) Avail: CASI HC A04/MF A01

SNES (Scalable Nonlinear Equations Solvers) is a software package for the numerical solution of large-scale systems of nonlinear equations on both uniprocessors and parallel architectures. SNES also contains a component for the solution of unconstrained minimization problems, called SUMS (Scalable Unconstrained Minimization Solvers). Newton-like methods, which are known for their efficiency and robustness, constitute the core of the package. As part of the multilevel PETSc library, SNES incorporates many features and options from other parts of PETSc. In keeping with the spirit of the PETSc library, the nonlinear solution routines are data-structure-neutral, making them flexible and easily extensible. This users guide contains a detailed description of uniprocessor usage of SNES, with some added comments regarding multiprocessor usage. At this time the parallel version is undergoing refinement and extension, as we work toward a common interface for the uniprocessor and parallel cases. Thus, forthcoming versions of the software will contain additional features, and changes to parallel interface may result at any time. The new parallel version will employ the MPI (Message Passing Interface) standard for interprocessor communication. Since most of these details will be hidden, users will need to perform only minimal message-passing programming. DOE

N95-28074# Sandia National Labs., Albuquerque, NM.
SANDIA'S NETWORK FOR SUPERCOMPUTING '94: LINKING THE LOS ALAMOS, LAWRENCE LIVERMORE, AND SANDIA NATIONAL LABORATORIES USING SWITCHED MULTIMEGABIT DATA SERVICE
M. O. Vahle, S. A. Gossage, and J. P. Brenkosh Jan. 1995 14 p
(Contract DE-AC04-94AL-85000)
(DE95-007717; SAND-94-3096) Avail: CASI HC A03/MF A01

Supercomputing '94, a high-performance computing and communications conference, was held November 14th through 18th, 1994 in Washington

DC. For the past four years, Sandia National Laboratories has used this conference to showcase and focus its communications and networking endeavors. At the 1994 conference, Sandia built a Switched Multimegabit Data Service (SMDS) network running at 44.736 megabits per second linking its private SMDS network between its facilities in Albuquerque, New Mexico and Livermore, California to the convention center in Washington, D.C. For the show, the network was also extended from Sandia, New Mexico to Los Alamos National Laboratory and from Sandia, California to Lawrence Livermore National Laboratory. This paper documents and describes this network and how it was used at the conference. DOE

N95-28093 Selskapet for Industriell og Teknisk Forskning, Trondheim (Norway). Dept. of Instrumentation.
SIMULATOR REPORT FOR SCI SYSTEMS WITH HIC-ROUTER
J. Bothner and E. Kristiansen 14 Sep. 1994 34 p
(PB95-196580; STF31-A94038) Avail: Issuing Activity (National Technical Information Service (NTIS))

The report presents a simulator for studying the use of Heterogenous Interprocessor Communication (HIC) technology to connect together Scalable Coherent Interface (SCI) rings. In other words, HIC technology is used to transport SCI packets. HIC is part of the European Open Microprocessor Systems Initiative (OMI) program. It is a definition of a link in various ranges of cost and performance. SCIs main attributes are strong mechanisms in a multiprocessor environment and speed. NTIS

N95-28335 Naval Surface Warfare Center, Dahlgren, VA.
PARALLEL BLOCK IMPLICIT INTEGRATION TECHNIQUE FOR TRAJECTORY PARALLELISM
Alan E. Rufty Dec. 1994 39 p Limited Reproducibility: More than 20% of this document may be affected by microfiche quality
(AD-A288961; NSWCDD/TR-94/217) Avail: Issuing Activity (Defense Technical Information Center (DTIC))

This report describes the evaluation of a Parallel Block Implicit (PBI) integration technique in a simplified missile trajectory. This project was carried out to ascertain the suitability of PBI techniques when modest amounts of parallelism are available; that is, when 3 to 10 processors are allocated per missile trajectory. The PBI technique was first evaluated on a serial mainframe computer before it was implemented in parallel on an INMOS TRANSPUTER with four parallel central processing units. While the serial implementation of the four-node PBI technique indicated that a speedup of a factor of three to four was possible with ideal hardware, in practice only a modest gain (approximately 30 percent) was obtained because of systems-related overhead. DTIC

N95-28502 Selskapet for Industriell og Teknisk Forskning, Trondheim (Norway).
INTERNATIONAL NETWORKS
S. Haug 26 Sep. 1994 40 p
(PB95-196366; STF13-S94005) Avail: Issuing Activity (National Technical Information Service (NTIS))

The document is a collection of transparencies from a presentation on international networks at the NORUG conference held April 25-27, 1994. NTIS

N95-28665 Selskapet for Industriell og Teknisk Forskning, Trondheim (Norway).
PRACTICAL CONSIDERATIONS FOR NETWORK ADDRESSING USING CIDR Journal Article
H. Eidnes 26 Sep. 1994 7 p
(PB95-195335; STF13-S94006) Avail: Issuing Activity (National Technical Information Service (NTIS))

Due to the continually increasing popularity of the Transmission Control Protocol/Internet Protocol (TCP/IP) protocol suite, the Internet community is currently facing three related major problems: The Class B address space is in danger of exhaustion; The Internet routing explosion is a problem for those routers on the Internet that do not use a default route and have to carry a routing entry for each and every network they need connectivity to; Eventual exhaustion of the entire IP address space is a real, though not imminent danger. The proposed solution is through the deployment of two mechanisms: (1) Development of new routing protocols for interdomain routing, implementing Classless Inter-Domain Routing (CIDR); (2) Start to assign IP network numbers based on the Internet topology, in order to make effective use of CIDR routing technology. NTIS

63 CYBERNETICS

Includes feedback and control theory, artificial intelligence, robotics and expert systems.

For related information see also *54 Man/System Technology and Life Support.*

N95-26421 Naval Postgraduate School, Monterey, CA.
SCALABLE MULTICAST TREE CONSTRUCTION FOR WIDE AREA NETWORKS M.S. Thesis
James Eric Klinker Sep. 1994 114 p Limited Reproducibility: More than 20% of this document may be affected by microfiche quality
(AD-A288318) Avail: Issuing Activity (Defense Technical Information Center (DTIC))

In this thesis, we address the problem of multicast tree construction with guaranteed quality of service (QoS) in networks with asymmetric link costs. We describe a protocol to locate distribution centers for an interaction based on network load and participant location. We then describe the protocol for constructing a shared tree around the selected center. We compare the quality of the resultant trees on large hypothetical networks with that of source based trees. Additional comparisons are made with other multicast techniques such as Protocol Independent Multicasting (PIM) and Core Based Trees (CBT). Our results show that the shared trees built using our approach represent a significant improvement over other techniques when the network topology contains a large degree of asymmetry in link cost. This makes our approach the most general of all other techniques proposed to date. DTIC

N95-26443# Los Alamos National Lab., NM.
INTEGRATION OF VIDEO AND RADIATION ANALYSIS DATA
H. O. Menlove, J. A. Howell, C. A. Rodriguez, G. W. Eccleston, D. Beddingfield, J. E. Smith, and C. W. Baumgart (EG and G Energy Measurements, Inc., Los Alamos, NM.) 1995 10 p
(Contract DE-AC08-93NV-11265)
(DE95-004165; EGG-11265-5025) Avail: CASI HC A02/MF A01

The authors have introduced a new method to integrate spatial (digital video) with time (radiation monitoring) information. This technology is based on pattern recognition by neural networks, provides significant capability to analyze complex data, and has the ability to learn and adapt to changing situations. This technique has the potential of significantly reducing the frequency of inspection visits to key facilities without a loss of safeguards effectiveness. safeguards effectiveness. DOE

N95-26449# Helsinki Univ. of Technology, Espoo (Finland). Control Engineering Lab.
SELF-ORGANIZING ARTIFICIAL NEURAL NETWORKS IN DYNAMIC SYSTEMS MODELING AND CONTROL Ph.D. Thesis
Heikki Hyoetyniemi Nov. 1994 141 p
(ISSN 0356-0872)
(PB95-185120; ISBN-951-22-2362-7) Avail: CASI HC A07/MF A02

This thesis discusses the potential of self-organizing networks applied to the modeling and control of dynamic systems. A general framework is created for self-organizing networks applications that is especially suited to control engineering. Apart from the traditional time-domain features, linear operators can be mapped in the network. Efficient algorithms are derived for adapting the parameters in the self-organizing net. These algorithms are motivated as solutions to well-founded optimization problems. Two prototypical approaches to realizing controllers based on the neural network representations are presented with simple application examples. The theoretical problems of combining self-organizing networks with dynamic systems are discussed extensively. The algorithms that are derived for self-organization are not limited only to control engineering applications. On the other hand, the theoretical analyses of dynamic systems are not limited to neural networks applications--for example, the identification algorithms and the results achieved on the systems identifiability are applicable to the general parameter estimation tasks. NTIS

N95-26468 Houston Univ., TX. Dept. of Electrical Engineering.
ROBUST HYBRID STATE-SPACE SELF-TUNING CONTROL USING DUAL-RATE SAMPLING Final Report, 1 May 1991 - 31 Aug. 1994
L. S. Shieh and C. K. Koc 31 Aug. 1994 10 p Limited Reproducibility: More than 20% of this document may be affected by microfiche quality
(Contract DAAL03-91-G-0106)
(AD-A288359; ARO-28511.27-MA) Avail: Issuing Activity (Defense Technical Information Center (DTIC))

This report presents a hybrid state-space self-tuner using a new dual-rate sampling scheme for digital adaptive control of continuous-time uncertain linear systems. A state-space-based recursive least-squares algorithm, together with a variable forgetting factor, is used for direct estimation of both the equivalent discrete-time uncertain linear system parameters and associated discrete-time state of a continuous-time uncertain linear system from the sampled input and output data. An analog optimal regional pole-placement design method is used for designing an optimal observer-based analoque controller. A sub-optimal observer-based digital controller is then designed from the designed analoque controller using digital redesign technique. To enhance the robustness of parameter identification and state estimation algorithms, a dynamic bound for a class of uncertain bilinear parameters and a fast-rate digital controller are developed at each fast-sampling period. Also, to accommodate computation loads and computation delay for developing the advance hybrid self-tuner, the designed analoque controller and observer gains are both updated at each slow-sampling period. This control technique has been successfully applied to benchmark control problems. DTIC

N95-26475 Rome Lab., Griffiss AFB, NY.
ENCODING USER-DEFINED PROBLEMS WITH SIPE-2 Report, Jun. 1993 - Mar. 1994
Karen M. Alguire Oct. 1994 44 p Limited Reproducibility: More than 20% of this document may be affected by microfiche quality
(AF Proj. 5581)
(AD-A288390; RL-TR-94-165) Avail: Issuing Activity (Defense Technical Information Center (DTIC))

This report describes work related to some experiments performed at Rome Laboratory with generative planners. The main objective of the project was to provide an understanding of generative planners and familiarization with two different generative planners, O-Plan2 and SIPE-2. The approach was to become proficient in the use of the generative planning systems to define and solve new problems representative of basic planning capability requirements. The Missionaries and Cannibals (MC) puzzle was selected as a starting point because of its simplicity and it deals with simple numerical calculations, an aspect we felt was relevant to application interests. This report focuses on the work with SIPE-2, specifically, our experience encoding the MC puzzle. The process of encoding problems in general is also addressed for providing guidance in defining and solving user-defined problems with SIPE-2. DTIC

N95-26480 Maryland Univ., College Park, MD. Dept. of Electrical Engineering.
STOCHASTIC ADAPTIVE ESTIMATION AND CONTROL Final Report
Steven I. Marcus 26 Oct. 1994 11 p Limited Reproducibility: More than 20% of this document may be affected by microfiche quality
(Contract F49620-92-J-0045)
(AD-A289088; AFOSR-94-0759TR) Avail: Issuing Activity (Defense Technical Information Center (DTIC))

Significant progress was made in a number of aspects of stochastic and discrete event systems. A controlled switching diffusion model was developed to study systems with multiple modes or failure modes, such as aircraft with multiple operating modes, the hierarchical control of flexible manufacturing systems, and large scale interconnected power networks. In addition, a number of other optimal stochastic control problems with long time horizans were solved. An important problem in the adaptive control of a finite state Markov chain was solved, and significant progress was made along more general directions. New results on the risk-sensitive control of hidden Markov processes were obtained. Motivated by applications in hierarchical intelligent control, some important problems in the area of discrete event systems were solved. DTIC

N95-26492 Institute of Electrical and Electronics Engineers, Pasadena, CA. Information Theory Society.
THE 1994 IEEE-IMS WORKSHOP ON INFORMATION THEORY AND STATISTICS
29 Oct. 1994 111 p Workshop held in Alexandria, VA, 27-29 Oct. 1994; sponsored by IEEE Information Theory Society Institute of Mathematical Statistics Sponsored by the Office of Naval Research; the National Security Agency; and the National Science Foundation Limited Reproducibility: More than 20% of this document may be affected by microfiche quality
(AD-A288808) Avail: Issuing Activity (Defense Technical Information Center (DTIC))

The idea of a workshop on information theory and statistics was born from a recent series of exciting interactions between researchers from both communities covering a wide range of topics including data compression, complexity, Markov fields, large deviations, nonparametrics and sampling and wavelets. Our aim has been to provide a forum for the presentation and discussion of new technical results at the interface of these two disciplines. We hope that this Workshop will be the first of a series of many which will serve to promote a better understanding of the interplay between information theory and statistics. DTIC

N95-26530 Boston Univ., MA. Center for Adaptive Systems.
NEURAL MODELS OF SPATIAL ORIENTATION IN NOVEL ENVIRONMENTS Annual Technical Report, 1 Sep. 1993 - 31 Aug. 1994
Stephen Grossberg Oct. 1994 29 p Limited Reproducibility: More than 20% of this document may be affected by microfiche quality
(Contract F49620-92-J-0499)
(AD-A288420; AFOSR-94-0677TR) Avail: Issuing Activity (Defense Technical Information Center (DTIC))

Completed work on this grant analyzes problems of 3-D vision, visual search, spatial mapping, planning and action, all of which utilize spatial representations to control adaptive behaviors in real time. Highlights include significant contributions towards solving the classical figure-ground problem for biological vision, the problem of self-organizing body-centered spatial representations for movement planning and spatial orientation, and the problem of carrying out fast visual search for targets among multiple distractors. New research directions include projects which have been developed to frontally attack core problems concerning how a rapidly moving agent can self-organize spatial representations, use these representations for real-time movement planning, and transform spatial movement plans into appropriate motor commands for movement control and real-time navigation. Specific projects include retinal image processing, formation of egocentric maps of object positions from optic flow, detection of moving objects from optic flow, integration of egocentric and allocentric representations for autonomous navigation, and investigation of spatial reference frames and transformations between frames for real-time flexible speech articulator control. DTIC

N95-26638 Galaxy Scientific Corp., Pleasantville, NJ.
DIGITAL SYSTEMS VALIDATION. CHAPTER 20 ARTIFICIAL INTELLIGENGE WITH APPLICATIONS FOR AIRCRAFT. HANDBBOOK, VOLUME 2
L. Harrison, P. Saunders, and J. Janowitz Jul. 1994 200 p Limited Reproducibility: More than 20% of this document may be affected by microfiche quality
(Contract DTFA03-89-C-00043)
(AD-A288492; DOT/FAA/CT-88/10-Vol-2) Avail: Issuing Activity (Defense Technical Information Center (DTIC))

This chapter provides an overview of Artificial Intelligence (AI) technology, one of the more complex applications of digital systems. This chapter examines AI-based technology, focusing on three fields: neural networks, 'fuzzy' logic, and Expert Systems. This chapter provides the reader with the background and a basic understanding of the fundamental at those fields. Another section examines aspects of the AI development environment, including languages, tools, and AI-based hardware components. Some of the proposed aviation-related applications for both civil and military aircraft, including pilot assistants and diagnostic aids, are surveyed. Additionally, certification issues, including regulations, guidelines, and verification and validation techniques are examined. Human factors issues relating to the use of this technology are identified and reviewed. In addition, this chapter identifies safety issues and concerns over the use of this technology in airborne systems. DTIC

N95-26920 Air Force Inst. of Tech., Wright-Patterson AFB, OH.
A GAIN SCHEDULING OPTIMIZATION METHOD USING GENETIC ALGORITHMS M.S. Thesis
Robert C. Martin, IV Dec. 1994 153 p Limited Reproducibility: More than 20% of this document may be affected by microfiche quality
(AD-A289306; AFIT/GAE/ENY/94D-3) Avail: Issuing Activity (Defense Technical Information Center (DTIC))

Gain scheduling, the traditional method of providing adaptive control to a nonlinear system, has long been an ad hoc design process. Until recently, little theoretical guidance directed this practitioners' art. For this reason a systematic study of this design process and its potential for optimization has never been accomplished. Additionally, the nonlinearities and the large search space involved in gain scheduling also precluded such an optimization study. Traditionally, the gain scheduling process has been some variation of a linear interpolation between discrete design points. By using powerful non-traditional optimization tools such as genetic algorithms there are ways of improving this design process. This thesis utilizes the power of genetic algorithms to optimally design a gain schedule. First, a design methodology is validated on a simple pole placement problem, then demonstrated for an F-18 Super-maneuverable Fighter. From this experience, a general gain scheduling design process is developed and presented. DTIC

N95-26990 Air Force Inst. of Tech., Wright-Patterson AFB, OH. School of Engineering.
SURVEY AND IMPLEMENTATION OF COMMERCIAL MANUAL CONTROLLERS FOR A GENERIC TELEROBOTICS ARCHITECTURE M.S. Thesis
Thomas E. Deeter Dec. 1994 128 p Limited Reproducibility: More than 20% of this document may be affected by microfiche quality
(AD-A289215; AFIT/GE/ENG/94D-04) Avail: Issuing Activity (Defense Technical Information Center (DTIC))

The purpose of this study is to determine an input device for the Air Force's generic telerobotics architecture for large aircraft maintenance and repair. One area of concern is the human to machine interface, more specifically, which manual controller should be used for the specified tasks in this architecture. The authors mailed a survey to 68 companies in order to compile a list of possible input devices that the telerobotics architecture could use. Thirty-two companies responded which gave enough data to generate a list that described the physical traits of the input devices. The required tasks were divided into actions and analyzed to generate a list of traits required by an input device. Both the task analysis and device listings were combined mathematically to form a performance table which revealed the possible devices that could perform each individual action. To aid in development of the Air Force's generic telerobotics architecture, four input devices were integrated into a VME based operating system called CHIMERA. These four devices represent the four different sensor types that are currently available in today's market. The first device is a mouse which relays position changes of the mouse to the computer. The second device is a joystick that can be used in two different ways. The joystick can measure position data of the hand position or it can measure the displacement of the hand from the center of the total movement. The third device is a six degree- of-freedom (DOF) spaceball that measures the amount of force for position data and rotational data. The fourth device is a Schilling manual controller which has a one-to-one mapping from the controller joints to the manipulator joints. DTIC

N95-27007 Air Force Inst. of Tech., Wright-Patterson AFB, OH. School of Engineering.
NEXT GENERATION REAL-TIME SYSTEMS: INVESTIGATING THE POTENTIAL OF PARTIAL-SOLUTION TASKS M.S. Thesis
Robert E. Caley Dec. 1994 139 p Limited Reproducibility: More than 20% of this document may be affected by microfiche quality
(AD-A289203; AFIT/GCS/ENG/94D-01) Avail: Issuing Activity (Defense Technical Information Center (DTIC))

While the cyclic executive and fixed-priority scheduling strategies have been sufficient to handle traditional real-time requirements. They are insufficient for dealing with the complexities of next-generation real-time systems. New methods of intelligent control must be developed for guaranteeing on-time task completion for real-time systems that are faced with unpredictable and dynamically changing requirements. Implementing real-time processes as partial-solution tasks is one technique that may be beneficial. This type of task, when combined with intelligent control, has the potential for increasing pre-runtime schedulability, system maintainability, and runtime robustness. This research investigates the benefits of partial-solution tasks by experimentally measuring the change in performance of 11 simulated real-time systems when converted from all-or-nothing tasks to partial-solution tasks. Results from the experiments indicate that partial-solution tasks have the potential to decrease missed deadlines and increase a systems' average solution quality. The results also suggest that best performance gains can be achieved using Optimistic partial-solution tasks where the bulk of solution quality is achieved early during task execution. The framework used in this research was developed to measure the general case performance characteristics of partial-solution tasks. As a by-product, the research resulted in a framework that can also be used to measure specific case characteristics. DTIC

N95-27025# International Centre for Theoretical Physics, Trieste (Italy).
A MODIFIED BACKPROPAGATION ALGORITHM FOR TRAINING NEURAL NETWORKS ON DATA WITH ERROR BARS
K. A. Gernoth and J. W. Clark Aug. 1994 41 p
(DE95-608729; IC-94/229) Avail: CASI HC A03/MF A01 (US Sales Only)

A method is proposed for training multilayer feedforward neural networks on data contaminated with noise. Specifically, we consider the case that the artificial neural system is required to learn a physical mapping when the available values of the target variable are subject to experimental uncertainties, but are characterized by error bars. The proposed method, based on maximum likelihood criterion for parameter estimation, involves simple modifications of the on-line backpropagation learning algorithm. These include incorporation of the error-bar assignments in a pattern-specific learning rate, together with epochal updating of a new measure of model accuracy that replaces the usual mean-square error. The extended backpropagation algorithm is successfully tested on two problems relevant to the modeling of atomic-mass systematics by neural networks. Provided the underlying mapping is reasonably smooth, neural nets trained with the new procedure are able to learn the true function to a good approximation even in the presence of high levels of Gaussian noise. DOE

N95-27041 Carnegie-Mellon Univ., Pittsburgh, PA. Robotics Inst.
ELVIS: EIGENVECTORS FOR LAND VEHICLE IMAGE SYSTEM
John A. Hancock and Charles E. Thorpe Dec. 1994 26 p Limited Reproducibility: More than 20% of this document may be affected by microfiche quality
(Contracts DACA76-89-C-0014; DAAB07-90-C-R059)
(AD-A289297; CMU-RI-TR-94-43) Avail: Issuing Activity (Defense Technical Information Center (DTIC))

ELVIS (Eigenvectors for Land Vehicle Image System) is a road-following system designed to drive the CMU Navlabs. It is based on ALVINN, the neural network road-following system built by Dean Pomerleau at CMU. ALVINN provided the motivation for creating ELVIS: although ALVINN is successful, it is not entirely clear why the system works. ELVIS is an attempt to more fully understand ALVINN and to determine whether it is possible to design a system that can rival ALVINN using the same input and output, but without using a neural network. Like ALVINN, ELVIS observes the road through a video camera and observes human steering response through encoders mounted on the steering column. After a few minutes of observing the human trainer, ELVIS can take control. ELVIS learns the eigenvectors of the image and steering training set via principal component analysis. These eigenvectors roughly correspond to the primary features of the image set and their correlations to steering. Road-following is then performed by projecting new images onto the previously calculated eigenspace. ELVIS architecture and experiments will be discussed as well as implications for eigenvector-based systems and how they compare with neural network-based systems. DTIC

N95-27044# International Centre for Theoretical Physics, Trieste (Italy).
HIGHER-ORDER PROBABILISTIC PERCEPTRONS AS BAYESIAN INFERENCE ENGINES
J. W. Clark, K. A. Gernoth, and M. L. Ristig Aug. 1994 10 p
(DE95-608730; IC-94/236) Avail: CASI HC A02/MF A01 (US Sales Only)

This letter makes explicit a structural connection between the Bayes optimal classifier operating on K binary input variables and corresponding two-layer perceptron having normalized output activities and couplings from input to output units of all orders up to K. Given a large and unbiased training set and an effective learning algorithm, such a neural network should be able to learn the statistics of the classification problem and match the a posteriori probabilities given by the Bayes optimal classifier.
DOE

N95-27045# International Centre for Theoretical Physics, Trieste (Italy).
OPTIMAL CONTROL OF TWO QUEUES IN SERIES
M. S. Moustafa and R. M. Mohammed Aug. 1994 15 p
(DE95-608731; IC-94/256) Avail: CASI HC A03/MF A01 (US Sales Only)

We give a fairly complete survey of the available results on the control of arrival and service rates for both single queue and networks of queues. We also study two M/M/1 queues in series. At the first queue, the arrival and the service rates are chosen in pair from a finite set whenever the queue lengths at both queues change. Each choice has a switching cost depending on the chosen rates and the queue lengths. At the second queue, the arrival and the service rates are fixed. Our objective is to find a policy for dynamically choosing rates, based on the current rates and queues lengths that minimizes the expected total discounted cost over a finite horizon; numerical results are given. DOE

N95-27066 Carnegie-Mellon Univ., Pittsburgh, PA. School of Computer Science.
REDUCING NETWORK DEPTH IN THE CASCADE-CORRELATION LEARNING ARCHITECTURE
Shumeet Baluja and Scott E. Fahlman 17 Oct. 1994 12 p Limited Reproducibility: More than 20% of this document may be affected by microfiche quality
(Contract N00014-93-1-0806; NSF IRI-92-14873)
(AD-A289352; CMU-CS-94-209) Avail: Issuing Activity (Defense Technical Information Center (DTIC))

The Cascade-Correlation learning algorithm constructs a multi-layer artificial neural network as it learns to perform a given task. The resulting network's size and topology are chosen specifically for this task. In the resulting 'cascade' networks, each new hidden unit receives incoming connections from all input and pre-existing hidden units. In effect, each new unit adds a new layer to the network. This allows Cascade-Correlation to create complex feature detectors, but it typically results in a network that is deeper, in terms of the longest path from input to output, than is necessary to solve the problem efficiently. In this paper we investigate a simple variation of Cascade-Correlation that will build deep nets if necessary, but that is biased toward minimizing network depth. We demonstrate empirically, across a range of problems, that this simple technique can reduce network depth, often dramatically. However, we show that this technique does not, in general, reduce the total number of weights or improve the generalization ability of the resulting networks. DTIC

N95-27145 Air Force Inst. of Tech., Wright-Patterson AFB, OH. School of Engineering.
HEAD RELATED TRANSFER FUNCTION APPROXIMATION USING NEURAL NETWORKS M.S. Thesis
John K. Millhouse Dec. 1994 156 p Limited Reproducibility: More than 20% of this document may be affected by microfiche quality
(AD-A289422; AFIT/GE/ENG/94D-21) Avail: Issuing Activity (Defense Technical Information Center (DTIC))

This thesis determines whether an artificial neural network (ANN) can approximate the Armstrong Aerospace Medical Research Laboratories (AAMRL) head related transfer functions (HRTF) data obtained from research at AAMRL during the fall of 1988. The first test determines whether HRTF lends any support in sound localization when compared to no HRTF (Interaural Time Delay only). There is a statistically significant interaction between the location of the sound and whether the HRTF or no HRTF is used. When this interaction is removed using the alternate F.Value, the statistics give the result of equal means for the filters and azimuth. This means that at certain angles of azimuth, the HRTF either provides no advantage at all or hinders localization capabilities. Adding in the corrections for reversals changes the results to where the means of the azimuth are not statistically equal. The reversal corrections will inherently reduce the error results. However, comparing the number of reversals indicates an advantage of using the HRTF over no HRTF. The second test determines whether HRTF and ANN lend the same amount of information in sound localization when compared to each other. With reversal corrections included, a statistical advantage is not indicated, and the means of the two filters are statistically equal. Also there is a statistically significant interaction between the location of the sound and whether the AAMRL HRTF or ANN HRTF is used. Comparing the number of reversals does not indicate a large difference between the AAMRL HRTF and the RBF HRTF. DTIC

N95-27293 Air Force Inst. of Tech., Wright-Patterson AFB, OH. School of Engineering.
AN ANALYSIS OF BAYESIAN NETWORKS AS CLASSIFIERS M.S. Thesis
Gregory C. Ahlquist Dec. 1994 198 p Limited Reproducibility: More than 20% of this document may be affected by microfiche quality
(AD-A289316; AFIT/GCE/ENG/94D-01) Avail: Issuing Activity (Defense Technical Information Center (DTIC))

An analysis of Bayesian networks as classifiers is presented. This analysis results in an algorithm and several tools related to Bayesian network classifiers. The tools calculate and display the decision regions for two level Bayesian network classifiers. They collectively provide an approach to analyze the effects of changing network parameters on the network's decision regions. The algorithm defines a Bayesian network classifier to solve traditional classification problems. The algorithm is data driven, meaning that the resulting Bayesian network classifier is uniquely tuned to the classification problem at hand. Also, the algorithm contains procedures for defining the topology of a Bayesian network classifier and for precisely deriving the required conditional probabilities. A brief tutorial on Bayesian networks is also presented. DTIC

N95-27375*# National Aeronautics and Space Administration. Goddard Space Flight Center, Greenbelt, MD.
THE 1995 GODDARD CONFERENCE ON SPACE APPLICATIONS OF ARTIFICIAL INTELLIGENCE AND EMERGING INFORMATION TECHNOLOGIES
Carl F. Hostetter, ed. May 1995 367 p Conference held in Greenbelt, MD, 9-11 May 1995
(RTOP 510-00-00)
(NASA-CP-3296; Rept-93B00058; NAS 1.55:3296) Avail: CASI HC A16/MF A03

This publication comprises the papers presented at the 1995 Goddard Conference on Space Applications of Artificial Intelligence and Emerging Information Technologies held at the NASA/Goddard Space Flight Center, Greenbelt, Maryland, on May 9-11, 1995. The purpose of this annual conference is to provide a forum in which current research and development directed at space applications of artificial intelligence can be presented and discussed. For individual titles, see N95-27376 through N95-27397.

N95-27376*# GTE Government Systems Corp., Colorado Springs, CO.
APPLYING AI TOOLS TO OPERATIONAL SPACE ENVIRONMENTAL ANALYSIS
Mike Krajnak, Lisa Jesse, and John Mucks (Rome Lab., Griffiss AFB, NY.) *In* NASA. Goddard Space Flight Center, The 1995 Goddard Conference on Space Applications of Artificial Intelligence and Emerging Information Technologies May 1995 p 3-13 (For primary document see N95-27375 09-63)
Avail: CASI HC A03/MF A03

The U.S. Air Force and National Oceanic Atmospheric Agency (NOAA) space environmental operations centers are facing increasingly complex challenges meeting the needs of their growing user community. These centers provide current space environmental information and short term forecasts of geomagnetic activity. Recent advances in modeling and data access have provided sophisticated tools for making accurate and timely forecasts, but have introduced new problems associated with handling and analyzing large quantities of complex data. AI (Artificial Intelligence) techniques have been considered as potential solutions to some of these problems. Fielding AI systems has proven more difficult than expected, in part because of operational constraints. Using systems which have been demonstrated successfully in the operational environment will provide a basis for a useful data fusion and analysis capability. Our approach uses a general purpose AI system already in operational use within the military intelligence community, called the Temporal Analysis System (TAS). TAS is an operational suite of tools supporting data processing, data visualization, historical analysis, situation assessment and predictive analysis. TAS includes expert system tools to analyze incoming events for indications of particular situations and predicts future activity. The expert system operates on a knowledge base of temporal patterns encoded using a knowledge representation called Temporal Transition Models (TTM's) and an event database maintained by the other TAS tools. The system also includes a robust knowledge acquisition and maintenance tool for creating TTM's using a graphical specification language. The ability to manipulate TTM's in a graphical format gives non-computer specialists an intuitive way of accessing and editing the knowledge base. To support space environmental analyses, we used TAS's ability to define domain specific event analysis abstractions. The prototype system defines events covering reports of natural phenomena such as solar flares, bursts, geomagnetic storms, and five others pertinent to space environmental analysis. With our preliminary event definitions we experimented with TAS's support for temporal pattern analysis using X-ray flare and geomagnetic storm forecasts as case studies. We are currently working on a framework for integrating advanced graphics and space environmental models into this analytical environment. Author

N95-27377*# Commonwealth Scientific and Industrial Research Organization, Ryde (Australia). Div. of Information Technology.

AN ARCHITECTURE AND PROTOCOL FOR COMMUNICATIONS SATELLITE CONSTELLATIONS REGARDED AS MULTI-AGENT SYSTEMS

c18

Craig A. Lindley *In* NASA. Goddard Space Flight Center, The 1995 Goddard Conference on Space Applications of Artificial Intelligence and Emerging Information Technologies May 1995 p 15-28 (For primary document see N95-27375 09-63)
Avail: CASI HC A03/MF A03

This paper presents an architecture for satellites regarded as intercommunicating agents. The architecture is based upon a postmodern paradigm of artificial intelligence in which represented knowledge is regarded as text, inference procedures are regarded as social discourse and decision making conventions and the semantics of representations are grounded in the situated behaviour and activity of agents. A particular protocol is described for agent participation in distributed search and retrieval operations conducted as joint activities. Author

N95-27378*# National Aeronautics and Space Administration. John F. Kennedy Space Center, Cocoa Beach, FL.

AUTOMATED DATABASE DESIGN FROM NATURAL LANGUAGE INPUT

c82

Fernando Gomez (University of Central Florida, Orlando, FL.), Carlos Segami (Barry Univ., Miami Shores, FL.), and Carl Delaune *In* NASA. Goddard Space Flight Center, The 1995 Goddard Conference on Space Applications of Artificial Intelligence and Emerging Information Technologies May 1995 p 29-44 (For primary document see N95-27375 09-63)
(Contract NAS10-120)
Avail: CASI HC A03/MF A03

Users and programmers of small systems typically do not have the skills needed to design a database schema from an English description of a problem. This paper describes a system that automatically designs databases for such small applications from English descriptions provided by end-users. Although the system has been motivated by the space applications at Kennedy Space Center, and portions of it have been designed with that idea in mind, it can be applied to different situations. The system consists of two major components: a natural language understander and a problem-solver. The paper describes briefly the knowledge representation structures constructed by the natural language understander, and, then, explains the problem-solver in detail. Author

N95-27379*# Bowie State Univ., MD. Dept. of Computer Science.

A USER-SYSTEM INTERFACE AGENT

Nagi T. Wakim, Sadanand Srivastava, Mehdi Bousaidi, and Gin-Hua Goh *In* NASA. Goddard Space Flight Center, The 1995 Goddard Conference on Space Applications of Artificial Intelligence and Emerging Information Technologies May 1995 p 45-55 (For primary document see N95-27375 09-63)
Avail: CASI HC A03/MF A03

Agent-based technologies answer to several challenges posed by additional information processing requirements in today's computing environments. In particular, (1) users desire interaction with computing devices in a mode which is similar to that used between people, (2) the efficiency and successful completion of information processing tasks often require a high-level of expertise in complex and multiple domains, (3) information processing tasks often require handling of large volumes of data and, therefore, continuous and endless processing activities. The concept of an agent is an attempt to address these new challenges by introducing information processing environments in which (1) users can communicate with a system in a natural way, (2) an agent is a specialist and a self-learner and, therefore, it qualifies to be trusted to perform tasks independent of the human user, and (3) an agent is an entity that is continuously active performing tasks that are either delegated to it or self-imposed. The work described in this paper focuses on the development of an interface agent for users of a complex information processing environment (IPE). This activity is part of an on-going effort to build a model for developing agent-based information systems. Such systems will be highly applicable to environments which require a high degree of automation, such as, flight control operations and/or processing of large volumes of data in complex domains, such as the EOSDIS environment and other multidisciplinary, scientific data systems. The concept of an agent as an information processing entity is fully described with emphasis on characteristics of special interest to the User-System Interface Agent (USIA). Issues such as agent 'existence' and 'qualification' are discussed in this paper. Based on a definition of an agent and its main characteristics, we propose an architecture for the development of interface agents for users of an IPE that is agent-oriented and whose resources are likely to be distributed and heterogeneous in nature. The architecture of USIA is outlined in two main components: (1) the user interface which is concerned with issues as user dialog and interaction, user modeling, and adaptation to user profile, and (2) the system interface part which deals with identification of IPE capabilities, task understanding and feasibility assessment, and task delegation and coordination of assistant agents. Author

N95-27380*# George Mason Univ., Fairfax, VA. Dept. of Computer Science.

BUILDING AN ADAPTIVE AGENT TO MONITOR AND REPAIR THE ELECTRICAL POWER SYSTEM OF AN ORBITAL SATELLITE

Gheorghe Tecuci, Michael R. Hieb, and Tomasz Dybala *In* NASA. Goddard Space Flight Center, The 1995 Goddard Conference on Space Applications of Artificial Intelligence and Emerging Information Technologies May 1995 p 57-71 (For primary document see N95-27375 09-63)
Avail: CASI HC A03/MF A03

Over several years we have developed a multistrategy apprenticeship learning methodology for building knowledge-based systems. Recently we have developed and applied our methodology to building intelligent agents. This methodology allows a subject matter expert to build an agent in the same way in which the expert would teach a human apprentice. The expert will give the agent specific examples of problems and solutions, explanations of these solutions, or supervise the agent as it solves new problems. During such interactions, the agent learns general rules and concepts, continuously extending and improving its knowledge base. In this paper we present initial results on applying this methodology to build an intelligent adaptive agent for monitoring and repair of the electrical power system of an orbital satellite, stressing the interaction with the expert during apprenticeship learning. Author

N95-27381*# Maastricht Univ. (Netherlands). Dept. of Computer Science.

LIMITS TO GROUND CONTROL IN AUTONOMOUS SPACECRAFT

Alfred D. M. Wan, Peter J. Braspenning, and Gerrard A. W. Vreeswijk *In* NASA. Goddard Space Flight Center, The 1995 Goddard Conference on Space Applications of Artificial Intelligence and Emerging Information Technologies May 1995 p 75-89 (For primary document see N95-27375 09-63)
Avail: CASI HC A03/MF A03

In this paper the autonomy concept used by ESA and NASA is critically evaluated. Moreover, a more proper ground control/spacecraft organizational structure is proposed on the basis of a new, more elaborated concept of autonomy. In an extended theoretical discussion its definitional properties and functionalities are established. The rather basic property of adaptivity leads to the categorization of behaviour into the modes of satisfaction and avoidance behaviour. However, the autonomy property with the most profound consequences is goal-robustness. The mechanism that implements goal-robustness tests newly generated goals and externally received goals on consistency with high-level goals. If goals appear not to be good instantiations or more acceptable replacements of existing goals, they are rejected. This means that ground control has to cooperate with the spacecraft instead of (intermittently) commanding it. Author

N95-27382*# National Aeronautics and Space Administration. Goddard Space Flight Center, Greenbelt, MD.
INTEGRATED PLANNING AND SCHEDULING FOR EARTH SCIENCE DATA PROCESSING **c82**
Mark Boddy (Honeywell Technology Center, Minneapolis, MN.), Jim White (Honeywell Technology Center, Minneapolis, MN.), Robert Goldman (Honeywell Technology Center, Minneapolis, MN.), and Nick Short, Jr. *In its* The 1995 Goddard Conference on Space Applications of Artificial Intelligence and Emerging Information Technologies May 1995 p 91-101 (For primary document see N95-27375 09-63)
Avail: CASI HC A03/MF A03

Several current NASA programs such as the EOSDIS Core System (ECS) have data processing and data management requirements that call for an integrated planning and scheduling capability. In this paper, we describe the experience of applying advanced scheduling technology operationally, in terms of what was accomplished, lessons learned, and what remains to be done in order to achieve similar successes in ECS and other programs. We discuss the importance and benefits of advanced scheduling tools, and our progress toward realizing them, through examples and illustrations based on ECS requirements. The first part of the paper focuses on the Data Archive and Distribution (DADS) V0 Scheduler. We then discuss system integration issues ranging from communication with the scheduler to the monitoring of system events and re-scheduling in response to them. The challenge of adapting the scheduler to domain-specific features and scheduling policies is also considered. Extrapolation to the ECS domain raises issues of integrating scheduling with a product-generation planner (such as PlaSTiC), and implementing conditional planning in an operational system. We conclude by briefly noting ongoing technology development and deployment projects being undertaken by HTC and the ISTB. Derived from text

N95-27383*# Aerospace Corp., Los Angeles, CA.
A SUSTAINABLE GENETIC ALGORITHM FOR SATELLITE RESOURCE ALLOCATION **c61**
R. J. Abbott (California State Univ., Los Angeles, CA.), M. L. Campbell, and W. C. Krenz *In* NASA. Goddard Space Flight Center, The 1995 Goddard Conference on Space Applications of Artificial Intelligence and Emerging Information Technologies May 1995 p 103-117 (For primary document see N95-27375 09-63)
Avail: CASI HC A03/MF A03

A hybrid genetic algorithm is used to schedule tasks for 8 satellites, which can be modelled as a robot whose task is to retrieve objects from a two dimensional field. The objective is to find a schedule that maximizes the value of objects retrieved. Typical of the real-world tasks to which this corresponds is the scheduling of ground contacts for a communications satellite. An important feature of our application is that the amount of time available for running the scheduler is not necessarily known in advance. This requires that the scheduler produce reasonably good results after a short period but that it also continue to improve its results if allowed to run for a longer period. We satisfy this requirement by developing what we call a sustainable genetic algorithm. Author

N95-27384*# Space Telescope Science Inst., Baltimore, MD.
A RULE-BASED SHELL TO HIERARCHICALLY ORGANIZE HST OBSERVATIONS **c82**
Ashim Bose and Andrew Gerb *In* NASA. Goddard Space Flight Center, The 1995 Goddard Conference on Space Applications of Artificial Intelligence and Emerging Information Technologies May 1995 p 119-130 (For primary document see N95-27375 09-63)
Avail: CASI HC A03/MF A03

An observing program on the Hubble Space Telescope (HST) is described in terms of exposures that are obtained by one or more of the instruments onboard the HST. These exposures are organized into a hierarchy of structures for purposes of efficient scheduling of observations. The process by which exposures get organized into the higher-level structures is called merging. This process relies on rules to determine which observations can be 'merged' into the same higher level structure, and which cannot. The TRANSformation expert system converts proposals for astronomical observations with HST into detailed observing plans. The conversion process includes the task of merging. Within TRANS, we have implemented a declarative shell to facilitate merging. This shell offers the following features: (1) an easy way of specifying rules on when to merge and when not to merge, (2) a straightforward priority mechanism for resolving conflicts among rules, (3) an explanation facility for recording the merging history, (4) a report generating mechanism to help users understand the reasons for merging, and (5) a self-documenting mechanism that documents all the merging rules that have been defined in the shell, ordered by priority. The merging shell is implemented using an object-oriented paradigm in CLOS. It has been a part of operational TRANS (after extensive testing) since July 1993. It has fulfilled all performance expectations, and has considerably simplified the process of implementing new or changed requirements for merging. The users are pleased with its report-generating and self-documenting features. Author

N95-27385*# Maryland Univ., College Park, MD. Dept. of Aerospace Engineering and Space Systems Lab.
STABLE ADAPTIVE NEUROCONTROLLERS FOR SPACECRAFT AND SPACE ROBOTS
Robert M. Sanner *In* NASA. Goddard Space Flight Center, The 1995 Goddard Conference on Space Applications of Artificial Intelligence and Emerging Information Technologies May 1995 p 131-142 (For primary document see N95-27375 09-63)
Avail: CASI HC A03/MF A03

This paper reviews recently developed techniques of adaptive nonlinear control using neural networks, and demonstrates their application to two important practical problems in orbital operations. An adaptive neurocontroller is first developed for spacecraft attitude control applications, and then the same design, slightly modified, is shown to be effective in the control of free-floating orbital manipulators. The algorithms discussed have guaranteed stability and convergence properties, and thus constitute viable alternatives to existing control methodologies. Simulation results are presented demonstrating the performance of each algorithm with representative dynamic models. Author

N95-27386*# European Space Agency. European Space Operations Center, Darmstadt (Germany).
FUZZY LOGIC TECHNIQUES FOR RENDEZVOUS AND DOCKING OF TWO GEOSTATIONARY SATELLITES
Guillermo Ortega *In* NASA. Goddard Space Flight Center, The 1995 Goddard Conference on Space Applications of Artificial Intelligence and Emerging Information Technologies May 1995 p 143-152 (For primary document see N95-27375 09-63)
Avail: CASI HC A02/MF A03

Large assemblings in space require the ability to manage rendezvous and docking operations. In future these techniques will be required for the gradual build up of big telecommunication platforms in the geostationary orbit. The paper discusses the use of fuzzy logic to model and implement a control system for the docking/berthing of two satellites in geostationary orbit. The system mounted in a chaser vehicle determines the actual state of both satellites and generates torques to execute maneuvers to establish the structural latching. The paper describes the proximity operations to collocate the two satellites in the same orbital window, the fuzzy guidance and navigation of the chaser approaching the target and the final Fuzzy berthing. The fuzzy logic system represents a knowledge based controller that realizes the close loop operations autonomously replacing the conventional control algorithms. The goal is to produce smooth control actions in the proximity of the target and during the docking to avoid disturbance torques in the final assembly orbit. The knowledge of the fuzzy controller consists of a data base of rules and the definitions of the fuzzy sets. The knowledge of an experienced spacecraft controller is captured into a set of rules forming the Rules Data Base. Author

N95-27387*# Aerospace Corp., Los Angeles, CA.
A HYBRID GENETIC ALGORITHM FOR RESOLVING CLOSELY SPACED OBJECTS

R. J. Abbott (California State Univ., Los Angeles, CA.), W. E. Lillo, and N. Schulenburg *In* NASA. Goddard Space Flight Center, The 1995 Goddard Conference on Space Applications of Artificial Intelligence and Emerging Information Technologies May 1995 p 155-162 (For primary document see N95-27375 09-63)
Avail: CASI HC A02/MF A03

A hybrid genetic algorithm is described for performing the difficult optimization task of resolving closely spaced objects appearing in space based and ground based surveillance data. This application of genetic algorithms is unusual in that it uses a powerful domain-specific operation as a genetic operator. Results of applying the algorithm to real data from telescopic observations of a star field are presented. Author

N95-27388*# Aerospace Corp., Los Angeles, CA.
IMPROVED REDUCED-RESOLUTION SATELLITE IMAGERY **c61**
James Ellison and Jaime Milstein *In* NASA. Goddard Space Flight Center, The 1995 Goddard Conference on Space Applications of Artificial Intelligence and Emerging Information Technologies May 1995 p 163-178 (For primary document see N95-27375 09-63)
Avail: CASI HC A03/MF A03

The resolution of satellite imagery is often traded-off to satisfy transmission time and bandwidth, memory, and display limitations. Although there are many ways to achieve the same reduction in resolution, algorithms vary in their ability to preserve the visual quality of the original imagery. These issues are investigated in the context of the Landsat browse system, which permits the user to preview a reduced resolution version of a Landsat image. Wavelets-based techniques for resolution reduction are proposed as alternatives to subsampling used in the current system. Experts judged imagery generated by the wavelets-based methods visually superior, confirming initial quantitative results. In particular, compared to subsampling, the wavelets-based techniques were much less likely to obscure roads, transmission lines, and other linear features present in the original image, introduce artifacts and noise, and otherwise reduce the usefulness of the image. The wavelets-based techniques afford multiple levels of resolution reduction and computational speed. This study is applicable to a wide range of reduced resolution applications in satellite imaging systems, including low resolution display, spaceborne browse, emergency image transmission, and real-time video downlinking. Author

N95-27389*# Science Applications International Corp., McLean, VA.
RECONSTRUCTION OF AN INFRARED BAND OF METEOROLOGICAL SATELLITE IMAGERY WITH ABDUCTIVE NETWORKS **c47**
Harvey A. Singer, John E. Cockayne, and Peter L. Versteegen *In* NASA. Goddard Space Flight Center, The 1995 Goddard Conference on Space Applications of Artificial Intelligence and Emerging Information Technologies May 1995 p 179-191 (For primary document see N95-27375 09-63)
(SAIC-94/1062) Avail: CASI HC A03/MF A03

As the current fleet of meteorological satellites age, the accuracy of the imagery sensed on a spectral channel of the image scanning system is continually and progressively degraded by noise. In time, that data may even become unusable. We describe a novel approach to the reconstruction of the noisy satellite imagery according to empirical functional relationships that tie the spectral channels together. Abductive networks are applied to automatically learn the empirical functional relationships between the data sensed on the other spectral channels to calculate the data that should have been sensed on the corrupted channel. Using imagery unaffected by noise, it is demonstrated that abductive networks correctly predict the noise-free observed data. Author

N95-27390*# Organisatie voor Toegepast Natuurwetenschappelijk Onderzoek, Delft (Netherlands). Instrumentation Dept.
MODEL-BASED MONITORING AND DIAGNOSIS OF A SATELLITE-BASED INSTRUMENT **c19**
Andre Bos, Jorg Callies (European Space Agency. European Space Research and Technology Center, ESTEC, Noordwijk, Netherlands.), and Alain Lefebvre (European Space Agency. European Space Research and Technology Center, ESTEC, Noordwijk, Netherlands.) *In* NASA. Goddard Space Flight Center, The 1995 Goddard Conference on Space Applications of Artificial Intelligence and Emerging Information Technologies May 1995 p 195-207 (For primary document see N95-27375 09-63)
Avail: CASI HC A03/MF A03

For about a decade model-based reasoning has been propounded by a number of researchers. Maybe one of the most convincing arguments in favor of this kind of reasoning has been given by Davis in his paper on diagnosis from first principles (Davis 1984). Following their guidelines we have developed a system to verify the behavior of a satellite-based instrument GOME (which will be measuring Ozone concentrations in the near future (1995)). We start by giving a description of model-based monitoring. Besides recognizing that something is wrong, we also like to find the cause for misbehaving automatically. Therefore, we show how the monitoring technique can be extended to model-based diagnosis. Author

N95-27391*# Morgan State Univ., Baltimore, MD. Dept. of Mathematics.
LINEAR AND NONLINEAR TRENDING AND PREDICTION FOR AVHRR TIME SERIES DATA **c82**
J. Smid, P. Volf (Ceskoslovenska Akademie Ved, Prague.), M. Slama (Ceskoslovenska Akademie Ved, Prague.), and M. Palus (Santa Fe Inst., NM.) *In* NASA. Goddard Space Flight Center, The 1995 Goddard Conference on Space Applications of Artificial Intelligence and Emerging Information Technologies May 1995 p 209-220 (For primary document see N95-27375 09-63)
(Grant NAG5-2686)
Avail: CASI HC A03/MF A03

The variability of AVHRR calibration coefficient in time was analyzed using algorithms of linear and non-linear time series analysis. Specifically we have used the spline trend modeling, autoregressive process analysis, incremental neural network learning algorithm and redundancy functional testing. The analysis performed on available AVHRR data sets revealed that (1) the calibration data have nonlinear dependencies, (2) the calibration data depend strongly on the target temperature, (3) both calibration coefficients and the temperature time series can be modeled, in the first approximation, as autonomous dynamical systems, (4) the high frequency residuals of the analyzed data sets can be best modeled as an autoregressive process of the 10th degree. We have dealt with a nonlinear identification problem and the problem of noise filtering (data smoothing). The system identification and filtering are significant problems for AVHRR data sets. The algorithms outlined in this study can be used for the future EOS missions. Prediction and smoothing algorithms for time series of calibration data provide a functional characterization of the data. Those algorithms can be particularly useful when calibration data are incomplete or sparse. Author

N95-27392*# GeoControl Systems, Inc., Houston, TX.
A FUZZY LOGIC INTELLIGENT DIAGNOSTIC SYSTEM FOR SPACECRAFT INTEGRATED VEHICLE HEALTH MANAGEMENT
G. Gordon Wu *In* NASA. Goddard Space Flight Center, The 1995 Goddard Conference on Space Applications of Artificial Intelligence and Emerging Information Technologies May 1995 p 221-227 (For primary document see N95-27375 09-63)
(Contract NAS9-19266)
Avail: CASI HC A02/MF A03

Due to the complexity of future space missions and the large amount of data involved, greater autonomy in data processing is demanded for mission operations, training, and vehicle health management. In this paper, we develop a fuzzy logic intelligent diagnostic system to perform data reduction, data analysis, and fault diagnosis for spacecraft vehicle health management applications. The diagnostic system contains a data filter and an inference engine. The data filter is designed to intelligently select only the necessary data for analysis, while the inference engine is designed for failure detection, warning, and decision on corrective actions using fuzzy logic synthesis. Due to its adaptive nature and on-line learning ability, the diagnostic system is capable of dealing with environmental noise, uncertainties, conflict information, and sensor faults. Author

N95-27393*# California Univ., Berkeley, CA. Center for EUV Astrophysics.
LESSONS LEARNED FROM THE INTRODUCTION OF AUTONOMOUS MONITORING TO THE EUVE SCIENCE OPERATIONS CENTER
M. Lewis, F. Girouard, F. Kronberg, P. Ringrose, A. Abedini, D. Biroscak, T. Morgan, and R. F. Malina *In* NASA. Goddard Space Flight Center, The 1995 Goddard Conference on Space Applications of Artificial Intelligence and Emerging Information Technologies May 1995 p 229-235 (For

primary document see N95-27375 09-63)
(Contracts NAS5-29298; NCC2-838)
Avail: CASI HC A02/MF A03

The University of California at Berkeley's (UCB) Center for Extreme Ultraviolet Astrophysics (CEA), in conjunction with NASA's Ames Research Center (ARC), has implemented an autonomous monitoring system in the Extreme Ultraviolet Explorer (EUVE) science operations center (ESOC). The implementation was driven by a need to reduce operations costs and has allowed the ESOC to move from continuous, three-shift, human-tended monitoring of the science payload to a one-shift operation in which the off shifts are monitored by an autonomous anomaly detection system. This system includes Eworks, an artificial intelligence (AI) payload telemetry monitoring package based on RTworks, and Epage, an automatic paging system to notify ESOC personnel of detected anomalies. In this age of shrinking NASA budgets, the lessons learned on the EUVE project are useful to other NASA missions looking for ways to reduce their operations budgets. The process of knowledge capture, from the payload controllers for implementation in an expert system, is directly applicable to any mission considering a transition to autonomous monitoring in their control center. The collaboration with ARC demonstrates how a project with limited programming resources can expand the breadth of its goals without incurring the high cost of hiring additional, dedicated programmers. This dispersal of expertise across NASA centers allows future missions to easily access experts for collaborative efforts of their own. Even the criterion used to choose an expert system has widespread impacts on the implementation, including the completion time and the final cost. In this paper we discuss, from inception to completion, the areas where our experiences in moving from three shifts to one shift may offer insights for other NASA missions.

Author

N95-27394*# California Univ., Davis, CA. Computer Science Dept.

COMPREHENSION AND RETRIEVAL OF FAILURE CASES IN AIRBORNE OBSERVATORIES c12

Sergio J. Alvarado and Kenrick J. Mock *In* NASA. Goddard Space Flight Center, The 1995 Goddard Conference on Space Applications of Artificial Intelligence and Emerging Information Technologies May 1995 p 237-251 (For primary document see N95-27375 09-63)
(Contract NCA2-721)
Avail: CASI HC A03/MF A03

This paper describes research dealing with the computational problem of analyzing and repairing failures of electronic and mechanical systems of telescopes in NASA's airborne observatories, such as KAO (Kuiper Airborne Observatory) and SOFIA (Stratospheric Observatory for Infrared Astronomy). The research has resulted in the development of an experimental system that acquires knowledge of failure analysis from input text, and answers questions regarding failure detection and correction. The system's design builds upon previous work on text comprehension and question answering, including: knowledge representation for conceptual analysis of failure descriptions, strategies for mapping natural language into conceptual representations, case-based reasoning strategies for memory organization and indexing, and strategies for memory search and retrieval. These techniques have been combined into a model that accounts for: (a) how to build a knowledge base of system failures and repair procedures from descriptions that appear in telescope-operators' logbooks and FMEA (failure modes and effects analysis) manuals; and (b) how to use that knowledge base to search and retrieve answers to questions about causes and effects of failures, as well as diagnosis and repair procedures. This model has been implemented in FANSYS (Failure ANalysis SYStem), a prototype text comprehension and question answering program for failure analysis.

Author

N95-27395*# National Aeronautics and Space Administration. Langley Research Center, Hampton, VA.

A PATH-ORIENTED KNOWLEDGE REPRESENTATION SYSTEM: DEFUSING THE COMBINATORIAL SYSTEM

Stamos T. Karamouzis, John S. Barry (Lockheed Engineering and Sciences Co., Hampton, VA.), Steven L. Smith (Lockheed Engineering and Sciences Co., Hampton, VA.), and Stefan Feyock (College of William and Mary, Williamsburg, VA.) *In* NASA. Goddard Space Flight Center, The 1995 Goddard Conference on Space Applications of Artificial Intelligence and Emerging Information Technologies May 1995 p 253-262 (For primary document see N95-27375 09-63)
(Contracts NAS1-19000; NCC1-159)
Avail: CASI HC A02/MF A03

LIMAP is a programming system oriented toward efficient information manipulation over fixed finite domains, and quantification over paths and predicates. A generalization of Warshall's Algorithm to precompute paths in a sparse matrix representation of semantic nets is employed to allow questions involving paths between components to be posed and answered easily. LIMAP's ability to cache all paths between two components in a matrix cell proved to be a computational obstacle, however, when the semantic net grew to realistic size. The present paper describes a means of mitigating this combinatorial explosion to an extent that makes the use of the LIMAP representation feasible for problems of significant size. The technique we describe radically reduces the size of the search space in which LIMAP must operate; semantic nets of more than 500 nodes have been attacked successfully. Furthermore, it appears that the procedure described is applicable not only to LIMAP, but to a number of other combinatorially explosive search space problems found in AI as well.

Author

N95-27396*# Oregon State Univ., Corvallis, OR. Dept. of Computer Science.

REAL-TIME VALUE-DRIVEN DIAGNOSIS

Bruce DAmbrosio *In* NASA. Goddard Space Flight Center, The 1995 Goddard Conference on Space Applications of Artificial Intelligence and Emerging Information Technologies May 1995 p 263-278 (For primary document see N95-27375 09-63)
(Contract NSF 91-00530)
Avail: CASI HC A03/MF A03

Diagnosis is often thought of as an isolated task in theoretical reasoning (reasoning with the goal of updating our beliefs about the world). We present a decision-theoretic interpretation of diagnosis as a task in practical reasoning (reasoning with the goal of acting in the world), and sketch components of our approach to this task. These components include an abstract problem description, a decision-theoretic model of the basic task, a set of inference methods suitable for evaluating the decision representation in real-time, and a control architecture to provide the needed continuing coordination between the agent and its environment. A principal contribution of this work is the representation and inference methods we have developed, which extend previously available probabilistic inference methods and narrow, somewhat, the gap between probabilistic and logical models of diagnosis.

Author

N95-27397*# Colorado Univ., Denver, CO. Dept. of Computer Science and Engineering.

A LINGUISTIC GEOMETRY FOR 3D STRATEGIC PLANNING

Boris Stilman *In* NASA. Goddard Space Flight Center, The 1995 Goddard Conference on Space Applications of Artificial Intelligence and Emerging Information Technologies May 1995 p 279-295 (For primary document see N95-27375 09-63)
Avail: CASI HC A03/MF A03

This paper is a new step in the development and application of the Linguistic Geometry. This formal theory is intended to discover the inner properties of human expert heuristics, which have been successful in a certain class of complex control systems, and apply them to different systems. In this paper we investigate heuristics extracted in the form of hierarchical networks of planning paths of autonomous agents. Employing Linguistic Geometry tools the dynamic hierarchy of networks is represented as a hierarchy of formal attribute languages. The main ideas of this methodology are shown in this paper on the new pilot example of the solution of the extremely complex 3D optimization problem of strategic planning for the space combat of autonomous vehicles. This example demonstrates deep and highly selective search in comparison with conventional search algorithms.

Author

N95-27400 Air Force Inst. of Tech., Wright-Patterson AFB, OH. School of Engineering.

IMPROVED NUMERICAL SOLUTION OF MIXED H2/H(INFINITY) OPTIMIZATION WITH APPLICATIONS M.S. Thesis

Linda D. Smith Dec. 1994 171 p Limited Reproducibility: More than 20% of this document may be affected by microfiche quality

(AD-A289315; AFIT/GAE/ENY/94D-01) Avail: Issuing Activity (Defense Technical Information Center (DTIC))

This study improved the numerical optimization technique used to compute mixed H2/H(infinity) controllers. The run time to generate the full curve of an H2/H(infinity) design was reduced by a factor of almost 200 for a specific example. This was accomplished by improving gradient calculations, upgrading the H infinity norm calculation to capture multiple peaks in the singular value plot and using routines that minimized processing time. The optimization routine used was the MATLAB 'CONSTR' Sequential Quadratic Programming (SQP) routine. This SQP routine was compared to a FORTRAN SQP numerical optimizer, IMSL/DNCONG. The method was applied to an F-16 SISO example and a missile MIMO example. The mixed H2/H(infinity) controller for both these examples are compared to previous controller designs created using the LQG/LTR technique. DTIC

N95-28217 Tetra Precision, Inc., Gainesville, FL.

NEURAL NETWORK ERROR COMPENSATION OF MACHINE TOOLS Final Report, 12 May - 12 Nov. 1994

Christopher D. Mize, John C. Ziegert, and N. Srinivasa 16 Dec. 1994 51 p Limited Reproducibility: More than 20% of this document may be affected by microfiche quality
(Contract F33615-94-C-4438)
(AD-A289300; Rept-0001AF) Avail: Issuing Activity (Defense Technical Information Center (DTIC))

Thermally induced errors have been identified as a major contributor to the overall inaccuracy of machine tools. The main objective of this research was to provide a fast and accurate method for identifying and compensating these errors. A direct workspace identification technique was adopted where the total error at cutting tool is measured directly using a new calibration device called the Laser Ball Bar. This device was used in conjunction with a neural network to rapidly build a model of the mach tool for a thermal duty cycle that simulated machining of large workpieces. The overall prediction accuracy of the network was found to be within 3 microns. The network was then integrated with a PC based error compensation system. Final the performance of the overall system was tested by machining test parts under a variety thermal conditions. Substantial improvements in the accuracy of the machined parts were achieved using the error compensation system. DTIC

N95-28336 Pennsylvania Univ., Philadelphia, PA.

COGNITIVE NETWORKS FOR ATR: THE ROLES OF BIFURCATION AND CHAOS Quarterly Report No. 2, 1 Oct. 1994 - 1 Jan. 1995

N. H. Farhat 19 Dec. 1994 5 p Limited Reproducibility: More than 20% of this document may be affected by microfiche quality
(Contract N00014-94-1-0931)
(AD-A289010) Avail: Issuing Activity (Defense Technical Information Center (DTIC))

In previous work we established the importance of developing neural networks that compute with diverse attractors as means for introducing cognition in neural networks. Cognition is the ability of a network to distinguish, on its own, between novel and familiar objects, the latter being the set of objects on which the network is trained and the former being the set of all objects never seen by the network before. Bifurcation between different kinds of attractors in such cognitive networks is the mechanism by which cognition is achieved. Cognition is essential in networks intended to operate in complex uncontrolled environment like that encountered in most automated target recognition (ATR) scenarios. For these reasons we began exploring neural net models that could exhibit all three types of attractors: point, periodic, and chaotic. There is mounting evidence from biology to indicate that the study of such networks can help understand higher-level brain functions such as feature-linking, cognition, separation of object from background, inferencing, and other higher-level functions and can lead to the development of higher-level neural networks with enhanced capabilities. DTIC

N95-28461 Massachusetts Inst. of Tech., Cambridge, MA.

PIECEMEAL LEARNING OF AN UNKNOWN ENVIRONMENT

Margrit Betke, Ronald L. Rivest, and Mona Singh Mar. 1994 15 p Limited Reproducibility: More than 20% of this document may be affected by microfiche quality
(Grants NSF CCR-89-14428; NSF ASC-92-17041; NSF CCR-93-10888)
(AD-A291683; AIM-1474; CBCL-93) Avail: Issuing Activity (Defense Technical Information Center (DTIC))

We introduce a new learning problem: learning a graph by piecemeal search, in which the learner must return every so often to its starting point (for refueling, say). We present two linear-time piecemeal-search algorithms for learning city-block graphs: grid graphs with rectangular obstacles. DTIC

N95-28527 Texas A&M Univ., College Station, TX. Dept. of Mathematics.

WAVELET ANALYSIS AND ITS APPLICATIONS Final Report, 1 Apr. 1993 - 30 Nov. 1994

Charles K. Chui 24 Jan. 1995 5 p Limited Reproducibility: More than 20% of this document may be affected by microfiche quality
(Contract DAAH04-93-G-0047)
(AD-A291735; ARO-31003.1-MA-SDI) Avail: Issuing Activity (Defense Technical Information Center (DTIC))

Time-frequency localization is one of the most essential features of the wavelet transform. It was shown that while high order Daubechies and Battle-Lemarie wavelets give poor time-frequency localizations, the Chui-Wang spline-wavelets provide asymptotically optimal time-frequency windows. On the other hand, we also showed that by using the scale 3 instead of 2, symmetry can be achieved by orthonormal wavelets with compact support. Multivariate wavelets, particularly those with matrix dilation, were studied, and the theory of oversampling frames was extended to this setting. Interpolating wavelets have distributional duals that lead to the notion of functional wavelet transform. Other extensions required a study of the stability issue and algorithmic construction in multivariate splines. Applications to systems theory lead to the study of Hankel approximation and localization of neural networks. DTIC

N95-28536# Oak Ridge National Lab., TN.

ALLIANCE: AN ARCHITECTURE FOR FAULT TOLERANT, COOPERATIVE CONTROL OF HETEROGENEOUS MOBILE ROBOTS

L. E. Parker 1995 9 p Presented at the IEEE/RSJ/GI International Conference on Intelligent Robots and Systems (IROS), Munich, Germany, 12-16 Sep. 1994
(Contract DE-AC05-84OR-21400)
(DE95-007374; CONF-9409306-1) Avail: CASI HC A02/MF A01

This research addresses the problem of achieving fault tolerant cooperation within small- to medium-sized teams of heterogeneous mobile robots. The author describes a novel behavior-based, fully distributed architecture, called ALLIANCE, that utilizes adaptive action selection to achieve fault tolerant cooperative control in robot missions involving loosely coupled, largely independent tasks. The robots in this architecture possess a variety of high-level functions that they can perform during a mission, and must at all times select an appropriate action based on the requirements of the mission, the activities of other robots, the current environmental conditions, and their own internal states. Since such cooperative teams often work in dynamic and unpredictable environments, the software architecture allows the team members to respond robustly and reliably to unexpected environmental changes and modifications in the robot team that may occur due to mechanical failure, the learning of new skills, or the addition or removal of robots from the team by human intervention. After presenting ALLIANCE, the author describes in detail experimental results of an implementation of this architecture on a team of physical mobile robots performing a cooperative box pushing demonstration. These experiments illustrate the ability of ALLIANCE to achieve adaptive, fault-tolerant cooperative control amidst dynamic changes in the capabilities of the robot team. DOE

N95-28545 Naval Postgraduate School, Monterey, CA.

BILATERAL FORCE FEEDBACK FOR HYDRAULICALLY ACTUATED SYSTEMS M.S. Thesis

Gregory S. Johnson Dec. 1994 120 p Limited Reproducibility: More than 20% of this document may be affected by microfiche quality
(AD-A291632) Avail: Issuing Activity (Defense Technical Information Center (DTIC))

This thesis report discusses the design, construction, and experimentation of force feedback in one and two degrees of freedom, hydraulically actuated systems. A master hydraulic unit is used to positionally control a remotely located slave hydraulic unit. An obstruction in the path of the slave unit is used as a force control to the master unit, reducing the power assist to the operator. An analysis was conducted to predict the performance and stability of the system for various amplifier gain settings. One and two degrees of freedom models were constructed to verify the analysis and to physically observe the force feedback. DTIC

N95-26943# Wichita State Univ., Wichita, KS.
AN EXPLORATORY APPLICATION OF NEURAL NETWORKS FOR AIRFOIL DESIGN Abstract Only
Steve Huang, L. S. Miller, and J. E. Steck *In its* AIAA Techfest 20 Proceedings 1994 26 p (For primary document see N95-26941 09-01)
Avail: CASI HC A03/MF A03

64 NUMERICAL ANALYSIS

Includes iteration, difference equations, and numerical approximation.

N95-26395*# Institute for Computer Applications in Science and Engineering, Hampton, VA.
INTRODUCTION TO MULTIGRID METHODS Final Report
P. Wesseling Feb. 1995 137 p
(Contract NAS1-19480; RTOP 505-90-52-01)
(NASA-CR-195045; NAS 1.26:195045; ICASE-95-11) Avail: CASI HC A07/MF A02

These notes were written for an introductory course on the application of multigrid methods to elliptic and hyperbolic partial differential equations for engineers, physicists and applied mathematicians. The use of more advanced mathematical tools, such as functional analysis, is avoided. The course is intended to be accessible to a wide audience of users of computational methods. We restrict ourselves to finite volume and finite difference discretization. The basic principles are given. Smoothing methods and Fourier smoothing analysis are reviewed. The fundamental multigrid algorithm is studied. The smoothing and coarse grid approximation properties are discussed. Multigrid schedules and structured programming of multigrid algorithms are treated. Robustness and efficiency are considered. Author

N95-26459 Tulane Univ., New Orleans, LA. Dept. of Electrical Engineering.
THE fBm INTERPOLATOR Final Report
Andrew B. Martinez 4 Nov. 1994 16 p Limited Reproducibility: More than 20% of this document may be affected by microfiche quality
(DA Proj. R03-5)
(AD-A288996; NRL-MR/7441-93-7079) Avail: Issuing Activity (Defense Technical Information Center (DTIC))

A technique for interpolating an irregularly sampled multidimensional field is presented. The method assumes that the field to be interpolated is a fractional Brownian motion surface with additive measurement error. There are several advantages to this method: data sets with different mean-squared measurement errors can be optimally merged, and the variance of the estimator can be easily computed at each interpolation point. An iterative algorithm is given for implementing the estimator with the advantage of allowing a stopping rule to be used to terminate the iteration after a predetermined level of performance is achieved. Furthermore, at each stage, multiple points can be tested, the resulting performance evaluated, and that point which most decreases the variance of the estimator selected. Using the iterative algorithm produces a low order estimator based on a small, carefully selected set of points with a reasonable level of performance. DTIC

N95-26495# Helsinki Univ. of Technology, Espoo (Finland). Inst. of Computational Dynamics.
GENERAL PURPOSE FINITE ELEMENT SOLVER
J. Freund and A. Lempinen Oct. 1994 82 p
(ISSN 1237-4903)
(PB95-185062; ISBN-951-22-2334-1) Avail: CASI HC A05/MF A01

The manual describes a finite element method based program for second order partial differential equations. The program handles sets of non-linear non-stationary problems; and it can be used to solve problems of elliptic, parabolic and hyperbolic type whenever a proper weak (weighted residual) formulation is known. Similar approximations are used for all of the unknowns, which means that the burden for stability will be on the weak form. As spatial and temporal coordinates are handled truly on the same footing, the treatment of moving domain or boundaries is straightforward. The constituent parts of the solution method are explained in detail. Then the solution algorithm showing how to put the parts together is given in pseudo language. Only the finite element solver part of the program is considered here. The selected algorithm led to a quite compact solver consisting of about 3,000 lines of FORTRAN 77. NTIS

N95-26514# Institut des Hautes Etudes Scientifiques, Bures-sur-Yvette (France).
HYPERKAEHLER METRICS ASSOCIATED TO COMPACT LIE GROUPS
Andrew Dancer and Andrew Swann (Odense Univ., Denmark.) Dec. 1994 16 p
(PB95-185161; IHES/M/94/66) Avail: CASI HC A03/MF A01

In this paper we study a moduli space of solutions to Nahm's equations. We recall that a hyperkahler structure on a manifold is a quadruple (g, I, J, K), where g is a Riemannian metric and I, J, K are complex structures satisfying the quaternionic relations IJ = K = -IJ etc., and such that (g, I), (g, J), (g, K) are Kahler structures. One can show that such a metric g is necessarily Ricci-flat, and in fact all the hyperkahler metrics we discuss are also complete. NTIS

N95-26515# Institut des Hautes Etudes Scientifiques, Bures-sur-Yvette (France).
COMPACTIFICATION OF MODULI SPACES OF MONOPOLES
R. G. Wang Nov. 1994 28 p See also PB95-165528
(PB95-185179; IHES/M/94/57) Avail: CASI HC A03/MF A01

In 1987, A. Floer suggested that Yang-Mills-Higgs theory should be studied on asymptotically Euclidean 3-manifolds M and it has been proved a rich subject in recent years. The focus of interest is the geometry of the moduli space of monopoles on M and its applications. To apply the theory of monopoles to study the topology of M, a main problem is the non-compactness of moduli space M(sub m, sup k). Although it is clearly clarified, M(sub m, sup k) itself seems not to have an immediate, natural compactification. The problem is discussed in this paper. NTIS

N95-26516# Institut des Hautes Etudes Scientifiques, Bures-sur-Yvette (France).
YANG-BAXTER TYPE EQUATIONS AND POSETS OF MAXIMAL CHAINS
R. J. Lawrence (Michigan Univ., Ann Arbor, MI.) Nov. 1994 33 p
Presented at the 3rd Ann Arbor Conference on Combinatories and Algebra, Ann Arbor, MI, 8-12 Jun. 1994
(PB95-185195; IHES/M/94/59) Avail: CASI HC A03/MF A01

The usual Yang-Baxter equation may be viewed as a commutativity relation on faces of a permutahedron. These polyhedra are related via extension posets to certain arrangements of hyperplanes and their vertices are in 1-1 correspondence with maximal chains in the Boolean poset B(sub n). In this paper, similar constructions are performed in one dimension higher, the associated algebraic relations replacing the Yang-Baxter equation being similar to the permutahedron equation. The geometric structure of the poset of maximal chains in S (sub(alpha sub 1)) X...X S (sub (alpha sub k)) is discussed in some detail, and cell types are found to be classified by a poset of 'partitions of partitions' in much the same way as those for permutahedra are classified by ordinary partitions. NTIS

N95-26539# Institut des Hautes Etudes Scientifiques, Bures-sur-Yvette (France).
GENERALIZED SCHWARZIANS IN SEVERAL VARIABLES AND MOEBIUS INVARIANT DIFFERENTIAL OPERATORS
Robert Molzon (Kentucky Univ., Lexington, KY.) and Hirotaka Tamanoi (Kentucky Univ., Lexington, KY.) Dec. 1994 49 p
(PB95-185211; IHES/M/94/64) Avail: CASI HC A03/MF A01

We introduce certain Mobius invariant differential operators in several variables, which in many ways correctly generalize the classical Schwarzian derivative in one variable. We show that these generalized Schwarzians generate the entire set of Mobius invariant differential operators acting on local biholomorphisms. We then prove the composition formula for generalized Schwarzians from the point of view of connections in vector bundles. We also give the necessary and sufficient condition to prescribe generalized Schwarzians and give the formula for the solution. NTIS

N95-26609 Army Armament Research, Development and Engineering Center, Watervliet, NY. Benet Lab.

ADAPTIVE FINITE ELEMENT METHOD I: SOLUTION ALGORITHM AND COMPUTATIONAL EXAMPLES Final Report

J. M. Coyle and J. E. Flaherty Aug. 1994 57 p Limited Reproducibility: More than 20% of this document may be affected by microfiche quality
(AD-A288979; ARCCB-TR-94033) Avail: Issuing Activity (Defense Technical Information Center (DTIC))

An adaptive finite element method is developed to solve initial boundary value problems for vector systems of parabolic partial differential equations in one space dimension and time. The differential equations are discretized in space using piecewise linear finite element approximations. Superconvergence properties and quadratic polynomials are used to derive a computationally inexpensive approximation to the spatial component of the error. This technique is coupled with time integration schemes of successively higher orders to obtain an approximation of the temporal and total discretization errors. These approximate errors are used to control an adaptive mesh refinement strategy. Refinement is performed in space, time, or both space and time depending on the dominant component of the error estimate. A computer code coupling this refinement strategy and stable mesh movement has been written and applied to a number of problems. These computations confirm that proper mesh movement can reduce the computational efforts associated with mesh refinement. DTIC

N95-26663*# National Aeronautics and Space Administration. Lewis Research Center, Cleveland, OH.

THE METHOD OF SPACE-TIME CONSERVATION ELEMENT AND SOLUTION ELEMENT-APPLICATIONS TO ONE-DIMENSIONAL AND TWO-DIMENSIONAL TIME-MARCHING FLOW PROBLEMS

Sin-Chung Chang, Xiao-Yen Wang (Colorado Univ., Boulder, CO.), and Chuen-Yen Chow (Colorado Univ., Boulder, CO.) May 1995 37 p Presented at the 12th Computational Fluid Dynamics Conference, San Diego, CA, 19-22 Jun. 1995; sponsored by AIAA
(RTOP 505-62-52)
(NASA-TM-106915; E-9623; NAS 1.15:106915; AIAA Paper 95-1754)
Avail: CASI HC A03/MF A01

A nontraditional numerical method for solving conservation laws is being developed. The new method is designed from a physicist's perspective, i.e., its development is based more on physics than numerics. Even though it uses only the simplest approximation techniques, a 2D time-marching Euler solver developed recently using the new method is capable of generating nearly perfect solutions for a 2D shock reflection problem used by Helen Yee and others. Moreover, a recent application of this solver to computational aeroacoustics (CAA) problems reveals that: (1) accuracy of its results is comparable to that of a 6th order compact difference scheme even though nominally the current solver is only of 2nd-order accuracy; (2) generally, the non-reflecting boundary condition can be implemented in a simple way without involving characteristic variables; and (3) most importantly, the current solver is capable of handling both continuous and discontinuous flows very well and thus provides a unique numerical tool for solving those flow problems where the interactions between sound waves and shocks are important, such as the noise field around a supersonic over- or under-expansion jet. Author

N95-26672*# Institute for Computer Applications in Science and Engineering, Hampton, VA.

CONTRIBUTION TO THE OPTIMAL SHAPE DESIGN OF TWO-DIMENSIONAL INTERNAL FLOWS WITH EMBEDDED SHOCKS

Angelo Iollo (Politecnico di Torino, Torino, Italy.) and Manuel D. Salas (National Aeronautics and Space Administration. Langley Research Center, Hampton, VA.) Mar. 1995 23 p Submitted for publication
(Contract NAS1-19480; RTOP 505-90-52-01)
(NASA-CR-195062; NAS 1.26:195062; ICASE-95-20) Avail: CASI HC A03/MF A01

We explore the practicability of optimal shape design for flows modeled by the Euler equations. We define a functional whose minimum represents the optimality condition. The gradient of the functional with respect to the geometry is calculated with the Lagrange multipliers, which are determined by solving a co-state equation. The optimization problem is then examined by comparing the performance of several gradient-based optimization algorithms. In this formulation, the flow field can be computed to an arbitrary order of accuracy. Finally, some results for internal flows with embedded shocks are presented, including a case for which the solution to the inverse problem does not belong to the design space. Author

N95-26772 Carnegie-Mellon Univ., Pittsburgh, PA. School of Computer Science.

CONTROL-FLOW ANALYSIS AND TYPE SYSTEMS

Nevin Heintze Dec. 1994 20 p Limited Reproducibility: More than 20% of this document may be affected by microfiche quality
(Contract F19628-91-C-0168; ARPA Order 8313)
(AD-A289338; CMU-CS-94-227; CMU-CS-FOX-94-09) Avail: Issuing Activity (Defense Technical Information Center (DTIC))

We establish a series of equivalences between type systems and control-flow analyses. Specifically, we take four type systems from the literature (involving simple types, subtypes and recursion) and conservatively enrich them to reason about control-flow information. Similarly, we take four standard control-flow systems and conservatively enrich them to reason about type consistency. Our main result is that for each type system, there is a control-flow system with equivalent reasoning power. In essence, type systems and control-flow analysis can be viewed as complementary approaches for addressing questions of type consistency and control-flow. DTIC

N95-26882 Carnegie-Mellon Univ., Pittsburgh, PA. Management Sciences Research Group.

USING THE DIMENSION REDUCTION TECHNIQUE TO PROVE THAT CLIQUE TREES DEFINE FACETS FOR THE ASYMMETRIC TRAVELING SALESMAN POLYTOPE Research Report

Bob Carr 14 Sep. 1994 59 p Limited Reproducibility: More than 20% of this document may be affected by microfiche quality
(Contract N00014-85-K-0198)
(AD-A289397; MSR-608) Avail: Issuing Activity (Defense Technical Information Center (DTIC))

In this paper the author develops a new general approach to proving that a given inequality is facet-defining. This approach is then used to show that clique tree inequalities define facets for the asymmetric traveling salesman problem. DTIC

N95-26910 Helsinki Univ. of Technology, Espoo (Finland). Systems Analysis Lab.

RANDOM RELAXATION OF FIXED POINT ITERATION

M. Verkama Oct. 1994 17 p Limited Reproducibility: More than 20% of this document may be affected by microfiche quality
(PB95-185013; RR-A54) Avail: CASI HC A03

This paper considers a stochastic fixed point iteration where each coordinate is updated with a certain probability and otherwise left unchanged. The iteration is interesting from the viewpoint of parallel distributed computation because the realized sequences belong to the class of asynchronous fixed point iterations. It is demonstrated with a linear system that the convergence conditions for randomly relaxed iterations are less stringent than their asynchronous counterparts, and that they can illuminate the tightness of the convergence conditions for asynchronous iterations, which are typically worst-case conditions. NTIS

N95-26915 Institut des Hautes Etudes Scientifiques, Bures-sur-Yvette (France).

GROMOV-LAWSON-ROSENBERG CONJECTURE FOR GROUPS WITH PERIODIC COHOMOLOGY

B. Botvinnik, P. Gilkey, and S. Stolz 26 Nov. 1994 24 p Prepared in cooperation with Oregon Univ. Limited Reproducibility: More than 20% of this document may be affected by microfiche quality
(Grant NSF DMS-94-03360)
(PB95-185203; IHES/M/94/62) Avail: CASI HC A03

The Gromov-Lawson-Rosenberg conjecture claims that a spin manifold M with fundamental group pi admits a metric with positive scalar if and only if a generalized index of the Dirac operator with values in the real K-theory of the C(sup *)-algebra C(sub tau, sup *)pi vanishes. We prove this conjecture for groups with periodic cohomology. NTIS

N95-27020 Naval Command, Control and Ocean Surveillance Center, San Diego, CA. Research, Development, Technology and Evaluation Div.
EVOLVING CASCADE-CORRELATION NETWORKS FOR TIME-SERIES FORECASTING
J. R. McDonnell and D. E. Waagen Oct. 1994 12 p Limited Reproducibility: More than 20% of this document may be affected by microfiche quality
(AD-A289197) Avail: Issuing Activity (Defense Technical Information Center (DTIC))

This investigation applies evolutionary search to the cascade-correlation learning network. Evolutionary search is used to find both the input weights and input connectivity of candidate hidden units. A time-series prediction example is used to demonstrate the capabilities of the proposed approach. DTIC

N95-27029*# Institute for Computer Applications in Science and Engineering, Hampton, VA.
A 3D AGGLOMERATION MULTIGRID SOLVER FOR THE REYNOLDS-AVERAGED NAVIER-STOKES EQUATIONS ON UNSTRUCTURED MESHES Final Report
D. J. Marvriplis and V. Venkatakrishnan Apr. 1995 30 p
(Contract NAS1-19480; RTOP 505-90-52-01)
(NASA-CR-195073; NAS 1.26:195073; ICASE-95-30) Avail: CASI HC A03/MF A01

An agglomeration multigrid strategy is developed and implemented for the solution of three-dimensional steady viscous flows. The method enables convergence acceleration with minimal additional memory overheads, and is completely automated, in that it can deal with grids of arbitrary construction. The multigrid technique is validated by comparing the delivered convergence rates with those obtained by a previously developed overset-mesh multigrid approach, and by demonstrating grid independent convergence rates for aerodynamic problems on very large grids. Prospects for further increases in multigrid efficiency for high-Reynolds number viscous flows on highly stretched meshes are discussed. Author

N95-27092# International Centre for Theoretical Physics, Trieste (Italy).
ON COMPACT MULTIPLIERS OF TOPOLOGICAL ALGEBRAS
N. Mohammad Aug. 1994 3 p
(DE95-608751; IC-94/237) Avail: CASI HC A01/MF A01 (US Sales Only)

It is shown that if the maximal ideal space (Delta)(A) of a semisimple commutative complete metrizable locally convex algebra contains no isolated points, then every compact multiplier is trivial. Particularly, compact multipliers on semisimple commutative Frechet algebras whose maximal ideal space has no isolated points are identically zero. DOE

N95-27299# International Centre for Theoretical Physics, Trieste (Italy).
SPECTRAL PROPERTIES OF MULTIPLIERS ON TOPOLOGICAL ALGEBRAS
M. Noor Jul. 1994 6 p
(DE95-608747; IC-94/187) Avail: CASI HC A02/MF A01 (US Sales Only)

We investigate the spectral properties of a multiplier T on a Hausdorff topological algebra A possessing an orthogonal basis. We show that each multiplier T on A is determined by a sequence of complex numbers which are precisely the eigenvalues of T. It is further proved here that the point spectrum of T coincides with this sequence and the residual spectrum of T is empty. DOE

N95-27301# International Centre for Theoretical Physics, Trieste (Italy).
q-STRUCTURE ALGEBRA OF U(SUB q)(g-CIRCUMFLEX) FROM ITS ADJOINT ACTION
A. ElHassouni, Y. Hassouni, and M. Zakkari Aug. 1994 5 p
(DE95-608749; IC-94/206) Avail: CASI HC A01/MF A01 (US Sales Only)

We prove that the adjoint action of the quantum affine Lie algebra U(sub q)(g-circumflex), where g is a simple finite dimensional Lie algebra, reproduces the q-commutation relationship of U(sub q)(g-circumflex) if and only if g is of type A(sub n), n greater than or equal to 1. DOE

N95-27302# International Centre for Theoretical Physics, Trieste (Italy).
SOME COMMUTATIVITY THEOREMS FOR A CERTAIN CLASS OF RINGS
M. A. Khan Aug. 1994 14 p
(DE95-608750; IC-94/235) Avail: CASI HC A03/MF A01 (US Sales Only)

We first establish the commutativity theorem for semiprime ring satisfying the polynomial identity (x(sup n), y) x(sup r) = +/- y(sup s) (x, y(sup m)) y(sup t) for all x,y in R, where m, n, r, s, and t are fixed nonnegative integers, and further, we investigate commutativity of rings with unity under some additional hypothesis. It is also shown that the above result is true for s-unital. We provide some counter examples which show that the hypothesis of our theorems are not altogether superfluous. The results generalize some of the well-known commutativity theorems for rings which are right s-unital. DOE

N95-27304# Los Alamos National Lab., NM.
THE COMPARISON OF P(SUB 1) AND SIMPLIFIED P(SUB 2) SYNTHETIC ACCELERATION FOR ITERATIVE METHODS IN TRANSPORT SOLUTIONS
Taewan Noh and Warren F. Miller 1994 12 p Presented at the International Conference on Mathematics and Computations, Reactor Physics, and Environmental Analyses, Portland, OR, 30 Apr. - 4 May 1995
(Contract W-7405-eng-36)
(DE94-018306; LA-UR-94-2848; CONF-950420-1) Avail: CASI HC A03/MF A01

Using an operator form of a synthetic acceleration method, we derive the P(sub 1) and a new second-moment P(sub 2) acceleration schemes. We analyze the convergence rate of each scheme by performing a Fourier analysis. The second-moment P(sub 2) acceleration outperforms an earlier third-moment P(sub 2) acceleration method by Miller and Larsen. However, it is still less efficient than P(sub 1) acceleration (diffusion synthetic acceleration: DSA). These results confirm that one cannot simply assume that replacement of the DSA method with a higher order operator will lead to a smaller spectral radius. We get similar results for the P(sub 1) and simplified P(sub 2) acceleration in two-dimensional x-y geometry. DOE

N95-27311# International Centre for Theoretical Physics, Trieste (Italy).
INTRODUCTION TO DUBOIS-VIOLETTE'S NON-COMMUTATIVE DIFFERENTIAL GEOMETRY
A. E. F. Djemai Jul. 1994 123 p
(DE95-608801; IC-94/218) Avail: CASI HC A06/MF A02 (US Sales Only)

In this work, we present a detailed review of the Dubois-Violette et al. approach to non-commutative differential calculus. The non-commutative differential geometry of matrix algebras and the non-commutative Poisson structures are treated in some detail. We also present the analog of the Maxwell theory and the new models of Yang-Mills-Higgs theories that can be constructed in this framework. In particular, some simple models are compared with the standard model. Finally, we discuss some perspectives and open questions. DOE

N95-27330# International Centre for Theoretical Physics, Trieste (Italy).
ON COMMUTATIVITY OF RIGHT s-UNITAL RINGS WITH SOME POLYNOMIAL CONSTRAINTS
M. A. Khan Aug. 1994 5 p
(DE95-608752; IC-94/248) Avail: CASI HC A01/MF A01 (US Sales Only)

We study the commutativity of a certain class of rings, namely rings with unity 1 and right s-unital rings under each of the following properties yx(sup m) - x(sup n) f(y)x(sup p), x = 0, yx(sup m) + x(sup n)f(y)x(sup p), x = 0, where f(t) is a polynomial in t(sup 2)Zyt varying with pair of ring elements x, y and m, n, p are fixed non-negative integers. Moreover, the results have been extended to the case when m and n depend on the choice of x and y and the ring satisfies the Chacron's Theorem. DOE

N95-27331# International Centre for Theoretical Physics, Trieste (Italy).
MEAN VALUE THEOREM IN TOPOLOGICAL VECTOR SPACES
L. A. Khan Aug. 1994 3 p
(DE95-608753; IC-94/249) Avail: CASI HC A01/MF A01 (US Sales Only)

The aim of this note is to give shorter proofs of the mean value theorem, the mean value inequality, and the mean value inclusion for the class of Gateaux differentiable functions having values in a topological vector space. DOE

N95-27432# Sandia National Labs., Albuquerque, NM. System Studies Dept.

FUZZY-ALGEBRA UNCERTAINTY ASSESSMENT

J. Arlin Cooper and Douglas K. Cooper (Naval Research Lab., Washington, DC.) Dec. 1994 10 p Presented at the Winter Fuzzy and Neural Networks Conference, Washington, DC, 9 Dec. 1994
(Contract DE-AC04-94AL-85000)
(DE95-005426; SAND-95-0013C; CONF-941262-1) Avail: CASI HC A02/MF A01

A significant number of analytical problems (for example, abnormal-environment safety analysis) depend on data that are partly or mostly subjective. Since fuzzy algebra depends on subjective operands, we have been investigating its applicability to these forms of assessment, particularly for portraying uncertainty in the results of PRA (probabilistic risk analysis) and in risk-analysis-aided decision-making. Since analysis results can be a major contributor to a safety-measure decision process, risk management depends on relating uncertainty to only known (not assumed) information. The uncertainties due to abnormal environments are even more challenging than those in normal-environment safety assessments; and therefore require an even more judicious approach. Fuzzy algebra matches these requirements well. One of the most useful aspects of this work is that we have shown the potential for significant differences (especially in perceived margin relative to a decision threshold) between fuzzy assessment and probabilistic assessment based on subtle factors inherent in the choice of probability distribution models. We have also shown the relation of fuzzy algebra assessment to 'bounds' analysis, as well as a description of how analyses can migrate from bounds analysis to fuzzy-algebra analysis, and to probabilistic analysis as information about the process to be analyzed is obtained. Instructive examples are used to illustrate the points. DOE

N95-27433*# Institute for Computer Applications in Science and Engineering, Hampton, VA.

MULTIGRID TECHNIQUES FOR UNSTRUCTURED MESHES Final Report

D. J. Mavriplis Apr. 1995 62 p Presented at the 26th Computational Fluid Dynamics Lecture Series Program, Rhode-Saint-Genese, Belgium, 13-17 Mar. 1995
(Contract NAS1-19480; RTOP 505-90-52-01)
(NASA-CR-195070; NAS 1.26:195070; ICASE-95-27) Avail: CASI HC A04/MF A01

An overview of current multigrid techniques for unstructured meshes is given. The basic principles of the multigrid approach are first outlined. Application of these principles to unstructured mesh problems is then described, illustrating various different approaches, and giving examples of practical applications. Advanced multigrid topics, such as the use of algebraic multigrid methods, and the combination of multigrid techniques with adaptive meshing strategies are dealt with in subsequent sections. These represent current areas of research, and the unresolved issues are discussed. The presentation is organized in an educational manner, for readers familiar with computational fluid dynamics, wishing to learn more about current unstructured mesh techniques. Author

N95-27489 Carnegie-Mellon Univ., Pittsburgh, PA. School of Computer Science.

THE ASSEMBLY TOWER AND SOME CATEGORICAL AND ALGEBRAIC ASPECTS OF FRAME THEORY Ph.D. Thesis

J. Todd Wilson May 1994 138 p Sponsored in part by the Johannes Kepler Universitat Linz and the Medlar Project Limited Reproducibility: More than 20% of this document may be affected by microfiche quality
(AD-A289360; CMU-CS-94-186) Avail: Issuing Activity (Defense Technical Information Center (DTIC))

This thesis studies the framework arising in the algebraic and categorical description of general (or point-set) topology. Classically, a topological space is a set with structure, the structure being its collection of open sets, which taken together determine an abstract notion of proximity. The collection of all such open sets forms a special kind of complete lattice, and it is a class of complete lattices (frames) motivated by these examples that is the focus of algebraic study-in short, one dispenses with the points and studies the algebra of open sets. This method has had successes not only in general topology, but has also found application in such diverse areas as logic, topos theory, and even computer science. It is not these specific areas of application, however, with which the thesis is primarily concerned; rather, it is that part of the theory which they all share: the category of frames. This category has as a sub-category the category of complete Boolean algebras, and these two categories stand in much the same relation as do the categories of topological spaces and sets. As with sets and spaces, complete Boolean algebras are in some ways better behaved categorically than frames, and so the former provides a potential source of information about the latter. For the purpose of obtaining this information, a construction for frames, called the assembly tower and present already at the beginnings of the subject, is studied systematically and, in this way, found to be a key tool for uncovering both structural and and algebraic properties of frames. DTIC

N95-27714# Joint Inst. for Nuclear Research, Dubna (USSR).

AN INVARIANT MEASURE FOR A NONLINEAR SCHROEDINGER EQUATION

P. E. Zhidkov 1994 20 p
(DE95-610166; JINR-R-5-94-199) Avail: CASI HC A03/MF A01 (US Sales Only)

We construct an invariant measure for the dynamical system generated by a nonlinear Schroedinger equation. Conditions of the boundedness of the measure constructed are obtained. The result allows us to apply the Poincare recurrence theorem which (partially) explains the Fermi-Pasta-Ulam phenomenon well-known in the theory of nonlinear waves. DOE

N95-27715# Joint Inst. for Nuclear Research, Dubna (USSR).

PROOFS OF CONTRACTED LENGTH NON-COVARIANCE

V. N. Streltsov 1994 4 p
(DE95-610175; JINR-D-2-94-179) Avail: CASI HC A01/MF A01 (US Sales Only)

Different proofs of contracted length non-covariance are discussed. The way based on the establishment of interval inconstancy (dependence on velocity) seems to be the most convincing one. It is stressed that the known non-covariance of the electromagnetic field energy and momentum of a moving charge (the problem 4/3) is a direct consequence of contracted length non-covariance. DOE

N95-27726*# National Aeronautics and Space Administration. Lewis Research Center, Cleveland, OH.

THE ORIGIN OF SPURIOUS SOLUTIONS IN COMPUTATIONAL ELECTROMAGNETICS

Bo-nan Jiang, Jie Wu, and L. A. Povinelli May 1995 46 p
(Contract NCC3-370; RTOP 505-90-5K)
(NASA-TM-106921; E-9633; ICOMP-95-8; NAS 1.15:106921) Avail: CASI HC A03/MF A01

The origin of spurious solutions in computational electromagnetics, which violate the divergence equations, is deeply rooted in a misconception about the first-order Maxwell's equations and in an incorrect derivation and use of the curl-curl equations. The divergence equations must be always included in the first-order Maxwell's equations to maintain the ellipticity of the system in the space domain and to guarantee the uniqueness of the solution and/or the accuracy of the numerical solutions. The div-curl method and the least-squares method provide rigorous derivation of the equivalent second-order Maxwell's equations and their boundary conditions. The node-based least-squares finite element method (LSFEM) is recommended for solving the first-order full Maxwell equations directly. Examples of the numerical solutions by LSFEM for time-harmonic problems are given to demonstrate that the LSFEM is free of spurious solutions. Author

N95-27739# International Centre for Theoretical Physics, Trieste (Italy).

SCALING OF LOCALIZATION LENGTH OF A QUASI 1D SYSTEM WITH LONGITUDINAL BOUNDARY ROUGHNESS

Kar Gupta Abhijit and A. K. Sen (Saha Inst. of Nuclear Physics, Calcutta, India.) Aug. 1994 9 p
(DE95-609148; IC-94/213) Avail: CASI HC A02/MF A01 (US Sales Only)

We introduce irregularities on one of the longitudinal boundaries of a quasi 1D strip which has no bulk disorder. We calculate the localization length of such a system within the scope of tight-binding formalism and see how it behaves with the roughness introduced on the boundary and with the strip-width. We find that localization length scales with a composite one parameter. DOE

N95-27742# Argonne National Lab., IL.
TWO-BODY BOUND STATES AND THE BETHE-SALPETER EQUATION
M. Pichowsky, M. Kennedy (New Hampshire Univ., Durham, NH.), and M. Strickland (Duke Univ., Durham, NC.) 18 Jan. 1995 28 p Presented at the HUGS At CEBAF '94, Hampton, VA, 31 May - 17 Jun. 1994
(Contract W-31-109-eng-38)
(DE95-008302; ANL/PHY/CP-85493; CONF-9405297-1) Avail: CASI HC A03/MF A01

The Bethe-Salpeter formalism is used to study two-body bound states within a scalar theory: two scalar fields interacting via the exchange of a third massless scalar field. The Schwinger-Dyson equation is derived using functional and diagrammatic techniques, and the Bethe-Salpeter equation is obtained in an analogous way, showing it to be a two-particle generalization of the Schwinger-Dyson equation. The authors also present a numerical method for solving the Bethe-Salpeter equation without three-dimensional reduction. The ground and first excited state masses and wavefunctions are computed within the ladder approximation and space-like form factors are calculated. DOE

N95-28010 Institut des Hautes Etudes Scientifiques, Bures-sur-Yvette (France).
SYMMETRIES OF THE KAC-PETERSON MODULAR MATRICES OF AFFINE ALGEBRAS
T. Gannon Sep. 1994 19 p Limited Reproducibility: More than 20% of this document may be affected by microfiche quality
(PB95-190138; IHES/P/94/53) Avail: CASI HC A03

The author classifies an important subset of the A(sub r, sup (1)) physical invariants, called automorphism invariants. NTIS

N95-28012# Institut des Hautes Etudes Scientifiques, Bures-sur-Yvette (France).
LIE GROUP WEIGHT MULTIPLICITIES FROM CONFORMAL FIELD THEORY
T. Gannon, C. Jakovljevic, and M. A. Walton Nov. 1994 15 p Prepared in cooperation with Lethbridge Univ.
(PB95-190153; IHES/P/94/58) Avail: CASI HC A03/MF A01

Dominant weight multiplicities of simple Lie groups are expressed in terms of the modular matrices of Wess-Zumino-Witten conformal field theories, and related objects. Symmetries of the modular matrices give rise to new relations among multiplicities. At least for some Lie groups, these new relations are strong enough to completely fix all multiplicities. NTIS

N95-28110# Oak Ridge National Lab., TN.
ONE DIMENSIONAL GLOBAL AND LOCAL SOLUTION FOR ICRF HEATING
C. Y. Wang, D. B. Batchelor, E. F. Jaeger, and M. D. Carter Feb. 1995 30 p
(Contract DE-AC05-84OR-21400)
(DE95-007984; ORNL/TM-12923) Avail: CASI HC A03/MF A01

A numerical code GLOSI (Global and Local One-dimensional Solution for Ion cyclotron range of frequencies (ICRF) heating) is developed to solve one-dimensional wave equations resulting from the use of radio frequency (RF) waves to heat plasmas. The code uses a finite difference method. Due to its numerical stability, the code can be used to find both global and local solutions when imposed with appropriate boundary conditions. Three types of boundary conditions are introduced to describe wave scattering, antenna wave excitation, and fixed tangential wave magnetic field. The scattering boundary conditions are especially useful for local solutions. The antenna wave excitation boundary conditions can be used to excite fast and slow waves in a plasma. The tangential magnetic field boundary conditions are used to calculate impedance matrices, which describe plasma and antenna coupling and can be used by an antenna code to calculate antenna loading. These three types of boundary conditions can also be combined to describe various physical situations in RF plasma heating. The code also includes plasma thermal effects and calculates collisionless power absorption and kinetic energy flux. The plasma current density is approximated by a second-order Larmor radius expansion, which results in a sixth-order ordinary differential equation. DOE

N95-28162# Lawrence Livermore National Lab., Livermore, CA.
A METHOD FOR GENERATING SKEWED RANDOM NUMBERS USING TWO OVERLAPPING UNIFORM DISTRIBUTIONS
Donald L. Ermak and John S. Nasstrom (EG and G Energy Measurements, Inc., Pleasanton, CA.) Feb. 1995 31 p Submitted for publication
(Contract W-7405-eng-48)
(DE95-008747; UCRL-ID-120424) Avail: CASI HC A03/MF A01

The objective was to implement and evaluate a method for generating skewed random numbers using a combination of uniform random numbers. The method provides a simple and accurate way of generating skewed random numbers from the specified first three moments without an a priori specification of the probability density function. We describe the procedure for generating skewed random numbers from uniform random numbers, and show that it accurately produces random numbers with the desired first three moments over a range of skewness values. We also show that in the limit of zero skewness, the distribution of random numbers is an accurate approximation to the Gaussian probability density function. DOE

N95-28173# Argonne National Lab., IL.
A CASE STUDY IN AUTOMATED THEOREM PROVING: A DIFFICULT PROBLEM ABOUT COMMUTATORS
W. McCune Feb. 1995 12 p
(Contract W-31-109-eng-38)
(DE95-008392; ANL/MCS-TM-202) Avail: CASI HC A03/MF A01

This paper shows how the automated deduction system OTTER was used to prove the group theory theorem chi(exp 3) = e implies (((y, z), u), v) = e, where e is the identity, and (chi, y) is is the commutator chi'y'(chi)y. This is a difficult problem for automated provers, and several lengthy searches were run before a proof was found. Problem formulation and search strategy played a key role in the success. I believe that ours is the first automated proof of the theorem. DOE

N95-28215*# National Aeronautics and Space Administration. Marshall Space Flight Center, Huntsville, AL.
CORSSTOL: CYLINDER OPTIMIZATION OF RINGS, SKIN, AND STRINGERS WITH TOLERANCE SENSITIVITY
J. Finckenor and M. Bevill Washington May 1995 37 p
(NASA-TP-3551; M-779; NAS 1.60:3551) Avail: CASI HC A03/MF A01

Cylinder Optimization of Rings, Skin, and Stringers with Tolerance (CORSSTOL) sensitivity is a design optimization program incorporating a method to examine the effects of user-provided manufacturing tolerances on weight and failure. CORSSTOL gives designers a tool to determine tolerances based on need. This is a decisive way to choose the best design among several manufacturing methods with differing capabilities and costs. CORSSTOL initially optimizes a stringer-stiffened cylinder for weight without tolerances. The skin and stringer geometry are varied, subject to stress and buckling constraints. Then the same analysis and optimization routines are used to minimize the maximum material condition weight subject to the least favorable combination of tolerances. The adjusted optimum dimensions are provided with the weight and constraint sensitivities of each design variable. The designer can immediately identify critical tolerances. The safety of parts made out of tolerance can also be determined. During design and development of weight-critical systems, design/analysis tools that provide product-oriented results are of vital significance. The development of this program and methodology provides designers with an effective cost- and weight-saving design tool. The tolerance sensitivity method can be applied to any system defined by a set of deterministic equations. Author

N95-28232# Lawrence Livermore National Lab., Livermore, CA.
A POINT-CENTERED DIFFUSION DIFFERENCING FOR UNSTRUCTURED MESHES IN 3-D
T. S. Palmer 22 Sep. 1994 10 p Presented at the International Conference on Mathematics and Computations, Reactor Physics, and Environmental Analyses, Portland, OR, 30 Apr. - 4 May 1995
(Contract W-7405-eng-48)
(DE95-008382; UCRL-JC-118730; CONF-950420-21) Avail: CASI HC A02/MF A01

We describe a point-centered diffusion discretization for 3-D unstructured meshes of polyhedra. The method has several attractive qualities, including second-order accuracy and preservation of linear solutions. A potential drawback to the scheme is that the diffusion matrix is asymmetric, in general. Results of numerical test problems illustrate the behavior of the scheme. DOE

N95-28393# Sandia National Labs., Albuquerque, NM.
APPLICATIONS OF BOUNDARY ELEMENT METHODS ON THE INTEL PARAGON
D. E. Womble, D. S. Greenberg, S. R. Wheat, R. E. Benner, M. S. Ingber (New Mexico Univ., Albuquerque, NM.), G. Henry (INTEL Corp., Beaverton, OR.), and S. Gutpa (INTEL Corp., Beaverton, OR.) 1994 7 p Presented at the Supercomputing 1994 Meeting, Washington, DC, 14-18 Nov. 1994
(Contract DE-AC04-94AL-85000)
(DE94-014135; SAND-94-1566C; CONF-941118-5) Avail: CASI HC A02/MF A01

This paper describes three applications of the boundary element method and their implementations on the Intel Paragon supercomputer. Each of these applications sustains over 99 Gflops/s based on wall-clock time for the entire application and an actual count of flops executed; one application sustains over 140 Gflops/s. These implementations are production quality: each accepts the description of an arbitrary geometry as input and computes the solution to a problem of commercial and research interest. The serial versions of the codes used in one of our applications are in commercial and government use at over forty-five sites for one code and at almost 200 sites for the second code. The common kernel for these applications is a dense equation solver based on LU factorization. It is generally accepted that good performance can be achieved by dense matrix algorithms, but achieving the excellent performance demonstrated here required the development of a variety of special techniques to take full advantage of the power of the Intel Paragon. DOE

N95-28499# Helsinki Univ. of Technology, Espoo (Finland).
LOCAL OPERATORS IN KRYLOV SUBSPACES Research Report
M. Huhtanen Nov. 1994 28 p See also PB94-133170
(PB95-195525; RR-A-339) Avail: CASI HC A03/MF A01

In this paper we shall first collect some definitions and results from the local spectral theory. A motivation is to find a relation between these concepts and the spectrum of the restricted operator on its Krylov subspace. NTIS

N95-28501# Institut des Hautes Etudes Scientifiques, Bures-sur-Yvette (France).
COLLAPSING AND SOLVMANIFOLDS
W. Tuschmann Jan. 1995 21 p
(PB95-196267; IHES/M/95/7) Avail: CASI HC A03/MF A01

The paper is concerned with the study of solv- and infrasolvmanifolds from the point of view of the theory of convergence and collapsing of Riemannian manifolds. NTIS

N95-28507 George Mason Univ., Fairfax, VA. Center for Computational Statistics.
VISUALIZATION METHODS FOR THE EXPLORATION OF HIGH DIMENSIONAL DATA Final Report, 4 Feb. 1991 - 30 Jun. 1994
Edward J. Wegman 16 Feb. 1995 10 p Limited Reproducibility: More than 20% of this document may be affected by microfiche quality
(Contract DAAL03-91-G-0039)
(AD-A291717; ARO-28309.9-MA) Avail: Issuing Activity (Defense Technical Information Center (DTIC))

This project focused on the development of data analysis and statistical methodology which may be characterized by one or more of the properties that they are large in size, high in dimension, and nonhomogeneous. The major thrust is in visualization on of both point clouds and mathematical structures in high dimensions. The specific advances made under this project are three dimensional generalizations of the Andrews plot, the grand tour in k-dimensions, fast algorithms for the pseudo-Grand Tour and structural inference using ridge estimation. DTIC

N95-28611# Institut des Hautes Etudes Scientifiques, Bures-sur-Yvette (France).
KORTEWEG-DE VRIES EQUATION: CONVERGENT BIRKHOFF NORMAL FORM
D. Baettig, T. Kappeler, and B. Mityagin Jan. 1995 27 p Prepared in cooperation with Ohio State Univ.
(PB95-196275; IHES/M/95/5) Avail: CASI HC A03/MF A01

The Korteweg-de Vries equation is a completely integrable Hamiltonian system with the phase space, Hamiltonian and Poisson structure. The function q identically equal to O is an elliptic fixed point. We prove that in a neighborhood of q identically equal to O the Hamiltonian admits a convergent Birkhoff normal form. To the best of our knowledge, this is the first such example in infinite dimension. NTIS

N95-28653# Helsinki Univ. of Technology, Espoo (Finland).
REMARKS ON THE GROWTH OF THE RESOLVENT OPERATORS FOR POWER BOUNDED OPERATORS
O. Nevanlinna Dec. 1994 26 p
(PB95-195418; RR-A-340) Avail: CASI HC A03/MF A01

In this paper the author discusses some quantitative aspects related to power bounded operators T and to the decay of T(sup n)(T-1). First, if the decay of T(sup n)(T-1) is as fast as O(1/n) then quite strong conclusions can be made. The situation can be thought of as a discrete version of analytic semigroups; the author tries to motivate this in section 1 by demonstrating the similarity and lack of it between power boundedness of T and uniform boundedness of e(sup t)(sup cT-1) where c is a constant of modulus 1 and t greater than 0. Section 2 then contains the main result in this direction. Secondly, the so called Kreiss matrix theorem relates bounds for the powers to bounds for the resolvent. The estimate is proportional to the dimension of the space and thus has as such no generalization to operators. However, qualitatively such a result holds in Banach spaces for e.g. Riesz operators: if the resolvent satisfies the resolvent condition, then the operator is power bounded (but without an estimate). The author introduces in section 3 a growth function for bounded operators. This allows one to obtain a result of the form: if the resolvent condition holds and if the growth function is finite at 1, then the powers are bounded and can be estimated. In section 4, in addition to the Kreiss matrix theorem, two other applications of the growth function are given. NTIS

N95-27800*# National Aeronautics and Space Administration. Goddard Space Flight Center, Greenbelt, MD.
A NEW ANGLE ON THE EULER ANGLES
F. Landis Markley and Malcolm D. Shuster (Florida Univ., Gainesville, FL.) *In its* Flight Mechanics/Estimation Theory Symposium 1995 May 1995 p 395-403 (For primary document see N95-27763 09-13)
Avail: CASI HC A02/MF A04

65 STATISTICS AND PROBABILITY

Includes data sampling and smoothing; Monte Carlo method; and stochastic processes.

N95-26347 Institute for Defense Analyses, Alexandria, VA.
A METHOD FOR SIMULATING CORRELATED RANDOM VARIABLES FROM PARTIALLY SPECIFIED DISTRIBUTIONS Final Report, Jan. - Oct. 1994
Philip M. Lurie and Matthew S. Goldberg Oct. 1994 27 p Limited Reproducibility: More than 20% of this document may be affected by microfiche quality
(AD-A288820; IDA-P-2998) Avail: Issuing Activity (Defense Technical Information Center (DTIC))

Historical data from which to develop reliable estimates of the statistical relationships among cost elements are often scarce. Typically, information comes from many different subject-matter experts, who provide at most the moments (mean or median or mode, and possibly variance), distributional form (e.g., beta or triangular), bounds (lowest and highest possible cost), if applicable, and correlation matrix. Eliciting a fully specified multivariate distribution for the entire set of cost elements comprising a system is usually impossible. Therefore, an algorithm is needed for simulating correlated random variables from partially specified, non-normal distributions. This paper presents such an algorithm and explains how it was developed. DTIC

N95-26413 George Mason Univ., Fairfax, VA. Center for Computational Statistics.

FILTERED KERNEL DENSITY ESTIMATION

David J. Marchette (Naval Surface Warfare Center, Dahlgren, VA.), Carey E. Priebe (Johns Hopkins Univ., Baltimore, MD.), George W. Rogers (Naval Surface Warfare Center, Dahlgren, VA.), and Jeffrey L. Solka (Naval Surface Warfare Center, Dahlgren, VA.) Oct. 1994 36 p Limited Reproducibility: More than 20% of this document may be affected by microfiche quality
(Contracts N00014-93-1-0527; N00014-92-J-1303; DAAH04-94-G-0267; DAAL03-94-G-0039)
(AD-A288293; TR-104) Avail: Issuing Activity (Defense Technical Information Center (DTIC))

A modification of the kernel estimator for density estimation is proposed which allows the incorporation of local information about the smoothness of the density. The estimator used a small set of local bandwidths rather than a single global one as in the standard kernel estimator. It uses a set of filtering functions which determines the extent of influence of the local bandwidths. Various versions of the idea are discussed. The estimator is shown to be consistent and is illustrated by comparison to the single bandwidth kernel estimator for the case in which the filter functions are derived from finite mixture models. DTIC

N95-26414 George Mason Univ., Fairfax, VA. Center for Computational Statistics.

PARALLELIZING LOCALLY-WEIGHTED REGRESSION

Julia Corbin Fauntleroy and Edward J. Wegman Oct. 1994 22 p Limited Reproducibility: More than 20% of this document may be affected by microfiche quality
(Contracts N00014-92-J-1303; N00014-93-I-0527; DAAH04-94-G-2067; DAAL03-91-G-0039)
(AD-A288294; TR-102) Avail: Issuing Activity (Defense Technical Information Center (DTIC))

This paper focuses on a nonparametric regression technique known as locally-weighted regression or LOESS. LOESS is a computationally intensive technique which makes it naturally amenable to exploiting high performance computers. In this paper, we explore domain decomposition techniques for LOESS and study the performance of our algorithm on an Intel Paragon XP/S A4 machine. We study both speedup and efficiency as a function of the number of nodes. Certain segments of the LOESS computation are shown to be fruitfully parallelized while others are essentially sequential and cannot be parallelized effectively. DTIC

N95-26415 George Mason Univ., Fairfax, VA. Center for Computational Statistics.

A METHOD TO DETERMINE THE STRUCTURE OF AN UNKNOWN MIXTURE USING THE AKAIKE INFORMATION CRITERION AND THE BOOTSTRAP

Jeffrey L. Solka (Naval Surface Warfare Center, Dahlgren, VA.), Edward J. Wegman, Carey E. Priebe (Johns Hopkins Univ., Baltimore, MD.), Wendy L. Poston (Naval Surface Warfare Center, Dahlgren, VA.), and George W. Rogers (Naval Surface Warfare Center, Dahlgren, VA.) Oct. 1994 30 p Limited Reproducibility: More than 20% of this document may be affected by microfiche quality
(Contracts N00014-92-J-1303; N00014-93-1-0527; DAAH04-94-G-0267; DAAL03-91-G-0039)
(AD-A288295; TR-105) Avail: Issuing Activity (Defense Technical Information Center (DTIC))

Given i.i.d. observations x1,x2,x3,,,,xn drawn from a mixture of normal terms one is often interested in determining the number of terms in the mixture and their defining parameters. Although the problem of determining the number of terms is intractable under the most general assumptions there is hope of elucidating the mixture structure given appropriate caveats on the underlying mixture. This paper examines a new approach to this problem based on the use of Akaike Information Criterion (AIC) based pruning of data driven mixture models which are obtained from resampled data sets. Results of the application of this procedure to artificially generated and real world data sets are provided. DTIC

N95-26457 George Mason Univ., Fairfax, VA. Center for Computational Statistics.

FAST MULTIDIMENSIONAL DENSITY ESTIMATION BASED ON RANDOM-WIDTH BINS

Leonard B. Hearne and Edward J. Wegman Oct. 1994 10 p Limited Reproducibility: More than 20% of this document may be affected by microfiche quality
(Contracts N00014-92-J-1303; MDA904-92-H-3082; DAAL03-91-G-0039; NSF DMS-90-02237)
(AD-A288286) Avail: Issuing Activity (Defense Technical Information Center (DTIC))

Histogram-type density estimators have some notable computational advantages over other forms of density estimation by virtue of the WARPing algorithm. However, traditional fixed-bin-width have less than satisfactory smoothing properties, being too coarse in regions of high density and too fine in regions of low density. Scott (1992) suggests the ASH algorithm as a means of overcoming these problems, but the ASH algorithm is computationally intensive, somewhat negating the benefits of WARPing. Wegman (1975) proposed a variable bin-width technique for one dimensional density estimators and used sieve type methods to show strong consistency results that did not depend on smoothness properties of the underlying density. In this paper, we extend the idea to high-dimensional, variable bin-width meshes. The boundaries of the bins are determined by a random subsampling of the observations. An extension of the WARPing algorithm may still be used for fast computation. We give combinatorial arguments for calculating the number of bins and also the conditional expectation and variance of the number of observations per bin. Conditional on the random hyper-rectangular tessellation, we calculate the maximum likelihood density estimator. DTIC

N95-26478 Maryland Univ., College Park, MD. Computer Vision Lab.

NONLINEAR SCALESPACE VIA HIERARCHICAL STATISTICAL MODELING Technical Report

David Shulman and Tomas Brodsky Oct. 1994 28 p Limited Reproducibility: More than 20% of this document may be affected by microfiche quality
(Contract N00014-93-1-0257)
(AD-A289057; CAR-TR-742; CS-TR-3366) Avail: Issuing Activity (Defense Technical Information Center (DTIC))

Nonlinear scalespace should be based on a hierarchical statistical model of the image intensity function. This model should contain an explicit representation of the multiscale structure of edges and corners. Using this model we can have a non-ad-hoc basis for computing the parameters we need to determine how much smoothing we should do at points that appear to be edge points. We also have a basis for computing the apparent error in our scalespace calculations. Hierarchical statistical modeling is a technique that can be applied to other problems in low-level vision, but in this introductory paper we just present the application of our scalespace theory to image smoothing. DTIC

N95-26733 Missouri Univ., Columbia, MO. Dept. of Statistics.

STATISTICAL THEORY AND RELIABILITY Final Technical Report, 1 Oct. 1992 - 30 Jun. 1994

Asit P. Basu 1 Sep. 1994 3 p Limited Reproducibility: More than 20% of this document may be affected by microfiche quality
(Contract F49620-92-J-0371)
(AD-A288519; TR-1; AFOSR-94-0750TR) Avail: Issuing Activity (Defense Technical Information Center (DTIC))

Here we submit the final report for research carried out at the Department of Statistics, University of Missouri-Columbia during the period October 1, 1992 - July 31, 1994. During this period the Principal Investigator, A. P. Basu, along with his collaborators considered a number of problems in reliability theory. A. P. Basu edited the research monograph Advances in Reliability. Six refereed papers also were published. The titles of these papers are given below: (1) Life Testing and Reliability Estimation with Asymmetric Loss Function; (2) On a test for exponentiality against Monotone Failure Rate; (3) Bayesian Approach to Some Problems in Life Testing and Reliability Estimation; (4) Characterizations of a Family of Bivariate Exponential Distribution; (5) Bayesian Reliability of Stress-Strength Systems; and (6) Some Problems of Safe Dose Estimation. DTIC

N95-26892 Air Force Inst. of Tech., Wright-Patterson AFB, OH. School of Engineering.

EMBEDOLOGY AND NEURAL ESTIMATION FOR TIME SERIES PREDICTION M.S. Thesis

Robert E. Garza Dec. 1994 179 p Limited Reproducibility: More than

20% of this document may be affected by microfiche quality
(AD-A289312; AFIT/GE/ENG/94D-11) Avail: Issuing Activity (Defense Technical Information Center (DTIC))

Time series prediction has widespread application, ranging from predicting the stock market to trying to predict future locations of scud missiles. Recent work by Sauer and Casdagli has developed into the embedology theorem, which sets forth the procedures for state space manipulation and reconstruction for time series prediction. This includes embedding the time series into a higher dimensional space in order to form an attractor, a structure defined by the embedded vectors. Embedology is combined with neural technologies in an effort to create a more accurate prediction algorithm. These algorithms consist of embedology, neural networks, Euclidean space nearest neighbors, and spectral estimation techniques in an effort to surpass the prediction accuracy of conventional methods. Local linear training methods are also examined through the use of the nearest neighbors as the training set for a neural network. Fusion methodologies are also examined in an attempt to combine several algorithms in order to increase prediction accuracy. The results of these experiments determine that the neural network algorithms have the best individual prediction accuracies, and both fusion methodologies can determine the best performance. The performance of the nearest neighbor trained neural network validates the applicability of the local linear training set. DTIC

N95-26913 Helsinki Univ. of Technology, Espoo (Finland). Inst. of Mathematics.
PROBABILISTIC GROWTH MODEL
K. Eloranta Nov. 1994 20 p Limited Reproducibility: More than 20% of this document may be affected by microfiche quality
(PB95-185054; RR-A-338) Avail: CASI HC A03

We study a one-parameter family of probabilistic cellular automata on square and triangular lattices. Above a critical parameter value, a new dominant invariant phase appears, resulting in domain growth. In the growth regime, a second critical threshold is found, above which the expanding domains facet. This phenomenon is shown to be equivalent to a certain one-dimensional directed percolation problem studied by Domany and Kinzel. Tight bounds are given to the critical probabilities which depend on the lattice. These models are of special interest as their behavior corresponds extremely closely to that of certain simple purely deterministic cellular automata. NTIS

N95-27016 Air Force Inst. of Tech., Wright-Patterson AFB, OH.
GENERALIZED PROBABILISTIC REASONING AND EMPIRICAL STUDIES ON COMPUTATIONAL EFFICIENCY AND SCALABILITY M.S. Thesis
Eric P. Baenen Dec. 1994 77 p Limited Reproducibility: More than 20% of this document may be affected by microfiche quality
(AD-A289185; AFIT/GCE/ENG/94D-02) Avail: Issuing Activity (Defense Technical Information Center (DTIC))

Expert systems are tools that can be very useful for diagnostic purposes; however current methods of storing and reasoning with knowledge have significant limitations. One set of limitations involves how to store and manipulate uncertain knowledge: much of the knowledge we are dealing with has some degree of uncertainty. These limitations include lack of complete information, not being able to model cyclic information, and limitations on the size and complexity of the problems to be solved. If expert systems are ever going to be able to tackle significant real world problems then these deficiencies must be corrected. This paper describes a new method of reasoning with uncertain knowledge which improves the computational efficiency as well as scalability over current methods. The cornerstone of this method involves incorporating and exploiting information about the structure of the knowledge representation to reduce the problem size and complexity. Additionally, a new knowledge representation is discussed that will further increase the capability of expert systems to model a wider variety of real world problems. Finally, benchmarking studies of the new algorithm against the old have led to insights into the graph structure of very large knowledge bases. DTIC

N95-27340# International Centre for Theoretical Physics, Trieste (Italy).
ALGEBRAIC STRUCTURE OF THE GREEN'S ANSATZ AND ITS q-DEFORMED ANALOGUE
T. D. Palev Aug. 1994 15 p
(DE95-608780; IC-94/260) Avail: CASI HC A03/MF A01 (US Sales Only)

The algebraic structure of the Green's ansatz is analyzed in such a way that its generalization to the case of q-deformed para-Bose and para-Fermi operators is becoming evident. To this end the underlying Lie (super) algebraic properties of the parastatistics are essentially used. DOE

N95-27417* Carnegie-Mellon Univ., Pittsburgh, PA. Robotics Inst.
TRUNCATED GAUSSIANS AS TOLERANCE SETS
Fabio Cozman and Eric Krotkov 28 Sep. 1994 33 p Limited Reproducibility: More than 20% of this document may be affected by microfiche quality
(Grant NAGw-1175)
(NASA-CR-197732; NAS 1.26:197732; AD-A289357; CMU-RI-TR-94-35)
Avail: Issuing Activity (Defense Technical Information Center (DTIC))

This work focuses on the use of truncated Gaussian distributions as models for bounded data measurements that are constrained to appear between fixed limits. The authors prove that the truncated Gaussian can be viewed as a maximum entropy distribution for truncated bounded data, when mean and covariance are given. The characteristic function for the truncated Gaussian is presented; from this, algorithms are derived for calculation of mean, variance, summation, application of Bayes rule and filtering with truncated Gaussians. As an example of the power of their methods, a derivation of the disparity constraint (used in computer vision) from their models is described. The authors' approach complements results in Statistics, but their proposal is not only to use the truncated Gaussian as a model for selected data; they propose to model measurements as fundamentally in terms of truncated Gaussians. DTIC

N95-27684# Sandia National Labs., Albuquerque, NM.
FITTING: SUBROUTINE TO FIT FOUR-MOMENT PROBABILITY DISTRIBUTIONS TO DATA
S. R. Winterstein, C. H. Lange, and S. Kumar (Stanford Univ., CA.) Jan. 1995 44 p
(Contract DE-AC04-94AL-85000)
(DE95-007722; SAND-94-3039) Avail: CASI HC A03/MF A01

FITTING is a Fortran subroutine that constructs a smooth, generalized four-parameter probability distribution model. It is fit to the first four statistical moments of the random variable X (i.e., average values of X, X(exp 2), X(exp 3), and X(exp 4)) which can be calculated from data using the associated subroutine CALMOM. The generalized model is produced from a cubic distortion of the parent model, calibrated to match the first four moments of the data. This four-moment matching is intended to provide models that are more faithful to the data in the upper tail of the distribution. Examples are shown for two specific cases. DOE

N95-28510 Hampton Univ., VA. Dept. of Mathematics.
A STUDY OF NON-STATIONARY PROCESSES AND THEIR APPLICATIONS Final Report, 1 Sep. 1991 - 31 Jan. 1995
Abol G. Miamee 31 Jan. 1995 6 p Limited Reproducibility: More than 20% of this document may be affected by microfiche quality
(Contract DAAL03-91-G-0238)
(AD-A291725; ARO-28689.4-MA-SDI) Avail: Issuing Activity (Defense Technical Information Center (DTIC))

Some prediction problems of an important class of non-stationary processes, namely periodically correlated processes were studied. DTIC

N95-28526 Columbia Univ., New York, NY. Dept. of Statistics.
STOCHASTIC CONTROL AND TOPICS IN APPLIED PROBABILITY Final Report, 1 Jun. 1991 - 30 Nov. 1994
Ioannis Karatzas Feb. 1995 5 p Limited Reproducibility: More than 20% of this document may be affected by microfiche quality
(Contract DAAL03-91-G-0170)
(AD-A291712; ARO-28715.17-MA) Avail: Issuing Activity (Defense Technical Information Center (DTIC))

Research findings achieved under the auspices of the Army research grant on these topics: Stochastic control under partial observations; Dynamic allocation and Multi-armed Bandit Problems; Deterministic and anticipative aspects of stochastic optimization; Predictable representation properties for semimartingales; The stochastic version of Pontryagin's maximum principle; and Representation of additive functionals of Markov processes are outlined in the final report. DTIC

66 SYSTEMS ANALYSIS

Includes mathematical modeling; network analysis; and operations research.

N95-26613# Helsinki Univ. of Technology, Espoo (Finland). Systems Analysis Lab.
DISTRIBUTED COMPUTATION OF PARETO SOLUTIONS FOR TWO DECISION MAKERS
Harri Ehtamo, Markku Verkama, and Raimo P. Haemaelaeinen Oct. 1994 24 p Sponsored by Vano Tanner Foundation; Finnish Cultural Foundation; Swedish Foundation of Culture in Finland; and Academy of Finland
(ISSN 0782-2030)
(PB95-185047; ISBN-951-22-2337-6) Avail: CASI HC A03/MF A01

The problem of computing Pareto optimal solutions with distributed methods is considered in games with two decision makers (DMs). Distributed computation schemes do not require the DM's to know each others' objective functions. Such procedures are especially relevant in real life situations where the DM's are unwilling or unable to disclose their goals. Problems of this kind include negotiations as well as hierarchical optimization of large-scale systems. NTIS

N95-26912 Helsinki Univ. of Technology, Espoo (Finland). Systems Analysis Lab.
DISTRIBUTED COMPUTATION OF PARETO SOLUTIONS IN N-PLAYER GAMES
M. Verkama, H. Ehtamo, and R. P. Haemaelaeinen Oct. 1994 30 p Limited Reproducibility: More than 20% of this document may be affected by microfiche quality
(PB95-185039; ISBN-951-22-2338-4) Avail: Issuing Activity (National Technical Information Service (NTIS))

The problem of computing Pareto optimal solutions with distributed algorithms is considered in N-player games. We shall first formulate a new geometric problem for finding Pareto solutions. It involves solving joint tangents for the players' objective functions. This problem can then be solved with distributed iterative methods, and two such methods are presented. The principal results are related to the analysis of the geometric problem. We give conditions under which its solutions are Pareto optimal, characterize the solutions, and prove an existence theorem. There are two important reasons for the interest in distributed algorithms. First, they can carry computational advantages over centralized schemes. Second, they can be used in situations where the players do not know each others' objective functions. NTIS

N95-28352# Helsinki Univ. of Technology, Espoo (Finland). Systems Analysis Lab.
DISTRIBUTED METHODS AND PROCESSES IN GAMES OF INCOMPLETE INFORMATION Ph.D. Thesis
M. Verkama Oct. 1994 21 p
(PB95-184842; ISBN-951-22-2340-6) Avail: CASI HC A03/MF A01

One factor limiting the applicability of game theory has been the inadequacy of computational tools for handling real world problems where decision makers have incomplete information. The thesis presents the first approach to computing Pareto optimal game solutions under such circumstances, and thus opens new research possibilities. Moreover, the reachability of Pareto optimal agreements in negotiations is studied under realistic assumptions about information. The methods developed in the thesis may find applications in problems where independent decision makers, each having limited information about the situation, need to cooperate or to reach a joint decision. Another main topic of the thesis is the illumination of the interdisciplinary nature of this problem type. The third topic is the stability of asynchronous iterations that are relevant in game-related reaction processes and in distributed computation. This volume contains a summary of the thesis and lists the titles of the six papers included in PB95-184859. NTIS

N95-28353# Helsinki Univ. of Technology, Espoo (Finland). Systems Analysis Lab.
DISTRIBUTED METHODS AND PROCESSES IN GAMES OF INCOMPLETE INFORMATION Research Report
M. Verkama Oct. 1994 147 p
(PB95-184859; RR-A55) Avail: CASI HC A07/MF A02

One factor limiting the applicability of game theory has been the inadequacy of computational tools for handling real world problems where decision makers have incomplete information. The thesis presents the first approach to computing Pareto optimal game solutions under such circumstances, and thus opens new research possibilities. Moreover, the reachability of Pareto optimal agreements in negotiations is studied under realistic assumptions about information. The methods developed in the thesis may find applications in problems where independent decision makers, each having limited information about the situation, need to cooperate or to reach a joint decision. Another main topic of the thesis is the illumination of the interdisciplinary nature of this problem type. The third topic is the stability of asynchronous iterations that are relevant in game-related reaction processes and in distributed computation. The thesis consists of a summary and the six papers included in this volume. NTIS

67 THEORETICAL MATHEMATICS

Includes topology and number theory.

N95-26538# Institut des Hautes Etudes Scientifiques, Bures-sur-Yvette (France).
NONEXISTENCE OF BILIPSCHITZ PARAMETERIZATIONS AND GEOMETRIC PROBLEMS ABOUT A(SUB INFINITY) WEIGHTS
Stephen Semmes Oct. 1994 45 p
(PB95-185187; IHES/M/94/54) Avail: CASI HC A03/MF A01

How one can recognize when a metric space is bilipschitz equivalent to a Euclidean space is considered. One should not take the abstraction of metric spaces too seriously here; subsets of R(sup n) are already quite interesting. It is easy to generate geometric conditions which are necessary for bilipschitz equivalence, but it is not clear that such conditions should ever be sufficient. The main point of this paper is that the optimistic conjectures about the existence of bilipschitz parameterizations are wrong. In other words, there are spaces whose geometry is very similar to, but still distinct from, Euclidean geometry. Related questions of bilipschitz equivalence and embeddings are addressed for metric spaces obtained by deforming the Euclidean metric on R(sup n) using an A(sub infinity) weight. NTIS

N95-27300# International Centre for Theoretical Physics, Trieste (Italy).
HOLOMORPHIC CURVES IN ABELIAN VARIETIES, PART 1
R. Kobayashi Jul. 1994 10 p
(DE95-608748; IC-94/198) Avail: CASI HC A02/MF A01 (US Sales Only)

We introduce a new technique transforming a holomorphic curve in Abelian varieties into a family of holomorphic maps between appropriate Riemann surfaces. Applying this transformation, we establish the second main theorem for holomorphic curves in Abelian varieties. DOE

N95-27337# Joint Inst. for Nuclear Research, Dubna (USSR). Lab. of Theoretical Physics.
THE HURWITZ-EULERIAN REDUCTION [REDUKTSIYA GURVITSA-EHJLERA]
A. N. Sisakyan and V. M. Ter-Antonyan 1994 6 p In RUSSIAN Submitted for publication
(DE95-608760; JINR-R-5-94-220) Avail: CASI HC A02/MF A01 (US Sales Only)

We show in this paper that the Hurwitz transformation acting in 8-dimensional configuration space induces in a space of the state vectors the rule of reduction identical to the angular momentum addition rule of quantum mechanics. DOE

N95-27341# International Centre for Theoretical Physics, Trieste (Italy).
THE CANONICAL q-TRANSFORMATIONS WITH TWO q-PARA-BOSE OSCILLATORS

Ha Huy Bang Sep. 1994 9 p
(DE95-608781; IC-94/282) Avail: CASI HC A02/MF A01 (US Sales Only)

The canonical q-transformations with two q-para-Bose oscillators are described. It turns out that the two q-oscillators are not exactly independent. DOE

N95-27344# Joint Inst. for Nuclear Research, Dubna (USSR). Lab. of Theoretical Physics.

TRACE ANOMALIES AND COCYCLES OF WEYL AND DIFFEOMORPHISM GROUPS

D. R. Karakhanyan, R. P. Manvelyan, and R. L. Mkrtchyan (Academy of Sciences of the Armenian SSR, Erivan, Armenia.) 1994 6 p Submitted for publication
(DE95-608793; JINR-E-2-94-190) Avail: CASI HC A02/MF A01 (US Sales Only)

The cocycles for the Weyl group, connected with trace anomaly in d = 2 k dimensions are constructed. The general rule for transformation of these cocycles into the cocycles of diffeomorphisms group is found. The general structure of trace anomaly is shown to be a consequence of the Wess-Zumino consistency condition. DOE

N95-27485# International Centre for Theoretical Physics, Trieste (Italy).

HARMONIC MAPS OF THE BOUNDED SYMMETRIC DOMAINS

Y. L. Xin Jun. 1994 19 p
(DE95-608798; IC-94/123) Avail: CASI HC A03/MF A01 (US Sales Only)

A shrinking property of harmonic maps into R(sub IV)(2) is proved which is used to classify complete spacelike surfaces of the parallel mean curvature in R(sup 4)(sub 2) with a reasonable condition on the Gauss image. Liouville-type theorems of harmonic maps from the higher dimensional bounded symmetric domains are also established. DOE

N95-28011 Institut des Hautes Etudes Scientifiques, Bures-sur-Yvette (France).

CRUSHING SINGULARITIES IN SPACETIMES WITH SPHERICAL, PLANE AND HYPERBOLIC SYMMETRY

A. D. Rendall Oct. 1994 21 p Prepared in cooperation with Max-Planck-Inst. Limited Reproducibility: More than 20% of this document may be affected by microfiche quality
(PB95-190146; IHES/P/94/55) Avail: CASI HC A03

It is shown that the initial singularities in spatially compact spacetimes with spherical, plane or hyperbolic symmetry admitting a compact constant mean curvature hypersurface are crushing singularities when the matter content of spacetime is described by the Vlasov equation (collisionless matter) or the wave equation (massless scalar field). In the spherically symmetric case, it is further shown that if the spacetime admits a maximal slice, then there are crushing singularities both in the past and in the future. The essential properties of the matter models chosen are that their energy-momentum tensors satisfy certain inequalities and that they do not develop singularities in a given regular background spacetime. NTIS

N95-28174# Institut des Hautes Etudes Scientifiques, Bures-sur-Yvette (France).

PHOTON ROCKETS AND GRAVITATIONAL RADIATION

T. Damour Nov. 1994 22 p Submitted for publication
(PB95-190161; IHES/P/94/60) Avail: CASI HC A03/MF A01

The absence of gravitational radiation in Kinnersley's 'photon rocket' solution of Einstein's equations is clarified by studying the mathematically well-defined problem of point-like photon rockets in Minkowski space (i.e. massive particles emitting null fluid anisotropically and accelerating because of the recoil). We explicitly compute the (uniquely defined) linearized retarded gravitational waves emitted by such objects, which are the coherent superposition of the gravitational waves generated by the motion of the massive point-like rocket and of those generated by the energy-momentum distribution of the photon fluid. In the special case (corresponding to Kinnersley's solution) where the anisotropy of the photon emission is purely dipolar, we find that the gravitational wave amplitude generated by the energy-momentum of the photons exactly cancels the usual $1/r$ gravitational wave amplitude generated by the accelerated motion of the rocket. More general photon anisotropies would, however, generate genuine gravitational radiation at infinity. Our explicit calculations show the compatibility between the non-radiative character of Kinnersley's solution and the currently used gravitational wave generation formalisms based on post-Minkowskian perturbation theory. NTIS

N95-28234# Texas Univ., Austin, TX. Center for Particle Physics.

COORDINATES OF THE QUANTUM PLANE AS q-TENSOR OPERATORS IN U(SUB q) (su(2) * su(2))

L. C. Biedenharn and M. A. Lohe (Northern Territory Univ., Casuarina, Australia.) 13 Jan. 1995 18 p
(Contract DE-FG03-93ER-40757)
(DE95-007100; DOE/ER-40757/058) Avail: CASI HC A03/MF A01

The relation between the set of transformations M(sub q)(2) of the quantum plane and the quantum universal enveloping algebra U(sub q)(u(2)) is investigated by constructing representations of the factor algebra U(sub q) (u(2) * u(2)). The non-commuting coordinates of M(sub q)(2), on which U(sub q)(2) * U(sub q)(2) acts, are realized as q-spinors with respect to each U(sub q)(u(2)) algebra. The representation matrices of U(sub q)(2) are constructed as polynomials in these spinor components. This construction allows a derivation of the commutation relations of the noncommuting coordinates of M(sub q)(2) directly from properties of U(sub q)(u(2)). The generalization of these results to U(sub q)(u(n)) and M(sub q)(n) is also discussed. DOE

N95-28238 Helsinki Univ., Helsinki (Finland). Dept. of Mathematics.

ABSOLUTE LOGICS Thesis

Jyrki Akkanen and Olli Lehto, ed. 1995 87 p Repr. from Annales Academie Scientiarum Fennice, Series A. 1: Mathematica Dissertationes, 100 (Helsinki, Finland), 1995 p 1-83
(ISSN 0355-0087)
(ISBN-951-41-0775-6) Copyright Avail: Issuing Activity (Helsinki Univ., Helsinki, Finland)

An abstract logic is a formal language which describes mathematical structures. its syntax is formulated by defining which objects are sentences; a semantics for the sentences is introduced by defining when a sentence is true in a structure. Often the semantic overrides the syntax: one is more concerned about the expressive power of a logic than about what objects the sentences really are. However, when necessary, a metatheory is introduced to make things clear in this respect, too. The most used metatheory is set theory: sentences and structures are sets, and abstract logics are defined by set-theoretical predicates. A logic is said to be absolute if its syntax is persistent (every object which is a sentence in a set-theoretical universe is a sentence in extensions of the universe), and if its semantics are absolute (the truth of a sentence in a structure is independent of the set-theoretical universe). In a sense, absoluteness is an abstract notion of 'first-order'. The set-theoretical methods are most useful when applied to absolute logics, especially to those absolute relative to a standard set theory. The first part of this work presents concepts in order to fix terminology and to lay a firm foundation for this study. The second part discusses and proves the absoluteness of several logics. The third part presents the new construction method for translating sentences of an absolute logic into sentences of L(sub infinity omega), a game quantifier logic, or into sentences of the infinitely deep language M(sub infinity infinity). The final part of this work presents applications of this construction method. Derived from text

N95-28518# Joint Inst. for Nuclear Research, Dubna (USSR). Lab. of Theoretical Physics.

THE STRUCTURE OF THE HURWITZ TRANSFORMATION [STRUKTURA PREOBRAZOVANIYA GURVITSA]

A. N. Sisakyan and V. M. Ter-Antonyan 1994 6 p In RUSSIAN Submitted for publication
(DE95-608759; JINR-R-5-94-219) Avail: CASI HC A02/MF A01 (US Sales Only)

It is shown that the Hurwitz transformation includes two structural elements: the conformal transformation of Levi-Civita and the unitary unimodular transformation acting in the space of the Eulerian angular coordinates. DOE

70 PHYSICS (GENERAL)

For precision time and time interval (PTTI) see *35 Instrumentation and Photography;* for geophysics, astrophysics or solar physics see *46 Geophysics, 90 Astrophysics,* or *92 Solar Physics.*

N95-26345 Yale Univ., New Haven, CT. Dept. of Computer Science.
ON THE AZIMUTHAL FOURIER COMPONENTS OF THE GREEN'S FUNCTION FOR THE HELMHOLTZ EQUATION IN THREE DIMENSIONS Research Report
Gregory Matviyenko 9 Dec. 1994 16 p Limited Reproducibility: More than 20% of this document may be affected by microfiche quality
(Contract N00014-89-J-1527; NSF DMS-90-12135)
(AD-A288775; YALEU/DCS/RR-1055) Avail: Issuing Activity (Defense Technical Information Center (DTIC))

Many algorithms that compute acoustic or electromagnetic fields scattered by surfaces of revolution require fast evaluation of the azimuthal Fourier components Gm of the Green's function for the Helmholtz equation in three dimensions. In this paper we derive a recurrence relation for the functions Gm and obtain explicit formulae for their partial derivatives. These observations significantly reduce the complexity of the computation of the scattered fields generated by axisymmetric scatterers. DTIC

N95-26518 Polish Academy of Sciences, Warsaw (Poland). Independent Applied Dynamics Lab.
THE PHENOMENA OF SUBHARMONIC BIFURCATIONS, RUNAWAY, AND TRANSITION TO CHAOS IN A NON-LINEAR OSCILLATOR: PERTURBATION METHODS AND A NUMERICAL EXPERIMENT Ph.D. Thesis [ZJAWISKA BIFURKACJI SUBHARMONICZNYCH, UCIECZKI I PRZEJSCIA DO CHAOSU W NIELINIOWYM OSCYLATORZE METODY PERTURBACYJNE A EKSPERYMENT NUMERCZNY]
Krzysztof L. Janicki Cooperative Publishing House Ltd. Jul. 1994 128 p In POLISH
(ISSN 0208-5658)
(IFTR-16/1994) Avail: Issuing Activity

The importance of non-linear dynamic systems has grown significantly in recent years. And this statement does not merely apply to the development of the discipline per se, but most importantly to the extension of its concepts and results to other sciences, including engineering, biology, and economics. Its results which have demonstrated the complexity of the behavior of relatively simple systems have been especially spectacular. These advances have given researchers the hope that relatively compact non-linear mathematical models might be used for largely qualitative descriptions of a variety of complex phenomena such as hydrodynamic instabilities, population dynamics, or ship disasters. Studies of simple models also seem to constitute a necessary preliminary step for gaining knowledge of the phenomena which occur in more complex systems.
Transl. by Schreiber Translations Inc.

N95-26598# Australian and New Zealand Inst. of Physics (Australia).
THE 18TH ANNUAL CONDENSED MATTER PHYSICS MEETING
Don Chaplin, ed., Wayne Hutchinson, ed., Nick Yazidjoglou, ed., and Glen Stewart, ed. 1994 227 p Conference held in Wagga Wagga, Australia, 9-11 Feb. 1994
(DE95-605568; INIS-MF-14386; CONF-9402112) Avail: CASI HC A11/MF A03 (US Sales Only)

The Handbook contains abstracts of oral and poster presentations covering various aspects of condensed matter physics such as magnetism, superconductivity, semiconductor materials and their properties, as well as the use of nuclear techniques in studies of these materials. 162 contributions have been considered to be in the INIS subject scope and were indexed separately. DOE

N95-26614 National Physical Lab., Teddington (England). Div. of Quantum Metrology.
BIPM PROJECT: INTERCOMPARISON OF WATER TRIPLE-POINT CELLS
M. V. Chattle and J. Butler Dec. 1994 15 p See also PB95-166583
(PB95-185237; NPL-QU-104) Copyright Avail: Issuing Activity (National Technical Information Service (NTIS))

The paper presents the results of an intercomparison between 3 triple point of water cells circulated by the Bureau International des Poids et Measures (BIPM), and a cell which is one of those used as a reference cell at the National Physical Laboratory (NPL). All 4 cells were prepared, stored and measured in the manner normally adopted at NPL. The results of the intercomparison show that over the course of about 6 weeks the temperatures of the 3 circulated cells generally agreed within 0.20 mK, with a maximum difference of 0.27(7) mK. Over the same period, the total variations of temperature measured in the 3 individual cells were 0.04 mK, 0.08 mK and 0.18 mK, respectively; the NPL cell varied by 0.10 mK. Gallium point measurements made over a similar period confirmed that these differences were partly due to small drifts in the thermometer resistance or in the measuring system. NTIS

N95-26687 Rheology Research, Gaithersburg, MD.
VIBRATION CONTROL USING CHAOTIC MOTION STABILIZERS Final Report, Jun. - Dec. 1994
David L. Don and Edward S. Regan 20 Dec. 1994 30 p Limited Reproducibility: More than 20% of this document may be affected by microfiche quality
(Contract DASG60-94-C-0059)
(AD-A289576) Avail: Issuing Activity (Defense Technical Information Center (DTIC))

Chaotic motion stabilizers transform chaotic behavior into predictable periodic motion. Our product enhances the performance of active damping systems, eliminates the need for damping devices in some applications, and increases the variability of passive damping methods. We have based our product on the observance that chaotic attractors typically have infinite numbers of unstable periodic orbits. The device attempts to stabilize existing orbits in the attractor - not create new ones. The process is straight forward. First, determine unstable periodic orbits embedded in the chaotic attractor. Examine these orbits and choose ones that yield improved system performance. Finally, tailor small-time dependent parameter perturbations to stabilize the orbit. To make the necessary system parameter changes that transform chaotic motion into periodic motion, we will utilize electrorheological (ER) materials. For Phase 1 research we modeled the behavior of an ER magnetoelastic system and incorporated our control algorithm into the model. We then compared the theoretical results with experimental testing where similarities were observed. DTIC

N95-27160# International Centre for Theoretical Physics, Trieste (Italy).
THE CONSIDERATION OF A BRIGHT RELATIVE BEAM DYNAMICS IN THE MAGNETIC FOCUSING FIELD
A. I. Borodich Aug. 1994 7 p
(DE95-608377; IC-94/209) Avail: CASI HC A02/MF A01 (US Sales Only)

A bright relative beam being transported by the magnetic focusing field is considered. The description of its dynamics is based on the Lie algebraic methods and the distribution function of particles of a beam is used. The results of numerical simulations in the case of solenoid magnetic focusing are given as a simple example. DOE

N95-27239# Joint Inst. for Nuclear Research, Dubna (USSR).
MATHEMATICAL SIMULATION OF THREE-DIMENSIONAL MAGNETIC FIELD OF SPECTROMETRIC MAGNET SP-40
E. P. Zhidkov, M. B. Yuldasheva, I. P. Yudin, and O. I. Yuldashev 1994 12 p In RUSSIAN
(DE95-608736; JINR-R-11-94-160) Avail: CASI HC A03/MF A01 (US Sales Only)

The results of mathematical simulation of three-dimensional magnetic field of spectrometric magnet SP-40, which is the important part of the experimental setup EXCHARM, are presented. The aims of the communication are the comparison of numerical analysis with data of the measurements and the investigation of distribution of the magnetic field near end region. It has been shown that, in limits of length of the magnet, the computed by program MSFE3D main relative field component and the results of the measurement are agreed on OZ axis with the accuracy approximately equal 10(exp -3). The computations also showed that the absolute values of the relative field components B(sub x)/B(sub 0) and B(sub z)/B(sub 0) near the magnet end are less than 2.7% and 4% accordingly. DOE

N95-27298# Joint Inst. for Nuclear Research, Dubna (USSR).
VECTOR ALGORITHMS FOR SOLVING 3D NONLINEAR MAGNETOSTATIC PROBLEMS
E. P. Zhidkov, M. B. Yuldasheva, and O. I. Yuldashev 1994 18 p
(DE95-608737; JINR-R-11-94-161) Avail: CASI HC A03/MF A01 (US Sales Only)

The differential formulation of the magnetostatic problem using two scalar potentials is considered. The discretization by finite element method reduces the problem to system of the nonlinear equations with sparse matrix. To solve the system some iteration process is used and on each iteration step the solving linearized system is required. For this purpose the vector algorithms are elaborated based on the incomplete Choleski factorization with conjugate gradient method. The use of combination of natural and suggested multicolor ordering of unknowns in the nodes of regular grid allowed one to keep the good qualities of the preconditioner and essentially to increase the degree of vectorization of matrix-vector multiplication and of solving the system with preconditioner. The advantages of the suggested approach are demonstrated on the example of three-dimensional spectrometric magnet field simulation on vector computer CONVEX C 120. The comparison of the computed results for grid consisting of 42120 nodes, when the suggested vector algorithms and the standard algorithms compiled with the vector option are used, showed that the processor time of solving the nonlinear system in the first case is 2.3 times less than in second case. DOE

N95-27398 Army Research Lab., Watertown, MA. Materials Directorate.
A NEW METHOD OF EVALUATING THE EXPLICIT MAGNETIC-STATE-DEPENDENT ENERGY IN SEMI-EMPIRICAL CALCULATIONS OF IRON Final Report, Jul. 1994
Genrich L. Krasko Nov. 1994 20 p Limited Reproducibility: More than 20% of this document may be affected by microfiche quality
(AD-A289098; ARL-TR-650) Avail: Issuing Activity (Defense Technical Information Center (DTIC))

The existing semi-empirical methods for use in atomic computer simulations in iron (such as various modifications of the Embedded Atom Method) have not explicitly taken account of the ferromagnetism per se. Rather, the adjustable parameters just have been fitted to mechanical and thermal properties of iron. However, when the magnetic properties are essential in affecting localized atomic behavior (e.g. in the vicinity of crystal defects), these methods may be inadequate. To remedy the situation, a procedure is suggested of explicitly calculating the magnetic contribution to the energy of individual atoms, as a function of their atomic environment. The method uses the Stoner approach, as previously developed in, and a data base obtained by the LMTO-Stoner calculations on BCC Fe under hydrostatic and tetragonal deformations, and Fe free surfaces. The procedure may be incorporated in any semi-empirical method: the ferromagnetic contributions to the bulk moduli, C11, C12 and C44 are easily calculated and may be subsequently used in adjusting the semi-empirical Method parameters. Preliminary testing shows a good agreement with the magnetic properties obtained by the LMTO-Stoner calculations. DTIC

N95-27530# Fermi National Accelerator Lab., Batavia, IL.
MEASUREMENT OF THE D0 WAMUS MAGNET INDUCTANCE
A. Kristalinski, R. Hance, and W. Jaskierny Dec. 1994 7 p
(Contract DE-AC02-76CH-03000)
(DE95-005128; FNAL-TM-1917) Avail: CASI HC A02/MF A01

Historically, the term inductance, as it relates to magnets, has been relatively obscure at Fermilab. Confusion resulted from the typical engineering approach to the matter, whereby distinction may not have been made between analytical and beam line magnets, and distribution transformers. The latter always have a laminated core to reduce eddy currents which makes their inductance in a transitional state very close to that in a steady state. This is true only if the core material is not in saturation, which is once again the case for transformers, but not for magnets, especially the analytical ones. Based on the traditional 'transformer' thinking, an incorrect method to measure magnet inductance was initially employed. The characteristics of a tank circuit including the magnet under test were observed. Then based on the resonant frequency and quality factor, the inductance was calculated. This method represents a very valuable tool for magnet testing where you can compare newly built magnets to a reference magnet and see if there is any difference. Although electrically correct, this method unfortunately does not reveal any valuable information which could be used to anticipate the magnet behavior under the normal working conditions. Another method of measuring inductance, based on a freewheeling discharge of the magnet, is also widely used in the Lab. To measure the inductance, a magnet is powered from a small power supply from 100 A up to 200 A, then the power is turned off and the current decay in the magnet is recorded. Based on the dc resistance measurements and the magnet current decay data, one can determine the magnet inductance. In order to do so, the inductance is assumed to be constant and current decay is assumed to be exponential. To find out how well the effective inductance represents the real process taking place in the magnet was one of the purposes of the experiment. DOE

N95-27548# Washington Univ., Seattle, WA.
MAGNETIZATION OF FERROMAGNETIC CLUSTERS
Naoki Onishi (Tokyo Univ., Japan.), G. Bertsch, and Kazuhiro Yabana (Niigata Univ., Japan.) 1995 11 p
(Contract DE-FG06-90ER-40561)
(DE95-006878; DOE/ER-40561/179) Avail: CASI HC A03/MF A01

The magnetization and deflection profiles of magnetic clusters in a Stern-Gerlach magnet are calculated for conditions under which the magnetic moment is fixed in the intrinsic frame of the cluster, and the clusters enter the magnetic field adiabatically. The predicted magnetization is monotonic in the Langevin parameter, the ratio of magnetic energy (mu)(sub 0)B to thermal energy k(sub B)T. In low field the average magnetization is 2/3 of the Langevin function. The high-field moment approaches saturation asymptotically as B(sup -1/2) instead of the B(sup -1) dependence in the Langevin function. DOE

N95-27852*# Stanford Research Inst., Menlo Park, CA. Molecular Physics Lab.
SPACE PHYSICS EDUCATIONAL OUTREACH Final Report
Richard A. Copeland May 1995 12 p
(Contract NASw-4621; NAGw-3673; SRI Proj. 4854)
(NASA-CR-198649; NAS 1.26:198649; MP-95-068) Avail: CASI HC A03/MF A01

The goal of this Space Physics Educational Outreach project was to develop a laboratory experiment and classroom lecture on Earth's aurora for use in lower division college physics courses, with the particular aim of implementing the experiment and lecture at Saint Mary's College of California. The strategy is to teach physics in the context of an interesting natural phenomenon by investigating the physical principles that are important in Earth's aurora, including motion of charged particles in electric and magnetic fields, particle collisions and chemical reactions, and atomic and molecular spectroscopy. As a by-product, the undergraduate students would develop an appreciation for naturally occurring space physics phenomena.
Derived from text

N95-28108# Lawrence Livermore National Lab., Livermore, CA.
WHIRL PLUS TILT
T. K. Fowler 12 Oct. 1994 14 p
(Contract W-7405-eng-48)
(DE95-007948; UCRL-ID-118981) Avail: CASI HC A03/MF A01

It is shown that, for an idealized rotor with identical magnetic bearings of negligible mass, precession and rotation are decoupled from the center-of-mass motion so that stabilization of whirl instabilities can be designed independent of tilt. The bearing torques that cause whirl also apply torques on the free-body-rotational motion in a tilted state. The rotational equations of motion including these torques are given in the paper. An approximate solution for a special case suggests the possibility of tilt instability above a critical frequency. DOE

N95-28109# Lawrence Livermore National Lab., Livermore, CA.
PERFORMANCE ANALYSIS OF BULLET TRAJECTORY ESTIMATION: APPROACH, SIMULATION, AND EXPERIMENTS
L. C. Ng and T. J. Karr Nov. 1994 35 p
(Contract W-7405-eng-48)
(DE95-007949; UCRL-ID-119289) Avail: CASI HC A03/MF A01

This paper describes an approach to estimate a bullet's trajectory from a time sequence of angles-only observations from a high-speed camera, and analyzes its performance. The technique is based on fitting a ballistic model of a bullet in flight along with unknown source location parameters to a time series of angular observations. The theory is developed to precisely reconstruct, from firing range geometry, the actual bullet trajectory as it appeared on the focal plane array and in real space. A metric for measuring the effective trajectory track error is also presented. Detailed Monte-Carlo simulations assuming different bullet ranges, shot-angles, camera frame rates, and angular noise show that angular track error can be as small as 100 micro rad for a 2 meter rad/pixel sensor. It is also shown that if actual values of bullet ballistic parameters were available, the bullet s source location variables, and the angles of flight information could also be determined. DOE

N95-28350# International Centre for Theoretical Physics, Trieste (Italy).
TEMPERATURE DEPENDENCE OF THE STATIC DIELECTRIC RESPONSE IN A Q1D ELECTRON GAS
J. Tutor, P. Pajon, and F. Comas Aug. 1994 8 p
(DE95-609269; IC-94/222) Avail: CASI HC A02/MF A01 (US Sales Only)

We show results for the Static Polarization and Static Dielectric Function of a Q1DEG (Quasi-One-Dimensional-Electron-Gas) in the finite temperature case. Calculations are made in a Lindhard-like approach considering the Q1DEG of a semiconductor Quantum-Wire including some simplifying assumptions of the electron band structure. Temperature dependence is discussed using two different approaches: the Maldague's approximation and the 'exact' calculation considering Fermi-Dirac statistics directly. Both kinds of results are compared in details in the low temperature range. DOE

N95-28579 Air Force Inst. of Tech., Wright-Patterson AFB, OH.
VISUALIZATION OF FINITE ELEMENT MODEL SOLUTIONS FOR DEFIBRILLATION VOLTAGE AND CURRENT DISTRIBUTIONS M.S. Thesis
Steven J. Jantz Dec. 1994 70 p Limited Reproducibility: More than 20% of this document may be affected by microfiche quality
(AD-A289836; AFIT/CI/CIA/94-161) Avail: Issuing Activity (Defense Technical Information Center (DTIC))

The objective of this project was to begin filling the need for visualization. A set of tools has been developed to aid in analyzing the results of our FEM computations. Tools facilitating the display of both scalar and vector quantities were included. The toolset was developed utilizing the graphics routines and features available in a commercial scientific visualization package - the Application Visualization System (AVS) . The attempt was made to give the user as much control over the visualization environment as possible with a minimum amount of knowledge of the underlying software. The project was begun on an IBM RS6OOO computer. During the toolset development, the work was ported to a SUN SPARCstation 20 and it was completed there. This thesis describes the development of these visualization tools for use in the AVS environment. DTIC

N95-27801*# National Aeronautics and Space Administration. Goddard Space Flight Center, Greenbelt, MD.
A MAGNETIC HYSTERESIS MODEL
Thomas W. Flatley and Debra A. Henretty *In its* Flight Mechanics/Estimation Theory Symposium 1995 May 1995 p 405-415
(For primary document see N95-27763 09-13)
Avail: CASI HC A03/MF A04

71 ACOUSTICS

Includes sound generation, transmission and attenuation.
For noise pollution see *45 Environmental Pollution.*

N95-26358 Polish Academy of Sciences, Warsaw (Poland).
SELF-EXCITED OSCILLATIONS IN A DUCT WITH CLOSED BRANCES [OSCYLACJE SAMOWZBUDNE W RUROCIAGU Z ZAMKNIETYMI ODGALEZIENIAMI]
Miroslaw Meissner 1994 41 p In POLISH
(ISSN 0208-5658)
(IFTR-18/1994) Avail: Issuing Activity (Polish Academy of Sciences, Warsaw, Poland)

This article contains the results of studies of the generation of self-excited oscillations in a duct with closed branches. The study involved measuring the frequency and amplitude of acoustic oscillations in three different experimental systems, namely a duct with one branch, a duct with two differently oriented branches, and a duct with three branches. Tests of the duct with two branches revealed that significant variations of the frequency of the oscillations occur in the same ranges of branch lengths where the excitation of acoustic oscillations occurs in the case of a duct with a single branch. This means that these frequency variations are due to feedback between the acoustic signals in the two branches. For certain branch lengths, this effect either results in greater or lower amplitude for the oscillations. This is especially obvious for a duct with three branches, where with certain branch lengths the oscillations are either greatly amplified (about 5 dB) or completely damped (about 25 dB for the discrete component). Under damping conditions, the reduction in the overall noise level in the duct is approximately 15 dB. Transl. by Schreiber Translations Inc.

N95-26392*# National Aeronautics and Space Administration. Langley Research Center, Hampton, VA.
AIRCRAFT NOISE PREDICTION PROGRAM THEORETICAL MANUAL: ROTORCRAFT SYSTEM NOISE PREDICTION SYSTEM (ROTONET), PART 4
Donald S. Weir (Lockheed Engineering and Sciences Co., Hampton, VA.), Stephen J. Jumper (Lockheed Engineering and Sciences Co., Hampton, VA.), Casey L. Burley (Lockheed Engineering and Sciences Co., Hampton, VA.), and Robert A. Golub Apr. 1995 270 p
(RTOP 532-06-37-01)
(NASA-TM-83199-Pt-4; L-16700-Pt-4; NAS 1.15:83199-Pt-4) Avail: CASI HC A12/MF A03

This document describes the theoretical methods used in the rotorcraft noise prediction system (ROTONET), which is a part of the NASA Aircraft Noise Prediction Program (ANOPP). The ANOPP code consists of an executive, database manager, and prediction modules for jet engine, propeller, and rotor noise. The ROTONET subsystem contains modules for the prediction of rotor airloads and performance with momentum theory and prescribed wake aerodynamics, rotor tone noise with compact chordwise and full-surface solutions to the Ffowcs-Williams-Hawkings equations, semiempirical airfoil broadband noise, and turbulence ingestion broadband noise. Flight dynamics, atmosphere propagation, and noise metric calculations are covered in NASA TM-83199, Parts 1, 2, and 3. Author

N95-26394*# National Aeronautics and Space Administration. Langley Research Center, Hampton, VA.
A FINITE ELEMENT PROPAGATION MODEL FOR EXTRACTING NORMAL INCIDENCE IMPEDANCE IN NONPROGRESSIVE ACOUSTIC WAVE FIELDS
Willie R. Watson, Michael G. Jones (Lockheed Engineering and Sciences Co., Hampton, VA.), Sharon E. Tanner, and Tony L. Parrott Apr. 1995 21 p
(RTOP 537-02-22-02)
(NASA-TM-110160; NAS 1.15:110160) Avail: CASI HC A03/MF A01

A propagation model method for extracting the normal incidence impedance of an acoustic material installed as a finite length segment in a wall of a duct carrying a nonprogressive wave field is presented. The method recasts the determination of the unknown impedance as the minimization of the normalized wall pressure error function. A finite element propagation model is combined with a coarse/fine grid impedance plane search technique to extract the impedance of the material. Results are presented for three different materials for which the impedance is known. For each material, the input data required for the prediction scheme was computed from modal theory and then contaminated by random error. The finite element method reproduces the known impedance of each material almost exactly for random errors typical of those found in many measurement environments. Thus, the method developed here provides a means for determining the impedance of materials in a nonprogressirve wave environment such as that usually encountered in a commercial aircraft engine and most laboratory settings. Author

N95-26502 Department of the Navy, Washington, DC.
ULTRASONIC TEST SYSTEM Patent
Anthony Smith, inventor (to Navy), Dan Goff, inventor (to Navy), Roman Kruchowy, inventor (to Navy), and Carl Rhoads, inventor (to Navy) 23 Aug. 1994 62 p Filed 13 Oct. 1993
(AD-D017261; US-Patent-5,339,691; US-Patent-Appl-SN-138042; US-Patent-Class-73-597) Avail: US Patent and Trademark Office

An ultrasonic system for determining the quality of concrete under water without inaccuracies caused by electromagnetic interference from the ultrasonic generator. An ultrasonic generator applies pulses to the concrete. An ultrasonic detector detects the ultrasonic pulses and produces corresponding signals that are indicative of ultrasonic pulses that have passed through the material. Signal processing circuitry processes the signals to determine the transit time of the ultrasonic pulses through the material. The signal processing circuitry is disabled for a predetermined time after application of each ultrasonic pulse to the material to prevent noise produced by the means for applying ultrasonic pulses to the material from entering the signal processing circuitry and causing spurious measurements. DTIC

N95-26519 Polish Academy of Sciences, Warsaw (Poland). Acoustoelectronics Center.
THE USE OF ACOUSTIC METHODS TO DETERMINE THE PARAMETERS OF POROUS MATERIALS [WYZNACZANIE PARAMETROW MATERIALOW POROWATYCH METODAMI AKUSTYCZNYMI]
Ignacy Malecki and Jerzy Ranachowski 1994 22 p In POLISH
(ISSN 0208-5658)
(IFTR-40/1994) Avail: Issuing Activity (Polish Academy of Sciences, Warsaw, Poland)

Porous media are a subject of research in a variety of scientific disciplines, including physics, mechanics, electrical engineering, materials science, and acoustics. The subject of this article is a comparison of the methods used in theoretical mechanics with standard acoustic methods. The authors start by examining the method of static averaging of the mechanical properties of porous media. This method makes it possible to determine substitute static moduli of elasticity, which, however, does not meet the needs of acoustics. More suitable methods include the dynamic methods developed in the works of J. Lewandowski, among others. These methods are based on a motion equation in which the tensor of elasticity is assigned a complex value which accounts for the medium's dynamic properties and losses. The transition from a complex tensor of elasticity to the velocity and damping of an acoustic wave poses no particular problems. On the backdrop of the theory of porous materials used in mechanics, the authors present their own theory for the acoustic properties of these materials. They call it the theory of 'compound obstacles', which initially examines the interference offered by a solitary inclusion in a homogeneous medium to the propagation of an acoustic wave. This is followed by the calculation of the interference caused by a group of inclusions using the concept of the density of obstacles. In turn, this leads to general formulas for acoustic wave velocity and damping as functions of obstacle density. The authors consider examples of a spherical inclusion in a liquid and a hollow spheroidal inclusion in a solid. The article also contains the results of experiments conducted to verify the 'compound obstacles' theory. The authors measured the velocity of an ultrasound wave in electrical engineering porcelain with varying degrees of porosity and in glycerine in which glass balls were suspended. Transl. by Schreiber Translations Inc.

N95-26615 National Physical Lab., Teddington (England). Div. of Radiation Science and Acoustics.
UNCERTAINTIES IN THE CALIBRATION OF HYDROPHONES AT NPL BY THE THREE-TRANSDUCER SPHERICAL-WAVE RECIPROCITY METHOD IN THE FREQUENCY RANGE 10 kHz ON 500 kHz
S. P. Robinson and G. R. Dore Nov. 1994 58 p
(PB95-185245; NPL-RSA(EXT)0054) Avail: Issuing Activity (National Technical Information Service (NTIS))

A description is given of the calibration of hydrophones at NPL by the method of three-transducer spherical-wave reciprocity in the frequency range 10-500 kHz. This is used as the primary standard method for the calibration of hydrophones for underwater acoustics. An assessment is given of the sources of uncertainty present in the method and it is shown that with careful implementation, it is possible to calibrate reference hydrophones over this frequency range to an accuracy of +/- 0.5 dB or better (expressed for a confidence probability of 95%). In addition, a comparison has been made of hydrophone calibrations performed by the reciprocity method and the method of optical interferometry, in the frequency range 200-500 kHz. The comparison has shown agreement within the combined uncertainties of the two methods. NTIS

N95-26801*# National Aeronautics and Space Administration. Lewis Research Center, Cleveland, OH.
SUPERSONIC COAXIAL JET NOISE PREDICTIONS
Milo D. Dahl and Philip J. Morris (Pennsylvania State Univ., University Park, PA.) May 1995 12 p Presented at the First Joint Aeroacoustics Conference, Munich, Germany, 12-15 Jun. 1995; sponsored by CEAS and AIAA
(RTOP 505-62-52)
(NASA-TM-106917; E-9584; NAS 1.15:106917; CEAS/AIAA-95-171) Avail: CASI HC A03/MF A01

Predictions are made for the noise radiation from supersonic, coaxial jets. These predictions are based on the assumption that the noise radiation in the downstream direction of supersonic jets is dominated by sound generated by instability waves with supersonic phase velocities relative to ambient. Since the analysis requires a known mean flow and the coaxial jet mean flow is not described easily in terms of analytical functions, a numerical prediction is made for its development. The compressible, Reynolds averaged, boundary layer equations are solved with a modified mixing length turbulence model. The model has been calibrated to account for compressibility and temperature effects on the rate of mixing. Both normal and inverted velocity profile jets are considered. Predictions are made for the differences between the noise radiated by coaxial jets with difference operating conditions and a single reference jet with the same thrust, mass flow, and exit area. The effects of area ratio changes and simulated enhanced mixing on noise radiation are also considered. Author

N95-26857 Air Force Systems Command, Wright-Patterson AFB, OH. National Air Intelligence Center.
MODULATION EFFECT OF A BRAGG ACOUSTO-OPTIC BISTABLE SYSTEM
Zhiren Zheng and Jinyue Gao 10 Nov. 1994 14 p Transl. into ENGLISH from Guangxue Xuebao (China), v. 10, no. 1, Jan. 1990 p 7-13 Limited Reproducibility: More than 20% of this document may be affected by microfiche quality
(AD-A289622; NAIC-ID(RS)T-0382-94) Avail: Issuing Activity (Defense Technical Information Center (DTIC))

The linear stability and the modulation effect of Bragg acousto-optic bistable systems are analyzed. According to the dynamic and stationary equations describing the system, the boundary for instability has been calculated. When the input intensity undergoes a sinusoidal modulation, we predict the resonance and shift of resonance peak of the output intensity in the stable region and the appearance of frequency looping phenomena in the unstable region. DTIC

N95-26925 Catholic Univ. of America, Washington, DC.
[NUMERICAL ANALYSIS OF WAVE SCATTERING] Progress Report, 1 Nov. - 31 Dec. 1994
Mark J. Beran 31 Dec. 1994 5 p Limited Reproducibility: More than 20% of this document may be affected by microfiche quality
(Contract N00014-94-1-0201)
(AD-A289478) Avail: Issuing Activity (Defense Technical Information Center (DTIC))

The following topics were studied in detail during the report period: (1) Combined volume and surface scattering in a channel, using a modal formulation. (2) Two-way formulation to account for backscattering in a channel. (3) Data analysis to determine vertical and horizontal correlation lengths of the random index-of-refraction fluctuations in a channel. (4) The effect of random fluctuations on the two-frequency coherence function in a shallow channel. (5) Approximate eigenfunctions and eigenvalues for linear sound-speed profiles. (6) The effect of sea-water absorption on scattering in a shallow channel. DTIC

N95-27908*# National Aeronautics and Space Administration. Langley Research Center, Hampton, VA.
A NUMERICAL STUDY OF FUNDAMENTAL SHOCK NOISE MECHANISMS Ph.D. Thesis - Cornell Univ.
Kristine R. Meadows May 1995 193 p Original contains color illustrations
(NASA-TM-110608; NAS 1.15:110608) Copyright Avail: CASI HC A09/MF A03; 17 functional color pages

The results of this thesis demonstrate that direct numerical simulation can predict sound generation in unsteady aerodynamic flows containing shock waves. Shock waves can be significant sources of sound in high speed jet flows, on helicopter blades, and in supersonic combustion inlets. Direct computation of sound permits the prediction of noise levels in the preliminary design stage and can be used as a tool to focus experimental studies, thereby reducing cost and increasing the probability of a successfully quiet product in less time. This thesis reveals and investigates two mechanisms fundamental to sound generation by shocked flows: shock motion and shock deformation. Shock motion is modeled by the interaction of a sound wave with a shock. During the interaction, the shock wave begins to move and the sound pressure is amplified as the wave passes through the shock. The numerical approach presented in this thesis is validated by the comparison of results obtained in a quasi-one dimensional simulation with linear theory. Analysis of the perturbation energy demonstrated for the first time that acoustic energy is generated by the interaction. Shock deformation is investigated by the numerical simulation of a ring vortex interacting with a shock. This interaction models the passage of turbulent structures through the shock wave. The simulation demonstrates that both acoustic waves and contact surfaces are generated downstream during the interaction. Analysis demonstrates that the acoustic wave spreads cylindrically, that the sound intensity is highly directional, and that the sound pressure level increases significantly with increasing shock strength. The effect of shock strength on sound pressure level is consistent with experimental observations of shock noise, indicating that the interaction of a ring vortex with a shock wave correctly models a dominant mechanism of shock noise generation. Author (revised)

N95-28073*# Douglas Aircraft Co., Inc., Long Beach, CA.
AIRCRAFT IR/ACOUSTIC DETECTION EVALUATION. VOLUME 2: DEVELOPMENT OF A GROUND-BASED ACOUSTIC SENSOR SYSTEM FOR THE DETECTION OF SUBSONIC JET-POWERED AIRCRAFT
Robert E. Kraft (General Electric Co., Cincinnati, OH.) Dec. 1992 85 p
(Contract NAS1-19060; RTOP 505-63-70-02)
(NASA-CR-189705-Vol-2; NAS 1.26:189705-Vol-2) Avail: CASI HC A05/MF A01

The design and performance of a ground-based acoustic sensor system for the detection of subsonic jet-powered aircraft is described and specified. The acoustic detection system performance criteria will subsequently be used to determine target detection ranges for the subject contract. Although the defined system has never been built and demonstrated in the field, the design parameters were chosen on the basis of achievable technology and overall system practicality. Areas where additional information is needed to substantiate the design are identified. Author

N95-28264*# United Technologies Research Center, East Hartford, CT.
EVALUATION OF A DOUBLY-SWEPT BLADE TIP FOR ROTORCRAFT NOISE REDUCTION Report, 20 Nov. 1990 - 15 Oct. 1992
Brian E. Wake and T. Alan Egolf Oct. 1992 65 p
(Contract NAS1-19143)
(NASA-CR-189677; NAS 1.26:189677) Avail: CASI HC A04/MF A01

A computational study was performed for a doubly-swept rotor blade tip to determine its benefit for high-speed impulsive (HSI) and blade-vortex interaction (BVI) noise. This design consists of aft and forward sweep. For the HSI-noise computations, unsteady Euler calculations were performed for several variations to a rotor blade geometry. A doubly-swept planform was predicted to increase the delocalizing Mach number to 0.94 (representative of a 200+ kt helicopter). For the BVI-noise problem, it had been hypothesized that the doubly-swept blade tip, by producing a leading-edge vortex, would reduce the tip-vortex effect on BVI noise. A procedure was used in which the tip vortex velocity profile computed by a Navier-Stokes solver was used to compute the inflow associated with BVI. This inflow was used by a Euler solver to compute the unsteady pressures for an acoustic analysis. The results of this study were inconclusive due to the difficulty in accurately predicting the viscous tip vortex downstream of the blade. Also, for the condition studied, no leading-edge vortex formed at the tip. Author

N95-28505 Rensselaer Polytechnic Inst., Troy, NY.
ANALYTICAL INVESTIGATIONS OF THE ACCELERATION SENSITIVITY OF ACOUSTIC BULK AND SURFACE WAVE RESONATORS Final Report, 1 May 1991 - 30 Sep. 1994
Harry F. Tiersten Feb. 1995 5 p Limited Reproducibility: More than 20% of this document may be affected by microfiche quality
(Contract DAAL03-91-G-0120)
(AD-A291715; ARO-28591.8-PH) Avail: Issuing Activity (Defense Technical Information Center (DTIC))

Earlier work has shown that the acceleration sensitivity of contoured SC-cut quartz resonators vanishes for perfect symmetry of the resonator plus support system. Since it is impossible to construct such a configuration in practice, a stiffened structure which reduces the increase in acceleration sensitivity with fabrication error hag been investigated. Calculations of the increase in acceleration sensitivity with fabrication error have been performed. The calculations reveal that a rectangular support configuration with an aspect ratio of 1.5 oriented in a specific direction yields optimal results. The calculations also show that two clips should be used on each of the large sides with one on each of the small sides. Optimal clip sizes and spacings between the clips were established. The use of this stiffened configuration should enable consistently low acceleration sensitivities to be obtained. Analyses of flat and contoured quartz resonators with beveled edges has been performed. The influence of the contouring and the beveling on the radial dependence of the modes was obtained. DTIC

N95-28622 Sonoquest/Advanced Ultrasonics Research, Wellesley Hills, MA.
ULTRASONIC STUDIES OF LIQUID/SOLID SEIMOACOUSTIC WAVE PHENOMENA Final Report, Apr. 1992 - Oct. 1994
Jacques R. Chamuel Nov. 1994 76 p Limited Reproducibility: More than 20% of this document may be affected by microfiche quality
(Contract N00014-92-C-0028)
(AD-A289644; JRC-36-94) Avail: Issuing Activity (Defense Technical Information Center (DTIC))

New ultrasonic modeling findings are presented contributing to ten fundamental problems related to low-frequency seismoacoustic wave phenomena resulting from the interaction of underwater acoustic waves with heterogeneous elastic boundaries such as the ice cover and/or ocean bottom. The results are described in ten independent sections covering the following problems: (1) backscattering of Scholte waves and grazing underwater acoustic waves by a trench at a liquid/solid interface; (2) explanation for observed underwater acoustic backscatter from the Canada Basin near 73.2 deg N, 139 deg W where recent bathymetric charts do not reveal the existence of large bathymetric highs nearby; (3) effect of a thin low-velocity layer underneath a floating plate on flexural wave dispersion; (4) effect of viscous waves from suspended particles in a thin layer under sea ice on low-frequency underwater acoustic wave reflectivity; (5) comparison of experimental and theoretical results on the dispersion of antisymmetric edge waves along apex of truncated elastic wedge; (6) wave propagation along apex of free and immersed elastic wedge with range-dependent apex angle and cross section; (7) shear wave coupling to ice cores; (8) ultrasonic characterization of sea ice cores; (9) monostatic seismic profiling using scattering from 45 deg oblique cylindrical hole in ice plate using one compressional transducer; and (10) sea ice finger-rafting and ice thickness. DTIC

N95-28670*# Boeing Commercial Airplane Co., Seattle, WA.
NOISE EXPOSURE REDUCTION OF ADVANCED HIGH-LIFT SYSTEMS
Stephen W. Haffner May 1995 22 p
(Contract NAS1-20090; RTOP 538-03-15-01)
(NASA-CR-195077; NAS 1.26:195077) Avail: CASI HC A03/MF A01

The purpose of NASA Contract NAS1-20090 Task 3 was to investigate the potential for noise reduction that would result from improving the high-lift performance of conventional subsonic transports. The study showed that an increase in lift-to-drag ratio of 15 percent would reduce certification noise levels by about 2 EPNdB on approach, 1.5 EPNdB on cutback, and zero EPNdB on sideline. In most cases, noise contour areas would be reduced by 10 to 20 percent. Author

N95-28671 Air Force Systems Command, Wright-Patterson AFB, OH. National Air Intelligence Center.
METHOD OF SPACE-TIME SEQUENCE TRANSFORM USED TO MEASURE ACOUSTO-OPTIC DEFLECTION AND MODULATION
Feng Bihua, Pen Zhiping, and Huang Zonghua 16 Dec. 1994 13 p
Transl. into ENGLISH from Nanjing Daxue Xuebao, China, v. 27, no. 3, Jul. 1991 p 599-603 Limited Reproducibility: More than 20% of this

document may be affected by microfiche quality
(AD-A289612; NAIC-ID(RS)T-0384-94) Avail: Issuing Activity (Defense Technical Information Center (DTIC))

This paper describes that the method of spatial sequence to be transformed into time sequence is used to measure the complete picture of the a-f curve that is of realtime. series and stability. This method is also used to measure dynamical process of variation in distribution of relative intensity of light, which varies with plate current as Bragg's diffraction. The experimental results coincide with the theory of acousto-optics interaction. DTIC

N95-27990*# Bionetics Corp., Hampton, VA.
MEASUREMENT AND PREDICTION OF BROADBAND NOISE FROM LARGE HORIZONTAL AXIS WIND TURBINE GENERATORS
F. W. Grosveld, K. P. Shepherd, and H. H. Hubbard (College of William and Mary, Williamsburg, VA.) *In* DASCON Engineering, Collected Papers on Wind Turbine Technology May 1995 p 211-220 (For primary document see N95-27970 09-44)
Avail: CASI HC A02/MF A03

N95-27991*# Midwest Research Inst., Golden, CO.
OBSERVED ACOUSTIC AND AEROELASTIC SPECTRAL RESPONSES OF A MOD-2 TURBINE BLADE TO TURBULENCE EXCITATION
N. D. Kelley, H. E. McKenna, and E. W. Jacobs *In* DASCON Engineering, Collected Papers on Wind Turbine Technology May 1995 p 221-227 (For primary document see N95-27970 09-44)
(Contracts DE-AC02-83CH-10093; EG-77-C-01-4042)
Avail: CASI HC A02/MF A03

N95-27992*# Massachusetts Inst. of Tech., Cambridge, MA.
ANECHOIC WIND TUNNEL STUDY OF TURBULENCE EFFECTS ON WIND TURBINE BROADBAND NOISE
B. Loyd and W. L. Harris *In* DASCON Engineering, Collected Papers on Wind Turbine Technology May 1995 p 229-236 Presented at the DOE/NASA Workshop on Horizontal Axis Wind Turbine Technology, Cleveland, OH, 8-10 May 1984 (For primary document see N95-27970 09-44)
(Grant NAG3-378)
Avail: CASI HC A02/MF A03

72 ATOMIC AND MOLECULAR PHYSICS

Includes atomic structure, electron properties, and molecular spectra.

N95-26437# International Centre for Theoretical Physics, Trieste (Italy).
ATOMIC AND ELECTRONIC STRUCTURE OF CLUSTERS FROM CAR-PARRINELLO METHOD
Vijay Kumar Jun. 1994 53 p Sponsored by the International Atomic Energy Agency and the United Nations Educational Scientific and Cultural Organization
(DE94-634463; IC-94/127) Avail: CASI HC A04/MF A01 (US Sales Only)

With the development of ab-initio molecular dynamics method, it has now become possible to study the static and dynamical properties of clusters containing up to a few tens of atoms. Here I present a review of the method within the framework of the density functional theory and pseudopotential approach to represent the electron-ion interaction and discuss some of its applications to clusters. Particular attention is focussed on the structure and bonding properties of clusters as a function of their size. Applications to clusters of alkali metals and Al, non-metal - metal transition in divalent metal clusters, molecular clusters of carbon and Sb are discussed in detail. Some results are also presented on mixed clusters. DOE

N95-26466 Denver Univ., Denver, CO. Dept. of Chemistry.
ENERGY TRANSFER FROM EXCITED NITRENES AT HIGH DENSITY Final Report
Robert D. Coombe 4 Nov. 1994 23 p Limited Reproducibility: More than 20% of this document may be affected by microfiche quality
(Contract F49620-93-1-0187)
(AD-A288352; AFOSR-94-0753TR) Avail: Issuing Activity (Defense Technical Information Center (DTIC))

This report describes the results of a sixteen month program which supplemented a broader effort dealing with reactions and energy transfer processes of excited nitrenes (AFOSR grant no. F4962O-92-J-027O). This supplemental program was directed specifically toward the generation of NCl(a(1)delta) at high densities, and its energy transfer process with iodine atoms. In one task, NCl(a(1)delta) was created by pulsed photolysis of ClN3. This effort was quite successful in that high densities of both NCl(a(1)delta) and excited I(5()2P) were generated. A second task involved continuous generation of NCl(a(1)delta) by the H + NCl3 reaction in a fast discharge-flow reactor. Although high densities of reagents were achieved, the yield of NCl(a)1)delta) was small. Extensive modeling indicated that the low yield was likely caused by loss of NCl(a(1)delta), NCl3, or NCl2 at the reactor walls. DTIC

N95-26491 Northwestern Univ., Evanston, IL. Dept. of Chemistry.
TOWARD MOLECULAR SELECTIVITY WITH CHEMICALLY MODIFIED ELECTRODES: CAN ELECTROACTIVITY AND PERMEABILITY THROUGH AN OVERLAYING METALLOPOLYMER FILM BE CONTROLLED VIA RATIONAL MANIPULATION OF INTERNAL ARCHITECTURE?
Susan G. Yan and Joseph T. Hupp 30 Nov. 1994 26 p Submitted for publication Limited Reproducibility: More than 20% of this document may be affected by microfiche quality
(Contract N00014-91-J-1035)
(AD-A288719; TR-21) Avail: Issuing Activity (Defense Technical Information Center (DTIC))

Metallopolymeric films featuring widely varying metal-to-metal linkage lengths have been prepared via a combination of oxidative and reductive electropolymerization schemes. Each of the film materials exhibits strong size selective permeability behavior towards molecular reactants - providing a primitive physical basis, therefore, for selectivity with respect to reactivity at an underlying electrode. Surprisingly, the observed molecular size cutoffs are essentially independent of film composition, implying that a uniform molecular cavity or pore size exists. Attempts to modify effective pore sizes by introducing large ligand substituents (phenyl groups) at the monomer synthesis stage have failed to alter the pattern of size selectivity. We speculate that: (1) potential pore size expansion effects expected from linkage length extension are offset by enhanced cross linking, and/or (2) electrolyte anion templating effects during film synthesis may be defining the effective minimum pore size, thereby yielding uniform permeation size cutoffs. DTIC

N95-26542# International Centre for Theoretical Physics, Trieste (Italy).
MONTE CARLO STUDY OF ELECTRON-PLASMON SCATTERING EFFECTS ON HOT ELECTRON TRANSPORT IN GaAs
V. V. Popov, T. Yu. Bagaeva (Academy of Sciences, Russia, Saratov, Russia.), and T. I. Solodkaya (Academy of Sciences, Russia, Saratov, Russia.) Jul. 1994 19 p Sponsored by Russian Fundamental Research Foundation
(DE95-607768; IC-94/205) Avail: CASI HC A03/MF A01 (US Sales Only)

It is shown using a Monte Carlo simulation that electron-plasmon scattering substantially affects the hot-electron energy distribution function and transport properties in bulk GaAs. However, this effect is found to be much less than that predicted in an earlier paper by other authors. DOE

N95-26560# Sussex Univ., Brighton (England).
DETECTION OF CHARGED PARTICLES IN SUPERFLUID HELIUM Ph.D. Thesis
Simon R. Bandler Dec. 1994 143 p Prepared in cooperation with Brown Univ., Providence, RI
(Contract DE-FG02-88ER-40452)
(DE95-007354; DOE/ER-40452/11) Avail: CASI HC A07/MF A02

This thesis is concerned with the use of a large superfluid helium detector for the detection of solar neutrinos. A small-scale prototype of this type of detector has been constructed and tested. In this thesis the author discussed in detail the design of the apparatus, the experiments which have been carried out, and what has been learned about the important physical processes involved in this type of detector. These processes

include the anisotropic generation of phonons and rotons by the recoiling particle, the propagation of the phonons and rotons in the liquid, the evaporation process at the liquid surface, and the adsorption of the helium atoms onto the wafers. In addition he discusses the generation and detection of fluorescent photons from recoiling particles. The implications of these results to the design of a full-scale detector of neutrinos are discussed.
DOE

N95-26574 California Univ., San Diego, La Jolla, CA. Dept. of Chemistry.
CHEMICAL PHYSICS OF UNIFORM CYCLIC ETCHING Annual Report, 1 Jan. - 30 Sep. 1994
Andrew C. Kummel 1994 3 p Limited Reproducibility: More than 20% of this document may be affected by microfiche quality
(Contract F49620-94-1-0075)
(AD-A288975; AFOSR-94-0762TR) Avail: Issuing Activity (Defense Technical Information Center (DTIC))

The chemisorption mechanisms of Cl2, Br2, and I2 on Si(100) 2x1 are very similar while those of F2 and O2 are very distinct. For the heavy diatomic halogens (Cl2, Br2, and I2), the sticking probability increases with incident translation energies above 0.1 eV, and the largest initial sticking probabilities are obtained at the highest incident energies, with So equal to 95-100% for I2 and Br2, and 80-85% for Cl2. At low incident energies the initial sticking probability, So decreases with increasing surface temperature while at high incident energies the sticking probability is independent of surface temperature. In addition, for Cl2 very low energy molecular beams can be prepared, and the sticking probability is observed to decrease with increasing incident energies between 0.02 eV and 0.06 eV. Therefore, all three heavy diatomic halogens can adsorb via precursor - mediated chemisorption at low incident translational energy and via direct - activated chemisorption activated chemisorption at high incident translational energy 1,2. DTIC

N95-26632 Iowa State Univ. of Science and Technology, Ames, IA. Dept. of Chemistry.
THEORETICAL STUDIES OF REACTION SURFACES Annual Report, 1 Sep. 1993 - 31 Aug. 1994
Mark S. Gordon 31 Aug. 1994 26 p Limited Reproducibility: More than 20% of this document may be affected by microfiche quality
(Contract F49620-93-1-0556)
(AD-A288458; AFOSR-94-0751TR) Avail: Issuing Activity (Defense Technical Information Center (DTIC))

The main goals in the previous grant period have been to develop new, more effective methods for performing accurate ab initio electronic structure calculations and to use these methods for the prediction of molecular structure, bonding and reactivity, especially for main group species and reactions of interest to the Air Force. From the theoretical point of view, the principle accomplishments have been extensive development of approaches and codes for performing electronic structure calculations in parallel, continued development of methods for interfacing electronic structure calculations with dynamics, initial studies of the possibility of splicing together different levels of electronic structure theory, and the development of a new model for treating solvation. Applications have ranged from the development of very accurate and extensive potential energy surfaces for A +HB reactions (to interface with the experiments) to the role of catalysts in the hydrosilation reaction to extensive studies of reactions involved in both main group and transition metal chemical vapor deposition (CVD) to broad-based studies of cage molecules (using our new parallel capabilities) that are potential precursors for new materials electronic and optical devices and catalysts. A new area that we have entered into is a series of systematic calculations on transition metal(TM)-main group (MG) compounds and their roles and catalysts and in such important area as CVD. DTIC

N95-26748 National Physical Lab., Teddington (England). Div. of Radiation Science and Acoustics.
BILATERAL INTERCOMPARISON OF THE NEUTRON EMISSION RATE OF A (252)Cf SPONTANEOUS FISSION SOURCE BETWEEN THE NATIONAL PHYSICAL LABORATORY, TEDDINGTON, UK AND THE PHYSIKALISCH-TECHNISCHE BUNDESANSTALT, BRAUNSCHWEIG, GERMANY Final Report
A. G. Bardell, K. J. Zieba, R. Boettger, and H. Klein Sep. 1994 18 p
Prepared in cooperation with Physikalisch-Technische Bundesanstalt, Berlin, Germany
(EUROMET Proj. 221)
(PB95-190120; NPL-RSA(EXT)47) Copyright Avail: Issuing Activity (National Technical Information Service (NTIS))

The neutron emission rate of a small Cf-252 fission source, incorporated into a fission counter, has been measured by two different methods. The fission rate of the source was measured at Physikalisch-Technische Bundesanstalt (PTB), the neutron emission rate being obtained by means of the neutron multiplicity factor nu(bar). The manganese sulphate bath method was used at the National Physical Laboratory (NPL) to determine the total neutron emission from the chamber assembly. Agreement between the two independent methods was found to be within 1%. NTIS

N95-26861*# National Aeronautics and Space Administration. Pasadena Office, CA.
EXTENDED LINEAR ION TRAP FREQUENCY STANDARD APPARATUS Patent Application
John D. Prestage, inventor (to NASA) (Jet Propulsion Lab., California Inst. of Tech., Pasadena, CA.) 12 May 1994 42 p
(NASA-Case-NPO-19081-1-CU; NAS 1.71:NPO-19081-1-CU; US-Patent-Appl-SN-246041) Avail: CASI HC A03/MF A01

A linear ion trap for frequency standard applications is provided with a plurality of trapping rods equally spaced and applied quadruple rf voltages for radial confinement of atomic ions and biased level pins at each end for axial confinement of the ions. The trapping rods are divided into two linear ion trap regions by a gap in each rod in a common radial plane to provide dc discontinuity, thus dc isolating one region from the other. A first region for ion-loading and preparation fluorescence is biased with a dc voltage to transport ions into a second region for resonance frequency comparison with a local oscillator derived frequency while the second region is held at zero voltage. The dc bias voltage of the regions is reversed for transporting the ions back into the first region for fluorescence measurement. The dual mode cycle is repeated continuously for comparison and feedback control of the local oscillator derived frequency. Only the second region requires magnetic shielding for the resonance function which is sensitive to any ambient magnetic fields. NASA

N95-26960 New Orleans Univ., LA. Dept. of Chemistry.
A DENSITY FUNCTIONAL/MOLECULAR DYNAMICS STUDY OF THE STRUCTURE OF LIQUID NITROMETHANE
Jorge M. Seminario, Monica C. Concha, and Peter Politzer 20 Dec. 1994 8 p Limited Reproducibility: More than 20% of this document may be affected by microfiche quality
(Contract N00014-95-1-0028)
(AD-A289224; TR-77) Avail: Issuing Activity (Defense Technical Information Center (DTIC))

A molecular dynamics simulation of liquid nitromethane has been carried out in which a density functional (DF) procedure was used to compute the properties needed to establish the intermolecular force field. The latter was subsequently updated by further DF calculations. The first and second shells of neighbors are found to be at radii of about 6 A and 11 A from a given nitromethane molecule. OH partial pair correlation functions are determined, and Indicate the presence of C-H...0 hydrogen bonding. DTIC

N95-26979 Air Force Inst. of Tech., Wright-Patterson AFB, OH. School of Engineering.
MEASUREMENT OF N2(+) MOBILITY He VIA FOURIER TRANSFORM EMISSION SPECTROSCOPY M.S. Thesis
Patrick D. Kee Dec. 1994 105 p Limited Reproducibility: More than 20% of this document may be affected by microfiche quality
(AD-A289266; AFIT/GAP/EN/94D-4) Avail: Issuing Activity (Defense Technical Information Center (DTIC))

Recently, Hong and Miller used Fourier Transform Emission (FTE) spectroscopy to determine the N2+ mobility in helium by relating the observed Doppler shift of the N2+ (B-X) transition to the measured electric field in the discharge as determined by probes. In order to establish the technique in-house, this effort duplicated that experiment and investigated the sensitivity and utility of the method. Doppler shift measurements in this experiment disagreed significantly with those reported by Hong and Miller. Attempts to reduce the data (and thus determine the mobility) using a model developed by Hong and Miller were unsuccessful. The model did not qualitatively or quantitatively describe the Doppler shifts observed in this work. At this time, an explanation of the differences between the two experiments is not known. Possibilities include effects of striations on the Doppler shift measurements, competition between one- and two-step excitation of the N2+ (B-X) state, and failure to interpret the Hong and Miller model correctly. Subsequent attempts to model Hong and Miller's own data (taken from their figures) yielded mobility parameters which disagreed with their published results. DTIC

N95-27010# Instituto Tecnologico de Toluca, Toluca (Mexico).
RADON INTEGRAL MEASUREMENT SYSTEM Ph.D. Thesis [SISTEMA DE MEDICION INTEGRAL DE RADON]
J. M. GarciaH 1994 240 p In SPANISH
(DE95-608074; INIS-mf-14401) Avail: CASI HC A11/MF A03 (US Sales Only)

The Radon Integral Measurement System (SMIR) is a device designed specially to detect, count and store data relating to the acquisition of alpha particles emitted by Radon-222 coming from underground. The system includes a detection chamber, a radiation detector, a digital system with battery backup and an auxiliary photovoltaic cell. A personal computer fixes the mode in which the system works, transmitting the commands to the system by the serial port. The heart of the system is a microprocessor working with interrupts by hardware. Every external device of the microprocessor sends its own interrupt request and the microprocessor handles the interrupts with a defined priority. The system uses a real time clock, compatible with the microprocessor, to take care of the real timing and date of the acquisition. A non volatile RAM is used to store data of two bytes every 15 minutes with 41 days as a maximum. After the setting up the system with the computer, it can operate by itself for up 41 days in the working mode without the loss of any data. If the memory is full, incoming data will be written in the first location of the memory. The memory is divided into pages corresponding to a different day of the acquisition. The counting time for every acquisition can be programmed by the user from 15 minutes to 65535 minutes, but it is recommended that the time should not reach the limit of 65535 counts in every acquisition period. We can take information from the system without affecting the acquisition process in the field by using a lap top computer, the information can then be stored in a file. There is a program in the computer that can show the information in a table of values or in a bar graph. DOE

N95-27017 Wisconsin Univ., Madison, WI. Dept. of Chemistry.
ATOMIC STRUCTURE AND BONDING OF BORON-INDUCED RECONSTRUCTIONS ON Si(001) Interim Technical Report
Yajun Wang, Robert J. Hamers, and Efthimios Kaxiras 20 Dec. 1994 17 p Limited Reproducibility: More than 20% of this document may be affected by microfiche quality
(Contract N00014-91-J-1629)
(AD-A289187; UWIS/DC-22) Avail: Issuing Activity (Defense Technical Information Center (DTIC))

Scanning tunneling microscopy and tunneling spectroscopy have been used to investigate the local structural and electronic properties of boron-induced reconstructions on Si(001). Thermal decomposition of diborane produces three ordered reconstructions, which arise from ordered arrangements of three structural subunits, with a local boron coverage of 1/2 monolayer. A structural model is proposed which accounts for the observed STM features. The principal structural subunit is shown to be an ordered arrangement of four boron atoms at substitutional sites in the first bulk-like silicon layer, which is then capped with ordered arrangements of silicon dimers and dimer vacancies. DTIC

N95-27034 Edgewood Research Development and Engineering Center, Aberdeen Proving Ground, MD.
CHLORODIFLUOROMETHANE EQUILIBRIUM ON 13X MOLECULAR SIEVE Final Report, Sep. 1992 - Mar. 1993
Donna L. Carlile, John J. Mahle, Leonard C. Buettner, David E. Tevault, and David K. Friday Aug. 1994 21 p Limited Reproducibility: More than 20% of this document may be affected by microfiche quality
(DA Proj. 101-62622-A-553)
(AD-A289282; ERDEC-TR-195) Avail: Issuing Activity (Defense Technical Information Center (DTIC))

Adsorption phase equilibrium data are required for evaluating any adsorption-based gas separation process. The U.S. Army Edgewood Research, Development and Engineering Center is currently measuring adsorption phase equilibrium data for a variety of chemical warfare agents and their surrogates on adsorbent materials to correlate physical properties to filtration/separation efficiencies of each vapor on each adsorbent. This report details the adsorption phase equilibrium data measured for chlorodifluoromethane (R-22) on 13X Molecular Sieve. The 13X Molecular Sieve is a candidate adsorbent for future military air purification systems employing the pressure-swing adsorption separation process. DTIC

N95-27081# Los Alamos National Lab., NM.
STUDY OF PARITY AND TIME REVERSAL VIOLATION IN NEUTRON-NUCLEUS INTERACTIONS
Yi-Fen Yen, J. D. Bowman, C. M. Frankle, and B. E. Crawford 1994 17 p Presented at the International Symposia on High Energy Spin Physics and Polarization Phenomena in Nuclear Physics, Bloomington, IN, 15-22 Sep. 1994
(Contract W-7405-eng-36)
(DE95-005158; LA-UR-94-4242; CONF-9409103-14) Avail: CASI HC A03/MF A01

The parity and time-reversal symmetries can be studied in neutron-nucleus interactions. Parity non-conserving asymmetries have been observed for many p-wave resonances in a compound nucleus and measurements were performed on several nuclei in the mass region of A approximately 100 and A approximately 230. The statistical model of the compound nucleus provides a theoretical basis for extracting mean-squared matrix elements from the experimental asymmetry data, and for interpreting the mean-squared matrix elements. The constraints on the weak meson-exchange couplings calculated from the compound-nucleus asymmetry data agree qualitatively with the results from few-body and light-nuclei experiments. The tests of time-reversal invariance in various experiments using thermal, epithermal and MeV neutrons are being developed. DOE

N95-27159# Bhabha Atomic Research Centre, Bombay (India).
SELECTED BIBLIOGRAPHY ON HEAVY WATER, TRITIATED WATER AND HYDROGEN ISOTOPES (1981-1992)
V. T. Gopalakrishnan, U. B. Sutawane, and B. N. Rathi (Bhabha Atomic Research Centre, Bombay, India.) 1994 460 p
(DE95-608331; BARC-1994/E/004) Avail: CASI HC A20/MF A04 (US Sales Only)

A selected bibliography on heavy water, tritiated water and hydrogen isotopes is presented. This bibliography covers the period 1981-1992 and is in continuation to Division's earlier report BARC-1192 (1983). The sources of information for this compilation are Chemical Abstracts, INIS Atom Index and also some scattered search through journals and reports available in our library. No claim is made towards exhaustiveness of this bibliography even though sincere attempts have been made for a wide coverage. The bibliography is arranged under the headings: (1) production, purification, recovery, reprocessing and storage; (2) isotope exchange; (3) isotope analysis; (4) properties; and (5) miscellaneous. Total number of references in the bibliography are 1762. DOE

N95-27211# Universidad Nacional Autonoma de Mexico, Mexico City (Mexico).
DETERMINATION OF THE FIRST HYDROLYSIS CONSTANT OF EUROPIUM (3) IN 3 M OF IONIC STRENGTH Ph.D. Thesis [DETERMINACION DE LA PRIMERA CONSTANTE DE HIDROLISIS DEL EUROPIO (3) EN UN MEDIO DE FUERZA IONICA 3M]
Maria Elena RamirezBernal 1994 74 p In SPANISH
(DE95-607912; INIS-mf-14396) Avail: CASI HC A04/MF A01 (US Sales Only)

The first hydrolysis constant of Eu(sup 3+) has been determined at 303 K and 3 M (NaCl) ionic strength. A solvent extraction method was used, the extractant was dibenzoylmethane in benzene and di glycolate anion in the aqueous phase provided competitive complexation. The tracer solution was (sup 152m1) Eu (III) in water. The radioactive solution of europium was obtained by neutron irradiation of europium nitrate solutions at pH 3.0, in a TRIGA Mark III nuclear reactor at a neutron flux of 1 x 10(exp 13) cm(sup -2) s(sup -1). The half life of the produced isotope, (sup 152m1) Eu (9.3 h), was verified by means of a Ge H detector and no interfering radiations were observed in the spectra. DOE

N95-27212# Bhabha Atomic Research Centre, Bombay (India).
PROGRAMMING FOR TIME RESOLVED SPECTRUM IN PULSE RADIOLYSIS EXPERIMENTS
C. A. Betty, M. S. Panajkar (Bhabha Atomic Research Centre, Bombay, India.), and N. D. Shirke (Bhabha Atomic Research Centre, Bombay, India.) 1993 19 p
(DE95-607929; BARC-1993/E/021) Avail: CASI HC A03/MF A01 (US Sales Only)

A user friendly program in Pascal has been developed for data acquisition and subsequent processing of time resolved spectra of transient species produced in pulse radiolysis experiments. The salient features of the program are thiocyanate dosimetry and spectrum acquisition. The thiocyanate dosimetry is carried out to normalize experimental conditions to a standard value as determined by computing absorbance of the transient signal CNS(sub -2) that is produced from thiocyanate solution by a 7 MeV electron pulse. Spectrum acquisition allows the acquisition of the time resolved data at 20 different time points and subsequent display of the plots of absorbance vs. wavelength for the desired time points during the experiment. It is also possible to plot single time point spectrum as well as superimposed spectra for different time points. Printing, editing and merging facilities are also provided. DOE

N95-27307# Oak Ridge National Lab., TN.
PHYSICS WITH RELATIVISTIC HEAVY IONS: QGP AND OTHER DELICACIES
G. R. Young 1995 16 p Presented at the Meeting of the Division of Particles and Fields of the American Physical Society, Albuquerque, NM, 2-6 Aug. 1994
(Contract DE-AC05-84OR-21400)
(DE95-007014; CONF-940816-89) Avail: CASI HC A03/MF A01

Conditions favorable to formation and observation of a deconfined state of quarks and gluons, often called the quark-gluon plasma (QGP), are thought to exist following the collision of very heavy nuclei at center-of-mass energies exceeding several tens of GeV/nucleon. The Relativistic Heavy Ion Collider under construction at BNL since 1991 is designed to provide such collisions at energies up to (square root of s)/A = 200 GeV. Two large dedicated experiments are being built to operate there; these two experiments take rather different approaches to the problem of classifying such collisions and probing for signals of QGP formation. Two smaller experiments are proposed to focus on specific aspects of these collisions. Recent developments in the understanding of the initial state formed in such collisions include, particularly, the possible rapid equilibration of the gluon density, leading in an equilibrium picture to such high temperatures that sizable thermal excitation of charm becomes probable. Recent theoretical conjectures have focussed on the possible formation of a disordered chiral condensate following chiral symmetry restoration in heavy-nucleus collisions, which might be a consequence of nonequilibrium deexcitation of a dense partonic state. DOE

N95-27309# International Centre for Theoretical Physics, Trieste (Italy).
EXTENDED BRST SYMMETRY FOR THE RELATIVISTIC PARTICLE WITH CURVATURE
D. Constantinescu (Craiova Univ., Romania.), R. Constantinescu, and M. Negrea (Craiova Univ., Romania.) Aug. 1994 6 p
(DE95-608799; IC-94/214) Avail: CASI HC A02/MF A01 (US Sales Only)

The model of a massive relativistic particle with rigidity is analyzed with the methods of the dynamical systems with constraints. A special physical significance is proposed and the ghost spectrum in the case 'off shell' is constructed. DOE

N95-27314# Joint Inst. for Nuclear Research, Dubna (USSR). Lab. of Theoretical Physics.
THE PHOTON STRUCTURE FUNCTION F2 IN QCD WITH NONLOCAL VACUUM QUARK CONDENSATES
A. P. Bakulev and S. V. Mikhajlov 1994 7 p Submitted for publication
(DE95-608829; JINR-E-2-94-208) Avail: CASI HC A02/MF A01 (US Sales Only)

We calculate the contribution from nonlocal vacuum condensates of quark fields to the hadronic part of the photon structure function F(sub 2)(x) in the operator product expansion approach to QCD and as a result we obtain a substantial improvement of the agreement with experimental data for the standard value of the parameter lambda(sub q)(sup 2) = (anti-qD(sup 2)q)/(anti-qq) approx. 0.5 GeV(sup 2). DOE

N95-27316# International Centre for Theoretical Physics, Trieste (Italy).
A NOTE ON THE CONSTITUENT QUARK RESONANCES
Kuang-Ta Chao and Hanqing Zheng Sep. 1994 6 p
(DE95-608831; IC-94/275) Avail: CASI HC A02/MF A01 (US Sales Only)

If there exists a constituent quark resonance, we find that, by using the Adler-Weisberger relation and the finite-energy sum rule for pion quark scattering, it must be very massive and have a large decay width. Our results indicate that the presence of the constituent quark excitations does not contradict the observed low lying hadron spectrum. DOE

N95-27317# International Centre for Theoretical Physics, Trieste (Italy).
MODEL INDEPENDENT CONSTRAINTS ON ANOMALOUS GAUGE BOSON SELF-COUPLINGS FROM e(+)e(-) COLLIDERS WITH LONGITUDINALLY POLARIZED BEAMS
A. A. Pankov and N. Paver (Trieste Univ., Italy.) Sep. 1994 15 p
(DE95-608844; IC-94/274; UTS-DTF-94-10) Avail: CASI HC A03/MF A01 (US Sales Only)

We explore the possibility of deriving model independent limits on the anomalous trilinear electroweak gauge boson couplings from high energy e(+)e(-) yields W(+)W(-), by combining the cross sections for the different initial and final states polarizations integrated with suitable kinematical cuts. In the case of the CP conserving couplings the limits can be disentangled, and are given by simple mathematical expressions. Numerical results show the advantages of this approach, in particular the important role of polarization in improving the bound. DOE

N95-27318# International Centre for Theoretical Physics, Trieste (Italy).
A SIMPLE RELATIVISTIC MODEL OF pp-BAR YIELDS K(+)K(-)
T. Frederico (Centro Tecnico Aerospacial, San Jose dos Campos, Brazil.), J. Dey, and L. Tomio Aug. 1994 15 p
(DE95-608852; IC-94/244) Avail: CASI HC A03/MF A01 (US Sales Only)

We compare a model calculation with some available experimental data (LEAP 92) of KK-bar production. We believe the simplicity of the model makes it a useful tool for studying charm and beauty baryon production, for which also experimental data will soon be profuse. DOE

N95-27399 Air Force Inst. of Tech., Wright-Patterson AFB, OH. School of Engineering.
DETECTING ALPHA PARTICLES THROUGH SCINTILLATION IN POROUS MATERIALS M.S. Thesis
Martin E. Keillor Dec. 1994 114 p Limited Reproducibility: More than 20% of this document may be affected by microfiche quality
(AD-A289313; AFIT/GAP/ENP/94D-05) Avail: Issuing Activity (Defense Technical Information Center (DTIC))

This thesis presents the results of a preliminary study of parameters essential to the development of a scintillation flow-cell detector with improved characteristics over existing cells. Such a detector with better than 10% alpha energy resolution could provide in situ capability to detect and identify important alpha-emitting radionuclides in dilute aqueous solutions. Gel-silica is a potential candidate that may provide the needed improvement in resolution while maintaining 100% detection efficiency; however, gel-silica with useful light output is yet to be developed. As a step toward realizing the system described, the dependence of alpha detection efficiency and intrinsic energy resolution on the phase dimensions in heterogeneous scintillation detectors is examined. Two main areas of this research are: (1) computer modeling of the geometric detection efficiency and intrinsic energy resolution in porous glass scintillation detectors, and (2) experiments designed to test model predictions and provide data on the detection of alphas in porous glass structures. Experimental emphasis is on alpha detection in gel-silica filled with liquid scintillant. Results show that phase dimensions must be considered in constructing a flow-cell detector for alpha spectroscopy, and that the dimensions available in gel-silica provide for excellent intrinsic energy resolution, as well as 100% detection efficiency. DTIC

N95-27406# Weizmann Inst. of Science, Rehovot (Israel). Dept. of Physics.

IMPLICATIONS OF HORIZONTAL SYMMETRIES ON BARYON NUMBER VIOLATION IN SUPERSYMMETRIC MODELS

V. Ben-Hamo and Y. Nir Aug. 1994 11 p
(DE95-610202; WIS-PH-94-34; Hep-ph-9408315) Avail: CASI HC A03/MF A01 (US Sales Only)

The smallness of the quark and lepton parameters and the hierarchy between them could be the result of selection rules due to a horizontal symmetry broken by a small parameter. The same selection rules apply to baryon number violating terms. Consequently, the problem of baryon number violation in supersymmetry may be solved naturally, without invoking any especially-designed extra symmetry. This mechanism is efficient enough even for low-scale flavor physics. Proton decay is likely to be dominated by the modes K(+)bar-nu(sub i) or K(o) mu(+) (e(+)), and may proceed at observable rates. DOE

N95-27407# Academy of Sciences (USSR), Novosibirsk (USSR).

MEASUREMENT OF INCLUSIVE LAMBDA PRODUCTION IN ELECTRON-POSITRON INTERACTIONS AT THE UPSILON ENERGIES

A. E. Blinov, V. E. Blinov, and A. E. Bondar 1993 12 p
(DE95-610302; BUDKERINP-93-53; IYaF-93-53) Avail: CASI HC A03/MF A01 (US Sales Only)

Using the MD-1 detector at the VEPP-4 e(+)e(-) storage ring the inclusive production rate of the Lambda and Xi(-) baryons in direct Upsilon(1S) decays are measured. The Lambda momentum spectrum in direct Upsilon(1S) decays is obtained. The inclusive production rate of the Lambda baryon in the continuum at center of mass energies 7.2-10.0 GeV is measured. DOE

N95-27408# Academy of Sciences (USSR), Novosibirsk (USSR).

MEASUREMENT OF R IN e(+)e(-)-ANNIHILATION AT CENTER-OF-MASS ENERGIES BETWEEN 7.2 AND 10.34 GeV

A. E. Blinov, V. E. Blinov, and A. E. Bondar 1993 22 p
(DE95-610303; BUDKERINP-93-54; IYaF-93-54) Avail: CASI HC A03/MF A01 (US Sales Only)

The total cross section of the process e(+)e(-) yields hadrons has been measured in the center-of-mass energy range between 7.23 and 10.34 GeV using the MD-1 detector at the VEPP-4 collider. The ratio R = sigma(e(+)e(-) yields hadrons)/sigma (e(+)e(-) yields mu(+) mu(-)) was found to be constant in this energy range with the average value of 3.58 +/- 0.02 +/- 0.14. DOE

N95-27409# Weizmann Inst. of Science, Rehovot (Israel).

TRANSVERSE TAU POLARIZATION IN INCLUSIVE BAR-B YIELDS TAU BAR-NU X DECAYS

Y. Grossman and Z. Ligeti (California Inst. of Tech., Pasadena, CA.) Sep. 1994 12 p
(DE95-610325; WIS-PH-94-39; CALT-68-1952; Hep-ph-9409418) Avail: CASI HC A03/MF A01 (US Sales Only)

We calculate, in the framework of multi Higgs doublet models, the C P violating transverse tau polarization, P perpendicular, in inclusive semileptonic B meson decays. We find that P perpendicular diverges at Omicron(1/m(exp 2)(sub b)) of the heavy quark expansion. We discuss the physical reasons for this divergence and show how to regularize it. We find large 1/m(exp 2)(sub b) corrections that can suppress the C P asymmetry is a(sub CP) approx. 0.34. We discuss how the allowed range is expected to change in the future. DOE

N95-27410# Academy of Sciences (USSR), Novosibirsk (USSR).

COUPLINGS OF HEAVY HADRONS WITH SOFT PIONS FROM QCD SUM RULES

A. G. Grozin and O. I. Yakovlev 1994 16 p
(DE95-610349; BUDKERINP-94-3; IYaF-94-3) Avail: CASI HC A03/MF A01 (US Sales Only)

The couplings in the Heavy Hadron Chiral theory Lagrangian from the QCD sum rules in an external axial field are estimated. Stability of the sum rules at moderate values of the Borel parameter is poor that probably signals slow convergence of the OPE series. At large values of the Borel parameter they stabilize, and yield the couplings much lower than the constituent quark model expectations. DOE

N95-27411# Academy of Sciences (USSR), Novosibirsk (USSR).

MAGNETIC QUADRUPOLE MOMENT OF W-BOSON IN KOBAYASHI-MASKAWA MODEL

I. B. Khriplovich and M. E. Pospelov 1993 12 p
(DE95-610355; BUDKERINP-93-88) Avail: CASI HC A03/MF A01 (US Sales Only)

The W-boson magnetic quadrupole moment in calculated in the Kobayashi-Maskawa model. This is the only known CP-odd moment arising in this model in two-loop approximation. DOE

N95-27412# Academy of Sciences (USSR), Novosibirsk (USSR).

LARGE RELATIVISTIC CORRECTIONS TO THE POSITRONIUM DECAY RATE

I. B. Khriplovich and A. I. Milstejn 1994 10 p
(DE95-610470; BUDKERINP-94-30; IYaF-94-30) Avail: CASI HC A02/MF A01 (US Sales Only)

Relativistic corrections to the positronium decay rate are calculated. They are close to 40(alpha/ pi)(exp 2) and 46(alpha/pi)(exp 2) for singlet and triplet states respectively. DOE

N95-27430# Fermi National Accelerator Lab., Batavia, IL.

SEARCH FOR SUSY AT CDF

Teruki Kamon Sep. 1994 7 p Presented at the 8th Meeting of the Division of Particles and Fields of the American Physical Society, Albuquerque, NM, 2-6 Aug. 1994 Sponsored by the National Science Foundation, the Italian Instituto Nazionale di Fisica Nucleare; the Ministry of Education, Science and Culture of Japan; the Natural Sciences and Engineering ResearchCouncil of Canada; the National Science Council of the Republic of China; the A.P. Sloan Foundation; and the Alexander von Humboldt-Stiftung
(Contract DE-AC02-76CH-03000)
(DE95-005109; FNAL/C-94/270-E; CONF-940816-86) Avail: CASI HC A02/MF A01

We have searched supersymmetry (SUSY) using trilepton events in p(bar p) collisions at (radical)s = 1.8 TeV. In the Minimal Supersymmetric Standard Model (MSSM), trilepton events are expected from chargino-neutralino ((tilde (chi))(sub 1)(sup (+/-))(tilde (chi))(sub 2)(sup o)) pair production, with subsequent decay into leptons. In all possible combinations of electron and muon channels in 19 pb(sup -1)data, we observe no events which pass our trilepton selection criteria. Assuming the GUT hypothesis within the framework of the MSSM, our preliminary analysis excludes M((tilde (chi))(sub 1)(sup (+/-))(tilde (chi))(sub 2)(sup o)) less than 46 Ge0/c(sup 2) for -500 less than (mu) less than -400 GeV, 2.0 less than tan (beta) less than 15.0, and M((bar q)) = 1.2 (times) M((bar g)). DOE

N95-27431# Los Alamos National Lab., NM. Materials Science and Technology Div.

THE PHYSICS AND CHEMISTRY OF HEAVY FERMIONS

Z. Fisk (Florida State Univ., Tallahassee, FL.), J. L. Sarrao (Florida State Univ., Tallahassee, FL.), J. L. Smith, and J. D. Thompson 1994 29 p Presented at the National Academy of Sciences Colloquiom, Physics: The Opening to Complexity, Irvine, CA, Jun. 1994
(Contract W-7405-eng-36)
(DE95-005277; LA-UR-94-4280; CONF-9406310-1) Avail: CASI HC A03/MF A01

The heavy Fermions are a subset of the f-element intermetallics straddling the magnetic/non-magnetic boundary. Their low temperature properties are characterized by an electronic energy scale of order 1-10 K. Among the low temperature ground states observed in heavy Fermion compounds are exotic superconductors and magnets, as well as unusual semiconductors. We review here the current experimental and theoretical understanding of these systems. DOE

N95-27439# Kansas State Univ., Manhattan, KS. J.R. Macdonald Lab.

ATOMIC PHYSICS WITH HIGHLY CHARGED IONS Progress Report

Patrick Richard Aug. 1994 126 p
(Contract DE-FG02-86ER-13491)
(DE95-007325; DOE/ER-13491/709) Avail: CASI HC A07/MF A02

The study of inelastic collision phenomena with highly charged projectile ions and the interpretation of spectral features resulting from these collisions remain as the major focal points in the atomic physics research at the

J.R. Macdonald Laboratory, Kansas State University, Manhattan, Kansas. The title of the research project, 'Atomic Physics with Highly Charged Ions,' speaks to these points. The experimental work in the past few years has divided into collisions at high velocity using the primary beams from the tandem and LINAC accelerators and collisions at low velocity using the CRYEBIS facility. Theoretical calculations have been performed to accurately describe inelastic scattering processes of the one-electron and many-electron type, and to accurately predict atomic transition energies and intensities for x rays and Auger electrons. Brief research summaries are given for the following: (1) electron production in ion-atom collisions; (2) role of electron-electron interactions in two-electron processes; (3) multi-electron processes; (4) collisions with excited, aligned, Rydberg targets; (5) ion-ion collisions; (6) ion-molecule collisions; (7) ion-atom collision theory; and (8) ion-surface interactions. DOE

N95-27444# Fermi National Accelerator Lab., Batavia, IL.
A STUDY OF PARTON DISTRIBUTION FUNCTIONS WITH THE USE OF PHOTON + JET EVENT KINEMATICS IN p(BAR p) COLLISIONS AT (RADICAL)s = TeV
C. Hawk Aug. 1994 5 p Presented at the Meeting of the Division of Particles and Fields of the American Physical Society, Albuquerque, NM, 2-6 Aug. 1994
(Contract DE-AC02-76CH-03000)
(DE95-005127; FNAL/C-94/226-E; CONF-940816-85) Avail: CASI HC A01/MF A01

We have measured the leading jet pseudorapidity distribution in photon + jet events selected from the inclusive direct photon event sample. The data are from p(bar p) collisions at (radical)s = 1.8 TeV recorded with CDF in the 1992-1993 run. This measurement has been used to study the behavior of current parton distribution sets in selected kinematic regions. The parton distribution sets CTEQ2M and MRSD0 are currently favored by this measurement. DOE

N95-27453# Argonne National Lab., IL.
OBSERVATIONS OF CEF-SPLIT INTERMULTIPLET TRANSITIONS IN OPTICALLY OPAQUE EuBa2Cu3O7 USING INELASTIC NEUTRON SCATTERING
U. Staub, L. Soderholm, R. Osborn, E. Balcar (Atominstitut der Oesterreichischen Hochschulen, Vienna, Austria.), and V. Trunov (Saint Petersburg Nuclear Physics Inst., Saint Petersburg, Russia.) 1995 7 p Presented at the 1994 Fall Meeting of the Materials Research Society (MRS), Boston, MA, 28 Nov. - 2 Dec. 1994
(Contract W-31-109-eng-38)
(DE95-007135; ANL/CHM/CP-85153; CONF-941144-70) Avail: CASI HC A02/MF A01

Inelastic neutron scattering (INS) results on the intermultiplet transitions J=0 (yields) 1 and J=l (yields) 2 in optically opaque EuBa2Cu3O7 are reported. Whereas these multiplets are split by the crystalline electric field (CEF), their low J values are influenced to first order only by the 2 second-order (J=l) and additional fourth-order (J=2) CEF parameters. B(sub 0)(sup 2), B2(sup 2) and the spin-orbit coupling parameter were obtained by fitting the splitting of the J=1 multiplet and the energy separation between the J=0 and 1 multiplets. The J=0 to 1 splitting observed here is smaller than previously seen by optical spectroscopic studies on a variety of transparent, ionic compounds, necessitating fitting of the free-ion parameter. Additional spectroscopic information on the J=2 multiplet indicates that additional fitting of free ion parameters must be included to adequately model the observed low energy separation between the two lowest J-multiplets. Preliminary calculation on the Q-dependence of the CEF split J=0 to 1 transitions and the comparison with observations are presented. DOE

N95-27456# Oak Ridge National Lab., TN.
INTEGRATING THE QMR METHOD WITH FIRST PRINCIPLES MATERIAL SCIENCE APPLICATION CODE
N. M. Nachtigal, W. A. Shelton, G. M. Stocks, D. M. C. Nicholson, and Y. Wang 1995 6 p Presented at the 7th Society for Industrial and Applied Mathematics (SIAM) Conference on Parallel Processing for Scientific Computing, San Francisco, CA, 15-17 Feb. 1995
(Contract DE-AC05-84OR-21400)
(DE95-007380; CONF-950212-5) Avail: CASI HC A02/MF A01

First principles methods are used to aid the material designers and metallurgists in the investigation and design of new materials. These methods suffer from a divergent O(N(sup 3)) scaling which restricts the problem sizes that can be addressed. It will be demonstrated that the O(N(sup 3)) scaling problem can be overcome by employing real-space multiple scattering techniques to calculate the scattering properties, combined with the QMR algorithm. By incorporating the QMR method into our real-sp ce multiple scattering code, we observed O(N) scaling for the large problem sizes of interest. This advancement will provide researchers with the necessary tools to treat large systems. DOE

N95-27466# Los Alamos National Lab., NM.
INTERMEDIATE ENERGY NEUTRONS AT WNR. SPIN-ISOSPIN AND ENERGY DEPENDENCE OF THE NN INTERACTION AND THE NUCLEAR RESPONSE
T. N. Taddeucci 1995 12 p Presented at the DNP/NSAC Town Meeting on Nuclear Physics With Intermediate Energy and High-energy Hadron Probes, Chicago, IL, 29-30 Jan. 1995
(Contract W-7405-eng-36)
(DE95-006291; LA-UR-95-373; CONF-950165-1) Avail: CASI HC A03/MF A01

This report summarizes results of nuclear physics studies using intermediate energy (50-800 MeV) neutron probes carried out over the past five years using the Neutron Time-of-Flight (NTOF) Facility and Optically-Pumped Ion Source (OPPIS) at LAMPF and the 'white' neutron source at the Weapons Neutron Research (WNR) facility. LAMPF did significant work in polarization transfer, while WNR took advantage of the wide neutron energy spectrum available to study energy dependent effects. The major focus of experiments with intermediate energy neutron probes for the next five years will be to explore fundamental details of the spin-isospin and energy dependence of the NN interaction and the nuclear response. To achieve this goal, the WNR white neutron source will be used for nucleon-nucleon and nucleon-nucleus interaction studies over a broad continuous range of incident neutron energy. Measurement of polarization observables using polarized targets or polarized beam should be possible, and will add an important extra dimension to these studies. DOE

N95-27478# Fermi National Accelerator Lab., Batavia, IL.
STUDIES OF KINEMATIC DISTRIBUTIONS AND MASS RECONSTRUCTION OF CDF TOP CANDIDATE EVENTS
Brian D. Harral (Pennsylvania Univ., Philadelphia, PA.) Aug. 1994 6 p Presented at the 8th Meeting of the Division of Particles and Fields of the American Physical Society, Albuquerque, NM, 2-6 Aug. 1994
(Contract DE-AC02-76CH-03000)
(DE95-005108; FNAL/C-94/238-E; CONF-940816-87) Avail: CASI HC A02/MF A01

We present analyses of CDF top-candidate events which study the separation of signal from background using easily-defined kinematic variables, and which study invariant masses of three-body systems to fully reconstruct the top quark decay products. DOE

N95-27534# Sandia National Labs., Albuquerque, NM.
ATOMISTIC CALCULATIONS OF HYDROGEN INTERACTIONS WITH NI3AI GRAIN BOUNDARIES AND NI/NI/NI3AI INTERFACES
M. I. Baskes, J. E. Angelo, and N. R. Moody 1995 14 p Presented at the 5th International Conference on Hydrogen Effects on Material Behavior, Moran, WY, 11-15 Sep. 1994
(Contracts DE-AC04-94AL-85000; DE-AC04-76DR-00789)
(DE95-006497; SAND-94-8741C; CONF-940945-7) Avail: CASI HC A03/MF A01

Embedded Atom Method (EAM) potentials have been developed for the Ni/Al/H system. The potentials have been fit to numerous properties of this system. For example, these potentials represent the structural and elastic properties of bulk Ni, Al, Ni3Al, and NiAl quite well. In addition the potentials describe the solution and migration behavior of hydrogen in both nickel and aluminum. A number of calculations using these potentials have been performed. It is found that hydrogen strongly prefers sites in Ni3Al that are surrounded by 6 Ni atoms. Calculations of the trapping of hydrogen to a number of grain boundaries in Ni3Al have been performed as a function of hydrogen chemical potential at room temperature. The failure of these bicrystals under tensile stress has been examined and will be compared to the failure of pure Ni3Al boundaries. Boundaries containing a preponderance of nickel are severely weakened by hydrogen. In order to investigate the potential embrittlement of gamma/gamma(prime) alloys, trapping of hydrogen to a spherical Ni3Al precipitate in nickel as a function of chemical potential at room temperature has been calculated. It appears that the boundary is not a strong trap for hydrogen, hence embrittlement in these alloys is not primarily due to interactions of hydrogen with the gamma/gamma(prime) interface. DOE

N95-27551# Oak Ridge National Lab., TN.
PROJECTILE IMAGE ACCELERATION, NEUTRALIZATION AND ELECTRON EMISSION DURING GRAZING INTERACTIONS OF MULTICHARGED IONS WITH Au(110)
F. W. Meyer, L. Folkerts, H. O. Folkerts (Groningen Rijksuniv., Netherlands.), and S. Schippers (Groningen Rijksuniv., Netherlands.) 1995 14 p Presented at the 7th International Conference on Physics of Highly Charged Ions, Vienna, Austria, 19-23 Sep. 1994
(Contract DE-AC05-84OR-21400)
(DE95-007394; CONF-940922-4) Avail: CASI HC A03/MF A01

Recent Oak Ridge work is summarized on projectile energy gain by image charge acceleration, scattered ion charge distributions, and K-Auger electron emission during low energy grazing interactions of highly charged Pb, I, O, and Ar ions with a Au(110) surface. DOE

N95-27552# Brookhaven National Lab., Upton, NY.
PRELIMINARY HEAVY-LIGHT DECAY CONSTANTS FROM THE MILC COLLABORATION
C. Bernard (Washington Univ., Saint Louis, MO.), A. De (Washington Univ., Saint Louis, MO.), N. Ishizuka (Washington Univ., Saint Louis, MO.), T. Blum (Arizona Univ., Tucson, AZ.), L. Karkkainen (Arizona Univ., Tucson, AZ.), D. Toussaint (Arizona Univ., Tucson, AZ.), T. DeGrand (Colorado Univ., Boulder, CO.), D. DeTar (Utah Univ., Salt Lake City, UT.), Steven Gottlieb (Indiana Univ., Bloomington, IN.), and U. M. Heller (Florida State Univ., Tallahassee, FL.) et al Dec. 1994 3 p Presented at the Lattice '94 Conference, Bielefeld, Germany, 25 Sep. - 1 Oct. 1994
(Contract DE-AC02-76CH-00016)
(DE95-005685; BNL-61140; CONF-9409269-5) Avail: CASI HC A01/MF A01

Preliminary results from the MILC Collaboration for f(sub B), f(sub B(sub s)), f(sub D), f(sub D(sub s)) and their ratios are presented. We compute in the quenched approximation at (beta) = 6.3, 6.0 and 5.7 with Wilson light quarks and static and Wilson heavy quarks. We attempt to quantify all systematic errors other than quenching. DOE

N95-27676# California Univ., Berkeley. Lawrence Berkeley Lab, CA. Physics Div.
THE PHYSICS PROGRAM AND STATUS OF THE SLAC B-FACTORY AND DETECTOR
C. Hearty May 1994 6 p Presented at the 5th Conference on the Intersections of Particle and Nuclear Physics, St. Petersburg, FL, 31 May - 6 Jun. 1994
(Contract DE-AC03-76SF-00098)
(DE95-006562; LBL-36360; CONF-940514-18) Avail: CASI HC A02/MF A01

The goal of the SLAC B-Factory is to measure CP violation in the decay of B-mesons and to test the standard model description of CP violation. Work is now underway in upgrading the PEP collider for this project, and much of the preliminary detector design has been done. The physics goals and design of PEP-2 are briefly discussed, and the current plans for the detector are outlined. DOE

N95-27689# Fermi National Accelerator Lab., Batavia, IL.
SEARCH FOR THE TOP QUARK IN DILEPTON DECAY MODES AT D(PHI)
S. J. Wimpenny (California Univ., Riverside, CA.) Feb. 1995 5 p Presented at the 27th International Conference on High Energy Physics, Glasgow, England, 21-27 Jul. 1994
(Contract DE-AC02-76CH-03000)
(DE95-007764; FNAL/C-95/016-E; CONF-940722-43) Avail: CASI HC A01/MF A01

The authors present preliminary results on the search for the top quark in p(bar p) collisions at (radical)s = 1.8 TeV by the D0 collaboration at the Fermilab Tevatron. The results are based on an integrated luminosity of 13.5 pb(sup -1) of data collected by the D0 detector during the 1992-3 Tevatron collider run. They have searched for Standard Model t(bar t) decays into the dilepton decay modes ee + X, e(mu) + X and (mu)(mu) + X. No significant signal is observed for top quark production in these channels. They find one candidate event in the e(mu) + X channel and no events in the other two channels with an estimated non-top background of 0.76 (+-) 0.16 events. DOE

N95-27744# California Univ., Berkeley. Lawrence Berkeley Lab, CA. Structural Biology Div.
STRUCTURAL OXIDATION STATE STUDIES OF THE MANGANESE CLUSTER IN THE OXYGEN EVOLVING COMPLEX OF PHOTOSYSTEM II Ph.D. Thesis
Wenchuan Liang Nov. 1994 158 p
(Contract DE-AC03-76SF-00098)
(DE95-008488; LBL-36632) Avail: CASI HC A08/MF A02

X-ray absorption spectroscopy (XAS) was performed on Photosystem II (PSII)-enriched membranes prepared from spinach to explore: (1) the correlation between structure and magnetic spin state of the Mn cluster in the oxygen evolving complex (OEC) in the S(sub 2) state; and (2) the oxidation state changes of the Mn cluster in the flash-induced S-states. The structure of the Mn cluster in the S(sub 2) state with the g approx. 4electron paramagnetic resonance (EPR) signal (S(sub 2)-g4 state) was compared with that in the S(sub 2) state with multiline signal (S(sub 2)-MLS state) and the S(sub 1) state. The S(sub 2)-g4 state has a higher XAS inflection point energy than that of the S(sub 1) state, indicating the oxidation of Mn in the advance from the S(sub 1) to the S(sub 2)-g4 state. Differences in the edge shape and in the extended X-ray absorption fine structure (EXAFS) show that the structure of the Mn cluster in the S(sub 2)-g4 state is different from that in the S(sub 2)-MLS or the S(sub 1) state. In the S(sub 2)-g4 state, the second shell of backscatterers from the Mn absorber contains two Mn-Mn distances of 2.73 angstrom and 2.85 angstrom. Very little distance disorder exists in the second shell of the S(sub 1) or S(sub 2)-MLS states. The third shell of the S(sub 2)-g4 state at about 3.3 angstrom also contains increased heterogeneity relative to that of the S(sub 2)-MLS or the S(sub 1) state. Various S-states were prepared at room-temperature by saturating, single-turnover flashes. The flash-dependent oscillation in the amplitude of the MLS was used to characterize the S-state composition and to construct (pure) S-state Mn K-edge spectra. The edge position shifts to higher energy by 1.8 eV upon the S(sub 1) yields S(sub 2) transition. DOE

N95-27747# Fermi National Accelerator Lab., Batavia, IL.
EXCITED CHARM STATES
Shekhar Shukla 1994 14 p Presented at the 2nd International Workshop on Heavy Quark Physics in Fixed Targets, Charlottesville, VA, 6-10 Oct. 1994
(Contract DE-AC02-76CH-03000)
(DE95-005749; FNAL/C-94/401; CONF-9410285-2) Avail: CASI HC A03/MF A01

Characteristics of mass spectra and decays of orbitally excited charm mesons and baryons, expected on the basis of quark models and Heavy Quark Symmetry, are briefly described. The difficulties associated with measurements on these excited states are discussed. The accuracy and reliability of currently available experimental information is examined. The reasons, for the widely accepted spin-parity assignments to the observed excited mesons and baryons, are stated. Finally, the experimental data, with the accepted spin-parity assignments, is compared with expectations based on quark models and Heavy Quark Symmetry. DOE

N95-27753# Argonne National Lab., IL.
EXPERIMENTAL DETERMINATION OF CLUSTER GEOMETRICAL STRUCTURE
S. J. Riley 1995 23 p Presented at the Workshop on Clusters and Nanostructured Materials, Bhubaneswar, India, 29 Dec. 1994 - 4 Jan. 1995
(Contract W-31-109-eng-38)
(DE95-007089; ANL/CHM/CP-83631; CONF-941257-1) Avail: CASI HC A03/MF A01

Chemical probes have been developed to provide insight into the geometrical structure of isolated transition metal clusters. By determining as a function of cluster size the number of adsorbate molecules that saturate a cluster, and/or the binding energy of molecules to cluster surfaces,

it is often possible to propose geometrical structures consistent with the experimental observations. The authors review recent studies of the reactions of cobalt, nickel, and copper clusters with ammonia, water, and nitrogen that provide structural information. It is found that small (between 50 and 150 atoms) cobalt, nickel, and copper clusters generally adopt icosahedral packing. However, for even smaller (less than 20 atoms) clusters, cobalt and nickel differ in their structure. The authors also see evidence for adsorbate-induced structural changes. These changes may allow the properties of materials fabricated from such clusters to be tailored to specific needs. A preliminary illustration of the dramatic effect that heteroatoms can have on metal cluster chemical properties is presented.
DOE

N95-27871# Fermi National Accelerator Lab., Batavia, IL.
SEARCH FOR SUPERSYMMETRY AND LEPTOQUARK STATES AT FNAL
Sharon Hagopian Sep. 1994 4 p Presented at the 27th International Conference on High Energy Physics, Glasgow, Scotland, 21-27 Jul. 1994
(Contract DE-AC02-76CH-03000)
(DE95-003381; FNAL/C-94/331-E; CONF-940722-32) Avail: CASI HC A01/MF A01

Searches have been made for first generation scalar and vector leptoquarks by the D0 collaboration and for second generation scalar leptoquarks by the CDF collaboration. The data sample is from the 1992-93 p bar-p run at radical s = 1.8 TeV at the Fermilab Tevatron Collider. Assuming that leptoquarks are pair produced and decay into charged leptons and quarks with branching fraction beta, mass limits at the 95% Confidence Level (CL) have been obtained. For first generation scalar leptoquarks the lower mass limit is 130 GeV/c(exp 2) for beta = 1.0 and 116 GeV/c(exp 2) for beta = 0.5. For first generation vector leptoquarks with kappa, the anomalous coupling, of 1.0 and beta = 1.0, the lower mass limit is 240 GeV/c(exp 2) and for kappa = 1.0, beta = 0.5, the lower mass limit is 240 GeV/c(exp 2). For kappa = 0 and beta = 1.0, the lower mass limits is 190 GeV/c(exp 2) and for kappa = 0, beta = 0.5, the lower mass limit is 185 GeV/c(exp 2). For second generation scalar leptoquarks, the mass limits are 133 GeV/c(exp 2) for beta = 1.0 and 98 GeV/c(exp 2) for beta = 0.5. A search for squarks and gluinos, predicted by Supersymmetric models, was made by D0 in the three or more jets plus E(sub t) channel. The number of events observed was consistent with background. For heavy squarks, a lower gluino mass limit of 146 GeV/c(exp 2) was obtained, and for equal squark and gluino masses a mass limit of 205 GeV/c(exp 2) was obtained at the 95% CL. DOE

N95-27872# Fermi National Accelerator Lab., Batavia, IL.
A STUDY OF EVENTS WITH LARGE TOTAL TRANSVERSE ENERGY PRODUCED IN PROTON-ANTIPROTON COLLISIONS AT (RADICAL)s = 1.8 TeV
Henryk Piekarz Sep. 1994 7 p Presented at the Meeting of the Division of Particles and Fields of the American Physical Society, Albuquerque, NM, 2-6 Aug. 1994
(Contract DE-AC02-76CH-03000)
(DE95-003382; FNAL/C-94/330-E; CONF-940816-61) Avail: CASI HC A02/MF A01

Properties of events originating from proton-antiproton interactions in which the total transverse energy, Sigma(E(sub T)), of the event exceeded 400 GeV are presented. These events were produced at the Fermilab Tevatron Collider operating at a center-of-mass energy of 1.8 TeV and recorded in the D0 detector. The authors describe their analysis method which minimizes the effect of multiple interactions in the data sample. Based on a data sample of 5.45 +/- 0.65 pb(sup -1), the topology of these hard scattering events as well as preliminary results for the cross-section, d sigma/d Sigma(E(sub T)), are presented and discussed.
DOE

N95-27874# Oak Ridge National Lab., TN.
POSITRON MICROSCOPY
L. D. Hulett, Jr. and J. Xu 1995 9 p Presented at the 10th International Conference on Positron Annihilation, Beijing, China, 23-29 May 1994
(Contract DE-AC05-84OR-21400)
(DE95-007042; CONF-9405170-9) Avail: CASI HC A02/MF A01

The negative work function property that some materials have for positrons make possible the development of positron reemission microscopy (PRM). Because of the low energies with which the positrons are emitted, some unique applications, such as the imaging of defects, can be made. The history of the concept of PRM, and its present state of development will be reviewed. The potential of positron microprobe techniques will be discussed also. DOE

N95-27881# International Centre for Theoretical Physics, Trieste (Italy).
A DIAGRAM TECHNIQUE FOR STRONGLY INTERACTING FERMION SYSTEMS. ONE-AND TWO-BAND HUBBARD MODELS
V. A. Moskalenko, S. P. Cojocaru, and M. I. Vladimir (Academy of Sciences, USSR, Moscow, USSR.) Jul. 1994 34 p
(DE95-609437; IC-94/182) Avail: CASI HC A03/MF A01 (US Sales Only)

The basic notions of a diagram method for the one-band Hubbard model, including Green functions, generalized Wick theorem and Dyson equation are discussed. The study of Mott-Hubbard and superconducting transitions is based on a localized approximation for the irreducible two-particle Green function. A similar technique is developed for the two-band Hubbard model which is more closely related to the structure of CuO2 planes of high-Tc superconductors and to find the criterion of metal-insulator transition. DOE

N95-27922# Cornell Univ., Ithaca, NY.
ON THE PHYSICS OF ION RING GENERATION FOR THE STABILIZATION OF FRX DISCHARGES Final Report
H. Fleischmann 1995 36 p
(Contract DE-AC02-76ET-53017)
(DE95-007105; DOE/ET-53017/T3) Avail: CASI HC A03/MF A01

As envisioned in the respective proposals, the author's work over the final periods of this contract centered on experimental and related theoretical investigations of the physics of the generation of ion rings which might be used for a tilt stabilization of FRX rings, with experiments centering around the new MICE equipment constructed during the earlier parts of the work. In particular, the work mainly consisted of the following: (1) investigations concerning the operation of the ion beam driver constructed earlier, especially of the magnetically insulated ion diode and possible improvements of that diode; (2) theoretical analyses on the propagation and neutralization of the ion beam during its injection into the confinement tank; and (3) experimental investigations on the physics of ion beam injection and ring formation in the MICE device; in these latter experiments very significant discrepancies of various observed data and those predicted from single-particle orbit calculations were found. Unfortunately, the work could not be completed due to stop in funding, but a semiquantitative analysis of these discrepancies indicated insufficient space charge neutralization of the ion beam in the tank and/or charge-exchange effects in the diode are considered the most likely reasons. In contrast to claims by its authors, a similar discrepancy also was found in the published data of the earlier IREX experiment. The results of their investigations, which together with the design and construction of the equipment provided the basis for two PhD theses, will be briefly described in this report; the full details can be obtained from the two theses. DOE

N95-27927# Missouri Univ., Columbia, MO.
HIGH PRESSURE OPTICAL STUDIES OF SEMICONDUCTORS AND HETEROSTRUCTURES Final Report
H. R. Chandrasekhar 1995 14 p
(Contract DE-FG02-89ER-45402)
(DE95-007119; DOE/ER-45402/T1) Avail: CASI HC A03/MF A01

The authors have studied the effects of hydrostatic pressure on the confined transitions in quantum well heterostructures, using lattice matched GaAs/Al(x)GaAs(1-x)As, strained layer narrow band gap GaSb/AlSb and In(x)Ga(1-x)As/GaAs, and strained layer wide gap Zn(1-x)Cd(x)Se/ZnSe as examples. Precise values of the energies, pressure coefficients and band alignments are determined. In strained epilayers the interfacial strains, deformation potential constants and compressibilities are deduced. Strain compensation, structural stability and phase transitions are probed. The authors have observed a novel type of Fano resonance of excitons in GaAs associated with the (Gamma) conduction band as they hybridize with the X and L continua via electron-phonon coupling. This effect is used to extract the intervalley electron-phonon deformation potential D(sub (Gamma)X) to be 10.7 (+/-) 0.7 eV/(angstrom). They have observed a new electron trap state in Al(0.3)Ga(0.7)As doped with silicon at pressure of 60 kbar. They postulate that this new trap state has a large lattice relaxation with the trap energy well above the X CB. These trap states may be present in all Al(x)Ga(x)As materials and may be dominant at large x values (0.7 less than x less than 1). DOE

N95-27930# International Centre for Theoretical Physics, Trieste (Italy).
HYDROGEN-LIKE ATOM IN LASER FIELD: INVARIANT ATOMIC PARAMETERS IN THE GROUND STATE
I. V. Bondarev and S. A. Kuten (Belarussian State Univ., Minsk, Belarus.) Jul. 1994 15 p
(DE95-609036; IC-94/217) Avail: CASI HC A03/MF A01 (US Sales Only)

The invariant atomic parameters (dynamical vector and tensor polarizabilities) of hydrogen-like atom in the ground 1S(sub 1/2) state are calculated analytically by means of the Laplace transform of the radial Schroedinger equation. The obtained analytical expressions have been written in the compact form as a sum of linear and squared combinations of Gauss hypergeometric functions (sub 2)F(sub 1). The frequency dependence of the invariant atomic parameters is analyzed. DOE

N95-27933# Fermi National Accelerator Lab., Batavia, IL.
SEARCH FOR EXOTIC PARTICLES AT CDF
R. M. Harris Feb. 1995 5 p Presented at the 4th International Conference on Physics Beyond the Standard Model, Lake Tahoe, CA, 13-18 Dec. 1994
(Contract DE-AC02-76CH-03000)
(DE95-008383; FNAL/C-95/024-E; CONF-941251-3) Avail: CASI HC A01/MF A01

CDF has searched for 2nd generation leptoquarks, new gauge bosons W(prime) and Z(prime), axigluons, excited quarks, color octet technirhos and E(sub 6) diquarks. We place the most stringent limits on direct production of these exotic particles. DOE

N95-27945# Fermi National Accelerator Lab., Batavia, IL.
THE TOP...IS IT THERE? A SURVEY OF THE CDF AND D0 EXPERIMENTS
A. V. Tollestrup Dec. 1994 71 p Presented at the Frontiers in Particle Physics, Cargese, France, 1-13 Aug. 1994
(Contract DE-AC02-76CH-03000)
(DE95-005746; FNAL/C-94-419-E; CONF-9408221-1) Avail: CASI HC A04/MF A01

This paper describes: (1) features that the top quark must have if it exists, and how those features are inferred from various experiments; (2) how top quarks may be produced; (3) what must be accomplished to directly establish that the top quark has been produced in an experiment. Relevant features of the CDF and D0 detectors are described, as are methods useful in a top-quark search for identifying and detecting various kinds of particles. The author reviews data found by both CDF and D0, and discusses differences between the detectors and the data found with each. DOE

N95-27953# Arizona Univ., Tucson, AZ. Dept. of Chemistry.
SINGLE MOLECULE DETECTION USING CHARGE-COUPLED DEVICE ARRAY TECHNOLOGY Final Report
M. B. Denton Apr. 1994 17 p
(Contract DE-FG02-90ER-60986)
(DE95-006425; DOE/ER-60986/T2) Avail: CASI HC A03/MF A01

An ultra sensitive technique for the detection of fluorescent species in a flowing stream has been developed. The extension of this technique to the detection of fluorescently tagged nucleotides will be a significant benefit to one of the novel approaches for DNA sequencing being developed at Los Alamos National Laboratories. The detection scheme is based on a novel mode of operating a charge-coupled device (CCD) which greatly enhances the discrimination between fluorescence from the analyte and the background Raman scattering from the solvent. Register shifts between rows in the CCD are synchronized with the sample flow velocity so that fluorescence from a single species is collected in a single moving charge packet occupying an area approaching that of a single pixel while the background is spread evenly among a large number of pixels. This research has demonstrated that this technique is highly effective for the detection of fluorescently labelled latex microspheres. With additional development, the authors believe that this technique will achieve single molecule detection. DOE

N95-28004# Argonne National Lab., IL. Materials Science Div.
REFLECTION OF NEUTRONS FROM AN OPTICAL GRATING
Alan E. Munter, S. Adenwalla, G. F. Felcher, and X. L. Zhou (Massachusetts Inst. of Tech., Cambridge, MA.) Dec. 1994 5 p Presented at the 1994 Fall Meeting of the Materials Research Society, Boston, MA, 28 Nov. - 2 Dec. 1994
(Contract W-31-109-eng-38)
(DE95-007145; ANL/MSD/CP-85268; CONF-941144-79) Avail: CASI HC A01/MF A01

Specular and off-specular neutron intensities were measured at grazing incidence from an optical grating. The periodicity of the grating was determined from the locations of the intensity peaks in the off-specular data. An analysis of the widths of the off-specular intensity peaks showed that the effect of the coherence length of the neutron beam on the determination of a surface length scale (approximately)30 (mu)m was negligible compared to that of the instrument resolution. Although the structure of an optical grating used in this paper is simple, it has served to illustrate the simple relationship between the off-specular data structure and the real-space properties. For more general rough systems, a practical theoretical model will be needed to relate the off-specular data to the real-space roughness structure so that the diffusive data can be analyzed. Owing to the intrinsic complexity of diffuse scattering, the development of such a theoretical model will be a significant technical challenge, and its solution will constitute a major breakthrough in the development of the diffuse reflectivity technique for rough surface/interface characterization. DOE

N95-28020# Massachusetts Inst. of Tech., Cambridge, MA.
MEASUREMENT OF PARTICLE TRANSPORT COEFFICIENTS ON ALCATOR C-MOD Ph.D. Thesis
T. C. T. Luke Oct. 1994 171 p
(Contract DE-AC02-78ET-51013)
(DE95-007763; DOE/ET-51013/307; PFC/RR-94-12) Avail: CASI HC A08/MF A02

The goal of this thesis was to study the behavior of the plasma transport during the divertor detachment in order to explain the central electron density rise. The measurement of particle transport coefficients requires sophisticated diagnostic tools. A two color interferometer system was developed and installed on Alcator C-Mod to measure the electron density with high spatial (approximately) 2 cm and high temporal (less than or equal to 1.0 ms) resolution. The system consists of 10 CO2 (10.6 micrometer) and 4 HeNe (.6328 micrometer) chords that are used to measure the line integrated density to within 0.08 CO2 degrees or 2.3 x 10(exp 16)/sq m theoretically. Using the two color interferometer, a series of gas puffing experiments were conducted. The density was varied above and below the threshold density for detachment at a constant magnetic field and plasma current. Using a gas modulation technique, the particle diffusion, D, and the convective velocity, V, were determined. Profiles were inverted using a SVD inversion and the transport coefficients were extracted with a time regression analysis and a transport simulation analysis. Results from each analysis were in good agreement. Measured profiles of the coefficients increased with the radius and the values were consistent with measurements from other experiments. The values exceeded neoclassical predictions by a factor of 10. The profiles also exhibited an inverse dependence with plasma density. The scaling of both attached and detached plasmas agreed well with this inverse scaling. This result and the lack of change in the energy and impurity transport indicate that there was no change in the underlying transport processes after detachment. DOE

N95-28024# Los Alamos National Lab., NM.
ALPHA CHARACTERIZATION INSIDE PIPES USING ION-TRANSPORT TECHNOLOGY
S. P. Rojas, M. W. Rawool-Sullivan, K. G. Williams, and J. A. Vaccarella 1995 9 p Presented at the Waste Management '95, Tucson, AZ, 26 Feb. - 2 Mar. 1995
(Contract W-7405-eng-36)
(DE95-007869; LA-UR-95-174; CONF-950216-69) Avail: CASI HC A02/MF A01

Many DOE facilities have several miles of waste pipe systems that are internally contaminated with various and often undetermined radio nuclides. Unfortunately, currently acceptable alpha detection technologies are inefficient, time consuming, and do not address the problems presented by small diameter or curved pipes. In general, the problem of detecting alpha contamination on the inside surface of pipes is complicated by the fact that alphas do not penetrate the pipe walls. Unlike their conventional counterparts, alpha detectors based on ion transport technology sense alpha particles by collecting the ions created in ambient air as the particle loses its kinetic energy. The ions inside the pipe are transported by a fan-generated air current to an electrode inside the detector, which is attached to one end of the pipe. The collected charge at the electrode is proportional to the number of ions created inside the pipe, which in turn is proportional to the number of alphas emitted. Typically, monitoring for alpha contamination inside pipes or ductwork involves disrupting the operation to access as much surface area as possible for standard alpha monitoring. The detector based on ion transport technology effectively minimizes such disruption and in many circumstances will allow for in situ monitoring of a system that might otherwise not be practically accessible to standard methods. DOE

N95-28028# Stanford Linear Accelerator Center, Stanford, CA.
THE TAU-CHARM FACTORY IN THE ERA OF B-FACTORIES AND CESR
L. V. Beers, ed. and M. L. Perl, ed. Oct. 1994 784 p Presented at the Tau-Charm Factory in the Era of B-factories and CESR Conference, Stanford, CA, 15-16 Aug. 1994
(Contract DE-AC03-76SF-00515)
(DE95-007894; SU-SLAC-451; CONF-9408190) Avail: CASI HC A99/MF A10

This paper is a collection of presentations made at a conference on tau-charm factories, held at the Stanford Linear Accelerator Center and Stanford University on August 15-16, 1994. The papers presented summarize the physics which can be learned from such a facility, the advantages it would present over planned B-factories and large centers such as CESR, and the types of decay modes which could be observed. More detailed studies of tau physics are opened up, as well as charmonium and charmed systems. Separate presentations to the proceedings are indexed individually into the database. DOE

N95-28041# Weizmann Inst. of Science, Rehovot (Israel).
SUPERSYMMETRY AND LIGHT QUARK MASSES IN A REALISTIC SUPERSTRING MODEL
Edi Halyo Aug. 1994 15 p
(DE95-610201; WIS-PH-94-29) Avail: CASI HC A03/MF A01 (US Sales Only)

We show that supersymmetry can be broken mainly by hidden matter condensates in the observable matter direction in generic superstring models. This happens only when the fields whose VEV's give masses to hidden matter do not decouple at the condensation scale. We find how the parameters of the string model and the vacuum determine whether supersymmetry is broken mainly by hidden matter or gaugino condensates and in the matter or moduli direction. DOE

N95-28045# Oak Ridge National Lab., TN.
ERROR ANALYSIS OF THE QUARTIC NODAL EXPANSION METHOD FOR SLAB GEOMETRY
R. C. Penland (North Carolina Univ., Raleigh, NC.), P. J. Turinsky (North Carolina Univ., Raleigh, NC.), and Y. Y. Azmy 1995 10 p Presented at the International Conference on Mathematics and Computations, Reactor Physics, and Environmental Analyses, Portland, OR, 30 Apr. - 4 May 1995
(Contract DE-AC05-84OR-21400)
(DE95-007373; CONF-950420-19) Avail: CASI HC A02/MF A01

This paper presents an analysis of the quartic polynomial Nodal Expansion Method (NEM) for one-dimensional neutron diffusion calculations. As part of an ongoing effort to develop an adaptive mesh refinement strategy for use in state-of-the-art nodal kinetics codes, we derive a priori error bounds on the computed solution for uniform meshes and validate them using a simple test problem. Predicted error bounds are found to be greater than computed maximum absolute errors by no more than a factor of six allowing mesh size selection to reflect desired accuracy. We also quantify the rapid convergence in the NEM computed solution as a function of mesh size. DOE

N95-28051# Los Alamos National Lab., NM.
AN INVESTIGATION OF THE APPLICABILITY OF THE NEW REILLEX(TM)-HPQ ANION EXCHANGE RESIN SYSTEM FOR TECHNETIUM/RHENIUM AND URANIUM IN THE HANFORD WASTE TANKS Final Report
K. R. Ashley, J. R. Ball, S. L. Cobb, J. M. Adams, and D. A. Young 30 Sep. 1994 84 p
(Contract W-7405-eng-36)
(DE95-007643; LA-SUB-95-28) Avail: CASI HC A05/MF A01

Results of the measurements of the exchange capacity and K(sub d) values for ReO4(-) on Reillex(tm)-HPQ as a function of nitric acid and hydroxide concentration, temperature, and ten months time will be reported. Results of the breakthrough volumes for UO2(2+) on Reillex-HPQ chromatography columns as a function of carbonate ion concentration in high nitrate ion concentrations and various column sizes will be reported. Individual sections of this report describe the following: the sorption behavior of ReO4(-) on the Reillex-HPQ between pH 2 and 12 in 1.00 M NaNO3; results of the measurements of the K(sub d) values for ReO4(-) on Reillex-HPQ and on Reillex-HP as a function of nitrate and hydroxide ion concentrations; the sorption behavior of ReO4(-) on Reillex-HPQ resin in base with time as a variable; the results of the early attempts at determining the K(sub d) values for Na4UO2(CO3)3 on Reillex-HPQ resin; and the breakthrough of UO2(NO3)2 in varying nitric acid solutions on Reillex-HPQ columns. DOE

N95-28057# Los Alamos National Lab., NM.
OFF-SPECULAR SCATTERING IN NEUTRON REFLECTOMETRY
R. Pynn, S. M. Baker, G. Smith, and M. Fitzsimmons 1995 22 p Presented at the Workshop on Neutron Applications in Materials Science and Engineering, Chalk River, Canada, 17 Aug. 1994
(Contract W-7405-eng-36)
(DE95-007835; LA-UR-95-754; CONF-9408211-1) Avail: CASI HC A03/MF A01

When neutrons are scattered at small angles from planar, laterally homogeneous, stratified media, only specular (mirror like) reflection is observed. Sample inhomogeneities, such as interfacial roughness or voids, give rise to off-specular scattering which has been observed in many experiments with neutrons and x-rays. The easiest way to describe this scattering theoretically is based on the distorted-wave Born approximation (DWBA), which uses the neutron wavefunctions that describe reflection from a smooth surface as the basis functions for perturbation theory. From the DWBA one may obtain a number of qualitative results which are supported by experiment. Examples include the Yoneda fringes observed in reflection experiments with microscopically rough surfaces and the constant-q(sub z) fringes observed for multilayers with correlated, rough interfaces. One must, however, use the DWBA with care. When the correlation range within the reflecting interfaces is large--for example, when a surface is composed of misoriented facets--the approximation breaks down. Some authors have also reported a lack of quantitative agreement between versions of the DWBA calculations and the scattering observed with microscopically rough surfaces. A remarkable feature of neutron (or x-ray) reflectometry is the length scales that are probed within reflecting surfaces. These range from a few hundred Angstroms up to several microns, allowing neutron scattering to probe objects of a size normally visible by optical microscopy! The intent of this paper is to provide a simple description of scattering from rough surfaces that is accessible to a wide audience. Mathematical completeness is sacrificed in favor of intuitive arguments and experimental examples. DOE

N95-28063# Los Alamos National Lab., NM.
MEASUREMENT OF THE REACTION C(NU(SUB MU), MU(-)) X NEAR THRESHOLD
F. J. Federspiel 1994 6 p Presented at the 5th Conference on Intersections Between Particle and Nuclear Physics, St. Petersburg, FL, 31 May - 6 Jun. 1994
(Contract W-7405-eng-36)
(DE95-007888; LA-UR-95-597; CONF-940514-20) Avail: CASI HC A02/MF A01

Using the decay-in-flight nu(sub mu) beam from the Los Alamos Meson

Physics Facility and a massive liquid scintillator neutrino detector (LSND), the reaction C(nu(sub mu), mu(-))X has been studied near threshold. Preliminary results for the visible energy distribution of the final state and the flux integrated cross section are presented and compared with the results of several nuclear model calculations. DOE

N95-28066# Oak Ridge National Lab., TN.
RECENT NEUTRON SCATTERING RESULTS ON HIGH-TEMPERATURE SUPERCONDUCTORS
H. A. Mook, P. Dai, G. Aeppli (Bell Telephone Labs., Inc., Murray Hill, NJ.), T. E. Mason (Toronto Univ., Ontario.), N. E. Hecker (Harvard Univ., Cambridge, MA.), J. A. Harvey (Harvard Univ., Cambridge, MA.), T. Armstrong (Battelle Northwest Labs., Richland, WA.), K. Salama (Houston Univ., TX.), and D. Lee (Houston Univ., TX.) 16 Sep. 1994 29 p Presented at the Neutron Scattering, Sendai, Japan, 11-14 Oct. 1994 Sponsored by Martin Marietta Energy Systems, Inc.
(Contract DE-AC05-84OR-21400)
(DE95-007028; CONF-9410165-11) Avail: CASI HC A03/MF A01

Triple-axis spectrometry has been used to determine the magnetic excitations in YBa2Cu3O7. Polarized measurements at 100 K show the scattering consists of a peak near 40 MeV superposed on a small relatively flat background. The 40-MeV peak is found to be sharp in energy and anisotropic in momentum occupying a square portion of the Cu-O reciprocal lattice plane. The temperature dependence of the scattering is identical at the square side and corner. Polarized measurements show that the small background scattering observed at 100 K disappears below the superconducting transition. Resonant absorption measurements made to examine the Cu phonons show that no changes in the phonons occur at the superconducting transition. DOE

N95-28067# Texas Univ., Austin, TX. Center for Particle Physics.
PROBING STRONGLY-INTERACTING ELECTROWEAK DYNAMICS THROUGH W(+)W(-)/ZZ RATIOS AT FUTURE E(+)E(-) COLLIDERS
V. Barger, Kingman Cheung, T. Han, and R. J. N. Phillips Jan. 1995 32 p Prepared in cooperation with California Univ., Davis, CA; Wisconsin Univ., Madison, WI; and Rutherford Appleton Lab., Chilton, England
(Contracts DE-FG03-93ER-40757; DE-FG03-91ER-40674; DE-FG02-95ER-40896)
(DE95-007202; DOE/ER-40757/061; UCD-95-2; RAL-95-003) Avail: CASI HC A03/MF A01

The authors point out that the ratio of W(+)W(-) yields W(+)W(-) and W(+)W(-) yields ZZ cross sections is a sensitive probe of the dynamics of electroweak symmetry breaking, in the CM energy region square root of s(sub ww) approximately greater than 1 TeV where vector boson scattering may well become strong. They suggest ways in which this ratio can be extracted at a 1.5 TeV e(+)e(-) linear collider, using W(+/-), Z yields jj hadronic decays and relying on dijet mass resolution to provide statistical discrimination between W(+/-) and Z. WW fusion processes studied here are unique for exploring scalar resonances of mass about 1 TeV and are complementary to studies via the direct channel e(+)e(-) yields W(+)W(-) for the vector and nonresonant cases. With an integrated luminosity of 200 fb(exp -1), the signals obtained are statistically significant. Comparison with a study of e(-)e(-) yields nu nu W(-)W(-) process is made. Enhancements of the signal rate from using a polarized electron beam, or at a 2 TeV e(+)e(-) linear collider and possible higher energy mu(+) mu(-) colliders, are also presented. DOE

N95-28077# Oak Ridge National Lab., TN. Center for Computationally Intensive Physics.
LATTICE CALCULATION FOR LEPTON CAPTURE FROM VACUUM-PAIR PRODUCTION IN RELATIVISTIC HEAVY-ION COLLISIONS
J. C. Wells, V. E. Oberacker, A. S. Umar, and M. R. Strayer 1994 12 p Presented at the 13th International Conference on the Application of Accelerators in Research and Industry, Denton, TX, 7-10 Nov. 1994 Sponsored by Martin Marietta Energy Systems, Inc.
(Contracts DE-AC05-84OR-21400; DE-FG05-87ER-40376)
(DE95-007392; CONF-941129-16) Avail: CASI HC A03/MF A01

The new colliding-beam heavy-ion accelerators, designed to investigate nuclear matter at high temperatures and densities, have motivated great interest during the last decade concerning possible new electromagnetic phenomena. One of the most interesting of these processes is the sparking of the vacuum to produce lepton-antilepton pairs. The process of electron capture from vacuum pair production is a principal beam-loss mechanism for highly charged relativistic ions in a storage ring, and thus must be considered in the design and the operation of these machines. In this paper, I present calculated impact-parameter-dependent probabilities and cross sections for muon capture from vacuum production in collisions of relativistic heavy ions by solving the time-dependent Dirac equation in unrestricted three-dimensional space using lattice-collocation techniques. Calculations are performed for muonpair production with capture into the K-shell in collisions of Au-197 + Au-197 at collider kinetic energies of 2 GeV per nucleon. DOE

N95-28078# Oak Ridge National Lab., TN.
COLLISIONS OF HIGHLY CHARGED IONS WITH ELECTRONS, ATOMS AND SURFACES
C. C. Havener, M. E. Bannister, L. Folkerts, J. W. Hale, M. Pieksma, J. Shinpaugh, and F. W. Meyer 30 Sep. 1994 15 p Presented at the 13th International Conference on the Application of Accelerators in Research and Industry, Denton, TX, 7-10 Nov. 1994 Sponsored by Martin Marietta Energy Systems, Inc.
(Contract DE-AC05-84OR-21400)
(DE95-007393; CONF-941129-17) Avail: CASI HC A03/MF A01

At the Oak Ridge Multicharged Ion Source Facility, an experimental atomic collisions physics program is centered around a recently upgraded Electron Cyclotron Resonance (ECR) multicharged ion source. The 10 GHz CAPRICE source has been in operation since October 22, 1992, and has provided more intense, higher charge ion beams than our previous ECR ion source. Intense metallic beams have recently become available with the installation of a metallic oven on the source. In addition to measurements of electron-impact excitation, carried out in collaboration with the Joint Institute for Laboratory Astrophysics (JILA), experiments are presently on-line to study electron-impact ionization, low-energy ion-atom collisions, and ion-surface interactions. A brief summary of our various activities with an emphasis on the new capabilities is presented. DOE

N95-28091# California Univ., Berkeley. Lawrence Berkeley Lab, CA.
INFRARED SPECTROSCOPY OF NONCLASSICAL IONS AND THEIR COMPLEXES Ph.D. Thesis
D. W. Boo Jan. 1995 190 p
(Contract DE-AC03-76SF-00098)
(DE95-008487; LBL-36702) Avail: CASI HC A09/MF A02

This thesis describes an infrared spectroscopic study on the structures and dynamics of the nonclassical ions and their complexes, using ion trap vibrational predissociation spectroscopy. Chapter One provides an introduction to the experimental apparatus used in this work. Chapter Two describes the previous theoretical and experimental works on the carbonium ion CH(5+) and infrared spectroscopic and theoretical works on CH(5+). CH(5+) was predicted to scramble constantly without possessing a stable structure. In Chapter Three, the infrared spectroscopy for the molecular hydrogen solvated carbonium ions CH(5+)(H2)(sub n) (n=1-6) in the frequency region of 2700-4200/sq cm are presented and compared with the results of ab initio molecular dynamics simulation on CH(5+)(H2)(sub n) (n=0-3). The results suggested that the scrambling of CH(5+) slowed down considerably by the stabilization effects of the solvent H2 molecules, and it was completely frozen out when the first three H2 molecules were bound to the core CH(5+). Chapter Four presents the complete infrared spectra for the solvated carbonium ions, CH(5+)(A)(x)(B)(y) A,B=H2, Ar, N2, CH4 : x,y=(0-5) in the frequency region of 2500-3200/cm. As the binding affinities of the solvent molecules and the number of the solvent molecules in the clusters increased, the scrambling of CH(5+) slowed down substantially. The structures of the solvated carbonium ions and the evidence for rapid proton transfer in CH(5+)(CH4) were also presented. Chapter Five presents the vib-rotational spectrum for the H-H stretching mode of the silanium ion SiH(5+). The results suggested that SiH(5+) can be described as a complex of SiH(3+) and a freely internally rotating H2, analogous to, but distinct from CH(5+). DOE

N95-28101 McCrone Associates, Inc., Westmont, IL.
ANALYTICAL ELECTRON MICROSCOPY OF NANOMETER-SIZED PARTICLES Quarterly Report No. 3, 1 Sep. - 30 Nov. 1994
Stephen B. Rice 19 Dec. 1994 18 p Limited Reproducibility: More than 20% of this document may be affected by microfiche quality

(Contract F08650-94-C-0034)
(AD-A289124) Avail: Issuing Activity (Defense Technical Information Center (DTIC))

During the past quarter, despite lengthy downtime for the JEOL 4000FX, two aspects of our research plan were initiated: microdiffraction; and the effects of prolonged beam exposure on the EELS signature of U oxides. While obtaining microdiffraction patterns, it was recognized that high resolution electron microscope images can be obtained on thin sections produced by ultramicrotomy. DTIC

N95-28142# Stanford Linear Accelerator Center, Stanford, CA.
POLARIZATION AS A PROBE TO THE PRODUCTION MECHANISMS OF CHARMONIUM IN (pi)N COLLISIONS
W. K. Tang, S. J. Brodsky, M. Vaenttinen (Helsinki Univ., Helsinki, Finland.), and P. Hoyer (Helsinki Univ., Helsinki, Finland.) Jul. 1994 8 p Presented at the Workshop on the Future of High Sensitivity Charm Experiments, Batavia, IL, 7-9 Jun. 1994
(Contract DE-AC03-76SF-00515)
(DE95-008136; SU-SLAC-PUB-6576; CONF-9406242-6) Avail: CASI HC A02/MF A01

Measurements of the polarization of J/(psi) produced in pion-nucleus collisions are in disagreement with leading twist QCD prediction where J/(psi) is observed to have negligible polarization whereas theory predicts substantial polarization. The authors argue that this discrepancy cannot be due to poorly known structure functions nor the relative production rates of J/(psi) and (chi)(sub j). The disagreement between theory and experiment suggests important higher twist corrections, as has earlier been surmised from the anomalous non-factorized nuclear A-dependence of the J/(psi) cross section. DOE

N95-28158# Stanford Linear Accelerator Center, Stanford, CA.
PRECISE MEASUREMENT OF THE LEFT-RIGHT CROSS SECTION ASYMMETRY IN Z BOSON PRODUCTION BY e(+)e(-) COLLISIONS
A. Lath (Massachusetts Inst. of Tech., Cambridge, MA.) Sep. 1994 4 p Presented at the Meeting of the Division of Particles and Fields of the American Physical Society, Albuquerque, NM, 2-6 Aug. 1994
(Contract DE-AC03-76SF-00515)
(DE95-008591; SU-SLAC-PUB-6667; CONF-940816-90) Avail: CASI HC A01/MF A01

The authors present a precise measurement of the left-right cross section asymmetry (A(sub LR)) for Z boson production by e(+)e(-) collisions. The measurement was performed at a center-of-mass energy of 91.26 GeV with the SLD detector at the SLAC Linear Collider (SLC). The luminosity-weighted average polarization of the SLC electron beam was (63.0 +/- 1.1)%. Using a sample of 49,392 Z decays, they measure A(sub LR) to be 0.1628 +/- 0.0071 (stat.) +/- 0.0028(syst.) which determines the effective weak mixing angle to be sin(sup 2) (theta)(sub W)(sup eff) = 0.2292 +/- 0.0009(stat.) +/- 0.0004(syst.). They combine this result with the result obtained in 1992 and obtain sin(sup 2) (theta)(sub W)(sup eff) = 0.2294 +/- 0.0010, which constitutes the best measurement of sin(sup 2) (theta)(sub W)(sup eff) in a single experiment presently available. DOE

N95-28169# Brookhaven National Lab., Upton, NY.
ASPECTS OF STRANGENESS
C. B. Dover 1995 14 p Presented at the Quark Matter 1995, Monterey, CA, 9-13 Jan. 1995
(Contract DE-AC02-76CH-00016)
(DE95-008314; BNL-61490; CONF-950173-1) Avail: CASI HC A03/MF A01

We review various aspects of strangeness production in relativistic heavy ion collisions from AGS to CERN energies. The experimental data are briefly summarized and various possible theoretical interpretations of these data are evaluated, such as quark-gluon-plasma (QGP), hadron gas (HG) thermal models, or event generators (cascade models). Some comments on the production of strange clusters are offered. DOE

N95-28170# Brookhaven National Lab., Upton, NY.
ASPECTS OF STRANGE MATTER
C. B. Dover Feb. 1995 14 p Presented at the Strangeness 1995 Conference, Tucson, AZ, 4-6 Jan. 1995
(Contract DE-AC02-76CH-00016)
(DE95-008316; BNL-61487; CONF-950172-1) Avail: CASI HC A03/MF A01

We discuss the stability of multiply strange baryonic systems, in the context of a mean field approach obtained from an underlying set of phenomenological meson-baryon interactions. The coupling parameters which determine the conventional sigma + omega mean fields (Hartree potentials) seen by various baryon species (N, lambda, Xi) in the many-body system are constrained by reproducing the trend of observed binding energies of single particle (N, lambda, Xi) states, as well as the energy per particle and density of non- strange nuclear matter. We also consider additional scalar (sigma*) and vector (phi) fields which couple strongly to strange baryons. The couplings of these fields are adjusted to produce strong hyperon-hyperon interactions, as suggested by the data on (Lambda)(Lambda) hypernuclei. Extrapolating this approach to systems of large strangeness S, we find a broad class of objects composed of neutrons, protons, Lambda's and Xi's, which are stable against strong decay. In these systems, the presence of filled Lambda orbitals blocks the strong decay (Xi)N yields (Lambda)(Lambda), leading to a strangeness fraction f(sub s) = (absolute value of S)/A approximately equal to 1, density rho approximately equal to (2 - 3)(sub rho), and charge fraction f(sub q) in the range -0.1less than q/A less than 0.1, comparable to that of hypothetical stable strange quark matter ('strangelets'), but with a low binding energy per particle E(sub B)/A approximately equal to -10 to -20 MeV. Such weakly bound multi-strange objects can be stable for very large A, unlike ordinary nuclei, since the Coulomb repulsion generated by the protons is largely cancelled by the presence of a comparable number of (Xi)'s, leading to a small net charge (positive or negative) of order A(sup 1/3). DOE

N95-28171# Lawrence Livermore National Lab., Livermore, CA.
BEGET: THE B-FACTORY EVENT GENERATOR VERSION 21
D. M. Wright 15 Aug. 1994 25 p
(Contract W-7405-eng-48)
(DE95-008329; UCRL-ID-117982) Avail: CASI HC A03/MF A01

This note is a reference manual for the B-Factory Event Generator (BEGET V21) software package which generates physics events relevant to B-Factory detector studies. The package provides a standard framework that can easily interface to various external generators and simulation applications. Version 21 of BEGET contains a number of physics and background generators and is interfaced to the JETSET and KORALB generators and the GEANT and ASLUND simulation programs. DOE

N95-28184# Joint Inst. for Nuclear Research, Dubna (USSR). Lab. of Nuclear Reactions.
ON IONIC CHARGE DISTRIBUTIONS OF HEAVY EVAPORATION RESIDUES PASSING THROUGH A CARBON FOIL
R. N. Sagajdak and A. V. Eremin 1993 10 p Submitted for publication
(DE94-629016; JINR-E-7-93-356) Avail: CASI HC A02/MF A01 (US Sales Only)

Parameters of the ionic charge distributions, i.e. mean charge values and charge distribution widths, for very heavy (Z greater than or equal to 53) ions passing through a carbon foil were analyzed from the view point of applicability of known empirical systematics. Strong deviations (up to 60%) for experimental mean charge values were obtained from those deduced from empirical formulae at energies of ions less than 0.1 MeV/a mu. Corrections providing a general agreement with the experimental data within of +/- 6% at the energies of ions 0.001 less than or equal E less than or equal 10 MeV/a mu to the formula of Shima et al. are proposed. New systematics of the widths for charge distributions is also presented. The obtained systematics were used in ion-optical calculations of transportation of evaporation residues through the electrostatic recoil separator VASSILISSA. DOE

N95-28199# Massachusetts Inst. of Tech., Cambridge, MA.
SPECTROSCOPIC AND DYNAMICAL STUDIES OF HIGHLY ENERGIZED SMALL POLYATOMIC MOLECULES Technical Progress Report, 1 Jul. 1993 - 31 Oct. 1994
R. W. Field and R. J. Silbey 1995 11 p
(Contract DE-FG02-87ER-13671)
(DE95-006640; DOE/ER-13671/8) Avail: CASI HC A03/MF A01

This is a progress report on a project to spectroscopically study small polyatomic molecules which are highly excited. The authors describe work on acetylene (HCCH) and HCO. Their work involves dispersed fluorescence spectroscopy, and the development and application of superpolyad models for studying intramolecular vibrational redistribution. DOE

N95-28204# Oak Ridge National Lab., TN.
SENSOR FOR MEASURING THE ATOMIC FRACTION IN HIGHLY DISSOCIATED HYDROGEN
W. L. Gardner 1994 16 p Presented at the 41th Annual American Vacuum Society Symposium, Denver, CO, 24-28 Oct. 1994
(Contract DE-AC05-84OR-21400)
(DE95-006531; CONF-941001-13) Avail: CASI HC A03/MF A01

Atomic hydrogen is a very important constituent for processes ranging from cleaning oxide from GaAs and annealing amorphous silicon to the deposition of diamond. Because the usual techniques for measuring atomic fraction are either expensive and cumbersome to use, or unsuitable for application to highly dissociated hydrogen, a specially designed sensor was developed. Sensor design is based on a diffusion tube with noncatalytic walls, having one end open to the atom source and a catalytic closure at the other end. The sensor is simple and inexpensive to fabricate, and determining atom density is straightforward. Sensor design also inhibits thermal runaway, which occurs when atom density is high enough to impart enough recombination energy to the non-catalytic surface to substantially raise its temperature. While recombination coefficients for such surfaces are very low near room temperature, they increase nearly exponentially with temperature unless actively cooled. With the use of a straightforward calibration scheme to determine the variation in species fraction along the diffusion tube, the atomic fraction at the tube opening is determined. Design strategy, implementation considerations, and calibration method are presented. In addition, data obtained from an atomic hydrogen source are compared to relevant published data. DOE

N95-28210# Argonne National Lab., IL.
THE HIGH ENERGY BEHAVIOR OF THE FORWARD SCATTERING PARAMETERS – (SIGMA)(SUB TOT), (RHO), AND B
Martin M. Block, F. Halzen (Wisconsin Univ., Madison, WI.), B. Margolis (McGill Univ., Montreal, Quebec.), and A. R. White Oct. 1994 12 p Presented at the 24th International Symposium on Multiparticle Dynamics, Vietri sul Mare, Italy, 12-19 Sep. 1994 Prepared in cooperation with Northwestern Univ., Evanston, IL
(Contracts W-31-109-eng-38; DE-AC02-76ER-02289; DE-AC02-76ER-00088)
(DE95-007075; ANL/HEP/CP-94-81; CONF-9409257-4) Avail: CASI HC A03/MF A01

Utilizing the most recent experimental data, the authors reanalyze high energy (anti p)p and pp data, using, two distinct (and dissimilar) analysis techniques: (1) asymptotic amplitude analysis, under the assumption that they have reached 'asymptopia'; and (2) an eikonal model whose amplitudes are designed to mimic real QCD amplitudes. The former gives strong evidence for a log(s/s(sub o)) dependence at current energies and not log(sup 2)(s/s(sub o)), and demonstrates that odderons are not necessary to explain the experimental data. The latter gives a unitary model for extrapolation into true 'asymptopia' from current energies, allowing the authors to predict the values of the total cross section at future supercolliders. Using the QCD-model, they obtain (sigma)(sub tot)(16 TeV) = 109 (+/-) 4 mb and (sigma)(sub tot)(40 TeV) = 124 (+/-) 4 mb. DOE

N95-28221# Fermi National Accelerator Lab., Batavia, IL.
COSMIC RAY TEST RESULTS OF THE D0 PROTOTYPE SCINTILLATING FIBER TRACKER
D. Adams (Rice Univ., Houston, TX.), I. Bertram (Rice Univ., Houston, TX.), M. Adams (Illinois Univ., Chicago, IL.), M. Chung (Illinois Univ., Chicago, IL.), B. Baumbaugh (Notre Dame Univ., IN.), and A. Bross Jan. 1995 10 p Presented at the 4th International Conference on Advanced Technology and Particle Physics, Como, Italy, 3-7 Oct. 1994
(Contract DE-AC02-76CH-03000)
(DE95-007215; FNAL/C-95/012-E; CONF-941060-4) Avail: CASI HC A02/MF A01

The performance of a large scale scintillating fiber tracker with VLPC readout has been studied in a cosmic-ray test. Approximately 9.6 photoelectrons per single layer per trigger were detected at a VLPC bias voltage of 6.5V. The doublet efficiency was nearly 100% at a 0.1% noise level and a position resolution of about 140 micron was measured. The authors also studied the relationship between VLPC performance and VLPC bias voltage by measuring single fiber efficiency as a function of VLPC bias in the range 6.2V to 7.0V at a fixed temperature of 6.5 K. They observed no significant variation in VLPC performance within this bias range. DOE

N95-28245# Joint Inst. for Nuclear Research, Dubna (USSR). Lab. of Nuclear Problems.
SOME ASPECTS OF THE OZI-RULE VIOLATION IN THE REACTION ANTI-pp YIELDS PHI PI(0)
D. Buzatu and F. M. Lev 1994 26 p
(DE95-608853; JINR-E-4-94-158) Avail: CASI HC A03/MF A01 (US Sales Only)

We consider the problem whether the violation of the OZI-rule in the reaction anti-pp yields phi pi(0) can be explained as the effect of rescattering in the processes anti-pp yields (K* anti-K + anti-K* K) yields K anti-K pi(0) yields phi pi(0) and/or anti-p p yields rho(+) rho(-) yields rho(+) pi(-) + rho(-) pi(+) pi(0) yields phi pi(0). If this effect is important then it is possible to give theoretical predictions concerning the energy dependence of the quantity BR(anti-p p yields phi pi(0))/BR(anti-p p yields K* anti-K) and the value of this quantity in the annihilation at rest from the P state. At the same time the analogous effect in the reaction anti-p p yields f(sub 2)'pi(0) is negligible. DOE

N95-28246# Melbourne Univ., Parkville (Australia). Research Center for High Energy Physics.
CONSTRAINTS ON THE ANOMALOUS WW GAMMA COUPLINGS FROM b VECTOR s GAMMA
Xiao-Gang He and Bruce McKellar 1993 11 p
(DE95-608866; UM-P-93/52; OZ-93/14) Avail: CASI HC A03/MF A01 (US Sales Only)

The contributions to b yields s gamma from anomalous WW gamma interactions are analyzed. Although these anomalous interactions are not renormalizable, the contributions are cut-off independent. Recent results from the CLEO collaboration on inclusive radiative B decays are used to obtain bounds for the anomalous CP conserving and CP violating couplings. The constraints on the CP conserving couplings are comparable with or better than constraints from other experiments. DOE

N95-28247# Joint Inst. for Nuclear Research, Dubna (USSR). Lab. of Neutron Physics.
SITUATION IN STUDY OF ELECTRIC POLARIZABILITY AND MEAN SQUARE CHARGE RADIUS OF THE NEUTRON
Yu. A. Aleksandrov 1994 3 p Presented at the International Conference on Nuclear Data for Science and Technology, Gatlinburg, TN, 9-13 May 1994
(DE95-608869; JINR-E-3-94-169) Avail: CASI HC A01/MF A01 (US Sales Only)

The paper discusses the status of the study of electric polarizability and intrinsic charge radius of the neutron as for the end of 20th century. Recent experimental data in the field of low energy physics are presented. The current theoretical version of the problem interpreting these data is also discussed. DOE

N95-28248# Joint Inst. for Nuclear Research, Dubna (USSR). Lab. of High Energy.
THE BREMSSTRAHLUNG OF SOFT GAMMA-QUANTA CREATED BY ELASTIC pp- AND np-SCATTERINGS AND THE DIBARYON RESONANCE PROBLEM [TORMOZNOE IZLUCHENIE MYAGKIKH GAMMA-KVANTOV PRI UPRUGOM PP- I NP-RASSEYANII I PROBLEMA DIBARIONNYKH REZONANSOV]
V. L. Lyuboshits and M. I. Podgoretskij 1994 18 p In RUSSIAN
(DE95-608870; JINR-R-2-94-181) Avail: CASI HC A03/MF A01 (US Sales Only)

It is shown that the investigation of the Bremsstrahlung spectrum of soft gamma-quanta in pp- and np-collisions allows, in principle, to solve the question of the existence of dibaryon resonances and to determine their parameters. The features of the Bremsstrahlung connected with the resonance elastic scattering at small angles are analyzed in detail. DOE

N95-28249# International Centre for Theoretical Physics, Trieste (Italy).
NEUTRINO OSCILLATIONS IN STRONG MAGNETIC FIELDS
G. G. Likhachev (Moscow State Univ., Russia.) and A. I. Studenikin Jul. 1994 8 p
(DE95-608876; IC-94/170) Avail: CASI HC A02/MF A01 (US Sales Only)

Neutrino conversion processes between two neutrino species and the corresponding oscillations induced by strong magnetic fields are considered. The value of the critical strength of magnetic field B(sub cr) as a function of characteristics of neutrinos in vacuum (Delta m(sup 2)(sub nu), mixing angle theta), effective particle density of matter n(sub eff), neutrino (transition) magnetic moment mu-tilde and energy E is introduced. It is shown that the neutrino conversion and oscillations effects induced by magnetic fields B greater or equal than B(sub cr) are important and may result in the depletion of the initial type of nu's in the bunch. A possible increase of these effects in the case when neutrinos pass through a sudden decrease of density of matter ('cross-boundary effect') and applications to neutrinos from neutron stars and supernova are discussed. DOE

N95-28251# International Centre for Theoretical Physics, Trieste (Italy).
QUANTUM EFFECTS INDUCED BY A GAP IN THE SPECTRUM OF ATOM-BATH COUPLING CONSTANTS: FREEZING OF ATOMIC DECAY AND MONOCHROMATIC COLLECTIVE RADIATION
D. S. Mogilevtsev and S. Ya. Kilin (Akademiya Nauk BSSR, Minsk, Russia.) Aug. 1994 29 p
(DE95-609037; IC-94/219) Avail: CASI HC A03/MF A01 (US Sales Only)

A specific kind of inhibition of atomic decay ('freezing' of decay) and intense monochromatic collective radiation are predicted for a single two-level atom and for a system of atoms interacting with the field bath having the gap in the spectrum of coupling constants. DOE

N95-28252# Joint Inst. for Nuclear Research, Dubna (USSR). Lab. of Nuclear Problems.
SEARCH FOR DEEPLY BOUND PIONIC ATOMS WITH HIGH-PURITY GERMANIUM TAGGING SPECTROMETER
B. A. Chernyshev (Moscow Physical-Engineering Inst., Russia.), M. G. Gornov (Moscow Physical-Engineering Inst., Russia.), V. N. Grebenev (Moscow Physical-Engineering Inst., Russia.), Yu. B. Gurov (Moscow Physical-Engineering Inst., Russia.), R. R. Shafigulin, S. V. Dovgun, S. L. Katulina, and V. G. Sandukovskij 1994 6 p
(DE95-609072; JINR-E-13-94-198) Avail: CASI HC A02/MF A01 (US Sales Only)

The experimental search and study of the deeply bound pionic atoms of xenon are proposed. The levels of pionic atoms produced in two-body channels of the reaction (sub N)Xe(d, He-3)(sub (N-1)) Xe(sub (pi))-can be identified by observing peaks in the He-3 energy spectrum measured at Theta = 0 deg where the cross section must reach the largest value. It is supposed that the experiment will be carried out with the zero-angle high-purity germanium spectrometer ('tagging system' of WASA) at the CELSIUS storage ring. The estimations show that an experimental run of about 100 hours will be enough for the observation of pionic atoms if the production cross section is not less than several micro b/sr/MeV. DOE

N95-28329# General Atomics Co., San Diego, CA.
TRANSPORT SIMULATION OF NEGATIVE MAGNETIC SHEAR DISCHARGES
H. St.John, T. S. Taylor, Y. R. Lin-Liu, and A. D. Turnbull Oct. 1994 12 p Presented at the 15th International Conference on Plasma Physics and Controlled Nuclear Fusion Research, Seville, Spain, 26 Sep. - 1 Oct. 1994
(Contract DE-AC03-89ER-51114; GA Proj. 3466)
(DE95-003941; GA-A-21847; IAEA-CN-60/D-D-II-8; CONF-940933-20)
Avail: CASI HC A03/MF A01

In the present work the authors present simulations which show that the hollow current profile can be maintained in quasi-steady state through a self-consistently determined combination of bootstrap current and neutral beam and rf current drive. Controllability of the q profile is demonstrated by eliminating low m/n mode number instabilities from these discharges by maintaining q greater than 1.5 at all times, starting from appropriate initial conditions. At moderately high beta(sub p), the bootstrap current can be a substantial fraction of the total current and the ability to maintain the proper total current density profile depends on the bootstrap current profile and the availability of suitable localized heating and current drive. In these simulations, they use electron cyclotron heating, ion cyclotron heating, and electron cyclotron and fast wave current drive. The ability to maintain the profiles is demonstrated using several energy transport models. Self-consistent transport simulations are used to model the SSC discharges using the ONETWO transport code coupled to RF heating and current drive packages FASTWAVE and TORAY. To accurately model inductive and driven current profile evolution, the additional source terms that arise in Faraday's law due to internal flux surface motion are included by coupling the transport calculations to a fixed boundary equilibrium code. To test the sensitivity of the results to the transport model used, they model DIII-D discharges using thermal conductivities consistent with improved confinement DIII-D discharges, and with the Rebut-Lallia-Watkins model of energy transport. DOE

N95-28338# Brookhaven National Lab., Upton, NY.
RARE DECAYS/CP: THE PERSPECTIVE OF A KAON PHYSICIST
L. Littenberg 1994 29 p Presented at the Meeting of the Division of Particles and Fields of the American Physical Society, Albuquerque, NM, 2-6 Aug. 1994
(Contract DE-AC02-76CH-00016)
(DE95-005964; BNL-61193; CONF-940816-84) Avail: CASI HC A03/MF A01

The status and future prospects of searches for and studies of forbidden and highly suppressed K decays are reviewed as is the search for charge parity time (CPT) violation in K decays. DOE

N95-28348* National Aeronautics and Space Administration. Pasadena Office, CA.
EXTENDED LINEAR ION TRAP FREQUENCY STANDARD APPARATUS Patent
John D. Prestage, inventor (to NASA) (Jet Propulsion Lab., California Inst. of Tech., Pasadena, CA.) 30 May 1995 42 p Filed 13 May 1994 Prepared in cooperation with Jet Propulsion Lab., California Inst. of Tech., Pasadena, CA
(NASA-Case-NPO-19081-1-CU; US-Patent-5,420,549;
US-Patent-Appl-SN-246041; US-Patent-Class-331-94.1;
US-Patent-Class-331-3; US-Patent-Class-324-304;
Int-Patent-Class-H03L-7/26) Avail: US Patent and Trademark Office

A linear ion trap for frequency standard applications is provided with a plurality of trapping rods equally spaced and applied quadruple rf voltages for radial confinement of atomic ions and biased level pins at each end for axial confinement of the ions. The trapping rods are divided into two linear ion trap regions by a gap in each rod in a common radial plane to provide dc discontinuity, thus dc isolating one region from the other. A first region for ion-loading and preparation fluorescence is biased with a dc voltage to transport ions into a second region for resonance frequency comparison with a local oscillator derived frequency while the second region is held at zero voltage. The dc bias voltage of the regions is reversed for transporting the ions back into the first region for fluorescence measurement. The dual mode cycle is repeated continuously for comparison and feedback control of the local oscillator derived frequency. Only the second region requires magnetic shielding for the resonance function which is sensitive to any ambient magnetic fields.

Official Gazette of the U.S. Patent and Trademark Office

N95-28355# Brookhaven National Lab., Upton, NY.
WEAK MATRIX ELEMENTS EFFORTS ON THE LATTICE: STATUS AND PROSPECTS
A. Soni Jan. 1995 19 p Presented at the 1994 International Workshop on B Physics, Physics Beyond the Standard Model At the B Factory, Nagoya, Japan, 26-28 Oct. 1994
(Contract DE-AC02-76CH-00016)
(DE95-007701; BNL-61378; CONF-9410248-2) Avail: CASI HC A03/MF A01

Lattice approach to weak matrix elements is reviewed. Recent progress in treating heavy quarks on the lattice is briefly discussed. Illustrative sample of results obtained so far is given. Among them I elaborate on B(sub K), line integral of B and B yields K*(sub gamma). Experimental implications especially with regard to constraints on the Standard Model (i.e. Wolfenstein) parameters, V(sub td) measurements and expectations for B(sub s)- bar-B(sub s), oscillations are briefly discussed. DOE

N95-28447# Oak Ridge National Lab., TN.
RECENT STATUS IN THE SEARCH FOR THE QUARK-GLUON PLASMA
Cheuk-Yin Wong 1995 15 p Presented at the International Symposium on Medium Energy Physics, Beijing, China, 22-26 Aug. 1994
(Contract DE-AC05-84OR-21400)
(DE95-007036; CONF-9408185-2) Avail: CASI HC A03/MF A01

The author reviews recent experimental results in the search for the quark-gluon plasma. Because the magnitudes of many signals for the plasma are directly proportional to the reaction cross sections, the author examines the corrections to the commonly used lowest-order cross sections. The author finds that the corrections are often significant and should be properly taken into account. The use of dileptons and photons with large transverse momenta is suggested as a means to study the boundary of the quark-gluon plasma. DOE

N95-28495# Fermi National Accelerator Lab., Batavia, IL.
B-PHYSICS RESULTS FROM D0
D. Hedin (University of Northern Illinois, De Kalb, IL.) and L. Markosky (Arizona Univ., Tucson, AZ.) Dec. 1994 5 p Presented at the 27th International Conference on High Energy Physics, Glasgow, Scotland, 21-27 Jul. 1994
(Contract DE-AC02-76CH-03000)
(DE95-005126; FNAL/C-94/415-E; CONF-940722-42) Avail: CASI HC A01/MF A01

We report on preliminary measurements of the inclusive single muon and dimuon cross sections in p(bar p) collisions at (radical)s = 1.8 TeV using the D0 detector at the Fermilab collider. From these results, we extract the cross section for b-quark production for the kinematic range (vert bar)yb(vert bar) less than 1.0 and 6 less than p(sub t)(sup b) less than 50 GeV/c. We also report measurements on the J/(psi) production, and correlations between muons in dimuon events. DOE

N95-28572 Northwestern Univ., Evanston, IL. Dept. of Chemistry.
HIGH ENERGY DENSITY SYSTEMS IN CRYOGENIC MEDIA: THE PRODUCTION AND REACTIONS OF ATOMS AND RADICALS Final Report, 21 May 1990 - 1 Oct. 1994
Eric Weitz Nov. 1994 44 p Limited Reproducibility: More than 20% of this document may be affected by microfiche quality
(Contract F29601-91-C-0016)
(AD-A289818; PL-TR-94-3050) Avail: Issuing Activity (Defense Technical Information Center (DTIC))

The work in this study has been directed towards developing an understanding of the factors that affect the production and storage of energetic species in a cryogenic environment and to evaluate the feasibility of employing such a medium for use as a high energy density material. Matrix isolation techniques have been employed to produce and attempt to store reactive species, specifically atoms in cryogenic solids, with a focus on storage of O and H atoms. Factors that must be considered in optimizing the storage of photolytically produced atoms include: matrix temperature, photolysis wavelength, spin state of the atoms, reactions with co-fragments and parent, the relative mass of the photofragments, and diffusion and photoinduced diffusion of the photofragments and/or the parent molecule. The interplay between these factors and their effect on atom storage is considered. O atom storage in solid Xe at a 32 mmolar concentration has been achieved with a number of enumerated strategies possible for increasing this concentration. H atoms have been successfully isolated and are stable in solid Xe for days at a temperature of 10 K. Progress directed towards storing O atoms in solid O2 is reported on. DTIC

N95-28594# Stanford Linear Accelerator Center, Stanford, CA.
MEASUREMENT OF ALPHA(s) IN e(+)e(-) ANNIHILATION AT E(cm) = 29 GeV
D. A. Bauer (California Univ., Santa Barbara, CA.), R. Belcinski (Massachusetts Univ., Amherst, MA.), R. C. Berg (California Univ., Los Angeles, CA.), H. H. Bingham (California Univ., Berkeley, CA.), E. D. Bloom, C. D. Buchanan (California Univ., Los Angeles, CA.), D. O. Caldwell (California Univ., Santa Barbara, CA.), S.-B. Chun (California Univ., Los Angeles, CA.), A. R. Clark (California Univ., Berkeley. Lawrence Berkeley Lab, CA.), and G. D. Cowan (Gesamthochschule, Siegen, Germany.) et al Jul. 1994 8 p Presented at the 27th International Conference on High Energy Physics, Glasgow, Scotland, 21-27 Jul. 1994
(Contracts DE-FG03-91ER-40674; DE-AS03-76ER-70285; DE-FG03-91ER-40662; DE-AT03-87ER-40327; DE-AM03-76SF-00010; DE-AC03-76SF-00098; DE-FG02-92ER-40730; DE-FG02-92ER-40715; DE-AC03-76SF-00515; NSF PHY-91-19849)
(DE95-006486; SU-SLAC-PUB-6518; LBL-35812; CONF-940722-41) Avail: CASI HC A02/MF A01

A measurement of the strong coupling constant alpha(sub s) using the event-shape variable y(sub 3) (the differential two-jet rate) in the reaction e(+)e(-) yields hadrons is presented. The analysis is based on data from the TPC/Two-Gamma detector at the PEP e(+)e(-) storage ring taken between 1984 and 1986 at a center-of-mass energy of E(sub cm) = 29 GeV. A value of alpha(sub s)(29 GeV) = 0.160 +/- 0.012 is obtained, where the error is the quadratic sum of experimental and theoretical uncertainties. The procedure for determining alpha(sub s) is the same as that used by the ALEPH and TOPAZ experiments, which allows for a consistent comparison of the alpha(sub s) values obtained at different center-of-mass energies. The observed energy dependence 'running' of alpha(sub s) is found to be in good agreement with the QCD prediction, and is clearly incompatible with a constant value. DOE

N95-28595# Oak Ridge National Lab., TN.
RESONANT COHERENT EXCITATION OF N6(+) AND Mg11(+) IN PLANAR CHANNELING: ANISOTROPIES IN IONIZATION PROBABILITIES AND X-RAY EMISSION
S. Datz, P. F. Dittner, H. F. Krause, C. R. Vane, O. H. Crawford, J. S. Forster, G. S. Ball, W. G. Davies, and J. S. Geiger 1994 24 p Presented at the 10th International Workshop of Inelastic Ion-Surface Collisions, Grand Targhee Resort, WY, 8-12 Aug. 1994
(Contract DE-AC05-84OR-21400)
(DE95-006732; CONF-9408150-3) Avail: CASI HC A03/MF A01

The thrust of the conference in which this paper is presented is toward inelastic interactions of ions with surfaces. The work described in this paper deals with inelastic interactions of ions in planar channeling inside the crystal. The authors are, however, not too far off the mark because the planar channeling potential is made up from the sum of two (sheet) surface potentials. For the nitrogen experiment, a beam of N(6+) ions at an energy of 3.25 MeV/amu was supplied by the ORNL EN Tandem accelerator. After suitable collimation, it was passed through an Au crystal (1,800 angstrom thick). The emergent charge-state distribution was analyzed by electrostatic deflection followed by a solid-state position-sensitive detector. Charge states 5, 6 and 7 were simultaneously detected. In the case of Mg(11+) the beam was supplied at an energy of 25 MeV/amu by the CSCC Tandem Cyclotron Facility at Chalk River, Canada, and passed through an Ni crystal 4,000 angstrom thick which was epitaxially grown with the surface parallel to a (100) plane. The beam was charge state analyzed by a Q3D magnetic analyzer in which charges 11+ and 12+ were registered. At the energy in question, almost no 10+ fraction is visible. Two Si(Li) X-ray detectors aimed at 90 deg and 45 deg recorded the emission of Mg(11+) Ly alpha (n = 2 yields n = 1) X-rays. In conclusion, there is strong evidence that once a given ionic state is excited, a large fraction of the ions remain in that state and are either ionized or radiate from that state. The result is counter to the expectation that electron-ion collisions in the channel would have a large enough cross section to destroy the alignment before either of these two events could take place. At this point, the reasons for the observed retention of anisotropy are open to conjecture. DOE

N95-28607# International Centre for Theoretical Physics, Trieste (Italy).
NONLINEAR DYNAMICS OF A COHERENT POLARITON-BIEXCITON SYSTEM
Nguyen Trung Dan and Vo Tinh (Hue Coll., Viet Nam.) Aug. 1994 16 p
(DE95-609150; IC-94/230) Avail: CASI HC A03/MF A01 (US Sales Only)

The nonlinear dynamics of a coherent interacting polariton-biexciton system in optically excited semiconductors is investigated. We consider the case when two macroscopically coherent modes - a lower branch polariton and a biexciton existing simultaneously in a direct-gap semiconductor. The conditions for exhibiting optical bistability in stationary regime are obtained. Numerical simulation for the nonlinear dynamics equations of the system is also carried out. DOE

N95-28638# Technische Univ., Delft (Netherlands).
CRITICAL BEHAVIOUR OF SPIN MODELS: A TRANSFER-MATRIX APPROACH Ph.D. Thesis
Y. M. M. Knops 27 Oct. 1994 137 p Sponsored by Stichting voor Fundamenteel Onderzoek der Materie, and Nederlandse Organisatie voor Wetenschappelijk Onderzoek
(PB95-192456) Avail: CASI HC A07/MF A02

This thesis presents a study of several two-dimensional models. Critical and multicritical behavior are considered of the q-state Potts model, the O(n) model (variables are n-component vectors) and the fully frustrated XY model (O(2) model with frustration). These models are introduced in section 1.3. In chapter 2 we study the phase diagram of a generalized q-state Potts model with multispin interactions. In chapter 3 we describe a method to obtain some critical branches of the O(n) model on the triangular lattice. Chapter 4 contains an interpretation for the exotic exponents, exponents with a conformal classification but just outside the unitary grid, which describes the thermodynamic singularities. In Chapter 5 we describe a different kind of spin model; the fully frustrated XY model. Apart from a discrete Ising-like degree of freedom (the chirality) this model has also a continuous degree of freedom (the XY spin). Therefore, two kinds of phase transitions are expected, which happen to be at the same temperature. NTIS

N95-28640 Rutherford Appleton Lab., Oxford (England).
PRODUCTION AND DECAY OF HYBRID MESONS BY FLUX-TUBE BREAKING
F. E. Close and P. R. Page Nov. 1994 24 p Prepared in cooperation with Oxford Univ.
(PB95-192837; RAL-94-116) Avail: Issuing Activity (National Technical Information Service (NTIS))

An analytic calculation of the breaking of excited chromoelectric flux-tubes is performed in a harmonic oscillator approximation and applied to predict the dynamics of all J(sup PC) low-lying gluonic excitations of mesons (hybrids). Widths, branching ratios and production dynamics of some recently discovered J(sup PC) = 1(- +), 0(- +), and 1(- -) mesons are found to be in remarkable agreement with these results. We introduce the selection rules that can be used to understand the systematics of numerical decay calculations, and we find possible significant breaking of these rules for specific channels that may enable enhanced production and detection of hybrids. NTIS

N95-28641 Rutherford Appleton Lab., Oxford (England).
MUON SPIN RELAXATION IN FERROMAGNETS: THEORETICAL RESULTS FOR PARAMAGNETIC EuO AND EuS
S. W. Lovesey and E. Engdahl Nov. 1994 20 p See also PB95-192878
(PB95-192860; RAL-94-121) Avail: Issuing Activity (National Technical Information Service (NTIS))

The relaxation rate for depolarization of a positive muon implanted in an isotropic magnetic salt with ferromagnetic exchange interactions is studied theoretically, on the basis of the coupled-mode theory of critical and paramagnetic spin fluctuations and a full numerical evaluation of the dipole field experienced by the muon. The main findings from studies of realistic models of EuO and EuS are (1) a significant dependence of the relaxation rate, lambda, on the assumed position of the implanted muon and (2) a monotonic temperature dependence, with lambda approx xi(sup 3/2) in the approach to the critical temperature at which the correlation length, xi, diverges. In contrast, previous results for a model of an isotropic magnet with an antiferromagnetic exchange, RbMnF3, show that lambda for this magnet is not a monotonic function of the temperature, and in the precursor region to T(c) lambda increases with decreasing temperature with a power law behavior lambda approx xi(sup 1/2). The calculated values of lambda for EuO are consistent with data from preliminary experiments on the same salt. NTIS

N95-28642 Rutherford Appleton Lab., Oxford (England).
MUON SPIN RELAXATION IN ANTIFERROMAGNETS: A STUDY OF RbMnF3 BASED ON THE COUPLED-MODE THEORY OF PARAMAGNETIC AND CRITICAL SPIN FLUCTUATIONS
S. W. Lovesey, E. Balcar, and A. Cuccoli Oct. 1994 34 p See also PB95-192860 Prepared in cooperation with Atominstitut der Oesterreichischen Univ., and Florence Univ.
(PB95-192878; RAL-94-110) Avail: Issuing Activity (National Technical Information Service (NTIS))

The relaxation rate for the depolarization of a positive muon implanted in an antiferromagnetically coupled Heisenberg magnet is studied on the basis of a coupled-mode theory of critical and paramagnetic spin fluctuations, which gives overall an unrivaled account of spin fluctuations. The paper includes the first comprehensive treatment of the dipole field that couples the muon and atomic (spin) magnetic moments. An analytical calculation of the relaxation rate is feasible in the vicinity of the critical temperature, because of the dominant role of the critical fluctuations, whereas in general numerical methods are required to calculate the spin response function and the dipole field. In the approach to the critical temperature, the muon relaxation rate increases as the square root of the correlation length. Results for the isotropic antiferromagnet RbMnF3 demonstrate that, the relaxation rate is not a monotonic function of the temperature, and the magnitude and temperature variation of the relaxation rate depend to a significant degree on the site of the implanted muon. A theoretical framework for the interpretation of the muon relaxation rate is reviewed in a set of appendices. NTIS

N95-28648 Army Research Lab., Aberdeen Proving Ground, MD.
OPTIMIZATION STRATEGIES FOR MOLECULAR DYNAMICS PROGRAMS ON CRAY COMPUTERS AND SCALAR WORK STATIONS Final Report, Aug. - Dec. 1993
Michael J. Unekis and Betsy M. Rice Dec. 1994 42 p Limited Reproducibility: More than 20% of this document may be affected by microfiche quality
(AD-A289574; ARL-TR-661) Avail: Issuing Activity (Defense Technical Information Center (DTIC))

We present results of timing runs and different optimization strategies for a prototype molecular dynamics program that simulates shock waves in a two-dimensional (2-D) model of a reactive energetic solid. The performance of the program may be improved substantially by simple changes to the Fortran or by employing various vendor-supplied compiler optimizations. The optimum strategy varies among the machines used and will vary depending upon the details of the program. The effect of various compiler options and vendor-supplied subroutine calls is demonstrated. Comparison is made between two scalar workstations (IBM RS/6000 Model 370 and Model 530) and several Cray supercomputers (X-MP/48, Y-MP8/128, and C-90/16256). We find that for a scientific application program dominated by sequential, scalar statements, a relatively inexpensive high-end work station such as the IBM RS/60006 RISC series will outperform single processor performance of the Cray X-MP/48 and perform competitively with single processor performance of the Y-MP8/128 and C-9O/16256. DTIC

N95-28657 Rutherford Appleton Lab., Oxford (England).
FUTURE OPPORTUNITIES AND PRESENT POSSIBILITIES FOR COHERENT INELASTIC SINGLE CRYSTAL MEASUREMENTS ON PULSED NEUTRON SOURCES
M. Hagan, U. Steigenberger, C. Petrillo, and F. Sacchetti Jan. 1995 32 p
(PB95-195798; RAL-95-006) Avail: Issuing Activity (National Technical Information Service (NTIS))

The triple axis spectrometer (TAS) has long been the mainstay for measuring excitations in single crystal samples. In a recent paper, Dorner has claimed that the TAS would be the instrument of choice for such measurements at any future high flux spallation neutron source. However, a comparison of the operational characteristics of a TAS and those of direct and indirect geometry time of flight spectrometers for this type of measurement at a pulsed source shows that the TAS would not in fact be a particularly competitive instrument for this purpose. NTIS

N95-27634*# National Aeronautics and Space Administration. Marshall Space Flight Center, Huntsville, AL.
ATOMIC OXYGEN DOSIMETRY MEASUREMENTS MADE ON STS-46 BY CONCAP 2
J. C. Gregory (Alabama Univ., Huntsville, AL.), G. P. Miller (Alabama Univ., Huntsville, AL.), P. J. Pettigrew (Alabama Univ., Huntsville, AL.), G. N.

Raikar (Alabama Univ., Huntsville, AL.), Jon B. Cross (Lockheed Engineering and Sciences Co., Houston, TX.), E. Lan (McDonnell-Douglas Space Systems Co., Huntington Beach, CA.), C. L. Renschler (Sandia National Labs., Albuquerque, NM.), and W. T. Sutherland *In* NASA. Langley Research Center, LDEF: 69 Months in Space. Third Post-Retrieval Symposium, Part 3 Feb. 1995 p 957-970 Sponsored by Consortium for Materials Development in Space (For primary document see N95-27629 09-99)
Avail: CASI HC A03/MF A04

N95-27637*# National Aeronautics and Space Administration. Marshall Space Flight Center, Huntsville, AL.
ORBITAL ATOMIC OXYGEN EFFECTS ON MATERIALS: AN OVERVIEW OF MSFC EXPERIMENTS ON THE STS-46 EOIM-3
Roger C. Linton, Jason A. Vaughn, Miria M. Finckenor, Rachel R. Kamenetzky, Robert F. DeHaye, and Ann F. Whitaker *In* NASA. Langley Research Center, LDEF: 69 Months in Space. Third Post-Retrieval Symposium, Part 3 Feb. 1995 p 999-1010 (For primary document see N95-27629 09-99)
Avail: CASI HC A03/MF A04

N95-27643*# Jet Propulsion Lab., California Inst. of Tech., Pasadena, CA.
MOLECULAR BEAM SCATTERING FROM C-13 ENRICHED KAPTON AND CORRELATION WITH THE EOIM-3 CAROUSEL EXPERIMENT
Timothy K. Minton and Teresa A. Moore *In* NASA. Langley Research Center, LDEF: 69 Months in Space. Third Post-Retrieval Symposium, Part 3 Feb. 1995 p 1095-1114 (For primary document see N95-27629 09-99)
Avail: CASI HC A03/MF A04

73 NUCLEAR AND HIGH-ENERGY PHYSICS

Includes elementary and nuclear particles; and reactor theory.
For space radiation see *93 Space Radiation.*

N95-26584# National Inst. for Fusion Science, Nagoya (Japan).
PROPOSED HIGH SPEED PELLET INJECTION SYSTEM HIPEL FOR LARGE HELICAL DEVICE
S. Sudo, M. Kanno (Kobe Steel Ltd., Japan.), H. Kaneko, S. Saka (Kobe Steel Ltd., Japan.), T. Shirai (Kyoto Univ., Uji, Japan.), and T. Baba Nov. 1993 18 p Presented at the IEEE/NPSS 15th Symposium on Fusion Engineering, Cape Cod, MA, 1993
(ISSN 0915-633X)
(NIFS-255) Avail: CASI HC A03/MF A01

From the results of the simulation study including pellet ablation and 1-D transport code, it is found that a high speed pellet injector with pellet velocity of more than 3 km/s is necessary for the penetration of the pellet with diameter of 3 mm into the core region under the expected plasma condition of Large Helical Device (LHD) of heliotron/stellarator type with superconducting coils at NIFS in Japan. Therefore, a two stage pellet injector was constructed and tested successfully in order to obtain the pellet velocity range of 3 km/s. Based upon the above results, a high speed flexible multiple-pellet injection system 'HIPEL' for LHD is proposed. HIPEL consists of independent 10 two-stage gun barrels and 10 single-stage gun barrels. It has multi purposes such as refueling and flexible density profile control, diagnostics and other functions. Author

N95-27089# Texas Univ., Austin, TX.
SIGNATURES OF HIGGS-TRIPLET REPRESENTATIONS AT TeV-e(+)e(-) COLLIDERS
Kingman Cheung, R. J. N. Phillips, and A. Pilaftsis Nov. 1994 20 p
(Contract DE-FG03-93ER-40757)
(DE95-007201; DOE/ER-40757/057; RAL-94-119) Avail: CASI HC A03/MF A01

The authors investigate the potential of future TeV linear e(+)e(-) colliders to observe singly-charged Higgs bosons (H(+/-) via the coupling H(+/-)W(-/+))Z, which would signal the existence of exotic Higgs representations. In the context of a Higgs-triplet model compatible with the electroweak oblique parameters, they estimate the cross section for producing charged Higgs-triplet bosons that couple predominantly to W and Z bosons in 0.5-2 TeV-e(+)e(-) colliders. The principal backgrounds are evaluated and the viability of the signal is discussed and illustrated. DOE

N95-27091# Fermi National Accelerator Lab., Batavia, IL.
ORBIT ANALYSIS
L. Michelotti Jan. 1995 10 p Presented at the Workshop on Nonlinear Dynamics in Particle Accelerators: Theory and Experiments, Arcidosso, Italy, 4-9 Sep. 1994
(Contract DE-AC02-76CH-03000)
(DE95-007216; FNAL/C-95/005; CONF-9409258-3) Avail: CASI HC A02/MF A01

The past fifteen years have witnessed a remarkable development of methods for analyzing single particle orbit dynamics in accelerators. Unlike their more classic counterparts, which act upon differential equations, these methods proceed by manipulating Poincare maps directly. This attribute makes them well matched for studying accelerators whose physics is most naturally modelled in terms of maps, an observation that has been championed most vigorously by Forest. In the following sections the author sketchs a little background, explains some of the physics underlying these techniques, and discusses the best computing strategy for implementing them in conjunction with modeling accelerators. DOE

N95-27158# European Organization for Nuclear Research, Geneva (Switzerland).
CAS CERN ACCELERATOR SCHOOL 5TH GENERAL ACCELERATOR PHYSICS COURSE
S. Turner, ed. 26 Jan. 1994 537 p Course held in Jyvaeskylae, Finland, 7-18 Sep. 1992
(ISSN 0007-8328)
(DE95-608324; CERN-94-01-Vol-2; CONF-9209485; ISBN 92-9083-058-1)
Avail: CASI HC A23/MF A04 (US Sales Only)

The fifth CERN Accelerator School (CAS) basic course on General Accelerator Physics was given at the University of Jyvaeskylae, Finland, from 7 to 18 September 1992. Its syllabus was based on the previous similar courses held at Gif-sur-Yvette in 1984, Aarhus 1986, Salamanca 1988 and Juelich 1990, and whose proceedings were published as CERN Reports 85-19, 87-10, 89-05 and 91-04, respectively. However, certain topics were treated in a different way, improved or extended, while new subjects were introduced. As far as the proceedings of this school are concerned the opportunity was taken not only to include the lectures presented but also to select and revise the most appropriate chapters from the previous similar schools. In this way the present volumes constitute a rather complete introduction to all aspects of the design and construction of particle accelerators, including optics, emittance, luminosity, longitudinal and transverse beam dynamics, insertions, chromaticity, transfer lines, resonances, accelerating structures, tune shifts, coasting beams, lifetime, synchrotron radiation, radiation damping, beam-beam effects, diagnostics, cooling, ion and positron sources, RF and vacuum systems, injection and extraction, conventional, permanent and superconducting magnets, cyclotrons, RF linear accelerators, microtrons, as well as applications of particle accelerators (including therapy) and the history of accelerators. See hints under the relevant topics. DOE

N95-27161# Joint Inst. for Nuclear Research, Dubna (USSR).
THE SYSTEMS OF THE PROPORTIONAL CHAMBERS REGISTRATION ELECTRONICS FOR PRESENT EXPERIMENTS IN NUCLEAR PHYSICS
V. A. Kalinnikov 1994 22 p In RUSSIAN
(DE95-608559; JINR-R-1-94-166) Avail: CASI HC A03/MF A01 (US Sales Only)

The main direction of the development of present systems of the proportional chambers registration electronics for experiments in nuclear physics is described. The following features of each type of systems and their future are considered in the review. DOE

N95-27321# European Organization for Nuclear Research, Geneva (Switzerland).
ADDENDUM TO THE 1993 EUROPEAN SCHOOL OF HIGH-ENERGY PHYSICS
N. Ellis, ed. 30 Jun. 1994 105 p Presented at the European School of High-energy Physics, Zakopane, Poland, 12-25 Sep. 1993

(DE95-610313; CERN-94-04-Add; CONF-9309446) Avail: CASI HC A06/MF A02 (US Sales Only)

The use of energetic electrons (and other leptons) to probe the structure of hadronic matter has had a long and extremely successful history. We begin with a quick pictorial review and then introduce the Quark Parton Model with its prediction of scaling for deep inelastic ep yields eX and nu N yields mu X scattering. Here by 'scaling' we mean that the structure functions F(sub i)(x, Q(sup 2)) depend only on the Bjorken variable x, and not on Q(sup 2). A study of the QCD-improved parton model is preceded by an introductory discussion of QCD, renormalization, and the running of the coupling constant alpha(sub s). We indicate how the running of alpha(sub s), governed by the universal beta function, can, in principle, sum all the logarithmic ultraviolet divergences associated with the quark-gluon vertices. In an analogous way we indicate how universal running parton densities, governed by Altarelli-Parisi evolution equations, can, in principle, sum all the logarithmic initial state collinear singularities. DOE

N95-27372*# National Aeronautics and Space Administration. Langley Research Center, Hampton, VA.

ABRASION-ABLATION MODEL FOR NEUTRON PRODUCTION IN HEAVY ION REACTIONS

Francis A. Cucinotta, John W. Wilson, and Lawrence W. Townsend Jun. 1995 16 p
(RTOP 199-45-16-12)
(NASA-TM-4656; L-17455; NAS 1.15:4656) Avail: CASI HC A03/MF A01

In heavy ion reactions, neutron production at forward angles is observed to occur with a Gaussian shape that is centered near the beam energy and extends to energies well above that of the beam. This paper presents an abrasion-ablation model for making quantitative predictions of the neutron spectrum. To describe neutrons produced from the abrasion step of the reaction where the projectile and target overlap, the authors use the Glauber model and include effects of final-state interactions. They then use the prefragment mass distribution from abrasion with a statistical evaporation model to estimate the neutron spectrum resulting from ablation. Measurements of neutron production from Ne and Nb beams are compared with calculations, and good agreement is found. Author

N95-27425# Los Alamos National Lab., NM.

HEAT PIPE COOLED REACTORS FOR MULTI-KILOWATT SPACE POWER SUPPLIES

W. A. Ranken and M. G. Houts 1995 7 p Presented at the 9th International Heat Pipe Conference, Albuquerque, NM, 1-5 May 1995
(Contract W-7405-eng-36)
(DE95-005211; LA-UR-94-4199; CONF-9505155-1) Avail: CASI HC A02/MF A01

Three nuclear reactor space power system designs are described that demonstrate how the use of high temperature heat pipes for reactor heat transport, combined with direct conversion of heat to electricity, can result in eliminating pumped heat transport loops for both primary reactor cooling and heat rejection. The result is a significant reduction in system complexity that leads to very low mass systems with high reliability, especially in the power range of 1 to 20 kWe. In addition to removing heat exchangers, electromagnetic pumps, and coolant expansion chambers, the heat pipe/direct conversion combination provides such capabilities as startup from the frozen state, automatic rejection of reactor decay heat in the event of emergency or accidental reactor shutdown, and the elimination of single point failures in the reactor cooling system. The power system designs described include a thermoelectric system that can produce 1 to 2 kWe, a bimodal modification of this system to increase its power level to 5 kWe and incorporate high temperature hydrogen propulsion capability, and a moderated thermionic reactor concept with 5 to 20 kWe power output that is based on beryllium modules that thermally couple cylindrical thermionic fuel elements (TFE's) to radiator heat pipes. DOE

N95-27427# Oak Ridge National Lab., TN.

MONOLITHIC ELECTRONICS FOR NUCLEAR AND HIGH-ENERGY PHYSICS EXPERIMENTS

G. R. Young 1994 11 p Presented at the Intersections of Particle and Nuclear Physics, St. Petersburg, FL, 31 May - 6 Jun. 1994
(Contract DE-AC05-84OR-21400)
(DE95-005393; CONF-940514-19) Avail: CASI HC A03/MF A01

Electronic instrumentation for large fixed-target and collider experiments is rapidly moving to the use of highly integrated electronics wherever it is cost effective. This trend is aided by the development of circuit building blocks useful for nuclear and high-energy physics instrumentation and has accelerated recently with the development of monolithic silicon chips with multiple functions on one substrate. Examples of recent developments are given, together with remarks on the rationale for use of monolithic electronics and economic considerations. DOE

N95-27470# California Univ., Berkeley. Lawrence Berkeley Lab, CA.

CRAB CROSSING IN A GAMMA-GAMMA COLLIDER

M. Xie, K. J. Kim, and A. Sessler Aug. 1994 8 p Presented at the Workshop on Gamma-gamma Colliders, Berkeley, CA, 28-31 Mar. 1994
(Contract DE-AC03-76SF-00098)
(DE95-006580; LBL-35997; CONF-940351-6) Avail: CASI HC A02/MF A01

The crabbing of an incident photon beam from a laser, and the electron beam with which it interacts at the conversion point, is shown to have the same efficiency as in head-on Compton scattering, but with the advantages of a crossing geometry. The resulting gamma-ray beam is also crabbed, which allows for a crossing collision point, while maintaining the luminosity at the same value it would have in a head-on collision. DOE

N95-27480# Sandia National Labs., Albuquerque, NM.

HIGH ENERGY ELECTRON BEAMS FOR CERAMIC JOINING

B. N. Turman, S. J. Glass, J. A. Halbleib, D. R. Helmich, R. E. Loehman, and J. R. Clifford (Titan Corp., Albuquerque, NM.) 1994 11 p Presented at the SPIE 1995: SPIE Conference on Optics, Electro-Optics, and Laser Application in Science, Engineering and Medicine, San Jose, CA, 5-10 Feb. 1995
(Contract DE-AC04-94AL-85000)
(DE95-006316; SAND-94-2145C; CONF-950226-4) Avail: CASI HC A03/MF A01

Joining of structural ceramics is possible using high melting point metals such as Mo and Pt that are heated with a high energy electron beam, with the potential for high temperature joining. A 10 MeV electron beam can penetrate through 1 cm of ceramic, offering the possibility of buried interface joining. Because of transient heating and the lower heat capacity of the metal relative to the ceramic, a pulsed high power beam has the potential for melting the metal without decomposing or melting the ceramic. We have demonstrated the feasibility of the process with a series of 10 MeV, 1 kW electron beam experiments. Shear strengths up to 28 MPa have been measured. This strength is comparable to that reported in the literature for bonding silicon nitride to molybdenum with copper-silver-titanium braze, but weaker than that reported for Si3N4-Si3N4 with gold-nickel braze. The bonding mechanism appears to be a thin silicide layer. DOE

N95-27484# Brookhaven National Lab., Upton, NY.

ACCELERATION THEOREMS

R. Palmer Jun. 1994 12 p Presented at the Advanced Accelerator Concepts Workshop, Lake Geneva, WI, 13-18 Jun. 1994
(Contracts DE-AC02-76CH-00016; DE-AC03-76SF-00515)
(DE95-007300; BNL-61317; CONF-940681-8) Avail: CASI HC A03/MF A01

Electromagnetic fields can be separated into near and far components. Near fields are extensions of static fields. They do not radiate, and they fall off more rapidly from a source than far fields. Near fields can accelerate particles, but the ratio of acceleration to source fields at a distance R is always less than R/lambda or 1, whichever is smaller. Far fields can be represented as sums of plane parallel, transversely polarized waves that travel at the velocity of light. A single such wave in a vacuum cannot give continuous acceleration, and it is shown that no sum of such waves can give net first order acceleration. This theorem is proven in three different ways, each method showing a different aspect of the situation. DOE

N95-27494# Los Alamos National Lab., NM.

BUBBLE FUSION: PRELIMINARY ESTIMATES

R. A. Krakowski 1995 21 p
(Contract W-7405-eng-36)
(DE95-006337; LA-UR-95-100) Avail: CASI HC A03/MF A01

The collapse of a gas-filled bubble in disequilibrium (i.e., internal pressure much less than external pressure) can occur with a significant focusing of energy onto the entrapped gas in the form of pressure-volume work and/or acoustical shocks; the resulting heating can be sufficient to cause ionization and the emission of atomic radiations. The suggestion that extreme conditions necessary for thermonuclear fusion to occur may be possible has been examined parametrically in terms of the ratio of initial bubble pressure relative to that required for equilibrium. In this sense, the disequilibrium bubble is viewed as a three-dimensional 'sling shot' that is 'loaded' to an extent allowed by the maximum level of disequilibrium that can stably be achieved. Values of this disequilibrium ratio in the range 10(exp -5) to 10(exp -6) are predicted by an idealized bubble-dynamics model as necessary to achieve conditions where nuclear fusion of deuterium-tritium might be observed. Harmonic and aharmonic pressurizations/decompressions are examined as means to achieve the required levels of disequilibrium required to create fusion conditions. A number of phenomena not included in the analysis reported herein could enhance or reduce the small levels of nuclear fusions predicted. DOE

N95-27531# Fermi National Accelerator Lab., Batavia, IL.

COUPLING IN THE TEVATRON

N. M. Gelfand Dec. 1994 36 p
(Contract DE-AC02-76CH-03000)
(DE95-005129; FNAL-TM-1916) Avail: CASI HC A03/MF A01

The performance of the Fermilab Tevatron Collider at the commencement of run Ib was far below expectations. After a frustrating period of several months, a low-beta quad downstream of the interaction point at B0 was found to be rolled. This rolled quadrupole coupled the horizontal and vertical motion of the Tevatron beams. It also made matching the beam from the Main Ring to the Tevatron impossible, resulting in emittance blow up on injection. The net result of the roll was a significant reduction in the Tevatron luminosity. When the roll in the quadrupole was corrected the performance of the Tevatron improved dramatically. This note will discuss the experimental data indicating the presence of coupling and subsequent calculations which show how coupling can affect the luminosity. It is not intended to exhaust a discussion of coupling, which hopefully will be understood well enough to be discussed in a subsequent note. DOE

N95-27679# California Univ., Berkeley. Lawrence Berkeley Lab, CA. Life Sciences Div.

SCINTILLATOR MATERIALS FOR CALORIMETRY

Marvin J. Weber Sep. 1994 19 p Presented at the 5th International Conference on Calorimetry in High Energy Physics, Upton, NY, 26-30 Sep. 1994 Sponsored by the National Cancer Institute, Dept. of Health and Human Services
(Contract DE-AC03-76SF-00098)
(DE95-006570; LBL-36535; CONF-9409268-6) Avail: CASI HC A03/MF A01

Requirements for fast, dense scintillator materials for calorimetry in high energy physics and approaches to satisfying these requirements are reviewed with respect to possible hosts and luminescent species. Special attention is given to cerium-activated crystals, core-valence luminescence, and glass scintillators. The present state of the art, limitations, and suggestions for possible new scintillator materials are presented. DOE

N95-27735# Los Alamos National Lab., NM.

SILICON SUBSYSTEM MECHANICAL ENGINEERING CLOSEOUT REPORT FOR THE SOLENOIDAL DETECTOR COLLABORATION

J. Hanlon, R. W. Christensen, G. Hayman, D. C. Jones, R. Ross, W. Wilds, S. Yeamans, and H. J. Ziock 1995 60 p
(Contract W-7405-eng-36)
(DE95-006336; LA-UR-95-156) Avail: CASI HC A04/MF A01

The authors' group at Los Alamos National Laboratory was responsible for the mechanical engineering of the silicon tracking system of the Solenoidal Detector Collaboration (SDC) experiment of the Superconducting Super Collider (SSC) project. The responsibility included the overall design of the system from the mechanical point of view, development and integration of the cooling system, which was required to remove the heat generated by the front-end electronics, assembly of the system to extremely tight tolerances, and verification that the construction and operational stability and alignment tolerances would be met. In addition to the mechanical engineering work, they also performed activation, background, and shielding studies for the SSC program. Much of the work they performed was potentially useful for other future high energy physics (HEP) projects. This report describes the closeout work that was performed for the Los Alamos SDC project. Four major tasks were identified for completion: (1) integration of the semi-automated assembly station being developed and construction of a precision part to demonstrate solutions to important general assembly problems (the station was designed to build precision silicon tracker subassemblies); (2) build a state-of-the-art TV holography (TVH) system to use for detector assembly stability tests; (3) design, build, and test a water based cooling system for a full silicon shell prototype; and (4) complete and oocument the activation, background, and shielding studies, which is covered in a separate report. DOE

N95-27923# Iowa Univ., Iowa City, IA.

POLARIZING MATTER AND ANTIMATTER: A NEW METHOD Final Report

Y. Onel Dec. 1994 62 p
(Contract DE-FG02-91ER-40644)
(DE95-007109; DOE/ER-40644/T1) Avail: CASI HC A04/MF A01

Several years ago a self-polarization effect for stored (anti-)protons and ions was investigated theoretically. The effect is based on the well-known Stern-Gerlach effect in gradient fields. The aim of the ongoing measurements at the Indiana University Cyclotron Facility (IUCF) is to verify experimentally the various assumptions on which this effect is based. The final goal is to demonstrate this new polarization effect. The proposed effect could be a powerful tool to produce polarized stored hadron beams both in the low-energy range and at SSC and LHC energies. In this progress report the authors will describe the progress in three parts: (1) experimental work at IUCF Cooler Ring; (2) the extensive computer simulations of the spin stability for the IUCF Cooler Ring; and (3) theoretical studies. DOE

N95-28017# Brookhaven National Lab., Upton, NY.

SOME NOTES ON LONG-RANGE BEAM-BEAM EFFECTS FOR THE 2 TeV COLLIDER

M. J. Syphers 1994 5 p Presented at the Workshop on Future Hadron Facilities in the United States, Bloomington, IN, 6-10 Jul. 1994
(Contract DE-AC02-76CH-00016)
(DE95-006771; BNL-61291; CONF-9407128-3) Avail: CASI HC A01/MF A01

The 2 TeV (bar p)-p collider discussed at this workshop would necessarily have hundreds of long-range interactions between the counter-rotating bunches and some of the low-order effects of these interactions are estimated below. We discuss in this paper how the helical orbit around the accelerator will help alleviate some of these effects, though the tune spread due to the long-range interactions will be present. DOE

N95-28040# European Organization for Nuclear Research, Geneva (Switzerland).

THE 1993 EUROPEAN SCHOOL OF HIGH-ENERGY PHYSIS

N. Ellis, ed. 30 Jun. 1994 498 p Presented at the European School of High-Energy Physics, Zakopane, Poland, 12-25 Sep. 1993
(DE95-610196; CERN-94-04; CONF-9309446) Avail: CASI HC A21/MF A04 (US Sales Only)

The European School of High-Energy Physics is intended to give young experimental physicists an introduction to the theoretical aspects of recent advances in elementary particle physics. These proceedings contain lectures on quantum field theory, quantum chromodynamics, CP violation, radiative corrections, cosmology, particle detectors and e(+)e(-) accelerators, as well as reports on results from Hadron - Electron - Ring - Accelerator (HERA) and Laboratory for Extraterrestial Physics (LEP) and accounts of particle physics research at CERN and in Poland and Russia. DOE

N95-28107# Fermi National Accelerator Lab., Batavia, IL.

THE CDF UPGRADE

C. Newman-Holmes Jan. 1995 9 p Presented at the 4th International Conference on Advanced Technology and Particle Physics, Como, Italy, 3-7 Oct. 1994
(Contract DE-AC02-76CH-03000)
(DE95-006683; FNAL/C-95/003-E; CONF-941060-2) Avail: CASI HC A02/MF A01

The Collider Detector at Fermilab (CDF) has been used to study proton-antiproton collisions at the Fermilab Tevatron since 1985. Over the years, the detector has evolved steadily to increase its physics capability and to keep pace with improvements to the Tevatron. Fermilab is currently building a new Main Injector accelerator which will lead to even larger luminosity values. This paper describes upgrades to CDF that will allow one to exploit the higher luminosity of the Main Injector. DOE

N95-28115# Brookhaven National Lab., Upton, NY.
SKEW CHROMATICITY
S. Peggs and G. F. Dell 1994 22 p Presented at the Collective Effects in Large Hadron Collider Conference, Montreux, Switzerland, 17-22 Oct. 1994
(Contract DE-AC02-76CH-00016)
(DE95-007677; BNL-61420; CONF-9410315-1) Avail: CASI HC A03/MF A01

The on-momentum description of linear coupling between horizontal and vertical betatron motion is extended to include off-momentum particles, introducing a vector quantity called the 'skew chromaticity.' This vector tends to be long in large superconducting storage rings, where it restricts the available working space in the tune plane, and modifies collective effect stability criteria. Skew chromaticity measurements at the Cornell Electron Storage Ring (CESR) and at the Fermilab Tevatron are reported, as well as tracking results from the Relativistic Heavy Ion Collider (RHIC). The observation of anomalous head-tail beam losses near the tune diagonal in the Tevatron are explained in terms of the extended theory, including modified criteria for head-tail stability. These results are confirmed in head-tail simulations. Sources of skew chromaticity are investigated. DOE

N95-28122# Stanford Linear Accelerator Center, Stanford, CA.
NONLINEAR BEAM DYNAMICS EXPERIMENTAL PROGRAM AT SPEAR
P. Tran (California Univ., Los Angeles, CA.), C. Pellegrini (California Univ., Los Angeles, CA.), M. Cornacchia, M. Lee, and W. Corbett 1995 6 p Presented at the Workshop on Nonlinear Dynamics in Particle Accelerators: Theory and Experiments, Arcidosso, Italy, 4-9 Sep. 1994
(Contract DE-AC03-76SF-00515)
(DE95-007823; SU-SLAC-PUB-95-6720; CONF-9409258-5) Avail: CASI HC A02/MF A01

Since nonlinear effects can impose strict performance limitations on modern colliders and storage rings, future performance improvements depend on further understanding of nonlinear beam dynamics. Experimental studies of nonlinear beam motion in three-dimensional space have begun in SPEAR using turn-by-turn transverse and longitudinal phase-space monitors. This paper presents preliminary results from an on-going experiment in SPEAR. DOE

N95-28123# Stanford Linear Accelerator Center, Stanford, CA.
BEAM-BEAM INTERACTION WORKING GROUP SUMMARY
R. H. Siemann 1995 6 p Presented at the Workshop on Nonlinear Dynamics in Particle Accelerators: Theory and Experiments, Arcidosso, Italy, 4-9 Sep. 1994
(Contract DE-AC03-76SF-00515)
(DE95-007824; SU-SLAC-PUB-95-6763; CONF-9409258-4) Avail: CASI HC A02/MF A01

The limit in hadron colliders is understood phenomenologically. The beam-beam interaction produces nonlinear resonances and makes the transverse tunes amplitude dependent. Tune spreads result from the latter, and as long as these tune spreads do not overlap low order resonances, the lifetime and performance is acceptable. Experience is that tenth and sometimes twelfth order resonances must be avoided, and the hadron collider limit corresponds roughly to the space available between resonances of that and lower order when operating near the coupling resonance. The beam-beam interaction in e(+)e(-) colliders is not understood well. This affects the performance of existing colliders and could lead to surprises in new ones. For example. a substantial amount of operator tuning is usually required to reach the performance limit given above, and this tuning has to be repeated after each major shutdown. The usual interpretation is that colliding beam performance is sensitive to small lattice errors, and these are being reduced during tuning. It is natural to ask what these errors are, how can a lattice be characterized to minimize tuning time, and what aspects of a lattice should receive particular attention when a new collider is being designed. The answers to this type of question are not known, and developing ideas for calculations, simulations and experiments that could illuminate the details of the beam-beam interaction was the primary working group activity. DOE

N95-28159# Stanford Linear Accelerator Center, Stanford, CA.
MEASUREMENT OF WAKEFIELD SUPPRESSION IN A DETUNED X-BAND ACCELERATOR STRUCTURE
C. Adolphsen, K. Bane, T. Higo, K. Kubo, R. Miller, R. Ruth, K. Thompson, and J. Wang Aug. 1994 4 p Presented at the 17th International LINAC Conference, Tsukuba, Japan, 21-26 Aug. 1994
(Contract DE-AC03-76SF-00515)
(DE95-008592; SU-SLAC-PUB-6629; CONF-9408125-49) Avail: CASI HC A01/MF A01

Research is underway at SLAC to develop accelerator structures for a next generation linear collider. A full-scale prototype X-band structure has been built in which the dipole mode frequencies were detuned to suppress the long-range transverse wakefield by about two orders of magnitude. To verify that the detuning works as expected, a facility to measure the long-range wakefield, called the Accelerator Structure SETup, or ASSET, was constructed in the SLAC Linear Collider (SLC). This paper presents the results from the measurement of the prototype X-band structure with this facility. DOE

N95-28195# Brookhaven National Lab., Upton, NY.
OPTICAL DESIGN AND PERFORMANCE OF THE INELASTIC SCATTERING BEAMLINE AT THE NATIONAL SYNCHROTRON LIGHT SOURCE
C. C. Kao, D. P. Siddons, T. Oversluizen, J. B. Hastings, K. Hamalainen, and M. Krisch (European Synchrotron Radiation Facility, Grenoble, France.) 1994 13 p Presented at the International Meeting on Synchrotron Radiation Instrumentation, Stony Brook, NY, 18-22 Jul. 1994
(Contract DE-AC02-76CH-00016)
(DE95-007679; BNL-61410; CONF-940714-50) Avail: CASI HC A03/MF A01

Phase 1 of the X21 beamline at the National Synchrotron Light Source was commissioned during 1993. The research program at the X21 beamline is focused on the study of electronic excitations in condensed matter with total energy resolution of 0.1 eV to 1.0 eV. The source is a 27 pole hybrid wiggler. A water-cooled horizontal focusing Si(220) monochromator and a spherically bent Si(444) analyzer were installed and commissioned. At 8 keV the energy resolution of the monochromator is about 0.7 eV, and the energy resolution of the analyzer is about 0.1 eV. Results from several selected experiments are also discussed. DOE

N95-28205# Oak Ridge National Lab., TN.
RECENT HIGH-SPEED BALLISTICS EXPERIMENTS AT ORNL
S. K. Combs, M. J. Gouge, L. R. Baylor, P. W. Fisher, C. A. Foster, C. R. Foust, S. L. Milora, and A. L. Qualls 1994 14 p Presented at the 45th Aeroballistic Range Association (ARA) Meeting, Huntsville, AL, 10-14 Oct. 1994
(Contract DE-AC05-84OR-21400)
(DE95-006534; CONF-9410305-1) Avail: CASI HC A03/MF A01

Oak Ridge National Laboratory (ORNL) has been developing pellet injectors for plasma fueling experiments on magnetic confinement devices for almost 20 years. With these devices, pellets (1 to 8 mm in diameter) composed of hydrogen isotopes are formed (at temperatures less than 20 K) and typically accelerated to speeds of (approximately) 1.0 to 2.0 km/s for injection into plasmas of experimental fusion devices. A variety of pellet injector designs have been developed at ORNL, including repeating pneumatic injectors (single- and multiple-barrel light gas guns) that can inject up to hundreds of pellets for long-pulse plasma operation. The repeating pneumatic injectors are of particular importance because long-pulse fueling is required for present large experimental fusion devices, with steady-state operation the objective for future fusion reactors. In this paper, recent advancements in the development of repeating pneumatic injectors are described, including (1) a small-bore (1.8-mm), high-firing-rate (10-Hz) version of a single-stage light gas gun; (2) a repeating single-stage light gas gun for 8-mm-diam tritium pellets; (3) a repeating two-stage light gas gun for operation at higher pellet velocities; and (4) a steady-state hydrogen extruder feed system. DOE

N95-28346# Fermi National Accelerator Lab., Batavia, IL.
THE 132 NSEC BUNCH SPACING IN THE TEVATRON PROTON-ANTIPROTON COLLIDER
S. D. Holmes, J. Holt, J. A. Johnstone, J. Marriner, M. Martens, and D.

McGinnis 23 Dec. 1994 23 p
(Contract DE-AC02-76CH-03000)
(DE95-005750; FNAL-TM-1920) Avail: CASI HC A03/MF A01

Following completion of the Fermilab Main Injector, it is expected that the Tevatron proton-antiproton collider will be operating at a luminosity in excess of 5 x 10(exp 31)/sq cm/sec with 36 proton and antiproton bunches spaced at 396 nsec. At this luminosity, each of the experimental detectors will see approximately 1.3 interactions per crossing. Potential improvements to the collider low beta and rf systems could push the luminosity beyond 10 x 10(exp 31)/sq cm/sec, resulting in more than three interactions per crossing if the bunch separation is left unchanged. This paper discusses issues related to moving to approx. 100 bunch operation, with bunch spacings of 132 nsec, in the Tevatron. Specific scenarios and associated hardware requirements are described. DOE

N95-28452 Rutherford Appleton Lab., Oxford (England).
PIPELINED FIRST-LEVEL TRIGGER FOR THE H1 FORWARD-MUON SPECTROMETER
T. Ahmed, J. D. Dowell, N. Ellis, J. Garvey, and P. Jovanovic Jan. 1995 29 p Prepared in cooperation with Birmingham Univ.
(PB95-196242; RAL-94-126) Avail: Issuing Activity (National Technical Information Service (NTIS))

We have built a fast, pipelined first-level trigger processor for the H1 experiment at HERA. The trigger finds tracks in the forward-muon spectrometer which point back to the interaction vertex. The inputs to the trigger come from drift chambers with a 6-cm drift space corresponding to maximum drift time of 1.2 microsec. These chambers consist of two layers of drift cells whose staggered configuration makes it possible to extract the time at which a particle traversed the chambers to better than one HERA bunch-crossing period, 96 ns. The trigger hardware exploits this characteristic in a real-time operation, and is able to find pointing tracks and associate them to production in a specific electron-proton crossing. NTIS

N95-28551# Superconducting Super Collider Lab., Dallas, TX.
BEAM INSTABILITY STUDIES FOR THE SSC
W. Chou Sep. 1994 22 p
(Contract DE-AC35-89ER-40486)
(DE95-008024; SSCL-680) Avail: CASI HC A03/MF A01

Beam instability studies of the Superconducting Super Collider (SSC) during the period 1989-1993 are briefly reviewed in this paper. Various topics are covered: single bunch and multi-bunch; single beam and beam-beam; parasitic heating and active feedback; etc. Although the SSC will not be built, many of the results obtained from these studies remain as useful references to the accelerator community. DOE

74 OPTICS

Includes light phenomena; and optical devices.
For lasers see *36 Lasers and Masers.*

N95-26385* National Aeronautics and Space Administration. Marshall Space Flight Center, Huntsville, AL.
RADIATION SENSITIVE AREA DETECTION DEVICE AND METHOD Patent
Daniel C. Carter, inventor (to NASA), Diana L. Hecht, inventor (to NASA), and William K. Witherow, inventor (to NASA) et al 21 Mar. 1995 10 p Filed 6 May 1994
(NASA-Case-MFS-28563-3; US-Patent-5,399,877;
US-Patent-Appl-SN-243602; US-Patent-Class-250-581;
US-Patent-Class-250-584; US-Patent-Class-250-585;
US-Patent-Class-250-586; US-Patent-Class-250-228;
US-Patent-Class-356-236; Int-Patent-Class-G03B-42/02) Avail: US Patent and Trademark Office

An area detection device for use with x-ray or ultraviolet radiation wherein light from an integrating device is passed through an optical fiber to fall on a phosphor-containing film which is capable of storing a diffraction pattern formed by the transmission of x-rays or ultraviolet radiation through a sample when the diffraction pattern is projected onto the film and also being capable of fluorescing in correspondence to the diffraction pattern. Fluoresced light from the film is directed back along the fiber and into the integrating device and is fed from the integrating device to photomultiplier which sends a signal from which the diffraction pattern can be detected.
Official Gazette of the U.S. Patent and Trademark Office

N95-26532 Naval Postgraduate School, Monterey, CA.
SOOT PARTICLE DENSITY DETERMINATION FROM A LASER EXTINCTION MULTIPASS TECHNIQUE M.S. Thesis
Gregory E. Glaros Sep. 1994 46 p Limited Reproducibility: More than 20% of this document may be affected by microfiche quality
(Contract N00421-94-WR-01539)
(AD-A288551) Avail: Issuing Activity (Defense Technical Information Center (DTIC))

Methods of measuring soot particle densities have been of interest for several decades. Plume signature determination of both rocket and air-breathing engines is of concern when applied to pollution and theater missile ballistic defense strategies. Application of non-intrusive traditional techniques employing Bouguer's law relied on Sauter mean diameter statistical deviation and the probability density function in order to compensate for the ambiguities present in the extension of classical Mie theory. Our investigation developed an apparatus which will determine soot particle densities by measuring extinction from absorption of light energy transmitted through an exhaust plume. The method used was a two-pass technique using an optical phase conjugator (OPC) which returned the non-absorbed portion of light energy. When the apparatus was used with a retroreflector, it produced accurate results but did not compensate for thermal blooming or beam steering. Characteristics of a photorefractive crystal used in the OPC process allowed for the return of an incident beam corrected for aberrations. Although the OPC returned the phase conjugate of the incident beam its size precluded the return of all of the transmitted data because data was lost on the blossomed beam. DTIC

N95-26549 Department of the Navy, Washington, DC.
PRELIMINARY DESIGN STUDY OF THE BEAM COLLAPSER AND CERTAIN OPTOMECHANICAL ASPECTS OF THE SIDEROSTAT
1994 125 p Limited Reproducibility: More than 20% of this document may be affected by microfiche quality
(AD-A288423) Avail: Issuing Activity (Defense Technical Information Center (DTIC))

Four topics were studied during this phase of the design of the USNO astrometric interferometer: (1) the optical configuration of the beam collapser; (2) the mirror mount for the primary mirror of the beam collapser; (3) the beam collapser structure, and (4) bearings for use in the siderostat. A Gregorian beam collapser configuration, with a 750-mm diameter f/2.7 primary mirror, a 1 16-mm diameter secondary mirror, with a radius of curvature of 623 mm, and a vertex-to-vertex spacing 2337 mm is recommended. Use of a Gregorian beam collapser reduces optical fabrication costs, with a small impact in overall system length and weight. A solid primary mirror, 100-mm thick and oversized, with a 85% mm diameter, is the simplest and most economical mirror to fabricate and mount. A roller chain would provide radial support for the primary mirror; a six-point whiffle tree located outside the optical clear aperture would provide axial support. A modified Serrurier truss connects the secondary mirror to the primary mirror; the upper forward section of the truss is removed to allow better sky coverage for the siderostat. Use of a modified Serrurier truss permits testing of the system in the optical axis horizontal position, and without loss of alignment in the 100 down position. In addition, this type of truss is center supported, permitting the use of a tapered pier to minimize concrete volume on site. Spacing from the primary mirror to the secondary mirror, a critical parameter for system performance, is controlled by a pair of metering rods made from the same type of material as the optics. Rolling element bearings, oil pad bearings, and air bearings were considered for use in the siderostat. Although an extensive literature survey was performed, and a number of vendors contacted, it is not yet established which bearings are optimum for the siderostat. DTIC

N95-26679 Electro-Optek Corp., Torrance, CA.
FABRICATION OF LONG WAVELENGTH ARRAY BY IN-SITU MOLECULAR BEAM EPITAXY Monthly Report No. 1
12 Dec. 1994 3 p Limited Reproducibility: More than 20% of this document may be affected by microfiche quality
(Contract DAAB07-91-C-K762)

(AD-A288599) Avail: Issuing Activity (Defense Technical Information Center (DTIC))

In this reporting period, we have designed and constructed the major components of a MBE system for fabrication of long wavelength IR (LWIR) detector arrays. Among these components, the high temperature effusion cells were specially designed for alkaline earth fluoride (CaF2 and BaF2) growth. In the meantime, several multiple-layered fluoride films were grown on Si substrate to test out their crystallinities. The purpose of introducing the fluoride epilayers in this project is to form a buffer layer to accommodate a large lattice mismatch between LWIR detector layer and Si substrate. Since the growth of fluoride epilayers requires high source temperature (1200 C - 1300 C) to obtain reasonable growth rates (0.3 - 2A/sec), the specially designed effusion cell has been made. The designed structure and the power consumption of the high temperature effusion cell is shown, measured, and plotted versus the cell temperature. The shadowed area provides the applicable cell temperature ranges required for the fluoride epilayer growth. Our data show that the power consumption corresponding to the shadowed area is still at a feasible level. DTIC

N95-26860 Air Force Systems Command, Wright-Patterson AFB, OH. National Air Intelligence Center.

STUDY OF FREQUENCY DOUBLING ANTIREFLECTION COATING

Mingli Wang and Zhengxiu Fan 15 Dec. 1994 19 p Transl. into ENGLISH from Houang Hshu (China), v. 16, no. 3, 1992 p 167-172 Limited Reproducibility: More than 20% of this document may be affected by microfiche quality

(AD-A289634; NAIC-ID(RS)T-0102-93) Avail: Issuing Activity (Defense Technical Information Center (DTIC))

This article carries out detailed study and discussion, both theoretically and in terms of experimentation, on frequency doubling dual wavelength increased transparency or antireflection films or coatings. It puts forth film or coating series designs and error analysis, as well as production processes, and solves problems of film or coating uniformity and waveband width. DTIC

N95-26894*# National Aeronautics and Space Administration. Pasadena Office, CA.

SOLID-STATE IMAGE SENSOR WITH FOCAL-PLANE DIGITAL PHOTON-COUNTING PIXEL ARRAY Patent Application

Eric R. Fossum, inventor (to NASA) (Jet Propulsion Lab., California Inst. of Tech., Pasadena, CA.) and Bedabrata Pain, inventor (to NASA) (Jet Propulsion Lab., California Inst. of Tech., Pasadena, CA.) 12 Jan. 1995 67 p

(NASA-Case-NPO-18518-1-CU; NAS 1.71:NPO-18518-1-CU; US-Patent-Appl-SN-372640) Avail: CASI HC A04/MF A01

A photosensitive layer such as a-Si for a UV/visible wavelength band is provided for low light level imaging with at least a separate CMOS amplifier directly connected to each PIN photodetector diode to provide a focal-plane array of NxN pixels, and preferably a separate photon-counting CMOS circuit directly connected to each CMOS amplifier, although one row of counters may be time shared for reading out the photon flux rate of each diode in the array, together with a buffer memory for storing all rows of the NxN image frame before transfer to suitable storage. All CMOS circuitry is preferably fabricated in the same silicon layer as the PIN photodetector diode for a monolithic structure, but when the wavelength band of interest requires photosensitive material different from silicon, the focal-plane array may be fabricated separately on a different semiconductor layer bump-bonded or otherwise bonded for a virtually monolithic structure with one free terminal of each diode directly connected to the input terminal of its CMOS amplifier and digital counter for integration of the photon flux rate at each photodetector of the array. NASA

N95-26900 Carnegie-Mellon Univ., Pittsburgh, PA. Robotics Inst.

AN ILLUMINATION PLANNER FOR LAMBERTIAN POLYHEDRAL OBJECTS

Fredric Solomon and Katsushi Ikeuchi 4 Oct. 1994 39 p Limited Reproducibility: More than 20% of this document may be affected by microfiche quality

(Contract F33615-90-C-1465; ARPA Order 7597)

(AD-A289332; CMU-RI-TR-94-26) Avail: Issuing Activity (Defense Technical Information Center (DTIC))

The measurement of shape is a basic object inspection task. We use a noncontact method to determine shape called photometric stereo. The method uses three light sources which sequentially illuminate the object under inspection and a video camera for taking intensity images of the object. A significant problem with using photometric stereo is determining where to place the three light sources and the video camera. In order to solve this problem, we have developed an illumination planner that determines how to position the three light sources and the video camera around the object. The planner determines how to position light sources around an object so that we illuminate a specified set of faces in an efficient manner, and so that we obtain an accurate measurement. We predict the uncertainty in our measurements due to sensor noise by performing a statistical simulation in our planner. This gives us the capability to determine when a measured shape differs in a statistically significant way from what we expect. From a high level, our planner has three major inputs: the CAD model of the object to be inspected, a noise model for our sensor, and a reflectance model for the object to be inspected. We have experimentally verified that the plans generated by the planner are valid and accurate. In most cases, the uncertainty predictions made by the planner were accurate to within 10%. DTIC

N95-26965 Air Force Inst. of Tech., Wright-Patterson AFB, OH.

FRAME SELECTION PERFORMANCE LIMITS FOR STATISTICAL IMAGE RECONSTRUCTION OF ADAPTIVE OPTICS COMPENSATED IMAGES M.S. Thesis

Stephen D. Ford Dec. 1994 200 p Limited Reproducibility: More than 20% of this document may be affected by microfiche quality

(AD-A289240; AFIT/GEO/ENP/94D-03) Avail: Issuing Activity (Defense Technical Information Center (DTIC))

The U.S. Air Force uses adaptive optics systems to collect images of extended objects beyond the atmosphere. These systems use wavefront sensors and deformable mirrors to compensate for atmospheric turbulence induced aberrations. Adaptive optics greatly enhance image quality, however, wavefront aberrations are not completely eliminated. Therefore, post-detection processing techniques are employed to further improve the compensated images. Typically, many short exposure images are collected, recentered to compensate for tilt, and then averaged to overcome randomness in the images and improve signal-to-noise ratio. Experience shows that some short exposure images in a data set are better than others. Frame selection exploits this fact by using a quality metric to discard low quality frames. A composite image is then created by averaging only the best frames. Performance limits associated with the frame selection technique are investigated in this thesis. Limits imposed by photon noise result in a minimum object brightness of visual magnitude +8 for point sources and +4 for a typical satellite model. Effective average point spread functions for point source and extended objects after frame selection processing are almost identical across a wide range of conditions. This discovery allows the use of deconvolution techniques to sharpen images after using the frame selection technique. A new post-detection processing method, frame weighting, is investigated and may offer some improvement for dim objects during poor atmospheric seeing. Frame selection is demonstrated for the first time on actual imagery from an adaptive optics system. Data analysis indicates that signal-to-noise ratio improvements are degraded for exposure times longer than that allowed to 'freeze' individual realizations of the turbulence effects. DTIC

N95-26971 Air Force Inst. of Tech., Wright-Patterson AFB, OH. School of Engineering.

ROC ANALYSIS OF IR SEGMENTATION TECHNIQUES M.S. Thesis

Georgia K. Harrup Dec. 1994 112 p Limited Reproducibility: More than 20% of this document may be affected by microfiche quality

(AD-A289252; AFIT/GE/ENG/94D-15) Avail: Issuing Activity (Defense Technical Information Center (DTIC))

Receiver Operating Characteristic (ROC) curves are used to compare the effectiveness of IR image processing techniques. Two non-parametric error estimation techniques (k-Nearest Neighbor and Parzen Window) are used to create estimates of the probability density functions for the data. These pdfs are used in the creation of the ROC curves for both resubstitution and leave-one-out estimates. These estimates generate the upper and lower bounds, respectively, on the ROC curves. The ROC curve analysis is performed on the outputs of various image processing techniques and the resulting ROC curves are used to compare the techniques. Of the image processing techniques used in this thesis, the close minus open (CMO) morphological filter operation produced the best results. DTIC

N95-27038 Carnegie-Mellon Univ., Pittsburgh, PA. Robotics Inst.
MOMENT AND HYPERGEOMETRIC FILTERS FOR HIGH PRECISION COMPUTATION OF FOCUS, STEREO AND OPTICAL FLOW Technical Report
Yalin Xiong and Steven A. Shafer Sep. 1994 79 p Limited Reproducibility: More than 20% of this document may be affected by microfiche quality
(AD-A289293; CMU-RI-TR-94-28) Avail: Issuing Activity (Defense Technical Information Center (DTIC))

Many low level visual computation problems such as focus, stereo, optical flow, etc. can be formulated as problems of extracting one or more parameters of a non-stationary transformation between two images. Because of the non-stationary nature, finite-width windows are widely used in various algorithms to extract spatially local information from images. While the choice of window width has a very profound impact on the quality of results of algorithms, there has been no quantitative way to measure or eliminate the negative effects of finite-width windows. To address this problem, we introduce two sets of filters, 'moment' filters and 'hypergeometric' filters. Due to their recursive properties, these filters allow the effects of finite-width windows and foreshortening to be explicitly analyzed and eliminated. We develop one paradigm to solve general one-parameter extraction problems using moment filters, and another one to solve general multiple parameter extraction problem using hypergeometric filters. We apply these paradigms to problems of focus and stereo, in which one parameter is extracted at every pixel location, and optical flow, in which two parameters are extracted. We demonstrate that our algorithms based on moment filters and hypergeometric filters achieve much higher precision than other techniques. DTIC

N95-27482# Sandia National Labs., Albuquerque, NM.
DIRECT ULTRASHORT-PULSE RETRIEVAL USING FREQUENCY-RESOLVED OPTICAL GATING AND A COMPUTATIONAL NEURAL NETWORK
C. L. Ladera, K. W. DeLong, R. Trebino, and D. N. Fittinghoff 1995 4 p Presented at the Signal Recovery and Synthesis Conference, Salt Lake City, UT, 12 Mar. 1995
(Contract DE-AC04-94AL-85000)
(DE95-007148; SAND-95-8491C; CONF-950396-1) Avail: CASI HC A01/MF A01

Previously, ultrashort-laser-pulse retrieval in frequency-resolved optical gating required an iterative algorithm. Here we use a computational neural network for directly recovering pulses. DOE

N95-27490# Brookhaven National Lab., Upton, NY.
SPECIFICATION OF THE FIGURE AND FINISH OF EUV MIRRORS IN TERMS OF PERFORMANCE REQUIREMENTS, REVISED NOV. 1994
E. L. Church and P. Z. Takacs Nov. 1994 6 p Presented at the Optical Society of America Conference on Extreme Ultraviolet Lithography, Monterey, CA, 19-21 Sep. 1994
(Contract DE-AC02-76CH-00016)
(DE95-005689; BNL-60902-Rev-11/94; CONF-9409177-4-Rev-11/94) Avail: CASI HC A02/MF A01

All manufacturing processes involve errors. In the case of bare and multilayer mirrors these unavoidable errors introduce near-field fluctuations in the reflected wavefront which propagate to the far field and degrade imaging performance. In order to specify manufacturing tolerances in terms of performance requirements we must know the connection between the two -- the finish-function relationship. This paper discusses the form of that relationship derived using elementary statistical diffraction theory. It tells us what statistical properties of the surface errors are relevant, it spells out the important role of the system parameters for EUV mirrors which is absent for conventional mirrors, and it leads to simple good-bad tests for mirror quality. These results are an extension of previous work in this area. DOE

N95-27539# California Univ., Berkeley. Lawrence Berkeley Lab, CA. Materials Sciences Div.
PHOTOEMISSION AND OPTICAL PROPERTIES OF C60 FULLERITES
Eric L. Shirley (National Inst. of Standards and Technology, Gaithersburg, MD.) and Steven G. Louie Aug. 1994 15 p Presented at the Quantum Theory of Real Materials, Berkeley, CA, 13 Aug. 1994 Sponsored in part by the Miller Inst. for Basic Research in Science
(Contracts DE-AC03-76SF-00098; NSF DMR-91-20269; W-7405-eng-48)
(DE95-006588; LBL-36517; CONF-9408212-1) Avail: CASI HC A03/MF A01

A theory is presented for excitations in undoped, solid C60 involving addition or removal of an electron, as well as creation of an electron-hole pair. Excitation energies are computed using a quasiparticle description of electrons and holes, plus a model for electron-hole interactions. Results are compared with those of direct and inverse photoelectron and optical absorption spectroscopy studies. Reasonable agreement is found in such comparisons, while more complete modeling of experimental spectra might include neglected matrix-element and vibrational effects. These results give values for simple, conceptual parameters, such as a molecular Hubbard U. Some results could also be relevant in doped fullerites. DOE

N95-27675# California Univ., Berkeley. Lawrence Berkeley Lab, CA. Accelerator and Fusion Research Div.
OBSERVATION OF NONLINEAR RESONANCES IN THE ADVANCED LIGHT SOURCE
D. Robin, H. Collins, W. Decking, G. Portmann, L. Schachinger, and A. Zholents Sep. 1994 6 p Presented at the Workshop on Nonlinear Dynamics in Particle Accelerators: Theory and Experiments, Arcidosso, Italy, 4-9 Sep. 1994 Sponsored in part by the German Academic Exchange Service
(Contract DE-AC03-76SF-00098)
(DE95-006561; LBL-36427; CONF-9409258-6) Avail: CASI HC A02/MF A01

Observations of nonlinear resonances in the Advanced Light Source have been made by scanning betatron tunes and observing count rates in a beam-loss radiation monitor placed down stream of a beam scraper. The authors have found that it is possible to see structural resonances which are unallowed as well as those which are allowed by the ring's natural 12-fold symmetry. By systematically breaking the amount of symmetry they see that the widths of the unallowed resonances grow while the widths of the allowed resonances do not. In this paper the authors briefly discuss the importance of symmetry and its effect on resonances in the design of the ALS. Next they describe their experimental setup and discuss the performance of the beam loss monitor which they used to view the resonances. They then present scans of the tune space where one can see the presence of the structural resonances and their evolution when the lattice symmetry is systematically broken. DOE

N95-27734# Los Alamos National Lab., NM.
MEASUREMENT OF HIGH ACIDITY USING A RENEWABLE-REAGENT FIBER OPTIC SENSOR
K. J. Kuhn and J. T. Dyke 1995 24 p Presented at the International Forum Process Analytical Chemistry (IFPAC), Houston, TX, 22-25 Jan. 1995
(Contract W-7405-eng-36)
(DE95-006327; LA-UR-95-191; CONF-950158-1) Avail: CASI HC A03/MF A01

The renewable-reagent sensor concept was initially developed to address shortcomings in fiber optic chemical sensors dependent on immobilized, reversible reagents to produce analyte specific responses. The renewable-reagent sensor incorporates semi-selective membranes, analyte specific reagents, and remote spectroscopic detection to extract selective responses. While renewable-reagent fiber optic sensors have been demonstrated for a number of chemical sensing applications, the transfer of laboratory prototypes to real world applications require devices which oversample the measurement matrix to differentiate among environmental and analyte specific response components. For example, optical sensors which acquire broadband rather than single wavelength spectroscopic data provide diagnostics regarding the identity of and measurement error associated with matrix interferences. The following describes the fabrication and evaluation of two renewable-reagent fiber optic sensor designs for the measurement of HNO3 in the 0.1 M to 10.0 M concentration range. Both sensor designs employ an internal pH indicator reagent and broadband visible spectroscopic detection to characterize HNO3 concentration. DOE

N95-27843* National Aeronautics and Space Administration. Pasadena Office, CA.

DISPLAY SYSTEM EMPLOYING ACOUSTO-OPTIC TUNABLE FILTER Patent

James L. Lambert, inventor (to NASA) (Jet Propulsion Lab., California Inst. of Tech., Pasadena, CA.) 25 Apr. 1995 10 p Filed 7 Jun. 1993 Supersedes N94-15933 (32 - 3, p 1190)
(Contract NAS7-918)
(NASA-Case-NPO-18736-1-CU; US-Patent-5,410,371; US-Patent-Appl-SN-073235; US-Patent-Class-348-769; US-Patent-Class-348-754; US-Patent-Class-359-285; Int-Patent-Class-H04N-5/74) Avail: US Patent and Trademark Office

An acousto-optic tunable filter (AOTF) is employed to generate a display by driving the AOTF with a RF electrical signal comprising modulated red, green, and blue video scan line signals and scanning the AOTF with a linearly polarized, pulsed light beam, resulting in encoding of color video columns (scan lines) of an input video image into vertical columns of the AOTF output beam. The AOTF is illuminated periodically as each acoustically-encoded scan line fills the cell aperture of the AOTF. A polarizing beam splitter removes the unused first order beam component of the AOTF output and, if desired, overlays a real world scene on the output plane. Resolutions as high as 30,000 lines are possible, providing holographic display capability.

Official Gazette of the U.S. Patent and Trademark Office

N95-27906*# National Aeronautics and Space Administration. Lewis Research Center, Cleveland, OH.

FUNDAMENTAL CONCEPTS OF INTEGRATED AND FIBER OPTIC SENSORS

Margaret L. Tuma May 1995 37 p
(RTOP 505-62-50)
(NASA-TM-106920; E-9632; NAS 1.15:106920) Avail: CASI HC A03/MF A01

This chapter discusses fiber optic and integrated optic sensor concepts. Unfortunately, there is no standard method to categorize these sensor concepts. Here, fiber optic and integrated optic sensor concepts will be categorized by the primary modulation technique. These modulation techniques have been classified as: intensity, phase, wavelength, polarization, and time/frequency modulation. All modulate the output light with respect to changes in the physical or chemical property to be measured. Each primary modulation technique is then divided into fiber optic and integrated optic sections which are treated independently. For each sensor concept, possible sensor applications are discussed. The sensors and references discussed are not exhaustive, but sufficient to give the reader an overview of sensor concepts developed to date. Sensor multiplexing techniques such as wavelength division, time division, and frequency division will not be discussed as they are beyond the scope of this report. Author

N95-27913*# Tennessee Technological Univ., Cookeville, TN. Dept. of Electrical Engineering.

INVESTIGATION OF THE COLLISION LINE BROADENING PROBLEM AS APPLICABLE TO THE NASA OPTICAL PLUME ANOMALY DETECTION (OPAD) SYSTEM, PHASE 1 Final Report

Timothy C. Dean and Carl A. Ventrice 31 May 1995 39 p
(Grant NAG8-206)
(NASA-CR-198605; NAS 1.26:198605; D-V-95-1) Avail: CASI HC A03/MF A01

As a final report for phase 1 of the project, the researchers are submitting to the Tennessee Tech Office of Research the following two papers (reprinted in this report): 'Collision Line Broadening Effects on Spectrometric Data from the Optical Plume Anomaly System (OPAD),' presented at the 30th AIAA/ASME/SAE/ASEE Joint Propulsion Conference, 27-29 June 1994, and 'Calculation of Collision Cross Sections for Atomic Line Broadening in the Plume of the Space Shuttle Main Engine (SSME),' presented at the IEEE Southeastcon '95, 26-29 March 1995. These papers fully state the problem and the progress made up to the end of NASA Fiscal Year 1994. The NASA OPAD system was devised to predict concentrations of anomalous species in the plume of the Space Shuttle Main Engine (SSME) through analysis of spectrometric data. The self absorption of the radiation of these plume anomalies is highly dependent on the line shape of the atomic transition of interest. The Collision Line Broadening paper discusses the methods used to predict line shapes of atomic transitions in the environment of a rocket plume. The Voigt profile is used as the line shape factor since both Doppler and collisional line broadening are significant. Methods used to determine the collisional cross sections are discussed and the results are given and compared with experimental data. These collisional cross sections are then incorporated into the current self absorbing radiative model and the predicted spectrum is compared to actual spectral data collected from the Stennis Space Center Diagnostic Test Facility rocket engine. The second paper included in this report investigates an analytical method for determining the cross sections for collision line broadening by molecular perturbers, using effective central force interaction potentials. These cross sections are determined for several atomic species with H2, one of the principal constituents of the SSME plume environment, and compared with experimental data.

Derived from text

N95-28018# Los Alamos National Lab., NM.

NONLINEAR OPTICAL MICROSCOPY FOR IMAGING THIN FILMS AND SURFACES

L. B. Smilowitz, D. W. McBranch, and J. M. Robinson 1995 12 p Presented at the SPIE 1995: SPIE Conference on Optics, Electro-optics, and Laser Application in Science, Engineering and Medicine, San Jose, CA, 5-10 Feb. 1995
(Contract W-7405-eng-36)
(DE95-007872; LA-UR-95-405; CONF-950226-22) Avail: CASI HC A03/MF A01

We have used the inherent surface sensitivity of second harmonic generation to develop an instrument for nonlinear optical microscopy of surfaces and interfaces. We have demonstrated the use of several nonlinear optical responses for imaging thin films. The second harmonic response of a thin film of C60 has been used to image patterned films. Two photon absorption light induced fluorescence has been used to image patterned thin films of Rhodamine 6G. Applications of nonlinear optical microscopy include the imaging of charge injection and photoinduced charge transfer between layers in semiconductor heterojunction devices as well as across membranes in biological systems. DOE

N95-28022# Los Alamos National Lab., NM.

DEVELOPMENT OF AN OPTICAL TRAP AS AN ULTRA-SENSITIVE ANALYTICAL TOOL

D. J. Vieira, V. Sandberg, D. Tupa, J. M. Wouters, R. Guckert (Justus Liebig-Univ., Giessen, Germany.), and D. W. Preston (California State Univ., Hayward, CA.) 1995 7 p Presented at the SPIE '95: SPIE Conference on Optics, Electro-optics, and Laser Application in Science, Engineering and Medicine, San Jose, CA, 5-10 Feb. 1995
(Contract W-7405-eng-36)
(DE95-007843; LA-UR-95-837; CONF-950226-16) Avail: CASI HC A02/MF A01

The use of an optical trap for the quantitative detection of small numbers of radioactive atoms is featured. Presently under construction is a system consisting of a high-efficiency magneto-optical trap (MOT) coupled to a mass separator. Mass-separated samples will be implanted into a thin platinum foil, subsequently released from the foil by heating, and resonantly trapped in the MOT. The number of atoms in the trap will be quantitatively deduced from the amplitude of the fluorescence signal. Measurements for different isotopes are planned by appropriately shifting the trapping and repumping laser frequencies of the optical trap. Our initial investigations will concentrate on the determination of trace amounts of Cs-135 and Cs-137. DOE

N95-28196# Brookhaven National Lab., Upton, NY.

FLAT PANEL PLANAR OPTIC DISPLAY

J. T. Veligdan Nov. 1994 12 p Presented at the Technology 2004, Washington, DC, 8-10 Nov. 1994
(Contract DE-AC02-76CH-00016)
(DE95-007686; BNL-61332; CONF-9411151-2) Avail: CASI HC A03/MF A01

A prototype 10 inch flat panel Planar Optic Display, (POD), screen has been constructed and tested. This display screen is comprised of hundreds of planar optic class sheets bonded together with a cladding layer between each sheet where each glass sheet represents a vertical line of resolution. The display is 9 inches wide by 5 inches high and approximately 1 inch thick. A 3 milliwatt HeNe laser is used as the illumination source and a vector scanning technique is employed. DOE

N95-28363* National Aeronautics and Space Administration. Pasadena Office, CA.

OPTICAL IMPLEMENTATION OF INNER PRODUCT NEURAL ASSOCIATIVE MEMORY Patent

Hua-Kuang Liu, inventor (to NASA) 2 May 1995 9 p Filed 8 Feb. 1994
(NASA-Case-NPO-18491-2-CU; US-Patent-5,412,755;
US-Patent-Appl-SN-195737; US-Patent-Class-395-25;
Int-Patent-Class-G06F-15/18) Avail: US Patent and Trademark Office

An optical implementation of an inner-product neural associative memory is realized with a first spatial light modulator for entering an initial two-dimensional N-tuple vector and for entering a thresholded output vector image after each iteration until convergence is reached, and a second spatial light modulator for entering M weighted vectors of inner-product scalars multiplied with each of the M stored vectors, where the inner-product scalars are produced by multiplication of the initial input vector in the first iterative cycle (and thresholded vectors in subsequent iterative cycles) with each of the M stored vectors, and the weighted vectors are produced by multiplication of the scalars with corresponding ones of the stored vectors. A Hughes liquid crystal light valve is used for the dual function of summing the weighted vectors and thresholding the sum vector. The thresholded vector is then entered through the first spatial light modulator for reiteration of the process cycle until convergence is reached.
Official Gazette of the U.S. Patent and Trademark Office

N95-28384* National Aeronautics and Space Administration. Lyndon B. Johnson Space Center, Houston, TX.

FULL COMPLEX MODULATION USING TWO ONE-PARAMETER SPATIAL LIGHT MODULATORS Patent

Richard D. Juday, inventor (to NASA) 16 May 1995 37 p Filed 10 Nov. 1992
(NASA-Case-MSC-22255-1; US-Patent-5,416,618;
US-Patent-Appl-SN-977302; US-Patent-Class-359-53;
US-Patent-Class-359-247; US-Patent-Class-359-250;
US-Patent-Class-359-259; US-Patent-Class-359-279;
Int-Patent-Class-G02F-1/01) Avail: US Patent and Trademark Office

Full complex spatial light modulation is enabled by an optically additive combination of the actions of separate and independent spatial light modulators, even though the independent modulators can each express only a one-parameter subset of complex values called its operating curve. Similarly the operating curve of a single modulator can be shifted (biased) by optically adding a constant complex value.
Official Gazette of the U.S. Patent and Trademark Office

N95-28408 Arnold Engineering Development Center, Arnold AFS, TN.

CRYOGENIC BRDF MEASUREMENTS AT 10.6 MICROMETERS AND 0.63 MICROMETERS ON CONTAMINATED MIRRORS Final Report, Oct. 1993 - Sep. 1994

B. L. Seiber, R. J. Bryson, W. T. Bertrand, and B. E. Wood Feb. 1995 88 p Limited Reproducibility: More than 20% of this document may be affected by microfiche quality
(AD-A291611; AEDC-TR-94-16) Avail: Issuing Activity (Defense Technical Information Center (DTIC))

Effects of contaminants on optical surface are concern for space-based systems. Many systems contain cryogenic optical systems that operate at temperatures where gases condense. This study presents experimental results of the effects of condensed gases and spacecraft contaminants on highly polished (superpolished) mirror surfaces cooled, under vacuum to temperatures near 16 K and 70 K. After condensing contaminants on the mirror, the change in the bidirectional reflectance distribution function (BRDF) was obtained at wavelengths of 10.6 and 0.6328 um for various contaminant thicknesses up to 15 um. For a mirror surface of 16 K, BRDF changes for the following contaminant films were obtained: air, N_2, O_2, H_2O, CO, CO_2, and Ar. For a mirror surface near 70 K, the BRDF changes from condensed films of the following outgassing effluents were measured: RS12M polycyanate, Nusil CV2500 silicone, Solithane 113/Cl 13-300 urethane, RTVS60 silicone, and 1120. In addition, using measured optical properties and the thin-film interference theory-based computer program CALCRT, the spectral reflectance of an 80 K aluminum mirror was calculated for H_2O, CO and RTV560. This report was sponsored by the Ballistic Missile Defense Organization (BMDO) through Johns Hopkins Applied Physics Laboratory (JHU/APL) and by the Jet Propulsion Laboratory (JPL) Space Environmental Effects Program. DTIC

N95-28516# Sandia National Labs., Albuquerque, NM.

RETROFITTING A FINE-POINTING SYSTEM TO SATELLITE OPTICS

R. O. Woods 1994 9 p Presented at the 29th Aerospace Mechanisms Symposium, Houston, TX, 17-19 May 1995 See also N95-27277
(Contract DE-AC04-94AL-85000)
(DE95-004529; SAND-94-2920C; CONF-9505124-1) Avail: CASI HC A02/MF A01

This paper describes a system that was added to an existing satellite-borne telescope design for the purpose of compensating the boresight errors that had been observed in earlier flights of similar instruments. Those errors had been found to be caused by thermal distortion of the spaceframe. This retrofit design was subject to severe volume restrictions because it was fitted into an already tightly-packaged instrument envelope. It was found practical to improve the basic design by converting a redundant structure into a statically-determinate one. It was also possible to use portions of the mechanical actuation system to facilitate the position encoding needed for computer interfacing. DOE

N95-28524 Colorado Univ., Boulder, CO. Dept. of Electrical and Computer Engineering.

PERTURBATIONS ON EFFECTIVE INDEX OF REFRACTION FROM PRISM COUPLING Report No. 66

Stephen L. Kwiatkowski and Alan R. Mickelson Feb. 1995 52 p Limited Reproducibility: More than 20% of this document may be affected by microfiche quality
(Contracts N00014-92-J-1190; DAAL03-92-G-0289; NSF ECS-90-15752)
(AD-A291700) Avail: Issuing Activity (Defense Technical Information Center (DTIC))

We investigate the accuracy and precision of effective index of refraction measurements using prism coupling. The coupling gap's geometry is critical to predicting the accuracy and resolution of measurements. We provide experimental evidence that there are advantages to using high coupling pressures that yield long coupling lengths. Furthermore, effective index perturbations vary with mode number in some cases. We present and evaluate an experimental technique aimed at reducing the effects of perturbation and find that it may not be applicable to all situations. We extend a previous model of prism coupling to include a finite coupling length. This allows us to explain some of our experimental observations of m-line characteristics. We find disagreements between previous models when predicting effective index perturbations. Also, we introduce an alternative model of prism coupling based upon a local normal-mode expansion and present its preliminary numerical results. Finally, our results indicate that using prism coupling to measure effective index beyond the fourth decimal place will require additional experimental techniques and theoretical models. DTIC

N95-28552# Oak Ridge National Lab., TN.

DESIGN AND FABRICATION OF A DIAMOND-TURNED HYBRID DIFFRACTIVE/REFRACTIVE SINGLET FOR VISIBLE APPLICATIONS AT ORNL

B. E. Bernacki, A. C. Miller, and L. C. Maxey 1995 15 p Presented at the Conference on Manufacturing Redstone Arsenal, Huntsville, AL, 1-2 Nov. 1994
(Contract DE-AC05-84OR-21400)
(DE95-007007; CONF-9411198-1) Avail: CASI HC A03/MF A01

Hybrid diffractive/refractive optics can be fabricated using traditional lithographic methods involving masks or holographic techniques as well as direct-write approaches that include electron-beam lithography, single-point diamond turning, and laser beam lithography. Only the direct-write methods have proven to be practical in producing continuous-form diffractive surfaces, or kinoforms, and among these methods, only diamond turning can easily produce large kinoforms on curved base surfaces. In this paper, we describe design and fabrication issues for a hybrid singlet produced by single-point diamond turning that functions in the visible portion of the spectrum and takes advantage of all of the degrees of freedom available from diamond turning: aspheric front surface to control spherical aberration; curved rear surface for elimination of coma; and kinoform surface placed on either curved base surface for control of primary chromatic aberration. DOE

N95-28557# California Univ., Berkeley. Lawrence Berkeley Lab, CA.
NONLINEAR OPTICAL STUDIES OF SURFACES
Y. R. Shen Jul. 1994 8 p Presented at the Surface Studies By Nonlinear Optical Spectroscopy Conference, Kassel, Germany, 29 May - 2 Jun. 1994
(Contract DE-AC03-76SF-00098)
(DE95-006574; LBL-35991; CONF-9405289-1) Avail: CASI HC A02/MF A01

The possibility of using nonlinear optical processes for surface studies has attracted increasing attention in recent years. Optical second harmonic generation (SHG) and sum frequency generation (SFG), in particular, have been well accepted as viable surface probes. They have many advantages over the conventional techniques. By nature, they are highly surface-specific and has a submonolayer sensitivity. As coherent optical processes, they are capable of in-situ probing of surfaces in hostile environment as well as applicable to all interfaces accessible by light. With ultrafast pump laser pulses, they can be employed to study surface dynamic processes with a subpicosecond time resolution. These advantages have opened the door to many exciting research opportunities in surface science and technology. This paper gives a brief overview of this fast-growing new area of research. Optical SHG from a surface was first studied theoretically and experimentally in the sixties. Even the submonolayer surface sensitivity of the process was noticed fairly early. The success was, however, limited because of difficulties in controlling the experimental conditions. It was not until the early 1980's that the potential of the process for surface analysis was duly recognized. The first surface study by SHG was actually motivated by the then active search for an understanding of the intriguing surface enhanced Raman scattering (SERS). It had been suspected that the enhancement in SERS mainly came from the local-field enhancement due to local plasmon resonances and pointing rod effect on rough metal surfaces. In our view, Raman scattering is a two-photon process and is therefore a nonlinear optical effect. DOE

N95-28617 Air Force Systems Command, Wright-Patterson AFB, OH. National Air Intelligence Center.
ATMOSPHERIC DISPERSION IN ADAPTIVE OPTICS
Yuezhong Feng, Zhengfang Song, and Zhiben Gong 16 Dec. 1994 14 p Transl. into ENGLISH from Hongwai Yu Haomibo Xuebao, China, v. 10, no. 3, Jun. 1991 p 217-221 Limited Reproducibility: More than 20% of this document may be affected by microfiche quality
(AD-A289639; NAIC-ID(RS)T-0893-92) Avail: Issuing Activity (Defense Technical Information Center (DTIC))

Using methods associated with Zernicke's polynomial expansion, we discussed atmospheric dispersion effects in dual wavelength adaptive optics systems. On the basis of dual frequency correlations associated with phase expansion coefficients, we solved for residual phase errors produced by atmospheric dispersion. The results clearly showed that, although atmospheric dispersion will cause phase compensation to be imperfect, the use, however, of light sources with wavelengths even shorter than the transmitting lasers as beacons, and, in conjunction with that, taking the product of the amount of beacon phase distortion and the specific value of the ratio (lambda 2)/(lambda 1) (the beacon wavelength/ transmitted wavelength) to be the phase predistortion, it is possible to rectify relatively well the phase distortion of transmitted light beams. DTIC

N95-27270*# SSG, Inc., Waltham, MA.
ULTRA-HIGH, RESOLUTION, MODULAR OPTICAL ANGLE ENCODER FOR SPACE-BASED OPTO-MECHANICAL APPLICATIONS
Holger Luther, Paul Beard, Donald Mitchell (BEI Sensors and Systems Co., Needham, MA.), and William Thorburn (BEI Sensors and Systems Co., Needham, MA.) *In* NASA. Johnson Space Center, The 29th Aerospace Mechanisms Symposium May 1995 p 136-146 (For primary document see N95-27260 09-15)
Avail: CASI HC A01/MF A04

N95-27277*# Sandia National Labs., Albuquerque, NM. Intelligent Systems and Robotics Center.
RETROFITTING A FINE-POINTING SYSTEM TO SATELLITE OPTICS
Robert O. Woods *In* NASA. Johnson Space Center, The 29th Aerospace Mechanisms Symposium May 1995 p 175-182 (For primary document see N95-27260 09-15)
(Contract DE-AC04-94AL-85000)
Avail: CASI HC A02/MF A04

N95-27288*# Ball Corp., Boulder, CO. Aerospace Systems Div.
HIGH-PERFORMANCE REACTIONLESS SCAN MECHANISM
Ellen I. Williams, Richard T. Summers, and Miroslaw A. Ostaszewski *In* NASA. Johnson Space Center, The 29th Aerospace Mechanisms Symposium May 1995 p 334-349 Sponsored by Dick Maxwell (For primary document see N95-27260 09-15)
Avail: CASI HC A03/MF A04

N95-27646*# National Aeronautics and Space Administration. Marshall Space Flight Center, Huntsville, AL.
POINT DEFECT FORMATION IN OPTICAL MATERIALS EXPOS ED TO THE SPACE ENVIRONMENT
J. L. Allen (Vanderbilt Univ., Nashville, TN.), N. Seifert (Vanderbilt Univ., Nashville, TN.), Y. Yao (Vanderbilt Univ., Nashville, TN.), R. G. Albridge (Vanderbilt Univ., Nashville, TN.), A. V. Barnes (Vanderbilt Univ., Nashville, TN.), N. H. Tolk (Vanderbilt Univ., Nashville, TN.), A. M. Strauss (Vanderbilt Univ., Nashville, TN.), Roger C. Linton, R. R. Kamenetzky, and Jason A. Vaughn et al *In* NASA. Langley Research Center, LDEF: 69 Months in Space. Third Post-Retrieval Symposium, Part 3 Feb. 1995 p 1131-1145 (For primary document see N95-27629 09-99)
(Contracts N00014-87-C-0146; N00014-91-C-0109; N00014-91-J-4040)
Avail: CASI HC A03/MF A04

N95-27650*# Georgia Inst. of Tech., Atlanta, GA. Research Center.
A FINAL LOOK AT LDEF ELECTRO-OPTIC SYSTEMS COMPONENTS
M. D. Blue *In* NASA. Langley Research Center, LDEF: 69 Months in Space. Third Post-Retrieval Symposium, Part 3 Feb. 1995 p 1179-1188 (For primary document see N95-27629 09-99)
Avail: CASI HC A02/MF A04

N95-27651*# National Aeronautics and Space Administration. Goddard Space Flight Center, Greenbelt, MD.
EFFECTS OF THE LDEF ORBITAL ENVIRONMENT ON THE REFLECTANCE OF OPTICAL MIRROR MATERIALS
Howard Herzig and Charles Fleetwood, Jr. *In* NASA. Langley Research Center, LDEF: 69 Months in Space. Third Post-Retrieval Symposium, Part 3 Feb. 1995 p 1189-1203 (For primary document see N95-27629 09-99)
Avail: CASI HC A03/MF A04

N95-27652*# Donovan (Terence), Palo Alto, CA.
EFFECTS OF LOW EARTH ORBIT ON THE OPTICAL PERFORMANCE OF MULTI-LAYER ENHANCED HIGH REFLECTANCE MIRRORS
Terence Donovan, Linda Johnson (Naval Air Warfare Center, China Lake, CA.), Karl Klemm (Naval Air Warfare Center, China Lake, CA.), Rick Scheri (Naval Air Warfare Center, China Lake, CA.), Jean Bennett (Naval Air Warfare Center, China Lake, CA.), Jon Erickson (Evans, Charles and Associates, Redwood City, CA.), and Filippo diBrozolo (Evans, Charles and Associates, Redwood City, CA.) *In* NASA. Langley Research Center, LDEF: 69 Months in Space. Third Post-Retrieval Symposium, Part 3 Feb. 1995 p 1205-1225 Sponsored by DARPA; and Wright Labs. (For primary document see N95-27629 09-99)
Avail: CASI HC A03/MF A04

N95-27653*# Eastman Kodak Co., Rochester, NY.
EFFECTS OF LONG TERM SPACE ENVIRONMENT EXPOSURE ON OPTICAL SUBSTRATES AND COATINGS Abstract Only
John Vallimont, E. Steven Brandt, Keith Havey, and Arthur Mustico *In* NASA. Langley Research Center, LDEF: 69 Months in Space. Third Post-Retrieval Symposium, Part 3 Feb. 1995 p 1227 (For primary document see N95-27629 09-99)
Avail: CASI HC A01/MF A04

N95-27654*# Phillips Lab., Kirtland AFB, NM. Space and Missiles Technology Directorate.
LONG DURATION EXPOSURE FACILITY (LDEF) SPACE OPTICS HANDBOOK Abstract Only

William T. Kemp, Edward Taylor, Robert Champetier (Science Applications International Corp., Santa Monica, CA.), Alan Watts (POD Associates, Inc., Albuquerque, NM.), and Dale Atkinson (POD Associates, Inc., Albuquerque, NM.) *In* NASA. Langley Research Center, LDEF: 69 Months in Space. Third Post-Retrieval Symposium, Part 3 Feb. 1995 p 1229 (For primary document see N95-27629 09-99)
Avail: CASI HC A01/MF A04

75 PLASMA PHYSICS

Includes magnetohydrodynamics and plasma fusion.
For ionospheric plasmas see *46 Geophysics*. For space plasmas see *90 Astrophysics*.

N95-26438# Ceskoslovenska Akademie Ved, Prague. Institute of Plasma Physics.
ON HELICON WAVE INDUCED RADIAL PLASMA TRANSPORT
V. Petrzilka Apr. 1993 12 p
(DE94-634477; IPPCZ-333) Avail: CASI HC A03/MF A01 (US Sales Only)

Estimates of helicon wave induced radial plasma transport are presented. The wave induced transport grows or decreases in dependence on the sign of the azimuthal wave number; these changes in transport may play an important role in helicon wave plasma sources. DOE

N95-26439# International Centre for Theoretical Physics, Trieste (Italy).
WAKE FIELDS IN SEMICONDUCTOR PLASMAS
V. I. Berezhiani and S. M. Mahajan May 1994 9 p
(Contract DE-FG05-80ET-53088)
(DE94-634523; IC-94/90) Avail: CASI HC A02/MF A01 (US Sales Only)

It is shown that an intense short laser pulse propagating through a semiconductor plasma will generate longitudinal Langmuir waves in its wake. The measurable wake field can be used as a diagnostic to study nonlinear optical phenomena. For narrow gap semiconductors (for examples InSb) with Kane-type dispersion relation, the system can simulate, at currently available laser powers, the physics underlying wake-field accelerators. DOE

N95-26444# California Inst. of Tech., Pasadena, CA.
FLUCTUATIONS AND TRANSPORT IN FUSION PLASMA Progress Report, 1 Oct. - 30 Sep. 1990
1995 32 p
(Contract DE-FG03-84ER-53173)
(DE95-004178; DOE/ER-53173/T4) Avail: CASI HC A03/MF A01

In the study of plasma collection by obstacles in a tokamak edge plasma, the effect of anomalous transport have been examined using an extension of the 2D fluid code developed here previously (Appendices A and B). The origin of the anomalous transport is assumed to be a randomly fluctuating electric field such as would be caused by drift waves. As before, the magnetic field is assumed to be uniform and perpendicular to the obstacle, which is taken to be an infinite strip. In the absence of ambient plasma flow, the numerical results indicate that ion viscous heating is important near the tip of the obstacle, where there is a large velocity gradient in the flow. For typical plasma parameters, the maximum ion temperature near the tip is up to 85% higher than the ambient ion temperature. When there is a subsonic plasma flow past the obstacle, the numerical results indicate that, near the tip of the obstacle, the ions on the downstream side are hotter than those on the upstream side. Furthermore, the ion density is higher on the upstream side. A detailed report of this work has been prepared and will be submitted as part of the Annual Progress Report. Recently, the 2D parallel electrostatic plasma particle-in-cell (PIC) code has been upgraded to a 2D fully electromagnetic PIC code. This code has been successfully tested on the JPL/Caltech Mark III Hypercube concurrent computers and can be used to simulate interactions of electromagnetic waves with a magnetized plasma. It is currently applied to investigate the decay of large amplitude Alfven waves, such as those observed in the solar wind. Large amplitude Alfven waves, propagating parallel to the magnetic field, are predicted to decay into obliquely propagating daughter waves and standing magnetosonic waves. Results from the simulations will be compared with theoretical predictions.Moreover, it will be possible to study the influence of kinetic effects on the decy instability which are very difficult to included in analytic models. DOE

N95-26720 Phillips Lab., Kirtland AFB, NM.
RADIATION PRODUCTION FROM STAGNATING COMPACT TOROIDS EMPLOYING A NONEQUILIBRIUM RADIATION DIFFUSION MODEL Final Report, Sep. 1990 - May 1994
Melissa R. Douglas Dec. 1994 260 p Limited Reproducibility: More than 20% of this document may be affected by microfiche quality
(AD-A289602; PL-TR-94-1126) Avail: Issuing Activity (Defense Technical Information Center (DTIC))

The stagnation of a high Z, high velocity compact toroidal plasma against a stationary object has been shown computationally to be an efficient radiation source. To obtain a better understanding of the stagnation process and the influence of various prestagnation properties on radiation production, the 2 1/2 dimensional radiation magnetohydrodynamic code, MACH2, was used to simulate the stagnation physics. To perform these calculations, a flux-limited non-equilibrium radiation diffusion model was incorporated into the MACH2 code. In this model the radiation field evolves separately from the material components of the fluid and is described by a Plankian distribution at the radiation temperature, TR. This introduced a dynamic equation for the radiation field and modifications to both the momentum and electron energy equations. A flux-limited version of the radiative conductivity was formulated to extend this model into the optically thin regime. Detailed benchmarking of the radiation diffusion and electron-radiation coupling using a set of radiation MHD test problems was conducted. DTIC

N95-26800 Pittsburgh Univ., Pittsburgh, PA.
BOW SHOCK DATA ANALYSIS Final Report
Edward C. Zipf and Peeter W. Erdman 19 Aug. 1994 12 p Limited Reproducibility: More than 20% of this document may be affected by microfiche quality
(Contract DAAL03-92-G-0311)
(AD-A288432; ARO-30419.1-EG-SDI) Avail: Issuing Activity (Defense Technical Information Center (DTIC))

The University of Pittsburgh Space Physics Group in collaboration with the Army Research Office (ARO) modeling team has completed a systematic organization of the shock and plume spectral data and the electron temperature and density measurements obtained during the BowShock I and II rocket flights which have been submitted to the AEDC Data Center, has verified the presence of CO Cameron band emission during the Antares engine burn and for an extended period of time in the post-burn plume, and have adapted 3-D radiation entrapment codes developed by the University of Pittsburgh to study aurora and other atmospheric phenomena that involve significant spatial effects to investigate the vacuum ultraviolet (VUV) and extreme ultraviolet (EUV) envelope surrounding the re-entry that create an extensive plasma cloud by photoionization. DTIC

N95-26940 Wisconsin Univ., Madison, WI. Dept. of Physics.
MHD SIMULATIONS OF DC HELICITY INJECTION FOR CURRENT DRIVE IN TOKAMAKS
C. R. Sovinec and S. C. Prager Dec. 1994 28 p Limited Reproducibility: More than 20% of this document may be affected by microfiche quality
(Contract DE-FG02-85ER-53212)
(DE95-007018; DOE/ER-53212/255) Avail: CASI HC A03

MHD computations of DC helicity injection in tokamak-like configurations show current drive with no 'loop voltage' in a resistive, pressureless plasma. The self-consistently generated current profiles are unstable to resistive modes that partially relax the profile through the MHD dynamo mechanism. The current driven by the fluctuations leads to closed contours of average poloidal flux. However, the 1% fluctuation level is large enough to produce a region of stochastic magnetic field. A limited Lundquist number (S) scan from 2.5 x 10(exp 3) to 4 x 10(exp 4) indicates that both the fluctuation level and relaxation increase with S. DOE

N95-27084# Texas Univ., Austin, TX.
NONLINEAR INSTABILITY AND CHAOS IN PLASMA WAVE-WAVE INTERACTIONS. I. INTRODUCTION
C. S. Kueny and P. J. Morrison Nov. 1994 53 p

(Contract DE-FG05-80ET-53088)
(DE95-005529; DOE/ET-53088/682) Avail: CASI HC A04/MF A01

Conventional linear stability analyses may fail for fluid systems with an indefinite free energy functional. When such a system is linearly stable, it is said to possess negative energy modes. Instability may then occur either via dissipation of the negative energy modes, or nonlinearly via resonant wave-wave coupling, leading to explosive growth. In the dissipationless case, it is conjectured that intrinsic chaotic behavior may allow initially nonresonant systems to reach resonance by diffusion in phase space. In this and a companion paper, this phenomenon is demonstrated for a simple equilibrium involving cold counterstreaming ions. The system is described in the fluid approximation by a Hamiltonian functional and associated noncanonical Poisson bracket. By Fourier decomposition and appropriate coordinate transformations, the Hamiltonian for the perturbed energy is expressed in action-angle form. The normal modes correspond to Doppler-shifted ion-acoustic waves of positive and negative energy. Nonlinear coupling leads to decay instability via two-wave interactions, and to either decay or explosive instability via three-wave interactions. These instabilities are described for various (integrable) systems of waves interacting via single nonlinear terms. This discussion provides the foundation for the treatment of nonintegrable systems in the companion paper. DOE

N95-27190 Science Research Lab., Inc., Somerville, MA.
HIGH-DENSITY PLASMA SOURCE FOR LARGE-AREA CHEMICAL VAPOR DEPOSITION OF DIAMOND FILMS Monthly Report, 1 Nov. - 30 Nov. 1994
Xing Chen 15 Dec. 1994 4 p Limited Reproducibility: More than 20% of this document may be affected by microfiche quality
(Contract N00014-94-C-0199)
(AD-A289053) Avail: Issuing Activity (Defense Technical Information Center (DTIC))

During this program Science Research Laboratory (SRL) and the Plasma Processing Group in the Department of Chemical Engineering at MIT are developing a large-area, directed plasma/atomic beam source for diamond deposition. The plasma source is based on an inductively-driven plasma accelerator that efficiently produces a high density (1014-1017 cu cm) plasma over an area of 0.1-1 sq m. The goal of this effort is to experimentally demonstrate the technical feasibility of employing the plasma source for high-throughput diamond deposition, through characterization of plasma parameters and preliminary diamond deposition experiments. A reactor design study will also be completed during Phase 1, leading to an engineering design of a large-area plasma reactor for Phase H implementation. The period of performance is from 30 September 1994 to 31 March 1995. DTIC

N95-27237# Idaho Univ., Moscow, ID.
MAGNETICALLY CONTROLLED DEPOSITION OF METALS USING GAS PLASMA Quarterly Progress Report, Oct. - Dec. 1994
1995 22 p
(Contract DE-FG07-93ID-13220)
(DE95-007248; DOE/ID-13220/T3) Avail: CASI HC A03/MF A01

The objective of the grant is to develop a method of spraying materials on a substrate in a controlled manner to eliminate the waste inherent in present plating processes. The process under consideration is magnetically controlled plasma spraying. The project continues to be on schedule. The field equations have been developed and were reported in the April-June 1994 Progress Report. The equations for the external magnetic field were reported in the July-September 1994 progress report. The field equations have been cast in a format that allows solution using Finite Element (FE) techniques. The development of the computer code that will allow evaluation of the proposed technique and design of an experiment to prove the proposed process is underway. DOE

N95-27306# Oak Ridge National Lab., TN.
DYNAMICS OF THE L YIELDS H TRANSITION, VH-MODE EVOLUTION, EDGE LOCALIZED MODES AND R.F. DRIVEN CONFINEMENT CONTROL IN TOKAMAKS
P. H. Diamond (California Univ., San Diego, CA.), V. B. Lebedev (California Univ., San Diego, CA.), Y. M. Liang (California Univ., San Diego, CA.), A. V. Gruzinov (California Univ., San Diego, CA.), I. Gruzinov (California Univ., San Diego, CA.), M. Medvedev (California Univ., San Diego, CA.), B. A. Carreras, D. E. Newman, L. Charlton, and K. L. Sidikman 1995 35 p Presented at the 15th International Conference on Plasma Physics and Controlled Nuclear Fusion Research, Seville, Spain, 26 Sep. - 1 Oct. 1994
(Contract DE-AC05-84OR-21400)
(DE95-007012; CONF-940933-30; IAEA-CN-60/D-2-II-6) Avail: CASI HC A03/MF A01

Several novel theoretical results related to L yields H transition physics, VH-mode evolution, edge localized modes, and active confinement control are presented. Critical issues are identified, results are discussed, and important unresolved questions are listed. The basic physics is discussed in the contexts of current experiments and of ITER. DOE

N95-27308# Oak Ridge National Lab., TN.
EVALUATION OF CURRENT DRIVE REQUIREMENTS AND OPERATING CHARACTERISTICS OF A HIGH BOOTSTRAP FRACTION ADVANCED TOKAMAK REACTOR
W. A. Houlberg and S. E. Attenberger 1995 6 p Presented at the 11th Topical Meeting on the Technology of Fusion Energy, New Orleans, LA, 19-24 Jun. 1994
(Contract DE-AC05-84OR-21400)
(DE95-007041; CONF-940630-54) Avail: CASI HC A02/MF A01

The reactor potential of some advanced physics operating modes proposed for the TPX physics program are examined. A moderate aspect ratio (A = 4.5 as in TPX), 2 GW reactor is analyzed because of its potential for steady-state, noninductive operation with high bootstrap current fraction. Particle, energy, and toroidal current equations are evolved to steady-state conditions using the 1 1/2-D time-dependent WHIST transport code. The solutions are therefore consistent with particle, energy, and current sources and assumed transport models. Fast wave current drive (FWCD) provides the axial seed current. The bootstrap current typically provides 80-90% of the current, while feedback on the lower hybrid current drive (LHCD) power maintains the total current. The sensitivity of the plasma power amplification factor, Q equivalent to P(sub fus)/P(sub aux), to variations in the plasma properties is examined. The auxiliary current drive power, P(sub aux) = P(sub LH) + P(sub FW); bootstrap current fraction; current drive efficiency; and other parameters are evaluated. The plasma is thermodynamically stable for the energy confinement model assumed (a multiple of ITER89P). The FWCD and LHCD sources provide attractive control possibilities, not only for the current profile, but also for the total fusion power since the gain on the incremental auxiliary power is typically 10-30 in these calculations when overall Q approximately equals 30. DOE

N95-27327# Los Alamos National Lab., NM.
INDIRECTLY DRIVEN TARGETS FOR IGNITION
D. C. Wilson and W. J. Krauser 1994 5 p Presented at the ECLIM 23: Laser Interaction With Matter, Oxford, England, 19-23 Sep. 1994
(Contracts W-7405-eng-36; W-7405-eng-48)
(DE95-006451; LA-UR-94-3115; CONF-9409226-4) Avail: CASI HC A01/MF A01

Both Los Alamos and Lawrence Livermore Laboratories have studied capsule and laser driven target designs for the National Ignition Facility. The current hohlraum design is a 2.76mm radius, 9.5mm long gold cylinder with 1.39mm radius laser entrance holes covered by 1 micro m thick plastic foils. Laser beams strike the inside cylinder wall from two separate cones with a peak power less than 400 TW. The problem with a pressure pulse caused by wall plasma stagnating on axis has been overcome by filling the hohlraum with gas. Currently this is equi-molar hydrogen-helium gas at 0.83 mg/cc density. One capsule uses a 160 micro m plastic ablator doped with oxygen and bromine surrounding an 80 micro m thick DT ice layer with an inner radius of 0.87 mm. Los Alamos integrated calculations of the hohlraum and this capsule using 1.4 MJ of laser energy achieve yields of 4.9 MJ using LTE atomic physics, and 3.5 MJ with non-LTE. This confirms Livermore calculations of ignition. For radiation driven implosions, a beryllium ablator offers a viable alternative to plastic. It is strong enough to contain high DT pressures. Copper, soluble at required levels, is an excellent dopant to add opacity. A beryllium capsule with a 155 micro m thick ablator doped with 0.9 atom% copper, and the same inner dimensions as the plastic capsule, placed in a similar hohlraum , yields 6.9 MJ with LTE. Although these calculations show the designs are sensitive, they add to the confidence that NIF can achieve ignition. Using their best integrated calculations which are not yet fully optimized, they confirm Livermore calculations of ignition with a plastic capsule, and have added an alternate capsule design with a beryllium ablator. DOE

N95-27414# Japan Atomic Energy Research Inst., Tokyo (Japan).
OUTLINE AND HANDLING MANUAL OF FUSION EXPERIMENTAL DATA MONITOR SYSTEM DAISY, VERSION 2
Hirofumi Haginoya, Tetsuo Aoyagi, Keiji Tani, Yuichi Watanabe, and Mari Yamanaka Mar. 1994 96 p
(DE95-703895; JAERI-M-94-040) • Avail: CASI HC A05/MF A01 (US Sales Only)

DAISY (version 1), which was developed about 7 years ago, has been used as a main experimental data monitor system for JT-60 and JT-60U. Through many years use, the system has been improved by complying with users requests. This report summarizes a brief explanation and the usage of the new 'DAISY (version 2)'. DOE

N95-27419# Oak Ridge National Lab., TN.
ENERGETIC PARTICLE DESTABILIZATION OF SHEAR ALFVEN WAVES IN STELLARATORS AND TOKAMAKS
D. A. Spong, B. A. Carreras, C. L. Hedrick, J. N. Leboeuf, and A. Weller (Max-Planck-Inst. fuer Plasmaphysik, Garching, Germany.) 1994 55 p Presented at the 15th International Conference on Plasma Physics and Controlled Nuclear Fusion Research, Seville, Spain, 26 Sep. - 1 Oct. 1994
(Contract DE-AC05-84OR-21400)
(DE95-006393; CONF-940933-26; IAEA-CN-60/D-P-II-3) Avail: CASI HC A04/MF A01

An important issue for ignited devices is the resonant destabilization of shear Alfven waves by energetic populations. These instabilities have been observed in a variety of toroidal plasma experiments in recent years, including: beam-destabilized toroidal Alfven instabilities (TAE) in low magnetic field tokamaks, ICRF destabilized TAE's in higher field tokamaks, and global Alfven instabilities (GAE) in low shear stellarators. In addition, excitation and study of these modes is a significant goal of the TFIR-DT program and a component of the ITER physics tasks. The authors have developed a gyrofluid model which includes the wave-particle resonances necessary to excite such instabilities. The TAE linear mode structure is calculated nonperturbatively, including many of the relevant damping mechanisms, such as: continuum damping, non-ideal effects (ion FLR and electron collisionality), and ion/electron Landau damping. This model has been applied to both linear and nonlinear regimes for a range of experimental cases using measured profiles. DOE

N95-27441# General Atomics Co., San Diego, CA.
FAST WAVE CURRENT DRIVE IN D3-D
C. C. Petty, R. W. Callis, S. C. Chiu, J. S. deGrassie, C. B. Forest, R. L. Freeman, P. Gohil, R. W. Harvey, H. Ikezi, and Y. -R. Lin-Liu et al Feb. 1995 10 p Presented at the Meeting of the Division of Plasma Physics of the American Physical Society, Minneapolis, MN, 7-11 Nov. 1994
(Contracts DE-AC03-89ER-51114; W-7405-eng-48)
(DE95-007582; GA-A-21904; CONF-941101-4) Avail: CASI HC A02/MF A01

The non-inductive current drive from fast Alfven waves launched by a directional four-element antenna was measured in the D3-D tokamak. The fast wave frequency (60 MHz) was eight times the deuterium cyclotron frequency at the plasma center. An array of RF pickup loops at several locations around the torus was used to verify the directivity of the four-element antenna. Complete non-inductive current drive was achieved using a combination of fast wave current drive (FWCD) and electron cyclotron current drive (ECCD) in discharges for which the total plasma current was inductively ramped down from 400 to 170 kA. For discharges with steady plasma current, up to 110 kA of FWCD was inferred from an analysis of the loop voltage, with a maximum non-inductive current (FWCD, ECCD, and bootstrap) of 195 out of 310 kA. The FWCD efficiency increased linearly with central electron temperature. For low current discharges, the FWCD efficiency was degraded due to incomplete fast wave damping. The experimental FWCD was found to agree with predictions from the CURRAY ray-tracing code only when a parasitic loss of 4% per pass was included in the modeling along with multiple pass damping. DOE

N95-27497# Oak Ridge National Lab., TN.
NONLINEAR PHENOMENA, TURBULENCE AND ANOMALOUS TRANSPORT IN FUSION PLASMAS
C. Hidalgo, T. Estrada, E. Sanchez, B. Branas, I. Garcia-Cortes, B. P. VanMilligen, R. Balbin, M. A. Pedrosa, J. Sanchez, and B. A. Carreras 1995 11 p Presented at the 15th International Conference on Plasma Physics and Controlled Nuclear Fusion Research, Seville, 26 Sep. - 1 Oct. 1994
(Contract DE-AC05-84OR-21400)
(DE95-007044; CONF-940933-29) Avail: CASI HC A03/MF A01

The nonlinear nature of the plasma turbulence, as measured by bicoherence analysis, has been studied in stellarator (ATF and W7AS) and tokamak (PBXM) devices. In ATF, little nonlinear interaction is found in the scrape-off layer region whereas the strength of the coupling is enhanced in the edge plasma region where the level of fluctuations is consistent with the theoretical expectations from resistive interchange modes. In W7AS the level of bicoherence is significantly smaller than in ATF. The comparison ATF/W7AS/PBXM suggests the important role of the magnetic shear to determine nonlinear behavior of the turbulence. The level of bicoherence also depends on the plasma conditions: in particular, it increases at the H-mode transition. The comparison between the nonlinear behavior of the turbulence in tokamaks and stellarators allows experimental verification of theoretical turbulence models. DOE

N95-27498# Oak Ridge National Lab., TN.
PHYSICS ASSESSMENT OF STELLARATORS AS FUSION POWER PLANTS
J. F. Lyon, J. A. Rome, P. R. Garabedian (New York Univ., New York, NY.), D. T. Anderson (Wisconsin Univ., Madison, WI.), and S. L. Painter (Australian National Univ., Canberra, Australia.) 1995 8 p Presented at the 15th International Conference on Plasma Physics and Controlled Nuclear Fusion Research, Seville, 26 Sep. - 1 Oct. 1994
(Contract DE-AC05-84OR-21400)
(DE95-007045; CONF-940933-28; IAEA-CN-60/F-1-I-4) Avail: CASI HC A02/MF A01

Four different stellarator configurations (a compact torsatron, a new modular torsatron, Helias, and a new modular Helias-like heliac) were analyzed as fusion power plants and compared with the second-stability ARIES-4 tokamak. The device and plasma parameters were determined by minimizing the projected cost of electricity subject to various constraints. The stellarators were competitive with ARIES-4 for a range of assumptions on confinement models, alpha-particle losses, and beta. One dimensional power balance equations were solved for both Lackner-Gottardi confinement scaling with an assumed n(sub e)(r) and for helical-ripple-induced transport with both assumed and calculated forms for n(sub e)(r) and E(sub r)(r). DOE

N95-27536# Oak Ridge National Lab., TN.
DITHERING TRANSITIONS IN RESISTIVE PRESSURE-GRADIENT-DRIVEN TURBULENCE
L. Garcia (Madrid Univ., Spain.), B. A. Carreras, V. E. Lynch, and P. H. Diamond (California Univ., San Diego, CA.) 1994 7 p Presented at the 15th International Conference on Plasma Physics and Controlled Nuclear Fusion Researh, Seville, Spain, 26 Sep. - 1 Oct. 1994
(Contracts DE-AC05-84OR-21400; DE-FG03-88ER-53275)
(DE95-006737; CONF-940933-27; IAEA-CN-60/D-P-I-12) Avail: CASI HC A02/MF A01

A self-consistent model of the L to H transition has been derived from coupled nonlinear envelope equations for the fluctuation level, and radial electric field shear, E(prime)(sub r). This model is based on general properties of the coupling between turbulence and averaged sheared flows. To extract these generic properties several turbulence models have been investigated. Here, some of the results obtained with the resistive pressure-gradient-driven turbulence are presented with special emphasis on the structure of the Reynolds stress and the existence of limit cycle solutions. DOE

N95-27537# Oak Ridge National Lab., TN.
PARALLEL PLASMA FLUID TURBULENCE CALCULATIONS
J. N. Leboeuf, B. A. Carreras, L. A. Charlton, J. B. Drake, V. E. Lynch, D. E. Newman, K. L. Sidikman, and D. A. Spong 1994 8 p Presented at the 2nd DOE-Energy Research Power Users Symposium, Rockville, MD, 12 Jul. 1994
(Contract DE-AC05-84OR-21400)
(DE95-006741; CONF-9407126-3) Avail: CASI HC A02/MF A01

The study of plasma turbulence and transport is a complex problem of critical importance for fusion-relevant plasmas. To this day, the fluid treatment of plasma dynamics is the best approach to realistic physics at the high resolution required for certain experimentally relevant calculations. Core and edge turbulence in a magnetic fusion device have been modeled using state-of-the-art, nonlinear, three-dimensional, initial-value fluid and gyrofluid codes. Parallel implementation of these models on diverse platforms--vector parallel (National Energy Research Supercomputer Center's CRAY Y-MP C90), massively parallel (Intel Paragon XP/S 35), and serial parallel (clusters of high-performance workstations using the Parallel Virtual Machine protocol)--offers a variety of paths to high resolution and significant improvements in real-time efficiency, each with its own advantages. The largest and most efficient calculations have been performed at the 200 Mword memory limit on the C90 in dedicated mode, where an overlap of 12 to 13 out of a maximum of 16 processors has been achieved with a gyrofluid model of core fluctuations. The richness of the physics captured by these calculations is commensurate with the increased resolution and efficiency and is limited only by the ingenuity brought to the analysis of the massive amounts of data generated. DOE

N95-27673# Los Alamos National Lab., NM.
THE ROLE OF MICROPROCESSES IN MACROSCALE MAGNETOTAIL DYNAMICS
Joachim Birn, S. Peter Gary, and Michael Hesse (National Aeronautics and Space Administration. Goddard Space Flight Center, Greenbelt, MD.) 1995 22 p Presented at the 1994 Huntsville Workshop on Coupling of Micro- and Mesoscale Processes in Space Plasma Transport, Guntersville, AL, 16-19 Oct. 1995
(Contract W-7405-eng-36)
(DE95-006288; LA-UR-95-416; CONF-9410243-2) Avail: CASI HC A03/MF A01

Microphysical processes influence the behavior of macroscopic variables and hence the dynamical processes on larger scales through the isotropization of the pressure tensor and through anomalous transport processes which affect the conservation and transport of momentum, energy, and magnetic flux. Using MHD simulations of the dynamic evolution of the magnetotail with deviations from ideal, isotropic, and isentropic MHD, it is demonstrated that each of these deviations may have drastic effects on the stability and dynamic behavior of the magnetotail. DOE

N95-27688# Massachusetts Inst. of Tech., Cambridge, MA.
NEUTRAL GAS COMPRESSION IN THE ALCATOR C-MOD DIVERTOR. EXPERIMENTAL OBSERVATIONS
A. Niemczewski, B. LaBombard, B. Lipschultz, and G. McCracken Nov. 1994 21 p Presented at the Meeting of the Division of Plasma Physics of the American Physical Society, Minneapolis, MN, 7-11 Nov. 1994
(Contract DE-AC02-78ET-51013)
(DE95-007762; DOE/ET-51013/308; PFC/RR-94-13; CONF-941101-6)
Avail: CASI HC A03/MF A01

One of the high heat flux solutions envisioned for ITER is the gas target divertor. This scheme requires high neutral pressure to be sustained in the divertor chamber with a minimal effect on the pressure in the main tokamak chamber (i.e. high gas compression). The neutral gas compression has been studied in the Alcator C-Mod closed divertor under various central and edge plasma conditions. The neutral pressure measured by a fast, in-situ, ionization gauge, installed behind the divertor target plate was compared with the midplane pressure, measured by a shielded Bayard-Alpert gauge. Divertor pressures up to 30 mTorr with compression factors p(sub div)/p(sub mid) less than or equal to 70 have been observed. It has been found that the neutral pressure in the divertor does not depend strongly on the fueling location but rather on the core plasma density and the resulting divertor plasma regime. Divertor detachment leads to a considerable drop in the compression ratio, suggesting a partial 'unplugging' of the divertor volume. An examination of the local particle flux balance in the divertor indicates that the single most important factor determining divertor pressure and compression is the private-flux plasma channel opacity to neutrals. DOE

N95-27710# Lawrence Livermore National Lab., Livermore, CA.
FLUCTUATIONS IN HIGH BETA(SUB p) PLASMAS IN DIII-D
T. A. Casper, M. S. Chu (California Univ., Irvine, CA.), and C. P. Gohil (California Univ., Irvine, CA.) Jun. 1994 7 p Presented at the 21st EPS Conference on Controlled Fusion and Plasma Physics, Montpellier, France, 27 Jun. - 1 Jul. 1994
(Contract W-7405-eng-48)
(DE95-008071; UCRL-JC-116862; CONF-9406270-4) Avail: CASI HC A02/MF A01

In our investigation of improved confinement in high poloidal beta (beta(sub p) = 2 to 4) advanced tokamak experiments, coincident with q(sub 0) rising above 2, we observe the internal MHD activity to evolve from an m/n = 2/1 to a 3/1 structure consistent with the GATO code stability analysis. The plasma eventually evolves to a quiescent state at which time the stored energy increases, mostly as a result of improved particle confinement. The measured plasma pressure profiles during this time are also calculated to be stable to high-n ballooning modes consistent with operation of the core in the second stable regime. The sustained improvement in confinement is ultimately limited by our ability to control the toroidal current profile of which the bootstrap current contributes a large fraction (up to 80%). DOE

N95-27869# Nagoya Univ., Nagoya (Japan). Plasma Science Center.
GLOBAL DYNAMO IN A REVERSED FIELD PINCH PLASMA
K. I. Sato, A. Nagata, S. Kubota, T. Ando, H. Arimoto, T. Amano, K. Saito, S. Shiina, A. Matsuoka, and M. Nagatsu et al Oct. 1993 23 p
(DE94-765441; PSC-31) Avail: CASI HC A03/MF A01

We found that an RFP dynamo uniformly generates most of the toroidal flux along the toroidal direction in an RFP plasma with a high magnetic Reynolds (S) number. Hereafter we call it the global dynamo. The toroidal flux generated by the global dynamo is proportional to the plasma current. The effective inductance (proportional constant) increases with the S number and is kept at a constant value against the change of the plasma current. This means that the pinch parameter Theta is held constant; that is, the global dynamo has a self-organizing effect sustaining a particular RFP magnetic field configuration. By comparison with simulation results and analysis of magnetic fluctuations. We confirmed that the global dynamo is generated by the single helicity m (poloidal mode number) = 1 mode alone. DOE

N95-27870# Nagoya Univ., Nagoya (Japan). Plasma Science Center.
BURST OF ENERGETIC IONS FROM REVERSED FIELD PINCH PLASMA
A. Matsuoka, M. Sugawara, Y. Kondoh (Gunma Univ., Kiryu, Japan.), K. Aoto, K. I. Sato, S. Kubota, H. Arimoto, A. Nagata, M. Nagatsu, and S. Masamune Nov. 1993 29 p
(DE94-765447; PSC-32) Avail: CASI HC A03/MF A01

In a reversed field pinch (RFP), behavior of edge plasma is investigated by an energy analyzer and movable electrostatic probes scanning from the boundary of the core plasma to 122 mm outside in order to separate effects of ions and electrons. We clearly confirmed the behavior of the edge plasma and found that the energetic ions with a monochromatic energy distribution of about 3 keV were emitted from the core plasma. Its particle flux is 10(exp 17) - 10(exp 18) cm(exp -2) sec(exp -1). The energetic ion burst does not synchronize with the RFP dynamo. It is accompanied with the generation of the island overlapping. DOE

N95-27873# General Atomics Co., San Diego, CA.
EXPERIMENTAL ASPECTS OF EFFECTS OF HIGH-ENERGY PARTICLES ON ALFVEN MODES
W. W. Heidbrink (California Univ., Irvine, CA.) Oct. 1994 16 p Presented at the ISPP Workshop on the Theory of Fusion Plasmas, Varenna, Italy, 22-26 Aug. 1994
(Contract DE-AC03-89ER-51114)
(DE95-003383; GA-A-21811; CONF-9408176-3) Avail: CASI HC A03/MF A01

Global Alfven modes are observed in a number of tokamaks, including DIII-D and TFTR. Instabilities occur during neutral-beam injection and during fast-wave ICRF heating, and may recently have been observed during alpha-particle heating. Identification of toroidicity-induced Alfven eigenmodes (TAE) is based primarily on the scaling of the real frequency of the mode. Other modes, including the beta-induced Alfven eigenmode (BAE), are also observed. The stability threshold of TAE modes agree (to within a factor of two) with theoretical predictions. Toroidal mode numbers of n = 2-6 are usually most unstable, as theoretically expected. Measurements of the poloidal and radial mode structure are consistent with theoretical predictions, but the uncertainties are large. Both TAE and BAE modes can cause large, concentrated losses of fast ions. Phenomenologically, beam-driven Alfven modes usually 'saturate' through bursts that expel beam ions, while modes observed during ICPF heating approach a steady saturation amplitude. DOE

N95-27924# California Inst. of Tech., Pasadena, CA.
FLUCTUATIONS AND TRANSPORT IN FUSION PLASMAS Final Report
R. W. Gould and P. C. Liewer 1995 20 p
(Contract DE-FG03-84ER-53173)
(DE95-007111; DOE/ER-53173/T6) Avail: CASI HC A03/MF A01

The energy confinement in tokamaks in thought to be limited by transport caused by plasma turbulence. Three dimensional plasma particle-in-cell (PIC) codes are used to model the turbulent transport in tokamaks to attempt to understand this phenomena so that tokamaks can be made more efficient. Presently, hundreds of hours of Cray time are used to model these experiments and much bigger and longer runs are desired, to model a large tokamak with realistic parameters is beyond the capability of existing sequential supercomputers. Parallel supercomputers might be a cost effect tool for performing such large scale 3D tokamak simulations. The goal of the work was to develop algorithms for performing PIC codes on coarse-grained message passing parallel computers and to evaluate the performance of such parallel computers on PIC codes. This algorithm would be used in a large scale PIC production code such as the UCLA 3D gyrokinetic code. DOE

N95-28052# Maryland Univ., College Park, MD.
DEVELOPMENT OF DENSITY AND TEMPERATURE PROFILE DIAGNOSTICS FOR ICF TARGETS Final Report, 30 Sep. 1993 - 31 Dec. 1994
H. R. Griem and R. C. Elton Mar. 1995 6 p
(Contract DE-FG03-93SF-20142)
(DE95-007664; DOE/SF-20142/1) Avail: CASI HC A02/MF A01

In the authors' research for the period of September 30, 1993 through December 31, 1994, they have upgraded their equipment in anticipation of the restart of the upgraded lasers at the University of Rochester Laboratory for Laser Energetics/National Laser User Facility (LLE/NLUF) and elsewhere. As a direct result of cooperation with Dr. Paul Jaanimagi of LLE, they have modified the cathode on a LLE-designed front-illuminated streak camera so as to operate over a wavelength range extending from the x-ray (greater or equal 0.3 nm) into the vacuum ultraviolet (greater 100 nm) spectral regions. They have accomplished this with (coated) screen cathodes which permit the photoelectrons to freely penetrate through the openings after emission from the mesh surfaces. Such cathodes were studied, compared and optimized. In anticipation of the development of these long-wavelength photocathodes, they assembled and tested a xuv flat-field streak spectrograph using a varied-spacing grating and covering the 4-30 nm wavelength region. They successfully obtained spectra of highly-ionized boron and carbon. They have also installed a new 300 grooves/mm, 4.2 deg blazed grating in their 'McPig' microchannel plate equipped grazing incidence spectrograph, and obtained test spectra extending from 3 to 140 nm wavelength. DOE

N95-28054# Lawrence Livermore National Lab., Livermore, CA.
SCRAPE-OFF LAYER PLASMA MODELING FOR THE DIII-D TOKAMAK
G. D. Porter, T. D. Rognlien, and S. L. Allen Sep. 1994 12 p Presented at the 15th International Conference on Plasma Physics and Controlled Nuclear Fusion Research, Seville, Spain, 26 Sep. - 1 Oct. 1994
(Contract W-7405-eng-48)
(DE95-008059; UCRL-JC-117107; CONF-940933-38) Avail: CASI HC A03/MF A01

The behavior of the scrape-off layer (SOL) region in tokamaks is believed to play an important role determining the overall device performance. In addition, control of the exhaust power has become one of the most important issues in the design of future devices such as ITER and TPX. This paper presents the results of application of 2-D fluid models to the DII-D tokamak, and research into the importance of processes which are inadequately treated in the fluid models. Comparison of measured and simulated profiles of SOL plasma parameters suggest the physics model contained in the UEDGE code is sufficient to simulate plasmas which are attached to the divertor plates. Experimental evidence suggests the presence of enhanced plasma recombination and momentum removal leading to the existence of detached plasma states. UEDGE simulation of these plasmas obtains a bifurcation to a low temperature plasma at the divertor, but the plasma remains attached. Understanding the physics of this detachment is important for the design of future devices. Analytic studies of the behavior of SOL plasmas enhance our understanding beyond that achieved with fluid modeling. Analysis of the effect of drifts on sheath structure suggest these drifts may play a role in the detachment process. Analysis of the turbulent-transport equations indicate a bifurcation which is qualitatively similar to the experimentally different behavior of the L- and H-mode SOL. Electrostatic simulations of conducting wall modes suggest possible control of the SOL width by biasing. DOE

N95-28065# Lawrence Livermore National Lab., Livermore, CA.
UEDGE AND DEGAS MODELING OF THE DIII-D SCRAPE-OFF LAYER PLASMA, REVISION 1
M. E. Fenstermacher, G. D. Porter, M. E. Rensink, T. D. Rognlien, S. L. Allen, D. N. Hill, C. J. Lasnier, T. Leonard, and T. Petrie May 1994 18 p Presented at the 11th International Conference on Plasma Surface Interactions in Controlled Fusion Devices, Mito, Japan, 23-27 May 1994
(Contract W-7405-eng-48)
(DE95-008052; UCRL-JC-115491-Rev-1; CONF-940580-23-Rev-1) Avail: CASI HC A03/MF A01

This paper presents work to develop benchmarked theoretical models of scrape-off-layer (SOL) characteristics in diverted tokamaks by comparing shot simulations using the UEDGE plasma fluid and DEGAS neutral transport codes to measurements of the DIII-D SOL plasma. The experimental data include the radial profiles of n(sub e) T(sub e), and T(sub i), the divertor exhaust power, the intensity of H(sub alpha) emission, and profiles of the radiated power. A very simple model of the anomalous perpendicular transport rates produces consistency between the calculated and measured radial profiles of the divertor power, and of the midplane densities and temperatures. Experimentally, the measured exhaust power is now 80-90% of the input power. The simulated peak power on the outer leg of the divertor floor is now within 20% of the measured power. Various sensitivities of these comparisons to model assumptions are described. Finally, these benchmarked models have been used to examine the effects of various baffle configurations for the Radiative Divertor Upgrade in DIII-D. DOE

N95-28106# General Atomics Co., San Diego, CA.
EFFECT OF TOROIDAL PLASMA FLOW AND FLOW SHEAR ON GLOBAL MHD MODES
M. S. Chu, J. M. Greene, T. H. Jensen, R. L. Miller, A. Bondeson, and R. W. Johnson Jan. 1995 25 p Presented at the Meeting of the Division of Plasma Physics of the American Physical Society, Minneapolis, MN, 7-11 Nov. 1994
(Contract DE-AC03-89ER-51114)
(DE95-006676; GA-A-21903; CONF-941101-3) Avail: CASI HC A03/MF A01

The effect of a subsonic toroidal flow on the linear magnetohydrodynamic stability of a tokamak plasma surrounded by an external resistive wall is studied. A complex non-self-adjoint eigenvalue problem for the stability of general kink and tearing modes is formulated, solved numerically, and applied to high (beta) tokamaks. Results indicate that toroidal plasma flow, in conjunction with dissipation in the plasma, can open a window of stability for the position of the external wall. In this window, stable plasma beta values can significantly exceed those predicted by the Troyon scaling law with no wall. Computations utilizing experimental data indicate good agreement with observations. DOE

N95-28111# Texas Univ., Austin, TX. Inst. for Fusion Studies.
MAGNETIC VISCOSITY BY LOCALIZED SHEAR FLOW INSTABILITY IN MAGNETIZED ACCRETION DISKS
R. Matsumoto and T. Tajima Jan. 1995 45 p
(Contract DE-FG05-80ET-53088)
(DE95-006879; DOE/ET-53088/684; IFSR-684) Avail: CASI HC A03/MF A01

Differentially rotating disks are subject to the axisymmetric instability for perfectly conducting plasma in the presence of poloidal magnetic fields. For nonaxisymmetric perturbations, the authors find localized unstable eigenmodes whose eigenfunction is confined between two Alfven singularities at omega(d) = +/- omega(A), where omega(d) is the Doppler-shifted wave frequency, and omega(A) = k(parallel bars)v(A) is the Alfven frequency. The radial width of the unstable eigenfunction is Delta x approximately to omega(A)/(Ak(y)), where A is the Oort's constant, and k(y) is the azimuthal wave number. The growth rate of the fundamental mode is larger for smaller value of k(y)/k(z). The maximum growth rate when k(y)/k(z) approximately 0.1 is approximately 0.2 Omega for the Keplerian disk with local angular velocity Omega. It is found that the purely growing mode disappears when k(y)/k(z) greater than 0.12. In a perfectly conducting disk, the instability grows even when the seed magnetic field is infinitesimal. Inclusion of the resistivity, however, leads to the appearance of an instability threshold. When the resistivity eta depends on the instability-induced turbulent magnetic fields delta B as eta ((delta B(exp 2))), the marginal stability condition self-consistently determines the alpha parameter of the angular momentum transport due to the magnetic stress. For fully ionized disks, the magnetic viscosity parameter alpha(B) is between 0.001 and 1. The authors' three-dimensional MHD simulation confirms these unstable eigenmodes. It also shows that the alpha parameter observed in simulation is between 0.01 and 1, in agreement with theory. The observationally required smaller alpha in the quiescent phase of accretion disks in dwarf novae may be explained by the decreased ionization due to the temperature drop. DOE

N95-28138# Lawrence Livermore National Lab., Livermore, CA.
ADVANCED TOKAMAK OPERATING MODES IN TPX AND ITER
W. M. Nevins 1994 14 p Presented at the ISPP Workshop on Tokamak Concept Improvement, Varenna, Italy, 29 Aug. - 3 Sep. 1994
(Contract W-7405-eng-48)
(DE95-008058; UCRL-JC-118673; CONF-9408189-4) Avail: CASI HC A03/MF A01

A program is described to develop the advanced tokamak physics required for an economic steady-state fusion reactor on existing (short-pulse) tokamak experiments; to extend these operating modes to long-pulse on TPX; and finally to demonstrate them in a long-pulse D-T plasma on ITER. DOE

N95-28140# Lawrence Livermore National Lab., Livermore, CA.
ENGINEERING DESIGN OF THE ITER RF SYSTEMS
M. Makowski, G. Bosia, T. Nagashima, and D. Remsen 1994 6 p Presented at the 18th European Symposium on Fusion Technology, Karlsruhe, Germany, 22-26 Aug. 1994
(Contract W-7405-eng-48)
(DE95-008064; UCRL-JC-118999; CONF-940843-16) Avail: CASI HC A02/MF A01

Parallel conceptual design efforts for auxiliary heating systems on ITER are being carried out in both the electron cyclotron range of frequencies (ECRF) and ion cyclotron range of frequencies (ICRF). These systems are required to deliver a minimum of 50 MW of CW power to the plasma for the primary purpose of heating and the secondary purpose of current drive. Current designs of the two systems are presented and the primary design issues are discussed. DOE

N95-28141# Lawrence Livermore National Lab., Livermore, CA.
OBSERVATION ON RADIATION TRANSFER EXPERIMENTS USING k-SHELL ABSORPTION SPECTRA
C. A. Iglesias, M. H. Chen, D. L. McWilliams, J. K. Nash, and F. J. Rogers Jan. 1995 18 p Presented at the 6th International Workshop on Radiative Properties of Hot Dense Matter, Sarasota, FL, 31 Oct. - 4 Nov. 1994
(Contract W-7405-eng-48)
(DE95-008068; UCRL-JC-119309; CONF-9410314-2) Avail: CASI HC A03/MF A01

Recent laser-produced plasma experiments have relied on spectroscopic comparisons with models to infer plasma temperatures. Here, the technique is applied to study thermal radiation transfer experiments. The transmission model combines high-quality atomic data with an ionization balance obtained from systematic expansions of the grand canonical ensemble. The latter avoids the ad hoc cutoffs required in free energy minimization schemes and includes Coulomb corrections usually neglected in other models. It is shown that the improved equation of state significantly affects inferred temperatures at the higher densities expected in the heat flow experiments. Even though good agreement is obtained between the experimental and theoretical transmission spectrum, the experimental uncertainties are sufficiently large that is compromises the intended bench marking of the thermal transport models. DOE

N95-28161# Stanford Linear Accelerator Center, Stanford, CA.
PLASMA LENS EXPERIMENTS AT THE FINAL FOCUS TEST BEAM
W. Barletta, S. Chattopadhyay, and P. Chen Feb. 1995 6 p Presented at the Advanced Accelerator Concepts Workshop, Lake Geneva, WI, 13-18 Jun. 1994
(Contracts DE-AC03-76SF-00515; DE-FG03-92ER-40695)
(DE95-008595; SU-SLAC-PUB-95-6756; CONF-940681-11) Avail: CASI HC A02/MF A01

The authors intend to carry out a series of plasma lens experiments at the Final Focus Test Beam facility at SLAC. These experiments will be the first to study the focusing of particle beams by plasma focusing devices in the parameter regime of interest for high energy colliders, and is expected to lead to plasma lens designs capable of unprecedented spot sizes. Plasma focusing of positron beams will be attempted for the first time. They will study the effects of lens aberrations due to various lens imperfections. Several approaches will be applied to create the plasma required including laser ionization and beam induced tunneling ionization of a working gas-the latter which has never been observed before. The compactness of the device should prove to be of interest for applications at the SLC and the next generation linear colliders. DOE

N95-28185# General Atomics Co., San Diego, CA.
DIVERTOR RESEARCH ON THE DIII-D TOKAMAK
D. N. Hill (Lawrence Livermore National Lab., Livermore, CA.), S. L. Allen (Lawrence Livermore National Lab., Livermore, CA.), N. H. Brooks, D. Buchenauer (Sandia National Labs., Albuquerque, NM.), J. W. Cuthbertson (California Univ., Los Angeles, CA.), T. E. Evans, M. E. Fenstermacher (Lawrence Livermore National Lab., Livermore, CA.), Ph. Ghendrih (Association Euratom-CEA, Cadarache, France.), D. L. Hillis (Oak Ridge National Lab., TN.), and J. T. Hogan (Oak Ridge National Lab., TN.) Oct. 1994 15 p Presented at the 15th International Conference on Plasma Physics and Controlled Nuclear Fusion Research, Seville, Spain, 26 Sep. - 1 Oct. 1994
(Contracts DE-AC03-89ER-51114; DE-AC05-84OR-21400; DE-AC04-94AL-85000; DE-FG03-89ER-51121; DE-FG03-86ER-53225; GA Proj. 3466; W-7405-eng-48)
(DE95-003942; GA-A-21851; IAEA-CN-60/A-4-I-2; CONF-940933-21) Avail: CASI HC A03/MF A01

In this paper the authors summarize recent progress on DIII-D in developing techniques for divertor power and particle control relevant to next generation tokamaks such as the proposed ITER and TPX devices. Density control and helium removal by divertor pumping have been demonstrated for the first time in high confinement ELMing H-mode discharges (tau is approximately 2 times tau(sub ITER-89P)) following installation of a divertor cryopumping system. The peak divertor heat flux in similar H-mode discharges has been reduced through production of a radiating mantle with neon or argon puffing (reductions of 3-5). A number of diagnostics have been added to improve the understanding of the physical processes involved. They are now designing modified double-null divertor structures for DIII-D that will provide improved particle control for high-triangularity VH-mode plasmas while at the same time allowing for gas puffing to reduce the divertor heat flux. DOE

N95-28224# Argonne National Lab., IL.
FARADAY SCREEN SPUTTERING ON TPX
D. A. Ehst Dec. 1994 40 p
(Contract W-31-109-eng-38)
(DE95-008347; ANL/FPP/TM-274) Avail: CASI HC A03/MF A01

The TPX design stipulates that the ion-cyclotron resonance frequency (ICRF) antenna must have a Faraday screen (FS). The author considers here possible low Z coatings for the screen, as well as sputtering behavior of the Ni and Ti substrates. The theory of RF-induced sputtering has been developed, and follows those theoretical approaches. The author's emphasis will be on both impurity generation as a possible source of increased Z(sub eff), and also on actual erosion-lifetime of the materials under worst case conditions. DOE

N95-28233# Argonne National Lab., IL. Physics Div.
ORDERED ONE-COMPONENT PLASMAS: PHASE TRANSITIONS, NORMAL MODES, LARGE SYSTEMS, AND EXPERIMENTS IN A STORAGE RING
J. P. Schiffer 1994 13 p Presented at the Non Neutral Plasma

Physics, Berkeley, CA, 17-20 Jul. 1994
(Contract W-31-109-eng-38)
(DE95-007077; ANL/PHY/CP-85173; CONF-9407163-1) Avail: CASI HC A03/MF A01

The property of cold one-component plasmas, confined by external forces, to form an ordered array has been known for some time both from simulations and from experiment. The purpose of this talk is to summarize some recent work on simulations and some new experimental results. The author discusses some experimental work on real storage rings, magnetic storage devices in which partials circulate with large kinetic energies and for which laser cooling is used on partially ionized ions to attain temperatures ten or more orders of magnitude lower than their kinetic energies. DOE

N95-28356# Lawrence Livermore National Lab., Livermore, CA.
ATTRACTIVE CHARACTERISTICS OF MIRRORS
R. F. Post and D. D. Ryutov 15 Dec. 1994 8 p Presented at the 6th International Toki Conference on Plasma Physics and Controlled Nuclear Fusion: Research for Advanced Concepts in Magnetic Fusion, Toki-City, Japan, 29 Nov. - 2 Dec. 1994
(Contract W-7405-eng-48)
(DE95-008073; UCRL-JC-118719; CONF-941182-2) Avail: CASI HC A02/MF A01

A summary of the attractive characteristics of mirror devices is presented. Recent progress in development of axisymmetric mirror devices is described. Potentialities of mirrors as a basis for D(3)He fusion power generators and high-flux neutron sources for fusion material tests are discussed. DOE

N95-28406# General Atomics Co., San Diego, CA.
WALL STABILIZATION OF ROTATING HIGH (BETA) DISCHARGES IN D3-D
A. D. Turnbull, T. S. Taylor, and E. J. Strait Oct. 1994 12 p Presented at the 15th International Conference on Plasma Physics and Controlled Nuclear Fusion Research, Madrid, Spain, 26 Sep. - 1 Oct. 1994
(Contracts DE-AC03-89ER-51114; DE-FG03-92ER-54150; W-7405-eng-48)
(DE95-008207; GA-A-21819; CONF-940933-37) Avail: CASI HC A03/MF A01

Wall stabilization of the ideal $n = 1$ external kink mode is shown to be possible in high (beta), rotating D3-D plasmas for times much longer than the resistive wall penetration time. The gain in (ss) can be more than 30% above the calculated stability limit with no wall stabilization. Stabilization from the resistive wall is found to require plasma rotation speeds of several kHz; otherwise, unstable locked or slowly rotating modes appear, with growth times of the order of the wall penetration time, which ultimately lead to termination of the discharge. The slowly rotating modes have the characteristics expected of the theoretically predicted resistive wall mode in an ideal plasma. DOE

N95-28542# Lawrence Livermore National Lab., Livermore, CA.
THEORETICAL ASPECTS OF ENERGY CONFINEMENT IN SPHEROMAKS
T. K. Fowler 16 Nov. 1994 10 p Presented at the Workshop on Establishing the Hysics Basis Needed To Access the Potential of Compact Toroidal Reactors, Oak Ridge, TN, 19-31 Jul. 1994
(Contract W-7405-eng-48)
(DE95-008079; UCRL-JC-119307; CONF-9407169-1) Avail: CASI HC A02/MF A01

It is shown that, despite the poor global energy confinement observed in spheromak experiments to date, the long-term prospects may be favorable as spheromaks are scaled to larger size and higher temperatures. The present performance is traced to excessive magnetic energy loss at the edge compared to tokamaks and heat transport due to magnetic fluctuations, both of which should scale away as the temperature increases. DOE

N95-28553# Oak Ridge National Lab., TN.
OPERATING POINTS AND FEEDBACK CONTROL OF PLASMA CHARACTERISTICS IN TOKAMAKS WITH FULL CURRENT DRIVE
D. W. Swain, S. E. Attenberger, W. A. Houlberg, P. T. Bonoli (Massachusetts Inst. of Tech., Cambridge, MA.), and W. M. Nevins (Lawrence Livermore National Lab., Livermore, CA.) 1994 5 p Presented at the 18th European Symposium on Fusion Technology, Karlsruhe, Germany, 22-26 Aug. 1994
(Contracts DE-AC05-84OR-21400; DE-AC02-76CH-03073)
(DE95-007037; CONF-940843-15) Avail: CASI HC A01/MF A01

Tokamak operation using advanced tokamak modes with steady-state current drive may provide better performance, thereby improving the prospects of power-producing fusion reactors. Scenarios for such operation in TPX and in an ITER-like scale-up of TPX are modeled. Results indicate that the heating and current drive power and feedback control requirements may be achievable. DOE

N95-28562# Instituto de Pesquisas Espaciais, Sao Jose dos Campos (Brazil).
TOKAMAK ETE ENGINEERING PRELIMINARY PROJECT [ANTEPROJETO DE ENGENHARIA DO TOKAMAK ETE]
Gerson Otto Ludwig Nov. 1993 53 p In PORTUGUESE
(INPE-5529-PRE/1796) Avail: CASI HC A04/MF A01

This report introduces the tokamak ETE engineering preliminary project (Spheric Toroidal Experiment of the Associated Laboratory of Plasma of the National Institute for Space Research (LAP/INPE). The tokamak ETE appears to be a machine of small proportions, or spheric tokamak, which was created by the ETA project (Advanced Toroidal Experiment), developed in 1986 by the Associated Laboratory of Plasma. This project presented several unknown characteristics at the time, and, in 1987, the tokamak ETE was approved as the main experiment in the field of fusion to be built at the future National Laboratory of Plasma (LNP). However, when it became clear that the implementation of the National Laboratory of Plasma would not take place in a short period of time, the National Laboratory of Plasma proposed the construction of the Proto-ETA in 1988, which would be utilized as a prototype for the ETA machine at a much smaller cost. The conceptual project and the tokamak Proto-ETA engineering preliminary project were developed with the intense participation of national and foreign specialists during a series of work meetings which took place in 1989 and 1990. Even though the project was rendered important, unfortunately, it did not have the backing of the financial institutions for its implementation. At the end of 1990, the Proto-ETA was utilized as the foundation for the design of the tokamak TBR-E which kept the main characteristics of the spheric tokamak, and it was proposed as a joint endeavor of the largest active groups in the field of experimental physics of plasma in the country. Again, it was verified that there would not be any means to build an important machine like Proto-ETA or TBR-E. In the middle of 1991, therefore, the Associated Laboratory of Plasma began to work on the development of the current project, based on the premise that it would be necessary to utilize available energy sources at an extremely reduced cost and to make the most of the material and human resources of the institution. Author

N95-28596# Oak Ridge National Lab., TN.
PELLET INJECTOR RESEARCH AND DEVELOPMENT AT ORNL
S. K. Combs, G. C. Barber, and L. R. Baylor 1994 5 p Presented at the 18th European Symposium on Fusion Technology, Karlsruhe, Germany, 22-26 Aug. 1994
(Contract DE-AC05-84OR-21400)
(DE95-006736; CONF-940843-14) Avail: CASI HC A01/MF A01

Oak Ridge National Laboratory has been developing pellet injectors for plasma fueling experiments on magnetic confinement devices for more than 15 years. Recent major applications of the ORNL development program include: (1) a tritium-compatible four-shot pneumatic injector for the Tokamak Fusion Test Reactor; (2) a centrifuge pellet injector for the Tore Supra tokamak, and most recently; (3) a three-barrel repeating pneumatic injector for the DIII-D tokamak. In addition to applications, ORNL is developing advanced technologies, including high-speed pellet injectors, tritium injectors, and long-pulse pellet feed systems. The high-speed research involves a collaboration between ORNL and ENEA-Frascati in the development of a repeating two-stage light gas gun based on an extrusion-type pellet feed system. Construction of a new tritium-compatible, extruder-based repeating pneumatic injector (8-mm-diam) is complete and will replace the pipe gun in the original tritium proof-of-principle experiment. The development of a steady-state feed system in which three standard extruders operate in tandem is under way. These research and development activities are relevant to the International Thermonuclear Experimental Reactor and are briefly described in this paper. DOE

N95-28654 Helsinki Univ. of Technology, Espoo (Finland).
SIMULATION OF BURNING TOKAMAK PLASMAS

M. J. Mantsinen 2 Dec. 1994 118 p Limited Reproducibility: More than 20% of this document may be affected by microfiche quality
(PB95-195426; TKK-F-B155) Avail: CASI HC A06

In this thesis, time-dependent behavior of near-term experimental DT tokamak-fusion reactors and advanced D(3)He-tokamaks is studied. To do this, a zero-dimensional (volume-averaged using prescribed profiles for plasma parameters) time-dependent particle and power balance code has been developed. The predictions of the code are compared with experimental data and with transport calculations of a higher dimensionality. In all comparisons, a good agreement is found. The advantage of a zero-dimensional code, as compared to higher-dimensional transport codes, is the possibility to quickly scan the interdependencies between reactor parameters. The structure of the thesis is as follows: In Chapter 2, an overview on tokamak physics relevant to burning plasmas is presented and the tokamaks considered in the thesis are introduced. In Chapter 3 the zero-dimensional model for the simulations is described and in Chapter 4 results from the simulations are presented. In Chapter 5, the zero-dimensional calculations are compared with experiments and higher-dimensional transport calculations. In Chapter 6, transport of charged fusion products and cyclotron radiation are included in the zero-dimensional model, and their effects on the plasma behavior are studied. Chapter 7 consists of conclusions and a discussion. NTIS

N95-28668 University of South Florida, Tampa, FL.
PROCEEDINGS OF THE INTERNATIONAL WORKSHOP ON ACCELERATION AND RADIATION GENERATION IN SPACE AND LABORATORY PLASMAS Final Technical Report, 2 Feb. 1993 - 31 Jan. 1994
R. Bingham, J. M. Dawson, T. Katsouleas, and L. Stenflo 14 Feb. 1995 165 p Workshop held in Kardamyli, Greece, 29 Aug. - 4 Sep. 1993 Limited Reproducibility: More than 20% of this document may be affected by microfiche quality
(Contract N00014-93-1-0814)
(AD-A291673) Avail: Issuing Activity (Defense Technical Information Center (DTIC))

Workshop proceedings-Papers presented at the International Workshop on Acceleration and Radiation Generation in Space and Laboratory. Plasmas Kardamyli, Greece, August 29 - September 4, 1993. DTIC

76 SOLID-STATE PHYSICS

Includes superconductivity.

For related information, see also *33 Electronics and Electrical Engineering* and *36 Lasers and Masers.*

N95-26440# Nebraska Univ., Lincoln, NE. Dept. of Physics.
RESONANT PHOTOEMISSION STUDIES OF THICKNESS DEPENDENCE OF THE UNOCCUPIED Gd 5d BANDS
P. A. Dowben, Dongqi Li (Argonne National Lab., IL.), Jiandi Zhang, and M. Onellion (Wisconsin Univ., Madison, WI.) 1994 14 p Presented at the 41st Annual American Vacuum Society Symposium, Denver, CO, 24-28 Oct. 1994 Submitted for publication
(Contract W-31-109-eng-38; NSF DMR-92-21655)
(DE95-004127; ANL/MSD/CP-84783; CONF-941001-8) Avail: CASI HC A03/MF A01

Ultrathin Gd films have been studied with constant initial-state spectroscopy (CIS) of photoemission utilizing linearly polarized light of synchrotron radiation. The photoemission cross-section of the 5d surface state near E(sub F) shows strong photon energy dependence, i.e. sharp peaks in CIS spectra near the Gd 5p(sub 1/2) adsorption edge. These peaks originate from resonant photoemission processes involving the occupied 5p and unoccupied 5d levels of the surface atoms. The symmetry of the unoccupied states were determined experimentally by changing the polarization of light, where p-polarized light excites only to the unoccupied d(sub z(sup 2)) or d(sub xz,yz) states and s-polarized light to all the d states including d(sub x(sup 2) - (sup 2)) and d(sub xy) states. Based on the symmetry assignments, the lower bound of the exchange splitting of the Gd 5d(sub z(sup 2)) surface state can be abstracted, which increases when the thickness of Gd film decreases and reach maximum at the monolayer limit. DOE

N95-26442# Argonne National Lab., IL. Materials Science Div.
ROTOR PHASES IN COMPOUND SEMICONDUCTORS
David Long Price, Marie-Louise Saboungi, and W. Spencer Howells (Rutherford Appleton Lab., Chilton, England.) Nov. 1994 16 p Presented at the Neutron Scattering Conference, Sendai, Japan, 11-14 Oct. 1994 Submitted for publication
(Contract W-31-109-eng-38)
(DE95-004139; ANL/MSD/CP-84837; CONF-9410165-9) Avail: CASI HC A03/MF A01

Quasi-elastic neutron scattering is used to study the disordering processes in two classes of semiconductor: 1-4 Zintl compounds and the phosphorus-selenium system. Two alkali-metal-polyvalent metal Zintl compounds, CsPb and NaSn, exhibit a two-stage melting process with high-temperature solid phases characterized by rapid dynamical disorder. In CsPb this disorder is clearly associated with rapid reorientations of polyanions with the cations participating in the dynamical disorder on the same time scale. In NaSn the disorder is associated with fast reorientations of the polyanions closely coupled to a slower migration of the cations. The two high-temperature solid phases of the molecular crystal P4Se3 are confirmed to be rotor phases with small but significant differences in the reorientational motions in the two phases. DOE

N95-26462 University of Northern Illinois, De Kalb, IL.
DESIGN STRATEGIES FOR THE PREPARATION OF POLYMERIC ORGANIC SUPERCONDUCTORS Annual Research Report, 30 Sep. 1993 - 29 Sep. 1994
Charles W. Spangler 8 Nov. 1994 11 p Sponsored by Air Force Office of Scientific Research Limited Reproducibility: More than 20% of this document may be affected by microfiche quality
(Contract F49620-92-J-0533)
(AD-A289022; AFOSR-94-0761TR) Avail: Issuing Activity (Defense Technical Information Center (DTIC))

During the past year strategies were developed to synthesize ET monomers containing one functionalized side chain (for pendant attachment) and two functionalized side chains (for main chain copolymer incorporation). The redox behavior of these ET monomers and polymers is identical to ET itself. DTIC

N95-26473 Duke Univ., Durham, NC. Dept. of Chemistry.
CHEMISTRY INVOLVING THE SEPARATION, ISOLATION, AND IMMOBILIZATION OF 3-5 COMPOUND SEMICONDUCTOR NANOCRYSTALS AND QUANTUM DOTS Annual Technical Report, 1 Oct. 1993 - 20 Sep. 1994
Richard L. Wells and Louis A. Coury 14 Sep. 1994 11 p Limited Reproducibility: More than 20% of this document may be affected by microfiche quality
(Contract F49620-93-1-0004)
(AD-A288381; DU/DC/ATR-02; AFOSR-94-0685TR) Avail: Issuing Activity (Defense Technical Information Center (DTIC))

The facile thermolysis of Cl2GaP(SiMe3)22 to eliminate Me3 SiX and yield nanocrystalline GaP has been studied via thermal gravimetric analysis (TGA) and it has been found that the Me3SiCl is eliminated in a step-wise manner. Also, the new ternary single-source precursor Ga2(As,P)C13n has been synthesized and thermolyzed to yield the ternary 3-5 GaAsxPy. In addition, nanocrystalline GaAs and GaP, prepared by the Kher/Wells low temperature solution phase method, have been studied by transmission electron microscopy (TEM) and, in the TEM's of both, the lattice fringes of nanocrystalline material are clearly evident. Using a host of analytical techniques, it has been shown that the GaAs has crystalline regions of 12 +/- 2 nm. In addition, efforts in immobilization of particles have involved all binary permutations of In and Ga phosphides and arsenides. The materials have been cast onto electrode surfaces from volatile solvents to give uniform deposits. Dispersions can also be created in the presence of monomers which are subsequently electropolymerized to prepare composite films. In an STM plot of InAs immobilized in a poly(pyrrole) film, the nanocrystals appear as yellow dots embedded in the brown film, indicating that they extend above the film, and/or have a higher conductivity than the polymer. DTIC

N95-26513# Helsinki Univ. of Technology, Espoo (Finland). Dept. of Technical Physics.

INVESTIGATIONS OF THE HYPERFINE INTERACTIONS IN COPPER-OXIDE PEROVSKITES USING Eu-151 AND Fe-57 MOESSBAUER SPECTROSCOPY Ph.D. Thesis

Johan Linden 1994 93 p Sponsored by Emil Aaltonen Foundation; Alfred Kordelin Foundation; Heikki and Hilma Honkanen Foundation; and Jenny and Antti Wihuri Foundation

(PB95-185138; ISBN-951-22-2354-6) Avail: CASI HC A05/MF A01

In 1986, superconductivity was discovered in a perovskite-type material at an unprecedentedly high temperature. As no satisfactory theory describing high-Tc superconductivity has been developed and since not all the perovskite phases exhibiting superconducting properties have been explored, the field is still the focus of active research. This work strives to promote the basic understanding of the high-Tc superconducting materials. It is suggested that the results obtained here are part of those boundary conditions that any successful theory of high-Tc superconductivity must take into account. This overview begins with a survey of the various phases studied in the work, followed by the theory behind the methods used to characterize the materials. Finally the experimental conditions and the results are presented. NTIS

N95-26553 Illinois Univ., Urbana, IL. Dept. of Materials Science and Engineering.

MOLECULAR OBJECT LIQUID CRYSTALS: AN APPROACH TO NEW MATERIALS Technical Report, 1 May 1993 - 30 Apr. 1994

Samuel I. Stupp, Kenneth A. Walker, Vassou LeBonheur, John L. Wu, Leonard Radzilowski, Sehwan Son, Kevin E. Huggins, Li-Sheng Li, and Milan Keser 1 Dec. 1994 4 p Presented at the American Chemical Society Meeting, Anaheim, CA, 2-7 Apr. 1995 Limited Reproducibility: More than 20% of this document may be affected by microfiche quality

(Contracts N00014-93-1-0534; DE-AC02-76ER-01198; NSF DMR-89-20548; NSF DMR-93-12601)

(AD-A288905; TR-2) Avail: Issuing Activity (Defense Technical Information Center (DTIC))

The one aspect of the field of liquid crystals which remains largely undeveloped is the supermolecular dimension of self ordering oligomers and polymers. In our opinion it is here that many of the potential opportunities exist for truly novel materials. An example of super-molecular chemistry is the use of liquid crystallinity as a tool to form molecular object polymers of persistent shape. This will be illustrated through the bulk synthesis of two-dimensional (2D) polymers which may be described as nanometer-thick flat objects. One exciting observation has been the formation of 'macroscopic' films from the layered assemblies with two completely different surfaces which reflect directly the chemical nature of opposite surfaces of the 'molecular' assemblies. Other systems give rise to films with remarkably stable nonlinear optical properties and high thresholds for laser damage. A different example to be described by the lecture is that of discrete molecular aggregates of rodcoil polymers which form superlattices and melt into liquid crystalline phases. These systems should be of interest in the manufacturing of patterned surfaces for a wide variety of technologies. DTIC

N95-26756 North Carolina Univ., Raleigh, NC. Dept. of Materials Science and Engineering.

PSEUDOMORPHIC SEMICONDUCTING HETEROSTRUCTURES FROM COMBINATIONS OF AlN, GaN AND SELECTED SiC POLYTYPES: THEORETICAL ADVANCEMENT AND ITS COORDINATION WITH EXPERIMENTAL STUDIES OF NUCLEATION, GROWTH, CHARACTERIZATION AND DEVICE DEVELOPMENT Semiannual Technical Report, 1 Jul. - 31 Dec. 1994

Robert F. Davis, S. Kern, K. Linthicum, R. Patterson, and S. Tanaka Dec. 1994 42 p Limited Reproducibility: More than 20% of this document may be affected by microfiche quality

(Contract N00014-90-J-1427)

(AD-A289550) Avail: Issuing Activity (Defense Technical Information Center (DTIC))

Beta(3C)-SiC nucleation and 2H-SiC step flow growth have been achieved on 2H-AlN thin film templates using gas-source (GS) MBE and C2H4/ Si2H6 gas flow ratios of 1 and 5, respectively. In addition, thin epitaxial films of AlN and SiC/AlN multilayers have been grown by plasma-assisted, GSMBE at 1050 C using Si2H6, C2H4 and N2. RHEED and high-resolution TEM revealed monocrystalline layers and pseudomorphic interfacial relationships at the substrate/film and the film/film interfaces. X-ray rocking curve measurements on the (0002) Bragg peak of the AlN films indicate they are the highest quality ever reported. Auger spectroscopy, TEM and electron energy loss spectroscopy have been used to show that the solid solubility between AlN and SiC is very limited below 1950 C. Results regarding the high temperature growth and the use of graded buffer layers for optimizing the microstructural quality of GaN grown by ECR-assisted GSMBE is also reported. The use of supersonic jets (SSJ) to produce GaN thin films has also been incorporated into this program. Highly oriented wurtzite GaN(001) films were grown on sapphire(0001) in the temperature range of 500 C to 650 C by SSJ. The film growth was controlled by the decomposition rate of NH3. Growth rates as high as 4.5microns/hr were achieved. The films had a columnar morphology. DTIC

N95-26780*# Florida Inst. of Tech., Melbourne, FL.

ELECTRONIC CHARACTERIZATION OF DEFECTS IN NARROW GAP SEMICONDUCTORS: COMPARISON OF ELECTRONIC ENERGY LEVELS AND FORMATION ENERGIES IN MERCURY CADMIUM TELLURIDE, MERCURY ZINC TELLURIDE, AND MERCURY ZINC SELENIDE Semiannual Report, 19 Sep. 1994 - 19 Mar. 1995

James D. Patterson and Wei-Gang Li 19 Mar. 1995 74 p

(Grant NAG8-1094)

(NASA-CR-197835; NAS 1.26:197835) Avail: CASI HC A04/MF A01

The project has evolved to that of using Green's functions to predict properties of deep defects in narrow gap materials. Deep defects are now defined as originating from short range potentials and are often located near the middle of the energy gap. They are important because they affect the lifetime of charge carriers and hence the switching time of transistors. We are now moving into the arena of predicting formation energies of deep defects. This will also allow us to make predictions about the relative concentrations of the defects that could be expected at a given temperature. The narrow gap materials mercury cadmium telluride (MCT), mercury zinc telluride (MZT), and mercury zinc selenide (MZS) are of interest to NASA because they have commercial value for infrared detecting materials, and because there is a good possibility that they can be grown better in a microgravity environment. The uniform growth of these crystals on earth is difficult because of convection (caused by solute depletion just ahead of the growing interface, and also due to thermal gradients). In general it is very difficult to grow crystals with both radial and axial homogeneity. Derived from text

N95-26818 Materials Research Society, Pittsburg, PA.

MATERIALS RESEARCH SOCIETY SYMPOSIUM PROCEEDINGS. VOLUME 339: DIAMOND, SiC AND NITRIDE WIDE BANDGAP SEMICONDUCTORS

Calvin H. Carter (Cree Research, Inc., Durham, NC.), Gennady Gildenblat (Pennsylvania State Univ., University Park, PA.), Shuji Nakamura (Nichia Chemical Industries Ltd., Tokushima, Japan.), and Robert J. Nemanich (North Carolina State Univ., Raleigh, NC.) 8 Apr. 1994 754 p Symposium held in San Francisco, CA, 4-8 Apr. 1994 Sponsored by the US Navy Limited Reproducibility: More than 20% of this document may be affected by microfiche quality

(AD-A288690) Avail: Issuing Activity (Defense Technical Information Center (DTIC))

This symposium was directed toward the potential of using diamond, SiC, and nitride wide bandgap semiconductors. The symposium emphasized materials issues related to the semiconducting properties of these wide bandgap materials. Both experimental and theoretical studies were presented. Solid advances were reported in the growth techniques of all three materials groups. Contributions demonstrated the critical importance of surfaces, interfaces, doping, defects, and impurities Reports demonstrated potential device applications ranging from unique electronic devices to blue/UV light emitters/detectors and even novel structures employing a negative electron affinity. The overall theme of the symposium was that materials research into wide bandgap semiconductors will make available exciting new applications, and that we are just beginning to understand the potential of these materials. DTIC

N95-26872 Harvard Univ., Cambridge, MA. Dept. of Physics.
[DEMONSTRATION OF PHOTO-ASSISTED TUNNELING PROCESS ACROSS THE COULOMB BLOCKADE ENERGY GAP IN MESOSCOPIC TUNNEL JUNCTIONS] Annual Report, 15 Sep. 1993 - 14 Sep. 1994
M. Tinkham 14 Sep. 1994 4 p Limited Reproducibility: More than 20% of this document may be affected by microfiche quality
(Contracts N00014-93-1-1134; N00014-89-J-1565)
(AD-A289534) Avail: Issuing Activity (Defense Technical Information Center (DTIC))

The specific project demonstrates the photon-assisted tunneling process across the Coulomb blockade energy gap in mesoscopic tunnel junctions. Photon-assisted tunneling is well established in conventional macroscopic tunnel junctions, and forms the basis of very sensitive millimeter wave detectors for astrophysics applications. In this case, the photons supply the energy needed to tunnel in the presence of the superconducting energy gap, which is a single-particle property. We are trying to see if the same Tien-Gordon formalism that describes this process can also be applied to the case of the Coulomb blockade, where the energy barrier stems from the charging energy of an electron on a mesoscopic metallic island, which is a collective property of the configuration, not of a single electron's energy levels. DTIC

N95-26959 Wisconsin Univ., Madison, WI. Dept. of Chemistry.
BORON-INDUCED RECONSTRUCTIONS OF Si(100) INVESTIGATED BY SCANNING TUNNELING MICROSCOPY Interim Technical Report
Yajun Wang and Robert J. Hamers 20 Dec. 1994 15 p Limited Reproducibility: More than 20% of this document may be affected by microfiche quality
(Contract N00014-91-J-1629)
(AD-A289222; TR-23) Avail: Issuing Activity (Defense Technical Information Center (DTIC))

The local geometric and electronic structures of boron-induced reconstructions produced by thermal decomposition of diborane and decaborane on Si(001) has been investigated using scanning tunneling microscopy. STM images show that boron induces several related reconstructions, arising from ordered arrangements of simple structural subunits. These boron-induced atomic rearrangements order even at very low boron exposures, leading to a striking spatial segregation of boron on the surface. Similar reconstructions are observed using diborane and decaborane as boron precursors. Annealing at 1000 Kelvin for 90 seconds substantially improves the surface ordering, without significant diffusion of boron from the surface to the bulk. DTIC

N95-26997 Auburn Univ., AL. Dept. of Physics.
MODELING THE GROWTH OF ELECTRONIC MATERIALS Final Technical Report
An-Ban Chen Dec. 1994 17 p Limited Reproducibility: More than 20% of this document may be affected by microfiche quality
(Contract N00014-93-1-1105)
(AD-A289137) Avail: Issuing Activity (Defense Technical Information Center (DTIC))

Through the DEPSCoR program, this grant allowed Auburn University to acquire a dedicated workstation to simulate properties of semiconductors and their alloys. We have acquired a HP9000/735 workstation (named SOLID) with sufficient speed, memory, storage, and graphic capability to perform realistic simulations. The biggest advantage of having this machine is that we are not constrained by the turn-around and CPU time imposed by a general-purpose supercomputer. Since the installation of this machine in January 1994, we have made progress in several directions. These include (1) obtaining criteria for convergence in molecular-dynamic (MD) simulations of disordered zincblende alloys, (2) obtaining accurate information about bond lengths and excess energies of disordered zincblende alloys, (3) achieving a reliable method for obtaining bulk alloy free energies and phase diagrams from finite-size Monte-Carlo (MC) simulations, and (4) establishing an effective iterative method for calculating the density matrix in an order-N algorithm. In the last step we have demonstrated the validity of the density matrix approach. Using this method, we do not need to diagonalize the one electron Hamiltonian. Thus the computing time is reduced from N(exp 3) to N, where N is the number of atoms per unit cell used in the simulation. These studies have demonstrated the ability of SOLID for performing realistic MD and MC simulations. These results are being used to investigate a new class of III-V infrared materials and the wide-gap semiconductors SiC, GaN, AlN, and their alloys. DTIC

N95-27040 Naval Command, Control and Ocean Surveillance Center, San Diego, CA.
MICROWAVE CHARACTERIZATION OF SUB-MICRON N- AND P-CHANNEL MOSFET'S FABRICATED WITH THIN FILM SILICON-ON-SAPPHIRE
C. E. Chang, P. M. Asbeck, P. R. delaHoussaye, G. Imthurn, and G. A. Garcia Jun. 1994 6 p Limited Reproducibility: More than 20% of this document may be affected by microfiche quality
(AD-A289296) Avail: Issuing Activity (Defense Technical Information Center (DTIC))

This paper reports on microwave characteristics for n- and p- MOS transistors fabricated with thin-film Silicon-on-Sapphire technology. The gates were defined with I-line optical lithography, and ranged down to 0.5 micrometer (drawn dimension). The f sub t values of the transistors reach 22 GHz for the n-channel structures and 21 GEz for the p- channel devices. The PMOS results are significantly higher than found with other Si or III-V technologies, and can potentially lead to high performance complementary microwave circuits. Small signal transistor models are similar to the ones for GaAs FETs. Dependence of model parameters on gate length were determined. DTIC

N95-27061 Wisconsin Univ., Madison, WI. Dept. of Chemistry.
ATOMICALLY RESOLVED STM STUDY OF THE ADSORPTION AND DISSOCIATION OF METHYL CHLORIDE ON Si(001) Interim Technical Report
Michael Bronikowski and Robert J. Hamers 20 Dec. 1994 24 p Limited Reproducibility: More than 20% of this document may be affected by microfiche quality
(Contract N00014-91-J-1629)
(AD-A289218; TR-25) Avail: Issuing Activity (Defense Technical Information Center (DTIC))

The authors have studied the room-temperature adsorption and dissociation of methyl chloride (CH3Cl) on Si(001) using Scanning Tunneling Microscopy (STM). Fragments are identified by the symmetry of their binding on the underlying Si(001) lattice. Methyl chloride adsorbs dissociatively at room temperature, yielding a methyl group and a chlorine atom bound to the surface. Chlorine atoms bind in a variety of geometries, the most common being two chlorine atoms bonded to a single silicon dimer (silicon monochloride dimers). When the surface is heated to 150 C, all Cl rearranges to this monochloride-type bonding configuration, and images reveal the beginnings of monochloride island formation. The Cl:CH3 ratio on the surface is found to be approximately 2:1, implying that not all methyl groups are bound to the surface in the reaction. Consideration of the relative bond strengths involved leads us to propose a reaction mechanism in which the surface sometimes abstracts a Cl atom from the CH3Cl molecule, ejecting a methyl group back into the vacuum. DTIC

N95-27085# Argonne National Lab., IL.
SURFACE ENERGY DRIVEN CRYSTALLIZATION OF AMORPHOUS Ni69Cr14P17 ALLOY
G. Schumacher, N. Wanderka, and R. P. Wahi Nov. 1994 6 p Presented at the 1994 Fall Meeting of the Materials Research Society (MRS), Boston, MA, 28 Nov. - 2 Dec. 1994
(Contract W-31-109-eng-38)
(DE95-005543; ANL/MSD/CP-83327; CONF-941144-55) Avail: CASI HC A02/MF A01

Amorphous Ni69Cr14P17 specimens thinned for transmission electron microscopy have been studied in situ during thermal treatment. In the thinnest regions of the specimens (thickness d less than 50 nm), a metastable hexagonal (Ni,Cr)(sub 3)P phase nucleates at the perforation edge with the c-axis perpendicular to the specimen surface. The crystal width of this phase grows linearly with time. Above 530 C the hexagonal phase transforms into a stable b.c.t. (Ni,Cr)(sub 3)P phase. It is concluded that the surface and grain boundary energies dominate nucleation and growth. DOE

N95-27087# Pacific Northwest Lab., Richland, WA.
TEMPERATURE DEPENDENCE OF ION-BEAM-INDUCED AMORPHIZATION IN (BETA)-SiC

W. J. Weber and L. M. Wang Feb. 1995 15 p Presented at the 9th International Conference on Ion Beam Modification of Materials, Canberra, Australia, 5-10 Feb. 1995
(Contract DE-AC06-76RL-01830)
(DE95-007164; PNL-SA-25545; CONF-950220-1) Avail: CASI HC A03/MF A01

The ion-beam-induced crystalline-to-amorphous transition in monolithic (beta)-SIC has been studied as a function of irradiation temperature using the HVEM-Tandem Facility at Argonne National Laboratory. Specimens were irradiated with 1.5 MeV Xe(+) ions over the temperature range from 40 to 550 K, and the evolution of the amorphous state was followed in situ using the HVEM. At 40 K, the displacement dose for complete amorphization in (beta)-SIC is 0.34 dpa and increases with temperature in two stages. The simultaneous recovery process associated with the high-temperature stage (above 100 K) has an activation energy of 0.097 +/- 0.019 eV. The critical temperature above which complete amorphization does not occur is 498 K under these irradiation conditions. DOE

N95-27201# International Centre for Theoretical Physics, Trieste (Italy).
DNA DENATURATION THROUGH A MODEL OF THE PARTITION POINTS ON A ONE-DIMENSIONAL LATTICE
R. Mejdani and H. Huseini Aug. 1994 12 p
(DE95-607909; IC-94/227) Avail: CASI HC A03/MF A01 (US Sales Only)

We have shown that by using a model of the partition points gas on a one-dimensional lattice, we can study, besides the saturation curves obtained before for the enzyme kinetics, also the denaturation process, i.e. the breaking of the hydrogen bonds connecting the two strands, under treatment by heat of DNA. We think that this model, as a very simple model and mathematically transparent, can be advantageous for pedagogic goals or other theoretical investigations in chemistry or modern biology. DOE

N95-27413# International Centre for Theoretical Physics, Trieste (Italy).
HALL EFFECT AND RESISTIVITY IN THE NORMAL STATE OF HIGH-T(SUB c) CUPRATES IN THE ELECTRON-FRACTON MODEL
Q. Jiang, Z. H. Zhang, X. B. Wang, D. C. Tian, and T. Chui Aug. 1994 15 p
(DE95-610612; IC-94/239) Avail: CASI HC A03/MF A01 (US Sales Only)

Based on the electron-fracton interaction, the Hall effect and resistivity in the normal states of high-T(sub c) oxides are calculated by solving the quantum transport equations. The numerical results show that, under certain conditions, the inplane resistivity exhibits a nearly temperature dependence and the Hall angle exhibits a quadratic temperature dependence. DOE

N95-27416 North Carolina State Univ., Raleigh, NC. Dept. of Materials Science and Engineering.
GROWTH, CHARACTERIZATION AND DEVICE DEVELOPMENT IN MONOCRYSTALLINE DIAMOND FILMS Quarterly Technical Report, 1 Oct. - 31 Dec. 1994
Robert F. Davis, Jeffrey T. Glass, and R. J. Nemanich Dec. 1994 18 p Sponsored by the Ballistic Missile Defense Organization/Innovative Science and Technology program Limited Reproducibility: More than 20% of this document may be affected by microfiche quality
(Contract N00014-93-1-0437)
(AD-A289356) Avail: Issuing Activity (Defense Technical Information Center (DTIC))

Bias-enhanced nucleation (BEN) has been employed with TiC(111) substrates for the disposition of oriented diamond particles. The orientation of all the particles was the same, as observed via SEM. Some particles showed evidence of azimuthal twist and tilt, most likely due to the approx. 18% lattice mismatch with the TiC. Raman spectra exhibited a strong feature at 1332 cm(exp -1) indicative of diamond, and smaller features at 1480 cm(exp -1) and 1602 cm(exp -1) due to sp(2)-bonded carbon. An increase in the duration of the BEN step and a reduction in the twinning are expected to increase the density of oriented particles. An optical analysis of the strain fields of point and line defects, and the distributions of these defects as well as the distribution of the optical centers in the diamond films has also been conducted. The nitrogen optical centers were uniformly distributed. Calculations indicated that line-type defects are far more detrimental to the stress than point defects. DTIC

N95-27429# Sandia National Labs., Albuquerque, NM.
NEUTRON DIFFRACTION STUDIES ON RECRYSTALLIZATION OF SOLUTION DERIVED LEAD ZIRCONATE TITANATES
B. Morosin, B. A. Tuttle, J. A. Voigt, A. C. Lawson (Los Alamos National Lab., NM.), and G. H. Kwei (Lawrence Livermore National Lab., Livermore, CA.) 1994 6 p Presented at the Annual Meeting of the Division of High Polymer Physics of the American Physical Society, San Jose, CA, 20-24 Mar. 1995
(Contracts DE-AC04-94AL-85000; W-7405-eng-36; W-31-109-eng-38; DE-AC04-76DP-00789)
(DE95-004771; SAND-94-2986C; CONF-950380-1) Avail: CASI HC A02/MF A01

We performed neutron powder diffraction on solution-derived lead zirconate titanates (PZT). Three compositions, PZT 45/55, PZT 20/80 and PbTiO3, were investigated. The materials were annealed so that the perovskite phase had just begun to grow from the precursor phase. In our materials this precursor phase is the pyrochlore rather than fluorite phase. The results show that in the pyrochlore phase, the (Ti,Zr) and the Pb are ordered in their crystallographic sites while the O are essentially disordered in both of the two usual pyrochlore anion sites. DOE

N95-27443# Brookhaven National Lab., Upton, NY.
STOICHIOMETRY, STRUCTURE, AND PROPERTIES OF La2NiO(4+(DELTA)) AND La(2-x)Sr(x)NiO(4+/-(DELTA))
D. J. Buttrey, V. Sachan, J. M. Tranquada, and J. E. Lorenzo 1995 7 p Presented at the 7th International Symposium on Superconductivity, Kita Kiyushu, Japan, 8-11 Nov. 1994
(Contract DE-AC02-76CH-00016)
(DE95-007682; BNL-61393; CONF-941176-2) Avail: CASI HC A02/MF A01

The oxygen content phase diagram of La2NiO(4+(delta)) has been studied in detail using x ray and neutron diffraction data from well-characterized specimens. There are numerous phase separations and phase transitions which are observed with changes in temperature and composition. The complexity of the phase diagram arises primarily from oxygen defect interactions, however the authors have also obtained evidence for coupled charge and spin ordering at (delta) = 0.125 corresponding to organization of holes into ordered domain walls. These domain walls act as antiphase boundaries between stripes of antiferromagnetically ordered nickel moments. Neutron scattering data on Sr-substituted compositions with well-defined oxygen content indicate incommensurate charge and spin correlations closely related to those in the x=0, (delta) = 0.125 composition. The incommensurability approaches 1/4 and the correlation length increases as the hole concentration approaches p = x+2(delta) = 0.25. DOE

N95-27452# Argonne National Lab., IL.
CRYSTAL STRUCTURE, SHORT-RANGE OXYGEN DEFECTS, AND WATER ADSORPTION IN La- AND Nd-MODIFIED ZrO2
C. K. Loong, J. W. Richardson, Jr., L. E. Iton, and M. Ozawa (Nagoya Inst. of Tech., Japan.) 1995 7 p Presented at the 1994 Fall Meeting of the Materials Research Society (MRS), Boston, MA, 28 Nov. - 2 Dec. 1994
(Contract W-31-109-eng-38)
(DE95-007134; ANL/IPNS/CP-83321; CONF-941144-71) Avail: CASI HC A02/MF A01

Doping Rare-earth (RE) elements to ZrO2 helps stabilize the cubic and tetragonal phases and improves resistance to thermal shock and sintering at high temperatures. Since a RE ion has a lower valency 3(+) than Zr ion 4(+), oxygen vacancies are formed to preserve electroneutrality. We have studied the crystal structure of La(0.1)Zr(0.9)O(1.95) and Nd(0.1)Zr(0.9)O(1.95) by neutron diffraction and examined the associated oxygen defects by a Fourier transform of the filtered residual diffuse scattering. The hydration process was investigated by inelastic neutron-scattering measurements of the hydrogen vibrational density of states of the surface hydroxyl groups and physisorbed water on these fine powders. We compare the O-H stretch vibrations for samples from with only surface hydroxyl groups to multilayer coverage of water molecules. The decreasing energies and increasing widths of the O-H stretch bands with increasing H2O coverage indicate the influence of hydrogen bonding on the motion of water molecules. Similar elastic and inelastic experiments were also performed on a high surface-area pure ZrO2 powder. DOE

N95-27471# California Univ., Berkeley. Lawrence Berkeley Lab, CA.
CHARACTERIZATION AND CONTROL OF WAFER CHARGING EFFECTS DURING HIGH-CURRENT ION IMPLANTATION
M. I. Current (Applied Materials, Santa Clara, CA.), W. Lukaszek (Stanford Univ., CA.), W. Dixon (Stanford Univ., CA.), M. C. Vella, C. Messick (National Semiconductor Corp., West Jordan, UT.), J. Shideler (National Semiconductor Corp., West Jordan, UT.), and S. Reno (National Semiconductor Corp., West Jordan, UT.) Feb. 1994 12 p Presented at the 185th Electrochemical Society Meeting, San Francisco, CA, 22-27 May 1994
(Contract DE-AC03-76SF-00098)
(DE95-006587; LBL-35962; CONF-940529-27) Avail: CASI HC A03/MF A01

EEPROM-based sense and memory devices provide direct measures of the charge flow and potentials occurring on the surface of wafers during ion beam processing. Sensor design and applications for high current ion implantation are discussed. DOE

N95-27487# Oak Ridge National Lab., TN.
CRYSTAL AND MAGNETIC STRUCTURE OF STOICHIOMETRIC YFe2O4
S. Katano (Japan Atomic Energy Research Inst., Tokai, Japan.), S. Funahashi (Japan Atomic Energy Research Inst., Tokai, Japan.), T. Matsumoto (National Research Inst. for Metals, Tsukuba, Japan.), J. Iida (Ochanomizu Women's Univ., Tokyo, Japan.), M. Tanaka (Ochanomizu Women's Univ., Tokyo, Japan.), and J. W. Cable 1 Aug. 1994 12 p Presented at the Neutron Scattering, Sendai, Japan, 11-14 Oct. 1994
(Contract DE-AC05-84OR-21400)
(DE95-006627; CONF-9410165-14) Avail: CASI HC A03/MF A01

Crystal structure of stoichiometric YFe2O4 powder was studied by high-resolution neutron diffraction at room temperature, 225 K and 80 K. Rietveld refinements of the diffraction patterns give reasonable fits with space group R(bar 3)m (hexagonal) for room temperature, and with P(bar 1) (triclinic) for 225 K. However, the 80 K pattern cannot be fitted at all with the same triclinic symmetry, indicating that the structure is much more complicated. The magnetic reflection has been separated from those complex nuclear peaks by the polarization analysis. The magnetic structure is also fairly complicated both at 225 K and at 80 K. DOE

N95-27491# Pacific Northwest Lab., Richland, WA.
CHARACTERIZATION OF COLLISION CASCADE DAMAGE IN Ca2La8(SiO4)6O2 BY HRTEM
W. J. Weber and L. M. Wang Dec. 1994 6 p Presented at the 1994 Fall Meeting of the Materials Research Society (MRS), Boston, MA, 28 Nov. - 2 Dec. 1994
(Contract DE-AC06-76RL-01830)
(DE95-005719; PNL-SA-25554; CONF-941144-45) Avail: CASI HC A02/MF A01

Ca2La8(SiO4)6O2 thin crystals become amorphous under ion beam irradiation. The ion dose required for complete amorphization of the thin crystal (critical amorphization dose, D(sub c)) increased with the increasing irradiation temperature and decreased with ion mass at elevated temperatures. Samples irradiated with 1-1.5 MeV Ar(+), Kr(+) and Xe(+) ions to doses much lower than D(sub c), in the temperature range from 20 to 498 K were used for a detailed HRTEM study to better understand the amorphization process. The residual collision cascade damage after irradiation appeared as manometer scale amorphous domains. The images of these domains are extremely sensitive to the sample thickness. Small domains of cascade size were only found at the very thin edge of the sample. In thicker regions, amorphous domains appear after higher doses as the result of cascade overlap in projection. At higher temperatures, the observed amorphous domains are smaller indicating thermal recovery at the amorphous/crystalline interface. The amorphous domains are also larger in size after irradiation with ions of higher mass at a fixed ion dose. These results are consistent with the D(sub c) temperature curves determined by in situ TEM with the HVEM-Tandem Facility at Argonne National Laboratory. The width of the amorphous rim along the edge of the specimen grew with increasing ion dose suggesting that amorphization also proceeds from the sample surface. Images of the collision cascade damage were compared to the cascade sizes calculated with the TRIM code. Some digitally acquired HRTEM images of the cascade damage were processed to reveal more detailed information. DOE

N95-27535# Brookhaven National Lab., Upton, NY.
SURFACE CRYSTALLIZATION AND THIN FILM MELTING IN NORMAL ALKANES
X. Z. Wu and H. H. Shao 1994 12 p Presented at the 1994 Fall Meeting of the Materials Research Society (MRS), Boston, MA, 28 Nov. - 2 Dec. 1994
(Contract DE-AC02-76CH-00016)
(DE95-006694; BNL-61312; CONF-941144-57) Avail: CASI HC A03/MF A01

Normal alkanes of carbon number n greater than 14 exhibit surface crystallization at their liquid-vapor interface. This has been investigated with x-ray reflectivity, grazing incidence scattering and surface tension measurements. The structure and thermodynamics of the surface layer is consistent with a monolayer of the bulk rotator phase occurring at the surface above the bulk melting temperature. On the other hand, thin films of alkanes on SiO2, exhibit a reduction of the melting temperature. The surface crystalline phase is observed for carbon number n greater than 14. The vanishing of surface phase for small n may be due to a transition from surface freezing to surface melting behavior. These measurements can yield the relative surface energies of the various phases. DOE

N95-27538# California Univ., Berkeley. Lawrence Berkeley Lab, CA. Accelerator and Fusion Research Div.
CHARACTERIZATION OF WAFER CHARGING MECHANISMS AND OXIDE SURVIVAL PREDICTION METHODOLOGY
Wes Lukaszek (Stanford Univ., CA.), William Dixon (Stanford Univ., CA.), Michael Vella, Cleston Messick (National Semiconductor Corp., West Jordan, UT.), Steve Reno (National Semiconductor Corp., West Jordan, UT.), and Jay Shideler (National Semiconductor Corp., West Jordan, UT.) Apr. 1994 12 p Presented at the International Reliability Physics Symposium, San Jose, CA, 11-14 Apr. 1994
(Contract DE-AC03-76SF-00098)
(DE95-006583; LBL-35961; CONF-940453-5) Avail: CASI HC A03/MF A01

Unipolar, EEPROM-based peak potential sensors and current sensors have been used to characterize the I-V relationship of charging transients which devices normally experience during the course of ion implantation. The results indicate that the charging sources may appear to behave like current-sources or voltage-sources, depending on the impedance of the load. This behavior may be understood in terms of plasma concepts. The ability to empirically characterize the I-V characteristics of charging sources using the CHARM-2 monitor wafers opens the way for prediction of failure rates of oxides subjected to specific processes, if the oxide Q(sub bd) distributions are known. DOE

N95-27542# Argonne National Lab., IL.
SYNCHROTRON X-RAY SCATTERING STUDIES AT MINERAL-WATER INTERFACES
Ronald P. Chiarello and Neil C. Sturchio 1995 6 p Presented at the 1994 Fall Meeting of the Materials Research Society, Boston, MA, 28 Nov. - 2 Dec. 1994
(Contract W-31-109-eng-38)
(DE95-008303; ANL/CMT/CP-85560; CONF-941144-88) Avail: CASI HC A02/MF A01

Synchrotron X-ray scattering techniques provide a powerful tool for the in situ study of atomic scale processes occurring at solid-liquid interfaces. We have applied these techniques to characterize and study reactions at mineral-water interfaces. Here we present two examples. The first is the characterization of the calcite (CaCO3)(101'4) cleavage surface, in equilibrium with deionized water, by crystal truncation rod measurements. The second is the in situ study of the heteroepitaxial growth of otavite (CdCO3) on the calcite (101'4) cleavage surface. The results of such studies will lead to significant progress in understanding mineral-water interface geochemistry. DOE

N95-27712# International Centre for Theoretical Physics, Trieste (Italy).
NUMERICAL STUDY OF THE SINGLET-TRIPLET MODEL FOR CUPRATE SUPERCONDUCTORS
M. E. Simon and A. A. Aligia Aug. 1994 20 p
(DE95-609438; IC-94/208) Avail: CASI HC A03/MF A01 (US Sales Only)

We perform a low-energy reduction of the three-band Hubbard

Hamiltonian (H(sub 3b)), keeping in the relevant Hilbert subspace not only local singlets (Zhang-Rice singlets), but also triple states between Cu holes and O holes at the Wannier function of the same site, with x(sup 2) - y(sup 2) symmetry. We solve exactly the resulting Hamiltonian in a system of 2 x 2 unit cells. We find that the local triplet states can be practically neglected for finite O-Cu on-site energy difference (Delta), very large Cu on-site Coulomb repulsion U(sub d), and O-O hopping t(sub pp)=0. This fact is in contrast with the mapping of H(sub 3b) to a one-band model using non-orthogonal singlets, which is very accurate when the Cu(+) configuration can be neglected. Although the amount of local triplet states in the low-energy eigenstates is in general small, it increases with t(sub pp) and for large t(sub pp) it is necessary to introduce higher order corrections in the one-band model to accurately represent the low-energy physics. In all cases even when local triplets are not important, the t-J model should be supplemented with other terms to describe the lowest energy levels. We also discuss briefly the effect of non-bonding O orbitals. DOE

N95-27720# California Univ., Berkeley. Lawrence Berkeley Lab, CA.

MICROMAGNETICS AND MICROSTRUCTURE OF EPITAXIALLY GROWN Co AND Co-Cr FILMS FOR PERPENDICULAR MAGNETIC RECORDING

K. M. Krishnan, T. Takeuchi (Hitachi Ltd., Tokyo, Japan.), Y. Hirayama (Hitachi Ltd., Tokyo, Japan.), D. M. Donnet (Hitachi Ltd., Tokyo, Japan.), Y. Honda (Hitachi Ltd., Tokyo, Japan.), and M. Futamoto (Hitachi Ltd., Tokyo, Japan.) Jul. 1994 4 p Presented at the Magnetic Recording Conference, Tokyo, Japan, 10-14 Oct. 1994
(Contract DE-AC03-76SF-00098)
(DE95-004681; LBL-35986; CONF-9410278-1) Avail: CASI HC A01/MF A01

Highly c-axis oriented, single crystal films of Co(1-x)Cr(x) (0 less than or equal to x less than 0.3) have been grown epitaxially on mica substrates by e-beam evaporation. Films grown on Ru underlayers have an average grain size of 50-80 nm, negligibe fcc content, and very narrow c-axis dispersions. For Co films (x = 0), the as-grown magnetization structure are mainly 180 degree domain walls with a uniform distribution of cross-ties for thinner samples (less than or equal to 300 Angstrom), while thicker (greater than 400 Angstrom) ones show stripe domains. These images were analyzed in detail to measure the wall widths and associated energy densities for as-grown, remanent, and ac-magnetized samples. As expected, the magnetic properties of these films are composition dependent. However, for any Cr concentration, these films exhibit the largest saturation magnetization when compared with either sputtered or evaporated samples. This enhancement can be attributed to a nanometer-scale segregation of Cr, which in these samples could be particularly aided by the diffusion on the close-packed planes of the films with very narrow c-axis dispersions. Preliminary x-ray microanalysis and NMR data support this interpretation. DOE

N95-27740# International Centre for Theoretical Physics, Trieste (Italy).

MOLECULAR DYNAMICS SIMULATIONS OF GAY-BERNE NEMATIC LIQUID CRYSTAL: ELASTIC PROPERTIES FROM DIRECT CORRELATION FUNCTIONS

J. Stelzer, H. R. Trebin (Stuttgart Univ., Germany.), and L. Longa Aug. 1994 27 p
(DE95-609149; IC-94/220) Avail: CASI HC A03/MF A01 (US Sales Only)

We report NVT and NPT molecular dynamics simulations of a Gay-Berne nematic liquid crystal using generalization of recently proposed algorithm by Toxvaerd (Phys. Rev. E47, 343, 1993). On the basis of these simulations the Oseen-Zoher-Frank elastic constants K(sub 11), K(sub 22) and K(sub 33) as well as the surface constants K(sub 13) and K(sub 24) have been calculated within the framework of the direct correlation function approach of Lipkin et al. (J. Chem. Phys. 82, 472 (1985)). The angular coefficients of the direct pair correlation function, which enter the final formulas, have been determined from the computer simulation data for the pair correlation function of the nematic by combining the Ornstein-Zernike relation and the Wienier-Hopf factorization scheme. The unoriented nematic approximation has been assumed when constructing the reference, isotropic state of Lipkin et al. By an extensive study of the model over a wide range of temperatures, densities and pressures a very detailed information has been provided about elastic behaviour of the Gay-Berne nematic. Interestingly, it is found that the results for the surface elastic constants are qualitatively different than those obtained with the help of analytical approximations for the isotropic, direct pair correlation function. For example, the values of the surface elastic constants are negative and an order of magnitude smaller than the bulk elasticity. DOE

N95-27867# Joint Inst. for Nuclear Research, Dubna (USSR). Lab. of Nuclear Problems.

OBSERVATION OF ASYMMETRICAL TWO-CONE VAVILOV-CHERENKOV RADIATION IN BIAXIAL CRYSTAL OF TRIGLYCINESULPHATE EMITTED BY 658 MeV PROTONS PASSING ALONG BI NORMAL

V. P. Zrelov, V. P. Lupiltsev, and J. Ruzicka (Comenius Univ., Bratislava, Czechoslovakia.) 1993 11 p Submitted for publication
(DE94-629017; JINR-R-1-93-213) Avail: CASI HC A03/MF A01 (US Sales Only)

The paper deals with the directivity and polarization properties of the Vavilov-Cherenkov radiation (VChR) produced in passage of 658 MeV protons along an optical axis (bi normal) crystal of triglycinesulphate (TGS). The azimuthal distribution of the radiation turned out to be rather peculiar. First, it was asymmetrical about the plane running through the velocity vector of the beam particles perpendicularly to the plane of optical axes (POA). This VChR asymmetry was not observed in three earlier studied cases of 660 MeV protons passing through the main dielectric axes of a biaxial TGS crystal (i.e. when particles move along the small and the large bisectrix and perpendicularly to the plane of optical axes). Secondly, the azimuthal distribution of the VChR has a form of two symmetrical semi cones with different cone angles (their sections perpendicular to the proton beam axis resemble half-horseshoes inserted into each with their arcs outward). It also appeared that the outer VChR cone, F(sub -), is practically polarized only in the POA, while the inner cone, F(sub +), has more complicated polarization, i.e. in the angular region phi approx. 90 deg perpendicularly to the POA. Formulae are obtained for radiation directivity at any angle phi for this asymmetrical two-cone radiation. Comparison of the VChR emission angles calculated by these formulae and measured in experiment shows good agreement (within the measurement errors for the azimuthal) wave distribution of F(sub +) (inner cone) and some systematic excess (approx. 0.5 deg) for wave angles of F(sub -) (outer cone). DOE

N95-27925# National Academy of Sciences - National Research Council, Washington, DC.

TECHNICAL PROGRESS REPORT TO THE DEPARTMENT OF ENERGY ON THE SOLID STATE SCIENCES COMMITTEE (SSSC)

1995 6 p
(Contract DE-FG05-91ER-45442)
(DE95-007113; DOE/ER-45442/T1) Avail: CASI HC A02/MF A01

The Solid State Sciences Committee (SSSC) of the National Research Council (NRC) is charged with monitoring the health of the field of materials science in the United States. Accordingly, the Committee identifies and examines both broad and specific issues affecting the field. Regular meetings, teleconferences, briefings from agencies and the scientific community, the formation of study panels to prepare reports, and special forums are among the mechanisms used by the SSSC to meet its charge. This progress report presents a review of SSSC activities from May 1, 1992 through April 30, 1993. The details of prior activities are discussed in earlier reports. During the above period, the SSSC has continued to track and participate, when requested, in the development of a Federal initiative on advanced materials and processing. Specifically, the SSSC is presently planning the 1993 SSSC Forum (to be cosponsored with the National Materials Advisory Board (NMAB) and the Washington Materials Forum (WNM)). The thrust will be to highlight the Federal Advanced Materials and Processing Program (AMPP). In keeping with its charge to identify and highlight specific areas for scientific and technological opportunities, the SSSC continued to oversee the conduct of a study on biomolecular materials. Preliminary plans also have been developed for studies on neutron scattering science, on ultrasmall devices, and on molecular routes to materials. DOE

N95-27928# Argonne National Lab., IL.

DENSITY CHANGES IN AMORPHOUS Pd80Si20 DURING LOW TEMPERATURE ION IRRADIATION

G. Schumacher, R. C. Birtcher, and L. E. Rehn Nov. 1994 5 p
Presented at the 1994 Fall Meeting of the Materials Research Society

N95-27471# California Univ., Berkeley. Lawrence Berkeley Lab, CA.

CHARACTERIZATION AND CONTROL OF WAFER CHARGING EFFECTS DURING HIGH-CURRENT ION IMPLANTATION

M. I. Current (Applied Materials, Santa Clara, CA.), W. Lukaszek (Stanford Univ., CA.), W. Dixon (Stanford Univ., CA.), M. C. Vella, C. Messick (National Semiconductor Corp., West Jordan, UT.), J. Shideler (National Semiconductor Corp., West Jordan, UT.), and S. Reno (National Semiconductor Corp., West Jordan, UT.) Feb. 1994 12 p Presented at the 185th Electrochemical Society Meeting, San Francisco, CA, 22-27 May 1994

(Contract DE-AC03-76SF-00098)

(DE95-006587; LBL-35962; CONF-940529-27) Avail: CASI HC A03/MF A01

EEPROM-based sense and memory devices provide direct measures of the charge flow and potentials occurring on the surface of wafers during ion beam processing. Sensor design and applications for high current ion implantation are discussed. DOE

N95-27487# Oak Ridge National Lab., TN.

CRYSTAL AND MAGNETIC STRUCTURE OF STOICHIOMETRIC YFe2O4

S. Katano (Japan Atomic Energy Research Inst., Tokai, Japan.), S. Funahashi (Japan Atomic Energy Research Inst., Tokai, Japan.), T. Matsumoto (National Research Inst. for Metals, Tsukuba, Japan.), J. Iida (Ochanomizu Women's Univ., Tokyo, Japan.), M. Tanaka (Ochanomizu Women's Univ., Tokyo, Japan.), and J. W. Cable 1 Aug. 1994 12 p Presented at the Neutron Scattering, Sendai, Japan, 11-14 Oct. 1994

(Contract DE-AC05-84OR-21400)

(DE95-006627; CONF-9410165-14) Avail: CASI HC A03/MF A01

Crystal structure of stoichiometric YFe2O4 powder was studied by high-resolution neutron diffraction at room temperature, 225 K and 80 K. Rietveld refinements of the diffraction patterns give reasonable fits with space group R(bar 3)m (hexagonal) for room temperature, and with P(bar 1) (triclinic) for 225 K. However, the 80 K pattern cannot be fitted at all with the same triclinic symmetry, indicating that the structure is much more complicated. The magnetic reflection has been separated from those complex nuclear peaks by the polarization analysis. The magnetic structure is also fairly complicated both at 225 K and at 80 K. DOE

N95-27491# Pacific Northwest Lab., Richland, WA.

CHARACTERIZATION OF COLLISION CASCADE DAMAGE IN Ca2La8(SiO4)6O2 BY HRTEM

W. J. Weber and L. M. Wang Dec. 1994 6 p Presented at the 1994 Fall Meeting of the Materials Research Society (MRS), Boston, MA, 28 Nov. - 2 Dec. 1994

(Contract DE-AC06-76RL-01830)

(DE95-005719; PNL-SA-25554; CONF-941144-45) Avail: CASI HC A02/MF A01

Ca2La8(SiO4)6O2 thin crystals become amorphous under ion beam irradiation. The ion dose required for complete amorphization of the thin crystal (critical amorphization dose, D(sub c)) increased with the increasing irradiation temperature and decreased with ion mass at elevated temperatures. Samples irradiated with 1-1.5 MeV Ar(+), Kr(+) and Xe(+) ions to doses much lower than D(sub c), in the temperature range from 20 to 498 K were used for a detailed HRTEM study to better understand the amorphization process. The residual collision cascade damage after irradiation appeared as manometer scale amorphous domains. The images of these domains are extremely sensitive to the sample thickness. Small domains of cascade size were only found at the very thin edge of the sample. In thicker regions, amorphous domains appear after higher doses as the result of cascade overlap in projection. At higher temperatures, the observed amorphous domains are smaller indicating thermal recovery at the amorphous/crystalline interface. The amorphous domains are also larger in size after irradiation with ions of higher mass at a fixed ion dose. These results are consistent with the D(sub c) temperature curves determined by in situ TEM with the HVEM-Tandem Facility at Argonne National Laboratory. The width of the amorphous rim along the edge of the specimen grew with increasing ion dose suggesting that amorphization also proceeds from the sample surface. Images of the collision cascade damage were compared to the cascade sizes calculated with the TRIM code. Some digitally acquired HRTEM images of the cascade damage were processed to reveal more detailed information. DOE

N95-27535# Brookhaven National Lab., Upton, NY.

SURFACE CRYSTALLIZATION AND THIN FILM MELTING IN NORMAL ALKANES

X. Z. Wu and H. H. Shao 1994 12 p Presented at the 1994 Fall Meeting of the Materials Research Society (MRS), Boston, MA, 28 Nov. - 2 Dec. 1994

(Contract DE-AC02-76CH-00016)

(DE95-006694; BNL-61312; CONF-941144-57) Avail: CASI HC A03/MF A01

Normal alkanes of carbon number n greater than 14 exhibit surface crystallization at their liquid-vapor interface. This has been investigated with x-ray reflectivity, grazing incidence scattering and surface tension measurements. The structure and thermodynamics of the surface layer is consistent with a monolayer of the bulk rotator phase occurring at the surface above the bulk melting temperature. On the other hand, thin films of alkanes on SiO2, exhibit a reduction of the melting temperature. The surface crystalline phase is observed for carbon number n greater than 14. The vanishing of surface phase for small n may be due to a transition from surface freezing to surface melting behavior. These measurements can yield the relative surface energies of the various phases. DOE

N95-27538# California Univ., Berkeley. Lawrence Berkeley Lab, CA. Accelerator and Fusion Research Div.

CHARACTERIZATION OF WAFER CHARGING MECHANISMS AND OXIDE SURVIVAL PREDICTION METHODOLOGY

Wes Lukaszek (Stanford Univ., CA.), William Dixon (Stanford Univ., CA.), Michael Vella, Cleston Messick (National Semiconductor Corp., West Jordan, UT.), Steve Reno (National Semiconductor Corp., West Jordan, UT.), and Jay Shideler (National Semiconductor Corp., West Jordan, UT.) Apr. 1994 12 p Presented at the International Reliability Physics Symposium, San Jose, CA, 11-14 Apr. 1994

(Contract DE-AC03-76SF-00098)

(DE95-006583; LBL-35961; CONF-940453-5) Avail: CASI HC A03/MF A01

Unipolar, EEPROM-based peak potential sensors and current sensors have been used to characterize the I-V relationship of charging transients which devices normally experience during the course of ion implantation. The results indicate that the charging sources may appear to behave like current-sources or voltage-sources, depending on the impedance of the load. This behavior may be understood in terms of plasma concepts. The ability to empirically characterize the I-V characteristics of charging sources using the CHARM-2 monitor wafers opens the way for prediction of failure rates of oxides subjected to specific processes, if the oxide Q(sub bd) distributions are known. DOE

N95-27542# Argonne National Lab., IL.

SYNCHROTRON X-RAY SCATTERING STUDIES AT MINERAL-WATER INTERFACES

Ronald P. Chiarello and Neil C. Sturchio 1995 6 p Presented at the 1994 Fall Meeting of the Materials Research Society, Boston, MA, 28 Nov. - 2 Dec. 1994

(Contract W-31-109-eng-38)

(DE95-008303; ANL/CMT/CP-85560; CONF-941144-88) Avail: CASI HC A02/MF A01

Synchrotron X-ray scattering techniques provide a powerful tool for the in situ study of atomic scale processes occurring at solid-liquid interfaces. We have applied these techniques to characterize and study reactions at mineral-water interfaces. Here we present two examples. The first is the characterization of the calcite (CaCO3)(101'4) cleavage surface, in equilibrium with deionized water, by crystal truncation rod measurements. The second is the in situ study of the heteroepitaxial growth of otavite (CdCO3) on the calcite (101'4) cleavage surface. The results of such studies will lead to significant progress in understanding mineral-water interface geochemistry. DOE

N95-27712# International Centre for Theoretical Physics, Trieste (Italy).

NUMERICAL STUDY OF THE SINGLET-TRIPLET MODEL FOR CUPRATE SUPERCONDUCTORS

M. E. Simon and A. A. Aligia Aug. 1994 20 p

(DE95-609438; IC-94/208) Avail: CASI HC A03/MF A01 (US Sales Only)

We perform a low-energy reduction of the three-band Hubbard

Hamiltonian (H(sub 3b)), keeping in the relevant Hilbert subspace not only local singlets (Zhang-Rice singlets), but also triple states between Cu holes and O holes at the Wannier function of the same site, with x(sup 2) - y(sup 2) symmetry. We solve exactly the resulting Hamiltonian in a system of 2 x 2 unit cells. We find that the local triplet states can be practically neglected for finite O-Cu on-site energy difference (Delta), very large Cu on-site Coulomb repulsion U(sub d), and O-O hopping t(sub pp)=0. This fact is in contrast with the mapping of H(sub 3b) to a one-band model using non-orthogonal singlets, which is very accurate when the Cu(+) configuration can be neglected. Although the amount of local triplet states in the low-energy eigenstates is in general small, it increases with t(sub pp) and for large t(sub pp) it is necessary to introduce higher order corrections in the one-band model to accurately represent the low-energy physics. In all cases even when local triplets are not important, the t-J model should be supplemented with other terms to describe the lowest energy levels. We also discuss briefly the effect of non-bonding O orbitals. DOE

N95-27720# California Univ., Berkeley. Lawrence Berkeley Lab, CA.

MICROMAGNETICS AND MICROSTRUCTURE OF EPITAXIALLY GROWN Co AND Co-Cr FILMS FOR PERPENDICULAR MAGNETIC RECORDING

K. M. Krishnan, T. Takeuchi (Hitachi Ltd., Tokyo, Japan.), Y. Hirayama (Hitachi Ltd., Tokyo, Japan.), D. M. Donnet (Hitachi Ltd., Tokyo, Japan.), Y. Honda (Hitachi Ltd., Tokyo, Japan.), and M. Futamoto (Hitachi Ltd., Tokyo, Japan.) Jul. 1994 4 p Presented at the Magnetic Recording Conference, Tokyo, Japan, 10-14 Oct. 1994
(Contract DE-AC03-76SF-00098)
(DE95-004681; LBL-35986; CONF-9410278-1) Avail: CASI HC A01/MF A01

Highly c-axis oriented, single crystal films of Co(1-x)Cr(x) (0 less than or equal to x less than 0.3) have been grown epitaxially on mica substrates by e-beam evaporation. Films grown on Ru underlayers have an average grain size of 50-80 nm, negligibe fcc content, and very narrow c-axis dispersions. For Co films (x = 0), the as-grown magnetization structure are mainly 180 degree domain walls with a uniform distribution of cross-ties for thinner samples (less than or equal to 300 Angstrom), while thicker (greater than 400 Angstrom) ones show stripe domains. These images were analyzed in detail to measure the wall widths and associated energy densities for as-grown, remanent, and ac-magnetized samples. As expected, the magnetic properties of these films are composition dependent. However, for any Cr concentration, these films exhibit the largest saturation magnetization when compared with either sputtered or evaporated samples. This enhancement can be attributed to a nanometer-scale segregation of Cr, which in these samples could be particularly aided by the diffusion on the close-packed planes of the films with very narrow c-axis dispersions. Preliminary x-ray microanalysis and NMR data support this interpretation. DOE

N95-27740# International Centre for Theoretical Physics, Trieste (Italy).

MOLECULAR DYNAMICS SIMULATIONS OF GAY-BERNE NEMATIC LIQUID CRYSTAL: ELASTIC PROPERTIES FROM DIRECT CORRELATION FUNCTIONS

J. Stelzer, H. R. Trebin (Stuttgart Univ., Germany.), and L. Longa Aug. 1994 27 p
(DE95-609149; IC-94/220) Avail: CASI HC A03/MF A01 (US Sales Only)

We report NVT and NPT molecular dynamics simulations of a Gay-Berne nematic liquid crystal using generalization of recently proposed algorithm by Toxvaerd (Phys. Rev. E47, 343, 1993). On the basis of these simulations the Oseen-Zoher-Frank elastic constants K(sub 11), K(sub 22) and K(sub 33) as well as the surface constants K(sub 13) and K(sub 24) have been calculated within the framework of the direct correlation function approach of Lipkin et al. (J. Chem. Phys. 82, 472 (1985)). The angular coefficients of the direct pair correlation function, which enter the final formulas, have been determined from the computer simulation data for the pair correlation function of the nematic by combining the Ornstein-Zernike relation and the Wienier-Hopf factorization scheme. The unoriented nematic approximation has been assumed when constructing the reference, isotropic state of Lipkin et al. By an extensive study of the model over a wide range of temperatures, densities and pressures a very detailed information has been provided about elastic behaviour of the Gay-Berne nematic. Interestingly, it is found that the results for the surface elastic constants are qualitatively different than those obtained with the help of analytical approximations for the isotropic, direct pair correlation function. For example, the values of the surface elastic constants are negative and an order of magnitude smaller than the bulk elasticity. DOE

N95-27867# Joint Inst. for Nuclear Research, Dubna (USSR). Lab. of Nuclear Problems.

OBSERVATION OF ASYMMETRICAL TWO-CONE VAVILOV-CHERENKOV RADIATION IN BIAXIAL CRYSTAL OF TRIGLYCINESULPHATE EMITTED BY 658 MeV PROTONS PASSING ALONG BI NORMAL

V. P. Zrelov, V. P. Lupiltsev, and J. Ruzicka (Comenius Univ., Bratislava, Czechoslovakia.) 1993 11 p Submitted for publication
(DE94-629017; JINR-R-1-93-213) Avail: CASI HC A03/MF A01 (US Sales Only)

The paper deals with the directivity and polarization properties of the Vavilov-Cherenkov radiation (VChR) produced in passage of 658 MeV protons along an optical axis (bi normal) crystal of triglycinesulphate (TGS). The azimuthal distribution of the radiation turned out to be rather peculiar. First, it was asymmetrical about the plane running through the velocity vector of the beam particles perpendicularly to the plane of optical axes (POA). This VChR asymmetry was not observed in three earlier studied cases of 660 MeV protons passing through the main dielectric axes of a biaxial TGS crystal (i.e. when particles move along the small and the large bisectrix and perpendicularly to the plane of optical axes). Secondly, the azimuthal distribution of the VChR has a form of two symmetrical semi cones with different cone angles (their sections perpendicular to the proton beam axis resemble half-horseshoes inserted into each with their arcs outward). It also appeared that the outer VChR cone, F(sub -), is practically polarized only in the POA, while the inner cone, F(sub +), has more complicated polarization, i.e. in the angular region phi approx. 90 deg perpendicularly to the POA. Formulae are obtained for radiation directivity at any angle phi for this asymmetrical two-cone radiation. Comparison of the VChR emission angles calculated by these formulae and measured in experiment shows good agreement (within the measurement errors for the azimuthal) wave distribution of F(sub +) (inner cone) and some systematic excess (approx. 0.5 deg) for wave angles of F(sub -) (outer cone). DOE

N95-27925# National Academy of Sciences - National Research Council, Washington, DC.

TECHNICAL PROGRESS REPORT TO THE DEPARTMENT OF ENERGY ON THE SOLID STATE SCIENCES COMMITTEE (SSSC)

1995 6 p
(Contract DE-FG05-91ER-45442)
(DE95-007113; DOE/ER-45442/T1) Avail: CASI HC A02/MF A01

The Solid State Sciences Committee (SSSC) of the National Research Council (NRC) is charged with monitoring the health of the field of materials science in the United States. Accordingly, the Committee identifies and examines both broad and specific issues affecting the field. Regular meetings, teleconferences, briefings from agencies and the scientific community, the formation of study panels to prepare reports, and special forums are among the mechanisms used by the SSSC to meet its charge. This progress report presents a review of SSSC activities from May 1, 1992 through April 30, 1993. The details of prior activities are discussed in earlier reports. During the above period, the SSSC has continued to track and participate, when requested, in the development of a Federal initiative on advanced materials and processing. Specifically, the SSSC is presently planning the 1993 SSSC Forum (to be cosponsored with the National Materials Advisory Board (NMAB) and the Washington Materials Forum (WNM)). The thrust will be to highlight the Federal Advanced Materials and Processing Program (AMPP). In keeping with its charge to identify and highlight specific areas for scientific and technological opportunities, the SSSC continued to oversee the conduct of a study on biomolecular materials. Preliminary plans also have been developed for studies on neutron scattering science, on ultrasmall devices, and on molecular routes to materials. DOE

N95-27928# Argonne National Lab., IL.

DENSITY CHANGES IN AMORPHOUS Pd80Si20 DURING LOW TEMPERATURE ION IRRADIATION

G. Schumacher, R. C. Birtcher, and L. E. Rehn Nov. 1994 5 p Presented at the 1994 Fall Meeting of the Materials Research Society

(MRS), Boston, MA, 28 Nov. - 2 Dec. 1994
(Contract W-31-109-eng-38)
(DE95-007132; ANL/MSD/CP-83380; CONF-941144-67) Avail: CASI HC A01/MF A01

Density changes in amorphous Pd(80)Si(20) during ion irradiation below 100K were detected by in situ HVEM measurements of the changes in specimen length as a function of ion fluence. A decrease in mass density as a function of the ion fluence was observed. The saturation value of the change in mass density was determined to be approximately -1.2%. DOE

N95-27932# Brookhaven National Lab., Upton, NY. Physics Dept.
MAGNETIC STRUCTURES IN RNI2B2C (R = Ho, Er) SUPERCONDUCTORS
C. Stassis (Iowa State Univ. of Science and Technology, Ames, IA.), A. I. Goldman (Iowa State Univ. of Science and Technology, Ames, IA.), P. Dervenagas (Iowa State Univ. of Science and Technology, Ames, IA.), J. Zarestky (Iowa State Univ. of Science and Technology, Ames, IA.), P. C. Canfield (Iowa State Univ. of Science and Technology, Ames, IA.), B. K. Cho (Iowa State Univ. of Science and Technology, Ames, IA.), D. C. Johnston (Iowa State Univ. of Science and Technology, Ames, IA.), and B. Sternlieb 1994 5 p Presented at the 1994 Fall Meeting of the Materials Research Society (MRS), Boston, MA, 28 Nov. - 2 Dec. 1994
(Contract DE-AC02-76CH-00016)
(DE95-008370; BNL-61459; CONF-941144-89) Avail: CASI HC A01/MF A01

Single crystal neutron diffraction techniques have been employed to study the evolution of magnetic structures in RNi2B2C compounds in an attempt to understand the relationship between magnetic ordering and superconductivity in several members of this series. For HoNi2B2C, below the superconducting transition (T(sub c) = 8 K), an incommensurate magnetic structure characterized by two wave vectors (0.585 a(*) and 0.915 c(*)) is found in a narrow temperature range between 4.7 K and 6 K. This is the same temperature range where bulk measurements find a deep minimum in the upper critical field, H(sub c2). Below 4.7 K, HoNi2B2C is a simple collinear antiferromagnet. ErNi2B2C (T(sub c) = 11 K) orders in an incommensurate modulated antiferromagnetic state characterized by an ordering wave vector 0.553 a(*) below 7 K, which coexists with superconductivity. DOE

N95-27950# Argonne National Lab., IL.
SINTERING OF TEXTURED YBa2Cu3O(7-x) UNDER INTENSIVE Co-60 GAMMA IRRADIATION
E. M. Ibragimova (Institute of Nuclear Physics, Tashkent, Uzbekistan.), E. M. Gasanov (Institute of Nuclear Physics, Tashkent, Uzbekistan.), M. O. Kalanov (Institute of Nuclear Physics, Tashkent, Uzbekistan.), M. A. Kirk, and K. C. Goretta Dec. 1994 6 p Presented at the 1994 Fall Meeting of the Materials Research Society (MRS), Boston, MA, 28 Nov. - 2 Dec. 1994
(Contract W-31-109-eng-38)
(DE95-007098; ANL/MSD/CP-83324; CONF-941144-62) Avail: CASI HC A02/MF A01

A study of structural and superconducting characteristics of YBa2Cu3O(7-x) ceramics sintered after and in the course of gamma-irradiation is reported. Using x-diffraction and SEM analyses and transport measurements, it has been shown that mainly the subsurface layer of crystallites and intergrain contacts are affected by the irradiation by means of sorption/desorption of oxygen and ordering/disordering in oxygen sublattice, which depends on gamma dose rate and dose. The irradiation provides the sintering process with an additional superthermal energy to form the orthorhombic well-ordered structure and to obtain dense ceramics possessing strong intergrain contacts and improved and stable superconducting properties. DOE

N95-27959# Oak Ridge National Lab., TN.
THE DIFFUSION PROPERTIES OF ION IMPLANTED SPECIES IN SELECTED TARGET MATERIALS
G. D. Alton, J. Dellwo, H. K. Carter, J. Kormicki, G. diBartolo, J. C. Batchelder, J. Breitenbach, J. A. Chediak, K. Jentoff-Nilsen, and S. Ichikawa 1995 14 p Presented at the 4th International Conference on Applications of Nuclear Techniques: Neutrons and Their Applications, Crete, Greece, 12-18 Jun. 1994
(Contract DE-AC05-84OR-21400)
(DE95-007006; CONF-9406176-5) Avail: CASI HC A03/MF A01

Experiments important to the future success of the Holifield Radioactive Ion Beam Facility (HRIBF) are in progress at the Oak Ridge National Laboratory which are designed to select the most appropriate target material for generating a particular radioactive ion beam (RIB). The 25-MV HHIRF tandem accelerator is used to implant stable complements of interesting radioactive elements into refractory targets mounted in a high-temperature FEBIAD ion source which is 'on-line' at the UNISOR facility. The intensity versus time of implanted species, which diffuse from the high-temperature target material (approximately 1700 C) and are ionized in the FEBIAD ion source, is used to determine release times for a particular projectile/target material combination. From such release data, diffusion coefficients can be derived by fitting the theoretical results obtained by computational solution of Fick's second equation to experimental data. The diffusion coefficient can be used subsequently to predict the release properties of the particular element from the same material in other target geometries and at other temperatures, provided that the activation energy is also known. Diffusion coefficients for Cl implanted into and diffused from CeS and Zr5Si3 and As, Br, and Se implanted into and diffused from Zr5Ge3 have been derived from the resulting intensity versus time profiles. Brief descriptions of the experimental apparatus and procedures utilized in the present experiments and plans for future related experiments are presented. DOE

N95-27963# Argonne National Lab., IL.
ELECTRON SPECTROSCOPY STUDIES OF ARGON K-SHELL EXCITATION AND VACANCY CASCADES
S. H. Southworth (National Inst. of Standards and Technology, Gaithersburg, MD.), M. A. MacDonald (Science Research Council, Daresbury, England.), T. LeBrun, and Y. Azuma (National Lab. for High Energy Physics, Tsukuba, Japan.) 1995 11 p Presented at the Workshop on Atomic Physics At High Brilliance Synchrotron Sources, Argonne, IL, 23-24 Apr. 1994
(Contract W-31-109-eng-38)
(DE95-007096; ANL/PHY/CP-85306; CONF-9404198-5) Avail: CASI HC A03/MF A01

Electron spectroscopy combined with tunable synchrotron radiation has been used for studies of Ar K-shell excitation and vacancy decay processes. In addition, electrons and fluorescent X-rays have been recorded in coincidence to select subsets of the ejected electron spectra. Examples are presented for Ar 1s photoelectrons and KLL and LMM Auger spectra. DOE

N95-27964# Universidad Autonoma del Estado de Mexico, Toluca (Mexico).
DETERMINATION OF PHASE TRANSITIONS IN A LYOTROPIC LIQUID CRYSTAL BY POSITRON ANNIHILATION TECHNIQUE Ph.D. Thesis
V. M. Castillo 1994 80 p
(DE95-609162; INIS-MF-14400) Avail: CASI HC A05/MF A01 (US Sales Only)

Positron annihilation technique was used to determine the phase transitions in a lyotropic liquid crystal, as a function of temperature. Seven different concentrations of the surfactant cetyl dimethyl ethyl ammonium bromide were studied. The liquid crystal studied consisted of a binary system, formed by the surfactant and water. Positron annihilation technique has a very high sensitivity toward changes in the microstructure, in condensed matter; this is useful in order to detect the temperatures at which phase transitions occur and the number of these, in a liquid crystalline system. Thus, phase transitions are related with changes occurred in the ortho-positronium parameters: lifetime (tau(sub 3)) and intensity of formation (I(sub 3)). Six different kinds of phases were detected in the system studied in a temperature range of 35 to 140 C; those phases were: hexagonal, hexagonal-lamellae, lamellae, lamellae-cubic, nematic, and anisotropic. Using optical microscopes the textures of these phases were assigned. DOE

N95-27994# Los Alamos National Lab., NM. Theoretical Div.
PHENOMENOLOGY FROM 100 LARGE LATTICES
Tammoy Bhattacharya and Rajan Gupta 1995 7 p Presented at the Lattice 1994, Bielefeld, Germany, 25 Sep. - 1 Oct. 1994
(Contract W-7405-eng-36)
(DE95-006349; LA-UR-95-72; CONF-9409269-8) Avail: CASI HC A02/MF A01

The authors present a status report on simulations being done on 32(sup 3) x 64 lattices at (beta) = 6.0 using quenched Wilson fermions. Phenomenologically relevant results for the spectrum, decay constants, the kaon B-parameter B(sub K), B(sub 7), B(sub s), semi-leptonic and B (yields) K(sup *)(gamma) form factors are given based on a statistical sample of 100 configurations. DOE

N95-28016# International Centre for Theoretical Physics, Trieste (Italy).
MULTIFRACTAL CHARACTER OF THE ELECTRONIC STATES IN DISORDERED TWO-DIMENSIONAL SYSTEMS
N. Tit and M. Schreiber (Mainz Univ., Germany.) Aug. 1994 28 p
(DE95-609153; IC-94/246) Avail: CASI HC A03/MF A01 (US Sales Only)

The nature of electronic states in disordered two-dimensional (2D) systems is investigated. To this aim, we present our calculations of both density of states and dc-conductivity for square lattices modelling the Anderson Hamiltonian with on-site energies randomly chosen from a box distribution of width W. For weak disorder (W), the eigenfunctions calculated by means of the Lanczos diagonalization algorithm display spatial fluctuations reflecting their (multi)fractal behaviour. For increasing disorder or energy the observed increase of the curdling of the wavefunction reflects its stronger localization. Our dc-conductivity results suggest a critical fractal dimension d(sup *)(sub c)=1.48 +/- 0.05 todiscriminate between the exponentially and the power-law localized states. Consequences of the localization on transport properties are also discussed. DOE

N95-28023# Los Alamos National Lab., NM.
AN INVESTIGATION OF THE CHEMICAL AND PHYSICAL PROPERTIES OF PRISTINE, ELECTROCHROMICALLY DAMAGED, AND PHOTOCHROMICALLY DAMAGED KTiOPO4 (KTP) USING SURFACE ANALYTICAL AND OPTICAL SPECTROSCOPIC TECHNIQUES
J. R. Quagliano, R. R. Petrin, T. C. Trujillo, N. J. Cockroft, M. T. Paffett, C. J. Maggiore, and J. C. Jacco 1995 9 p Presented at the Advanced Solid-state Laser Conference, Memphis, TN, 29 Jan. - 1 Feb. 1995
(Contract W-7405-eng-36)
(DE95-007865; LA-UR-95-684; CONF-950101-4) Avail: CASI HC A02/MF A01

A variety of experimental techniques were employed to study the properties of electrochromically (EC) damaged, photochromically (PC) damaged, and pristine KTiOP04 (KTP). Additionally, nonlinear optical calculations were performed to complement the experimental work in an effort to elucidate the respective mechanisms operative in producing EC and PC damage to KTP. Several independent experiments indicate that there is Ti deficiency in the EC damaged material, which is due to migration of these ions to the electrode surface. The laser experiments indicate that UV radiation can produce reversible PC damage. UV-producing SFG processes accidentally occurring in SHG cut KTP may lead to macroscopic damage. It must be emphasized that a fundamentally different mechanism is responsible for EC damaged versus PC damaged KTP. DOE

N95-28033*# Alabama A & M Univ., Normal, AL. Dept. of Physics.
GROWTH AND CHARACTERIZATION OF CRYSTALS FOR ROOM TEMPERATURE I.R. DETECTORS AND SECOND HARMONIC GENERATION DEVICES
R. B. Lal Mar. 1995 15 p Sponsored by the Center of Commercial Crystal Growth, Clarkson Univ., Potsdam, NY
(Grant NAGw-976)
(NASA-CR-198598; NAS 1.26:198598) Avail: CASI HC A03/MF A01

One of the major objectives of this program was to modify the triglycine sulfate (TGS) crystals with suitable dopants and variants to achieve better pyroelectric properties and improved infrared detectivities (D(sup *)), and higher Curie transition temperature compared to undoped TGS crystals. Towards these objectives, many promising dopants, both inorganic and organic, were investigated in the last few years. These dopants gave significant improvement in the D(sup *) value of the infrared detectors fabricated from the grown crystals with no significant increase in the Curie temperature (49 C). The IR detectors were fabricated at EDO/Barnes Engineering Division, Shelton, CT. In the last one year many TGS crystals doped with urea were grown using the low temperature solution crystal growth facility. It is found that doping with urea, the normalized growth yield increased significantly compared to pure TGS crystals and there is an improvement in the pyroelectric and dielectric constant values of doped crystals. This gave a significant increase in the materials figure of merits. The Vicker's hardness of 10 wt percent urea doped crystals is found to be about three times higher in the (010) direction compared to undoped crystals. This report describes in detail the results of urea doped TGS crystals. Derived from text

N95-28050# Carnegie-Mellon Univ., Pittsburgh, PA.
PHASE SEPARATION AND ORDERING IN InGaAsP AND InGaAs MATERIALS Final Report
23 Feb. 1995 8 p
(Contract DE-FG02-87ER-45329)
(DE95-007493; DOE/ER-45329/1) Avail: CASI HC A02/MF A01

This report highlights the advances in the understanding of phase separation and atomic ordering in mixed III-V layers. Specifically, the following issues were addressed in the grant period (August 1987 to February 1992): (1) bulk vs surface phase separation; (2) influence of growth technique on phase separation; (3) origin of coarse contrast modulations; (4) influence of dopant diffusion on phase separated microstructures; (5) influence of annealing on carrier mobility in InGaAsP layers; (6) co-existence of CuPt-type ordering and phase separation; (7) influence of growth conditions on ordering; (8) influence of surface reconstruction on atomic ordering. DOE

N95-28060# Los Alamos National Lab., NM.
ASPECTS OF MACROSCOPIC PHASE SEPARATION AND INTERSTITIAL OXYGEN ORDERING IN OXYGEN DOPED La2CuO(4+DELTA)
P. C. Hammel, Z. Fisk, B. W. Statt (Ames Lab., IA.), F. C. Chou (Ames Lab., IA.), D. C. Johnston (Ames Lab., IA.), and S. W. Cheong (Bell Telephone Labs., Inc., Murray Hill, NJ.) 1994 15 p Presented at the International Workshop on the Anharmonic Properties of High-Tc Cuprates, Bled, Slovenia, 1-6 Sep. 1994
(Contract W-7405-eng-36)
(DE95-007864; LA-UR-95-677; CONF-940968-1) Avail: CASI HC A03/MF A01

NMR and neutron diffraction measurements reveal that macroscopic phase separation and the tetragonal to orthorhombic (TO) structural phase coincide at two distinct points in the temperature-doping phase plot for oxygen doped La2CuO(4+delta). Thus the TO phase line coincides with the phase separation line. This is evidence that the macroscopic phase separation is inhibited in the tetragonal phase. We propose that the interstitial oxygen has higher mobility in the orthorhombic phase and that insufficient mobility suppresses macroscopic phase separation in the tetragonal phase. Neutron diffraction measurements also reveal superlattice peaks which indicate ordering of the interstitial oxygen. Our NMR measurements, have demonstrated a distribution of tilts of the CuO6 octahedra. We propose a sawtooth modulation of the octahedral tilt in which the sign of the tilt changes when the tilt reaches a maximum value can explain this distribution. The large openings in the La-O layer resulting from the abrupt switch of the sign of the tilt provide an attractive location for the interstitial oxygen. This mechanism would lead to stripe ordering of the interstitial oxygen. DOE

N95-28076# Oak Ridge National Lab., TN.
SOLID STATE SINTERING OF SILICON NITRIDE ARL-CR-114 Final Report
John Mangels and Bilijana Mikijelj Sep. 1994 78 p Prepared in cooperation with Ceradyne, Inc., Cost a Mesa, CA Sponsored by Martin Marietta Energy Systems, Inc.
(Contracts DE-AC05-84OR-21400; DE-IA05-840R-21411)
(DE95-007291; ORNL/M-4021) Avail: CASI HC A05/MF A01

This report describes the development of Si3N4 material compositions in the Si3N4-Y2O3-SiO2-Mo2C system with good high temperature stress rupture properties which could be used in engine components. Two distinct processing routes were examined in the course of the program: SSN and SRBSN. SRBSN was chosen for material property optimization. After characterization of two optimized compositions in the above system, demonstration engine components (exhaust valve blanks) were manufactured using the established processing procedures. Dimensional tolerance capabilities of the process were established and material properties of the components were shown to be comparable to those established during material development. DOE

N95-28079# Oak Ridge National Lab., TN. Chemical and Analytical Sciences Div.
FORMATION OF ANISOTROPIC Tl-1212, Tl-2212, Tl-1223 AND Tl-2223 PARTICLES USING AEROSOL FLOW REACTED POWDERS
M. Paranthaman, A. Goyal, D. E. Heatherly, and D. M. Kroeger 1994 4 p Presented at the Applied Superconductivity Conference, Boston, MA, 16-21 Oct. 1994 Sponsored by Martin Marietta Energy Systems, Inc.
(Contract DE-AC05-84OR-21400)
(DE95-007400; CONF-941013-28) Avail: CASI HC A01/MF A01

Highly anisotropic particles of Tl-1212, Tl-2212, Tl-1223 and Tl-2223 superconductors were grown. The Tl-free precursor powders with the compositions Ba1Ca2Cu3Ag(0.37)O6 and Ba2Ca2Cu3Ag(0.37)O7 were prepared using an aerosol flow reactor. These precursor powders were then post-annealed in 0.1 atm oxygen at 700 C for 4h to reduce the carbon present and mixed with Tl2O3 (typical composition of Tl(x);x = 0.6-1.0). The Tl-containing powders were heated in sealed gold tubes between 650-890 C for various times. X ray diffraction showed that the Tl-2212 and Tl-2223 phases were stable over a wide range of temperatures. Scanning electron microscopy showed evidence for the presence of high aspect-ratio particles. These highly anisotropic particles may be of interest for the preparation of powder-in-tube and other powder deposited conductors, for current leads, and for grain alignment studies. DOE

N95-28081# Oak Ridge National Lab., TN. Solid State Div.
COHERENT V2O3 PRECIPITATES IN ALPHA-Al2O3CO- IMPLANTED WITH VANADIUM AND OXYGEN
Laurence A. Gea, L. A. Boatner, J. D. Budai, and Janet Rankin (Brown Univ., Providence, RI.) 1994 6 p Presented at the 1994 Fall Meeting of the Materials Research Society, Boston, MA, 28 Nov. - 2 Dec. 1994
(Contract DE-AC05-84OR-21400)
(DE95-007404; CONF-941144-74) Avail: CASI HC A02/MF A01

The oxides of vanadium VO2 and V2O3 are of fundamental and practical interest since they undergo structural phase transitions during which large variations in their optical and electronic properties are observed. In the present work, the authors report the formation of buried precipitates of V2O3 in sapphire by ion implantation and thermal annealing. It was found that the co-implantation of oxygen and vanadium was required in order to form nanophase V2O3 precipitates. Additionally, these precipitates, which formed only following an anneal of the co-implanted sample under reducing conditions, are coherent with the sapphire lattice. Two epitaxial relationships were observed: (0001)V2O3 //(0001) (alpha)-Al2O3 and (11-20)V2O3//(0001) (alpha)-Al2O3. This finding is in agreement with results obtained elsewhere for thin films of V2O3 deposited on c-axis-oriented sapphire. DOE

N95-28092# California Univ., Berkeley. Lawrence Berkeley Lab, CA.
LOW TEMPERATURE CARRIER TRANSPORT PROPERTIES IN ISOTOPICALLY CONTROLLED GERMANIUM Ph.D. Thesis
K. Itoh Dec. 1994 193 p
(Contract DE-AC03-76SF-00098)
(DE95-008489; LBL-36683) Avail: CASI HC A09/MF A03

Investigations of electronic and optical properties of semiconductors often require specimens with extremely homogeneous dopant distributions and precisely controlled net-carrier concentrations and compensation ratios. The previous difficulties in fabricating such samples are overcome as reported in this thesis by growing high-purity Ge single crystals of controlled Ge-75 and Ge-70 isotopic compositions, and doping these crystals by the neutron transmutation doping (NTD) technique. The resulting net-impurity concentrations and the compensation ratios are precisely determined by the thermal neutron fluence and the (Ge-74)/(Ge-70) ratios of the starting Ge materials, respectively. This method also guarantees unprecedented doping uniformity. Using such samples the authors have conducted four types of electron (hole) transport studies probing the nature of (1) free carrier scattering by neutral impurities, (2) free carrier scattering by ionized impurities, (3) low temperature hopping conduction, and (4) free carrier transport in samples close to the metal-insulator transition. DOE

N95-28103# Sandia National Labs., Albuquerque, NM.
CONTROL OF THIN FILM PROCESSING BEHAVIOR THROUGH PRECURSOR STRUCTURAL MODIFICATIONS
R. W. Schwartz, J. A. Voigt, T. J. Boyle, T. A. Christenson, and C. D. Buchheit 1995 15 p Presented at the 19th Annual Conference on Advanced Ceramics, Materials and Structures, Cocoa Beach, FL, 9-12 Jan. 1995
(Contract DE-AC04-94AL-85000)
(DE95-006468; SAND-95-0090C; CONF-950129-2) Avail: CASI HC A03/MF A01

In the sol-gel processing of ceramic thin films it has been frequently noted that the processing behavior, microstructure and properties of the films are dependent on the nature of the coating solution. In an attempt to understand such thin film processing-property relationships, the authors have systematically investigated the effects of varying the precursor nature on thin film densification and crystallization for ZrO2 and TiO2 films. Metal alkoxide starting compounds, e.g., zirconium n-butoxide (center dot) n-butanol and titanium i-propoxide, were reacted with acetic acid and 2,4-pentanedione to prepare coating solutions for thin film deposition. The use of these chelating ligands resulted in solution oligomeric species of different nature. Studies of thin film processing indicated that film processing characteristics, i.e., consolidation, densification and crystallization, were strongly dependent on solution precursor nature. Ligand steric size, pyrolysis behavior, extent of chelation, and precursor reactivity were found to be key variables in controlling film processing characteristics. DOE

N95-28112# International Centre for Theoretical Physics, Trieste (Italy).
A CORRELATED WALKS' THEORY FOR DNA DENATURATION
R. Mejdani Aug. 1994 13 p Prepared in cooperation with the Univ. of Tirana, Tirana, Albania
(DE95-607910; IC-94/228) Avail: CASI HC A03/MF A01 (US Sales Only)

We have shown that by using a correlated Walks' theory for the lattice gas model on a one-dimensional lattice, we can study, beside the saturation curves obtained before for the enzyme kinetics, also the DNA denaturation process. In the limit of no interactions between sites the equation for melting curves of DNA reduces to the random model equation. Thus our leads naturally to this classical equation in the limiting case. DOE

N95-28125# Los Alamos National Lab., NM.
PLASMA SOURCE ION IMPLANTATION OF AMMONIA INTO ELECTROPLATED CHROMIUM
J. T. Scheuer, K. C. Walter, D. J. Rej, M. Nastasi, and J. P. Blanchard (Wisconsin Univ., Madison, WI.) 1995 7 p Presented at the Annual Meeting and Exhibition of the Minerals, Metals and Materials Society, Las Vegas, NV, 12-16 Feb. 1995
(Contract W-7405-eng-36)
(DE95-006275; LA-UR-95-341; CONF-950201-4) Avail: CASI HC A02/MF A01

Ammonia gas (NH3) has been used as a nitrogen source for plasma source ion implantation processing of electroplated chromium. No evidence was found of increased hydrogen concentrations in the bulk material, implying that ammonia can be used without risking hydrogen embrittlement. The retained nitrogen dose of 2.1 x 10(exp 17)N-at/sq cm is sufficient to increase the surface hardness of electroplated Cr by 24% and decrease the wear rate by a factor of 4. DOE

N95-28127# Sandia National Labs., Albuquerque, NM.
CAVITY FORMATION AND IMPURITY GETTERING IN He-IMPLANTED Si
D. M. Follstaedt, S. M. Myers, G. A. Petersen, and J. W. Medernach 1994 36 p Presented at the Annual Meeting and Exhibition of the Minerals, Metals and Materials Society, Las Vegas, NV, 12-16 Feb. 1995
(Contract DE-AC04-94AL-85000)
(DE95-007744; SAND-94-2049C; CONF-950201-3) Avail: CASI HC A03/MF A01

Cavity microstructures formed in Si after ion implantation of He and annealing at 700 C or above are examined with cross-section transmission electron microscopy. A threshold concentration of 1.6 at.% He is identified to form cavities that survive such anneals. The cavities coarsen with a constant volume of 15 nm(exp 3)/nm(exp 2) (per wafer surface area), corresponding to approximately 0.75 lattice sites per implanted He atom. The internal area of the cavities is 3-7 times that of the wafer surface area for fluences of 1 x 10(exp 17) He/cm(exp 2). Transition metal atoms (Cu, Ni, Co, Fe, Au) are shown to be strongly trapped (1.5-2.2 eV) on the cavity walls by chemisorption. Whereas Cu, Au and Ni are bound more strongly to the cavity sites than to their respective precipitated phases, Co and Fe are more strongly bound to their silicides; nonetheless, appreciable trapping of Co and Fe does occur in equilibrium with the silicides. Cavity trapping appears to be an effective gettering mechanism at low impurity levels, as needed to meet future microelectronics device requirements. DOE

N95-28144# Sandia National Labs., Albuquerque, NM.
LOW RESISTIVITY OHMIC CONTACTS TO MODERATELY DOPED n-GaAs WITH LOW TEMPERATURE PROCESSING
M. L. Lovejoy, A. J. Howard, K. R. Zavadil, D. J. Rieger, R. J. Shul, and P. A. Barnes 1994 16 p Presented at the 41st Annual American Vacuum Society Symposium, Denver, CO, 24-28 Oct. 1994
(Contract DE-AC04-94AL-85000)
(DE95-008507; SAND-94-1367C; CONF-941001-14) Avail: CASI HC A03/MF A01

A low-temperature process for forming ohmic contacts to moderately doped GaAs has been optimized using a PdGe metallization scheme. Minimum specific contact resistivity of 1.5 x 10(exp -6)/sq cm has been obtained with a low anneal temperature of 250 C. Results for optimizing both time and temperature are reported and compared to GeAu n-GaAs contacts. Material compositions was analyzed by x ray photoelectron spectroscopy and circuit metal interconnect contact resistivity to the low-temperature processed PdGe contacts is reported. For the lowest temperature anneals considered, excess Ge on the ohmic contact layer is suspected of degrading interconnect metal contacts, while higher temperature anneals permitted interconnect metal formation with negligible contact resistivity. Atomic force microscopy measurements showed that the PdGe surface morphology is much more uniform than standard GeAu contacts. DOE

N95-28165# Brookhaven National Lab., Upton, NY.
VACANCY RELATED DEFECTS IN THIN FILM Pb(Zr,Ti)O3 MATERIALS
A. Krishnan (Michigan Technological Univ., Houghton, MI.), D. J. Keeble (Michigan Technological Univ., Houghton, MI.), R. Ramesh (Bell Communications Research, Inc., Red Bank, NJ.), W. L. Warren (Sandia National Labs., Albuquerque, NM.), B. A. Tuttle (Sandia National Labs., Albuquerque, NM.), R. L. Pfeffer (Army Research Lab., Fort Monmouth, NJ.), B. Nielsen, and K. G. Lynn 1994 6 p Presented at the 1994 Fall Meeting of the Materials Research Society (MRS), Boston, MA, 28 Nov. - 2 Dec. 1994
(Contracts DE-AC02-76CH-00016; DE-AC04-94AL-85000)
(DE95-007696; BNL-60717; CONF-941144-65) Avail: CASI HC A02/MF A01

Positron annihilation techniques have been applied to characterize vacancy-related defects in ferroelectric thin film structures. Variable energy positron beam measurements were carried out on doped and undoped Pb(Zr,Ti)O3 (PZT) samples subjected to different post-deposition cool down and anneal conditions. The PZT was deposited by sol-gel with either with platinum or RuO2 electrodes, or by laser ablation with La(0.5)Sr(0.5)CoO3 electrodes. The RuO2 and La(0.5)Sr(0.5)CoO3 electrode samples showed a smaller S-parameter compared to those deposited with Pt electrodes consistent with an improved PZT layer quality. For laser ablated samples cooled in a reducing ambient an increase in S-parameter for both the PZT and La(0.5)Sr(0.5)CoO3 layers was observed indicating an increase in neutral or negatively charged open-volume defects. DOE

N95-28179# National Academy of Sciences - National Research Council, Washington, DC. Solid State Sciences Committee.
[RESEARCH ACTIVITIES OF THE SOLID STATE SCIENCES COMMITTEE IN THE DEVELOPMENT OF A FEDERAL INITIATIVE ON ADVANCED MATERIALS AND PROCESSING] Technical Progress Report, 1 May 1992 - 30 Apr. 1993
Ronald Taylor 1995 6 p
(Contract DE-FG05-91ER-45442)
(DE95-009328; DOE/ER-45442/T2) Avail: CASI HC A02/MF A01

The Solid State Sciences Committee (SSSC) of the National Research Council (NRC) is charged with monitoring the health of the field of materials science in the United States. Accordingly, the committee identifies and examines both broad and specific issues affecting the field. Regular meetings, teleconferences, briefings from agencies and the scientific community, the formation of study panels to prepare reports, and special forums are among the mechanisms used by the SSSC to meet its charge. This progress report presents a review of SSSC activities from May 1, 1992 through April 30, 1993. The details of prior activities are discussed in earlier reports. During the above period, the SSSC has continued to track and participate, when requested, in the development of a federal initiative on advanced materials and processing. Specifically, the SSSC is presently planning the 1993 SSSC Forum (to be cosponsored with the National Materials Advisory Board (NMAB) and the Washington Materials Forum (WMF)). The thrust will be to highlight the Federal Advanced Materials and Processing Program (AMPP). In keeping with its charge to identify and highlight specific areas for scientific and technological opportunities, the SSSC continued to oversee the conduct of a study on biomolecular materials. Preliminary plans also were developed for a study on neutron science; however, further activity is pending. A proposed study on ultrasmall devices has been expanded and absorbed into a broader context; the Board on Physics and Astronomy (BPA), with SSSC participation, is preparing to hold a program initiation meeting to evaluate the need for a study on information technology and hardware. DOE

N95-28186# Brookhaven National Lab., Upton, NY.
THE REAL STRUCTURE OF COLUMNAR PINNING CENTERS IN HEAVY-ION-IRRADIATED CUPRATE SUPERCONDUCTORS
D. O. Welch, Y. Zhu, and R. C. Budhani (Indian Inst. of Tech., Kanpur.) 1995 4 p Presented at the Topical Conference on the Critical State in Superconductors, Honolulu, HI, 24-26 Oct. 1994
(Contract DE-AC02-76CH-00016)
(DE95-003948; BNL-60429; CONF-941014-2) Avail: CASI HC A01/MF A01

There has been considerable recent interest in the use of columnar defects produced by irradiation with energetic heavy ions to raise the irreversibility line and improve the critical current density of cuprate superconductors. In the interpretation and theoretical modeling of the flux-pinning characteristics of heavy-ion tracks, it is generally assumed that they are simply columns of non-superconducting material. In this paper we present a more realistic description, based both on resistivity measurements and on detailed, quantitative transmission electron microscope methods (both imaging and analytical studies), of the nature of heavy-ion damage, including defects, disorder, strain fields, and oxygen deficiencies in the matrix of the superconductor surrounding the amorphous columns. The presence of such disorder appears to be a consequence of the mechanism of track formation, which involves partial epitaxial regrowth of a molten region which follows the passage of sufficiently energetic ions. DOE

N95-28206# Sandia National Labs., Albuquerque, NM.
CHEMICAL AND ELECTRICAL PROPERTIES OF CAVITIES IN SILICON AND GERMANIUM
S. M. Myers, D. M. Follstaedt, G. A. Petersen, C. H. Seager, H. J. Stein, and W. R. Wampler 1994 23 p Presented at the 9th International Conference on Ion Beam Modification of Materials, Canberra, Australia, 5-10 Feb. 1995
(Contract DE-AC04-94AL-85000)
(DE95-006812; SAND-94-2299C; CONF-950220-4) Avail: CASI HC A03/MF A01

Cavities were formed in Si and Ge by He ion implantation and annealing, and resultant chemical and electrical properties were investigated. The dissociation energies for Si-H and Ge-H surface monohydride bonds were determined, showing that H chemisorption on Si is energetically stable with respect H2 gas whereas H chemisorption on Ge is not. Cavity walls in Si were found to trap transition metals strongly, suggesting application to impurity gettering in devices. Measurement and modeling of cavity electrical properties elucidated surface electronic states and indicated a potential for controlled electrical isolation in devices. DOE

N95-28240# Los Alamos National Lab., NM.
TOPOLOGICAL DENSITY AND INSTANTONS ON A LATTICE
J. Grandy (Ohio State Univ., Columbus, OH.) and R. Gupta 1995 3 p Presented at the Lattice '94, Bielefeld, Germany, 25 Sep. - 1 Oct. 1994
(Contract W-7405-eng-36)
(DE95-006348; LA-UR-95-73; CONF-9409269-7) Avail: CASI HC A01/MF A01

The authors present an update on the study of topological structure of QCD. Issues addressed include a comparison between the plaquette and the geometric methods of calculating the topological density. They show that the improved gauge action based on square root of 3 blocking transformation suppresses the formation of topologically charged dislocations with low action. Using a cooling method they identify the instantons location, estimate their size and density, and calculate the renormalization constant Z(sub Q) for the plaquette method. DOE

N95-28242# Pacific Northwest Lab., Richland, WA.
FEMTOSECOND OPO'S AT 3 MICRONS AND BEYOND: DESIGN AND PERFORMANCE ISSUES RELATED TO THE CRYSTAL PROPERTIES OF KTP AND SIMILAR MATERIALS
G. R. Holtom, R. A. Crowell, and L. K. Cheng (Du Pont de Nemours, E. I. and Co., Wilmington, DE.) Feb. 1995 6 p Presented at the SPIE '95: SPIE Conference on Optics, Electro-optics, and Laser Application in Science, Engineering and Medicine, San Jose, CA, 5-10 Feb. 1995
(Contract DE-AC06-76RL-01830)
(DE95-007286; PNL-SA-25742; CONF-950226-7) Avail: CASI HC A02/MF A01

Femtosecond optical parametric oscillators (OPO's), synchronously pumped by Ti:Sapphire lasers, operating in the near infrared (IR) region are an important light source now under active development. The authors report the results of Ti:Sapphire synchronously pumped noncritically phase matched femtosecond OPO's that are based upon several crystals from the KTP (KTiOPO4) family. The newly developed nonlinear crystal niobium doped KTP (Nb:KTP) has a greater birefringence than undoped KTP and is shown to extend the wavelength farther into the mid-IR. The authors report the first operation of a femtosecond OPO utilizing the solid-solution grown crystal Nb:KTP. Additionally, it is shown that CTA is very useful in mid-IR angle tuned OPO's. DOE

N95-28255# International Centre for Theoretical Physics, Trieste (Italy).
THE OFF-CENTER EFFECT ON THE DIFFUSION COEFFICIENT OF Cu(+) AND Li(+) IN THE KCl LATTICE
F. Despa Jul. 1994 24 p
(DE95-609146; IC-94/176) Avail: CASI HC A03/MF A01 (US Sales Only)

It is well known that the diffusion coefficients of the Cu(+) cation in the NaCl and KCl lattices exceeds by three or four orders of magnitude the corresponding self-diffusion coefficients in the intrinsic temperature regions. This fast diffusion of the Cu(+) has been explained in many papers as an interstitial diffusion although the optical spectra do not confirm the existence of interstitial Cu(+). In this paper we propose a new mechanism for fast diffusion. The model assumes that the equilibrium positions of the cationic impurities are noncentral and that the diffusion proceeds by hopping across the potential barrier along the nonlinear paths with the highest probability. The main result shows that the off-center position enhances considerably the diffusion. Theoretical diffusion coefficients have been obtained by modelling the potential barrier. Changes of the configuration entropy and the vibration spectra due to the presence of the noncentral impurity have been included in the model. We proceeded in the Li(+) cation case as in the case of Cu(+) cation. We emphasize the good agreement of the model with the experimental data and we show that if the impurity is placed close to the central site the due diffusion coefficient is close to that for the cationic self-diffusion. DOE

N95-28327 North Carolina State Univ., Raleigh, NC. Dept. of Materials Science and Engineering.
ATOMIC LAYER EPITAXY OF GROUP 4 MATERIALS: SURFACE PROCESSES, THIN FILMS, DEVICES AND THEIR CHARACTERIZATION Semiannual Technical Report, 1 Jul. - 31 Dec. 1994
Robert F. Davis, S. Bedair, N. A. El-Masry, J. T. Glass, and S. King Dec. 1994 54 p Limited Reproducibility: More than 20% of this document may be affected by microfiche quality
(Contract N00014-91-J-1416)
(AD-A289092) Avail: Issuing Activity (Defense Technical Information Center (DTIC))

Residual surface contaminants were removed from vicinal 6H-SiC(0001) surfaces in UHV via high temperature annealing in SiH4. Characterization via AES, EELS, LEED, XPS, and UPS was conducted. At T greater than 850 C, the surface oxide was rapidly removed. Exposure to approx. 400 Langmuir (10(exp -6) Torr(dot)liter/s) of SiH4 resulted in complete surface oxide removal and a nearly stoichiometric (l x l) 6H-SiC surface suitable for ALE of SiC. Further exposure resulted in a (3 x 3)R30 deg Si-rich reconstructed surface. Subsequent annealing in UHV resulted in a (square root of 3 x square root of 3)R30 deg Si deficient/graphitic reconstructed surface. The first set of wafers containing HBT device structures were fabricated on SiC films grown via ALE. No transistor activity was detected. Electrical characterization and SEM showed the most likely fault to be inaccurate etching of the SiC emitter. Nucleation and growth of oriented diamond particles on seeded, group of zone axes (0001) oriented single crystal Co substrates was achieved via multi-step, hot-filament CVD process involving seeding, annealing, nucleation and growth. Diamond particles oriented group of zone axes (111) were obtained. Micro-Raman showed a FWHM of 4.3/cm. A very weak graphitic peak was observed on regions of the substrate not covered by the diamond particles. A nucleation model has been proposed. Initial results showed that CeO2 film grows epitaxially on (111) Si substrates. The CeO2 films had density of interfacial traps and fixed oxide charge values comparable to that of amorphous SiO2/Si. DTIC

N95-28399# Sandia National Labs., Albuquerque, NM.
HETEROSTRUCTURES AND INFRARED EMITTERS WITH COMPRESSED InAsSb LAYERS
S. R. Kurtz and R. M. Biefeld 1995 7 p Presented at the International Conference on Narrow Gap Semiconductors, Santa Fe, NM, 9-12 Jan. 1995
(Contract DE-AC04-94AL-85000)
(DE95-008157; SAND-94-2478C; CONF-950167-1) Avail: CASI HC A02/MF A01

An overview is presented of strained InAsSb heterostructures and infrared emitters. InAsSb/InGaAs strained-layer superlattices (SLS) and InAsSb quantum wells were characterized using magneto-photoluminescence and compared with unstrained InAsSb and InAs alloys. In heterostructures with biaxially compressed InAsSb, large quantum confinement energies were observed, and the holes exhibited a decrease in effective mass, approaching that of the electrons. This study demonstrates that the electrons and holes in the InAsSb heterostructures are confined in the InAsSb layers, and the band offsets are type I. A large increase in the Auger-1 threshold energy should accompany the strain-induced change in valence-band symmetry of the InAsSb layers. Correspondingly, the InAsSb heterostructures display high radiative efficiencies and increased activation energies for nonradiative recombination compared with the unstrained alloys. LED's and L-mrs with InAsSb heterostructure active regions are described. InAsSb/InGaAs SLS LED's operating at 300 K at wavelengths less than or equal to 5 pm have been demonstrated. Optically pumped InAsSb/InGaAs SLS lasers, with InPSb cladding, had a maximum operating temperature of 100 K. DOE

N95-28522 Cornell Univ., Ithaca, NY. Lab. of Atomic and Solid State Physics.
FELLOWSHIP IN PHYSICS Final Report, Jan. 1993 - Dec. 1994
A. J. Sievers 2 Jan. 1995 11 p Limited Reproducibility: More than 20% of this document may be affected by microfiche quality
(Contract DAAL03-92-G-0349)
(AD-A291691; ARO-30627.1-RT-NDF) Avail: Issuing Activity (Defense Technical Information Center (DTIC))

The relaxation of molecular impurities in glasses has been gaining attention in recent years, partly due to the availability of novel spectroscopic techniques in the infrared region, including the development of powerful tunable infrared lasers needed to excite the vibrational transitions that are about 4 orders of magnitude weaker than electronic transitions. In general, glassy hosts offer the possibility to study the influence of a distribution the local environments on the static and dynamic properties of impurity atoms and molecules. Both persistent hole burning and picosecond IR pump-probe measurements show that the low temperature vibrational relaxation time of SH in As2S3 is also quite fast (approximately 10(exp-10) sec) even though temperature dependent measurements indicate that it corresponds to a seven phonon process. Equally interesting is that the relaxation time varies by a factor 6 across the inhomogeneously broadened band indicating a site-dependent interaction of the molecule with the host. A temperature dependence study indicated that the stretch mode relaxes through a multi-vibrational decay into modes of the glass host. We have also investigated the site-dependent vibrational relaxation dynamics of the OH molecular impurity in amorphous SiO2. At low temperatures, a short relaxation time of the order of 10(exp-10) sec is found that varies strongly across the inhomogeneously broadened absorption line, decreasing with increasing perturbation of the molecule by the host, similar to the results observed from As2S3:SH. A simple relation between the vibrational lifetime and the site-dependent frequency shift is found for both defect: glass systems by assuming that the molecule-host coupling determines both the shift of the vibrational frequency and the relaxation dynamics. DTIC

N95-28537# Oak Ridge National Lab., TN.
STRUCTURAL CHEMISTRY OF SOME PHASES IN THE YC-NI-B SYSTEM
B. C. Chakoumakos 1994 6 p Presented at the 1994 Fall Meeting of the Materials Research Society (MRS), Boston, MA, 28 Nov. - 2 Dec. 1994
(Contract DE-AC05-84OR-21400)
(DE95-007403; CONF-941144-76) Avail: CASI HC A02/MF A01

NiB, monoclinic Ni4B3, Ni2B and Ni3B were prepared by arc-melting and their room-temperature crystal structures were refined by Rietveld analysis of neutron powder diffraction data. The NiB refinement is altogether new data. Although the B atoms in NiB form characteristic zigzag chains, the primary coordination of each atom by atoms of the other kind is similar and distinctively sevenfold, with one short (2.117 angstrom), two intermediate (2.152 angstrom), and four long (2.163 angstrom) bonds. Other samples with stoichiometries (YC)(n)Ni2B2, n = 3, 4, did not yield single-phase material, but both x-ray and neutron powder diffraction suggest that the n = 4 structure is present in both of these samples. Phase-pure samples of these homologues may require non-stoichiometry and a more controlled thermal history than is attainable by arc melting. To screen samples for superconductivity, ac susceptibility measurements were made using the mutual inductance method with ac signal of 200 Hz. DOE

N95-28541# Los Alamos National Lab., NM.
SURFACE STRUCTURE OF MX-CHAINS STUDIED BY ATOMIC FORCE MICROSCOPY
G. Bar, B. Scott, S. R. Johnson, G. S. Kanner, and B. I. Swanson 1995 3 p Presented at the International Conference on Synthetic Metals (ICSM '94), Seoul, Korea, Aug. 1994
(Contract W-7405-eng-36)
(DE95-007881; LA-UR-95-539; CONF-9408219-1) Avail: CASI HC A01/MF A01

The surfaces of mixed-valence halogen-bridged transition metal linear chain compounds (Pt(en)2)(Pt(en))2(X(1-y)X'(y))2 (ClO4)(sub 4) (X, X' = Cl, Br, or I; en = C2H8N2; y = 0.0 - 1.0) were examined by atomic force microscopy (AFM). The AFM images are consistent with the surfaces expected from the bulk crystal structure. The surface unit cell parameters of the images correspond to the lattice constants of the bulk crystals. The patterns of the atomic-scale AFM images are dominated by the most protruded H atoms of the en ligands and the most protruded O atoms of the ClO4(-) anions. DOE

N95-28606# Oak Ridge National Lab., TN.
LOCAL TEXTURE AND GRAIN BOUNDARY MISORIENTATIONS IN HIGH H(C) OXIDE SUPERCONDUCTORS
D. M. Kroeger, A. Goyal, E. D. Specht, J. E. Tkaczyk (General Electric Co., Schenectady, NY.), J. Sutliff (General Electric Co., Schenectady, NY.), J. A. DeLuca (General Electric Co., Schenectady, NY.), Z. L. Wang (National Inst. of Standards and Technology, Gaithersburg, MD.), and G. N. Riley, Jr. (American Superconductor Corp., Westborough, MA.) 1995 27 p Presented at the 7th Conference on Superconductivity and Applications, Buffalo, NY, 7-9 Sep. 1994
(Contract DE-AC05-84OR-21400)
(DE95-007004; CONF-940926-5) Avail: CASI HC A03/MF A01

The orientations of hundreds of contiguous grains in high J(C) TlBa2Ca2Cu3O(x) deposits and (Bi, Pb)2 Sr2Ca2Cu3O(y) powder-in-tube tapes have been determined from electron back scatter diffraction patterns (EBSP). The misorientation angles and axes of rotation (angle/axis pairs) for grain boundaries connecting these grains were calculated. For both materials the population of low angle boundaries was found to be much larger than expected from calculations based on the macroscopic texture. The TlBa2Ca2Cu3O(x) deposits exhibit pronounced local texture which has been defined by EBSP and x-ray diffraction. Locally grains show significant in-plane (a-axis) alignment even though macroscopically a-axes are random, indicating the presence of colonies of grains with similar a-axis orientations. In (Bi, Pb)2 Sr2Ca2Cu3O(x) tapes no local texture was observed. In both materials the existence of connected networks of small angle grain boundaries can be inferred. Coincident site lattice (CSL) grain boundaries are also present in higher than expected numbers. Grain boundary energy thus appears to play a significant role in enhancing the population of potentially strongly-linked boundaries. We propose that long range strongly-linked conduction occurs through a percolative network small angle (and perhaps CSL) grain boundaries. DOE

N95-28608# International Centre for Theoretical Physics, Trieste (Italy).
SUBHARMONIC PHONON TRANSMISSION AND KAPITZA CONDUCTANCE BETWEEN CRYSTALS WITH VERY DIFFERENT VIBRATIONAL SPECTRA
Y. A. Kosevich Aug. 1994 12 p
(DE95-609151; IC-94/231) Avail: CASI HC A03/MF A01 (US Sales Only)

The low frequency resonant intrinsic vibrational modes are predicted to exist at the interface between two crystals with strongly different elastic properties. The interface resonant mode can stimulate the subharmonic nonlinear transmission of acoustic phonons and generation of the phonons with frequencies multiple to the resonant frequency. These inelastic processes can substantially contribute to the Kapitza thermal boundary conductance between solids with very different vibrational spectra (such as diamond and soft crystal) and to the thermal conductance across a helium-solid interface also. DOE

N95-28618 Ohio Univ., Athens, OH.
THE IN SITU OBSERVATION OF EPITAXIAL DIAMOND THIN FILM NUCLEATION AND GROWTH USING EMISSION ELECTRON MICROSCOPY Semiannual Technical Report, 1 Jan. - 30 Jun. 1994
Martin E. Kordesch 2 Jan. 1995 70 p Limited Reproducibility: More than 20% of this document may be affected by microfiche quality
(Contract N00014-91-J-1596)
(AD-A289841) Avail: Issuing Activity (Defense Technical Information Center (DTIC))

A variety of natural and chemical vapor deposited diamond surfaces have been imaged using a photoelectron emission microscope and synchrotron radiation in the 4-18 eV and 250-350 eV range. Both images and spatially resolved total electron yield curves were acquired simultaneously. Near-edge spectra at the carbon 1s edge show a resonance due to graphite; the image intensity varies uniformly in proportion to the C 1s edge intensity. In the 4-18 eV range, no sharp features related to a photoemission threshold were observed below 7 eV in the electron yield curves on any of the specimens. The image contrast was not strongly dependent on the illumination energy. Natural type 2a diamond showed severe charging effects. DTIC

77 THERMODYNAMICS AND STATISTICAL PHYSICS

Includes quantum mechanics; theoretical physics; and Bose and Fermi statistics.

For related information see also *25 Inorganic and Physical Chemistry* and *34 Fluid Mechanics and Heat Transfer.*

N95-26510 Polish Academy of Sciences, Warsaw (Poland). Energy-Saving Construction Design Methods Lab.
MATHEMATICAL MODELLING OF THE THERMODYNAMIC PROPERTIES OF COOLANTS AND WORKING MEDIA OF HEAT PUMPS [MATEMATYCZNE MODELOWANIE TERMODYNAMICZNYCH WLASCIWOSCI CZYNNIKOW CHLODNICZYCH I ROBOCZYCH POMP CIEPLA]
Hanna Jedrzejuk 1994 48 p In POLISH
(ISSN 0208-5658)
(IFTR-6/1994) Avail: Issuing Activity (Polish Academy of Sciences, Warsaw, Poland)

Equations for calculating the thermodynamic properties of coolants and working media of heat pumps are presented. The constants for these equations for properties R11, R12, R12B1, R13, R13B1, R22, R23, R113, R114, R115, R133a, R142b, R500, R502, and R503 are provided. The author describes a simplified method for determining the R12, R22, R114, R502, and R717 properties. Transl. by Schreiber Translations Inc.

N95-26563 Carnegie-Mellon Univ., Pittsburgh, PA. Dept. of Mathematics.
STABILITY AND THERMAL INFLUENCES IN NONLINEAR CONTINUUM MECHANICS AND MATERIAL SCIENCE Final Report
Morton E. Gurtin Jul. 1994 6 p Limited Reproducibility: More than 20% of this document may be affected by microfiche quality
(Contract DAAL03-91-G-0180)
(AD-A288333; ARO-28514.1-MA) Avail: Issuing Activity (Defense Technical Information Center (DTIC))

The final report summarizes the research efforts on stability and thermal influences in nonlinear continuum mechanics and material science. Research on phase transitions included solid-solid phase transitions in deformable continua, evolution of interfacial curves and generalized Stefen problems. Studies were also made of general continuum mechanics. DTIC

N95-26603# International Centre for Theoretical Physics, Trieste (Italy).
ANALYTIC FORMULAE FOR THE HARTREE-FOCK ORDER PARAMETER AT ARBITRARY p/q FILLING FACTORS FOR THE 2DEG IN A MAGNETIC FIELD
Alejandro CaboMontesdeOca Jul. 1994 15 p
(DE95-607805; IC-94/183) Avail: CASI HC A03/MF A01 (US Sales Only)

Analytic expressions for order parameters are given for the previously introduced general class of Hartree Fock states at arbitrary filling factors nu =p/q for odd q values. The order parameters are expressed as sums of magnetic translations eigenvalues over the filled single electron states. Simple summation formulae for the band spectra in terms of the same eigenvalues are also presented. The energy per particle at nu =1/3 is calculated for various states differing in the way of filling of the 1/3 of the orbitals. The calculated energies are not competing with the usual charge-density wave (CDW) results. However the high degree of electron overlapping allows for the next corrections to modify this situation. The discussion suggests these Hartree-Fock Slater determinants as interesting alternatives for the Tao-Thouless parent states which may correct their anomalous symmetry and correlation functions properties. DOE

N95-27310# International Centre for Theoretical Physics, Trieste (Italy).
FIELD THEORY OF POINT-LIKE SYSTEMS WITH HIGHER-ORDER DERIVATIVES
R. Constantinescu (Craiova Univ., Romania.) Aug. 1994 7 p
(DE95-608800; IC-94/215) Avail: CASI HC A02/MF A01 (US Sales Only)

Some similitudes between a point-like system and a field theory are pointed out. For the general case of a singular Lagrangian with higher-order derivatives the possibilities reducing the order are presented and the quantization on the basis of the extended BRST symmetry is done. The general theory is applied to the model of the relativistic particle with curvature. DOE

N95-27312# International Centre for Theoretical Physics, Trieste (Italy).
FINITE FERMION DENSITY EFFECTS ON THE ELECTROWEAK STRING
G. Bimonte and G. Lozano Aug. 1994 10 p
(DE95-608802; IC-94/224) Avail: CASI HC A02/MF A01 (US Sales Only)

We consider an electroweak string in the background of a uniform distribution of cold fermionic matter. As a consequence of the fermion number non-conservation in the Weinberg-Salam model, the string produces a long-range magnetic field. DOE

N95-27315# Joint Inst. for Nuclear Research, Dubna (USSR). Lab. of Theoretical Physics.
BOGOLYUBOV RENORMALIZATION GROUP [RENORMGRUPPA BOGOLYUBOVA]
D. V. Shirkov 1994 28 p In RUSSIAN Submitted for publication
(DE95-608830; JINR-R-2-94-310) Avail: CASI HC A03/MF A01 (US Sales Only)

We begin with personal notes addressing the birth of the 'Bogolyubov renormalization group.' Then we expose the history of the renormalization group (RG) discovery in QFT and of the RG method devised in the mid-fifties. Part three is devoted to the proliferation of the RG ideas into diverse parts of theoretical physics. We conclude with a discussion of the perspectives of the RG method, further development and its application in mathematical physics. DOE

N95-27332# International Centre for Theoretical Physics, Trieste (Italy).
QUANTUM k-POINCARE 1994
J. Lukierski, H. Ruegg (Geneva Univ., Geneva, Switzerland.), and V. N. Tolstoy (Moscow State Univ., Russia.) Aug. 1994 20 p
(DE95-608754; IC-94/250) Avail: CASI HC A03/MF A01 (US Sales Only)

After a description of three distinguished bases proposed for k-Poincare algebra, the representations of the k-deformed Poincare algebra as differential operators acting on the functions of commuting moments are considered. Further, the duality between the k-Poincare algebra U(sub n)(P(sub 4)) and the quantum Poincare group P(sub k) is discussed. The recent developments of the k-deformed formalism are presented in conclusion. DOE

N95-27333# International Centre for Theoretical Physics, Trieste (Italy).
ON THE HOPF STRUCTURE OF U(p,q)(gl(1/1)) AND THE UNIVERSAL TAU-MATRIX OF Fun(p,q)(GL(1/1))
R. Chakrabarti (Madras Univ., India.) and R. Jagannathan Aug. 1994 9 p
(DE95-608755; IC-94/254) Avail: CASI HC A02/MF A01 (US Sales Only)

Using the technique developed by Fronsdal and Galindo for studying the Hopf duality between the quantum algebras Fun(sub p,q)(GL(2)) and U(sub p,q)(gl(2)), the Hopf structure of U(sub p,q)(gl(1/1)), dual to Fun(sub p,q)(GL(1/1)), is derived and the corresponding universal (Tau)-matrix of Fun(sub p,q)(GL(1/1)), embodying the suitably modified exponential relationship U(sub p,q)(gl(1/1)) (yields) Fun(sub p,q)(GL(1/1)), is obtained. DOE

N95-27334# International Centre for Theoretical Physics, Trieste (Italy).
WIGNER QUANTUM OSCILLATORS. OSP (3/2) OSCILLATORS
T. D. Palev and N. I. Stoilova Aug. 1994 19 p
(DE95-608756; IC-94/259) Avail: CASI HC A03/MF A01 (US Sales Only)

The properties of the three-dimensional noncanonical osp(3/2) oscillators are further studied. The angular momentum M of the oscillators can take at most three values M = p-1, p, p+1, which are either all integers or all half-integers. The coordinates anticommute with each other. Depending on the state space the energy spectrum can coincide or can be essentially different from those of the canonical oscillators. The ground state is in general degenerated. DOE

N95-27336# Joint Inst. for Nuclear Research, Dubna (USSR). Lab. of High Energy.
THE ELECTRIC FIELD OF BOHR'S ATOM
V. N. Streltsov 1994 6 p
(DE95-608758; JINR-D-2-94-212) Avail: CASI HC A02/MF A01 (US Sales Only)

On the basis of the Lienard-Wiechert potential it is shown that the electric field of the simplest Bohr atom oscillates though the mean (per period) value is equal to zero. The calculation with the use of the generally accepted presentation of the moving charge field (in the form of spheroid) gives the mean value of electric potential different from zero. A detailed answer to the criticism of our approach to the known problem of the electric potential of a neutral current-carrying ring is given. DOE

N95-27447# Joint Inst. for Nuclear Research, Dubna (USSR).
N. N. BOGOLYUBOV AND PARTICLE PHYSICS [N. N. BOGOLYUBOV I FIZIKA CHASTITS]
A. N. Tavkhelidze (Academy of Sciences of the Georgian SSR, Tbilisi, Georgia.) 1994 15 p In RUSSIAN Presented at the Bogolyubov International Symposium on Fundamental Problems of Theoretical and Mathematical Physics, Dubna, Russia, 18-21 Aug. 1994
(DE95-608794; JINR-R-2-94-336) Avail: CASI HC A03/MF A01 (US Sales Only)

In this brief review I dwell upon the ideas belonging to N.N.Bogolyubov, which, in my opinion, made for the creation and development of the modern theory of strong interactions. DOE

N95-27448# Argonne National Lab., IL.
LATTICE QCD CALCULATION USING VPP500
Seyong Kim and Shigemi Ohta (Institute of Physical and Chemical Research, Saitama, Japan.) 1995 3 p Presented at the Lattice '94, Bielefeld, Germany, 25 Sep. - 1 Oct. 1994
(DE95-007076; ANL/HEP/CP-94-92; CONF-9409269-9) Avail: CASI HC A01/MF A01

A new vector parallel supercomputer, Fujitsu VPP500, was installed at RIKEN earlier this year. It consists of 30 vector computers, each with 1.6 GFLOPS peak speed and 256 MB memory, connected by a crossbar switch with 400 MB/s peak data transfer rate each way between any pair of nodes. The authors developed a Fortran lattice QCD simulation code for it. It runs at about 1.1 GFLOPS sustained per node for Metropolis pure-gauge update, and about 0.8 GFLOPS sustained per node for conjugate gradient inversion of staggered fermion matrix. DOE

N95-27449# Argonne National Lab., IL.
THE FREE ENERGY OF HOT QED AT THREE AND A HALF LOOPS
R. R. Parwani and C. Coriano 1995 4 p Presented at the Workshop on Quantum Infrared Physics, Paris, France, Jun. 1994
(DE95-007079; ANL/HEP/CP-94-52; CONF-9406248-6) Avail: CASI HC A01/MF A01

The computation of order e(sup 4) and e(sup 5) contributions to the pressure of massless quantum electrodynamics at a temperature T is overviewed. DOE

N95-27546# Oak Ridge National Lab., TN.
THERMODYNAMICS OF AQUEOUS ELECTROLYTES AT HIGH TEMPERATURES BY THE ISOPIESTIC TECHNIQUE
H. F. Holmes and R. E. Mesmer 1994 16 p Presented at the Conference on Properties of Water and Steam, Orlando, FL, 12 Sep. 1994
(Contract DE-AC05-84OR-21400)
(DE95-006747; CONF-9409219-4) Avail: CASI HC A03/MF A01

Excess thermodynamic properties of a wide variety of aqueous electrolyte solutions at elevated temperatures have been determined with the ORNL high-temperature isopiestic facility. This unique experimental apparatus provides very precise results over the useful temperature range of 110 to 250 C. The isopiestic method is a comparative technique which, in the present case, uses the Pitzer-Peiper-Busey formulation for NaCl(aq) as the reference electrolyte. At elevated temperatures the ion-interaction model of Pitzer continues to be the most useful description of the experimental results. The authors experimental program has included the alkali metal chlorides, sulfates, hydroxides, bromides, and bisulfates, the alkaline earth metal chlorides, and several specific compounds of scientific and practical interest. Numerous common-ion mixed electrolyte solutions have also been investigated in this program. In general, the activity coefficients of all the studied electrolytes decrease with increasing temperature. However, prominent differences between members of the same family remain, particularly when considered as the excess Gibbs free energy. The tendency for ion association increases with increasing temperature and becomes a factor at the higher temperatures. Trends and specific effects are illustrated with examples taken from the database generated in their high-temperature thermodynamic program. DOE

N95-27547# Washington Univ., Seattle, WA.
THE GLUON PROPAGATOR IN NON-ABELIAN WEIZSAECKER-WILLIAMS FIELDS
A. Ayala, J. Jalilian-Marian, L. McLerran, and R. Venugopalan Jan. 1995 23 p
(Contract DE-FG06-90ER-40561)
(DE95-006877; DOE/ER-40561/175) Avail: CASI HC A03/MF A01

The authors carefully compute the gluon propagator in the background of a non-Abelian Weizsaecker-Williams field. This background field is generated by the valence quarks in very large nuclei. They find contact terms in the small fluctuation equations of motion which induce corrections to a previously incorrect result for the gluon propagator in such a background field. The well known problem of the Hermiticity of certain operators in Light Cone gauge is resolved for the Weizsaecker-Williams background field. This is achieved by working in a gauge where singular terms in the equations of motion are absent and then gauge transforming the small fluctuation fields to Light Cone gauge. DOE

N95-27877# California Univ., Berkeley. Lawrence Berkeley Lab, CA.
REALIZATION OF VECTOR FIELDS FOR QUANTUM GROUPS AS PSEUDODIFFERENTIAL OPERATORS ON QUANTUM SPACES
Chong-Sun Chu and B. Zumino 24 Jan. 1995 16 p Presented at the 20th International Conference on Group Theory Methods in Physics, Toyonak, 24 Jan. 1995
(Contract DE-AC03-76SF-00098)
(DE95-008485; LBL-36746; CONF-950175-1) Avail: CASI HC A03/MF A01

The vector fields of the quantum Lie algebra are described for the quantum groups GL(sub q)(n), SL(sub q)(N) and SO(sub q)(N) as pseudodifferential operators on the linear quantum spaces covariant under the corresponding quantum group. Their expressions are simple and compact. It is pointed out that these vector fields satisfy certain characteristic polynomial identities. The real forms SU(sub q)(N) and SO(sub q)(N,R) are discussed in detail. DOE

N95-28137# Stanford Linear Accelerator Center, Menlo Park, CA
BIT-STRING PHYSICS: A NOVEL THEORY OF EVERYTHING
H. P. Noyes Aug. 1994 8 p Presented at PhysComp 1994: Workshop on Physics and Computation, Dallas, TX, 17-20 Nov. 1994
(Contract DE-AC03-76SF-00515)
(DE95-005941; SU-SLAC-PUB-6509; CONF-9411171-1) Avail: CASI HC A02/MF A01

We encode the quantum numbers of the standard model of quarks and leptons using constructed bitstrings of length 256. These label a grouting universe of bit-strings of growing length that eventually construct a finite and discrete space-time with reasonable cosmological properties. Coupling constants and mass ratios, computed from closure under XOR and a statistical hypothesis, using only (h bar), c and m(sub p) to fix our units of mass, length and time in terms of standard (meterkilogram-second) metrology, agree with the first four to seven significant figures of accepted experimental results. Finite and discrete conservation laws and commutation relations insure the essential characteristics of relativistic quantum mechanics, including particle-antiparticle pair creation. The correspondence limit in (free space) Maxwell electromagnetism and Einstein gravitation is consistent with the Feynman-Dyson-Tanimura proof. DOE

N95-28160# Stanford Linear Accelerator Center, Stanford, CA.
EFFICIENT ANALYTIC COMPUTATION OF HIGHER-ORDER QCD AMPLITUDES
Z. Bern, G. Chalmers, L. Dixon, D. C. Dunbar, and D. A Kosower 1995 3 p Presented at the 4th International Conference on Physics Beyond the Standard Model, Lake Tahoe, CA, 13-18 Dec. 1994
(Contracts DE-AC03-76SF-00515; DE-FG03-91ER-40662)
(DE95-008593; SU-SLAC-PUB-95-6771; CONF-941251-2) Avail: CASI HC A01/MF A01

The authors review techniques simplifying the analytic calculation of one-loop QCD amplitudes with many external legs, for use in next-to-leading-order corrections to multi-jet processes. Particularly useful are the constraints imposed by perturbative unitarity, collinear singularities and a supersymmetry-inspired organization of helicity amplitudes. Certain sequences of one-loop helicity amplitudes with an arbitrary number of external gluons have been obtained using these constraints. DOE

N95-28175# Institut des Hautes Etudes Scientifiques, Bures-sur-Yvette (France).
WAS EINSTEIN 100% RIGHT?
T. Damour Nov. 1994 17 p Prepared in cooperation with Observatoire de Paris, France
(PB95-190179; IHES/P/94/61) Avail: CASI HC A03/MF A01

The confrontation between General Relativity and experimental results, notably binary pulsar data, is summarized and its significance discussed. The agreement between experiment and theory is numerically very impressive. However, some recent theoretical findings (existence of non-perturbative strong-field effects, natural cosmological attraction toward zero scalar couplings) suggest that the present agreement between Einstein's theory and experiment might be a red herring and provide new motivations for improving the experimental tests of gravity. NTIS

N95-28183# Joint Inst. for Nuclear Research, Dubna (USSR).
QUANTUM RETRODICTION AND CAUSALITY PRINCIPLE
M. I. Shirokov 1994 12 p
(DE94-628438; JINR-E-4-94-4) Avail: CASI HC A03/MF A01 (US Sales Only)

Quantum mechanics is factually a predictive science. But quantum retrodiction may also be needed, e.g., for the experimental verification of the validity of the Schroedinger equation for the wave function in the past if the present state is given. It is shown that in the retrodictive analog of the prediction the measurement must be replaced by another physical process called the retromeasurement. In this process, the reduction of a state vector into eigenvectors of a measured observable must proceed in the opposite direction of time as compared to the usual reduction. Examples of such processes are unknown. Moreover, they are shown to be forbidden by the causality principle stating that the later event cannot influence the earlier one. So quantum retrodiction seems to be unrealizable. It is demonstrated that the approach to the retrodiction given by S.Watanabe and F.Belinfante must be considered as an unsatisfactory ersatz of retrodicting. DOE

N95-28260*# Rockwell International Corp., Downey, CA. Space Systems Div.
TASK 4 SUPPORTING TECHNOLOGY. DENSIFICATION REQUIREMENTS DEFINITION AND TEST OBJECTIVES. PROPELLANT DENSIFICATION REQUIREMENTS DEFINITION
Tibor Lak and D. P. Weeks 30 May 1995 22 p
(Contract NCC8-79)
(NASA-CR-198629; NAS 1.26:198629; SSD95D0241) Avail: CASI HC A03/MF A01

The primary challenge of the X-33 CAN is to build and test a prototype LO2 and LH2 densification ground support equipment (GSE) unit, and perform tank thermodynamic testing within the 15 month phase 1 period. The LO2 and LH2 propellant densification system will be scaled for the IPTD LO2 and LH2 tank configurations. The IPTD tanks were selected for the propellant technology demonstration because of the potential benefits to the phase 1 plan: tanks will be built in time to support thermodynamic testing; minimum cost; minimum schedule risk; future testing at MSFC will build on phase 1 data base; and densification system will be available to support X-33 and RLV engine test at IPTD. The objective of the task 1 effort is to define the preliminary requirements of the propellant densification GSE and tank recirculation system. The key densification system design parameters to be established in Task 1 are: recirculation flow rate; heat exchanger inlet temperature; heat exchanger outlet temperature; maximum heat rejection rate; vent flow rate (GN2 and GH2); densification time; and tank pressure level. Derived from text

N95-28664# Institut des Hautes Etudes Scientifiques, Bures-sur-Yvette (France).
GENERAL RELATIVITY AND EXPERIMENT
T. Damour Oct. 1994 16 p See also PB92-125012 Prepared in cooperation with Observatoire de Paris
(PB95-192894; IHES/P/94/56) Avail: CASI HC A03/MF A01

The confrontation between Einstein's theory of gravitation and experiment is summarized. Although all the current experimental data are compatible with General Relativity, the importance of pursuing the quest for possible deviations from Einstein's theory is emphasized. NTIS

80 SOCIAL SCIENCES (GENERAL)

Includes educational matters.

N95-26803# Technische Univ., Delft (Netherlands). Faculty of Technical Mathematics and Informatics.
NEXTSTEP: THE NEXT STEP IN THE RIGHT DIRECTION? PART 2: SOFTWARE DEVELOPMENT WITH NEXTSTEP [NEXTSTEP: DE VOLGENDE STAP IN DE GOEDE RICHTING? PART 2: SOFTWARE ONTWIKKELEN MET NEXTSTEP]
D. B. Tischenko and B. R. Sodoyer 1994 36 p In DUTCH
(Rept-94-33-Pt-2; ETN-95-97538) Copyright Avail: CASI HC A03/MF A01

Software development using the development environment NEXTSTEP for computer aided education is presented. The NEXTSTEP development tools and software architecture are described, with emphasis on one of the most important development tools, the NEXTSTEP Interface Builder. The available object libraries and the standard NEXTSTEP programming language, Objective C, are described. Possible application domains for NEXTSTEP as development environment are given. The first experience shows that NEXTSTEP opens perspectives for object oriented development and maintenance of software. Author

81 ADMINISTRATION AND MANAGEMENT

Includes management planning and research.

N95-26353# Advisory Group for Aerospace Research and Development, Neuilly-Sur-Seine (France).
AGARD MEMBERSHIP, 1995 [LES MEMBRES DE L'AGARD, 1995]
Mar. 1995 76 p
(AGARD-Memb-95) Copyright Avail: CASI HC A05/MF A01

This publication contains lists of members of the National Delegates Board of AGARD; the Steering Committee; AGARD national coordinators; technical panels; the Technical Information Committee; and the Aerospace Applications Studies Committee as of 1 Feb. 1995. It also contains a list of the staff of AGARD headquarters. Each list is separated by participating country and contains address, phone number, and fax number with each name. Derived from text

N95-27064 Carnegie-Mellon Univ., Pittsburgh, PA. School of Computer Science.
AUTOMATICALLY SELECTING AND USING PRIMARY EFFECTS IN PLANNING: THEORY AND EXPERIMENTS
Eugene Fink and Qiang Yang Oct. 1994 41 p Sponsored in part by the Natural Science and Engineering Research Council of Canada Limited Reproducibility: More than 20% of this document may be affected by microfiche quality
(Contract F33615-93-1-1330)
(AD-A289347; CMU-CS-94-206) Avail: Issuing Activity (Defense Technical Information Center (DTIC))

Using primary effects of operators in planning is an effective approach to reducing planning time and improving solution quality. However, the characterization of 'good' primary effects has remained at an informal level. In addition, no method has previously been known to automatically learn the primary effects of operators from a given domain specification. In this paper we formalize the use of primary effects in planning, present a criterion for selecting useful primary effects that guarantee the efficiency and completeness of planning, and prove the near-optimality of solutions found by planning with primary effects. Based on the formalization, we describe an inductive learning algorithm that automatically selects primary effects of operators. We show that the learning algorithm performs efficiently, producing plans that are near-optimal with high probability. We also empirically demonstrate the effectiveness of the learned primary effects in reducing search. DTIC

N95-27169*# Procurement Automation Inst., Arlington, VA.
AUTOMATED PROCUREMENT SYSTEM (APS) REVISED PROJECT MANAGEMENT PLAN (DS-03) Final Report
Diane R. Murphy 3 May 1995 61 p
(Contract NAS8-39897)
(NASA-CR-196605; NAS 1.26:196605; NASA-04) Avail: CASI HC A04/MF A01

The Project Plan is the governing document for the implementation of the Automated Procurement System (APS). It includes a description of the proposed system, describes the work to be done, establishes a schedule of deliverables, and discusses the major standards and procedures to be followed. Author

N95-27202 National Inst. of Standards and Technology, Gaithersburg, MD.
STANDARDS FOR EXCELLENCE (Videotape)
1992 Videotape: 28 min. playing time, in color, with sound
(NONP-NASA-VT-95-49096) Avail: CASI VHS A02/BETA A22

A history of the development of standard units and regulations of measurement are discussed in this educational video. John Aston narrates the historical background, from colonial times to the present, of the need for measurement standardization and discusses the conception of the National Bureau of Standards (1901), of the United States Department of Commerce. Historical photography and film footage is included. CASI

N95-27205 National Inst. of Standards and Technology, Gaithersburg, MD.
QUEST FOR EXCELLENCE 5 (Videotape)
1992 Videotape: 18 min. 30 sec. playing time, in color, with sound
(NONP-NASA-VT-95-49099) Avail: CASI VHS A02/BETA A22

The highlights of the 1992 Malcolm Baldrige National Quality Award winners - AT and T Network Systems Group, Transmission Systems Business Unit; Texas Instrument Defense Systems and Electronics Group; AT and T Universal Card Services; The Ritz Hotel CO; and The Granite Rock Company are presented, along with brief information about the company and their beliefs and business and production strategies for quality manufacturing and products. Author (revised)

N95-27206 National Inst. of Standards and Technology, Gaithersburg, MD.
GETTING IT RIGHT, MAKING IT BETTER (Videotape)
1992 Videotape: 15 min. 5 sec. playing time, in color, with sound
(NONP-NASA-VT-95-49118) Avail: CASI VHS A02/BETA A22

The research into the advancement of software error compensation techniques is discussed in this video. Although these techniques were originally designed for coordinate measuring machines, they are now used for machine tools as well. Author (revised)

N95-27207 National Inst. of Standards and Technology, Gaithersburg, MD.
MALCOLM BALDRIGE NATIONAL QUALITY AWARD WINNERS 1989 (Videotape)
1990 Videotape: 14 min. 30 sec. playing time, in color, with sound
(NONP-NASA-VT-95-49119) Avail: CASI VHS A02/BETA A22

The 1989 Malcolm Baldrige award winners - Milliken and Company; and Xerox Business Products and Services are highlighted in this video. Their strategies for producing quality products are discussed, along with their applications and importance in today's competitive workplace. CASI

N95-27209 National Inst. of Standards and Technology, Gaithersburg, MD.
STEP: A FUTUREVISION, TODAY (Videotape)
[1994] Videotape: 9 min. 50 sec. playing time, in color, with sound
(NONP-NASA-VT-95-49121) Avail: CASI VHS A02/BETA A22

STEP (STandard for the Exchange of Product Model Data) is an innovative software tool that allows the exchange of data between different programming systems to occur and helps speed up the designing in various process industries. This exchange occurs easily between those companies that have STEP, and many industries and government agencies are requiring that their vendors utilize STEP in their computer aided design projects, such as in the areas of mechanical, aeronautical, and electrical engineering. STEP allows the process of concurrent engineering to occur and increases the quality of the design product. One example of the STEP program is the Boeing 777, the first paperless airplane. CASI

N95-28025# Los Alamos National Lab., NM.
IMPLEMENTING AN INTEGRATED STANDARDS-BASED MANAGEMENT SYSTEM TO ENSURE COMPLIANCE AT LOS ALAMOS NATIONAL LABORATORY
D. Hjeresen, S. Roybal, P. Bertino, C. Gherman, and B. Hosteny 1995 10 p Presented at the Waste Management 1995, Tucson, AZ, 26 Feb. - 2 Mar. 1995
(Contract W-7405-eng-36)
(DE95-007873; LA-UR-95-420; CONF-950216-71) Avail: CASI HC A02/MF A01

Los Alamos National Laboratory (LANL or the Laboratory) is developing and implementing a comprehensive, Integrated Standards-Based Management System (ISBMS) to enhance environmental, safety, and health (ESH) compliance efforts and streamline management of ESH throughout the Laboratory. The Laboratory recognizes that to be competitive in today's business environment and attractive to potential Partnerships, Laboratory operations must be efficient and cost-effective. The Laboratory also realizes potential growth opportunities for developing ESH as a strength in providing new or improved services to its customers. Overall, the Laboratory desires to establish and build upon an ESH management system which ensures continuous improvement in protecting public health and safety and the environment and which fosters a working relationship with stakeholders. A team of process experts from the LANL Environmental Management (EM) Program Office, worked with management system consultants, and the Department of Energy (DOE) to develop an ESH management systems process to compare current LANL ESH management Systems and programs against leading industry standards. The process enabled the Laboratory to gauge its performance in each of the following areas: Planning and Policy Setting; Systems and Procedures; Implementation and Education; and Monitoring and Reporting. The information gathered on ESH management systems enabled LANL to pinpoint and prioritize opportunities for improvement in the provision of ESH services throughout the Laboratory and ultimately overall ESH compliance. DOE

N95-28135# Helsinki Univ. of Technology, Espoo (Finland). Dept. of Mechanical Engineering.
LABORATORY OF PRODUCTION ENGINEERING
M. Seppaelae 1994 9 p
(PB95-184834; KPT-7-94) Avail: CASI HC A02/MF A01

The operation of the laboratory consists of two main areas: education and research. The aim of the education area is to provide capable engineers for the Finnish manufacturing industry. The aim of the research is to support the Finnish manufacturing industry with its research and development, and to create new technologies in the field of manufacturing engineering. The clients of the laboratory are students, industry and the scientific world. NTIS

N95-28308 Edgerton, Germeshausen and Grier, Inc., Cocoa Beach, FL.
CAPE CANAVERAL AIR STATION LAUNCH EMERGENCY RESPONSE FORCES AND TOXIC MATERIALS RELEASE CONTINGENCY PLANS
S. W. Brown *In* Johns Hopkins Univ., The 1994 JANNAF Safety and Environmental Protection Subcommittee Meeting, Volume 1 Aug. 1994 p 143-148 (For primary document see N95-28294 09-20)
Avail: CPIA, 10630 Little Patuxent Pkwy., Suite 202, Columbia, MD 21044-3200 HC

N95-28316 Martin Marietta Corp., San Diego, CA.
DEVELOPMENT AND IMPLEMENTATION OF A SYSTEM SAFETY PROGRAM FOR THE SPACE LAUNCH COMPLEX 3 EAST (SLC-3E) GROUND SUPPORT SYSTEM PROJECT TO SUPPORT ATLAS 2 FAMILY OF SPACE LAUNCH VEHICLES
S. Iyengar and M. McCombs (Air Force Systems Command, Vandenberg AFB, CA.) *In* Johns Hopkins Univ., The 1994 JANNAF Safety and Environmental Protection Subcommittee Meeting, Volume 1 Aug. 1994 p 239-249 (For primary document see N95-28294 09-20)
(Contract F04701-92-C-0019)
Avail: CPIA, 10630 Little Patuxent Pkwy., Suite 202, Columbia, MD 21044-3200 HC

82 DOCUMENTATION AND INFORMATION SCIENCE

Includes information management; information storage and retrieval technology; technical writing; graphic arts; and micrography.

For computer documentation see *61 Computer Programming and Software.*

N95-26535 Carnegie-Mellon Univ., Pittsburgh, PA. Dept. of Computer Science.
LONG TERM DISTRIBUTED FILE REFERENCE TRACING: IMPLEMENTATION AND EXPERIENCE
L. Mummert and M. Satyanarayanan Nov. 1994 32 p Sponsored by Digital Equipment Corp.; and IBM Limited Reproducibility: More than 20% of this document may be affected by microfiche quality
(Contract F19628-93-C-0193; NSF ECD-89-07068)
(AD-A288585; CMU-CS-94-213) Avail: Issuing Activity (Defense Technical Information Center (DTIC))

DFSTrace is a system to collect and analyze long-term file reference data in a distributed UNIX workstation environment. The design of DFSTrace is unique in that it pays particular attention to efficiency, extensibility, and the logistics of long-term trace data collection in a distributed environment. The components of DFSTrace are a set of kernel hooks, a kernel buffer mechanism, a data extraction agent, a set of collection servers, and post-processing tools. Our experience with DFSTrace has been highly positive. Tracing has been virtually unnoticeable, degrading performance 3-7%, depending on the level of detail of tracing. We have collected file reference traces from approximately 30 workstations continuously for over two years. We have implemented a post-processing library to provide a convenient programmer interface to the traces, and have created an on-line database of results from a suite of analysis programs to aid trace selection. Our data has been used for a wide variety of purposes, including file system studies, performance measurement and tuning, and debugging. Extensions of DFSTrace have enabled its use in applications such as field reliability testing and determining disk geometry. This paper presents the design, implementation, and evaluation of DFSTrace and associated tools, and describes how they have been used. DTIC

N95-26607 Defense Mapping Agency Aerospace Center, Saint Louis, MO. Directorate of Production Systems.
VECTOR SMART MAP LEVEL 1: A NEW DMA PRODUCT
Tony Moore, Richard Glass, David Wesloh, and Joyce A. Hoffman 1994 12 p Limited Reproducibility: More than 20% of this document may be affected by microfiche quality
(AD-A288920) Avail: Issuing Activity (Defense Technical Information Center (DTIC))

The capability to produce Vector Smart Map Level 1 (VMap Level 1) is a new development within the Defense Mapping Agency (DMA). VMap Level 1 is a vector-based product currently derived from 1:250,000 cartographic source and designed to support Geographic Information System (GIS) applications with geographic data at medium resolutions. This paper will discuss the purpose, data structure, and content of the VMap Level 1 data base. This paper will further describe the extraction, finishing, and distribution processes involved in the creation of VMap Level 1. DTIC

N95-26631# Helsinki Univ. of Technology, Espoo (Finland). Dept. of Computer Science.
[ACTIVITIES OF THE LABORATORY OF INFORMATION PROCESSING SCIENCE] Annual Report, 1993
Vesa Hirvisalo, ed. 1994 52 p
(PB95-184982; TKO-C67) Avail: CASI HC A04/MF A01

The report covers the activities in the laboratory during the year 1993. It is meant to give an overview of the laboratory. It does not discuss the various activities of the laboratory in detail. The report concentrates on describing the research done in the laboratory. Research projects are grouped together to form research areas. Organization and personnel of the laboratory are only briefly shown. The annual bibliography is included. NTIS

N95-26673*# National Aeronautics and Space Administration, Washington, DC.
INDEX TO NASA NEWS RELEASES AND SPEECHES 1994
Apr. 1995 78 p
(NASA-TM-110650; NAS 1.15:110650) Avail: CASI HC A05/MF A01

This index contains a listing of news releases distributed by the Office of Public Affairs, NASA Headquarters, and a selected listing of speeches presented by members of the Headquarters staff during 1994. Author

N95-26721 Massachusetts Inst. of Tech., Lexington, MA.
BIBLIOGRAPHY OF PATENTS AND LICENSES 1951-1990. 1991 EDITION
Robert G. Hall, Jean E. King, and Mary L. Murphy 1994 77 p Limited Reproducibility: More than 20% of this document may be affected by microfiche quality
(Contract F19628-90-C-0002)
(AD-A289603; Rept-17-1015; ESC-TR-94-101) Avail: Issuing Activity (Defense Technical Information Center (DTIC))

Since its establishment in 1951, MIT Lincoln Laboratory has actively pursued its mission to 'Carry out a program of research and development pertinent to national defense with particular emphasis on advanced electronics.' Toward this end, the Laboratory promotes scientific and technological research providing the best solutions to address the needs of the nation. By patenting anti licensing inventions, technology originally developed to meet the specific needs of the Department of Defense and other government agencies can be applied to solve problems in the civilian sector; this substantially benefits the nation's economy and serves as an impetus for improving society worldwide. DTIC

N95-26752 Carnegie-Mellon Univ., Pittsburgh, PA. School of Computer Science.
FLEXIBLE AND SAFE RESOLUTION OF FILE CONFLICTS
Puneet Kumar and Mahadev Satyanarayanan Nov. 1994 16 p Submitted for publication Limited Reproducibility: More than 20% of this document may be affected by microfiche quality
(Contract F19628-93-C-0193)
(AD-A289342; CMU-CS-94-214) Avail: Issuing Activity (Defense Technical Information Center (DTIC))

In this paper we describe the support provided by the Coda File System for transparent resolution of conflicts arising from concurrent updates to a file in different network partitions. Such partitions often occur in mobile computing environments. Coda provides a framework for invoking customized pieces of code called application-specific resolvers (ASR's) that encapsulate the knowledge needed for file resolution. If resolution succeeds, the user notices nothing more than a slight performance delay. Only if resolution fails does the user have to resort to manual repair. Our design combines a rule-based approach to ASR selection with transactional encapsulation of ASR execution. This paper shows how such an approach leads to flexible and efficient file resolution without loss of security or robustness. DTIC

N95-26758 Naval Postgraduate School, Monterey, CA.
ANALYSIS, DESIGN AND IMPLEMENTATION OF A DATABASE SYSTEM FOR THE SYSTEMS MANAGEMENT CURRICULUM OFFICE M.S. Thesis
Sufian I. Althawadi and Barry D. Hubbard Sep. 1994 142 p Limited Reproducibility: More than 20% of this document may be affected by microfiche quality
(AD-A289656) Avail: Issuing Activity (Defense Technical Information Center (DTIC))

The Systems Management Curricular Office at the Naval Postgraduate School is burdened with the enormous administrative task of managing files for over 500 students. In a time of drastic military downsizing and funding cuts, this task will require more work of a smaller staff with less money. The burden of paper management could be lessened through automation of record keeping, while increasing efficiency and effectiveness. Valuable time for the students could be saved through elimination of excessive paperwork which they were required to prepare. Based on requirements from the Systems Management Curricular Office, this thesis designs and implements a database management system. The primary objective is to allow the incoming class of students to enroll using this system instead of traditional paper forms, enabling the staff to focus on more non-administrative tasks. This system will store, sort and compare data relevant to all students while minimizing the need to maintain hardcopy files. Additionally, the staff will be able to query reports and generate letters with minimal effort. The system is also analyzed to determine possible enhancements that could be added in the future. The Systems Management Database Systems (SMDS) is designed using Borland's PARADOX version 4.0. DTIC

N95-26864 Arizona State Univ., Tempe, AZ.
A DEMONSTRATION OF CLIENT/SERVER TECHNOLOGY USING REMOTE PROCEDURE CALLS FOR AN APPLICATION OF FILE MIGRATION FOR MOVING RECORDS BASED ON LOCATION M.S. Thesis
Andrea Miller 1 Dec. 1994 65 p Limited Reproducibility: More than 20% of this document may be affected by microfiche quality
(AD-A289391) Avail: Issuing Activity (Defense Technical Information Center (DTIC))

Client/Server Computing is one of the newest technologies in distributed systems. It allows different computers to communicate and share resources. The idea is relatively simple however, the underlying factors make it difficult. This paper explores the use of remote procedure calls (RPC) to create a distributed, client/server application. The presentation includes a discussion of RPC along with a simple application that introduces the reader to RPC. Finally, an application in the area of file migration is presented. The program is designed to receive a requested file from the user, it then accesses a file to find the location of the requested record and then the record is retrieved. For the purpose of the simulation the file is transferred when it is located in a different place than that of its owner. While this is not a complex file migration algorithm it lends itself to such applications as moving personnel records, dynamically, so that they reside in the same location as their owner in order to facilitate communication and reduce costs. Similarly, another application might involve having medical records follow a person from place to place. It is easy to see that client/server computing has the potential to be powerful and tools such as remote procedure calls are essential to this technology. DTIC

N95-26866 Air Force Inst. of Tech., Wright-Patterson AFB, OH. School of Engineering.
THE RE-ENGINEERING OF THE AIR FORCE INSTITUTE OF TECHNOLOGY STUDENT INFORMATION SYSTEM M.S. Thesis
Douglas J. Wu Dec. 1994 142 p Limited Reproducibility: More than 20% of this document may be affected by microfiche quality
(AD-A289426; AFIT/GCS/ENG/94D-27) Avail: Issuing Activity (Defense Technical Information Center (DTIC))

This research describes the design and implementation issues associated with re-engineering the Air Force Institute of Technology Student Information System (AFITSIS). Currently, AFITSIS executes on aging relational database technology and has unfriendly user interface mechanisms. The two research objectives met were to research current AFITSIS requirements, design, and implementation, and use object-oriented methods to design an alternative implementation based on proposed object database management system standards. This research explores how AFITSIS performance and capabilities might be enhanced by taking advantage of new object-oriented software engineering techniques. One of the primary benefits of this research is a detailed object modeling technique analysis and design that may be used as a foundation for upgrading the current AFITSIS. DTIC

N95-26879 Air Force Inst. of Tech., Wright-Patterson AFB, OH.
A DEMONSTRATION OF CLIENT-SERVER TECHNOLOGY USING REMOTE PROCEDURE CALLS WITH AN APPLICATION OF FILE MIGRATION FOR MOVING RECORDS BASED ON TIME M.S. Thesis
Andrew C. Jank Dec. 1994 71 p Limited Reproducibility: More than 20% of this document may be affected by microfiche quality
(AD-A289392; AFIT/CI/CIA/94-155) Avail: Issuing Activity (Defense Technical Information Center (DTIC))

As the computing resources of the world are quickly becoming integrated into a vast network of interconnected machines, client/server technology is becoming more prevalent as a method to utilize unused resources and to distribute complex systems. Remote Procedure Calls (RPC's) serve as one of the means to implement this technology. This report, combined with those produced by 2nd Lt. Andrea Miller and 2nd Lt. Eric DeLange, provide an overview of both the complexity and the benefits of using RPC in a distributed environment. The report initially investigates the fundamentals of RPC and follows with a discourse of RPC's suitability for implementation as a means for computer-integrated file migration. The report presents an application involving RPC for timed file migration and concludes with a discussion of implementing user-friendly front-ends to hide the complex nature of RPC from the user. This specific application investigates the applicability of RPC to developing a distributed file migration application. The application allows the user to access files that may reside on various hosts by querying a central database for a file's location via RPC. Some of the files, however, are dynamically relocated, based on a timing procedure. This could be very advantageous for global organizations that maintain a core set of organization files that must be accessed at a specific time of day (which, of course varies, depending on the time zone of the requester). DTIC

N95-27004 Army Engineer Waterways Experiment Station, Vicksburg, MS. Information Technology Lab.
RESEARCH AND DEVELOPMENT MANAGEMENT INFORMATION SYSTEM, SYSTEM USER MANUAL Final Report
Jennifer Rabert, Peggy Wright, and Phyllis Krug Nov. 1994 36 p Limited Reproducibility: More than 20% of this document may be affected by microfiche quality
(AD-A289151; WES/IR/ITL-94-3) Avail: Issuing Activity (Defense Technical Information Center (DTIC))

The Research and Development Management Information System (RDMIS) is a multi-user system. Each site requires a system user who is the RDMIS point of contact to support the needs of the RDMIS users. A system user is responsible for maintaining site access, security, and administration of RDMIS whether networked or stand alone. This document provides the system user with information necessary to effectively maintain RDMIS. DTIC

N95-27014 Naval Command, Control and Ocean Surveillance Center, San Diego, CA. Research, Development, Technology and Evaluation Div.
SEMANTIC HETEROGENEITY IN DATABASE AND DATA DICTIONARY INTEGRATION FOR COMMAND AND CONTROL SYSTEMS
M. G. Ceruti and M. N. Kamel Oct. 1994 27 p Limited Reproducibility: More than 20% of this document may be affected by microfiche quality
(AD-A289180) Avail: Issuing Activity (Defense Technical Information Center (DTIC))

Semantic heterogeneity has been investigated in connection with the database and data dictionary integration efforts that support Command, Control, Communications and Intelligence (C3I) systems. Based on this investigation, a systematic approach to the resolution of semantic heterogeneity has been developed and illustrated with examples derived from the component C3I system databases in a federation. A methodology is introduced for resolving semantic conflicts to construct a tightly coupled federated database system by facilitating the development of a global schema derived from the individual schemas of the component databases. This methodology of resolving semantic conflicts results in the formation and modification of synonym-homonym groups (SHG), a concept introduced and developed in the paper. A detailed analysis using a three-phased procedure is introduced, with each phase exploring semantic heterogeneity at progressively finer levels of information granularity. For the purpose of illustration, the simplest case of a two-component database integration into a tightly coupled federated database system is considered, but the methodology can be generalized to include three or more component databases in a federated system. It also can be applied in the case of a fully merged database integration involving any number of component databases. A variety of inconsistencies were identified using the heuristics implemented in the algorithm. Resolutions of the problems arising from semantic heterogeneity are suggested, and directions for future research are explored. DTIC

N95-27063 Carnegie-Mellon Univ., Pittsburgh, PA. Dept. of Computer Science.
SCALABILITY IN PRODUCTION SYSTEM PROGRAMS Ph.D. Thesis
Anurag Acharya 1994 368 p Limited Reproducibility: More than 20% of this document may be affected by microfiche quality
(AD-A289345; CMU-CS-94-211) Avail: Issuing Activity (Defense Technical Information Center (DTIC))

Production system programs have been notorious for their inability to handle large data sets. The primary cause of their poor scalability is the combinatorial explosion in the number of possible matches which arises from the need to match conjunctive conditions where each conjunct can match the whole data set. This dissertation investigates two approaches for handling large data sets in production system programs - scalable parallelism and scalable match algorithms. The primary limitation on parallelism in production system programs is the data-dependent nature of the computation combined with a lack of information about the run-time contents of the tuple-space. This dissertation argues that effective parallelization of production system programs requires information about the run-time contents of the tuple-space. Results from a simulation study show that simple extensions to existing production system languages can provide sufficient information to parallelize a wide variety of programs. These results also show that, in general, there is no program-independent bound on the speedup that can be achieved by parallel production system programs and that speedups in such programs can scale with data set size. DTIC

N95-27090# Fermi National Accelerator Lab., Batavia, IL.
STATISTICAL DATA ANALYSIS
A. A. Hahn Nov. 1994 21 p Presented at the Beam Instrumentation Workshop, Vancouver, Canada, 2-6 Oct. 1994
(Contract DE-AC02-76CH-03000)
(DE95-007214; FNAL/C-94/358; CONF-9410219-24) Avail: CASI HC A03/MF A01

The complexity of instrumentation sometimes requires data analysis to be done before the result is presented to the control room. This tutorial reviews some of the theoretical assumptions underlying the more popular forms of data analysis and presents simple examples to illuminate the advantages and hazards of different techniques. DOE

N95-27208 National Inst. of Standards and Technology, Gaithersburg, MD.
NIST: INFORMATION MANAGEMENT IN THE AMRF (Videotape)
George Callaghan, ed. Nov. 1991 Videotape: 12 min. 30 sec. playing time, in color, with sound
(NONP-NASA-VT-95-49120) Avail: CASI VHS A02/BETA A22

The information management strategies developed for the NIST Automated Manufacturing Research Facility (AMRF) - a prototype small batch manufacturing facility used for integration and measurement related standards research are outlined in this video. The five major manufacturing functions - design, process planning, off-line programming, shop floor control, and materials processing are explained and their applications demonstrated. Author (revised)

N95-27243*# National Aeronautics and Space Administration. John F. Kennedy Space Center, Cocoa Beach, FL.
SPACEPORT NEWS INDEX: JANUARY 1990 - DECEMBER 1994
Apr. 1995 218 p
(NASA-TM-110653; NAS 1.15:110653) Avail: CASI HC A10/MF A03

This index is intended to serve as a ready reference tool for the names, places, and events that comprise the history of John F. Kennedy Space Center. The arrangement is alphabetical by subject with entries arranged alphabetically by title. To facilitate use, cross references have been provided. Author

N95-27461# Westinghouse Hanford Co., Richland, WA.
AN UGLY DUCKLING BECOMES A SWAN (HOR ELLIPSIS): HOW AN ORGANIZATION BECOMES CUSTOMER FOCUSED THROUGH LISTENING
R. E. Asercion and V. J. Myer (Boeing Computer Services Co., Richland, WA.) Apr. 1995 10 p Presented at the 17th National Industrial Energy Technology Conference - Serving Industry's Needs, in Conjunction With the Spring Regional Conference of the Gulf Coast Cogeneration Association, Houston, TX, 4-6 Apr. 1995
(Contract DE-AC06-87RL-10930)
(DE95-004974; WHC-SA-2753; CONF-950464-1) Avail: CASI HC A02/MF A01

The story we're about to tell is true and the names have not been changed to protect the innocent because BCS Richland, Inc. (BCSR), a subsidiary of the Boeing Company, is proud of its metamorphosis from the ugly duckling of computer support to the shining swan-like star of the Help Desk industry. The transformation occurred in the midst of an all but antiquated computer technology environment, rapid technology changes, low employee morale, and high amount of customer frustration. BCSR, located at the Hanford site in the southeastern corner of Washington State, provides information resource management and computer support to the Department of Energy (DOE) complex located at the site. The primary mission of DOE is environmental restoration and waste clean-up. End User Support (EUS), an organization within BCSR, is tasked with all aspects of microcomputer support, both hardware and software. EUS efficiently and effectively supports approximately 12,000 computer users across the entire 560 square mile site. With a small staff of 50 consultants and technicians, EUS provides support to a diverse customer base that includes engineers and scientists, as well as financial personnel, managers, and clerical support. But it wasn't always this way. BCSR management recognized it and empowered the EUS staff to make the necessary changes. DOE

N95-27483# Pacific Northwest Lab., Richland, WA.
TRANSPARENT ACCESS TO DISTRIBUTED, HETEROGENEOUS ENVIRONMENTAL INFORMATION SYSTEMS
J. C. Brown and B. A. Kissinger Sep. 1994 14 p Presented at the 5th International Conference on Database and Expert Systems Applications, Athens, Greece, 7-9 Sep. 1994
(Contract DE-AC06-76RL-01830)
(DE95-007268; PNL-SA-23947; CONF-9409293-1) Avail: CASI HC A03/MF A01

Quality situation assessment and decision making require access to multiple sources of data and information. The question facing today's analyst is not so much 'Is the data I need to do my work available?' as 'How can I get to the data I need to make an informed decision?' Insufficient accessibility to data exists for many large corporations and government agencies. By utilizing current advances in computer technology, today's situation analysts have a wealth of information at their disposal. There are many potential solutions to the information accessibility problem using today's technology. The United States Department of Energy (US-DOE) faced this situation when dealing with the problem of high level radioactive waste (HLW) tanks in the United States. The result of their efforts has been the creation of the Tank Waste Information Network System - TWINS. The TWINS solution combines many technologies to address problems in several areas such as user interfaces, transparent access to multiple data sources, and integrated data access. Data related to the HLW tank complex is currently distributed throughout several US-DOE installations. Over time, each installation has adopted its own set of standards for information management, hardware, and software platforms. These factors contribute to the complexity of accessing information in a manner that enhances the performance and decision making process of the analysts. This paper presents one approach taken by the US-DOE to resolve the problem of distributed, heterogeneous, multimedia information management through the development of multilevel architectural controls and access mechanisms for the HLW Tank complex. The information system architecture developed for the US-DOE by the TWINS effort is one that is adaptable to other problem domains and uses. DOE

N95-27529 Carnegie-Mellon Univ., Pittsburgh, PA. Dept. of Computer Science.
A CASE FOR DYNAMIC SETS IN OPERATING SYSTEMS
David Steere and M. Satyanarayanan 30 Nov. 1994 20 p Sponsored in part by the IBM Corp., Digital Equipment Corp., and Intel Corp. Limited Reproducibility: More than 20% of this document may be affected by microfiche quality
(Contract F196828-93-C-0193)
(AD-A289354; CMU-CS-94-216) Avail: Issuing Activity (Defense Technical Information Center (DTIC))

Recent trends have exposed three key problems in today's operating systems. The first is the emergence of I/O latency as the dominant factor in the performance of many applications. The second is the need to cope with mobile communication environments where bandwidth and latency may be highly variable. The third is the importance of search activity to locating files of interest in a distributed system. In this paper we describe a single unifying abstraction called dynamic sets which can offer substantial benefits in the solution of these problems. These benefits include greater opportunity in the I/O subsystem to aggressively exploit prefetching and parallelism, as well as support for associative naming to complement the hierarchical naming in typical file systems. This paper motivates dynamic sets, presents the design of a system that embodies this abstraction, and evaluates a prototype implementation of the system via measurements and an analytical model. DTIC

N95-27701*# National Aeronautics and Space Administration. Langley Research Center, Hampton, VA.
DEVELOPMENT AND IMPLEMENTATION OF AN ELECTRONIC LIBRARY TOUR FOR THE NASA LANGLEY TECHNICAL LIBRARY M.S. Thesis, North Carlolna Univ., Jul. 1994
Nancy A. Rinker Jul. 1994 66 p
(NASA-TM-110619; NAS 1.15:110619) Avail: CASI HC A04/MF A01

The role of librarians today is drastically influenced by the changing nature of information and library services. The museum-like libraries of yesterday are a thing of the past: today's libraries are bustling with life, activity, and the sounds of new technologies. Libraries are replacing their paper card catalogs with state-of-the-art online systems, which provide faster and more comprehensive search capabilities. Even the resources themselves are changing. New formats for information, such as CD-ROM's, are becoming popular for all types of publications, from bibliographic tools to encyclopedias to electronic journals, even replacing print materials completely in some cases. Today it is almost impossible to walk into a library and find the information you need without coming into contact with at least one computer system. Librarians are not only struggling to keep up with the technological advancements of the day, but they are becoming information intermediaries: they must teach library users how to use all of the new systems and electronic resources. Not surprisingly, bibliographic instruction itself has taken on a new look and feel in these electronically advanced libraries. Many libraries are experimenting with the development of expert systems and other computer aided instruction interfaces for teaching patrons how to use the library and its resources. One popular type of interface in library instruction programs is hypertext, which utilizes 'stacks' or linked pages of information. Hypertext stacks can incorporate color graphics along with text to provide a more interesting interface and entice users into trying out the system. Another advantage of hypertext is that it is generally easy to use, even for those unfamiliar with computers. As such, it lends itself well to application in libraries, which often serve a broad range of clientele. This paper will discuss the design, development, and implementation of a hypertext library tour in a special library setting. The library featured in the electronic library tour is the National Aeronautics and Space Administration's Technical Library at Langley Research Center in Hampton, Virginia. Derived from text

N95-27847# Los Alamos National Lab., NM.
THE SUNRISE PROJECT: AN R&D PROJECT FOR A NATIONAL INFORMATION INFRASTRUCTURE PROTOTYPE
Juhnyoung Lee 1995 14 p
(Contract W-7405-eng-36)
(DE95-006340; LA-UR-95-35) Avail: CASI HC A03/MF A01

Sunrise is a Los Alamos National Laboratory (LANL) project started in October 1993. It is intended to a prototype National Information Infrastructure (NII) development project. A main focus of Sunrise is to tie together enabling technologies (networking, object-oriented distributed computing, graphical interfaces, security, multimedia technologies, and data mining technologies) with several specific applications. A diverse set of application areas was chosen to ensure that the solutions developed in the project are as generic as possible. Some of the application areas are materials modeling, medical records and image analysis, transportation simulations, and education. This paper provides a description of Sunrise and a view of the architecture and objectives of this evolving project. The primary objectives of Sunrise are three-fold: (1) to develop common information-enabling tools for advanced scientific research and its applications to industry; (2) to enhance the capabilities of important research programs at the laboratory; and (3) to define a new way of collaboration between computer science and industrially relevant research. DOE

N95-27949# Sandia National Labs., Albuquerque, NM.
REAL-TIME DATA COMPRESSION USING A FIXED HUFFMAN ENCODING SCHEME
R. E. Kidner Jan. 1995 40 p
(Contract DE-AC04-94AL-85000)
(DE95-006159; SAND-94-3172) Avail: CASI HC A03/MF A01

A common limitation to performance in data acquisition systems is storage of the collected data. Compressing the data would increase the amount of data that could be stored. However, most compression routines require that the data be collected and analyzed before compression is performed. Also, these compression routines often store the information required for decompression along with the data, thus decreasing the storage available for data. One solution to this problem is to create an encoding tree known to both the encoder and the decoder based on apriori knowledge of the data. Once the tree is created, optimal encoding schemes such as the Huffman algorithm may be used on the data as it is being collected. In this way the data is compressed as each byte is received and there is no overhead associated with storing decompression data. In this paper the idea of using a fixed Huffman tree is explored and the results are compared to a defacto standard in data compression, PKZIP. DOE

N95-27957# Sandia National Labs., Albuquerque, NM.
BROWSING THE WORLD WIDE WEB FROM BEHIND A FIREWALL
R. W. Simons 1995 9 p Presented at the DOE Computer Security Training Conference, Milwaukee, WI, 2-4 May 1995
(Contract DE-AC04-94AL-85000)
(DE95-006805; SAND-95-0121C; CONF-9505162-1) Avail: CASI HC A02/MF A01

The World Wide Web provides a unified method of access to various information services on the Internet via a variety of protocols. Mosaic and other browsers give users a graphical interface to the Web that is easier to use and more visually pleasing than any other common Internet information service today. The availability of information via the Web and the number of users accessing it have both grown rapidly in the last year. The interest and investment of commercial firms in this technology suggest that in the near future, access to the Web may become as necessary to doing business as a telephone. This is problematical for organizations that use firewalls to protect their internal networks from the Internet. Allowing all the protocols and types of information found in the Web to pass their firewall will certainly increase the risk of attack by hackers on the Internet. But not allowing access to the Web could be even more dangerous, as frustrated users of the internal network are either unable to do their jobs, or find creative new ways to get around the firewall. The solution to this dilemma adopted at Sandia National Laboratories is described. Discussion also covers risks of accessing the Web, design alternatives considered, and trade-offs used to find the proper balance between access and protection. DOE

N95-28085# Lawrence Livermore National Lab., Livermore, CA.
BEGINNING TO EDIT PHYSICS
P. W. Murphy 1 Feb. 1995 16 p Presented at the 42nd Society for Technical Communication Annual Conference, Washington, DC, 23-26 Apr. 1995
(Contract W-7405-eng-48)
(DE95-008374; UCRL-JC-119872; CONF-9504128-1) Avail: CASI HC A03/MF A01

A physicist-turned-editor shows the basics required for copy-editing physics papers (physical quantities, symbols, units, scientific notation, the structure of mathematical expressions, the nature of graphs), and points the way to learning enough 'editorial physics' to begin substantive editing. DOE

N95-28113# EG and G Energy Measurements, Inc., Las Vegas, NV. Remote Sensing Lab.
APPLICATION OF A GEOGRAPHIC INFORMATION SYSTEM FOR RADIOLOGIC EMERGENCY RESPONSE
R. G. Best and J. F. Doyle 1995 5 p Presented at the 5th ANS Topical Meeting on Emergency Preparedness and Response, Savannah, GA, 18-21 Apr. 1995
(Contract DE-AC08-93NV-11265)
(DE95-007624; EGG-11265-1123; CONF-950430-4) Avail: CASI HC A01/MF A01

A geographic information system (GIS) is a multifunctional analytical tool that can be used to compile available data and derive information. A GIS is a computerized database management system for the capture, storage, retrieval, analysis, and display of spatial data. Maps are the most common type of spatial data, but any type of data that can be referenced by an x-y location or geographic coordinate can be used in a GIS. In a radiological emergency, it is critical that data of all types be rapidly compiled into a common format in order to make accurate observations and informed decisions. Developing a baseline GIS for nuclear facilities would offer a significant incentive for all organizations to contribute to and utilize this powerful data management tool. The system being developed could integrate all elements of emergency planning, from the initial protective actions based on models through the emergency monitoring phase, and finally ending with the complex reentry and recovery phase. Within the Federal Radiological Monitoring and Assessment Center (FRMAC), there is a continuing effort to improve the data management and communication process. To demonstrate the potential of GIS for emergency response, the system has been utilized in interagency FRMAC exercises. An interactive GIS system has been deployed and used to analyze the available spatial data to help determine the impact of a hypothetical radiological release and to develop mitigation plans. For this application, both hardcopy and real-time spatial displays were generated with the GIS. Composite maps with different sizes, scales, and themes were produced to support the exercises. DOE

N95-28172# Oak Ridge National Lab., TN.
PROJECT RECORDS INFORMATION SYSTEM (PRIS) USER'S MANUAL, REVISION 3
R. K. Schwarz, ed. Jan. 1995 80 p
(Contract DE-AC05-84OR-21400)
(DE95-008330; K/CSD/TM-93-Rev-3) Avail: CASI HC A05/MF A01

The Project Records Information System (PRIS) is an interactive system developed for the Information Management Services (IMS) of Martin Marietta Energy Systems, Inc., to perform indexing, maintenance, and retrieval of information about Engineering project record documents for which they are responsible. This PRIS User's Manual provides instruction on the use of this system. Section 2.0 of this manual presents an overview of PRIS, describing the system's purpose; the data that it handles; functions it performs; hardware, software, and access; and help and error functions. Section 3.0 describes the interactive menu-driven operation of PRIS. Appendixes A, B, and C contain help screens, report descriptions, and the data dictionary, respectively. DOE

N95-28555# Oak Ridge National Lab., TN.
MANAGING ELECTRONIC RECORDS: A GUIDELINE
J. G. Stewart 25 Oct. 1994 6 p Presented at the Office of Scientific and Technical Information INFOTECH '94, Oak Ridge, TN, 25-26 Oct. 1994
(Contract DE-AC05-84OR-21400)
(DE95-007038; CONF-9410141-7) Avail: CASI HC A02/MF A01

A committee at Martin Marietta Energy Systems (MMES) has drafted a guideline to assist offices in the management of electronic records. This paper will address the activities surrounding its creating. The guideline is for use by creators, users, and custodians of any type of electronic information. The guideline supports and supplements requirements from DOE and the National Archives and Records Administration (NARA), other internal processes such as system reviews, and the comprehensive records management program. While an in-house publication, it could prove useful to other organizations implementing an electronic records management program. DOE

N95-28587 Air Force Inst. of Tech., Wright-Patterson AFB, OH. School of Logistics and Acquisition Management.
EVALUATION OF AN AIR FORCE INFORMATION RESOURCES MANAGEMENT (IRM) OVERVIEW COURSE M.S. Thesis
Joseph L. Cox and Brenda R. Forcht Dec. 1994 102 p Limited Reproducibility: More than 20% of this document may be affected by microfiche quality
(AD-A288746; AFIT/GIR/LAR/94D-3) Avail: Issuing Activity (Defense Technical Information Center (DTIC))

The federal government has passed laws and issued directives recognizing that information is a valuable national resource. To help assure that Air Force information managers are capable of implementing policy in support of such laws and directives, the Secretary of the Air Force's Directorate of Information Management (SAF/AAI) directed a team from the Air Force Institute of Technology (AFIT) to design and construct an exportable course to provide an overview of information resources management (IRM) concepts and principles. Such an IRM overview course was completed in the Summer of 1994. The authors evaluated this course quantitatively and qualitatively. During a pilot administration of the course, the authors used a quantitative measurement instrument and a pre-test/posttest research design to assess effectiveness of the instructional system. The authors also gathered feedback from students and instructors to provide a summative evaluation of the course as a whole. Based on test scores and qualitative feedback, the authors concluded that the course did provide a useful overview of IRM concepts and principles. Additionally, they were able to recommend several changes to the course presentation, content, and measurement instrument. DTIC

N95-28589 Naval Command, Control and Ocean Surveillance Center, San Diego, CA. Research, Development, Technology and Evaluation Div.
DOWNLOADING ENVIRONMENTAL DATA IN THE NEW MOODS FORMAT Final Report
Alvan Fisher, Jr. Sep. 1994 18 p Limited Reproducibility: More than 20% of this document may be affected by microfiche quality
(AD-A288835; NCCOSC/RDT/E-TD-2697) Avail: Issuing Activity (Defense Technical Information Center (DTIC))

Oceanic data in the revised master oceanographic observation data set (MOODS) format require transformation into a modified format before they can be used by various processing and analysis routines resident at the NCCOSC RDT&E Division. This document describes a technique developed to modify small data sets into the desired format using an IBM compatible personal computer. Depth increments may be reduced using a smoothing routine to a number of points compatible with the requirements of standard Navy acoustic performance prediction systems. Data editing routines are available. DTIC

N95-28600*# Illinois Univ., Urbana-Champaign, IL. School of Library and Information Science.
NASA/DOD AEROSPACE KNOWLEDGE DIFFUSION RESEARCH PROJECT. REPORT 35: THE USE OF COMPUTER NETWORKS IN AEROSPACE ENGINEERING
Ann P. Bishop and Thomas E. Pinelli (National Aeronautics and Space Administration. Langley Research Center, Hampton, VA.) Jun. 1995 403 p
(NASA Order L-45107; RTOP 505-90-00)
(NASA-CR-198170; NAS 1.26:198170) Avail: CASI HC A18/MF A04

This research used survey research to explore and describe the use of computer networks by aerospace engineers. The study population included 2000 randomly selected U.S. aerospace engineers and scientists who subscribed to Aerospace Engineering. A total of 950 usable questionnaires were received by the cutoff date of July 1994. Study results contribute to existing knowledge about both computer network use and the nature of engineering work and communication. We found that 74 percent of mail survey respondents personally used computer networks. Electronic mail, file transfer, and remote login were the most widely used applications. Networks were used less often than face-to-face interactions in performing work tasks, but about equally with reading and telephone conversations, and more often than mail or fax. Network use was associated with a range of technical, organizational, and personal factors: lack of compatibility across systems, cost, inadequate access and training, and unwillingness to embrace new technologies and modes of work appear to discourage network use. The greatest positive impacts from networking appear to be increases in the amount of accurate and timely information available, better exchange of ideas across organizational boundaries, and enhanced work flexibility, efficiency, and quality. Involvement with classified or proprietary data and type of organizational structure did not distinguish network users from nonusers. The findings can be used by people involved in the design and implementation of networks in engineering communities to inform the development of more effective networking systems, services, and policies. Author

N95-28631# Los Alamos National Lab., NM.
QUERY BY IMAGE EXAMPLE: THE CANDID APPROACH
P. M. Kelly, M. Cannon, and D. R. Hush 1995 12 p Presented at the SPIE 1995 Conference on Optics, Electro-optics, and Laser Application in Science, Engineering and Medicine, San Jose, CA, 5-10 Feb. 1995
(Contract W-7405-eng-36)
(DE95-006284; LA-UR-95-374; CONF-950226-12) Avail: CASI HC A03/MF A01

CANDID (Comparison Algorithm for Navigating Digital Image Databases) was developed to enable content-based retrieval of digital imagery from large databases using a query-by-example methodology. A user provides an example image to the system, and images in the database that are similar to that example are retrieved. The development of CANDID was inspired by the N-gram approach to document fingerprinting, where a 'global signature' is computed for every document in a database and these signatures are compared to one another to determine the similarity between any two documents. CANDID computes a global signature for every image in a database, where the signature is derived from various image features such as localized texture, shape, or color information. A distance between probability density functions of feature vectors is then used to compare signatures. In this paper, the authors present CANDID and highlight two results from their current research: subtracting a 'background' signature from every signature in a database in an attempt to improve system performance when using inner-product similarity measures, and visualizing the contribution of individual pixels in the matching process. These ideas are applicable to any histogram-based comparison technique. DOE

N95-28675# Department of Energy, Oak Ridge, TN. Office of Scientific and Technical Information.
GUIDE FOR TRANSMITTING STANDARD GENERALIZED MARKUP LANGUAGE (SGML) ENCODED BIBLIOGRAPHIC RECORDS
Sep. 1994 71 p
(DOE/OSTI-11685; DE95-000568) Avail: CASI HC A04/MF A01

This document provides the guidance necessary to transmit to the Department of Energy Office of Scientific and Technical Information (OSTI) an encoded bibliographic record that conforms to International Standard ISO 8879, Information Processing--Text and office systems--Standard Generalized Markup Language (SGML). Included in this document are element and attribute tag definitions, sample bibliographic records, the bibliographic document type definition, and instructions on how to transmit a bibliographic record electronically to OSTI. Derived from text

N95-28677*# National Aeronautics and Space Administration. Ames Research Center, Moffett Field, CA.
SPACE SCIENCE DIVISION CUMULATIVE BIBLIOGRAPHY: 1989-1994
D. Morrison May 1995 47 p
(NASA-TM-110355; A-950068; NAS 1.15:110355) Avail: CASI HC A03/MF A01

The Space Science Division at NASA's Ames Research Center is dedicated to research in astrophysics, exobiology, and planetary science. These research programs are structured around the study of origins and evolution of stars, planets, planetary atmospheres, and life, and address some of the most fundamental questions pursued by science; questions that examine the origin of life and of our place in the universe. This bibliography is the accumulation of peer-reviewed publications authored by Division scientists for the years 1989 through 1994. The list includes 777 papers published in over 5 dozen scientific journals representing the high productivity and interdisciplinary nature of the Space Science Division. Author

N95-26950# Wichita State Univ., Wichita, KS.
THE AEROSPACE DATABASE: AN INTRODUCTION TO AIAA'S COMPUTERIZED SOURCE FOR IDENTIFYING SCIENTIFIC AND TECHNICAL INFORMATION Abstract Only
Thomas G. DePetro *In its* AIAA Techfest 20 Proceedings 1994 2 p (For primary document see N95-26941 09-01)
Avail: CASI HC A01/MF A03

N95-27378*# National Aeronautics and Space Administration. John F. Kennedy Space Center, Cocoa Beach, FL.
AUTOMATED DATABASE DESIGN FROM NATURAL LANGUAGE INPUT
Fernando Gomez (University of Central Florida, Orlando, FL.), Carlos Segami (Barry Univ., Miami Shores, FL.), and Carl Delaune *In* NASA. Goddard Space Flight Center, The 1995 Goddard Conference on Space Applications of Artificial Intelligence and Emerging Information Technologies May 1995 p 29-44 (For primary document see N95-27375 09-63)
(Contract NAS10-120)
Avail: CASI HC A03/MF A03

N95-27382*# National Aeronautics and Space Administration. Goddard Space Flight Center, Greenbelt, MD.
INTEGRATED PLANNING AND SCHEDULING FOR EARTH SCIENCE DATA PROCESSING
Mark Boddy (Honeywell Technology Center, Minneapolis, MN.), Jim White (Honeywell Technology Center, Minneapolis, MN.), Robert Goldman (Honeywell Technology Center, Minneapolis, MN.), and Nick Short, Jr. *In its* The 1995 Goddard Conference on Space Applications of Artificial Intelligence and Emerging Information Technologies May 1995 p 91-101 (For primary document see N95-27375 09-63)
Avail: CASI HC A03/MF A03

N95-27384*# Space Telescope Science Inst., Baltimore, MD.
A RULE-BASED SHELL TO HIERARCHICALLY ORGANIZE HST OBSERVATIONS
Ashim Bose and Andrew Gerb *In* NASA. Goddard Space Flight Center, The 1995 Goddard Conference on Space Applications of Artificial Intelligence and Emerging Information Technologies May 1995 p 119-130 (For primary document see N95-27375 09-63)
Avail: CASI HC A03/MF A03

N95-27391*# Morgan State Univ., Baltimore, MD. Dept. of Mathematics.
LINEAR AND NONLINEAR TRENDING AND PREDICTION FOR AVHRR TIME SERIES DATA
J. Smid, P. Volf (Ceskoslovenska Akademie Ved, Prague.), M. Slama (Ceskoslovenska Akademie Ved, Prague.), and M. Palus (Santa Fe Inst., NM.) *In* NASA. Goddard Space Flight Center, The 1995 Goddard Conference on Space Applications of Artificial Intelligence and Emerging Information Technologies May 1995 p 209-220 (For primary document see N95-27375 09-63)
(Grant NAG5-2686)
Avail: CASI HC A03/MF A03

N95-27658*# Boeing Aerospace Operations, Inc., Hampton, VA.
LONG DURATION EXPOSURE FACILITY (LDEF) ARCHIVE SYSTEM
Brenda K. Wilson *In* NASA. Langley Research Center, LDEF: 69 Months in Space. Third Post-Retrieval Symposium, Part 3 Feb. 1995 p 1249-1262 (For primary document see N95-27629 09-99)
Avail: CASI HC A03/MF A04

N95-27659*# National Aeronautics and Space Administration. Langley Research Center, Hampton, VA.
THE LONG DURATION EXPOSURE FACILITY (LDEF) ANNOTATED BIBLIOGRAPHY
Arlene S. Levine *In its* LDEF: 69 Months in Space. Third Post-Retrieval Symposium, Part 3 Feb. 1995 p 1263-1265 (For primary document see N95-27629 09-99)
Avail: CASI HC A01/MF A04

N95-27660*# National Aeronautics and Space Administration. Langley Research Center, Hampton, VA.
THE LONG DURATION EXPOSURE FACILITY (LDEF) PHOTOGRAPHIC SURVEY SPECIAL PUBLICATION
Robert L. ONeal (O'Neal, Robert L., Hampton, VA.), Arlene S. Levine, and Carol C. Kiser (Kiser, Carol C., Hampton, VA.) *In its* LDEF: 69 Months in Space. Third Post-Retrieval Symposium, Part 3 Feb. 1995 p 1267-1269 (For primary document see N95-27629 09-99)
Avail: CASI HC A01/MF A04

N95-28465*# Analytical Services and Materials, Inc., Hampton, VA.
COINS: A COMPOSITES INFORMATION DATABASE SYSTEM
Shahid Siddiqi, Louis F. Vosteen, Ralph Edlow, and Teck-Seng Kwa *In* FAA, Ninth DOD/NASA/FAA Conference on Fibrous Composites in Structural Design, Volume 2 Sep. 1992 p 621-62 Previously announced as X92-10407 (For primary document see N95-28462 09-24)
Avail: CASI HC A02/MF A04

83 ECONOMICS AND COST ANALYSIS

Includes cost effectiveness studies.

No abstracts in this category.

84 LAW, POLITICAL SCIENCE AND SPACE POLICY

Includes NASA appropriation hearings; aviation law; space law and policy; international law; international cooperation; and patent policy.

No abstracts in this category.

85 URBAN TECHNOLOGY AND TRANSPORTATION

Includes applications of space technology to urban problems; technology transfer; technology assessment; and surface and mass transportation.

For related information see also *03 Air Transportation and Safety, 16 Space Transportation,* and *44 Energy Production and Conversion.*

N95-27937# New Energy and Industrial Technology Development Organization, Tokyo (Japan).
RESEARCH ON THE ESTABLISHMENT OF THE DATABASE SYSTEM FOR R AND D ON THE INNOVATIVE TECHNOLOGY FOR THE EARTH
Mar. 1994 101 p In JAPANESE
(DE95-759244; NEDO-GET-9310-4) Avail: CASI HC A06/MF A02

For the purpose of structuring a database system of technical information about the earth environmental issues, the 'database system for R and D of the earth environmental industrial technology' was operationally evaluated, and study was made to open it and structure a prototype of database. In the present state as pointed out in the operational evaluation, the utilization frequency is not heightened due to lack of UNIX experience, absence of system managers and shortage of utilizable articles listed, so that the renewal of database does not ideally progress. Therefore, study was then made to introduce tools utilizable by the initiators and open the information access terminal to the researchers at headquarters utilizing the internet. In order for the earth environment-related researchers to easily obtain the information, a database was prototypically structured to support the research exchange. Tasks were made clear to be taken for selecting the fields of research and compiling common thesauri in Japanese, Western and other languages. DOE

88 SPACE SCIENCES (GENERAL)

No abstracts in this category.

89 ASTRONOMY

Includes radio, gamma-ray, and infrared astronomy, and astrometry.

N95-27068*# National Aeronautics and Space Administration, Washington, DC.
CATACLYSMIC VARIABLES AND RELATED OBJECTS
Margherita Hack (Osservatorio Astronomico, Trieste, Italy.), Constanze laDous (Osservatorio Astronomico, Trieste, Italy.), Stuart D. Jordan, ed. (National Aeronautics and Space Administration. Goddard Space Flight Center, Greenbelt, MD.), Richard N. Thomas, ed. (Radiophysics, Inc., Boulder, CO.), Leo Goldberg (Kitt Peak National Observatory, Tucson, AZ.), and Jean-Claude Pecker (College de France, Paris, France.) Sep. 1993 902 p Prepared in cooperation with CNRS, Paris, France Its Monograph Series on Nonthermal Phenomena in Stellar Atmospheres
(NASA-SP-507; NAS 1.21:507; LC-92-7619; QB835.H27) Avail: CASI HC A99/MF A10; SOD HC

This volume begins with an introductory chapter on general properties of cataclysmic variables. Chapters 2 through 5 of Part 1 are devoted to observations and interpretation of dwarf novae and nova-like stars. Chapters 6 through 10, Part 2, discuss the general observational properties of classical and recurrent novae, the theoretical models, and the characteristics and models for some well observed classical novae and recurrent novae. Chapters 11 through 14 of Part 3 are devoted to an overview of the observations of symbiotic stars, to a description of the various models proposed for explaining the symbiotic phenomenon, and to a discussion of a few selected objects, respectively. Chapter 15 briefly examines the many unsolved problems posed by the observations of the different classes of cataclysmic variables and symbiotic stars. For individual titles, see N95-27069 through N95-27078.

N95-27069*# Osservatorio Astronomico, Trieste (Italy).
DWARF NOVAE
Constanze laDous *In* NASA, Washington, Cataclysmic Variables and Related Objects Sep. 1993 p 15-94 (For primary document see N95-27068 09-89)
Avail: CASI HC A05/MF A10; SOD HC

Dwarf novae are defined on grounds of their semi-regular brightness variations of some two to five magnitudes on time scales of typically 10 to 100 days. Historically several different classification schemes have been used. Today, dwarf novae are divided into three sub-classes: the U Geminorum stars, the SU Ursae Majoris stars, and the Z Camelopardalis stars. Outbursts of dwarf novae occur at semi-periodic intervals of time, typically every 10 to 100 days; amplitudes range from typically 2 to 5 mag. Within certain limits values are characteristic for each object. Relations between the outburst amplitude, or the total energy released during outburst, and the recurrence time have been found, as well as relations between the orbital period and the outburst decay time, the absolute magnitude during outburst maximum, and the widths of long and short outbursts, respectively. Some dwarf novae are known to have suspended their normal outburst activity altogether for a while. They later resumed it without having undergone any observable changes. The optical colors of dwarf novae all are quite similar during outburst, considerably bluer than during the quiescent state. During the outburst cycle, characteristic loops in the two color diagram are performed. At a time resolution on the order of minutes, strictly periodic photometric changes due to orbital motion become visible in the light curves of dwarf novae. These are characteristic for each system. Remarkably little is known about orbital variations during the course of an outburst. On time-scales of minutes and seconds, further more or less periodic types of variability are seen in dwarf novae. Appreciable flux is emitted by dwarf novae at all wavelengths from the X-rays to the longest IR wavelengths, and in some cases even in the radio. Most dwarf novae exhibit strong emission line spectra in the optical and UV during quiescence, although some have only very weak emissions in the optical and/or weak absorptions at UV wavelengths. Derived from text

N95-27070*# Osservatorio Astronomico, Trieste (Italy).
NOVA-LIKE VARIABLES
Constanze laDous *In* NASA, Wasington, Cataclysmic Variables and Related Objects Sep. 1993 p 95-143 (For primary document see

N95-27068 09-89)
Avail: CASI HC A03/MF A10; SOD HC

On grounds of different observable characteristics five classes of nova-like objects are distinguished: the UX Ursae Majoris stars, the antidwarf novae, the DQ Herculis stars, the AM Herculis stars, and the AM Canum Venaticorum stars. Some objects have not been classified specifically. Nova-like stars share most observable features with dwarf novae, except for the outburst behavior. The understanding is that dwarf novae, UX Ursae Majoris stars, and anti-dwarf novae are basically the same sort of objects. The difference between them is that in UX Ursae Majoris stars the mass transfer through the accretion disc always is high so the disc is stationary all the time; in anti-dwarf novae for some reason the mass transfer occasionally drops considerably for some time, and in dwarf novae it is low enough for the disc to undergo semiperiodic changes between high and low accretion events. DQ Herculis stars are believed to possess weakly magnetic white dwarfs which disrupt the inner disc at some distance from the central star; the rotation of the white dwarf can be seen as an additional photometric period. In AM Herculis stars, a strongly magnetic white dwarf entirely prevents the formation of an accretion disk and at the same time locks the rotation of the white dwarf to the binary orbit. Finally, AM Canum Venaticorum stars are believed to be cataclysmic variables that consist of two white dwarf components. Derived from text

N95-27071*# Osservatorio Astronomico, Trieste (Italy).

MODELS FOR VARIOUS ASPECTS OF DWARF NOVAE AND NOVA-LIKE STARS

Constanze laDous *In* NASA, Washington, Cataclysmic Variables and Related Objects Sep. 1993 p 145-231 (For primary document see N95-27068 09-89)
Avail: CASI HC A05/MF A10; SOD HC

The first attempts to explain the nature of dwarf novae were based on the assumption of single-star phenomena, in which emission lines were assumed to be caused by circumstellar gas shells. The outburst behavior was tentatively ascribed to the kind of (also not understood) mechanism leading to nova outbursts. The realization that some, and possibly all, dwarf novae and nova-like stars (and novae) are binaries eventually led to models which bore more and more similarities to the modern interpretation on the basis of the Roche model. Not all cataclysmic variables are known binaries. In fact, with respect to the entire number of known objects, the proven binaries are still the minority, but all the brightest variables are in fact known to binaries. Not a single system is known which exhibits the usual characteristics of a cataclysmic variable and at the same time can be declared with certainty to be a single star. Two systems are known, the dwarf nova EY Cyg and the recurrent nova V1017 Sgr, in which, in spite of intensive search, no radial velocity variations have been found; but they still exhibit composite spectra consisting of a bright continuum, an emission spectrum, and a cool absorption spectrum. If the Roche model is correct, it is to be expected that a small percentage of objects is viewed pole-on, so orbital motions do not make themselves felt as Doppler shifts of spectral lines. So even these two systems support the hypothesis that all cataclysmic variables (with the possible exception of symbiotic stars) are binaries. In cataclysmic variables, it seems that the brightness changes observed in dwarf novae and nova-like stars in the optical and the UV are due directly to changes in the accretion disks. The study and understanding of accretion disks in these systems can bear potentially valuable consequences for many other fields in astronomy. The observed spectra of dwarf novae and nova-like stars comprise a fairly large range: pure emission spectra, pure absorption spectra, a mixture of both, asymmetric line profiles, very different slopes of the continuous flux distribution -- and one single system may exhibit all of these features at different times. Agreement and disagreement between computed and observed spectra should show whether or not the Roche model is applicable and where it probably will have to be modified and improved. Except for their outburst behavior and its immediate consequences, novae, dwarf novae, and nova-like stars cannot be physically distinguished from each other.
Derived from text

N95-27072*# Osservatorio Astronomico, Trieste (Italy).

CLASSICAL NOVAE AND RECURRENT NOVAE: GENERAL PROPERTIES

Margherita Hack, Pierluigi Selvelli, and Hilmar W. Duerbeck (Muenster Univ., Germany.) *In* NASA, Washington, Cataclysmic Variables and Related Objects Sep. 1993 p 261-369 (For primary document see N95-27068 09-89)
Avail: CASI HC A06/MF A10; SOD HC

We describe the observable characteristics of classical novae and recurrent novae obtained by different techniques (photometry, spectroscopy, and imaging) in all the available spectral ranges. We consider the three stages in the life of a nova: quiescence (pre- and post-outburst), outburst, final decline and nebular phase. We describe the photometric properties during the quiescent phase. We describe the photometric properties during outburst, the classification according the rate of decline (magnitudes per day), which permits us to define very fast, fast, intermediate, slow, and very slow novae and the correlation between luminosity and speed class. We report the scanty data on the spectra of the few known prenovae and those on the spectra of old novae and those of dwarf novae and nova-like, which, however, are almost undistinguishable. We describe the typical spectra appearing from the beginning of the outburst, just before maximum, up to the nebular phase and the correlation between spectral type at maximum, expansional velocity, and speed class of the nova. We report the existing infrared observations, which permit us to explain some of the characteristics of the outburst light curve, and give evidence of the formation of a dust shell in slow and intermediate novae (with the important exception of the very slow nova HR Del 1967) and its absence or quasi-absence in fast novae. The ultraviolet and X-ray observations are described. The X ray observations of novae, mainly from the two satellites EINSTEIN and EXOSAT, are reported. Observations of the final decline and of the envelopes appearing several months after outburst are also reported.
Derived from text

N95-27073*# Institut d'Astrophysique, Paris (France).

MODELS OF CLASSICAL AND RECURRENT NOVAE

Michael Friedjung and Hilmar W. Duerbeck (Muenster Univ., Germany.) *In* NASA, Washington, Cataclysmic Variables and Related Objects Sep. 1993 p 371-412 (For primary document see N95-27068 09-89)
Avail: CASI HC A03/MF A10; SOD HC

The behavior of novae may be divided roughly into two separate stages: quiescence and outburst. However, at closer inspection, both stages cannot be separated. It should be attempted to explain features in both stages with a similar model. Various simple models to explain the observed light and spectral observations during post optical maximum activity are conceivable. In instantaneous ejection models, all or nearly all material is ejected in a time that is short compared with the duration of post optical maximum activity. Instantaneous ejection type 1 models are those where the ejected material is in a fairly thin shell, the thickness of which remains small. In the instantaneous ejection type 2 model ('Hubble Flow'), a thick envelope is ejected instantaneously. This envelope remains thick as different parts have different velocities. Continued ejection models emphasize the importance of winds from the nova after optical maximum. Ejection is supposed to occur from one of the components of the central binary, and one can imagine a general swelling of one of the components, so that something resembling a normal, almost stationary, stellar photosphere is observed after optical maximum. The observed characteristics of recurrent novae in general are rather different from those of classical novae, thus, models for these stars need not be the same. Derived from text

N95-27074*# Osservatorio Astronomico, Trieste (Italy).

TYPICAL EXAMPLES OF CLASSICAL NOVAE

Margherita Hack, Pierluigi Selvelli, Antonio Bianchini (Osservatorio Astrofisico, Asiago, Italy.), and Hilmar W. Duerbeck (Muenster Univ., Germany.) *In* NASA, Washington, Cataclysmic Variables and Related Objects Sep. 1993 p 413-510 (For primary document see N95-27068 09-89)
Avail: CASI HC A05/MF A10; SOD HC

Because of the very complicated individualistic behavior of each nova, we think it necessary to review the observations of a few well-observed individuals. We have selected a few objects of different speed classes, which have been extensively observed. They are: V1500 Cygni 1975, a very fast nova; V603 Aql 1918, fast nova; CP Pup 1942, fast nova; GK Per 1901, fast nova; V 1668 Cyg 1979, moderately fast nova; FH Ser 1970, slow nova; DQ Her 1934, slow nova; T Aur 1891, slow nova; RR Pic 1925, slow nova; and HR Del 1967, very slow nova.
Derived from text

N95-27075*# Osservatorio Astronomico, Trieste (Italy).
RECURRENT NOVAE
Margherita Hack and Pierluigi Selvelli *In* NASA, Washington, Cataclysmic Variables and Related Objects Sep. 1993 p 511-559 (For primary document see N95-27068 09-89)
Avail: CASI HC A03/MF A10; SOD HC

Recurrent novae seem to be a rather inhomogeneous group: T CrB is a binary with a M III companion; U Sco probably has a late dwarf as companion. Three are fast novae; two are slow novae. Some of them appear to have normal chemical composition; others may present He and CNO excess. Some present a mass-loss that is lower by two orders of magnitude than classical novae. However, our sample is too small for saying whether there are several classes of recurrent novae, which may be related to the various classes of classical novae, or whether the low mass-loss is a general property of the class or just a peculiarity of one member of the larger class of classical novae and recurrent novae.
Derived from text

N95-27076*# Consiglio Nazionale delle Ricerche, Frascati (Italy). Ist. di Astrofisica Spaziale.
OVERVIEW OF THE OBSERVATIONS OF SYMBIOTIC STARS
Roberto Viotti *In* NASA, Washington, Cataclysmic Variables and Related Objects Sep. 1993 p 583-645 (For primary document see N95-27068 09-89)
Avail: CASI HC A04/MF A10; SOD HC

The term Symbiotic stars commonly denotes variable stars whose optical spectra simultaneously present a cool absorption spectrum (typically TiO absorption bands) and emission lines of high ionization energy. This term is now used for the category of variable stars with composite spectrum. The main spectral features of these objects are: (1) the presence of the red continuum typical of a cool star, (2) the rich emission line spectrum, and (3) the UV excess, frequently with the Balmer continuum in emission. In addition to the peculiar spectrum, the very irregular photometric and spectroscopic variability is the major feature of the symbiotic stars. Moreover, the light curve is basic to identify the different phases of activity in a symbiotic star. The physical mechanisms that cause the symbiotic phenomenon and its variety are the focus of this paper. An astronomical phenomenon characterized by a composite stellar spectrum with two apparently conflicting features, and large variability has been observed. Our research set out to find the origin of this behavior and, in particular, to identify and measure the physical mechanism(s) responsible for the observed phenomena. Derived from text

N95-27077*# Institut d'Astrophysique, Paris (France).
MODELS OF SYMBIOTIC STARS
Michael Friedjung *In* NASA, Washington, Cataclysmic Variables and Related Objects Sep. 1993 p 647-662 (For primary document see N95-27068 09-89)
Avail: CASI HC A05/MF A10; SOD HC

One of the most important features of symbiotic stars is the coexistence of a cool spectral component that is apparently very similar to the spectrum of a cool giant, with at least one hot continuum, and emission lines from very different stages of ionization. The cool component dominates the infrared spectrum of S-type symbiotics; it tends to be veiled in this wavelength range by what appears to be excess emission in D-type symbiotics, this excess usually being attributed to circumstellar dust. The hot continuum (or continua) dominates the ultraviolet. X-rays have sometimes also been observed. Another important feature of symbiotic stars that needs to be explained is the variability. Different forms occur, some variability being periodic. This type of variability can, in a few cases, strongly suggest the presence of eclipses of a binary system. One of the most characteristic forms of variability is that characterizing the active phases. This basic form of variation is traditionally associated in the optical with the veiling of the cool spectrum and the disappearance of high-ionization emission lines, the latter progressively appearing (in classical cases, reappearing) later. Such spectral changes recall those of novae, but spectroscopic signatures of the high-ejection velocities observed for novae are not usually detected in symbiotic stars. However, the light curves of the 'symbiotic nova' subclass recall those of novae. We may also mention in this connection that radio observations (or, in a few cases, optical observations) of nebulae indicate ejection from symbiotic stars, with deviations from spherical symmetry. We shall give a historical overview of the proposed models for symbiotic stars and make a critical analysis in the light of the observations of symbiotic stars. We describe the empirical approach to models and use the observational data to diagnose the physical conditions in the symbiotics stars. Finally, we compare the results of this empirical approach with existing models and discuss unresolved problems requiring new observational and theoretical work.
Derived from text

N95-27078*# Consiglio Nazionale delle Ricerche, Frascati (Italy). Ist. di Astrofisica Spaziale.
DISCUSSION ON SELECTED SYMBIOTIC STARS
Roberto Viotti and Margherita Hack (Osservatorio Astronomico, Trieste, Italy.) *In* NASA, Washington, Cataclysmic Variables and Related Objects Sep. 1993 p 663-724 (For primary document see N95-27068 09-89)
Avail: CASI HC A04/MF A10; SOD HC

Because of its large variety of aspects, the symbiotic phenomenon is not very suitable for a statistical treatment. It is also not clear whether symbiotic stars really represent a homogeneous group of astrophysical objects or a collection of objects of different natures but showing similar phenomena. However we are especially interested in the symbiotic phenomenon, i.e., in those physical processes occurring in the atmosphere of each individual object and in their time dependence. Such a research can be performed through the detailed analysis of individual objects. This study should be done for a time long enough to cover all the different phases of their activity, in all the spectral ranges. Since the typical time scale of the symbiotic phenomena is up to several years and decades, this represents a problem since, for instance, making astronomy outside the visual region is a quite new field of research. It was a fortunate case that a few symbiotic stars (Z And, AG Dra, CH Cyg, AX Per, and PU Vul) had undergone remarkable light variations (or 'outbursts') in recent years, which could have been followed in the space ultraviolet with IUE, and simultaneously in the optical and IR with ground-based telescopes. But, in general, the time coverage of most of the symbiotic objects is too short to have a complete picture of their behavior. In this regard, one should recall Mayall's remark about the light curve of Z And: 'Z Andromedae is another variable that shows it will require several hundred years of observations before a good analysis can be made of its variations'. This pessimistic remark should be considered as a note of caution for those involved in the interpretation of the observations. We shall discuss a number of individual symbiotic stars for which the amount of observational data is large enough to draw a rather complete picture of their general behavior and to make consistent models. We shall especially illustrate the necessary steps toward an empirical model and take the discussion of the individual objects as a useful occasion to describe different techniques of diagnosis.
Derived from text

N95-28197# California Univ., Berkeley. Lawrence Berkeley Lab, CA.
DISCOVERY OF THE MOST DISTANT SUPERNOVAE AND THE QUEST FOR (OMEGA)
G. Goldhaber, S. Perlmutter, S. Gabi, A. Goobar, A. Kim, M. Kim, R. Pain, C. Pennypacker, I. Small, and B. Boyle (Institute of Astronomy, Cambridge, England.) May 1994 8 p Presented at the 1st Artic Workshop on Furture Physics and Accelerators, Saariselka, Finland, 21-26 Aug. 1994
(Contract DE-AC03-76SF-00098)
(DE95-006569; LBL-36361; CONF-9408217-2) Avail: CASI HC A02/MF A01

A search for cosmological supernovae has discovered a number of a type Ia supernovae. In particular, one at z = 0.458 is the most distant supernovae yet observed. There is strong evidence from measurements of nearby type Ia supernovae that they can be considered as 'standard candles'. The authors plan to use these supernovae to measure the deceleration in the general expansion of the universe. The aim of their experiment is to try and observe and measure about 30 such distant supernovae in order to obtain a measurement of the deceleration parameter q(sub o) which is related to (Omega). Here (Omega) is the ratio of the density of the universe to the critical density, and they expect a measurement with an accuracy of about 30%. DOE

90 ASTROPHYSICS

Includes cosmology; celestial mechanics; space plasmas; and interstellar and interplanetary gases and dust.

For related information see also *75 Plasma Physics.*

N95-26522# Onsala Space Observatory (Sweden).
CO, HCO(+) AND HCN ABSORPTION IN THE GRAVITATIONAL LENS CANDIDATE B0218+357 AT $z=0.685$
T. Wiklind and F. Combes (Observatoire de Paris, France.) Dec. 1994 10 p
(PB95-185146) Avail: CASI HC A02/MF A01

Absorption lines of CO(1-2), CO(2-3), HCO+(1-2) and HCN(1-2) have been detected at a redshift of Z(a) = 0.68466 towards the background BL Lac object B0218+357. The CO and HCN lines are strongly saturated, while the HCO+ line is mildly saturated. Lower limits to the column densities are given. The filling factor for the background source is larger than 0.7-0.8. The absorption line profile is asymmetric with a width of approximately 30 km/s B0218+357 is a gravitational lens candidate with two compact continuum sources separated by 335 mas (1.8 kpc). The small linewidth of the molecular absorption puts constraints on the inclination and position angle of the lensing galaxy. We also report a search for quasi stellar objects (QSO's) molecular absorption lines in 12 other redshifted systems; none were detected. NTIS

N95-26593*# Smithsonian Astrophysical Observatory, Cambridge, MA.
A LONG-TERM SPACE ASTROPHYSICS RESEARCH PROGRAM: AN X-RAY PERSPECTIVE OF THE COMPONENTS AND STRUCTURE OF GALAXIES Annual Progress Report, 1 May 1994 - 30 Apr. 1995
G. Fabbiano Apr. 1995 184 p
(Grant NAGw-2681)
(NASA-CR-197787; NAS 1.26:197787) Avail: CASI HC A09/MF A02

X-ray studies of galaxies by the Smithsonian Astrophysical Observatory (SAO) and MIT are described. Activities at SAO include ROSAT PSPC x-ray data reduction and analysis pipeline; x-ray sources in nearby Sc galaxies; optical, x-ray, and radio study of ongoing galactic merger; a radio, far infrared, optical, and x-ray study of the Sc galaxy NGC247; and a multiparametric analysis of the Einstein sample of early-type galaxies. Activities at MIT included continued analysis of observations with ROSAT and ASCA, and continued development of new approaches to spectral analysis with ASCA and AXAF. Also, a new method for characterizing structure in galactic clusters was developed and applied to ROSAT images of a large sample of clusters. An appendix contains preprints generated by the research. CASI

N95-27131 Air Force Inst. of Tech., Wright-Patterson AFB, OH. School of Engineering.
SPACE MODELER: AN EXPANDED, DISTRIBUTED, VIRTUAL ENVIRONMENT FOR SPACE VISUALIZATION M.S. Thesis
John C. Vanderburgh Dec. 1994 93 p Limited Reproducibility: More than 20% of this document may be affected by microfiche quality
(AD-A289409; AFIT/GCS/ENG/94D-23) Avail: Issuing Activity (Defense Technical Information Center (DTIC))

The Space Modeler is the first truly immersive virtual environment that models the solar system, models satellites in near-Earth orbit, and can operate in a Distributed Interactive Simulation (DIS) environment. It increases the capabilities of the 1993 Satellite Modeler by expanding the physical limits of the environment and by implementing a new three-dimensional user interface. Satellite orbits are modeled using NASA two line element sets. The positions of the Sun, Moon and planets are computed using an algorithm based on planetary orbital element sets using a linear polynomial fit. For higher precision, the planetary orbits can be computed using an algorithm based on VSOP87 planetary theory. The user interface is a three-dimensional array of panels, with buttons for controlling all aspects of the environment. The interface is easily accessible to an immersed user, and provides interactive movement controls for five. degrees of freedom, attachment to objects in the environment, setting the rate at which the simulation runs, and toggling the display of all visual features. The Space Modeler can model the solar system and render up to 50 satellites in near-Earth orbit using magnetic head tracking with a 20-30 Hz frame update rate. DTIC

N95-27166*# Johns Hopkins Univ., Baltimore, MD. Bloomberg Center for Physics and Astronomy.
OBSERVATIONS OF COMETS WITH THE IUE Final Report, 1 Dec. 1992 - 31 Jan. 1995
Paul D. Feldman 31 Jan. 1995 8 p
(Grant NAG5-2141)
(NASA-CR-197816; NAS 1.26:197816) Avail: CASI HC A02/MF A01

This is the final report for Observation of Comets with the IUE, which began in December 1992 and was completed in January 1995. This grant continued our IUE program which began in July 1979 and was terminated in September 1992. Attached in Appendix A is a complete list of publications related to IUE observations of comets from 1980 to the present. Publication numbers 51-53 appeared during the December 1992 - January 1995 period and copies of these are being forwarded to the NSSDC along with this report. Papers presented at recent scientific meetings are listed in Appendix B. During this period we have concentrated our effort into two distinct areas: new observations of comets of interest and continuing analysis of the data from previous observations. Derived from text

N95-27303 Air Force Inst. of Tech., Wright-Patterson AFB, OH. School of Engineering.
TRACKING AND IMPACT PREDICTION OF EARTH-CROSSING-OBJECTS (ECO'S) ON A COLLISION COURSE WITH EARTH M.S. Thesis
Gregory A. Bishop Dec. 1994 108 p Limited Reproducibility: More than 20% of this document may be affected by microfiche quality
(AD-A289321; AFIT/GSO/ENY/94D-01) Avail: Issuing Activity (Defense Technical Information Center (DTIC))

This study investigated the effectiveness of earth-based angles only observations in determining the orbit of various hypothetical earth-crossing-objects (ECO's). 'True' trajectories were simulated specifically for earth-crossing-comets (ECC's) by numerically integrating in a restricted three body system. Starting at earth impact points, the state vectors were 'reverse-propagated' to a proposed detection time. Observations (obs), with state-of-the-art accuracy, were then simulated with error induced by a Gaussian random number generator; these were used in a least-squares differential corrector to estimate the positions of the ECO's. State vectors and covariance matrices were then propagated to the impact times and axis lengths of the one sigma impact footprint were calculated. Varied amounts of data were fed into the differential corrector and it was determined that earth-based obs alone may be ineffective in predicting an ECC's orbit. DTIC

N95-27320 Observatoire de Paris-Meudon (France).
MOLECULAR CLOUD CONTENT OF EARLY-TYPE GALAXIES. V. CO IN ELLIPTICAL GALAXIES
T. Wiklind, F. Combes, and C. Henkel 25 Oct. 1994 19 p See also PB93-151074 Prepared in cooperation with Observatoire de Paris, Meudon France, Max-Planck-Inst. fuer Radioastronomie, Bonn, Germany Limited Reproducibility: More than 20% of this document may be affected by microfiche quality
(PB95-185153) Avail: CASI HC A03/MF A01

A survey of CO emission in 29 far-IR selected elliptical galaxies resulted in 16 detections, of which 3 remain tentative. The molecular gas masses range from 2 x 10(exp 6) solar masses to 1 x 10(exp 9) solar masses, and appear to be unrelated to the underlying stellar population. This suggests an external origin of the gas. Most of the elliptical galaxies with a molecular gas component have a gas-to-dust mass ratio of about 700, where dust masses are derived from the Infrared Astronomy Satellite (IRAS) fluxes, but some appear to have a ratio as low as 50. A small apparent gas-to-dust mass ratio is also found for some late-type galaxies, and is correlated with a low dust temperature. NTIS

N95-27326# Los Alamos National Lab., NM.
VIEWS OF THE SOLAR SYSTEM
C. Hamilton 1995 199 p
(Contract W-7405-eng-36)
(DE95-006446; LA-UR-94-3033) Avail: CASI HC A09/MF A03

Views of the Solar System has been created as an educational tour of the solar system. It contains images and information about the Sun, planets, moons, asteroids and comets found within the solar system. The image processing for many of the images was done by the author. This tour uses hypertext to allow space travel by simply clicking on a desired planet. This causes information and images about the planet to appear on screen. While on a planet page, hyperlinks travel to pages about the moons and other relevant available resources. Unusual terms are linked to and defined in the Glossary page. Statistical information of the planets and satellites can be browsed through lists sorted by name, radius and distance. History of Space Exploration contains information about rocket history, early astronauts, space missions, spacecraft and detailed chronology tables of space exploration. The Table of Contents page has links to all of the various pages within Views of the Solar System. DOE

N95-27343# Joint Inst. for Nuclear Research, Dubna (USSR). Lab. of Theoretical Physics.
ON HIGHER DERIVATIVE GRAVITY IN TWO DIMENSIONS
S. N. Solodukhin 1994 26 p Submitted for publication
(DE95-608789; JINR-E-2-94-185) Avail: CASI HC A03/MF A01 (US Sales Only)

The 2 D gravity described by the action which is as arbitrary function of the scalar curvature f(R) is considered. The classical vacuum solutions are analyzed. The one-loop renormalizability is studied. For the function f R1nR the model coupled with scalar (conformal) matter is exactly integrated and is shown to describe a black hole of the 2 D dilaton gravity type. The influence of one-loop quantum corrections on a classical black hole configuration is studied by including the Liouville-Polyakov term. The resulting model turns out to be exactly solvable. The general solution is analyzed and shown to be free from the space-time singularities for a certain number of scalar fields. DOE

N95-27445# Los Alamos National Lab., NM.
THE SECOND COMING OF COLD DARK MATTER?
W. H. Zurek, B. C. Bromley, and M. S. Warren 1994 11 p Presented at the 5th Astrophysics Conference: Dark Matter, College Park, MD, 10-12 Oct. 1994
(Contract W-7405-eng-36)
(DE95-005156; LA-UR-94-4268; CONF-9410287-2) Avail: CASI HC A03/MF A01

While the standard cold dark matter (CDM) model has received numerous marks against it on the basis of a variety of observational data, the prediction of high (Sigma)(Upsilon), the pairwise-velocity dispersion between galaxies, on small (megaparsec) scales was reported as perhaps one of its greatest failings. Here, we reexamine the case of CDM and (Sigma)(Upsilon), with high-resolution numerical simulations. The statistic was measured in simulations, in artificial galaxy catalogs, and in the CfA North Forty redshift survey. In our reanalysis of the CfA data, we found that (Sigma)(Upsilon) (approximately) 500 km/s, significantly higher than the original estimates of Davis & Peebles (1983). This new value, along with our estimate of the velocity bias, leads to a virial measure of the cosmological density parameter, (Omega) (approximately) 0.9, which is more than four times the traditionally cited CfA result. Analysis of the simulations indicates that while the method of Davis and Peebles works well, the (Sigma)(Upsilon) statistic itself is not generally robust: there is large scatter from catalog to catalog and evidence that the recovered (Sigma)(Upsilon) value depends strongly on a small fraction of galaxies in the central regions of rare, massive clusters. Thus, at present the CDM model cannot be deemed incompatible with observed small-scale peculiar velocities. DOE

N95-28013# Lawrence Livermore National Lab., Livermore, CA.
LABORATORY HIGH-ENERGY ASTROPHYSICS ON LASERS
W. H. Goldstein, D. A. Liedahl, R. S. Walling, M. E. Foord, A. L. Osterheld, and B. G. Wilson Dec. 1994 7 p Presented at the ECLIM 23: Laser Interaction With Matter, Oxford, United Kingdom, 19-23 Sep. 1994
(Contract W-7405-eng-48)
(DE95-008062; UCRL-JC-119288; CONF-9409226-5) Avail: CASI HC A02/MF A01

The tremendous range of temperatures and densities spanned by astrophysical plasmas has significant overlap with conditions attainable using high-power laser facilities. These facilities provide an opportunity to create, control, and characterize plasmas in the laboratory that mirror conditions in some of the most important cosmological systems. Moreover, laboratory experiments can enhance astrophysical understanding by focusing on and isolating important physical processes, without necessarily reproducing the exact conditions of the integral system. Basic study of radiative properties, transport phenomena, thermodynamic response and hydrodynamic evolution in plasmas under properly scaled conditions leads both directly and indirectly to improved models of complex astrophysical systems. In this paper, we will discuss opportunities for current and planned highpower lasers to contribute to the study of high-energy astrophysics. DOE

N95-28056# Los Alamos National Lab., NM.
PRECISION ASTEROSEISMOLOGY OF DAV (ZZ CETI) WHITE DWARF STARS
P. A. Bradley 1995 18 p Presented at the Astrophysical Applications of Stellar Pulsation, Cape Town, South Africa, 6-10 Feb. 1995
(DE95-006265; LA-UR-95-281; CONF-950278-1-Vugraphs) Avail: CASI HC A03/MF A01

This paper discusses the evolution of DA variable White Dwarf stars. Such objects are called DAV or ZZ Ceti white dwarfs. The author presents a model which allows the chemical composition profile, and the stellar mass and T(sub eff) to vary. With this model the author argues he can constrain the stellar mass, the composition profile, including hydrogen and helium mass, C/O ratios in the core and C/O composition profiles, composition gradients, the luminosity, and from this the effective temperature and distance, and the rotation rate and/or magnetic field strength based on fine structure splittings. DOE

N95-28062# Los Alamos National Lab., NM.
A NEW METHOD OF DETERMINING THE EJECTED MASS OF NOVAE
W. M. Sparks 1994 6 p Presented at the Padova-Abano Conference on Cataclysmic Variables: Inter Class Relations, Abano, Italy, 19-25 Jun. 1994
(Contract W-7405-eng-36)
(DE95-007884; LA-UR-95-568; CONF-9406308-1) Avail: CASI HC A02/MF A01

A new method of determining the ejected mass of novae based on simple, reasonable assumptions is presented. This method assumes that the remnant mass on the white dwarf is the same as that from the previous nova outburst. The hydrogen, helium, and metal abundances of the accreted material from the secondary must also be known or assumed. The white dwarf's mass has a small effect because the amount of hydrogen consumed during the thermonuclear runaway only depends weakly upon this mass. If the composition of the ejecta and the time of the remnant shell burnout are determined from observations, then the ejected and remnant masses can be deduced. At present only a sharp decrease in the X-rays observed by ROSAT has been attributed to this remnant burnout and only for two novae: GQ Mus and V1974 Cyg. The ejected and remnant masses for these two novae are calculated. If other indicators of nova remnant burnout, such as a rapid decrease in high-ionization lines, can be identified, then this method could be applied to additional novae. DOE

N95-28216*# Institute for Scientific Research, Lexington, MA.
THEORETICAL STUDIES OF INTERSTELLAR PROCESSES Final Report, 1 Dec. 1991 - 28 Feb. 1995
Steven L. Guberman 28 Feb. 1995 5 p
(Grant NAGw-2832)
(NASA-CR-198647; NAS 1.26:198647) Avail: CASI HC A01/MF A01

We have been studying the dissociative recombination (DR) of HeH(+) with an electron with the goal of calculating accurate cross sections and rate coefficients to allow for the accurate modelling of the abundance of HeH(+) in planetary nebulae and supernova envelopes. A unique feature of the HeH potential curves is that none of the neutral states cross the ion curve. This required a new approach to the calculation of DR cross sections and rate coefficients that had not yet appeared in the literature. Because of the lack of a potential curve crossing, the initial electron capture occurs by Born-Oppenheimer breakdown, i.e. by the interaction of the motion of the incoming electron with the nuclear motion. This same mechanism also drives DR in H3(+) and the methods developed and described below for HeH(+) DR will be used for the future calculation of H3(+) DR. Derived from text

N95-28222*# Pennsylvania State Univ., Erie, PA. Div. of Science.
SEARCH FOR MOLECULAR ABSORPTIONS WITH THE FOURIER TRANSFORM SPECTROMETER Final Report
Roger F. Knacke 21 May 1995 3 p Prepared for The State Univ. of

NY, Stony Brook, NY
(Grant NAG2-495)
(NASA-CR-198648; NAS 1.26:198648) Avail: CASI HC A01/MF A01

The objective of this research was a search for water molecules in the gas phase in molecular clouds. Water should be among the most abundant gases in the clouds and is of fundamental importance in gas chemistry, cloud cooling, shock wave chemistry, and gas-grain interactions of interstellar dust. Detection of water in Comet Halley in the 2.7 micron v(3) band in 1986 had shown that airborne H2O observations are feasible (ground-based observations of H2O are impossible because of the massive water content of the atmosphere). We planned to observe the v(3) band in interstellar clouds where a number of lines of this band should be in absorption. The search for H2O commenced in 1988 with a two flight program on the KAO. this resulted in a detection of interstellar H2O with S/N of 2-4 in the v(3) 1(01)-2(02) line at 3801.42/cm. A subsequent flight series of two flights in 1989 resulted in confirmation to the 3801.42/cm line detection and the detection of altogether four strong lines in the 000-001 v(3) vibration-rotation band of H2O. Derived from text

__N95-28328*__ National Aeronautics and Space Administration. Goddard Space Flight Center, Greenbelt, MD.
INTERNATIONAL ULTRAVIOLET EXPLORER ATLAS OF B-TYPE SPECTRA FROM 1200 TO 1900 A
Nolan R. Walborn, Joel William Parker, and Joy S. Nichols Apr. 1995 101 p
(RTOP 680-00-00)
(NASA-RP-1363; Rept-95B00054; NAS 1.61:1363) Avail: Issuing Activity (Goddard Space Flight Center, Greenbelt, MD)

An Atlas of B-type spectra observed at high resolution by the International Ultraviolet Explorer is presented. It is designed to complement the widely used O-type Atlas (NASA RP-1155). The purpose is to complete the OB natural group, i.e., to spectral type B3 on the main sequence and B8 at luminosity class Ia, in order to chart the gradual disappearance of the stellar-wind features in normal spectra as a function of spectral type and luminosity class. As in the O Atlas, the primary selection criterion is well-defined optical classifications to derive a consistent ultraviolet (UV) reference frame of normal objects. Some peculiar categories are also included, particularly types BN/BC and superluminous objects. Spectrograms of 86 stars are arranged in 20 spectral-type, luminosity-class, or peculiar-object sequences. The processing and presentation are similar to the O Atlas: the 1200-l900 A range has been rectified, rebinned to a uniform resolution of 0.25A, and plotted at 10 A/cm. The conclusions from the B Atlas are similar to those from the O Atlas, namely, that the UV stellar-wind features display strong systematic trends as a function of spectral type and luminosity class, and a high degree of correlation with the optical classifications as the winds decline toward the later types. A somewhat higher rate of exceptions to these correlations can be recognized among the B spectra (11 percent) than the O (2 percent), but they remain a small fraction of the total sample and do not prevent clear delineation of the normal behavior. Indeed, it is only as a result of the latter that the exceptions can be identified and described. Author

__N95-28357#__ California Univ., Berkeley. Lawrence Berkeley Lab, CA.
STABILITY OF STRANGE QUARK STARS WITH NUCLEAR CRUSTS AGAINST RADIAL OSCILLATIONS
Ch. Kettner, M. K. Weigel (Ludwig-Maximilians-Univ., Munich, Germany.), F. Weber (Ludwig-Maximilians-Univ., Munich, Germany.), and N. K. Glendenning Dec. 1994 10 p Presented at the Symposium on Strangeness and Quark Matter, Crete, Greece, 1-5 Sep. 1994
(Contract DE-AC03-76SF-00098)
(DE95-008484; LBL-36209; CONF-9409310-1) Avail: CASI HC A02/MF A01

This paper investigates the stability of the complete sequence of strange-matter stars with nuclear crusts against radial pulsations (acoustical modes). It is found that a broad class of white dwarf- like strange stars is stable against such pulsations. The same holds for the much denser strange stars, which are the strange counter-parts of neutron stars. All stars possessing still higher central densities (e.g., charm stars) turn out to be unstable. DOE

__N95-28558#__ Lawrence Livermore National Lab., Livermore, CA.
STATIONARY NEUTRINO RADIATION TRANSPORT BY MAXIMUM ENTROPY CLOSURE
S. A. Bludman (California Univ., Berkeley. Lawrence Berkeley Lab, CA.) and J. Cernohorsky (California Univ., Berkeley. Lawrence Berkeley Lab, CA.) Nov. 1994 18 p Presented at the Physics of Supernovae, Philadelphia, PA, 6-8 Apr. 1994
(Contract DE-AC03-76SF-00098)
(DE95-006579; LBL-36135; UPR-0631T; CONF-9404245-1) Avail: CASI HC A03/MF A01

The authors obtain the angular distributions that maximize the entropy functional for Maxwell-Boltzmann (classical), Bose-Einstein, and Fermi-Dirac radiation. In the low and high occupancy limits, the maximum entropy closure is bounded by previously known variable Eddington factors that depend only on the flux. For intermediate occupancy, the maximum entropy closure depends on both the occupation density and the flux. The Fermi-Dirac maximum entropy variable Eddington factor shows a scale invariance, which leads to a simple, exact analytic closure for fermions. This two-dimensional variable Eddington factor gives results that agree well with exact (Monte Carlo) neutrino transport calculations out of a collapse residue during early phases of hydrostatic neutron star formation. DOE

__N95-27668*#__ National Aeronautics and Space Administration. Langley Research Center, Hampton, VA.
ORBITING METEOROID AND DEBRIS COUNTING EXPERIMENT
William H. Kinard, Dwayne Armstrong, Sharon K. Crockett, James L. Jones, Jr., Philip C. Kassel, Jr., and J. J. Wortman (North Carolina State Univ., Raleigh, NC.) *In its* LDEF: 69 Months in Space. Third Post-Retrieval Symposium, Part 3 Feb. 1995 p 1331-1340 (For primary document see N95-27629 09-99)
Avail: CASI HC A02/MF A04

91 LUNAR AND PLANETARY EXPLORATION

Includes planetology; and manned and unmanned flights.
For spacecraft design or space stations see *18 Spacecraft Design, Testing and Performance.*

__N95-27700*#__ Michigan Univ., Ann Arbor, MI. Radiation Lab.
THEORETICAL AND EXPERIMENTAL MODELS OF THE DIFFUSE RADAR BACKSCATTER FROM MARS Final Report, 1 Jul. 1990 - 30 Jun. 1994
A. W. England 19 May 1995 84 p
(Grant NAGw-2199)
(NASA-CR-198650; NAS 1.26:198650) Avail: CASI HC A05/MF A01

The general objective for this work was to develop a theoretically and experimentally consistent explanation for the diffuse component of radar backscatter from Mars. The strength, variability, and wavelength independence of Mars' diffuse backscatter are unique among our Moon and the terrestrial planets. This diffuse backscatter is generally attributed to wavelength-scale surface roughness and to rock clasts within the Martian regolith. Through the combination of theory and experiment, the authors attempted to bound the range of surface characteristics that could produce the observed diffuse backscatter. Through these bounds they gained a limited capability for data inversion. Within this umbrella, specific objectives were: (1) To better define the statistical roughness parameters of Mars' surface so that they are consistent with observed radar backscatter data, and with the physical and chemical characteristics of Mars' surface as inferred from Mariner 9, the Viking probes, and Earth-based spectroscopy; (2) To better understand the partitioning between surface and volume scattering in the Mars regolith; (3) To develop computational models of Mars' radio emission that incorporate frequency dependent, surface and volume scattering. Author

__N95-27916*#__ Colorado Univ., Boulder, CO. Dept. of Astrophysical, Planetary and Atmospheric Sciences.
STUDIES OF PLANETARY SCALE WAVES AND INSTABILITIES IN SUPPORT OF THE GEOPHYSICAL FLUID FLOW CELL EXPERIMENT ON USML-2 Final Technical Report
J. E. Hart 30 May 1995 35 p Original contains color illustrations

(Grants NAG8-190; NAG8-1077)
(NASA-CR-198646; NAS 1.26:198646) Avail: CASI HC A03/MF A01; 2 functional color pages

High resolution numerical simulations of thermal convection in a rapidly rotating channel with gravity perpendicular to the rotation vector are described. The convecting columns are subject to a beta-effect resulting from cross-channel topographic vortex stretching. The symmetries of the problem allow many invariant wavenumber sets, and this property is associated with the existence of stable multiple-equilibria at modest supercriticality. The transition to chaotic behavior involves the production of intermittent unstable orbits off a two-torus in energy space. At very high Rayleigh number (of order 10(exp 6) to 10(exp 7)) the motion can be turbulent, depending on the size of beta. However, the turbulence is usually characterized by an almost-periodic formation of patches of small scale convection that cause regular pulsations in the accompanying strong zonal jets. The processes maintaining these flows may be related to those responsible for the zonal currents on Jupiter and for cyclic variability on the Sun. Author

N95-28009*# National Aeronautics and Space Administration, Washington, DC.
TOPS: TOWARD OTHER PLANETARY SYSTEMS. A REPORT BY THE SOLAR SYSTEM EXPLORATION DIVISION
1995 138 p
(NASA-TM-110609; NAS 1.15:110609; PB95-184024) Avail: CASI HC A07/MF A02

This report describes a general plan and the pertinent technological requirements for TOPS (Toward Other Planetary Systems), a staged program to ascertain the prevalence and character of other planetary systems and to construct a definitive picture of the formation of stars and their planets. The first stages focus on discovering and studying a significant number of fully formed planetary systems, as well as expanding current studies of protoplanetary systems. As the TOPS Program evolves, emphasis will shift toward intensive study of the discovered systems and of individual planets. Early stages of the TOPS Program can be undertaken with ground-based observations and space missions comparable in scale to those now being performed. In the long term, however, TOPS will become an ambitious program that challenges our capabilities and provides impetus for major space initiatives and new technologies. NTIS

N95-27265*# Jet Propulsion Lab., California Inst. of Tech., Pasadena, CA.
THE ALPHA-PROTON-X-RAY SPECTROMETER DEPLOYMENT MECHANISM: AN ANTHROPOMORPHIC APPROACH TO SENSOR PLACEMENT ON MARTIAN ROCKS AND SOIL
Richard S. Blomquist *In* NASA. Johnson Space Center, The 29th Aerospace Mechanisms Symposium May 1995 p 61-78 (For primary document see N95-27260 09-15)
Avail: CASI HC A03/MF A04

92 SOLAR PHYSICS

Includes solar activity, solar flares, solar radiation and sunspots.
For related information see *93 Space Radiation.*

N95-26671*# Lockheed Missiles and Space Co., Palo Alto, CA. Research Lab.
CORONAL ABUNDANCES AND THEIR VARIATION Final Annual Progress Report, 15 Apr. 1994 - 15 Apr. 1995
Julia L. R. Saba 28 Apr. 1995 19 p
(Contract NASw-4814)
(NASA-CR-197788; NAS 1.26:197788) Avail: CASI HC A03/MF A01

This contract supports the investigation of elemental abundances in the solar corona, principally through analysis of high-resolution soft X-ray spectra from the Flat Crystal Spectrometer on the Solar Maximum Mission. The goals of the study are a characterization of the mean values of relative abundances of elements accessible in the FCS data, and information on the extent and circumstances of their variability. This report is a summation of the data analysis and reporting activities which occurred during the period of 15 April 1994 to 15 April 1995. Author

N95-27184 Army Cold Regions Research and Engineering Lab., Hanover, NH.
SOLAR TERRESTRIAL RADIATION DATA FROM THE SLEEPERS RIVER RESEARCH WATERSHED
Janet P. Hardy Aug. 1994 30 p Limited Reproducibility: More than 20% of this document may be affected by microfiche quality
(AD-A288444; CRREL-SR-94-24) Avail: Issuing Activity (Defense Technical Information Center (DTIC))

A long-term (24-year) database of solar and terrestrial radiation, as monitored in northern Vermont, has been compiled. This extensive database is a result of cooperative efforts among many different government agencies. This report summarizes the present status of the solar and terrestrial radiation database, the instrumentation and calibration, and methods of data measurement, acquisition and analysis. DTIC

N95-27342# International Centre for Theoretical Physics, Trieste (Italy).
AXIONIC FUEL FOR SUN
V. S. Vanyashin Aug. 1994 5 p
(DE95-608788; IC-94/223) Avail: CASI HC A01/MF A01 (US Sales Only)

If a Bose condensate of relic hypothetical axions is sufficiently accumulated by the Sun during its evolution, it may be a noticeable source of solar energy, complementary to the thermonuclear one. For the rate of the condensate relaxation in the solar plasma medium an adequate kinetic Boltzmann equation has been derived. Fortunately, the effect depends on first rather than second power of the small coupling constant, that is typical for the quantum parametric resonance phenomena. DOE

N95-27858*# Hughes STX, Inc., Lanham, MD.
PLASMA PROPERTIES AND MAGNETIC FIELD STRUCTURE OF THE SOLAR CORONA, BASED ON COORDINATED MAX 1991 OBSERVATIONS FROM SERTS, THE VLA, AND MAGNETOGRAPHS Annual Report, 12 Jul. 1994 - 11 Jul. 1995
Jeffrey W. Brosius 11 Jul. 1995 44 p
(Contract NASw-4933)
(NASA-CR-198592; NAS 1.26:198592) Avail: CASI HC A03/MF A01

The purposes of this investigation are to use existing, calibrated, coaligned sets of coordinated multiwaveband observations of the Sun to determine the coronal magnetic field strength and structure, and interpret the collective observations in terms of a self-consistent model of the coronal plasma and magnetic field. This information is vital to understanding processes such as coronal heating, solar wind acceleration, pre-flare energy storage, and active region evolution. Understanding these processes is the central theme of Max '91, the NASA-supported series of solar observing campaigns under which the observations acquired for this work were obtained. The observations came from NASA/GSFC's Solar EUV Rocket Telescope and Spectrograph (SERTS), the Very Large Array (VLA), and magnetographs. The technique of calculating the coronal magnetic field is to establish the contributions to the microwave emission from the two main emission mechanisms: thermal bremsstrahlung and thermal gyroemission. This is done by using the EUV emission to determine values of the coronal plasma quantities needed to calculate the thermal bremsstrahlung contribution to the microwave emission. Once the microwave emission mechanism(s) are determined, the coronal magnetic field can be calculated. A comparison of the coronal magnetic field derived from the coordinated multiwaveband observations with extrapolations from photospheric magnetograms will provide insight into the nature of the coronal magnetic field. Derived from text

N95-28007# National Oceanic and Atmospheric Administration, Boulder, CO.
SOLAR UV FLUX MEASUREMENTS FROM THE SBUV2 MONITOR ON THE NOAA9 SATELLITE. PART 1: Mg II h AND k LINE CORE-TO-WING RATIOS FOR 1986-1988 Technical Memo
R. F. Donnelly, L. C. Puga, J. Barrett, S. D. Bouwer, J. Pap, D. E. Stevens, and W. K. Tobiska Dec. 1994 220 p Prepared in cooperation with Colorado Univ.
(PB95-181962; NOAA-TM-ERL-SEL-85) Avail: CASI HC A10/MF A03

Analyses of the discrete-wavelength mode of observations of the solar full-disk MG 2 h and k line spectral irradiance measured by the Solar Backscatter UV Monitor (SBUV2) on the NOAA9 satellite are presented. Relative photometry techniques were used to derive a core-to-wing. This ratio has been modified, relative to that used by Heath and Schlesinger's (1986) classical MG 2 ratio derived for solar UV measurements made by their SBUV experiment aboard the Nimbus-7 satellite, to avoid inter-range instrumentation drifts encountered in the NOAA9 SBUV2 monitor. Prior research of the solar MG 2 h and k lines is reviewed. The raw measurements and observational parameters, such as the angle of the Sun as seen at the SBUV2 monitor are discussed. Temporal interpolations among the sets of discrete-mode measurements are used to account for most of the Sun-angle dependence and to reduce the sensitivity of the results to any errors in the Sun angles. Wavelength 'jitter' and long-term drift are studied, and intensity linearity and inter-range drift are analyzed. The NOAA9 results are compared with same-day Nimbus-7 data, the Kitt Peak Ca K1 angstrom index, the Canadian 10.7 cm solar radio flux, and observations of the solar H Lyman alpha line. NTIS

N95-28087# National Geophysical Data Center, Boulder, CO.

SOLAR-GEOPHYSICAL DATA NUMBER 604, DECEMBER 1994. PART 1: (PROMPT REPORTS). DATA FOR NOVEMBER, OCTOBER 1994, AND LATE DATA

H. E. Coffey Dec. 1994 134 p

(PB95-181848; SGD-604-Pt-1) Avail: CASI HC A07/MF A02

The following topics are discussed: (1) Solar-Terrestrial Environment - Plots of GOES satellite X-rays, Particles and Magnetometer data with ground-based Boulder Magnetometer and Deep River Neutron Monitor; (2) IUWDS Alert Periods (Advance and Worldwide); (3) Solar Activity Indices - Daily Sunspot Numbers (12 Months), Daily 2800 MHz Solar Flux (12 Months), Daily Solar Indices (Sunspot Numbers and Solar Flux); (4) Smoothed Observed and Predicted Sunspot Numbers, Graph and Table of Monthly Mean Solar Radio Flux 1950-present, Plot of Monthly Mean Sunspot Numbers Jan. 1749-Nov. 1994; (5) Solar Flares; (6) Solar Radio Emission; (7) Stanford Mean Solar Magnetic Field; and (8) GOES-7 Daily Electron Fluence. NTIS

N95-28500 Rutherford Appleton Lab., Oxford (England).

THREEFOLD MAXIMAL LEPTON MIXING AND THE SOLAR AND ATMOSPHERIC NEUTRINO DEFICITS

P. F. Harrison, D. H. Perkins, and W. G. Scott Dec. 1994 29 p

Prepared in cooperation with Queen Mary and Westfield Coll. and Oxford Univ.

(PB95-196259; RAL-94-125) Avail: Issuing Activity

Threefold maximal mixing would imply a cyclic permutation symmetry among the generations. The data from solar and atmospheric neutrino experiments are consistent with such mixing, and require a hierarchical spectrum of mass-squared differences for the neutrinos. A fit for the two independent mass-squared differences (excluding only the HOMESTAKE solar neutrino result) yields: Delta(m squared) = (0.72 + or - 0.18) x 10(exp -2)e(V squared) and Delta(m' squared) less than 0.9 x 10(exp -11)e(V squared) at 90% confidence. In the case that the neutrino mass spectrum is qualitatively similar to that of the charged leptons and quarks, these results can be re-expressed in terms of the neutrino masses as follows: m(3) approx = 85 + or - 10 meV, and m(1), m(2) less than 3(micro)eV at 90% confidence. Implications for future experiments are discussed. NTIS

93 SPACE RADIATION

Includes cosmic radiation; and inner and outer earth's radiation belts.

For biological effects of radiation see *52 Aerospace Medicine*. For theory see *73 Nuclear and High-Energy Physics.*

N95-26427*# National Aeronautics and Space Administration. Langley Research Center, Hampton, VA.

RADIATION SAFETY ASPECTS OF COMMERCIAL HIGH-SPEED FLIGHT TRANSPORTATION

John W. Wilson, John E. Nealy, Francis A. Cucinotta, Judy L. Shinn, Ferenc Hajnal (Department of Energy, New York, NY.), Marcel Reginatto (Department of Energy, New York, NY.), and Paul Goldhagen (Department of Energy, New York, NY.) May 1995 33 p

(RTOP 537-09-21-05)

(NASA-TP-3524; L-17450; NAS 1.60:3524) Avail: CASI HC A03/MF A01

High-speed commercial flight transportation is being studied for intercontinental operations in the 21st century, the projected operational characteristics for these aircraft are examined, the radiation environment as it is now known is presented, and the relevant health issues are discussed. Based on a critical examination of the data, a number of specific issues need to be addressed to ensure an adequate knowledge of the ionizing radiation health risks of these aircraft operations. Large uncertainties in our knowledge of the physical fields for high-energy neutrons and multiply-charged ion components need to be reduced. Improved methods for estimating risks in prenatal exposure need to be developed. A firm basis for solar flare monitoring and forecasting needs to be developed with means of exposure abatement. Author

N95-26630*# Columbia Univ., New York, NY. Dept. of Astronomy and Physics.

MULTIWAVELENGTH OBSERVATIONS OF UNIDENTIFIED HIGH ENERGY GAMMA-RAY SOURCES Annual Status Report, 15 Feb. 1994 - 14 Feb. 1995

Jules P. Halpern May 1995 17 p

(Grant NAG5-2051)

(NASA-CR-197840; NAS 1.26:197840; CAL-2314) Avail: CASI HC A03/MF A01

As was the case for COS B, the majority of high-energy (greater than 100 MeV) gamma-ray sources detected by the EGRET instrument on GRO are not immediately identifiable with catalogued objects at other wavelengths. These persistent gamma-ray sources are, next to the gamma-ray bursts, the least understood objects in the universe. This two year investigation is intended to support the analysis, correlation, and theoretical interpretation of data that we are obtaining at x-ray, optical, and radio wavelengths in order to render the gamma-ray data interpretable. This second year was devoted to studies of unidentified gamma-ray sources from the first EGRET catalog, similar to previous observations. Efforts have concentrated on the sources at low and intermediate Galactic latitudes, which are the most plausible pulsar candidates. Derived from text

N95-28530*# National Aeronautics and Space Administration. Langley Research Center, Hampton, VA.

HZETRN: DESCRIPTION OF A FREE-SPACE ION AND NUCLEON TRANSPORT AND SHIELDING COMPUTER PROGRAM

John W. Wilson, Francis F. Badavi (Christopher Newport Coll., Newport News, VA.), Francis A. Cucinotta, Judy L. Shinn, Gautam D. Badhwar (National Aeronautics and Space Administration. Lyndon B. Johnson Space Center, Houston, TX.), R. Silberberg (Universities Space Research Association, Washington, DC.), C. H. Tsao (Naval Research Lab., Washington, DC.), Lawrence W. Townsend, and Ram K. Tripathi (Christopher Newport Coll., Newport News, VA.) May 1995 148 p

(RTOP 199-45-16-11)

(NASA-TP-3495; L-17417; NAS 1.60:3495) Avail: CASI HC A07/MF A02

The high-charge-and energy (HZE) transport computer program HZETRN is developed to address the problems of free-space radiation transport and shielding. The HZETRN program is intended specifically for the design engineer who is interested in obtaining fast and accurate dosimetric information for the design and construction of space modules and devices. The program is based on a one-dimensional space-marching formulation of the Boltzmann transport equation with a straight-ahead approximation. The effect of the long-range Coulomb force and electron interaction is treated as a continuous slowing-down process. Atomic (electronic) stopping power coefficients with energies above a few A MeV are calculated by using Bethe's theory including Bragg's rule, Ziegler's shell corrections, and effective charge. Nuclear absorption cross sections are obtained from fits to quantum calculations and total cross sections are obtained with a Ramsauer formalism. Nuclear fragmentation cross sections are calculated with a semiempirical abrasion-ablation fragmentation model. The relation of the final computer code to the Boltzmann equation is discussed in the context of simplifying assumptions. A detailed description of the flow of the computer code, input requirements, sample output, and compatibility requirements for non-VAX platforms are provided. Author

99 GENERAL

N95-26604 Princeton Univ., NJ. Dept. of Mechanical and Aerospace Engineering.

FUNDING FOR AFRAPT STUDENT TRAINEES FOR ACADEMIC YEAR 1992-1993 Annual Technical Report, 1 Oct. 1992 - 30 Sep. 1993

Chung K. Law 30 Aug. 1994 16 p Sponsored by United Technologies Corp. and the Air Force Office of Scientific Research AFRAPT Program Limited Reproducibility: More than 20% of this document may be affected by microfiche quality
(Grant AF-AFOSR-0473-89)
(AD-A288461; Rept-2308; AFOSR-94-0693TR) Avail: Issuing Activity (Defense Technical Information Center (DTIC))

The progress of seven AFRAPT (Air Force Research in Aero Propulsion Technology) student trainees for the academic year 1992-1993 is reported. DTIC

N95-26823 Naval Research Lab., Washington, DC.

BIBLIOGRAPHY OF NRL PUBLICATIONS - 1990

Eileen A. Pickenpaugh, Kenneth L. Thoenes, Alice B. Cox, and Richard W. Peacock 6 Dec. 1994 88 p Limited Reproducibility: More than 20% of this document may be affected by microfiche quality
(AD-A289483; NRL/FR/5220-94-9378) Avail: Issuing Activity (Defense Technical Information Center (DTIC))

This report lists Naval Research Laboratory papers published in periodicals, books, and proceedings, and Naval Research Laboratory in-house publications including formal and memorandum reports, which became available in 1990. Patents received by Naval Research Laboratory personnel in the year of 1990 are also listed as they appeared in Patent Issue Report published by the Naval Research Laboratory Patent Office. The papers are listed in the following broad subject categories: acoustics; artificial intelligence; atmospheric sciences; biosciences; ceramics, glasses, and plastics; chemistry; communications; computer sciences; electronics and electricity; fluid mechanics; geosciences; information; instrumentation; laser science; magnetism; mathematics; mechanics; metallurgy; nuclear science; ocean science and technology; optical sciences; physics; plasma physics; radar; radiation technology; solid state; space science and technology; and structure research. Within each subject category, papers are listed alphabetically by title as are the in-house publications and patents appearing after the listing of papers. An asterisk following an author's name indicates that author was not an employee of the Naval Research Laboratory. An author index is included. DTIC

N95-26856 Air Force Systems Command, Wright-Patterson AFB, OH. National Air Intelligence Center.

CHINESE SPACE SCIENCE AND TECHNOLOGY

13 Dec. 1994 141 p Transl. into ENGLISH from Zhongguo Kongjian Kexue Jishu (Russia), v. 10, no. 6, Dec. 1990 p 1-29 and 34-70 Limited Reproducibility: More than 20% of this document may be affected by microfiche quality
(AD-A289618; NAIC-ID(RS)T-0661-94) Avail: Issuing Activity (Defense Technical Information Center (DTIC))

Contents are: ablative thermal protective mechanism and numerical simulation for returnable satellite; ablative thermal protection structure design of ballistic return module; thermal control design of returnable satellite; main factors affecting photographic quality of prism scanning panoramic camera; electric power system of returnable satellites; development of return technology and returnable spacecraft; China's returnable satellites; deriving recovery motion equations of satellite with quaternion rule; and digital attitude control system and flight test results of china's returnable satellites. DTIC

N95-27367*# National Aeronautics and Space Administration. Ames Research Center, Moffett Field, CA.

NAS TECHNICAL SUMMARIES, MARCH 1993 - FEBRUARY 1994

Jan. 1995 136 p
(RTOP 536-01-11)
(NASA-RP-1355; A-94140; NAS 1.61:1355) Avail: CASI HC A07/MF A02

NASA created the Numerical Aerodynamic Simulation (NAS) Program in 1987 to focus resources on solving critical problems in aeroscience and related disciplines by utilizing the power of the most advanced supercomputers available. The NAS Program provides scientists with the necessary computing power to solve today's most demanding computational fluid dynamics problems and serves as a pathfinder in integrating leading-edge supercomputing technologies, thus benefitting other supercomputer centers in government and industry. The 1993-94 operational year concluded with 448 high-speed processor projects and 95 parallel projects representing NASA, the Department of Defense, other government agencies, private industry, and universities. This document provides a glimpse at some of the significant scientific results for the year. Author

N95-27629*# National Aeronautics and Space Administration. Langley Research Center, Hampton, VA.

LDEF: 69 MONTHS IN SPACE. THIRD POST-RETRIEVAL SYMPOSIUM, PART 3

Arlene S. Levine, ed. Feb. 1995 515 p Symposium held in Williamsburg, VA, 8-12 Nov. 1993; sponsored by NASA, Washington and AIAA
(RTOP 233-03-02-03)
(NASA-CP-3275-Pt-3; L-17430C-Pt-3; NAS 1.55:3275-Pt-3) Avail: CASI HC A22/MF A04

This volume is a compilation of papers presented at the Third Long Duration Exposure Facility (LDEF) Post-Retrieval Symposium. The papers represent the data analysis of the 57 experiments flown on the LDEF. The experiments include materials, coatings, thermal systems, power and propulsion, science (cosmic ray, interstellar gas, heavy ions, micrometeoroid, etc.), electronics, optics, and life science. In addition, papers on preliminary data analysis of EURECA, EOIM-3, and other spacecraft are included. For individual titles, see N95-27630 through N95-27671.

N95-27630*# National Aeronautics and Space Administration. Lyndon B. Johnson Space Center, Houston, TX.

AN OVERVIEW OF THE EVALUATION OF OXYGEN INTERACTIONS WITH MATERIALS 3 EXPERIMENT: SPACE SHUTTLE MISSION 46, JULY-AUGUST 1992 **c25**

Steven L. Koontz, Lubert J. Leger, James T. Visentine, Don E. Hunton (Phillips Lab., Hanscom AFB, MA.), Jon B. Cross (Los Alamos National Lab., NM.), and Charles L. Hakes (Lockheed Engineering and Sciences Co., Houston, TX.) *In* NASA. Langley Research Center, LDEF: 69 Months in Space. Third Post-Retrieval Symposium, Part 3 Feb. 1995 p 869-902 (For primary document see N95-27629 09-99)
Avail: CASI HC A03/MF A04

The Evaluation of Oxygen Interactions with Materials 3 (EOIM-3) flight experiment was developed to obtain benchmark atomic oxygen reactivity data and was conducted during Space Transportation System Mission 46 (STS-46), July 31 to August 7, 1992. In this paper, we present an overview of EOIM-3 and the results of the Lyndon B. Johnson Space Center (JSC) materials reactivity and mass spectrometer/carousel experiments. Mass spectrometer calibration methods are discussed briefly, as a prelude to a detailed discussion of the mass spectrometric results produced during STS-46. Mass spectrometric measurements of ambient O-atom flux and fluence are in good agreement with the values calculated using the MSIS-86 model of the thermosphere as well as estimates based on the extent of O-atom reaction with Kapton polyimide. Mass spectrometric measurements of gaseous products formed by O-atom reaction with C(13) labeled Kapton revealed CO, CO2, H2O, NO, and NO2. Finally, by operating the mass spectrometer so as to detect naturally occurring ionospheric species, we characterized the ambient ionosphere at various times during EOIM-3 and detected the gaseous reaction products formed when ambient ions interacted with the C(13) Kapton carousel sector. By direct comparison of the results of on-orbit O-atom exposures with those conducted in ground-based laboratory systems, which provide known O-atom fluences and translational energies, we have demonstrated the strong translational energy dependence of O-atom reactions with a variety of polymers. A 'line-of-centers' reactive scattering model was shown to provide a reasonably accurate description of the translational energy dependence of polymer reactions with O atoms at high atom kinetic energies while a Beckerle-Ceyer model provided an accurate description of O-atom reactivity over a three order-of-magnitude range in translational energy and a four order-of-magnitude range in reaction efficiency. Postflight studies of the polymer samples by x-ray photoelectron spectroscopy and infrared spectroscopy demonstrate that O-atom attack is confined to the near-surface region of the sample, i.e. within 50 to 100 A of the surface. Author

N95-27631*# National Aeronautics and Space Administration. Lyndon B. Johnson Space Center, Houston, TX.

EVALUATION OF OXYGEN INTERACTIONS WITH MATERIALS 3: MISSION AND INDUCED ENVIRONMENTS c25

Steven L. Koontz, Lubert J. Leger, Steven L. Rickman, Charles L. Hakes (Los Alamos National Lab., NM.), David T. Bui (Los Alamos National Lab., NM.), Donald Hunton (Phillips Lab., Hanscom AFB, MA.), and Jon B. Cross (Lockheed Engineering and Sciences Co., Houston, TX.) *In* NASA. Langley Research Center, LDEF: 69 Months in Space. Third Post-Retrieval Symposium, Part 3 Feb. 1995 p 903-916 (For primary document see N95-27629 09-99)

Avail: CASI HC A03/MF A04

The Evaluation of Oxygen Interactions with Materials 3 (EOIM-3) flight experiment was developed to obtain benchmark atomic oxygen/material reactivity data. The experiment was conducted during Space Shuttle mission 46 (STS-46), which flew July 31 to August 7, 1992. Quantitative interpretation of the materials reactivity measurements requires a complete and accurate definition of the space environment exposure, including the thermal history of the payload, the solar ultraviolet exposure, the atomic oxygen fluence, and any spacecraft outgassing contamination effects. The thermal history of the payload was measured using twelve thermocouple sensors placed behind selected samples and on the EOIM-3 payload structure. The solar ultraviolet exposure history of the EOIM-3 payload was determined by analysis of the as-flown orbit and vehicle attitude combined with daily average solar ultraviolet and vacuum ultraviolet (UV/VUV) fluxes. The atomic oxygen fluence was assessed in three different ways. First, the O-atom fluence was calculated using a program that incorporates the MSIS-86 atmospheric model, the as-flown Space Shuttle trajectory, and solar activity parameters. Second, the oxygen atom fluence was estimated directly from Kapton film erosion. Third, ambient oxygen atom measurements were made using the quadrupole mass spectrometer on the EOIM-3 payload. Our best estimate of the oxygen atom fluence as of this writing is 2.3 +/- 0.3 x 10(exp 20) atoms/sq cm. Finally, results of post-flight X-ray photoelectron spectroscopy (XPS) surface analyses of selected samples indicate low levels of contamination on the payload surface. Author

N95-27632*# Aerospace Corp., El Segundo, CA. Mechanics and Materials Technology Center.

SPACECRAFT MATERIALS STUDIES ON THE AEROSPACE CORPORATION TRAY ON EOIM-3 c25

Wayne K. Stuckey, Carol S. Hemminger, Gary L. Steckel, Malina M. Hills, and Michael R. Hilton *In* NASA. Langley Research Center, LDEF: 69 Months in Space. Third Post-Retrieval Symposium, Part 3 Feb. 1995 p 917-930 (For primary document see N95-27629 09-99)

(Contract F04701-93-C-0094)

Avail: CASI HC A03/MF A04

A passive tray was flown on the Effects of Oxygen Interaction with Materials experiment on STS-46 (EOIM-3) with 82 samples from The Aerospace Corporation. A variety of advanced materials related to potential uses on future spacecraft were included for evaluation representing optical coatings, lubricants, polymers, composites, carbon-carbon composite protective coatings, graphite protective coatings, thermal-control materials, and some samples of current materials. An overview of the available results from the investigations of these materials is presented. Author

N95-27633*# Aerospace Corp., El Segundo, CA. Mechanics and Materials Technology Center.

EXPOSURE OF LDEF MATERIALS TO ATOMIC OXYGEN: RESULTS OF EOIM 3 c25

C. H. Jaggers and M. J. Meshishnek *In* NASA. Langley Research Center, LDEF: 69 Months in Space. Third Post-Retrieval Symposium, Part 3 Feb. 1995 p 931-955 (For primary document see N95-27629 09-99)

Avail: CASI HC A03/MF A04

The third Effects of Oxygen Atom Interaction with Materials (EOIM 3) experiment flew on STS-46 from July 31 to August 8, 1992. The EOIM-3 sample tray was exposed to the low-earth orbit space environment for 58.55 hours at an altitude of 124 nautical miles resulting in a calculated total atomic oxygen (AO) fluence of 1.99 x 10(exp 20) atoms/sq cm. Five samples previously flown on the Long Duration Exposure Facility (LDEF) Experiment M0003 were included on the Aerospace EOIM 3 experimental tray: (1) Chemglaze A276 white thermal control paint from the LDEF trailing edge (TE); (2) S13GLO white thermal control paint from the LDEF TE; (3) S13GLO from the LDEF leading edge (LE) with a visible contamination layer from the LDEF mission; (4) Z306 black thermal control paint from the LDEF TE with a contamination layer from the LDEF mission; and (5) anodized aluminum from the LDEF TE with a contamination layer from the LDEF mission. The purpose of this experiment was twofold: (l) investigate the response of trailing edge LDEF materials to atomic oxygen exposure, thereby simulating LDEF leading edge phenomena; (2) investigate the response of contaminated LDEF samples to atomic oxygen in attempts to understand LDEF contamination-atomic oxygen interactions. This paper describes the response of these materials to atomic oxygen exposure, and compares the results of the EOIM 3 experiment to the LDEF mission and to ground-based atomic oxygen exposure studies. Author

N95-27634*# National Aeronautics and Space Administration. Marshall Space Flight Center, Huntsville, AL.

ATOMIC OXYGEN DOSIMETRY MEASUREMENTS MADE ON STS-46 BY CONCAP 2 c72

J. C. Gregory (Alabama Univ., Huntsville, AL.), G. P. Miller (Alabama Univ., Huntsville, AL.), P. J. Pettigrew (Alabama Univ., Huntsville, AL.), G. N. Raikar (Alabama Univ., Huntsville, AL.), Jon B. Cross (Lockheed Engineering and Sciences Co., Houston, TX.), E. Lan (McDonnell-Douglas Space Systems Co., Huntington Beach, CA.), C. L. Renschler (Sandia National Labs., Albuquerque, NM.), and W. T. Sutherland *In* NASA. Langley Research Center, LDEF: 69 Months in Space. Third Post-Retrieval Symposium, Part 3 Feb. 1995 p 957-970 Sponsored by Consortium for Materials Development in Space (For primary document see N95-27629 09-99)

Avail: CASI HC A03/MF A04

With increasing flight duration and the possibility of a permanent facility in space, long-term monitoring of material degradation due to atomic oxygen is increasing in importance. Reliance on models to determine the fluence of atomic oxygen is not only necessarily complex but also imprecise due to the strong dependence of oxygen concentration on day/night, latitude and solar activity. Mass-spectroscopy, the traditional method for determining the gas phase species densities at low pressure, is not only expensive but is limited in the area that it can monitor. Our group has developed a simple and inexpensive dosimeter to measure the atomic oxygen fluence via the change in resistance as the sensor element is gradually oxidized. The sensors consisted of thin-film circuit elements deposited on a suitable substrate. Four-point resistance measurements were used to monitor the change in resistance. Results obtained using silver and carbon dosimeters flown on STS-46 (CONCAP 2-01) will be discussed. Author

N95-27635*# National Aeronautics and Space Administration. Marshall Space Flight Center, Huntsville, AL.

INFLIGHT RESISTANCE MEASUREMENT ON HIGH-T(SUB c) SUPERCONDUCTING THIN FILMS EXPOSED TO ORBITAL ATOMIC OXYGEN ON CONCAP-2 (STS-46) c33

J. C. Gregory (Alabama Univ., Huntsville, AL.), G. N. Raiker (Alabama Univ., Huntsville, AL.), J. A. Bijvoet (Alabama Univ., Huntsville, AL.), P. D. Nerren (Alabama Univ., Huntsville, AL.), W. T. Sutherland, A. Mogro-Camperso (General Electric Co., Schenectady, NY.), L. G. Turner (General Electric Co., Schenectady, NY.), Hoi Kwok (State Univ. of New York, Buffalo, NY.), I. D. Raistrick (Lockheed Engineering and Sciences Co., Houston, TX.), and J. B. Cross (Lockheed Engineering and Sciences Co., Houston, TX.) et al *In* NASA. Langley Research Center, LDEF: 69 Months in Space. Third Post-Retrieval Symposium, Part 3 Feb. 1995 p 971-988 (For primary document see N95-27629 09-99)

Avail: CASI HC A03/MF A04

In 1992, UAH (University of Alabama in Huntsville) conducted a unique experiment on STS-46 in which YBa2Cu3O7 (commonly known as '1-2-3' superconductor) high-T(c) superconducting thin film samples prepared at three different laboratories were exposed to 5 eV atomic oxygen in low Earth orbit on the ambient and 320 C hot plate during the first flight of the CONCAP-2 (Complex Autonomous Payload) experiment carrier. The resistance of the thin films was measured in flight during the atomic oxygen exposure and heating cycle. Superconducting properties were measured in the laboratory before and after the flight by the individual experimenters. Films with good superconducting properties, and which were exposed to the oxygen flux, survived the flight including those heated to 320 C (600 K) with properties essentially unchanged, while other samples which were heated but not exposed to oxygen were degraded. The properties of other flight controls held at ambient temperature appear unchanged and indistinguishable from those of ground controls, whether exposed to oxygen or not. Author

N95-27636*# Nebraska Univ., Lincoln, NE. Dept. of Electrical Engineering.

LEO DEGRADATION OF GRAPHITE AND CARBON-BASED COMPOSITES ABOARD SPACE SHUTTLE FLIGHT STS-46 c24

Blaine R. Spady, R. A. Synowicki, Jeffrey S. Hale, M. J. DeVries, John A. Woollam, Arthur W. Moore (Union Carbide Corp., Parma, OH.), and Max Lake (Applied Sciences, Inc., Cedarville, OH.) *In* NASA. Langley Research Center, LDEF: 69 Months in Space. Third Post-Retrieval Symposium, Part 3 Feb. 1995 p 989-997 (For primary document see N95-27629 09-99)
(Grant NAG3-95)
Avail: CASI HC A02/MF A04

Six different types of carbon and carbon-boron nitride composites were exposed to low Earth orbit aboard Space Shuttle flight STS-46. The samples received a nominal atomic oxygen fluence of 2.2 x 10(exp 20) atoms/sq cm in 42 hours of exposure. Pyrolytic graphite and highly oriented pyrolytic graphite showed significant degradation, and the measured erosion yield was within a factor of two of published values. The erosion yield of pyrolytic boron nitride was found to be 2.6 x 10(exp 26) cu cm/atom in plasma asher exposure, over 42 times lower than that of pyrolytic graphite. This low erosion yield makes graphite plus boron nitride mixtures quite resistant to low Earth orbit exposure. Evidence suggests that the graphitic component was preferentially etched, leaving the surface boron nitride rich. Degradation resistance increases with boron nitride composition. Carbon fiber/carbon composites degraded in low Earth orbit, and the carbon pitch binder was found to etch more easily than the graphite fibers which have much higher degradation resistance. Derived from text

N95-27637*# National Aeronautics and Space Administration. Marshall Space Flight Center, Huntsville, AL.

ORBITAL ATOMIC OXYGEN EFFECTS ON MATERIALS: AN OVERVIEW OF MSFC EXPERIMENTS ON THE STS-46 EOIM-3 c72

Roger C. Linton, Jason A. Vaughn, Miria M. Finckenor, Rachel R. Kamenetzky, Robert F. DeHaye, and Ann F. Whitaker *In* NASA. Langley Research Center, LDEF: 69 Months in Space. Third Post-Retrieval Symposium, Part 3 Feb. 1995 p 999-1010 (For primary document see N95-27629 09-99)
Avail: CASI HC A03/MF A04

The third Evaluation of Oxygen Interaction with Materials experiment was flown on Space Shuttle Mission STS-46 (July 31 - August 8, 1992), representing a joint effort of several NASA centers, universities, and contractors. This array of active instrumentation and material exposure sub-assemblies was integrated as a Shuttle cargo bay pallet experiment for investigating the effects of orbital atomic oxygen on candidate space materials. Marshall Space Flight Center contributed several passive exposure trays of material specimens, uniform stress and static stress material exposure fixtures, the Atomic Oxygen Resistance Monitor (AORM), and specimens of thermal coatings for the EOIM-3 variable exposure mechanisms. As a result of 42 hours of spacecraft velocity vector-oriented exposure during the later phases of the STS-46 mission in LEO, EOIM-3 materials were exposed to an atomic oxygen fluence of 2.2 x 10(exp 20) atoms/sq cm. In this paper, an overview is presented of the technical approaches and results from analyses of the MSFC flight specimens, fixtures, and the AORM. More detailed results from earlier EOIM missions, the LDEF, and from laboratory testing are included in associated papers of this conference session. Author

N95-27638*# National Aeronautics and Space Administration. Marshall Space Flight Center, Huntsville, AL.

EFFECTS OF ATOMIC OXYGEN ON POLYMERIC MATERIALS FLOWN ON EOIM-3 c27

Rachel R. Kamenetzky, Roger C. Linton, Miria M. Finckenor, and Jason A. Vaughn *In* NASA. Langley Research Center, LDEF: 69 Months in Space. Third Post-Retrieval Symposium, Part 3 Feb. 1995 p 1011-1023 (For primary document see N95-27629 09-99)
Avail: CASI HC A03/MF A04

Diverse polymeric materials, including several variations of Kapton, were flown on STS-46 as part of the Evaluation of Oxygen Interaction with Materials Experiment (EOIM-3). These materials were flown in the cargo bay and exposed to the space environment July 31 - August 8, 1992, including 40 hours of direct atomic oxygen impingement. The atomic oxygen exposure was approximately 2.2 x 10(exp 20) atoms/sq cm. Polymeric materials flown on EOIM-3 include coated and uncoated Kapton, Tefzel ETFE, Lexan, FEP and TFE Teflon, bulk Halar and PEEK, S383 silicone and Viton elastomeric seal material. Analyses performed included thickness measurements using Dektak and eddy current methods, mass loss, resistance, permeability, hardness, and FTIR. The effects of stress and the space environment on Kapton were also evaluated. Previous EOIM missions on STS-5 and STS-8 and the Long Duration Exposure Facility also contained polymeric material samples. Data from these previous flights are shown for comparison, as well as ground simulation of space environment effects using both thermal energy flow tubes and 5 eV neutral atomic oxygen beam facilities. Reaction efficiencies for the various atomic oxygen exposure conditions are discussed. Author

N95-27639*# National Aeronautics and Space Administration. Marshall Space Flight Center, Huntsville, AL.

THERMAL CONTROL MATERIALS ON EOIM-3 c27

Miria M. Finckenor, Roger C. Linton, Rachel R. Kamenetzky, and Jason A. Vaughn *In* NASA. Langley Research Center, LDEF: 69 Months in Space. Third Post-Retrieval Symposium, Part 3 Feb. 1995 p 1025-1035 (For primary document see N95-27629 09-99)
Avail: CASI HC A03/MF A04

Thermal control paints, anodized aluminum, and beta cloth samples were flown on STS-46 as part of the Evaluation of Oxygen Interaction with Materials Experiment (EOIM-3). The thermal control paints flown on EOIM-3 include ceramic and polyurethane-based paints. Passively exposed samples are compared to actively heated samples and controlled exposure samples. Optical property measurements of absorptivity, emissivity, and spectrofluorescence are presented for each paint. Several variations of anodized aluminum, including chromic acid anodize, sulfuric acid anodize, and boric/sulfuric acid anodize were flown on the actively heated trays and the passive exposure trays. The post-flight optical properties are within tolerances for these materials. Also flown were two samples of yellow anodized aluminum. The yellow anodized aluminum samples darkened noticeably. Samples of aluminized and unaluminized beta cloth, a fiberglass woven mat impregnated with TFE Teflon, were flown with passive exposure to the space environment. Data from this part of the experiment is correlated to observations from LDEF and erosion of the Teflon thin film samples also flown on EOIM-3 and LDEF. Author

N95-27640*# McDonnell-Douglas Aerospace, Huntington Beach, CA. Materials and Processes.

SOLID FILM LUBRICANTS AND THERMAL CONTROL COATINGS FLOWN ABOARD THE EOIM-3 MDA SUB-EXPERIMENT c27

Taylor J. Murphy, Kaia E. David, and Hank W. Babel *In* NASA. Langley Research Center, LDEF: 69 Months in Space. Third Post-Retrieval Symposium, Part 3 Feb. 1995 p 1037-1052 (For primary document see N95-27629 09-99)
Avail: CASI HC A03/MF A04

Additional experimental data were desired to support the selection of candidate thermal control coatings and solid film lubricants for the McDonnell Douglas Aerospace (MDA) Space Station hardware. The third Evaluation of Oxygen Interactions With Materials Mission (EOIM-3) flight experiment presented an opportunity to study the effects of the low Earth orbit environment on thermal control coatings and solid film lubricants. MDA provided five solid film lubricants and two anodic thermal control coatings for EOIM-3. The lubricant sample set consisted of three solid film lubricants with organic binders one solid film lubricant with an inorganic binder, and one solid film lubricant with no binder. The anodize coating sample set consisted of undyed sulfuric acid anodize and cobalt sulfide dyed sulfuric acid anodize, each on two different substrate aluminum alloys. The organic and inorganic binders in the solid film lubricants experienced erosion, and the lubricating pigments experienced oxidation. MDA is continuing to assess the effect of exposure to the low Earth orbit environment on the life and friction properties of the lubricants. Results to date support the design practice of shielding solid film lubricants from the low Earth orbit environment. Post-flight optical property analysis of the anodized specimens indicated that there were limited contamination effects and some atomic oxygen and ultraviolet radiation effects. These effects appeared to be within the values predicted by simulated ground testing and analysis of these materials, and they were different for each coating and substrate. Author

N95-27641*# National Aeronautics and Space Administration. Marshall Space Flight Center, Huntsville, AL.
EVALUATION OF SPACE ENVIRONMENTAL EFFECTS ON METALS AND OPTICAL THIN FILMS ON EOIM-3 c25
Jason A. Vaughn, Roger C. Linton, Miria M. Finckenor, and Rachel R. Kamenetzky *In* NASA. Langley Research Center, LDEF: 69 Months in Space. Third Post-Retrieval Symposium, Part 3 Feb. 1995 p 1053-1065 (For primary document see N95-27629 09-99)
Avail: CASI HC A03/MF A04

Metals and optical thin films exposed to the space environment on the Third Flight of the Evaluation of Oxygen Interactions with Materials (EOIM-3) payload, onboard Space Shuttle mission STS-46 were evaluated. The materials effects described in this paper include the effects of space exposure on various pure metals, optical thin films, and optical thin film metals. The changes induced by exposure to the space environment in the material properties were evaluated using bidirectional reflectance distribution function (BRDF), specular reflectance (250 nm to 2500 nm), ESCA, VUV reflectance (120 nm to 200 nm), ellipsometry, FTIR and optical properties. Using these analysis techniques gold optically thin film metal mirrors with nickel undercoats were observed to darken due to nickel diffusion through the gold to the surface. Also, thin film nickel mirrors formed nickel oxide due to exposure to both the atmosphere and space. Author

N95-27642*# Boeing Defense and Space Group, Seattle, WA.
ANALYSIS OF SELECTED SPECIMENS FROM THE STS-46 ENERGETIC OXYGEN INTERACTION WITH MATERIALS-3 EXPERIMENT c25
Johnny L. Golden, Roger J. Bourassa, Harry W. Dursch, and H. Gary Pippin *In* NASA. Langley Research Center, LDEF: 69 Months in Space. Third Post-Retrieval Symposium, Part 3 Feb. 1995 p 1067-1094 (For primary document see N95-27629 09-99)
Avail: CASI HC A03/MF A04

The Energetic Oxygen Interaction with Materials 3 (EOIM-3) experiment was flown on the STS-46 mission, which was launched on 31 Jul. 1992 and returned 8 Aug. 1992. Boeing specimens were located on both the NASA Marshall Space Flight Center (MSFC) tray and the Ballistic Missile Defense Organization (BMDO) tray integrated by the Jet Propulsion Laboratory (JPL). The EOIM-3 pallet was mounted in the Space Shuttle payload bay near the aft bulkhead. During the mission, the atomic oxygen (AO) exposure levels of specimens in these passive sample trays was about 2.3 x 10(exp 20) atoms/sq cm. The specimens also received an estimated 22 equivalent sun hours of solar exposure. In addition, it appears that the EOIM-3 pallet was exposed to a silicone contamination source and many specimens had a thin layer of silicon based deposit on their surfaces after the flight. The specimens on the MSFC tray included seven solid film lubricants, a selection of butyl rubber (B612) and silicone (S383) o-rings, three indirect scatter surfaces, and Silver/Fluorinated Ethylene Propylene (Ag/FEP) and Chemglaze A276 specimens which had previously flown on trailing edge locations of the Long Duration Exposure Facility (LDEF). The specimens on the JPL tray included composites previously flown on LDEF and two indirect scattering surfaces. Derived from text

N95-27643*# Jet Propulsion Lab., California Inst. of Tech., Pasadena, CA.
MOLECULAR BEAM SCATTERING FROM C-13 ENRICHED KAPTON AND CORRELATION WITH THE EOIM-3 CAROUSEL EXPERIMENT c72
Timothy K. Minton and Teresa A. Moore *In* NASA. Langley Research Center, LDEF: 69 Months in Space. Third Post-Retrieval Symposium, Part 3 Feb. 1995 p 1095-1114 (For primary document see N95-27629 09-99)
Avail: CASI HC A03/MF A04

Mass spectra of products emerging from identical samples of a C-13-enriched polyimide polymer (chemically equivalent to Kapton) under atomic oxygen bombardment in space and in the laboratory were collected. Reaction products unambiguously detected in space were CO-13, NO, (12)CO2, and (13)CO2. These reaction products and two others, H2O and CO-12, were detected in the laboratory, along with inelastically scattered atomic and molecular oxygen. Qualitative agreement was seen in the mass spectra taken in space and in the laboratory; the agreement may be improved by reducing the fraction of O2 in the laboratory molecular beam. Both laboratory and space data indicated that CO and CO2 products come preferentially from reaction with the imide component of the polymer chain, raising the possibility that the either component may degrade in part by the 'evaporation' of higher molecular weight fragments. Laboratory time-of-flight distributions showed: (1) incomplete energy accommodation of impinging O and O2 species that do not react with the surface; and (2) both hyperthermal and thermal CO and CO2 products, suggesting two distinct reaction mechanisms with the surface. Author

N95-27644*# Jet Propulsion Lab., California Inst. of Tech., Pasadena, CA.
BMDO MATERIALS TESTING IN THE EOIM-3 EXPERIMENT c25
Shirley Y. Chung, David E. Brinza, Timothy K. Minton, and Ranty H. Liang *In* NASA. Langley Research Center, LDEF: 69 Months in Space. Third Post-Retrieval Symposium, Part 3 Feb. 1995 p 1115-1128 (For primary document see N95-27629 09-99)
Avail: CASI HC A03/MF A04

The NASA Evaluation of Oxygen Interactions with Materials-3 (EOIM-3) experiment served as a testbed for a variety of materials that are candidates for Ballistic Missile Defense Organization (BMDO) space assets. The materials evaluated on this flight experiment were provided by BMDO contractors and technology laboratories. A parallel ground-based exposure evaluation was conducted using the Fast Atom Sample Tester (FAST) atomic-oxygen simulation facility at Physical Sciences, Inc. The EOIM-3 flight materials were exposed to an atomic oxygen fluence of approximately 2.3 x 10(exp 20) atoms/sq cm. The ground-based exposure fluence of 2.0 - 2.5 x 10(exp 20) atoms/sq cm permits direct comparison with that of the flight-exposed specimens. The results from the flight test conducted aboard STS-46 and the correlative ground-based exposure are summarized here. A more detailed correlation study is presented in the JPL Publication 93-31 entitled 'Flight-and Ground-Test Correlation Study of BMDO SDS Materials: Phase 1 Report'. In general, the majority of the materials survived the AO environment with their performance tolerances maintained for the duration of the exposure. Optical materials, baffles, and coatings performed extremely well as did most of the thermal coatings and tribological materials. A few of the candidate radiator, threat shielding, and structural materials showed significant degradation. Many of the coatings designed to protect against AO erosion of sensitive materials performed this function well. Author

N95-27645*# National Aeronautics and Space Administration. Lyndon B. Johnson Space Center, Houston, TX.
STS-46 PLASMA COMPOSITION MEASUREMENTS USING THE EOIM-3 MASS SPECTROMETER Abstract Only c25
Donald E. Hunton, Edmund Trzcinski, Roger Gosselin, Steven Koontz, Lubert Leger, and James T. Visentine *In* NASA. Langley Research Center, LDEF: 69 Months in Space. Third Post-Retrieval Symposium, Part 3 Feb. 1995 p 1129 (For primary document see N95-27629 09-99)
Avail: CASI HC A01/MF A04

One of the active instruments incorporated into the Evaluation of Oxygen Interactions with Materials - 3 experiment was a quadrupole mass spectrometer. The primary objectives for this instrument, which was built by the Air Force Phillips Laboratory and was a veteran of the STS-4 flight in 1982, were to quantify the flux of atomic oxygen striking the test surfaces in the EOIM-3 payload and to detect surface reaction products from the materials in the carousel. Other speakers in this session have covered the results of these experiments. Prior to the 40-hour-long dedicated EOIM-3 mission segment at the end of the STS-46 flight, the authors used the mass spectrometer to make measurements of ion and neutral gas composition in the shuttle environment. About 25 hours of data were collected during a variety of mission events, including Eureca deployment at high altitude and many tethered satellite system operations. Author

N95-27646*# National Aeronautics and Space Administration. Marshall Space Flight Center, Huntsville, AL.
POINT DEFECT FORMATION IN OPTICAL MATERIALS EXPOS ED TO THE SPACE ENVIRONMENT c74
J. L. Allen (Vanderbilt Univ., Nashville, TN.), N. Seifert (Vanderbilt Univ., Nashville, TN.), Y. Yao (Vanderbilt Univ., Nashville, TN.), R. G. Albridge (Vanderbilt Univ., Nashville, TN.), A. V. Barnes (Vanderbilt Univ., Nashville,

TN.), N. H. Tolk (Vanderbilt Univ., Nashville, TN.), A. M. Strauss (Vanderbilt Univ., Nashville, TN.), Roger C. Linton, R. R. Kamenetzky, and Jason A. Vaughn et al *In* NASA. Langley Research Center, LDEF: 69 Months in Space. Third Post-Retrieval Symposium, Part 3 Feb. 1995 p 1131-1145 (For primary document see N95-27629 09-99)
(Contracts N00014-87-C-0146; N00014-91-C-0109; N00014-91-J-4040)
Avail: CASI HC A03/MF A04

Point defect formation associated with early stages of optical damage was observed unexpectedly in two, and possibly three, different optical materials subjected to short-duration space exposure. Three calcium fluoride, two lithium fluoride, and three magnesium fluoride samples were flown on Space Shuttle flight STS-46 as part of the Evaluation of Oxygen Interactions with Materials - Third Phase experiment. One each of the calcium and magnesium fluoride samples was held at a fixed temperature of 60 C during the space exposure, while the temperatures of the other samples were allowed to vary with the ambient temperature of the shuttle cargo bay. Pre-flight and post-flight optical absorption measurements were performed on all of the samples. With the possible exception of the magnesium fluoride samples, every sample clearly showed the formation of F-centers in that section of the sample that was exposed to the low earth orbit environment. Solar vacuum ultraviolet radiation is the most probable primary cause of the defect formation; however, the resulting surface metallization may be synergistically altered by the atomic oxygen environment. Author

N95-27647*# National Aeronautics and Space Administration. Goddard Space Flight Center, Greenbelt, MD.
LDEF SYSTEMS SPECIAL INVESTIGATION GROUP OVERVIEW
Jim Mason and Harry Dursch (Boeing Defense and Space Group, Seattle, WA.) *In* NASA. Langley Research Center, LDEF: 69 Months in Space. Third Post-Retrieval Symposium, Part 3 Feb. 1995 p 1149-1151 (For primary document see N95-27629 09-99)
(Contracts NAS1-18224; NAS1-19247)
Avail: CASI HC A01/MF A04

The Systems Special Investigation Group (Systems SIG), formed by the LDEF Project Office to perform post-flight analysis of LDEF systems hardware, was chartered to investigate the effects of the extended LDEF mission on both satellite and experiment systems and to coordinate and integrate all systems related analyses performed during post-flight investigations. The Systems SIG published a summary report in April, 1992 titled 'Analysis of Systems Hardware Flown on LDEF - Results of the Systems Special Investigation Group' that described findings through the end of 1991. The Systems SIG, unfunded in FY 92 and FY93, has been funded in FY 94 to update this report with all new systems related findings. This paper provides a brief summary of the highlights of earlier Systems SIG accomplishments and describes tasks the Systems SIG has been funded to accomplish in FY 94. Derived from text

N95-27648*# Centre National d'Etudes Spatiales, Toulouse (France).
SYSTEM RESULTS FROM FRECOPA **c25**
Christian Durin, Lucinda Berthoud, and Jean-Claude Mandeville *In* NASA. Langley Research Center, LDEF: 69 Months in Space. Third Post-Retrieval Symposium, Part 3 Feb. 1995 p 1153-1165 (For primary document see N95-27629 09-99)
Avail: CASI HC A03/MF A04

The work carried out over the past three years on FRECOPA and the LDEF has enabled a large quantity of information to be collected, part of which has already been exploited. As far as CNES is concerned, the major spin-offs of this mission mainly focus on the orbital environment and the behavior of materials in such an environment. With respect to the environment, the authors shall develop the lessons learned from expert appraisals on impacts by microparticles, which are the main feature observed in this area. As for the materials, the results show a variety of behavior when subjected to the space environment and even now constitute a wealth of information for the designing and validation of future mechanical systems. Apart from these direct spin-offs, there are repercussions on in-flight and ground testing, the calibration of test benches and improvements to simulation models. Author

N95-27649*# Boeing Defense and Space Group, Seattle, WA.
SPACE ENVIRONMENTAL EFFECT ON SOLAR CELLS: LDEF AND OTHER FLIGHT TESTS **c44**
Peter Gruenbaum and Harry Dursch *In* NASA. Langley Research Center, LDEF: 69 Months in Space. Third Post-Retrieval Symposium, Part 3 Feb. 1995 p 1167-1177 (For primary document see N95-27629 09-99)
(Contract NAS1-19247)
Avail: CASI HC A03/MF A04

This paper summarizes results of several experiments flown on the Long Duration Exposure Facility (LDEF) to examine the effects of the space environment on materials and technologies to be used in solar arrays. The various LDEF experiments are compared to each other as well as to other solar cell flight data published in the literature. Data on environmental effects such as atomic oxygen, ultraviolet light, micrometeoroids and debris, and charged particles are discussed in detail. The results from the LDEF experiments allow us to draw several conclusions. Atomic oxygen erodes unprotected silver interconnects, unprotected Kapton, and polymer cell covers, but certain dielectric coatings can protect both silver and Kapton. Cells that had wrap-around silver contacts sometimes showed erosion at the edges, but more recently developed wrap-through cells are not expected to have these problems. Micrometeoroid and debris damage is limited to the area close to the impact, and microsheet covers provide the cells with some protection. Damage from charged particles was as predicted, and the cell covers provided adequate protection. In general, silicon cells with microsheet covers showed very little degradation, and solar modules showed less than 3 percent degradation, except when mechanically damaged. The solar cell choices for the Space Station solar array are supported by the data from LDEF. Author

N95-27650*# Georgia Inst. of Tech., Atlanta, GA. Research Center.
A FINAL LOOK AT LDEF ELECTRO-OPTIC SYSTEMS COMPONENTS **c74**
M. D. Blue *In* NASA. Langley Research Center, LDEF: 69 Months in Space. Third Post-Retrieval Symposium, Part 3 Feb. 1995 p 1179-1188 (For primary document see N95-27629 09-99)
Avail: CASI HC A02/MF A04

Postrecovery characteristics of LDEF electro-optic components from the GTRI tray are compared with their prelaunch characteristics and with the characteristics of similar components from related experiments. Components considered here include lasers, light-emitting diodes, semiconducting radiation detectors and arrays, optical substrates, filters, and mirrors, and specialized coatings. Our understanding of the physical effects resulting from low earth orbit are described, and guidelines and recommendations for component and materials choices are presented. Author

N95-27651*# National Aeronautics and Space Administration. Goddard Space Flight Center, Greenbelt, MD.
EFFECTS OF THE LDEF ORBITAL ENVIRONMENT ON THE REFLECTANCE OF OPTICAL MIRROR MATERIALS **c74**
Howard Herzig and Charles Fleetwood, Jr. *In* NASA. Langley Research Center, LDEF: 69 Months in Space. Third Post-Retrieval Symposium, Part 3 Feb. 1995 p 1189-1203 (For primary document see N95-27629 09-99)
Avail: CASI HC A03/MF A04

Specimens of eight different optical mirror materials were flown in low earth orbit as part of the Long Duration Exposure Facility (LDEF) manifest to determine their ability to withstand exposure to the residual atomic oxygen and other environmental effects at those altitudes. Optical thin films of aluminum, gold, iridium, osmium, platinum, magnesium fluoride-overcoated aluminum and reactively deposited, silicon monoxide-protected aluminum, all of which were vacuum deposited on polished fused silica substrates, were included as part of Experiment S0010, Exposure of Spacecraft Coatings. Two specimens of polished, chemical vapor deposited (CVD) silicon carbide were installed in sites available in Experiment A0114, Interaction of Atomic Oxygen with Solid Surfaces at Orbital Altitudes, which included trays in two of the spacecraft bays, one on the leading edge and the other on the trailing edge. One of the silicon carbide samples was located in each of these trays. This paper will compare specular reflectance data from the preflight and postflight measurements made on each of these samples and attempt to explain the changes in light of the specific environments to which the experiments were exposed. Author

N95-27652*# Donovan (Terence), Palo Alto, CA.

EFFECTS OF LOW EARTH ORBIT ON THE OPTICAL PERFORMANCE OF MULTI-LAYER ENHANCED HIGH REFLECTANCE MIRRORS c74

Terence Donovan, Linda Johnson (Naval Air Warfare Center, China Lake, CA.), Karl Klemm (Naval Air Warfare Center, China Lake, CA.), Rick Scheri (Naval Air Warfare Center, China Lake, CA.), Jean Bennett (Naval Air Warfare Center, China Lake, CA.), Jon Erickson (Evans, Charles and Associates, Redwood City, CA.), and Filippo diBrozolo (Evans, Charles and Associates, Redwood City, CA.) *In* NASA. Langley Research Center, LDEF: 69 Months in Space. Third Post-Retrieval Symposium, Part 3 Feb. 1995 p 1205-1225 Sponsored by DARPA; and Wright Labs. (For primary document see N95-27629 09-99)

Avail: CASI HC A03/MF A04

Two mirror designs developed for space applications were flown along with a standard mid-infrared design on the leading and trailing edges of the Long Duration Exposure Facility (LDEF). Preliminary observations of induced changes in optical performance of ZnS-coated mirrors and impact-related microstructural and microchemical effects are described in the proceedings of the First LDEF Post-Retrieval Symposium. In this paper, effects of the induced environment and meteoroid/debris impacts on mirror performance are described in more detail. Also, an analysis of reflectance spectra using the results of Auger and secondary ion mass spectroscopy (SIMS) profiling measurements are used to identify an optical-degradation mechanism for the ZnS-coated mirrors. Structural damage associated with a high-velocity impact on a (Si/Al_2O_3)-coated mirror was imaged optically and with scanning electron and atomic force microscopy (SEM and AFM). Scanning Auger and SIMS analysis provided chemical mapping of selected impact sites. The impact data suggest design and fabrication modifications for obtaining improved mechanical performance using a design variation identified in preflight laboratory simulations. Auger surface profile and SIMS imaging data verified the conclusion that secondary impacts are the source of contamination associated with the dendrites grown on the leading-edge ZnS-coated test samples. It was also found that dendrites can be grown in the laboratory by irradiating contaminated sites on a trailing-edge ZnS-coated sample with a rastered electron beam. These results suggest a mechanism for dendrite growth. Author

N95-27653*# Eastman Kodak Co., Rochester, NY.

EFFECTS OF LONG TERM SPACE ENVIRONMENT EXPOSURE ON OPTICAL SUBSTRATES AND COATINGS Abstract Only c74

John Vallimont, E. Steven Brandt, Keith Havey, and Arthur Mustico *In* NASA. Langley Research Center, LDEF: 69 Months in Space. Third Post-Retrieval Symposium, Part 3 Feb. 1995 p 1227 (For primary document see N95-27629 09-99)

Avail: CASI HC A01/MF A04

At the time of our Second LDEF Post-Retrieval Symposium report, we had completed cleaning and measuring the post flight spectral performance of all of the samples except for the fused silica substrate with an antireflection (SiO_2/TiO_2) coating. As was documented in that report, after cleaning, all of the samples returned to their original pre-flight performance, with the exception of the fused silica anti-reflectance coated sample, which had significant degraded performance. All normal methods of removing the contaminant from the surface of this sample failed except for oxygen plasma etch. At the time of the previous report, we had only exposed the sample to three hours of plasma etch. We have since continued the plasma etch for a total of 32 hours, after which time, the transmission of the sample almost reached its pre-flight values. The peak areas of the transmission curves remained shifted approximately 150 nm. Of interest is the fact that the control samples, which hadn't flown, did not exhibit any spectral shifting. In summary, after the 6 yr exposure to the space environment, all of the coatings and substrates returned to their pre-flight performance after cleaning, with the exception of the antireflection coated fused silica sample. On this sample, the spectral transmission curves shifted approximately 150 nm. Author (revised)

N95-27654*# Phillips Lab., Kirtland AFB, NM. Space and Missiles Technology Directorate.

LONG DURATION EXPOSURE FACILITY (LDEF) SPACE OPTICS HANDBOOK Abstract Only c74

William T. Kemp, Edward Taylor, Robert Champetier (Science Applications International Corp., Santa Monica, CA.), Alan Watts (POD Associates, Inc., Albuquerque, NM.), and Dale Atkinson (POD Associates, Inc., Albuquerque, NM.) *In* NASA. Langley Research Center, LDEF: 69 Months in Space. Third Post-Retrieval Symposium, Part 3 Feb. 1995 p 1229 (For primary document see N95-27629 09-99)

Avail: CASI HC A01/MF A04

The overall objective of this effort is to construct a top-level space optics handbook that provides design guidelines based upon data collected from the Long Duration Exposure Facility (LDEF) experiment. The content of the handbook would cover optical coatings, surfaces, fiber optics, and fabricating process for lenses, windows and mirrors that were used on LDEF. The goal of this program (and handbook) is to ensure that the space community can derive the maximum benefit from the LDEF experiment relative to future optics designs for space applications. The summary of this handbook is 'What did we learn from the LDEF experiment?' Author

N95-27655*# National Aeronautics and Space Administration. Goddard Space Flight Center, Greenbelt, MD.

SPACE ENVIRONMENTAL EFFECTS OBSERVED ON THE HUBBLE SPACE TELESCOPE c27

Joel E. Edelman (Long Duration Exposure Facility Newsletter, Silver Spring, MD.) and James B. Mason *In* NASA. Langley Research Center, LDEF: 69 Months in Space. Third Post-Retrieval Symposium, Part 3 Feb. 1995 p 1231-1236 (For primary document see N95-27629 09-99)

Avail: CASI HC A02/MF A04

The Hubble Space Telescope (HST) Repair Mission of December, 1993, was first and foremost a mission to improve the performance of the observatory. But for a specialized segment of the aerospace industry, the primary interest is in the return to Earth of numerous pieces of the HST hardware, pieces which have been replaced, repaired, improved, or superseded. The returned hardware is of interest because of the information it potentially carries about the effects of exposure to the space environment for three and a half years. Like the LDEF retrieval mission four years ago, the HST repair mission is of interest to many engineering disciplines, including all of the disciplines represented by the LDEF Special Investigation Groups (SIG's). There is particular interest in the evaluation of specific materials and systems in the returned components. Some coated surfaces have been processed with materials which are newer and still in use by, or under consideration for, other spacecraft in a variety of stages of development. Several of the systems are being returned because a specific failure or anomaly has been observed and thus there is, at the outset, a specific investigative trail that needs to be followed. These systems are much more complex than those flown on LDEF and, in two instances, comprised state-of-the-art science instruments. Further, the parts used in these systems generally were characterized more rigorously prior to flight than were those in the LDEF systems, and thus post flight testing may yield more significant results. Author

N95-27656*# National Aeronautics and Space Administration. Langley Research Center, Hampton, VA.

HARDWARE CLEANLINESS METHODOLOGY AND CERTIFICATION c25

Gale A. Harvey, Thomas J. Lash, and J. Richard Rawls *In its* LDEF: 69 Months in Space. Third Post-Retrieval Symposium, Part 3 Feb. 1995 p 1237-1243 (For primary document see N95-27629 09-99)

Avail: CASI HC A02/MF A04

Inadequacy of mass loss cleanliness criteria for selection of materials for contamination sensitive uses, and processing of flight hardware for contamination sensitive instruments is discussed. Materials selection for flight hardware is usually based on mass loss (ASTM E-595). However, flight hardware cleanliness (MIL 1246A) is a surface cleanliness assessment. It is possible for materials (e.g. Sil-Pad 2000) to pass ASTM E-595 and fail MIL 1246A class A by orders of magnitude. Conversely, it is possible for small amounts of nonconforming material (Huma-Seal conformal coating) to not present significant cleanliness problems to an optical flight instrument. Effective cleaning (precleaning, precision cleaning, and ultra cleaning) and cleanliness verification are essential for contamination sensitive flight instruments. Polish cleaning of hardware, e.g. vacuum baking for vacuum applications, and storage of clean hardware, e.g. laser optics, is discussed. Silicone materials present special concerns for use in space because of the rapid conversion of the outgassed residues to glass by solar ultraviolet radiation and/or atomic oxygen. Non ozone depleting solvent cleaning and institutional support for cleaning and certification are also discussed. Author

N95-27657*# National Aeronautics and Space Administration. Langley Research Center, Hampton, VA.

FROM LDEF TO A NATIONAL SPACE ENVIRONMENT AND EFFECTS (SEE) PROGRAM: A NATURAL PROGRESSION Abstract Only c12

David E. Bowles, Robert L. Calloway, Joan G. Funk, William H. Kinard, and Arlene S. Levine *In its* LDEF: 69 Months in Space. Third Post-Retrieval Symposium, Part 3 Feb. 1995 p 1247-1248 (For primary document see N95-27629 09-99)

Avail: CASI HC A01/MF A04

As the LDEF program draws to a close, it leaves in place the fundamental building blocks for a Space Environment and Effects (SEE) program. Results from LDEF data analyses and investigations now form a substantial core of knowledge on the long term effects of the space environment on materials, system and structures. In addition, these investigations form the basic structure of a critically-needed SEE archive and database system. An agency-wide effort is required to capture all elements of a SEE program to provide a more comprehensive and focused approach to understanding the space environment, determining the best techniques for both flight and ground-based experimentation, updating the models which predict both the environments and those effects on subsystems and spacecraft, and, finally, ensuring that this multitudinous information is properly maintained, and inserted into spacecraft design programs. Many parts and pieces of a SEE program already exist at various locations to fulfill specific needs. The primary purpose of this program, under the direction of the Office of Advanced Concepts and Technology (OACT) in NASA Headquarters, is to take advantage of these parts; apply synergisms where possible; identify and when possible fill-in gaps; coordinate and advocate a comprehensive SEE program. The SEE program must coordinate and support the efforts of well-established technical communities wherein the bulk of the work will continue to be done. The SEE program will consist of a NASA-led SEE Steering Committee, consisting of government and industry users, with the responsibility for coordination between technology developers and NASA customers; and Technical Working Groups with primary responsibility for program technical content in response to user needs. The Technical Working Groups are as follows: Materials and Processes; Plasma and Fields; Ionizing Radiation; Meteoroids and Orbital Debris; Neutral External Contamination; Thermosphere, Thermal, and Solar Conditions; Electromagnetic Effects; Integrated Assessments and Databases. Specific technology development tasks will be solicited through a NASA Research Announcement to be released in May of 1994. The areas in which tasks are solicited include: (1) engineering environment definitions, (2) environments and effects design guidelines, (3) environments and effects assessment models and databases, and (4) flight/ground simulation/technology assessment data. Author (revised)

N95-27658*# Boeing Aerospace Operations, Inc., Hampton, VA.

LONG DURATION EXPOSURE FACILITY (LDEF) ARCHIVE SYSTEM c82

Brenda K. Wilson *In* NASA. Langley Research Center, LDEF: 69 Months in Space. Third Post-Retrieval Symposium, Part 3 Feb. 1995 p 1249-1262 (For primary document see N95-27629 09-99)

Avail: CASI HC A03/MF A04

The Long Duration Exposure Facility (LDEF) Archive System is designed to provide spacecraft designers and space environment researchers single point access to all available resources from LDEF. These include data, micrographs, photographs, technical reports, papers, hardware and test specimens, as well as technical expertise. Further, the LDEF Archive System is planned such that it could be the foundation for a NASA Space Environments and Effects (SEE) Archive System, with the addition of other spaceflight, laboratory and theoretical space environments and effects data and associated materials. This paper describes the current status and plans of the LDEF Archive System. Author

N95-27659*# National Aeronautics and Space Administration. Langley Research Center, Hampton, VA.

THE LONG DURATION EXPOSURE FACILITY (LDEF) ANNOTATED BIBLIOGRAPHY c82

Arlene S. Levine *In its* LDEF: 69 Months in Space. Third Post-Retrieval Symposium, Part 3 Feb. 1995 p 1263-1265 (For primary document see N95-27629 09-99)

Avail: CASI HC A01/MF A04

A major objective of the Space Act of 1958 which led to the establishment of the National Aeronautics and Space Administration (NASA) was the dissemination of science and technology. Today, under NASA administrator Daniel Goldin and the White House, there is a reemphasis on the dissemination and transfer of NASA science and technology to U.S. industry: both aerospace and non aerospace. The goal of this transfer of science and technology is to aid U.S. industries, making them more competitive in the global economy. After 69 months in space, LDEF provided new and important information on the space environment and how this hostile environment impacts spacecraft materials and systems. The space environment investigated by the LDEF researchers included: ionizing radiation, ultraviolet radiation, meteoroid and debris, atomic oxygen, thermal cycling, vacuum, microgravity, induced contamination and various synergistic effects. The materials used as part of LDEF and its experiments include polymers, metals, glass, paints and coatings. Fiber optic, mechanical, electrical, and optical systems were also used on LDEF. As part of the effort to disseminate and transfer LDEF science and technology, an annotated bibliographic database is being developed. This bibliography will be available electronically, as well as in hard copy. All LDEF domestic and foreign publications in the open literature, including scientific journals, the NASA LDEF Symposia volumes, books, technical reports and unrestricted contractor reports will be included in this database. The hard copy, as well as the electronic database, will be categorized by section in the scientific and technical discipline. Derived from text

N95-27660*# National Aeronautics and Space Administration. Langley Research Center, Hampton, VA.

THE LONG DURATION EXPOSURE FACILITY (LDEF) PHOTOGRAPHIC SURVEY SPECIAL PUBLICATION c82

Robert L. ONeal (O'Neal, Robert L., Hampton, VA.), Arlene S. Levine, and Carol C. Kiser (Kiser, Carol C., Hampton, VA.) *In its* LDEF: 69 Months in Space. Third Post-Retrieval Symposium, Part 3 Feb. 1995 p 1267-1269 (For primary document see N95-27629 09-99)

Avail: CASI HC A01/MF A04

During the construction, integration, launch, retrieval and deintegration of the Long Duration Exposure Facility (LDEF), photographic surveys were made. Approximately 10,000 photographs were taken during the various phases of the LDEF project. These surveys are of technical and scientific importance because they revealed the pre and post flight conditions of the experiment trays as well as the spacecraft. Visual inspection of the photographs reveal valuable data such as space environment's effects and the earth atmosphere's effects post-retrieval. Careful files and records have been kept of these photographs. Each photograph has a Kennedy Space Center photo number or a Johnson Spaceflight Center photo number as well as a Langley Research Center photo number. The tray number, row number, and experiment number are also noted. Out of the 10,000 photographs taken, approximately 700 selected photographs were chosen for publication in a NASA Special Publication (SP) because they reveal the effects of space exposure to the viewer. These photographs will give researchers and spacecraft designers visual images of the effects of the space environment on specific materials, systems and spacecraft in general. One can visually see the degradation of thermal blankets, meteoroid craters, outgassing discoloration, atomic oxygen erosion, etc. Derived from text

N95-27661*# McDonnell-Douglas Space Systems Co., Huntington Beach, CA. Space Station Program.

LDEF'S CONTRIBUTION TO THE SELECTION OF THERMAL CONTROL COATINGS FOR THE SPACE STATION c27

Henry W. Babel *In* NASA. Langley Research Center, LDEF: 69 Months in Space. Third Post-Retrieval Symposium, Part 3 Feb. 1995 p 1273-1283 (For primary document see N95-27629 09-99)

Avail: CASI HC A03/MF A04

The design of the Space Station presented new challenges in the selection and qualification of thermal control materials that would survive in low Earth orbit for a duration of up to 30 years. Prior to LDEF, flight data were obtained from Orbiting Solar Observatory (OSO) satellites, a number of Orbiter flights, and limited ground tests. The excellent data obtained from the OSO satellites were based on calorimetry and temperature measurements which were transmitted to Earth; these satellites were not recovered. For some of these flight experiments it was difficult to distinguish between changes due to contamination, atomic oxygen (AO), ultraviolet radiation (UV), particle radiation and the synergistic effects between them. The data from Shuttle flights were primarily focused on developing a better understanding of atomic oxygen (AO) effects. Although UV and AO were present, the relatively short duration of the Orbiter flights, about one week, was viewed as too short to show the effects from UV or possible synergistic interactions with AO and contamination. At the beginning of the program in 1989 there was no established design data base for AO resistant thermal control coatings for the Space Station. Then came the Long Duration Exposure Facility (LDEF). It provided the first long life data for materials exposed and recovered from space with a characterized environment. Post flight analysis proved data on the effects of contamination on optical properties in the ram (velocity) and wake directions and the erosion of Teflon and multilayer insulation (MLI) covers. The results from LDEF confirmed and, in some cases, modified the approach used for the Space Station, as well as helped to focus our development activities. These development activities resulted in a number of new technical solutions which are applicable to many spacecraft surfaces and missions. LDEF also showed the detrimental effects that could occur from silicone contamination, an issue that has not been completely resolved. An investigation was initiated in 1993 on the effects of silicone contamination and was continuing at the time this paper was prepared. Author

N95-27662*# National Aeronautics and Space Administration. Lyndon B. Johnson Space Center, Houston, TX.

SPACE STATION PROGRAM STATUS AND RESEARCH CAPABILITIES **c18**

Alan C. Holt *In* NASA. Langley Research Center, LDEF: 69 Months in Space. Third Post-Retrieval Symposium, Part 3 Feb. 1995 p 1285-1288 (For primary document see N95-27629 09-99)

Avail: CASI HC A01/MF A04

Space Station will be a permanent orbiting laboratory in space which will provide researchers with unprecedented opportunities for access to the space environment. Space Station is designed to provide essential resources of volume, crew, power, data handling and communications to accommodate experiments for long-duration studies in technology, materials and the life sciences. Materials and coatings for exposure research will be supported by Space Station, providing new knowledge for applications in Earthbased technology and future space missions. Space Station has been redesigned at the direction of the President. The redesign was performed to significantly reduce development, operations and utilization costs while achieving many of the original goals for long duration scientific research. An overview of the Space Station Program and capabilities for research following the redesign is presented below. Accommodations for pressurized and external payloads are described. Derived from text

N95-27663*# McDonnell-Douglas Space Systems Co., Huntington Beach, CA. Space Station Div.

SPACE STATION AS A LONG DURATION EXPOSURE FACILITY **c18**

Adrienne Folley and Jim Scheib *In* NASA. Langley Research Center, LDEF: 69 Months in Space. Third Post-Retrieval Symposium, Part 3 Feb. 1995 p 1289-1300 (For primary document see N95-27629 09-99)

Avail: CASI HC A03/MF A04

There is need for a space platform for experiments investigating long duration exposure to space. This platform should be maintainable in the event of a malfunction, and experiments should be easily recoverable for analysis on Earth. The International Space Station provides such a platform. The current Space Station configuration has six external experiment attachment sites, providing utilities and data support distributed along the external truss. There are also other sites that could potentially support long duration exposure experiments. This paper describes the resources provided to payloads at these sites, and cites examples of integration of proposed long duration exposure experiments on these sites. The environments to which external attached payloads will be exposed are summarized. Author

N95-27664*# National Aeronautics and Space Administration. Langley Research Center, Hampton, VA.

A MATERIALS EXPOSURE FACILITY **c18**

Wayne S. Slemp and Don E. Avery *In its* LDEF: 69 Months in Space. Third Post-Retrieval Symposium, Part 3 Feb. 1995 p 1301-1304 (For primary document see N95-27629 09-99)

Avail: CASI HC A01/MF A04

The objective of the Materials Exposure Facility (MEF) is to provide a test bed in space for conducting long-term (greater than one year) materials experiments which require exposure to the low Earth orbit (LEO) space environment. The proposed MEF is planned to be an integral part of the agency's Space Environments and Effects Research Program. The facility will provide experiment trays similar to the Long Duration Exposure Facility (LDEF). Each tray location is planned to have a power and data interface and robotic installation and removal provisions. Space environmental monitoring for each side of the MEF will also be provided. Since routine access to MEF for specimen retrieval is extremely important to the materials research, Space Station Freedom has been chosen as the preferred MEF carrier. Derived from text

N95-27665*# National Aeronautics and Space Administration. Marshall Space Flight Center, Huntsville, AL.

AN LDEF FOLLOW-ON SPACECRAFT CONCEPT Abstract Only **c18**

Vernon Keller, Larry Breazeale, Don Perkinson, and William H. Kinard (National Aeronautics and Space Administration. Langley Research Center, Hampton, VA.) *In* NASA. Langley Research Center, LDEF: 69 Months in Space. Third Post-Retrieval Symposium, Part 3 Feb. 1995 p 1307 (For primary document see N95-27629 09-99)

Avail: CASI HC A01/MF A04

The successful flight, retrieval, and analyses of the Long Duration Exposure Facility (LDEF) experiments demonstrated the value of long duration space exposure for a broad spectrum of science and engineering investigations. The original LDEF was an excellent gravity gradient spacecraft, but because of its 9 m length and 9,700 kg mass it was difficult to manifest on the Shuttle, for either launch or retrieval, in conjunction with other payloads. This paper discusses an LDEF follow-on spacecraft concept whose short stowed length (approximately 3 m) greatly improves Shuttle manifesting opportunities while still providing very large surface area exposure for experiments. Deployable 'wings' on each end of the short, 'cylindrical' main body of this new spacecraft provide the means for gravity gradient stabilization while greatly increasing the spacecraft surface area. The center section of the spacecraft is oriented with the end faces of the twelve sided, 4.2 m diameter 'cylinder' perpendicular to the velocity vector thus providing large areas for experiments in both the ram and anti-ram directions as well as additional exposure area around the periphery of the cylinder. When deployed and properly oriented with the Shuttle's Remote Manipulator System (RMS), both wings of the spacecraft are oriented edge on to the direction of motion and lie in the plane which contains the local gravity vector. The relatively thin wings readily accommodate dual side exposure of glass plate stacks for cosmic ray detection. Flat surfaces mounted normal to and on the periphery of the wings provide additional areas in both the ram and anti-ram directions for cosmic dust, micrometeoroid, and orbital debris collection free of contamination from 'splatter' off secondary surfaces. The baseline concept provides enhancements not available on the original LDEF such as solar array generated electrical power and data telemetry. Status of the efforts to promote support for and ultimately space flight of this concept will be presented. Suggestions for improvements in the spacecraft design and proposed utilization are solicited. Author

N95-27666*# National Aeronautics and Space Administration. Goddard Space Flight Center, Greenbelt, MD.

LONG DURATION EXPOSURE FACILITY POST-FLIGHT DATA AS IT INFLUENCES THE TROPICAL RAINFALL MEASURING MISSION **c47**

Sharon A. Straka *In* NASA. Langley Research Center, LDEF: 69 Months in Space. Third Post-Retrieval Symposium, Part 3 Feb. 1995 p 1309-1318 (For primary document see N95-27629 09-99)

Avail: CASI HC A02/MF A04

The Tropical Rainfall Measuring Mission (TRMM) is an earth observing satellite that will be in a low earth orbit (350 kilometers) during the next period of maximum solar activity. The TRMM observatory is expected to experience an atomic oxygen fluence of 8.9 x 10(exp 22) atoms per square centimeter. This fluence is ten times higher than the atomic oxygen impingement incident to the Long Duration Exposure Facility (LDEF). Other environmental concerns on TRMM include: spacecraft glow, silicon oxide contaminant build-up, severe spacecraft material degradation, and contamination deposition resulting from molecular interactions with the dense ambient atmosphere. Because of TRMM's predicted harsh environment, TRMM faces many unique material concerns and subsystem design issues. The LDEF data has influenced the design of TRMM and the TRMM material selection process. Author

N95-27667*# Ishikawajima-Harima Heavy Industries Co. Ltd., Tokyo (Japan).
ELEMENT MATERIAL EXPERIMENT BY EFFU **c12**
Yoshihiro Hashimoto, Masaaki Ichikawa, Mitsuru Takei (National Space Development Agency, Tsukuba, Japan.), Yoshihiro Torii (National Space Development Agency, Tsukuba, Japan.), and Kazuo Ota (National Space Development Agency, Tsukuba, Japan.) *In* NASA. Langley Research Center, LDEF: 69 Months in Space. Third Post-Retrieval Symposium, Part 3 Feb. 1995 p 1321-1329 (For primary document see N95-27629 09-99)
Avail: CASI HC A02/MF A04

National Space Development Agency of JAPAN (NASDA) is planning to perform Element Material Exposure Experiment using Exposed Facility Flyer Unit (EFFU). Several materials which will be used on JEM (Japanese Experiment Module for the space station) will be exposed. Space environment monitoring is also planned in this experiment. Several ground based tests are now being performed and getting useful data. Author

N95-27668*# National Aeronautics and Space Administration. Langley Research Center, Hampton, VA.
ORBITING METEOROID AND DEBRIS COUNTING EXPERIMENT **c90**
William H. Kinard, Dwayne Armstrong, Sharon K. Crockett, James L. Jones, Jr., Philip C. Kassel, Jr., and J. J. Wortman (North Carolina State Univ., Raleigh, NC.) *In its* LDEF: 69 Months in Space. Third Post-Retrieval Symposium, Part 3 Feb. 1995 p 1331-1340 (For primary document see N95-27629 09-99)
Avail: CASI HC A02/MF A04

The Orbiting Meteoroid and Debris Counting Experiment (OMDC) flew for approximately 90 days in a highly elliptical earth orbit onboard the Clementine Interstage Adapter (ISA) Spacecraft. This experiment obtained data on the impact flux of natural micrometeoroids and it provided limited information on the population of small mass man-made debris as a function of altitude in near earth space. The flight of the OMDC experiment on the ISA spacecraft also demonstrated that the ultra-lightweight, low-power, particle impact detector system that was used is a viable system for flights on future spacecraft to monitor the population of small mass man-made debris particles and to map the cosmic dust environment encountered on interplanetary missions. An overview of the ISA spacecraft mission, the approach to the OMDC experiment, and the data obtained by the experiment are presented. Author

N95-27669*# Canadian Space Agency, Saint Hubert (Quebec). Strategic Technologies for Automation and Robotics Program.
THE STRATEGIC TECHNOLOGIES FOR AUTOMATION AND ROBOTICS (STEAR) PROGRAM: PROTECTION OF MATERIALS IN THE SPACE ENVIRONMENT SUBPROGRAM **c27**
Lorne R. Schmidt, J. Francoeur, Alina Aguero (Cametoid Advanced Technologies, Inc., Whitby, Ontario.), Michael R. Wertheimer (Ecole Polytechnique, Montreal, Quebec.), J. E. Klemberg-Sapieha (Ecole Polytechnique, Montreal, Quebec.), L. Martinu (Ecole Polytechnique, Montreal, Quebec.), J. W. Blezius (MPB Technologies, Inc., Pointe Claire, Quebec.), M. Oliver (MPB Technologies, Inc., Pointe Claire, Quebec.), and A. Singh (National Optics Inst., Ste-Foy, Quebec.) *In* NASA. Langley Research Center, LDEF: 69 Months in Space. Third Post-Retrieval Symposium, Part 3 Feb. 1995 p 1341-1359 (For primary document see N95-27629 09-99)
Avail: CASI HC A03/MF A04

Three projects are currently underway for the development of new coatings for the protection of materials in the space environment. These coatings are based on vacuum deposition technologies. The projects will go as far as the proof-of-concept stage when the commercial potential for the technology will be demonstrated on pilot-scale fabrication facilities in 1996. These projects are part of a subprogram to develop supporting technologies for automation and robotics technologies being developed under the Canadian Space Agency's STEAR Program, part of the Canadian Space Station Program. Author

N95-27670*# Institute for Space Science and Technology, Inc., Gainesville, FL.
THE ORBITAL DEBRIS DETECTOR CONSORTIUM: SUPPLIERS OF INSTRUMENTS FOR IN-SITU MEASUREMENTS OF SMALL-PARTICLES IN THE SPACE ENVIRONMENT **c35**
C. G. Simon, R. Muenzenmeyer (Technical Univ. of Munich, Muchen, Germany.), W. G. Tanner, Jr. (Baylor Univ., Waco, TX.), O. M. Uy (Johns Hopkins Univ., Laurel, MD.), R. A. Skrivanek (Visidyne, Inc., Burlington, MA.), A. J. Tuzzolino (Chicago Univ., Chicago, IL.), C. Maag (T and M Engineering, Glendora, CA.), and J. J. Wortman (North Carolina State Univ., Raleigh, NC.) *In* NASA. Langley Research Center, LDEF: 69 Months in Space. Third Post-Retrieval Symposium, Part 3 Feb. 1995 p 1361-1377 (For primary document see N95-27629 09-99)
Avail: CASI HC A03/MF A04

Industry and university participants have joined together to form the IMPA:Ct consortium (In-situ Monitors of the Particulate Ambient: Circumterrestrial) which offers a broad range of flight qualified instruments for monitoring the small particle (0.1 micron to 10 cm) environment in space. Instruments are available in 12 months or less at costs ranging from 0.5 to 1.5 million dollars (US) for the total program. Detector technologies represented by these groups are: impact-induced capacitor-discharge (MOS, metal-oxide-silicon), cratering or penetration of electroactive thin film (polyvinylidene fluoride (PVDF)), impact-plasma detection, acoustic detection, CCD tracking of optical scatter of sunlight, and photodiode detection of optical scatter of laser light. The operational characteristics, general spacecraft interface and resource requirements (mass/power/telemetry), cost and delivery schedules, and points of contact for seven different instruments are presented. Author

N95-27671*# Phillips Lab., Kirtland AFB, NM.
A NEW TECHNIQUE FOR GROUND SIMULATION OF HYPERVELOCITY DEBRIS **c14**
R. Roybal, J. Shively, C. Stein, C. Miglionico, and R. Robertson *In* NASA. Langley Research Center, LDEF: 69 Months in Space. Third Post-Retrieval Symposium, Part 3 Feb. 1995 p 1379-1388 (For primary document see N95-27629 09-99)
Avail: CASI HC A02/MF A04

A series of hypervelocity damage experiments were preformed on spacecraft materials. These experiments employed a technique which accelerates micro flyer plates simulating space debris traveling at 3 to 8 km/sec. The apparatus used to propel the micro flyer plates was compact and fit well into a space environmental chamber equipped with instrumentation capable of analyzing the vapor ejected from the sample. Mechanical damage to the sample was also characterized using optical and scanning electron microscpopy. Data for this work was obtained from hypervelocity impacts on a polysulfone resin and a graphite polysulfone composite. Polysulfone was selected because it was flown on the Long Duration Exposure Facility (LDEF) which spent several years in low earth orbit (LEO). Chemistry of the vapor produced by the impact was analyzed with a time of flight mass spectrometer, (TOFMS). This represents the first time that ejected vapors from hypervelocity collisions were trapped and analyzed with a mass spectrometer. With this approach we are able to study changes in the vapor chemistry as a function of time after impact, obtain a velocity measurement of the vapor, and estimate a temperature of the surface at time of impact using dynamic gas equations. Samples of the vapor plume may be captured and examined by transmission electron microscopy. Studies were also conducted to determine mechanical damage to a graphite polysulfone composite and a polysulfone resin. Impact craters were examined under optical and scanning electron microscopes. The collision craters in the matrix were typical of those shown in conventional shock experiments. However, the hypervelocity collisions with the graphite polysulfone composite were remarkably different than those with the resin. Author

N95-27685*# National Aeronautics and Space Administration, Washington, DC.
SPACEFLIGHT REVOLUTION: NASA LANGLEY RESEARCH CENTER FROM SPUTNIK TO APOLLO
James R. Hansen 1995 563 p
(NASA-SP-4308; NAS 1.21:4308; LC-94-24592) Avail: CASI HC A24/MF A04; SOD HC

As part of the transition to the broad research scope of the National Aeronautics and Space Administration (NASA) starting in the late 1950's, the Langley Research Center underwent many changes in program content, organization and management, and areas of personnel expertise. This book describes and evaluates the evolution and activities of the Langley Research Center during the seventeen-year period from 1958 to 1975. The book was based on the analysis of hundreds of written records, both published and unpublished, as well as numerous personal interviews with many of the key individuals involved in the transition of Langley. Some of the projects and research areas covered include Project Echo, magnetoplasmadynamics research, Scout Rocket Program, lunar-orbit rendezvous research, manned space laboratory development, and Apollo and the Lunar Orbiter Project. CASI

N95-28002*# National Aeronautics and Space Administration, Washington, DC.

RESEARCH AND TECHNOLOGY OBJECTIVES AND PLANS SUMMARY (RTOPS) Research and Technology Program, FY 1993

Mar. 1993 202 p

(NASA-TM-108574; NAS 1.15:108574) Avail: CASI HC A10/MF A03

This publication represents the NASA research and technology program for FY-93. It is a compilation of the Summary portions of each of the RTOP's (Research and Technology Objectives and Plans) used for management review and control of research currently in progress throughout NASA. The RTOP Summary is designed to facilitate communication and coordination among concerned technical personnel in government, in industry, and in universities. The first section containing citations and abstracts of the RTOP's is followed by four indexes: Subject, Technical Monitor, Responsible NASA Organization, and RTOP Number. Author

N95-28038*# Loyola Coll., Baltimore, MD. International Technology Research Inst.

JTEC/WTEC ANNUAL REPORT AND PROGRAM SUMMARY: 1993/94

Geoffrey M. Holdridge, ed. Mar. 1994 204 p

(Grants NSF ECS-89-02528; NSF ECS-89-22947; NSF ENG-91-11333; NSF ENG-92-17849)

(NASA-CR-198563; NAS 1.26:198563; ISBN-1-883-71231-9; PB94-155702)

Avail: CASI HC A10/MF A03

The JTEC/WTEC (Japanese Technology Evaluation Center/World Technology Evaluation Center) Program at Loyola College is overviewed. A review of activities for 1993 and early 1994 is discussed along with plans for the following year. The bulk of the report consists of the summaries of completed projects in Information and Communication Technology; Materials; Manufacturing and Construction; Aeronautics, Space, and Ocean Technology; Energy; and Biotechnology. CASI

SUBJECT INDEX

SCIENTIFIC AND TECHNICAL AEROSPACE REPORTS VOLUME 33 NUMBER 9

Typical Subject Index Listing

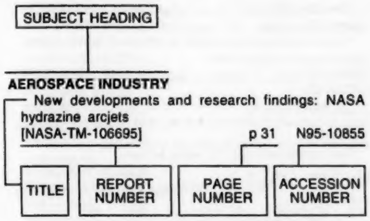

The subject heading is a key to the subject content of the document. Titles, report numbers, and accession numbers of pertinent documents are provided under each subject heading. When the title is insufficiently descriptive of the document content, a title extension is added, separated from the title by three hyphens. The report number helps to indicate the type of document cited (e.g., NASA report, NASA translation, NASA contractor report). The accession number is the number by which the document abstracts are arranged in this journal and by which the document is sold or requested. The page number helps you locate the citation in the abstract section. The titles, with title extensions if present, are arranged under each subject heading in ascending accession number order. The subject headings have been selected from the latest revision of the *NASA Thesaurus.*

A

ABERRATION
Frame selection performance limits for statistical image reconstruction of adaptive optics compensated images
[AD-A289240] p 2424 N95-26965
Plasma lens experiments at the final focus test beam
[DE95-008595] p 2434 N95-28161

ABLATION
Engineering calculations associated with the ablative thermal protective structures of returnable satellites
[AD-A289593] p 2162 N95-26715
Abrasion-ablation model for neutron production in heavy ion reactions
[NASA-TM-4656] p 2420 N95-27372

ABLATIVE MATERIALS
A high velocity electromagnetic mass launcher having an ablation resistant insulator
[AD-A288231] p 2154 N95-26524
Engineering calculations associated with the ablative thermal protective structures of returnable satellites
[AD-A289593] p 2162 N95-26715
Indirectly driven targets for ignition
[DE95-006451] p 2430 N95-27327
Task 4 supporting technology. Part 1: Detailed test plan for leading edge tile development. Leading edge material development and testing
[NASA-CR-198633] p 2160 N95-28258

ABNORMALITIES
Fuzzy-algebra uncertainty assessment
[DE95-005426] p 2391 N95-27432

ABRASION
Abrasion-ablation model for neutron production in heavy ion reactions
[NASA-TM-4656] p 2420 N95-27372

ABSORBENTS
Chlorodifluoromethane equilibrium on 13X molecular sieve
[AD-A289282] p 2405 N95-27034

ABSORBERS (MATERIALS)
Particle fallout/activity sensor
[NASA-CASE-KSC-11687-1] p 2293 N95-28362

ABSORPTION
Analysis of gas absorption to a thin liquid film in the presence of a zero-order chemical reaction
p 2280 N95-27348

ABSORPTION SPECTRA
CO, HCO(+) and HCN absorption in the gravitational lens candidate B0218+357 at z=0.685
[PB95-185146] p 2461 N95-26522
Overview of the observations of symbiotic stars
p 2460 N95-27076
Ionizing radiation measurements on LDEF: A0015 Free flyer biostack experiment
[NASA-CR-196603] p 2202 N95-27168
Analytical spectroscopy
[DE95-607896] p 2203 N95-27200
Programming for time resolved spectrum in pulse radiolysis experiments
[DE95-607929] p 2406 N95-27212
Particle-like absorption spectra in small transition metal clusters
[DE95-007082] p 2218 N95-27752
Observation on radiation transfer experiments using k-shell absorption spectra
[DE95-008068] p 2434 N95-28141
Multivariate classification of BPSG thin films using Mahalanobis distances
[DE95-008519] p 2267 N95-28148
Search for molecular absorptions with the Fourier Transform Spectrometer
[NASA-CR-198648] p 2462 N95-28222

ABSORPTION SPECTROSCOPY
Continuously-tunable, narrow-linewidth, Q-switched Cr:LiSAF laser for lidar applications
[DE95-006285] p 2296 N95-27672
High temperature kinetic study of the reactions H + O2 = OH + O and O + H2 = OH + H in H2/O2 system by shock tube-laser absorption spectroscopy
[NASA-CR-195473] p 2206 N95-27695
Structural oxidation state studies of the manganese cluster in the oxygen evolving complex of Photosystem II
[DE95-008488] p 2409 N95-27744
Bubble chamber spectroscopy for chemical analysis: A new concept
[DE95-006350] p 2209 N95-28088
Application of modern diagnostic methods to environmental improvement
[DE95-005797] p 2330 N95-28119

ABSORPTIVITY
Time-dependent model for vertical-cavity surface-emitting laser
[DE95-007880] p 2298 N95-28027

ABSTRACTS
Selected bibliography on heavy water, tritiated water and hydrogen isotopes (1981-1992)
[DE95-608331] p 2405 N95-27159

ABUNDANCE
Coronal abundances and their variation
[NASA-CR-197788] p 2464 N95-26671
Theoretical studies of interstellar processes
[NASA-CR-198647] p 2462 N95-28216

ACCELERATED LIFE TESTS
Progress towards computer simulation of NiH2 battery performance over life p 2272 N95-26786
Long life 80Ah standard IPV NiH2 battery cell
p 2272 N95-26787
Hubble Space Telescope nickel-hydrogen battery testing: An update p 2272 N95-26794

ACCELERATION (PHYSICS)
Analytical investigations of the acceleration sensitivity of acoustic bulk and surface wave resonators
[AD-A291715] p 2402 N95-28505

ACCELEROMETERS
Bearing defect signature analysis using advanced nonlinear signal analysis in a controlled environment
[NASA-TM-108491] p 2304 N95-28364
Material characterization system
[AD-D017385] p 2210 N95-28584

ACCEPTOR MATERIALS
Photoinduced dipoles and charge pairs in condensed phase
[DE95-007071] p 2207 N95-27921

ACCIDENT PREVENTION
Prevention and control of inlet unstart using an SR-71 simulation p 2119 N95-26948
Computational studies of projectile melt in impact with typical whipple shields
[DE95-005916] p 2311 N95-28337

ACCRETION DISKS
Nova-like variables p 2458 N95-27070
Models for various aspects of dwarf novae and nova-like stars p 2459 N95-27071
Magnetic viscosity by localized shear flow instability in magnetized accretion disks
[DE95-006879] p 2433 N95-28111

ACCUMULATORS
Replicator for characterization of cirrus and polar stratospheric cloud particles
[NASA-CR-197785] p 2341 N95-26669
To develop an aerosoling immunomagnetic device for rapid medical diagnosis from clinical samples
[AD-A288504] p 2354 N95-27059

ACCURACY
Micron Accuracy Deployment Experiment (MADE), phase A. Volume 1
[NASA-CR-197792] p 2144 N95-26426
Accurate orbit determination strategies for the tracking and data relay satellites p 2147 N95-27768
Operational improvements of long-term predicted ephemerides of the Tracking and Data Relay Satellites (TDRSs) p 2147 N95-27769
Earth horizon modeling and application to static Earth sensors on TRMM spacecraft p 2150 N95-27783
Perturbations on effective index of refraction from prism coupling
[AD-A291700] p 2427 N95-28524

ACEE PROGRAM
NASA-ACEE/Boeing 737 graphite-epoxy horizontal stabilizer service p 2138 N95-28489

ACETONITRILE
Applications of Second Harmonic and Sum Frequency Generation to graphite and silica type interfaces
[AD-A288228] p 2201 N95-26544

ACETYLENE
JPRS report: Science and technology. Central Eurasia
[JPRS-UST-95-015] p 2246 N95-27213
Spectroscopic and dynamical studies of highly energized small polyatomic molecules
[DE95-006640] p 2414 N95-28199

ACIDITY
Measurement of high acidity using a renewable-reagent fiber optic sensor
[DE95-006327] p 2425 N95-27734
Porosity in hexylene-bridged polysilsesquioxanes: Effects of monomer concentration
[DE95-005421] p 2240 N95-28531
Comparison of bridged polysilsesquioxane xerogels prepared from methoxy- and ethoxy-silyl monomers
[DE95-005422] p 2240 N95-28532

ACOUSTIC ATTENUATION
Suppressor of oscillations in airframe cavities
[AD-D017265] p 2128 N95-26507
The use of acoustic methods to determine the parameters of porous materials
[IFTR-40/1994] p 2401 N95-26519

ACOUSTIC EMISSION
Bearing defect signature analysis using advanced nonlinear signal analysis in a controlled environment
[NASA-TM-108491] p 2304 N95-28364

ACOUSTIC EXCITATION
Self-excited oscillations in a duct with closed brances
[IFTR-18/1994] p 2400 N95-26358

ACOUSTIC IMPEDANCE
A finite element propagation model for extracting normal incidence impedance in nonprogressive acoustic wave fields
[NASA-TM-110160] p 2400 N95-26394

ACOUSTIC PROPERTIES
A finite element propagation model for extracting normal incidence impedance in nonprogressive acoustic wave fields
[NASA-TM-110160] p 2400 N95-26394
Analysis of historical oceanographic data on a personal computer. Program MDS
[AD-A288965] p 2363 N95-26447
The use of acoustic methods to determine the parameters of porous materials
[IFTR-40/1994] p 2401 N95-26519
Photoacoustic chambers for studying solids and gases: Theory and practical examples
[IFTR-39/1994] p 2143 N95-26837
The noise reduction potential of dual-stream coaxial rectangular improperly expanded jet flows
[NASA-CR-197820] p 2277 N95-26995
Anechoic wind tunnel study of turbulence effects on wind turbine broadband noise p 2325 N95-27992
Evaluation of a doubly-swept blade tip for rotorcraft noise reduction
[NASA-CR-189677] p 2402 N95-28264

ACOUSTIC SCATTERING
On the azimuthal Fourier components of the Green's function for the Helmholtz equation in three dimensions
[AD-A288775] p 2398 N95-26345

ACOUSTIC SOUNDING
Basic principles and recent observations of rotationally sampled wind p 2321 N95-27971

ACOUSTIC VELOCITY
Numerical analysis of wave scattering
[AD-A289478] p 2401 N95-26925

ACOUSTICS
Valve mechanism for an acoustic modulator
[AD-D017263] p 2300 N95-26504
The use of acoustic methods to determine the parameters of porous materials
[IFTR-40/1994] p 2401 N95-26519
Acoustic field in unsteady moving media
[NASA-CR-198162] p 2279 N95-27179
Material characterization system
[AD-D017385] p 2210 N95-28584
Subharmonic phonon transmission and Kapitza conductance between crystals with very different vibrational spectra
[DE95-609151] p 2447 N95-28608

ACOUSTO-OPTICS
Signals processing using acousto-optical technology
[AD-A289597] p 2250 N95-26717
Modulation effect of a Bragg acousto-optic bistable system
[AD-A289622] p 2401 N95-26857
Display system employing acousto-optic tunable filter
[NASA-CASE-NPO-18736-1-CU] p 2426 N95-27843
Method of space-time sequence transform used to measure acousto-optic deflection and modulation
[AD-A289612] p 2402 N95-28671

ACTIVATION (BIOLOGY)
The electrical behaviour of an excitable cell at different conditions
[DE95-607911] p 2351 N95-27254

ACTIVATION ENERGY
The effects of temperature on Schottky diode barrier height and evidence of multiple barrier
[DE95-609147] p 2264 N95-27405
Hydrogen induced C-C, C-N, and C-S bond activities on Pi and Ni surfaces
[DE95-006251] p 2206 N95-27838
Polarization relaxation in zinc oxide varistors from 77 K to 450 K
[DE95-007761] p 2268 N95-28156
Heterostructures and infrared emitters with compressed InAsSb layers
[DE95-008157] p 2446 N95-28399

ACTIVE CONTROL
Vibration control using chaotic motion stabilizers
[AD-A289576] p 2398 N95-26687
Analysis of modal behavior at frequency cross-over
[AD-A289304] p 2162 N95-26918
A state-space model of a large, lightly damped space structure using the Eigensystem realization algorithm
[AD-A289251] p 2163 N95-26970
Dynamics of the L yields H transition, VH-mode evolution, edge localized modes and R.F. driven confinement control in tokamaks
[DE95-007012] p 2430 N95-27306
Beam instability studies for the SSC
[DE95-008024] p 2423 N95-28551

ACTIVITY (BIOLOGY)
Magnetic resonance imaging of solvent transport in polymer networks
[DE95-007142] p 2234 N95-27455
Cognitive networks for ATR: The roles of bifurcation and chaos
[AD-A289010] p 2387 N95-28336

ACTUATORS
Design and development of a test rig for the high frequency testing of rolling sleeve airsprings
[DSTO-TN-0001] p 2142 N95-26378
Silicon based microactuators for telerobotic tactile stimulation
[AD-A289340] p 2260 N95-26767
Electro-hydrostatic actuator controller design using quantitative feedback theory
[AD-A289220] p 2141 N95-26957
Dynamic coupling of underactuated manipulators
[AD-A289404] p 2301 N95-27098
The 29th Aerospace Mechanisms Symposium
[NASA-CP-3293] p 2154 N95-27260
Advanced development for space robotics with emphasis on fault tolerance p 2155 N95-27263
Development of a miniature actuator/controller system
p 2156 N95-27272
Non-explosive actuation for the ORBCOMM (TM) satellite p 2156 N95-27274
A rotating arm using shape-memory alloy
p 2157 N95-27276
Electromechanical rotary actuator
p 2157 N95-27278
Linear Proof Mass Actuator p 2158 N95-27290
Autonomous control system reconfiguration for spacecraft with non-redundant actuators
p 2153 N95-27802
JTEC Panel report on microelectromechanical systems in Japan
[NASA-CR-197831] p 2268 N95-28239
Composite flight-control actuator development
p 2142 N95-28281

ADA (PROGRAMMING LANGUAGE)
EASY-SIM: A visual simulation system software architecture with an Ada 9X application framework
[AD-A289325] p 2368 N95-26895
Multiple model adaptive estimation and head motion tracking in a virtual environment: An engineering approach
[AD-A289299] p 2359 N95-27046
Software technology for adaptable, reliable systems (STARS). AdaWise user's manual
[AD-A289655] p 2375 N95-28635

ADAPTIVE CONTROL
Robust hybrid state-space self-tuning control using dual-rate sampling
[AD-A288359] p 2380 N95-26468
Stochastic adaptive estimation and control
[AD-A289088] p 2380 N95-26480
Control of a large space structure using multiple model adaptive estimation and control techniques
[AD-A289309] p 2162 N95-26916
A gain scheduling optimization method using genetic algorithms
[AD-A289306] p 2381 N95-26920
Unstructured mesh generation and adaptivity
[NASA-CR-195069] p 2278 N95-27027
Stable adaptive neurocontrollers for spacecraft and space robots p 2384 N95-27385

ADAPTIVE FILTERS
ACT adaptive filters
[AD-A288385] p 2363 N95-26474
Attitude determination using an adaptive multiple model filtering Scheme p 2148 N95-27772

ADAPTIVE OPTICS
Compensated deconvolution from wavefront sensing
[AD-A289490] p 2336 N95-26824
Frame selection performance limits for statistical image reconstruction of adaptive optics compensated images
[AD-A289240] p 2424 N95-26965
Atmospheric dispersion in adaptive optics
[AD-A289639] p 2428 N95-28617

ADDITIVES
The fBm Interpolator
[AD-A288996] p 2388 N95-26459
Materials Research Society Symposium Proceedings. Volume 339: Diamond, SiC and nitride wide bandgap semiconductors
[AD-A288690] p 2437 N95-26818
Photoluminescence spectroscopy of 4H- and 6H-SiC
[AD-A289326] p 2202 N95-26896
Modeling of trapping and abrupt doping effects in MESFET's using R-dynamic element
[PB95-184891] p 2262 N95-27050
Use of CTFE as an additive to enhance fire resistance of single hydraulic fluid
[AD-A289377] p 2233 N95-27325
The effect of aviation fuels containing low amounts of static dissipater additive on electrostatic charge generation
[AD-A280075] p 2243 N95-28152

ADHESION
Processing and properties of chromate-free conversion coatings on aluminum
[DE95-004768] p 2218 N95-27722
Effects of interlayers on the scratch adhesion performance of ultra-thin films of copper and gold on silicon substrates
[DE95-007367] p 2220 N95-28044
Functionalized block copolymers as adhesion promoters
[DE95-008158] p 2239 N95-28400

ADHESION TESTS
Effects of interlayers on the scratch adhesion performance of ultra-thin films of copper and gold on silicon substrates
[DE95-007367] p 2220 N95-28044

ADHESIVE BONDING
Adhesively bonded composite patch repair of cracked aluminum alloy structures p 2132 N95-27507
Field repair materials for naval aircraft
p 2133 N95-27514
The development of an engineering standard for composite repairs p 2135 N95-27528
Fracture testing and analysis of adhesively bonded joints for automotive applications
[DE95-007024] p 2184 N95-28207

ADHESIVES
Sceening, down selection, and implementation of environmentally compliant cleaning and insulation bonding for MNASA p 2165 N95-27124
Field repair materials for naval aircraft
p 2133 N95-27514
Repair of high temperature composite aircraft structure p 2134 N95-27520
Fracture testing and analysis of adhesively bonded joints for automotive applications
[DE95-007024] p 2184 N95-28207
Mechanical properties of Hysol EA-9394 structural adhesive
[DE95-008187] p 2240 N95-28405

ADIABATIC CONDITIONS
Adiabatic charging of nickel-hydrogen batteries
p 2272 N95-26795

ADJUSTING
Aircraft fuel system lightning protection design and qualification test procedures development
[AD-A288401] p 2125 N95-26497

ADSORBENTS
Chlorodifluoromethane equilibrium on 13X molecular sieve
[AD-A289282] p 2405 N95-27034

ADSORPTION
Stabilization and control of high energy intermediates through adsorption of restricted spaces
[AD-A288552] p 2201 N95-26606
Chlorodifluoromethane equilibrium on 13X molecular sieve
[AD-A289282] p 2405 N95-27034
Atomically resolved STM study of the adsorption and dissociation of methyl chloride on Si(001)
[AD-A289218] p 2438 N95-27061
Crystal structure, short-range oxygen defects, and water adsorption in La- and Nd-modified ZrO2
[DE95-007134] p 2439 N95-27452
FTIR studies of CH3OH on porous silicon
[AD-A289038] p 2207 N95-27904
Kinetics and dynamics of oxidation reactions involving adsorbed CO species on bulk supported Pt and copper oxides
[DE95-006420] p 2207 N95-27952
The role of hydrogen in the hydrogenation and hydrogenolysis of aniline on the nickel single crystal surfaces: Its implication on the mechanisms of HDN reactions
[DE95-006687] p 2222 N95-28134

ADVANCED VERY HIGH RESOLUTION RADIOMETER
Performance modeling of hyperspectral imaging sensors for atmospheric studies
[AD-A289017] p 2289 N95-26461
Linear and nonlinear trending and prediction for AVHRR time series data p 2385 N95-27391

ADVECTION
A numerical model to predict the fate of jettisoned aviation fuel
[AD-A289336] p 2242 N95-26842

AERIAL RECONNAISSANCE
Geophex airborne unmanned survey system
[DE95-007566] p 2131 N95-27440
Radon transform and its applications in gridding airborne geophysical survey data
[PB95-195533] p 2315 N95-28643

AEROACOUSTICS
Aircraft noise prediction program theoretical manual: Rotorcraft System Noise Prediction System (ROTONET), part 4
[NASA-TM-83199-PT-4] p 2400 N95-26392
The method of space-time conservation element and solution element-applications to one-dimensional and two-dimensional time-marching flow problems
[NASA-TM-106915] p 2389 N95-26663

Turbomachinery design and tonal acoustics computations [NASA-CR-197749] p 2139 N95-26777
Supersonic coaxial jet noise predictions [NASA-TM-106917] p 2401 N95-26801
An outflow boundary condition for aeroacoustic computations [NASA-TM-106930] p 2279 N95-27175
A numerical study of fundamental shock noise mechanisms [NASA-TM-110608] p 2401 N95-27908
Anechoic wind tunnel study of turbulence effects on wind turbine broadband noise p 2325 N95-27992
Evaluation of a doubly-swept blade tip for rotorcraft noise reduction [NASA-CR-189677] p 2402 N95-28264
Noise exposure reduction of advanced high-lift systems [NASA-CR-195077] p 2402 N95-28670
Response of multi-panel assembly to noise from a jet in forward motion [NASA-CR-198164] p 2289 N95-28673

AEROBRAKING
Rarefied gas effects on aerobraking/reentry vehicles with wakes [NASA-CR-196586] p 2164 N95-27093

AERODYNAMIC BALANCE
An easy way to analyze longitudinal and lateral-directional trim problems with AEO or OEI p 2119 N95-26949

AERODYNAMIC BRAKES
Comparative wind tunnel tests of NACA 23024 airfoils with several aileron and spoiler configurations p 2124 N95-27976

AERODYNAMIC CHARACTERISTICS
Simulation model of the integrated flight/propulsion control system, displays, and propulsion system for ASTOVL lift-fan aircraft [NASA-TM-108866] p 2139 N95-26412
Suppressor of oscillations in airframe cavities [AD-D017265] p 2128 N95-26507
Development and validation of a blade-element mathematical model for the AH-64A Apache helicopter [NASA-TM-108863] p 2118 N95-26710
AIAA Techfest 20 Proceedings [NIAR-94-1] p 2118 N95-26941
Modeling of aircraft unsteady aerodynamic characteristics. Part 2: Parameters estimated from wind tunnel data [NASA-TM-110161] p 2142 N95-27839
Comparative wind tunnel test at high Reynolds numbers of NACA 64 621 airfoils with two aileron configurations p 2124 N95-27977

AERODYNAMIC COEFFICIENTS
User documentation of the CTA program [AD-A289508] p 2121 N95-26854
Wind-tunnel test of the S814 thick root airfoil [DE95-000268] p 2122 N95-27541

AERODYNAMIC CONFIGURATIONS
Aeroelasticity of wing and wing-body configurations on parallel computers [NASA-CR-197756] p 2129 N95-26590
Design and testing of low sonic boom configurations and an oblique all-wing supersonic transport [NASA-CR-197744] p 2129 N95-26651
Supersonic civil airplane study and design: Performance and sonic boom [NASA-CR-197745] p 2130 N95-26813
An exploratory application of neural networks for airfoil design p 2118 N95-26943
The noise reduction potential of dual-stream coaxial rectangular improperly expanded jet flows [NASA-CR-197820] p 2277 N95-26995
The lift-fan aircraft: Lessons learned [NASA-CR-196694] p 2131 N95-27143
NAS Technical Summaries, March 1993 - February 1994 [NASA-RP-1355] p 2466 N95-27367

AERODYNAMIC DRAG
A new drag measurement system for wind tunnel testing of the racing bicycle and rider to determine a low drag configuration [AD-A289375] p 2122 N95-26875
Comparative wind tunnel test at high Reynolds numbers of NACA 64 621 airfoils with two aileron configurations p 2124 N95-27977
A hybrid vehicle evaluation code and its application to vehicle design. Revision 1 [DE95-008053] p 2303 N95-28029
A hybrid vehicle evaluation code and its application to vehicle design, revision 2 [DE95-008060] p 2303 N95-28139
Construction and wind tunnel test of a 1/12th scale helicopter model [AD-A288487] p 2123 N95-28331
Study of potential aerodynamic benefits from spanwise blowing at wingtip [NASA-TP-3515] p 2124 N95-28669

AERODYNAMIC HEATING
Engineering calculations associated with the ablative thermal protective structures of returnable satellites [AD-A289593] p 2162 N95-26715
Viscous shock-layer analysis on hypersonic flow over reentry capsule with nonequilibrium chemistry [ISAS-R-656] p 2274 N95-26739
Rarefied gas effects on aerobraking/reentry vehicles with wakes [NASA-CR-196586] p 2164 N95-27093

AERODYNAMIC LOADS
F/A-18 IFOSTP Fatigue test airbag load determination on the vertical and horizontal tails [DSTO-TR-0135] p 2128 N95-26389
Computational analysis of forebody tangential slot blowing on the high alpha research vehicle [NASA-CR-197754] p 2129 N95-26591
Preliminary analysis of dynamic stall effects on a 91-meter wind turbine rotor p 2124 N95-27975
Observed acoustic and aeroelastic spectral responses of a MOD-2 turbine blade to turbulence excitation p 2324 N95-27991
Aeroelasticity and structural optimization of composite helicopter rotor blades with swept tips [NASA-CR-4665] p 2136 N95-28262

AERODYNAMIC NOISE
Aircraft noise prediction program theoretical manual: Rotorcraft System Noise Prediction System (ROTONET), part 4 [NASA-TM-83199-PT-4] p 2400 N95-26392
A numerical study of fundamental shock noise mechanisms [NASA-TM-110608] p 2401 N95-27908
Anechoic wind tunnel study of turbulence effects on wind turbine broadband noise p 2325 N95-27992
Noise exposure reduction of advanced high-lift systems [NASA-CR-195077] p 2402 N95-28670
Response of multi-panel assembly to noise from a jet in forward motion [NASA-CR-198164] p 2289 N95-28673

AERODYNAMIC STABILITY
AIAA Techfest 20 Proceedings [NIAR-94-1] p 2118 N95-26941
A magnetic hysteresis model p 2153 N95-27801

AERODYNAMIC STALLING
Stall precursor study of high frequency data for three high speed, swept compressor rotors [AD-A289379] p 2139 N95-26878
Horizontal axis wind turbine post stall airfoil characteristics synthesization p 2124 N95-27974
Preliminary analysis of dynamic stall effects on a 91-meter wind turbine rotor p 2124 N95-27975

AERODYNAMICS
Suppressor of oscillations in airframe cavities [AD-D017265] p 2128 N95-26507
Wind-tunnel test of the S814 thick root airfoil [DE95-000268] p 2122 N95-27541
Aeronautical engineering: A continuing bibliography with indexes (supplement 318) [NASA-SP-7037(318)] p 2120 N95-27543
The Global Positioning System (GPS) and attitude determination: Applications and activities in the Flight Dynamics Division p 2152 N95-27795
Study of potential aerodynamic benefits from spanwise blowing at wingtip [NASA-TP-3515] p 2124 N95-28669

AEROELASTIC RESEARCH WINGS
Structural design optimization with survivability dependent constraints application: Primary wing box of a multi-role fighter p 2137 N95-28440

AEROELASTICITY
A non-iterative grid deformation algorithm for computational fluid dynamics for aeroelasticity [AD-A288298] p 2273 N95-26418
Aeroelasticity of wing and wing-body configurations on parallel computers [NASA-CR-197756] p 2129 N95-26590
Aeroelastic stability of wind turbine blade/aileron systems p 2124 N95-27981
Observed acoustic and aeroelastic spectral responses of a MOD-2 turbine blade to turbulence excitation p 2324 N95-27991
Aeroelasticity and structural optimization of composite helicopter rotor blades with swept tips [NASA-CR-4665] p 2136 N95-28262
Unique considerations in the design and experimental evaluation of tailored wings with elastically produced chordwise camber p 2192 N95-28436
Nonlinear dynamics and aeroelasticity of rotorcraft in forward flight [AD-A291714] p 2136 N95-28504

AEROGELS
The experience of CF Technologies, Inc. (CF Tech) in critical fluid processing p 2232 N95-27128
Ambient-pressure silica aerogel films [DE95-008161] p 2237 N95-28090

AERONAUTICAL ENGINEERING
Asian Aeronautics: Technology acquisition drives industry development. Report to Congressional requesters [GAO/NSIAD-94-140] p 2118 N95-26817
The noise reduction potential of dual-stream coaxial rectangular improperly expanded jet flows [NASA-CR-197820] p 2277 N95-26995
Aeronautical engineering: A continuing bibliography with indexes (supplement 318) [NASA-SP-7037(318)] p 2120 N95-27543
A review of Australian and New Zealand investigations on aeronautical fatigue during the period Apr. 1993 - Mar. 1995 [AR-009-202] p 2136 N95-27918
JTEC/WTEC annual report and program summary: 1993/94 [NASA-CR-198563] p 2475 N95-28038

AERONAUTICS
Research and Technology Objectives and Plans Summary (RTOPS) [NASA-TM-108574] p 2475 N95-28002

AEROSOLS
Transport phenomena and interfacial kinetics in multiphase combustion systems [AD-A288297] p 2199 N95-26417
Natural aerosol extinction module: XSCALE 1992 user's guide [AD-A289029] p 2340 N95-26463
Measurement of heterogeneous chemical processes relevant to aerosol surfaces and trace gases active in the marine environment [DE95-008337] p 2328 N95-27743
Formation of anisotropic Tl-1212, Tl-2212, Tl-1223 and Tl-2223 particles using aerosol flow reacted powders [DE95-007400] p 2444 N95-28079
Carbonaceous aerosols influencing atmospheric radiation: Black and organic carbon [DE95-006437] p 2330 N95-28118
Proceedings of the 1993 Scientific Conference on Obscuration and Aerosol Research [AD-A280084] p 2331 N95-28153
Towards the detection and attribution of an anthropogenic effect on climate [DE95-008589] p 2331 N95-28157
Toxicity assessment of liquid propellant XM46 p 2175 N95-28319
Laser beam aerosol interactions [AD-A291723] p 2300 N95-28509

AEROSPACE ENGINEERING
AGARD membership, 1995 [AGARD-MEMB-95] p 2450 N95-26353
Space Commerce 1994 Forum: The 10th National Space Symposium. Proceedings report [NASA-CR-198031] p 2144 N95-26583
The aerospace database: An introduction to AIAA'S computerized source for identifying scientific and technical information p 2119 N95-26950
The 29th Aerospace Mechanisms Symposium [NASA-CP-3293] p 2154 N95-27260
High performance stepper motors for space mechanisms p 2156 N95-27271
Thermal neutral format based on the step technology p 2283 N95-27363
Spaceflight revolution: NASA Langley Research Center from Sputnik to Apollo [NASA-SP-4308] p 2474 N95-27685
High-stakes aviation: US-Japan technology linkages in transport aircraft [LC-94-65759] p 2126 N95-27907
Research and Technology Objectives and Plans Summary (RTOPS) [NASA-TM-108574] p 2475 N95-28002
JPRS Report: Science and Technology. Central Eurasia [JPRS-UST-95-020] p 2145 N95-28257
The importance of propulsion engineers in protecting the global environment p 2170 N95-28295
Probabilistic design of advanced composite structure p 2193 N95-28443
Probabilistic evaluation of fuselage-type composite structures p 2137 N95-28444
Post impact compressive strength in composites p 2198 N95-28485
NASA/DOD Aerospace Knowledge Diffusion Research Project. Report 35: The use of computer networks in aerospace engineering [NASA-CR-198170] p 2456 N95-28600

AEROSPACE ENVIRONMENTS
Air Force Ni-H2 cell test program: State of Charge test p 2272 N95-26789

Deployment and retraction of a cable-driven solar array: Testing and simulation p 2158 N95-27283
LDEF: 69 Months in Space. Third Post-Retrieval Symposium, part 3 [NASA-CP-3275-PT-3] p 2466 N95-27629
Evaluation of Oxygen Interactions with Materials 3: Mission and induced environments p 2210 N95-27631
Exposure of LDEF materials to atomic oxygen: Results of EOIM 3 p 2210 N95-27633
Inflight resistance measurement on high-T(sub c) superconducting thin films exposed to orbital atomic oxygen on CONCAP-2 (STS-46) p 2272 N95-27635
Orbital atomic oxygen effects on materials: An overview of MSFC experiments on the STS-46 EOIM-3 p 2419 N95-27637
Effects of atomic oxygen on polymeric materials flown on EOIM-3 p 2242 N95-27638
Point defect formation in optical materials expos ed to the space environment p 2428 N95-27646
System results from FRECOPA p 2211 N95-27648
Space environmental effect on solar cells: LDEF and other flight tests p 2326 N95-27649
Effects of the LDEF orbital environment on the reflectance of optical mirror materials p 2428 N95-27651
Effects of long term space environment exposure on optical substrates and coatings p 2428 N95-27653
Space environmental effects observed on the Hubble Space Telescope p 2242 N95-27655
From LDEF to a national Space Environment and Effects (SEE) program: A natural progression p 2145 N95-27657
The Long Duration Exposure Facility (LDEF) photographic survey special publication p 2457 N95-27660
Space Station program status and research capabilities p 2166 N95-27662
Space Station as a Long Duration Exposure Facility p 2166 N95-27663
A Materials Exposure Facility p 2166 N95-27664
An LDEF follow-on spacecraft concept p 2166 N95-27665
The orbital debris detector consortium: Suppliers of instruments for in-situ measurements of small-particles in the space environment p 2294 N95-27670
PRISM validation [AD-A288476] p 2337 N95-27703

AEROSPACE INDUSTRY
Asian Aeronautics: Technology acquisition drives industry development. Report to Congressional requesters [GAO/NSIAD-94-140] p 2118 N95-26817
Spaceport news index: January 1990 - December 1994 [NASA-TM-110653] p 2454 N95-27243
High-stakes aviation: US-Japan technology linkages in transport aircraft [LC-94-65759] p 2126 N95-27907
The importance of propulsion engineers in protecting the global environment p 2170 N95-28295

AEROSPACE MEDICINE
Aerospace medicine [AD-A289691] p 2353 N95-26763
Aerospace medicine and biology: A continuing bibliography with indexes (supplement 402) [NASA-SP-7011(402)] p 2354 N95-27502
Acute and subacute toxicity of ammonium dinitramide (ADN) p 2175 N95-28318
Toxicity assessment of liquid propellant XM46 p 2175 N95-28319
A study of heart rate and heart rate variability during rapid decompression to 50,000 ft [AD-A291598] p 2355 N95-28561
Manikin integrated data acquisition system (MIDAS) initial modifications [AD-A291662] p 2361 N95-28667

AEROSPACE PLANES
Free Electron Laser Physical Process Code (FELPPC) [DE95-006276] p 2296 N95-27557

AEROSPACE SAFETY
Probabilistic risk assessment of the Space Shuttle. Phase 3: A study of the potential of losing the vehicle during nominal operation. Volume 2: Integrated loss of vehicle model [NASA-CR-197809] p 2159 N95-26399
Computational studies of projectile melt in impact with typical whipple shields [DE95-005916] p 2311 N95-28337

AEROSPACE SCIENCES
The aerospace database: An introduction to AIAA'S computerized source for identifying scientific and technical information p 2119 N95-26950
NAS Technical Summaries, March 1993 - February 1994 [NASA-RP-1355] p 2466 N95-27367
Research and Technology Objectives and Plans Summary (RTOPS) [NASA-TM-108574] p 2475 N95-28002
JPRS Report: Science and Technology. Central Eurasia [JPRS-UST-95-020] p 2145 N95-28257

AEROSPACE SYSTEMS
A methodology to assess the utility of future space systems [AD-A289414] p 2144 N95-27133
Design, testing and evaluation of latching end effector p 2155 N95-27261
ORION: A Supersynchronous Transfer Orbit mission p 2154 N95-27804

AEROSPACE TECHNOLOGY TRANSFER
Space Commerce 1994 Forum: The 10th National Space Symposium. Proceedings report [NASA-CR-198031] p 2144 N95-26583

AEROTHERMODYNAMICS
Viscous shock-layer analysis on hypersonic flow over reentry capsule with nonequilibrium chemistry [ISAS-R-656] p 2274 N95-26739

AEROZINE
Alternative cleaning solvents and lubricants at the Air Force PJKS facility p 2228 N95-27108
Chemical reactions identified in the Titan 2, Titan 4, and Delta 2 propellant systems and their application to source modeling p 2172 N95-28304

AFRICA
Southern Africa: A climatological study [AD-A289466] p 2342 N95-27148

AGGLOMERATION
A 3D agglomeration multigrid solver for the Reynolds-averaged Navier-Stokes equations on unstructured meshes [NASA-CR-195073] p 2390 N95-27029

AGGREGATES
Variation of solvent scattering-length density small-angle neutron scattering as a means of determining structure of composite materials [DE95-005394] p 2183 N95-27428
Small angle x ray scattering studies of reverse micelles in supercritical fluids [DE95-007803] p 2287 N95-28021

AGING (MATERIALS)
Creep recovery of PVC and polypropylene [PB95-185112] p 2224 N95-26448
The effect of proteins on the aging properties of radiation vulcanized Natural Rubber Latex [DE95-603357] p 2225 N95-26599
Can TMAE photocathode be used for high rate applications? [DE95-008594] p 2293 N95-28178

AGRICULTURE
Survey on bio-chemical complex harmonized with global environment [DE95-759252] p 2331 N95-28535
Models used to forecast agricultural corn crops in the micro-region of Ribeirao Preto-SP [INPE-5513-NTC/309] p 2315 N95-28554

AH-64 HELICOPTER
Development and validation of a blade-element mathematical model for the AH-64A Apache helicopter [NASA-TM-108863] p 2118 N95-26710

AILERONS
Full span flaperons for a biplane p 2119 N95-26954
Comparative wind tunnel test at high Reynolds numbers of NACA 64 621 airfoils with two aileron configurations p 2124 N95-27977
Aeroelastic stability of wind turbine blade/aileron systems p 2124 N95-27981

AIR BAG RESTRAINT DEVICES
F/A-18 IFOSTP Fatigue test airbag load determination on the vertical and horizontal tails [DSTO-TR-0135] p 2128 N95-26389

AIR CARGO
Incorporating biplane wing theory into a large, subsonic, all-cargo transport p 2120 N95-26956
Enplanement and all cargo activity [AD-A280074] p 2144 N95-28151

AIR CONDITIONING
Research on combustion processes relevant to burners in HVAC systems [PB95-179735] p 2208 N95-28006
Methods development for measuring and classifying flammability/combustibility of refrigerants. Task 1: Annotated bibliography [DE95-007232] p 2238 N95-28133
Planning, design and construction of the cavern arena: Heating, ventilation and air conditioning [PB95-196382] p 2361 N95-28659

AIR FILTERS
Evaluation of microporous carbon filters as catalysts for ozone decomposition [DE95-006498] p 2331 N95-28548

AIR FLOW
Flutter clearance flight tests of an OV-10A airplane modified for wake vortex flight experiments [NASA-TM-109168] p 2117 N95-26381
Valve mechanism for an acoustic modulator [AD-D017263] p 2300 N95-26504
A continuous emissions monitor for airborne metals p 2174 N95-28313

AIR LAND INTERACTIONS
Measurement and analysis of the surface energy budget for ARM field experiments [DE95-007646] p 2338 . N95-28114

AIR LAUNCHING
Cape Canaveral air station launch emergency response forces and toxic materials release contingency plans p 2172 N95-28308

AIR NAVIGATION
Design and synthesis of a real-time controller for an unmanned air vehicle [AD-A289134] p 2141 N95-26555

AIR POLLUTION
Soot particle density determination from a laser extinction multipass technique [AD-A288551] p 2423 N95-26532
Live from Antarctica, volume 4 [NASA-CR-197828] p 2335 N95-26596
Cleanliness verification process at Martin Marietta Astronautics p 2165 N95-27104
Reducing cold-start emissions by catalytic converter thermal management [DE95-000256] p 2327 N95-27540
Absorption of sparingly soluble gases by reactive media in self-aerated gas-liquid contactors: A scale-up procedure [DE95-006429] p 2206 N95-27707
Evaluation and qualification of environmentally conscious manufacturing processes for commercial and military applications [DE95-008520] p 2329 N95-27878
Application of modern diagnostic methods to environmental improvement [DE95-005797] p 2330 N95-28119
FY 1994 ambient air monitoring report for McMurdo Station, Antarctica [DE95-008565] p 2331 N95-28149
SIHTI 2: Energy and environmental technology. Yearbook 1993 of the research programme [DE95-755135] p 2331 N95-28202
The 1994 JANNAF Safety and Environmental Protection Subcommittee Meeting, volume 1 [CPIA-PUBL-614-VOL-1] p 2170 N95-28294
The importance of propulsion engineers in protecting the global environment p 2170 N95-28295
OB/OD treatment: The effective use of measured field data and air modeling to support an environmental assessment p 2170 N95-28296
Use of SURFACE CHEMKIN to model multiphase atmospheric chemistry: Application to nitrogen tetroxide spills p 2172 N95-28305
Prototype development and test results of a continuous ambient air monitoring system for hydrazine at the 110 ppb level p 2173 N95-28310
A continuous emissions monitor for airborne metals p 2174 N95-28313
Evaluation of microporous carbon filters as catalysts for ozone decomposition [DE95-006498] p 2331 N95-28548
A comparison of NH3 point monitoring and diode laser based path integrated measurements [DE95-006892] p 2332 N95-28602
The Global Historical Climatology Network: A preview of version 2 [DE95-007003] p 2332 N95-28605

AIR PURIFICATION
Chlorodifluoromethane equilibrium on 13X molecular sieve [AD-A289282] p 2405 N95-27034
Radiant exchange considerations in design and scaleup of photocatalytic reactors for purification of nitroglycerine-contaminated air p 2171 N95-28300

AIR QUALITY
Electromagnetic devices and processes in environment protection [AD-A288656] p 2141 N95-26487
Cleanliness verification process at Martin Marietta Astronautics p 2165 N95-27104
Wipe solvent substitutions for 1,1,1-trichloroethane (TCA) and methyl ethyl ketone (MEK) at Hill Air Force Base p 2228 N95-27107
Three objective indices for clear-air turbulence reconsidered [KNMI-TR-160] p 2342 N95-27366

AIR SAMPLING
Live from Antarctica, volume 4 [NASA-CR-197828] p 2335 N95-26596

Basic principles and recent observations of rotationally sampled wind p 2321 N95-27971
A model of rotationally-sampled wind turbulence for predicting fatigue loads in wind turbines p 2312 N95-27972
Comparison of measured and calculated dynamic loads for the Mod-2 2.5 mW wind turbine system p 2312 N95-27983
FY 1994 ambient air monitoring report for McMurdo Station, Antarctica [DE95-008565] p 2331 N95-28149
Prototype development and test results of a continuous ambient air monitoring system for hydrazine at the 110 ppb level p 2173 N95-28310
The sensitive detection of hydrazine using chemiluminescence p 2173 N95-28311

AIR SEA ICE INTERACTIONS
A parallel coupled oceanic-atmospheric general circulation model [DE95-005918] p 2335 N95-26622
Measurement of heterogeneous chemical processes relevant to aerosol surfaces and trace gases active in the marine environment [DE95-008337] p 2328 N95-27743

AIR TRAFFIC
Air traffic operational inventory CY 1994 [AD-A288281] p 2126 N95-26454
The 1994 updated National Airspace System performance assessment for year 2005 [AD-A288652] p 2125 N95-26485
Enplanement and all cargo activity [AD-A280074] p 2144 N95-28151

AIR TRAFFIC CONTROL
Weather And Radar Processor (WARP) Test and Evaluation Master Plan (TEMP) [AD-A288280] p 2340 N95-26453
Air traffic operational inventory CY 1994 [AD-A288281] p 2126 N95-26454
The 1994 updated National Airspace System performance assessment for year 2005 [AD-A288652] p 2125 N95-26485
The controller memory guide. Concepts from the field [AD-A289263] p 2127 N95-26978
Advanced interactive display formats for terminal area traffic control [NASA-CR-198576] p 2127 N95-28188
Development of a coding form for approach control/pilot voice communications [DOT/FAA/AM-95/15] p 2128 N95-28540
Proceedings of the AIAA/FAA joint symposium on general aviation systems [AD-A289830] p 2120 N95-28610

AIR TRAFFIC CONTROLLERS (PERSONNEL)
The controller memory guide. Concepts from the field [AD-A289263] p 2127 N95-26978
Practical color vision tests for air traffic control applicants: En route center and terminal facilities [DOT/FAA/AM-95/13] p 2357 N95-27323
Development of a coding form for approach control/pilot voice communications [DOT/FAA/AM-95/15] p 2128 N95-28540

AIR TRANSPORTATION
The high speed civil transport and NASA's High Speed Research (HSR) program p 2118 N95-26945
Enplanement and all cargo activity [AD-A280074] p 2144 N95-28151

AIR WATER INTERACTIONS
Hindcasting wind-driven anomalies using reduced-gravity global ocean models with 1/2 deg and 1/4 deg resolution [AD-A289060] p 2345 N95-26406
Infrared field measurements of sea surface temperature: Analysis of wake signatures and comparison of skin layer models [NASA-CR-197849] p 2346 N95-26533
Deep convection in the Mediterranean Sea [AD-A288497] p 2346 N95-26647
Meteorological and oceanographic data collected during the ASREX 91 field experiment [AD-A289492] p 2342 N95-26826
Nonlinear problems in fluid dynamics and inverse scattering: Langmuir circulations and spiral flows [AD-A289194] p 2278 N95-27019
Study of the response of a three-dimensional coupled ice-ocean model to daily varying atmospheric forcing [AD-A289050] p 2347 N95-27189

AIRBORNE EQUIPMENT
Radiometer measurements of snow in Sodankylae, 1991-1993 [PB95-184966] p 2313 N95-26645
Hardware cleanliness methodology and certification p 2211 N95-27656

AIRBORNE/SPACEBORNE COMPUTERS
Advanced flight computer. Special study [NASA-CR-198165] p 2371 N95-27246

AIRCRAFT ACCIDENT INVESTIGATION
Aircraft accident report: Controlled collision with Terrain Transportes Aereos Ejecutivos, S.A. (TAESA) Learjet 25D, XA-BBA Dulles International Airport Chantilly, Virginia, June 18, 1994 [NTSB/AAR-95/02] p 2125 N95-26498

AIRCRAFT ACCIDENTS
Aircraft accident report: Controlled collision with Terrain Transportes Aereos Ejecutivos, S.A. (TAESA) Learjet 25D, XA-BBA Dulles International Airport Chantilly, Virginia, June 18, 1994 [NTSB/AAR-95/02] p 2125 N95-26498
Prevention and control of inlet unstart using an SR-71 simulation p 2119 N95-26948

AIRCRAFT CARRIERS
Benefits and limitations of composites in carrier-based aircraft p 2189 N95-28422

AIRCRAFT COMMUNICATION
Development of a coding form for approach control/pilot voice communications [DOT/FAA/AM-95/15] p 2128 N95-28540

AIRCRAFT CONFIGURATIONS
Aeroelasticity of wing and wing-body configurations on parallel computers [NASA-CR-197756] p 2129 N95-26590
Comparison of fixed wing aircraft algorithms for JANUS [AD-A288503] p 2129 N95-26652
Supersonic civil airplane study and design: Performance and sonic boom [NASA-CR-197745] p 2130 N95-26813
A quantitative feedback theory FCS design for the subsonic envelope of the VISTA F-16 including configuration variation [AD-A289221] p 2141 N95-26958
Test operations procedure (TOP) 7-3-534 airworthiness testing of fixed wing aircraft: Asymmetric power testing [AD-A289458] p 2130 N95-26994

AIRCRAFT CONSTRUCTION MATERIALS
Static and fatigue testing of full-scale fuselage panels fabricated using a Therm-X(R) process p 2185 N95-28270
ACT/ICAPS: Thermoplastic composite activities p 2185 N95-28274
Development of composite carrythrough bulkhead p 2192 N95-28438
Effects of floor location on response of composite fuselage frames p 2192 N95-28439
Navy composite maintenance and repair experience p 2193 N95-28446
Ninth DOD/NASA/FAA Conference on Fibrous Composites in Structural Design, volume 2 [NASA-CR-198722] p 2193 N95-28462
Overview of the ACT program p 2193 N95-28463
Characterization and manufacture of braided composites for large commercial aircraft structures p 2196 N95-28478
Impact damage resistance of composite fuselage structure, part 1 p 2138 N95-28482
Fundamental concepts in the suppression of delamination buckling by stitching p 2198 N95-28486
Advanced wing design survivability testing and results p 2138 N95-28488

AIRCRAFT CONTROL
Simulation model of the integrated flight/propulsion control system, displays, and propulsion system for ASTOVL lift-fan aircraft [NASA-TM-108866] p 2139 N95-26412
Development of a nonlinear simulation for the McDonnell Douglas F-15 Eagle with a longitudinal TECS control-law [AD-A288610] p 2128 N95-26481
A comparison of the Neal-Smith and omega Tau function, zeta function and tau function flying qualities criteria [AD-A289503] p 2130 N95-26844
Pilot opinions on high level flight deck automation issues: Toward the development of a design philosophy [NASA-CR-4669] p 2357 N95-28253

AIRCRAFT DESIGN
Aircraft fuel system lightning protection design and qualification test procedures development [AD-A288401] p 2125 N95-26497
Balanced on air aircraft [AD-D017251] p 2129 N95-26537
Aeroelasticity of wing and wing-body configurations on parallel computers [NASA-CR-197756] p 2129 N95-26590
Supersonic civil airplane study and design: Performance and sonic boom [NASA-CR-197745] p 2130 N95-26813
AIAA Techfest 20 Proceedings [NIAR-94-1] p 2118 N95-26941
Preliminary design problems and solutions for a supersonic oblique all-wing transport aircraft p 2118 N95-26942
An exploratory application of neural networks for airfoil design p 2118 N95-26943
Creating an alternative parameter optimization method (APO) p 2118 N95-26946
Design of a high altitude long endurance aircraft with manufacturing considerations p 2119 N95-26947
Incorporating biplane wing theory into a large, subsonic, all-cargo transport p 2120 N95-26956
The lift-fan aircraft: Lessons learned [NASA-CR-196694] p 2131 N95-27143
Rapid repair of large area damage to contoured aircraft structures p 2133 N95-27516
Wind-tunnel test of the S814 thick root airfoil [DE95-000268] p 2122 N95-27541
JPRS report: Science and technology. Central Eurasia [JPRS-UST-94-022] p 2246 N95-27699
Propulsion system assessment for very high UAV under ERAST [NASA-CR-195469] p 2140 N95-27866
Evaluation of all-electric secondary power for transport aircraft [NASA-CR-189077] p 2266 N95-27999
Performance study for inlet installations [NASA-CR-189714] p 2140 N95-28227
Ninth DOD/NASA/FAA Conference on Fibrous Composites in Structural Design, volume 3 [NASA-CR-198718] p 2184 N95-28266
Ninth DOD/NASA/FAA Conference on Fibrous Composites in Structural Design, volume 1 [NASA-CR-198723] p 2189 N95-28420
Benefits and limitations of composites in carrier-based aircraft p 2189 N95-28422
Development of composite carrythrough bulkhead p 2192 N95-28438
Structural design optimization with survivability dependent constraints application: Primary wing box of a multi-role fighter p 2137 N95-28440
Probabilistic design of advanced composite structure p 2193 N95-28443
Probabilistic evaluation of fuselage-type composite structures p 2137 N95-28444
Ninth DOD/NASA/FAA Conference on Fibrous Composites in Structural Design, volume 2 [NASA-CR-198722] p 2193 N95-28462
Overview of the ACT program p 2193 N95-28463
Designers' unified cost model p 2194 N95-28464
COINS: A composites information database system p 2194 N95-28465
Structural testing of the technology integration box beam p 2194 N95-28467
Technology integration box beam failure study p 2194 N95-28468
Recent progress in NASA Langley textile reinforced composites program p 2196 N95-28475
Advanced textile applications for primary aircraft structures p 2138 N95-28476
Applications of a damage tolerance analysis methodology in aircraft design and production p 2197 N95-28483
Advanced wing design survivability testing and results p 2138 N95-28488

AIRCRAFT DETECTION
Aircraft IR/acoustic detection evaluation. Volume 2: Development of a ground-based acoustic sensor system for the detection of subsonic jet-powered aircraft [NASA-CR-189705-VOL-2] p 2402 N95-28073
Performance study for inlet installations [NASA-CR-189714] p 2140 N95-28227

AIRCRAFT ENGINES
Design of a high altitude long endurance aircraft with manufacturing considerations p 2119 N95-26947
Prevention and control of inlet unstart using an SR-71 simulation p 2119 N95-26948
Analysis of aircraft engine blade subject to ice impact p 2141 N95-28277
Application of fiber-reinforced bismaleimide materials to aircraft nacelle structures p 2137 N95-28278

AIRCRAFT EQUIPMENT
Aircraft nosewheel steering simulation p 2118 N95-26944

AIRCRAFT FUEL SYSTEMS
Aircraft fuel system lightning protection design and qualification test procedures development [AD-A288401] p 2125 N95-26497

AIRCRAFT FUELS
A numerical model to predict the fate of jettisoned aviation fuel [AD-A289336] p 2242 N95-26842
The effect of aviation fuels containing low amounts of static dissipater additive on electrostatic charge generation [AD-A280075] p 2243 N95-28152

AIRCRAFT GUIDANCE
Flight evaluation of GPS/DGPS sensor systems installed in NAL Do228 [NAL-TR-1230] p 2126 N95-26585

AIRCRAFT HAZARDS
Further investigations of icing effects on an advanced high-lift multi-element airfoil
[NASA-TM-106947] p 2125 N95-27762
A review of falconry as a bird control technique with recommendations for use at the Shuttle Landing Facility, John F. Kennedy Space Center, Florida, USA
[NASA-TM-110142] p 2126 N95-27859
AIRCRAFT INDUSTRY
Strategy in the commercial aircraft industry in the United States: A comparison of decisionmaking by McDonnell-Douglas and Boeing aircraft companies from 1977-1983
[AD-A288289] p 2117 N95-26409
Surviving the peace. Lessons learned from the aircraft industry in the 1920s and 1930s
[AD-A288284] p 2117 N95-26455
AIRCRAFT INSTRUMENTS
Flight evaluation of GPS/DGPS sensor systems installed in NAL Do228
[NAL-TR-1230] p 2126 N95-26585
AIRCRAFT LANDING
Flightpath synthesis and HUD scaling for V/STOL terminal area operations
[NASA-TM-110348] p 2127 N95-26587
An integrated GPS/INS/BARO and radar altimeter system for aircraft precision approach landings
[AD-A289280] p 2127 N95-26985
AIRCRAFT MAINTENANCE
Survey and implementation of commercial manual controllers for a generic telerobotics architecture
[AD-A289215] p 2381 N95-26990
AH-1F COBRA rewire program MANPRINT analysis
[AD-A289190] p 2130 N95-27018
Composite Repair of Military Aircraft Structures
[AGARD-CP-550] p 2131 N95-27504
Bonded composite repair of metallic aircraft components: Overview of Australian activities
p 2132 N95-27505
Status of bonded boron/epoxy doublers for military and commercial aircraft structures p 2132 N95-27506
Adhesively bonded composite patch repair of cracked aluminum alloy structures p 2132 N95-27507
Composite repair of metallic airframe: Twenty years of experience p 2132 N95-27508
Bonded composite repair of thin metallic materials: Variable load amplitude and temperature cycling effects
p 2132 N95-27509
Design and structural validation of CF116 upper wing skin boron doubler p 2132 N95-27510
A FEAM based methodology for analyzing composite patch repairs of metallic structures
p 2133 N95-27511
Structural modification and repair of C-130 wing structure using bonded composites p 2133 N95-27512
Evaluation of patch effectiveness in repairing aircraft components p 2133 N95-27513
Field repair materials for naval aircraft
p 2133 N95-27514
On aircraft repair verification of a fighter A/C integrally stiffened fuselage skin p 2133 N95-27515
Rapid repair of large area damage to contoured aircraft structures p 2133 N95-27516
Composite repair of a CF18: Vertical stabilizer leading edge p 2134 N95-27517
Composite repair issues on the CF-18 aircraft
p 2134 N95-27518
Repair technology for thermoplastic aircraft structures
p 2134 N95-27519
Repair of high temperature composite aircraft structure p 2134 N95-27520
Composite repair of composite structures
p 2134 N95-27521
External patch repair of CFRP/honeycomb sandwich
p 2134 N95-27522
Scarf joint technique with cocured and precured patches for composite repair p 2135 N95-27524
Composite or metallic bolted repairs on self-stiffened carbon wing panel of the commuter ATR72 design criteria, analysis, verification by test p 2135 N95-27525
Damage occurrence on composites during testing and fleet service: Repair of Airbus aircraft
p 2135 N95-27526
Repairs of CFC primary structures
p 2135 N95-27527
The development of an engineering standard for composite repairs p 2135 N95-27528
Human factors in aviation maintenance, phase 4
[DOT/FAA/AM-95/14] p 2360 N95-27696
Proceedings of the AIAA/FAA joint symposium on general aviation systems
[AD-A289830] p 2120 N95-28610
AIRCRAFT MODELS
Airfoil modification effects on subsonic and transonic pressure distributions and performance for the EA-6B airplane
[NASA-TP-3516] p 2120 N95-26382
Simulation model of the integrated flight/propulsion control system, displays, and propulsion system for ASTOVL lift-fan aircraft
[NASA-TM-108866] p 2139 N95-26412
Experimental investigation of static and dynamic ground effect on HOPE ALFLEX vehicle
[NAL-TR-1236] p 2128 N95-26525
Comparison of fixed wing aircraft algorithms for JANUS
[AD-A288503] p 2129 N95-26652
A verification procedure for MSC/NASTRAN Finite Element Models
[NASA-CR-4675] p 2131 N95-27371
Modeling of aircraft unsteady aerodynamic characteristics. Part 2: Parameters estimated from wind tunnel data
[NASA-TM-110161] p 2142 N95-27839
AIRCRAFT NOISE
Aircraft noise prediction program theoretical manual: Rotorcraft System Noise Prediction System (ROTONET), part 4
[NASA-TM-83199-PT-4] p 2400 N95-26392
Evaluation of a doubly-swept blade tip for rotorcraft noise reduction
[NASA-CR-189677] p 2402 N95-28264
Noise exposure reduction of advanced high-lift systems
[NASA-CR-195077] p 2402 N95-28670
AIRCRAFT PERFORMANCE
Supersonic civil airplane study and design: Performance and sonic boom
[NASA-CR-197745] p 2130 N95-26813
A comparison of the Neal-Smith and omega Tau function, zeta function and tau function flying qualities criteria
[AD-A289503] p 2130 N95-26844
Performance study for inlet installations
[NASA-CR-189714] p 2140 N95-28227
Benefits and limitations of composites in carrier-based aircraft p 2189 N95-28422
AIRCRAFT PILOTS
Development of injury preventing helmet servo-support system for high performance aircraft
[AD-A289547] p 2359 N95-26755
Pilot opinions on high level flight deck automation issues: Toward the development of a design philosophy
[NASA-CR-4669] p 2357 N95-28253
AIRCRAFT POWER SUPPLIES
Evaluation of all-electric secondary power for transport aircraft
[NASA-CR-189077] p 2266 N95-27999
AIRCRAFT PRODUCTION
Overview of the ACT program p 2193 N95-28463
AIRCRAFT PRODUCTION COSTS
Designers' unified cost model p 2194 N95-28464
COINS: A composites information database system
p 2194 N95-28465
Composite fuselage crown panel manufacturing technology p 2137 N95-28474
AIRCRAFT RELIABILITY
Test operations procedure (TOP) 7-3-534 airworthiness testing of fixed wing aircraft: Asymmetric power testing
[AD-A289458] p 2130 N95-26994
Composite or metallic bolted repairs on self-stiffened carbon wing panel of the commuter ATR72 design criteria, analysis, verification by test p 2135 N95-27525
AIRCRAFT SAFETY
WINCLR: A computer code for heat transfer and clearance calculation in a compressor
[NASA-CR-195436] p 2117 N95-26363
Aircraft accident report: Controlled collision with Terrain Transportes Aereos Ejecutivos, S.A. (TAESA) Learjet 25D, XA-BBA Dulles International Airport Chantilly, Virginia, June 18, 1994
[NTSB/AAR-95/02] p 2125 N95-26498
AIAA Techfest 20 Proceedings
[NIAR-94-1] p 2118 N95-26941
Prevention and control of inlet unstart using an SR-71 simulation p 2119 N95-26948
Precision landing system mathematical modeling study report for Andrews Air Force Base, runway 19L, Camp Springs, MD
[AD-A289015] p 2127 N95-27903
AIRCRAFT STABILITY
An easy way to analyze longitudinal and lateral-directional trim problems with AEO or OEI
p 2119 N95-26949
AIRCRAFT STRUCTURES
A verification procedure for MSC/NASTRAN Finite Element Models
[NASA-CR-4675] p 2131 N95-27371
Composite Repair of Military Aircraft Structures
[AGARD-CP-550] p 2131 N95-27504
Bonded composite repair of metallic aircraft components: Overview of Australian activities
p 2132 N95-27505
Status of bonded boron/epoxy doublers for military and commercial aircraft structures p 2132 N95-27506
Adhesively bonded composite patch repair of cracked aluminum alloy structures p 2132 N95-27507
Design and structural validation of CF116 upper wing skin boron doubler p 2132 N95-27510
A FEAM based methodology for analyzing composite patch repairs of metallic structures
p 2133 N95-27511
Structural modification and repair of C-130 wing structure using bonded composites p 2133 N95-27512
Evaluation of patch effectiveness in repairing aircraft components p 2133 N95-27513
Rapid repair of large area damage to contoured aircraft structures p 2133 N95-27516
Repair technology for thermoplastic aircraft structures
p 2134 N95-27519
Repair of high temperature composite aircraft structure p 2134 N95-27520
External patch repair of CFRP/honeycomb sandwich
p 2134 N95-27522
Scarf joint technique with cocured and precured patches for composite repair p 2135 N95-27524
Damage occurrence on composites during testing and fleet service: Repair of Airbus aircraft
p 2135 N95-27526
Repairs of CFC primary structures
p 2135 N95-27527
The development of an engineering standard for composite repairs p 2135 N95-27528
Ninth DOD/NASA/FAA Conference on Fibrous Composites in Structural Design, volume 3
[NASA-CR-198718] p 2184 N95-28266
Process and control systems for composites manufacturing p 2184 N95-28267
Advanced tow placement of composite fuselage structure p 2185 N95-28271
Through-the Thickness(R) braided composites for aircraft applications p 2185 N95-28273
Resin transfer molding of textile preforms for aircraft structural applications p 2185 N95-28276
Application of fiber-reinforced bismaleimide materials to aircraft nacelle structures p 2137 N95-28278
Analysis techniques for the prediction of springback in formed and bonded composite components
p 2188 N95-28289
The effect of material heterogeneity in curved composite beams for use in aircraft structures
p 2190 N95-28426
Vibrational behavior of adaptive aircraft wing structures modelled as composite thin-walled beams
p 2191 N95-28435
Development of composite carrythrough bulkhead
p 2192 N95-28438
Probabilistic design of advanced composite structure
p 2193 N95-28443
Probabilistic evaluation of fuselage-type composite structures p 2137 N95-28444
Navy composite maintenance and repair experience
p 2193 N95-28446
Ninth DOD/NASA/FAA Conference on Fibrous Composites in Structural Design, volume 2
[NASA-CR-198722] p 2193 N95-28462
Overview of the ACT program p 2193 N95-28463
COINS: A composites information database system
p 2194 N95-28465
Composite fuselage shell structures research at NASA Langley Research Center p 2194 N95-28466
Technology integration box beam failure study
p 2194 N95-28468
Development of stitched/RTM composite primary structures p 2195 N95-28469
Recent progress in NASA Langley textile reinforced composites program p 2196 N95-28475
Advanced textile applications for primary aircraft structures p 2138 N95-28476
Comparison of resin film infusion, resin transfer molding, and consolidation of textile preforms for primary aircraft structure p 2196 N95-28477
Characterization and manufacture of braided composites for large commercial aircraft structures
p 2196 N95-28478
Application of damage tolerance methodology in certification of the Piaggio P-180 Avanti
p 2138 N95-28480
Effect of low-speed impact damage and damage location on behavior of composite panels p 2197 N95-28481
AIRCRAFT SURVIVABILITY
Structural design optimization with survivability dependent constraints application: Primary wing box of a multi-role fighter p 2137 N95-28440

Advanced wing design survivability testing and results
p 2138 N95-28488

AIRCRAFT TIRES

Aircraft nosewheel steering simulation
p 2118 N95-26944

AIRDROPS

The performance of cargo airdrop systems using g-12E parachutes: Statistical determination of minimum altitude
[AD-A291666] p 2126 N95-28454

AIRFOIL OSCILLATIONS

Nonlinear dynamics and aeroelasticity of rotorcraft in forward flight
[AD-A291714] p 2136 N95-28504

AIRFOIL PROFILES

An exploratory application of neural networks for airfoil design p 2118 N95-26943

Comparative wind tunnel tests of NACA 23024 airfoils with several aileron and spoiler configurations
p 2124 N95-27976

Comparative wind tunnel test at high Reynolds numbers of NACA 64 621 airfoils with two aileron configurations
p 2124 N95-27977

Numerical study to assess sulfur hexafluoride as a medium for testing multielement airfoils
[NASA-TP-3496] p 2124 N95-28674

AIRFOILS

Airfoil modification effects on subsonic and transonic pressure distributions and performance for the EA-6B airplane
[NASA-TP-3516] p 2120 N95-26382

Computational fluid dynamics and transonic flow
[AD-A288962] p 2273 N95-26405

An exploratory application of neural networks for airfoil design p 2118 N95-26943

Creating an alternative parameter optimization method (APO) p 2118 N95-26946

The near-wake flow behavior of an oscillating airfoil with modified trailing edge p 2119 N95-26953

Wind-tunnel test of the S814 thick root airfoil
[DE95-000268] p 2122 N95-27541

Further investigations of icing effects on an advanced high-lift multi-element airfoil
[NASA-TM-106947] p 2125 N95-27762

Horizontal axis wind turbine post stall airfoil characteristics synthesization p 2124 N95-27974

AIRFRAMES

Suppressor of oscillations in airframe cavities
[AD-D017265] p 2128 N95-26507

Composite repair of metallic airframe: Twenty years of experience p 2132 N95-27508

Resin transfer molding of textile preforms for aircraft structural applications p 2185 N95-28276

Applications of a damage tolerance analysis methodology in aircraft design and production
p 2197 N95-28483

NASA-ACEE/Boeing 737 graphite-epoxy horizontal stabilizer service p 2138 N95-28489

Rotorcraft crashworthy airframe and fuel system technology development program
[AD-A289986] p 2126 N95-28630

AIRLINE OPERATIONS

An integrated GPS/INS/BARO and radar altimeter system for aircraft precision approach landings
[AD-A289280] p 2127 N95-26985

The effects of Crew Resource Management (CRM) training in airline maintenance: Results following three year's experience
[NASA-CR-196696] p 2358 N95-28676

AIRPORT TOWERS

Air traffic operational inventory CY 1994
[AD-A288281] p 2126 N95-26454

AIRPORTS

The 1994 updated National Airspace System performance assessment for year 2005
[AD-A288652] p 2125 N95-26485

AIRSPACE

The 1994 updated National Airspace System performance assessment for year 2005
[AD-A288652] p 2125 N95-26485

Unmanned aerial vehicles, 1994 master plan
[AD-A291628] p 2136 N95-28411

AIRSPEED

Advanced formation flight control
[AD-A289271] p 2142 N95-26981

ALCOHOLS

Probe molecule studies: Active species in alcohol synthesis
[DE95-003514] p 2203 N95-27420

NQR-NMR studies of higher alcohol synthesis Cu-Co catalysts
[DE95-007926] p 2205 N95-27680

ALGEBRA

On compact multipliers of topological algebras
[DE95-608751] p 2390 N95-27092

Spectral properties of multipliers on topological algebras
[DE95-608747] p 2390 N95-27299

Some commutativity theorems for a certain class of rings
[DE95-608750] p 2390 N95-27302

Introduction to Dubois-Violette's non-commutative differential geometry
[DE95-608801] p 2390 N95-27311

On commutativity of right s-unital rings with some polynomial constraints
[DE95-608752] p 2390 N95-27330

Quantum k-Poincare 1994
[DE95-608754] p 2448 N95-27332

Algebraic structure of the Green's ansatz and its q-deformed analogue
[DE95-608780] p 2395 N95-27340

Fuzzy-algebra uncertainty assessment
[DE95-005426] p 2391 N95-27432

The assembly tower and some categorical and algebraic aspects of frame theory
[AD-A289360] p 2391 N95-27489

Symmetries of the KAC-Peterson modular matrices of affine algebras
[PB95-190138] p 2392 N95-28010

Lie group weight multiplicities from conformal field theory
[PB95-190153] p 2392 N95-28012

Coordinates of the quantum plane as q-tensor operators in U(sub q) (su(2) * su(2))
[DE95-007100] p 2397 N95-28234

ALGORITHMS

A method for simulating correlated random variables from partially specified distributions
[AD-A288820] p 2393 N95-26347

Modified Gaussian elimination for adaptive beamforming using RNS arithmetic
[AD-A288809] p 2248 N95-26356

A fully implicit time accurate method for hypersonic combustion: Application to shock-induced combustion instability
[NASA-TM-106707] p 2273 N95-26380

Parallelizing locally-weighted regression
[AD-A288294] p 2394 N95-26414

A non-iterative grid deformation algorithm for computational fluid dynamics for aeroelasticity
[AD-A288298] p 2273 N95-26418

An introduction to software architecture
[AD-A288963] p 2363 N95-26446

Fast multidimensional density estimation based on Random-width bins
[AD-A288286] p 2394 N95-26457

An introduction to software architecture
[AD-A288356] p 2363 N95-26467

Robust hybrid state-space self-tuning control using dual-rate sampling
[AD-A288359] p 2380 N95-26468

ACT adaptive filters
[AD-A288385] p 2363 N95-26474

Modified eigenvalue problems with applications to structural dynamic re-analysis on parallel computers
[AD-A288257] p 2307 N95-26547

Grain size management in repetitive task graphs for multiprocessor computer scheduling
[AD-A288575] p 2377 N95-26551

A fast numerical method for isothermal resin transfer mold filling
[AD-A288944] p 2179 N95-26565

Flightpath synthesis and HUD scaling for V/STOL terminal area operations
[NASA-TM-110348] p 2127 N95-26587

Algorithms for parallel flow solvers on message passing architectures
[NASA-CR-197758] p 2274 N95-26588

Adaptive finite element method I: Solution algorithm and computational examples
[AD-A288979] p 2389 N95-26609

Activities of the Laboratory of Information Processing Science
[PB95-184982] p 2452 N95-26631

Comparison of fixed wing aircraft algorithms for JANUS
[AD-A288503] p 2129 N95-26652

Com(sup 3): A composite-compatible component coding system
[BBC-RD-1994/17] p 2249 N95-26670

Design tool for multiprocessor scheduling and evaluation of iterative dataflow algorithms
[NASA-TP-3491] p 2366 N95-26685

The D* algorithm for real-time planning of optimal traverses
[AD-A289361] p 2367 N95-26754

Computation of electromagnetic scattering parameters for lognormal distributions of magnetic spheres: Theory and algorithms
[AD-A289672] p 2250 N95-26759

Development of an upwind, finite-volume code with finite-rate chemistry
[NASA-CR-197747] p 2121 N95-26760

Performance and policy dimensions in internet routing
[NASA-CR-197772] p 2367 N95-26770

Addressing tension instability in SPH methods
[AD-A289531] p 2276 N95-26852

Do we fully understand the symmetric Lanczos algorithm yet?
[AD-A289614] p 2368 N95-26855

A demonstration of Client/Server technology using remote procedure calls for an application of file migration for moving records based on location
[AD-A289391] p 2453 N95-26864

Random relaxation of fixed point iteration
[PB95-185013] p 2389 N95-26910

Distributed computation of Pareto solutions in N-player games
[PB95-185039] p 2396 N95-26912

Image perception wavelet simulation and enhancement for the visually impaired
[AD-A289303] p 2353 N95-26917

Analysis of modal behavior at frequency cross-over
[AD-A289304] p 2162 N95-26918

A state-space model of a large, lightly damped space structure using the Eigensystem realization algorithm
[AD-A289251] p 2163 N95-26970

Nonlinear problems in fluid dynamics and inverse scattering: Propagation and capturing of singularities in problems of fluid dynamics and inverse scattering
[AD-A289146] p 2277 N95-26999

A modified backpropagation algorithm for training neural networks on data with error bars
[DE95-608729] p 2381 N95-27025

Unstructured mesh generation and adaptivity
[NASA-CR-195069] p 2278 N95-27027

Moment and hypergeometric filters for high precision computation of focus, stereo and optical flow
[AD-A289293] p 2425 N95-27038

Implementation and demonstration of a multiple model adaptive estimation failure detection system for the F-16
[AD-A289301] p 2131 N95-27042

Reducing network depth in the Cascade-Correlation learning architecture
[AD-A289352] p 2382 N95-27066

Efficient generation of counterexamples and witnesses in symbolic model checking
[AD-A288583] p 2370 N95-27095

Development of numerical methods for overset grids with applications for the integrated Space Shuttle vehicle
[NASA-CR-197759] p 2160 N95-27154

Vector algorithms for solving 3D nonlinear magnetostatic problems
[DE95-608737] p 2399 N95-27298

Single-drop reactive extraction/extractive reaction with forced convective diffusion and interphase mass transfer
p 2282 N95-27358

A spectral algorithm for the seriation problem
[DE95-004775] p 2372 N95-27436

Integrating the QMR method with first principles material science application code
[DE95-007380] p 2408 N95-27456

Parallel algorithms for semi-Lagrangian transport in global atmospheric circulation models
[DE95-007385] p 2327 N95-27457

Sequence comparison on a cluster of workstations using the PVM system
[DE95-006527] p 2378 N95-27709

Molecular dynamics simulations of Gay-Berne nematic liquid crystal: Elastic properties from direct correlation functions
[DE95-609149] p 2441 N95-27740

Kepler Equation solver p 2147 N95-27767

A PC-based magnetometer-only attitude and rate determination system for gyroless spacecraft
p 2147 N95-27770

An MME-based attitude estimator using vector observations p 2148 N95-27775

Development of a Robust star identification technique for use in attitude determination of the ACE spacecraft
p 2149 N95-27777

Experience from the in-flight calibration of the Extreme Ultraviolet Explorer (EUVE) and Upper Atmosphere Research Satellite (UARS) fixed head star trackers (FHSTs) p 2149 N95-27779

Use of nonlinear identification in robust attitude and attitude rate estimation for SAMPEX
p 2149 N95-27781

A simple method for verifying the deployment of the TOMS-EP solar arrays p 2150 N95-27782

Earth horizon modeling and application to static Earth sensors on TRMM spacecraft p 2150 N95-27783

A magnetic hysteresis model p 2153 N95-27801

Contingency designs for attitude determination of TRMM p 2154 N95-27803

Modeling of aircraft unsteady aerodynamic characteristics. Part 2: Parameters estimated from wind tunnel data
[NASA-TM-110161] p 2142 N95-27839
The applicability of turbulence models to aerodynamic and propulsion flowfields at McDonnell-Douglas Aerospace p 2285 N95-27886
Algorithm to describe the spread of a wall fire under a ceiling
[PB95-182259] p 2247 N95-28008
A numerical study of ultra-short-pulse reflectometry
[DE95-008070] p 2266 N95-28015
Multifractal character of the electronic states in disordered two-dimensional systems
[DE95-609153] p 2443 N95-28016
Robust integration schemes for generalized viscoplasticity with internal-state variables. Part 1: Theoretical developments and applications
[NASA-CR-195452-PT-1] p 2310 N95-28031
Robust integration schemes for generalized viscoplasticity with internal-state variables. Part 2: Algorithmic developments and implementation
[NASA-CR-195453-PT-2] p 2310 N95-28032
A new algorithm for generating highly accurate benchmark solutions to transport test problems
[DE95-007397] p 2373 N95-28047
Analysis of forward and inverse problems in chemical dynamics and spectroscopy
[DE95-009309] p 2209 N95-28164
Ultrashort Pulse retrieval using FROG trace irradiance moments and the adaptive neural networks backpropagation algorithm
[DE95-007153] p 2299 N95-28220
The concentration-estimation problem for multiple-wavelength differential absorption lidar
[DE95-008375] p 2256 N95-28231
Altimeter analysis of ocean currents
[AD-A290167] p 2315 N95-28392
Applications of boundary element methods on the Intel Paragon
[DE94-014135] p 2393 N95-28393
Denoising and robust non-linear wavelet analysis
[AD-A291668] p 2257 N95-28455
Piecemeal learning of an unknown environment
[AD-A291683] p 2387 N95-28461
Local design optimization for composite transport fuselage crown panels p 2137 N95-28473
Visualization methods for the exploration of high dimensional data
[AD-A291717] p 2393 N95-28507
Weighting the recursive spectral bisection algorithm for unstructured grids
[DE95-008080] p 2373 N95-28521
HZETRN: Description of a free-space ion and nucleon transport and shielding computer program
[NASA-TP-3495] p 2465 N95-28530
Cloud classification using whole-sky imager data
[DE95-006501] p 2344 N95-28556
Binary segmentation of SAR images by the ICM algorithm
[INPE-5464-PRE/1772] p 2258 N95-28559
A genuinely multidimensional upwind scheme and efficient multigrid solver for the compressible Euler equations
[NASA-CR-195000] p 2288 N95-28571
Low-angle tracking in the presence of ducting, coherent and incoherent multipath
[AD-A289838] p 2258 N95-28580
Exploiting parallelism in a Monte Carlo image-matching algorithm
[AD-A289872] p 2374 N95-28625
Query by image example: The CANDID approach
[DE95-006284] p 2456 N95-28631

ALIGNMENT
Nondestructive testing apparatus for determining the orientation of reinforcing bars within a concrete structure
[AD-D017267] p 2245 N95-26508
Isolated digit recognition without time alignment
[AD-A289344] p 2254 N95-27062
Experience from the in-flight calibration of the Extreme Ultraviolet Explorer (EUVE) and Upper Atmosphere Research Satellite (UARS) fixed head star trackers (FHSTs) p 2149 N95-27779

ALIPHATIC HYDROCARBONS
Wipe solvent substitutions for 1,1,1-trichloroethane (TCA) and methyl ethyl ketone (MEK) at Hill Air Force Base p 2228 N95-27107

ALKALI METAL COMPOUNDS
Rotor phases in compound semiconductors
[DE95-004139] p 2436 N95-26442

ALKALI METALS
Molecular approach to mesoporous metal sulfides
[DE95-005418] p 2202 N95-27137
Thermodynamics of aqueous electrolytes at high temperatures by the isopiestic technique
[DE95-006747] p 2449 N95-27546
Polybenzimidazoles via aromatic nucleophilic displacement
[NASA-CASE-LAR-14924-1-CU] p 2179 N95-28361

ALKALINE EARTH COMPOUNDS
Fabrication of long wavelength array by in-situ molecular beam epitaxy
[AD-A288599] p 2423 N95-26679

ALKANES
Surface crystallization and thin film melting in normal alkanes
[DE95-006694] p 2440 N95-27535

ALKENES
Porosity in hexylene-bridged polysilsesquioxanes: Effects of monomer concentration
[DE95-005421] p 2240 N95-28531

ALKYL COMPOUNDS
Comparison of bridged polysilsesquioxane xerogels prepared from methoxy- and ethoxy-silyl monomers
[DE95-005422] p 2240 N95-28532

ALL SKY PHOTOGRAPHY
Cloud classification using whole-sky imager data
[DE95-006501] p 2344 N95-28556

ALLOYING
Spin-density-wave magnetism in dilute copper-manganese alloys
[DE95-005121] p 2215 N95-27462
Laser ultrasonic generation at the surface of a liquid metal
[DE95-004999] p 2216 N95-27477
Systematic study of the ion beam mixing of oxide markers into alumina
[DE95-006262] p 2217 N95-27555

ALLOYS
Current programmes on physical metallurgy and related areas in BARC
[DE95-607939] p 2214 N95-27255
AMCC casting development. Volume 1: Executive Summary
[NASA-CR-196597] p 2247 N95-28419

ALPHA PARTICLES
Radon integral measurement system
[DE95-608074] p 2405 N95-27010
Detecting alpha particles through scintillation in porous materials
[AD-A289313] p 2406 N95-27399
Alpha characterization inside pipes using ion-transport technology
[DE95-007869] p 2411 N95-28024

ALTERNATING CURRENT
Alternate charging profiles for the onboard nickel cadmium batteries of the Explorer Platform/Extreme Ultraviolet Explorer p 2272 N95-26796
Automated integration of genomic physical mapping data via parallel simulated annealing
[DE95-008057] p 2351 N95-27725
OBIC analysis of stressed, thermally-isolated polysilicon resistors
[DE95-008511] p 2268 N95-28201
Surface scanning techniques to locate and study defects in painted zinc and zinc alloy coated steels
[DE95-006099] p 2240 N95-28547

ALTERNATIVES
Cleanliness verification process at Martin Marietta Astronautics p 2165 N95-27104
Life cycle costs of alternatives for F-16 printed circuit board diagnosis equipment
[AD-A288744] p 2138 N95-28586

ALTIMETERS
An in situ evaluation of TOPEX/Poseidon altimetric measurements versus meaurements made by moorings and inverted echo sounders for sea surface height
[NASA-CR-198621] p 2347 N95-27805
Altimeter analysis of ocean currents
[AD-A290167] p 2315 N95-28392

ALTIMETRY
An in situ evaluation of TOPEX/Poseidon altimetric measurements versus meaurements made by moorings and inverted echo sounders for sea surface height
[NASA-CR-198621] p 2347 N95-27805

ALUMINIDES
Lattice parameters and Debye-Waller factors of gamma-TiAl alloys
[AD-A288843] p 2213 N95-26681

ALUMINUM
The response of hydrotalcite coated aluminum to sealing with transition metal salt solutions
[DE95-004767] p 2234 N95-27460
Advanced neutron source materials surveillance program
[DE95-005700] p 2215 N95-27464
Atomistic calculations of hydrogen interactions with Ni3Al grain boundaries and Ni/Ni/Ni3Al interfaces
[DE95-006497] p 2408 N95-27534
Scaling issues in dynamic fragmentation
[DE95-008509] p 2309 N95-27745
Chromate-free corrosion resistant conversion coatings for aluminum alloys
[DE95-007742] p 2238 N95-28117
Hazards analysis of an integral class 1.1/1.3 rocket motor demilitarization and ingredient recovery system using ammonia p 2174 N95-28315
Computational studies of projectile melt in impact with typical whipple shields
[DE95-005916] p 2311 N95-28337
Photoemission study of solid state reaction and initial oxidation of the Ce/Al(100) system
[PB95-195368] p 2210 N95-28652

ALUMINUM ALLOYS
Identification of the plastic anisotropy of an aluminum alloy
[IFTR-26/1994] p 2212 N95-26512
Changes in the anisotropy parameters of an aluminum alloy caused by cyclical deformation
[IFTR-27/1994] p 2212 N95-26666
Lattice parameters and Debye-Waller factors of gamma-TiAl alloys
[AD-A288843] p 2213 N95-26681
Annealing-induced changes in the anisotropy of an aluminum alloy
[IFTR-24/1994] p 2213 N95-26838
Ductile - ductile beryllium aluminum metal matrix composite manufactured by extrusion
[AD-A289519] p 2181 N95-26848
A study of internal damage of metal matrix composites by neutron diffraction
[DE95-005157] p 2182 N95-27080
Tensile properties of Fe-16 at. % Al alloys
[DE95-007102] p 2215 N95-27450
Atomistic calculations of hydrogen interactions with Ni3Al grain boundaries and Ni/Ni/Ni3Al interfaces
[DE95-006497] p 2408 N95-27534
Thermal control materials on EOIM-3
p 2242 N95-27639
Solid film lubricants and thermal control coatings flown aboard the EOIM-3 MDA sub-experiment
p 2242 N95-27640
Processing and properties of chromate-free conversion coatings on aluminum
[DE95-004768] p 2218 N95-27722
A new technique for measuring the separation of closely spaced dislocations using residual contrast conditions
[DE95-007147] p 2219 N95-27968
Trace elements and the mechanical properties of intermetallic compounds
[DE95-007378] p 2220 N95-28046
Pulsed ion beam surface treatment for preparing rapidly solidified corrosion resistant steel and aluminum surfaces
[DE95-007741] p 2221 N95-28116
Chromate-free corrosion resistant conversion coatings for aluminum alloys
[DE95-007742] p 2238 N95-28117
Bases for extrapolating materials durability in fuel storage pools
[DE95-007748] p 2222 N95-28129
Electronic structure of ordered and disordered transition metal aluminides
[DE95-609034] p 2223 N95-28250
Surface scanning techniques to locate and study defects in painted zinc and zinc alloy coated steels
[DE95-006099] p 2240 N95-28547
Fatigue properties of an A356 (AlSi7Mg) aluminum alloy for automotive applications: Fatigue life prediction
[PB95-196424] p 2224 N95-28660

ALUMINUM BORON COMPOSITES
Composite flexible insulation for thermal protection of space vehicles p 2166 N95-28293

ALUMINUM GALLIUM ARSENIDES
Dimensionally self regulating materials
[AD-A291671] p 2257 N95-28456

ALUMINUM NITRIDES
Pseudomorphic semiconducting heterostructures from combinations of AlN, GaN and selected SiC polytypes: Theoretical advancement and its coordination with experimental studies of nucleation, growth, characterization and device development
[AD-A289550] p 2437 N95-26756
First-principles calculations for AlN, GaN, and InN: Bulk and alloy properties
[DE95-006822] p 2219 N95-27958

ALUMINUM OXIDES
A study of the use beta-alumina as a weak interface in alumina fiber composites
[AD-A288629] p 2179 N95-26484
Mechanical performance of fiber reinforced metal matrix composites and microstructural development of polycrystalline alumina fibers synthesized from liquid precursors
[AD-A289518] p 2181 N95-26847

Systematic study of the ion beam mixing of oxide markers into alumina
[DE95-006262] p 2217 N95-27555
ECR plasma-assisted deposition of Al2O3 and dispersion-strengthened AlO2
[DE95-007743] p 2235 N95-27687
High-temperature deformation of ZrO2-Al2O3/SiC whisker composites fabricated by two techniques
[DE95-008273] p 2183 N95-28069
Task 4 supporting technology. Part 1: Detailed test plan for leading edge tile development. Leading edge material development and testing
[NASA-CR-198633] p 2160 N95-28258
Stratospheric ozone reactive chemicals generated by space launches worldwide
[AD-A289852] p 2332 N95-28623

ALUMINUM SILICATES
Ceramic fiber-reinforced monoclinic celsian phase glass-ceramic matrix composite material
[NASA-CASE-LEW-15714-1] p 2183 N95-27717

ALUMINUM-LITHIUM ALLOYS
A first principles approach to phase stability and order-disorder transformation: Application to Li-Al alloys
[DE95-609152] p 2218 N95-27756

AMBIENCE
FY 1994 ambient air monitoring report for McMurdo Station, Antarctica
[DE95-008565] p 2331 N95-28149
Prototype development and test results of a continuous ambient air monitoring system for hydrazine at the 110 ppb level p 2173 N95-28310
Development and application of low-temperature AFM
[AD-A291704] p 2352 N95-28525

AMBIENT TEMPERATURE
Precision parts cleaning with supercritical carbon dioxide p 2229 N95-27114
Laser ultrasonic generation at the surface of a liquid metal
[DE95-004999] p 2216 N95-27477
Effect of internal hydrogen on the mixed-mode 1/3 fracture toughness of a ferrific/martensitic stainless steel
[DE95-005722] p 2216 N95-27479
Inflight resistance measurement on high-T(sub c) superconducting thin films exposed to orbital atomic oxygen on CONCAP-2 (STS-46) p 2272 N95-27635
Cryogenic washout of solid rocket propellants
p 2176 N95-28324

AMBIPOLAR DIFFUSION
Energization and transport of ions of ionospheric origin in the terrestrial magnetosphere
[NASA-CR-197813] p 2336 N95-26699

AMINO ACIDS
Hydrogen-ion titrations of amino acids and proteins in solutions containing concentrated electrolyte
[DE95-008356] p 2209 N95-28229

AMMONIA
Superior catalysts for selective catalytic reduction of nitric oxide
[DE95-007903] p 2205 N95-27691
Plasma source ion implantation of ammonia into electroplated chromium
[DE95-006275] p 2444 N95-28125
A comparison of NH3 point monitoring and diode laser based path integrated measurements
[DE95-006892] p 2332 N95-28602

AMMONIUM COMPOUNDS
Acute and subacute toxicity of ammonium dinitramide (ADN) p 2175 N95-28318

AMMONIUM PERCHLORATES
Hazards analysis of an integral class 1.1/1.3 rocket motor demilitarization and ingredient recovery system using ammonia p 2174 N95-28315
Acute and subacute toxicity of ammonium dinitramide (ADN) p 2175 N95-28318
The demilitarization of class 1.1 rocket motors using high pressure waterjets p 2176 N95-28322

AMMUNITION
Performance analysis of bullet trajectory estimation: Approach, simulation, and experiments
[DE95-007949] p 2399 N95-28109

AMORPHOUS MATERIALS
Surface energy driven crystallization of amorphous Ni69Cr14P17 alloy
[DE95-005543] p 2438 N95-27085
Temperature dependence of ion-beam-induced amorphization in (Beta)-SiC
[DE95-007164] p 2438 N95-27087
Variation of solvent scattering-length density small-angle neutron scattering as a means of determining structure of composite materials
[DE95-005394] p 2183 N95-27428
Characterization of collision cascade damage in Ca2La8(SiO4)6O2 by HRTEM
[DE95-005719] p 2440 N95-27491
Repair technology for thermoplastic aircraft structures
p 2134 N95-27519
Systematic study of the ion beam mixing of oxide markers into alumina
[DE95-006262] p 2217 N95-27555
Amorphization of complex ceramics by heavy-particle irradiations
[DE95-005725] p 2236 N95-27733
Density changes in amorphous Pd80Si20 during low temperature ion irradiation
[DE95-007132] p 2441 N95-27928
Pulsed laser deposition of zeolitic membranes
[DE95-006274] p 2298 N95-28124
The real structure of columnar pinning centers in heavy-ion-irradiated cuprate superconductors
[DE95-003948] p 2445 N95-28186

AMORPHOUS SILICON
Growth of hydrogenated amorphous silicon (a-Si:H) on patterned substrates for increased mechanical stability
[DE95-006589] p 2234 N95-27472
Amorphous silicon pixel radiation detectors and associated thin film transistor electronics readout
[DE95-006568] p 2265 N95-27678
Sensor for measuring the atomic fraction in highly dissociated hydrogen
[DE95-006531] p 2415 N95-28204
Atomic layer epitaxy of group 4 materials: Surface processes, thin films, devices and their characterization
[AD-A289092] p 2446 N95-28327

AMPHIBIOUS VEHICLES
Air cushioned landing craft (LCAC) based ship to shore movement simulation: A decision aid for the amphibious commander. A (SMMAT) application
[AD-A289635] p 2246 N95-26722

AMPLIFICATION
Low noise monolithic Si JFETS for operation in the 90-300K range and in high radiation environments
[DE95-007303] p 2269 N95-28244

AMPLITUDE MODULATION
High-speed coherent laser arrays
[AD-A289373] p 2295 N95-26906
Full complex modulation using two one-parameter spatial light modulators
[NASA-CASE-MSC-22255-1] p 2427 N95-28384

AMPLITUDES
Ball bearing vibrations amplitude modeling and test comparisons p 2158 N95-27286

ANALOG CIRCUITS
Modeling of trapping and abrupt doping effects in MESFET's using R-dynamic element
[PB95-184891] p 2262 N95-27050
Novel field effect transistors for low power electronics
[AD-A289929] p 2271 N95-28629

ANALOG SIMULATION
Modeling of trapping and abrupt doping effects in MESFET's using R-dynamic element
[PB95-184891] p 2262 N95-27050

ANALOG TO DIGITAL CONVERTERS
The systems of the proportional chambers registration electronics for present experiments in nuclear physics
[DE95-608559] p 2419 N95-27161
Method and apparatus for maintaining linearity and frequency accuracy of an FM chirp waveform
[AD-D017398] p 2258 N95-28615

ANALOGIES
Unification of LARCH and Z-based object models to support algebraically-based design refinement: The Z perspective
[AD-A289234] p 2369 N95-26962

ANALOGS
Algebraic structure of the Green's ansatz and its q-deformed analogue
[DE95-608780] p 2395 N95-27340
Leak detection utilizing analog binaural (VLSI) techniques
[NASA-CASE-NPO-18399-1-CU] p 2271 N95-28599

ANALYSIS (MATHEMATICS)
Efficient analytic computation of higher-order QCD amplitudes
[DE95-008593] p 2449 N95-28160

ANALYTIC FUNCTIONS
Generalized Schwarzians in several variables and Moebius invariant differential operators
[PB95-185211] p 2388 N95-26539
Holomorphic curves in Abelian varieties, part 1
[DE95-608748] p 2396 N95-27300

ANALYTICAL CHEMISTRY
Observations on the solvating power of supercritical fluids p 2228 N95-27106

ANDROMEDA CONSTELLATION
Discussion on selected symbiotic stars
p 2460 N95-27078

ANECHOIC CHAMBERS
Anechoic wind tunnel study of turbulence effects on wind turbine broadband noise p 2325 N95-27992
Data acquisition software for DREO's near-field antenna measurement facility
[AD-A289819] p 2258 N95-28573

ANGLE OF ATTACK
Numerical simulation of the flow about the F-18 HARV at high angle of attack
[NASA-CR-197755] p 2121 N95-26735

ANGLES (GEOMETRY)
A new angle on the Euler angles
p 2153 N95-27800

ANGULAR DISTRIBUTION
Radiation of a uniformly moving charge
[DE95-608757] p 2255 N95-27335
Laser ultrasonic generation at the surface of a liquid metal
[DE95-004999] p 2216 N95-27477

ANGULAR MOMENTUM
Wigner quantum oscillators. OSP (3/2) oscillators
[DE95-608756] p 2448 N95-27334
The Hurwitz-Eulerian reduction
[DE95-608760] p 2396 N95-27337
Magnetic viscosity by localized shear flow instability in magnetized accretion disks
[DE95-006879] p 2433 N95-28111
Coordinates of the quantum plane as q-tensor operators in U(sub q) (su(2) * su(2))
[DE95-007100] p 2397 N95-28234

ANGULAR VELOCITY
Electro-hydrostatic actuator controller design using quantitative feedback theory
[AD-A289220] p 2141 N95-26957
Preliminary analysis of dynamic stall effects on a 91-meter wind turbine rotor p 2124 N95-27975

ANILINE
The role of hydrogen in the hydrogenation and hydrogenolysis of aniline on the nickel single crystal surfaces: Its implication on the mechanisms of HDN reactions
[DE95-006687] p 2222 N95-28134

ANIMATION
Virtual Prototyping as an aid for control system analysis
[AD-A288819] p 2362 N95-28346

ANIONS
Molecular approach to mesoporous metal sulfides
[DE95-005418] p 2202 N95-27137
Atomistic study of energy and structure of surfaces in NiO
[DE95-005207] p 2215 N95-27446
Synthesis and properties of lanthanide-exchanged Preyssler's heteropolyanions
[DE95-007136] p 2238 N95-28235

ANISOTROPIC MEDIA
Conditions for the parameter dyadics of lossless bi-anisotropic media
[PB95-185104] p 2252 N95-26914
Dip-moveout processing by Fourier transform in anisotropic media
[DE95-007668] p 2339 N95-28190
Internal electric field of anisotropic and bi-anisotropic spheres
[PB95-195491] p 2257 N95-28449

ANISOTROPIC PLATES
Buckling behavior of long symmetrically laminated plates subjected to combined loads p 2190 N95-28430

ANISOTROPY
Determination of the cyclical properties of 18G2A steel on the basis of skeleton curves for a planar stress state
[IFTR-32/1994] p 2211 N95-26359
The development of the anisotropic properties of copper under plastic deformation induced by creep and monotonic loading
[IFTR-23/1994] p 2212 N95-26517
Changes in the anisotropy parameters of an aluminum alloy caused by cyclical deformation
[IFTR-27/1994] p 2212 N95-26666
Annealing-induced changes in the anisotropy of an aluminum alloy
[IFTR-24/1994] p 2213 N95-26838
Micromechanical modeling of damage and inelasticity of composite materials in macroscopic structural analysis
[DE95-003668] p 2182 N95-27421
Formation of anisotropic Tl-1212, Tl-2212, Tl-1223 and Tl-2223 particles using aerosol flow reacted powders
[DE95-007400] p 2444 N95-28079
Photon rockets and gravitational radiation
[PB95-190161] p 2397 N95-28174
Analysis of stresses in finite anisotropic panels with centrally located cutouts p 2187 N95-28286

ANNEALING
Annealing of radiation damaged gallium arsenide solar cells by laser illumination
[AD-A289683] p 2316 N95-26762

Annealing-induced changes in the anisotropy of an aluminum alloy
[IFTR-24/1994] p 2213 N95-26838
Effects of helium pre-implantation on the microstructure and mechanical properties of irradiated 316 stainless steel
[DE95-007162] p 2214 N95-27086
Neutron diffraction studies on recrystallization of solution derived lead zirconate titanates
[DE95-004771] p 2439 N95-27429
Characterization of defects in deuterium-implanted beryllium
[DE95-005688] p 2217 N95-27553
Modification of the optical properties of glass by sequential ion implantation
[DE95-007401] p 2237 N95-28080
Low resistivity ohmic contacts to moderately doped n-GaAs with low temperature processing
[DE95-008507] p 2445 N95-28144
Sensor for measuring the atomic fraction in highly dissociated hydrogen
[DE95-006531] p 2415 N95-28204
Chemical and electrical properties of cavities in silicon and germanium
[DE95-006812] p 2445 N95-28206

ANNIHILATION REACTIONS
A simple relativistic model of pp-bar yields K(+)K(-)
[DE95-608852] p 2406 N95-27318
Some aspects of the OZI-rule violation in the reaction anti-pp yields phi pi(0)
[DE95-608853] p 2415 N95-28245
B-Physics results from D0
[DE95-005126] p 2417 N95-28495

ANNUAL VARIATIONS
Hindcasting wind-driven anomalies using reduced-gravity global ocean models with 1/2 deg and 1/4 deg resolution
[AD-A289060] p 2345 N95-26406
Temporal and spatial decorrelation scales of the Yellow Sea thermal fields
[AD-A288617] p 2346 N95-26483
Spectral analyses, climatology, and interannual variability of Nimbus-7 TOMS version 6 total column ozone
[NASA-RP-1360] p 2341 N95-26689
Variability study of foF2 for an equatorial station
[DE95-608080] p 2337 N95-27157
Research project on CO2-induced climate change
[DE95-008339] p 2330 N95-28084

ANODES
Electrolyte effects in Li(Si)/FeS2 thermal batteries
[DE95-001614] p 2264 N95-27474

ANODIC COATINGS
Thermal control materials on EOIM-3
p 2242 N95-27639
Solid film lubricants and thermal control coatings flown aboard the EOIM-3 MDA sub-experiment
p 2242 N95-27640

ANOMALIES
Hindcasting wind-driven anomalies using reduced-gravity global ocean models with 1/2 deg and 1/4 deg resolution
[AD-A289060] p 2345 N95-26406
Parallelism detection and scheduling strategies for reliable and efficient execution on multicomputers
[AD-A288370] p 2376 N95-26471
Trace anomalies and cocycles of Weyl and diffeomorphism groups
[DE95-608793] p 2397 N95-27344
Geophex airborne unmanned survey system
[DE95-007566] p 2131 N95-27440
Kepler Equation solver p 2147 N95-27767

ANTARCTIC REGIONS
Live from Antarctica: Then and now
[NASA-CR-197829] p 2335 N95-26594
Live from Antarctica: The coldest, windiest place on Earth
[NASA-CR-197737] p 2335 N95-26595
Live from Antarctica, volume 4
[NASA-CR-197828] p 2335 N95-26596
FY 1994 ambient air monitoring report for McMurdo Station, Antarctica
[DE95-008565] p 2331 N95-28149

ANTENNA ARRAYS
Joint services electronics program
[AD-A289594] p 2260 N95-26716
Active antennas with periodic structures
[AD-A289437] p 2252 N95-26924
Adaptive beamforming in frequency-dispersive multipath environments
[AD-A289206] p 2254 N95-27009
Linearly tapered slot antenna impedance characteristics
[NASA-TM-106912] p 2266 N95-27853
Theoretical and experimental study of low-loss, High-efficiency monolithic antenna structures at 94 GHz
[AD-A291785] p 2257 N95-28513
JPRS report: Science and technology. Central Eurasia
[JPRS-UST-95-019] p 2270 N95-28565

ANTENNA COMPONENTS
FORTE antenna element and release mechanism design p 2157 N95-27282
Theoretical and experimental study of low-loss, High-efficiency monolithic antenna structures at 94 GHz
[AD-A291785] p 2257 N95-28513

ANTENNA COUPLERS
One dimensional global and local solution for ICRF heating
[DE95-007984] p 2392 N95-28110
Shear Alfven wave excitation by direct antenna coupling and fast wave resonant mode conversion
[DE95-609109] p 2256 N95-28254

ANTENNA DESIGN
Improving the performance of spiral antennas by using passive scatterers
[AD-A289324] p 2251 N95-26893
Active antennas with periodic structures
[AD-A289437] p 2252 N95-26924
Low-cost tubular antenna deployer for WISP-2
p 2156 N95-27269
Design, development and testing of the x-ray timing explorer High Gain Antenna System
p 2157 N95-27279
Special features of the CLUSTER antenna and radial booms design, development and verification
p 2157 N95-27281
FORTE antenna element and release mechanism design p 2157 N95-27282
Linearly tapered slot antenna impedance characteristics
[NASA-TM-106912] p 2266 N95-27853
Faraday screen sputtering on TPX
[DE95-008347] p 2434 N95-28224
Data acquisition software for DREO's near-field antenna measurement facility
[AD-A289819] p 2258 N95-28573

ANTENNA RADIATION PATTERNS
Improving the performance of spiral antennas by using passive scatterers
[AD-A289324] p 2251 N95-26893
Active antennas with periodic structures
[AD-A289437] p 2252 N95-26924
FDTD-ANT user manual
[NASA-CR-195444] p 2372 N95-27729
Linearly tapered slot antenna impedance characteristics
[NASA-TM-106912] p 2266 N95-27853

ANTHROPOMETRY
The Alpha-Proton-X-ray Spectrometer deployment mechanism: An anthropomorphic approach to sensor placement on Martian rocks and soil
p 2155 N95-27265

ANTIBODIES
Cofactor-assisted antibody catalysis
[AD-A288929] p 2349 N95-26608

ANTIFERROMAGNETISM
Magnetic structures in RNi2B2C (R = Ho, Er) superconductors
[DE95-008370] p 2442 N95-27932
Muon spin relaxation in antiferromagnets: A study of RbMnF3 based on the coupled-mode theory of paramagnetic and critical spin fluctuations
[PB95-192878] p 2418 N95-28642

ANTIGENS
Anti-idiotype probes for toxin detection
[AD-A288955] p 2348 N95-26435
Diagnostic antigens of Leishmania
[AD-A288605] p 2350 N95-27097

ANTIMATTER
Polarizing matter and antimatter: A new method
[DE95-007109] p 2421 N95-27923

ANTIMONY
Analysis of the dimerized Sb/Si(001)-(2x1) surface by x-ray standing waves
[DE95-007097] p 2208 N95-27965

ANTIPROTONS
A study of events with large total transverse energy produced in proton-antiproton collisions at (radical)s = 1.8 TeV
[DE95-003382] p 2410 N95-27872
The CDF upgrade
[DE95-006683] p 2421 N95-28107
Some aspects of the OZI-rule violation in the reaction anti-pp yields phi pi(0)
[DE95-608853] p 2415 N95-28245
The 132 nsec bunch spacing in the Tevatron proton-antiproton collider
[DE95-005750] p 2422 N95-28346

ANTIREFLECTION COATINGS
Study of frequency doubling antireflection coating
[AD-A289634] p 2424 N95-26860
Effects of long term space environment exposure on optical substrates and coatings p 2428 N95-27653

APERTURES
Preliminary design study of the beam collapser and certain optomechanical aspects of the siderostat
[AD-A288423] p 2423 N95-26549

APOGEE BOOST MOTORS
Development test of a liquid Apogee engine for the ETS-6
[NAL-TR-1250] p 2167 N95-26799

APPLICATIONS PROGRAMS (COMPUTERS)
Manual for SHOCK3D, version 2.0. Computer program for non-linear shock response
[AD-A288631] p 2307 N95-26342
An evaluation of the Software Through Pictures/T Tool (StP/T) for the Software Support Activity (SSA)
[AD-A288822] p 2362 N95-26348
WINCLR: A computer code for heat transfer and clearance calculation in a compressor
[NASA-CR-195436] p 2117 N95-26363
Hindcasting wind-driven anomalies using reduced-gravity global ocean models with 1/2 deg and 1/4 deg resolution
[AD-A289060] p 2345 N95-26406
FREZCHEM: A chemical-thermodynamic model for aqueous solutions at subzero temperatures
[AD-A288456] p 2200 N95-26432
Analysis of historical oceanographic data on a personal computer. Program MDS
[AD-A288965] p 2363 N95-26447
Long term distributed file reference tracing: Implementation and experience
[AD-A288585] p 2452 N95-26535
Design tool for multiprocessor scheduling and evaluation of iterative dataflow algorithms
[NASA-TP-3491] p 2366 N95-26685
Software packager user's guide
[NASA-CR-197763] p 2366 N95-26693
The multidimensional Self-Adaptive Grid code, SAGE, version 2
[NASA-TM-110350] p 2367 N95-26726
NEXTSTEP: The next step in the right direction? Part 2: Software development with NEXTSTEP
[REPT-94-33-PT-2] p 2450 N95-26803
User documentation of the CTA program
[AD-A289508] p 2121 N95-26854
EASY-SIM: A visual simulation system software architecture with an Ada 9X application framework
[AD-A289325] p 2368 N95-26895
An exploratory application of neural networks for airfoil design p 2118 N95-26943
Measuring fault tolerance with the FTAPE fault injection tool
[NASA-CR-197773] p 2306 N95-27253
Computer program BL2D for solving two-dimensional and axisymmetric boundary layers
[NASA-CR-4668] p 2279 N95-27257
Thermal neutral format based on the step technology
p 2283 N95-27363
Automated database design from natural language input p 2383 N95-27378
Outline and handling manual of fusion experimental data monitor system DAISY, version 2
[DE95-703895] p 2431 N95-27414
Energetic particle destabilization of shear Alfven waves in stellarators and tokamaks
[DE95-006393] p 2431 N95-27419
Lattice QCD calculation using VPP500
[DE95-007076] p 2449 N95-27448
Scientific statistics and graphics on the Macintosh
[DE95-006445] p 2372 N95-27533
Numerical methods for determining interstitial oxygen in silicon
[DE95-007710] p 2205 N95-27683
PRISM validation
[AD-A288476] p 2337 N95-27703
Multimedia Environmental Pollutant Assessment System (MEPAS) application guidance. Guidelines for evaluating MEPAS input parameters for Version 3.1
[DE95-007525] p 2328 N95-27749
Development of a direct match technique for star identification on the SWAS mission
p 2148 N95-27771
Determining GPS average performance metrics
p 2128 N95-27791
Improvements and new features in the PDF module
p 2287 N95-27902
Scrape-off layer plasma modeling for the DIII-D tokamak
[DE95-008059] p 2433 N95-28054
UEDGE and DEGAS modeling of the DIII-D scrape-off layer plasma, revision 1
[DE95-008052] p 2433 N95-28065

Using the scalable nonlinear equations solvers package
[DE95-008323] p 2378 N95-28071
Preliminary flight software specification for the petite amateur Navy satellite (PANSAT)
[AD-A280068] p 2165 N95-28150
BEGET: The B-Factory Event Generator version 21
[DE95-008329] p 2414 N95-28171
Transport simulation of negative magnetic shear discharges
[DE95-003941] p 2416 N95-28329
Measurement-based MESFET model in APLAC
[PB95-195483] p 2269 N95-28448
HZETRN: Description of a free-space ion and nucleon transport and shielding computer program
[NASA-TP-3495] p 2465 N95-28530
ALLIANCE: An architecture for fault tolerant, cooperative control of heterogeneous mobile robots
[DE95-007374] p 2387 N95-28536
Development of a TECS control-law for the lateral directional axis of the McDonnell Douglas F-15 Eagle
[AD-A289771] p 2142 N95-28598
Radon transform and its applications in gridding airborne geophysical survey data
[PB95-195533] p 2315 N95-28643
Using COLETTE. (A simple guide)
[PB95-195806] p 2375 N95-28658

APPROACH CONTROL
Development of a coding form for approach control/pilot voice communications
[DOT/FAA/AM-95/15] p 2128 N95-28540

APPROXIMATION
Analysis and development of finite element methods for the study of nonlinear thermomechanical behavior of structural components
[NASA-CR-195354] p 2307 N95-26387
A mathematical framework for an improved search model
[AD-A288858] p 2358 N95-26552
The attenuation of microwave radiation by fog and rain
[AD-A288326] p 2249 N95-26562
Adaptive finite element method I: Solution algorithm and computational examples
[AD-A288979] p 2389 N95-26609
Truncated Gaussians as tolerance sets
[NASA-CR-197732] p 2395 N95-27417
Solving recursive domain equations with enriched categories
[AD-A289358] p 2371 N95-27418
An automated method of tuning an attitude estimator
p 2148 N95-27774
Optimal attitude maneuver execution for the Advanced Composition Explorer (ACE) mission
p 2149 N95-27778
Ulysses orbit determination at high declinations
p 2151 N95-27787
A magnetic hysteresis model p 2153 N95-27801
Generalized CNF satisfiability, local reductions and complexity of succinctly specified problems
[DE95-006343] p 2372 N95-27849
Deformation limits on two-parameter fracture mechanics in terms of higher order asymptotics
[AD-A289113] p 2310 N95-28098
Modeling the shock response of submerged structures
[AD-A289082] p 2288 N95-28351
Evaluation of defect-related diffusion in semiconductors by electrooptical sampling
[AD-A291630] p 2270 N95-28544

AQUEOUS SOLUTIONS
FREZCHEM: A chemical-thermodynamic model for aqueous solutions at subzero temperatures
[AD-A288456] p 2200 N95-26432
Applications of Second Harmonic and Sum Frequency Generation to graphite and silica type interfaces
[AD-A288228] p 2201 N95-26544
Survey of environmentally benign cleaning methodologies and materials p 2231 N95-27122
Sceening, down selection, and implementation of environmentally compliant cleaning and insulation bonding for MNASA p 2165 N95-27124
The response of hydrotalcite coated aluminum to sealing with transition metal salt solutions
[DE95-004767] p 2234 N95-27460
Thermodynamics of aqueous electrolytes at high temperatures by the isopiestic technique
[DE95-006747] p 2449 N95-27546
Absorption of sparingly soluble gases by reactive media in self-aerated gas-liquid contactors: A scale-up procedure
[DE95-006429] p 2206 N95-27707
Electrical conductivity measurements of aqueous electrolyte solutions at high temperatures and high pressures
[DE95-006748] p 2208 N95-27956
Aqueous electrolyte modeling in ASPEN PLUS(trademark)
[DE95-007008] p 2208 N95-27960

AQUIFERS
Numerical simulation of coupled flow and transport with TOUGH2: A verification study
[DE95-008351] p 2287 N95-28225

ARAMID FIBER COMPOSITES
Proof test methodology for composites
p 2193 N95-28445

ARC JET ENGINES
Electric propulsion for geostationary orbit insertion
[NASA-TM-106942] p 2168 N95-27727

ARC MELTING
Structural chemistry of some phases in the YC-Ni-B system
[DE95-007403] p 2447 N95-28537

ARC SPRAYING
Magnetically controlled deposition of metals using gas plasma
[DE95-007248] p 2430 N95-27237

ARCHES
Investigation into the behavior of geometrically nonlinear composite arches
[AD-A289258] p 2308 N95-26975

ARCHITECTURE
Advanced development for space robotics with emphasis on fault tolerance p 2155 N95-27263
Building-integrated photovoltaics: A case study
[DE95-004032] p 2325 N95-28396

ARCHITECTURE (COMPUTERS)
Using machine learning to derive efficient cost and performance estimates in VLSI CAD designs
[AD-A288254] p 2363 N95-26408
Massively parallel self-consistent-field calculations
[DE95-004128] p 2376 N95-26441
An introduction to software architecture
[AD-A288963] p 2363 N95-26446
Performance prediction: A case study using a multi-ring KSR-1 machine
[NASA-CR-195066] p 2361 N95-26697
Using an architectural approach to integrate heterogeneous, distributed software components
[NASA-CR-197766] p 2366 N95-26711
Control-flow analysis and type systems
[AD-A289338] p 2389 N95-26772
Progress towards computer simulation of NiH2 battery performance over life p 2272 N95-26786
An architecture for optimal all-to-all personalized communication
[AD-A288532] p 2377 N95-26840
Next generation controller specification for an open systems architecture standard - overview
[AD-A289507] p 2368 N95-26853
EASY-SIM: A visual simulation system software architecture with an Ada 9X application framework
[AD-A289325] p 2368 N95-26895
An exploratory application of neural networks for airfoil design p 2118 N95-26943
Design and implementation of a software communication architecture for the JANUS-3D Visualizer
[AD-A288509] p 2370 N95-27150
Advanced flight computer. Special study
[NASA-CR-198165] p 2371 N95-27246
An architecture and protocol for communications satellite constellations regarded as multi-agent systems
p 2166 N95-27377
A user-system interface agent p 2383 N95-27379
Design of a real-time wind turbine simulator using a custom parallel architecture p 2322 N95-27979
Teaching interdisciplinary computational science from an electronic book on the Internet
[DE95-006525] p 2373 N95-28498
Next generation controller specification for an open systems architecture standard
[AD-A289567] p 2375 N95-28647

ARGON
Cryogenic and simulated fuel jet breakup in argon, helium and nitrogen gas flows
[NASA-TM-106923] p 2291 N95-27030
Electron spectroscopy studies of argon K-shell excitation and vacancy cascades
[DE95-007096] p 2442 N95-27963
Low noise monolithic Si JFETS for operation in the 90-300K range and in high radiation environments
[DE95-007303] p 2269 N95-28244

ARID LANDS
Measurement and analysis of the surface energy budget for ARM field experiments
[DE95-007646] p 2338 N95-28114

ARITHMETIC
Modified Gaussian elimination for adaptive beamforming using RNS arithmetic
[AD-A288809] p 2248 N95-26356

ARMATURES
AFC generator development
[DE95-007094] p 2266 N95-27754

ARMED FORCES
Myers-Briggs type indicators and Kirton adaption-innovation inventory correlations
[AD-A288435] p 2357 N95-27181

ARMED FORCES (UNITED STATES)
Utilization of composite materials by the US Army: A look ahead p 2189 N95-28421

ARMOR
Improved hardness RHA weldability and material property testing
[AD-A289127] p 2221 N95-28102

ARRAYS
Fabrication of long wavelength array by in-situ molecular beam epitaxy
[AD-A288599] p 2423 N95-26679

ARSENIDES
Isolation and x-ray crystal structures of (Li(mu2-As(SiMe3)2) (mu3-As(SiMe3)2)(THF))2 and ((Me3Si)2AsLi(THF)2)2
[AD-A288870] p 2241 N95-28661

ARTIFICIAL INTELLIGENCE
Self-organizing artificial neural networks in dynamic systems modeling and control
[PB95-185120] p 2379 N95-26449
Encoding user-defined problems with SIPE-2
[AD-A288390] p 2380 N95-26475
Intelligent computer based reliability assessment of multichip modules
[AD-A288833] p 2259 N95-26550
Design and synthesis of a real-time controller for an unmanned air vehicle
[AD-A289134] p 2141 N95-26555
Digital systems validation. Chapter 20 Artificial Intelligenge with applications for aircraft. Handbbook, volume 2
[AD-A288492] p 2380 N95-26638
Multi-agent perception for Human/Robot interaction: A framework for intuitive trajectory modification
[AD-A289399] p 2359 N95-26884
Next generation real-time systems: Investigating the potential of partial-solution tasks
[AD-A289203] p 2381 N95-27007
Head related transfer function approximation using neural networks
[AD-A289422] p 2382 N95-27145
The 1995 Goddard Conference on Space Applications of Artificial Intelligence and Emerging Information Technologies
[NASA-CP-3296] p 2382 N95-27375
Applying AI tools to operational space environmental analysis p 2382 N95-27376
An architecture and protocol for communications satellite constellations regarded as multi-agent systems
p 2166 N95-27377
Building an adaptive agent to monitor and repair the electrical power system of an orbital satellite
p 2383 N95-27380
Limits to ground control in autonomous spacecraft
p 2383 N95-27381
Lessons learned from the introduction of autonomous monitoring to the EUVE science operations center
p 2385 N95-27393
Real-time value-driven diagnosis
p 2386 N95-27396
A linguistic geometry for 3D strategic planning
p 2386 N95-27397
Human factors in aviation maintenance, phase 4
[DOT/FAA/AM-95/14] p 2360 N95-27696
Operator modeling in commerical aviation: Cognitive models, intelligent displays, and pilot's assistants
[NASA-CR-198609] p 2138 N95-28203
Piecemeal learning of an unknown environment
[AD-A291683] p 2387 N95-28461
TRAINS: Dialogue transcription tools
[AD-A289869] p 2259 N95-28624

ARTIFICIAL SATELLITES
Engineering calculations associated with the ablative thermal protective structures of returnable satellites
[AD-A289593] p 2162 N95-26715
Optimization of a nutation damper attached to a spin-stabilized satellite
[AD-A289424] p 2162 N95-26887
A multi-attribute-utility-theory model that minimizes interview-data requirements: A consolidation of space launch decisions
[AD-A289421] p 2164 N95-27144
Non-explosive actuation for the ORBCOMM (TM) satellite p 2156 N95-27274
A sustainable genetic algorithm for satellite resource allocation p 2376 N95-27383
The combined release and radiation effects satellite time history data base system
[AD-A289835] p 2165 N95-28578

ASCENT PROPULSION SYSTEMS

Summary of EOS flight dynamics analysis p 2152 N95-27797

ASCENT TRAJECTORIES

Geostationary Operational Environmental Satellite (GOES)-8 mission flight experience p 2153 N95-27798

ASIA

An observational study on the onset of the summer monsoon over eastern Asia in 1979 [AD-A289637] p 2341 N95-26723

Synoptic features of the Yunan rainy season before the onset of the tropical monsoons [AD-A289641] p 2342 N95-26724

Asian Aeronautics: Technology acquisition drives industry development. Report to Congressional requesters [GAO/NSIAD-94-140] p 2118 N95-26817

JPRS report: Science and technology. Central Eurasia [JPRS-UST-95-016] p 2262 N95-27170

JPRS report: Science and technology. Central Eurasia [JPRS-UST-95-014] p 2145 N95-27171

JPRS report: Science and technology. Central Eurasia [JPRS-UST-95-019] p 2270 N95-28565

ASPECT RATIO

Analytical investigations of the acceleration sensitivity of acoustic bulk and surface wave resonators [AD-A291715] p 2402 N95-28505

ASPHALT

Layer coefficients for NHDOT pavement materials [AD-A288262] p 2246 N95-26548

ASPHERIC OPTICS

Design and fabrication of a diamond-turned hybrid diffractive/refractive singlet for visible applications at ORNL [DE95-007007] p 2427 N95-28552

ASSAYING

Microbial treatment for shipboard collection, hold ing, and transfer system tanks p 2179 N95-27119

ASSEMBLING

Automated integration of genomic physical mapping data via parallel simulated annealing [DE95-008057] p 2351 N95-27725

JTEC Panel report on microelectromechanical systems in Japan [NASA-CR-197831] p 2268 N95-28239

ASSEMBLY

Electronics manufacturing and assembly in Japan p 2263 N95-27231

ASSESSMENTS

Probabilistic risk assessment of the Space Shuttle. Phase 3: A study of the potential of losing the vehicle during nominal operation, volume 1 [NASA-CR-197808] p 2159 N95-26398

Probabilistic risk assessment of the Space Shuttle. Phase 3: A study of the potential of losing the vehicle during nominal operation. Volume 2: Integrated loss of vehicle model [NASA-CR-197809] p 2159 N95-26399

An introductory guide to uncertainty analysis in environmental and health risk assessment. Environmental Restoration Program [DE95-008097] p 2354 N95-28136

ASSIMILATION

Technical report series on global modeling and data assimilation. Volume 6: A multiyear assimilation with the GEOS-1 system: Overview and results [NASA-TM-104606-VOL-6] p 2334 N95-26423

ASSOCIATIVE PROCESSING (COMPUTERS)

Optical implementation of inner product neural associative memory [NASA-CASE-NPO-18491-2-CU] p 2427 N95-28363

ASTEROIDS

Tracking and impact prediction of Earth-Crossing-Objects (ECO's) on a collision course with Earth [AD-A289321] p 2461 N95-27303

ASTROMETRY

Preliminary design study of the beam collapser and certain optomechanical aspects of the siderostat [AD-A288423] p 2423 N95-26549

ASTRONAUTICS

Aeronautical engineering: A continuing bibliography with indexes (supplement 318) [NASA-SP-7037(318)] p 2120 N95-27543

ASTRONAUTS

Views of the solar system [DE95-006446] p 2461 N95-27326

ASTRONOMICAL MODELS

The second coming of cold dark matter? [DE95-005156] p 2462 N95-27445

ASTRONOMICAL POLARIMETRY

Classical novae and recurrent novae: General properties p 2459 N95-27072

ASTRONOMICAL SPECTROSCOPY

International Ultraviolet Explorer Atlas of B-type spectra from 1200 to 1900 A [NASA-RP-1363] p 2463 N95-28328

ASTROPHYSICS

Discussion on selected symbiotic stars p 2460 N95-27078

Airborne geophysics and precise positioning: Scientific issues and future directions [LC-94-68678] p 2314 N95-27156

Laboratory high-energy astrophysics on lasers [DE95-008062] p 2462 N95-28013

Normal modes and continuous spectra [DE95-006166] p 2287 N95-28055

Search for molecular absorptions with the Fourier Transform Spectrometer [NASA-CR-198648] p 2462 N95-28222

Neutrino oscillations in strong magnetic fields [DE95-608876] p 2416 N95-28249

Proceedings of the International Workshop on Acceleration and Radiation Generation in Space and Laboratory Plasmas [AD-A291673] p 2436 N95-28668

Space Science Division cumulative bibliography: 1989-1994 [NASA-TM-110355] p 2457 N95-28677

ASYMMETRY

Scalable multicast tree construction for wide area networks [AD-A288318] p 2379 N95-26421

Using the dimension reduction technique to prove that clique trees define facets for the asymmetric traveling salesman polytope [AD-A289397] p 2389 N95-26882

Study of parity and time reversal violation in neutron-nucleus interactions [DE95-005158] p 2405 N95-27081

Precise measurement of the left-right cross section asymmetry in Z boson production by e(+)e(-) collisions [DE95-008591] p 2414 N95-28158

ASYMPTOTIC METHODS

Modeling the shock response of submerged structures [AD-A289082] p 2288 N95-28351

ASYMPTOTIC SERIES

Deformation limits on two-parameter fracture mechanics in terms of higher order asymptotics [AD-A289113] p 2310 N95-28098

The high energy behavior of the forward scattering parameters -- (sigma)(sub tot), (rho), and B [DE95-007075] p 2415 N95-28210

ATMOSPHERIC ATTENUATION

Prediction of rain attenuation and total atmospheric attenuation for low-availability satellite communications in Europe [PB95-184925] p 2252 N95-26908

A study of surface temperatures, clouds and net radiation [NASA-CR-198589] p 2329 N95-27864

ATMOSPHERIC CHEMISTRY

Applications of Second Harmonic and Sum Frequency Generation to graphite and silica type interfaces [AD-A288228] p 2201 N95-26544

Engineering photochemical smog through convection towers [DE95-007727] p 2328 N95-27686

Dynamics and control of SEDSAT tethered multi-probe for thermospheric research flight data analysis of SEDS-2 satellite: Tethered systems dynamics and flight data analysis [NASA-CR-198653] p 2165 N95-27836

Issues relevant to the development of coupled chemistry/climate models [DE95-006441] p 2330 N95-27954

Emerging applications of probability (stochastic models in geosystems) [AD-A289117] p 2313 N95-28099

Use of SURFACE CHEMKIN to model multiphase atmospheric chemistry: Application to nitrogen tetroxide spills p 2172 N95-28305

Site scientific mission plan for the Southern Great Plains CART site, January-June 1995 [DE95-008393] p 2344 N95-28340

Remote sensing of the atmosphere by resonance Raman LIDAR [DE95-007312] p 2315 N95-28520

Measurements of daytime and upper tropospheric water vapor profiles by Raman lidar [DE95-007640] p 2344 N95-28538

A black carbon emission data base for atmospheric chemistry and climate studies [DE95-006436] p 2332 N95-28662

ATMOSPHERIC CIRCULATION

Meso-beta scale numerical simulation studies of terrain-induced jet streak mass/momentum perturbations [NASA-CR-197804] p 2335 N95-26592

Indexing meso-beta surface wind site representative [AD-A288501] p 2341 N95-26650

An observational study on the onset of the summer monsoon over eastern Asia in 1979 [AD-A289637] p 2341 N95-26723

Parallel algorithms for semi-Lagrangian transport in global atmospheric circulation models [DE95-007385] p 2327 N95-27457

Emerging applications of probability (stochastic models in geosystems) [AD-A289117] p 2313 N95-28099

OB/OD treatment: The effective use of measured field data and air modeling to support an environmental assessment p 2170 N95-28296

Three-dimensional forecast models for emergency response management p 2172 N95-28303

The northern wintertime divergence extrema at 200 hPa and surface cyclones as simulated in the integration of the ECMWF general circulation model [DE95-007946] p 2332 N95-28550

ATMOSPHERIC COMPOSITION

Live from Antarctica, volume 4 [NASA-CR-197828] p 2335 N95-26596

Integrated assessment and the relation between land-use change and climate change [DE95-006533] p 2327 N95-27469

Coupled chemistry/climate issues [DE95-006443] p 2327 N95-27532

Measurement of heterogeneous chemical processes relevant to aerosol surfaces and trace gases active in the marine environment [DE95-008337] p 2328 N95-27743

Carbonaceous aerosols influencing atmospheric radiation: Black and organic carbon [DE95-006437] p 2330 N95-28118

Mars Sample Return mission utilizing in-situ propellant production [NASA-CR-188371] p 2145 N95-28261

Stratospheric ozone reactive chemicals generated by space launches worldwide [AD-A289852] p 2332 N95-28623

A black carbon emission data base for atmospheric chemistry and climate studies [DE95-006436] p 2332 N95-28662

ATMOSPHERIC EFFECTS

The attenuation of microwave radiation by fog and rain [AD-A288326] p 2249 N95-26562

Study of development and utilization of a multipurpose atmospheric corrosion sensor [NASA-CR-198595] p 2292 N95-27368

Orbital atomic oxygen effects on materials: An overview of MSFC experiments on the STS-46 EOIM-3 p 2419 N95-27637

Basic principles and recent observations of rotationally sampled wind p 2321 N95-27971

Weightless Environment Training Facility (WETF) materials coating evaluation, volume 1 [NASA-CR-188366-VOL-1] p 2239 N95-28385

Atmospheric dispersion in adaptive optics [AD-A289639] p 2428 N95-28617

ATMOSPHERIC ELECTRICITY

A brief history of laser guided lightning discharge models and experiments [AD-A289448] p 2295 N95-27022

ATMOSPHERIC ENTRY

Composite flexible insulation for thermal protection of space vehicles p 2166 N95-28293

ATMOSPHERIC GENERAL CIRCULATION MODELS

Technical report series on global modeling and data assimilation. Volume 6: A multiyear assimilation with the GEOS-1 system: Overview and results [NASA-TM-104606-VOL-6] p 2334 N95-26423

A parallel coupled oceanic-atmospheric general circulation model [DE95-005918] p 2335 N95-26622

Parallel algorithms for semi-Lagrangian transport in global atmospheric circulation models [DE95-007385] p 2327 N95-27457

Issues relevant to the development of coupled chemistry/climate models [DE95-006441] p 2330 N95-27954

Research project on CO2-induced climate change [DE95-008339] p 2330 N95-28084

Anomalous cloud absorption? A critique of the paper entitled Absorption of Solar Radiation by Clouds: Observations Versus Models [DE95-007703] p 2331 N95-28121

The northern wintertime divergence extrema at 200 hPa and surface cyclones as simulated in the integration of the ECMWF general circulation model [DE95-007946] p 2332 N95-28550

Cloud classification using whole-sky imager data [DE95-006501] p 2344 N95-28556

ATMOSPHERIC LASERS

A novel sensitive detector of atmospheric nitrocompounds based on laser photofragmentation/ionization spectrometry p 2174 N95-28314

ATMOSPHERIC MODELS

A study of magnetic activity effects on the thermospheric winds in the low ionosphere [AD-A288677] p 2334 N95-26488

An improved model of high-latitude f-region scintillation (WBMOD version 13) [AD-A288558] p 2334 N95-26520

A mathematical analysis of the Janus combat simulation weather effects models and sensitivity analysis of sky-to-ground brightness ratio on target detection [AD-A289629] p 2336 N95-26858

Prediction of rain attenuation and total atmospheric attenuation for low-availability satellite communications in Europe [PB95-184925] p 2252 N95-26908

Assessment of the AN/FPS-118 Ionospheric model and proposed improvements [AD-A289439] p 2337 N95-27146

Evaluation of Oxygen Interactions with Materials 3: Mission and induced environments p 2210 N95-27631

PRISM validation [AD-A288476] p 2337 N95-27703

Differenced Range Versus Integrated Doppler (DRVID) ionospheric analysis of metric tracking in the Tracking and Data Relay Satellite System (TDRSS) p 2147 N95-27766

A summary documentation of the AMIP models [DE95-008343] p 2338 N95-27931

Remote measurement of ground temperature and emissivity [DE95-008055] p 2314 N95-28053

Three-dimensional forecast models for emergency response management p 2172 N95-28303

ATMOSPHERIC MOISTURE

Continuously-tunable, narrow-linewidth, Q-switched Cr:LiSAF laser for lidar applications [DE95-006285] p 2296 N95-27672

Millimeter-wave imaging radiometer data processing and development of water vapor retrieval algorithms [NASA-CR-198593] p 2343 N95-27997

Measurements of daytime and upper tropospheric water vapor profiles by Raman lidar [DE95-007640] p 2344 N95-28538

ATMOSPHERIC OPTICS

Atmospheric dispersion in adaptive optics [AD-A289639] p 2428 N95-28617

ATMOSPHERIC PHYSICS

Natural aerosol extinction module: XSCALE 1992 user's guide [AD-A289029] p 2340 N95-26463

Space physics educational outreach [NASA-CR-198649] p 2399 N95-27852

Emerging applications of probability (stochastic models in geosystems) [AD-A289117] p 2313 N95-28099

Site scientific mission plan for the Southern Great Plains CART site, January-June 1995 [DE95-008393] p 2344 N95-28340

ATMOSPHERIC REFRACTION

VOCAR: An experiment in Variability of Coastal Atmospheric Refractivity [AD-A289202] p 2253 N95-27006

ATMOSPHERIC SOUNDING

Indexing meso-beta surface wind site representative [AD-A288501] p 2341 N95-26650

ATMOSPHERIC TEMPERATURE

Synthetic 3-D atmospheric temperature structure: A model for known geophysical power spectra using a hybrid autoregression and Fourier technique [AD-A289058] p 2340 N95-26479

Infrared field measurements of sea surface temperature: Analysis of wake signatures and comparison of skin layer models [NASA-CR-197849] p 2346 N95-26533

Southern Africa: A climatological study [AD-A289466] p 2342 N95-27148

Dynamics and control of SEDSAT tethered multi-probe for thermospheric research flight data analysis of SEDS-2 satellite: Tethered systems dynamics and flight data analysis [NASA-CR-198653] p 2165 N95-27836

ATMOSPHERIC TURBULENCE

The small-scale structure of dispersing clouds in the atmosphere [AD-A288256] p 2341 N95-26546

Compensated deconvolution from wavefront sensing [AD-A289490] p 2336 N95-26824

Frame selection performance limits for statistical image reconstruction of adaptive optics compensated images [AD-A289240] p 2424 N95-26965

Laser beam propagation in non-Kolmogorov atmospheric turbulence [AD-A289256] p 2295 N95-26974

Studies of radar backscatter as a function of wave properties and the winds in the turbulent marine atmosphere [NASA-CR-198608] p 2315 N95-28209

ATOMIC BEAMS

Experimental aspects of effects of high-energy particles on Alfven modes [DE95-003383] p 2432 N95-27873

ATOMIC CLUSTERS

Atomic and electronic structure of clusters from Car-Parrinello method [DE94-634463] p 2403 N95-26437

Photoemission and optical properties of C60 fullerites [DE95-006588] p 2425 N95-27539

Particle-like absorption spectra in small transition metal clusters [DE95-007082] p 2218 N95-27752

Experimental determination of cluster geometrical structure [DE95-007089] p 2409 N95-27753

ATOMIC COLLISIONS

Collisions of highly charged ions with electrons, atoms and surfaces [DE95-007393] p 2413 N95-28078

ATOMIC ENERGY LEVELS

Quantum effects induced by a gap in the spectrum of atom-bath coupling constants: Freezing of atomic decay and monochromatic collective radiation [DE95-609037] p 2416 N95-28251

ATOMIC EXCITATIONS

Electron spectroscopy studies of argon K-shell excitation and vacancy cascades [DE95-007096] p 2442 N95-27963

ATOMIC FORCE MICROSCOPY

Electrocrystallization of an ordered organic monolayer: Selective epitaxial growth of beta(ET)213 ongraphite [AD-A288942] p 2178 N95-26569

Non-destructive inter-level dielectric via in-line process monitoring by atomic force microscopy [DE95-008516] p 2267 N95-28146

Functionalized block copolymers as adhesion promoters [DE95-008158] p 2239 N95-28400

Development and application of low-temperature AFM [AD-A291704] p 2352 N95-28525

Surface structure of MX-chains studied by atomic force microscopy [DE95-007881] p 2447 N95-28541

ATOMIC INTERACTIONS

Temperature dependence of ion-beam-induced amorphization in (Beta)-SiC [DE95-007164] p 2438 N95-27087

ATOMIC PHYSICS

Toward coherent excitation: Development of a single-source pump for the rubidium hyperfine ground state doublet [AD-A289413] p 2295 N95-27132

A new method of evaluating the explicit magnetic-state-dependent energy in semi-empirical calculations of iron [AD-A289098] p 2399 N95-27398

Atomic physics with highly charged ions [DE95-007325] p 2407 N95-27439

Basic and applied research in the field of electronics and communications [AD-A291727] p 2270 N95-28512

ATOMIC SPECTRA

Analytical spectroscopy [DE95-607896] p 2203 N95-27200

A continuous emissions monitor for airborne metals p 2174 N95-28313

Atomic layer epitaxy of group 4 materials: Surface processes, thin films, devices and their characterization [AD-A289092] p 2446 N95-28327

ATOMIC STRUCTURE

Atomic and electronic structure of clusters from Car-Parrinello method [DE94-634463] p 2403 N95-26437

Resonant photoemission studies of thickness dependence of the unoccupied Gd 5d bands [DE95-004127] p 2436 N95-26440

Massively parallel self-consistent-field calculations [DE95-004128] p 2376 N95-26441

Structure of ordinary ice Ih. Part 2: Defects in ice. Volume 1: Point defects [AD-A288279] p 2200 N95-26452

Investigations of the hyperfine interactions in copper-oxide perovskites using Eu-151 and Fe-57 Moessbauer spectroscopy [PB95-185138] p 2437 N95-26513

Analytic formulae for the Hartree-Fock order parameter at arbitrary p/q filling factors for the 2DEG in a magnetic field [DE95-607805] p 2448 N95-26603

Theoretical studies of reaction surfaces [AD-A288458] p 2404 N95-26632

Materials Research Society Symposium Proceedings. Volume 339: Diamond, SiC and nitride wide bandgap semiconductors [AD-A288690] p 2437 N95-26818

Boron-induced reconstructions of Si(100) investigated by scanning tunneling microscopy [AD-A289222] p 2438 N95-26959

Atomic structure and bonding of boron-induced reconstructions on Si(001) [AD-A289187] p 2405 N95-27017

Integrating the QMR method with first principles material science application code [DE95-007380] p 2408 N95-27456

PXAMS: Projectile X ray AMS: X ray yields and applications [DE95-006438] p 2204 N95-27496

Particle-like absorption spectra in small transition metal clusters [DE95-007082] p 2218 N95-27752

Electronic structure of disordered Cu-Ag alloys [DE95-609156] p 2219 N95-27758

Analysis of the dimerized Sb/Si(001)-(2x1) surface by x-ray standing waves [DE95-007097] p 2208 N95-27965

Electronic structure of ordered and disordered transition metal aluminides [DE95-609034] p 2223 N95-28250

The unusual properties of beryllium surfaces [DE95-006471] p 2223 N95-28593

ATOMIC WEIGHTS

PXAMS: Projectile X ray AMS: X ray yields and applications [DE95-006438] p 2204 N95-27496

ATOMS

Hydrogen-like atom in laser field: Invariant atomic parameters in the ground state [DE95-609036] p 2411 N95-27930

Observation on radiation transfer experiments using k-shell absorption spectra [DE95-008068] p 2434 N95-28141

Sensor for measuring the atomic fraction in highly dissociated hydrogen [DE95-006531] p 2415 N95-28204

Quantum effects induced by a gap in the spectrum of atom-bath coupling constants: Freezing of atomic decay and monochromatic collective radiation [DE95-609037] p 2416 N95-28251

High energy density systems in cryogenic media: The production and reactions of atoms and radicals [AD-A289818] p 2417 N95-28572

ATTACK AIRCRAFT

AH-1F COBRA rewire program MANPRINT analysis [AD-A289190] p 2130 N95-27018

ATTENUATION COEFFICIENTS

The attenuation of microwave radiation by fog and rain [AD-A288326] p 2249 N95-26562

ATTENUATORS

An optoelectronic attenuator for the high-speed control of microwave integrated circuits [AD-A289579] p 2260 N95-26690

ATTITUDE (INCLINATION)

Neural models of spatial orientation in novel environments [AD-A288420] p 2380 N95-26530

Frame selection performance limits for statistical image reconstruction of adaptive optics compensated images [AD-A289240] p 2424 N95-26965

Polarization sensitivity of monopulse radar boresight error induced by large, ogive radomes [AD-A289254] p 2252 N95-26972

A PC-based magnetometer-only attitude and rate determination system for gyroless spacecraft p 2147 N95-27770

Attitude determination using an adaptive multiple model filtering Scheme p 2148 N95-27772

An MME-based attitude estimator using vector observations p 2148 N95-27775

Development of a Robust star identification technique for use in attitude determination of the ACE spacecraft p 2149 N95-27777

Optimal attitude maneuver execution for the Advanced Composition Explorer (ACE) mission p 2149 N95-27778

Use of nonlinear identification in robust attitude and attitude rate estimation for SAMPEX p 2149 N95-27781

The Global Positioning System (GPS) and attitude determination: Applications and activities in the Flight Dynamics Division p 2152 N95-27795

Geostationary Operational Environmental Satellite (GOES)-8 mission flight experience
p 2153 N95-27798
Contingency designs for attitude determination of TRMM p 2154 N95-27803
ORION: A Supersynchronous Transfer Orbit mission
p 2154 N95-27804
On the physics of ion ring generation for the stabilization of FRX discharges
[DE95-007105] p 2410 N95-27922
Whirl plus tilt
[DE95-007948] p 2399 N95-28108

ATTITUDE CONTROL
Analysis of modal behavior at frequency cross-over
[AD-A289304] p 2162 N95-26918
High-precision buffer circuit for suppression of regenerative oscillation
[NASA-TM-4658] p 2291 N95-27259
Evaluation and modeling of autonomous attitude thrust control for the Geostation Operational Environmental Satellite (GOES)-8 orbit determination
p 2146 N95-27765
Optimal attitude maneuver execution for the Advanced Composition Explorer (ACE) mission
p 2149 N95-27778
Geostationary Operational Environmental Satellite (GOES)-8 mission flight experience
p 2153 N95-27798
Estimation of attitude sensor timetag biases
p 2153 N95-27799
Autonomous control system reconfiguration for spacecraft with non-redundant actuators
p 2153 N95-27802

ATTITUDE GYROS
Estimation of attitude sensor timetag biases
p 2153 N95-27799

ATTITUDE INDICATORS
High-precision buffer circuit for suppression of regenerative oscillation
[NASA-TM-4658] p 2291 N95-27259
Development of a Robust star identification technique for use in attitude determination of the ACE spacecraft
p 2149 N95-27777

ATTITUDE STABILITY
An automated method of tuning an attitude estimator
p 2148 N95-27774

AUDIO EQUIPMENT
Research and development report. Digital audio broadcasting: Comparison of coverage at Band 2 and Band 3
[BBC-RD-1994/16] p 2248 N95-26493
Research and development report. Eureka 147: Tests of the error performance of the DAB system
[BBC-RD-1994/18] p 2249 N95-26696

AUDIO SIGNALS
Research and development report. Digital audio broadcasting: Comparison of coverage at Band 2 and Band 3
[BBC-RD-1994/16] p 2248 N95-26493
The automatic extraction of selected speech spectral characteristics
[IFTR-2/1994] p 2250 N95-26835
An experimental version of the MZT (speech-from-text) system with external F(sub 0) control
[IFTR-14/1994] p 2250 N95-26836

AUGER SPECTROSCOPY
NO decomposition in non-reducing atmospheres
[DE95-007895] p 2205 N95-27690
Electron spectroscopy studies of argon K-shell excitation and vacancy cascades
[DE95-007096] p 2442 N95-27963

AUGMENTATION
Natural aerosol extinction module: XSCALE 1992 user's guide
[AD-A289029] p 2340 N95-26463
Performance enhancing ration components program: Supplemental carbohydrate test
[AD-A288560] p 2358 N95-26558

AURORAS
Measurements of HF auroral clutter using the Verona Ava Linear Array Radar (VALAR)
[AD-A289442] p 2337 N95-27147
Space physics educational outreach
[NASA-CR-198649] p 2399 N95-27852

AUSTENITE
Fatigue fracture analysis in medium carbon structural steel and austenitic stainless steel by X-ray fractography
[DE95-601504] p 2213 N95-26675
Radiation-induced segregation: A microchemical gauge to quantify fundamental defect parameters
[DE95-005720] p 2216 N95-27492

AUSTENITIC STAINLESS STEELS
Recycle of radiologically contaminated austenitic stainless steels
[DE95-006484] p 2215 N95-27328
Radiation-induced grain boundary segregation in austenitic stainless steels
[DE95-005721] p 2216 N95-27493
Toward a mechanistic understanding of radiation effects in materials
[DE95-006530] p 2221 N95-28120

AUSTRALIA
Comparison of fixed wing aircraft algorithms for JANUS
[AD-A288503] p 2129 N95-26652
A review of Australian and New Zealand investigations on aeronautical fatigue during the period Apr. 1993 - Mar. 1995
[AR-009-202] p 2136 N95-27918
Geothermal development in Australia
[DE95-007837] p 2325 N95-28058

AUTOCLAVES
ACT/ICAPS: Thermoplastic composite activities
p 2185 N95-28274

AUTOCORRELATION
Prediction of fatigue crack growth under constant amplitude and random loading using specimens with multiple cracks
[AD-A291614] p 2136 N95-28409

AUTOMATA THEORY
Probabilistic growth model
[PB95-185054] p 2395 N95-26913
An automated method of tuning an attitude estimator
p 2148 N95-27774

AUTOMATIC CONTROL
Automated Procurement System (APS) revised project management plan (DS-03)
[NASA-CR-198605] p 2450 N95-27169
NIST Automated Manufacturing Research Facility (AMRF): March 1987
[NONP-NASA-VT-95-49097] p 2246 N95-27203
NIST: Information management in the AMRF
[NONP-NASA-VT-95-49120] p 2454 N95-27208
Evaluation and modeling of autonomous attitude thrust control for the Geostation Operational Environmental Satellite (GOES)-8 orbit determination
p 2146 N95-27765
Autonomous control system reconfiguration for spacecraft with non-redundant actuators
p 2153 N95-27802
Operator modeling in commerical aviation: Cognitive models, intelligent displays, and pilot's assistants
[NASA-CR-198609] p 2138 N95-28203
Automated remedial assessment methodology software system
[DE95-007287] p 2373 N95-28243
Dimensionally self regulating materials
[AD-A291671] p 2257 N95-28456

AUTOMATIC FLIGHT CONTROL
Development of a TECS control-law for the lateral directional axis of the McDonnell Douglas F-15 Eagle
[AD-A289771] p 2142 N95-28598

AUTOMATIC PILOTS
Advanced formation flight control
[AD-A289271] p 2142 N95-26981

AUTOMATIC TEST EQUIPMENT
Life cycle costs of alternatives for F-16 printed circuit board diagnosis equipment
[AD-A288744] p 2138 N95-28586

AUTOMATION
Electronics manufacturing and assembly in Japan
p 2263 N95-27231
Limits to ground control in autonomous spacecraft
p 2383 N95-27381
Pilot opinions on high level flight deck automation issues: Toward the development of a design philosophy
[NASA-CR-4669] p 2357 N95-28253

AUTOMOBILES
Spray-formed tooling
[DE95-005031] p 2246 N95-27404
Reducing cold-start emissions by catalytic converter thermal management
[DE95-000256] p 2327 N95-27540
Fracture testing and analysis of adhesively bonded joints for automotive applications
[DE95-007024] p 2184 N95-28207
Fatigue properties of an A356 (AlSi7Mg) aluminum alloy for automotive applications: Fatigue life prediction
[PB95-196424] p 2224 N95-28660
Manikin integrated data acquisition system (MIDAS) initial modifications
[AD-A291662] p 2361 N95-28667

AUTOMORPHISMS
Symmetries of the KAC-Peterson modular matrices of affine algebras
[PB95-190138] p 2392 N95-28010

AUTONOMOUS NAVIGATION
Neural models of spatial orientation in novel environments
[AD-A288420] p 2380 N95-26530
A systems engineering approach to electro-mechanical reconfiguration for mobility autonomy
[AD-A289479] p 2301 N95-26926
Using virtual active vision tools to improve autonomous driving tasks
[AD-A289175] p 2356 N95-27013

AUTONOMY
Limits to ground control in autonomous spacecraft
p 2383 N95-27381
A fuzzy logic intelligent diagnostic system for spacecraft integrated vehicle health management
p 2385 N95-27392
Lessons learned from the introduction of autonomous monitoring to the EUVE science operations center
p 2385 N95-27393
A linguistic geometry for 3D strategic planning
p 2386 N95-27397
Preliminary flight software specification for the petite amateur Navy satellite (PANSAT)
[AD-A280068] p 2165 N95-28150

AUTOREGRESSIVE PROCESSES
Evolving cascade-correlation networks for time-series forecasting
[AD-A289197] p 2390 N95-27020
Linear and nonlinear trending and prediction for AVHRR time series data p 2385 N95-27391

AUXILIARY POWER SOURCES
Probabilistic risk assessment of the Space Shuttle. Phase 3: A study of the potential of losing the vehicle during nominal operation. Volume 4: System models and data analysis
[NASA-CR-197811] p 2160 N95-26401

AVAILABILITY
Report to the Chairman and Ranking Minority Member, Committee on Science, House of Representatives. Weather forecasting: Radar availability requirement not being met
[GAO/AIMD-95-132] p 2342 N95-27912

AVALANCHE DIODES
An acoustic charge transport imager for high definition television applications
[NASA-CR-197841] p 2249 N95-26708

AVIONICS
Micro-time stress measurement device development
[AD-A289511] p 2361 N95-26845
An analysis of the KC-135 three-person cockpit
[AD-A289540] p 2130 N95-26873

AWARDS
Quest for excellence 5
[NONP-NASA-VT-95-49099] p 2451 N95-27205
Malcolm Baldrige National Quality Award winners 1989
[NONP-NASA-VT-95-49119] p 2451 N95-27207

AXES OF ROTATION
Horizontal axis wind turbine post stall airfoil characteristics synthesization p 2124 N95-27974
A NASTRAN-based computer program for structural dynamic analysis of Horizontal Axis Wind Turbines
p 2312 N95-27980
Measurement and prediction of broadband noise from large horizontal axis wind turbine generators
p 2324 N95-27990
Local texture and grain boundary misorientations in high H(C) oxide superconductors
[DE95-007004] p 2447 N95-28606

AXIAL FLOW
The effects of transverse vibration on the performance of an axial groove wick heat pipe
[AD-A289349] p 2278 N95-27065
A general theory of two- and three-dimensional rotational flow in subsonic and transonic turbomachines
[NASA-CR-4496] p 2123 N95-28003

AXIAL LOADS
Reactor pressure vessel structural integrity research
[DE95-007034] p 2223 N95-28208

AXIAL STRESS
Stress transfer from axially loaded fiber to matrix in a microcomposite
[DE95-007366] p 2183 N95-28043
The role of biaxial stresses in discriminating between meaningful and illusory composite failure theories
p 2187 N95-28287

AXISYMMETRIC FLOW
An outflow boundary condition for aeroacoustic computations
[NASA-TM-106930] p 2279 N95-27175
Computer program BL2D for solving two-dimensional and axisymmetric boundary layers
[NASA-CR-4668] p 2279 N95-27257

AZIMUTH
Electromagnetic hysteretic response calculation for superconductors in demagnetizing geometries
[DE95-005028] p 2264 N95-27403

B

B STARS
International Ultraviolet Explorer Atlas of B-type spectra from 1200 to 1900 A
[NASA-RP-1363] p 2463 N95-28328

BACKGROUND RADIATION
Low energy neutral atom imaging: Remote observations of the magnetosphere
[DE95-006342] p 2337 N95-27848

BACKSCATTERING
Numerical analysis of wave scattering
[AD-A289478] p 2401 N95-26925
Assessment of the AN/FPS-118 Ionospheric model and proposed improvements
[AD-A289439] p 2337 N95-27146
Measurements of HF auroral clutter using the Verona Ava Linear Array Radar (VALAR)
[AD-A289442] p 2337 N95-27147
Material analysis using combined Elastic Recoil Detection and Rutherford/Enhanced Rutherford Backscattering Spectrometry
[DE95-005415] p 2205 N95-27681
Theoretical and experimental models of the diffuse radar backscatter from Mars
[NASA-CR-198650] p 2463 N95-27700
Solar UV flux measurements from the SBUV2 monitor on the NOAA9 satellite. Part 1: Mg II h and k line core-to-wing ratios for 1986-1988
[PB95-181962] p 2464 N95-28007
Studies of radar backscatter as a function of wave properties and the winds in the turbulent marine atmosphere
[NASA-CR-198608] p 2315 N95-28209
Local texture and grain boundary misorientations in high H(C) oxide superconductors
[DE95-007004] p 2447 N95-28606
Ultrasonic studies of liquid/solid seimoacoustic wave phenomena
[AD-A289644] p 2402 N95-28622

BACTERIA
Flow cytometry as a means of detecting, enumerating and characterizing bacteria for monitoring of the environment
[AD-A288997] p 2326 N95-26610
To develop an aerosoling immunomagnetic device for rapid medical diagnosis from clinical samples
[AD-A288504] p 2354 N95-27059
Microbial treatment for shipboard collection, hold ing, and transfer system tanks p 2179 N95-27119
Application of bacterial bioemusifiers to in situ maintenance of oil/water separators
p 2179 N95-27120
Investigation on energy conversion technology using biochemical reaction elements, 2
[DE95-759250] p 2321 N95-27940

BACTERIOLOGY
Environmentally Benign Cleaning and Degreasing Technology: JANNAF Safety and Protection Subcommittee and Propellant Development and Characterization Subcommittee Joint Workshop
[CPIA-PUBL-611] p 2227 N95-27101

BAINITIC STEEL
Characterization of Ultra-Low Carbon Baintic steels for use as weld wire consumables
[AD-A288292] p 2212 N95-26411

BALANCING
Balanced on air aircraft
[AD-D017251] p 2129 N95-26537
Parallel algorithms for semi-Lagrangian transport in global atmospheric circulation models
[DE95-007385] p 2327 N95-27457

BALL BEARINGS
Comparison of life theories for rolling-element bearings
[NASA-TM-106585] p 2301 N95-26774
Effect of hoop stress on ball bearing life prediction
[NASA-TM-106874] p 2301 N95-27178
Effects of bearing cleaning and lube environment on bearing performance p 2158 N95-27285
Ball bearing vibrations amplitude modeling and test comparisons p 2158 N95-27286
Developmental problems and their solution for the Space Shuttle main engine alternate liquid oxygen high-pressure turbopump: Anomaly or failure investigation the key
[NASA-TP-3553] p 2169 N95-28263

BALLISTIC MISSILES
Reusable launch vehicle development research
[NASA-CR-196614] p 2154 N95-27245

BALLISTIC TRAJECTORIES
Performance analysis of bullet trajectory estimation: Approach, simulation, and experiments
[DE95-007949] p 2399 N95-28109

BALLISTICS
Scale model experiments with ceramic laminate targets
[AD-A288322] p 2225 N95-26561
Recent high-speed ballistics experiments at ORNL
[DE95-006534] p 2422 N95-28205

BALTIC SEA
On the persistence of the oceanic background of apparent sea level changes in the Baltic Sea
[REPT-94:5] p 2348 N95-27996

BANACH SPACE
On permanent capillar-heavy waves in circular shaped channels
[DE95-608779] p 2280 N95-27339

BAND STRUCTURE OF SOLIDS
Numerical study of the singlet-triplet model for cuprate superconductors
[DE95-609438] p 2440 N95-27712
First-principles calculations for AIN, GaN, and InN: Bulk and alloy properties
[DE95-006822] p 2219 N95-27958

BANDWIDTH
Electrical performance characterisation of single-shot switches in high speed, high voltage and high current applications
[DSTO-RR-0010] p 2259 N95-26425
A foveated system to reduce transmission bandwidth of video images from remote camera systems
[AD-A288516] p 2254 N95-27060
Ring-plane traveling-wave tube slow-wave circuit design simulations at V-Band frequencies
[NASA-TM-106949] p 2371 N95-27370

BARIUM COMPOUNDS
Growth and evaluation of nonlinear optical crystals for laser applications: Lithium borate, barium borate and silver gallium selenide
[AD-A289147] p 2277 N95-27000
Ceramic fiber-reinforced monoclinic celsian phase glass-ceramic matrix composite material
[NASA-CASE-LEW-15714-1] p 2183 N95-27717
The oxidation state and magnetic behaviour of Tb in high-(Tc) related materials
[DE95-007129] p 2219 N95-27966

BARIUM OXIDES
Observations of CEF-split intermultiplet transitions in optically opaque EuBa2Cu3O7 using inelastic neutron scattering
[DE95-007135] p 2408 N95-27453
Review of activities in USA on HTS materials
[DE95-006404] p 2234 N95-27468

BARRIER LAYERS
The effects of temperature on Schottky diode barrier height and evidence of multiple barrier
[DE95-609147] p 2264 N95-27405

BARYONS
A simple relativistic model of pp-bar yields K(+)K(-)
[DE95-608852] p 2406 N95-27318
Implications of horizontal symmetries on baryon number violation in supersymmetric models
[DE95-610202] p 2407 N95-27406
Measurement of inclusive Lambda production in electron-positron interactions at the upsilon energies
[DE95-610302] p 2407 N95-27407
Excited Charm States
[DE95-005749] p 2409 N95-27747
Aspects of strange matter
[DE95-008316] p 2414 N95-28170

BASE FLOW
Effect of turbulence models on criticality conditions in swirling flows p 2282 N95-27356

BASE PRESSURE
Unsteady base pressure measurements in the near wake of a cylinder with imposed three-dimensional disturbances
[AD-A289498] p 2276 N95-26827

BATHYMETERS
Ultrasonic studies of liquid/solid seimoacoustic wave phenomena
[AD-A289644] p 2402 N95-28622

BATTERY CHARGERS
The 1994 27th Annual NASA Aerospace Battery Workshop
[NASA-CP-3292] p 2317 N95-26785
Calorimetric evaluation of commercial Ni-MH cells and charges p 2272 N95-26790
Alternate charging profiles for the onboard nickel cadmium batteries of the Explorer Platform/Extreme Ultraviolet Explorer p 2272 N95-26796

BAYARD-ALPERT IONIZATION GAGES
Neutral gas compression in the Alcator C-Mod divertor. Experimental observations
[DE95-007762] p 2432 N95-27688

BAYES THEOREM
Statistical theory and reliability
[AD-A288519] p 2394 N95-26733
Higher-order probabilistic perceptrons as Bayesian inference engines
[DE95-608730] p 2381 N95-27044
An analysis of Bayesian networks as classifiers
[AD-A289316] p 2382 N95-27293

BEADS
Contact micromechanics in granular media with clay
[DE95-006566] p 2340 N95-28583

BEAM CURRENTS
OBIC analysis of stressed, thermally-isolated polysilicon resistors
[DE95-008511] p 2268 N95-28201
Low power limits in ultrashort pulse measurement using Frequency-Resolved Optical Gating
[DE95-007150] p 2299 N95-28219
Transport simulation of negative magnetic shear discharges
[DE95-003941] p 2416 N95-28329

BEAM INJECTION
Coupling in the Tevatron
[DE95-005129] p 2421 N95-27531
Experimental aspects of effects of high-energy particles on Alfven modes
[DE95-003383] p 2432 N95-27873
On the physics of ion ring generation for the stabilization of FRX discharges
[DE95-007105] p 2410 N95-27922

BEAM INTERACTIONS
Orbit analysis
[DE95-007216] p 2419 N95-27091
Some notes on long-range beam-beam effects for the 2 TeV collider
[DE95-006771] p 2421 N95-28017
Nonlinear beam dynamics experimental program at SPEAR
[DE95-007823] p 2422 N95-28122
Beam-beam interaction working group summary
[DE95-007824] p 2422 N95-28123
Laser beam aerosol interactions
[AD-A291723] p 2300 N95-28509
Beam instability studies for the SSC
[DE95-008024] p 2423 N95-28551

BEAM SPLITTERS
Display system employing acousto-optic tunable filter
[NASA-CASE-NPO-18736-1-CU] p 2426 N95-27843
Phase retrieval and time-frequency methods in the measurement of ultrashort laser pulses
[DE95-006499] p 2300 N95-28549

BEAMFORMING
Modified Gaussian elimination for adaptive beamforming using RNS arithmetic
[AD-A288809] p 2248 N95-26356
Adaptive beamforming in frequency-dispersive multipath environments
[AD-A289206] p 2254 N95-27009

BEAMS
User's guide: Computer program for analysis of beam-column structures with nonlinear supports (CBEAMC)
[AD-A289031] p 2307 N95-26464

BEAMS (RADIATION)
CAS CERN Accelerator School 5th General Accelerator Physics Course
[DE95-608324] p 2419 N95-27158
Some notes on long-range beam-beam effects for the 2 TeV collider
[DE95-006771] p 2421 N95-28017
Optical design and performance of the inelastic scattering beamline at the National Synchrotron Light Source
[DE95-007679] p 2422 N95-28195
Ultrashort Pulse retrieval using FROG trace irradiance moments and the adaptive neural networks backpropagation algorithm
[DE95-007153] p 2299 N95-28220

BEAMS (SUPPORTS)
Preliminary design study of the beam collapser and certain optomechanical aspects of the siderostat
[AD-A288423] p 2423 N95-26549
Experimental studies to test simple flexural neutralizers fitted to beams
[ISVR-TR-239] p 2309 N95-27846
Vibrational behavior of adaptive aircraft wing structures modelled as composite thin-walled beams
p 2191 N95-28435

BEARINGS
Bearing defect signature analysis using advanced nonlinear signal analysis in a controlled environment
[NASA-TM-108491] p 2304 N95-28364

BEHAVIOR
Research activities on somatosensory (SI) cortical neurons
[AD-A288794] p 2348 N95-26360

BELIEF NETWORKS
A path-oriented knowledge representation system: Defusing the combinatorial system p 2386 N95-27395

BELL AIRCRAFT
Rotorcraft crashworthy airframe and fuel system technology development program
[AD-A289986] p 2126 N95-28630
BENARD CELLS
The Benard problem: A comparison of finite difference and spectral collocation eigen value solutions
p 2283 N95-27364
BEND TESTS
Interfacial mobility and its effect on flexural strength and fracture toughness in glass-fiber fabric reinforced epoxy laminates
[AD-A288344] p 2180 N95-26572
On aircraft repair verification of a fighter A/C integrally stiffened fuselage skin p 2133 N95-27515
BENDING
Interfacial mobility and its effect on flexural strength and fracture toughness in glass-fiber fabric reinforced epoxy laminates
[AD-A288344] p 2180 N95-26572
Study of damage evolutions in composite plates subjected to bending loads using micro-macro analysis
[AD-A288523] p 2308 N95-26839
Analysis of composite structures with delaminations under combined bending and compression
p 2190 N95-28429
BENDING MOMENTS
Technology integration box beam failure study
p 2194 N95-28468
BENZENE
Poly(N-arylenbenzimidazoles) via aromatic nucleophilic displacement
[NASA-CASE-LAR-14939-1] p 2179 N95-28360
BERYLLIUM
Characterization of defects in deuterium-implanted beryllium
[DE95-005688] p 2217 N95-27553
FY 1994 ambient air monitoring report for McMurdo Station, Antarctica
[DE95-008565] p 2331 N95-28149
The elevated temperature tensile properties of S-200E commercially pure beryllium
[DE95-009331] p 2223 N95-28534
The unusual properties of beryllium surfaces
[DE95-006471] p 2223 N95-28593
BERYLLIUM ALLOYS
Ductile - ductile beryllium aluminum metal matrix composite manufactured by extrusion
[AD-A289519] p 2181 N95-26848
BETA PARTICLES
Determination of the first hydrolysis constant of Europium (3) in 3 M of ionic strength
[DE95-607912] p 2405 N95-27211
Beta-dynamics in simple liquid metal
[DE95-609154] p 2220 N95-28039
BETATRONS
Observation of nonlinear resonances in the advanced light source
[DE95-006561] p 2425 N95-27675
Skew chromaticity
[DE95-007677] p 2422 N95-28115
Measurement of wakefield suppression in a detuned X-band accelerator structure
[DE95-008592] p 2422 N95-28159
BETHE-SALPETER EQUATION
Two-body bound states and the Bethe-Salpeter equation
[DE95-008302] p 2392 N95-27742
BIAS
Extended linear ion trap frequency standard apparatus
[NASA-CASE-NPO-19081-1-CU] p 2404 N95-26861
Estimation of attitude sensor timetag biases
p 2153 N95-27799
Extended linear ion trap frequency standard apparatus
[NASA-CASE-NPO-19081-1-CU] p 2416 N95-28348
Full complex modulation using two one-parameter spatial light modulators
[NASA-CASE-MSC-22255-1] p 2427 N95-28384
BIBLIOGRAPHIES
Bibliography of patents and licenses 1951-1990. 1991 edition
[AD-A289603] p 2452 N95-26721
Bibliography of NASA-related publications on wind turbine technology 1973-1995
[NASA-CR-195462] p 2316 N95-26734
Bibliography of NRL publications - 1990
[AD-A289483] p 2466 N95-26823
Selected bibliography on heavy water, tritiated water and hydrogen isotopes (1981-1992)
[DE95-608331] p 2405 N95-27159
Aerospace medicine and biology: A continuing bibliography with indexes (supplement 402)
[NASA-SP-7011(402)] p 2354 N95-27502
Aeronautical engineering: A continuing bibliography with indexes (supplement 318)
[NASA-SP-7037(318)] p 2120 N95-27543
The Long Duration Exposure Facility (LDEF) annotated bibliography p 2457 N95-27659
Methods development for measuring and classifying flammability/combustibility of refrigerants. Task 1: Annotated bibliography
[DE95-007232] p 2238 N95-28133
Microgravity science and applications. Program tasks and bibliography for FY 1994
[NASA-TM-4677] p 2245 N95-28460
Space Science Division cumulative bibliography: 1989-1994
[NASA-TM-110355] p 2457 N95-28677
BICRYSTALS
Atomistic calculations of hydrogen interactions with Ni3Al grain boundaries and Ni/Ni/Ni3Al interfaces
[DE95-006497] p 2408 N95-27534
BIDIRECTIONAL REFLECTANCE
Cryogenic BRDF measurements at 10.6 micrometers and 0.63 micrometers on contaminated mirrors
[AD-A291611] p 2427 N95-28408
BIFURCATION (BIOLOGY)
Cognitive networks for ATR: The roles of bifurcation and chaos
[AD-A289010] p 2387 N95-28336
BINARY ALLOYS
Modeling the growth of electronic materials
[AD-A289137] p 2438 N95-26997
Study of the phase transformations and microstructures of uranium rich alloys of the binary uranium-gallium system
[DE95-609624] p 2217 N95-27713
A first principles approach to phase stability and order-disorder transformation: Application to Li-Al alloys
[DE95-609152] p 2218 N95-27756
Electronic structure of disordered Cu-Ag alloys
[DE95-609156] p 2219 N95-27758
The effects of processing variables on reaction synthesis of Fe-Al alloys
[DE95-007405] p 2221 N95-28082
BINARY CODES
Method of phased magnitude correlation using binary sequences
[AD-D017257] p 2248 N95-26465
BINARY DATA
Method of phased magnitude correlation using binary sequences
[AD-D017257] p 2248 N95-26465
First-principles study of intermetallic phase stability in the ternary Ti-Al-Nb alloy system
[DE95-005259] p 2213 N95-27082
Laser ionization of molecular clusters
[DE95-007011] p 2296 N95-27550
Binary segmentation of SAR images by the ICM algorithm
[INPE-5464-PRE/1772] p 2258 N95-28559
Vocoded KING data base
[AD-A289827] p 2258 N95-28576
BINARY STARS
Recurrent novae p 2460 N95-27075
Was Einstein 100% right?
[PB95-190179] p 2449 N95-28175
BINARY SYSTEMS (MATERIALS)
Bimaterial interlaces and their role in the mechanical performance of the in-situ composites
[AD-A288973] p 2182 N95-27188
BINAURAL HEARING
Leak detection utilizing analog binaural (VLSI) techniques
[NASA-CASE-NPO-18399-1-CU] p 2271 N95-28599
BINDERS (MATERIALS)
Thermal control materials on EOIM-3
p 2242 N95-27639
BINOCULAR VISION
Image perception wavelet simulation and enhancement for the visually impaired
[AD-A289303] p 2353 N95-26917
BIOASSAY
Modeling and statistical analysis of bioassay data: Medaka cell proliferation under DEN and TCE
[AD-A289998] p 2352 N95-28519
BIOCHEMISTRY
Biochemically vulnerable sites for antifungal intercession in the control of fungal growth
[AD-A288345] p 2348 N95-26573
Predicting protein structure using parallel genetic algorithms
[AD-A289305] p 2369 N95-26919
Investigation on energy conversion technology using biochemical reaction elements, 2
[DE95-759250] p 2321 N95-27940
Survey on bio-chemical complex harmonized with global environment
[DE95-759252] p 2331 N95-28535
BIOCONVERSION
Review and analysis of the 1980-1989 biomass thermochemical conversion program
[DE95-000287] p 2325 N95-28394
BIODEGRADABILITY
JTEC monograph on biodegradable polymers and plastics in Japan: Research, development, and applications
[NASA-CR-198562] p 2235 N95-27694
BIODEGRADATION
Environmentally Benign Cleaning and Degreasing Technology: JANNAF Safety and Protection Subcommittee and Propellant Development and Characterization Subcommittee Joint Workshop
[CPIA-PUBL-611] p 2227 N95-27101
The biodegradation of fuels in soils and sediments: Differences as a function of mineralogy
p 2230 N95-27116
Bioremediation of chlorinated organics: PCBs, TCE, HCFCs p 2179 N95-27117
Combined use of ground water circulation (UVB) technology and in situ bioreactors for enhanced bioremediation of subsurface contamination
p 2230 N95-27118
Microbial treatment for shipboard collection, hold ing, and transfer system tanks p 2179 N95-27119
Application of bacterial bioemusifiers to in situ maintenance of oil/water separators
p 2179 N95-27120
Biodegradation of nitrate esters p 2171 N95-28299
Survey on bio-chemical complex harmonized with global environment
[DE95-759252] p 2331 N95-28535
BIOELECTRIC POTENTIAL
The electrical behaviour of an excitable cell at different conditions
[DE95-607911] p 2351 N95-27254
BIOELECTRICITY
The electrical behaviour of an excitable cell at different conditions
[DE95-607911] p 2351 N95-27254
BIOLOGICAL EFFECTS
Radiation in everyday life
[DE95-604111] p 2349 N95-26597
Aerospace medicine and biology: A continuing bibliography with indexes (supplement 402)
[NASA-SP-7011(402)] p 2354 N95-27502
Toxicity assessment of liquid propellant XM46
p 2175 N95-28319
BIOLOGICAL MODELS (MATHEMATICS)
Modeling and statistical analysis of bioassay data: Medaka cell proliferation under DEN and TCE
[AD-A289998] p 2352 N95-28519
BIOLOGY
Live from Antarctica: Then and now
[NASA-CR-197829] p 2335 N95-26594
BIOMASS
Hydrogen program
[DE94-011827] p 2242 N95-27415
Biomass Pyrolysis Oil Properties and Combustion Meeting
[DE95-004017] p 2204 N95-27438
Review and analysis of the 1980-1989 biomass thermochemical conversion program
[DE95-000287] p 2325 N95-28394
Survey on bio-chemical complex harmonized with global environment
[DE95-759252] p 2331 N95-28535
BIOMASS ENERGY PRODUCTION
Review and analysis of the 1980-1989 biomass thermochemical conversion program
[DE95-000287] p 2325 N95-28394
BIOMETRICS
Long-range eye tracking: A feasibility study
[DE95-008587] p 2357 N95-28176
BIONICS
A model of the neural basis of the rat's sense of direction
[AD-A289678] p 2350 N95-26761
BIOPOLYMER DENATURATION
DNA denaturation through a model of the partition points on a one-dimensional lattice
[DE95-607909] p 2439 N95-27201
A correlated Walks' theory for DNA denaturation
[DE95-607910] p 2444 N95-28112
BIOPOLYMERS
Materials design and processing by biomimicking. Section 1: Research progress
[AD-A288229] p 2226 N95-26623
Research activities of the Solid State Sciences Committee in the development of a Federal initiative on advanced materials and processing
[DE95-009328] p 2445 N95-28179

BIOREACTORS
Combined use of ground water circulation (UVB) technology and in situ bioreactors for enhanced bioremediation of subsurface contamination p 2230 N95-27118
BIOSPHERE
Nonlinear dynamics of global atmospheric and earth system processes [NASA-CR-197926] p 2326 N95-26429
BIOTECHNOLOGY
Microgravity Sciences Biotechnology Facility assessment [NASA-CR-196602] p 2351 N95-27329
Investigation on technology for increasing the biological CO2 sink and technology for CO2 fixation and reutilization [DE95-759251] p 2329 N95-27941
Physical interpretation and development of ultrasonic nondestructive evaluation techniques applied to the quantitative characterization of textile composite materials [NASA-CR-198591] p 2306 N95-28034
JTEC/WTEC annual report and program summary: 1993/94 [NASA-CR-198563] p 2475 N95-28038
Survey on bio-chemical complex harmonized with global environment [DE95-759252] p 2331 N95-28535
BIPLANES
Full span flaperons for a biplane p 2119 N95-26954
Incorporating biplane wing theory into a large, subsonic, all-cargo transport p 2120 N95-26956
BIPOLAR TRANSISTORS
Atomic layer epitaxy of group 4 materials: Surface processes, thin films, devices and their characterization [AD-A289092] p 2446 N95-28327
BIRD-AIRCRAFT COLLISIONS
Development of repair processes and sources for C/KC-135 aircraft windows/windshields [AD-A288348] p 2117 N95-26629
A review of falconry as a bird control technique with recommendations for use at the Shuttle Landing Facility, John F. Kennedy Space Center, Florida, USA [NASA-TM-110142] p 2126 N95-27859
BIRDS
A review of falconry as a bird control technique with recommendations for use at the Shuttle Landing Facility, John F. Kennedy Space Center, Florida, USA [NASA-TM-110142] p 2126 N95-27859
BISMALEIMIDE
Application of fiber-reinforced bismaleimide materials to aircraft nacelle structures p 2137 N95-28278
Post impact compressive strength in composites p 2198 N95-28485
BISTABLE CIRCUITS
Modulation effect of a Bragg acousto-optic bistable system [AD-A289622] p 2401 N95-26857
BIVARIATE ANALYSIS
Statistical theory and reliability [AD-A288519] p 2394 N95-26733
BL LACERTAE OBJECTS
CO, HCO(+) and HCN absorption in the gravitational lens candidate B0218+357 at z=0.685 [PB95-185146] p 2461 N95-26522
BLACK HOLES (ASTRONOMY)
On higher derivative gravity in two dimensions [DE95-608789] p 2462 N95-27343
BLADE SLAP NOISE
Flow structure generated by perpendicular blade vortex interaction and implications for helicopter noise predictions [NASA-CR-198590] p 2123 N95-28193
Evaluation of a doubly-swept blade tip for rotorcraft noise reduction [NASA-CR-189677] p 2402 N95-28264
BLADE TIPS
Evaluation of a doubly-swept blade tip for rotorcraft noise reduction [NASA-CR-189677] p 2402 N95-28264
BLADE-VORTEX INTERACTION
Comparative performance tests on the Mod-2, 2.5-mW wind turbine with and without vortex generators p 2124 N95-27978
Measurement and prediction of broadband noise from large horizontal axis wind turbine generators p 2324 N95-27990
Flow structure generated by perpendicular blade vortex interaction and implications for helicopter noise predictions [NASA-CR-198590] p 2123 N95-28193
Evaluation of a doubly-swept blade tip for rotorcraft noise reduction [NASA-CR-189677] p 2402 N95-28264
BLANKETS (FISSION REACTORS)
Toward a mechanistic understanding of radiation effects in materials [DE95-006530] p 2221 N95-28120
BLAST LOADS
Pressure vessel burst test study p 2175 N95-28317
BLOCK COPOLYMERS
Small angle neutron scattering study of the micelle structure of amphiphilic block copolymers [DE95-006625] p 2234 N95-27486
Functionalized block copolymers as adhesion promoters [DE95-008158] p 2239 N95-28400
BLOCKING
Precision landing system mathematical modeling study report for Andrews Air Force Base, runway 19L, Camp Springs, MD [AD-A289015] p 2127 N95-27903
Bilateral force feedback for hydraulically actuated systems [AD-A291632] p 2387 N95-28545
BLOCKS
Reference manual: Naive physics simulator [PB95-184917] p 2369 N95-26907
BLOOD
Mechanisms of hypertension after cross-linked hemoglobin blood-substitute transfusion [AD-A289558] p 2352 N95-26680
BLOWING
Computational analysis of forebody tangential slot blowing on the high alpha research vehicle [NASA-CR-197754] p 2129 N95-26591
Investigation of boundary layer and performance effects of transpiration cooling through a porous plate in a rocket nozzle [AD-A289393] p 2167 N95-26880
Performance characterization of a highly-offset diffuser with and without blowing vortex generator jets [AD-A289334] p 2122 N95-26901
BLUFF BODIES
Effects of three-dimensional imposed 3-D disturbances on bluff-body near wake flows [AD-A289553] p 2121 N95-26757
BODY CENTERED CUBIC LATTICES
First-principles study of intermetallic phase stability in the ternary Ti-Al-Nb alloy system [DE95-005259] p 2213 N95-27082
The role of edge dislocations in the deformation of BCC metals [DE95-609157] p 2219 N95-27759
BODY-WING CONFIGURATIONS
Aeroelasticity of wing and wing-body configurations on parallel computers [NASA-CR-197756] p 2129 N95-26590
Preliminary design problems and solutions for a supersonic oblique all-wing transport aircraft p 2118 N95-26942
BOEING AIRCRAFT
Strategy in the commercial aircraft industry in the United States: A comparison of decisionmaking by McDonnell-Douglas and Boeing aircraft companies from 1977-1983 [AD-A288289] p 2117 N95-26409
Report to Congressional Committees. Comanche Helicopter: Testing needs to be completed prior to production decisions [GAO/NSIAD-95-112] p 2135 N95-27910
BOEING 737 AIRCRAFT
NASA-ACEE/Boeing 737 graphite-epoxy horizontal stabilizer service p 2138 N95-28489
BOEING 747 AIRCRAFT
Numerical simulation of the SOFIA flow field [NASA-CR-197757] p 2274 N95-26589
BOEING 757 AIRCRAFT
The determination of the constitutive parameters of a medium with application to a reinforced concrete pad [NASA-CR-4674] p 2268 N95-28181
BOHR THEORY
The electric field of Bohr's atom [DE95-608758] p 2448 N95-27336
BOILERS
Measurements of the volatilities of electrolytes: Application to water/steam cycles [DE95-007103] p 2204 N95-27451
BOLTS
Evaluation of composite joints [AD-A289247] p 2181 N95-26967
BOLTZMANN TRANSPORT EQUATION
Axionic fuel for sun [DE95-608788] p 2464 N95-27342
Hall effect and resistivity in the normal state of high-T(sub c) cuprates in the electron-fracton model [DE95-610612] p 2439 N95-27413
HZETRN: Description of a free-space ion and nucleon transport and shielding computer program [NASA-TP-3495] p 2465 N95-28530
BOMBER AIRCRAFT
Performance study for inlet installations [NASA-CR-189714] p 2140 N95-28227
BONDED JOINTS
Split pipe testing device for the measurement of bond of reinforcement under controlled confinement [AD-D017258] p 2245 N95-26500
Bimaterial interlaces and their role in the mechanical performance of the in-situ composites [AD-A288973] p 2182 N95-27188
Design and structural validation of CF116 upper wing skin boron doubler p 2132 N95-27510
Composite repair issues on the CF-18 aircraft p 2134 N95-27518
The development of an engineering standard for composite repairs p 2135 N95-27528
Fracture testing and analysis of adhesively bonded joints for automotive applications [DE95-007024] p 2184 N95-28207
BONDING
Sceening, down selection, and implementation of environmentally compliant cleaning and insulation bonding for MNASA p 2165 N95-27124
Status of bonded boron/epoxy doublers for military and commercial aircraft structures p 2132 N95-27506
Evaluation of patch effectiveness in repairing aircraft components p 2133 N95-27513
Repair technology for thermoplastic aircraft structures p 2134 N95-27519
Analysis of the dimerized Sb/Si(001)-(2x1) surface by x-ray standing waves [DE95-007097] p 2208 N95-27965
Fracture testing and analysis of adhesively bonded joints for automotive applications [DE95-007024] p 2184 N95-28207
BOOLEAN ALGEBRA
The assembly tower and some categorical and algebraic aspects of frame theory [AD-A289360] p 2391 N95-27489
BOOMS (EQUIPMENT)
Special features of the CLUSTER antenna and radial booms design, development and verification p 2157 N95-27281
Development and testing of the rack insertion device p 2158 N95-27289
BORANES
Boron-induced reconstructions of Si(100) investigated by scanning tunneling microscopy [AD-A289222] p 2438 N95-26959
BORATES
Growth and evaluation of nonlinear optical crystals for laser applications: Lithium borate, barium borate and silver gallium selenide [AD-A289147] p 2277 N95-27000
BORESIGHT ERROR
Reduction of off-boresight fields for a TEM horn antenna [AD-A289708] p 2250 N95-26738
Polarization sensitivity of monopulse radar boresight error induced by large, ogive radomes [AD-A289254] p 2252 N95-26972
Retrofitting a fine-pointing system to satellite optics [DE95-004529] p 2427 N95-28516
BORESIGHTS
Reduction of off-boresight fields for a TEM horn antenna [AD-A289708] p 2250 N95-26738
SAMPEX special pointing mode p 2149 N95-27780
BORIDES
Structural chemistry of some phases in the YC-Ni-B system [DE95-007403] p 2447 N95-28537
BORN APPROXIMATION
Off-specular scattering in neutron reflectometry [DE95-007835] p 2412 N95-28057
BORON
Boron-induced reconstructions of Si(100) investigated by scanning tunneling microscopy [AD-A289222] p 2438 N95-26959
Boron-induced morphology changes in silicon CVD growth: A scanning tunneling microscopy study [AD-A289275] p 2290 N95-26982
Atomic structure and bonding of boron-induced reconstructions on Si(001) [AD-A289187] p 2405 N95-27017
Trace elements and the mechanical properties of intermetallic compounds [DE95-007378] p 2220 N95-28046
BORON COMPOUNDS
Boron-carbon-silicon polymers and the ceramic thereof [NASA-CASE-ARC-11891-1-SB] p 2238 N95-28212
BORON FIBERS
Composite repair of metallic airframe: Twenty years of experience p 2132 N95-27508

BORON REINFORCED MATERIALS

Adhesively bonded composite patch repair of cracked aluminum alloy structures p 2132 N95-27507

Bonded composite repair of thin metallic materials: Variable load amplitude and temperature cycling effects p 2132 N95-27509

BORON-EPOXY COMPOSITES

Bonded composite repair of metallic aircraft components: Overview of Australian activities p 2132 N95-27505

Status of bonded boron/epoxy doublers for military and commercial aircraft structures p 2132 N95-27506

Bonded composite repair of thin metallic materials: Variable load amplitude and temperature cycling effects p 2132 N95-27509

Design and structural validation of CF116 upper wing skin boron doubler p 2132 N95-27510

Structural modification and repair of C-130 wing structure using bonded composites p 2133 N95-27512

BOSONS

Model independent constraints on anomalous gauge boson self-couplings from e(+)e(-) colliders with longitudinally polarized beams [DE95-608844] p 2406 N95-27317

Magnetic quadrupole moment of W-boson in Kobayashi-Maskawa model [DE95-610355] p 2407 N95-27411

Search for exotic particles at CDF [DE95-008383] p 2411 N95-27933

Probing strongly-interacting electroweak dynamics through W(+)W(-)/ZZ ratios at future e(+)e(-) colliders [DE95-007202] p 2413 N95-28067

Precise measurement of the left-right cross section asymmetry in Z boson production by e(+)e(-) collisions [DE95-008591] p 2414 N95-28158

Constraints on the anomalous WW gamma couplings from b vector s gamma [DE95-608866] p 2415 N95-28246

BOTANY

Live from Antarctica: Then and now [NASA-CR-197829] p 2335 N95-26594

BOUNDARIES

A non-iterative grid deformation algorithm for computational fluid dynamics for aeroelasticity [AD-A288298] p 2273 N95-26418

The physics and chemistry of heavy Fermions [DE95-005277] p 2407 N95-27431

Advanced neutron source materials surveillance program [DE95-005700] p 2215 N95-27464

Comparison of the calculated and measured stability of a NbTi cable-in-conduit conductor [DE95-007964] p 2265 N95-27693

Scaling of localization length of a quasi 1D system with longitudinal boundary roughness [DE95-609148] p 2391 N95-27739

Molecular engineering of thin polymer films prepared from functionally-terminated oligomers [AD-A291681] p 2240 N95-28457

Piecemeal learning of an unknown environment [AD-A291683] p 2387 N95-28461

BOUNDARY CONDITIONS

Fluxes across the west coast resolved by Picket Fence observations during stormfest [AD-A288511] p 2341 N95-26653

User's and test case manual for FEMATS [NASA-CR-197803] p 2366 N95-26694

Material modeling in the CRALE code. Users' manual [AD-A288988] p 2178 N95-26712

An outflow boundary condition for aeroacoustic computations [NASA-TM-106930] p 2279 N95-27175

Features and applications of the Groove Analysis Program (GAP) p 2281 N95-27349

Validation of the SINDA/FLUINT code using several analytical solutions p 2281 N95-27350

Transient studies of G-induced capillary dryout and rewet p 2281 N95-27351

Single-drop reactive extraction/extractive reaction with forced convective diffusion and interphase mass transfer p 2282 N95-27358

Turbulance boundary conditions for shear flow analysis, using the DTNS flow solver p 2283 N95-27362

Single-drop reactive extraction/extractive reaction with forced convective diffusion and interphase mass transfer p 2283 N95-27365

A magnetic hysteresis model p 2153 N95-27801

A summary documentation of the AMIP models [DE95-008343] p 2338 N95-27931

BOUNDARY ELEMENT METHOD

Applications of boundary element methods on the Intel Paragon [DE94-014135] p 2393 N95-28393

BOUNDARY LAYER CONTROL

Performance characterization of a highly-offset diffuser with and without blowing vortex generator jets [AD-A289334] p 2122 N95-26901

Comparative performance tests on the Mod-2, 2.5-mW wind turbine with and without vortex generators p 2124 N95-27978

BOUNDARY LAYER EQUATIONS

Supersonic coaxial jet noise predictions [NASA-TM-106917] p 2401 N95-26801

BOUNDARY LAYER FLOW

Wavenumber selection for small-wavelength Goertler vortices in curved channel flows [NASA-CR-195063] p 2273 N95-26576

Direct numerical simulation of transitional and turbulent flow over a heated flat plate using finite-difference schemes [NASA-CR-197753] p 2275 N95-26776

Investigation of boundary layer and performance effects of transpiration cooling through a porous plate in a rocket nozzle [AD-A289393] p 2167 N95-26880

Computer program BL2D for solving two-dimensional and axisymmetric boundary layers [NASA-CR-4668] p 2279 N95-27257

Computation of three-dimensional mixed convective boundary layer flow p 2280 N95-27347

Response of multi-panel assembly to noise from a jet in forward motion [NASA-CR-198164] p 2289 N95-28673

BOUNDARY LAYER SEPARATION

Performance characterization of a highly-offset diffuser with and without blowing vortex generator jets [AD-A289334] p 2122 N95-26901

BOUNDARY LAYER STABILITY

Analysis of hypersonic boundary layer second mode instability over a 7 deg cone [AD-A289471] p 2276 N95-26819

On the modulational instability of large amplitude waves in supersonic boundary layers [NASA-CR-195072] p 2284 N95-27760

BOUNDARY LAYER TRANSITION

Direct numerical simulation of transitional and turbulent flow over a heated flat plate using finite-difference schemes [NASA-CR-197753] p 2275 N95-26776

Analysis of hypersonic boundary layer second mode instability over a 7 deg cone [AD-A289471] p 2276 N95-26819

BOUNDARY LAYERS

Transport phenomena and interfacial kinetics in multiphase combustion systems [AD-A288297] p 2199 N95-26417

Direct numerical simulation of transitional and turbulent flow over a heated flat plate using finite-difference schemes [NASA-CR-197753] p 2275 N95-26776

Compressible turbulence measurements in a supersonic flow with adverse pressure gradient [AD-A289477] p 2276 N95-26822

Investigation of boundary layer and performance effects of transpiration cooling through a porous plate in a rocket nozzle [AD-A289393] p 2167 N95-26880

BOUNDARY LUBRICATION

Deformation behavior of thin lubricant films at elevated pressure [AD-A288906] p 2241 N95-28592

BOUNDARY VALUE PROBLEMS

Analysis and development of finite element methods for the study of nonlinear thermomechanical behavior of structural components [NASA-CR-195354] p 2307 N95-26387

Balanced data focusing: Direction of arrival estimation with maximum likelihood performance [AD-A288252] p 2248 N95-26407

General purpose finite element solver [PB95-185062] p 2388 N95-26495

Adaptive finite element method I: Solution algorithm and computational examples [AD-A288979] p 2389 N95-26609

On permanent capillar-heavy waves in circular shaped channels [DE95-608779] p 2280 N95-27339

Extensional flow convecting a reactant undergoing a first order homogeneous reaction and diffusional mass transfer from a sphere at low to intermediate Peclet and Damkohler numbers p 2280 N95-27346

A Navier-Stokes boundary element solver p 2283 N95-27361

Parallel plasma fluid turbulence calculations [DE95-006741] p 2431 N95-27537

BOW WAVES

Bow shock data analysis [AD-A288432] p 2429 N95-26800

BOX BEAMS

C-130 Advanced Technology Center wing box conceptual design/cost study p 2192 N95-28437

Structural testing of the technology integration box beam p 2194 N95-28467

Technology integration box beam failure study p 2194 N95-28468

BRAGG ANGLE

Modulation effect of a Bragg acousto-optic bistable system [AD-A289622] p 2401 N95-26857

A numerical study of ultra-short-pulse reflectometry [DE95-008070] p 2266 N95-28015

BRAIDED COMPOSITES

Through-the Thickness(R) braided composites for aircraft applications p 2185 N95-28273

Mechanical properties of triaxially braided composites: Experimental and analytical results p 2189 N95-28423

Characterization and manufacture of braided composites for large commercial aircraft structures p 2196 N95-28478

BRAIN

Experimental definition for implantation of the AFIT cortical multielectrode array [AD-A289216] p 2354 N95-26991

Characterization and redesign of the AFIT multielectrode array [AD-A289295] p 2354 N95-27039

BRANCHING (PHYSICS)

Search for the top quark in dilepton decay modes at D(PHI) [DE95-007764] p 2409 N95-27689

Search for exotic particles at CDF [DE95-008383] p 2411 N95-27933

BRAZIL

Models used to forecast agricultural corn crops in the micro-region of Ribeirao Preto-SP [INPE-5513-NTC/309] p 2315 N95-28554

BRAZING

High energy electron beams for ceramic joining [DE95-006316] p 2420 N95-27480

BREADBOARD MODELS

Characterization of corrosion and development of a breadboard of a D sight aircraft inspection system, phase 1 [AD-A288347] p 2125 N95-26527

Hubble Space Telescope nickel-hydrogen battery testing: An update p 2272 N95-26794

BREEDER REACTORS

Toward a mechanistic understanding of radiation effects in materials [DE95-006530] p 2221 N95-28120

BREMSSTRAHLUNG

Comparative experimental study of PIXE and X-ray fluorescence analysis [DE95-607868] p 2327 N95-27198

The Bremsstrahlung of soft gamma-quanta created by elastic pp- and np-scatterings and the dibaryon resonance problem [DE95-608870] p 2415 N95-28248

BRIDGES (STRUCTURES)

The effects of finite element grid density on model correlation and damage detection of a bridge [DE94-018895] p 2309 N95-27305

BRIGHTNESS

Coronal abundances and their variation [NASA-CR-197788] p 2464 N95-26671

Dwarf novae p 2458 N95-27069

BRIGHTNESS TEMPERATURE

Radiometer measurements of snow in Sodankylae, 1991-1993 [PB95-184966] p 2313 N95-26645

Method and apparatus for polaradiometric pyrometer [NASA-CASE-NPO-19064-1-CU] p 2290 N95-26765

Modeling and retrieval of snow and sea ice characteristics in the frequency range 6 to 90 GHz [PB95-195467] p 2316 N95-28656

BRINES

Tomographic observations of deep convection and the thermal evolution of the Greenland Sea Gyre 1988-1989 [AD-A289104] p 2348 N95-28096

BRITISH COLUMBIA

Meteorological and oceanographic data collected during the ASREX 91 field experiment [AD-A289492] p 2342 N95-26826

BRITTLE MATERIALS

The development of mechanical strength in a ceramic material during firing [DE95-004925] p 2234 N95-27476

Prediction of material strength and fracture of glass using the SPHINX smooth particle hydrodynamics code [DE95-004869] p 2236 N95-27943

BRITTLENESS
Trace elements and the mechanical properties of intermetallic compounds
[DE95-007378] p 2220 N95-28046
BROADBAND
Measurement and prediction of broadband noise from large horizontal axis wind turbine generators
p 2324 N95-27990
Anechoic wind tunnel study of turbulence effects on wind turbine broadband noise p 2325 N95-27992
BROADBAND AMPLIFIERS
High power, broadband folded waveguide Gyrotron-Traveling-Wave-Amplifier
[AD-A288847] p 2259 N95-26433
BROADCASTING
Joint Services Electronics Program (JSEP)
[AD-A288299] p 2345 N95-26419
Research and development report. Digital audio broadcasting: Comparison of coverage at Band 2 and Band 3
[BBC-RD-1994/16] p 2248 N95-26493
Com(sup 3): A composite-compatible component coding system
[BBC-RD-1994/17] p 2249 N95-26670
Research and development report. Eureka 147: Tests of the error performance of the DAB system
[BBC-RD-1994/18] p 2249 N95-26696
Information superhighway: Issues affecting development
[AD-A289434] p 2252 N95-26923
Replacing the message service component in an integration framework
[AD-A289928] p 2375 N95-28628
BROKEN SYMMETRY
Supersymmetry and light quark masses in a realistic superstring model
[DE95-610201] p 2412 N95-28041
Probing strongly-interacting electroweak dynamics through W(+)W(-)/ZZ ratios at future e(+)e(-) colliders
[DE95-007202] p 2413 N95-28067
Rare decays/CP: The perspective of a kaon physicist
[DE95-005964] p 2416 N95-28338
BROMIDES
High resolution Fourier transform spectroscopy of the first overtone of the N-O stretch in nitrosyl bromide
[AD-A289318] p 2203 N95-27295
Thermodynamics of aqueous electrolytes at high temperatures by the isopiestic technique
[DE95-006747] p 2449 N95-27546
BROWNIAN MOVEMENTS
The fBm Interpolator
[AD-A288996] p 2388 N95-26459
BRUSHES
Water driven turbine/brush pipe cleaner
[NASA-CASE-KSC-11669-1] p 2304 N95-28359
BUBBLE CHAMBERS
Bubble chamber spectroscopy for chemical analysis: A new concept
[DE95-006350] p 2209 N95-28088
BUBBLES
The stability of the flow in a laminar separation bubble
[CUED/A-AERO/TR-22] p 2275 N95-26809
A model of bubble evolution during decompression based on a Monte Carlo simulation of inert gas diffusion
[AD-A289400] p 2353 N95-26885
Bubble fusion: Preliminary estimates
[DE95-006337] p 2420 N95-27494
Bubble chamber spectroscopy for chemical analysis: A new concept
[DE95-006350] p 2209 N95-28088
BUCKLING
Buckling behavior of long symmetrically laminated plates subjected to combined loads p 2190 N95-28430
Effect of low-speed impact damage and damage location on behavior of composite panels p 2197 N95-28481
Fundamental concepts in the suppression of delamination buckling by stitching p 2198 N95-28486
Damage tolerance of a geodesically stiffened advanced composite structural concept for aircraft structural applications p 2138 N95-28487
BULK MODULUS
First-principles calculations for AIN, GaN, and InN: Bulk and alloy properties
[DE95-006822] p 2219 N95-27958
The minimum pore size obtainable in a silica gel during drying
[DE95-008162] p 2239 N95-28401
BULKHEADS
Development of composite carrythrough bulkhead
p 2192 N95-28438
BUNCHING
Time-dependent multi-dimensional simulation studies of the electron output scheme for high power FELs
[DE95-006593] p 2297 N95-27737
Some notes on long-range beam-beam effects for the 2 TeV collider
[DE95-006771] p 2421 N95-28017
Measurement of wakefield suppression in a detuned X-band accelerator structure
[DE95-008592] p 2422 N95-28159
BUOYS
Radio telemetry buoy for long-range communication
[AD-D017269] p 2161 N95-28581
BURNERS
Research on combustion processes relevant to burners in HVAC systems
[PB95-179735] p 2208 N95-28006
BY-PRODUCTS
SIHTI 2: Energy and environmental technology. Yearbook 1993 of the research programme
[DE95-755135] p 2331 N95-28202

C

C BAND
Studies of radar backscatter as a function of wave properties and the winds in the turbulent marine atmosphere
[NASA-CR-198608] p 2315 N95-28209
C++ (PROGRAMMING LANGUAGE)
Multiple model adaptive estimation and head motion tracking in a virtual environment: An engineering approach
[AD-A289299] p 2359 N95-27046
C-130 AIRCRAFT
C-130 Advanced Technology Center wing box conceptual design/cost study p 2192 N95-28437
C-135 AIRCRAFT
Development of repair processes and sources for C/KC-135 aircraft windows/windshields
[AD-A288348] p 2117 N95-26629
An analysis of the KC-135 three-person cockpit
[AD-A289540] p 2130 N95-26873
Two-phase flow research using the learjet apparatus
[NASA-TM-106814] p 2284 N95-27854
CABLES
FENIX experimental results of large-scale CICC made of bronze-processed Nb3Sn strands
[DE95-007965] p 2222 N95-28167
CABLES (ROPES)
Deployment and retraction of a cable-driven solar array: Testing and simulation p 2158 N95-27283
CADMIUM
FY 1994 ambient air monitoring report for McMurdo Station, Antarctica
[DE95-008565] p 2331 N95-28149
CADMIUM ALLOYS
Precursor phenomenon of martensitic transformation in Au-49.5at%Cd alloy
[DE95-007698] p 2222 N95-28166
CADMIUM COMPOUNDS
Synchrotron X-ray scattering studies at mineral-water interfaces
[DE95-008303] p 2440 N95-27542
Health and environmental hazards of CdTe photovoltaic module production, use and decommissioning
[DE95-006688] p 2320 N95-27682
CADMIUM TELLURIDES
Health and environmental hazards of CdTe photovoltaic module production, use and decommissioning
[DE95-006688] p 2320 N95-27682
Recent progress in the Photovoltaic Manufacturing Technology Project (PVMaT)
[DE95-000279] p 2320 N95-27704
Strategies for recycling CdTe photovoltaic modules
[DE95-006776] p 2325 N95-28517
CALCITE
Synchrotron X-ray scattering studies at mineral-water interfaces
[DE95-008303] p 2440 N95-27542
CALCIUM
Large area smart piezoelectric and pyroelectric sensors
[AD-A288565] p 2290 N95-26541
Ash-based ceramic materials
[AD-D017272] p 2241 N95-28582
CALCIUM FLUORIDES
Point defect formation in optical materials expos ed to the space environment p 2428 N95-27646
CALCIUM OXIDES
Characterization of collision cascade damage in Ca2La8(SiO4)6O2 by HRTEM
[DE95-005719] p 2440 N95-27491
Ash-based ceramic materials
[AD-D017272] p 2241 N95-28582
CALCULUS
Modal event calculus in Lolli
[AD-A288544] p 2365 N95-26605
A parallel complexity model for functional languages
[AD-A288589] p 2365 N95-26656
CALDERAS
Seismic constraints on shallow crustal processes at the East Pacific rise
[AD-A289055] p 2338 N95-28094
CALIBRATING
Micron Accuracy Deployment Experiment (MADE), phase A. Volume 1
[NASA-CR-197792] p 2144 N95-26426
Aircraft fuel system lightning protection design and qualification test procedures development
[AD-A288401] p 2125 N95-26497
Uncertainties in the calibration of hydrophones at NPL by the three-transducer spherical-wave reciprocity method in the frequency range 10 kHz on 500 kHz
[PB95-185245] p 2401 N95-26615
Stability of reference masses 4: Growth of carbonaceous contamination on platinum-iridium mass standard surfaces, and its cleaning by UV/ozone treatment
[PB95-190096] p 2226 N95-26745
Telepresent spacecraft docking with object-based bilateral control (OBBC)
[AD-A289268] p 2163 N95-26980
Notes on the calibration of the JHU-APL solar vector magnetograph at NSO-Sec peak
[AD-A289277] p 2253 N95-26983
Solar terrestrial radiation data from the Sleepers River Research Watershed
[AD-A288444] p 2464 N95-27184
Linear and nonlinear trending and prediction for AVHRR time series data p 2385 N95-27391
The KTeV pure CsI calorimeter
[DE95-005747] p 2292 N95-27751
Observational magnetometer calibration with the Hubble Space Telescope's new magnetometers
p 2148 N95-27773
Experience from the in-flight calibration of the Extreme Ultraviolet Explorer (EUVE) and Upper Atmosphere Research Satellite (UARS) fixed head star trackers (FHSTs) p 2149 N95-27779
The installation of and first results from the superconducting gravimeter GWR20 at the Metsahovi Station, Finland
[REPT-95:1] p 2338 N95-27995
Remote sensing of hydrologic variables in boreal areas, phase 2
[NASA-CR-198717] p 2314 N95-27998
CALIFORNIA
Molten Carbonate Fuel Cell (MCFC) product development test
[DE95-007345] p 2316 N95-26543
CALIFORNIUM ISOTOPES
Bilateral intercomparison of the neutron emission rate of a (252)Cf spontaneous fission source between the National Physical Laboratory, Teddington, UK and the Physikalisch-Technische Bundesanstalt, Braunschweig, Germany
[PB95-190120] p 2404 N95-26748
CALORIMETERS
Large area smart piezoelectric and pyroelectric sensors
[AD-A288565] p 2290 N95-26541
Calorimetric evaluation of commercial Ni-MH cells and charges p 2272 N95-26790
Precision electromagnetic calorimetry with liquid krypton
[DE95-006685] p 2292 N95-27677
Performance of an accordion electromagnetic calorimeter with liquid krypton
[DE95-006693] p 2292 N95-27738
The KTeV pure CsI calorimeter
[DE95-005747] p 2292 N95-27751
CAMERAS
An illumination planner for Lambertian polyhedral objects
[AD-A289332] p 2424 N95-26900
ELVIS: Eigenvectors for land vehicle image system
[AD-A289297] p 2381 N95-27041
A foveated system to reduce transmission bandwidth of video images from remote camera systems
[AD-A288516] p 2254 N95-27060
SXI Prototype mirror mount
[NASA-CR-196613] p 2301 N95-27244
CANADA
Characterization of corrosion and development of a breadboard of a D sight aircraft inspection system, phase 1
[AD-A288347] p 2125 N95-26527
CANADIAN SPACE PROGRAM
The Strategic Technologies for Automation and Robotics (STEAR) program: Protection of materials in the space environment subprogram p 2242 N95-27669

CANARD CONFIGURATIONS
Design and testing of low sonic boom configurations and an oblique all-wing supersonic transport [NASA-CR-197744] p 2129 N95-26651

CANCER
A 3-D finite difference time domain investigation of microwave propagation through inhomogeneous biological materials [AD-A289431] p 2251 N95-26869

CANONICAL FORMS
The canonical q-transformations with two q-para-Bose oscillators [DE95-608781] p 2396 N95-27341

CANYONS
Comparison of the activities of fine-particle size catalysts [DE95-004773] p 2203 N95-27423

CAPACITANCE
Nickel metal hydride LEO cycle testing p 2272 N95-26791
Unique features of a new nickel-hydrogen 2-cell CPV p 2272 N95-26793
Efficient modeling of interconnects and capacitive discontinuities in high-speed digital circuits [NASA-CR-198728] p 2270 N95-28570
Characterization of a fused silica capacitance standard [DE95-006457] p 2270 N95-28597

CAPACITORS
A hybrid vehicle evaluation code and its application to vehicle design. Revision 1 [DE95-008053] p 2303 N95-28029
Forback DC-to-DC converter [NASA-CASE-GSC-13404-1] p 2269 N95-28341
Characterization of a fused silica capacitance standard [DE95-006457] p 2270 N95-28597

CAPE KENNEDY LAUNCH COMPLEX
Spaceport news index: January 1990 - December 1994 [NASA-TM-110653] p 2454 N95-27243
A review of falconry as a bird control technique with recommendations for use at the Shuttle Landing Facility, John F. Kennedy Space Center, Florida, USA [NASA-TM-110142] p 2126 N95-27859
Weather hazards to a Titan 4 on-pad destack-restack operation p 2172 N95-28307
Cape Canaveral air station launch emergency response forces and toxic materials release contingency plans p 2172 N95-28308

CAPILLARY FLOW
Measurement of viscosity by capillary rheometry: Dwell time effects [PB95-190203] p 2201 N95-26750
On permanent capillar-heavy waves in circular shaped channels [DE95-608779] p 2280 N95-27339
Transient studies of G-induced capillary dryout and rewet p 2281 N95-27351

CAPILLARY WAVES
New developments for sol-gel film and fiber processing [DE95-008175] p 2240 N95-28404

CARBIDES
JPRS report: Science and technology. Central Eurasia [JPRS-UST-95-015] p 2246 N95-27213
Engineered materials for appliation in severe metallurgical environments: Tantalum-carbon alloy development [DE95-006838] p 2216 N95-27488
Structural chemistry of some phases in the YC-Ni-B system [DE95-007403] p 2447 N95-28537

CARBOHYDRATES
Performance enhancing ration components program: Supplemental carbohydrate test [AD-A288560] p 2358 N95-26558

CARBON
Variation of solvent scattering-length density small-angle neutron scattering as a means of determining structure of composite materials [DE95-005394] p 2183 N95-27428
Engineered materials for appliation in severe metallurgical environments: Tantalum-carbon alloy development [DE95-006838] p 2216 N95-27488
Photoemission and optical properties of C60 fullerites [DE95-006588] p 2425 N95-27539
Atomic oxygen dosimetry measurements made on STS-46 by CONCAP 2 p 2418 N95-27634
Hydrogen induced C-C, C-N, and C-S bond activities on Pi and Ni surfaces [DE95-006251] p 2206 N95-27838
Formation of anisotropic Tl-1212, Tl-2212, Tl-1223 and Tl-2223 particles using aerosol flow reacted powders [DE95-007400] p 2444 N95-28079
Carbonaceous aerosols influencing atmospheric radiation: Black and organic carbon [DE95-006437] p 2330 N95-28118
On ionic charge distributions of heavy evaporation residues passing through a carbon foil [DE94-629016] p 2414 N95-28184
Evaluation of microporous carbon filters as catalysts for ozone decomposition [DE95-006498] p 2331 N95-28548
A black carbon emission data base for atmospheric chemistry and climate studies [DE95-006436] p 2332 N95-28662

CARBON COMPOUNDS
Statistical analysis of tensile mechanical property data of carbon/polyimide composites [NAL-TR-1238] p 2180 N95-26667
Investigation on energy conversion technology using biochemical reaction elements, 2 [DE95-759250] p 2321 N95-27940
Boron-carbon-silicon polymers and the ceramic thereof [NASA-CASE-ARC-11891-1-SB] p 2238 N95-28212

CARBON DIOXIDE
A summary of ODS replacement technologies at Litton Poly-Scientific p 2228 N95-27105
Observations on the solvating power of supercritical fluids p 2228 N95-27106
CO2 pellet blast cleaning and degreasing: The true environmentally benign technology p 2229 N95-27109
The use of supercritical carbon dioxide for contaminant removal from solid waste p 2229 N95-27110
Precision parts cleaning with supercritical CO2: Practical applications and solutions p 2229 N95-27111
Corrosive effects of supercritical carbon dioxide and cosolvents on metals p 2224 N95-27113
Precision parts cleaning with supercritical carbon dioxide p 2229 N95-27114
Survey of environmentally benign cleaning methodologies and materials p 2231 N95-27122
Fluid dynamic effects on precision cleaning with supercritical fluids p 2232 N95-27129
Integrated assessment and the relation between land-use change and climate change [DE95-006533] p 2327 N95-27469
Investigation on comprehensive fossil fuel cycle analysis and assessment approach as viewed from the global environment [DE95-759241] p 2329 N95-27935
Investigation on working out the global regeneration plan [DE95-759246] p 2329 N95-27938
Survey on researches related to ocean disposal of carbon dioxide [DE95-759247] p 2329 N95-27939
Investigation on energy conversion technology using biochemical reaction elements, 2 [DE95-759250] p 2321 N95-27940
Investigation on technology for increasing the biological CO2 sink and technology for CO2 fixation and reutilization [DE95-759251] p 2329 N95-27941
Measurement of particle transport coefficients on Alcator C-Mod [DE95-007763] p 2411 N95-28020
Mars Sample Return mission utilizing in-situ propellant production [NASA-CR-188371] p 2145 N95-28261
Cryogenic BRDF measurements at 10.6 micrometers and 0.63 micrometers on contaminated mirrors [AD-A291611] p 2427 N95-28408

CARBON DIOXIDE CONCENTRATION
Research project on CO2-induced climate change [DE95-008339] p 2330 N95-28084

CARBON DIOXIDE LASERS
Far-infrared laser interferometry measurements on the STP-3(M) reversed-field pinch [DE94-765440] p 2297 N95-27868
Applications of lasers and electro-optics [DE95-600841] p 2299 N95-28330
Thermally-induced unsymmetric optical distortion of output window of high-power CO2 laser [AD-A289604] p 2300 N95-28650

CARBON DIOXIDE REMOVAL
The use of supercritical carbon dioxide for contaminant removal from solid waste p 2229 N95-27110

CARBON FIBER REINFORCED PLASTICS
Adhesively bonded composite patch repair of cracked aluminum alloy structures p 2132 N95-27507
External patch repair of CFRP/honeycomb sandwich p 2134 N95-27522

CARBON FIBERS
Composite or metallic bolted repairs on self-stiffened carbon wing panel of the commuter ATR72 design criteria, analysis, verification by test p 2135 N95-27525
Failure analysis of thick composite cylinders under external pressure p 2187 N95-28284

CARBON MONOXIDE
CO, HCO(+) and HCN absorption in the gravitational lens candidate B0218+357 at z=0.685 [PB95-185146] p 2461 N95-26522
Photo and thermal excitation of surface chemistry on model catalyst surfaces [AD-A288541] p 2200 N95-26528
Molecular cloud content of early-type galaxies. V. CO in elliptical galaxies [PB95-185153] p 2461 N95-27320
Preconversion catalytic deoxygenation of phenolic functional groups [DE95-007556] p 2204 N95-27458
Coupled chemistry/climate issues [DE95-006443] p 2327 N95-27532
Kinetics and dynamics of oxidation reactions involving adsorbed CO species on bulk supported Pt and copper oxides [DE95-006420] p 2207 N95-27952
FY 1994 ambient air monitoring report for McMurdo Station, Antarctica [DE95-008565] p 2331 N95-28149

CARBON STEELS
Characterization of Ultra-Low Carbon Baintic steels for use as weld wire consumables [AD-A288292] p 2212 N95-26411
Fatigue fracture analysis in medium carbon structural steel and austenitic stainless steel by X-ray fractography [DE95-601504] p 2213 N95-26675
Stress corrosion cracking susceptibility of the earthquake resistant NOM B457 Mexican steel [DE95-607956] p 2214 N95-27256
Non-metallic oxide inclusion formation in C-Mnlow alloy steel welds [DE94-019160] p 2215 N95-27319
Effects of hydrogen on carbon steels at the Multi-Function Waste Tank Facility [DE95-007194] p 2219 N95-28005

CARBON 13
Molecular beam scattering from C-13 enriched Kapton and correlation with the EOIM-3 carousel experiment p 2419 N95-27643

CARBON-CARBON COMPOSITES
Composite heat pipe development status: Development of lightweight prototype carbon-carbon heat pipe with integral fins and metal foil liner [NASA-TM-106909] p 2283 N95-27369
LEO degradation of graphite and carbon-based composites aboard Space Shuttle Flight STS-46 p 2199 N95-27636

CARBONACEOUS MATERIALS
Carbonaceous aerosols influencing atmospheric radiation: Black and organic carbon [DE95-006437] p 2330 N95-28118

CARBONATES
Molten Carbonate Fuel Cell (MCFC) product development test [DE95-007345] p 2316 N95-26543
The US Molten Carbonate Fuel-Cell development and commercialization effort [DE95-008580] p 2320 N95-27746

CARCINOGENS
An introductory guide to uncertainty analysis in environmental and health risk assessment. Environmental Restoration Program [DE95-008097] p 2354 N95-28136

CARGO
The performance of cargo airdrop systems using g-12E parachutes: Statistical determination of minimum altitude [AD-A291666] p 2126 N95-28454

CARGO AIRCRAFT
Incorporating biplane wing theory into a large, subsonic, all-cargo transport p 2120 N95-26956

CARRIER DENSITY (SOLID STATE)
Time-dependent model for vertical-cavity surface-emitting laser [DE95-007880] p 2298 N95-28027

CARRIER FREQUENCIES
Nonlinear optical studies of surfaces [DE95-006574] p 2428 N95-28557

CARTESIAN COORDINATES
User documentation of the CTA program [AD-A289508] p 2121 N95-26854

CASE BONDED PROPELLANTS
A comprehensive energetic materials resource recovery and recycling program p 2176 N95-28323

CASES (CONTAINERS)
Composite intermediate case manufacturing scale-up for advanced engines p 2141 N95-28275

CASSINI MISSION

Briefing Report to the Ranking Minority Member, Subcommittee on Space and Aeronautics, Committee on Science, House of Representatives. Cassini Mission: Estimated launch costs for NASA's mission to Saturn [GAO/NSIAD-95-141BR] p 2145 N95-27856

CAST ALLOYS

Ductile - ductile beryllium aluminum metal matrix composite manufactured by extrusion [AD-A289519] p 2181 N95-26848

Fatigue properties of an A356 (AlSi7Mg) aluminum alloy for automotive applications: Fatigue life prediction [PB95-196424] p 2224 N95-28660

CASTING

Magnetic resonance imaging of solvent transport in polymer networks [DE95-007142] p 2234 N95-27455

AMCC casting development. Volume 1: Executive Summary [NASA-CR-196597] p 2247 N95-28419

CASTINGS

AMCC casting development. Volume 1: Executive Summary [NASA-CR-196597] p 2247 N95-28419

CATACLYSMIC VARIABLES

Cataclysmic variables and related objects [NASA-SP-507] p 2458 N95-27068

Models for various aspects of dwarf novae and nova-like stars p 2459 N95-27071

Classical novae and recurrent novae: General properties p 2459 N95-27072

Typical examples of classical novae p 2459 N95-27074

Recurrent novae p 2460 N95-27075

Overview of the observations of symbiotic stars p 2460 N95-27076

Models of symbiotic stars p 2460 N95-27077

CATALYSIS

Cofactor-assisted antibody catalysis [AD-A288929] p 2349 N95-26608

Synthesis and properties of lanthanide-exchanged Preyssler's heteropolyanions [DE95-007136] p 2238 N95-28235

The minimum pore size obtainable in a silica gel during drying [DE95-008162] p 2239 N95-28401

CATALYSTS

International Space Station Alpha trace contaminant control subassembly life test report [NASA-TM-108488] p 2358 N95-26364

Photo and thermal excitation of surface chemistry on model catalyst surfaces [AD-A288541] p 2200 N95-26528

Theoretical studies of reaction surfaces [AD-A288458] p 2404 N95-26632

Probe molecule studies: Active species in alcohol synthesis [DE95-003514] p 2203 N95-27420

Comparison of the activities of fine-particle size catalysts [DE95-004773] p 2203 N95-27423

Preconversion catalytic deoxygenation of phenolic functional groups [DE95-007556] p 2204 N95-27458

Reducing cold-start emissions by catalytic converter thermal management [DE95-000256] p 2327 N95-27540

Charge distribution analysis of catalysts under simulated reaction conditions [DE95-006943] p 2204 N95-27549

NQR-NMR studies of higher alcohol synthesis Cu-Co catalysts [DE95-007926] p 2205 N95-27680

Superior catalysts for selective catalytic reduction of nitric oxide [DE95-007903] p 2205 N95-27691

Transient studies of low temperature catalyst for methane conversion [DE95-007913] p 2205 N95-27692

Kinetics and dynamics of oxidation reactions involving adsorbed CO species on bulk supported Pt and copper oxides [DE95-006420] p 2207 N95-27952

Synthesis and properties of lanthanide-exchanged Preyssler's heteropolyanions [DE95-007136] p 2238 N95-28235

Comparison of bridged polysilsesquioxane xerogels prepared from methoxy- and ethoxy-silyl monomers [DE95-005422] p 2240 N95-28532

Evaluation of microporous carbon filters as catalysts for ozone decomposition [DE95-006498] p 2331 N95-28548

CATALYTIC ACTIVITY

Cofactor-assisted antibody catalysis [AD-A288929] p 2349 N95-26608

Comparison of the activities of fine-particle size catalysts [DE95-004773] p 2203 N95-27423

Synthesis and properties of lanthanide-exchanged Preyssler's heteropolyanions [DE95-007136] p 2238 N95-28235

Radiant exchange considerations in design and scaleup of photocatalytic reactors for purification of nitroglycerine-contaminated air p 2171 N95-28300

CATHODE RAY TUBES

Image quality metrics for color CRT displays [AD-A288934] p 2262 N95-27196

CATIONS

AEM investigation of tetrahedrally coordinated Ti(4+) in nickel-titanate spinel [DE95-006624] p 2215 N95-27473

The off-center effect on the diffusion coefficient of Cu(+) and Li(+) in the KCl lattice [DE95-609146] p 2446 N95-28255

CAVITATION FLOW

Scaling issues in dynamic fragmentation [DE95-008509] p 2309 N95-27745

CAVITIES

Suppressor of oscillations in airframe cavities [AD-D017265] p 2128 N95-26507

Numerical simulation of the SOFIA flow field [NASA-CR-197757] p 2274 N95-26589

Comparison of numerical results and multicavity purge and rim seal data with extensions to dynamics [NASA-TM-106685] p 2168 N95-27434

Cavity formation and impurity gettering in He-implanted Si [DE95-007744] p 2444 N95-28127

Chemical and electrical properties of cavities in silicon and germanium [DE95-006812] p 2445 N95-28206

Measurements of store forces and moments and cavity pressures for a generic store in and near a box cavity at subsonic and transonic speeds [NASA-TM-4611] p 2123 N95-28241

Investigation of HE driven cylindrical liner [DE95-007866] p 2311 N95-28539

CAVITONS

Proceedings of the International Workshop on Acceleration and Radiation Generation in Space and Laboratory Plasmas [AD-A291673] p 2436 N95-28668

CAVITY FLOW

Calculation of three-dimensional (3-D) internal flow by means of the velocity-vorticity formulation on a staggered grid [NASA-TM-110352] p 2122 N95-27258

A Navier-Stokes boundary element solver p 2283 N95-27361

Numerical analysis of intrs cavity and power-stream flow interaction in multiple gas-turbine disk-cavities [NASA-TM-106886] p 2140 N95-28344

Experimental study on transition characteristics of natural-convection flow [PB95-192423] p 2289 N95-28637

CAVITY RESONATORS

Design and characterization of resonant cavity light-emitting diodes [AD-A289307] p 2261 N95-26921

Thermally-induced unsymmetric optical distortion of output window of high-power CO2 laser [AD-A289604] p 2300 N95-28650

CCD STAR TRACKER

Development of a Robust star identification technique for use in attitude determination of the ACE spacecraft p 2149 N95-27777

CELESTIAL MECHANICS

Space modeler: An expanded, distributed, virtual environment for space visualization [AD-A289409] p 2461 N95-27131

Tracking and impact prediction of Earth-Crossing-Objects (ECO's) on a collision course with Earth [AD-A289321] p 2461 N95-27303

CELL DIVISION

Modeling and statistical analysis of bioassay data: Medaka cell proliferation under DEN and TCE [AD-A289998] p 2352 N95-28519

CELLS (BIOLOGY)

Comparative Transduction Mechanisms of Vestibular Otolith Hair Cells [NASA-CR-197980] p 2349 N95-26727

Regional differences in lectin binding patterns of vestibular hair cells p 2349 N95-26728

Hair cell regeneration in the bullfrog vestibular otolith organs following aminoglycoside toxicity p 2349 N95-26729

Peripheral innervation patterns of vestibular nerve afferents in the bullfrog utriculus p 2349 N95-26730

Comparative transduction mechanisms of hair cells in the bullfrog utriculus. 1: Responses to intracellular current p 2350 N95-26731

Comparative transduction mechanisms of hair cells in the bullfrog uticulus. 2: Sensitivity and response dynamics to hair bundle displacement p 2350 N95-26732

Hippocampal place fields, the internal compass, and the learning of landmark stability [AD-A289406] p 2350 N95-27100

The electrical behaviour of an excitable cell at different conditions [DE95-607911] p 2351 N95-27254

Mutagenesis in human cells with accelerated H and Fe ions [NASA-CR-198599] p 2351 N95-28177

Third international congress of plant molecular biology: Molecular biology of plant growth and development [DE95-006482] p 2352 N95-28496

CELLULOSE NITRATE

A comprehensive energetic materials resource recovery and recycling program p 2176 N95-28323

CEMENTS

Method and apparatus for measuring temperatures in fabrics and flexible thermal insulations [NASA-CASE-ARC-11984-1] p 2293 N95-28345

CENTAUR LAUNCH VEHICLE

Electromechanical rotary actuator p 2157 N95-27278

CENTER OF GRAVITY

A quantitative feedback theory FCS design for the subsonic envelope of the VISTA F-16 including configuration variation [AD-A289221] p 2141 N95-26958

CENTRAL NERVOUS SYSTEM

Research activities on somatosensory (SI) cortical neurons [AD-A288794] p 2348 N95-26360

CENTRAL PROCESSING UNITS

Testing of Uninterruptible Power Supplies with nonlinear loads [AD-A289353] p 2262 N95-27067

The transition of GTDS to the Unix workstation environment p 2151 N95-27789

Parallel block implicit integration technique for trajectory parallelism [AD-A288961] p 2379 N95-28335

CERAMIC FIBERS

Ceramic fiber-reinforced monoclinic celsian phase glass-ceramic matrix composite material [NASA-CASE-LEW-15714-1] p 2183 N95-27717

Ceramic composite combustor cans for expendable turbine engines [AD-A289551] p 2140 N95-28646

CERAMIC MATRIX COMPOSITES

Micromechanical prediction of tensile damage for ceramic matrix composites under high temperature [AD-A288238] p 2180 N95-26626

Characterization of fatigue behavior of 2-D woven fabric reinforced ceramic matrix composite at elevated temperature [AD-A289423] p 2181 N95-26886

Fatigue behavior of a cross-ply ceramic matrix composite at elevated temperature under tension-tension loading [AD-A289250] p 2182 N95-26969

Fatigue behavior of a cross-ply ceramic matrix composite subjected to tension-tension cycling with hold time [AD-A289418] p 2182 N95-27134

Structural ceramics incorporating whiskers, platelets, and particulate phases [DE95-007048] p 2235 N95-27499

Ceramic fiber-reinforced monoclinic celsian phase glass-ceramic matrix composite material [NASA-CASE-LEW-15714-1] p 2183 N95-27717

Thermal shock behavior of fiber-reinforced composites [DE95-006746] p 2183 N95-27955

Stress transfer from axially loaded fiber to matrix in a microcomposite [DE95-007366] p 2183 N95-28043

Effects of high-temperature environments on flaw generation and fracture behavior of SiC/SiC composites [DE95-008270] p 2183 N95-28068

High-temperature deformation of ZrO2-Al2O3/SiC whisker composites fabricated by two techniques [DE95-008273] p 2183 N95-28069

Ceramic composite combustor cans for expendable turbine engines [AD-A289551] p 2140 N95-28646

CERAMICS

Scale model experiments with ceramic laminate targets [AD-A288322] p 2225 N95-26561

Materials design and processing by biomimicking. Section 1: Research progress [AD-A288229] p 2226 N95-26623

Design and processing of materials by biomimicking. Section 2. Publications
[AD-A288230] p 2226 N95-26624
Bimaterial interlaces and their role in the mechanical performance of the in-situ composites
[AD-A288973] p 2182 N95-27188
Japan's electronic packaging technologies
p 2263 N95-27230
Current programmes on physical metallurgy and related areas in BARC
[DE95-607939] p 2214 N95-27255
The development of mechanical strength in a ceramic material during firing
[DE95-004925] p 2234 N95-27476
High energy electron beams for ceramic joining
[DE95-006316] p 2420 N95-27480
Thermal control materials on EOIM-3
p 2242 N95-27639
Amorphization of complex ceramics by heavy-particle irradiations
[DE95-005725] p 2236 N95-27733
Tungsten carbide fragmentation: Experimental characterization and numerical modelling
[DE95-008521] p 2236 N95-27879
Prediction of material strength and fracture of glass using the SPHINX smooth particle hydrodynamics code
[DE95-004869] p 2236 N95-27943
The development and testing of ceramic components in piston engines
[DE95-005759] p 2236 N95-27946
Sintering of textured YBa2Cu3O(7-x) under intensive Co-60 gamma irradiation
[DE95-007098] p 2442 N95-27950
Manufacturing tailored property ceramic composites
[DE95-006303] p 2237 N95-27993
Control of thin film processing behavior through precursor structural modifications
[DE95-006468] p 2444 N95-28103
Boron-carbon-silicon polymers and the ceramic thereof
[NASA-CASE-ARC-11891-1-SB] p 2238 N95-28212
Task 4 supporting technology. Part 1: Detailed test plan for leading edge tile development. Leading edge material development and testing
[NASA-CR-198633] p 2160 N95-28258
Method and apparatus for measuring temperatures in fabrics and flexible thermal insulations
[NASA-CASE-ARC-11984-1] p 2293 N95-28345
Development of low-expansion ceramics with strength retention to elevated temperatures
[DE95-005760] p 2239 N95-28397
An overview of activities and accomplishments of the Metals and Ceramics Division
[DE95-007020] p 2241 N95-28560
Ash-based ceramic materials
[AD-D017272] p 2241 N95-28582
Coatings of non-oxide ceramics for improved corrosion resistance in high temperature coal combustion
[DE95-006932] p 2241 N95-28604

CERENKOV COUNTERS
Measurement of the reaction C(nu(sub mu), mu(-)) X near threshold
[DE95-007888] p 2412 N95-28063
Can TMAE photocathode be used for high rate applications?
[DE95-008594] p 2293 N95-28178

CERENKOV RADIATION
Radiation of a uniformly moving charge
[DE95-608757] p 2255 N95-27335
Observation of asymmetrical two-cone Vavilov-Cherenkov radiation in biaxial crystal of triglycinesulphate emitted by 658 MeV protons passing along bi normal
[DE94-629017] p 2441 N95-27867

CERIUM OXIDES
Atomic layer epitaxy of group 4 materials: Surface processes, thin films, devices and their characterization
[AD-A289092] p 2446 N95-28327

CERTIFICATION
Bonded composite repair of metallic aircraft components: Overview of Australian activities
p 2132 N95-27505
Hardware cleanliness methodology and certification
p 2211 N95-27656
Application of damage tolerance methodology in certification of the Piaggio P-180 Avanti
p 2138 N95-28480

CESIUM
Cesium/oxide interactions for ultrathin films on (alpha)-Al2O3(001) and (alpha)-Al2O3(1(bar 1)O2)
[DE95-008159] p 2238 N95-28358
Photoemission study of solid state reaction and initial oxidation of the Ce/Al(100) system
[PB95-195368] p 2210 N95-28652

CESIUM IODIDES
The KTeV pure CsI calorimeter
[DE95-005747] p 2292 N95-27751

CHAINS
Design strategies for the preparation of polymeric organic superconductors
[AD-A289022] p 2436 N95-26462

CHANGE DETECTION
Search for molecular absorptions with the Fourier Transform Spectrometer
[NASA-CR-198648] p 2462 N95-28222
The sensitive detection of hydrazine using chemiluminescence p 2173 N95-28311
A new method for measuring hypergol scrubber emissions p 2174 N95-28312
In situ dynamic material property measurement system
[AD-D017387] p 2210 N95-28585

CHANNEL FLOW
A fixed time performance evaluation of parallel CFD applications
[DE94-014240] p 2273 N95-26445
Wavenumber selection for small-wavelength Goertler vortices in curved channel flows
[NASA-CR-195063] p 2273 N95-26576
Resonant coherent excitation of N6(+) and Mg11(+) in planer channeling: Anisotropies in ionization probabilities and X-ray emission
[DE95-006732] p 2417 N95-28595

CHAOS
The phenomena of subharmonic bifurcations, runaway, and transition to chaos in a non-linear oscillator: perturbation methods and a numerical experiment
[IFTR-16/1994] p 2398 N95-26518
Vibration control using chaotic motion stabilizers
[AD-A289576] p 2398 N95-26687
Nonlinear instability and chaos in plasma wave-wave interactions. I. Introduction
[DE95-005529] p 2429 N95-27084
Cognitive networks for ATR: The roles of bifurcation and chaos
[AD-A289010] p 2387 N95-28336
Chua's circuits: Phenomena and applications
[AD-A291638] p 2271 N95-28666

CHARACTERIZATION
Automatically selecting and using primary effects in planning: Theory and experiments
[AD-A289347] p 2450 N95-27064
Iron oxides characterization by Moessbauer spectroscopy
[DE95-607869] p 2202 N95-27199
Matrix kernels for MEG and EEG source localization and imaging
[DE95-005238] p 2354 N95-27426
Alpha characterization inside pipes using ion-transport technology
[DE95-007869] p 2411 N95-28024
High temperature Hexoloy(trademark) SX silicon carbide
[DE95-007290] p 2221 N95-28075
Improved hardness RHA weldability and material property testing
[AD-A289127] p 2221 N95-28102
Proceedings of the 1993 Scientific Conference on Obscuration and Aerosol Research
[AD-A280084] p 2331 N95-28153
Material characterization system
[AD-D017385] p 2210 N95-28584

CHARGE CARRIERS
On helicon wave induced radial plasma transport
[DE94-634477] p 2429 N95-26438
Low temperature deposition and characterization of N- and P-type silicon carbide thin films and associated Ohmic and Schottky contacts
[AD-A289107] p 2237 N95-28097
Comprehensive numerical model for CW vertical-cavity surface-emitting lasers
[DE95-007758] p 2299 N95-28132

CHARGE COUPLED DEVICES
The systems of the proportional chambers registration electronics for present experiments in nuclear physics
[DE95-608559] p 2419 N95-27161
Development of a Robust star identification technique for use in attitude determination of the ACE spacecraft
p 2149 N95-27777
Single molecule detection using charge-coupled device array technology
[DE95-006425] p 2411 N95-27953

CHARGE DISTRIBUTION
Simple equivalent dipole distributions for dielectric spheroidal scatterers
[PB95-184883] p 2254 N95-27049
Charge distribution analysis of catalysts under simulated reaction conditions
[DE95-006943] p 2204 N95-27549
Projectile image acceleration, neutralization and electron emission during grazing interactions of multicharged ions with Au(110)
[DE95-007394] p 2409 N95-27551
On ionic charge distributions of heavy evaporation residues passing through a carbon foil
[DE94-629016] p 2414 N95-28184

CHARGE TRANSFER
ACT adaptive filters
[AD-A288385] p 2363 N95-26474
An acoustic charge transport imager for high definition television applications
[NASA-CR-197841] p 2249 N95-26708
Photoinduced dipoles and charge pairs in condensed phase
[DE95-007071] p 2207 N95-27921

CHARGE TRANSFER DEVICES
An acoustic charge transport imager for high definition television applications
[NASA-CR-197841] p 2249 N95-26708

CHARGED PARTICLES
Detection of charged particles in superfluid helium
[DE95-007354] p 2403 N95-26560
Simulating the production of free defects in irradiated metals
[DE95-007165] p 2214 N95-27088
Acceleration theorems
[DE95-007300] p 2420 N95-27484
Amorphous silicon pixel radiation detectors and associated thin film transistor electronics readout
[DE95-006568] p 2265 N95-27678
Burst of energetic ions from reversed field pinch plasma
[DE94-765447] p 2432 N95-27870
Nonlinear beam dynamics experimental program at SPEAR
[DE95-007823] p 2422 N95-28122
Rare decays/CP: The perspective of a kaon physicist
[DE95-005964] p 2416 N95-28338
Resonant coherent excitation of N6(+) and Mg11(+) in planar channeling: Anisotropies in ionization probabilities and X-ray emission
[DE95-006732] p 2417 N95-28595
Supercooled liquid dynamics for the charged hard-sphere model
[DE95-609158] p 2241 N95-28609
Proceedings of the International Workshop on Acceleration and Radiation Generation in Space and Laboratory Plasmas
[AD-A291673] p 2436 N95-28668

CHARM (PARTICLE PHYSICS)
Excited Charm States
[DE95-005749] p 2409 N95-27747
The Tau-Charm Factory in the ERA of B-Factories and CESR
[DE95-007894] p 2412 N95-28028
Polarization as a probe to the production mechanisms of charmonium in (pi)N collisions
[DE95-008136] p 2414 N95-28142
Recent status in the search for the quark-gluon plasma
[DE95-007036] p 2417 N95-28447
B-Physics results from D0
[DE95-005126] p 2417 N95-28495

CHARTS
Digital mapping, charting, and geodesy analysis program: Initial technical review of Raster Product Format
[AD-A289039] p 2313 N95-26476
A video strip chart program
[DE95-006389] p 2372 N95-27495
Ultrasonic studies of liquid/solid seimoacoustic wave phenomena
[AD-A289644] p 2402 N95-28622

CHEBYSHEV APPROXIMATION
The Benard problem: A comparison of finite difference and spectral collocation eigen value solutions
p 2283 N95-27364

CHELATION
Non-covalent immobilization of proteins and enzymes on polymerized lipid assemblies
[AD-A288234] p 2225 N95-26526

CHEMICAL ANALYSIS
The 18th Annual Condensed Matter Physics Meeting
[DE95-605568] p 2398 N95-26598
Determining nanoscale physical properties of materials by microscopy and spectroscopy
[AD-A289532] p 2201 N95-26870
The evaluation of a fluorochemical drying process for an electrical contact p 2227 N95-27103
Cleanliness verification process at Martin Marietta Astronautics p 2165 N95-27104
A summary of ODS replacement technologies at Litton Poly-Scientific p 2228 N95-27105
Ethyl lactate as a solvent alternative for cleaning metal parts p 2229 N95-27112

Corrosive effects of supercritical carbon dioxide and cosolvents on metals p 2224 N95-27113
Evaluations of the effectiveness of environmentally benign cleaning methodologies p 2230 N95-27115
Superior catalysts for selective catalytic reduction of nitric oxide
[DE95-007903] p 2205 N95-27691
Investigation on comprehensive fossil fuel cycle analysis and assessment approach as viewed from the global environment
[DE95-759241] p 2329 N95-27935
The structure of lead-indium phosphate glass
[DE95-007130] p 2237 N95-27967
Recovery, evaluation, and decontamination of landfilled pentaborane cylinders, former liquid propellant rocket engine test facility, Washoe County, Nevada
p 2171 N95-28302

CHEMICAL BONDS
Stabilization and control of high energy intermediates through adsorption of restricted spaces
[AD-A288552] p 2201 N95-26606
Theoretical studies of reaction surfaces
[AD-A288458] p 2404 N95-26632
Modeling the growth of electronic materials
[AD-A289137] p 2438 N95-26997
Atomic structure and bonding of boron-induced reconstructions on Si(001)
[AD-A289187] p 2405 N95-27017
High resolution Fourier transform spectroscopy of the first overtone of the N-O stretch in nitrosyl bromide
[AD-A289318] p 2203 N95-27295
Hydrogen induced C-C, C-N, and C-S bond activities on Pi and Ni surfaces
[DE95-006251] p 2206 N95-27838
The structure of lead-indium phosphate glass
[DE95-007130] p 2237 N95-27967

CHEMICAL CLEANING
Effects of bearing cleaning and lube environment on bearing performance p 2158 N95-27285

CHEMICAL COMPOSITION
Characterization of Ultra-Low Carbon Baintic steels for use as weld wire consumables
[AD-A288292] p 2212 N95-26411
Replicator for characterization of cirrus and polar stratospheric cloud particles
[NASA-CR-197785] p 2341 N95-26669
Recurrent novae p 2460 N95-27075

CHEMICAL ENERGY
Investigation on energy conversion technology using biochemical reaction elements, 2
[DE95-759250] p 2321 N95-27940

CHEMICAL ENGINEERING
Chemical engineering: Measurements for a competitive age
[NONP-NASA-VT-95-49098] p 2203 N95-27204
JPRS report: Science and technology. Central Eurasia
[JPRS-UST-95-015] p 2246 N95-27213
Intrusive multi-probe system
[DE95-006258] p 2292 N95-27465
The importance of propulsion engineers in protecting the global environment p 2170 N95-28295

CHEMICAL EQUILIBRIUM
Chlorodifluoromethane equilibrium on 13X molecular sieve
[AD-A289282] p 2405 N95-27034
Measurements of the volatilities of electrolytes: Application to water/steam cycles
[DE95-007103] p 2204 N95-27451
Transport coefficients for the NASA Lewis Chemical Equilibrium Program
[NASA-TM-4647] p 2209 N95-28182

CHEMICAL EXPLOSIONS
A compatibility study of containment materials in FEFO, bis-(2-fluoro-2,2-dinitroethyl) formal
[DE95-007548] p 2206 N95-27750
Investigation of HE driven cylindrical liner
[DE95-007866] p 2311 N95-28539

CHEMICAL PROPERTIES
Photoacoustic chambers for studying solids and gases: Theory and practical examples
[IFTR-39/1994] p 2143 N95-26837
Fundamental concepts of integrated and fiber optic sensors
[NASA-TM-106920] p 2426 N95-27906

CHEMICAL PROPULSION
The importance of propulsion engineers in protecting the global environment p 2170 N95-28295

CHEMICAL REACTIONS
Environmental effects on high energy density materials
[AD-A288296] p 2199 N95-26416
The use of electrochemistry and ellipsometry for identifying and evaluating corrosion on aircraft
[AD-A288536] p 2125 N95-27186
Analysis of gas absorption to a thin liquid film in the presence of a zero-order chemical reaction
p 2280 N95-27348
The influence of surface structure on the interaction of water with TiO2(100)
[DE95-004927] p 2203 N95-27401
Probe molecule studies: Active species in alcohol synthesis
[DE95-003514] p 2203 N95-27420
Charge distribution analysis of catalysts under simulated reaction conditions
[DE95-006943] p 2204 N95-27549
An overview of the Evaluation of Oxygen Interactions with Materials 3 experiment: Space Shuttle Mission 46, July-August 1992 p 2210 N95-27630
Evaluation of Oxygen Interactions with Materials 3: Mission and induced environments
p 2210 N95-27631
Investigation on LCA (Life Cycle Analysis/assessment)
[DE95-759260] p 2330 N95-27942
Beyond transition state theory: Rigorous quantum approaches for determining chemical reaction rates
[DE95-008483] p 2208 N95-28086
Analysis of forward and inverse problems in chemical dynamics and spectroscopy
[DE95-009309] p 2209 N95-28164
Chemical reactions identified in the Titan 2, Titan 4, and Delta 2 propellant systems and their application to source modeling p 2172 N95-28304
Poly(N-arylenbenzimidazoles) via aromatic nucleophilic displacement
[NASA-CASE-LAR-14939-1] p 2179 N95-28360
Polybenzimidazoles via aromatic nucleophilic displacement
[NASA-CASE-LAR-14924-1-CU] p 2179 N95-28361

CHEMICAL REACTORS
Absorption of sparingly soluble gases by reactive media in self-aerated gas-liquid contactors: A scale-up procedure
[DE95-006429] p 2206 N95-27707
Radiant exchange considerations in design and scaleup of photocatalytic reactors for purification of nitroglycerine-contaminated air p 2171 N95-28300

CHEMICAL TESTS
Measurement of high acidity using a renewable-reagent fiber optic sensor
[DE95-006327] p 2425 N95-27734

CHEMICAL VAPOR INFILTRATION
Ceramic composite combustor cans for expendable turbine engines
[AD-A289551] p 2140 N95-28646

CHEMICAL WARFARE
Chlorodifluoromethane equilibrium on 13X molecular sieve
[AD-A289282] p 2405 N95-27034

CHEMILUMINESCENCE
The sensitive detection of hydrazine using chemiluminescence p 2173 N95-28311
A comparison of NH3 point monitoring and diode laser based path integrated measurements
[DE95-006892] p 2332 N95-28602

CHEMISORPTION
Chemical physics of uniform cyclic etching
[AD-A288975] p 2404 N95-26574
Analysis of the dimerized Sb/Si(001)-(2x1) surface by x-ray standing waves
[DE95-007097] p 2208 N95-27965
Chemical and electrical properties of cavities in silicon and germanium
[DE95-006812] p 2445 N95-28206
Cesium/oxide interactions for ultrathin films on (alpha)-Al2O3(001) and (alpha)-Al2O3(1(bar 1)O2)
[DE95-008159] p 2236 N95-28358

CHEMORECEPTORS
Anti-idiotype probes for toxin detection
[AD-A288955] p 2348 N95-26435

CHINA
An observational study on the onset of the summer monsoon over eastern Asia in 1979
[AD-A289637] p 2341 N95-26723

CHINESE SPACECRAFT
Chinese space science and technology
[AD-A289618] p 2466 N95-26856

CHIPS
Orbital impacts and the Space Shuttle windshield
[NASA-TM-110594] p 2159 N95-26379
Monolithic electronics for nuclear and high-energy physics experiments
[DE95-005393] p 2420 N95-27427

CHIPS (ELECTRONICS)
Intelligent computer based reliability assessment of multichip modules
[AD-A288833] p 2259 N95-26550
An acoustic charge transport imager for high definition television applications
[NASA-CR-197841] p 2249 N95-26708
Construction of a connectionist network supercomputer
[AD-A288439] p 2377 N95-27182
Chua's circuits: Phenomena and applications
[AD-A291638] p 2271 N95-28666

CHIRALITY
Analysis of electromagnetic problems involving chiral, bi-isotropic, and uniaxial bianisotropic media
[PB95-185096] p 2248 N95-26450
Conditions for the parameter dyadics of lossless bi-anisotropic media
[PB95-185104] p 2252 N95-26914

CHIRP
Method and apparatus for maintaining linearity and frequency accuracy of an FM chirp waveform
[AD-D017398] p 2258 N95-28615

CHLORIDES
Atomically resolved STM study of the adsorption and dissociation of methyl chloride on Si(001)
[AD-A289218] p 2438 N95-27061
Thermodynamics of aqueous electrolytes at high temperatures by the isopiestic technique
[DE95-006747] p 2449 N95-27546

CHLORINATION
Bioremediation of chlorinated organics: PCBs, TCE, HCFCs p 2179 N95-27117

CHLORINE COMPOUNDS
Stratospheric ozone reactive chemicals generated by space launches worldwide
[AD-A289852] p 2332 N95-28623

CHLORINE FLUORIDES
Use of CTFE as an additive to enhance fire resistance of single hydraulic fluid
[AD-A289377] p 2233 N95-27325

CHLOROETHYLENE
Use of CTFE as an additive to enhance fire resistance of single hydraulic fluid
[AD-A289377] p 2233 N95-27325

CHLOROFLUOROCARBONS
Extended equation-of-state for dichlorodifluoromethane (CCl2F2)
[AD-A288885] p 2177 N95-26434
The evaluation of a fluorochemical drying process for an electrical contact p 2227 N95-27103
Methods development for measuring and classifying flammability/combustibility of refrigerants. Task 2: Test plan
[DE95-007066] p 2234 N95-27481
Vapor pressures of mixtures of CFC-114 with the potential replacement coolants C4F(10) andc-C4F 8
[DE95-003444] p 2208 N95-28042

CHLOROPHYLLS
Energy transfer in real and artificial photosynthetic systems
[DE95-005824] p 2351 N95-27948

CHOLESKY FACTORIZATION
Vector algorithms for solving 3D nonlinear magnetostatic problems
[DE95-608737] p 2399 N95-27298

CHOLESTEROL
Biochemically vulnerable sites for antifungal intercession in the control of fungal growth
[AD-A288345] p 2348 N95-26573

CHROMATOGRAPHY
An investigation of the applicability of the new Reillex(tm)-HPQ anion exchange resin system for technetium/rhenium and uranium in the Hanford waste tanks
[DE95-007643] p 2412 N95-28051

CHROMITES
Stability of chromite interconnections in dual environments
[DE95-007755] p 2267 N95-28131

CHROMIUM
NQR-NMR studies of higher alcohol synthesis Cu-Co catalysts
[DE95-007926] p 2205 N95-27680
Micromagnetics and microstructure of epitaxially grown Co and Co-Cr films for perpendicular magnetic recording
[DE95-004681] p 2441 N95-27720
Plasma source ion implantation of ammonia into electroplated chromium
[DE95-006275] p 2444 N95-28125

CHROMIUM ALLOYS
Surface energy driven crystallization of amorphous Ni69Cr14P17 alloy
[DE95-005543] p 2438 N95-27085

CHROMOPHORES
Applications of Second Harmonic and Sum Frequency Generation to graphite and silica type interfaces
[AD-A288228] p 2201 N95-26544

CHROMOSOMES
Automated integration of genomic physical mapping data via parallel simulated annealing
[DE95-008057] p 2351 N95-27725

CHRONIC CONDITIONS
Acute and subacute toxicity of ammonium dinitramide (ADN) p 2175 N95-28318
CIRCADIAN RHYTHMS
Research activities on somatosensory (SI) cortical neurons [AD-A288794] p 2348 N95-26360
Basic mechanisms and implications of non-photic entrainment of circadian rhythmicity [AD-A288433] p 2353 N95-26779
Crew adaptation evaluation of the Norwegian Crew Concept (NOROREW) [AD-A288478] p 2360 N95-27058
CIRCUIT BOARDS
Construction of a connectionist network supercomputer [AD-A288439] p 2377 N95-27182
CAE for thermal management of aerospace electronic boards using the BETAsoft program p 2272 N95-27354
Life cycle costs of alternatives for F-16 printed circuit board diagnosis equipment [AD-A288744] p 2138 N95-28586
CIRCUIT BREAKERS
Partial discharge testing of high voltage wiring harness for airborne displays [AD-A289150] p 2138 N95-27003
CIRCUIT PROTECTION
Characteristics of the standard current trip circuit [PB95-192886] p 2271 N95-28663
CIRCUIT RELIABILITY
Self-checking state machine realization in CMOS [AD-A289149] p 2261 N95-27002
I(sub DDQ) testing and defect classes: A tutorial [DE95-005467] p 2306 N95-27723
CIRCUITS
Calorimetric evaluation of commercial Ni-MH cells and charges p 2272 N95-26790
Characterization and redesign of the AFIT multielectrode array [AD-A289295] p 2354 N95-27039
Efficient generation of counterexamples and witnesses in symbolic model checking [AD-A288583] p 2370 N95-27095
High-precision buffer circuit for suppression of regenerative oscillation [NASA-TM-4658] p 2291 N95-27259
Monolithic electronics for nuclear and high-energy physics experiments [DE95-005393] p 2420 N95-27427
Atomic oxygen dosimetry measurements made on STS-46 by CONCAP 2 p 2418 N95-27634
Manufacturing tailored property ceramic composites [DE95-006303] p 2237 N95-27993
Low-power, parallel photonic interconnections for Multi-Chip Module applications [DE95-008518] p 2267 N95-28147
Novel field effect transistors for low power electronics [AD-A289929] p 2271 N95-28629
Chua's circuits: Phenomena and applications [AD-A291638] p 2271 N95-28666
CIRCULAR CYLINDERS
Unsteady base pressure measurements in the near wake of a cylinder with imposed three-dimensional disturbances [AD-A289498] p 2276 N95-26827
CIRCULAR ORBITS
Contingency maneuver strategies for the Total Ozone Mapping Spectrometer-Earth Probe (TOMS-EP) p 2152 N95-27796
CIRCULATION
Diagnostic system Cryo-D for the determination of parameters of vapor-liquid currents of the coolant [DE95-608775] p 2280 N95-27338
CIRRUS CLOUDS
Replicator for characterization of cirrus and polar stratospheric cloud particles [NASA-CR-197785] p 2341 N95-26669
Subvisual cirrus: What it is and where you find it [AD-A289329] p 2342 N95-26899
CIVIL AVIATION
CFD research, parallel computation and aerodynamic optimization [NASA-CR-197748] p 2120 N95-26649
The high speed civil transport and NASA's High Speed Research (HSR) program p 2118 N95-26945
An integrated GPS/INS/BARO and radar altimeter system for aircraft precision approach landings [AD-A289280] p 2127 N95-26985
A review of Australian and New Zealand investigations on aeronautical fatigue during the period Apr. 1993 - Mar. 1995 [AR-009-202] p 2136 N95-27918
Rotorcraft crashworthy airframe and fuel system technology development program [AD-A289986] p 2126 N95-28630
CLADDING
Bases for extrapolating materials durability in fuel storage pools [DE95-007748] p 2222 N95-28129
CLAMPS
Changing paradigms: Manufacturing vs. fabricating a high volume Hold Down and Release Mechanism p 2155 N95-27267
The Clementine mechanisms p 2156 N95-27268
Non-explosive actuation for the ORBCOMM (TM) satellite p 2156 N95-27274
CLASSICAL MECHANICS
Magnetization of ferromagnetic clusters [DE95-006878] p 2399 N95-27548
CLASSIFICATIONS
Dwarf novae p 2458 N95-27069
Classical novae and recurrent novae: General properties p 2459 N95-27072
A comparison of error categorization schemes for use in software system safety programs [AD-A288741] p 2371 N95-27251
Multivariate classification of BPSG thin films using Mahalanobis distances [DE95-008519] p 2267 N95-28148
Cloud classification using whole-sky imager data [DE95-006501] p 2344 N95-28556
CLASSIFIERS
Isolated digit recognition without time alignment [AD-A289344] p 2254 N95-27062
CLAYS
The biodegradation of fuels in soils and sediments: Differences as a function of mineralogy p 2230 N95-27116
The development of mechanical strength in a ceramic material during firing [DE95-004925] p 2234 N95-27476
The PCMDI Visualization and Computation System (VCS): A workbench for climate data display and analysis [DE95-008586] p 2328 N95-27558
Superior catalysts for selective catalytic reduction of nitric oxide [DE95-007903] p 2205 N95-27691
CLEANERS
Environmentally Benign Cleaning and Degreasing Technology: JANNAF Safety and Protection Subcommittee and Propellant Development and Characterization Subcommittee Joint Workshop [CPIA-PUBL-611] p 2227 N95-27101
Wipe solvent substitutions for 1,1,1-trichloroethane (TCA) and methyl ethyl ketone (MEK) at Hill Air Force Base p 2228 N95-27107
Alternative cleaning solvents and lubricants at the Air Force PJKS facility p 2228 N95-27108
Microbial treatment for shipboard collection, hold ing, and transfer system tanks p 2179 N95-27119
Survey of environmentally benign cleaning methodologies and materials p 2231 N95-27122
Sceening, down selection, and implementation of environmentally compliant cleaning and insulation bonding for MNASA p 2165 N95-27124
Water driven turbine/brush pipe cleaner [NASA-CASE-KSC-11669-1] p 2304 N95-28359
CLEANING
Stability of reference masses 4: Growth of carbonaceous contamination on platinum-iridium mass standard surfaces, and its cleaning by UV/ozone treatment [PB95-190096] p 2226 N95-26745
The evaluation of a fluorochemical drying process for an electrical contact p 2227 N95-27103
Cleanliness verification process at Martin Marietta Astronautics p 2165 N95-27104
A summary of ODS replacement technologies at Litton Poly-Scientific p 2228 N95-27105
Observations on the solvating power of supercritical fluids p 2228 N95-27106
Wipe solvent substitutions for 1,1,1-trichloroethane (TCA) and methyl ethyl ketone (MEK) at Hill Air Force Base p 2228 N95-27107
Alternative cleaning solvents and lubricants at the Air Force PJKS facility p 2228 N95-27108
CO2 pellet blast cleaning and degreasing: The true environmentally benign technology p 2229 N95-27109
Precision parts cleaning with supercritical CO2: Practical applications and solutions p 2229 N95-27111
Ethyl lactate as a solvent alternative for cleaning metal parts p 2229 N95-27112
Corrosive effects of supercritical carbon dioxide and cosolvents on metals p 2224 N95-27113
Precision parts cleaning with supercritical carbon dioxide p 2229 N95-27114
Evaluations of the effectiveness of environmentally benign cleaning methodologies p 2230 N95-27115
Microbial treatment for shipboard collection, hold ing, and transfer system tanks p 2179 N95-27119
Application of bacterial bioemusifiers to in situ maintenance of oil/water separators p 2179 N95-27120
Aqueous degreasing, precision cleaning, and cleanliness verification p 2231 N95-27121
Survey of environmentally benign cleaning methodologies and materials p 2231 N95-27122
Cleaning of parts for new manufacturing and parts rebuilding p 2231 N95-27123
Sceening, down selection, and implementation of environmentally compliant cleaning and insulation bonding for MNASA p 2165 N95-27124
Design considerations in supercritical fluid technology p 2232 N95-27126
Retrofitting conventional vapor degreasers to use a solvent wash/fluorochemical rinse process p 2232 N95-27127
The experience of CF Technologies, Inc. (CF Tech) in critical fluid processing p 2232 N95-27128
Fluid dynamic effects on precision cleaning with supercritical fluids p 2232 N95-27129
The application of waterjets for cleaning p 2233 N95-27130
Hardware cleanliness methodology and certification p 2211 N95-27656
Sensor for measuring the atomic fraction in highly dissociated hydrogen [DE95-006531] p 2415 N95-28204
The demilitarization of class 1.1 rocket motors using high pressure waterjets p 2176 N95-28322
Cryogenic washout of solid rocket propellants p 2176 N95-28324
Water driven turbine/brush pipe cleaner [NASA-CASE-KSC-11669-1] p 2304 N95-28359
CLEANLINESS
Cleanliness verification process at Martin Marietta Astronautics p 2165 N95-27104
Aqueous degreasing, precision cleaning, and cleanliness verification p 2231 N95-27121
Hardware cleanliness methodology and certification p 2211 N95-27656
CLEAR AIR TURBULENCE
Three objective indices for clear-air turbulence reconsidered [KNMI-TR-160] p 2342 N95-27366
CLEARANCES
WINCLR: A computer code for heat transfer and clearance calculation in a compressor [NASA-CR-195436] p 2117 N95-26363
CLEAVAGE
An experimental and numerical investigation of specimen size requirements for cleavage fracture toughness [AD-A289120] p 2311 N95-28100
CLIMATE
Subvisual cirrus: What it is and where you find it [AD-A289329] p 2342 N95-26899
The PCMDI Visualization and Computation System (VCS): A workbench for climate data display and analysis [DE95-008586] p 2328 N95-27558
Calculations of downward IR surface fluxes in the 500-3,000 cm(exp -1) wavenumber range for the 1994 ICRCCM model intercomparison study [DE95-006430] p 2328 N95-27708
A study of surface temperatures, clouds and net radiation [NASA-CR-198589] p 2329 N95-27864
Towards the detection and attribution of an anthropogenic effect on climate [DE95-008589] p 2331 N95-28157
Measurements of daytime and upper tropospheric water vapor profiles by Raman lidar [DE95-007640] p 2344 N95-28538
The Global Historical Climatology Network: A preview of version 2 [DE95-007003] p 2332 N95-28605
CLIMATE CHANGE
Technical report series on global modeling and data assimilation. Volume 6: A multiyear assimilation with the GEOS-1 system: Overview and results [NASA-TM-104606-VOL-6] p 2334 N95-26423
A parallel coupled oceanic-atmospheric general circulation model [DE95-005918] p 2335 N95-26622
Integrated assessment and the relation between land-use change and climate change [DE95-006533] p 2327 N95-27469
Coupled chemistry/climate issues [DE95-006443] p 2327 N95-27532
Issues relevant to the development of coupled chemistry/climate models [DE95-006441] p 2330 N95-27954
Research project on CO2-induced climate change [DE95-008339] p 2330 N95-28084

The Global Historical Climatology Network: A preview of version 2
[DE95-007003] p 2332 N95-28605

CLIMATE MODELS
A parallel coupled oceanic-atmospheric general circulation model
[DE95-005918] p 2335 N95-26622
The PCMDI Visualization and Computation System (VCS): A workbench for climate data display and analysis
[DE95-008586] p 2328 N95-27558
Calculations of downward IR surface fluxes in the 500-3,000 cm(exp -1) wavenumber range for the 1994 ICRCCM model intercomparison study
[DE95-006430] p 2328 N95-27708
Issues relevant to the development of coupled chemistry/climate models
[DE95-006441] p 2330 N95-27954
Advances in scientific visualization
[DE95-008065] p 2343 N95-28014
Models used to forecast agricultural corn crops in the micro-region of Ribeirao Preto-SP
[INPE-5513-NTC/309] p 2315 N95-28554

CLIMATOLOGY
Technical report series on global modeling and data assimilation. Volume 6: A multiyear assimilation with the GEOS-1 system: Overview and results
[NASA-TM-104606-VOL-6] p 2334 N95-26423
Spectral analyses, climatology, and interannual variability of Nimbus-7 TOMS version 6 total column ozone
[NASA-RP-1360] p 2341 N95-26689
Southern Africa: A climatological study
[AD-A289466] p 2342 N95-27148
Integrated assessment and the relation between land-use change and climate change
[DE95-006533] p 2327 N95-27469
Coupled chemistry/climate issues
[DE95-006443] p 2327 N95-27532
PRISM validation
[AD-A288476] p 2337 N95-27703
A study of surface temperatures, clouds and net radiation
[NASA-CR-198589] p 2329 N95-27864
The distribution of cloud cover over the former USSR as derived from the RIHMI 223-Station 3-hourly meteorological database
[DE95-007046] p 2343 N95-27920
A summary documentation of the AMIP models
[DE95-008343] p 2338 N95-27931
Issues relevant to the development of coupled chemistry/climate models
[DE95-006441] p 2330 N95-27954
The program for calculating sunshine duration from global radiation
[KNMI-TR-158] p 2343 N95-28237
The northern wintertime divergence extrema at 200 hPa and surface cyclones as simulated in the integration of the ECMWF general circulation model
[DE95-007946] p 2332 N95-28550
The Global Historical Climatology Network: A preview of version 2
[DE95-007003] p 2332 N95-28605
A black carbon emission data base for atmospheric chemistry and climate studies
[DE95-006436] p 2332 N95-28662

CLOUD COVER
Longterm infrared cloud clutter research
[AD-A288632] p 2340 N95-26343
Diagnosing cloudiness from global numerical weather prediction model forecasts
[AD-A289456] p 2356 N95-26992
The distribution of cloud cover over the former USSR as derived from the RIHMI 223-Station 3-hourly meteorological database
[DE95-007046] p 2343 N95-27920
Advances in scientific visualization
[DE95-008065] p 2343 N95-28014
Cloud classification using whole-sky imager data
[DE95-006501] p 2344 N95-28556

CLOUD DISPERSAL
The small-scale structure of dispersing clouds in the atmosphere
[AD-A288256] p 2341 N95-26546

CLOUD GLACIATION
Replicator for characterization of cirrus and polar stratospheric cloud particles
[NASA-CR-197785] p 2341 N95-26669

CLOUD PHYSICS
Longterm infrared cloud clutter research
[AD-A288632] p 2340 N95-26343
The small-scale structure of dispersing clouds in the atmosphere
[AD-A288256] p 2341 N95-26546

CLOUDS
Site scientific mission plan for the Southern Great Plains CART site, January-June 1995
[DE95-008393] p 2344 N95-28340

CLOUDS (METEOROLOGY)
The small-scale structure of dispersing clouds in the atmosphere
[AD-A288256] p 2341 N95-26546
Prediction of rain attenuation and total atmospheric attenuation for low-availability satellite communications in Europe
[PB95-184925] p 2252 N95-26908
A study of surface temperatures, clouds and net radiation
[NASA-CR-198589] p 2329 N95-27864
The distribution of cloud cover over the former USSR as derived from the RIHMI 223-Station 3-hourly meteorological database
[DE95-007046] p 2343 N95-27920
Anomalous cloud absorption? A critique of the paper entitled Absorption of Solar Radiation by Clouds: Observations Versus Models
[DE95-007703] p 2331 N95-28121
Cloud classification using whole-sky imager data
[DE95-006501] p 2344 N95-28556

CLUSTERS
Optical features of nanosize iron and molybdenum sulfide clusters
[DE95-005417] p 2202 N95-27136

CLUTTER
Longterm infrared cloud clutter research
[AD-A288632] p 2340 N95-26343
Auto-processing of OTH radar amplitude/range/Doppler data
[AD-A289152] p 2253 N95-27005
Measurements of HF auroral clutter using the Verona Ava Linear Array Radar (VALAR)
[AD-A289442] p 2337 N95-27147
Nonlinear signal processing schemes for robust target detection in radar
[AD-A288449] p 2255 N95-27185

CMOS
Silicon based microactuators for telerobotic tactile stimulation
[AD-A289340] p 2260 N95-26767
Solid-state image sensor with focal-plane digital photon-counting pixel array
[NASA-CASE-NPO-18518-1-CU] p 2424 N95-26894
Self-checking state machine realization in CMOS
[AD-A289149] p 2261 N95-27002
I(sub DDQ) testing and defect classes: A tutorial
[DE95-005467] p 2306 N95-27723

COAL
Comparison of the activities of fine-particle size catalysts
[DE95-004773] p 2203 N95-27423
Ash-based ceramic materials
[AD-D017272] p 2241 N95-28582
Coatings of non-oxide ceramics for improved corrosion resistance in high temperature coal combustion
[DE95-006932] p 2241 N95-28604

COAL LIQUEFACTION
Comparison of the activities of fine-particle size catalysts
[DE95-004773] p 2203 N95-27423

COASTAL WATER
Performance modeling of hyperspectral imaging sensors for atmospheric studies
[AD-A289017] p 2289 N95-26461
VOCAR: An experiment in Variability of Coastal Atmospheric Refractivity
[AD-A289202] p 2253 N95-27006

COASTS
Fluxes across the west coast resolved by Picket Fence observations during stormfest
[AD-A288511] p 2341 N95-26653
Meteorological and oceanographic data collected during the ASREX 91 field experiment
[AD-A289492] p 2342 N95-26826

COATING
Characterization of optical polymers for multi-layered electro-optic devices
[AD-A289255] p 2227 N95-26973
The response of hydrotalcite coated aluminum to sealing with transition metal salt solutions
[DE95-004767] p 2234 N95-27460
Processing and properties of chromate-free conversion coatings on aluminum
[DE95-004768] p 2218 N95-27722
Control of thin film processing behavior through precursor structural modifications
[DE95-006468] p 2444 N95-28103
Chromate-free corrosion resistant conversion coatings for aluminum alloys
[DE95-007742] p 2238 N95-28117
Weightless Environment Training Facility (WETF) materials coating evaluation, volume 2
[NASA-CR-188366-VOL-2] p 2239 N95-28386

COATINGS
The response of hydrotalcite coated aluminum to sealing with transition metal salt solutions
[DE95-004767] p 2234 N95-27460
Faraday screen sputtering on TPX
[DE95-008347] p 2434 N95-28224
Task 4 supporting technology. Part 1: Detailed test plan for leading edge tile development. Leading edge material development and testing
[NASA-CR-198633] p 2160 N95-28258
Contact micromechanics in granular media with clay
[DE95-006566] p 2340 N95-28583
Mechanism of deposit formation on fuel-wetted hot metal surfaces
[AD-A289847] p 2210 N95-28621

COAXIAL FLOW
Supersonic coaxial jet noise predictions
[NASA-TM-106917] p 2401 N95-26801

COAXIAL NOZZLES
The noise reduction potential of dual-stream coaxial rectangular improperly expanded jet flows
[NASA-CR-197820] p 2277 N95-26995

COBALT
Probe molecule studies: Active species in alcohol synthesis
[DE95-003514] p 2203 N95-27420
Solid film lubricants and thermal control coatings flown aboard the EOIM-3 MDA sub-experiment
p 2242 N95-27640

COBALT ALLOYS
Micromagnetics and microstructure of epitaxially grown Co and Co-Cr films for perpendicular magnetic recording
[DE95-004681] p 2441 N95-27720
Electronic structure of ordered and disordered transition metal aluminides
[DE95-609034] p 2223 N95-28250

COBALT COMPOUNDS
Experimental determination of cluster geometrical structure
[DE95-007089] p 2409 N95-27753

COCKPIT SIMULATORS
The photo-realistic AFIT virtual cockpit
[AD-A289376] p 2130 N95-26876

COCKPITS
Integrated mission precision attack cockpit technology (IMPACT). Phase 1: Identifying technologies for air-to-ground fighter integration
[AD-A289562] p 2129 N95-26684
An analysis of the KC-135 three-person cockpit
[AD-A289540] p 2130 N95-26873
The photo-realistic AFIT virtual cockpit
[AD-A289376] p 2130 N95-26876
Operator modeling in commerical aviation: Cognitive models, intelligent displays, and pilot's assistants
[NASA-CR-198609] p 2138 N95-28203

CODERS
ELVIS: Eigenvectors for land vehicle image system
[AD-A289297] p 2381 N95-27041
Ultra-high, resolution, modular optical angle encoder for space-based opto-mechanical applications
p 2156 N95-27270
Pulse Code Modulation (PCM) encoder handbook for Aydin Vector MMP-900 series system
[NASA-RP-1365] p 2255 N95-27435
Vocoded KING data base
[AD-A289827] p 2258 N95-28576

CODING
Encoding user-defined problems with SIPE-2
[AD-A288390] p 2380 N95-26475
Com(sup 3): A composite-compatible component coding system
[BBC-RD-1994/17] p 2249 N95-26670
Computing NORAD mean orbital elements from a state vector
[AD-A289281] p 2146 N95-27033
Real-time data compression using a fixed Huffman encoding scheme
[DE95-006159] p 2455 N95-27949
Modeling helicopter blade dynamics using a modified Myklestad-Prohl transfer matrix method
[AD-A289891] p 2136 N95-28626

COEFFICIENTS
Performance evaluation of a new parallel preconditioner
[AD-A288563] p 2376 N95-26529
Layer coefficients for NHDOT pavement materials
[AD-A288262] p 2246 N95-26548
Characterization of optical polymers for multi-layered electro-optic devices
[AD-A289255] p 2227 N95-26973
Time-dependent model for vertical-cavity surface-emitting laser
[DE95-007880] p 2298 N95-28027

Transport coefficients for the NASA Lewis Chemical Equilibrium Program
[NASA-TM-4647] p 2209 N95-28182
Atmospheric dispersion in adaptive optics
[AD-A289639] p 2428 N95-28617

COGNITION
Handbook of perception and human performance, volume 2. Cognitive processes and performance
[AD-A289587] p 2355 N95-26692
Myers-Briggs type indicators and Kirton adaption-innovation inventory correlations
[AD-A288435] p 2357 N95-27181
Operator modeling in commerical aviation: Cognitive models, intelligent displays, and pilot's assistants
[NASA-CR-198609] p 2138 N95-28203
Cognitive networks for ATR: The roles of bifurcation and chaos
[AD-A289010] p 2387 N95-28336

COHERENT LIGHT
Nonlinear dynamics of a coherent polariton-biexciton system
[DE95-609150] p 2417 N95-28607

COLD PLASMAS
Electromagnetic devices and processes in environment protection
[AD-A288656] p 2141 N95-26487
Ordered one-component plasmas: Phase transitions, normal modes, large systems, and experiments in a storage ring
[DE95-007077] p 2434 N95-28233
Proceedings of the International Workshop on Acceleration and Radiation Generation in Space and Laboratory Plasmas
[AD-A291673] p 2436 N95-28668

COLD ROLLING
Composite prepreg application device
[NASA-CASE-LAR-15259-1] p 2182 N95-27192

COLD STRENGTH
Layer coefficients for NHDOT pavement materials
[AD-A288262] p 2246 N95-26548

COLD WEATHER
Lightweight cold weather underwear investigation
[AD-A288506] p 2358 N95-26736

COLD WORKING
Effects of helium pre-implantation on the microstructure and mechanical properties of irradiated 316 stainless steel
[DE95-007162] p 2214 N95-27086

COLLAPSE
The collapse of composite cylindrical panels with various thickness using finite element analysis
[AD-A289370] p 2308 N95-26905
The minimum pore size obtainable in a silica gel during drying
[DE95-008162] p 2239 N95-28401

COLLINEARITY
Magnetic structures in RNi2B2C (R = Ho, Er) superconductors
[DE95-008370] p 2442 N95-27932
Efficient analytic computation of higher-order QCD amplitudes
[DE95-008593] p 2449 N95-28160

COLLISION PARAMETERS
Collisional dynamics and spectroscopic studies of highly excited rovibrational levels of I2(X)(0(+)(sub g)) via stimulated emission pumping
[AD-A289447] p 2295 N95-27172
Recent status in the search for the quark-gluon plasma
[DE95-007036] p 2417 N95-28447
B-Physics results from D0
[DE95-005126] p 2417 N95-28495

COLLISION RATES
Anomalous collision rate in the time counter scheme of the direct simulation Monte Carlo method for rarefied gas flow analysis
[ISAS-R-653] p 2275 N95-26742
Some notes on long-range beam-beam effects for the 2 TeV collider
[DE95-006771] p 2421 N95-28017

COLLISIONS
A study of parton distribution functions with the use of photon + jet event kinematics in p(bar p) collisions at (radical)s = TeV
[DE95-005127] p 2408 N95-27444
Collisions of highly charged ions with electrons, atoms and surfaces
[DE95-007393] p 2413 N95-28078
Polarization as a probe to the production mechanisms of charmonium in (pi)N collisions
[DE95-008136] p 2414 N95-28142
Precise measurement of the left-right cross section asymmetry in Z boson production by e(+)e(-) collisions
[DE95-008591] p 2414 N95-28158.
Time-resolved FTIR emission studies of laser photofragmentation and radical reactions
[DE95-008125] p 2300 N95-28398
Monte-Carlo simulation methods for finite flat plate winding flows
[AD-A289842] p 2289 N95-28619

COLLOCATION
The Benard problem: A comparison of finite difference and spectral collocation eigen value solutions
p 2283 N95-27364

COLOR
Image quality metrics for color CRT displays
[AD-A288934] p 2262 N95-27196
Search for exotic particles at CDF
[DE95-008383] p 2411 N95-27933
Measurement of particle transport coefficients on Alcator C-Mod
[DE95-007763] p 2411 N95-28020

COLOR VISION
Factors in human-computer interface design (a pilot study)
[AD-A288908] p 2360 N95-27195
Practical color vision tests for air traffic control applicants: En route center and terminal facilities
[DOT/FAA/AM-95/13] p 2357 N95-27323

COMBAT
A mathematical analysis of the Janus combat simulation weather effects models and sensitivity analysis of sky-to-ground brightness ratio on target detection
[AD-A289629] p 2336 N95-26858

COMBINATORIAL ANALYSIS
Yang-Baxter type equations and posets of maximal chains
[PB95-185195] p 2388 N95-26516
Scalability in production system programs
[AD-A289345] p 2453 N95-27063
A path-oriented knowledge representation system: Defusing the combinatorial system p 2386 N95-27395
A spectral algorithm for the seriation problem
[DE95-004775] p 2372 N95-27436
Symmetries of the KAC-Peterson modular matrices of affine algebras
[PB95-190138] p 2392 N95-28010

COMBINED STRESS
The role of biaxial stresses in discriminating between meaningful and illusory composite failure theories
p 2187 N95-28287

COMBUSTIBLE FLOW
Numerical simulation of combustion flow around a flame holder with hydrogen injection
[NAL-TR-1233] p 2200 N95-26523
A laboratory scale supersonic combustive flow system
[DE95-006347] p 2206 N95-27851

COMBUSTION
Transport phenomena and interfacial kinetics in multiphase combustion systems
[AD-A288297] p 2199 N95-26417
Numerical simulation of combustion flow around a flame holder with hydrogen injection
[NAL-TR-1233] p 2200 N95-26523
Ram accelerator performance calculations using a modified version of the NASA CET89 equilibrium chemistry code
[AD-A289554] p 2201 N95-26678
Design and development of experimental facilities for short duration, low-gravity combustion and fire experiments
[NASA-CR-195458] p 2244 N95-26709
Biomass Pyrolysis Oil Properties and Combustion Meeting
[DE95-004017] p 2204 N95-27438
Methods development for measuring and classifying flammability/combustibility of refrigerants. Task 2: Test plan
[DE95-007066] p 2234 N95-27481
Evaluating the environmental viability of open burning/open detonation operations
p 2170 N95-28297
Upgrade of the computer modeling programs POLU10 and POLU13A for open burning and open detonation of energetic materials p 2172 N95-28306

COMBUSTION CHAMBERS
Experiment on a rectangular cross section scramjet combustor. 2: Effects of fuel injector geometry
[NAL-TR-1220] p 2139 N95-26600
NASA Lewis Research Center's combustor test facilities and capabilities
[NASA-TM-106903] p 2143 N95-27176
Three-dimensional computer modeling of hydrogen injection and combustion
[DE95-006261] p 2203 N95-27437
Three-dimensional visualization of reactive flows in complex geometries
[DE95-006332] p 2284 N95-27845
Turbulence models for gas turbine combustors
p 2285 N95-27888
Combustion system CFD modeling at GE Aircraft Engines p 2285 N95-27889
Experimental investigation of inlet-combustor isolators for a dual-mode scramjet at a Mach number of 4
[NASA-TP-3502] p 2140 N95-28343
AMCC casting development. Volume 1: Executive Summary
[NASA-CR-196597] p 2247 N95-28419
Ceramic composite combustor cans for expendable turbine engines
[AD-A289551] p 2140 N95-28646

COMBUSTION CHEMISTRY
Transport phenomena and interfacial kinetics in multiphase combustion systems
[AD-A288297] p 2199 N95-26417
Design and development of experimental facilities for short duration, low-gravity combustion and fire experiments
[NASA-CR-195458] p 2244 N95-26709
Chemical engineering: Measurements for a competitive age
[NONP-NASA-VT-95-49098] p 2203 N95-27204
High temperature kinetic study of the reactions H + O2 = OH + O and O + H2 = OH + H in H2/O2 system by shock tube-laser absorption spectroscopy
[NASA-CR-195473] p 2206 N95-27695
Recent progress in the joint velocity-scalar PDF method p 2285 N95-27890
Experience with turbulence interaction and turbulence-chemistry models at Fluent Inc.
p 2286 N95-27893

COMBUSTION EFFICIENCY
High pressure Earth storable rocket technology program: Basic program
[NASA-CR-195449] p 2166 N95-26390
Experiment on a rectangular cross section scramjet combustor. 2: Effects of fuel injector geometry
[NAL-TR-1220] p 2139 N95-26600

COMBUSTION PHYSICS
Chemical engineering: Measurements for a competitive age
[NONP-NASA-VT-95-49098] p 2203 N95-27204
Turbulence program for propulsion systems
p 2285 N95-27883
Research on combustion processes relevant to burners in HVAC systems
[PB95-179735] p 2208 N95-28006
Application of modern diagnostic methods to environmental improvement
[DE95-005797] p 2330 N95-28119
Coatings of non-oxide ceramics for improved corrosion resistance in high temperature coal combustion
[DE95-006932] p 2241 N95-28604

COMBUSTION STABILITY
A fully implicit time accurate method for hypersonic combustion: Application to shock-induced combustion instability
[NASA-TM-106707] p 2273 N95-26380

COMBUSTION TEMPERATURE
NASA Lewis Research Center's combustor test facilities and capabilities
[NASA-TM-106903] p 2143 N95-27176

COMETARY COLLISIONS
Tracking and impact prediction of Earth-Crossing-Objects (ECO's) on a collision course with Earth
[AD-A289321] p 2461 N95-27303

COMETS
Observations of comets with the IUE
[NASA-CR-197816] p 2461 N95-27166
Tracking and impact prediction of Earth-Crossing-Objects (ECO's) on a collision course with Earth
[AD-A289321] p 2461 N95-27303

COMMAND AND CONTROL
The controller memory guide. Concepts from the field
[AD-A289263] p 2127 N95-26978
Semantic heterogeneity in database and data dictionary integration for command and control systems
[AD-A289180] p 2453 N95-27014
Design and implementation of a software communication architecture for the JANUS-3D Visualizer
[AD-A288509] p 2370 N95-27150

COMMERCE
Implementing an integrated standards-based management system to ensure compliance at Los Alamos National Laboratory
[DE95-007873] p 2451 N95-28025

COMMERCIAL AIRCRAFT
Strategy in the commercial aircraft industry in the United States: A comparison of decisionmaking by McDonnell-Douglas and Boeing aircraft companies from 1977-1983
[AD-A288289] p 2117 N95-26409

Radiation safety aspects of commercial high-speed flight transportation
[NASA-TP-3524] p 2465 N95-26427

An integrated GPS/INS/BARO and radar altimeter system for aircraft precision approach landings
[AD-A289280] p 2127 N95-26985

Pilot opinions on high level flight deck automation issues: Toward the development of a design philosophy
[NASA-CR-4669] p 2357 N95-28253

Study of potential aerodynamic benefits from spanwise blowing at wingtip
[NASA-TP-3515] p 2124 N95-28669

COMMERCIAL SPACECRAFT

Solar array deployment mechanism
p 2155 N95-27266

Global trade in satellites and launch services
[GPO-84-811] p 2165 N95-28342

COMMUNICATION

The effects of Crew Resource Management (CRM) training in airline maintenance: Results following three year's experience
[NASA-CR-196696] p 2358 N95-28676

COMMUNICATION EQUIPMENT

Testing of Uninterruptible Power Supplies with nonlinear loads
[AD-A289353] p 2262 N95-27067

The evolution and impact of PCS technology
[AD-A288606] p 2255 N95-27249

COMMUNICATION NETWORKS

Assessment of long-distance HF radio and satellite communication assets for RNLAF out-of-area operations
[AD-A288633] p 2247 N95-26344

Scalable multicast tree construction for wide area networks
[AD-A288318] p 2379 N95-26421

Design and implementation of a software communication architecture for the JANUS-3D Visualizer
[AD-A288509] p 2370 N95-27150

Radio telemetry buoy for long-range communication
[AD-D017269] p 2161 N95-28581

COMMUNICATION SATELLITES

An architecture and protocol for communications satellite constellations regarded as multi-agent systems
p 2166 N95-27377

ORION: A Supersynchronous Transfer Orbit mission
p 2154 N95-27804

Preliminary flight software specification for the petite amateur Navy satellite (PANSAT)
[AD-A280068] p 2165 N95-28150

Global trade in satellites and launch services
[GPO-84-811] p 2165 N95-28342

COMMUTATION

Dynamically timed electric motor
[NASA-CASE-MFS-28958-1] p 2261 N95-26890

On compact multipliers of topological algebras
[DE95-608751] p 2390 N95-27092

q-structure algebra of U(sub q)(g-circumflex) from its adjoint action
[DE95-608749] p 2390 N95-27301

Some commutativity theorems for a certain class of rings
[DE95-608750] p 2390 N95-27302

Realization of vector fields for quantum groups as pseudodifferential operators on quantum spaces
[DE95-008485] p 2449 N95-27877

Coordinates of the quantum plane as q-tensor operators in U(sub q) (su(2) * su(2))
[DE95-007100] p 2397 N95-28234

COMMUTATORS

A case study in automated theorem proving: A difficult problem about commutators
[DE95-008392] p 2392 N95-28173

COMPACTING

Compactification of moduli spaces of monopoles
[PB95-185179] p 2388 N95-26515

The effects of processing variables on reaction synthesis of Fe-Al alloys
[DE95-007405] p 2221 N95-28082

Residual stress, strain, and faults in nanocrystalline palladium and copper
[DE95-008294] p 2223 N95-28543

COMPARISON

An in situ evaluation of TOPEX/Poseidon altimetric measurements versus meaurements made by moorings and inverted echo sounders for sea surface height
[NASA-CR-198621] p 2347 N95-27805

COMPATIBILITY

Wipe solvent substitutions for 1,1,1-trichloroethane (TCA) and methyl ethyl ketone (MEK) at Hill Air Force Base p 2228 N95-27107

Alternative cleaning solvents and lubricants at the Air Force PJKS facility p 2228 N95-27108

COMPETITION

Information superhighway: Issues affecting development
[AD-A289434] p 2252 N95-26923

Global trade in satellites and launch services
[GPO-84-811] p 2165 N95-28342

COMPILERS

Control-flow analysis and type systems
[AD-A289338] p 2389 N95-26772

High performance hardware and software for pattern recognition and image processing
[AD-A289153] p 2370 N95-27031

COMPLEX COMPOUNDS

Structural oxidation state studies of the manganese cluster in the oxygen evolving complex of Photosystem II
[DE95-008488] p 2409 N95-27744

COMPLEX NUMBERS

Spectral properties of multipliers on topological algebras
[DE95-608747] p 2390 N95-27299

COMPLEX SYSTEMS

Nonlinear dynamics of global atmospheric and earth system processes
[NASA-CR-197926] p 2326 N95-26429

The phenomena of subharmonic bifurcations, runaway, and transition to chaos in a non-linear oscillator: perturbation methods and a numerical experiment
[IFTR-16/1994] p 2398 N95-26518

Digital systems validation. Chapter 20 Artificial Intelligenge with applications for aircraft. Handbbook, volume 2
[AD-A288492] p 2380 N95-26638

The controller memory guide. Concepts from the field
[AD-A289263] p 2127 N95-26978

Model-based monitoring and diagnosis of a satellite-based instrument p 2166 N95-27390

COMPLEXITY

Generalized CNF satisfiability, local reductions and complexity of succinctly specified problems
[DE95-006343] p 2372 N95-27849

COMPOSITE MATERIALS

Split pipe testing device for the measurement of bond of reinforcement under controlled confinement
[AD-D017258] p 2245 N95-26500

Molecular object liquid crystals: An approach to new materials
[AD-A288905] p 2437 N95-26553

The 18th Annual Condensed Matter Physics Meeting
[DE95-605568] p 2398 N95-26598

Design and processing of materials by biomimicking. Section 2. Publications
[AD-A288230] p 2226 N95-26624

Materials with self organized surfaces: 2D polymer assemblies
[AD-A288928] p 2226 N95-26627

Microengineered conducting composites from nanochannel templates
[AD-A289573] p 2180 N95-26686

Analysis of plate-twist test for in-plane shear modulus of composite materials (revised)
[PB95-190195] p 2308 N95-26749

Materials Research Society Symposium Proceedings. Volume 339: Diamond, SiC and nitride wide bandgap semiconductors
[AD-A288690] p 2437 N95-26818

Evaluation of composite joints
[AD-A289247] p 2181 N95-26967

Chlorodifluoromethane equilibrium on 13X molecular sieve
[AD-A289282] p 2405 N95-27034

Modeling considerations in the prediction of residual strength in composite laminates
[AD-A289128] p 2182 N95-27142

Bimaterial interlaces and their role in the mechanical performance of the in-situ composites
[AD-A288973] p 2182 N95-27188

A cryogenic scan mechanism for use in Fourier transform spectrometers p 2158 N95-27287

A FEAM based methodology for analyzing composite patch repairs of metallic structures
p 2133 N95-27511

Rapid repair of large area damage to contoured aircraft structures p 2133 N95-27516

Repair of high temperature composite aircraft structure p 2134 N95-27520

Composite repair of composite structures
p 2134 N95-27521

Damage occurrence on composites during testing and fleet service: Repair of Airbus aircraft
p 2135 N95-27526

The development of an engineering standard for composite repairs p 2135 N95-27528

Manufacturing tailored property ceramic composites
[DE95-006303] p 2237 N95-27993

The determination of the constitutive parameters of a medium with application to a reinforced concrete pad
[NASA-CR-4674] p 2268 N95-28181

Process and control systems for composites manufacturing p 2184 N95-28267

Advanced tow placement of composite fuselage structure p 2185 N95-28271

ACT/ICAPS: Thermoplastic composite activities
p 2185 N95-28274

Resin transfer molding of textile preforms for aircraft structural applications p 2185 N95-28276

Analysis techniques for the prediction of springback in formed and bonded composite components
p 2188 N95-28289

Atomic layer epitaxy of group 4 materials: Surface processes, thin films, devices and their characterization
[AD-A289092] p 2446 N95-28327

Utilization of composite materials by the US Army: A look ahead p 2189 N95-28421

Benefits and limitations of composites in carrier-based aircraft p 2189 N95-28422

Development of composite carrythrough bulkhead
p 2192 N95-28438

Reliability analysis of composite structures
p 2192 N95-28441

Navy composite maintenance and repair experience
p 2193 N95-28446

Overview of the ACT program p 2193 N95-28463

Technology integration box beam failure study
p 2194 N95-28468

Tension fracture of laminates for transport fuselage. Part 1: Material screening p 2137 N95-28471

Recent progress in NASA Langley textile reinforced composites program p 2196 N95-28475

Impact damage resistance of composite fuselage structure, part 1 p 2138 N95-28482

Applications of a damage tolerance analysis methodology in aircraft design and production
p 2197 N95-28483

The 18th Asilomar Conference on Polymeric Materials
[AD-A291721] p 2240 N95-28508

COMPOSITE STRUCTURES

A fast numerical method for isothermal resin transfer mold filling
[AD-A288944] p 2179 N95-26565

Composite sandwich structure and method for making same
[NASA-CASE-LAR-14898-1] p 2180 N95-26764

Study of damage evolutions in composite plates subjected to bending loads using micro-macro analysis
[AD-A288523] p 2308 N95-26839

The collapse of composite cylindrical panels with various thickness using finite element analysis
[AD-A289370] p 2308 N95-26905

Composite Repair of Military Aircraft Structures
[AGARD-CP-550] p 2131 N95-27504

Bonded composite repair of metallic aircraft components: Overview of Australian activities
p 2132 N95-27505

Composite repair of metallic airframe: Twenty years of experience p 2132 N95-27508

A FEAM based methodology for analyzing composite patch repairs of metallic structures
p 2133 N95-27511

Structural modification and repair of C-130 wing structure using bonded composites p 2133 N95-27512

Field repair materials for naval aircraft
p 2133 N95-27514

Rapid repair of large area damage to contoured aircraft structures p 2133 N95-27516

Composite repair of a CF18: Vertical stabilizer leading edge p 2134 N95-27517

Composite repair issues on the CF-18 aircraft
p 2134 N95-27518

Repair technology for thermoplastic aircraft structures
p 2134 N95-27519

Repair of high temperature composite aircraft structure p 2134 N95-27520

Composite repair of composite structures
p 2134 N95-27521

Scarf joint technique with cocured and precured patches for composite repair p 2135 N95-27524

Damage occurrence on composites during testing and fleet service: Repair of Airbus aircraft
p 2135 N95-27526

Repairs of CFC primary structures
p 2135 N95-27527

The development of an engineering standard for composite repairs p 2135 N95-27528

Load transfer in the stiffener-to-skin joints of a pressurized fuselage
[NASA-CR-198610] p 2310 N95-27865

Aeroelasticity and structural optimization of composite helicopter rotor blades with swept tips
[NASA-CR-4665] p 2136 N95-28262

Design of fabric preforms for double diaphragm forming p 2184 N95-28269

Static and fatigue testing of full-scale fuselage panels fabricated using a Therm-X(R) process
p 2185 N95-28270

Advanced tow placement of composite fuselage structure p 2185 N95-28271
Service tough composite structures using the Z-direction reinforcement process p 2185 N95-28272
ACT/ICAPS: Thermoplastic composite activities p 2185 N95-28274
Composite intermediate case manufacturing scale-up for advanced engines p 2141 N95-28275
Resin transfer molding of textile preforms for aircraft structural applications p 2185 N95-28276
Analysis of aircraft engine blade subject to ice impact p 2141 N95-28277
Application of fiber-reinforced bismaleimide materials to aircraft nacelle structures p 2137 N95-28278
Assembly induced delaminations in composite structures p 2186 N95-28279
Composite flight-control actuator development p 2142 N95-28281
Failure analysis of thick composite cylinders under external pressure p 2187 N95-28284
Analysis techniques for the prediction of springback in formed and bonded composite components p 2188 N95-28289
Design prediction for long term stress rupture service of composite pressure vessels p 2188 N95-28291
Ninth DOD/NASA/FAA Conference on Fibrous Composites in Structural Design, volume 1 [NASA-CR-198723] p 2189 N95-28420
Mechanical properties of triaxially braided composites: Experimental and analytical results p 2189 N95-28423
The effect of material heterogeneity in curved composite beams for use in aircraft structures p 2190 N95-28426
Analysis of composite structures with delaminations under combined bending and compression p 2190 N95-28429
Application of advanced material systems to composite frame elements p 2191 N95-28432
Unique considerations in the design and experimental evaluation of tailored wings with elastically produced chordwise camber p 2192 N95-28436
Effects of floor location on response of composite fuselage frames p 2192 N95-28439
Structural design optimization with survivability dependent constraints application: Primary wing box of a multi-role fighter p 2137 N95-28440
Reliability analysis of composite structures p 2192 N95-28441
Probabilistic design of advanced composite structure p 2193 N95-28443
Navy composite maintenance and repair experience p 2193 N95-28446
Ninth DOD/NASA/FAA Conference on Fibrous Composites in Structural Design, volume 2 [NASA-CR-198722] p 2193 N95-28462
Overview of the ACT program p 2193 N95-28463
COINS: A composites information database system p 2194 N95-28465
Composite fuselage shell structures research at NASA Langley Research Center p 2194 N95-28466
Structural testing of the technology integration box beam p 2194 N95-28467
Technology integration box beam failure study p 2194 N95-28468
Development of stitched/RTM composite primary structures p 2195 N95-28469
Test and analysis results for composite transport fuselage and wing structures p 2137 N95-28470
Local design optimization for composite transport fuselage crown panels p 2137 N95-28473
Composite fuselage crown panel manufacturing technology p 2137 N95-28474
Recent progress in NASA Langley textile reinforced composites program p 2196 N95-28475
Advanced textile applications for primary aircraft structures p 2138 N95-28476
Characterization and manufacture of braided composites for large commercial aircraft structures p 2196 N95-28478
The use of impact force as a scale parameter for the impact response of composite laminates p 2197 N95-28479
Application of damage tolerance methodology in certification of the Piaggio P-180 Avanti p 2138 N95-28480
Compressive strength of damaged and repaired composite plates p 2198 N95-28484
Post impact compressive strength in composites p 2198 N95-28485
Damage tolerance of a geodesically stiffened advanced composite structural concept for aircraft structural applications p 2138 N95-28487
Advanced wing design survivability testing and results p 2138 N95-28488
NASA-ACEE/Boeing 737 graphite-epoxy horizontal stabilizer service p 2138 N95-28489
SMART materials: Surfaces, transforms and interfaces. The commensurate engineering dimension [AD-A289598] p 2312 N95-28649

COMPOSITION (PROPERTY)
Satellite surface material composition from synthetic spectra [AD-A289236] p 2163 N95-26963
Advances in welding science: A perspective [DE95-006745] p 2302 N95-27545
Low temperature carrier transport properties in isotopically controlled germanium [DE95-008489] p 2444 N95-28092

COMPRESSIBILITY
Turbulence modeling [NASA-CR-197751] p 2274 N95-26665
Overview of through-thickness test methods for polymer matrix composites [PB95-190112] p 2227 N95-26747
High pressure optical studies of semiconductors and heterostructures [DE95-007119] p 2410 N95-27927

COMPRESSIBILITY EFFECTS
Compressible turbulence measurements in a supersonic boundary layer including favorable pressure gradient effects [AD-A289475] p 2276 N95-26821
Compressible turbulence measurements in a supersonic flow with adverse pressure gradient [AD-A289477] p 2276 N95-26822

COMPRESSIBLE BOUNDARY LAYER
Compressible turbulence measurements in a supersonic boundary layer including favorable pressure gradient effects [AD-A289475] p 2276 N95-26821
Nonlinear stability of non-stationary cross-flow vortices in compressible boundary layers [NASA-CR-189184] p 2279 N95-27242
On the modulational instability of large amplitude waves in supersonic boundary layers [NASA-CR-195072] p 2284 N95-27760

COMPRESSIBLE FLOW
Development of numerical methods for overset grids with applications for the integrated Space Shuttle vehicle [NASA-CR-197759] p 2160 N95-27154
Second-order closures for compressible turbulence p 2286 N95-27898
TranAir: A full-potential, solution-adaptive, rectangular grid code for predicting subsonic, transonic, and supersonic flows about arbitrary configurations. User's manual [NASA-CR-4349] p 2123 N95-28230

COMPRESSING
Real-time data compression using a fixed Huffman encoding scheme [DE95-006159] p 2455 N95-27949

COMPRESSION LOADS
Composite repair issues on the CF-18 aircraft p 2134 N95-27518
The high strain rate deformation of tungsten single crystals [AD-A288874] p 2223 N95-28189
Compression failure of angle-ply laminates p 2190 N95-28428
Analysis of composite structures with delaminations under combined bending and compression p 2190 N95-28429
Buckling behavior of long symmetrically laminated plates subjected to combined loads p 2190 N95-28430
Cryogenic temperature control and tension/compression attachment stage for an electron microscope [AD-D017390] p 2294 N95-28612

COMPRESSION TESTS
External patch repair of CFRP/honeycomb sandwich p 2134 N95-27522
High-temperature deformation of ZrO2-Al2O3/SiC whisker composites fabricated by two techniques [DE95-008273] p 2183 N95-28069
Task 4 supporting technology. Part 2: Detailed test plan for thermal seals. Thermal seals evaluation, improvement and test. CAN8-1, Reusable Launch Vehicle (RLV), advanced technology demonstrator: X-33. Leading edge and seals thermal protection system technology demonstration [NASA-CR-198628] p 2304 N95-28259
Test and analysis results for composite transport fuselage and wing structures p 2137 N95-28470

COMPRESSIVE STRENGTH
Identification of the plastic anisotropy of an aluminum alloy [IFTR-26/1994] p 2212 N95-26512
Service tough composite structures using the Z-direction reinforcement process p 2185 N95-28272
Failure analysis of thick composite cylinders under external pressure p 2187 N95-28284
Mechanisms of compressive failure in woven composites and stitched laminates p 2189 N95-28424
Investigation of static and cyclic bearing failure mechanisms for GR/EP laminates p 2190 N95-28427
Compression failure of angle-ply laminates p 2190 N95-28428
Compressive residual strength of graphite/epoxy laminates after impact p 2191 N95-28431
Compressive strength of damaged and repaired composite plates p 2198 N95-28484
Post impact compressive strength in composites p 2198 N95-28485

COMPRESSOR ROTORS
Stall precursor study of high frequency data for three high speed, swept compressor rotors [AD-A289379] p 2139 N95-26878
A general theory of two- and three-dimensional rotational flow in subsonic and transonic turbomachines [NASA-CR-4496] p 2123 N95-28003

COMPRESSORS
Cryogenic temperature control and tension/compression attachment stage for an electron microscope [AD-D017390] p 2294 N95-28612

COMPTON EFFECT
Comparative experimental study of PIXE and X-ray fluorescence analysis [DE95-607868] p 2327 N95-27198

COMPUTATION
Parallelizing locally-weighted regression [AD-A288294] p 2394 N95-26414
User's guide: Computer program for analysis of beam-column structures with nonlinear supports (CBEAMC) [AD-A289031] p 2307 N95-26464
An introduction to software architecture [AD-A288356] p 2363 N95-26467
Grain size management in repetitive task graphs for multiprocessor computer scheduling [AD-A288575] p 2377 N95-26551
CFD research, parallel computation and aerodynamic optimization [NASA-CR-197748] p 2120 N95-26649
Construction of arbitrary order schemes for many dimensional wave equation [PB95-184818] p 2276 N95-26928
Moment and hypergeometric filters for high precision computation of focus, stereo and optical flow [AD-A289293] p 2425 N95-27038
Scalability in production system programs [AD-A289345] p 2453 N95-27063
An outflow boundary condition for aeroacoustic computations [NASA-TM-106930] p 2279 N95-27175
A study of workstation computational performance for real-time flight simulation [NASA-TM-109184] p 2362 N95-27241
The PCMDI Visualization and Computation System (VCS): A workbench for climate data display and analysis [DE95-008586] p 2328 N95-27558

COMPUTATIONAL CHEMISTRY
Theoretical studies of reaction surfaces [AD-A288458] p 2404 N95-26632
Atomistic calculations of hydrogen interactions with Ni3Al grain boundaries and Ni/Ni/Ni3Al interfaces [DE95-006497] p 2408 N95-27534
Molecular modeling: An approach for the study of piezoelectric polymers [AD-A289821] p 2241 N95-28574

COMPUTATIONAL ELECTROMAGNETICS
The origin of spurious solutions in computational electromagnetics [NASA-TM-106921] p 2391 N95-27726
FDTD-ANT user manual [NASA-CR-195444] p 2372 N95-27729

COMPUTATIONAL FLUID DYNAMICS
A fully implicit time accurate method for hypersonic combustion: Application to shock-induced combustion instability [NASA-TM-106707] p 2273 N95-26380
Analysis and development of finite element methods for the study of nonlinear thermomechanical behavior of structural components [NASA-CR-195354] p 2307 N95-26387
Computational fluid dynamics and transonic flow [AD-A288962] p 2273 N95-26405
A non-iterative grid deformation algorithm for computational fluid dynamics for aeroelasticity [AD-A288298] p 2273 N95-26418
A fixed time performance evaluation of parallel CFD applications [DE94-014240] p 2273 N95-26445

Parallel computing on various platforms: A case study
[AD-A289008] p 2376 N95-26460
Numerical simulation of combustion flow around a flame holder with hydrogen injection
[NAL-TR-1233] p 2200 N95-26523
Algorithms for parallel flow solvers on message passing architectures
[NASA-CR-197758] p 2274 N95-26588
Supersonic transport grid generation, validation, and optimization
[NASA-CR-197752] p 2365 N95-26648
CFD research, parallel computation and aerodynamic optimization
[NASA-CR-197748] p 2120 N95-26649
The method of space-time conservation element and solution element-applications to one-dimensional and two-dimensional time-marching flow problems
[NASA-TM-106915] p 2389 N95-26663
Contribution to the optimal shape design of two-dimensional internal flows with embedded shocks
[NASA-CR-195062] p 2389 N95-26672
Ram accelerator performance calculations using a modified version of the NASA CET89 equilibrium chemistry code
[AD-A289554] p 2201 N95-26678
SUPG finite numerical element solutions for non-compressible Navier-Stokes equation sets
[AD-A289600] p 2274 N95-26718
The multidimensional Self-Adaptive Grid code, SAGE, version 2
[NASA-TM-110350] p 2367 N95-26726
Numerical simulation of the flow about the F-18 HARV at high angle of attack
[NASA-CR-197755] p 2121 N95-26735
Development of an upwind, finite-volume code with finite-rate chemistry
[NASA-CR-197747] p 2121 N95-26760
Progress in incompressible Navier-Stokes computations for propulsion flows and its dual-use applications
[NASA-CR-197746] p 2275 N95-26766
Computational support of the laminar flow supersonic wind tunnel, CNSFV code development, Maglev, and grid generation
[NASA-CR-197750] p 2143 N95-26775
Supersonic civil airplane study and design: Performance and sonic boom
[NASA-CR-197745] p 2130 N95-26813
A numerical method for unsteady transonic flow about wings with control surfaces
[AD-A289631] p 2121 N95-26859
Rarefied gas effects on aerobraking/reentry vehicles with wakes
[NASA-CR-196586] p 2164 N95-27093
Development of numerical methods for overset grids with applications for the integrated Space Shuttle vehicle
[NASA-CR-197759] p 2160 N95-27154
Flow control
[AD-A289262] p 2279 N95-27197
Application of CFD to the analysis and design of high-speed inlets
[NASA-CR-198574] p 2279 N95-27240
Nonlinear stability of non-stationary cross-flow vortices in compressible boundary layers
[NASA-CR-189184] p 2279 N95-27242
Computer program BL2D for solving two-dimensional and axisymmetric boundary layers
[NASA-CR-4668] p 2279 N95-27257
The Sixth Annual Thermal and Fluids Analysis Workshop
[NASA-CP-10161] p 2280 N95-27345
Numerical solution of fluid flow and heat tranfer problems with surface radiation p 2282 N95-27357
NAS Technical Summaries, March 1993 - February 1994
[NASA-RP-1355] p 2466 N95-27367
Multigrid techniques for unstructured meshes
[NASA-CR-195070] p 2391 N95-27433
Three-dimensional computer modeling of hydrogen injection and combustion
[DE95-006261] p 2203 N95-27437
A new finite element formulation for incompressible flow
[DE95-007141] p 2284 N95-27454
Optimization of wave rotors for use as gas turbine engine topping cycles
[NASA-TM-106951] p 2140 N95-27860
Industry-Wide Workshop on Computational Turbulence Modeling
[NASA-CP-10165] p 2285 N95-27882
A summary of computational experience at GE Aircraft Engines for complex turbulent flows in gas turbines
p 2285 N95-27885
The applicability of turbulence models to aerodynamic and propulsion flowfields at McDonnell-Douglas Aerospace p 2285 N95-27886
Experience with k-epsilon turbulence models for heat transfer computations in rotating p 2285 N95-27887
Combustion system CFD modeling at GE Aircraft Engines p 2285 N95-27889
Overview of turbulence model development and applications at Rocketdyne p 2286 N95-27891
Experience with turbulence interaction and turbulence-chemistry models at Fluent Inc.
p 2286 N95-27893
Experiences with two-equation turbulence models
p 2286 N95-27894
Progress in simulating industrial flows using two-equation models: Can more be achieved with further research?
p 2286 N95-27895
Turbulence modeling needs of commercial CFD codes: Complex flows in the aerospace and automotive industries p 2286 N95-27896
Turbulence requirements of a commerical CFD code
p 2286 N95-27897
A numerical method for solving the three-dimensional parabolized Navier-Stokes equations
[NASA-CR-198159] p 2287 N95-27917
Large HAWT wake measurement and analysis
p 2289 N95-27973
A NASTRAN-based computer program for structural dynamic analysis of Horizontal Axis Wind Turbines
p 2312 N95-27980
TranAir: A full-potential, solution-adaptive, rectangular grid code for predicting subsonic, transonic, and supersonic flows about arbitrary configurations. Theory document
[NASA-CR-4348] p 2123 N95-28265
Numerical analysis of intra-cavity and power-stream flow interaction in multiple gas-turbine disk-cavities
[NASA-TM-106886] p 2140 N95-28344
Modeling the shock response of submerged structures
[AD-A289082] p 2288 N95-28351
Numerical study to assess sulfur hexafluoride as a medium for testing multielement airfoils
[NASA-TP-3496] p 2124 N95-28674

COMPUTATIONAL GEOMETRY
Unstructured mesh generation and adaptivity
[NASA-CR-195069] p 2278 N95-27027
Uncertainties in obtaining high reliability from stress-strength models p 2193 N95-28442

COMPUTATIONAL GRIDS
Algorithms for parallel flow solvers on message passing architectures
[NASA-CR-197758] p 2274 N95-26588
Computational analysis of forebody tangential slot blowing on the high alpha research vehicle
[NASA-CR-197754] p 2129 N95-26591
Adaptive finite element method I: Solution algorithm and computational examples
[AD-A288979] p 2389 N95-26609
The multidimensional Self-Adaptive Grid code, SAGE, version 2
[NASA-TM-110350] p 2367 N95-26726
A 3D agglomeration multigrid solver for the Reynolds-averaged Navier-Stokes equations on unstructured meshes
[NASA-CR-195073] p 2390 N95-27029
Development of numerical methods for overset grids with applications for the integrated Space Shuttle vehicle
[NASA-CR-197759] p 2160 N95-27154
Global flowfield about the V-22 Tiltrotor Aircraft
[NASA-CR-198603] p 2122 N95-27248
Calculation of three-dimensional (3-D) internal flow by means of the velocity-vorticity formulation on a staggered grid
[NASA-TM-110352] p 2122 N95-27258
The effects of finite element grid density on model correlation and damage detection of a bridge
[DE94-018895] p 2309 N95-27305
Analysis of developing laminar flows in circular pipes using a higher-order finite-difference technique
p 2281 N95-27352
Error analysis of the quartic nodal expansion method for slab geometry
[DE95-007373] p 2412 N95-28045
TranAir: A full-potential, solution-adaptive, rectangular grid code for predicting subsonic, transonic, and supersonic flows about arbitrary configurations. User's manual
[NASA-CR-4349] p 2123 N95-28230
TranAir: A full-potential, solution-adaptive, rectangular grid code for predicting subsonic, transonic, and supersonic flows about arbitrary configurations. Theory document
[NASA-CR-4348] p 2123 N95-28265
Radon transform and its applications in gridding airborne geophysical survey data
[PB95-195533] p 2315 N95-28643

COMPUTER AIDED DESIGN
Virtual Prototyping as an aid for control system analysis
[AD-A288819] p 2362 N95-26346
Using machine learning to derive efficient cost and performance estimates in VLSI CAD designs
[AD-A288254] p 2363 N95-26408
User's guide: Computer program for analysis of beam-column structures with nonlinear supports (CBEAMC)
[AD-A289031] p 2307 N95-26464
Intelligent computer based reliability assessment of multichip modules
[AD-A288833] p 2259 N95-26550
The development of a feature-based concurrent engineering system
[AD-A288424] p 2364 N95-26557
Aeroelasticity of wing and wing-body configurations on parallel computers
[NASA-CR-197756] p 2129 N95-26590
Turbulence modeling
[NASA-CR-197751] p 2274 N95-26665
User's and test case manual for FEMATS
[NASA-CR-197803] p 2366 N95-26694
Turbomachinery design and tonal acoustics computations
[NASA-CR-197749] p 2139 N95-26777
Supersonic civil airplane study and design: Performance and sonic boom
[NASA-CR-197745] p 2130 N95-26813
Naval Aviation System TEAM mapping, charting, and geodesy handbook
[AD-A288590] p 2314 N95-26841
Creating an alternative parameter optimization method (APO) p 2118 N95-26946
NIST: Information management in the AMRF
[NONP-NASA-VT-95-49120] p 2454 N95-27208
STEP: A futurevision, today
[NONP-NASA-VT-95-49121] p 2451 N95-27209
Application of CFD to the analysis and design of high-speed inlets
[NASA-CR-198574] p 2279 N95-27240
Advanced flight computer. Special study
[NASA-CR-198165] p 2371 N95-27246
CAE for thermal management of aerospace electronic boards using the BETAsoft program
p 2272 N95-27354
Thermal neutral format based on the step technology
p 2283 N95-27363
PC Software graphics tool for conceptual design of space/planetary electrical power systems
[NASA-TM-106908] p 2372 N95-27905
A NASTRAN-based computer program for structural dynamic analysis of Horizontal Axis Wind Turbines
p 2312 N95-27980
Designers' unified cost model p 2194 N95-28464
COINS: A composites information database system
p 2194 N95-28465
Structural optimisation of cage induction motors using finite element analysis
[PB95-195434] p 2271 N95-28655

COMPUTER AIDED MANUFACTURING
The development of a feature-based concurrent engineering system
[AD-A288424] p 2364 N95-26557
Next generation controller specification for an open systems architecture standard - overview
[AD-A289507] p 2368 N95-26853
Advanced educational methods in the Department of Defense: Application of case theory and computer-assisted instruction to business process reengineering
[AD-A288881] p 2374 N95-28590
Next generation controller specification for an open systems architecture standard
[AD-A289567] p 2375 N95-28647

COMPUTER AIDED MAPPING
Digital mapping, charting, and geodesy analysis program: Initial technical review of Raster Product Format
[AD-A289039] p 2313 N95-26476
Digital mapping, charting, and geodesy analysis program technical review of Vector Quantization (VQ) Decompression for the National Imagery Transmission Format Standard (NITFS)
[AD-A288998] p 2314 N95-26682

COMPUTER AIDED TOMOGRAPHY
JPRS report: Science and technology. Central Eurasia
[JPRS-UST-95-016] p 2262 N95-27170

COMPUTER ASSISTED INSTRUCTION
The value of simulation for training
[AD-A289174] p 2143 N95-26556
NEXTSTEP: The next step in the right direction? Part 2: Software development with NEXTSTEP
[REPT-94-33-PT-2] p 2450 N95-26803
Human factors in aviation maintenance, phase 4
[DOT/FAA/AM-95/14] p 2360 N95-27696

Development and implementation of an electronic library tour for the NASA Langley Technical Library
[NASA-TM-110619] p 2455 N95-27701
Advanced educational methods in the Department of Defense: Application of case theory and computer-assisted instruction to business process reengineering
[AD-A288881] p 2374 N95-28590

COMPUTER COMPONENTS
A decentralized software bus based on IP multicasting
[NASA-CR-197768] p 2366 N95-26695

COMPUTER DESIGN
Construction of a connectionist network supercomputer
[AD-A288439] p 2377 N95-27182
Advanced flight computer. Special study
[NASA-CR-198165] p 2371 N95-27246

COMPUTER GRAPHICS
An evaluation of the Software Through Pictures/T Tool (StP/T) for the Software Support Activity (SSA)
[AD-A288822] p 2362 N95-26348
EASY-SIM: A visual simulation system software architecture with an Ada 9X application framework
[AD-A289325] p 2368 N95-26895
Image quality metrics for color CRT displays
[AD-A288934] p 2262 N95-27196
Performance of a stand-alone wind-electric ice maker for remote villages
[DE95-004006] p 2320 N95-27475
A video strip chart program
[DE95-006389] p 2372 N95-27495
Scientific statistics and graphics on the Macintosh
[DE95-006445] p 2372 N95-27533
PC Software graphics tool for conceptual design of space/planetary electrical power systems
[NASA-TM-106908] p 2372 N95-27905

COMPUTER INFORMATION SECURITY
Flexible and safe resolution of file conflicts
[AD-A289342] p 2452 N95-26752
Research and development management information system, system user manual
[AD-A289151] p 2453 N95-27004
The Sunrise project: An R&D project for a national information infrastructure prototype
[DE95-006340] p 2455 N95-27847
Browsing the World Wide Web from behind a firewall
[DE95-006805] p 2455 N95-27957

COMPUTER NETWORKS
A software bus for thread objects
[NASA-CR-197764] p 2365 N95-26575
An architecture for optimal all-to-all personalized communication
[AD-A288532] p 2377 N95-26840
A demonstration of Client/Server technology using remote procedure calls for an application of file migration for moving records based on location
[AD-A289391] p 2453 N95-26864
A demonstration of Client-Server technology using remote procedure calls with an application of file migration for moving records based on time
[AD-A289392] p 2453 N95-26879
Weighting scheme for the space surveillance network automated tasker
[AD-A289285] p 2146 N95-27035
Reducing network depth in the Cascade-Correlation learning architecture
[AD-A289352] p 2382 N95-27066
A demonstration of client-server technology using remote procedure calls with an application in file migration using heuristics
[AD-A289467] p 2255 N95-27149
Design and implementation of a software communication architecture for the JANUS-3D Visualizer
[AD-A288509] p 2370 N95-27150
Construction of a connectionist network supercomputer
[AD-A288439] p 2377 N95-27182
Gigabit LAN issues: HIPPI, Fibre Channel, or ATM?
[DE95-003673] p 2378 N95-27422
Transparent access to distributed, heterogeneous environmental information systems
[DE95-007268] p 2454 N95-27483
A case for dynamic sets in operating systems
[AD-A289354] p 2454 N95-27529
The Sunrise project: An R&D project for a national information infrastructure prototype
[DE95-006340] p 2455 N95-27847
Sandia's network for Supercomputing '94: Linking the Los Alamos, Lawrence Livermore, and Sandia National Laboratories using switched multimegabit data service
[DE95-007717] p 2378 N95-28074
Optical implementation of inner product neural associative memory
[NASA-CASE-NPO-18491-2-CU] p 2427 N95-28363
International networks
[PB95-196366] p 2379 N95-28502
NASA/DOD Aerospace Knowledge Diffusion Research Project. Report 35: The use of computer networks in aerospace engineering
[NASA-CR-198170] p 2456 N95-28600
Two implementation relations and the correctness of communicating replicated processes
[PB95-195640] p 2375 N95-28645

COMPUTER PROGRAM INTEGRITY
Using an architectural approach to integrate heterogeneous, distributed software components
[NASA-CR-197766] p 2366 N95-26711

COMPUTER PROGRAMMING
An introduction to software architecture
[AD-A288963] p 2363 N95-26446
Application-aware adaptation for mobile computing
[AD-A288366] p 2363 N95-26469
Nonlinear scalespace via hierarchical statistical modeling
[AD-A289057] p 2394 N95-26478
A system dynamics based study of software reuse and its determinants
[AD-A288578] p 2364 N95-26554
Software packager user's guide
[NASA-CR-197763] p 2366 N95-26693
A process improvement model for software verification and validation
[NASA-CR-197761] p 2367 N95-26814
A demonstration of Client/Server technology using remote procedure calls for an application of file migration for moving records based on location
[AD-A289391] p 2453 N95-26864
User-centric development. Version 01.00.04
[AD-A289363] p 2368 N95-26903
Multiple model adaptive estimation and head motion tracking in a virtual environment: An engineering approach
[AD-A289299] p 2359 N95-27046
A demonstration of client-server technology using remote procedure calls with an application in file migration using heuristics
[AD-A289467] p 2255 N95-27149
Factors in human-computer interface design (a pilot study)
[AD-A288908] p 2360 N95-27195
STEP: A futurevision, today
[NONP-NASA-VT-95-49121] p 2451 N95-27209
Overview of megaprogramming course: Lectures and eexercises. Version 02.00.03
[AD-A286723] p 2370 N95-27235
Automated database design from natural language input p 2383 N95-27378
Contingency designs for attitude determination of TRMM p 2154 N95-27803
Control system design for the MOD-5A 7.3 mW wind turbine generator p 2306 N95-27985
An automated cost uncertainty program
[AD-A288747] p 2374 N95-28588
Advanced educational methods in the Department of Defense: Application of case theory and computer-assisted instruction to business process reengineering
[AD-A288881] p 2374 N95-28590
A correlational study of the SEI's capability maturity model and software development performance in DOD contracts
[AD-A288890] p 2374 N95-28591
Software process improvement in the NASA software engineering laboratory
[AD-A289912] p 2374 N95-28627

COMPUTER PROGRAMS
A non-iterative grid deformation algorithm for computational fluid dynamics for aeroelasticity
[AD-A288298] p 2273 N95-26418
Natural aerosol extinction module: XSCALE 1992 user's guide
[AD-A289029] p 2340 N95-26463
User's guide: Computer program for analysis of beam-column structures with nonlinear supports (CBEAMC)
[AD-A289031] p 2307 N95-26464
Software risk management through independent verification and validation
[NASA-CR-197767] p 2364 N95-26486
General purpose finite element solver
[PB95-185062] p 2388 N95-26495
An improved model of high-latitude f-region scintillation (WBMOD version 13)
[AD-A288558] p 2334 N95-26520
A system dynamics based study of software reuse and its determinants
[AD-A288578] p 2364 N95-26554
Design and synthesis of a real-time controller for an unmanned air vehicle
[AD-A289134] p 2141 N95-26555
Comparison of fixed wing aircraft algorithms for JANUS
[AD-A288503] p 2129 N95-26652
Turbulence modeling
[NASA-CR-197751] p 2274 N95-26665
Using SCR methods to analyze requirements documentation
[NASA-CR-197760] p 2365 N95-26668
User's and test case manual for FEMATS
[NASA-CR-197803] p 2366 N95-26694
Using an architectural approach to integrate heterogeneous, distributed software components
[NASA-CR-197766] p 2366 N95-26711
Development of an upwind, finite-volume code with finite-rate chemistry
[NASA-CR-197747] p 2121 N95-26760
Progress in incompressible Navier-Stokes computations for propulsion flows and its dual-use applications
[NASA-CR-197746] p 2275 N95-26766
Performance and policy dimensions in internet routing
[NASA-CR-197772] p 2367 N95-26770
Control-flow analysis and type systems
[AD-A289338] p 2389 N95-26772
Study of damage evolutions in composite plates subjected to bending loads using micro-macro analysis
[AD-A288523] p 2308 N95-26839
An architecture for optimal all-to-all personalized communication
[AD-A288532] p 2377 N95-26840
A 3-D finite difference time domain investigation of microwave propagation through inhomogeneous biological materials
[AD-A289431] p 2251 N95-26869
User-centric development. Version 01.00.04
[AD-A289363] p 2368 N95-26903
Calculation of suspended sediment transport by combined wave-current flows
[AD-A289368] p 2346 N95-26904
Predicting protein structure using parallel genetic algorithms
[AD-A289305] p 2369 N95-26919
Diagnosing cloudiness from global numerical weather prediction model forecasts
[AD-A289456] p 2356 N95-26992
Weighting scheme for the space surveillance network automated tasker
[AD-A289285] p 2146 N95-27035
A general object model transformation system
[AD-A289289] p 2370 N95-27037
Novel field effect transistors for low power electronics
[AD-A288650] p 2262 N95-27096
Design and implementation of a software communication architecture for the JANUS-3D Visualizer
[AD-A288509] p 2370 N95-27150
Development of numerical methods for overset grids with applications for the integrated Space Shuttle vehicle
[NASA-CR-197759] p 2160 N95-27154
The calculation of the mass moment of inertia of a fluid in a rotating rectangular tank
[NASA-CR-197777] p 2278 N95-27165
STEP: A futurevision, today
[NONP-NASA-VT-95-49121] p 2451 N95-27209
Computer Systems Division software system metrics approach
[AD-A288837] p 2370 N95-27210
Programming for time resolved spectrum in pulse radiolysis experiments
[DE95-607929] p 2406 N95-27212
Application of CFD to the analysis and design of high-speed inlets
[NASA-CR-198574] p 2279 N95-27240
Global flowfield about the V-22 Tiltrotor Aircraft
[NASA-CR-198603] p 2122 N95-27248
Spinning a web: Publishing the SEI software configuration management research on the world wide web
[AD-A288708] p 2377 N95-27250
Views of the solar system
[DE95-006446] p 2461 N95-27326
CAE for thermal management of aerospace electronic boards using the BETAsoft program
p 2272 N95-27354
RTE: A computer code for Rocket Thermal Evaluation
p 2177 N95-27355
Ring-plane traveling-wave tube slow-wave circuit design simulations at V-Band frequencies
[NASA-TM-106949] p 2371 N95-27370
Three-dimensional computer modeling of hydrogen injection and combustion
[DE95-006261] p 2203 N95-27437
An ugly duckling becomes a swan (hor ellipsis): How an organization becomes customer focused through listening
[DE95-004974] p 2454 N95-27461
A video strip chart program
[DE95-006389] p 2372 N95-27495
Flight Mechanics/Estimation Theory Symposium 1995
[NASA-CP-3299] p 2146 N95-27763
Kepler Equation solver p 2147 N95-27767

A PC-based magnetometer-only attitude and rate determination system for gyroless spacecraft p 2147 N95-27770
An MME-based attitude estimator using vector observations p 2148 N95-27775
Ulysses orbit determination at high declinations p 2151 N95-27787
Application of non-coherent Doppler data types for deep space navigation p 2151 N95-27788
PC Software graphics tool for conceptual design of space/planetary electrical power systems [NASA-TM-106908] p 2372 N95-27905
A model of rotationally-sampled wind turbulence for predicting fatigue loads in wind turbines p 2312 N95-27972
A NASTRAN-based computer program for structural dynamic analysis of Horizontal Axis Wind Turbines p 2312 N95-27980
Aeroelastic stability of wind turbine blade/aileron systems p 2124 N95-27981
Calculation of design load for the MOD-5A 7.3 mW wind turbine system p 2312 N95-27982
Control system design for the MOD-5A 7.3 mW wind turbine generator p 2306 N95-27985
Error analysis of the quartic nodal expansion method for slab geometry [DE95-007373] p 2412 N95-28045
Simulator report for SCI systems with HIC-router [PB95-196580] p 2379 N95-28093
Project Records Information System (PRIS) user's manual, revision 3 [DE95-008330] p 2456 N95-28172
Operator modeling in commerical aviation: Cognitive models, intelligent displays, and pilot's assistants [NASA-CR-198609] p 2138 N95-28203
TranAir: A full-potential, solution-adaptive, rectangular grid code for predicting subsonic, transonic, and supersonic flows about arbitrary configurations. User's manual [NASA-CR-4349] p 2123 N95-28230
TranAir: A full-potential, solution-adaptive, rectangular grid code for predicting subsonic, transonic, and supersonic flows about arbitrary configurations. Theory document [NASA-CR-4348] p 2123 N95-28265
Three-dimensional forecast models for emergency response management p 2172 N95-28303
Use of SURFACE CHEMKIN to model multiphase atmospheric chemistry: Application to nitrogen tetroxide spills p 2172 N95-28305
Upgrade of the computer modeling programs POLU10 and POLU13A for open burning and open detonation of energetic materials p 2172 N95-28306
Probabilistic evaluation of fuselage-type composite structures p 2137 N95-28444
An automated cost uncertainty program [AD-A288747] p 2374 N95-28588
Advanced educational methods in the Department of Defense: Application of case theory and computer-assisted instruction to business process reengineering [AD-A288881] p 2374 N95-28590
A correlational study of the SEI's capability maturity model and software development performance in DOD contracts [AD-A288890] p 2374 N95-28591
Computational and experimental studies of hydrodynamic instabilities and turbulent mixing [DE95-006837] p 2288 N95-28603
The Global Historical Climatology Network: A preview of version 2 [DE95-007003] p 2332 N95-28605
TRAINS: Dialogue transcription tools [AD-A289869] p 2259 N95-28624
Software process improvement in the NASA software engineering laboratory [AD-A289912] p 2374 N95-28627
Replacing the message service component in an integration framework [AD-A289928] p 2375 N95-28628
Manikin integrated data acquisition system (MIDAS) initial modifications [AD-A291662] p 2361 N95-28667
Guide for transmitting Standard Generalized Markup Language (SGML) encoded bibliographic records [DOE/OSTI-11685] p 2457 N95-28675

COMPUTER STORAGE DEVICES
Characterization and control of wafer charging effects during high-current ion implantation [DE95-006587] p 2440 N95-27471
Downloading environmental data in the new MOODS format [AD-A288835] p 2456 N95-28589

COMPUTER SYSTEMS DESIGN
Operating system support for coexistence of real-time and conventional scheduling [AD-A288584] p 2364 N95-26534
Control-flow analysis and type systems [AD-A289338] p 2389 N95-26772
Next generation controller specification for an open systems architecture standard - overview [AD-A289507] p 2368 N95-26853
Design considerations for FrankTalk: A distributed group support system [AD-A289386] p 2359 N95-26863
Self-checking state machine realization in CMOS [AD-A289149] p 2261 N95-27002
Advanced flight computer. Special study [NASA-CR-198165] p 2371 N95-27246
An ugly duckling becomes a swan (hor ellipsis): How an organization becomes customer focused through listening [DE95-004974] p 2454 N95-27461
Transparent access to distributed, heterogeneous environmental information systems [DE95-007268] p 2454 N95-27483
A case for dynamic sets in operating systems [AD-A289354] p 2454 N95-27529
Human factors in aviation maintenance, phase 4 [DOT/FAA/AM-95/14] p 2360 N95-27696
Design of a real-time wind turbine simulator using a custom parallel architecture p 2322 N95-27979
Next generation controller specification for an open systems architecture standard [AD-A289567] p 2375 N95-28647

COMPUTER SYSTEMS PERFORMANCE
Digital systems validation. Chapter 20 Artificial Intelligenge with applications for aircraft. Handbbook, volume 2 [AD-A288492] p 2380 N95-26638
Performance prediction: A case study using a multi-ring KSR-1 machine [NASA-CR-195066] p 2361 N95-26697
Measuring fault tolerance with the FTAPE fault injection tool [NASA-CR-197773] p 2306 N95-27253
Accelerating conservative parallel simulation of VHDL circuits [AD-A289317] p 2264 N95-27294
A case for dynamic sets in operating systems [AD-A289354] p 2454 N95-27529
Human factors in aviation maintenance, phase 4 [DOT/FAA/AM-95/14] p 2360 N95-27696
Development of a direct match technique for star identification on the SWAS mission p 2148 N95-27771
Observational magnetometer calibration with the Hubble Space Telescope's new magnetometers p 2148 N95-27773
Flight dynamics software in a distributed network environment p 2151 N95-27790
Control system design for the MOD-5A 7.3 mW wind turbine generator p 2306 N95-27985
Optimization strategies for molecular dynamics programs on Cray computers and scalar work stations [AD-A289574] p 2418 N95-28648

COMPUTER SYSTEMS PROGRAMS
Design considerations for FrankTalk: A distributed group support system [AD-A289386] p 2359 N95-26863
Research and development management information system, system user manual [AD-A289151] p 2453 N95-27004
Measuring fault tolerance with the FTAPE fault injection tool [NASA-CR-197773] p 2306 N95-27253
Sequence comparison on a cluster of workstations using the PVM system [DE95-006527] p 2378 N95-27709
Development of a direct match technique for star identification on the SWAS mission p 2148 N95-27771

COMPUTER TECHNIQUES
Long term distributed file reference tracing: Implementation and experience [AD-A288585] p 2452 N95-26535
The development of a feature-based concurrent engineering system [AD-A288424] p 2364 N95-26557
Activities of the Laboratory of Information Processing Science [PB95-184982] p 2452 N95-26631
Transitional flow in thin tubes for space station freedom radiator p 2282 N95-27360

COMPUTER VISION
Learning Hand/Eye coordination by an active observer. part 1: Organizing centers [AD-A289502] p 2356 N95-26843
EASY-SIM: A visual simulation system software architecture with an Ada 9X application framework [AD-A289325] p 2368 N95-26895
An illumination planner for Lambertian polyhedral objects [AD-A289332] p 2424 N95-26900
Using virtual active vision tools to improve autonomous driving tasks [AD-A289175] p 2356 N95-27013
The detection and tracking of motion by means of time-space pattern modelling using random fields [IFTR-37/1994] p 2374 N95-28566

COMPUTERIZED SIMULATION
Manual for SHOCK3D, version 2.0. Computer program for non-linear shock response [AD-A288631] p 2307 N95-26342
Virtual Prototyping as an aid for control system analysis [AD-A288819] p 2362 N95-26346
A method for simulating correlated random variables from partially specified distributions [AD-A288820] p 2393 N95-26347
Hindcasting wind-driven anomalies using reduced-gravity global ocean models with 1/2 deg and 1/4 deg resolution [AD-A289060] p 2345 N95-26406
The 1994 updated National Airspace System performance assessment for year 2005 [AD-A288652] p 2125 N95-26485
Microwave circuit simulation using higher-order dynamic elements [PB95-185088] p 2259 N95-26496
Analysis of fatigue fractographic data of a rod end housing using a Monte Carlo simulation [NAL-TR-1225] p 2307 N95-26521
Numerical simulation of combustion flow around a flame holder with hydrogen injection [NAL-TR-1233] p 2200 N95-26523
The small-scale structure of dispersing clouds in the atmosphere [AD-A288256] p 2341 N95-26546
Intelligent computer based reliability assessment of multichip modules [AD-A288833] p 2259 N95-26550
A system dynamics based study of software reuse and its determinants [AD-A288578] p 2364 N95-26554
The value of simulation for training [AD-A289174] p 2143 N95-26556
Indexing meso-beta surface wind site representative [AD-A288501] p 2341 N95-26650
Comparison of fixed wing aircraft algorithms for JANUS [AD-A288503] p 2129 N95-26652
Turbulence modeling [NASA-CR-197751] p 2274 N95-26665
Signals processing using acousto-optical technology [AD-A289597] p 2250 N95-26717
Numerical simulation of the flow about the F-18 HARV at high angle of attack [NASA-CR-197755] p 2121 N95-26735
Anomalous collision rate in the time counter scheme of the direct simulation Monte Carlo method for rarefied gas flow analysis [ISAS-R-653] p 2275 N95-26742
Soil moisture prediction during freeze and thaw using a coupled heat and moisture flow model [AD-A289343] p 2336 N95-26753
Progress towards computer simulation of NiH2 battery performance over life p 2272 N95-26786
A numerical model to predict the fate of jettisoned aviation fuel [AD-A289336] p 2242 N95-26842
A mathematical analysis of the Janus combat simulation weather effects models and sensitivity analysis of sky-to-ground brightness ratio on target detection [AD-A289629] p 2336 N95-26858
The photo-realistic AFIT virtual cockpit [AD-A289376] p 2130 N95-26876
Analysis of instability growth and collisionless relaxation in thermionic converters using 1-D PIC simulations [AD-A289310] p 2319 N95-26891
EASY-SIM: A visual simulation system software architecture with an Ada 9X application framework [AD-A289325] p 2368 N95-26895
Analysis and simulation of narrowband GPS jamming using digital excision temporal filtering [AD-A289328] p 2127 N95-26898
Reference manual: Naive physics simulator [PB95-184917] p 2369 N95-26907
Predicting protein structure using parallel genetic algorithms [AD-A289305] p 2369 N95-26919
Aircraft nosewheel steering simulation p 2118 N95-26944
Minimizing the impact of synchronization overhead in parallel discrete event simulations [AD-A289278] p 2377 N95-26984

Distributed interactive simulation virtual cassette recorder (DIS VCR); A datalogger with variable speed replay
[AD-A289212] p 2290 N95-26989

Implementation and demonstration of a multiple model adaptive estimation failure detection system for the F-16
[AD-A289301] p 2131 N95-27042

Simulating the production of free defects in irradiated metals
[DE95-007165] p 2214 N95-27088

Space modeler: An expanded, distributed, virtual environment for space visualization
[AD-A289409] p 2461 N95-27131

A finite element based technique for simulation helix TWT interaction circuit thermal behavior
[AD-A289552] p 2262 N95-27152

Probabilistic simulation of long term behavior in polymer matrix composites
[NASA-TM-106893] p 2309 N95-27174

Simulating a multi-target acoustic array on the Intel Paragon
[AD-A288443] p 2377 N95-27183

Mathematical simulation of three-dimensional magnetic field of spectrometric magnet SP-40
[DE95-608736] p 2398 N95-27239

Ball bearing vibrations amplitude modeling and test comparisons p 2158 N95-27286

Accelerating conservative parallel simulation of VHDL circuits
[AD-A289317] p 2264 N95-27294

CAE for thermal management of aerospace electronic boards using the BETAsoft program
p 2272 N95-27354

Transitional flow in thin tubes for space station freedom radiator p 2282 N95-27360

NAS Technical Summaries, March 1993 - February 1994
[NASA-RP-1355] p 2466 N95-27367

Ring-plane traveling-wave tube slow-wave circuit design simulations at V-Band frequencies
[NASA-TM-106949] p 2371 N95-27370

Three-dimensional computer modeling of hydrogen injection and combustion
[DE95-006261] p 2203 N95-27437

The second coming of cold dark matter?
[DE95-005156] p 2462 N95-27445

Lattice QCD calculation using VPP500
[DE95-007076] p 2449 N95-27448

Comparison of the calculated and measured stability of a NbTi cable-in-conduit conductor
[DE95-007964] p 2265 N95-27693

Time-dependent multi-dimensional simulation studies of the electron output scheme for high power FELs
[DE95-006593] p 2297 N95-27737

Molecular dynamics simulations of Gay-Berne nematic liquid crystal: Elastic properties from direct correlation functions
[DE95-609149] p 2441 N95-27740

Simulations of metal dissolution and corrosion
[DE95-007486] p 2218 N95-27748

Development of a direct match technique for star identification on the SWAS mission
p 2148 N95-27771

Precision landing system mathematical modeling study report for Andrews Air Force Base, runway 19L, Camp Springs, MD
[AD-A289015] p 2127 N95-27903

Studies of planetary scale waves and instabilities in support of the geophysical fluid flow cell experiment on USML-2
[NASA-CR-198646] p 2463 N95-27916

Polarizing matter and antimatter: A new method
[DE95-007109] p 2421 N95-27923

Aqueous electrolyte modeling in ASPEN PLUS(trademark)
[DE95-007008] p 2208 N95-27960

A NASTRAN-based computer program for structural dynamic analysis of Horizontal Axis Wind Turbines
p 2312 N95-27980

Aeroelastic stability of wind turbine blade/aileron systems p 2124 N95-27981

Phenomenology from 100 large lattices
[DE95-006349] p 2442 N95-27994

Algorithm to describe the spread of a wall fire under a ceiling
[PB95-182259] p 2247 N95-28008

A hybrid vehicle evaluation code and its application to vehicle design. Revision 1
[DE95-008053] p 2303 N95-28029

Beta-dynamics in simple liquid metal
[DE95-609154] p 2220 N95-28039

Scrape-off layer plasma modeling for the DIII-D tokamak
[DE95-008050] p 2433 N95-28054

Performance analysis of bullet trajectory estimation: Approach, simulation, and experiments
[DE95-007949] p 2399 N95-28109

An introductory guide to uncertainty analysis in environmental and health risk assessment. Environmental Restoration Program
[DE95-008097] p 2354 N95-28136

A hybrid vehicle evaluation code and its application to vehicle design, revision 2
[DE95-008060] p 2303 N95-28139

Developments in the electron gun simulation program, EGUN
[DE95-008137] p 2267 N95-28143

DNS, LES and stochastic modeling of turbulent reacting flows
[AD-A280099] p 2287 N95-28155

BEGET: The B-Factory Event Generator version 21
[DE95-008329] p 2414 N95-28171

Neural network error compensation of machine tools
[AD-A289300] p 2387 N95-28217

Numerical simulation of coupled flow and transport with TOUGH2: A verification study
[DE95-008351] p 2287 N95-28225

Automated remedial assessment methodology software system
[DE95-007287] p 2373 N95-28243

Analysis of aircraft engine blade subject to ice impact
p 2141 N95-28277

Upgrade of the computer modeling programs POLU10 and POLU13A for open burning and open detonation of energetic materials p 2172 N95-28306

Transport simulation of negative magnetic shear discharges
[DE95-003941] p 2416 N95-28329

Computational studies of projectile melt in impact with typical whipple shields
[DE95-005916] p 2311 N95-28337

Modeling the shock response of submerged structures
[AD-A289082] p 2288 N95-28351

Unmanned aerial vehicles, 1994 master plan
[AD-A291628] p 2136 N95-28411

Investigation of HE driven cylindrical liner
[DE95-007866] p 2311 N95-28539

The northern wintertime divergence extrema at 200 hPa and surface cyclones as simulated in the integration of the ECMWF general circulation model
[DE95-007946] p 2332 N95-28550

Numerical simulation of crack growth in pressurized fuselages
[PB95-192415] p 2137 N95-28636

Optimization strategies for molecular dynamics programs on Cray computers and scalar work stations
[AD-A289574] p 2418 N95-28648

Chua's circuits: Phenomena and applications
[AD-A291638] p 2271 N95-28666

COMPUTERS

Parallelizing locally-weighted regression
[AD-A288294] p 2394 N95-26414

A demonstration of client-server technology using remote procedure calls with an application in file migration using heuristics
[AD-A289467] p 2255 N95-27149

Factors in human-computer interface design (a pilot study)
[AD-A288908] p 2360 N95-27195

Lattice QCD calculation using VPP500
[DE95-007076] p 2449 N95-27448

Developments in the electron gun simulation program, EGUN
[DE95-008137] p 2267 N95-28143

CONCENTRATION (COMPOSITION)

Ethyl lactate as a solvent alternative for cleaning metal parts p 2229 N95-27112

Spacecraft materials studies on the Aerospace Corporation tray on EOIM-3 p 2210 N95-27632

Towards the detection and attribution of an anthropogenic effect on climate
[DE95-008589] p 2331 N95-28157

The sensitive detection of hydrazine using chemiluminescence p 2173 N95-28311

A new method for measuring hypergol scrubber emissions p 2174 N95-28312

The minimum pore size obtainable in a silica gel during drying
[DE95-008162] p 2239 N95-28401

High temperature oxidation of nickel concentrates
[PB95-195586] p 2224 N95-28644

CONCENTRATORS

Solar concentrator technology development for space based applications, volume 1
[NASA-CR-197723] p 2319 N95-27193

Solar concentrator technology development for space based applications, volume 2
[NASA-CR-197724] p 2319 N95-27194

Direct drive options for electric propulsion systems
[NASA-TM-106576] p 2168 N95-27861

Analysis of solar receiver flux distributions for US/Russian solar dynamic system demonstration on the MIR Space Station
[NASA-TM-106933] p 2169 N95-28036

CONCRETE STRUCTURES

Nondestructive testing apparatus for determining the orientation of reinforcing bars within a concrete structure
[AD-D017267] p 2245 N95-26508

CONCRETES

Split pipe testing device for the measurement of bond of reinforcement under controlled confinement
[AD-D017258] p 2245 N95-26500

Ultrasonic test system
[AD-D017261] p 2400 N95-26502

Nondestructive testing apparatus for determining the orientation of reinforcing bars within a concrete structure
[AD-D017267] p 2245 N95-26508

Layer coefficients for NHDOT pavement materials
[AD-A288262] p 2246 N95-26548

The determination of the constitutive parameters of a medium with application to a reinforced concrete pad
[NASA-CR-4674] p 2268 N95-28181

CONCURRENT ENGINEERING

Concurrent engineering research center
[NASA-CR-197726] p 2362 N95-26386

The development of a feature-based concurrent engineering system
[AD-A288424] p 2364 N95-26557

NIST: Information management in the AMRF
[NONP-NASA-VT-95-49120] p 2454 N95-27208

STEP: A futurevision, today
[NONP-NASA-VT-95-49121] p 2451 N95-27209

Thermal neutral format based on the step technology
p 2283 N95-27363

CONCURRENT PROCESSING

Two implementation relations and the correctness of communicating replicated processes
[PB95-195640] p 2375 N95-28645

CONDENSATES

Axionic fuel for sun
[DE95-608788] p 2464 N95-27342

CONDENSED MATTER PHYSICS

The 18th Annual Condensed Matter Physics Meeting
[DE95-605568] p 2398 N95-26[illegible]98

Optical design and performance of the inelastic scattering beamline at the National Synchrotron Light Source
[DE95-007679] p 2422 N95-28195

International journal of quantum chemistry
[AD-A291633] p 2352 N95-28546

CONDENSERS (LIQUEFIERS)

Experimental investigation of the effects of relative physical orientation between evaporator and condenser for a loop heat pipe
[AD-A289248] p 2277 N95-26968

CONDENSING

The surface of liquid He-4 at nonzero temperatures
[DE95-607841] p 2207 N95-27880

Cryogenic BRDF measurements at 10.6 micrometers and 0.63 micrometers on contaminated mirrors
[AD-A291611] p 2427 N95-28408

CONDUCTING POLYMERS

Current status of environmental, health, and safety issues of lithium polymer electric vehicle batteries
[DE95-004005] p 2265 N95-27719

CONDUCTIVE HEAT TRANSFER

Validation of the SINDA/FLUINT code using several analytical solutions p 2281 N95-27350

CAE for thermal management of aerospace electronic boards using the BETAsoft program
p 2272 N95-27354

CONDUCTIVITY

High pressure conductivity study of template synthesized polypyrrole: Observation of a crossover from three to one dimensional variable range hopping
[AD-A288367] p 2224 N95-26470

The effect of aviation fuels containing low amounts of static dissipater additive on electrostatic charge generation
[AD-A280075] p 2243 N95-28152

CONDUCTORS

Matrix kernels for MEG and EEG source localization and imaging
[DE95-005238] p 2354 N95-27426

Induced axial oscillations in superconducting dipole windings
[DE95-005690] p 2265 N95-27554

Comparison of the calculated and measured stability of a NbTi cable-in-conduit conductor
[DE95-007964] p 2265 N95-27693

FENIX experimental results of large-scale CICC made of bronze-processed Nb3Sn strands
[DE95-007965] p 2222 N95-28167

Numerical and theoretical studies of rough surface scattering
[AD-A291748] p 2257 N95-28528

CONFERENCES

The 1994 IEEE-IMS Workshop on Information Theory and Statistics
[AD-A288808] p 2380 N95-26492

Space Commerce 1994 Forum: The 10th National Space Symposium. Proceedings report
[NASA-CR-198031] p 2144 N95-26583

The 18th Annual Condensed Matter Physics Meeting
[DE95-605568] p 2398 N95-26598

Proceedings: Workshop on Research Needs in Wind Engineering
[PB95-189528] p 2308 N95-26743

The 1994 27th Annual NASA Aerospace Battery Workshop
[NASA-CP-3292] p 2317 N95-26785

Materials Research Society Symposium Proceedings. Volume 339: Diamond, SiC and nitride wide bandgap semiconductors
[AD-A288690] p 2437 N95-26818

Second International Conference on Software for Multiprocessors and Supercomputers Theory, Practice, Experience
[AD-A289474] p 2368 N95-26820

Determining nanoscale physical properties of materials by microscopy and spectroscopy
[AD-A289532] p 2201 N95-26870

AIAA Techfest 20 Proceedings
[NIAR-94-1] p 2118 N95-26941

Environmentally Benign Cleaning and Degreasing Technology: JANNAF Safety and Protection Subcommittee and Propellant Development and Characterization Subcommittee Joint Workshop
[CPIA-PUBL-611] p 2227 N95-27101

CAS CERN Accelerator School 5th General Accelerator Physics Course
[DE95-608324] p 2419 N95-27158

The 29th Aerospace Mechanisms Symposium
[NASA-CP-3293] p 2154 N95-27260

The Sixth Annual Thermal and Fluids Analysis Workshop
[NASA-CP-10161] p 2280 N95-27345

The 1995 Goddard Conference on Space Applications of Artificial Intelligence and Emerging Information Technologies
[NASA-CP-3296] p 2382 N95-27375

Advanced Earth-to-orbit propulsion technology information, dissemination and research
[NASA-CR-196582] p 2168 N95-27424

Biomass Pyrolysis Oil Properties and Combustion Meeting
[DE95-004017] p 2204 N95-27438

Composite Repair of Military Aircraft Structures
[AGARD-CP-550] p 2131 N95-27504

LDEF: 69 Months in Space. Third Post-Retrieval Symposium, part 3
[NASA-CP-3275-PT-3] p 2466 N95-27629

Flight Mechanics/Estimation Theory Symposium 1995
[NASA-CP-3299] p 2146 N95-27763

Industry-Wide Workshop on Computational Turbulence Modeling
[NASA-CP-10165] p 2285 N95-27882

The Tau-Charm Factory in the ERA of B-Factories and CESR
[DE95-007894] p 2412 N95-28028

The 1993 European school of high-energy physis
[DE95-610196] p 2421 N95-28040

Proceedings of the 1993 Scientific Conference on Obscuration and Aerosol Research
[AD-A280084] p 2331 N95-28153

Ninth DOD/NASA/FAA Conference on Fibrous Composites in Structural Design, volume 3
[NASA-CR-198718] p 2184 N95-28266

The 1994 JANNAF Safety and Environmental Protection Subcommittee Meeting, volume 1
[CPIA-PUBL-614-VOL-1] p 2170 N95-28294

Ninth DOD/NASA/FAA Conference on Fibrous Composites in Structural Design, volume 1
[NASA-CR-198723] p 2189 N95-28420

Ninth DOD/NASA/FAA Conference on Fibrous Composites in Structural Design, volume 2
[NASA-CR-198722] p 2193 N95-28462

Third international congress of plant molecular biology: Molecular biology of plant growth and development
[DE95-006482] p 2352 N95-28496

The 18th Asilomar Conference on Polymeric Materials
[AD-A291721] p 2240 N95-28508

International journal of quantum chemistry
[AD-A291633] p 2352 N95-28546

Proceedings of the AIAA/FAA joint symposium on general aviation systems
[AD-A289830] p 2120 N95-28610

Chua's circuits: Phenomena and applications
[AD-A291638] p 2271 N95-28666

Proceedings of the International Workshop on Acceleration and Radiation Generation in Space and Laboratory Plasmas
[AD-A291673] p 2436 N95-28668

CONFIGURATION MANAGEMENT

Spinning a web: Publishing the SEI software configuration management research on the world wide web
[AD-A288708] p 2377 N95-27250

Report to Congressional Committees. Comanche Helicopter: Testing needs to be completed prior to production decisions
[GAO/NSIAD-95-112] p 2135 N95-27910

CONFINEMENT

On the physics of ion ring generation for the stabilization of FRX discharges
[DE95-007105] p 2410 N95-27922

Fluctuations and transport in fusion plasmas
[DE95-007111] p 2433 N95-27924

High pressure optical studies of semiconductors and heterostructures
[DE95-007119] p 2410 N95-27927

Ordered one-component plasmas: Phase transitions, normal modes, large systems, and experiments in a storage ring
[DE95-007077] p 2434 N95-28233

Heterostructures and infrared emitters with compressed InAsSb layers
[DE95-008157] p 2446 N95-28399

Theoretical aspects of energy confinement in spheromaks
[DE95-008079] p 2435 N95-28542

CONFORMAL MAPPING

The structure of the Hurwitz transformation
[DE95-608759] p 2397 N95-28518

CONGRESSIONAL REPORTS

Report to Congressional Committees. Comanche Helicopter: Testing needs to be completed prior to production decisions
[GAO/NSIAD-95-112] p 2135 N95-27910

Report to the Chairman and Ranking Minority Member, Committee on Science, House of Representatives. Weather forecasting: Radar availability requirement not being met
[GAO/AIMD-95-132] p 2342 N95-27912

Global trade in satellites and launch services
[GPO-84-811] p 2165 N95-28342

CONICAL BODIES

Optimization of a nutation damper attached to a spin-stabilized satellite
[AD-A289424] p 2162 N95-26887

CONIFERS

Unification of LARCH and Z-based object models to support algebraically-based design refinement: The Z perspective
[AD-A289234] p 2369 N95-26962

CONJUGATE GRADIENT METHOD

Vector algorithms for solving 3D nonlinear magnetostatic problems
[DE95-608737] p 2399 N95-27298

CONJUGATION

Near-resonant properties of nonlinear organic materials for optical devices
[AD-A288339] p 2178 N95-26570

CONSECUTIVE EVENTS

Modal event calculus in Lolli
[AD-A288544] p 2365 N95-26605

CONSERVATION

The role of microprocesses in macroscale magnetotail dynamics
[DE95-006288] p 2432 N95-27673

CONSERVATION LAWS

The method of space-time conservation element and solution element-applications to one-dimensional and two-dimensional time-marching flow problems
[NASA-TM-106915] p 2389 N95-26663

Transient studies of G-induced capillary dryout and rewet p 2281 N95-27351

The 1993 European school of high-energy physis
[DE95-610196] p 2421 N95-28040

CONSISTENCY

Building the electronic industry's roadmaps
p 2263 N95-27228

Trace anomalies and cocycles of Weyl and diffeomorphism groups
[DE95-608793] p 2397 N95-27344

CONSTELLATIONS

Changing paradigms: Manufacturing vs. fabricating a high volume Hold Down and Release Mechanism
p 2155 N95-27267

CONSTITUTIVE EQUATIONS

Accuracy issues in modeling superplastic metal forming
[DE95-008934] p 2222 N95-28163

CONSTRUCTION

Process control of microstructure in manufacturing
[AD-A288291] p 2245 N95-26410

Scalable multicast tree construction for wide area networks
[AD-A288318] p 2379 N95-26421

Development of an optical trap as an ultra-sensitive analytical tool
[DE95-007843] p 2426 N95-28022

Design, construction, test and evaluation of a frequency scanning radiometer for measuring oil slick thicknesses
[AD-A290040] p 2293 N95-28389

Bilateral force feedback for hydraulically actuated systems
[AD-A291632] p 2387 N95-28545

A genuinely multidimensional upwind scheme and efficient multigrid solver for the compressible Euler equations
[NASA-CR-195000] p 2288 N95-28571

CONSTRUCTION MATERIALS

Pre-integrated truss space station and method of assembly
[NASA-CASE-MSC-22015-1] p 2165 N95-27842

CONSUMABLES (SPACECRAFT)

Characterization of Ultra-Low Carbon Baintic steels for use as weld wire consumables
[AD-A288292] p 2212 N95-26411

CONSUMERS

Successful product realization strategies
p 2264 N95-27233

Lithium ion rechargeable systems studies
[DE95-006810] p 2268 N95-28200

CONTACT RESISTANCE

Processing and properties of chromate-free conversion coatings on aluminum
[DE95-004768] p 2218 N95-27722

CONTACTORS

Discharge ignition behavior of the Space Station plasma contactor
[NASA-TM-106925] p 2168 N95-27862

CONTAINMENT

A compatibility study of containment materials in FEFO, bis-(2-fluoro-2,2-dinitroethyl) formal
[DE95-007548] p 2206 N95-27750

CONTAMINANTS

The evaluation of a fluorochemical drying process for an electrical contact p 2227 N95-27103

The use of supercritical carbon dioxide for contaminant removal from solid waste p 2229 N95-27110

Ethyl lactate as a solvent alternative for cleaning metal parts p 2229 N95-27112

Cleaning of parts for new manufacturing and parts rebuilding p 2231 N95-27123

Fluid dynamic effects on precision cleaning with supercritical fluids p 2232 N95-27129

Laser ultrasonic generation at the surface of a liquid metal
[DE95-004999] p 2216 N95-27477

Effects of long term space environment exposure on optical substrates and coatings p 2428 N95-27653

Fracture testing and analysis of adhesively bonded joints for automotive applications
[DE95-007024] p 2184 N95-28207

Automated remedial assessment methodology software system
[DE95-007287] p 2373 N95-28243

Atomic layer epitaxy of group 4 materials: Surface processes, thin films, devices and their characterization
[AD-A289092] p 2446 N95-28327

Cryogenic BRDF measurements at 10.6 micrometers and 0.63 micrometers on contaminated mirrors
[AD-A291611] p 2427 N95-28408

CONTAMINATION

Stability of reference masses 4: Growth of carbonaceous contamination on platinum-iridium mass standard surfaces, and its cleaning by UV/ozone treatment
[PB95-190096] p 2226 N95-26745

Combined use of ground water circulation (UVB) technology and in situ bioreactors for enhanced bioremediation of subsurface contamination
p 2230 N95-27118

Community relations plan: Galena Airport and Camp ion Air Force Station, Alaska
[AD-A286722] p 2327 N95-27234

Recycle of radiologically contaminated austenitic stainless steels
[DE95-006464] p 2215 N95-27328

Spacecraft materials studies on the Aerospace Corporation tray on EOIM-3 p 2210 N95-27632

Space environmental effects observed on the Hubble Space Telescope p 2242 N95-27655

Hardware cleanliness methodology and certification
p 2211 N95-27656

From LDEF to a national Space Environment and Effects (SEE) program: A natural progression
p 2145 N95-27657

LDEF's contribution to the selection of thermal control coatings for the Space Station p 2242 N95-27661
Alpha characterization inside pipes using ion-transport technology
[DE95-007869] p 2411 N95-28024
Cryogenic BRDF measurements at 10.6 micrometers and 0.63 micrometers on contaminated mirrors
[AD-A291611] p 2427 N95-28408

CONTINENTAL SHELVES
On the persistence of the oceanic background of apparent sea level changes in the Baltic Sea
[REPT-94:5] p 2348 N95-27996

CONTINGENCY
Contingency maneuver strategies for the Total Ozone Mapping Spectrometer-Earth Probe (TOMS-EP)
p 2152 N95-27796
Contingency designs for attitude determination of TRMM p 2154 N95-27803
Cape Canaveral air station launch emergency response forces and toxic materials release contingency plans
p 2172 N95-28308

CONTINUITY
Crew adaptation evaluation of the Norwegian Crew Concept (NOROREW)
[AD-A288478] p 2360 N95-27058

CONTINUITY EQUATION
A new finite element formulation for incompressible flow
[DE95-007141] p 2284 N95-27454

CONTINUOUS RADIATION
ACT adaptive filters
[AD-A288385] p 2363 N95-26474
Evaluation of the FMICW waveform in HF surface radar applications
[AD-A288245] p 2249 N95-26545

CONTINUOUS SPECTRA
FTIR measurements of thermal infrared sky radiance and transmission
[DE95-003642] p 2334 N95-26436
Synthetic 3-D atmospheric temperature structure: A model for known geophysical power spectra using a hybrid autoregression and Fourier technique
[AD-A289058] p 2340 N95-26479
A continuous emissions monitor for airborne metals
p 2174 N95-28313

CONTINUOUS WAVE LASERS
Comprehensive numerical model for CW vertical-cavity surface-emitting lasers
[DE95-007758] p 2299 N95-28132

CONTINUOUS WAVE RADAR
Evaluation of the FMICW waveform in HF surface radar applications
[AD-A288245] p 2249 N95-26545

CONTINUUM FLOW
NO decomposition in non-reducing atmospheres
[DE95-007695] p 2205 N95-27690

CONTINUUM MECHANICS
Continuum mechanical modeling of solids undergoing a phase transformation
[AD-A288274] p 2200 N95-26451
Stability and thermal influences in nonlinear continuum mechanics and material science
[AD-A288333] p 2448 N95-26563
Material modeling in the CRALE code. Users' manual
[AD-A288988] p 2178 N95-26712

CONTINUUM MODELING
Continuum mechanical modeling of solids undergoing a phase transformation
[AD-A288274] p 2200 N95-26451

CONTOURS
Advances in scientific visualization
[DE95-008065] p 2343 N95-28014

CONTRACT MANAGEMENT
Automated Procurement System (APS) revised project management plan (DS-03)
[NASA-CR-196605] p 2450 N95-27169
A correlational study of the SEI's capability maturity model and software development performance in DOD contracts
[AD-A288890] p 2374 N95-28591

CONTRAST
Image quality metrics for color CRT displays
[AD-A288934] p 2262 N95-27198

CONTROL BOARDS
Gloved operator performance study. The effects of hand wear and elastic resistance of a control during tracking performance
[AD-A289405] p 2360 N95-27099

CONTROL EQUIPMENT
Simulation model of the integrated flight/propulsion control system, displays, and propulsion system for ASTOVL lift-fan aircraft
[NASA-TM-108866] p 2139 N95-26412
Plate manipulators
[AD-A289601] p 2121 N95-26719
Calorimetric evaluation of commercial Ni-MH cells and charges p 2272 N95-26790
NIST: Information management in the AMRF
[NONP-NASA-VT-95-49120] p 2454 N95-27208
Bilateral force feedback for hydraulically actuated systems
[AD-A291632] p 2387 N95-28545

CONTROL SIMULATION
Development of a nonlinear simulation for the McDonnell Douglas F-15 Eagle with a longitudinal TECS control-law
[AD-A288610] p 2128 N95-26481
Hubble Space Telescope nickel-hydrogen battery testing: An update p 2272 N95-26794

CONTROL STABILITY
Stable adaptive neurocontrollers for spacecraft and space robots p 2384 N95-27385
Use of blade pitch control to provide power train damping for the Mod-2, 2.5-mW wind turbine
p 2306 N95-27986

CONTROL STICKS
Gloved operator performance study. The effects of hand wear and elastic resistance of a control during tracking performance
[AD-A289405] p 2360 N95-27099

CONTROL SURFACES
Plate manipulators
[AD-A289601] p 2121 N95-26719
A numerical method for unsteady transonic flow about wings with control surfaces
[AD-A289631] p 2121 N95-26859
Implementation and demonstration of a multiple model adaptive estimation failure detection system for the F-16
[AD-A289301] p 2131 N95-27042

CONTROL SYSTEMS DESIGN
Virtual Prototyping as an aid for control system analysis
[AD-A288819] p 2362 N95-26346
Demonstration study of hierarchical control of fluid-dynamic phenomena
[AD-A289341] p 2275 N95-26751
Control of a large space structure using multiple model adaptive estimation and control techniques
[AD-A289309] p 2162 N95-26916
A gain scheduling optimization method using genetic algorithms
[AD-A289306] p 2381 N95-26920
Prevention and control of inlet unstart using an SR-71 simulation p 2119 N95-26948
Generic satellite monitoring expert system
[AD-A289209] p 2163 N95-26987
NIST: Information management in the AMRF
[NONP-NASA-VT-95-49120] p 2454 N95-27208
Fuzzy logic techniques for rendezvous and docking of two geostationary satellites p 2384 N95-27386
A linguistic geometry for 3D strategic planning
p 2386 N95-27397
Time-optimal control of the magnetically levitated photolithography platen
[DE95-005493] p 2266 N95-27724
Collected papers on wind turbine technology
[NASA-CR-195432] p 2321 N95-27970
Analysis methods for wind turbine control and electrical system dynamics p 2273 N95-27984
Control system design for the MOD-5A 7.3 mW wind turbine generator p 2306 N95-27985
Use of blade pitch control to provide power train damping for the Mod-2, 2.5-mW wind turbine
p 2306 N95-27986
Variable speed generator technology options for wind turbine generators p 2273 N95-27988
Variable speed generator application on the MOD-5A 7.3 mW wind turbine generator p 2273 N95-27989
Application of modern diagnostic methods to environmental improvement
[DE95-005797] p 2330 N95-28119
The solar array-induced disturbance of the Hubble Space Telescope pointing system
[NASA-TP-3556] p 2311 N95-28214
Pilot opinions on high level flight deck automation issues: Toward the development of a design philosophy
[NASA-CR-4669] p 2357 N95-28253
Functionalized block copolymers as adhesion promoters
[DE95-008158] p 2239 N95-28400
Development of a TECS control-law for the lateral directional axis of the McDonnell Douglas F-15 Eagle
[AD-A289771] p 2142 N95-28598

CONTROL THEORY
A class of stabilizing controllers for flexible multibody systems
[NASA-TP-3494] p 2161 N95-26428
Development of a nonlinear simulation for the McDonnell Douglas F-15 Eagle with a longitudinal TECS control-law
[AD-A288610] p 2128 N95-26481
A comparison of the Neal-Smith and omega Tau function, zeta function and tau function flying qualities criteria
[AD-A289503] p 2130 N95-26844
Advanced formation flight control
[AD-A289271] p 2142 N95-26981
Optimal control of two queues in series
[DE95-608731] p 2382 N95-27045
Flow control
[AD-A289262] p 2279 N95-27197
High-precision buffer circuit for suppression of regenerative oscillation
[NASA-TM-4658] p 2291 N95-27259
Improved numerical solution of mixed H2/H(infinity) optimization with applications
[AD-A289315] p 2386 N95-27400
Dynamics and control of SEDSAT tethered multi-probe for thermospheric research flight data analysis of SEDS-2 satellite: Tethered systems dynamics and flight data analysis
[NASA-CR-198653] p 2165 N95-27836
Development of a TECS control-law for the lateral directional axis of the McDonnell Douglas F-15 Eagle
[AD-A289771] p 2142 N95-28598

CONTROLLABILITY
An investigation of the effects of pitch-roll (de)coupling on helicopter handling qualities
[NASA-TM-110349] p 2141 N95-26773
A comparison of the Neal-Smith and omega Tau function, zeta function and tau function flying qualities criteria
[AD-A289503] p 2130 N95-26844
Test operations procedure (TOP) 7-3-534 airworthiness testing of fixed wing aircraft: Asymmetric power testing
[AD-A289458] p 2130 N95-26994

CONTROLLERS
A class of stabilizing controllers for flexible multibody systems
[NASA-TP-3494] p 2161 N95-26428
Robust hybrid state-space self-tuning control using dual-rate sampling
[AD-A288359] p 2380 N95-26468
Design and synthesis of a real-time controller for an unmanned air vehicle
[AD-A289134] p 2141 N95-26555
Next generation controller specification for an open systems architecture standard - overview
[AD-A289507] p 2368 N95-26853
Electro-hydrostatic actuator controller design using quantitative feedback theory
[AD-A289220] p 2141 N95-26957
Telepresent spacecraft docking with object-based bilateral control (OBBC)
[AD-A289268] p 2163 N95-26980
Survey and implementation of commercial manual controllers for a generic telerobotics architecture
[AD-A289215] p 2381 N95-26990
Flight control design using mixed H2/micron optimization
[AD-A289288] p 2142 N95-27036
Development of a miniature actuator/controller system
p 2156 N95-27272
Fuzzy logic techniques for rendezvous and docking of two geostationary satellites p 2384 N95-27386
Improved numerical solution of mixed H2/H(infinity) optimization with applications
[AD-A289315] p 2386 N95-27400
A hybrid vehicle evaluation code and its application to vehicle design. Revision 1
[DE95-008053] p 2303 N95-28029
Functionalized block copolymers as adhesion promoters
[DE95-008158] p 2239 N95-28400
Replacing the message service component in an integration framework
[AD-A289928] p 2375 N95-28628
Next generation controller specification for an open systems architecture standard
[AD-A289567] p 2375 N95-28647

CONVECTION
Single-drop reactive extraction/extractive reaction with forced convective diffusion and interphase mass transfer
p 2282 N95-27358
Single-drop reactive extraction/extractive reaction with forced convective diffusion and interphase mass transfer
p 2283 N95-27365
Engineering photochemical smog through convection towers
[DE95-007727] p 2328 N95-27686
Algorithm to describe the spread of a wall fire under a ceiling
[PB95-182259] p 2247 N95-28008

CONVECTION CLOUDS
A study of lightning in winter thunderstorms and the analysis of thunderstorm overflight data
[NASA-CR-198577] p 2343 N95-28191

CONVECTION-DIFFUSION EQUATION

Extensional flow convecting a reactant undergoing a first order homogeneous reaction and diffusional mass transfer from a sphere at low to intermediate Peclet and Damkohler numbers p 2280 N95-27346

Single-drop reactive extraction/extractive reaction with forced convective diffusion and interphase mass transfer p 2283 N95-27365

CONVECTIVE FLOW

Two-layer or free surface shear flows and viscoelastic shear flows and the relationship between stability and eigenvalues --- viscoelastic, shear, and convective flows [AD-A289510] p 2278 N95-27047

Computation of three-dimensional mixed convective boundary layer flow p 2280 N95-27347

Single-drop reactive extraction/extractive reaction with forced convective diffusion and interphase mass transfer p 2283 N95-27365

Experimental study on transition characteristics of natural-convection flow [PB95-192423] p 2289 N95-28637

CONVECTIVE HEAT TRANSFER

Deep convection in the Mediterranean Sea [AD-A288497] p 2346 N95-26647

Adiabatic charging of nickel-hydrogen batteries p 2272 N95-26795

CAE for thermal management of aerospace electronic boards using the BETAsoft program p 2272 N95-27354

Tomographic observations of deep convection and the thermal evolution of the Greenland Sea Gyre 1988-1989 [AD-A289104] p 2348 N95-28096

Composite flexible insulation for thermal protection of space vehicles p 2166 N95-28293

CONVERGENCE

ACT adaptive filters [AD-A288385] p 2363 N95-26474

The comparison of P(sub 1) and simplified P(sub 2) synthetic acceleration for iterative methods in transport solutions [DE94-018306] p 2390 N95-27304

Optical implementation of inner product neural associative memory [NASA-CASE-NPO-18491-2-CU] p 2427 N95-28363

Korteweg-de Vries equation: Convergent Birkhoff normal form [PB95-196275] p 2393 N95-28611

COOLANTS

Mathematical modelling of the thermodynamic properties of coolants and working media of heat pumps [IFTR-6/1994] p 2447 N95-26510

Experimental investigation of the effects of relative physical orientation between evaporator and condenser for a loop heat pipe [AD-A289248] p 2277 N95-26968

Diagnostic system Cryo-D for the determination of parameters of vapor-liquid currents of the coolant [DE95-608775] p 2280 N95-27338

Vapor pressures of mixtures of CFC-114 with the potential replacement coolants C4F(10) andc-C4F 8 [DE95-003444] p 2208 N95-28042

Cooling apparatus and couplings therefor [NASA-CASE-ARC-11921-1] p 2304 N95-28256

COOLING

Ultra high purity, dimensionally stable INVAR 36 [NASA-CASE-NPO-19358-1-CU] p 2213 N95-26862

CAE for thermal management of aerospace electronic boards using the BETAsoft program p 2272 N95-27354

Heat pipe cooled reactors for multi-kilowatt space power supplies [DE95-005211] p 2420 N95-27425

Towards the detection and attribution of an anthropogenic effect on climate [DE95-008589] p 2331 N95-28157

Cooling apparatus and couplings therefor [NASA-CASE-ARC-11921-1] p 2304 N95-28256

COOLING SYSTEMS

Silicon subsystem mechanical engineering closeout report for the Solenoidal Detector Collaboration [DE95-006336] p 2421 N95-27735

Vapor pressures of mixtures of CFC-114 with the potential replacement coolants C4F(10) andc-C4F 8 [DE95-003444] p 2208 N95-28042

Cooling apparatus and couplings therefor [NASA-CASE-ARC-11921-1] p 2304 N95-28256

COORDINATE TRANSFORMATIONS

User documentation of the CTA program [AD-A289508] p 2121 N95-26854

The structure of the Hurwitz transformation [DE95-608759] p 2397 N95-28518

COORDINATES

Wigner quantum oscillators. OSP (3/2) oscillators [DE95-608756] p 2448 N95-27334

A simple method for verifying the deployment of the TOMS-EP solar arrays p 2150 N95-27782

Coordinates of the quantum plane as q-tensor operators in U(sub q) (su(2) * su(2)) [DE95-007100] p 2397 N95-28234

Three-dimensional photogrammetry for laboratory applications [AD-A291624] p 2294 N95-28410

COORDINATION

AEM investigation of tetrahedrally coordinated Ti(4+) in nickel-titanate spinel [DE95-006624] p 2215 N95-27473

COPOLYMERS

Design strategies for the preparation of polymeric organic superconductors [AD-A289022] p 2436 N95-26462

Fractionation studies of polyethylene using DSC-technique [PB95-185252] p 2200 N95-26540

Small angle neutron scattering study of the micelle structure of amphiphilic block copolymers [DE95-006625] p 2234 N95-27486

JTEC monograph on biodegradable polymers and plastics in Japan: Research, development, and applications [NASA-CR-198562] p 2235 N95-27694

Feasibility studies for separation processes using environmentally sensitive hydrogels [DE95-008355] p 2238 N95-28226

Functionalized block copolymers as adhesion promoters [DE95-008158] p 2239 N95-28400

Molecular modeling: An approach for the study of piezoelectric polymers [AD-A289821] p 2241 N95-28574

COPPER

The development of the anisotropic properties of copper under plastic deformation induced by creep and monotonic loading [IFTR-23/1994] p 2212 N95-26517

Characteristics of thermal lens in a copper-vapor laser [AD-A289545] p 2294 N95-26874

Simulating the production of free defects in irradiated metals [DE95-007165] p 2214 N95-27088

Probe molecule studies: Active species in alcohol synthesis [DE95-003514] p 2203 N95-27420

A new technique for measuring the separation of closely spaced dislocations using residual contrast conditions [DE95-007147] p 2219 N95-27968

Effects of interlayers on the scratch adhesion performance of ultra-thin films of copper and gold on silicon substrates [DE95-007367] p 2220 N95-28044

Copper CVD using liquid coinjection of (hfac)Cu(TMVS) and TMVS [DE95-008155] p 2237 N95-28089

The off-center effect on the diffusion coefficient of Cu(+) and Li(+) in the KCl lattice [DE95-609146] p 2446 N95-28255

Residual stress, strain, and faults in nanocrystalline palladium and copper [DE95-008294] p 2223 N95-28543

COPPER ALLOYS

Spin-density-wave magnetism in dilute copper-manganese alloys [DE95-005121] p 2215 N95-27462

A new Cu-8 Cr-4 Nb alloy for high temperature applications [NASA-TM-106910] p 2218 N95-27728

Electronic structure of disordered Cu-Ag alloys [DE95-609156] p 2219 N95-27758

COPPER COMPOUNDS

Experimental determination of cluster geometrical structure [DE95-007089] p 2409 N95-27753

The oxidation state and magnetic behaviour of Tb in high-(Tc) related materials [DE95-007129] p 2219 N95-27966

Indentability of conventional and negative Poisson's ratio foams p 2195 N95-28472

COPPER OXIDES

Investigations of the hyperfine interactions in copper-oxide perovskites using Eu-151 and Fe-57 Moessbauer spectroscopy [PB95-185138] p 2437 N95-26513

Hall effect and resistivity in the normal state of high-T(sub c) cuprates in the electron-fracton model [DE95-610612] p 2439 N95-27413

Observations of CEF-split intermultiplet transitions in optically opaque EuBa2Cu3O7 using inelastic neutron scattering [DE95-007135] p 2408 N95-27453

Numerical study of the singlet-triplet model for cuprate superconductors [DE95-609438] p 2440 N95-27712

Kinetics and dynamics of oxidation reactions involving adsorbed CO species on bulk supported Pt and copper oxides [DE95-006420] p 2207 N95-27952

Aspects of macroscopic phase separation and interstitial oxygen ordering in oxygen doped La2CuO(4+delta) [DE95-007864] p 2443 N95-28060

The real structure of columnar pinning centers in heavy-ion-irradiated cuprate superconductors [DE95-003948] p 2445 N95-28186

CORNER FLOW

A numerical method for solving the three-dimensional parabolized Navier-Stokes equations [NASA-CR-198159] p 2287 N95-27917

CORRECTION

Computing NORAD mean orbital elements from a state vector [AD-A289281] p 2146 N95-27033

The gluon propagator in non-Abelian Weizsaecker-Williams fields [DE95-006877] p 2449 N95-27547

Polarization as a probe to the production mechanisms of charmonium in (pi)N collisions [DE95-008136] p 2414 N95-28142

Efficient analytic computation of higher-order QCD amplitudes [DE95-008593] p 2449 N95-28160

CORRELATION

Method of phased magnitude correlation using binary sequences [AD-D017257] p 2248 N95-26465

Temporal and spatial decorrelation scales of the Yellow Sea thermal fields [AD-A288617] p 2346 N95-26483

A spectral algorithm for the seriation problem [DE95-004775] p 2372 N95-27436

A study of non-stationary processes and their applications [AD-A291725] p 2395 N95-28510

Atmospheric dispersion in adaptive optics [AD-A289639] p 2428 N95-28617

CORROSION

Alternative cleaning solvents and lubricants at the Air Force PJKS facility p 2228 N95-27108

Corrosive effects of supercritical carbon dioxide and cosolvents on metals p 2224 N95-27113

The use of electrochemistry and ellipsometry for identifying and evaluating corrosion on aircraft [AD-A288536] p 2125 N95-27186

Iron oxides characterization by Moessbauer spectroscopy [DE95-607869] p 2202 N95-27199

Current programmes on physical metallurgy and related areas in BARC [DE95-607939] p 2214 N95-27255

Study of development and utilization of a multipurpose atmospheric corrosion sensor [NASA-CR-198595] p 2292 N95-27368

Measurements of the volatilities of electrolytes: Application to water/steam cycles [DE95-007103] p 2204 N95-27451

Engineered materials for appliation in severe metallurgical environments: Tantalum-carbon alloy development [DE95-006838] p 2216 N95-27488

Effects of hydrogen on carbon steels at the Multi-Function Waste Tank Facility [DE95-007194] p 2219 N95-28005

An overview of activities and accomplishments of the Metals and Ceramics Division [DE95-007020] p 2241 N95-28560

CORROSION PREVENTION

Characterization of corrosion and development of a breadboard of a D sight aircraft inspection system, phase 1 [AD-A288347] p 2125 N95-26527

Stress corrosion cracking susceptibility of the earthquake resistant NOM B457 Mexican steel [DE95-607956] p 2214 N95-27256

Processing and properties of chromate-free conversion coatings on aluminum [DE95-004768] p 2218 N95-27722

Chromate-free corrosion resistant conversion coatings for aluminum alloys [DE95-007742] p 2238 N95-28117

CORROSION RESISTANCE

Engineered materials for appliation in severe metallurgical environments: Tantalum-carbon alloy development [DE95-006838] p 2216 N95-27488

Processing and properties of chromate-free conversion coatings on aluminum [DE95-004768] p 2218 N95-27722

Pulsed ion beam surface treatment for preparing rapidly solidified corrosion resistant steel and aluminum surfaces
[DE95-007741] p 2221 N95-28116
Chromate-free corrosion resistant conversion coatings for aluminum alloys
[DE95-007742] p 2238 N95-28117
Bases for extrapolating materials durability in fuel storage pools
[DE95-007748] p 2222 N95-28129
Coatings of non-oxide ceramics for improved corrosion resistance in high temperature coal combustion
[DE95-006932] p 2241 N95-28604

CORROSION TESTS
Study of development and utilization of a multipurpose atmospheric corrosion sensor
[NASA-CR-198595] p 2292 N95-27368

COSMIC DUST
Molecular cloud content of early-type galaxies. V. CO in elliptical galaxies
[PB95-185153] p 2461 N95-27320

COSMIC RAYS
Cosmic ray test results of the D0 prototype scintillating fiber tracker
[DE95-007215] p 2415 N95-28221

COSMOLOGY
Laboratory high-energy astrophysics on lasers
[DE95-008062] p 2462 N95-28013
The 1993 European school of high-energy physis
[DE95-610196] p 2421 N95-28040
Was Einstein 100% right?
[PB95-190179] p 2449 N95-28175
Discovery of the most distant supernovae and the quest for (Omega)
[DE95-006569] p 2460 N95-28197

COST ANALYSIS
Development of repair processes and sources for C/KC-135 aircraft windows/windshields
[AD-A288348] p 2117 N95-26629
An analysis of the KC-135 three-person cockpit
[AD-A289540] p 2130 N95-26873
Accelerating conservative parallel simulation of VHDL circuits
[AD-A289317] p 2264 N95-27294
Physics assessment of stellarators as fusion power plants
[DE95-007045] p 2431 N95-27498
Briefing Report to the Ranking Minority Member, Subcommittee on Space and Aeronautics, Committee on Science, House of Representatives. Cassini Mission: Estimated launch costs for NASA's mission to Saturn
[GAO/NSIAD-95-141BR] p 2145 N95-27856
C-130 Advanced Technology Center wing box conceptual design/cost study p 2192 N95-28437
Designers' unified cost model p 2194 N95-28464
An automated cost uncertainty program
[AD-A288747] p 2374 N95-28588

COST EFFECTIVENESS
Successful product realization strategies
p 2264 N95-27233
Monolithic electronics for nuclear and high-energy physics experiments
[DE95-005393] p 2420 N95-27427
Report to Congressional Committees. Comanche Helicopter: Testing needs to be completed prior to production decisions
[GAO/NSIAD-95-112] p 2135 N95-27910
Implementing an integrated standards-based management system to ensure compliance at Los Alamos National Laboratory
[DE95-007873] p 2451 N95-28025

COST ESTIMATES
Briefing Report to the Ranking Minority Member, Subcommittee on Space and Aeronautics, Committee on Science, House of Representatives. Cassini Mission: Estimated launch costs for NASA's mission to Saturn
[GAO/NSIAD-35-141BR] p 2145 N95-27856
Report to Congressional Committees. Comanche Helicopter: Testing needs to be completed prior to production decisions
[GAO/NSIAD-95-112] p 2135 N95-27910
Report to the Chairman and Ranking Minority Member, Committee on Science, House of Representatives. Weather forecasting: Radar availability requirement not being met
[GAO/AIMD-95-132] p 2342 N95-27912

COST REDUCTION
A system dynamics based study of software reuse and its determinants
[AD-A288578] p 2364 N95-26554
Using SCR methods to analyze requirements documentation
[NASA-CR-197760] p 2365 N95-26668
Development and analysis of SCR requirements tables for system scenarios
[NASA-CR-197769] p 2367 N95-26802
Briefing Report to the Ranking Minority Member, Subcommittee on Space and Aeronautics, Committee on Science, House of Representatives. Cassini Mission: Estimated launch costs for NASA's mission to Saturn
[GAO/NSIAD-95-141BR] p 2145 N95-27856
Low-power, parallel photonic interconnections for Multi-Chip Module applications
[DE95-008518] p 2267 N95-28147
C-130 Advanced Technology Center wing box conceptual design/cost study p 2192 N95-28437
Composite fuselage crown panel manufacturing technology p 2137 N95-28474

COSTS
Using machine learning to derive efficient cost and performance estimates in VLSI CAD designs
[AD-A288254] p 2363 N95-26408
Weightless Environment Training Facility (WETF) materials coating evaluation, volume 3
[NASA-CR-188366-VOL-3] p 2239 N95-28387
The U.S. Department of Energy Wind Turbine Development Program
[DE95-000292] p 2325 N95-28395
Building-integrated photovoltaics: A case study
[DE95-004032] p 2325 N95-28396
Strategies for recycling CdTe photovoltaic modules
[DE95-006776] p 2325 N95-28517

COUNTER ROTATION
Some notes on long-range beam-beam effects for the 2 TeV collider
[DE95-006771] p 2421 N95-28017

COUNTERS
Solid-state image sensor with focal-plane digital photon-counting pixel array
[NASA-CASE-NPO-18518-1-CU] p 2424 N95-26894
Orbiting meteoroid and debris counting experiment
p 2463 N95-27668
Precision electromagnetic calorimetry with liquid krypton
[DE95-006685] p 2292 N95-27677

COUPLED MODES
Supercooled liquid dynamics for the charged hard-sphere model
[DE95-609158] p 2241 N95-28609

COUPLING
An investigation of the effects of pitch-roll (de)coupling on helicopter handling qualities
[NASA-TM-110349] p 2141 N95-26773
Couplings of heavy hadrons with soft pions from QCD sum rules
[DE95-610349] p 2407 N95-27410
Skew chromaticity
[DE95-007677] p 2422 N95-28115
Constraints on the anomalous WW gamma couplings from b vector s gamma
[DE95-608866] p 2415 N95-28246

COUPLINGS
Dynamic coupling of underactuated manipulators
[AD-A289404] p 2301 N95-27098
Cooling apparatus and couplings therefor
[NASA-CASE-ARC-11921-1] p 2304 N95-28256

COVALENT BONDS
Non-covalent immobilization of proteins and enzymes on polymerized lipid assemblies
[AD-A288234] p 2225 N95-26526

COVARIANCE
Analysis of filter tuning techniques for sequential orbit determination p 2146 N95-27764
Accurate orbit determination strategies for the tracking and data relay satellites p 2147 N95-27768
Experience from the in-flight calibration of the Extreme Ultraviolet Explorer (EUVE) and Upper Atmosphere Research Satellite (UARS) fixed head star trackers (FHSTs) p 2149 N95-27779
Application of non-coherent Doppler data types for deep space navigation p 2151 N95-27788
A demonstration of unified TDRS/GPS tracking and orbit determination p 2151 N95-27792

CRACK BRIDGING
Structural ceramics incorporating whiskers, platelets, and particulate phases
[DE95-007048] p 2235 N95-27499

CRACK INITIATION
Fatigue properties of an A356 (AlSi7Mg) aluminum alloy for automotive applications: Fatigue life prediction
[PB95-196424] p 2224 N95-28660

CRACK OPENING DISPLACEMENT
An experimental and numerical investigation of specimen size requirements for cleavage fracture toughness
[AD-A289120] p 2311 N95-28100

CRACK PROPAGATION
Analysis of fatigue fractographic data of a rod end housing using a Monte Carlo simulation
[NAL-TR-1225] p 2307 N95-26521
Fatigue fracture analysis in medium carbon structural steel and austenitic stainless steel by X-ray fractography
[DE95-601504] p 2213 N95-26675
Stress corrosion cracking susceptibility of the earthquake resistant NOM B457 Mexican steel
[DE95-607956] p 2214 N95-27256
Adhesively bonded composite patch repair of cracked aluminum alloy structures p 2132 N95-27507
An experimental and numerical investigation of specimen size requirements for cleavage fracture toughness
[AD-A289120] p 2311 N95-28100
Prediction of fatigue crack growth under constant amplitude and random loading using specimens with multiple cracks
[AD-A291614] p 2136 N95-28409
Characteristics of laminates with delamination control strips p 2191 N95-28434
Numerical simulation of crack growth in pressurized fuselages
[PB95-192415] p 2137 N95-28636

CRACK TIPS
Fatigue fracture analysis in medium carbon structural steel and austenitic stainless steel by X-ray fractography
[DE95-601504] p 2213 N95-26675
Environmentally assisted cracking of high strength beta titanium alloys
[AD-A289156] p 2213 N95-27032
Deformation limits on two-parameter fracture mechanics in terms of higher order asymptotics
[AD-A289113] p 2310 N95-28098
An experimental and numerical investigation of specimen size requirements for cleavage fracture toughness
[AD-A289120] p 2311 N95-28100

CRACKING (FRACTURING)
Micromechanical prediction of tensile damage for ceramic matrix composites under high temperature
[AD-A288238] p 2180 N95-26626
Characterization of fatigue behavior of 2-D woven fabric reinforced ceramic matrix composite at elevated temperature
[AD-A289423] p 2181 N95-26886
Evaluation of patch effectiveness in repairing aircraft components p 2133 N95-27513
Deformation limits on two-parameter fracture mechanics in terms of higher order asymptotics
[AD-A289113] p 2310 N95-28098
An experimental and numerical investigation of specimen size requirements for cleavage fracture toughness
[AD-A289120] p 2311 N95-28100
Numerical simulation of crack growth in pressurized fuselages
[PB95-192415] p 2137 N95-28636

CRACKS
Bonded composite repair of metallic aircraft components: Overview of Australian activities
p 2132 N95-27505
Design and structural validation of CF116 upper wing skin boron doubler p 2132 N95-27510
Evaluation of patch effectiveness in repairing aircraft components p 2133 N95-27513
Prediction of fatigue crack growth under constant amplitude and random loading using specimens with multiple cracks
[AD-A291614] p 2136 N95-28409

CRASHES
Rotorcraft crashworthy airframe and fuel system technology development program
[AD-A289986] p 2126 N95-28630

CRASHWORTHINESS
Rotorcraft crashworthy airframe and fuel system technology development program
[AD-A289986] p 2126 N95-28630

CRATERS
A new technique for ground simulation of hypervelocity debris p 2154 N95-27671

CRAY COMPUTERS
Fluctuations and transport in fusion plasmas
[DE95-007111] p 2433 N95-27924
Optimization strategies for molecular dynamics programs on Cray computers and scalar work stations
[AD-A289574] p 2418 N95-28648

CREEP PROPERTIES
Creep recovery of PVC and polypropylene
[PB95-185112] p 2224 N95-26448
The development of the anisotropic properties of copper under plastic deformation induced by creep and monotonic loading
[IFTR-23/1994] p 2212 N95-26517
Probabilistic material strength degradation model for Inconel 718 components subjected to high temperature, high-cycle and low-cycle mechanical fatigue, creep and thermal fatigue effects
[NASA-CR-197832] p 2214 N95-27167

Scarf repairs to graphite/epoxy components
p 2135 N95-27523

CREEP STRENGTH

A new Cu-8 Cr-4 Nb alloy for high temperature applications
[NASA-TM-106910] p 2218 N95-27728

CREWS

Crew adaptation evaluation of the Norwegian Crew Concept (NOROREW)
[AD-A288478] p 2360 N95-27058

CRITERIA

A method to determine the structure of an unknown mixture using the Akaike Information Criterion and the bootstrap
[AD-A288295] p 2394 N95-26415

Automatically selecting and using primary effects in planning: Theory and experiments
[AD-A289347] p 2450 N95-27064

CRITICAL EXPERIMENTS

The experience of CF Technologies, Inc. (CF Tech) in critical fluid processing p 2232 N95-27128

CRITICAL FREQUENCIES

Variability study of foF2 for an equatorial station
[DE95-608080] p 2337 N95-27157

CRITICAL LOADING

Comparison of life theories for rolling-element bearings
[NASA-TM-106585] p 2301 N95-26774

Testing of Uninterruptible Power Supplies with nonlinear loads
[AD-A289353] p 2262 N95-27067

Fundamental concepts in the suppression of delamination buckling by stitching p 2198 N95-28486

CRITICAL POINT

Critical behaviour of spin models: A transfer-matrix approach
[PB95-192456] p 2418 N95-28638

CRITICAL PRESSURE

Precision parts cleaning with supercritical carbon dioxide p 2229 N95-27114

Design considerations in supercritical fluid technology
p 2232 N95-27126

CRITICAL TEMPERATURE

Precision parts cleaning with supercritical carbon dioxide p 2229 N95-27114

Design considerations in supercritical fluid technology
p 2232 N95-27126

Comparison of the calculated and measured stability of a NbTi cable-in-conduit conductor
[DE95-007964] p 2265 N95-27693

Beta-dynamics in simple liquid metal
[DE95-609154] p 2220 N95-28039

CROP GROWTH

Third international congress of plant molecular biology: Molecular biology of plant growth and development
[DE95-006482] p 2352 N95-28496

Models used to forecast agricultural corn crops in the micro-region of Ribeirao Preto-SP
[INPE-5513-NTC/309] p 2315 N95-28554

CROP IDENTIFICATION

Method for determining surface coverage by materials exhibiting different fluorescent properties
[NASA-CASE-GSC-13539-1] p 2315 N95-28211

CROSS CORRELATION

Fuzzy inference enhanced information recovery from digital PIV using cross-correlation combined with particle tracking
[NASA-TM-106896] p 2291 N95-27173

CROSS COUPLING

Coupling in the Tevatron
[DE95-005129] p 2421 N95-27531

CROSS FLOW

Nonlinear stability of non-stationary cross-flow vortices in compressible boundary layers
[NASA-CR-189184] p 2279 N95-27242

Computation of three-dimensional mixed convective boundary layer flow p 2280 N95-27347

CROSS SECTIONS

Measurement of R in e(+)e(-)-annihilation at center-of-mass energies between 7.2 and 10.34 GeV
[DE95-610303] p 2407 N95-27408

A study of events with large total transverse energy produced in proton-antiproton collisions at (radical)s = 1.8 TeV
[DE95-003382] p 2410 N95-27872

CROSSINGS

Crab crossing in a gamma-gamma collider
[DE95-006580] p 2420 N95-27470

CROSSLINKING

Radiation vulcanization of natural rubber latex
[DE95-600026] p 2226 N95-26637

Mechanisms of hypertension after cross-linked hemoglobin blood-substitute transfusion
[AD-A289558] p 2352 N95-26680

CRRES (SATELLITE)

The combined release and radiation effects satellite time history data base system
[AD-A289835] p 2165 N95-28578

CRUDE OIL

The biodegradation of fuels in soils and sediments: Differences as a function of mineralogy
p 2230 N95-27116

Investigation on energy conversion technology using biochemical reaction elements, 2
[DE95-759250] p 2321 N95-27940

CRUSHING

Crushing singularities in spacetimes with spherical, plane and hyperbolic symmetry
[PB95-190146] p 2397 N95-28011

CRUSTS

Stability of strange quark stars with nuclear crusts against radial oscillations
[DE95-008484] p 2463 N95-28357

CRYOGENIC FLUIDS

Precision electromagnetic calorimetry with liquid krypton
[DE95-006685] p 2292 N95-27677

Tank pressure control in low gravity by jet mixing
[NASA-CR-191012] p 2243 N95-28001

CRYOGENIC TEMPERATURE

Diagnostic system Cryo-D for the determination of parameters of vapor-liquid currents of the coolant
[DE95-608775] p 2280 N95-27338

Cryogenic washout of solid rocket propellants
p 2176 N95-28324

Development and application of low-temperature AFM
[AD-A291704] p 2352 N95-28525

Cryogenic temperature control and tension/compression attachment stage for an electron microscope
[AD-D017390] p 2294 N95-28612

CRYOGENICS

Cryogenic and simulated fuel jet breakup in argon, helium and nitrogen gas flows
[NASA-TM-106923] p 2291 N95-27030

Multi-channel electronically scanned cryogenic pressure sensor
[NASA-CASE-LAR-15062-1] p 2291 N95-27138

A cryogenic scan mechanism for use in Fourier transform spectrometers p 2158 N95-27287

Tank pressure control in low gravity by jet mixing
[NASA-CR-191012] p 2243 N95-28001

Cryogenic washout of solid rocket propellants
p 2176 N95-28324

Cryogenic BRDF measurements at 10.6 micrometers and 0.63 micrometers on contaminated mirrors
[AD-A291611] p 2427 N95-28408

High energy density systems in cryogenic media: The production and reactions of atoms and radicals
[AD-A289818] p 2417 N95-28572

Cryogenic temperature control and tension/compression attachment stage for an electron microscope
[AD-D017390] p 2294 N95-28612

CRYOPUMPING

Pumping characteristics of a cryopump with Ar sorbent in He and in D2/He mixture
[DE95-007049] p 2302 N95-27875

Divertor research on the DIII-D tokamak
[DE95-003942] p 2434 N95-28185

CRYSTAL DEFECTS

Electronic characterization of defects in narrow gap semiconductors: Comparison of electronic energy levels and formation energies in mercury cadmium telluride, mercury zinc telluride, and mercury zinc selenide
[NASA-CR-197835] p 2437 N95-26780

Effects of helium pre-implantation on the microstructure and mechanical properties of irradiated 316 stainless steel
[DE95-007162] p 2214 N95-27086

Simulating the production of free defects in irradiated metals
[DE95-007165] p 2214 N95-27088

A new method of evaluating the explicit magnetic-state-dependent energy in semi-empirical calculations of iron
[AD-A289098] p 2399 N95-27398

Crystal structure, short-range oxygen defects, and water adsorption in La- and Nd-modified ZrO2
[DE95-007134] p 2439 N95-27452

The real structure of columnar pinning centers in heavy-ion-irradiated cuprate superconductors
[DE95-003948] p 2445 N95-28186

CRYSTAL GROWTH

Probabilistic growth model
[PB95-185054] p 2395 N95-26913

Growth and evaluation of nonlinear optical crystals for laser applications: Lithium borate, barium borate and silver gallium selenide
[AD-A289147] p 2277 N95-27000

Low temperature materials growth and processing development for flat panel display technology applications
[AD-A288970] p 2233 N95-27187

Growth, characterization and device development in monocrystalline diamond films
[AD-A289356] p 2439 N95-27416

Effects of low earth orbit on the optical performance of multi-layer enhanced high reflectance mirrors
p 2428 N95-27652

Growth and characterization of crystals for room temperature I.R. detectors and second harmonic generation devices
[NASA-CR-198598] p 2443 N95-28033

Pulsed laser deposition of zeolitic membranes
[DE95-006274] p 2298 N95-28124

Self-assembly of low-dimensional molecular nanoclusters on Au(111) surfaces
[AD-A288936] p 2178 N95-28334

CRYSTAL LATTICES

Structure of ordinary ice Ih. Part 2: Defects in ice. Volume 1: Point defects
[AD-A288279] p 2200 N95-26452

Atomically resolved STM study of the adsorption and dissociation of methyl chloride on Si(001)
[AD-A289218] p 2438 N95-27061

A correlated Walks' theory for DNA denaturation
[DE95-607910] p 2444 N95-28112

The high strain rate deformation of tungsten single crystals
[AD-A288874] p 2223 N95-28189

The off-center effect on the diffusion coefficient of Cu(+) and Li(+) in the KCl lattice
[DE95-609146] p 2446 N95-28255

Local texture and grain boundary misorientations in high H(C) oxide superconductors
[DE95-007004] p 2447 N95-28606

Isolation and x-ray crystal structures of (Li(mu2-As(SiMe3)2) (mu3-As(SiMe3)2)(THF))2 and ((Me3Si)2AsLi(THF)2)2
[AD-A288870] p 2241 N95-28661

CRYSTAL OPTICS

Nonlinear dynamics of a coherent polariton-biexciton system
[DE95-609150] p 2417 N95-28607

CRYSTAL OSCILLATORS

Femtosecond OPO's at 3 microns and beyond: Design and performance issues related to the crystal properties of KTP and similar materials
[DE95-007286] p 2446 N95-28242

CRYSTAL STRUCTURE

The influence of surface structure on the interaction of water with TiO2(100)
[DE95-004927] p 2203 N95-27401

Crystal structure, short-range oxygen defects, and water adsorption in La- and Nd-modified ZrO2
[DE95-007134] p 2439 N95-27452

Crystal and magnetic structure of stoichiometric YFe2O4
[DE95-006627] p 2440 N95-27487

Surface crystallization and thin film melting in normal alkanes
[DE95-006694] p 2440 N95-27535

Amorphization of complex ceramics by heavy-particle irradiations
[DE95-005725] p 2236 N95-27733

The structure of lead-indium phosphate glass
[DE95-007130] p 2237 N95-27967

Precursor phenomenon of martensitic transformation in Au-49.5at%Cd alloy
[DE95-007698] p 2222 N95-28166

Structural chemistry of some phases in the YC-Ni-B system
[DE95-007403] p 2447 N95-28537

Surface structure of MX-chains studied by atomic force microscopy
[DE95-007881] p 2447 N95-28541

The unusual properties of beryllium surfaces
[DE95-006471] p 2223 N95-28593

Isolation and x-ray crystal structures of (Li(mu2-As(SiMe3)2) (mu3-As(SiMe3)2)(THF))2 and ((Me3Si)2AsLi(THF)2)2
[AD-A288870] p 2241 N95-28661

CRYSTAL SURFACES

Surface chemistry of silicon
[AD-A288893] p 2224 N95-26351

The role of hydrogen in the hydrogenation and hydrogenolysis of aniline on the nickel single crystal surfaces: Its implication on the mechanisms of HDN reactions
[DE95-006687] p 2222 N95-28134

CRYSTALLINITY

Chemistry involving the separation, isolation, and immobilization of 3-5 compound semiconductor nanocrystals and quantum dots
[AD-A288381] p 2436 N95-26473

Fractionation studies of polyethylene using DSC-technique
[PB95-185252] p 2200 N95-26540
Observations of CEF-split intermultiplet transitions in optically opaque EuBa2Cu3O7 using inelastic neutron scattering
[DE95-007135] p 2408 N95-27453
The 18th Asilomar Conference on Polymeric Materials
[AD-A291721] p 2240 N95-28508
Surfactants and desensitizing wax substitutes for TNT-Based systems
[AD-A289652] p 2243 N95-28634

CRYSTALLITES
Pulsed laser deposition of zeolitic membranes
[DE95-006274] p 2298 N95-28124

CRYSTALLIZATION
Electrocrystallization of an ordered organic monolayer: Selective epitaxial growth of beta(ET)213 ongraphite
[AD-A288942] p 2178 N95-26569
Device and method for screening crystallization conditions in solution crystal growth
[NASA-CASE-MFS-28985-1] p 2245 N95-26888
Surface energy driven crystallization of amorphous Ni69Cr14P17 alloy
[DE95-005543] p 2438 N95-27085
Surface crystallization and thin film melting in normal alkanes
[DE95-006694] p 2440 N95-27535
Control of thin film processing behavior through precursor structural modifications
[DE95-006468] p 2444 N95-28103
Vacancy related defects in thin film Pb(Zr,Ti)O3 materials
[DE95-007696] p 2445 N95-28165
The 18th Asilomar Conference on Polymeric Materials
[AD-A291721] p 2240 N95-28508

CRYSTALLOGRAPHY
Stiffness and strength tailoring in uniform space-filling truss structures p 2188 N95-28290

CRYSTALS
Growth and evaluation of nonlinear optical crystals for laser applications: Lithium borate, barium borate and silver gallium selenide
[AD-A289147] p 2277 N95-27000
Temperature dependence of ion-beam-induced amorphization in (Beta)-SiC
[DE95-007164] p 2438 N95-27087
The influence of surface structure on the interaction of water with TiO2(100)
[DE95-004927] p 2203 N95-27401
Characterization of collision cascade damage in Ca2La8(SiO4)6O2 by HRTEM
[DE95-005719] p 2440 N95-27491
Scintillator materials for calorimetry
[DE95-006570] p 2421 N95-27679
Observation of asymmetrical two-cone Vavilov-Cherenkov radiation in biaxial crystal of triglycinesulphate emitted by 658 MeV protons passing along bi normal
[DE94-629017] p 2441 N95-27867
Characterization of solid state laser and nonlinear optical materials
[AD-A291684] p 2300 N95-28458
Subharmonic phonon transmission and Kapitza conductance between crystals with very different vibrational spectra
[DE95-609151] p 2447 N95-28608

CUBIC EQUATIONS
Kepler Equation solver p 2147 N95-27767

CUES
Role of somatosensory and vestibular cues in attenuating visually induced human postural sway
[NASA-CR-197845] p 2357 N95-27697

CULTURE TECHNIQUES
Comparative Transduction Mechanisms of Vestibular Otolith Hair Cells
[NASA-CR-197980] p 2349 N95-26727
Hair cell regeneration in the bullfrog vestibular otolith organs following aminoglycoside toxicity
p 2349 N95-26729

CURING
External patch repair of CFRP/honeycomb sandwich
p 2134 N95-27522
Mechanical properties of Hysol EA-9394 structural adhesive
[DE95-008187] p 2240 N95-28405

CURRENT ALGEBRA
N. N. Bogolyubov and particle physics
[DE95-608794] p 2448 N95-27447

CURRENT DENSITY
Nickel metal hydride LEO cycle testing
p 2272 N95-26791
OBIC analysis of stressed, thermally-isolated polysilicon resistors
[DE95-008511] p 2268 N95-28201
Surface scanning techniques to locate and study defects in painted zinc and zinc alloy coated steels
[DE95-006099] p 2240 N95-28547
Local texture and grain boundary misorientations in high H(C) oxide superconductors
[DE95-007004] p 2447 N95-28606

CURRENT DISTRIBUTION
FENIX experimental results of large-scale CICC made of bronze-processed Nb3Sn strands
[DE95-007965] p 2222 N95-28167
Visualization of finite element model solutions for defibrillation voltage and current distributions
[AD-A289836] p 2400 N95-28579

CURVATURE
Preliminary design study of the beam collapser and certain optomechanical aspects of the siderostat
[AD-A288423] p 2423 N95-26549
Extended BRST symmetry for the relativistic particle with curvature
[DE95-608799] p 2406 N95-27309
On higher derivative gravity in two dimensions
[DE95-608789] p 2462 N95-27343
Crushing singularities in spacetimes with spherical, plane and hyperbolic symmetry
[PB95-190146] p 2397 N95-28011

CURVED BEAMS
The effect of material heterogeneity in curved composite beams for use in aircraft structures
p 2190 N95-28426

CURVED PANELS
Rapid repair of large area damage to contoured aircraft structures p 2133 N95-27516
Static and fatigue testing of full-scale fuselage panels fabricated using a Therm-X(R) process
p 2185 N95-28270

CURVES (GEOMETRY)
Holomorphic curves in Abelian varieties, part 1
[DE95-608748] p 2396 N95-27300
Theoretical studies of interstellar processes
[NASA-CR-198647] p 2462 N95-28216

CUTTING
The application of waterjets for cleaning
p 2233 N95-27130
SIHTI 2: Energy and environmental technology. Yearbook 1993 of the research programme
[DE95-755135] p 2331 N95-28202

CYCLES
Determination of the cyclical properties of 18G2A steel on the basis of skeleton curves for a planar stress state
[IFTR-32/1994] p 2211 N95-26359
Life prediction methodology for composite laminates. Part 1: Constant amplitude and two-stress level fatigue
[AD-A288343] p 2180 N95-26571
Measurements of the volatilities of electrolytes: Application to water/steam cycles
[DE95-007103] p 2204 N95-27451

CYCLIC LOADS
Determination of the cyclical properties of 18G2A steel on the basis of skeleton curves for a planar stress state
[IFTR-32/1994] p 2211 N95-26359
Changes in the anisotropy parameters of an aluminum alloy caused by cyclical deformation
[IFTR-27/1994] p 2212 N95-26666
Air Force Ni-H2 cell test program: State of Charge test
p 2272 N95-26789
Nickel metal hydride LEO cycle testing
p 2272 N95-26791
The 50 Ah NiH2 CPV qualification tests
p 2272 N95-26792
Hubble Space Telescope nickel-hydrogen battery testing: An update p 2272 N95-26794
Characterization of fatigue behavior of 2-D woven fabric reinforced ceramic matrix composite at elevated temperature
[AD-A289423] p 2181 N95-26886
Fatigue behavior of a cross-ply ceramic matrix composite subjected to tension-tension cycling with hold time
[AD-A289418] p 2182 N95-27134
Probabilistic material strength degradation model for Inconel 718 components subjected to high temperature, high-cycle and low-cycle mechanical fatigue, creep and thermal fatigue effects
[NASA-CR-197832] p 2214 N95-27167
A model of rotationally-sampled wind turbulence for predicting fatigue loads in wind turbines
p 2312 N95-27972
Preliminary analysis of dynamic stall effects on a 91-meter wind turbine rotor p 2124 N95-27975
Calculation of design load for the MOD-5A 7.3 mW wind turbine system p 2312 N95-27982
Comparison of measured and calculated dynamic loads for the Mod-2 2.5 mW wind turbine system
p 2312 N95-27983
Investigation of static and cyclic bearing failure mechanisms for GR/EP laminates p 2190 N95-28427

CYCLOHEXANE
Variation of solvent scattering-length density small-angle neutron scattering as a means of determining structure of composite materials
[DE95-005394] p 2183 N95-27428

CYCLONES
Systematic and integrated approach to Tropical Cyclone track forecasting. Part 1: Approach overview and description of meteorological basis
[AD-A291775] p 2344 N95-28459
The northern wintertime divergence extrema at 200 hPa and surface cyclones as simulated in the integration of the ECMWF general circulation model
[DE95-007946] p 2332 N95-28550

CYCLOTRON FREQUENCY
Fast wave current drive in D3-D
[DE95-007582] p 2431 N95-27441
One dimensional global and local solution for ICRF heating
[DE95-007984] p 2392 N95-28110
Engineering design of the ITER RF systems
[DE95-008064] p 2434 N95-28140

CYCLOTRON RADIATION
Fast wave current drive in D3-D
[DE95-007582] p 2431 N95-27441
ECR plasma-assisted deposition of Al2O3 and dispersion-strengthened AlO2
[DE95-007743] p 2235 N95-27687
Collisions of highly charged ions with electrons, atoms and surfaces
[DE95-007393] p 2413 N95-28078
Engineering design of the ITER RF systems
[DE95-008064] p 2434 N95-28140

CYCLOTRON RESONANCE
A BATSE investigation of radiation belt electrons precipitated by VLF waves
[NASA-CR-197780] p 2336 N95-26922
ECR plasma-assisted deposition of Al2O3 and dispersion-strengthened AlO2
[DE95-007743] p 2235 N95-27687
Process for non-contact removal of organic coatings from the surface of paintings
[NASA-CASE-LEW-15896-1] p 2235 N95-27702
Collisions of highly charged ions with electrons, atoms and surfaces
[DE95-007393] p 2413 N95-28078

CYCLOTRON RESONANCE DEVICES
High power, broadband folded waveguide Gyrotron-Traveling-Wave-Amplifier
[AD-A288847] p 2259 N95-26433

CYCLOTRONS
Polarizing matter and antimatter: A new method
[DE95-007109] p 2421 N95-27923

CYGNUS CONSTELLATION
Discussion on selected symbiotic stars
p 2460 N95-27078

CYLINDERS
Stress analysis and failure of an internally pressurized composite-jacketed steel cylinder p 2186 N95-28280

CYLINDRICAL BODIES
Template synthesis of electronically conductive polymer nanostructures
[AD-A288373] p 2225 N95-26472
Valve mechanism for an acoustic modulator
[AD-D017263] p 2300 N95-26504
Effects of three-dimensional imposed 3-D disturbances on bluff-body near wake flows
[AD-A289553] p 2121 N95-26757
A magnetic hysteresis model p 2153 N95-27801
Investigation of HE driven cylindrical liner
[DE95-007866] p 2311 N95-28539

CYLINDRICAL SHELLS
The collapse of composite cylindrical panels with various thickness using finite element analysis
[AD-A289370] p 2308 N95-26905
Load transfer in the stiffener-to-skin joints of a pressurized fuselage
[NASA-CR-198610] p 2310 N95-27865

CYTOCHROMES
Feasibility studies for separation processes using environmentally sensitive hydrogels
[DE95-008355] p 2238 N95-28226

CYTOMETRY
Flow cytometry as a means of detecting, enumerating and characterizing bacteria for monitoring of the environment
[AD-A288997] p 2326 N95-26610

CZOCHRALSKI METHOD
Numerical methods for determining interstitial oxygen in silicon
[DE95-007710] p 2205 N95-27683

D

DAMAGE

Synthesis and characterization of polymeric materials [AD-A288613] p 2225 N95-26482

A study of internal damage of metal matrix composites by neutron diffraction [DE95-005157] p 2182 N95-27080

Modeling considerations in the prediction of residual strength in composite laminates [AD-A289128] p 2182 N95-27142

Micromechanical modeling of damage and inelasticity of composite materials in macroscopic structural analysis [DE95-003666] p 2182 N95-27421

Radiation-induced segregation: A microchemical gauge to quantify fundamental defect parameters [DE95-005720] p 2216 N95-27492

Radiation-induced grain boundary segregation in austenitic stainless steels [DE95-005721] p 2216 N95-27493

Scarf repairs to graphite/epoxy components p 2135 N95-27523

Damage occurrence on composites during testing and fleet service: Repair of Airbus aircraft p 2135 N95-27526

An investigation of the chemical and physical properties of pristine, electrochromically damaged, and photochromically damaged KTiOPO4 (KTP) using surface analytical and optical spectroscopic techniques [DE95-007865] p 2443 N95-28023

Comparison of resin film infusion, resin transfer molding, and consolidation of textile preforms for primary aircraft structure p 2196 N95-28477

Application of damage tolerance methodology in certification of the Piaggio P-180 Avanti p 2138 N95-28480

DAMAGE ASSESSMENT

Probabilistic risk assessment of the Space Shuttle. Phase 3: A study of the potential of losing the vehicle during nominal operation. Volume 3: Basic events and minimal cutsets [NASA-CR-197810] p 2160 N95-26400

Study of damage evolutions in composite plates subjected to bending loads using micro-macro analysis [AD-A288523] p 2308 N95-26839

Debris/Ice/TPS assessment and integrated photographic analysis of Shuttle mission STS-67 [NASA-TM-110651] p 2160 N95-27238

The effects of finite element grid density on model correlation and damage detection of a bridge [DE94-018895] p 2309 N95-27305

Multimedia Environmental Pollutant Assessment System (MEPAS) application guidance. Guidelines for evaluating MEPAS input parameters for Version 3.1 [DE95-007525] p 2328 N95-27749

Assay of weathering effects on protective polymer coatings using positron annihilation spectroscopy [DE95-007040] p 2236 N95-27962

Gamma ray-induced embrittlement of pressure vessel alloys [DE95-007133] p 2220 N95-28072

OB/OD treatment: The effective use of measured field data and air modeling to support an environmental assessment p 2170 N95-28296

Toxicity assessment of liquid propellant XM46 p 2175 N95-28319

Weightless Environment Training Facility (WETF) materials coating evaluation, volume 3 [NASA-CR-188366-VOL-3] p 2239 N95-28387

Navy composite maintenance and repair experience p 2193 N95-28446

Compressive strength of damaged and repaired composite plates p 2198 N95-28484

SMART materials: Surfaces, transforms and interfaces. The commensurate engineering dimension [AD-A289598] p 2312 N95-28649

DAMPING

A state-space model of a large, lightly damped space structure using the Eigensystem realization algorithm [AD-A289251] p 2163 N95-26970

Use of blade pitch control to provide power train damping for the Mod-2, 2.5-mW wind turbine p 2306 N95-27986

DARK MATTER

The second coming of cold dark matter? [DE95-005156] p 2462 N95-27445

Supersymmetry and light quark masses in a realistic superstring model [DE95-610201] p 2412 N95-28041

DARKNESS

Basic mechanisms and implications of non-photic entrainment of circadian rhythmicity [AD-A288433] p 2353 N95-26779

DATA ACQUISITION

Longterm infrared cloud clutter research [AD-A288632] p 2340 N95-26343

Technical report series on global modeling and data assimilation. Volume 6: A multiyear assimilation with the GEOS-1 system: Overview and results [NASA-TM-104606-VOL-6] p 2334 N95-26423

Analysis of historical oceanographic data on a personal computer. Program MDS [AD-A288965] p 2363 N95-26447

Weather And Radar Processor (WARP) Test and Evaluation Master Plan (TEMP) [AD-A288280] p 2340 N95-26453

Long term distributed file reference tracing: Implementation and experience [AD-A288585] p 2452 N95-26535

Auto-processing of OTH radar amplitude/range/Doppler data [AD-A289152] p 2253 N95-27005

Radon integral measurement system [DE95-608074] p 2405 N95-27010

Measurements of HF auroral clutter using the Verona Ava Linear Array Radar (VALAR) [AD-A289442] p 2337 N95-27147

The systems of the proportional chambers registration electronics for present experiments in nuclear physics [DE95-608559] p 2419 N95-27161

Programming for time resolved spectrum in pulse radiolysis experiments [DE95-607929] p 2406 N95-27212

Spinning a web: Publishing the SEI software configuration management research on the world wide web [AD-A288708] p 2377 N95-27250

A video strip chart program [DE95-006389] p 2372 N95-27495

Development of a direct match technique for star identification on the SWAS mission p 2148 N95-27771

Real-time data compression using a fixed Huffman encoding scheme [DE95-006159] p 2455 N95-27949

The installation of and first results from the superconducting gravimeter GWR20 at the Metsahovi Station, Finland [REPT-95:1] p 2338 N95-27995

Remote measurement of ground temperature and emissivity [DE95-008055] p 2314 N95-28053

Particle fallout/activity sensor [NASA-CASE-KSC-11687-1] p 2293 N95-28362

Data acquisition software for DREO's near-field antenna measurement facility [AD-A289819] p 2258 N95-28573

Manikin integrated data acquisition system (MIDAS) initial modifications [AD-A291662] p 2361 N95-28667

DATA BASE MANAGEMENT SYSTEMS

Analysis, design and implementation of a database system for the systems management curriculum office [AD-A289656] p 2452 N95-26758

The re-engineering of the Air Force Institute of Technology Student Information System [AD-A289426] p 2453 N95-26866

A demonstration of Client-Server technology using remote procedure calls with an application of file migration for moving records based on time [AD-A289392] p 2453 N95-26879

Research and development management information system, system user manual [AD-A289151] p 2453 N95-27004

The transition of GTDS to the Unix workstation environment p 2151 N95-27789

The Sunrise project: An R&D project for a national information infrastructure prototype [DE95-006340] p 2455 N95-27847

Research on the establishment of the database system for R and D on the innovative technology for the Earth [DE95-759244] p 2458 N95-27937

Methods development for measuring and classifying flammability/combustibility of refrigerants. Task 1: Annotated bibliography [DE95-007232] p 2238 N95-28133

Managing electronic records: A guideline [DE95-007038] p 2456 N95-28555

The Global Historical Climatology Network: A preview of version 2 [DE95-007003] p 2332 N95-28605

Query by image example: The CANDID approach [DE95-006284] p 2456 N95-28631

A black carbon emission data base for atmospheric chemistry and climate studies [DE95-006436] p 2332 N95-28662

DATA BASES

Long Duration Exposure Facility Mini-Data Base User's Guide: Macintosh version [NASA-CR-4656] p 2177 N95-26391

A method to determine the structure of an unknown mixture using the Akaike Information Criterion and the bootstrap [AD-A288295] p 2394 N95-26415

Technical report series on global modeling and data assimilation. Volume 6: A multiyear assimilation with the GEOS-1 system: Overview and results [NASA-TM-104606-VOL-6] p 2334 N95-26423

The re-engineering of the Air Force Institute of Technology Student Information System [AD-A289426] p 2453 N95-26866

AIAA Techfest 20 Proceedings [NIAR-94-1] p 2118 N95-26941

The aerospace database: An introduction to AIAA'S computerized source for identifying scientific and technical information p 2119 N95-26950

Semantic heterogeneity in database and data dictionary integration for command and control systems [AD-A289180] p 2453 N95-27014

Isolated digit recognition without time alignment [AD-A289344] p 2254 N95-27062

Solar terrestrial radiation data from the Sleepers River Research Watershed [AD-A288444] p 2464 N95-27184

Automated database design from natural language input p 2383 N95-27378

Modeling precipitation from concentrated solutions with the EQ3/6 chemical speciation codes [DE95-006264] p 2204 N95-27556

From LDEF to a national Space Environment and Effects (SEE) program: A natural progression p 2145 N95-27657

Long Duration Exposure Facility (LDEF) Archive System p 2457 N95-27658

The Long Duration Exposure Facility (LDEF) annotated bibliography p 2457 N95-27659

The distribution of cloud cover over the former USSR as derived from the RIHMI 223-Station 3-hourly meteorological database [DE95-007046] p 2343 N95-27920

Research on the establishment of the database system for R and D on the innovative technology for the Earth [DE95-759244] p 2458 N95-27937

Horizontal axis wind turbine post stall airfoil characteristics synthesization p 2124 N95-27974

The Tau-Charm Factory in the ERA of B-Factories and CESR [DE95-007894] p 2412 N95-28028

High temperature Hexoloy(trademark) SX silicon carbide [DE95-007290] p 2221 N95-28075

Application of a Geographic Information System for radiologic emergency response [DE95-007624] p 2455 N95-28113

Methods development for measuring and classifying flammability/combustibility of refrigerants. Task 1: Annotated bibliography [DE95-007232] p 2238 N95-28133

Enplanement and all cargo activity [AD-A280074] p 2144 N95-28151

The program for calculating sunshine duration from global radiation [KNMI-TR-158] p 2343 N95-28237

Overview of the ACT program p 2193 N95-28463

COINS: A composites information database system p 2194 N95-28465

Managing electronic records: A guideline [DE95-007038] p 2456 N95-28555

Vocoded KING data base [AD-A289827] p 2258 N95-28576

The combined release and radiation effects satellite time history data base system [AD-A289835] p 2165 N95-28578

Downloading environmental data in the new MOODS format [AD-A288835] p 2456 N95-28589

Proceedings of the AIAA/FAA joint symposium on general aviation systems [AD-A289830] p 2120 N95-28610

TRAINS: Dialogue transcription tools [AD-A289869] p 2259 N95-28624

Query by image example: The CANDID approach [DE95-006284] p 2456 N95-28631

A black carbon emission data base for atmospheric chemistry and climate studies [DE95-006436] p 2332 N95-28662

DATA COMPRESSION

Digital mapping, charting, and geodesy analysis program technical review of Vector Quantization (VQ) Decompression for the National Imagery Transmission Format Standard (NITFS) [AD-A288998] p 2314 N95-26682

Auto-processing of OTH radar amplitude/range/Doppler data
[AD-A289152] p 2253 N95-27005
Real-time data compression using a fixed Huffman encoding scheme
[DE95-006159] p 2455 N95-27949

DATA CONVERSION ROUTINES
User documentation of the CTA program
[AD-A289508] p 2121 N95-26854
A simple method for verifying the deployment of the TOMS-EP solar arrays p 2150 N95-27782

DATA CORRELATION
The effects of finite element grid density on model correlation and damage detection of a bridge
[DE94-018895] p 2309 N95-27305

DATA FLOW ANALYSIS
Automatic test data generation tool for large-scale software systems
[AD-A289081] p 2365 N95-26611
Design tool for multiprocessor scheduling and evaluation of iterative dataflow algorithms
[NASA-TP-3491] p 2366 N95-26685
Control-flow analysis and type systems
[AD-A289338] p 2389 N95-26772

DATA INTEGRATION
Finding the forest in the trees. The challenge of combining diverse environmental data
[NASA-CR-197798] p 2326 N95-26362
Semantic heterogeneity in database and data dictionary integration for command and control systems
[AD-A289180] p 2453 N95-27014
Replacing the message service component in an integration framework
[AD-A289928] p 2375 N95-28628

DATA LINKS
Low-power, parallel photonic interconnections for Multi-Chip Module applications
[DE95-008518] p 2267 N95-28147
Radio telemetry buoy for long-range communication
[AD-D017269] p 2161 N95-28581

DATA MANAGEMENT
Finding the forest in the trees. The challenge of combining diverse environmental data
[NASA-CR-197798] p 2326 N95-26362
Digital mapping, charting, and geodesy analysis program: Initial technical review of Raster Product Format
[AD-A289039] p 2313 N95-26476
Activities of the Laboratory of Information Processing Science
[PB95-184982] p 2452 N95-26631
Flexible and safe resolution of file conflicts
[AD-A289342] p 2452 N95-26752
Analysis, design and implementation of a database system for the systems management curriculum office
[AD-A289656] p 2452 N95-26758
Scalability in production system programs
[AD-A289345] p 2453 N95-27063
A multi-attribute-utility-theory model that minimizes interview-data requirements: A consolidation of space launch decisions
[AD-A289421] p 2164 N95-27144
Solar terrestrial radiation data from the Sleepers River Research Watershed
[AD-A288444] p 2464 N95-27184
Integrated planning and scheduling for Earth science data processing p 2384 N95-27382
Flight dynamics software in a distributed network environment p 2151 N95-27790
Application of a Geographic Information System for radiologic emergency response
[DE95-007624] p 2455 N95-28113
Visualization methods for the exploration of high dimensional data
[AD-A291717] p 2393 N95-28507
Downloading environmental data in the new MOODS format
[AD-A288835] p 2456 N95-28589

DATA PROCESSING
SeaWiFS technical report series. Volume 26: Results of the SeaWiFS Data Analysis Round-Robin, July 1994 (DARR-1994)
[NASA-TM-104566-VOL-26] p 2345 N95-26430
Integration of video and radiation analysis data
[DE95-004165] p 2379 N95-26443
Analysis of historical oceanographic data on a personal computer. Program MDS
[AD-A288965] p 2363 N95-26447
Weather And Radar Processor (WARP) Test and Evaluation Master Plan (TEMP)
[AD-A288280] p 2340 N95-26453
Digital mapping, charting, and geodesy analysis program: Initial technical review of Raster Product Format
[AD-A289039] p 2313 N95-26476
Modal event calculus in Lolli
[AD-A288544] p 2365 N95-26605
Activities of the Laboratory of Information Processing Science
[PB95-184982] p 2452 N95-26631
Using SCR methods to analyze requirements documentation
[NASA-CR-197760] p 2365 N95-26668
Space tether-radar data processing
[AD-A289654] p 2250 N95-26725
Flexible and safe resolution of file conflicts
[AD-A289342] p 2452 N95-26752
Analysis, design and implementation of a database system for the systems management curriculum office
[AD-A289656] p 2452 N95-26758
Performance and policy dimensions in internet routing
[NASA-CR-197772] p 2367 N95-26770
Bow shock data analysis
[AD-A288432] p 2429 N95-26800
Conversion of sunflower multiband radiometer polarization measurements to polarization parameters
[NASA-CR-197774] p 2314 N95-26815
Stall precursor study of high frequency data for three high speed, swept compressor rotors
[AD-A289379] p 2139 N95-26878
Auto-processing of OTH radar amplitude/range/Doppler data
[AD-A289152] p 2253 N95-27005
A modified backpropagation algorithm for training neural networks on data with error bars
[DE95-608729] p 2381 N95-27025
Statistical data analysis
[DE95-007214] p 2454 N95-27090
STEP: A futurevision, today
[NONP-NASA-VT-95-49121] p 2451 N95-27209
Computer Systems Division software system metrics approach
[AD-A288837] p 2370 N95-27210
A user-system interface agent p 2383 N95-27379
Integrated planning and scheduling for Earth science data processing p 2384 N95-27382
A fuzzy logic intelligent diagnostic system for spacecraft integrated vehicle health management
p 2385 N95-27392
Scientific statistics and graphics on the Macintosh
[DE95-006445] p 2372 N95-27533
A simple method for verifying the deployment of the TOMS-EP solar arrays p 2150 N95-27782
Millimeter-wave imaging radiometer data processing and development of water vapor retrieval algorithms
[NASA-CR-198593] p 2343 N95-27997
Dip-moveout processing by Fourier transform in anisotropic media
[DE95-007668] p 2339 N95-28190
Transformation to zero offset in transversely isotropic media
[DE95-007669] p 2339 N95-28192
Bilateral force feedback for hydraulically actuated systems
[AD-A291632] p 2387 N95-28545
Guide for transmitting Standard Generalized Markup Language (SGML) encoded bibliographic records
[DOE/OSTI-11685] p 2457 N95-28675

DATA RECORDERS
Micro-time stress measurement device development
[AD-A289511] p 2361 N95-26845

DATA REDUCTION
SeaWiFS technical report series. Volume 26: Results of the SeaWiFS Data Analysis Round-Robin, July 1994 (DARR-1994)
[NASA-TM-104566-VOL-26] p 2345 N95-26430
Using SCR methods to analyze requirements documentation
[NASA-CR-197760] p 2365 N95-26668
Statistical data analysis
[DE95-007214] p 2454 N95-27090
A fuzzy logic intelligent diagnostic system for spacecraft integrated vehicle health management
p 2385 N95-27392
A simple method for verifying the deployment of the TOMS-EP solar arrays p 2150 N95-27782
Using COLETTE. (A simple guide)
[PB95-195806] p 2375 N95-28658

DATA RETRIEVAL
A demonstration of Client-Server technology using remote procedure calls with an application of file migration for moving records based on time
[AD-A289392] p 2453 N95-26879

DATA STORAGE
Distributed interactive simulation virtual cassette recorder (DIS VCR); A datalogger with variable speed replay
[AD-A289212] p 2290 N95-26989

DATA STRUCTURES
Parallel computing on various platforms: A case study
[AD-A289008] p 2376 N95-26460
An introduction to software architecture
[AD-A288356] p 2363 N95-26467
Vector Smart Map Level 1: A new DMA product
[AD-A288920] p 2452 N95-26607
Reflection of neutrons from an optical grating
[DE95-007145] p 2411 N95-28004

DATA SYSTEMS
Distributed interactive simulation virtual cassette recorder (DIS VCR); A datalogger with variable speed replay
[AD-A289212] p 2290 N95-26989
Outline and handling manual of fusion experimental data monitor system DAISY, version 2
[DE95-703895] p 2431 N95-27414

DATA TRANSFER (COMPUTERS)
A decentralized software bus based on IP multicasting
[NASA-CR-197768] p 2366 N95-26695
A demonstration of Client/Server technology using remote procedure calls for an application of file migration for moving records based on location
[AD-A289391] p 2453 N95-26864
A demonstration of Client-Server technology using remote procedure calls with an application of file migration for moving records based on time
[AD-A289392] p 2453 N95-26879
STEP: A futurevision, today
[NONP-NASA-VT-95-49121] p 2451 N95-27209
Preliminary flight software specification for the petite amateur Navy satellite (PANSAT)
[AD-A280068] p 2165 N95-28150

DATA TRANSMISSION
Joint Services Electronics Program (JSEP)
[AD-A288299] p 2345 N95-26419
A decentralized software bus based on IP multicasting
[NASA-CR-197768] p 2366 N95-26695
Information superhighway: Issues affecting development
[AD-A289434] p 2252 N95-26923
The systems of the proportional chambers registration electronics for present experiments in nuclear physics
[DE95-608559] p 2419 N95-27161
Sandia's network for Supercomputing '94: Linking the Los Alamos, Lawrence Livermore, and Sandia National Laboratories using switched multimegabit data service
[DE95-007717] p 2378 N95-28074
Guide for transmitting Standard Generalized Markup Language (SGML) encoded bibliographic records
[DOE/OSTI-11685] p 2457 N95-28675

DAYTIME
Parallel plasma fluid turbulence calculations
[DE95-006741] p 2431 N95-27537
Measurements of daytime and upper tropospheric water vapor profiles by Raman lidar
[DE95-007640] p 2344 N95-28538

DEBONDING (MATERIALS)
Micromechanical prediction of tensile damage for ceramic matrix composites under high temperature
[AD-A288238] p 2180 N95-26626
Micromechanical modeling of damage and inelasticity of composite materials in macroscopic structural analysis
[DE95-003666] p 2182 N95-27421
Evaluation of patch effectiveness in repairing aircraft components p 2133 N95-27513
Composite repair issues on the CF-18 aircraft
p 2134 N95-27518

DECELERATION
Discovery of the most distant supernovae and the quest for (Omega)
[DE95-006569] p 2460 N95-28197

DECISION MAKING
Using machine learning to derive efficient cost and performance estimates in VLSI CAD designs
[AD-A288254] p 2363 N95-26408
Strategy in the commercial aircraft industry in the United States: A comparison of decisionmaking by McDonnell-Douglas and Boeing aircraft companies from 1977-1983
[AD-A288289] p 2117 N95-26409
Distributed computation of Pareto solutions for two decision makers
[PB95-185047] p 2396 N95-26613
Analysis of group performance in visual signal detection
[AD-A289561] p 2355 N95-26683
A multi-attribute-utility-theory model that minimizes interview-data requirements: A consolidation of space launch decisions
[AD-A289421] p 2164 N95-27144
Myers-Briggs type indicators and Kirton adaption-innovation inventory correlations
[AD-A288435] p 2357 N95-27181

Community relations plan: Galena Airport and Camp ion Air Force Station, Alaska
[AD-A286722] p 2327 N95-27234
An analysis of Bayesian networks as classifiers
[AD-A289316] p 2382 N95-27293
Fuzzy-algebra uncertainty assessment
[DE95-005426] p 2391 N95-27432
An introductory guide to uncertainty analysis in environmental and health risk assessment. Environmental Restoration Program
[DE95-008097] p 2354 N95-28136
Automated remedial assessment methodology software system
[DE95-007287] p 2373 N95-28243
Distributed methods and processes in games of incomplete information
[PB95-184842] p 2396 N95-28352
Distributed methods and processes in games of incomplete information
[PB95-184859] p 2396 N95-28353
Severe weather guide mediterranean
[AD-A289829] p 2344 N95-28577

DECISION THEORY
Classification of ultra high range resolution radar using decision boundary analysis
[AD-A289378] p 2251 N95-26877
Real-time value-driven diagnosis
p 2386 N95-27396
Automated remedial assessment methodology software system
[DE95-007287] p 2373 N95-28243

DECLINATION
Ulysses orbit determination at high declinations
p 2151 N95-27787

DECODERS
Vocoded KING data base
[AD-A289827] p 2258 N95-28576

DECODING
The automatic extraction of selected speech spectral characteristics
[IFTR-2/1994] p 2250 N95-26835

DECOMMISSIONING
Health and environmental hazards of CdTe photovoltaic module production, use and decommissioning
[DE95-006688] p 2320 N95-27682

DECOMPOSITION
Parallelizing locally-weighted regression
[AD-A288294] p 2394 N95-26414
NO decomposition in non-reducing atmospheres
[DE95-007895] p 2205 N95-27690
Effects of hydrogen on carbon steels at the Multi-Function Waste Tank Facility
[DE95-007194] p 2219 N95-28005
Evaluation of microporous carbon filters as catalysts for ozone decomposition
[DE95-006498] p 2331 N95-28548

DECONTAMINATION
A practical approach to soil remediation
p 2232 N95-27125
Automated remedial assessment methodology software system
[DE95-007287] p 2373 N95-28243
Biodegradation of nitrate esters p 2171 N95-28299
Radiant exchange considerations in design and scaleup of photocatalytic reactors for purification of nitroglycerine-contaminated air p 2171 N95-28300
Recovery, evaluation, and decontamination of landfilled pentaborane cylinders, former liquid propellant rocket engine test facility, Washoe County, Nevada
p 2171 N95-28302

DECOUPLING
An investigation of the effects of pitch-roll (de)coupling on helicopter handling qualities
[NASA-TM-110349] p 2141 N95-26773

DEEP SPACE
Application of non-coherent Doppler data types for deep space navigation p 2151 N95-27788

DEEP SPACE NETWORK
Application of non-coherent Doppler data types for deep space navigation p 2151 N95-27788

DEEP WATER
Tomographic observations of deep convection and the thermal evolution of the Greenland Sea Gyre 1988-1989
[AD-A289104] p 2348 N95-28096

DEFECTS
A book and series of monographs on ice physics
[AD-A288319] p 2200 N95-26422
Combined investigation of Eddy current and ultrasonic techniques for composite materials NDE
[NASA-TM-110599] p 2306 N95-26778
Materials Research Society Symposium Proceedings. Volume 339: Diamond, SiC and nitride wide bandgap semiconductors
[AD-A288690] p 2437 N95-26818
Radiation-induced segregation: A microchemical gauge to quantify fundamental defect parameters
[DE95-005720] p 2216 N95-27492
Characterization of defects in deuterium-implanted beryllium
[DE95-005688] p 2217 N95-27553
I(sub DDQ) testing and defect classes: A tutorial
[DE95-005467] p 2306 N95-27723
Defect characterization of electronic conducting pseudo-perovskite systems
[DE95-007487] p 2220 N95-28049
Effects of high-temperature environments on flaw generation and fracture behavior of SiC/SiC composites
[DE95-008270] p 2183 N95-28068
Reactor pressure vessel structural integrity research
[DE95-007034] p 2223 N95-28208
Evaluation of defect-related diffusion in semiconductors by electrooptical sampling
[AD-A291630] p 2270 N95-28544

DEFENSE INDUSTRY
Surviving the peace. Lessons learned from the aircraft industry in the 1920s and 1930s
[AD-A288284] p 2117 N95-26455

DEFENSE PROGRAM
An integrated GPS/INS/BARO and radar altimeter system for aircraft precision approach landings
[AD-A289280] p 2127 N95-26985
OB/OD treatment: The effective use of measured field data and air modeling to support an environmental assessment p 2170 N95-28296
Hazards analysis of an integral class 1.1/1.3 rocket motor demilitarization and ingredient recovery system using ammonia p 2174 N95-28315
Recovery and reuse of rocket motor propellant ingredients p 2177 N95-28326
Unmanned aerial vehicles, 1994 master plan
[AD-A291628] p 2136 N95-28411
Inspection methods for underwater cables
[AD-A289610] p 2312 N95-28616

DEFLECTION
A non-iterative grid deformation algorithm for computational fluid dynamics for aeroelasticity
[AD-A288298] p 2273 N95-26418
Evaluation of composite joints
[AD-A289247] p 2181 N95-26967
Magnetization of ferromagnetic clusters
[DE95-006878] p 2399 N95-27548
Resonant coherent excitation of N6(+) and Mg11(+) in planar channeling: Anisotropies in ionization probabilities and X-ray emission
[DE95-006732] p 2417 N95-28595
Method of space-time sequence transform used to measure acousto-optic deflection and modulation
[AD-A289612] p 2402 N95-28671

DEFORESTATION
Investigation on technology for increasing the biological CO2 sink and technology for CO2 fixation and reutilization
[DE95-759251] p 2329 N95-27941

DEFORMATION
Process control of microstructure in manufacturing
[AD-A288291] p 2245 N95-26410
A non-iterative grid deformation algorithm for computational fluid dynamics for aeroelasticity
[AD-A288298] p 2273 N95-26418
Stability and thermal influences in nonlinear continuum mechanics and material science
[AD-A288333] p 2448 N95-26563
Frame selection performance limits for statistical image reconstruction of adaptive optics compensated images
[AD-A289240] p 2424 N95-26965
Investigation into the behavior of geometrically nonlinear composite arches
[AD-A289258] p 2308 N95-26975
The role of edge dislocations in the deformation of BCC metals
[DE95-609157] p 2219 N95-27759
The high strain rate deformation of tungsten single crystals
[AD-A288874] p 2223 N95-28189
Designing for time-dependent material response in spacecraft structures p 2166 N95-28292
Deformation behavior of thin lubricant films at elevated pressure
[AD-A288906] p 2241 N95-28592

DEGRADATION
Progress towards computer simulation of NiH2 battery performance over life p 2272 N95-26786
Fatigue behavior of a cross-ply ceramic matrix composite at elevated temperature under tension-tension loading
[AD-A289250] p 2182 N95-26969
Probabilistic material strength degradation model for Inconel 718 components subjected to high temperature, high-cycle and low-cycle mechanical fatigue, creep and thermal fatigue effects
[NASA-CR-197832] p 2214 N95-27167
Systematic study of the ion beam mixing of oxide markers into alumina
[DE95-006262] p 2217 N95-27555
Atomic oxygen dosimetry measurements made on STS-46 by CONCAP 2 p 2418 N95-27634
LEO degradation of graphite and carbon-based composites aboard Space Shuttle Flight STS-46
p 2199 N95-27636
Evaluation of laser-protective eyewear dyes in UVEX lenses
[AD-A290076] p 2361 N95-28390

DEGREES OF FREEDOM
Dynamic coupling of underactuated manipulators
[AD-A289404] p 2301 N95-27098
Aeroelastic stability of wind turbine blade/aileron systems p 2124 N95-27981
Bilateral force feedback for hydraulically actuated systems
[AD-A291632] p 2387 N95-28545

DEICING
Replicator for characterization of cirrus and polar stratospheric cloud particles
[NASA-CR-197785] p 2341 N95-26669

DEIONIZATION
Aqueous degreasing, precision cleaning, and cleanliness verification p 2231 N95-27121

DELAMINATING
Growth of hydrogenated amorphous silicon (a-Si:H) on patterned substrates for increased mechanical stability
[DE95-006589] p 2234 N95-27472
Composite repair issues on the CF-18 aircraft
p 2134 N95-27518
Repair technology for thermoplastic aircraft structures
p 2134 N95-27519
Service tough composite structures using the Z-direction reinforcement process p 2185 N95-28272
Through-the Thickness(R) braided composites for aircraft applications p 2185 N95-28273
Assembly induced delaminations in composite structures p 2186 N95-28279
Analysis of composite structures with delaminations under combined bending and compression
p 2190 N95-28429
Characteristics of laminates with delamination control strips p 2191 N95-28434
Fundamental concepts in the suppression of delamination buckling by stitching p 2198 N95-28486

DELAY
Crushing the delay: Tools for fractional delay filter design
[PB95-195509] p 2257 N95-28450

DELAY LINES
Generation of a single-lobe, far-field intensity pattern from a laser diode array using an optical delay line
[AD-A289226] p 2295 N95-26961

DELTA LAUNCH VEHICLE
Chemical reactions identified in the Titan 2, Titan 4, and Delta 2 propellant systems and their application to source modeling p 2172 N95-28304

DEMAGNETIZATION
Electromagnetic hysteretic response calculation for superconductors in demagnetizing geometries
[DE95-005028] p 2264 N95-27403

DEMAND (ECONOMICS)
Alternative fuels and vehicles choice model
[DE95-005695] p 2243 N95-27944

DEMOGRAPHY
Enhancing the effects of diversity awareness training: A review of the research literature
[DOT/FAA/AM-95/10] p 2355 N95-28361

DENITROGENATION
Biodegradation of nitrate esters p 2171 N95-28299

DENSIFICATION
Control of thin film processing behavior through precursor structural modifications
[DE95-006468] p 2444 N95-28103
Task 4 supporting technology. Densification requirements definition and test objectives. Propellant densification requirements definition
[NASA-CR-198629] p 2450 N95-28260
Ceramic composite combustor cans for expendable turbine engines
[AD-A289551] p 2140 N95-28646

DENSITY MEASUREMENT
A new technique for measuring the separation of closely spaced dislocations using residual contrast conditions
[DE95-007147] p 2219 N95-27968

DEOXYGENATION
Preconversion catalytic deoxygenation of phenolic functional groups
[DE95-007556] p 2204 N95-27458

DEOXYRIBONUCLEIC ACID
DNA denaturation through a model of the partition points on a one-dimensional lattice
[DE95-807909] p 2439 N95-27201

Sequence comparison on a cluster of workstations using the PVM system
[DE95-006527] p 2378 N95-27709
A correlated Walks' theory for DNA denaturation
[DE95-607910] p 2444 N95-28112

DEPLOYMENT
The Alpha-Proton-X-ray Spectrometer deployment mechanism: An anthropomorphic approach to sensor placement on Martian rocks and soil
p 2155 N95-27265
Solar array deployment mechanism
p 2155 N95-27266
Deployment and retraction of a cable-driven solar array: Testing and simulation p 2158 N95-27283
Development of the solar array deployment and drive system for the XTE spacecraft p 2158 N95-27284
A simple method for verifying the deployment of the TOMS-EP solar arrays p 2150 N95-27782
Report to the Chairman and Ranking Minority Member, Committee on Science, House of Representatives. Weather forecasting: Radar availability requirement not being met
[GAO/AIMD-95-132] p 2342 N95-27912

DEPOLARIZATION
Muon spin relaxation in ferromagnets: Theoretical results for paramagnetic EuO and EuS
[PB95-192860] p 2418 N95-28641
Muon spin relaxation in antiferromagnets: A study of RbMnF3 based on the coupled-mode theory of paramagnetic and critical spin fluctuations
[PB95-192878] p 2418 N95-28642

DEPOSITION
Advanced solid lubricant films by Ion-Beam Assisted Deposition
[AD-A288866] p 2225 N95-26499
Effect of processing parameters on surface finish for fused deposition machinable wax patterns
[NASA-TP-3550] p 2244 N95-26769
Magnetically controlled deposition of metals using gas plasma
[DE95-007248] p 2430 N95-27237
Growth of hydrogenated amorphous silicon (a-Si:H) on patterned substrates for increased mechanical stability
[DE95-006589] p 2234 N95-27472
ECR plasma-assisted deposition of Al2O3 and dispersion-strengthened AlO2
[DE95-007743] p 2235 N95-27687
Copper CVD using liquid coinjection of (hfac)Cu(TMVS) and TMVS
[DE95-008155] p 2237 N95-28089
Sensor for measuring the atomic fraction in highly dissociated hydrogen
[DE95-006531] p 2415 N95-28204
A model of the diurnal variation in magnesium ion density and radiance in the thermosphere
[AD-A289824] p 2339 N95-28575

DEPOSITS
Mechanism of deposit formation on fuel-wetted hot metal surfaces
[AD-A289847] p 2210 N95-28621

DEPTH
ACT adaptive filters
[AD-A288385] p 2363 N95-26474
Reducing network depth in the Cascade-Correlation learning architecture
[AD-A289352] p 2382 N95-27066
Depth migration in transversely isotropic media with explicit operators
[DE95-007670] p 2337 N95-27442
Non-destructive inter-level dielectric via in-line process monitoring by atomic force microscopy
[DE95-008516] p 2267 N95-28146

DERIVATION
Notes on the calibration of the JHU-APL solar vector magnetograph at NSO-Sec peak
[AD-A289277] p 2253 N95-26983
On higher derivative gravity in two dimensions
[DE95-608789] p 2462 N95-27343
Developments in the electron gun simulation program, EGUN
[DE95-008137] p 2267 N95-28143

DESCENT
Engineering photochemical smog through convection towers
[DE95-007727] p 2328 N95-27686

DESENSITIZING
Surfactants and desensitizing wax substitutes for TNT-Based systems
[AD-A289652] p 2243 N95-28634

DESIGN
Monolithic electronics for nuclear and high-energy physics experiments
[DE95-005393] p 2420 N95-27427

DESIGN ANALYSIS
An introduction to software architecture
[AD-A288963] p 2363 N95-26446
An introduction to software architecture
[AD-A288356] p 2363 N95-26467
Supersonic transport grid generation, validation, and optimization
[NASA-CR-197752] p 2365 N95-26648
CFD research, parallel computation and aerodynamic optimization
[NASA-CR-197748] p 2120 N95-26649
Design and testing of low sonic boom configurations and an oblique all-wing supersonic transport
[NASA-CR-197744] p 2129 N95-26651
The re-engineering of the Air Force Institute of Technology Student Information System
[AD-A289426] p 2453 N95-26866
Design and characterization of resonant cavity light-emitting diodes
[AD-A289307] p 2261 N95-26921
Active antennas with periodic structures
[AD-A289437] p 2252 N95-26924
A systems engineering approach to electro-mechanical reconfiguration for mobility autonomy
[AD-A289479] p 2301 N95-26926
Preliminary design problems and solutions for a supersonic oblique all-wing transport aircraft
p 2118 N95-26942
An exploratory application of neural networks for airfoil design p 2118 N95-26943
Distributed interactive simulation virtual cassette recorder (DIS VCR); A datalogger with variable speed replay
[AD-A289212] p 2290 N95-26989
A foveated system to reduce transmission bandwidth of video images from remote camera systems
[AD-A288516] p 2254 N95-27060
Design considerations in supercritical fluid technology
p 2232 N95-27126
A review of nickel hydrogen battery technology
[NASA-TM-106918] p 2167 N95-27177
Successful product realization strategies
p 2264 N95-27233
Design, testing and evaluation of latching end effector
p 2155 N95-27261
Some mechanical design aspects of the European Robotic Arm p 2155 N95-27262
Solar array deployment mechanism
p 2155 N95-27266
Changing paradigms: Manufacturing vs. fabricating a high volume Hold Down and Release Mechanism
p 2155 N95-27267
Ultra-high, resolution, modular optical angle encoder for space-based opto-mechanical applications
p 2156 N95-27270
High performance stepper motors for space mechanisms p 2156 N95-27271
Electromechanical rotary actuator
p 2157 N95-27278
Special features of the CLUSTER antenna and radial booms design, development and verification
p 2157 N95-27281
FORTE antenna element and release mechanism design p 2157 N95-27282
Development of the solar array deployment and drive system for the XTE spacecraft p 2158 N95-27284
High-performance reactionless scan mechanism
p 2158 N95-27288
Linear Proof Mass Actuator p 2158 N95-27290
Micromechanisms for optimism seismometer
p 2159 N95-27292
Composite heat pipe development status: Development of lightweight prototype carbon-carbon heat pipe with integral fins and metal foil liner
[NASA-TM-106909] p 2283 N95-27369
A verification procedure for MSC/NASTRAN Finite Element Models
[NASA-CR-4675] p 2131 N95-27371
Wind-tunnel test of the S814 thick root airfoil
[DE95-000268] p 2122 N95-27541
Performance of an accordion electromagnetic calorimeter with liquid krypton
[DE95-006693] p 2292 N95-27738
The KTeV pure CsI calorimeter
[DE95-005747] p 2292 N95-27751
Vibration analysis of a split path gearbox
[NASA-TM-106875] p 2302 N95-27855
Use of blade pitch control to provide power train damping for the Mod-2, 2.5-mW wind turbine
p 2306 N95-27986
A conceptual framework for evaluating variable speed generator options for wind energy applications
p 2273 N95-27987
Variable speed generator technology options for wind turbine generators p 2273 N95-27988
Variable speed generator application on the MOD-5A 7.3 mW wind turbine generator p 2273 N95-27989
A phase-stepped point diffraction interferometer using liquid crystals
[NASA-TM-106922] p 2293 N95-28037
FENIX experimental results of large-scale CICC made of bronze-processed Nb3Sn strands
[DE95-007965] p 2222 N95-28167
Advanced interactive display formats for terminal area traffic control
[NASA-CR-198576] p 2127 N95-28188
Optical design and performance of the inelastic scattering beamline at the National Synchrotron Light Source
[DE95-007679] p 2422 N95-28195
CORSSTOL: Cylinder Optimization of Rings, Skin, and Stringers with Tolerance sensitivity
[NASA-TP-3551] p 2392 N95-28215
Performance study for inlet installations
[NASA-CR-189714] p 2140 N95-28227
Femtosecond OPO's at 3 microns and beyond: Design and performance issues related to the crystal properties of KTP and similar materials
[DE95-007286] p 2446 N95-28242
Radiant exchange considerations in design and scaleup of photocatalytic reactors for purification of nitroglycerine-contaminated air p 2171 N95-28300
Design, analysis, and testing of a metal matrix composite web/flange intersection p 2191 N95-28433
Unique considerations in the design and experimental evaluation of tailored wings with elastically produced chordwise camber p 2192 N95-28436
C-130 Advanced Technology Center wing box conceptual design/cost study p 2192 N95-28437
Probabilistic design of advanced composite structure
p 2193 N95-28443
Nonlinear dynamics and aeroelasticity of rotorcraft in forward flight
[AD-A291714] p 2136 N95-28504

DESORPTION
The role of hydrogen in the hydrogenation and hydrogenolysis of aniline on the nickel single crystal surfaces: Its implication on the mechanisms of HDN reactions
[DE95-006687] p 2222 N95-28134

DESTABILIZATION
Energetic particle destabilization of shear Alfven waves in stellarators and tokamaks
[DE95-006393] p 2431 N95-27419

DESTRUCTION
Photo and thermal excitation of surface chemistry on model catalyst surfaces
[AD-A288541] p 2200 N95-26528

DETACHMENT
Measurement of particle transport coefficients on Alcator C-Mod
[DE95-007763] p 2411 N95-28020

DETECTION
Anti-idiotype probes for toxin detection
[AD-A288955] p 2348 N95-26435
Detection of charged particles in superfluid helium
[DE95-007354] p 2403 N95-26560
Compiler-assisted debugging and multiple instruction retry
[NASA-CR-197729] p 2365 N95-26628
Subvisual cirrus: What it is and where you find it
[AD-A289329] p 2342 N95-26899
Lessons learned from the introduction of autonomous monitoring to the EUVE science operations center
p 2385 N95-27393
Detecting alpha particles through scintillation in porous materials
[AD-A289313] p 2406 N95-27399
Single molecule detection using charge-coupled device array technology
[DE95-006425] p 2411 N95-27953
Alpha characterization inside pipes using ion-transport technology
[DE95-007869] p 2411 N95-28024
Particle fallout/activity sensor
[NASA-CASE-KSC-11687-1] p 2293 N95-28362
The detection and tracking of motion by means of time-space pattern modelling using random fields
[IFTR-37/1994] p 2374 N95-28566
Leak detection utilizing analog binaural (VLSI) techniques
[NASA-CASE-NPO-18399-1-CU] p 2271 N95-28599

DETECTORS
The Top...is it There? A Survey of the CDF and D0 Experiments
[DE95-005746] p 2411 N95-27945

DETERMINANTS
A system dynamics based study of software reuse and its determinants
[AD-A288578] p 2364 N95-26554

DETONATION

Evaluating the environmental viability of open burning/open detonation operations p 2170 N95-28297

Upgrade of the computer modeling programs POLU10 and POLU13A for open burning and open detonation of energetic materials p 2172 N95-28306

Recovery and reuse of rocket motor propellant ingredients p 2177 N95-28326

DETONATION WAVES

Pressure vessel burst test study p 2175 N95-28317

Investigation of HE driven cylindrical liner [DE95-007866] p 2311 N95-28539

DEUTERIUM

Fast wave current drive in D3-D [DE95-007582] p 2431 N95-27441

Characterization of defects in deuterium-implanted beryllium [DE95-005688] p 2217 N95-27553

Pumping characteristics of a cryopump with Ar sorbent in He and in D2/He mixture [DE95-007049] p 2302 N95-27875

DEUTERIUM COMPOUNDS

Small angle neutron scattering study of the micelle structure of amphiphilic block copolymers [DE95-006625] p 2234 N95-27486

DEUTERIUM FLUORIDES

A density functional/molecular dynamics study of the structure of liquid nitromethane [AD-A289224] p 2404 N95-26960

DEUTERONS

Search for deeply bound pionic atoms with high-purity germanium tagging spectrometer [DE95-609072] p 2416 N95-28252

DEVELOPING NATIONS

Environmental pollution-effects on national development [DE95-600439] p 2326 N95-26639

DIAGNOSIS

To develop an aerosoling immunomagnetic device for rapid medical diagnosis from clinical samples [AD-A288504] p 2354 N95-27059

Model-based monitoring and diagnosis of a satellite-based instrument p 2166 N95-27390

Real-time value-driven diagnosis p 2386 N95-27396

The PCMDI Visualization and Computation System (VCS): A workbench for climate data display and analysis [DE95-008586] p 2328 N95-27558

Fault tolerant features and experiments of ANTS distributed real-time system [AD-A290133] p 2256 N95-28391

Phase retrieval and time-frequency methods in the measurement of ultrashort laser pulses [DE95-006499] p 2300 N95-28549

DIALYSIS

Apparatus for diffusion controlled dialysis under microgravity conditions [NASA-CASE-MFS-28986-1] p 2245 N95-27500

DIAMOND FILMS

High-density plasma source for large-area chemical vapor deposition of diamond films [AD-A289053] p 2430 N95-27190

Growth, characterization and device development in monocrystalline diamond films [AD-A289356] p 2439 N95-27416

The in situ observation of epitaxial diamond thin film nucleation and growth using emission electron microscopy [AD-A289841] p 2447 N95-28618

DIAMONDS

Materials Research Society Symposium Proceedings. Volume 339: Diamond, SiC and nitride wide bandgap semiconductors [AD-A288690] p 2437 N95-26818

Growth, characterization and device development in monocrystalline diamond films [AD-A289356] p 2439 N95-27416

Sensor for measuring the atomic fraction in highly dissociated hydrogen [DE95-006531] p 2415 N95-28204

Atomic layer epitaxy of group 4 materials: Surface processes, thin films, devices and their characterization [AD-A289092] p 2446 N95-28327

Design and fabrication of a diamond-turned hybrid diffractive/refractive singlet for visible applications at ORNL [DE95-007007] p 2427 N95-28552

The in situ observation of epitaxial diamond thin film nucleation and growth using emission electron microscopy [AD-A289841] p 2447 N95-28618

DIATOMIC MOLECULES

Chemical physics of uniform cyclic etching [AD-A288975] p 2404 N95-26574

DIBORANE

Boron-induced reconstructions of Si(100) investigated by scanning tunneling microscopy [AD-A289222] p 2438 N95-26959

DIELECTRIC POLARIZATION

Simple equivalent dipole distributions for dielectric spheroidal scatterers [PB95-184883] p 2254 N95-27049

DIELECTRIC PROPERTIES

Temperature dependence of the static dielectric response in a Q1D electron gas [DE95-609269] p 2400 N95-28350

DIELECTRICS

A book and series of monographs on ice physics [AD-A288319] p 2200 N95-26422

Microengineered conducting composites from nanochannel templates [AD-A289573] p 2180 N95-26686

Materials, structures, and devices for high-speed electronics [NASA-CR-197815] p 2260 N95-26816

Improving the performance of spiral antennas by using passive scatterers [AD-A289324] p 2251 N95-26893

Simple equivalent dipole distributions for dielectric spheroidal scatterers [PB95-184883] p 2254 N95-27049

Observation of asymmetrical two-cone Vavilov-Cherenkov radiation in biaxial crystal of triglycinesulphate emitted by 658 MeV protons passing along bi normal [DE94-629017] p 2441 N95-27867

Time-dependent model for vertical-cavity surface-emitting laser [DE95-007880] p 2298 N95-28027

Non-destructive inter-level dielectric via in-line process monitoring by atomic force microscopy [DE95-008516] p 2267 N95-28146

Quantum effects induced by a gap in the spectrum of atom-bath coupling constants: Freezing of atomic decay and monochromatic collective radiation [DE95-609037] p 2416 N95-28251

Temperature dependence of the static dielectric response in a Q1D electron gas [DE95-609269] p 2400 N95-28350

Method of images applied to electromagnetic problems involving spherical, spheroidal and planar geometries [PB95-195517] p 2257 N95-28451

Theoretical and experimental study of low-loss, High-efficiency monolithic antenna structures at 94 GHz [AD-A291785] p 2257 N95-28513

Efficient modeling of interconnects and capacitive discontinuities in high-speed digital circuits [NASA-CR-198728] p 2270 N95-28570

Characterization of a fused silica capacitance standard [DE95-006457] p 2270 N95-28597

DIESEL FUELS

The biodegradation of fuels in soils and sediments: Differences as a function of mineralogy p 2230 N95-27116

DIFFERENCE EQUATIONS

Robust integration schemes for generalized viscoplasticity with internal-state variables. Part 1: Theoretical developments and applications [NASA-CR-195452-PT-1] p 2310 N95-28031

Robust integration schemes for generalized viscoplasticity with internal-state variables. Part 2: Algorithmic developments and implementation [NASA-CR-195453-PT-2] p 2310 N95-28032

DIFFERENTIAL ABSORPTION LIDAR

The concentration-estimation problem for multiple-wavelength differential absorption lidar [DE95-008375] p 2256 N95-28231

DIFFERENTIAL EQUATIONS

Generalized Schwarzians in several variables and Moebius invariant differential operators [PB95-185211] p 2388 N95-26539

Adaptive finite element method I: Solution algorithm and computational examples [AD-A288979] p 2389 N95-26609

Quantum k-Poincare 1994 [DE95-608754] p 2448 N95-27332

A genuinely multidimensional upwind scheme and efficient multigrid solver for the compressible Euler equations [NASA-CR-195000] p 2288 N95-28571

DIFFERENTIAL GEOMETRY

Gromov-Lawson-Rosenberg conjecture for groups with periodic cohomology [PB95-185203] p 2389 N95-26915

Introduction to Dubois-Violette's non-commutative differential geometry [DE95-608801] p 2390 N95-27311

DIFFRACTION

A phase-stepped point diffraction interferometer using liquid crystals [NASA-TM-106922] p 2293 N95-28037

Design and fabrication of a diamond-turned hybrid diffractive/refractive singlet for visible applications at ORNL [DE95-007007] p 2427 N95-28552

Method of space-time sequence transform used to measure acousto-optic deflection and modulation [AD-A289612] p 2402 N95-28671

DIFFRACTION PATTERNS

Radiation sensitive area detection device and method [NASA-CASE-MFS-28563-3] p 2423 N95-26385

DIFFUSE RADIATION

A case study of view-factor rectification procedures for diffuse-gray radiation enclosure computations p 2281 N95-27353

Reflection of neutrons from an optical grating [DE95-007145] p 2411 N95-28004

DIFFUSION

Stochastic adaptive estimation and control [AD-A289088] p 2380 N95-26480

On-axis polarization coupling in y-cut titanium in-diffused lithium niobate slab waveguides [AD-A289260] p 2253 N95-26977

Boron-induced morphology changes in silicon CVD growth: A scanning tunneling microscopy study [AD-A289275] p 2290 N95-26982

New radiation stable and long-lived plastic scintillators [DE95-608622] p 2233 N95-27163

Single-drop reactive extraction/extractive reaction with forced convective diffusion and interphase mass transfer p 2282 N95-27358

Single-drop reactive extraction/extractive reaction with forced convective diffusion and interphase mass transfer p 2283 N95-27365

Magnetic resonance imaging of solvent transport in polymer networks [DE95-007142] p 2234 N95-27455

Apparatus for diffusion controlled dialysis under microgravity conditions [NASA-CASE-MFS-28986-1] p 2245 N95-27500

The diffusion properties of ion implanted species in selected target materials [DE95-007006] p 2442 N95-27959

Error analysis of the quartic nodal expansion method for slab geometry [DE95-007373] p 2412 N95-28045

Sensor for measuring the atomic fraction in highly dissociated hydrogen [DE95-006531] p 2415 N95-28204

A point-centered diffusion differencing for unstructured meshes in 3-D [DE95-008382] p 2392 N95-28232

The off-center effect on the diffusion coefficient of Cu(+) and Li(+) in the KCl lattice [DE95-609146] p 2446 N95-28255

Evaluation of defect-related diffusion in semiconductors by electrooptical sampling [AD-A291630] p 2270 N95-28544

High energy density systems in cryogenic media: The production and reactions of atoms and radicals [AD-A289818] p 2417 N95-28572

Monte-Carlo simulation methods for finite flat plate winding flows [AD-A289842] p 2289 N95-28619

DIFFUSION COEFFICIENT

The diffusion properties of ion implanted species in selected target materials [DE95-007006] p 2442 N95-27959

The off-center effect on the diffusion coefficient of Cu(+) and Li(+) in the KCl lattice [DE95-609146] p 2446 N95-28255

DIFFUSION THEORY

The comparison of P(sub 1) and simplified P(sub 2) synthetic acceleration for iterative methods in transport solutions [DE94-018306] p 2390 N95-27304

DIFFUSIVITY

Survey on researches related to ocean disposal of carbon dioxide [DE95-759247] p 2329 N95-27939

DIGITAL COMMAND SYSTEMS

Advanced flight computer. Special study [NASA-CR-198165] p 2371 N95-27246

DIGITAL COMPUTERS

Digital optical computing [AD-A289395] p 2368 N95-26881

DIGITAL DATA

Digital mapping, charting, and geodesy analysis program technical review of Vector Quantization (VQ) Decompression for the National Imagery Transmission Format Standard (NITFS) [AD-A288998] p 2314 N95-26682

DIGITAL ELECTRONICS
Digital optical computing
[AD-A289395] p 2368 N95-26881
Novel field effect transistors for low power electronics
[AD-A288650] p 2262 N95-27096
Advanced flight computer. Special study
[NASA-CR-198165] p 2371 N95-27246
Efficient modeling of interconnects and capacitive discontinuities in high-speed digital circuits
[NASA-CR-198728] p 2270 N95-28570
Novel field effect transistors for low power electronics
[AD-A289929] p 2271 N95-28629
DIGITAL FILTERS
Analysis and simulation of narrowband GPS jamming using digital excision temporal filtering
[AD-A289328] p 2127 N95-26898
Structures for time-reversed inversion in filter banks
[AD-A289238] p 2261 N95-26964
Crushing the delay: Tools for fractional delay filter design
[PB95-195509] p 2257 N95-28450
DIGITAL SIMULATION
Design of a real-time wind turbine simulator using a custom parallel architecture p 2322 N95-27979
Parallel block implicit integration technique for trajectory parallelism
[AD-A288961] p 2379 N95-28335
DIGITAL SYSTEMS
Robust hybrid state-space self-tuning control using dual-rate sampling
[AD-A288359] p 2380 N95-26468
Research and development report. Digital audio broadcasting: Comparison of coverage at Band 2 and Band 3
[BBC-RD-1994/16] p 2248 N95-26493
Multipurpose bus interface utilizing a digital signal processor
[AD-D017264] p 2248 N95-26505
Target detection for vision systems
[AD-D017271] p 2249 N95-26509
Digital systems validation. Chapter 20 Artificial Intelligenge with applications for aircraft. Handbbook, volume 2
[AD-A288492] p 2380 N95-26638
Design tool for multiprocessor scheduling and evaluation of iterative dataflow algorithms
[NASA-TP-3491] p 2366 N95-26685
Research and development report. Eureka 147: Tests of the error performance of the DAB system
[BBC-RD-1994/18] p 2249 N95-26696
High-speed coherent laser arrays
[AD-A289373] p 2295 N95-26906
The KTeV pure CsI calorimeter
[DE95-005747] p 2292 N95-27751
Radio telemetry buoy for long-range communication
[AD-D017269] p 2161 N95-28581
Query by image example: The CANDID approach
[DE95-006284] p 2456 N95-28631
DIGITAL TECHNIQUES
Robust hybrid state-space self-tuning control using dual-rate sampling
[AD-A288359] p 2380 N95-26468
Long-range eye tracking: A feasibility study
[DE95-008587] p 2357 N95-28176
High performance ground penetrating radar survey of TA-49/Area 2
[DE95-006856] p 2258 N95-28601
DIGITAL TELEVISION
Integration of video and radiation analysis data
[DE95-004165] p 2379 N95-26443
DIGITAL TO ANALOG CONVERTERS
Method and apparatus for maintaining linearity and frequency accuracy of an FM chirp waveform
[AD-D017398] p 2258 N95-28615
DIGITS
Isolated digit recognition without time alignment
[AD-A289344] p 2254 N95-27062
DIMENSIONAL ANALYSIS
Parallel algorithms for semi-Lagrangian transport in global atmospheric circulation models
[DE95-007385] p 2327 N95-27457
DIMENSIONAL STABILITY
Ultra high purity, dimensionally stable INVAR 36
[NASA-CASE-NPO-19358-1-CU] p 2213 N95-26862
DIMERS
Analysis of the dimerized Sb/Si(001)-(2x1) surface by x-ray standing waves
[DE95-007097] p 2208 N95-27965
On the synthesis of mixed-metal and mixed-pnicogen13-15 ring-systems
[AD-A288869] p 2223 N95-28332
Isolation and x-ray crystal structures of (Li(mu2-As(SiMe3)2) (mu3-As(SiMe3)2)(THF))2 and ((Me3Si)2AsLi(THF)2)2
[AD-A288870] p 2241 N95-28661
DIMETHYLHYDRAZINES
Evaluation of a conductive polymer-based sensor for detection of hydrazines at the part-per-billion level
p 2173 N95-28309
DINITRATES
Biodegradation of nitrate esters p 2171 N95-28299
DIODES
Solid-state image sensor with focal-plane digital photon-counting pixel array
[NASA-CASE-NPO-18518-1-CU] p 2424 N95-26894
On the physics of ion ring generation for the stabilization of FRX discharges
[DE95-007105] p 2410 N95-27922
A comparison of NH3 point monitoring and diode laser based path integrated measurements
[DE95-006892] p 2332 N95-28602
DIOXIDES
Small angle x ray scattering studies of reverse micelles in supercritical fluids
[DE95-007803] p 2287 N95-28021
DIPOLE ANTENNAS
Low-cost tubular antenna deployer for WISP-2
p 2156 N95-27269
DIRECT CURRENT
Extended linear ion trap frequency standard apparatus
[NASA-CASE-NPO-19081-1-CU] p 2404 N95-26861
Dynamically timed electric motor
[NASA-CASE-MFS-28958-1] p 2261 N95-26890
MHD simulations of DC helicity injection for current drive in tokamaks
[DE95-007018] p 2429 N95-26940
Surface scanning techniques to locate and study defects in painted zinc and zinc alloy coated steels
[DE95-006099] p 2240 N95-28547
DIRECTIONAL ANTENNAS
Fast wave current drive in D3-D
[DE95-007582] p 2431 N95-27441
DIRECTIONAL COUPLERS
Design, fabrication, modeling, and optical characterization of organic polymer nonlinear directional couplers
[AD-A289327] p 2227 N95-26897
DIRECTIONAL STABILITY
An easy way to analyze longitudinal and lateral-directional trim problems with AEO or OEI
p 2119 N95-26949
DIRECTIVITY
Observation of asymmetrical two-cone Vavilov-Cherenkov radiation in biaxial crystal of triglycinesulphate emitted by 658 MeV protons passing along bi normal
[DE94-629017] p 2441 N95-27867
DIRECTORIES
AGARD membership, 1995
[AGARD-MEMB-95] p 2450 N95-26353
DISASTERS
Cape Canaveral air station launch emergency response forces and toxic materials release contingency plans
p 2172 N95-28308
DISCONNECT DEVICES
Partial discharge testing of high voltage wiring harness for airborne displays
[AD-A289150] p 2138 N95-27003
Development of a high force thermal latch
p 2157 N95-27275
DISCOVERY (ORBITER)
Debris/Ice/TPS assessment and integrated photographic analysis of Shuttle mission STS-67
[NASA-TM-110651] p 2160 N95-27238
DISCRIMINATION
Grayscale/resolution trade-off for text: Model predictions and psychophysical results for letter confusion and letter discrimination
[NASA-CR-197784] p 2369 N95-26930
DISLOCATIONS (MATERIALS)
A new technique for measuring the separation of closely spaced dislocations using residual contrast conditions
[DE95-007147] p 2219 N95-27968
DISORIENTATION
Rotor phases in compound semiconductors
[DE95-004139] p 2436 N95-26442
DISPERSING
Materials design and processing by biomimicking. Section 1: Research progress
[AD-A288229] p 2226 N95-26623
Design and processing of materials by biomimicking. Section 2. Publications
[AD-A288230] p 2226 N95-26624
A numerical model to predict the fate of jettisoned aviation fuel
[AD-A289336] p 2242 N95-26842
DISPLACEMENT
User's guide: Computer program for analysis of beam-column structures with nonlinear supports (CBEAMC)
[AD-A289031] p 2307 N95-26464
Temperature dependence of ion-beam-induced amorphization in (Beta)-SiC
[DE95-007164] p 2438 N95-27087
Visualization and direct comparison of large displacements using difference holographic interferometry
[DE95-608782] p 2292 N95-27711
An improved plate theory of order (1,2) for thick composite laminates p 2187 N95-28283
Poly(N-arylenbenzimidazoles) via aromatic nucleophilic displacement
[NASA-CASE-LAR-14939-1] p 2179 N95-28360
Polybenzimidazoles via aromatic nucleophilic displacement
[NASA-CASE-LAR-14924-1-CU] p 2179 N95-28361
DISPLACEMENT MEASUREMENT
TV-holography at high temperatures: In situ observations of the oxidation of advanced materials
[PB95-195343] p 2294 N95-28651
DISPLAY DEVICES
Grayscale/resolution trade-off for text: Model predictions and psychophysical results for letter confusion and letter discrimination
[NASA-CR-197784] p 2369 N95-26930
Visual system operational evaluation
[AD-A289173] p 2356 N95-27012
Multiple model adaptive estimation and head motion tracking in a virtual environment: An engineering approach
[AD-A289299] p 2359 N95-27046
Image quality metrics for color CRT displays
[AD-A288934] p 2262 N95-27196
Programming for time resolved spectrum in pulse radiolysis experiments
[DE95-607929] p 2406 N95-27212
Display system employing acousto-optic tunable filter
[NASA-CASE-NPO-18736-1-CU] p 2426 N95-27843
Advanced interactive display formats for terminal area traffic control
[NASA-CR-198576] p 2127 N95-28188
Operator modeling in commerical aviation: Cognitive models, intelligent displays, and pilot's assistants
[NASA-CR-198609] p 2138 N95-28203
DISSECTION
Variation of solvent scattering-length density small-angle neutron scattering as a means of determining structure of composite materials
[DE95-005394] p 2183 N95-27428
DISSIPATION
The effect of aviation fuels containing low amounts of static dissipater additive on electrostatic charge generation
[AD-A280075] p 2243 N95-28152
DISSOCIATION
Atomically resolved STM study of the adsorption and dissociation of methyl chloride on Si(001)
[AD-A289218] p 2438 N95-27061
Chemical and electrical properties of cavities in silicon and germanium
[DE95-006812] p 2445 N95-28206
DISSOLVING
Precision parts cleaning with supercritical CO2: Practical applications and solutions p 2229 N95-27111
Modeling precipitation from concentrated solutions with the EQ3/6 chemical speciation codes
[DE95-006264] p 2204 N95-27556
Simulations of metal dissolution and corrosion
[DE95-007486] p 2218 N95-27748
DISTANCE
Multivariate classification of BPSG thin films using Mahalanobis distances
[DE95-008519] p 2267 N95-28148
DISTANCE MEASURING EQUIPMENT
Precision landing system mathematical modeling study report for Andrews Air Force Base, runway 19L, Camp Springs, MD
[AD-A289015] p 2127 N95-27903
DISTRIBUTED PARAMETER SYSTEMS
Design considerations for FrankTalk: A distributed group support system
[AD-A289386] p 2359 N95-26863
Multi-agent perception for Human/Robot interaction: A framework for intuitive trajectory modification
[AD-A289399] p 2359 N95-26884
DISTRIBUTED PROCESSING
Using machine learning to derive efficient cost and performance estimates in VLSI CAD designs
[AD-A288254] p 2363 N95-26408
Long term distributed file reference tracing: Implementation and experience
[AD-A288585] p 2452 N95-26535
A demonstration of Client/Server technology using remote procedure calls for an application of file migration for moving records based on location
[AD-A289391] p 2453 N95-26864

A demonstration of Client-Server technology using remote procedure calls with an application of file migration for moving records based on time
[AD-A289392] p 2453 N95-26879
Distributed computation of Pareto solutions in N-player games
[PB95-185039] p 2396 N95-26912
A demonstration of client-server technology using remote procedure calls with an application in file migration using heuristics
[AD-A289467] p 2255 N95-27149
XTP as a transport protocol for distributed parallel processing
[DE95-004992] p 2378 N95-27402
A case for dynamic sets in operating systems
[AD-A289354] p 2454 N95-27529
Sequence comparison on a cluster of workstations using the PVM system
[DE95-006527] p 2378 N95-27709
Flight dynamics software in a distributed network environment p 2151 N95-27790
The Sunrise project: An R&D project for a national information infrastructure prototype
[DE95-006340] p 2455 N95-27847
Distributed methods and processes in games of incomplete information
[PB95-184842] p 2396 N95-28352
Distributed methods and processes in games of incomplete information
[PB95-184859] p 2396 N95-28353
Fault tolerant features and experiments of ANTS distributed real-time system
[AD-A290133] p 2256 N95-28391
Two implementation relations and the correctness of communicating replicated processes
[PB95-195640] p 2375 N95-28645

DISTRIBUTION FUNCTIONS
Anomalous collision rate in the time counter scheme of the direct simulation Monte Carlo method for rarefied gas flow analysis
[ISAS-R-653] p 2275 N95-26742
A study of parton distribution functions with the use of photon + jet event kinematics in p(bar p) collisions at (radical)s = TeV
[DE95-005127] p 2408 N95-27444
The structure of lead-indium phosphate glass
[DE95-007130] p 2237 N95-27967
Cryogenic BRDF measurements at 10.6 micrometers and 0.63 micrometers on contaminated mirrors
[AD-A291611] p 2427 N95-28408

DISTRIBUTION MOMENTS
Fitting: Subroutine to fit four-moment probability distributions to data
[DE95-007722] p 2395 N95-27684

DITHERS
Dithering transitions in resistive pressure-gradient-driven turbulence
[DE95-006737] p 2431 N95-27536

DIURNAL VARIATIONS
A model of the diurnal variation in magnesium ion density and radiance in the thermosphere
[AD-A289824] p 2339 N95-28575

DIVERGENCE
The northern wintertime divergence extrema at 200 hPa and surface cyclones as simulated in the integration of the ECMWF general circulation model
[DE95-007946] p 2332 N95-28550

DIVERTERS
Neutral gas compression in the Alcator C-Mod divertor. Experimental observations
[DE95-007762] p 2432 N95-27688
Pumping characteristics of a cryopump with Ar sorbent in He and in D2/He mixture
[DE95-007049] p 2302 N95-27875
Measurement of particle transport coefficients on Alcator C-Mod
[DE95-007763] p 2411 N95-28020

DIVERTORS (FUSION REACTORS)
UEDGE and DEGAS modeling of the DIII-D scrape-off layer plasma, revision 1
[DE95-008052] p 2433 N95-28065
Divertor research on the DIII-D tokamak
[DE95-003942] p 2434 N95-28185

DMSP SATELLITES
Development of welded solar arrays for DMSP and GPS satellites
[AD-A289512] p 2318 N95-26846

DOCUMENTATION
Using SCR methods to analyze requirements documentation
[NASA-CR-197760] p 2365 N95-26668
Index to NASA news releases and speeches 1994
[NASA-TM-110650] p 2452 N95-26673

DOCUMENTS
A book and series of monographs on ice physics
[AD-A288319] p 2200 N95-26422
Managing electronic records: A guideline
[DE95-007038] p 2456 N95-28555

DOMESTIC ENERGY
Hydrogen program
[DE94-011827] p 2242 N95-27415

DONOR MATERIALS
Photoinduced dipoles and charge pairs in condensed phase
[DE95-007071] p 2207 N95-27921

DOORS
The Solar X-ray Imager Vacuum Door Assembly
p 2157 N95-27280

DOPED CRYSTALS
Microwave circuit simulation using higher-order dynamic elements
[PB95-185088] p 2259 N95-26496
Silicate gel dye laser
[AD-D017262] p 2294 N95-26503
Photoluminescence spectroscopy of 4H- and 6H-SiC
[AD-A289326] p 2202 N95-26896
Atomic structure and bonding of boron-induced reconstructions on Si(001)
[AD-A289187] p 2405 N95-27017
Numerical methods for determining interstitial oxygen in silicon
[DE95-007710] p 2205 N95-27683
Growth and characterization of crystals for room temperature I.R. detectors and second harmonic generation devices
[NASA-CR-198598] p 2443 N95-28033
Aspects of macroscopic phase separation and interstitial oxygen ordering in oxygen doped La2CuO(4+delta)
[DE95-007864] p 2443 N95-28060
Low resistivity ohmic contacts to moderately doped n-GaAs with low temperature processing
[DE95-008507] p 2445 N95-28144
Vacancy related defects in thin film Pb(Zr,Ti)O3 materials
[DE95-007696] p 2445 N95-28165
Femtosecond OPO's at 3 microns and beyond: Design and performance issues related to the crystal properties of KTP and similar materials
[DE95-007286] p 2446 N95-28242

DOPPLER EFFECT
Evaluation of a new laboratory acoustic Doppler velocimeter
[AD-A289592] p 2290 N95-26714
Measurement of N2(+) mobility He via Fourier transform emission spectroscopy
[AD-A289266] p 2404 N95-26979
Telemetry down-link Doppler as an attitude sensor for spin stabilized spacecraft p 2150 N95-27785
Multi-spacecraft coherent Doppler and ranging for interplanetary-navigation p 2150 N95-27786

DOPPLER RADAR
Evaluation of the FMICW waveform in HF surface radar applications
[AD-A288245] p 2249 N95-26545
Measurements of HF auroral clutter using the Verona Ava Linear Array Radar (VALAR)
[AD-A289442] p 2337 N95-27147
Differenced Range Versus Integrated Doppler (DRVID) ionospheric analysis of metric tracking in the Tracking and Data Relay Satellite System (TDRSS)
p 2147 N95-27766
Telemetry down-link Doppler as an attitude sensor for spin stabilized spacecraft p 2150 N95-27785
Application of non-coherent Doppler data types for deep space navigation p 2151 N95-27788
Report to the Chairman and Ranking Minority Member, Committee on Science, House of Representatives. Weather forecasting: Radar availability requirement not being met
[GAO/AIMD-95-132] p 2342 N95-27912
Basic principles and recent observations of rotationally sampled wind p 2321 N95-27971

DOSAGE
Modification of the optical properties of glass by sequential ion implantation
[DE95-007401] p 2237 N95-28080
Acute and subacute toxicity of ammonium dinitramide (ADN) p 2175 N95-28318
Toxicity assessment of liquid propellant XM46
p 2175 N95-28319
The ELF controversy
[DE95-008283] p 2256 N95-28407

DOSIMETERS
Atomic oxygen dosimetry measurements made on STS-46 by CONCAP 2 p 2418 N95-27634
Evaluation of a conductive polymer-based sensor for detection of hydrazines at the part-per-billion level
p 2173 N95-28309

DOUGLAS AIRCRAFT
Evaluation of all-electric secondary power for transport aircraft
[NASA-CR-189077] p 2266 N95-27999

DOWNLINKING
Telemetry down-link Doppler as an attitude sensor for spin stabilized spacecraft p 2150 N95-27785
Multi-spacecraft coherent Doppler and ranging for interplanetary-navigation p 2150 N95-27786

DRAG
Computing NORAD mean orbital elements from a state vector
[AD-A289281] p 2146 N95-27033

DRAG MEASUREMENT
A new drag measurement system for wind tunnel testing of the racing bicycle and rider to determine a low drag configuration
[AD-A289375] p 2122 N95-26875

DRAG REDUCTION
Plate manipulators
[AD-A289601] p 2121 N95-26719

DREDGED MATERIALS
Calculation of suspended sediment transport by combined wave-current flows
[AD-A289368] p 2346 N95-26904

DROP SIZE
Structure of high-speed sprays
[AD-A291696] p 2288 N95-28523

DROP TOWERS
Design and development of experimental facilities for short duration, low-gravity combustion and fire experiments
[NASA-CR-195458] p 2244 N95-26709

DROPS (LIQUIDS)
The attenuation of microwave radiation by fog and rain
[AD-A288326] p 2249 N95-26562
Single-drop reactive extraction/extractive reaction with forced convective diffusion and interphase mass transfer
p 2283 N95-27365
Engineering photochemical smog through convection towers
[DE95-007727] p 2328 N95-27686

DRYING
The evaluation of a fluorochemical drying process for an electrical contact p 2227 N95-27103
Cleaning of parts for new manufacturing and parts rebuilding p 2231 N95-27123
Retrofitting conventional vapor degreasers to use a solvent wash/fluorochemical rinse process
p 2232 N95-27127
The experience of CF Technologies, Inc. (CF Tech) in critical fluid processing p 2232 N95-27128
Ambient-pressure silica aerogel films
[DE95-008161] p 2237 N95-28090
The minimum pore size obtainable in a silica gel during drying
[DE95-008162] p 2239 N95-28401

DUCTS
Self-excited oscillations in a duct with closed brances
[IFTR-18/1994] p 2400 N95-26358
A finite element propagation model for extracting normal incidence impedance in nonprogressive acoustic wave fields
[NASA-TM-110160] p 2400 N95-26394
The effect of infrared sea surface temperature measurements on evaporation duct height estimation
[AD-A289045] p 2346 N95-26477
Low-angle tracking in the presence of ducting, coherent and incoherent multipath
[AD-A289838] p 2258 N95-28580

DURABILITY
Bases for extrapolating materials durability in fuel storage pools
[DE95-007748] p 2222 N95-28129
Development of stitched/RTM composite primary structures p 2195 N95-28469

DUST
Effects of dust from storage heaters on ignition in scramjets
[NAL-TR-1234] p 2139 N95-26706
Particle fallout/activity sensor
[NASA-CASE-KSC-11687-1] p 2293 N95-28362

DWARF NOVAE
Cataclysmic variables and related objects
[NASA-SP-507] p 2458 N95-27068
Dwarf novae p 2458 N95-27069
Nova-like variables p 2458 N95-27070
Models for various aspects of dwarf novae and nova-like stars p 2459 N95-27071
Magnetic viscosity by localized shear flow instability in magnetized accretion disks
[DE95-006879] p 2433 N95-28111

DWARF STARS
Stability of strange quark stars with nuclear crusts against radial oscillations
[DE95-008484] p 2463 N95-28357

DWELL
N. N. Bogolyubov and particle physics
[DE95-608794] p 2448 N95-27447

DYADICS
Conditions for the parameter dyadics of lossless bi-anisotropic media
[PB95-185104] p 2252 N95-26914

DYE LASERS
Silicate gel dye laser
[AD-D017262] p 2294 N95-26503
New radiation stable and long-lived plastic scintillators
[DE95-608622] p 2233 N95-27163

DYES
Flow cytometry as a means of detecting, enumerating and characterizing bacteria for monitoring of the environment
[AD-A288997] p 2326 N95-26610
Evaluation of laser-protective eyewear dyes in UVEX lenses
[AD-A290076] p 2361 N95-28390

DYNAMIC CHARACTERISTICS
Dynamics and control of SEDSAT tethered multi-probe for thermospheric research flight data analysis of SEDS-2 satellite: Tethered systems dynamics and flight data analysis
[NASA-CR-198653] p 2165 N95-27836
A conceptual framework for evaluating variable speed generator options for wind energy applications
p 2273 N95-27987
Fellowship in physics
[AD-A291691] p 2446 N95-28522
In situ dynamic material property measurement system
[AD-D017387] p 2210 N95-28585

DYNAMIC CONTROL
Self-organizing artificial neural networks in dynamic systems modeling and control
[PB95-185120] p 2379 N95-26449
Analysis of modal behavior at frequency cross-over
[AD-A289304] p 2162 N95-26918
Dynamics and control of SEDSAT tethered multi-probe for thermospheric research flight data analysis of SEDS-2 satellite: Tethered systems dynamics and flight data analysis
[NASA-CR-198653] p 2165 N95-27836
A review of falconry as a bird control technique with recommendations for use at the Shuttle Landing Facility, John F. Kennedy Space Center, Florida, USA
[NASA-TM-110142] p 2126 N95-27859
Analysis methods for wind turbine control and electrical system dynamics p 2273 N95-27984
A conceptual framework for evaluating variable speed generator options for wind energy applications
p 2273 N95-27987

DYNAMIC LOADS
Using hob offset to balance dynamic strength in spur gears
[NASA-TM-106934] p 2302 N95-27698
System identification of damped truss-like space structures
[NASA-TM-106638] p 2303 N95-27911
A NASTRAN-based computer program for structural dynamic analysis of Horizontal Axis Wind Turbines
p 2312 N95-27980

DYNAMIC MODELS
Extension to the dynamic modeling of the large angle magnetic suspension test fixture
[NASA-CR-197801] p 2143 N95-26768
Optimal attitude maneuver execution for the Advanced Composition Explorer (ACE) mission
p 2149 N95-27778

DYNAMIC MODULUS OF ELASTICITY
In situ dynamic material property measurement system
[AD-D017387] p 2210 N95-28585

DYNAMIC PRESSURE
Wind tunnel experiments on wake flow field behind a reentry capsule from a viewpoint of parachute deployment at supersonic speeds
[ISAS-R-655] p 2121 N95-26740
Comparative wind tunnel tests of NACA 23024 airfoils with several aileron and spoiler configurations
p 2124 N95-27976
Pressure vessel burst test study p 2175 N95-28317

DYNAMIC RESPONSE
Effect of surface coating on one-dimensional system subjected to unit step pressure wave
[AD-A288237] p 2308 N95-26625
Dynamic coupling of underactuated manipulators
[AD-A289404] p 2301 N95-27098
Observed acoustic and aeroelastic spectral responses of a MOD-2 turbine blade to turbulence excitation
p 2324 N95-27991
Aeroelasticity and structural optimization of composite helicopter rotor blades with swept tips
[NASA-CR-4665] p 2136 N95-28262
Cape Canaveral air station launch emergency response forces and toxic materials release contingency plans
p 2172 N95-28308
Impact damage resistance of composite fuselage structure, part 1 p 2138 N95-28482
Non-linear viscoelastic behaviour
[PB95-192811] p 2199 N95-28639

DYNAMIC STABILITY
Beam instability studies for the SSC
[DE95-008024] p 2423 N95-28551

DYNAMIC STRUCTURAL ANALYSIS
Modified eigenvalue problems with applications to structural dynamic re-analysis on parallel computers
[AD-A288257] p 2307 N95-26547
The effects of finite element grid density on model correlation and damage detection of a bridge
[DE94-018895] p 2309 N95-27305
Vibration analysis of a split path gearbox
[NASA-TM-106875] p 2302 N95-27855
Collected papers on wind turbine technology
[NASA-CR-195432] p 2321 N95-27970
A NASTRAN-based computer program for structural dynamic analysis of Horizontal Axis Wind Turbines
p 2312 N95-27980
Structural design optimization with survivability dependent constraints application: Primary wing box of a multi-role fighter p 2137 N95-28440
Reliability analysis of composite structures
p 2192 N95-28441
Technology integration box beam failure study
p 2194 N95-28468

DYNAMIC TESTS
Experimental investigation of static and dynamic ground effect on HOPE ALFLEX vehicle
[NAL-TR-1236] p 2128 N95-26525

DYNAMICAL SYSTEMS
Self-organizing artificial neural networks in dynamic systems modeling and control
[PB95-185120] p 2379 N95-26449
The phenomena of subharmonic bifurcations, runaway, and transition to chaos in a non-linear oscillator: perturbation methods and a numerical experiment
[IFTR-16/1994] p 2398 N95-26518
Reference manual: Naive physics simulator
[PB95-184917] p 2369 N95-26907
An invariant measure for a nonlinear Schroedinger equation
[DE95-610166] p 2391 N95-27714
Nonlinear beam dynamics experimental program at SPEAR
[DE95-007823] p 2422 N95-28122

DYSON THEORY
A diagram technique for strongly interacting fermion systems. One-and two-band Hubbard models
[DE95-609437] p 2410 N95-27881

E

EARTH ATMOSPHERE
Nonlinear dynamics of global atmospheric and earth system processes
[NASA-CR-197926] p 2326 N95-26429
The Long Duration Exposure Facility (LDEF) photographic survey special publication
p 2457 N95-27660
Contingency maneuver strategies for the Total Ozone Mapping Spectrometer-Earth Probe (TOMS-EP)
p 2152 N95-27796
Mission to Planet Earth. Strategic enterprise plan, 1995-2000
[NASA-TM-110620] p 2145 N95-27919
Remote sensing of the atmosphere by resonance Raman LIDAR
[DE95-007312] p 2315 N95-28520

EARTH CRUST
Very low frequency seismo-acoustic noise below the sea floor (0.2-10 Hz)
[AD-A289164] p 2347 N95-27011
Seismic constraints on shallow crustal processes at the East Pacific rise
[AD-A289055] p 2338 N95-28094

EARTH ENVIRONMENT
Mission to Planet Earth. Strategic enterprise plan, 1995-2000
[NASA-TM-110620] p 2145 N95-27919

EARTH HYDROSPHERE
Nonlinear dynamics of global atmospheric and earth system processes
[NASA-CR-197926] p 2326 N95-26429

EARTH IONOSPHERE
An improved model of high-latitude f-region scintillation (WBMOD version 13)
[AD-A288558] p 2334 N95-26520
Space tether-radar data processing
[AD-A289654] p 2250 N95-26725
Assessment of the AN/FPS-118 Ionospheric model and proposed improvements
[AD-A289439] p 2337 N95-27146
PRISM validation
[AD-A288476] p 2337 N95-27703

EARTH MAGNETOSPHERE
SAMPEX special pointing mode p 2149 N95-27780
Low energy neutral atom imaging: Remote observations of the magnetosphere
[DE95-006342] p 2337 N95-27848
Relativistic electrons in the outer-zone: An 11 year cycle, their relation to the solar wind
[DE95-007882] p 2338 N95-28061

EARTH OBSERVATIONS (FROM SPACE)
Earth horizon modeling and application to static Earth sensors on TRMM spacecraft p 2150 N95-27783

EARTH OBSERVING SYSTEM (EOS)
Technical report series on global modeling and data assimilation. Volume 6: A multiyear assimilation with the GEOS-1 system: Overview and results
[NASA-TM-104606-VOL-6] p 2334 N95-26423
Development and analysis of SCR requirements tables for system scenarios
[NASA-CR-197769] p 2367 N95-26802
Summary of EOS flight dynamics analysis
p 2152 N95-27797

EARTH ORBITAL ENVIRONMENTS
Space Debris Research Phase One Program: Abstracts from published papers (1990-1993)
[AD-A289504] p 2162 N95-26850
Thermal control materials on EOIM-3
p 2242 N95-27639
Solid film lubricants and thermal control coatings flown aboard the EOIM-3 MDA sub-experiment
p 2242 N95-27640
Evaluation of space environmental effects on metals and optical thin films on EOIM-3 p 2210 N95-27641
Analysis of selected specimens from the STS-46 Energetic Oxygen Interaction with Materials-3 experiment p 2210 N95-27642
Molecular beam scattering from C-13 enriched Kapton and correlation with the EOIM-3 carousel experiment
p 2419 N95-27643
LDEF systems special investigation group overview
p 2470 N95-27647
A Materials Exposure Facility p 2166 N95-27664
Long Duration Exposure Facility post-flight data as it influences the Tropical Rainfall Measuring Mission
p 2345 N95-27666
Element material experiment by EFFU
p 2145 N95-27667
The Strategic Technologies for Automation and Robotics (STEAR) program: Protection of materials in the space environment subprogram p 2242 N95-27669

EARTH ORBITS
Orbital impacts and the Space Shuttle windshield
[NASA-TM-110594] p 2159 N95-26379

EARTH RADIATION BUDGET
A study of surface temperatures, clouds and net radiation
[NASA-CR-198589] p 2329 N95-27864
Cloud classification using whole-sky imager data
[DE95-006501] p 2344 N95-28556

EARTH RESOURCES
Materials design and processing by biomimicking. Section 1: Research progress
[AD-A288229] p 2226 N95-26623
Design and processing of materials by biomimicking. Section 2. Publications
[AD-A288230] p 2226 N95-26624
Mission to Planet Earth. Strategic enterprise plan, 1995-2000
[NASA-TM-110620] p 2145 N95-27919

EARTH SCIENCES
Airborne geophysics and precise positioning: Scientific issues and future directions
[LC-94-68678] p 2314 N95-27156

EARTH SURFACE
Naval Aviation System TEAM mapping, charting, and geodesy handbook
[AD-A288590] p 2314 N95-26841

EARTHQUAKE RESISTANT STRUCTURES
Stress corrosion cracking susceptibility of the earthquake resistant NOM B457 Mexican steel
[DE95-607956] p 2214 N95-27256

EARTHQUAKES
Live from Antarctica, volume 4
[NASA-CR-197828] p 2335 N95-26596
Investigation of rifting processes in the Rio Grande Rift using data from an unusually large earthquake swarm
[DE95-007623] p 2339 N95-28126

ECLIPTIC
Ulysses orbit determination at high declinations
p 2151 N95-27787

ECOLOGY
Finding the forest in the trees. The challenge of combining diverse environmental data
[NASA-CR-197798] p 2326 N95-26362

ECONOMIC ANALYSIS
Physics assessment of stellarators as fusion power plants
[DE95-007045] p 2431 N95-27498
ECONOMICS
Monolithic electronics for nuclear and high-energy physics experiments
[DE95-005393] p 2420 N95-27427
Commercial reformulation: An economic and environmentally neutral means of managing explosives and solid propellants p 2175 N95-28320
ECOSYSTEMS
Survey on researches related to ocean disposal of carbon dioxide
[DE95-759247] p 2329 N95-27939
EDDINGTON APPROXIMATION
Stationary neutrino radiation transport by maximum entropy closure
[DE95-006579] p 2463 N95-28558
EDDY CURRENTS
Extension to the dynamic modeling of the large angle magnetic suspension test fixture
[NASA-CR-197801] p 2143 N95-26768
Combined investigation of Eddy current and ultrasonic techniques for composite materials NDE
[NASA-TM-110599] p 2306 N95-26778
EDDY VISCOSITY
Computational analysis of forebody tangential slot blowing on the high alpha research vehicle
[NASA-CR-197754] p 2129 N95-26591
Calculation of suspended sediment transport by combined wave-current flows
[AD-A289368] p 2346 N95-26904
Progress in simulating industrial flows using two-equation models: Can more be achieved with further research?
p 2286 N95-27895
EDGE DETECTION
User's and test case manual for FEMATS
[NASA-CR-197803] p 2366 N95-26694
Edge detection by nonlinear dynamics
[DE95-008076] p 2373 N95-28168
EDGE DISLOCATIONS
The role of edge dislocations in the deformation of BCC metals
[DE95-609157] p 2219 N95-27759
EDGES
Nonlinear scalespace via hierarchical statistical modeling
[AD-A289057] p 2394 N95-26478
EDITING
Beginning to edit physics
[DE95-008374] p 2455 N95-28085
EDUCATION
Enhancing the effects of diversity awareness training: A review of the research literature
[DOT/FAA/AM-95/10] p 2355 N95-26361
Compiler-assisted debugging and multiple instruction retry
[NASA-CR-197729] p 2365 N95-26628
NEXTSTEP: The next step in the right direction? Part 2: Software development with NEXTSTEP
[REPT-94-33-PT-2] p 2450 N95-26803
Can there be reliability without reliability?
[AD-A289480] p 2306 N95-26927
Overview of megaprogramming course: Lectures and eexercises. Version 02.00.03
[AD-A286723] p 2370 N95-27235
Views of the solar system
[DE95-006446] p 2461 N95-27326
Space physics educational outreach
[NASA-CR-198649] p 2399 N95-27852
Laboratory of production engineering
[PB95-184834] p 2451 N95-28135
Teaching interdisciplinary computational science from an electronic book on the Internet
[DE95-006525] p 2373 N95-28498
Evaluation of an Air Force Information Resources Management (IRM) overview course
[AD-A288746] p 2456 N95-28587
Advanced educational methods in the Department of Defense: Application of case theory and computer-assisted instruction to business process reengineering
[AD-A288881] p 2374 N95-28590
Building an electronic book on the Internet. CSEP:An interdisciplinary syllabus for teaching computational science at the graduate level
[DE95-006526] p 2375 N95-28632
The effects of Crew Resource Management (CRM) training in airline maintenance: Results following three year's experience
[NASA-CR-196696] p 2358 N95-28676
EFFICIENCY
Automatically selecting and using primary effects in planning: Theory and experiments
[AD-A289347] p 2450 N95-27064
Heterostructures and infrared emitters with compressed InAsSb layers
[DE95-008157] p 2446 N95-28399
EFFLUENTS
Hydrothermal oxidation of solid rocket propellant and other department of defense hazardous wastes
p 2177 N95-28325
EIGENVALUES
Modified eigenvalue problems with applications to structural dynamic re-analysis on parallel computers
[AD-A288257] p 2307 N95-26547
Do we fully understand the symmetric Lanczos algorithm yet?
[AD-A289614] p 2368 N95-26855
Optimization of a nutation damper attached to a spin-stabilized satellite
[AD-A289424] p 2162 N95-26887
Adaptive beamforming in frequency-dispersive multipath environments
[AD-A289206] p 2254 N95-27009
Spectral properties of multipliers on topological algebras
[DE95-608747] p 2390 N95-27299
Aeroelastic stability of wind turbine blade/aileron systems p 2124 N95-27981
EIGENVECTORS
Optimization of a nutation damper attached to a spin-stabilized satellite
[AD-A289424] p 2162 N95-26887
ELVIS: Eigenvectors for land vehicle image system
[AD-A289297] p 2381 N95-27041
Extensional flow convecting a reactant undergoing a first order homogeneous reaction and diffusional mass transfer from a sphere at low to intermediate Peclet and Damkohler numbers p 2280 N95-27346
Multifractal character of the electronic states in disordered two-dimensional systems
[DE95-609153] p 2443 N95-28016
EJECTA
A new method of determining the ejected mass of novae
[DE95-007884] p 2462 N95-28062
ELASTIC BENDING
Deformation limits on two-parameter fracture mechanics in terms of higher order asymptotics
[AD-A289113] p 2310 N95-28098
ELASTIC BODIES
Manual for SHOCK3D, version 2.0. Computer program for non-linear shock response
[AD-A288631] p 2307 N95-26342
ELASTIC DEFORMATION
Characterization of the membrane theory of a clamped shell. The hyperbolic case
[PB95-185021] p 2308 N95-26911
Load transfer in the stiffener-to-skin joints of a pressurized fuselage
[NASA-CR-198610] p 2310 N95-27865
High-temperature deformation of ZrO2-Al2O3/SiC whisker composites fabricated by two techniques
[DE95-008273] p 2183 N95-28069
Unique considerations in the design and experimental evaluation of tailored wings with elastically produced chordwise camber p 2192 N95-28436
ELASTIC MEDIA
Emerging applications of probability (stochastic models in geosystems)
[AD-A289117] p 2313 N95-28099
ELASTIC PROPERTIES
Elastic properties of metallic superlattices
[AD-A288699] p 2212 N95-26490
C15 intermetallic compounds HfV2+Nb
[DE95-005264] p 2215 N95-27463
Atomistic calculations of hydrogen interactions with Ni3Al grain boundaries and Ni/Ni/Ni3Al interfaces
[DE95-006497] p 2408 N95-27534
ECR plasma-assisted deposition of Al2O3 and dispersion-strengthened AlO2
[DE95-007743] p 2235 N95-27687
Molecular dynamics simulations of Gay-Berne nematic liquid crystal: Elastic properties from direct correlation functions
[DE95-609149] p 2441 N95-27740
Phase stability and elasticity of C15 transition-metal intermetallic compounds
[DE95-007876] p 2219 N95-28026
An improved plate theory of order (1,2) for thick composite laminates p 2187 N95-28283
ELASTIC SCATTERING
Comparative experimental study of PIXE and X-ray fluorescence analysis
[DE95-607868] p 2327 N95-27198
The Bremsstrahlung of soft gamma-quanta created by elastic pp- and np-scatterings and the dibaryon resonance problem
[DE95-608870] p 2415 N95-28248
Laser beam aerosol interactions
[AD-A291723] p 2300 N95-28509
ELASTIC WAVES
Effect of surface coating on one-dimensional system subjected to unit step pressure wave
[AD-A288237] p 2308 N95-26625
ELASTOHYDRODYNAMICS
Deformation behavior of thin lubricant films at elevated pressure
[AD-A288906] p 2241 N95-28592
ELASTOMERS
Siloxane-based ferroelectric liquid crystal elastomers and Self-Assembled Mono- and multilayers
[AD-A288285] p 2224 N95-26456
Variation of solvent scattering-length density small-angle neutron scattering as a means of determining structure of composite materials
[DE95-005394] p 2183 N95-27428
Effects of atomic oxygen on polymeric materials flown on EOIM-3 p 2242 N95-27638
Development of a low-cost, modified resin transfer molding process using elastomeric tooling and automated preform fabrication p 2184 N95-28268
ELASTOSTATICS
Analysis of stresses in finite anisotropic panels with centrally located cutouts p 2187 N95-28286
ELECTRIC BATTERIES
Thermodynamics of electrolyte solutions for use in high energy lithium batteries
[AD-A288897] p 2199 N95-26352
Electrolyte effects in Li(Si)/FeS2 thermal batteries
[DE95-001614] p 2264 N95-27474
Current status of environmental, health, and safety issues of lithium polymer electric vehicle batteries
[DE95-004005] p 2265 N95-27719
Development of an ultra-safe rechargeable lithium-ion battery
[AD-A288959] p 2269 N95-28349
Thermal analysis of PANSAT batteries and Electrical Power Subsystem
[AD-A290013] p 2269 N95-28388
ELECTRIC CELLS
The 1994 27th Annual NASA Aerospace Battery Workshop
[NASA-CP-3292] p 2317 N95-26785
ELECTRIC CHARGE
Nickel metal hydride LEO cycle testing
p 2272 N95-26791
Adiabatic charging of nickel-hydrogen batteries
p 2272 N95-26795
Radiation of a uniformly moving charge
[DE95-608757] p 2255 N95-27335
Characterization of wafer charging mechanisms and oxide survival prediction methodology
[DE95-006583] p 2440 N95-27538
ELECTRIC CONDUCTORS
Microengineered conducting composites from nanochannel templates
[AD-A289573] p 2180 N95-26686
ELECTRIC CONNECTORS
Partial discharge testing of high voltage wiring harness for airborne displays
[AD-A289150] p 2138 N95-27003
ELECTRIC CONTACTS
The evaluation of a fluorochemical drying process for an electrical contact p 2227 N95-27103
Low temperature deposition and characterization of N- and P-type silicon carbide thin films and associated Ohmic and Schottky contacts
[AD-A289107] p 2237 N95-28097
ELECTRIC CURRENT
Room-temperature photocurrent spectroscopy of GaAs/GaAlAs multiple quantum wells
[AD-A289607] p 2201 N95-26707
The electric field of Bohr's atom
[DE95-608758] p 2448 N95-27336
Photoinduced dipoles and charge pairs in condensed phase
[DE95-007071] p 2207 N95-27921
Can TMAE photocathode be used for high rate applications?
[DE95-008594] p 2293 N95-28178
Energy-measuring resistor bank
[AD-D017392] p 2271 N95-28613
ELECTRIC DIPOLES
Scattering by a small object close to an interface. 3. Buried object
[PB95-184909] p 2256 N95-28354
Method of images applied to electromagnetic problems involving spherical, spheroidal and planar geometries
[PB95-195517] p 2257 N95-28451
ELECTRIC DISCHARGES
High-rate/high-temperature capability of a single-layer zicar-separator nickel-hydrogen cell
p 2272 N95-26788

Air Force Ni-H2 cell test program: State of Charge test
p 2272 N95-26789
The 50 Ah NiH2 CPV qualification tests
p 2272 N95-26792
Partial discharge testing of high voltage wiring harness for airborne displays
[AD-A289150] p 2138 N95-27003
Effect of internal hydrogen on the mixed-mode 1/3 fracture toughness of a ferrific/martensitic stainless steel
[DE95-005722] p 2216 N95-27479
The protection of electro-explosive devices (EEDs) and electronics from electrostatic discharge (ESD) hazards
[DSTO-TR-0100] p 2258 N95-28568

ELECTRIC ENERGY STORAGE
Investigation of high-temperature superconducting flywheel energy storage devices
[DE95-759242] p 2320 N95-27936

ELECTRIC EQUIPMENT
Analysis of magnetic field levels at KSC
[NASA-CR-197678] p 2326 N95-26808

ELECTRIC EQUIPMENT TESTS
The 1994 27th Annual NASA Aerospace Battery Workshop
[NASA-CP-3292] p 2317 N95-26785
Long life 80Ah standard IPV NiH2 battery cell
p 2272 N95-26787
Test operations procedure (TOP) 2-2-613, electromagnetic interference testing and electrical subsystem - non-communication
[AD-A289521] p 2251 N95-26851
Partial discharge testing of high voltage wiring harness for airborne displays
[AD-A289150] p 2138 N95-27003

ELECTRIC FIELDS
Room-temperature photocurrent spectroscopy of GaAs/GaAlAs multiple quantum wells
[AD-A289607] p 2201 N95-26707
Polarization sensitivity of monopulse radar boresight error induced by large, ogive radomes
[AD-A289254] p 2252 N95-26972
Measurement of N2(+) mobility He via Fourier transform emission spectroscopy
[AD-A289266] p 2404 N95-26979
Model of a single impurity in a wide bandgap semiconductor describing electric field screening
[AD-A289322] p 2264 N95-27296
The electric field of Bohr's atom
[DE95-608758] p 2448 N95-27336
Observations of CEF-split intermultiplet transitions in optically opaque EuBa2Cu3O7 using inelastic neutron scattering
[DE95-007135] p 2408 N95-27453
Dithering transitions in resistive pressure-gradient-driven turbulence
[DE95-006737] p 2431 N95-27536
Internal electric field of anisotropic and bi-anisotropic spheres
[PB95-195491] p 2257 N95-28449
Evaluation of defect-related diffusion in semiconductors by electrooptical sampling
[AD-A291630] p 2270 N95-28544

ELECTRIC GENERATORS
Test operations procedure (TOP) 2-2-613, electromagnetic interference testing and electrical subsystem - non-communication
[AD-A289521] p 2251 N95-26851
AFC generator development
[DE95-007094] p 2266 N95-27754
A hybrid vehicle evaluation code and its application to vehicle design. Revision 1
[DE95-008053] p 2303 N95-28029
The U.S. Department of Energy Wind Turbine Development Program
[DE95-000292] p 2325 N95-28395

ELECTRIC MOTOR VEHICLES
Current status of environmental, health, and safety issues of lithium polymer electric vehicle batteries
[DE95-004005] p 2265 N95-27719
DOE/KEURP Site Operator Program
[DE95-007116] p 2266 N95-27926
Electric vehicle activities
[DE95-006648] p 2267 N95-28105

ELECTRIC MOTORS
Dynamically timed electric motor
[NASA-CASE-MFS-28958-1] p 2261 N95-26890

ELECTRIC NETWORKS
Microengineered conducting composites from nanochannel templates
[AD-A289573] p 2180 N95-26686
Reference manual: Naive physics simulator
[PB95-184917] p 2369 N95-26907
Non-linear resistive grid kernel estimator useful in single feature, two-class pattern classification
[AD-D017394] p 2271 N95-28614

ELECTRIC POTENTIAL
Electrical performance characterisation of single-shot switches in high speed, high voltage and high current applications
[DSTO-RR-0010] p 2259 N95-26425
High-rate/high-temperature capability of a single-layer zicar-separator nickel-hydrogen cell
p 2272 N95-26788
Air Force Ni-H2 cell test program: State of Charge test
p 2272 N95-26789
Micro-time stress measurement device development
[AD-A289511] p 2361 N95-26845
MHD simulations of DC helicity injection for current drive in tokamaks
[DE95-007018] p 2429 N95-26940
The electric field of Bohr's atom
[DE95-608758] p 2448 N95-27336
Electromagnetic hysteretic response calculation for superconductors in demagnetizing geometries
[DE95-005028] p 2264 N95-27403
Matrix kernels for MEG and EEG source localization and imaging
[DE95-005238] p 2354 N95-27426
Performance of a stand-alone wind-electric ice maker for remote villages
[DE95-004006] p 2320 N95-27475
Visualization of finite element model solutions for defibrillation voltage and current distributions
[AD-A289836] p 2400 N95-28579
Non-linear resistive grid kernel estimator useful in single feature, two-class pattern classification
[AD-D017394] p 2271 N95-28614
Mechanism of deposit formation on fuel-wetted hot metal surfaces
[AD-A289847] p 2210 N95-28621

ELECTRIC POWER
Probabilistic risk assessment of the Space Shuttle. Phase 3: A study of the potential of losing the vehicle during nominal operation. Volume 4: System models and data analysis
[NASA-CR-197811] p 2160 N95-26401
Molten Carbonate Fuel Cell (MCFC) product development test
[DE95-007345] p 2316 N95-26543

ELECTRIC POWER SUPPLIES
Analysis methods for wind turbine control and electrical system dynamics p 2273 N95-27984
Evaluation of all-electric secondary power for transport aircraft
[NASA-CR-189077] p 2266 N95-27999

ELECTRIC POWER TRANSMISSION
Hydrogen program
[DE94-011827] p 2242 N95-27415

ELECTRIC PROPULSION
Direct drive options for electric propulsion systems
[NASA-TM-106576] p 2168 N95-27861
Micro electric propulsion feasibility
[NASA-CR-189139] p 2168 N95-28000

ELECTRIC ROCKET ENGINES
Micro electric propulsion feasibility
[NASA-CR-189139] p 2168 N95-28000

ELECTRIC SWITCHES
Electrical performance characterisation of single-shot switches in high speed, high voltage and high current applications
[DSTO-RR-0010] p 2259 N95-26425
Forback DC-to-DC converter
[NASA-CASE-GSC-13404-1] p 2269 N95-28341

ELECTRIC TERMINALS
Unique features of a new nickel-hydrogen 2-cell CPV
p 2272 N95-26793

ELECTRICAL ENGINEERING
Basic and applied research in the field of electronics and communications
[AD-A291727] p 2270 N95-28512

ELECTRICAL IMPEDANCE
Joint services electronics program
[AD-A289594] p 2260 N95-26716
Nickel metal hydride LEO cycle testing
p 2272 N95-26791
Characterization of wafer charging mechanisms and oxide survival prediction methodology
[DE95-006583] p 2440 N95-27538
Linearly tapered slot antenna impedance characteristics
[NASA-TM-106912] p 2266 N95-27853

ELECTRICAL MEASUREMENT
Micro-time stress measurement device development
[AD-A289511] p 2361 N95-26845
A study of lightning in winter thunderstorms and the analysis of thunderstorm overflight data
[NASA-CR-198577] p 2343 N95-28191
OBIC analysis of stressed, thermally-isolated polysilicon resistors
[DE95-008511] p 2268 N95-28201
Manufacture and testing of the superconducting wire and cable for the RHIC dipoles and quadrupoles
[DE95-006000] p 2270 N95-28515
Energy-measuring resistor bank
[AD-D017392] p 2271 N95-28613

ELECTRICAL PROPERTIES
A book and series of monographs on ice physics
[AD-A288319] p 2200 N95-26422
Electrical performance characterisation of single-shot switches in high speed, high voltage and high current applications
[DSTO-RR-0010] p 2259 N95-26425
Microengineered conducting composites from nanochannel templates
[AD-A289573] p 2180 N95-26686
Review of activities in USA on HTS materials
[DE95-006404] p 2234 N95-27468
I(sub DDQ) testing and defect classes: A tutorial
[DE95-005467] p 2306 N95-27723
Stability measurements on a 1-T high temperature superconducting magnet
[DE95-007411] p 2267 N95-28048
A study of lightning in winter thunderstorms and the analysis of thunderstorm overflight data
[NASA-CR-198577] p 2343 N95-28191
Chemical and electrical properties of cavities in silicon and germanium
[DE95-006812] p 2445 N95-28206

ELECTRICAL RESISTIVITY
Hall effect and resistivity in the normal state of high-T(sub c) cuprates in the electron-fracton model
[DE95-610612] p 2439 N95-27413
Atomic oxygen dosimetry measurements made on STS-46 by CONCAP 2 p 2418 N95-27634
Inflight resistance measurement on high-T(sub c) superconducting thin films exposed to orbital atomic oxygen on CONCAP-2 (STS-46) p 2272 N95-27635
Electrical conductivity measurements of aqueous electrolyte solutions at high temperatures and high pressures
[DE95-006748] p 2208 N95-27956
Defect characterization of electronic conducting pseudo-perovskite systems
[DE95-007487] p 2220 N95-28049
Low resistivity ohmic contacts to moderately doped n-GaAs with low temperature processing
[DE95-008507] p 2445 N95-28144

ELECTRICITY
Hydrogen program
[DE94-011827] p 2242 N95-27415
Heat pipe cooled reactors for multi-kilowatt space power supplies
[DE95-005211] p 2420 N95-27425

ELECTRO-OPTICS
Characterization of optical polymers for multi-layered electro-optic devices
[AD-A289255] p 2227 N95-26973
Toward coherent excitation: Development of a single-source pump for the rubidium hyperfine ground state doublet
[AD-A289413] p 2295 N95-27132
A final look at LDEF electro-optic systems components p 2428 N95-27650
Applications of lasers and electro-optics
[DE95-600841] p 2299 N95-28330
Passive spatial beam control, appendix
[AD-A288913] p 2300 N95-28333
Perturbations on effective index of refraction from prism coupling
[AD-A291700] p 2427 N95-28524
Evaluation of defect-related diffusion in semiconductors by electrooptical sampling
[AD-A291630] p 2270 N95-28544

ELECTROCHEMICAL CELLS
Progress towards computer simulation of NiH2 battery performance over life p 2272 N95-26786
High-rate/high-temperature capability of a single-layer zicar-separator nickel-hydrogen cell
p 2272 N95-26788
Air Force Ni-H2 cell test program: State of Charge test
p 2272 N95-26789
Calorimetric evaluation of commercial Ni-MH cells and charges p 2272 N95-26790
Nickel metal hydride LEO cycle testing
p 2272 N95-26791
Adiabatic charging of nickel-hydrogen batteries
p 2272 N95-26795
Alternate charging profiles for the onboard nickel cadmium batteries of the Explorer Platform/Extreme Ultraviolet Explorer p 2272 N95-26796

ELECTROCHEMICAL CORROSION
Environmentally Benign Cleaning and Degreasing Technology: JANNAF Safety and Protection Subcommittee and Propellant Development and Characterization Subcommittee Joint Workshop
[CPIA-PUBL-611] p 2227 N95-27101

Simulations of metal dissolution and corrosion
[DE95-007486] p 2218 N95-27748

ELECTROCHEMICAL OXIDATION
Absorption of sparingly soluble gases by reactive media in self-aerated gas-liquid contactors: A scale-up procedure
[DE95-006429] p 2206 N95-27707

ELECTROCHEMISTRY
Investigation of the interface between immiscible electrolytes applied to membrane electrochemistry
[AD-A288887] p 2199 N95-26350
Electrocrystallization of an ordered organic monolayer: Selective epitaxial growth of beta(ET)213 ongraphite
[AD-A288942] p 2178 N95-26569
The use of electrochemistry and ellipsometry for identifying and evaluating corrosion on aircraft
[AD-A288536] p 2125 N95-27186
Simulations of metal dissolution and corrosion
[DE95-007486] p 2218 N95-27748

ELECTRODES
Toward molecular selectivity with chemically modified electrodes: Can electroactivity and permeability through an overlaying metallopolymer film be controlled via rational manipulation of internal architecture?
[AD-A288719] p 2403 N95-26491
Experimental definition for implantation of the AFIT cortical multielectrode array
[AD-A289216] p 2354 N95-26991
An investigation of the chemical and physical properties of pristine, electrochromically damaged, and photochromically damaged KTiOPO4 (KTP) using surface analytical and optical spectroscopic techniques
[DE95-007865] p 2443 N95-28023

ELECTRODYNAMICS
Radiation of a uniformly moving charge
[DE95-608757] p 2255 N95-27335

ELECTROENCEPHALOGRAPHY
Experimental definition for implantation of the AFIT cortical multielectrode array
[AD-A289216] p 2354 N95-26991
Matrix kernels for MEG and EEG source localization and imaging
[DE95-005238] p 2354 N95-27426

ELECTROLUMINESCENCE
JTEC panel on display technologies in Japan
[NASA-CR-198564] p 2292 N95-27863

ELECTROLYTES
Investigation of the interface between immiscible electrolytes applied to membrane electrochemistry
[AD-A288887] p 2199 N95-26350
Thermodynamics of electrolyte solutions for use in high energy lithium batteries
[AD-A288897] p 2199 N95-26352
FREZCHEM: A chemical-thermodynamic model for aqueous solutions at subzero temperatures
[AD-A288456] p 2200 N95-26432
Materials design and processing by biomimicking. Section 1: Research progress
[AD-A288229] p 2226 N95-26623
Design and processing of materials by biomimicking. Section 2. Publications
[AD-A288230] p 2226 N95-26624
Measurements of the volatilities of electrolytes: Application to water/steam cycles
[DE95-007103] p 2204 N95-27451
Electrolyte effects in Li(Si)/FeS2 thermal batteries
[DE95-001614] p 2264 N95-27474
Thermodynamics of aqueous electrolytes at high temperatures by the isopiestic technique
[DE95-006747] p 2449 N95-27546
Simulations of metal dissolution and corrosion
[DE95-007486] p 2218 N95-27748
Electrical conductivity measurements of aqueous electrolyte solutions at high temperatures and high pressures
[DE95-006748] p 2208 N95-27956
Aqueous electrolyte modeling in ASPEN PLUS(trademark)
[DE95-007008] p 2208 N95-27960
Hydrogen-ion titrations of amino acids and proteins in solutions containing concentrated electrolyte
[DE95-008356] p 2209 N95-28229

ELECTROLYTIC CELLS
Long life 80Ah standard IPV NiH2 battery cell
p 2272 N95-26787

ELECTROMAGNETIC ABSORPTION
Soot particle density determination from a laser extinction multipass technique
[AD-A288551] p 2423 N95-26532
Particle-like absorption spectra in small transition metal clusters
[DE95-007082] p 2218 N95-27752
Nonlinear optical microscopy for imaging thin films and surfaces
[DE95-007872] p 2426 N95-28018
SeaWiFS technical report series. Volume 27: Case studies for SeaWiFS calibration and validation, part 3
[NASA-TM-104566-VOL-27] p 2348 N95-28030

ELECTROMAGNETIC ACCELERATION
A high velocity electromagnetic mass launcher having an ablation resistant insulator
[AD-A288231] p 2154 N95-26524

ELECTROMAGNETIC FIELDS
Analysis of electromagnetic problems involving chiral, bi-isotropic, and uniaxial bianisotropic media
[PB95-185096] p 2248 N95-26450
Radiation of a uniformly moving charge
[DE95-608757] p 2255 N95-27335
Acceleration theorems
[DE95-007300] p 2420 N95-27484
Proofs of contracted length non-covariance
[DE95-610175] p 2391 N95-27715
Landau quasi-energy spectrum destruction for an electron in both a static magnetic field and a resonant electromagnetic wave
[DE95-610176] p 2256 N95-27716
The ELF controversy
[DE95-008283] p 2256 N95-28407

ELECTROMAGNETIC INTERACTIONS
A high velocity electromagnetic mass launcher having an ablation resistant insulator
[AD-A288231] p 2154 N95-26524
A model of the extended electron and its nonlocal electromagnetic interaction: Gauge invariance of the nonlocal theory
[DE95-608803] p 2255 N95-27313

ELECTROMAGNETIC INTERFERENCE
Electromagnetic spectrum occupancy study of a potential transmitter site for the HF Active Auroral Research Program (HAARP)
[AD-A288909] p 2249 N95-26564
Test operations procedure (TOP) 2-2-613, electromagnetic interference testing and electrical subsystem - non-communication
[AD-A289521] p 2251 N95-26851

ELECTROMAGNETIC PROPERTIES
Reduction of off-boresight fields for a TEM horn antenna
[AD-A289708] p 2250 N95-26738

ELECTROMAGNETIC PUMPS
Heat pipe cooled reactors for multi-kilowatt space power supplies
[DE95-005211] p 2420 N95-27425

ELECTROMAGNETIC RADIATION
The attenuation of microwave radiation by fog and rain
[AD-A288326] p 2249 N95-26562
A BATSE investigation of radiation belt electrons precipitated by VLF waves
[NASA-CR-197780] p 2336 N95-26922
New trends and ideas in the fields of microwave technology
[AD-A291663] p 2257 N95-28453

ELECTROMAGNETIC SCATTERING
On the azimuthal Fourier components of the Green's function for the Helmholtz equation in three dimensions
[AD-A288775] p 2398 N95-26345
Joint services electronics program
[AD-A289594] p 2260 N95-26716
Computation of electromagnetic scattering parameters for lognormal distributions of magnetic spheres: Theory and algorithms
[AD-A289672] p 2250 N95-26759
Simple equivalent dipole distributions for dielectric spheroidal scatterers
[PB95-184883] p 2254 N95-27049
Internal electric field of anisotropic and bi-anisotropic spheres
[PB95-195491] p 2257 N95-28449
Method of images applied to electromagnetic problems involving spherical, spheroidal and planar geometries
[PB95-195517] p 2257 N95-28451
Numerical and theoretical studies of rough surface scattering
[AD-A291748] p 2257 N95-28528

ELECTROMAGNETIC SPECTRA
Electromagnetic spectrum occupancy study of a potential transmitter site for the HF Active Auroral Research Program (HAARP)
[AD-A288909] p 2249 N95-26564

ELECTROMAGNETIC WAVE TRANSMISSION
Electromagnetic spectrum occupancy study of a potential transmitter site for the HF Active Auroral Research Program (HAARP)
[AD-A288909] p 2249 N95-26564
Joint services electronics program
[AD-A289594] p 2260 N95-26716
New trends and ideas in the fields of microwave technology
[AD-A291663] p 2257 N95-28453

ELECTROMAGNETISM
Analysis of electromagnetic problems involving chiral, bi-isotropic, and uniaxial bianisotropic media
[PB95-185096] p 2248 N95-26450
Conditions for the parameter dyadics of lossless bi-anisotropic media
[PB95-185104] p 2252 N95-26914

ELECTROMAGNETS
Extension to the dynamic modeling of the large angle magnetic suspension test fixture
[NASA-CR-197801] p 2143 N95-26768
Magnetic field measurement for the spectrometric magnet of the ISTRA-M setup
[DE95-608560] p 2362 N95-27162

ELECTROMECHANICAL DEVICES
Feasibility of flywheel energy storage systems for applications in future space missions
[NASA-CR-195422] p 2316 N95-26393
Valve mechanism for an acoustic modulator
[AD-D017263] p 2300 N95-26504
A systems engineering approach to electro-mechanical reconfiguration for mobility autonomy
[AD-A289479] p 2301 N95-26926
Non-explosive actuation for the ORBCOMM (TM) satellite p 2156 N95-27274
A rotating arm using shape-memory alloy
p 2157 N95-27276
Electromechanical rotary actuator
p 2157 N95-27278
High-performance reactionless scan mechanism
p 2158 N95-27288
JTEC Panel report on microelectromechanical systems in Japan
[NASA-CR-197831] p 2268 N95-28239

ELECTRON BEAMS
The consideration of a bright relative beam dynamics in the magnetic focusing field
[DE95-608377] p 2398 N95-27160
Crab crossing in a gamma-gamma collider
[DE95-006580] p 2420 N95-27470
High energy electron beams for ceramic joining
[DE95-006316] p 2420 N95-27480
Femtosecond X-ray generation through 90 degrees T homson scattering: Status of the LBL experiment
[DE95-006560] p 2296 N95-27674
Precision electromagnetic calorimetry with liquid krypton
[DE95-006685] p 2292 N95-27677
ECR plasma-assisted deposition of Al2O3 and dispersion-strengthened AlO2
[DE95-007743] p 2235 N95-27687
Process for non-contact removal of organic coatings from the surface of paintings
[NASA-CASE-LEW-15896-1] p 2235 N95-27702
Application of conventional laser technology to gamma-gamma colliders
[DE95-006341] p 2297 N95-27736
Time-dependent multi-dimensional simulation studies of the electron output scheme for high power FELs
[DE95-006593] p 2297 N95-27737
Performance of an accordion electromagnetic calorimeter with liquid krypton
[DE95-006693] p 2292 N95-27738
Finite pulse effects in self-amplified-spontaneous emission
[DE95-006585] p 2298 N95-28104
Precise measurement of the left-right cross section asymmetry in Z boson production by e(+)e(-) collisions
[DE95-008591] p 2414 N95-28158
Beam instability studies for the SSC
[DE95-008024] p 2423 N95-28551

ELECTRON BOMBARDMENT
Molecular beam scattering from C-13 enriched Kapton and correlation with the EOIM-3 carousel experiment
p 2419 N95-27643

ELECTRON BUNCHING
Beam instability studies for the SSC
[DE95-008024] p 2423 N95-29551

ELECTRON CAPTURE
Lattice calculation for lepton capture from vacuum-pair production in relativistic heavy-ion collisions
[DE95-007392] p 2413 N95-28077

ELECTRON DENSITY (CONCENTRATION)
Measurement of particle transport coefficients on Alcator C-Mod
[DE95-007763] p 2411 N95-28020
Finite pulse effects in self-amplified-spontaneous emission
[DE95-006585] p 2298 N95-28104

ELECTRON DENSITY PROFILES
Far-infrared laser interferometry measurements on the STP-3(M) reversed-field pinch
[DE94-765440] p 2297 N95-27868
Finite pulse effects in self-amplified-spontaneous emission
[DE95-006585] p 2298 N95-28104

ELECTRON EMISSION

Projectile image acceleration, neutralization and electron emission during grazing interactions of multicharged ions with Au(110)
[DE95-007394] p 2409 N95-27551

ELECTRON ENERGY

Resonant photoemission studies of thickness dependence of the unoccupied Gd 5d bands
[DE95-004127] p 2436 N95-26440

Electronic characterization of defects in narrow gap semiconductors: Comparison of electronic energy levels and formation energies in mercury cadmium telluride, mercury zinc telluride, and mercury zinc selenide
[NASA-CR-197835] p 2437 N95-26780

Measurement of R in e(+)e(-)-annihilation at center-of-mass energies between 7.2 and 10.34 GeV
[DE95-610303] p 2407 N95-27408

Landau quasi-energy spectrum destruction for an electron in both a static magnetic field and a resonant electromagnetic wave
[DE95-610176] p 2256 N95-27716

Electron spectroscopy studies of argon K-shell excitation and vacancy cascades
[DE95-007096] p 2442 N95-27963

Phase stability and elasticity of C15 transition-metal intermetallic compounds
[DE95-007876] p 2219 N95-28026

Theory of exotic superconductivity and normal states of heavy electron and high temperature superconductivity materials
[DE95-006637] p 2268 N95-28198

ELECTRON GAS

Wake fields in semiconductor plasmas
[DE94-634523] p 2429 N95-26439

Monte Carlo study of electron-plasmon scattering effects on hot electron transport in GaAs
[DE95-607768] p 2403 N95-26542

Temperature dependence of the static dielectric response in a Q1D electron gas
[DE95-609269] p 2400 N95-28350

ELECTRON GUNS

Developments in the electron gun simulation program, EGUN
[DE95-008137] p 2267 N95-28143

ELECTRON IRRADIATION

Annealing of radiation damaged gallium arsenide solar cells by laser illumination
[AD-A289683] p 2316 N95-26762

ELECTRON MICROSCOPES

Cryogenic temperature control and tension/compression attachment stage for an electron microscope
[AD-D017390] p 2294 N95-28612

ELECTRON MICROSCOPY

Boron-induced reconstructions of Si(100) investigated by scanning tunneling microscopy
[AD-A289222] p 2438 N95-26959

Density changes in amorphous Pd80Si20 during low temperature ion irradiation
[DE95-007132] p 2441 N95-27928

Analytical electron microscopy of nanometer-sized particles
[AD-A289124] p 2413 N95-28101

The in situ observation of epitaxial diamond thin film nucleation and growth using emission electron microscopy
[AD-A289841] p 2447 N95-28618

ELECTRON MOBILITY

Comprehensive numerical model for CW vertical-cavity surface-emitting lasers
[DE95-007758] p 2299 N95-28132

ELECTRON PLASMA

Process for non-contact removal of organic coatings from the surface of paintings
[NASA-CASE-LEW-15896-1] p 2235 N95-27702

ELECTRON PRECIPITATION

A BATSE investigation of radiation belt electrons precipitated by VLF waves
[NASA-CR-197780] p 2336 N95-26922

ELECTRON RADIATION

Long-term variability of electron radiation dose in geosynchronous orbit
[AD-A289335] p 2162 N95-26902

ELECTRON SCATTERING

Monte Carlo study of electron-plasmon scattering effects on hot electron transport in GaAs
[DE95-607768] p 2403 N95-26542

A BATSE investigation of radiation belt electrons precipitated by VLF waves
[NASA-CR-197780] p 2336 N95-26922

Crab crossing in a gamma-gamma collider
[DE95-006580] p 2420 N95-27470

Molecular beam scattering from C-13 enriched Kapton and correlation with the EOIM-3 carousel experiment
p 2419 N95-27643

HZETRN: Description of a free-space ion and nucleon transport and shielding computer program
[NASA-TP-3495] p 2465 N95-28530

ELECTRON SPECTROSCOPY

Electron spectroscopy studies of argon K-shell excitation and vacancy cascades
[DE95-007096] p 2442 N95-27963

ELECTRON STATES

Analytic formulae for the Hartree-Fock order parameter at arbitrary p/q filling factors for the 2DEG in a magnetic field
[DE95-607805] p 2448 N95-26603

Multifractal character of the electronic states in disordered two-dimensional systems
[DE95-609153] p 2443 N95-28016

Chemical and electrical properties of cavities in silicon and germanium
[DE95-006812] p 2445 N95-28206

ELECTRON TRANSFER

Monte Carlo study of electron-plasmon scattering effects on hot electron transport in GaAs
[DE95-607768] p 2403 N95-26542

Photoemission and optical properties of C60 fullerites
[DE95-006588] p 2425 N95-27539

Photoinduced dipoles and charge pairs in condensed phase
[DE95-007071] p 2207 N95-27921

ELECTRON TRANSITIONS

Atomic physics with highly charged ions
[DE95-007325] p 2407 N95-27439

ELECTRON TUNNELING

Demonstration of photo-assisted tunneling process across the coulomb blockade energy gap in mesoscopic tunnel junctions --- photon-assisted tunneling
[AD-A289534] p 2438 N95-26872

ELECTRON-POSITRON PAIRS

Measurement of inclusive Lambda production in electron-positron interactions at the upsilon energies
[DE95-610302] p 2407 N95-27407

Measurement of R in e(+)e(-)-annihilation at center-of-mass energies between 7.2 and 10.34 GeV
[DE95-610303] p 2407 N95-27408

Measurement of alpha(s) in e(+)e(-) annihilation at E(cm) = 29 GeV
[DE95-006486] p 2417 N95-28594

ELECTRONIC CONTROL

Laser with optically driven Q-switch
[NASA-CASE-NPO-18470-1-CU] p 2297 N95-27731

ELECTRONIC EQUIPMENT

Test operations procedure (TOP) 2-2-613, electromagnetic interference testing and electrical subsystem - non-communication
[AD-A289521] p 2251 N95-26851

Multi-channel electronically scanned cryogenic pressure sensor
[NASA-CASE-LAR-15062-1] p 2291 N95-27138

JTEC Panel report on electronic manufacturing and packaging in Japan
[NASA-CR-197830] p 2263 N95-27226

Microelectronics in Japan p 2263 N95-27227

Building the electronic industry's roadmaps
p 2263 N95-27228

Japan's technology and manufacturing infrastructure
p 2263 N95-27229

Electronics manufacturing and assembly in Japan
p 2263 N95-27231

Quality assurance and reliability in the Japanese electronics industry p 2263 N95-27232

Successful product realization strategies
p 2264 N95-27233

CAE for thermal management of aerospace electronic boards using the BETAsoft program
p 2272 N95-27354

Monolithic electronics for nuclear and high-energy physics experiments
[DE95-005393] p 2420 N95-27427

Evaluation and qualification of environmentally conscious manufacturing processes for commercial and military applications
[DE95-008520] p 2329 N95-27878

Lithium ion rechargeable systems studies
[DE95-006810] p 2268 N95-28200

Basic and applied research in the field of electronics and communications
[AD-A291727] p 2270 N95-28512

The protection of electro-explosive devices (EEDs) and electronics from electrostatic discharge (ESD) hazards
[DSTO-TR-0100] p 2258 N95-28568

ELECTRONIC EQUIPMENT TESTS

Test operations procedure (TOP) 2-2-613, electromagnetic interference testing and electrical subsystem - non-communication
[AD-A289521] p 2251 N95-26851

Efficient generation of counterexamples and witnesses in symbolic model checking
[AD-A288583] p 2370 N95-27095

ELECTRONIC MODULES

Intelligent computer based reliability assessment of multichip modules
[AD-A288833] p 2259 N95-26550

Managing electronic records: A guideline
[DE95-007038] p 2456 N95-28555

ELECTRONIC PACKAGING

JTEC Panel report on electronic manufacturing and packaging in Japan
[NASA-CR-197830] p 2263 N95-27226

Microelectronics in Japan p 2263 N95-27227

Building the electronic industry's roadmaps
p 2263 N95-27228

Japan's technology and manufacturing infrastructure
p 2263 N95-27229

Japan's electronic packaging technologies
p 2263 N95-27230

Successful product realization strategies
p 2264 N95-27233

Manufacturing tailored property ceramic composites
[DE95-006303] p 2237 N95-27993

ELECTRONIC SPECTRA

Analytical spectroscopy
[DE95-607896] p 2203 N95-27200

Electron spectroscopy studies of argon K-shell excitation and vacancy cascades
[DE95-007096] p 2442 N95-27963

ELECTRONICS

Template synthesis of electronically conductive polymer nanostructures
[AD-A288373] p 2225 N95-26472

JPRS report: Science and technology. Central Eurasia
[JPRS-UST-95-016] p 2262 N95-27170

ELECTRONS

Long-term variability of electron radiation dose in geosynchronous orbit
[AD-A289335] p 2162 N95-26902

A BATSE investigation of radiation belt electrons precipitated by VLF waves
[NASA-CR-197780] p 2336 N95-26922

A model of the extended electron and its nonlocal electromagnetic interaction: Gauge invariance of the nonlocal theory
[DE95-608803] p 2255 N95-27313

Integrating the QMR method with first principles material science application code
[DE95-007380] p 2408 N95-27456

Photoemission and optical properties of C60 fullerites
[DE95-006588] p 2425 N95-27539

Search for the top quark in dilepton decay modes at D(PHI)
[DE95-007764] p 2409 N95-27689

Burst of energetic ions from reversed field pinch plasma
[DE94-765447] p 2432 N95-27870

Relativistic electrons in the outer-zone: An 11 year cycle, their relation to the solar wind
[DE95-007882] p 2338 N95-28061

Collisions of highly charged ions with electrons, atoms and surfaces
[DE95-007393] p 2413 N95-28078

Heterostructures and infrared emitters with compressed InAsSb layers
[DE95-008157] p 2446 N95-28399

ELECTROPLATING

The evaluation of a fluorochemical drying process for an electrical contact p 2227 N95-27103

Plasma source ion implantation of ammonia into electroplated chromium
[DE95-006275] p 2444 N95-28125

ELECTRORHEOLOGICAL FLUIDS

Vibration control using chaotic motion stabilizers
[AD-A289576] p 2398 N95-26687

ELECTROSTATIC CHARGE

Simple equivalent dipole distributions for dielectric spheroidal scatterers
[PB95-184883] p 2254 N95-27049

The effect of aviation fuels containing low amounts of static dissipater additive on electrostatic charge generation
[AD-A280075] p 2243 N95-28152

The protection of electro-explosive devices (EEDs) and electronics from electrostatic discharge (ESD) hazards
[DSTO-TR-0100] p 2258 N95-28568

ELECTROWEAK INTERACTIONS (FIELD THEORY)

Signatures of Higgs-Triplet representations at TeV-e(+)e(-) colliders
[DE95-007201] p 2419 N95-27089

Finite fermion density effects on the electroweak string
[DE95-608802] p 2448 N95-27312

Model independent constraints on anomalous gauge boson self-couplings from e(+)e(-) colliders with longitudinally polarized beams
[DE95-608844] p 2406 N95-27317

Probing strongly-interacting electroweak dynamics through W(+)W(-)/ZZ ratios at future e(+)e(-) colliders
[DE95-007202] p 2413 N95-28067
Constraints on the anomalous WW gamma couplings from b vector s gamma
[DE95-608866] p 2415 N95-28246

ELECTROWEAK MODEL
Weak matrix elements efforts on the lattice: Status and prospects
[DE95-007701] p 2416 N95-28355

ELEMENTARY EXCITATIONS
Photoemission and optical properties of C60 fullerites
[DE95-006588] p 2425 N95-27539
The surface of liquid He-4 at nonzero temperatures
[DE95-607841] p 2207 N95-27880

ELEMENTARY PARTICLE INTERACTIONS
Measurement of inclusive Lambda production in electron-positron interactions at the upsilon energies
[DE95-610302] p 2407 N95-27407
Application of conventional laser technology to gamma-gamma colliders
[DE95-006341] p 2297 N95-27736
Search for supersymmetry and leptoquark states at FNAL
[DE95-003381] p 2410 N95-27871
A study of events with large total transverse energy produced in proton-antiproton collisions at (radical)s = 1.8 TeV
[DE95-003382] p 2410 N95-27872
Beam-beam interaction working group summary
[DE95-007824] p 2422 N95-28123
Some aspects of the OZI-rule violation in the reaction anti-pp yields phi pi(0)
[DE95-608853] p 2415 N95-28245
Situation in study of electric polarizability and mean square charge radius of the neutron
[DE95-608869] p 2415 N95-28247
The Bremsstrahlung of soft gamma-quanta created by elastic pp- and np-scatterings and the dibaryon resonance problem
[DE95-608870] p 2415 N95-28248

ELEMENTARY PARTICLES
Extended BRST symmetry for the relativistic particle with curvature
[DE95-608799] p 2406 N95-27309
Field theory of point-like systems with higher-order derivatives
[DE95-608800] p 2448 N95-27310
N. N. Bogolyubov and particle physics
[DE95-608794] p 2448 N95-27447
The 1993 European school of high-energy physis
[DE95-610196] p 2421 N95-28040

ELLIPSES
An ugly duckling becomes a swan (hor ellipsis): How an organization becomes customer focused through listening
[DE95-004974] p 2454 N95-27461

ELLIPSOMETRY
Materials, structures, and devices for high-speed electronics
[NASA-CR-197815] p 2260 N95-26816
The use of electrochemistry and ellipsometry for identifying and evaluating corrosion on aircraft
[AD-A288536] p 2125 N95-27186
Ambient-pressure silica aerogel films
[DE95-008161] p 2237 N95-28090
New developments for sol-gel film and fiber processing
[DE95-008175] p 2240 N95-28404

ELLIPTIC DIFFERENTIAL EQUATIONS
Introduction to multigrid methods
[NASA-CR-195045] p 2388 N95-26395

ELLIPTICAL GALAXIES
Molecular cloud content of early-type galaxies. V. CO in elliptical galaxies
[PB95-185153] p 2461 N95-27320

ELLIPTICAL ORBITS
Kepler Equation solver p 2147 N95-27767

EMBEDDING
Contribution to the optimal shape design of two-dimensional internal flows with embedded shocks
[NASA-CR-195062] p 2389 N95-26672
Atomistic calculations of hydrogen interactions with Ni3Al grain boundaries and Ni/Ni/Ni3Al interfaces
[DE95-006497] p 2408 N95-27534
Pulsed laser deposition of zeolitic membranes
[DE95-006274] p 2298 N95-28124

EMBRITTLEMENT
Materials considerations for molten salt accelerator-based plutonium conversion systems
[DE95-006743] p 2217 N95-27544
Effects of hydrogen on carbon steels at the Multi-Function Waste Tank Facility
[DE95-007194] p 2219 N95-28005
Gamma ray-induced embrittlement of pressure vessel alloys
[DE95-007133] p 2220 N95-28072

EMERGENCIES
Application of a Geographic Information System for radiologic emergency response
[DE95-007624] p 2455 N95-28113

EMISSION
Photon rockets and gravitational radiation
[PB95-190161] p 2397 N95-28174
A black carbon emission data base for atmospheric chemistry and climate studies
[DE95-006436] p 2332 N95-28662

EMISSION SPECTRA
FTIR measurements of thermal infrared sky radiance and transmission
[DE95-003642] p 2334 N95-26436
Measurement of N2(+) mobility He via Fourier transform emission spectroscopy
[AD-A289266] p 2404 N95-26979
Overview of the observations of symbiotic stars
p 2460 N95-27076
Analytical spectroscopy
[DE95-607896] p 2203 N95-27200
Superior catalysts for selective catalytic reduction of nitric oxide
[DE95-007903] p 2205 N95-27691
Evaluation of a conductive polymer-based sensor for detection of hydrazines at the part-per-billion level
p 2173 N95-28309
A continuous emissions monitor for airborne metals
p 2174 N95-28313

EMISSIVITY
Remote measurement of ground temperature and emissivity
[DE95-008055] p 2314 N95-28053

EMITTANCE
Coupling in the Tevatron
[DE95-005129] p 2421 N95-27531
Observation of asymmetrical two-cone Vavilov-Cherenkov radiation in biaxial crystal of triglycinesulphate emitted by 658 MeV protons passing along bi normal
[DE94-629017] p 2441 N95-27867
Burst of energetic ions from reversed field pinch plasma
[DE94-765447] p 2432 N95-27870
Positron microscopy
[DE95-007042] p 2410 N95-27874
Gamma ray-induced embrittlement of pressure vessel alloys
[DE95-007133] p 2220 N95-28072

EMITTERS
Heterostructures and infrared emitters with compressed InAsSb layers
[DE95-008157] p 2446 N95-28399

EMULSIONS
Application of bacterial bioemusifiers to in situ maintenance of oil/water separators
p 2179 N95-27120

ENCAPSULATING
Parallelism detection and scheduling strategies for reliable and efficient execution on multicomputers
[AD-A288370] p 2376 N95-26471

END EFFECTORS
Multi-agent perception for Human/Robot interaction: A framework for intuitive trajectory modification
[AD-A289399] p 2359 N95-26884
Design, testing and evaluation of latching end effector
p 2155 N95-27261
Some mechanical design aspects of the European Robotic Arm p 2155 N95-27262
Development and testing of the rack insertion device
p 2158 N95-27289

END-TO-END DATA SYSTEMS
Performance modeling of hyperspectral imaging sensors for atmospheric studies
[AD-A289017] p 2289 N95-26461

ENERGETIC PARTICLES
Ionizing radiation measurements on LDEF: A0015 Free flyer biostack experiment
[NASA-CR-196603] p 2202 N95-27168
Energetic particle destabilization of shear Alfven waves in stellarators and tokamaks
[DE95-006393] p 2431 N95-27419

ENERGY
A new method of evaluating the explicit magnetic-state-dependent energy in semi-empirical calculations of iron
[AD-A289098] p 2399 N95-27398

ENERGY BUDGETS
Measurement and analysis of the surface energy budget for ARM field experiments
[DE95-007646] p 2338 N95-28114

ENERGY CONSERVATION
Rarefied gas effects on aerobraking/reentry vehicles with wakes
[NASA-CR-196586] p 2164 N95-27093
Investigation on working out the global regeneration plan
[DE95-759246] p 2329 N95-27938
Investigation on energy conversion technology using biochemical reaction elements, 2
[DE95-759250] p 2321 N95-27940
Electric vehicle activities
[DE95-006648] p 2267 N95-28105

ENERGY CONSUMPTION
Fabrication of long wavelength array by in-situ molecular beam epitaxy
[AD-A288599] p 2423 N95-26679
Novel field effect transistors for low power electronics
[AD-A288650] p 2262 N95-27096
Performance of a stand-alone wind-electric ice maker for remote villages
[DE95-004006] p 2320 N95-27475
Survey on bio-chemical complex harmonized with global environment
[DE95-759252] p 2331 N95-28535
Novel field effect transistors for low power electronics
[AD-A289929] p 2271 N95-28629

ENERGY CONVERSION
Investigation on energy conversion technology using biochemical reaction elements, 2
[DE95-759250] p 2321 N95-27940

ENERGY CONVERSION EFFICIENCY
Solar concentrator technology development for space based applications, volume 1
[NASA-CR-197723] p 2319 N95-27193
NQR-NMR studies of higher alcohol synthesis Cu-Co catalysts
[DE95-007926] p 2205 N95-27680

ENERGY DISSIPATION
Photoacoustic chambers for studying solids and gases: Theory and practical examples
[IFTR-39/1994] p 2143 N95-26837
Energy-measuring resistor bank
[AD-D017392] p 2271 N95-28613

ENERGY DISTRIBUTION
A study of events with large total transverse energy produced in proton-antiproton collisions at (radical)s = 1.8 TeV
[DE95-003382] p 2410 N95-27872

ENERGY GAPS (SOLID STATE)
Optical features of nanosize iron and molybdenum sulfide clusters
[DE95-005417] p 2202 N95-27136
Model of a single impurity in a wide bandgap semiconductor describing electric field screening
[AD-A289322] p 2264 N95-27296

ENERGY LEVELS
Electronic characterization of defects in narrow gap semiconductors: Comparison of electronic energy levels and formation energies in mercury cadmium telluride, mercury zinc telluride, and mercury zinc selenide
[NASA-CR-197835] p 2437 N95-26780
Numerical study of the singlet-triplet model for cuprate superconductors
[DE95-609438] p 2440 N95-27712
Electron spectroscopy studies of argon K-shell excitation and vacancy cascades
[DE95-007096] p 2442 N95-27963

ENERGY METHODS
First-principles study of intermetallic phase stability in the ternary Ti-Al-Nb alloy system
[DE95-005259] p 2213 N95-27082

ENERGY OF FORMATION
Electronic characterization of defects in narrow gap semiconductors: Comparison of electronic energy levels and formation energies in mercury cadmium telluride, mercury zinc telluride, and mercury zinc selenide
[NASA-CR-197835] p 2437 N95-26780

ENERGY POLICY
Alternative fuels and vehicles choice model
[DE95-005695] p 2243 N95-27944

ENERGY REQUIREMENTS
Geothermal direct-heat utilization assistance
[DE95-007247] p 2319 N95-27236

ENERGY SOURCES
The U.S. Department of Energy Wind Turbine Development Program
[DE95-000292] p 2325 N95-28395

ENERGY SPECTRA
Wigner quantum oscillators. OSP (3/2) oscillators
[DE95-608756] p 2448 N95-27334
Landau quasi-energy spectrum destruction for an electron in both a static magnetic field and a resonant electromagnetic wave
[DE95-610176] p 2256 N95-27716

Electron spectroscopy studies of argon K-shell excitation and vacancy cascades
[DE95-007096] p 2442 N95-27963
A phenomenological treatment of rotating turbulence
[NASA-CR-198168] p 2288 N95-28228

ENERGY STORAGE
Feasibility of flywheel energy storage systems for applications in future space missions
[NASA-CR-195422] p 2316 N95-26393
A review of nickel hydrogen battery technology
[NASA-TM-106918] p 2167 N95-27177
Investigation of high-temperature superconducting flywheel energy storage devices
[DE95-759242] p 2320 N95-27936

ENERGY TECHNOLOGY
Molten Carbonate Fuel Cell (MCFC) product development test
[DE95-007345] p 2316 N95-26543
Solar concentrator technology development for space based applications, volume 1
[NASA-CR-197723] p 2319 N95-27193
Parallel plasma fluid turbulence calculations
[DE95-006741] p 2431 N95-27537
Current status of environmental, health, and safety issues of lithium polymer electric vehicle batteries
[DE95-004005] p 2265 N95-27719
Investigation on technology for increasing the biological CO2 sink and technology for CO2 fixation and reutilization
[DE95-759251] p 2329 N95-27941
Analysis methods for wind turbine control and electrical system dynamics p 2273 N95-27984
Variable speed generator technology options for wind turbine generators p 2273 N95-27988
Transportation R and D included in thermal and mechanical sciences program
[DE95-008275] p 2303 N95-28070
SIHTI 2: Energy and environmental technology. Yearbook 1993 of the research programme
[DE95-755135] p 2331 N95-28202
Review and analysis of the 1980-1989 biomass thermochemical conversion program
[DE95-000287] p 2325 N95-28394

ENERGY TRANSFER
Energy transfer from excited nitrenes at high density
[AD-A288352] p 2403 N95-26466
Statistical model for molecular internal energy exchange in DSMC method for rarefied flow analysis
[ISAS-R-654] p 2274 N95-26741
Energy transfer in real and artificial photosynthetic systems
[DE95-005824] p 2351 N95-27948
Bubble chamber spectroscopy for chemical analysis: A new concept
[DE95-006350] p 2209 N95-28088
A phenomenological treatment of rotating turbulence
[NASA-CR-198168] p 2288 N95-28228
Time-resolved FTIR emission studies of laser photofragmentation and radical reactions
[DE95-008125] p 2300 N95-28398

ENGINE AIRFRAME INTEGRATION
Development of an upwind, finite-volume code with finite-rate chemistry
[NASA-CR-197747] p 2121 N95-26760
Performance study for inlet installations
[NASA-CR-189714] p 2140 N95-28227

ENGINE CONTROL
Prevention and control of inlet unstart using an SR-71 simulation p 2119 N95-26948

ENGINE DESIGN
Experiment on a rectangular cross section scramjet combustor. 2: Effects of fuel injector geometry
[NAL-TR-1220] p 2139 N95-26600
Prevention and control of inlet unstart using an SR-71 simulation p 2119 N95-26948
Preliminary results and research capabilities of a new jet facility at the University of Kansas
p 2119 N95-26951
Application of CFD to the analysis and design of high-speed inlets
[NASA-CR-198574] p 2279 N95-27240
Comparison of numerical results and multicavity purge and rim seal data with extensions to dynamics
[NASA-TM-106685] p 2168 N95-27434
Composite intermediate case manufacturing scale-up for advanced engines p 2141 N95-28275

ENGINE INLETS
Characteristics of the turbine inlet temperature sensing circuit for the T56 turbo-prop engine
[DSTO-TR-0095] p 2139 N95-26424
Performance characterization of a highly-offset diffuser with and without blowing vortex generator jets
[AD-A289334] p 2122 N95-26901
Prevention and control of inlet unstart using an SR-71 simulation p 2119 N95-26948
Application of CFD to the analysis and design of high-speed inlets
[NASA-CR-198574] p 2279 N95-27240
Performance study for inlet installations
[NASA-CR-189714] p 2140 N95-28227
Experimental investigation of inlet-combustor isolators for a dual-mode scramjet at a Mach number of 4
[NASA-TP-3502] p 2140 N95-28343

ENGINE MONITORING INSTRUMENTS
Characteristics of the turbine inlet temperature sensing circuit for the T56 turbo-prop engine
[DSTO-TR-0095] p 2139 N95-26424

ENGINE NOISE
Aircraft noise prediction program theoretical manual: Rotorcraft System Noise Prediction System (ROTONET), part 4
[NASA-TM-83199-PT-4] p 2400 N95-26392

ENGINE PARTS
Electromechanical rotary actuator
p 2157 N95-27278
Solid state sintering of silicon nitride ARL-CR-114
[DE95-007291] p 2443 N95-28076
Composite intermediate case manufacturing scale-up for advanced engines p 2141 N95-28275
Application of fiber-reinforced bismaleimide materials to aircraft nacelle structures p 2137 N95-28278

ENGINE TESTS
High pressure Earth storable rocket technology program: Basic program
[NASA-CR-195449] p 2166 N95-26390
Effects of dust from storage heaters on ignition in scramjets
[NAL-TR-1234] p 2139 N95-26706
Prevention and control of inlet unstart using an SR-71 simulation p 2119 N95-26948

ENGINEERS
NASA/DOD Aerospace Knowledge Diffusion Research Project. Report 35: The use of computer networks in aerospace engineering
[NASA-CR-198170] p 2456 N95-28600

ENTRAINMENT
Research on combustion processes relevant to burners in HVAC systems
[PB95-179735] p 2208 N95-28006

ENTROPY
The surface of liquid He-4 at nonzero temperatures
[DE95-607841] p 2207 N95-27880

ENUMERATION
Flow cytometry as a means of detecting, enumerating and characterizing bacteria for monitoring of the environment
[AD-A288997] p 2326 N95-26610

ENVIRONMENT EFFECTS
Finding the forest in the trees. The challenge of combining diverse environmental data
[NASA-CR-197798] p 2326 N95-26362
Environmental effects on high energy density materials
[AD-A288296] p 2199 N95-26416
Environmental pollution-effects on national development
[DE95-600439] p 2326 N95-26639
Space environmental effect on solar cells: LDEF and other flight tests p 2326 N95-27649
Effects of the LDEF orbital environment on the reflectance of optical mirror materials
p 2428 N95-27651
Current status of environmental, health, and safety issues of lithium polymer electric vehicle batteries
[DE95-004005] p 2265 N95-27719
Evaluation and qualification of environmentally conscious manufacturing processes for commercial and military applications
[DE95-008520] p 2329 N95-27878
Research project on CO2-induced climate change
[DE95-008339] p 2330 N95-28084
Carbonaceous aerosols influencing atmospheric radiation: Black and organic carbon
[DE95-006437] p 2330 N95-28118
Towards the detection and attribution of an anthropogenic effect on climate
[DE95-008589] p 2331 N95-28157
Survey on bio-chemical complex harmonized with global environment
[DE95-759252] p 2331 N95-28535

ENVIRONMENT MANAGEMENT
Multimedia Environmental Pollutant Assessment System (MEPAS) application guidance. Guidelines for evaluating MEPAS input parameters for Version 3.1
[DE95-007525] p 2328 N95-27749
Implementing an integrated standards-based management system to ensure compliance at Los Alamos National Laboratory
[DE95-007873] p 2451 N95-28025

ENVIRONMENT MODELS
Quantitative modeling and analysis in environmental studies
[AD-A288451] p 2326 N95-26431

ENVIRONMENT POLLUTION
Quantitative modeling and analysis in environmental studies
[AD-A288451] p 2326 N95-26431
Environmental pollution-effects on national development
[DE95-600439] p 2326 N95-26639
Subsurface radar investigations at the Pegasus Glacial-ice Runway and Williams Field, McMurdo Station, Antarctica
[AD-A289323] p 2144 N95-27297
Multimedia Environmental Pollutant Assessment System (MEPAS) application guidance. Guidelines for evaluating MEPAS input parameters for Version 3.1
[DE95-007525] p 2328 N95-27749
Three-dimensional forecast models for emergency response management p 2172 N95-28303

ENVIRONMENT PROTECTION
Concurrent engineering research center
[NASA-CR-197726] p 2362 N95-26386
Electromagnetic devices and processes in environment protection
[AD-A288656] p 2141 N95-26487
Environmentally Benign Cleaning and Degreasing Technology: JANNAF Safety and Protection Subcommittee and Propellant Development and Characterization Subcommittee Joint Workshop
[CPIA-PUBL-611] p 2227 N95-27101
Cleanliness verification process at Martin Marietta Astronautics p 2165 N95-27104
Wipe solvent substitutions for 1,1,1-trichloroethane (TCA) and methyl ethyl ketone (MEK) at Hill Air Force Base p 2228 N95-27107
CO2 pellet blast cleaning and degreasing: The true environmentally benign technology
p 2229 N95-27109
Evaluations of the effectiveness of environmentally benign cleaning methodologies p 2230 N95-27115
Sceening, down selection, and implementation of environmentally compliant cleaning and insulation bonding for MNASA p 2165 N95-27124
Marshall Space Flight Center solid waste characterization and recycling improvement study
[NASA-CR-196594] p 2360 N95-27164
Community relations plan: Galena Airport and Camp ion Air Force Station, Alaska
[AD-A286722] p 2327 N95-27234
Application of modern diagnostic methods to environmental improvement
[DE95-005797] p 2330 N95-28119
SIHTI 2: Energy and environmental technology. Yearbook 1993 of the research programme
[DE95-755135] p 2331 N95-28202
The 1994 JANNAF Safety and Environmental Protection Subcommittee Meeting, volume 1
[CPIA-PUBL-614-VOL-1] p 2170 N95-28294
The importance of propulsion engineers in protecting the global environment p 2170 N95-28295
Three-dimensional forecast models for emergency response management p 2172 N95-28303
Commercial reformulation: An economic and environmentally neutral means of managing explosives and solid propellants p 2175 N95-28320
A comprehensive energetic materials resource recovery and recycling program p 2176 N95-28323
Cryogenic washout of solid rocket propellants
p 2176 N95-28324
Strategies for recycling CdTe photovoltaic modules
[DE95-006776] p 2325 N95-28517
A comparison of NH3 point monitoring and diode laser based path integrated measurements
[DE95-006892] p 2332 N95-28602

ENVIRONMENT SIMULATION
LDEF: 69 Months in Space. Third Post-Retrieval Symposium, part 3
[NASA-CP-3275-PT-3] p 2466 N95-27629
Exposure of LDEF materials to atomic oxygen: Results of EOIM 3 p 2210 N95-27633
Solid film lubricants and thermal control coatings flown aboard the EOIM-3 MDA sub-experiment
p 2242 N95-27640

ENVIRONMENT SIMULATORS
The value of simulation for training
[AD-A289174] p 2143 N95-26556

ENVIRONMENTAL CHEMISTRY
Cleanliness verification process at Martin Marietta Astronautics p 2165 N95-27104
Chemical engineering: Measurements for a competitive age
[NONP-NASA-VT-95-49098] p 2203 N95-27204

ENVIRONMENTAL CONTROL

International Space Station Alpha trace contaminant control subassembly life test report [NASA-TM-108488] p 2358 N95-26364

ENVIRONMENTAL MONITORING

Finding the forest in the trees. The challenge of combining diverse environmental data [NASA-CR-197798] p 2326 N95-26362

Using SCR methods to analyze requirements documentation [NASA-CR-197760] p 2365 N95-26668

Subsurface radar investigations at the Pegasus Glacial-ice Runway and Williams Field, McMurdo Station, Antarctica [AD-A289323] p 2144 N95-27297

Element material experiment by EFFU p 2145 N95-27667

Evaluation and qualification of environmentally conscious manufacturing processes for commercial and military applications [DE95-008520] p 2329 N95-27878

FY 1994 ambient air monitoring report for McMurdo Station, Antarctica [DE95-008565] p 2331 N95-28149

The 1994 JANNAF Safety and Environmental Protection Subcommittee Meeting, volume 1 [CPIA-PUBL-614-VOL-1] p 2170 N95-28294

OB/OD treatment: The effective use of measured field data and air modeling to support an environmental assessment p 2170 N95-28296

Use of mussels in biomonitoring of environmental impacts of propellants, projectiles, explosives, and pyrotechnics p 2170 N95-28298

Destruction of pyrotechnics manufacture wastewater treatment sludge by plasma arc pyrolysis p 2171 N95-28301

Three-dimensional forecast models for emergency response management p 2172 N95-28303

Prototype development and test results of a continuous ambient air monitoring system for hydrazine at the 110 ppb level p 2173 N95-28310

A comparison of NH3 point monitoring and diode laser based path integrated measurements [DE95-006892] p 2332 N95-28602

The Global Historical Climatology Network: A preview of version 2 [DE95-007003] p 2332 N95-28605

ENVIRONMENTAL QUALITY

Transparent access to distributed, heterogeneous environmental information systems [DE95-007268] p 2454 N95-27483

ENVIRONMENTAL SURVEYS

Multimedia Environmental Pollutant Assessment System (MEPAS) application guidance. Guidelines for evaluating MEPAS input parameters for Version 3.1 [DE95-007525] p 2328 N95-27749

ENVIRONMENTAL TESTS

Design and development of experimental facilities for short duration, low-gravity combustion and fire experiments [NASA-CR-195458] p 2244 N95-26709

The 1994 27th Annual NASA Aerospace Battery Workshop [NASA-CP-3292] p 2317 N95-26785

Air Force Ni-H2 cell test program: State of Charge test p 2272 N95-26789

Nickel metal hydride LEO cycle testing p 2272 N95-26791

Adiabatic charging of nickel-hydrogen batteries p 2272 N95-26795

Thermal control materials on EOIM-3 p 2242 N95-27639

Solid film lubricants and thermal control coatings flown aboard the EOIM-3 MDA sub-experiment p 2242 N95-27640

Evaluation of space environmental effects on metals and optical thin films on EOIM-3 p 2210 N95-27641

Analysis of selected specimens from the STS-46 Energetic Oxygen Interaction with Materials-3 experiment p 2210 N95-27642

Effects of low earth orbit on the optical performance of multi-layer enhanced high reflectance mirrors p 2428 N95-27652

Space Station as a Long Duration Exposure Facility p 2166 N95-27663

A Materials Exposure Facility p 2166 N95-27664

Use of mussels in biomonitoring of environmental impacts of propellants, projectiles, explosives, and pyrotechnics p 2170 N95-28298

ENZYME ACTIVITY

Microbial treatment for shipboard collection, hold ing, and transfer system tanks p 2179 N95-27119

ENZYMES

Non-covalent immobilization of proteins and enzymes on polymerized lipid assemblies [AD-A288234] p 2225 N95-26526

DNA denaturation through a model of the partition points on a one-dimensional lattice [DE95-607909] p 2439 N95-27201

A correlated Walks' theory for DNA denaturation [DE95-607910] p 2444 N95-28112

Biodegradation of nitrate esters p 2171 N95-28299

EOS DATA AND INFORMATION SYSTEM

Development and analysis of SCR requirements tables for system scenarios [NASA-CR-197769] p 2367 N95-26802

EPHEMERIDES

Operational improvements of long-term predicted ephemerides of the Tracking and Data Relay Satellites (TDRSs) p 2147 N95-27769

EPITAXY

Electrocrystallization of an ordered organic monolayer: Selective epitaxial growth of beta(ET)213 ongraphite [AD-A288942] p 2178 N95-26569

Preferentially etched epitaxial liftoff of InP material [NASA-CASE-LEW-15760-1] p 2235 N95-27503

Atomic layer epitaxy of group 4 materials: Surface processes, thin films, devices and their characterization [AD-A289092] p 2446 N95-28327

Basic and applied research in the field of electronics and communications [AD-A291727] p 2270 N95-28512

The in situ observation of epitaxial diamond thin film nucleation and growth using emission electron microscopy [AD-A289841] p 2447 N95-28618

EPOXY COMPOUNDS

Stress transfer from axially loaded fiber to matrix in a microcomposite [DE95-007366] p 2183 N95-28043

EPOXY MATRIX COMPOSITES

Characterization of fatigue behavior of 2-D woven fabric reinforced ceramic matrix composite at elevated temperature [AD-A289423] p 2181 N95-26886

Service tough composite structures using the Z-direction reinforcement process p 2185 N95-28272

Failure analysis of thick composite cylinders under external pressure p 2187 N95-28284

Mechanical properties of triaxially braided composites: Experimental and analytical results p 2189 N95-28423

EPOXY RESINS

Interfacial mobility and its effect on flexural strength and fracture toughness in glass-fiber fabric reinforced epoxy laminates [AD-A288344] p 2180 N95-26572

Scarf joint technique with cocured and precured patches for composite repair p 2135 N95-27524

EQUATIONS OF MOTION

Optimization of a nutation damper attached to a spin-stabilized satellite [AD-A289424] p 2162 N95-26887

The gluon propagator in non-Abelian Weizsaecker-Williams fields [DE95-006877] p 2449 N95-27547

EQUATIONS OF STATE

Extended equation-of-state for dichlorodifluoromethane (CCl2F2) [AD-A288885] p 2177 N95-26434

Material modeling in the CRALE code. Users' manual [AD-A288988] p 2178 N95-26712

SUPG finite numerical element solutions for non-compressible Navier-Stokes equation sets [AD-A289600] p 2274 N95-26718

EQUILIBRIUM FLOW

Normal modes and continuous spectra [DE95-006166] p 2287 N95-28055

EQUIPMENT

Cleaning of parts for new manufacturing and parts rebuilding p 2231 N95-27123

EQUIPMENT SPECIFICATIONS

Next generation controller specification for an open systems architecture standard - overview [AD-A289507] p 2368 N95-26853

Dynamically timed electric motor [NASA-CASE-MFS-28958-1] p 2261 N95-26890

A cryogenic scan mechanism for use in Fourier transform spectrometers p 2158 N95-27287

Next generation controller specification for an open systems architecture standard [AD-A289567] p 2375 N95-28647

EQUIVALENCE

Nonexistence of bilipschitz parameterizations and geometric problems about A(sub infinity) weights [PB95-185187] p 2396 N95-26538

EQUIVALENT CIRCUITS

Survey on step recovery diode and its applications [PB95-184974] p 2260 N95-26646

EROSION

Faraday screen sputtering on TPX [DE95-008347] p 2434 N95-28224

ERROR ANALYSIS

The attenuation of microwave radiation by fog and rain [AD-A288326] p 2249 N95-26562

Adaptive finite element method I: Solution algorithm and computational examples [AD-A288979] p 2389 N95-26609

Using SCR methods to analyze requirements documentation [NASA-CR-197760] p 2365 N95-26668

ROC analysis of IR segmentation techniques [AD-A289252] p 2424 N95-26971

Getting it right, making it better [NONP-NASA-VT-95-49118] p 2451 N95-27206

Analysis of filter tuning techniques for sequential orbit determination p 2146 N95-27764

An MME-based attitude estimator using vector observations p 2148 N95-27775

Error analysis of the quartic nodal expansion method for slab geometry [DE95-007373] p 2412 N95-28045

Bearing defect signature analysis using advanced nonlinear signal analysis in a controlled environment [NASA-TM-108491] p 2304 N95-28364

ERROR CORRECTING CODES

A comparison of error categorization schemes for use in software system safety programs [AD-A288741] p 2371 N95-27251

Neural network error compensation of machine tools [AD-A289300] p 2387 N95-28217

ERROR DETECTION CODES

ALLIANCE: An architecture for fault tolerant, cooperative control of heterogeneous mobile robots [DE95-007374] p 2387 N95-28536

ERRORS

The fBm Interpolator [AD-A288996] p 2388 N95-26459

Nonlinear scalespace via hierarchical statistical modeling [AD-A289057] p 2394 N95-26478

Compiler-assisted debugging and multiple instruction retry [NASA-CR-197729] p 2365 N95-26628

Preliminary heavy-light decay constants from the MILC Collaboration [DE95-005685] p 2409 N95-27552

Error analysis of the quartic nodal expansion method for slab geometry [DE95-007373] p 2412 N95-28045

A new algorithm for generating highly accurate benchmark solutions to transport test problems [DE95-007397] p 2373 N95-28047

Neural network error compensation of machine tools [AD-A289300] p 2387 N95-28217

ERS-1 (ESA SATELLITE)

Speckle spectrum of the ERS-1 wavemode product [PB95-196564] p 2315 N95-28180

ESA SATELLITES

Altimeter analysis of ocean currents [AD-A290167] p 2315 N95-28392

ESSENTIALLY NON-OSCILLATORY SCHEMES

A numerical method for solving the three-dimensional parabolized Navier-Stokes equations [NASA-CR-198159] p 2287 N95-27917

ESTERS

Evaluation of high ester content PAO based single hydraulic fluid in high humidity conditions [AD-A289374] p 2233 N95-27324

Use of CTFE as an additive to enhance fire resistance of single hydraulic fluid [AD-A289377] p 2233 N95-27325

ESTIMATES

Using machine learning to derive efficient cost and performance estimates in VLSI CAD designs [AD-A288254] p 2363 N95-26408

Satellite surface material composition from synthetic spectra [AD-A289236] p 2163 N95-26963

Design, construction, test and evaluation of a frequency scanning radiometer for measuring oil slick thicknesses [AD-A290040] p 2293 N95-28389

ESTIMATING

Filtered kernel density estimation [AD-A288293] p 2394 N95-26413

SeaWiFS technical report series. Volume 26: Results of the SeaWiFS Data Analysis Round-Robin, July 1994 (DARR-1994) [NASA-TM-104566-VOL-26] p 2345 N95-26430

The fBm Interpolator [AD-A288996] p 2388 N95-26459

Embedology and neural estimation for time series prediction [AD-A289312] p 2394 N95-26892

ROC analysis of IR segmentation techniques [AD-A289252] p 2424 N95-26971

Multiple model adaptive estimation and head motion tracking in a virtual environment: An engineering approach
[AD-A289299] p 2359 N95-27046
Characterization of defects in deuterium-implanted beryllium
[DE95-005688] p 2217 N95-27553
An automated method of tuning an attitude estimator
p 2148 N95-27774
Non-linear resistive grid kernel estimator useful in single feature, two-class pattern classification
[AD-D017394] p 2271 N95-28614
ETCHING
Chemical physics of uniform cyclic etching
[AD-A288975] p 2404 N95-26574
Preferentially etched epitaxial liftoff of InP material
[NASA-CASE-LEW-15760-1] p 2235 N95-27503
Non-destructive inter-level dielectric via in-line process monitoring by atomic force microscopy
[DE95-008516] p 2267 N95-28146
ETHERS
Small angle neutron scattering study of the micelle structure of amphiphilic block copolymers
[DE95-006625] p 2234 N95-27486
ETHYL ALCOHOL
Comparison of bridged polysilsesquioxane xerogels prepared from methoxy- and ethoxy-silyl monomers
[DE95-005422] p 2240 N95-28532
ETHYL COMPOUNDS
A summary of ODS replacement technologies at Litton Poly-Scientific p 2228 N95-27105
Ethyl lactate as a solvent alternative for cleaning metal parts p 2229 N95-27112
ETHYLENE
Use of CTFE as an additive to enhance fire resistance of single hydraulic fluid
[AD-A289377] p 2233 N95-27325
EUCLIDEAN GEOMETRY
Compactification of moduli spaces of monopoles
[PB95-185179] p 2388 N95-26515
Nonexistence of bilipschitz parameterizations and geometric problems about A(sub infinity) weights
[PB95-185187] p 2396 N95-26538
EULER EQUATIONS OF MOTION
Computational fluid dynamics and transonic flow
[AD-A288962] p 2273 N95-26405
A fixed time performance evaluation of parallel CFD applications
[DE94-014240] p 2273 N95-26445
The method of space-time conservation element and solution element-applications to one-dimensional and two-dimensional time-marching flow problems
[NASA-TM-106915] p 2389 N95-26663
Contribution to the optimal shape design of two-dimensional internal flows with embedded shocks
[NASA-CR-195062] p 2389 N95-26672
Flow control
[AD-A289262] p 2279 N95-27197
A new angle on the Euler angles
p 2153 N95-27800
Evaluation of a doubly-swept blade tip for rotorcraft noise reduction
[NASA-CR-189677] p 2402 N95-28264
EULER-LAGRANGE EQUATION
The surface of liquid He-4 at nonzero temperatures
[DE95-607841] p 2207 N95-27880
EURECA (ESA)
LDEF: 69 Months in Space. Third Post-Retrieval Symposium, part 3
[NASA-CP-3275-PT-3] p 2466 N95-27629
EUROPE
Prediction of rain attenuation and total atmospheric attenuation for low-availability satellite communications in Europe
[PB95-184925] p 2252 N95-26908
JPRS report: Science and technology. Central Eurasia
[JPRS-UST-95-016] p 2262 N95-27170
JPRS report: Science and technology. Central Eurasia
[JPRS-UST-95-014] p 2145 N95-27171
JPRS report: Science and technology. Central Eurasia
[JPRS-UST-95-019] p 2270 N95-28565
EUROPEAN SPACE AGENCY
Altimeter analysis of ocean currents
[AD-A290167] p 2315 N95-28392
EUROPIUM COMPOUNDS
Muon spin relaxation in ferromagnets: Theoretical results for paramagnetic EuO and EuS
[PB95-192860] p 2418 N95-28641
EUROPIUM ISOTOPES
Determination of the first hydrolysis constant of Europium (3) in 3 M of ionic strength
[DE95-607912] p 2405 N95-27211
EUTECTICS
Electrolyte effects in Li(Si)/FeS2 thermal batteries
[DE95-001614] p 2264 N95-27474
EVALUATION
Performance evaluation of a new parallel preconditioner
[AD-A288563] p 2376 N95-26529
Overview of through-thickness test methods for polymer matrix composites
[PB95-190112] p 2227 N95-26747
Evaluation of high ester content PAO based single hydraulic fluid in high humidity conditions
[AD-A289374] p 2233 N95-27324
Engineered materials for appliation in severe metallurgical environments: Tantalum-carbon alloy development
[DE95-006866] p 2216 N95-27488
Evaluation of an Air Force Information Resources Management (IRM) overview course
[AD-A288746] p 2456 N95-28587
EVAPORATION
FREZCHEM: A chemical-thermodynamic model for aqueous solutions at subzero temperatures
[AD-A288456] p 2200 N95-26432
The effect of infrared sea surface temperature measurements on evaporation duct height estimation
[AD-A289045] p 2346 N95-26477
A numerical model to predict the fate of jettisoned aviation fuel
[AD-A289336] p 2242 N95-26842
Transient studies of G-induced capillary dryout and rewet p 2281 N95-27351
Engineering photochemical smog through convection towers
[DE95-007727] p 2328 N95-27686
On ionic charge distributions of heavy evaporation residues passing through a carbon foil
[DE94-629016] p 2414 N95-28184
EVAPORATION RATE
Wipe solvent substitutions for 1,1,1-trichloroethane (TCA) and methyl ethyl ketone (MEK) at Hill Air Force Base p 2228 N95-27107
EVAPORATORS
Experimental investigation of the effects of relative physical orientation between evaporator and condenser for a loop heat pipe
[AD-A289248] p 2277 N95-26968
EVASIVE ACTIONS
Severe weather guide mediterranean
[AD-A289829] p 2344 N95-28577
EVOLUTION (DEVELOPMENT)
A model of bubble evolution during decompression based on a Monte Carlo simulation of inert gas diffusion
[AD-A289400] p 2353 N95-26885
The evolution and impact of PCS technology
[AD-A288606] p 2255 N95-27249
EXCIMER LASERS
Swords to plowshares: Shock wave applications to advanced lithography
[DE95-008154] p 2299 N95-28223
EXCITATION
Photo and thermal excitation of surface chemistry on model catalyst surfaces
[AD-A288541] p 2200 N95-26528
Toward coherent excitation: Development of a single-source pump for the rubidium hyperfine ground state doublet
[AD-A289413] p 2295 N95-27132
Excited Charm States
[DE95-005749] p 2409 N95-27747
Recent neutron scattering results on high-temperature superconductors
[DE95-007028] p 2413 N95-28066
Optical design and performance of the inelastic scattering beamline at the National Synchrotron Light Source
[DE95-007679] p 2422 N95-28195
Resonant coherent excitation of N6(+) and Mg11(+) in planar channeling: Anisotropies in ionization probabilities and X-ray emission
[DE95-006732] p 2417 N95-28595
EXCITONS
Nonlinear dynamics of a coherent polariton-biexciton system
[DE95-609150] p 2417 N95-28607
EXHAUST DIFFUSERS
Performance characterization of a highly-offset diffuser with and without blowing vortex generator jets
[AD-A289334] p 2122 N95-26901
EXHAUST EMISSION
Bow shock data analysis
[AD-A288432] p 2429 N95-26800
CO2 pellet blast cleaning and degreasing: The true environmentally benign technology
p 2229 N95-27109
Reducing cold-start emissions by catalytic converter thermal management
[DE95-000256] p 2327 N95-27540
Fracture testing and analysis of adhesively bonded joints for automotive applications
[DE95-007024] p 2184 N95-28207
Destruction of pyrotechnics manufacture wastewater treatment sludge by plasma arc pyrolysis
p 2171 N95-28301
A new method for measuring hypergol scrubber emissions p 2174 N95-28312
EXHAUST GASES
Plume measurements with the T5 xenon ion thruster
[AD-A288697] p 2167 N95-26489
Soot particle density determination from a laser extinction multipass technique
[AD-A288551] p 2423 N95-26532
CO2 pellet blast cleaning and degreasing: The true environmentally benign technology
p 2229 N95-27109
Reducing cold-start emissions by catalytic converter thermal management
[DE95-000256] p 2327 N95-27540
Pumping characteristics of a cryopump with Ar sorbent in He and in D2/He mixture
[DE95-007049] p 2302 N95-27875
EXHAUST NOZZLES
Preliminary results and research capabilities of a new jet facility at the University of Kansas
p 2119 N95-26951
EXOBIOLOGY
Space Science Division cumulative bibliography: 1989-1994
[NASA-TM-110355] p 2457 N95-28677
EXPERIMENT DESIGN
Micron Accuracy Deployment Experiment (MADE), phase A. Volume 1
[NASA-CR-197792] p 2144 N95-26426
Balanced on air aircraft
[AD-D017251] p 2129 N95-26537
The design and implementation of the Military Applications of Shiptracks experiment on Space Transportation System - 65
[AD-A288488] p 2160 N95-26634
Comparison of the activities of fine-particle size catalysts
[DE95-004773] p 2203 N95-27423
Weightless Environment Training Facility (WETF) materials coating evaluation, volume 3
[NASA-CR-188366-VOL-3] p 2239 N95-28387
EXPERIMENTATION
A brief history of laser guided lightning discharge models and experiments
[AD-A289448] p 2295 N95-27022
General relativity and experiment
[PB95-192894] p 2450 N95-28664
EXPERT SYSTEMS
Digital systems validation. Chapter 20 Artificial Intelligenge with applications for aircraft. Handbbook, volume 2
[AD-A288492] p 2380 N95-26638
Generic satellite monitoring expert system
[AD-A289209] p 2163 N95-26987
Generalized probabilistic reasoning and empirical studies on computational efficiency and scalability
[AD-A289185] p 2395 N95-27016
The 1995 Goddard Conference on Space Applications of Artificial Intelligence and Emerging Information Technologies
[NASA-CP-3296] p 2382 N95-27375
Applying AI tools to operational space environmental analysis p 2382 N95-27376
Building an adaptive agent to monitor and repair the electrical power system of an orbital satellite
p 2383 N95-27380
A rule-based shell to hierarchically organize HST observations p 2384 N95-27384
Lessons learned from the introduction of autonomous monitoring to the EUVE science operations center
p 2385 N95-27393
Development and implementation of an electronic library tour for the NASA Langley Technical Library
[NASA-TM-110619] p 2455 N95-27701
EXPLORATION
TOPS: Toward Other Planetary Systems. A report by the solar system exploration division
[NASA-TM-110609] p 2464 N95-28009
EXPLORER SATELLITES
Development of the solar array deployment and drive system for the XTE spacecraft p 2158 N95-27284
Development of a Robust star identification technique for use in attitude determination of the ACE spacecraft
p 2149 N95-27777
Optimal attitude maneuver execution for the Advanced Composition Explorer (ACE) mission
p 2149 N95-27778
SAMPEX special pointing mode p 2149 N95-27780

Use of nonlinear identification in robust attitude and attitude rate estimation for SAMPEX p 2149 N95-27781

EXPLOSIVE DEVICES

The protection of electro-explosive devices (EEDs) and electronics from electrostatic discharge (ESD) hazards [DSTO-TR-0100] p 2258 N95-28568

EXPLOSIVES

A compatibility study of containment materials in FEFO, bis-(2-fluoro-2,2-dinitroethyl) formal [DE95-007548] p 2206 N95-27750

Use of mussels in biomonitoring of environmental impacts of propellants, projectiles, explosives, and pyrotechnics p 2170 N95-28298

Commercial reformulation: An economic and environmentally neutral means of managing explosives and solid propellants p 2175 N95-28320

Alternate use of rocket propellants as ingredients in commercial watergel explosives p 2176 N95-28321

EXPONENTIAL FUNCTIONS

A mathematical framework for an improved search model [AD-A288858] p 2358 N95-26552

EXPOSURE

A practical approach to soil remediation p 2232 N95-27125

The response of hydrotalcite coated aluminum to sealing with transition metal salt solutions [DE95-004767] p 2234 N95-27460

Adhesively bonded composite patch repair of cracked aluminum alloy structures p 2132 N95-27507

Evaluation of Oxygen Interactions with Materials 3: Mission and induced environments p 2210 N95-27631

Exposure of LDEF materials to atomic oxygen: Results of EOIM 3 p 2210 N95-27633

Inflight resistance measurement on high-T(sub c) superconducting thin films exposed to orbital atomic oxygen on CONCAP-2 (STS-46) p 2272 N95-27635

LEO degradation of graphite and carbon-based composites aboard Space Shuttle Flight STS-46 p 2199 N95-27636

Orbital atomic oxygen effects on materials: An overview of MSFC experiments on the STS-46 EOIM-3 p 2419 N95-27637

Effects of atomic oxygen on polymeric materials flown on EOIM-3 p 2242 N95-27638

Analysis of selected specimens from the STS-46 Energetic Oxygen Interaction with Materials-3 experiment p 2210 N95-27642

BMDO materials testing in the EOIM-3 experiment p 2211 N95-27644

Effects of long term space environment exposure on optical substrates and coatings p 2428 N95-27653

Space environmental effects observed on the Hubble Space Telescope p 2242 N95-27655

From LDEF to a national Space Environment and Effects (SEE) program: A natural progression p 2145 N95-27657

A Materials Exposure Facility p 2166 N95-27664

Acute and subacute toxicity of ammonium dinitramide (ADN) p 2175 N95-28318

Toxicity assessment of liquid propellant XM46 p 2175 N95-28319

Weightless Environment Training Facility (WETF) materials coating evaluation, volume 1 [NASA-CR-188366-VOL-1] p 2239 N95-28385

Weightless Environment Training Facility (WETF) materials coating evaluation, volume 2 [NASA-CR-188366-VOL-2] p 2239 N95-28386

Weightless Environment Training Facility (WETF) materials coating evaluation, volume 3 [NASA-CR-188366-VOL-3] p 2239 N95-28387

EXTERNAL TANKS

Debris/Ice/TPS assessment and integrated photographic analysis of Shuttle mission STS-67 [NASA-TM-110651] p 2160 N95-27238

EXTINCTION

Natural aerosol extinction module: XSCALE 1992 user's guide [AD-A289029] p 2340 N95-26463

Computation of electromagnetic scattering parameters for lognormal distributions of magnetic spheres: Theory and algorithms [AD-A289672] p 2250 N95-26759

EXTRACTION

Processing of wide-angle synthetic aperture radar signals for detection of obscured ground targets [AD-A289243] p 2253 N95-26976

Moment and hypergeometric filters for high precision computation of focus, stereo and optical flow [AD-A289293] p 2425 N95-27038

Junkyard chemistry p 2227 N95-27102

Design considerations in supercritical fluid technology p 2232 N95-27126

The experience of CF Technologies, Inc. (CF Tech) in critical fluid processing p 2232 N95-27128

Investigation on working out the global regeneration plan [DE95-759246] p 2329 N95-27938

Novel field effect transistors for low power electronics [AD-A289929] p 2271 N95-28629

EXTRAPOLATION

Depth migration in transversely isotropic media with explicit operators [DE95-007670] p 2337 N95-27442

Spin-density-wave magnetism in dilute copper-manganese alloys [DE95-005121] p 2215 N95-27462

Bases for extrapolating materials durability in fuel storage pools [DE95-007748] p 2222 N95-28129

The high energy behavior of the forward scattering parameters -- (sigma)(sub tot), (rho), and B [DE95-007075] p 2415 N95-28210

EXTRATERRESTRIAL MATTER

The second coming of cold dark matter? [DE95-005156] p 2462 N95-27445

EXTREME ULTRAVIOLET EXPLORER SATELLITE

Experience from the in-flight calibration of the Extreme Ultraviolet Explorer (EUVE) and Upper Atmosphere Research Satellite (UARS) fixed head star trackers (FHSTs) p 2149 N95-27779

EXTREME ULTRAVIOLET RADIATION

Specification of the figure and finish of EUV mirrors in terms of performance requirements, revised Nov. 1994 [DE95-005689] p 2425 N95-27490

Plasma properties and magnetic field structure of the solar corona, based on coordinated Max 1991 observations from SERTS, the VLA, and magnetographs [NASA-CR-198592] p 2464 N95-27858

Swords to plowshares: Shock wave applications to advanced lithography [DE95-008154] p 2299 N95-28223

EXTREMELY HIGH FREQUENCIES

Prediction of rain attenuation and total atmospheric attenuation for low-availability satellite communications in Europe [PB95-184925] p 2252 N95-26908

Ring-plane traveling-wave tube slow-wave circuit design simulations at V-Band frequencies [NASA-TM-106949] p 2371 N95-27370

Search for molecular absorptions with the Fourier Transform Spectrometer [NASA-CR-198648] p 2462 N95-28222

Design, construction, test and evaluation of a frequency scanning radiometer for measuring oil slick thicknesses [AD-A290040] p 2293 N95-28389

EXTREMELY LOW FREQUENCIES

The ELF controversy [DE95-008283] p 2256 N95-28407

EXTRUDING

Ductile - ductile beryllium aluminum metal matrix composite manufactured by extrusion [AD-A289519] p 2181 N95-26848

The development of mechanical strength in a ceramic material during firing [DE95-004925] p 2234 N95-27476

EYE MOVEMENTS

Long-range eye tracking: A feasibility study [DE95-008587] p 2357 N95-28176

F

F REGION

A study of magnetic activity effects on the thermospheric winds in the low ionosphere [AD-A288677] p 2334 N95-26488

An improved model of high-latitude f-region scintillation (WBMOD version 13) [AD-A288558] p 2334 N95-26520

F 2 REGION

Variability study of foF2 for an equatorial station [DE95-608080] p 2337 N95-27157

F-14 AIRCRAFT

Navy composite maintenance and repair experience p 2193 N95-28446

F-15 AIRCRAFT

Development of a nonlinear simulation for the McDonnell Douglas F-15 Eagle with a longitudinal TECS control-law [AD-A288610] p 2128 N95-26481

Development of a TECS control-law for the lateral directional axis of the McDonnell Douglas F-15 Eagle [AD-A289771] p 2142 N95-28598

F-16 AIRCRAFT

A quantitative feedback theory FCS design for the subsonic envelope of the VISTA F-16 including configuration variation [AD-A289221] p 2141 N95-26958

Flight control design using mixed H2/micron optimization [AD-A289288] p 2142 N95-27036

Implementation and demonstration of a multiple model adaptive estimation failure detection system for the F-16 [AD-A289301] p 2131 N95-27042

Improved numerical solution of mixed H2/H(infinity) optimization with applications [AD-A289315] p 2386 N95-27400

Life cycle costs of alternatives for F-16 printed circuit board diagnosis equipment [AD-A288744] p 2138 N95-28586

F-18 AIRCRAFT

F/A-18 IFOSTP Fatigue test airbag load determination on the vertical and horizontal tails [DSTO-TR-0135] p 2128 N95-26389

Numerical simulation of the flow about the F-18 HARV at high angle of attack [NASA-CR-197755] p 2121 N95-26735

Composite repair of a CF18: Vertical stabilizer leading edge p 2134 N95-27517

Composite flight-control actuator development p 2142 N95-28281

FABRICATION

Fabrication of long wavelength array by in-situ molecular beam epitaxy [AD-A288599] p 2423 N95-26679

Composite sandwich structure and method for making same [NASA-CASE-LAR-14898-1] p 2180 N95-26764

Silicon based microactuators for telerobotic tactile stimulation [AD-A289340] p 2260 N95-26767

Design, fabrication, modeling, and optical characterization of organic polymer nonlinear directional couplers [AD-A289327] p 2227 N95-26897

Current programmes on physical metallurgy and related areas in BARC [DE95-607939] p 2214 N95-27255

Linear Proof Mass Actuator p 2158 N95-27290

The development and testing of ceramic components in piston engines [DE95-005759] p 2236 N95-27946

Manufacturing tailored property ceramic composites [DE95-006303] p 2237 N95-27993

Stability measurements on a 1-T high temperature superconducting magnet [DE95-007411] p 2267 N95-28048

TEM characterization of Al/Al2O3 composite fabricated by reactive metal infiltration [DE95-008506] p 2184 N95-28145

Flat panel planar optic display [DE95-007686] p 2426 N95-28196

Swords to plowshares: Shock wave applications to advanced lithography [DE95-008154] p 2299 N95-28223

Development of a low-cost, modified resin transfer molding process using elastomeric tooling and automated preform fabrication p 2184 N95-28268

Static and fatigue testing of full-scale fuselage panels fabricated using a Therm-X(R) process p 2185 N95-28270

Advanced tow placement of composite fuselage structure p 2185 N95-28271

Resin transfer molding of textile preforms for aircraft structural applications p 2185 N95-28276

Molecular engineering of thin polymer films prepared from functionally-terminated oligomers [AD-A291681] p 2240 N95-28457

Evaluation of defect-related diffusion in semiconductors by electrooptical sampling [AD-A291630] p 2270 N95-28544

Design and fabrication of a diamond-turned hybrid diffractive/refractive singlet for visible applications at ORNL [DE95-007007] p 2427 N95-28552

Novel field effect transistors for low power electronics [AD-A289929] p 2271 N95-28629

FABRICS

Interfacial mobility and its effect on flexural strength and fracture toughness in glass-fiber fabric reinforced epoxy laminates [AD-A288344] p 2180 N95-26572

Design of fabric preforms for double diaphragm forming p 2184 N95-28269

Method and apparatus for measuring temperatures in fabrics and flexible thermal insulations [NASA-CASE-ARC-11984-1] p 2293 N95-28345

FACSIMILE COMMUNICATION

NASA/DOD Aerospace Knowledge Diffusion Research Project. Report 35: The use of computer networks in aerospace engineering [NASA-CR-198170] p 2456 N95-28600

FACTORIAL DESIGN
Comparison of the activities of fine-particle size catalysts
[DE95-004773] p 2203 N95-27423
FACTORIZATION
Modified eigenvalue problems with applications to structural dynamic re-analysis on parallel computers
[AD-A288257] p 2307 N95-26547
FAILURE
Life prediction methodology for composite laminates. Part 1: Constant amplitude and two-stress level fatigue
[AD-A288343] p 2180 N95-26571
Compiler-assisted debugging and multiple instruction retry
[NASA-CR-197729] p 2365 N95-26628
FAILURE ANALYSIS
Probabilistic risk assessment of the Space Shuttle. Phase 3: A study of the potential of losing the vehicle during nominal operation. Volume 4: System models and data analysis
[NASA-CR-197811] p 2160 N95-26401
Synthesis and characterization of polymeric materials
[AD-A288613] p 2225 N95-26482
Specifying weak sets
[AD-A288587] p 2364 N95-26536
Micromechanical prediction of tensile damage for ceramic matrix composites under high temperature
[AD-A288238] p 2180 N95-26626
Research and development report. Eureka 147: Tests of the error performance of the DAB system
[BBC-RD-1994/18] p 2249 N95-26696
Study of damage evolutions in composite plates subjected to bending loads using micro-macro analysis
[AD-A288523] p 2308 N95-26839
Characterization of fatigue behavior of 2-D woven fabric reinforced ceramic matrix composite at elevated temperature
[AD-A289423] p 2181 N95-26886
Implementation and demonstration of a multiple model adaptive estimation failure detection system for the F-16
[AD-A289301] p 2131 N95-27042
Fatigue behavior of a cross-ply ceramic matrix composite subjected to tension-tension cycling with hold time
[AD-A289418] p 2182 N95-27134
An experimental investigation of sandwich flat panels under low velocity impact
[AD-A289420] p 2309 N95-27135
Comprehension and retrieval of failure cases in airborne observatories p 2145 N95-27394
I(sub DDQ) testing and defect classes: A tutorial
[DE95-005467] p 2306 N95-27723
Static stability of a three-dimensional space truss
[NASA-TM-106944] p 2164 N95-27730
Stress analysis and failure of an internally pressurized composite-jacketed steel cylinder p 2186 N95-28280
Failure analysis of thick composite cylinders under external pressure p 2187 N95-28284
The role of biaxial stresses in discriminating between meaningful and illusory composite failure theories
p 2187 N95-28287
Design prediction for long term stress rupture service of composite pressure vessels p 2188 N95-28291
Bearing defect signature analysis using advanced nonlinear signal analysis in a controlled environment
[NASA-TM-106491] p 2304 N95-28364
Mechanisms of compressive failure in woven composites and stitched laminates p 2189 N95-28424
Compression failure of angle-ply laminates
p 2190 N95-28428
Technology integration box beam failure study
p 2194 N95-28468
Tension fracture of laminates for transport fuselage. Part 1: Material screening p 2137 N95-28471
Application of damage tolerance methodology in certification of the Piaggio P-180 Avanti
p 2138 N95-28480
FAILURE MODES
Stochastic adaptive estimation and control
[AD-A289088] p 2380 N95-26480
Modeling considerations in the prediction of residual strength in composite laminates
[AD-A289128] p 2182 N95-27142
Static stability of a three-dimensional space truss
[NASA-TM-106944] p 2164 N95-27730
Contingency designs for attitude determination of TRMM p 2154 N95-27803
Static and fatigue testing of full-scale fuselage panels fabricated using a Therm-X(R) process
p 2185 N95-28270
Static and dynamic strain energy release rates in toughened thermosetting composite laminates
p 2188 N95-28288
Proof test methodology for composites
p 2193 N95-28445
Coatings of non-oxide ceramics for improved corrosion resistance in high temperature coal combustion
[DE95-006932] p 2241 N95-28604
Numerical simulation of crack growth in pressurized fuselages
[PB95-192415] p 2137 N95-28636
FALLOUT
Particle fallout/activity sensor
[NASA-CASE-KSC-11687-1] p 2293 N95-28362
FALSE ALARMS
Processing of wide-angle synthetic aperture radar signals for detection of obscured ground targets
[AD-A289243] p 2253 N95-26976
FAR FIELDS
Generation of a single-lobe, far-field intensity pattern from a laser diode array using an optical delay line
[AD-A289226] p 2295 N95-26961
Acceleration theorems
[DE95-007300] p 2420 N95-27484
Data acquisition software for DREO's near-field antenna measurement facility
[AD-A289819] p 2258 N95-28573
FAR INFRARED RADIATION
Far-infrared laser interferometry measurements on the STP-3(M) reversed-field pinch
[DE94-765440] p 2297 N95-27868
FAR ULTRAVIOLET RADIATION
Evaluation of Oxygen Interactions with Materials 3: Mission and induced environments
p 2210 N95-27631
FARM CROPS
Measurement and analysis of the surface energy budget for ARM field experiments
[DE95-007646] p 2338 N95-28114
Models used to forecast agricultural corn crops in the micro-region of Ribeirao Preto-SP
[INPE-5513-NTC/309] p 2315 N95-28554
FAST FOURIER TRANSFORMATIONS
Nonlinear problems in fluid dynamics and inverse scattering: Propagation and capturing of singularities in problems of fluid dynamics and inverse scattering
[AD-A289146] p 2277 N95-26999
FAST NEUTRONS
Comparison of the resistance of the MOS integrated circuits with various types of nuclear radiation
[DE95-608623] p 2261 N95-27023
Investigation of radiation resistance of transistors and integrated circuits using the heavy ions beam of energy higher than 1 MeV/amu and fast neutrons
[DE95-608624] p 2261 N95-27024
FAST NUCLEAR REACTORS
Energy transfer from excited nitrenes at high density
[AD-A288352] p 2403 N95-26466
Toward a mechanistic understanding of radiation effects in materials
[DE95-006530] p 2221 N95-28120
FASTENERS
Basic space payload fastener p 2156 N95-27273
Non-explosive actuation for the ORBCOMM (TM) satellite p 2156 N95-27274
Assembly induced delaminations in composite structures p 2186 N95-28279
FATIGUE (MATERIALS)
Fatigue fracture analysis in medium carbon structural steel and austenitic stainless steel by X-ray fractography
[DE95-601504] p 2213 N95-26675
Fatigue behavior of a cross-ply ceramic matrix composite at elevated temperature under tension-tension loading
[AD-A289250] p 2182 N95-26969
A review of Australian and New Zealand investigations on aeronautical fatigue during the period Apr. 1993 - Mar. 1995
[AR-009-202] p 2136 N95-27918
Comparison of measured and calculated dynamic loads for the Mod-2 2.5 mW wind turbine system
p 2312 N95-27963
Prediction of fatigue crack growth under constant amplitude and random loading using specimens with multiple cracks
[AD-A291614] p 2136 N95-28409
Investigation of static and cyclic bearing failure mechanisms for GR/EP laminates p 2190 N95-28427
Applications of a damage tolerance analysis methodology in aircraft design and production
p 2197 N95-28483
FATIGUE LIFE
Analysis of fatigue fractographic data of a rod end housing using a Monte Carlo simulation
[NAL-TR-1225] p 2307 N95-26521
Comparison of life theories for rolling-element bearings
[NASA-TM-106585] p 2301 N95-26774
Fatigue behavior of a cross-ply metal matrix composite at elevated temperature under strain controlled mode
[AD-A289425] p 2181 N95-26865
Viscoplastic characterization and fatigue modeling of titanium based metal matrix composites
[AD-A289430] p 2181 N95-26868
Probabilistic simulation of long term behavior in polymer matrix composites
[NASA-TM-106893] p 2309 N95-27174
Fatigue properties of an A356 (AlSi7Mg) aluminum alloy for automotive applications: Fatigue life prediction
[PB95-196424] p 2224 N95-28660
FATIGUE TESTS
Design and development of a test rig for the high frequency testing of rolling sleeve airsprings
[DSTO-TN-0001] p 2142 N95-26378
F/A-18 IFOSTP Fatigue test airbag load determination on the vertical and horizontal tails
[DSTO-TR-0135] p 2128 N95-26389
Development of welded solar arrays for DMSP and GPS satellites
[AD-A289512] p 2318 N95-26846
Fatigue behavior of a cross-ply metal matrix composite at elevated temperature under strain controlled mode
[AD-A289425] p 2181 N95-26865
Characterization of fatigue behavior of 2-D woven fabric reinforced ceramic matrix composite at elevated temperature
[AD-A289423] p 2181 N95-26886
Composite repair of metallic airframe: Twenty years of experience p 2132 N95-27508
External patch repair of CFRP/honeycomb sandwich
p 2134 N95-27522
Damage occurrence on composites during testing and fleet service: Repair of Airbus aircraft
p 2135 N95-27526
Static and fatigue testing of full-scale fuselage panels fabricated using a Therm-X(R) process
p 2185 N95-28270
Design, analysis, and testing of a metal matrix composite web/flange intersection p 2191 N95-28433
Proof test methodology for composites
p 2193 N95-28445
Applications of a damage tolerance analysis methodology in aircraft design and production
p 2197 N95-28483
FAULT DETECTION
Measuring fault tolerance with the FTAPE fault injection tool
[NASA-CR-197773] p 2306 N95-27253
Diagnosis of helicopter gearboxes using structure-based networks
[NASA-TM-106932] p 2302 N95-27373
I(sub DDQ) testing and defect classes: A tutorial
[DE95-005467] p 2306 N95-27723
SMART materials: Surfaces, transforms and interfaces. The commensurate engineering dimension
[AD-A289598] p 2312 N95-28649
FAULT TOLERANCE
Self-checking state machine realization in CMOS
[AD-A289149] p 2261 N95-27002
Measuring fault tolerance with the FTAPE fault injection tool
[NASA-CR-197773] p 2306 N95-27253
Advanced development for space robotics with emphasis on fault tolerance p 2155 N95-27263
Autonomous control system reconfiguration for spacecraft with non-redundant actuators
p 2153 N95-27802
Fault tolerant features and experiments of ANTS distributed real-time system
[AD-A290133] p 2256 N95-28391
ALLIANCE: An architecture for fault tolerant, cooperative control of heterogeneous mobile robots
[DE95-007374] p 2387 N95-28536
Two implementation relations and the correctness of communicating replicated processes
[PB95-195640] p 2375 N95-28645
FAULT TREES
Using the dimension reduction technique to prove that clique trees define facets for the asymmetric traveling salesman polytope
[AD-A289397] p 2389 N95-26882
FEASIBILITY
The development of a feature-based concurrent engineering system
[AD-A288424] p 2364 N95-26557
FEASIBILITY ANALYSIS
Multipoint multirate signal processing
[AD-A289211] p 2253 N95-26988
Report to the Chairman and Ranking Minority Member, Committee on Science, House of Representatives. Weather forecasting: Radar availability requirement not being met
[GAO/AIMD-95-132] p 2342 N95-27912
Long-range eye tracking: A feasibility study
[DE95-008587] p 2357 N95-28176

Evaluating the environmental viability of open burning/open detonation operations
p 2170 N95-28297
Alternate use of rocket propellants as ingredients in commercial watergel explosives p 2176 N95-28321

FEDERAL BUDGETS
Briefing Report to the Ranking Minority Member, Subcommittee on Space and Aeronautics, Committee on Science, House of Representatives. Cassini Mission: Estimated launch costs for NASA's mission to Saturn
[GAO/NSIAD-95-141BR] p 2145 N95-27856

FEEDBACK
Electro-hydrostatic actuator controller design using quantitative feedback theory
[AD-A289220] p 2141 N95-26957
A quantitative feedback theory FCS design for the subsonic envelope of the VISTA F-16 including configuration variation
[AD-A289221] p 2141 N95-26958
Telepresent spacecraft docking with object-based bilateral control (OBBC)
[AD-A289268] p 2163 N95-26980
Bilateral force feedback for hydraulically actuated systems
[AD-A291632] p 2387 N95-28545

FEEDBACK CONTROL
Extended linear ion trap frequency standard apparatus
[NASA-CASE-NPO-19081-1-CU] p 2404 N95-26861
A gain scheduling optimization method using genetic algorithms
[AD-A289306] p 2381 N95-26920
Telepresent spacecraft docking with object-based bilateral control (OBBC)
[AD-A289268] p 2163 N95-26980
Advanced formation flight control
[AD-A289271] p 2142 N95-26981
High-precision buffer circuit for suppression of regenerative oscillation
[NASA-TM-4658] p 2291 N95-27259
Time-optimal control of the magnetically levitated photolithography platen
[DE95-005493] p 2266 N95-27724
Extended linear ion trap frequency standard apparatus
[NASA-CASE-NPO-19081-1-CU] p 2416 N95-28348
Beam instability studies for the SSC
[DE95-008024] p 2423 N95-28551
Operating points and feedback control of plasma characteristics in tokamaks with full current drive
[DE95-007037] p 2435 N95-28553

FEMALES
Toxicity assessment of liquid propellant XM46
p 2175 N95-28319

FERMI SURFACES
Electronic structure of disordered Cu-Ag alloys
[DE95-609156] p 2219 N95-27758

FERMI-DIRAC STATISTICS
Stationary neutrino radiation transport by maximum entropy closure
[DE95-006579] p 2463 N95-28558

FERMIONS
Finite fermion density effects on the electroweak string
[DE95-608802] p 2448 N95-27312
The physics and chemistry of heavy Fermions
[DE95-005277] p 2407 N95-27431
A diagram technique for strongly interacting fermion systems. One-and two-band Hubbard models
[DE95-609437] p 2410 N95-27881
Phenomenology from 100 large lattices
[DE95-006349] p 2442 N95-27994
Theory of exotic superconductivity and normal states of heavy electron and high temperature superconductivity materials
[DE95-006637] p 2268 N95-28198
Stationary neutrino radiation transport by maximum entropy closure
[DE95-006579] p 2463 N95-28558

FERRITES
Effect of internal hydrogen on the mixed-mode 1/3 fracture toughness of a ferrific/martensitic stainless steel
[DE95-005722] p 2216 N95-27479

FERROELECTRICITY
Siloxane-based ferroelectric liquid crystal elastomers and Self-Assembled Mono- and multilayers
[AD-A288285] p 2224 N95-26456
Vacancy related defects in thin film Pb(Zr,Ti)O3 materials
[DE95-007696] p 2445 N95-28165

FERROMAGNETIC MATERIALS
Magnetization of ferromagnetic clusters
[DE95-006878] p 2399 N95-27548
Muon spin relaxation in ferromagnets: Theoretical results for paramagnetic EuO and EuS
[PB95-192860] p 2418 N95-28641

FERROMAGNETISM
A new method of evaluating the explicit magnetic-state-dependent energy in semi-empirical calculations of iron
[AD-A289098] p 2399 N95-27398

FERTILIZERS
Investigation on technology for increasing the biological CO2 sink and technology for CO2 fixation and reutilization
[DE95-759251] p 2329 N95-27941

FIBER COMPOSITES
A study of the use beta-alumina as a weak interface in alumina fiber composites
[AD-A288629] p 2179 N95-26484
Interfacial mobility and its effect on flexural strength and fracture toughness in glass-fiber fabric reinforced epoxy laminates
[AD-A288344] p 2180 N95-26572
Micromechanical prediction of tensile damage for ceramic matrix composites under high temperature
[AD-A288238] p 2180 N95-26626
Rheological measurement methods for fibre filled plastics
[PB95-190088] p 2226 N95-26744
Mechanical performance of fiber reinforced metal matrix composites and microstructural development of polycrystalline alumina fibers synthesized from liquid precursors
[AD-A289518] p 2181 N95-26847
On aircraft repair verification of a fighter A/C integrally stiffened fuselage skin p 2133 N95-27515
Composite repair of a CF18: Vertical stabilizer leading edge p 2134 N95-27517
Scarf joint technique with cocured and precured patches for composite repair p 2135 N95-27524
Composite or metallic bolted repairs on self-stiffened carbon wing panel of the commuter ATR72 design criteria, analysis, verification by test p 2135 N95-27525
Repairs of CFC primary structures
p 2135 N95-27527
Ceramic fiber-reinforced monoclinic celsian phase glass-ceramic matrix composite material
[NASA-CASE-LEW-15714-1] p 2183 N95-27717
Design of a unidirectional composite momentum wheel rim
[NASA-TM-106911] p 2164 N95-27761
Thermal shock behavior of fiber-reinforced composites
[DE95-006746] p 2183 N95-27955
Stress transfer from axially loaded fiber to matrix in a microcomposite
[DE95-007366] p 2183 N95-28043
Effects of high-temperature environments on flaw generation and fracture behavior of SiC/SiC composites
[DE95-008270] p 2183 N95-28068
Ninth DOD/NASA/FAA Conference on Fibrous Composites in Structural Design, volume 3
[NASA-CR-198718] p 2184 N95-28266
Service tough composite structures using the Z-direction reinforcement process p 2185 N95-28272
Analysis of aircraft engine blade subject to ice impact
p 2141 N95-28277
Application of fiber-reinforced bismaleimide materials to aircraft nacelle structures p 2137 N95-28278
Stress analysis and failure of an internally pressurized composite-jacketed steel cylinder p 2186 N95-28280
Failure analysis of thick composite cylinders under external pressure p 2187 N95-28284
The role of biaxial stresses in discriminating between meaningful and illusory composite failure theories
p 2187 N95-28287
Designing for time-dependent material response in spacecraft structures p 2166 N95-28292
Ninth DOD/NASA/FAA Conference on Fibrous Composites in Structural Design, volume 1
[NASA-CR-198723] p 2189 N95-28420
Effect of the fiber-matrix interphase on the transverse tensile strength of the unidirectional composite material
p 2190 N95-28425
Application of advanced material systems to composite frame elements p 2191 N95-28432
Design, analysis, and testing of a metal matrix composite web/flange intersection p 2191 N95-28433
Characteristics of laminates with delamination control strips p 2191 N95-28434
Ninth DOD/NASA/FAA Conference on Fibrous Composites in Structural Design, volume 2
[NASA-CR-198722] p 2193 N95-28462
Advanced wing design survivability testing and results
p 2138 N95-28488
Non-linear viscoelastic behaviour
[PB95-192811] p 2199 N95-28639
Ceramic composite combustor cans for expendable turbine engines
[AD-A289551] p 2140 N95-28646

FIBER OPTICS
Measurement of high acidity using a renewable-reagent fiber optic sensor
[DE95-006327] p 2425 N95-27734
Fundamental concepts of integrated and fiber optic sensors
[NASA-TM-106920] p 2426 N95-27906
Flat panel planar optic display
[DE95-007686] p 2426 N95-28196
SMART materials: Surfaces, transforms and interfaces. The commensurate engineering dimension
[AD-A289598] p 2312 N95-28649

FIBER ORIENTATION
Characteristics of laminates with delamination control strips p 2191 N95-28434

FIBER STRENGTH
Effects of high-temperature environments on flaw generation and fracture behavior of SiC/SiC composites
[DE95-008270] p 2183 N95-28068

FIBER VOLUME FRACTION
Design of a unidirectional composite momentum wheel rim
[NASA-TM-106911] p 2164 N95-27761

FIBER-MATRIX INTERFACES
A study of the use beta-alumina as a weak interface in alumina fiber composites
[AD-A288629] p 2179 N95-26484
Ceramic fiber-reinforced monoclinic celsian phase glass-ceramic matrix composite material
[NASA-CASE-LEW-15714-1] p 2183 N95-27717
Stress transfer from axially loaded fiber to matrix in a microcomposite
[DE95-007366] p 2183 N95-28043
Effect of the fiber-matrix interphase on the transverse tensile strength of the unidirectional composite material
p 2190 N95-28425

FIBERS
Gigabit LAN issues: HIPPI, Fibre Channel, or ATM?
[DE95-003673] p 2378 N95-27422

FIBRILLATION
Visualization of finite element model solutions for defibrillation voltage and current distributions
[AD-A289836] p 2400 N95-28579

FIELD EFFECT TRANSISTORS
Microwave circuit simulation using higher-order dynamic elements
[PB95-185088] p 2259 N95-26496
Active antennas with periodic structures
[AD-A289437] p 2252 N95-26924
Characterization of microwave MESFET circuits under laser illumination. Applications to phased array radar, microwave communications, and digital clock control
[AD-A289181] p 2261 N95-27015
Microwave characterization of sub-micron N- and P-channel MOSFET's fabricated with thin film silicon-on-sapphire
[AD-A289296] p 2438 N95-27040
Modeling of trapping and abrupt doping effects in MESFET's using R-dynamic element
[PB95-184891] p 2262 N95-27050
Novel field effect transistors for low power electronics
[AD-A288650] p 2262 N95-27096
Measurement-based MESFET model in APLAC
[PB95-195483] p 2269 N95-28448
Basic and applied research in the field of electronics and communications
[AD-A291727] p 2270 N95-28512
Quasi-optical millimeter wave power combining
[AD-A291767] p 2270 N95-28529
Novel field effect transistors for low power electronics
[AD-A289929] p 2271 N95-28629

FIELD INTENSITY METERS
A PC-based magnetometer-only attitude and rate determination system for gyroless spacecraft
p 2147 N95-27770

FIELD OF VIEW
SeaWiFS technical report series. Volume 27: Case studies for SeaWiFS calibration and validation, part 3
[NASA-TM-104566-VOL-27] p 2348 N95-28030

FIELD STRENGTH
Radiation of a uniformly moving charge
[DE95-608757] p 2255 N95-27335

FIELD THEORY (ALGEBRA)
Symmetries of the KAC-Peterson modular matrices of affine algebras
[PB95-190138] p 2392 N95-28010
Lie group weight multiplicities from conformal field theory
[PB95-190153] p 2392 N95-28012

FIELD THEORY (PHYSICS)
A density functional/molecular dynamics study of the structure of liquid nitromethane
[AD-A289224] p 2404 N95-26960
Field theory of point-like systems with higher-order derivatives
[DE95-608800] p 2448 N95-27310

Bogolyubov renormalization group
[DE95-608830] p 2448 N95-27315

FIGHTER AIRCRAFT

Integrated mission precision attack cockpit technology (IMPACT). Phase 1: Identifying technologies for air-to-ground fighter integration
[AD-A289562] p 2129 N95-26684

Performance study for inlet installations
[NASA-CR-189714] p 2140 N95-28227

Structural design optimization with survivability dependent constraints application: Primary wing box of a multi-role fighter p 2137 N95-28440

FILE MAINTENANCE (COMPUTERS)

Long term distributed file reference tracing: Implementation and experience
[AD-A288585] p 2452 N95-26535

Flexible and safe resolution of file conflicts
[AD-A289342] p 2452 N95-26752

A demonstration of Client/Server technology using remote procedure calls for an application of file migration for moving records based on location
[AD-A289391] p 2453 N95-26864

A demonstration of Client-Server technology using remote procedure calls with an application of file migration for moving records based on time
[AD-A289392] p 2453 N95-26879

A case for dynamic sets in operating systems
[AD-A289354] p 2454 N95-27529

The transition of GTDS to the Unix workstation environment p 2151 N95-27789

FILM COOLING

Investigation of boundary layer and performance effects of transpiration cooling through a porous plate in a rocket nozzle
[AD-A289393] p 2167 N95-26880

A summary of computational experience at GE Aircraft Engines for complex turbulent flows in gas turbines
p 2285 N95-27885

FILM THICKNESS

Copper CVD using liquid coinjection of (hfac)Cu(TMVS) and TMVS
[DE95-008155] p 2237 N95-28089

Influences of film structures on laser damage thresholds
[AD-A289647] p 2300 N95-28633

FILTRATION

Cleaning of parts for new manufacturing and parts rebuilding p 2231 N95-27123

FINE STRUCTURE

Observations of CEF-split intermultiplet transitions in optically opaque EuBa2Cu3O7 using inelastic neutron scattering
[DE95-007135] p 2408 N95-27453

Precision asteroseismology of DAV (ZZ CETI) white dwarf stars
[DE95-006265] p 2462 N95-28056

FINITE DIFFERENCE THEORY

Performance evaluation of a new parallel preconditioner
[AD-A288563] p 2376 N95-26529

Material modeling in the CRALE code. Users' manual
[AD-A288988] p 2178 N95-26712

Reduction of off-boresight fields for a TEM horn antenna
[AD-A289708] p 2250 N95-26738

Development of an upwind, finite-volume code with finite-rate chemistry
[NASA-CR-197747] p 2121 N95-26760

Direct numerical simulation of transitional and turbulent flow over a heated flat plate using finite-difference schemes
[NASA-CR-197753] p 2275 N95-26776

A numerical method for unsteady transonic flow about wings with control surfaces
[AD-A289631] p 2121 N95-26859

A 3-D finite difference time domain investigation of microwave propagation through inhomogeneous biological materials
[AD-A289431] p 2251 N95-26869

Analysis of modal behavior at frequency cross-over
[AD-A289304] p 2162 N95-26918

Validation of the SINDA/FLUINT code using several analytical solutions p 2281 N95-27350

Analysis of developing laminar flows in circular pipes using a higher-order finite-difference technique
p 2281 N95-27352

The Benard problem: A comparison of finite difference and spectral collocation eigen value solutions
p 2283 N95-27364

FDTD-ANT user manual
[NASA-CR-195444] p 2372 N95-27729

Scaling issues in dynamic fragmentation
[DE95-008509] p 2309 N95-27745

Time-dependent model for vertical-cavity surface-emitting laser
[DE95-007880] p 2298 N95-28027

FINITE ELEMENT METHOD

Analysis and development of finite element methods for the study of nonlinear thermomechanical behavior of structural components
[NASA-CR-195354] p 2307 N95-26387

A finite element propagation model for extracting normal incidence impedance in nonprogressive acoustic wave fields
[NASA-TM-110160] p 2400 N95-26394

Process control of microstructure in manufacturing
[AD-A288291] p 2245 N95-26410

General purpose finite element solver
[PB95-185062] p 2388 N95-26495

Performance evaluation of a new parallel preconditioner
[AD-A288563] p 2376 N95-26529

Intelligent computer based reliability assessment of multichip modules
[AD-A288833] p 2259 N95-26550

A fast numerical method for isothermal resin transfer mold filling
[AD-A288944] p 2179 N95-26565

Adaptive finite element method I: Solution algorithm and computational examples
[AD-A288979] p 2389 N95-26609

User's and test case manual for FEMATS
[NASA-CR-197803] p 2366 N95-26694

SUPG finite numerical element solutions for non-compressible Navier-Stokes equation sets
[AD-A289600] p 2274 N95-26718

The collapse of composite cylindrical panels with various thickness using finite element analysis
[AD-A289370] p 2308 N95-26905

Analysis of modal behavior at frequency cross-over
[AD-A289304] p 2162 N95-26918

Investigation into the behavior of geometrically nonlinear composite arches
[AD-A289258] p 2308 N95-26975

A finite element based technique for simulation helix TWT interaction circuit thermal behavior
[AD-A289552] p 2262 N95-27152

Effect of hoop stress on ball bearing life prediction
[NASA-TM-106874] p 2301 N95-27178

Magnetically controlled deposition of metals using gas plasma
[DE95-007248] p 2430 N95-27237

High performance stepper motors for space mechanisms p 2156 N95-27271

Vector algorithms for solving 3D nonlinear magnetostatic problems
[DE95-608737] p 2399 N95-27298

The effects of finite element grid density on model correlation and damage detection of a bridge
[DE94-018895] p 2309 N95-27305

A probabilistic model of a porous heat exchanger
p 2282 N95-27359

A verification procedure for MSC/NASTRAN Finite Element Models
[NASA-CR-4675] p 2131 N95-27371

Micromechanical modeling of damage and inelasticity of composite materials in macroscopic structural analysis
[DE95-003666] p 2182 N95-27421

A new finite element formulation for incompressible flow
[DE95-007141] p 2284 N95-27454

A FEAM based methodology for analyzing composite patch repairs of metallic structures
p 2133 N95-27511

Scarf repairs to graphite/epoxy components
p 2135 N95-27523

The origin of spurious solutions in computational electromagnetics
[NASA-TM-106921] p 2391 N95-27726

Scaling issues in dynamic fragmentation
[DE95-008509] p 2309 N95-27745

System identification of damped truss-like space structures
[NASA-TM-106638] p 2303 N95-27911

A NASTRAN-based computer program for structural dynamic analysis of Horizontal Axis Wind Turbines
p 2312 N95-27980

Robust integration schemes for generalized viscoplasticity with internal-state variables. Part 1: Theoretical developments and applications
[NASA-CR-195452-PT-1] p 2310 N95-28031

Robust integration schemes for generalized viscoplasticity with internal-state variables. Part 2: Algorithmic developments and implementation
[NASA-CR-195453-PT-2] p 2310 N95-28032

Deformation limits on two-parameter fracture mechanics in terms of higher order asymptotics
[AD-A289113] p 2310 N95-28098

Accuracy issues in modeling superplastic metal forming
[DE95-008934] p 2222 N95-28163

Reactor pressure vessel structural integrity research
[DE95-007034] p 2223 N95-28208

Aeroelasticity and structural optimization of composite helicopter rotor blades with swept tips
[NASA-CR-4665] p 2136 N95-28262

TranAir: A full-potential, solution-adaptive, rectangular grid code for predicting subsonic, transonic, and supersonic flows about arbitrary configurations. Theory document
[NASA-CR-4348] p 2123 N95-28265

Higher order finite element analysis of thick composite laminates p 2186 N95-28282

Failure analysis of thick composite cylinders under external pressure p 2187 N95-28284

Analysis techniques for the prediction of springback in formed and bonded composite components
p 2188 N95-28289

Design, analysis, and testing of a metal matrix composite web/flange intersection p 2191 N95-28433

Visualization of finite element model solutions for defibrillation voltage and current distributions
[AD-A289836] p 2400 N95-28579

Structural optimisation of cage induction motors using finite element analysis
[PB95-195434] p 2271 N95-28655

FINITE VOLUME METHOD

Numerical investigation to S-inlet flows (Numerical simulation study of S-inlet flows)
[AD-A289590] p 2120 N95-26713

Transitional flow in thin tubes for space station freedom radiator p 2282 N95-27360

FINLAND

Milestones in telecommunications in some selected countries
[PB95-184826] p 2252 N95-26929

WTEC panel report on research submersibles and undersea technologies
[NASA-CR-198565] p 2247 N95-27909

Laboratory of production engineering
[PB95-184834] p 2451 N95-28135

FINS

Application of damage tolerance methodology in certification of the Piaggio P-180 Avanti
p 2138 N95-28480

FIR FILTERS

Crushing the delay: Tools for fractional delay filter design
[PB95-195509] p 2257 N95-28450

FIRE EXTINGUISHERS

Engineering Technical Letter (ETL) 94-5: Fire protection engineering criteria and technical guidance. Emergency lighting and marking of exits
[AD-A288953] p 2246 N95-26566

FIRE PREVENTION

Engineering Technical Letter (ETL) 94-5: Fire protection engineering criteria and technical guidance. Emergency lighting and marking of exits
[AD-A288953] p 2246 N95-26566

FIRES

Design and development of experimental facilities for short duration, low-gravity combustion and fire experiments
[NASA-CR-195458] p 2244 N95-26709

Algorithm to describe the spread of a wall fire under a ceiling
[PB95-182259] p 2247 N95-28008

FISHES

Modeling and statistical analysis of bioassay data: Medaka cell proliferation under DEN and TCE
[AD-A289998] p 2352 N95-28519

FISSION

Bilateral intercomparison of the neutron emission rate of a (252)Cf spontaneous fission source between the National Physical Laboratory, Teddington, UK and the Physikalisch-Technische Bundesanstalt, Braunschweig, Germany
[PB95-190120] p 2404 N95-26748

FITTING

Fitting: Subroutine to fit four-moment probability distributions to data
[DE95-007722] p 2395 N95-27684

FIXED POINTS (MATHEMATICS)

Random relaxation of fixed point iteration
[PB95-185013] p 2389 N95-26910

FIXED WINGS

Comparison of fixed wing aircraft algorithms for JANUS
[AD-A288503] p 2129 N95-26652

Test operations procedure (TOP) 7-3-534 airworthiness testing of fixed wing aircraft: Asymmetric power testing
[AD-A289458] p 2130 N95-26994

FIXING

Compressive strength of damaged and repaired composite plates p 2198 N95-28484

FIXTURES
Extension to the dynamic modeling of the large angle magnetic suspension test fixture
[NASA-CR-197801] p 2143 N95-26768
FLAME HOLDERS
Numerical simulation of combustion flow around a flame holder with hydrogen injection
[NAL-TR-1233] p 2200 N95-26523
FLAME PROPAGATION
Funding for AFRAPT student trainees for academic year 1992-1993
[AD-A288461] p 2466 N95-26604
FLAMES
A composition joint PDF method for the modeling of spray flames p 2287 N95-27901
Research on combustion processes relevant to burners in HVAC systems
[PB95-179735] p 2208 N95-28006
FLAMMABILITY
Use of CTFE as an additive to enhance fire resistance of single hydraulic fluid
[AD-A289377] p 2233 N95-27325
Methods development for measuring and classifying flammability/combustibility of refrigerants. Task 2: Test plan
[DE95-007066] p 2234 N95-27461
Methods development for measuring and classifying flammability/combustibility of refrigerants. Task 1: Annotated bibliography
[DE95-007232] p 2238 N95-28133
FLANGES
Application of advanced material systems to composite frame elements p 2191 N95-28432
Design, analysis, and testing of a metal matrix composite web/flange intersection p 2191 N95-28433
FLAPERONS
Full span flaperons for a biplane
p 2119 N95-26954
FLAPPING
Visualization of the multiple supersonic jet oscillations by swept focused strobed schlieren technique
p 2119 N95-26952
Full span flaperons for a biplane
p 2119 N95-26954
FLAPS (CONTROL SURFACES)
Comparative wind tunnel tests of NACA 23024 airfoils with several aileron and spoiler configurations
p 2124 N95-27976
FLAT PANEL DISPLAYS
Low temperature materials growth and processing development for flat panel display technology applications
[AD-A288970] p 2233 N95-27187
Flat panel display development activities at Sandia National Laboratories
[DE95-005442] p 2265 N95-27706
JTEC panel on display technologies in Japan
[NASA-CR-198564] p 2292 N95-27863
Flat panel planar optic display
[DE95-007686] p 2426 N95-28196
FLAT PLATES
Plate manipulators
[AD-A289601] p 2121 N95-26719
Direct numerical simulation of transitional and turbulent flow over a heated flat plate using finite-difference schemes
[NASA-CR-197753] p 2275 N95-26776
Measurements of store forces and moments and cavity pressures for a generic store in and near a box cavity at subsonic and transonic speeds
[NASA-TM-4611] p 2123 N95-28241
Construction and wind tunnel test of a 1/12th scale helicopter model
[AD-A288487] p 2123 N95-28331
Monte-Carlo simulation methods for finite flat plate winding flows
[AD-A289842] p 2289 N95-28619
FLAT SURFACES
Atomistic study of energy and structure of surfaces in NiO
[DE95-005207] p 2215 N95-27446
FLAVOR (PARTICLE PHYSICS)
The Top...is it There? A Survey of the CDF and D0 Experiments
[DE95-005746] p 2411 N95-27945
FLEXIBLE BODIES
Method and apparatus for measuring temperatures in fabrics and flexible thermal insulations
[NASA-CASE-ARC-11984-1] p 2293 N95-28345
FLEXIBLE SPACECRAFT
A class of stabilizing controllers for flexible multibody systems
[NASA-TP-3494] p 2161 N95-26428
Analysis of modal behavior at frequency cross-over
[AD-A289304] p 2162 N95-26918
Static stability of a three-dimensional space truss
[NASA-TM-106944] p 2164 N95-27730
FLEXING
Interfacial mobility and its effect on flexural strength and fracture toughness in glass-fiber fabric reinforced epoxy laminates
[AD-A288344] p 2180 N95-26572
Experimental studies to test simple flexural neutralizers fitted to beams
[ISVR-TR-239] p 2309 N95-27846
Analytical and experimental evaluation of joining silicon carbide to silicon carbide and silicon nitride to silicon nitride for advanced heat engine applications, phase 2
[DE95-005761] p 2303 N95-27947
FLIGHT CHARACTERISTICS
Simulation model of the integrated flight/propulsion control system, displays, and propulsion system for ASTOVL lift-fan aircraft
[NASA-TM-108866] p 2139 N95-26412
A comparison of the Neal-Smith and omega Tau function, zeta function and tau function flying qualities criteria
[AD-A289503] p 2130 N95-26844
FLIGHT CLOTHING
Development of injury preventing helmet servo-support system for high performance aircraft
[AD-A289547] p 2359 N95-26755
FLIGHT CONDITIONS
Electro-hydrostatic actuator controller design using quantitative feedback theory
[AD-A289220] p 2141 N95-26957
Construction and wind tunnel test of a 1/12th scale helicopter model
[AD-A288487] p 2123 N95-28331
FLIGHT CONTROL
Development of a nonlinear simulation for the McDonnell Douglas F-15 Eagle with a longitudinal TECS control-law
[AD-A288610] p 2128 N95-26481
Design and synthesis of a real-time controller for an unmanned air vehicle
[AD-A289134] p 2141 N95-26555
An investigation of the effects of pitch-roll (de)coupling on helicopter handling qualities
[NASA-TM-110349] p 2141 N95-26773
A comparison of the Neal-Smith and omega Tau function, zeta function and tau function flying qualities criteria
[AD-A289503] p 2130 N95-26844
Electro-hydrostatic actuator controller design using quantitative feedback theory
[AD-A289220] p 2141 N95-26957
A quantitative feedback theory FCS design for the subsonic envelope of the VISTA F-16 including configuration variation
[AD-A289221] p 2141 N95-26958
Advanced formation flight control
[AD-A289271] p 2142 N95-26981
Flight control design using mixed H2/micron optimization
[AD-A289288] p 2142 N95-27036
Advanced flight computer. Special study
[NASA-CR-198165] p 2371 N95-27246
JPRS report: Science and technology. Central Eurasia
[JPRS-UST-94-022] p 2246 N95-27699
Operator modeling in commerical aviation: Cognitive models, intelligent displays, and pilot's assistants
[NASA-CR-198609] p 2138 N95-28203
Composite flight-control actuator development
p 2142 N95-28281
FLIGHT CREWS
An analysis of the KC-135 three-person cockpit
[AD-A289540] p 2130 N95-26873
FLIGHT ENVELOPES
Flutter clearance flight tests of an OV-10A airplane modified for wake vortex flight experiments
[NASA-TM-109168] p 2117 N95-26381
Bow shock data analysis
[AD-A288432] p 2429 N95-26800
A quantitative feedback theory FCS design for the subsonic envelope of the VISTA F-16 including configuration variation
[AD-A289221] p 2141 N95-26958
FLIGHT HAZARDS
A review of falconry as a bird control technique with recommendations for use at the Shuttle Landing Facility, John F. Kennedy Space Center, Florida, USA
[NASA-TM-110142] p 2126 N95-27859
Weather hazards to a Titan 4 on-pad destack-restack operation p 2172 N95-28307
FLIGHT INSTRUMENTS
Hardware cleanliness methodology and certification
p 2211 N95-27656
FLIGHT MANAGEMENT SYSTEMS
Operator modeling in commerical aviation: Cognitive models, intelligent displays, and pilot's assistants
[NASA-CR-198609] p 2138 N95-28203
Pilot opinions on high level flight deck automation issues: Toward the development of a design philosophy
[NASA-CR-4669] p 2357 N95-28253
FLIGHT MECHANICS
Flight Mechanics/Estimation Theory Symposium 1995
[NASA-CP-3299] p 2146 N95-27763
Flight dynamics software in a distributed network environment p 2151 N95-27790
The Global Positioning System (GPS) and attitude determination: Applications and activities in the Flight Dynamics Division p 2152 N95-27795
Summary of EOS flight dynamics analysis
p 2152 N95-27797
FLIGHT OPERATIONS
Weather hazards to a Titan 4 on-pad destack-restack operation p 2172 N95-28307
FLIGHT PATHS
Flightpath synthesis and HUD scaling for V/STOL terminal area operations
[NASA-TM-110348] p 2127 N95-26587
FLIGHT SAFETY
Probabilistic risk assessment of the Space Shuttle. Phase 3: A study of the potential of losing the vehicle during nominal operation, volume 1
[NASA-CR-197808] p 2159 N95-26398
The 1994 updated National Airspace System performance assessment for year 2005
[AD-A288652] p 2125 N95-26485
The effect of aviation fuels containing low amounts of static dissipater additive on electrostatic charge generation
[AD-A280075] p 2243 N95-28152
Development and implementation of a system safety program for the space launch complex 3 east (SLC-3E) ground support system project to support Atlas 2 family of space launch vehicles p 2174 N95-28316
FLIGHT SIMULATION
Simulation model of the integrated flight/propulsion control system, displays, and propulsion system for ASTOVL lift-fan aircraft
[NASA-TM-108866] p 2139 N95-26412
Development of a nonlinear simulation for the McDonnell Douglas F-15 Eagle with a longitudinal TECS control-law
[AD-A288610] p 2128 N95-26481
Integrated mission precision attack cockpit technology (IMPACT). Phase 1: Identifying technologies for air-to-ground fighter integration
[AD-A289562] p 2129 N95-26684
The photo-realistic AFIT virtual cockpit
[AD-A289376] p 2130 N95-26876
Visual system operational evaluation
[AD-A289173] p 2356 N95-27012
Implementation and demonstration of a multiple model adaptive estimation failure detection system for the F-16
[AD-A289301] p 2131 N95-27042
The lift-fan aircraft: Lessons learned
[NASA-CR-196694] p 2131 N95-27143
A study of workstation computational performance for real-time flight simulation
[NASA-TM-109184] p 2362 N95-27241
FLIGHT SIMULATORS
The photo-realistic AFIT virtual cockpit
[AD-A289376] p 2130 N95-26876
The effects of UH-1 experience on UH-6O simulator performance: A preliminary study
[AD-A289457] p 2130 N95-26993
Visual system operational evaluation
[AD-A289173] p 2356 N95-27012
Flight control design using mixed H2/micron optimization
[AD-A289288] p 2142 N95-27036
FLIGHT TESTS
Flutter clearance flight tests of an OV-10A airplane modified for wake vortex flight experiments
[NASA-TM-109168] p 2117 N95-26381
Flight evaluation of GPS/DGPS sensor systems installed in NAL Do228
[NAL-TR-1230] p 2126 N95-26585
Hubble Space Telescope nickel-hydrogen battery testing: An update p 2272 N95-26794
The effects of UH-1 experience on UH-6O simulator performance: A preliminary study
[AD-A289457] p 2130 N95-26993
Test operations procedure (TOP) 7-3-534 airworthiness testing of fixed wing aircraft: Asymmetric power testing
[AD-A289458] p 2130 N95-26994
Status of bonded boron/epoxy doublers for military and commercial aircraft structures p 2132 N95-27506
Space environmental effect on solar cells: LDEF and other flight tests p 2326 N95-27649
Analysis of solar receiver flux distributions for US/Russian solar dynamic system demonstration on the MIR Space Station
[NASA-TM-106933] p 2169 N95-28036

Analysis of shadowing effects on MIR photovoltaic and solar dynamic power systems [NASA-TM-106940] p 2169 N95-28213

The solar array-induced disturbance of the Hubble Space Telescope pointing system [NASA-TP-3556] p 2311 N95-28214

Unmanned aerial vehicles, 1994 master plan [AD-A291628] p 2136 N95-28411

Proceedings of the AIAA/FAA joint symposium on general aviation systems [AD-A289830] p 2120 N95-28610

FLIGHT TRAINING

The value of simulation for training [AD-A289174] p 2143 N95-26556

FLOATING

Ultrasonic studies of liquid/solid seimoacoustic wave phenomena [AD-A289644] p 2402 N95-28622

FLOORS

Effects of floor location on response of composite fuselage frames p 2192 N95-28439

FLOQUET THEOREM

Aeroelasticity and structural optimization of composite helicopter rotor blades with swept tips [NASA-CR-4665] p 2136 N95-28262

FLOW CHARACTERISTICS

Viscous shock-layer analysis on hypersonic flow over reentry capsule with nonequilibrium chemistry [ISAS-R-656] p 2274 N95-26739

Wind tunnel experiments on wake flow field behind a reentry capsule from a viewpoint of parachute deployment at supersonic speeds [ISAS-R-655] p 2121 N95-26740

FLOW DISTRIBUTION

Numerical simulation of the SOFIA flow field [NASA-CR-197757] p 2274 N95-26589

CFD research, parallel computation and aerodynamic optimization [NASA-CR-197748] p 2120 N95-26649

Wind tunnel experiments on wake flow field behind a reentry capsule from a viewpoint of parachute deployment at supersonic speeds [ISAS-R-655] p 2121 N95-26740

Rarefied gas effects on aerobraking/reentry vehicles with wakes [NASA-CR-196586] p 2164 N95-27093

Fuzzy inference enhanced information recovery from digital PIV using cross-correlation combined with particle tracking [NASA-TM-106896] p 2291 N95-27173

Schlieren System and method for moving objects [NASA-CASE-LAR-15053-1] p 2291 N95-27191

Global flowfield about the V-22 Tiltrotor Aircraft [NASA-CR-198603] p 2122 N95-27248

Single-drop reactive extraction/extractive reaction with forced convective diffusion and interphase mass transfer p 2283 N95-27365

Measurements of store forces and moments and cavity pressures for a generic store in and near a box cavity at subsonic and transonic speeds [NASA-TM-4611] p 2123 N95-28241

TranAir: A full-potential, solution-adaptive, rectangular grid code for predicting subsonic, transonic, and supersonic flows about arbitrary configurations. Theory document [NASA-CR-4348] p 2123 N95-28265

Numerical analysis of intra-cavity and power-stream flow interaction in multiple gas-turbine disk-cavities [NASA-TM-106886] p 2140 N95-28344

FLOW EQUATIONS

A Navier-Stokes boundary element solver p 2283 N95-27361

Three-dimensional computer modeling of hydrogen injection and combustion [DE95-006261] p 2203 N95-27437

Robust integration schemes for generalized viscoplasticity with internal-state variables. Part 1: Theoretical developments and applications [NASA-CR-195452-PT-1] p 2310 N95-28031

Robust integration schemes for generalized viscoplasticity with internal-state variables. Part 2: Algorithmic developments and implementation [NASA-CR-195453-PT-2] p 2310 N95-28032

A genuinely multidimensional upwind scheme and efficient multigrid solver for the compressible Euler equations [NASA-CR-195000] p 2288 N95-28571

FLOW MEASUREMENT

Compressible turbulence measurements in a supersonic flow with adverse pressure gradient [AD-A289477] p 2276 N95-26822

FLOW RESISTANCE

Features and applications of the Groove Analysis Program (GAP) p 2281 N95-27349

FLOW STABILITY

The stability of the flow in a laminar separation bubble [CUED/A-AERO/TR-22] p 2275 N95-26809

On the nonlinear stability of the unsteady, viscous flow of an incompressible fluid in a curved pipe [NASA-CR-195065] p 2278 N95-27028

The Benard problem: A comparison of finite difference and spectral collocation eigen value solutions p 2283 N95-27364

Magnetic viscosity by localized shear flow instability in magnetized accretion disks [DE95-006879] p 2433 N95-28111

Computational and experimental studies of hydrodynamic instabilities and turbulent mixing [DE95-006837] p 2288 N95-28603

Experimental study on transition characteristics of natural-convection flow [PB95-192423] p 2289 N95-28637

FLOW VELOCITY

Evaluation of a new laboratory acoustic Doppler velocimeter [AD-A289592] p 2290 N95-26714

An investigation of the AFIT 2-inch shock tube as a flow source for supersonic testing [AD-A289246] p 2143 N95-26966

Observations of near-bottom flow in a wave-dominated nearshore environment [AD-A289331] p 2347 N95-27043

NASA Dryden flow visualization facility [NASA-TM-4631] p 2362 N95-27914

Energization and transport of ions of ionospheric origin in the terrestrial magnetosphere [NASA-CR-198618-REV] p 2338 N95-28035

Water driven turbine/brush pipe cleaner [NASA-CASE-KSC-11669-1] p 2304 N95-28359

Evaluation of microporous carbon filters as catalysts for ozone decomposition [DE95-006498] p 2331 N95-28548

FLOW VISUALIZATION

Plate manipulators [AD-A289601] p 2121 N95-26719

The stability of the flow in a laminar separation bubble [CUED/A-AERO/TR-22] p 2275 N95-26809

Visualization of the multiple supersonic jet oscillations by swept focused strobed schlieren technique p 2119 N95-26952

Flow visualization of a turbulent shear flow using an optical wavefront sensor [AD-A289208] p 2277 N95-26986

Schlieren System and method for moving objects [NASA-CASE-LAR-15053-1] p 2291 N95-27191

NASA Dryden flow visualization facility [NASA-TM-4631] p 2362 N95-27914

DNS, LES and stochastic modeling of turbulent reacting flows [AD-A280099] p 2287 N95-28155

Measurements of store forces and moments and cavity pressures for a generic store in and near a box cavity at subsonic and transonic speeds [NASA-TM-4611] p 2123 N95-28241

FLUENCE

Evaluation of Oxygen Interactions with Materials 3: Mission and induced environments p 2210 N95-27631

Spacecraft materials studies on the Aerospace Corporation tray on EOIM-3 p 2210 N95-27632

Exposure of LDEF materials to atomic oxygen: Results of EOIM 3 p 2210 N95-27633

Atomic oxygen dosimetry measurements made on STS-46 by CONCAP 2 p 2418 N95-27634

FLUID DYNAMICS

A non-iterative grid deformation algorithm for computational fluid dynamics for aeroelasticity [AD-A288298] p 2273 N95-26418

Demonstration study of hierarchical control of fluid-dynamic phenomena [AD-A289341] p 2275 N95-26751

Basic studies in turbulent shear flows [AD-A289145] p 2277 N95-26998

Nonlinear problems in fluid dynamics and inverse scattering: Nonlinear waves and inverse scattering [AD-A289148] p 2278 N95-27001

Nonlinear problems in fluid dynamics and inverse scattering: Langmuir circulations and spiral flows [AD-A289194] p 2278 N95-27019

Junkyard chemistry p 2227 N95-27102

Parallel plasma fluid turbulence calculations [DE95-006741] p 2431 N95-27537

FLUID FILMS

Transport phenomena and interfacial kinetics in multiphase combustion systems [AD-A288297] p 2199 N95-26417

Analysis of gas absorption to a thin liquid film in the presence of a zero-order chemical reaction p 2280 N95-27348

FLUID FILTERS

Application of bacterial bioemusifiers to in situ maintenance of oil/water separators p 2179 N95-27120

FLUID FLOW

Validation of the SINDA/FLUINT code using several analytical solutions p 2281 N95-27350

Transient studies of G-induced capillary dryout and rewet p 2281 N95-27351

Analysis of developing laminar flows in circular pipes using a higher-order finite-difference technique p 2281 N95-27352

Numerical solution of fluid flow and heat tranfer problems with surface radiation p 2282 N95-27357

The Benard problem: A comparison of finite difference and spectral collocation eigen value solutions p 2283 N95-27364

Studies of planetary scale waves and instabilities in support of the geophysical fluid flow cell experiment on USML-2 [NASA-CR-198646] p 2463 N95-27916

Computational and experimental studies of hydrodynamic instabilities and turbulent mixing [DE95-006837] p 2288 N95-28603

FLUID PRESSURE

Apparatus for testing high pressure injector elements [NASA-CASE-MFS-28773-1] p 2304 N95-28347

FLUIDICS

Flow control [AD-A289262] p 2279 N95-27197

FLUORESCENCE

Radiation sensitive area detection device and method [NASA-CASE-MFS-28563-3] p 2423 N95-26385

Flow cytometry as a means of detecting, enumerating and characterizing bacteria for monitoring of the environment [AD-A288997] p 2326 N95-26610

To develop an aerosoling immunomagnetic device for rapid medical diagnosis from clinical samples [AD-A288504] p 2354 N95-27059

Testing of Uninterruptible Power Supplies with nonlinear loads [AD-A289353] p 2262 N95-27067

Automated integration of genomic physical mapping data via parallel simulated annealing [DE95-008057] p 2351 N95-27725

Energy transfer in real and artificial photosynthetic systems [DE95-005824] p 2351 N95-27948

Single molecule detection using charge-coupled device array technology [DE95-006425] p 2411 N95-27953

Nonlinear optical microscopy for imaging thin films and surfaces [DE95-007872] p 2426 N95-28018

Development of an optical trap as an ultra-sensitive analytical tool [DE95-007843] p 2426 N95-28022

Spectroscopic and dynamical studies of highly energized small polyatomic molecules [DE95-006640] p 2414 N95-28199

Method for determining surface coverage by materials exhibiting different fluorescent properties [NASA-CASE-GSC-13539-1] p 2315 N95-28211

New developments for sol-gel film and fiber processing [DE95-008175] p 2240 N95-28404

FLUORIDES

Molecular modeling: An approach for the study of piezoelectric polymers [AD-A289821] p 2241 N95-28574

FLUORO COMPOUNDS

Retrofitting conventional vapor degreasers to use a solvent wash/fluorochemical rinse process p 2232 N95-27127

FLUOROCARBONS

The evaluation of a fluorochemical drying process for an electrical contact p 2227 N95-27103

FLUOROHYDROCARBONS

Extended equation-of-state for dichlorodifluoromethane (CCl2F2) [AD-A288885] p 2177 N95-26434

FLUTTER

Aeroelasticity of wing and wing-body configurations on parallel computers [NASA-CR-197756] p 2129 N95-26590

Nonlinear dynamics and aeroelasticity of rotorcraft in forward flight [AD-A291714] p 2136 N95-28504

FLUTTER ANALYSIS

Flutter clearance flight tests of an OV-10A airplane modified for wake vortex flight experiments [NASA-TM-109168] p 2117 N95-26381

FLUX DENSITY

The 50 Ah NiH2 CPV qualification tests p 2272 N95-26792

The role of microprocesses in macroscale magnetotail dynamics
[DE95-006288] p 2432 N95-27673
Aspects of strange matter
[DE95-008316] p 2414 N95-28170

FLUX DIFFERENCE SPLITTING
A numerical method for solving the three-dimensional parabolized Navier-Stokes equations
[NASA-CR-198159] p 2287 N95-27917

FLUX PINNING
The real structure of columnar pinning centers in heavy-ion-irradiated cuprate superconductors
[DE95-003948] p 2445 N95-28186

FLUX TRANSFER EVENTS
Energization and transport of ions of ionospheric origin in the terrestrial magnetosphere
[NASA-CR-197813] p 2336 N95-26699

FLY ASH
Ash-based ceramic materials
[AD-D017272] p 2241 N95-28582

FLY BY WIRE CONTROL
Evaluation of all-electric secondary power for transport aircraft
[NASA-CR-189077] p 2266 N95-27999

FLYWHEELS
Feasibility of flywheel energy storage systems for applications in future space missions
[NASA-CR-195422] p 2316 N95-26393
Investigation of high-temperature superconducting flywheel energy storage devices
[DE95-759242] p 2320 N95-27936
A hybrid vehicle evaluation code and its application to vehicle design. Revision 1
[DE95-008053] p 2303 N95-28029

FOAMING
Use of CTFE as an additive to enhance fire resistance of single hydraulic fluid
[AD-A289377] p 2233 N95-27325

FOCAL PLANE DEVICES
Performance analysis of bullet trajectory estimation: Approach, simulation, and experiments
[DE95-007949] p 2399 N95-28109

FOCUSING
The consideration of a bright relative beam dynamics in the magnetic focusing field
[DE95-608377] p 2398 N95-27160
Plasma lens experiments at the final focus test beam
[DE95-008595] p 2434 N95-28161

FOG
The attenuation of microwave radiation by fog and rain
[AD-A288326] p 2249 N95-26562

FOILS (MATERIALS)
Indirectly driven targets for ignition
[DE95-006451] p 2430 N95-27327
Development of an optical trap as an ultra-sensitive analytical tool
[DE95-007843] p 2426 N95-28022
On ionic charge distributions of heavy evaporation residues passing through a carbon foil
[DE94-629016] p 2414 N95-28184

FOREBODIES
Computational analysis of forebody tangential slot blowing on the high alpha research vehicle
[NASA-CR-197754] p 2129 N95-26591

FORECASTING
Evolving cascade-correlation networks for time-series forecasting
[AD-A289197] p 2390 N95-27020
Calculations of downward IR surface fluxes in the 500-3,000 cm(exp -1) wavenumber range for the 1994 ICRCCM model intercomparison study
[DE95-006430] p 2328 N95-27708
Models used to forecast agricultural corn crops in the micro-region of Ribeirao Preto-SP
[INPE-5513-NTC/309] p 2315 N95-28554
Severe weather guide mediterranean
[AD-A289829] p 2344 N95-28577

FORESTS
Survey on bio-chemical complex harmonized with global environment
[DE95-759252] p 2331 N95-28535

FORGING
Process control of microstructure in manufacturing
[AD-A288291] p 2245 N95-26410

FORM FACTORS
Phenomenology from 100 large lattices
[DE95-006349] p 2442 N95-27994

FORMALISM
Specifying weak sets
[AD-A288587] p 2364 N95-26536

FORMAT
Digital mapping, charting, and geodesy analysis program: Initial technical review of Raster Product Format
[AD-A289039] p 2313 N95-26476
Thermal neutral format based on the step technology
p 2283 N95-27363

FORMING TECHNIQUES
Forming metallurgy: Supervised drawing course, NTH
[PB95-196507] p 2219 N95-27934
Accuracy issues in modeling superplastic metal forming
[DE95-008934] p 2222 N95-28163
Design of fabric preforms for double diaphragm forming p 2184 N95-28269

FORTRAN
Computing NORAD mean orbital elements from a state vector
[AD-A289281] p 2146 N95-27033
Lattice QCD calculation using VPP500
[DE95-007076] p 2449 N95-27448
Fitting: Subroutine to fit four-moment probability distributions to data
[DE95-007722] p 2395 N95-27684

FORWARD SCATTERING
The high energy behavior of the forward scattering parameters -- (sigma)(sub tot), (rho), and B
[DE95-007075] p 2415 N95-28210

FOSSIL FUELS
Magnetic resonance imaging of solvent transport in polymer networks
[DE95-007142] p 2234 N95-27455
Investigation on comprehensive fossil fuel cycle analysis and assessment approach as viewed from the global environment
[DE95-759241] p 2329 N95-27935
A black carbon emission data base for atmospheric chemistry and climate studies
[DE95-006436] p 2332 N95-28662

FOURIER ANALYSIS
On the azimuthal Fourier components of the Green's function for the Helmholtz equation in three dimensions
[AD-A288775] p 2398 N95-26345
The comparison of P(sub 1) and simplified P(sub 2) synthetic acceleration for iterative methods in transport solutions
[DE94-018306] p 2390 N95-27304

FOURIER SERIES
Load transfer in the stiffener-to-skin joints of a pressurized fuselage
[NASA-CR-198610] p 2310 N95-27865

FOURIER TRANSFORMATION
FTIR measurements of thermal infrared sky radiance and transmission
[DE95-003642] p 2334 N95-26436
Synthetic 3-D atmospheric temperature structure: A model for known geophysical power spectra using a hybrid autoregression and Fourier technique
[AD-A289058] p 2340 N95-26479
Satellite surface material composition from synthetic spectra
[AD-A289236] p 2163 N95-26963
Measurement of N2(+) mobility He via Fourier transform emission spectroscopy
[AD-A289266] p 2404 N95-26979
A cryogenic scan mechanism for use in Fourier transform spectrometers p 2158 N95-27287
Crystal structure, short-range oxygen defects, and water adsorption in La- and Nd-modified ZrO2
[DE95-007134] p 2439 N95-27452
An introduction to wavelet transforms
[AD-A289083] p 2256 N95-28095
Dip-moveout processing by Fourier transform in anisotropic media
[DE95-007668] p 2339 N95-28190
Radon transform and its applications in gridding airborne geophysical survey data
[PB95-195533] p 2315 N95-28643

FRACTALS
The small-scale structure of dispersing clouds in the atmosphere
[AD-A288256] p 2341 N95-26546

FRACTIONATION
Fractionation studies of polyethylene using DSC-technique
[PB95-185252] p 2200 N95-26540
Design considerations in supercritical fluid technology
p 2232 N95-27126

FRACTOGRAPHY
Analysis of fatigue fractographic data of a rod end housing using a Monte Carlo simulation
[NAL-TR-1225] p 2307 N95-26521
Fatigue fracture analysis in medium carbon structural steel and austenitic stainless steel by X-ray fractography
[DE95-601504] p 2213 N95-26675

FRACTURE MECHANICS
Interfacial mobility and its effect on flexural strength and fracture toughness in glass-fiber fabric reinforced epoxy laminates
[AD-A288344] p 2180 N95-26572
Fatigue fracture analysis in medium carbon structural steel and austenitic stainless steel by X-ray fractography
[DE95-601504] p 2213 N95-26675
Characterization of fatigue behavior of 2-D woven fabric reinforced ceramic matrix composite at elevated temperature
[AD-A289423] p 2181 N95-26886
Fatigue behavior of a cross-ply ceramic matrix composite subjected to tension-tension cycling with hold time
[AD-A289418] p 2182 N95-27134
Effect of internal hydrogen on the mixed-mode 1/3 fracture toughness of a ferrific/martensitic stainless steel
[DE95-005722] p 2216 N95-27479
Deformation limits on two-parameter fracture mechanics in terms of higher order asymptotics
[AD-A289113] p 2310 N95-28098
Reactor pressure vessel structural integrity research
[DE95-007034] p 2223 N95-28208
An overview of activities and accomplishments of the Metals and Ceramics Division
[DE95-007020] p 2241 N95-28560

FRACTURE STRENGTH
Interfacial mobility and its effect on flexural strength and fracture toughness in glass-fiber fabric reinforced epoxy laminates
[AD-A288344] p 2180 N95-26572
Effect of internal hydrogen on the mixed-mode 1/3 fracture toughness of a ferrific/martensitic stainless steel
[DE95-005722] p 2216 N95-27479
Structural ceramics incorporating whiskers, platelets, and particulate phases
[DE95-007048] p 2235 N95-27499
Effects of high-temperature environments on flaw generation and fracture behavior of SiC/SiC composites
[DE95-008270] p 2183 N95-28068
An experimental and numerical investigation of specimen size requirements for cleavage fracture toughness
[AD-A289120] p 2311 N95-28100
Reactor pressure vessel structural integrity research
[DE95-007034] p 2223 N95-28208
Service tough composite structures using the Z-direction reinforcement process p 2185 N95-28272
Effect of the fiber-matrix interphase on the transverse tensile strength of the unidirectional composite material
p 2190 N95-28425

FRACTURING
Interfacial mobility and its effect on flexural strength and fracture toughness in glass-fiber fabric reinforced epoxy laminates
[AD-A288344] p 2180 N95-26572
Fatigue fracture analysis in medium carbon structural steel and austenitic stainless steel by X-ray fractography
[DE95-601504] p 2213 N95-26675
Scaling issues in dynamic fragmentation
[DE95-008509] p 2309 N95-27745
Prediction of material strength and fracture of glass using the SPHINX smooth particle hydrodynamics code
[DE95-004869] p 2236 N95-27943
Fracture testing and analysis of adhesively bonded joints for automotive applications
[DE95-007024] p 2184 N95-28207
Tension fracture of laminates for transport fuselage. Part 1: Material screening p 2137 N95-28471

FRAGMENTATION
Environmental effects on high energy density materials
[AD-A288296] p 2199 N95-26416
Scaling issues in dynamic fragmentation
[DE95-008509] p 2309 N95-27745
Tungsten carbide fragmentation: Experimental characterization and numerical modelling
[DE95-008521] p 2236 N95-27879
A novel sensitive detector of atmospheric nitrocompounds based on laser photofragmentation/ionization spectrometry
p 2174 N95-28314
Pressure vessel burst test study p 2175 N95-28317

FRAGMENTS
Automated integration of genomic physical mapping data via parallel simulated annealing
[DE95-008057] p 2351 N95-27725

FRAMES
Application of advanced material systems to composite frame elements p 2191 N95-28432
Effects of floor location on response of composite fuselage frames p 2192 N95-28439

FRANCE
WTEC panel report on research submersibles and undersea technologies
[NASA-CR-198565] p 2247 N95-27909

FREE CONVECTION
Studies of planetary scale waves and instabilities in support of the geophysical fluid flow cell experiment on USML-2
[NASA-CR-198646] p 2463 N95-27916
Experimental study on transition characteristics of natural-convection flow
[PB95-192423] p 2289 N95-28637
FREE ELECTRON LASERS
Free Electron Laser Physical Process Code (FELPPC)
[DE95-006276] p 2296 N95-27557
Time-dependent multi-dimensional simulation studies of the electron output scheme for high power FELs
[DE95-006593] p 2297 N95-27737
High power free-electron laser concepts and problems
[DE95-007841] p 2298 N95-28059
Finite pulse effects in self-amplified-spontaneous emission
[DE95-006585] p 2298 N95-28104
FREE ELECTRONS
Landau quasi-energy spectrum destruction for an electron in both a static magnetic field and a resonant electromagnetic wave
[DE95-610176] p 2256 N95-27716
FREE ENERGY
Modeling the growth of electronic materials
[AD-A289137] p 2438 N95-26997
The free energy of hot QED at three and a half loops
[DE95-007079] p 2449 N95-27449
A first principles approach to phase stability and order-disorder transformation: Application to Li-Al alloys
[DE95-609152] p 2218 N95-27756
Observation on radiation transfer experiments using k-shell absorption spectra
[DE95-008068] p 2434 N95-28141
FREE FLIGHT
Ionizing radiation measurements on LDEF: A0015 Free flyer biostack experiment
[NASA-CR-196603] p 2202 N95-27168
FREE JETS
Preliminary results and research capabilities of a new jet facility at the University of Kansas
p 2119 N95-26951
FREEZING
FREZCHEM: A chemical-thermodynamic model for aqueous solutions at subzero temperatures
[AD-A288456] p 2200 N95-26432
Quantum effects induced by a gap in the spectrum of atom-bath coupling constants: Freezing of atomic decay and monochromatic collective radiation
[DE95-609037] p 2416 N95-28251
FREQUENCIES
Applications of Second Harmonic and Sum Frequency Generation to graphite and silica type interfaces
[AD-A288228] p 2201 N95-26544
Fast wave current drive in D3-D
[DE95-007582] p 2431 N95-27441
Research on the establishment of the database system for R and D on the innovative technology for the Earth
[DE95-759244] p 2458 N95-27937
A numerical study of ultra-short-pulse reflectometry
[DE95-008070] p 2266 N95-28015
Infrared spectroscopy of nonclassical ions and their complexes
[DE95-008487] p 2413 N95-28091
Design, construction, test and evaluation of a frequency scanning radiometer for measuring oil slick thicknesses
[AD-A290040] p 2293 N95-28389
Prediction of fatigue crack growth under constant amplitude and random loading using specimens with multiple cracks
[AD-A291614] p 2136 N95-28409
Atmospheric dispersion in adaptive optics
[AD-A289639] p 2428 N95-28617
FREQUENCY HOPPING
Characterization of solid state laser and nonlinear optical materials
[AD-A291684] p 2300 N95-28458
FREQUENCY MODULATION
Evaluation of the FMICW waveform in HF surface radar applications
[AD-A288245] p 2249 N95-26545
Fundamental concepts of integrated and fiber optic sensors
[NASA-TM-106920] p 2426 N95-27906
Method and apparatus for maintaining linearity and frequency accuracy of an FM chirp waveform
[AD-D017398] p 2258 N95-28615
FREQUENCY MULTIPLIERS
Survey on step recovery diode and its applications
[PB95-184974] p 2260 N95-26646
Study of frequency doubling antireflection coating
[AD-A289634] p 2424 N95-26860
FREQUENCY RANGES
Uncertainties in the calibration of hydrophones at NPL by the three-transducer spherical-wave reciprocity method in the frequency range 10 kHz on 500 kHz
[PB95-185245] p 2401 N95-26615
A study of heart rate and heart rate variability during rapid decompression to 50,000 ft
[AD-A291598] p 2355 N95-28561
FREQUENCY RESPONSE
A state-space model of a large, lightly damped space structure using the Eigensystem realization algorithm
[AD-A289251] p 2163 N95-26970
Modeling of trapping and abrupt doping effects in MESFET's using R-dynamic element
[PB95-184891] p 2262 N95-27050
Effect of noise on Frequency-Resolved Optical Gating measurements of ultrashort pulses
[DE95-007149] p 2298 N95-27969
Low power limits in ultrashort pulse measurement using Frequency-Resolved Optical Gating
[DE95-007150] p 2299 N95-28219
FREQUENCY SCANNING
Design, construction, test and evaluation of a frequency scanning radiometer for measuring oil slick thicknesses
[AD-A290040] p 2293 N95-28389
FREQUENCY STANDARDS
Extended linear ion trap frequency standard apparatus
[NASA-CASE-NPO-19081-1-CU] p 2404 N95-26861
Extended linear ion trap frequency standard apparatus
[NASA-CASE-NPO-19081-1-CU] p 2416 N95-28348
FRICTION
Advanced solid lubricant films by Ion-Beam Assisted Deposition
[AD-A288866] p 2225 N95-26499
Accuracy issues in modeling superplastic metal forming
[DE95-008934] p 2222 N95-28163
FUEL CELL POWER PLANTS
The US Molten Carbonate Fuel-Cell development and commercialization effort
[DE95-008580] p 2320 N95-27746
FUEL CELLS
Molten Carbonate Fuel Cell (MCFC) product development test
[DE95-007345] p 2316 N95-26543
The US Molten Carbonate Fuel-Cell development and commercialization effort
[DE95-008580] p 2320 N95-27746
Stability of chromite interconnections in dual environments
[DE95-007755] p 2267 N95-28131
FUEL COMBUSTION
Coatings of non-oxide ceramics for improved corrosion resistance in high temperature coal combustion
[DE95-006932] p 2241 N95-28604
A black carbon emission data base for atmospheric chemistry and climate studies
[DE95-006436] p 2332 N95-28662
FUEL CORROSION
Characterization of corrosion and development of a breadboard of a D sight aircraft inspection system, phase 1
[AD-A288347] p 2125 N95-26527
Coatings of non-oxide ceramics for improved corrosion resistance in high temperature coal combustion
[DE95-006932] p 2241 N95-28604
FUEL INJECTION
Numerical simulation of combustion flow around a flame holder with hydrogen injection
[NAL-TR-1233] p 2200 N95-26523
Experiment on a rectangular cross section scramjet combustor. 2: Effects of fuel injector geometry
[NAL-TR-1220] p 2139 N95-26600
Propellant injection systems and processes
[NASA-TM-110632] p 2242 N95-26781
Apparatus for testing high pressure injector elements
[NASA-CASE-MFS-28773-1] p 2304 N95-28347
FUEL PRODUCTION
Alternative fuels and vehicles choice model
[DE95-005695] p 2243 N95-27944
FUEL SPRAYS
Cryogenic and simulated fuel jet breakup in argon, helium and nitrogen gas flows
[NASA-TM-106923] p 2291 N95-27030
FUEL SYSTEMS
Pellet injector research and development at ORNL
[DE95-006736] p 2435 N95-28596
Rotorcraft crashworthy airframe and fuel system technology development program
[AD-A289986] p 2126 N95-28630
FUEL TANKS
Bases for extrapolating materials durability in fuel storage pools
[DE95-007748] p 2222 N95-28129
FUELS
Transport phenomena and interfacial kinetics in multiphase combustion systems
[AD-A288297] p 2199 N95-26417
Alternative fuels and vehicles choice model
[DE95-005695] p 2243 N95-27944
Proceedings of the AIAA/FAA joint symposium on general aviation systems
[AD-A289830] p 2120 N95-28610
FULL SCALE TESTS
Structural modification and repair of C-130 wing structure using bonded composites p 2133 N95-27512
Report to Congressional Committees. Comanche Helicopter: Testing needs to be completed prior to production decisions
[GAO/NSIAD-95-112] p 2135 N95-27910
Comparative wind tunnel tests of NACA 23024 airfoils with several aileron and spoiler configurations
p 2124 N95-27976
FULLERENES
Photoemission and optical properties of C60 fullerites
[DE95-006588] p 2425 N95-27539
FUNCTION SPACE
Local operators in Krylov subspaces
[PB95-195525] p 2393 N95-28499
FUNCTIONALS
Contribution to the optimal shape design of two-dimensional internal flows with embedded shocks
[NASA-CR-195062] p 2389 N95-26672
FUNCTIONS (MATHEMATICS)
Studies of radar backscatter as a function of wave properties and the winds in the turbulent marine atmosphere
[NASA-CR-198608] p 2315 N95-28209
FUNGI
Biochemically vulnerable sites for antifungal intercession in the control of fungal growth
[AD-A288345] p 2348 N95-26573
FUNGICIDES
Biochemically vulnerable sites for antifungal intercession in the control of fungal growth
[AD-A288345] p 2348 N95-26573
FURNACES
Junkyard chemistry p 2227 N95-27102
A practical approach to soil remediation
p 2232 N95-27125
The effects of processing variables on reaction synthesis of Fe-Al alloys
[DE95-007405] p 2221 N95-28082
FUSELAGES
Characterization of corrosion and development of a breadboard of a D sight aircraft inspection system, phase 1
[AD-A288347] p 2125 N95-26527
On aircraft repair verification of a fighter A/C integrally stiffened fuselage skin p 2133 N95-27515
Load transfer in the stiffener-to-skin joints of a pressurized fuselage
[NASA-CR-198610] p 2310 N95-27865
Static and fatigue testing of full-scale fuselage panels fabricated using a Therm-X(R) process
p 2185 N95-28270
Advanced tow placement of composite fuselage structure p 2185 N95-28271
ACT/ICAPS: Thermoplastic composite activities
p 2185 N95-28274
The effect of material heterogeneity in curved composite beams for use in aircraft structures
p 2190 N95-28426
Effects of floor location on response of composite fuselage frames p 2192 N95-28439
Probabilistic evaluation of fuselage-type composite structures p 2137 N95-28444
Composite fuselage shell structures research at NASA Langley Research Center p 2194 N95-28466
Test and analysis results for composite transport fuselage and wing structures p 2137 N95-28470
Tension fracture of laminates for transport fuselage. Part 1: Material screening p 2137 N95-28471
Local design optimization for composite transport fuselage crown panels p 2137 N95-28473
Composite fuselage crown panel manufacturing technology p 2137 N95-28474
Advanced textile applications for primary aircraft structures p 2138 N95-28476
Characterization and manufacture of braided composites for large commercial aircraft structures
p 2196 N95-28478
Impact damage resistance of composite fuselage structure, part 1 p 2138 N95-28482
Damage tolerance of a geodesically stiffened advanced composite structural concept for aircraft structural applications p 2138 N95-28487
Rotorcraft crashworthy airframe and fuel system technology development program
[AD-A289986] p 2126 N95-28630

Numerical simulation of crack growth in pressurized fuselages
[PB95-192415] p 2137 N95-28636

FUSION REACTORS
Experimental aspects of effects of high-energy particles on Alfven modes
[DE95-003383] p 2432 N95-27873
Pumping characteristics of a cryopump with Ar sorbent in He and in D2/He mixture
[DE95-007049] p 2302 N95-27875
Advanced tokamak operating modes in TPX and ITER
[DE95-008058] p 2434 N95-28138
Recent high-speed ballistics experiments at ORNL
[DE95-006534] p 2422 N95-28205
Operating points and feedback control of plasma characteristics in tokamaks with full current drive
[DE95-007037] p 2435 N95-28553
Tokamak ETE engineering preliminary project
[INPE-5529-PRE/1796] p 2435 N95-28562

FUZZY SYSTEMS
Digital systems validation. Chapter 20 Artificial Intelligenge with applications for aircraft. Handbbook, volume 2
[AD-A288492] p 2380 N95-26638
Fuzzy inference enhanced information recovery from digital PIV using cross-correlation combined with particle tracking
[NASA-TM-106896] p 2291 N95-27173
Fuzzy logic techniques for rendezvous and docking of two geostationary satellites p 2384 N95-27386
A fuzzy logic intelligent diagnostic system for spacecraft integrated vehicle health management
p 2385 N95-27392

G

GADOLINIUM
Resonant photoemission studies of thickness dependence of the unoccupied Gd 5d bands
[DE95-004127] p 2436 N95-26440

GALACTIC COSMIC RAYS
Abrasion-ablation model for neutron production in heavy ion reactions
[NASA-TM-4656] p 2420 N95-27372

GALACTIC EVOLUTION
A long-term space astrophysics research program: An x-ray perspective of the components and structure of galaxies
[NASA-CR-197787] p 2461 N95-26593

GALACTIC STRUCTURE
A long-term space astrophysics research program: An x-ray perspective of the components and structure of galaxies
[NASA-CR-197787] p 2461 N95-26593

GALAXIES
A long-term space astrophysics research program: An x-ray perspective of the components and structure of galaxies
[NASA-CR-197787] p 2461 N95-26593
The second coming of cold dark matter?
[DE95-005156] p 2462 N95-27445

GALERKIN METHOD
Spectral methods on arbitrary grids
[NASA-CR-198158] p 2279 N95-27247
A probabilistic model of a porous heat exchanger
p 2282 N95-27359
Numerical study to assess sulfur hexafluoride as a medium for testing multielement airfoils
[NASA-TP-3496] p 2124 N95-28674

GALLIUM
BIPM project: Intercomparison of water triple-point cells
[PB95-185237] p 2398 N95-26614

GALLIUM ALLOYS
Study of the phase transformations and microstructures of uranium rich alloys of the binary uranium-gallium system
[DE95-609624] p 2217 N95-27713

GALLIUM ARSENIDES
Chemistry involving the separation, isolation, and immobilization of 3-5 compound semiconductor nanocrystals and quantum dots
[AD-A288381] p 2436 N95-26473
Monte Carlo study of electron-plasmon scattering effects on hot electron transport in GaAs
[DE95-607768] p 2403 N95-26542
Room-temperature photocurrent spectroscopy of GaAs/GaAlAs multiple quantum wells
[AD-A289607] p 2201 N95-26707
Annealing of radiation damaged gallium arsenide solar cells by laser illumination
[AD-A289683] p 2316 N95-26762
Characterization of optical polymers for multi-layered electro-optic devices
[AD-A289255] p 2227 N95-26973
Low resistivity ohmic contacts to moderately doped n-GaAs with low temperature processing
[DE95-008507] p 2445 N95-28144
Sensor for measuring the atomic fraction in highly dissociated hydrogen
[DE95-006531] p 2415 N95-28204
Evaluation of defect-related diffusion in semiconductors by electrooptical sampling
[AD-A291630] p 2270 N95-28544

GALLIUM NITRIDES
Pseudomorphic semiconducting heterostructures from combinations of AlN, GaN and selected SiC polytypes: Theoretical advancement and its coordination with experimental studies of nucleation, growth, characterization and device development
[AD-A289550] p 2437 N95-26756
First-principles calculations for AlN, GaN, and InN: Bulk and alloy properties
[DE95-006822] p 2219 N95-27958

GALLIUM SELENIDES
Growth and evaluation of nonlinear optical crystals for laser applications: Lithium borate, barium borate and silver gallium selenide
[AD-A289147] p 2277 N95-27000

GAME THEORY
Distributed computation of Pareto solutions for two decision makers
[PB95-185047] p 2396 N95-26613
Distributed computation of Pareto solutions in N-player games
[PB95-185039] p 2396 N95-26912
Absolute logics
[ISBN-951-41-0775-6] p 2397 N95-28238
Distributed methods and processes in games of incomplete information
[PB95-184842] p 2396 N95-28352
Distributed methods and processes in games of incomplete information
[PB95-184859] p 2396 N95-28353

GAMMA RAY ASTRONOMY
Multiwavelength observations of unidentified high energy gamma-ray sources
[NASA-CR-197840] p 2465 N95-26630

GAMMA RAY OBSERVATORY
A BATSE investigation of radiation belt electrons precipitated by VLF waves
[NASA-CR-197780] p 2336 N95-26922

GAMMA RAY SPECTRA
Multiwavelength observations of unidentified high energy gamma-ray sources
[NASA-CR-197840] p 2465 N95-26630

GAMMA RAY TELESCOPES
Multiwavelength observations of unidentified high energy gamma-ray sources
[NASA-CR-197840] p 2465 N95-26630

GAMMA RAYS
The effect of proteins on the aging properties of radiation vulcanized Natural Rubber Latex
[DE95-603357] p 2225 N95-26599
Multiwavelength observations of unidentified high energy gamma-ray sources
[NASA-CR-197840] p 2465 N95-26630
Amorphous silicon pixel radiation detectors and associated thin film transistor electronics readout
[DE95-006568] p 2265 N95-27678
Sintering of textured YBa2Cu3O(7-x) under intensive Co-60 gamma irradiation
[DE95-007098] p 2442 N95-27950
Remote sensing of hydrologic variables in boreal areas, phase 2
[NASA-CR-198717] p 2314 N95-27998
Gamma ray-induced embrittlement of pressure vessel alloys
[DE95-007133] p 2220 N95-28072
The Bremsstrahlung of soft gamma-quanta created by elastic pp- and np-scatterings and the dibaryon resonance problem
[DE95-608870] p 2415 N95-28248

GAS ATOMIZATION
Cryogenic and simulated fuel jet breakup in argon, helium and nitrogen gas flows
[NASA-TM-106923] p 2291 N95-27030

GAS DETECTORS
Evaluation of a conductive polymer-based sensor for detection of hydrazines at the part-per-billion level
p 2173 N95-28309
The sensitive detection of hydrazine using chemiluminescence p 2173 N95-28311

GAS DYNAMICS
A genuinely multidimensional upwind scheme and efficient multigrid solver for the compressible Euler equations
[NASA-CR-195000] p 2288 N95-28571
Computational and experimental studies of hydrodynamic instabilities and turbulent mixing
[DE95-006837] p 2288 N95-28603

GAS EXCHANGE
A model of bubble evolution during decompression based on a Monte Carlo simulation of inert gas diffusion
[AD-A289400] p 2353 N95-26885

GAS EXPANSION
A model of bubble evolution during decompression based on a Monte Carlo simulation of inert gas diffusion
[AD-A289400] p 2353 N95-26885
The noise reduction potential of dual-stream coaxial rectangular improperly expanded jet flows
[NASA-CR-197820] p 2277 N95-26995

GAS FLOW
Cryogenic and simulated fuel jet breakup in argon, helium and nitrogen gas flows
[NASA-TM-106923] p 2291 N95-27030

GAS HEATING
Research on combustion processes relevant to burners in HVAC systems
[PB95-179735] p 2208 N95-28006

GAS INJECTION
Three-dimensional computer modeling of hydrogen injection and combustion
[DE95-006261] p 2203 N95-27437

GAS MIXTURES
High temperature kinetic study of the reactions H + O2 = OH + O and O + H2 = OH + H in H2/O2 system by shock tube-laser absorption spectroscopy
[NASA-CR-195473] p 2206 N95-27695

GAS PRESSURE
An investigation of the AFIT 2-inch shock tube as a flow source for supersonic testing
[AD-A289246] p 2143 N95-26966

GAS TUNGSTEN ARC WELDING
Characterization of Ultra-Low Carbon Baintic steels for use as weld wire consumables
[AD-A288292] p 2212 N95-26411

GAS TURBINE ENGINES
Transport phenomena and interfacial kinetics in multiphase combustion systems
[AD-A288297] p 2199 N95-26417
Optimization of wave rotors for use as gas turbine engine topping cycles
[NASA-TM-106951] p 2140 N95-27860
A summary of computational experience at GE Aircraft Engines for complex turbulent flows in gas turbines
p 2285 N95-27865
Composite intermediate case manufacturing scale-up for advanced engines p 2141 N95-28275

GAS TURBINES
Turbulence models for gas turbine combustors
p 2285 N95-27888
Numerical analysis of intra-cavity and power-stream flow interaction in multiple gas-turbine disk-cavities
[NASA-TM-106886] p 2140 N95-28344

GAS VISCOSITY
Magnetic viscosity by localized shear flow instability in magnetized accretion disks
[DE95-006879] p 2433 N95-28111

GAS-METAL INTERACTIONS
Cesium/oxide interactions for ultrathin films on (alpha)-Al2O3(001) and (alpha)-Al2O3(1(bar 1)O2)
[DE95-008159] p 2238 N95-28358

GAS-SOLID INTERACTIONS
Modeling the shock response of submerged structures
[AD-A289082] p 2288 N95-28351

GASEOUS DIFFUSION
A model of bubble evolution during decompression based on a Monte Carlo simulation of inert gas diffusion
[AD-A289400] p 2353 N95-26885
Vapor pressures of mixtures of CFC-114 with the potential replacement coolants C4F(10) andc-C4F 8
[DE95-003444] p 2208 N95-28042

GASES
Development of an upwind, finite-volume code with finite-rate chemistry
[NASA-CR-197747] p 2121 N95-26760
Photoacoustic chambers for studying solids and gases: Theory and practical examples
[IFTR-39/1994] p 2143 N95-26837
Measurement of heterogeneous chemical processes relevant to aerosol surfaces and trace gases active in the marine environment
[DE95-008337] p 2328 N95-27743

GASIFICATION
JPRS report: Science and technology. Central Eurasia
[JPRS-UST-95-021] p 2202 N95-27155
Review and analysis of the 1980-1989 biomass thermochemical conversion program
[DE95-000287] p 2325 N95-28394

GASOLINE
A hybrid vehicle evaluation code and its application to vehicle design. Revision 1
[DE95-008053] p 2303 N95-28029

GAUGE INVARIANCE
A model of the extended electron and its nonlocal electromagnetic interaction: Gauge invariance of the nonlocal theory
[DE95-608803] p 2255 N95-27313
Model independent constraints on anomalous gauge boson self-couplings from e(+)e(-) colliders with longitudinally polarized beams
[DE95-608844] p 2406 N95-27317

GAUGE THEORY
Addendum to the 1993 European school of high-energy physics
[DE95-610313] p 2419 N95-27321

GAUSS EQUATION
Truncated Gaussians as tolerance sets
[NASA-CR-197732] p 2395 N95-27417

GAUSSIAN ELIMINATION
Modified Gaussian elimination for adaptive beamforming using RNS arithmetic
[AD-A288809] p 2248 N95-26356

GEAR TEETH
Using hob offset to balance dynamic strength in spur gears
[NASA-TM-106934] p 2302 N95-27698

GEARS
Diagnosis of helicopter gearboxes using structure-based networks
[NASA-TM-106932] p 2302 N95-27373
Using hob offset to balance dynamic strength in spur gears
[NASA-TM-106934] p 2302 N95-27698
Vibration analysis of a split path gearbox
[NASA-TM-106875] p 2302 N95-27855

GELS
Silicate gel dye laser
[AD-D017262] p 2294 N95-26503
Variation of solvent scattering-length density small-angle neutron scattering as a means of determining structure of composite materials
[DE95-005394] p 2183 N95-27428
Feasibility studies for separation processes using environmentally sensitive hydrogels
[DE95-008355] p 2238 N95-28226
Alternate use of rocket propellants as ingredients in commercial watergel explosives p 2176 N95-28321
The minimum pore size obtainable in a silica gel during drying
[DE95-008162] p 2239 N95-28401
Porosity in hexylene-bridged polysilsesquioxanes: Effects of monomer concentration
[DE95-005421] p 2240 N95-28531
Comparison of bridged polysilsesquioxane xerogels prepared from methoxy- and ethoxy-silyl monomers
[DE95-005422] p 2240 N95-28532

GENE EXPRESSION
Toxicity assessment of liquid propellant XM46
p 2175 N95-28319

GENERAL AVIATION AIRCRAFT
Proceedings of the AIAA/FAA joint symposium on general aviation systems
[AD-A289830] p 2120 N95-28610

GENERAL OVERVIEWS
Building an electronic book on the Internet. CSEP:An interdisciplinary syllabus for teaching computational science at the graduate level
[DE95-006526] p 2375 N95-28632

GENES
Third international congress of plant molecular biology: Molecular biology of plant growth and development
[DE95-006482] p 2352 N95-28496

GENETIC ALGORITHMS
Predicting protein structure using parallel genetic algorithms
[AD-A289305] p 2369 N95-26919
A gain scheduling optimization method using genetic algorithms
[AD-A289306] p 2381 N95-26920
A sustainable genetic algorithm for satellite resource allocation p 2376 N95-27383
A hybrid genetic algorithm for resolving closely spaced objects p 2384 N95-27387

GENETICS
Comparative Transduction Mechanisms of Vestibular Otolith Hair Cells
[NASA-CR-197980] p 2349 N95-26727
Comparative transduction mechanisms of hair cells in the bullfrog utriculus. 1: Responses to intracellular current p 2350 N95-26731
Predicting protein structure using parallel genetic algorithms
[AD-A289305] p 2369 N95-26919
Investigation on technology for increasing the biological CO2 sink and technology for CO2 fixation and reutilization
[DE95-759251] p 2329 N95-27941
Toxicity assessment of liquid propellant XM46
p 2175 N95-28319

GEOCENTRIC COORDINATES
Ulysses orbit determination at high declinations
p 2151 N95-27787

GEOCHEMISTRY
Synchrotron X-ray scattering studies at mineral-water interfaces
[DE95-008303] p 2440 N95-27542
Testing the correlation between seismic stratigraphy, diagenesis and physical rock properties: Evaluation of fluid flow during early and late diagenesis
[DE95-008338] p 2338 N95-28083

GEODESIC LINES
Damage tolerance of a geodesically stiffened advanced composite structural concept for aircraft structural applications p 2138 N95-28487

GEODESY
Digital mapping, charting, and geodesy analysis program: Initial technical review of Raster Product Format
[AD-A289039] p 2313 N95-26476
Naval Aviation System TEAM mapping, charting, and geodesy handbook
[AD-A288590] p 2314 N95-26841
On the persistence of the oceanic background of apparent sea level changes in the Baltic Sea
[REPT-94:5] p 2348 N95-27996

GEODYNAMICS
On the persistence of the oceanic background of apparent sea level changes in the Baltic Sea
[REPT-94:5] p 2348 N95-27996

GEOGRAPHIC INFORMATION SYSTEMS
Application of a Geographic Information System for radiologic emergency response
[DE95-007624] p 2455 N95-28113

GEOGRAPHY
Live from Antarctica: The coldest, windiest place on Earth
[NASA-CR-197737] p 2335 N95-26595
Southern Africa: A climatological study
[AD-A289466] p 2342 N95-27148

GEOLOGICAL FAULTS
Investigation of rifting processes in the Rio Grande Rift using data from an unusually large earthquake swarm
[DE95-007623] p 2339 N95-28126
Dip-moveout processing by Fourier transform in anisotropic media
[DE95-007668] p 2339 N95-28190
Transformation to zero offset in transversely isotropic media
[DE95-007669] p 2339 N95-28192

GEOLOGICAL SURVEYS
High performance ground penetrating radar survey of TA-49/Area 2
[DE95-006656] p 2258 N95-28601

GEOLOGY
Live from Antarctica: The coldest, windiest place on Earth
[NASA-CR-197737] p 2335 N95-26595
Contact micromechanics in granular media with clay
[DE95-006566] p 2340 N95-28583

GEOMAGNETISM
Applying AI tools to operational space environmental analysis p 2382 N95-27376
SAMPEX special pointing mode p 2149 N95-27780

GEOMETRIC DILUTION OF PRECISION
Determining GPS average performance metrics
p 2128 N95-27791

GEOMETRICAL OPTICS
Full complex modulation using two one-parameter spatial light modulators
[NASA-CASE-MSC-22255-1] p 2427 N95-28384

GEOPHYSICS
Finding the forest in the trees. The challenge of combining diverse environmental data
[NASA-CR-197798] p 2326 N95-26362
A geo-acoustic and oceanographic description of several shallow water experimental sites on the Scotian Shelf
[AD-A288300] p 2345 N95-26420
Synthetic 3-D atmospheric temperature structure: A model for known geophysical power spectra using a hybrid autoregression and Fourier technique
[AD-A289058] p 2340 N95-26479
Airborne geophysics and precise positioning: Scientific issues and future directions
[LC-94-68678] p 2314 N95-27156
Geophex airborne unmanned survey system
[DE95-007566] p 2131 N95-27440
Studies of planetary scale waves and instabilities in support of the geophysical fluid flow cell experiment on USML-2
[NASA-CR-198646] p 2463 N95-27916
Solar-geophysical data number 604, December 1994. Part 1: (Prompt reports). Data for November, October 1994, and late data
[PB95-181848] p 2465 N95-28087
Emerging applications of probability (stochastic models in geosystems)
[AD-A289117] p 2313 N95-28099
Radon transform and its applications in gridding airborne geophysical survey data
[PB95-195533] p 2315 N95-28643

GEOSYNCHRONOUS ORBITS
Development test of a liquid Apogee engine for the ETS-6
[NAL-TR-1250] p 2167 N95-26799
Long-term variability of electron radiation dose in geosynchronous orbit
[AD-A289335] p 2162 N95-26902
Electric propulsion for geostationary orbit insertion
[NASA-TM-106942] p 2168 N95-27727
Accurate orbit determination strategies for the tracking and data relay satellites p 2147 N95-27768
Geostationary Operational Environmental Satellite (GOES)-8 mission flight experience
p 2153 N95-27798
ORION: A Supersynchronous Transfer Orbit mission
p 2154 N95-27804
The combined release and radiation effects satellite time history data base system
[AD-A289835] p 2165 N95-28578

GEOTHERMAL ENERGY CONVERSION
Geothermal direct-heat utilization assistance
[DE95-007247] p 2319 N95-27236

GEOTHERMAL ENERGY EXTRACTION
Geothermal direct-heat utilization assistance
[DE95-007247] p 2319 N95-27236

GEOTHERMAL ENERGY UTILIZATION
Geothermal direct-heat utilization assistance
[DE95-007247] p 2319 N95-27236
Geothermal development in Australia
[DE95-007837] p 2325 N95-28058

GEOTHERMAL RESOURCES
Geothermal direct-heat utilization assistance
[DE95-007247] p 2319 N95-27236

GEOTHERMAL TECHNOLOGY
Geothermal direct-heat utilization assistance
[DE95-007247] p 2319 N95-27236
Geothermal development in Australia
[DE95-007837] p 2325 N95-28058

GERMANIUM
Low temperature carrier transport properties in isotopically controlled germanium
[DE95-008489] p 2444 N95-28092
Chemical and electrical properties of cavities in silicon and germanium
[DE95-006812] p 2445 N95-28206
Search for deeply bound pionic atoms with high-purity germanium tagging spectrometer
[DE95-609072] p 2416 N95-28252

GETTERS
Cavity formation and impurity gettering in He-implanted Si
[DE95-007744] p 2444 N95-28127

GIBBS FREE ENERGY
Thermodynamics of electrolyte solutions for use in high energy lithium batteries
[AD-A288897] p 2199 N95-26352

GLASS
Orbital impacts and the Space Shuttle windshield
[NASA-TM-110594] p 2159 N95-26379
Silicate gel dye laser
[AD-D017262] p 2294 N95-26503
Scintillator materials for calorimetry
[DE95-006570] p 2421 N95-27679
Ceramic fiber-reinforced monoclinic celsian phase glass-ceramic matrix composite material
[NASA-CASE-LEW-15714-1] p 2183 N95-27717
Prediction of material strength and fracture of glass using the SPHINX smooth particle hydrodynamics code
[DE95-004869] p 2236 N95-27943
Modification of the optical properties of glass by sequential ion implantation
[DE95-007401] p 2237 N95-28080
Characterization of solid state laser and nonlinear optical materials
[AD-A291684] p 2300 N95-28458
Fellowship in physics
[AD-A291691] p 2446 N95-28522
Contact micromechanics in granular media with clay
[DE95-006566] p 2340 N95-28583
Supercooled liquid dynamics for the charged hard-sphere model
[DE95-609158] p 2241 N95-28609

GLASS FIBERS
Interfacial mobility and its effect on flexural strength and fracture toughness in glass-fiber fabric reinforced epoxy laminates
[AD-A288344] p 2180 N95-26572
Scarf joint technique with cocured and precured patches for composite repair p 2135 N95-27524
Thermal control materials on EOIM-3
p 2242 N95-27639
Design prediction for long term stress rupture service of composite pressure vessels p 2188 N95-28291
Utilization of composite materials by the US Army: A look ahead p 2189 N95-28421

GLASS LASERS
Trident as an ultrahigh irradiance laser
[DE95-006345] p 2297 N95-27850

GLIDERS
Sailplane glide performance and control using fixed and articulating winglets
[NASA-CR-198579] p 2131 N95-27180

GLIDING
Sailplane glide performance and control using fixed and articulating winglets
[NASA-CR-198579] p 2131 N95-27180

GLOBAL POSITIONING SYSTEM
Flight evaluation of GPS/DGPS sensor systems installed in NAL Do228
[NAL-TR-1230] p 2126 N95-26585
Analysis and simulation of narrowband GPS jamming using digital excision temporal filtering
[AD-A289328] p 2127 N95-26898
Flight Mechanics/Estimation Theory Symposium 1995
[NASA-CP-3299] p 2146 N95-27763
Determining GPS average performance metrics
p 2128 N95-27791
A demonstration of unified TDRS/GPS tracking and orbit determination p 2151 N95-27792
GPS as an orbit determination subsystems
p 2152 N95-27793
Operational considerations of using GPS for spacecraft navigation p 2152 N95-27794
The Global Positioning System (GPS) and attitude determination: Applications and activities in the Flight Dynamics Division p 2152 N95-27795

GLOBAL WARMING
Investigation on working out the global regeneration plan
[DE95-759246] p 2329 N95-27938
Research project on CO2-induced climate change
[DE95-008339] p 2330 N95-28084
The importance of propulsion engineers in protecting the global environment p 2170 N95-28295

GLOVES
Gloved operator performance study. The effects of hand wear and elastic resistance of a control during tracking performance
[AD-A289405] p 2360 N95-27099

GLUONS
Physics with relativistic heavy ions: QGP and other delicacies
[DE95-007014] p 2406 N95-27307
The gluon propagator in non-Abelian Weizsaecker-Williams fields
[DE95-006877] p 2449 N95-27547
Recent status in the search for the quark-gluon plasma
[DE95-007036] p 2417 N95-28447

GLYCINE
Growth and characterization of crystals for room temperature I.R. detectors and second harmonic generation devices
[NASA-CR-198598] p 2443 N95-28033

GLYCOLS
Biodegradation of nitrate esters p 2171 N95-28299

GODDARD TRAJECTORY DETERMINATION SYSTEM
Accurate orbit determination strategies for the tracking and data relay satellites p 2147 N95-27768
The transition of GTDS to the Unix workstation environment p 2151 N95-27789

GOES SATELLITES
Flight Mechanics/Estimation Theory Symposium 1995
[NASA-CP-3299] p 2146 N95-27763
Evaluation and modeling of autonomous attitude thrust control for the Geostation Operational Environmental Satellite (GOES)-8 orbit determination
p 2146 N95-27765
Geostationary Operational Environmental Satellite (GOES)-8 mission flight experience
p 2153 N95-27798
Solar-geophysical data number 604, December 1994. Part 1: (Prompt reports). Data for November, October 1994, and late data
[PB95-181848] p 2465 N95-28087

GOGGLES
An image quality analysis of ANVIS-6 night vision goggles
[AD-A289398] p 2359 N95-26883
Evaluation of laser-protective eyewear dyes in UVEX lenses
[AD-A290076] p 2361 N95-28390

GOLD
Indirectly driven targets for ignition
[DE95-006451] p 2430 N95-27327
Evaluation of space environmental effects on metals and optical thin films on EOIM-3 p 2210 N95-27641
Effects of interlayers on the scratch adhesion performance of ultra-thin films of copper and gold on silicon substrates
[DE95-007367] p 2220 N95-28044
Formation of anisotropic Tl-1212, Tl-2212, Tl-1223 and Tl-2223 particles using aerosol flow reacted powders
[DE95-007400] p 2444 N95-28079
Self-assembly of low-dimensional molecular nanoclusters on Au(111) surfaces
[AD-A288936] p 2178 N95-28334

GOLD ALLOYS
Precursor phenomenon of martensitic transformation in Au-49.5at%Cd alloy
[DE95-007698] p 2222 N95-28166

GOODNESS OF FIT
Statistical analysis of tensile mechanical property data of carbon/polyimide composites
[NAL-TR-1238] p 2180 N95-26667

GOVERNMENT PROCUREMENT
Surviving the peace. Lessons learned from the aircraft industry in the 1920s and 1930s
[AD-A288284] p 2117 N95-26455
Report to the Chairman and Ranking Minority Member, Committee on Science, House of Representatives. Weather forecasting: Radar availability requirement not being met
[GAO/AIMD-95-132] p 2342 N95-27912

GOVERNMENT/INDUSTRY RELATIONS
NIST Automated Manufacturing Research Facility (AMRF): March 1987
[NONP-NASA-VT-95-49097] p 2246 N95-27203
Quest for excellence 5
[NONP-NASA-VT-95-49099] p 2451 N95-27205
Malcolm Baldrige National Quality Award winners 1989
[NONP-NASA-VT-95-49119] p 2451 N95-27207
NIST: Information management in the AMRF
[NONP-NASA-VT-95-49120] p 2454 N95-27208
STEP: A futurevision, today
[NONP-NASA-VT-95-49121] p 2451 N95-27209
Collected papers on wind turbine technology
[NASA-CR-195432] p 2321 N95-27970

GRADIENTS
Polarizing matter and antimatter: A new method
[DE95-007109] p 2421 N95-27923

GRAFTING
The 18th Asilomar Conference on Polymeric Materials
[AD-A291721] p 2240 N95-28508

GRAIN BOUNDARIES
Radiation-induced grain boundary segregation in austenitic stainless steels
[DE95-005721] p 2216 N95-27493
Atomistic calculations of hydrogen interactions with Ni3Al grain boundaries and Ni/Ni/Ni3Al interfaces
[DE95-006497] p 2408 N95-27534
Trace elements and the mechanical properties of intermetallic compounds
[DE95-007378] p 2220 N95-28046
Local texture and grain boundary misorientations in high H(C) oxide superconductors
[DE95-007004] p 2447 N95-28606

GRAIN SIZE
Grain size management in repetitive task graphs for multiprocessor computer scheduling
[AD-A288575] p 2377 N95-26551
Solid-state sintering of tungsten heavy alloys
[DE95-007749] p 2222 N95-28130

GRAND UNIFIED THEORY
Bit-string physics: A novel theory of everything
[DE95-005941] p 2449 N95-28137

GRANULAR MATERIALS
Contact micromechanics in granular media with clay
[DE95-006566] p 2340 N95-28583

GRAPHICAL USER INTERFACE
NEXTSTEP: The next step in the right direction? Part 2: Software development with NEXTSTEP
[REPT-94-33-PT-2] p 2450 N95-26803
The transition of GTDS to the Unix workstation environment p 2151 N95-27789
The Sunrise project: An R&D project for a national information infrastructure prototype
[DE95-006340] p 2455 N95-27847

GRAPHITE
Applications of Second Harmonic and Sum Frequency Generation to graphite and silica type interfaces
[AD-A288228] p 2201 N95-26544
Evaluation of composite joints
[AD-A289247] p 2181 N95-26967

GRAPHITE-EPOXY COMPOSITES
Combined investigation of Eddy current and ultrasonic techniques for composite materials NDE
[NASA-TM-110599] p 2306 N95-26778
The collapse of composite cylindrical panels with various thickness using finite element analysis
[AD-A289370] p 2308 N95-26905
An experimental investigation of sandwich flat panels under low velocity impact
[AD-A289420] p 2309 N95-27135
Probabilistic simulation of long term behavior in polymer matrix composites
[NASA-TM-106893] p 2309 N95-27174
Structural modification and repair of C-130 wing structure using bonded composites p 2133 N95-27512
Scarf repairs to graphite/epoxy components
p 2135 N95-27523
Analysis of selected specimens from the STS-46 Energetic Oxygen Interaction with Materials-3 experiment p 2210 N95-27642
Load transfer in the stiffener-to-skin joints of a pressurized fuselage
[NASA-CR-198610] p 2310 N95-27865
Mechanical properties of triaxially braided composites: Experimental and analytical results
p 2189 N95-28423
Investigation of static and cyclic bearing failure mechanisms for GR/EP laminates p 2190 N95-28427
Compressive residual strength of graphite/epoxy laminates after impact p 2191 N95-28431
Effects of floor location on response of composite fuselage frames p 2192 N95-28439
Structural testing of the technology integration box beam p 2194 N95-28467
Effect of low-speed impact damage and damage location on behavior of composite panels p 2197 N95-28481
Compressive strength of damaged and repaired composite plates p 2198 N95-28484
Post impact compressive strength in composites
p 2198 N95-28485
Fundamental concepts in the suppression of delamination buckling by stitching p 2198 N95-28486
NASA-ACEE/Boeing 737 graphite-epoxy horizontal stabilizer service p 2138 N95-28489

GRAPHS (CHARTS)
Naval Aviation System TEAM mapping, charting, and geodesy handbook
[AD-A288590] p 2314 N95-26841
Using the dimension reduction technique to prove that clique trees define facets for the asymmetric traveling salesman polytope
[AD-A289397] p 2389 N95-26882

GRASSLANDS
Measurement and analysis of the surface energy budget for ARM field experiments
[DE95-007646] p 2338 N95-28114

GRAVIMETERS
The installation of and first results from the superconducting gravimeter GWR20 at the Metsahovi Station, Finland
[REPT-95:1] p 2338 N95-27995

GRAVIRECEPTORS
Comparative transduction mechanisms of hair cells in the bullfrog utriculus. 1: Responses to intracellular current p 2350 N95-26731

GRAVITATION
On higher derivative gravity in two dimensions
[DE95-608789] p 2462 N95-27343
General relativity and experiment
[PB95-192894] p 2450 N95-28664

GRAVITATIONAL EFFECTS
Device and method for screening crystallization conditions in solution crystal growth
[NASA-CASE-MFS-28985-1] p 2245 N95-26888
Transient studies of G-induced capillary dryout and rewet p 2281 N95-27351
Photon rockets and gravitational radiation
[PB95-190161] p 2397 N95-28174

GRAVITATIONAL LENSES
CO, HCO(+) and HCN absorption in the gravitational lens candidate B0218+357 at z=0.685
[PB95-185146] p 2461 N95-26522

GRAVITATIONAL WAVES
Photon rockets and gravitational radiation
[PB95-190161] p 2397 N95-28174

GRAVITY WAVES
Meso-beta scale numerical simulation studies of terrain-induced jet streak mass/momentum perturbations
[NASA-CR-197804] p 2335 N95-26592

GRAY SCALE
Grayscale/resolution trade-off for text: Model predictions and psychophysical results for letter confusion and letter discrimination [NASA-CR-197784] p 2369 N95-26930
GRAZING
Projectile image acceleration, neutralization and electron emission during grazing interactions of multicharged ions with Au(110) [DE95-007394] p 2409 N95-27551
GRAZING INCIDENCE
Reflection of neutrons from an optical grating [DE95-007145] p 2411 N95 28004
GREASES
Environmentally Benign Cleaning and Degreasing Technology: JANNAF Safety and Protection Subcommittee and Propellant Development and Characterization Subcommittee Joint Workshop [CPIA-PUBL-611] p 2227 N95-27101
CO2 pellet blast cleaning and degreasing: The true environmentally benign technology p 2229 N95-27109
Aqueous degreasing, precision cleaning, and cleanliness verification p 2231 N95-27121
GREAT PLAINS CORRIDOR (NORTH AMERICA)
Site scientific mission plan for the Southern Great Plains CART site, January-June 1995 [DE95-008393] p 2344 N95-28340
GREEN'S FUNCTIONS
On the azimuthal Fourier components of the Green's function for the Helmholtz equation in three dimensions [AD-A288775] p 2398 N95-26345
Scaling of localization length of a quasi 1D system with longitudinal boundary roughness [DE95-609148] p 2391 N95-27739
A diagram technique for strongly interacting fermion systems. One-and two-band Hubbard models [DE95-609437] p 2410 N95-27881
Scattering by a small object close to an interface. 3. Buried object [PB95-184909] p 2256 N95-28354
Efficient modeling of interconnects and capacitive discontinuities in high-speed digital circuits [NASA-CR-198728] p 2270 N95-28570
GREENHOUSE EFFECT
Measurement of heterogeneous chemical processes relevant to aerosol surfaces and trace gases active in the marine environment [DE95-008337] p 2328 N95-27743
Towards the detection and attribution of an anthropogenic effect on climate [DE95-008589] p 2331 N95-28157
GREENLAND
Tomographic observations of deep convection and the thermal evolution of the Greenland Sea Gyre 1988-1989 [AD-A289104] p 2348 N95-28096
GRID GENERATION (MATHEMATICS)
Adaptive finite element method I: Solution algorithm and computational examples [AD-A288979] p 2389 N95-26609
Supersonic transport grid generation, validation, and optimization [NASA-CR-197752] p 2365 N95-26648
User's and test case manual for FEMATS [NASA-CR-197803] p 2366 N95-26694
The multidimensional Self-Adaptive Grid code, SAGE, version 2 [NASA-TM-110350] p 2367 N95-26726
Numerical simulation of the flow about the F-18 HARV at high angle of attack [NASA-CR-197755] p 2121 N95-26735
Computational support of the laminar flow supersonic wind tunnel, CNSFV code development, Maglev, and grid generation [NASA-CR-197750] p 2143 N95-26775
Unstructured mesh generation and adaptivity [NASA-CR-195069] p 2278 N95-27027
A 3D agglomeration multigrid solver for the Reynolds-averaged Navier-Stokes equations on unstructured meshes [NASA-CR-195073] p 2390 N95-27029
Development of numerical methods for overset grids with applications for the integrated Space Shuttle vehicle [NASA-CR-197759] p 2160 N95-27154
Global flowfield about the V-22 Tiltrotor Aircraft [NASA-CR-198603] p 2122 N95-27248
Calculation of three-dimensional (3-D) internal flow by means of the velocity-vorticity formulation on a staggered grid [NASA-TM-110352] p 2122 N95-27258
Error analysis of the quartic nodal expansion method for slab geometry [DE95-007373] p 2412 N95-28045
A new algorithm for generating highly accurate benchmark solutions to transport test problems [DE95-007397] p 2373 N95-28047
TranAir: A full-potential, solution-adaptive, rectangular grid code for predicting subsonic, transonic, and supersonic flows about arbitrary configurations. Theory document [NASA-CR-4348] p 2123 N95-28265
Weighting the recursive spectral bisection algorithm for unstructured grids [DE95-008080] p 2373 N95-28521
Radon transform and its applications in gridding airborne geophysical survey data [PB95-195533] p 2315 N95-28643
GROOVES
The effects of transverse vibration on the performance of an axial groove wick heat pipe [AD-A289349] p 2278 N95-27065
Features and applications of the Groove Analysis Program (GAP) p 2281 N95-27349
Transient studies of G-induced capillary dryout and rewet p 2281 N95-27351
GROUND BASED CONTROL
Air traffic operational inventory CY 1994 [AD-A288281] p 2126 N95-26454
Limits to ground control in autonomous spacecraft p 2383 N95-27381
Optimal attitude maneuver execution for the Advanced Composition Explorer (ACE) mission p 2149 N95-27778
GROUND EFFECT (AERODYNAMICS)
Experimental investigation of static and dynamic ground effect on HOPE ALFLEX vehicle [NAL-TR-1236] p 2128 N95-26525
GROUND EFFECT MACHINES
Air cushioned landing craft (LCAC) based ship to shore movement simulation: A decision aid for the amphibious commander. A (SMMAT) application [AD-A289635] p 2246 N95-26722
GROUND STATE
Hydrogen-like atom in laser field: Invariant atomic parameters in the ground state [DE95-609036] p 2411 N95-27930
GROUND STATIONS
A demonstration of unified TDRS/GPS tracking and orbit determination p 2151 N95-27792
GROUND SUPPORT EQUIPMENT
Aqueous degreasing, precision cleaning, and cleanliness verification p 2231 N95-27121
The 29th Aerospace Mechanisms Symposium [NASA-CP-3293] p 2154 N95-27260
GROUND SUPPORT SYSTEMS
Development and implementation of a system safety program for the space launch complex 3 east (SLC-3E) ground support system project to support Atlas 2 family of space launch vehicles p 2174 N95-28316
GROUND TESTS
The 1994 27th Annual NASA Aerospace Battery Workshop [NASA-CP-3292] p 2317 N95-26785
A new technique for ground simulation of hypervelocity debris p 2154 N95-27671
GROUND WATER
Combined use of ground water circulation (UVB) technology and in situ bioreactors for enhanced bioremediation of subsurface contamination p 2230 N95-27118
Biodegradation of nitrate esters p 2171 N95-28299
GROUND WIND
Indexing meso-beta surface wind site representative [AD-A288501] p 2341 N95-26650
GROUP DYNAMICS
Analysis of group performance in visual signal detection [AD-A289561] p 2355 N95-26683
GROUP THEORY
Gromov-Lawson-Rosenberg conjecture for groups with periodic cohomology [PB95-185203] p 2389 N95-26915
Trace anomalies and cocycles of Weyl and diffeomorphism groups [DE95-608793] p 2397 N95-27344
Realization of vector fields for quantum groups as pseudodifferential operators on quantum spaces [DE95-008485] p 2449 N95-27877
A case study in automated theorem proving: A difficult problem about commutators [DE95-008392] p 2392 N95-28173
GROWTH
Modeling the growth of electronic materials [AD-A289137] p 2438 N95-26997
GUN LAUNCHERS
A high velocity electromagnetic mass launcher having an ablation resistant insulator [AD-A288231] p 2154 N95-26524
GUNS (ORDNANCE)
Stress analysis and failure of an internally pressurized composite-jacketed steel cylinder p 2186 N95-28280
GUST LOADS
Calculation of design load for the MOD-5A 7.3 mW wind turbine system p 2312 N95-27982
Comparison of measured and calculated dynamic loads for the Mod-2 2.5 mW wind turbine system p 2312 N95-27983
GUSTS
A model of rotationally-sampled wind turbulence for predicting fatigue loads in wind turbines p 2312 N95-27972
Calculation of design load for the MOD-5A 7.3 mW wind turbine system p 2312 N95-27982
GYRES
Tomographic observations of deep convection and the thermal evolution of the Greenland Sea Gyre 1988-1989 [AD-A289104] p 2348 N95-28096

H

H LINES
Solar UV flux measurements from the SBUV2 monitor on the NOAA9 satellite. Part 1: Mg II h and k line core-to-wing ratios for 1986-1988 [PB95-181962] p 2464 N95-28007
HADRONS
The photon structure function F2 in QCD with nonlocal vacuum quark condensates [DE95-608829] p 2406 N95-27314
Measurement of R in e(+)e(-)-annihilation at center-of-mass energies between 7.2 and 10.34 GeV [DE95-610303] p 2407 N95-27408
Couplings of heavy hadrons with soft pions from QCD sum rules [DE95-610349] p 2407 N95-27410
Polarizing matter and antimatter: A new method [DE95-007109] p 2421 N95-27923
Beam-beam interaction working group summary [DE95-007824] p 2422 N95-28123
Measurement of alpha(s) in e(+)e(-) annihilation at E(cm) = 29 GeV [DE95-006486] p 2417 N95-28594
HAIR
Comparative Transduction Mechanisms of Vestibular Otolith Hair Cells [NASA-CR-197980] p 2349 N95-26727
Regional differences in lectin binding patterns of vestibular hair cells p 2349 N95-26728
Hair cell regeneration in the bullfrog vestibular otolith organs following aminoglycoside toxicity p 2349 N95-26729
Peripheral innervation patterns of vestibular nerve afferents in the bullfrog utriculus p 2349 N95-26730
Comparative transduction mechanisms of hair cells in the bullfrog utriculus. 1: Responses to intracellular current p 2350 N95-26731
Comparative transduction mechanisms of hair cells in the bullfrog uticulus. 2: Sensitivity and response dynamics to hair bundle displacement p 2350 N95-26732
HALIDES
Poly(N-arylenbenzimidazoles) via aromatic nucleophilic displacement [NASA-CASE-LAR-14939-1] p 2179 N95-28360
HALL EFFECT
Hall effect and resistivity in the normal state of high-T(sub c) cuprates in the electron-fracton model [DE95-610612] p 2439 N95-27413
HALLEY'S COMET
Search for molecular absorptions with the Fourier Transform Spectrometer [NASA-CR-198648] p 2462 N95-28222
HALOGENS
Chemical physics of uniform cyclic etching [AD-A288975] p 2404 N95-26574
HAMILTONIAN FUNCTIONS
DNA denaturation through a model of the partition points on a one-dimensional lattice [DE95-607909] p 2439 N95-27201
Wigner quantum oscillators. OSP (3/2) oscillators [DE95-608756] p 2448 N95-27334
Numerical study of the singlet-triplet model for cuprate superconductors [DE95-609438] p 2440 N95-27712
Scaling of localization length of a quasi 1D system with longitudinal boundary roughness [DE95-609148] p 2391 N95-27739
Multifractal character of the electronic states in disordered two-dimensional systems [DE95-609153] p 2443 N95-28016
Aeroelasticity and structural optimization of composite helicopter rotor blades with swept tips [NASA-CR-4665] p 2136 N95-28262
Korteweg-de Vries equation: Convergent Birkhoff normal form [PB95-196275] p 2393 N95-28611

HANDBOOKS
Naval Aviation System TEAM mapping, charting, and geodesy handbook
[AD-A288590] p 2314 N95-26841
Long Duration Exposure Facility (LDEF) space optics handbook p 2428 N95-27654
Severe weather guide mediterranean
[AD-A289829] p 2344 N95-28577

HARDNESS
New radiation stable and long-lived plastic scintillators
[DE95-608622] p 2233 N95-27163

HARDWARE
Pulse Code Modulation (PCM) encoder handbook for Aydin Vector MMP-900 series system
[NASA-RP-1365] p 2255 N95-27435
Building an electronic book on the Internet. CSEP:An interdisciplinary syllabus for teaching computational science at the graduate level
[DE95-006526] p 2375 N95-28632

HARDWARE DESCRIPTION LANGUAGES
Accelerating conservative parallel simulation of VHDL circuits
[AD-A289317] p 2264 N95-27294

HARMONIC GENERATIONS
Applications of Second Harmonic and Sum Frequency Generation to graphite and silica type interfaces
[AD-A288228] p 2201 N95-26544
A new growth technology for highly non-linear, optical quality organic films: Organic vapor phase deposition
[AD-A289006] p 2178 N95-26567
Nonlinear optical microscopy for imaging thin films and surfaces
[DE95-007872] p 2426 N95-28018
Growth and characterization of crystals for room temperature I.R. detectors and second harmonic generation devices
[NASA-CR-198598] p 2443 N95-28033
Vibrational spectroscopy of water interfaces
[DE95-006592] p 2209 N95-28218
Nonlinear optical studies of surfaces
[DE95-006574] p 2428 N95-28557

HARMONIC OSCILLATORS
The canonical q-transformations with two q-para-Bose oscillators
[DE95-608781] p 2396 N95-27341

HARMONICS
Field quality improvements in superconducting magnets for RHIC
[DE95-006096] p 2269 N95-28339

HARNESSES
Partial discharge testing of high voltage wiring harness for airborne displays
[AD-A289150] p 2138 N95-27003

HARRIER AIRCRAFT
Navy composite maintenance and repair experience
p 2193 N95-28446

HARTREE APPROXIMATION
Analytic formulae for the Hartree-Fock order parameter at arbitrary p/q filling factors for the 2DEG in a magnetic field
[DE95-607805] p 2448 N95-26603

HASTELLOY (TRADEMARK)
Materials considerations for molten salt accelerator-based plutonium conversion systems
[DE95-006743] p 2217 N95-27544

HAZARDS
Space Debris Research Phase One Program: Abstracts from published papers (1990-1993)
[AD-A289504] p 2162 N95-26850
Measurements of the volatilities of electrolytes: Application to water/steam cycles
[DE95-007103] p 2204 N95-27451
The effect of aviation fuels containing low amounts of static dissipater additive on electrostatic charge generation
[AD-A280075] p 2243 N95-28152
Hazards analysis of an integral class 1.1/1.3 rocket motor demilitarization and ingredient recovery system using ammonia p 2174 N95-28315
The protection of electro-explosive devices (EEDs) and electronics from electrostatic discharge (ESD) hazards
[DSTO-TR-0100] p 2258 N95-28568

HEAD MOVEMENT
Multiple model adaptive estimation and head motion tracking in a virtual environment: An engineering approach
[AD-A289299] p 2359 N95-27046

HEAD-UP DISPLAYS
Simulation model of the integrated flight/propulsion control system, displays, and propulsion system for ASTOVL lift-fan aircraft
[NASA-TM-108866] p 2139 N95-26412

HEALTH
Implementing an integrated standards-based management system to ensure compliance at Los Alamos National Laboratory
[DE95-007873] p 2451 N95-28025
An introductory guide to uncertainty analysis in environmental and health risk assessment. Environmental Restoration Program
[DE95-008097] p 2354 N95-28136

HEART
Progress in incompressible Navier-Stokes computations for propulsion flows and its dual-use applications
[NASA-CR-197746] p 2275 N95-26766
A study of heart rate and heart rate variability during rapid decompression to 50,000 ft
[AD-A291598] p 2355 N95-28561

HEART RATE
A study of heart rate and heart rate variability during rapid decompression to 50,000 ft
[AD-A291598] p 2355 N95-28561

HEAT ENGINES
Analytical and experimental evaluation of joining silicon carbide to silicon carbide and silicon nitride to silicon nitride for advanced heat engine applications, phase 2
[DE95-005761] p 2303 N95-27947

HEAT EXCHANGERS
A probabilistic model of a porous heat exchanger
p 2282 N95-27359
Heat pipe cooled reactors for multi-kilowatt space power supplies
[DE95-005211] p 2420 N95-27425
Task 4 supporting technology. Densification requirements definition and test objectives. Propellant densification requirements definition
[NASA-CR-198629] p 2450 N95-28260
Coatings of non-oxide ceramics for improved corrosion resistance in high temperature coal combustion
[DE95-006932] p 2241 N95-28604
Cryogenic temperature control and tension/compression attachment stage for an electron microscope
[AD-D017390] p 2294 N95-28612
Mechanism of deposit formation on fuel-wetted hot metal surfaces
[AD-A289847] p 2210 N95-28621

HEAT FLUX
Fluxes across the west coast resolved by Picket Fence observations during stormfest
[AD-A288511] p 2341 N95-26653
Radiation production from stagnating compact toroids employing a nonequilibrium radiation diffusion model
[AD-A289602] p 2429 N95-26720
RTE: A computer code for Rocket Thermal Evaluation
p 2177 N95-27355
Neutral gas compression in the Alcator C-Mod divertor. Experimental observations
[DE95-007762] p 2432 N95-27688
Measurement and analysis of the surface energy budget for ARM field experiments
[DE95-007646] p 2338 N95-28114

HEAT MEASUREMENT
Fractionation studies of polyethylene using DSC-technique
[PB95-185252] p 2200 N95-26540
Scintillator materials for calorimetry
[DE95-008570] p 2421 N95-27679

HEAT PIPES
Experimental investigation of the effects of relative physical orientation between evaporator and condenser for a loop heat pipe
[AD-A289248] p 2277 N95-26968
The effects of transverse vibration on the performance of an axial groove wick heat pipe
[AD-A289349] p 2278 N95-27065
Features and applications of the Groove Analysis Program (GAP) p 2281 N95-27349
Composite heat pipe development status: Development of lightweight prototype carbon-carbon heat pipe with integral fins and metal foil liner
[NASA-TM-106909] p 2283 N95-27369
Heat pipe cooled reactors for multi-kilowatt space power supplies
[DE95-005211] p 2420 N95-27425

HEAT PUMPS
Mathematical modelling of the thermodynamic properties of coolants and working media of heat pumps
[IFTR-6/1994] p 2447 N95-26510

HEAT RESISTANT ALLOYS
Atomistic calculations of hydrogen interactions with Ni3Al grain boundaries and Ni/Ni/Ni3Al interfaces
[DE95-006497] p 2408 N95-27534
A new Cu-8 Cr-4 Nb alloy for high temperature applications
[NASA-TM-106910] p 2218 N95-27728

HEAT SHIELDING
Engineering calculations associated with the ablative thermal protective structures of returnable satellites
[AD-A289593] p 2162 N95-26715

HEAT TRANSFER
WINCLR: A computer code for heat transfer and clearance calculation in a compressor
[NASA-CR-195436] p 2117 N95-26363
Progress in incompressible Navier-Stokes computations for propulsion flows and its dual-use applications
[NASA-CR-197746] p 2275 N95-26766
Experimental investigation of the effects of relative physical orientation between evaporator and condenser for a loop heat pipe
[AD-A289248] p 2277 N95-26968
A finite element based technique for simulation helix TWT interaction circuit thermal behavior
[AD-A289552] p 2262 N95-27152
Effects of blowing ratio on heat transfer to the throat region of a porous-walled nozzle
[AD-A289459] p 2167 N95-27153
Computation of three-dimensional mixed convective boundary layer flow p 2280 N95-27347
Features and applications of the Groove Analysis Program (GAP) p 2281 N95-27349
RTE: A computer code for Rocket Thermal Evaluation
p 2177 N95-27355
Numerical solution of fluid flow and heat tranfer problems with surface radiation p 2282 N95-27357
A probabilistic model of a porous heat exchanger
p 2282 N95-27359
Transitional flow in thin tubes for space station freedom radiator p 2282 N95-27360
Heat pipe cooled reactors for multi-kilowatt space power supplies
[DE95-005211] p 2420 N95-27425
Advances in welding science: A perspective
[DE95-006745] p 2302 N95-27545
Experience with k-epsilon turbulence models for heat transfer computations in rotating p 2285 N95-27887
Cooling apparatus and couplings therefor
[NASA-CASE-ARC-11921-1] p 2304 N95-28256
Radiant exchange considerations in design and scaleup of photocatalytic reactors for purification of nitroglycerine-contaminated air p 2171 N95-28300
Thermal analysis of PANSAT batteries and Electrical Power Subsystem
[AD-A290013] p 2269 N95-28388

HEAT TRANSMISSION
Phase stability and elasticity of C15 transition-metal intermetallic compounds
[DE95-007876] p 2219 N95-28026
Thermal analysis of PANSAT batteries and Electrical Power Subsystem
[AD-A290013] p 2269 N95-28388

HEAT TREATMENT
The development of mechanical strength in a ceramic material during firing
[DE95-004925] p 2234 N95-27476

HEATING
Composite prepreg application device
[NASA-CASE-LAR-15259-1] p 2182 N95-27192
Development of an optical trap as an ultra-sensitive analytical tool
[DE95-007843] p 2426 N95-28022
Engineering design of the ITER RF systems
[DE95-008064] p 2434 N95-28140

HEAVY IONS
Investigation of radiation resistance of transistors and integrated circuits using the heavy ions beam of energy higher than 1 MeV/amu and fast neutrons
[DE95-608624] p 2261 N95-27024
Physics with relativistic heavy ions: QGP and other delicacies
[DE95-007014] p 2406 N95-27307
Abrasion-ablation model for neutron production in heavy ion reactions
[NASA-TM-4656] p 2420 N95-27372
Aspects of strangeness
[DE95-008314] p 2414 N95-28169
Aspects of strange matter
[DE95-008316] p 2414 N95-28170
Mutagenesis in human cells with accelerated H and Fe ions
[NASA-CR-198599] p 2351 N95-28177
On ionic charge distributions of heavy evaporation residues passing through a carbon foil
[DE94-629016] p 2414 N95-28184
The real structure of columnar pinning centers in heavy-ion-irradiated cuprate superconductors
[DE95-003948] p 2445 N95-28186

HEAVY WATER
Selected bibliography on heavy water, tritiated water and hydrogen isotopes (1981-1992)
[DE95-608331] p 2405 N95-27159

HELICOPTER CONTROL
An investigation of the effects of pitch-roll (de)coupling on helicopter handling qualities
[NASA-TM-110349] p 2141 N95-26773
HELICOPTER DESIGN
Construction and wind tunnel test of a 1/12th scale helicopter model
[AD-A288487] p 2123 N95-28331
Modeling helicopter blade dynamics using a modified Myklestad-Prohl transfer matrix method
[AD-A289891] p 2136 N95-28626
HELICOPTER PERFORMANCE
An investigation of the effects of pitch-roll (de)coupling on helicopter handling qualities
[NASA-TM-110349] p 2141 N95-26773
HELICOPTER WAKES
An experimental investigation of helicopter downwash and tailboom interaction at the Wichita State University 7x10 foot wind tunnel p 2120 N95-26955
HELICOPTERS
Aircraft noise prediction program theoretical manual: Rotorcraft System Noise Prediction System (ROTONET), part 4
[NASA-TM-83199-PT-4] p 2400 N95-26392
An investigation of the effects of pitch-roll (de)coupling on helicopter handling qualities
[NASA-TM-110349] p 2141 N95-26773
Flow structure generated by perpendicular blade vortex interaction and implications for helicopter noise predictions
[NASA-CR-198590] p 2123 N95-28193
Aeroelasticity and structural optimization of composite helicopter rotor blades with swept tips
[NASA-CR-4665] p 2136 N95-28262
Construction and wind tunnel test of a 1/12th scale helicopter model
[AD-A288487] p 2123 N95-28331
Modeling helicopter blade dynamics using a modified Myklestad-Prohl transfer matrix method
[AD-A289891] p 2136 N95-28626
Rotorcraft crashworthy airframe and fuel system technology development program
[AD-A289986] p 2126 N95-28630
HELIUM
Measurement of N2(+) mobility He via Fourier transform emission spectroscopy
[AD-A289266] p 2404 N95-26979
Cryogenic and simulated fuel jet breakup in argon, helium and nitrogen gas flows
[NASA-TM-106923] p 2291 N95-27030
Effects of helium pre-implantation on the microstructure and mechanical properties of irradiated 316 stainless steel
[DE95-007162] p 2214 N95-27086
Diagnostic system Cryo-D for the determination of parameters of vapor-liquid currents of the coolant
[DE95-608775] p 2280 N95-27338
Comparison of the calculated and measured stability of a NbTi cable-in-conduit conductor
[DE95-007964] p 2265 N95-27693
The surface of liquid He-4 at nonzero temperatures
[DE95-607841] p 2207 N95-27880
Divertor research on the DIII-D tokamak
[DE95-003942] p 2434 N95-28185
HELIUM HYDROGEN ATMOSPHERES
Theoretical studies of interstellar processes
[NASA-CR-198647] p 2462 N95-28216
HELIUM IONS
Cavity formation and impurity gettering in He-implanted Si
[DE95-007744] p 2444 N95-28127
Theoretical studies of interstellar processes
[NASA-CR-198647] p 2462 N95-28216
HELIUM ISOTOPES
Search for deeply bound pionic atoms with high-purity germanium tagging spectrometer
[DE95-609072] p 2416 N95-28252
HELIUM-NEON LASERS
Flat panel planar optic display
[DE95-007686] p 2426 N95-28196
HELMET MOUNTED DISPLAYS
Development of injury preventing helmet servo-support system for high performance aircraft
[AD-A289547] p 2359 N95-26755
Partial discharge testing of high voltage wiring harness for airborne displays
[AD-A289150] p 2138 N95-27003
HELMETS
Development of injury preventing helmet servo-support system for high performance aircraft
[AD-A289547] p 2359 N95-26755
HELMHOLTZ VORTICITY EQUATION
On the azimuthal Fourier components of the Green's function for the Helmholtz equation in three dimensions
[AD-A288775] p 2398 N95-26345
HEMOGLOBIN
Mechanisms of hypertension after cross-linked hemoglobin blood-substitute transfusion
[AD-A289558] p 2352 N95-26680
Acute and subacute toxicity of ammonium dinitramide (ADN) p 2175 N95-28318
HERMITIAN POLYNOMIAL
The gluon propagator in non-Abelian Weizsaecker-Williams fields
[DE95-006877] p 2449 N95-27547
HETEROGENEITY
Charge distribution analysis of catalysts under simulated reaction conditions
[DE95-006943] p 2204 N95-27549
Synthesis and properties of lanthanide-exchanged Preyssler's heteropolyanions
[DE95-007136] p 2238 N95-28235
The effect of material heterogeneity in curved composite beams for use in aircraft structures
p 2190 N95-28426
Ultrasonic studies of liquid/solid seimoacoustic wave phenomena
[AD-A289644] p 2402 N95-28622
HETEROJUNCTION DEVICES
Atomic layer epitaxy of group 4 materials: Surface processes, thin films, devices and their characterization
[AD-A289092] p 2446 N95-28327
HEURISTIC METHODS
Grain size management in repetitive task graphs for multiprocessor computer scheduling
[AD-A288575] p 2377 N95-26551
Accelerating conservative parallel simulation of VHDL circuits
[AD-A289317] p 2264 N95-27294
A linguistic geometry for 3D strategic planning
p 2386 N95-27397
A spectral algorithm for the seriation problem
[DE95-004775] p 2372 N95-27436
An automated cost uncertainty program
[AD-A288747] p 2374 N95-28588
HIERARCHIES
A rule-based shell to hierarchically organize HST observations p 2384 N95-27384
Generalized CNF satisfiability, local reductions and complexity of succinctly specified problems
[DE95-006343] p 2372 N95-27849
HIGGS BOSONS
Signatures of Higgs-Triplet representations at TeV-e(+)e(-) colliders
[DE95-007201] p 2419 N95-27089
HIGH ALTITUDE
Design of a high altitude long endurance aircraft with manufacturing considerations p 2119 N95-26947
Propulsion system assessment for very high UAV under ERAST
[NASA-CR-195469] p 2140 N95-27866
HIGH CURRENT
Electrical performance characterisation of single-shot switches in high speed, high voltage and high current applications
[DSTO-RR-0010] p 2259 N95-26425
Evaluation of current drive requirements and operating characteristics of a high bootstrap fraction advanced tokamak reactor
[DE95-007041] p 2430 N95-27308
Characterization and control of wafer charging effects during high-current ion implantation
[DE95-006587] p 2440 N95-27471
Comparison of the calculated and measured stability of a NbTi cable-in-conduit conductor
[DE95-007964] p 2265 N95-27693
HIGH DEFINITION TELEVISION
An acoustic charge transport imager for high definition television applications
[NASA-CR-197841] p 2249 N95-26708
HIGH ELECTRON MOBILITY TRANSISTORS
Quasi-optical millimeter wave power combining
[AD-A291767] p 2270 N95-28529
HIGH ENERGY ELECTRONS
High energy electron beams for ceramic joining
[DE95-006316] p 2420 N95-27480
Relativistic electrons in the outer-zone: An 11 year cycle, their relation to the solar wind
[DE95-007882] p 2338 N95-28061
HIGH ENERGY INTERACTIONS
Addendum to the 1993 European school of high-energy physics
[DE95-610313] p 2419 N95-27321
Scintillator materials for calorimetry
[DE95-006570] p 2421 N95-27679
The 1993 European school of high-energy physis
[DE95-610196] p 2421 N95-28040
The 132 nsec bunch spacing in the Tevatron proton-antiproton collider
[DE95-005750] p 2422 N95-28346
B-Physics results from D0
[DE95-005126] p 2417 N95-28495
Beam instability studies for the SSC
[DE95-008024] p 2423 N95-28551
HIGH FREQUENCIES
Design and development of a test rig for the high frequency testing of rolling sleeve airsprings
[DSTO-TN-0001] p 2142 N95-26378
Evaluation of the FMICW waveform in HF surface radar applications
[AD-A288245] p 2249 N95-26545
Com(sup 3): A composite-compatible component coding system
[BBC-RD-1994/17] p 2249 N95-26670
HIGH GAIN
OBIC analysis of stressed, thermally-isolated polysilicon resistors
[DE95-008511] p 2268 N95-28201
HIGH LEVEL LANGUAGES
Software technology for adaptable, reliable systems (STARS). AdaWise user's manual
[AD-A289655] p 2375 N95-28635
HIGH POLYMERS
JTEC monograph on biodegradable polymers and plastics in Japan: Research, development, and applications
[NASA-CR-198562] p 2235 N95-27694
HIGH POWER LASERS
Trident as an ultrahigh irradiance laser
[DE95-006345] p 2297 N95-27850
Laboratory high-energy astrophysics on lasers
[DE95-008062] p 2462 N95-28013
High power free-electron laser concepts and problems
[DE95-007841] p 2298 N95-28059
Thermally-induced unsymmetric optical distortion of output window of high-power CO2 laser
[AD-A289604] p 2300 N95-28650
HIGH PRESSURE
High pressure Earth storable rocket technology program: Basic program
[NASA-CR-195449] p 2166 N95-26390
Extended equation-of-state for dichlorodifluoromethane (CCl2F2)
[AD-A288885] p 2177 N95-26434
High pressure conductivity study of template synthesized polypyrrole: Observation of a crossover from three to one dimensional variable range hopping
[AD-A288367] p 2224 N95-26470
An investigation of the AFIT 2-inch shock tube as a flow source for supersonic testing
[AD-A289246] p 2143 N95-26966
Sceening, down selection, and implementation of environmentally compliant cleaning and insulation bonding for MNASA p 2165 N95-27124
The application of waterjets for cleaning
p 2233 N95-27130
NASA Lewis Research Center's combustor test facilities and capabilities
[NASA-TM-106903] p 2143 N95-27176
Neutral gas compression in the Alcator C-Mod divertor. Experimental observations
[DE95-007762] p 2432 N95-27688
High pressure optical studies of semiconductors and heterostructures
[DE95-007119] p 2410 N95-27927
Survey on researches related to ocean disposal of carbon dioxide
[DE95-759247] p 2329 N95-27939
Electrical conductivity measurements of aqueous electrolyte solutions at high temperatures and high pressures
[DE95-006748] p 2208 N95-27956
The demilitarization of class 1.1 rocket motors using high pressure waterjets p 2176 N95-28322
Apparatus for testing high pressure injector elements
[NASA-CASE-MFS-28773-1] p 2304 N95-28347
HIGH RESOLUTION
The ambiguity function of the stepped frequency radar
[AD-A289533] p 2251 N95-26871
Classification of ultra high range resolution radar using decision boundary analysis
[AD-A289378] p 2251 N95-26877
The second coming of cold dark matter?
[DE95-005156] p 2462 N95-27445
Crystal and magnetic structure of stoichiometric YFe2O4
[DE95-006627] p 2440 N95-27487
Parallel plasma fluid turbulence calculations
[DE95-006741] p 2431 N95-27537
Automated integration of genomic physical mapping data via parallel simulated annealing
[DE95-008057] p 2351 N95-27725
Studies of planetary scale waves and instabilities in support of the geophysical fluid flow cell experiment on USML-2
[NASA-CR-198646] p 2463 N95-27916

Analytical electron microscopy of nanometer-sized particles
[AD-A289124] p 2413 N95-28101
A genuinely multidimensional upwind scheme and efficient multigrid solver for the compressible Euler equations
[NASA-CR-195000] p 2288 N95-28571

HIGH REYNOLDS NUMBER
Analysis of hypersonic boundary layer second mode instability over a 7 deg cone
[AD-A289471] p 2276 N95-26819
Comparative wind tunnel test at high Reynolds numbers of NACA 64 621 airfoils with two aileron configurations
p 2124 N95-27977

HIGH SPEED
Electrical performance characterisation of single-shot switches in high speed, high voltage and high current applications
[DSTO-RR-0010] p 2259 N95-26425
Characterization of optical polymers for multi-layered electro-optic devices
[AD-A289255] p 2227 N95-26973
Application of CFD to the analysis and design of high-speed inlets
[NASA-CR-198574] p 2279 N95-27240
Overview of turbulence model development and applications at Rocketdyne p 2286 N95-27891
The effects of processing variables on reaction synthesis of Fe-Al alloys
[DE95-007405] p 2221 N95-28082
Recent high-speed ballistics experiments at ORNL
[DE95-006534] p 2422 N95-28205
Structure of high-speed sprays
[AD-A291696] p 2288 N95-28523

HIGH STRENGTH
The development of mechanical strength in a ceramic material during firing
[DE95-004925] p 2234 N95-27476
Repairs of CFC primary structures
p 2135 N95-27527
Modeling precipitation from concentrated solutions with the EQ3/6 chemical speciation codes
[DE95-006264] p 2204 N95-27556
A new Cu-8 Cr-4 Nb alloy for high temperature applications
[NASA-TM-106910] p 2218 N95-27728

HIGH STRENGTH ALLOYS
Lattice parameters and Debye-Waller factors of gamma-TiAl alloys
[AD-A288843] p 2213 N95-26681
Environmentally assisted cracking of high strength beta titanium alloys
[AD-A289156] p 2213 N95-27032

HIGH STRENGTH STEELS
Determination of the cyclical properties of 18G2A steel on the basis of skeleton curves for a planar stress state
[IFTR-32/1994] p 2211 N95-26359
Non-metallic oxide inclusion formation in C-Mnlow alloy steel welds
[DE94-019160] p 2215 N95-27319

HIGH TEMPERATURE
International Space Station Alpha trace contaminant control subassembly life test report
[NASA-TM-108488] p 2358 N95-26364
Extended equation-of-state for dichlorodifluoromethane (CCl2F2)
[AD-A288885] p 2177 N95-26434
High-rate/high-temperature capability of a single-layer zicar-separator nickel-hydrogen cell
p 2272 N95-26788
Fatigue behavior of a cross-ply metal matrix composite at elevated temperature under strain controlled mode
[AD-A289425] p 2181 N95-26865
Fatigue behavior of a cross-ply ceramic matrix composite at elevated temperature under tension-tension loading
[AD-A289250] p 2182 N95-26969
Alternative cleaning solvents and lubricants at the Air Force PJKS facility p 2228 N95-27108
Heat pipe cooled reactors for multi-kilowatt space power supplies
[DE95-005211] p 2420 N95-27425
Measurements of the volatilities of electrolytes: Application to water/steam cycles
[DE95-007103] p 2204 N95-27451
Crystal structure, short-range oxygen defects, and water adsorption in La- and Nd-modified ZrO2
[DE95-007134] p 2439 N95-27452
High energy electron beams for ceramic joining
[DE95-006316] p 2420 N95-27480
Materials considerations for molten salt accelerator-based plutonium conversion systems
[DE95-006743] p 2217 N95-27544
Thermodynamics of aqueous electrolytes at high temperatures by the isopiestic technique
[DE95-006747] p 2449 N95-27546
Inflight resistance measurement on high-T(sub c) superconducting thin films exposed to orbital atomic oxygen on CONCAP-2 (STS-46) p 2272 N95-27635
Analytical and experimental evaluation of joining silicon carbide to silicon carbide and silicon nitride to silicon nitride for advanced heat engine applications, phase 2
[DE95-005761] p 2303 N95-27947
Electrical conductivity measurements of aqueous electrolyte solutions at high temperatures and high pressures
[DE95-006748] p 2208 N95-27956
High-temperature deformation of ZrO2-Al2O3/SiC whisker composites fabricated by two techniques
[DE95-008273] p 2183 N95-28069
High temperature Hexoloy(trademark) SX silicon carbide
[DE95-007290] p 2221 N95-28075
Solid state sintering of silicon nitride ARL-CR-114
[DE95-007291] p 2443 N95-28076
Lattice calculation for lepton capture from vacuum-pair production in relativistic heavy-ion collisions
[DE95-007392] p 2413 N95-28077
Review and analysis of the 1980-1989 biomass thermochemical conversion program
[DE95-000287] p 2325 N95-28394
Development of low-expansion ceramics with strength retention to elevated temperatures
[DE95-005760] p 2239 N95-28397
TV-holography at high temperatures: In situ observations of the oxidation of advanced materials
[PB95-195343] p 2294 N95-28651

HIGH TEMPERATURE ENVIRONMENTS
Effects of high-temperature environments on flaw generation and fracture behavior of SiC/SiC composites
[DE95-008270] p 2183 N95-28068
Hydrothermal oxidation of solid rocket propellant and other department of defense hazardous wastes
p 2177 N95-28325

HIGH TEMPERATURE GASES
Algorithm to describe the spread of a wall fire under a ceiling
[PB95-182259] p 2247 N95-28008

HIGH TEMPERATURE PLASMAS
Application of modern diagnostic methods to environmental improvement
[DE95-005797] p 2330 N95-28119

HIGH TEMPERATURE RESEARCH
High temperature oxidation of nickel concentrates
[PB95-195566] p 2224 N95-28644

HIGH TEMPERATURE SUPERCONDUCTORS
Investigations of the hyperfine interactions in copper-oxide perovskites using Eu-151 and Fe-57 Moessbauer spectroscopy
[PB95-185138] p 2437 N95-26513
Hall effect and resistivity in the normal state of high-T(sub c) cuprates in the electron-fracton model
[DE95-610612] p 2439 N95-27413
Review of activities in USA on HTS materials
[DE95-006404] p 2234 N95-27468
Numerical study of the singlet-triplet model for cuprate superconductors
[DE95-609438] p 2440 N95-27712
A diagram technique for strongly interacting fermion systems. One-and two-band Hubbard models
[DE95-609437] p 2410 N95-27881
Investigation of high-temperature superconducting flywheel energy storage devices
[DE95-759242] p 2320 N95-27936
The oxidation state and magnetic behaviour of Tb in high-(Tc) related materials
[DE95-007129] p 2219 N95-27966
Stability measurements on a 1-T high temperature superconducting magnet
[DE95-007411] p 2267 N95-28048
Aspects of macroscopic phase separation and interstitial oxygen ordering in oxygen doped La2CuO(4+delta)
[DE95-007864] p 2443 N95-28060
Local texture and grain boundary misorientations in high H(C) oxide superconductors
[DE95-007004] p 2447 N95-28606

HIGH TEMPERATURE TESTS
Calorimetric evaluation of commercial Ni-MH cells and charges p 2272 N95-26790
High temperature kinetic study of the reactions H + O2 = OH + O and O + H2 = OH + H in H2/O2 system by shock tube-laser absorption spectroscopy
[NASA-CR-195473] p 2206 N95-27695
Task 4 supporting technology. Part 2: Detailed test plan for thermal seals. Thermal seals evaluation, improvement and test. CAN8-1, Reusable Launch Vehicle (RLV), advanced technology demonstrator: X-33. Leading edge and seals thermal protection system technology demonstration
[NASA-CR-198628] p 2304 N95-28259
Coatings of non-oxide ceramics for improved corrosion resistance in high temperature coal combustion
[DE95-006932] p 2241 N95-28604
High temperature oxidation of nickel concentrates
[PB95-195566] p 2224 N95-28644

HIGH VOLTAGES
Electrical performance characterisation of single-shot switches in high speed, high voltage and high current applications
[DSTO-RR-0010] p 2259 N95-26425
Partial discharge testing of high voltage wiring harness for airborne displays
[AD-A289150] p 2138 N95-27003
AFC generator development
[DE95-007094] p 2266 N95-27754

HILL METHOD
Dynamics and control of SEDSAT tethered multi-probe for thermospheric research flight data analysis of SEDS-2 satellite: Tethered systems dynamics and flight data analysis
[NASA-CR-198653] p 2165 N95-27836

HIPPOCAMPUS
Hippocampal place fields, the internal compass, and the learning of landmark stability
[AD-A289406] p 2350 N95-27100

HISTORIES
Live from Antarctica: Then and now
[NASA-CR-197829] p 2335 N95-26594
Live from Antarctica, volume 4
[NASA-CR-197828] p 2335 N95-26596
Standards for excellence
[NONP-NASA-VT-95-49096] p 2451 N95-27202
Application of CFD to the analysis and design of high-speed inlets
[NASA-CR-198574] p 2279 N95-27240
Spaceport news index: January 1990 - December 1994
[NASA-TM-110653] p 2454 N95-27243
Spaceflight revolution: NASA Langley Research Center from Sputnik to Apollo
[NASA-SP-4308] p 2474 N95-27685
The Global Historical Climatology Network: A preview of version 2
[DE95-007003] p 2332 N95-28605

HMX
Hazards analysis of an integral class 1.1/1.3 rocket motor demilitarization and ingredient recovery system using ammonia p 2174 N95-28315
A comprehensive energetic materials resource recovery and recycling program p 2176 N95-28323

HOHLRAUMS
Indirectly driven targets for ignition
[DE95-006451] p 2430 N95-27327

HOLES (ELECTRON DEFICIENCIES)
Photoemission and optical properties of C60 fullerites
[DE95-006588] p 2425 N95-27539

HOLES (MECHANICS)
Assembly induced delaminations in composite structures p 2186 N95-28279

HOLLOW CATHODES
Discharge ignition behavior of the Space Station plasma contactor
[NASA-TM-106925] p 2168 N95-27862

HOLOGRAPHIC INTERFEROMETRY
Visualization and direct comparison of large displacements using difference holographic interferometry
[DE95-608782] p 2292 N95-27711

HOLOGRAPHY
JPRS report: Science and technology. Central Eurasia
[JPRS-UST-95-016] p 2262 N95-27170
Visualization and direct comparison of large displacements using difference holographic interferometry
[DE95-608782] p 2292 N95-27711
TV-holography at high temperatures: In situ observations of the oxidation of advanced materials
[PB95-195343] p 2294 N95-28651

HOMODYNE RECEPTION
Method and apparatus for maintaining linearity and frequency accuracy of an FM chirp waveform
[AD-D017398] p 2258 N95-28615

HOMOGENEITY
Improved hardness RHA weldability and material property testing
[AD-A289127] p 2221 N95-28102
Scattering by a small object close to an interface. 3. Buried object
[PB95-184909] p 2256 N95-28354

HOMOLOGY
Gromov-Lawson-Rosenberg conjecture for groups with periodic cohomology
[PB95-185203] p 2389 N95-26915

HOMOTOPY THEORY
Compactification of moduli spaces of monopoles
[PB95-185179] p 2388 N95-26515

HONEYCOMB CORES

An experimental investigation of sandwich flat panels under low velocity impact [AD-A289420] p 2309 N95-27135

HONEYCOMB STRUCTURES

An experimental investigation of sandwich flat panels under low velocity impact [AD-A289420] p 2309 N95-27135

Development of the solar array deployment and drive system for the XTE spacecraft p 2158 N95-27284

Field repair materials for naval aircraft p 2133 N95-27514

Composite repair of a CF18: Vertical stabilizer leading edge p 2134 N95-27517

Composite repair issues on the CF-18 aircraft p 2134 N95-27518

External patch repair of CFRP/honeycomb sandwich p 2134 N95-27522

Scarf repairs to graphite/epoxy components p 2135 N95-27523

HORIZON

Earth horizon modeling and application to static Earth sensors on TRMM spacecraft p 2150 N95-27783

HORIZONTAL ORIENTATION

Large HAWT wake measurement and analysis p 2289 N95-27973

Horizontal axis wind turbine post stall airfoil characteristics synthesization p 2124 N95-27974

A NASTRAN-based computer program for structural dynamic analysis of Horizontal Axis Wind Turbines p 2312 N95-27980

Measurement and prediction of broadband noise from large horizontal axis wind turbine generators p 2324 N95-27990

HORN ANTENNAS

Reduction of off-boresight fields for a TEM horn antenna [AD-A289708] p 2250 N95-26738

HOT ELECTRONS

Monte Carlo study of electron-plasmon scattering effects on hot electron transport in GaAs [DE95-607768] p 2403 N95-26542

HOT ISOSTATIC PRESSING

Analytical and experimental evaluation of joining silicon carbide to silicon carbide and silicon nitride to silicon nitride for advanced heat engine applications, phase 2 [DE95-005761] p 2303 N95-27947

HOT SURFACES

Mechanism of deposit formation on fuel-wetted hot metal surfaces [AD-A289847] p 2210 N95-28621

HOVERING

An experimental investigation of helicopter downwash and tailboom interaction at the Wichita State University 7x10 foot wind tunnel p 2120 N95-26955

HUBBLE SPACE TELESCOPE

Hubble Space Telescope nickel-hydrogen battery testing: An update p 2272 N95-26794

A rule-based shell to hierarchically organize HST observations p 2384 N95-27384

Space environmental effects observed on the Hubble Space Telescope p 2242 N95-27655

Observational magnetometer calibration with the Hubble Space Telescope's new magnetometers p 2148 N95-27773

The solar array-induced disturbance of the Hubble Space Telescope pointing system [NASA-TP-3556] p 2311 N95-28214

HUMAN BEHAVIOR

Enhancing the effects of diversity awareness training: A review of the research literature [DOT/FAA/AM-95/10] p 2355 N95-26361

HUMAN BODY

Non-invasive method and apparatus for monitoring intracranial pressure and pressure volume index in humans [NASA-CASE-LAR-13894-1] p 2353 N95-26889

HUMAN FACTORS ENGINEERING

A perspective on the Human-Rating process of US spacecraft: Both past and present [NASA-SP-6104] p 2162 N95-26586

US Coast Guard Human Systems Integration (HSI) process model [AD-A289172] p 2358 N95-26612

Digital systems validation. Chapter 20 Artificial Intelligenge with applications for aircraft. Handbbook, volume 2 [AD-A288492] p 2380 N95-26638

Integrated mission precision attack cockpit technology (IMPACT). Phase 1: Identifying technologies for air-to-ground fighter integration [AD-A289562] p 2129 N95-26684

Development of injury preventing helmet servo-support system for high performance aircraft [AD-A289547] p 2359 N95-26755

Multi-agent perception for Human/Robot interaction: A framework for intuitive trajectory modification [AD-A289399] p 2359 N95-26884

Change, Learning and Mental Work in Organizations: Working papers of the 3rd Otaniemi-Dresden Workshop [PB95-184941] p 2356 N95-26909

Crew adaptation evaluation of the Norwegian Crew Concept (NOROREW) [AD-A288478] p 2360 N95-27058

Factors in human-computer interface design (a pilot study) [AD-A288908] p 2360 N95-27195

Image quality metrics for color CRT displays [AD-A288934] p 2262 N95-27196

Human factors in aviation maintenance, phase 4 [DOT/FAA/AM-95/14] p 2360 N95-27696

HUMAN PERFORMANCE

A mathematical framework for an improved search model [AD-A288858] p 2358 N95-26552

A perspective on the Human-Rating process of US spacecraft: Both past and present [NASA-SP-6104] p 2162 N95-26586

Analysis of group performance in visual signal detection [AD-A289561] p 2355 N95-26683

Codes of processing and multiple resources: Model and methodology [AD-A289583] p 2355 N95-26691

Handbook of perception and human performance, volume 2. Cognitive processes and performance [AD-A289587] p 2355 N95-26692

HUMAN REACTIONS

ELVIS: Eigenvectors for land vehicle image system [AD-A289297] p 2381 N95-27041

HUMAN TOLERANCES

Radiation in everyday life [DE95-604111] p 2349 N95-26597

HUMAN-COMPUTER INTERFACE

Enhanced visual user interface support for domain-oriented application composition systems [AD-A289337] p 2359 N95-26737

A demonstration of Client-Server technology using remote procedure calls with an application of file migration for moving records based on time [AD-A289392] p 2453 N95-26879

Multi-agent perception for Human/Robot interaction: A framework for intuitive trajectory modification [AD-A289399] p 2359 N95-26884

Factors in human-computer interface design (a pilot study) [AD-A288908] p 2360 N95-27195

A user-system interface agent p 2383 N95-27379

Building an adaptive agent to monitor and repair the electrical power system of an orbital satellite p 2383 N95-27380

Development and implementation of an electronic library tour for the NASA Langley Technical Library [NASA-TM-110619] p 2455 N95-27701

HUMIDITY

Evaluation of high ester content PAO based single hydraulic fluid in high humidity conditions [AD-A289374] p 2233 N95-27324

Millimeter-wave imaging radiometer data processing and development of water vapor retrieval algorithms [NASA-CR-198593] p 2343 N95-27997

Evaluation of a conductive polymer-based sensor for detection of hydrazines at the part-per-billion level p 2173 N95-28309

HYBRID STRUCTURES

Design and fabrication of a diamond-turned hybrid diffractive/refractive singlet for visible applications at ORNL [DE95-007007] p 2427 N95-28552

HYDRATES

Survey on researches related to ocean disposal of carbon dioxide [DE95-759247] p 2329 N95-27939

HYDRAULIC EQUIPMENT

Composite flight-control actuator development p 2142 N95-28281

Water driven turbine/brush pipe cleaner [NASA-CASE-KSC-11669-1] p 2304 N95-28359

HYDRAULIC FLUIDS

Evaluation of high ester content PAO based single hydraulic fluid in high humidity conditions [AD-A289374] p 2233 N95-27324

Use of CTFE as an additive to enhance fire resistance of single hydraulic fluid [AD-A289377] p 2233 N95-27325

HYDRAULIC JETS

Environmentally Benign Cleaning and Degreasing Technology: JANNAF Safety and Protection Subcommittee and Propellant Development and Characterization Subcommittee Joint Workshop [CPIA-PUBL-611] p 2227 N95-27101

The application of waterjets for cleaning p 2233 N95-27130

The demilitarization of class 1.1 rocket motors using high pressure waterjets p 2176 N95-28322

HYDRAULIC TEST TUNNELS

Demonstration study of hierarchical control of fluid-dynamic phenomena [AD-A289341] p 2275 N95-26751

HYDRAZINE ENGINES

Electric propulsion for geostationary orbit insertion [NASA-TM-106942] p 2168 N95-27727

HYDRAZINES

Evaluation of a conductive polymer-based sensor for detection of hydrazines at the part-per-billion level p 2173 N95-28309

Prototype development and test results of a continuous ambient air monitoring system for hydrazine at the 110 ppb level p 2173 N95-28310

The sensitive detection of hydrazine using chemiluminescence p 2173 N95-28311

A new method for measuring hypergol scrubber emissions p 2174 N95-28312

HYDRIDES

The 1994 27th Annual NASA Aerospace Battery Workshop [NASA-CP-3292] p 2317 N95-26785

HYDROCARBONS

A summary of ODS replacement technologies at Litton Poly-Scientific p 2228 N95-27105

Coupled chemistry/climate issues [DE95-006443] p 2327 N95-27532

NQR-NMR studies of higher alcohol synthesis Cu-Co catalysts [DE95-007926] p 2205 N95-27680

HYDROCHLORIC ACID

Molecular approach to mesoporous metal sulfides [DE95-005418] p 2202 N95-27137

Measurements of the volatilities of electrolytes: Application to water/steam cycles [DE95-007103] p 2204 N95-27451

HYDROCLIMATOLOGY

Deep convection in the Mediterranean Sea [AD-A288497] p 2346 N95-26647

HYDROCYANIC ACID

CO, HCO(+) and HCN absorption in the gravitational lens candidate B0218+357 at z=0.685 [PB95-185146] p 2461 N95-26522

HYDRODYNAMICS

Addressing tension instability in SPH methods [AD-A289531] p 2276 N95-26852

Calculation of suspended sediment transport by combined wave-current flows [AD-A289368] p 2346 N95-26904

Validation of the SINDA/FLUINT code using several analytical solutions p 2281 N95-27350

Single-drop reactive extraction/extractive reaction with forced convective diffusion and interphase mass transfer p 2282 N95-27358

Three-dimensional computer modeling of hydrogen injection and combustion [DE95-006261] p 2203 N95-27437

WTEC panel report on research submersibles and undersea technologies [NASA-CR-198565] p 2247 N95-27909

Prediction of material strength and fracture of glass using the SPHINX smooth particle hydrodynamics code [DE95-004869] p 2236 N95-27943

Numerical simulation of coupled flow and transport with TOUGH2: A verification study [DE95-008351] p 2287 N95-28225

Computational and experimental studies of hydrodynamic instabilities and turbulent mixing [DE95-006837] p 2288 N95-28603

HYDROGEN

Environmental effects on high energy density materials [AD-A288296] p 2199 N95-26416

Hydrogen program [DE94-011827] p 2242 N95-27415

Three-dimensional computer modeling of hydrogen injection and combustion [DE95-006261] p 2203 N95-27437

Effect of internal hydrogen on the mixed-mode 1/3 fracture toughness of a ferrific/martensitic stainless steel [DE95-005722] p 2216 N95-27479

Atomistic calculations of hydrogen interactions with Ni3Al grain boundaries and Ni/Ni/Ni3Al interfaces [DE95-006497] p 2408 N95-27534

High temperature kinetic study of the reactions H + O2 = OH + O and O + H2 = OH + H in H2/O2 system by shock tube-laser absorption spectroscopy [NASA-CR-195473] p 2206 N95-27695

FTIR studies of CH3OH on porous silicon [AD-A289038] p 2207 N95-27904

Investigation on energy conversion technology using biochemical reaction elements, 2
[DE95-759250] p 2321 N95-27940

Effects of hydrogen on carbon steels at the Multi-Function Waste Tank Facility
[DE95-007194] p 2219 N95-28005

A hybrid vehicle evaluation code and its application to vehicle design. Revision 1
[DE95-008053] p 2303 N95-28029

LLNL input to FY94 hydrogen annual report
[DE95-007950] p 2243 N95-28064

Infrared spectroscopy of nonclassical ions and their complexes
[DE95-008487] p 2413 N95-28091

The role of hydrogen in the hydrogenation and hydrogenolysis of aniline on the nickel single crystal surfaces: Its implication on the mechanisms of HDN reactions
[DE95-006687] p 2222 N95-28134

Sensor for measuring the atomic fraction in highly dissociated hydrogen
[DE95-006531] p 2415 N95-28204

HYDROGEN BONDS

A density functional/molecular dynamics study of the structure of liquid nitromethane
[AD-A289224] p 2404 N95-26960

HYDROGEN EMBRITTLEMENT

Environmentally assisted cracking of high strength beta titanium alloys
[AD-A289156] p 2213 N95-27032

Stress corrosion cracking susceptibility of the earthquake resistant NOM B457 Mexican steel
[DE95-607956] p 2214 N95-27256

Atomistic calculations of hydrogen interactions with Ni3Al grain boundaries and Ni/Ni/Ni3Al interfaces
[DE95-006497] p 2408 N95-27534

HYDROGEN ENGINES

A hybrid vehicle evaluation code and its application to vehicle design. Revision 1
[DE95-008053] p 2303 N95-28029

A hybrid vehicle evaluation code and its application to vehicle design, revision 2
[DE95-008060] p 2303 N95-28139

HYDROGEN FUELS

LLNL input to FY94 hydrogen annual report
[DE95-007950] p 2243 N95-28064

HYDROGEN IONS

Infrared spectroscopy of nonclassical ions and their complexes
[DE95-008487] p 2413 N95-28091

Theoretical studies of interstellar processes
[NASA-CR-198647] p 2462 N95-28216

HYDROGEN ISOTOPES

Selected bibliography on heavy water, tritiated water and hydrogen isotopes (1981-1992)
[DE95-608331] p 2405 N95-27159

D/H and O-18/O-16 partitioning between water liquid and vapor in the system H2O-Na-K-Mg-Ca-Cl-SO4 from 0 to 350 C
[DE95-007013] p 2208 N95-27961

Recent high-speed ballistics experiments at ORNL
[DE95-006534] p 2422 N95-28205

HYDROGEN PRODUCTION

Investigation on energy conversion technology using biochemical reaction elements, 2
[DE95-759250] p 2321 N95-27940

HYDROGENATION

Growth of hydrogenated amorphous silicon (a-Si:H) on patterned substrates for increased mechanical stability
[DE95-006589] p 2234 N95-27472

Amorphous silicon pixel radiation detectors and associated thin film transistor electronics readout
[DE95-006568] p 2265 N95-27678

The role of hydrogen in the hydrogenation and hydrogenolysis of aniline on the nickel single crystal surfaces: Its implication on the mechanisms of HDN reactions
[DE95-006687] p 2222 N95-28134

HYDROGENOLYSIS

Hydrogen induced C-C, C-N, and C-S bond activities on Pt and Ni surfaces
[DE95-006251] p 2206 N95-27838

The role of hydrogen in the hydrogenation and hydrogenolysis of aniline on the nickel single crystal surfaces: Its implication on the mechanisms of HDN reactions
[DE95-006687] p 2222 N95-28134

HYDROLYSIS

Determination of the first hydrolysis constant of Europium (3) in 3 M of ionic strength
[DE95-607912] p 2405 N95-27211

Measurements of the volatilities of electrolytes: Application to water/steam cycles
[DE95-007103] p 2204 N95-27451

HYDROMETEOROLOGY

The distribution of cloud cover over the former USSR as derived from the RIHMI 223-Station 3-hourly meteorological database
[DE95-007046] p 2343 N95-27920

HYDROPHONES

Uncertainties in the calibration of hydrophones at NPL by the three-transducer spherical-wave reciprocity method in the frequency range 10 kHz on 500 kHz
[PB95-185245] p 2401 N95-26615

Simulating a multi-target acoustic array on the Intel Paragon
[AD-A288443] p 2377 N95-27183

Molecular modeling: An approach for the study of piezoelectric polymers
[AD-A289821] p 2241 N95-28574

Inspection methods for underwater cables
[AD-A289610] p 2312 N95-28616

HYDROSTATIC PRESSURE

High pressure optical studies of semiconductors and heterostructures
[DE95-007119] p 2410 N95-27927

HYDROSTATICS

Electro-hydrostatic actuator controller design using quantitative feedback theory
[AD-A289220] p 2141 N95-26957

Stationary neutrino radiation transport by maximum entropy closure
[DE95-006579] p 2463 N95-28558

HYDROTHERMAL SYSTEMS

Geothermal development in Australia
[DE95-007837] p 2325 N95-28058

Hydrothermal oxidation of solid rocket propellant and other department of defense hazardous wastes
p 2177 N95-28325

HYDROXIDES

Thermodynamics of aqueous electrolytes at high temperatures by the isopiestic technique
[DE95-006747] p 2449 N95-27546

Photochemistry in constrained spaces: Zeolites and layered double metal hydroxides
[DE95-006417] p 2207 N95-27951

HYDROXYL RADICALS

High temperature kinetic study of the reactions H + O2 = OH + O and O + H2 = OH + H in H2/O2 system by shock tube-laser absorption spectroscopy
[NASA-CR-195473] p 2206 N95-27695

HYPERBOLAS

Characterization of the membrane theory of a clamped shell. The hyperbolic case
[PB95-185021] p 2308 N95-26911

HYPERBOLIC DIFFERENTIAL EQUATIONS

Introduction to multigrid methods
[NASA-CR-195045] p 2388 N95-26395

HYPERCUBE MULTIPROCESSORS

A fixed time performance evaluation of parallel CFD applications
[DE94-014240] p 2273 N95-26445

HYPERFINE STRUCTURE

Investigations of the hyperfine interactions in copper-oxide perovskites using Eu-151 and Fe-57 Moessbauer spectroscopy
[PB95-185138] p 2437 N95-26513

Toward coherent excitation: Development of a single-source pump for the rubidium hyperfine ground state doublet
[AD-A289413] p 2295 N95-27132

HYPERGEOMETRIC FUNCTIONS

Moment and hypergeometric filters for high precision computation of focus, stereo and optical flow
[AD-A289293] p 2425 N95-27038

HYPERGOLIC ROCKET PROPELLANTS

A new method for measuring hypergol scrubber emissions p 2174 N95-28312

HYPERPLANES

Yang-Baxter type equations and posets of maximal chains
[PB95-185195] p 2388 N95-26516

HYPERSONIC BOUNDARY LAYER

Analysis of hypersonic boundary layer second mode instability over a 7 deg cone
[AD-A289471] p 2276 N95-26819

HYPERSONIC COMBUSTION

A fully implicit time accurate method for hypersonic combustion: Application to shock-induced combustion instability
[NASA-TM-106707] p 2273 N95-26380

HYPERSONIC FLOW

Turbulence modeling
[NASA-CR-197751] p 2274 N95-26665

Viscous shock-layer analysis on hypersonic flow over reentry capsule with nonequilibrium chemistry
[ISAS-R-656] p 2274 N95-26739

Analysis of hypersonic boundary layer second mode instability over a 7 deg cone
[AD-A289471] p 2276 N95-26819

HYPERSONIC REENTRY

Viscous shock-layer analysis on hypersonic flow over reentry capsule with nonequilibrium chemistry
[ISAS-R-656] p 2274 N95-26739

HYPERSONIC SHOCK

Turbulence modeling
[NASA-CR-197751] p 2274 N95-26665

HYPERSONIC SPEED

A fully implicit time accurate method for hypersonic combustion: Application to shock-induced combustion instability
[NASA-TM-106707] p 2273 N95-26380

Turbulence modeling
[NASA-CR-197751] p 2274 N95-26665

Application of CFD to the analysis and design of high-speed inlets
[NASA-CR-198574] p 2279 N95-27240

HYPERTENSION

Mechanisms of hypertension after cross-linked hemoglobin blood-substitute transfusion
[AD-A289558] p 2352 N95-26680

HYPERTHERMIA

A 3-D finite difference time domain investigation of microwave propagation through inhomogeneous biological materials
[AD-A289431] p 2251 N95-26869

HYPERVELOCITY

A high velocity electromagnetic mass launcher having an ablation resistant insulator
[AD-A288231] p 2154 N95-26524

HYPERVELOCITY GUNS

A high velocity electromagnetic mass launcher having an ablation resistant insulator
[AD-A288231] p 2154 N95-26524

Ram accelerator performance calculations using a modified version of the NASA CET89 equilibrium chemistry code
[AD-A289554] p 2201 N95-26678

HYPERVELOCITY IMPACT

Orbital impacts and the Space Shuttle windshield
[NASA-TM-110594] p 2159 N95-26379

A new technique for ground simulation of hypervelocity debris p 2154 N95-27671

HYPERVELOCITY PROJECTILES

A high velocity electromagnetic mass launcher having an ablation resistant insulator
[AD-A288231] p 2154 N95-26524

HYSTERESIS

Fatigue behavior of a cross-ply ceramic matrix composite at elevated temperature under tension-tension loading
[AD-A289250] p 2182 N95-26969

Electromagnetic hysteretic response calculation for superconductors in demagnetizing geometries
[DE95-005028] p 2264 N95-27403

A magnetic hysteresis model p 2153 N95-27801

I

ICE

A book and series of monographs on ice physics
[AD-A288319] p 2200 N95-26422

Structure of ordinary ice Ih. Part 2: Defects in ice. Volume 1: Point defects
[AD-A288279] p 2200 N95-26452

Subsurface radar investigations at the Pegasus Glacial-ice Runway and Williams Field, McMurdo Station, Antarctica
[AD-A289323] p 2144 N95-27297

Performance of a stand-alone wind-electric ice maker for remote villages
[DE95-004006] p 2320 N95-27475

Analysis of aircraft engine blade subject to ice impact
p 2141 N95-28277

Ultrasonic studies of liquid/solid seimoacoustic wave phenomena
[AD-A289644] p 2402 N95-28622

ICE CLOUDS

Replicator for characterization of cirrus and polar stratospheric cloud particles
[NASA-CR-197785] p 2341 N95-26669

Subvisual cirrus: What it is and where you find it
[AD-A289329] p 2342 N95-26899

ICE FORMATION

Structure of ordinary ice Ih. Part 2: Defects in ice. Volume 1: Point defects
[AD-A288279] p 2200 N95-26452

Replicator for characterization of cirrus and polar stratospheric cloud particles
[NASA-CR-197785] p 2341 N95-26669

Debris/Ice/TPS assessment and integrated photographic analysis of Shuttle mission STS-67
[NASA-TM-110651] p 2160 N95-27238

Further investigations of icing effects on an advanced high-lift multi-element airfoil
[NASA-TM-106947] p 2125 N95-27762

Tomographic observations of deep convection and the thermal evolution of the Greenland Sea Gyre 1988-1989
[AD-A289104] p 2348 N95-28096

IDEAL FLUIDS

Computational and experimental studies of hydrodynamic instabilities and turbulent mixing
[DE95-006837] p 2288 N95-28603

IDENTIFYING

A study of the use beta-alumina as a weak interface in alumina fiber composites
[AD-A288629] p 2179 N95-26484

The use of electrochemistry and ellipsometry for identifying and evaluating corrosion on aircraft
[AD-A288536] p 2125 N95-27186

PXAMS: Projectile X ray AMS: X ray yields and applications
[DE95-006438] p 2204 N95-27496

IGNITION

Effects of dust from storage heaters on ignition in scramjets
[NAL-TR-1234] p 2139 N95-26706

Indirectly driven targets for ignition
[DE95-006451] p 2430 N95-27327

Discharge ignition behavior of the Space Station plasma contactor
[NASA-TM-106925] p 2168 N95-27862

IGNITION LIMITS

Methods development for measuring and classifying flammability/combustibility of refrigerants. Task 2: Test plan
[DE95-007066] p 2234 N95-27481

IGNITION TEMPERATURE

Use of CTFE as an additive to enhance fire resistance of single hydraulic fluid
[AD-A289377] p 2233 N95-27325

High temperature oxidation of nickel concentrates
[PB95-195566] p 2224 N95-28644

ILLITE

The biodegradation of fuels in soils and sediments: Differences as a function of mineralogy
p 2230 N95-27116

ILLUMINATING

Testing of Uninterruptible Power Supplies with nonlinear loads
[AD-A289353] p 2262 N95-27067

Visualization and direct comparison of large displacements using difference holographic interferometry
[DE95-608782] p 2292 N95-27711

ILLUMINATION

An illumination planner for Lambertian polyhedral objects
[AD-A289332] p 2424 N95-26900

IMAGE ANALYSIS

Neural models of spatial orientation in novel environments
[AD-A288420] p 2380 N95-26530

Schlieren System and method for moving objects
[NASA-CASE-LAR-15053-1] p 2291 N95-27191

Characterization of collision cascade damage in Ca2La8(SiO4)6O2 by HRTEM
[DE95-005719] p 2440 N95-27491

Physical interpretation and development of ultrasonic nondestructive evaluation techniques applied to the quantitative characterization of textile composite materials
[NASA-CR-198591] p 2306 N95-28034

Scattering by a small object close to an interface. 3. Buried object
[PB95-184909] p 2256 N95-28354

The detection and tracking of motion by means of time-space pattern modelling using random fields
[IFTR-37/1994] p 2374 N95-28566

IMAGE CLASSIFICATION

An analysis of Bayesian networks as classifiers
[AD-A289316] p 2382 N95-27293

Neural networks in the classification of uses of the soil in satellite images
[INPE-5478-PRE/1777] p 2316 N95-28672

IMAGE CONTRAST

Performance modeling of hyperspectral imaging sensors for atmospheric studies
[AD-A289017] p 2289 N95-26461

IMAGE ENHANCEMENT

Image perception wavelet simulation and enhancement for the visually impaired
[AD-A289303] p 2353 N95-26917

IMAGE FILTERS

SAR noise reduction through the utilization of robust filters
[INPE-5504-PRE/1787] p 2258 N95-28569

IMAGE PROCESSING

Longterm infrared cloud clutter research
[AD-A288632] p 2340 N95-26343

Joint Services Electronics Program (JSEP)
[AD-A288299] p 2345 N95-26419

Digital mapping, charting, and geodesy analysis program: Initial technical review of Raster Product Format
[AD-A289039] p 2313 N95-26476

Nonlinear scalespace via hierarchical statistical modeling
[AD-A289057] p 2394 N95-26478

Neural models of spatial orientation in novel environments
[AD-A288420] p 2380 N95-26530

Digital mapping, charting, and geodesy analysis program technical review of Vector Quantization (VQ) Decompression for the National Imagery Transmission Format Standard (NITFS)
[AD-A288998] p 2314 N95-26682

User's and test case manual for FEMATS
[NASA-CR-197803] p 2366 N95-26694

Compensated deconvolution from wavefront sensing
[AD-A289490] p 2336 N95-26824

Perceptual based image fusion with applications to hyperspectral image data
[AD-A289429] p 2251 N95-26867

Frame selection performance limits for statistical image reconstruction of adaptive optics compensated images
[AD-A289240] p 2424 N95-26965

ROC analysis of IR segmentation techniques
[AD-A289252] p 2424 N95-26971

Using virtual active vision tools to improve autonomous driving tasks
[AD-A289175] p 2356 N95-27013

A foveated system to reduce transmission bandwidth of video images from remote camera systems
[AD-A288516] p 2254 N95-27060

A hybrid genetic algorithm for resolving closely spaced objects p 2384 N95-27387

Improved reduced-resolution satellite imagery
p 2376 N95-27388

Effect of noise on Frequency-Resolved Optical Gating measurements of ultrashort pulses
[DE95-007149] p 2298 N95-27969

An introduction to wavelet transforms
[AD-A289083] p 2256 N95-28095

Edge detection by nonlinear dynamics
[DE95-008076] p 2373 N95-28168

Speckle spectrum of the ERS-1 wavemode product
[PB95-196564] p 2315 N95-28180

Full complex modulation using two one-parameter spatial light modulators
[NASA-CASE-MSC-22255-1] p 2427 N95-28384

Binary segmentation of SAR images by the ICM algorithm
[INPE-5464-PRE/1772] p 2258 N95-28559

The detection and tracking of motion by means of time-space pattern modelling using random fields
[IFTR-37/1994] p 2374 N95-28566

Exploiting parallelism in a Monte Carlo image-matching algorithm
[AD-A289872] p 2374 N95-28625

IMAGE RECONSTRUCTION

Frame selection performance limits for statistical image reconstruction of adaptive optics compensated images
[AD-A289240] p 2424 N95-26965

JPRS report: Science and technology. Central Eurasia
[JPRS-UST-95-016] p 2262 N95-27170

Visualization and direct comparison of large displacements using difference holographic interferometry
[DE95-608782] p 2292 N95-27711

An introduction to wavelet transforms
[AD-A289083] p 2256 N95-28095

IMAGE RESOLUTION

An image quality analysis of ANVIS-6 night vision goggles
[AD-A289398] p 2359 N95-26883

Grayscale/resolution trade-off for text: Model predictions and psychophysical results for letter confusion and letter discrimination
[NASA-CR-197784] p 2369 N95-26930

Frame selection performance limits for statistical image reconstruction of adaptive optics compensated images
[AD-A289240] p 2424 N95-26965

Factors in human-computer interface design (a pilot study)
[AD-A288908] p 2360 N95-27195

Image quality metrics for color CRT displays
[AD-A288934] p 2262 N95-27196

Improved reduced-resolution satellite imagery
p 2376 N95-27388

Reconstruction of an infrared band of meteorological satellite imagery with abductive networks
[SAIC-94/1062] p 2345 N95-27389

Effect of noise on Frequency-Resolved Optical Gating measurements of ultrashort pulses
[DE95-007149] p 2298 N95-27969

Low power limits in ultrashort pulse measurement using Frequency-Resolved Optical Gating
[DE95-007150] p 2299 N95-28219

IMAGERY

Digital mapping, charting, and geodesy analysis program technical review of Vector Quantization (VQ) Decompression for the National Imagery Transmission Format Standard (NITFS)
[AD-A288998] p 2314 N95-26682

Three-dimensional photogrammetry for laboratory applications
[AD-A291624] p 2294 N95-28410

IMAGES

Grayscale/resolution trade-off for text: Model predictions and psychophysical results for letter confusion and letter discrimination
[NASA-CR-197784] p 2369 N95-26930

Views of the solar system
[DE95-006446] p 2461 N95-27326

Free Electron Laser Physical Process Code (FELPPC)
[DE95-006276] p 2296 N95-27557

TOPS: Toward Other Planetary Systems. A report by the solar system exploration division
[NASA-TM-110609] p 2464 N95-28009

Query by image example: The CANDID approach
[DE95-006284] p 2456 N95-28631

Method of space-time sequence transform used to measure acousto-optic deflection and modulation
[AD-A289612] p 2402 N95-28671

IMAGING RADAR

High performance ground penetrating radar survey of TA-49/Area 2
[DE95-006856] p 2258 N95-28601

IMAGING SPECTROMETERS

Perceptual based image fusion with applications to hyperspectral image data
[AD-A289429] p 2251 N95-26867

IMAGING TECHNIQUES

Radiation sensitive area detection device and method
[NASA-CASE-MFS-28563-3] p 2423 N95-26385

Analysis of electromagnetic problems involving chiral, bi-isotropic, and uniaxial bianisotropic media
[PB95-185096] p 2248 N95-26450

Performance modeling of hyperspectral imaging sensors for atmospheric studies
[AD-A289017] p 2289 N95-26461

Replicator for characterization of cirrus and polar stratospheric cloud particles
[NASA-CR-197785] p 2341 N95-26669

The development of infrared detectors and mechanisms for use in future infrared space missions
[NASA-CR-197819] p 2290 N95-26702

An acoustic charge transport imager for high definition television applications
[NASA-CR-197841] p 2249 N95-26708

Combined investigation of Eddy current and ultrasonic techniques for composite materials NDE
[NASA-TM-110599] p 2306 N95-26778

Compensated deconvolution from wavefront sensing
[AD-A289490] p 2336 N95-26824

Perceptual based image fusion with applications to hyperspectral image data
[AD-A289429] p 2251 N95-26867

Determining nanoscale physical properties of materials by microscopy and spectroscopy
[AD-A289532] p 2201 N95-26870

Solid-state image sensor with focal-plane digital photon-counting pixel array
[NASA-CASE-NPO-18518-1-CU] p 2424 N95-26894

Image perception wavelet simulation and enhancement for the visually impaired
[AD-A289303] p 2353 N95-26917

Grayscale/resolution trade-off for text: Model predictions and psychophysical results for letter confusion and letter discrimination
[NASA-CR-197784] p 2369 N95-26930

Notes on the calibration of the JHU-APL solar vector magnetograph at NSO-Sec peak
[AD-A289277] p 2253 N95-26983

Schlieren System and method for moving objects
[NASA-CASE-LAR-15053-1] p 2291 N95-27191

SXI Prototype mirror mount
[NASA-CR-196613] p 2301 N95-27244

Matrix kernels for MEG and EEG source localization and imaging
[DE95-005238] p 2354 N95-27426

Magnetic resonance imaging of solvent transport in polymer networks
[DE95-007142] p 2234 N95-27455

Specification of the figure and finish of EUV mirrors in terms of performance requirements, revised Nov. 1994
[DE95-005689] p 2425 N95-27490

Visualization and direct comparison of large displacements using difference holographic interferometry
[DE95-608782] p 2292 N95-27711

Low energy neutral atom imaging: Remote observations of the magnetosphere

[DE95-006342] p 2337 N95-27848

Positron microscopy

[DE95-007042] p 2410 N95-27874

Nonlinear optical microscopy for imaging thin films and surfaces

[DE95-007872] p 2426 N95-28018

Physical interpretation and development of ultrasonic nondestructive evaluation techniques applied to the quantitative characterization of textile composite materials

[NASA-CR-198591] p 2306 N95-28034

Remote measurement of ground temperature and emissivity

[DE95-008055] p 2314 N95-28053

Ambient-pressure silica aerogel films

[DE95-008161] p 2237 N95-28090

Analytical electron microscopy of nanometer-sized particles

[AD-A289124] p 2413 N95-28101

Surface-emitting semiconductor laser for intracavity spectroscopy and microscopy

[DE95-007745] p 2299 N95-28128

Transformation to zero offset in transversely isotropic media

[DE95-007669] p 2339 N95-28192

Fowler DMO and time migration for transversely isotropic media with explicit operators

[DE95-007671] p 2339 N95-28194

OBIC analysis of stressed, thermally-isolated polysilicon resistors

[DE95-008511] p 2268 N95-28201

New developments for sol-gel film and fiber processing

[DE95-008175] p 2240 N95-28404

Development and application of low-temperature AFM

[AD-A291704] p 2352 N95-28525

Query by image example: The CANDID approach

[DE95-006284] p 2456 N95-28631

TV-holography at high temperatures: In situ observations of the oxidation of advanced materials

[PB95-195343] p 2294 N95-28651

IMMOBILIZATION

Chemistry involving the separation, isolation, and immobilization of 3-5 compound semiconductor nanocrystals and quantum dots

[AD-A288381] p 2436 N95-26473

Non-covalent immobilization of proteins and enzymes on polymerized lipid assemblies

[AD-A288234] p 2225 N95-26526

IMMUNE SYSTEMS

Diagnostic antigens of Leishmania

[AD-A288805] p 2350 N95-27097

IMMUNOLOGY

Anti-idiotype probes for toxin detection

[AD-A288955] p 2348 N95-26435

Diagnostic antigens of Leishmania

[AD-A288805] p 2350 N95-27097

IMPACT

Scale model experiments with ceramic laminate targets

[AD-A288322] p 2225 N95-26561

IMPACT DAMAGE

Orbital impacts and the Space Shuttle windshield

[NASA-TM-110594] p 2159 N95-26379

Combined investigation of Eddy current and ultrasonic techniques for composite materials NDE

[NASA-TM-110599] p 2306 N95-26778

Effects of low earth orbit on the optical performance of multi-layer enhanced high reflectance mirrors

p 2428 N95-27652

Space environmental effects observed on the Hubble Space Telescope p 2242 N95-27655

A new technique for ground simulation of hypervelocity debris p 2154 N95-27671

Analysis of aircraft engine blade subject to ice impact

p 2141 N95-28277

Characteristics of laminates with delamination control strips p 2191 N95-28434

The use of impact force as a scale parameter for the impact response of composite laminates

p 2197 N95-28479

Effect of low-speed impact damage and damage location on behavior of composite panels p 2197 N95-28481

Impact damage resistance of composite fuselage structure, part 1 p 2138 N95-28482

Applications of a damage tolerance analysis methodology in aircraft design and production

p 2197 N95-28483

Compressive strength of damaged and repaired composite plates p 2198 N95-28484

Post impact compressive strength in composites

p 2198 N95-28485

Fundamental concepts in the suppression of delamination buckling by stitching p 2198 N95-28486

Damage tolerance of a geodesically stiffened advanced composite structural concept for aircraft structural applications p 2138 N95-28487

Advanced wing design survivability testing and results

p 2138 N95-28488

IMPACT LOADS

Layer coefficients for NHDOT pavement materials

[AD-A288262] p 2246 N95-26548

Effects of floor location on response of composite fuselage frames p 2192 N95-28439

IMPACT MELTS

Computational studies of projectile melt in impact with typical whipple shields

[DE95-005916] p 2311 N95-28337

IMPACT PREDICTION

Tracking and impact prediction of Earth-Crossing-Objects (ECO's) on a collision course with Earth

[AD-A289321] p 2461 N95-27303

IMPACT RESISTANCE

Static and dynamic strain energy release rates in toughened thermosetting composite laminates

p 2188 N95-28288

IMPACT STRENGTH

Orbital impacts and the Space Shuttle windshield

[NASA-TM-110594] p 2159 N95-26379

Layer coefficients for NHDOT pavement materials

[AD-A288262] p 2246 N95-26548

Compressive residual strength of graphite/epoxy laminates after impact p 2191 N95-28431

Effects of floor location on response of composite fuselage frames p 2192 N95-28439

The use of impact force as a scale parameter for the impact response of composite laminates

p 2197 N95-28479

Post impact compressive strength in composites

p 2198 N95-28485

IMPACT TESTS

Layer coefficients for NHDOT pavement materials

[AD-A288262] p 2246 N95-26548

Development of repair processes and sources for C/KC-135 aircraft windows/windshields

[AD-A288348] p 2117 N95-26629

An experimental investigation of sandwich flat panels under low velocity impact

[AD-A289420] p 2309 N95-27135

Scaling issues in dynamic fragmentation

[DE95-008509] p 2309 N95-27745

Analysis of aircraft engine blade subject to ice impact

p 2141 N95-28277

Computational studies of projectile melt in impact with typical whipple shields

[DE95-005916] p 2311 N95-28337

The use of impact force as a scale parameter for the impact response of composite laminates

p 2197 N95-28479

Effect of low-speed impact damage and damage location on behavior of composite panels p 2197 N95-28481

Impact damage resistance of composite fuselage structure, part 1 p 2138 N95-28482

Applications of a damage tolerance analysis methodology in aircraft design and production

p 2197 N95-28483

Damage tolerance of a geodesically stiffened advanced composite structural concept for aircraft structural applications p 2138 N95-28487

Rotorcraft crashworthy airframe and fuel system technology development program

[AD-A289986] p 2126 N95-28630

IMPACT TOLERANCES

Through-the Thickness(R) braided composites for aircraft applications p 2185 N95-28273

Compressive residual strength of graphite/epoxy laminates after impact p 2191 N95-28431

IMPEDANCE

Surface scanning techniques to locate and study defects in painted zinc and zinc alloy coated steels

[DE95-006099] p 2240 N95-28547

IMPINGEMENT

Load measurement system with load cell lock-out mechanism p 2159 N95-27291

IMPLANTATION

Characterization and redesign of the AFIT multielectrode array

[AD-A289295] p 2354 N95-27039

Characterization of defects in deuterium-implanted beryllium

[DE95-005688] p 2217 N95-27553

Modification of the optical properties of glass by sequential ion implantation

[DE95-007401] p 2237 N95-28080

IMPLOSIONS

Bubble fusion: Preliminary estimates

[DE95-006337] p 2420 N95-27494

Investigation of HE driven cylindrical liner

[DE95-007866] p 2311 N95-28539

IMPULSES

ACT adaptive filters

[AD-A288385] p 2363 N95-26474

IMPURITIES

A new growth technology for highly non-linear, optical quality organic films: Organic vapor phase deposition

[AD-A289006] p 2178 N95-26567

Materials Research Society Symposium Proceedings. Volume 339: Diamond, SiC and nitride wide bandgap semiconductors

[AD-A288690] p 2437 N95-26818

Ultra high purity, dimensionally stable INVAR 36

[NASA-CASE-NPO-19358-1-CU] p 2213 N95-26862

Photoluminescence spectroscopy of 4H- and 6H-SiC

[AD-A289326] p 2202 N95-26896

Model of a single impurity in a wide bandgap semiconductor describing electric field screening

[AD-A289322] p 2264 N95-27296

Cavity formation and impurity gettering in He-implanted Si

[DE95-007744] p 2444 N95-28127

Theory of exotic superconductivity and normal states of heavy electron and high temperature superconductivity materials

[DE95-006637] p 2268 N95-28198

Chemical and electrical properties of cavities in silicon and germanium

[DE95-006812] p 2445 N95-28206

The off-center effect on the diffusion coefficient of Cu(+) and Li(+) in the KCl lattice

[DE95-609146] p 2446 N95-28255

Fellowship in physics

[AD-A291691] p 2446 N95-28522

IN SITU MEASUREMENT

Electrocrystallization of an ordered organic monolayer: Selective epitaxial growth of beta(ET)213 ongraphite

[AD-A288942] p 2178 N95-26569

Replicator for characterization of cirrus and polar stratospheric cloud particles

[NASA-CR-197785] p 2341 N95-26660

Fabrication of long wavelength array by in-situ molecular beam epitaxy

[AD-A288599] p 2423 N95-26679

Surface scanning techniques to locate and study defects in painted zinc and zinc alloy coated steels

[DE95-006099] p 2240 N95-28547

In situ dynamic material property measurement system

[AD-D017387] p 2210 N95-28585

TV-holography at high temperatures: In situ observations of the oxidation of advanced materials

[PB95-195343] p 2294 N95-28651

IN-FLIGHT MONITORING

Inflight resistance measurement on high-T(sub c) superconducting thin films exposed to orbital atomic oxygen on CONCAP-2 (STS-46) p 2272 N95-27635

A PC-based magnetometer-only attitude and rate determination system for gyroless spacecraft

p 2147 N95-27770

Experience from the in-flight calibration of the Extreme Ultraviolet Explorer (EUVE) and Upper Atmosphere Research Satellite (UARS) fixed head star trackers (FHSTs) p 2149 N95-27779

INCLUSIONS

Non-metallic oxide inclusion formation in C-Mnlow alloy steel welds

[DE94-019160] p 2215 N95-27319

Engineered materials for appliation in severe metallurgical environments: Tantalum-carbon alloy development

[DE95-006838] p 2216 N95-27488

Advances in welding science: A perspective

[DE95-006745] p 2302 N95-27545

INCOMPRESSIBLE FLOW

CFD research, parallel computation and aerodynamic optimization

[NASA-CR-197748] p 2120 N95-26649

Progress in incompressible Navier-Stokes computations for propulsion flows and its dual-use applications

[NASA-CR-197746] p 2275 N95-26766

Flow control

[AD-A289262] p 2279 N95-27197

A new finite element formulation for incompressible flow

[DE95-007141] p 2284 N95-27454

Computational and experimental studies of hydrodynamic instabilities and turbulent mixing

[DE95-006837] p 2288 N95-28603

INCOMPRESSIBLE FLUIDS

A fast numerical method for isothermal resin transfer mold filling

[AD-A288944] p 2179 N95-26565

On the nonlinear stability of the unsteady, viscous flow of an incompressible fluid in a curved pipe

[NASA-CR-195065] p 2278 N95-27028

The calculation of the mass moment of inertia of a fluid in a rotating rectangular tank
[NASA-CR-197777] p 2278 N95-27165

INCONEL (TRADEMARK)

Probabilistic material strength degradation model for Inconel 718 components subjected to high temperature, high-cycle and low-cycle mechanical fatigue, creep and thermal fatigue effects
[NASA-CR-197832] p 2214 N95-27167

INDENTATION

Indentability of conventional and negative Poisson's ratio foams p 2195 N95-28472

In situ dynamic material property measurement system
[AD-D017387] p 2210 N95-28585

INDEXES (DOCUMENTATION)

Index to NASA news releases and speeches 1994
[NASA-TM-110650] p 2452 N95-26673

Spaceport news index: January 1990 - December 1994
[NASA-TM-110653] p 2454 N95-27243

Aerospace medicine and biology: A continuing bibliography with indexes (supplement 402)
[NASA-SP-7011(402)] p 2354 N95-27502

Aeronautical engineering: A continuing bibliography with indexes (supplement 318)
[NASA-SP-7037(318)] p 2120 N95-27543

INDIAN OCEAN

The northern wintertime divergence extrema at 200 hPa and surface cyclones as simulated in the integration of the ECMWF general circulation model
[DE95-007946] p 2332 N95-28550

INDIUM

The structure of lead-indium phosphate glass
[DE95-007130] p 2237 N95-27967

INDIUM COMPOUNDS

First-principles calculations for AlN, GaN, and InN: Bulk and alloy properties
[DE95-006822] p 2219 N95-27958

INDIUM GALLIUM ARSENIDES

Phase separation and ordering in InGaAsP and InGaAs materials
[DE95-007493] p 2443 N95-28050

INDIUM PHOSPHIDES

Preferentially etched epitaxial liftoff of InP material
[NASA-CASE-LEW-15760-1] p 2235 N95-27503

Phase separation and ordering in InGaAsP and InGaAs materials
[DE95-007493] p 2443 N95-28050

INDUCTANCE

Measurement of the D0 WAMUS magnet inductance
[DE95-005126] p 2399 N95-27530

Global dynamo in a reversed field pinch plasma
[DE94-765441] p 2432 N95-27869

Forback DC-to-DC converter
[NASA-CASE-GSC-13404-1] p 2269 N95-28341

INDUCTION MOTORS

Structural optimisation of cage induction motors using finite element analysis
[PB95-195434] p 2271 N95-28655

INDUCTORS

Forback DC-to-DC converter
[NASA-CASE-GSC-13404-1] p 2269 N95-28341

INDUSTRIAL MANAGEMENT

Asian Aeronautics: Technology acquisition drives industry development. Report to Congressional requesters
[GAO/NSIAD-94-140] p 2118 N95-26817

Change, Learning and Mental Work in Organizations: Working papers of the 3rd Otaniemi-Dresden Workshop
[PB95-184941] p 2356 N95-26909

INDUSTRIAL PLANTS

Molten Carbonate Fuel Cell (MCFC) product development test
[DE95-007345] p 2316 N95-26543

Electro-hydrostatic actuator controller design using quantitative feedback theory
[AD-A289220] p 2141 N95-26957

NIST Automated Manufacturing Research Facility (AMRF): March 1987
[NONP-NASA-VT-95-49097] p 2246 N95-27203

Building the electronic industry's roadmaps p 2263 N95-27228

Electronics manufacturing and assembly in Japan p 2263 N95-27231

The Tau-Charm Factory in the ERA of B-Factories and CESR
[DE95-007894] p 2412 N95-28028

INDUSTRIAL SAFETY

Concurrent engineering research center
[NASA-CR-197726] p 2362 N95-26386

INDUSTRIAL WASTES

Marshall Space Flight Center solid waste characterization and recycling improvement study
[NASA-CR-196594] p 2360 N95-27164

INDUSTRIES

Quest for excellence 5
[NONP-NASA-VT-95-49099] p 2451 N95-27205

JTEC Panel report on electronic manufacturing and packaging in Japan
[NASA-CR-197830] p 2263 N95-27226

Building the electronic industry's roadmaps p 2263 N95-27228

Japan's electronic packaging technologies p 2263 N95-27230

Electronics manufacturing and assembly in Japan p 2263 N95-27231

Quality assurance and reliability in the Japanese electronics industry p 2263 N95-27232

An ugly duckling becomes a swan (hor ellipsis): How an organization becomes customer focused through listening
[DE95-004974] p 2454 N95-27461

SIHTI 2: Energy and environmental technology. Yearbook 1993 of the research programme
[DE95-755135] p 2331 N95-28202

The U.S. Department of Energy Wind Turbine Development Program
[DE95-000292] p 2325 N95-28395

INELASTIC COLLISIONS

Atomic physics with highly charged ions
[DE95-007325] p 2407 N95-27439

INELASTIC SCATTERING

Comparative experimental study of PIXE and X-ray fluorescence analysis
[DE95-607868] p 2327 N95-27198

A note on the constituent quark resonances
[DE95-608831] p 2406 N95-27316

Addendum to the 1993 European school of high-energy physics
[DE95-610313] p 2419 N95-27321

Atomic physics with highly charged ions
[DE95-007325] p 2407 N95-27439

Observations of CEF-split intermultiplet transitions in optically opaque EuBa2Cu3O7 using inelastic neutron scattering
[DE95-007135] p 2408 N95-27453

Molecular beam scattering from C-13 enriched Kapton and correlation with the EOIM-3 carousel experiment p 2419 N95-27643

Optical design and performance of the inelastic scattering beamline at the National Synchrotron Light Source
[DE95-007679] p 2422 N95-28195

Resonant coherent excitation of N6(+) and Mg11(+) in planar channeling: Anisotropies in ionization probabilities and X-ray emission
[DE95-006732] p 2417 N95-28595

Future opportunities and present possibilities for coherent inelastic single crystal measurements on pulsed neutron sources
[PB95-195798] p 2418 N95-28657

INERTIAL CONFINEMENT FUSION

Development of density and temperature profile diagnostics for ICF targets
[DE95-007664] p 2433 N95-28052

INERTIAL NAVIGATION

A modified proportional navigation scheme for rendezvous and docking with tumbling targets: The Planar case p 2150 N95-27784

INFECTIOUS DISEASES

Diagnostic antigens of Leishmania
[AD-A288805] p 2350 N95-27097

INFERENCE

Generalized probabilistic reasoning and empirical studies on computational efficiency and scalability
[AD-A289185] p 2395 N95-27016

INFILTRATION

Polymer infiltration studies
[NASA-CR-198601] p 2236 N95-27857

TEM characterization of Al/Al2O3 composite fabricated by reactive metal infiltration
[DE95-008508] p 2184 N95-28145

INFORMATION

The distribution of cloud cover over the former USSR as derived from the RIHMI 223-Station 3-hourly meteorological database
[DE95-007046] p 2343 N95-27920

INFORMATION DISSEMINATION

The aerospace database: An introduction to AIAA'S computerized source for identifying scientific and technical information p 2119 N95-26950

Geothermal direct-heat utilization assistance
[DE95-007247] p 2319 N95-27236

Advanced Earth-to-orbit propulsion technology information, dissemination and research
[NASA-CR-196582] p 2168 N95-27424

Teaching interdisciplinary computational science from an electronic book on the Internet
[DE95-006525] p 2373 N95-28498

NASA/DOD Aerospace Knowledge Diffusion Research Project. Report 35: The use of computer networks in aerospace engineering
[NASA-CR-198170] p 2456 N95-28600

Building an electronic book on the Internet. CSEP:An interdisciplinary syllabus for teaching computational science at the graduate level
[DE95-006526] p 2375 N95-28632

INFORMATION MANAGEMENT

Concurrent engineering research center
[NASA-CR-197726] p 2362 N95-26386

NIST: Information management in the AMRF
[NONP-NASA-VT-95-49120] p 2454 N95-27208

An ugly duckling becomes a swan (hor ellipsis): How an organization becomes customer focused through listening
[DE95-004974] p 2454 N95-27461

Project Records Information System (PRIS) user's manual, revision 3
[DE95-008330] p 2456 N95-28172

Evaluation of an Air Force Information Resources Management (IRM) overview course
[AD-A288746] p 2456 N95-28587

INFORMATION PROCESSING (BIOLOGY)

Codes of processing and multiple resources: Model and methodology
[AD-A289583] p 2355 N95-26691

INFORMATION RETRIEVAL

Specifying weak sets
[AD-A288587] p 2364 N95-26536

A demonstration of Client/Server technology using remote procedure calls for an application of file migration for moving records based on location
[AD-A289391] p 2453 N95-26864

Transparent access to distributed, heterogeneous environmental information systems
[DE95-007268] p 2454 N95-27483

Development and implementation of an electronic library tour for the NASA Langley Technical Library
[NASA-TM-110619] p 2455 N95-27701

The Sunrise project: An R&D project for a national information infrastructure prototype
[DE95-006340] p 2455 N95-27847

Query by image example: The CANDID approach
[DE95-006284] p 2456 N95-28631

INFORMATION SYSTEMS

Long term distributed file reference tracing: Implementation and experience
[AD-A288585] p 2452 N95-26535

Specifying weak sets
[AD-A288587] p 2364 N95-26536

Activities of the Laboratory of Information Processing Science
[PB95-184982] p 2452 N95-26631

The aerospace database: An introduction to AIAA'S computerized source for identifying scientific and technical information p 2119 N95-26950

Selected bibliography on heavy water, tritiated water and hydrogen isotopes (1981-1992)
[DE95-608331] p 2405 N95-27159

A user-system interface agent p 2383 N95-27379

Outline and handling manual of fusion experimental data monitor system DAISY, version 2
[DE95-703895] p 2431 N95-27414

Transparent access to distributed, heterogeneous environmental information systems
[DE95-007268] p 2454 N95-27483

Long Duration Exposure Facility (LDEF) Archive System p 2457 N95-27658

Human factors in aviation maintenance, phase 4
[DOT/FAA/AM-95/14] p 2360 N95-27696

Development and implementation of an electronic library tour for the NASA Langley Technical Library
[NASA-TM-110619] p 2455 N95-27701

The distribution of cloud cover over the former USSR as derived from the RIHMI 223-Station 3-hourly meteorological database
[DE95-007046] p 2343 N95-27920

Research on the establishment of the database system for R and D on the innovative technology for the Earth
[DE95-759244] p 2458 N95-27937

Project Records Information System (PRIS) user's manual, revision 3
[DE95-008330] p 2456 N95-28172

International networks
[PB95-196366] p 2379 N95-28502

Query by image example: The CANDID approach
[DE95-006284] p 2456 N95-28631

INFORMATION THEORY

The 1994 IEEE-IMS Workshop on Information Theory and Statistics
[AD-A288808] p 2380 N95-26492

Distributed methods and processes in games of incomplete information
[PB95-184842] p 2396 N95-28352

Distributed methods and processes in games of incomplete information
[PB95-184859] p 2396 N95-28353

INFORMATION TRANSFER

A demonstration of Client/Server technology using remote procedure calls for an application of file migration for moving records based on location
[AD-A289391] p 2453 N95-28864

Integrated planning and scheduling for Earth science data processing p 2384 N95-27382

Teaching interdisciplinary computational science from an electronic book on the Internet
[DE95-006525] p 2373 N95-28498

Downloading environmental data in the new MOODS format
[AD-A288835] p 2456 N95-28589

INFRARED ASTRONOMY

The development of infrared detectors and mechanisms for use in future infrared space missions
[NASA-CR-197819] p 2290 N95-26702

Typical examples of classical novae
p 2459 N95-27074

Molecular cloud content of early-type galaxies. V. CO in elliptical galaxies
[PB95-185153] p 2461 N95-27320

INFRARED DETECTORS

Longterm infrared cloud clutter research
[AD-A288632] p 2340 N95-26343

A probabilistic target classification and description model for seismic sensors
[AD-A288548] p 2335 N95-26531

Fabrication of long wavelength array by in-situ molecular beam epitaxy
[AD-A288599] p 2423 N95-26679

The development of infrared detectors and mechanisms for use in future infrared space missions
[NASA-CR-197819] p 2290 N95-26702

Subvisual cirrus: What it is and where you find it
[AD-A289329] p 2342 N95-26899

Growth and characterization of crystals for room temperature I.R. detectors and second harmonic generation devices
[NASA-CR-198598] p 2443 N95-28033

Dimensionally self regulating materials
[AD-A291671] p 2257 N95-28456

INFRARED IMAGERY

Infrared field measurements of sea surface temperature: Analysis of wake signatures and comparison of skin layer models
[NASA-CR-197849] p 2346 N95-26533

Perceptual based image fusion with applications to hyperspectral image data
[AD-A289429] p 2251 N95-26867

ROC analysis of IR segmentation techniques
[AD-A289252] p 2424 N95-26971

Reconstruction of an infrared band of meteorological satellite imagery with abductive networks
[SAIC-94/1062] p 2345 N95-27389

INFRARED LASERS

Generation of a single-lobe, far-field intensity pattern from a laser diode array using an optical delay line
[AD-A289226] p 2295 N95-26961

Improved performance 1590 nm Er:YLF laser
[DE95-003691] p 2296 N95-27705

Fellowship in physics
[AD-A291691] p 2446 N95-28522

INFRARED RADIATION

Longterm infrared cloud clutter research
[AD-A288632] p 2340 N95-26343

The effect of infrared sea surface temperature measurements on evaporation duct height estimation
[AD-A289045] p 2346 N95-26477

Infrared field measurements of sea surface temperature: Analysis of wake signatures and comparison of skin layer models
[NASA-CR-197849] p 2346 N95-26533

The development of infrared detectors and mechanisms for use in future infrared space missions
[NASA-CR-197819] p 2290 N95-26702

Calculations of downward IR surface fluxes in the 500-3,000 cm(exp -1) wavenumber range for the 1994 ICRCCM model intercomparison study
[DE95-006430] p 2328 N95-27708

Remote measurement of ground temperature and emissivity
[DE95-008055] p 2314 N95-28053

Heterostructures and infrared emitters with compressed InAsSb layers
[DE95-008157] p 2446 N95-28399

INFRARED SPECTRA

FTIR measurements of thermal infrared sky radiance and transmission
[DE95-003642] p 2334 N95-26436

FTIR studies of CH3OH on porous silicon
[AD-A289038] p 2207 N95-27904

Multivariate classification of BPSG thin films using Mahalanobis distances
[DE95-008519] p 2267 N95-28148

Weightless Environment Training Facility (WETF) materials coating evaluation, volume 2
[NASA-CR-188366-VOL-2] p 2239 N95-28386

Time-resolved FTIR emission studies of laser photofragmentation and radical reactions
[DE95-008125] p 2300 N95-28398

INFRARED SPECTROMETERS

Perceptual based image fusion with applications to hyperspectral image data
[AD-A289429] p 2251 N95-26867

A cryogenic scan mechanism for use in Fourier transform spectrometers p 2158 N95-27287

High-performance reactionless scan mechanism
p 2158 N95-27288

INFRARED SPECTROSCOPY

FTIR measurements of thermal infrared sky radiance and transmission
[DE95-003642] p 2334 N95-26436

Analytical spectroscopy
[DE95-607896] p 2203 N95-27200

High resolution Fourier transform spectroscopy of the first overtone of the N-O stretch in nitrosyl bromide
[AD-A289318] p 2203 N95-27295

FTIR studies of CH3OH on porous silicon
[AD-A289038] p 2207 N95-27904

Infrared spectroscopy of nonclassical ions and their complexes
[DE95-008487] p 2413 N95-28091

INGESTION (ENGINES)

WINCLR: A computer code for heat transfer and clearance calculation in a compressor
[NASA-CR-195436] p 2117 N95-26363

Comparison of numerical results and multicavity purge and rim seal data with extensions to dynamics
[NASA-TM-106685] p 2168 N95-27434

INITIATION

Comparison of the calculated and measured stability of a NbTi cable-in-conduit conductor
[DE95-007964] p 2265 N95-27693

INITIATORS (EXPLOSIVES)

The protection of electro-explosive devices (EEDs) and electronics from electrostatic discharge (ESD) hazards
[DSTO-TR-0100] p 2258 N95-28568

INJECTION

Proposed high speed pellet injection system HIPEL for large helical device
[NIFS-255] p 2419 N95-26584

MHD simulations of DC helicity injection for current drive in tokamaks
[DE95-007018] p 2429 N95-26940

On the physics of ion ring generation for the stabilization of FRX discharges
[DE95-007105] p 2410 N95-27922

Fault tolerant features and experiments of ANTS distributed real-time system
[AD-A290133] p 2256 N95-28391

INJECTORS

Experiment on a rectangular cross section scramjet combustor. 2: Effects of fuel injector geometry
[NAL-TR-1220] p 2139 N95-26600

Propellant injection systems and processes
[NASA-TM-110632] p 2242 N95-26781

The CDF upgrade
[DE95-006683] p 2421 N95-28107

Recent high-speed ballistics experiments at ORNL
[DE95-006534] p 2422 N95-28205

Apparatus for testing high pressure injector elements
[NASA-CASE-MFS-28773-1] p 2304 N95-28347

Pellet injector research and development at ORNL
[DE95-006736] p 2435 N95-28596

INJURIES

Development of injury preventing helmet servo-support system for high performance aircraft
[AD-A289547] p 2359 N95-26755

INLET AIRFRAME CONFIGURATIONS

Performance study for inlet installations
[NASA-CR-189714] p 2140 N95-28227

INLET FLOW

Numerical investigation to S-inlet flows (Numerical simulation study of S-inlet flows)
[AD-A289590] p 2120 N95-26713

INLET TEMPERATURE

Characteristics of the turbine inlet temperature sensing circuit for the T56 turbo-prop engine
[DSTO-TR-0095] p 2139 N95-26424

INNER RADIATION BELT

A BATSE investigation of radiation belt electrons precipitated by VLF waves
[NASA-CR-197780] p 2336 N95-26922

INORGANIC COMPOUNDS

On the synthesis of mixed-metal and mixed-pnicogen13-15 ring-systems
[AD-A288869] p 2223 N95-28332

Stratospheric ozone reactive chemicals generated by space launches worldwide
[AD-A289852] p 2332 N95-28623

INPUT/OUTPUT ROUTINES

Reducing network depth in the Cascade-Correlation learning architecture
[AD-A289352] p 2382 N95-27066

A case for dynamic sets in operating systems
[AD-A289354] p 2454 N95-27529

INSECTS

Fault tolerant features and experiments of ANTS distributed real-time system
[AD-A290133] p 2256 N95-28391

INSERTION

CAS CERN Accelerator School 5th General Accelerator Physics Course
[DE95-608324] p 2419 N95-27158

INSOLATION

A study of surface temperatures, clouds and net radiation
[NASA-CR-198589] p 2329 N95-27864

INSPECTION

Integration of video and radiation analysis data
[DE95-004165] p 2379 N95-26443

Synthesis and characterization of polymeric materials
[AD-A288613] p 2225 N95-26482

Characterization of corrosion and development of a breadboard of a D sight aircraft inspection system, phase 1
[AD-A288347] p 2125 N95-26527

An illumination planner for Lambertian polyhedral objects
[AD-A289332] p 2424 N95-26900

Evaluations of the effectiveness of environmentally benign cleaning methodologies p 2230 N95-27115

Performance of the Satellite Test Assistant Robot in JPL's Space Simulation Facility p 2154 N95-27264

Inspection methods for underwater cables
[AD-A289610] p 2312 N95-28616

INSTALLING

Development and testing of the rack insertion device
p 2158 N95-27289

The installation of and first results from the superconducting gravimeter GWR20 at the Metsahovi Station, Finland
[REPT-95:1] p 2338 N95-27995

INSTANTONS

Topological density and instantons on a lattice
[DE95-006348] p 2445 N95-28240

INSTRUMENT ERRORS

Flight evaluation of GPS/DGPS sensor systems installed in NAL Do228
[NAL-TR-1230] p 2126 N95-26585

INSTRUMENT LANDING SYSTEMS

An integrated GPS/INS/BARO and radar altimeter system for aircraft precision approach landings
[AD-A289280] p 2127 N95-26985

INSULATION

Sceening, down selection, and implementation of environmentally compliant cleaning and insulation bonding for MNASA p 2165 N95-27124

Reducing cold-start emissions by catalytic converter thermal management
[DE95-000256] p 2327 N95-27540

INSULATORS

A high velocity electromagnetic mass launcher having an ablation resistant insulator
[AD-A288231] p 2154 N95-26524

INTEGERS

On commutativity of right s-unital rings with some polynomial constraints
[DE95-608752] p 2390 N95-27330

Wigner quantum oscillators. OSP (3/2) oscillators
[DE95-608756] p 2448 N95-27334

INTEGRAL EQUATIONS

Electromagnetic hysteretic response calculation for superconductors in demagnetizing geometries
[DE95-005028] p 2264 N95-27403

INTEGRATED CIRCUITS

An optoelectronic attenuator for the high-speed control of microwave integrated circuits
[AD-A289579] p 2260 N95-26690

Comparison of the resistance of the MOS integrated circuits with various types of nuclear radiation
[DE95-608623] p 2261 N95-27023

Investigation of radiation resistance of transistors and integrated circuits using the heavy ions beam of energy higher than 1 MeV/amu and fast neutrons
[DE95-608624] p 2261 N95-27024

Novel field effect transistors for low power electronics
[AD-A288650] p 2262 N95-27096

Pulse Code Modulation (PCM) encoder handbook for Aydin Vector MMP-900 series system
[NASA-RP-1365] p 2255 N95-27435

Characterization of wafer charging mechanisms and oxide survival prediction methodology
[DE95-006583] p 2440 N95-27538
Numerical methods for determining interstitial oxygen in silicon
[DE95-007710] p 2205 N95-27683
I(sub DDQ) testing and defect classes: A tutorial
[DE95-005467] p 2306 N95-27723
Research activities of the Solid State Sciences Committee in the development of a Federal initiative on advanced materials and processing
[DE95-009328] p 2445 N95-28179
JTEC Panel report on microelectromechanical systems in Japan
[NASA-CR-197831] p 2268 N95-28239
Novel field effect transistors for low power electronics
[AD-A289929] p 2271 N95-28629
Characteristics of the standard current trip circuit
[PB95-192886] p 2271 N95-28663

INTEGRATED LIBRARY SYSTEMS
The Global Historical Climatology Network: A preview of version 2
[DE95-007003] p 2332 N95-28605

INTEGRATED OPTICS
Digital optical computing
[AD-A289395] p 2368 N95-26881
Fundamental concepts of integrated and fiber optic sensors
[NASA-TM-106920] p 2426 N95-27906

INTEGRATORS
Robust integration schemes for generalized viscoplasticity with internal-state variables. Part 1: Theoretical developments and applications
[NASA-CR-195452-PT-1] p 2310 N95-28031
Robust integration schemes for generalized viscoplasticity with internal-state variables. Part 2: Algorithmic developments and implementation
[NASA-CR-195453-PT-2] p 2310 N95-28032

INTERFACE STABILITY
Static and dynamic strain energy release rates in toughened thermosetting composite laminates
p 2188 N95-28288

INTERFACES
Bimaterial interlaces and their role in the mechanical performance of the in-situ composites
[AD-A288973] p 2182 N95-27188

INTERFACIAL ENERGY
Bimaterial interlaces and their role in the mechanical performance of the in-situ composites
[AD-A288973] p 2182 N95-27188

INTERFACIAL TENSION
Investigation of the interface between immiscible electrolytes applied to membrane electrochemistry
[AD-A288887] p 2199 N95-26350

INTERFERENCE FIT
Design and structural validation of CF116 upper wing skin boron doubler p 2132 N95-27510

INTERFEROMETERS
Preliminary design study of the beam collapser and certain optomechanical aspects of the siderostat
[AD-A288423] p 2423 N95-26549
Satellite surface material composition from synthetic spectra
[AD-A289236] p 2163 N95-26963
Flow visualization of a turbulent shear flow using an optical wavefront sensor
[AD-A289208] p 2277 N95-26986
Ultrasonic study on ternary liquid systems by laser-sound interaction
[DE95-608783] p 2207 N95-27929
Measurement of particle transport coefficients on Alcator C-Mod
[DE95-007763] p 2411 N95-28020
A phase-stepped point diffraction interferometer using liquid crystals
[NASA-TM-106922] p 2293 N95-28037

INTERFEROMETRY
Uncertainties in the calibration of hydrophones at NPL by the three-transducer spherical-wave reciprocity method in the frequency range 10 kHz on 500 kHz
[PB95-185245] p 2401 N95-26615
Satellite surface material composition from synthetic spectra
[AD-A289236] p 2163 N95-26963

INTERGRANULAR CORROSION
Environmentally assisted cracking of high strength beta titanium alloys
[AD-A289156] p 2213 N95-27032

INTERIOR BALLISTICS
Ram accelerator performance calculations using a modified version of the NASA CET89 equilibrium chemistry code
[AD-A289554] p 2201 N95-26678

INTERLAYERS
Materials Research Society Symposium Proceedings. Volume 339: Diamond, SiC and nitride wide bandgap semiconductors
[AD-A288690] p 2437 N95-26818
Effects of interlayers on the scratch adhesion performance of ultra-thin films of copper and gold on silicon substrates
[DE95-007367] p 2220 N95-28044

INTERMETALLICS
First-principles study of intermetallic phase stability in the ternary Ti-Al-Nb alloy system
[DE95-005259] p 2213 N95-27082
The physics and chemistry of heavy Fermions
[DE95-005277] p 2407 N95-27431
The response of hydrotalcite coated aluminum to sealing with transition metal salt solutions
[DE95-004767] p 2234 N95-27460
C15 intermetallic compounds HfV2+Nb
[DE95-005264] p 2215 N95-27463
A new technique for measuring the separation of closely spaced dislocations using residual contrast conditions
[DE95-007147] p 2219 N95-27968
Phase stability and elasticity of C15 transition-metal intermetallic compounds
[DE95-007876] p 2219 N95-28026
Trace elements and the mechanical properties of intermetallic compounds
[DE95-007378] p 2220 N95-28046
Electronic structure of ordered and disordered transition metal aluminides
[DE95-609034] p 2223 N95-28250

INTERMOLECULAR FORCES
A density functional/molecular dynamics study of the structure of liquid nitromethane
[AD-A289224] p 2404 N95-26960

INTERNAL COMBUSTION ENGINES
Biomass Pyrolysis Oil Properties and Combustion Meeting
[DE95-004017] p 2204 N95-27438
A hybrid vehicle evaluation code and its application to vehicle design. Revision 1
[DE95-008053] p 2303 N95-28029
A hybrid vehicle evaluation code and its application to vehicle design, revision 2
[DE95-008060] p 2303 N95-28139

INTERNAL ENERGY
Statistical model for molecular internal energy exchange in DSMC method for rarefied flow analysis
[ISAS-R-654] p 2274 N95-26741
Burst of energetic ions from reversed field pinch plasma
[DE94-765447] p 2432 N95-27870

INTERNAL FLOW
A fixed time performance evaluation of parallel CFD applications
[DE94-014240] p 2273 N95-26445
Contribution to the optimal shape design of two-dimensional internal flows with embedded shocks
[NASA-CR-195062] p 2389 N95-26672
Calculation of three-dimensional (3-D) internal flow by means of the velocity-vorticity formulation on a staggered grid
[NASA-TM-110352] p 2122 N95-27258
Comparison of numerical results and multicavity purge and rim seal data with extensions to dynamics
[NASA-TM-106685] p 2168 N95-27434

INTERNAL FRICTION
Stress transfer from axially loaded fiber to matrix in a microcomposite
[DE95-007366] p 2183 N95-28043

INTERNAL PRESSURE
Stress analysis and failure of an internally pressurized composite-jacketed steel cylinder p 2186 N95-28280
Composite fuselage shell structures research at NASA Langley Research Center p 2194 N95-28466

INTERNATIONAL COOPERATION
AGARD membership, 1995
[AGARD-MEMB-95] p 2450 N95-26353
High-stakes aviation: US-Japan technology linkages in transport aircraft
[LC-94-65759] p 2126 N95-27907
JTEC/WTEC annual report and program summary: 1993/94
[NASA-CR-198563] p 2475 N95-28038
SIHTI 2: Energy and environmental technology. Yearbook 1993 of the research programme
[DE95-755135] p 2331 N95-28202
Global trade in satellites and launch services
[GPO-84-811] p 2165 N95-28342

INTERNATIONAL SPACE STATION
International Space Station Alpha trace contaminant control subassembly life test report
[NASA-TM-108488] p 2358 N95-26364
Feasibility of flywheel energy storage systems for applications in future space missions
[NASA-CR-195422] p 2316 N95-26393
Some mechanical design aspects of the European Robotic Arm p 2155 N95-27262
Microgravity Sciences Biotechnology Facility assessment
[NASA-CR-196602] p 2351 N95-27329

INTERNATIONAL TRADE
Global trade in satellites and launch services
[GPO-84-811] p 2165 N95-28342

INTERNETS
A decentralized software bus based on IP multicasting
[NASA-CR-197768] p 2366 N95-26695
Performance and policy dimensions in internet routing
[NASA-CR-197772] p 2367 N95-26770
Spinning a web: Publishing the SEI software configuration management research on the world wide web
[AD-A288708] p 2377 N95-27250
A high performance totally ordered multicast protocol
[NASA-CR-197765] p 2371 N95-27252
Sequence comparison on a cluster of workstations using the PVM system
[DE95-006527] p 2378 N95-27709
Browsing the World Wide Web from behind a firewall
[DE95-006805] p 2455 N95-27957
Teaching interdisciplinary computational science from an electronic book on the Internet
[DE95-006525] p 2373 N95-28498
Building an electronic book on the Internet. CSEP:An interdisciplinary syllabus for teaching computational science at the graduate level
[DE95-006526] p 2375 N95-28632
Practical considerations for network addressing using CIDR
[PB95-195335] p 2379 N95-28665

INTERPLANETARY MEDIUM
Differenced Range Versus Integrated Doppler (DRVID) ionospheric analysis of metric tracking in the Tracking and Data Relay Satellite System (TDRSS)
p 2147 N95-27766

INTERPLANETARY NAVIGATION
Multi-spacecraft coherent Doppler and ranging for interplanetary-navigation p 2150 N95-27786

INTERPLANETARY SPACECRAFT
Application of non-coherent Doppler data types for deep space navigation p 2151 N95-27788

INTERPLANETARY TRAJECTORIES
Application of non-coherent Doppler data types for deep space navigation p 2151 N95-27788

INTERPOLATION
The fBm Interpolator
[AD-A288996] p 2388 N95-26459
SUPG finite numerical element solutions for non-compressible Navier-Stokes equation sets
[AD-A289600] p 2274 N95-26718

INTERPROCESSOR COMMUNICATION
An architecture for optimal all-to-all personalized communication
[AD-A288532] p 2377 N95-26840
A demonstration of Client/Server technology using remote procedure calls for an application of file migration for moving records based on location
[AD-A289391] p 2453 N95-26864
Digital optical computing
[AD-A289395] p 2368 N95-26881
A demonstration of client-server technology using remote procedure calls with an application in file migration using heuristics
[AD-A289467] p 2255 N95-27149
Simulator report for SCI systems with HIC-router
[PB95-196580] p 2379 N95-28093
Two implementation relations and the correctness of communicating replicated processes
[PB95-195640] p 2375 N95-28645

INTERSTELLAR CHEMISTRY
Search for molecular absorptions with the Fourier Transform Spectrometer
[NASA-CR-198648] p 2462 N95-28222

INTERSTELLAR GAS
Molecular cloud content of early-type galaxies. V. CO in elliptical galaxies
[PB95-185153] p 2461 N95-27320
Theoretical studies of interstellar processes
[NASA-CR-198647] p 2462 N95-28216

INTERSTELLAR MATTER
CO, HCO(+) and HCN absorption in the gravitational lens candidate B0218+357 at z=0.685
[PB95-185146] p 2461 N95-26522
A long-term space astrophysics research program: An x-ray perspective of the components and structure of galaxies
[NASA-CR-197787] p 2461 N95-26593

INTERSTITIALS
Numerical methods for determining interstitial oxygen in silicon
[DE95-007710] p 2205 N95-27683
Aspects of macroscopic phase separation and interstitial oxygen ordering in oxygen doped La2CuO(4+delta)
[DE95-007864] p 2443 N95-28060
INTRACRANIAL PRESSURE
Non-invasive method and apparatus for monitoring intracranial pressure and pressure volume index in humans
[NASA-CASE-LAR-13894-1] p 2353 N95-26889
INTRUSION
Numerical simulation of coupled flow and transport with TOUGH2: A verification study
[DE95-008351] p 2287 N95-28225
INVARIANCE
Generalized Schwarzians in several variables and Moebius invariant differential operators
[PB95-185211] p 2388 N95-26539
Transverse tau polarization in inclusive bar-B yields tau bar-nu X decays
[DE95-610325] p 2407 N95-27409
INVENTORIES
Investigation on LCA (Life Cycle Analysis/assessment)
[DE95-759260] p 2330 N95-27942
INVERSE SCATTERING
Nonlinear problems in fluid dynamics and inverse scattering: Nonlinear waves and inverse scattering
[AD-A289148] p 2278 N95-27001
INVERSIONS
Structures for time-reversed inversion in filter banks
[AD-A289238] p 2261 N95-26964
Far-infrared laser interferometry measurements on the STP-3(M) reversed-field pinch
[DE94-765440] p 2297 N95-27868
INVESTMENT CASTING
Effect of processing parameters on surface finish for fused deposition machinable wax patterns
[NASA-TP-3550] p 2244 N95-26769
INVISCID FLOW
A fixed time performance evaluation of parallel CFD applications
[DE94-014240] p 2273 N95-26445
The calculation of the mass moment of inertia of a fluid in a rotating rectangular tank
[NASA-CR-197777] p 2278 N95-27165
A numerical method for solving the three-dimensional parabolized Navier-Stokes equations
[NASA-CR-198159] p 2287 N95-27917
IODINE
Energy transfer from excited nitrenes at high density
[AD-A288352] p 2403 N95-26466
Collisional dynamics and spectroscopic studies of highly excited rovibrational levels of I2(X)(0(+)(sub g)) via stimulated emission pumping
[AD-A289447] p 2295 N95-27172
IODINE LASERS
Collisional dynamics and spectroscopic studies of highly excited rovibrational levels of I2(X)(0(+)(sub g)) via stimulated emission pumping
[AD-A289447] p 2295 N95-27172
ION ACOUSTIC WAVES
Nonlinear instability and chaos in plasma wave-wave interactions. I. Introduction
[DE95-005529] p 2429 N95-27084
ION ATOM INTERACTIONS
Atomic and electronic structure of clusters from Car-Parrinello method
[DE94-634463] p 2403 N95-26437
Resonant coherent excitation of N6(+) and Mg11(+) in planar channeling: Anisotropies in ionization probabilities and X-ray emission
[DE95-006732] p 2417 N95-28595
ION BEAMS
Advanced solid lubricant films by Ion-Beam Assisted Deposition
[AD-A288866] p 2225 N95-26499
Temperature dependence of ion-beam-induced amorphization in (Beta)-SiC
[DE95-007164] p 2438 N95-27087
Characterization and control of wafer charging effects during high-current ion implantation
[DE95-006587] p 2440 N95-27471
Systematic study of the ion beam mixing of oxide markers into alumina
[DE95-006262] p 2217 N95-27555
On the physics of ion ring generation for the stabilization of FRX discharges
[DE95-007105] p 2410 N95-27922
The diffusion properties of ion implanted species in selected target materials
[DE95-007006] p 2442 N95-27959
Collisions of highly charged ions with electrons, atoms and surfaces
[DE95-007393] p 2413 N95-28078
Pulsed ion beam surface treatment for preparing rapidly solidified corrosion resistant steel and aluminum surfaces
[DE95-007741] p 2221 N95-28116
Mutagenesis in human cells with accelerated H and Fe ions
[NASA-CR-198599] p 2351 N95-28177
On ionic charge distributions of heavy evaporation residues passing through a carbon foil
[DE94-629016] p 2414 N95-28184
ION CHARGE
Projectile image acceleration, neutralization and electron emission during grazing interactions of multicharged ions with Au(110)
[DE95-007394] p 2409 N95-27551
ION CYCLOTRON RADIATION
Energetic particle destabilization of shear Alfven waves in stellarators and tokamaks
[DE95-006393] p 2431 N95-27419
Experimental aspects of effects of high-energy particles on Alfven modes
[DE95-003383] p 2432 N95-27873
One dimensional global and local solution for ICRF heating
[DE95-007984] p 2392 N95-28110
Engineering design of the ITER RF systems
[DE95-008064] p 2434 N95-28140
Faraday screen sputtering on TPX
[DE95-008347] p 2434 N95-28224
ION DENSITY (CONCENTRATION)
Energization and transport of ions of ionospheric origin in the terrestrial magnetosphere
[NASA-CR-197813] p 2336 N95-26699
A model of the diurnal variation in magnesium ion density and radiance in the thermosphere
[AD-A289824] p 2339 N95-28575
ION DISTRIBUTION
Modification of the optical properties of glass by sequential ion implantation
[DE95-007401] p 2237 N95-28080
ION EMISSION
Energization and transport of ions of ionospheric origin in the terrestrial magnetosphere
[NASA-CR-198618-REV] p 2338 N95-28035
ION ENGINES
Plume measurements with the T5 xenon ion thruster
[AD-A288697] p 2167 N95-26489
ION EXCHANGE RESINS
An investigation of the applicability of the new Reillex(tm)-HPQ anion exchange resin system for technetium/rhenium and uranium in the Hanford waste tanks
[DE95-007643] p 2412 N95-28051
ION EXCHANGING
Investigation of the interface between immiscible electrolytes applied to membrane electrochemistry
[AD-A288887] p 2199 N95-26350
Molecular approach to mesoporous metal sulfides
[DE95-005418] p 2202 N95-27137
NO decomposition in non-reducing atmospheres
[DE95-007895] p 2205 N95-27690
An investigation of the applicability of the new Reillex(tm)-HPQ anion exchange resin system for technetium/rhenium and uranium in the Hanford waste tanks
[DE95-007643] p 2412 N95-28051
ION IMPLANTATION
Effects of helium pre-implantation on the microstructure and mechanical properties of irradiated 316 stainless steel
[DE95-007162] p 2214 N95-27086
Characterization and control of wafer charging effects during high-current ion implantation
[DE95-006587] p 2440 N95-27471
Characterization of wafer charging mechanisms and oxide survival prediction methodology
[DE95-006583] p 2440 N95-27538
Characterization of defects in deuterium-implanted beryllium
[DE95-005688] p 2217 N95-27553
The diffusion properties of ion implanted species in selected target materials
[DE95-007006] p 2442 N95-27959
Modification of the optical properties of glass by sequential ion implantation
[DE95-007401] p 2237 N95-28080
Coherent V2O3 precipitates in alpha-Al2O3CO-implanted with vanadium and oxygen
[DE95-007404] p 2444 N95-28081
Plasma source ion implantation of ammonia into electroplated chromium
[DE95-006275] p 2444 N95-28125
Cavity formation and impurity gettering in He-implanted Si
[DE95-007744] p 2444 N95-28127
Chemical and electrical properties of cavities in silicon and germanium
[DE95-006812] p 2445 N95-28206
ION IRRADIATION
Amorphization of complex ceramics by heavy-particle irradiations
[DE95-005725] p 2236 N95-27733
Density changes in amorphous Pd80Si20 during low temperature ion irradiation
[DE95-007132] p 2441 N95-27928
Toward a mechanistic understanding of radiation effects in materials
[DE95-006530] p 2221 N95-28120
ION PROPULSION
Plume measurements with the T5 xenon ion thruster
[AD-A288697] p 2167 N95-26489
ION SCATTERING
An overview of the Evaluation of Oxygen Interactions with Materials 3 experiment: Space Shuttle Mission 46, July-August 1992 p 2210 N95-27630
ION SOURCES
Intermediate energy neutrons at WNR. Spin-isospin and energy dependence of the NN interaction and the nuclear response
[DE95-006291] p 2408 N95-27466
Collisions of highly charged ions with electrons, atoms and surfaces
[DE95-007393] p 2413 N95-28078
ION STORAGE
Extended linear ion trap frequency standard apparatus
[NASA-CASE-NPO-19081-1-CU] p 2404 N95-26861
Extended linear ion trap frequency standard apparatus
[NASA-CASE-NPO-19081-1-CU] p 2416 N95-28348
ION TEMPERATURE
Energization and transport of ions of ionospheric origin in the terrestrial magnetosphere
[NASA-CR-197813] p 2336 N95-26699
ION TRAPS (INSTRUMENTATION)
Extended linear ion trap frequency standard apparatus
[NASA-CASE-NPO-19081-1-CU] p 2416 N95-28348
IONIC COLLISIONS
Physics with relativistic heavy ions: QGP and other delicacies
[DE95-007014] p 2406 N95-27307
Characterization of collision cascade damage in Ca2La8(SiO4)6O2 by HRTEM
[DE95-005719] p 2440 N95-27491
Lattice calculation for lepton capture from vacuum-pair production in relativistic heavy-ion collisions
[DE95-007392] p 2413 N95-28077
Aspects of strangeness
[DE95-008314] p 2414 N95-28169
IONIZATION
Comparison of the resistance of the MOS integrated circuits with various types of nuclear radiation
[DE95-608623] p 2261 N95-27023
Models of symbiotic stars p 2460 N95-27077
Laser ionization of molecular clusters
[DE95-007011] p 2296 N95-27550
Observation on radiation transfer experiments using k-shell absorption spectra
[DE95-008068] p 2434 N95-28141
IONIZATION GAGES
Neutral gas compression in the Alcator C-Mod divertor. Experimental observations
[DE95-007762] p 2432 N95-27688
IONIZING RADIATION
Radiation safety aspects of commercial high-speed flight transportation
[NASA-TP-3524] p 2465 N95-26427
Ionizing radiation measurements on LDEF: A0015 Free flyer biostack experiment
[NASA-CR-196603] p 2202 N95-27168
Low noise monolithic Si JFETS for operation in the 90-300K range and in high radiation environments
[DE95-007303] p 2269 N95-28244
IONOSPHERIC COMPOSITION
Energization and transport of ions of ionospheric origin in the terrestrial magnetosphere
[NASA-CR-198618-REV] p 2338 N95-28035
IONOSPHERIC CONDUCTIVITY
PRISM validation
[AD-A288476] p 2337 N95-27703
IONOSPHERIC DISTURBANCES
Space tether-radar data processing
[AD-A289654] p 2250 N95-26725
IONS
Energization and transport of ions of ionospheric origin in the terrestrial magnetosphere
[NASA-CR-197813] p 2336 N95-26699
Atomic physics with highly charged ions
[DE95-007325] p 2407 N95-27439
PXAMS: Projectile X ray AMS: X ray yields and applications
[DE95-006438] p 2204 N95-27496

Projectile image acceleration, neutralization and electron emission during grazing interactions of multicharged ions with Au(110)
[DE95-007394] p 2409 N95-27551

Burst of energetic ions from reversed field pinch plasma
[DE94-765447] p 2432 N95-27870

Polarizing matter and antimatter: A new method
[DE95-007109] p 2421 N95-27923

An investigation of the chemical and physical properties of pristine, electrochromically damaged, and photochromically damaged KTiOPO4 (KTP) using surface analytical and optical spectroscopic techniques
[DE95-007865] p 2443 N95-28023

Lattice calculation for lepton capture from vacuum-pair production in relativistic heavy-ion collisions
[DE95-007392] p 2413 N95-28077

Infrared spectroscopy of nonclassical ions and their complexes
[DE95-008487] p 2413 N95-28091

Resonant coherent excitation of N6(+) and Mg11(+) in planar channeling: Anisotropies in ionization probabilities and X-ray emission
[DE95-006732] p 2417 N95-28595

IRIDIUM ALLOYS

Stability of reference masses 4: Growth of carbonaceous contamination on platinum-iridium mass standard surfaces, and its cleaning by UV/ozone treatment
[PB95-190096] p 2226 N95-26745

IRON

Optical features of nanosize iron and molybdenum sulfide clusters
[DE95-005417] p 2202 N95-27136

A new method of evaluating the explicit magnetic-state-dependent energy in semi-empirical calculations of iron
[AD-A289098] p 2399 N95-27398

Electrolyte effects in Li(Si)/FeS2 thermal batteries
[DE95-001614] p 2264 N95-27474

Magnetic and structural properties of Fe/Pd multilayers studied by magnetic x-ray dichroism and x-ray absorption spectroscopy
[DE95-007095] p 2206 N95-27755

Mutagenesis in human cells with accelerated H and Fe ions
[NASA-CR-198599] p 2351 N95-28177

IRON ALLOYS

Ultra high purity, dimensionally stable INVAR 36
[NASA-CASE-NPO-19358-1-CU] p 2213 N95-26862

Electronic structure of ordered and disordered transition metal aluminides
[DE95-609034] p 2223 N95-28250

IRON OXIDES

Iron oxides characterization by Moessbauer spectroscopy
[DE95-607869] p 2202 N95-27199

Charge distribution analysis of catalysts under simulated reaction conditions
[DE95-006943] p 2204 N95-27549

Superior catalysts for selective catalytic reduction of nitric oxide
[DE95-007903] p 2205 N95-27691

IRRADIANCE

SeaWiFS technical report series. Volume 26: Results of the SeaWiFS Data Analysis Round-Robin, July 1994 (DARR-1994)
[NASA-TM-104566-VOL-26] p 2345 N95-26430

The attenuation of microwave radiation by fog and rain
[AD-A288326] p 2249 N95-26562

Calculations of downward IR surface fluxes in the 500-3,000 cm(exp -1) wavenumber range for the 1994 ICRCCM model intercomparison study
[DE95-006430] p 2328 N95-27708

SeaWiFS technical report series. Volume 27: Case studies for SeaWiFS calibration and validation, part 3
[NASA-TM-104566-VOL-27] p 2348 N95-28030

Ultrashort Pulse retrieval using FROG trace irradiance moments and the adaptive neural networks backpropagation algorithm
[DE95-007153] p 2299 N95-28220

IRRADIATION

Radiation in everyday life
[DE95-604111] p 2349 N95-26597

Investigation of radiation resistance of transistors and integrated circuits using the heavy ions beam of energy higher than 1 MeV/amu and fast neutrons
[DE95-608624] p 2261 N95-27024

Effects of helium pre-implantation on the microstructure and mechanical properties of irradiated 316 stainless steel
[DE95-007162] p 2214 N95-27086

Temperature dependence of ion-beam-induced amorphization in (Beta)-SiC
[DE95-007184] p 2438 N95-27087

Density changes in amorphous Pd80Si20 during low temperature ion irradiation
[DE95-007132] p 2441 N95-27928

Sintering of textured YBa2Cu3O(7-x) under intensive Co-60 gamma irradiation
[DE95-007098] p 2442 N95-27950

The real structure of columnar pinning centers in heavy-ion-irradiated cuprate superconductors
[DE95-003948] p 2445 N95-28186

ISING MODEL

DNA denaturation through a model of the partition points on a one-dimensional lattice
[DE95-607909] p 2439 N95-27201

ISLANDS

Automated integration of genomic physical mapping data via parallel simulated annealing
[DE95-008057] p 2351 N95-27725

ISOLATION

Chemistry involving the separation, isolation, and immobilization of 3-5 compound semiconductor nanocrystals and quantum dots
[AD-A288381] p 2436 N95-26473

Computational and matrix isolation studies of (2- and 3-furyl)methylene
[AD-A280085] p 2178 N95-28154

High energy density systems in cryogenic media: The production and reactions of atoms and radicals
[AD-A289818] p 2417 N95-28572

ISOLATORS

Experimental investigation of inlet-combustor isolators for a dual-mode scramjet at a Mach number of 4
[NASA-TP-3502] p 2140 N95-28343

ISOMERS

Iron oxides characterization by Moessbauer spectroscopy
[DE95-607869] p 2202 N95-27199

ISOTHERMAL FLOW

A fast numerical method for isothermal resin transfer mold filling
[AD-A288944] p 2179 N95-26565

Testing the correlation between seismic stratigraphy, diagenesis and physical rock properties: Evaluation of fluid flow during early and late diagenesis
[DE95-008338] p 2338 N95-28083

ISOTOPE RATIOS

D/H and O-18/O-16 partitioning between water liquid and vapor in the system H2O-Na-K-Mg-Ca-Cl-SO4 from 0 to 350 C
[DE95-007013] p 2208 N95-27961

ISOTOPIC LABELING

Low temperature carrier transport properties in isotopically controlled germanium
[DE95-008489] p 2444 N95-28092

ISOTROPIC MEDIA

Analysis of electromagnetic problems involving chiral, bi-isotropic, and uniaxial bianisotropic media
[PB95-185096] p 2248 N95-26450

Analysis of plate-twist test for in-plane shear modulus of composite materials (revised)
[PB95-190195] p 2308 N95-26749

Depth migration in transversely isotropic media with explicit operators
[DE95-007670] p 2337 N95-27442

Transformation to zero offset in transversely isotropic media
[DE95-007669] p 2339 N95-28192

Fowler DMO and time migration for transversely isotropic media with explicit operators
[DE95-007671] p 2339 N95-28194

Scattering by a small object close to an interface. 3. Buried object
[PB95-184909] p 2256 N95-28354

ISOTROPIC TURBULENCE

A phenomenological treatment of rotating turbulence
[NASA-CR-198168] p 2288 N95-28228

ISOTROPY

Transformation to zero offset in transversely isotropic media
[DE95-007669] p 2339 N95-28192

Fowler DMO and time migration for transversely isotropic media with explicit operators
[DE95-007671] p 2339 N95-28194

ITERATION

Random relaxation of fixed point iteration
[PB95-185013] p 2389 N95-26910

Computing NORAD mean orbital elements from a state vector
[AD-A289281] p 2146 N95-27033

Optical implementation of inner product neural associative memory
[NASA-CASE-NPO-18491-2-CU] p 2427 N95-28363

Remarks on the growth of the resolvent operators for power bounded operators
[PB95-195418] p 2393 N95-28653

ITERATIVE SOLUTION

Introduction to multigrid methods
[NASA-CR-195045] p 2388 N95-26395

Distributed computation of Pareto solutions in N-player games
[PB95-185039] p 2396 N95-26912

An easy way to analyze longitudinal and lateral-directional trim problems with AEO or OEI
p 2119 N95-26949

Vector algorithms for solving 3D nonlinear magnetostatic problems
[DE95-608737] p 2399 N95-27298

The comparison of P(sub 1) and simplified P(sub 2) synthetic acceleration for iterative methods in transport solutions
[DE94-018306] p 2390 N95-27304

IUE

Observations of comets with the IUE
[NASA-CR-197816] p 2461 N95-27166

J

J INTEGRAL

Effect of internal hydrogen on the mixed-mode 1/3 fracture toughness of a ferrific/martensitic stainless steel
[DE95-005722] p 2216 N95-27479

JACKETS

The effect on stability and thermal hydraulic quenchback of perforating the jacket of a cable-in-conduit conductor
[DE95-005392] p 2262 N95-27083

AMCC casting development. Volume 1: Executive Summary
[NASA-CR-196597] p 2247 N95-28419

JAMMING

Analysis and simulation of narrowband GPS jamming using digital excision temporal filtering
[AD-A289328] p 2127 N95-26898

Nonlinear signal processing schemes for robust target detection in radar
[AD-A288449] p 2255 N95-27185

JAPAN

JTEC Panel report on electronic manufacturing and packaging in Japan
[NASA-CR-197830] p 2263 N95-27226

Microelectronics in Japan p 2263 N95-27227

Building the electronic industry's roadmaps
p 2263 N95-27228

Japan's technology and manufacturing infrastructure
p 2263 N95-27229

Japan's electronic packaging technologies
p 2263 N95-27230

Electronics manufacturing and assembly in Japan
p 2263 N95-27231

Quality assurance and reliability in the Japanese electronics industry p 2263 N95-27232

JTEC monograph on biodegradable polymers and plastics in Japan: Research, development, and applications
[NASA-CR-198562] p 2235 N95-27694

High-stakes aviation: US-Japan technology linkages in transport aircraft
[LC-94-65759] p 2126 N95-27907

JTEC/WTEC annual report and program summary: 1993/94
[NASA-CR-198563] p 2475 N95-28038

JTEC Panel report on microelectromechanical systems in Japan
[NASA-CR-197831] p 2268 N95-28239

JAPANESE SPACECRAFT

Element material experiment by EFFU
p 2145 N95-27667

JET AIRCRAFT

Aircraft IR/acoustic detection evaluation. Volume 2: Development of a ground-based acoustic sensor system for the detection of subsonic jet-powered aircraft
[NASA-CR-189705-VOL-2] p 2402 N95-28073

JET AIRCRAFT NOISE

Supersonic coaxial jet noise predictions
[NASA-TM-106917] p 2401 N95-26801

Preliminary results and research capabilities of a new jet facility at the University of Kansas
p 2119 N95-26951

Basic studies in turbulent shear flows
[AD-A289145] p 2277 N95-26998

A numerical study of fundamental shock noise mechanisms
[NASA-TM-110608] p 2401 N95-27908

Response of multi-panel assembly to noise from a jet in forward motion
[NASA-CR-198164] p 2289 N95-28673

JET CONTROL

The application of waterjets for cleaning
p 2233 N95-27130

JET ENGINE FUELS
Mechanism of deposit formation on fuel-wetted hot metal surfaces
[AD-A289847] p 2210 N95-28621

JET ENGINES
Performance characterization of a highly-offset diffuser with and without blowing vortex generator jets
[AD-A289334] p 2122 N95-26901
Preliminary results and research capabilities of a new jet facility at the University of Kansas
p 2119 N95-26951

JET FLOW
The noise reduction potential of dual-stream coaxial rectangular improperly expanded jet flows
[NASA-CR-197820] p 2277 N95-26995
The application of waterjets for cleaning
p 2233 N95-27130
An outflow boundary condition for aeroacoustic computations
[NASA-TM-106930] p 2279 N95-27175
Response of multi-panel assembly to noise from a jet in forward motion
[NASA-CR-198164] p 2289 N95-28673

JET MIXING FLOW
Tank pressure control in low gravity by jet mixing
[NASA-CR-191012] p 2243 N95-28001
DNS, LES and stochastic modeling of turbulent reacting flows
[AD-A280099] p 2287 N95-28155

JET NOZZLES
Visualization of the multiple supersonic jet oscillations by swept focused strobed schlieren technique
p 2119 N95-26952

JET STREAMS (METEOROLOGY)
Meso-beta scale numerical simulation studies of terrain-induced jet streak mass/momentum perturbations
[NASA-CR-197804] p 2335 N95-26592
An observational study on the onset of the summer monsoon over eastern Asia in 1979
[AD-A289637] p 2341 N95-26723

JETTISONING
A numerical model to predict the fate of jettisoned aviation fuel
[AD-A289336] p 2242 N95-26842

JFET
Low noise monolithic Si JFETS for operation in the 90-300K range and in high radiation environments
[DE95-007303] p 2269 N95-28244

JOINTS (ANATOMY)
Automatic locking knee brace joint
[NASA-CASE-MFS-28997-1] p 2360 N95-27501

JOINTS (JUNCTIONS)
Status of bonded boron/epoxy doublers for military and commercial aircraft structures p 2132 N95-27506
Load transfer in the stiffener-to-skin joints of a pressurized fuselage
[NASA-CR-198610] p 2310 N95-27865
Design, analysis, and testing of a metal matrix composite web/flange intersection p 2191 N95-28433

JUNCTION DIODES
Survey on step recovery diode and its applications
[PB95-184974] p 2260 N95-26646
Amorphous silicon pixel radiation detectors and associated thin film transistor electronics readout
[DE95-006568] p 2265 N95-27678

JUNCTION TRANSISTORS
Demonstration of photo-assisted tunneling process across the coulomb blockade energy gap in mesoscopic tunnel junctions — photon-assisted tunneling
[AD-A289534] p 2438 N95-26872

K

K LINES
Solar UV flux measurements from the SBUV2 monitor on the NOAA9 satellite. Part 1: Mg II h and k line core-to-wing ratios for 1986-1988
[PB95-181962] p 2464 N95-28007

K-EPSILON TURBULENCE MODEL
Experience with k-epsilon turbulence models for heat transfer computations in rotating p 2285 N95-27887
Experiences with two-equation turbulence models
p 2286 N95-27894

KALMAN FILTERS
Control of a large space structure using multiple model adaptive estimation and control techniques
[AD-A289309] p 2162 N95-26916
Multiple model adaptive estimation and head motion tracking in a virtual environment: An engineering approach
[AD-A289299] p 2359 N95-27046
Analysis of filter tuning techniques for sequential orbit determination p 2146 N95-27764
A PC-based magnetometer-only attitude and rate determination system for gyroless spacecraft
p 2147 N95-27770
Attitude determination using an adaptive multiple model filtering Scheme p 2148 N95-27772
An automated method of tuning an attitude estimator
p 2148 N95-27774
Post Kalman progress p 2148 N95-27776
Estimation of attitude sensor timetag biases
p 2153 N95-27799
Autonomous control system reconfiguration for spacecraft with non-redundant actuators
p 2153 N95-27802
Contingency designs for attitude determination of TRMM p 2154 N95-27803

KAONS
A simple relativistic model of pp-bar yields K(+)K(-)
[DE95-608852] p 2406 N95-27318
The KTeV pure CsI calorimeter
[DE95-005747] p 2292 N95-27751
Rare decays/CP: The perspective of a kaon physicist
[DE95-005964] p 2416 N95-28338

KAPITZA RESISTANCE
Subharmonic phonon transmission and Kapitza conductance between crystals with very different vibrational spectra
[DE95-609151] p 2447 N95-28608

KAPTON (TRADEMARK)
An overview of the Evaluation of Oxygen Interactions with Materials 3 experiment: Space Shuttle Mission 46, July-August 1992 p 2210 N95-27630
Evaluation of Oxygen Interactions with Materials 3: Mission and induced environments
p 2210 N95-27631
Effects of atomic oxygen on polymeric materials flown on EOIM-3 p 2242 N95-27638
Molecular beam scattering from C-13 enriched Kapton and correlation with the EOIM-3 carousel experiment
p 2419 N95-27643

KELVIN WAVES
Spectral analyses, climatology, and interannual variability of Nimbus-7 TOMS version 6 total column ozone
[NASA-RP-1360] p 2341 N95-26689

KELVIN-HELMHOLTZ INSTABILITY
Computational and experimental studies of hydrodynamic instabilities and turbulent mixing
[DE95-006837] p 2288 N95-28603

KEPLER LAWS
Kepler Equation solver p 2147 N95-27767

KERNEL FUNCTIONS
Filtered kernel density estimation
[AD-A288293] p 2394 N95-26413
Applications of boundary element methods on the Intel Paragon
[DE94-014135] p 2393 N95-28393
Non-linear resistive grid kernel estimator useful in single feature, two-class pattern classification
[AD-D017394] p 2271 N95-28614

KEVLAR (TRADEMARK)
Design prediction for long term stress rupture service of composite pressure vessels p 2188 N95-28291
Utilization of composite materials by the US Army: A look ahead p 2189 N95-28421

KINEMATIC EQUATIONS
A new angle on the Euler angles
p 2153 N95-27800

KINEMATICS
Learning Hand/Eye coordination by an active observer. part 1: Organizing centers
[AD-A289502] p 2356 N95-26843
Telepresent spacecraft docking with object-based bilateral control (OBBC)
[AD-A289268] p 2163 N95-26980
Studies of kinematic distributions and mass reconstruction of CDF top candidate events
[DE95-005108] p 2408 N95-27478
An MME-based attitude estimator using vector observations p 2148 N95-27775

KINETIC ENERGY
Deep convection in the Mediterranean Sea
[AD-A288497] p 2346 N95-26647
The role of microprocesses in macroscale magnetotail dynamics
[DE95-006288] p 2432 N95-27673

KINETIC EQUATIONS
Axionic fuel for sun
[DE95-608788] p 2464 N95-27342

KINETICS
DNA denaturation through a model of the partition points on a one-dimensional lattice
[DE95-607909] p 2439 N95-27201

KINOFORM
Design and fabrication of a diamond-turned hybrid diffractive/refractive singlet for visible applications at ORNL
[DE95-007007] p 2427 N95-28552

KLYSTRONS
Time-dependent multi-dimensional simulation studies of the electron output scheme for high power FELs
[DE95-006593] p 2297 N95-27737

KNEE (ANATOMY)
Automatic locking knee brace joint
[NASA-CASE-MFS-28997-1] p 2360 N95-27501

KNOWLEDGE BASED SYSTEMS
A knowledge highway for integrated modelling from manufacturing to design
[AD-A288872] p 2247 N95-28187

KNOWLEDGE BASES (ARTIFICIAL INTELLIGENCE)
Digital systems validation. Chapter 20 Artificial Intelligenge with applications for aircraft. Handbbook, volume 2
[AD-A288492] p 2380 N95-26638
Generalized probabilistic reasoning and empirical studies on computational efficiency and scalability
[AD-A289185] p 2395 N95-27016

KNOWLEDGE REPRESENTATION
Generalized probabilistic reasoning and empirical studies on computational efficiency and scalability
[AD-A289185] p 2395 N95-27016
Applying AI tools to operational space environmental analysis p 2382 N95-27376
Automated database design from natural language input p 2383 N95-27378
Comprehension and retrieval of failure cases in airborne observatories p 2145 N95-27394
A path-oriented knowledge representation system: Defusing the combinatorial system p 2386 N95-27395

KOLMOGOROV-SMIRNOV TEST
Statistical analysis of tensile mechanical property data of carbon/polyimide composites
[NAL-TR-1238] p 2180 N95-26667

KORTEWEG-DEVRIES EQUATION
Korteweg-de Vries equation: Convergent Birkhoff normal form
[PB95-196275] p 2393 N95-28611

KRYPTON
Precision electromagnetic calorimetry with liquid krypton
[DE95-006685] p 2292 N95-27677
Performance of an accordion electromagnetic calorimeter with liquid krypton
[DE95-006693] p 2292 N95-27738
Low noise monolithic Si JFETS for operation in the 90-300K range and in high radiation environments
[DE95-007303] p 2269 N95-28244

KRYPTON FLUORIDE LASERS
Spectral broadening of KrF laser radiation by self-seeded Raman amplification in long air paths
[DE95-003697] p 2297 N95-27718

KRYPTON ISOTOPES
Photon burst mass spectrometry--ultrasensitive detection of rare isotopes
[DE95-006403] p 2204 N95-27467

L

LABORATORIES
Implementing an integrated standards-based management system to ensure compliance at Los Alamos National Laboratory
[DE95-007873] p 2451 N95-28025
Sandia's network for Supercomputing '94: Linking the Los Alamos, Lawrence Livermore, and Sandia National Laboratories using switched multimegabit data service
[DE95-007717] p 2378 N95-28074
Laboratory of production engineering
[PB95-184834] p 2451 N95-28135

LABORATORY EQUIPMENT
A laboratory scale supersonic combustive flow system
[DE95-006347] p 2206 N95-27851

LABYRINTH
Hair cell regeneration in the bullfrog vestibular otolith organs following aminoglycoside toxicity
p 2349 N95-26729

LACTATES
A summary of ODS replacement technologies at Litton Poly-Scientific p 2228 N95-27105
Ethyl lactate as a solvent alternative for cleaning metal parts p 2229 N95-27112

LAGRANGIAN FUNCTION
Field theory of point-like systems with higher-order derivatives
[DE95-608800] p 2448 N95-27310
Parallel algorithms for semi-Lagrangian transport in global atmospheric circulation models
[DE95-007385] p 2327 N95-27457

Subharmonic phonon transmission and Kapitza conductance between crystals with very different vibrational spectra
[DE95-609151] p 2447 N95-28608

LAMINAR FLOW

Computational support of the laminar flow supersonic wind tunnel, CNSFV code development, Maglev, and grid generation
[NASA-CR-197750] p 2143 N95-26775

The stability of the flow in a laminar separation bubble
[CUED/A-AERO/TR-22] p 2275 N95-26809

Analysis of developing laminar flows in circular pipes using a higher-order finite-difference technique
p 2281 N95-27352

Research on combustion processes relevant to burners in HVAC systems
[PB95-179735] p 2208 N95-28006

LAMINATES

A high velocity electromagnetic mass launcher having an ablation resistant insulator
[AD-A288231] p 2154 N95-26524

Scale model experiments with ceramic laminate targets
[AD-A288322] p 2225 N95-26561

Life prediction methodology for composite laminates. Part 1: Constant amplitude and two-stress level fatigue
[AD-A288343] p 2180 N95-26571

Interfacial mobility and its effect on flexural strength and fracture toughness in glass-fiber fabric reinforced epoxy laminates
[AD-A288344] p 2180 N95-26572

Composite sandwich structure and method for making same
[NASA-CASE-LAR-14898-1] p 2180 N95-26764

Fatigue behavior of a cross-ply ceramic matrix composite subjected to tension-tension cycling with hold time
[AD-A289418] p 2182 N95-27134

An experimental investigation of sandwich flat panels under low velocity impact
[AD-A289420] p 2309 N95-27135

Modeling considerations in the prediction of residual strength in composite laminates
[AD-A289128] p 2182 N95-27142

Scarf repairs to graphite/epoxy components
p 2135 N95-27523

Scarf joint technique with cocured and precured patches for composite repair p 2135 N95-27524

Measurement of the D0 WAMUS magnet inductance
[DE95-005128] p 2399 N95-27530

Superior catalysts for selective catalytic reduction of nitric oxide
[DE95-007903] p 2205 N95-27691

Analysis of aircraft engine blade subject to ice impact
p 2141 N95-28277

Assembly induced delaminations in composite structures p 2186 N95-28279

Higher order finite element analysis of thick composite laminates p 2186 N95-28282

An improved plate theory of order (1,2) for thick composite laminates p 2187 N95-28283

On the thermally-induced residual stresses in thick fiber-thermoplastic matrix (PEEK) cross-ply laminated plates p 2187 N95-28285

Analysis of stresses in finite anisotropic panels with centrally located cutouts p 2187 N95-28286

The role of biaxial stresses in discriminating between meaningful and illusory composite failure theories
p 2187 N95-28287

Static and dynamic strain energy release rates in toughened thermosetting composite laminates
p 2188 N95-28288

Mechanisms of compressive failure in woven composites and stitched laminates p 2189 N95-28424

Investigation of static and cyclic bearing failure mechanisms for GR/EP laminates p 2190 N95-28427

Compression failure of angle-ply laminates
p 2190 N95-28428

Buckling behavior of long symmetrically laminated plates subjected to combined loads p 2190 N95-28430

Compressive residual strength of graphite/epoxy laminates after impact p 2191 N95-28431

Characteristics of laminates with delamination control strips p 2191 N95-28434

Probabilistic evaluation of fuselage-type composite structures p 2137 N95-28444

Development of stitched/RTM composite primary structures p 2195 N95-28469

Tension fracture of laminates for transport fuselage. Part 1: Material screening p 2137 N95-28471

The use of impact force as a scale parameter for the impact response of composite laminates
p 2197 N95-28479

Effect of low-speed impact damage and damage location on behavior of composite panels p 2197 N95-28481

Impact damage resistance of composite fuselage structure, part 1 p 2138 N95-28482

Applications of a damage tolerance analysis methodology in aircraft design and production
p 2197 N95-28483

Post impact compressive strength in composites
p 2198 N95-28485

Fundamental concepts in the suppression of delamination buckling by stitching p 2198 N95-28486

LAND USE

Integrated assessment and the relation between land-use change and climate change
[DE95-006533] p 2327 N95-27469

LANDING

Full span flaperons for a biplane
p 2119 N95-26954

LANDING AIDS

Precision landing system mathematical modeling study report for Andrews Air Force Base, runway 19L, Camp Springs, MD
[AD-A289015] p 2127 N95-27903

LANDING GEAR

Aircraft nosewheel steering simulation
p 2118 N95-26944

Rotorcraft crashworthy airframe and fuel system technology development program
[AD-A289986] p 2126 N95-28630

LANGEVIN FORMULA

Magnetization of ferromagnetic clusters
[DE95-006878] p 2399 N95-27548

LANGUAGES

An introduction to software architecture
[AD-A288356] p 2363 N95-26467

Unification of LARCH and Z-based object models to support algebraically-based design refinement: The Z perspective
[AD-A289234] p 2369 N95-26962

LANTHANUM ALLOYS

Aspects of macroscopic phase separation and interstitial oxygen ordering in oxygen doped La2CuO(4+delta)
[DE95-007864] p 2443 N95-28060

LANTHANUM OXIDES

Characterization of collision cascade damage in Ca2La8(SiO4)6O2 by HRTEM
[DE95-005719] p 2440 N95-27491

LAP JOINTS

Characterization of corrosion and development of a breadboard of a D sight aircraft inspection system, phase 1
[AD-A288347] p 2125 N95-26527

Evaluation of composite joints
[AD-A289247] p 2181 N95-26967

LAPLACE TRANSFORMATION

Hydrogen-like atom in laser field: Invariant atomic parameters in the ground state
[DE95-609036] p 2411 N95-27930

LARGE SPACE STRUCTURES

A class of stabilizing controllers for flexible multibody systems
[NASA-TP-3494] p 2161 N95-26428

Control of a large space structure using multiple model adaptive estimation and control techniques
[AD-A289309] p 2162 N95-26916

A state-space model of a large, lightly damped space structure using the Eigensystem realization algorithm
[AD-A289251] p 2163 N95-26970

Static stability of a three-dimensional space truss
[NASA-TM-106944] p 2164 N95-27730

System identification of damped truss-like space structures
[NASA-TM-106638] p 2303 N95-27911

LASER ABLATION

Analysis of surfaces, films and multilayers by resonant laser ablation
[DE95-006295] p 2297 N95-27841

Vacancy related defects in thin film Pb(Zr,Ti)O3 materials
[DE95-007696] p 2445 N95-28165

LASER APPLICATIONS

Soot particle density determination from a laser extinction multipass technique
[AD-A288551] p 2423 N95-26532

Design and development of experimental facilities for short duration, low-gravity combustion and fire experiments
[NASA-CR-195458] p 2244 N95-26709

Continuously-tunable, narrow-linewidth, Q-switched Cr:LiSAF laser for lidar applications
[DE95-006285] p 2296 N95-27672

Application of conventional laser technology to gamma-gamma colliders
[DE95-006341] p 2297 N95-27736

Applications of lasers and electro-optics
[DE95-600841] p 2299 N95-28330

Structural design optimization with survivability dependent constraints application: Primary wing box of a multi-role fighter p 2137 N95-28440

LASER ARRAYS

High-speed coherent laser arrays
[AD-A289373] p 2295 N95-26906

LASER BEAMS

Laser beam propagation in non-Kolmogorov atmospheric turbulence
[AD-A289256] p 2295 N95-26974

Surface damage effects generated by a fast-pulse laser beam
[AD-A289131] p 2295 N95-26996

JPRS report: Science and technology. Central Eurasia
[JPRS-UST-95-015] p 2246 N95-27213

Indirectly driven targets for ignition
[DE95-006451] p 2430 N95-27327

Crab crossing in a gamma-gamma collider
[DE95-006580] p 2420 N95-27470

Femtosecond X-ray generation through 90 degrees T homson scattering: Status of the LBL experiment
[DE95-006560] p 2296 N95-27674

Spectral broadening of KrF laser radiation by self-seeded Raman amplification in long air paths
[DE95-003697] p 2297 N95-27718

High power free-electron laser concepts and problems
[DE95-007841] p 2298 N95-28059

Flat panel planar optic display
[DE95-007686] p 2426 N95-28196

Ultrashort Pulse retrieval using FROG trace irradiance moments and the adaptive neural networks backpropagation algorithm
[DE95-007153] p 2299 N95-28220

Femtosecond OPO's at 3 microns and beyond: Design and performance issues related to the crystal properties of KTP and similar materials
[DE95-007286] p 2446 N95-28242

Laser beam aerosol interactions
[AD-A291723] p 2300 N95-28509

A comparison of NH3 point monitoring and diode laser based path integrated measurements
[DE95-006892] p 2332 N95-28602

LASER CAVITIES

Comprehensive numerical model for CW vertical-cavity surface-emitting lasers
[DE95-007758] p 2299 N95-28132

Thermally-induced unsymmetric optical distortion of output window of high-power CO2 laser
[AD-A289604] p 2300 N95-28650

LASER DAMAGE

Surface damage effects generated by a fast-pulse laser beam
[AD-A289131] p 2295 N95-26996

Influences of film structures on laser damage thresholds
[AD-A289647] p 2300 N95-28633

LASER GUIDANCE

A brief history of laser guided lightning discharge models and experiments
[AD-A289448] p 2295 N95-27022

LASER HEATING

Surface damage effects generated by a fast-pulse laser beam
[AD-A289131] p 2295 N95-26996

LASER INDUCED FLUORESCENCE

Laser beam aerosol interactions
[AD-A291723] p 2300 N95-28509

LASER INTERFEROMETRY

Far-infrared laser interferometry measurements on the STP-3(M) reversed-field pinch
[DE94-765440] p 2297 N95-27868

LASER MATERIALS

Growth and evaluation of nonlinear optical crystals for laser applications: Lithium borate, barium borate and silver gallium selenide
[AD-A289147] p 2277 N95-27000

New radiation stable and long-lived plastic scintillators
[DE95-608622] p 2233 N95-27163

Characterization of solid state laser and nonlinear optical materials
[AD-A291684] p 2300 N95-28458

LASER MICROSCOPY

Surface-emitting semiconductor laser for intracavity spectroscopy and microscopy
[DE95-007745] p 2299 N95-28128

LASER MODE LOCKING

Characterization of microwave MESFET circuits under laser illumination. Applications to phased array radar, microwave communications, and digital clock control
[AD-A289181] p 2261 N95-27015

LASER OUTPUTS

Laser ultrasonic generation at the surface of a liquid metal
[DE95-004999] p 2216 N95-27477

Direct ultrashort-pulse retrieval using frequency-resolved optical gating and a computational neural network
[DE95-007148] p 2425 N95-27482

Femtosecond X-ray generation through 90 degrees T homson scattering: Status of the LBL experiment
[DE95-006560] p 2296 N95-27674
Laser with optically driven Q-switch
[NASA-CASE-NPO-18470-1-CU] p 2297 N95-27731
Application of conventional laser technology to gamma-gamma colliders
[DE95-006341] p 2297 N95-27736
Trident as an ultrahigh irradiance laser
[DE95-006345] p 2297 N95-27850
Ultrasonic study on ternary liquid systems by laser-sound interaction
[DE95-608783] p 2207 N95-27929
Hydrogen-like atom in laser field: Invariant atomic parameters in the ground state
[DE95-609036] p 2411 N95-27930
High power free-electron laser concepts and problems
[DE95-007841] p 2298 N95-28059
Inspection methods for underwater cables
[AD-A289610] p 2312 N95-28616

LASER PUMPING
Silicate gel dye laser
[AD-D017262] p 2294 N95-26503
Collisional dynamics and spectroscopic studies of highly excited rovibrational levels of I2(X)(0(+)(sub g)) via stimulated emission pumping
[AD-A289447] p 2295 N95-27172
Improved performance 1590 nm Er:YLF laser
[DE95-003691] p 2296 N95-27705
Low power limits in ultrashort pulse measurement using Frequency-Resolved Optical Gating
[DE95-007150] p 2299 N95-28219

LASER SPECTROSCOPY
Analytical spectroscopy
[DE95-607896] p 2203 N95-27200
High temperature kinetic study of the reactions H + O2 = OH + O and O + H2 = OH + H in H2/O2 system by shock tube-laser absorption spectroscopy
[NASA-CR-195473] p 2206 N95-27695
Analysis of surfaces, films and multilayers by resonant laser ablation
[DE95-006295] p 2297 N95-27841
Single molecule detection using charge-coupled device array technology
[DE95-006425] p 2411 N95-27953
Bubble chamber spectroscopy for chemical analysis: A new concept
[DE95-006350] p 2209 N95-28088
Surface-emitting semiconductor laser for intracavity spectroscopy and microscopy
[DE95-007745] p 2299 N95-28128
A novel sensitive detector of atmospheric nitrocompounds based on laser photofragmentation/ionization spectrometry
p 2174 N95-28314

LASER TARGETS
Indirectly driven targets for ignition
[DE95-006451] p 2430 N95-27327
A magnetic hysteresis model p 2153 N95-27801
Development of density and temperature profile diagnostics for ICF targets
[DE95-007664] p 2433 N95-28052
Pulsed laser deposition of zeolitic membranes
[DE95-006274] p 2298 N95-28124
A novel sensitive detector of atmospheric nitrocompounds based on laser photofragmentation/ionization spectrometry
p 2174 N95-28314

LASER WINDOWS
Characteristics of thermal lens in a copper-vapor laser
[AD-A289545] p 2294 N95-26874

LASERS
Annealing of radiation damaged gallium arsenide solar cells by laser illumination
[AD-A289683] p 2316 N95-26762
Design and characterization of resonant cavity light-emitting diodes
[AD-A289307] p 2261 N95-26921
Laser ultrasonic generation at the surface of a liquid metal
[DE95-004999] p 2216 N95-27477
Laser ionization of molecular clusters
[DE95-007011] p 2296 N95-27550
Continuously-tunable, narrow-linewidth, Q-switched Cr:LiSAF laser for lidar applications
[DE95-006285] p 2296 N95-27672
Application of conventional laser technology to gamma-gamma colliders
[DE95-006341] p 2297 N95-27736
Portable laser laboratory
[DE95-008376] p 2298 N95-27876
Laboratory high-energy astrophysics on lasers
[DE95-008062] p 2462 N95-28013
Evaluation of laser-protective eyewear dyes in UVEX lenses
[AD-A290076] p 2361 N95-28390
Time-resolved FTIR emission studies of laser photofragmentation and radical reactions
[DE95-008125] p 2300 N95-28398

LASING
Toward coherent excitation: Development of a single-source pump for the rubidium hyperfine ground state doublet
[AD-A289413] p 2295 N95-27132
Surface-emitting semiconductor laser for intracavity spectroscopy and microscopy
[DE95-007745] p 2299 N95-28128

LATCH-UP
Characteristics of the standard current trip circuit
[PB95-192886] p 2271 N95-28663

LATCHES
Changing paradigms: Manufacturing vs. fabricating a high volume Hold Down and Release Mechanism
p 2155 N95-27267
Development of a high force thermal latch
p 2157 N95-27275

LATERAL STABILITY
An easy way to analyze longitudinal and lateral-directional trim problems with AEO or OEI
p 2119 N95-26949

LATEX
The effect of proteins on the aging properties of radiation vulcanized Natural Rubber Latex
[DE95-603357] p 2225 N95-26599
Radiation vulcanization of natural rubber latex
[DE95-600026] p 2226 N95-26637

LATTICE PARAMETERS
Lattice parameters and Debye-Waller factors of gamma-TiAl alloys
[AD-A288843] p 2213 N95-26681
First-principles calculations for AlN, GaN, and InN: Bulk and alloy properties
[DE95-006822] p 2219 N95-27958
Phenomenology from 100 large lattices
[DE95-006349] p 2442 N95-27994
Local texture and grain boundary misorientations in high H(C) oxide superconductors
[DE95-007004] p 2447 N95-28606

LATTICE VIBRATIONS
The unusual properties of beryllium surfaces
[DE95-006471] p 2223 N95-28593

LATTICES (MATHEMATICS)
Probabilistic growth model
[PB95-185054] p 2395 N95-26913
Phenomenology from 100 large lattices
[DE95-006349] p 2442 N95-27994
Topological density and instantons on a lattice
[DE95-006348] p 2445 N95-28240

LAUNCH VEHICLES
Stratospheric ozone reactive chemicals generated by space launches worldwide
[AD-A289852] p 2332 N95-28623

LAUNCHING BASES
Development and implementation of a system safety program for the space launch complex 3 east (SLC-3E) ground support system project to support Atlas 2 family of space launch vehicles p 2174 N95-28316

LAUNCHING PADS
Weather hazards to a Titan 4 on-pad destack-restack operation p 2172 N95-28307

LAY-UP
Field repair materials for naval aircraft
p 2133 N95-27514
Design of fabric preforms for double diaphragm forming p 2184 N95-28269
Advanced tow placement of composite fuselage structure p 2185 N95-28271

LEAD (METAL)
The structure of lead-indium phosphate glass
[DE95-007130] p 2237 N95-27967

LEAD ALLOYS
A microstructurally based model of solder joints under conditions of thermomechanical fatigue
[DE95-006226] p 2309 N95-27837
Vacancy related defects in thin film Pb(Zr,Ti)O3 materials
[DE95-007696] p 2445 N95-28165

LEAD COMPOUNDS
The oxidation state and magnetic behaviour of Tb in high-(Tc) related materials
[DE95-007129] p 2219 N95-27966

LEAD TITANATES
Large area smart piezoelectric and pyroelectric sensors
[AD-A288565] p 2290 N95-26541

LEAD ZIRCONATE TITANATES
Neutron diffraction studies on recrystallization of solution derived lead zirconate titanates
[DE95-004771] p 2439 N95-27429

LEADING EDGES
Airfoil modification effects on subsonic and transonic pressure distributions and performance for the EA-6B airplane
[NASA-TP-3516] p 2120 N95-26382
Composite repair of a CF18: Vertical stabilizer leading edge p 2134 N95-27517
Wind-tunnel test of the S814 thick root airfoil
[DE95-000268] p 2122 N95-27541
Task 4 supporting technology. Part 1: Detailed test plan for leading edge tile development. Leading edge material development and testing
[NASA-CR-198633] p 2160 N95-28258

LEAKAGE
Leak detection utilizing analog binaural (VLSI) techniques
[NASA-CASE-NPO-18399-1-CU] p 2271 N95-28599

LEAR JET AIRCRAFT
Aircraft accident report: Controlled collision with Terrain Transportes Aereos Ejecutivos, S.A. (TAESA) Learjet 25D, XA-BBA Dulles International Airport Chantilly, Virginia, June 18, 1994
[NTSB/AAR-95/02] p 2125 N95-26498
Two-phase flow research using the learjet apparatus
[NASA-TM-106814] p 2284 N95-27854

LEARNING
Change, Learning and Mental Work in Organizations: Working papers of the 3rd Otaniemi-Dresden Workshop
[PB95-184941] p 2356 N95-26909
Hippocampal place fields, the internal compass, and the learning of landmark stability
[AD-A289406] p 2350 N95-27100
Piecemeal learning of an unknown environment
[AD-A291683] p 2387 N95-28461

LEARNING THEORY
Piecemeal learning of an unknown environment
[AD-A291683] p 2387 N95-28461

LEAST SQUARES METHOD
The origin of spurious solutions in computational electromagnetics
[NASA-TM-106921] p 2391 N95-27726
Accurate orbit determination strategies for the tracking and data relay satellites p 2147 N95-27768
Use of nonlinear identification in robust attitude and attitude rate estimation for SAMPEX
p 2149 N95-27781
Ulysses orbit determination at high declinations
p 2151 N95-27787

LECTURES
Index to NASA news releases and speeches 1994
[NASA-TM-110650] p 2452 N95-26673
CAS CERN Accelerator School 5th General Accelerator Physics Course
[DE95-608324] p 2419 N95-27158
The 1993 European school of high-energy physis
[DE95-610196] p 2421 N95-28040
International journal of quantum chemistry
[AD-A291633] p 2352 N95-28546

LENGTH
Reflection of neutrons from an optical grating
[DE95-007145] p 2411 N95-28004

LENNARD-JONES POTENTIAL
A new shared-memory programming paradigm for molecular dynamics simulations on the Intel Paragon
[DE95-007289] p 2378 N95-28019
Beta-dynamics in simple liquid metal
[DE95-609154] p 2220 N95-28039

LENSES
Characteristics of thermal lens in a copper-vapor laser
[AD-A289545] p 2294 N95-26874
Plasma lens experiments at the final focus test beam
[DE95-008595] p 2434 N95-28161
Evaluation of laser-protective eyewear dyes in UVEX lenses
[AD-A290076] p 2361 N95-28390

LEPTONS
Implications of horizontal symmetries on baryon number violation in supersymmetric models
[DE95-610202] p 2407 N95-27406
Search for SUSY at CDF
[DE95-005109] p 2407 N95-27430
Search for supersymmetry and leptoquark states at FNAL
[DE95-003381] p 2410 N95-27871
Lattice calculation for lepton capture from vacuum-pair production in relativistic heavy-ion collisions
[DE95-007392] p 2413 N95-28077
Bit-string physics: A novel theory of everything
[DE95-005941] p 2449 N95-28137
Threefold maximal lepton mixing and the solar and atmospheric neutrino deficits
[PB95-196259] p 2465 N95-28500

LEUKOCYTES
Anti-idiotype probes for toxin detection
[AD-A288955] p 2348 N95-26435

LEVITATION
Time-optimal control of the magnetically levitated photolithography platen
[DE95-005493] p 2266 N95-27724
LEXAN (TRADEMARK)
Effects of atomic oxygen on polymeric materials flown on EOIM-3 p 2242 N95-27638
LIBRARIES
Development and implementation of an electronic library tour for the NASA Langley Technical Library
[NASA-TM-110619] p 2455 N95-27701
A new shared-memory programming paradigm for molecular dynamics simulations on the Intel Paragon
[DE95-007289] p 2378 N95-28019
LICENSING
Bibliography of patents and licenses 1951-1990. 1991 edition
[AD-A289603] p 2452 N95-26721
Global trade in satellites and launch services
[GPO-84-811] p 2165 N95-28342
LIE GROUPS
Hyperkaehler metrics associated to compact Lie groups
[PB95-185161] p 2388 N95-26514
q-structure algebra of U(sub q)(g-circumflex) from its adjoint action
[DE95-608749] p 2390 N95-27301
Introduction to Dubois-Violette's non-commutative differential geometry
[DE95-608801] p 2390 N95-27311
On the Hopf structure of U(p,q)(gl(1/1)) and the universal Tau-matrix of Fun(p,q)(GL(1/1))
[DE95-608755] p 2448 N95-27333
Algebraic structure of the Green's ansatz and its q-deformed analogue
[DE95-608780] p 2395 N95-27340
Realization of vector fields for quantum groups as pseudodifferential operators on quantum spaces
[DE95-008485] p 2449 N95-27877
Symmetries of the KAC-Peterson modular matrices of affine algebras
[PB95-190138] p 2392 N95-28010
Lie group weight multiplicities from conformal field theory
[PB95-190153] p 2392 N95-28012
Coordinates of the quantum plane as q-tensor operators in U(sub q) (su(2) * su(2))
[DE95-007100] p 2397 N95-28234
LIFE (DURABILITY)
Life prediction methodology for composite laminates. Part 1: Constant amplitude and two-stress level fatigue
[AD-A288343] p 2180 N95-26571
Statistical theory and reliability
[AD-A288519] p 2394 N95-26733
A review of nickel hydrogen battery technology
[NASA-TM-106918] p 2167 N95-27177
Effect of hoop stress on ball bearing life prediction
[NASA-TM-106874] p 2301 N95-27178
Investigation on LCA (Life Cycle Analysis/assessment)
[DE95-759260] p 2330 N95-27942
Electric vehicle activities
[DE95-006648] p 2267 N95-28105
Lithium ion rechargeable systems studies
[DE95-006810] p 2268 N95-28200
LIFE CYCLE COSTS
Life cycle costs of alternatives for F-16 printed circuit board diagnosis equipment
[AD-A288744] p 2138 N95-28586
LIFE SCIENCES
JPRS report: Science and technology. Central Eurasia
[JPRS-UST-95-015] p 2246 N95-27213
JPRS report: Science and technology. Central Eurasia
[JPRS-UST-94-022] p 2246 N95-27699
LIFE SUPPORT SYSTEMS
International Space Station Alpha trace contaminant control subassembly life test report
[NASA-TM-108488] p 2358 N95-26364
LIFT
Wind-tunnel test of the S814 thick root airfoil
[DE95-000268] p 2122 N95-27541
Study of potential aerodynamic benefits from spanwise blowing at wingtip
[NASA-TP-3515] p 2124 N95-28669
Noise exposure reduction of advanced high-lift systems
[NASA-CR-195077] p 2402 N95-28670
LIFT DRAG RATIO
Noise exposure reduction of advanced high-lift systems
[NASA-CR-195077] p 2402 N95-28670
LIFT FANS
The lift-fan aircraft: Lessons learned
[NASA-CR-196694] p 2131 N95-27143
LIGHT (VISIBLE RADIATION)
Solar UV flux measurements from the SBUV2 monitor on the NOAA9 satellite. Part 1: Mg II h and k line core-to-wing ratios for 1986-1988
[PB95-181962] p 2464 N95-28007
LIGHT BEAMS
Preliminary design study of the beam collapser and certain optomechanical aspects of the siderostat
[AD-A288423] p 2423 N95-26549
Ultrasonic study on ternary liquid systems by laser-sound interaction
[DE95-608783] p 2207 N95-27929
OBIC analysis of stressed, thermally-isolated polysilicon resistors
[DE95-008511] p 2268 N95-28201
Inspection methods for underwater cables
[AD-A289610] p 2312 N95-28616
LIGHT CURVE
Models of classical and recurrent novae
p 2459 N95-27073
Overview of the observations of symbiotic stars
p 2460 N95-27076
Discussion on selected symbiotic stars
p 2460 N95-27078
LIGHT EMITTING DIODES
An organic thin film laser diode: A novel light source
[AD-A289007] p 2294 N95-26568
Design and characterization of resonant cavity light-emitting diodes
[AD-A289307] p 2261 N95-26921
Laser with optically driven Q-switch
[NASA-CASE-NPO-18470-1-CU] p 2297 N95-27731
LIGHT GAS GUNS
Pellet injector research and development at ORNL
[DE95-006736] p 2435 N95-28596
LIGHT MODULATION
Modulation effect of a Bragg acousto-optic bistable system
[AD-A289622] p 2401 N95-26857
Optical implementation of inner product neural associative memory
[NASA-CASE-NPO-18491-2-CU] p 2427 N95-28363
Full complex modulation using two one-parameter spatial light modulators
[NASA-CASE-MSC-22255-1] p 2427 N95-28384
LIGHT SCATTERING
Visualization and direct comparison of large displacements using difference holographic interferometry
[DE95-608782] p 2292 N95-27711
Advances in scientific visualization
[DE95-008065] p 2343 N95-28014
Scattering by a small object close to an interface. 3. Buried object
[PB95-184909] p 2256 N95-28354
New developments for sol-gel film and fiber processing
[DE95-008175] p 2240 N95-28404
LIGHT SOURCES
An organic thin film laser diode: A novel light source
[AD-A289007] p 2294 N95-26568
An illumination planner for Lambertian polyhedral objects
[AD-A289332] p 2424 N95-26900
Observation of nonlinear resonances in the advanced light source
[DE95-006561] p 2425 N95-27675
Laser with optically driven Q-switch
[NASA-CASE-NPO-18470-1-CU] p 2297 N95-27731
Atmospheric dispersioh in adaptive optics
[AD-A289639] p 2428 N95-28617
LIGHTHILL METHOD
A numerical study of fundamental shock noise mechanisms
[NASA-TM-110608] p 2401 N95-27908
LIGHTING EQUIPMENT
Engineering Technical Letter (ETL) 94-5: Fire protection engineering criteria and technical guidance. Emergency lighting and marking of exits
[AD-A288953] p 2246 N95-26566
LIGHTNING
Aircraft fuel system lightning protection design and qualification test procedures development
[AD-A288401] p 2125 N95-26497
A brief history of laser guided lightning discharge models and experiments
[AD-A289448] p 2295 N95-27022
A study of lightning in winter thunderstorms and the analysis of thunderstorm overflight data
[NASA-CR-198577] p 2343 N95-28191
Weather hazards to a Titan 4 on-pad destack-restack operation p 2172 N95-28307
LIGHTNING SUPPRESSION
A brief history of laser guided lightning discharge models and experiments
[AD-A289448] p 2295 N95-27022
LIMESTONE
Ash-based ceramic materials
[AD-D017272] p 2241 N95-28582
LIMITER CIRCUITS
Characteristics of the standard current trip circuit
[PB95-192886] p 2271 N95-28663
LINE OF SIGHT
A modified proportional navigation scheme for rendezvous and docking with tumbling targets: The Planar case p 2150 N95-27784
LINE SHAPE
Investigation of the collision line broadening problem as applicable to the NASA Optical Plume Anomaly Detection (OPAD) system, phase 1
[NASA-CR-198605] p 2426 N95-27913
LINE SPECTRA
CO, HCO(+) and HCN absorption in the gravitational lens candidate B0218+357 at z=0.685
[PB95-185146] p 2461 N95-26522
Coronal abundances and their variation
[NASA-CR-197788] p 2464 N95-26671
Spectral broadening of KrF laser radiation by self-seeded Raman amplification in long air paths
[DE95-003697] p 2297 N95-27718
Investigation of the collision line broadening problem as applicable to the NASA Optical Plume Anomaly Detection (OPAD) system, phase 1
[NASA-CR-198605] p 2426 N95-27913
LINEAR ACCELERATORS
Atomic physics with highly charged ions
[DE95-007325] p 2407 N95-27439
LINEAR ARRAYS
Balanced data focusing: Direction of arrival estimation with maximum likelihood performance
[AD-A288252] p 2248 N95-26407
Satellite surface material composition from synthetic spectra
[AD-A289236] p 2163 N95-26963
Simulating a multi-target acoustic array on the Intel Paragon
[AD-A288443] p 2377 N95-27183
Physical interpretation and development of ultrasonic nondestructive evaluation techniques applied to the quantitative characterization of textile composite materials
[NASA-CR-198591] p 2306 N95-28034
LINEAR ENERGY TRANSFER (LET)
Ionizing radiation measurements on LDEF: A0015 Free flyer biostack experiment
[NASA-CR-196603] p 2202 N95-27168
LINEAR EQUATIONS
Electromagnetic hysteretic response calculation for superconductors in demagnetizing geometries
[DE95-005028] p 2264 N95-27403
LINEAR FILTERS
Filtered kernel density estimation
[AD-A288293] p 2394 N95-26413
LINEAR OPERATORS
Local operators in Krylov subspaces
[PB95-195525] p 2393 N95-28499
LINEAR POLARIZATION
Scattering by a small object close to an interface. 3. Buried object
[PB95-184909] p 2256 N95-28354
LINEAR PROGRAMMING
Modal event calculus in Lolli
[AD-A288544] p 2365 N95-26605
LINEAR QUADRATIC GAUSSIAN CONTROL
Control of a large space structure using multiple model adaptive estimation and control techniques
[AD-A289309] p 2162 N95-26916
Post Kalman progress p 2148 N95-27776
LINEAR SYSTEMS
Robust hybrid state-space self-tuning control using dual-rate sampling
[AD-A288359] p 2380 N95-26468
Performance evaluation of a new parallel preconditioner
[AD-A288563] p 2376 N95-26529
Random relaxation of fixed point iteration
[PB95-185013] p 2389 N95-26910
Control of a large space structure using multiple model adaptive estimation and control techniques
[AD-A289309] p 2162 N95-26916
Linear and nonlinear trending and prediction for AVHRR time series data p 2385 N95-27391
Post Kalman progress p 2148 N95-27776
Method and apparatus for maintaining linearity and frequency accuracy of an FM chirp waveform
[AD-D017398] p 2258 N95-28615
LINEAR TRANSFORMATIONS
Three-dimensional photogrammetry for laboratory applications
[AD-A291624] p 2294 N95-28410

LINGUISTICS
Factors in human-computer interface design (a pilot study)
[AD-A288908] p 2360 N95-27195
A linguistic geometry for 3D strategic planning
p 2386 N95-27397
LININGS
Composite heat pipe development status: Development of lightweight prototype carbon-carbon heat pipe with integral fins and metal foil liner
[NASA-TM-106909] p 2283 N95-27369
Investigation of HE driven cylindrical liner
[DE95-007866] p 2311 N95-28539
LIPIDS
Non-covalent immobilization of proteins and enzymes on polymerized lipid assemblies
[AD-A288234] p 2225 N95-26526
LIQUEFIED GASES
Low noise monolithic Si JFETS for operation in the 90-300K range and in high radiation environments
[DE95-007303] p 2269 N95-28244
LIQUEFIED NATURAL GAS
Investigation on comprehensive fossil fuel cycle analysis and assessment approach as viewed from the global environment
[DE95-759241] p 2329 N95-27935
LIQUID AMMONIA
Hazards analysis of an integral class 1.1/1.3 rocket motor demilitarization and ingredient recovery system using ammonia p 2174 N95-28315
LIQUID COOLING
Supercooled liquid dynamics for the charged hard-sphere model
[DE95-609158] p 2241 N95-28609
LIQUID CRYSTALS
Siloxane-based ferroelectric liquid crystal elastomers and Self-Assembled Mono- and multilayers
[AD-A288285] p 2224 N95-26456
Molecular object liquid crystals: An approach to new materials
[AD-A288905] p 2437 N95-26553
Surface crystallization and thin film melting in normal alkanes
[DE95-006694] p 2440 N95-27535
Molecular dynamics simulations of Gay-Berne nematic liquid crystal: Elastic properties from direct correlation functions
[DE95-609149] p 2441 N95-27740
JTEC panel on display technologies in Japan
[NASA-CR-198564] p 2292 N95-27863
Determination of phase transitions in a lyotropic liquid crystal by positron annihilation technique
[DE95-609162] p 2442 N95-27964
A phase-stepped point diffraction interferometer using liquid crystals
[NASA-TM-106922] p 2293 N95-28037
LIQUID FUELS
Alternative fuels and vehicles choice model
[DE95-005695] p 2243 N95-27944
Mechanism of deposit formation on fuel-wetted hot metal surfaces
[AD-A289847] p 2210 N95-28621
LIQUID HELIUM
Detection of charged particles in superfluid helium
[DE95-007354] p 2403 N95-26560
Pumping characteristics of a cryopump with Ar sorbent in He and in D2/He mixture
[DE95-007049] p 2302 N95-27875
LIQUID HYDROGEN
Task 4 supporting technology. Densification requirements definition and test objectives. Propellant densification requirements definition
[NASA-CR-198629] p 2450 N95-28260
LIQUID INJECTION
Propellant injection systems and processes
[NASA-TM-110632] p 2242 N95-26781
LIQUID METALS
Spray-formed tooling
[DE95-005031] p 2246 N95-27404
Laser ultrasonic generation at the surface of a liquid metal
[DE95-004999] p 2216 N95-27477
Crossover integral equation theory for the liquid structure study
[DE95-609155] p 2218 N95-27757
Beta-dynamics in simple liquid metal
[DE95-609154] p 2220 N95-28039
LIQUID NITROGEN
Cryogenic and simulated fuel jet breakup in argon, helium and nitrogen gas flows
[NASA-TM-106923] p 2291 N95-27030
The 77 K operation of a multi-resonant power converter
[NASA-TM-106941] p 2264 N95-27374
Cryogenic washout of solid rocket propellants
p 2176 N95-28324
LIQUID OXYGEN
Task 4 supporting technology. Densification requirements definition and test objectives. Propellant densification requirements definition
[NASA-CR-198629] p 2450 N95-28260
Developmental problems and their solution for the Space Shuttle main engine alternate liquid oxygen high-pressure turbopump: Anomaly or failure investigation the key
[NASA-TP-3553] p 2169 N95-28263
Chemical reactions identified in the Titan 2, Titan 4, and Delta 2 propellant systems and their application to source modeling p 2172 N95-28304
LIQUID PHASES
Molecular object liquid crystals: An approach to new materials
[AD-A288905] p 2437 N95-26553
LIQUID PROPELLANT ROCKET ENGINES
Progress in incompressible Navier-Stokes computations for propulsion flows and its dual-use applications
[NASA-CR-197746] p 2275 N95-26766
LIQUID ROCKET PROPELLANTS
Funding for AFRAPT student trainees for academic year 1992-1993
[AD-A288461] p 2466 N95-26604
Propellant injection systems and processes
[NASA-TM-110632] p 2242 N95-26781
Development test of a liquid Apogee engine for the ETS-6
[NAL-TR-1250] p 2167 N95-26799
Alternative cleaning solvents and lubricants at the Air Force PJKS facility p 2228 N95-27108
Task 4 supporting technology. Densification requirements definition and test objectives. Propellant densification requirements definition
[NASA-CR-198629] p 2450 N95-28260
Mars Sample Return mission utilizing in-situ propellant production
[NASA-CR-188371] p 2145 N95-28261
Toxicity assessment of liquid propellant XM46
p 2175 N95-28319
LIQUID WASTES
Recovery, evaluation, and decontamination of landfilled pentaborane cylinders, former liquid propellant rocket engine test facility, Washoe County, Nevada
p 2171 N95-28302
LIQUID-GAS MIXTURES
Two-phase flow research using the learjet apparatus
[NASA-TM-106814] p 2284 N95-27854
LIQUID-LIQUID INTERFACES
Investigation of the interface between immiscible electrolytes applied to membrane electrochemistry
[AD-A288887] p 2199 N95-26350
Vibrational spectroscopy of water interfaces
[DE95-006592] p 2209 N95-28218
LIQUID-SOLID INTERFACES
Synchrotron X-ray scattering studies at mineral-water interfaces
[DE95-008303] p 2440 N95-27542
Vibrational spectroscopy of water interfaces
[DE95-006592] p 2209 N95-28218
Cooling apparatus and couplings therefor
[NASA-CASE-ARC-11921-1] p 2304 N95-28256
LIQUID-VAPOR EQUILIBRIUM
Bubble fusion: Preliminary estimates
[DE95-006337] p 2420 N95-27494
LIQUID-VAPOR INTERFACES
Applications of Second Harmonic and Sum Frequency Generation to graphite and silica type interfaces
[AD-A288228] p 2201 N95-26544
Surface crystallization and thin film melting in normal alkanes
[DE95-006694] p 2440 N95-27535
LIQUIDS
Observations on the solvating power of supercritical fluids p 2228 N95-27106
The surface of liquid He-4 at nonzero temperatures
[DE95-607841] p 2207 N95-27880
LITHIUM
The 1994 27th Annual NASA Aerospace Battery Workshop
[NASA-CP-3292] p 2317 N95-26785
Current status of environmental, health, and safety issues of lithium polymer electric vehicle batteries
[DE95-004005] p 2265 N95-27719
Lithium ion rechargeable systems studies
[DE95-006810] p 2268 N95-28200
The off-center effect on the diffusion coefficient of Cu(+) and Li(+) in the KCl lattice
[DE95-609146] p 2446 N95-28255
Development of an ultra-safe rechargeable lithium-ion battery
[AD-A288959] p 2269 N95-28349
Isolation and x-ray crystal structures of (Li(mu2-As(SiMe3)2) (mu3-As(SiMe3)2)(THF))2 and ((Me3Si)2AsLi(THF)2)2
[AD-A288870] p 2241 N95-28661
LITHIUM ALLOYS
Electrolyte effects in Li(Si)/FeS2 thermal batteries
[DE95-001614] p 2264 N95-27474
LITHIUM BORATES
Growth and evaluation of nonlinear optical crystals for laser applications: Lithium borate, barium borate and silver gallium selenide
[AD-A289147] p 2277 N95-27000
LITHIUM COMPOUNDS
Thermodynamics of electrolyte solutions for use in high energy lithium batteries
[AD-A288897] p 2199 N95-26352
Processing and properties of chromate-free conversion coatings on aluminum
[DE95-004768] p 2218 N95-27722
LITHIUM FLUORIDES
Point defect formation in optical materials expos ed to the space environment p 2428 N95-27646
LITHIUM NIOBATES
On-axis polarization coupling in y-cut titanium in-diffused lithium niobate slab waveguides
[AD-A289260] p 2253 N95-26977
LITHOGRAPHY
Swords to plowshares: Shock wave applications to advanced lithography
[DE95-008154] p 2299 N95-28223
LIVER
Modeling and statistical analysis of bioassay data: Medaka cell proliferation under DEN and TCE
[AD-A289998] p 2352 N95-28519
LOAD DISTRIBUTION (FORCES)
Analysis of plate-twist test for in-plane shear modulus of composite materials (revised)
[PB95-190195] p 2308 N95-26749
LOAD TESTS
Stress corrosion cracking susceptibility of the earthquake resistant NOM B457 Mexican steel
[DE95-607956] p 2214 N95-27258
On aircraft repair verification of a fighter A/C integrally stiffened fuselage skin p 2133 N95-27515
Comparison of measured and calculated dynamic loads for the Mod-2 2.5 mW wind turbine system
p 2312 N95-27983
Buckling behavior of long symmetrically laminated plates subjected to combined loads p 2190 N95-28430
Design, analysis, and testing of a metal matrix composite web/flange intersection p 2191 N95-28433
Development of composite carrythrough bulkhead
p 2192 N95-28438
Structural testing of the technology integration box beam p 2194 N95-28467
Technology integration box beam failure study
p 2194 N95-28468
LOADS (FORCES)
Process control of microstructure in manufacturing
[AD-A288291] p 2245 N95-26410
Identification of the plastic anisotropy of an aluminum alloy
[IFTR-26/1994] p 2212 N95-26512
Evaluation of composite joints
[AD-A289247] p 2181 N95-26967
Testing of Uninterruptible Power Supplies with nonlinear loads
[AD-A289353] p 2262 N95-27067
Load measurement system with load cell lock-out mechanism p 2159 N95-27291
A comparison of measured wind park load histories with the WISPER and WISPERX load spectra
[DE95-000295] p 2319 N95-27459
Load transfer in the stiffener-to-skin joints of a pressurized fuselage
[NASA-CR-198610] p 2310 N95-27865
Investigation on technology for increasing the biological CO2 sink and technology for CO2 fixation and reutilization
[DE95-759251] p 2329 N95-27941
Investigation on LCA (Life Cycle Analysis/assessment)
[DE95-759260] p 2330 N95-27942
A hybrid vehicle evaluation code and its application to vehicle design. Revision 1
[DE95-008053] p 2303 N95-28029
A hybrid vehicle evaluation code and its application to vehicle design, revision 2
[DE95-008060] p 2303 N95-28139
Local design optimization for composite transport fuselage crown panels p 2137 N95-28473
Comparison of resin film infusion, resin transfer molding, and consolidation of textile preforms for primary aircraft structure p 2196 N95-28477
LOCAL AREA NETWORKS
A high performance totally ordered multicast protocol
[NASA-CR-197765] p 2371 N95-27252
Gigabit LAN issues: HIPPI, Fibre Channel, or ATM?
[DE95-003673] p 2378 N95-27422

LOG PERIODIC ANTENNAS
Improving the performance of spiral antennas by using passive scatterers
[AD-A289324] p 2251 N95-26893
FORTE antenna element and release mechanism design p 2157 N95-27282

LOGIC CIRCUITS
Novel field effect transistors for low power electronics
[AD-A289929] p 2271 N95-28629

LOGIC PROGRAMMING
Modal event calculus in Lolli
[AD-A288544] p 2365 N95-26605
Reference manual: Naive physics simulator
[PB95-184917] p 2369 N95-26907

LOGISTICS
The value of simulation for training
[AD-A289174] p 2143 N95-26556
US Coast Guard Human Systems Integration (HSI) process model
[AD-A289172] p 2358 N95-26612

LONG DURATION EXPOSURE FACILITY
Long Duration Exposure Facility Mini-Data Base User's Guide: Macintosh version
[NASA-CR-4656] p 2177 N95-26391
Ionizing radiation measurements on LDEF: A0015 Free flyer biostack experiment
[NASA-CR-196603] p 2202 N95-27168
LDEF: 69 Months in Space. Third Post-Retrieval Symposium, part 3
[NASA-CP-3275-PT-3] p 2466 N95-27629
Exposure of LDEF materials to atomic oxygen: Results of EOIM 3 p 2210 N95-27633
LDEF systems special investigation group overview
p 2470 N95-27647
System results from FRECOPA p 2211 N95-27648
Space environmental effect on solar cells: LDEF and other flight tests p 2326 N95-27649
A final look at LDEF electro-optic systems components p 2428 N95-27650
Effects of the LDEF orbital environment on the reflectance of optical mirror materials
p 2428 N95-27651
Long Duration Exposure Facility (LDEF) space optics handbook p 2428 N95-27654
Long Duration Exposure Facility (LDEF) Archive System p 2457 N95-27658
The Long Duration Exposure Facility (LDEF) annotated bibliography p 2457 N95-27659
The Long Duration Exposure Facility (LDEF) photographic survey special publication
p 2457 N95-27660
LDEF's contribution to the selection of thermal control coatings for the Space Station p 2242 N95-27661
Space Station as a Long Duration Exposure Facility
p 2166 N95-27663
A Materials Exposure Facility p 2166 N95-27664
An LDEF follow-on spacecraft concept
p 2166 N95-27665

LONG TERM EFFECTS
From LDEF to a national Space Environment and Effects (SEE) program: A natural progression
p 2145 N95-27657

LONG WAVE RADIATION
A study of surface temperatures, clouds and net radiation
[NASA-CR-198589] p 2329 N95-27864

LONGITUDINAL CONTROL
A comparison of the Neal-Smith and omega Tau function, zeta function and tau function flying qualities criteria
[AD-A289503] p 2130 N95-26844
Use of blade pitch control to provide power train damping for the Mod-2, 2.5-mW wind turbine
p 2306 N95-27986

LONGITUDINAL STABILITY
An easy way to analyze longitudinal and lateral-directional trim problems with AEO or OEI
p 2119 N95-26949

LOOPS
The free energy of hot QED at three and a half loops
[DE95-007079] p 2449 N95-27449

LORENTZ TRANSFORMATIONS
Mean value theorem in topological vector spaces
[DE95-608753] p 2390 N95-27331

LOSSES
Investigation of high-temperature superconducting flywheel energy storage devices
[DE95-759242] p 2320 N95-27936

LOSSLESS MATERIALS
Conditions for the parameter dyadics of lossless bi-anisotropic media
[PB95-185104] p 2252 N95-26914

LOW ALTITUDE
Visual system operational evaluation
[AD-A289173] p 2356 N95-27012

LOW CONCENTRATIONS
Modeling precipitation from concentrated solutions with the EQ3/6 chemical speciation codes
[DE95-006264] p 2204 N95-27556

LOW COST
Adaptive finite element method I: Solution algorithm and computational examples
[AD-A288979] p 2389 N95-26609
Design of a high altitude long endurance aircraft with manufacturing considerations p 2119 N95-26947
Optical features of nanosize iron and molybdenum sulfide clusters
[DE95-005417] p 2202 N95-27136
Successful product realization strategies
p 2264 N95-27233
Spray-formed tooling
[DE95-005031] p 2246 N95-27404
Development of a low-cost, modified resin transfer molding process using elastomeric tooling and automated preform fabrication p 2184 N95-28268
Commercial reformulation: An economic and environmentally neutral means of managing explosives and solid propellants p 2175 N95-28320

LOW CURRENTS
Comparison of the calculated and measured stability of a NbTi cable-in-conduit conductor
[DE95-007964] p 2265 N95-27693

LOW EARTH ORBITS
An analysis of orbital propagators for Low Earth Orbit Rendezvous
[AD-A288883] p 2161 N95-26458
Space tether-radar data processing
[AD-A289654] p 2250 N95-26725
Nickel metal hydride LEO cycle testing
p 2272 N95-26791
Space Debris Research Phase One Program: Abstracts from published papers (1990-1993)
[AD-A289504] p 2162 N95-26850
Computing NORAD mean orbital elements from a state vector
[AD-A289281] p 2146 N95-27033
Solar concentrator technology development for space based applications, volume 1
[NASA-CR-197723] p 2319 N95-27193
LEO degradation of graphite and carbon-based composites aboard Space Shuttle Flight STS-46
p 2199 N95-27636
Orbital atomic oxygen effects on materials: An overview of MSFC experiments on the STS-46 EOIM-3
p 2419 N95-27637
Solid film lubricants and thermal control coatings flown aboard the EOIM-3 MDA sub-experiment
p 2242 N95-27640
Effects of the LDEF orbital environment on the reflectance of optical mirror materials
p 2428 N95-27651
Effects of low earth orbit on the optical performance of multi-layer enhanced high reflectance mirrors
p 2428 N95-27652
LDEF's contribution to the selection of thermal control coatings for the Space Station p 2242 N95-27661
Long Duration Exposure Facility post-flight data as it influences the Tropical Rainfall Measuring Mission
p 2345 N95-27666

LOW FREQUENCIES
Ultrasonic studies of liquid/solid seimoacoustic wave phenomena
[AD-A289644] p 2402 N95-28622

LOW NOISE
Low noise monolithic Si JFETS for operation in the 90-300K range and in high radiation environments
[DE95-007303] p 2269 N95-28244

LOW PASS FILTERS
The installation of and first results from the superconducting gravimeter GWR20 at the Metsahovi Station, Finland
[REPT-95:1] p 2338 N95-27995

LOW SPEED
Atomic physics with highly charged ions
[DE95-007325] p 2407 N95-27439
Overview of turbulence model development and applications at Rocketdyne p 2286 N95-27891
Effect of low-speed impact damage and damage location on behavior of composite panels p 2197 N95-28481
Post impact compressive strength in composites
p 2198 N95-28485
Damage tolerance of a geodesically stiffened advanced composite structural concept for aircraft structural applications p 2138 N95-28487
Ultrasonic studies of liquid/solid seimoacoustic wave phenomena
[AD-A289644] p 2402 N95-28622

LOW TEMPERATURE
High pressure conductivity study of template synthesized polypyrrole: Observation of a crossover from three to one dimensional variable range hopping
[AD-A288367] p 2224 N95-26470
Chemistry involving the separation, isolation, and immobilization of 3-5 compound semiconductor nanocrystals and quantum dots
[AD-A288381] p 2436 N95-26473
First-principles study of intermetallic phase stability in the ternary Ti-Al-Nb alloy system
[DE95-005259] p 2213 N95-27082
Fluid dynamic effects on precision cleaning with supercritical fluids p 2232 N95-27129
Low temperature materials growth and processing development for flat panel display technology applications
[AD-A288970] p 2233 N95-27187
The 77 K operation of a multi-resonant power converter
[NASA-TM-106941] p 2264 N95-27374
Transient studies of low temperature catalyst for methane conversion
[DE95-007913] p 2205 N95-27692
Comparison of the calculated and measured stability of a NbTi cable-in-conduit conductor
[DE95-007964] p 2265 N95-27693
Density changes in amorphous Pd80Si20 during low temperature ion irradiation
[DE95-007132] p 2441 N95-27928
Phase stability and elasticity of C15 transition-metal intermetallic compounds
[DE95-007876] p 2219 N95-28026
Low temperature carrier transport properties in isotopically controlled germanium
[DE95-008489] p 2444 N95-28092
Low temperature deposition and characterization of N- and P-type silicon carbide thin films and associated Ohmic and Schottky contacts
[AD-A289107] p 2237 N95-28097
Low resistivity ohmic contacts to moderately doped n-GaAs with low temperature processing
[DE95-008507] p 2445 N95-28144

LOW THRUST PROPULSION
Micro electric propulsion feasibility
[NASA-CR-189139] p 2168 N95-28000

LUBRICANT TESTS
Deformation behavior of thin lubricant films at elevated pressure
[AD-A288906] p 2241 N95-28592

LUBRICANTS
Environmentally Benign Cleaning and Degreasing Technology: JANNAF Safety and Protection Subcommittee and Propellant Development and Characterization Subcommittee Joint Workshop
[CPIA-PUBL-611] p 2227 N95-27101
Alternative cleaning solvents and lubricants at the Air Force PJKS facility p 2228 N95-27108
Effects of bearing cleaning and lube environment on bearing performance p 2158 N95-27285
Molecular engineering of thin polymer films prepared from functionally-terminated oligomers
[AD-A291681] p 2240 N95-28457
Deformation behavior of thin lubricant films at elevated pressure
[AD-A288906] p 2241 N95-28592

LUBRICATION
Advanced solid lubricant films by Ion-Beam Assisted Deposition
[AD-A288866] p 2225 N95-26499
Effects of bearing cleaning and lube environment on bearing performance p 2158 N95-27285

LUGS
Higher order finite element analysis of thick composite laminates p 2186 N95-28282

LUMINANCE
Com(sup 3): A composite-compatible component coding system
[BBC-RD-1994/17] p 2249 N95-26670

LUMINESCENCE
Scintillator materials for calorimetry
[DE95-006570] p 2421 N95-27679
Optimization of measurements with pressure sensitive paints
[NASA-TM-4695] p 2293 N95-27915

LUMINOSITY
CAS CERN Accelerator School 5th General Accelerator Physics Course
[DE95-608324] p 2419 N95-27158
The CDF upgrade
[DE95-006683] p 2421 N95-28107
The 132 nsec bunch spacing in the Tevatron proton-antiproton collider
[DE95-005750] p 2422 N95-28346

LUMINOUS INTENSITY

Fundamental concepts of integrated and fiber optic sensors
[NASA-TM-106920] p 2426 N95-27906

LUNAR EXPLORATION

The Clementine mechanisms p 2156 N95-27268

LYSOZYME

Hydrogen-ion titrations of amino acids and proteins in solutions containing concentrated electrolyte
[DE95-008356] p 2209 N95-28229

M

MACH NUMBER

On the modulational instability of large amplitude waves in supersonic boundary layers
[NASA-CR-195072] p 2284 N95-27760

Comparative wind tunnel test at high Reynolds numbers of NACA 64 621 airfoils with two aileron configurations
p 2124 N95-27977

Measurements of store forces and moments and cavity pressures for a generic store in and near a box cavity at subsonic and transonic speeds
[NASA-TM-4611] p 2123 N95-28241

Surfactants and desensitizing wax substitutes for TNT-Based systems
[AD-A289652] p 2243 N95-28634

MACHINE LEARNING

Using machine learning to derive efficient cost and performance estimates in VLSI CAD designs
[AD-A288254] p 2363 N95-26408

Evolving cascade-correlation networks for time-series forecasting
[AD-A289197] p 2390 N95-27020

A modified backpropagation algorithm for training neural networks on data with error bars
[DE95-608729] p 2381 N95-27025

Higher-order probabilistic perceptrons as Bayesian inference engines
[DE95-608730] p 2381 N95-27044

Building an adaptive agent to monitor and repair the electrical power system of an orbital satellite
p 2383 N95-27380

A fuzzy logic intelligent diagnostic system for spacecraft integrated vehicle health management
p 2385 N95-27392

MACHINE TOOLS

Neural network error compensation of machine tools
[AD-A289300] p 2387 N95-28217

MACHINING

Neural network error compensation of machine tools
[AD-A289300] p 2387 N95-28217

JTEC Panel report on microelectromechanical systems in Japan
[NASA-CR-197831] p 2268 N95-28239

MACINTOSH PERSONAL COMPUTERS

Scientific statistics and graphics on the Macintosh
[DE95-006445] p 2372 N95-27533

MACROMOLECULES

Materials with self organized surfaces: 2D polymer assemblies
[AD-A288928] p 2226 N95-26627

MACROPHAGES

Anti-idiotype probes for toxin detection
[AD-A288955] p 2348 N95-26435

MAGNESIUM

A model of the diurnal variation in magnesium ion density and radiance in the thermosphere
[AD-A289824] p 2339 N95-28575

MAGNESIUM FLUORIDES

Point defect formation in optical materials expos ed to the space environment p 2428 N95-27646

MAGNETIC BEARINGS

Whirl plus tilt
[DE95-007948] p 2399 N95-28108

MAGNETIC COILS

Extension to the dynamic modeling of the large angle magnetic suspension test fixture
[NASA-CR-197801] p 2143 N95-26768

MAGNETIC DIPOLES

Simple equivalent dipole distributions for dielectric spheroidal scatterers
[PB95-184883] p 2254 N95-27049

Field quality improvements in superconducting magnets for RHIC
[DE95-006096] p 2269 N95-28339

Manufacture and testing of the superconducting wire and cable for the RHIC dipoles and quadrupoles
[DE95-006000] p 2270 N95-28515

MAGNETIC EFFECTS

The oxidation state and magnetic behaviour of Tb in high-(Tc) related materials
[DE95-007129] p 2219 N95-27966

Transport simulation of negative magnetic shoar discharges
[DE95-003941] p 2416 N95-28329

Theoretical aspects of energy confinement in spheromaks
[DE95-008079] p 2435 N95-28542

MAGNETIC FIELD CONFIGURATIONS

Magnetically controlled deposition of metals using gas plasma
[DE95-007248] p 2430 N95-27237

Crystal and magnetic structure of stoichiometric YFe2O4
[DE95-006627] p 2440 N95-27487

SAMPEX special pointing mode p 2149 N95-27780

Plasma properties and magnetic field structure of the solar corona, based on coordinated Max 1991 observations from SERTS, the VLA, and magnetographs
[NASA-CR-198592] p 2464 N95-27858

Magnetic structures in RNi2B2C (R = Ho, Er) superconductors
[DE95-008370] p 2442 N95-27932

MAGNETIC FIELDS

A study of magnetic activity effects on the thermospheric winds in the low ionosphere
[AD-A288677] p 2334 N95-26488

Analytic formulae for the Hartree-Fock order parameter at arbitrary p/q filling factors for the 2DEG in a magnetic field
[DE95-607805] p 2448 N95-26603

Joint services electronics program
[AD-A289594] p 2260 N95-26716

Computation of electromagnetic scattering parameters for lognormal distributions of magnetic spheres: Theory and algorithms
[AD-A289672] p 2250 N95-26759

Analysis of magnetic field levels at KSC
[NASA-CR-197678] p 2326 N95-26808

Notes on the calibration of the JHU-APL solar vector magnetograph at NSO-Sec peak
[AD-A289277] p 2253 N95-26983

The consideration of a bright relative beam dynamics in the magnetic focusing field
[DE95-608377] p 2398 N95-27160

Magnetic field measurement for the spectrometric magnet of the ISTRA-M setup
[DE95-608560] p 2362 N95-27162

Mathematical simulation of three-dimensional magnetic field of spectrometric magnet SP-40
[DE95-608736] p 2398 N95-27239

Energetic particle destabilization of shear Alfven waves in stellarators and tokamaks
[DE95-006393] p 2431 N95-27419

Magnetization of ferromagnetic clusters
[DE95-006878] p 2399 N95-27548

Landau quasi-energy spectrum destruction for an electron in both a static magnetic field and a resonant electromagnetic wave
[DE95-610176] p 2256 N95-27716

A PC-based magnetometer-only attitude and rate determination system for gyroless spacecraft
p 2147 N95-27770

Measurement of particle transport coefficients on Alcator C-Mod
[DE95-007763] p 2411 N95-28020

Solar-geophysical data number 604, December 1994. Part 1: (Prompt reports). Data for November, October 1994, and late data
[PB95-181848] p 2465 N95-28087

One dimensional global and local solution for ICRF heating
[DE95-007984] p 2392 N95-28110

Neutrino oscillations in strong magnetic fields
[DE95-608876] p 2416 N95-28249

Field quality improvements in superconducting magnets for RHIC
[DE95-006096] p 2269 N95-28339

MAGNETIC FLUX

Magnetically controlled deposition of metals using gas plasma
[DE95-007248] p 2430 N95-27237

The role of microprocesses in macroscale magnetotail dynamics
[DE95-006288] p 2432 N95-27673

A magnetic hysteresis model p 2153 N95-27801

MAGNETIC INDUCTION

Measurement of the D0 WAMUS magnet inductance
[DE95-005128] p 2399 N95-27530

MAGNETIC LENSES

The consideration of a bright relative beam dynamics in the magnetic focusing field
[DE95-608377] p 2398 N95-27160

MAGNETIC LEVITATION VEHICLES

Computational support of the laminar flow supersonic wind tunnel, CNSFV code development, Maglev, and grid generation
[NASA-CR-197750] p 2143 N95-26775

MAGNETIC MEASUREMENT

Analysis of magnetic field levels at KSC
[NASA-CR-197678] p 2326 N95-26808

Measurement of the D0 WAMUS magnet inductance
[DE95-005128] p 2399 N95-27530

Manufacture and testing of the superconducting wire and cable for the RHIC dipoles and quadrupoles
[DE95-006000] p 2270 N95-28515

MAGNETIC MIRRORS

Attractive characteristics of mirrors
[DE95-008073] p 2435 N95-28356

MAGNETIC MOMENTS

Magnetic quadrupole moment of W-boson in Kobayashi-Maskawa model
[DE95-610355] p 2407 N95-27411

Magnetization of ferromagnetic clusters
[DE95-006878] p 2399 N95-27548

Magnetic and structural properties of Fe/Pd multilayers studied by magnetic x-ray dichroism and x-ray absorption spectroscopy
[DE95-007095] p 2206 N95-27755

Observational magnetometer calibration with the Hubble Space Telescope's new magnetometers
p 2148 N95-27773

MAGNETIC PERMEABILITY

The oxidation state and magnetic behaviour of Tb in high-(Tc) related materials
[DE95-007129] p 2219 N95-27966

MAGNETIC PROPERTIES

A new method of evaluating the explicit magnetic-state-dependent energy in semi-empirical calculations of iron
[AD-A289098] p 2399 N95-27398

Spin-density-wave magnetism in dilute copper-manganese alloys
[DE95-005121] p 2215 N95-27462

Measurement of the D0 WAMUS magnet inductance
[DE95-005128] p 2399 N95-27530

Micromagnetics and microstructure of epitaxially grown Co and Co-Cr films for perpendicular magnetic recording
[DE95-004681] p 2441 N95-27720

Recent neutron scattering results on high-temperature superconductors
[DE95-007028] p 2413 N95-28066

MAGNETIC RECORDING

Micromagnetics and microstructure of epitaxially grown Co and Co-Cr films for perpendicular magnetic recording
[DE95-004681] p 2441 N95-27720

MAGNETIC RELAXATION

Muon spin relaxation in ferromagnets: Theoretical results for paramagnetic EuO and EuS
[PB95-192860] p 2418 N95-28641

Muon spin relaxation in antiferromagnets: A study of RbMnF3 based on the coupled-mode theory of paramagnetic and critical spin fluctuations
[PB95-192878] p 2418 N95-28642

MAGNETIC RESONANCE

Magnetic resonance imaging of solvent transport in polymer networks
[DE95-007142] p 2234 N95-27455

MAGNETIC SHIELDING

Analysis of magnetic field levels at KSC
[NASA-CR-197678] p 2326 N95-26808

Extended linear ion trap frequency standard apparatus
[NASA-CASE-NPO-19081-1-CU] p 2404 N95-26861

Extended linear ion trap frequency standard apparatus
[NASA-CASE-NPO-19081-1-CU] p 2416 N95-28348

MAGNETIC SIGNATURES

Plasma properties and magnetic field structure of the solar corona, based on coordinated Max 1991 observations from SERTS, the VLA, and magnetographs
[NASA-CR-198592] p 2464 N95-27858

MAGNETIC SUSPENSION

Extension to the dynamic modeling of the large angle magnetic suspension test fixture
[NASA-CR-197801] p 2143 N95-26768

Time-optimal control of the magnetically levitated photolithography platen
[DE95-005493] p 2266 N95-27724

MAGNETIC VARIATIONS

A study of magnetic activity effects on the thermospheric winds in the low ionosphere
[AD-A288677] p 2334 N95-26488

Energization and transport of ions of ionospheric origin in the terrestrial magnetosphere
[NASA-CR-197813] p 2336 N95-26699

MAGNETIZATION

Magnetization of ferromagnetic clusters
[DE95-006878] p 2399 N95-27548

Micromagnetics and microstructure of epitaxially grown Co and Co-Cr films for perpendicular magnetic recording
[DE95-004681] p 2441 N95-27720

Magnetic and structural properties of Fe/Pd multilayers studied by magnetic x-ray dichroism and x-ray absorption spectroscopy
[DE95-007095] p 2206 N95-27755

MAGNETO-OPTICS
Development of an optical trap as an ultra-sensitive analytical tool
[DE95-007843] p 2426 N95-28022
MAGNETOHYDRODYNAMIC FLOW
Fluctuations and transport in fusion plasma
[DE95-004178] p 2429 N95-26444
Effect of toroidal plasma flow and flow shear on global MHD modes
[DE95-006676] p 2433 N95-28106
MAGNETOHYDRODYNAMIC STABILITY
Analysis of instability growth and collisionless relaxation in thermionic converters using 1-D PIC simulations
[AD-A289310] p 2319 N95-26891
Nonlinear instability and chaos in plasma wave-wave interactions. I. Introduction
[DE95-005529] p 2429 N95-27084
Fluctuations in high beta(sub p) plasmas in DIII-D
[DE95-008071] p 2432 N95-27710
MAGNETOHYDRODYNAMIC TURBULENCE
Magnetic viscosity by localized shear flow instability in magnetized accretion disks
[DE95-006879] p 2433 N95-28111
A phenomenological treatment of rotating turbulence
[NASA-CR-198168] p 2288 N95-28228
MAGNETOHYDRODYNAMIC WAVES
Energetic particle destabilization of shear Alfven waves in stellarators and tokamaks
[DE95-006393] p 2431 N95-27419
Fast wave current drive in D3-D
[DE95-007582] p 2431 N95-27441
Experimental aspects of effects of high-energy particles on Alfven modes
[DE95-003383] p 2432 N95-27873
Magnetic viscosity by localized shear flow instability in magnetized accretion disks
[DE95-006879] p 2433 N95-28111
Shear Alfven wave excitation by direct antenna coupling and fast wave resonant mode conversion
[DE95-609109] p 2256 N95-28254
Proceedings of the International Workshop on Acceleration and Radiation Generation in Space and Laboratory Plasmas
[AD-A291673] p 2436 N95-28668
MAGNETOHYDRODYNAMICS
MHD simulations of DC helicity injection for current drive in tokamaks
[DE95-007018] p 2429 N95-26940
Intrusive multi-probe system
[DE95-006258] p 2292 N95-27465
The role of microprocesses in macroscale magnetotail dynamics
[DE95-006288] p 2432 N95-27673
Global dynamo in a reversed field pinch plasma
[DE94-765441] p 2432 N95-27869
Effect of toroidal plasma flow and flow shear on global MHD modes
[DE95-006676] p 2433 N95-28106
Magnetic viscosity by localized shear flow instability in magnetized accretion disks
[DE95-006879] p 2433 N95-28111
A phenomenological treatment of rotating turbulence
[NASA-CR-198168] p 2288 N95-28228
Third-order-accurate numerical methods for efficient, large time-step solutions of mixed linear and nonlinear problems
[DE95-009184] p 2288 N95-28533
MAGNETOMETERS
Notes on the calibration of the JHU-APL solar vector magnetograph at NSO-Sec peak
[AD-A289277] p 2253 N95-26983
Flight Mechanics/Estimation Theory Symposium 1995
[NASA-CP-3299] p 2146 N95-27763
A PC-based magnetometer-only attitude and rate determination system for gyroless spacecraft
p 2147 N95-27770
Observational magnetometer calibration with the Hubble Space Telescope's new magnetometers
p 2148 N95-27773
An automated method of tuning an attitude estimator
p 2148 N95-27774
SAMPEX special pointing mode p 2149 N95-27780
Solar-geophysical data number 604, December 1994. Part 1: (Prompt reports). Data for November, October 1994, and late data
[PB95-181848] p 2465 N95-28087
MAGNETOSPHERE-IONOSPHERE COUPLING
Energization and transport of ions of ionospheric origin in the terrestrial magnetosphere
[NASA-CR-197813] p 2336 N95-26699
MAGNETOSTATICS
Vector algorithms for solving 3D nonlinear magnetostatic problems
[DE95-608737] p 2399 N95-27298
MAGNETS
Mathematical simulation of three-dimensional magnetic field of spectrometric magnet SP-40
[DE95-608736] p 2398 N95-27239
MAGNITUDE
Weighting scheme for the space surveillance network automated tasker
[AD-A289265] p 2146 N95-27035
MAINTAINABILITY
Design of a high altitude long endurance aircraft with manufacturing considerations p 2119 N95-26947
Report to Congressional Committees. Comanche Helicopter: Testing needs to be completed prior to production decisions
[GAO/NSIAD-95-112] p 2135 N95-27910
MAINTENANCE
Alternative cleaning solvents and lubricants at the Air Force PJKS facility p 2228 N95-27108
Application of bacterial bioemusifiers to in situ maintenance of oil/water separators
p 2179 N95-27120
Cleaning of parts for new manufacturing and parts rebuilding p 2231 N95-27123
Comprehension and retrieval of failure cases in airborne observatories p 2145 N95-27394
Life cycle costs of alternatives for F-16 printed circuit board diagnosis equipment
[AD-A288744] p 2138 N95-28586
The effects of Crew Resource Management (CRM) training in airline maintenance: Results following three year's experience
[NASA-CR-196696] p 2358 N95-28676
MAINTENANCE TRAINING
The value of simulation for training
[AD-A289174] p 2143 N95-26556
MALAYSIA
Environmental pollution-effects on national development
[DE95-600439] p 2326 N95-26639
MAN ENVIRONMENT INTERACTIONS
Quantitative modeling and analysis in environmental studies
[AD-A288451] p 2326 N95-26431
Towards the detection and attribution of an anthropogenic effect on climate
[DE95-008589] p 2331 N95-28157
MAN MACHINE SYSTEMS
A perspective on the Human-Rating process of US spacecraft: Both past and present
[NASA-SP-6104] p 2162 N95-26586
US Coast Guard Human Systems Integration (HSI) process model
[AD-A289172] p 2358 N95-26612
Integrated mission precision attack cockpit technology (IMPACT). Phase 1: Identifying technologies for air-to-ground fighter integration
[AD-A289562] p 2129 N95-26684
Telepresent spacecraft docking with object-based bilateral control (OBBC)
[AD-A289268] p 2163 N95-26980
Survey and implementation of commercial manual controllers for a generic telerobotics architecture
[AD-A289215] p 2381 N95-26990
MANAGEMENT INFORMATION SYSTEMS
Analysis, design and implementation of a database system for the systems management curriculum office
[AD-A289656] p 2452 N95-26758
Design considerations for FrankTalk: A distributed group support system
[AD-A289386] p 2359 N95-26863
A demonstration of Client/Server technology using remote procedure calls for an application of file migration for moving records based on location
[AD-A289391] p 2453 N95-26864
The re-engineering of the Air Force Institute of Technology Student Information System
[AD-A289426] p 2453 N95-26866
Research and development management information system, system user manual
[AD-A289151] p 2453 N95-27004
Managing electronic records: A guideline
[DE95-007038] p 2456 N95-28555
A correlational study of the SEI's capability maturity model and software development performance in DOD contracts
[AD-A288890] p 2374 N95-28591
The Global Historical Climatology Network: A preview of version 2
[DE95-007003] p 2332 N95-28605
MANAGEMENT METHODS
Distributed computation of Pareto solutions for two decision makers
[PB95-185047] p 2396 N95-26613
Change, Learning and Mental Work in Organizations: Working papers of the 3rd Otaniemi-Dresden Workshop
[PB95-184941] p 2356 N95-26909
Performance of a stand-alone wind-electric ice maker for remote villages
[DE95-004006] p 2320 N95-27475
The 1994 JANNAF Safety and Environmental Protection Subcommittee Meeting, volume 1
[CPIA-PUBL-614-VOL-1] p 2170 N95-28294
MANAGEMENT PLANNING
Air traffic operational inventory CY 1994
[AD-A288281] p 2126 N95-26454
Automated Procurement System (APS) revised project management plan (DS-03)
[NASA-CR-196605] p 2450 N95-27169
A linguistic geometry for 3D strategic planning
p 2386 N95-27397
Cape Canaveral air station launch emergency response forces and toxic materials release contingency plans
p 2172 N95-28308
Evaluation of an Air Force Information Resources Management (IRM) overview course
[AD-A288746] p 2456 N95-28587
MANAGEMENT SYSTEMS
Automated Procurement System (APS) revised project management plan (DS-03)
[NASA-CR-196605] p 2450 N95-27169
Implementing an integrated standards-based management system to ensure compliance at Los Alamos National Laboratory
[DE95-007873] p 2451 N95-28025
Automated remedial assessment methodology software system
[DE95-007287] p 2373 N95-28243
Cape Canaveral air station launch emergency response forces and toxic materials release contingency plans
p 2172 N95-28308
Replacing the message service component in an integration framework
[AD-A289928] p 2375 N95-28628
MANEUVERABILITY
Airfoil modification effects on subsonic and transonic pressure distributions and performance for the EA-6B airplane
[NASA-TP-3516] p 2120 N95-26382
MANEUVERS
Full span flaperons for a biplane
p 2119 N95-26954
MANGANESE
Structural oxidation state studies of the manganese cluster in the oxygen evolving complex of Photosystem II
[DE95-008488] p 2409 N95-27744
MANGANESE ALLOYS
Spin-density-wave magnetism in dilute copper-manganese alloys
[DE95-005121] p 2215 N95-27462
MANGANESE COMPOUNDS
Muon spin relaxation in antiferromagnets: A study of RbMnF3 based on the coupled-mode theory of paramagnetic and critical spin fluctuations
[PB95-192878] p 2418 N95-28642
MANIFOLDS (MATHEMATICS)
Compactification of moduli spaces of monopoles
[PB95-185179] p 2388 N95-26515
Generalized Schwarzians in several variables and Moebius invariant differential operators
[PB95-185211] p 2388 N95-26539
Gromov-Lawson-Rosenberg conjecture for groups with periodic cohomology
[PB95-185203] p 2389 N95-26915
Collapsing and solvmanifolds
[PB95-196267] p 2393 N95-28501
MANIPULATORS
Plate manipulators
[AD-A289601] p 2121 N95-26719
Learning Hand/Eye coordination by an active observer. part 1: Organizing centers
[AD-A289502] p 2356 N95-26843
Telepresent spacecraft docking with object-based bilateral control (OBBC)
[AD-A289268] p 2163 N95-26980
Survey and implementation of commercial manual controllers for a generic telerobotics architecture
[AD-A289215] p 2381 N95-26990
Dynamic coupling of underactuated manipulators
[AD-A289404] p 2301 N95-27098
MANNED SPACE FLIGHT
International Space Station Alpha trace contaminant control subassembly life test report
[NASA-TM-108488] p 2358 N95-26364
A perspective on the Human-Rating process of US spacecraft: Both past and present
[NASA-SP-6104] p 2162 N95-26586
Spaceflight revolution: NASA Langley Research Center from Sputnik to Apollo
[NASA-SP-4308] p 2474 N95-27685

MANNED SPACECRAFT
Long-term variability of electron radiation dose in geosynchronous orbit
[AD-A289335] p 2162 N95-26902
MANPOWER
Free Electron Laser Physical Process Code (FELPPC)
[DE95-006276] p 2296 N95-27557
MANUFACTURING
Process control of microstructure in manufacturing
[AD-A288291] p 2245 N95-26410
Stochastic adaptive estimation and control
[AD-A289088] p 2380 N95-26480
Design of a high altitude long endurance aircraft with manufacturing considerations p 2119 N95-26947
JTEC Panel report on electronic manufacturing and packaging in Japan
[NASA-CR-197830] p 2263 N95-27226
Microelectronics in Japan p 2263 N95-27227
Japan's technology and manufacturing infrastructure
p 2263 N95-27229
Electronics manufacturing and assembly in Japan
p 2263 N95-27231
Specification of the figure and finish of EUV mirrors in terms of performance requirements, revised Nov. 1994
[DE95-005689] p 2425 N95-27490
Recent progress in the Photovoltaic Manufacturing Technology Project (PVMaT)
[DE95-000279] p 2320 N95-27704
JTEC panel on display technologies in Japan
[NASA-CR-198564] p 2292 N95-27863
Evaluation and qualification of environmentally conscious manufacturing processes for commercial and military applications
[DE95-008520] p 2329 N95-27878
A knowledge highway for integrated modelling from manufacturing to design
[AD-A288872] p 2247 N95-28187
Process and control systems for composites manufacturing p 2184 N95-28267
ACT/ICAPS: Thermoplastic composite activities
p 2185 N95-28274
Composite intermediate case manufacturing scale-up for advanced engines p 2141 N95-28275
Composite fuselage crown panel manufacturing technology p 2137 N95-28474
Manufacture and testing of the superconducting wire and cable for the RHIC dipoles and quadrupoles
[DE95-006000] p 2270 N95-28515
MAPPING
Longterm infrared cloud clutter research
[AD-A288632] p 2340 N95-26343
Digital mapping, charting, and geodesy analysis program: Initial technical review of Raster Product Format
[AD-A289039] p 2313 N95-26476
Vector Smart Map Level 1: A new DMA product
[AD-A288920] p 2452 N95-26607
On compact multipliers of topological algebras
[DE95-608751] p 2390 N95-27092
Harmonic maps of the bounded symmetric domains
[DE95-608798] p 2397 N95-27485
MARINE BIOLOGY
Biological/physical modeling of upper ocean processes
[AD-A289468] p 2347 N95-27151
MARINE ENVIRONMENTS
Transport phenomena and interfacial kinetics in multiphase combustion systems
[AD-A288297] p 2199 N95-26417
Environmentally assisted cracking of high strength beta titanium alloys
[AD-A289156] p 2213 N95-27032
Biological/physical modeling of upper ocean processes
[AD-A289468] p 2347 N95-27151
Measurement of heterogeneous chemical processes relevant to aerosol surfaces and trace gases active in the marine environment
[DE95-008337] p 2328 N95-27743
Benefits and limitations of composites in carrier-based aircraft p 2189 N95-28422
Downloading environmental data in the new MOODS format
[AD-A288835] p 2456 N95-28589
MARINE METEOROLOGY
Live from Antarctica: The coldest, windiest place on Earth
[NASA-CR-197737] p 2335 N95-26595
Live from Antarctica, volume 4
[NASA-CR-197828] p 2335 N95-26596
Deep convection in the Mediterranean Sea
[AD-A288497] p 2346 N95-26647
Study of the response of a three-dimensional coupled ice-ocean model to daily varying atmospheric forcing
[AD-A289050] p 2347 N95-27189
Tomographic observations of deep convection and the thermal evolution of the Greenland Sea Gyre 1988-1989
[AD-A289104] p 2348 N95-28096
Studies of radar backscatter as a function of wave properties and the winds in the turbulent marine atmosphere
[NASA-CR-198608] p 2315 N95-28209
MARINE TECHNOLOGY
JTEC/WTEC annual report and program summary: 1993/94
[NASA-CR-198563] p 2475 N95-28038
Modeling the shock response of submerged structures
[AD-A289082] p 2288 N95-28351
MARKERS
Systematic study of the ion beam mixing of oxide markers into alumina
[DE95-006262] p 2217 N95-27555
MARKET RESEARCH
Electronics manufacturing and assembly in Japan
p 2263 N95-27231
JTEC monograph on biodegradable polymers and plastics in Japan: Research, development, and applications
[NASA-CR-198562] p 2235 N95-27694
MARKOV PROCESSES
A mathematical framework for an improved search model
[AD-A288858] p 2358 N95-26552
Stochastic control and topics in applied probability
[AD-A291712] p 2395 N95-28526
MARS (PLANET)
Micromechanisms for optimism seismometer
p 2159 N95-27292
MARS ATMOSPHERE
Mars Sample Return mission utilizing in-situ propellant production
[NASA-CR-188371] p 2145 N95-28261
MARS EXPLORATION
A rotating arm using shape-memory alloy
p 2157 N95-27276
MARS SAMPLE RETURN MISSIONS
Mars Sample Return mission utilizing in-situ propellant production
[NASA-CR-188371] p 2145 N95-28261
MARS SURFACE
The Alpha-Proton-X-ray Spectrometer deployment mechanism: An anthropomorphic approach to sensor placement on Martian rocks and soil
p 2155 N95-27265
Theoretical and experimental models of the diffuse radar backscatter from Mars
[NASA-CR-198650] p 2463 N95-27700
MARTENSITE
Precursor phenomenon of martensitic transformation in Au-49.5at%Cd alloy
[DE95-007698] p 2222 N95-28166
MARTENSITIC STAINLESS STEELS
Effect of internal hydrogen on the mixed-mode 1/3 fracture toughness of a ferrific/martensitic stainless steel
[DE95-005722] p 2216 N95-27479
MARTENSITIC TRANSFORMATION
Precursor phenomenon of martensitic transformation in Au-49.5at%Cd alloy
[DE95-007698] p 2222 N95-28166
MASS DISTRIBUTION
The calculation of the mass moment of inertia of a fluid in a rotating rectangular tank
[NASA-CR-197777] p 2278 N95-27165
MASS DRIVERS
A high velocity electromagnetic mass launcher having an ablation resistant insulator
[AD-A288231] p 2154 N95-26524
MASS RATIOS
Molecular cloud content of early-type galaxies. V. CO in elliptical galaxies
[PB95-185153] p 2461 N95-27320
MASS SPECTRA
Measurement of inclusive Lambda production in electron-positron interactions at the upsilon energies
[DE95-610302] p 2407 N95-27407
Molecular beam scattering from C-13 enriched Kapton and correlation with the EOIM-3 carousel experiment
p 2419 N95-27643
Excited Charm States
[DE95-005749] p 2409 N95-27747
MASS SPECTROMETERS
Plume measurements with the T5 xenon ion thruster
[AD-A288697] p 2167 N95-26489
Photon burst mass spectrometry--ultrasensitive detection of rare isotopes
[DE95-006403] p 2204 N95-27467
STS-46 plasma composition measurements using the EOIM-3 mass spectrometer p 2211 N95-27645
MASS SPECTROSCOPY
Photon burst mass spectrometry--ultrasensitive detection of rare isotopes
[DE95-006403] p 2204 N95-27467
PXAMS: Projectile X ray AMS: X ray yields and applications
[DE95-006438] p 2204 N95-27496
Laser ionization of molecular clusters
[DE95-007011] p 2296 N95-27550
Analysis of surfaces, films and multilayers by resonant laser ablation
[DE95-006295] p 2297 N95-27841
D/H and O-18/O-16 partitioning between water liquid and vapor in the system H2O-Na-K-Mg-Ca-Cl-SO4 from 0 to 350 C
[DE95-007013] p 2208 N95-27961
MASS TRANSFER
Nova-like variables p 2458 N95-27070
Models for various aspects of dwarf novae and nova-like stars p 2459 N95-27071
Extensional flow convecting a reactant undergoing a first order homogeneous reaction and diffusional mass transfer from a sphere at low to intermediate Peclet and Damkohler numbers p 2280 N95-27346
Computation of three-dimensional mixed convective boundary layer flow p 2280 N95-27347
Analysis of gas absorption to a thin liquid film in the presence of a zero-order chemical reaction
p 2280 N95-27348
Single-drop reactive extraction/extractive reaction with forced convective diffusion and interphase mass transfer
p 2282 N95-27358
Single-drop reactive extraction/extractive reaction with forced convective diffusion and interphase mass transfer
p 2283 N95-27365
Survey on researches related to ocean disposal of carbon dioxide
[DE95-759247] p 2329 N95-27939
MATCHING
Development of a direct match technique for star identification on the SWAS mission
p 2148 N95-27771
MATERIALS RECOVERY
Hazards analysis of an integral class 1.1/1.3 rocket motor demilitarization and ingredient recovery system using ammonia p 2174 N95-28315
Commercial reformulation: An economic and environmentally neutral means of managing explosives and solid propellants p 2175 N95-28320
Alternate use of rocket propellants as ingredients in commercial watergel explosives p 2176 N95-28321
A comprehensive energetic materials resource recovery and recycling program p 2176 N95-28323
Recovery and reuse of rocket motor propellant ingredients p 2177 N95-28326
MATERIALS SCIENCE
JPRS report: Science and technology. Central Eurasia
[JPRS-UST-94-022] p 2246 N95-27699
Research activities of the Solid State Sciences Committee in the development of a Federal initiative on advanced materials and processing
[DE95-009328] p 2445 N95-28179
An overview of activities and accomplishments of the Metals and Ceramics Division
[DE95-007020] p 2241 N95-28560
MATERIALS TESTS
Integrating the QMR method with first principles material science application code
[DE95-007380] p 2408 N95-27456
LDEF: 69 Months in Space. Third Post-Retrieval Symposium, part 3
[NASA-CP-3275-PT-3] p 2466 N95-27629
An overview of the Evaluation of Oxygen Interactions with Materials 3 experiment: Space Shuttle Mission 46, July-August 1992 p 2210 N95-27630
Evaluation of Oxygen Interactions with Materials 3: Mission and induced environments
p 2210 N95-27631
Spacecraft materials studies on the Aerospace Corporation tray on EOIM-3 p 2210 N95-27632
Exposure of LDEF materials to atomic oxygen: Results of EOIM 3 p 2210 N95-27633
LEO degradation of graphite and carbon-based composites aboard Space Shuttle Flight STS-46
p 2199 N95-27636
Orbital atomic oxygen effects on materials: An overview of MSFC experiments on the STS-46 EOIM-3
p 2419 N95-27637
Effects of atomic oxygen on polymeric materials flown on EOIM-3 p 2242 N95-27638
Thermal control materials on EOIM-3
p 2242 N95-27639
Solid film lubricants and thermal control coatings flown aboard the EOIM-3 MDA sub-experiment
p 2242 N95-27640

Evaluation of space environmental effects on metals and optical thin films on EOIM-3 p 2210 N95-27641
Analysis of selected specimens from the STS-46 Energetic Oxygen Interaction with Materials-3 experiment p 2210 N95-27642
Alternate use of rocket propellants as ingredients in commercial watergel explosives p 2176 N95-28321
Recovery and reuse of rocket motor propellant ingredients p 2177 N95-28326
Proof test methodology for composites p 2193 N95-28445
Impact damage resistance of composite fuselage structure, part 1 p 2138 N95-28482
NASA-ACEE/Boeing 737 graphite-epoxy horizontal stabilizer service p 2138 N95-28489
Nonlinear optical studies of surfaces [DE95-006574] p 2428 N95-28557
Material characterization system [AD-D017385] p 2210 N95-28584
In situ dynamic material property measurement system [AD-D017387] p 2210 N95-28585

MATHEMATICAL LOGIC
Digital systems validation. Chapter 20 Artificial Intelligenge with applications for aircraft. Handbbook, volume 2 [AD-A288492] p 2380 N95-26638
A case study in automated theorem proving: A difficult problem about commutators [DE95-008392] p 2392 N95-28173
Absolute logics [ISBN-951-41-0775-6] p 2397 N95-28238

MATHEMATICAL MODELS
Manual for SHOCK3D, version 2.0. Computer program for non-linear shock response [AD-A288631] p 2307 N95-26342
A finite element propagation model for extracting normal incidence impedance in nonprogressive acoustic wave fields [NASA-TM-110160] p 2400 N95-26394
Simulation model of the integrated flight/propulsion control system, displays, and propulsion system for ASTOVL lift-fan aircraft [NASA-TM-108866] p 2139 N95-26412
Quantitative modeling and analysis in environmental studies [AD-A288451] p 2326 N95-26431
FREZCHEM: A chemical-thermodynamic model for aqueous solutions at subzero temperatures [AD-A288456] p 2200 N95-26432
Atomic and electronic structure of clusters from Car-Parrinello method [DE94-634463] p 2403 N95-26437
Massively parallel self-consistent-field calculations [DE95-004128] p 2376 N95-26441
User's guide: Computer program for analysis of beam-column structures with nonlinear supports (CBEAMC) [AD-A289031] p 2307 N95-26464
Nonlinear scalespace via hierarchical statistical modeling [AD-A289057] p 2394 N95-26478
Development of a nonlinear simulation for the McDonnell Douglas F-15 Eagle with a longitudinal TECS control-law [AD-A288610] p 2128 N95-26481
The 1994 updated National Airspace System performance assessment for year 2005 [AD-A288652] p 2125 N95-26485
Development of an acuity-based nurse staffing system for the post anesthesia care unit [AD-A288831] p 2352 N95-26494
Intelligent computer based reliability assessment of multichip modules [AD-A288833] p 2259 N95-26550
A mathematical framework for an improved search model [AD-A288858] p 2358 N95-26552
Distributed computation of Pareto solutions for two decision makers [PB95-185047] p 2396 N95-26613
Theoretical studies of reaction surfaces [AD-A288458] p 2404 N95-26632
A parallel complexity model for functional languages [AD-A288589] p 2365 N95-26656
Development and validation of a blade-element mathematical model for the AH-64A Apache helicopter [NASA-TM-108863] p 2118 N95-26710
Numerical investigation to S-inlet flows (Numerical simulation study of S-inlet flows) [AD-A289590] p 2120 N95-26713
Joint services electronics program [AD-A289594] p 2260 N95-26716
Radiation production from stagnating compact toroids employing a nonequilibrium radiation diffusion model . [AD-A289602] p 2429 N95-26720
Numerical simulation of the flow about the F-18 HARV at high angle of attack [NASA-CR-197755] p 2121 N95-26735
Statistical model for molecular internal energy exchange in DSMC method for rarefied flow analysis [ISAS-R-654] p 2274 N95-26741
Soil moisture prediction during freeze and thaw using a coupled heat and moisture flow model [AD-A289343] p 2336 N95-26753
Progress towards computer simulation of NiH2 battery performance over life p 2272 N95-26786
Photoacoustic chambers for studying solids and gases: Theory and practical examples [IFTR-39/1994] p 2143 N95-26837
Study of damage evolutions in composite plates subjected to bending loads using micro-macro analysis [AD-A288523] p 2308 N95-26839
A numerical model to predict the fate of jettisoned aviation fuel [AD-A289336] p 2242 N95-26842
Viscoplastic characterization and fatigue modeling of titanium based metal matrix composites [AD-A289430] p 2181 N95-26868
A model of bubble evolution during decompression based on a Monte Carlo simulation of inert gas diffusion [AD-A289400] p 2353 N95-26885
Calculation of suspended sediment transport by combined wave-current flows [AD-A289368] p 2346 N95-26904
Control of a large space structure using multiple model adaptive estimation and control techniques [AD-A289309] p 2162 N95-26916
A gain scheduling optimization method using genetic algorithms [AD-A289306] p 2381 N95-26920
Design and characterization of resonant cavity light-emitting diodes [AD-A289307] p 2261 N95-26921
Aircraft nosewheel steering simulation p 2118 N95-26944
A state-space model of a large, lightly damped space structure using the Eigensystem realization algorithm [AD-A289251] p 2163 N95-26970
A brief history of laser guided lightning discharge models and experiments [AD-A289448] p 2295 N95-27022
Computing NORAD mean orbital elements from a state vector [AD-A289281] p 2146 N95-27033
Implementation and demonstration of a multiple model adaptive estimation failure detection system for the F-16 [AD-A289301] p 2131 N95-27042
Modeling of trapping and abrupt doping effects in MESFET's using R-dynamic element [PB95-184891] p 2262 N95-27050
A study of internal damage of metal matrix composites by neutron diffraction [DE95-005157] p 2182 N95-27080
Space modeler: An expanded, distributed, virtual environment for space visualization [AD-A289409] p 2461 N95-27131
A methodology to assess the utility of future space systems [AD-A289414] p 2144 N95-27133
Modeling considerations in the prediction of residual strength in composite laminates [AD-A289128] p 2182 N95-27142
A multi-attribute-utility-theory model that minimizes interview-data requirements: A consolidation of space launch decisions [AD-A289421] p 2164 N95-27144
Assessment of the AN/FPS-118 Ionospheric model and proposed improvements [AD-A289439] p 2337 N95-27146
A finite element based technique for simulation helix TWT interaction circuit thermal behavior [AD-A289552] p 2262 N95-27152
Probabilistic material strength degradation model for Inconel 718 components subjected to high temperature, high-cycle and low-cycle mechanical fatigue, creep and thermal fatigue effects [NASA-CR-197832] p 2214 N95-27167
Flow control [AD-A289262] p 2279 N95-27197
Mathematical simulation of three-dimensional magnetic field of spectrometric magnet SP-40 [DE95-608736] p 2398 N95-27239
Effects of bearing cleaning and lube environment on bearing performance p 2158 N95-27285
Ball bearing vibrations amplitude modeling and test comparisons p 2158 N95-27286
Model of a single impurity in a wide bandgap semiconductor describing electric field screening [AD-A289322] p 2264 N95-27296
Analysis of gas absorption to a thin liquid film in the presence of a zero-order chemical reaction p 2280 N95-27348
Features and applications of the Groove Analysis Program (GAP) p 2281 N95-27349
RTE: A computer code for Rocket Thermal Evaluation p 2177 N95-27355
A probabilistic model of a porous heat exchanger p 2282 N95-27359
A verification procedure for MSC/NASTRAN Finite Element Models [NASA-CR-4675] p 2131 N95-27371
Improved numerical solution of mixed H2/H(infinity) optimization with applications [AD-A289315] p 2386 N95-27400
Micromechanical modeling of damage and inelasticity of composite materials in macroscopic structural analysis [DE95-003666] p 2182 N95-27421
A new finite element formulation for incompressible flow [DE95-007141] p 2284 N95-27454
A case for dynamic sets in operating systems [AD-A289354] p 2454 N95-27529
LDEF: 69 Months in Space. Third Post-Retrieval Symposium, part 3 [NASA-CP-3275-PT-3] p 2466 N95-27629
An overview of the Evaluation of Oxygen Interactions with Materials 3 experiment: Space Shuttle Mission 46, July-August 1992 p 2210 N95-27630
Theoretical and experimental models of the diffuse radar backscatter from Mars [NASA-CR-198650] p 2463 N95-27700
Crossover integral equation theory for the liquid structure study [DE95-609155] p 2218 N95-27757
Flight Mechanics/Estimation Theory Symposium 1995 [NASA-CP-3299] p 2146 N95-27763
Evaluation and modeling of autonomous attitude thrust control for the Geostation Operational Environmental Satellite (GOES)-8 orbit determination p 2146 N95-27765
Accurate orbit determination strategies for the tracking and data relay satellites p 2147 N95-27768
Attitude determination using an adaptive multiple model filtering Scheme p 2148 N95-27772
An automated method of tuning an attitude estimator p 2148 N95-27774
An MME-based attitude estimator using vector observations p 2148 N95-27775
Post Kalman progress p 2148 N95-27776
Optimal attitude maneuver execution for the Advanced Composition Explorer (ACE) mission p 2149 N95-27778
Use of nonlinear identification in robust attitude and attitude rate estimation for SAMPEX p 2149 N95-27781
Earth horizon modeling and application to static Earth sensors on TRMM spacecraft p 2150 N95-27783
Telemetry down-link Doppler as an attitude sensor for spin stabilized spacecraft p 2150 N95-27785
Application of non-coherent Doppler data types for deep space navigation p 2151 N95-27788
A magnetic hysteresis model p 2153 N95-27801
A microstructurally based model of solder joints under conditions of thermomechanical fatigue [DE95-006226] p 2309 N95-27837
Vibration analysis of a split path gearbox [NASA-TM-106875] p 2302 N95-27855
Load transfer in the stiffener-to-skin joints of a pressurized fuselage [NASA-CR-198610] p 2310 N95-27865
Tungsten carbide fragmentation: Experimental characterization and numerical modelling [DE95-008521] p 2236 N95-27879
A diagram technique for strongly interacting fermion systems. One-and two-band Hubbard models [DE95-609437] p 2410 N95-27881
Precision landing system mathematical modeling study report for Andrews Air Force Base, runway 19L, Camp Springs, MD [AD-A289015] p 2127 N95-27903
A summary documentation of the AMIP models [DE95-008343] p 2338 N95-27931
Collected papers on wind turbine technology [NASA-CR-195432] p 2321 N95-27970
Large HAWT wake measurement and analysis p 2289 N95-27973
Preliminary analysis of dynamic stall effects on a 91-meter wind turbine rotor p 2124 N95-27975
Comparative wind tunnel tests of NACA 23024 airfoils with several aileron and spoiler configurations p 2124 N95-27976
Comparative performance tests on the Mod-2, 2.5-mW wind turbine with and without vortex generators p 2124 N95-27978

Design of a real-time wind turbine simulator using a custom parallel architecture p 2322 N95-27979
Aeroelastic stability of wind turbine blade/aileron systems p 2124 N95-27981
UEDGE and DEGAS modeling of the DIII-D scrape-off layer plasma, revision 1
[DE95-008052] p 2433 N95-28065
Testing the correlation between seismic stratigraphy, diagenesis and physical rock properties: Evaluation of fluid flow during early and late diagenesis
[DE95-008338] p 2338 N95-28083
Beyond transition state theory: Rigorous quantum approaches for determining chemical reaction rates
[DE95-008483] p 2208 N95-28086
Deformation limits on two-parameter fracture mechanics in terms of higher order asymptotics
[AD-A289113] p 2310 N95-28098
Whirl plus tilt
[DE95-007948] p 2399 N95-28108
One dimensional global and local solution for ICRF heating
[DE95-007984] p 2392 N95-28110
Anomalous cloud absorption? A critique of the paper entitled Absorption of Solar Radiation by Clouds: Observations Versus Models
[DE95-007703] p 2331 N95-28121
Beam-beam interaction working group summary
[DE95-007824] p 2422 N95-28123
Comprehensive numerical model for CW vertical-cavity surface-emitting lasers
[DE95-007758] p 2299 N95-28132
An introductory guide to uncertainty analysis in environmental and health risk assessment. Environmental Restoration Program
[DE95-008097] p 2354 N95-28136
Accuracy issues in modeling superplastic metal forming
[DE95-008934] p 2222 N95-28163
The real structure of columnar pinning centers in heavy-ion-irradiated cuprate superconductors
[DE95-003948] p 2445 N95-28186
Fowler DMO and time migration for transversely isotropic media with explicit operators
[DE95-007671] p 2339 N95-28194
Operator modeling in commerical aviation: Cognitive models, intelligent displays, and pilot's assistants
[NASA-CR-198609] p 2138 N95-28203
Aeroelasticity and structural optimization of composite helicopter rotor blades with swept tips
[NASA-CR-4665] p 2136 N95-28262
Analysis of aircraft engine blade subject to ice impact
p 2141 N95-28277
Higher order finite element analysis of thick composite laminates p 2186 N95-28282
OB/OD treatment: The effective use of measured field data and air modeling to support an environmental assessment p 2170 N95-28296
Use of SURFACE CHEMKIN to model multiphase atmospheric chemistry: Application to nitrogen tetroxide spills p 2172 N95-28305
Modeling the shock response of submerged structures
[AD-A289082] p 2288 N95-28351
Effect of the fiber-matrix interphase on the transverse tensile strength of the unidirectional composite material
p 2190 N95-28425
Structural design optimization with survivability dependent constraints application: Primary wing box of a multi-role fighter p 2137 N95-28440
Uncertainties in obtaining high reliability from stress-strength models p 2193 N95-28442
Proof test methodology for composites
p 2193 N95-28445
Measurement-based MESFET model in APLAC
[PB95-195483] p 2269 N95-28448
Designers' unified cost model p 2194 N95-28464
Local design optimization for composite transport fuselage crown panels p 2137 N95-28473
Nonlinear dynamics and aeroelasticity of rotorcraft in forward flight
[AD-A291714] p 2136 N95-28504
Visualization methods for the exploration of high dimensional data
[AD-A291717] p 2393 N95-28507
Structure of high-speed sprays
[AD-A291696] p 2288 N95-28523
Stochastic control and topics in applied probability
[AD-A291712] p 2395 N95-28526
Bilateral force feedback for hydraulically actuated systems
[AD-A291632] p 2387 N95-28545
Models used to forecast agricultural corn crops in the micro-region of Ribeirao Preto-SP
[INPE-5513-NTC/309] p 2315 N95-28554
Visualization of finite element model solutions for defibrillation voltage and current distributions
[AD-A289836] p 2400 N95-28579
Development of a TECS control-law for the lateral directional axis of the McDonnell Douglas F-15 Eagle
[AD-A289771] p 2142 N95-28598
Critical behaviour of spin models: A transfer-matrix approach
[PB95-192456] p 2418 N95-28638
Simulation of burning tokamak plasmas
[PB95-195426] p 2435 N95-28654
Chua's circuits: Phenomena and applications
[AD-A291638] p 2271 N95-28666

MATHEMATICAL PROGRAMMING
Improved numerical solution of mixed H2/H(infinity) optimization with applications
[AD-A289315] p 2386 N95-27400
Solving recursive domain equations with enriched categories
[AD-A289358] p 2371 N95-27418
Building an electronic book on the Internet. CSEP:An interdisciplinary syllabus for teaching computational science at the graduate level
[DE95-006526] p 2375 N95-28632

MATRICES (MATHEMATICS)
Performance evaluation of a new parallel preconditioner
[AD-A288563] p 2376 N95-26529
Structures for time-reversed inversion in filter banks
[AD-A289238] p 2261 N95-26964
A path-oriented knowledge representation system: Defusing the combinatorial system p 2386 N95-27395
Estimation of attitude sensor timetag biases
p 2153 N95-27799
Symmetries of the KAC-Peterson modular matrices of affine algebras
[PB95-190138] p 2392 N95-28010
Computational and matrix isolation studies of (2- and 3-furyl)methylene
[AD-A280085] p 2178 N95-28154
Coordinates of the quantum plane as q-tensor operators in U(sub q) (su(2) * su(2))
[DE95-007100] p 2397 N95-28234
Applications of boundary element methods on the Intel Paragon
[DE94-014135] p 2393 N95-28393
The structure of the Hurwitz transformation
[DE95-608759] p 2397 N95-28518
Modeling helicopter blade dynamics using a modified Myklestad-Prohl transfer matrix method
[AD-A289891] p 2136 N95-28626

MATRIX MATERIALS
Design of a unidirectional composite momentum wheel rim
[NASA-TM-106911] p 2164 N95-27761

MATRIX METHODS
Analysis and development of finite element methods for the study of nonlinear thermomechanical behavior of structural components
[NASA-CR-195354] p 2307 N95-26387
Modified eigenvalue problems with applications to structural dynamic re-analysis on parallel computers
[AD-A288257] p 2307 N95-26547
The effects of finite element grid density on model correlation and damage detection of a bridge
[DE94-018895] p 2309 N95-27305
Modeling helicopter blade dynamics using a modified Myklestad-Prohl transfer matrix method
[AD-A289891] p 2136 N95-28626

MATRIX THEORY
Do we fully understand the symmetric Lanczos algorithm yet?
[AD-A289614] p 2368 N95-26855
The surface of liquid He-4 at nonzero temperatures
[DE95-607841] p 2207 N95-27880

MATTER (PHYSICS)
Lattice calculation for lepton capture from vacuum-pair production in relativistic heavy-ion collisions
[DE95-007392] p 2413 N95-28077

MAXIMUM ENTROPY METHOD
Truncated Gaussians as tolerance sets
[NASA-CR-197732] p 2395 N95-27417
Stationary neutrino radiation transport by maximum entropy closure
[DE95-006579] p 2463 N95-28558
A study of heart rate and heart rate variability during rapid decompression to 50,000 ft
[AD-A291598] p 2355 N95-28561

MAXIMUM LIKELIHOOD ESTIMATES
Balanced data focusing: Direction of arrival estimation with maximum likelihood performance
[AD-A288252] p 2248 N95-26407
A method to determine the structure of an unknown mixture using the Akaike Information Criterion and the bootstrap
[AD-A288295] p 2394 N95-26415
Fast multidimensional density estimation based on Random-width bins
[AD-A288286] p 2394 N95-26457
Low-angle tracking in the presence of ducting, coherent and incoherent multipath
[AD-A289838] p 2258 N95-28580

MAXIMUM PRINCIPLE
Stochastic control and topics in applied probability
[AD-A291712] p 2395 N95-28526

MAXWELL EQUATION
Matrix kernels for MEG and EEG source localization and imaging
[DE95-005238] p 2354 N95-27426
The origin of spurious solutions in computational electromagnetics
[NASA-TM-106921] p 2391 N95-27726
Time-dependent model for vertical-cavity surface-emitting laser
[DE95-007880] p 2298 N95-28027
Finite pulse effects in self-amplified-spontaneous emission
[DE95-006585] p 2298 N95-28104

MCDONNELL AIRCRAFT
Performance study for inlet installations
[NASA-CR-189714] p 2140 N95-28227

MCDONNELL DOUGLAS AIRCRAFT
Strategy in the commercial aircraft industry in the United States: A comparison of decisionmaking by McDonnell-Douglas and Boeing aircraft companies from 1977-1983
[AD-A288289] p 2117 N95-26409

MCMURDO SOUND
Live from Antarctica: The coldest, windiest place on Earth
[NASA-CR-197737] p 2335 N95-26595
Live from Antarctica, volume 4
[NASA-CR-197828] p 2335 N95-26596
Subsurface radar investigations at the Pegasus Glacial-ice Runway and Williams Field, McMurdo Station, Antarctica
[AD-A289323] p 2144 N95-27297
FY 1994 ambient air monitoring report for McMurdo Station, Antarctica
[DE95-008565] p 2331 N95-28149

MEAN SQUARE VALUES
The fBm Interpolator
[AD-A288996] p 2388 N95-26459
Study of parity and time reversal violation in neutron-nucleus interactions
[DE95-005158] p 2405 N95-27081
Situation in study of electric polarizability and mean square charge radius of the neutron
[DE95-608869] p 2415 N95-28247

MEASURE AND INTEGRATION
Adaptive finite element method I: Solution algorithm and computational examples
[AD-A288979] p 2389 N95-26609
Robust integration schemes for generalized viscoplasticity with internal-state variables. Part 1: Theoretical developments and applications
[NASA-CR-195452-PT-1] p 2310 N95-28031
Robust integration schemes for generalized viscoplasticity with internal-state variables. Part 2: Algorithmic developments and implementation
[NASA-CR-195453-PT-2] p 2310 N95-28032

MEASURING INSTRUMENTS
Flutter clearance flight tests of an OV-10A airplane modified for wake vortex flight experiments
[NASA-TM-109168] p 2117 N95-26381
Split pipe testing device for the measurement of bond of reinforcement under controlled confinement
[AD-D017258] p 2245 N95-26500
Nondestructive testing apparatus for determining the orientation of reinforcing bars within a concrete structure
[AD-D017267] p 2245 N95-26508
Rheological measurement methods for fibre filled plastics
[PB95-190088] p 2226 N95-26744
Multi-channel electronically scanned cryogenic pressure sensor
[NASA-CASE-LAR-15062-1] p 2291 N95-27138
Load measurement system with load cell lock-out mechanism p 2159 N95-27291
The gluon propagator in non-Abelian Weizsaecker-Williams fields
[DE95-006877] p 2449 N95-27547
The orbital debris detector consortium: Suppliers of instruments for in-situ measurements of small-particles in the space environment p 2294 N95-27670
Search for exotic particles at CDF
[DE95-008383] p 2411 N95-27933

MECHANICAL DEVICES
Ultra-high, resolution, modular optical angle encoder for space-based opto-mechanical applications
p 2156 N95-27270
Development of a high force thermal latch
p 2157 N95-27275
The Solar X-ray Imager Vacuum Door Assembly
p 2157 N95-27280

FORTE antenna element and release mechanism design p 2157 N95-27282
Development and testing of the rack insertion device p 2158 N95-27289
Linear Proof Mass Actuator p 2158 N95-27290
Automatic locking knee brace joint
[NASA-CASE-MFS-28997-1] p 2360 N95-27501

MECHANICAL DRIVES
Testing of Uninterruptible Power Supplies with nonlinear loads
[AD-A289353] p 2262 N95-27067
Direct drive options for electric propulsion systems
[NASA-TM-106576] p 2168 N95-27861
Control system design for the MOD-5A 7.3 mW wind turbine generator p 2306 N95-27985
Variable speed generator application on the MOD-5A 7.3 mW wind turbine generator p 2273 N95-27989
Low-power, parallel photonic interconnections for Multi-Chip Module applications
[DE95-008518] p 2267 N95-28147

MECHANICAL ENGINEERING
Intelligent computer based reliability assessment of multichip modules
[AD-A288833] p 2259 N95-26550
Getting it right, making it better
[NONP-NASA-VT-95-49118] p 2451 N95-27206
NIST: Information management in the AMRF
[NONP-NASA-VT-95-49120] p 2454 N95-27208

MECHANICAL IMPEDANCE
One dimensional global and local solution for ICRF heating
[DE95-007984] p 2392 N95-28110

MECHANICAL MEASUREMENT
Power train torque measurement
[AD-A289577] p 2301 N95-26688

MECHANICAL PROPERTIES
Determination of the cyclical properties of 18G2A steel on the basis of skeleton curves for a planar stress state
[IFTR-32/1994] p 2211 N95-26359
Material modeling in the CRALE code. Users' manual
[AD-A288988] p 2178 N95-26712
Mechanical performance of fiber reinforced metal matrix composites and microstructural development of polycrystalline alumina fibers synthesized from liquid precursors
[AD-A289518] p 2181 N95-26847
Effects of helium pre-implantation on the microstructure and mechanical properties of irradiated 316 stainless steel
[DE95-007162] p 2214 N95-27086
Fatigue behavior of a cross-ply ceramic matrix composite subjected to tension-tension cycling with hold time
[AD-A289418] p 2182 N95-27134
Bimaterial interlaces and their role in the mechanical performance of the in-situ composites
[AD-A288973] p 2182 N95-27188
Current programmes on physical metallurgy and related areas in BARC
[DE95-607939] p 2214 N95-27255
Review of activities in USA on HTS materials
[DE95-006404] p 2234 N95-27468
ECR plasma-assisted deposition of Al2O3 and dispersion-strengthened AlO2
[DE95-007743] p 2235 N95-27687
Using hob offset to balance dynamic strength in spur gears
[NASA-TM-106934] p 2302 N95-27698
Prediction of material strength and fracture of glass using the SPHINX smooth particle hydrodynamics code
[DE95-004869] p 2236 N95-27943
Trace elements and the mechanical properties of intermetallic compounds
[DE95-007378] p 2220 N95-28046
High temperature Hexoloy(trademark) SX silicon carbide
[DE95-007290] p 2221 N95-28075
Through-the Thickness(R) braided composites for aircraft applications p 2185 N95-28273
Designing for time-dependent material response in spacecraft structures p 2166 N95-28292
Functionalized block copolymers as adhesion promoters
[DE95-008158] p 2239 N95-28400
Mechanical properties of Hysol EA-9394 structural adhesive
[DE95-008187] p 2240 N95-28405
Application of advanced material systems to composite frame elements p 2191 N95-28432

MECHANICAL SHOCK
Manual for SHOCK3D, version 2.0. Computer program for non-linear shock response
[AD-A288631] p 2307 N95-26342

MECHANICS (PHYSICS)
Stability and thermal influences in nonlinear continuum mechanics and material science
[AD-A288333] p 2448 N95-26563

MEDIAN (STATISTICS)
Variability study of foF2 for an equatorial station
[DE95-608080] p 2337 N95-27157

MEDICAL PERSONNEL
Aerospace medicine
[AD-A289691] p 2353 N95-26763

MEDICAL SERVICES
Development of an acuity-based nurse staffing system for the post anesthesia care unit
[AD-A288831] p 2352 N95-26494
Aerospace medicine
[AD-A289691] p 2353 N95-26763

MEDITERRANEAN SEA
Deep convection in the Mediterranean Sea
[AD-A288497] p 2346 N95-26647

MELTING
Tensile properties of Fe-16 at. % Al alloys
[DE95-007102] p 2215 N95-27450
Electrolyte effects in Li(Si)/FeS2 thermal batteries
[DE95-001614] p 2264 N95-27474
Surface crystallization and thin film melting in normal alkanes
[DE95-006694] p 2440 N95-27535

MELTING POINTS
BIPM project: Intercomparison of water triple-point cells
[PB95-185237] p 2398 N95-26614
Electrolyte effects in Li(Si)/FeS2 thermal batteries
[DE95-001614] p 2264 N95-27474
High energy electron beams for ceramic joining
[DE95-006316] p 2420 N95-27480

MEMBRANES
Investigation of the interface between immiscible electrolytes applied to membrane electrochemistry
[AD-A288887] p 2199 N95-26350
Template synthesis of electronically conductive polymer nanostructures
[AD-A288373] p 2225 N95-26472

MEMORY
Codes of processing and multiple resources: Model and methodology
[AD-A289583] p 2355 N95-26691
Subjective workload assessment in a spatial memory task
[AD-A289491] p 2356 N95-26825

MEMORY (COMPUTERS)
JPRS report: Science and technology. Central Eurasia
[JPRS-UST-95-019] p 2270 N95-28565

MENTAL PERFORMANCE
Performance enhancing ration components program: Supplemental carbohydrate test
[AD-A288560] p 2358 N95-26558
Codes of processing and multiple resources: Model and methodology
[AD-A289583] p 2355 N95-26691
Handbook of perception and human performance, volume 2. Cognitive processes and performance
[AD-A289587] p 2355 N95-26692
Subjective workload assessment in a spatial memory task
[AD-A289491] p 2356 N95-26825
Change, Learning and Mental Work in Organizations: Working papers of the 3rd Otaniemi-Dresden Workshop
[PB95-184941] p 2356 N95-26909

MERCURY CADMIUM TELLURIDES
Electronic characterization of defects in narrow gap semiconductors: Comparison of electronic energy levels and formation energies in mercury cadmium telluride, mercury zinc telluride, and mercury zinc selenide
[NASA-CR-197835] p 2437 N95-26780

MERCURY LAMPS
Radiant exchange considerations in design and scaleup of photocatalytic reactors for purification of nitroglycerine-contaminated air p 2171 N95-28300

MERCURY TELLURIDES
Electronic characterization of defects in narrow gap semiconductors: Comparison of electronic energy levels and formation energies in mercury cadmium telluride, mercury zinc telluride, and mercury zinc selenide
[NASA-CR-197835] p 2437 N95-26780

MESOMETEOROLOGY
Fluxes across the west coast resolved by Picket Fence observations during stormfest
[AD-A288511] p 2341 N95-26653
Three-dimensional forecast models for emergency response management p 2172 N95-28303

MESONS
Preliminary heavy-light decay constants from the MILC Collaboration
[DE95-005685] p 2409 N95-27552
The physics program and status of the SLAC B-Factory and detector
[DE95-006562] p 2409 N95-27676
Excited Charm States
[DE95-005749] p 2409 N95-27747
Phenomenology from 100 large lattices
[DE95-006349] p 2442 N95-27994
Measurement of the reaction C(nu(sub mu), mu(-)) X near threshold
[DE95-007888] p 2412 N95-28063
Polarization as a probe to the production mechanisms of charmonium in (pi)N collisions
[DE95-008136] p 2414 N95-28142
Aspects of strange matter
[DE95-008316] p 2414 N95-28170
Some aspects of the OZI-rule violation in the reaction anti-pp yields phi pi(0)
[DE95-608853] p 2415 N95-28245
Constraints on the anomalous WW gamma couplings from b vector s gamma
[DE95-608866] p 2415 N95-28246
Weak matrix elements efforts on the lattice: Status and prospects
[DE95-007701] p 2416 N95-28355
Production and decay of hybrid mesons by flux-tube breaking
[PB95-192837] p 2418 N95-28640

MESOSCALE PHENOMENA
Indexing meso-beta surface wind site representative
[AD-A288501] p 2341 N95-26650
Fluxes across the west coast resolved by Picket Fence observations during stormfest
[AD-A288511] p 2341 N95-26653
Three-dimensional forecast models for emergency response management p 2172 N95-28303

MESSAGE PROCESSING
Two implementation relations and the correctness of communicating replicated processes
[PB95-195640] p 2375 N95-28645

MESSAGES
Replacing the message service component in an integration framework
[AD-A289928] p 2375 N95-28628

METAL BONDING
Theoretical studies of reaction surfaces
[AD-A288458] p 2404 N95-26632

METAL CLUSTERS
Atomic and electronic structure of clusters from Car-Parrinello method
[DE94-634463] p 2403 N95-26437
Particle-like absorption spectra in small transition metal clusters
[DE95-007082] p 2218 N95-27752
Experimental determination of cluster geometrical structure
[DE95-007089] p 2409 N95-27753

METAL COATINGS
Effect of surface coating on one-dimensional system subjected to unit step pressure wave
[AD-A288237] p 2308 N95-26625
Weightless Environment Training Facility (WETF) materials coating evaluation, volume 1
[NASA-CR-188366-VOL-1] p 2239 N95-28385
Surface scanning techniques to locate and study defects in painted zinc and zinc alloy coated steels
[DE95-006099] p 2240 N95-28547

METAL CRYSTALS
The high strain rate deformation of tungsten single crystals
[AD-A288874] p 2223 N95-28189

METAL FATIGUE
Changes in the anisotropy parameters of an aluminum alloy caused by cyclical deformation
[IFTR-27/1994] p 2212 N95-26666
Comparison of life theories for rolling-element bearings
[NASA-TM-106585] p 2301 N95-26774
Viscoplastic characterization and fatigue modeling of titanium based metal matrix composites
[AD-A289430] p 2181 N95-26868
Adhesively bonded composite patch repair of cracked aluminum alloy structures p 2132 N95-27507
A new Cu-8 Cr-4 Nb alloy for high temperature applications
[NASA-TM-106910] p 2218 N95-27728
Fatigue properties of an A356 (AlSi7Mg) aluminum alloy for automotive applications: Fatigue life prediction
[PB95-196424] p 2224 N95-28660

METAL FILMS
Elastic properties of metallic superlattices
[AD-A288699] p 2212 N95-26490
Toward molecular selectivity with chemically modified electrodes: Can electroactivity and permeability through an overlaying metallopolymer film be controlled via rational manipulation of internal architecture?
[AD-A288719] p 2403 N95-26491
Bimaterial interlaces and their role in the mechanical performance of the in-situ composites
[AD-A288973] p 2182 N95-27188
Evaluation of space environmental effects on metals and optical thin films on EOIM-3 p 2210 N95-27641

Cesium/oxide interactions for ultrathin films on (alpha)-Al2O3(001) and (alpha)-Al2O3(1(bar 1)O2)
[DE95-008159] p 2238 N95-28358

METAL FINISHING
Precision parts cleaning with supercritical carbon dioxide p 2229 N95-27114
Plasma source ion implantation of ammonia into electroplated chromium
[DE95-006275] p 2444 N95-28125

METAL FLUORIDES
Muon spin relaxation in antiferromagnets: A study of RbMnF3 based on the coupled-mode theory of paramagnetic and critical spin fluctuations
[PB95-192878] p 2418 N95-28642

METAL FOAMS
Indentability of conventional and negative Poisson's ratio foams p 2195 N95-28472

METAL FOILS
Composite heat pipe development status: Development of lightweight prototype carbon-carbon heat pipe with integral fins and metal foil liner
[NASA-TM-106909] p 2283 N95-27369
Characterization of defects in deuterium-implanted beryllium
[DE95-005688] p 2217 N95-27553
Development of an optical trap as an ultra-sensitive analytical tool
[DE95-007843] p 2426 N95-28022

METAL HYDRIDES
Calorimetric evaluation of commercial Ni-MH cells and charges p 2272 N95-26790
Nickel metal hydride LEO cycle testing
p 2272 N95-26791

METAL IONS
Plume measurements with the T5 xenon ion thruster
[AD-A288697] p 2167 N95-26489
Non-covalent immobilization of proteins and enzymes on polymerized lipid assemblies
[AD-A288234] p 2225 N95-26526
Ethyl lactate as a solvent alternative for cleaning metal parts p 2229 N95-27112
Defect characterization of electronic conducting pseudo-perovskite systems
[DE95-007487] p 2220 N95-28049
Mutagenesis in human cells with accelerated H and Fe ions
[NASA-CR-198599] p 2351 N95-28177
Lithium ion rechargeable systems studies
[DE95-006810] p 2268 N95-28200
Development of an ultra-safe rechargeable lithium-ion battery
[AD-A288959] p 2269 N95-28349
Characterization of solid state laser and nonlinear optical materials
[AD-A291684] p 2300 N95-28458
A model of the diurnal variation in magnesium ion density and radiance in the thermosphere
[AD-A289824] p 2339 N95-28575

METAL MATRIX COMPOSITES
Concurrent engineering research center
[NASA-CR-197726] p 2362 N95-26386
Mechanical performance of fiber reinforced metal matrix composites and microstructural development of polycrystalline alumina fibers synthesized from liquid precursors
[AD-A289518] p 2181 N95-26847
Ductile - ductile beryllium aluminum metal matrix composite manufactured by extrusion
[AD-A289519] p 2181 N95-26848
Fatigue behavior of a cross-ply metal matrix composite at elevated temperature under strain controlled mode
[AD-A289425] p 2181 N95-26865
Viscoplastic characterization and fatigue modeling of titanium based metal matrix composites
[AD-A289430] p 2181 N95-26868
A study of internal damage of metal matrix composites by neutron diffraction
[DE95-005157] p 2182 N95-27080
Design, analysis, and testing of a metal matrix composite web/flange intersection p 2191 N95-28433

METAL OXIDE SEMICONDUCTORS
Comparison of the resistance of the MOS integrated circuits with various types of nuclear radiation
[DE95-608623] p 2261 N95-27023
Microwave characterization of sub-micron N- and P-channel MOSFET's fabricated with thin film silicon-on-sapphire
[AD-A289296] p 2438 N95-27040

METAL OXIDES
Material analysis using combined Elastic Recoil Detection and Rutherford/Enhanced Rutherford Backscattering Spectrometry
[DE95-005415] p 2205 N95-27681
Defect characterization of electronic conducting pseudo-perovskite systems
[DE95-007487] p 2220 N95-28049

METAL POWDER
Lattice parameters and Debye-Waller factors of gamma-TiAl alloys
[AD-A288843] p 2213 N95-26681
Ultra high purity, dimensionally stable INVAR 36
[NASA-CASE-NPO-19358-1-CU] p 2213 N95-26862
Electrolyte effects in Li(Si)/FeS2 thermal batteries
[DE95-001614] p 2264 N95-27474

METAL SURFACES
Ethyl lactate as a solvent alternative for cleaning metal parts p 2229 N95-27112
Corrosive effects of supercritical carbon dioxide and cosolvents on metals p 2224 N95-27113
Precision parts cleaning with supercritical carbon dioxide p 2229 N95-27114
Fluid dynamic effects on precision cleaning with supercritical fluids p 2232 N95-27129
Laser ultrasonic generation at the surface of a liquid metal
[DE95-004999] p 2216 N95-27477
Simulations of metal dissolution and corrosion
[DE95-007486] p 2218 N95-27748
Hydrogen induced C-C, C-N, and C-S bond activities on Pi and Ni surfaces
[DE95-006251] p 2206 N95-27838
Pulsed ion beam surface treatment for preparing rapidly solidified corrosion resistant steel and aluminum surfaces
[DE95-007741] p 2221 N95-28116
Plasma source ion implantation of ammonia into electroplated chromium
[DE95-006275] p 2444 N95-28125
The role of hydrogen in the hydrogenation and hydrogenolysis of aniline on the nickel single crystal surfaces: Its implication on the mechanisms of HDN reactions
[DE95-006687] p 2222 N95-28134
Surface scanning techniques to locate and study defects in painted zinc and zinc alloy coated steels
[DE95-006099] p 2240 N95-28547
Nonlinear optical studies of surfaces
[DE95-006574] p 2428 N95-28557
Mechanism of deposit formation on fuel-wetted hot metal surfaces
[AD-A289847] p 2210 N95-28621
TV-holography at high temperatures: In situ observations of the oxidation of advanced materials
[PB95-195343] p 2294 N95-28651

METAL VAPOR LASERS
Characteristics of thermal lens in a copper-vapor laser
[AD-A289545] p 2294 N95-26874

METAL VAPORS
Theoretical studies of reaction surfaces
[AD-A288458] p 2404 N95-26632
Copper CVD using liquid coinjection of (hfac)Cu(TMVS) and TMVS
[DE95-008155] p 2237 N95-28089

METAL WORKING
Forming metallurgy: Supervised drawing course, NTH
[PB95-196507] p 2219 N95-27934
Accuracy issues in modeling superplastic metal forming
[DE95-008934] p 2222 N95-28163

METAL-METAL BONDING
Development of an ultra-safe rechargeable lithium-ion battery
[AD-A288959] p 2269 N95-28349

METALLIC GLASSES
The structure of lead-indium phosphate glass
[DE95-007130] p 2237 N95-27967

METALLIC PLASMAS
A continuous emissions monitor for airborne metals
p 2174 N95-28313

METALLIZING
Magnetically controlled deposition of metals using gas plasma
[DE95-007248] p 2430 N95-27237
Low resistivity ohmic contacts to moderately doped n-GaAs with low temperature processing
[DE95-008507] p 2445 N95-28144
Non-destructive inter-level dielectric via in-line process monitoring by atomic force microscopy
[DE95-008516] p 2267 N95-28146

METALLURGY
Current programmes on physical metallurgy and related areas in BARC
[DE95-607939] p 2214 N95-27255
Improved hardness RHA weldability and material property testing
[AD-A289127] p 2221 N95-28102

METALS
Corrosive effects of supercritical carbon dioxide and cosolvents on metals p 2224 N95-27113
Molecular approach to mesoporous metal sulfides
[DE95-005418] p 2202 N95-27137
High energy electron beams for ceramic joining
[DE95-006316] p 2420 N95-27480
The role of edge dislocations in the deformation of BCC metals
[DE95-609157] p 2219 N95-27759
A diagram technique for strongly interacting fermion systems. One-and two-band Hubbard models
[DE95-609437] p 2410 N95-27881
Forming metallurgy: Supervised drawing course, NTH
[PB95-196507] p 2219 N95-27934
A continuous emissions monitor for airborne metals
p 2174 N95-28313
On the synthesis of mixed-metal and mixed-pnicogen13-15 ring-systems
[AD-A288869] p 2223 N95-28332
Investigation of HE driven cylindrical liner
[DE95-007866] p 2311 N95-28539
An overview of activities and accomplishments of the Metals and Ceramics Division
[DE95-007020] p 2241 N95-28560

METASTABLE STATE
AEM investigation of tetrahedrally coordinated Ti(4+) in nickel-titanate spinel
[DE95-006624] p 2215 N95-27473

METEORITE COLLISIONS
Tracking and impact prediction of Earth-Crossing-Objects (ECO's) on a collision course with Earth
[AD-A289321] p 2461 N95-27303

METEOROID CONCENTRATION
Orbiting meteoroid and debris counting experiment
p 2463 N95-27668

METEOROLOGICAL BALLOONS
Live from Antarctica, volume 4
[NASA-CR-197828] p 2335 N95-26596

METEOROLOGICAL PARAMETERS
Weather And Radar Processor (WARP) Test and Evaluation Master Plan (TEMP)
[AD-A288280] p 2340 N95-26453
Meteorological and oceanographic data collected during the ASREX 91 field experiment
[AD-A289492] p 2342 N95-26826
VOCAR: An experiment in Variability of Coastal Atmospheric Refractivity
[AD-A289202] p 2253 N95-27006
The distribution of cloud cover over the former USSR as derived from the RIHMI 223-Station 3-hourly meteorological database
[DE95-007046] p 2343 N95-27920
Models used to forecast agricultural corn crops in the micro-region of Ribeirao Preto-SP
[INPE-5513-NTC/309] p 2315 N95-28554

METEOROLOGICAL RADAR
Weather And Radar Processor (WARP) Test and Evaluation Master Plan (TEMP)
[AD-A288280] p 2340 N95-26453
Assessment of the AN/FPS-118 Ionospheric model and proposed improvements
[AD-A289439] p 2337 N95-27146
Report to the Chairman and Ranking Minority Member, Committee on Science, House of Representatives. Weather forecasting: Radar availability requirement not being met
[GAO/AIMD-95-132] p 2342 N95-27912

METEOROLOGICAL RESEARCH AIRCRAFT
Design of a high altitude long endurance aircraft with manufacturing considerations p 2119 N95-26947

METEOROLOGICAL SATELLITES
Reconstruction of an infrared band of meteorological satellite imagery with abductive networks
[SAIC-94/1062] p 2345 N95-27389
Earth horizon modeling and application to static Earth sensors on TRMM spacecraft p 2150 N95-27783
Contingency designs for attitude determination of TRMM p 2154 N95-27803

METEOROLOGY
Live from Antarctica: Then and now
[NASA-CR-197829] p 2335 N95-26594
An observational study on the onset of the summer monsoon over eastern Asia in 1979
[AD-A289637] p 2341 N95-26723
Emerging applications of probability (stochastic models in geosystems)
[AD-A289117] p 2313 N95-28099
Site scientific mission plan for the Southern Great Plains CART site, January-June 1995
[DE95-008393] p 2344 N95-28340

METHANE
Coupled chemistry/climate issues
[DE95-006443] p 2327 N95-27532
Transient studies of low temperature catalyst for methane conversion
[DE95-007913] p 2205 N95-27692
Mars Sample Return mission utilizing in-situ propellant production
[NASA-CR-188371] p 2145 N95-28261

METHODOLOGY
Fundamental concepts of integrated and fiber optic sensors
[NASA-TM-106920] p 2426 N95-27906
METHYL ALCOHOL
Corrosive effects of supercritical carbon dioxide and cosolvents on metals p 2224 N95-27113
Molecular approach to mesoporous metal sulfides
[DE95-005418] p 2202 N95-27137
NQR-NMR studies of higher alcohol synthesis Cu-Co catalysts
[DE95-007926] p 2205 N95-27680
FTIR studies of CH3OH on porous silicon
[AD-A289038] p 2207 N95-27904
Comparison of bridged polysilsesquioxane xerogels prepared from methoxy- and ethoxy-silyl monomers
[DE95-005422] p 2240 N95-28532
METHYL CHLORIDE
Atomically resolved STM study of the adsorption and dissociation of methyl chloride on Si(001)
[AD-A289218] p 2438 N95-27061
METHYL COMPOUNDS
Atomically resolved STM study of the adsorption and dissociation of methyl chloride on Si(001)
[AD-A289218] p 2438 N95-27061
On the synthesis of mixed-metal and mixed-pnicogen13-15 ring-systems
[AD-A288869] p 2223 N95-28332
Poly(N-arylenbenzimidazoles) via aromatic nucleophilic displacement
[NASA-CASE-LAR-14939-1] p 2179 N95-28360
METHYLENE
Computational and matrix isolation studies of (2- and 3-furyl)methylene
[AD-A280085] p 2178 N95-28154
METHYLHYDRAZINE
High pressure Earth storable rocket technology program: Basic program
[NASA-CR-195449] p 2166 N95-26390
A new method for measuring hypergol scrubber emissions p 2174 N95-28312
METRIC SPACE
Hyperkaehler metrics associated to compact Lie groups
[PB95-185161] p 2388 N95-26514
Nonexistence of bilipschitz parameterizations and geometric problems about A(sub infinity) weights
[PB95-185187] p 2396 N95-26538
An image quality analysis of ANVIS-6 night vision goggles
[AD-A289398] p 2359 N95-26883
METRICATION
Standards for excellence
[NONP-NASA-VT-95-49096] p 2451 N95-27202
METROLOGY
Standards for excellence
[NONP-NASA-VT-95-49096] p 2451 N95-27202
Getting it right, making it better
[NONP-NASA-VT-95-49118] p 2451 N95-27206
Methods development for measuring and classifying flammability/combustibility of refrigerants. Task 2: Test plan
[DE95-007066] p 2234 N95-27481
MICROANALYSIS
Positron microscopy
[DE95-007042] p 2410 N95-27874
Analytical electron microscopy of nanometer-sized particles
[AD-A289124] p 2413 N95-28101
MICROBEAMS
Analytical electron microscopy of nanometer-sized particles
[AD-A289124] p 2413 N95-28101
MICROBIOLOGY
Live from Antarctica: The coldest, windiest place on Earth
[NASA-CR-197737] p 2335 N95-26595
Environmentally Benign Cleaning and Degreasing Technology: JANNAF Safety and Protection Subcommittee and Propellant Development and Characterization Subcommittee Joint Workshop
[CPIA-PUBL-611] p 2227 N95-27101
Bioremediation of chlorinated organics: PCBs, TCE, HCFCs p 2179 N95-27117
Microbial treatment for shipboard collection, hold ing, and transfer system tanks p 2179 N95-27119
MICROCOMPUTERS
Magnetic field measurement for the spectrometric magnet of the ISTRA-M setup
[DE95-606560] p 2362 N95-27162
An ugly duckling becomes a swan (hor ellipsis): How an organization becomes customer focused through listening
[DE95-004974] p 2454 N95-27461
Control system design for the MOD-5A 7.3 mW wind turbine generator p 2306 N95-27985
MICROCRACKS
On the thermally-induced residual stresses in thick fiber-thermoplastic matrix (PEEK) cross-ply laminated plates p 2187 N95-28285
MICROCRYSTALS
Surfactants and desensitizing wax substitutes for TNT-Based systems
[AD-A289652] p 2243 N95-28634
MICROELECTRONICS
Microengineered conducting composites from nanochannel templates
[AD-A289573] p 2180 N95-26686
Microelectronics in Japan p 2263 N95-27227
Japan's technology and manufacturing infrastructure p 2263 N95-27229
The 77 K operation of a multi-resonant power converter
[NASA-TM-106941] p 2264 N95-27374
Manufacturing tailored property ceramic composites
[DE95-006303] p 2237 N95-27993
Swords to plowshares: Shock wave applications to advanced lithography
[DE95-008154] p 2299 N95-28223
JTEC Panel report on microelectromechanical systems in Japan
[NASA-CR-197831] p 2268 N95-28239
MICROGRAVITY
Design and development of experimental facilities for short duration, low-gravity combustion and fire experiments
[NASA-CR-195458] p 2244 N95-26709
Device and method for screening crystallization conditions in solution crystal growth
[NASA-CASE-MFS-28985-1] p 2245 N95-26888
Apparatus for diffusion controlled dialysis under microgravity conditions
[NASA-CASE-MFS-28986-1] p 2245 N95-27500
Two-phase flow research using the learjet apparatus
[NASA-TM-106814] p 2284 N95-27854
Tank pressure control in low gravity by jet mixing
[NASA-CR-191012] p 2243 N95-28001
Microgravity science and applications. Program tasks and bibliography for FY 1994
[NASA-TM-4677] p 2245 N95-28460
MICROGRAVITY APPLICATIONS
Microgravity science and applications. Program tasks and bibliography for FY 1994
[NASA-TM-4677] p 2245 N95-28460
MICROMECHANICS
Micron Accuracy Deployment Experiment (MADE), phase A. Volume 1
[NASA-CR-197792] p 2144 N95-26426
Micromechanical prediction of tensile damage for ceramic matrix composites under high temperature
[AD-A288238] p 2180 N95-26626
Study of damage evolutions in composite plates subjected to bending loads using micro-macro analysis
[AD-A288523] p 2308 N95-26839
Micromechanisms for optimism seismometer p 2159 N95-27292
Micromechanical modeling of damage and inelasticity of composite materials in macroscopic structural analysis
[DE95-003666] p 2182 N95-27421
Contact micromechanics in granular media with clay
[DE95-006566] p 2340 N95-28583
MICROMETEOROIDS
LDEF: 69 Months in Space. Third Post-Retrieval Symposium, part 3
[NASA-CP-3275-PT-3] p 2466 N95-27629
Orbiting meteoroid and debris counting experiment p 2463 N95-27668
MICROMETEOROLOGY
A study of lightning in winter thunderstorms and the analysis of thunderstorm overflight data
[NASA-CR-198577] p 2343 N95-28191
MICROMINIATURIZATION
JTEC Panel report on microelectromechanical systems in Japan
[NASA-CR-197831] p 2268 N95-28239
MICROORGANISMS
Bioremediation of chlorinated organics: PCBs, TCE, HCFCs p 2179 N95-27117
Microbial treatment for shipboard collection, hold ing, and transfer system tanks p 2179 N95-27119
Investigation on energy conversion technology using biochemical reaction elements, 2
[DE95-759250] p 2321 N95-27940
MICROPARTICLES
The 18th Asilomar Conference on Polymeric Materials
[AD-A291721] p 2240 N95-28508
MICROPOROSITY
Superior catalysts for selective catalytic reduction of nitric oxide
[DE95-007903] p 2205 N95-27691
Evaluation of microporous carbon filters as catalysts for ozone decomposition
[DE95-006498] p 2331 N95-28548
MICROPROCESSORS
Micro-time stress measurement device development
[AD-A289511] p 2361 N95-26845
MICROROCKET ENGINES
Micro electric propulsion feasibility
[NASA-CR-189139] p 2168 N95-28000
MICROSCOPES
The in situ observation of epitaxial diamond thin film nucleation and growth using emission electron microscopy
[AD-A289841] p 2447 N95-28618
MICROSCOPY
Determining nanoscale physical properties of materials by microscopy and spectroscopy
[AD-A289532] p 2201 N95-26870
Positron microscopy
[DE95-007042] p 2410 N95-27874
Nonlinear optical microscopy for imaging thin films and surfaces
[DE95-007872] p 2426 N95-28018
MICROSEISMS
Very low frequency seismo-acoustic noise below the sea floor (0.2-10 Hz)
[AD-A289164] p 2347 N95-27011
MICROSTRUCTURE
Process control of microstructure in manufacturing
[AD-A288291] p 2245 N95-26410
Characterization of Ultra-Low Carbon Baintic steels for use as weld wire consumables
[AD-A288292] p 2212 N95-26411
Survey of sub-micrometre powder size measurement for ceramic and cermet powders
[PB95-190104] p 2227 N95-26746
Mechanical performance of fiber reinforced metal matrix composites and microstructural development of polycrystalline alumina fibers synthesized from liquid precursors
[AD-A289518] p 2181 N95-26847
Effects of helium pre-implantation on the microstructure and mechanical properties of irradiated 316 stainless steel
[DE95-007162] p 2214 N95-27086
Current programmes on physical metallurgy and related areas in BARC
[DE95-607939] p 2214 N95-27255
Non-metallic oxide inclusion formation in C-Mnlow alloy steel welds
[DE94-019160] p 2215 N95-27319
Engineered materials for appliation in severe metallurgical environments: Tantalum-carbon alloy development
[DE95-006838] p 2216 N95-27488
Radiation-induced segregation: A microchemical gauge to quantify fundamental defect parameters
[DE95-005720] p 2216 N95-27492
Advances in welding science: A perspective
[DE95-006745] p 2302 N95-27545
LEO degradation of graphite and carbon-based composites aboard Space Shuttle Flight STS-46 p 2199 N95-27636
Effects of atomic oxygen on polymeric materials flown on EOIM-3 p 2242 N95-27638
ECR plasma-assisted deposition of Al2O3 and dispersion-strengthened AlO2
[DE95-007743] p 2235 N95-27687
Study of the phase transformations and microstructures of uranium rich alloys of the binary uranium-gallium system
[DE95-609624] p 2217 N95-27713
Ceramic fiber-reinforced monoclinic celsian phase glass-ceramic matrix composite material
[NASA-CASE-LEW-15714-1] p 2183 N95-27717
Micromagnetics and microstructure of epitaxially grown Co and Co-Cr films for perpendicular magnetic recording
[DE95-004681] p 2441 N95-27720
A microstructurally based model of solder joints under conditions of thermomechanical fatigue
[DE95-006226] p 2309 N95-27837
Sintering of textured YBa2Cu3O(7-x) under intensive Co-60 gamma irradiation
[DE95-007098] p 2442 N95-27950
Phase separation and ordering in InGaAsP and InGaAs materials
[DE95-007493] p 2443 N95-28050
Pulsed laser deposition of zeolitic membranes
[DE95-006274] p 2298 N95-28124
Cavity formation and impurity gettering in He-implanted Si
[DE95-007744] p 2444 N95-28127
Solid-state sintering of tungsten heavy alloys
[DE95-007749] p 2222 N95-28130

TEM characterization of Al/Al2O3 composite fabricated by reactive metal infiltration
[DE95-008508] p 2184 N95-28145
New developments for sol-gel film and fiber processing
[DE95-008175] p 2240 N95-28404
Local texture and grain boundary misorientations in high H(C) oxide superconductors
[DE95-007004] p 2447 N95-28606

MICROWAVE AMPLIFIERS
High power, broadband folded waveguide Gyrotron-Traveling-Wave-Amplifier
[AD-A288847] p 2259 N95-26433

MICROWAVE ATTENUATION
The attenuation of microwave radiation by fog and rain
[AD-A288326] p 2249 N95-26562
An optoelectronic attenuator for the high-speed control of microwave integrated circuits
[AD-A289579] p 2260 N95-26690
Prediction of rain attenuation and total atmospheric attenuation for low-availability satellite communications in Europe
[PB95-184925] p 2252 N95-26908

MICROWAVE CIRCUITS
Microwave circuit simulation using higher-order dynamic elements
[PB95-185088] p 2259 N95-26496
An optoelectronic attenuator for the high-speed control of microwave integrated circuits
[AD-A289579] p 2260 N95-26690
Characterization of microwave MESFET circuits under laser illumination. Applications to phased array radar, microwave communications, and digital clock control
[AD-A289181] p 2261 N95-27015

MICROWAVE EQUIPMENT
Survey on step recovery diode and its applications
[PB95-184974] p 2260 N95-26646
New trends and ideas in the fields of microwave technology
[AD-A291663] p 2257 N95-28453

MICROWAVE FREQUENCIES
Ring-plane traveling-wave tube slow-wave circuit design simulations at V-Band frequencies
[NASA-TM-106949] p 2371 N95-27370

MICROWAVE IMAGERY
Millimeter-wave imaging radiometer data processing and development of water vapor retrieval algorithms
[NASA-CR-198593] p 2343 N95-27997
Modeling and retrieval of snow and sea ice characteristics in the frequency range 6 to 90 GHz
[PB95-195467] p 2316 N95-28656

MICROWAVE LANDING SYSTEMS
An integrated GPS/INS/BARO and radar altimeter system for aircraft precision approach landings
[AD-A289280] p 2127 N95-26985
Precision landing system mathematical modeling study report for Andrews Air Force Base, runway 19L, Camp Springs, MD
[AD-A289015] p 2127 N95-27903

MICROWAVE RADIOMETERS
Radiometer measurements of snow in Sodankylae, 1991-1993
[PB95-184966] p 2313 N95-26645
Design, construction, test and evaluation of a frequency scanning radiometer for measuring oil slick thicknesses
[AD-A290040] p 2293 N95-28389
Modeling and retrieval of snow and sea ice characteristics in the frequency range 6 to 90 GHz
[PB95-195467] p 2316 N95-28656

MICROWAVE SCATTERING
Precision landing system mathematical modeling study report for Andrews Air Force Base, runway 19L, Camp Springs, MD
[AD-A289015] p 2127 N95-27903
Studies of radar backscatter as a function of wave properties and the winds in the turbulent marine atmosphere
[NASA-CR-198608] p 2315 N95-28209

MICROWAVE SENSORS
Millimeter-wave imaging radiometer data processing and development of water vapor retrieval algorithms
[NASA-CR-198593] p 2343 N95-27997

MICROWAVES
The attenuation of microwave radiation by fog and rain
[AD-A288326] p 2249 N95-26562
A 3-D finite difference time domain investigation of microwave propagation through inhomogeneous biological materials
[AD-A289431] p 2251 N95-26869
Microwave characterization of sub-micron N- and P-channel MOSFET's fabricated with thin film silicon-on-sapphire
[AD-A289296] p 2438 N95-27040
A numerical study of ultra-short-pulse reflectometry
[DE95-008070] p 2266 N95-28015
New trends and ideas in the fields of microwave technology
[AD-A291663] p 2257 N95-28453
Data acquisition software for DREO's near-field antenna measurement facility
[AD-A289819] p 2258 N95-28573

MID-OCEAN RIDGES
Seismic constraints on shallow crustal processes at the East Pacific rise
[AD-A289055] p 2338 N95-28094

MIE SCATTERING
Soot particle density determination from a laser extinction multipass technique
[AD-A288551] p 2423 N95-26532
The attenuation of microwave radiation by fog and rain
[AD-A288326] p 2249 N95-26562

MIGRATION
A demonstration of client-server technology using remote procedure calls with an application in file migration using heuristics
[AD-A289467] p 2255 N95-27149
Depth migration in transversely isotropic media with explicit operators
[DE95-007670] p 2337 N95-27442
An investigation of the chemical and physical properties of pristine, electrochromically damaged, and photochromically damaged KTiOPO4 (KTP) using surface analytical and optical spectroscopic techniques
[DE95-007865] p 2443 N95-28023

MILITARY AIRCRAFT
Digital systems validation. Chapter 20 Artificial Intelligenge with applications for aircraft. Handbbook, volume 2
[AD-A288492] p 2380 N95-26638
Naval Aviation System TEAM mapping, charting, and geodesy handbook
[AD-A288590] p 2314 N95-26841
A review of Australian and New Zealand investigations on aeronautical fatigue during the period Apr. 1993 - Mar. 1995
[AR-009-202] p 2136 N95-27918
Aircraft IR/acoustic detection evaluation. Volume 2: Development of a ground-based acoustic sensor system for the detection of subsonic jet-powered aircraft
[NASA-CR-189705-VOL-2] p 2402 N95-28073

MILITARY HELICOPTERS
AH-1F COBRA rewire program MANPRINT analysis
[AD-A289190] p 2130 N95-27018
Report to Congressional Committees. Comanche Helicopter: Testing needs to be completed prior to production decisions
[GAO/NSIAD-95-112] p 2135 N95-27910
Construction and wind tunnel test of a 1/12th scale helicopter model
[AD-A288487] p 2123 N95-28331
Tie-down trials involving a Sikorsky S-70B-2 helicopter
[DSTO-TR-0132] p 2136 N95-28567

MILITARY OPERATIONS
The value of simulation for training
[AD-A289174] p 2143 N95-26556
Digital systems validation. Chapter 20 Artificial Intelligenge with applications for aircraft. Handbbook, volume 2
[AD-A288492] p 2380 N95-26638
Air cushioned landing craft (LCAC) based ship to shore movement simulation: A decision aid for the amphibious commander. A (SMMAT) application
[AD-A289635] p 2246 N95-26722
Aqueous degreasing, precision cleaning, and cleanliness verification p 2231 N95-27121

MILITARY SPACECRAFT
Assessment of long-distance HF radio and satellite communication assets for RNLAF out-of-area operations
[AD-A288633] p 2247 N95-26344

MILITARY TECHNOLOGY
The design and implementation of the Military Applications of Shiptracks experiment on Space Transportation System - 65
[AD-A288488] p 2160 N95-26634

MILITARY VEHICLES
Improved hardness RHA weldability and material property testing
[AD-A289127] p 2221 N95-28102
Thermal analysis of PANSAT batteries and Electrical Power Subsystem
[AD-A290013] p 2269 N95-28388

MILLIMETER WAVES
High power, broadband folded waveguide Gyrotron-Traveling-Wave-Amplifier
[AD-A288847] p 2259 N95-26433
Millimeter-wave imaging radiometer data processing and development of water vapor retrieval algorithms
[NASA-CR-198593] p 2343 N95-27997
Quasi-optical millimeter wave power combining
[AD-A291767] p 2270 N95-28529
Data acquisition software for DREO's near-field antenna measurement facility
[AD-A289819] p 2258 N95-28573

MIMD (COMPUTERS)
Algorithms for parallel flow solvers on message passing architectures
[NASA-CR-197758] p 2274 N95-26588

MINERALOGY
The biodegradation of fuels in soils and sediments: Differences as a function of mineralogy
p 2230 N95-27116

MINERALS
Synchrotron X-ray scattering studies at mineral-water interfaces
[DE95-008303] p 2440 N95-27542

MINIATURIZATION
Multi-channel electronically scanned cryogenic pressure sensor
[NASA-CASE-LAR-15062-1] p 2291 N95-27138
Microelectronics in Japan p 2263 N95-27227

MINIMA
Prediction of fatigue crack growth under constant amplitude and random loading using specimens with multiple cracks
[AD-A291614] p 2136 N95-28409

MINKOWSKI SPACE
Mean value theorem in topological vector spaces
[DE95-608753] p 2390 N95-27331
Quantum k-Poincare 1994
[DE95-608754] p 2448 N95-27332
Photon rockets and gravitational radiation
[PB95-190161] p 2397 N95-28174

MIR SPACE STATION
Analysis of solar receiver flux distributions for US/Russian solar dynamic system demonstration on the MIR Space Station
[NASA-TM-106933] p 2169 N95-28036
Analysis of shadowing effects on MIR photovoltaic and solar dynamic power systems
[NASA-TM-106940] p 2169 N95-28213

MIRRORS
Preliminary design study of the beam collapser and certain optomechanical aspects of the siderostat
[AD-A288423] p 2423 N95-26549
Frame selection performance limits for statistical image reconstruction of adaptive optics compensated images
[AD-A289240] p 2424 N95-26965
SXI Prototype mirror mount
[NASA-CR-196613] p 2301 N95-27244
High-performance reactionless scan mechanism
p 2158 N95-27288
Specification of the figure and finish of EUV mirrors in terms of performance requirements, revised Nov. 1994
[DE95-005689] p 2425 N95-27490
Evaluation of space environmental effects on metals and optical thin films on EOIM-3 p 2210 N95-27641
Effects of the LDEF orbital environment on the reflectance of optical mirror materials
p 2428 N95-27651
Effects of low earth orbit on the optical performance of multi-layer enhanced high reflectance mirrors
p 2428 N95-27652
Laboratory high-energy astrophysics on lasers
[DE95-008062] p 2462 N95-28013
Particle fallout/activity sensor
[NASA-CASE-KSC-11687-1] p 2293 N95-28362
Cryogenic BRDF measurements at 10.6 micrometers and 0.63 micrometers on contaminated mirrors
[AD-A291611] p 2427 N95-28408

MISALIGNMENT
Local texture and grain boundary misorientations in high H(C) oxide superconductors
[DE95-007004] p 2447 N95-28606

MISSILE DEFENSE
Reusable launch vehicle development research
[NASA-CR-196614] p 2154 N95-27245

MISSILE STRUCTURES
Development of a low-cost, modified resin transfer molding process using elastomeric tooling and automated preform fabrication p 2184 N95-28268

MISSILE TRAJECTORIES
Parallel block implicit integration technique for trajectory parallelism
[AD-A288961] p 2379 N95-28335

MISSILES
User documentation of the CTA program
[AD-A289508] p 2121 N95-26854
Improved numerical solution of mixed H2/H(infinity) optimization with applications
[AD-A289315] p 2386 N95-27400

MISSION PLANNING
The development of infrared detectors and mechanisms for use in future infrared space missions
[NASA-CR-197819] p 2290 N95-26702

Micromechanisms for optimism seismometer p 2159 N95-27292

Limits to ground control in autonomous spacecraft p 2383 N95-27381

A rule-based shell to hierarchically organize HST observations p 2384 N95-27384

Electric propulsion for geostationary orbit insertion [NASA-TM-106942] p 2168 N95-27727

Operational considerations of using GPS for spacecraft navigation p 2152 N95-27794

Contingency maneuver strategies for the Total Ozone Mapping Spectrometer-Earth Probe (TOMS-EP) p 2152 N95-27796

Summary of EOS flight dynamics analysis p 2152 N95-27797

ORION: A Supersynchronous Transfer Orbit mission p 2154 N95-27804

Mission to Planet Earth. Strategic enterprise plan, 1995-2000 [NASA-TM-110620] p 2145 N95-27919

MISSION TO PLANET EARTH

Mission to Planet Earth. Strategic enterprise plan, 1995-2000 [NASA-TM-110620] p 2145 N95-27919

MIST

Engineering photochemical smog through convection towers [DE95-007727] p 2328 N95-27686

MIXERS

Apparatus for diffusion controlled dialysis under microgravity conditions [NASA-CASE-MFS-28986-1] p 2245 N95-27500

MIXING

Apparatus for diffusion controlled dialysis under microgravity conditions [NASA-CASE-MFS-28986-1] p 2245 N95-27500

Tank pressure control in low gravity by jet mixing [NASA-CR-191012] p 2243 N95-28001

MIXING LAYERS (FLUIDS)

Basic studies in turbulent shear flows [AD-A289145] p 2277 N95-26998

MIXING LENGTH FLOW THEORY

Supersonic coaxial jet noise predictions [NASA-TM-106917] p 2401 N95-26801

MIXTURES

Ultra high purity, dimensionally stable INVAR 36 [NASA-CASE-NPO-19358-1-CU] p 2213 N95-26862

A summary of ODS replacement technologies at Litton Poly-Scientific p 2228 N95-27105

MOBILE COMMUNICATION SYSTEMS

The evolution and impact of PCS technology [AD-A288606] p 2255 N95-27249

MOBILITY

Interfacial mobility and its effect on flexural strength and fracture toughness in glass-fiber fabric reinforced epoxy laminates [AD-A288344] p 2180 N95-26572

A systems engineering approach to electro-mechanical reconfiguration for mobility autonomy [AD-A289479] p 2301 N95-26926

Measurement of N2(+) mobility He via Fourier transform emission spectroscopy [AD-A289266] p 2404 N95-26979

MODELS

A process improvement model for software verification and validation [NASA-CR-197761] p 2367 N95-26814

Unification of LARCH and Z-based object models to support algebraically-based design refinement: The Z perspective [AD-A289234] p 2369 N95-26962

A knowledge highway for integrated modelling from manufacturing to design [AD-A288872] p 2247 N95-28187

Efficient modeling of interconnects and capacitive discontinuities in high-speed digital circuits [NASA-CR-198728] p 2270 N95-28570

MODULATION

Fundamental concepts of integrated and fiber optic sensors [NASA-TM-106920] p 2426 N95-27906

Method of space-time sequence transform used to measure acousto-optic deflection and modulation [AD-A289612] p 2402 N95-28671

MODULATORS

Valve mechanism for an acoustic modulator [AD-D017263] p 2300 N95-26504

Full complex modulation using two one-parameter spatial light modulators [NASA-CASE-MSC-22255-1] p 2427 N95-28384

MODULES

Low-power, parallel photonic interconnections for Multi-Chip Module applications [DE95-008518] p 2267 N95-28147

MODULUS OF ELASTICITY

Elastic properties of metallic superlattices [AD-A288699] p 2212 N95-26490

Fatigue behavior of a cross-ply ceramic matrix composite at elevated temperature under tension-tension loading [AD-A289250] p 2182 N95-26969

MOISTURE

Bonded composite repair of thin metallic materials: Variable load amplitude and temperature cycling effects p 2132 N95-27509

MOISTURE CONTENT

Soil moisture prediction during freeze and thaw using a coupled heat and moisture flow model [AD-A289343] p 2336 N95-26753

Remote sensing of hydrologic variables in boreal areas, phase 2 [NASA-CR-198717] p 2314 N95-27998

MOLDING MATERIALS

Japan's electronic packaging technologies p 2263 N95-27230

MOLECULAR ABSORPTION

CO, HCO(+) and HCN absorption in the gravitational lens candidate B0218+357 at z=0.685 [PB95-185146] p 2461 N95-26522

Search for molecular absorptions with the Fourier Transform Spectrometer [NASA-CR-198648] p 2462 N95-28222

MOLECULAR BEAM EPITAXY

Fabrication of long wavelength array by in-situ molecular beam epitaxy [AD-A288599] p 2423 N95-26679

Pseudomorphic semiconducting heterostructures from combinations of AlN, GaN and selected SiC polytypes: Theoretical advancement and its coordination with experimental studies of nucleation, growth, characterization and device development [AD-A289550] p 2437 N95-26756

Materials Research Society Symposium Proceedings. Volume 339: Diamond, SiC and nitride wide bandgap semiconductors [AD-A288690] p 2437 N95-26818

MOLECULAR BEAMS

Fabrication of long wavelength array by in-situ molecular beam epitaxy [AD-A288599] p 2423 N95-26679

Molecular beam scattering from C-13 enriched Kapton and correlation with the EOIM-3 carousel experiment p 2419 N95-27643

MOLECULAR BIOLOGY

Third international congress of plant molecular biology: Molecular biology of plant growth and development [DE95-006482] p 2352 N95-28496

MOLECULAR CLOUDS

Molecular cloud content of early-type galaxies. V. CO in elliptical galaxies [PB95-185153] p 2461 N95-27320

Search for molecular absorptions with the Fourier Transform Spectrometer [NASA-CR-198648] p 2462 N95-28222

MOLECULAR CLUSTERS

Atomic and electronic structure of clusters from Car-Parrinello method [DE94-634463] p 2403 N95-26437

Photoemission and optical properties of C60 fullerites [DE95-006588] p 2425 N95-27539

Laser ionization of molecular clusters [DE95-007011] p 2296 N95-27550

Self-assembly of low-dimensional molecular nanoclusters on Au(111) surfaces [AD-A288936] p 2178 N95-28334

MOLECULAR COLLISIONS

Statistical model for molecular internal energy exchange in DSMC method for rarefied flow analysis [ISAS-R-654] p 2274 N95-26741

MOLECULAR DYNAMICS

Atomic and electronic structure of clusters from Car-Parrinello method [DE94-634463] p 2403 N95-26437

Theoretical studies of reaction surfaces [AD-A288458] p 2404 N95-26632

A density functional/molecular dynamics study of the structure of liquid nitromethane [AD-A289224] p 2404 N95-26960

Modeling the growth of electronic materials [AD-A289137] p 2438 N95-26997

Simulating the production of free defects in irradiated metals [DE95-007165] p 2214 N95-27088

Molecular dynamics simulations of Gay-Berne nematic liquid crystal: Elastic properties from direct correlation functions [DE95-609149] p 2441 N95-27740

A new shared-memory programming paradigm for molecular dynamics simulations on the Intel Paragon [DE95-007289] p 2378 N95-28019

Beyond transition state theory: Rigorous quantum approaches for determining chemical reaction rates [DE95-008483] p 2208 N95-28086

Infrared spectroscopy of nonclassical ions and their complexes [DE95-008487] p 2413 N95-28091

Analysis of forward and inverse problems in chemical dynamics and spectroscopy [DE95-009309] p 2209 N95-28164

Optimization strategies for molecular dynamics programs on Cray computers and scalar work stations [AD-A289574] p 2418 N95-28648

MOLECULAR ENERGY LEVELS

High resolution Fourier transform spectroscopy of the first overtone of the N-O stretch in nitrosyl bromide [AD-A289318] p 2203 N95-27295

Analysis of forward and inverse problems in chemical dynamics and spectroscopy [DE95-009309] p 2209 N95-28164

MOLECULAR EXCITATION

Fellowship in physics [AD-A291691] p 2446 N95-28522

MOLECULAR GASES

Applications of Second Harmonic and Sum Frequency Generation to graphite and silica type interfaces [AD-A288228] p 2201 N95-26544

Infrared spectroscopy of nonclassical ions and their complexes [DE95-008487] p 2413 N95-28091

Self-assembly of low-dimensional molecular nanoclusters on Au(111) surfaces [AD-A288936] p 2178 N95-28334

MOLECULAR ORBITALS

Computational and matrix isolation studies of (2- and 3-furyl)methylene [AD-A280085] p 2178 N95-28154

MOLECULAR RELAXATION

Fellowship in physics [AD-A291691] p 2446 N95-28522

MOLECULAR STRUCTURE

Template synthesis of electronically conductive polymer nanostructures [AD-A288373] p 2225 N95-26472

Toward molecular selectivity with chemically modified electrodes: Can electroactivity and permeability through an overlaying metallopolymer film be controlled via rational manipulation of internal architecture? [AD-A288719] p 2403 N95-26491

Molecular object liquid crystals: An approach to new materials [AD-A288905] p 2437 N95-26553

Theoretical studies of reaction surfaces [AD-A288458] p 2404 N95-26632

Structural oxidation state studies of the manganese cluster in the oxygen evolving complex of Photosystem II [DE95-008488] p 2409 N95-27744

Experimental determination of cluster geometrical structure [DE95-007089] p 2409 N95-27753

Crossover integral equation theory for the liquid structure study [DE95-609155] p 2218 N95-27757

Surface structure of MX-chains studied by atomic force microscopy [DE95-007881] p 2447 N95-28541

MOLECULES

Near-resonant properties of nonlinear organic materials for optical devices [AD-A288339] p 2178 N95-26570

Molecular approach to mesoporous metal sulfides [DE95-005418] p 2202 N95-27137

International journal of quantum chemistry [AD-A291633] p 2352 N95-28546

Monte-Carlo simulation methods for finite flat plate winding flows [AD-A289842] p 2289 N95-28619

MOLLUSKS

Use of mussels in biomonitoring of environmental impacts of propellants, projectiles, explosives, and pyrotechnics p 2170 N95-28298

MOLTEN SALTS

Molten Carbonate Fuel Cell (MCFC) product development test [DE95-007345] p 2316 N95-26543

Materials considerations for molten salt accelerator-based plutonium conversion systems [DE95-006743] p 2217 N95-27544

MOLYBDENUM

High energy electron beams for ceramic joining [DE95-006316] p 2420 N95-27480

MOLYBDENUM DISULFIDES

Advanced solid lubricant films by Ion-Beam Assisted Deposition [AD-A288866] p 2225 N95-26499

Optical features of nanosize iron and molybdenum sulfide clusters
[DE95-005417] p 2202 N95-27136

MOLYBDENUM SULFIDES
Optical features of nanosize iron and molybdenum sulfide clusters
[DE95-005417] p 2202 N95-27136

MOMENTS OF INERTIA
A quantitative feedback theory FCS design for the subsonic envelope of the VISTA F-16 including configuration variation
[AD-A289221] p 2141 N95-26958
The calculation of the mass moment of inertia of a fluid in a rotating rectangular tank
[NASA-CR-197777] p 2278 N95-27165

MOMENTUM
Performance analysis of bullet trajectory estimation: Approach, simulation, and experiments
[DE95-007949] p 2399 N95-28109

MOMENTUM THEORY
Rarefied gas effects on aerobraking/reentry vehicles with wakes
[NASA-CR-196586] p 2164 N95-27093

MOMENTUM TRANSFER
Magnetic viscosity by localized shear flow instability in magnetized accretion disks
[DE95-006879] p 2433 N95-28111

MONITORS
Model-based monitoring and diagnosis of a satellite-based instrument p 2166 N95-27390
Lessons learned from the introduction of autonomous monitoring to the EUVE science operations center
p 2385 N95-27393
Prototype development and test results of a continuous ambient air monitoring system for hydrazine at the 110 ppb level p 2173 N95-28310
A continuous emissions monitor for airborne metals
p 2174 N95-28313

MONOCHROMATIC RADIATION
Quantum effects induced by a gap in the spectrum of atom-bath coupling constants: Freezing of atomic decay and monochromatic collective radiation
[DE95-609037] p 2416 N95-28251

MONOCHROMATORS
Optical design and performance of the inelastic scattering beamline at the National Synchrotron Light Source
[DE95-007679] p 2422 N95-28195

MONOMERS
Design strategies for the preparation of polymeric organic superconductors
[AD-A289022] p 2436 N95-26462
Poly(N-arylenbenzimidazoles) via aromatic nucleophilic displacement
[NASA-CASE-LAR-14939-1] p 2179 N95-28360
Polybenzimidazoles via aromatic nucleophilic displacement
[NASA-CASE-LAR-14924-1-CU] p 2179 N95-28361
Functionalized block copolymers as adhesion promoters
[DE95-008158] p 2239 N95-28400
Porosity in hexylene-bridged polysilsesquioxanes: Effects of monomer concentration
[DE95-005421] p 2240 N95-28531
Comparison of bridged polysilsesquioxane xerogels prepared from methoxy- and ethoxy-silyl monomers
[DE95-005422] p 2240 N95-28532

MONOMOLECULAR FILMS
Electrocrystallization of an ordered organic monolayer: Selective epitaxial growth of beta(ET)213 ongraphite
[AD-A288942] p 2178 N95-26569

MONOPLANES
Incorporating biplane wing theory into a large, subsonic, all-cargo transport p 2120 N95-26956

MONOPOLES
Compactification of moduli spaces of monopoles
[PB95-185179] p 2388 N95-26515

MONOPULSE RADAR
Polarization sensitivity of monopulse radar boresight error induced by large, ogive radomes
[AD-A289254] p 2252 N95-26972

MONSOONS
An observational study on the onset of the summer monsoon over eastern Asia in 1979
[AD-A289637] p 2341 N95-26723
Synoptic features of the Yunan rainy season before the onset of the tropical monsoons
[AD-A289641] p 2342 N95-26724

MONTE CARLO METHOD
Analysis of fatigue fractographic data of a rod end housing using a Monte Carlo simulation
[NAL-TR-1225] p 2307 N95-26521
Monte Carlo study of electron-plasmon scattering effects on hot electron transport in GaAs
[DE95-607768] p 2403 N95-26542
Statistical model for molecular internal energy exchange in DSMC method for rarefied flow analysis
[ISAS-R-654] p 2274 N95-26741
Anomalous collision rate in the time counter scheme of the direct simulation Monte Carlo method for rarefied gas flow analysis
[ISAS-R-653] p 2275 N95-26742
A model of bubble evolution during decompression based on a Monte Carlo simulation of inert gas diffusion
[AD-A289400] p 2353 N95-26885
Modeling the growth of electronic materials
[AD-A289137] p 2438 N95-26997
A case study of view-factor rectification procedures for diffuse-gray radiation enclosure computations
p 2281 N95-27353
Recent advances in PDF modeling of turbulent reacting flows p 2286 N95-27892
Remote measurement of ground temperature and emissivity
[DE95-008055] p 2314 N95-28053
Performance analysis of bullet trajectory estimation: Approach, simulation, and experiments
[DE95-007949] p 2399 N95-28109
Stationary neutrino radiation transport by maximum entropy closure
[DE95-006579] p 2463 N95-28558
Measurement of alpha(s) in e(+)e(-) annihilation at E(cm) = 29 GeV
[DE95-006486] p 2417 N95-28594
Monte-Carlo simulation methods for finite flat plate winding flows
[AD-A289842] p 2289 N95-28619
Exploiting parallelism in a Monte Carlo image-matching algorithm
[AD-A289872] p 2374 N95-28625
Chua's circuits: Phenomena and applications
[AD-A291638] p 2271 N95-28666

MONTMORILLONITE
Contact micromechanics in granular media with clay
[DE95-006566] p 2340 N95-28583

MOORING
An in situ evaluation of TOPEX/Poseidon altimetric measurements versus meaurements made by moorings and inverted echo sounders for sea surface height
[NASA-CR-198621] p 2347 N95-27805

MORPHOLOGY
Boron-induced morphology changes in silicon CVD growth: A scanning tunneling microscopy study
[AD-A289275] p 2290 N95-26982
Simulations of metal dissolution and corrosion
[DE95-007486] p 2218 N95-27748
Effects of interlayers on the scratch adhesion performance of ultra-thin films of copper and gold on silicon substrates
[DE95-007367] p 2220 N95-28044
Self-assembly of low-dimensional molecular nanoclusters on Au(111) surfaces
[AD-A288936] p 2178 N95-28334

MOSSBAUER EFFECT
Iron oxides characterization by Moessbauer spectroscopy
[DE95-607869] p 2202 N95-27199

MOTION SIMULATION
Air cushioned landing craft (LCAC) based ship to shore movement simulation: A decision aid for the amphibious commander. A (SMMAT) application
[AD-A289635] p 2246 N95-26722

MOTION SIMULATORS
Collected papers on wind turbine technology
[NASA-CR-195432] p 2321 N95-27970
Design of a real-time wind turbine simulator using a custom parallel architecture p 2322 N95-27979

MOTIVATION
ELVIS: Eigenvectors for land vehicle image system
[AD-A289297] p 2381 N95-27041

MULLITES
TEM characterization of Al/Al2O3 composite fabricated by reactive metal infiltration
[DE95-008508] p 2184 N95-28145
Development of low-expansion ceramics with strength retention to elevated temperatures
[DE95-005760] p 2239 N95-28397

MULTIDISCIPLINARY DESIGN OPTIMIZATION
Structural design optimization with survivability dependent constraints application: Primary wing box of a multi-role fighter p 2137 N95-28440

MULTIGRID METHODS
introduction to multigrid methods
[NASA-CR-195045] p 2388 N95-26395
A 3D agglomeration multigrid solver for the Reynolds-averaged Navier-Stokes equations on unstructured meshes
[NASA-CR-195073] p 2390 N95-27029
Multigrid techniques for unstructured meshes
[NASA-CR-195070] p 2391 N95-27433

MULTIMEDIA
Transparent access to distributed, heterogeneous environmental information systems
[DE95-007268] p 2454 N95-27483

MULTIPATH TRANSMISSION
Adaptive beamforming in frequency-dispersive multipath environments
[AD-A289206] p 2254 N95-27009
A high performance totally ordered multicast protocol
[NASA-CR-197765] p 2371 N95-27252
Precision landing system mathematical modeling study report for Andrews Air Force Base, runway 19L, Camp Springs, MD
[AD-A289015] p 2127 N95-27903
Low-angle tracking in the presence of ducting, coherent and incoherent multipath
[AD-A289838] p 2258 N95-28580

MULTIPHASE FLOW
Computation of three-dimensional mixed convective boundary layer flow p 2280 N95-27347

MULTIPHOTON ABSORPTION
Laser ionization of molecular clusters
[DE95-007011] p 2296 N95-27550

MULTIPLE TARGET TRACKING
A mathematical framework for an improved search model
[AD-A288858] p 2358 N95-26552

MULTIPLEXING
Multipurpose bus interface utilizing a digital signal processor
[AD-D017264] p 2248 N95-26505
Experimental definition for implantation of the AFIT cortical multielectrode array
[AD-A289216] p 2354 N95-26991
Characterization and redesign of the AFIT multielectrode array
[AD-A289295] p 2354 N95-27039

MULTIPLIERS
On compact multipliers of topological algebras
[DE95-608751] p 2390 N95-27092
Spectral properties of multipliers on topological algebras
[DE95-608747] p 2390 N95-27299

MULTIPROCESSING (COMPUTERS)
Parallelism detection and scheduling strategies for reliable and efficient execution on multicomputers
[AD-A288370] p 2376 N95-26471
Grain size management in repetitive task graphs for multiprocessor computer scheduling
[AD-A288575] p 2377 N95-26551
Design tool for multiprocessor scheduling and evaluation of iterative dataflow algorithms
[NASA-TP-3491] p 2366 N95-26685
Second International Conference on Software for Multiprocessors and Supercomputers Theory, Practice, Experience
[AD-A289474] p 2368 N95-26820

MULTISPECTRAL BAND SCANNERS
Conversion of sunflower multiband radiometer polarization measurements to polarization parameters
[NASA-CR-197774] p 2314 N95-26815

MULTIVARIATE STATISTICAL ANALYSIS
A method for simulating correlated random variables from partially specified distributions
[AD-A288820] p 2393 N95-26347
Parallelizing locally-weighted regression
[AD-A288294] p 2394 N95-26414
A method to determine the structure of an unknown mixture using the Akaike Information Criterion and the bootstrap
[AD-A288295] p 2394 N95-26415
Wavelet analysis and its applications
[AD-A291735] p 2387 N95-28527

MUON SPIN ROTATION
Muon spin relaxation in ferromagnets: Theoretical results for paramagnetic EuO and EuS
[PB95-192860] p 2418 N95-28641
Muon spin relaxation in antiferromagnets: A study of RbMnF3 based on the coupled-mode theory of paramagnetic and critical spin fluctuations
[PB95-192878] p 2418 N95-28642

MUONS
Search for SUSY at CDF
[DE95-005109] p 2407 N95-27430
Search for the top quark in dilepton decay modes at D(PHI)
[DE95-007764] p 2409 N95-27689
Measurement of the reaction C(nu(sub mu), mu(-)) X near threshold
[DE95-007888] p 2412 N95-28063
B-Physics results from D0
[DE95-005126] p 2417 N95-28495
Muon spin relaxation in ferromagnets: Theoretical results for paramagnetic EuO and EuS
[PB95-192860] p 2418 N95-28641

MUTATIONS
Mutagenesis in human cells with accelerated H and Fe ions
[NASA-CR-198599] p 2351 N95-28177
MYLAR (TRADEMARK)
An overview of the Evaluation of Oxygen Interactions with Materials 3 experiment: Space Shuttle Mission 46, July-August 1992 p 2210 N95-27630

N

N-TYPE SEMICONDUCTORS
Photoluminescence spectroscopy of 4H- and 6H-SiC
[AD-A289326] p 2202 N95-26896
Defect characterization of electronic conducting pseudo-perovskite systems
[DE95-007487] p 2220 N95-28049
Low temperature deposition and characterization of N- and P-type silicon carbide thin films and associated Ohmic and Schottky contacts
[AD-A289107] p 2237 N95-28097
NACELLES
Application of fiber-reinforced bismaleimide materials to aircraft nacelle structures p 2137 N95-28278
NARROWBAND
Analysis and simulation of narrowband GPS jamming using digital excision temporal filtering
[AD-A289328] p 2127 N95-26898
High pressure optical studies of semiconductors and heterostructures
[DE95-007119] p 2410 N95-27927
NASA PROGRAMS
Probabilistic risk assessment of the Space Shuttle. Phase 3: A study of the potential of losing the vehicle during nominal operation, volume 1
[NASA-CR-197808] p 2159 N95-26398
AIAA Techfest 20 Proceedings
[NIAR-94-1] p 2118 N95-26941
The high speed civil transport and NASA's High Speed Research (HSR) program p 2118 N95-26945
The aerospace database: An introduction to AIAA'S computerized source for identifying scientific and technical information p 2119 N95-26950
Spaceflight revolution: NASA Langley Research Center from Sputnik to Apollo
[NASA-SP-4308] p 2474 N95-27685
Mission to Planet Earth. Strategic enterprise plan, 1995-2000
[NASA-TM-110620] p 2145 N95-27919
Research and Technology Objectives and Plans Summary (RTOPS)
[NASA-TM-108574] p 2475 N95-28002
Overview of the ACT program p 2193 N95-28463
NASA/DOD Aerospace Knowledge Diffusion Research Project. Report 35: The use of computer networks in aerospace engineering
[NASA-CR-198170] p 2456 N95-28600
Software process improvement in the NASA software engineering laboratory
[AD-A289912] p 2374 N95-28627
NASA SPACE PROGRAMS
Reusable launch vehicle development research
[NASA-CR-196614] p 2154 N95-27245
Briefing Report to the Ranking Minority Member, Subcommittee on Space and Aeronautics, Committee on Science, House of Representatives. Cassini Mission: Estimated launch costs for NASA's mission to Saturn
[GAO/NSIAD-95-141BR] p 2145 N95-27856
NASTRAN
A NASTRAN-based computer program for structural dynamic analysis of Horizontal Axis Wind Turbines
p 2312 N95-27980
Applications of a damage tolerance analysis methodology in aircraft design and production
p 2197 N95-28483
NATIONAL AIRSPACE SYSTEM
The 1994 updated National Airspace System performance assessment for year 2005
[AD-A288652] p 2125 N95-26485
NATURAL GAS
Research on combustion processes relevant to burners in HVAC systems
[PB95-179735] p 2208 N95-28006
NATURAL LANGUAGE (COMPUTERS)
TRAINS: Dialogue transcription tools
[AD-A289869] p 2259 N95-28624
NAVIER-STOKES EQUATION
Computational analysis of forebody tangential slot blowing on the high alpha research vehicle
[NASA-CR-197754] p 2129 N95-26591
Turbulence modeling
[NASA-CR-197751] p 2274 N95-26665
SUPG finite numerical element solutions for non-compressible Navier-Stokes equation sets
[AD-A289600] p 2274 N95-26718
Progress in incompressible Navier-Stokes computations for propulsion flows and its dual-use applications
[NASA-CR-197746] p 2275 N95-26766
A 3D agglomeration multigrid solver for the Reynolds-averaged Navier-Stokes equations on unstructured meshes
[NASA-CR-195073] p 2390 N95-27029
Development of numerical methods for overset grids with applications for the integrated Space Shuttle vehicle
[NASA-CR-197759] p 2160 N95-27154
Flow control
[AD-A289262] p 2279 N95-27197
Effect of turbulence models on criticality conditions in swirling flows p 2282 N95-27356
A Navier-Stokes boundary element solver
p 2283 N95-27361
Turbulance boundary conditions for shear flow analysis, using the DTNS flow solver p 2283 N95-27362
Multigrid techniques for unstructured meshes
[NASA-CR-195070] p 2391 N95-27433
A new finite element formulation for incompressible flow
[DE95-007141] p 2284 N95-27454
A numerical method for solving the three-dimensional parabolized Navier-Stokes equations
[NASA-CR-198159] p 2287 N95-27917
Study of potential aerodynamic benefits from spanwise blowing at wingtip
[NASA-TP-3515] p 2124 N95-28669
Numerical study to assess sulfur hexafluoride as a medium for testing multielement airfoils
[NASA-TP-3496] p 2124 N95-28674
NAVIGATION
Operator modeling in commerical aviation: Cognitive models, intelligent displays, and pilot's assistants
[NASA-CR-198609] p 2138 N95-28203
NAVIGATION INSTRUMENTS
Flight evaluation of GPS/DGPS sensor systems installed in NAL Do228
[NAL-TR-1230] p 2126 N95-26585
NAVIGATION SATELLITES
Development of welded solar arrays for DMSP and GPS satellites
[AD-A289512] p 2318 N95-26846
Analysis and simulation of narrowband GPS jamming using digital excision temporal filtering
[AD-A289328] p 2127 N95-26898
Determining GPS average performance metrics
p 2128 N95-27791
NAVIGATION TECHNOLOGY SATELLITES
A demonstration of unified TDRS/GPS tracking and orbit determination p 2151 N95-27792
NAVIGATORS
An analysis of the KC-135 three-person cockpit
[AD-A289540] p 2130 N95-26873
NAVY
Naval Aviation System TEAM mapping, charting, and geodesy handbook
[AD-A288590] p 2314 N95-26841
Navy composite maintenance and repair experience
p 2193 N95-28446
NEAR FIELDS
Data acquisition software for DREO's near-field antenna measurement facility
[AD-A289819] p 2258 N95-28573
NEAR WAKES
Effects of three-dimensional imposed 3-D disturbances on bluff-body near wake flows
[AD-A289553] p 2121 N95-26757
Unsteady base pressure measurements in the near wake of a cylinder with imposed three-dimensional disturbances
[AD-A289498] p 2276 N95-26827
The near-wake flow behavior of an oscillating airfoil with modified trailing edge p 2119 N95-26953
NEGATIVE IONS
Molecular approach to mesoporous metal sulfides
[DE95-005418] p 2202 N95-27137
NEODYMIUM LASERS
Trident as an ultrahigh irradiance laser
[DE95-006345] p 2297 N95-27850
NERVES
Peripheral innervation patterns of vestibular nerve afferents in the bullfrog utriculus p 2349 N95-26730
NERVOUS SYSTEM
A model of the neural basis of the rat's sense of direction
[AD-A289678] p 2350 N95-26761
NETWORK ANALYSIS
The reliable multicast protocol application programming interface
[NASA-CR-197762] p 2363 N95-26388
Reference manual: Naive physics simulator
[PB95-184917] p 2369 N95-26907
An analysis of Bayesian networks as classifiers
[AD-A289316] p 2382 N95-27293
An architecture and protocol for communications satellite constellations regarded as multi-agent systems
p 2166 N95-27377
Linear and nonlinear trending and prediction for AVHRR time series data p 2385 N95-27391
Non-linear resistive grid kernel estimator useful in single feature, two-class pattern classification
[AD-D017394] p 2271 N95-28614
NETWORK CONTROL
The reliable multicast protocol application programming interface
[NASA-CR-197762] p 2363 N95-26388
An architecture and protocol for communications satellite constellations regarded as multi-agent systems
p 2166 N95-27377
NEUMANN PROBLEM
A probabilistic model of a porous heat exchanger
p 2282 N95-27359
NEURAL NETS
Using machine learning to derive efficient cost and performance estimates in VLSI CAD designs
[AD-A288254] p 2363 N95-26408
Joint Services Electronics Program (JSEP)
[AD-A288299] p 2345 N95-26419
Integration of video and radiation analysis data
[DE95-004165] p 2379 N95-26443
Self-organizing artificial neural networks in dynamic systems modeling and control
[PB95-185120] p 2379 N95-26449
Digital systems validation. Chapter 20 Artificial Intelligenge with applications for aircraft. Handbbook, volume 2
[AD-A288492] p 2380 N95-26638
Embedology and neural estimation for time series prediction
[AD-A289312] p 2394 N95-26892
Long-term variability of electron radiation dose in geosynchronous orbit
[AD-A289335] p 2162 N95-26902
An exploratory application of neural networks for airfoil design p 2118 N95-26943
Using virtual active vision tools to improve autonomous driving tasks
[AD-A289175] p 2356 N95-27 13
Evolving cascade-correlation networks for time-series forecasting
[AD-A289197] p 2390 N95-27020
A modified backpropagation algorithm for training neural networks on data with error bars
[DE95-608729] p 2381 N95-27025
ELVIS: Eigenvectors for land vehicle image system
[AD-A289297] p 2381 N95-27041
Higher-order probabilistic perceptrons as Bayesian inference engines
[DE95-608730] p 2381 N95-27044
Reducing network depth in the Cascade-Correlation learning architecture
[AD-A289352] p 2382 N95-27066
Head related transfer function approximation using neural networks
[AD-A289422] p 2382 N95-27145
An analysis of Bayesian networks as classifiers
[AD-A289316] p 2382 N95-27293
Diagnosis of helicopter gearboxes using structure-based networks
[NASA-TM-106932] p 2302 N95-27373
Stable adaptive neurocontrollers for spacecraft and space robots p 2384 N95-27385
Linear and nonlinear trending and prediction for AVHRR time series data p 2385 N95-27391
Direct ultrashort-pulse retrieval using frequency-resolved optical gating and a computational neural network
[DE95-007148] p 2425 N95-27482
Classification of RF transients in space using digital signal processing and neural network techniques
[DE95-006287] p 2256 N95-27840
Neural network error compensation of machine tools
[AD-A289300] p 2387 N95-28217
Ultrashort Pulse retrieval using FROG trace irradiance moments and the adaptive neural networks backpropagation algorithm
[DE95-007153] p 2299 N95-28220
Neural networks versus linear regression: Research into the value of neural networks in meteorological practice
[KNMI-TR-165] p 2343 N95-28236
Cognitive networks for ATR: The roles of bifurcation and chaos
[AD-A289010] p 2387 N95-28336
Optical implementation of inner product neural associative memory
[NASA-CASE-NPO-18491-2-CU] p 2427 N95-28363
JPRS report: Science and technology. Central Eurasia
[JPRS-UST-95-019] p 2270 N95-28565

Neural networks in the classification of uses of the soil in satellite images
[INPE-5478-PRE/1777] p 2316 N95-28672

NEURONS
Research activities on somatosensory (SI) cortical neurons
[AD-A288794] p 2348 N95-26360
Cognitive networks for ATR: The roles of bifurcation and chaos
[AD-A289010] p 2387 N95-28336

NEUROPHYSIOLOGY
Research activities on somatosensory (SI) cortical neurons
[AD-A288794] p 2348 N95-26360

NEUTRAL ATOMS
Low energy neutral atom imaging: Remote observations of the magnetosphere
[DE95-006342] p 2337 N95-27848

NEUTRAL GASES
Neutral gas compression in the Alcator C-Mod divertor. Experimental observations
[DE95-007762] p 2432 N95-27688

NEUTRALIZERS
Experimental studies to test simple flexural neutralizers fitted to beams
[ISVR-TR-239] p 2309 N95-27846

NEUTRINOS
Measurement of the reaction C(nu(sub mu), mu(-)) X near threshold
[DE95-007888] p 2412 N95-28063
Neutrino oscillations in strong magnetic fields
[DE95-608876] p 2416 N95-28249
Threefold maximal lepton mixing and the solar and atmospheric neutrino deficits
[PB95-196259] p 2465 N95-28500
Stationary neutrino radiation transport by maximum entropy closure
[DE95-006579] p 2463 N95-28558

NEUTRON BEAMS
Reflection of neutrons from an optical grating
[DE95-007145] p 2411 N95-28004

NEUTRON COUNTERS
Solar-geophysical data number 604, December 1994. Part 1: (Prompt reports). Data for November, October 1994, and late data
[PB95-181848] p 2465 N95-28087

NEUTRON DIFFRACTION
A study of internal damage of metal matrix composites by neutron diffraction
[DE95-005157] p 2182 N95-27080
Neutron diffraction studies on recrystallization of solution derived lead zirconate titanates
[DE95-004771] p 2439 N95-27429
Stoichiometry, structure, and properties of La2NiO(4+(delta)) and La(2-x)Sr(x)NiO(4+/-(delta))
[DE95-007682] p 2439 N95-27443
Crystal structure, short-range oxygen defects, and water adsorption in La- and Nd-modified ZrO2
[DE95-007134] p 2439 N95-27452
Crystal and magnetic structure of stoichiometric YFe2O4
[DE95-006627] p 2440 N95-27487
Magnetic structures in RNi2B2C (R = Ho, Er) superconductors
[DE95-008370] p 2442 N95-27932
Structural chemistry of some phases in the YC-Ni-B system
[DE95-007403] p 2447 N95-28537

NEUTRON EMISSION
Bilateral intercomparison of the neutron emission rate of a (252)Cf spontaneous fission source between the National Physical Laboratory, Teddington, UK and the Physikalisch-Technische Bundesanstalt, Braunschweig, Germany
[PB95-190120] p 2404 N95-26748

NEUTRON IRRADIATION
Simulating the production of free defects in irradiated metals
[DE95-007165] p 2214 N95-27088
Determination of the first hydrolysis constant of Europium (3) in 3 M of ionic strength
[DE95-607912] p 2405 N95-27211

NEUTRON SCATTERING
Rotor phases in compound semiconductors
[DE95-004139] p 2436 N95-26442
Variation of solvent scattering-length density small-angle neutron scattering as a means of determining structure of composite materials
[DE95-005394] p 2183 N95-27428
Observations of CEF-split intermultiplet transitions in optically opaque EuBa2Cu3O7 using inelastic neutron scattering
[DE95-007135] p 2408 N95-27453
Spin-density-wave magnetism in dilute copper-manganese alloys
[DE95-005121] p 2215 N95-27462
Small angle neutron scattering study of the micelle structure of amphiphilic block copolymers
[DE95-006625] p 2234 N95-27486
Technical progress report to the Department of Energy on the Solid State Sciences Committee (SSSC)
[DE95-007113] p 2441 N95-27925
The structure of lead-indium phosphate glass
[DE95-007130] p 2237 N95-27967
Off-specular scattering in neutron reflectometry
[DE95-007835] p 2412 N95-28057
Recent neutron scattering results on high-temperature superconductors
[DE95-007028] p 2413 N95-28066
Research activities of the Solid State Sciences Committee in the development of a Federal initiative on advanced materials and processing
[DE95-009328] p 2445 N95-28179
Situation in study of electric polarizability and mean square charge radius of the neutron
[DE95-608869] p 2415 N95-28247
Future opportunities and present possibilities for coherent inelastic single crystal measurements on pulsed neutron sources
[PB95-195798] p 2418 N95-28657
Using COLETTE. (A simple guide)
[PB95-195806] p 2375 N95-28658

NEUTRON SOURCES
Bilateral intercomparison of the neutron emission rate of a (252)Cf spontaneous fission source between the National Physical Laboratory, Teddington, UK and the Physikalisch-Technische Bundesanstalt, Braunschweig, Germany
[PB95-190120] p 2404 N95-26748
Advanced neutron source materials surveillance program
[DE95-005700] p 2215 N95-27464
Intermediate energy neutrons at WNR. Spin-isospin and energy dependence of the NN interaction and the nuclear response
[DE95-006291] p 2408 N95-27466
The structure of lead-indium phosphate glass
[DE95-007130] p 2237 N95-27967
Future opportunities and present possibilities for coherent inelastic single crystal measurements on pulsed neutron sources
[PB95-195798] p 2418 N95-28657
Using COLETTE. (A simple guide)
[PB95-195806] p 2375 N95-28658

NEUTRON SPECTRA
Abrasion-ablation model for neutron production in heavy ion reactions
[NASA-TM-4656] p 2420 N95-27372
Intermediate energy neutrons at WNR. Spin-isospin and energy dependence of the NN interaction and the nuclear response
[DE95-006291] p 2408 N95-27466

NEUTRON SPECTROMETERS
Future opportunities and present possibilities for coherent inelastic single crystal measurements on pulsed neutron sources
[PB95-195798] p 2418 N95-28657

NEUTRON STARS
Neutrino oscillations in strong magnetic fields
[DE95-608876] p 2416 N95-28249
Stationary neutrino radiation transport by maximum entropy closure
[DE95-006579] p 2463 N95-28558

NEUTRONS
Abrasion-ablation model for neutron production in heavy ion reactions
[NASA-TM-4656] p 2420 N95-27372
Intermediate energy neutrons at WNR. Spin-isospin and energy dependence of the NN interaction and the nuclear response
[DE95-006291] p 2408 N95-27466
Reflection of neutrons from an optical grating
[DE95-007145] p 2411 N95-28004
Error analysis of the quartic nodal expansion method for slab geometry
[DE95-007373] p 2412 N95-28045
A new algorithm for generating highly accurate benchmark solutions to transport test problems
[DE95-007397] p 2373 N95-28047
Situation in study of electric polarizability and mean square charge radius of the neutron
[DE95-608869] p 2415 N95-28247
Functionalized block copolymers as adhesion promoters
[DE95-008158] p 2239 N95-28400

NEVADA
Recovery, evaluation, and decontamination of landfilled pentaborane cylinders, former liquid propellant rocket engine test facility, Washoe County, Nevada
p 2171 N95-28302

NEW ZEALAND
A review of Australian and New Zealand investigations on aeronautical fatigue during the period Apr. 1993 - Mar. 1995
[AR-009-202] p 2136 N95-27918

NEWS
Index to NASA news releases and speeches 1994
[NASA-TM-110650] p 2452 N95-26673

NICKEL
Calorimetric evaluation of commercial Ni-MH cells and charges p 2272 N95-26790
Atomistic calculations of hydrogen interactions with Ni3Al grain boundaries and Ni/Ni/Ni3Al interfaces
[DE95-006497] p 2408 N95-27534
Evaluation of space environmental effects on metals and optical thin films on EOIM-3 p 2210 N95-27641
Particle-like absorption spectra in small transition metal clusters
[DE95-007082] p 2218 N95-27752
Hydrogen induced C-C, C-N, and C-S bond activities on Pi and Ni surfaces
[DE95-006251] p 2206 N95-27838
The role of hydrogen in the hydrogenation and hydrogenolysis of aniline on the nickel single crystal surfaces: Its implication on the mechanisms of HDN reactions
[DE95-006687] p 2222 N95-28134
Structural chemistry of some phases in the YC-Ni-B system
[DE95-007403] p 2447 N95-28537

NICKEL ALLOYS
Ultra high purity, dimensionally stable INVAR 36
[NASA-CASE-NPO-19358-1-CU] p 2213 N95-26862
Surface energy driven crystallization of amorphous Ni69Cr14P17 alloy
[DE95-005543] p 2438 N95-27085
Atomistic calculations of hydrogen interactions with Ni3Al grain boundaries and Ni/Ni/Ni3Al interfaces
[DE95-006497] p 2408 N95-27534
A new technique for measuring the separation of closely spaced dislocations using residual contrast conditions
[DE95-007147] p 2219 N95-27968
Trace elements and the mechanical properties of intermetallic compounds
[DE95-007378] p 2220 N95-28046
Electronic structure of ordered and disordered transition metal aluminides
[DE95-609034] p 2223 N95-28250

NICKEL CADMIUM BATTERIES
The 1994 27th Annual NASA Aerospace Battery Workshop
[NASA-CP-3292] p 2317 N95-26785
Alternate charging profiles for the onboard nickel cadmium batteries of the Explorer Platform/Extreme Ultraviolet Explorer p 2272 N95-26796

NICKEL COMPOUNDS
Nickel metal hydride LEO cycle testing
p 2272 N95-26791
Experimental determination of cluster geometrical structure
[DE95-007089] p 2409 N95-27753
High temperature oxidation of nickel concentrates
[PB95-195566] p 2224 N95-28644

NICKEL HYDROGEN BATTERIES
The 1994 27th Annual NASA Aerospace Battery Workshop
[NASA-CP-3292] p 2317 N95-26785
Progress towards computer simulation of NiH2 battery performance over life p 2272 N95-26786
Long life 80Ah standard IPV NiH2 battery cell
p 2272 N95-26787
High-rate/high-temperature capability of a single-layer zicar-separator nickel-hydrogen cell
p 2272 N95-26788
Air Force Ni-H2 cell test program: State of Charge test
p 2272 N95-26789
The 50 Ah NiH2 CPV qualification tests
p 2272 N95-26792
Unique features of a new nickel-hydrogen 2-cell CPV
p 2272 N95-26793
Hubble Space Telescope nickel-hydrogen battery testing: An update p 2272 N95-26794
Adiabatic charging of nickel-hydrogen batteries
p 2272 N95-26795
A review of nickel hydrogen battery technology
[NASA-TM-106918] p 2167 N95-27177

NICKEL OXIDES
Atomistic study of energy and structure of surfaces in NiO
[DE95-005207] p 2215 N95-27446

NIGHT VISION
An image quality analysis of ANVIS-6 night vision goggles
[AD-A289398] p 2359 N95-26883

NIMBUS 7 SATELLITE
Contingency maneuver strategies for the Total Ozone Mapping Spectrometer-Earth Probe (TOMS-EP)
p 2152 N95-27796
Solar UV flux measurements from the SBUV2 monitor on the NOAA9 satellite. Part 1: Mg II h and k line core-to-wing ratios for 1986-1988
[PB95-181962] p 2464 N95-28007
NIOBIUM
Particle-like absorption spectra in small transition metal clusters
[DE95-007082] p 2218 N95-27752
Femtosecond OPO's at 3 microns and beyond: Design and performance issues related to the crystal properties of KTP and similar materials
[DE95-007286] p 2446 N95-28242
NIOBIUM ALLOYS
FENIX experimental results of large-scale CICC made of bronze-processed Nb3Sn strands
[DE95-007965] p 2222 N95-28167
NITRATE ESTERS
Biodegradation of nitrate esters p 2171 N95-28299
NITRIC ACID
Absorption of sparingly soluble gases by reactive media in self-aerated gas-liquid contactors: A scale-up procedure
[DE95-006429] p 2206 N95-27707
Measurement of high acidity using a renewable-reagent fiber optic sensor
[DE95-006327] p 2425 N95-27734
NITRIC OXIDE
Mechanisms of hypertension after cross-linked hemoglobin blood-substitute transfusion
[AD-A289558] p 2352 N95-26680
High resolution Fourier transform spectroscopy of the first overtone of the N-O stretch in nitrosyl bromide
[AD-A289318] p 2203 N95-27295
Laser ionization of molecular clusters
[DE95-007011] p 2296 N95-27550
Superior catalysts for selective catalytic reduction of nitric oxide
[DE95-007903] p 2205 N95-27691
Absorption of sparingly soluble gases by reactive media in self-aerated gas-liquid contactors: A scale-up procedure
[DE95-006429] p 2206 N95-27707
NITRIDES
Materials Research Society Symposium Proceedings. Volume 339: Diamond, SiC and nitride wide bandgap semiconductors
[AD-A288690] p 2437 N95-26818
First-principles calculations for AlN, GaN, and InN: Bulk and alloy properties
[DE95-006822] p 2219 N95-27958
NITROBENZENES
A novel sensitive detector of atmospheric nitrocompounds based on laser photofragmentation/ionization spectrometry
p 2174 N95-28314
NITROGEN
Hydrogen induced C-C, C-N, and C-S bond activities on Pi and Ni surfaces
[DE95-006251] p 2206 N95-27838
The minimum pore size obtainable in a silica gel during drying
[DE95-008162] p 2239 N95-28401
Cryogenic BRDF measurements at 10.6 micrometers and 0.63 micrometers on contaminated mirrors
[AD-A291611] p 2427 N95-28408
NITROGEN IONS
Plasma source ion implantation of ammonia into electroplated chromium
[DE95-006275] p 2444 N95-28125
NITROGEN OXIDES
High pressure Earth storable rocket technology program: Basic program
[NASA-CR-195449] p 2166 N95-26390
Coupled chemistry/climate issues
[DE95-006443] p 2327 N95-27532
Absorption of sparingly soluble gases by reactive media in self-aerated gas-liquid contactors: A scale-up procedure
[DE95-006429] p 2206 N95-27707
FY 1994 ambient air monitoring report for McMurdo Station, Antarctica
[DE95-008565] p 2331 N95-28149
NITROGEN PLASMA
Plasma source ion implantation of ammonia into electroplated chromium
[DE95-006275] p 2444 N95-28125
NITROGEN TETROXIDE
Development test of a liquid Apogee engine for the ETS-6
[NAL-TR-1250] p 2167 N95-26799
Chemical reactions identified in the Titan 2, Titan 4, and Delta 2 propellant systems and their application to source modeling p 2172 N95-28304
Use of SURFACE CHEMKIN to model multiphase atmospheric chemistry: Application to nitrogen tetroxide spills p 2172 N95-28305
A new method for measuring hypergol scrubber emissions p 2174 N95-28312
NITROGLYCERIN
Biodegradation of nitrate esters p 2171 N95-28299
Radiant exchange considerations in design and scaleup of photocatalytic reactors for purification of nitroglycerine-contaminated air p 2171 N95-28300
NITROMETHANE
A density functional/molecular dynamics study of the structure of liquid nitromethane
[AD-A289224] p 2404 N95-26960
Probe molecule studies: Active species in alcohol synthesis
[DE95-003514] p 2203 N95-27420
NITROSYLS
High resolution Fourier transform spectroscopy of the first overtone of the N-O stretch in nitrosyl bromide
[AD-A289318] p 2203 N95-27295
NITROUS ACID
Absorption of sparingly soluble gases by reactive media in self-aerated gas-liquid contactors: A scale-up procedure
[DE95-006429] p 2206 N95-27707
NITROUS OXIDES
A novel sensitive detector of atmospheric nitrocompounds based on laser photofragmentation/ionization spectrometry
p 2174 N95-28314
NOAA SATELLITES
The design and implementation of the Military Applications of Shiptracks experiment on Space Transportation System - 65
[AD-A288488] p 2160 N95-26634
NOISE INTENSITY
Analysis of filter tuning techniques for sequential orbit determination p 2146 N95-27764
NOISE MEASUREMENT
Attitude determination using an adaptive multiple model filtering Scheme p 2148 N95-27772
NOISE PREDICTION
A numerical study of fundamental shock noise mechanisms
[NASA-TM-110608] p 2401 N95-27908
Measurement and prediction of broadband noise from large horizontal axis wind turbine generators
p 2324 N95-27990
Flow structure generated by perpendicular blade vortex interaction and implications for helicopter noise predictions
[NASA-CR-198590] p 2123 N95-28193
Response of multi-panel assembly to noise from a jet in forward motion
[NASA-CR-198164] p 2289 N95-28673
NOISE PREDICTION (AIRCRAFT)
Aircraft noise prediction program theoretical manual: Rotorcraft System Noise Prediction System (ROTONET), part 4
[NASA-TM-83199-PT-4] p 2400 N95-26392
Supersonic coaxial jet noise predictions
[NASA-TM-106917] p 2401 N95-26801
NOISE PROPAGATION
Very low frequency seismo-acoustic noise below the sea floor (0.2-10 Hz)
[AD-A289164] p 2347 N95-27011
NOISE REDUCTION
Electromagnetic devices and processes in environment protection
[AD-A288656] p 2141 N95-26487
Supersonic coaxial jet noise predictions
[NASA-TM-106917] p 2401 N95-26801
The noise reduction potential of dual-stream coaxial rectangular improperly expanded jet flows
[NASA-CR-197820] p 2277 N95-26995
Reconstruction of an infrared band of meteorological satellite imagery with abductive networks
[SAIC-94/1062] p 2345 N95-27389
Evaluation of a doubly-swept blade tip for rotorcraft noise reduction
[NASA-CR-189677] p 2402 N95-28264
SAR noise reduction through the utilization of robust filters
[INPE-5504-PRE/1787] p 2258 N95-28569
Noise exposure reduction of advanced high-lift systems
[NASA-CR-195077] p 2402 N95-28670
NOISE SPECTRA
Effect of noise on Frequency-Resolved Optical Gating measurements of ultrashort pulses
[DE95-007149] p 2298 N95-27969
Measurement and prediction of broadband noise from large horizontal axis wind turbine generators
p 2324 N95-27990
Observed acoustic and aeroelastic spectral responses of a MOD-2 turbine blade to turbulence excitation
p 2324 N95-27991
NONDESTRUCTIVE TESTS
Synthesis and characterization of polymeric materials
[AD-A288613] p 2225 N95-26482
Nondestructive testing apparatus for determining the orientation of reinforcing bars within a concrete structure
[AD-D017267] p 2245 N95-26508
Characterization of corrosion and development of a breadboard of a D sight aircraft inspection system, phase 1
[AD-A288347] p 2125 N95-26527
Combined investigation of Eddy current and ultrasonic techniques for composite materials NDE
[NASA-TM-110599] p 2306 N95-26778
Assay of weathering effects on protective polymer coatings using positron annihilation spectroscopy
[DE95-007040] p 2236 N95-27962
Physical interpretation and development of ultrasonic nondestructive evaluation techniques applied to the quantitative characterization of textile composite materials
[NASA-CR-198591] p 2306 N95-28034
Non-destructive inter-level dielectric via in-line process monitoring by atomic force microscopy
[DE95-008516] p 2267 N95-28146
AMCC casting development. Volume 1: Executive Summary
[NASA-CR-196597] p 2247 N95-28419
NONEQUILIBRIUM CONDITIONS
Anomalous collision rate in the time counter scheme of the direct simulation Monte Carlo method for rarefied gas flow analysis
[ISAS-R-653] p 2275 N95-26742
NONEQUILIBRIUM FLOW
Viscous shock-layer analysis on hypersonic flow over reentry capsule with nonequilibrium chemistry
[ISAS-R-656] p 2274 N95-26739
NONEQUILIBRIUM RADIATION
Radiation production from stagnating compact toroids employing a nonequilibrium radiation diffusion model
[AD-A289602] p 2429 N95-26720
NONFLAMMABLE MATERIALS
Design considerations in supercritical fluid technology
p 2232 N95-27126
NONLINEAR EQUATIONS
Development of a nonlinear simulation for the McDonnell Douglas F-15 Eagle with a longitudinal TECS control-law
[AD-A288610] p 2128 N95-26481
General purpose finite element solver
[PB95-185062] p 2388 N95-26495
An easy way to analyze longitudinal and lateral-directional trim problems with AEO or OEI
p 2119 N95-26949
Nonlinear problems in fluid dynamics and inverse scattering: Nonlinear waves and inverse scattering
[AD-A289148] p 2278 N95-27001
Nonlinear problems in fluid dynamics and inverse scattering: Langmuir circulations and spiral flows
[AD-A289194] p 2278 N95-27019
Nonlinear stability of non-stationary cross-flow vortices in compressible boundary layers
[NASA-CR-189184] p 2279 N95-27242
A Navier-Stokes boundary element solver
p 2283 N95-27361
Dithering transitions in resistive pressure-gradient-driven turbulence
[DE95-006737] p 2431 N95-27536
An invariant measure for a nonlinear Schroedinger equation
[DE95-610166] p 2391 N95-27714
Using the scalable nonlinear equations solvers package
[DE95-008323] p 2378 N95-28071
NONLINEAR EVOLUTION EQUATIONS
Nonlinear problems in fluid dynamics and inverse scattering: Propagation and capturing of singularities in problems of fluid dynamics and inverse scattering
[AD-A289146] p 2277 N95-26999
NONLINEAR FILTERS
Edge detection by nonlinear dynamics
[DE95-008076] p 2373 N95-28168
NONLINEAR OPTICS
Wake fields in semiconductor plasmas
[DE94-634523] p 2429 N95-26439
Near-resonant properties of nonlinear organic materials for optical devices
[AD-A288339] p 2178 N95-26570
Design, fabrication, modeling, and optical characterization of organic polymer nonlinear directional couplers
[AD-A289327] p 2227 N95-26897

Growth and evaluation of nonlinear optical crystals for laser applications: Lithium borate, barium borate and silver gallium selenide
[AD-A289147] p 2277 N95-27000
Edge detection by nonlinear dynamics
[DE95-008076] p 2373 N95-28168
Vibrational spectroscopy of water interfaces
[DE95-006592] p 2209 N95-28218
Low power limits in ultrashort pulse measurement using Frequency-Resolved Optical Gating
[DE95-007150] p 2299 N95-28219
Ultrashort Pulse retrieval using FROG trace irradiance moments and the adaptive neural networks backpropagation algorithm
[DE95-007153] p 2299 N95-28220
Passive spatial beam control, appendix
[AD-A288913] p 2300 N95-28333
Phase retrieval and time-frequency methods in the measurement of ultrashort laser pulses
[DE95-006499] p 2300 N95-28549
Nonlinear optical studies of surfaces
[DE95-006574] p 2428 N95-28557
Nonlinear dynamics of a coherent polariton-biexciton system
[DE95-609150] p 2417 N95-28607

NONLINEAR SYSTEMS
Analysis and development of finite element methods for the study of nonlinear thermomechanical behavior of structural components
[NASA-CR-195354] p 2307 N95-26387
A class of stabilizing controllers for flexible multibody systems
[NASA-TP-3494] p 2161 N95-26428
Nonlinear dynamics of global atmospheric and earth system processes
[NASA-CR-197926] p 2326 N95-26429
The phenomena of subharmonic bifurcations, runaway, and transition to chaos in a non-linear oscillator: perturbation methods and a numerical experiment
[IFTR-16/1994] p 2398 N95-26518
Stability and thermal influences in nonlinear continuum mechanics and material science
[AD-A288333] p 2448 N95-26563
A gain scheduling optimization method using genetic algorithms
[AD-A289306] p 2381 N95-26920
On the nonlinear stability of the unsteady, viscous flow of an incompressible fluid in a curved pipe
[NASA-CR-195065] p 2278 N95-27028
Nonlinear instability and chaos in plasma wave-wave interactions. I. Introduction
[DE95-005529] p 2429 N95-27084
Vector algorithms for solving 3D nonlinear magnetostatic problems
[DE95-608737] p 2399 N95-27298
Stable adaptive neurocontrollers for spacecraft and space robots p 2384 N95-27385
Linear and nonlinear trending and prediction for AVHRR time series data p 2385 N95-27391
A new finite element formulation for incompressible flow
[DE95-007141] p 2284 N95-27454
An invariant measure for a nonlinear Schroedinger equation
[DE95-610166] p 2391 N95-27714
Using the scalable nonlinear equations solvers package
[DE95-008323] p 2378 N95-28071
Nonlinear dynamics and aeroelasticity of rotorcraft in forward flight
[AD-A291714] p 2136 N95-28504
Non-linear resistive grid kernel estimator useful in single feature, two-class pattern classification
[AD-D017394] p 2271 N95-28614
Non-linear viscoelastic behaviour
[PB95-192811] p 2199 N95-28639

NONLINEARITY
Process control of microstructure in manufacturing
[AD-A288291] p 2245 N95-26410
Nonlinear scalespace via hierarchical statistical modeling
[AD-A289057] p 2394 N95-26478
A new growth technology for highly non-linear, optical quality organic films: Organic vapor phase deposition
[AD-A289006] p 2178 N95-26567
Near-resonant properties of nonlinear organic materials for optical devices
[AD-A288339] p 2178 N95-26570
A state-space model of a large, lightly damped space structure using the Eigensystem realization algorithm
[AD-A289251] p 2163 N95-26970
Characterization of optical polymers for multi-layered electro-optic devices
[AD-A289255] p 2227 N95-26973
Investigation into the behavior of geometrically nonlinear composite arches
[AD-A289258] p 2308 N95-26975
Testing of Uninterruptible Power Supplies with nonlinear loads
[AD-A289353] p 2262 N95-27067
A study of internal damage of metal matrix composites by neutron diffraction
[DE95-005157] p 2182 N95-27080
Nonlinear signal processing schemes for robust target detection in radar
[AD-A288449] p 2255 N95-27185
Micromechanical modeling of damage and inelasticity of composite materials in macroscopic structural analysis
[DE95-003666] p 2182 N95-27421
Integrating the QMR method with first principles material science application code
[DE95-007380] p 2408 N95-27456
Parallel plasma fluid turbulence calculations
[DE95-006741] p 2431 N95-27537
Observation of nonlinear resonances in the advanced light source
[DE95-006561] p 2425 N95-27675
Use of nonlinear identification in robust attitude and attitude rate estimation for SAMPEX
p 2149 N95-27781
Nonlinear optical microscopy for imaging thin films and surfaces
[DE95-007872] p 2426 N95-28018
An investigation of the chemical and physical properties of pristine, electrochromically damaged, and photochromically damaged KTiOPO4 (KTP) using surface analytical and optical spectroscopic techniques
[DE95-007865] p 2443 N95-28023
Modification of the optical properties of glass by sequential ion implantation
[DE95-007401] p 2237 N95-28080
Nonlinear beam dynamics experimental program at SPEAR
[DE95-007823] p 2422 N95-28122
Beam-beam interaction working group summary
[DE95-007824] p 2422 N95-28123
Bearing defect signature analysis using advanced nonlinear signal analysis in a controlled environment
[NASA-TM-108491] p 2304 N95-28364
Denoising and robust non-linear wavelet analysis
[AD-A291668] p 2257 N95-28455
Characterization of solid state laser and nonlinear optical materials
[AD-A291684] p 2300 N95-28458
Chua's circuits: Phenomena and applications
[AD-A291638] p 2271 N95-28666

NONPARAMETRIC STATISTICS
A method to determine the structure of an unknown mixture using the Akaike Information Criterion and the bootstrap
[AD-A288295] p 2394 N95-26415
The 1994 IEEE-IMS Workshop on Information Theory and Statistics
[AD-A288808] p 2380 N95-26492

NONUNIFORM MAGNETIC FIELDS
Electromagnetic hysteretic response calculation for superconductors in demagnetizing geometries
[DE95-005028] p 2264 N95-27403

NORMAL DENSITY FUNCTIONS
Truncated Gaussians as tolerance sets
[NASA-CR-197732] p 2395 N95-27417
A method for generating skewed random numbers using two overlapping uniform distributions
[DE95-008747] p 2392 N95-28162

NORTH ATLANTIC TREATY ORGANIZATION (NATO)
AGARD membership, 1995
[AGARD-MEMB-95] p 2450 N95-26353

NORTHERN HEMISPHERE
The northern wintertime divergence extrema at 200 hPa and surface cyclones as simulated in the integration of the ECMWF general circulation model
[DE95-007946] p 2332 N95-28550

NOTCH SENSITIVITY
Tension fracture of laminates for transport fuselage. Part 1: Material screening p 2137 N95-28471

NOVAE
Classical novae and recurrent novae: General properties p 2459 N95-27072
Models of classical and recurrent novae
p 2459 N95-27073
Typical examples of classical novae
p 2459 N95-27074
Recurrent novae p 2460 N95-27075
A new method of determining the ejected mass of novae
[DE95-007884] p 2462 N95-28062

NOZZLE DESIGN
The noise reduction potential of dual-stream coaxial rectangular improperly expanded jet flows
[NASA-CR-197820] p 2277 N95-26995
The application of waterjets for cleaning
p 2233 N95-27130

NOZZLE FLOW
An investigation of the AFIT 2-inch shock tube as a flow source for supersonic testing
[AD-A289246] p 2143 N95-26966
Effects of blowing ratio on heat transfer to the throat region of a porous-walled nozzle
[AD-A289459] p 2167 N95-27153
A laboratory scale supersonic combustive flow system
[DE95-006347] p 2206 N95-27851
Structure of high-speed sprays
[AD-A291696] p 2288 N95-28523

NOZZLE GEOMETRY
Effects of blowing ratio on heat transfer to the throat region of a porous-walled nozzle
[AD-A289459] p 2167 N95-27153

NUCLEAR BINDING ENERGY
Aspects of strange matter
[DE95-008316] p 2414 N95-28170

NUCLEAR FUELS
An overview of activities and accomplishments of the Metals and Ceramics Division
[DE95-007020] p 2241 N95-28560

NUCLEAR FUSION
Bubble fusion: Preliminary estimates
[DE95-006337] p 2420 N95-27494
Parallel plasma fluid turbulence calculations
[DE95-006741] p 2431 N95-27537

NUCLEAR MAGNETIC RESONANCE
NQR-NMR studies of higher alcohol synthesis Cu-Co catalysts
[DE95-007926] p 2205 N95-27680

NUCLEAR PHYSICS
Signatures of Higgs-Triplet representations at TeV-e(+)e(-) colliders
[DE95-007201] p 2419 N95-27089
The systems of the proportional chambers registration electronics for present experiments in nuclear physics
[DE95-608559] p 2419 N95-27161
Monolithic electronics for nuclear and high-energy physics experiments
[DE95-005393] p 2420 N95-27427
Intermediate energy neutrons at WNR. Spin-isospin and energy dependence of the NN interaction and the nuclear response
[DE95-006291] p 2408 N95-27466

NUCLEAR POWER PLANTS
Physics assessment of stellarators as fusion power plants
[DE95-007045] p 2431 N95-27498

NUCLEAR RADIATION
Comparison of the resistance of the MOS integrated circuits with various types of nuclear radiation
[DE95-608623] p 2261 N95-27023

NUCLEAR REACTIONS
Search for deeply bound pionic atoms with high-purity germanium tagging spectrometer
[DE95-609072] p 2416 N95-28252

NUCLEAR REACTORS
Heat pipe cooled reactors for multi-kilowatt space power supplies
[DE95-005211] p 2420 N95-27425
Gamma ray-induced embrittlement of pressure vessel alloys
[DE95-007133] p 2220 N95-28072
Reactor pressure vessel structural integrity research
[DE95-007034] p 2223 N95-28208

NUCLEAR STRUCTURE
Measurement of the reaction C(nu(sub mu), mu(-)) X near threshold
[DE95-007888] p 2412 N95-28063

NUCLEATION
Pseudomorphic semiconducting heterostructures from combinations of AlN, GaN and selected SiC polytypes: Theoretical advancement and its coordination with experimental studies of nucleation, growth, characterization and device development
[AD-A289550] p 2437 N95-26756
Growth, characterization and device development in monocrystalline diamond films
[AD-A289356] p 2439 N95-27416
Bubble chamber spectroscopy for chemical analysis: A new concept
[DE95-006350] p 2209 N95-28088
Atomic layer epitaxy of group 4 materials: Surface processes, thin films, devices and their characterization
[AD-A289092] p 2446 N95-28327
The in situ observation of epitaxial diamond thin film nucleation and growth using emission electron microscopy
[AD-A289841] p 2447 N95-28618

NUCLEIC ACIDS
DNA denaturation through a model of the partition points on a one-dimensional lattice
[DE95-607909] p 2439 N95-27201
NUCLEON-NUCLEON INTERACTIONS
Recent status in the search for the quark-gluon plasma
[DE95-007036] p 2417 N95-28447
NUCLEON-NUCLEON SCATTERING
Measurement of the reaction C(nu(sub mu), mu(-)) X near threshold
[DE95-007888] p 2412 N95-28063
NUCLEONS
Lattice calculation for lepton capture from vacuum-pair production in relativistic heavy-ion collisions
[DE95-007392] p 2413 N95-28077
HZETRN: Description of a free-space ion and nucleon transport and shielding computer program
[NASA-TP-3495] p 2465 N95-28530
NUCLEOTIDES
Single molecule detection using charge-coupled device array technology
[DE95-006425] p 2411 N95-27953
NUCLIDES
Alpha characterization inside pipes using ion-transport technology
[DE95-007869] p 2411 N95-28024
NUMERICAL ANALYSIS
Encoding user-defined problems with SIPE-2
[AD-A288390] p 2380 N95-26475
Addressing tension instability in SPH methods
[AD-A289531] p 2276 N95-26852
Numerical analysis of wave scattering
[AD-A289478] p 2401 N95-26925
Mathematical simulation of three-dimensional magnetic field of spectrometric magnet SP-40
[DE95-608736] p 2398 N95-27239
Spectral methods on arbitrary grids
[NASA-CR-198158] p 2279 N95-27247
Numerical methods for determining interstitial oxygen in silicon
[DE95-007710] p 2205 N95-27683
A numerical study of fundamental shock noise mechanisms
[NASA-TM-110608] p 2401 N95-27908
Prediction of material strength and fracture of glass using the SPHINX smooth particle hydrodynamics code
[DE95-004869] p 2236 N95-27943
Numerical analysis of intra-cavity and power-stream flow interaction in multiple gas-turbine disk-cavities
[NASA-TM-106886] p 2140 N95-28344
Third-order-accurate numerical methods for efficient, large time-step solutions of mixed linear and nonlinear problems
[DE95-009184] p 2288 N95-28533
NUMERICAL CONTROL
Robust hybrid state-space self-tuning control using dual-rate sampling
[AD-A288359] p 2380 N95-26468
Next generation controller specification for an open systems architecture standard - overview
[AD-A289507] p 2368 N95-26853
To develop an aerosoling immunomagnetic device for rapid medical diagnosis from clinical samples
[AD-A288504] p 2354 N95-27059
Statistical data analysis
[DE95-007214] p 2454 N95-27090
Process and control systems for composites manufacturing p 2184 N95-28267
Particle fallout/activity sensor
[NASA-CASE-KSC-11687-1] p 2293 N95-28362
ALLIANCE: An architecture for fault tolerant, cooperative control of heterogeneous mobile robots
[DE95-007374] p 2387 N95-28536
Next generation controller specification for an open systems architecture standard
[AD-A289567] p 2375 N95-28647
NUMERICAL DATA BASES
Indexing meso-beta surface wind site representative
[AD-A288501] p 2341 N95-26650
NUMERICAL FLOW VISUALIZATION
Three-dimensional visualization of reactive flows in complex geometries
[DE95-006332] p 2284 N95-27845
NUMERICAL INTEGRATION
Analysis and development of finite element methods for the study of nonlinear thermomechanical behavior of structural components
[NASA-CR-195354] p 2307 N95-26387
The attenuation of microwave radiation by fog and rain
[AD-A288326] p 2249 N95-26562
A numerical study of ultra-short-pulse reflectometry
[DE95-006070] p 2266 N95-28015
NUMERICAL STABILITY
Analysis and development of finite element methods for the study of nonlinear thermomechanical behavior of structural components
[NASA-CR-195354] p 2307 N95-26387
Spectral methods on arbitrary grids
[NASA-CR-198158] p 2279 N95-27247
NUMERICAL WEATHER FORECASTING
Diagnosing cloudiness from global numerical weather prediction model forecasts
[AD-A289456] p 2356 N95-26992
NUTATION
Optimal attitude maneuver execution for the Advanced Composition Explorer (ACE) mission
p 2149 N95-27778
NUTATION DAMPERS
Optimization of a nutation damper attached to a spin-stabilized satellite
[AD-A289424] p 2162 N95-26887
NUTRITION
Performance enhancing ration components program: Supplemental carbohydrate test
[AD-A288560] p 2358 N95-26558

O

OBJECT-ORIENTED PROGRAMMING
Specifying weak sets
[AD-A288587] p 2364 N95-26536
User's and test case manual for FEMATS
[NASA-CR-197803] p 2366 N95-26694
NEXTSTEP: The next step in the right direction? Part 2: Software development with NEXTSTEP
[REPT-94-33-PT-2] p 2450 N95-26803
The re-engineering of the Air Force Institute of Technology Student Information System
[AD-A289426] p 2453 N95-26866
EASY-SIM: A visual simulation system software architecture with an Ada 9X application framework
[AD-A289325] p 2368 N95-26895
Flight dynamics software in a distributed network environment p 2151 N95-27790
OBLATE SPHEROIDS
Simple equivalent dipole distributions for dielectric spheroidal scatterers
[PB95-184883] p 2254 N95-27049
OBLIQUE WINGS
Preliminary design problems and solutions for a supersonic oblique all-wing transport aircraft
p 2118 N95-26942
OBSERVATORIES
Long Duration Exposure Facility post-flight data as it influences the Tropical Rainfall Measuring Mission
p 2345 N95-27666
The installation of and first results from the superconducting gravimeter GWR20 at the Metsahovi Station, Finland
[REPT-95:1] p 2338 N95-27995
OCCULTATION
Proceedings of the 1993 Scientific Conference on Obscuration and Aerosol Research
[AD-A280084] p 2331 N95-28153
OCEAN BOTTOM
Very low frequency seismo-acoustic noise below the sea floor (0.2-10 Hz)
[AD-A289164] p 2347 N95-27011
Observations of near-bottom flow in a wave-dominated nearshore environment
[AD-A289331] p 2347 N95-27043
Investigation on comprehensive fossil fuel cycle analysis and assessment approach as viewed from the global environment
[DE95-759241] p 2329 N95-27935
On the persistence of the oceanic background of apparent sea level changes in the Baltic Sea
[REPT-94:5] p 2348 N95-27996
Seismic constraints on shallow crustal processes at the East Pacific rise
[AD-A289055] p 2338 N95-28094
Ultrasonic studies of liquid/solid seimoacoustic wave phenomena
[AD-A289644] p 2402 N95-28622
OCEAN CURRENTS
A geo-acoustic and oceanographic description of several shallow water experimental sites on the Scotian Shelf
[AD-A288300] p 2345 N95-26420
Calculation of suspended sediment transport by combined wave-current flows
[AD-A289368] p 2346 N95-26904
Nonlinear problems in fluid dynamics and inverse scattering: Langmuir circulations and spiral flows
[AD-A289194] p 2278 N95-27019
Observations of near-bottom flow in a wave-dominated nearshore environment
[AD-A289331] p 2347 N95-27043
Biological/physical modeling of upper ocean processes
[AD-A289468] p 2347 N95-27151
Study of the response of a three-dimensional coupled ice-ocean model to daily varying atmospheric forcing
[AD-A289050] p 2347 N95-27189
Tomographic observations of deep convection and the thermal evolution of the Greenland Sea Gyre 1988-1989
[AD-A289104] p 2348 N95-28096
Altimeter analysis of ocean currents
[AD-A290167] p 2315 N95-28392
OCEAN DYNAMICS
Nonlinear problems in fluid dynamics and inverse scattering: Langmuir circulations and spiral flows
[AD-A289194] p 2278 N95-27019
OCEAN MODELS
Hindcasting wind-driven anomalies using reduced-gravity global ocean models with 1/2 deg and 1/4 deg resolution
[AD-A289060] p 2345 N95-26406
Infrared field measurements of sea surface temperature: Analysis of wake signatures and comparison of skin layer models
[NASA-CR-197849] p 2346 N95-26533
A parallel coupled oceanic-atmospheric general circulation model
[DE95-005918] p 2335 N95-26622
Biological/physical modeling of upper ocean processes
[AD-A289468] p 2347 N95-27151
Study of the response of a three-dimensional coupled ice-ocean model to daily varying atmospheric forcing
[AD-A289050] p 2347 N95-27189
Testing the correlation between seismic stratigraphy, diagenesis and physical rock properties: Evaluation of fluid flow during early and late diagenesis
[DE95-008338] p 2338 N95-28083
OCEAN SURFACE
SeaWiFS technical report series. Volume 26: Results of the SeaWiFS Data Analysis Round-Robin, July 1994 (DARR-1994)
[NASA-TM-104566-VOL-26] p 2345 N95-26430
Infrared field measurements of sea surface temperature: Analysis of wake signatures and comparison of skin layer models
[NASA-CR-197849] p 2346 N95-26533
Deep convection in the Mediterranean Sea
[AD-A288497] p 2346 N95-26647
Fluxes across the west coast resolved by Picket Fence observations during stormfest
[AD-A288511] p 2341 N95-26653
Modeling surface effects with the parabolic equation method
[AD-A289199] p 2254 N95-27021
Biological/physical modeling of upper ocean processes
[AD-A289468] p 2347 N95-27151
Study of the response of a three-dimensional coupled ice-ocean model to daily varying atmospheric forcing
[AD-A289050] p 2347 N95-27189
An in situ evaluation of TOPEX/Poseidon altimetric measurements versus meaurements made by moorings and inverted echo sounders for sea surface height
[NASA-CR-198621] p 2347 N95-27805
Tomographic observations of deep convection and the thermal evolution of the Greenland Sea Gyre 1988-1989
[AD-A289104] p 2348 N95-28096
The northern wintertime divergence extrema at 200 hPa and surface cyclones as simulated in the integration of the ECMWF general circulation model
[DE95-007946] p 2332 N95-28550
OCEAN TEMPERATURE
Temporal and spatial decorrelation scales of the Yellow Sea thermal fields
[AD-A288617] p 2346 N95-26483
Infrared field measurements of sea surface temperature: Analysis of wake signatures and comparison of skin layer models
[NASA-CR-197849] p 2346 N95-26533
OCEANOGRAPHIC PARAMETERS
A geo-acoustic and oceanographic description of several shallow water experimental sites on the Scotian Shelf
[AD-A288300] p 2345 N95-26420
Analysis of historical oceanographic data on a personal computer. Program MDS
[AD-A288965] p 2363 N95-26447
Meteorological and oceanographic data collected during the ASREX 91 field experiment
[AD-A289492] p 2342 N95-26826
Downloading environmental data in the new MOODS format
[AD-A288835] p 2456 N95-28589

OCEANOGRAPHY

Hindcasting wind-driven anomalies using reduced-gravity global ocean models with 1/2 deg and 1/4 deg resolution [AD-A289060] p 2345 N95-26406

A geo-acoustic and oceanographic description of several shallow water experimental sites on the Scotian Shelf [AD-A288300] p 2345 N95-26420

SeaWiFS technical report series. Volume 26: Results of the SeaWiFS Data Analysis Round-Robin, July 1994 (DARR-1994) [NASA-TM-104566-VOL-26] p 2345 N95-26430

Analysis of historical oceanographic data on a personal computer. Program MDS [AD-A288965] p 2363 N95-26447

The effect of infrared sea surface temperature measurements on evaporation duct height estimation [AD-A289045] p 2346 N95-26477

Infrared field measurements of sea surface temperature: Analysis of wake signatures and comparison of skin layer models [NASA-CR-197849] p 2346 N95-26533

Biological/physical modeling of upper ocean processes [AD-A289468] p 2347 N95-27151

Airborne geophysics and precise positioning: Scientific issues and future directions [LC-94-68678] p 2314 N95-27156

WTEC panel report on research submersibles and undersea technologies [NASA-CR-198565] p 2247 N95-27909

Tomographic observations of deep convection and the thermal evolution of the Greenland Sea Gyre 1988-1989 [AD-A289104] p 2348 N95-28096

Emerging applications of probability (stochastic models in geosystems) [AD-A289117] p 2313 N95-28099

OCEANS

Observations of near-bottom flow in a wave-dominated nearshore environment [AD-A289331] p 2347 N95-27043

Measurement of heterogeneous chemical processes relevant to aerosol surfaces and trace gases active in the marine environment [DE95-008337] p 2328 N95-27743

Survey on researches related to ocean disposal of carbon dioxide [DE95-759247] p 2329 N95-27939

Inspection methods for underwater cables [AD-A289610] p 2312 N95-28616

OCTETS

Search for exotic particles at CDF [DE95-008383] p 2411 N95-27933

OGIVES

Polarization sensitivity of monopulse radar boresight error induced by large, ogive radomes [AD-A289254] p 2252 N95-26972

OH-58 HELICOPTER

Diagnosis of helicopter gearboxes using structure-based networks [NASA-TM-106932] p 2302 N95-27373

OHMIC DISSIPATION

OBIC analysis of stressed, thermally-isolated polysilicon resistors [DE95-008511] p 2268 N95-28201

OIL SLICKS

Design, construction, test and evaluation of a frequency scanning radiometer for measuring oil slick thicknesses [AD-A290040] p 2293 N95-28389

OILS

Biomass Pyrolysis Oil Properties and Combustion Meeting [DE95-004017] p 2204 N95-27438

Design, construction, test and evaluation of a frequency scanning radiometer for measuring oil slick thicknesses [AD-A290040] p 2293 N95-28389

OLIGOMERS

Molecular object liquid crystals: An approach to new materials [AD-A288905] p 2437 N95-26553

Materials with self organized surfaces: 2D polymer assemblies [AD-A288928] p 2226 N95-26627

Phenylethynyl terminated imide oligomers [NASA-CASE-LAR-15175-1] p 2235 N95-27732

Molecular engineering of thin polymer films prepared from functionally-terminated oligomers [AD-A291681] p 2240 N95-28457

ON-LINE SYSTEMS

Long term distributed file reference tracing: Implementation and experience [AD-A288585] p 2452 N95-26535

The systems of the proportional chambers registration electronics for present experiments in nuclear physics [DE95-608559] p 2419 N95-27161

Magnetic field measurement for the spectrometric magnet of the ISTRA-M setup [DE95-608560] p 2362 N95-27162

Real-time value-driven diagnosis p 2386 N95-27396

Transparent access to distributed, heterogeneous environmental information systems [DE95-007268] p 2454 N95-27483

Long Duration Exposure Facility (LDEF) Archive System p 2457 N95-27658

Development and implementation of an electronic library tour for the NASA Langley Technical Library [NASA-TM-110619] p 2455 N95-27701

Flight dynamics software in a distributed network environment p 2151 N95-27790

Methods development for measuring and classifying flammability/combustibility of refrigerants. Task 1: Annotated bibliography [DE95-007232] p 2238 N95-28133

Teaching interdisciplinary computational science from an electronic book on the Internet [DE95-006525] p 2373 N95-28498

Building an electronic book on the Internet. CSEP:An interdisciplinary syllabus for teaching computational science at the graduate level [DE95-006526] p 2375 N95-28632

ONBOARD DATA PROCESSING

Classification of RF transients in space using digital signal processing and neural network techniques [DE95-006287] p 2256 N95-27840

ONBOARD EQUIPMENT

Alternate charging profiles for the onboard nickel cadmium batteries of the Explorer Platform/Extreme Ultraviolet Explorer p 2272 N95-26796

Analysis of filter tuning techniques for sequential orbit determination p 2146 N95-27764

ONE DIMENSIONAL FLOW

The method of space-time conservation element and solution element-applications to one-dimensional and two-dimensional time-marching flow problems [NASA-TM-106915] p 2389 N95-26663

The use of wavelet transforms in the solution of two-phase flow problems [DE95-004688] p 2284 N95-27721

OPEN CIRCUIT VOLTAGE

Adiabatic charging of nickel-hydrogen batteries p 2272 N95-26795

OPENINGS

Analysis of stresses in finite anisotropic panels with centrally located cutouts p 2187 N95-28286

OPERATING COSTS

Lessons learned from the introduction of autonomous monitoring to the EUVE science operations center p 2385 N95-27393

OPERATING SYSTEMS (COMPUTERS)

Application-aware adaptation for mobile computing [AD-A288366] p 2363 N95-26469

Operating system support for coexistence of real-time and conventional scheduling [AD-A288584] p 2364 N95-26534

Energetic particle destabilization of shear Alfven waves in stellarators and tokamaks [DE95-006393] p 2431 N95-27419

OPERATING TEMPERATURE

Comparison of the calculated and measured stability of a NbTi cable-in-conduit conductor [DE95-007964] p 2265 N95-27693

OPERATIONAL PROBLEMS

Air traffic operational inventory CY 1994 [AD-A288281] p 2126 N95-26454

OPERATOR PERFORMANCE

Subjective workload assessment in a spatial memory task [AD-A289491] p 2356 N95-26825

Generic satellite monitoring expert system [AD-A289209] p 2163 N95-26987

Gloved operator performance study. The effects of hand wear and elastic resistance of a control during tracking performance [AD-A289405] p 2360 N95-27099

Image quality metrics for color CRT displays [AD-A288934] p 2262 N95-27196

OPERATORS (MATHEMATICS)

Gromov-Lawson-Rosenberg conjecture for groups with periodic cohomology [PB95-185203] p 2389 N95-26915

Quantum k-Poincare 1994 [DE95-608754] p 2448 N95-27332

The assembly tower and some categorical and algebraic aspects of frame theory [AD-A289360] p 2391 N95-27489

Remarks on the growth of the resolvent operators for power bounded operators [PB95-195418] p 2393 N95-28653

OPERATORS (PERSONNEL)

Handbook of perception and human performance, volume 2. Cognitive processes and performance [AD-A289587] p 2355 N95-26692

OPTICAL COMPUTERS

Digital optical computing [AD-A289395] p 2368 N95-26881

OPTICAL CONTROL

An optoelectronic attenuator for the high-speed control of microwave integrated circuits [AD-A289579] p 2260 N95-26690

Characterization of microwave MESFET circuits under laser illumination. Applications to phased array radar, microwave communications, and digital clock control [AD-A289181] p 2261 N95-27015

OPTICAL CORRECTION PROCEDURE

Experience from the in-flight calibration of the Extreme Ultraviolet Explorer (EUVE) and Upper Atmosphere Research Satellite (UARS) fixed head star trackers (FHSTs) p 2149 N95-27779

OPTICAL DATA PROCESSING

Digital optical computing [AD-A289395] p 2368 N95-26881

Nonlinear dynamics of a coherent polariton-biexciton system [DE95-609150] p 2417 N95-28607

OPTICAL DENSITY

Evaluation of laser-protective eyewear dyes in UVEX lenses [AD-A290076] p 2361 N95-28390

OPTICAL EQUIPMENT

Near-resonant properties of nonlinear organic materials for optical devices [AD-A288339] p 2178 N95-26570

The development of infrared detectors and mechanisms for use in future infrared space missions [NASA-CR-197819] p 2290 N95-26702

Ultra-high, resolution, modular optical angle encoder for space-based opto-mechanical applications p 2156 N95-27270

Direct ultrashort-pulse retrieval using frequency-resolved optical gating and a computational neural network [DE95-007148] p 2425 N95-27482

Long Duration Exposure Facility (LDEF) space optics handbook p 2428 N95-27654

Optical design and performance of the inelastic scattering beamline at the National Synchrotron Light Source [DE95-007679] p 2422 N95-28195

OPTICAL FIBERS

JPRS report: Science and technology. Central Eurasia [JPRS-UST-95-016] p 2262 N95-27170

OPTICAL FILTERS

Display system employing acousto-optic tunable filter [NASA-CASE-NPO-18736-1-CU] p 2426 N95-27843

OPTICAL FLOW (IMAGE ANALYSIS)

Schlieren System and method for moving objects [NASA-CASE-LAR-15053-1] p 2291 N95-27191

OPTICAL MATERIALS

A new growth technology for highly non-linear, optical quality organic films: Organic vapor phase deposition [AD-A289006] p 2178 N95-26567

Study of frequency doubling antireflection coating [AD-A289634] p 2424 N95-26860

Growth and evaluation of nonlinear optical crystals for laser applications: Lithium borate, barium borate and silver gallium selenide [AD-A289147] p 2277 N95-27000

Evaluation of space environmental effects on metals and optical thin films on EOIM-3 p 2210 N95-27641

BMDO materials testing in the EOIM-3 experiment p 2211 N95-27644

Point defect formation in optical materials expos ed to the space environment p 2428 N95-27646

Effects of the LDEF orbital environment on the reflectance of optical mirror materials p 2428 N95-27651

Passive spatial beam control, appendix [AD-A288913] p 2300 N95-28333

Characterization of solid state laser and nonlinear optical materials [AD-A291684] p 2300 N95-28458

Influences of film structures on laser damage thresholds [AD-A289647] p 2300 N95-28633

OPTICAL MEASUREMENT

Flow visualization of a turbulent shear flow using an optical wavefront sensor [AD-A289208] p 2277 N95-26986

Investigation of the collision line broadening problem as applicable to the NASA Optical Plume Anomaly Detection (OPAD) system, phase 1 [NASA-CR-198605] p 2426 N95-27913

Effect of noise on Frequency-Resolved Optical Gating measurements of ultrashort pulses
[DE95-007149] p 2298 N95-27969
A numerical study of ultra-short-pulse reflectometry
[DE95-008070] p 2266 N95-28015
Analysis of solar receiver flux distributions for US/Russian solar dynamic system demonstration on the MIR Space Station
[NASA-TM-106933] p 2169 N95-28036
Off-specular scattering in neutron reflectometry
[DE95-007835] p 2412 N95-28057
Low power limits in ultrashort pulse measurement using Frequency-Resolved Optical Gating
[DE95-007150] p 2299 N95-28219
Particle fallout/activity sensor
[NASA-CASE-KSC-11687-1] p 2293 N95-28362

OPTICAL MEASURING INSTRUMENTS
Measurement of high acidity using a renewable-reagent fiber optic sensor
[DE95-006327] p 2425 N95-27734
Passive spatial beam control, appendix
[AD-A288913] p 2300 N95-28333

OPTICAL MEMORY (DATA STORAGE)
Optical implementation of inner product neural associative memory
[NASA-CASE-NPO-18491-2-CU] p 2427 N95-28363

OPTICAL POLARIZATION
Conversion of sunflower multiband radiometer polarization measurements to polarization parameters
[NASA-CR-197774] p 2314 N95-26815
Fundamental concepts of integrated and fiber optic sensors
[NASA-TM-106920] p 2426 N95-27906

OPTICAL PROPERTIES
Molecular object liquid crystals: An approach to new materials
[AD-A288905] p 2437 N95-26553
Design, fabrication, modeling, and optical characterization of organic polymer nonlinear directional couplers
[AD-A289327] p 2227 N95-26897
Growth, characterization and device development in monocrystalline diamond films
[AD-A289356] p 2439 N95-27416
Photoemission and optical properties of C60 fullerites
[DE95-006588] p 2425 N95-27539
Evaluation of space environmental effects on metals and optical thin films on EOIM-3 p 2210 N95-27641
Observation of asymmetrical two-cone Vavilov-Cherenkov radiation in biaxial crystal of triglycinesulphate emitted by 658 MeV protons passing along bi normal
[DE94-629017] p 2441 N95-27867
Modification of the optical properties of glass by sequential ion implantation
[DE95-007401] p 2237 N95-28080
Coherent V2O3 precipitates in alpha-Al2O3CO-implanted with vanadium and oxygen
[DE95-007404] p 2444 N95-28081
Low temperature carrier transport properties in isotopically controlled germanium
[DE95-008489] p 2444 N95-28092
Proceedings of the 1993 Scientific Conference on Obscuration and Aerosol Research
[AD-A280084] p 2331 N95-28153
Characterization of solid state laser and nonlinear optical materials
[AD-A291684] p 2300 N95-28458
Laser beam aerosol interactions
[AD-A291723] p 2300 N95-28509
Influences of film structures on laser damage thresholds
[AD-A289647] p 2300 N95-28633

OPTICAL RADAR
Continuously-tunable, narrow-linewidth, Q-switched Cr:LiSAF laser for lidar applications
[DE95-006285] p 2296 N95-27672
The concentration-estimation problem for multiple-wavelength differential absorption lidar
[DE95-008375] p 2256 N95-28231
Remote sensing of the atmosphere by resonance Raman LIDAR
[DE95-007312] p 2315 N95-28520
Measurements of daytime and upper tropospheric water vapor profiles by Raman lidar
[DE95-007640] p 2344 N95-28538

OPTICAL REFLECTION
Phase retrieval and time-frequency methods in the measurement of ultrashort laser pulses
[DE95-006499] p 2300 N95-28549

OPTICAL RESONATORS
Thermally-induced unsymmetric optical distortion of output window of high-power CO2 laser
[AD-A289604] p 2300 N95-28650

OPTICAL SCANNERS
Characterization of Ultra-Low Carbon Baintic steels for use as weld wire consumables
[AD-A288292] p 2212 N95-26411
Tensile properties of Fe-16 at. % Al alloys
[DE95-007102] p 2215 N95-27450

OPTICAL SWITCHING
An optoelectronic attenuator for the high-speed control of microwave integrated circuits
[AD-A289579] p 2260 N95-26690

OPTICAL TRACKING
An image quality analysis of ANVIS-6 night vision goggles
[AD-A289398] p 2359 N95-26883
Long-range eye tracking: A feasibility study
[DE95-008587] p 2357 N95-28176

OPTICAL WAVEGUIDES
Design, fabrication, modeling, and optical characterization of organic polymer nonlinear directional couplers
[AD-A289327] p 2227 N95-26897
Perturbations on effective index of refraction from prism coupling
[AD-A291700] p 2427 N95-28524

OPTICS
Retrofitting a fine-pointing system to satellite optics
p 2157 N95-27277
The 132 nsec bunch spacing in the Tevatron proton-antiproton collider
[DE95-005750] p 2422 N95-28346
Basic and applied research in the field of electronics and communications
[AD-A291727] p 2270 N95-28512

OPTIMAL CONTROL
Flight control design using mixed H2/micron optimization
[AD-A289288] p 2142 N95-27036
Optimal control of two queues in series
[DE95-608731] p 2382 N95-27045
Optimal attitude maneuver execution for the Advanced Composition Explorer (ACE) mission
p 2149 N95-27778
Use of nonlinear identification in robust attitude and attitude rate estimation for SAMPEX
p 2149 N95-27781

OPTIMIZATION
Supersonic transport grid generation, validation, and optimization
[NASA-CR-197752] p 2365 N95-26648
Contribution to the optimal shape design of two-dimensional internal flows with embedded shocks
[NASA-CR-195062] p 2389 N95-26672
Alternate charging profiles for the onboard nickel cadmium batteries of the Explorer Platform/Extreme Ultraviolet Explorer p 2272 N95-26796
A process improvement model for software verification and validation
[NASA-CR-197761] p 2367 N95-26814
Creating an alternative parameter optimization method (APO) p 2118 N95-26946
Observations on the solvating power of supercritical fluids p 2228 N95-27106
A sustainable genetic algorithm for satellite resource allocation p 2376 N95-27383
Improved numerical solution of mixed H2/H(infinity) optimization with applications
[AD-A289315] p 2386 N95-27400
Optimization of wave rotors for use as gas turbine engine topping cycles
[NASA-TM-106951] p 2140 N95-27860
CORSSTOL: Cylinder Optimization of Rings, Skin, and Stringers with Tolerance sensitivity
[NASA-TP-3551] p 2392 N95-28215
Upgrade of the computer modeling programs POLU10 and POLU13A for open burning and open detonation of energetic materials p 2172 N95-28306
Distributed methods and processes in games of incomplete information
[PB95-184842] p 2396 N95-28352
Distributed methods and processes in games of incomplete information
[PB95-184859] p 2396 N95-28353
Local design optimization for composite transport fuselage crown panels p 2137 N95-28473
Optimization strategies for molecular dynamics programs on Cray computers and scalar work stations
[AD-A289574] p 2418 N95-28648
Structural optimisation of cage induction motors using finite element analysis
[PB95-195434] p 2271 N95-28655

OPTOELECTRONIC DEVICES
Characterization of optical polymers for multi-layered electro-optic devices
[AD-A289255] p 2227 N95-26973

ORBIT CALCULATION
Flight Mechanics/Estimation Theory Symposium 1995
[NASA-CP-3299] p 2146 N95-27763
Analysis of filter tuning techniques for sequential orbit determination p 2146 N95-27764
Evaluation and modeling of autonomous attitude thrust control for the Geostation Operational Environmental Satellite (GOES)-8 orbit determination
p 2146 N95-27765
Differenced Range Versus Integrated Doppler (DRVID) ionospheric analysis of metric tracking in the Tracking and Data Relay Satellite System (TDRSS)
p 2147 N95-27766
Accurate orbit determination strategies for the tracking and data relay satellites p 2147 N95-27768
Operational improvements of long-term predicted ephemerides of the Tracking and Data Relay Satellites (TDRSs) p 2147 N95-27769
Observational magnetometer calibration with the Hubble Space Telescope's new magnetometers
p 2148 N95-27773
Ulysses orbit determination at high declinations
p 2151 N95-27787
A demonstration of unified TDRS/GPS tracking and orbit determination p 2151 N95-27792
GPS as an orbit determination subsystems
p 2152 N95-27793
Operational considerations of using GPS for spacecraft navigation p 2152 N95-27794
Geostationary Operational Environmental Satellite (GOES)-8 mission flight experience
p 2153 N95-27798
ORION: A Supersynchronous Transfer Orbit mission
p 2154 N95-27804
On the physics of ion ring generation for the stabilization of FRX discharges
[DE95-007105] p 2410 N95-27922

ORBIT INSERTION
Electric propulsion for geostationary orbit insertion
[NASA-TM-106942] p 2168 N95-27727

ORBIT PERTURBATION
Orbit analysis
[DE95-007216] p 2419 N95-27091
Evaluation and modeling of autonomous attitude thrust control for the Geostation Operational Environmental Satellite (GOES)-8 orbit determination
p 2146 N95-27765

ORBITAL ASSEMBLY
Pre-integrated truss space station and method of assembly
[NASA-CASE-MSC-22015-1] p 2165 N95-27842

ORBITAL ELEMENTS
Computing NORAD mean orbital elements from a state vector
[AD-A289281] p 2146 N95-27033

ORBITAL MANEUVERS
Contingency maneuver strategies for the Total Ozone Mapping Spectrometer-Earth Probe (TOMS-EP)
p 2152 N95-27796

ORBITAL MECHANICS
Kepler Equation solver p 2147 N95-27767
Operational improvements of long-term predicted ephemerides of the Tracking and Data Relay Satellites (TDRSs) p 2147 N95-27769
Summary of EOS flight dynamics analysis
p 2152 N95-27797
Dynamics and control of SEDSAT tethered multi-probe for thermospheric research flight data analysis of SEDS-2 satellite: Tethered systems dynamics and flight data analysis
[NASA-CR-198653] p 2165 N95-27836

ORBITAL POSITION ESTIMATION
Analysis of filter tuning techniques for sequential orbit determination p 2146 N95-27764
Accurate orbit determination strategies for the tracking and data relay satellites p 2147 N95-27768
Operational improvements of long-term predicted ephemerides of the Tracking and Data Relay Satellites (TDRSs) p 2147 N95-27769
A PC-based magnetometer-only attitude and rate determination system for gyroless spacecraft
p 2147 N95-27770
Observational magnetometer calibration with the Hubble Space Telescope's new magnetometers
p 2148 N95-27773
A demonstration of unified TDRS/GPS tracking and orbit determination p 2151 N95-27792
Estimation of attitude sensor timetag biases
p 2153 N95-27799
Contingency designs for attitude determination of TRMM p 2154 N95-27803

ORBITAL RENDEZVOUS
Fuzzy logic techniques for rendezvous and docking of two geostationary satellites p 2384 N95-27386

A modified proportional navigation scheme for rendezvous and docking with tumbling targets: The Planar case p 2150 N95-27784

ORDER-DISORDER TRANSFORMATIONS

Rotor phases in compound semiconductors [DE95-004139] p 2436 N95-26442

A first principles approach to phase stability and order-disorder transformation: Application to Li-Al alloys [DE95-609152] p 2218 N95-27756

Multifractal character of the electronic states in disordered two-dimensional systems [DE95-609153] p 2443 N95-28016

Phase separation and ordering in InGaAsP and InGaAs materials [DE95-007493] p 2443 N95-28050

Aspects of macroscopic phase separation and interstitial oxygen ordering in oxygen doped La2CuO(4+delta) [DE95-007864] p 2443 N95-28060

Electronic structure of ordered and disordered transition metal aluminides [DE95-609034] p 2223 N95-28250

ORDNANCE

A comprehensive energetic materials resource recovery and recycling program p 2176 N95-28323

ORGANIC CHARGE TRANSFER SALTS

Electrocrystallization of an ordered organic monolayer: Selective epitaxial growth of beta(ET)213 ongraphite [AD-A288942] p 2178 N95-26569

ORGANIC CHEMISTRY

Environmentally Benign Cleaning and Degreasing Technology: JANNAF Safety and Protection Subcommittee and Propellant Development and Characterization Subcommittee Joint Workshop [CPIA-PUBL-611] p 2227 N95-27101

ORGANIC COMPOUNDS

Design, fabrication, modeling, and optical characterization of organic polymer nonlinear directional couplers [AD-A289327] p 2227 N95-26897

Bioremediation of chlorinated organics: PCBs, TCE, HCFCs p 2179 N95-27117

On the synthesis of mixed-metal and mixed-pnicogen13-15 ring-systems [AD-A288869] p 2223 N95-28332

Self-assembly of low-dimensional molecular nanoclusters on Au(111) surfaces [AD-A288936] p 2178 N95-28334

ORGANIC LASERS

An organic thin film laser diode: A novel light source [AD-A289007] p 2294 N95-26568

ORGANIC MATERIALS

Photo and thermal excitation of surface chemistry on model catalyst surfaces [AD-A288541] p 2200 N95-26528

An organic thin film laser diode: A novel light source [AD-A289007] p 2294 N95-26568

Near-resonant properties of nonlinear organic materials for optical devices [AD-A288339] p 2178 N95-26570

Process for non-contact removal of organic coatings from the surface of paintings [NASA-CASE-LEW-15896-1] p 2235 N95-27702

A compatibility study of containment materials in FEFO, bis-(2-fluoro-2,2-dinitroethyl) formal [DE95-007548] p 2206 N95-27750

Passive spatial beam control, appendix [AD-A288913] p 2300 N95-28333

ORGANIC SUPERCONDUCTORS

Design strategies for the preparation of polymeric organic superconductors [AD-A289022] p 2436 N95-26462

ORGANISMS

Live from Antarctica: The coldest, windiest place on Earth [NASA-CR-197737] p 2335 N95-26595

Survey on researches related to ocean disposal of carbon dioxide [DE95-759247] p 2329 N95-27939

Energy transfer in real and artificial photosynthetic systems [DE95-005824] p 2351 N95-27948

ORGANIZATIONS

Change, Learning and Mental Work in Organizations: Working papers of the 3rd Otaniemi-Dresden Workshop [PB95-184941] p 2356 N95-26909

Investigation on LCA (Life Cycle Analysis/assessment) [DE95-759260] p 2330 N95-27942

Fracture testing and analysis of adhesively bonded joints for automotive applications [DE95-007024] p 2184 N95-28207

ORGANOMETALLIC COMPOUNDS

On the synthesis of mixed-metal and mixed-pnicogen13-15 ring-systems [AD-A288869] p 2223 N95-28332

ORR-SOMMERFELD EQUATIONS

The stability of the flow in a laminar separation bubble [CUED/A-AERO/TR-22] p 2275 N95-26809

ORTHOPEDICS

Automatic locking knee brace joint [NASA-CASE-MFS-28997-1] p 2360 N95-27501

OSCILLATION DAMPERS

High-precision buffer circuit for suppression of regenerative oscillation [NASA-TM-4658] p 2291 N95-27259

OSCILLATIONS

Self-excited oscillations in a duct with closed brances [IFTR-18/1994] p 2400 N95-26358

Suppressor of oscillations in airframe cavities [AD-D017265] p 2128 N95-26507

Visualization of the multiple supersonic jet oscillations by swept focused strobed schlieren technique p 2119 N95-26952

The near-wake flow behavior of an oscillating airfoil with modified trailing edge p 2119 N95-26953

Induced axial oscillations in superconducting dipole windings [DE95-005690] p 2265 N95-27554

Neutrino oscillations in strong magnetic fields [DE95-608876] p 2416 N95-28249

Stability of strange quark stars with nuclear crusts against radial oscillations [DE95-008484] p 2463 N95-28357

OSCILLATORS

The phenomena of subharmonic bifurcations, runaway, and transition to chaos in a non-linear oscillator: perturbation methods and a numerical experiment [IFTR-16/1994] p 2398 N95-26518

Wigner quantum oscillators. OSP (3/2) oscillators [DE95-608756] p 2448 N95-27334

Time-dependent multi-dimensional simulation studies of the electron output scheme for high power FELs [DE95-006593] p 2297 N95-27737

High power free-electron laser concepts and problems [DE95-007841] p 2298 N95-28059

Theoretical and experimental study of low-loss, High-efficiency monolithic antenna structures at 94 GHz [AD-A291785] p 2257 N95-28513

Method and apparatus for maintaining linearity and frequency accuracy of an FM chirp waveform [AD-D017398] p 2258 N95-28615

OTOLITH ORGANS

Comparative Transduction Mechanisms of Vestibular Otolith Hair Cells [NASA-CR-197980] p 2349 N95-26727

Regional differences in lectin binding patterns of vestibular hair cells p 2349 N95-26728

Hair cell regeneration in the bullfrog vestibular otolith organs following aminoglycoside toxicity p 2349 N95-26729

Peripheral innervation patterns of vestibular nerve afferents in the bullfrog utriculus p 2349 N95-26730

Comparative transduction mechanisms of hair cells in the bullfrog utriculus. 1: Responses to intracellular current p 2350 N95-26731

Comparative transduction mechanisms of hair cells in the bullfrog uticulus. 2: Sensitivity and response dynamics to hair bundle displacement p 2350 N95-26732

OUTGASSING

Evaluation of Oxygen Interactions with Materials 3: Mission and induced environments p 2210 N95-27631

Cryogenic BRDF measurements at 10.6 micrometers and 0.63 micrometers on contaminated mirrors [AD-A291611] p 2427 N95-28408

OV-10 AIRCRAFT

Flutter clearance flight tests of an OV-10A airplane modified for wake vortex flight experiments [NASA-TM-109168] p 2117 N95-26381

OVER-THE-HORIZON RADAR

Auto-processing of OTH radar amplitude/range/Doppler data [AD-A289152] p 2253 N95-27005

Assessment of the AN/FPS-118 Ionospheric model and proposed improvements [AD-A289439] p 2337 N95-27146

Measurements of HF auroral clutter using the Verona Ava Linear Array Radar (VALAR) [AD-A289442] p 2337 N95-27147

OXIDASE

Peripheral innervation patterns of vestibular nerve afferents in the bullfrog utriculus p 2349 N95-26730

OXIDATION

Iron oxides characterization by Moessbauer spectroscopy [DE95-607869] p 2202 N95-27199

Systematic study of the ion beam mixing of oxide markers into alumina [DE95-006262] p 2217 N95-27555

Spacecraft materials studies on the Aerospace Corporation tray on EOIM-3 p 2210 N95-27632

Orbital atomic oxygen effects on materials: An overview of MSFC experiments on the STS-46 EOIM-3 p 2419 N95-27637

Effects of atomic oxygen on polymeric materials flown on EOIM-3 p 2242 N95-27638

BMDO materials testing in the EOIM-3 experiment p 2211 N95-27644

Structural oxidation state studies of the manganese cluster in the oxygen evolving complex of Photosystem II [DE95-008488] p 2409 N95-27744

A compatibility study of containment materials in FEFO, bis-(2-fluoro-2,2-dinitroethyl) formal [DE95-007548] p 2206 N95-27750

Kinetics and dynamics of oxidation reactions involving adsorbed CO species on bulk supported Pt and copper oxides [DE95-006420] p 2207 N95-27952

The oxidation state and magnetic behaviour of Tb in high-(Tc) related materials [DE95-007129] p 2219 N95-27966

Hydrothermal oxidation of solid rocket propellant and other department of defense hazardous wastes p 2177 N95-28325

Mechanism of deposit formation on fuel-wetted hot metal surfaces [AD-A289847] p 2210 N95-28621

High temperature oxidation of nickel concentrates [PB95-195566] p 2224 N95-28644

TV-holography at high temperatures: In situ observations of the oxidation of advanced materials [PB95-195343] p 2294 N95-28651

Photoemission study of solid state reaction and initial oxidation of the Ce/Al(100) system [PB95-195368] p 2210 N95-28652

OXIDATION RESISTANCE

Stability of chromite interconnections in dual environments [DE95-007755] p 2267 N95-28131

OXIDATION-REDUCTION REACTIONS

Design strategies for the preparation of polymeric organic superconductors [AD-A289022] p 2436 N95-26462

Defect characterization of electronic conducting pseudo-perovskite systems [DE95-007487] p 2220 N95-28049

OXIDE FILMS

Transport phenomena and interfacial kinetics in multiphase combustion systems [AD-A288297] p 2199 N95-26417

Coatings of non-oxide ceramics for improved corrosion resistance in high temperature coal combustion [DE95-006932] p 2241 N95-28604

OXIDES

Non-metallic oxide inclusion formation in C-Mnlow alloy steel welds [DE94-019160] p 2215 N95-27319

Systematic study of the ion beam mixing of oxide markers into alumina [DE95-006262] p 2217 N95-27555

The oxidation state and magnetic behaviour of Tb in high-(Tc) related materials [DE95-007129] p 2219 N95-27966

Coherent V2O3 precipitates in alpha-Al2O3CO-implanted with vanadium and oxygen [DE95-007404] p 2444 N95-28081

Sensor for measuring the atomic fraction in highly dissociated hydrogen [DE95-006531] p 2415 N95-28204

Development of low-expansion ceramics with strength retention to elevated temperatures [DE95-005760] p 2239 N95-28397

Characterization of solid state laser and nonlinear optical materials [AD-A291684] p 2300 N95-28458

Local texture and grain boundary misorientations in high H(C) oxide superconductors [DE95-007004] p 2447 N95-28606

Muon spin relaxation in ferromagnets: Theoretical results for paramagnetic EuO and EuS [PB95-192860] p 2418 N95-28641

OXIDIZERS

International Space Station Alpha trace contaminant control subassembly life test report [NASA-TM-108488] p 2358 N95-26364

A new method for measuring hypergol scrubber emissions p 2174 N95-28312

OXYGEN

Environmental effects on high energy density materials [AD-A288296] p 2199 N95-26416

Chemical physics of uniform cyclic etching [AD-A288975] p 2404 N95-26574

Prediction of rain attenuation and total atmospheric attenuation for low-availability satellite communications in Europe
[PB95-184925] p 2252 N95-26908

Stoichiometry, structure, and properties of La2NiO(4+(delta)) and La(2-x)Sr(x)NiO(4+/-(delta))
[DE95-007682] p 2439 N95-27443

Crystal structure, short-range oxygen defects, and water adsorption in La- and Nd-modified ZrO2
[DE95-007134] p 2439 N95-27452

LDEF: 69 Months in Space. Third Post-Retrieval Symposium, part 3
[NASA-CP-3275-PT-3] p 2466 N95-27629

Molecular beam scattering from C-13 enriched Kapton and correlation with the EOIM-3 carousel experiment
p 2419 N95-27643

Numerical methods for determining interstitial oxygen in silicon
[DE95-007710] p 2205 N95-27683

ECR plasma-assisted deposition of Al2O3 and dispersion-strengthened AlO2
[DE95-007743] p 2235 N95-27687

High temperature kinetic study of the reactions H + O2 = OH + O and O + H2 = OH + H in H2/O2 system by shock tube-laser absorption spectroscopy
[NASA-CR-195473] p 2206 N95-27695

Absorption of sparingly soluble gases by reactive media in self-aerated gas-liquid contactors: A scale-up procedure
[DE95-006429] p 2206 N95-27707

Structural oxidation state studies of the manganese cluster in the oxygen evolving complex of Photosystem II
[DE95-008488] p 2409 N95-27744

Aspects of macroscopic phase separation and interstitial oxygen ordering in oxygen doped La2CuO(4+delta)
[DE95-007864] p 2443 N95-28060

Formation of anisotropic Tl-1212, Tl-2212, Tl-1223 and Tl-2223 particles using aerosol flow reacted powders
[DE95-007400] p 2444 N95-28079

Modification of the optical properties of glass by sequential ion implantation
[DE95-007401] p 2237 N95-28080

Coherent V2O3 precipitates in alpha-Al2O3CO-implanted with vanadium and oxygen
[DE95-007404] p 2444 N95-28081

Mars Sample Return mission utilizing in-situ propellant production
[NASA-CR-188371] p 2145 N95-28261

High energy density systems in cryogenic media: The production and reactions of atoms and radicals
[AD-A289818] p 2417 N95-28572

High temperature oxidation of nickel concentrates
[PB95-195566] p 2224 N95-28644

OXYGEN ATOMS

An overview of the Evaluation of Oxygen Interactions with Materials 3 experiment: Space Shuttle Mission 46, July-August 1992 p 2210 N95-27630

Evaluation of Oxygen Interactions with Materials 3: Mission and induced environments
p 2210 N95-27631

Spacecraft materials studies on the Aerospace Corporation tray on EOIM-3 p 2210 N95-27632

Exposure of LDEF materials to atomic oxygen: Results of EOIM 3 p 2210 N95-27633

Atomic oxygen dosimetry measurements made on STS-46 by CONCAP 2 p 2418 N95-27634

Inflight resistance measurement on high-T(sub c) superconducting thin films exposed to orbital atomic oxygen on CONCAP-2 (STS-46) p 2272 N95-27635

LEO degradation of graphite and carbon-based composites aboard Space Shuttle Flight STS-46
p 2199 N95-27636

Orbital atomic oxygen effects on materials: An overview of MSFC experiments on the STS-46 EOIM-3
p 2419 N95-27637

Effects of atomic oxygen on polymeric materials flown on EOIM-3 p 2242 N95-27638

Analysis of selected specimens from the STS-46 Energetic Oxygen Interaction with Materials-3 experiment p 2210 N95-27642

Molecular beam scattering from C-13 enriched Kapton and correlation with the EOIM-3 carousel experiment
p 2419 N95-27643

BMDO materials testing in the EOIM-3 experiment
p 2211 N95-27644

STS-46 plasma composition measurements using the EOIM-3 mass spectrometer p 2211 N95-27645

Effects of the LDEF orbital environment on the reflectance of optical mirror materials
p 2428 N95-27651

LDEF's contribution to the selection of thermal control coatings for the Space Station p 2242 N95-27661

Process for non-contact removal of organic coatings from the surface of paintings
[NASA-CASE-LEW-15896-1] p 2235 N95-27702

OXYGEN ISOTOPES

LEO degradation of graphite and carbon-based composites aboard Space Shuttle Flight STS-46
p 2199 N95-27636

D/H and O-18/O-16 partitioning between water liquid and vapor in the system H2O-Na-K-Mg-Ca-Cl-SO4 from 0 to 350 C
[DE95-007013] p 2208 N95-27961

OXYGEN-HYDROCARBON ROCKET ENGINES

Advanced Earth-to-orbit propulsion technology information, dissemination and research
[NASA-CR-196582] p 2168 N95-27424

OZONE

Electromagnetic devices and processes in environment protection
[AD-A288656] p 2141 N95-26487

Spectral analyses, climatology, and interannual variability of Nimbus-7 TOMS version 6 total column ozone
[NASA-RP-1360] p 2341 N95-26689

Coupled chemistry/climate issues
[DE95-006443] p 2327 N95-27532

Evaluation of microporous carbon filters as catalysts for ozone decomposition
[DE95-006498] p 2331 N95-28548

Stratospheric ozone reactive chemicals generated by space launches worldwide
[AD-A289852] p 2332 N95-28623

OZONE DEPLETION

Live from Antarctica, volume 4
[NASA-CR-197828] p 2335 N95-26596

The importance of propulsion engineers in protecting the global environment p 2170 N95-28295

OZONOSPHERE

The importance of propulsion engineers in protecting the global environment p 2170 N95-28295

P

P WAVES

Study of parity and time reversal violation in neutron-nucleus interactions
[DE95-005158] p 2405 N95-27081

Fowler DMO and time migration for transversely isotropic media with explicit operators
[DE95-007671] p 2339 N95-28194

P-I-N JUNCTIONS

Amorphous silicon pixel radiation detectors and associated thin film transistor electronics readout
[DE95-006568] p 2265 N95-27678

P-TYPE SEMICONDUCTORS

Photoluminescence spectroscopy of 4H- and 6H-SiC
[AD-A289326] p 2202 N95-26896

Defect characterization of electronic conducting pseudo-perovskite systems
[DE95-007487] p 2220 N95-28049

Low temperature deposition and characterization of N- and P-type silicon carbide thin films and associated Ohmic and Schottky contacts
[AD-A289107] p 2237 N95-28097

PACIFIC OCEAN

Fluxes across the west coast resolved by Picket Fence observations during stormfest
[AD-A288511] p 2341 N95-26653

Meteorological and oceanographic data collected during the ASREX 91 field experiment
[AD-A289492] p 2342 N95-26826

PACKAGING

JTEC Panel report on microelectromechanical systems in Japan
[NASA-CR-197831] p 2268 N95-28239

Development of an ultra-safe rechargeable lithium-ion battery
[AD-A288959] p 2269 N95-28349

PACKET TRANSMISSION

A high performance totally ordered multicast protocol
[NASA-CR-197765] p 2371 N95-27252

PACKETS (COMMUNICATION)

The reliable multicast protocol application programming interface
[NASA-CR-197762] p 2363 N95-26388

A high performance totally ordered multicast protocol
[NASA-CR-197765] p 2371 N95-27252

Simulator report for SCI systems with HIC-router
[PB95-196580] p 2379 N95-28093

PAINTS

Thermal control materials on EOIM-3
p 2242 N95-27639

Optimization of measurements with pressure sensitive paints
[NASA-TM-4695] p 2293 N95-27915

Assay of weathering effects on protective polymer coatings using positron annihilation spectroscopy
[DE95-007040] p 2236 N95-27962

Surface scanning techniques to locate and study defects in painted zinc and zinc alloy coated steels
[DE95-006099] p 2240 N95-28547

PAIR PRODUCTION

Search for SUSY at CDF
[DE95-005109] p 2407 N95-27430

Search for supersymmetry and leptoquark states at FNAL
[DE95-003381] p 2410 N95-27871

Lattice calculation for lepton capture from vacuum-pair production in relativistic heavy-ion collisions
[DE95-007392] p 2413 N95-28077

PALLADIUM

Magnetic and structural properties of Fe/Pd multilayers studied by magnetic x-ray dichroism and x-ray absorption spectroscopy
[DE95-007095] p 2206 N95-27755

Residual stress, strain, and faults in nanocrystalline palladium and copper
[DE95-008294] p 2223 N95-28543

PALLADIUM COMPOUNDS

Density changes in amorphous Pd80Si20 during low temperature ion irradiation
[DE95-007132] p 2441 N95-27928

PANEL METHOD (FLUID DYNAMICS)

TranAir: A full-potential, solution-adaptive, rectangular grid code for predicting subsonic, transonic, and supersonic flows about arbitrary configurations. Theory document
[NASA-CR-4348] p 2123 N95-28265

PANELS

The collapse of composite cylindrical panels with various thickness using finite element analysis
[AD-A289370] p 2308 N95-26905

Weightless Environment Training Facility (WETF) materials coating evaluation, volume 3
[NASA-CR-188366-VOL-3] p 2239 N95-28387

Composite fuselage crown panel manufacturing technology p 2137 N95-28474

Effect of low-spe[illegible]pact damage and damage location on behavior of composite panels p 2197 N95-28481

Response of multi-panel assembly to noise from a jet in forward motion
[NASA-CR-198164] p 2289 N95-28673

PARABOLIC DIFFERENTIAL EQUATIONS

Adaptive finite element method I: Solution algorithm and computational examples
[AD-A288979] p 2389 N95-26609

Modeling surface effects with the parabolic equation method
[AD-A289199] p 2254 N95-27021

PARACHUTES

Wind tunnel experiments on wake flow field behind a reentry capsule from a viewpoint of parachute deployment at supersonic speeds
[ISAS-R-655] p 2121 N95-26740

The performance of cargo airdrop systems using g-12E parachutes: Statistical determination of minimum altitude
[AD-A291666] p 2126 N95-28454

PARALLEL COMPUTERS

Grain size management in repetitive task graphs for multiprocessor computer scheduling
[AD-A288575] p 2377 N95-26551

Aeroelasticity of wing and wing-body configurations on parallel computers
[NASA-CR-197756] p 2129 N95-26590

Minimizing the impact of synchronization overhead in parallel discrete event simulations
[AD-A289278] p 2377 N95-26984

Language constructs and runtime systems for compositional parallel programming
[DE95-008298] p 2378 N95-27741

PARALLEL PLATES

Energy-measuring resistor bank
[AD-D017392] p 2271 N95-28613

PARALLEL PROCESSING (COMPUTERS)

Parallelizing locally-weighted regression
[AD-A288294] p 2394 N95-26414

Massively parallel self-consistent-field calculations
[DE95-004128] p 2376 N95-26441

A fixed time performance evaluation of parallel CFD applications
[DE94-014240] p 2273 N95-26445

Parallel computing on various platforms: A case study
[AD-A289008] p 2376 N95-26460

Parallelism detection and scheduling strategies for reliable and efficient execution on multicomputers
[AD-A288370] p 2376 N95-26471

Modified eigenvalue problems with applications to structural dynamic re-analysis on parallel computers
[AD-A288257] p 2307 N95-26547

Algorithms for parallel flow solvers on message passing architectures
[NASA-CR-197758] p 2274 N95-26588

Aeroelasticity of wing and wing-body configurations on parallel computers
[NASA-CR-197756] p 2129 N95-26590
A parallel coupled oceanic-atmospheric general circulation model
[DE95-005918] p 2335 N95-26622
A parallel complexity model for functional languages
[AD-A288589] p 2365 N95-26656
Performance prediction: A case study using a multi-ring KSR-1 machine
[NASA-CR-195066] p 2361 N95-26697
Second International Conference on Software for Multiprocessors and Supercomputers Theory, Practice, Experience
[AD-A289474] p 2368 N95-26820
An architecture for optimal all-to-all personalized communication
[AD-A288532] p 2377 N95-26840
An exploratory application of neural networks for airfoil design p 2118 N95-26943
Minimizing the impact of synchronization overhead in parallel discrete event simulations
[AD-A289278] p 2377 N95-26984
Scalability in production system programs
[AD-A289345] p 2453 N95-27063
The systems of the proportional chambers registration electronics for present experiments in nuclear physics
[DE95-608559] p 2419 N95-27161
Accelerating conservative parallel simulation of VHDL circuits
[AD-A289317] p 2264 N95-27294
NAS Technical Summaries, March 1993 - February 1994
[NASA-RP-1355] p 2466 N95-27367
XTP as a transport protocol for distributed parallel processing
[DE95-004992] p 2378 N95-27402
Parallel algorithms for semi-Lagrangian transport in global atmospheric circulation models
[DE95-007385] p 2327 N95-27457
Language constructs and runtime systems for compositional parallel programming
[DE95-008298] p 2378 N95-27741
Design of a real-time wind turbine simulator using a custom parallel architecture p 2322 N95-27979
Parallel block implicit integration technique for trajectory parallelism
[AD-A288961] p 2379 N95-28335
Exploiting parallelism in a Monte Carlo image-matching algorithm
[AD-A289872] p 2374 N95-28625

PARALLEL PROGRAMMING
A parallel complexity model for functional languages
[AD-A288589] p 2365 N95-26656
Second International Conference on Software for Multiprocessors and Supercomputers Theory, Practice, Experience
[AD-A289474] p 2368 N95-26820
Language constructs and runtime systems for compositional parallel programming
[DE95-008298] p 2378 N95-27741
A new shared-memory programming paradigm for molecular dynamics simulations on the Intel Paragon
[DE95-007289] p 2378 N95-28019
Parallel block implicit integration technique for trajectory parallelism
[AD-A288961] p 2379 N95-28335

PARAMETER IDENTIFICATION
Use of nonlinear identification in robust attitude and attitude rate estimation for SAMPEX
p 2149 N95-27781

PARAMETERIZATION
A new angle on the Euler angles
p 2153 N95-27800

PARAMETRIC AMPLIFIERS
Femtosecond OPO's at 3 microns and beyond: Design and performance issues related to the crystal properties of KTP and similar materials
[DE95-007286] p 2446 N95-28242

PARITY
Study of parity and time reversal violation in neutron-nucleus interactions
[DE95-005158] p 2405 N95-27081
Rare decays/CP: The perspective of a kaon physicist
[DE95-005964] p 2416 N95-28338

PARKING ORBITS
Contingency maneuver strategies for the Total Ozone Mapping Spectrometer-Earth Probe (TOMS-EP)
p 2152 N95-27796

PARSING ALGORITHMS
Unification of LARCH and Z-based object models to support algebraically-based design refinement: The Z perspective
[AD-A289234] p 2369 N95-26962

PARTIAL DIFFERENTIAL EQUATIONS
Introduction to multigrid methods
[NASA-CR-195045] p 2388 N95-26395
General purpose finite element solver
[PB95-185062] p 2388 N95-26495
Performance evaluation of a new parallel preconditioner
[AD-A288563] p 2376 N95-26529
Adaptive finite element method I: Solution algorithm and computational examples
[AD-A288979] p 2389 N95-26609
A model of bubble evolution during decompression based on a Monte Carlo simulation of inert gas diffusion
[AD-A289400] p 2353 N95-26885
Nonlinear problems in fluid dynamics and inverse scattering: Propagation and capturing of singularities in problems of fluid dynamics and inverse scattering
[AD-A289146] p 2277 N95-26999
Nonlinear problems in fluid dynamics and inverse scattering: Langmuir circulations and spiral flows
[AD-A289194] p 2278 N95-27019
Spectral methods on arbitrary grids
[NASA-CR-198158] p 2279 N95-27247
Extensional flow convecting a reactant undergoing a first order homogeneous reaction and diffusional mass transfer from a sphere at low to intermediate Peclet and Damkohler numbers p 2280 N95-27346
The use of wavelet transforms in the solution of two-phase flow problems
[DE95-004688] p 2284 N95-27721

PARTIAL PRESSURE
Stability of chromite interconnections in dual environments
[DE95-007755] p 2267 N95-28131

PARTICLE ACCELERATION
Acceleration theorems
[DE95-007300] p 2420 N95-27484

PARTICLE ACCELERATOR TARGETS
PXAMS: Projectile X ray AMS: X ray yields and applications
[DE95-006438] p 2204 N95-27496

PARTICLE ACCELERATORS
Signatures of Higgs-Triplet representations at TeV-e(+)e(-) colliders
[DE95-007201] p 2419 N95-27089
Statistical data analysis
[DE95-007214] p 2454 N95-27090
Orbit analysis
[DE95-007216] p 2419 N95-27091
CAS CERN Accelerator School 5th General Accelerator Physics Course
[DE95-608324] p 2419 N95-27158
The CDF upgrade
[DE95-006683] p 2421 N95-28107
Beam-beam interaction working group summary
[DE95-007824] p 2422 N95-28123

PARTICLE BEAMS
Signatures of Higgs-Triplet representations at TeV-e(+)e(-) colliders
[DE95-007201] p 2419 N95-27089
Orbit analysis
[DE95-007216] p 2419 N95-27091
Coupling in the Tevatron
[DE95-005129] p 2421 N95-27531
Beam-beam interaction working group summary
[DE95-007824] p 2422 N95-28123
Plasma lens experiments at the final focus test beam
[DE95-008595] p 2434 N95-28161
The 132 nsec bunch spacing in the Tevatron proton-antiproton collider
[DE95-005750] p 2422 N95-28346

PARTICLE COLLISIONS
Anomalous collision rate in the time counter scheme of the direct simulation Monte Carlo method for rarefied gas flow analysis
[ISAS-R-653] p 2275 N95-26742
Simulating the production of free defects in irradiated metals
[DE95-007165] p 2214 N95-27088
Signatures of Higgs-Triplet representations at TeV-e(+)e(-) colliders
[DE95-007201] p 2419 N95-27089
A study of events with large total transverse energy produced in proton-antiproton collisions at (radical)s = 1.8 TeV
[DE95-003382] p 2410 N95-27872
Investigation of the collision line broadening problem as applicable to the NASA Optical Plume Anomaly Detection (OPAD) system, phase 1
[NASA-CR-198605] p 2426 N95-27913
The CDF upgrade
[DE95-006683] p 2421 N95-28107
Constraints on the anomalous WW gamma couplings from b vector s gamma
[DE95-608866] p 2415 N95-28246
The 132 nsec bunch spacing in the Tevatron proton-antiproton collider
[DE95-005750] p 2422 N95-28346
Recent status in the search for the quark-gluon plasma
[DE95-007036] p 2417 N95-28447
B-Physics results from D0
[DE95-005126] p 2417 N95-28495

PARTICLE DECAY
Physics with relativistic heavy ions: QGP and other delicacies
[DE95-007014] p 2406 N95-27307
Implications of horizontal symmetries on baryon number violation in supersymmetric models
[DE95-610202] p 2407 N95-27406
Transverse tau polarization in inclusive bar-B yields tau bar-nu X decays
[DE95-610325] p 2407 N95-27409
Large relativistic corrections to the positronium decay rate
[DE95-610470] p 2407 N95-27412
Studies of kinematic distributions and mass reconstruction of CDF top candidate events
[DE95-005108] p 2408 N95-27478
Measurement of the D0 WAMUS magnet inductance
[DE95-005128] p 2399 N95-27530
Preliminary heavy-light decay constants from the MILC Collaboration
[DE95-005685] p 2409 N95-27552
Search for the top quark in dilepton decay modes at D(PHI)
[DE95-007764] p 2409 N95-27689
Probing strongly-interacting electroweak dynamics through W(+)W(-)/ZZ ratios at future e(+)e(-) colliders
[DE95-007202] p 2413 N95-28067
Precise measurement of the left-right cross section asymmetry in Z boson production by e(+)e(-) collisions
[DE95-008591] p 2414 N95-28158
Weak matrix elements efforts on the lattice: Status and prospects
[DE95-007701] p 2416 N95-28355
Production and decay of hybrid mesons by flux-tube breaking
[PB95-192837] p 2418 N95-28640

PARTICLE DIFFUSION
Measurement of particle transport coefficients on Alcator C-Mod
[DE95-007763] p 2411 N95-28020

PARTICLE IMAGE VELOCIMETRY
Fuzzy inference enhanced information recovery from digital PIV using cross-correlation combined with particle tracking
[NASA-TM-106896] p 2291 N95-27173

PARTICLE INTERACTIONS
Abrasion-ablation model for neutron production in heavy ion reactions
[NASA-TM-4656] p 2420 N95-27372
Supersymmetry and light quark masses in a realistic superstring model
[DE95-610201] p 2412 N95-28041
Aspects of strange matter
[DE95-008316] p 2414 N95-28170

PARTICLE MASS
Measurement of inclusive Lambda production in electron-positron interactions at the upsilon energies
[DE95-610302] p 2407 N95-27407
Search for supersymmetry and leptoquark states at FNAL
[DE95-003381] p 2410 N95-27871

PARTICLE MOTION
Skew chromaticity
[DE95-007677] p 2422 N95-28115

PARTICLE PRODUCTION
A simple relativistic model of pp-bar yields K(+)K(-)
[DE95-608852] p 2406 N95-27318
Abrasion-ablation model for neutron production in heavy ion reactions
[NASA-TM-4656] p 2420 N95-27372
Measurement of inclusive Lambda production in electron-positron interactions at the upsilon energies
[DE95-610302] p 2407 N95-27407
Precise measurement of the left-right cross section asymmetry in Z boson production by e(+)e(-) collisions
[DE95-008591] p 2414 N95-28158
Aspects of strangeness
[DE95-008314] p 2414 N95-28169
Recent status in the search for the quark-gluon plasma
[DE95-007036] p 2417 N95-28447
B-Physics results from D0
[DE95-005126] p 2417 N95-28495
Production and decay of hybrid mesons by flux-tube breaking
[PB95-192837] p 2418 N95-28640

PARTICLE SIZE DISTRIBUTION
Survey of sub-micrometre powder size measurement for ceramic and cermet powders
[PB95-190104] p 2227 N95-26746
Analytical electron microscopy of nanometer-sized particles
[AD-A289124] p 2413 N95-28101
PARTICLE SPIN
Excited Charm States
[DE95-005749] p 2409 N95-27747
PARTICLE THEORY
The 1993 European school of high-energy physis
[DE95-610196] p 2421 N95-28040
PARTICLE TRACKS
Fuzzy inference enhanced information recovery from digital PIV using cross-correlation combined with particle tracking
[NASA-TM-106896] p 2291 N95-27173
PARTICULATE REINFORCED COMPOSITES
Structural ceramics incorporating whiskers, platelets, and particulate phases
[DE95-007048] p 2235 N95-27499
PARTICULATES
The orbital debris detector consortium: Suppliers of instruments for in-situ measurements of small-particles in the space environment p 2294 N95-27670
Engineering photochemical smog through convection towers
[DE95-007727] p 2328 N95-27686
A compatibility study of containment materials in FEFO, bis-(2-fluoro-2,2-dinitroethyl) formal
[DE95-007548] p 2206 N95-27750
PARTITIONS (MATHEMATICS)
Yang-Baxter type equations and posets of maximal chains
[PB95-185195] p 2388 N95-26516
Symmetries of the KAC-Peterson modular matrices of affine algebras
[PB95-190138] p 2392 N95-28010
PARTONS
A study of parton distribution functions with the use of photon + jet event kinematics in p(bar p) collisions at (radical)s = TeV
[DE95-005127] p 2408 N95-27444
PASCAL (PROGRAMMING LANGUAGE)
Programming for time resolved spectrum in pulse radiolysis experiments
[DE95-607929] p 2406 N95-27212
PASSENGERS
Enplanement and all cargo activity
[AD-A280074] p 2144 N95-28151
PASSIVITY
FTIR studies of CH3OH on porous silicon
[AD-A289038] p 2207 N95-27904
Energy-measuring resistor bank
[AD-D017392] p 2271 N95-28613
PASTES
A compatibility study of containment materials in FEFO, bis-(2-fluoro-2,2-dinitroethyl) formal
[DE95-007548] p 2206 N95-27750
Mechanical properties of Hysol EA-9394 structural adhesive
[DE95-008187] p 2240 N95-28405
PATENTS
Bibliography of patents and licenses 1951-1990. 1991 edition
[AD-A289603] p 2452 N95-26721
PATHOGENS
Anti-idiotype probes for toxin detection
[AD-A288955] p 2348 N95-26435
PATHS
Piecemeal learning of an unknown environment
[AD-A291683] p 2387 N95-28461
PATTERN RECOGNITION
Integration of video and radiation analysis data
[DE95-004165] p 2379 N95-26443
Non-linear resistive grid kernel estimator useful in single feature, two-class pattern classification
[AD-D017394] p 2271 N95-28614
TRAINS: Dialogue transcription tools
[AD-A289869] p 2259 N95-28624
PAVEMENTS
Layer coefficients for NHDOT pavement materials
[AD-A288262] p 2246 N95-26548
Silicone joint sealants for pavements
[AD-A289843] p 2241 N95-28620
PAYLOADS
Basic space payload fastener p 2156 N95-27273
Development and testing of the rack insertion device
p 2158 N95-27289
Lessons learned from the introduction of autonomous monitoring to the EUVE science operations center
p 2385 N95-27393
Electric propulsion for geostationary orbit insertion
[NASA-TM-106942] p 2168 N95-27727
System identification of damped truss-like space structures
[NASA-TM-106638] p 2303 N95-27911
PEACETIME
Surviving the peace. Lessons learned from the aircraft industry in the 1920s and 1930s
[AD-A288284] p 2117 N95-26455
PEEK
An overview of the Evaluation of Oxygen Interactions with Materials 3 experiment: Space Shuttle Mission 46, July-August 1992 p 2210 N95-27630
Effects of atomic oxygen on polymeric materials flown on EOIM-3 p 2242 N95-27638
On the thermally-induced residual stresses in thick fiber-thermoplastic matrix (PEEK) cross-ply laminated plates p 2187 N95-28285
PELLETS
Proposed high speed pellet injection system HIPEL for large helical device
[NIFS-255] p 2419 N95-26584
CO2 pellet blast cleaning and degreasing: The true environmentally benign technology
p 2229 N95-27109
Recent high-speed ballistics experiments at ORNL
[DE95-006534] p 2422 N95-28205
Pellet injector research and development at ORNL
[DE95-006736] p 2435 N95-28596
PELVIS
Manikin integrated data acquisition system (MIDAS) initial modifications
[AD-A291662] p 2361 N95-28667
PENETRATION
Proposed high speed pellet injection system HIPEL for large helical device
[NIFS-255] p 2419 N95-26584
High energy electron beams for ceramic joining
[DE95-006316] p 2420 N95-27480
Effects of hydrogen on carbon steels at the Multi-Function Waste Tank Facility
[DE95-007194] p 2219 N95-28005
Alpha characterization inside pipes using ion-transport technology
[DE95-007869] p 2411 N95-28024
PENTABORANES
Recovery, evaluation, and decontamination of landfilled pentaborane cylinders, former liquid propellant rocket engine test facility, Washoe County, Nevada
p 2171 N95-28302
PERCOLATION
Probabilistic growth model
[PB95-185054] p 2395 N95-26913
PERFORATING
The effect on stability and thermal hydraulic quenchback of perforating the jacket of a cable-in-conduit conductor
[DE95-005392] p 2262 N95-27083
PERFORMANCE
Femtosecond OPO's at 3 microns and beyond: Design and performance issues related to the crystal properties of KTP and similar materials
[DE95-007286] p 2446 N95-28242
PERFORMANCE PREDICTION
Probabilistic risk assessment of the Space Shuttle. Phase 3: A study of the potential of losing the vehicle during nominal operation. Volume 3: Basic events and minimal cutsets
[NASA-CR-197810] p 2160 N95-26400
Performance modeling of hyperspectral imaging sensors for atmospheric studies
[AD-A289017] p 2289 N95-26461
Ram accelerator performance calculations using a modified version of the NASA CET89 equilibrium chemistry code
[AD-A289554] p 2201 N95-26678
Performance prediction: A case study using a multi-ring KSR-1 machine
[NASA-CR-195066] p 2361 N95-26697
Air cushioned landing craft (LCAC) based ship to shore movement simulation: A decision aid for the amphibious commander. A (SMMAT) application
[AD-A289635] p 2246 N95-26722
The 1994 27th Annual NASA Aerospace Battery Workshop
[NASA-CP-3292] p 2317 N95-26785
Progress towards computer simulation of NiH2 battery performance over life p 2272 N95-26786
Long life 80Ah standard IPV NiH2 battery cell
p 2272 N95-26787
Grayscale/resolution trade-off for text: Model predictions and psychophysical results for letter confusion and letter discrimination
[NASA-CR-197784] p 2369 N95-26930
A study of workstation computational performance for real-time flight simulation
[NASA-TM-109184] p 2362 N95-27241
Effects of bearing cleaning and lube environment on bearing performance p 2158 N95-27285
Transitional flow in thin tubes for space station freedom radiator p 2282 N95-27360
Attitude determination using an adaptive multiple model filtering Scheme p 2148 N95-27772
Determining GPS average performance metrics
p 2128 N95-27791
The vibration transmission of lift truck suspension seats
[ISVR-TR-245] p 2302 N95-27844
Experimental studies to test simple flexural neutralizers fitted to beams
[ISVR-TR-239] p 2309 N95-27846
Horizontal axis wind turbine post stall airfoil characteristics synthesization p 2124 N95-27974
Calculation of design load for the MOD-5A 7.3 mW wind turbine system p 2312 N95-27982
Analysis of solar receiver flux distributions for US/Russian solar dynamic system demonstration on the MIR Space Station
[NASA-TM-106933] p 2169 N95-28036
Performance analysis of bullet trajectory estimation: Approach, simulation, and experiments
[DE95-007949] p 2399 N95-28109
PERFORMANCE TESTS
Weather And Radar Processor (WARP) Test and Evaluation Master Plan (TEMP)
[AD-A288280] p 2340 N95-26453
An analysis of orbital propagators for Low Earth Orbit Rendezvous
[AD-A288883] p 2161 N95-26458
Aircraft fuel system lightning protection design and qualification test procedures development
[AD-A288401] p 2125 N95-26497
Performance evaluation of a new parallel preconditioner
[AD-A288563] p 2376 N95-26529
Development of repair processes and sources for C/KC-135 aircraft windows/windshields
[AD-A288348] p 2117 N95-26629
Design and testing of low sonic boom configurations and an oblique all-wing supersonic transport
[NASA-CR-197744] p 2129 N95-26651
Research and development report. Eureka 147: Tests of the error performance of the DAB system
[BBC-RD-1994/18] p 2249 N95-26696
High-rate/high-temperature capability of a single-layer zicar-separator nickel-hydrogen cell
p 2272 N95-26788
Air Force Ni-H2 cell test program: State of Charge test
p 2272 N95-26789
Calorimetric evaluation of commercial Ni-MH cells and charges p 2272 N95-26790
The 50 Ah NiH2 CPV qualification tests
p 2272 N95-26792
Unique features of a new nickel-hydrogen 2-cell CPV
p 2272 N95-26793
Hubble Space Telescope nickel-hydrogen battery testing: An update p 2272 N95-26794
Adiabatic charging of nickel-hydrogen batteries
p 2272 N95-26795
Alternate charging profiles for the onboard nickel cadmium batteries of the Explorer Platform/Extreme Ultraviolet Explorer p 2272 N95-26796
Development test of a liquid Apogee engine for the ETS-6
[NAL-TR-1250] p 2167 N95-26799
The effects of UH-1 experience on UH-6O simulator performance: A preliminary study
[AD-A289457] p 2130 N95-26993
The noise reduction potential of dual-stream coaxial rectangular improperly expanded jet flows
[NASA-CR-197820] p 2277 N95-26995
Visual system operational evaluation
[AD-A289173] p 2356 N95-27012
Sceening, down selection, and implementation of environmentally compliant cleaning and insulation bonding for MNASA p 2165 N95-27124
Effects of blowing ratio on heat transfer to the throat region of a porous-walled nozzle
[AD-A289459] p 2167 N95-27153
Ionizing radiation measurements on LDEF: A0015 Free flyer biostack experiment
[NASA-CR-196603] p 2202 N95-27168
A review of nickel hydrogen battery technology
[NASA-TM-106918] p 2167 N95-27177
Sailplane glide performance and control using fixed and articulating winglets
[NASA-CR-198579] p 2131 N95-27180
Measuring fault tolerance with the FTAPE fault injection tool
[NASA-CR-197773] p 2306 N95-27253
Design, testing and evaluation of latching end effector
p 2155 N95-27261
Deployment and retraction of a cable-driven solar array: Testing and simulation p 2158 N95-27283

Practical color vision tests for air traffic control applicants: En route center and terminal facilities
[DOT/FAA/AM-95/13] p 2357 N95-27323

Evaluation of high ester content PAO based single hydraulic fluid in high humidity conditions
[AD-A289374] p 2233 N95-27324

Use of CTFE as an additive to enhance fire resistance of single hydraulic fluid
[AD-A289377] p 2233 N95-27325

Performance of a stand-alone wind-electric ice maker for remote villages
[DE95-004006] p 2320 N95-27475

Engineered materials for appliation in severe metallurgical environments: Tantalum-carbon alloy development
[DE95-006838] p 2216 N95-27488

Atomic oxygen dosimetry measurements made on STS-46 by CONCAP 2 p 2418 N95-27634

Inflight resistance measurement on high-T(sub c) superconducting thin films exposed to orbital atomic oxygen on CONCAP-2 (STS-46) p 2272 N95-27635

Improved performance 1590 nm Er:YLF laser
[DE95-003691] p 2296 N95-27705

AFC generator development
[DE95-007094] p 2266 N95-27754

GPS as an orbit determination subsystems
p 2152 N95-27793

Propulsion system assessment for very high UAV under ERAST
[NASA-CR-195469] p 2140 N95-27866

DOE/KEURP Site Operator Program
[DE95-007116] p 2266 N95-27926

The development and testing of ceramic components in piston engines
[DE95-005759] p 2236 N95-27946

Collected papers on wind turbine technology
[NASA-CR-195432] p 2321 N95-27970

Comparative performance tests on the Mod-2, 2.5-mW wind turbine with and without vortex generators
p 2124 N95-27978

FENIX experimental results of large-scale CICC made of bronze-processed Nb3Sn strands
[DE95-007965] p 2222 N95-28167

Cosmic ray test results of the D0 prototype scintillating fiber tracker
[DE95-007215] p 2415 N95-28221

Evaluation of a conductive polymer-based sensor for detection of hydrazines at the part-per-billion level
p 2173 N95-28309

Prototype development and test results of a continuous ambient air monitoring system for hydrazine at the 110 ppb level p 2173 N95-28310

A new method for measuring hypergol scrubber emissions p 2174 N95-28312

A continuous emissions monitor for airborne metals
p 2174 N95-28313

Pressure vessel burst test study p 2175 N95-28317

Experimental investigation of inlet-combustor isolators for a dual-mode scramjet at a Mach number of 4
[NASA-TP-3502] p 2140 N95-28343

Manufacture and testing of the superconducting wire and cable for the RHIC dipoles and quadrupoles
[DE95-006000] p 2270 N95-28515

PERIGEES

Evaluation and modeling of autonomous attitude thrust control for the Geostation Operational Environmental Satellite (GOES)-8 orbit determination
p 2146 N95-27765

PERIODIC FUNCTIONS

Generalized CNF satisfiability, local reductions and complexity of succinctly specified problems
[DE95-006343] p 2372 N95-27849

A study of non-stationary processes and their applications
[AD-A291725] p 2395 N95-28510

PERIODIC VARIATIONS

Typical examples of classical novae
p 2459 N95-27074

Induced axial oscillations in superconducting dipole windings
[DE95-005690] p 2265 N95-27554

Determining GPS average performance metrics
p 2128 N95-27791

Reflection of neutrons from an optical grating
[DE95-007145] p 2411 N95-28004

A study of heart rate and heart rate variability during rapid decompression to 50,000 ft
[AD-A291598] p 2355 N95-28561

PERMANENT MAGNETS

Investigation of high-temperature superconducting flywheel energy storage devices
[DE95-759242] p 2320 N95-27936

PERMEABILITY

Toward molecular selectivity with chemically modified electrodes: Can electroactivity and permeability through an overlaying metallopolymer film be controlled via rational manipulation of internal architecture?
[AD-A288719] p 2403 N95-26491

Computation of electromagnetic scattering parameters for lognormal distributions of magnetic spheres: Theory and algorithms
[AD-A289672] p 2250 N95-26759

The electrical behaviour of an excitable cell at different conditions
[DE95-607911] p 2351 N95-27254

PERMITTIVITY

A book and series of monographs on ice physics
[AD-A288319] p 2200 N95-26422

Characterization of optical polymers for multi-layered electro-optic devices
[AD-A289255] p 2227 N95-26973

PERMUTATIONS

Symmetries of the KAC-Peterson modular matrices of affine algebras
[PB95-190138] p 2392 N95-28010

PEROVSKITES

Investigations of the hyperfine interactions in copper-oxide perovskites using Eu-151 and Fe-57 Moessbauer spectroscopy
[PB95-185138] p 2437 N95-26513

Neutron diffraction studies on recrystallization of solution derived lead zirconate titanates
[DE95-004771] p 2439 N95-27429

Material analysis using combined Elastic Recoil Detection and Rutherford/Enhanced Rutherford Backscattering Spectrometry
[DE95-005415] p 2205 N95-27681

Transient studies of low temperature catalyst for methane conversion
[DE95-007913] p 2205 N95-27692

Defect characterization of electronic conducting pseudo-perovskite systems
[DE95-007487] p 2220 N95-28049

PERSONAL COMPUTERS

Analysis of historical oceanographic data on a personal computer. Program MDS
[AD-A288965] p 2363 N95-26447

PC Software graphics tool for conceptual design of space/planetary electrical power systems
[NASA-TM-106908] p 2372 N95-27905

PERSONALITY TESTS

Myers-Briggs type indicators and Kirton adaption-innovation inventory correlations
[AD-A288435] p 2357 N95-27181

PERSONNEL

AGARD membership, 1995
[AGARD-MEMB-95] p 2450 N95-26353

The effect of infrared sea surface temperature measurements on evaporation duct height estimation
[AD-A289045] p 2346 N95-26477

Myers-Briggs type indicators and Kirton adaption-innovation inventory correlations
[AD-A288435] p 2357 N95-27181

An ugly duckling becomes a swan (hor ellipsis): How an organization becomes customer focused through listening
[DE95-004974] p 2454 N95-27461

Building-integrated photovoltaics: A case study
[DE95-004032] p 2325 N95-28396

PERSONNEL DEVELOPMENT

Enhancing the effects of diversity awareness training: A review of the research literature
[DOT/FAA/AM-95/10] p 2355 N95-26361

PERSONNEL MANAGEMENT

Enhancing the effects of diversity awareness training: A review of the research literature
[DOT/FAA/AM-95/10] p 2355 N95-26361

Change, Learning and Mental Work in Organizations: Working papers of the 3rd Otaniemi-Dresden Workshop
[PB95-184941] p 2356 N95-26909

PERTURBATION

Suppressor of oscillations in airframe cavities
[AD-D017265] p 2128 N95-26507

The phenomena of subharmonic bifurcations, runaway, and transition to chaos in a non-linear oscillator: perturbation methods and a numerical experiment
[IFTR-16/1994] p 2398 N95-26518

Meso-beta scale numerical simulation studies of terrain-induced jet streak mass/momentum perturbations
[NASA-CR-197804] p 2335 N95-26592

Perturbations on effective index of refraction from prism coupling
[AD-A291700] p 2427 N95-28524

PERTURBATION THEORY

A diagram technique for strongly interacting fermion systems. One-and two-band Hubbard models
[DE95-609437] p 2410 N95-27881

Numerical and theoretical studies of rough surface scattering
[AD-A291748] p 2257 N95-28528

PETRI NETS

Design tool for multiprocessor scheduling and evaluation of iterative dataflow algorithms
[NASA-TP-3491] p 2366 N95-26685

PH

Measurement of high acidity using a renewable-reagent fiber optic sensor
[DE95-006327] p 2425 N95-27734

Hydrogen-ion titrations of amino acids and proteins in solutions containing concentrated electrolyte
[DE95-008356] p 2209 N95-28229

PH FACTOR

Feasibility studies for separation processes using environmentally sensitive hydrogels
[DE95-008355] p 2238 N95-28226

PHASE CONTROL

Generation of a single-lobe, far-field intensity pattern from a laser diode array using an optical delay line
[AD-A289226] p 2295 N95-26961

PHASE DETECTORS

The sensitive detection of hydrazine using chemiluminescence p 2173 N95-28311

PHASE DIAGRAMS

Modeling the growth of electronic materials
[AD-A289137] p 2438 N95-26997

Stoichiometry, structure, and properties of La2NiO(4+(delta)) and La(2-x)Sr(x)NiO(4+/-(delta))
[DE95-007682] p 2439 N95-27443

PHASE ERROR

A phase-stepped point diffraction interferometer using liquid crystals
[NASA-TM-106922] p 2293 N95-28037

Atmospheric dispersion in adaptive optics
[AD-A289639] p 2428 N95-28617

PHASE MODULATION

Fundamental concepts of integrated and fiber optic sensors
[NASA-TM-106920] p 2426 N95-27906

Full complex modulation using two one-parameter spatial light modulators
[NASA-CASE-MSC-22255-1] p 2427 N95-28384

PHASE SEPARATION (MATERIALS)

Phase separation and ordering in InGaAsP and InGaAs materials
[DE95-007493] p 2443 N95-28050

Aspects of macroscopic phase separation and interstitial oxygen ordering in oxygen doped La2CuO(4+delta)
[DE95-007864] p 2443 N95-28060

PHASE SHIFT

A phase-stepped point diffraction interferometer using liquid crystals
[NASA-TM-106922] p 2293 N95-28037

PHASE STABILITY (MATERIALS)

A first principles approach to phase stability and order-disorder transformation: Application to Li-Al alloys
[DE95-609152] p 2218 N95-27756

PHASE TRANSFORMATIONS

Rotor phases in compound semiconductors
[DE95-004139] p 2436 N95-26442

Continuum mechanical modeling of solids undergoing a phase transformation
[AD-A288274] p 2200 N95-26451

Applications of Second Harmonic and Sum Frequency Generation to graphite and silica type interfaces
[AD-A288228] p 2201 N95-26544

Stability and thermal influences in nonlinear continuum mechanics and material science
[AD-A288333] p 2448 N95-26563

Lattice parameters and Debye-Waller factors of gamma-TiAl alloys
[AD-A288843] p 2213 N95-26681

Temperature dependence of ion-beam-induced amorphization in (Beta)-SiC
[DE95-007164] p 2438 N95-27087

Stoichiometry, structure, and properties of La2NiO(4+(delta)) and La(2-x)Sr(x)NiO(4+/-(delta))
[DE95-007682] p 2439 N95-27443

Surface crystallization and thin film melting in normal alkanes
[DE95-006694] p 2440 N95-27535

Study of the phase transformations and microstructures of uranium rich alloys of the binary uranium-gallium system
[DE95-609624] p 2217 N95-27713

Ceramic fiber-reinforced monoclinic celsian phase glass-ceramic matrix composite material
[NASA-CASE-LEW-15714-1] p 2183 N95-27717

Amorphization of complex ceramics by heavy-particle irradiations
[DE95-005725] p 2236 N95-27733

High pressure optical studies of semiconductors and heterostructures
[DE95-007119] p 2410 N95-27927

Determination of phase transitions in a lyotropic liquid crystal by positron annihilation technique
[DE95-609162] p 2442 N95-27964
Coherent V2O3 precipitates in alpha-Al2O3CO-implanted with vanadium and oxygen
[DE95-007404] p 2444 N95-28081
Ordered one-component plasmas: Phase transitions, normal modes, large systems, and experiments in a storage ring
[DE95-007077] p 2434 N95-28233
Cooling apparatus and couplings therefor
[NASA-CASE-ARC-11921-1] p 2304 N95-28256
Use of SURFACE CHEMKIN to model multiphase atmospheric chemistry: Application to nitrogen tetroxide spills p 2172 N95-28305
Supercooled liquid dynamics for the charged hard-sphere model
[DE95-609158] p 2241 N95-28609
Critical behaviour of spin models: A transfer-matrix approach
[PB95-192456] p 2418 N95-28638

PHASED ARRAYS
Active antennas with periodic structures
[AD-A289437] p 2252 N95-26924
Quasi-optical millimeter wave power combining
[AD-A291767] p 2270 N95-28529

PHENANTHRENE
Comparison of the activities of fine-particle size catalysts
[DE95-004773] p 2203 N95-27423

PHENOLS
Preconversion catalytic deoxygenation of phenolic functional groups
[DE95-007556] p 2204 N95-27458

PHENOMENOLOGY
Theory of exotic superconductivity and normal states of heavy electron and high temperature superconductivity materials
[DE95-006637] p 2268 N95-28198
A phenomenological treatment of rotating turbulence
[NASA-CR-198168] p 2288 N95-28228

PHONONS
Precursor phenomenon of martensitic transformation in Au-49.5at%Cd alloy
[DE95-007698] p 2222 N95-28166
Subharmonic phonon transmission and Kapitza conductance between crystals with very different vibrational spectra
[DE95-609151] p 2447 N95-28608

PHOSPHATES
A study of the use beta-alumina as a weak interface in alumina fiber composites
[AD-A288629] p 2179 N95-26484
The structure of lead-indium phosphate glass
[DE95-007130] p 2237 N95-27967
Femtosecond OPO's at 3 microns and beyond: Design and performance issues related to the crystal properties of KTP and similar materials
[DE95-007286] p 2446 N95-28242
Ash-based ceramic materials
[AD-D017272] p 2241 N95-28582

PHOSPHORS
Radiation sensitive area detection device and method
[NASA-CASE-MFS-28563-3] p 2423 N95-26385
Flat panel display development activities at Sandia National Laboratories
[DE95-005442] p 2265 N95-27706

PHOSPHORUS
Photo and thermal excitation of surface chemistry on model catalyst surfaces
[AD-A288541] p 2200 N95-26528

PHOSPHORUS COMPOUNDS
Surface energy driven crystallization of amorphous Ni69Cr14P17 alloy
[DE95-005543] p 2438 N95-27085

PHOTOACOUSTIC SPECTROSCOPY
Photoacoustic chambers for studying solids and gases: Theory and practical examples
[IFTR-39/1994] p 2143 N95-26837

PHOTOCATHODES
Can TMAE photocathode be used for high rate applications?
[DE95-008594] p 2293 N95-28178

PHOTOCHEMICAL REACTIONS
Photo and thermal excitation of surface chemistry on model catalyst surfaces
[AD-A288541] p 2200 N95-26528
Stabilization and control of high energy intermediates through adsorption of restricted spaces
[AD-A288552] p 2201 N95-26606
Coupled chemistry/climate issues
[DE95-006443] p 2327 N95-27532
Engineering photochemical smog through convection towers
[DE95-007727] p 2328 N95-27686
Photochemistry in constrained spaces: Zeolites and layered double metal hydroxides
[DE95-006417] p 2207 N95-27951
Radiant exchange considerations in design and scaleup of photocatalytic reactors for purification of nitroglycerine-contaminated air p 2171 N95-28300

PHOTOCONDUCTIVITY
Characterization of microwave MESFET circuits under laser illumination. Applications to phased array radar, microwave communications, and digital clock control
[AD-A289181] p 2261 N95-27015

PHOTOELECTRIC EMISSION
Resonant photoemission studies of thickness dependence of the unoccupied Gd 5d bands
[DE95-004127] p 2436 N95-26440
Photoemission and optical properties of C60 fullerites
[DE95-006588] p 2425 N95-27539
Finite pulse effects in self-amplified-spontaneous emission
[DE95-006585] p 2298 N95-28104
Photoemission study of solid state reaction and initial oxidation of the Ce/Al(100) system
[PB95-195368] p 2210 N95-28652

PHOTOELECTRICITY
Room-temperature photocurrent spectroscopy of GaAs/GaAlAs multiple quantum wells
[AD-A289607] p 2201 N95-26707

PHOTOELECTRON SPECTROSCOPY
Room-temperature photocurrent spectroscopy of GaAs/GaAlAs multiple quantum wells
[AD-A289607] p 2201 N95-26707
Probe molecule studies: Active species in alcohol synthesis
[DE95-003514] p 2203 N95-27420
NO decomposition in non-reducing atmospheres
[DE95-007895] p 2205 N95-27690
Low resistivity ohmic contacts to moderately doped n-GaAs with low temperature processing
[DE95-008507] p 2445 N95-28144

PHOTOELECTRONS
Development of density and temperature profile diagnostics for ICF targets
[DE95-007664] p 2433 N95-28052
The in situ observation of epitaxial diamond thin film nucleation and growth using emission electron microscopy
[AD-A289841] p 2447 N95-28618

PHOTOEXCITATION
Photoinduced dipoles and charge pairs in condensed phase
[DE95-007071] p 2207 N95-27921

PHOTOGRAMMETRY
Three-dimensional photogrammetry for laboratory applications
[AD-A291624] p 2294 N95-28410

PHOTOGRAPHIC RECORDING
Debris/Ice/TPS assessment and integrated photographic analysis of Shuttle mission STS-67
[NASA-TM-110651] p 2160 N95-27238

PHOTOGRAPHS
The Long Duration Exposure Facility (LDEF) photographic survey special publication
p 2457 N95-27660
Three-dimensional photogrammetry for laboratory applications
[AD-A291624] p 2294 N95-28410

PHOTOIONIZATION
Laser ionization of molecular clusters
[DE95-007011] p 2296 N95-27550
A novel sensitive detector of atmospheric nitrocompounds based on laser photofragmentation/ionization spectrometry
p 2174 N95-28314

PHOTOLITHOGRAPHY
Time-optimal control of the magnetically levitated photolithography platen
[DE95-005493] p 2266 N95-27724

PHOTOLUMINESCENCE
Photoluminescence spectroscopy of 4H- and 6H-SiC
[AD-A289326] p 2202 N95-26896

PHOTOLYSIS
Energy transfer from excited nitrenes at high density
[AD-A288352] p 2403 N95-26466
High energy density systems in cryogenic media: The production and reactions of atoms and radicals
[AD-A289818] p 2417 N95-28572

PHOTOMAPPING
Frame selection performance limits for statistical image reconstruction of adaptive optics compensated images
[AD-A289240] p 2424 N95-26965

PHOTOMETERS
Solid-state image sensor with focal-plane digital photon-counting pixel array
[NASA-CASE-NPO-18518-1-CU] p 2424 N95-26894
Method for determining surface coverage by materials exhibiting different fluorescent properties
[NASA-CASE-GSC-13539-1] p 2315 N95-28211

PHOTOMETRY
An illumination planner for Lambertian polyhedral objects
[AD-A289332] p 2424 N95-26900
Solar UV flux measurements from the SBUV2 monitor on the NOAA9 satellite. Part 1: Mg II h and k line core-to-wing ratios for 1986-1988
[PB95-181962] p 2464 N95-28007

PHOTON BEAMS
Crab crossing in a gamma-gamma collider
[DE95-006580] p 2420 N95-27470

PHOTONICS
Design and characterization of resonant cavity light-emitting diodes
[AD-A289307] p 2261 N95-26921

PHOTONS
Demonstration of photo-assisted tunneling process across the coulomb blockade energy gap in mesoscopic tunnel junctions --- photon-assisted tunneling
[AD-A289534] p 2438 N95-26872
Solid-state image sensor with focal-plane digital photon-counting pixel array
[NASA-CASE-NPO-18518-1-CU] p 2424 N95-26894
The photon structure function F2 in QCD with nonlocal vacuum quark condensates
[DE95-608829] p 2406 N95-27314
A study of parton distribution functions with the use of photon + jet event kinematics in p(bar p) collisions at (radical)s = TeV
[DE95-005127] p 2408 N95-27444
Photon burst mass spectrometry--ultrasensitive detection of rare isotopes
[DE95-006403] p 2204 N95-27467
Application of conventional laser technology to gamma-gamma colliders
[DE95-006341] p 2297 N95-27736
Nonlinear optical microscopy for imaging thin films and surfaces
[DE95-007872] p 2426 N95-28018
Finite pulse effects in self-amplified-spontaneous emission
[DE95-006585] p 2298 N95-28104
Photon rockets and gravitational radiation
[PB95-190161] p 2397 N95-28174
Low noise monolithic Si JFETS for operation in the 90-300K range and in high radiation environments
[DE95-007303] p 2269 N95-28244
Constraints on the anomalous WW gamma couplings from b vector s gamma
[DE95-608866] p 2415 N95-28246
The Bremsstrahlung of soft gamma-quanta created by elastic pp- and np-scatterings and the dibaryon resonance problem
[DE95-608870] p 2415 N95-28248
Nonlinear dynamics of a coherent polariton-biexciton system
[DE95-609150] p 2417 N95-28607

PHOTOSYNTHESIS
Structural oxidation state studies of the manganese cluster in the oxygen evolving complex of Photosystem II
[DE95-008488] p 2409 N95-27744
Photoinduced dipoles and charge pairs in condensed phase
[DE95-007071] p 2207 N95-27921
Investigation on energy conversion technology using biochemical reaction elements, 2
[DE95-759250] p 2321 N95-27940
Energy transfer in real and artificial photosynthetic systems
[DE95-005824] p 2351 N95-27948

PHOTOTHERMAL CONVERSION
Solar concentrator technology development for space based applications, volume 1
[NASA-CR-197723] p 2319 N95-27193

PHOTOVOLTAIC CELLS
Analysis of shadowing effects on MIR photovoltaic and solar dynamic power systems
[NASA-TM-106940] p 2169 N95-28213
Strategies for recycling CdTe photovoltaic modules
[DE95-006776] p 2325 N95-28517

PHOTOVOLTAIC CONVERSION
Recent progress in the Photovoltaic Manufacturing Technology Project (PVMaT)
[DE95-000279] p 2320 N95-27704
Building-integrated photovoltaics: A case study
[DE95-004032] p 2325 N95-28396

PHYSICAL CHEMISTRY
Theoretical studies of reaction surfaces
[AD-A288458] p 2404 N95-26632
Evaluations of the effectiveness of environmentally benign cleaning methodologies p 2230 N95-27115

Analysis of the dimerized Sb/Si(001)-(2x1) surface by x-ray standing waves
[DE95-007097] p 2208 N95-27965

PHYSICAL EXERCISE
Basic mechanisms and implications of non-photic entrainment of circadian rhythmicity
[AD-A288433] p 2353 N95-26779

PHYSICAL PROPERTIES
Lightweight cold weather underwear investigation
[AD-A288506] p 2358 N95-26736

PHYSICS
Beginning to edit physics
[DE95-008374] p 2455 N95-28085

PHYSIOLOGICAL EFFECTS
Biochemically vulnerable sites for antifungal intercession in the control of fungal growth
[AD-A288345] p 2348 N95-26573
Acute and subacute toxicity of ammonium dinitramide (ADN) p 2175 N95-28318
Toxicity assessment of liquid propellant XM46
p 2175 N95-28319
Development and application of low-temperature AFM
[AD-A291704] p 2352 N95-28525

PHYSIOLOGICAL RESPONSES
A study of heart rate and heart rate variability during rapid decompression to 50,000 ft
[AD-A291598] p 2355 N95-28561

PHYTOPLANKTON
Investigation on technology for increasing the biological CO2 sink and technology for CO2 fixation and reutilization
[DE95-759251] p 2329 N95-27941

PIEZOELECTRICITY
Large area smart piezoelectric and pyroelectric sensors
[AD-A288565] p 2290 N95-26541
Vibrational behavior of adaptive aircraft wing structures modelled as composite thin-walled beams
p 2191 N95-28435
Molecular modeling: An approach for the study of piezoelectric polymers
[AD-A289821] p 2241 N95-28574

PILOT PERFORMANCE
The effects of UH-1 experience on UH-60 simulator performance: A preliminary study
[AD-A289457] p 2130 N95-26993

PILOT PLANTS
Molten Carbonate Fuel Cell (MCFC) product development test
[DE95-007345] p 2316 N95-26543

PILOT TRAINING
Visual system operational evaluation
[AD-A289173] p 2356 N95-27012

PILOTLESS AIRCRAFT
Design and synthesis of a real-time controller for an unmanned air vehicle
[AD-A289134] p 2141 N95-26555
Propulsion system assessment for very high UAV under ERAST
[NASA-CR-195469] p 2140 N95-27866
Unmanned aerial vehicles, 1994 master plan
[AD-A291628] p 2136 N95-28411

PILOTS (PERSONNEL)
Development of a coding form for approach control/pilot voice communications
[DOT/FAA/AM-95/15] p 2128 N95-28540

PINS
Extended linear ion trap frequency standard apparatus
[NASA-CASE-NPO-19081-1-CU] p 2404 N95-26861
The development and testing of ceramic components in piston engines
[DE95-005759] p 2236 N95-27946
Extended linear ion trap frequency standard apparatus
[NASA-CASE-NPO-19081-1-CU] p 2416 N95-28348

PIONS
Couplings of heavy hadrons with soft pions from QCD sum rules
[DE95-610349] p 2407 N95-27410
Some aspects of the OZI-rule violation in the reaction anti-pp yields phi pi(0)
[DE95-608853] p 2415 N95-28245
Search for deeply bound pionic atoms with high-purity germanium tagging spectrometer
[DE95-609072] p 2416 N95-28252

PIPE FLOW
Validation of the SINDA/FLUINT code using several analytical solutions p 2281 N95-27350
Analysis of developing laminar flows in circular pipes using a higher-order finite-difference technique
p 2281 N95-27352

PIPES (TUBES)
Split pipe testing device for the measurement of bond of reinforcement under controlled confinement
[AD-D017258] p 2245 N95-26500
Experimental investigation of the effects of relative physical orientation between evaporator and condenser for a loop heat pipe
[AD-A289248] p 2277 N95-26968
On the nonlinear stability of the unsteady, viscous flow of an incompressible fluid in a curved pipe
[NASA-CR-195065] p 2278 N95-27028
Alpha characterization inside pipes using ion-transport technology
[DE95-007869] p 2411 N95-28024
Water driven turbine/brush pipe cleaner
[NASA-CASE-KSC-11669-1] p 2304 N95-28359

PISTON ENGINES
The development and testing of ceramic components in piston engines
[DE95-005759] p 2236 N95-27946

PISTONS
The development and testing of ceramic components in piston engines
[DE95-005759] p 2236 N95-27946

PITCH (INCLINATION)
An investigation of the effects of pitch-roll (de)coupling on helicopter handling qualities
[NASA-TM-110349] p 2141 N95-26773

PITCHING MOMENTS
A comparison of the Neal-Smith and omega Tau function, zeta function and tau function flying qualities criteria
[AD-A289503] p 2130 N95-26844

PITTING
Pulsed ion beam surface treatment for preparing rapidly solidified corrosion resistant steel and aluminum surfaces
[DE95-007741] p 2221 N95-28116
Chromate-free corrosion resistant conversion coatings for aluminum alloys
[DE95-007742] p 2238 N95-28117

PIVOTS
Status of bonded boron/epoxy doublers for military and commercial aircraft structures p 2132 N95-27506

PIXELS
Solid-state image sensor with focal-plane digital photon-counting pixel array
[NASA-CASE-NPO-18518-1-CU] p 2424 N95-26894
Moment and hypergeometric filters for high precision computation of focus, stereo and optical flow
[AD-A289293] p 2425 N95-27038
Amorphous silicon pixel radiation detectors and associated thin film transistor electronics readout
[DE95-006568] p 2265 N95-27678

PLANAR STRUCTURES
Theoretical and experimental study of low-loss, High-efficiency monolithic antenna structures at 94 GHz
[AD-A291785] p 2257 N95-28513
Evaluation of defect-related diffusion in semiconductors by electrooptical sampling
[AD-A291630] p 2270 N95-28544

PLANE WAVES
Laser beam propagation in non-Kolmogorov atmospheric turbulence
[AD-A289256] p 2295 N95-26974

PLANETARY GEOLOGY
The Alpha-Proton-X-ray Spectrometer deployment mechanism: An anthropomorphic approach to sensor placement on Martian rocks and soil
p 2155 N95-27265

PLANETARY MAGNETOSPHERES
Energization and transport of ions of ionospheric origin in the terrestrial magnetosphere
[NASA-CR-198618-REV] p 2338 N95-28035

PLANETARY MAPPING
Naval Aviation System TEAM mapping, charting, and geodesy handbook
[AD-A288590] p 2314 N95-26841

PLANETARY NEBULAE
Theoretical studies of interstellar processes
[NASA-CR-198647] p 2462 N95-28216

PLANETARY ORBITS
Space modeler: An expanded, distributed, virtual environment for space visualization
[AD-A289409] p 2461 N95-27131

PLANETARY SYSTEMS
TOPS: Toward Other Planetary Systems. A report by the solar system exploration division
[NASA-TM-110609] p 2464 N95-28009

PLANETARY WAVES
Spectral analyses, climatology, and interannual variability of Nimbus-7 TOMS version 6 total column ozone
[NASA-RP-1360] p 2341 N95-26689
Studies of planetary scale waves and instabilities in support of the geophysical fluid flow cell experiment on USML-2
[NASA-CR-198646] p 2463 N95-27916

PLANETS
TOPS: Toward Other Planetary Systems. A report by the solar system exploration division
[NASA-TM-110609] p 2464 N95-28009
Space Science Division cumulative bibliography: 1989-1994
[NASA-TM-110355] p 2457 N95-28677

PLANNING
Integrated planning and scheduling for Earth science data processing p 2384 N95-27382

PLANT DESIGN
Molten Carbonate Fuel Cell (MCFC) product development test
[DE95-007345] p 2316 N95-26543

PLANTING
Investigation on technology for increasing the biological CO2 sink and technology for CO2 fixation and reutilization
[DE95-759251] p 2329 N95-27941

PLANTS (BOTANY)
Third international congress of plant molecular biology: Molecular biology of plant growth and development
[DE95-006482] p 2352 N95-28496

PLASMA ACCELERATION
Proceedings of the International Workshop on Acceleration and Radiation Generation in Space and Laboratory Plasmas
[AD-A291673] p 2436 N95-28668

PLASMA ACCELERATORS
Proposed high speed pellet injection system HIPEL for large helical device
[NIFS-255] p 2419 N95-26584
High-density plasma source for large-area chemical vapor deposition of diamond films
[AD-A289053] p 2430 N95-27190
Proceedings of the International Workshop on Acceleration and Radiation Generation in Space and Laboratory Plasmas
[AD-A291673] p 2436 N95-28668

PLASMA ANTENNAS
One dimensional global and local solution for ICRF heating
[DE95-007984] p 2392 N95-28110

PLASMA CLOUDS
Space tether-radar data processing
[AD-A289654] p 2250 N95-26725
Bow shock data analysis
[AD-A288432] p 2429 N95-26800

PLASMA COMPOSITION
STS-46 plasma composition measurements using the EOIM-3 mass spectrometer p 2211 N95-27645

PLASMA CONTROL
Analysis of instability growth and collisionless relaxation in thermionic converters using 1-D PIC simulations
[AD-A289310] p 2319 N95-26891
Magnetically controlled deposition of metals using gas plasma
[DE95-007248] p 2430 N95-27237
Dynamics of the L yields H transition, VH-mode evolution, edge localized modes and R.F. driven confinement control in tokamaks
[DE95-007012] p 2430 N95-27306
Fluctuations in high beta(sub p) plasmas in DIII-D
[DE95-008071] p 2432 N95-27710
Application of modern diagnostic methods to environmental improvement
[DE95-005797] p 2330 N95-28119
Divertor research on the DIII-D tokamak
[DE95-003942] p 2434 N95-28185
Recent high-speed ballistics experiments at ORNL
[DE95-006534] p 2422 N95-28205
Transport simulation of negative magnetic shear discharges
[DE95-003941] p 2416 N95-28329
Theoretical aspects of energy confinement in spheromaks
[DE95-008079] p 2435 N95-28542
Operating points and feedback control of plasma characteristics in tokamaks with full current drive
[DE95-007037] p 2435 N95-28553
Simulation of burning tokamak plasmas
[PB95-195426] p 2435 N95-28654

PLASMA CURRENTS
Global dynamo in a reversed field pinch plasma
[DE94-765441] p 2432 N95-27869
Measurement of particle transport coefficients on Alcator C-Mod
[DE95-007763] p 2411 N95-28020
One dimensional global and local solution for ICRF heating
[DE95-007984] p 2392 N95-28110

PLASMA DENSITY
Proposed high speed pellet injection system HIPEL for large helical device
[NIFS-255] p 2419 N95-26584

Development of density and temperature profile diagnostics for ICF targets
[DE95-007664] p 2433 N95-28052
Transport simulation of negative magnetic shear discharges
[DE95-003941] p 2416 N95-28329
PLASMA DIAGNOSTICS
Proposed high speed pellet injection system HIPEL for large helical device
[NIFS-255] p 2419 N95-26584
Low energy neutral atom imaging: Remote observations of the magnetosphere
[DE95-006342] p 2337 N95-27848
Development of density and temperature profile diagnostics for ICF targets
[DE95-007664] p 2433 N95-28052
Application of modern diagnostic methods to environmental improvement
[DE95-005797] p 2330 N95-28119
PLASMA DIFFUSION
Nonlinear phenomena, turbulence and anomalous transport in fusion plasmas
[DE95-007044] p 2431 N95-27497
Fluctuations and transport in fusion plasmas
[DE95-007111] p 2433 N95-27924
PLASMA DRIFT
Fluctuations and transport in fusion plasma
[DE95-004178] p 2429 N95-26444
Effect of toroidal plasma flow and flow shear on global MHD modes
[DE95-006676] p 2433 N95-28106
PLASMA DYNAMICS
Dynamics of the L yields H transition, VH-mode evolution, edge localized modes and R.F. driven confinement control in tokamaks
[DE95-007012] p 2430 N95-27306
Parallel plasma fluid turbulence calculations
[DE95-006741] p 2431 N95-27537
PLASMA EQUILIBRIUM
Fluctuations in high beta(sub p) plasmas in DIII-D
[DE95-008071] p 2432 N95-27710
PLASMA GENERATORS
Electromagnetic devices and processes in environment protection
[AD-A288656] p 2141 N95-26487
PLASMA HEATING
Energetic particle destabilization of shear Alfven waves in stellarators and tokamaks
[DE95-006393] p 2431 N95-27419
Experimental aspects of effects of high-energy particles on Alfven modes
[DE95-003383] p 2432 N95-27673
One dimensional global and local solution for ICRF heating
[DE95-007984] p 2392 N95-28110
Engineering design of the ITER RF systems
[DE95-008064] p 2434 N95-28140
Faraday screen sputtering on TPX
[DE95-008347] p 2434 N95-28224
Operating points and feedback control of plasma characteristics in tokamaks with full current drive
[DE95-007037] p 2435 N95-28553
PLASMA INTERACTIONS
Nonlinear instability and chaos in plasma wave-wave interactions. I. Introduction
[DE95-005529] p 2429 N95-27084
Special features of the CLUSTER antenna and radial booms design, development and verification
p 2157 N95-27281
PLASMA JETS
Destruction of pyrotechnics manufacture wastewater treatment sludge by plasma arc pyrolysis
p 2171 N95-28301
PLASMA LAYERS
Scrape-off layer plasma modeling for the DIII-D tokamak
[DE95-008059] p 2433 N95-28054
UEDGE and DEGAS modeling of the DIII-D scrape-off layer plasma, revision 1
[DE95-008052] p 2433 N95-28065
PLASMA PHYSICS
Radiation production from stagnating compact toroids employing a nonequilibrium radiation diffusion model
[AD-A289602] p 2429 N95-26720
Tokamak ETE engineering preliminary project
[INPE-5529-PRE/1796] p 2435 N95-28562
Proceedings of the International Workshop on Acceleration and Radiation Generation in Space and Laboratory Plasmas
[AD-A291673] p 2436 N95-28668
PLASMA RESONANCE
Nonlinear optical studies of surfaces
[DE95-006574] p 2428 N95-28557
PLASMA SPRAYING
Magnetically controlled deposition of metals using gas plasma
[DE95-007248] p 2430 N95-27237
PLASMA TEMPERATURE
Observation on radiation transfer experiments using k-shell absorption spectra
[DE95-008068] p 2434 N95-28141
PLASMA TORCHES
Application of modern diagnostic methods to environmental improvement
[DE95-005797] p 2330 N95-28119
PLASMA TURBULENCE
Nonlinear phenomena, turbulence and anomalous transport in fusion plasmas
[DE95-007044] p 2431 N95-27497
Parallel plasma fluid turbulence calculations
[DE95-006741] p 2431 N95-27537
Fluctuations and transport in fusion plasmas
[DE95-007111] p 2433 N95-27924
PLASMA WAVES
On helicon wave induced radial plasma transport
[DE94-634477] p 2429 N95-26438
Fluctuations and transport in fusion plasma
[DE95-004178] p 2429 N95-26444
Nonlinear instability and chaos in plasma wave-wave interactions. I. Introduction
[DE95-005529] p 2429 N95-27084
PLASMAS (PHYSICS)
On helicon wave induced radial plasma transport
[DE94-634477] p 2429 N95-26438
Wake fields in semiconductor plasmas
[DE94-634523] p 2429 N95-26439
Fluctuations and transport in fusion plasma
[DE95-004178] p 2429 N95-26444
Proposed high speed pellet injection system HIPEL for large helical device
[NIFS-255] p 2419 N95-26584
Analysis of instability growth and collisionless relaxation in thermionic converters using 1-D PIC simulations
[AD-A289310] p 2319 N95-26891
MHD simulations of DC helicity injection for current drive in tokamaks
[DE95-007018] p 2429 N95-26940
Analytical spectroscopy
[DE95-607896] p 2203 N95-27200
Evaluation of current drive requirements and operating characteristics of a high bootstrap fraction advanced tokamak reactor
[DE95-007041] p 2430 N95-27308
Indirectly driven targets for ignition
[DE95-006451] p 2430 N95-27327
Axionic fuel for sun
[DE95-608788] p 2464 N95-27342
Fast wave current drive in D3-D
[DE95-007582] p 2431 N95-27441
Parallel plasma fluid turbulence calculations
[DE95-006741] p 2431 N95-27537
ECR plasma-assisted deposition of Al2O3 and dispersion-strengthened AlO2
[DE95-007743] p 2235 N95-27687
Neutral gas compression in the Alcator C-Mod divertor. Experimental observations
[DE95-007762] p 2432 N95-27688
Global dynamo in a reversed field pinch plasma
[DE94-765441] p 2432 N95-27869
Pumping characteristics of a cryopump with Ar sorbent in He and in D2/He mixture
[DE95-007049] p 2302 N95-27875
Fluctuations and transport in fusion plasmas
[DE95-007111] p 2433 N95-27924
Laboratory high-energy astrophysics on lasers
[DE95-008062] p 2462 N95-28013
A numerical study of ultra-short-pulse reflectometry
[DE95-008070] p 2266 N95-28015
Measurement of particle transport coefficients on Alcator C-Mod
[DE95-007763] p 2411 N95-28020
Normal modes and continuous spectra
[DE95-006166] p 2287 N95-28055
Advanced tokamak operating modes in TPX and ITER
[DE95-008058] p 2434 N95-28138
Observation on radiation transfer experiments using k-shell absorption spectra
[DE95-008068] p 2434 N95-28141
Plasma lens experiments at the final focus test beam
[DE95-008595] p 2434 N95-28161
Divertor research on the DIII-D tokamak
[DE95-003942] p 2434 N95-28185
Recent high-speed ballistics experiments at ORNL
[DE95-006534] p 2422 N95-28205
Ordered one-component plasmas: Phase transitions, normal modes, large systems, and experiments in a storage ring
[DE95-007077] p 2434 N95-28233
Shear Alfven wave excitation by direct antenna coupling and fast wave resonant mode conversion
[DE95-609109] p 2256 N95-28254
Third-order-accurate numerical methods for efficient, large time-step solutions of mixed linear and nonlinear problems
[DE95-009184] p 2288 N95-28533
Operating points and feedback control of plasma characteristics in tokamaks with full current drive
[DE95-007037] p 2435 N95-28553
Pellet injector research and development at ORNL
[DE95-006736] p 2435 N95-28596
Supercooled liquid dynamics for the charged hard-sphere model
[DE95-609158] p 2241 N95-28609
PLASMONS
Monte Carlo study of electron-plasmon scattering effects on hot electron transport in GaAs
[DE95-607768] p 2403 N95-26542
Nonlinear optical studies of surfaces
[DE95-006574] p 2428 N95-28557
Proceedings of the International Workshop on Acceleration and Radiation Generation in Space and Laboratory Plasmas
[AD-A291673] p 2436 N95-28668
PLASTIC ANISOTROPY
Identification of the plastic anisotropy of an aluminum alloy
[IFTR-26/1994] p 2212 N95-26512
PLASTIC COATINGS
Analysis of selected specimens from the STS-46 Energetic Oxygen Interaction with Materials-3 experiment p 2210 N95-27642
Weightless Environment Training Facility (WETF) materials coating evaluation, volume 1
[NASA-CR-188366-VOL-1] p 2239 N95-28385
PLASTIC DEFORMATION
Determination of the cyclical properties of 18G2A steel on the basis of skeleton curves for a planar stress state
[IFTR-32/1994] p 2211 N95-26359
Identification of the plastic anisotropy of an aluminum alloy
[IFTR-26/1994] p 2212 N95-26512
The development of the anisotropic properties of copper under plastic deformation induced by creep and monotonic loading
[IFTR-23/1994] p 2212 N95-26517
Changes in the anisotropy parameters of an aluminum alloy caused by cyclical deformation
[IFTR-27/1994] p 2212 N95-26666
Forming metallurgy: Supervised drawing course, NTH
[PB95-196507] p 2219 N95-27934
High-temperature deformation of ZrO2-Al2O3/SiC whisker composites fabricated by two techniques
[DE95-008273] p 2183 N95-28069
Residual stress, strain, and faults in nanocrystalline palladium and copper
[DE95-008294] p 2223 N95-28543
PLASTIC PROPERTIES
Changes in the anisotropy parameters of an aluminum alloy caused by cyclical deformation
[IFTR-27/1994] p 2212 N95-26666
PLASTICS
Japan's electronic packaging technologies
p 2263 N95-27230
Indirectly driven targets for ignition
[DE95-006451] p 2430 N95-27327
JTEC monograph on biodegradable polymers and plastics in Japan: Research, development, and applications
[NASA-CR-198562] p 2235 N95-27694
Deformation limits on two-parameter fracture mechanics in terms of higher order asymptotics
[AD-A289113] p 2310 N95-28098
PLATE THEORY
An improved plate theory of order (1,2) for thick composite laminates p 2187 N95-28283
PLATENS
Time-optimal control of the magnetically levitated photolithography platen
[DE95-005493] p 2266 N95-27724
PLATES (STRUCTURAL MEMBERS)
Study of damage evolutions in composite plates subjected to bending loads using micro-macro analysis
[AD-A288523] p 2308 N95-26839
An improved plate theory of order (1,2) for thick composite laminates p 2187 N95-28283
On the thermally-induced residual stresses in thick fiber-thermoplastic matrix (PEEK) cross-ply laminated plates p 2187 N95-28285
Compressive strength of damaged and repaired composite plates p 2198 N95-28484
Fundamental concepts in the suppression of delamination buckling by stitching p 2198 N95-28486

PLATES (TECTONICS)
Live from Antarctica, volume 4
[NASA-CR-197828] p 2335 N95-26596
PLATING
Magnetically controlled deposition of metals using gas plasma
[DE95-007248] p 2430 N95-27237
PLATINUM
Hydrogen induced C-C, C-N, and C-S bond activities on Pi and Ni surfaces
[DE95-006251] p 2206 N95-27838
Kinetics and dynamics of oxidation reactions involving adsorbed CO species on bulk supported Pt and copper oxides
[DE95-006420] p 2207 N95-27952
Development of an optical trap as an ultra-sensitive analytical tool
[DE95-007843] p 2426 N95-28022
PLATINUM ALLOYS
Stability of reference masses 4: Growth of carbonaceous contamination on platinum-iridium mass standard surfaces, and its cleaning by UV/ozone treatment
[PB95-190096] p 2226 N95-26745
PLUMES
Plume measurements with the T5 xenon ion thruster
[AD-A288697] p 2167 N95-26489
Soot particle density determination from a laser extinction multipass technique
[AD-A288551] p 2423 N95-26532
The small-scale structure of dispersing clouds in the atmosphere
[AD-A288256] p 2341 N95-26546
Load measurement system with load cell lock-out mechanism p 2159 N95-27291
PLUTONIUM
Engineered materials for appliation in severe metallurgical environments: Tantalum-carbon alloy development
[DE95-006838] p 2216 N95-27488
Materials considerations for molten salt accelerator-based plutonium conversion systems
[DE95-006743] p 2217 N95-27544
PLY ORIENTATION
Compression failure of angle-ply laminates
p 2190 N95-28428
PNEUMATIC EQUIPMENT
Design and development of a test rig for the high frequency testing of rolling sleeve airsprings
[DSTO-TN-0001] p 2142 N95-26378
PNEUMATICS
Pressure vessel burst test study p 2175 N95-28317
POINCARE SPHERES
Orbit analysis
[DE95-007216] p 2419 N95-27091
POINT DEFECTS
A book and series of monographs on ice physics
[AD-A288319] p 2200 N95-26422
Structure of ordinary ice Ih. Part 2: Defects in ice. Volume 1: Point defects
[AD-A288279] p 2200 N95-26452
Point defect formation in optical materials expos ed to the space environment p 2428 N95-27646
POINTING CONTROL SYSTEMS
SAMPEX special pointing mode p 2149 N95-27780
POISSON RATIO
Indentability of conventional and negative Poisson's ratio foams p 2195 N95-28472
POLAR COORDINATES
User documentation of the CTA program
[AD-A289508] p 2121 N95-26854
POLAR METEOROLOGY
Replicator for characterization of cirrus and polar stratospheric cloud particles
[NASA-CR-197785] p 2341 N95-26669
POLAR REGIONS
An improved model of high-latitude f-region scintillation (WBMOD version 13)
[AD-A288558] p 2334 N95-26520
Contingency maneuver strategies for the Total Ozone Mapping Spectrometer-Earth Probe (TOMS-EP)
p 2152 N95-27796
POLARIMETRY
Processing of wide-angle synthetic aperture radar signals for detection of obscured ground targets
[AD-A289243] p 2253 N95-26976
POLARITONS
Nonlinear dynamics of a coherent polariton-biexciton system
[DE95-609150] p 2417 N95-28607
POLARITY
Observations on the solvating power of supercritical fluids p 2228 N95-27106
POLARIZATION
On-axis polarization coupling in y-cut titanium in-diffused lithium niobate slab waveguides
[AD-A289260] p 2253 N95-26977
POLARIZATION (CHARGE SEPARATION)
Photoinduced dipoles and charge pairs in condensed phase
[DE95-007071] p 2207 N95-27921
Situation in study of electric polarizability and mean square charge radius of the neutron
[DE95-608869] p 2415 N95-28247
POLARIZATION (SPIN ALIGNMENT)
Transverse tau polarization in inclusive bar-B yields tau bar-nu X decays
[DE95-610325] p 2407 N95-27409
Observation of asymmetrical two-cone Vavilov-Cherenkov radiation in biaxial crystal of triglycinesulphate emitted by 658 MeV protons passing along bi normal
[DE94-629017] p 2441 N95-27867
POLARIZATION (WAVES)
Method and apparatus for polaradiometric pyrometer
[NASA-CASE-NPO-19064-1-CU] p 2290 N95-26765
Conversion of sunflower multiband radiometer polarization measurements to polarization parameters
[NASA-CR-197774] p 2314 N95-26815
Modeling surface effects with the parabolic equation method
[AD-A289199] p 2254 N95-27021
POLARIZATION CHARACTERISTICS
Hydrogen-like atom in laser field: Invariant atomic parameters in the ground state
[DE95-609036] p 2411 N95-27930
Scattering by a small object close to an interface. 3. Buried object
[PB95-184909] p 2256 N95-28354
Internal electric field of anisotropic and bi-anisotropic spheres
[PB95-195491] p 2257 N95-28449
POLARIZATION MODULATION
Fundamental concepts of integrated and fiber optic sensors
[NASA-TM-106920] p 2426 N95-27906
POLARIZED ELECTROMAGNETIC RADIATION
Conversion of sunflower multiband radiometer polarization measurements to polarization parameters
[NASA-CR-197774] p 2314 N95-26815
POLARIZED LIGHT
Resonant photoemission studies of thickness dependence of the unoccupied Gd 5d bands
[DE95-004127] p 2436 N95-26440
Display system employing acousto-optic tunable filter
[NASA-CASE-NPO-18736-1-CU] p 2426 N95-27843
POLARIZERS
Conversion of sunflower multiband radiometer polarization measurements to polarization parameters
[NASA-CR-197774] p 2314 N95-26815
POLICIES
Space Commerce 1994 Forum: The 10th National Space Symposium. Proceedings report
[NASA-CR-198031] p 2144 N95-26583
Global trade in satellites and launch services
[GPO-84-811] p 2165 N95-28342
POLLUTION
Community relations plan: Galena Airport and Camp ion Air Force Station, Alaska
[AD-A286722] p 2327 N95-27234
POLLUTION CONTROL
Absorption of sparingly soluble gases by reactive media in self-aerated gas-liquid contactors: A scale-up procedure
[DE95-006429] p 2206 N95-27707
Automated remedial assessment methodology software system
[DE95-007287] p 2373 N95-28243
Use of mussels in biomonitoring of environmental impacts of propellants, projectiles, explosives, and pyrotechnics p 2170 N95-28298
Commercial reformulation: An economic and environmentally neutral means of managing explosives and solid propellants p 2175 N95-28320
Evaluation of microporous carbon filters as catalysts for ozone decomposition
[DE95-006498] p 2331 N95-28548
POLLUTION MONITORING
Application of modern diagnostic methods to environmental improvement
[DE95-005797] p 2330 N95-28119
Use of SURFACE CHEMKIN to model multiphase atmospheric chemistry: Application to nitrogen tetroxide spills p 2172 N95-28305
Survey on bio-chemical complex harmonized with global environment
[DE95-759252] p 2331 N95-28535
POLLUTION TRANSPORT
A method for generating skewed random numbers using two overlapping uniform distributions
[DE95-008747] p 2392 N95-28162
POLYATOMIC MOLECULES
Spectroscopic and dynamical studies of highly energized small polyatomic molecules
[DE95-006640] p 2414 N95-28199
POLYBENZIMIDAZOLE
Polybenzimidazoles via aromatic nucleophilic displacement
[NASA-CASE-LAR-14924-1-CU] p 2179 N95-28361
POLYCARBONATES
Evaluation of laser-protective eyewear dyes in UVEX lenses
[AD-A290076] p 2361 N95-28390
POLYCRYSTALS
Forming metallurgy: Supervised drawing course, NTH
[PB95-196507] p 2219 N95-27934
POLYESTERS
JTEC monograph on biodegradable polymers and plastics in Japan: Research, development, and applications
[NASA-CR-198562] p 2235 N95-27694
POLYETHYLENES
Fractionation studies of polyethylene using DSC-technique
[PB95-185252] p 2200 N95-26540
POLYHEDRONS
Yang-Baxter type equations and posets of maximal chains
[PB95-185195] p 2388 N95-26516
A point-centered diffusion differencing for unstructured meshes in 3-D
[DE95-008382] p 2392 N95-28232
POLYIMIDE RESINS
Phenylethynyl terminated imide oligomers
[NASA-CASE-LAR-15175-1] p 2235 N95-27732
POLYIMIDES
Statistical analysis of tensile mechanical property data of carbon/polyimide composites
[NAL-TR-1238] p 2180 N95-26667
Wipe solvent substitutions for 1,1,1-trichloroethane (TCA) and methyl ethyl ketone (MEK) at Hill Air Force Base p 2228 N95-27107
Phenylethynyl terminated imide oligomers
[NASA-CASE-LAR-15175-1] p 2235 N95-27732
POLYMER BLENDS
Evaluation of a conductive polymer-based sensor for detection of hydrazines at the part-per-billion level
p 2173 N95-28309
POLYMER CHEMISTRY
Synthesis and characterization of polymeric materials
[AD-A288613] p 2225 N95-26482
Molecular object liquid crystals: An approach to new materials
[AD-A288905] p 2437 N95-26553
Stabilization and control of high energy intermediates through adsorption of restricted spaces
[AD-A288552] p 2201 N95-26606
Materials with self organized surfaces: 2D polymer assemblies
[AD-A288928] p 2226 N95-26627
JPRS report: Science and technology. Central Eurasia
[JPRS-UST-95-015] p 2246 N95-27213
Polymer infiltration studies
[NASA-CR-198601] p 2236 N95-27857
POLYMER MATRIX COMPOSITES
Overview of through-thickness test methods for polymer matrix composites
[PB95-190112] p 2227 N95-26747
Probabilistic simulation of long term behavior in polymer matrix composites
[NASA-TM-106893] p 2309 N95-27174
Polymer infiltration studies
[NASA-CR-198601] p 2236 N95-27857
Designing for time-dependent material response in spacecraft structures p 2166 N95-28292
Mechanisms of compressive failure in woven composites and stitched laminates p 2189 N95-28424
Advanced wing design survivability testing and results
p 2138 N95-28488
POLYMER PHYSICS
Synthesis and characterization of polymeric materials
[AD-A288613] p 2225 N95-26482
The 18th Asilomar Conference on Polymeric Materials
[AD-A291721] p 2240 N95-28508
POLYMERIC FILMS
Toward molecular selectivity with chemically modified electrodes: Can electroactivity and permeability through an overlaying metallopolymer film be controlled via rational manipulation of internal architecture?
[AD-A288719] p 2403 N95-26491
Assay of weathering effects on protective polymer coatings using positron annihilation spectroscopy
[DE95-007040] p 2236 N95-27962
POLYMERIZATION
Synthesis and characterization of polymeric materials
[AD-A288613] p 2225 N95-26482

Toward molecular selectivity with chemically modified electrodes: Can electroactivity and permeability through an overlaying metallopolymer film be controlled via rational manipulation of internal architecture?
[AD-A288719] p 2403 N95-26491

Non-covalent immobilization of proteins and enzymes on polymerized lipid assemblies
[AD-A288234] p 2225 N95-26526

Small angle neutron scattering study of the micelle structure of amphiphilic block copolymers
[DE95-006625] p 2234 N95-27486

Poly(N-arylenbenzimidazoles) via aromatic nucleophilic displacement
[NASA-CASE-LAR-14939-1] p 2179 N95-28360

The 18th Asilomar Conference on Polymeric Materials
[AD-A291721] p 2240 N95-28508

Porosity in hexylene-bridged polysilsesquioxanes: Effects of monomer concentration
[DE95-005421] p 2240 N95-28531

Comparison of bridged polysilsesquioxane xerogels prepared from methoxy- and ethoxy-silyl monomers
[DE95-005422] p 2240 N95-28532

POLYMORPHISM

Fractionation studies of polyethylene using DSC-technique
[PB95-185252] p 2200 N95-26540

POLYNOMIALS

Adaptive finite element method I: Solution algorithm and computational examples
[AD-A288979] p 2389 N95-26609

On commutativity of right s-unital rings with some polynomial constraints
[DE95-608752] p 2390 N95-27330

Coordinates of the quantum plane as q-tensor operators in U(sub q) (su(2) * su(2))
[DE95-007100] p 2397 N95-28234

Atmospheric dispersion in adaptive optics
[AD-A289639] p 2428 N95-28617

POLYPEPTIDES

Materials design and processing by biomimicking. Section 1: Research progress
[AD-A288229] p 2226 N95-26623

Design and processing of materials by biomimicking. Section 2. Publications
[AD-A288230] p 2226 N95-26624

Predicting protein structure using parallel genetic algorithms
[AD-A289305] p 2369 N95-26919

POLYPHENYLS

Design, fabrication, modeling, and optical characterization of organic polymer nonlinear directional couplers
[AD-A289327] p 2227 N95-26897

POLYPROPYLENE

Creep recovery of PVC and polypropylene
[PB95-185112] p 2224 N95-26448

Application of bacterial bioemusifiers to in situ maintenance of oil/water separators
p 2179 N95-27120

POLYSACCHARIDES

Materials design and processing by biomimicking. Section 1: Research progress
[AD-A288229] p 2226 N95-26623

JTEC monograph on biodegradable polymers and plastics in Japan: Research, development, and applications
[NASA-CR-198562] p 2235 N95-27694

POLYSTYRENE

New radiation stable and long-lived plastic scintillators
[DE95-608622] p 2233 N95-27163

Surface-emitting semiconductor laser for intracavity spectroscopy and microscopy
[DE95-007745] p 2299 N95-28128

POLYSULFIDES

Wipe solvent substitutions for 1,1,1-trichloroethane (TCA) and methyl ethyl ketone (MEK) at Hill Air Force Base p 2228 N95-27107

POLYTOPES

Yang-Baxter type equations and posets of maximal chains
[PB95-185195] p 2388 N95-26516

Using the dimension reduction technique to prove that clique trees define facets for the asymmetric traveling salesman polytope
[AD-A289397] p 2389 N95-26882

POLYVINYL CHLORIDE

Creep recovery of PVC and polypropylene
[PB95-185112] p 2224 N95-26448

POROSITY

Template synthesis of electronically conductive polymer nanostructures
[AD-A288373] p 2225 N95-26472

Ambient-pressure silica aerogel films
[DE95-008161] p 2237 N95-28090

Porosity in hexylene-bridged polysilsesquioxanes: Effects of monomer concentration
[DE95-005421] p 2240 N95-28531

POROUS MATERIALS

The use of acoustic methods to determine the parameters of porous materials
[IFTR-40/1994] p 2401 N95-26519

Investigation of boundary layer and performance effects of transpiration cooling through a porous plate in a rocket nozzle
[AD-A289393] p 2167 N95-26880

A probabilistic model of a porous heat exchanger
p 2282 N95-27359

Detecting alpha particles through scintillation in porous materials
[AD-A289313] p 2406 N95-27399

FTIR studies of CH3OH on porous silicon
[AD-A289038] p 2207 N95-27904

Evaluation of microporous carbon filters as catalysts for ozone decomposition
[DE95-006498] p 2331 N95-28548

POROUS PLATES

Investigation of boundary layer and performance effects of transpiration cooling through a porous plate in a rocket nozzle
[AD-A289393] p 2167 N95-26880

PORTABLE EQUIPMENT

Test operations procedure (TOP) 2-2-613, electromagnetic interference testing and electrical subsystem - non-communication
[AD-A289521] p 2251 N95-26851

Portable laser laboratory
[DE95-008376] p 2298 N95-27876

Lithium ion rechargeable systems studies
[DE95-006810] p 2268 N95-28200

POSITION (LOCATION)

Scalable multicast tree construction for wide area networks
[AD-A288318] p 2379 N95-26421

An illumination planner for Lambertian polyhedral objects
[AD-A289332] p 2424 N95-26900

Electro-hydrostatic actuator controller design using quantitative feedback theory
[AD-A289220] p 2141 N95-26957

Matrix kernels for MEG and EEG source localization and imaging
[DE95-005236] p 2354 N95-27426

Scaling of localization length of a quasi 1D system with longitudinal boundary roughness
[DE95-609148] p 2391 N95-27739

Development of a direct match technique for star identification on the SWAS mission
p 2148 N95-27771

Reflection of neutrons from an optical grating
[DE95-007145] p 2411 N95-28004

FY 1994 ambient air monitoring report for McMurdo Station, Antarctica
[DE95-008565] p 2331 N95-28149

Effects of floor location on response of composite fuselage frames p 2192 N95-28439

POSITION ERRORS

Flight evaluation of GPS/DGPS sensor systems installed in NAL Do228
[NAL-TR-1230] p 2126 N95-26585

Observational magnetometer calibration with the Hubble Space Telescope's new magnetometers
p 2148 N95-27773

Estimation of attitude sensor timetag biases
p 2153 N95-27799

POSITIONING

Airborne geophysics and precise positioning: Scientific issues and future directions
[LC-94-68678] p 2314 N95-27156

The Alpha-Proton-X-ray Spectrometer deployment mechanism: An anthropomorphic approach to sensor placement on Martian rocks and soil
p 2155 N95-27265

POSITRON ANNIHILATION

Model independent constraints on anomalous gauge boson self-couplings from e(+)e(-) colliders with longitudinally polarized beams
[DE95-608844] p 2406 N95-27317

Measurement of R in e(+)e(-)-annihilation at center-of-mass energies between 7.2 and 10.34 GeV
[DE95-610303] p 2407 N95-27408

Assay of weathering effects on protective polymer coatings using positron annihilation spectroscopy
[DE95-007040] p 2236 N95-27962

Determination of phase transitions in a lyotropic liquid crystal by positron annihilation technique
[DE95-609162] p 2442 N95-27964

Probing strongly-interacting electroweak dynamics through W(+)W(-)/ZZ ratios at future e(+)e(-) colliders
[DE95-007202] p 2413 N95-28067

Vacancy related defects in thin film Pb(Zr,Ti)O3 materials
[DE95-007696] p 2445 N95-28165

Measurement of alpha(s) in e(+)e(-) annihilation at E(cm) = 29 GeV
[DE95-006486] p 2417 N95-28594

POSITRONIUM

Large relativistic corrections to the positronium decay rate
[DE95-610470] p 2407 N95-27412

POSITRONS

Characterization of defects in deuterium-implanted beryllium
[DE95-005688] p 2217 N95-27553

Positron microscopy
[DE95-007042] p 2410 N95-27874

Plasma lens experiments at the final focus test beam
[DE95-008595] p 2434 N95-28161

POSTFLIGHT ANALYSIS

Debris/Ice/TPS assessment and integrated photographic analysis of Shuttle mission STS-67
[NASA-TM-110651] p 2160 N95-27238

Thermal control materials on EOIM-3
p 2242 N95-27639

Molecular beam scattering from C-13 enriched Kapton and correlation with the EOIM-3 carousel experiment
p 2419 N95-27643

LDEF systems special investigation group overview
p 2470 N95-27647

Geostationary Operational Environmental Satellite (GOES)-8 mission flight experience
p 2153 N95-27798

POSTMISSION ANALYSIS (SPACECRAFT)

LDEF: 69 Months in Space. Third Post-Retrieval Symposium, part 3
[NASA-CP-3275-PT-3] p 2466 N95-27629

A final look at LDEF electro-optic systems components p 2428 N95-27650

Long Duration Exposure Facility (LDEF) Archive System p 2457 N95-27658

The Long Duration Exposure Facility (LDEF) annotated bibliography p 2457 N95-27659

Geostationary Operational Environmental Satellite (GOES)-8 mission flight experience
p 2153 N95-27798

POSTURE

Role of somatosensory and vestibular cues in attenuating visually induced human postural sway
[NASA-CR-197845] p 2357 N95-27697

POTASSIUM CHLORIDES

The off-center effect on the diffusion coefficient of Cu(+) and Li(+) in the KCl lattice
[DE95-609146] p 2446 N95-28255

POTASSIUM HYDROXIDES

Long life 80Ah standard IPV NiH2 battery cell
p 2272 N95-26787

Electrical conductivity measurements of aqueous electrolyte solutions at high temperatures and high pressures
[DE95-006748] p 2208 N95-27956

POTASSIUM OXIDES

Femtosecond OPO's at 3 microns and beyond: Design and performance issues related to the crystal properties of KTP and similar materials
[DE95-007286] p 2446 N95-28242

POTENTIAL ENERGY

Investigation into the behavior of geometrically nonlinear composite arches
[AD-A289258] p 2308 N95-26975

Analysis of forward and inverse problems in chemical dynamics and spectroscopy
[DE95-009309] p 2209 N95-28164

Theoretical studies of interstellar processes
[NASA-CR-198647] p 2462 N95-28216

POTENTIAL FIELDS

The electric field of Bohr's atom
[DE95-608758] p 2448 N95-27336

POTENTIAL FLOW

Computational fluid dynamics and transonic flow
[AD-A288962] p 2273 N95-26405

POWDER (PARTICLES)

Lattice parameters and Debye-Waller factors of gamma-TiAl alloys
[AD-A288843] p 2213 N95-26681

Survey of sub-micrometre powder size measurement for ceramic and cermet powders
[PB95-190104] p 2227 N95-26746

Neutron diffraction studies on recrystallization of solution derived lead zirconate titanates
[DE95-004771] p 2439 N95-27429

Crystal and magnetic structure of stoichiometric YFe2O4
[DE95-006627] p 2440 N95-27487

Formation of anisotropic Tl-1212, Tl-2212, Tl-1223 and Tl-2223 particles using aerosol flow reacted powders
[DE95-007400] p 2444 N95-28079

The effects of processing variables on reaction synthesis of Fe-Al alloys
[DE95-007405] p 2221 N95-28082

POWDER METALLURGY
Review of activities in USA on HTS materials
[DE95-006404] p 2234 N95-27468

POWDERED ALUMINUM
Ceramic fiber-reinforced monoclinic celsian phase glass-ceramic matrix composite material
[NASA-CASE-LEW-15714-1] p 2183 N95-27717

POWER AMPLIFIERS
Material characterization system
[AD-D017385] p 2210 N95-28584

POWER CONVERTERS
The 77 K operation of a multi-resonant power converter
[NASA-TM-106941] p 2264 N95-27374
Forback DC-to-DC converter
[NASA-CASE-GSC-13404-1] p 2269 N95-28341

POWER FACTOR CONTROLLERS
Control system design for the MOD-5A 7.3 mW wind turbine generator p 2306 N95-27985

POWER LIMITERS
Low power limits in ultrashort pulse measurement using Frequency-Resolved Optical Gating
[DE95-007150] p 2299 N95-28219

POWER SERIES
Construction of arbitrary order schemes for many dimensional wave equation
[PB95-184818] p 2276 N95-26928

POWER SPECTRA
Synthetic 3-D atmospheric temperature structure: A model for known geophysical power spectra using a hybrid autoregression and Fourier technique
[AD-A289058] p 2340 N95-26479
Laser beam propagation in non-Kolmogorov atmospheric turbulence
[AD-A289256] p 2295 N95-26974
Post Kalman progress p 2148 N95-27776
Basic principles and recent observations of rotationally sampled wind p 2321 N95-27971

POWER SUPPLIES
Hubble Space Telescope nickel-hydrogen battery testing: An update p 2272 N95-26794

PREAMPLIFIERS
Low noise monolithic Si JFETS for operation in the 90-300K range and in high radiation environments
[DE95-007303] p 2269 N95-28244

PRECIPITATES
Modeling precipitation from concentrated solutions with the EQ3/6 chemical speciation codes
[DE95-006264] p 2204 N95-27556
ECR plasma-assisted deposition of Al2O3 and dispersion-strengthened AlO2
[DE95-007743] p 2235 N95-27687
Coherent V2O3 precipitates in alpha-Al2O3CO-implanted with vanadium and oxygen
[DE95-007404] p 2444 N95-28081

PRECISION
An integrated GPS/INS/BARO and radar altimeter system for aircraft precision approach landings
[AD-A289280] p 2127 N95-26985
Moment and hypergeometric filters for high precision computation of focus, stereo and optical flow
[AD-A289293] p 2425 N95-27038
Perturbations on effective index of refraction from prism coupling
[AD-A291700] p 2427 N95-28524

PREDICTION ANALYSIS TECHNIQUES
Aircraft noise prediction program theoretical manual: Rotorcraft System Noise Prediction System (ROTONET), part 4
[NASA-TM-83199-PT-4] p 2400 N95-26392
Intelligent computer based reliability assessment of multichip modules
[AD-A288833] p 2259 N95-26550
A mathematical framework for an improved search model
[AD-A288858] p 2358 N95-26552
Life prediction methodology for composite laminates. Part 1: Constant amplitude and two-stress level fatigue
[AD-A288343] p 2180 N95-26571
Deep convection in the Mediterranean Sea
[AD-A288497] p 2346 N95-26647
Embedology and neural estimation for time series prediction
[AD-A289312] p 2394 N95-26892
Study of the response of a three-dimensional coupled ice-ocean model to daily varying atmospheric forcing
[AD-A289050] p 2347 N95-27189
Applying AI tools to operational space environmental analysis p 2382 N95-27376
Accurate orbit determination strategies for the tracking and data relay satellites p 2147 N95-27768
Operational improvements of long-term predicted ephemerides of the Tracking and Data Relay Satellites (TDRSs) p 2147 N95-27769
Attitude determination using an adaptive multiple model filtering Scheme p 2148 N95-27772
A model of rotationally-sampled wind turbulence for predicting fatigue loads in wind turbines p 2312 N95-27972
A NASTRAN-based computer program for structural dynamic analysis of Horizontal Axis Wind Turbines p 2312 N95-27980
Calculation of design load for the MOD-5A 7.3 mW wind turbine system p 2312 N95-27982
Comparison of measured and calculated dynamic loads for the Mod-2 2.5 mW wind turbine system p 2312 N95-27983
Neural networks versus linear regression: Research into the value of neural networks in meteorological practice
[KNMI-TR-165] p 2343 N95-28236
Chemical reactions identified in the Titan 2, Titan 4, and Delta 2 propellant systems and their application to source modeling p 2172 N95-28304
Applications of a damage tolerance analysis methodology in aircraft design and production p 2197 N95-28483
A study of non-stationary processes and their applications
[AD-A291725] p 2395 N95-28510

PREDICTIONS
Life prediction methodology for composite laminates. Part 1: Constant amplitude and two-stress level fatigue
[AD-A288343] p 2180 N95-26571
Embedology and neural estimation for time series prediction
[AD-A289312] p 2394 N95-26892
Prediction of material strength and fracture of glass using the SPHINX smooth particle hydrodynamics code
[DE95-004869] p 2236 N95-27943
Analytical and experimental evaluation of joining silicon carbide to silicon carbide and silicon nitride to silicon nitride for advanced heat engine applications, phase 2
[DE95-005761] p 2303 N95-27947

PREFLIGHT ANALYSIS
Debris/Ice/TPS assessment and integrated photographic analysis of Shuttle mission STS-67
[NASA-TM-110651] p 2160 N95-27238

PREFORMS
TEM characterization of Al/Al2O3 composite fabricated by reactive metal infiltration
[DE95-008508] p 2184 N95-28145
Design of fabric preforms for double diaphragm forming p 2184 N95-28269
Through-the Thickness(R) braided composites for aircraft applications p 2185 N95-28273
Resin transfer molding of textile preforms for aircraft structural applications p 2185 N95-28276
Recent progress in NASA Langley textile reinforced composites program p 2196 N95-28475
Advanced textile applications for primary aircraft structures p 2138 N95-28476
Comparison of resin film infusion, resin transfer molding, and consolidation of textile preforms for primary aircraft structure p 2196 N95-28477

PREPOLYMERS
Boron-carbon-silicon polymers and the ceramic thereof
[NASA-CASE-ARC-11891-1-SB] p 2238 N95-28212

PREPREGS
Composite prepreg application device
[NASA-CASE-LAR-15259-1] p 2182 N95-27192
Scarf joint technique with cocured and precured patches for composite repair p 2135 N95-27524
Polymer infiltration studies
[NASA-CR-198601] p 2236 N95-27857
Design of fabric preforms for double diaphragm forming p 2184 N95-28269
Advanced tow placement of composite fuselage structure p 2185 N95-28271

PRESSURE BREATHING
A study of heart rate and heart rate variability during rapid decompression to 50,000 ft
[AD-A291598] p 2355 N95-28561

PRESSURE DEPENDENCE
The effect on stability and thermal hydraulic quenchback of perforating the jacket of a cable-in-conduit conductor
[DE95-005392] p 2262 N95-27083

PRESSURE DISTRIBUTION
Airfoil modification effects on subsonic and transonic pressure distributions and performance for the EA-6B airplane
[NASA-TP-3516] p 2120 N95-26382
Wind tunnel experiments on wake flow field behind a reentry capsule from a viewpoint of parachute deployment at supersonic speeds
[ISAS-R-655] p 2121 N95-26740
Analysis of developing laminar flows in circular pipes using a higher-order finite-difference technique p 2281 N95-27352
Comparative wind tunnel test at high Reynolds numbers of NACA 64 621 airfoils with two aileron configurations p 2124 N95-27977
Measurements of store forces and moments and cavity pressures for a generic store in and near a box cavity at subsonic and transonic speeds
[NASA-TM-4611] p 2123 N95-28241

PRESSURE EFFECTS
Compressible turbulence measurements in a supersonic boundary layer including favorable pressure gradient effects
[AD-A289475] p 2276 N95-26821
Load transfer in the stiffener-to-skin joints of a pressurized fuselage
[NASA-CR-198610] p 2310 N95-27865
High pressure optical studies of semiconductors and heterostructures
[DE95-007119] p 2410 N95-27927
Composite fuselage shell structures research at NASA Langley Research Center p 2194 N95-28466

PRESSURE GRADIENTS
A study of magnetic activity effects on the thermospheric winds in the low ionosphere
[AD-A288677] p 2334 N95-26488
Compressible turbulence measurements in a supersonic boundary layer including favorable pressure gradient effects
[AD-A289475] p 2276 N95-26821
Compressible turbulence measurements in a supersonic flow with adverse pressure gradient
[AD-A289477] p 2276 N95-26822

PRESSURE MEASUREMENT
Unsteady base pressure measurements in the near wake of a cylinder with imposed three-dimensional disturbances
[AD-A289498] p 2276 N95-26827
Stall precursor study of high frequency data for three high speed, swept compressor rotors
[AD-A289379] p 2139 N95-26878
Non-invasive method and apparatus for monitoring intracranial pressure and pressure volume index in humans
[NASA-CASE-LAR-13894-1] p 2353 N95-26889
Optimization of measurements with pressure sensitive paints
[NASA-TM-4695] p 2293 N95-27915

PRESSURE PULSES
Pressure vessel burst test study p 2175 N95-28317

PRESSURE RATIO
The noise reduction potential of dual-stream coaxial rectangular improperly expanded jet flows
[NASA-CR-197820] p 2277 N95-26995
High pressure optical studies of semiconductors and heterostructures
[DE95-007119] p 2410 N95-27927

PRESSURE REDUCTION
A model of bubble evolution during decompression based on a Monte Carlo simulation of inert gas diffusion
[AD-A289400] p 2353 N95-26885
Real-time data compression using a fixed Huffman encoding scheme
[DE95-006159] p 2455 N95-27949
A study of heart rate and heart rate variability during rapid decompression to 50,000 ft
[AD-A291598] p 2355 N95-28561

PRESSURE SENSORS
Multi-channel electronically scanned cryogenic pressure sensor
[NASA-CASE-LAR-15062-1] p 2291 N95-27138
Process and control systems for composites manufacturing p 2184 N95-28267

PRESSURE VESSEL DESIGN
Long life 80Ah standard IPV NiH2 battery cell p 2272 N95-26787
The 50 Ah NiH2 CPV qualification tests p 2272 N95-26792
Unique features of a new nickel-hydrogen 2-cell CPV p 2272 N95-26793

PRESSURE VESSELS
Long life 80Ah standard IPV NiH2 battery cell p 2272 N95-26787
The 50 Ah NiH2 CPV qualification tests p 2272 N95-26792
Unique features of a new nickel-hydrogen 2-cell CPV p 2272 N95-26793
Gamma ray-induced embrittlement of pressure vessel alloys
[DE95-007133] p 2220 N95-28072
Reactor pressure vessel structural integrity research
[DE95-007034] p 2223 N95-28208
Process and control systems for composites manufacturing p 2184 N95-28267

Design prediction for long term stress rupture service of composite pressure vessels p 2188 N95-28291
Pressure vessel burst test study p 2175 N95-28317

PRESTRESSING
Stress corrosion cracking susceptibility of the earthquake resistant NOM B457 Mexican steel
[DE95-607956] p 2214 N95-27256

PREVENTION
Investigation on technology for increasing the biological CO2 sink and technology for CO2 fixation and reutilization
[DE95-759251] p 2329 N95-27941

PRINTED CIRCUITS
Life cycle costs of alternatives for F-16 printed circuit board diagnosis equipment
[AD-A288744] p 2138 N95-28586

PRIORITIES
Operating system support for coexistence of real-time and conventional scheduling
[AD-A288584] p 2364 N95-26534

PRISMS
Perturbations on effective index of refraction from prism coupling
[AD-A291700] p 2427 N95-28524

PROBABILITY DENSITY FUNCTIONS
A method to determine the structure of an unknown mixture using the Akaike Information Criterion and the bootstrap
[AD-A288295] p 2394 N95-26415
Fast multidimensional density estimation based on Random-width bins
[AD-A288286] p 2394 N95-26457
Soot particle density determination from a laser extinction multipass technique
[AD-A288551] p 2423 N95-26532
ROC analysis of IR segmentation techniques
[AD-A289252] p 2424 N95-26971
Recent progress in the joint velocity-scalar PDF method p 2285 N95-27890
Recent advances in PDF modeling of turbulent reacting flows p 2286 N95-27892
PDF methods for turbulent reactive flows
p 2287 N95-27900
A composition joint PDF method for the modeling of spray flames p 2287 N95-27901
Improvements and new features in the PDF module
p 2287 N95-27902
Uncertainties in obtaining high reliability from stress-strength models p 2193 N95-28442

PROBABILITY DISTRIBUTION FUNCTIONS
Fast multidimensional density estimation based on Random-width bins
[AD-A288286] p 2394 N95-26457
Statistical theory and reliability
[AD-A288519] p 2394 N95-26733
Probabilistic simulation of long term behavior in polymer matrix composites
[NASA-TM-106893] p 2309 N95-27174
Probabilistic evaluation of fuselage-type composite structures p 2137 N95-28444

PROBABILITY THEORY
Probabilistic risk assessment of the Space Shuttle. Phase 3: A study of the potential of losing the vehicle during nominal operation. Volume 2: Integrated loss of vehicle model
[NASA-CR-197809] p 2159 N95-26399
Probabilistic risk assessment of the Space Shuttle. Phase 3: A study of the potential of losing the vehicle during nominal operation. Volume 5: Auxiliary shuttle risk analyses
[NASA-CR-197812] p 2160 N95-26403
A mathematical framework for an improved search model
[AD-A288858] p 2358 N95-26552
Life prediction methodology for composite laminates. Part 1: Constant amplitude and two-stress level fatigue
[AD-A288343] p 2180 N95-26571
Chemical physics of uniform cyclic etching
[AD-A288975] p 2404 N95-26574
Probabilistic growth model
[PB95-185054] p 2395 N95-26913
Automatically selecting and using primary effects in planning: Theory and experiments
[AD-A289347] p 2450 N95-27064
Fitting: Subroutine to fit four-moment probability distributions to data
[DE95-007722] p 2395 N95-27684
Emerging applications of probability (stochastic models in geosystems)
[AD-A289117] p 2313 N95-28099
Cesium/oxide interactions for ultrathin films on (alpha)-Al2O3(001) and (alpha)-Al2O3(1(bar 1)O2)
[DE95-008159] p 2238 N95-28358
Probabilistic design of advanced composite structure
p 2193 N95-28443
Proof test methodology for composites
p 2193 N95-28445
Stochastic control and topics in applied probability
[AD-A291712] p 2395 N95-28526
An automated cost uncertainty program
[AD-A288747] p 2374 N95-28588

PROBLEM SOLVING
Modified Gaussian elimination for adaptive beamforming using RNS arithmetic
[AD-A288809] p 2248 N95-26356
Parallel computing on various platforms: A case study
[AD-A289008] p 2376 N95-26460
Encoding user-defined problems with SIPE-2
[AD-A288390] p 2380 N95-26475
Hyperkaehler metrics associated to compact Lie groups
[PB95-185161] p 2388 N95-26514
Neural models of spatial orientation in novel environments
[AD-A288420] p 2380 N95-26530
Modified eigenvalue problems with applications to structural dynamic re-analysis on parallel computers
[AD-A288257] p 2307 N95-26547
Automatic test data generation tool for large-scale software systems
[AD-A289081] p 2365 N95-26611
Contribution to the optimal shape design of two-dimensional internal flows with embedded shocks
[NASA-CR-195062] p 2389 N95-26672
A process improvement model for software verification and validation
[NASA-CR-197761] p 2367 N95-26814
Using the dimension reduction technique to prove that clique trees define facets for the asymmetric traveling salesman polytope
[AD-A289397] p 2389 N95-26882
Multi-agent perception for Human/Robot interaction: A framework for intuitive trajectory modification
[AD-A289399] p 2359 N95-26884
Automatically selecting and using primary effects in planning: Theory and experiments
[AD-A289347] p 2450 N95-27064
Myers-Briggs type indicators and Kirton adaption-innovation inventory correlations
[AD-A288435] p 2357 N95-27181
Automated database design from natural language input p 2383 N95-27378
Limits to ground control in autonomous spacecraft
p 2383 N95-27381
Solving recursive domain equations with enriched categories
[AD-A289358] p 2371 N95-27418
Two-body bound states and the Bethe-Salpeter equation
[DE95-008302] p 2392 N95-27742
A new algorithm for generating highly accurate benchmark solutions to transport test problems
[DE95-007397] p 2373 N95-28047
Using the scalable nonlinear equations solvers package
[DE95-008323] p 2378 N95-28071
Developmental problems and their solution for the Space Shuttle main engine alternate liquid oxygen high-pressure turbopump: Anomaly or failure investigation the key
[NASA-TP-3553] p 2169 N95-28263
Stochastic control and topics in applied probability
[AD-A291712] p 2395 N95-28526

PROCESS CONTROL (INDUSTRY)
NIST: Information management in the AMRF
[NONP-NASA-VT-95-49120] p 2454 N95-27208
STEP: A futurevision, today
[NONP-NASA-VT-95-49121] p 2451 N95-27209
Application of modern diagnostic methods to environmental improvement
[DE95-005797] p 2330 N95-28119

PROCUREMENT
Automated Procurement System (APS) revised project management plan (DS-03)
[NASA-CR-196605] p 2450 N95-27169

PRODUCT DEVELOPMENT
The development of a feature-based concurrent engineering system
[AD-A288424] p 2364 N95-26557
Microelectronics in Japan p 2263 N95-27227
Building the electronic industry's roadmaps
p 2263 N95-27228
Japan's technology and manufacturing infrastructure
p 2263 N95-27229
Successful product realization strategies
p 2264 N95-27233
Development of a miniature actuator/controller system
p 2156 N95-27272
SIHTI 2: Energy and environmental technology. Yearbook 1993 of the research programme
[DE95-755135] p 2331 N95-28202

PRODUCTION ENGINEERING
Laboratory of production engineering
[PB95-184834] p 2451 N95-28135

PRODUCTIVITY
A system dynamics based study of software reuse and its determinants
[AD-A288578] p 2364 N95-26554
Advances in welding science: A perspective
[DE95-006745] p 2302 N95-27545

PROGRAM VERIFICATION (COMPUTERS)
An evaluation of the Software Through Pictures/T Tool (StP/T) for the Software Support Activity (SSA)
[AD-A288822] p 2362 N95-26348
Concurrent engineering research center
[NASA-CR-197726] p 2362 N95-26386
Compiler-assisted debugging and multiple instruction retry
[NASA-CR-197729] p 2365 N95-26628
Turbulence modeling
[NASA-CR-197751] p 2274 N95-26665
Com(sup 3): A composite-compatible component coding system
[BBC-RD-1994/17] p 2249 N95-26670
A process improvement model for software verification and validation
[NASA-CR-197761] p 2367 N95-26814
High performance hardware and software for pattern recognition and image processing
[AD-A289153] p 2370 N95-27031
A verification procedure for MSC/NASTRAN Finite Element Models
[NASA-CR-4675] p 2131 N95-27371
Scientific statistics and graphics on the Macintosh
[DE95-006445] p 2372 N95-27533
PRISM validation
[AD-A288476] p 2337 N95-27703
A simple method for verifying the deployment of the TOMS-EP solar arrays p 2150 N95-27782
Calculation of design load for the MOD-5A 7.3 mW wind turbine system p 2312 N95-27982

PROGRAMMING ENVIRONMENTS
A software bus for thread objects
[NASA-CR-197764] p 2365 N95-26575
Unification of LARCH and Z-based object models to support algebraically-based design refinement: The Z perspective
[AD-A289234] p 2369 N95-26962

PROGRAMMING LANGUAGES
An introduction to software architecture
[AD-A288963] p 2363 N95-26446
Specifying weak sets
[AD-A288587] p 2364 N95-26536
Modal event calculus in Lolli
[AD-A288544] p 2365 N95-26605
A parallel complexity model for functional languages
[AD-A288589] p 2365 N95-26656
Using an architectural approach to integrate heterogeneous, distributed software components
[NASA-CR-197766] p 2366 N95-26711
Scalability in production system programs
[AD-A289345] p 2453 N95-27063
Language constructs and runtime systems for compositional parallel programming
[DE95-008298] p 2378 N95-27741
Guide for transmitting Standard Generalized Markup Language (SGML) encoded bibliographic records
[DOE/OSTI-11685] p 2457 N95-28675

PROGRESS
Review of activities in USA on HTS materials
[DE95-006404] p 2234 N95-27468

PROJECT MANAGEMENT
Software risk management through independent verification and validation
[NASA-CR-197767] p 2364 N95-26486
Automated Procurement System (APS) revised project management plan (DS-03)
[NASA-CR-196605] p 2450 N95-27169

PROJECT PLANNING
Automated Procurement System (APS) revised project management plan (DS-03)
[NASA-CR-196605] p 2450 N95-27169
Electric vehicle activities
[DE95-006648] p 2267 N95-28105

PROJECTILES
Ram accelerator performance calculations using a modified version of the NASA CET89 equilibrium chemistry code
[AD-A289554] p 2201 N95-26678
Atomic physics with highly charged ions
[DE95-007325] p 2407 N95-27439
PXAMS: Projectile X ray AMS: X ray yields and applications
[DE95-006438] p 2204 N95-27496

Projectile image acceleration, neutralization and electron emission during grazing interactions of multicharged ions with Au(110)
[DE95-007394] p 2409 N95-27551

Use of mussels in biomonitoring of environmental impacts of propellants, projectiles, explosives, and pyrotechnics p 2170 N95-28298

Computational studies of projectile melt in impact with typical whipple shields
[DE95-005916] p 2311 N95-28337

PROLATE SPHEROIDS

Simple equivalent dipole distributions for dielectric spheroidal scatterers
[PB95-184883] p 2254 N95-27049

PROPAGATION MODES

Depth migration in transversely isotropic media with explicit operators
[DE95-007670] p 2337 N95-27442

PROPANE

Small angle x ray scattering studies of reverse micelles in supercritical fluids
[DE95-007803] p 2287 N95-28021

PROPELLANT ADDITIVES

Mars Sample Return mission utilizing in-situ propellant production
[NASA-CR-188371] p 2145 N95-28261

PROPELLANT CHEMISTRY

Mars Sample Return mission utilizing in-situ propellant production
[NASA-CR-188371] p 2145 N95-28261

PROPELLANT COMBUSTION

Propellant injection systems and processes
[NASA-TM-110632] p 2242 N95-26781

Chemical reactions identified in the Titan 2, Titan 4, and Delta 2 propellant systems and their application to source modeling p 2172 N95-28304

PROPELLANT SENSITIVITY

Cryogenic washout of solid rocket propellants
p 2176 N95-28324

PROPELLANT STORAGE

Task 4 supporting technology. Densification requirements definition and test objectives. Propellant densification requirements definition
[NASA-CR-198629] p 2450 N95-28260

PROPELLANT TESTS

Chemical reactions identified in the Titan 2, Titan 4, and Delta 2 propellant systems and their application to source modeling p 2172 N95-28304

Acute and subacute toxicity of ammonium dinitramide (ADN) p 2175 N95-28318

PROPELLANTS

Use of mussels in biomonitoring of environmental impacts of propellants, projectiles, explosives, and pyrotechnics p 2170 N95-28298

PROPELLER BLADES

Development and validation of a blade-element mathematical model for the AH-64A Apache helicopter
[NASA-TM-108863] p 2118 N95-26710

Analysis of aircraft engine blade subject to ice impact
p 2141 N95-28277

PROPULSION

Progress in incompressible Navier-Stokes computations for propulsion flows and its dual-use applications
[NASA-CR-197746] p 2275 N95-26766

The lift-fan aircraft: Lessons learned
[NASA-CR-196694] p 2131 N95-27143

NAS Technical Summaries, March 1993 - February 1994
[NASA-RP-1355] p 2466 N95-27367

Turbulence program for propulsion systems
p 2285 N95-27883

A knowledge highway for integrated modelling from manufacturing to design
[AD-A288872] p 2247 N95-28187

PROPULSION SYSTEM CONFIGURATIONS

Simulation model of the integrated flight/propulsion control system, displays, and propulsion system for ASTOVL lift-fan aircraft
[NASA-TM-108866] p 2139 N95-26412

Funding for AFRAPT student trainees for academic year 1992-1993
[AD-A288461] p 2466 N95-26604

Direct drive options for electric propulsion systems
[NASA-TM-106576] p 2168 N95-27861

Propulsion system assessment for very high UAV under ERAST
[NASA-CR-195469] p 2140 N95-27866

PROPULSION SYSTEM PERFORMANCE

Funding for AFRAPT student trainees for academic year 1992-1993
[AD-A288461] p 2466 N95-26604

Micro electric propulsion feasibility
[NASA-CR-189139] p 2168 N95-28000

PROPULSIVE EFFICIENCY

Propulsion system assessment for very high UAV under ERAST
[NASA-CR-195469] p 2140 N95-27866

PROTECTION

Aircraft fuel system lightning protection design and qualification test procedures development
[AD-A288401] p 2125 N95-26497

The protection of electro-explosive devices (EEDs) and electronics from electrostatic discharge (ESD) hazards
[DSTO-TR-0100] p 2258 N95-28568

PROTECTIVE CLOTHING

Lightweight cold weather underwear investigation
[AD-A288506] p 2358 N95-26736

PROTECTIVE COATINGS

Engineering calculations associated with the ablative thermal protective structures of returnable satellites
[AD-A289593] p 2162 N95-26715

The response of hydrotalcite coated aluminum to sealing with transition metal salt solutions
[DE95-004767] p 2234 N95-27460

Orbital atomic oxygen effects on materials: An overview of MSFC experiments on the STS-46 EOIM-3
p 2419 N95-27637

Effects of atomic oxygen on polymeric materials flown on EOIM-3 p 2242 N95-27638

The Strategic Technologies for Automation and Robotics (STEAR) program: Protection of materials in the space environment subprogram p 2242 N95-27669

Process for non-contact removal of organic coatings from the surface of paintings
[NASA-CASE-LEW-15896-1] p 2235 N95-27702

Processing and properties of chromate-free conversion coatings on aluminum
[DE95-004768] p 2218 N95-27722

Assay of weathering effects on protective polymer coatings using positron annihilation spectroscopy
[DE95-007040] p 2236 N95-27962

Chromate-free corrosion resistant conversion coatings for aluminum alloys
[DE95-007742] p 2238 N95-28117

Weightless Environment Training Facility (WETF) materials coating evaluation, volume 1
[NASA-CR-188366-VOL-1] p 2239 N95-28385

Weightless Environment Training Facility (WETF) materials coating evaluation, volume 2
[NASA-CR-188366-VOL-2] p 2239 N95-28386

Weightless Environment Training Facility (WETF) materials coating evaluation, volume 3
[NASA-CR-188366-VOL-3] p 2239 N95-28387

Coatings of non-oxide ceramics for improved corrosion resistance in high temperature coal combustion
[DE95-006932] p 2241 N95-28604

PROTEIN CRYSTAL GROWTH

Device and method for screening crystallization conditions in solution crystal growth
[NASA-CASE-MFS-28985-1] p 2245 N95-26888

Apparatus for diffusion controlled dialysis under microgravity conditions
[NASA-CASE-MFS-28986-1] p 2245 N95-27500

PROTEIN SYNTHESIS

Device and method for screening crystallization conditions in solution crystal growth
[NASA-CASE-MFS-28985-1] p 2245 N95-26888

PROTEINS

Non-covalent immobilization of proteins and enzymes on polymerized lipid assemblies
[AD-A288234] p 2225 N95-26526

The effect of proteins on the aging properties of radiation vulcanized Natural Rubber Latex
[DE95-603357] p 2225 N95-26599

Regional differences in lectin binding patterns of vestibular hair cells p 2349 N95-26728

Predicting protein structure using parallel genetic algorithms
[AD-A289305] p 2369 N95-26919

Advances in scientific visualization
[DE95-008065] p 2343 N95-28014

Feasibility studies for separation processes using environmentally sensitive hydrogels
[DE95-008355] p 2238 N95-28226

Hydrogen-ion titrations of amino acids and proteins in solutions containing concentrated electrolyte
[DE95-008356] p 2209 N95-28229

PROTOCOL (COMPUTERS)

The reliable multicast protocol application programming interface
[NASA-CR-197762] p 2363 N95-26388

Scalable multicast tree construction for wide area networks
[AD-A288318] p 2379 N95-26421

A decentralized software bus based on IP multicasting
[NASA-CR-197768] p 2366 N95-26695

Minimizing the impact of synchronization overhead in parallel discrete event simulations
[AD-A289278] p 2377 N95-26984

A foveated system to reduce transmission bandwidth of video images from remote camera systems
[AD-A288516] p 2254 N95-27060

Efficient generation of counterexamples and witnesses in symbolic model checking
[AD-A288583] p 2370 N95-27095

Design and implementation of a software communication architecture for the JANUS-3D Visualizer
[AD-A288509] p 2370 N95-27150

Construction of a connectionist network supercomputer
[AD-A288439] p 2377 N95-27182

A high performance totally ordered multicast protocol
[NASA-CR-197765] p 2371 N95-27252

An architecture and protocol for communications satellite constellations regarded as multi-agent systems
p 2168 N95-27377

XTP as a transport protocol for distributed parallel processing
[DE95-004992] p 2378 N95-27402

Practical considerations for network addressing using CIDR
[PB95-195335] p 2379 N95-28665

PROTON BEAMS

Observation of asymmetrical two-cone Vavilov-Cherenkov radiation in biaxial crystal of triglycinesulphate emitted by 658 MeV protons passing along bi normal
[DE94-629017] p 2441 N95-27867

PROTON DAMAGE

Radiation-induced segregation: A microchemical gauge to quantify fundamental defect parameters
[DE95-005720] p 2216 N95-27492

PROTON RESONANCE

Beam-beam interaction working group summary
[DE95-007824] p 2422 N95-28123

PROTON-PROTON REACTIONS

The CDF upgrade
[DE95-006683] p 2421 N95-28107

The Bremsstrahlung of soft gamma-quanta created by elastic pp- and np-scatterings and the dibaryon resonance problem
[DE95-608870] p 2415 N95-28248

PROTONS

Implications of horizontal symmetries on baryon number violation in supersymmetric models
[DE95-610202] p 2407 N95-27406

A study of events with large total transverse energy produced in proton-antiproton collisions at (radical)s = 1.8 TeV
[DE95-003382] p 2410 N95-27872

Some aspects of the OZI-rule violation in the reaction anti-pp yields phi pi(0)
[DE95-608853] p 2415 N95-28245

The 132 nsec bunch spacing in the Tevatron proton-antiproton collider
[DE95-005750] p 2422 N95-28346

PROTOTYPES

Effect of processing parameters on surface finish for fused deposition machinable wax patterns
[NASA-TP-3550] p 2244 N95-26769

Design considerations for FrankTalk: A distributed group support system
[AD-A289386] p 2359 N95-26863

Unification of LARCH and Z-based object models to support algebraically-based design refinement: The Z perspective
[AD-A289234] p 2369 N95-26962

Weighting scheme for the space surveillance network automated tasker
[AD-A289285] p 2146 N95-27035

A general object model transformation system
[AD-A289289] p 2370 N95-27037

NIST: Information management in the AMRF
[NONP-NASA-VT-95-49120] p 2454 N95-27208

SXI Prototype mirror mount
[NASA-CR-198613] p 2301 N95-27244

Spray-formed tooling
[DE95-005031] p 2246 N95-27404

JTEC panel on display technologies in Japan
[NASA-CR-198564] p 2292 N95-27863

Research on the establishment of the database system for R and D on the innovative technology for the Earth
[DE95-759244] p 2458 N95-27937

Measurement of wakefield suppression in a detuned X-band accelerator structure
[DE95-008592] p 2422 N95-28159

Cosmic ray test results of the D0 prototype scintillating fiber tracker
[DE95-007215] p 2415 N95-28221

Prototype development and test results of a continuous ambient air monitoring system for hydrazine at the 110 ppb level p 2173 N95-28310

Dimensionally self regulating materials
[AD-A291671] p 2257 N95-28456
Manikin integrated data acquisition system (MIDAS) initial modifications
[AD-A291662] p 2361 N95-28667

PROVING
Supersonic transport grid generation, validation, and optimization
[NASA-CR-197752] p 2365 N95-26648
Cleanliness verification process at Martin Marietta Astronautics p 2165 N95-27104
Evaluations of the effectiveness of environmentally benign cleaning methodologies p 2230 N95-27115
On permanent capillar-heavy waves in circular shaped channels
[DE95-608779] p 2280 N95-27339
DOE/KEURP Site Operator Program
[DE95-007116] p 2266 N95-27926
Proof test methodology for composites
p 2193 N95-28445

PSYCHOLOGICAL EFFECTS
Basic mechanisms and implications of non-photic entrainment of circadian rhythmicity
[AD-A288433] p 2353 N95-26779

PSYCHOLOGICAL TESTS
Codes of processing and multiple resources: Model and methodology
[AD-A289583] p 2355 N95-26691
Handbook of perception and human performance, volume 2. Cognitive processes and performance
[AD-A289587] p 2355 N95-26692
Myers-Briggs type indicators and Kirton adaption-innovation inventory correlations
[AD-A288435] p 2357 N95-27181

PSYCHOLOGY
Enhancing the effects of diversity awareness training: A review of the research literature
[DOT/FAA/AM-95/10] p 2355 N95-26361
Change, Learning and Mental Work in Organizations: Working papers of the 3rd Otaniemi-Dresden Workshop
[PB95-184941] p 2356 N95-26909

PUBLIC HEALTH
Concurrent engineering research center
[NASA-CR-197726] p 2362 N95-26386
Health and environmental hazards of CdTe photovoltaic module production, use and decommissioning
[DE95-006688] p 2320 N95-27682
Current status of environmental, health, and safety issues of lithium polymer electric vehicle batteries
[DE95-004005] p 2265 N95-27719
Implementing an integrated standards-based management system to ensure compliance at Los Alamos National Laboratory
[DE95-007873] p 2451 N95-28025
Evaluating the environmental viability of open burning/open detonation operations
p 2170 N95-28297

PUBLIC RELATIONS
Community relations plan: Galena Airport and Camp ion Air Force Station, Alaska
[AD-A286722] p 2327 N95-27234

PULSARS
Multiwavelength observations of unidentified high energy gamma-ray sources
[NASA-CR-197840] p 2465 N95-26630
Was Einstein 100% right?
[PB95-190179] p 2449 N95-28175

PULSE CODE MODULATION
Pulse Code Modulation (PCM) encoder handbook for Aydin Vector MMP-900 series system
[NASA-RP-1365] p 2255 N95-27435

PULSE COMPRESSION
Method of phased magnitude correlation using binary sequences
[AD-D017257] p 2248 N95-26465

PULSE DURATION
Low power limits in ultrashort pulse measurement using Frequency-Resolved Optical Gating
[DE95-007150] p 2299 N95-28219
Ultrashort Pulse retrieval using FROG trace irradiance moments and the adaptive neural networks backpropagation algorithm
[DE95-007153] p 2299 N95-28220
Phase retrieval and time-frequency methods in the measurement of ultrashort laser pulses
[DE95-006499] p 2300 N95-28549

PULSE GENERATORS
AFC generator development
[DE95-007094] p 2266 N95-27754

PULSE RADAR
The ambiguity function of the stepped frequency radar
[AD-A289533] p 2251 N95-26871

PULSED LASER DEPOSITION
Pulsed laser deposition of zeolitic membranes
[DE95-006274] p 2298 N95-28124

PULSED LASERS
Wake fields in semiconductor plasmas
[DE94-634523] p 2429 N95-26439
Femtosecond X-ray generation through 90 degrees T homson scattering: Status of the LBL experiment
[DE95-006560] p 2296 N95-27674
Spectral broadening of KrF laser radiation by self-seeded Raman amplification in long air paths
[DE95-003697] p 2297 N95-27718
Laser with optically driven Q-switch
[NASA-CASE-NPO-18470-1-CU] p 2297 N95-27731
Bubble chamber spectroscopy for chemical analysis: A new concept
[DE95-006350] p 2209 N95-28088
Passive spatial beam control, appendix
[AD-A288913] p 2300 N95-28333

PULSED RADIATION
Surface damage effects generated by a fast-pulse laser beam
[AD-A289131] p 2295 N95-26996
Direct ultrashort-pulse retrieval using frequency-resolved optical gating and a computational neural network
[DE95-007148] p 2425 N95-27482
Phase retrieval and time-frequency methods in the measurement of ultrashort laser pulses
[DE95-006499] p 2300 N95-28549

PURGING
Comparison of numerical results and multicavity purge and rim seal data with extensions to dynamics
[NASA-TM-106685] p 2168 N95-27434

PURIFICATION
To develop an aerosoling immunomagnetic device for rapid medical diagnosis from clinical samples
[AD-A288504] p 2354 N95-27059

PURITY
Ultra high purity, dimensionally stable INVAR 36
[NASA-CASE-NPO-19358-1-CU] p 2213 N95-26862

PYROELECTRICITY
Large area smart piezoelectric and pyroelectric sensors
[AD-A288565] p 2290 N95-26541
Growth and characterization of crystals for room temperature I.R. detectors and second harmonic generation devices
[NASA-CR-198598] p 2443 N95-28033

PYROLYSIS
Junkyard chemistry p 2227 N95-27102
A practical approach to soil remediation
p 2232 N95-27125
Biomass Pyrolysis Oil Properties and Combustion Meeting
[DE95-004017] p 2204 N95-27438
Boron-carbon-silicon polymers and the ceramic thereof
[NASA-CASE-ARC-11891-1-SB] p 2238 N95-28212
Destruction of pyrotechnics manufacture wastewater treatment sludge by plasma arc pyrolysis
p 2171 N95-28301
Review and analysis of the 1980-1989 biomass thermochemical conversion program
[DE95-000287] p 2325 N95-28394

PYROLYTIC GRAPHITE
Electrocrystallization of an ordered organic monolayer: Selective epitaxial growth of beta(ET)213 ongraphite
[AD-A288942] p 2178 N95-26569
LEO degradation of graphite and carbon-based composites aboard Space Shuttle Flight STS-46
p 2199 N95-27636

PYROTECHNICS
Use of mussels in biomonitoring of environmental impacts of propellants, projectiles, explosives, and pyrotechnics p 2170 N95-28298
Destruction of pyrotechnics manufacture wastewater treatment sludge by plasma arc pyrolysis
p 2171 N95-28301
A comprehensive energetic materials resource recovery and recycling program p 2176 N95-28323

PYRROLES
High pressure conductivity study of template synthesized polypyrrole: Observation of a crossover from three to one dimensional variable range hopping
[AD-A288367] p 2224 N95-26470

Q

Q SWITCHED LASERS
Continuously-tunable, narrow-linewidth, Q-switched Cr:LiSAF laser for lidar applications
[DE95-006285] p 2296 N95-27672
Laser with optically driven Q-switch
[NASA-CASE-NPO-18470-1-CU] p 2297 N95-27731

QUADRUPOLES
Iron oxides characterization by Moessbauer spectroscopy
[DE95-607869] p 2202 N95-27199
Magnetic quadrupole moment of W-boson in Kobayashi-Maskawa model
[DE95-610355] p 2407 N95-27411
Coupling in the Tevatron
[DE95-005129] p 2421 N95-27531
STS-46 plasma composition measurements using the EOIM-3 mass spectrometer p 2211 N95-27645
Field quality improvements in superconducting magnets for RHIC
[DE95-006096] p 2269 N95-28339
Manufacture and testing of the superconducting wire and cable for the RHIC dipoles and quadrupoles
[DE95-006000] p 2270 N95-28515

QUALITY CONTROL
Evaluations of the effectiveness of environmentally benign cleaning methodologies p 2230 N95-27115
Quest for excellence 5
[NONP-NASA-VT-95-49099] p 2451 N95-27205
Malcolm Baldrige National Quality Award winners 1989
[NONP-NASA-VT-95-49119] p 2451 N95-27207
STEP: A futurevision, today
[NONP-NASA-VT-95-49121] p 2451 N95-27209
Quality assurance and reliability in the Japanese electronics industry p 2263 N95-27232
The development of an engineering standard for composite repairs p 2135 N95-27528
I(sub DDQ) testing and defect classes: A tutorial
[DE95-005467] p 2306 N95-27723
Field quality improvements in superconducting magnets for RHIC
[DE95-006096] p 2269 N95-28339

QUANTITATIVE ANALYSIS
Chemistry involving the separation, isolation, and immobilization of 3-5 compound semiconductor nanocrystals and quantum dots
[AD-A288381] p 2436 N95-26473
Corrosive effects of supercritical carbon dioxide and cosolvents on metals p 2224 N95-27113
Analysis of surfaces, films and multilayers by resonant laser ablation
[DE95-006295] p 2297 N95-27841
On the physics of ion ring generation for the stabilization of FRX discharges
[DE95-007105] p 2410 N95-27922

QUANTUM CHEMISTRY
Beyond transition state theory: Rigorous quantum approaches for determining chemical reaction rates
[DE95-008483] p 2208 N95-28086
International journal of quantum chemistry
[AD-A291633] p 2352 N95-28546

QUANTUM CHROMODYNAMICS
The photon structure function F2 in QCD with nonlocal vacuum quark condensates
[DE95-608829] p 2406 N95-27314
Addendum to the 1993 European school of high-energy physics
[DE95-610313] p 2419 N95-27321
Couplings of heavy hadrons with soft pions from QCD sum rules
[DE95-610349] p 2407 N95-27410
A study of parton distribution functions with the use of photon + jet event kinematics in p(bar p) collisions at (radical)s = TeV
[DE95-005127] p 2408 N95-27444
N. N. Bogolyubov and particle physics
[DE95-608794] p 2448 N95-27447
Lattice QCD calculation using VPP500
[DE95-007076] p 2449 N95-27448
Studies of kinematic distributions and mass reconstruction of CDF top candidate events
[DE95-005108] p 2408 N95-27478
The 1993 European school of high-energy physis
[DE95-610196] p 2421 N95-28040
Skew chromaticity
[DE95-007677] p 2422 N95-28115
Polarization as a probe to the production mechanisms of charmonium in (pi)N collisions
[DE95-008136] p 2414 N95-28142
Efficient analytic computation of higher-order QCD amplitudes
[DE95-008593] p 2449 N95-28160
The high energy behavior of the forward scattering parameters -- (sigma)(sub tot), (rho), and B
[DE95-007075] p 2415 N95-28210
Topological density and instantons on a lattice
[DE95-006348] p 2445 N95-28240
Weak matrix elements efforts on the lattice: Status and prospects
[DE95-007701] p 2416 N95-28355

Measurement of alpha(s) in e(+)e(-) annihilation at E(cm) = 29 GeV
[DE95-006486] p 2417 N95-28594
QUANTUM ELECTRODYNAMICS
The free energy of hot QED at three and a half loops
[DE95-007079] p 2449 N95-27449
The 1993 European school of high-energy physis
[DE95-610196] p 2421 N95-28040
QUANTUM MECHANICS
Mean value theorem in topological vector spaces
[DE95-608753] p 2390 N95-27331
Quantum k-Poincare 1994
[DE95-608754] p 2448 N95-27332
Wigner quantum oscillators. OSP (3/2) oscillators
[DE95-608756] p 2448 N95-27334
The Hurwitz-Eulerian reduction
[DE95-608760] p 2396 N95-27337
Realization of vector fields for quantum groups as pseudodifferential operators on quantum spaces
[DE95-008485] p 2449 N95-27877
Phase stability and elasticity of C15 transition-metal intermetallic compounds
[DE95-007876] p 2219 N95-28026
Beyond transition state theory: Rigorous quantum approaches for determining chemical reaction rates
[DE95-008483] p 2208 N95-28086
Bit-string physics: A novel theory of everything
[DE95-005941] p 2449 N95-28137
Quantum retrodiction and causality principle
[DE94-628438] p 2450 N95-28183
Some aspects of the OZI-rule violation in the reaction anti-pp yields phi pi(0)
[DE95-608853] p 2415 N95-28245
Quantum effects induced by a gap in the spectrum of atom-bath coupling constants: Freezing of atomic decay and monochromatic collective radiation
[DE95-609037] p 2416 N95-28251
QUANTUM NUMBERS
Bit-string physics: A novel theory of everything
[DE95-005941] p 2449 N95-28137
QUANTUM OPTICS
Toward coherent excitation: Development of a single-source pump for the rubidium hyperfine ground state doublet
[AD-A289413] p 2295 N95-27132
Basic and applied research in the field of electronics and communications
[AD-A291727] p 2270 N95-28512
QUANTUM STATISTICS
Algebraic structure of the Green's ansatz and its q-deformed analogue
[DE95-608780] p 2395 N95-27340
The canonical q-transformations with two q-para-Bose oscillators
[DE95-608781] p 2396 N95-27341
QUANTUM THEORY
Environmental effects on high energy density materials
[AD-A288296] p 2199 N95-26416
Analytic formulae for the Hartree-Fock order parameter at arbitrary p/q filling factors for the 2DEG in a magnetic field
[DE95-607805] p 2448 N95-26603
Toward coherent excitation: Development of a single-source pump for the rubidium hyperfine ground state doublet
[AD-A289413] p 2295 N95-27132
q-structure algebra of U(sub q)(g-circumflex) from its adjoint action
[DE95-608749] p 2390 N95-27301
Bogolyubov renormalization group
[DE95-608830] p 2448 N95-27315
Excited Charm States
[DE95-005749] p 2409 N95-27747
The 1993 European school of high-energy physis
[DE95-610196] p 2421 N95-28040
Rare decays/CP: The perspective of a kaon physicist
[DE95-005964] p 2416 N95-28338
International journal of quantum chemistry
[AD-A291633] p 2352 N95-28546
QUANTUM WELL LASERS
Comprehensive numerical model for CW vertical-cavity surface-emitting lasers
[DE95-007758] p 2299 N95-28132
QUANTUM WELLS
Joint Services Electronics Program (JSEP)
[AD-A288299] p 2345 N95-26419
Room-temperature photocurrent spectroscopy of GaAs/GaAlAs multiple quantum wells
[AD-A289607] p 2201 N95-26707
Materials, structures, and devices for high-speed electronics
[NASA-CR-197815] p 2260 N95-26816
Design and characterization of resonant cavity light-emitting diodes
[AD-A289307] p 2261 N95-26921
High pressure optical studies of semiconductors and heterostructures
[DE95-007119] p 2410 N95-27927
Time-dependent model for vertical-cavity surface-emitting laser
[DE95-007880] p 2298 N95-28027
Heterostructures and infrared emitters with compressed InAsSb layers
[DE95-008157] p 2446 N95-28399
QUARK MODELS
A simple relativistic model of pp-bar yields K(+)K(-)
[DE95-608852] p 2406 N95-27318
Implications of horizontal symmetries on baryon number violation in supersymmetric models
[DE95-610202] p 2407 N95-27406
Excited Charm States
[DE95-005749] p 2409 N95-27747
QUARK PARTON MODEL
Addendum to the 1993 European school of high-energy physics
[DE95-610313] p 2419 N95-27321
QUARKS
Physics with relativistic heavy ions: QGP and other delicacies
[DE95-007014] p 2406 N95-27307
The photon structure function F2 in QCD with nonlocal vacuum quark condensates
[DE95-608829] p 2406 N95-27314
A note on the constituent quark resonances
[DE95-608831] p 2406 N95-27316
Implications of horizontal symmetries on baryon number violation in supersymmetric models
[DE95-610202] p 2407 N95-27406
Transverse tau polarization in inclusive bar-B yields tau bar-nu X decays
[DE95-610325] p 2407 N95-27409
Studies of kinematic distributions and mass reconstruction of CDF top candidate events
[DE95-005108] p 2408 N95-27478
The gluon propagator in non-Abelian Weizsaecker-Williams fields
[DE95-006877] p 2449 N95-27547
Preliminary heavy-light decay constants from the MILC Collaboration
[DE95-005685] p 2409 N95-27552
Search for the top quark in dilepton decay modes at D(PHI)
[DE95-007764] p 2409 N95-27689
Search for supersymmetry and leptoquark states at FNAL
[DE95-003381] p 2410 N95-27871
Search for exotic particles at CDF
[DE95-008383] p 2411 N95-27933
The Top...is it There? A Survey of the CDF and D0 Experiments
[DE95-005746] p 2411 N95-27945
Supersymmetry and light quark masses in a realistic superstring model
[DE95-610201] p 2412 N95-28041
Bit-string physics: A novel theory of everything
[DE95-005941] p 2449 N95-28137
Aspects of strangeness
[DE95-008314] p 2414 N95-28169
Stability of strange quark stars with nuclear crusts against radial oscillations
[DE95-008484] p 2463 N95-28357
Recent status in the search for the quark-gluon plasma
[DE95-007036] p 2417 N95-28447
B-Physics results from D0
[DE95-005126] p 2417 N95-28495
QUARTZ
The biodegradation of fuels in soils and sediments: Differences as a function of mineralogy
p 2230 N95-27116
The effects of processing variables on reaction synthesis of Fe-Al alloys
[DE95-007405] p 2221 N95-28082
QUARTZ CRYSTALS
Analytical investigations of the acceleration sensitivity of acoustic bulk and surface wave resonators
[AD-A291715] p 2402 N95-28505
QUENCHING
The effect on stability and thermal hydraulic quenchback of perforating the jacket of a cable-in-conduit conductor
[DE95-005392] p 2262 N95-27083
QUENCHING (COOLING)
On the thermally-induced residual stresses in thick fiber-thermoplastic matrix (PEEK) cross-ply laminated plates p 2187 N95-28285
QUERY LANGUAGES
Specifying weak sets
[AD-A288587] p 2364 N95-26536
Query by image example: The CANDID approach
[DE95-006284] p 2456 N95-28631
QUEUEING THEORY
Optimal control of two queues in series
[DE95-608731] p 2382 N95-27045

R

RABBITS
Advanced formation flight control
[AD-A289271] p 2142 N95-26981
RACE FACTORS
Enhancing the effects of diversity awareness training: A review of the research literature
[DOT/FAA/AM-95/10] p 2355 N95-26361
RADAR DATA
Space tether-radar data processing
[AD-A289654] p 2250 N95-26725
Classification of ultra high range resolution radar using decision boundary analysis
[AD-A289378] p 2251 N95-26877
Processing of wide-angle synthetic aperture radar signals for detection of obscured ground targets
[AD-A289243] p 2253 N95-26976
Auto-processing of OTH radar amplitude/range/Doppler data
[AD-A289152] p 2253 N95-27005
Theoretical and experimental models of the diffuse radar backscatter from Mars
[NASA-CR-198650] p 2463 N95-27700
High performance ground penetrating radar survey of TA-49/Area 2
[DE95-006856] p 2258 N95-28601
RADAR DETECTION
Processing of wide-angle synthetic aperture radar signals for detection of obscured ground targets
[AD-A289243] p 2253 N95-26976
Nonlinear signal processing schemes for robust target detection in radar
[AD-A288449] p 2255 N95-27185
RADAR IMAGERY
Speckle spectrum of the ERS-1 wavemode product
[PB95-196564] p 2315 N95-28180
Binary segmentation of SAR images by the ICM algorithm
[INPE-5464-PRE/1772] p 2258 N95-28559
SAR noise reduction through the utilization of robust filters
[INPE-5504-PRE/1787] p 2258 N95-28569
RADAR MEASUREMENT
Measurements of HF auroral clutter using the Verona Ava Linear Array Radar (VALAR)
[AD-A289442] p 2337 N95-27147
Subsurface radar investigations at the Pegasus Glacial-ice Runway and Williams Field, McMurdo Station, Antarctica
[AD-A289323] p 2144 N95-27297
Continuously-tunable, narrow-linewidth, Q-switched Cr:LiSAF laser for lidar applications
[DE95-006285] p 2296 N95-27672
A study of lightning in winter thunderstorms and the analysis of thunderstorm overflight data
[NASA-CR-198577] p 2343 N95-28191
The concentration-estimation problem for multiple-wavelength differential absorption lidar
[DE95-008375] p 2256 N95-28231
RADAR NAVIGATION
GPS as an orbit determination subsystems
p 2152 N95-27793
Operational considerations of using GPS for spacecraft navigation p 2152 N95-27794
RADAR NETWORKS
Report to the Chairman and Ranking Minority Member, Committee on Science, House of Representatives. Weather forecasting: Radar availability requirement not being met
[GAO/AIMD-95-132] p 2342 N95-27912
RADAR RECEIVERS
GPS as an orbit determination subsystems
p 2152 N95-27793
Operational considerations of using GPS for spacecraft navigation p 2152 N95-27794
RADAR RESOLUTION
The ambiguity function of the stepped frequency radar
[AD-A289533] p 2251 N95-26871
RADAR SCATTERING
Theoretical and experimental models of the diffuse radar backscatter from Mars
[NASA-CR-198650] p 2463 N95-27700
Studies of radar backscatter as a function of wave properties and the winds in the turbulent marine atmosphere
[NASA-CR-198608] p 2315 N95-28209
RADAR TARGETS
Evaluation of the FMICW waveform in HF surface radar applications
[AD-A288245] p 2249 N95-26545

Processing of wide-angle synthetic aperture radar signals for detection of obscured ground targets
[AD-A289243] p 2253 N95-26976
RADAR TRACKING
Evaluation of the FMICW waveform in HF surface radar applications
[AD-A288245] p 2249 N95-26545
The design and implementation of the Military Applications of Shiptracks experiment on Space Transportation System - 65
[AD-A288488] p 2160 N95-26634
Fluxes across the west coast resolved by Picket Fence observations during stormfest
[AD-A288511] p 2341 N95-26653
Classification of ultra high range resolution radar using decision boundary analysis
[AD-A289378] p 2251 N95-26877
Measurements of HF auroral clutter using the Verona Ava Linear Array Radar (VALAR)
[AD-A289442] p 2337 N95-27147
Differenced Range Versus Integrated Doppler (DRVID) ionospheric analysis of metric tracking in the Tracking and Data Relay Satellite System (TDRSS)
p 2147 N95-27768
Telemetry down-link Doppler as an attitude sensor for spin stabilized spacecraft p 2150 N95-27785
GPS as an orbit determination subsystems
p 2152 N95-27793
Operational considerations of using GPS for spacecraft navigation p 2152 N95-27794
RADIAL DISTRIBUTION
The structure of lead-indium phosphate glass
[DE95-007130] p 2237 N95-27967
RADIAL FLOW
A general theory of two- and three-dimensional rotational flow in subsonic and transonic turbomachines
[NASA-CR-4496] p 2123 N95-28003
RADIANCE
SeaWiFS technical report series. Volume 26: Results of the SeaWiFS Data Analysis Round-Robin, July 1994 (DARR-1994)
[NASA-TM-104566-VOL-26] p 2345 N95-26430
Performance modeling of hyperspectral imaging sensors for atmospheric studies
[AD-A289017] p 2289 N95-26461
SeaWiFS technical report series. Volume 27: Case studies for SeaWiFS calibration and validation, part 3
[NASA-TM-104566-VOL-27] p 2348 N95-28030
A model of the diurnal variation in magnesium ion density and radiance in the thermosphere
[AD-A289824] p 2339 N95-28575
RADIANT HEATING
Radiant exchange considerations in design and scaleup of photocatalytic reactors for purification of nitroglycerine-contaminated air p 2171 N95-28300
RADIATION
Radiation in everyday life
[DE95-604111] p 2349 N95-26597
RADIATION ABSORPTION
The attenuation of microwave radiation by fog and rain
[AD-A288326] p 2249 N95-26562
Investigation of the collision line broadening problem as applicable to the NASA Optical Plume Anomaly Detection (OPAD) system, phase 1
[NASA-CR-198605] p 2426 N95-27913
Carbonaceous aerosols influencing atmospheric radiation: Black and organic carbon
[DE95-006437] p 2330 N95-28118
Anomalous cloud absorption? A critique of the paper entitled Absorption of Solar Radiation by Clouds: Observations Versus Models
[DE95-007703] p 2331 N95-28121
RADIATION CHEMISTRY
The effect of proteins on the aging properties of radiation vulcanized Natural Rubber Latex
[DE95-603357] p 2225 N95-26599
RADIATION COUNTERS
Silicon subsystem mechanical engineering closeout report for the Solenoidal Detector Collaboration
[DE95-006336] p 2421 N95-27735
The 1993 European school of high-energy physis
[DE95-610196] p 2421 N95-28040
RADIATION DAMAGE
Radiation in everyday life
[DE95-604111] p 2349 N95-26597
Annealing of radiation damaged gallium arsenide solar cells by laser illumination
[AD-A289683] p 2316 N95-26762
Toward a mechanistic understanding of radiation effects in materials
[DE95-006530] p 2221 N95-28120
RADIATION DETECTORS
Radiation sensitive area detection device and method
[NASA-CASE-MFS-28563-3] p 2423 N95-26385
Integration of video and radiation analysis data
[DE95-004165] p 2379 N95-26443
Detection of charged particles in superfluid helium
[DE95-007354] p 2403 N95-26560
Ionizing radiation measurements on LDEF: A0015 Free flyer biostack experiment
[NASA-CR-196603] p 2202 N95-27168
The physics program and status of the SLAC B-Factory and detector
[DE95-006562] p 2409 N95-27676
BEGET: The B-Factory Event Generator version 21
[DE95-008329] p 2414 N95-28171
Can TMAE photocathode be used for high rate applications?
[DE95-008594] p 2293 N95-28178
Cosmic ray test results of the D0 prototype scintillating fiber tracker
[DE95-007215] p 2415 N95-28221
RADIATION DISTRIBUTION
Radiation in everyday life
[DE95-604111] p 2349 N95-26597
A study of surface temperatures, clouds and net radiation
[NASA-CR-198589] p 2329 N95-27864
Carbonaceous aerosols influencing atmospheric radiation: Black and organic carbon
[DE95-006437] p 2330 N95-28118
International Ultraviolet Explorer Atlas of B-type spectra from 1200 to 1900 A
[NASA-RP-1363] p 2463 N95-28328
RADIATION DOSAGE
Radiation in everyday life
[DE95-604111] p 2349 N95-26597
The effect of proteins on the aging properties of radiation vulcanized Natural Rubber Latex
[DE95-603357] p 2225 N95-26599
Long-term variability of electron radiation dose in geosynchronous orbit
[AD-A289335] p 2162 N95-26902
Ionizing radiation measurements on LDEF: A0015 Free flyer biostack experiment
[NASA-CR-196603] p 2202 N95-27168
Materials considerations for molten salt accelerator-based plutonium conversion systems
[DE95-006743] p 2217 N95-27544
RADIATION EFFECTS
The effect of proteins on the aging properties of radiation vulcanized Natural Rubber Latex
[DE95-603357] p 2225 N95-26599
Radiation vulcanization of natural rubber latex
[DE95-600026] p 2226 N95-26637
Annealing of radiation damaged gallium arsenide solar cells by laser illumination
[AD-A289683] p 2316 N95-26762
Comparison of the resistance of the MOS integrated circuits with various types of nuclear radiation
[DE95-608623] p 2261 N95-27023
Investigation of radiation resistance of transistors and integrated circuits using the heavy ions beam of energy higher than 1 MeV/amu and fast neutrons
[DE95-608624] p 2261 N95-27024
Simulating the production of free defects in irradiated metals
[DE95-007165] p 2214 N95-27088
CAS CERN Accelerator School 5th General Accelerator Physics Course
[DE95-608324] p 2419 N95-27158
Numerical solution of fluid flow and heat tranfer problems with surface radiation p 2282 N95-27357
Radiation-induced grain boundary segregation in austenitic stainless steels
[DE95-005721] p 2216 N95-27493
Amorphization of complex ceramics by heavy-particle irradiations
[DE95-005725] p 2236 N95-27733
Density changes in amorphous Pd80Si20 during low temperature ion irradiation
[DE95-007132] p 2441 N95-27928
Sintering of textured YBa2Cu3O(7-x) under intensive Co-60 gamma irradiation
[DE95-007098] p 2442 N95-27950
Gamma ray-induced embrittlement of pressure vessel alloys
[DE95-007133] p 2220 N95-28072
Toward a mechanistic understanding of radiation effects in materials
[DE95-006530] p 2221 N95-28120
The real structure of columnar pinning centers in heavy-ion-irradiated cuprate superconductors
[DE95-003948] p 2445 N95-28186
The combined release and radiation effects satellite time history data base system
[AD-A289835] p 2165 N95-28578
RADIATION HAZARDS
Application of a Geographic Information System for radiologic emergency response
[DE95-007624] p 2455 N95-28113
RADIATION MEASUREMENT
Radon integral measurement system
[DE95-608074] p 2405 N95-27010
Ionizing radiation measurements on LDEF: A0015 Free flyer biostack experiment
[NASA-CR-196603] p 2202 N95-27168
Solar terrestrial radiation data from the Sleepers River Research Watershed
[AD-A288444] p 2464 N95-27184
LDEF: 69 Months in Space. Third Post-Retrieval Symposium, part 3
[NASA-CP-3275-PT-3] p 2466 N95-27629
RADIATION MEASURING INSTRUMENTS
The program for calculating sunshine duration from global radiation
[KNMI-TR-158] p 2343 N95-28237
RADIATION PROTECTION
Radiation safety aspects of commercial high-speed flight transportation
[NASA-TP-3524] p 2465 N95-26427
RADIATION PYROMETERS
Method and apparatus for polaradiometric pyrometer
[NASA-CASE-NPO-19064-1-CU] p 2290 N95-26765
RADIATION SHIELDING
Ionizing radiation measurements on LDEF: A0015 Free flyer biostack experiment
[NASA-CR-196603] p 2202 N95-27168
HZETRN: Description of a free-space ion and nucleon transport and shielding computer program
[NASA-TP-3495] p 2465 N95-28530
RADIATION SPECTRA
SeaWiFS technical report series. Volume 26: Results of the SeaWiFS Data Analysis Round-Robin, July 1994 (DARR-1994)
[NASA-TM-104566-VOL-26] p 2345 N95-26430
Cosmic ray test results of the D0 prototype scintillating fiber tracker
[DE95-007215] p 2415 N95-28221
RADIATION TOLERANCE
Radiation in everyday life
[DE95-604111] p 2349 N95-26597
Toward a mechanistic understanding of radiation effects in materials
[DE95-006530] p 2221 N95-28120
RADIATION TRANSPORT
HZETRN: Description of a free-space ion and nucleon transport and shielding computer program
[NASA-TP-3495] p 2465 N95-28530
Stationary neutrino radiation transport by maximum entropy closure
[DE95-006579] p 2463 N95-28558
RADIATIVE HEAT TRANSFER
Validation of the SINDA/FLUINT code using several analytical solutions p 2281 N95-27350
A case study of view-factor rectification procedures for diffuse-gray radiation enclosure computations
p 2281 N95-27353
CAE for thermal management of aerospace electronic boards using the BETAsoft program
p 2272 N95-27354
RADIATIVE TRANSFER
FTIR measurements of thermal infrared sky radiance and transmission
[DE95-003642] p 2334 N95-26436
Calculations of downward IR surface fluxes in the 500-3,000 cm(exp -1) wavenumber range for the 1994 ICRCCM model intercomparison study
[DE95-006430] p 2328 N95-27708
Observation on radiation transfer experiments using k-shell absorption spectra
[DE95-008068] p 2434 N95-28141
RADICALS
Engineering photochemical smog through convection towers
[DE95-007727] p 2328 N95-27686
On the synthesis of mixed-metal and mixed-pnicogen13-15 ring-systems
[AD-A288869] p 2223 N95-28332
Time-resolved FTIR emission studies of laser photofragmentation and radical reactions
[DE95-008125] p 2300 N95-28398
High energy density systems in cryogenic media: The production and reactions of atoms and radicals
[AD-A289818] p 2417 N95-28572
RADII
Preliminary design study of the beam collapser and certain optomechanical aspects of the siderostat
[AD-A288423] p 2423 N95-26549
Situation in study of electric polarizability and mean square charge radius of the neutron
[DE95-608869] p 2415 N95-28247

The minimum pore size obtainable in a silica gel during drying
[DE95-008162] p 2239 N95-28401

RADIO ALTIMETERS
An integrated GPS/INS/BARO and radar altimeter system for aircraft precision approach landings
[AD-A289280] p 2127 N95-26985

RADIO ASTRONOMY
Multiwavelength observations of unidentified high energy gamma-ray sources
[NASA-CR-197840] p 2465 N95-26630

RADIO COMMUNICATION
Assessment of long-distance HF radio and satellite communication assets for RNLAF out-of-area operations
[AD-A288633] p 2247 N95-26344

RADIO DIRECTION FINDERS
JPRS report: Science and technology. Central Eurasia
[JPRS-UST-95-019] p 2270 N95-28565

RADIO EMISSION
Theoretical and experimental models of the diffuse radar backscatter from Mars
[NASA-CR-198650] p 2463 N95-27700

RADIO EQUIPMENT
The evolution and impact of PCS technology
[AD-A288606] p 2255 N95-27249

RADIO FREQUENCIES
Electromagnetic spectrum occupancy study of a potential transmitter site for the HF Active Auroral Research Program (HAARP)
[AD-A288909] p 2249 N95-26564
Fast wave current drive in D3-D
[DE95-007582] p 2431 N95-27441
Multi-spacecraft coherent Doppler and ranging for interplanetary-navigation p 2150 N95-27786
One dimensional global and local solution for ICRF heating
[DE95-007984] p 2392 N95-28110
Engineering design of the ITER RF systems
[DE95-008064] p 2434 N95-28140
Method and apparatus for maintaining linearity and frequency accuracy of an FM chirp waveform
[AD-D017398] p 2258 N95-28615

RADIO FREQUENCY HEATING
Experimental aspects of effects of high-energy particles on Alfven modes
[DE95-003383] p 2432 N95-27873
One dimensional global and local solution for ICRF heating
[DE95-007984] p 2392 N95-28110
Faraday screen sputtering on TPX
[DE95-008347] p 2434 N95-28224

RADIO NAVIGATION
Analysis and simulation of narrowband GPS jamming using digital excision temporal filtering
[AD-A289328] p 2127 N95-26898
Multi-spacecraft coherent Doppler and ranging for interplanetary-navigation p 2150 N95-27786

RADIO OBSERVATION
Models of symbiotic stars p 2460 N95-27077

RADIO RECEIVERS
Flight evaluation of GPS/DGPS sensor systems installed in NAL Do228
[NAL-TR-1230] p 2126 N95-26585
VOCAR: An experiment in Variability of Coastal Atmospheric Refractivity
[AD-A289202] p 2253 N95-27006
Method and apparatus for maintaining linearity and frequency accuracy of an FM chirp waveform
[AD-D017398] p 2258 N95-28615

RADIO SIGNALS
An improved model of high-latitude f-region scintillation (WBMOD version 13)
[AD-A288558] p 2334 N95-26520
VOCAR: An experiment in Variability of Coastal Atmospheric Refractivity
[AD-A289202] p 2253 N95-27006

RADIO SOURCES (ASTRONOMY)
Multiwavelength observations of unidentified high energy gamma-ray sources
[NASA-CR-197840] p 2465 N95-26630

RADIO TELEMETRY
Radio telemetry buoy for long-range communication
[AD-D017269] p 2161 N95-28581

RADIO TRACKING
Radio telemetry buoy for long-range communication
[AD-D017269] p 2161 N95-28581

RADIO TRANSMISSION
An improved model of high-latitude f-region scintillation (WBMOD version 13)
[AD-A288558] p 2334 N95-26520
Information superhighway: Issues affecting development
[AD-A289434] p 2252 N95-26923
Modeling surface effects with the parabolic equation method
[AD-A289199] p 2254 N95-27021

RADIO TRANSMITTERS
Electromagnetic spectrum occupancy study of a potential transmitter site for the HF Active Auroral Research Program (HAARP)
[AD-A288909] p 2249 N95-26564
VOCAR: An experiment in Variability of Coastal Atmospheric Refractivity
[AD-A289202] p 2253 N95-27006

RADIO WAVES
Classification of RF transients in space using digital signal processing and neural network techniques
[DE95-006287] p 2256 N95-27840

RADIOACTIVE DECAY
Determination of the first hydrolysis constant of Europium (3) in 3 M of ionic strength
[DE95-607912] p 2405 N95-27211
Rare decays/CP: The perspective of a kaon physicist
[DE95-005964] p 2416 N95-28338

RADIOACTIVE ISOTOPES
Photon burst mass spectrometry--ultrasensitive detection of rare isotopes
[DE95-006403] p 2204 N95-27467
Search for deeply bound pionic atoms with high-purity germanium tagging spectrometer
[DE95-609072] p 2416 N95-28252

RADIOACTIVE MATERIALS
Recycle of radiologically contaminated austenitic stainless steels
[DE95-006464] p 2215 N95-27328

RADIOACTIVE WASTES
Recycle of radiologically contaminated austenitic stainless steels
[DE95-006464] p 2215 N95-27328
Transparent access to distributed, heterogeneous environmental information systems
[DE95-007268] p 2454 N95-27483
Multimedia Environmental Pollutant Assessment System (MEPAS) application guidance. Guidelines for evaluating MEPAS input parameters for Version 3.1
[DE95-007525] p 2328 N95-27749
Automated remedial assessment methodology software system
[DE95-007287] p 2373 N95-28243

RADIOACTIVITY
Determination of the first hydrolysis constant of Europium (3) in 3 M of ionic strength
[DE95-607912] p 2405 N95-27211
Development of an optical trap as an ultra-sensitive analytical tool
[DE95-007843] p 2426 N95-28022

RADIOLYSIS
Programming for time resolved spectrum in pulse radiolysis experiments
[DE95-607929] p 2406 N95-27212
Effects of hydrogen on carbon steels at the Multi-Function Waste Tank Facility
[DE95-007194] p 2219 N95-28005

RADIOMETERS
Conversion of sunflower multiband radiometer polarization measurements to polarization parameters
[NASA-CR-197774] p 2314 N95-26815
Solar terrestrial radiation data from the Sleepers River Research Watershed
[AD-A288444] p 2464 N95-27184
Millimeter-wave imaging radiometer data processing and development of water vapor retrieval algorithms
[NASA-CR-198593] p 2343 N95-27997
SeaWiFS technical report series. Volume 27: Case studies for SeaWiFS calibration and validation, part 3
[NASA-TM-104566-VOL-27] p 2348 N95-28030
Design, construction, test and evaluation of a frequency scanning radiometer for measuring oil slick thicknesses
[AD-A290040] p 2293 N95-28389

RADIUM
Flow cytometry as a means of detecting, enumerating and characterizing bacteria for monitoring of the environment
[AD-A288997] p 2326 N95-26610

RADOMES
Polarization sensitivity of monopulse radar boresight error induced by large, ogive radomes
[AD-A289254] p 2252 N95-26972

RADON
Radon integral measurement system
[DE95-608074] p 2405 N95-27010

RAILGUN ACCELERATORS
A high velocity electromagnetic mass launcher having an ablation resistant insulator
[AD-A288231] p 2154 N95-26524

RAIN
The attenuation of microwave radiation by fog and rain
[AD-A288326] p 2249 N95-26562
Synoptic features of the Yunan rainy season before the onset of the tropical monsoons
[AD-A289641] p 2342 N95-26724
Prediction of rain attenuation and total atmospheric attenuation for low-availability satellite communications in Europe
[PB95-184925] p 2252 N95-26908

RAM ACCELERATORS
Ram accelerator performance calculations using a modified version of the NASA CET89 equilibrium chemistry code
[AD-A289554] p 2201 N95-26678

RAMAN LASERS
Remote sensing of the atmosphere by resonance Raman LIDAR
[DE95-007312] p 2315 N95-28520

RAMAN SPECTRA
Spectral broadening of KrF laser radiation by self-seeded Raman amplification in long air paths
[DE95-003697] p 2297 N95-27718
Single molecule detection using charge-coupled device array technology
[DE95-006425] p 2411 N95-27953
Remote sensing of the atmosphere by resonance Raman LIDAR
[DE95-007312] p 2315 N95-28520

RAMAN SPECTROSCOPY
Analytical spectroscopy
[DE95-607896] p 2203 N95-27200
Remote sensing of the atmosphere by resonance Raman LIDAR
[DE95-007312] p 2315 N95-28520

RAMJET ENGINES
Transport phenomena and interfacial kinetics in multiphase combustion systems
[AD-A288297] p 2199 N95-26417
Numerical simulation of combustion flow around a flame holder with hydrogen injection
[NAL-TR-1233] p 2200 N95-26523

RANDOM NOISE
Balanced data focusing: Direction of arrival estimation with maximum likelihood performance
[AD-A288252] p 2248 N95-26407
A modified backpropagation algorithm for training neural networks on data with error bars
[DE95-608729] p 2381 N95-27025
Analysis of filter tuning techniques for sequential orbit determination p 2146 N95-27764
An automated method of tuning an attitude estimator
p 2148 N95-27774
An MME-based attitude estimator using vector observations p 2148 N95-27775
Post Kalman progress p 2148 N95-27776
Material characterization system
[AD-D017385] p 2210 N95-28584

RANDOM NUMBERS
A method for generating skewed random numbers using two overlapping uniform distributions
[DE95-008747] p 2392 N95-28162

RANDOM VARIABLES
A method for simulating correlated random variables from partially specified distributions
[AD-A288820] p 2393 N95-26347

RANGE (EXTREMES)
A comparison of measured wind park load histories with the WISPER and WISPERX load spectra
[DE95-000295] p 2319 N95-27459

RANGEFINDING
Multi-spacecraft coherent Doppler and ranging for interplanetary-navigation p 2150 N95-27786

RAPID QUENCHING (METALLURGY)
Spray-formed tooling
[DE95-005031] p 2246 N95-27404

RARE EARTH ELEMENTS
Crystal structure, short-range oxygen defects, and water adsorption in La- and Nd-modified ZrO2
[DE95-007134] p 2439 N95-27452
Defect characterization of electronic conducting pseudo-perovskite systems
[DE95-007487] p 2220 N95-28049
Characterization of solid state laser and nonlinear optical materials
[AD-A291684] p 2300 N95-28458

RARE GAS-HALIDE LASERS
A novel sensitive detector of atmospheric nitrocompounds based on laser photofragmentation/ionization spectrometry
p 2174 N95-28314

RARE GASES
A model of bubble evolution during decompression based on a Monte Carlo simulation of inert gas diffusion
[AD-A289400] p 2353 N95-26885

RAREFIED GAS DYNAMICS
Statistical model for molecular internal energy exchange in DSMC method for rarefied flow analysis
[ISAS-R-654] p 2274 N95-26741

Anomalous collision rate in the time counter scheme of the direct simulation Monte Carlo method for rarefied gas flow analysis
[ISAS-R-653] p 2275 N95-26742
A model of bubble evolution during decompression based on a Monte Carlo simulation of inert gas diffusion
[AD-A289400] p 2353 N95-26885

RAREFIED GASES
Rarefied gas effects on aerobraking/reentry vehicles with wakes
[NASA-CR-196586] p 2164 N95-27093

RATIONS
Performance enhancing ration components program: Supplemental carbohydrate test
[AD-A288560] p 2358 N95-26558

RATIOS
Investigation of boundary layer and performance effects of transpiration cooling through a porous plate in a rocket nozzle
[AD-A289393] p 2167 N95-26880

RATS
A model of the neural basis of the rat's sense of direction
[AD-A289678] p 2350 N95-26761
Hippocampal place fields, the internal compass, and the learning of landmark stability
[AD-A289406] p 2350 N95-27100

RAY TRACING
Transformation to zero offset in transversely isotropic media
[DE95-007669] p 2339 N95-28192

RAYLEIGH SCATTERING
Comparative experimental study of PIXE and X-ray fluorescence analysis
[DE95-607868] p 2327 N95-27198

RAYLEIGH WAVES
Very low frequency seismo-acoustic noise below the sea floor (0.2-10 Hz)
[AD-A289164] p 2347 N95-27011

RAYLEIGH-RITZ METHOD
Do we fully understand the symmetric Lanczos algorithm yet?
[AD-A289614] p 2368 N95-26855

RDX
Hazards analysis of an integral class 1.1/1.3 rocket motor demilitarization and ingredient recovery system using ammonia p 2174 N95-28315
A comprehensive energetic materials resource recovery and recycling program p 2176 N95-28323
Recovery and reuse of rocket motor propellant ingredients p 2177 N95-28326

REACTING FLOW
A fully implicit time accurate method for hypersonic combustion: Application to shock-induced combustion instability
[NASA-TM-106707] p 2273 N95-26380
Three-dimensional visualization of reactive flows in complex geometries
[DE95-006332] p 2284 N95-27845
Recent advances in PDF modeling of turbulent reacting flows p 2286 N95-27892
Modeling of turbulent chemical reaction
p 2286 N95-27899
PDF methods for turbulent reactive flows
p 2287 N95-27900
DNS, LES and stochastic modeling of turbulent reacting flows
[AD-A280099] p 2287 N95-28155

REACTION BONDING
Theoretical studies of reaction surfaces
[AD-A288458] p 2404 N95-26632

REACTION KINETICS
Transport phenomena and interfacial kinetics in multiphase combustion systems
[AD-A288297] p 2199 N95-26417
Stabilization and control of high energy intermediates through adsorption of restricted spaces
[AD-A288552] p 2201 N95-26606
Theoretical studies of reaction surfaces
[AD-A288458] p 2404 N95-26632
Stress corrosion cracking susceptibility of the earthquake resistant NOM B457 Mexican steel
[DE95-607956] p 2214 N95-27256
Non-metallic oxide inclusion formation in C-Mnlow alloy steel welds
[DE94-019160] p 2215 N95-27319
Analysis of gas absorption to a thin liquid film in the presence of a zero-order chemical reaction
p 2280 N95-27348
Single-drop reactive extraction/extractive reaction with forced convective diffusion and interphase mass transfer
p 2282 N95-27358
Single-drop reactive extraction/extractive reaction with forced convective diffusion and interphase mass transfer
p 2283 N95-27365
Intrusive multi-probe system
[DE95-006258] p 2292 N95-27465
Engineered materials for appliation in severe metallurgical environments: Tantalum-carbon alloy development
[DE95-006838] p 2216 N95-27488
High temperature kinetic study of the reactions H + O2 = OH + O and O + H2 = OH + H in H2/O2 system by shock tube-laser absorption spectroscopy
[NASA-CR-195473] p 2206 N95-27695
Kinetics and dynamics of oxidation reactions involving adsorbed CO species on bulk supported Pt and copper oxides
[DE95-006420] p 2207 N95-27952
Beyond transition state theory: Rigorous quantum approaches for determining chemical reaction rates
[DE95-008483] p 2208 N95-28086
The role of hydrogen in the hydrogenation and hydrogenolysis of aniline on the nickel single crystal surfaces: Its implication on the mechanisms of HDN reactions
[DE95-006687] p 2222 N95-28134
DNS, LES and stochastic modeling of turbulent reacting flows
[AD-A280099] p 2287 N95-28155
Polarization relaxation in zinc oxide varistors from 77 K to 450 K
[DE95-007761] p 2268 N95-28156
Analysis of forward and inverse problems in chemical dynamics and spectroscopy
[DE95-009309] p 2209 N95-28164
Use of SURFACE CHEMKIN to model multiphase atmospheric chemistry: Application to nitrogen tetroxide spills p 2172 N95-28305
Time-resolved FTIR emission studies of laser photofragmentation and radical reactions
[DE95-008125] p 2300 N95-28398
JPRS report: Science and technology. Central Eurasia
[JPRS-UST-95-019] p 2270 N95-28565
High temperature oxidation of nickel concentrates
[PB95-195566] p 2224 N95-28644

REACTION PRODUCTS
An overview of the Evaluation of Oxygen Interactions with Materials 3 experiment: Space Shuttle Mission 46, July-August 1992 p 2210 N95-27630
Molecular beam scattering from C-13 enriched Kapton and correlation with the EOIM-3 carousel experiment
p 2419 N95-27643

REACTION WHEELS
Design of a unidirectional composite momentum wheel rim
[NASA-TM-106911] p 2164 N95-27761

REACTION-DIFFUSION EQUATIONS
Single-drop reactive extraction/extractive reaction with forced convective diffusion and interphase mass transfer
p 2282 N95-27358

REACTIVITY
Spacecraft materials studies on the Aerospace Corporation tray on EOIM-3 p 2210 N95-27632
Atomic oxygen dosimetry measurements made on STS-46 by CONCAP 2 p 2418 N95-27634
Photochemistry in constrained spaces: Zeolites and layered double metal hydroxides
[DE95-006417] p 2207 N95-27951
TEM characterization of Al/Al2O3 composite fabricated by reactive metal infiltration
[DE95-008508] p 2184 N95-28145
High energy density systems in cryogenic media: The production and reactions of atoms and radicals
[AD-A289818] p 2417 N95-28572
Stratospheric ozone reactive chemicals generated by space launches worldwide
[AD-A289852] p 2332 N95-28623

REACTOR DESIGN
Evaluation of current drive requirements and operating characteristics of a high bootstrap fraction advanced tokamak reactor
[DE95-007041] p 2430 N95-27308
Heat pipe cooled reactors for multi-kilowatt space power supplies
[DE95-005211] p 2420 N95-27425
Hydrothermal oxidation of solid rocket propellant and other department of defense hazardous wastes
p 2177 N95-28325

REACTOR MATERIALS
FENIX experimental results of large-scale CICC made of bronze-processed Nb3Sn strands
[DE95-007965] p 2222 N95-28167
Attractive characteristics of mirrors
[DE95-008073] p 2435 N95-28356

REACTOR SAFETY
Application of a Geographic Information System for radiologic emergency response
[DE95-007624] p 2455 N95-28113

READERS
Multiclassifier fusion of an ultrasonic lip reader in automatic speech recognition
[AD-A289207] p 2254 N95-27079

READOUT
The KTeV pure CsI calorimeter
[DE95-005747] p 2292 N95-27751

REAGENTS
Energy transfer from excited nitrenes at high density
[AD-A288352] p 2403 N95-26466

REAL TIME OPERATION
Neural models of spatial orientation in novel environments
[AD-A288420] p 2380 N95-26530
Operating system support for coexistence of real-time and conventional scheduling
[AD-A288584] p 2364 N95-26534
Design and synthesis of a real-time controller for an unmanned air vehicle
[AD-A289134] p 2141 N95-26555
The D* algorithm for real-time planning of optimal traverses
[AD-A289361] p 2367 N95-26754
Next generation real-time systems: Investigating the potential of partial-solution tasks
[AD-A289203] p 2381 N95-27007
Application of bacterial bioemusifiers to in situ maintenance of oil/water separators
p 2179 N95-27120
A study of workstation computational performance for real-time flight simulation
[NASA-TM-109184] p 2362 N95-27241
SXI Prototype mirror mount
[NASA-CR-196613] p 2301 N95-27244
Real-time value-driven diagnosis
p 2386 N95-27396
Geophex airborne unmanned survey system
[DE95-007566] p 2131 N95-27440
PRISM validation
[AD-A288476] p 2337 N95-27703
Development of a Robust star identification technique for use in attitude determination of the ACE spacecraft
p 2149 N95-27777
Real-time data compression using a fixed Huffman encoding scheme
[DE95-006159] p 2455 N95-27949
Design of a real-time wind turbine simulator using a custom parallel architecture p 2322 N95-27979
Control system design for the MOD-5A 7.3 mW wind turbine generator p 2306 N95-27985
Application of modern diagnostic methods to environmental improvement
[DE95-005797] p 2330 N95-28119
Fault tolerant features and experiments of ANTS distributed real-time system
[AD-A290133] p 2256 N95-28391
Method of space-time sequence transform used to measure acousto-optic deflection and modulation
[AD-A289612] p 2402 N95-28671

RECEIVERS
Research and development report. Eureka 147: Tests of the error performance of the DAB system
[BBC-RD-1994/18] p 2249 N95-26696
ROC analysis of IR segmentation techniques
[AD-A289252] p 2424 N95-26971

RECLAMATION
A comprehensive energetic materials resource recovery and recycling program p 2176 N95-28323
Recovery and reuse of rocket motor propellant ingredients p 2177 N95-28326

RECOMBINATION COEFFICIENT
Theoretical studies of interstellar processes
[NASA-CR-198647] p 2462 N95-28216

RECOMBINATION REACTIONS
Theoretical studies of interstellar processes
[NASA-CR-198647] p 2462 N95-28216

RECOMMENDATIONS
High-stakes aviation: US-Japan technology linkages in transport aircraft
[LC-94-65759] p 2126 N95-27907
Report to Congressional Committees. Comanche Helicopter: Testing needs to be completed prior to production decisions
[GAO/NSIAD-95-112] p 2135 N95-27910
Report to the Chairman and Ranking Minority Member, Committee on Science, House of Representatives. Weather forecasting: Radar availability requirement not being met
[GAO/AIMD-95-132] p 2342 N95-27912

RECORDS MANAGEMENT
A demonstration of Client-Server technology using remote procedure calls with an application of file migration for moving records based on time
[AD-A289392] p 2453 N95-26879
Managing electronic records: A guideline
[DE95-007038] p 2456 N95-28555

RECOVERABLE SPACECRAFT

Chinese space science and technology [AD-A289618] p 2466 N95-26856

RECRYSTALLIZATION

Neutron diffraction studies on recrystallization of solution derived lead zirconate titanates [DE95-004771] p 2439 N95-27429

RECTANGULAR PANELS

Analysis of stresses in finite anisotropic panels with centrally located cutouts p 2187 N95-28286

RECTIFICATION

A case study of view-factor rectification procedures for diffuse-gray radiation enclosure computations p 2281 N95-27353

RECURSIVE FUNCTIONS

Solving recursive domain equations with enriched categories [AD-A289358] p 2371 N95-27418

RECYCLING

Marshall Space Flight Center solid waste characterization and recycling improvement study [NASA-CR-196594] p 2360 N95-27164

Recycle of radiologically contaminated austenitic stainless steels [DE95-006464] p 2215 N95-27328

Alternate use of rocket propellants as ingredients in commercial watergel explosives p 2176 N95-28321

A comprehensive energetic materials resource recovery and recycling program p 2176 N95-28323

Strategies for recycling CdTe photovoltaic modules [DE95-006776] p 2325 N95-28517

RED SHIFT

CO, HCO(+) and HCN absorption in the gravitational lens candidate B0218+357 at z=0.685 [PB95-185146] p 2461 N95-26522

The second coming of cold dark matter? [DE95-005156] p 2462 N95-27445

REDUCTION (CHEMISTRY)

Junkyard chemistry p 2227 N95-27102

REDUNDANCY

Autonomous control system reconfiguration for spacecraft with non-redundant actuators p 2153 N95-27802

REDUNDANT COMPONENTS

Retrofitting a fine-pointing system to satellite optics p 2157 N95-27277

REENTRY

Bow shock data analysis [AD-A288432] p 2429 N95-26800

REENTRY SHIELDING

Task 4 supporting technology. Part 1: Detailed test plan for leading edge tile development. Leading edge material development and testing [NASA-CR-198633] p 2160 N95-28258

Task 4 supporting technology. Part 2: Detailed test plan for thermal seals. Thermal seals evaluation, improvement and test. CAN8-1, Reusable Launch Vehicle (RLV), advanced technology demonstrator: X-33. Leading edge and seals thermal protection system technology demonstration [NASA-CR-198628] p 2304 N95-28259

REFINING

Structural chemistry of some phases in the YC-Ni-B system [DE95-007403] p 2447 N95-28537

Low-angle tracking in the presence of ducting, coherent and incoherent multipath [AD-A289838] p 2258 N95-28580

REFLECTANCE

Effects of the LDEF orbital environment on the reflectance of optical mirror materials p 2428 N95-27651

Functionalized block copolymers as adhesion promoters [DE95-008158] p 2239 N95-28400

REFLECTION

A spectral algorithm for the seriation problem [DE95-004775] p 2372 N95-27436

Multifractal character of the electronic states in disordered two-dimensional systems [DE95-609153] p 2443 N95-28016

Transformation to zero offset in transversely isotropic media [DE95-007669] p 2339 N95-28192

REFLECTORS

Micron Accuracy Deployment Experiment (MADE), phase A. Volume 1 [NASA-CR-197792] p 2144 N95-26426

Advanced neutron source materials surveillance program [DE95-005700] p 2215 N95-27464

REFRACTION

Design and fabrication of a diamond-turned hybrid diffractive/refractive singlet for visible applications at ORNL [DE95-007007] p 2427 N95-28552

REFRACTIVITY

Computation of electromagnetic scattering parameters for lognormal distributions of magnetic spheres: Theory and algorithms [AD-A289672] p 2250 N95-26759

Laser beam propagation in non-Kolmogorov atmospheric turbulence [AD-A289256] p 2295 N95-26974

Ambient-pressure silica aerogel films [DE95-008161] p 2237 N95-28090

Seismic constraints on shallow crustal processes at the East Pacific rise [AD-A289055] p 2338 N95-28094

Passive spatial beam control, appendix [AD-A288913] p 2300 N95-28333

Perturbations on effective index of refraction from prism coupling [AD-A291700] p 2427 N95-28524

REFRACTORY MATERIALS

Theory of exotic superconductivity and normal states of heavy electron and high temperature superconductivity materials [DE95-006637] p 2268 N95-28198

Boron-carbon-silicon polymers and the ceramic thereof [NASA-CASE-ARC-11891-1-SB] p 2238 N95-28212

An overview of activities and accomplishments of the Metals and Ceramics Division [DE95-007020] p 2241 N95-28560

REFRIGERANTS

Methods development for measuring and classifying flammability/combustibility of refrigerants. Task 2: Test plan [DE95-007066] p 2234 N95-27481

Methods development for measuring and classifying flammability/combustibility of refrigerants. Task 1: Annotated bibliography [DE95-007232] p 2238 N95-28133

REFUELING

Recent high-speed ballistics experiments at ORNL [DE95-006534] p 2422 N95-28205

Piecemeal learning of an unknown environment [AD-A291683] p 2387 N95-28461

REGRESSION ANALYSIS

Parallelizing locally-weighted regression [AD-A288294] p 2394 N95-26414

Analysis of fatigue fractographic data of a rod end housing using a Monte Carlo simulation [NAL-TR-1225] p 2307 N95-26521

REGULATIONS

Standards for excellence [NONP-NASA-VT-95-49096] p 2451 N95-27202

REGULATORS

Post Kalman progress p 2148 N95-27776

REINFORCED PLASTICS

Rheological measurement methods for fibre filled plastics [PB95-190088] p 2226 N95-26744

REINFORCED SHELLS

Load transfer in the stiffener-to-skin joints of a pressurized fuselage [NASA-CR-198610] p 2310 N95-27865

REINFORCEMENT (STRUCTURES)

Nondestructive testing apparatus for determining the orientation of reinforcing bars within a concrete structure [AD-D017267] p 2245 N95-26508

Recent progress in NASA Langley textile reinforced composites program p 2196 N95-28475

REINFORCING FIBERS

Rheological measurement methods for fibre filled plastics [PB95-190088] p 2226 N95-26744

Mechanical performance of fiber reinforced metal matrix composites and microstructural development of polycrystalline alumina fibers synthesized from liquid precursors [AD-A289518] p 2181 N95-26847

Composite repair of metallic airframe: Twenty years of experience p 2132 N95-27508

Ceramic fiber-reinforced monoclinic celsian phase glass-ceramic matrix composite material [NASA-CASE-LEW-15714-1] p 2183 N95-27717

Design of a unidirectional composite momentum wheel rim [NASA-TM-106911] p 2164 N95-27761

Service tough composite structures using the Z-direction reinforcement process p 2185 N95-28272

Mechanical properties of triaxially braided composites: Experimental and analytical results p 2189 N95-28423

Application of advanced material systems to composite frame elements p 2191 N95-28432

Comparison of resin film infusion, resin transfer molding, and consolidation of textile preforms for primary aircraft structure p 2196 N95-28477

Fundamental concepts in the suppression of delamination buckling by stitching p 2198 N95-28486

REINFORCING MATERIALS

Split pipe testing device for the measurement of bond of reinforcement under controlled confinement [AD-D017258] p 2245 N95-26500

Recent progress in NASA Langley textile reinforced composites program p 2196 N95-28475

RELATIVISTIC EFFECTS

Proofs of contracted length non-covariance [DE95-610175] p 2391 N95-27715

Was Einstein 100% right? [PB95-190179] p 2449 N95-28175

RELATIVISTIC ELECTRON BEAMS

Femtosecond X-ray generation through 90 degrees Thomson scattering: Status of the LBL experiment [DE95-006560] p 2296 N95-27674

High power free-electron laser concepts and problems [DE95-007841] p 2298 N95-28059

RELATIVISTIC PARTICLES

Long-term variability of electron radiation dose in geosynchronous orbit [AD-A289335] p 2162 N95-26902

Extended BRST symmetry for the relativistic particle with curvature [DE95-608799] p 2406 N95-27309

Field theory of point-like systems with higher-order derivatives [DE95-608800] p 2448 N95-27310

Large relativistic corrections to the positronium decay rate [DE95-610470] p 2407 N95-27412

Relativistic electrons in the outer-zone: An 11 year cycle, their relation to the solar wind [DE95-007882] p 2338 N95-28061

RELATIVITY

The method of space-time conservation element and solution element-applications to one-dimensional and two-dimensional time-marching flow problems [NASA-TM-106915] p 2389 N95-26663

Was Einstein 100% right? [PB95-190179] p 2449 N95-28175

General relativity and experiment [PB95-192894] p 2450 N95-28664

RELAXATION (MECHANICS)

Analysis of instability growth and collisionless relaxation in thermionic converters using 1-D PIC simulations [AD-A289310] p 2319 N95-26891

High-speed coherent laser arrays [AD-A289373] p 2295 N95-26906

RELAXATION METHOD (MATHEMATICS)

A fully implicit time accurate method for hypersonic combustion: Application to shock-induced combustion instability [NASA-TM-106707] p 2273 N95-26380

Random relaxation of fixed point iteration [PB95-185013] p 2389 N95-26910

RELIABILITY

Compiler-assisted debugging and multiple instruction retry [NASA-CR-197729] p 2365 N95-26628

Statistical theory and reliability [AD-A288519] p 2394 N95-26733

Comparison of life theories for rolling-element bearings [NASA-TM-106585] p 2301 N95-26774

Can there be reliability without reliability? [AD-A289480] p 2306 N95-26927

Quest for excellence 5 [NONP-NASA-VT-95-49099] p 2451 N95-27205

Malcolm Baldrige National Quality Award winners 1989 [NONP-NASA-VT-95-49119] p 2451 N95-27207

Quality assurance and reliability in the Japanese electronics industry p 2263 N95-27232

Electric vehicle activities [DE95-006648] p 2267 N95-28105

Low-power, parallel photonic interconnections for Multi-Chip Module applications [DE95-008518] p 2267 N95-28147

Software technology for adaptable, reliable systems (STARS). AdaWise user's manual [AD-A289655] p 2375 N95-28635

RELIABILITY ANALYSIS

Probabilistic risk assessment of the Space Shuttle. Phase 3: A study of the potential of losing the vehicle during nominal operation. Volume 5: Auxiliary shuttle risk analyses [NASA-CR-197812] p 2160 N95-26403

The 1994 updated National Airspace System performance assessment for year 2005 [AD-A288652] p 2125 N95-26485

Using SCR methods to analyze requirements documentation [NASA-CR-197760] p 2365 N95-26668

I(sub DDQ) testing and defect classes: A tutorial
[DE95-005467] p 2306 N95-27723
Performance analysis of bullet trajectory estimation: Approach, simulation, and experiments
[DE95-007949] p 2399 N95-28109
Reliability analysis of composite structures
p 2192 N95-28441
Uncertainties in obtaining high reliability from stress-strength models p 2193 N95-28442

RELIABILITY ENGINEERING
Intelligent computer based reliability assessment of multichip modules
[AD-A288833] p 2259 N95-26550
Digital optical computing
[AD-A289395] p 2368 N95-26881
Human factors in aviation maintenance, phase 4
[DOT/FAA/AM-95/14] p 2360 N95-27696
Reliability analysis of composite structures
p 2192 N95-28441
Uncertainties in obtaining high reliability from stress-strength models p 2193 N95-28442
Probabilistic design of advanced composite structure
p 2193 N95-28443
Proof test methodology for composites
p 2193 N95-28445
Post impact compressive strength in composites
p 2198 N95-28485

RELIEF MAPS
Naval Aviation System TEAM mapping, charting, and geodesy handbook
[AD-A288590] p 2314 N95-26841

REMOTE CONTROL
A foveated system to reduce transmission bandwidth of video images from remote camera systems
[AD-A288516] p 2254 N95-27060
Performance of the Satellite Test Assistant Robot in JPL's Space Simulation Facility p 2154 N95-27264
Geophex airborne unmanned survey system
[DE95-007566] p 2131 N95-27440
Pre-integrated truss space station and method of assembly
[NASA-CASE-MSC-22015-1] p 2165 N95-27842

REMOTE MANIPULATOR SYSTEM
Design, testing and evaluation of latching end effector
p 2155 N95-27261

REMOTE SENSING
FTIR measurements of thermal infrared sky radiance and transmission
[DE95-003642] p 2334 N95-26436
Radiometer measurements of snow in Sodankylae, 1991-1993
[PB95-184966] p 2313 N95-26645
Subvisual cirrus: What it is and where you find it
[AD-A289329] p 2342 N95-26899
VOCAR: An experiment in Variability of Coastal Atmospheric Refractivity
[AD-A289202] p 2253 N95-27006
Structures and materials technology needs for communications and remote sensing spacecraft
[NASA-CR-198166] p 2163 N95-27026
Design, development and testing of the x-ray timing explorer High Gain Antenna System
p 2157 N95-27279
Improved performance 1590 nm Er:YLF laser
[DE95-003691] p 2296 N95-27705
Portable laser laboratory
[DE95-008376] p 2298 N95-27876
Remote sensing of hydrologic variables in boreal areas, phase 2
[NASA-CR-198717] p 2314 N95-27998
Remote measurement of ground temperature and emissivity
[DE95-008055] p 2314 N95-28053
Method for determining surface coverage by materials exhibiting different fluorescent properties
[NASA-CASE-GSC-13539-1] p 2315 N95-28211
Altimeter analysis of ocean currents
[AD-A290167] p 2315 N95-28392
Remote sensing of the atmosphere by resonance Raman LIDAR
[DE95-007312] p 2315 N95-28520
Binary segmentation of SAR images by the ICM algorithm
[INPE-5464-PRE/1772] p 2258 N95-28559
High performance ground penetrating radar survey of TA-49/Area 2
[DE95-006856] p 2258 N95-28601
Modeling and retrieval of snow and sea ice characteristics in the frequency range 6 to 90 GHz
[PB95-195467] p 2316 N95-28656
Neural networks in the classification of uses of the soil in satellite images
[INPE-5478-PRE/1777] p 2316 N95-28672

REMOTE SENSORS
A probabilistic target classification and description model for seismic sensors
[AD-A288548] p 2335 N95-26531
Earth horizon modeling and application to static Earth sensors on TRMM spacecraft p 2150 N95-27783
WTEC panel report on research submersibles and undersea technologies
[NASA-CR-198565] p 2247 N95-27909
Large HAWT wake measurement and analysis
p 2289 N95-27973

REMOTELY PILOTED VEHICLES
Design and synthesis of a real-time controller for an unmanned air vehicle
[AD-A289134] p 2141 N95-26555
Reactor pressure vessel structural integrity research
[DE95-007034] p 2223 N95-28208
Unmanned aerial vehicles, 1994 master plan
[AD-A291628] p 2136 N95-28411

REMOVAL
CO2 pellet blast cleaning and degreasing: The true environmentally benign technology
p 2229 N95-27109
Aqueous degreasing, precision cleaning, and cleanliness verification p 2231 N95-27121
Preferentially etched epitaxial liftoff of InP material
[NASA-CASE-LEW-15760-1] p 2235 N95-27503
Process for non-contact removal of organic coatings from the surface of paintings
[NASA-CASE-LEW-15896-1] p 2235 N95-27702
Cryogenic washout of solid rocket propellants
p 2176 N95-28324

RENDEZVOUS GUIDANCE
An analysis of orbital propagators for Low Earth Orbit Rendezvous
[AD-A288883] p 2161 N95-26458

RENDEZVOUS TRAJECTORIES
An analysis of orbital propagators for Low Earth Orbit Rendezvous
[AD-A288883] p 2161 N95-26458

REPLACING
A summary of ODS replacement technologies at Litton Poly-Scientific p 2228 N95-27105
Vapor pressures of mixtures of CFC-114 with the potential replacement coolants C4F(10) andc-C4F 8
[DE95-003444] p 2208 N95-28042

REPLICAS
Scale model experiments with ceramic laminate targets
[AD-A288322] p 2225 N95-26561
Two implementation relations and the correctness of communicating replicated processes
[PB95-195640] p 2375 N95-28645

RESEARCH
Bibliography of NRL publications - 1990
[AD-A289483] p 2466 N95-26823
The high speed civil transport and NASA's High Speed Research (HSR) program p 2118 N95-26945
Laboratory of production engineering
[PB95-184834] p 2451 N95-28135

RESEARCH AIRCRAFT
Flightpath synthesis and HUD scaling for V/STOL terminal area operations
[NASA-TM-110348] p 2127 N95-26587

RESEARCH AND DEVELOPMENT
Concurrent engineering research center
[NASA-CR-197726] p 2362 N95-26386
Performance enhancing ration components program: Supplemental carbohydrate test
[AD-A288560] p 2358 N95-26558
Development test of á liquid Apogee engine for the ETS-6
[NAL-TR-1250] p 2167 N95-26799
The aerospace database: An introduction to AIAA'S computerized source for identifying scientific and technical information p 2119 N95-26950
JPRS report: Science and technology. Central Eurasia
[JPRS-UST-95-021] p 2202 N95-27155
JPRS report: Science and technology. Central Eurasia
[JPRS-UST-95-016] p 2262 N95-27170
JPRS report: Science and technology. Central Eurasia
[JPRS-UST-95-014] p 2145 N95-27171
NIST Automated Manufacturing Research Facility (AMRF): March 1987
[NONP-NASA-VT-95-49097] p 2246 N95-27203
JPRS report: Science and technology. Central Eurasia
[JPRS-UST-95-015] p 2246 N95-27213
Building the electronic industry's roadmaps
p 2263 N95-27228
Japan's technology and manufacturing infrastructure
p 2263 N95-27229
Successful product realization strategies
p 2264 N95-27233
Current programmes on physical metallurgy and related areas in BARC
[DE95-607939] p 2214 N95-27255
Advanced Earth-to-orbit propulsion technology information, dissemination and research
[NASA-CR-196582] p 2168 N95-27424
Advances in welding science: A perspective
[DE95-006745] p 2302 N95-27545
Spaceflight revolution: NASA Langley Research Center from Sputnik to Apollo
[NASA-SP-4308] p 2474 N95-27685
JTEC monograph on biodegradable polymers and plastics in Japan: Research, development, and applications
[NASA-CR-198562] p 2235 N95-27694
JPRS report: Science and technology. Central Eurasia
[JPRS-UST-94-022] p 2246 N95-27699
Recent progress in the Photovoltaic Manufacturing Technology Project (PVMaT)
[DE95-000279] p 2320 N95-27704
WTEC panel report on research submersibles and undersea technologies
[NASA-CR-198565] p 2247 N95-27909
Collected papers on wind turbine technology
[NASA-CR-195432] p 2321 N95-27970
Research and Technology Objectives and Plans Summary (RTOPS)
[NASA-TM-108574] p 2475 N95-28002
JTEC/WTEC annual report and program summary: 1993/94
[NASA-CR-198563] p 2475 N95-28038
LLNL input to FY94 hydrogen annual report
[DE95-007950] p 2243 N95-28064
Transportation R and D included in thermal and mechanical sciences program
[DE95-008275] p 2303 N95-28070
Methods development for measuring and classifying flammability/combustibility of refrigerants. Task 1: Annotated bibliography
[DE95-007232] p 2238 N95-28133
JPRS Report: Science and Technology. Central Eurasia
[JPRS-UST-95-020] p 2145 N95-28257
Development of an ultra-safe rechargeable lithium-ion battery
[AD-A288959] p 2269 N95-28349
Attractive characteristics of mirrors
[DE95-008073] p 2435 N95-28356
An overview of activities and accomplishments of the Metals and Ceramics Division
[DE95-007020] p 2241 N95-28560
JPRS report: Science and technology. Central Eurasia
[JPRS-UST-95-019] p 2270 N95-28565

RESEARCH FACILITIES
Live from Antarctica: Then and now
[NASA-CR-197829] p 2335 N95-26594
Design and development of experimental facilities for short duration, low-gravity combustion and fire experiments
[NASA-CR-195458] p 2244 N95-26709
Preliminary results and research capabilities of a new jet facility at the University of Kansas
p 2119 N95-26951
NIST Automated Manufacturing Research Facility (AMRF): March 1987
[NONP-NASA-VT-95-49097] p 2246 N95-27203
NIST: Information management in the AMRF
[NONP-NASA-VT-95-49120] p 2454 N95-27208
Microgravity Sciences Biotechnology Facility assessment
[NASA-CR-196602] p 2351 N95-27329
Three-dimensional computer modeling of hydrogen injection and combustion
[DE95-006261] p 2203 N95-27437
Intermediate energy neutrons at WNR. Spin-isospin and energy dependence of the NN interaction and the nuclear response
[DE95-006291] p 2408 N95-27466
A review of Australian and New Zealand investigations on aeronautical fatigue during the period Apr. 1993 - Mar. 1995
[AR-009-202] p 2136 N95-27918
An overview of activities and accomplishments of the Metals and Ceramics Division
[DE95-007020] p 2241 N95-28560

RESEARCH MANAGEMENT
Funding for AFRAPT student trainees for academic year 1992-1993
[AD-A288461] p 2466 N95-26604
Bibliography of patents and licenses 1951-1990. 1991 edition
[AD-A289603] p 2452 N95-26721
Research and Technology Objectives and Plans Summary (RTOPS)
[NASA-TM-108574] p 2475 N95-28002

RESEARCH PROJECTS
Activities of the Laboratory of Information Processing Science
[PB95-184982] p 2452 N95-26631

Automated Procurement System (APS) revised project management plan (DS-03)
[NASA-CR-196605] p 2450 N95-27169
Chemical engineering: Measurements for a competitive age
[NONP-NASA-VT-95-49098] p 2203 N95-27204
Spaceflight revolution: NASA Langley Research Center from Sputnik to Apollo
[NASA-SP-4308] p 2474 N95-27685
A review of Australian and New Zealand investigations on aeronautical fatigue during the period Apr. 1993 - Mar. 1995
[AR-009-202] p 2136 N95-27918
Collected papers on wind turbine technology
[NASA-CR-195432] p 2321 N95-27970
A comprehensive energetic materials resource recovery and recycling program p 2176 N95-28323

RESEARCH VEHICLES
Computational analysis of forebody tangential slot blowing on the high alpha research vehicle
[NASA-CR-197754] p 2129 N95-26591
Numerical simulation of the flow about the F-18 HARV at high angle of attack
[NASA-CR-197755] p 2121 N95-26735
Electric vehicle activities
[DE95-006648] p 2267 N95-28105

RESIDUAL STRENGTH
Life prediction methodology for composite laminates. Part 1: Constant amplitude and two-stress level fatigue
[AD-A288343] p 2180 N95-26571
Modeling considerations in the prediction of residual strength in composite laminates
[AD-A289128] p 2182 N95-27142
Assembly induced delaminations in composite structures p 2186 N95-28279
Investigation of static and cyclic bearing failure mechanisms for GR/EP laminates p 2190 N95-28427
Compressive residual strength of graphite/epoxy laminates after impact p 2191 N95-28431

RESIDUAL STRESS
Fatigue fracture analysis in medium carbon structural steel and austenitic stainless steel by X-ray fractography
[DE95-601504] p 2213 N95-26675
Growth of hydrogenated amorphous silicon (a-Si:H) on patterned substrates for increased mechanical stability
[DE95-006589] p 2234 N95-27472
On the thermally-induced residual stresses in thick fiber-thermoplastic matrix (PEEK) cross-ply laminated plates p 2187 N95-28285
Residual stress, strain, and faults in nanocrystalline palladium and copper
[DE95-008294] p 2223 N95-28543

RESIDUES
CO2 pellet blast cleaning and degreasing: The true environmentally benign technology
p 2229 N95-27109
Ethyl lactate as a solvent alternative for cleaning metal parts p 2229 N95-27112
Hardware cleanliness methodology and certification
p 2211 N95-27656

RESIN MATRIX COMPOSITES
Stress analysis and failure of an internally pressurized composite-jacketed steel cylinder p 2186 N95-28280
Static and dynamic strain energy release rates in toughened thermosetting composite laminates
p 2188 N95-28288
Characteristics of laminates with delamination control strips p 2191 N95-28434

RESIN TRANSFER MOLDING
A fast numerical method for isothermal resin transfer mold filling
[AD-A288944] p 2179 N95-26565
Development of a low-cost, modified resin transfer molding process using elastomeric tooling and automated preform fabrication p 2184 N95-28268
Resin transfer molding of textile preforms for aircraft structural applications p 2185 N95-28276
Development of stitched/RTM composite primary structures p 2195 N95-28469
Test and analysis results for composite transport fuselage and wing structures p 2137 N95-28470
Composite fuselage crown panel manufacturing technology p 2137 N95-28474
Advanced textile applications for primary aircraft structures p 2138 N95-28476
Comparison of resin film infusion, resin transfer molding, and consolidation of textile preforms for primary aircraft structure p 2196 N95-28477
Characterization and manufacture of braided composites for large commercial aircraft structures
p 2196 N95-28478

RESINS
Fractionation studies of polyethylene using DSC-technique
[PB95-185252] p 2200 N95-26540
Composite repair of metallic airframe: Twenty years of experience p 2132 N95-27508
Field repair materials for naval aircraft
p 2133 N95-27514
A new technique for ground simulation of hypervelocity debris p 2154 N95-27671
Polymer infiltration studies
[NASA-CR-198801] p 2236 N95-27857
Development of stitched/RTM composite primary structures p 2195 N95-28469
Surfactants and desensitizing wax substitutes for TNT-Based systems
[AD-A289652] p 2243 N95-28634

RESISTANCE HEATING
OBIC analysis of stressed, thermally-isolated polysilicon resistors
[DE95-008511] p 2268 N95-28201

RESISTORS
OBIC analysis of stressed, thermally-isolated polysilicon resistors
[DE95-008511] p 2268 N95-28201
Energy-measuring resistor bank
[AD-D017392] p 2271 N95-28613

RESONANCE
Study of parity and time reversal violation in neutron-nucleus interactions
[DE95-005158] p 2405 N95-27081
CAS CERN Accelerator School 5th General Accelerator Physics Course
[DE95-608324] p 2419 N95-27158
A note on the constituent quark resonances
[DE95-608831] p 2406 N95-27316
Observation of nonlinear resonances in the advanced light source
[DE95-006561] p 2425 N95-27675
NQR-NMR studies of higher alcohol synthesis Cu-Co catalysts
[DE95-007926] p 2205 N95-27680
A numerical study of ultra-short-pulse reflectometry
[DE95-008070] p 2266 N95-28015
Shear Alfven wave excitation by direct antenna coupling and fast wave resonant mode conversion
[DE95-609109] p 2256 N95-28254
Subharmonic phonon transmission and Kapitza conductance between crystals with very different vibrational spectra
[DE95-609151] p 2447 N95-28608

RESONANCE SCATTERING
The Bremsstrahlung of soft gamma-quanta created by elastic pp- and np-scatterings and the dibaryon resonance problem
[DE95-608870] p 2415 N95-28248
Remote sensing of the atmosphere by resonance Raman LIDAR
[DE95-007312] p 2315 N95-28520

RESONANT FREQUENCIES
Extended linear ion trap frequency standard apparatus
[NASA-CASE-NPO-19081-1-CU] p 2404 N95-26861
Extended linear ion trap frequency standard apparatus
[NASA-CASE-NPO-19081-1-CU] p 2416 N95-28348
Material characterization system
[AD-D017385] p 2210 N95-28584

RESONANT VIBRATION
Material characterization system
[AD-D017385] p 2210 N95-28584

RESONATORS
Analytical investigations of the acceleration sensitivity of acoustic bulk and surface wave resonators
[AD-A291715] p 2402 N95-28505

RESOURCES MANAGEMENT
An ugly duckling becomes a swan (hor ellipsis): How an organization becomes customer focused through listening
[DE95-004974] p 2454 N95-27461
Evaluating the environmental viability of open burning/open detonation operations
p 2170 N95-28297
Commercial reformulation: An economic and environmentally neutral means of managing explosives and solid propellants p 2175 N95-28320

RESPIRATORY RATE
A study of heart rate and heart rate variability during rapid decompression to 50,000 ft
[AD-A291598] p 2355 N95-28561

RESTORATION
Process for non-contact removal of organic coatings from the surface of paintings
[NASA-CASE-LEW-15896-1] p 2235 N95-27702

RETINAL IMAGES
Neural models of spatial orientation in novel environments
[AD-A288420] p 2380 N95-26530

RETROFITTING
Retrofitting conventional vapor degreasers to use a solvent wash/fluorochemical rinse process
p 2232 N95-27127
Retrofitting a fine-pointing system to satellite optics
p 2157 N95-27277
Retrofitting a fine-pointing system to satellite optics
[DE95-004529] p 2427 N95-28516

REUSABLE HEAT SHIELDING
Task 4 supporting technology. Part 1: Detailed test plan for leading edge tile development. Leading edge material development and testing
[NASA-CR-198633] p 2160 N95-28258

REUSABLE LAUNCH VEHICLES
Reusable launch vehicle development research
[NASA-CR-196614] p 2154 N95-27245
Task 4 supporting technology. Part 1: Detailed test plan for leading edge tile development. Leading edge material development and testing
[NASA-CR-198633] p 2160 N95-28258
Task 4 supporting technology. Part 2: Detailed test plan for thermal seals. Thermal seals evaluation, improvement and test. CAN8-1, Reusable Launch Vehicle (RLV), advanced technology demonstrator: X-33. Leading edge and seals thermal protection system technology demonstration
[NASA-CR-198628] p 2304 N95-28259
Task 4 supporting technology. Densification requirements definition and test objectives. Propellant densification requirements definition
[NASA-CR-198629] p 2450 N95-28260

REVERBERATION CHAMBERS
Photoacoustic chambers for studying solids and gases: Theory and practical examples
[IFTR-39/1994] p 2143 N95-26837

REVERSE FIELD PINCH
Far-infrared laser interferometry measurements on the STP-3(M) reversed-field pinch
[DE94-765440] p 2297 N95-27868
Global dynamo in a reversed field pinch plasma
[DE94-765441] p 2432 N95-27869
Burst of energetic ions from reversed field pinch plasma
[DE94-765447] p 2432 N95-27870

REYNOLDS EQUATION
Computational analysis of forebody tangential slot blowing on the high alpha research vehicle
[NASA-CR-197754] p 2129 N95-26591
A 3D agglomeration multigrid solver for the Reynolds-averaged Navier-Stokes equations on unstructured meshes
[NASA-CR-195073] p 2390 N95-27029

REYNOLDS NUMBER
Comparative wind tunnel test at high Reynolds numbers of NACA 64 621 airfoils with two aileron configurations
p 2124 N95-27977

REYNOLDS STRESS
Effect of turbulence models on criticality conditions in swirling flows p 2282 N95-27356
Dithering transitions in resistive pressure-gradient-driven turbulence
[DE95-006737] p 2431 N95-27536

RHENIUM COMPOUNDS
An investigation of the applicability of the new Reillex(tm)-HPQ anion exchange resin system for technetium/rhenium and uranium in the Hanford waste tanks
[DE95-007643] p 2412 N95-28051

RHEOLOGY
Rheological measurement methods for fibre filled plastics
[PB95-190088] p 2226 N95-26744

RHEOMETERS
Measurement of viscosity by capillary rheometry: Dwell time effects
[PB95-190203] p 2201 N95-26750

RIBS (SUPPORTS)
Composite sandwich structure and method for making same
[NASA-CASE-LAR-14898-1] p 2180 N95-26764

RICHARDSON NUMBER
Three objective indices for clear-air turbulence reconsidered
[KNMI-TR-160] p 2342 N95-27366

RIEMANN MANIFOLD
Hyperkaehler metrics associated to compact Lie groups
[PB95-185161] p 2388 N95-26514
Holomorphic curves in Abelian varieties, part 1
[DE95-608749] p 2396 N95-27300
Harmonic maps of the bounded symmetric domains
[DE95-608798] p 2397 N95-27485
Collapsing and solvmanifolds
[PB95-196267] p 2393 N95-28501

RIGID STRUCTURES
Manual for SHOCK3D, version 2.0. Computer program for non-linear shock response
[AD-A288631] p 2307 N95-28342

A modified proportional navigation scheme for rendezvous and docking with tumbling targets: The Planar case p 2150 N95-27764
Composite fuselage shell structures research at NASA Langley Research Center p 2194 N95-28466
RIMS
Comparison of numerical results and multicavity purge and rim seal data with extensions to dynamics
[NASA-TM-106685] p 2168 N95-27434
Design of a unidirectional composite momentum wheel rim
[NASA-TM-106911] p 2164 N95-27761
RING STRUCTURES
Ball bearing vibrations amplitude modeling and test comparisons p 2158 N95-27286
RINGS (MATHEMATICS)
Some commutativity theorems for a certain class of rings
[DE95-608750] p 2390 N95-27302
RIO GRANDE (NORTH AMERICA)
Investigation of rifting processes in the Rio Grande Rift using data from an unusually large earthquake swarm
[DE95-007623] p 2339 N95-28126
RISC PROCESSORS
Optimization strategies for molecular dynamics programs on Cray computers and scalar work stations
[AD-A289574] p 2418 N95-28648
RISK
Probabilistic risk assessment of the Space Shuttle. Phase 3: A study of the potential of losing the vehicle during nominal operation, volume 1
[NASA-CR-197808] p 2159 N95-26398
Probabilistic risk assessment of the Space Shuttle. Phase 3: A study of the potential of losing the vehicle during nominal operation. Volume 2: Integrated loss of vehicle model
[NASA-CR-197809] p 2159 N95-26399
Probabilistic risk assessment of the Space Shuttle. Phase 3: A study of the potential of losing the vehicle during nominal operation. Volume 3: Basic events and minimal cutsets
[NASA-CR-197810] p 2160 N95-26400
Probabilistic risk assessment of the Space Shuttle. Phase 3: A study of the potential of losing the vehicle during nominal operation. Volume 4: System models and data analysis
[NASA-CR-197811] p 2160 N95-26401
Probabilistic risk assessment of the Space Shuttle. Phase 3: A study of the potential of losing the vehicle during nominal operation. Volume 5: Auxiliary shuttle risk analyses
[NASA-CR-197812] p 2160 N95-26403
Software risk management through independent verification and validation
[NASA-CR-197767] p 2364 N95-26486
Fuzzy-algebra uncertainty assessment
[DE95-005426] p 2391 N95-27432
An introductory guide to uncertainty analysis in environmental and health risk assessment. Environmental Restoration Program
[DE95-008097] p 2354 N95-28136
ROADS
Using virtual active vision tools to improve autonomous driving tasks
[AD-A289175] p 2356 N95-27013
ELVIS: Eigenvectors for land vehicle image system
[AD-A289297] p 2381 N95-27041
ROBOT ARMS
Dynamic coupling of underactuated manipulators
[AD-A289404] p 2301 N95-27098
Some mechanical design aspects of the European Robotic Arm p 2155 N95-27262
Advanced development for space robotics with emphasis on fault tolerance p 2155 N95-27263
A rotating arm using shape-memory alloy
p 2157 N95-27276
ROBOT CONTROL
Learning Hand/Eye coordination by an active observer. part 1: Organizing centers
[AD-A289502] p 2356 N95-26843
Multi-agent perception for Human/Robot interaction: A framework for intuitive trajectory modification
[AD-A289399] p 2359 N95-26884
Advanced development for space robotics with emphasis on fault tolerance p 2155 N95-27263
Performance of the Satellite Test Assistant Robot in JPL's Space Simulation Facility p 2154 N95-27264
Stable adaptive neurocontrollers for spacecraft and space robots p 2384 N95-27385
A linguistic geometry for 3D strategic planning
p 2386 N95-27397
ROBOTICS
The D* algorithm for real-time planning of optimal traverses
[AD-A289361] p 2367 N95-26754
Learning Hand/Eye coordination by an active observer. part 1: Organizing centers
[AD-A289502] p 2356 N95-26843
Multi-agent perception for Human/Robot interaction: A framework for intuitive trajectory modification
[AD-A289399] p 2359 N95-26884
A systems engineering approach to electro-mechanical reconfiguration for mobility autonomy
[AD-A289479] p 2301 N95-26926
Survey and implementation of commercial manual controllers for a generic telerobotics architecture
[AD-A289215] p 2381 N95-26990
The 29th Aerospace Mechanisms Symposium
[NASA-CP-3293] p 2154 N95-27260
Design, testing and evaluation of latching end effector
p 2155 N95-27261
Some mechanical design aspects of the European Robotic Arm p 2155 N95-27262
Advanced development for space robotics with emphasis on fault tolerance p 2155 N95-27263
The Strategic Technologies for Automation and Robotics (STEAR) program: Protection of materials in the space environment subprogram p 2242 N95-27669
ALLIANCE: An architecture for fault tolerant, cooperative control of heterogeneous mobile robots
[DE95-007374] p 2387 N95-28536
Bilateral force feedback for hydraulically actuated systems
[AD-A291632] p 2387 N95-28545
ROBOTS
The D* algorithm for real-time planning of optimal traverses
[AD-A289361] p 2367 N95-26754
A systems engineering approach to electro-mechanical reconfiguration for mobility autonomy
[AD-A289479] p 2301 N95-26926
Dynamic coupling of underactuated manipulators
[AD-A289404] p 2301 N95-27098
Performance of the Satellite Test Assistant Robot in JPL's Space Simulation Facility p 2154 N95-27264
ALLIANCE: An architecture for fault tolerant, cooperative control of heterogeneous mobile robots
[DE95-007374] p 2387 N95-28536
ROBUSTNESS (MATHEMATICS)
Intelligent computer based reliability assessment of multichip modules
[AD-A288833] p 2259 N95-26550
Attitude determination using an adaptive multiple model filtering Scheme p 2148 N95-27772
Development of a Robust star identification technique for use in attitude determination of the ACE spacecraft
p 2149 N95-27777
SAR noise reduction through the utilization of robust filters
[INPE-5504-PRE/1787] p 2258 N95-28569
ROCHE LIMIT
Models for various aspects of dwarf novae and nova-like stars p 2459 N95-27071
ROCK INTRUSIONS
Seismic constraints on shallow crustal processes at the East Pacific rise
[AD-A289055] p 2338 N95-28094
ROCK MECHANICS
Planning, design and construction of the cavern arena: Heating, ventilation and air conditioning
[PB95-196382] p 2361 N95-28659
ROCKET ENGINE DESIGN
Propellant injection systems and processes
[NASA-TM-110632] p 2242 N95-26781
Advanced Earth-to-orbit propulsion technology information, dissemination and research
[NASA-CR-196582] p 2168 N95-27424
Micro electric propulsion feasibility
[NASA-CR-189139] p 2168 N95-28000
ROCKET ENGINES
Electromechanical rotary actuator
p 2157 N95-27278
RTE: A computer code for Rocket Thermal Evaluation
p 2177 N95-27355
The demilitarization of class 1.1 rocket motors using high pressure waterjets p 2176 N95-28322
ROCKET EXHAUST
Bow shock data analysis
[AD-A288432] p 2429 N95-26800
Investigation of the collision line broadening problem as applicable to the NASA Optical Plume Anomaly Detection (OPAD) system, phase 1
[NASA-CR-198605] p 2426 N95-27913
ROCKET FLIGHT
Bow shock data analysis
[AD-A288432] p 2429 N95-26800
ROCKET LAUNCHING
Development and implementation of a system safety program for the space launch complex 3 east (SLC-3E) ground support system project to support Atlas 2 family of space launch vehicles p 2174 N95-28316
ROCKET PROPELLANTS
High pressure Earth storable rocket technology program: Basic program
[NASA-CR-195449] p 2166 N95-26390
The demilitarization of class 1.1 rocket motors using high pressure waterjets p 2176 N95-28322
ROCKS
The Alpha-Proton-X-ray Spectrometer deployment mechanism: An anthropomorphic approach to sensor placement on Martian rocks and soil
p 2155 N95-27265
ROCKWELL HARDNESS
Improved hardness RHA weldability and material property testing
[AD-A289127] p 2221 N95-28102
ROCKY MOUNTAINS (NORTH AMERICA)
Meso-beta scale numerical simulation studies of terrain-induced jet streak mass/momentum perturbations
[NASA-CR-197804] p 2335 N95-26592
RODS
Identification of the plastic anisotropy of an aluminum alloy
[IFTR-26/1994] p 2212 N95-26512
Analysis of fatigue fractographic data of a rod end housing using a Monte Carlo simulation
[NAL-TR-1225] p 2307 N95-26521
Extended linear ion trap frequency standard apparatus
[NASA-CASE-NPO-19081-1-CU] p 2404 N95-26861
Extended linear ion trap frequency standard apparatus
[NASA-CASE-NPO-19081-1-CU] p 2416 N95-28348
Nonlinear optical studies of surfaces
[DE95-006574] p 2428 N95-28557
ROLL
Compiler-assisted debugging and multiple instruction retry
[NASA-CR-197729] p 2365 N95-26628
An investigation of the effects of pitch-roll (de)coupling on helicopter handling qualities
[NASA-TM-110349] p 2141 N95-26773
ROLLERS
Preliminary design study of the beam collapser and certain optomechanical aspects of the siderostat
[AD-A288423] p 2423 N95-26549
Composite prepreg application device
[NASA-CASE-LAR-15259-1] p 2182 N95-27192
The development and testing of ceramic components in piston engines
[DE95-005759] p 2236 N95-27946
ROLLING CONTACT LOADS
Design and development of a test rig for the high frequency testing of rolling sleeve airsprings
[DSTO-TN-0001] p 2142 N95-26378
Comparison of life theories for rolling-element bearings
[NASA-TM-106585] p 2301 N95-26774
ROOFS
Building-integrated photovoltaics: A case study
[DE95-004032] p 2325 N95-28396
ROOM TEMPERATURE
Optical features of nanosize iron and molybdenum sulfide clusters
[DE95-005417] p 2202 N95-27136
Molecular approach to mesoporous metal sulfides
[DE95-005418] p 2202 N95-27137
Laser ultrasonic generation at the surface of a liquid metal
[DE95-004999] p 2216 N95-27477
Characterization of defects in deuterium-implanted beryllium
[DE95-005688] p 2217 N95-27553
High temperature Hexoloy(trademark) SX silicon carbide
[DE95-007290] p 2221 N95-28075
Mechanical properties of Hysol EA-9394 structural adhesive
[DE95-008187] p 2240 N95-28405
ROSS ICE SHELF
Subsurface radar investigations at the Pegasus Glacial-ice Runway and Williams Field, McMurdo Station, Antarctica
[AD-A289323] p 2144 N95-27297
ROTARY STABILITY
Comparison of numerical results and multicavity purge and rim seal data with extensions to dynamics
[NASA-TM-106685] p 2168 N95-27434
Whirl plus tilt
[DE95-007948] p 2399 N95-28108
ROTARY WING AIRCRAFT
Vibration analysis of a split path gearbox
[NASA-TM-106875] p 2302 N95-27855
Evaluation of a doubly-swept blade tip for rotorcraft noise reduction
[NASA-CR-189677] p 2402 N95-28264
Application of advanced material systems to composite frame elements p 2191 N95-28432

Rotorcraft crashworthy airframe and fuel system technology development program [AD-A289986] p 2126 N95-28630

ROTARY WINGS

An experimental investigation of helicopter downwash and tailboom interaction at the Wichita State University 7x10 foot wind tunnel p 2120 N95-26955

Flow structure generated by perpendicular blade vortex interaction and implications for helicopter noise predictions [NASA-CR-198590] p 2123 N95-28193

Aeroelasticity and structural optimization of composite helicopter rotor blades with swept tips [NASA-CR-4665] p 2136 N95-28262

Evaluation of a doubly-swept blade tip for rotorcraft noise reduction [NASA-CR-189677] p 2402 N95-28264

Nonlinear dynamics and aeroelasticity of rotorcraft in forward flight [AD-A291714] p 2136 N95-28504

Modeling helicopter blade dynamics using a modified Myklestad-Prohl transfer matrix method [AD-A289891] p 2136 N95-28626

ROTATING BODIES

The calculation of the mass moment of inertia of a fluid in a rotating rectangular tank [NASA-CR-197777] p 2278 N95-27165

ROTATING DISKS

Magnetic viscosity by localized shear flow instability in magnetized accretion disks [DE95-006879] p 2433 N95-28111

ROTATING FLUIDS

A phenomenological treatment of rotating turbulence [NASA-CR-198168] p 2288 N95-28228

ROTATING PLASMAS

Effect of toroidal plasma flow and flow shear on global MHD modes [DE95-006676] p 2433 N95-28106

Wall stabilization of rotating high (Beta) discharges in D3-D [DE95-008207] p 2435 N95-28406

ROTATING SHAFTS

Use of blade pitch control to provide power train damping for the Mod-2, 2.5-mW wind turbine p 2306 N95-27986

ROTATION

Investigation into the behavior of geometrically nonlinear composite arches [AD-A289258] p 2308 N95-26975

A new angle on the Euler angles p 2153 N95-27800

Whirl plus tilt [DE95-007948] p 2399 N95-28108

Wall stabilization of rotating high (Beta) discharges in D3-D [DE95-008207] p 2435 N95-28406

Modeling helicopter blade dynamics using a modified Myklestad-Prohl transfer matrix method [AD-A289891] p 2136 N95-28626

ROTATIONAL SPECTRA

Basic principles and recent observations of rotationally sampled wind p 2321 N95-27971

A model of rotationally-sampled wind turbulence for predicting fatigue loads in wind turbines p 2312 N95-27972

ROTOR AERODYNAMICS

Aircraft noise prediction program theoretical manual: Rotorcraft System Noise Prediction System (ROTONET), part 4 [NASA-TM-83199-PT-4] p 2400 N95-26392

Development and validation of a blade-element mathematical model for the AH-64A Apache helicopter [NASA-TM-108863] p 2118 N95-26710

Preliminary analysis of dynamic stall effects on a 91-meter wind turbine rotor p 2124 N95-27975

ROTOR BLADES (TURBOMACHINERY)

Comparison of numerical results and multicavity purge and rim seal data with extensions to dynamics [NASA-TM-106685] p 2168 N95-27434

Preliminary analysis of dynamic stall effects on a 91-meter wind turbine rotor p 2124 N95-27975

Comparative wind tunnel tests of NACA 23024 airfoils with several aileron and spoiler configurations p 2124 N95-27976

ROTOR DYNAMICS

Aircraft noise prediction program theoretical manual: Rotorcraft System Noise Prediction System (ROTONET), part 4 [NASA-TM-83199-PT-4] p 2400 N95-26392

Development and validation of a blade-element mathematical model for the AH-64A Apache helicopter [NASA-TM-108863] p 2118 N95-26710

Stall precursor study of high frequency data for three high speed, swept compressor rotors [AD-A289379] p 2139 N95-26878

Whirl plus tilt [DE95-007948] p 2399 N95-28108

Modeling helicopter blade dynamics using a modified Myklestad-Prohl transfer matrix method [AD-A289891] p 2136 N95-28626

ROTORS

Optimization of wave rotors for use as gas turbine engine topping cycles [NASA-TM-106951] p 2140 N95-27860

Comparative wind tunnel tests of NACA 23024 airfoils with several aileron and spoiler configurations p 2124 N95-27976

Whirl plus tilt [DE95-007948] p 2399 N95-28108

RUBBER

The effect of proteins on the aging properties of radiation vulcanized Natural Rubber Latex [DE95-603357] p 2225 N95-26599

Radiation vulcanization of natural rubber latex [DE95-600026] p 2226 N95-26637

Variation of solvent scattering-length density small-angle neutron scattering as a means of determining structure of composite materials [DE95-005394] p 2183 N95-27428

RUBIDIUM

Toward coherent excitation: Development of a single-source pump for the rubidium hyperfine ground state doublet [AD-A289413] p 2295 N95-27132

RUBIDIUM COMPOUNDS

Muon spin relaxation in antiferromagnets: A study of RbMnF3 based on the coupled-mode theory of paramagnetic and critical spin fluctuations [PB95-192878] p 2418 N95-28642

RUN TIME (COMPUTERS)

A demonstration of Client-Server technology using remote procedure calls with an application of file migration for moving records based on time [AD-A289392] p 2453 N95-26879

Design of a real-time wind turbine simulator using a custom parallel architecture p 2322 N95-27979

RUNGE-KUTTA METHOD

Parallel block implicit integration technique for trajectory parallelism [AD-A288961] p 2379 N95-28335

Third-order-accurate numerical methods for efficient, large time-step solutions of mixed linear and nonlinear problems [DE95-009184] p 2288 N95-28533

Numerical study to assess sulfur hexafluoride as a medium for testing multielement airfoils [NASA-TP-3496] p 2124 N95-28674

RUNWAY CONDITIONS

Subsurface radar investigations at the Pegasus Glacial-ice Runway and Williams Field, McMurdo Station, Antarctica [AD-A289323] p 2144 N95-27297

RUNWAYS

Precision landing system mathematical modeling study report for Andrews Air Force Base, runway 19L, Camp Springs, MD [AD-A289015] p 2127 N95-27903

RUPTURING

Design prediction for long term stress rupture service of composite pressure vessels p 2188 N95-28291

RUSSIAN FEDERATION

JPRS report: Science and technology. Central Eurasia [JPRS-UST-95-021] p 2202 N95-27155

JPRS report: Science and technology. Central Eurasia [JPRS-UST-95-016] p 2262 N95-27170

JPRS report: Science and technology. Central Eurasia [JPRS-UST-95-014] p 2145 N95-27171

JPRS report: Science and technology. Central Eurasia [JPRS-UST-95-015] p 2246 N95-27213

JPRS report: Science and technology. Central Eurasia [JPRS-UST-94-022] p 2246 N95-27699

WTEC panel report on research submersibles and undersea technologies [NASA-CR-198565] p 2247 N95-27909

The distribution of cloud cover over the former USSR as derived from the RIHMI 223-Station 3-hourly meteorological database [DE95-007046] p 2343 N95-27920

JPRS Report: Science and Technology. Central Eurasia [JPRS-UST-95-020] p 2145 N95-28257

JPRS report: Science and technology. Central Eurasia [JPRS-UST-95-019] p 2270 N95-28565

Computational and experimental studies of hydrodynamic instabilities and turbulent mixing [DE95-006837] p 2288 N95-28603

RUTHENIUM COMPOUNDS

Photochemistry in constrained spaces: Zeolites and layered double metal hydroxides [DE95-006417] p 2207 N95-27951

RUTILE

The influence of surface structure on the interaction of water with TiO2(100) [DE95-004927] p 2203 N95-27401

S

S MATRIX THEORY

On the Hopf structure of U(p,q)(gl(1/1)) and the universal Tau-matrix of Fun(p,q)(GL(1/1)) [DE95-608755] p 2448 N95-27333

S WAVES

Energetic particle destabilization of shear Alfven waves in stellarators and tokamaks [DE95-006393] p 2431 N95-27419

Shear Alfven wave excitation by direct antenna coupling and fast wave resonant mode conversion [DE95-609109] p 2256 N95-28254

SACCHAROMYCES

Biochemically vulnerable sites for antifungal intercession in the control of fungal growth [AD-A288345] p 2348 N95-26573

SAFEGUARD SYSTEM

Development and implementation of a system safety program for the space launch complex 3 east (SLC-3E) ground support system project to support Atlas 2 family of space launch vehicles p 2174 N95-28316

SAFETY

Fuzzy-algebra uncertainty assessment [DE95-005426] p 2391 N95-27432

Current status of environmental, health, and safety issues of lithium polymer electric vehicle batteries [DE95-004005] p 2265 N95-27719

Implementing an integrated standards-based management system to ensure compliance at Los Alamos National Laboratory [DE95-007873] p 2451 N95-28025

Lithium ion rechargeable systems studies [DE95-006810] p 2268 N95-28200

Reactor pressure vessel structural integrity research [DE95-007034] p 2223 N95-28208

Development of an ultra-safe rechargeable lithium-ion battery [AD-A288959] p 2269 N95-28349

SAFETY FACTORS

Probabilistic risk assessment of the Space Shuttle. Phase 3: A study of the potential of losing the vehicle during nominal operation, volume 1 [NASA-CR-197808] p 2159 N95-26398

A comparison of error categorization schemes for use in software system safety programs [AD-A288741] p 2371 N95-27251

Development and implementation of a system safety program for the space launch complex 3 east (SLC-3E) ground support system project to support Atlas 2 family of space launch vehicles p 2174 N95-28316

SAFETY MANAGEMENT

Evaluating the environmental viability of open burning/open detonation operations p 2170 N95-28297

Cape Canaveral air station launch emergency response forces and toxic materials release contingency plans p 2172 N95-28306

Development and implementation of a system safety program for the space launch complex 3 east (SLC-3E) ground support system project to support Atlas 2 family of space launch vehicles p 2174 N95-28316

SAMPLED DATA SYSTEMS

Robust hybrid state-space self-tuning control using dual-rate sampling [AD-A288359] p 2380 N95-26468

SAMPLING

Robust hybrid state-space self-tuning control using dual-rate sampling [AD-A288359] p 2380 N95-26468

Use of mussels in biomonitoring of environmental impacts of propellants, projectiles, explosives, and pyrotechnics p 2170 N95-28298

Design, construction, test and evaluation of a frequency scanning radiometer for measuring oil slick thicknesses [AD-A290040] p 2293 N95-28389

Evaluation of defect-related diffusion in semiconductors by electrooptical sampling [AD-A291630] p 2270 N95-28544

SANDS

The biodegradation of fuels in soils and sediments: Differences as a function of mineralogy p 2230 N95-27116

SANDWICH STRUCTURES

Composite sandwich structure and method for making same [NASA-CASE-LAR-14898-1] p 2180 N95-26764

An experimental investigation of sandwich flat panels under low velocity impact [AD-A289420] p 2309 N95-27135

Composite repair issues on the CF-18 aircraft
p 2134 N95-27518
External patch repair of CFRP/honeycomb sandwich
p 2134 N95-27522
Application of fiber-reinforced bismaleimide materials to aircraft nacelle structures
p 2137 N95-28278

SAPPHIRE
Coherent V2O3 precipitates in alpha-Al2O3CO-implanted with vanadium and oxygen
[DE95-007404] p 2444 N95-28081
Cesium/oxide interactions for ultrathin films on (alpha)-Al2O3(001) and (alpha)-Al2O3(1(bar 1)O2)
[DE95-008159] p 2238 N95-28358

SATELLITE ANTENNAS
Telemetry down-link Doppler as an attitude sensor for spin stabilized spacecraft
p 2150 N95-27785

SATELLITE ATTITUDE CONTROL
Autonomous control system reconfiguration for spacecraft with non-redundant actuators
p 2153 N95-27802
Micro electric propulsion feasibility
[NASA-CR-189139] p 2168 N95-28000

SATELLITE COMMUNICATION
Assessment of long-distance HF radio and satellite communication assets for RNLAF out-of-area operations
[AD-A288633] p 2247 N95-26344
Prediction of rain attenuation and total atmospheric attenuation for low-availability satellite communications in Europe
[PB95-184925] p 2252 N95-26908
Preliminary flight software specification for the petite amateur Navy satellite (PANSAT)
[AD-A280068] p 2165 N95-28150

SATELLITE CONSTELLATIONS
An architecture and protocol for communications satellite constellations regarded as multi-agent systems
p 2166 N95-27377

SATELLITE CONTROL
Generic satellite monitoring expert system
[AD-A289209] p 2163 N95-26987
An architecture and protocol for communications satellite constellations regarded as multi-agent systems
p 2166 N95-27377
GPS as an orbit determination subsystems
p 2152 N95-27793
Dynamics and control of SEDSAT tethered multi-probe for thermospheric research flight data analysis of SEDS-2 satellite: Tethered systems dynamics and flight data analysis
[NASA-CR-198653] p 2165 N95-27836

SATELLITE DESIGN
Structures and materials technology needs for communications and remote sensing spacecraft
[NASA-CR-198166] p 2163 N95-27026
Low-cost tubular antenna deployer for WISP-2
p 2156 N95-27269
Non-explosive actuation for the ORBCOMM (TM) satellite
p 2156 N95-27274
Long Duration Exposure Facility post-flight data as it influences the Tropical Rainfall Measuring Mission
p 2345 N95-27666

SATELLITE IMAGERY
The design and implementation of the Military Applications of Shiptracks experiment on Space Transportation System - 65
[AD-A288488] p 2160 N95-26634
The Solar X-ray Imager Vacuum Door Assembly
p 2157 N95-27280
Improved reduced-resolution satellite imagery
p 2376 N95-27388
Reconstruction of an infrared band of meteorological satellite imagery with abductive networks
[SAIC-94/1062] p 2345 N95-27389
Speckle spectrum of the ERS-1 wavemode product
[PB95-196564] p 2315 N95-28180
Neural networks in the classification of uses of the soil in satellite images
[INPE-5478-PRE/1777] p 2316 N95-28672

SATELLITE INSTRUMENTS
Model-based monitoring and diagnosis of a satellite-based instrument
p 2166 N95-27390
Solar UV flux measurements from the SBUV2 monitor on the NOAA9 satellite. Part 1: Mg II h and k line core-to-wing ratios for 1986-1988
[PB95-181962] p 2464 N95-28007

SATELLITE LIFETIME
Dynamics and control of SEDSAT tethered multi-probe for thermospheric research flight data analysis of SEDS-2 satellite: Tethered systems dynamics and flight data analysis
[NASA-CR-198653] p 2165 N95-27836

SATELLITE OBSERVATION
Technical report series on global modeling and data assimilation. Volume 6: A multiyear assimilation with the GEOS-1 system: Overview and results
[NASA-TM-104606-VOL-6] p 2334 N95-26423
The design and implementation of the Military Applications of Shiptracks experiment on Space Transportation System - 65
[AD-A288488] p 2160 N95-26634
Deep convection in the Mediterranean Sea
[AD-A288497] p 2346 N95-26647
Differenced Range Versus Integrated Doppler (DRVID) ionospheric analysis of metric tracking in the Tracking and Data Relay Satellite System (TDRSS)
p 2147 N95-27766
An in situ evaluation of TOPEX/Poseidon altimetric measurements versus meaurements made by moorings and inverted echo sounders for sea surface height
[NASA-CR-198621] p 2347 N95-27805
Studies of radar backscatter as a function of wave properties and the winds in the turbulent marine atmosphere
[NASA-CR-198608] p 2315 N95-28209
Altimeter analysis of ocean currents
[AD-A290167] p 2315 N95-28392

SATELLITE ORBITS
Space modeler: An expanded, distributed, virtual environment for space visualization
[AD-A289409] p 2461 N95-27131
Earth horizon modeling and application to static Earth sensors on TRMM spacecraft
p 2150 N95-27783
Determining GPS average performance metrics
p 2128 N95-27791
Estimation of attitude sensor timetag biases
p 2153 N95-27799

SATELLITE ORIENTATION
Optimization of a nutation damper attached to a spin-stabilized satellite
[AD-A289424] p 2162 N95-26887
Evaluation and modeling of autonomous attitude thrust control for the Geostation Operational Environmental Satellite (GOES)-8 orbit determination
p 2146 N95-27765
An MME-based attitude estimator using vector observations
p 2148 N95-27775
Earth horizon modeling and application to static Earth sensors on TRMM spacecraft
p 2150 N95-27783
Telemetry down-link Doppler as an attitude sensor for spin stabilized spacecraft
p 2150 N95-27785
Estimation of attitude sensor timetag biases
p 2153 N95-27799
Autonomous control system reconfiguration for spacecraft with non-redundant actuators
p 2153 N95-27802

SATELLITE TRACKING
Generic satellite monitoring expert system
[AD-A289209] p 2163 N95-26987
Flight Mechanics/Estimation Theory Symposium 1995
[NASA-CP-3299] p 2146 N95-27763
Evaluation and modeling of autonomous attitude thrust control for the Geostation Operational Environmental Satellite (GOES)-8 orbit determination
p 2146 N95-27765
Differenced Range Versus Integrated Doppler (DRVID) ionospheric analysis of metric tracking in the Tracking and Data Relay Satellite System (TDRSS)
p 2147 N95-27766
Accurate orbit determination strategies for the tracking and data relay satellites
p 2147 N95-27768
Use of nonlinear identification in robust attitude and attitude rate estimation for SAMPEX
p 2149 N95-27781
Determining GPS average performance metrics
p 2128 N95-27791
A demonstration of unified TDRS/GPS tracking and orbit determination
p 2151 N95-27792
GPS as an orbit determination subsystems
p 2152 N95-27793

SATELLITE-BORNE INSTRUMENTS
Retrofitting a fine-pointing system to satellite optics
p 2157 N95-27277
Design, development and testing of the x-ray timing explorer High Gain Antenna System
p 2157 N95-27279
The Solar X-ray Imager Vacuum Door Assembly
p 2157 N95-27280
SAMPEX special pointing mode
p 2149 N95-27780
A simple method for verifying the deployment of the TOMS-EP solar arrays
p 2150 N95-27782
Retrofitting a fine-pointing system to satellite optics
[DE95-004529] p 2427 N95-28516

SATELLITE-BORNE RADAR
Telemetry down-link Doppler as an attitude sensor for spin stabilized spacecraft
p 2150 N95-27785
A demonstration of unified TDRS/GPS tracking and orbit determination
p 2151 N95-27792

SATURATION
Measurement of the D0 WAMUS magnet inductance
[DE95-005128] p 2399 N95-27530

SCALARS
On higher derivative gravity in two dimensions
[DE95-608789] p 2462 N95-27343
Two-body bound states and the Bethe-Salpeter equation
[DE95-008302] p 2392 N95-27742
Advances in scientific visualization
[DE95-008065] p 2343 N95-28014

SCALE EFFECT
Scaling issues in dynamic fragmentation
[DE95-008509] p 2309 N95-27745

SCALE MODELS
Scale model experiments with ceramic laminate targets
[AD-A288322] p 2225 N95-26561
Spray-formed tooling
[DE95-005031] p 2246 N95-27404
Large HAWT wake measurement and analysis
p 2289 N95-27973
Comparative wind tunnel tests of NACA 23024 airfoils with several aileron and spoiler configurations
p 2124 N95-27976

SCALING LAWS
Scaling of localization length of a quasi 1D system with longitudinal boundary roughness
[DE95-609148] p 2391 N95-27739
Theoretical aspects of energy confinement in spheromaks
[DE95-008079] p 2435 N95-28542

SCANNERS
MHD simulations of DC helicity injection for current drive in tokamaks
[DE95-007018] p 2429 N95-26940
A cryogenic scan mechanism for use in Fourier transform spectrometers
p 2158 N95-27287
High-performance reactionless scan mechanism
p 2158 N95-27288
Reconstruction of an infrared band of meteorological satellite imagery with abductive networks
[SAIC-94/1062] p 2345 N95-27389

SCANNING ELECTRON MICROSCOPY
Tensile properties of Fe-16 at. % Al alloys
[DE95-007102] p 2215 N95-27450
C15 intermetallic compounds HfV2+Nb
[DE95-005264] p 2215 N95-27463
Formation of anisotropic Tl-1212, Tl-2212, Tl-1223 and Tl-2223 particles using aerosol flow reacted powders
[DE95-007400] p 2444 N95-28079
Ambient-pressure silica aerogel films
[DE95-008161] p 2237 N95-28090

SCANNING TUNNELING MICROSCOPY
Boron-induced reconstructions of Si(100) investigated by scanning tunneling microscopy
[AD-A289222] p 2438 N95-26959
Boron-induced morphology changes in silicon CVD growth: A scanning tunneling microscopy study
[AD-A289275] p 2290 N95-26982

SCATTERING
User's and test case manual for FEMATS
[NASA-CR-197803] p 2366 N95-26694
Improving the performance of spiral antennas by using passive scatterers
[AD-A289324] p 2251 N95-26893
Variation of solvent scattering-length density small-angle neutron scattering as a means of determining structure of composite materials
[DE95-005394] p 2183 N95-27428
Integrating the QMR method with first principles material science application code
[DE95-007380] p 2408 N95-27456
Femtosecond X-ray generation through 90 degrees T homson scattering: Status of the LBL experiment
[DE95-006560] p 2296 N95-27674

SCATTERING CROSS SECTIONS
Statistical model for molecular internal energy exchange in DSMC method for rarefied flow analysis
[ISAS-R-654] p 2274 N95-26741

SCATTEROMETERS
Studies of radar backscatter as a function of wave properties and the winds in the turbulent marine atmosphere
[NASA-CR-198608] p 2315 N95-28209

SCHEDULES
A hybrid vehicle evaluation code and its application to vehicle design. Revision 1
[DE95-008053] p 2303 N95-28029
A hybrid vehicle evaluation code and its application to vehicle design, revision 2
[DE95-008060] p 2303 N95-28139
International journal of quantum chemistry
[AD-A291633] p 2352 N95-28546

SCHEDULING
Parallelism detection and scheduling strategies for reliable and efficient execution on multicomputers
[AD-A288370] p 2376 N95-26471

Operating system support for coexistence of real-time and conventional scheduling
[AD-A288584] p 2364 N95-26534

Grain size management in repetitive task graphs for multiprocessor computer scheduling
[AD-A288575] p 2377 N95-26551

Design tool for multiprocessor scheduling and evaluation of iterative dataflow algorithms
[NASA-TP-3491] p 2366 N95-26685

A gain scheduling optimization method using genetic algorithms
[AD-A289306] p 2381 N95-26920

Integrated planning and scheduling for Earth science data processing p 2384 N95-27382

A sustainable genetic algorithm for satellite resource allocation p 2376 N95-27383

A rule-based shell to hierarchically organize HST observations p 2384 N95-27384

SCHLIEREN PHOTOGRAPHY

Visualization of the multiple supersonic jet oscillations by swept focused strobed schlieren technique
p 2119 N95-26952

Schlieren System and method for moving objects
[NASA-CASE-LAR-15053-1] p 2291 N95-27191

SCHOOLS

CAS CERN Accelerator School 5th General Accelerator Physics Course
[DE95-608324] p 2419 N95-27158

SCHOTTKY DIODES

The effects of temperature on Schottky diode barrier height and evidence of multiple barrier
[DE95-609147] p 2264 N95-27405

Low temperature deposition and characterization of N- and P-type silicon carbide thin films and associated Ohmic and Schottky contacts
[AD-A289107] p 2237 N95-28097

JPRS report: Science and technology. Central Eurasia
[JPRS-UST-95-019] p 2270 N95-28565

SCHROEDINGER EQUATION

An invariant measure for a nonlinear Schroedinger equation
[DE95-610166] p 2391 N95-27714

Hydrogen-like atom in laser field: Invariant atomic parameters in the ground state
[DE95-609036] p 2411 N95-27930

Quantum retrodiction and causality principle
[DE94-628438] p 2450 N95-28183

SCIENTIFIC SATELLITES

A magnetic hysteresis model p 2153 N95-27801

SCIENTIFIC VISUALIZATION

Three-dimensional visualization of reactive flows in complex geometries
[DE95-006332] p 2284 N95-27845

Advances in scientific visualization
[DE95-008065] p 2343 N95-28014

Visualization methods for the exploration of high dimensional data
[AD-A291717] p 2393 N95-28507

SCIENTISTS

NASA/DOD Aerospace Knowledge Diffusion Research Project. Report 35: The use of computer networks in aerospace engineering
[NASA-CR-198170] p 2456 N95-28600

SCINTILLATING FIBERS

Cosmic ray test results of the D0 prototype scintillating fiber tracker
[DE95-007215] p 2415 N95-28221

SCINTILLATION

An improved model of high-latitude f-region scintillation (WBMOD version 13)
[AD-A288558] p 2334 N95-26520

Detecting alpha particles through scintillation in porous materials
[AD-A289313] p 2406 N95-27399

SCINTILLATION COUNTERS

New radiation stable and long-lived plastic scintillators
[DE95-608622] p 2233 N95-27163

Detecting alpha particles through scintillation in porous materials
[AD-A289313] p 2406 N95-27399

Scintillator materials for calorimetry
[DE95-006570] p 2421 N95-27679

Measurement of the reaction C(nu(sub mu), mu(-)) X near threshold
[DE95-007888] p 2412 N95-28063

Cosmic ray test results of the D0 prototype scintillating fiber tracker
[DE95-007215] p 2415 N95-28221

SCRAPERS

Observation of nonlinear resonances in the advanced light source
[DE95-006561] p 2425 N95-27675

SCREWS

Basic space payload fastener p 2156 N95-27273

SCRUBBERS

A new method for measuring hypergol scrubber emissions p 2174 N95-28312

SEA FLOOR SPREADING

Seismic constraints on shallow crustal processes at the East Pacific rise
[AD-A289055] p 2338 N95-28094

SEA ICE

Study of the response of a three-dimensional coupled ice-ocean model to daily varying atmospheric forcing
[AD-A289050] p 2347 N95-27189

Tomographic observations of deep convection and the thermal evolution of the Greenland Sea Gyre 1988-1989
[AD-A289104] p 2348 N95-28096

Modeling and retrieval of snow and sea ice characteristics in the frequency range 6 to 90 GHz
[PB95-195467] p 2316 N95-28656

SEA LEVEL

An in situ evaluation of TOPEX/Poseidon altimetric measurements versus meaurements made by moorings and inverted echo sounders for sea surface height
[NASA-CR-198621] p 2347 N95-27805

On the persistence of the oceanic background of apparent sea level changes in the Baltic Sea
[REPT-94:5] p 2348 N95-27996

Testing the correlation between seismic stratigraphy, diagenesis and physical rock properties: Evaluation of fluid flow during early and late diagenesis
[DE95-008338] p 2338 N95-28083

SEA ROUGHNESS

Meteorological and oceanographic data collected during the ASREX 91 field experiment
[AD-A289492] p 2342 N95-26826

SEA SURFACE TEMPERATURE

The effect of infrared sea surface temperature measurements on evaporation duct height estimation
[AD-A289045] p 2346 N95-26477

Infrared field measurements of sea surface temperature: Analysis of wake signatures and comparison of skin layer models
[NASA-CR-197849] p 2346 N95-26533

SEA WATER

FREZCHEM: A chemical-thermodynamic model for aqueous solutions at subzero temperatures
[AD-A288456] p 2200 N95-26432

Temporal and spatial decorrelation scales of the Yellow Sea thermal fields
[AD-A288617] p 2346 N95-26483

Investigation on comprehensive fossil fuel cycle analysis and assessment approach as viewed from the global environment
[DE95-759241] p 2329 N95-27935

Numerical simulation of coupled flow and transport with TOUGH2: A verification study
[DE95-008351] p 2287 N95-28225

SEALERS

Task 4 supporting technology. Part 2: Detailed test plan for thermal seals. Thermal seals evaluation, improvement and test. CAN8-1, Reusable Launch Vehicle (RLV), advanced technology demonstrator: X-33. Leading edge and seals thermal protection system technology demonstration
[NASA-CR-198628] p 2304 N95-28259

Silicone joint sealants for pavements
[AD-A289843] p 2241 N95-28620

SEALING

The response of hydrotalcite coated aluminum to sealing with transition metal salt solutions
[DE95-004767] p 2234 N95-27460

SEALS (STOPPERS)

Comparison of numerical results and multicavity purge and rim seal data with extensions to dynamics
[NASA-TM-106685] p 2168 N95-27434

Numerical analysis of intra-cavity and power-stream flow interaction in multiple gas-turbine disk-cavities
[NASA-TM-106886] p 2140 N95-28344

SEARCHING

Piecemeal learning of an unknown environment
[AD-A291683] p 2387 N95-28461

SEAS

Temporal and spatial decorrelation scales of the Yellow Sea thermal fields
[AD-A288617] p 2346 N95-26483

Tomographic observations of deep convection and the thermal evolution of the Greenland Sea Gyre 1988-1989
[AD-A289104] p 2348 N95-28096

SECONDARY EMISSION

Ionizing radiation measurements on LDEF: A0015 Free flyer biostack experiment
[NASA-CR-196603] p 2202 N95-27168

SECONDARY FLOW

Turbomachinery design and tonal acoustics computations
[NASA-CR-197749] p 2139 N95-26777

Numerical analysis of intra-cavity and power-stream flow interaction in multiple gas-turbine disk-cavities
[NASA-TM-106886] p 2140 N95-28344

SEDIMENT TRANSPORT

A geo-acoustic and oceanographic description of several shallow water experimental sites on the Scotian Shelf
[AD-A288300] p 2345 N95-26420

Calculation of suspended sediment transport by combined wave-current flows
[AD-A289368] p 2346 N95-26904

Testing the correlation between seismic stratigraphy, diagenesis and physical rock properties: Evaluation of fluid flow during early and late diagenesis
[DE95-008338] p 2338 N95-28083

SEDIMENTARY ROCKS

Testing the correlation between seismic stratigraphy, diagenesis and physical rock properties: Evaluation of fluid flow during early and late diagenesis
[DE95-008338] p 2338 N95-28083

Contact micromechanics in granular media with clay
[DE95-006566] p 2340 N95-28583

SEDIMENTS

Calculation of suspended sediment transport by combined wave-current flows
[AD-A289368] p 2346 N95-26904

The biodegradation of fuels in soils and sediments: Differences as a function of mineralogy
p 2230 N95-27116

SEEDS

Intrusive multi-probe system
[DE95-006258] p 2292 N95-27465

SEGMENTS

ROC analysis of IR segmentation techniques
[AD-A289252] p 2424 N95-26971

SEISMIC WAVES

Seismic constraints on shallow crustal processes at the East Pacific rise
[AD-A289055] p 2338 N95-28094

Emerging applications of probability (stochastic models in geosystems)
[AD-A289117] p 2313 N95-28099

Dip-moveout processing by Fourier transform in anisotropic media
[DE95-007668] p 2339 N95-28190

Transformation to zero offset in transversely isotropic media
[DE95-007669] p 2339 N95-28192

Fowler DMO and time migration for transversely isotropic media with explicit operators
[DE95-007671] p 2339 N95-28194

Contact micromechanics in granular media with clay
[DE95-006566] p 2340 N95-28583

SEISMOGRAPHS

Micromechanisms for optimism seismometer
p 2159 N95-27292

SEISMOLOGY

A probabilistic target classification and description model for seismic sensors
[AD-A288548] p 2335 N95-26531

Micromechanisms for optimism seismometer
p 2159 N95-27292

Seismic constraints on shallow crustal processes at the East Pacific rise
[AD-A289055] p 2338 N95-28094

Investigation of rifting processes in the Rio Grande Rift using data from an unusually large earthquake swarm
[DE95-007623] p 2339 N95-28126

Fowler DMO and time migration for transversely isotropic media with explicit operators
[DE95-007671] p 2339 N95-28194

Contact micromechanics in granular media with clay
[DE95-006566] p 2340 N95-28583

SELECTION

Moment and hypergeometric filters for high precision computation of focus, stereo and optical flow
[AD-A289293] p 2425 N95-27038

Alternative fuels and vehicles choice model
[DE95-005695] p 2243 N95-27944

SELECTIVE DISSEMINATION OF INFORMATION

Browsing the World Wide Web from behind a firewall
[DE95-006805] p 2455 N95-27957

SELF CONSISTENT FIELDS

Massively parallel self-consistent-field calculations
[DE95-004128] p 2376 N95-26441

SELF EXCITATION

Nonlinear dynamics and aeroelasticity of rotorcraft in forward flight
[AD-A291714] p 2136 N95-28504

SELF ORGANIZING SYSTEMS

Self-organizing artificial neural networks in dynamic systems modeling and control
[PB95-185120] p 2379 N95-26449

Higher-order probabilistic perceptrons as Bayesian inference engines
[DE95-608730] p 2381 N95-27044

SEMANTICS

A parallel complexity model for functional languages
[AD-A288589] p 2365 N95-26656

Semantic heterogeneity in database and data dictionary integration for command and control systems
[AD-A289180] p 2453 N95-27014

Solving recursive domain equations with enriched categories
[AD-A289358] p 2371 N95-27418

SEMICIRCULAR CANALS

Regional differences in lectin binding patterns of vestibular hair cells p 2349 N95-26728

SEMICONDUCTING FILMS

Materials, structures, and devices for high-speed electronics
[NASA-CR-197815] p 2260 N95-26816

SEMICONDUCTOR DEVICES

Technical progress report to the Department of Energy on the Solid State Sciences Committee (SSSC)
[DE95-007113] p 2441 N95-27925

SEMICONDUCTOR DIODES

An organic thin film laser diode: A novel light source
[AD-A289007] p 2294 N95-26568

High-speed coherent laser arrays
[AD-A289373] p 2295 N95-26906

SEMICONDUCTOR JUNCTIONS

Pseudomorphic semiconducting heterostructures from combinations of AlN, GaN and selected SiC polytypes: Theoretical advancement and its coordination with experimental studies of nucleation, growth, characterization and device development
[AD-A289550] p 2437 N95-26756

Demonstration of photo-assisted tunneling process across the coulomb blockade energy gap in mesoscopic tunnel junctions — photon-assisted tunneling
[AD-A289534] p 2438 N95-26872

SEMICONDUCTOR LASERS

An organic thin film laser diode: A novel light source
[AD-A289007] p 2294 N95-26568

High-speed coherent laser arrays
[AD-A289373] p 2295 N95-26906

Generation of a single-lobe, far-field intensity pattern from a laser diode array using an optical delay line
[AD-A289226] p 2295 N95-26961

Laser with optically driven Q-switch
[NASA-CASE-NPO-18470-1-CU] p 2297 N95-27731

Surface-emitting semiconductor laser for intracavity spectroscopy and microscopy
[DE95-007745] p 2299 N95-28128

SEMICONDUCTOR PLASMAS

Wake fields in semiconductor plasmas
[DE94-634523] p 2429 N95-26439

SEMICONDUCTORS (MATERIALS)

Joint Services Electronics Program (JSEP)
[AD-A288299] p 2345 N95-26419

Wake fields in semiconductor plasmas
[DE94-634523] p 2429 N95-26439

Rotor phases in compound semiconductors
[DE95-004139] p 2436 N95-26442

Template synthesis of electronically conductive polymer nanostructures
[AD-A288373] p 2225 N95-26472

Chemistry involving the separation, isolation, and immobilization of 3-5 compound semiconductor nanocrystals and quantum dots
[AD-A288381] p 2436 N95-26473

The 18th Annual Condensed Matter Physics Meeting
[DE95-605568] p 2398 N95-26598

Pseudomorphic semiconducting heterostructures from combinations of AlN, GaN and selected SiC polytypes: Theoretical advancement and its coordination with experimental studies of nucleation, growth, characterization and device development
[AD-A289550] p 2437 N95-26756

Electronic characterization of defects in narrow gap semiconductors: Comparison of electronic energy levels and formation energies in mercury cadmium telluride, mercury zinc telluride, and mercury zinc selenide
[NASA-CR-197835] p 2437 N95-26780

Materials Research Society Symposium Proceedings. Volume 339: Diamond, SiC and nitride wide bandgap semiconductors
[AD-A288690] p 2437 N95-26818

Solid-state image sensor with focal-plane digital photon-counting pixel array
[NASA-CASE-NPO-18518-1-CU] p 2424 N95-26894

Modeling the growth of electronic materials
[AD-A289137] p 2438 N95-26997

Atomic structure and bonding of boron-induced reconstructions on Si(001)
[AD-A289187] p 2405 N95-27017

Modeling of trapping and abrupt doping effects in MESFET's using R-dynamic element
[PB95-184891] p 2262 N95-27050

Optical features of nanosize iron and molybdenum sulfide clusters
[DE95-005417] p 2202 N95-27136

Model of a single impurity in a wide bandgap semiconductor describing electric field screening
[AD-A289322] p 2264 N95-27296

The physics and chemistry of heavy Fermions
[DE95-005277] p 2407 N95-27431

Characterization of wafer charging mechanisms and oxide survival prediction methodology
[DE95-006583] p 2440 N95-27538

Technical progress report to the Department of Energy on the Solid State Sciences Committee (SSSC)
[DE95-007113] p 2441 N95-27925

High pressure optical studies of semiconductors and heterostructures
[DE95-007119] p 2410 N95-27927

First-principles calculations for AlN, GaN, and InN: Bulk and alloy properties
[DE95-006822] p 2219 N95-27958

Phase separation and ordering in InGaAsP and InGaAs materials
[DE95-007493] p 2443 N95-28050

Low temperature carrier transport properties in isotopically controlled germanium
[DE95-008489] p 2444 N95-28092

Research activities of the Solid State Sciences Committee in the development of a Federal initiative on advanced materials and processing
[DE95-009328] p 2445 N95-28179

Low noise monolithic Si JFETS for operation in the 90-300K range and in high radiation environments
[DE95-007303] p 2269 N95-28244

Temperature dependence of the static dielectric response in a Q1D electron gas
[DE95-609269] p 2400 N95-28350

Evaluation of defect-related diffusion in semiconductors by electrooptical sampling
[AD-A291630] p 2270 N95-28544

Nonlinear dynamics of a coherent polariton-biexciton system
[DE95-609150] p 2417 N95-28607

SENSITIVITY

Comparative transduction mechanisms of hair cells in the bullfrog utriculus. 1: Responses to intracellular current p 2350 N95-26731

Comparative transduction mechanisms of hair cells in the bullfrog uticulus. 2: Sensitivity and response dynamics to hair bundle displacement p 2350 N95-26732

Polarization sensitivity of monopulse radar boresight error induced by large, ogive radomes
[AD-A289254] p 2252 N95-26972

Measurement of N2(+) mobility He via Fourier transform emission spectroscopy
[AD-A289266] p 2404 N95-26979

Design considerations in supercritical fluid technology
p 2232 N95-27126

Optimization of measurements with pressure sensitive paints
[NASA-TM-4695] p 2293 N95-27915

Nonlinear optical microscopy for imaging thin films and surfaces
[DE95-007872] p 2426 N95-28018

CORSSTOL: Cylinder Optimization of Rings, Skin, and Stringers with Tolerance sensitivity
[NASA-TP-3551] p 2392 N95-28215

Analytical investigations of the acceleration sensitivity of acoustic bulk and surface wave resonators
[AD-A291715] p 2402 N95-28505

SENSORS

Fundamental concepts of integrated and fiber optic sensors
[NASA-TM-106920] p 2426 N95-27906

JTEC Panel report on microelectromechanical systems in Japan
[NASA-CR-197831] p 2268 N95-28239

SENSORY DEPRIVATION

A model of the neural basis of the rat's sense of direction
[AD-A289678] p 2350 N95-26761

SENSORY PERCEPTION

Research activities on somatosensory (SI) cortical neurons
[AD-A288794] p 2348 N95-26360

Handbook of perception and human performance, volume 2. Cognitive processes and performance
[AD-A289587] p 2355 N95-26692

SENTENCES

Absolute logics
[ISBN-951-41-0775-6] p 2397 N95-28238

SEPARATED FLOW

Turbulence modeling
[NASA-CR-197751] p 2274 N95-26665

Demonstration study of hierarchical control of fluid-dynamic phenomena
[AD-A289341] p 2275 N95-26751

Performance characterization of a highly-offset diffuser with and without blowing vortex generator jets
[AD-A289334] p 2122 N95-26901

Computation of three-dimensional mixed convective boundary layer flow p 2280 N95-27347

SEPARATORS

High-rate/high-temperature capability of a single-layer zicar-separator nickel-hydrogen cell
p 2272 N95-26788

Development of an optical trap as an ultra-sensitive analytical tool
[DE95-007843] p 2426 N95-28022

SEQUENCING

Modal event calculus in Lolli
[AD-A288544] p 2365 N95-26605

Evaluation of composite joints
[AD-A289247] p 2181 N95-26967

A spectral algorithm for the seriation problem
[DE95-004775] p 2372 N95-27436

A comparison of measured wind park load histories with the WISPER and WISPERX load spectra
[DE95-000295] p 2319 N95-27459

Sequence comparison on a cluster of workstations using the PVM system
[DE95-006527] p 2378 N95-27709

SEQUENTIAL ANALYSIS

Analysis of filter tuning techniques for sequential orbit determination p 2146 N95-27764

SERVICE LIFE

The 1994 27th Annual NASA Aerospace Battery Workshop
[NASA-CP-3292] p 2317 N95-26785

Progress towards computer simulation of NiH2 battery performance over life p 2272 N95-26786

Long life 80Ah standard IPV NiH2 battery cell
p 2272 N95-26787

The 50 Ah NiH2 CPV qualification tests
p 2272 N95-26792

Hubble Space Telescope nickel-hydrogen battery testing: An update p 2272 N95-26794

Summary of EOS flight dynamics analysis
p 2152 N95-27797

SERVOMECHANISMS

Design and synthesis of a real-time controller for an unmanned air vehicle
[AD-A289134] p 2141 N95-26555

SET THEORY

The assembly tower and some categorical and algebraic aspects of frame theory
[AD-A289360] p 2391 N95-27489

A case for dynamic sets in operating systems
[AD-A289354] p 2454 N95-27529

Absolute logics
[ISBN-951-41-0775-6] p 2397 N95-28238

SEWAGE

Ash-based ceramic materials
[AD-D017272] p 2241 N95-28582

SEWAGE TREATMENT

Microbial treatment for shipboard collection, holding, and transfer system tanks p 2179 N95-27119

SEWING

Development of stitched/RTM composite primary structures p 2195 N95-28469

Test and analysis results for composite transport fuselage and wing structures p 2137 N95-28470

SHADOWS

Analysis of shadowing effects on MIR photovoltaic and solar dynamic power systems
[NASA-TM-106940] p 2169 N95-28213

SHAFTS (MACHINE ELEMENTS)

Analytical and experimental evaluation of joining silicon carbide to silicon carbide and silicon nitride to silicon nitride for advanced heat engine applications, phase 2
[DE95-005761] p 2303 N95-27947

SHAKERS

In situ dynamic material property measurement system
[AD-D017387] p 2210 N95-28585

SHALLOW WATER

A geo-acoustic and oceanographic description of several shallow water experimental sites on the Scotian Shelf
[AD-A288300] p 2345 N95-26420

Temporal and spatial decorrelation scales of the Yellow Sea thermal fields
[AD-A288617] p 2346 N95-26483

SHAPE FUNCTIONS

Investigation into the behavior of geometrically nonlinear composite arches
[AD-A289258] p 2308 N95-26975

SHAPE MEMORY ALLOYS

A rotating arm using shape-memory alloy
p 2157 N95-27276

SMART materials: Surfaces, transforms and interfaces. The commensurate engineering dimension
[AD-A289598] p 2312 N95-28649

SHAPES
Contribution to the optimal shape design of two-dimensional internal flows with embedded shocks
[NASA-CR-195062] p 2389 N95-26672
SHEAR FLOW
Flow visualization of a turbulent shear flow using an optical wavefront sensor
[AD-A289208] p 2277 N95-26986
Basic studies in turbulent shear flows
[AD-A289145] p 2277 N95-26998
Two-layer or free surface shear flows and viscoelastic shear flows and the relationship between stability and eigenvalues --- viscoelastic, shear, and convective flows
[AD-A289510] p 2278 N95-27047
Turbulance boundary conditions for shear flow analysis, using the DTNS flow solver p 2283 N95-27362
Magnetic viscosity by localized shear flow instability in magnetized accretion disks
[DE95-006879] p 2433 N95-28111
Computational and experimental studies of hydrodynamic instabilities and turbulent mixing
[DE95-006837] p 2288 N95-28603
SHEAR LAYERS
The stability of the flow in a laminar separation bubble
[CUED/A-AERO/TR-22] p 2275 N95-26809
Flow visualization of a turbulent shear flow using an optical wavefront sensor
[AD-A289208] p 2277 N95-26986
Turbulance boundary conditions for shear flow analysis, using the DTNS flow solver p 2283 N95-27362
SHEAR PROPERTIES
Overview of through-thickness test methods for polymer matrix composites
[PB95-190112] p 2227 N95-26747
Stress transfer from axially loaded fiber to matrix in a microcomposite
[DE95-007366] p 2183 N95-28043
SHEAR STRENGTH
Analysis of plate-twist test for in-plane shear modulus of composite materials (revised)
[PB95-190195] p 2308 N95-26749
Scarf joint technique with cocured and precured patches for composite repair p 2135 N95-27524
Tungsten carbide fragmentation: Experimental characterization and numerical modelling
[DE95-008521] p 2236 N95-27879
SHEAR STRESS
Studies of radar backscatter as a function of wave properties and the winds in the turbulent marine atmosphere
[NASA-CR-198608] p 2315 N95-28209
SHELL THEORY
The collapse of composite cylindrical panels with various thickness using finite element analysis
[AD-A289370] p 2308 N95-26905
Characterization of the membrane theory of a clamped shell. The hyperbolic case
[PB95-185021] p 2308 N95-26911
SHELLS (STRUCTURAL FORMS)
Composite fuselage shell structures research at NASA Langley Research Center p 2194 N95-28466
SHIPS
The design and implementation of the Military Applications of Shiptracks experiment on Space Transportation System - 65
[AD-A288488] p 2160 N95-26634
Tie-down trials involving a Sikorsky S-70B-2 helicopter
[DSTO-TR-0132] p 2136 N95-28567
Severe weather guide mediterranean
[AD-A289829] p 2344 N95-28577
SHOCK HEATING
High temperature kinetic study of the reactions H + O2 = OH + O and O + H2 = OH + H in H2/O2 system by shock tube-laser absorption spectroscopy
[NASA-CR-195473] p 2206 N95-27695
Investigation of HE driven cylindrical liner
[DE95-007866] p 2311 N95-28539
SHOCK LAYERS
Viscous shock-layer analysis on hypersonic flow over reentry capsule with nonequilibrium chemistry
[ISAS-R-656] p 2274 N95-26739
SHOCK MEASURING INSTRUMENTS
Micro-time stress measurement device development
[AD-A289511] p 2361 N95-26845
SHOCK RESISTANCE
Development of low-expansion ceramics with strength retention to elevated temperatures
[DE95-005760] p 2239 N95-28397
SHOCK TUBES
An investigation of the AFIT 2-inch shock tube as a flow source for supersonic testing
[AD-A289246] p 2143 N95-26966
Computational and experimental studies of hydrodynamic instabilities and turbulent mixing
[DE95-006837] p 2288 N95-28603
SHOCK WAVE INTERACTION
A fully implicit time accurate method for hypersonic combustion: Application to shock-induced combustion instability
[NASA-TM-106707] p 2273 N95-26380
Compressible turbulence measurements in a supersonic flow with adverse pressure gradient
[AD-A289477] p 2276 N95-26822
A numerical study of fundamental shock noise mechanisms
[NASA-TM-110608] p 2401 N95-27908
Response of multi-panel assembly to noise from a jet in forward motion
[NASA-CR-198164] p 2289 N95-28673
SHOCK WAVE PROPAGATION
A numerical study of fundamental shock noise mechanisms
[NASA-TM-110608] p 2401 N95-27908
SHOCK WAVES
Contribution to the optimal shape design of two-dimensional internal flows with embedded shocks
[NASA-CR-195062] p 2389 N95-26672
Bow shock data analysis
[AD-A288432] p 2429 N95-26800
An investigation of the AFIT 2-inch shock tube as a flow source for supersonic testing
[AD-A289246] p 2143 N95-26966
A numerical study of fundamental shock noise mechanisms
[NASA-TM-110608] p 2401 N95-27908
Swords to plowshares: Shock wave applications to advanced lithography
[DE95-008154] p 2299 N95-28223
Modeling the shock response of submerged structures
[AD-A289082] p 2288 N95-28351
SHORT WAVE RADIATION
A study of surface temperatures, clouds and net radiation
[NASA-CR-198589] p 2329 N95-27864
SHRINKAGE
The minimum pore size obtainable in a silica gel during drying
[DE95-008162] p 2239 N95-28401
SIGNAL ANALYSIS
Speech analysis and synthesis based on pitch-synchronous segmentation of the speech waveform
[AD-A288824] p 2248 N95-26349
The automatic extraction of selected speech spectral characteristics
[IFTR-2/1994] p 2250 N95-26835
An introduction to wavelet transforms
[AD-A289083] p 2256 N95-28095
Bearing defect signature analysis using advanced nonlinear signal analysis in a controlled environment
[NASA-TM-108491] p 2304 N95-28364
SIGNAL ANALYZERS
Multipurpose bus interface utilizing a digital signal processor
[AD-D017264] p 2248 N95-26505
An introduction to wavelet transforms
[AD-A289083] p 2256 N95-28095
Low-power, parallel photonic interccnnections for Multi-Chip Module applications
[DE95-008518] p 2267 N95-28147
SIGNAL DETECTION
Research and development report. Digital audio broadcasting: Comparison of coverage at Band 2 and Band 3
[BBC-RD-1994/16] p 2248 N95-26493
Target detection for vision systems
[AD-D017271] p 2249 N95-26509
Analysis of group performance in visual signal detection
[AD-A289561] p 2355 N95-26683
Nonlinear signal processing schemes for robust target detection in radar
[AD-A288449] p 2255 N95-27185
The concentration-estimation problem for multiple-wavelength differential absorption lidar
[DE95-008375] p 2256 N95-28231
SIGNAL ENCODING
An experimental version of the MZT (speech-from-text) system with external F(sub 0) control
[IFTR-14/1994] p 2250 N95-26836
An introduction to wavelet transforms
[AD-A289083] p 2256 N95-28095
SIGNAL PROCESSING
Balanced data focusing: Direction of arrival estimation with maximum likelihood performance
[AD-A288252] p 2248 N95-26407
Joint Services Electronics Program (JSEP)
[AD-A288299] p 2345 N95-26419
Ultrasonic test system
[AD-D017261] p 2400 N95-26502
Multipurpose bus interface utilizing a digital signal processor
[AD-D017264] p 2248 N95-26505
Target detection for vision systems
[AD-D017271] p 2249 N95-26509
Evaluation of the FMICW waveform in HF surface radar applications
[AD-A288245] p 2249 N95-26545
Design tool for multiprocessor scheduling and evaluation of iterative dataflow algorithms
[NASA-TP-3491] p 2366 N95-26685
Signals processing using acousto-optical technology
[AD-A289597] p 2250 N95-26717
Enhanced visual user interface support for domain-oriented application composition systems
[AD-A289337] p 2359 N95-26737
The ambiguity function of the stepped frequency radar
[AD-A289533] p 2251 N95-26871
Multipoint multirate signal processing
[AD-A289211] p 2253 N95-26988
Voice analysis using the bispectrum
[AD-A289204] p 2254 N95-27008
Head related transfer function approximation using neural networks
[AD-A289422] p 2382 N95-27145
JPRS report: Science and technology. Central Eurasia
[JPRS-UST-95-016] p 2262 N95-27170
Nonlinear signal processing schemes for robust target detection in radar
[AD-A288449] p 2255 N95-27185
Classification of RF transients in space using digital signal processing and neural network techniques
[DE95-006287] p 2256 N95-27840
An introduction to wavelet transforms
[AD-A289083] p 2256 N95-28095
Long-range eye tracking: A feasibility study
[DE95-008587] p 2357 N95-28176
Full complex modulation using two one-parameter spatial light modulators
[NASA-CASE-MSC-22255-1] p 2427 N95-28384
Method and apparatus for maintaining linearity and frequency accuracy of an FM chirp waveform
[AD-D017398] p 2258 N95-28615
Manikin integrated data acquisition system (MIDAS) initial modifications
[AD-A291662] p 2361 N95-28667
SIGNAL TO NOISE RATIOS
Balanced data focusing: Direction of arrival estimation with maximum likelihood performance
[AD-A288252] p 2248 N95-26407
Performance modeling of hyperspectral imaging sensors for atmospheric studies
[AD-A289017] p 2289 N95-26461
Signals processing using acousto-optical technology
[AD-A289597] p 2250 N95-26717
Frame selection performance limits for statistical image reconstruction of adaptive optics compensated images
[AD-A289240] p 2424 N95-26965
SIGNAL TRANSMISSION
Self-excited oscillations in a duct with closed brances
[IFTR-18/1994] p 2400 N95-26358
Research and development report. Digital audio broadcasting: Comparison of coverage at Band 2 and Band 3
[BBC-RD-1994/16] p 2248 N95-26493
Signals processing using acousto-optical technology
[AD-A289597] p 2250 N95-26717
The automatic extraction of selected speech spectral characteristics
[IFTR-2/1994] p 2250 N95-26835
Simulating a multi-target acoustic array on the Intel Paragon
[AD-A288443] p 2377 N95-27183
SIGNATURE ANALYSIS
Bearing defect signature analysis using advanced nonlinear signal analysis in a controlled environment
[NASA-TM-108491] p 2304 N95-28364
SIGNATURES
Unification of LARCH and Z-based object models to support algebraically-based design refinement: The Z perspective
[AD-A289234] p 2369 N95-26962
SIGNS AND SYMPTOMS
Diagnostic antigens of Leishmania
[AD-A288805] p 2350 N95-27097
SIKORSKY AIRCRAFT
Report to Congressional Committees. Comanche Helicopter: Testing needs to be completed prior to production decisions
[GAO/NSIAD-95-112] p 2135 N95-27910
Tie-down trials involving a Sikorsky S-70B-2 helicopter
[DSTO-TR-0132] p 2136 N95-28567
SILICA GEL
The minimum pore size obtainable in a silica gel during drying
[DE95-008162] p 2239 N95-28401

SILICA GLASS
Characteristics of thermal lens in a copper-vapor laser
[AD-A289545] p 2294 N95-26874
Effects of long term space environment exposure on optical substrates and coatings p 2428 N95-27653
SILICATES
Silicate gel dye laser
[AD-D017262] p 2294 N95-26503
Investigation on technology for increasing the biological CO2 sink and technology for CO2 fixation and reutilization
[DE95-759251] p 2329 N95-27941
The structure of lead-indium phosphate glass
[DE95-007130] p 2237 N95-27967
SILICON
Surface chemistry of silicon
[AD-A288893] p 2224 N95-26351
Silicon based microactuators for telerobotic tactile stimulation
[AD-A289340] p 2260 N95-26767
Boron-induced morphology changes in silicon CVD growth: A scanning tunneling microscopy study
[AD-A289275] p 2290 N95-26982
Surface damage effects generated by a fast-pulse laser beam
[AD-A289131] p 2295 N95-26996
Atomic structure and bonding of boron-induced reconstructions on Si(001)
[AD-A289187] p 2405 N95-27017
Atomically resolved STM study of the adsorption and dissociation of methyl chloride on Si(001)
[AD-A289218] p 2438 N95-27061
Monolithic electronics for nuclear and high-energy physics experiments
[DE95-005393] p 2420 N95-27427
Numerical methods for determining interstitial oxygen in silicon
[DE95-007710] p 2205 N95-27683
Silicon subsystem mechanical engineering closeout report for the Solenoidal Detector Collaboration
[DE95-006336] p 2421 N95-27735
FTIR studies of CH3OH on porous silicon
[AD-A289038] p 2207 N95-27904
Analysis of the dimerized Sb/Si(001)-(2x1) surface by x-ray standing waves
[DE95-007097] p 2208 N95-27965
Effects of interlayers on the scratch adhesion performance of ultra-thin films of copper and gold on silicon substrates
[DE95-007367] p 2220 N95-28044
Cavity formation and impurity gettering in He-implanted Si
[DE95-007744] p 2444 N95-28127
Chemical and electrical properties of cavities in silicon and germanium
[DE95-006812] p 2445 N95-28206
Comparison of bridged polysilsesquioxane xerogels prepared from methoxy- and ethoxy-silyl monomers
[DE95-005422] p 2240 N95-28532
Leak detection utilizing analog binaural (VLSI) techniques
[NASA-CASE-NPO-18399-1-CU] p 2271 N95-28599
SILICON ALLOYS
Electrolyte effects in Li(Si)/FeS2 thermal batteries
[DE95-001614] p 2264 N95-27474
SILICON CARBIDES
Pseudomorphic semiconducting heterostructures from combinations of AlN, GaN and selected SiC polytypes: Theoretical advancement and its coordination with experimental studies of nucleation, growth, characterization and device development
[AD-A289550] p 2437 N95-26756
Materials Research Society Symposium Proceedings. Volume 339: Diamond, SiC and nitride wide bandgap semiconductors
[AD-A288690] p 2437 N95-26818
Characterization of fatigue behavior of 2-D woven fabric reinforced ceramic matrix composite at elevated temperature
[AD-A289423] p 2181 N95-26886
Photoluminescence spectroscopy of 4H- and 6H-SiC
[AD-A289326] p 2202 N95-26896
A study of internal damage of metal matrix composites by neutron diffraction
[DE95-005157] p 2182 N95-27080
Temperature dependence of ion-beam-induced amorphization in (Beta)-SiC
[DE95-007164] p 2438 N95-27087
Fatigue behavior of a cross-ply ceramic matrix composite subjected to tension-tension cycling with hold time
[AD-A289418] p 2182 N95-27134
Analytical and experimental evaluation of joining silicon carbide to silicon carbide and silicon nitride to silicon nitride for advanced heat engine applications, phase 2
[DE95-005761] p 2303 N95-27947
Thermal shock behavior of fiber-reinforced composites
[DE95-006746] p 2183 N95-27955
Effects of high-temperature environments on flaw generation and fracture behavior of SiC/SiC composites
[DE95-008270] p 2183 N95-28068
High-temperature deformation of ZrO2-Al2O3/SiC whisker composites fabricated by two techniques
[DE95-008273] p 2183 N95-28069
High temperature Hexoloy(trademark) SX silicon carbide
[DE95-007290] p 2221 N95-28075
Low temperature deposition and characterization of N- and P-type silicon carbide thin films and associated Ohmic and Schottky contacts
[AD-A289107] p 2237 N95-28097
Composite flexible insulation for thermal protection of space vehicles p 2166 N95-28293
SILICON COMPOUNDS
Boron-carbon-silicon polymers and the ceramic thereof
[NASA-CASE-ARC-11891-1-SB] p 2238 N95-28212
SILICON DIOXIDE
Applications of Second Harmonic and Sum Frequency Generation to graphite and silica type interfaces
[AD-A288228] p 2201 N95-26544
Ambient-pressure silica aerogel films
[DE95-008161] p 2237 N95-28090
Atomic layer epitaxy of group 4 materials: Surface processes, thin films, devices and their characterization
[AD-A289092] p 2446 N95-28327
Characterization of a fused silica capacitance standard
[DE95-006457] p 2270 N95-28597
SILICON FILMS
Growth of hydrogenated amorphous silicon (a-Si:H) on patterned substrates for increased mechanical stability
[DE95-006589] p 2234 N95-27472
SILICON JUNCTIONS
Low noise monolithic Si JFETS for operation in the 90-300K range and in high radiation environments
[DE95-007303] p 2269 N95-28244
SILICON NITRIDES
Analytical and experimental evaluation of joining silicon carbide to silicon carbide and silicon nitride to silicon nitride for advanced heat engine applications, phase 2
[DE95-005761] p 2303 N95-27947
Solid state sintering of silicon nitride ARL-CR-114
[DE95-007291] p 2443 N95-28076
SILICON OXIDES
Characterization of collision cascade damage in Ca2La8(SiO4)6O2 by HRTEM
[DE95-005719] p 2440 N95-27491
Surface crystallization and thin film melting in normal alkanes
[DE95-006694] p 2440 N95-27535
SILICON POLYMERS
Low temperature materials growth and processing development for flat panel display technology applications
[AD-A288970] p 2233 N95-27187
Recent progress in the Photovoltaic Manufacturing Technology Project (PVMaT)
[DE95-000279] p 2320 N95-27704
OBIC analysis of stressed, thermally-isolated polysilicon resistors
[DE95-008511] p 2268 N95-28201
SILICON RADIATION DETECTORS
Amorphous silicon pixel radiation detectors and associated thin film transistor electronics readout
[DE95-006568] p 2265 N95-27678
SILICON TRANSISTORS
Low temperature materials growth and processing development for flat panel display technology applications
[AD-A288970] p 2233 N95-27187
SILICONE RUBBER
Design and development of experimental facilities for short duration, low-gravity combustion and fire experiments
[NASA-CR-195458] p 2244 N95-26709
Analysis of selected specimens from the STS-46 Energetic Oxygen Interaction with Materials-3 experiment p 2210 N95-27642
SILICONES
Effects of atomic oxygen on polymeric materials flown on EOIM-3 p 2242 N95-27638
Hardware cleanliness methodology and certification
p 2211 N95-27656
Task 4 supporting technology. Part 1: Detailed test plan for leading edge tile development. Leading edge material development and testing
[NASA-CR-198633] p 2160 N95-28258
Silicone joint sealants for pavements
[AD-A289843] p 2241 N95-28620
SILOXANES
Siloxane-based ferroelectric liquid crystal elastomers and Self-Assembled Mono- and multilayers
[AD-A288285] p 2224 N95-26456
A summary of ODS replacement technologies at Litton Poly-Scientific p 2228 N95-27105
SILVER
Atomic oxygen dosimetry measurements made on STS-46 by CONCAP 2 p 2418 N95-27634
SILVER ALLOYS
Electronic structure of disordered Cu-Ag alloys
[DE95-609156] p 2219 N95-27758
SILVER COMPOUNDS
Growth and evaluation of nonlinear optical crystals for laser applications: Lithium borate, barium borate and silver gallium selenide
[AD-A289147] p 2277 N95-27000
SIMPLIFICATION
Efficient analytic computation of higher-order QCD amplitudes
[DE95-008593] p 2449 N95-28160
SIMULATED ANNEALING
Weighting scheme for the space surveillance network automated tasker
[AD-A289285] p 2146 N95-27035
Simulating the production of free defects in irradiated metals
[DE95-007165] p 2214 N95-27088
Automated integration of genomic physical mapping data via parallel simulated annealing
[DE95-008057] p 2351 N95-27725
SIMULATION
Balanced data focusing: Direction of arrival estimation with maximum likelihood performance
[AD-A288252] p 2248 N95-26407
Performance modeling of hyperspectral imaging sensors for atmospheric studies
[AD-A289017] p 2289 N95-26461
Statistical model for molecular internal energy exchange in DSMC method for rarefied flow analysis
[ISAS-R-654] p 2274 N95-26741
Image perception wavelet simulation and enhancement for the visually impaired
[AD-A289303] p 2353 N95-26917
MHD simulations of DC helicity injection for current drive in tokamaks
[DE95-007018] p 2429 N95-26940
The near-wake flow behavior of an oscillating airfoil with modified trailing edge p 2119 N95-26953
Advanced formation flight control
[AD-A289271] p 2142 N95-26981
Study of the response of a three-dimensional coupled ice-ocean model to daily varying atmospheric forcing
[AD-A289050] p 2347 N95-27189
Deployment and retraction of a cable-driven solar array: Testing and simulation p 2158 N95-27283
A new shared-memory programming paradigm for molecular dynamics simulations on the Intel Paragon
[DE95-007289] p 2378 N95-28019
A hybrid vehicle evaluation code and its application to vehicle design. Revision 1
[DE95-008053] p 2303 N95-28029
A hybrid vehicle evaluation code and its application to vehicle design, revision 2
[DE95-008060] p 2303 N95-28139
Developments in the electron gun simulation program, EGUN
[DE95-008137] p 2267 N95-28143
Monte-Carlo simulation methods for finite flat plate winding flows
[AD-A289842] p 2289 N95-28619
SIMULATORS
Construction of a connectionist network supercomputer
[AD-A288439] p 2377 N95-27182
Simulator report for SCI systems with HIC-router
[PB95-196580] p 2379 N95-28093
SIMULTANEOUS EQUATIONS
An easy way to analyze longitudinal and lateral-directional trim problems with AEO or OEI
p 2119 N95-26949
SINE WAVES
The effects of transverse vibration on the performance of an axial groove wick heat pipe
[AD-A289349] p 2278 N95-27065
SINGLE CRYSTALS
Surface chemistry of silicon
[AD-A288893] p 2224 N95-26351
Pseudomorphic semiconducting heterostructures from combinations of AlN, GaN and selected SiC polytypes: Theoretical advancement and its coordination with experimental studies of nucleation, growth, characterization and device development
[AD-A289550] p 2437 N95-26756

Materials Research Society Symposium Proceedings. Volume 339: Diamond, SiC and nitride wide bandgap semiconductors
[AD-A288690] p 2437 N95-26818
JPRS report: Science and technology. Central Eurasia
[JPRS-UST-95-021] p 2202 N95-27155
Growth, characterization and device development in monocrystalline diamond films
[AD-A289356] p 2439 N95-27416
Micromagnetics and microstructure of epitaxially grown Co and Co-Cr films for perpendicular magnetic recording
[DE95-004681] p 2441 N95-27720
Magnetic structures in RNi2B2C (R = Ho, Er) superconductors
[DE95-008370] p 2442 N95-27932
Low temperature carrier transport properties in isotopically controlled germanium
[DE95-008489] p 2444 N95-28092
Low temperature deposition and characterization of N- and P-type silicon carbide thin films and associated Ohmic and Schottky contacts
[AD-A289107] p 2237 N95-28097
The role of hydrogen in the hydrogenation and hydrogenolysis of aniline on the nickel single crystal surfaces: Its implication on the mechanisms of HDN reactions
[DE95-006687] p 2222 N95-28134
Precursor phenomenon of martensitic transformation in Au-49.5at%Cd alloy
[DE95-007698] p 2222 N95-28166
The high strain rate deformation of tungsten single crystals
[AD-A288874] p 2223 N95-28189
Femtosecond OPO's at 3 microns and beyond: Design and performance issues related to the crystal properties of KTP and similar materials
[DE95-007286] p 2446 N95-28242
Atomic layer epitaxy of group 4 materials: Surface processes, thin films, devices and their characterization
[AD-A289092] p 2446 N95-28327
Future opportunities and present possibilities for coherent inelastic single crystal measurements on pulsed neutron sources
[PB95-195798] p 2418 N95-28657

SINGLE STAGE TO ORBIT VEHICLES
Reusable launch vehicle development research
[NASA-CR-198614] p 2154 N95-27245

SINGULARITY (MATHEMATICS)
On higher derivative gravity in two dimensions
[DE95-608789] p 2462 N95-27343
Crushing singularities in spacetimes with spherical, plane and hyperbolic symmetry
[PB95-190146] p 2397 N95-28011
Normal modes and continuous spectra
[DE95-006166] p 2287 N95-28055
Efficient analytic computation of higher-order QCD amplitudes
[DE95-008593] p 2449 N95-28160

SINTERING
Ultra high purity, dimensionally stable INVAR 36
[NASA-CASE-NPO-19358-1-CU] p 2213 N95-26862
Crystal structure, short-range oxygen defects, and water adsorption in La- and Nd-modified ZrO2
[DE95-007134] p 2439 N95-27452
Sintering of textured YBa2Cu3O(7-x) under intensive Co-60 gamma irradiation
[DE95-007098] p 2442 N95-27950
Manufacturing tailored property ceramic composites
[DE95-006303] p 2237 N95-27993
High temperature Hexoloy(trademark) SX silicon carbide
[DE95-007290] p 2221 N95-28075
Solid state sintering of silicon nitride ARL-CR-114
[DE95-007291] p 2443 N95-28076
Solid-state sintering of tungsten heavy alloys
[DE95-007749] p 2222 N95-28130

SIZE (DIMENSIONS)
Using the dimension reduction technique to prove that clique trees define facets for the asymmetric traveling salesman polytope
[AD-A289397] p 2389 N95-26882
Reducing network depth in the Cascade-Correlation learning architecture
[AD-A289352] p 2382 N95-27066

SIZE DISTRIBUTION
Characterization of Ultra-Low Carbon Baintic steels for use as weld wire consumables
[AD-A288292] p 2212 N95-26411
Computation of electromagnetic scattering parameters for lognormal distributions of magnetic spheres: Theory and algorithms
[AD-A289672] p 2250 N95-26759
Performance of a stand-alone wind-electric ice maker for remote villages
[DE95-004006] p 2320 N95-27475

SKEWNESS
A method for generating skewed random numbers using two overlapping uniform distributions
[DE95-008747] p 2392 N95-28162

SKIN (STRUCTURAL MEMBER)
On aircraft repair verification of a fighter A/C integrally stiffened fuselage skin p 2133 N95-27515

SKY BRIGHTNESS
A mathematical analysis of the Janus combat simulation weather effects models and sensitivity analysis of sky-to-ground brightness ratio on target detection
[AD-A289629] p 2336 N95-26858

SLABS
On-axis polarization coupling in y-cut titanium in-diffused lithium niobate slab waveguides
[AD-A289260] p 2253 N95-26977
Error analysis of the quartic nodal expansion method for slab geometry
[DE95-007373] p 2412 N95-28045

SLEEVES
Design and development of a test rig for the high frequency testing of rolling sleeve airsprings
[DSTO-TN-0001] p 2142 N95-26378

SLIDING
Prediction of fatigue crack growth under constant amplitude and random loading using specimens with multiple cracks
[AD-A291614] p 2136 N95-28409

SLOPES
Natural aerosol extinction module: XSCALE 1992 user's guide
[AD-A289029] p 2340 N95-26463
Synthetic 3-D atmospheric temperature structure: A model for known geophysical power spectra using a hybrid autoregression and Fourier technique
[AD-A289058] p 2340 N95-26479

SLOT ANTENNAS
Linearly tapered slot antenna impedance characteristics
[NASA-TM-106912] p 2266 N95-27853
Theoretical and experimental study of low-loss, High-efficiency monolithic antenna structures at 94 GHz
[AD-A291785] p 2257 N95-28513

SLOTS
Computational analysis of forebody tangential slot blowing on the high alpha research vehicle
[NASA-CR-197754] p 2129 N95-26591

SLUDGE
Application of bacterial bioemusifiers to in situ maintenance of oil/water separators
p 2179 N95-27120
Destruction of pyrotechnics manufacture wastewater treatment sludge by plasma arc pyrolysis
p 2171 N95-28301

SMART STRUCTURES
SMART materials: Surfaces, transforms and interfaces. The commensurate engineering dimension
[AD-A289598] p 2312 N95-28649

SMOG
Engineering photochemical smog through convection towers
[DE95-007727] p 2328 N95-27686

SMOKE
Proceedings of the 1993 Scientific Conference on Obscuration and Aerosol Research
[AD-A280084] p 2331 N95-28153

SMOOTHING
Nonlinear scalespace via hierarchical statistical modeling
[AD-A289057] p 2394 N95-26478
Denoising and robust non-linear wavelet analysis
[AD-A291668] p 2257 N95-28455

SNOW
Radiometer measurements of snow in Sodankylae, 1991-1993
[PB95-184966] p 2313 N95-26645

SNOW COVER
Subsurface radar investigations at the Pegasus Glacial-ice Runway and Williams Field, McMurdo Station, Antarctica
[AD-A289323] p 2144 N95-27297
Modeling and retrieval of snow and sea ice characteristics in the frequency range 6 to 90 GHz
[PB95-195467] p 2316 N95-28656

SODIUM
Ash-based ceramic materials
[AD-D017272] p 2241 N95-28582

SODIUM CHLORIDES
Electrical conductivity measurements of aqueous electrolyte solutions at high temperatures and high pressures
[DE95-006748] p 2208 N95-27956

SODIUM HYDROXIDES
Electrical conductivity measurements of aqueous electrolyte solutions at high temperatures and high pressures
[DE95-006748] p 2208 N95-27956

SOFIA (AIRBORNE OBSERVATORY)
Numerical simulation of the SOFIA flow field
[NASA-CR-197757] p 2274 N95-26589

SOFTENING
Precursor phenomenon of martensitic transformation in Au-49.5at%Cd alloy
[DE95-007698] p 2222 N95-28166

SOFTWARE DEVELOPMENT TOOLS
An evaluation of the Software Through Pictures/T Tool (StP/T) for the Software Support Activity (SSA)
[AD-A288822] p 2362 N95-26348
Software risk management through independent verification and validation
[NASA-CR-197767] p 2364 N95-26486
Long term distributed file reference tracing: Implementation and experience
[AD-A288585] p 2452 N95-26535
Intelligent computer based reliability assessment of multichip modules
[AD-A288833] p 2259 N95-26550
A software bus for thread objects
[NASA-CR-197764] p 2365 N95-26575
Automatic test data generation tool for large-scale software systems
[AD-A289081] p 2365 N95-26611
Design tool for multiprocessor scheduling and evaluation of iterative dataflow algorithms
[NASA-TP-3491] p 2366 N95-26685
Software packager user's guide
[NASA-CR-197763] p 2366 N95-26693
User-centric development. Version 01.00.04
[AD-A289363] p 2368 N95-26903
High performance hardware and software for pattern recognition and image processing
[AD-A289153] p 2370 N95-27031
Getting it right, making it better
[NONP-NASA-VT-95-49118] p 2451 N95-27206
STEP: A futurevision, today
[NONP-NASA-VT-95-49121] p 2451 N95-27209
Measuring fault tolerance with the FTAPE fault injection tool
[NASA-CR-197773] p 2306 N95-27253
Automated database design from natural language input p 2383 N95-27378
Determining GPS average performance metrics
p 2128 N95-27791
PC Software graphics tool for conceptual design of space/planetary electrical power systems
[NASA-TM-106908] p 2372 N95-27905
Calculation of design load for the MOD-5A 7.3 mW wind turbine system p 2312 N95-27982

SOFTWARE ENGINEERING
An evaluation of the Software Through Pictures/T Tool (StP/T) for the Software Support Activity (SSA)
[AD-A288822] p 2362 N95-26348
An introduction to software architecture
[AD-A288963] p 2363 N95-26446
An introduction to software architecture
[AD-A288356] p 2363 N95-26467
Application-aware adaptation for mobile computing
[AD-A288366] p 2363 N95-26469
Digital mapping, charting, and geodesy analysis program: Initial technical review of Raster Product Format
[AD-A289039] p 2313 N95-26476
Software risk management through independent verification and validation
[NASA-CR-197767] p 2364 N95-26486
Operating system support for coexistence of real-time and conventional scheduling
[AD-A288584] p 2364 N95-26534
Intelligent computer based reliability assessment of multichip modules
[AD-A288833] p 2259 N95-26550
Automatic test data generation tool for large-scale software systems
[AD-A289081] p 2365 N95-26611
Software packager user's guide
[NASA-CR-197763] p 2366 N95-26693
Using an architectural approach to integrate heterogeneous, distributed software components
[NASA-CR-197766] p 2366 N95-26711
Development and analysis of SCR requirements tables for system scenarios
[NASA-CR-197769] p 2367 N95-26802
A process improvement model for software verification and validation
[NASA-CR-197761] p 2367 N95-26814

Second International Conference on Software for Multiprocessors and Supercomputers Theory, Practice, Experience
[AD-A289474] p 2368 N95-26820
User-centric development. Version 01.00.04
[AD-A289363] p 2368 N95-26903
High performance hardware and software for pattern recognition and image processing
[AD-A289153] p 2370 N95-27031
Multiple model adaptive estimation and head motion tracking in a virtual environment: An engineering approach
[AD-A289299] p 2359 N95-27046
Design and implementation of a software communication architecture for the JANUS-3D Visualizer
[AD-A288509] p 2370 N95-27150
Development of numerical methods for overset grids with applications for the integrated Space Shuttle vehicle
[NASA-CR-197759] p 2160 N95-27154
Construction of a connectionist network supercomputer
[AD-A288439] p 2377 N95-27182
Getting it right, making it better
[NONP-NASA-VT-95-49118] p 2451 N95-27206
Computer Systems Division software system metrics approach
[AD-A288837] p 2370 N95-27210
Overview of megaprogramming course: Lectures and eexercises. Version 02.00.03
[AD-A286723] p 2370 N95-27235
A comparison of error categorization schemes for use in software system safety programs
[AD-A288741] p 2371 N95-27251
Human factors in aviation maintenance, phase 4
[DOT/FAA/AM-95/14] p 2360 N95-27696
Flight dynamics software in a distributed network environment p 2151 N95-27790
Contingency designs for attitude determination of TRMM p 2154 N95-27803
A NASTRAN-based computer program for structural dynamic analysis of Horizontal Axis Wind Turbines
p 2312 N95-27980
Control system design for the MOD-5A 7.3 mW wind turbine generator p 2306 N95-27985
Operator modeling in commerical aviation: Cognitive models, intelligent displays, and pilot's assistants
[NASA-CR-198609] p 2138 N95-28203
Three-dimensional forecast models for emergency response management p 2172 N95-28303
Upgrade of the computer modeling programs POLU10 and POLU13A for open burning and open detonation of energetic materials p 2172 N95-28306
Unmanned aerial vehicles, 1994 master plan
[AD-A291628] p 2136 N95-28411
A correlational study of the SEI's capability maturity model and software development performance in DOD contracts
[AD-A288890] p 2374 N95-28591
TRAINS: Dialogue transcription tools
[AD-A289869] p 2259 N95-28624
Software process improvement in the NASA software engineering laboratory
[AD-A289912] p 2374 N95-28627
Replacing the message service component in an integration framework
[AD-A289928] p 2375 N95-28628
Building an electronic book on the Internet. CSEP:An interdisciplinary syllabus for teaching computational science at the graduate level
[DE95-006526] p 2375 N95-28632
Software technology for adaptable, reliable systems (STARS). AdaWise user's manual
[AD-A289655] p 2375 N95-28635

SOFTWARE RELIABILITY
Computer Systems Division software system metrics approach
[AD-A288837] p 2370 N95-27210

SOFTWARE REUSE
A system dynamics based study of software reuse and its determinants
[AD-A288578] p 2364 N95-26554

SOIL MECHANICS
Soil moisture prediction during freeze and thaw using a coupled heat and moisture flow model
[AD-A289343] p 2336 N95-26753
The biodegradation of fuels in soils and sediments: Differences as a function of mineralogy
p 2230 N95-27116

SOIL MOISTURE
Soil moisture prediction during freeze and thaw using a coupled heat and moisture flow model
[AD-A289343] p 2336 N95-26753
Remote sensing of hydrologic variables in boreal areas, phase 2
[NASA-CR-198717] p 2314 N95-27998

SOILS
Soil moisture prediction during freeze and thaw using a coupled heat and moisture flow model
[AD-A289343] p 2336 N95-26753
Combined use of ground water circulation (UVB) technology and in situ bioreactors for enhanced bioremediation of subsurface contamination
p 2230 N95-27118
A practical approach to soil remediation
p 2232 N95-27125
The Alpha-Proton-X-ray Spectrometer deployment mechanism: An anthropomorphic approach to sensor placement on Martian rocks and soil
p 2155 N95-27265
Method for determining surface coverage by materials exhibiting different fluorescent properties
[NASA-CASE-GSC-13539-1] p 2315 N95-28211
Biodegradation of nitrate esters p 2171 N95-28299
Neural networks in the classification of uses of the soil in satellite images
[INPE-5478-PRE/1777] p 2316 N95-28672

SOL-GEL PROCESSES
Control of thin film processing behavior through precursor structural modifications
[DE95-006468] p 2444 N95-28103
Vacancy related defects in thin film Pb(Zr,Ti)O3 materials
[DE95-007696] p 2445 N95-28165
New developments for sol-gel film and fiber processing
[DE95-008175] p 2240 N95-28404
Porosity in hexylene-bridged polysilsesquioxanes: Effects of monomer concentration
[DE95-005421] p 2240 N95-28531
Comparison of bridged polysilsesquioxane xerogels prepared from methoxy- and ethoxy-silyl monomers
[DE95-005422] p 2240 N95-28532
Coatings of non-oxide ceramics for improved corrosion resistance in high temperature coal combustion
[DE95-006932] p 2241 N95-28604

SOLAR ACTIVITY
Coronal abundances and their variation
[NASA-CR-197788] p 2464 N95-26671
Variability study of foF2 for an equatorial station
[DE95-608080] p 2337 N95-27157
Solar-geophysical data number 604, December 1994. Part 1: (Prompt reports). Data for November, October 1994, and late data
[PB95-181848] p 2465 N95-28087

SOLAR ARRAYS
Alternate charging profiles for the onboard nickel cadmium batteries of the Explorer Platform/Extreme Ultraviolet Explorer p 2272 N95-26796
Development of welded solar arrays for DMSP and GPS satellites
[AD-A289512] p 2318 N95-26846
Solar array deployment mechanism
p 2155 N95-27266
Deployment and retraction of a cable-driven solar array: Testing and simulation p 2158 N95-27283
Development of the solar array deployment and drive system for the XTE spacecraft p 2158 N95-27284
Space environmental effect on solar cells: LDEF and other flight tests p 2326 N95-27649
A simple method for verifying the deployment of the TOMS-EP solar arrays p 2150 N95-27782
Direct drive options for electric propulsion systems
[NASA-TM-106576] p 2168 N95-27861
The solar array-induced disturbance of the Hubble Space Telescope pointing system
[NASA-TP-3556] p 2311 N95-28214

SOLAR BACKSCATTER UV SPECTROMETER
Solar UV flux measurements from the SBUV2 monitor on the NOAA9 satellite. Part 1: Mg II h and k line core-to-wing ratios for 1986-1988
[PB95-181962] p 2464 N95-28007

SOLAR CELLS
Annealing of radiation damaged gallium arsenide solar cells by laser illumination
[AD-A289683] p 2316 N95-26762
A state-space model of a large, lightly damped space structure using the Eigensystem realization algorithm
[AD-A289251] p 2163 N95-26970
Heat pipe cooled reactors for multi-kilowatt space power supplies
[DE95-005211] p 2420 N95-27425
Space environmental effect on solar cells: LDEF and other flight tests p 2326 N95-27649
Health and environmental hazards of CdTe photovoltaic module production, use and decommissioning
[DE95-006688] p 2320 N95-27682
Recent progress in the Photovoltaic Manufacturing Technology Project (PVMaT)
[DE95-000279] p 2320 N95-27704

SOLAR COLLECTORS
Solar concentrator technology development for space based applications, volume 1
[NASA-CR-197723] p 2319 N95-27193
Solar concentrator technology development for space based applications, volume 2
[NASA-CR-197724] p 2319 N95-27194
Analysis of solar receiver flux distributions for US/Russian solar dynamic system demonstration on the MIR Space Station
[NASA-TM-106933] p 2169 N95-28036

SOLAR CORONA
Coronal abundances and their variation
[NASA-CR-197788] p 2464 N95-26671
Plasma properties and magnetic field structure of the solar corona, based on coordinated Max 1991 observations from SERTS, the VLA, and magnetographs
[NASA-CR-198592] p 2464 N95-27858

SOLAR CYCLES
Relativistic electrons in the outer-zone: An 11 year cycle, their relation to the solar wind
[DE95-007882] p 2338 N95-28061

SOLAR DYNAMIC POWER SYSTEMS
Analysis of shadowing effects on MIR photovoltaic and solar dynamic power systems
[NASA-TM-106940] p 2169 N95-28213

SOLAR ELECTRIC PROPULSION
Solar concentrator technology development for space based applications, volume 1
[NASA-CR-197723] p 2319 N95-27193
Solar concentrator technology development for space based applications, volume 2
[NASA-CR-197724] p 2319 N95-27194
Electric propulsion for geostationary orbit insertion
[NASA-TM-106942] p 2168 N95-27727

SOLAR ENERGY
Axionic fuel for sun
[DE95-608788] p 2464 N95-27342

SOLAR ENERGY CONVERSION
Investigation on technology for increasing the biological CO2 sink and technology for CO2 fixation and reutilization
[DE95-759251] p 2329 N95-27941

SOLAR FLUX
Solar UV flux measurements from the SBUV2 monitor on the NOAA9 satellite. Part 1: Mg II h and k line core-to-wing ratios for 1986-1988
[PB95-181962] p 2464 N95-28007
Analysis of solar receiver flux distributions for US/Russian solar dynamic system demonstration on the MIR Space Station
[NASA-TM-106933] p 2169 N95-28036
Solar-geophysical data number 604, December 1994. Part 1: (Prompt reports). Data for November, October 1994, and late data
[PB95-181848] p 2465 N95-28087

SOLAR GENERATORS
Heat pipe cooled reactors for multi-kilowatt space power supplies
[DE95-005211] p 2420 N95-27425
PC Software graphics tool for conceptual design of space/planetary electrical power systems
[NASA-TM-106908] p 2372 N95-27905

SOLAR HEATING
A study of surface temperatures, clouds and net radiation
[NASA-CR-198589] p 2329 N95-27864

SOLAR INSTRUMENTS
Notes on the calibration of the JHU-APL solar vector magnetograph at NSO-Sec peak
[AD-A289277] p 2253 N95-26983

SOLAR MAGNETIC FIELD
Plasma properties and magnetic field structure of the solar corona, based on coordinated Max 1991 observations from SERTS, the VLA, and magnetographs
[NASA-CR-198592] p 2464 N95-27858

SOLAR NEUTRINOS
Detection of charged particles in superfluid helium
[DE95-007354] p 2403 N95-26560
Threefold maximal lepton mixing and the solar and atmospheric neutrino deficits
[PB95-196259] p 2465 N95-28500

SOLAR PHYSICS
Coronal abundances and their variation
[NASA-CR-197788] p 2464 N95-26671
Solar-geophysical data number 604, December 1994. Part 1: (Prompt reports). Data for November, October 1994, and late data
[PB95-181848] p 2465 N95-28087

SOLAR RADIATION
Solar terrestrial radiation data from the Sleepers River Research Watershed
[AD-A288444] p 2464 N95-27184
Analysis of selected specimens from the STS-46 Energetic Oxygen Interaction with Materials-3 experiment p 2210 N95-27642

Calculations of downward IR surface fluxes in the 500-3,000 cm(exp -1) wavenumber range for the 1994 ICRCCM model intercomparison study
[DE95-006430] p 2328 N95-27708

A study of surface temperatures, clouds and net radiation
[NASA-CR-198589] p 2329 N95-27864

Carbonaceous aerosols influencing atmospheric radiation: Black and organic carbon
[DE95-006437] p 2330 N95-28118

Anomalous cloud absorption? A critique of the paper entitled Absorption of Solar Radiation by Clouds: Observations Versus Models
[DE95-007703] p 2331 N95-28121

SOLAR SENSORS

Development of a Robust star identification technique for use in attitude determination of the ACE spacecraft
p 2149 N95-27777

SOLAR SYSTEM

Space modeler: An expanded, distributed, virtual environment for space visualization
[AD-A289409] p 2461 N95-27131

Views of the solar system
[DE95-006446] p 2461 N95-27326

TOPS: Toward Other Planetary Systems. A report by the solar system exploration division
[NASA-TM-110609] p 2464 N95-28009

SOLAR THERMAL PROPULSION

Solar concentrator technology development for space based applications, volume 1
[NASA-CR-197723] p 2319 N95-27193

Solar concentrator technology development for space based applications, volume 2
[NASA-CR-197724] p 2319 N95-27194

SOLAR WIND

Plasma properties and magnetic field structure of the solar corona, based on coordinated Max 1991 observations from SERTS, the VLA, and magnetographs
[NASA-CR-198592] p 2464 N95-27858

SOLAR X-RAYS

SXI Prototype mirror mount
[NASA-CR-196613] p 2301 N95-27244

The Solar X-ray Imager Vacuum Door Assembly
p 2157 N95-27280

SOLDERED JOINTS

Development of welded solar arrays for DMSP and GPS satellites
[AD-A289512] p 2318 N95-26846

A microstructurally based model of solder joints under conditions of thermomechanical fatigue
[DE95-006226] p 2309 N95-27837

SOLDERS

A microstructurally based model of solder joints under conditions of thermomechanical fatigue
[DE95-006226] p 2309 N95-27837

SOLENOIDS

The consideration of a bright relative beam dynamics in the magnetic focusing field
[DE95-608377] p 2398 N95-27160

SOLID ELECTROLYTES

Current status of environmental, health, and safety issues of lithium polymer electric vehicle batteries
[DE95-004005] p 2265 N95-27719

SOLID LUBRICANTS

Advanced solid lubricant films by Ion-Beam Assisted Deposition
[AD-A288866] p 2225 N95-26499

Solid film lubricants and thermal control coatings flown aboard the EOIM-3 MDA sub-experiment
p 2242 N95-27640

Analysis of selected specimens from the STS-46 Energetic Oxygen Interaction with Materials-3 experiment p 2210 N95-27642

SOLID PHASES

Rotor phases in compound semiconductors
[DE95-004139] p 2436 N95-26442

SOLID PROPELLANT ROCKET ENGINES

Hazards analysis of an integral class 1.1/1.3 rocket motor demilitarization and ingredient recovery system using ammonia p 2174 N95-28315

SOLID ROCKET PROPELLANTS

Chemical reactions identified in the Titan 2, Titan 4, and Delta 2 propellant systems and their application to source modeling p 2172 N95-28304

Hazards analysis of an integral class 1.1/1.3 rocket motor demilitarization and ingredient recovery system using ammonia p 2174 N95-28315

Commercial reformulation: An economic and environmentally neutral means of managing explosives and solid propellants p 2175 N95-28320

Alternate use of rocket propellants as ingredients in commercial watergel explosives p 2176 N95-28321

Cryogenic washout of solid rocket propellants
p 2176 N95-28324

Hydrothermal oxidation of solid rocket propellant and other department of defense hazardous wastes
p 2177 N95-28325

SOLID SOLUTIONS

Pseudomorphic semiconducting heterostructures from combinations of AlN, GaN and selected SiC polytypes: Theoretical advancement and its coordination with experimental studies of nucleation, growth, characterization and device development
[AD-A289550] p 2437 N95-26756

Survey of environmentally benign cleaning methodologies and materials p 2231 N95-27122

Engineered materials for appliation in severe metallurgical environments: Tantalum-carbon alloy development
[DE95-006838] p 2216 N95-27488

Synthesis and properties of lanthanide-exchanged Preyssler's heteropolyanions
[DE95-007136] p 2238 N95-28235

SOLID STATE

Technical progress report to the Department of Energy on the Solid State Sciences Committee (SSSC)
[DE95-007113] p 2441 N95-27925

Solid state sintering of silicon nitride ARL-CR-114
[DE95-007291] p 2443 N95-28076

Solid-state sintering of tungsten heavy alloys
[DE95-007749] p 2222 N95-28130

Research activities of the Solid State Sciences Committee in the development of a Federal initiative on advanced materials and processing
[DE95-009328] p 2445 N95-28179

SOLID STATE DEVICES

Solid-state image sensor with focal-plane digital photon-counting pixel array
[NASA-CASE-NPO-18518-1-CU] p 2424 N95-26894

Active antennas with periodic structures
[AD-A289437] p 2252 N95-26924

Quasi-optical millimeter wave power combining
[AD-A291767] p 2270 N95-28529

SOLID STATE LASERS

Silicate gel dye laser
[AD-D017262] p 2294 N95-26503

Characterization of solid state laser and nonlinear optical materials
[AD-A291684] p 2300 N95-28458

SOLID WASTES

The use of supercritical carbon dioxide for contaminant removal from solid waste p 2229 N95-27110

Marshall Space Flight Center solid waste characterization and recycling improvement study
[NASA-CR-196594] p 2360 N95-27164

Recovery, evaluation, and decontamination of landfilled pentaborane cylinders, former liquid propellant rocket engine test facility, Washoe County, Nevada
p 2171 N95-28302

Ash-based ceramic materials
[AD-D017272] p 2241 N95-28582

SOLID-SOLID INTERFACES

Photoemission study of solid state reaction and initial oxidation of the Ce/Al(100) system
[PB95-195368] p 2210 N95-28652

SOLIDS

Photoacoustic chambers for studying solids and gases: Theory and practical examples
[IFTR-39/1994] p 2143 N95-26837

High energy density systems in cryogenic media: The production and reactions of atoms and radicals
[AD-A289818] p 2417 N95-28572

SOLITARY WAVES

Nonlinear problems in fluid dynamics and inverse scattering: Nonlinear waves and inverse scattering
[AD-A289148] p 2278 N95-27001

Proceedings of the International Workshop on Acceleration and Radiation Generation in Space and Laboratory Plasmas
[AD-A291673] p 2436 N95-28668

SOLUBILITY

Junkyard chemistry p 2227 N95-27102

Observations on the solvating power of supercritical fluids p 2228 N95-27106

Precision parts cleaning with supercritical CO2: Practical applications and solutions p 2229 N95-27111

Fluid dynamic effects on precision cleaning with supercritical fluids p 2232 N95-27129

Absorption of sparingly soluble gases by reactive media in self-aerated gas-liquid contactors: A scale-up procedure
[DE95-006429] p 2206 N95-27707

SOLUTES

Bubble chamber spectroscopy for chemical analysis: A new concept
[DE95-006350] p 2209 N95-28088

SOLUTIONS

Automatically selecting and using primary effects in planning: Theory and experiments
[AD-A289347] p 2450 N95-27064

Apparatus for diffusion controlled dialysis under microgravity conditions
[NASA-CASE-MFS-28986-1] p 2245 N95-27500

SOLVATION

Observations on the solvating power of supercritical fluids p 2228 N95-27106

Ethyl lactate as a solvent alternative for cleaning metal parts p 2229 N95-27112

SOLVENT EXTRACTION

Determination of the first hydrolysis constant of Europium (3) in 3 M of ionic strength
[DE95-607912] p 2405 N95-27211

SOLVENTS

Environmentally Benign Cleaning and Degreasing Technology: JANNAF Safety and Protection Subcommittee and Propellant Development and Characterization Subcommittee Joint Workshop
[CPIA-PUBL-611] p 2227 N95-27101

Cleanliness verification process at Martin Marietta Astronautics p 2165 N95-27104

A summary of ODS replacement technologies at Litton Poly-Scientific p 2228 N95-27105

Wipe solvent substitutions for 1,1,1-trichloroethane (TCA) and methyl ethyl ketone (MEK) at Hill Air Force Base p 2228 N95-27107

Alternative cleaning solvents and lubricants at the Air Force PJKS facility p 2228 N95-27108

The use of supercritical carbon dioxide for contaminant removal from solid waste p 2229 N95-27110

Precision parts cleaning with supercritical CO2: Practical applications and solutions p 2229 N95-27111

Ethyl lactate as a solvent alternative for cleaning metal parts p 2229 N95-27112

Corrosive effects of supercritical carbon dioxide and cosolvents on metals p 2224 N95-27113

Precision parts cleaning with supercritical carbon dioxide p 2229 N95-27114

Evaluations of the effectiveness of environmentally benign cleaning methodologies p 2230 N95-27115

Aqueous degreasing, precision cleaning, and cleanliness verification p 2231 N95-27121

Design considerations in supercritical fluid technology
p 2232 N95-27126

Retrofitting conventional vapor degreasers to use a solvent wash/fluorochemical rinse process
p 2232 N95-27127

Fluid dynamic effects on precision cleaning with supercritical fluids p 2232 N95-27129

The application of waterjets for cleaning
p 2233 N95-27130

Variation of solvent scattering-length density small-angle neutron scattering as a means of determining structure of composite materials
[DE95-005394] p 2183 N95-27428

Magnetic resonance imaging of solvent transport in polymer networks
[DE95-007142] p 2234 N95-27455

Small angle x ray scattering studies of reverse micelles in supercritical fluids
[DE95-007803] p 2287 N95-28021

SOMMERFELD WAVES

Very low frequency seismo-acoustic noise below the sea floor (0.2-10 Hz)
[AD-A289164] p 2347 N95-27011

SONAR

Molecular modeling: An approach for the study of piezoelectric polymers
[AD-A289821] p 2241 N95-28574

SONIC BOOMS

Design and testing of low sonic boom configurations and an oblique all-wing supersonic transport
[NASA-CR-197744] p 2129 N95-26651

Supersonic civil airplane study and design: Performance and sonic boom
[NASA-CR-197745] p 2130 N95-26813

SOOT

Soot particle density determination from a laser extinction multipass technique
[AD-A288551] p 2423 N95-26532

SORPTION

An investigation of the applicability of the new Reillex(tm)-HPQ anion exchange resin system for technetium/rhenium and uranium in the Hanford waste tanks
[DE95-007643] p 2412 N95-28051

SORTING ALGORITHMS

A parallel complexity model for functional languages
[AD-A288589] p 2365 N95-26656

SOS (SEMICONDUCTORS)

Microwave characterization of sub-micron N- and P-channel MOSFET's fabricated with thin film silicon-on-sapphire
[AD-A289296] p 2438 N95-27040

SOUND DETECTING AND RANGING

Aircraft IR/acoustic detection evaluation. Volume 2: Development of a ground-based acoustic sensor system for the detection of subsonic jet-powered aircraft
[NASA-CR-189705-VOL-2] p 2402 N95-28073

SOUND FIELDS

Acoustic field in unsteady moving media
[NASA-CR-198162] p 2279 N95-27179

SOUND GENERATORS

Simulating a multi-target acoustic array on the Intel Paragon
[AD-A288443] p 2377 N95-27183

A numerical study of fundamental shock noise mechanisms
[NASA-TM-110608] p 2401 N95-27908

Molecular modeling: An approach for the study of piezoelectric polymers
[AD-A289821] p 2241 N95-28574

SOUND LOCALIZATION

Head related transfer function approximation using neural networks
[AD-A289422] p 2382 N95-27145

SOUND PRESSURE

Numerical simulation of the SOFIA flow field
[NASA-CR-197757] p 2274 N95-26589

Observed acoustic and aeroelastic spectral responses of a MOD-2 turbine blade to turbulence excitation
p 2324 N95-27991

Anechoic wind tunnel study of turbulence effects on wind turbine broadband noise p 2325 N95-27992

SOUND TRANSDUCERS

Aircraft IR/acoustic detection evaluation. Volume 2: Development of a ground-based acoustic sensor system for the detection of subsonic jet-powered aircraft
[NASA-CR-189705-VOL-2] p 2402 N95-28073

SOUND TRANSMISSION

An acoustic charge transport imager for high definition television applications
[NASA-CR-197841] p 2249 N95-26708

SOUND WAVES

Self-excited oscillations in a duct with closed brances
[IFTR-18/1994] p 2400 N95-26358

A finite element propagation model for extracting normal incidence impedance in nonprogressive acoustic wave fields
[NASA-TM-110160] p 2400 N95-26394

The use of acoustic methods to determine the parameters of porous materials
[IFTR-40/1994] p 2401 N95-26519

Evaluation of a new laboratory acoustic Doppler velocimeter
[AD-A289592] p 2290 N95-26714

Signals processing using acousto-optical technology
[AD-A289597] p 2250 N95-26717

The automatic extraction of selected speech spectral characteristics
[IFTR-2/1994] p 2250 N95-26835

Numerical analysis of wave scattering
[AD-A289478] p 2401 N95-26925

Head related transfer function approximation using neural networks
[AD-A289422] p 2382 N95-27145

Ultrasonic study on ternary liquid systems by laser-sound interaction
[DE95-606783] p 2207 N95-27929

Observed acoustic and aeroelastic spectral responses of a MOD-2 turbine blade to turbulence excitation
p 2324 N95-27991

Anechoic wind tunnel study of turbulence effects on wind turbine broadband noise p 2325 N95-27992

Ultrasonic studies of liquid/solid seimoacoustic wave phenomena
[AD-A289644] p 2402 N95-28622

SOUNDING

An in situ evaluation of TOPEX/Poseidon altimetric measurements versus meaurements made by moorings and inverted echo sounders for sea surface height
[NASA-CR-198621] p 2347 N95-27805

SOURCE PROGRAMS

Advanced neutron source materials surveillance program
[DE95-005700] p 2215 N95-27464

SPACE COMMERCIALIZATION

Structures and materials technology needs for communications and remote sensing spacecraft
[NASA-CR-198186] p 2163 N95-27026

SPACE DEBRIS

Orbital impacts and the Space Shuttle windshield
[NASA-TM-110594] p 2159 N95-26379

Space Debris Research Phase One Program: Abstracts from published papers (1990-1993)
[AD-A289504] p 2162 N95-26850

Debris/Ice/TPS assessment and integrated photographic analysis of Shuttle mission STS-67
[NASA-TM-110651] p 2160 N95-27238

LDEF: 69 Months in Space. Third Post-Retrieval Symposium, part 3
[NASA-CP-3275-PT-3] p 2466 N95-27629

Orbiting meteoroid and debris counting experiment
p 2463 N95-27668

The orbital debris detector consortium: Suppliers of instruments for in-situ measurements of small-particles in the space environment p 2294 N95-27670

A new technique for ground simulation of hypervelocity debris p 2154 N95-27671

Computational studies of projectile melt in impact with typical whipple shields
[DE95-005916] p 2311 N95-28337

SPACE ENVIRONMENT SIMULATION

A new technique for ground simulation of hypervelocity debris p 2154 N95-27671

SPACE ERECTABLE STRUCTURES

Static stability of a three-dimensional space truss
[NASA-TM-106944] p 2164 N95-27730

Pre-integrated truss space station and method of assembly
[NASA-CASE-MSC-22015-1] p 2165 N95-27842

SPACE EXPLORATION

A rotating arm using shape-memory alloy
p 2157 N95-27276

Views of the solar system
[DE95-006446] p 2461 N95-27326

Multi-spacecraft coherent Doppler and ranging for interplanetary-navigation p 2150 N95-27786

TOPS: Toward Other Planetary Systems. A report by the solar system exploration division
[NASA-TM-110609] p 2464 N95-28009

SPACE FLIGHT

The Long Duration Exposure Facility (LDEF) photographic survey special publication
p 2457 N95-27660

Spaceflight revolution: NASA Langley Research Center from Sputnik to Apollo
[NASA-SP-4308] p 2474 N95-27685

SPACE HEATING (BUILDINGS)

Research on combustion processes relevant to burners in HVAC systems
[PB95-179735] p 2208 N95-28006

Planning, design and construction of the cavern arena: Heating, ventilation and air conditioning
[PB95-196382] p 2361 N95-28659

SPACE LABORATORIES

Microgravity Sciences Biotechnology Facility assessment
[NASA-CR-196602] p 2351 N95-27329

SPACE MISSIONS

Feasibility of flywheel energy storage systems for applications in future space missions
[NASA-CR-195422] p 2316 N95-26393

A multi-attribute-utility-theory model that minimizes interview-data requirements: A consolidation of space launch decisions
[AD-A289421] p 2164 N95-27144

Special features of the CLUSTER antenna and radial booms design, development and verification
p 2157 N95-27281

Microgravity Sciences Biotechnology Facility assessment
[NASA-CR-196602] p 2351 N95-27329

Development of a direct match technique for star identification on the SWAS mission
p 2148 N95-27771

TOPS: Toward Other Planetary Systems. A report by the solar system exploration division
[NASA-TM-110609] . p 2464 N95-28009

SPACE NAVIGATION

An analysis of orbital propagators for Low Earth Orbit Rendezvous
[AD-A288883] p 2161 N95-26458

Flight Mechanics/Estimation Theory Symposium 1995
[NASA-CP-3299] p 2146 N95-27763

Analysis of filter tuning techniques for sequential orbit determination p 2146 N95-27764

Differenced Range Versus Integrated Doppler (DRVID) ionospheric analysis of metric tracking in the Tracking and Data Relay Satellite System (TDRSS)
p 2147 N95-27766

A modified proportional navigation scheme for rendezvous and docking with tumbling targets: The Planar case p 2150 N95-27784

Application of non-coherent Doppler data types for deep space navigation p 2151 N95-27788

Operational considerations of using GPS for spacecraft navigation p 2152 N95-27794

SPACE OBSERVATIONS (FROM EARTH)

Observations of comets with the IUE
[NASA-CR-197816] p 2461 N95-27166

Tracking and impact prediction of Earth-Crossing-Objects (ECO's) on a collision course with Earth
[AD-A289321] p 2461 N95-27303

SPACE PLASMAS

Special features of the CLUSTER antenna and radial booms design, development and verification
p 2157 N95-27281

Differenced Range Versus Integrated Doppler (DRVID) ionospheric analysis of metric tracking in the Tracking and Data Relay Satellite System (TDRSS)
p 2147 N95-27766

Laboratory high-energy astrophysics on lasers
[DE95-008062] p 2462 N95-28013

Energization and transport of ions of ionospheric origin in the terrestrial magnetosphere
[NASA-CR-199618-REV] p 2338 N95-28035

Magnetic viscosity by localized shear flow instability in magnetized accretion disks
[DE95-006879] p 2433 N95-28111

Proceedings of the International Workshop on Acceleration and Radiation Generation in Space and Laboratory Plasmas
[AD-A291673] p 2436 N95-28668

SPACE PLATFORMS

Alternate charging profiles for the onboard nickel cadmium batteries of the Explorer Platform/Extreme Ultraviolet Explorer p 2272 N95-26796

Space Station as a Long Duration Exposure Facility
p 2166 N95-27663

SPACE PROGRAMS

A methodology to assess the utility of future space systems
[AD-A289414] p 2144 N95-27133

SPACE SHUTTLE BOOSTERS

Probabilistic risk assessment of the Space Shuttle. Phase 3: A study of the potential of losing the vehicle during nominal operation. Volume 4: System models and data analysis
[NASA-CR-197811] p 2160 N95-26401

Probabilistic risk assessment of the Space Shuttle. Phase 3: A study of the potential of losing the vehicle during nominal operation. Volume 5: Auxiliary shuttle risk analyses
[NASA-CR-197812] p 2160 N95-26403

Debris/Ice/TPS assessment and integrated photographic analysis of Shuttle mission STS-67
[NASA-TM-110651] p 2160 N95-27238

SPACE SHUTTLE MAIN ENGINE

Probabilistic risk assessment of the Space Shuttle. Phase 3: A study of the potential of losing the vehicle during nominal operation. Volume 4: System models and data analysis
[NASA-CR-197811] p 2160 N95-26401

Probabilistic risk assessment of the Space Shuttle. Phase 3: A study of the potential of losing the vehicle during nominal operation. Volume 5: Auxiliary shuttle risk analyses
[NASA-CR-197812] p 2160 N95-26403

Developmental problems and their solution for the Space Shuttle main engine alternate liquid oxygen high-pressure turbopump: Anomaly or failure investigation the key
[NASA-TP-3553] p 2169 N95-28263

AMCC casting development. Volume 1: Executive Summary
[NASA-CR-196597] p 2247 N95-28419

SPACE SHUTTLE MISSIONS

An overview of the Evaluation of Oxygen Interactions with Materials 3 experiment: Space Shuttle Mission 46, July-August 1992 p 2210 N95-27630

Evaluation of Oxygen Interactions with Materials 3: Mission and induced environments
p 2210 N95-27631

Spacecraft materials studies on the Aerospace Corporation tray on EOIM-3 p 2210 N95-27632

Exposure of LDEF materials to atomic oxygen: Results of EOIM 3 p 2210 N95-27633

LEO degradation of graphite and carbon-based composites aboard Space Shuttle Flight STS-46
p 2199 N95-27636

Orbital atomic oxygen effects on materials: An overview of MSFC experiments on the STS-46 EOIM-3
p 2419 N95-27637

Observational magnetometer calibration with the Hubble Space Telescope's new magnetometers
p 2148 N95-27773

SPACE SHUTTLE ORBITERS

Probabilistic risk assessment of the Space Shuttle. Phase 3: A study of the potential of losing the vehicle during nominal operation. Volume 5: Auxiliary shuttle risk analyses
[NASA-CR-197812] p 2160 N95-26403

SPACE SHUTTLE PAYLOADS

Micron Accuracy Deployment Experiment (MADE), phase A. Volume 1
[NASA-CR-197792] p 2144 N95-26426

The design and implementation of the Military Applications of Shiptracks experiment on Space Transportation System - 65
[AD-A288488] p 2160 N95-26834

Space Station as a Long Duration Exposure Facility p 2166 N95-27663

SPACE SHUTTLES

Orbital impacts and the Space Shuttle windshield [NASA-TM-110594] p 2159 N95-26379

Probabilistic risk assessment of the Space Shuttle. Phase 3: A study of the potential of losing the vehicle during nominal operation, volume 1 [NASA-CR-197808] p 2159 N95-26398

Probabilistic risk assessment of the Space Shuttle. Phase 3: A study of the potential of losing the vehicle during nominal operation. Volume 2: Integrated loss of vehicle model [NASA-CR-197809] p 2159 N95-26399

Probabilistic risk assessment of the Space Shuttle. Phase 3: A study of the potential of losing the vehicle during nominal operation. Volume 3: Basic events and minimal cutsets [NASA-CR-197810] p 2160 N95-26400

Probabilistic risk assessment of the Space Shuttle. Phase 3: A study of the potential of losing the vehicle during nominal operation. Volume 4: System models and data analysis [NASA-CR-197811] p 2160 N95-26401

Probabilistic risk assessment of the Space Shuttle. Phase 3: A study of the potential of losing the vehicle during nominal operation. Volume 5: Auxiliary shuttle risk analyses [NASA-CR-197812] p 2160 N95-26403

Aqueous degreasing, precision cleaning, and cleanliness verification p 2231 N95-27121

Debris/Ice/TPS assessment and integrated photographic analysis of Shuttle mission STS-67 [NASA-TM-110651] p 2160 N95-27238

SPACE STATION FREEDOM

A Materials Exposure Facility p 2166 N95-27664

Pre-integrated truss space station and method of assembly [NASA-CASE-MSC-22015-1] p 2165 N95-27842

SPACE STATION POWER SUPPLIES

Feasibility of flywheel energy storage systems for applications in future space missions [NASA-CR-195422] p 2316 N95-26393

SPACE STATION STRUCTURES

Static stability of a three-dimensional space truss [NASA-TM-106944] p 2164 N95-27730

Pre-integrated truss space station and method of assembly [NASA-CASE-MSC-22015-1] p 2165 N95-27842

SPACE STATIONS

Development and testing of the rack insertion device p 2158 N95-27289

LDEF: 69 Months in Space. Third Post-Retrieval Symposium, part 3 [NASA-CP-3275-PT-3] p 2466 N95-27629

LDEF's contribution to the selection of thermal control coatings for the Space Station p 2242 N95-27661

Space Station program status and research capabilities p 2166 N95-27662

Space Station as a Long Duration Exposure Facility p 2166 N95-27663

Discharge ignition behavior of the Space Station plasma contactor [NASA-TM-106925] p 2168 N95-27862

SPACE SURVEILLANCE (GROUND BASED)

Compensated deconvolution from wavefront sensing [AD-A289490] p 2336 N95-26824

A hybrid genetic algorithm for resolving closely spaced objects p 2384 N95-27387

SPACE SURVEILLANCE (SPACEBORNE)

A hybrid genetic algorithm for resolving closely spaced objects p 2384 N95-27387

SPACE TRANSPORTATION SYSTEM FLIGHTS

The design and implementation of the Military Applications of Shiptracks experiment on Space Transportation System - 65 [AD-A288488] p 2160 N95-26634

Load measurement system with load cell lock-out mechanism p 2159 N95-27291

LEO degradation of graphite and carbon-based composites aboard Space Shuttle Flight STS-46 p 2199 N95-27636

Orbital atomic oxygen effects on materials: An overview of MSFC experiments on the STS-46 EOIM-3 p 2419 N95-27637

LDEF's contribution to the selection of thermal control coatings for the Space Station p 2242 N95-27661

Tank pressure control in low gravity by jet mixing [NASA-CR-191012] p 2243 N95-28001

SPACE-TIME FUNCTIONS

The method of space-time conservation element and solution element-applications to one-dimensional and two-dimensional time-marching flow problems [NASA-TM-106915] p 2389 N95-26663

Spectral analyses, climatology, and interannual variability of Nimbus-7 TOMS version 6 total column ozone [NASA-RP-1360] p 2341 N95-26689

Crushing singularities in spacetimes with spherical, plane and hyperbolic symmetry [PB95-190146] p 2397 N95-28011

SPACEBORNE ASTRONOMY

A long-term space astrophysics research program: An x-ray perspective of the components and structure of galaxies [NASA-CR-197787] p 2461 N95-26593

The development of infrared detectors and mechanisms for use in future infrared space missions [NASA-CR-197819] p 2290 N95-26702

A rule-based shell to hierarchically organize HST observations p 2384 N95-27384

Development of a direct match technique for star identification on the SWAS mission p 2148 N95-27771

Retrofitting a fine-pointing system to satellite optics [DE95-004529] p 2427 N95-28516

SPACEBORNE EXPERIMENTS

The design and implementation of the Military Applications of Shiptracks experiment on Space Transportation System - 65 [AD-A288488] p 2160 N95-26634

An overview of the Evaluation of Oxygen Interactions with Materials 3 experiment: Space Shuttle Mission 46, July-August 1992 p 2210 N95-27630

Evaluation of Oxygen Interactions with Materials 3: Mission and induced environments p 2210 N95-27631

Spacecraft materials studies on the Aerospace Corporation tray on EOIM-3 p 2210 N95-27632

Exposure of LDEF materials to atomic oxygen: Results of EOIM 3 p 2210 N95-27633

LEO degradation of graphite and carbon-based composites aboard Space Shuttle Flight STS-46 p 2199 N95-27636

Orbital atomic oxygen effects on materials: An overview of MSFC experiments on the STS-46 EOIM-3 p 2419 N95-27637

Thermal control materials on EOIM-3 p 2242 N95-27639

Evaluation of space environmental effects on metals and optical thin films on EOIM-3 p 2210 N95-27641

Analysis of selected specimens from the STS-46 Energetic Oxygen Interaction with Materials-3 experiment p 2210 N95-27642

STS-46 plasma composition measurements using the EOIM-3 mass spectrometer p 2211 N95-27645

System results from FRECOPA p 2211 N95-27648

Space environmental effect on solar cells: LDEF and other flight tests p 2326 N95-27649

A final look at LDEF electro-optic systems components p 2428 N95-27650

Long Duration Exposure Facility (LDEF) space optics handbook p 2428 N95-27654

Space Station program status and research capabilities p 2166 N95-27662

Space Station as a Long Duration Exposure Facility p 2166 N95-27663

Element material experiment by EFFU p 2145 N95-27667

Orbiting meteoroid and debris counting experiment p 2463 N95-27668

Classification of RF transients in space using digital signal processing and neural network techniques [DE95-006287] p 2256 N95-27840

SPACEBORNE TELESCOPES

Comprehension and retrieval of failure cases in airborne observatories p 2145 N95-27394

Retrofitting a fine-pointing system to satellite optics [DE95-004529] p 2427 N95-28516

SPACECRAFT

Composite flexible insulation for thermal protection of space vehicles p 2166 N95-28293

SPACECRAFT ANTENNAS

Solar concentrator technology development for space based applications, volume 2 [NASA-CR-197724] p 2319 N95-27194

SPACECRAFT CHARGING

Discharge ignition behavior of the Space Station plasma contactor [NASA-TM-106925] p 2168 N95-27862

SPACECRAFT COMPONENTS

The 29th Aerospace Mechanisms Symposium [NASA-CP-3293] p 2154 N95-27260

Performance of the Satellite Test Assistant Robot in JPL's Space Simulation Facility p 2154 N95-27264

Changing paradigms: Manufacturing vs. fabricating a high volume Hold Down and Release Mechanism p 2155 N95-27267

The Clementine mechanisms p 2156 N95-27268

SPACECRAFT CONFIGURATIONS

An LDEF follow-on spacecraft concept p 2166 N95-27665

SPACECRAFT CONSTRUCTION MATERIALS

Spacecraft materials studies on the Aerospace Corporation tray on EOIM-3 p 2210 N95-27632

Exposure of LDEF materials to atomic oxygen: Results of EOIM 3 p 2210 N95-27633

LEO degradation of graphite and carbon-based composites aboard Space Shuttle Flight STS-46 p 2199 N95-27636

Orbital atomic oxygen effects on materials: An overview of MSFC experiments on the STS-46 EOIM-3 p 2419 N95-27637

A Materials Exposure Facility p 2166 N95-27664

Long Duration Exposure Facility post-flight data as it influences the Tropical Rainfall Measuring Mission p 2345 N95-27666

Element material experiment by EFFU p 2145 N95-27667

The Strategic Technologies for Automation and Robotics (STEAR) program: Protection of materials in the space environment subprogram p 2242 N95-27669

A new technique for ground simulation of hypervelocity debris p 2154 N95-27671

SPACECRAFT CONTAMINATION

International Space Station Alpha trace contaminant control subassembly life test report [NASA-TM-108488] p 2358 N95-26364

Evaluation of Oxygen Interactions with Materials 3: Mission and induced environments p 2210 N95-27631

Exposure of LDEF materials to atomic oxygen: Results of EOIM 3 p 2210 N95-27633

Long Duration Exposure Facility post-flight data as it influences the Tropical Rainfall Measuring Mission p 2345 N95-27666

SPACECRAFT CONTROL

Limits to ground control in autonomous spacecraft p 2383 N95-27381

Stable adaptive neurocontrollers for spacecraft and space robots p 2384 N95-27385

Fuzzy logic techniques for rendezvous and docking of two geostationary satellites p 2384 N95-27386

Geostationary Operational Environmental Satellite (GOES)-8 mission flight experience p 2153 N95-27798

SPACECRAFT DESIGN

Chinese space science and technology [AD-A289618] p 2466 N95-26856

Structures and materials technology needs for communications and remote sensing spacecraft [NASA-CR-198166] p 2163 N95-27026

The Clementine mechanisms p 2156 N95-27268

Thermal neutral format based on the step technology p 2283 N95-27363

From LDEF to a national Space Environment and Effects (SEE) program: A natural progression p 2145 N95-27657

An LDEF follow-on spacecraft concept p 2166 N95-27665

JPRS report: Science and technology. Central Eurasia [JPRS-UST-94-022] p 2246 N95-27699

PC Software graphics tool for conceptual design of space/planetary electrical power systems [NASA-TM-106908] p 2372 N95-27905

SPACECRAFT DOCKING

Telepresent spacecraft docking with object-based bilateral control (OBBC) [AD-A289268] p 2163 N95-26980

Fuzzy logic techniques for rendezvous and docking of two geostationary satellites p 2384 N95-27386

A modified proportional navigation scheme for rendezvous and docking with tumbling targets: The Planar case p 2150 N95-27784

SPACECRAFT ELECTRONIC EQUIPMENT

Characteristics of the standard current trip circuit [PB95-192886] p 2271 N95-28663

SPACECRAFT EQUIPMENT

The 50 Ah NiH2 CPV qualification tests p 2272 N95-26792

LDEF: 69 Months in Space. Third Post-Retrieval Symposium, part 3 [NASA-CP-3275-PT-3] p 2466 N95-27629

SPACECRAFT INSTRUMENTS

Orbiting meteoroid and debris counting experiment p 2463 N95-27668

The orbital debris detector consortium: Suppliers of instruments for in-situ measurements of small-particles in the space environment p 2294 N95-27670

SPACECRAFT LAUNCHING

A multi-attribute-utility-theory model that minimizes interview-data requirements: A consolidation of space launch decisions [AD-A289421] p 2164 N95-27144

Geostationary Operational Environmental Satellite (GOES)-8 mission flight experience
p 2153 N95-27798
Autonomous control system reconfiguration for spacecraft with non-redundant actuators
p 2153 N95-27802
Weather hazards to a Titan 4 on-pad destack-restack operation p 2172 N95-28307
Cape Canaveral air station launch emergency response forces and toxic materials release contingency plans
p 2172 N95-28308
Stratospheric ozone reactive chemicals generated by space launches worldwide
[AD-A289852] p 2332 N95-28623

SPACECRAFT MAINTENANCE
Building an adaptive agent to monitor and repair the electrical power system of an orbital satellite
p 2383 N95-27380
A fuzzy logic intelligent diagnostic system for spacecraft integrated vehicle health management
p 2385 N95-27392

SPACECRAFT MANEUVERS
Evaluation and modeling of autonomous attitude thrust control for the Geostation Operational Environmental Satellite (GOES)-8 orbit determination
p 2146 N95-27765
Operational improvements of long-term predicted ephemerides of the Tracking and Data Relay Satellites (TDRSs) p 2147 N95-27769
Attitude determination using an adaptive multiple model filtering Scheme p 2148 N95-27772
Optimal attitude maneuver execution for the Advanced Composition Explorer (ACE) mission
p 2149 N95-27778
A modified proportional navigation scheme for rendezvous and docking with tumbling targets: The Planar case p 2150 N95-27784
Contingency maneuver strategies for the Total Ozone Mapping Spectrometer-Earth Probe (TOMS-EP)
p 2152 N95-27796
Geostationary Operational Environmental Satellite (GOES)-8 mission flight experience
p 2153 N95-27798
ORION: A Supersynchronous Transfer Orbit mission
p 2154 N95-27804

SPACECRAFT MODULES
Element material experiment by EFFU
p 2145 N95-27667

SPACECRAFT MOTION
Differenced Range Versus Integrated Doppler (DRVID) ionospheric analysis of metric tracking in the Tracking and Data Relay Satellite System (TDRSS)
p 2147 N95-27766

SPACECRAFT ORBITS
A PC-based magnetometer-only attitude and rate determination system for gyroless spacecraft
p 2147 N95-27770
Attitude determination using an adaptive multiple model filtering Scheme p 2148 N95-27772
Application of non-coherent Doppler data types for deep space navigation p 2151 N95-27788
Operational considerations of using GPS for spacecraft navigation p 2152 N95-27794
The Global Positioning System (GPS) and attitude determination: Applications and activities in the Flight Dynamics Division p 2152 N95-27795
Summary of EOS flight dynamics analysis
p 2152 N95-27797

SPACECRAFT POWER SUPPLIES
Alternate charging profiles for the onboard nickel cadmium batteries of the Explorer Platform/Extreme Ultraviolet Explorer p 2272 N95-26796
Heat pipe cooled reactors for multi-kilowatt space power supplies
[DE95-005211] p 2420 N95-27425
PC Software graphics tool for conceptual design of space/planetary electrical power systems
[NASA-TM-106908] p 2372 N95-27905

SPACECRAFT PROPULSION
Advanced Earth-to-orbit propulsion technology information, dissemination and research
[NASA-CR-196582] p 2168 N95-27424

SPACECRAFT RADIATORS
Transitional flow in thin tubes for space station freedom radiator p 2282 N95-27360
Composite heat pipe development status: Development of lightweight prototype carbon-carbon heat pipe with integral fins and metal foil liner
[NASA-TM-106909] p 2283 N95-27369

SPACECRAFT RECOVERY
Chinese space science and technology
[AD-A289618] p 2466 N95-26856

SPACECRAFT REENTRY
Viscous shock-layer analysis on hypersonic flow over reentry capsule with nonequilibrium chemistry
[ISAS-R-656] p 2274 N95-26739
Rarefied gas effects on aerobraking/reentry vehicles with wakes
[NASA-CR-196586] p 2164 N95-27093

SPACECRAFT RELIABILITY
Probabilistic risk assessment of the Space Shuttle. Phase 3: A study of the potential of losing the vehicle during nominal operation. Volume 2: Integrated loss of vehicle model
[NASA-CR-197809] p 2159 N95-26399
Probabilistic risk assessment of the Space Shuttle. Phase 3: A study of the potential of losing the vehicle during nominal operation. Volume 5: Auxiliary shuttle risk analyses
[NASA-CR-197812] p 2160 N95-26403

SPACECRAFT SHIELDING
Debris/Ice/TPS assessment and integrated photographic analysis of Shuttle mission STS-67
[NASA-TM-110651] p 2160 N95-27238
Computational studies of projectile melt in impact with typical whipple shields
[DE95-005916] p 2311 N95-28337

SPACECRAFT STRUCTURES
Control of a large space structure using multiple model adaptive estimation and control techniques
[AD-A289309] p 2162 N95-26916
Analysis of modal behavior at frequency cross-over
[AD-A289304] p 2162 N95-26918
A state-space model of a large, lightly damped space structure using the Eigensystem realization algorithm
[AD-A289251] p 2163 N95-26970
The Clementine mechanisms p 2156 N95-27268
Basic space payload fastener p 2156 N95-27273
System identification of damped truss-like space structures
[NASA-TM-106638] p 2303 N95-27911
Stiffness and strength tailoring in uniform space-filling truss structures p 2188 N95-28290
Designing for time-dependent material response in spacecraft structures p 2166 N95-28292

SPACECRAFT TRACKING
Flight Mechanics/Estimation Theory Symposium 1995
[NASA-CP-3299] p 2146 N95-27763
Multi-spacecraft coherent Doppler and ranging for interplanetary-navigation p 2150 N95-27786
Application of non-coherent Doppler data types for deep space navigation p 2151 N95-27788
Operational considerations of using GPS for spacecraft navigation p 2152 N95-27794

SPACECRAFT TRAJECTORIES
Ulysses orbit determination at high declinations
p 2151 N95-27787
Contingency designs for attitude determination of TRMM p 2154 N95-27803

SPACELAB
Space Station program status and research capabilities p 2166 N95-27662

SPACING
Preliminary design study of the beam collapser and certain optomechanical aspects of the siderostat
[AD-A288423] p 2423 N95-26549
Characterization and redesign of the AFIT multielectrode array
[AD-A289295] p 2354 N95-27039

SPANWISE BLOWING
Study of potential aerodynamic benefits from spanwise blowing at wingtip
[NASA-TP-3515] p 2124 N95-28669

SPARK IGNITION
Aircraft fuel system lightning protection design and qualification test procedures development
[AD-A288401] p 2125 N95-26497

SPATIAL DEPENDENCIES
Temporal and spatial decorrelation scales of the Yellow Sea thermal fields
[AD-A288617] p 2346 N95-26483

SPATIAL DISTRIBUTION
Neural models of spatial orientation in novel environments
[AD-A288420] p 2380 N95-26530
Codes of processing and multiple resources: Model and methodology
[AD-A289583] p 2355 N95-26691
Boron-induced reconstructions of Si(100) investigated by scanning tunneling microscopy
[AD-A289222] p 2438 N95-26959
Amorphous silicon pixel radiation detectors and associated thin film transistor electronics readout
[DE95-006568] p 2265 N95-27678
Full complex modulation using two one-parameter spatial light modulators
[NASA-CASE-MSC-22255-1] p 2427 N95-28384
Method of space-time sequence transform used to measure acousto-optic deflection and modulation
[AD-A289612] p 2402 N95-28671

SPATIAL RESOLUTION
Fluxes across the west coast resolved by Picket Fence observations during stormfest
[AD-A288511] p 2341 N95-26653
Grayscale/resolution trade-off for text: Model predictions and psychophysical results for letter confusion and letter discrimination
[NASA-CR-197784] p 2369 N95-26930
A hybrid genetic algorithm for resolving closely spaced objects p 2384 N95-27387
Improved reduced-resolution satellite imagery
p 2376 N95-27388
A new technique for measuring the separation of closely spaced dislocations using residual contrast conditions
[DE95-007147] p 2219 N95-27968

SPECIFIC HEAT
C15 intermetallic compounds HfV2+Nb
[DE95-005264] p 2215 N95-27463
High energy electron beams for ceramic joining
[DE95-006316] p 2420 N95-27480

SPECIFICATIONS
Generalized CNF satisfiability, local reductions and complexity of succinctly specified problems
[DE95-006343] p 2372 N95-27849

SPECIMEN GEOMETRY
Density changes in amorphous Pd80Si20 during low temperature ion irradiation
[DE95-007132] p 2441 N95-27928

SPECKLE PATTERNS
Speckle spectrum of the ERS-1 wavemode product
[PB95-196564] p 2315 N95-28180
SAR noise reduction through the utilization of robust filters
[INPE-5504-PRE/1787] p 2258 N95-28569

SPECTRA
A spectral algorithm for the seriation problem
[DE95-004775] p 2372 N95-27436

SPECTRAL BANDS
FTIR measurements of thermal infrared sky radiance and transmission
[DE95-003642] p 2334 N95-26436

SPECTRAL EMISSION
Solar UV flux measurements from the SBUV2 monitor on the NOAA9 satellite. Part 1: Mg II h and k line core-to-wing ratios for 1986-1988
[PB95-181962] p 2464 N95-28007

SPECTRAL METHODS
Spectral methods on arbitrary grids
[NASA-CR-198158] p 2279 N95-27247
The Benard problem: A comparison of finite difference and spectral collocation eigen value solutions
p 2283 N95-27364
Weighting the recursive spectral bisection algorithm for unstructured grids
[DE95-008080] p 2373 N95-28521

SPECTRAL REFLECTANCE
Effects of low earth orbit on the optical performance of multi-layer enhanced high reflectance mirrors
p 2428 N95-27652

SPECTRAL RESOLUTION
Reconstruction of an infrared band of meteorological satellite imagery with abductive networks
[SAIC-94/1062] p 2345 N95-27389

SPECTRAL SENSITIVITY
The sensitive detection of hydrazine using chemiluminescence p 2173 N95-28311
A novel sensitive detector of atmospheric nitrocompounds based on laser photofragmentation/ionization spectrometry
p 2174 N95-28314

SPECTRAL SIGNATURES
Infrared field measurements of sea surface temperature: Analysis of wake signatures and comparison of skin layer models
[NASA-CR-197849] p 2346 N95-26533
Signatures of Higgs-Triplet representations at TeV-e(+)e(-) colliders
[DE95-007201] p 2419 N95-27089
Method for determining surface coverage by materials exhibiting different fluorescent properties
[NASA-CASE-GSC-13539-1] p 2315 N95-28211

SPECTRAL THEORY
Laser beam propagation in non-Kolmogorov atmospheric turbulence
[AD-A289256] p 2295 N95-26974

SPECTROGRAMS
Isolated digit recognition without time alignment
[AD-A289344] p 2254 N95-27062

SPECTROMETERS
Magnetic field measurement for the spectrometric magnet of the ISTRA-M setup
[DE95-608560] p 2362 N95-27162
The Alpha-Proton-X-ray Spectrometer deployment mechanism: An anthropomorphic approach to sensor placement on Martian rocks and soil
p 2155 N95-27265

A cryogenic scan mechanism for use in Fourier transform spectrometers p 2158 N95-27287

Search for deeply bound pionic atoms with high-purity germanium tagging spectrometer [DE95-609072] p 2416 N95-28252

A continuous emissions monitor for airborne metals p 2174 N95-28313

Pipelined first-level trigger for the H1 forward-muon spectrometer [PB95-196242] p 2423 N95-28452

Dimensionally self regulating materials [AD-A291671] p 2257 N95-28456

SPECTROPHOTOMETRY

Classical novae and recurrent novae: General properties p 2459 N95-27072

SPECTROSCOPIC ANALYSIS

Plume measurements with the T5 xenon ion thruster [AD-A288697] p 2167 N95-26489

Large area smart piezoelectric and pyroelectric sensors [AD-A288565] p 2290 N95-26541

Coronal abundances and their variation [NASA-CR-197788] p 2464 N95-26671

Collisional dynamics and spectroscopic studies of highly excited rovibrational levels of I2(X)(0(+)(sub g)) via stimulated emission pumping [AD-A289447] p 2295 N95-27172

Iron oxides characterization by Moessbauer spectroscopy [DE95-607869] p 2202 N95-27199

Magnetic resonance imaging of solvent transport in polymer networks [DE95-007142] p 2234 N95-27455

Material analysis using combined Elastic Recoil Detection and Rutherford/Enhanced Rutherford Backscattering Spectrometry [DE95-005415] p 2205 N95-27681

High temperature kinetic study of the reactions H + O2 = OH + O and O + H2 = OH + H in H2/O2 system by shock tube-laser absorption spectroscopy [NASA-CR-195473] p 2206 N95-27695

Plasma properties and magnetic field structure of the solar corona, based on coordinated Max 1991 observations from SERTS, the VLA, and magnetographs [NASA-CR-198592] p 2464 N95-27858

Investigation of the collision line broadening problem as applicable to the NASA Optical Plume Anomaly Detection (OPAD) system, phase 1 [NASA-CR-198605] p 2426 N95-27913

Electron spectroscopy studies of argon K-shell excitation and vacancy cascades [DE95-007096] p 2442 N95-27963

Bubble chamber spectroscopy for chemical analysis: A new concept [DE95-006350] p 2209 N95-28088

Computational and matrix isolation studies of (2- and 3-furyl)methylene [AD-A280085] p 2178 N95-28154

Method for determining surface coverage by materials exhibiting different fluorescent properties [NASA-CASE-GSC-13539-1] p 2315 N95-28211

Use of mussels in biomonitoring of environmental impacts of propellants, projectiles, explosives, and pyrotechnics p 2170 N95-28298

Weightless Environment Training Facility (WETF) materials coating evaluation, volume 2 [NASA-CR-188366-VOL-2] p 2239 N95-28386

Fellowship in physics [AD-A291691] p 2446 N95-28522

SPECTROSCOPY

Materials, structures, and devices for high-speed electronics [NASA-CR-197815] p 2260 N95-26816

Determining nanoscale physical properties of materials by microscopy and spectroscopy [AD-A289532] p 2201 N95-26870

Photoluminescence spectroscopy of 4H- and 6H-SiC [AD-A289326] p 2202 N95-26896

Observations of CEF-split intermultiplet transitions in optically opaque EuBa2Cu3O7 using inelastic neutron scattering [DE95-007135] p 2408 N95-27453

Material analysis using combined Elastic Recoil Detection and Rutherford/Enhanced Rutherford Backscattering Spectrometry [DE95-005415] p 2205 N95-27681

Assay of weathering effects on protective polymer coatings using positron annihilation spectroscopy [DE95-007040] p 2236 N95-27962

An investigation of the chemical and physical properties of pristine, electrochromically damaged, and photochromically damaged KTiOPO4 (KTP) using surface analytical and optical spectroscopic techniques [DE95-007865] p 2443 N95-28023

Phase stability and elasticity of C15 transition-metal intermetallic compounds [DE95-007876] p 2219 N95-28026

Observation on radiation transfer experiments using k-shell absorption spectra [DE95-008068] p 2434 N95-28141

Analysis of forward and inverse problems in chemical dynamics and spectroscopy [DE95-009309] p 2209 N95-28164

Spectroscopic and dynamical studies of highly energized small polyatomic molecules [DE95-006640] p 2414 N95-28199

Vibrational spectroscopy of water interfaces [DE95-006592] p 2209 N95-28218

International journal of quantum chemistry [AD-A291633] p 2352 N95-28546

SPECTRUM ANALYSIS

SeaWiFS technical report series. Volume 26: Results of the SeaWiFS Data Analysis Round-Robin, July 1994 (DARR-1994) [NASA-TM-104566-VOL-26] p 2345 N95-26430

Spectral analyses, climatology, and interannual variability of Nimbus-7 TOMS version 6 total column ozone [NASA-RP-1360] p 2341 N95-26689

Voice analysis using the bispectrum [AD-A289204] p 2254 N95-27008

Programming for time resolved spectrum in pulse radiolysis experiments [DE95-607929] p 2406 N95-27212

Effects of low earth orbit on the optical performance of multi-layer enhanced high reflectance mirrors p 2428 N95-27652

Basic principles and recent observations of rotationally sampled wind p 2321 N95-27971

Low power limits in ultrashort pulse measurement using Frequency-Resolved Optical Gating [DE95-007150] p 2299 N95-28219

Search for molecular absorptions with the Fourier Transform Spectrometer [NASA-CR-198648] p 2462 N95-28222

A study of heart rate and heart rate variability during rapid decompression to 50,000 ft [AD-A291598] p 2355 N95-28561

Material characterization system [AD-D017385] p 2210 N95-28584

In situ dynamic material property measurement system [AD-D017387] p 2210 N95-28585

SPECULAR REFLECTION

Off-specular scattering in neutron reflectometry [DE95-007835] p 2412 N95-28057

SPEECH

The automatic extraction of selected speech spectral characteristics [IFTR-2/1994] p 2250 N95-26835

An experimental version of the MZT (speech-from-text) system with external F(sub 0) control [IFTR-14/1994] p 2250 N95-26836

Voice analysis using the bispectrum [AD-A289204] p 2254 N95-27008

TRAINS: Dialogue transcription tools [AD-A289869] p 2259 N95-28624

SPEECH RECOGNITION

Speech analysis and synthesis based on pitch-synchronous segmentation of the speech waveform [AD-A288824] p 2248 N95-26349

Isolated digit recognition without time alignment [AD-A289344] p 2254 N95-27062

Multiclassifier fusion of an ultrasonic lip reader in automatic speech recognition [AD-A289207] p 2254 N95-27079

Construction of a connectionist network supercomputer [AD-A288439] p 2377 N95-27182

SPEED REGULATORS

Variable speed generator technology options for wind turbine generators p 2273 N95-27988

Variable speed generator application on the MOD-5A 7.3 mW wind turbine generator p 2273 N95-27989

SPHERES

Extensional flow convecting a reactant undergoing a first order homogeneous reaction and diffusional mass transfer from a sphere at low to intermediate Peclet and Damkohler numbers p 2280 N95-27346

Internal electric field of anisotropic and bi-anisotropic spheres [PB95-195491] p 2257 N95-28449

Method of images applied to electromagnetic problems involving spherical, spheroidal and planar geometries [PB95-195517] p 2257 N95-28451

Monte-Carlo simulation methods for finite flat plate winding flows [AD-A289842] p 2289 N95-28619

SPHERICAL ANTENNAS

Data acquisition software for DREO's near-field antenna measurement facility [AD-A289819] p 2258 N95-28573

SPHERICAL WAVES

Uncertainties in the calibration of hydrophones at NPL by the three-transducer spherical-wave reciprocity method in the frequency range 10 kHz on 500 kHz [PB95-185245] p 2401 N95-26615

Laser beam propagation in non-Kolmogorov atmospheric turbulence [AD-A289256] p 2295 N95-26974

SPHEROMAKS

Theoretical aspects of energy confinement in spheromaks [DE95-008079] p 2435 N95-28542

SPHINX

Prediction of material strength and fracture of glass using the SPHINX smooth particle hydrodynamics code [DE95-004869] p 2236 N95-27943

SPILLING

Use of SURFACE CHEMKIN to model multiphase atmospheric chemistry: Application to nitrogen tetroxide spills p 2172 N95-28305

SPIN

Structural oxidation state studies of the manganese cluster in the oxygen evolving complex of Photosystem II [DE95-008488] p 2409 N95-27744

SPIN STABILIZATION

Optimization of a nutation damper attached to a spin-stabilized satellite [AD-A289424] p 2162 N95-26887

Telemetry down-link Doppler as an attitude sensor for spin stabilized spacecraft p 2150 N95-27785

SPINE

Manikin integrated data acquisition system (MIDAS) initial modifications [AD-A291662] p 2361 N95-28667

SPINEL

AEM investigation of tetrahedrally coordinated Ti(4+) in nickel-titanate spinel [DE95-006624] p 2215 N95-27473

SPIRAL ANTENNAS

Improving the performance of spiral antennas by using passive scatterers [AD-A289324] p 2251 N95-26893

SPOILER SLOT AILERONS

Comparative wind tunnel tests of NACA 23024 airfoils with several aileron and spoiler configurations p 2124 N95-27976

SPONTANEOUS EMISSION

Design and characterization of resonant cavity light-emitting diodes [AD-A289307] p 2261 N95-26921

SPRAY CHARACTERISTICS

Apparatus for testing high pressure injector elements [NASA-CASE-MFS-28773-1] p 2304 N95-28347

SPRAY NOZZLES

Structure of high-speed sprays [AD-A291696] p 2288 N95-28523

SPRAYERS

Spray-formed tooling [DE95-005031] p 2246 N95-27404

Structure of high-speed sprays [AD-A291696] p 2288 N95-28523

SPRAYING

A composition joint PDF method for the modeling of spray flames p 2287 N95-27901

SPRINGS (ELASTIC)

Reference manual: Naive physics simulator [PB95-184917] p 2369 N95-26907

Analysis techniques for the prediction of springback in formed and bonded composite components p 2188 N95-28289

SPUTTERING

Faraday screen sputtering on TPX [DE95-008347] p 2434 N95-28224

STABILITY

Stability and thermal influences in nonlinear continuum mechanics and material science [AD-A288333] p 2448 N95-26563

Construction of arbitrary order schemes for many dimensional wave equation [PB95-184818] p 2276 N95-26928

First-principles study of intermetallic phase stability in the ternary Ti-Al-Nb alloy system [DE95-005259] p 2213 N95-27082

The effect on stability and thermal hydraulic quenchback of perforating the jacket of a cable-in-conduit conductor [DE95-005392] p 2262 N95-27083

New radiation stable and long-lived plastic scintillators [DE95-608622] p 2233 N95-27163

Comparison of the calculated and measured stability of a NbTi cable-in-conduit conductor [DE95-007964] p 2265 N95-27693

Phase stability and elasticity of C15 transition-metal intermetallic compounds
[DE95-007876] p 2219 N95-28026
Stability measurements on a 1-T high temperature superconducting magnet
[DE95-007411] p 2267 N95-28048
Normal modes and continuous spectra
[DE95-006166] p 2287 N95-28055
Formation of anisotropic Tl-1212, Tl-2212, Tl-1223 and Tl-2223 particles using aerosol flow reacted powders
[DE95-007400] p 2444 N95-28079
Infrared spectroscopy of nonclassical ions and their complexes
[DE95-008487] p 2413 N95-28091
Stability of chromite interconnections in dual environments
[DE95-007755] p 2267 N95-28131
FENIX experimental results of large-scale CICC made of bronze-processed Nb3Sn strands
[DE95-007965] p 2222 N95-28167
Aspects of strange matter
[DE95-008316] p 2414 N95-28170
Stability of strange quark stars with nuclear crusts against radial oscillations
[DE95-008484] p 2463 N95-28357
Development of low-expansion ceramics with strength retention to elevated temperatures
[DE95-005760] p 2239 N95-28397
Bilateral force feedback for hydraulically actuated systems
[AD-A291632] p 2387 N95-28545
A genuinely multidimensional upwind scheme and efficient multigrid solver for the compressible Euler equations
[NASA-CR-195000] p 2288 N95-28571
High energy density systems in cryogenic media: The production and reactions of atoms and radicals
[AD-A289818] p 2417 N95-28572

STABILITY TESTS
On the nonlinear stability of the unsteady, viscous flow of an incompressible fluid in a curved pipe
[NASA-CR-195065] p 2278 N95-27028
Flight control design using mixed H2/micron optimization
[AD-A289288] p 2142 N95-27036

STABILIZATION
Environmental effects on high energy density materials
[AD-A288296] p 2199 N95-26416
On the physics of ion ring generation for the stabilization of FRX discharges
[DE95-007105] p 2410 N95-27922
Wall stabilization of rotating high (Beta) discharges in D3-D
[DE95-008207] p 2435 N95-28406

STABILIZERS (FLUID DYNAMICS)
Composite repair of a CF18: Vertical stabilizer leading edge p 2134 N95-27517
NASA-ACEE/Boeing 737 graphite-epoxy horizontal stabilizer service p 2138 N95-28489

STAINING
To develop an aerosoling immunomagnetic device for rapid medical diagnosis from clinical samples
[AD-A288504] p 2354 N95-27059

STAINLESS STEELS
Fatigue fracture analysis in medium carbon structural steel and austenitic stainless steel by X-ray fractography
[DE95-601504] p 2213 N95-26675
Effects of helium pre-implantation on the microstructure and mechanical properties of irradiated 316 stainless steel
[DE95-007162] p 2214 N95-27086
Fluid dynamic effects on precision cleaning with supercritical fluids p 2232 N95-27129
Effect of internal hydrogen on the mixed-mode 1/3 fracture toughness of a ferrific/martensitic stainless steel
[DE95-005722] p 2216 N95-27479
Radiation-induced segregation: A microchemical gauge to quantify fundamental defect parameters
[DE95-005720] p 2216 N95-27492
A compatibility study of containment materials in FEFO, bis-(2-fluoro-2,2-dinitroethyl) formal
[DE95-007548] p 2206 N95-27750
Pulsed ion beam surface treatment for preparing rapidly solidified corrosion resistant steel and aluminum surfaces
[DE95-007741] p 2221 N95-28116
Mechanism of deposit formation on fuel-wetted hot metal surfaces
[AD-A289847] p 2210 N95-28621

STANDARD MODEL (PARTICLE PHYSICS)
The physics program and status of the SLAC B-Factory and detector
[DE95-006562] p 2409 N95-27676
Supersymmetry and light quark masses in a realistic superstring model
[DE95-610201] p 2412 N95-28041
Constraints on the anomalous WW gamma couplings from b vector s gamma
[DE95-608866] p 2415 N95-28246
Weak matrix elements efforts on the lattice: Status and prospects
[DE95-007701] p 2416 N95-28355

STANDARDIZATION
Standards for excellence
[NONP-NASA-VT-95-49096] p 2451 N95-27202
A comparison of measured wind park load histories with the WISPER and WISPERX load spectra
[DE95-000295] p 2319 N95-27459
The development of an engineering standard for composite repairs p 2135 N95-27528

STANDARDS
Digital mapping, charting, and geodesy analysis program technical review of Vector Quantization (VQ) Decompression for the National Imagery Transmission Format Standard (NITFS)
[AD-A288998] p 2314 N95-26682
Stability of reference masses 4: Growth of carbonaceous contamination on platinum-iridium mass standard surfaces, and its cleaning by UV/ozone treatment
[PB95-190096] p 2226 N95-26745
Survey of sub-micrometre powder size measurement for ceramic and cermet powders
[PB95-190104] p 2227 N95-26746

STANDING WAVES
Analysis of the dimerized Sb/Si(001)-(2x1) surface by x-ray standing waves
[DE95-007097] p 2208 N95-27965
Material characterization system
[AD-D017385] p 2210 N95-28584

STAPHYLOCOCCUS
Anti-idiotype probes for toxin detection
[AD-A288955] p 2348 N95-26435

STAR DISTRIBUTION
Development of a direct match technique for star identification on the SWAS mission
p 2148 N95-27771

STAR TRACKERS
Development of a direct match technique for star identification on the SWAS mission
p 2148 N95-27771
Experience from the in-flight calibration of the Extreme Ultraviolet Explorer (EUVE) and Upper Atmosphere Research Satellite (UARS) fixed head star trackers (FHSTs) p 2149 N95-27779

STATE ESTIMATION
A PC-based magnetometer-only attitude and rate determination system for gyroless spacecraft
p 2147 N95-27770
An MME-based attitude estimator using vector observations p 2148 N95-27775
Post Kalman progress p 2148 N95-27776
Use of nonlinear identification in robust attitude and attitude rate estimation for SAMPEX
p 2149 N95-27781
Telemetry down-link Doppler as an attitude sensor for spin stabilized spacecraft p 2150 N95-27785
Estimation of attitude sensor timetag biases
p 2153 N95-27799
Performance analysis of bullet trajectory estimation: Approach, simulation, and experiments
[DE95-007949] p 2399 N95-28109

STATE VECTORS
Computing NORAD mean orbital elements from a state vector
[AD-A289281] p 2146 N95-27033
The Hurwitz-Eulerian reduction
[DE95-608760] p 2396 N95-27337
Post Kalman progress p 2148 N95-27776
Estimation of attitude sensor timetag biases
p 2153 N95-27799
Performance analysis of bullet trajectory estimation: Approach, simulation, and experiments
[DE95-007949] p 2399 N95-28109
Quantum retrodiction and causality principle
[DE94-628438] p 2450 N95-28183

STATIC AERODYNAMIC CHARACTERISTICS
Reliability analysis of composite structures
p 2192 N95-28441

STATIC CHARACTERISTICS
Effects of floor location on response of composite fuselage frames p 2192 N95-28439

STATIC DISCHARGERS
The protection of electro-explosive devices (EEDs) and electronics from electrostatic discharge (ESD) hazards
[DSTO-TR-0100] p 2258 N95-28568

STATIC ELECTRICITY
The effect of aviation fuels containing low amounts of static dissipater additive on electrostatic charge generation
[AD-A280075] p 2243 N95-28152

STATIC LOADS
Investigation of static and cyclic bearing failure mechanisms for GR/EP laminates p 2190 N95-28427

STATIC MODELS
Earth horizon modeling and application to static Earth sensors on TRMM spacecraft p 2150 N95-27783
Alternative fuels and vehicles choice model
[DE95-005695] p 2243 N95-27944

STATIC TESTS
Experimental investigation of static and dynamic ground effect on HOPE ALFLEX vehicle
[NAL-TR-1236] p 2128 N95-26525
On aircraft repair verification of a fighter A/C integrally stiffened fuselage skin p 2133 N95-27515
External patch repair of CFRP/honeycomb sandwich
p 2134 N95-27522
Static and fatigue testing of full-scale fuselage panels fabricated using a Therm-X(R) process
p 2185 N95-28270
Development of composite carrythrough bulkhead
p 2192 N95-28438

STATIONKEEPING
Electric propulsion for geostationary orbit insertion
[NASA-TM-106942] p 2168 N95-27727

STATISTICAL ANALYSIS
Filtered kernel density estimation
[AD-A288293] p 2394 N95-26413
Quantitative modeling and analysis in environmental studies
[AD-A288451] p 2326 N95-26431
Fast multidimensional density estimation based on Random-width bins
[AD-A288286] p 2394 N95-26457
Nonlinear scalespace via hierarchical statistical modeling
[AD-A289057] p 2394 N95-26478
Indexing meso-beta surface wind site representative
[AD-A288501] p 2341 N95-26650
Statistical analysis of tensile mechanical property data of carbon/polyimide composites
[NAL-TR-1238] p 2180 N95-26667
Spectral analyses, climatology, and interannual variability of Nimbus-7 TOMS version 6 total column ozone
[NASA-RP-1360] p 2341 N95-26689
Statistical model for molecular internal energy exchange in DSMC method for rarefied flow analysis
[ISAS-R-654] p 2274 N95-26741
Satellite surface material composition from synthetic spectra
[AD-A289236] p 2163 N95-26963
Diagnosing cloudiness from global numerical weather prediction model forecasts
[AD-A289456] p 2356 N95-26992
Multiple model adaptive estimation and head motion tracking in a virtual environment: An engineering approach
[AD-A289299] p 2359 N95-27046
Statistical data analysis
[DE95-007214] p 2454 N95-27090
Probabilistic material strength degradation model for Inconel 718 components subjected to high temperature, high-cycle and low-cycle mechanical fatigue, creep and thermal fatigue effects
[NASA-CR-197832] p 2214 N95-27167
A probabilistic model of a porous heat exchanger
p 2282 N95-27359
Scientific statistics and graphics on the Macintosh
[DE95-006445] p 2372 N95-27533
An automated method of tuning an attitude estimator
p 2148 N95-27774
An MME-based attitude estimator using vector observations p 2148 N95-27775
Experience from the in-flight calibration of the Extreme Ultraviolet Explorer (EUVE) and Upper Atmosphere Research Satellite (UARS) fixed head star trackers (FHSTs) p 2149 N95-27779
Use of nonlinear identification in robust attitude and attitude rate estimation for SAMPEX
p 2149 N95-27781
Calculation of design load for the MOD-5A 7.3 mW wind turbine system p 2312 N95-27982
Emerging applications of probability (stochastic models in geosystems)
[AD-A289117] p 2313 N95-28099
Reliability analysis of composite structures
p 2192 N95-28441
The performance of cargo airdrop systems using g-12E parachutes: Statistical determination of minimum altitude
[AD-A291666] p 2126 N95-28454

Modeling and statistical analysis of bioassay data: Medaka cell proliferation under DEN and TCE [AD-A289998] p 2352 N95-28519

STATISTICAL CORRELATION

Towards the detection and attribution of an anthropogenic effect on climate [DE95-008589] p 2331 N95-28157

STATISTICAL DISTRIBUTIONS

A method for simulating correlated random variables from partially specified distributions [AD-A288820] p 2393 N95-26347

STATISTICAL MECHANICS

Statistical theory and reliability [AD-A288519] p 2394 N95-26733

STATISTICAL TESTS

Uncertainties in obtaining high reliability from stress-strength models p 2193 N95-28442

STEADY FLOW

SUPG finite numerical element solutions for non-compressible Navier-Stokes equation sets [AD-A289600] p 2274 N95-26718

A 3D agglomeration multigrid solver for the Reynolds-averaged Navier-Stokes equations on unstructured meshes [NASA-CR-195073] p 2390 N95-27029

STEADY STATE

Experimental investigation of the effects of relative physical orientation between evaporator and condenser for a loop heat pipe [AD-A289248] p 2277 N95-26968

Features and applications of the Groove Analysis Program (GAP) p 2281 N95-27349

Measurement of the D0 WAMUS magnet inductance [DE95-005128] p 2399 N95-27530

Advanced tokamak operating modes in TPX and ITER [DE95-008058] p 2434 N95-28138

Thermal analysis of PANSAT batteries and Electrical Power Subsystem [AD-A290013] p 2269 N95-28388

Operating points and feedback control of plasma characteristics in tokamaks with full current drive [DE95-007037] p 2435 N95-28553

A genuinely multidimensional upwind scheme and efficient multigrid solver for the compressible Euler equations [NASA-CR-195000] p 2288 N95-28571

STEELS

Current programmes on physical metallurgy and related areas in BARC [DE95-607939] p 2214 N95-27255

Investigation on LCA (Life Cycle Analysis/assessment) [DE95-759260] p 2330 N95-27942

Effects of hydrogen on carbon steels at the Multi-Function Waste Tank Facility [DE95-007194] p 2219 N95-28005

Improved hardness RHA weldability and material property testing [AD-A289127] p 2221 N95-28102

Stress analysis and failure of an internally pressurized composite-jacketed steel cylinder p 2186 N95-28280

Surface scanning techniques to locate and study defects in painted zinc and zinc alloy coated steels [DE95-006099] p 2240 N95-28547

STEERING

Aircraft nosewheel steering simulation p 2118 N95-26944

ELVIS: Eigenvectors for land vehicle image system [AD-A289297] p 2381 N95-27041

STELLAR COLOR

Dwarf novae p 2458 N95-27069

STELLAR COMPOSITION

Precision asteroseismology of DAV (ZZ CETI) white dwarf stars [DE95-006265] p 2462 N95-28056

STELLAR ENVELOPES

Models of classical and recurrent novae p 2459 N95-27073

Models of symbiotic stars p 2460 N95-27077

STELLAR EVOLUTION

Precision asteroseismology of DAV (ZZ CETI) white dwarf stars [DE95-006265] p 2462 N95-28056

STELLAR LUMINOSITY

Dwarf novae p 2458 N95-27069

Models for various aspects of dwarf novae and nova-like stars p 2459 N95-27071

Classical novae and recurrent novae: General properties p 2459 N95-27072

Precision asteroseismology of DAV (ZZ CETI) white dwarf stars [DE95-006265] p 2462 N95-28056

International Ultraviolet Explorer Atlas of B-type spectra from 1200 to 1900 A [NASA-RP-1363] p 2463 N95-28328

STELLAR MAGNITUDE

Dwarf novae p 2458 N95-27069

Classical novae and recurrent novae: General properties p 2459 N95-27072

STELLAR MASS

Precision asteroseismology of DAV (ZZ CETI) white dwarf stars [DE95-006265] p 2462 N95-28056

A new method of determining the ejected mass of novae [DE95-007884] p 2462 N95-28062

STELLAR MASS EJECTION

Models of classical and recurrent novae p 2459 N95-27073

Typical examples of classical novae p 2459 N95-27074

Recurrent novae p 2460 N95-27075

Discussion on selected symbiotic stars p 2460 N95-27078

A new method of determining the ejected mass of novae [DE95-007884] p 2462 N95-28062

STELLAR MODELS

Cataclysmic variables and related objects [NASA-SP-507] p 2458 N95-27068

Dwarf novae p 2458 N95-27069

Models for various aspects of dwarf novae and nova-like stars p 2459 N95-27071

Models of classical and recurrent novae p 2459 N95-27073

Models of symbiotic stars p 2460 N95-27077

Precision asteroseismology of DAV (ZZ CETI) white dwarf stars [DE95-006265] p 2462 N95-28056

STELLAR ORBITS

Dwarf novae p 2458 N95-27069

Models for various aspects of dwarf novae and nova-like stars p 2459 N95-27071

STELLAR OSCILLATIONS

Dwarf novae p 2458 N95-27069

Typical examples of classical novae p 2459 N95-27074

STELLAR RADIATION

Models of classical and recurrent novae p 2459 N95-27073

STELLAR SPECTRA

Nova-like variables p 2458 N95-27070

Models for various aspects of dwarf novae and nova-like stars p 2459 N95-27071

Classical novae and recurrent novae: General properties p 2459 N95-27072

Models of classical and recurrent novae p 2459 N95-27073

Typical examples of classical novae p 2459 N95-27074

Recurrent novae p 2460 N95-27075

Overview of the observations of symbiotic stars p 2460 N95-27076

Models of symbiotic stars p 2460 N95-27077

Discussion on selected symbiotic stars p 2460 N95-27078

International Ultraviolet Explorer Atlas of B-type spectra from 1200 to 1900 A [NASA-RP-1363] p 2463 N95-28328

STELLAR SPECTROPHOTOMETRY

Nova-like variables p 2458 N95-27070

Overview of the observations of symbiotic stars p 2460 N95-27076

STELLAR SYSTEMS

Normal modes and continuous spectra [DE95-006166] p 2287 N95-28055

STELLAR WINDS

International Ultraviolet Explorer Atlas of B-type spectra from 1200 to 1900 A [NASA-RP-1363] p 2463 N95-28328

STELLARATORS

Energetic particle destabilization of shear Alfven waves in stellarators and tokamaks [DE95-006393] p 2431 N95-27419

Nonlinear phenomena, turbulence and anomalous transport in fusion plasmas [DE95-007044] p 2431 N95-27497

Physics assessment of stellarators as fusion power plants [DE95-007045] p 2431 N95-27498

STEP FUNCTIONS

The ambiguity function of the stepped frequency radar [AD-A289533] p 2251 N95-26871

STEP RECOVERY DIODES

Survey on step recovery diode and its applications [PB95-184974] p 2260 N95-26646

STEPPING MOTORS

High performance stepper motors for space mechanisms p 2156 N95-27271

STIFFENING

Analytical investigations of the acceleration sensitivity of acoustic bulk and surface wave resonators [AD-A291715] p 2402 N95-28505

STIFFNESS

Effect of surface coating on one-dimensional system subjected to unit step pressure wave [AD-A288237] p 2308 N95-26625

Stiffness and strength tailoring in uniform space-filling truss structures p 2188 N95-28290

Indentability of conventional and negative Poisson's ratio foams p 2195 N95-28472

Damage tolerance of a geodesically stiffened advanced composite structural concept for aircraft structural applications p 2138 N95-28487

STIMULATED EMISSION

Collisional dynamics and spectroscopic studies of highly excited rovibrational levels of I2(X)(0(+)(sub g)) via stimulated emission pumping [AD-A289447] p 2295 N95-27172

STIMULATION

Silicon based microactuators for telerobotic tactile stimulation [AD-A289340] p 2260 N95-26767

STOCHASTIC PROCESSES

A method to determine the structure of an unknown mixture using the Akaike Information Criterion and the bootstrap [AD-A288295] p 2394 N95-26415

Nonlinear scalespace via hierarchical statistical modeling [AD-A289057] p 2394 N95-26478

Stochastic adaptive estimation and control [AD-A289088] p 2380 N95-26480

Random relaxation of fixed point iteration [PB95-185013] p 2389 N95-26910

The electrical behaviour of an excitable cell at different conditions [DE95-607911] p 2351 N95-27254

A NASTRAN-based computer program for structural dynamic analysis of Horizontal Axis Wind Turbines p 2312 N95-27980

Emerging applications of probability (stochastic models in geosystems) [AD-A289117] p 2313 N95-28099

DNS, LES and stochastic modeling of turbulent reacting flows [AD-A280099] p 2287 N95-28155

A study of non-stationary processes and their applications [AD-A291725] p 2395 N95-28510

Stochastic control and topics in applied probability [AD-A291712] p 2395 N95-28526

Exploiting parallelism in a Monte Carlo image-matching algorithm [AD-A289872] p 2374 N95-28625

STOICHIOMETRY

Stoichiometry, structure, and properties of La2NiO(4+(delta)) and La(2-x)Sr(x)NiO(4+/-(delta)) [DE95-007682] p 2439 N95-27443

AEM investigation of tetrahedrally coordinated Ti(4+) in nickel-titanate spinel [DE95-006624] p 2215 N95-27473

Crystal and magnetic structure of stoichiometric YFe2O4 [DE95-006627] p 2440 N95-27487

Trace elements and the mechanical properties of intermetallic compounds [DE95-007378] p 2220 N95-28046

STORABLE PROPELLANTS

High pressure Earth storable rocket technology program: Basic program [NASA-CR-195449] p 2166 N95-26390

STORAGE RINGS (PARTICLE ACCELERATORS)

Coupling in the Tevatron [DE95-005129] p 2421 N95-27531

The physics program and status of the SLAC B-Factory and detector [DE95-006562] p 2409 N95-27676

Lattice calculation for lepton capture from vacuum-pair production in relativistic heavy-ion collisions [DE95-007392] p 2413 N95-28077

Skew chromaticity [DE95-007677] p 2422 N95-28115

Nonlinear beam dynamics experimental program at SPEAR [DE95-007823] p 2422 N95-28122

Ordered one-component plasmas: Phase transitions, normal modes, large systems, and experiments in a storage ring [DE95-007077] p 2434 N95-28233

Pipelined first-level trigger for the H1 forward-muon spectrometer [PB95-196242] p 2423 N95-28452

STORAGE TANKS

Tank pressure control in low gravity by jet mixing [NASA-CR-191012] p 2243 N95-28001

Bases for extrapolating materials durability in fuel storage pools [DE95-007748] p 2222 N95-28129

Recovery, evaluation, and decontamination of landfilled pentaborane cylinders, former liquid propellant rocket engine test facility, Washoe County, Nevada p 2171 N95-28302

STORMS

FORTE antenna element and release mechanism design p 2157 N95-27282

STOVL AIRCRAFT

Simulation model of the integrated flight/propulsion control system, displays, and propulsion system for ASTOVL lift-fan aircraft [NASA-TM-108866] p 2139 N95-26412

STOWAGE (ONBOARD EQUIPMENT)

Tie-down trials involving a Sikorsky S-70B-2 helicopter [DSTO-TR-0132] p 2136 N95-28567

STRAIN ENERGY METHODS

Evaluation of patch effectiveness in repairing aircraft components p 2133 N95-27513

STRAIN ENERGY RELEASE RATE

Static and dynamic strain energy release rates in toughened thermosetting composite laminates p 2188 N95-28288

Analysis of composite structures with delaminations under combined bending and compression p 2190 N95-28429

STRAIN GAGES

Power train torque measurement [AD-A289577] p 2301 N95-26688

STRAIN MEASUREMENT

Fatigue behavior of a cross-ply metal matrix composite at elevated temperature under strain controlled mode [AD-A289425] p 2181 N95-26865

SMART materials: Surfaces, transforms and interfaces. The commensurate engineering dimension [AD-A289598] p 2312 N95-28649

STRAIN RATE

The high strain rate deformation of tungsten single crystals [AD-A288674] p 2223 N95-28189

Technology integration box beam failure study p 2194 N95-28468

The elevated temperature tensile properties of S-200E commercially pure beryllium [DE95-009331] p 2223 N95-28534

STRANDS

FENIX experimental results of large-scale CICC made of bronze-processed Nb3Sn strands [DE95-007965] p 2222 N95-28167

STRANGE ATTRACTORS

Vibration control using chaotic motion stabilizers [AD-A289576] p 2398 N95-26687

STRANGENESS

Aspects of strangeness [DE95-008314] p 2414 N95-28169

Aspects of strange matter [DE95-008316] p 2414 N95-28170

Stability of strange quark stars with nuclear crusts against radial oscillations [DE95-008484] p 2463 N95-28357

STRATEGY

Malcolm Baldrige National Quality Award winners 1989 [NONP-NASA-VT-95-49119] p 2451 N95-27207

Strategies for recycling CdTe photovoltaic modules [DE95-006776] p 2325 N95-28517

STRATOSPHERE

Replicator for characterization of cirrus and polar stratospheric cloud particles [NASA-CR-197785] p 2341 N95-26669

Stratospheric ozone reactive chemicals generated by space launches worldwide [AD-A289852] p 2332 N95-28623

STRESS ANALYSIS

Creep recovery of PVC and polypropylene [PB95-185112] p 2224 N95-26448

Effect of surface coating on one-dimensional system subjected to unit step pressure wave [AD-A288237] p 2308 N95-26625

Statistical theory and reliability [AD-A288519] p 2394 N95-26733

Comparison of life theories for rolling-element bearings [NASA-TM-106585] p 2301 N95-26774

Addressing tension instability in SPH methods [AD-A289531] p 2276 N95-26852

Effect of hoop stress on ball bearing life prediction [NASA-TM-106874] p 2301 N95-27178

Design and structural validation of CF116 upper wing skin boron doubler p 2132 N95-27510

Evaluation of patch effectiveness in repairing aircraft components p 2133 N95-27513

Repair technology for thermoplastic aircraft structures p 2134 N95-27519

Scarf repairs to graphite/epoxy components p 2135 N95-27523

Damage occurrence on composites during testing and fleet service: Repair of Airbus aircraft p 2135 N95-27526

Using hob offset to balance dynamic strength in spur gears [NASA-TM-106934] p 2302 N95-27698

Stress transfer from axially loaded fiber to matrix in a microcomposite [DE95-007366] p 2183 N95-28043

Accuracy issues in modeling superplastic metal forming [DE95-008934] p 2222 N95-28163

Stress analysis and failure of an internally pressurized composite-jacketed steel cylinder p 2186 N95-28280

Analysis of stresses in finite anisotropic panels with centrally located cutouts p 2187 N95-28286

Compression failure of angle-ply laminates p 2190 N95-28428

Reliability analysis of composite structures p 2192 N95-28441

Uncertainties in obtaining high reliability from stress-strength models p 2193 N95-28442

Non-linear viscoelastic behaviour [PB95-192811] p 2199 N95-28639

STRESS CONCENTRATION

Tension fracture of laminates for transport fuselage. Part 1: Material screening p 2137 N95-28471

STRESS CORROSION CRACKING

Environmentally assisted cracking of high strength beta titanium alloys [AD-A289156] p 2213 N95-27032

Stress corrosion cracking susceptibility of the earthquake resistant NOM B457 Mexican steel [DE95-607956] p 2214 N95-27256

STRESS DISTRIBUTION

Fatigue fracture analysis in medium carbon structural steel and austenitic stainless steel by X-ray fractography [DE95-601504] p 2213 N95-26675

Comparison of life theories for rolling-element bearings [NASA-TM-106585] p 2301 N95-26774

Reactor pressure vessel structural integrity research [DE95-007034] p 2223 N95-28208

Tension fracture of laminates for transport fuselage. Part 1: Material screening p 2137 N95-28471

STRESS MEASUREMENT

Fatigue fracture analysis in medium carbon structural steel and austenitic stainless steel by X-ray fractography [DE95-601504] p 2213 N95-26675

STRESS-STRAIN RELATIONSHIPS

Fatigue behavior of a cross-ply metal matrix composite at elevated temperature under strain controlled mode [AD-A289425] p 2181 N95-26865

Viscoplastic characterization and fatigue modeling of titanium based metal matrix composites [AD-A289430] p 2181 N95-26868

Characterization of fatigue behavior of 2-D woven fabric reinforced ceramic matrix composite at elevated temperature [AD-A289423] p 2181 N95-26886

Fatigue behavior of a cross-ply ceramic matrix composite at elevated temperature under tension-tension loading [AD-A289250] p 2182 N95-26969

Forming metallurgy: Supervised drawing course, NTH [PB95-196507] p 2219 N95-27934

Deformation limits on two-parameter fracture mechanics in terms of higher order asymptotics [AD-A289113] p 2310 N95-28098

Residual stress, strain, and faults in nanocrystalline palladium and copper [DE95-008294] p 2223 N95-28543

STRESSES

Split pipe testing device for the measurement of bond of reinforcement under controlled confinement [AD-D017258] p 2245 N95-26500

STRETCH FORMING

Application of advanced material systems to composite frame elements p 2191 N95-28432

STRING THEORY

Finite fermion density effects on the electroweak string [DE95-608802] p 2448 N95-27312

Supersymmetry and light quark masses in a realistic superstring model [DE95-610201] p 2412 N95-28041

STRINGERS

Load transfer in the stiffener-to-skin joints of a pressurized fuselage [NASA-CR-198610] p 2310 N95-27865

STRONG INTERACTIONS (FIELD THEORY)

Measurement of alpha(s) in e(+)e(-) annihilation at E(cm) = 29 GeV [DE95-006486] p 2417 N95-28594

STRONTIUM COMPOUNDS

The oxidation state and magnetic behaviour of Tb in high-(Tc) related materials [DE95-007129] p 2219 N95-27966

STRUCTURAL ANALYSIS

Manual for SHOCK3D, version 2.0. Computer program for non-linear shock response [AD-A288631] p 2307 N95-26342

A non-iterative grid deformation algorithm for computational fluid dynamics for aeroelasticity [AD-A288298] p 2273 N95-26418

User's guide: Computer program for analysis of beam-column structures with nonlinear supports (CBEAMC) [AD-A289031] p 2307 N95-26464

Large area smart piezoelectric and pyroelectric sensors [AD-A288565] p 2290 N95-26541

Addressing tension instability in SPH methods [AD-A289531] p 2276 N95-26852

The collapse of composite cylindrical panels with various thickness using finite element analysis [AD-A289370] p 2308 N95-26905

Characterization of the membrane theory of a clamped shell. The hyperbolic case [PB95-185021] p 2308 N95-26911

Analysis of modal behavior at frequency cross-over [AD-A289304] p 2162 N95-26918

Structures and materials technology needs for communications and remote sensing spacecraft [NASA-CR-198166] p 2163 N95-27026

Summaries of theses for the degree of diploma engineer 1992-1993 [PB95-184867] p 2246 N95-27048

Fatigue behavior of a cross-ply ceramic matrix composite subjected to tension-tension cycling with hold time [AD-A289418] p 2182 N95-27134

An experimental investigation of sandwich flat panels under low velocity impact [AD-A289420] p 2309 N95-27135

The Solar X-ray Imager Vacuum Door Assembly p 2157 N95-27280

Micromechanical modeling of damage and inelasticity of composite materials in macroscopic structural analysis [DE95-003666] p 2182 N95-27421

Bonded composite repair of metallic aircraft components: Overview of Australian activities p 2132 N95-27505

Design and structural validation of CF116 upper wing skin boron doubler p 2132 N95-27510

Static stability of a three-dimensional space truss [NASA-TM-106944] p 2164 N95-27730

Load transfer in the stiffener-to-skin joints of a pressurized fuselage [NASA-CR-198610] p 2310 N95-27865

Trace elements and the mechanical properties of intermetallic compounds [DE95-007378] p 2220 N95-28046

Aeroelasticity and structural optimization of composite helicopter rotor blades with swept tips [NASA-CR-4665] p 2136 N95-28262

Static and fatigue testing of full-scale fuselage panels fabricated using a Therm-X(R) process p 2185 N95-28270

Higher order finite element analysis of thick composite laminates p 2186 N95-28282

Failure analysis of thick composite cylinders under external pressure p 2187 N95-28284

Analysis of stresses in finite anisotropic panels with centrally located cutouts p 2187 N95-28286

The role of biaxial stresses in discriminating between meaningful and illusory composite failure theories p 2187 N95-28287

Analysis techniques for the prediction of springback in formed and bonded composite components p 2188 N95-28289

Stiffness and strength tailoring in uniform space-filling truss structures p 2188 N95-28290

Mechanisms of compressive failure in woven composites and stitched laminates p 2189 N95-28424

Investigation of static and cyclic bearing failure mechanisms for GR/EP laminates p 2190 N95-28427

Analysis of composite structures with delaminations under combined bending and compression p 2190 N95-28429

Development of composite carrythrough bulkhead p 2192 N95-28438

Probabilistic evaluation of fuselage-type composite structures p 2137 N95-28444

Composite fuselage shell structures research at NASA Langley Research Center p 2194 N95-28466

Structural testing of the technology integration box beam p 2194 N95-28467

Development of stitched/RTM composite primary structures p 2195 N95-28469

Test and analysis results for composite transport fuselage and wing structures p 2137 N95-28470

STRUCTURAL DESIGN

Design and development of a test rig for the high frequency testing of rolling sleeve airsprings
[DSTO-TN-0001] p 2142 N95-26378

Fabrication of long wavelength array by in-situ molecular beam epitaxy
[AD-A288599] p 2423 N95-26679

Design and development of experimental facilities for short duration, low-gravity combustion and fire experiments
[NASA-CR-195458] p 2244 N95-26709

Calorimetric evaluation of commercial Ni-MH cells and charges p 2272 N95-26790

Unique features of a new nickel-hydrogen 2-cell CPV
p 2272 N95-26793

AIAA Techfest 20 Proceedings
[NIAR-94-1] p 2118 N95-26941

Summaries of theses for the degree of diploma engineer 1992-1993
[PB95-184867] p 2246 N95-27048

SXI Prototype mirror mount
[NASA-CR-198613] p 2301 N95-27244

Damage occurrence on composites during testing and fleet service: Repair of Airbus aircraft
p 2135 N95-27526

Space Station as a Long Duration Exposure Facility
p 2166 N95-27663

Load transfer in the stiffener-to-skin joints of a pressurized fuselage
[NASA-CR-198610] p 2310 N95-27865

Analytical and experimental evaluation of joining silicon carbide to silicon carbide and silicon nitride to silicon nitride for advanced heat engine applications, phase 2
[DE95-005761] p 2303 N95-27947

Horizontal axis wind turbine post stall airfoil characteristics synthesization p 2124 N95-27974

Calculation of design load for the MOD-5A 7.3 mW wind turbine system p 2312 N95-27982

Whirl plus tilt
[DE95-007948] p 2399 N95-28108

Ninth DOD/NASA/FAA Conference on Fibrous Composites in Structural Design, volume 3
[NASA-CR-198718] p 2184 N95-28266

Development of a low-cost, modified resin transfer molding process using elastomeric tooling and automated preform fabrication p 2184 N95-28268

Resin transfer molding of textile preforms for aircraft structural applications p 2185 N95-28276

Stiffness and strength tailoring in uniform space-filling truss structures p 2188 N95-28290

Ninth DOD/NASA/FAA Conference on Fibrous Composites in Structural Design, volume 1
[NASA-CR-198723] p 2189 N95-28420

Ninth DOD/NASA/FAA Conference on Fibrous Composites in Structural Design, volume 2
[NASA-CR-198722] p 2193 N95-28462

Overview of the ACT program p 2193 N95-28463

Development of stitched/RTM composite primary structures p 2195 N95-28469

Recent progress in NASA Langley textile reinforced composites program p 2196 N95-28475

Damage tolerance of a geodesically stiffened advanced composite structural concept for aircraft structural applications p 2138 N95-28487

Design and fabrication of a diamond-turned hybrid diffractive/refractive singlet for visible applications at ORNL
[DE95-007007] p 2427 N95-28552

STRUCTURAL DESIGN CRITERIA

Structural design optimization with survivability dependent constraints application: Primary wing box of a multi-role fighter p 2137 N95-28440

STRUCTURAL ENGINEERING

Summaries of theses for the degree of diploma engineer 1992-1993
[PB95-184867] p 2246 N95-27048

Probabilistic evaluation of fuselage-type composite structures p 2137 N95-28444

COINS: A composites information database system
p 2194 N95-28465

STRUCTURAL FAILURE

The collapse of composite cylindrical panels with various thickness using finite element analysis
[AD-A289370] p 2308 N95-26905

Design and structural validation of CF116 upper wing skin boron doubler p 2132 N95-27510

Repair technology for thermoplastic aircraft structures
p 2134 N95-27519

Static stability of a three-dimensional space truss
[NASA-TM-106944] p 2164 N95-27730

Reactor pressure vessel structural integrity research
[DE95-007034] p 2223 N95-28208

Applications of a damage tolerance analysis methodology in aircraft design and production
p 2197 N95-28483

Numerical simulation of crack growth in pressurized fuselages
[PB95-192415] p 2137 N95-28636

STRUCTURAL MEMBERS

Analysis and development of finite element methods for the study of nonlinear thermomechanical behavior of structural components
[NASA-CR-195354] p 2307 N95-26387

Comparison of resin film infusion, resin transfer molding, and consolidation of textile preforms for primary aircraft structure p 2196 N95-28477

STRUCTURAL RELIABILITY

Reliability analysis of composite structures
p 2192 N95-28441

Probabilistic design of advanced composite structure
p 2193 N95-28443

STRUCTURAL STABILITY

C15 intermetallic compounds HfV2+Nb
[DE95-005264] p 2215 N95-27463

Static stability of a three-dimensional space truss
[NASA-TM-106944] p 2164 N95-27730

High pressure optical studies of semiconductors and heterostructures
[DE95-007119] p 2410 N95-27927

Aeroelastic stability of wind turbine blade/aileron systems p 2124 N95-27981

STRUCTURAL STRAIN

A model of rotationally-sampled wind turbulence for predicting fatigue loads in wind turbines
p 2312 N95-27972

STRUCTURAL VIBRATION

Ball bearing vibrations amplitude modeling and test comparisons p 2158 N95-27286

Experimental studies to test simple flexural neutralizers fitted to beams
[ISVR-TR-239] p 2309 N95-27846

Vibration analysis of a split path gearbox
[NASA-TM-106875] p 2302 N95-27855

System identification of damped truss-like space structures
[NASA-TM-106638] p 2303 N95-27911

In situ dynamic material property measurement system
[AD-D017387] p 2210 N95-28585

STRUCTURAL WEIGHT

Structural design optimization with survivability dependent constraints application: Primary wing box of a multi-role fighter p 2137 N95-28440

STRUCTURED GRIDS (MATHEMATICS)

Introduction to multigrid methods
[NASA-CR-195045] p 2388 N95-26395

Unstructured mesh generation and adaptivity
[NASA-CR-195069] p 2278 N95-27027

STUDENTS

Funding for AFRAPT student trainees for academic year 1992-1993
[AD-A288461] p 2466 N95-26604

Characterization and redesign of the AFIT multielectrode array
[AD-A289295] p 2354 N95-27039

SUBDIVISIONS

Selected bibliography on heavy water, tritiated water and hydrogen isotopes (1981-1992)
[DE95-608331] p 2405 N95-27159

Current programmes on physical metallurgy and related areas in BARC
[DE95-607939] p 2214 N95-27255

SUBLIMATION

Self-assembly of low-dimensional molecular nanoclusters on Au(111) surfaces
[AD-A288936] p 2178 N95-28334

SUBMERGING

SeaWiFS technical report series. Volume 27: Case studies for SeaWiFS calibration and validation, part 3
[NASA-TM-104566-VOL-27] p 2348 N95-28030

SUBROUTINE LIBRARIES (COMPUTERS)

Using the scalable nonlinear equations solvers package
[DE95-008323] p 2378 N95-28071

SUBROUTINES

Fitting: Subroutine to fit four-moment probability distributions to data
[DE95-007722] p 2395 N95-27684

SUBSIDIARIES

An ugly duckling becomes a swan (hor ellipsis): How an organization becomes customer focused through listening
[DE95-004974] p 2454 N95-27461

Investigation on working out the global regeneration plan
[DE95-759246] p 2329 N95-27938

SUBSONIC FLOW

A fixed time performance evaluation of parallel CFD applications
[DE94-014240] p 2273 N95-26445

Effect of toroidal plasma flow and flow shear on global MHD modes
[DE95-006676] p 2433 N95-28106

TranAir: A full-potential, solution-adaptive, rectangular grid code for predicting subsonic, transonic, and supersonic flows about arbitrary configurations. User's manual
[NASA-CR-4349] p 2123 N95-28230

TranAir: A full-potential, solution-adaptive, rectangular grid code for predicting subsonic, transonic, and supersonic flows about arbitrary configurations. Theory document
[NASA-CR-4348] p 2123 N95-28265

Response of multi-panel assembly to noise from a jet in forward motion
[NASA-CR-198164] p 2289 N95-28673

SUBSONIC SPEED

Airfoil modification effects on subsonic and transonic pressure distributions and performance for the EA-6B airplane
[NASA-TP-3516] p 2120 N95-26382

Performance characterization of a highly-offset diffuser with and without blowing vortex generator jets
[AD-A289334] p 2122 N95-26901

A general theory of two- and three-dimensional rotational flow in subsonic and transonic turbomachines
[NASA-CR-4496] p 2123 N95-28003

Measurements of store forces and moments and cavity pressures for a generic store in and near a box cavity at subsonic and transonic speeds
[NASA-TM-4611] p 2123 N95-28241

Study of potential aerodynamic benefits from spanwise blowing at wingtip
[NASA-TP-3515] p 2124 N95-28669

Noise exposure reduction of advanced high-lift systems
[NASA-CR-195077] p 2402 N95-28670

Numerical study to assess sulfur hexafluoride as a medium for testing multielement airfoils
[NASA-TP-3496] p 2124 N95-28674

SUBSTITUTES

Mechanisms of hypertension after cross-linked hemoglobin blood-substitute transfusion
[AD-A289558] p 2352 N95-26680

Wipe solvent substitutions for 1,1,1-trichloroethane (TCA) and methyl ethyl ketone (MEK) at Hill Air Force Base p 2228 N95-27107

Investigation on energy conversion technology using biochemical reaction elements, 2
[DE95-759250] p 2321 N95-27940

Surfactants and desensitizing wax substitutes for TNT-Based systems
[AD-A289652] p 2243 N95-28834

SUBSTRATES

Electrocrystallization of an ordered organic monolayer: Selective epitaxial growth of beta(ET)213 ongraphite
[AD-A288942] p 2178 N95-26589

Monolithic electronics for nuclear and high-energy physics experiments
[DE95-005393] p 2420 N95-27427

Growth of hydrogenated amorphous silicon (a-Si:H) on patterned substrates for increased mechanical stability
[DE95-006589] p 2234 N95-27472

Preferentially etched epitaxial liftoff of InP material
[NASA-CASE-LEW-15760-1] p 2235 N95-27503

Atomic oxygen dosimetry measurements made on STS-46 by CONCAP 2 p 2418 N95-27634

Effects of long term space environment exposure on optical substrates and coatings p 2428 N95-27653

Flat panel display development activities at Sandia National Laboratories
[DE95-005442] p 2265 N95-27706

Analysis of the dimerized Sb/Si(001)-(2x1) surface by x-ray standing waves
[DE95-007097] p 2208 N95-27965

Effects of interlayers on the scratch adhesion performance of ultra-thin films of copper and gold on silicon substrates
[DE95-007367] p 2220 N95-28044

Pulsed laser deposition of zeolitic membranes
[DE95-006274] p 2298 N95-28124

Weightless Environment Training Facility (WETF) materials coating evaluation, volume 1
[NASA-CR-188366-VOL-1] p 2239 N95-28385

Weightless Environment Training Facility (WETF) materials coating evaluation, volume 2
[NASA-CR-188366-VOL-2] p 2239 N95-28386

Weightless Environment Training Facility (WETF) materials coating evaluation, volume 3
[NASA-CR-188366-VOL-3] p 2239 N95-28387

Functionalized block copolymers as adhesion promoters
[DE95-008158] p 2239 N95-28400

SUBSTRUCTURES
Micromechanical modeling of damage and inelasticity of composite materials in macroscopic structural analysis
[DE95-003666] p 2182 N95-27421

SUBZERO TEMPERATURE
FREZCHEM: A chemical-thermodynamic model for aqueous solutions at subzero temperatures
[AD-A288456] p 2200 N95-26432

SULFATES
Thermodynamics of aqueous electrolytes at high temperatures by the isopiestic technique
[DE95-006747] p 2449 N95-27546
Towards the detection and attribution of an anthropogenic effect on climate
[DE95-008589] p 2331 N95-28157

SULFIDES
Molecular approach to mesoporous metal sulfides
[DE95-005418] p 2202 N95-27137
Solid film lubricants and thermal control coatings flown aboard the EOIM-3 MDA sub-experiment
p 2242 N95-27640
Muon spin relaxation in ferromagnets: Theoretical results for paramagnetic EuO and EuS
[PB95-192860] p 2418 N95-28641

SULFONES
A new technique for ground simulation of hypervelocity debris p 2154 N95-27671

SULFUR
Hydrogen induced C-C, C-N, and C-S bond activities on Pi and Ni surfaces
[DE95-006251] p 2206 N95-27838
High temperature oxidation of nickel concentrates
[PB95-195566] p 2224 N95-28644

SULFUR COMPOUNDS
Measurement of heterogeneous chemical processes relevant to aerosol surfaces and trace gases active in the marine environment
[DE95-008337] p 2328 N95-27743

SULFUR DIOXIDES
FY 1994 ambient air monitoring report for McMurdo Station, Antarctica
[DE95-008565] p 2331 N95-28149
Remote sensing of the atmosphere by resonance Raman LIDAR
[DE95-007312] p 2315 N95-28520

SULFUR HEXAFLUORIDE
Numerical study to assess sulfur hexafluoride as a medium for testing multielement airfoils
[NASA-TP-3496] p 2124 N95-28674

SULFUR OXIDES
Measurement of heterogeneous chemical processes relevant to aerosol surfaces and trace gases active in the marine environment
[DE95-008337] p 2328 N95-27743

SULFURIC ACID
Solid film lubricants and thermal control coatings flown aboard the EOIM-3 MDA sub-experiment
p 2242 N95-27640

SUM RULES
Couplings of heavy hadrons with soft pions from QCD sum rules
[DE95-610349] p 2407 N95-27410

SUMMARIES
Summaries of theses for the degree of diploma engineer 1992-1993
[PB95-184867] p 2246 N95-27048

SUN
Coronal abundances and their variation
[NASA-CR-197788] p 2464 N95-26671
SXI Prototype mirror mount
[NASA-CR-196613] p 2301 N95-27244
Axionic fuel for sun
[DE95-608788] p 2464 N95-27342
Solar UV flux measurements from the SBUV2 monitor on the NOAA9 satellite. Part 1: Mg II h and k line core-to-wing ratios for 1986-1988
[PB95-181962] p 2464 N95-28007
Advances in scientific visualization
[DE95-008065] p 2343 N95-28014

SUNLIGHT
The program for calculating sunshine duration from global radiation
[KNMI-TR-158] p 2343 N95-28237

SUNSPOT CYCLE
Relativistic electrons in the outer-zone: An 11 year cycle, their relation to the solar wind
[DE95-007882] p 2338 N95-28061

SUNSPOTS
Solar-geophysical data number 604, December 1994. Part 1: (Prompt reports). Data for November, October 1994, and late data
[PB95-181848] p 2465 N95-28087

SUPERCOMPUTERS
Massively parallel self-consistent-field calculations
[DE95-004128] p 2376 N95-26441
Parallel computing on various platforms: A case study
[AD-A289008] p 2376 N95-26460
Performance prediction: A case study using a multi-ring KSR-1 machine
[NASA-CR-195068] p 2361 N95-26697
Performance and policy dimensions in internet routing
[NASA-CR-197772] p 2367 N95-26770
Second International Conference on Software for Multiprocessors and Supercomputers Theory, Practice, Experience
[AD-A289474] p 2368 N95-26820
Construction of a connectionist network supercomputer
[AD-A288439] p 2377 N95-27182
NAS Technical Summeries, March 1993 - February 1994
[NASA-RP-1355] p 2466 N95-27367
Gigabit LAN issues: HIPPI, Fibre Channel, or ATM?
[DE95-003673] p 2378 N95-27422
Lattice QCD calculation using VPP500
[DE95-007076] p 2449 N95-27448
Fluctuations and transport in fusion plasmas
[DE95-007111] p 2433 N95-27924
Sandia's network for Supercomputing '94: Linking the Los Alamos, Lawrence Livermore, and Sandia National Laboratories using switched multimegabit data service
[DE95-007717] p 2378 N95-28074
Applications of boundary element methods on the Intel Paragon
[DE94-014135] p 2393 N95-28393

SUPERCONDUCTING DEVICES
The effect on stability and thermal hydraulic quenchback of perforating the jacket of a cable-in-conduit conductor
[DE95-005392] p 2262 N95-27083
Investigation of high-temperature superconducting flywheel energy storage devices
[DE95-759242] p 2320 N95-27936

SUPERCONDUCTING MAGNETS
Measurement of the D0 WAMUS magnet inductance
[DE95-005128] p 2399 N95-27530
Induced axial oscillations in superconducting dipole windings
[DE95-005690] p 2265 N95-27554
Investigation of high-temperature superconducting flywheel energy storage devices
[DE95-759242] p 2320 N95-27936
Stability measurements on a 1-T high temperature superconducting magnet
[DE95-007411] p 2267 N95-28048
Field quality improvements in superconducting magnets for RHIC
[DE95-006096] p 2269 N95-28339
Manufacture and testing of the superconducting wire and cable for the RHIC dipoles and quadrupoles
[DE95-006000] p 2270 N95-28515

SUPERCONDUCTING SUPER COLLIDER
Silicon subsystem mechanical engineering closeout report for the Solenoidal Detector Collaboration
[DE95-006336] p 2421 N95-27735
Beam instability studies for the SSC
[DE95-008024] p 2423 N95-28551

SUPERCONDUCTIVITY
Investigations of the hyperfine interactions in copper-oxide perovskites using Eu-151 and Fe-57 Moessbauer spectroscopy
[PB95-185138] p 2437 N95-26513
The 18th Annual Condensed Matter Physics Meeting
[DE95-605568] p 2398 N95-26598
Diagnostic system Cryo-D for the determination of parameters of vapor-liquid currents of the coolant
[DE95-608775] p 2280 N95-27338
Electromagnetic hysteretic response calculation for superconductors in demagnetizing geometries
[DE95-005028] p 2264 N95-27403
Review of activities in USA on HTS materials
[DE95-006404] p 2234 N95-27468
Induced axial oscillations in superconducting dipole windings
[DE95-005690] p 2265 N95-27554
Inflight resistance measurement on high-T(sub c) superconducting thin films exposed to orbital atomic oxygen on CONCAP-2 (STS-46) p 2272 N95-27635
Magnetic structures in RNi2B2C (R = Ho, Er) superconductors
[DE95-008370] p 2442 N95-27932
Sintering of textured YBa2Cu3O(7-x) under intensive Co-60 gamma irradiation
[DE95-007098] p 2442 N95-27950
Recent neutron scattering results on high-temperature superconductors
[DE95-007028] p 2413 N95-28066
FENIX experimental results of large-scale CICC made of bronze-processed Nb3Sn strands
[DE95-007965] p 2222 N95-28167
Theory of exotic superconductivity and normal states of heavy electron and high temperature superconductivity materials
[DE95-006637] p 2268 N95-28198

SUPERCONDUCTORS (MATERIALS)
Electromagnetic hysteretic response calculation for superconductors in demagnetizing geometries
[DE95-005028] p 2264 N95-27403
The physics and chemistry of heavy Fermions
[DE95-005277] p 2407 N95-27431
Review of activities in USA on HTS materials
[DE95-006404] p 2234 N95-27468
Magnetic structures in RNi2B2C (R = Ho, Er) superconductors
[DE95-008370] p 2442 N95-27932
Formation of anisotropic Tl-1212, Tl-2212, Tl-1223 and Tl-2223 particles using aerosol flow reacted powders
[DE95-007400] p 2444 N95-28079
The real structure of columnar pinning centers in heavy-ion-irradiated cuprate superconductors
[DE95-003948] p 2445 N95-28186

SUPERCOOLING
Supercooled liquid dynamics for the charged hard-sphere model
[DE95-609158] p 2241 N95-28609

SUPERCRITICAL FLOW
Effect of turbulence models on criticality conditions in swirling flows p 2282 N95-27356

SUPERCRITICAL FLUIDS
Environmentally Benign Cleaning and Degreasing Technology: JANNAF Safety and Protection Subcommittee and Propellant Development and Characterization Subcommittee Joint Workshop
[CPIA-PUBL-611] p 2227 N95-27101
Observations on the solvating power of supercritical fluids p 2228 N95-27106
The use of supercritical carbon dioxide for contaminant removal from solid waste p 2229 N95-27110
Precision parts cleaning with supercritical CO2: Practical applications and solutions p 2229 N95-27111
Corrosive effects of supercritical carbon dioxide and cosolvents on metals p 2224 N95-27113
Precision parts cleaning with supercritical carbon dioxide p 2229 N95-27114
Survey of environmentally benign cleaning methodologies and materials p 2231 N95-27122
Design considerations in supercritical fluid technology
p 2232 N95-27126
The experience of CF Technologies, Inc. (CF Tech) in critical fluid processing p 2232 N95-27128
Fluid dynamic effects on precision cleaning with supercritical fluids p 2232 N95-27129
Small angle x ray scattering studies of reverse micelles in supercritical fluids
[DE95-007803] p 2287 N95-28021

SUPERFLUIDITY
Detection of charged particles in superfluid helium
[DE95-007354] p 2403 N95-26560

SUPERHIGH FREQUENCIES
Prediction of rain attenuation and total atmospheric attenuation for low-availability satellite communications in Europe
[PB95-184925] p 2252 N95-26908
Measurement of wakefield suppression in a detuned X-band accelerator structure
[DE95-008592] p 2422 N95-28159

SUPERLATTICES
Elastic properties of metallic superlattices
[AD-A288699] p 2212 N95-26490
Molecular object liquid crystals: An approach to new materials
[AD-A288905] p 2437 N95-26553
Materials, structures, and devices for high-speed electronics
[NASA-CR-197815] p 2260 N95-26816
Magnetic and structural properties of Fe/Pd multilayers studied by magnetic x-ray dichroism and x-ray absorption spectroscopy
[DE95-007095] p 2206 N95-27755
Heterostructures and infrared emitters with compressed InAsSb layers
[DE95-008157] p 2446 N95-28399

SUPERNOVAE
Discovery of the most distant supernovae and the quest for (Omega)
[DE95-006569] p 2460 N95-28197
Theoretical studies of interstellar processes
[NASA-CR-198647] p 2462 N95-28216

SUPERPLASTIC FORMING
Accuracy issues in modeling superplastic metal forming
[DE95-008934] p 2222 N95-28163

SUPERSONIC AIRCRAFT
Development of injury preventing helmet servo-support system for high performance aircraft
[AD-A289547] p 2359 N95-26755
SUPERSONIC BOUNDARY LAYERS
Compressible turbulence measurements in a supersonic boundary layer including favorable pressure gradient effects
[AD-A289475] p 2276 N95-26821
On the modulational instability of large amplitude waves in supersonic boundary layers
[NASA-CR-195072] p 2284 N95-27760
SUPERSONIC COMBUSTION RAMJET ENGINES
Experiment on a rectangular cross section scramjet combustor. 2: Effects of fuel injector geometry
[NAL-TR-1220] p 2139 N95-26600
Effects of dust from storage heaters on ignition in scramjets
[NAL-TR-1234] p 2139 N95-26706
Experimental investigation of inlet-combustor isolators for a dual-mode scramjet at a Mach number of 4
[NASA-TP-3502] p 2140 N95-28343
SUPERSONIC FLOW
A fixed time performance evaluation of parallel CFD applications
[DE94-014240] p 2273 N95-26445
Wind tunnel experiments on wake flow field behind a reentry capsule from a viewpoint of parachute deployment at supersonic speeds
[ISAS-R-655] p 2121 N95-26740
Development of an upwind, finite-volume code with finite-rate chemistry
[NASA-CR-197747] p 2121 N95-26760
Compressible turbulence measurements in a supersonic boundary layer including favorable pressure gradient effects
[AD-A289475] p 2276 N95-26821
Compressible turbulence measurements in a supersonic flow with adverse pressure gradient
[AD-A289477] p 2276 N95-26822
An investigation of the AFIT 2-inch shock tube as a flow source for supersonic testing
[AD-A289246] p 2143 N95-26966
A laboratory scale supersonic combustive flow system
[DE95-006347] p 2206 N95-27851
A numerical method for solving the three-dimensional parabolized Navier-Stokes equations
[NASA-CR-198159] p 2287 N95-27917
TranAir: A full-potential, solution-adaptive, rectangular grid code for predicting subsonic, transonic, and supersonic flows about arbitrary configurations. User's manual
[NASA-CR-4349] p 2123 N95-28230
TranAir: A full-potential, solution-adaptive, rectangular grid code for predicting subsonic, transonic, and supersonic flows about arbitrary configurations. Theory document
[NASA-CR-4348] p 2123 N95-28265
SUPERSONIC JET FLOW
Pseudomorphic semiconducting heterostructures from combinations of AlN, GaN and selected SiC polytypes: Theoretical advancement and its coordination with experimental studies of nucleation, growth, characterization and device development
[AD-A289550] p 2437 N95-26756
Supersonic coaxial jet noise predictions
[NASA-TM-106917] p 2401 N95-26801
Preliminary results and research capabilities of a new jet facility at the University of Kansas
p 2119 N95-26951
Visualization of the multiple supersonic jet oscillations by swept focused strobed schlieren technique
p 2119 N95-26952
A numerical study of fundamental shock noise mechanisms
[NASA-TM-110608] p 2401 N95-27908
SUPERSONIC SPEED
An investigation of the AFIT 2-inch shock tube as a flow source for supersonic testing
[AD-A289246] p 2143 N95-26966
Experimental investigation of inlet-combustor isolators for a dual-mode scramjet at a Mach number of 4
[NASA-TP-3502] p 2140 N95-28343
SUPERSONIC TRANSPORTS
Supersonic transport grid generation, validation, and optimization
[NASA-CR-197752] p 2365 N95-26648
CFD research, parallel computation and aerodynamic optimization
[NASA-CR-197748] p 2120 N95-26649
Design and testing of low sonic boom configurations and an oblique all-wing supersonic transport
[NASA-CR-197744] p 2129 N95-26651
Supersonic civil airplane study and design: Performance and sonic boom
[NASA-CR-197745] p 2130 N95-26813
Preliminary design problems and solutions for a supersonic oblique all-wing transport aircraft
p 2118 N95-26942
The high speed civil transport and NASA's High Speed Research (HSR) program p 2118 N95-26945
SUPERSONIC TURBINES
Turbomachinery design and tonal acoustics computations
[NASA-CR-197749] p 2139 N95-26777
SUPERSONIC WAKES
Wind tunnel experiments on wake flow field behind a reentry capsule from a viewpoint of parachute deployment at supersonic speeds
[ISAS-R-655] p 2121 N95-26740
SUPERSONIC WIND TUNNELS
Computational support of the laminar flow supersonic wind tunnel, CNSFV code development, Maglev, and grid generation
[NASA-CR-197750] p 2143 N95-26775
A laboratory scale supersonic combustive flow system
[DE95-006347] p 2206 N95-27851
SUPERSYMMETRY
q-structure algebra of U(sub q)(g-circumflex) from its adjoint action
[DE95-608749] p 2390 N95-27301
Extended BRST symmetry for the relativistic particle with curvature
[DE95-608799] p 2406 N95-27309
Field theory of point-like systems with higher-order derivatives
[DE95-608800] p 2448 N95-27310
Implications of horizontal symmetries on baryon number violation in supersymmetric models
[DE95-610202] p 2407 N95-27406
Search for SUSY at CDF
[DE95-005109] p 2407 N95-27430
Search for supersymmetry and leptoquark states at FNAL
[DE95-003381] p 2410 N95-27871
Supersymmetry and light quark masses in a realistic superstring model
[DE95-610201] p 2412 N95-28041
SUPPLYING
Alternative fuels and vehicles choice model
[DE95-005695] p 2243 N95-27944
SUPPORT SYSTEMS
Vector Smart Map Level 1: A new DMA product
[AD-A288920] p 2452 N95-26607
Design considerations for FrankTalk: A distributed group support system
[AD-A289386] p 2359 N95-26863
SUPPORTS
User's guide: Computer program for analysis of beam-column structures with nonlinear supports (CBEAMC)
[AD-A289031] p 2307 N95-26464
Preliminary design study of the beam collapser and certain optomechanical aspects of the siderostat
[AD-A288423] p 2423 N95-26549
SXI Prototype mirror mount
[NASA-CR-196613] p 2301 N95-27244
Tie-down trials involving a Sikorsky S-70B-2 helicopter
[DSTO-TR-0132] p 2136 N95-28567
SUPPRESSORS
Suppressor of oscillations in airframe cavities
[AD-D017265] p 2128 N95-26507
SURFACE CRACKS
New radiation stable and long-lived plastic scintillators
[DE95-608622] p 2233 N95-27163
SURFACE DEFECTS
Surface damage effects generated by a fast-pulse laser beam
[AD-A289131] p 2295 N95-26996
Reactor pressure vessel structural integrity research
[DE95-007034] p 2223 N95-28208
Surface scanning techniques to locate and study defects in painted zinc and zinc alloy coated steels
[DE95-006099] p 2240 N95-28547
SURFACE DISTORTION
Thermally-induced unsymmetric optical distortion of output window of high-power CO2 laser
[AD-A289604] p 2300 N95-28650
SURFACE EMITTING LASERS
Time-dependent model for vertical-cavity surface-emitting laser
[DE95-007880] p 2298 N95-28027
Surface-emitting semiconductor laser for intracavity spectroscopy and microscopy
[DE95-007745] p 2299 N95-28128
Comprehensive numerical model for CW vertical-cavity surface-emitting lasers
[DE95-007758] p 2299 N95-28132
SURFACE ENERGY
Surface energy driven crystallization of amorphous Ni69Cr14P17 alloy
[DE95-005543] p 2438 N95-27085
Atomistic study of energy and structure of surfaces in NiO
[DE95-005207] p 2215 N95-27446
Measurement and analysis of the surface energy budget for ARM field experiments
[DE95-007646] p 2338 N95-28114
The unusual properties of beryllium surfaces
[DE95-006471] p 2223 N95-28593
SURFACE FINISHING
Effect of processing parameters on surface finish for fused deposition machinable wax patterns
[NASA-TP-3550] p 2244 N95-26769
SURFACE LAYERS
Effect of processing parameters on surface finish for fused deposition machinable wax patterns
[NASA-TP-3550] p 2244 N95-26769
Satellite surface material composition from synthetic spectra
[AD-A289236] p 2163 N95-26963
Laser ultrasonic generation at the surface of a liquid metal
[DE95-004999] p 2216 N95-27477
Surface crystallization and thin film melting in normal alkanes
[DE95-006694] p 2440 N95-27535
Plasma source ion implantation of ammonia into electroplated chromium
[DE95-006275] p 2444 N95-28125
SURFACE NAVIGATION
Using virtual active vision tools to improve autonomous driving tasks
[AD-A289175] p 2356 N95-27013
SURFACE PROPERTIES
Surface chemistry of silicon
[AD-A288893] p 2224 N95-26351
Molecular object liquid crystals: An approach to new materials
[AD-A288905] p 2437 N95-26553
Materials with self organized surfaces: 2D polymer assemblies
[AD-A288928] p 2226 N95-26627
Numerical solution of fluid flow and heat tranfer problems with surface radiation p 2282 N95-27357
The influence of surface structure on the interaction of water with TiO2(100)
[DE95-004927] p 2203 N95-27401
LDEF's contribution to the selection of thermal control coatings for the Space Station p 2242 N95-27661
Simulations of metal dissolution and corrosion
[DE95-007486] p 2218 N95-27748
Analysis of surfaces, films and multilayers by resonant laser ablation
[DE95-006295] p 2297 N95-27841
Method for determining surface coverage by materials exhibiting different fluorescent properties
[NASA-CASE-GSC-13539-1] p 2315 N95-28211
Self-assembly of low-dimensional molecular nanoclusters on Au(111) surfaces
[AD-A286936] p 2178 N95-28334
Cesium/oxide interactions for ultrathin films on (alpha)-Al2O3(001) and (alpha)-Al2O3(1(bar 1)O2)
[DE95-008159] p 2238 N95-28358
Nonlinear optical studies of surfaces
[DE95-006574] p 2428 N95-28557
SURFACE REACTIONS
Surface chemistry of silicon
[AD-A288893] p 2224 N95-26351
Photo and thermal excitation of surface chemistry on model catalyst surfaces
[AD-A288541] p 2200 N95-26528
Theoretical studies of reaction surfaces
[AD-A288458] p 2404 N95-26632
Changes in the anisotropy parameters of an aluminum alloy caused by cyclical deformation
[IFTR-27/1994] p 2212 N95-26666
Materials Research Society Symposium Proceedings. Volume 339: Diamond, SiC and nitride wide bandgap semiconductors
[AD-A288690] p 2437 N95-26818
Iron oxides characterization by Moessbauer spectroscopy
[DE95-607869] p 2202 N95-27199
Spacecraft materials studies on the Aerospace Corporation tray on EOIM-3 p 2210 N95-27632
Exposure of LDEF materials to atomic oxygen: Results of EOIM 3 p 2210 N95-27633
Orbital atomic oxygen effects on materials: An overview of MSFC experiments on the STS-46 EOIM-3
p 2419 N95-27637
Effects of atomic oxygen on polymeric materials flown on EOIM-3 p 2242 N95-27638
Thermal control materials on EOIM-3
p 2242 N95-27639
Solid film lubricants and thermal control coatings flown aboard the EOIM-3 MDA sub-experiment
p 2242 N95-27640

Evaluation of space environmental effects on metals and optical thin films on EOIM-3 p 2210 N95-27641
Molecular beam scattering from C-13 enriched Kapton and correlation with the EOIM-3 carousel experiment
p 2419 N95-27643
BMDO materials testing in the EOIM-3 experiment
p 2211 N95-27644
STS-46 plasma composition measurements using the EOIM-3 mass spectrometer p 2211 N95-27645
Process for non-contact removal of organic coatings from the surface of paintings
[NASA-CASE-LEW-15896-1] p 2235 N95-27702
Hydrogen induced C-C, C-N, and C-S bond activities on Pi and Ni surfaces
[DE95-006251] p 2206 N95-27838
FTIR studies of CH3OH on porous silicon
[AD-A289038] p 2207 N95-27904
The role of hydrogen in the hydrogenation and hydrogenolysis of aniline on the nickel single crystal surfaces: Its implication on the mechanisms of HDN reactions
[DE95-006687] p 2222 N95-28134
Self-assembly of low-dimensional molecular nanoclusters on Au(111) surfaces
[AD-A288936] p 2178 N95-28334
Cesium/oxide interactions for ultrathin films on (alpha)-Al2O3(001) and (alpha)-Al2O3(1(bar 1)O2)
[DE95-008159] p 2238 N95-28358
Molecular engineering of thin polymer films prepared from functionally-terminated oligomers
[AD-A291681] p 2240 N95-28457
High temperature oxidation of nickel concentrates
[PB95-195566] p 2224 N95-28644
TV-holography at high temperatures: In situ observations of the oxidation of advanced materials
[PB95-195343] p 2294 N95-28651
Photoemission study of solid state reaction and initial oxidation of the Ce/Al(100) system
[PB95-195368] p 2210 N95-28652

SURFACE ROUGHNESS
Theoretical and experimental models of the diffuse radar backscatter from Mars
[NASA-CR-198650] p 2463 N95-27700
Scaling of localization length of a quasi 1D system with longitudinal boundary roughness
[DE95-609148] p 2391 N95-27739
Off-specular scattering in neutron reflectometry
[DE95-007835] p 2412 N95-28057
Numerical and theoretical studies of rough surface scattering
[AD-A291748] p 2257 N95-28528

SURFACE ROUGHNESS EFFECTS
Modeling surface effects with the parabolic equation method
[AD-A289199] p 2254 N95-27021

SURFACE TEMPERATURE
Chemical physics of uniform cyclic etching
[AD-A288975] p 2404 N95-26574
Laser ultrasonic generation at the surface of a liquid metal
[DE95-004999] p 2216 N95-27477
A study of surface temperatures, clouds and net radiation
[NASA-CR-198589] p 2329 N95-27864
Remote measurement of ground temperature and emissivity
[DE95-008055] p 2314 N95-28053

SURFACE TREATMENT
Stability of reference masses 4: Growth of carbonaceous contamination on platinum-iridium mass standard surfaces, and its cleaning by UV/ozone treatment
[PB95-190096] p 2226 N95-26745
Pulsed ion beam surface treatment for preparing rapidly solidified corrosion resistant steel and aluminum surfaces
[DE95-007741] p 2221 N95-28116
Weightless Environment Training Facility (WETF) materials coating evaluation, volume 2
[NASA-CR-188366-VOL-2] p 2239 N95-28386
Weightless Environment Training Facility (WETF) materials coating evaluation, volume 3
[NASA-CR-188366-VOL-3] p 2239 N95-28387

SURFACE VEHICLES
A new drag measurement system for wind tunnel testing of the racing bicycle and rider to determine a low drag configuration
[AD-A289375] p 2122 N95-26875

SURFACE WATER
Tomographic observations of deep convection and the thermal evolution of the Greenland Sea Gyre 1988-1989
[AD-A289104] p 2348 N95-28096
Vibrational spectroscopy of water interfaces
[DE95-006592] p 2209 N95-28218

SURFACE WAVES
Evaluation of the FMICW waveform in HF surface radar applications
[AD-A288245] p 2249 N95-26545
Nonlinear problems in fluid dynamics and inverse scattering: Langmuir circulations and spiral flows
[AD-A289194] p 2278 N95-27019
Analysis of the dimerized Sb/Si(001)-(2x1) surface by x-ray standing waves
[DE95-007097] p 2208 N95-27965
Modeling the shock response of submerged structures
[AD-A289082] p 2288 N95-28351
Analytical investigations of the acceleration sensitivity of acoustic bulk and surface wave resonators
[AD-A291715] p 2402 N95-28505
Numerical and theoretical studies of rough surface scattering
[AD-A291748] p 2257 N95-28528

SURFACTANTS
Application of bacterial bioemusifiers to in situ maintenance of oil/water separators
p 2179 N95-27120
Molecular approach to mesoporous metal sulfides
[DE95-005418] p 2202 N95-27137
Determination of phase transitions in a lyotropic liquid crystal by positron annihilation technique
[DE95-609162] p 2442 N95-27964
Surfactants and desensitizing wax substitutes for TNT-Based systems
[AD-A289652] p 2243 N95-28634

SURGES
Energy-measuring resistor bank
[AD-D017392] p 2271 N95-28613

SURVEILLANCE
Advanced neutron source materials surveillance program
[DE95-005700] p 2215 N95-27464

SURVEYS
Development of an acuity-based nurse staffing system for the post anesthesia care unit
[AD-A288831] p 2352 N95-26494
Survey and implementation of commercial manual controllers for a generic telerobotics architecture
[AD-A289215] p 2381 N95-26990
Crew adaptation evaluation of the Norwegian Crew Concept (NOROREW)
[AD-A288478] p 2360 N95-27058
Geophex airborne unmanned survey system
[DE95-007566] p 2131 N95-27440
Survey on researches related to ocean disposal of carbon dioxide
[DE95-759247] p 2329 N95-27939
Investigation on LCA (Life Cycle Analysis/assessment)
[DE95-759260] p 2330 N95-27942
The Top...is it There? A Survey of the CDF and D0 Experiments
[DE95-005746] p 2411 N95-27945
NASA/DOD Aerospace Knowledge Diffusion Research Project. Report 35: The use of computer networks in aerospace engineering
[NASA-CR-198170] p 2456 N95-28600

SUSPENSION SYSTEMS (VEHICLES)
The vibration transmission of lift truck suspension seats
[ISVR-TR-245] p 2302 N95-27844

SWEAT COOLING
Investigation of boundary layer and performance effects of transpiration cooling through a porous plate in a rocket nozzle
[AD-A289393] p 2167 N95-26880

SWEDEN
Milestones in telecommunications in some selected countries
[PB95-184826] p 2252 N95-26929

SWEEP EFFECT
Evaluation of a doubly-swept blade tip for rotorcraft noise reduction
[NASA-CR-189677] p 2402 N95-28264

SWELLING
Feasibility studies for separation processes using environmentally sensitive hydrogels
[DE95-008355] p 2238 N95-28226

SWEPT WINGS
Study of potential aerodynamic benefits from spanwise blowing at wingtip
[NASA-TP-3515] p 2124 N95-28669

SWIRLING
Effect of turbulence models on criticality conditions in swirling flows p 2282 N95-27356

SWITCHING
Stochastic adaptive estimation and control
[AD-A289088] p 2380 N95-26480
Optimal control of two queues in series
[DE95-608731] p 2382 N95-27045

SWITCHING CIRCUITS
Forback DC-to-DC converter
[NASA-CASE-GSC-13404-1] p 2269 N95-28341

SYMBIOTIC STARS
Cataclysmic variables and related objects
[NASA-SP-507] p 2458 N95-27068
Overview of the observations of symbiotic stars
p 2460 N95-27076
Models of symbiotic stars p 2460 N95-27077
Discussion on selected symbiotic stars
p 2460 N95-27078

SYMBOLS
High temperature Hexoloy(trademark) SX silicon carbide
[DE95-007290] p 2221 N95-28075

SYMMETRY
Electromagnetic hysteretic response calculation for superconductors in demagnetizing geometries
[DE95-005028] p 2264 N95-27403
Depth migration in transversely isotropic media with explicit operators
[DE95-007670] p 2337 N95-27442
Crushing singularities in spacetimes with spherical, plane and hyperbolic symmetry
[PB95-190146] p 2397 N95-28011
Lie group weight multiplicities from conformal field theory
[PB95-190153] p 2392 N95-28012
Heterostructures and infrared emitters with compressed InAsSb layers
[DE95-008157] p 2446 N95-28399
Wavelet analysis and its applications
[AD-A291735] p 2387 N95-28527

SYNAPSES
Comparative transduction mechanisms of hair cells in the bullfrog utriculus. 1: Responses to intracellular current p 2350 N95-26731

SYNCHRONISM
Minimizing the impact of synchronization overhead in parallel discrete event simulations
[AD-A289278] p 2377 N95-26984

SYNCHRONOUS PLATFORMS
ORION: A Supersynchronous Transfer Orbit mission
p 2154 N95-27804

SYNCHRONOUS SATELLITES
Long-term variability of electron radiation dose in geosynchronous orbit
[AD-A289335] p 2162 N95-26902
Accurate orbit determination strategies for the tracking and data relay satellites p 2147 N95-27768

SYNCHROTRON RADIATION
Resonant photoemission studies of thickness dependence of the unoccupied Gd 5d bands
[DE95-004127] p 2436 N95-26440
CAS CERN Accelerator School 5th General Accelerator Physics Course
[DE95-608324] p 2419 N95-27158

SYNCHROTRONS
Analytical spectroscopy
[DE95-607896] p 2203 N95-27200
Synchrotron X-ray scattering studies at mineral-water interfaces
[DE95-008303] p 2440 N95-27542
Performance of an accordion electromagnetic calorimeter with liquid krypton
[DE95-006693] p 2292 N95-27738

SYNOPTIC METEOROLOGY
Synoptic features of the Yunan rainy season before the onset of the tropical monsoons
[AD-A289641] p 2342 N95-26724

SYNTAX
Unification of LARCH and Z-based object models to support algebraically-based design refinement: The Z perspective
[AD-A289234] p 2369 N95-26962

SYNTHESIS
Template synthesis of electronically conductive polymer nanostructures
[AD-A288373] p 2225 N95-26472

SYNTHESIS (CHEMISTRY)
Stabilization and control of high energy intermediates through adsorption of restricted spaces
[AD-A288552] p 2201 N95-26606
Materials design and processing by biomimicking. Section 1: Research progress
[AD-A288229] p 2226 N95-26623
Design and processing of materials by biomimicking. Section 2. Publications
[AD-A288230] p 2226 N95-26624
Computational and matrix isolation studies of (2- and 3-furyl)methylene
[AD-A280085] p 2178 N95-28154
On the synthesis of mixed-metal and mixed-pnicogen13-15 ring-systems
[AD-A288869] p 2223 N95-28332

Ash-based ceramic materials
[AD-D017272] p 2241 N95-28582

SYNTHETIC APERTURE RADAR

Perceptual based image fusion with applications to hyperspectral image data
[AD-A289429] p 2251 N95-26867

Processing of wide-angle synthetic aperture radar signals for detection of obscured ground targets
[AD-A289243] p 2253 N95-26976

Speckle spectrum of the ERS-1 wavemode product
[PB95-196564] p 2315 N95-28180

Binary segmentation of SAR images by the ICM algorithm
[INPE-5464-PRE/1772] p 2258 N95-28559

SAR noise reduction through the utilization of robust filters
[INPE-5504-PRE/1787] p 2258 N95-28569

SYNTHETIC FIBERS

The 18th Asilomar Conference on Polymeric Materials
[AD-A291721] p 2240 N95-28508

SYNTHETIC FUELS

Biomass Pyrolysis Oil Properties and Combustion Meeting
[DE95-004017] p 2204 N95-27438

SYSTEM FAILURES

Probabilistic risk assessment of the Space Shuttle. Phase 3: A study of the potential of losing the vehicle during nominal operation. Volume 5: Auxiliary shuttle risk analyses
[NASA-CR-197812] p 2160 N95-26403

Comprehension and retrieval of failure cases in airborne observatories p 2145 N95-27394

SYSTEM IDENTIFICATION

System identification of damped truss-like space structures
[NASA-TM-106638] p 2303 N95-27911

SYSTEMS ANALYSIS

Long term distributed file reference tracing: Implementation and experience
[AD-A288585] p 2452 N95-26535

Structures and materials technology needs for communications and remote sensing spacecraft
[NASA-CR-198166] p 2163 N95-27026

LDEF: 69 Months in Space. Third Post-Retrieval Symposium, part 3
[NASA-CP-3275-PT-3] p 2466 N95-27629

LDEF systems special investigation group overview p 2470 N95-27647

The Global Positioning System (GPS) and attitude determination: Applications and activities in the Flight Dynamics Division p 2152 N95-27795

Summary of EOS flight dynamics analysis p 2152 N95-27797

Autonomous control system reconfiguration for spacecraft with non-redundant actuators p 2153 N95-27802

ORION: A Supersynchronous Transfer Orbit mission p 2154 N95-27804

Comparison of measured and calculated dynamic loads for the Mod-2 2.5 mW wind turbine system p 2312 N95-27983

Analysis methods for wind turbine control and electrical system dynamics p 2273 N95-27984

A conceptual framework for evaluating variable speed generator options for wind energy applications p 2273 N95-27987

Variable speed generator technology options for wind turbine generators p 2273 N95-27988

Variable speed generator application on the MOD-5A 7.3 mW wind turbine generator p 2273 N95-27989

SYSTEMS ENGINEERING

Aircraft fuel system lightning protection design and qualification test procedures development
[AD-A288401] p 2125 N95-26497

Design and synthesis of a real-time controller for an unmanned air vehicle
[AD-A289134] p 2141 N95-26555

Design considerations for FrankTalk: A distributed group support system
[AD-A289386] p 2359 N95-26863

A systems engineering approach to electro-mechanical reconfiguration for mobility autonomy
[AD-A289479] p 2301 N95-26926

Next generation real-time systems: Investigating the potential of partial-solution tasks
[AD-A289203] p 2381 N95-27007

Changing paradigms: Manufacturing vs. fabricating a high volume Hold Down and Release Mechanism p 2155 N95-27267

Development of a miniature actuator/controller system p 2156 N95-27272

Design, development and testing of the x-ray timing explorer High Gain Antenna System p 2157 N95-27279

Spray-formed tooling
[DE95-005031] p 2246 N95-27404

Magnetic resonance imaging of solvent transport in polymer networks
[DE95-007142] p 2234 N95-27455

Calculation of design load for the MOD-5A 7.3 mW wind turbine system p 2312 N95-27982

Evaluating the environmental viability of open burning/open detonation operations p 2170 N95-28297

Prototype development and test results of a continuous ambient air monitoring system for hydrazine at the 110 ppb level p 2173 N95-28310

Hazards analysis of an integral class 1.1/1.3 rocket motor demilitarization and ingredient recovery system using ammonia p 2174 N95-28315

Development and implementation of a system safety program for the space launch complex 3 east (SLC-3E) ground support system project to support Atlas 2 family of space launch vehicles p 2174 N95-28316

Unmanned aerial vehicles, 1994 master plan
[AD-A291628] p 2136 N95-28411

SYSTEMS INTEGRATION

US Coast Guard Human Systems Integration (HSI) process model
[AD-A289172] p 2358 N95-26612

Basic space payload fastener p 2156 N95-27273

Non-explosive actuation for the ORBCOMM (TM) satellite p 2156 N95-27274

Integrated planning and scheduling for Earth science data processing p 2384 N95-27382

A fuzzy logic intelligent diagnostic system for spacecraft integrated vehicle health management p 2385 N95-27392

Analysis methods for wind turbine control and electrical system dynamics p 2273 N95-27984

A conceptual framework for evaluating variable speed generator options for wind energy applications p 2273 N95-27987

A knowledge highway for integrated modelling from manufacturing to design
[AD-A288872] p 2247 N95-28187

SYSTEMS MANAGEMENT

Analysis, design and implementation of a database system for the systems management curriculum office
[AD-A289656] p 2452 N95-26758

Research and development management information system, system user manual
[AD-A289151] p 2453 N95-27004

SYSTEMS SIMULATION

Adiabatic charging of nickel-hydrogen batteries p 2272 N95-26795

Reference manual: Naive physics simulator
[PB95-184917] p 2369 N95-26907

SYSTEMS STABILITY

Modulation effect of a Bragg acousto-optic bistable system
[AD-A289622] p 2401 N95-26857

Design considerations in supercritical fluid technology p 2232 N95-27126

T

T-56 ENGINE

Characteristics of the turbine inlet temperature sensing circuit for the T56 turbo-prop engine
[DSTO-TR-0095] p 2139 N95-26424

TABLES (DATA)

Development and analysis of SCR requirements tables for system scenarios
[NASA-CR-197769] p 2367 N95-26802

Enplanement and all cargo activity
[AD-A280074] p 2144 N95-28151

TACTILE SENSORS (ROBOTICS)

Silicon based microactuators for telerobotic tactile stimulation
[AD-A289340] p 2260 N95-26767

TAIL ASSEMBLIES

F/A-18 IFOSTP Fatigue test airbag load determination on the vertical and horizontal tails
[DSTO-TR-0135] p 2128 N95-26389

Numerical simulation of the SOFIA flow field
[NASA-CR-197757] p 2274 N95-26589

Application of damage tolerance methodology in certification of the Piaggio P-180 Avanti p 2138 N95-28480

TANTALUM

Engineered materials for appliation in severe metallurgical environments: Tantalum-carbon alloy development
[DE95-006838] p 2216 N95-27488

TAPE RECORDERS

Distributed interactive simulation virtual cassette recorder (DIS VCR); A datalogger with variable speed replay
[AD-A289212] p 2290 N95-26989

TAPS

ACT adaptive filters
[AD-A288385] p 2363 N95-26474

TARGET ACQUISITION

Target detection for vision systems
[AD-D017271] p 2249 N95-26509

A probabilistic target classification and description model for seismic sensors
[AD-A288548] p 2335 N95-26531

A mathematical framework for an improved search model
[AD-A288858] p 2358 N95-26552

A mathematical analysis of the Janus combat simulation weather effects models and sensitivity analysis of sky-to-ground brightness ratio on target detection
[AD-A289629] p 2336 N95-26858

Classification of ultra high range resolution radar using decision boundary analysis
[AD-A289378] p 2251 N95-26877

An image quality analysis of ANVIS-6 night vision goggles
[AD-A289398] p 2359 N95-26883

Processing of wide-angle synthetic aperture radar signals for detection of obscured ground targets
[AD-A289243] p 2253 N95-26976

Nonlinear signal processing schemes for robust target detection in radar
[AD-A288449] p 2255 N95-27185

Aircraft IR/acoustic detection evaluation. Volume 2: Development of a ground-based acoustic sensor system for the detection of subsonic jet-powered aircraft
[NASA-CR-189705-VOL-2] p 2402 N95-28073

TARGET RECOGNITION

A probabilistic target classification and description model for seismic sensors
[AD-A288548] p 2335 N95-26531

Classification of ultra high range resolution radar using decision boundary analysis
[AD-A289378] p 2251 N95-26877

An image quality analysis of ANVIS-6 night vision goggles
[AD-A289398] p 2359 N95-26883

Cognitive networks for ATR: The roles of bifurcation and chaos
[AD-A289010] p 2387 N95-28336

TARGETS

Target detection for vision systems
[AD-D017271] p 2249 N95-26509

Neural models of spatial orientation in novel environments
[AD-A288420] p 2380 N95-26530

A probabilistic target classification and description model for seismic sensors
[AD-A288548] p 2335 N95-26531

Scale model experiments with ceramic laminate targets
[AD-A288322] p 2225 N95-26561

Classification of ultra high range resolution radar using decision boundary analysis
[AD-A289378] p 2251 N95-26877

Simulating a multi-target acoustic array on the Intel Paragon
[AD-A288443] p 2377 N95-27183

Nonlinear signal processing schemes for robust target detection in radar
[AD-A288449] p 2255 N95-27185

Neutral gas compression in the Alcator C-Mod divertor. Experimental observations
[DE95-007762] p 2432 N95-27688

A modified proportional navigation scheme for rendezvous and docking with tumbling targets: The Planar case p 2150 N95-27784

Investigation on LCA (Life Cycle Analysis/assessment)
[DE95-759260] p 2330 N95-27942

The diffusion properties of ion implanted species in selected target materials
[DE95-007006] p 2442 N95-27959

Three-dimensional photogrammetry for laboratory applications
[AD-A291624] p 2294 N95-28410

TASK PLANNING (ROBOTICS)

Advanced development for space robotics with emphasis on fault tolerance p 2155 N95-27263

A sustainable genetic algorithm for satellite resource allocation p 2376 N95-27383

TASKS

A sustainable genetic algorithm for satellite resource allocation p 2376 N95-27383

TAYLOR SERIES

Depth migration in transversely isotropic media with explicit operators
[DE95-007670] p 2337 N95-27442

TDR SATELLITES

Flight Mechanics/Estimation Theory Symposium 1995
[NASA-CP-3299] p 2146 N95-27763

Differenced Range Versus Integrated Doppler (DRVID) ionospheric analysis of metric tracking in the Tracking and Data Relay Satellite System (TDRSS) p 2147 N95-27766

Accurate orbit determination strategies for the tracking and data relay satellites p 2147 N95-27768

Operational improvements of long-term predicted ephemerides of the Tracking and Data Relay Satellites (TDRSs) p 2147 N95-27769

A demonstration of unified TDRS/GPS tracking and orbit determination p 2151 N95-27792

TECHNICAL WRITING

Beginning to edit physics [DE95-008374] p 2455 N95-28085

TECHNOLOGIES

Performance enhancing ration components program: Supplemental carbohydrate test [AD-A288560] p 2358 N95-26558

Bibliography of NRL publications - 1990 [AD-A289483] p 2466 N95-26823

JPRS report: Science and technology. Central Eurasia [JPRS-UST-95-021] p 2202 N95-27155

JPRS report: Science and technology. Central Eurasia [JPRS-UST-95-016] p 2262 N95-27170

JPRS report: Science and technology. Central Eurasia [JPRS-UST-95-014] p 2145 N95-27171

JPRS report: Science and technology. Central Eurasia [JPRS-UST-95-015] p 2246 N95-27213

Advances in welding science: A perspective [DE95-006745] p 2302 N95-27545

JPRS Report: Science and Technology. Central Eurasia [JPRS-UST-95-020] p 2145 N95-28257

TECHNOLOGY ASSESSMENT

Asian Aeronautics: Technology acquisition drives industry development. Report to Congressional requesters [GAO/NSIAD-94-140] p 2118 N95-26817

Junkyard chemistry p 2227 N95-27102

CO2 pellet blast cleaning and degreasing: The true environmentally benign technology p 2229 N95-27109

Precision parts cleaning with supercritical CO2: Practical applications and solutions p 2229 N95-27111

Bioremediation of chlorinated organics: PCBs, TCE, HCFCs p 2179 N95-27117

Aqueous degreasing, precision cleaning, and cleanliness verification p 2231 N95-27121

Survey of environmentally benign cleaning methodologies and materials p 2231 N95-27122

Cleaning of parts for new manufacturing and parts rebuilding p 2231 N95-27123

Sceening, down selection, and implementation of environmentally compliant cleaning and insulation bonding for MNASA p 2165 N95-27124

Fluid dynamic effects on precision cleaning with supercritical fluids p 2232 N95-27129

The application of waterjets for cleaning p 2233 N95-27130

High-density plasma source for large-area chemical vapor deposition of diamond films [AD-A289053] p 2430 N95-27190

NIST Automated Manufacturing Research Facility (AMRF): March 1987 [NONP-NASA-VT-95-49097] p 2246 N95-27203

Chemical engineering: Measurements for a competitive age [NONP-NASA-VT-95-49098] p 2203 N95-27204

Geothermal direct-heat utilization assistance [DE95-007247] p 2319 N95-27236

The evolution and impact of PCS technology [AD-A288606] p 2255 N95-27249

Spinning a web: Publishing the SEI software configuration management research on the world wide web [AD-A288708] p 2377 N95-27250

Microgravity Sciences Biotechnology Facility assessment [NASA-CR-196602] p 2351 N95-27329

Hydrogen program [DE94-011827] p 2242 N95-27415

JTEC monograph on biodegradable polymers and plastics in Japan: Research, development, and applications [NASA-CR-198562] p 2235 N95-27694

Recent progress in the Photovoltaic Manufacturing Technology Project (PVMaT) [DE95-000279] p 2320 N95-27704

Current status of environmental, health, and safety issues of lithium polymer electric vehicle batteries [DE95-004005] p 2265 N95-27719

The Global Positioning System (GPS) and attitude determination: Applications and activities in the Flight Dynamics Division p 2152 N95-27795

The Sunrise project: An R&D project for a national information infrastructure prototype [DE95-006340] p 2455 N95-27847

A review of falconry as a bird control technique with recommendations for use at the Shuttle Landing Facility, John F. Kennedy Space Center, Florida, USA [NASA-TM-110142] p 2126 N95-27859

Propulsion system assessment for very high UAV under ERAST [NASA-CR-195469] p 2140 N95-27866

High-stakes aviation: US-Japan technology linkages in transport aircraft [LC-94-65759] p 2126 N95-27907

WTEC panel report on research submersibles and undersea technologies [NASA-CR-198565] p 2247 N95-27909

Analysis methods for wind turbine control and electrical system dynamics p 2273 N95-27984

A conceptual framework for evaluating variable speed generator options for wind energy applications p 2273 N95-27987

Variable speed generator technology options for wind turbine generators p 2273 N95-27988

JTEC/WTEC annual report and program summary: 1993/94 [NASA-CR-198563] p 2475 N95-28038

Research activities of the Solid State Sciences Committee in the development of a Federal initiative on advanced materials and processing [DE95-009328] p 2445 N95-28179

Swords to plowshares: Shock wave applications to advanced lithography [DE95-008154] p 2299 N95-28223

JTEC Panel report on microelectromechanical systems in Japan [NASA-CR-197831] p 2268 N95-28239

Task 4 supporting technology. Part 2: Detailed test plan for thermal seals. Thermal seals evaluation, improvement and test. CAN8-1, Reusable Launch Vehicle (RLV), advanced technology demonstrator: X-33. Leading edge and seals thermal protection system technology demonstration [NASA-CR-198628] p 2304 N95-28259

OB/OD treatment: The effective use of measured field data and air modeling to support an environmental assessment p 2170 N95-28296

Evaluating the environmental viability of open burning/open detonation operations p 2170 N95-28297

Destruction of pyrotechnics manufacture wastewater treatment sludge by plasma arc pyrolysis p 2171 N95-28301

Recovery and reuse of rocket motor propellant ingredients p 2177 N95-28326

Navy composite maintenance and repair experience p 2193 N95-28446

Composite fuselage crown panel manufacturing technology p 2137 N95-28474

TECHNOLOGY TRANSFER

Proceedings: Workshop on Research Needs in Wind Engineering [PB95-189528] p 2308 N95-26743

Spray-formed tooling [DE95-005031] p 2246 N95-27404

High-stakes aviation: US-Japan technology linkages in transport aircraft [LC-94-65759] p 2126 N95-27907

Collected papers on wind turbine technology [NASA-CR-195432] p 2321 N95-27970

Applications of lasers and electro-optics [DE95-600841] p 2299 N95-28330

Global trade in satellites and launch services [GPO-84-811] p 2165 N95-28342

TECHNOLOGY UTILIZATION

Space Commerce 1994 Forum: The 10th National Space Symposium. Proceedings report [NASA-CR-198031] p 2144 N95-26583

Integrated mission precision attack cockpit technology (IMPACT). Phase 1: Identifying technologies for air-to-ground fighter integration [AD-A289562] p 2129 N95-26684

Structures and materials technology needs for communications and remote sensing spacecraft [NASA-CR-198166] p 2163 N95-27026

Novel field effect transistors for low power electronics [AD-A288650] p 2262 N95-27096

Cleaning of parts for new manufacturing and parts rebuilding p 2231 N95-27123

Low temperature materials growth and processing development for flat panel display technology applications [AD-A288970] p 2233 N95-27187

NIST Automated Manufacturing Research Facility (AMRF): March 1987 [NONP-NASA-VT-95-49097] p 2246 N95-27203

Microelectronics in Japan p 2263 N95-27227

Japan's technology and manufacturing infrastructure p 2263 N95-27229

Japan's electronic packaging technologies p 2263 N95-27230

High-performance reactionless scan mechanism p 2158 N95-27288

Thermal neutral format based on the step technology p 2283 N95-27363

The 1995 Goddard Conference on Space Applications of Artificial Intelligence and Emerging Information Technologies [NASA-CP-3296] p 2382 N95-27375

Recent progress in the Photovoltaic Manufacturing Technology Project (PVMaT) [DE95-000279] p 2320 N95-27704

The US Molten Carbonate Fuel-Cell development and commercialization effort [DE95-008580] p 2320 N95-27746

Transportation R and D included in thermal and mechanical sciences program [DE95-008275] p 2303 N95-28070

Utilization of composite materials by the US Army: A look ahead p 2189 N95-28421

NASA/DOD Aerospace Knowledge Diffusion Research Project. Report 35: The use of computer networks in aerospace engineering [NASA-CR-198170] p 2456 N95-28600

TEFLON (TRADEMARK)

Design and development of experimental facilities for short duration, low-gravity combustion and fire experiments [NASA-CR-195458] p 2244 N95-26709

Effects of atomic oxygen on polymeric materials flown on EOIM-3 p 2242 N95-27638

Thermal control materials on EOIM-3 p 2242 N95-27639

TELECOMMUNICATION

Assessment of long-distance HF radio and satellite communication assets for RNLAF out-of-area operations [AD-A288633] p 2247 N95-26344

Milestones in telecommunications in some selected countries [PB95-184826] p 2252 N95-26929

XTP as a transport protocol for distributed parallel processing [DE95-004992] p 2378 N95-27402

Low-power, parallel photonic interconnections for Multi-Chip Module applications [DE95-008518] p 2267 N95-28147

Inspection methods for underwater cables [AD-A289610] p 2312 N95-28616

TELECONFERENCING

Technical progress report to the Department of Energy on the Solid State Sciences Committee (SSSC) [DE95-007113] p 2441 N95-27925

TELEGRAPH SYSTEMS

Milestones in telecommunications in some selected countries [PB95-184826] p 2252 N95-26929

TELEMETRY

A simple method for verifying the deployment of the TOMS-EP solar arrays p 2150 N95-27782

Telemetry down-link Doppler as an attitude sensor for spin stabilized spacecraft p 2150 N95-27785

Preliminary flight software specification for the petite amateur Navy satellite (PANSAT) [AD-A280068] p 2165 N95-28150

TELEOPERATORS

Telepresent spacecraft docking with object-based bilateral control (OBBC) [AD-A289268] p 2163 N95-26980

TELEPHONES

Milestones in telecommunications in some selected countries [PB95-184826] p 2252 N95-26929

TELEROBOTICS

Silicon based microactuators for telerobotic tactile stimulation [AD-A289340] p 2260 N95-26767

Survey and implementation of commercial manual controllers for a generic telerobotics architecture [AD-A289215] p 2381 N95-26990

Performance of the Satellite Test Assistant Robot in JPL's Space Simulation Facility p 2154 N95-27264

TELESCOPES

Numerical simulation of the SOFIA flow field [NASA-CR-197757] p 2274 N95-26589

Compensated deconvolution from wavefront sensing [AD-A289490] p 2336 N95-26824

SXI Prototype mirror mount [NASA-CR-196613] p 2301 N95-27244

Retrofitting a fine-pointing system to satellite optics p 2157 N95-27277

The Solar X-ray Imager Vacuum Door Assembly p 2157 N95-27280

TELEVISION SYSTEMS

Information superhighway: Issues affecting development [AD-A289434] p 2252 N95-26923

TV-holography at high temperatures: In situ observations of the oxidation of advanced materials [PB95-195343] p 2294 N95-28651

TEMPERATURE CONTROL

Characteristics of the turbine inlet temperature sensing circuit for the T56 turbo-prop engine [DSTO-TR-0095] p 2139 N95-26424

CAE for thermal management of aerospace electronic boards using the BETAsoft program p 2272 N95-27354

Reducing cold-start emissions by catalytic converter thermal management [DE95-000256] p 2327 N95-27540

Thermal analysis of PANSAT batteries and Electrical Power Subsystem [AD-A290013] p 2269 N95-28388

Cryogenic temperature control and tension/compression attachment stage for an electron microscope [AD-D017390] p 2294 N95-28612

TEMPERATURE DEPENDENCE

Temperature dependence of ion-beam-induced amorphization in (Beta)-SiC [DE95-007164] p 2438 N95-27087

Simulating the production of free defects in irradiated metals [DE95-007165] p 2214 N95-27088

Spin-density-wave magnetism in dilute copper-manganese alloys [DE95-005121] p 2215 N95-27462

D/H and O-18/O-16 partitioning between water liquid and vapor in the system H2O-Na-K-Mg-Ca-Cl-SO4 from 0 to 350 C [DE95-007013] p 2208 N95-27961

Determination of phase transitions in a lyotropic liquid crystal by positron annihilation technique [DE95-609162] p 2442 N95-27964

Polarization relaxation in zinc oxide varistors from 77 K to 450 K [DE95-007761] p 2268 N95-28156

Low noise monolithic Si JFETS for operation in the 90-300K range and in high radiation environments [DE95-007303] p 2269 N95-28244

Temperature dependence of the static dielectric response in a Q1D electron gas [DE95-609269] p 2400 N95-28350

Fellowship in physics [AD-A291691] p 2446 N95-28522

TEMPERATURE DISTRIBUTION

Engineering calculations associated with the ablative thermal protective structures of returnable satellites [AD-A289593] p 2162 N95-26715

RTE: A computer code for Rocket Thermal Evaluation p 2177 N95-27355

TEMPERATURE EFFECTS

Process control of microstructure in manufacturing [AD-A288291] p 2245 N95-26410

Rotor phases in compound semiconductors [DE95-004139] p 2436 N95-26442

Micromechanical prediction of tensile damage for ceramic matrix composites under high temperature [AD-A288238] p 2180 N95-26626

Characteristics of thermal lens in a copper-vapor laser [AD-A289545] p 2294 N95-26874

The noise reduction potential of dual-stream coaxial rectangular improperly expanded jet flows [NASA-CR-197820] p 2277 N95-26995

A finite element based technique for simulation helix TWT interaction circuit thermal behavior [AD-A289552] p 2262 N95-27152

Probabilistic material strength degradation model for Inconel 718 components subjected to high temperature, high-cycle and low-cycle mechanical fatigue, creep and thermal fatigue effects [NASA-CR-197832] p 2214 N95-27167

The 77 K operation of a multi-resonant power converter [NASA-TM-106941] p 2264 N95-27374

The effects of temperature on Schottky diode barrier height and evidence of multiple barrier [DE95-609147] p 2264 N95-27405

Bonded composite repair of thin metallic materials: Variable load amplitude and temperature cycling effects p 2132 N95-27509

Repair of high temperature composite aircraft structure p 2134 N95-27520

Scarf joint technique with cocured and precured patches for composite repair p 2135 N95-27524

Point defect formation in optical materials expos ed to the space environment p 2428 N95-27646

Effects of high-temperature environments on flaw generation and fracture behavior of SiC/SiC composites [DE95-008270] p 2183 N95-28068

Stability of chromite interconnections in dual environments [DE95-007755] p 2267 N95-28131

Neural network error compensation of machine tools [AD-A289300] p 2387 N95-28217

On the thermally-induced residual stresses in thick fiber-thermoplastic matrix (PEEK) cross-ply laminated plates p 2187 N95-28285

Composite flexible insulation for thermal protection of space vehicles p 2166 N95-28293

Poly(N-arylenbenzimidazoles) via aromatic nucleophilic displacement [NASA-CASE-LAR-14939-1] p 2179 N95-28360

Polybenzimidazoles via aromatic nucleophilic displacement [NASA-CASE-LAR-14924-1-CU] p 2179 N95-28361

Characterization of a fused silica capacitance standard [DE95-006457] p 2270 N95-28597

High temperature oxidation of nickel concentrates [PB95-195566] p 2224 N95-28644

Thermally-induced unsymmetric optical distortion of output window of high-power CO2 laser [AD-A289604] p 2300 N95-28650

TEMPERATURE GRADIENTS

A finite element based technique for simulation helix TWT interaction circuit thermal behavior [AD-A289552] p 2262 N95-27152

Laser ultrasonic generation at the surface of a liquid metal [DE95-004999] p 2216 N95-27477

AMCC casting development. Volume 1: Executive Summary [NASA-CR-196597] p 2247 N95-28419

Experimental study on transition characteristics of natural-convection flow [PB95-192423] p 2289 N95-28637

TEMPERATURE MEASUREMENT

Characteristics of the turbine inlet temperature sensing circuit for the T56 turbo-prop engine [DSTO-TR-0095] p 2139 N95-26424

The effect of infrared sea surface temperature measurements on evaporation duct height estimation [AD-A289045] p 2346 N95-26477

Infrared field measurements of sea surface temperature: Analysis of wake signatures and comparison of skin layer models [NASA-CR-197849] p 2346 N95-26533

BIPM project: Intercomparison of water triple-point cells [PB95-185237] p 2398 N95-26614

Method and apparatus for polaradiometric pyrometer [NASA-CASE-NPO-19064-1-CU] p 2290 N95-26765

A phase-stepped point diffraction interferometer using liquid crystals [NASA-TM-106922] p 2293 N95-28037

Remote measurement of ground temperature and emissivity [DE95-008055] p 2314 N95-28053

TEMPERATURE MEASURING INSTRUMENTS

Micro-time stress measurement device development [AD-A289511] p 2361 N95-26845

TEMPERATURE PROFILES

Temporal and spatial decorrelation scales of the Yellow Sea thermal fields [AD-A288617] p 2346 N95-26483

Development of density and temperature profile diagnostics for ICF targets [DE95-007664] p 2433 N95-28052

TEMPERATURE SENSORS

Characteristics of the turbine inlet temperature sensing circuit for the T56 turbo-prop engine [DSTO-TR-0095] p 2139 N95-26424

Method and apparatus for measuring temperatures in fabrics and flexible thermal insulations [NASA-CASE-ARC-11984-1] p 2293 N95-28345

TEMPLATES

An introduction to software architecture [AD-A288356] p 2363 N95-26467

High pressure conductivity study of template synthesized polypyrrole: Observation of a crossover from three to one dimensional variable range hopping [AD-A288367] p 2224 N95-26470

Template synthesis of electronically conductive polymer nanostructures [AD-A288373] p 2225 N95-26472

TEMPORAL RESOLUTION

Fluxes across the west coast resolved by Picket Fence observations during stormfest [AD-A288511] p 2341 N95-26653

Measurement of particle transport coefficients on Alcator C-Mod [DE95-007763] p 2411 N95-28020

TENSILE PROPERTIES

Micromechanical prediction of tensile damage for ceramic matrix composites under high temperature [AD-A288238] p 2180 N95-26626

Statistical analysis of tensile mechanical property data of carbon/polyimide composites [NAL-TR-1238] p 2180 N95-26667

Overview of through-thickness test methods for polymer matrix composites [PB95-190112] p 2227 N95-26747

Tensile properties of Fe-16 at. % Al alloys [DE95-007102] p 2215 N95-27450

The development of mechanical strength in a ceramic material during firing [DE95-004925] p 2234 N95-27476

Tension fracture of laminates for transport fuselage. Part 1: Material screening p 2137 N95-28471

The elevated temperature tensile properties of S-200E commercially pure beryllium [DE95-009331] p 2223 N95-28534

TENSILE STRENGTH

Identification of the plastic anisotropy of an aluminum alloy [IFTR-26/1994] p 2212 N95-26512

Status of bonded boron/epoxy doublers for military and commercial aircraft structures p 2132 N95-27506

Tungsten carbide fragmentation: Experimental characterization and numerical modelling [DE95-008521] p 2236 N95-27879

Service tough composite structures using the Z-direction reinforcement process p 2185 N95-28272

Mechanical properties of triaxially braided composites: Experimental and analytical results p 2189 N95-28423

Effect of the fiber-matrix interphase on the transverse tensile strength of the unidirectional composite material p 2190 N95-28425

TENSILE STRESS

Creep recovery of PVC and polypropylene [PB95-185112] p 2224 N95-26448

Addressing tension instability in SPH methods [AD-A289531] p 2276 N95-26852

Fatigue behavior of a cross-ply ceramic matrix composite subjected to tension-tension cycling with hold time [AD-A289418] p 2182 N95-27134

Deployment and retraction of a cable-driven solar array: Testing and simulation p 2158 N95-27283

Composite repair issues on the CF-18 aircraft p 2134 N95-27518

The elevated temperature tensile properties of S-200E commercially pure beryllium [DE95-009331] p 2223 N95-28534

TENSILE TESTS

On aircraft repair verification of a fighter A/C integrally stiffened fuselage skin p 2133 N95-27515

TENSIOMETERS

Cryogenic temperature control and tension/compression attachment stage for an electron microscope [AD-D017390] p 2294 N95-28612

TENSORS

The role of microprocesses in macroscale magnetotail dynamics [DE95-006288] p 2432 N95-27673

Hydrogen-like atom in laser field: Invariant atomic parameters in the ground state [DE95-609036] p 2411 N95-27930

TERBIUM COMPOUNDS

The oxidation state and magnetic behaviour of Tb in high-(Tc) related materials [DE95-007129] p 2219 N95-27966

TERMINAL BALLISTICS

Scale model experiments with ceramic laminate targets [AD-A288322] p 2225 N95-26561

TERMS

The PCMDI Visualization and Computation System (VCS): A workbench for climate data display and analysis [DE95-008586] p 2328 N95-27558

TERNARY ALLOYS

First-principles study of intermetallic phase stability in the ternary Ti-Al-Nb alloy system [DE95-005259] p 2213 N95-27082

TERNARY SYSTEMS

Ultrasonic study on ternary liquid systems by laser-sound interaction [DE95-608783] p 2207 N95-27929

TERPENES

A summary of ODS replacement technologies at Litton Poly-Scientific p 2228 N95-27105

TERRACES (LANDFORMS)

Boron-induced morphology changes in silicon CVD growth: A scanning tunneling microscopy study [AD-A289275] p 2290 N95-26982

TERRAIN
Meso-beta scale numerical simulation studies of terrain-induced jet streak mass/momentum perturbations
[NASA-CR-197804] p 2335 N95-26592

TERRESTRIAL RADIATION
Solar terrestrial radiation data from the Sleepers River Research Watershed
[AD-A288444] p 2464 N95-27184
Classification of RF transients in space using digital signal processing and neural network techniques
[DE95-006287] p 2256 N95-27840
Cloud classification using whole-sky imager data
[DE95-006501] p 2344 N95-28556

TEST CHAMBERS
NASA Lewis Research Center's combustor test facilities and capabilities
[NASA-TM-106903] p 2143 N95-27176
Two-phase flow research using the learjet apparatus
[NASA-TM-106814] p 2284 N95-27854
NASA Dryden flow visualization facility
[NASA-TM-4631] p 2362 N95-27914

TEST FACILITIES
Stall precursor study of high frequency data for three high speed, swept compressor rotors
[AD-A289379] p 2139 N95-26878
NASA Lewis Research Center's combustor test facilities and capabilities
[NASA-TM-106903] p 2143 N95-27176
Femtosecond X-ray generation through 90 degrees T homson scattering: Status of the LBL experiment
[DE95-006560] p 2296 N95-27674
Plasma lens experiments at the final focus test beam
[DE95-008595] p 2434 N95-28161

TEST STANDS
Design and development of a test rig for the high frequency testing of rolling sleeve airsprings
[DSTO-TN-0001] p 2142 N95-26378
Fluid dynamic effects on precision cleaning with supercritical fluids p 2232 N95-27129

TEST VEHICLES
Electric vehicle activities
[DE95-006648] p 2267 N95-28105

TESTS
JTEC monograph on biodegradable polymers and plastics in Japan: Research, development, and applications
[NASA-CR-198562] p 2235 N95-27694

TETHERED SATELLITES
Space tether-radar data processing
[AD-A289654] p 2250 N95-26725
Dynamics and control of SEDSAT tethered multi-probe for thermospheric research flight data analysis of SEDS-2 satellite: Tethered systems dynamics and flight data analysis
[NASA-CR-198653] p 2165 N95-27836

TETHERING
Dynamics and control of SEDSAT tethered multi-probe for thermospheric research flight data analysis of SEDS-2 satellite: Tethered systems dynamics and flight data analysis
[NASA-CR-198653] p 2165 N95-27836

TETRAHEDRONS
AEM investigation of tetrahedrally coordinated Ti(4+) in nickel-titanate spinel
[DE95-006624] p 2215 N95-27473

TETRAHYDROFURAN
Isolation and x-ray crystal structures of (Li(mu2-As(SiMe3)2) (mu3-As(SiMe3)2)(THF))2 and ((Me3Si)2AsLi(THF)2)2
[AD-A288870] p 2241 N95-28661

TEXTILES
Polymer infiltration studies
[NASA-CR-198601] p 2236 N95-27857
Physical interpretation and development of ultrasonic nondestructive evaluation techniques applied to the quantitative characterization of textile composite materials
[NASA-CR-198591] p 2306 N95-28034
Recent progress in NASA Langley textile reinforced composites program p 2196 N95-28475
Advanced textile applications for primary aircraft structures p 2138 N95-28476

TEXTS
Digital mapping, charting, and geodesy analysis program: Initial technical review of Raster Product Format
[AD-A289039] p 2313 N95-26476
Grayscale/resolution trade-off for text: Model predictions and psychophysical results for letter confusion and letter discrimination
[NASA-CR-197784] p 2369 N95-26930
The controller memory guide. Concepts from the field
[AD-A289263] p 2127 N95-26978

TEXTURES
Forming metallurgy: Supervised drawing course, NTH
[PB95-196507] p 2219 N95-27934
Advances in scientific visualization
[DE95-008065] p 2343 N95-28014
Local texture and grain boundary misorientations in high H(C) oxide superconductors
[DE95-007004] p 2447 N95-28606

THEOREM PROVING
A case study in automated theorem proving: A difficult problem about commutators
[DE95-008392] p 2392 N95-28173
Absolute logics
[ISBN-951-41-0775-6] p 2397 N95-28238

THEOREMS
Using the dimension reduction technique to prove that clique trees define facets for the asymmetric traveling salesman polytope
[AD-A289397] p 2389 N95-26882
Some commutativity theorems for a certain class of rings
[DE95-608750] p 2390 N95-27302
On commutativity of right s-unital rings with some polynomial constraints
[DE95-608752] p 2390 N95-27330
Mean value theorem in topological vector spaces
[DE95-608753] p 2390 N95-27331
Acceleration theorems
[DE95-007300] p 2420 N95-27484

THEORETICAL PHYSICS
The use of acoustic methods to determine the parameters of porous materials
[IFTR-40/1994] p 2401 N95-26519
Bogolyubov renormalization group
[DE95-608830] p 2448 N95-27315
Space physics educational outreach
[NASA-CR-198649] p 2399 N95-27852
The 1993 European school of high-energy physis
[DE95-610196] p 2421 N95-28040
Nonlinear beam dynamics experimental program at SPEAR
[DE95-007823] p 2422 N95-28122
General relativity and experiment
[PB95-192894] p 2450 N95-28664

THEORIES
Horizontal axis wind turbine post stall airfoil characteristics synthesization p 2124 N95-27974

THERMAL ANALYSIS
Chemistry involving the separation, isolation, and immobilization of 3-5 compound semiconductor nanocrystals and quantum dots
[AD-A288381] p 2436 N95-26473
Energization and transport of ions of ionospheric origin in the terrestrial magnetosphere
[NASA-CR-197813] p 2336 N95-26699
The Sixth Annual Thermal and Fluids Analysis Workshop
[NASA-CP-10161] p 2280 N95-27345
Validation of the SINDA/FLUINT code using several analytical solutions p 2281 N95-27350
CAE for thermal management of aerospace electronic boards using the BETAsoft program
p 2272 N95-27354
RTE: A computer code for Rocket Thermal Evaluation
p 2177 N95-27355
Numerical solution of fluid flow and heat tranfer problems with surface radiation p 2282 N95-27357
Thermal neutral format based on the step technology
p 2283 N95-27363
Thermal analysis of PANSAT batteries and Electrical Power Subsystem
[AD-A290013] p 2269 N95-28388

THERMAL BATTERIES
Electrolyte effects in Li(Si)/FeS2 thermal batteries
[DE95-001614] p 2264 N95-27474

THERMAL BOUNDARY LAYER
Direct numerical simulation of transitional and turbulent flow over a heated flat plate using finite-difference schemes
[NASA-CR-197753] p 2275 N95-26776

THERMAL CONDUCTIVITY
A new Cu-8 Cr-4 Nb alloy for high temperature applications
[NASA-TM-106910] p 2218 N95-27728
Subharmonic phonon transmission and Kapitza conductance between crystals with very different vibrational spectra
[DE95-609151] p 2447 N95-28608

THERMAL CONTROL COATINGS
Orbital atomic oxygen effects on materials: An overview of MSFC experiments on the STS-46 EOIM-3
p 2419 N95-27637
Thermal control materials on EOIM-3
p 2242 N95-27639
Solid film lubricants and thermal control coatings flown aboard the EOIM-3 MDA sub-experiment
p 2242 N95-27640
LDEF's contribution to the selection of thermal control coatings for the Space Station p 2242 N95-27661

THERMAL CYCLING TESTS
Composite repair of metallic airframe: Twenty years of experience p 2132 N95-27508
Bonded composite repair of thin metallic materials: Variable load amplitude and temperature cycling effects
p 2132 N95-27509

THERMAL DECOMPOSITION
Boron-induced reconstructions of Si(100) investigated by scanning tunneling microscopy
[AD-A289222] p 2438 N95-26959
Hydrogen induced C-C, C-N, and C-S bond activities on Pi and Ni surfaces
[DE95-006251] p 2206 N95-27838

THERMAL DEGRADATION
Combined investigation of Eddy current and ultrasonic techniques for composite materials NDE
[NASA-TM-110599] p 2306 N95-26778
Evaluation of high ester content PAO based single hydraulic fluid in high humidity conditions
[AD-A289374] p 2233 N95-27324

THERMAL DIFFUSION
Radiation production from stagnating compact toroids employing a nonequilibrium radiation diffusion model
[AD-A289602] p 2429 N95-26720

THERMAL ENERGY
Magnetization of ferromagnetic clusters
[DE95-006878] p 2399 N95-27548
Polarization relaxation in zinc oxide varistors from 77 K to 450 K
[DE95-007761] p 2268 N95-28156

THERMAL EXPANSION
Ultra high purity, dimensionally stable INVAR 36
[NASA-CASE-NPO-19358-1-CU] p 2213 N95-26862
Density changes in amorphous Pd80Si20 during low temperature ion irradiation
[DE95-007132] p 2441 N95-27928
Development of low-expansion ceramics with strength retention to elevated temperatures
[DE95-005760] p 2239 N95-28397

THERMAL FATIGUE
Development of welded solar arrays for DMSP and GPS satellites
[AD-A289512] p 2318 N95-26846
Characterization of fatigue behavior of 2-D woven fabric reinforced ceramic matrix composite at elevated temperature
[AD-A289423] p 2181 N95-26886
Probabilistic material strength degradation model for Inconel 718 components subjected to high temperature, high-cycle and low-cycle mechanical fatigue, creep and thermal fatigue effects
[NASA-CR-197832] p 2214 N95-27167
A microstructurally based model of solder joints under conditions of thermomechanical fatigue
[DE95-006226] p 2309 N95-27837

THERMAL INSULATION
Task 4 supporting technology. Part 2: Detailed test plan for thermal seals. Thermal seals evaluation, improvement and test. CAN8-1, Reusable Launch Vehicle (RLV), advanced technology demonstrator: X-33. Leading edge and seals thermal protection system technology demonstration
[NASA-CR-198628] p 2304 N95-28259
Composite flexible insulation for thermal protection of space vehicles p 2166 N95-28293
Method and apparatus for measuring temperatures in fabrics and flexible thermal insulations
[NASA-CASE-ARC-11984-1] p 2293 N95-28345
AMCC casting development. Volume 1: Executive Summary
[NASA-CR-196597] p 2247 N95-28419

THERMAL NEUTRONS
Materials considerations for molten salt accelerator-based plutonium conversion systems
[DE95-006743] p 2217 N95-27544

THERMAL PROTECTION
Probabilistic risk assessment of the Space Shuttle. Phase 3: A study of the potential of losing the vehicle during nominal operation. Volume 5: Auxiliary shuttle risk analyses
[NASA-CR-197812] p 2160 N95-26403
Chinese space science and technology
[AD-A289618] p 2466 N95-26856
Debris/Ice/TPS assessment and integrated photographic analysis of Shuttle mission STS-67
[NASA-TM-110651] p 2160 N95-27238
Task 4 supporting technology. Part 1: Detailed test plan for leading edge tile development. Leading edge material development and testing
[NASA-CR-198633] p 2160 N95-28258

Task 4 supporting technology. Part 2: Detailed test plan for thermal seals. Thermal seals evaluation, improvement and test. CAN8-1, Reusable Launch Vehicle (RLV), advanced technology demonstrator: X-33. Leading edge and seals thermal protection system technology demonstration
[NASA-CR-198628] p 2304 N95-28259
Composite flexible insulation for thermal protection of space vehicles p 2166 N95-28293

THERMAL RADIATION
Method and apparatus for polaradiometric pyrometer
[NASA-CASE-NPO-19064-1-CU] p 2290 N95-26765
A case study of view-factor rectification procedures for diffuse-gray radiation enclosure computations
p 2281 N95-27353
Observation on radiation transfer experiments using k-shell absorption spectra
[DE95-008068] p 2434 N95-28141

THERMAL RESISTANCE
Engineering calculations associated with the ablative thermal protective structures of returnable satellites
[AD-A289593] p 2162 N95-26715

THERMAL SHOCK
Crystal structure, short-range oxygen defects, and water adsorption in La- and Nd-modified ZrO2
[DE95-007134] p 2439 N95-27452
The development of mechanical strength in a ceramic material during firing
[DE95-004925] p 2234 N95-27476
Thermal shock behavior of fiber-reinforced composites
[DE95-006746] p 2183 N95-27955
Development of low-expansion ceramics with strength retention to elevated temperatures
[DE95-005760] p 2239 N95-28397

THERMAL STABILITY
International Space Station Alpha trace contaminant control subassembly life test report
[NASA-TM-108488] p 2358 N95-26364
Use of CTFE as an additive to enhance fire resistance of single hydraulic fluid
[AD-A289377] p 2233 N95-27325
Field repair materials for naval aircraft
p 2133 N95-27514
Stability of chromite interconnections in dual environments
[DE95-007755] p 2267 N95-28131

THERMAL STRESSES
Composite repair of metallic airframe: Twenty years of experience p 2132 N95-27508

THERMIONIC CONVERTERS
Analysis of instability growth and collisionless relaxation in thermionic converters using 1-D PIC simulations
[AD-A289310] p 2319 N95-26891

THERMOCHEMICAL PROPERTIES
Extended equation-of-state for dichlorodifluoromethane (CCl2F2)
[AD-A288885] p 2177 N95-26434

THERMOCHEMISTRY
Review and analysis of the 1980-1989 biomass thermochemical conversion program
[DE95-000287] p 2325 N95-28394

THERMOCOUPLES
Characteristics of the turbine inlet temperature sensing circuit for the T56 turbo-prop engine
[DSTO-TR-0095] p 2139 N95-26424
Process and control systems for composites manufacturing p 2184 N95-28267

THERMODYNAMIC PROPERTIES
Thermodynamics of electrolyte solutions for use in high energy lithium batteries
[AD-A288897] p 2199 N95-26352
Mathematical modelling of the thermodynamic properties of coolants and working media of heat pumps
[IFTR-6/1994] p 2447 N95-26510
Photo and thermal excitation of surface chemistry on model catalyst surfaces
[AD-A288541] p 2200 N95-26528
Lightweight cold weather underwear investigation
[AD-A288506] p 2358 N95-26736
JPRS report: Science and technology. Central Eurasia
[JPRS-UST-95-021] p 2202 N95-27155
RTE: A computer code for Rocket Thermal Evaluation
p 2177 N95-27355
Thermodynamics of aqueous electrolytes at high temperatures by the isopiestic technique
[DE95-006747] p 2449 N95-27546
Aqueous electrolyte modeling in ASPEN PLUS(trademark)
[DE95-007008] p 2208 N95-27960
Critical behaviour of spin models: A transfer-matrix approach
[PB95-192456] p 2418 N95-28638

THERMODYNAMICS
Analysis and development of finite element methods for the study of nonlinear thermomechanical behavior of structural components
[NASA-CR-195354] p 2307 N95-26387
FREZCHEM: A chemical-thermodynamic model for aqueous solutions at subzero temperatures
[AD-A288456] p 2200 N95-26432
Continuum mechanical modeling of solids undergoing a phase transformation
[AD-A288274] p 2200 N95-26451
Surface crystallization and thin film melting in normal alkanes
[DE95-006694] p 2440 N95-27535
Thermodynamics of aqueous electrolytes at high temperatures by the isopiestic technique
[DE95-006747] p 2449 N95-27546
Systematic study of the ion beam mixing of oxide markers into alumina
[DE95-006262] p 2217 N95-27555
Modeling precipitation from concentrated solutions with the EQ3/6 chemical speciation codes
[DE95-006264] p 2204 N95-27556
Development of low-expansion ceramics with strength retention to elevated temperatures
[DE95-005760] p 2239 N95-28397

THERMOELECTRIC POWER GENERATION
Solar concentrator technology development for space based applications, volume 2
[NASA-CR-197724] p 2319 N95-27194

THERMOGRAVIMETRY
Chemistry involving the separation, isolation, and immobilization of 3-5 compound semiconductor nanocrystals and quantum dots
[AD-A288381] p 2436 N95-26473

THERMONUCLEAR POWER GENERATION
Transport simulation of negative magnetic shear discharges
[DE95-003941] p 2416 N95-28329
Attractive characteristics of mirrors
[DE95-008073] p 2435 N95-28356

THERMONUCLEAR REACTIONS
A new method of determining the ejected mass of novae
[DE95-007884] p 2462 N95-28062

THERMOPLASTIC RESINS
Composite prepreg application device
[NASA-CASE-LAR-15259-1] p 2182 N95-27192
Higher order finite element analysis of thick composite laminates p 2186 N95-28282
Analysis techniques for the prediction of springback in formed and bonded composite components
p 2188 N95-28289
Characterization and manufacture of braided composites for large commercial aircraft structures
p 2196 N95-28478
Advanced wing design survivability testing and results
p 2138 N95-28488

THERMOPLASTICITY
Evaluation of composite joints
[AD-A289247] p 2181 N95-26967
Repair technology for thermoplastic aircraft structures
p 2134 N95-27519
ACT/ICAPS: Thermoplastic composite activities
p 2185 N95-28274
The 18th Asilomar Conference on Polymeric Materials
[AD-A291721] p 2240 N95-28508

THERMOSETTING RESINS
Phenylethynyl terminated imide oligomers
[NASA-CASE-LAR-15175-1] p 2235 N95-27732
Static and dynamic strain energy release rates in toughened thermosetting composite laminates
p 2188 N95-28288

THERMOSIPHONS
Numerical solution of fluid flow and heat tranfer problems with surface radiation p 2282 N95-27357

THERMOSPHERE
A study of magnetic activity effects on the thermospheric winds in the low ionosphere
[AD-A288677] p 2334 N95-26488
Dynamics and control of SEDSAT tethered multi-probe for thermospheric research flight data analysis of SEDS-2 satellite: Tethered systems dynamics and flight data analysis
[NASA-CR-198653] p 2165 N95-27836
A model of the diurnal variation in magnesium ion density and radiance in the thermosphere
[AD-A289824] p 2339 N95-28575

THESES
Advanced formation flight control
[AD-A289271] p 2142 N95-26981
Summaries of theses for the degree of diploma engineer 1992-1993
[PB95-184867] p 2246 N95-27048
Distributed methods and processes in games of incomplete information
[PB95-184842] p 2396 N95-28352
Distributed methods and processes in games of incomplete information
[PB95-184859] p 2396 N95-28353

THETA PINCH
Far-infrared laser interferometry measurements on the STP-3(M) reversed-field pinch
[DE94-765440] p 2297 N95-27868
Global dynamo in a reversed field pinch plasma
[DE94-765441] p 2432 N95-27869
Burst of energetic ions from reversed field pinch plasma
[DE94-765447] p 2432 N95-27870

THICK FILMS
ECR plasma-assisted deposition of Al2O3 and dispersion-strengthened AlO2
[DE95-007743] p 2235 N95-27687

THICK PLATES
Higher order finite element analysis of thick composite laminates p 2186 N95-28282

THICKNESS
Resonant photoemission studies of thickness dependence of the unoccupied Gd 5d bands
[DE95-004127] p 2436 N95-26440
Overview of through-thickness test methods for polymer matrix composites
[PB95-190112] p 2227 N95-26747
Scarf repairs to graphite/epoxy components
p 2135 N95-27523
Using hob offset to balance dynamic strength in spur gears
[NASA-TM-106934] p 2302 N95-27698
An improved plate theory of order (1,2) for thick composite laminates p 2187 N95-28283
Molecular engineering of thin polymer films prepared from functionally-terminated oligomers
[AD-A291681] p 2240 N95-28457

THIN FILMS
Radiation sensitive area detection device and method
[NASA-CASE-MFS-28563-3] p 2423 N95-26385
Joint Services Electronics Program (JSEP)
[AD-A288299] p 2345 N95-26419
Resonant photoemission studies of thickness dependence of the unoccupied Gd 5d bands
[DE95-004127] p 2436 N95-26440
High pressure conductivity study of template synthesized polypyrrole: Observation of a crossover from three to one dimensional variable range hopping
[AD-A288367] p 2224 N95-26470
Advanced solid lubricant films by Ion-Beam Assisted Deposition
[AD-A288866] p 2225 N95-26499
Pseudomorphic semiconducting heterostructures from combinations of AlN, GaN and selected SiC polytypes: Theoretical advancement and its coordination with experimental studies of nucleation, growth, characterization and device development
[AD-A289550] p 2437 N95-26756
Materials, structures, and devices for high-speed electronics
[NASA-CR-197815] p 2260 N95-26816
Materials Research Society Symposium Proceedings. Volume 339: Diamond, SiC and nitride wide bandgap semiconductors
[AD-A288690] p 2437 N95-26818
Study of frequency doubling antireflection coating
[AD-A289634] p 2424 N95-26860
Microwave characterization of sub-micron N- and P-channel MOSFET's fabricated with thin film silicon-on-sapphire
[AD-A289296] p 2438 N95-27040
Effects of blowing ratio on heat transfer to the throat region of a porous-walled nozzle
[AD-A289459] p 2167 N95-27153
Low temperature materials growth and processing development for flat panel display technology applications
[AD-A288970] p 2233 N95-27187
Analysis of gas absorption to a thin liquid film in the presence of a zero-order chemical reaction
p 2280 N95-27348
Surface crystallization and thin film melting in normal alkanes
[DE95-006694] p 2440 N95-27535
Atomic oxygen dosimetry measurements made on STS-46 by CONCAP 2 p 2418 N95-27634
Inflight resistance measurement on high-T(sub c) superconducting thin films exposed to orbital atomic oxygen on CONCAP-2 (STS-46) p 2272 N95-27635
Solid film lubricants and thermal control coatings flown aboard the EOIM-3 MDA sub-experiment
p 2242 N95-27640
Evaluation of space environmental effects on metals and optical thin films on EOIM-3 p 2210 N95-27641

Analysis of selected specimens from the STS-46 Energetic Oxygen Interaction with Materials-3 experiment
p 2210 N95-27642

Amorphous silicon pixel radiation detectors and associated thin film transistor electronics readout
[DE95-006568] p 2265 N95-27678

Micromagnetics and microstructure of epitaxially grown Co and Co-Cr films for perpendicular magnetic recording
[DE95-004681] p 2441 N95-27720

Analysis of surfaces, films and multilayers by resonant laser ablation
[DE95-006295] p 2297 N95-27841

Nonlinear optical microscopy for imaging thin films and surfaces
[DE95-007872] p 2426 N95-28018

Effects of interlayers on the scratch adhesion performance of ultra-thin films of copper and gold on silicon substrates
[DE95-007367] p 2220 N95-28044

Low temperature deposition and characterization of N- and P-type silicon carbide thin films and associated Ohmic and Schottky contacts
[AD-A289107] p 2237 N95-28097

Control of thin film processing behavior through precursor structural modifications
[DE95-006468] p 2444 N95-28103

Pulsed laser deposition of zeolitic membranes
[DE95-006274] p 2298 N95-28124

Multivariate classification of BPSG thin films using Mahalanobis distances
[DE95-008519] p 2267 N95-28148

Atomic layer epitaxy of group 4 materials: Surface processes, thin films, devices and their characterization
[AD-A289092] p 2446 N95-28327

Cesium/oxide interactions for ultrathin films on (alpha)-Al2O3(001) and (alpha)-Al2O3(1(bar 1)O2)
[DE95-008159] p 2238 N95-28358

Molecular engineering of thin polymer films prepared from functionally-terminated oligomers
[AD-A291681] p 2240 N95-28457

Deformation behavior of thin lubricant films at elevated pressure
[AD-A288906] p 2241 N95-28592

The in situ observation of epitaxial diamond thin film nucleation and growth using emission electron microscopy
[AD-A289841] p 2447 N95-28618

Influences of film structures on laser damage thresholds
[AD-A289647] p 2300 N95-28633

Photoemission study of solid state reaction and initial oxidation of the Ce/Al(100) system
[PB95-195368] p 2210 N95-28652

THIN WALLED SHELLS

Characterization of the membrane theory of a clamped shell. The hyperbolic case
[PB95-185021] p 2308 N95-26911

Models of classical and recurrent novae
p 2459 N95-27073

THIN WALLS

Determination of the cyclical properties of 18G2A steel on the basis of skeleton curves for a planar stress state
[IFTR-32/1994] p 2211 N95-26359

Identification of the plastic anisotropy of an aluminum alloy
[IFTR-26/1994] p 2212 N95-26512

Vibrational behavior of adaptive aircraft wing structures modelled as composite thin-walled beams
p 2191 N95-28435

THREADS

A software bus for thread objects
[NASA-CR-197764] p 2365 N95-26575

THREE AXIS STABILIZATION

An MME-based attitude estimator using vector observations p 2148 N95-27775

SAMPEX special pointing mode p 2149 N95-27780

THREE BODY PROBLEM

Tracking and impact prediction of Earth-Crossing-Objects (ECO's) on a collision course with Earth
[AD-A289321] p 2461 N95-27303

THREE DIMENSIONAL BODIES

Development of an upwind, finite-volume code with finite-rate chemistry
[NASA-CR-197747] p 2121 N95-26760

THREE DIMENSIONAL BOUNDARY LAYER

Nonlinear stability of non-stationary cross-flow vortices in compressible boundary layers
[NASA-CR-189184] p 2279 N95-27242

Computation of three-dimensional mixed convective boundary layer flow p 2280 N95-27347

THREE DIMENSIONAL FLOW

Computational fluid dynamics and transonic flow
[AD-A288962] p 2273 N95-26405

Effects of three-dimensional imposed 3-D disturbances on bluff-body near wake flows
[AD-A289553] p 2121 N95-26757

Turbomachinery design and tonal acoustics computations
[NASA-CR-197749] p 2139 N95-26777

A 3D agglomeration multigrid solver for the Reynolds-averaged Navier-Stokes equations on unstructured meshes
[NASA-CR-195073] p 2390 N95-27029

Global flowfield about the V-22 Tiltrotor Aircraft
[NASA-CR-198603] p 2122 N95-27248

Calculation of three-dimensional (3-D) internal flow by means of the velocity-vorticity formulation on a staggered grid
[NASA-TM-110352] p 2122 N95-27258

Three-dimensional computer modeling of hydrogen injection and combustion
[DE95-006261] p 2203 N95-27437

Three-dimensional visualization of reactive flows in complex geometries
[DE95-006332] p 2284 N95-27845

A numerical method for solving the three-dimensional parabolized Navier-Stokes equations
[NASA-CR-198159] p 2287 N95-27917

A general theory of two- and three-dimensional rotational flow in subsonic and transonic turbomachines
[NASA-CR-4496] p 2123 N95-28003

TranAir: A full-potential, solution-adaptive, rectangular grid code for predicting subsonic, transonic, and supersonic flows about arbitrary configurations. User's manual
[NASA-CR-4349] p 2123 N95-28230

THREE DIMENSIONAL MODELS

Manual for SHOCK3D, version 2.0. Computer program for non-linear shock response
[AD-A288631] p 2307 N95-26342

Progress towards computer simulation of NiH2 battery performance over life p 2272 N95-26786

Study of the response of a three-dimensional coupled ice-ocean model to daily varying atmospheric forcing
[AD-A289050] p 2347 N95-27189

Three-dimensional computer modeling of hydrogen injection and combustion
[DE95-006261] p 2203 N95-27437

A point-centered diffusion differencing for unstructured meshes in 3-D
[DE95-008382] p 2392 N95-28232

Three-dimensional forecast models for emergency response management p 2172 N95-28303

Cloud classification using whole-sky imager data
[DE95-006501] p 2344 N95-28556

THROATS

Effects of blowing ratio on heat transfer to the throat region of a porous-walled nozzle
[AD-A289459] p 2167 N95-27153

THRUST CHAMBERS

High pressure Earth storable rocket technology program: Basic program
[NASA-CR-195449] p 2166 N95-26390

THRUST CONTROL

Evaluation and modeling of autonomous attitude thrust control for the Geostation Operational Environmental Satellite (GOES)-8 orbit determination
p 2146 N95-27765

Optimal attitude maneuver execution for the Advanced Composition Explorer (ACE) mission
p 2149 N95-27778

THRUST VECTOR CONTROL

Plume measurements with the T5 xenon ion thruster
[AD-A288697] p 2167 N95-26489

THUNDERSTORMS

A study of lightning in winter thunderstorms and the analysis of thunderstorm overflight data
[NASA-CR-198577] p 2343 N95-28191

TIDES

Observations of near-bottom flow in a wave-dominated nearshore environment
[AD-A289331] p 2347 N95-27043

TILES

Task 4 supporting technology. Part 1: Detailed test plan for leading edge tile development. Leading edge material development and testing
[NASA-CR-198633] p 2160 N95-28258

TIME

Modal event calculus in Lolli
[AD-A288544] p 2365 N95-26605

TIME DEPENDENCE

Operating system support for coexistence of real-time and conventional scheduling
[AD-A288584] p 2364 N95-26534

Anomalous collision rate in the time counter scheme of the direct simulation Monte Carlo method for rarefied gas flow analysis
[ISAS-R-653] p 2275 N95-26742

Measurement of viscosity by capillary rheometry: Dwell time effects
[PB95-190203] p 2201 N95-26750

Single-drop reactive extraction/extractive reaction with forced convective diffusion and interphase mass transfer
p 2283 N95-27365

Time-dependent model for vertical-cavity surface-emitting laser
[DE95-007880] p 2298 N95-28027

Lattice calculation for lepton capture from vacuum-pair production in relativistic heavy-ion collisions
[DE95-007392] p 2413 N95-28077

Designing for time-dependent material response in spacecraft structures p 2166 N95-28292

TIME DIVISION MULTIPLEXING

Pulse Code Modulation (PCM) encoder handbook for Aydin Vector MMP-900 series system
[NASA-RP-1365] p 2255 N95-27435

TIME FUNCTIONS

Programming for time resolved spectrum in pulse radiolysis experiments
[DE95-607929] p 2406 N95-27212

TIME LAG

A numerical study of ultra-short-pulse reflectometry
[DE95-008070] p 2266 N95-28015

TIME MARCHING

The method of space-time conservation element and solution element-applications to one-dimensional and two-dimensional time-marching flow problems
[NASA-TM-106915] p 2389 N95-26663

Numerical investigation to S-inlet flows (Numerical simulation study of S-inlet flows)
[AD-A289590] p 2120 N95-26713

TIME MEASUREMENT

Estimation of attitude sensor timetag biases
p 2153 N95-27799

Particle fallout/activity sensor
[NASA-CASE-KSC-11687-1] p 2293 N95-28362

TIME OF FLIGHT SPECTROMETERS

Future opportunities and present possibilities for coherent inelastic single crystal measurements on pulsed neutron sources
[PB95-195798] p 2418 N95-28657

TIME OPTIMAL CONTROL

Time-optimal control of the magnetically levitated photolithography platen
[DE95-005493] p 2266 N95-27724

TIME SERIES ANALYSIS

Embedology and neural estimation for time series prediction
[AD-A289312] p 2394 N95-26892

Evolving cascade-correlation networks for time-series forecasting
[AD-A289197] p 2390 N95-27020

Linear and nonlinear trending and prediction for AVHRR time series data p 2385 N95-27391

On the persistence of the oceanic background of apparent sea level changes in the Baltic Sea
[REPT-94:5] p 2348 N95-27996

Chua's circuits: Phenomena and applications
[AD-A291638] p 2271 N95-28666

TIME SHARING

Operating system support for coexistence of real-time and conventional scheduling
[AD-A288584] p 2364 N95-26534

TIME TEMPERATURE PARAMETER

Low resistivity ohmic contacts to moderately doped n-GaAs with low temperature processing
[DE95-008507] p 2445 N95-28144

Polarization relaxation in zinc oxide varistors from 77 K to 450 K
[DE95-007761] p 2268 N95-28156

TIN ALLOYS

A microstructurally based model of solder joints under conditions of thermomechanical fatigue
[DE95-006226] p 2309 N95-27837

TISSUES (BIOLOGY)

A 3-D finite difference time domain investigation of microwave propagation through inhomogeneous biological materials
[AD-A289431] p 2251 N95-26869

TITAN 4 LAUNCH VEHICLE

Chemical reactions identified in the Titan 2, Titan 4, and Delta 2 propellant systems and their application to source modeling p 2172 N95-28304

Weather hazards to a Titan 4 on-pad destack-restack operation p 2172 N95-28307

TITANIUM

On-axis polarization coupling in y-cut titanium in-diffused lithium niobate slab waveguides
[AD-A289260] p 2253 N95-26977

AEM investigation of tetrahedrally coordinated Ti(4+) in nickel-titanate spinel
[DE95-006624] p 2215 N95-27473

TITANIUM ALLOYS

Viscoplastic characterization and fatigue modeling of titanium based metal matrix composites
[AD-A289430] p 2181 N95-26868

Environmentally assisted cracking of high strength beta titanium alloys
[AD-A289156] p 2213 N95-27032

JPRS report: Science and technology. Central Eurasia
[JPRS-UST-95-019] p 2270 N95-28565

TITANIUM COMPOUNDS

Lattice parameters and Debye-Waller factors of gamma-TiAl alloys
[AD-A288843] p 2213 N95-26681

TITANIUM ISOTOPES

Lattice parameters and Debye-Waller factors of gamma-TiAl alloys
[AD-A288843] p 2213 N95-26681

TITANIUM OXIDES

The influence of surface structure on the interaction of water with TiO2(100)
[DE95-004927] p 2203 N95-27401

Control of thin film processing behavior through precursor structural modifications
[DE95-006468] p 2444 N95-28103

Femtosecond OPO's at 3 microns and beyond: Design and performance issues related to the crystal properties of KTP and similar materials
[DE95-007286] p 2446 N95-28242

Radiant exchange considerations in design and scaleup of photocatalytic reactors for purification of nitroglycerine-contaminated air p 2171 N95-28300

TITRATION

Hydrogen-ion titrations of amino acids and proteins in solutions containing concentrated electrolyte
[DE95-008356] p 2209 N95-28229

TOKAMAK DEVICES

Fluctuations and transport in fusion plasma
[DE95-004178] p 2429 N95-26444

MHD simulations of DC helicity injection for current drive in tokamaks
[DE95-007018] p 2429 N95-26940

Dynamics of the L yields H transition, VH-mode evolution, edge localized modes and R.F. driven confinement control in tokamaks
[DE95-007012] p 2430 N95-27306

Evaluation of current drive requirements and operating characteristics of a high bootstrap fraction advanced tokamak reactor
[DE95-007041] p 2430 N95-27308

Outline and handling manual of fusion experimental data monitor system DAISY, version 2
[DE95-703895] p 2431 N95-27414

Energetic particle destabilization of shear Alfven waves in stellarators and tokamaks
[DE95-006393] p 2431 N95-27419

Fast wave current drive in D3-D
[DE95-007582] p 2431 N95-27441

Nonlinear phenomena, turbulence and anomalous transport in fusion plasmas
[DE95-007044] p 2431 N95-27497

Neutral gas compression in the Alcator C-Mod divertor. Experimental observations
[DE95-007762] p 2432 N95-27688

Fluctuations in high beta(sub p) plasmas in DIII-D
[DE95-008071] p 2432 N95-27710

Experimental aspects of effects of high-energy particles on Alfven modes
[DE95-003383] p 2432 N95-27873

Pumping characteristics of a cryopump with Ar sorbent in He and in D2/He mixture
[DE95-007049] p 2302 N95-27875

Fluctuations and transport in fusion plasmas
[DE95-007111] p 2433 N95-27924

Measurement of particle transport coefficients on Alcator C-Mod
[DE95-007763] p 2411 N95-28020

Scrape-off layer plasma modeling for the DIII-D tokamak
[DE95-008059] p 2433 N95-28054

UEDGE and DEGAS modeling of the DIII-D scrape-off layer plasma, revision 1
[DE95-008052] p 2433 N95-28065

Effect of toroidal plasma flow and flow shear on global MHD modes
[DE95-006676] p 2433 N95-28106

Advanced tokamak operating modes in TPX and ITER
[DE95-008058] p 2434 N95-28138

Divertor research on the DIII-D tokamak
[DE95-003942] p 2434 N95-28185

Faraday screen sputtering on TPX
[DE95-008347] p 2434 N95-28224

Transport simulation of negative magnetic shear discharges
[DE95-003941] p 2416 N95-28329

Operating points and feedback control of plasma characteristics in tokamaks with full current drive
[DE95-007037] p 2435 N95-28553

Tokamak ETE engineering preliminary project
[INPE-5529-PRE/1796] p 2435 N95-28562

Pellet injector research and development at ORNL
[DE95-006736] p 2435 N95-28596

Simulation of burning tokamak plasmas
[PB95-195426] p 2435 N95-28654

TOLERANCES (MECHANICS)

CORSSTOL: Cylinder Optimization of Rings, Skin, and Stringers with Tolerance sensitivity
[NASA-TP-3551] p 2392 N95-28215

Tension fracture of laminates for transport fuselage. Part 1: Material screening p 2137 N95-28471

Application of damage tolerance methodology in certification of the Piaggio P-180 Avanti
p 2138 N95-28480

Applications of a damage tolerance analysis methodology in aircraft design and production
p 2197 N95-28483

Damage tolerance of a geodesically stiffened advanced composite structural concept for aircraft structural applications p 2138 N95-28487

TOLLMIEN-SCHLICHTING WAVES

Analysis of hypersonic boundary layer second mode instability over a 7 deg cone
[AD-A289471] p 2276 N95-26819

On the modulational instability of large amplitude waves in supersonic boundary layers
[NASA-CR-195072] p 2284 N95-27760

TOMOGRAPHY

Tomographic observations of deep convection and the thermal evolution of the Greenland Sea Gyre 1988-1989
[AD-A289104] p 2348 N95-28096

Radon transform and its applications in gridding airborne geophysical survey data
[PB95-195533] p 2315 N95-28643

TOOLING

Spray-formed tooling
[DE95-005031] p 2246 N95-27404

TOPOGRAPHY

Deep convection in the Mediterranean Sea
[AD-A288497] p 2346 N95-26647

Naval Aviation System TEAM mapping, charting, and geodesy handbook
[AD-A288590] p 2314 N95-26841

Airborne geophysics and precise positioning: Scientific issues and future directions
[LC-94-68678] p 2314 N95-27156

TOPOLOGY

Live from Antarctica, volume 4
[NASA-CR-197828] p 2335 N95-26596

On compact multipliers of topological algebras
[DE95-608751] p 2390 N95-27092

Spectral properties of multipliers on topological algebras
[DE95-608747] p 2390 N95-27299

Holomorphic curves in Abelian varieties, part 1
[DE95-608748] p 2396 N95-27300

Harmonic maps of the bounded symmetric domains
[DE95-608798] p 2397 N95-27485

The assembly tower and some categorical and algebraic aspects of frame theory
[AD-A289360] p 2391 N95-27489

Topological density and instantons on a lattice
[DE95-006348] p 2445 N95-28240

TOPPING CYCLE ENGINES

Optimization of wave rotors for use as gas turbine engine topping cycles
[NASA-TM-106951] p 2140 N95-27860

TOROIDAL PLASMAS

Radiation production from stagnating compact toroids employing a nonequilibrium radiation diffusion model
[AD-A289602] p 2429 N95-26720

Energetic particle destabilization of shear Alfven waves in stellarators and tokamaks
[DE95-006393] p 2431 N95-27419

Burst of energetic ions from reversed field pinch plasma
[DE94-765447] p 2432 N95-27870

Scrape-off layer plasma modeling for the DIII-D tokamak
[DE95-008059] p 2433 N95-28054

UEDGE and DEGAS modeling of the DIII-D scrape-off layer plasma, revision 1
[DE95-008052] p 2433 N95-28065

Effect of toroidal plasma flow and flow shear on global MHD modes
[DE95-006676] p 2433 N95-28106

TORQUE

Identification of the plastic anisotropy of an aluminum alloy
[IFTR-26/1994] p 2212 N95-26512

Power train torque measurement
[AD-A289577] p 2301 N95-26688

Effects of bearing cleaning and lube environment on bearing performance p 2158 N95-27285

Whirl plus tilt
[DE95-007948] p 2399 N95-28108

TORQUE MOTORS

Structural optimisation of cage induction motors using finite element analysis
[PB95-195434] p 2271 N95-28655

TORQUE SENSORS (ROBOTICS)

Multi-agent perception for Human/Robot interaction: A framework for intuitive trajectory modification
[AD-A289399] p 2359 N95-26884

TORQUEMETERS

Power train torque measurement
[AD-A289577] p 2301 N95-26688

TORQUERS

Observational magnetometer calibration with the Hubble Space Telescope's new magnetometers
p 2148 N95-27773

TORSION

Analysis of plate-twist test for in-plane shear modulus of composite materials (revised)
[PB95-190195] p 2308 N95-26749

TORUSES

Fast wave current drive in D3-D
[DE95-007582] p 2431 N95-27441

TOTAL ENERGY SYSTEMS

Development of a TECS control-law for the lateral directional axis of the McDonnell Douglas F-15 Eagle
[AD-A289771] p 2142 N95-28598

TOTAL OZONE MAPPING SPECTROMETER

Spectral analyses, climatology, and interannual variability of Nimbus-7 TOMS version 6 total column ozone
[NASA-RP-1360] p 2341 N95-26689

A simple method for verifying the deployment of the TOMS-EP solar arrays p 2150 N95-27782

Contingency maneuver strategies for the Total Ozone Mapping Spectrometer-Earth Probe (TOMS-EP)
p 2152 N95-27796

TOUGHNESS

Structural ceramics incorporating whiskers, platelets, and particulate phases
[DE95-007048] p 2235 N95-27499

High temperature Hexoloy(trademark) SX silicon carbide
[DE95-007290] p 2221 N95-28075

An experimental and numerical investigation of specimen size requirements for cleavage fracture toughness
[AD-A289120] p 2311 N95-28100

TOWERS

Engineering photochemical smog through convection towers
[DE95-007727] p 2328 N95-27888

TOXIC HAZARDS

Electromagnetic devices and processes in environment protection
[AD-A288656] p 2141 N95-26487

The use of supercritical carbon dioxide for contaminant removal from solid waste p 2229 N95-27110

Health and environmental hazards of CdTe photovoltaic module production, use and decommissioning
[DE95-006688] p 2320 N95-27682

The 1994 JANNAF Safety and Environmental Protection Subcommittee Meeting, volume 1
[CPIA-PUBL-614-VOL-1] p 2170 N95-28294

Destruction of pyrotechnics manufacture wastewater treatment sludge by plasma arc pyrolysis
p 2171 N95-28301

Cape Canaveral air station launch emergency response forces and toxic materials release contingency plans
p 2172 N95-28308

Toxicity assessment of liquid propellant XM46
p 2175 N95-28319

Hydrothermal oxidation of solid rocket propellant and other department of defense hazardous wastes
p 2177 N95-28325

Recovery and reuse of rocket motor propellant ingredients p 2177 N95-28326

TOXICITY

Retrofitting conventional vapor degreasers to use a solvent wash/fluorochemical rinse process
p 2232 N95-27127

Acute and subacute toxicity of ammonium dinitramide (ADN) p 2175 N95-28318

Toxicity assessment of liquid propellant XM46
p 2175 N95-28319

TOXICOLOGY

Acute and subacute toxicity of ammonium dinitramide (ADN) p 2175 N95-28318

TOXINS AND ANTITOXINS

Anti-idiotype probes for toxin detection
[AD-A288955] p 2348 N95-26435

TRACE CONTAMINANTS

International Space Station Alpha trace contaminant control subassembly life test report
[NASA-TM-108488] p 2358 N95-26364

TRACE ELEMENTS

Comparative experimental study of PIXE and X-ray fluorescence analysis
[DE95-607868] p 2327 N95-27198

Coupled chemistry/climate issues
[DE95-006443] p 2327 N95-27532

Measurement of heterogeneous chemical processes relevant to aerosol surfaces and trace gases active in the marine environment
[DE95-008337] p 2328 N95-27743

Trace elements and the mechanical properties of intermetallic compounds
[DE95-007378] p 2220 N95-28046

TRACING

Ultrashort Pulse retrieval using FROG trace irradiance moments and the adaptive neural networks backpropagation algorithm
[DE95-007153] p 2299 N95-28220

TRACKED VEHICLES

Power train torque measurement
[AD-A289577] p 2301 N95-26688

TRACKING (POSITION)

Gloved operator performance study. The effects of hand wear and elastic resistance of a control during tracking performance
[AD-A289405] p 2360 N95-27099

The detection and tracking of motion by means of time-space pattern modelling using random fields
[IFTR-37/1994] p 2374 N95-28566

TRADEOFFS

Specifying weak sets
[AD-A288587] p 2364 N95-26536

Grayscale/resolution trade-off for text: Model predictions and psychophysical results for letter confusion and letter discrimination
[NASA-CR-197784] p 2369 N95-26930

Free Electron Laser Physical Process Code (FELPPC)
[DE95-006276] p 2296 N95-27557

TRAILING EDGES

Airfoil modification effects on subsonic and transonic pressure distributions and performance for the EA-6B airplane
[NASA-TP-3516] p 2120 N95-26382

Unsteady base pressure measurements in the near wake of a cylinder with imposed three-dimensional disturbances
[AD-A289498] p 2276 N95-26827

The near-wake flow behavior of an oscillating airfoil with modified trailing edge p 2119 N95-26953

TRAINING ANALYSIS

Enhancing the effects of diversity awareness training: A review of the research literature
[DOT/FAA/AM-95/10] p 2355 N95-26361

TRAINING EVALUATION

Inspection methods for underwater cables
[AD-A289610] p 2312 N95-28616

TRAJECTORIES

Telepresent spacecraft docking with object-based bilateral control (OBBC)
[AD-A289268] p 2163 N95-26980

The performance of cargo airdrop systems using g-12E parachutes: Statistical determination of minimum altitude
[AD-A291666] p 2126 N95-28454

TRAJECTORY ANALYSIS

Tracking and impact prediction of Earth-Crossing-Objects (ECO's) on a collision course with Earth
[AD-A289321] p 2461 N95-27303

TRAJECTORY CONTROL

Multi-agent perception for Human/Robot interaction: A framework for intuitive trajectory modification
[AD-A289399] p 2359 N95-26884

Operational considerations of using GPS for spacecraft navigation p 2152 N95-27794

TRAJECTORY PLANNING

The D* algorithm for real-time planning of optimal traverses
[AD-A289361] p 2367 N95-26754

TRANSCENDENTAL FUNCTIONS

Kepler Equation solver p 2147 N95-27767

TRANSFER FUNCTIONS

Structures for time-reversed inversion in filter banks
[AD-A289238] p 2261 N95-26964

Head related transfer function approximation using neural networks
[AD-A289422] p 2382 N95-27145

TRANSFER ORBITS

ORION: A Supersynchronous Transfer Orbit mission
p 2154 N95-27804

Dynamics and control of SEDSAT tethered multi-probe for thermospheric research flight data analysis of SEDS-2 satellite: Tethered systems dynamics and flight data analysis
[NASA-CR-198653] p 2165 N95-27836

The combined release and radiation effects satellite time history data base system
[AD-A289835] p 2165 N95-28578

TRANSFERRING

Comparative transduction mechanisms of hair cells in the bullfrog uticulus. 2: Sensitivity and response dynamics to hair bundle displacement p 2350 N95-26732

TRANSFORMATIONS (MATHEMATICS)

Hyperkaehler metrics associated to compact Lie groups
[PB95-185161] p 2388 N95-26514

Generalized Schwarzians in several variables and Moebius invariant differential operators
[PB95-185211] p 2388 N95-26539

A general object model transformation system
[AD-A289289] p 2370 N95-27037

Holomorphic curves in Abelian varieties, part 1
[DE95-608748] p 2396 N95-27300

Denoising and robust non-linear wavelet analysis
[AD-A291668] p 2257 N95-28455

Wavelet analysis and its applications
[AD-A291735] p 2387 N95-28527

TRANSFORMERS

A general object model transformation system
[AD-A289289] p 2370 N95-27037

Forback DC-to-DC converter
[NASA-CASE-GSC-13404-1] p 2269 N95-28341

TRANSFUSION

Mechanisms of hypertension after cross-linked hemoglobin blood-substitute transfusion
[AD-A289558] p 2352 N95-26680

TRANSIENT HEATING

High energy electron beams for ceramic joining
[DE95-006316] p 2420 N95-27480

TRANSIENT RESPONSE

Transient studies of G-induced capillary dryout and rewet p 2281 N95-27351

TRANSISTOR CIRCUITS

Self-checking state machine realization in CMOS
[AD-A289149] p 2261 N95-27002

Characterization of microwave MESFET circuits under laser illumination. Applications to phased array radar, microwave communications, and digital clock control
[AD-A289181] p 2261 N95-27015

TRANSISTORS

Investigation of radiation resistance of transistors and integrated circuits using the heavy ions beam of energy higher than 1 MeV/amu and fast neutrons
[DE95-608624] p 2261 N95-27024

Amorphous silicon pixel radiation detectors and associated thin film transistor electronics readout
[DE95-006568] p 2265 N95-27678

Forback DC-to-DC converter
[NASA-CASE-GSC-13404-1] p 2269 N95-28341

TRANSITION FLOW

Turbulence modeling
[NASA-CR-197751] p 2274 N95-26665

The stability of the flow in a laminar separation bubble
[CUED/A-AERO/TR-22] p 2275 N95-26809

Transitional flow in thin tubes for space station freedom radiator p 2282 N95-27360

Experimental study on transition characteristics of natural-convection flow
[PB95-192423] p 2289 N95-28637

TRANSITION METALS

Theoretical studies of reaction surfaces
[AD-A288458] p 2404 N95-26632

The response of hydrotalcite coated aluminum to sealing with transition metal salt solutions
[DE95-004767] p 2234 N95-27460

Experimental determination of cluster geometrical structure
[DE95-007089] p 2409 N95-27753

Defect characterization of electronic conducting pseudo-perovskite systems
[DE95-007487] p 2220 N95-28049

Cavity formation and impurity gettering in He-implanted Si
[DE95-007744] p 2444 N95-28127

Chemical and electrical properties of cavities in silicon and germanium
[DE95-006812] p 2445 N95-28206

Surface structure of MX-chains studied by atomic force microscopy
[DE95-007881] p 2447 N95-28541

TRANSITION TEMPERATURE

High pressure conductivity study of template synthesized polypyrrole: Observation of a crossover from three to one dimensional variable range hopping
[AD-A288367] p 2224 N95-26470

Investigations of the hyperfine interactions in copper-oxide perovskites using Eu-151 and Fe-57 Moessbauer spectroscopy
[PB95-185138] p 2437 N95-26513

Recent neutron scattering results on high-temperature superconductors
[DE95-007028] p 2413 N95-28066

TRANSLATING

Chemical physics of uniform cyclic etching
[AD-A288975] p 2404 N95-26574

TRANSMISSION ELECTRON MICROSCOPY

Chemistry involving the separation, isolation, and immobilization of 3-5 compound semiconductor nanocrystals and quantum dots
[AD-A288381] p 2436 N95-26473

Characterization of collision cascade damage in Ca2La8(SiO4)6O2 by HRTEM
[DE95-005719] p 2440 N95-27491

Phase stability and elasticity of C15 transition-metal intermetallic compounds
[DE95-007876] p 2219 N95-28026

TRANSMISSION LOSS

Natural aerosol extinction module: XSCALE 1992 user's guide
[AD-A289029] p 2340 N95-26463

TRANSMISSIONS (MACHINE ELEMENTS)

Power train torque measurement
[AD-A289577] p 2301 N95-26688

Diagnosis of helicopter gearboxes using structure-based networks
[NASA-TM-106932] p 2302 N95-27373

Using hob offset to balance dynamic strength in spur gears
[NASA-TM-106934] p 2302 N95-27698

TRANSMITTER RECEIVERS

Radio telemetry buoy for long-range communication
[AD-D017269] p 2161 N95-28581

TRANSONIC COMPRESSORS

A general theory of two- and three-dimensional rotational flow in subsonic and transonic turbomachines
[NASA-CR-4496] p 2123 N95-28003

TRANSONIC FLOW

Computational fluid dynamics and transonic flow
[AD-A288962] p 2273 N95-26405

A numerical method for unsteady transonic flow about wings with control surfaces
[AD-A289631] p 2121 N95-26859

A general theory of two- and three-dimensional rotational flow in subsonic and transonic turbomachines
[NASA-CR-4496] p 2123 N95-28003

TranAir: A full-potential, solution-adaptive, rectangular grid code for predicting subsonic, transonic, and supersonic flows about arbitrary configurations. User's manual
[NASA-CR-4349] p 2123 N95-28230

TranAir: A full-potential, solution-adaptive, rectangular grid code for predicting subsonic, transonic, and supersonic flows about arbitrary configurations. Theory document
[NASA-CR-4348] p 2123 N95-28265

TRANSONIC SPEED

A fully implicit time accurate method for hypersonic combustion: Application to shock-induced combustion instability
[NASA-TM-106707] p 2273 N95-26380

Airfoil modification effects on subsonic and transonic pressure distributions and performance for the EA-6B airplane
[NASA-TP-3516] p 2120 N95-26382

Measurements of store forces and moments and cavity pressures for a generic store in and near a box cavity at subsonic and transonic speeds
[NASA-TM-4611] p 2123 N95-28241

TRANSPONDERS

Radio telemetry buoy for long-range communication
[AD-D017269] p 2161 N95-28581

Inspection methods for underwater cables
[AD-A289610] p 2312 N95-28616

TRANSPORT AIRCRAFT

Preliminary design problems and solutions for a supersonic oblique all-wing transport aircraft
p 2118 N95-26942

Load transfer in the stiffener-to-skin joints of a pressurized fuselage
[NASA-CR-198610] p 2310 N95-27865

High-stakes aviation: US-Japan technology linkages in transport aircraft
[LC-94-65759] p 2126 N95-27907

Evaluation of all-electric secondary power for transport aircraft
[NASA-CR-189077] p 2266 N95-27999

Overview of the ACT program p 2193 N95-28463

Designers' unified cost model p 2194 N95-28464

COINS: A composites information database system
p 2194 N95-28465

Composite fuselage shell structures research at NASA Langley Research Center p 2194 N95-28466
Test and analysis results for composite transport fuselage and wing structures p 2137 N95-28470

TRANSPORT PROPERTIES
Transport phenomena and interfacial kinetics in multiphase combustion systems
[AD-A288297] p 2199 N95-26417
Fluctuations and transport in fusion plasma
[DE95-004178] p 2429 N95-26444
RTE: A computer code for Rocket Thermal Evaluation
p 2177 N95-27355
Nonlinear phenomena, turbulence and anomalous transport in fusion plasmas
[DE95-007044] p 2431 N95-27497
Fluctuations and transport in fusion plasmas
[DE95-007111] p 2433 N95-27924
Survey on researches related to ocean disposal of carbon dioxide
[DE95-759247] p 2329 N95-27939
Laboratory high-energy astrophysics on lasers
[DE95-008062] p 2462 N95-28013
Multifractal character of the electronic states in disordered two-dimensional systems
[DE95-609153] p 2443 N95-28016
Measurement of particle transport coefficients on Alcator C-Mod
[DE95-007763] p 2411 N95-28020
A new algorithm for generating highly accurate benchmark solutions to transport test problems
[DE95-007397] p 2373 N95-28047
Low temperature carrier transport properties in isotopically controlled germanium
[DE95-008489] p 2444 N95-28092
Comprehensive numerical model for CW vertical-cavity surface-emitting lasers
[DE95-007758] p 2299 N95-28132
Transport coefficients for the NASA Lewis Chemical Equilibrium Program
[NASA-TM-4647] p 2209 N95-28182
On ionic charge distributions of heavy evaporation residues passing through a carbon foil
[DE94-629016] p 2414 N95-28184
Numerical simulation of coupled flow and transport with TOUGH2: A verification study
[DE95-008351] p 2287 N95-28225
Transport simulation of negative magnetic shear discharges
[DE95-003941] p 2416 N95-28329

TRANSPORT THEORY
On helicon wave induced radial plasma transport
[DE94-634477] p 2429 N95-26438
Monte Carlo study of electron-plasmon scattering effects on hot electron transport in GaAs
[DE95-607768] p 2403 N95-26542
The comparison of P(sub 1) and simplified P(sub 2) synthetic acceleration for iterative methods in transport solutions
[DE94-018306] p 2390 N95-27304
A composition joint PDF method for the modeling of spray flames p 2287 N95-27901

TRANSPORTATION
Alternative fuels and vehicles choice model
[DE95-005695] p 2243 N95-27944
Transportation R and D included in thermal and mechanical sciences program
[DE95-008275] p 2303 N95-28070
Review and analysis of the 1980-1989 biomass thermochemical conversion program
[DE95-000287] p 2325 N95-28394

TRANSPORTATION NETWORKS
Layer coefficients for NHDOT pavement materials
[AD-A288262] p 2246 N95-26548

TRANSPORTER
Pre-integrated truss space station and method of assembly
[NASA-CASE-MSC-22015-1] p 2165 N95-27842

TRANSPUTERS
Parallel block implicit integration technique for trajectory parallelism
[AD-A288961] p 2379 N95-28335

TRANSVERSE OSCILLATION
The effects of transverse vibration on the performance of an axial groove wick heat pipe
[AD-A289349] p 2278 N95-27065

TRAPPING
Extended linear ion trap frequency standard apparatus
[NASA-CASE-NPO-19081-1-CU] p 2404 N95-26861
Modeling of trapping and abrupt doping effects in MESFET's using R-dynamic element
[PB95-184891] p 2262 N95-27050
Extended linear ion trap frequency standard apparatus
[NASA-CASE-NPO-19081-1-CU] p 2416 N95-28348

TRAPS
Characterization of defects in deuterium-implanted beryllium
[DE95-005688] p 2217 N95-27553

TRAVELING SALESMAN PROBLEM
Using the dimension reduction technique to prove that clique trees define facets for the asymmetric traveling salesman polytope
[AD-A289397] p 2389 N95-26882

TRAVELING WAVE AMPLIFIERS
High power, broadband folded waveguide Gyrotron-Traveling-Wave-Amplifier
[AD-A286847] p 2259 N95-26433

TRAVELING WAVE TUBES
A finite element based technique for simulation helix TWT interaction circuit thermal behavior
[AD-A289552] p 2262 N95-27152
Ring-plane traveling-wave tube slow-wave circuit design simulations at V-Band frequencies
[NASA-TM-106949] p 2371 N95-27370

TRAYS
Spacecraft materials studies on the Aerospace Corporation tray on EOIM-3 p 2210 N95-27632

TREES
Scalable multicast tree construction for wide area networks
[AD-A288318] p 2379 N95-26421

TREND ANALYSIS
Linear and nonlinear trending and prediction for AVHRR time series data p 2385 N95-27391
A video strip chart program
[DE95-006389] p 2372 N95-27495

TRENDS
High-stakes aviation: US-Japan technology linkages in transport aircraft
[LC-94-65759] p 2126 N95-27907
New trends and ideas in the fields of microwave technology
[AD-A291663] p 2257 N95-28453

TRIANGULATION
Unstructured mesh generation and adaptivity
[NASA-CR-195069] p 2278 N95-27027

TRIGGER CIRCUITS
Pipelined first-level trigger for the H1 forward-muon spectrometer
[PB95-196242] p 2423 N95-28452

TRIGONOMETRIC FUNCTIONS
Kepler Equation solver p 2147 N95-27767

TRINITROTOLUENE
A novel sensitive detector of atmospheric nitrocompounds based on laser photofragmentation/ionization spectrometry
p 2174 N95-28314

TRITIUM
Recent high-speed ballistics experiments at ORNL
[DE95-006534] p 2422 N95-28205

TRIVALENT IONS
Synthesis and properties of lanthanide-exchanged Preyssler's heteropolyanions
[DE95-007136] p 2238 N95-28235

TROPICAL METEOROLOGY
Systematic and integrated approach to Tropical Cyclone track forecasting. Part 1: Approach overview and description of meteorological basis
[AD-A291775] p 2344 N95-28459

TROPICAL REGIONS
An observational study on the onset of the summer monsoon over eastern Asia in 1979
[AD-A289637] p 2341 N95-26723
Synoptic features of the Yunan rainy season before the onset of the tropical monsoons
[AD-A289641] p 2342 N95-26724
Contingency designs for attitude determination of TRMM p 2154 N95-27803
A study of lightning in winter thunderstorms and the analysis of thunderstorm overflight data
[NASA-CR-198577] p 2343 N95-28191

TROPICAL STORMS
Systematic and integrated approach to Tropical Cyclone track forecasting. Part 1: Approach overview and description of meteorological basis
[AD-A291775] p 2344 N95-28459

TROPOSPHERE
Coupled chemistry/climate issues
[DE95-006443] p 2327 N95-27532
Dynamics and control of SEDSAT tethered multi-probe for thermospheric research flight data analysis of SEDS-2 satellite: Tethered systems dynamics and flight data analysis
[NASA-CR-198653] p 2165 N95-27836
Use of SURFACE CHEMKIN to model multiphase atmospheric chemistry: Application to nitrogen tetroxide spills p 2172 N95-28305
Measurements of daytime and upper tropospheric water vapor profiles by Raman lidar
[DE95-007640] p 2344 N95-28538
Stratospheric ozone reactive chemicals generated by space launches worldwide
[AD-A289852] p 2332 N95-28623

TRUCKS
The vibration transmission of lift truck suspension seats
[ISVR-TR-245] p 2302 N95-27844

TRUSSES
Static stability of a three-dimensional space truss
[NASA-TM-106944] p 2164 N95-27730
Pre-integrated truss space station and method of assembly
[NASA-CASE-MSC-22015-1] p 2165 N95-27842
Stiffness and strength tailoring in uniform space-filling truss structures p 2188 N95-28290

TUBE LASERS
High temperature kinetic study of the reactions H + O2 = OH + O and O + H2 = OH + H in H2/O2 system by shock tube-laser absorption spectroscopy
[NASA-CR-195473] p 2206 N95-27695

TUMBLING MOTION
A modified proportional navigation scheme for rendezvous and docking with tumbling targets: The Planar case p 2150 N95-27784

TUNABLE LASERS
Toward coherent excitation: Development of a single-source pump for the rubidium hyperfine ground state doublet
[AD-A289413] p 2295 N95-27132
Fellowship in physics
[AD-A291691] p 2446 N95-28522

TUNERS
Display system employing acousto-optic tunable filter
[NASA-CASE-NPO-18736-1-CU] p 2426 N95-27843

TUNGSTEN
The high strain rate deformation of tungsten single crystals
[AD-A288874] p 2223 N95-28189

TUNGSTEN ALLOYS
Solid-state sintering of tungsten heavy alloys
[DE95-007749] p 2222 N95-28130

TUNGSTEN CARBIDES
Tungsten carbide fragmentation: Experimental characterization and numerical modelling
[DE95-008521] p 2236 N95-27879

TUNING
Analysis of filter tuning techniques for sequential orbit determination p 2146 N95-27764
An automated method of tuning an attitude estimator
p 2148 N95-27774

TUNNEL JUNCTIONS
Demonstration of photo-assisted tunneling process across the coulomb blockade energy gap in mesoscopic tunnel junctions — photon-assisted tunneling
[AD-A289534] p 2438 N95-26872

TURBINE BLADES
A summary of computational experience at GE Aircraft Engines for complex turbulent flows in gas turbines
p 2285 N95-27885
Basic principles and recent observations of rotationally sampled wind p 2321 N95-27971
A model of rotationally-sampled wind turbulence for predicting fatigue loads in wind turbines
p 2312 N95-27972
Comparative performance tests on the Mod-2, 2.5-mW wind turbine with and without vortex generators
p 2124 N95-27978
Aeroelastic stability of wind turbine blade/aileron systems p 2124 N95-27981
Comparison of measured and calculated dynamic loads for the Mod-2 2.5 mW wind turbine system
p 2312 N95-27983
Use of blade pitch control to provide power train damping for the Mod-2, 2.5-mW wind turbine
p 2306 N95-27986
Observed accustic and aeroelastic spectral responses of a MOD-2 turbine blade to turbulence excitation
p 2324 N95-27991
Mechanical properties of Hysol EA-9394 structural adhesive
[DE95-008187] p 2240 N95-28405

TURBINE ENGINES
Ceramic composite combustor cans for expendable turbine engines
[AD-A289551] p 2140 N95-28646

TURBINE PUMPS
Progress in incompressible Navier-Stokes computations for propulsion flows and its dual-use applications
[NASA-CR-197746] p 2275 N95-26766
Comparison of numerical results and multicavity purge and rim seal data with extensions to dynamics
[NASA-TM-106685] p 2168 N95-27434
Developmental problems and their solution for the Space Shuttle main engine alternate liquid oxygen high-pressure turbopump: Anomaly or failure investigation the key
[NASA-TP-3553] p 2169 N95-28263

TURBINE WHEELS

Preliminary analysis of dynamic stall effects on a 91-meter wind turbine rotor p 2124 N95-27975

Use of blade pitch control to provide power train damping for the Mod-2, 2.5-mW wind turbine p 2306 N95-27986

Variable speed generator application on the MOD-5A 7.3 mW wind turbine generator p 2273 N95-27989

TURBINES

Measurements of the volatilities of electrolytes: Application to water/steam cycles [DE95-007103] p 2204 N95-27451

A comparison of measured wind park load histories with the WISPER and WISPERX load spectra [DE95-000295] p 2319 N95-27459

Water driven turbine/brush pipe cleaner [NASA-CASE-KSC-11669-1] p 2304 N95-28359

TURBOCOMPRESSORS

WINCLR: A computer code for heat transfer and clearance calculation in a compressor [NASA-CR-195436] p 2117 N95-26363

TURBOJET ENGINES

Comparison of numerical results and multicavity purge and rim seal data with extensions to dynamics [NASA-TM-106685] p 2168 N95-27434

TURBOMACHINERY

A general theory of two- and three-dimensional rotational flow in subsonic and transonic turbomachines [NASA-CR-4496] p 2123 N95-28003

Bearing defect signature analysis using advanced nonlinear signal analysis in a controlled environment [NASA-TM-108491] p 2304 N95-28364

TURBULENCE

Fluctuations and transport in fusion plasma [DE95-004178] p 2429 N95-26444

Deep convection in the Mediterranean Sea [AD-A288497] p 2346 N95-26647

Compressible turbulence measurements in a supersonic boundary layer including favorable pressure gradient effects [AD-A289475] p 2276 N95-26821

Compressible turbulence measurements in a supersonic flow with adverse pressure gradient [AD-A289477] p 2276 N95-26822

Laser beam propagation in non-Kolmogorov atmospheric turbulence [AD-A289256] p 2295 N95-26974

Basic studies in turbulent shear flows [AD-A289145] p 2277 N95-26998

Turbulance boundary conditions for shear flow analysis, using the DTNS flow solver p 2283 N95-27362

NAS Technical Summaries, March 1993 - February 1994 [NASA-RP-1355] p 2466 N95-27367

Dithering transitions in resistive pressure-gradient-driven turbulence [DE95-006737] p 2431 N95-27536

Parallel plasma fluid turbulence calculations [DE95-006741] p 2431 N95-27537

Industry-Wide Workshop on Computational Turbulence Modeling [NASA-CP-10165] p 2285 N95-27882

Turbulence program for propulsion systems p 2285 N95-27883

Turbulence model development and application at Lockheed Fort Worth Company p 2285 N95-27884

Experiences with two-equation turbulence models p 2286 N95-27894

Second-order closures for compressible turbulence p 2286 N95-27898

Modeling of turbulent chemical reaction p 2286 N95-27899

Fluctuations and transport in fusion plasmas [DE95-007111] p 2433 N95-27924

Third-order-accurate numerical methods for efficient, large time-step solutions of mixed linear and nonlinear problems [DE95-009184] p 2288 N95-28533

Experimental study on transition characteristics of natural-convection flow [PB95-192423] p 2289 N95-28637

TURBULENCE EFFECTS

Compensated deconvolution from wavefront sensing [AD-A289490] p 2336 N95-26824

Flow visualization of a turbulent shear flow using an optical wavefront sensor [AD-A289208] p 2277 N95-26986

Effect of turbulence models on criticality conditions in swirling flows p 2282 N95-27356

Large HAWT wake measurement and analysis p 2289 N95-27973

Observed acoustic and aeroelastic spectral responses of a MOD-2 turbine blade to turbulence excitation p 2324 N95-27991

Anechoic wind tunnel study of turbulence effects on wind turbine broadband noise p 2325 N95-27992

TURBULENCE MODELS

Indexing meso-beta surface wind site representative [AD-A288501] p 2341 N95-26650

Turbulence modeling [NASA-CR-197751] p 2274 N95-26665

Supersonic coaxial jet noise predictions [NASA-TM-106917] p 2401 N95-26801

Effect of turbulence models on criticality conditions in swirling flows p 2282 N95-27356

Dithering transitions in resistive pressure-gradient-driven turbulence [DE95-006737] p 2431 N95-27536

Industry-Wide Workshop on Computational Turbulence Modeling [NASA-CP-10165] p 2285 N95-27882

Turbulence program for propulsion systems p 2285 N95-27883

Turbulence model development and application at Lockheed Fort Worth Company p 2285 N95-27884

A summary of computational experience at GE Aircraft Engines for complex turbulent flows in gas turbines p 2285 N95-27885

The applicability of turbulence models to aerodynamic and propulsion flowfields at McDonnell-Douglas Aerospace p 2285 N95-27886

Turbulence models for gas turbine combustors p 2285 N95-27888

Combustion system CFD modeling at GE Aircraft Engines p 2285 N95-27889

Recent progress in the joint velocity-scalar PDF method p 2285 N95-27890

Overview of turbulence model development and applications at Rocketdyne p 2286 N95-27891

Recent advances in PDF modeling of turbulent reacting flows p 2286 N95-27892

Experience with turbulence interaction and turbulence-chemistry models at Fluent Inc. p 2286 N95-27893

Progress in simulating industrial flows using two-equation models: Can more be achieved with further research? p 2286 N95-27895

Turbulence modeling needs of commercial CFD codes: Complex flows in the aerospace and automotive industries p 2286 N95-27896

Turbulence requirements of a commerical CFD code p 2286 N95-27897

Second-order closures for compressible turbulence p 2286 N95-27898

Modeling of turbulent chemical reaction p 2286 N95-27899

PDF methods for turbulent reactive flows p 2287 N95-27900

A composition joint PDF method for the modeling of spray flames p 2287 N95-27901

Improvements and new features in the PDF module p 2287 N95-27902

A model of rotationally-sampled wind turbulence for predicting fatigue loads in wind turbines p 2312 N95-27972

Measurement and prediction of broadband noise from large horizontal axis wind turbine generators p 2324 N95-27990

DNS, LES and stochastic modeling of turbulent reacting flows [AD-A280099] p 2287 N95-28155

Studies of radar backscatter as a function of wave properties and the winds in the turbulent marine atmosphere [NASA-CR-198608] p 2315 N95-28209

TURBULENT BOUNDARY LAYER

The small-scale structure of dispersing clouds in the atmosphere [AD-A288256] p 2341 N95-26546

The near-wake flow behavior of an oscillating airfoil with modified trailing edge p 2119 N95-26953

Turbulance boundary conditions for shear flow analysis, using the DTNS flow solver p 2283 N95-27362

Measurement and prediction of broadband noise from large horizontal axis wind turbine generators p 2324 N95-27990

TURBULENT COMBUSTION

Turbulence models for gas turbine combustors p 2285 N95-27888

Combustion system CFD modeling at GE Aircraft Engines p 2285 N95-27889

Recent progress in the joint velocity-scalar PDF method p 2285 N95-27890

Modeling of turbulent chemical reaction p 2286 N95-27899

PDF methods for turbulent reactive flows p 2287 N95-27900

TURBULENT DIFFUSION

A method for generating skewed random numbers using two overlapping uniform distributions [DE95-008747] p 2392 N95-28162

TURBULENT FLOW

The small-scale structure of dispersing clouds in the atmosphere [AD-A288256] p 2341 N95-26546

Plate manipulators [AD-A289601] p 2121 N95-26719

Direct numerical simulation of transitional and turbulent flow over a heated flat plate using finite-difference schemes [NASA-CR-197753] p 2275 N95-26776

Analysis of hypersonic boundary layer second mode instability over a 7 deg cone [AD-A289471] p 2276 N95-26819

Compressible turbulence measurements in a supersonic boundary layer including favorable pressure gradient effects [AD-A289475] p 2276 N95-26821

Compressible turbulence measurements in a supersonic flow with adverse pressure gradient [AD-A289477] p 2276 N95-26822

Calculation of suspended sediment transport by combined wave-current flows [AD-A289368] p 2346 N95-26904

Flow visualization of a turbulent shear flow using an optical wavefront sensor [AD-A289208] p 2277 N95-26986

Basic studies in turbulent shear flows [AD-A289145] p 2277 N95-26998

Flow control [AD-A289262] p 2279 N95-27197

Turbulence program for propulsion systems p 2285 N95-27883

A summary of computational experience at GE Aircraft Engines for complex turbulent flows in gas turbines p 2285 N95-27885

Experience with k-epsilon turbulence models for heat transfer computations in rotating p 2285 N95-27887

Recent advances in PDF modeling of turbulent reacting flows p 2286 N95-27892

Progress in simulating industrial flows using two-equation models: Can more be achieved with further research? p 2286 N95-27895

Turbulence modeling needs of commercial CFD codes: Complex flows in the aerospace and automotive industries p 2286 N95-27896

Modeling of turbulent chemical reaction p 2286 N95-27899

PDF methods for turbulent reactive flows p 2287 N95-27900

DNS, LES and stochastic modeling of turbulent reacting flows [AD-A280099] p 2287 N95-28155

A phenomenological treatment of rotating turbulence [NASA-CR-198168] p 2288 N95-28228

Computational and experimental studies of hydrodynamic instabilities and turbulent mixing [DE95-006837] p 2288 N95-28603

Numerical study to assess sulfur hexafluoride as a medium for testing multielement airfoils [NASA-TP-3496] p 2124 N95-28674

TURBULENT HEAT TRANSFER

Direct numerical simulation of transitional and turbulent flow over a heated flat plate using finite-difference schemes [NASA-CR-197753] p 2275 N95-26776

TURBULENT MIXING

Computational and experimental studies of hydrodynamic instabilities and turbulent mixing [DE95-006837] p 2288 N95-28603

TVD SCHEMES

A fully implicit time accurate method for hypersonic combustion: Application to shock-induced combustion instability [NASA-TM-106707] p 2273 N95-26380

Development of an upwind, finite-volume code with finite-rate chemistry [NASA-CR-197747] p 2121 N95-26760

TWO BODY PROBLEM

Two-body bound states and the Bethe-Salpeter equation [DE95-008302] p 2392 N95-27742

Kepler Equation solver p 2147 N95-27767

TWO DIMENSIONAL BODIES

Materials with self organized surfaces: 2D polymer assemblies [AD-A288928] p 2226 N95-26627

TWO DIMENSIONAL BOUNDARY LAYER

Computer program BL2D for solving two-dimensional and axisymmetric boundary layers [NASA-CR-4668] p 2279 N95-27257

TWO DIMENSIONAL FLOW

Numerical simulation of combustion flow around a flame holder with hydrogen injection [NAL-TR-1233] p 2200 N95-26523

The method of space-time conservation element and solution element-applications to one-dimensional and two-dimensional time-marching flow problems
[NASA-TM-106915] p 2389 N95-26663

Contribution to the optimal shape design of two-dimensional internal flows with embedded shocks
[NASA-CR-195062] p 2389 N95-26672

A general theory of two- and three-dimensional rotational flow in subsonic and transonic turbomachines
[NASA-CR-4496] p 2123 N95-28003

Numerical simulation of coupled flow and transport with TOUGH2: A verification study
[DE95-008351] p 2287 N95-28225

TWO DIMENSIONAL MODELS

Scrape-off layer plasma modeling for the DIII-D tokamak
[DE95-008059] p 2433 N95-28054

Critical behaviour of spin models: A transfer-matrix approach
[PB95-192456] p 2418 N95-28638

TWO PHASE FLOW

Cryogenic and simulated fuel jet breakup in argon, helium and nitrogen gas flows
[NASA-TM-106923] p 2291 N95-27030

Diagnostic system Cryo-D for the determination of parameters of vapor-liquid currents of the coolant
[DE95-608775] p 2280 N95-27338

The use of wavelet transforms in the solution of two-phase flow problems
[DE95-004688] p 2284 N95-27721

Two-phase flow research using the learjet apparatus
[NASA-TM-106814] p 2284 N95-27854

Structure of high-speed sprays
[AD-A291696] p 2288 N95-28523

U

UH-1 HELICOPTER

The effects of UH-1 experience on UH-6O simulator performance: A preliminary study
[AD-A289457] p 2130 N95-26993

UKRAINE

JPRS report: Science and technology. Central Eurasia
[JPRS-UST-94-022] p 2246 N95-27699

WTEC panel report on research submersibles and undersea technologies
[NASA-CR-198565] p 2247 N95-27909

ULTRAHIGH VACUUM

Low temperature deposition and characterization of N- and P-type silicon carbide thin films and associated Ohmic and Schottky contacts
[AD-A289107] p 2237 N95-28097

ULTRASHORT PULSED LASERS

Surface damage effects generated by a fast-pulse laser beam
[AD-A289131] p 2295 N95-26996

Direct ultrashort-pulse retrieval using frequency-resolved optical gating and a computational neural network
[DE95-007148] p 2425 N95-27482

Trident as an ultrahigh irradiance laser
[DE95-006345] p 2297 N95-27850

Effect of noise on Frequency-Resolved Optical Gating measurements of ultrashort pulses
[DE95-007149] p 2298 N95-27969

Phase retrieval and time-frequency methods in the measurement of ultrashort laser pulses
[DE95-006499] p 2300 N95-28549

ULTRASONIC AGITATION

Ethyl lactate as a solvent alternative for cleaning metal parts p 2229 N95-27112

ULTRASONIC TESTS

Ultrasonic test system
[AD-D017261] p 2400 N95-26502

Combined investigation of Eddy current and ultrasonic techniques for composite materials NDE
[NASA-TM-110599] p 2306 N95-26778

ULTRASONICS

Ultrasonic test system
[AD-D017261] p 2400 N95-26502

Multiclassifier fusion of an ultrasonic lip reader in automatic speech recognition
[AD-A289207] p 2254 N95-27079

The evaluation of a fluorochemical drying process for an electrical contact p 2227 N95-27103

JPRS report: Science and technology. Central Eurasia
[JPRS-UST-95-021] p 2202 N95-27155

Laser ultrasonic generation at the surface of a liquid metal
[DE95-004999] p 2216 N95-27477

Ultrasonic study on ternary liquid systems by laser-sound interaction
[DE95-608783] p 2207 N95-27929

Phase stability and elasticity of C15 transition-metal intermetallic compounds
[DE95-007876] p 2219 N95-28026

Physical interpretation and development of ultrasonic nondestructive evaluation techniques applied to the quantitative characterization of textile composite materials
[NASA-CR-198591] p 2306 N95-28034

ULTRAVIOLET ASTRONOMY

Typical examples of classical novae
p 2459 N95-27074

Recurrent novae p 2460 N95-27075

ULTRAVIOLET RADIATION

Radiation sensitive area detection device and method
[NASA-CASE-MFS-28563-3] p 2423 N95-26385

Method for determining surface coverage by materials exhibiting different fluorescent properties
[NASA-CASE-GSC-13539-1] p 2315 N95-28211

ULTRAVIOLET SPECTRA

Optical features of nanosize iron and molybdenum sulfide clusters
[DE95-005417] p 2202 N95-27136

International Ultraviolet Explorer Atlas of B-type spectra from 1200 to 1900 A
[NASA-RP-1363] p 2463 N95-28328

ULTRAVIOLET SPECTROSCOPY

International Ultraviolet Explorer Atlas of B-type spectra from 1200 to 1900 A
[NASA-RP-1363] p 2463 N95-28328

ULYSSES MISSION

Ulysses orbit determination at high declinations
p 2151 N95-27787

UNDERGROUND STORAGE

Recovery, evaluation, and decontamination of landfilled pentaborane cylinders, former liquid propellant rocket engine test facility, Washoe County, Nevada
p 2171 N95-28302

UNDERGROUND STRUCTURES

Planning, design and construction of the cavern arena: Heating, ventilation and air conditioning
[PB95-196382] p 2361 N95-28659

UNDERWATER ACOUSTICS

Ultrasonic test system
[AD-D017261] p 2400 N95-26502

Uncertainties in the calibration of hydrophones at NPL by the three-transducer spherical-wave reciprocity method in the frequency range 10 kHz on 500 kHz
[PB95-185245] p 2401 N95-26615

Very low frequency seismo-acoustic noise below the sea floor (0.2-10 Hz)
[AD-A289164] p 2347 N95-27011

Observations of near-bottom flow in a wave-dominated nearshore environment
[AD-A289331] p 2347 N95-27043

WTEC panel report on research submersibles and undersea technologies
[NASA-CR-198565] p 2247 N95-27909

Modeling the shock response of submerged structures
[AD-A289082] p 2288 N95-28351

Molecular modeling: An approach for the study of piezoelectric polymers
[AD-A289821] p 2241 N95-28574

Radio telemetry buoy for long-range communication
[AD-D017269] p 2161 N95-28581

Ultrasonic studies of liquid/solid seimoacoustic wave phenomena
[AD-A289644] p 2402 N95-28622

UNDERWATER COMMUNICATION

WTEC panel report on research submersibles and undersea technologies
[NASA-CR-198565] p 2247 N95-27909

UNDERWATER ENGINEERING

WTEC panel report on research submersibles and undersea technologies
[NASA-CR-198565] p 2247 N95-27909

UNDERWATER PROPULSION

WTEC panel report on research submersibles and undersea technologies
[NASA-CR-198565] p 2247 N95-27909

UNDERWATER STRUCTURES

Nondestructive testing apparatus for determining the orientation of reinforcing bars within a concrete structure
[AD-D017267] p 2245 N95-26508

UNDERWATER TESTS

Ultrasonic test system
[AD-D017261] p 2400 N95-26502

UNIQUENESS

On permanent capillar-heavy waves in circular shaped channels
[DE95-608779] p 2280 N95-27339

UNITED KINGDOM

Milestones in telecommunications in some selected countries
[PB95-184826] p 2252 N95-26929

WTEC panel report on research submersibles and undersea technologies
[NASA-CR-198565] p 2247 N95-27909

UNITED STATES

Strategy in the commercial aircraft industry in the United States: A comparison of decisionmaking by McDonnell-Douglas and Boeing aircraft companies from 1977-1983
[AD-A288289] p 2117 N95-26409

Comparison of fixed wing aircraft algorithms for JANUS
[AD-A288503] p 2129 N95-26652

Milestones in telecommunications in some selected countries
[PB95-184826] p 2252 N95-26929

UNITS OF MEASUREMENT

Standards for excellence
[NONP-NASA-VT-95-49096] p 2451 N95-27202

Chemical engineering: Measurements for a competitive age
[NONP-NASA-VT-95-49098] p 2203 N95-27204

Getting it right, making it better
[NONP-NASA-VT-95-49118] p 2451 N95-27206

UNIVERSE

Discovery of the most distant supernovae and the quest for (Omega)
[DE95-006569] p 2460 N95-28197

UNIVERSITIES

Summaries of theses for the degree of diploma engineer 1992-1993
[PB95-184867] p 2246 N95-27048

Intrusive multi-probe system
[DE95-006258] p 2292 N95-27465

UNIVERSITY PROGRAM

Space physics educational outreach
[NASA-CR-198649] p 2399 N95-27852

UNIX (OPERATING SYSTEM)

Beginner's guide to UNIX
[IFTR-17/1994] p 2364 N95-26511

Long term distributed file reference tracing: Implementation and experience
[AD-A288585] p 2452 N95-26535

A case for dynamic sets in operating systems
[AD-A289354] p 2454 N95-27529

The transition of GTDS to the Unix workstation environment p 2151 N95-27789

Research on the establishment of the database system for R and D on the innovative technology for the Earth
[DE95-759244] p 2458 N95-27937

Replacing the message service component in an integration framework
[AD-A289928] p 2375 N95-28628

UNMANNED SPACECRAFT

Analysis of modal behavior at frequency cross-over
[AD-A289304] p 2162 N95-26918

UNSTEADY AERODYNAMICS

An experimental investigation of helicopter downwash and tailboom interaction at the Wichita State University 7x10 foot wind tunnel p 2120 N95-26955

Modeling of aircraft unsteady aerodynamic characteristics. Part 2: Parameters estimated from wind tunnel data
[NASA-TM-110161] p 2142 N95-27839

A numerical study of fundamental shock noise mechanisms
[NASA-TM-110608] p 2401 N95-27908

UNSTEADY FLOW

A fully implicit time accurate method for hypersonic combustion: Application to shock-induced combustion instability
[NASA-TM-106707] p 2273 N95-26380

Progress in incompressible Navier-Stokes computations for propulsion flows and its dual-use applications
[NASA-CR-197746] p 2275 N95-26766

Turbomachinery design and tonal acoustics computations
[NASA-CR-197749] p 2139 N95-26777

Unsteady base pressure measurements in the near wake of a cylinder with imposed three-dimensional disturbances
[AD-A289498] p 2276 N95-26827

A numerical method for unsteady transonic flow about wings with control surfaces
[AD-A289631] p 2121 N95-26859

On the nonlinear stability of the unsteady, viscous flow of an incompressible fluid in a curved pipe
[NASA-CR-195065] p 2276 N95-27028

Global flowfield about the V-22 Tiltrotor Aircraft
[NASA-CR-198603] p 2122 N95-27248

Comparison of numerical results and multicavity purge and rim seal data with extensions to dynamics
[NASA-TM-106685] p 2168 N95-27434

A numerical study of fundamental shock noise mechanisms
[NASA-TM-110608] p 2401 N95-27908

UNSTEADY STATE
Acoustic field in unsteady moving media
[NASA-CR-198162] p 2279 N95-27179
UNSTRUCTURED GRIDS (MATHEMATICS)
Unstructured mesh generation and adaptivity
[NASA-CR-195069] p 2278 N95-27027
Spectral methods on arbitrary grids
[NASA-CR-198158] p 2279 N95-27247
Multigrid techniques for unstructured meshes
[NASA-CR-195070] p 2391 N95-27433
A point-centered diffusion differencing for unstructured meshes in 3-D
[DE95-008382] p 2392 N95-28232
Numerical study to assess sulfur hexafluoride as a medium for testing multielement airfoils
[NASA-TP-3496] p 2124 N95-28674
UPPER ATMOSPHERE RESEARCH SATELLITE (UARS)
Experience from the in-flight calibration of the Extreme Ultraviolet Explorer (EUVE) and Upper Atmosphere Research Satellite (UARS) fixed head star trackers (FHSTs) p 2149 N95-27779
UPWELLING WATER
SeaWiFS technical report series. Volume 26: Results of the SeaWiFS Data Analysis Round-Robin, July 1994 (DARR-1994)
[NASA-TM-104566-VOL-26] p 2345 N95-26430
URANIUM
An investigation of the applicability of the new Reillex(tm)-HPQ anion exchange resin system for technetium/rhenium and uranium in the Hanford waste tanks
[DE95-007643] p 2412 N95-28051
URANIUM ALLOYS
Study of the phase transformations and microstructures of uranium rich alloys of the binary uranium-gallium system
[DE95-609624] p 2217 N95-27713
URANIUM OXIDES
Analytical electron microscopy of nanometer-sized particles
[AD-A289124] p 2413 N95-28101
URBAN TRANSPORTATION
Layer coefficients for NHDOT pavement materials
[AD-A288262] p 2246 N95-26548
UREAS
Absorption of sparingly soluble gases by reactive media in self-aerated gas-liquid contactors: A scale-up procedure
[DE95-006429] p 2206 N95-27707
Growth and characterization of crystals for room temperature I.R. detectors and second harmonic generation devices
[NASA-CR-198598] p 2443 N95-28033
URETHANES
Cryogenic BRDF measurements at 10.6 micrometers and 0.63 micrometers on contaminated mirrors
[AD-A291611] p 2427 N95-28408
USER MANUALS (COMPUTER PROGRAMS)
Manual for SHOCK3D, version 2.0. Computer program for non-linear shock response
[AD-A288631] p 2307 N95-26342
WINCLR: A computer code for heat transfer and clearance calculation in a compressor
[NASA-CR-195436] p 2117 N95-26363
Long Duration Exposure Facility Mini-Data Base User's Guide: Macintosh version
[NASA-CR-4656] p 2177 N95-26391
Aircraft noise prediction program theoretical manual: Rotorcraft System Noise Prediction System (ROTONET), part 4
[NASA-TM-83199-PT-4] p 2400 N95-26392
Natural aerosol extinction module: XSCALE 1992 user's guide
[AD-A289029] p 2340 N95-26463
General purpose finite element solver
[PB95-185062] p 2388 N95-26495
Beginner's guide to UNIX
[IFTR-17/1994] p 2364 N95-26511
Software packager user's guide
[NASA-CR-197763] p 2366 N95-26693
User's and test case manual for FEMATS
[NASA-CR-197803] p 2366 N95-26694
Material modeling in the CRALE code. Users' manual
[AD-A288988] p 2178 N95-26712
The multidimensional Self-Adaptive Grid code, SAGE, version 2
[NASA-TM-110350] p 2367 N95-26726
User documentation of the CTA program
[AD-A289508] p 2121 N95-26854
Reference manual: Naive physics simulator
[PB95-184917] p 2369 N95-26907
Research and development management information system, system user manual
[AD-A289151] p 2453 N95-27004
Computer program BL2D for solving two-dimensional and axisymmetric boundary layers
[NASA-CR-4668] p 2279 N95-27257
Outline and handling manual of fusion experimental data monitor system DAISY, version 2
[DE95-703895] p 2431 N95-27414
FDTD-ANT user manual
[NASA-CR-195444] p 2372 N95-27729
Using the scalable nonlinear equations solvers package
[DE95-008323] p 2378 N95-28071
BEGET: The B-Factory Event Generator version 21
[DE95-008329] p 2414 N95-28171
Project Records Information System (PRIS) user's manual, revision 3
[DE95-008330] p 2456 N95-28172
TranAir: A full-potential, solution-adaptive, rectangular grid code for predicting subsonic, transonic, and supersonic flows about arbitrary configurations. User's manual
[NASA-CR-4349] p 2123 N95-28230
Software technology for adaptable, reliable systems (STARS). AdaWise user's manual
[AD-A289655] p 2375 N95-28635
Using COLETTE. (A simple guide)
[PB95-195806] p 2375 N95-28658
USER REQUIREMENTS
The value of simulation for training
[AD-A289174] p 2143 N95-26556
Enhanced visual user interface support for domain-oriented application composition systems
[AD-A289337] p 2359 N95-26737
User-centric development. Version 01.00.04
[AD-A289363] p 2368 N95-26903
A user-system interface agent p 2383 N95-27379
UTILITIES
DOE/KEURP Site Operator Program
[DE95-007116] p 2266 N95-27926

V

V-22 AIRCRAFT
Global flowfield about the V-22 Tiltrotor Aircraft
[NASA-CR-198603] p 2122 N95-27248
Navy composite maintenance and repair experience
p 2193 N95-28446
V/STOL AIRCRAFT
Flightpath synthesis and HUD scaling for V/STOL terminal area operations
[NASA-TM-110348] p 2127 N95-26587
VACANCIES (CRYSTAL DEFECTS)
Vacancy related defects in thin film Pb(Zr,Ti)O3 materials
[DE95-007696] p 2445 N95-28165
VACUUM
The influence of surface structure on the interaction of water with TiO2(100)
[DE95-004927] p 2203 N95-27401
Acceleration theorems
[DE95-007300] p 2420 N95-27484
Reducing cold-start emissions by catalytic converter thermal management
[DE95-000256] p 2327 N95-27540
Lattice calculation for lepton capture from vacuum-pair production in relativistic heavy-ion collisions
[DE95-007392] p 2413 N95-28077
The effects of processing variables on reaction synthesis of Fe-Al alloys
[DE95-007405] p 2221 N95-28082
Cryogenic BRDF measurements at 10.6 micrometers and 0.63 micrometers on contaminated mirrors
[AD-A291611] p 2427 N95-28408
VACUUM CHAMBERS
Process for non-contact removal of organic coatings from the surface of paintings
[NASA-CASE-LEW-15896-1] p 2235 N95-27702
VACUUM DEPOSITION
The Strategic Technologies for Automation and Robotics (STEAR) program: Protection of materials in the space environment subprogram p 2242 N95-27669
VACUUM FURNACES
The effects of processing variables on reaction synthesis of Fe-Al alloys
[DE95-007405] p 2221 N95-28082
VALENCE
The gluon propagator in non-Abelian Weizsaecker-Williams fields
[DE95-006877] p 2449 N95-27547
VALUE ENGINEERING
An analysis of the KC-135 three-person cockpit
[AD-A289540] p 2130 N95-26873
VALVES
Valve mechanism for an acoustic modulator
[AD-D017263] p 2300 N95-26504
The development and testing of ceramic components in piston engines
[DE95-005759] p 2236 N95-27946
VANADIUM
Photoluminescence spectroscopy of 4H- and 6H-SiC
[AD-A289326] p 2202 N95-26896
Coherent V2O3 precipitates in alpha-Al2O3CO-implanted with vanadium and oxygen
[DE95-007404] p 2444 N95-28081
VAPOR DEPOSITION
A new growth technology for highly non-linear, optical quality organic films: Organic vapor phase deposition
[AD-A289006] p 2178 N95-26567
Boron-induced morphology changes in silicon CVD growth: A scanning tunneling microscopy study
[AD-A289275] p 2290 N95-26982
High-density plasma source for large-area chemical vapor deposition of diamond films
[AD-A289053] p 2430 N95-27190
Copper CVD using liquid coinjection of (hfac)Cu(TMVS) and TMVS
[DE95-008155] p 2237 N95-28089
Low temperature deposition and characterization of N- and P-type silicon carbide thin films and associated Ohmic and Schottky contacts
[AD-A289107] p 2237 N95-28097
Atomic layer epitaxy of group 4 materials: Surface processes, thin films, devices and their characterization
[AD-A289092] p 2446 N95-28327
The in situ observation of epitaxial diamond thin film nucleation and growth using emission electron microscopy
[AD-A289841] p 2447 N95-28618
VAPOR PHASES
A new growth technology for highly non-linear, optical quality organic films: Organic vapor phase deposition
[AD-A289006] p 2178 N95-26567
Search for molecular absorptions with the Fourier Transform Spectrometer
[NASA-CR-198648] p 2462 N95-28222
The sensitive detection of hydrazine using chemiluminescence p 2173 N95-28311
Self-assembly of low-dimensional molecular nanoclusters on Au(111) surfaces
[AD-A288936] p 2178 N95-28334
VAPOR PRESSURE
Vapor pressures of mixtures of CFC-114 with the potential replacement coolants C4F(10) andc-C4F 8
[DE95-003444] p 2208 N95-28042
VAPORIZING
Structure of high-speed sprays
[AD-A291696] p 2288 N95-28523
VAPORS
Retrofitting conventional vapor degreasers to use a solvent wash/fluorochemical rinse process
p 2232 N95-27127
Diagnostic system Cryo-D for the determination of parameters of vapor-liquid currents of the coolant
[DE95-608775] p 2280 N95-27338
The surface of liquid He-4 at nonzero temperatures
[DE95-607841] p 2207 N95-27880
Evaluation of a conductive polymer-based sensor for detection of hydrazines at the part-per-billion level
p 2173 N95-28309
Prototype development and test results of a continuous ambient air monitoring system for hydrazine at the 110 ppb level p 2173 N95-28310
VARIABILITY
Coronal abundances and their variation
[NASA-CR-197788] p 2464 N95-26671
Long-term variability of electron radiation dose in geosynchronous orbit
[AD-A289335] p 2162 N95-26902
Overview of the observations of symbiotic stars
p 2460 N95-27076
Models of symbiotic stars p 2460 N95-27077
Variability study of foF2 for an equatorial station
[DE95-608080] p 2337 N95-27157
Study of the response of a three-dimensional coupled ice-ocean model to daily varying atmospheric forcing
[AD-A289050] p 2347 N95-27189
Variable speed generator technology options for wind turbine generators p 2273 N95-27988
VARIABLE AMPLITUDE LOADING
Bonded composite repair of thin metallic materials: Variable load amplitude and temperature cycling effects
p 2132 N95-27509
VARIANCE (STATISTICS)
Truncated Gaussians as tolerance sets
[NASA-CR-197732] p 2395 N95-27417
VARIATIONAL PRINCIPLES
First-principles study of intermetallic phase stability in the ternary Ti-Al-Nb alloy system
[DE95-005259] p 2213 N95-27082

VARISTORS

Polarization relaxation in zinc oxide varistors from 77 K to 450 K
[DE95-007761] p 2268 N95-28156

VAX COMPUTERS

Using COLETTE. (A simple guide)
[PB95-195806] p 2375 N95-28658

VECTOR ANALYSIS

Multipoint multirate signal processing
[AD-A289211] p 2253 N95-26988

VECTOR MESONS

Transverse tau polarization in inclusive bar-B yields tau bar-nu X decays
[DE95-610325] p 2407 N95-27409

VECTOR QUANTIZATION

Digital mapping, charting, and geodesy analysis program technical review of Vector Quantization (VQ) Decompression for the National Imagery Transmission Format Standard (NITFS)
[AD-A288998] p 2314 N95-26682

VECTOR SPACES

Hyperkaehler metrics associated to compact Lie groups
[PB95-185161] p 2388 N95-26514

Mean value theorem in topological vector spaces
[DE95-608753] p 2390 N95-27331

Harmonic maps of the bounded symmetric domains
[DE95-608798] p 2397 N95-27485

VECTORS (MATHEMATICS)

Vector Smart Map Level 1: A new DMA product
[AD-A288920] p 2452 N95-26607

Vector algorithms for solving 3D nonlinear magnetostatic problems
[DE95-608737] p 2399 N95-27298

On commutativity of right s-unital rings with some polynomial constraints
[DE95-608752] p 2390 N95-27330

Realization of vector fields for quantum groups as pseudodifferential operators on quantum spaces
[DE95-008485] p 2449 N95-27877

VEGETATION

Radiometer measurements of snow in Sodankylae, 1991-1993
[PB95-184966] p 2313 N95-26645

VELOCITY DISTRIBUTION

Indexing meso-beta surface wind site representative
[AD-A288501] p 2341 N95-26650

Fuzzy inference enhanced information recovery from digital PIV using cross-correlation combined with particle tracking
[NASA-TM-106896] p 2291 N95-27173

Analysis of developing laminar flows in circular pipes using a higher-order finite-difference technique
p 2281 N95-27352

Recovery and reuse of rocket motor propellant ingredients p 2177 N95-28326

VELOCITY MEASUREMENT

Flutter clearance flight tests of an OV-10A airplane modified for wake vortex flight experiments
[NASA-TM-109168] p 2117 N95-26381

Evaluation of a new laboratory acoustic Doppler velocimeter
[AD-A289592] p 2290 N95-26714

Calculation of three-dimensional (3-D) internal flow by means of the velocity-vorticity formulation on a staggered grid
[NASA-TM-110352] p 2122 N95-27258

VENTILATION

Research on combustion processes relevant to burners in HVAC systems
[PB95-179735] p 2208 N95-28006

Algorithm to describe the spread of a wall fire under a ceiling
[PB95-182259] p 2247 N95-28008

Planning, design and construction of the cavern arena: Heating, ventilation and air conditioning
[PB95-196382] p 2361 N95-28659

VERBAL COMMUNICATION

Codes of processing and multiple resources: Model and methodology
[AD-A289583] p 2355 N95-26691

VERTEBRATES

Biochemically vulnerable sites for antifungal intercession in the control of fungal growth
[AD-A288345] p 2348 N95-26573

VERTICAL DISTRIBUTION

The development of a feature-based concurrent engineering system
[AD-A288424] p 2364 N95-26557

VERTICAL TAKEOFF AIRCRAFT

Design and synthesis of a real-time controller for an unmanned air vehicle
[AD-A289134] p 2141 N95-26555

VERY LARGE SCALE INTEGRATION

Using machine learning to derive efficient cost and performance estimates in VLSI CAD designs
[AD-A288254] p 2363 N95-26408

Construction of a connectionist network supercomputer
[AD-A288439] p 2377 N95-27182

Leak detection utilizing analog binaural (VLSI) techniques
[NASA-CASE-NPO-18399-1-CU] p 2271 N95-28599

VERY LOW FREQUENCIES

A BATSE investigation of radiation belt electrons precipitated by VLF waves
[NASA-CR-197780] p 2336 N95-26922

VESTIBULAR TESTS

Role of somatosensory and vestibular cues in attenuating visually induced human postural sway
[NASA-CR-197845] p 2357 N95-27697

VESTIBULES

Comparative Transduction Mechanisms of Vestibular Otolith Hair Cells
[NASA-CR-197980] p 2349 N95-26727

Regional differences in lectin binding patterns of vestibular hair cells p 2349 N95-26728

Hair cell regeneration in the bullfrog vestibular otolith organs following aminoglycoside toxicity
p 2349 N95-26729

Peripheral innervation patterns of vestibular nerve afferents in the bullfrog utriculus p 2349 N95-26730

Comparative transduction mechanisms of hair cells in the bullfrog uticulus. 2: Sensitivity and response dynamics to hair bundle displacement p 2350 N95-26732

A model of the neural basis of the rat's sense of direction
[AD-A289678] p 2350 N95-26761

Role of somatosensory and vestibular cues in attenuating visually induced human postural sway
[NASA-CR-197845] p 2357 N95-27697

VHSIC (CIRCUITS)

Accelerating conservative parallel simulation of VHDL circuits
[AD-A289317] p 2264 N95-27294

VIABILITY

Unique features of a new nickel-hydrogen 2-cell CPV
p 2272 N95-26793

Preconversion catalytic deoxygenation of phenolic functional groups
[DE95-007556] p 2204 N95-27458

The demilitarization of class 1.1 rocket motors using high pressure waterjets p 2176 N95-28322

VIBRATION

Research activities on somatosensory (SI) cortical neurons
[AD-A288794] p 2348 N95-26360

Control of a large space structure using multiple model adaptive estimation and control techniques
[AD-A289309] p 2162 N95-26916

A state-space model of a large, lightly damped space structure using the Eigensystem realization algorithm
[AD-A289251] p 2163 N95-26970

Collisional dynamics and spectroscopic studies of highly excited rovibrational levels of I2(X)(0(+)(sub g)) via stimulated emission pumping
[AD-A289447] p 2295 N95-27172

Infrared spectroscopy of nonclassical ions and their complexes
[DE95-008487] p 2413 N95-28091

Spectroscopic and dynamical studies of highly energized small polyatomic molecules
[DE95-006640] p 2414 N95-28199

The solar array-induced disturbance of the Hubble Space Telescope pointing system
[NASA-TP-3556] p 2311 N95-28214

Vibrational spectroscopy of water interfaces
[DE95-006592] p 2209 N95-28218

Modeling helicopter blade dynamics using a modified Myklestad-Prohl transfer matrix method
[AD-A289891] p 2136 N95-28626

VIBRATION DAMPING

Vibration control using chaotic motion stabilizers
[AD-A289576] p 2398 N95-26687

Experimental studies to test simple flexural neutralizers fitted to beams
[ISVR-TR-239] p 2309 N95-27846

System identification of damped truss-like space structures
[NASA-TM-106638] p 2303 N95-27911

VIBRATION EFFECTS

The effects of transverse vibration on the performance of an axial groove wick heat pipe
[AD-A289349] p 2278 N95-27065

Developmental problems and their solution for the Space Shuttle main engine alternate liquid oxygen high-pressure turbopump: Anomaly or failure investigation the key
[NASA-TP-3553] p 2169 N95-28263

Vibrational behavior of adaptive aircraft wing structures modelled as composite thin-walled beams
p 2191 N95-28435

VIBRATION ISOLATORS

The vibration transmission of lift truck suspension seats
[ISVR-TR-245] p 2302 N95-27844

VIBRATION MEASUREMENT

Diagnosis of helicopter gearboxes using structure-based networks
[NASA-TM-106932] p 2302 N95-27373

The vibration transmission of lift truck suspension seats
[ISVR-TR-245] p 2302 N95-27844

TV-holography at high temperatures: In situ observations of the oxidation of advanced materials
[PB95-195343] p 2294 N95-28651

VIBRATION METERS

Micro-time stress measurement device development
[AD-A289511] p 2361 N95-28845

VIBRATION MODE

Aeroelastic stability of wind turbine blade/aileron systems p 2124 N95-27981

VIBRATION TESTS

The vibration transmission of lift truck suspension seats
[ISVR-TR-245] p 2302 N95-27844

Experimental studies to test simple flexural neutralizers fitted to beams
[ISVR-TR-239] p 2309 N95-27846

System identification of damped truss-like space structures
[NASA-TM-106638] p 2303 N95-27911

In situ dynamic material property measurement system
[AD-D017387] p 2210 N95-28585

VIBRATIONAL SPECTRA

The vibration transmission of lift truck suspension seats
[ISVR-TR-245] p 2302 N95-27844

Fellowship in physics
[AD-A291691] p 2446 N95-28522

Subharmonic phonon transmission and Kapitza conductance between crystals with very different vibrational spectra
[DE95-609151] p 2447 N95-28808

VIDEO COMMUNICATION

Information superhighway: Issues affecting development
[AD-A289434] p 2252 N95-26923

VIDEO DATA

Integration of video and radiation analysis data
[DE95-004165] p 2379 N95-26443

Information superhighway: Issues affecting development
[AD-A289434] p 2252 N95-26923

VIDEO SIGNALS

Target detection for vision systems
[AD-D017271] p 2249 N95-26509

Com(sup 3): A composite-compatible component coding system
[BBC-RD-1994/17] p 2249 N95-26670

Information superhighway: Issues affecting development
[AD-A289434] p 2252 N95-26923

A foveated system to reduce transmission bandwidth of video images from remote camera systems
[AD-A288516] p 2254 N95-27080

Display system employing acousto-optic tunable filter
[NASA-CASE-NPO-18736-1-CU] p 2426 N95-27843

Long-range eye tracking: A feasibility study
[DE95-008587] p 2357 N95-28176

VIDEO TAPES

The effects of processing variables on reaction synthesis of Fe-Al alloys
[DE95-007405] p 2221 N95-28082

VIEWING

Advanced interactive display formats for terminal area traffic control
[NASA-CR-198576] p 2127 N95-28188

VINYL COPOLYMERS

Small angle neutron scattering study of the micelle structure of amphiphilic block copolymers
[DE95-006625] p 2234 N95-27486

VINYL POLYMERS

Molecular modeling: An approach for the study of piezoelectric polymers
[AD-A289821] p 2241 N95-28574

VINYLIDENE

Molecular modeling: An approach for the study of piezoelectric polymers
[AD-A289821] p 2241 N95-28574

VIRTUAL REALITY

The photo-realistic AFIT virtual cockpit
[AD-A289376] p 2130 N95-26876

VISCOELASTICITY

Effect of surface coating on one-dimensional system subjected to unit step pressure wave [AD-A288237] p 2308 N95-26625

Two-layer or free surface shear flows and viscoelastic shear flows and the relationship between stability and eigenvalues — viscoelastic, shear, and convective flows [AD-A289510] p 2278 N95-27047

Junkyard chemistry p 2227 N95-27102

Designing for time-dependent material response in spacecraft structures p 2166 N95-28292

Non-linear viscoelastic behaviour [PB95-192811] p 2199 N95-28639

VISCOPLASTICITY

Viscoplastic characterization and fatigue modeling of titanium based metal matrix composites [AD-A289430] p 2181 N95-26868

Robust integration schemes for generalized viscoplasticity with internal-state variables. Part 1: Theoretical developments and applications [NASA-CR-195452-PT-1] p 2310 N95-28031

Robust integration schemes for generalized viscoplasticity with internal-state variables. Part 2: Algorithmic developments and implementation [NASA-CR-195453-PT-2] p 2310 N95-28032

VISCOSITY

Measurement of viscosity by capillary rheometry: Dwell time effects [PB95-190203] p 2201 N95-26750

Precision parts cleaning with supercritical carbon dioxide p 2229 N95-27114

Turbulance boundary conditions for shear flow analysis, using the DTNS flow solver p 2283 N95-27362

Surfactants and desensitizing wax substitutes for TNT-Based systems [AD-A289652] p 2243 N95-28634

VISCOUS FLOW

A fully implicit time accurate method for hypersonic combustion: Application to shock-induced combustion instability [NASA-TM-106707] p 2273 N95-26380

Development of an upwind, finite-volume code with finite-rate chemistry [NASA-CR-197747] p 2121 N95-26760

On the nonlinear stability of the unsteady, viscous flow of an incompressible fluid in a curved pipe [NASA-CR-195065] p 2278 N95-27028

A 3D agglomeration multigrid solver for the Reynolds-averaged Navier-Stokes equations on unstructured meshes [NASA-CR-195073] p 2390 N95-27029

Two-layer or free surface shear flows and viscoelastic shear flows and the relationship between stability and eigenvalues — viscoelastic, shear, and convective flows [AD-A289510] p 2278 N95-27047

Global flowfield about the V-22 Tiltrotor Aircraft [NASA-CR-198603] p 2122 N95-27248

Calculation of three-dimensional (3-D) internal flow by means of the velocity-vorticity formulation on a staggered grid [NASA-TM-110352] p 2122 N95-27258

A numerical method for solving the three-dimensional parabolized Navier-Stokes equations [NASA-CR-198159] p 2287 N95-27917

Numerical study to assess sulfur hexafluoride as a medium for testing multielement airfoils [NASA-TP-3496] p 2124 N95-28674

VISIBLE SPECTRUM

Design and fabrication of a diamond-turned hybrid diffractive/refractive singlet for visible applications at ORNL [DE95-007007] p 2427 N95-28552

VISUAL ACUITY

Image perception wavelet simulation and enhancement for the visually impaired [AD-A289303] p 2353 N95-26917

VISUAL AIDS

Image perception wavelet simulation and enhancement for the visually impaired [AD-A289303] p 2353 N95-26917

Views of the solar system [DE95-006446] p 2461 N95-27326

VISUAL CONTROL

Learning Hand/Eye coordination by an active observer. part 1: Organizing centers [AD-A289502] p 2356 N95-26843

VISUAL OBSERVATION

Nova-like variables p 2458 N95-27070

Classical novae and recurrent novae: General properties p 2459 N95-27072

VISUAL PERCEPTION

Characterization of corrosion and development of a breadboard of a D sight aircraft inspection system, phase 1 [AD-A288347] p 2125 N95-26527

A mathematical framework for an improved search model [AD-A288858] p 2358 N95-26552

Image quality metrics for color CRT displays [AD-A288934] p 2262 N95-27196

Practical color vision tests for air traffic control applicants: En route center and terminal facilities [DOT/FAA/AM-95/13] p 2357 N95-27323

VISUAL SIGNALS

Analysis of group performance in visual signal detection [AD-A289561] p 2355 N95-26683

Characterization and redesign of the AFIT multielectrode array [AD-A289295] p 2354 N95-27039

VISUAL STIMULI

Role of somatosensory and vestibular cues in attenuating visually induced human postural sway [NASA-CR-197845] p 2357 N95-27697

VISUAL TASKS

Analysis of group performance in visual signal detection [AD-A289561] p 2355 N95-26683

Subjective workload assessment in a spatial memory task [AD-A289491] p 2356 N95-26825

VITON RUBBER (TRADEMARK)

Effects of atomic oxygen on polymeric materials flown on EOIM-3 p 2242 N95-27638

VITRIFICATION

Application of modern diagnostic methods to environmental improvement [DE95-005797] p 2330 N95-28119

VLASOV EQUATIONS

Crushing singularities in spacetimes with spherical, plane and hyperbolic symmetry [PB95-190146] p 2397 N95-28011

VOICE COMMUNICATION

Speech analysis and synthesis based on pitch-synchronous segmentation of the speech waveform [AD-A288824] p 2248 N95-26349

An experimental version of the MZT (speech-from-text) system with external F(sub 0) control [IFTR-14/1994] p 2250 N95-26836

Information superhighway: Issues affecting development [AD-A289434] p 2252 N95-26923

Voice analysis using the bispectrum [AD-A289204] p 2254 N95-27008

Development of a coding form for approach control/pilot voice communications [DOT/FAA/AM-95/15] p 2128 N95-28540

VOICE DATA PROCESSING

Speech analysis and synthesis based on pitch-synchronous segmentation of the speech waveform [AD-A288824] p 2248 N95-26349

An experimental version of the MZT (speech-from-text) system with external F(sub 0) control [IFTR-14/1994] p 2250 N95-26836

VOLCANOES

Seismic constraints on shallow crustal processes at the East Pacific rise [AD-A289055] p 2338 N95-28094

VOLT-AMPERE CHARACTERISTICS

Characterization of wafer charging mechanisms and oxide survival prediction methodology [DE95-006583] p 2440 N95-27538

VOLTAGE CONTROLLED OSCILLATORS

Extended linear ion trap frequency standard apparatus [NASA-CASE-NPO-19061-1-CU] p 2416 N95-28348

VOLTAGE CONVERTERS (DC TO DC)

Forback DC-to-DC converter [NASA-CASE-GSC-13404-1] p 2269 N95-28341

VOLTAGE REGULATORS

Testing of Uninterruptible Power Supplies with nonlinear loads [AD-A289353] p 2262 N95-27067

VORTEX GENERATORS

Performance characterization of a highly-offset diffuser with and without blowing vortex generator jets [AD-A289334] p 2122 N95-26901

Collected papers on wind turbine technology [NASA-CR-195432] p 2321 N95-27970

Comparative performance tests on the Mod-2, 2.5-mW wind turbine with and without vortex generators p 2124 N95-27978

Comparison of measured and calculated dynamic loads for the Mod-2 2.5 mW wind turbine system p 2312 N95-27983

VORTEX SHEDDING

Unsteady base pressure measurements in the near wake of a cylinder with imposed three-dimensional disturbances [AD-A289498] p 2276 N95-26827

VORTICES

Flutter clearance flight tests of an OV-10A airplane modified for wake vortex flight experiments [NASA-TM-109168] p 2117 N95-26381

Suppressor of oscillations in airframe cavities [AD-D017265] p 2128 N95-26507

The small-scale structure of dispersing clouds in the atmosphere [AD-A288256] p 2341 N95-26546

Wavenumber selection for small-wavelength Goertler vortices in curved channel flows [NASA-CR-195063] p 2273 N95-26576

Numerical simulation of the flow about the F-18 HARV at high angle of attack [NASA-CR-197755] p 2121 N95-26735

Effects of three-dimensional imposed 3-D disturbances on bluff-body near wake flows [AD-A289553] p 2121 N95-26757

Performance characterization of a highly-offset diffuser with and without blowing vortex generator jets [AD-A289334] p 2122 N95-26901

The near-wake flow behavior of an oscillating airfoil with modified trailing edge p 2119 N95-26953

Nonlinear stability of non-stationary cross-flow vortices in compressible boundary layers [NASA-CR-189184] p 2279 N95-27242

Effect of turbulence models on criticality conditions in swirling flows p 2282 N95-27356

A general theory of two- and three-dimensional rotational flow in subsonic and transonic turbomachines [NASA-CR-4496] p 2123 N95-28003

VORTICITY

Basic studies in turbulent shear flows [AD-A289145] p 2277 N95-26998

Calculation of three-dimensional (3-D) internal flow by means of the velocity-vorticity formulation on a staggered grid [NASA-TM-110352] p 2122 N95-27258

VULCANIZING

The effect of proteins on the aging properties of radiation vulcanized Natural Rubber Latex [DE95-603357] p 2225 N95-26599

Radiation vulcanization of natural rubber latex [DE95-600026] p 2226 N95-26637

W

WAFERS

Characterization and control of wafer charging effects during high-current ion implantation [DE95-006587] p 2440 N95-27471

Characterization of wafer charging mechanisms and oxide survival prediction methodology [DE95-006583] p 2440 N95-27538

WAKES

Flutter clearance flight tests of an OV-10A airplane modified for wake vortex flight experiments [NASA-TM-109168] p 2117 N95-26381

Wake fields in semiconductor plasmas [DE94-634523] p 2429 N95-26439

Infrared field measurements of sea surface temperature: Analysis of wake signatures and comparison of skin layer models [NASA-CR-197849] p 2346 N95-26533

Rarefied gas effects on aerobraking/reentry vehicles with wakes [NASA-CR-196586] p 2164 N95-27093

Large HAWT wake measurement and analysis p 2289 N95-27973

WALL PRESSURE

Investigation of boundary layer and performance effects of transpiration cooling through a porous plate in a rocket nozzle [AD-A289393] p 2167 N95-26880

WALL TEMPERATURE

Viscous shock-layer analysis on hypersonic flow over reentry capsule with nonequilibrium chemistry [ISAS-R-656] p 2274 N95-26739

WALLS

Algorithm to describe the spread of a wall fire under a ceiling [PB95-182259] p 2247 N95-28008

Alpha characterization inside pipes using ion-transport technology [DE95-007869] p 2411 N95-28024

Wall stabilization of rotating high (Beta) discharges in D3-D [DE95-008207] p 2435 N95-28406

Monte-Carlo simulation methods for finite flat plate winding flows [AD-A289842] p 2289 N95-28619

WAR GAMES
Integrated mission precision attack cockpit technology (IMPACT). Phase 1: Identifying technologies for air-to-ground fighter integration
[AD-A289562] p 2129 N95-26684
A mathematical analysis of the Janus combat simulation weather effects models and sensitivity analysis of sky-to-ground brightness ratio on target detection
[AD-A289629] p 2336 N95-26858
WARFARE
Characterization of Ultra-Low Carbon Baintic steels for use as weld wire consumables
[AD-A288292] p 2212 N95-26411
WARNING SYSTEMS
Control system design for the MOD-5A 7.3 mW wind turbine generator p 2306 N95-27985
WASHING
Cleaning of parts for new manufacturing and parts rebuilding p 2231 N95-27123
Retrofitting conventional vapor degreasers to use a solvent wash/fluorochemical rinse process
p 2232 N95-27127
The application of waterjets for cleaning
p 2233 N95-27130
The demilitarization of class 1.1 rocket motors using high pressure waterjets p 2176 N95-28322
Cryogenic washout of solid rocket propellants
p 2176 N95-28324
WASTE DISPOSAL
Junkyard chemistry p 2227 N95-27102
The use of supercritical carbon dioxide for contaminant removal from solid waste p 2229 N95-27110
Microbial treatment for shipboard collection, holding, and transfer system tanks p 2179 N95-27119
A practical approach to soil remediation
p 2232 N95-27125
Design considerations in supercritical fluid technology
p 2232 N95-27126
The experience of CF Technologies, Inc. (CF Tech) in critical fluid processing p 2232 N95-27128
Marshall Space Flight Center solid waste characterization and recycling improvement study
[NASA-CR-196594] p 2360 N95-27164
The 1994 JANNAF Safety and Environmental Protection Subcommittee Meeting, volume 1
[CPIA-PUBL-614-VOL-1] p 2170 N95-28294
OB/OD treatment: The effective use of measured field data and air modeling to support an environmental assessment p 2170 N95-28296
Recovery, evaluation, and decontamination of landfilled pentaborane cylinders, former liquid propellant rocket engine test facility, Washoe County, Nevada
p 2171 N95-28302
Upgrade of the computer modeling programs POLU10 and POLU13A for open burning and open detonation of energetic materials p 2172 N95-28306
Hazards analysis of an integral class 1.1/1.3 rocket motor demilitarization and ingredient recovery system using ammonia p 2174 N95-28315
Commercial reformulation: An economic and environmentally neutral means of managing explosives and solid propellants p 2175 N95-28320
Hydrothermal oxidation of solid rocket propellant and other department of defense hazardous wastes
p 2177 N95-28325
Recovery and reuse of rocket motor propellant ingredients p 2177 N95-28326
Strategies for recycling CdTe photovoltaic modules
[DE95-006776] p 2325 N95-28517
WASTE ENERGY UTILIZATION
Intrusive multi-probe system
[DE95-006258] p 2292 N95-27465
Building-integrated photovoltaics: A case study
[DE95-004032] p 2325 N95-28396
WASTE HEAT
High power free-electron laser concepts and problems
[DE95-007841] p 2298 N95-28059
WASTE TREATMENT
Electromagnetic devices and processes in environment protection
[AD-A288656] p 2141 N95-26487
The use of supercritical carbon dioxide for contaminant removal from solid waste p 2229 N95-27110
A practical approach to soil remediation
p 2232 N95-27125
The experience of CF Technologies, Inc. (CF Tech) in critical fluid processing p 2232 N95-27128
Application of modern diagnostic methods to environmental improvement
[DE95-005797] p 2330 N95-28119
The 1994 JANNAF Safety and Environmental Protection Subcommittee Meeting, volume 1
[CPIA-PUBL-614-VOL-1] p 2170 N95-28294
Recovery, evaluation, and decontamination of landfilled pentaborane cylinders, former liquid propellant rocket engine test facility, Washoe County, Nevada
p 2171 N95-28302
Upgrade of the computer modeling programs POLU10 and POLU13A for open burning and open detonation of energetic materials p 2172 N95-28306
Hydrothermal oxidation of solid rocket propellant and other department of defense hazardous wastes
p 2177 N95-28325
WASTE UTILIZATION
Geothermal direct-heat utilization assistance
[DE95-007247] p 2319 N95-27236
WASTE WATER
The experience of CF Technologies, Inc. (CF Tech) in critical fluid processing p 2232 N95-27128
Biodegradation of nitrate esters p 2171 N95-28299
Destruction of pyrotechnics manufacture wastewater treatment sludge by plasma arc pyrolysis
p 2171 N95-28301
The demilitarization of class 1.1 rocket motors using high pressure waterjets p 2176 N95-28322
Hydrothermal oxidation of solid rocket propellant and other department of defense hazardous wastes
p 2177 N95-28325
WASTES
Hydrothermal oxidation of solid rocket propellant and other department of defense hazardous wastes
p 2177 N95-28325
WATER
Flow cytometry as a means of detecting, enumerating and characterizing bacteria for monitoring of the environment
[AD-A288997] p 2326 N95-26610
BIPM project: Intercomparison of water triple-point cells
[PB95-185237] p 2398 N95-26614
The influence of surface structure on the interaction of water with TiO_2(100)
[DE95-004927] p 2203 N95-27401
Synchrotron X-ray scattering studies at mineral-water interfaces
[DE95-008303] p 2440 N95-27542
D/H and O-18/O-16 partitioning between water liquid and vapor in the system H_2O-Na-K-Mg-Ca-Cl-SO_4 from 0 to 350 C
[DE95-007013] p 2208 N95-27961
Vibrational spectroscopy of water interfaces
[DE95-006592] p 2209 N95-28218
Cryogenic BRDF measurements at 10.6 micrometers and 0.63 micrometers on contaminated mirrors
[AD-A291611] p 2427 N95-28408
WATER CIRCULATION
Combined use of ground water circulation (UVB) technology and in situ bioreactors for enhanced bioremediation of subsurface contamination
p 2230 N95-27118
WATER DEPTH
Deep convection in the Mediterranean Sea
[AD-A288497] p 2346 N95-26647
WATER FLOW
Evaluation of a new laboratory acoustic Doppler velocimeter
[AD-A289592] p 2290 N95-26714
WATER INJECTION
Investigation on comprehensive fossil fuel cycle analysis and assessment approach as viewed from the global environment
[DE95-759241] p 2329 N95-27935
WATER POLLUTION
Combined use of ground water circulation (UVB) technology and in situ bioreactors for enhanced bioremediation of subsurface contamination
p 2230 N95-27118
The 1994 JANNAF Safety and Environmental Protection Subcommittee Meeting, volume 1
[CPIA-PUBL-614-VOL-1] p 2170 N95-28294
Destruction of pyrotechnics manufacture wastewater treatment sludge by plasma arc pyrolysis
p 2171 N95-28301
WATER PRESSURE
Water driven turbine/brush pipe cleaner
[NASA-CASE-KSC-11669-1] p 2304 N95-28359
WATER TEMPERATURE
FREZCHEM: A chemical-thermodynamic model for aqueous solutions at subzero temperatures
[AD-A288456] p 2200 N95-26432
WATER TREATMENT
Environmentally Benign Cleaning and Degreasing Technology: JANNAF Safety and Protection Subcommittee and Propellant Development and Characterization Subcommittee Joint Workshop
[CPIA-PUBL-611] p 2227 N95-27101
Corrosive effects of supercritical carbon dioxide and cosolvents on metals p 2224 N95-27113
Combined use of ground water circulation (UVB) technology and in situ bioreactors for enhanced bioremediation of subsurface contamination
p 2230 N95-27118
Sceening, down selection, and implementation of environmentally compliant cleaning and insulation bonding for MNASA p 2165 N95-27124
A practical approach to soil remediation
p 2232 N95-27125
Retrofitting conventional vapor degreasers to use a solvent wash/fluorochemical rinse process
p 2232 N95-27127
The application of waterjets for cleaning
p 2233 N95-27130
Destruction of pyrotechnics manufacture wastewater treatment sludge by plasma arc pyrolysis
p 2171 N95-28301
Evaluation of microporous carbon filters as catalysts for ozone decomposition
[DE95-006498] p 2331 N95-28548
WATER TUNNEL TESTS
NASA Dryden flow visualization facility
[NASA-TM-4631] p 2362 N95-27914
WATER VAPOR
Prediction of rain attenuation and total atmospheric attenuation for low-availability satellite communications in Europe
[PB95-184925] p 2252 N95-26908
D/H and O-18/O-16 partitioning between water liquid and vapor in the system H_2O-Na-K-Mg-Ca-Cl-SO_4 from 0 to 350 C
[DE95-007013] p 2208 N95-27961
Millimeter-wave imaging radiometer data processing and development of water vapor retrieval algorithms
[NASA-CR-198593] p 2343 N95-27997
Measurement and analysis of the surface energy budget for ARM field experiments
[DE95-007646] p 2338 N95-28114
Search for molecular absorptions with the Fourier Transform Spectrometer
[NASA-CR-198648] p 2462 N95-28222
Measurements of daytime and upper tropospheric water vapor profiles by Raman lidar
[DE95-007640] p 2344 N95-28538
WATER VEHICLES
Air cushioned landing craft (LCAC) based ship to shore movement simulation: A decision aid for the amphibious commander. A (SMMAT) application
[AD-A289635] p 2246 N95-26722
WATER WAVES
Calculation of suspended sediment transport by combined wave-current flows
[AD-A289368] p 2346 N95-26904
Observations of near-bottom flow in a wave-dominated nearshore environment
[AD-A289331] p 2347 N95-27043
Speckle spectrum of the ERS-1 wavemode product
[PB95-196564] p 2315 N95-28180
WATERSHEDS
Solar terrestrial radiation data from the Sleepers River Research Watershed
[AD-A288444] p 2464 N95-27184
WAVE DIFFRACTION
Ultrasonic study on ternary liquid systems by laser-sound interaction
[DE95-608783] p 2207 N95-27929
WAVE DISPERSION
Ultrasonic studies of liquid/solid seimoacoustic wave phenomena
[AD-A289644] p 2402 N95-28622
WAVE DRAG
Computational fluid dynamics and transonic flow
[AD-A288962] p 2273 N95-26405
WAVE EQUATIONS
Construction of arbitrary order schemes for many dimensional wave equation
[PB95-184818] p 2276 N95-26928
Nonlinear problems in fluid dynamics and inverse scattering: Nonlinear waves and inverse scattering
[AD-A289148] p 2278 N95-27001
WAVE EXCITATION
Shear Alfven wave excitation by direct antenna coupling and fast wave resonant mode conversion
[DE95-609109] p 2256 N95-28254
WAVE FRONTS
Compensated deconvolution from wavefront sensing
[AD-A289490] p 2336 N95-26824
Frame selection performance limits for statistical image reconstruction of adaptive optics compensated images
[AD-A289240] p 2424 N95-26965
Flow visualization of a turbulent shear flow using an optical wavefront sensor
[AD-A289208] p 2277 N95-26986
WAVE FUNCTIONS
Massively parallel self-consistent-field calculations
[DE95-004128] p 2376 N95-26441

Two-body bound states and the Bethe-Salpeter equation
[DE95-008302] p 2392 N95-27742
Off-specular scattering in neutron reflectometry
[DE95-007835] p 2412 N95-28057
Quantum retrodiction and causality principle
[DE94-628438] p 2450 N95-28183

WAVE GENERATION
Meso-beta scale numerical simulation studies of terrain-induced jet streak mass/momentum perturbations
[NASA-CR-197804] p 2335 N95-26592

WAVE PROPAGATION
Very low frequency seismo-acoustic noise below the sea floor (0.2-10 Hz)
[AD-A289164] p 2347 N95-27011
Modeling surface effects with the parabolic equation method
[AD-A289199] p 2254 N95-27021
Normal modes and continuous spectra
[DE95-006166] p 2287 N95-28055
Seismic constraints on shallow crustal processes at the East Pacific rise
[AD-A289055] p 2338 N95-28094
Emerging applications of probability (stochastic models in geosystems)
[AD-A289117] p 2313 N95-28099
Transformation to zero offset in transversely isotropic media
[DE95-007669] p 2339 N95-28192
Fowler DMO and time migration for transversely isotropic media with explicit operators
[DE95-007671] p 2339 N95-28194
Contact micromechanics in granular media with clay
[DE95-006566] p 2340 N95-28583

WAVE SCATTERING
Numerical analysis of wave scattering
[AD-A289478] p 2401 N95-26925
One dimensional global and local solution for ICRF heating
[DE95-007984] p 2392 N95-28110

WAVEFORMS
Speech analysis and synthesis based on pitch-synchronous segmentation of the speech waveform
[AD-A288824] p 2248 N95-26349
Evaluation of the FMICW waveform in HF surface radar applications
[AD-A288245] p 2249 N95-26545
Survey on step recovery diode and its applications
[PB95-184974] p 2260 N95-26646
A study of lightning in winter thunderstorms and the analysis of thunderstorm overflight data
[NASA-CR-198577] p 2343 N95-28191
Method and apparatus for maintaining linearity and frequency accuracy of an FM chirp waveform
[AD-D017398] p 2258 N95-28615

WAVEGUIDE ANTENNAS
Theoretical and experimental study of low-loss, High-efficiency monolithic antenna structures at 94 GHz
[AD-A291785] p 2257 N95-28513

WAVEGUIDES
High power, broadband folded waveguide Gyrotron-Traveling-Wave-Amplifier
[AD-A288847] p 2259 N95-26433
Analysis of electromagnetic problems involving chiral, bi-isotropic, and uniaxial bianisotropic media
[PB95-185096] p 2248 N95-26450
On-axis polarization coupling in y-cut titanium in-diffused lithium niobate slab waveguides
[AD-A289260] p 2253 N95-26977
Evaluation of defect-related diffusion in semiconductors by electrooptical sampling
[AD-A291630] p 2270 N95-28544

WAVELENGTHS
Multiwavelength observations of unidentified high energy gamma-ray sources
[NASA-CR-197840] p 2465 N95-26630
Fundamental concepts of integrated and fiber optic sensors
[NASA-TM-106920] p 2426 N95-27906

WAVELET ANALYSIS
Image perception wavelet simulation and enhancement for the visually impaired
[AD-A289303] p 2353 N95-26917
Multipoint multirate signal processing
[AD-A289211] p 2253 N95-26988
Nonlinear problems in fluid dynamics and inverse scattering: Propagation and capturing of singularities in problems of fluid dynamics and inverse scattering
[AD-A289146] p 2277 N95-26999
Improved reduced-resolution satellite imagery
p 2376 N95-27388
The use of wavelet transforms in the solution of two-phase flow problems
[DE95-004688] p 2284 N95-27721
An introduction to wavelet transforms
[AD-A289083] p 2256 N95-28095
Denoising and robust non-linear wavelet analysis
[AD-A291668] p 2257 N95-28455
Wavelet analysis and its applications
[AD-A291735] p 2387 N95-28527

WAXES
Effect of processing parameters on surface finish for fused deposition machinable wax patterns
[NASA-TP-3550] p 2244 N95-26769
Surfactants and desensitizing wax substitutes for TNT-Based systems
[AD-A289652] p 2243 N95-28634

WEAK ENERGY INTERACTIONS
Rare decays/CP: The perspective of a kaon physicist
[DE95-005964] p 2416 N95-28338

WEAK INTERACTIONS (FIELD THEORY)
Magnetic quadrupole moment of W-boson in Kobayashi-Maskawa model
[DE95-610355] p 2407 N95-27411

WEAPON SYSTEMS
A comparison of error categorization schemes for use in software system safety programs
[AD-A288741] p 2371 N95-27251
Time-dependent model for vertical-cavity surface-emitting laser
[DE95-007880] p 2298 N95-28027

WEAPONS DEVELOPMENT
Concurrent engineering research center
[NASA-CR-197726] p 2362 N95-26386
Report to Congressional Committees. Comanche Helicopter: Testing needs to be completed prior to production decisions
[GAO/NSIAD-95-112] p 2135 N95-27910

WEAR
Advanced solid lubricant films by Ion-Beam Assisted Deposition
[AD-A288866] p 2225 N95-26499

WEAR RESISTANCE
Gloved operator performance study. The effects of hand wear and elastic resistance of a control during tracking performance
[AD-A289405] p 2360 N95-27099

WEAR TESTS
Developmental problems and their solution for the Space Shuttle main engine alternate liquid oxygen high-pressure turbopump: Anomaly or failure investigation the key
[NASA-TP-3553] p 2169 N95-28263

WEATHER
WINCLR: A computer code for heat transfer and clearance calculation in a compressor
[NASA-CR-195436] p 2117 N95-26363
Synoptic features of the Yunan rainy season before the onset of the tropical monsoons
[AD-A289641] p 2342 N95-26724
A mathematical analysis of the Janus combat simulation weather effects models and sensitivity analysis of sky-to-ground brightness ratio on target detection
[AD-A289629] p 2336 N95-26858
Southern Africa: A climatological study
[AD-A289466] p 2342 N95-27148
Design, construction, test and evaluation of a frequency scanning radiometer for measuring oil slick thicknesses
[AD-A290040] p 2293 N95-28389
Severe weather guide mediterranean
[AD-A289829] p 2344 N95-28577

WEATHER FORECASTING
Live from Antarctica, volume 4
[NASA-CR-197828] p 2335 N95-26596
Indexing meso-beta surface wind site representative
[AD-A288501] p 2341 N95-26650
Fluxes across the west coast resolved by Picket Fence observations during stormfest
[AD-A288511] p 2341 N95-26653
Neural networks versus linear regression: Research into the value of neural networks in meteorological practice
[KNMI-TR-165] p 2343 N95-28236
Three-dimensional forecast models for emergency response management p 2172 N95-28303
Systematic and integrated approach to Tropical Cyclone track forecasting. Part 1: Approach overview and description of meteorological basis
[AD-A291775] p 2344 N95-28459

WEATHER STATIONS
Live from Antarctica: The coldest, windiest place on Earth
[NASA-CR-197737] p 2335 N95-26595

WEATHERING
The use of electrochemistry and ellipsometry for identifying and evaluating corrosion on aircraft
[AD-A288536] p 2125 N95-27186
Investigation on technology for increasing the biological CO2 sink and technology for CO2 fixation and reutilization
[DE95-759251] p 2329 N95-27941
Assay of weathering effects on protective polymer coatings using positron annihilation spectroscopy
[DE95-007040] p 2236 N95-27962
Weightless Environment Training Facility (WETF) materials coating evaluation, volume 1
[NASA-CR-188366-VOL-1] p 2239 N95-28385

WEAVING
Characterization and manufacture of braided composites for large commercial aircraft structures
p 2196 N95-28478

WEIBULL DENSITY FUNCTIONS
Proof test methodology for composites
p 2193 N95-28445

WEIGHTING FUNCTIONS
F/A-18 IFOSTP Fatigue test airbag load determination on the vertical and horizontal tails
[DSTO-TR-0135] p 2128 N95-26389
Weighting scheme for the space surveillance network automated tasker
[AD-A289285] p 2146 N95-27035
Ulysses orbit determination at high declinations
p 2151 N95-27787

WEIGHTLESSNESS
Weightless Environment Training Facility (WETF) materials coating evaluation, volume 1
[NASA-CR-188366-VOL-1] p 2239 N95-28385

WELD TESTS
Development of welded solar arrays for DMSP and GPS satellites
[AD-A289512] p 2318 N95-26846

WELDABILITY
Improved hardness RHA weldability and material property testing
[AD-A289127] p 2221 N95-28102

WELDED JOINTS
Characterization of Ultra-Low Carbon Baintic steels for use as weld wire consumables
[AD-A288292] p 2212 N95-26411
Development of welded solar arrays for DMSP and GPS satellites
[AD-A289512] p 2318 N95-26846
Non-metallic oxide inclusion formation in C-Mnlow alloy steel welds
[DE94-019160] p 2215 N95-27[illegible]19
Advances in welding science: A perspective
[DE95-006745] p 2302 N95-27545

WELDING
Advances in welding science: A perspective
[DE95-006745] p 2302 N95-27545

WETTING
Transient studies of G-induced capillary dryout and rewet p 2281 N95-27351

WHISKER COMPOSITES
Structural ceramics incorporating whiskers, platelets, and particulate phases
[DE95-007048] p 2235 N95-27499
High-temperature deformation of ZrO2-Al2O3/SiC whisker composites fabricated by two techniques
[DE95-008273] p 2183 N95-28069

WHITE DWARF STARS
Precision asteroseismology of DAV (ZZ CETI) white dwarf stars
[DE95-006265] p 2462 N95-28056
A new method of determining the ejected mass of novae
[DE95-007884] p 2462 N95-28062

WHITE NOISE
Post Kalman progress p 2148 N95-27776

WICKS
The effects of transverse vibration on the performance of an axial groove wick heat pipe
[AD-A289349] p 2278 N95-27065

WIGGLER MAGNETS
Free Electron Laser Physical Process Code (FELPPC)
[DE95-006276] p 2296 N95-27557

WIND (METEOROLOGY)
Proceedings: Workshop on Research Needs in Wind Engineering
[PB95-189528] p 2308 N95-26743
Basic principles and recent observations of rotationally sampled wind p 2321 N95-27971
Weather hazards to a Titan 4 on-pad destack-restack operation p 2172 N95-28307

WIND DIRECTION
Performance of a stand-alone wind-electric ice maker for remote villages
[DE95-004006] p 2320 N95-27475

WIND EFFECTS
Hindcasting wind-driven anomalies using reduced-gravity global ocean models with 1/2 deg and 1/4 deg resolution
[AD-A289060] p 2345 N95-26406
Proceedings: Workshop on Research Needs in Wind Engineering
[PB95-189528] p 2308 N95-26743

WIND MEASUREMENT

Indexing meso-beta surface wind site representative [AD-A288501] p 2341 N95-26650

Large HAWT wake measurement and analysis p 2289 N95-27973

WIND SHEAR

Studies of radar backscatter as a function of wave properties and the winds in the turbulent marine atmosphere [NASA-CR-198608] p 2315 N95-28209

WIND TUNNEL MODELS

Experimental investigation of static and dynamic ground effect on HOPE ALFLEX vehicle [NAL-TR-1236] p 2128 N95-26525

High-precision buffer circuit for suppression of regenerative oscillation [NASA-TM-4658] p 2291 N95-27259

WIND TUNNEL TESTS

Airfoil modification effects on subsonic and transonic pressure distributions and performance for the EA-6B airplane [NASA-TP-3516] p 2120 N95-26382

Experimental investigation of static and dynamic ground effect on HOPE ALFLEX vehicle [NAL-TR-1236] p 2128 N95-26525

Wind tunnel experiments on wake flow field behind a reentry capsule from a viewpoint of parachute deployment at supersonic speeds [ISAS-R-655] p 2121 N95-26740

Effects of three-dimensional imposed 3-D disturbances on bluff-body near wake flows [AD-A289553] p 2121 N95-26757

Analysis of hypersonic boundary layer second mode instability over a 7 deg cone [AD-A289471] p 2276 N95-26819

Compressible turbulence measurements in a supersonic boundary layer including favorable pressure gradient effects [AD-A289475] p 2276 N95-26821

Compressible turbulence measurements in a supersonic flow with adverse pressure gradient [AD-A289477] p 2276 N95-26822

Unsteady base pressure measurements in the near wake of a cylinder with imposed three-dimensional disturbances [AD-A289498] p 2276 N95-26827

A new drag measurement system for wind tunnel testing of the racing bicycle and rider to determine a low drag configuration [AD-A289375] p 2122 N95-26875

An experimental investigation of helicopter downwash and tailboom interaction at the Wichita State University 7x10 foot wind tunnel p 2120 N95-26955

Incorporating biplane wing theory into a large, subsonic, all-cargo transport p 2120 N95-26956

The lift-fan aircraft: Lessons learned [NASA-CR-196694] p 2131 N95-27143

Sailplane glide performance and control using fixed and articulating winglets [NASA-CR-198579] p 2131 N95-27180

Wind-tunnel test of the S814 thick root airfoil [DE95-000266] p 2122 N95-27541

Further investigations of icing effects on an advanced high-lift multi-element airfoil [NASA-TM-106947] p 2125 N95-27762

Modeling of aircraft unsteady aerodynamic characteristics. Part 2: Parameters estimated from wind tunnel data [NASA-TM-110161] p 2142 N95-27839

Optimization of measurements with pressure sensitive paints [NASA-TM-4695] p 2293 N95-27915

Collected papers on wind turbine technology [NASA-CR-195432] p 2321 N95-27970

Large HAWT wake measurement and analysis p 2289 N95-27973

Horizontal axis wind turbine post stall airfoil characteristics synthesization p 2124 N95-27974

Comparative wind tunnel tests of NACA 23024 airfoils with several aileron and spoiler configurations p 2124 N95-27976

Comparative wind tunnel test at high Reynolds numbers of NACA 64 621 airfoils with two aileron configurations p 2124 N95-27977

Flow structure generated by perpendicular blade vortex interaction and implications for helicopter noise predictions [NASA-CR-198590] p 2123 N95-28193

Performance study for inlet installations [NASA-CR-189714] p 2140 N95-28227

Measurements of store forces and moments and cavity pressures for a generic store in and near a box cavity at subsonic and transonic speeds [NASA-TM-4611] p 2123 N95-28241

Construction and wind tunnel test of a 1/12th scale helicopter model [AD-A288487] p 2123 N95-28331

Experimental investigation of inlet-combustor isolators for a dual-mode scramjet at a Mach number of 4 [NASA-TP-3502] p 2140 N95-28343

Study of potential aerodynamic benefits from spanwise blowing at wingtip [NASA-TP-3515] p 2124 N95-28669

Numerical study to assess sulfur hexafluoride as a medium for testing multielement airfoils [NASA-TP-3496] p 2124 N95-28674

WIND TUNNELS

Anechoic wind tunnel study of turbulence effects on wind turbine broadband noise p 2325 N95-27992

WIND TURBINES

Bibliography of NASA-related publications on wind turbine technology 1973-1995 [NASA-CR-195462] p 2316 N95-26734

A comparison of measured wind park load histories with the WISPER and WISPERX load spectra [DE95-000295] p 2319 N95-27459

Performance of a stand-alone wind-electric ice maker for remote villages [DE95-004006] p 2320 N95-27475

Collected papers on wind turbine technology [NASA-CR-195432] p 2321 N95-27970

Basic principles and recent observations of rotationally sampled wind p 2321 N95-27971

A model of rotationally-sampled wind turbulence for predicting fatigue loads in wind turbines p 2312 N95-27972

Large HAWT wake measurement and analysis p 2289 N95-27973

Horizontal axis wind turbine post stall airfoil characteristics synthesization p 2124 N95-27974

Preliminary analysis of dynamic stall effects on a 91-meter wind turbine rotor p 2124 N95-27975

Comparative wind tunnel test at high Reynolds numbers of NACA 64 621 airfoils with two aileron configurations p 2124 N95-27977

Comparative performance tests on the Mod-2, 2.5-mW wind turbine with and without vortex generators p 2124 N95-27978

Design of a real-time wind turbine simulator using a custom parallel architecture p 2322 N95-27979

A NASTRAN-based computer program for structural dynamic analysis of Horizontal Axis Wind Turbines p 2312 N95-27980

Aeroelastic stability of wind turbine blade/aileron systems p 2124 N95-27981

Calculation of design load for the MOD-5A 7.3 mW wind turbine system p 2312 N95-27982

Comparison of measured and calculated dynamic loads for the Mod-2 2.5 mW wind turbine system p 2312 N95-27983

Analysis methods for wind turbine control and electrical system dynamics p 2273 N95-27984

Control system design for the MOD-5A 7.3 mW wind turbine generator p 2306 N95-27985

Use of blade pitch control to provide power train damping for the Mod-2, 2.5-mW wind turbine p 2306 N95-27986

Variable speed generator technology options for wind turbine generators p 2273 N95-27988

Variable speed generator application on the MOD-5A 7.3 mW wind turbine generator p 2273 N95-27989

Measurement and prediction of broadband noise from large horizontal axis wind turbine generators p 2324 N95-27990

Observed acoustic and aeroelastic spectral responses of a MOD-2 turbine blade to turbulence excitation p 2324 N95-27991

Anechoic wind tunnel study of turbulence effects on wind turbine broadband noise p 2325 N95-27992

The U.S. Department of Energy Wind Turbine Development Program [DE95-000292] p 2325 N95-28395

Mechanical properties of Hysol EA-9394 structural adhesive [DE95-008187] p 2240 N95-28405

WIND VELOCITY

Indexing meso-beta surface wind site representative [AD-A288501] p 2341 N95-26650

Performance of a stand-alone wind-electric ice maker for remote villages [DE95-004006] p 2320 N95-27475

Basic principles and recent observations of rotationally sampled wind p 2321 N95-27971

A model of rotationally-sampled wind turbulence for predicting fatigue loads in wind turbines p 2312 N95-27972

Preliminary analysis of dynamic stall effects on a 91-meter wind turbine rotor p 2124 N95-27975

Comparative wind tunnel tests of NACA 23024 airfoils with several aileron and spoiler configurations p 2124 N95-27976

Comparative wind tunnel test at high Reynolds numbers of NACA 64 621 airfoils with two aileron configurations p 2124 N95-27977

Comparative performance tests on the Mod-2, 2.5-mW wind turbine with and without vortex generators p 2124 N95-27978

Comparison of measured and calculated dynamic loads for the Mod-2 2.5 mW wind turbine system p 2312 N95-27983

The performance of cargo airdrop systems using g-12E parachutes: Statistical determination of minimum altitude [AD-A291666] p 2126 N95-28454

WIND VELOCITY MEASUREMENT

Comparative performance tests on the Mod-2, 2.5-mW wind turbine with and without vortex generators p 2124 N95-27978

WINDING

Induced axial oscillations in superconducting dipole windings [DE95-005690] p 2265 N95-27554

Monte-Carlo simulation methods for finite flat plate winding flows [AD-A289842] p 2289 N95-28619

WINDOWS (APERTURES)

Development of repair processes and sources for C/KC-135 aircraft windows/windshields [AD-A288348] p 2117 N95-26629

Thermally-induced unsymmetric optical distortion of output window of high-power CO2 laser [AD-A289604] p 2300 N95-28650

WINDOWS (COMPUTER PROGRAMS)

High performance hardware and software for pattern recognition and image processing [AD-A289153] p 2370 N95-27031

WINDPOWER UTILIZATION

Bibliography of NASA-related publications on wind turbine technology 1973-1995 [NASA-CR-195462] p 2316 N95-26734

Collected papers on wind turbine technology [NASA-CR-195432] p 2321 N95-27970

Large HAWT wake measurement and analysis p 2289 N95-27973

Comparative performance tests on the Mod-2, 2.5-mW wind turbine with and without vortex generators p 2124 N95-27978

Design of a real-time wind turbine simulator using a custom parallel architecture p 2322 N95-27979

Analysis methods for wind turbine control and electrical system dynamics p 2273 N95-27984

A conceptual framework for evaluating variable speed generator options for wind energy applications p 2273 N95-27987

Variable speed generator technology options for wind turbine generators p 2273 N95-27988

WINDPOWERED GENERATORS

Collected papers on wind turbine technology [NASA-CR-195432] p 2321 N95-27970

Control system design for the MOD-5A 7.3 mW wind turbine generator p 2306 N95-27985

A conceptual framework for evaluating variable speed generator options for wind energy applications p 2273 N95-27987

Variable speed generator technology options for wind turbine generators p 2273 N95-27988

Variable speed generator application on the MOD-5A 7.3 mW wind turbine generator p 2273 N95-27989

Measurement and prediction of broadband noise from large horizontal axis wind turbine generators p 2324 N95-27990

WINDS ALOFT

A study of magnetic activity effects on the thermospheric winds in the low ionosphere [AD-A288677] p 2334 N95-26488

WINDSHIELDS

Orbital impacts and the Space Shuttle windshield [NASA-TM-110594] p 2159 N95-26379

Development of repair processes and sources for C/KC-135 aircraft windows/windshields [AD-A288348] p 2117 N95-26629

Prediction of material strength and fracture of glass using the SPHINX smooth particle hydrodynamics code [DE95-004869] p 2236 N95-27943

WING CAMBER

Unique considerations in the design and experimental evaluation of tailored wings with elastically produced chordwise camber p 2192 N95-28436

WING PANELS

Structural modification and repair of C-130 wing structure using bonded composites p 2133 N95-27512

Composite or metallic bolted repairs on self-stiffened carbon wing panel of the commuter ATR72 design criteria, analysis, verification by test p 2135 N95-27525

WING-FUSELAGE STORES
Airfoil modification effects on subsonic and transonic pressure distributions and performance for the EA-6B airplane
[NASA-TP-3516] p 2120 N95-26382
WINGLETS
Sailplane glide performance and control using fixed and articulating winglets
[NASA-CR-198579] p 2131 N95-27180
WINGS
Demonstration study of hierarchical control of fluid-dynamic phenomena
[AD-A289341] p 2275 N95-26751
A numerical method for unsteady transonic flow about wings with control surfaces
[AD-A289631] p 2121 N95-26859
Advanced formation flight control
[AD-A289271] p 2142 N95-26981
Design and structural validation of CF116 upper wing skin boron doubler p 2132 N95-27510
An LDEF follow-on spacecraft concept
p 2166 N95-27665
Vibrational behavior of adaptive aircraft wing structures modelled as composite thin-walled beams
p 2191 N95-28435
Unique considerations in the design and experimental evaluation of tailored wings with elastically produced chordwise camber p 2192 N95-28436
C-130 Advanced Technology Center wing box conceptual design/cost study p 2192 N95-28437
Structural testing of the technology integration box beam p 2194 N95-28467
Test and analysis results for composite transport fuselage and wing structures p 2137 N95-28470
Application of damage tolerance methodology in certification of the Piaggio P-180 Avanti
p 2138 N95-28480
Advanced wing design survivability testing and results
p 2138 N95-28488
WINTER
A study of lightning in winter thunderstorms and the analysis of thunderstorm overflight data
[NASA-CR-198577] p 2343 N95-28191
The northern wintertime divergence extrema at 200 hPa and surface cyclones as simulated in the integration of the ECMWF general circulation model
[DE95-007946] p 2332 N95-28550
WIRE
Characterization of Ultra-Low Carbon Baintic steels for use as weld wire consumables
[AD-A288292] p 2212 N95-26411
Iron oxides characterization by Moessbauer spectroscopy
[DE95-607869] p 2202 N95-27199
A rotating arm using shape-memory alloy
p 2157 N95-27276
Review of activities in USA on HTS materials
[DE95-006404] p 2234 N95-27468
Manufacture and testing of the superconducting wire and cable for the RHIC dipoles and quadrupoles
[DE95-006000] p 2270 N95-28515
WIRING
Design and development of experimental facilities for short duration, low-gravity combustion and fire experiments
[NASA-CR-195458] p 2244 N95-26709
Partial discharge testing of high voltage wiring harness for airborne displays
[AD-A289150] p 2138 N95-27003
AH-1F COBRA rewire program MANPRINT analysis
[AD-A289190] p 2130 N95-27018
WORDS (LANGUAGE)
Isolated digit recognition without time alignment
[AD-A289344] p 2254 N95-27062
Multiclassifier fusion of an ultrasonic lip reader in automatic speech recognition
[AD-A289207] p 2254 N95-27079
Free Electron Laser Physical Process Code (FELPPC)
[DE95-006276] p 2296 N95-27557
Simulator report for SCI systems with HIC-router
[PB95-196580] p 2379 N95-28093
WORK
Change, Learning and Mental Work in Organizations: Working papers of the 3rd Otaniemi-Dresden Workshop
[PB95-184941] p 2356 N95-26909
WORK HARDENING
Forming metallurgy: Supervised drawing course, NTH
[PB95-196507] p 2219 N95-27934
WORKING FLUIDS
Mathematical modelling of the thermodynamic properties of coolants and working media of heat pumps
[IFTR-6/1994] p 2447 N95-26510
The effects of transverse vibration on the performance of an axial groove wick heat pipe
[AD-A289349] p 2278 N95-27065
Features and applications of the Groove Analysis Program (GAP) p 2281 N95-27349
WORKLOADS (PSYCHOPHYSIOLOGY)
Development of an acuity-based nurse staffing system for the post anesthesia care unit
[AD-A288831] p 2352 N95-26494
Integrated mission precision attack cockpit technology (IMPACT). Phase 1: Identifying technologies for air-to-ground fighter integration
[AD-A289562] p 2129 N95-26684
Handbook of perception and human performance, volume 2. Cognitive processes and performance
[AD-A289587] p 2355 N95-26692
Enhanced visual user interface support for domain-oriented application composition systems
[AD-A289337] p 2359 N95-26737
Subjective workload assessment in a spatial memory task
[AD-A289491] p 2356 N95-26825
Full span flaperons for a biplane
p 2119 N95-26954
Human factors in aviation maintenance, phase 4
[DOT/FAA/AM-95/14] p 2360 N95-27696
Pilot opinions on high level flight deck automation issues: Toward the development of a design philosophy
[NASA-CR-4669] p 2357 N95-28253
WORKSTATIONS
Next generation controller specification for an open systems architecture standard - overview
[AD-A289507] p 2368 N95-26853
NIST Automated Manufacturing Research Facility (AMRF): March 1987
[NONP-NASA-VT-95-49097] p 2246 N95-27203
A study of workstation computational performance for real-time flight simulation
[NASA-TM-109184] p 2362 N95-27241
The transition of GTDS to the Unix workstation environment p 2151 N95-27789
Optimization strategies for molecular dynamics programs on Cray computers and scalar work stations
[AD-A289574] p 2418 N95-28648
WORLD METEOROLOGICAL ORGANIZATION
The Global Historical Climatology Network: A preview of version 2
[DE95-007003] p 2332 N95-28605
WOVEN COMPOSITES
Characterization of fatigue behavior of 2-D woven fabric reinforced ceramic matrix composite at elevated temperature
[AD-A289423] p 2181 N95-26886
Mechanisms of compressive failure in woven composites and stitched laminates p 2189 N95-28424
Development of stitched/RTM composite primary structures p 2195 N95-28469
WRIST
Research activities on somatosensory (SI) cortical neurons
[AD-A288794] p 2348 N95-26360

X

X RAY ABSORPTION
Structural oxidation state studies of the manganese cluster in the oxygen evolving complex of Photosystem II
[DE95-008488] p 2409 N95-27744
Magnetic and structural properties of Fe/Pd multilayers studied by magnetic x-ray dichroism and x-ray absorption spectroscopy
[DE95-007095] p 2206 N95-27755
X RAY ANALYSIS
Structure of ordinary ice Ih. Part 2: Defects in ice. Volume 1: Point defects
[AD-A288279] p 2200 N95-26452
Large area smart piezoelectric and pyroelectric sensors
[AD-A288565] p 2290 N95-26541
Comparative experimental study of PIXE and X-ray fluorescence analysis
[DE95-607868] p 2327 N95-27198
Basic and applied research in the field of electronics and communications
[AD-A291727] p 2270 N95-28512
X RAY ASTRONOMY
A long-term space astrophysics research program: An x-ray perspective of the components and structure of galaxies
[NASA-CR-197787] p 2461 N95-26593
Multiwavelength observations of unidentified high energy gamma-ray sources
[NASA-CR-197840] p 2465 N95-26630
A new method of determining the ejected mass of novae
[DE95-007884] p 2462 N95-28062
X RAY DIFFRACTION
Fatigue fracture analysis in medium carbon structural steel and austenitic stainless steel by X-ray fractography
[DE95-601504] p 2213 N95-26675
Stoichiometry, structure, and properties of La2NiO(4+(delta)) and La(2-x)Sr(x)NiO(4+/-(delta))
[DE95-007682] p 2439 N95-27443
C15 intermetallic compounds HfV2+Nb
[DE95-005264] p 2215 N95-27463
Superior catalysts for selective catalytic reduction of nitric oxide
[DE95-007903] p 2205 N95-27691
Formation of anisotropic Tl-1212, Tl-2212, Tl-1223 and Tl-2223 particles using aerosol flow reacted powders
[DE95-007400] p 2444 N95-28079
X RAY FLUORESCENCE
Comparative experimental study of PIXE and X-ray fluorescence analysis
[DE95-607868] p 2327 N95-27198
X RAY SCATTERING
Synchrotron X-ray scattering studies at mineral-water interfaces
[DE95-008303] p 2440 N95-27542
Small angle x ray scattering studies of reverse micelles in supercritical fluids
[DE95-007803] p 2287 N95-28021
X RAY SPECTRA
Multiwavelength observations of unidentified high energy gamma-ray sources
[NASA-CR-197840] p 2465 N95-26630
Coronal abundances and their variation
[NASA-CR-197788] p 2464 N95-26671
X RAY SPECTROSCOPY
Probe molecule studies: Active species in alcohol synthesis
[DE95-003514] p 2203 N95-27420
NO decomposition in non-reducing atmospheres
[DE95-007895] p 2205 N95-27690
Low resistivity ohmic contacts to moderately doped n-GaAs with low temperature processing
[DE95-008507] p 2445 N95-28144
X RAY TIMING EXPLORER
Design, development and testing of the x-ray timing explorer High Gain Antenna System
p 2157 N95-27279
Development of the solar array deployment and drive system for the XTE spacecraft p 2158 N95-27284
X RAYS
Radiation sensitive area detection device and method
[NASA-CASE-MFS-28563-3] p 2423 N95-26385
Fatigue fracture analysis in medium carbon structural steel and austenitic stainless steel by X-ray fractography
[DE95-601504] p 2213 N95-26675
PXAMS: Projectile X ray AMS: X ray yields and applications
[DE95-006438] p 2204 N95-27496
Femtosecond X-ray generation through 90 degrees T homson scattering: Status of the LBL experiment
[DE95-006560] p 2296 N95-27674
Amorphous silicon pixel radiation detectors and associated thin film transistor electronics readout
[DE95-006568] p 2265 N95-27678
Small angle x ray scattering studies of reverse micelles in supercritical fluids
[DE95-007803] p 2287 N95-28021
Solar-geophysical data number 604, December 1994. Part 1: (Prompt reports). Data for November, October 1994, and late data
[PB95-181848] p 2465 N95-28087
XENON
Temperature dependence of ion-beam-induced amorphization in (Beta)-SiC
[DE95-007164] p 2438 N95-27087
XENON ISOTOPES
Search for deeply bound pionic atoms with high-purity germanium tagging spectrometer
[DE95-609072] p 2416 N95-28252

Y

YANG-MILLS THEORY
Compactification of moduli spaces of monopoles
[PB95-185179] p 2388 N95-26515
YAWING MOMENTS
Sailplane glide performance and control using fixed and articulating winglets
[NASA-CR-198579] p 2131 N95-27180
YBCO SUPERCONDUCTORS
Inflight resistance measurement on high-T(sub c) superconducting thin films exposed to orbital atomic oxygen on CONCAP-2 (STS-46) p 2272 N95-27635
Sintering of textured YBa2Cu3O(7-x) under intensive Co-60 gamma irradiation
[DE95-007098] p 2442 N95-27950

Recent neutron scattering results on high-temperature superconductors
[DE95-007028] p 2413 N95-28066

YIELD POINT
The role of edge dislocations in the deformation of BCC metals
[DE95-609157] p 2219 N95-27759
The elevated temperature tensile properties of S-200E commercially pure beryllium
[DE95-009331] p 2223 N95-28534
Influences of film structures on laser damage thresholds
[AD-A289647] p 2300 N95-28633

YIELD STRENGTH
ECR plasma-assisted deposition of Al2O3 and dispersion-strengthened AlO2
[DE95-007743] p 2235 N95-27687
An experimental and numerical investigation of specimen size requirements for cleavage fracture toughness
[AD-A289120] p 2311 N95-28100
Uncertainties in obtaining high reliability from stress-strength models p 2193 N95-28442
Indentability of conventional and negative Poisson's ratio foams p 2195 N95-28472

YLF LASERS
Improved performance 1590 nm Er:YLF laser
[DE95-003691] p 2296 N95-27705

YTTRIUM
High temperature Hexoloy(trademark) SX silicon carbide
[DE95-007290] p 2221 N95-28075
Structural chemistry of some phases in the YC-Ni-B system
[DE95-007403] p 2447 N95-28537

YTTRIUM COMPOUNDS
The oxidation state and magnetic behaviour of Tb in high-(Tc) related materials
[DE95-007129] p 2219 N95-27966

YTTRIUM-ALUMINUM GARNET
Method and apparatus for maintaining linearity and frequency accuracy of an FM chirp waveform
[AD-D017398] p 2258 N95-28615

Z

ZEOLITES
NO decomposition in non-reducing atmospheres
[DE95-007695] p 2205 N95-27690
Photochemistry in constrained spaces: Zeolites and layered double metal hydroxides
[DE95-008417] p 2207 N95-27951
Pulsed laser deposition of zeolitic membranes
[DE95-006274] p 2298 N95-28124

ZINC ALLOYS
Surface scanning techniques to locate and study defects in painted zinc and zinc alloy coated steels
[DE95-006099] p 2240 N95-28547

ZINC OXIDES
Polarization relaxation in zinc oxide varistors from 77 K to 450 K
[DE95-007761] p 2268 N95-28156

ZINC SELENIDES
Electronic characterization of defects in narrow gap semiconductors: Comparison of electronic energy levels and formation energies in mercury cadmium telluride, mercury zinc telluride, and mercury zinc selenide
[NASA-CR-197835] p 2437 N95-26780

ZINC SULFIDES
Effects of low earth orbit on the optical performance of multi-layer enhanced high reflectance mirrors
p 2428 N95-27652

ZINC TELLURIDES
Electronic characterization of defects in narrow gap semiconductors: Comparison of electronic energy levels and formation energies in mercury cadmium telluride, mercury zinc telluride, and mercury zinc selenide
[NASA-CR-197835] p 2437 N95-26780

ZIRCONIUM ALLOYS
Bases for extrapolating materials durability in fuel storage pools
[DE95-007748] p 2222 N95-28129

ZIRCONIUM OXIDES
Long life 80Ah standard IPV NiH2 battery cell
p 2272 N95-26787
Crystal structure, short-range oxygen defects, and water adsorption in La- and Nd-modified ZrO2
[DE95-007134] p 2439 N95-27452
High-temperature deformation of ZrO2-Al2O3/SiC whisker composites fabricated by two techniques
[DE95-008273] p 2183 N95-28069
Control of thin film processing behavior through precursor structural modifications
[DE95-006468] p 2444 N95-28103

ZONAL FLOW (METEOROLOGY)
Spectral analyses, climatology, and interannual variability of Nimbus-7 TOMS version 6 total column ozone
[NASA-RP-1360] p 2341 N95-26689

PERSONAL AUTHOR INDEX

Typical Personal Author Index Listing

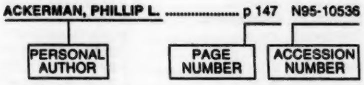

Listings in this index are arranged alphabetically by personal author. The page number helps you locate the citation in the abstract section. The accession number denotes the number by which the citation is identified.

A

AARONSON, PHILIP G. ..... p 2365 N95-26848
ABAD, LUCILLE V. ..... p 2225 N95-26599
ABBOTT, R. J. ..... p 2376 N95-27383
p 2384 N95-27387
ABE, TAKASHI ..... p 2274 N95-26739
p 2121 N95-26740
p 2274 N95-26741
p 2275 N95-26742
ABEDINI, A. ..... p 2385 N95-27393
ABEL, DEREK H. ..... p 2359 N95-26883
ABELES, JOSEPH H. ..... p 2295 N95-26906
ABEYARATNE, ROHAN ..... p 2200 N95-26451
ABHIJIT, KAR QUPTA ..... p 2391 N95-27739
ABLOWITZ, MARK J. ..... p 2278 N95-27001
ABRAMSON, E. ..... p 2331 N95-28121
ABTAHI, ALI A. ..... p 2290 N95-26765
ABUMERI, G. H. ..... p 2141 N95-28277
ACEVES, S. M. ..... p 2303 N95-28029
p 2303 N95-28139
ACHARYA, ANURAG ..... p 2453 N95-27063
ACKER, JAMES G. ..... p 2348 N95-28030
ADAMS, D. ..... p 2415 N95-28221
ADAMS, J. M. ..... p 2412 N95-28051
ADAMS, M. ..... p 2415 N95-28221
ADAMS, R. ..... p 2331 N95-28548
ADENIYI, J. O. ..... p 2337 N95-27157
ADENWALLA, S. ..... p 2411 N95-28004
ADIMULA, I. A. ..... p 2337 N95-27157
ADITYAWARMAN, YUDI ..... p 2289 N95-26461
ADKINS, CAROL L. J. ..... p 2229 N95-27110
p 2224 N95-27113
ADOLPHSEN, C. ..... p 2422 N95-28159
ADVANI, S. G. ..... p 2179 N95-26565
AEPPLI, G. ..... p 2413 N95-28066
AFEYAN, B. B. ..... p 2266 N95-28015
AGRAWAL, DHARMA P. ..... p 2376 N95-26471
AGRAWAL, O. P. ..... p 2282 N95-27359
AGRAWAL, YOGESH C. ..... p 2347 N95-27043
AGUERO, ALINA ..... p 2242 N95-27669
AHLQUIST, GREGORY C. ..... p 2382 N95-27293
AHMAD, HARITH ..... p 2299 N95-28330
AHMED, T. ..... p 2423 N95-28452
AHUJA, S. ..... p 2282 N95-27357
AIKEN, DONALD L. ..... p 2356 N95-26992
AIKEN, WAYNE LEE ..... p 2364 N95-26554
AIZED, D. ..... p 2267 N95-28048
AKKANEN, JYRKI ..... p 2397 N95-28238
ALBERS, R. C. ..... p 2213 N95-27082
ALBRIDGE, R. G. ..... p 2428 N95-27646
ALDYKIEWICZ, A. J., JR. ..... p 2240 N95-28547
ALEKSANDROV, YU. A. ..... p 2415 N95-28247
ALEM, NABIH M. ..... p 2294 N95-28410
p 2361 N95-28667
ALENITSKIJ, YU. G. ..... p 2280 N95-27338
ALEXANDER, D. E. ..... p 2220 N95-28072
ALEXANDER, K. B. ..... p 2235 N95-27499
ALGUIRE, KAREN M. ..... p 2380 N95-26475
ALIGIA, A. A. ..... p 2440 N95-27712
ALKHALIFAH, T. ..... p 2339 N95-28192
p 2339 N95-28194
ALLARD, GARY S. ..... p 2356 N95-27012
ALLEN, C. R. G. ..... p 2201 N95-26750
ALLEN, D. ..... p 2373 N95-28521
ALLEN, J. L. ..... p 2428 N95-27646
ALLEN, JAMES F. ..... p 2259 N95-28624
ALLEN, JONATHAN ..... p 2270 N95-28512
ALLEN, S. L. ..... p 2433 N95-28054
p 2433 N95-28065
p 2434 N95-28185
ALLEN, T. M. ..... p 2297 N95-27841
ALLENBY, M. ..... p 2271 N95-28663
ALLISON, DENNIS O. ..... p 2120 N95-26382
ALMAZAN, P. PLANAS ..... p 2283 N95-27363
ALME, M. L. ..... p 2311 N95-28337
ALPER, J. M. ..... p 2191 N95-28434
ALTHAWADI, SUFIAN I. ..... p 2452 N95-26758
ALTON, G. D. ..... p 2442 N95-27959
ALVARADO, SERGIO J. ..... p 2145 N95-27394
AMANO, T. ..... p 2432 N95-27869
AMBUR, DAMODAR R. ..... p 2194 N95-28468
p 2138 N95-28487
AMSDEN, ANTHONY A. ..... p 2203 N95-27437
ANAND, M. S. ..... p 2285 N95-27890
ANDERL, R. A. ..... p 2217 N95-27553
ANDERSEN, DWIGHT E. ..... p 2146 N95-27033
ANDERSEN, STEPHEN O. ..... p 2170 N95-28295
ANDERSON, CHARLES E., JR. ..... p 2225 N95-26561
ANDERSON, D. J. ..... p 2329 N95-27878
ANDERSON, D. T. ..... p 2431 N95-27498
ANDERSON, GLEN ..... p 2360 N95-27099
ANDERSON, H. U. ..... p 2220 N95-28049
ANDERSON, I. M. ..... p 2215 N95-27473
ANDERSON, J. ..... p 2339 N95-28190
p 2339 N95-28194
ANDERSON, J. E. ..... p 2297 N95-27841
ANDERSON, M. T. ..... p 2202 N95-27137
ANDERSON, MARK O. ..... p 2148 N95-27771
ANDERSON, ROBERT L. ..... p 2185 N95-28271
ANDERSON, T. L. ..... p 2310 N95-28098
p 2311 N95-28100
ANDERSON, W. KYLE ..... p 2124 N95-28674
ANDERTON, JAMES F. ..... p 2139 N95-26878
ANDO, T. ..... p 2432 N95-27869
ANDREWS, STEPHEN F. ..... p 2154 N95-27803
ANDRONOV, V. A. ..... p 2288 N95-28603
ANEMAAT, WILLIAM ..... p 2119 N95-26949
ANGELO, J. E. ..... p 2408 N95-27534
p 2219 N95-27968
ANTONIO, M. R. ..... p 2219 N95-27966
ANTONIO, MARK R. ..... p 2238 N95-28235
AOKI, SHINGO ..... p 2222 N95-28166
AOTO, K. ..... p 2432 N95-27870
AOYAGI, TETSUO ..... p 2431 N95-27414
APBLETT, C. A. ..... p 2237 N95-28089
APITZ, SABINE E. ..... p 2230 N95-27116
APPIGNANI, PETER L. ..... p 2159 N95-26398
p 2159 N95-26399
p 2160 N95-26400
p 2160 N95-26401
p 2160 N95-26403
ARAGON, LARRY ..... p 2144 N95-26583
ARATA, BERNARD H. ..... p 2346 N95-26647
ARCONE, STEVEN A. ..... p 2144 N95-27297
ARGANISJUAREZ, CARLOS ROSENDO
p 2214 N95-27256
ARIMOTO, H. ..... p 2432 N95-27869
p 2432 N95-27870
ARIMOTO, HIDEKI ..... p 2297 N95-27868
ARMAND, SASAN ..... p 2303 N95-27911
ARMANTROUT, JON D. ..... p 2272 N95-26787
ARMSTRONG, CARTER M. ..... p 2259 N95-26433
ARMSTRONG, DWAYNE ..... p 2463 N95-27668
ARMSTRONG, N. R. ..... p 2294 N95-26568
ARMSTRONG, ROBERT L. ..... p 2300 N95-28509
ARMSTRONG, T. ..... p 2413 N95-28066
ARMSTRONG, T. R. ..... p 2267 N95-28131
ARNOLD, RICHARD D. ..... p 2342 N95-27148
AROCHO, A. M. ..... p 2190 N95-28425
ARONE, R. ..... p 2136 N95-28409
ARYA, ASHOK ..... p 2218 N95-27756
ASBECK, P. M. ..... p 2438 N95-27040
ASERCION, R. E. ..... p 2454 N95-27461
ASHLEY, K. R. ..... p 2412 N95-28051
ASHTON, JOHN H. ..... p 2258 N95-28615
ASKEW, E. W. ..... p 2358 N95-26558
ASOKA-KUMAR, P. ..... p 2217 N95-27553
ASSINK, ROGER A. ..... p 2240 N95-28531
p 2240 N95-28532
ASTA, M. ..... p 2213 N95-27082
ASTON, GRAEME ..... p 2168 N95-28000
ASTON, MARTHA ..... p 2168 N95-28000
ATENCIO, JERRY H. ..... p 2209 N95-28088
ATHAVALE, M. M. ..... p 2140 N95-28344
ATHAVALE, MAHESH ..... p 2168 N95-27434
ATKINS, J. E. ..... p 2372 N95-27436
ATKINSON, DALE ..... p 2428 N95-27654
ATLURI, S. N. ..... p 2133 N95-27511
ATTENBERGER, S. E. ..... p 2430 N95-27308
p 2435 N95-28553
AUGUST, RICHARD ..... p 2301 N95-27178
AUSLENDER, AARON H. ..... p 2140 N95-28343
AUSTIN, J. ..... p 2330 N95-27954
AVERY, DON E. ..... p 2166 N95-27664
AVERY, W. B. ..... p 2137 N95-28471
p 2138 N95-28482
AVVA, RAM K. ..... p 2286 N95-27894
AXLER, K. M. ..... p 2216 N95-27488
AYALA, A. ..... p 2449 N95-27547
AYDIN, R. ..... p 2292 N95-27711
AYDIN, RAMAZAN ..... p 2207 N95-27929
AZMY, Y. Y. ..... p 2412 N95-28045
p 2373 N95-28047
AZUMA, Y. ..... p 2442 N95-27963

B

BAART, DOUGLAS ..... p 2125 N95-26485
BABA, T. ..... p 2419 N95-26584
BABEL, HANK W. ..... p 2242 N95-27640
BABEL, HENRY W. ..... p 2242 N95-27661
BABU, S. S. ..... p 2215 N95-27319
p 2302 N95-27545
BACA, A. G. ..... p 2267 N95-28146
BACON, DOUGLASS P. ..... p 2170 N95-28297
BADAVI, FRANCIS F. ..... p 2465 N95-28530
BADHWAR, GAUTAM D. ..... p 2465 N95-28530
BAENEN, ERIC P. ..... p 2395 N95-27016
BAER, ERIC ..... p 2240 N95-28508
BAETTIG, D. ..... p 2393 N95-28611
BAGAEVA, T. YU. ..... p 2403 N95-26542
BAHR, J. M. ..... p 2338 N95-28083
BAILEY, DAVE ..... p 2158 N95-27286
BAILEY, JIM ..... p 2127 N95-26978
BAILEY, JOHN C. ..... p 2308 N95-26975
BAILEY, SHEILA G. ..... p 2235 N95-27503
BAIR, SCOTT ..... p 2241 N95-28592
BAIRD, RICHARD A. ..... p 2349 N95-26727
p 2349 N95-26728
p 2349 N95-26729
p 2349 N95-26730
p 2350 N95-26731
p 2350 N95-26732
BAKER, A. A. ..... p 2132 N95-27505
p 2132 N95-27509
p 2135 N95-27523
BAKER, A. M. ..... p 2273 N95-26445
BAKER, DAVID ..... p 2149 N95-27778
BAKER, J. F. ..... p 2154 N95-27804
BAKER, S. M. ..... p 2412 N95-28057
BAKKER, HARRY ..... p 2342 N95-27366
BAKOWSKY, TED ..... p 2328 N95-27708
BAKULEV, A. P. ..... p 2406 N95-27314
BALBIN, R. ..... p 2431 N95-27497
BALCAR, E. ..... p 2408 N95-27453
p 2418 N95-28642
BALCH, ROBERT ..... p 2339 N95-28126
BALL, A. S. ..... p 2132 N95-27507
BALL, G. S. ..... p 2417 N95-28595
BALL, J. R. ..... p 2412 N95-28051
BALL, R. ..... p 2353 N95-26885
BALLESIO, JORGE ..... p 2159 N95-26398
p 2159 N95-26399

p 2160 N95-26400
p 2160 N95-26401
p 2160 N95-26403
BALMFORTH, N. J. p 2287 N95-28055
BALUJA, SHUMEET p 2382 N95-27066
BAN, V. S. p 2178 N95-26587
BANCROFT, J. p 2349 N95-26728
BANDLER, SIMON R. p 2403 N95-26560
BANE, K. p 2422 N95-28159
BANERJEE, I. p 2267 N95-28148
BANERJEE, SRIKUMAR p 2218 N95-27756
BANG, HA HUY p 2396 N95-27341
BANKS, BRUCE A. p 2235 N95-27702
BANNING, D. W. p 2172 N95-28304
BANNISTER, M. E. p 2413 N95-28078
BANOWETZ, VIRGIL p 2362 N95-26348
BANSAL, NAROTTAM P. p 2183 N95-27717
BAOZHEN, ZHU p 2342 N95-26724
BAR, G. p 2447 N95-28541
BARBASCH, C. A. p 2375 N95-28635
BARBATO, GREGORY J. p 2129 N95-26684
BARBER, G. C. p 2435 N95-28596
BARBOUR, J. C. p 2205 N95-27681
p 2235 N95-27687
BARDELL, A. G. p 2404 N95-26748
BARDINA, JORGE E. p 2274 N95-26665
BARGER, V. p 2413 N95-28067
BARILE, RON p 2173 N95-28310
p 2174 N95-28312
BARKATE, M. L. p 2358 N95-26558
BARLETTA, W. p 2434 N95-28161
BARNES, A. V. p 2428 N95-27646
BARNES, P. A. p 2445 N95-28144
BARNES, R. A. p 2348 N95-28030
BARNES, WILBERT L. p 2272 N95-26792
BARNEY, S. p 2228 N95-27107
BAROODY, EDWARD E. p 2172 N95-28306
BARRETT, J. p 2464 N95-28007
BARRIE, RONALD E. p 2138 N95-28476
BARRIOCARDABA, A. p 2135 N95-27527
BARRY, JOHN S. p 2386 N95-27395
BARTELL, S. M. p 2354 N95-28136
BARTLETT, RODNEY J. p 2352 N95-28546
BARTON, ROBERT S. p 2306 N95-27985
p 2273 N95-27989
BASILI, VICTOR p 2374 N95-28627
BASKES, M. I. p 2408 N95-27534
BAST, CALLIE C. p 2214 N95-27167
BASU, ASIT P. p 2394 N95-26733
BASURTOSANCHEZ, R. p 2202 N95-27199
BATCHELDER, J. C. p 2442 N95-27959
BATCHELOR, D. B. p 2392 N95-28110
BAUER, D. A. p 2417 N95-28594
BAUER, F. p 2279 N95-27179
BAUER, J. p 2133 N95-27515
BAUGHER, BRIGITTA p 2240 N95-28531
p 2240 N95-28532
BAUMBAUGH, B. p 2415 N95-28221
BAUMGART, C. W. p 2379 N95-26443
BAYLISS, A. p 2289 N95-28673
BAYLOR, L. R. p 2422 N95-28205
p 2435 N95-28596
BEARD, M. p 2179 N95-27120
BEARD, PAUL p 2156 N95-27270
BEARMAN, PETER W. p 2121 N95-26757
BEATON, ROBERT J. p 2262 N95-27196
BECHER, P. F. p 2235 N95-27499
BECHTLE, DANIEL W. p 2295 N95-26906
BECKMAN, R. M. p 2147 N95-27769
BEDAIR, S. p 2446 N95-28327
BEDDINGFIELD, D. p 2379 N95-26443
BEDZYK, M. J. p 2208 N95-27965
BEECHER, S. C. p 2183 N95-27955
BEERS, L. V. p 2412 N95-28028
BEFRUI, BIZHAN A. p 2286 N95-27896
BEHBOUDNIA, MEHDI p 2207 N95-27929
BELASON, E. B. p 2132 N95-27506
BELCINSKI, R. p 2417 N95-28594
BELIAN, R. D. p 2338 N95-28061
BELL, DAVID K. p 2193 N95-28445
BELLOCH, GUY p 2365 N95-26656
BELYAEV, A. L. p 2280 N95-27338
BEN-HAMO, V. p 2407 N95-27406
BENAK, T. J. p 2132 N95-27509
BENCH, G. S. p 2204 N95-27496
BENNER, R. E. p 2393 N95-28393
BENNER, WILLIAM p 2340 N95-26453
BENNETT, C. L. p 2334 N95-26436
BENNETT, JEAN p 2428 N95-27652
BENO, MICHAEL L. p 2212 N95-26411
BENOLKEN, MARTHA S. p 2357 N95-27697
BENSON, ROBERT H. p 2351 N95-27329
BENTALL, RICHARD H. p 2155 N95-27262
BENTLEY, J. p 2215 N95-27473
BENTON, E. R. p 2202 N95-27168
BENTON, E. V. p 2202 N95-27168
BENTZ, MICHAEL D. p 2243 N95-28001
BERAN, MARK J. p 2401 N95-26925
BEREZHIANI, V. I. p 2429 N95-26439
BERG, C. p 2210 N95-28652
BERG, R. C. p 2417 N95-28594
BERGERMAN, MARCEL p 2301 N95-27098
BERGEY, MICHAEL L. S. p 2320 N95-27475
BERGLUND, C. N. p 2233 N95-27187
BERGMAN, U. p 2343 N95-28237
BERKHOUT, JAN p 2360 N95-27099
BERN, Z. p 2449 N95-28160
BERNACKI, B. E. p 2427 N95-28552
BERNARD, C. p 2409 N95-27552
BERNARDON, EDWARD p 2184 N95-28269
BERRY, JOHN N. p 2227 N95-26897
BERTHOUD, LUCINDA p 2211 N95-27648
BERTINO, P. p 2451 N95-28025
BERTRAM, I. p 2415 N95-28221
BERTRAND, W. T. p 2427 N95-28408
BERTSCH, G. p 2399 N95-27548
BEST, R. G. p 2455 N95-28113
BETKE, MARGRIT p 2387 N95-28461
BETTNER, JAMES L. p 2140 N95-27866
BETTY, C. A. p 2406 N95-27212
BEVILL, M. p 2392 N95-28215
BEYLKIN, GREGORY p 2277 N95-26999
BHARTIA, P. K. p 2341 N95-26689
BHASKARAN, SHYAM p 2151 N95-27788
BHATIA, K. p 2282 N95-27357
BHATTACHARYA, P. K. p 2292 N95-27368
BHATTACHARYA, SANDEEPAN p 2259 N95-26550
BHATTACHARYA, TAMMOY p 2442 N95-27994
BIANCHINI, ANTONIO p 2459 N95-27074
BIANCO, JEAN p 2143 N95-27176
BIEDENHARN, L. C. p 2397 N95-28234
BIEFELD, R. M. p 2446 N95-28399
BIEHL, LARRY L. p 2314 N95-26815
BIEN, F. p 2332 N95-28602
BIER, KARLA p 2176 N95-28322
BIERNACKI, PAUL p 2270 N95-28544
BIETERMAN, M. B. p 2123 N95-28230
p 2123 N95-28265
BIGGAR, S. F. p 2348 N95-28030
BIGGERS, S. B. p 2191 N95-28433
BIGI, SUSAN R. p 2336 N95-26753
BIHUA, FENG p 2402 N95-28671
BIJVOET, J. A. p 2272 N95-27635
BILGUTAY, NIHAT M. p 2255 N95-27185
BILLON, HORACE p 2258 N95-28568
BIMONTE, G. p 2448 N95-27312
BINGAMAN, DONALD C. p 2140 N95-28227
BINGHAM, H. H. p 2417 N95-28594
BINGHAM, R. p 2436 N95-28668
BINMOHAMMEDIDRIS, MOHAMMED FAZIL
p 2326 N95-26639
BINRAHMAT, AZMI p 2213 N95-26675
BINRAMLI, MAHYUDDIN p 2326 N95-26639
BINTIMOHID, NORJANAH p 2226 N95-26637
BINWANZIN, WAN MANSHOL p 2226 N95-26637
BIRN, JOACHIM p 2432 N95-27673
BIROSCAK, D. p 2385 N95-27393
BIRTCHER, R. C. p 2441 N95-27928
BISHOP, ANN P. p 2456 N95-28600
BISHOP, GREGORY A. p 2461 N95-27303
BISSON, S. E. p 2344 N95-28538
BLACKMOND, D. G. p 2203 N95-27420
BLACKWELL, JEREMY p 2136 N95-28567
BLAIN, P. C. p 2256 N95-27840
BLAKE, J. B. p 2162 N95-26902
BLANCH, H. W. p 2238 N95-28226
p 2209 N95-28229
BLANCHARD, J. P. p 2444 N95-28125
BLANDFORD, CRAIG S. p 2140 N95-27866
BLANKEN, C. L. p 2141 N95-26773
BLAYLOCK, NEIL W. p 2225 N95-26561
BLEZIUS, J. W. p 2242 N95-27669
BLIDBERG, D. RICHARD p 2247 N95-27909
BLINOV, A. E. p 2407 N95-27407
p 2407 N95-27408
BLINOV, V. E. p 2407 N95-27407
p 2407 N95-27408
BLISSELL, W. A., JR. p 2306 N95-27986
BLOCK, MARTIN M. p 2415 N95-28210
BLOMQUIST, RICHARD S. p 2155 N95-27265
BLOOM, E. D. p 2417 N95-28594
BLOOM, E. E. p 2221 N95-28120
BLOOMINGBURG, G. F. p 2208 N95-27960
BLUDMAN, S. A. p 2463 N95-28558
BLUE, M. D. p 2428 N95-27650
BLUM, FRANK D. p 2180 N95-26572
BLUM, T. p 2409 N95-27552
BLUMENSTOCK, KENNETH A. p 2158 N95-27287
BOATNER, L. A. p 2237 N95-27967
p 2444 N95-28081
BOBISH, KIMBERLY p 2272 N95-27354
BODDY, DOUGLAS E. p 2281 N95-27352
BODDY, MARK p 2384 N95-27382
BOEMAN, RAYMOND G. p 2184 N95-28207
BOETTGER, R. p 2404 N95-26748
BOFF, KENNETH R. p 2355 N95-26692
BOGDANOV, V. I. p 2348 N95-27996
BOHLMANN, R. p 2186 N95-28279
BOHNHOFF-HLAVACEK, GAIL p 2177 N95-26391
BOHON, HERMAN L. p 2184 N95-28266
p 2189 N95-28420
p 2193 N95-28462
BOLAND, D. p 2151 N95-27790
BOLDUC, STEVEN J. p 2341 N95-26653
BOLSTER, ROBERT N. p 2225 N95-26499
BOLTRALIK, WILLIAM J. p 2130 N95-27018
BOLVIN, D. T. p 2147 N95-27768
BOMAN, E. G. p 2372 N95-27436
BOMAR, JOHN B., JR. p 2355 N95-28561
BONAM, RICHARD C. p 2342 N95-27148
BONCELET, CHARLES G. p 2367 N95-26770
BONDAR, A. E. p 2407 N95-27407
p 2407 N95-27408
BONDAREV, I. V. p 2411 N95-27930
BONDESON, A. p 2433 N95-28106
BONHAUS, DARYL L. p 2124 N95-28674
BONOLI, P. T. p 2435 N95-28553
BOO, D. W. p 2413 N95-28091
BORCHERS, PAUL F. p 2139 N95-26412
BORG, A. p 2210 N95-28652
BORG, G. G. p 2256 N95-28254
BORG, J. P. p 2276 N95-26827
BORGEN, GARY S. p 2300 N95-26504
BORGUET, E. p 2201 N95-26544
BORODICH, A. I. p 2398 N95-27160
BOS, ANDRE p 2166 N95-27390
BOSE, ASHIM p 2384 N95-27384
BOSE, T. K. p 2117 N95-26363
BOSIA, G. p 2434 N95-28140
BOSSE, ELOI p 2258 N95-28580
BOSSERT, J. E. p 2328 N95-27686
BOTHNER, J. p 2379 N95-28093
BOTT, RICHARD p 2185 N95-28272
p 2142 N95-28281
BOTTO, R. E. p 2234 N95-27455
BOTVINNIK, B. p 2389 N95-26915
BOUCHILLON, C. W. p 2292 N95-27465
BOULTON, WILLIAM R. p 2263 N95-27226
p 2263 N95-27227
p 2263 N95-27228
p 2263 N95-27229
p 2263 N95-27231
p 2263 N95-27232
p 2264 N95-27233
BOURASSA, ROGER J. p 2210 N95-27642
BOURGEOIS, AL J. p 2335 N95-26622
BOURKE, M. A. M. p 2182 N95-27080
BOUSAIDI, MEHDI p 2383 N95-27379
BOUWER, S. D. p 2464 N95-28007
BOWEN, BARRY C. p 2160 N95-27238
BOWLES, D. E. p 2166 N95-28292
BOWLES, DAVID E. p 2145 N95-27657
BOWMAN, J. D. p 2405 N95-27081
BOWMAN, W. J. p 2281 N95-27351
BOYCE, JOSEPH p 2185 N95-28272
BOYCE, LOLA p 2214 N95-27167
BOYD, B. F. p 2172 N95-28307
BOYLE, B. p 2460 N95-28197
BOYLE, J. S. p 2332 N95-28550
BOYLE, T. J. p 2444 N95-28103
BRAATEN, M. p 2265 N95-27889
BRACCO, FREDIANO V. p 2288 N95-28523
BRADLEY, CHRISTOPHER ROBERT
p 2347 N95-27011
BRADLEY, P. A. p 2462 N95-28056
BRADLEY, R. A. p 2241 N95-28560
BRADY, B. B. p 2332 N95-28623
BRADY, BRIAN B. p 2172 N95-28305
BRADY, M. J. p 2327 N95-27540
BRANAS, B. p 2431 N95-27497
BRANCART, CLAUDE P. p 2247 N95-27909
BRANDEMUEHL, MICHAEL J. p 2320 N95-27475
BRANDT, E. STEVEN p 2428 N95-27653
BRANKOVIC, ANDREJA p 2285 N95-27888
BRASEK, T. P. p 2308 N95-26625
BRASPENNING, PETER J. p 2383 N95-27381
BREAZEALE, LARRY p 2166 N95-27665
BRECKENRIDGE, JOHN p 2313 N95-28476
BREININGER, DAVID R. p 2126 N95-27859
BREITENBACH, J. p 2442 N95-27959
BRENKOSH, J. P. p 2378 N95-28074
BRENNAN, KEVIN F. p 2249 N95-26708
BRENNAN, P. C. p 2318 N95-26846
BRENNAN, PATRICK J. p 2281 N95-27349
BRENNAN, T. M. p 2299 N95-28128
BRESCIA, DAVID A. p 2144 N95-26583
BREWER, JEFF p 2272 N95-26795
BREWER, JEFFREY C. p 2317 N95-26785
p 2272 N95-26794

BREWSTER, WAYNE A. .... p 2250 N95-26725
BRIGGS, STEVE .... p 2262 N95-27067
BRILES, S. D. .... p 2256 N95-27840
BRINKER, C. J. .... p 2237 N95-28090
p 2239 N95-28401
BRINZA, DAVID E. .... p 2211 N95-27644
BRITCHER, COLIN P. .... p 2143 N95-26768
BRITT, VICKI O. .... p 2187 N95-28286
BRITTON, T. W. .... p 2128 N95-28540
BROCHU, CLAUDE J. .... p 2258 N95-28573
BRODSKY, S. J. .... p 2414 N95-28142
BRODSKY, TOMAS .... p 2394 N95-26478
BRODY, ERIC A. .... p 2345 N95-26430
BROMLEY, B. C. .... p 2462 N95-27445
BRONIKOWSKI, MICHAEL .... p 2438 N95-27061
BROOK, MARX .... p 2343 N95-28191
BROOKS, N. H. .... p 2434 N95-28185
BROSIUS, JEFFREY W. .... p 2464 N95-27858
BROSS, A. .... p 2415 N95-28221
BROUDE, SIDNEY M. .... p 2148 N95-27773
BROUGHTON, W. R. .... p 2227 N95-26747
BROWN, ALAN W. .... p 2375 N95-28628
BROWN, BRIAN A. .... p 2374 N95-28590
BROWN, C. S. .... p 2201 N95-26750
BROWN, E. R. .... p 2293 N95-28389
BROWN, J. C. .... p 2454 N95-27483
BROWN. J. J. .... p 2241 N95-28604
BROWN, J. J., JR. .... p 2239 N95-28397
BROWN, JAMES E. .... p 2356 N95-27012
BROWN, LEE F. .... p 2204 N95-27556
BROWN, LINCOLN D. .... p 2337 N95-27703
BROWN, RICHARD T. .... p 2185 N95-28273
BROWN, S. W. .... p 2172 N95-28308
BROWN, SUSAN M. .... p 2374 N95-28590
BROWN, T. .... p 2137 N95-28474
BROWNING, G. .... p 2155 N95-27263
BRUBAKER, KATHRYNE B. .... p 2361 N95-28390
BRUCE, ANDREW G. .... p 2257 N95-28455
BRUEMMER, S. M. .... p 2216 N95-27492
p 2216 N95-27493
BRUNO, J. .... p 2138 N95-28488
BRUNO, JOHN G. .... p 2354 N95-27059
BRUZZINI, MICHAEL A. .... p 2142 N95-28598
BRYANT, ROBERT G. .... p 2235 N95-27732
BRYSON, R. J. .... p 2427 N95-28408
BUCH, K. A., JR. .... p 2344 N95-28556
BUCHANAN, C. D. .... p 2417 N95-28594
BUCHENAUER, D. .... p 2434 N95-28185
BUCHHEIT, C. D. .... p 2444 N95-28103
BUCHHEIT, R. G. .... p 2234 N95-27460
p 2218 N95-27722
p 2221 N95-28116
p 2238 N95-28117
BUCK, J. W. .... p 2328 N95-27749
p 2289 N95-27973
BUCKINGHAM, N. W. .... p 2325 N95-28058
BUDAI, J. D. .... p 2444 N95-28081
BUDHANI, R. C. .... p 2445 N95-28186
BUETTNER, LEONARD C. .... p 2405 N95-27034
BUI, DAVID T. .... p 2210 N95-27631
BUNNELL, L. R. .... p 2234 N95-27476
BURCH, DAN .... p 2175 N95-28320
p 2176 N95-28322
p 2176 N95-28323
BURCH, S. D. .... p 2327 N95-27540
BURCHETT, S. N. .... p 2309 N95-27837
BURCHETT, STEVEN .... p 2265 N95-27706
BURKE, G. L. .... p 2268 N95-28181
BURKHALTER, P. G. .... p 2295 N95-26996
BURKHART, J. H. .... p 2205 N95-27681
BURLEY, CASEY L. .... p 2400 N95-26392
BURNS, K. L. .... p 2325 N95-28058
BURPO, S. J. .... p 2185 N95-28274
BURR, D. .... p 2315 N95-28520
BURRUS, D. .... p 2285 N95-27889
BUSKA, STEVEN .... p 2361 N95-26845
BUSSEY, ROBERT M. .... p 2334 N95-26520
BUSSOLETTI, J. E. .... p 2123 N95-28230
p 2123 N95-28265
BUTLER, J. .... p 2398 N95-26614
BUTLER, THOMAS A. .... p 2157 N95-27282
BUTTREY, D. J. .... p 2439 N95-27443
BUZATU, D. .... p 2415 N95-28245
BUZDAVIN, A. P. .... p 2280 N95-27338
BYUN, CHANSUP .... p 2129 N95-26590

C

CABLE, J. W. .... p 2440 N95-27487
CABOMONTESDEOCA, ALEJANDRO
p 2448 N95-26603
CAIAZZO, A. .... p 2187 N95-28284
CAIN, MAURICE R. .... p 2175 N95-28317
CAIRNS, DOUGLAS S. .... p 2188 N95-28288
CALASSA, MARK C. .... p 2155 N95-27266
CALDERONMORENO, J. M. .... p 2183 N95-28069
CALDWELL, D. O. .... p 2417 N95-28594
CALDWELL, DANIEL J. .... p 2175 N95-28319
CALDWELL, JOHN A., JR. .... p 2130 N95-26993
CALEY, ROBERT E. .... p 2381 N95-27007
CALLAGHAN, GEORGE .... p 2454 N95-27208
CALLAHAN, JOHN .... p 2365 N95-26668
p 2367 N95-26814
CALLAHAN, JOHN R. .... p 2362 N95-26386
p 2364 N95-26486
p 2365 N95-26575
p 2366 N95-26693
p 2366 N95-26695
p 2366 N95-26711
p 2367 N95-26802
CALLIES, JORG .... p 2166 N95-27390
CALLIS, R. W. .... p 2431 N95-27441
CALLOWAY, ROBERT L. .... p 2145 N95-27657
CAMPBELL, ANN N. .... p 2268 N95-28201
CAMPBELL, J. M. .... p 2267 N95-28048
CAMPBELL, M. L. .... p 2376 N95-27383
CANAKAPALLI, SRI .... p 2360 N95-27099
CANFIELD, P. C. .... p 2442 N95-27932
CANNON, M. .... p 2456 N95-28631
CANTRELL, JOHN H. .... p 2353 N95-26889
CAPASSO, MICHAEL A. .... p 2123 N95-28331
CARDEN, HUEY D. .... p 2192 N95-28439
CARIOLLE, D. .... p 2330 N95-27954
CARLILE, DONNA L. .... p 2405 N95-27034
CARLOS, W. C. .... p 2219 N95-28005
CARPENTER, KENNETH A. .... p 2278 N95-27065
CARPENTER, MARK H. .... p 2279 N95-27247
CARR, BOB .... p 2389 N95-26882
CARR, LESTER E., III .... p 2344 N95-28459
CARRERAS, B. A. .... p 2430 N95-27306
p 2431 N95-27419
p 2431 N95-27497
p 2431 N95-27536
p 2431 N95-27537
CARROLL, MONTY .... p 2159 N95-27291
CARROLL, THOMAS R. .... p 2314 N95-27998
CARSON, R. F. .... p 2267 N95-28147
CARTER, C. B. .... p 2215 N95-27473
CARTER, CALVIN H. .... p 2437 N95-26818
CARTER, D. .... p 2151 N95-27789
CARTER, DANIEL C. .... p 2423 N95-26385
p 2245 N95-26888
p 2245 N95-27500
CARTER, DOUGLAS W. .... p 2133 N95-27516
CARTER, H. K. .... p 2442 N95-27959
CARTER, K. DAVID, JR. .... p 2229 N95-27112
CARTER, M. D. .... p 2392 N95-28110
CARTER, SUSAN V. .... p 2313 N95-26476
p 2314 N95-26682
CARUSO, MICHAEL J. .... p 2315 N95-28392
CARVALHAIS, ANTONIO B. .... p 2360 N95-27058
CASPER, ANN M. .... p 2261 N95-26890
CASPER, T. A. .... p 2432 N95-27710
CASTILLO, V. M. .... p 2442 N95-27964
CASTLE, C. H. .... p 2319 N95-27193
p 2319 N95-27194
CASTLETON, K. J. .... p 2328 N95-27749
CASTRO, EDGAR O. .... p 2165 N95-27842
CAUDILL, EUGENE L. .... p 2163 N95-26963
CAULFIELD, H. J. .... p 2368 N95-26881
CAUZZI, GIANNA .... p 2253 N95-26983
CAYTON, T. E. .... p 2338 N95-28061
CEFOLA, P. .... p 2151 N95-27789
CERNOHORSKY, J. .... p 2463 N95-28558
CERUTI, M. G. .... p 2453 N95-27014
CERVESATO, ILIANO .... p 2365 N95-26605
CESS, R. D. .... p 2330 N95-28084
CHACKO, DABORAH .... p 2180 N95-26686
CHAIT, RICHARD .... p 2189 N95-28421
CHAKOUMAKOS, B. C. .... p 2447 N95-28537
CHAKRABARTI, R. .... p 2448 N95-27333
CHALLA, M. .... p 2147 N95-27770
p 2150 N95-27783
CHALMERS, G. .... p 2449 N95-28160
CHAMBERLIN, E. P. .... p 2204 N95-27467
CHAMIS, C. C. .... p 2309 N95-27174
p 2141 N95-28277
CHAMIS, CHRISTOS C. .... p 2137 N95-28444
CHAMPETIER, ROBERT .... p 2428 N95-27654
CHAMUEL, JACQUES R. .... p 2402 N95-28622
CHAN, HING C. .... p 2249 N95-26545
CHAN, K. C. D. .... p 2296 N95-27557
CHAN, WILLIAM M. .... p 2160 N95-27154
CHANDRASEKHAR, H. R. .... p 2410 N95-27927
CHANG, C. E. .... p 2438 N95-27040
CHANG, L. ARON .... p 2343 N95-27997
CHANG, S. Y. .... p 2241 N95-28609
CHANG, SIN-CHUNG .... p 2389 N95-26663
CHANG, STEPHEN .... p 2192 N95-28436
CHAO, KUANG-TA .... p 2406 N95-27316
CHAPARALA, PRASAD .... p 2268 N95-28201
CHAPES, S. K. .... p 2348 N95-26435
CHAPLIN, CHRISTOPHER P. .... p 2308 N95-26905
CHAPLIN, DON .... p 2398 N95-26598
CHAPMAN, JOHN J. .... p 2291 N95-27138
CHAPPELLE, EMMETT W. .... p 2315 N95-28211
CHARLOT, L. A. .... p 2216 N95-27493
CHARLTON, L. .... p 2430 N95-27306
CHARLTON, L. A. .... p 2431 N95-27537
CHATTERJEE, ARINDAM .... p 2366 N95-26694
CHATTLE, M. V. .... p 2398 N95-26614
CHATTOPADHYAY, S. .... p 2296 N95-27674
p 2434 N95-28161
CHAZEN, M. L. .... p 2166 N95-26390
CHEDIAK, J. A. .... p 2442 N95-27959
CHEN, AN-BAN .... p 2438 N95-26997
CHEN, C. L. .... p 2315 N95-28520
CHEN, CHIN-SHENG .... p 2364 N95-26557
CHEN, H. C. .... p 2218 N95-27757
CHEN, J. P. .... p 2205 N95-27691
CHEN, J.-Y. .... p 2286 N95-27899
CHEN, KUANG Y. .... p 2252 N95-26924
CHEN, M. H. .... p 2434 N95-28141
CHEN, P. .... p 2434 N95-28161
CHEN, PETER C. T. .... p 2186 N95-28280
CHEN, S. P. .... p 2215 N95-27446
p 2215 N95-27463
p 2219 N95-28026
CHEN, SHYH-KWEH .... p 2365 N95-26628
CHEN, TIMOTHY S. .... p 2238 N95-28212
CHEN, TSUHAN .... p 2261 N95-26964
CHEN, VICTOR L. .... p 2137 N95-28470
CHEN, XING .... p 2430 N95-27190
CHEN, Y. H. .... p 2299 N95-28330
CHEN, Z. .... p 2315 N95-28643
CHENG, A. H-D. .... p 2283 N95-27361
CHENG, L. K. .... p 2446 N95-28242
CHEONG, S. W. .... p 2443 N95-28060
CHEREPANOV, A. .... p 2257 N95-28449
CHERNYSHEV, B. A. .... p 2416 N95-28252
CHESTER, R. J. .... p 2135 N95-27523
CHEUNG, ANNY .... p 2125 N95-26485
CHEUNG, KINGMAN .... p 2419 N95-27089
p 2413 N95-28067
CHEUNG, SAMSON .... p 2130 N95-26813
CHIARELLO, RONALD P. .... p 2440 N95-27542
CHIN, A. .... p 2296 N95-27674
CHING, FRED .... p 2142 N95-28281
CHITTARO, LUCA .... p 2365 N95-26605
CHIU, S. AMANDA .... p 2166 N95-28293
CHIU, S. C. .... p 2431 N95-27441
CHLADEK, J. .... p 2155 N95-27263
CHO, B. K. .... p 2442 N95-27932
CHOI, DAVID S. .... p 2337 N95-27147
CHOI, JIN J. .... p 2259 N95-26433
CHOPP, C. S. .... p 2355 N95-28561
CHOQUETTE, K. D. .... p 2299 N95-28132
CHOU, A. E. .... p 2266 N95-28015
CHOU, F. C. .... p 2443 N95-28060
CHOU, JACK C. .... p 2185 N95-28270
CHOU, W. .... p 2423 N95-28551
CHOUCHEN, SHERRY .... p 2315 N95-28554
CHOUDHURY, D. .... p 2286 N95-27893
CHOW, CHUEN-YEN .... p 2389 N95-26663
CHRISTENSEN, R. A. .... p 2338 N95-28061
CHRISTENSEN, R. W. .... p 2421 N95-27735
CHRISTENSON, T. A. .... p 2444 N95-28103
CHRISTESON, GAIL L. .... p 2338 N95-28094
CHRISTODOULOU, CHRISTOS G.
p 2326 N95-26808
CHU, CHONG-SUN .... p 2449 N95-27877
CHU, F. .... p 2215 N95-27463
p 2219 N95-28026
CHU, M. S. .... p 2432 N95-27710
p 2433 N95-28106
CHUA, LEON O. .... p 2271 N95-26666
CHUI, CHARLES K. .... p 2387 N95-28527
CHUI, T. .... p 2439 N95-27413
CHUN, S.-B. .... p 2417 N95-28594
CHUNG, M. .... p 2415 N95-28221
CHUNG, SHIRLEY Y. .... p 2211 N95-27644
CHUNG, W. Y. WILLIAM .... p 2139 N95-26412
CHURCH, E. L. .... p 2425 N95-27490
CITTERIO, M. .... p 2269 N95-28244
CLARK, A. R. .... p 2417 N95-28594
CLARK, J. W. .... p 2381 N95-27025
p 2381 N95-27044
p 2207 N95-27880
CLARK, NOEL A. .... p 2224 N95-26456
CLARK, P. .... p 2309 N95-27846
CLARKE, E. .... p 2370 N95-27095
CLARKE, ROBERT A. .... p 2130 N95-27018
CLAYPOOLE, ROGER L., JR. .... p 2253 N95-26988
CLAYTON, CHRISTOPHER E. .... p 2297 N95-27736
CLEVELAND, JEFF I., II .... p 2362 N95-27241
CLIFFORD, J. R. .... p 2420 N95-27480
CLINE, R. E., JR. .... p 2378 N95-27402

CLOSE, F. E. p 2418 N95-28640
COBB, J. W. p 2288 N95-28533
COBB, S. L. p 2412 N95-28051
COBBLE, J. A. p 2297 N95-27850
COCHRAN, H. D. p 2208 N95-27960
COCHRAN, R. p 2133 N95-27514
COCHRAN, R. C. p 2193 N95-28446
COCKAYNE, JOHN E. p 2345 N95-27389
COCKROFT, N. J. p 2296 N95-27705
p 2443 N95-28023
COCKROFT, NIGEL J. p 2296 N95-27672
CODY, G. D. p 2234 N95-27455
COE, HAROLD H. p 2301 N95-27178
COFFEY, H. E. p 2465 N95-28087
COHEN, B. I. p 2266 N95-28015
COHEN, R. B. p 2332 N95-28623
COJOCARU, S. P. p 2410 N95-27881
COLE, D. R. p 2208 N95-27961
COLE, EDWARD I., JR. p 2268 N95-28201
COLEBAUGH, JAMES p 2360 N95-27164
COLLING, JAMES DAVID p 2131 N95-27180
COLLINS, ERIN P. p 2159 N95-26398
p 2159 N95-26399
p 2160 N95-26400
p 2160 N95-26401
p 2160 N95-26403
COLLINS, G. E. p 2173 N95-28311
COLLINS, H. p 2425 N95-27675
COLLINS, WILLIAM E. p 2357 N95-27323
COLTMAN, JOSEPH W. p 2126 N95-28630
COMAS, F. p 2400 N95-28350
COMBES, F. p 2461 N95-26522
p 2461 N95-27320
COMBS, S. K. p 2422 N95-28205
p 2435 N95-28596
CONANT, R. J. p 2216 N95-27477
CONCHA, MONICA C. p 2404 N95-26960
CONDE, M. p 2296 N95-27674
CONNELL, JAMES R. p 2321 N95-27971
CONNELL, JOHN W. p 2179 N95-28360
p 2179 N95-28361
CONNER, WM. C. p 2207 N95-27952
CONNOLLY, JEROME J. p 2134 N95-27520
CONSTANTINESCU, D. p 2406 N95-27309
CONSTANTINESCU, R. p 2406 N95-27309
p 2448 N95-27310
COO, DENNIS p 2371 N95-27246
COOK, KAREN L. p 2374 N95-28590
COOMBE, ROBERT D. p 2403 N95-26466
COOPER, DOUGLAS K. p 2391 N95-27432
COOPER, ELIZABETH A. p 2217 N95-27555
COOPER, J. ARLIN p 2391 N95-27432
COPELAND, RICHARD A. p 2399 N95-27852
CORBETT, W. p 2422 N95-28122
CORBUS, D. p 2265 N95-27719
CORIANO, C. p 2449 N95-27449
CORNACCHIA, M. p 2422 N95-28122
CORREA, S. p 2285 N95-27889
CORRELL, THOMAS E. p 2148 N95-27771
CORWIN, W. R. p 2223 N95-28208
CORZINE, S. W. p 2299 N95-28132
COSMO, MARIO L. p 2165 N95-27836
COSTA, ROBERT N., JR. p 2162 N95-26918
COSTELLO, R. J. p 2370 N95-27210
COUGHLAN, S. D. p 2313 N95-26476
COUGHLAN, S. DANETTE p 2314 N95-26682
COULTER, R. C. p 2301 N95-26926
COURTNEY, CRAIG p 2156 N95-27274
COURY, LOUIS A. p 2436 N95-26473
COUTTS, D. p 2331 N95-28548
COVINO-HRBACEK, JOSEPHINE p 2294 N95-26503
COWAN, G. D. p 2417 N95-28594
COX, ALICE B. p 2466 N95-26823
COX, B. N. p 2189 N95-28424
p 2198 N95-28486
COX, D. L. p 2268 N95-28198
COX, J. N. p 2267 N95-28148
COX, JOSEPH L. p 2456 N95-28587
COXON, B. R. p 2138 N95-28482
COYLE, J. M. p 2389 N95-26609
COZMAN, FABIO p 2395 N95-27417
CRAIG, D. F. p 2241 N95-28560
CRANE, D. L. p 2310 N95-28098
CRANWELL, R. M. p 2329 N95-27878
CRASSIDIS, JOHN L. p 2148 N95-27775
p 2154 N95-27803
CRAWFIS, R. p 2343 N95-28014
CRAWFORD, B. E. p 2405 N95-27081
CRAWFORD, O. H. p 2417 N95-28595
CREATH, KATHERINE p 2293 N95-28037
CREDELLE, THOMAS p 2292 N95-27863
CREEDON, W. P. p 2176 N95-28324
CREELMAN, R. A. p 2325 N95-28058
CREWS, LAVONNE p 2360 N95-27164
CROCKETT, SHARON K. p 2463 N95-27668
CROSS, J. B. p 2272 N95-27635
CROSS, JON B. p 2210 N95-27630
p 2210 N95-27631
p 2418 N95-27634
CROUCH, KEITH E. p 2125 N95-26497
CROWELL, PETER G. p 2177 N95-26434
CROWELL, R. A. p 2446 N95-28242
CROWLEY, JOHN S. p 2130 N95-26993
CSANAK, G. p 2298 N95-28027
CSIGE, I. p 2202 N95-27168
CUCCOLI, A. p 2418 N95-28642
CUCINOTTA, FRANCIS A. p 2465 N95-26427
p 2420 N95-27372
p 2465 N95-28530
CUESTA, JUAN D. p 2136 N95-28626
CUEVAS, O. O. p 2147 N95-27769
CULSHAW, BRIAN p 2312 N95-28649
CUMPSON, P. J. p 2226 N95-26745
CUNLIFFE, N. p 2199 N95-28639
CURFMAN, L. V. p 2284 N95-27454
CURRAN, DAN p 2173 N95-28309
p 2174 N95-28312
CURRAN, FRANCIS M. p 2168 N95-27727
CURRENT, M. I. p 2440 N95-27471
CURTIS, IHLEFELD M. p 2293 N95-28362
CUSTER, J. S. p 2237 N95-28089
CUTHBERTSON, J. W. p 2434 N95-28185
CUTLER, R. M. p 2271 N95-28663
CYGAN, RANDALL T. p 2268 N95-28200

D

DACRES, CHESTER M. p 2125 N95-27186
DADKHAH, M. S. p 2189 N95-28424
DAHL, MILO D. p 2401 N95-26801
DAHLMAN, CARL J. p 2143 N95-26556
DAI, F. p 2286 N95-27892
DAI, P. p 2413 N95-28066
DALE, V. H. p 2327 N95-27469
DAMBROSIO, BRUCE p 2386 N95-27396
DAMBROSIO, DOMENIC p 2287 N95-27917
DAMOUR, T. p 2397 N95-28174
p 2449 N95-28175
p 2450 N95-28664
DAN, NGUYEN TRUNG p 2417 N95-28607
DANAI, KOUROSH p 2302 N95-27373
DANCER, ANDREW p 2388 N95-26514
DANDEKAR, B. S. p 2337 N95-27146
DANDO, ANDREW p 2273 N95-26576
DANG, T. p 2267 N95-28148
DANIEL, M. G. p 2270 N95-28597
DANIEL, WALTER K. p 2148 N95-27771
DANIELL, ROBERT E. p 2337 N95-27703
DANIELS, CHARLES L., II p 2129 N95-26652
DANIELS, JOHN A. p 2198 N95-28485
DANILDEMAMOR, ANGELA F. p 2199 N95-26352
DANNEVIK, WILLIAM P. p 2335 N95-26622
DARCY, ERIC C. p 2272 N95-26790
DARENBERG, RICHARD G. p 2354 N95-27039
DAS-GUPTA, D. K. p 2290 N95-26541
DAS, G. P. p 2223 N95-28250
DAS, GOUR P. p 2218 N95-27756
DASGUPTA, I. p 2223 N95-28250
DASTIN, S. p 2196 N95-28477
DATLOWE, DAYTON W. p 2336 N95-26922
DATZ, S. p 2417 N95-28595
DAUGHTRY, CRAIG S. T. p 2315 N95-28211
DAVID, KAIA E. p 2242 N95-27640
DAVID, S. A. p 2215 N95-27319
p 2302 N95-27545
p 2221 N95-28082
DAVIDOVITS, P. p 2328 N95-27743
DAVIDSON, BARRY D. p 2180 N95-26571
DAVIDSON, K. L. p 2346 N95-26477
DAVIES, CAROL B. p 2367 N95-26726
DAVIES, W. G. p 2417 N95-28595
DAVILA, RICARDO CRUZ p 2334 N95-26488
DAVIS, C. W. p 2306 N95-26778
DAVIS, CABELL S. p 2347 N95-27151
DAVIS, CURTISS O. p 2345 N95-26430
DAVIS, D. D., JR. p 2194 N95-28468
DAVIS, HOLLY C. p 2320 N95-27475
DAVIS, J. BRADLEY p 2160 N95-27238
DAVIS, JOHN G., JR. p 2193 N95-28463
DAVIS, M. J. p 2135 N95-27528
DAVIS, R. C. p 2194 N95-28468
DAVIS, ROBERT F. p 2437 N95-26756
p 2439 N95-27416
p 2237 N95-28097
p 2446 N95-28327
DAVIS, WILLIAM A. p 2202 N95-26896
DAWKINS, WILLIAM P. p 2307 N95-26464
DAWSON, J. M. p 2436 N95-28668
DAYAN, DAVID p 2217 N95-27713
DAZEVEDO, E. F. p 2378 N95-28019
DE, A. p 2409 N95-27552
DEAN, TIMOTHY C. p 2426 N95-27913
DEANGELO, FRANK L. p 2235 N95-27503
DEARELLANO-LOPEZ, A. R. p 2183 N95-28069
DEATON, JERRY W. p 2137 N95-28470
DEBROY, T. p 2215 N95-27319
p 2302 N95-27545
DECKER, DOUGLAS D. p 2142 N95-27036
DECKERT, WALLACE H. p 2131 N95-27143
DECKING, W. p 2425 N95-27675
DECLEENE, DONALD F. p 2359 N95-26755
DEETER, THOMAS E. p 2381 N95-26990
DEFAZIO, R. L. p 2146 N95-27765
p 2153 N95-27798
DEFOREY, DENNIS E. p 2165 N95-28578
DEFREEZ, RICHARD p 2295 N95-26906
DEGNAN, FRANK p 2145 N95-27856
DEGRAND, T. p 2409 N95-27552
DEGRASSIE, J. S. p 2431 N95-27441
DEHAEMER, MICHAEL J. p 2263 N95-27226
DEHAYE, ROBERT F. p 2419 N95-27637
DEIVERT, ROBERT A. p 2130 N95-26873
DELAHOUSSAYE, P. R. p 2438 N95-27040
DELALE, F. p 2180 N95-26626
DELANEY, ALLAN J. p 2144 N95-27297
DELANGE, ERIC p 2255 N95-27149
DELAUNE, CARL p 2383 N95-27378
DELAVEGABALLESTEROS, LUIS RICARDO
p 2327 N95-27198
DELFRATE, JOHN H. p 2362 N95-27914
DELL, G. F. p 2422 N95-28115
DELLINGER, JOHN A. p 2355 N95-28561
DELLWO, J. p 2442 N95-27959
DELMONACO, J. L. p 2267 N95-28105
DELONG, K. W. p 2425 N95-27482
p 2298 N95-27969
p 2299 N95-28219
p 2299 N95-28220
p 2300 N95-28549
DELRE, S. p 2270 N95-28515
DELUCA, J. A. p 2447 N95-28606
DEMUTS, EDVINS p 2198 N95-28485
DENISON, A. B. p 2217 N95-27553
DENMARK, RAYMOND H. p 2145 N95-27856
DENNERY, RICHARD A. p 2276 N95-26819
DENNIS, LEON B. p 2181 N95-26865
DENTON, M. B. p 2411 N95-27953
DEPENA, JUAN p 2149 N95-27781
DEPETRO, THOMAS G. p 2119 N95-26950
DERVENAGAS, P. p 2442 N95-27932
DESAI, S. p 2296 N95-27550
DESPA, F. p 2446 N95-28255
DETAR, D. p 2409 N95-27552
DEUTSCHMANN, J. p 2147 N95-27770
DEVAN, J. H. p 2217 N95-27544
DEVENPORT, WILLIAM J. p 2123 N95-28193
DEVRIES, M. J. p 2199 N95-27636
DEWITT, KENNETH J. p 2206 N95-27695
DEWSON, T. p 2199 N95-28639
DEXTER, H. BENSON p 2185 N95-28276
p 2196 N95-28475
DEY, J. p 2406 N95-27318
DHURIA, HARBANS p 2329 N95-27864
DIAMOND, P. H. p 2430 N95-27306
p 2431 N95-27536
DIAZ, MILTON E. p 2130 N95-26876
DIBARTOLO, G. p 2442 N95-27959
DIBELLO, EDWARD G. p 2265 N95-27706
DIBERARDINO, M. p 2133 N95-27514
DIBROZOLO, FILIPPO p 2428 N95-27652
DICARLO, JAMES A. p 2183 N95-27717
DIDYK, A. YU. p 2261 N95-27023
p 2261 N95-27024
DIEGERT, K. V. p 2203 N95-27423
DIETRICH, LECH p 2212 N95-26512
p 2212 N95-26517
p 2212 N95-26666
p 2213 N95-26838
DIGNON, J. p 2332 N95-28662
DILLARD, ROBERT M. p 2361 N95-28667
DILLARD, T. W. p 2165 N95-27124
DILLS, ANTHONY N. p 2264 N95-27296
DIMICHELE, ROBERTO p 2120 N95-28610
DINICOLA, ALBERT J. p 2185 N95-28270
DINWIDDIE, R. B. p 2183 N95-27955
DION, DENIS p 2258 N95-28580
DISTEFANO, J. R. p 2217 N95-27544
DITTNER, P. F. p 2417 N95-28595
DIWAN, RAVINDER M. p 2292 N95-27368
DIXON, L. p 2449 N95-28160
DIXON, W. p 2440 N95-27471
DIXON, WILLIAM p 2440 N95-27538
DJEMAI, A. E. F. p 2390 N95-27311
DJOKOVIC, IGOR p 2256 N95-28095
DOANE, J. WILLIAM p 2292 N95-27863
DOANE, WILLIAM J. p 2184 N95-28268
DODDS, R. H., JR. p 2311 N95-28100

DOGGETT, ROBERT V., JR. p 2117 N95-26381
DOHERTY, JEFF p 2231 N95-27123
DOHERTY, P. J. p 2248 N95-26493
DOLL, C. E. p 2147 N95-27766
p 2147 N95-27768
DOLVIN, DOUGLAS J. p 2137 N95-28440
DOMINGUEZ-RODRIGUEZ, A. p 2183 N95-28069
DOMINIC-SAVIO, PATRICK p 2256 N95-28391
DON, DAVID L. p 2398 N95-26687
DONAHUE, CHRISTOPHER A. p 2342 N95-27148
DONATTO, U. A. p 2205 N95-27680
DONNELLAN, T. M. p 2193 N95-28446
DONNELLY, R. F. p 2464 N95-28007
DONNET, D. M. p 2441 N95-27720
DONOHO, DAVID L. p 2257 N95-28455
DONOVAN, TERENCE p 2428 N95-27652
DORE, G. R. p 2401 N95-26615
DOSANJH, DARSHAN p 2277 N95-26995
DOST, E. F. p 2138 N95-28482
DOTTER, JON W. p 2276 N95-26822
DOUGLAS, MELISSA R. p 2429 N95-26720
DOUGLASS, DEBORAH A. p 2254 N95-27008
DOVER, C. B. p 2414 N95-28169
p 2414 N95-28170
DOVGUN, S. V. p 2416 N95-28252
DOW, MARVIN B. p 2195 N95-28469
DOWBEN, P. A. p 2436 N95-26440
DOWELL, EARL H. p 2136 N95-28504
DOWELL, J. D. p 2423 N95-28452
DOWNEN, TROY p 2118 N95-26942
p 2119 N95-26947
p 2119 N95-26948
DOWNEY, K. W. p 2177 N95-28325
DOYLE, J. F. p 2455 N95-28113
DRAKE, J. B. p 2327 N95-27457
p 2431 N95-27537
DRESHFIELD, R. L. p 2218 N95-27728
DRESNER, L. p 2262 N95-27083
p 2267 N95-28048
DREWERY, J. p 2265 N95-27678
DREWIEN, C. A. p 2218 N95-27722
p 2238 N95-28117
DROPPO, J. G., JR. p 2328 N95-27749
DRUET, MICHELINE p 2132 N95-27508
DU, Q. p 2209 N95-28218
DUAN, HAILONG p 2201 N95-26707
DUBE, E. p 2373 N95-28521
DUERBECK, HILMAR W. p 2459 N95-27072
p 2459 N95-27073
p 2459 N95-27074
DUFFY, PHILLIP B. p 2335 N95-26622
DUMAS, PIERRE p 2159 N95-27292
DUNBAR, D. C. p 2449 N95-28160
DUNN, DAVID B., JR. p 2251 N95-26869
DURIN, CHRISTIAN p 2211 N95-27648
DURSCH, HARRY p 2470 N95-27647
p 2326 N95-27649
DURSCH, HARRY W. p 2177 N95-26391
p 2210 N95-27642
DUTTA, P. K. p 2207 N95-27951
DUTTON, JAMES P., JR. p 2128 N95-26481
DYBALA, TOMASZ p 2383 N95-27380
DYE, R. C. p 2298 N95-28124
DYKA, C. T. p 2276 N95-26852
DYKE, J. T. p 2425 N95-27734

E

EARHART, E. p 2304 N95-28364
EARLY, JAMES W. p 2296 N95-27672
EASTON, D. S. p 2221 N95-28082
EATHERLY, W. P. p 2217 N95-27544
EBERSPACHER, CHRIS p 2325 N95-28517
EBINGER, MICHAEL H. p 2204 N95-27556
ECCLESTON, G. W. p 2379 N95-26443
ECK, GARY p 2176 N95-28321
ECKLUND, ROWENA H. p 2141 N95-28275
EDDLEMAN, H. E. p 2332 N95-28662
EDEEN, GREGG A. p 2165 N95-27842
EDELMAN, JOEL E. p 2242 N95-27655
EDELSTEIN, KAREN S. p 2159 N95-26379
EDGAR, DAIVA p 2262 N95-27067
EDIGHOFFER, J. A. p 2297 N95-27737
EDLOW, RALPH p 2194 N95-28465
EDWARDS, S. p 2228 N95-27107
EGGEMEIER, F. T. p 2356 N95-26825
EGOLF, T. ALAN p 2402 N95-28264
EHLEN, R. J. p 2192 N95-28438
EHST, D. A. p 2434 N95-28224
EHTAMO, H. p 2396 N95-26912
EHTAMO, HARRI p 2396 N95-26613
EIDE, PETER K. p 2131 N95-27042
EIDEN, G. C. p 2297 N95-27841
EIDNES, H. p 2379 N95-28665
EISCHEID, J. K. p 2332 N95-28605
EISENBIES, CHRISTOPHER L. p 2251 N95-26877
EISENTHAL, K. B. p 2201 N95-26544
EL-MASRY, N. A. p 2446 N95-28327
EL-SAYED, M. p 2351 N95-27254
ELALDI, F. p 2135 N95-27524
ELEY, MICHAEL H. p 2360 N95-27164
ELHASSOUNI, A. p 2390 N95-27301
ELIAS, JOHN G. p 2367 N95-26770
ELLIOTT, J. P. p 2176 N95-28324
p 2177 N95-28325
ELLIOTT, S. p 2328 N95-27686
ELLIS, D. L. p 2218 N95-27728
ELLIS, N. p 2419 N95-27321
p 2421 N95-28040
p 2423 N95-28452
ELLISON, JAMES p 2376 N95-27388
ELMS, K. p 2195 N95-28472
ELORANTA, K. p 2395 N95-26913
ELSBERRY, RUSSELL L. p 2344 N95-28459
ELTGROTH, PETER G. p 2335 N95-26622
ELTON, R. C. p 2433 N95-28052
EMAMI, SAIED p 2140 N95-28343
ENGDAHL, E. p 2418 N95-28641
ENGLAND, A. W. p 2463 N95-27700
ENGLEBRETSON, RONALD E. p 2344 N95-28577
EPSTEIN, G. p 2270 N95-28515
ERDMAN, PEETER W. p 2429 N95-26800
EREMIN, A. V. p 2414 N95-28184
ERICKSON, JON p 2428 N95-27652
ERMAK, DONALD L. p 2392 N95-28162
ERMUTLU, M. E. p 2256 N95-28354
ESCOBEDO, RICHARD p 2371 N95-27251
ESTEVENON, CHRISTINE p 2156 N95-27271
ESTRADA, T. p 2431 N95-27497
EVANS, A. G. p 2181 N95-26847
p 2247 N95-28187
EVANS, ANTHONY G. p 2182 N95-27188
EVANS, T. E. p 2434 N95-28185
EWING, R. C. p 2236 N95-27733
EWSUK, K. G. p 2184 N95-28145
EWSUK, KEVIN G. p 2237 N95-27993

F

FABBIANO, G. p 2461 N95-26593
FAHLMAN, SCOTT E. p 2382 N95-27066
FAIRBANK, W. M., JR. p 2204 N95-27467
FAIRFIELD, M. S. p 2284 N95-27845
FALCO, CHARLES M. p 2212 N95-26490
FALEN, GERALD L. p 2127 N95-26898
FAN, ZHENGXIU p 2424 N95-26860
FARHAT, N. H. p 2387 N95-28336
FARLEY, G. L. p 2194 N95-28468
FARLEY, RODGER p 2158 N95-27284
FARLEY, WILLARD W. p 2262 N95-27196
FARNSWORTH, A. p 2299 N95-28223
FARRELL, K. p 2220 N95-28072
FASANELLA, EDWIN L. p 2192 N95-28439
FAUNTLEROY, JULIA CORBIN p 2394 N95-26414
FAWLEY, W. M. p 2297 N95-27737
FAY, RUSSELL p 2191 N95-28432
FEAREY, B. L. p 2204 N95-27467
FEDERSPIEL, F. J. p 2412 N95-28063
FEDRO, MARK J. p 2196 N95-28478
FEHRENBACHER, LARRY L. p 2140 N95-28646
FEIGELSON, ROBERT S. p 2277 N95-27000
FEIGERLE, C. S. p 2296 N95-27550
FEINER, L. J. p 2266 N95-27999
FELCHER, G. F. p 2411 N95-28004
FELDMAN, PAUL D. p 2461 N95-27166
FELISKY, MARC K. p 2295 N95-26906
FELKER, B. p 2222 N95-28167
FELTER, TOM p 2265 N95-27706
FENG, YUEZHONG p 2428 N95-28617
FENNESSEY, RICHARD p 2152 N95-27793
FENNO, C. C., JR. p 2289 N95-28673
FENSTERMACHER, M. E. p 2433 N95-28065
p 2434 N95-28185
FENTRESS, MICHAEL L. p 2192 N95-28436
FERGG, F. p 2209 N95-28229
FERGUSON, J. S. p 2134 N95-27518
FERRARA, GUS p 2120 N95-28610
FERRISS, D. H. p 2308 N95-26749
FETTERER, THOMAS A. p 2314 N95-26682
FETTERER, TOM p 2313 N95-26476
FETZER, G. J. p 2332 N95-28602
FEYOCK, STEFAN p 2386 N95-27395
FICKIE, K. D. p 2179 N95-26565
FIEGEL, ROBERT P. p 2340 N95-26463
FIELD, R. W. p 2414 N95-28199
FINCANNON, JAMES p 2169 N95-28036
p 2169 N95-28213
FINCKENOR, J. p 2392 N95-28215
FINCKENOR, MIRIA M. p 2419 N95-27637
p 2242 N95-27638
p 2242 N95-27639
p 2210 N95-27641
FINK, EUGENE p 2450 N95-27064
FINN, SCOTT R. p 2198 N95-28484
FIORUCCI, T. p 2304 N95-28364
FIRESTER, ARTHUR H. p 2292 N95-27863
FIRESTONE, ELAINE R. p 2345 N95-26430
p 2348 N95-28030
FISCHER, D. A. p 2222 N95-28134
FISHER, ALVAN, JR. p 2363 N95-26447
p 2456 N95-28589
FISHER, P. W. p 2422 N95-28205
FISK, Z. p 2407 N95-27431
p 2443 N95-28060
FITTINGHOFF, D. N. p 2425 N95-27482
p 2298 N95-27969
p 2299 N95-28219
p 2299 N95-28220
p 2300 N95-28549
FITZ-COY, NORMAN p 2150 N95-27784
FITZGERALD, THOMAS M. p 2261 N95-26921
FITZMAURICE, NESSAN p 2283 N95-27364
FITZSIMMONS, M. p 2412 N95-28057
FLABERTY, J. E. p 2389 N95-26609
FLANNERY, JACK p 2144 N95-26583
FLATLEY, THOMAS W. p 2149 N95-27780
p 2153 N95-27801
FLEETWOOD, CHARLES, JR. p 2428 N95-27651
FLEISCHMANN, H. p 2410 N95-27922
FLETCHER, DALE N. p 2374 N95-28588
FLORES, R. R. p 2266 N95-27999
FLOWE, ROBERT M. p 2374 N95-28591
FOLKERTS, H. O. p 2409 N95-27551
FOLKERTS, L. p 2409 N95-27551
p 2413 N95-28078
FOLLEY, ADRIENNE p 2166 N95-27663
FOLLSTAEDT, D. M. p 2235 N95-27687
p 2444 N95-28127
p 2445 N95-28206
FOLTA, DAVID C. p 2152 N95-27797
FOORD, M. E. p 2462 N95-28013
FOOS, MICHAEL L. p 2221 N95-28102
FORBES, JOHN C. p 2304 N95-28347
FORCEY, W. p 2146 N95-27765
FORCHT, BRENDA R. p 2456 N95-28587
FORD, STEPHEN D. p 2424 N95-26965
FORD, TERESA O. p 2165 N95-28150
FOREMAN, C. R. p 2192 N95-28437
FOREST, C. B. p 2431 N95-27441
FORINGER, MARK A. p 2181 N95-26868
FOROOZAN, S. p 2272 N95-26795
FORREST, WILLIAM C. p 2118 N95-26946
FORSTER, J. S. p 2417 N95-28595
FORTNER, JONATHAN L. p 2290 N95-26989
FOSSEY, ROBERT p 2233 N95-27130
FOSSUM, ERIC R. p 2424 N95-26894
FOSTER, C. A. p 2422 N95-28205
FOSTER, C. L. p 2311 N95-28214
FOSTER, I. T. p 2327 N95-27457
FOSTER, IAN p 2378 N95-27741
FOSTER, LUCAS E. p 2143 N95-26768
FOSTER, P. p 2206 N95-27750
FOURNIER, E. W. p 2332 N95-28623
FOUST, C. R. p 2422 N95-28205
FOUTS, CHRISTINE S. p 2232 N95-27127
FOWLER, C. M. p 2266 N95-27754
FOWLER, T. K. p 2399 N95-28108
p 2435 N95-28542
FOX, ALAN G. p 2213 N95-26681
FOYE, RAYMOND L. p 2189 N95-28423
FRAGOLA, JOSEPH R. p 2159 N95-26398
p 2159 N95-26399
p 2160 N95-26400
p 2160 N95-26401
p 2160 N95-26403
FRAILEY, JAMES A. p 2133 N95-27516
FRAME, C. S. p 2134 N95-27521
FRANCOEUR, J. p 2242 N95-27669
FRANGANILLO, A. p 2135 N95-27527
FRANK, A. L. p 2202 N95-27168
FRANK, JASON p 2119 N95-26951
FRANK, MICHAEL V. p 2159 N95-26398
p 2159 N95-26399
p 2160 N95-26400
p 2160 N95-26401
p 2160 N95-26403
FRANKE, J. E. p 2267 N95-28148
FRANKLE, C. M. p 2405 N95-27081
FRANKLIN, JAMES A. p 2139 N95-26412
FRANSEN, LAWRENCE J. p 2248 N95-26349
FRASER, K. F. p 2139 N95-26424
FRASER, R. S. p 2348 N95-28030
FRAUNBERG, M. p 2369 N95-26907
FREAR, D. R. p 2309 N95-27837
FREDERICK, D. p 2228 N95-27107
FREDERICKS, J. J. p 2347 N95-27043
FREDERICKSON, P. A. p 2346 N95-26477

FREDERICO, T. p 2406 N95-27318
FREEMAN, B. L. p 2266 N95-27754
FREEMAN, DONALD J. p 2171 N95-28301
FREEMAN, R. L. p 2431 N95-27441
FREEMAN, S. P. H. T. p 2204 N95-27496
FREEMAN, W. p 2194 N95-28464
FREITAS, GLENN p 2185 N95-28272
FRERY, A. C. p 2258 N95-28569
FRERY, ALEJANDRO C. p 2258 N95-28559
FREUND, F. p 2204 N95-27549
FREUND, J. p 2388 N95-26495
FRIDAY, DAVID K. p 2405 N95-27034
FRIEDJUNG, MICHAEL p 2459 N95-27073
p 2460 N95-27077
FRIEDMAN, AVNER p 2279 N95-27197
p 2313 N95-28099
FRIEDMANN, P. P. p 2136 N95-28262
FRIGO, L. A. p 2202 N95-27168
FRY, H. A. p 2206 N95-27851
FUJITA, TOSHIMI p 2128 N95-26525
FUK, MASATOSHI p 2271 N95-28613
FULLERTON, E. E. p 2206 N95-27755
FULTON, J. L. p 2287 N95-28021
FULTON, J. P. p 2306 N95-26778
FUNAHASHI, S. p 2440 N95-27487
FUNK, JOAN G. p 2145 N95-27657
FUNSTEN, H. O. p 2337 N95-27848
FURNEAUX, JOHN E. p 2257 N95-28456
FUTAMOTO, M. p 2441 N95-27720

G

GABAREE, C. L. p 2358 N95-26558
GABI, S. p 2460 N95-28197
GABL, E. F. p 2295 N95-26996
GABRUK, ROBERT S. p 2341 N95-26546
GADEPALLI, PRASHANDT p 2280 N95-27347
GAJJAR, J. S. B. p 2279 N95-27242
GALAL, K. p 2147 N95-27770
p 2150 N95-27783
GALAL, K. F. p 2153 N95-27798
GALBRAITH, NANCY R. p 2342 N95-26826
GALLAGHER-WETMORE, PAULA p 2229 N95-27111
GAMOTA, GEORGE p 2263 N95-27226
GANGLOGG, R. P. p 2213 N95-27032
GANGULY, ACHINTYA K. p 2259 N95-26433
GANNON, T. p 2392 N95-28010
p 2392 N95-28012
GANONG, GARY P. p 2177 N95-26434
GAO, HONG-YE p 2257 N95-28455
GAO, JINYUE p 2401 N95-26857
GAO, Y. p 2184 N95-28145
GARABEDIAN, P. R. p 2431 N95-27498
GARABEDIAN, PAUL R. p 2273 N95-26405
GARBER, M. G. p 2270 N95-28515
GARCIA-CORTES, I. p 2431 N95-27497
GARCIA, G. A. p 2438 N95-27040
GARCIA, L. p 2431 N95-27536
GARCIAH, J. M. p 2405 N95-27010
GARCIANUNEZ, H. p 2135 N95-27527
GARDINER, PETER T. p 2312 N95-28649
GARDNER, J. P. p 2182 N95-27421
GARDNER, W. L. p 2415 N95-28204
GARLAN, DAVID p 2363 N95-26446
p 2363 N95-26467
GARNER, J. C. p 2272 N95-26792
GARRETT, A. W. p 2297 N95-27841
GARRICK, JOE p 2152 N95-27795
GARVEY, J. p 2423 N95-28452
GARY, S. PETER p 2432 N95-27673
GARZA, ROBERT E. p 2394 N95-26892
GASANOV, E. M. p 2442 N95-27950
GASICK, MICHAEL F. p 2188 N95-28289
GATES, GEORGE H., JR. p 2369 N95-26919
GATSKI, THOMAS B. p 2282 N95-27356
GAUSE, L. W. p 2191 N95-28434
GAVER, DONALD P. p 2326 N95-26431
p 2352 N95-28519
GAY, CHARLES F. p 2325 N95-28517
GAY, JEFFREY MARK p 2254 N95-27062
GDOUTOS, E. E. p 2133 N95-27513
GEA, LAURENCE A. p 2444 N95-28081
GEE, J. p 2267 N95-28148
GEE, KEN p 2129 N95-26591
GEELHAAR, L. p 2171 N95-28299
GEIGER, J. S. p 2417 N95-28595
GEISINGER, J. p 2155 N95-27263
GEISLER, BILL p 2254 N95-27060
GELFAND, N. M. p 2421 N95-27531
GELLES, D. S. p 2216 N95-27479
GELOSH, DONALD S. p 2363 N95-26408
GENCO, SHERYL M. p 2261 N95-27015
GENTRY, LARRY L. p 2247 N95-27909
GEORGE, E. P. p 2220 N95-28046
GERB, ANDREW p 2384 N95-27384
GERBER, SCOTT S. p 2264 N95-27374
GEREZ, LUIS p 2159 N95-26398
p 2159 N95-26399
p 2160 N95-26400
p 2160 N95-26401
p 2160 N95-26403
GERNOTH, K. A. p 2381 N95-27025
p 2381 N95-27044
p 2207 N95-27880
GERSPACHER, M. p 2183 N95-27428
GHENDRIH, PH. p 2434 N95-28185
GHERMAN, C. p 2451 N95-28025
GHOSH, A. K. p 2265 N95-27554
p 2270 N95-28515
GIACHINO, JOSEPH M. p 2268 N95-28239
GIANFIGLIO, G. p 2157 N95-27281
GIBSON, R. B. p 2297 N95-27850
GILCHRIST, N. H. C. p 2249 N95-26696
GILDENBLAT, GENNADY p 2437 N95-26818
GILFORD, MICHAEL T. p 2342 N95-27148
GILION, J. BRENT p 2176 N95-28321
GILKEY, P. p 2389 N95-26915
GILL, C. G. p 2297 N95-27841
GILL, S. P. p 2316 N95-26393
GILLE, JENNIFER p 2369 N95-26930
GILLEPIE, PATTI L. p 2340 N95-26463
GILLETT, DAVE p 2117 N95-26409
GILMORE, RICHARD D. p 2344 N95-28577
GINSBURG, JERRY H. p 2288 N95-28351
GIORDANO, THOMAS J. p 2165 N95-27104
GIROUARD, F. p 2385 N95-27393
GIVI, PEYMAN p 2287 N95-28155
GLADDEN, HERBERT J. p 2281 N95-27352
GLAND, J. L. p 2206 N95-27838
p 2222 N95-28134
GLAROS, GREGORY E. p 2423 N95-26532
GLASS, J. T. p 2446 N95-28327
GLASS, JEFFREY T. p 2439 N95-27416
GLASS, JOHN A., JR. p 2207 N95-27904
GLASS, RICHARD p 2452 N95-26607
GLASS, S. J. p 2420 N95-27480
GLEGG, STEWART A. L. p 2123 N95-28193
GLENDENNING, N. K. p 2463 N95-28357
GLENN, WILLIAM E. p 2292 N95-27863
GLOVER, E. p 2296 N95-27674
GLUCK, R. p 2322 N95-27979
GNANADESIKAN, ANAND p 2342 N95-26826
GNAT, R. p 2171 N95-28302
GOERING, J. p 2186 N95-28279
p 2186 N95-28282
GOERING, J. C. p 2191 N95-28434
GOFF, DAN p 2400 N95-26502
p 2245 N95-26508
GOH, GIN-HUA p 2383 N95-27379
GOHIL, C. P. p 2432 N95-27710
GOHIL, P. p 2431 N95-27441
GOLD, J. p 2171 N95-28302
GOLDBERG, LEO p 2458 N95-27068
GOLDBERG, MATTHEW S. p 2393 N95-26347
GOLDEN, JOHNNY L. p 2210 N95-27642
GOLDHABER, G. p 2460 N95-28197
GOLDHAGEN, PAUL p 2465 N95-26427
GOLDMAN, A. I. p 2442 N95-27932
GOLDMAN, P. p 2325 N95-28395
GOLDMAN, ROBERT p 2384 N95-27382
GOLDSMITH, J. E. M. p 2344 N95-28538
GOLDSTEIN, J. C. p 2298 N95-28059
GOLDSTEIN, JOSEPH A. p 2249 N95-26564
GOLDSTEIN, N. p 2332 N95-28602
GOLDSTEIN, W. H. p 2462 N95-28013
GOLDSTONE, J. A. p 2182 N95-27080
GOLLAHALLI, S. R. p 2208 N95-28006
GOLUB, DAVID B. p 2364 N95-26534
GOLUB, GENE H. p 2307 N95-26547
GOLUB, ROBERT A. p 2400 N95-26392
GOMEZ, FERNANDO p 2383 N95-27378
GONG, ZHIBEN p 2428 N95-28617
GOOBAR, A. p 2460 N95-28197
GOODNOW, D. C. p 2203 N95-27423
GOODS, S. H. p 2206 N95-27750
GOPALAKRISHNAN, V. T. p 2405 N95-27159
GORDON, MARK S. p 2404 N95-26632
GORETTA, K. C. p 2442 N95-27950
GOREVAN, STEPHEN p 2156 N95-27273
GORNEY, D. J. p 2162 N95-26902
GORNOV, M. G. p 2416 N95-28252
GOSSAGE, S. A. p 2378 N95-28074
GOSSELIN, ROGER p 2211 N95-27645
GOTTLIEB, DAVID p 2279 N95-27247
GOTTLIEB, STEVEN p 2409 N95-27552
GOUGE, M. J. p 2422 N95-28205
GOULD, R. W. p 2433 N95-27924
GOURLEY, P. L. p 2299 N95-28128
GOVE, SANDRA D. p 2145 N95-27856
GOVIND, RAKESH p 2171 N95-28299
GOVINDARAJ, T. p 2138 N95-28203
GOWAYED, YASSER A. p 2189 N95-28423
GOYAL, A. p 2444 N95-28079
p 2447 N95-28606
GRADY, D. E. p 2236 N95-27879
p 2299 N95-28223
GRADY, DENNIS p 2309 N95-27745
GRAESSER, D. p 2137 N95-28473
GRANAAS, MICHAEL p 2360 N95-27099
GRANDAGE, J. M. p 2136 N95-27918
GRANDE, D. H. p 2138 N95-28482
GRANDELL, J. p 2316 N95-28656
GRANDHI, RAMANA V. p 2245 N95-26410
GRANDY, J. p 2445 N95-28240
GRANT, C. p 2137 N95-28474
GRANT, CARROLL G. p 2185 N95-28271
GRANT, CATHERINE p 2119 N95-26947
GRANT, KEITH E. p 2328 N95-27708
GRANT, SCOTT A. p 2182 N95-27134
GRANT, STEVEN A. p 2200 N95-26432
GRAY, P. M. p 2193 N95-28443
GRAY, ROBERT A. p 2127 N95-26985
GREBENEV, V. N. p 2416 N95-28252
GREEN, R. A. p 2292 N95-27465
GREENBERG, D. S. p 2393 N95-28393
GREENE, A. F. p 2270 N95-28515
GREENE, D. L. p 2243 N95-27944
GREENE, J. M. p 2433 N95-28106
GREENLY, J. B. p 2221 N95-28116
GREENWALD, E. p 2225 N95-26482
GREGOREK, G. M. p 2124 N95-27977
GREGORY, J. C. p 2418 N95-27634
p 2272 N95-27635
GREINER, JOHN p 2365 N95-26656
GREMBAN, KEITH D. p 2376 N95-26529
GRIEM, H. R. p 2433 N95-28052
GRIFFIN, C. F. p 2194 N95-28467
GRIFFIN, GORDON C., JR. p 2162 N95-26916
GRIFFIN, MICHAEL J. p 2302 N95-27844
GROFF, K. W. p 2332 N95-28602
GRONER, DANIEL J. p 2181 N95-26886
GRONET, M. J. p 2163 N95-27026
GROPP, W. D. p 2378 N95-28071
GROSKO, J. p 2133 N95-27512
GROSS, L. A. p 2169 N95-28263
GROSSBERG, STEPHEN p 2380 N95-26530
GROSSE, IAN R. p 2259 N95-26550
GROSSI, MARIO D. p 2165 N95-27836
GROSSMAN, ALLEN S. p 2328 N95-27708
GROSSMAN, WALTER p 2153 N95-27802
GROSSMAN, Y. p 2407 N95-27409
GROSSNICKLE, P. C. p 2258 N95-28576
GROSVELD, F. W. p 2324 N95-27990
GROTCH, S. L. p 2372 N95-27533
GROZIN, A. G. p 2407 N95-27410
GRUENBAUM, PETER p 2326 N95-27649
GRUMBERG, O. p 2370 N95-27095
GRUNWALD, ARTHUR J. p 2127 N95-28188
GRUZINOV, A. V. p 2430 N95-27306
GRUZINOV, I. p 2430 N95-27306
GUAN, X. p 2378 N95-27709
GUBERMAN, STEVEN L. p 2462 N95-28216
GUCKEL, HENRY p 2268 N95-28239
GUCKERT, R. p 2426 N95-28022
GUENTHER, G. p 2134 N95-27517
GUESS, T. R. p 2240 N95-28405
GUIDOTTI, RONALD A. p 2264 N95-27474
GUIDRY, RUTH A. p 2314 N95-26682
GUINTO, RICHARD A. p 2359 N95-26737
GULBEKYAN, G. G. p 2261 N95-27023
p 2261 N95-27024
GULDRY, RUTH p 2313 N95-26476
GULLAHORN, GORDON E. p 2165 N95-27836
GUPTA, R. p 2445 N95-28240
p 2269 N95-28339
GUPTA, RAJAN p 2442 N95-27994
GUROV, YU. B. p 2416 N95-28252
GURTIN, MORTON E. p 2448 N95-26563
GURWELL, W. E. p 2222 N95-28130
GUTMARK, EPHRAIM p 2128 N95-26507
GUTOWSKI, T. p 2194 N95-28464
GUTPA, S. p 2393 N95-28393
GUY, TERESA A. p 2191 N95-28431

H

HA, KONG p 2154 N95-27803
HAALAND, D. M. p 2267 N95-28148
HAAPALA, CHRISTINE p 2368 N95-26903
HACK, MARGHERITA p 2458 N95-27068
p 2459 N95-27072
p 2459 N95-27074
p 2460 N95-27075
p 2460 N95-27078
HACKETT, R. M. p 2182 N95-27421
HADID, A. H. p 2286 N95-27891

HADLEY, G. R. p 2299 N95-28132
HAEMAELAEINEN, R. P. p 2396 N95-26912
HAEMAELAEINEN, RAIMO P. p 2396 N95-26613
HAFFNER, STEPHEN W. p 2402 N95-28670
HAGAN, M. p 2418 N95-28657
HAGENIERS, O. L. p 2125 N95-26527
HAGERTY, JAMES D. p 2161 N95-28581
HAGINOYA, HIROFUMI p 2431 N95-27414
HAGOPIAN, SHARON p 2410 N95-27871
HAGSTROM, THOMAS p 2279 N95-27175
HAHN, A. A. p 2454 N95-27090
HAHN, DOUGLAS C. p 2356 N95-26992
HAHN, S. J. p 2297 N95-27737
HAHN, SANG JUNE p 2298 N95-28104
HAINES, B. p 2151 N95-27792
HAJNAL, FERENC p 2465 N95-26427
HAKES, CHARLES L. p 2210 N95-27630
p 2210 N95-27631
HAKUN, CLAEF F. p 2158 N95-27287
HALBLEIB, J. A. p 2420 N95-27480
HALE, J. W. p 2413 N95-28078
HALE, JEFFREY S. p 2199 N95-27636
HALL, H. p 2294 N95-26568
HALL, PHILIP p 2273 N95-26576
p 2278 N95-27028
p 2284 N95-27760
HALL, RICHARD p 2358 N95-26612
HALL, ROBERT G. p 2452 N95-26721
HALL, ROBERT J. p 2175 N95-28317
HALL, RONALD G. p 2184 N95-28268
HALL, WILLIAM p 2340 N95-26453
HALLETT, JOHN p 2341 N95-26669
HALLICK, RICHARD B. p 2352 N95-28496
HALLIKAINEN, M. p 2316 N95-28656
HALPERN, JULES P. p 2465 N95-26630
HALYO, EDI p 2412 N95-28041
HALZEN, F. p 2415 N95-28210
HAMAGUCHI, YASUMASA p 2180 N95-26667
HAMALAINEN, K. p 2422 N95-28195
HAMEED, S. p 2330 N95-28084
HAMERS, ROBERT J. p 2438 N95-26959
p 2290 N95-26982
p 2405 N95-27017
p 2438 N95-27061
HAMILTON, BRUCE HOWARD p 2308 N95-26839
HAMILTON, C. p 2461 N95-27326
HAMILTON, DAVID A. p 2165 N95-27842
HAMILTON, M. L. p 2214 N95-27086
HAMLEY, JOHN A. p 2168 N95-27861
p 2168 N95-27862
HAMMEL, C. J. p 2265 N95-27719
HAMMEL, P. C. p 2443 N95-28060
HAMMON, COLIN P. p 2143 N95-26556
HAMMONDS, J. S. p 2354 N95-28136
HAMMONS, B. E. p 2299 N95-28128
HAN, T. p 2413 N95-28067
HANADA, S. p 2234 N95-27486
HANAFEE, J. E. p 2223 N95-28534
HANCE, R. p 2399 N95-27530
HANCOCK, JOHN A. p 2381 N95-27041
HANIGOFSKY, JOHN A. p 2140 N95-28646
HANLON, J. p 2421 N95-27735
HANNON, J. B. p 2223 N95-28593
HANSEN, C. S. p 2204 N95-27467
HANSEN, JAMES R. p 2474 N95-27685
HARDEN, JOHN H., JR. p 2314 N95-26841
HARDER, D. p 2315 N95-28520
HARDING, JOY L. p 2342 N95-27148
HARDY, JANET P. p 2464 N95-27184
HARE, DAVID A. p 2291 N95-27259
HARELAND, WILLARD p 2265 N95-27706
HAROLD, M. p 2207 N95-27952
HAROUTUNIAN, VAHE p 2286 N95-27895
HARRAL, BRIAN D. p 2408 N95-27478
HARRINGTON, H. J. p 2325 N95-28058
HARRINGTON, TIMBERLYN M. p 2309 N95-27135
HARRIS, C. E. p 2137 N95-28471
HARRIS, CHARLES E. p 2196 N95-28475
HARRIS, H. M. p 2270 N95-28529
HARRIS, J. B. p 2345 N95-26419
HARRIS, R. M. p 2411 N95-27933
HARRIS, W. L. p 2325 N95-27992
HARRISON, L. p 2380 N95-26638
HARRISON, LARRY W. p 2237 N95-27993
HARRISON, P. F. p 2465 N95-28500
HARRUP, GEORGIA K. p 2424 N95-26971
HART-SMITH, L. J. p 2187 N95-28287
HART, J. E. p 2463 N95-27916
HART, ROGER C. p 2152 N95-27794
HARTLEY, FRANK T. p 2271 N95-28599
HARTMAN, KATHY R. p 2146 N95-27763
p 2152 N95-27794
HARTMANN, BRUCE p 2210 N95-28584
HARTSE, HANS p 2339 N95-28126
HARVEY, GALE A. p 2211 N95-27656
HARVEY, GARY p 2361 N95-26845
HARVEY, J. A. p 2413 N95-28066
HARVEY, R. W. p 2431 N95-27441
HASHIMOTO, YOSHIHIRO p 2145 N95-27667
HASKO, GREGORY H. p 2185 N95-28276
HASSOUNI, Y. p 2390 N95-27301
HASTINGS, J. B. p 2422 N95-28195
HAUBOLDT, BRADY P. p 2162 N95-26887
HAUG, S. p 2379 N95-28502
HAUGHT, DEBORAH A. p 2241 N95-28582
HAUN, ROBERT E. p 2171 N95-28301
HAUSLADEN, M. C. p 2205 N95-27691
HAVENER, C. C. p 2413 N95-28078
HAVENS, STEPHEN J. p 2235 N95-27732
HAVEY, KEITH p 2428 N95-27653
HAWK, C. p 2408 N95-27444
HAWKINS, CHARLES F. p 2306 N95-27723
HAYDER, M. EHTESHAM p 2279 N95-27175
HAYES, MICHAEL E. p 2232 N95-27127
HAYMAN, G. p 2421 N95-27735
HAYS, CHRISTOPHER J. p 2355 N95-26683
HAZLEBECK, D. A. p 2177 N95-28325
HAZLEWOOD, RICHARD p 2119 N95-26947
HE, XIAO-GANG p 2415 N95-28246
HEARNE, LEONARD B. p 2394 N95-26457
HEARTY, C. p 2409 N95-27676
HEATH, J. B. R. p 2132 N95-27509
HEATHERLY, D. E. p 2444 N95-28079
HEAVILIN, S. M. p 2215 N95-27464
HECHT, DIANA L. p 2423 N95-26385
HECKER, N. E. p 2413 N95-28066
HEDIN, D. p 2417 N95-28495
HEDRICK, C. L. p 2431 N95-27419
HEEMAN, PETER A. p 2259 N95-28624
HEENAN, R. K. p 2375 N95-28658
HEIDBRINK, W. W. p 2432 N95-27873
HEIMERDINGER, M. W. p 2134 N95-27519
HEINISCH, H. L. p 2214 N95-27088
HEINONEN, E. W. p 2234 N95-27481
p 2238 N95-28133
HEINTZE, NEVIN p 2389 N95-26772
HELLER, U. M. p 2409 N95-27552
HELMICH, D. R. p 2420 N95-27480
HEMBERGER, P. H. p 2297 N95-27841
HEMINGER, ALAN R. p 2359 N95-26863
HEMMATI, HAMID p 2297 N95-27731
HEMMINGER, CAROL S. p 2210 N95-27632
HEMSCH, MICHAEL J. p 2123 N95-28241
HENDERSON, J. R. p 2314 N95-28053
HENDERSON, M. A. p 2203 N95-27401
HENDRICKS, R. C. p 2140 N95-28344
HENDRICKS, ROBERT C. p 2168 N95-27434
HENDRICKSON, B. p 2372 N95-27436
HENDRICKSON, K. A. p 2174 N95-28315
HENDRIX, A. M. p 2128 N95-28540
HENDRY, S. D. p 2150 N95-27785
HENKEL, C. p 2461 N95-27320
HENMI, TEIZI p 2341 N95-26650
HENN, DOUGLAS S. p 2341 N95-26546
HENRETTY, DEBRA A. p 2153 N95-27801
HENRY, G. p 2393 N95-28393
HENRY, WENDELL A. p 2370 N95-27031
HENSEL, EDWARD p 2275 N95-26751
HENSHALL, G. A. p 2223 N95-28534
HERBERT, JUDITH E. p 2246 N95-27203
HERGENROTHER, PAUL M. p 2235 N95-27732
p 2179 N95-28360
p 2179 N95-28361
HERMAN, R. G. p 2205 N95-27690
HERNANDEZ, BECKY p 2353 N95-26763
HERRMANNSFELDT, W. B. p 2267 N95-28143
HERTEL, E. S., JR. p 2236 N95-27879
HERVE, JEAN-YVES p 2356 N95-26843
HERWIG, LLOYD O. p 2320 N95-27704
HERZIG, HOWARD p 2428 N95-27651
HESSE, MICHAEL p 2432 N95-27673
HESTER, L. R. p 2292 N95-27465
HEYDT, GERALD p 2262 N95-27067
HICKEN, A. p 2365 N95-26611
HICKMAN, GARY L. p 2272 N95-26792
HIDALGO, C. p 2431 N95-27497
HIEB, MICHAEL R. p 2383 N95-27380
HIGGINS, WAYNE p 2334 N95-26423
HIGHTOWER, RICHARD A., III p 2158 N95-27288
HIGO, T. p 2422 N95-28159
HILL, D. N. p 2433 N95-28065
p 2434 N95-28185
HILL, ELIZABETH A. p 2229 N95-27112
HILLIS, D. L. p 2302 N95-27875
p 2434 N95-28185
HILLS, MALINA M. p 2210 N95-27632
HILMES, C. L. p 2123 N95-28230
p 2123 N95-28265
HILTON, MICHAEL R. p 2210 N95-27632
HILVERT, DONALD p 2349 N95-26608
HIMM, J. p 2353 N95-26885
HIND, JOHN S. p 2179 N95-27119
p 2179 N95-27120
HINDMAN, J. C. p 2351 N95-27948
HINKLE, KARRIE p 2160 N95-28258
HINRICHS, SUSAN p 2377 N95-26840
HINRICHSEN, E. N. p 2273 N95-27984
p 2273 N95-27987
HIRAYAMA, Y. p 2441 N95-27720
HIRSCHFELD, D. A. p 2239 N95-28397
HIRTH, J. P. p 2216 N95-27479
HIRVISALO, VESA p 2452 N95-26631
HITNEY, HERBERT V. p 2254 N95-27021
HIXSON, J. p 2170 N95-28298
HJELM, R. P. p 2183 N95-27428
HJELME, DAG R. p 2253 N95-26977
HJERESEN, D. p 2451 N95-28025
HO, P. C. p 2208 N95-27956
HOARD, T. L. p 2205 N95-27680
HOCHBERG, A. K. p 2237 N95-28089
HOCHHEIMER, H. D. p 2224 N95-26470
HOCKER, G. BENJAMIN p 2268 N95-28239
HOEBERLING, R. F. p 2258 N95-28601
HOEFSLOOT, P. CH. p 2247 N95-26344
HOFFMAN, F. O. p 2354 N95-28136
HOFFMAN, JOHN A. p 2322 N95-27979
HOFFMAN, JOYCE A. p 2452 N95-26607
HOFFMAN, PETER M. p 2141 N95-26555
HOGAN, G. G. p 2293 N95-28389
HOGAN, J. T. p 2434 N95-28185
HOGAN, M. O. p 2232 N95-27129
HOGENSON, P. A. p 2160 N95-28258
p 2304 N95-28259
HOLCOMB, FRANKLIN p 2262 N95-27067
HOLDRIDGE, GEOFF p 2263 N95-27226
HOLDRIDGE, GEOFFREY M. p 2475 N95-28038
HOLLOWAY, S. E., III p 2158 N95-27290
HOLMES, A. W. p 2348 N95-28030
HOLMES, H. F. p 2449 N95-27546
HOLMES, S. D. p 2422 N95-28346
HOLT, ALAN C. p 2166 N95-27662
HOLT, J. p 2422 N95-28346
HOLTOM, G. R. p 2446 N95-28242
HOMER, L. D. p 2353 N95-26885
HONDA, Y. p 2441 N95-27720
HONG, S. p 2270 N95-28515
HONG, W. S. p 2234 N95-27472
p 2265 N95-27678
HOOKER, STANFORD B. p 2345 N95-26430
p 2348 N95-28030
HOOPER, R. p 2155 N95-27263
HOPSON, PURNELL, JR. p 2291 N95-27138
HORITA, J. p 2208 N95-27961
HORWATH, EDWARD J. p 2223 N95-28189
HORWATH, JOHN p 2138 N95-27003
HOSKINS, J. W. p 2163 N95-27026
HOSONO, F. p 2222 N95-28167
HOSP, THEODORE J. p 2306 N95-27985
HOSTENY, B. p 2451 N95-28025
HOSTETTER, CARL F. p 2382 N95-27375
HOTCHKISS, R. p 2298 N95-28027
HOTING, S. K. p 2370 N95-27210
HOUCK, JAMES R. p 2290 N95-26702
HOULBERG, CHRISTIAN L. p 2248 N95-26505
HOULBERG, W. A. p 2430 N95-27308
p 2435 N95-28553
HOUSE, LEIGH p 2339 N95-28126
HOUTS, M. G. p 2420 N95-27425
HOVER, G. L. p 2293 N95-28389
HOWARD, A. J. p 2445 N95-28144
p 2267 N95-28146
HOWELL, J. A. p 2379 N95-26443
HOWELL, W. F. p 2170 N95-28296
HOWELLS, W. SPENCER p 2436 N95-26442
HOYER, P. p 2414 N95-28142
HOYT, R. W. p 2358 N95-26558
HREBENAR, KEVIN R. p 2232 N95-27127
HSIEH, CHENG H. p 2213 N95-26862
HSU, ANDREW T. p 2287 N95-27900
HSU, MING-TA S. p 2238 N95-28212
HSUEH, C. H. p 2235 N95-27499
HSUEH, CHUN-HWAY p 2183 N95-28043
HU, H. p 2225 N95-26482
HU, SHOUFENG p 2187 N95-28285
HUANG, D. p 2166 N95-26390
HUANG, JEN-CHIH p 2251 N95-26871
HUANG, S. X. p 2222 N95-28134
HUANG, STEVE p 2118 N95-26943
HUBBARD, BARRY D. p 2452 N95-26758
HUBBARD, H. H. p 2324 N95-27990
HUBER, CARMEN A. p 2180 N95-26686
HUBER, TITO E. p 2180 N95-26686
HUDSON, T. L. p 2273 N95-27987
HUFF, CLIFFORD C. p 2377 N95-27250
HUGGINS, KEVIN E. p 2437 N95-26553
HUGHES, BRENT M. p 2272 N95-26790
HUGHES, MELANIE A. p 2357 N95-27181
HUGO, G. R. p 2135 N95-27523
HUGULEY, HAROLD, III p 2353 N95-26763

HUHTANEN, M. p 2393 N95-28499
HULETT, L. D., JR. p 2410 N95-27874
p 2236 N95-27962
HUNT, H. B., III p 2372 N95-27849
HUNT, J. E. p 2351 N95-27948
HUNT, W. D. p 2249 N95-26708
HUNTON, DON E. p 2210 N95-27630
HUNTON, DONALD p 2210 N95-27631
HUNTON, DONALD E. p 2211 N95-27645
HUPP, JOSEPH T. p 2403 N95-26491
HURD, A. J. p 2237 N95-28090
p 2240 N95-28404
HURFORD, JOEL F. p 2264 N95-27294
HURLBURT, HARLEY E. p 2345 N95-26406
HURLEY, J. A. p 2176 N95-28324
p 2177 N95-28325
HURLEY, MICHAEL p 2156 N95-27268
HUSEINI, H. p 2439 N95-27201
HUSH, D. R. p 2456 N95-28631
HUSSAIN, FAZLE p 2277 N95-26998
HUTCHENS, D. E. p 2165 N95-27124
HUTCHINSON, WAYNE p 2398 N95-26598
HWANG, SOON MUK p 2206 N95-27695
HYER, M. W. p 2166 N95-28292
p 2190 N95-28428
HYOETYNIEMI, HEIKKI p 2379 N95-26449

I

IANDOLO, JOHN J. p 2348 N95-26435
IBRAGIMOVA, E. M. p 2442 N95-27950
IBRAHIM, MOUNIR p 2282 N95-27360
ICHIKAWA, MASAAKI p 2145 N95-27667
ICHIKAWA, S. p 2442 N95-27959
IGLESIAS, C. A. p 2434 N95-28141
IIDA, J. p 2440 N95-27487
IKEUCHI, KATSUSHI p 2424 N95-26900
IKEZI, H. p 2431 N95-27441
ILCEWICZ, L. p 2194 N95-28464
ILCEWICZ, L. B. p 2137 N95-28471
p 2137 N95-28473
p 2138 N95-28482
IMAI, M. p 2234 N95-27486
IMAN, R. p 2329 N95-27878
IMRE, D. G. p 2331 N95-28121
IMRICH, K. J. p 2215 N95-27328
IMTHURN, G. p 2438 N95-27040
ING, J. L. p 2238 N95-28358
INGBER, M. S. p 2393 N95-28393
INGEBO, ROBERT D. p 2291 N95-27030
INGEL, R. P. p 2276 N95-26852
INGRAHAM, J. C. p 2338 N95-28061
INMAN, R. V. p 2189 N95-28424
IOLLO, ANGELO p 2389 N95-26672
IRELAND, M. W. p 2228 N95-27108
IRVING, A. D. p 2199 N95-28639
ISAACS, H. S. p 2240 N95-28547
ISAACSON, MICHAEL p 2201 N95-26870
ISHIKAWA, KAZUTOSHI p 2126 N95-26585
ISHIZUKA, N. p 2409 N95-27552
ISONO, T. p 2222 N95-28167
ITA, S. L. p 2340 N95-28583
ITO, JACKSON I. p 2242 N95-26781
ITOH, K. p 2444 N95-28092
ITOH, T. p 2257 N95-28453
ITON, L. E. p 2439 N95-27452
IVELAND, T. p 2219 N95-27934
IWASAKI, AKIHITO p 2128 N95-26525
IWATA, JIRO p 2119 N95-26953
IYENGAR, S. p 2174 N95-28316
IYER, N. C. p 2215 N95-27328
IYER, RAVISHANKAR K. p 2306 N95-27253
IYER, VENKIT p 2279 N95-27257

J

JACCO, J. C. p 2443 N95-28023
JACKSON, ALDEN W. p 2367 N95-26770
JACKSON, ANTHONY C. p 2138 N95-28476
JACKSON, LORNA p 2272 N95-26795
JACKSON, WADE C. p 2197 N95-28479
JACOBS, E. W. p 2324 N95-27991
JACOBS, GREGG A. p 2345 N95-26406
JACOBS, J. K. p 2269 N95-28349
JACOBS, PATRICIA A. p 2352 N95-28519
JACOBSEN, STEPHEN C. p 2268 N95-28239
JACOBSON, M. Z. p 2328 N95-27686
JAEGER, E. F. p 2392 N95-28110
JAGANNATHAN, R. p 2448 N95-27333
JAGGERS, C. H. p 2210 N95-27633
JAIN, A. p 2269 N95-28339
JAIN, AMOLAK C. p 2164 N95-27093
JAKOVLJEVIC, C. p 2392 N95-28012
JALILIAN-MARIAN, J. p 2449 N95-27547
JAMES, G. H. p 2309 N95-27305
JAMMU, VINAY B. p 2302 N95-27373
JANICKI, KRZYSZTOF L. p 2398 N95-26518
JANK, ANDREW C. p 2453 N95-26879
JANOO, VINCENT C. p 2246 N95-26548
JANOWITZ, J. p 2380 N95-26638
JANTZ, STEVEN J. p 2400 N95-28579
JASKIERNY, W. p 2399 N95-27530
JAYAWEERA, SURYA K. p 2357 N95-28176
JAYNE, J. T. p 2328 N95-27743
JEDRZEJUK, HANNA p 2447 N95-26510
JEGLEY, DAWN p 2197 N95-28481
JELETIC, J. p 2151 N95-27790
JENKINS, PHILLIP P. p 2157 N95-27276
JENNINGS, R. p 2299 N95-28219
p 2170 N95-28298
JENNNINGS, DAVID L. p 2254 N95-27079
JENSEN, BRIAN J. p 2235 N95-27732
JENSEN, D. D. p 2177 N95-28325
JENSEN, G. A. p 2163 N95-27026
JENSEN, J. P. p 2204 N95-27451
JENSEN, T. H. p 2433 N95-28106
JENTOFF-NILSEN, K. p 2442 N95-27959
JESKE, JAMES A. p 2127 N95-26587
JESSE, LISA p 2382 N95-27376
JEWELL, DANIEL W. p 2277 N95-26986
JIA, J. p 2184 N95-28145
JIAN, ZHANG p 2260 N95-26646
JIANG, BO-NAN p 2391 N95-27726
JIANG, Q. p 2439 N95-27413
JING, T. p 2265 N95-27678
JIRKA, I. p 2205 N95-27690
JOCHEM, TODD M. p 2356 N95-27013
JOHNSON, A. B., JR. p 2222 N95-28129
JOHNSON, A. F. p 2308 N95-26749
JOHNSON, BONNIE L. p 2119 N95-26954
JOHNSON, ERIC R. p 2310 N95-27865
JOHNSON, F. T. p 2123 N95-28230
p 2123 N95-28265
JOHNSON, GREGORY S. p 2387 N95-28545
JOHNSON, JERRY p 2138 N95-28480
JOHNSON, K. I. p 2222 N95-28163
JOHNSON, KEN p 2154 N95-27264
JOHNSON, LINDA p 2428 N95-27652
JOHNSON, MACDONALD B. p 2170 N95-28297
JOHNSON, MIKE p 2175 N95-28320
p 2176 N95-28322
JOHNSON, NORMAN L. p 2203 N95-27437
JOHNSON, R. P. p 2297 N95-27850
JOHNSON, R. W. p 2433 N95-28106
JOHNSON, S. R. p 2447 N95-28541
JOHNSTON, BEN p 2360 N95-27164
JOHNSTON, D. C. p 2442 N95-27932
p 2443 N95-28060
JOHNSTON, NORMAN J. p 2196 N95-28475
JOHNSTONE, J. A. p 2422 N95-28346
JOKILAAKSO, A. p 2224 N95-28644
JONES-MEEHAN, JOAN p 2179 N95-27119
p 2179 N95-27120
JONES, CHARLES A. p 2377 N95-27183
JONES, D. C. p 2421 N95-27735
JONES, F. K. p 2346 N95-26477
JONES, JAMES L., JR. p 2463 N95-27668
JONES, JESSE p 2127 N95-27903
JONES, L. T. p 2241 N95-28661
JONES, LEONIDAS J. p 2223 N95-28332
JONES, LISA E. p 2192 N95-28439
JONES, MICHAEL G. p 2400 N95-26394
JONES, N. L. p 2372 N95-27495
JONES, P. D. p 2331 N95-28157
JONES, R. G. p 2256 N95-27840
JONES, R. H. p 2216 N95-27479
JONES, ROBERT L., III p 2366 N95-26685
JONES, T. E. p 2358 N95-26558
JONES, WILLIAM K. p 2271 N95-28613
JONES, WILLIAM R. p 2179 N95-27119
JONES, WILLIAM R., JR. p 2164 N95-27761
JORDAN, STUART D. p 2458 N95-27068
JOSHI, SURESH M. p 2161 N95-26428
JOSLIN, D. L. p 2221 N95-28082
JOST, G. S. p 2136 N95-27918
JOVANOVIC, P. p 2423 N95-28452
JOYNER, MICHAEL J. p 2352 N95-26680
JUDAY, RICHARD D. p 2427 N95-28384
JUHASZ, ALBERT J. p 2283 N95-27369
JUMPER, STEPHEN J. p 2400 N95-26392
JUNLIN, QIU p 2300 N95-28650
JUSKO, J. p 2228 N95-27107

K

KAARIAINEN, JUSSI p 2338 N95-27995
KACKLEY, RUSSELL p 2155 N95-27266
KAHN, JON B. p 2165 N95-27842
KAHN, S. p 2269 N95-28339
KAISER, D. P. p 2343 N95-27920
KAKUTA, YOSHIAKI p 2307 N95-26521
p 2180 N95-26667
KALANOV, M. O. p 2442 N95-27950
KALINNIKOV, V. A. p 2419 N95-27161
KALVAITIS, ALGIS N. p 2247 N95-27909
KAMEL, M. N. p 2453 N95-27014
KAMENETZKY, R. R. p 2428 N95-27646
KAMENETZKY, RACHEL R. p 2419 N95-27637
p 2242 N95-27638
p 2242 N95-27639
p 2210 N95-27641
KAMON, TERUKI p 2407 N95-27430
KAN, HAN-PIN p 2190 N95-28429
p 2192 N95-28441
KANE, RICHARD p 2246 N95-27203
KANEKO, H. p 2419 N95-26584
KANG, GEORGE S. p 2248 N95-26349
KANG, KI HO p 2141 N95-26957
KANNER, G. S. p 2447 N95-28541
KANNO, M. p 2419 N95-26584
KAO, C. C. p 2422 N95-28195
KAPLAN, MICHAEL L. p 2335 N95-26592
KAPLAN, S. N. p 2265 N95-27678
KAPLAN, SIMON p 2371 N95-27252
KAPOOR, C. p 2155 N95-27263
KAPPELER, T. p 2393 N95-28611
KARAKHANYAN, D. R. p 2397 N95-27344
KARAMOUZIS, STAMOS T. p 2386 N95-27395
KARATZAS, IOANNIS p 2395 N95-28526
KARHU, S. p 2252 N95-26908
KARJALAINEN, M. p 2257 N95-28450
KARKKAINEN, L. p 2409 N95-27552
KARL, T. R. p 2343 N95-27920
KARNS, JAMES J. p 2159 N95-26398
p 2159 N95-26399
p 2160 N95-26400
p 2160 N95-26401
p 2160 N95-26403
KARPALA, F. p 2125 N95-26527
KARR, T. J. p 2399 N95-28109
KASSAPOGLOU, CHRISTOS p 2185 N95-28270
KASSEL, PHILIP C., JR. p 2463 N95-27668
KATANO, S. p 2440 N95-27487
KATEHI, LINDA p 2257 N95-28513
KATNIK, GREGORY N. p 2160 N95-27238
KATRAGADDA, PRASANNA p 2259 N95-26550
KATSOULEAS, T. p 2436 N95-28668
KATULINA, S. L. p 2416 N95-28252
KATZ, J. J. p 2351 N95-27948
KAUFMAN, LLOYD p 2355 N95-26692
KAUTZ, E. p 2186 N95-28279
KAUTZ, EDWARD p 2190 N95-28429
KAVARNOS, GEORGE J. p 2241 N95-28574
KAXIRAS, EFTHIMIOS p 2405 N95-27017
KAYLOE, JORDAN R. p 2368 N95-26895
KEARNS, EDWARD P., III p 2246 N95-26722
KEAT, J. p 2150 N95-27783
KEE, PATRICK D. p 2404 N95-26979
KEEBLE, D. J. p 2445 N95-28165
KEEN, JILL M. p 2165 N95-27124
KEENER, DAVID N. p 2167 N95-26880
KEILLOR, MARTIN E. p 2406 N95-27399
KEISER, J. R. p 2217 N95-27544
KELDER, H. p 2330 N95-27954
KELEMEN, LORETTA A. p 2163 N95-26987
KELKAR, ATUL G. p 2161 N95-26428
KELLER, JOHN R. p 2281 N95-27350
KELLER, VERNON p 2166 N95-27665
KELLEY, N. D. p 2319 N95-27459
p 2324 N95-27991
KELLEY, PAUL R. p 2271 N95-28613
KELLY, KATHRYN A. p 2315 N95-28392
KELLY, MICHAEL J. p 2263 N95-27226
KELLY, P. B. p 2297 N95-27841
KELLY, P. M. p 2456 N95-28631
KELLY, R. G. p 2213 N95-27032
KEMP, WILLIAM T. p 2428 N95-27654
KENNEDY, EDWARD J. p 2249 N95-26564
KENNEDY, M. p 2392 N95-27742
KENT, J. A. p 2138 N95-28489
KENT, M. S. p 2239 N95-28400
KERN, S. p 2437 N95-26756
KERSLAKE, THOMAS W. p 2169 N95-28036
KESER, MILAN p 2437 N95-26553
KESSELMAN, CARL p 2378 N95-27741
KESTLER, JAMES p 2152 N95-27796
KETCHUM, ELEANOR p 2150 N95-27782
p 2152 N95-27795
KETTNER, CH. p 2463 N95-28357
KEY, J. F. p 2246 N95-27404
KEYSER, M. A. p 2327 N95-27540
KHALEEL, M. A. p 2222 N95-28163
KHAN, L. A. p 2390 N95-27331
KHAN, M. A. p 2390 N95-27302
p 2390 N95-27330

KHODADOUST, ABDOLLAH p 2125 N95-27762
KHOSIA, PRADEEP K. p 2359 N95-26884
KHRIPLOVICH, I. B. p 2407 N95-27411
p 2407 N95-27412
KIDNER, R. E. p 2455 N95-27949
KIEL, JOHNATHAN L. p 2354 N95-27059
KIIRAS, J. p 2246 N95-27048
KILIAN, JOHN P. p 2354 N95-27059
KILIN, S. YA. p 2416 N95-28251
KIM, A. p 2460 N95-28197
KIM, H. J. p 2186 N95-28282
KIM, K. J. p 2420 N95-27470
p 2296 N95-27674
p 2297 N95-27737
KIM, KWANG-JE p 2298 N95-28104
KIM, M. p 2460 N95-28197
KIM, S. E. p 2286 N95-27893
KIM, SEYONG p 2449 N95-27448
KINARD, WILLIAM H. p 2145 N95-27657
p 2166 N95-27665
p 2463 N95-27668
KINDLE, JOHN C. p 2345 N95-26406
KING, ELIZABETH A. p 2165 N95-27104
KING, JEAN E. p 2452 N95-26721
KING, S. p 2446 N95-28327
KING, S. M. p 2375 N95-28658
KINKEAD, E. R. p 2175 N95-28318
KINKEAD, J. p 2325 N95-28396
KIPP, M. E. p 2299 N95-28223
KIRBY, JAMES, JR. p 2368 N95-26903
KIRIS, CETIN p 2275 N95-26766
KIRK, M. A. p 2442 N95-27950
KIRSCH, BARRY J. p 2248 N95-26356
KIRSCHBAUM, ANDREW R. p 2160 N95-26634
KIRYK, ROMUALD p 2212 N95-26512
p 2213 N95-26838
KISER, CAROL C. p 2457 N95-27660
KISH, BRIAN A. p 2130 N95-26844
KISS, G. p 2325 N95-28396
KISSINGER, B. A. p 2454 N95-27483
KIVINEN, K. p 2252 N95-26929
KLEIN, H. p 2404 N95-26748
KLEIN, VLADISLAV p 2142 N95-27839
KLEINMAN, LEONID S. p 2282 N95-27358
p 2283 N95-27365
KLEMBERG-SAPIEHA, J. E. p 2242 N95-27669
KLEMM, KARL p 2428 N95-27652
KLIER, K. p 2205 N95-27690
KLINGEL, E. J. p 2230 N95-27118
KLINKER, JAMES ERIC p 2379 N95-26421
KLOPFER, GOETZ H. p 2143 N95-26775
KLOTZ, STEPHEN P. p 2274 N95-26589
KLUEH, R. L. p 2217 N95-27544
KNACKE, ROGER F. p 2462 N95-28222
KNICKELBEIN, M. B. p 2218 N95-27752
KNIERIM, JAMES J. p 2350 N95-26761
p 2350 N95-27100
KNIGHT, N. F., JR. p 2191 N95-28433
KNIGHT, ROBIN p 2152 N95-27793
KNOPS, H. A. J. p 2137 N95-28636
KNOPS, Y. M. M. p 2418 N95-28638
KO, CHING L. p 2281 N95-27352
KOBA, V. p 2233 N95-27163
KOBAYASHI, R. p 2396 N95-27300
KOBERSTEIN, JEFFREY T. p 2240 N95-28457
KOC, C. K. p 2380 N95-26468
KOIVISTO, PAEIVI K p 2248 N95-26450
KOLAWA, A. p 2365 N95-26611
KOLB, C. E. p 2328 N95-27743
KOMURO, TOMOYUKI p 2139 N95-26600
KONDOH, Y. p 2432 N95-27870
KONDRATYEVA, YELENA p 2334 N95-26423
KONNERT, J. H. p 2295 N95-26996
KONNOFF, DANIEL A. p 2345 N95-26430
KOO, L. S. p 2264 N95-27403
KOONS, H. C. p 2162 N95-26902
KOONTZ, STEVEN p 2211 N95-27645
KOONTZ, STEVEN L. p 2210 N95-27630
p 2210 N95-27631
KOPPERSMITH, JAMES R. p 2150 N95-27782
KORDESCH, MARTIN E. p 2447 N95-28618
KORHONEN, M. p 2331 N95-28202
KORMICKI, J. p 2442 N95-27959
KORNEEVA, O. p 2233 N95-27163
KORY, CAROL L. p 2371 N95-27370
KOSAK, COREY p 2377 N95-26840
KOSEVICH, Y. A. p 2447 N95-28608
KOSOWER, D. A p 2449 N95-28160
KOSTOFF, J. L. p 2147 N95-27769
KOTAS, J. F. p 2316 N95-26393
KOURTIDES, DEMETRIUS A. p 2166 N95-28293
p 2293 N95-28345
KOUTNY, M. p 2375 N95-28645
KOWALEWSKI, ZBIGNIEW L. p 2211 N95-26359
p 2212 N95-26666
KOWALEWSKI, ZBNIGNIEW L. p 2212 N95-26517
KOZMA, MATTHEW A. p 2295 N95-27022
KRAFT, ROBERT E. p 2402 N95-28073
KRAJNAK, MIKE p 2382 N95-27376
KRAKOWSKI, R. A. p 2420 N95-27494
p 2328 N95-27686
KRAL, LINDA D. p 2285 N95-27886
KRAMER, RICHARD D. p 2316 N95-26762
KRANTZ, TIMOTHY L. p 2302 N95-27855
KRASKO, GENRICH L. p 2399 N95-27398
KRAUSE, H. F. p 2417 N95-28595
KRAUSER, W. J. p 2430 N95-27327
KREH, BRET B. p 2319 N95-26891
KRENZ, W. C. p 2376 N95-27383
KRISCH, M. p 2422 N95-28195
KRISHNAN, A. p 2445 N95-28165
KRISHNAN, K. M. p 2441 N95-27720
KRISTALINSKI, A. p 2399 N95-27530
KRISTIANSEN, E. p 2379 N95-28093
KROEGER, D. M. p 2444 N95-28079
p 2447 N95-28606
KRONBERG, F. p 2385 N95-27393
KRONENBERG, AMY p 2351 N95-28177
KROTKOV, ERIC p 2395 N95-27417
KRUCHOWY, ROMAN p 2400 N95-26502
p 2245 N95-26508
KRUEGER, A. J. p 2341 N95-26689
KRUG, PHYLLIS p 2453 N95-27004
KRUKONIS, V. p 2229 N95-27111
KRUSE, NANCY M. H. p 2291 N95-27138
KRUSE, SCOT p 2120 N95-26955
KRUSEMAN, A. C. p 2340 N95-26343
KU, JENTUNG p 2281 N95-27349
KUBIAK, C. P. p 2204 N95-27458
KUBIAK, G. D. p 2299 N95-28223
KUBO, K. p 2422 N95-28159
KUBOTA, S. p 2432 N95-27869
p 2432 N95-27870
KUBOTA, SHIGEYUKI p 2297 N95-27868
KUBZDELA, HENRYK p 2250 N95-26835
KUDER, STEVE p 2313 N95-26476
KUDOU, KENJI p 2139 N95-26600
KUDRIMOTI, HEMANT S. p 2350 N95-26761
p 2350 N95-27100
KUEHNER, D. E. p 2209 N95-28229
KUENY, C. S. p 2429 N95-27084
KUHN, K. J. p 2425 N95-27734
KUKOWSKI, JOHN p 2263 N95-27226
KUKOWSKI, JOHN A. p 2263 N95-27231
KULKARNI, SARANG p 2259 N95-26550
KULLERD, SUSAN M. p 2195 N95-28469
p 2137 N95-28470
KUMAR, M. LALITH p 2232 N95-27126
KUMAR, P. p 2158 N95-27283
KUMAR, PUNEET p 2363 N95-26469
p 2452 N95-26752
KUMAR, S. p 2395 N95-27684
KUMAR, VIJAY p 2403 N95-26437
KUMMEL, ANDREW C. p 2404 N95-26574
KUNG, HARRIET p 2217 N95-27555
KUNKEL, KENNETH E. p 2338 N95-28114
KUNZ, STEVEN E. p 2126 N95-28454
KUPIEC, S. p 2368 N95-26881
KURIANSKI, ADAM p 2374 N95-28566
KURNIT, N. A. p 2297 N95-27718
KURNIT, NORMAN A. p 2297 N95-27736
KURTZ, S. R. p 2446 N95-28399
KURVONEN, LAURI p 2313 N95-26645
KUSTRA, TODD W. p 2353 N95-26763
KUTEN, S. A. p 2411 N95-27930
KWA, TECK-SENG p 2194 N95-28465
KWEI, G. H. p 2439 N95-27429
KWIATKOWSKI, STEPHEN L. p 2253 N95-26977
p 2427 N95-28524
KWOK, HOI p 2272 N95-27635
KWON, Y. W. p 2308 N95-26625
KYLLING, A. p 2330 N95-27954

L

LAAKSO, T. I. p 2257 N95-28450
LABOMBARD, B. p 2432 N95-27688
LADD, JOHN A. p 2285 N95-27886
LADERA, C. L. p 2425 N95-27482
p 2298 N95-27969
p 2299 N95-28219
p 2299 N95-28220
p 2300 N95-28549
LADOUS, CONSTANZE p 2458 N95-27068
p 2458 N95-27069
p 2458 N95-27070
p 2459 N95-27071
LADVANSZKY, J. p 2262 N95-27050
LAEHEPELTO, M. p 2269 N95-28448
LAFE, O. p 2283 N95-27361
LAGACE, PAUL A. p 2191 N95-28431
LAI, S. K. p 2218 N95-27757
p 2220 N95-28039
p 2241 N95-28609
LAI, YONG G. p 2286 N95-27894
LAINE, U. K. p 2257 N95-28450
LAK, TIBOR p 2450 N95-28260
LAKE, MARK S. p 2144 N95-26426
p 2188 N95-28290
LAKE, MAX p 2199 N95-27636
LAKES, R. S. p 2195 N95-28472
LAL, R. B. p 2443 N95-28033
LALA, P. K. p 2261 N95-27002
LALL, UPMANU p 2326 N95-26429
LAM, QUANG p 2148 N95-27772
LAMB, P. J. p 2344 N95-28340
LAMBERT, JAMES L. p 2426 N95-27843
LAMBOOY, PETER J. p 2155 N95-27262
LAMELAS, F. J. p 2215 N95-27462
LAMPIO, P. p 2369 N95-26907
LAMPSON, ALAN I. p 2177 N95-26434
LAN, E. p 2418 N95-27634
LANDIS, GEOFFREY A. p 2157 N95-27276
LANDRUM, JERRY p 2313 N95-26476
LANE, MARC S. p 2213 N95-26862
LANGE, C. H. p 2395 N95-27684
LANGE, F. F. p 2181 N95-26847
LANGHALS, TAMMY p 2125 N95-27762
LARIMER, JAMES p 2369 N95-26930
LARSON, VICKIE L. p 2126 N95-27859
LASASSE, ROBERT R. p 2268 N95-28200
LASH, THOMAS J. p 2211 N95-27658
LASNIER, C. J. p 2433 N95-28065
LATH, A. p 2414 N95-28158
LAU, S. K. p 2221 N95-28075
LAUGHON, G. J. p 2302 N95-27875
LAVENDER, C. A. p 2222 N95-28163
LAW, CHUNG K. p 2466 N95-26604
LAW, G. E. p 2197 N95-28483
LAW, KINNCHO H. p 2307 N95-26547
LAWRENCE, R. J. p 2388 N95-26516
LAWSON, A. C. p 2439 N95-27429
LAWSON, JOHN R. p 2255 N95-27249
LAXSON, A. p 2325 N95-28395
LAZARUS, A. J. p 2338 N95-28061
LE, THANG p 2159 N95-27291
LEADER, D. H. p 2215 N95-27328
LEAHY, R. M. p 2354 N95-27426
LEAR, K. L. p 2299 N95-28132
p 2267 N95-28147
LEBEDEV, V. B. p 2430 N95-27306
LEBOEUF, J. N. p 2431 N95-27419
p 2431 N95-27537
LEBONHEUR, VASSOU p 2437 N95-26553
p 2226 N95-26627
LEBRUN, T. p 2442 N95-27963
LECHA, JAVIER p 2157 N95-27279
LEE, CHI H. p 2260 N95-26690
LEE, CHRISTOPHER p 2301 N95-27098
LEE, CHRISTOPHER A. p 2129 N95-26651
LEE, D. p 2413 N95-28066
LEE, D. W. p 2361 N95-28659
LEE, DAVID p 2360 N95-27164
LEE, GILBERT F. p 2210 N95-28584
LEE, H. p 2265 N95-27678
LEE, HENRY p 2270 N95-28544
LEE, ILZOO p 2294 N95-26503
LEE, J. p 2332 N95-28602
LEE, JUHNYOUNG p 2455 N95-27847
LEE, M. p 2422 N95-28122
LEE, M. F. p 2128 N95-26389
LEE, MARTIN E. p 2341 N95-26650
LEE, MICHAEL p 2149 N95-27779
LEE, MICHAEL J. p 2247 N95-27909
LEE, RICHARD Q. p 2266 N95-27853
LEE, S. p 2135 N95-27524
LEE, T. p 2146 N95-27764
p 2147 N95-27768
LEE, Y. K. p 2241 N95-28592
LEEMANS, W. p 2296 N95-27674
LEFEBVRE, ALAIN p 2166 N95-27390
LEGAL, J. L. p 2283 N95-27363
LEGER, LUBERT p 2211 N95-27645
LEGER, LUBERT J. p 2210 N95-27630
p 2210 N95-27631
LEHTO, OLLI p 2397 N95-28238
LEIGH, JAMES E. p 2120 N95-26955
LEMIRE, GEORGE W. p 2174 N95-28314
LEMPINEN, A. p 2388 N95-26495
LENERTZ, JOSEPH L. p 2167 N95-27153
LENZ, ROBERT W. p 2235 N95-27694
LEONARD, ANDREW D. p 2286 N95-27892
LEONARD, T. p 2433 N95-28065
LEOS, MELISSA J. p 2356 N95-27012
LEOUTSAKOS, THEODORE p 2149 N95-27780
LESTER, CHARLES S. p 2296 N95-27672
LEUNG, K. P. p 2315 N95-28520

LEV, F. M. .... p 2415 N95-28245
LEVASSEUR, LEONARD A. .... p 2361 N95-28390
LEVI, C. G. .... p 2181 N95-26847
LEVINE, ARLENE S. .... p 2466 N95-27629
p 2145 N95-27657
p 2457 N95-27659
p 2457 N95-27660
LEVOY, NANCY F. .... p 2181 N95-26848
LEVY, SAMUEL C. .... p 2268 N95-28200
LEWICKI, DAVID G. .... p 2302 N95-27373
LEWIS, CHRISTOPHER H. .... p 2302 N95-27844
LEWIS, GEORGE D. .... p 2151 N95-27787
LEWIS, JAMES A. .... p 2361 N95-28667
LEWIS, M. .... p 2385 N95-27393
LEWIS, M. J. .... p 2378 N95-27402
LEWIS, MICHAEL W. .... p 2229 N95-27109
LEWIS, P. S. .... p 2354 N95-27426
LI, DEHUAI .... p 2365 N95-26575
LI, DONGQI .... p 2436 N95-26440
LI, HUAXIN .... p 2216 N95-27479
LI, LI-SHENG .... p 2437 N95-26553
LI, NING .... p 2250 N95-26717
LI, WEI .... p 2310 N95-28031
p 2310 N95-28032
LI, WEI-GANG .... p 2437 N95-26780
LIANG, RANTY H. .... p 2211 N95-27644
LIANG, WENCHUAN .... p 2409 N95-27744
LIANG, Y. M. .... p 2430 N95-27306
LIAW, B. M. .... p 2180 N95-26626
LIBERATORE, FEDERICO .... p 2201 N95-26678
LIBESKIND, M. .... p 2192 N95-28438
LIBRESCU, L. .... p 2191 N95-28435
LICHTEN, S. .... p 2151 N95-27792
LICHTENWALNER, J. .... p 2270 N95-28515
LIEDAHL, D. A. .... p 2462 N95-28013
LIEWER, P. C. .... p 2433 N95-27924
LIGETI, Z. .... p 2407 N95-27409
LIKHACHEV, G. G. .... p 2416 N95-28249
LILLO, W. E. .... p 2384 N95-27387
LIN-LIU, Y. -R. .... p 2431 N95-27441
LIN-LIU, Y. R. .... p 2416 N95-28329
LIN, H. T. .... p 2235 N95-27499
LIN, HSI HSIANG .... p 2302 N95-27698
LIN, HUI .... p 2220 N95-28046
LIN, X. A. .... p 2282 N95-27359
LIN, YUH-LANG .... p 2335 N95-26592
LINCOURT, TIMOTHY J. .... p 2356 N95-27012
LINDELL, I. V. .... p 2252 N95-26914
p 2256 N95-28354
LINDEN, JOHAN .... p 2437 N95-26513
LINDLEY, CRAIG A. .... p 2166 N95-27377
LINK, H. .... p 2325 N95-28395
LINTHICUM, K. .... p 2437 N95-26756
LINTON, ROGER C. .... p 2419 N95-27637
p 2242 N95-27638
p 2242 N95-27639
p 2210 N95-27641
p 2428 N95-27646
LIOU, CHUEN-HUEI .... p 2302 N95-27698
LIPO, T. A. .... p 2273 N95-27987
p 2273 N95-27988
LIPSCHULTZ, B. .... p 2432 N95-27688
LIPSKIN, BETH ANN .... p 2144 N95-26583
LISSUAER, DAVID .... p 2292 N95-27738
LITTENBERG, L. .... p 2416 N95-28338
LITTLEFIELD, MARCIA D. .... p 2231 N95-27121
LIU, C. T. .... p 2215 N95-27463
p 2221 N95-28082
LIU, HUA-KUANG .... p 2427 N95-28363
LIU, JONATHAN .... p 2159 N95-27291
LIU, MING-CHENG .... p 2150 N95-27784
LLORENTE, STEVEN .... p 2191 N95-28432
LO, JIEN-CHUNG .... p 2256 N95-28391
LOBITZ, DON W. .... p 2312 N95-27980
LOCKHART, RONALD .... p 2127 N95-27903
LOEHMAN, R. E. .... p 2420 N95-27480
p 2184 N95-28145
LOEKBERG, O. J. .... p 2294 N95-28651
LOHE, M. A. .... p 2397 N95-28234
LOHRENZ, MAURA C. .... p 2314 N95-26682
LOMAX, CURTIS .... p 2304 N95-28256
LONEY, PATRICK .... p 2282 N95-27360
LONG, MARK .... p 2154 N95-27264
LONGA, L. .... p 2441 N95-27740
LOONG, C. K. .... p 2439 N95-27452
p 2237 N95-27967
LORAH, J. M. .... p 2147 N95-27768
LORENS, J. B. .... p 2172 N95-28307
LORENZ, B. .... p 2224 N95-26470
LORENZINI, ENRICO C. .... p 2165 N95-27836
LORENZO, J. E. .... p 2439 N95-27443
LOSEE, L. A. .... p 2174 N95-28315
LOTTS, C. G. .... p 2194 N95-28468
LOUER, JOHN W., III .... p 2342 N95-27148
LOUIE, STEVEN G. .... p 2425 N95-27539
LOUIS, STEVEN .... p 2361 N95-26845
LOUTHAN, M. R., JR. .... p 2215 N95-27328
LOVEJOY, M. L. .... p 2445 N95-28144
p 2267 N95-28147
LOVESEY, S. W. .... p 2418 N95-28641
p 2418 N95-28642
LOW, K. S. .... p 2299 N95-28330
LOWERY, ERIC .... p 2272 N95-26791
LOY, DOUGLAS A. .... p 2240 N95-28531
p 2240 N95-28532
LOYD, B. .... p 2325 N95-27992
LOZANO, G. .... p 2448 N95-27312
LU, SHIN-YEE .... p 2357 N95-28176
LU, TINA .... p 2304 N95-28259
LUBE, MICHAEL S. .... p 2223 N95-28332
LUBIN, JEFFREY .... p 2369 N95-26930
LUBY, STEVEN .... p 2184 N95-28269
LUCAS, G. E. .... p 2214 N95-27086
LUCK, ROGELIO .... p 2281 N95-27353
LUDWIG, GERSON OTTO .... p 2435 N95-28562
LUE, J. W. .... p 2267 N95-28048
LUECK, DALE .... p 2173 N95-28309
LUECK, DALE E. .... p 2173 N95-28310
p 2174 N95-28312
LUGAR, R. M. .... p 2331 N95-28149
LUHMANN, H. J. .... p 2157 N95-27281
LUKASZEK, W. .... p 2440 N95-27471
LUKASZEK, WES .... p 2440 N95-27538
LUKE, T. C. T. .... p 2411 N95-28020
LUKEMIRE, ALAN T. .... p 2269 N95-28341
LUKIERSKI, J. .... p 2448 N95-27332
LUMLEY, J. L. .... p 2286 N95-27898
LUMME, K. A. .... p 2256 N95-28354
LUNG, C. W. .... p 2219 N95-27759
LUO, XIN .... p 2209 N95-28088
LUPILTSEV, V. P. .... p 2441 N95-27867
LURIE, CHUCK .... p 2272 N95-26795
LURIE, PHILIP M. .... p 2393 N95-26347
LUTHER, HOLGER .... p 2156 N95-27270
LYMAN, P. F. .... p 2208 N95-27965
LYNCH, DAVID K. .... p 2342 N95-26899
LYNCH, E. D. .... p 2286 N95-27891
LYNCH, V. E. .... p 2431 N95-27536
p 2431 N95-27537
LYNN, K. G. .... p 2217 N95-27553
p 2236 N95-27962
p 2445 N95-28165
LYON, J. F. .... p 2431 N95-27498
LYUBOSHITS, V. L. .... p 2415 N95-28248

M

MAAG, C. .... p 2294 N95-27670
MACDONALD, M. A. .... p 2442 N95-27963
MACEK, R. W. .... p 2182 N95-27421
MACHACEK, O. .... p 2176 N95-28321
MADAN, RAM C. .... p 2137 N95-28470
MADAVAN, NATERI K. .... p 2275 N95-26776
MADDALON, JEFFREY M. .... p 2362 N95-27241
MADDOCKS, M. C. D. .... p 2248 N95-26493
MADIGOSKY, WALTER .... p 2210 N95-28585
MADSEN, OLE S. .... p 2346 N95-26904
MAESTAS, L. M. .... p 2221 N95-28116
MAESTRELLO, L. .... p 2279 N95-27179
p 2289 N95-28673
MAETHNER, SCOTT R. .... p 2162 N95-26850
MAGEE, CONSTANCE .... p 2185 N95-28272
MAGGIO, GASPARE .... p 2159 N95-26398
p 2159 N95-26399
p 2160 N95-26400
p 2160 N95-26401
p 2160 N95-26403
MAGGIORE, C. J. .... p 2443 N95-28023
MAGHAMI, PEIMAN G. .... p 2161 N95-26428
MAGRUDER, R. H., III .... p 2237 N95-28080
MAGURANY, CHARLES J. .... p 2180 N95-26764
MAHAJAN, S. M. .... p 2429 N95-26439
MAHDAVI, M. A. .... p 2302 N95-27875
MAHLE, JOHN J. .... p 2405 N95-27034
MAIER, A. .... p 2133 N95-27515
MAIER, A. E. .... p 2134 N95-27517
MAIER, R. S. .... p 2179 N95-26565
MAINGI, R. .... p 2302 N95-27875
MAJOR, R. W. .... p 2268 N95-28156
MAKOWSKI, M. .... p 2434 N95-28140
MALECKI, IGNACY .... p 2401 N95-26519
MALINA, R. F. .... p 2385 N95-27393
MALINSKY, J. .... p 2238 N95-28235
MALITSKY, CHRISTOPHER .... p 2340 N95-26453
MALMO, J. T. .... p 2294 N95-28651
MALVAR, JAVIER .... p 2245 N95-26500
MANCINI, L. V. .... p 2375 N95-28645
MANDELL, D. A. .... p 2236 N95-27943
MANDERSLOOT, WART M. .... p 2155 N95-27262
MANDEVILLE, JEAN-CLAUDE .... p 2211 N95-27648
MANFREDI, P. F. .... p 2269 N95-28244
MANGELS, JOHN .... p 2443 N95-28076
MANI, MORI .... p 2285 N95-27886
MANN, MICHAEL E. .... p 2326 N95-26429
MANSUR, L. K. .... p 2221 N95-28120
MANSUR, M. HOSSEIN .... p 2118 N95-26710
MANTSINEN, M. J. .... p 2435 N95-28654
MANVELYAN, R. P. .... p 2397 N95-27344
MARATHE, M. V. .... p 2372 N95-27849
MARCHBANKS, R. D. .... p 2296 N95-27705
MARCHELLO, JOSEPH M. .... p 2182 N95-27192
p 2236 N95-27857
MARCHETTE, DAVID J. .... p 2394 N95-26413
MARCUS, STEVEN I. .... p 2380 N95-26480
MARGOLIS, B. .... p 2415 N95-28210
MARION, GILES M. .... p 2200 N95-26432
MARKLEY, F. LANDIS .... p 2147 N95-27767
p 2148 N95-27775
p 2149 N95-27780
p 2153 N95-27800
p 2154 N95-27803
MARKOSKY, L. .... p 2417 N95-28495
MARQUES, ANTHONY M. .... p 2271 N95-28613
MARRINER, J. .... p 2422 N95-28346
MARSHALL, DAVID B. .... p 2179 N95-26484
MARSHALL, R. D. .... p 2308 N95-26743
MARSILIO, ROBERT .... p 2287 N95-27917
MARTENS, M. .... p 2422 N95-28346
MARTIN, CHARLES R. .... p 2225 N95-26472
MARTIN, CURTIS A. .... p 2241 N95-28582
MARTIN, L. R. .... p 2332 N95-28623
MARTIN, L. ROBBIN .... p 2172 N95-28305
MARTIN, R. D. .... p 2257 N95-28455
MARTIN, ROBERT C., IV .... p 2381 N95-26920
MARTIN, RUSSEL .... p 2369 N95-26930
MARTINEZ, ANDREW B. .... p 2388 N95-26459
MARTINEZ, M. A. .... p 2234 N95-27460
p 2218 N95-27722
p 2238 N95-28117
MARTINEZ, ROGER I. .... p 2258 N95-28615
MARTINU, L. .... p 2242 N95-27669
MARVRIPLIS, D. J. .... p 2390 N95-27029
MASAMUNE, S. .... p 2432 N95-27870
MASCARENHAS, NELSON D. A. p 2258 N95-28559
MASON, JAMES B. .... p 2242 N95-27655
MASON, JIM .... p 2470 N95-27647
MASON, PAUL A. C. .... p 2148 N95-27774
MASON, T. E. .... p 2413 N95-28066
MASTERS, JOHN E. .... p 2189 N95-28423
MATHISEN, H. M. .... p 2361 N95-28659
MATSUMOTO, R. .... p 2433 N95-28111
MATSUMOTO, SHUICHI .... p 2126 N95-26585
MATSUMOTO, T. .... p 2440 N95-27487
MATSUOKA, A. .... p 2432 N95-27869
p 2432 N95-27870
MATSUOKA, AKIO .... p 2297 N95-27868
MATSUOKA, H. .... p 2234 N95-27486
MATTHEWS, WILLIAM T. .... p 2193 N95-28442
MATVIYENKO, GREGORY .... p 2398 N95-26345
MAUS, DARYL .... p 2155 N95-27267
MAVRIPLIS, D. J. .... p 2278 N95-27027
p 2391 N95-27433
MAVRIPLIS, DIMITRI J. .... p 2124 N95-28674
MAX, N. .... p 2343 N95-28014
MAXEY, L. C. .... p 2427 N95-28552
MAXSON, JEFFREY B. .... p 2178 N95-26569
MAYES, R. L. .... p 2309 N95-27305
MAYFIELD, M. J. .... p 2320 N95-27746
MAYS, BOB .... p 2265 N95-27706
MAZIASZ, P. J. .... p 2221 N95-28120
MAZUMDAR, S. .... p 2294 N95-26568
MCADAMS, S. D. .... p 2220 N95-28044
MCAFFEE, DOUGLAS .... p 2154 N95-27264
MCANINCH, J. E. .... p 2204 N95-27496
MCBRANCH, D. W. .... p 2426 N95-28010
MCCAUGHAN, FRANCES E. .... p 2283 N95-27364
MCCHESNEY, D. .... p 2270 N95-28515
MCCOMAS, D. J. .... p 2337 N95-27848
MCCOMBS, M. .... p 2174 N95-28316
MCCOWN, ANDREW W. .... p 2209 N95-28088
MCCRACKEN, G. .... p 2432 N95-27688
MCCREARY, E. IAIN .... p 2209 N95-28088
MCCUNE, W. .... p 2392 N95-28173
MCDEDE, JAMES B. .... p 2165 N95-27842
MCDERMOTT, VINCENT A. .... p 2178 N95-28154
MCDONACH, ALASTER .... p 2312 N95-28649
MCDONALD, A. E. .... p 2299 N95-28128
MCDONALD, J. P. .... p 2328 N95-27749
MCDONNELL, J. R. .... p 2390 N95-27020
MCELRATH, TIMOTHY P. .... p 2151 N95-27787
MCENTIRE, B. J. .... p 2236 N95-27946
MCERLEAN, DONALD P. .... p 2189 N95-28422
MCEWEN, RON S. .... p 2312 N95-28649
MCFADDEN, RICHARD H. .... p 2159 N95-26398
p 2159 N95-26399
p 2160 N95-26400
p 2160 N95-26401
p 2160 N95-26403

MCGARRY, FRANK p 2374 N95-28627
MCGINNIS, D. p 2422 N95-28346
MCGOVERN, WILLIAM E. p 2229 N95-27114
p 2232 N95-27128
MCGOWN, MONROE Y. p 2249 N95-26564
MCGREEVY, J. L. p 2289 N95-28673
MCGUIRE, WILLIAM E. p 2228 N95-27108
MCHUGH, K. M. p 2246 N95-27404
MCINNES, L. C. p 2378 N95-28071
MCINNIS, LONA A. p 2210 N95-28621
MCINTOSH, R. J. p 2153 N95-27798
MCINTYRE, D. C. p 2221 N95-28116
MCKELLAR, BRUCE p 2415 N95-28246
MCKENNA, H. E. p 2324 N95-27991
MCKENZIE, A. p 2176 N95-28321
MCLERRAN, L. p 2449 N95-27547
MCMAHON, O. B. p 2293 N95-28389
MCMAHON, W. J. p 2157 N95-27278
MCMILLAN, K. p 2370 N95-27095
MCMILLAN, R. W. p 2270 N95-28529
MCMURTREY, JAMES E., III p 2315 N95-28211
MCNAUGHTON, BRUCE L. p 2350 N95-27100
MCNEIL, W. J. p 2339 N95-28575
MCPARTLAND, MICHAEL p 2149 N95-27781
MCPETERS, R. D. p 2341 N95-26689
MCPHAIL, A. T. p 2241 N95-28661
MCPHAIL, ANDREW T. p 2223 N95-28332
MCQUEEN, DONALD H., JR. p 2157 N95-27280
MCQUILLEN, JOHN B. p 2284 N95-27854
MCWILLIAMS, D. L. p 2434 N95-28141
MEADOWS, KRISTINE R. p 2401 N95-27908
MEAKIN, ROBERT L. p 2122 N95-27248
MEANEY, M. p 2155 N95-27263
MEDERNACH, J. W. p 2205 N95-27683
p 2444 N95-28127
MEDVEDEV, M. p 2430 N95-27306
MEDVEDEV, M. YU. p 2348 N95-27996
MEDWIN, STEVEN p 2191 N95-28432
MEGER, ROBERT A. p 2154 N95-26524
MEHRKAM, P. p 2133 N95-27514
MEIER, M. M. p 2338 N95-28061
MEIERAN, EUGENE S. p 2263 N95-27229
MEIERAN, GENE p 2263 N95-27226
MEISSNER, K. E. p 2299 N95-28128
MEISSNER, MIROSLAW p 2400 N95-26358
MEJDANI, R. p 2439 N95-27201
p 2444 N95-28112
MELTON, G. S. p 2231 N95-27121
MELVIN, R. G. p 2123 N95-28230
p 2123 N95-28265
MELVIN, WILLIAM S. p 2177 N95-28326
MENEGHELLI, BARRY p 2173 N95-28310
MENG, MIN p 2171 N95-28299
MENLOVE, H. O. p 2379 N95-26443
MENON, M. M. p 2302 N95-27875
MENON, SARATH K. p 2213 N95-26681
MENON, V. p 2224 N95-26470
MERCER, CAROLYN R. p 2293 N95-28037
MERRICK, VERNON K. p 2127 N95-26587
MERTENS, HENRY W. p 2357 N95-27323
MESHISHNEK, M. J. p 2210 N95-27633
MESKOV, E. E. p 2288 N95-28603
MESMER, R. E. p 2449 N95-27546
p 2208 N95-27960
MESSER, DALE C. p 2231 N95-27122
MESSICK, C. p 2440 N95-27471
MESSICK, CLESTON p 2440 N95-27538
METSCHAN, S. p 2137 N95-28474
METZGER, E. JOSEPH p 2345 N95-26406
METZINGER, R. p 2151 N95-27789
METZKO, JOHN p 2143 N95-26556
MEULEMAN, R. M. p 2343 N95-28236
MEYER, F. W. p 2409 N95-27551
p 2413 N95-28078
MEYERHOFER, DAVID D. p 2297 N95-27736
MEYERS-SCHULTE, KATHLEEN J.
p 2230 N95-27116
MEYERS, JENNIFER G. p 2355 N95-26361
MIAMEE, ABOL G. p 2395 N95-28510
MICHAELS, K. F. p 2327 N95-27540
MICHAL, G. M. p 2218 N95-27728
MICHALAKES, J. p 2327 N95-27457
MICHELOTTI, L. p 2419 N95-27091
MICKELSON, ALAN R. p 2253 N95-26977
p 2427 N95-28524
p 2270 N95-28544
MIGLIONICO, C. p 2154 N95-27671
MIGNERY, L. A. p 2197 N95-28483
MIKHAJLOV, S. V. p 2406 N95-27314
MIKIJELJ, BILIJANA p 2443 N95-28076
MILBURN, NELDA J. p 2357 N95-27323
MILHAM, MERRILL E. p 2250 N95-26759
MILLER, A. C. p 2427 N95-28552
MILLER, A. H. p 2289 N95-27973
MILLER, ANDREA p 2453 N95-26864
MILLER, ANDREW C. p 2178 N95-26569
MILLER, DEAN p 2125 N95-27762
MILLER, G. E. p 2124 N95-27978
MILLER, G. P. p 2418 N95-27634
MILLER, GARY L. p 2376 N95-26529
MILLER, H. VINCENT p 2313 N95-26476
p 2314 N95-26682
MILLER, J. C. p 2296 N95-27550
MILLER, JAMES G. p 2306 N95-28034
MILLER, L. S. p 2118 N95-26943
MILLER, R. p 2422 N95-28159
MILLER, R. D. p 2312 N95-27983
MILLER, R. L. p 2328 N95-27686
p 2433 N95-28106
MILLER, RAYMOND S. p 2276 N95-26821
MILLER, W. H. p 2208 N95-28086
MILLER, WARREN F. p 2390 N95-27304
MILLHOUSE, JOHN K. p 2382 N95-27145
MILLS, DAVID L. p 2367 N95-26770
MILLS, M. J. p 2219 N95-27968
MILORA, S. L. p 2422 N95-28205
MILSTEIN, JAIME p 2376 N95-27388
MILSTEJN, A. I. p 2407 N95-27412
MINECK, RAYMOND E. p 2124 N95-28669
MINENO, HITOSHI p 2126 N95-26585
MINGDE, ZHOU p 2121 N95-26719
MINGUET, PIERRE p 2191 N95-28432
MINI, S. M. p 2206 N95-27755
MINNIE, C. R. p 2146 N95-27765
MINTON, TIMOTHY K. p 2419 N95-27643
p 2211 N95-27644
MIRANDY, L. p 2124 N95-27981
p 2312 N95-27982
MIRESHGHI, A. p 2265 N95-27678
MISLEVY, ROBERT J. p 2306 N95-26927
MISSAGHI, M. p 2286 N95-27893
MITCHELL, C. M. p 2138 N95-28203
MITCHELL, D. H. p 2174 N95-28315
MITCHELL, DONALD p 2156 N95-27270
MITCHELL, RICHARD L. p 2320 N95-27704
MITCHELL, T. E. p 2215 N95-27446
p 2215 N95-27463
p 2219 N95-28026
MITLER, H. E. p 2247 N95-28008
MITYAGIN, B. p 2393 N95-28611
MIZE, CHRISTOPHER D. p 2387 N95-28217
MIZUKAMI, M. p 2283 N95-27362
MKRTCHYAN, R. L. p 2397 N95-27344
MOBLEY, ROBERT L. p 2328 N95-27558
MOCK, KENRICK J. p 2145 N95-27394
MODDEMAN, W. E. p 2206 N95-27750
MODINE, F. A. p 2268 N95-28156
MOEN, KENNON J. p 2359 N95-26863
MOERK, JOHN S. p 2293 N95-28362
MOGILEVTSEV, D. S. p 2416 N95-28251
MOGRO-CAMPERSO, A. p 2272 N95-27635
MOHAMMAD, N. p 2390 N95-27092
MOHAMMED, A. M. p 2351 N95-27254
MOHAMMED, R. M. p 2382 N95-27045
MOLLER, J. M. p 2222 N95-28167
MOLOD, ANDREA p 2334 N95-26423
MOLVIK, GREGORY A. p 2121 N95-26760
MOLZON, ROBERT p 2388 N95-26539
MONCUR, N. K. p 2297 N95-27850
MONGIA, H. p 2285 N95-27889
MONICK, DOUG p 2155 N95-27267
MONTANARI, ANGELO p 2365 N95-26605
MONTECALVO, ANTHONY J. p 2129 N95-26684
MONTGOMERY , TODD p 2363 N95-26388
MONTGOMERY, KENT R. p 2138 N95-28586
MONTGOMERY, TODD p 2366 N95-26695
p 2371 N95-27252
MOODY, N. R. p 2408 N95-27534
MOOK, D. JOSEPH p 2148 N95-27774
p 2149 N95-27781
MOOK, H. A. p 2413 N95-28066
MOOKERJEE, A. p 2223 N95-28250
MOONEY, BRAD p 2247 N95-27909
MOORE, ARNOTT S. p 2354 N95-27059
MOORE, ARTHUR W. p 2199 N95-27636
MOORE, BRUCE p 2272 N95-26789
MOORE, G. V. p 2128 N95-27791
MOORE, K. R. p 2256 N95-27840
p 2337 N95-27848
MOORE, KEVIN A. p 2120 N95-26955
MOORE, R. C. p 2208 N95-27960
MOORE, TERESA A. p 2419 N95-27643
MOORE, TONY p 2452 N95-26607
MORAN, S. G. p 2191 N95-28433
MORAN, TOM p 2156 N95-27274
MORGAN, G. p 2269 N95-28339
MORGAN, L. p 2176 N95-28321
MORGAN, PETER E. p 2179 N95-26484
MORGAN, T. p 2385 N95-27393
MORGILLO, A. p 2270 N95-28515
MORIDIS, G. J. p 2284 N95-27721
MORIN, GILBERT A. p 2258 N95-28573
MORINO, YOSHIKI p 2180 N95-26667
MOROSIN, B. p 2439 N95-27429
MORRIS, PHILIP J. p 2401 N95-26801
MORRIS, W. L. p 2189 N95-28424
MORRISON, D. p 2457 N95-28677
MORRISON, JEFFERY p 2365 N95-26668
MORRISON, JEFFERY L. p 2367 N95-26802
MORRISON, P. J. p 2429 N95-27084
p 2287 N95-28055
MOSES, J. M. p 2229 N95-27114
p 2232 N95-27128
MOSHER, J. C. p 2354 N95-27426
MOSKALENKO, V. A. p 2410 N95-27881
MOSKOWITZ, P. D. p 2320 N95-27682
MOSKOWITZ, PAUL D. p 2325 N95-28517
MOSSEY, ROBERTY p 2144 N95-26583
MOTYLEWSKI, JERZY p 2143 N95-26837
MOUSSA, N. p 2280 N95-27339
MOUSTAFA, M. S. p 2382 N95-27045
MOWERY, ROBERT L. p 2225 N95-26499
MOY, E. p 2229 N95-27111
MROZ, E. J. p 2328 N95-27686
MUCKS, JOHN p 2382 N95-27376
MUELLER, C. M. p 2286 N95-27897
MUELLER, J. L. p 2348 N95-28030
MUELLER, JAMES L. p 2345 N95-26430
MUELLER, T. p 2166 N95-26390
MUENCH, H. S. p 2356 N95-26992
MUENZENMEYER, R. p 2294 N95-27670
MUINONEN, K. p 2256 N95-28354
MULLANEY, JOHN P. p 2370 N95-27037
MULLER, JIM G. p 2230 N95-27118
MULLER, RICHARD S. p 2268 N95-28239
MULLIN, SCOTT A. p 2225 N95-26561
MUMMERT, L. p 2452 N95-26535
MUNDRA, K. p 2215 N95-27319
MUNTER, ALAN E. p 2411 N95-28004
MURADOV, NAZIM Z. p 2171 N95-28300
MURAKAMI, ATSUO p 2139 N95-26600
MURAL, R. J. p 2378 N95-27709
MURATA, MASAAKI p 2126 N95-26585
MURMAN, SCOTT M. p 2121 N95-26735
MURPHY, DIANE R. p 2450 N95-27169
MURPHY, J. p 2293 N95-28389
MURPHY, MARY L. p 2452 N95-26721
MURPHY, P. W. p 2455 N95-28085
MURPHY, T. C. p 2358 N95-26558
MURPHY, TAYLOR J. p 2242 N95-27640
MURRAY, DAVID A. p 2254 N95-27009
MURRAY, W. E. p 2266 N95-27999
MURTHY, P. L. N. p 2309 N95-27174
p 2141 N95-26277
MURTHY, S. N. B. p 2117 N95-26363
MURTY, A. N. p 2205 N95-27680
MUSTICO, ARTHUR p 2428 N95-27653
MYDOSH, J. p 2215 N95-27462
MYER, V. J. p 2454 N95-27461
MYERS, G. p 2256 N95-28407
MYERS, IRA T. p 2264 N95-27374
MYERS, LEMUEL R., JR. p 2353 N95-26917
MYERS, NEIL B. p 2337 N95-27147
MYERS, ROGER M. p 2168 N95-27727
MYERS, S. M. p 2235 N95-27687
p 2444 N95-28127
p 2445 N95-28206
MYERS, WILLIAM NEILL p 2304 N95-28347
MYOSE, ROY Y. p 2119 N95-26953

N

NABER, JEFF D. p 2203 N95-27437
NACHTIGAL, N. M. p 2408 N95-27456
NAGASHIMA, T. p 2434 N95-28140
NAGATA, A. p 2432 N95-27869
p 2432 N95-27870
NAGATSU, M. p 2432 N95-27869
p 2432 N95-27870
NAGATSU, MASAAKI p 2297 N95-27868
NAGODE, J. p 2225 N95-26482
NAGY, KORNEL p 2165 N95-27842
NAIRN, JOHN A. p 2187 N95-28285
NAKAMURA, SHUJI p 2437 N95-26818
NAKAYASU, HIDEHIKO p 2128 N95-26525
NAMKUNG, M. p 2306 N95-26778
NAMSRAI, KH. p 2255 N95-27313
NARAGHI, MOHAMMAD H. N. p 2177 N95-27355
NARAVAN, S. Y. p 2295 N95-26906
NASH, J. K. p 2434 N95-28141
NASRALLAH, M. p 2220 N95-28049
NASSTROM, JOHN S. p 2392 N95-28162
NASTASI, M. p 2444 N95-28125
NASTASI, MICHAEL p 2217 N95-27555
NATANSON, G. p 2147 N95-27770
NATH, S. p 2306 N95-26778
NATZKE, JOHN p 2366 N95-26694

NAZAROV, V. N. .... p 2261 N95-27024
NEAL, DONALD M. .... p 2193 N95-28442
NEALY, JOHN E. .... p 2465 N95-26427
NECATIECEVIT, F. .... p 2292 N95-27711
p 2207 N95-27929
NEGELSPACH, GREG L. .... p 2377 N95-26551
NEGREA, M. .... p 2406 N95-27309
NELSON, J. S. .... p 2219 N95-27958
NELSON, RANDALL J. .... p 2348 N95-26360
NEMANICH, R. J. .... p 2439 N95-27416
NEMANICH, ROBERT J. .... p 2437 N95-26818
p 2237 N95-28097
NEMETH, MICHAEL P. .... p 2190 N95-28430
NERI, LARRY .... p 2190 N95-28429
NERI, LAWRENCE M. .... p 2184 N95-28266
p 2186 N95-28279
p 2189 N95-28420
p 2193 N95-28462
NERREN, P. D. .... p 2272 N95-27635
NESVISZSKY, G. .... p 2136 N95-28409
NEUMANN, ERIC S. .... p 2284 N95-27854
NEVANLINNA, O. .... p 2393 N95-28653
NEVINS, W. M. .... p 2434 N95-28138
p 2435 N95-28553
NEVMERZHITSKII, N. V. .... p 2288 N95-28603
NEWCOMER, P. .... p 2202 N95-27136
p 2202 N95-27137
NEWMAN-HOLMES, C. .... p 2421 N95-28107
NEWMAN, D. E. .... p 2430 N95-27306
p 2431 N95-27537
NEWMAN, LAURI KRAFT .... p 2152 N95-27797
NG, L. C. .... p 2399 N95-28109
NGO, SON .... p 2158 N95-27284
NGUYEN, TU M. .... p 2281 N95-27349
NICHOLS, JOY S. .... p 2463 N95-28328
NICHOLSON, D. M. C. .... p 2408 N95-27456
NICOLL, JEFFREY .... p 2358 N95-26552
NIELSEN, B. .... p 2217 N95-27553
p 2236 N95-27962
p 2445 N95-28165
NIEMCZEWSKI, A. .... p 2432 N95-27688
NIEMCZYK, T. M. .... p 2267 N95-28148
NIETO, J. C. D. .... p 2234 N95-27472
NIEW, TAI RAN .... p 2275 N95-26809
NIKIFOROV, V. V. .... p 2288 N95-28603
NIKOLAOU, M. .... p 2284 N95-27721
NILES, STANLEY .... p 2249 N95-26562
NIMMO, W. .... p 2308 N95-26749
NIR, Y. .... p 2407 N95-27406
NISHI, M. .... p 2222 N95-28167
NOBLE, BRIAN .... p 2363 N95-26469
NODERER, KEITH D. .... p 2142 N95-27839
NOGAR, N. S. .... p 2204 N95-27467
p 2297 N95-27841
NOH, TAEWAN .... p 2390 N95-27304
NOONAN, C. H. .... p 2153 N95-27798
NOOR, M. .... p 2390 N95-27299
NORMAN, J. A. T. .... p 2237 N95-28089
NORQUIST, DONALD C. .... p 2356 N95-26992
NORRIS, ANDREW T. .... p 2287 N95-27902
NOVIKOV, A. V. .... p 2280 N95-27338
NOWAK, IGNACY .... p 2250 N95-26836
NOWLIN, MELVIN L. .... p 2295 N95-27172
NOYES, H. P. .... p 2449 N95-28137
NOYES, ROBIN Y. .... p 2312 N95-28616
NURMI, P. .... p 2224 N95-28644
NURNBERGER, MIKE .... p 2366 N95-26694
NURRE, G. S. .... p 2311 N95-28214
NYAMTSEREN, N. .... p 2255 N95-27313
NYGREN, WILLIAM D. .... p 2157 N95-27275

O

OBERACKER, V. E. .... p 2413 N95-28077
OBRIEN, MARGARET C. .... p 2345 N95-26430
OCKIER, C. J. .... p 2141 N95-26773
ODEN, J. TINSLEY .... p 2307 N95-26387
ODETTE, G. R. .... p 2214 N95-27086
ODONNELL, PATRICIA M. .... p 2167 N95-27177
ODONNELL, TIMOTHY P. .... p 2213 N95-26862
OEDEGARD, J. A. .... p 2224 N95-28660
OGLESBY, DONALD M. .... p 2293 N95-27915
OH, K. S. .... p 2270 N95-28570
OHALLARON, DAVID R. .... p 2377 N95-26840
OHBA, TAKUYA .... p 2222 N95-28166
OHNUKI, TAKESHI .... p 2128 N95-26525
OHTA, SHIGEMI .... p 2449 N95-27448
OLDENBURG, C. M. .... p 2287 N95-28225
OLEKSUK, LYNDA L. S. .... p 2166 N95-28292
OLESON, STEVEN R. .... p 2168 N95-27727
OLIVER, C. E. .... p 2373 N95-28498
p 2375 N95-28632
OLIVER, M. .... p 2242 N95-27669
OLIVER, W. C. .... p 2220 N95-28044
OLLIFFE, R. .... p 2191 N95-28433
OLSON, R. E. .... p 2299 N95-28223
OLSON, RICHARD J. .... p 2117 N95-26629
OLSON, RON B. .... p 2229 N95-27110
ONEAL, ROBERT L. .... p 2457 N95-27660
ONEL, Y. .... p 2421 N95-27923
ONELLION, M. .... p 2436 N95-26440
ONISHI, NAOKI .... p 2399 N95-27548
ONO, TAKATSUGU .... p 2126 N95-26585
OONA, H. .... p 2204 N95-27467
OPSTELTEN, I. J. .... p 2289 N95-28637
ORLANSKY, JESSE .... p 2143 N95-26556
ORMECI, A. .... p 2213 N95-27082
ORR, HORACE A. .... p 2129 N95-26684
ORTEGA, GUILLERMO .... p 2384 N95-27386
OSBORN, R. .... p 2408 N95-27453
OSBORNE, D. H., JR. .... p 2237 N95-28080
OSHRAT, J. .... p 2136 N95-28409
OSLER, JOHN C. .... p 2345 N95-26420
OSTASZEWSKI, MIROSLAW A. .. p 2158 N95-27288
OSTERHELD, A. L. .... p 2462 N95-28013
OSTOWARI, CYRUS .... p 2124 N95-27974
OSWALD, FRED B. .... p 2302 N95-27698
OTA, KAZUO .... p 2145 N95-27667
OTEY, M. G. .... p 2208 N95-28042
OTOOLE, BRENDAN J. .... p 2190 N95-28426
OTSUKA, KAZUHIRO .... p 2222 N95-28166
OUKACI, R. .... p 2203 N95-27420
OVERSLUIZEN, T. .... p 2422 N95-28195
OVIATT, HENRY .... p 2240 N95-28531
OWENS, S. D. .... p 2197 N95-28483
OZA, D. .... p 2146 N95-27764
OZA, D. H. .... p 2147 N95-27768
OZAWA, M. .... p 2439 N95-27452

P

PADIAS, A. .... p 2294 N95-26568
PAFFETT, M. T. .... p 2443 N95-28023
PAGE, GERALD .... p 2374 N95-28627
PAGE, P. R. .... p 2418 N95-28640
PAIN, BEDABRATA .... p 2424 N95-26894
PAIN, R. .... p 2460 N95-28197
PAINTER, CHARLES R. .... p 2171 N95-28300
PAINTER, S. L. .... p 2431 N95-27498
PAJERSKI, ROSE .... p 2374 N95-28627
PAJON, P. .... p 2400 N95-28350
PALEV, T. D. .... p 2448 N95-27334
p 2395 N95-27340
PALKO, S. .... p 2271 N95-28655
PALMER, D. A. .... p 2204 N95-27451
p 2208 N95-27956
PALMER, R. .... p 2420 N95-27484
PALMER, T. S. .... p 2392 N95-28232
PALUS, M. .... p 2385 N95-27391
PAN, X. J. .... p 2204 N95-27467
PANAJKAR, M. S. .... p 2406 N95-27212
PANDYA, D. A. .... p 2267 N95-28105
PANKOV, A. A. .... p 2406 N95-27317
PAP, J. .... p 2464 N95-28007
PAPAGEORGIOU, DEMETRIOS T.
p 2284 N95-27760
PAPPALARDO, G. .... p 2375 N95-28645
PARANTHAMAN, M. .... p 2444 N95-28079
PARK, CHUNG-KYU .... p 2334 N95-26423
PARK, JEFFREY .... p 2326 N95-26429
PARKER, BRIAN A. .... p 2122 N95-26875
PARKER, J. M. .... p 2222 N95-28167
PARKER, JOEL WILLIAM .... p 2463 N95-28328
PARKER, L. E. .... p 2387 N95-28536
PARKS, L. W. .... p 2348 N95-26573
PARLETT, BERESFORD N. .... p 2368 N95-26855
PARMETER, J. E. .... p 2237 N95-28089
PARRIS, P. E. .... p 2220 N95-28049
PARRISH, CLYDE .... p 2173 N95-28310
p 2174 N95-28312
PARROTT, TONY L. .... p 2400 N95-26394
PARSONS, EDWARD L., JR. .... p 2320 N95-27746
PARTHASARATHY, R. .... p 2224 N95-26470
PARWANI, R. R. .... p 2449 N95-27449
PASCHALL, R. .... p 2316 N95-26393
PASTORE, CHRISTOPHER M. .... p 2189 N95-28423
PATAL, ANEMI .... p 2171 N95-28299
PATTERSON, JAMES D. .... p 2437 N95-26780
PATTERSON, R. .... p 2437 N95-26756
PATTERSON, RICHARD L. .... p 2264 N95-27374
PATTERSON, SARA .... p 2144 N95-26583
PATTERSON, SHEILA A. .... p 2269 N95-28388
PAULIN, NICOLAS .... p 2159 N95-27292
PAULUS, RICHARD A. .... p 2253 N95-27006
PAUSDER, H. J. .... p 2141 N95-26773
PAVER, N. .... p 2406 N95-27317
PAWEL, J. E. .... p 2221 N95-28120
PAWLIKOWSKI, ELLEN M. .... p 2117 N95-26455
PAWLOWICZ, RYSZARD A. .... p 2348 N95-28096
PAXSON, DANIEL E. .... p 2140 N95-27860
PAYNE, A. N. .... p 2256 N95-28231
PAYNE, GREGORY .... p 2171 N95-28299
PEACHEY, N. M. .... p 2298 N95-28124
PEACOCK, RICHARD W. .... p 2466 N95-26823
PECHT, MICHAEL .... p 2263 N95-27226
p 2263 N95-27230
p 2263 N95-27232
PECK, EUGENE L. .... p 2314 N95-27998
PECKER, JEAN-CLAUDE .... p 2458 N95-27068
PEDERSEN, K. .... p 2224 N95-28660
PEDERSON, L. R. .... p 2267 N95-28131
PEDROSA, M. A. .... p 2431 N95-27497
PEEL, L. D. .... p 2190 N95-28428
PEEPLES, JOHN .... p 2263 N95-27226
p 2264 N95-27233
PEGGS, S. .... p 2422 N95-28115
PEIFENG, CHEN .... p 2300 N95-28650
PEIHUI, LIANG .... p 2294 N95-26874
PEKALA, R. W. .... p 2243 N95-28064
PELISCHEK, TIMOTHY E. .... p 2165 N95-27842
PELLEGRINI, C. .... p 2422 N95-28122
PELLEGRINO, S. .... p 2158 N95-27283
PELTONIEMI, M. .... p 2315 N95-28643
PENDER, MICHAEL .... p 2248 N95-26465
PENDLETON, J. D. .... p 2249 N95-26562
PENLAND, R. C. .... p 2412 N95-28045
PENNELL, W. E. .... p 2223 N95-28208
PENNER, J. E. .... p 2330 N95-27954
p 2330 N95-28118
p 2331 N95-28157
p 2332 N95-28662
PENNOCK, S. T. .... p 2268 N95-28181
PENNYPACKER, C. .... p 2460 N95-28197
PEREZ-MENDEZ, V. .... p 2234 N95-27472
p 2265 N95-27678
PERKINS, D. H. .... p 2465 N95-28500
PERKINSON, DON .... p 2166 N95-27665
PERL, M. L. .... p 2412 N95-28028
PERLMUTTER, S. .... p 2460 N95-28197
PEROS, VASILIOS .... p 2137 N95-28278
PERRY, J. L. .... p 2358 N95-26364
PERRY, R. .... p 2176 N95-28321
PERRYMAN, DENNIS C. .... p 2344 N95-28577
PETERKA, ROBERT J. .... p 2357 N95-27697
PETERS, STEVEN M. .... p 2301 N95-26774
PETERSEN, G. A. .... p 2237 N95-28089
p 2444 N95-28127
p 2445 N95-28206
PETERSON, D. E. .... p 2234 N95-27468
PETERSON, KENNETH A. .... p 2268 N95-28201
PETERSON, LEE D. .... p 2144 N95-26426
PETERSON, MARSHALL B. .... p 2225 N95-26499
PETERSON, T. C. .... p 2332 N95-28605
PETRENKO, VICTOR F. .... p 2200 N95-26422
p 2200 N95-26452
PETRICK, BETH L. .... p 2146 N95-27035
PETRIE, T. .... p 2433 N95-28065
PETRILLO, C. .... p 2418 N95-28657
PETRIN, R. R. .... p 2296 N95-27705
p 2443 N95-28023
PETRZILKA, V. .... p 2429 N95-26438
PETTIGREW, P. J. .... p 2418 N95-27634
PETTY, C. C. .... p 2431 N95-27441
PEW, RICHARD W. .... p 2357 N95-28253
PEYGHAMBARIAN, N. .... p 2294 N95-26568
PFAU, J. .... p 2236 N95-27962
PFEFFER, R. L. .... p 2445 N95-28165
PFEIFFER, KARL DURANT .... p 2242 N95-26842
PFUND, D. M. .... p 2287 N95-28021
PHAN, MINH .... p 2157 N95-27279
PHANEUF, TINA M. .... p 2358 N95-26736
PHARR, G. M. .... p 2220 N95-28044
PHELPS, MAX R. .... p 2232 N95-27129
PHILLIPS, R. J. N. .... p 2419 N95-27089
p 2413 N95-28067
PHILLIPS, SCOTT N. .... p 2141 N95-26958
PHILLIPS, T. J. .... p 2338 N95-27931
PICHOWSKY, M. .... p 2392 N95-27742
PICKENPAUGH, EILEEN A. .... p 2466 N95-26823
PICKETT, LORI A. .... p 2227 N95-27101
PICKETT, LORRI A. .... p 2170 N95-28294
PIEKARZ, HENRYK .... p 2410 N95-27872
PIEKSMA, M. .... p 2413 N95-28078
PIEKUTOWSKI, ANDREW J. .... p 2225 N95-26561
PIERCE, DONALD G. .... p 2268 N95-28201
PIERSON, WILLARD J., JR. .... p 2315 N95-28209
PIILA, J. .... p 2308 N95-26911
PIIPPO, S. W. .... p 2234 N95-27476
PILAFTSIS, A. .... p 2419 N95-27089
PINELLI, THOMAS E. .... p 2456 N95-28600
PINTZ, A. .... p 2319 N95-27193
p 2319 N95-27194
PIPKINS, D. S. .... p 2133 N95-27511
PIPPIN, H. GARY .... p 2177 N95-26391
p 2210 N95-27642
PLENTOVICH, E. B. .... p 2123 N95-28241

POCHARD, MARC p 2159 N95-27292
PODGORETSKIJ, M. I. p 2415 N95-28248
PODLESAK, MICHAEL p 2259 N95-26425
POE, C. C., JR. p 2137 N95-28471
p 2197 N95-28479
POE, DON R. p 2356 N95-27012
POGGIO, A. J. p 2268 N95-28181
POLITZER, PETER p 2404 N95-26960
POLLARD, JAMES E. p 2167 N95-26489
POLLMEIER, VINCENT M. p 2150 N95-27786
POLLOCK, KENNETH R. p 2161 N95-26458
POOLE, P. p 2132 N95-27507
POORMAN, KEVIN L. p 2225 N95-26561
POPE, D. P. p 2215 N95-27463
p 2219 N95-28026
p 2220 N95-28046
POPLAWSKI, JOSEPH V. p 2301 N95-26774
POPOV, V. V. p 2403 N95-26542
PORTER, G. D. p 2433 N95-28054
p 2433 N95-28065
PORTMANN, G. p 2425 N95-27675
POSPELOV, M. E. p 2407 N95-27411
POST, R. F. p 2435 N95-28356
POSTON, WENDY L. p 2394 N95-26415
p 2271 N95-28614
POTTER, T. F. p 2327 N95-27540
POULTER, G. A. p 2224 N95-27113
POVINELLI, L. A. p 2391 N95-27726
PRABAKAR, S. p 2240 N95-28531
p 2240 N95-28532
PRAGER, S. C. p 2429 N95-26940
PRAHL, JOSEPH M. p 2164 N95-27761
PRAKASH, CHANDER p 2285 N95-27885
PRAKASH, S. S. p 2237 N95-28090
PRATHER, M. J. p 2330 N95-27954
PRAUSNITZ, J. M. p 2238 N95-28226
p 2209 N95-28229
PRELLER, RUTH H. p 2347 N95-27189
PRESTAGE, JOHN D. p 2404 N95-26861
p 2416 N95-28348
PRESTON, D. W. p 2426 N95-28022
PRETTYMAN-LUKOSCHEK, JILL S.
p 2272 N95-26796
PRICE, D. L. p 2237 N95-27967
PRICE, DAVID LONG p 2436 N95-26442
PRICE, MORGAN p 2363 N95-26469
PRICE, STEVE p 2145 N95-28261
PRIEBE, CAREY E. p 2394 N95-26413
p 2394 N95-26415
p 2271 N95-28614
PRINCE, J. p 2225 N95-26482
PRINCE, S. P. p 2228 N95-27108
p 2172 N95-28304
PRINTY, MATTHEW p 2340 N95-26453
PRINZO, O. V. p 2128 N95-28540
PROCTOR, I. D. p 2204 N95-27496
PROULX, R. p 2151 N95-27789
PRUEITT, M. L. p 2328 N95-27686
PRUESS, K. p 2287 N95-28225
PRUNEAU, PAUL N. p 2165 N95-28578
PRYANICHNIKOV, V. I. p 2280 N95-27338
PRZEKWAS, A. J. p 2140 N95-28344
PRZEKWAS, ANDRZEJ J. p 2168 N95-27434
PUGA, L. C. p 2464 N95-28007
PUICH, M. p 2267 N95-28148
PULLEN, I. R. p 2248 N95-26493
PULLEN, MICHAEL W. p 2249 N95-26509
PURAM, CHITH K. p 2293 N95-27915
PURCELL, RICHARD G. p 2341 N95-26669
PURDY, ELLEN M. p 2233 N95-27324
p 2233 N95-27325
PURDY, WILLIAM p 2156 N95-27268
PURTILO, JAMES M. p 2366 N95-26711
PUSKA, P. p 2252 N95-26914
PYNN, R. p 2412 N95-28057

Q

QIAN, Y. p 2208 N95-27965
QUAGLIANO, J. R. p 2443 N95-28023
QUALLS, A. L. p 2422 N95-28205
QUICK, C. ROBERT p 2296 N95-27672
QUINLIVAN, J. T. p 2138 N95-28489
QUINTANA, C. p 2331 N95-28548
QUINZIO, M. V. p 2272 N95-26786
QURESHI, F. p 2241 N95-28592

R

RAAEN, S. p 2210 N95-28652
RABAH, K. V. O. p 2264 N95-27405
RABERT, JENNIFER p 2453 N95-27004
RABITZ, HERSCHEL p 2209 N95-28164
RACKERS, K. p 2155 N95-27263
RADEKA, V. p 2269 N95-28244
RADHAKRISHNAN, KRISHNAN p 2273 N95-26380
RADHAKRISHNAN, V. p 2372 N95-27849
RADICELLA, S. M. p 2337 N95-27157
RADOMSKI, M. S. p 2147 N95-27766
RADTKE, T. C. p 2135 N95-27523
RADZILOWSKI, LEONARD p 2437 N95-26553
RAEISAENEN, ANTTI p 2260 N95-26646
RAETY, T. p 2369 N95-26907
RAHMAN, M. M. p 2280 N95-27348
RAHMAN, MUHAMMAD M. p 2280 N95-27347
RAIKAR, G. N. p 2418 N95-27634
RAIKER, G. N. p 2272 N95-27635
RAISTRICK, I. D. p 2272 N95-27635
RAIZENNE, M. D. p 2132 N95-27509
RAJAGOPALAN, S. p 2280 N95-27348
RAJU, M. S. p 2287 N95-27901
RAMAN, A. p 2292 N95-27368
RAMAN, GANESH p 2119 N95-26952
RAMAN, M. p 2325 N95-28396
RAMBACH, G. p 2243 N95-28064
RAMESH, R. p 2445 N95-28165
RAMIREZBERNAL, MARIA ELENA
p 2405 N95-27211
RANACHOWSKI, JERZY p 2401 N95-26519
RANCOURT, JAMES D. p 2230 N95-27115
p 2231 N95-27122
RANDLE, SCOTT p 2120 N95-26955
RANEY, P. p 2267 N95-28131
RANGEL, M. J., III p 2258 N95-28601
RANGWALLA, AKIL A. p 2139 N95-26777
RANKEN, W. A. p 2420 N95-27425
RANKIN, JANET p 2444 N95-28081
RAO, GOPALAKRISHNA M. p 2272 N95-26796
RAO, N. N. p 2213 N95-26675
RAPHAEL, DAVID p 2255 N95-27435
RASHID, M. M. p 2309 N95-27837
RASHIDI, MAJID p 2302 N95-27855
RASHIDNIA, NASSER p 2293 N95-28037
RASMUSSEN, S. p 2228 N95-27107
RASTOGI, NAVEEN p 2310 N95-27865
RATHI, B. N. p 2405 N95-27159
RAW, M. J. p 2286 N95-27897
RAWLS, J. RICHARD p 2211 N95-27656
RAWOOL-SULLIVAN, M. W. p 2411 N95-28024
RAY, BISWAJIT p 2264 N95-27374
RAY, RONALD E. p 2292 N95-27751
RAY, SURENDRA N. p 2148 N95-27772
RAYNO, BRUCE p 2144 N95-27133
RAZEE, S. S. A. p 2219 N95-27758
RAZIN, A. N. p 2288 N95-28603
RAZUVAEV, V. N. p 2343 N95-27920
READ, B. E. p 2224 N95-26448
READ, BRITTON C., III p 2260 N95-26767
READ, WILLIAM J. L. p 2248 N95-26407
REAGAN, M. K. p 2281 N95-27351
REBEIZ, GABRIEL M. p 2257 N95-28513
RED, X. B., JR. p 2283 N95-27365
REDDEN, MARK C. p 2129 N95-26684
REDDOCH, T. W. p 2273 N95-27987
REDDY, D. R. p 2283 N95-27361
REDDY, E. S. p 2141 N95-28277
REDMOND, JIM p 2266 N95-27724
REED, CHARLES WILLIAM p 2227 N95-27103
p 2228 N95-27105
REED, M. H. p 2174 N95-28315
REED, STEVEN G. p 2350 N95-27097
REED, X. B., JR. p 2280 N95-27346
p 2282 N95-27358
REEDY, E. D. p 2240 N95-28405
REESE, G. M. p 2309 N95-27305
REEVES, G. D. p 2338 N95-28061
REEVES, JOHN p 2129 N95-26537
REGAN, CHRISTOPHER p 2144 N95-26583
REGAN, EDWARD S. p 2398 N95-26687
REGINATTO, MARCEL p 2465 N95-26427
REGOORD, R. p 2307 N95-26342
REHFIELD, LAWRENCE W. p 2192 N95-28436
REHN, L. E. p 2441 N95-27928
p 2220 N95-28072
REIMER, R. R. p 2319 N95-27193
p 2319 N95-27194
REINHARDT, FREDERICK W. p 2264 N95-27474
REJ, D. J. p 2444 N95-28125
REMSEN, D. p 2434 N95-28140
REN, BING p 2289 N95-28619
RENDALL, A. D. p 2397 N95-28011
RENIERI, GARY D. p 2188 N95-28289
RENIERI, M. P. p 2185 N95-28274
RENO, S. p 2440 N95-27471
RENO, STEVE p 2440 N95-27538
RENSCHLER, C. L. p 2418 N95-27634
RENSINK, M. E. p 2433 N95-28065
RENZHONG, HUA p 2294 N95-26874
RESCIA, S. p 2269 N95-28244
REYES, ROBERT p 2354 N95-27059
REYNOLDS, D. S. p 2253 N95-27005
REYNOLDS, GREGORY A. p 2275 N95-26751
REZY, BERNIE J. p 2140 N95-27866
RHEA, W. JOSEPH p 2345 N95-26430
RHOADES, C. E., JR. p 2311 N95-28337
RHOADS, CARL p 2400 N95-26502
RHOADS, GREGORY L. p 2138 N95-27003
RHODES, JANICE E. p 2331 N95-28153
RICCITIELLO, SALVATORE R. p 2238 N95-28212
RICE, BETSY M. p 2418 N95-28648
RICE, STEPHEN B. p 2413 N95-28101
RICHARD, PATRICK p 2407 N95-27439
RICHARDSON, J. H. p 2243 N95-28064
RICHARDSON, J. W., JR. p 2439 N95-27452
RICHTSMEIER, S. C. p 2332 N95-28602
RICKMAN, STEVEN L. p 2210 N95-27631
RIDES, M. p 2226 N95-26744
RIEDLINGER, SHELLEY K. p 2347 N95-27189
RIEGER, D. J. p 2445 N95-28144
RIES, P. D. p 2298 N95-28124
RILEY, G. N., JR. p 2447 N95-28606
RILEY, S. J. p 2409 N95-27753
RINGROSE, P. p 2385 N95-27393
RINKER, NANCY A. p 2455 N95-27701
RINOIE, KENICHI p 2128 N95-26525
RISING, S. A. p 2176 N95-28324
p 2177 N95-28325
RISKALLA, M. G. p 2193 N95-28443
RISTIG, M. L. p 2381 N95-27044
p 2207 N95-27880
RIVERA, JOSE A., JR. p 2117 N95-26381
RIVERS, JOHN V. p 2165 N95-27842
RIVEST, RONALD L. p 2387 N95-28461
ROACH, JOSEPH F. p 2361 N95-28390
ROBERTS, D. A. p 2237 N95-28089
ROBERTS, F. E., III p 2244 N95-26769
ROBERTS, M. L. p 2204 N95-27496
ROBERTS, PAT p 2152 N95-27793
ROBERTSON, M. M. p 2358 N95-28676
ROBERTSON, R. p 2154 N95-27671
ROBIN, D. p 2425 N95-27675
ROBINSON, ANTHONY p 2156 N95-27274
ROBINSON, ERNEST Y. p 2188 N95-28291
ROBINSON, J. M. p 2426 N95-28018
ROBINSON, S. P. p 2401 N95-26615
ROCCI, PETER J. p 2262 N95-27152
RODRIGUE, G. p 2373 N95-28521
RODRIGUEZ, C. A. p 2379 N95-26443
ROEDER, W. P. p 2172 N95-28307
ROGATCHEV, V. G. p 2288 N95-28603
ROGERS, C. A. p 2191 N95-28435
ROGERS, F. J. p 2434 N95-28141
ROGERS, GEORGE W. p 2394 N95-26413
p 2394 N95-26415
p 2271 N95-28614
ROGERS, WILLIAM H. p 2357 N95-28253
ROGNLIEN, T. D. p 2433 N95-28054
p 2433 N95-28065
ROHALY, T. F. p 2179 N95-26565
ROHLEV, LORI E. p 2227 N95-26973
ROHRBAUGH, DAVE p 2149 N95-27777
ROHWELLER, DAVID J. p 2157 N95-27282
ROJAS, S. P. p 2411 N95-28024
ROLEK, EVAN P. p 2129 N95-26684
ROME, J. A. p 2431 N95-27498
ROMINE, C. H. p 2378 N95-28019
ROOD, RICHARD p 2334 N95-26423
ROSE-PEHRSSON, S. L. p 2173 N95-28311
ROSE, KENNETH A., III p 2293 N95-28362
ROSE, WILLIAM C. p 2279 N95-27240
ROSEN, B. W. p 2187 N95-28284
ROSENZWEIG, E. L. p 2193 N95-28446
ROSKAM, JAN p 2119 N95-26949
ROSNER, DANIEL E. p 2199 N95-26417
ROSS, R. p 2421 N95-27735
ROTHER, S. L. p 2126 N95-26454
ROTMAN, D. A. p 2327 N95-27532
ROUNDY, L. M. p 2185 N95-28274
ROUSE, MARSHALL p 2138 N95-28487
ROUTBORT, J. L. p 2183 N95-28069
ROUTE, ROGER K. p 2277 N95-27000
ROVANG, RICHARD D. p 2283 N95-27369
ROWCLIFFE, A. F. p 2221 N95-28120
ROWE, J. N. p 2153 N95-27798
ROWE, SEAN P. p 2126 N95-27859
ROYBAL, R. p 2154 N95-27671
ROYBAL, S. p 2451 N95-28025
ROZAS, C. J. p 2171 N95-28302
RUBY, DOUGLAS S. p 2320 N95-27704
RUEGG, H. p 2448 N95-27332
RUFTY, ALAN E. p 2379 N95-28335
RUIZ, O. p 2234 N95-27472
RUOTANEN, L. H. p 2252 N95-26914
RUSHTON, ELLIOTT p 2127 N95-27903
RUSSELL, A. J. p 2134 N95-27518
RUSSELL, JAMES E. p 2359 N95-27046

RUSSICK, E. M. p 2224 N95-27113
RUSSICK, EDWARD M. p 2229 N95-27110
RUTH, JOHN p 2137 N95-28278
RUTH, R. p 2422 N95-28159
RUTLEDGE, SHARON K. p 2235 N95-27702
RUZICKA, J. p 2441 N95-27867
RYAN, JAMES S. p 2120 N95-26649
RYAN, R. p 2169 N95-28263
RYU, SI-OK p 2206 N95-27695
RYUTOV, D. D. p 2435 N95-28356

S

SABA, JULIA L. R. p 2464 N95-26671
SABOLISH, GEORGE p 2367 N95-26814
SABOUNGI, MARIE-LOUISE p 2436 N95-26442
SACCHETTI, F. p 2418 N95-28657
SACHAN, V. p 2439 N95-27443
SACKS, HOWARD p 2119 N95-26947
SADDOW, STEPHEN E. p 2260 N95-26690
SADOQI, MOSTAFA p 2180 N95-26686
SAENKO, V. A. p 2280 N95-27338
SAETHER, ERIC p 2182 N95-27142
SAGAJDAK, R. N. p 2414 N95-28184
SAGISAKA, MASAKAZU p 2128 N95-26525
SAHA, T. p 2223 N95-28250
SAITO, K. p 2432 N95-27869
SAKA, S. p 2419 N95-26584
SALAMA, K. p 2413 N95-28066
SALAS, MANUEL D. p 2389 N95-26672
SALEEB, ATEF F. p 2310 N95-28031
p 2310 N95-28032
SALES, B. C. p 2237 N95-27967
SALES, G. S. p 2253 N95-27005
SALINS, S. A. p 2175 N95-28318
SALONEN, E. p 2252 N95-26908
SALONEN, P. p 2369 N95-26907
SALTER, CHARLES A. p 2130 N95-26993
SALTZMAN, BARRY p 2326 N95-26429
SAMANT, S. S. p 2123 N95-28230
p 2123 N95-28265
SAMARA, G. p 2202 N95-27136
SAMPSON, W. B. p 2265 N95-27554
SAMS, E. C. p 2206 N95-27851
SANBONGI, SHIGEO p 2180 N95-26667
SANCHEZ, E. p 2431 N95-27497
SANCHEZ, J. p 2431 N95-27497
SANDBERG, V. p 2426 N95-28022
SANDER, ROBERT K. p 2209 N95-28088
SANDERS, MICHAEL L. p 2258 N95-28615
SANDERS, P. G. p 2223 N95-28543
SANDHU, RAGHBIR S. p 2198 N95-28485
SANDUKOVSKIJ, V. G. p 2416 N95-28252
SANDUSKY, DONALD A. p 2182 N95-27192
SANFORD, ALLAN p 2339 N95-28126
SANIIE, JAFAR p 2255 N95-27185
SANNER, ROBERT M. p 2384 N95-27385
SANTANNA, S. J. S. p 2258 N95-28569
SANTARE, MICHAEL H. p 2190 N95-28426
SANTER, B. D. p 2331 N95-28157
SANTO, G. ESPIRITU p 2316 N95-26393
SARIKAYA, MEHMET p 2226 N95-26623
p 2226 N95-26624
p 2201 N95-26870
SARRAO, J. L. p 2407 N95-27431
SARVER-VERHEY, TIMOTHY R. p 2168 N95-27862
SASSI, A. P. p 2238 N95-28226
SATHER, DUANE P. p 2278 N95-27019
SATO, C. p 2328 N95-27749
SATO, K. I. p 2432 N95-27869
p 2432 N95-27870
SATO, KOICHI p 2297 N95-27868
SATYANARAYANAN, M. p 2363 N95-26469
p 2452 N95-26535
p 2454 N95-27529
SATYANARAYANAN, MAHADEV p 2452 N95-26752
SAUNDERS, P. p 2380 N95-26638
SAUNDERS, R. p 2239 N95-28400
SAUSA, ROSARIO C. p 2174 N95-28314
SAVARESE, S. p 2286 N95-27898
SAVIHARJU, K. p 2331 N95-28202
SCHACHINGER, L. p 2425 N95-27675
SCHADOW, KLAUS C. p 2128 N95-26507
SCHAEFER, HENRY F., III p 2199 N95-26416
SCHAFF, JEFFERY R. p 2180 N95-26571
SCHANZENBACH, GEORGE P. p 2306 N95-27985
SCHAUB, A. p 2236 N95-27962
SCHEIB, JIM p 2166 N95-27663
SCHERI, RICK p 2428 N95-27652
SCHEUER, J. T. p 2444 N95-28125
SCHIFFER, J. P. p 2434 N95-28233
SCHILLING, T. J. p 2176 N95-28323
SCHINDLER, R. p 2134 N95-27522
SCHIPPERS, S. p 2409 N95-27551
SCHMIDT, LORNE R. p 2242 N95-27669
SCHMITT, M. J. p 2296 N95-27557
SCHMOYER, R. L. p 2332 N95-28605
SCHNEIDER, J. M. p 2344 N95-28340
SCHNEIDER, WILLIAM C. p 2154 N95-27260
SCHOCK, R. N. p 2243 N95-28064
SCHOENLEIN, R. p 2296 N95-27674
SCHOTT, JOACHIM HOSSICK p 2178 N95-28334
SCHOWENGERDT, R. A. p 2289 N95-26461
SCHRAGGER, PAUL A. p 2367 N95-26770
SCHREIBER, M. p 2443 N95-28016
SCHROEDER, S. p 2189 N95-28424
SCHUBERT, SIEGFRIED p 2334 N95-26423
SCHUFF, N. R. p 2349 N95-26728
p 2349 N95-26729
p 2349 N95-26730
SCHULENBURG, N. p 2384 N95-27387
SCHUMACHER, G. p 2438 N95-27085
p 2441 N95-27928
SCHUSTER, SHEL p 2178 N95-26712
SCHUTT-AINE, J. p 2270 N95-28570
SCHWALL, R. E. p 2267 N95-28048
SCHWARTZ, R. W. p 2444 N95-28103
SCHWARZ, R. K. p 2456 N95-28172
SCHWEICKART, DANIEL p 2138 N95-27003
SCHWENTERLY, S. W. p 2267 N95-28048
SCIME, E. E. p 2337 N95-27848
SCOTT, B. p 2447 N95-28541
SCOTT, EWELL M. p 2304 N95-28347
SCOTT, J. W. p 2299 N95-28132
SCOTT, R. F. p 2135 N95-27524
SCOTT, W. G. p 2465 N95-28500
SCULLY, J. R. p 2213 N95-27032
SEABLOM, MICHAEL p 2334 N95-26423
SEAGER, C. H. p 2445 N95-28206
SEAH, M. P. p 2226 N95-26745
SEARSON, P. C. p 2218 N95-27748
SECAN, JAMES A. p 2334 N95-26520
SEDLACEK, A. J. p 2315 N95-28520
SEDLAK, J. p 2153 N95-27799
SEGA, PATRICK p 2156 N95-27271
SEGAMI, CARLOS p 2383 N95-27378
SEIBER, B. L. p 2427 N95-28408
SEIFERT, N. p 2428 N95-27646
SEITZMAN, LARRY E. p 2225 N95-26499
SELL, ROBERT D. p 2232 N95-27127
SELLERS, RICK p 2320 N95-27704
SELNICK, ARNOLD P. p 2362 N95-26346
SELTZER, MICHAEL D. p 2174 N95-28313
SELVELLI, PIERLUIGI p 2459 N95-27072
p 2459 N95-27074
p 2460 N95-27075
SEMINARIO, JORGE M. p 2404 N95-26960
SEMMES, STEPHEN p 2396 N95-26538
SEN, A. K. p 2391 N95-27739
SENCHISHIN, V. p 2233 N95-27163
SENSENEY, MICHAEL B. p 2122 N95-26901
SEPPAELAE, M. p 2451 N95-28135
SESSLER, A. p 2420 N95-27470
SEWALL, WILLIAM G. p 2120 N95-26382
SEYMORE, RICHARD J. p 2247 N95-27909
SHABBIR, AAMIR p 2285 N95-27882
SHADOAN, MICHAEL D. p 2304 N95-28347
SHAFER, STEVEN A. p 2425 N95-27038
SHAFIGULIN, R. R. p 2416 N95-28252
SHAH, A. R. p 2309 N95-27174
SHAH, BHARAT M. p 2138 N95-28476
SHAH, N. Y. p 2280 N95-27346
SHAH, R. p 2270 N95-28515
SHAKER, JOHN F. p 2164 N95-27730
SHANK, C. V. p 2296 N95-27674
SHAO, H. H. p 2440 N95-27535
SHAO, ZHIFENG p 2352 N95-28525
SHAPIRO, S. M. p 2215 N95-27462
p 2222 N95-28166
SHAW, KEVIN B. p 2313 N95-26476
p 2314 N95-26682
SHAW, MARY p 2363 N95-26446
p 2363 N95-26467
SHAW, ROBERT J. p 2118 N95-26945
SHEA, KENNETH J. p 2240 N95-28531
p 2240 N95-28532
SHELDON, DAVID p 2125 N95-27762
SHELTON, W. A. p 2408 N95-27456
SHEN, C. p 2331 N95-28548
SHEN, S. S. p 2222 N95-28167
SHEN, Y. R. p 2428 N95-28557
SHENGXI, SHI p 2121 N95-26719
SHEPARD, W. S. p 2330 N95-28119
SHEPHERD, K. P. p 2324 N95-27990
SHEPHERD, WILLIAM T. p 2360 N95-27696
SHEPODD, T. J. p 2206 N95-27750
SHEPPARD, M. G. p 2266 N95-27754
SHERWOOD, TOM p 2119 N95-26951
SHESTAG, S. L. p 2171 N95-28302
SHGIMOKAWA, TOSHIYUKI p 2307 N95-26521
SHI, N. p 2182 N95-27080
SHI, YUZHONG p 2289 N95-28619
SHIAO, MICHAEL C. p 2137 N95-28444
SHIDELER, J. p 2440 N95-27471
SHIDELER, JAY p 2440 N95-27538
SHIEH, L. S. p 2380 N95-26468
SHIGEMI, MASASHI p 2128 N95-26525
SHIH, TSAN-HSING p 2285 N95-27883
SHIINA, S. p 2432 N95-27869
SHIMADA, TSUTOMU p 2296 N95-27672
SHIMOKAWA, TOSHIYUKI p 2180 N95-26667
SHIN, JAIWON p 2125 N95-27762
SHIN, Y. S. p 2308 N95-26625
SHINN, JUDY L. p 2465 N95-26427
p 2465 N95-28530
SHINPAUGH, J. p 2413 N95-28078
SHIPLEY, S. A. p 2312 N95-27983
SHIRAI, T. p 2419 N95-26584
SHIRES, DALE p 2374 N95-28625
SHIRKE, N. D. p 2406 N95-27212
SHIRKOV, D. V. p 2448 N95-27315
SHIRLEY, ERIC L. p 2425 N95-27539
SHIROKOV, M. I. p 2450 N95-28183
SHIVELY, J. p 2154 N95-27671
SHIXIU, HE p 2341 N95-26723
SHIYAN, TAO p 2341 N95-26723
SHOGRIN, BRADLEY p 2164 N95-27761
SHOOP, SALLY A. p 2336 N95-26753
SHORT, NICK, JR. p 2384 N95-27382
SHORTIS, TRUDI A. p 2278 N95-27028
SHORTS, VINCIENT F. p 2336 N95-26858
SHOWALTER, S. p 2331 N95-28548
SHUART, M. J. p 2190 N95-28428
SHUART, MARK J. p 2194 N95-28466
p 2194 N95-28468
SHUCHENG, ZHANG p 2120 N95-26713
SHUKLA, JAY G. p 2138 N95-28476
SHUKLA, SHEKHAR p 2409 N95-27747
SHUL, R. J. p 2445 N95-28144
p 2267 N95-28146
SHULMAN, DAVID p 2394 N95-26478
SHURMER, I. M. p 2154 N95-27804
SHUSTER, MALCOLM D. p 2153 N95-27800
SICHER, D. p 2166 N95-26390
SIDDIQI, SHAHID p 2194 N95-28465
SIDDONS, D. P. p 2422 N95-28195
SIDIKMAN, K. L. p 2430 N95-27306
p 2431 N95-27537
SIDILKOVER, DAVID p 2288 N95-28571
SIEBERS, DENNIS L. p 2203 N95-27437
SIEBES, GEORG p 2154 N95-27264
SIEGEL, DAVID A. p 2345 N95-26430
SIEGEL, R. W. p 2223 N95-28543
SIEGL, R. p 2219 N95-28026
SIEMANN, R. H. p 2422 N95-28123
SIEVERS, A. J. p 2446 N95-28522
SIH, G. C. p 2133 N95-27513
SIHVOLA, A. p 2257 N95-28449
SIHVOLA, A. H. p 2252 N95-26914
p 2256 N95-28354
SIKKA, V. K. p 2215 N95-27450
SILBERBERG, R. p 2465 N95-28530
SILBEY, R. J. p 2414 N95-28199
SILVA, K. p 2192 N95-28437
SILVA, L. J. p 2232 N95-27129
SIMEONSSON, JOSEF B. p 2174 N95-28314
SIMMERMACHER, TODD p 2309 N95-27305
SIMMONS, H. C. p 2170 N95-28296
SIMON, C. G. p 2294 N95-27670
SIMON, M. E. p 2440 N95-27712
SIMONEN, E. P. p 2216 N95-27492
p 2216 N95-27493
SIMONS, R. W. p 2455 N95-27957
SIMONS, RAINEE N. p 2266 N95-27853
SIMONSON, J. M. p 2204 N95-27451
p 2208 N95-27960
SIMPSON, D. L. p 2132 N95-27509
SIMPSON, T. C. p 2240 N95-28547
SIMS, G. D. p 2227 N95-26747
p 2308 N95-26749
SINDIR, MUNIR M. p 2286 N95-27891
SINGER, HARVEY A. p 2345 N95-27389
SINGER, IRWIN L. p 2225 N95-26499
SINGH, A. p 2242 N95-27669
SINGH, ALOK p 2225 N95-26526
SINGH, D. p 2183 N95-28068
SINGH, J. P. p 2183 N95-28068
SINGH, MAHAVIR p 2203 N95-27200
SINGH, MONA p 2387 N95-28461
SINGH, R. N. p 2183 N95-27955
SINGH, SANDIPA p 2315 N95-28392
SINGHAL, ASHOK K. p 2286 N95-27894
SINGHAL, S. N. p 2309 N95-27174
SISAKYAN, A. N. p 2396 N95-27337
p 2397 N95-28518
SISTERSON, D. L. p 2344 N95-28340
SITTON, OLIVER p 2176 N95-28322

SITTON, OLIVER C. .... p 2175 N95-28320
SKAGGS, WILLIAM E. .... p 2350 N95-26761
SKANTHAKUMAR, S. .... p 2219 N95-27966
SKARDA, J. RAYMOND LEE .... p 2283 N95-27364
SKIBINSKI, T. A. .... p 2358 N95-26558
SKOBLIN, A. A. .... p 2256 N95-27716
SKRIVANEK, R. A. .... p 2294 N95-27670
SLAMA, M. .... p 2385 N95-27391
SLATER, P. N. .... p 2348 N95-28030
SLEMP, WAYNE S. .... p 2166 N95-27664
SLEZAK, T. .... p 2351 N95-27725
SLIWOWSKI, MAREK .... p 2211 N95-26359
p 2212 N95-26512
p 2212 N95-26666
SMALL, I. .... p 2460 N95-28197
SMELLIE, DOUGLAS .... p 2272 N95-26789
SMID, J. .... p 2385 N95-27391
SMILOWITZ, L. B. .... p 2426 N95-28018
SMITH, ANTHONY .... p 2400 N95-26502
p 2245 N95-26508
SMITH, B. .... p 2325 N95-28395
SMITH, B. F. .... p 2378 N95-28071
SMITH, BRIAN R. .... p 2285 N95-27884
SMITH, C. H. .... p 2297 N95-27841
SMITH, D. M. .... p 2239 N95-28401
SMITH, G. .... p 2412 N95-28057
SMITH, G. M. .... p 2165 N95-27124
SMITH, H. MIKE .... p 2229 N95-27110
SMITH, J. .... p 2132 N95-27510
SMITH, J. E. .... p 2379 N95-26443
SMITH, J. L. .... p 2407 N95-27431
SMITH, J. R. .... p 2303 N95-28029
p 2243 N95-28064
p 2303 N95-28139
SMITH, JOSEPH G., JR. .... p 2179 N95-28360
p 2179 N95-28361
SMITH, LINDA D. .... p 2386 N95-27400
SMITH, M. T. .... p 2222 N95-28163
SMITH, P. M. .... p 2237 N95-28089
SMITH, ROBERT A. .... p 2128 N95-26507
SMITH, RONALD L. .... p 2130 N95-26993
SMITH, S. P. .... p 2157 N95-27278
SMITH, STEVEN L. .... p 2386 N95-27395
SMITHRICK, JOHN J. .... p 2167 N95-27177
SNELL, C. .... p 2298 N95-28027
SNYDER, ERIC S. .... p 2268 N95-28201
SNYDER, M. H. .... p 2124 N95-27976
SNYDER, PAUL G. .... p 2260 N95-26816
SOB, M. .... p 2219 N95-28026
SOCHA, GRZEGORZ .... p 2211 N95-26359
p 2212 N95-26512
SODEN, JERRY M. .... p 2306 N95-27723
SODERHOLM, L. .... p 2408 N95-27453
p 2219 N95-27966
p 2238 N95-28235
SODERQUIST, JOSEPH R. .... p 2184 N95-28266
p 2189 N95-28420
p 2193 N95-28462
SODOYER, B. R. .... p 2450 N95-26803
SOKOLOWSKI, WITOLD M. .... p 2213 N95-26862
SOLKA, JEFFREY L. .... p 2394 N95-26413
p 2394 N95-26415
p 2271 N95-28614
SOLODKAYA, T. I. .... p 2403 N95-26542
SOLODUKHIN, S. N. .... p 2462 N95-27343
SOLOMON, FREDRIC .... p 2424 N95-26900
SOMERS, D. M. .... p 2122 N95-27541
SON, SEHWAN .... p 2437 N95-26553
SONG, JIN-JOO .... p 2300 N95-28458
SONG, O. .... p 2191 N95-28435
SONG, ZHENGFANG .... p 2428 N95-28617
SONI, A. .... p 2416 N95-28355
SONNABEND, DAVID .... p 2148 N95-27776
SORENSEN, JEN C. .... p 2345 N95-26430
SORENSEN, N. R. .... p 2224 N95-27113
SOUTHAM, R. E. .... p 2236 N95-27946
SOUTHON, J. R. .... p 2204 N95-27496
SOUTHWORTH, S. H. .... p 2442 N95-27963
SOVINEC, C. R. .... p 2429 N95-26940
SOWDER, K. D. .... p 2266 N95-27754
SOWERS, C. H. .... p 2206 N95-27755
SPADY, BLAINE R. .... p 2199 N95-27636
SPALL, ROBERT E. .... p 2282 N95-27356
SPANGLER, CHARLES W. .... p 2436 N95-26462
SPARKS, W. M. .... p 2462 N95-28062
SPARLIN, D. M. .... p 2220 N95-28049
SPATZ, J. P. .... p 2224 N95-26470
SPECHT, E. D. .... p 2447 N95-28606
SPEEDIE, M. K. .... p 2171 N95-28299
SPEET, L. J. J. .... p 2199 N95-28639
SPENIK, ADAM G. .... p 2354 N95-26991
SPERA, DAVID A. .... p 2316 N95-26734
p 2321 N95-27970
p 2312 N95-27972
SPEZIALI, V. .... p 2269 N95-28244
SPINA, ERIC F. .... p 2277 N95-26995
SPONG, D. A. .... p 2431 N95-27419
p 2431 N95-27537
SPRINGER, GEORGE S. .... p 2198 N95-28484
SPRITZER, M. H. .... p 2176 N95-28324
p 2177 N95-28325
SREEVIJAYAN, D. .... p 2155 N95-27263
SRIDHAR, S. .... p 2322 N95-27979
SRINIVASA, N. .... p 2387 N95-28217
SRINIVASAN, G. V. .... p 2221 N95-28075
SRINIVASAN, J. .... p 2151 N95-27792
SRIVASTAVA, B. N. .... p 2376 N95-26460
SRIVASTAVA, SADANAND .... p 2383 N95-27379
ST.JOHN, H. .... p 2416 N95-28329
STAATS, RAYMOND W. .... p 2164 N95-27144
STACY, JOHNATHAN R. .... p 2171 N95-28299
STADLER, MICHAEL A. .... p 2355 N95-26691
p 2356 N95-26825
STAGG, C. H. .... p 2170 N95-28298
STALEY, JAMES T. .... p 2226 N95-26623
p 2226 N95-26624
STALLINGS, ROBERT L., JR. .... p 2123 N95-28241
STANFORD, J. L. .... p 2341 N95-26689
STANLEY, SCOTT P. .... p 2156 N95-27272
STARCK, P. .... p 2200 N95-26540
STARNES, JAMES H., JR. .... p 2194 N95-28466
STASSIS, C. .... p 2442 N95-27932
STASZAK, PAUL .... p 2160 N95-28258
STATT, B. W. .... p 2443 N95-28060
STATTON, GARY .... p 2243 N95-28634
STAUB, U. .... p 2408 N95-27453
p 2219 N95-27966
STAVIG, M. E. .... p 2240 N95-28405
STAVINOHA, LEO L. .... p 2210 N95-28621
STEARNS, R. E. .... p 2372 N95-27849
STECK, J. E. .... p 2118 N95-26943
STECKEL, GARY L. .... p 2210 N95-27632
STEEBY, KURT .... p 2144 N95-26583
STEELE, H. S. .... p 2297 N95-27718
STEELE, JOHN H. .... p 2347 N95-27151
STEERE, DAVID .... p 2454 N95-27529
STEERE, DAVID C. .... p 2364 N95-26536
STEGEMAN, GEORGE I. .... p 2212 N95-26490
p 2178 N95-26570
STEIGENBERGER, U. .... p 2418 N95-28657
STEIL, B. .... p 2330 N95-27954
STEIN, C. .... p 2154 N95-27671
STEIN, EARL S. .... p 2127 N95-26978
STEIN, H. J. .... p 2445 N95-28206
STEINBERGER, H. .... p 2320 N95-27682
STEINER, CRAIG D. .... p 2182 N95-26969
STEINETZ, B. M. .... p 2140 N95-28344
STEINETZ, BRUCE M. .... p 2168 N95-27434
STELZER, J. .... p 2441 N95-27740
STEMMER, G. .... p 2135 N95-27526
STEN, J. C. E. .... p 2254 N95-27049
p 2257 N95-28451
STENFLO, L. .... p 2436 N95-28668
STENTZ, ANTHONY .... p 2367 N95-26754
STERIN, E. .... p 2136 N95-28409
STERNLIEB, B. .... p 2442 N95-27932
STEVENS, D. E. .... p 2464 N95-28007
STEVENS, D. J. .... p 2325 N95-28394
STEVENS, PHILIP M. .... p 2174 N95-28315
STEVENSON, J. O. .... p 2205 N95-27683
STEVENSON, J. W. .... p 2267 N95-28131
STEWART, ERIC C. .... p 2117 N95-26381
STEWART, GLEN .... p 2398 N95-26598
STEWART, J. G. .... p 2456 N95-28555
STEWART, M. .... p 2227 N95-26746
STEWART, SUSAN .... p 2360 N95-27195
STILES, D. .... p 2373 N95-28243
STILMAN, BORIS .... p 2386 N95-27397
STINNETT, R. W. .... p 2221 N95-28116
STOCKS, G. M. .... p 2408 N95-27456
STOCKWELL, ALAN E. .... p 2131 N95-27371
STOHL, F. V. .... p 2203 N95-27423
STOILOVA, N. I. .... p 2448 N95-27334
STOLLER, H. M. .... p 2176 N95-28323
STOLLER, R. E. .... p 2214 N95-27086
p 2220 N95-28072
p 2221 N95-28120
STOLZ, S. .... p 2389 N95-26915
STONER, G. E. .... p 2218 N95-27722
p 2238 N95-28117
STORM, R. S. .... p 2221 N95-28075
STOUT, WAYNE .... p 2118 N95-26944
STRAIN, J. C. .... p 2124 N95-27981
p 2312 N95-27982
STRAIT, E. J. .... p 2435 N95-28406
STRAKA, SHARON A. .... p 2345 N95-27666
STRAUSS, A. M. .... p 2428 N95-27646
STRAYER, M. R. .... p 2413 N95-28077
p 2373 N95-28498
p 2375 N95-28632
STRAYER, W. T. .... p 2378 N95-27402
STREILE, G. P. .... p 2328 N95-27749
STRELTSOV, V. N. .... p 2255 N95-27335
p 2448 N95-27336
p 2391 N95-27715
STREMEL, PAUL M. .... p 2122 N95-27258
STRENGE, D. L. .... p 2328 N95-27749
STRIBLING, BRUCE E. .... p 2295 N95-26974
STRICKER, THOMAS M. .... p 2377 N95-26840
STRICKLAND, B. .... p 2365 N95-26611
STRICKLAND, G. SCOTT .... p 2158 N95-27289
STRICKLAND, M. .... p 2392 N95-27742
STROEMBERG, S. .... p 2224 N95-28644
STUCKEY, WAYNE K. .... p 2210 N95-27632
STUDENIKIN, A. I. .... p 2416 N95-28249
STUMPF, R. .... p 2223 N95-28593
STUPP, SAMUEL I. .... p 2437 N95-26553
p 2226 N95-26627
STURCHIO, NEIL C. .... p 2440 N95-27542
SUAREZ, J. .... p 2196 N95-28477
SUAREZ, MAX J. .... p 2334 N95-26423
SUDO, S. .... p 2419 N95-26584
SUEHLE, JOHN S. .... p 2268 N95-28201
SUELENASANTIAGOBARROS, MARIA
p 2316 N95-28672
SUGAWARA, M. .... p 2432 N95-27870
SUHR, STACY .... p 2144 N95-26583
SUKHANOV, V. I. .... p 2280 N95-27338
SULLIVAN, JAMES L. .... p 2300 N95-26504
SUMARU, K. .... p 2234 N95-27486
SUMMERS, C. J. .... p 2270 N95-28529
SUMMERS, D. A. .... p 2233 N95-27130
SUMMERS, DAVID .... p 2176 N95-28322
SUMMERS, RICHARD T. .... p 2158 N95-27288
SUMMERS, THOMAS A. .... p 2295 N95-26961
SUMNER, RICHARD J. .... p 2253 N95-26976
SUN, C. T. .... p 2191 N95-28434
SUN, CHEN-HUI .... p 2344 N95-28556
SUN, W. Q. .... p 2171 N95-28299
SUN, XIAN-HE .... p 2361 N95-26697
SUNDBERG, G. J. .... p 2303 N95-27947
SUNDET, J. K. .... p 2330 N95-27954
SUPEL, JERZY, A. .... p 2364 N95-26511
SUTAWANE, U. B. .... p 2405 N95-27159
SUTHERLAND, W. T. .... p 2418 N95-27634
p 2272 N95-27635
SUTLIFF, J. .... p 2447 N95-28606
SUZUKI, KOJIRO .... p 2274 N95-26739
p 2121 N95-26740
SUZUYA, K. .... p 2237 N95-27967
SVEHLA, ROGER A. .... p 2209 N95-28182
SWAIN, D. W. .... p 2435 N95-28553
SWANN, ANDREW .... p 2388 N95-26514
SWANSON, B. I. .... p 2447 N95-28541
SWANSON, G. .... p 2194 N95-28464
SWANSON, G. D. .... p 2137 N95-28473
SWANTON, G. .... p 2142 N95-26378
SWIFT, FRED W. .... p 2364 N95-26557
SYKES, R. IAN .... p 2341 N95-26546
SYLVESTER, WINFIELD B. .... p 2315 N95-28209
SYNDER, RICHARD D. .... p 2273 N95-26418
SYNOWICKI, R. A. .... p 2199 N95-27638
SYPHERS, M. J. .... p 2421 N95-28017
SZELES, CS. .... p 2236 N95-27962
SZEWCZYK, A. A. .... p 2276 N95-26827
SZEWCZYK, ALBIN A. .... p 2121 N95-26757
SZPALA, S. .... p 2217 N95-27553
SZU, HAROLD .... p 2271 N95-28614

T

T-RAISSI, ALI .... p 2171 N95-28300
TABRIZI, SIEMAK S. .... p 2363 N95-26474
TADDEUCCI, T. N. .... p 2408 N95-27466
TAGHAVI, RAY .... p 2119 N95-26951
p 2119 N95-26952
TAJIMA, T. .... p 2433 N95-28111
TAKACS, LAWRENCE .... p 2334 N95-26423
TAKACS, P. Z. .... p 2425 N95-27490
TAKAI, H. .... p 2292 N95-27677
TAKE, RIICHIRO .... p 2377 N95-26840
TAKEI, MITSURU .... p 2145 N95-27667
TAKEUCHI, T. .... p 2441 N95-27720
TALMY, INNA G. .... p 2241 N95-28582
TAMANOI, HIROTAKA .... p 2388 N95-26539
TAMARU, TAKASHI .... p 2200 N95-26523
TAN, B. C. .... p 2299 N95-28330
TAN, SENG C. .... p 2181 N95-26937
TAN, TAI-HO .... p 2311 N95-28539
TANAKA, M. .... p 2440 N95-27487
TANAKA, S. .... p 2437 N95-26756
TANG, W. K. .... p 2414 N95-28142
TANGLER, J. L. .... p 2122 N95-27541
TANGLER, JAMES L. .... p 2124 N95-27974
TANI, KEIJI .... p 2431 N95-27414
TANNAS, LAWRENCE E., JR. .... p 2292 N95-27863
TANNER, SHARON E. .... p 2400 N95-26394

TANNER, W. G., JR. p 2294 N95-27670
TAPSCOTT, R. E. p 2234 N95-27481
p 2238 N95-28133
TARMOVSKY, A. N. p 2201 N95-26544
TATARA, J. D. p 2358 N95-26364
TAVKHELIDZE, A. N. p 2448 N95-27447
TAYBATOROV, K. A. p 2348 N95-27996
TAYLOR, D. W. A. p 2131 N95-27440
TAYLOR, DALE E. p 2294 N95-28612
TAYLOR, EDWARD p 2428 N95-27654
TAYLOR, HENRY L. p 2143 N95-26556
TAYLOR, J. C. p 2358 N95-28676
TAYLOR, K. E. p 2331 N95-28157
TAYLOR, LARRY T. p 2228 N95-27106
TAYLOR, ROBERT C. p 2243 N95-28634
TAYLOR, ROBERT P. p 2281 N95-27353
TAYLOR, RONALD p 2445 N95-28179
TAYLOR, T. S. p 2416 N95-28329
p 2435 N95-28406
TCHENG, PING p 2291 N95-27259
TECUCI, GHEORGHE p 2383 N95-27380
TEDESKI, G. R. p 2214 N95-27086
TEIKARI, VEIKKO p 2356 N95-26909
TEKRIWAL, PRABBAT p 2285 N95-27887
TELSCHOW, K. L. p 2264 N95-27403
p 2216 N95-27477
TENNEY, YVETTE J. p 2357 N95-28253
TEPAS, DONALD I. p 2360 N95-27058
TER-ANTONYAN, V. M. p 2396 N95-27337
p 2397 N95-28518
TERRAY, EUGENE A. p 2342 N95-26826
TERRIE, GREG p 2313 N95-26476
TESAR, D. p 2155 N95-27263
TESSLER, A. p 2187 N95-28283
TEVAULT, DAVID E. p 2405 N95-27034
THALMANN, E. D. p 2353 N95-26885
THIERRY, D. p 2240 N95-28547
THODE, L. p 2298 N95-28027
THODE, L. E. p 2296 N95-27557
THOENES, KENNETH L. p 2466 N95-26823
THOMAS, G. A. p 2249 N95-26670
THOMAS, HOLLY p 2320 N95-27704
THOMAS, JAMES P. p 2355 N95-26692
THOMAS, JIM p 2371 N95-27251
THOMAS, R. J. p 2273 N95-27987
THOMAS, RICHARD N. p 2458 N95-27068
THOMAS, S. J. p 2297 N95-27718
THOME, K. J. p 2348 N95-28030
THOMPSON, BRAD R. p 2277 N95-26968
THOMPSON, D. C. p 2297 N95-27718
THOMPSON, J. D. p 2407 N95-27431
THOMPSON, K. p 2422 N95-28159
THOMPSON, MALCOLM p 2292 N95-27863
THOMPSON, P. p 2269 N95-28339
THORBURN, WILLIAM p 2156 N95-27270
THORDAHL, JAMES B. p 2374 N95-28591
THORPE, CHARLES E. p 2381 N95-27041
THORSON, LORI A. p 2336 N95-26824
THORSOS, ERIC I. p 2257 N95-28528
THORSTENSON, CLIFFORD B. p 2138 N95-28586
THUMM, W. p 2320 N95-27682
THYAGARAJAN, AJIT p 2367 N95-26770
TIAN, D. C. p 2439 N95-27413
TIEE, JOE J. p 2296 N95-27672
TIERSTEN, HARRY F. p 2402 N95-28505
TILL, W. A. p 2311 N95-28214
TILSON, JEFFREY L. p 2376 N95-26441
TING, L. p 2279 N95-27179
TINH, VO p 2417 N95-28607
TINKER, M. L. p 2311 N95-28214
TINKHAM, M. p 2438 N95-26872
TISCHENKO, D. B. p 2450 N95-26803
TIT, N. p 2443 N95-28016
TKACZYK, J. E. p 2447 N95-28606
TOBIAS, M. p 2138 N95-28488
TOBISKA, W. K. p 2464 N95-28007
TOBLASSON, WAYNE p 2144 N95-27297
TOCCO, D. R. p 2175 N95-28318
TODD, S. M. p 2185 N95-28274
TOLK, N. H. p 2428 N95-27646
TOLLESTRUP, A. V. p 2411 N95-27945
TOLMIE, D. E. p 2378 N95-27422
TOLOCZKO, M. B. p 2214 N95-27086
TOLPADI, ANIL K. p 2285 N95-27889
TOLSHMYAKOV, A. I. p 2288 N95-28603
TOLSTOY, V. N. p 2448 N95-27332
TOMIO, L. p 2406 N95-27318
TOMLINS, P. E. p 2224 N95-26448
TOMME, EDWARD B. p 2295 N95-27132
TOPE, T. J. p 2170 N95-28296
TORABI, A. p 2270 N95-28529
TORII, YOSHIHIRO p 2145 N95-27667
TORRES, M. A. p 2349 N95-26729
TORRES, S. G. p 2223 N95-28534
TOU, T. Y. p 2299 N95-28330
TOUSSAINT, D. p 2409 N95-27552
TOWNSEND, DENNIS P. p 2302 N95-27698
TOWNSEND, LAWRENCE W. p 2420 N95-27372
p 2465 N95-28530
TRABOCCO, R. p 2133 N95-27514
TRABOCCO, R. E. p 2193 N95-28446
TRACEWELL, D. p 2150 N95-27783
TRACY, M. B. p 2123 N95-28241
TRAN, HUY K. p 2166 N95-28293
TRAN, P. p 2422 N95-28122
TRANQUADA, J. M. p 2439 N95-27443
TRAWINSKI, DAVID p 2137 N95-28278
TRAXLER, KATHLEEN M. p 2342 N95-27148
TREBIN, H. R. p 2441 N95-27740
TREBINO, R. p 2425 N95-27482
p 2298 N95-27969
p 2299 N95-28219
p 2299 N95-28220
p 2300 N95-28549
TRENCHARD, MIKE E. p 2314 N95-26882
TREXLER, CARL A. p 2140 N95-28343
TRIPATHI, RAM K. p 2465 N95-28530
TRIPP, JOHN S. p 2291 N95-27259
TROPIS, A. p 2135 N95-27525
TROST, KELLY p 2149 N95-27781
TROWBRIDGE, JOHN H. p 2347 N95-27043
TROWBRIDGE, L. D. p 2208 N95-28042
TRUCANO, T. G. p 2299 N95-28223
TRUJILLO, T. C. p 2443 N95-28023
TRUNOV, V. p 2408 N95-27453
TRUONG, LONG V. p 2372 N95-27905
TRZCINSKI, EDMUND p 2211 N95-27645
TSAI, H. C. p 2190 N95-28425
TSAI, TIMOTHY K. p 2306 N95-27253
TSAO, C. H. p 2465 N95-28530
TSELEPIDAKIS, D. P. p 2286 N95-27893
TSIANG, T. H. p 2184 N95-28267
TSUI, T. Y. p 2220 N95-28044
TSUJII, TOSHIAKI p 2126 N95-26585
TSUKISHIMA, TAKASHIGE p 2297 N95-27868
TSVANKIN, I. p 2339 N95-28190
p 2339 N95-28194
TUCKER, SUSAN p 2266 N95-27724
TUFTS, DONALD W. p 2256 N95-28391
TUMA, MARGARET L. p 2426 N95-27906
TUMMALA, RAO p 2263 N95-27226
TUMMALA, RAO R. p 2263 N95-27229
p 2263 N95-27230
TUOMAS, J. p 2369 N95-26907
TUOMELA, J. p 2276 N95-26928
TUPA, D. p 2426 N95-28022
TUPPER, GEORGE H. p 2342 N95-26826
TURCO, R. P. p 2328 N95-27686
TURINSKY, P. J. p 2412 N95-28045
TURMAN, B. N. p 2420 N95-27480
TURNBULL, A. D. p 2416 N95-28329
p 2435 N95-28406
TURNER, L. G. p 2272 N95-27635
TURNER, PETER R. p 2248 N95-26356
TURNER, ROSS M. p 2258 N95-28580
TURNER, S. p 2419 N95-27158
TURRO, NICHOLAS J. p 2201 N95-26606
TURSKI, KAROL p 2213 N95-26838
TUSCHMANN, W. p 2393 N95-28501
TUTOR, J. p 2400 N95-28350
TUTTLE, B. A. p 2439 N95-27429
p 2445 N95-28165
TUTTLE, M. p 2137 N95-28473
TUTTLE, M. M. p 2190 N95-28427
TUZZOLINO, A. J. p 2294 N95-27670

U

UBERBACHER, E. C. p 2378 N95-27709
UMAR, A. S. p 2413 N95-28077
UMAR, V. M. p 2373 N95-28498
p 2375 N95-28632
UNDERWOOD, GARY N. p 2290 N95-26714
UNEKIS, MICHAEL J. p 2418 N95-28648
UNTERMAN, RONALD p 2179 N95-27117
UPCHURCH, BILLY T. p 2293 N95-27915
UPSON, CHRISTOPHER S. p 2370 N95-27150
USTILOVSKY, SH. p 2136 N95-28409
UY, O. M. p 2294 N95-27670
UZCATEGUI, O. p 2337 N95-27442

V

VACCARELLA, J. A. p 2411 N95-28024
VAELIMAEKI, V. p 2257 N95-28450
VAENTTINEN, M. p 2414 N95-28142
VAHLE, M. O. p 2378 N95-28074
VAIDYANATHAN, P. P. p 2261 N95-26964
p 2256 N95-28095
VALENTIN, JACK p 2349 N95-26597
VALIEV, R. Z. p 2223 N95-28543
VALLIMONT, JOHN p 2428 N95-27653
VALTONEN, M. p 2262 N95-27050
p 2269 N95-28448
VALTONEN, MARTTI p 2259 N95-26496
VANAKEN, R. p 2247 N95-26344
VANBUREN, P. D. p 2329 N95-27878
VANCAUTER, EVE p 2353 N95-26779
VANDERBURGH, JOHN C. p 2461 N95-27131
VANDERSLUIS, R. p 2155 N95-27261
VANDERWIJNGAART, ROB F. p 2274 N95-26588
VANDOORMAAL, J. P. p 2286 N95-27897
VANE, C. R. p 2417 N95-28595
VANGEL, MARK G. p 2193 N95-28442
VANKAN, MARK DAVID p 2335 N95-26531
VANMILLIGEN, B. P. p 2431 N95-27497
VANSTRYLAND, ERIC W. p 2300 N95-28333
VANVLIET, P. J. p 2247 N95-26344
VANVOLKINBURG, BART p 2152 N95-27793
VANYASHIN, V. S. p 2464 N95-27342
VANYSEK, PETR p 2199 N95-26350
VARTABEDIAN, A. M. p 2303 N95-27947
VARTIAINEN, MATTI p 2356 N95-26909
VAUGHN, JASON A. p 2419 N95-27637
p 2242 N95-27638
p 2242 N95-27639
p 2210 N95-27641
p 2428 N95-27646
VAVRA, J. p 2293 N95-28178
VELIGDAN, J. T. p 2426 N95-28196
VELLA, M. C. p 2440 N95-27471
VELLA, MICHAEL p 2440 N95-27538
VENKATAKRISHNAN, V. p 2390 N95-27029
VENKATAPATHY, ETHIRAJ p 2367 N95-26726
VENTRICE, CARL A. p 2426 N95-27913
VENUGOPALAN, R. p 2449 N95-27547
VERBITSKY, MIKHAIL p 2326 N95-26429
VERINDER, IRENE E. p 2165 N95-27842
VERKAMA, M. p 2389 N95-26910
p 2396 N95-26912
p 2396 N95-28352
p 2396 N95-28353
VERKAMA, MARKKU p 2396 N95-26613
VERSTEEGEN, PETER L. p 2345 N95-27389
VETH, MICHAEL J. p 2142 N95-26981
VETRANO, J. S. p 2216 N95-27493
VIDIC, J. p 2228 N95-27107
VIEIRA, D. J. p 2426 N95-28022
VIOTTI, ROBERTO p 2460 N95-27076
p 2460 N95-27078
VIRTANEN, HEIKKI p 2338 N95-27995
VISENTINE, JAMES T. p 2210 N95-27630
p 2211 N95-27645
VITEK, J. M. p 2215 N95-27319
p 2302 N95-27545
VLADIMIR, M. I. p 2410 N95-27881
VLCEK, KEVIN M. p 2143 N95-26966
VOGEL, J. S. p 2204 N95-27496
VOIGT, J. A. p 2439 N95-27429
p 2444 N95-28103
VOIGT, JAMES A. p 2268 N95-28200
VOLAKIS, JOHN p 2366 N95-26694
VOLF, P. p 2385 N95-27391
VOLKOV, A. D. p 2362 N95-27162
VOLTE, C. C. p 2286 N95-27898
VOSE, R. S. p 2343 N95-27920
p 2332 N95-28605
VOSKANYAN, A. V. p 2362 N95-27162
VOSTEEN, LOUIS F. p 2194 N95-28465
VOTER, A. F. p 2215 N95-27446
VOYLES, RICHARD M., JR. p 2359 N95-26884
VRANISH, J. M. p 2156 N95-27273
VREESWIJK, GERRARD A. W. p 2383 N95-27381

W

WAAGEN, D. E. p 2390 N95-27020
WABISZEWSKI, KATHLEEN M. p 2369 N95-26962
WADE, DONALD C. p 2165 N95-27842
WADE, J. A. p 2303 N95-27947
WADE, M. R. p 2302 N95-27875
WAGNER, KIM RITTER p 2371 N95-27418
WAHI, R. P. p 2438 N95-27085
WAHL, KATHRYN J. p 2225 N95-26499
WAITE, J. H., JR. p 2338 N95-28035
WAITE, J. HUNTER JR. p 2336 N95-26699
WAKE, BRIAN E. p 2402 N95-28264
WAKIM, NAGI T. p 2383 N95-27379
WALBA, DAVID M. p 2224 N95-26456
WALBORN, NOLAN R. p 2463 N95-28328
WALCH, M. p 2179 N95-27119
p 2179 N95-27120
WALIGORA, SHARON p 2374 N95-28627
WALKER, A. p 2261 N95-27002
WALKER, B. p 2155 N95-27261

WALKER, KENNETH A. p 2437 N95-26553
p 2226 N95-26627
WALKER, T. H. p 2137 N95-28471
p 2137 N95-28473
WALL, SARAH J. p 2331 N95-28153
WALLACE, S. p 2236 N95-27962
p 2239 N95-28401
WALLER, J. S. p 2272 N95-26787
WALLING, R. S. p 2462 N95-28013
WALLS, DONNA p 2152 N95-27796
WALSH, DON p 2247 N95-27909
WALTENBURG, HANNE N. p 2224 N95-26351
WALTER, J. B. p 2216 N95-27477
WALTER, K. C. p 2444 N95-28125
WALTER, R. W. p 2190 N95-28427
WALTERS, I. M. p 2154 N95-27804
WALTERS, KENNETH R., SR. p 2342 N95-27148
WALTON, ANDREW C. p 2377 N95-26984
WALTON, M. A. p 2392 N95-28012
WAMPLER, W. p 2183 N95-27428
WAMPLER, W. R. p 2445 N95-28206
WAN, ALFRED D. M. p 2383 N95-27381
WANAMAKER, JOHN L. p 2184 N95-28267
WANDERER, P. p 2269 N95-28339
WANDERKA, N. p 2438 N95-27085
WANG, C. Y. p 2392 N95-28110
WANG, H. p 2183 N95-27955
WANG, J. p 2422 N95-28159
WANG, J. T. p 2194 N95-28468
WANG, JIAN p 2203 N95-27420
WANG, L. M. p 2438 N95-27087
p 2440 N95-27491
p 2236 N95-27733
WANG, MINGLI p 2424 N95-26860
WANG, QIUNING p 2201 N95-26707
WANG, R. G. p 2388 N95-26515
WANG, TIMOTHY W. p 2180 N95-26572
WANG, X. p 2201 N95-26544
WANG, X. B. p 2439 N95-27413
WANG, XIAO-YEN p 2389 N95-26663
WANG, Y. p 2408 N95-27456
WANG, YAJUN p 2438 N95-26959
p 2290 N95-26982
p 2405 N95-27017
WANG, Z. L. p 2447 N95-28606
WANTHAL, S. p 2186 N95-28279
WANTUCK, P. J. p 2206 N95-27851
WARD, D. T. p 2147 N95-27769
WARD, MICHAEL D. p 2178 N95-26569
p 2178 N95-28334
WARD, PETER C. p 2158 N95-27285
WARDEN, ROBERT M. p 2156 N95-27269
WARREN, C. DAVID p 2184 N95-28207
WARREN, M. E. p 2299 N95-28132
WARREN, M. S. p 2462 N95-27445
WARREN, W. L. p 2445 N95-28165
WARTIK, STEVE p 2370 N95-27235
WARWICK, W. H. p 2235 N95-27499
WATANABE, YUICHI p 2431 N95-27414
WATERS, PAUL F. p 2227 N95-27102
p 2232 N95-27125
WATERS, S. B. p 2235 N95-27499
WATSON, S. J. p 2199 N95-28639
WATSON, WILLIE R. p 2400 N95-26394
WATT, R. G. p 2297 N95-27850
WATTS, ALAN p 2428 N95-27654
WAY, BRYAN S. p 2342 N95-26826
WEBBON, BRUCE p 2304 N95-28256
WEBER, D. C. p 2229 N95-27114
p 2232 N95-27128
WEBER, F. p 2463 N95-28357
WEBER, MARVIN J. p 2421 N95-27679
WEBER, W. J. p 2438 N95-27087
p 2440 N95-27491
p 2236 N95-27733
WEDDENDORF, BRUCE p 2360 N95-27501
WEEKS, D. P. p 2450 N95-28260
WEEMS, J. W. p 2172 N95-28307
WEERTMAN, J. R. p 2223 N95-28543
WEGAND, J. p 2225 N95-26482
WEGLEY, H. L. p 2289 N95-27973
WEGMAN, EDWARD J. p 2394 N95-26414
p 2394 N95-26415
p 2394 N95-26457
p 2393 N95-28507
WEHNER, MICHAEL F. p 2335 N95-26622
WEIDEMAN, MARK H. p 2185 N95-28276
WEIDNER, JOHN P. p 2140 N95-28343
WEIDOW, D. p 2151 N95-27790
WEIGEL, M. K. p 2463 N95-28357
WEIJERS, BERTUS p 2337 N95-27147
WEINSTEIN, LEONARD M. p 2291 N95-27191
WEIR, DONALD S. p 2400 N95-26392
WEIR, J. R., JR. p 2241 N95-28560
WEIR, J. T. p 2298 N95-27876
WEITZ, ERIC p 2417 N95-28572
WELCH, D. O. p 2445 N95-28186
WELCH, P. J. p 2231 N95-27121
WELLER, A. p 2431 N95-27419
WELLS, J. C. p 2413 N95-28077
WELLS, R. L. p 2241 N95-28661
WELLS, RICHARD L. p 2436 N95-26473
p 2223 N95-28332
WELLS, SUSAN K. p 2346 N95-26483
WEN, JUNG p 2149 N95-27781
WENDER, I. p 2203 N95-27420
WENGER, M. P. p 2290 N95-26541
WENTZ, W. H., JR. p 2124 N95-27976
WENTZ, WILLIAM H. p 2118 N95-26941
WERLINK, R. J. p 2231 N95-27121
WERLINK, RUDY J. p 2304 N95-28359
WERNER, A. E. p 2268 N95-28156
WERNER, S. A. p 2215 N95-27462
WERNET, MARK P. p 2291 N95-27173
WERTHEIMER, MICHAEL R. p 2242 N95-27669
WESLOH, DAVID p 2452 N95-26607
WESOLOWSKI, D. J. p 2208 N95-27961
WESSELING, P. p 2388 N95-26395
WESTBROOK, C. K. p 2243 N95-28064
WESTBROOK, STEVEN R. p 2210 N95-28621
WESTGEEST, B. Q. p 2307 N95-26342
WESTMORELAND, C. G. p 2235 N95-27499
WETMORE, ALAN E. p 2340 N95-26463
WHARTENBY, WILLIAM G. p 2337 N95-27703
WHEAT, S. R. p 2393 N95-28393
WHEELER, JAMES R. p 2272 N95-26788
p 2272 N95-26793
WHELAN, G. p 2328 N95-27749
WHETTEN, BRIAN p 2363 N95-26388
p 2371 N95-27252
WHINNERY, L. p 2331 N95-28548
WHITAKER, ANN F. p 2419 N95-27637
WHITE, A. R. p 2415 N95-28210
WHITE, C. S. p 2303 N95-27947
WHITE, JIM p 2384 N95-27382
WHITE, PETER S. p 2223 N95-28332
WHITE, R. G. p 2309 N95-27846
WHITEHEAD, R. S. p 2192 N95-28437
WHITING, M. p 2373 N95-28243
WHITT, THOMAS H. p 2272 N95-26794
WHITWORTH, ROBERT W. p 2200 N95-26452
WICKRAMASINGHE, H. K. p 2201 N95-26870
WIEST, TODD E. p 2203 N95-27295
WIGLEY, T. M. L. p 2331 N95-28157
WIGNALL, G. D. p 2234 N95-27486
WIKLIND, T. p 2461 N95-26522
p 2461 N95-27320
WIKRAMANAYAKE, PALITHA N. p 2346 N95-26904
WILCOX, PETER p 2125 N95-27762
WILCOXON, J. P. p 2202 N95-27136
WILDER, GREG p 2121 N95-26854
WILDS, W. p 2421 N95-27735
WILKINS, M. p 2373 N95-28243
WILLDEN, KURTIS p 2137 N95-28474
p 2196 N95-28478
WILLEN, E. p 2269 N95-28339
WILLIAMS, DEAN N. p 2328 N95-27558
WILLIAMS, ELLEN I. p 2158 N95-27288
WILLIAMS, K. G. p 2411 N95-28024
WILLIAMS, MARK C. p 2320 N95-27746
WILLIS, R. W. p 2236 N95-27946
WILLIS, ZDENKA S. p 2314 N95-26841
WILLS, J. M. p 2213 N95-27082
WILSON, B. G. p 2462 N95-28013
WILSON, BRENDA K. p 2457 N95-27658
WILSON, C. B. p 2268 N95-28156
WILSON, D. C. p 2430 N95-27327
WILSON, D. R. p 2138 N95-28489
WILSON, J. TODD p 2391 N95-27489
WILSON, JACK p 2140 N95-27860
WILSON, JEFFREY D. p 2371 N95-27370
WILSON, JOHN W. p 2465 N95-26427
p 2420 N95-27372
p 2465 N95-28530
WILSON, KELCE S. p 2252 N95-26972
WILSON, KENNETH J. p 2128 N95-26507
WILSON, ROBERT E. p 2124 N95-27975
WILSON, TERRY A. p 2251 N95-26867
WILT, DAVID M. p 2235 N95-27503
WILTSE, J. C. p 2270 N95-28529
WIMPENNY, S. J. p 2409 N95-27689
WINER, W. O. p 2241 N95-28592
WING, JEANNETTE M. p 2364 N95-26536
WINGATE, C. A. p 2236 N95-27943
WINTERSTEIN, S. R. p 2395 N95-27684
WISCHOW, PERRY B. p 2314 N95-26682
WISE, KENSALL D. p 2268 N95-28239
WISEMAN, F. L. p 2172 N95-28304
WITHEROW, WILLIAM K. p 2423 N95-26385
WITNEY, A. B. p 2223 N95-28543
WITT, C. EDWIN p 2320 N95-27704
WOLF, E. E. p 2205 N95-27692
WOLF, K. p 2134 N95-27522
WOLFE, MICHAEL p 2359 N95-26863
WOLFE, R. E. p 2175 N95-28318
WOLSTENHOLME, DENNIS J. p 2250 N95-26738
WOMBLE, D. E. p 2393 N95-28393
WON, I. J. p 2131 N95-27440
WONG, CHEUK-YIN p 2417 N95-28447
WONG, R. L. p 2265 N95-27693
WONG, YIU-FAI p 2373 N95-28168
WOOD, B. E. p 2427 N95-28408
WOOD, RALPH p 2364 N95-26486
WOODARD, MARK p 2149 N95-27777
WOODARD, MARK A. p 2149 N95-27778
WOODS, CLAUDIA p 2157 N95-27279
WOODS, R. O. p 2427 N95-28516
WOODS, ROBERT D. p 2163 N95-26970
WOODS, ROBERT O. p 2157 N95-27277
WOODWARD, M. R. p 2197 N95-28483
WOOLLAM, JOHN A. p 2260 N95-26816
p 2199 N95-27636
WORLEY, P. H. p 2327 N95-27457
WOROBEY, WALTER p 2265 N95-27706
WORSEY, PAUL p 2175 N95-28320
WORSEY, PAUL N. p 2176 N95-28322
WORSNOP, D. R. p 2328 N95-27743
WORTHINGTON, B. L. p 2228 N95-27108
WORTMAN, J. J. p 2463 N95-27668
p 2294 N95-27670
WOUTERS, J. M. p 2426 N95-28022
WOVCHKO, EDWARD A. p 2207 N95-27904
WOZNICK, PAUL p 2163 N95-26980
WRIGHT, A. F. p 2219 N95-27958
WRIGHT, D. M. p 2414 N95-28171
WRIGHT, JEFFERY S. p 2177 N95-28326
WRIGHT, PEGGY p 2453 N95-27004
WRIGHT, WAYNE p 2358 N95-26612
WRONSKI, W. p 2261 N95-27023
p 2261 N95-27024
WU, CHUNG-HUA p 2123 N95-28003
WU, CHUNG-YU p 2334 N95-26423
WU, DOUGLAS J. p 2453 N95-26866
WU, EDWARD M. p 2193 N95-28445
WU, G. GORDON p 2385 N95-27392
WU, JIE p 2391 N95-27726
WU, JOHN L. p 2437 N95-26553
WU, QIFEN p 2289 N95-28619
WU, S. T. p 2168 N95-27424
WU, X. Z. p 2440 N95-27535
WU, XUTING p 2302 N95-27844
WUEBBLES, D. J. p 2327 N95-27532
WULFMAN, DAVID S. p 2175 N95-28320

X

XIE, M. p 2420 N95-27470
XIJUN, HUANG p 2120 N95-26713
XIN, Y. L. p 2397 N95-27485
XING, LIANQUN p 2162 N95-26715
XIONG, YALIN p 2425 N95-27038
XU, GUOQUN p 2274 N95-26718
XU, J. p 2410 N95-27874
XU, JUN p 2236 N95-27962
XU, YANGSHENG p 2301 N95-27098

Y

YABANA, KAZUHIRO p 2399 N95-27548
YAKOVLEV, O. I. p 2407 N95-27410
YAMADA, TED p 2172 N95-28303
YAMAMOTO, MASATAKA p 2180 N95-26667
YAMAMOTO, TAKESHI p 2200 N95-26523
YAMANAKA, MARI p 2431 N95-27414
YAMAOKA, H. p 2234 N95-27486
YAN, M. p 2215 N95-27446
YAN, SUSAN G. p 2403 N95-26491
YANG, JIE p 2352 N95-28525
YANG, QIANG p 2450 N95-27064
YANG, R. T. p 2205 N95-27691
YANG, S. p 2241 N95-28604
YANILKIN, YU. V. p 2288 N95-28603
YAO, Y. p 2428 N95-27646
YASUKAWA, Y. p 2222 N95-28167
YATES, JOHN T., JR p 2224 N95-26351
YATES, JOHN T., JR. p 2200 N95-26528
p 2207 N95-27904
YAZIDJOGLOU, NICK p 2398 N95-26598
YEAMANS, S. p 2421 N95-27735
YEAW, C. T. p 2265 N95-27693
YEE, C. p 2146 N95-27764
YEN, YI-FEN p 2405 N95-27081
YING, S. X. p 2273 N95-26445
YIP, CHRISTOPHER M. p 2178 N95-28334
YORCK, M. p 2157 N95-27281
YOSEF, REUVEN p 2126 N95-27859

YOST, WILLIAM T. .... p 2353 N95-26889
YOU, YONG .... p 2284 N95-27721
YOUNG, A. .... p 2132 N95-27507
YOUNG, D. A. .... p 2412 N95-28051
YOUNG, D. P. .... p 2123 N95-28230
p 2123 N95-28265
YOUNG, G. R. .... p 2406 N95-27307
p 2420 N95-27427
YOUNG, L. .... p 2151 N95-27792
YOUNG, REBECCA C. .... p 2174 N95-28312
YOUNGBLUT, CHRISTINE .... p 2143 N95-26556
YOUNGQUIST, ROBERT C. .... p 2293 N95-28362
YU, TAO .... p 2121 N95-26859
YUAN, K. A. .... p 2136 N95-28262
YUDIN, I. P. .... p 2398 N95-27239
YULDASHEV, O. I. .... p 2398 N95-27239
p 2399 N95-27298
YULDASHEVA, M. B. .... p 2398 N95-27239
p 2399 N95-27298
YUNGSTER, SHAYE .... p 2273 N95-26380
YUXIANG, CHEN .... p 2342 N95-26724

Z

ZABINSKY, Z. .... p 2137 N95-28473
ZADINSKY, JULIE K. .... p 2352 N95-26494
ZAGHA, MARCO .... p 2376 N95-26529
ZAGHLOUL, HANY H. .... p 2171 N95-28301
ZAHNISER, M. S. .... p 2328 N95-27743
ZAKIN, MITCH .... p 2173 N95-28309
ZAKKARI, M. .... p 2390 N95-27301
ZALIKHANOV, B. ZH. .... p 2362 N95-27162
ZAPLATIN, N. L. .... p 2280 N95-27338
ZAPPA, CHRISTOPHER J. .... p 2346 N95-26533
ZAREN, JOSEPH S. .... p 2251 N95-26893
ZARESTKY, J. .... p 2442 N95-27932
ZARETSKY, ERWIN V. .... p 2301 N95-26774
p 2301 N95-27178
ZARRELLA, PAUL F. .... p 2375 N95-28628
ZAVADIL, K. R. .... p 2445 N95-28144
p 2238 N95-28358
ZELKOWITZ, MARVIN .... p 2374 N95-28627
ZERKLE, D. K. .... p 2206 N95-27851
ZERKLE, RONALD D. .... p 2285 N95-27885
ZHANG, D. .... p 2201 N95-26544
ZHANG, GUOFU .... p 2274 N95-26718
ZHANG, JIANBAI .... p 2121 N95-26859
ZHANG, JIANDI .... p 2436 N95-26440
ZHANG, S. .... p 2267 N95-28148
ZHANG, TAIPING .... p 2326 N95-26429
ZHANG, Z. H. .... p 2439 N95-27413
ZHAO, X. .... p 2370 N95-27095
ZHENG, HANQING .... p 2406 N95-27316
ZHENG, ZHIREN .... p 2401 N95-26857
ZHENGXIU, FAN .... p 2300 N95-28633
ZHIDKOV, E. P. .... p 2398 N95-27239
p 2399 N95-27298
ZHIDKOV, P. E. .... p 2391 N95-27714
ZHIDOV, I. G. .... p 2288 N95-28603
ZHIPING, PEN .... p 2402 N95-28671
ZHOLENTS, A. .... p 2425 N95-27675
ZHOU, TONG C. .... p 2364 N95-26486
ZHOU, X. L. .... p 2411 N95-28004
ZHOU, YE .... p 2288 N95-28228
ZHOULING, WU .... p 2300 N95-28633
ZHU, JIANPING .... p 2361 N95-26697
ZHU, Y. .... p 2445 N95-28186
ZIEBA, K. J. .... p 2404 N95-26748
ZIEGERT, JOHN C. .... p 2387 N95-28217
ZIEMKE, J. R. .... p 2341 N95-26689
ZIMKAS, CHUCK .... p 2144 N95-26583
ZIMMERMAN, ALBERT H. .... p 2272 N95-26786
ZIMMERMAN, D. K. .... p 2312 N95-27983
ZIMMERMAN, DAVID .... p 2309 N95-27305
ZIMMERMAN, MARTIN L. .... p 2372 N95-27729
ZINKLE, S. J. .... p 2221 N95-28120
ZIOCK, H. J. .... p 2421 N95-27735
ZIPF, EDWARD C. .... p 2429 N95-26800
ZISCHKA, PETER J. .... p 2192 N95-28436
ZMIERCZAK, TOMASZ .... p 2143 N95-26837
ZOK, F. .... p 2181 N95-26847
ZOLADZ, T. .... p 2304 N95-28364
ZONGHUA, HUANG .... p 2402 N95-28671
ZRELOV, V. P. .... p 2441 N95-27867
ZUBRIN, ROBERT .... p 2145 N95-28261
ZUFANG, YANG .... p 2341 N95-26723
ZUHOSKI, P. B., JR. .... p 2315 N95-28520
ZUHR, R. A. .... p 2237 N95-28080
ZUMINO, B. .... p 2449 N95-27877
ZUNDELEVICH, YURY .... p 2206 N95-27707
ZUPP, GEORGE .... p 2162 N95-26586
ZUREK, W. H. .... p 2462 N95-27445
ZYSKOWSKI, MICHAEL K. .... p 2120 N95-28956

CORPORATE SOURCE INDEX

Typical Corporate Source Index Listing

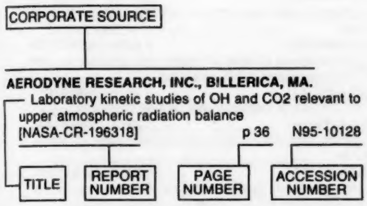
CORPORATE SOURCE
AERODYNE RESEARCH, INC., BILLERICA, MA.
Laboratory kinetic studies of OH and CO2 relevant to upper atmospheric radiation balance
[NASA-CR-196318] p 36 N95-10128
TITLE
REPORT NUMBER
PAGE NUMBER
ACCESSION NUMBER

Listings in this index are arranged alphabetically by corporate source. The title of the document provides the user with a brief description of the subject matter. The report number helps to indicate the type of document cited (e.g., NASA report, translation, NASA contractor report). The accession number denotes the number by which the citation is identified. The page number helps you locate the citation in the abstract section. The titles are arranged under each corporate source in ascending accession number order.

A

ACADEMY OF SCIENCES (USSR), KRASNOYARSK (USSR).

Second International Conference on Software for Multiprocessors and Supercomputers Theory, Practice, Experience
[AD-A289474] p 2368 N95-26820

ACADEMY OF SCIENCES (USSR), NOVOSIBIRSK (USSR).

Measurement of inclusive Lambda production in electron-positron interactions at the upsilon energies
[DE95-610302] p 2407 N95-27407

Measurement of R in e(+)e(-)-annihilation at center-of-mass energies between 7.2 and 10.34 GeV
[DE95-610303] p 2407 N95-27408

Couplings of heavy hadrons with soft pions from QCD sum rules
[DE95-610349] p 2407 N95-27410

Magnetic quadrupole moment of W-boson in Kobayashi-Maskawa model
[DE95-610355] p 2407 N95-27411

Large relativistic corrections to the positronium decay rate
[DE95-610470] p 2407 N95-27412

ACE-ABLE ENGINEERING CO., INC., GOLETA, CA.

Low-cost tubular antenna deployer for WISP-2
p 2156 N95-27269

ADAPTIVE SOLUTIONS, INC., BEAVERTON, OR.

High performance hardware and software for pattern recognition and image processing
[AD-A289153] p 2370 N95-27031

ADVANCED DEVICE TECHNOLOGIES, INC., CHARLOTTESVILLE, VA.

Novel field effect transistors for low power electronics
[AD-A288650] p 2262 N95-27096

Novel field effect transistors for low power electronics
[AD-A289929] p 2271 N95-28629

ADVANCED SCIENTIFIC COMPUTING LTD., WATERLOO (ONTARIO).

Turbulence requirements of a commerical CFD code
p 2286 N95-27897

ADVISORY GROUP FOR AEROSPACE RESEARCH AND DEVELOPMENT, NEUILLY-SUR-SEINE (FRANCE).

AGARD membership, 1995
[AGARD-MEMB-95] p 2450 N95-26353

Composite Repair of Military Aircraft Structures
[AGARD-CP-550] p 2131 N95-27504

AEPCO, INC., ROCKVILLE, MD.

AH-1F COBRA rewire program MANPRINT analysis
[AD-A289190] p 2130 N95-27018

AERONAUTICAL SYSTEMS DIV., EGLIN AFB, FL.

User documentation of the CTA program
[AD-A289508] p 2121 N95-26854

AERONAUTICAL SYSTEMS DIV., WRIGHT-PATTERSON AFB, OH.

Visual system operational evaluation
[AD-A289173] p 2356 N95-27012

AEROSPACE CORP., EL SEGUNDO, CA.

Plume measurements with the T5 xenon ion thruster
[AD-A288697] p 2167 N95-26489

Progress towards computer simulation of NiH2 battery performance over life p 2272 N95-26786

Development of welded solar arrays for DMSP and GPS satellites
[AD-A289512] p 2318 N95-26846

Subvisual cirrus: What it is and where you find it
[AD-A289329] p 2342 N95-26899

Long-term variability of electron radiation dose in geosynchronous orbit
[AD-A289335] p 2162 N95-26902

Computer Systems Division software system metrics approach
[AD-A288837] p 2370 N95-27210

Spacecraft materials studies on the Aerospace Corporation tray on EOIM-3 p 2210 N95-27632

Exposure of LDEF materials to atomic oxygen: Results of EOIM 3 p 2210 N95-27633

Design prediction for long term stress rupture service of composite pressure vessels p 2188 N95-28291

Stratospheric ozone reactive chemicals generated by space launches worldwide
[AD-A289852] p 2332 N95-28623

AEROSPACE CORP., LOS ANGELES, CA.

A sustainable genetic algorithm for satellite resource allocation p 2376 N95-27383

A hybrid genetic algorithm for resolving closely spaced objects p 2384 N95-27387

Improved reduced-resolution satellite imagery
p 2376 N95-27388

Use of SURFACE CHEMKIN to model multiphase atmospheric chemistry: Application to nitrogen tetroxide spills p 2172 N95-28305

AEROSPACE MEDICAL RESEARCH LABS., WRIGHT-PATTERSON AFB, OH.

Handbook of perception and human performance, volume 2. Cognitive processes and performance
[AD-A289587] p 2355 N95-26692

Design considerations for FrankTalk: A distributed group support system
[AD-A289386] p 2359 N95-26863

Acute and subacute toxicity of ammonium dinitramide (ADN) p 2175 N95-28318

AEROSPATIALE, TOULOUSE (FRANCE).

Composite or metallic bolted repairs on self-stiffened carbon wing panel of the commuter ATR72 design criteria, analysis, verification by test p 2135 N95-27525

AIR FORCE CIVIL ENGINEERING CENTER, TYNDALL AFB, FL.

Engineering Technical Letter (ETL) 94-5: Fire protection engineering criteria and technical guidance. Emergency lighting and marking of exits
[AD-A288953] p 2246 N95-26566

Silicone joint sealants for pavements
[AD-A289843] p 2241 N95-28620

AIR FORCE ENVIRONMENTAL TECHNICAL APPLICATIONS CENTER, SCOTT AFB, IL.

Southern Africa: A climatological study
[AD-A289466] p 2342 N95-27148

AIR FORCE INST. OF AVIATION MEDICINE, MANCHING (GERMANY).

Transient studies of G-induced capillary dryout and rewet p 2281 N95-27351

AIR FORCE INST. OF TECH., WRIGHT-PATTERSON AFB, OH.

Using machine learning to derive efficient cost and performance estimates in VLSI CAD designs
[AD-A288254] p 2363 N95-26408

Development of a nonlinear simulation for the McDonnell Douglas F-15 Eagle with a longitudinal TECS control-law
[AD-A288610] p 2128 N95-26481

A study of magnetic activity effects on the thermospheric winds in the low ionosphere
[AD-A288677] p 2334 N95-26488

Analysis of group performance in visual signal detection
[AD-A289561] p 2355 N95-26683

Enhanced visual user interface support for domain-oriented application composition systems
[AD-A289337] p 2359 N95-26737

Reduction of off-boresight fields for a TEM horn antenna
[AD-A289708] p 2250 N95-26738

Silicon based microactuators for telerobotic tactile stimulation
[AD-A289340] p 2260 N95-26767

Analysis of hypersonic boundary layer second mode instability over a 7 deg cone
[AD-A289471] p 2276 N95-26819

Compressible turbulence measurements in a supersonic boundary layer including favorable pressure gradient effects
[AD-A289475] p 2276 N95-26821

Compressible turbulence measurements in a supersonic flow with adverse pressure gradient
[AD-A289477] p 2276 N95-26822

Compensated deconvolution from wavefront sensing
[AD-A289490] p 2336 N95-26824

A numerical model to predict the fate of jettisoned aviation fuel
[AD-A289336] p 2242 N95-26842

A comparison of the Neal-Smith and omega Tau function, zeta function and tau function flying qualities criteria
[AD-A289503] p 2130 N95-26844

Fatigue behavior of a cross-ply metal matrix composite at elevated temperature under strain controlled mode
[AD-A289425] p 2181 N95-26865

The re-engineering of the Air Force Institute of Technology Student Information System
[AD-A289426] p 2453 N95-26866

Perceptual based image fusion with applications to hyperspectral image data
[AD-A289429] p 2251 N95-26867

Viscoplastic characterization and fatigue modeling of titanium based metal matrix composites
[AD-A289430] p 2181 N95-26868

A 3-D finite difference time domain investigation of microwave propagation through inhomogeneous biological materials
[AD-A289431] p 2251 N95-26869

An analysis of the KC-135 three-person cockpit
[AD-A289540] p 2130 N95-26873

A new drag measurement system for wind tunnel testing of the racing bicycle and rider to determine a low drag configuration
[AD-A289375] p 2122 N95-26875

The photo-realistic AFIT virtual cockpit
[AD-A289376] p 2130 N95-26876

Classification of ultra high range resolution radar using decision boundary analysis
[AD-A289378] p 2251 N95-26877

Stall precursor study of high frequency data for three high speed, swept compressor rotors
[AD-A289379] p 2139 N95-26878

A demonstration of Client-Server technology using remote procedure calls with an application of file migration for moving records based on time
[AD-A289392] p 2453 N95-26879

Investigation of boundary layer and performance effects of transpiration cooling through a porous plate in a rocket nozzle
[AD-A289393] p 2167 N95-26880

An image quality analysis of ANVIS-6 night vision goggles
[AD-A289398] p 2359 N95-26883

Characterization of fatigue behavior of 2-D woven fabric reinforced ceramic matrix composite at elevated temperature
[AD-A289423] p 2181 N95-26886

Optimization of a nutation damper attached to a spin-stabilized satellite
[AD-A289424] p 2162 N95-26887

Analysis of instability growth and collisionless relaxation in thermionic converters using 1-D PIC simulations
[AD-A289310] p 2319 N95-26891

Embedology and neural estimation for time series prediction
[AD-A289312] p 2394 N95-26892

Improving the performance of spiral antennas by using passive scatterers
[AD-A289324] p 2251 N95-26893

EASY-SIM: A visual simulation system software architecture with an Ada 9X application framework
[AD-A289325] p 2368 N95-26895

Photoluminescence spectroscopy of 4H- and 6H-SiC
[AD-A289326] p 2202 N95-26896

Design, fabrication, modeling, and optical characterization of organic polymer nonlinear directional couplers
[AD-A289327] p 2227 N95-26897

Analysis and simulation of narrowband GPS jamming using digital excision temporal filtering
[AD-A289328] p 2127 N95-26898

Performance characterization of a highly-offset diffuser with and without blowing vortex generator jets
[AD-A289334] p 2122 N95-26901

The collapse of composite cylindrical panels with various thickness using finite element analysis
[AD-A289370] p 2308 N95-26905

Control of a large space structure using multiple model adaptive estimation and control techniques
[AD-A289309] p 2162 N95-26916

Image perception wavelet simulation and enhancement for the visually impaired
[AD-A289303] p 2353 N95-26917

Analysis of modal behavior at frequency cross-over
[AD-A289304] p 2162 N95-26918

Predicting protein structure using parallel genetic algorithms
[AD-A289305] p 2369 N95-26919

A gain scheduling optimization method using genetic algorithms
[AD-A289306] p 2381 N95-26920

Design and characterization of resonant cavity light-emitting diodes
[AD-A289307] p 2261 N95-26921

Electro-hydrostatic actuator controller design using quantitative feedback theory
[AD-A289220] p 2141 N95-26957

A quantitative feedback theory FCS design for the subsonic envelope of the VISTA F-16 including configuration variation
[AD-A289221] p 2141 N95-26958

Generation of a single-lobe, far-field intensity pattern from a laser diode array using an optical delay line
[AD-A289226] p 2295 N95-26961

Unification of LARCH and Z-based object models to support algebraically-based design refinement: The Z perspective
[AD-A289234] p 2369 N95-26962

Satellite surface material composition from synthetic spectra
[AD-A289236] p 2163 N95-26963

Frame selection performance limits for statistical image reconstruction of adaptive optics compensated images
[AD-A289240] p 2424 N95-26965

An investigation of the AFIT 2-inch shock tube as a flow source for supersonic testing
[AD-A289246] p 2143 N95-26966

Experimental investigation of the effects of relative physical orientation between evaporator and condenser for a loop heat pipe
[AD-A289248] p 2277 N95-26968

Fatigue behavior of a cross-ply ceramic matrix composite at elevated temperature under tension-tension loading
[AD-A289250] p 2182 N95-26969

A state-space model of a large, lightly damped space structure using the Eigensystem realization algorithm
[AD-A289251] p 2163 N95-26970

ROC analysis of IR segmentation techniques
[AD-A289252] p 2424 N95-26971

Polarization sensitivity of monopulse radar boresight error induced by large, ogive radomes
[AD-A289254] p 2252 N95-26972

Laser beam propagation in non-Kolmogorov atmospheric turbulence
[AD-A289256] p 2295 N95-26974

Investigation into the behavior of geometrically nonlinear composite arches
[AD-A289258] p 2308 N95-26975

Processing of wide-angle synthetic aperture radar signals for detection of obscured ground targets
[AD-A289243] p 2253 N95-26976

Measurement of N2(+) mobility He via Fourier transform emission spectroscopy
[AD-A289266] p 2404 N95-26979

Telepresent spacecraft docking with object-based bilateral control (OBBC)
[AD-A289268] p 2163 N95-26980

Advanced formation flight control
[AD-A289271] p 2142 N95-26981

Minimizing the impact of synchronization overhead in parallel discrete event simulations
[AD-A289278] p 2377 N95-26984

An integrated GPS/INS/BARO and radar altimeter system for aircraft precision approach landings
[AD-A289280] p 2127 N95-26985

Flow visualization of a turbulent shear flow using an optical wavefront sensor
[AD-A289208] p 2277 N95-26986

Generic satellite monitoring expert system
[AD-A289209] p 2163 N95-26987

Multipoint multirate signal processing
[AD-A289211] p 2253 N95-26988

Distributed interactive simulation virtual cassette recorder (DIS VCR); A datalogger with variable speed replay
[AD-A289212] p 2290 N95-26989

Survey and implementation of commercial manual controllers for a generic telerobotics architecture
[AD-A289215] p 2381 N95-26990

Experimental definition for implantation of the AFIT cortical multielectrode array
[AD-A289216] p 2354 N95-26991

Next generation real-time systems: Investigating the potential of partial-solution tasks
[AD-A289203] p 2381 N95-27007

Voice analysis using the bispectrum
[AD-A289204] p 2254 N95-27008

Adaptive beamforming in frequency-dispersive multipath environments
[AD-A289206] p 2254 N95-27009

Generalized probabilistic reasoning and empirical studies on computational efficiency and scalability
[AD-A289185] p 2395 N95-27016

Computing NORAD mean orbital elements from a state vector
[AD-A289281] p 2146 N95-27033

Weighting scheme for the space surveillance network automated tasker
[AD-A289285] p 2146 N95-27035

Flight control design using mixed H2/micron optimization
[AD-A289288] p 2142 N95-27036

A general object model transformation system
[AD-A289289] p 2370 N95-27037

Characterization and redesign of the AFIT multielectrode array
[AD-A289295] p 2354 N95-27039

Implementation and demonstration of a multiple model adaptive estimation failure detection system for the F-16
[AD-A289301] p 2131 N95-27042

Multiple model adaptive estimation and head motion tracking in a virtual environment: An engineering approach
[AD-A289299] p 2359 N95-27046

Isolated digit recognition without time alignment
[AD-A289344] p 2254 N95-27062

The effects of transverse vibration on the performance of an axial groove wick heat pipe
[AD-A289349] p 2278 N95-27065

Multiclassifier fusion of an ultrasonic lip reader in automatic speech recognition
[AD-A289207] p 2254 N95-27079

Space modeler: An expanded, distributed, virtual environment for space visualization
[AD-A289409] p 2461 N95-27131

Toward coherent excitation: Development of a single-source pump for the rubidium hyperfine ground state doublet
[AD-A289413] p 2295 N95-27132

A methodology to assess the utility of future space systems
[AD-A289414] p 2144 N95-27133

Fatigue behavior of a cross-ply ceramic matrix composite subjected to tension-tension cycling with hold time
[AD-A289418] p 2182 N95-27134

An experimental investigation of sandwich flat panels under low velocity impact
[AD-A289420] p 2309 N95-27135

A multi-attribute-utility-theory model that minimizes interview-data requirements: A consolidation of space launch decisions
[AD-A289421] p 2164 N95-27144

Head related transfer function approximation using neural networks
[AD-A289422] p 2382 N95-27145

A demonstration of client-server technology using remote procedure calls with an application in file migration using heuristics
[AD-A289467] p 2255 N95-27149

Effects of blowing ratio on heat transfer to the throat region of a porous-walled nozzle
[AD-A289459] p 2167 N95-27153

Collisional dynamics and spectroscopic studies of highly excited rovibrational levels of I2(X)(0(+)(sub g)) via stimulated emission pumping
[AD-A289447] p 2295 N95-27172

Factors in human-computer interface design (a pilot study)
[AD-A288908] p 2360 N95-27195

A comparison of error categorization schemes for use in software system safety programs
[AD-A288741] p 2371 N95-27251

An analysis of Bayesian networks as classifiers
[AD-A289316] p 2382 N95-27293

Accelerating conservative parallel simulation of VHDL circuits
[AD-A289317] p 2264 N95-27294

High resolution Fourier transform spectroscopy of the first overtone of the N-O stretch in nitrosyl bromide
[AD-A289318] p 2203 N95-27295

Model of a single impurity in a wide bandgap semiconductor describing electric field screening
[AD-A289322] p 2264 N95-27296

Tracking and impact prediction of Earth-Crossing-Objects (ECO's) on a collision course with Earth
[AD-A289321] p 2461 N95-27303

Detecting alpha particles through scintillation in porous materials
[AD-A289313] p 2406 N95-27399

Improved numerical solution of mixed H2/H(infinity) optimization with applications
[AD-A289315] p 2386 N95-27400

Visualization of finite element model solutions for defibrillation voltage and current distributions
[AD-A289836] p 2400 N95-28579

Life cycle costs of alternatives for F-16 printed circuit board diagnosis equipment
[AD-A288744] p 2138 N95-28586

Evaluation of an Air Force Information Resources Management (IRM) overview course
[AD-A288746] p 2456 N95-28587

An automated cost uncertainty program
[AD-A288747] p 2374 N95-28588

Advanced educational methods in the Department of Defense: Application of case theory and computer-assisted instruction to business process reengineering
[AD-A288881] p 2374 N95-28590

A correlational study of the SEI's capability maturity model and software development performance in DOD contracts
[AD-A288890] p 2374 N95-28591

Development of a TECS control-law for the lateral directional axis of the McDonnell Douglas F-15 Eagle
[AD-A289771] p 2142 N95-28598

AIR FORCE OCCUPATIONAL MEASUREMENT CENTER, RANDOLPH AFB, TX.

Aerospace medicine
[AD-A289691] p 2353 N95-26763

AIR FORCE SYSTEMS COMMAND, WRIGHT-PATTERSON AFB, OH.

Room-temperature photocurrent spectroscopy of GaAs/GaAlAs multiple quantum wells
[AD-A289607] p 2201 N95-26707

Numerical investigation to S-inlet flows (Numerical simulation study of S-inlet flows)
[AD-A289590] p 2120 N95-26713

Engineering calculations associated with the ablative thermal protective structures of returnable satellites
[AD-A289593] p 2162 N95-26715

Signals processing using acousto-optical technology
[AD-A289597] p 2250 N95-26717

SUPG finite numerical element solutions for non-compressible Navier-Stokes equation sets
[AD-A289600] p 2274 N95-26718

Plate manipulators
[AD-A289601] p 2121 N95-26719

An observational study on the onset of the summer monsoon over eastern Asia in 1979
[AD-A289637] p 2341 N95-26723

Synoptic features of the Yunan rainy season before the onset of the tropical monsoons
[AD-A289641] p 2342 N95-26724

Chinese space science and technology
[AD-A289618] p 2466 N95-26856

Modulation effect of a Bragg acousto-optic bistable system
[AD-A289622] p 2401 N95-26857

A numerical method for unsteady transonic flow about wings with control surfaces
[AD-A289631] p 2121 N95-26859

Study of frequency doubling antireflection coating
[AD-A289634] p 2424 N95-26860

Characteristics of thermal lens in a copper-vapor laser
[AD-A289545] p 2294 N95-26874

Atmospheric dispersion in adaptive optics
[AD-A289639] p 2428 N95-28617

Influences of film structures on laser damage thresholds
[AD-A289647] p 2300 N95-28633

Thermally-induced unsymmetric optical distortion of output window of high-power CO2 laser
[AD-A289604] p 2300 N95-28650

Method of space-time sequence transform used to measure acousto-optic deflection and modulation
[AD-A289612] p 2402 N95-28671

AKRON UNIV., AKRON, OH.

Robust integration schemes for generalized viscoplasticity with internal-state variables. Part 1: Theoretical developments and applications
[NASA-CR-195452-PT-1] p 2310 N95-28031

Robust integration schemes for generalized viscoplasticity with internal-state variables. Part 2: Algorithmic developments and implementation
[NASA-CR-195453-PT-2] p 2310 N95-28032

ALABAMA A & M UNIV., NORMAL, AL.

Growth and characterization of crystals for room temperature I.R. detectors and second harmonic generation devices
[NASA-CR-198598] p 2443 N95-28033

ALABAMA AGRICULTURAL AND MECHANICAL COLL., NORMAL, AL.

Digital optical computing
[AD-A289395] p 2368 N95-26881

ALABAMA UNIV., HUNTSVILLE, AL.

Marshall Space Flight Center solid waste characterization and recycling improvement study
[NASA-CR-196594] p 2360 N95-27164

SXI Prototype mirror mount
[NASA-CR-196613] p 2301 N95-27244

Advanced Earth-to-orbit propulsion technology information, dissemination and research
[NASA-CR-196582] p 2168 N95-27424

ALLIED-SIGNAL CORP., MORRISTOWN, NJ.

Observational magnetometer calibration with the Hubble Space Telescope's new magnetometers
p 2148 N95-27773

ALLIED-SIGNAL TECHNICAL SERVICES CORP., COLUMBIA, MD.

Telemetry down-link Doppler as an attitude sensor for spin stabilized spacecraft p 2150 N95-27785

ALLISON ENGINE CO., INDIANAPOLIS, IN.

Propulsion system assessment for very high UAV under ERAST
[NASA-CR-195469] p 2140 N95-27866

Recent progress in the joint velocity-scalar PDF method p 2285 N95-27890

AMERICAN INST. OF AERONAUTICS AND ASTRONAUTICS, WASHINGTON, DC.

Proceedings of the AIAA/FAA joint symposium on general aviation systems
[AD-A289830] p 2120 N95-28610

AMERICAN UNIV., WASHINGTON, DC.

Junkyard chemistry p 2227 N95-27102

A practical approach to soil remediation
p 2232 N95-27125

ANALEX CORP., BROOK PARK, OH.

FDTD-ANT user manual
[NASA-CR-195444] p 2372 N95-27729

ANALYSIS AND DESIGN APPLICATION CO. LTD., MELVILLE, NY.

Turbulence modeling needs of commercial CFD codes: Complex flows in the aerospace and automotive industries p 2286 N95-27896

ANALYTICAL ENGINEERING CORP., BOULDER, CO.

Post Kalman progress p 2148 N95-27776

ANALYTICAL SERVICES AND MATERIALS, INC., HAMPTON, VA.

COINS: A composites information database system
p 2194 N95-28465

ARGONNE NATIONAL LAB., IL.

Massively parallel self-consistent-field calculations
[DE95-004128] p 2376 N95-26441

Rotor phases in compound semiconductors
[DE95-004139] p 2436 N95-26442

Surface energy driven crystallization of amorphous Ni69Cr14P17 alloy
[DE95-005543] p 2438 N95-27085

Lattice QCD calculation using VPP500
[DE95-007076] p 2449 N95-27448

The free energy of hot QED at three and a half loops
[DE95-007079] p 2449 N95-27449

Crystal structure, short-range oxygen defects, and water adsorption in La- and Nd-modified ZrO2
[DE95-007134] p 2439 N95-27452

Observations of CEF-split intermultiplet transitions in optically opaque EuBa2Cu3O7 using inelastic neutron scattering
[DE95-007135] p 2408 N95-27453

A new finite element formulation for incompressible flow
[DE95-007141] p 2284 N95-27454

Magnetic resonance imaging of solvent transport in polymer networks
[DE95-007142] p 2234 N95-27455

Synchrotron X-ray scattering studies at mineral-water interfaces
[DE95-008303] p 2440 N95-27542

Language constructs and runtime systems for compositional parallel programming
[DE95-008298] p 2378 N95-27741

Two-body bound states and the Bethe-Salpeter equation
[DE95-008302] p 2392 N95-27742

Particle-like absorption spectra in small transition metal clusters
[DE95-007082] p 2218 N95-27752

Experimental determination of cluster geometrical structure
[DE95-007089] p 2409 N95-27753

Magnetic and structural properties of Fe/Pd multilayers studied by magnetic x-ray dichroism and x-ray absorption spectroscopy
[DE95-007095] p 2206 N95-27755

Density changes in amorphous Pd80Si20 during low temperature ion irradiation
[DE95-007132] p 2441 N95-27928

Energy transfer in real and artificial photosynthetic systems
[DE95-005824] p 2351 N95-27948

Sintering of textured YBa2Cu3O(7-x) under intensive Co-60 gamma irradiation
[DE95-007098] p 2442 N95-27950

Electron spectroscopy studies of argon K-shell excitation and vacancy cascades
[DE95-007096] p 2442 N95-27963

Analysis of the dimerized Sb/Si(001)-(2x1) surface by x-ray standing waves
[DE95-007097] p 2208 N95-27965

The oxidation state and magnetic behaviour of Tb in high-(Tc) related materials
[DE95-007129] p 2219 N95-27966

The structure of lead-indium phosphate glass
[DE95-007130] p 2237 N95-27967

Reflection of neutrons from an optical grating
[DE95-007145] p 2411 N95-28004

Effects of high-temperature environments on flaw generation and fracture behavior of SiC/SiC composites
[DE95-008270] p 2183 N95-28068

High-temperature deformation of ZrO2-Al2O3/SiC whisker composites fabricated by two techniques
[DE95-008273] p 2183 N95-28069

Transportation R and D included in thermal and mechanical sciences program
[DE95-008275] p 2303 N95-28070

Using the scalable nonlinear equations solvers package
[DE95-008323] p 2378 N95-28071

Gamma ray-induced embrittlement of pressure vessel alloys
[DE95-007133] p 2220 N95-28072

A case study in automated theorem proving: A difficult problem about commutators
[DE95-008392] p 2392 N95-28173

The high energy behavior of the forward scattering parameters -- (sigma)(sub tot), (rho), and B
[DE95-007075] p 2415 N95-28210

The high energy behavior of the forward scattering parameters -- (sigma)(sub tot), (rho), and B
[DE95-007075] p 2415 N95-28210

Faraday screen sputtering on TPX
[DE95-008347] p 2434 N95-28224

Ordered one-component plasmas: Phase transitions, normal modes, large systems, and experiments in a storage ring
[DE95-007077] p 2434 N95-28233

Synthesis and properties of lanthanide-exchanged Preyssler's heteropolyanions
[DE95-007136] p 2238 N95-28235

Site scientific mission plan for the Southern Great Plains CART site, January-June 1995
[DE95-008393] p 2344 N95-28340

The ELF controversy
[DE95-008283] p 2256 N95-28407

Residual stress, strain, and faults in nanocrystalline palladium and copper
[DE95-008294] p 2223 N95-28543

ARIZONA STATE UNIV., TEMPE, AZ.

A demonstration of Client/Server technology using remote procedure calls for an application of file migration for moving records based on location
[AD-A289391] p 2453 N95-26864

Monte-Carlo simulation methods for finite flat plate winding flows
[AD-A289842] p 2289 N95-28619

ARIZONA UNIV., TUCSON, AZ.

Performance modeling of hyperspectral imaging sensors for atmospheric studies
[AD-A289017] p 2289 N95-26461

Elastic properties of metallic superlattices
[AD-A288699] p 2212 N95-26490

An organic thin film laser diode: A novel light source
[AD-A289007] p 2294 N95-26568

A model of the neural basis of the rat's sense of direction
[AD-A289678] p 2350 N95-26761

Hippocampal place fields, the internal compass, and the learning of landmark stability
[AD-A289406] p 2350 N95-27100

Single molecule detection using charge-coupled device array technology
[DE95-006425] p 2411 N95-27953

ARMY AEROMEDICAL RESEARCH LAB., FORT RUCKER, AL.

The effects of UH-1 experience on UH-6O simulator performance: A preliminary study
[AD-A289457] p 2130 N95-26993

Three-dimensional photogrammetry for laboratory applications
[AD-A291624] p 2294 N95-28410

Manikin integrated data acquisition system (MIDAS) initial modifications
[AD-A291662] p 2361 N95-28667

ARMY ARMAMENT RESEARCH, DEVELOPMENT AND ENGINEERING CENTER, PICATINNY ARSENAL, NJ.

Destruction of pyrotechnics manufacture wastewater treatment sludge by plasma arc pyrolysis
p 2171 N95-28301

ARMY ARMAMENT RESEARCH, DEVELOPMENT AND ENGINEERING CENTER, WATERVLIET, NY.

Adaptive finite element method I: Solution algorithm and computational examples
[AD-A288979] p 2389 N95-26609

Stress analysis and failure of an internally pressurized composite-jacketed steel cylinder p 2186 N95-28280

ARMY AVIATION SYSTEMS COMMAND, HAMPTON, VA.

Development and validation of a blade-element mathematical model for the AH-64A Apache helicopter
[NASA-TM-108863] p 2118 N95-26710

ARMY AVIATION SYSTEMS COMMAND, MOFFETT FIELD, CA.

An investigation of the effects of pitch-roll (de)coupling on helicopter handling qualities
[NASA-TM-110349] p 2141 N95-26773

ARMY AVIATION TECHNICAL TEST CENTER, FORT RUCKER, AL.

Test operations procedure (TOP) 7-3-534 airworthiness testing of fixed wing aircraft: Asymmetric power testing
[AD-A289458] p 2130 N95-26994

ARMY COLD REGIONS RESEARCH AND ENGINEERING LAB., HANOVER, NH.

FREZCHEM: A chemical-thermodynamic model for aqueous solutions at subzero temperatures
[AD-A288456] p 2200 N95-26432

Layer coefficients for NHDOT pavement materials
[AD-A288262] p 2246 N95-26548

Soil moisture prediction during freeze and thaw using a coupled heat and moisture flow model
[AD-A289343] p 2336 N95-26753

Solar terrestrial radiation data from the Sleepers River Research Watershed
[AD-A288444] p 2464 N95-27184

Subsurface radar investigations at the Pegasus Glacial-ice Runway and Williams Field, McMurdo Station, Antarctica
[AD-A289323] p 2144 N95-27297

ARMY COMBAT SYSTEMS TEST ACTIVITY (PROVISIONAL), ABERDEEN PROVING GROUND, MD.

Test operations procedure (TOP) 2-2-613, electromagnetic interference testing and electrical subsystem - non-communication
[AD-A289521] p 2251 N95-26851

ARMY CONSTRUCTION ENGINEERING RESEARCH LAB., CHAMPAIGN, IL.

Testing of Uninterruptible Power Supplies with nonlinear loads
[AD-A289353] p 2262 N95-27067

ARMY ENGINEER WATERWAYS EXPERIMENT STATION, VICKSBURG, MS.
Research and development management information system, system user manual
[AD-A289151] p 2453 N95-27004

ARMY MATERIALS TECHNOLOGY LAB., WATERTOWN, MA.
An improved plate theory of order (1,2) for thick composite laminates p 2187 N95-28283
Uncertainties in obtaining high reliability from stress-strength models p 2193 N95-28442

ARMY MATERIEL COMMAND, ABERDEEN PROVING GROUND, MD.
Utilization of composite materials by the US Army: A look ahead p 2189 N95-28421

ARMY MEDICAL DEPT. CENTER AND SCHOOL, FORT SAM HOUSTON, TX.
Development of an acuity-based nurse staffing system for the post anesthesia care unit
[AD-A288831] p 2352 N95-26494

ARMY MISSILE RESEARCH AND DEVELOPMENT COMMAND, REDSTONE ARSENAL, AL.
Recovery and reuse of rocket motor propellant ingredients p 2177 N95-28326

ARMY NATICK RESEARCH AND DEVELOPMENT COMMAND, MA.
Evaluation of laser-protective eyewear dyes in UVEX lenses
[AD-A290076] p 2361 N95-28390
The performance of cargo airdrop systems using g-12E parachutes: Statistical determination of minimum altitude
[AD-A291686] p 2126 N95-28454

ARMY RESEARCH INST. OF ENVIRONMENTAL MEDICINE, NATICK, MA.
Performance enhancing ration components program: Supplemental carbohydrate test
[AD-A288560] p 2358 N95-26558

ARMY RESEARCH LAB., ABERDEEN PROVING GROUND, MD.
Parallel computing on various platforms: A case study
[AD-A289008] p 2376 N95-26460
A fast numerical method for isothermal resin transfer mold filling
[AD-A288944] p 2179 N95-26565
Ram accelerator performance calculations using a modified version of the NASA CET89 equilibrium chemistry code
[AD-A289554] p 2201 N95-26678
Gloved operator performance study. The effects of hand wear and elastic resistance of a control during tracking performance
[AD-A289405] p 2360 N95-27099
The high strain rate deformation of tungsten single crystals
[AD-A288874] p 2223 N95-28189
A novel sensitive detector of atmospheric nitrocompounds based on laser photofragmentation/ionization spectrometry
p 2174 N95-28314
Exploiting parallelism in a Monte Carlo image-matching algorithm
[AD-A289872] p 2374 N95-28625
Optimization strategies for molecular dynamics programs on Cray computers and scalar work stations
[AD-A289574] p 2418 N95-28648

ARMY RESEARCH LAB., ADELPHI, MD.
An optoelectronic attenuator for the high-speed control of microwave integrated circuits
[AD-A289579] p 2260 N95-26690

ARMY RESEARCH LAB., CLEVELAND, OH.
Vibration analysis of a split path gearbox
[NASA-TM-106875] p 2302 N95-27855

ARMY RESEARCH LAB., WATERTOWN, MA.
Modeling considerations in the prediction of residual strength in composite laminates
[AD-A289128] p 2182 N95-27142
A new method of evaluating the explicit magnetic-state-dependent energy in semi-empirical calculations of iron
[AD-A289098] p 2399 N95-27398

ARMY RESEARCH LAB., WHITE SANDS MISSLE RANGE, NM.
Natural aerosol extinction module: XSCALE 1992 user's guide
[AD-A289029] p 2340 N95-26463
The attenuation of microwave radiation by fog and rain
[AD-A288326] p 2249 N95-26562
Indexing meso-beta surface wind site representative
[AD-A288501] p 2341 N95-26650

ARMY TANK-AUTOMOTIVE RESEARCH AND DEVELOPMENT COMMAND, WARREN, MI.
Evaluation of high ester content PAO based single hydraulic fluid in high humidity conditions
[AD-A289374] p 2233 N95-27324
Use of CTFE as an additive to enhance fire resistance of single hydraulic fluid
[AD-A289377] p 2233 N95-27325

ARMY TEST AND EVALUATION COMMAND, ABERDEEN PROVING GROUND, MD.
Power train torque measurement
[AD-A289577] p 2301 N95-26688

ARNOLD ENGINEERING DEVELOPMENT CENTER, ARNOLD AFS, TN.
Cryogenic BRDF measurements at 10.6 micrometers and 0.63 micrometers on contaminated mirrors
[AD-A291611] p 2427 N95-28408

ASTRO AEROSPACE CORP., CARPINTERIA, CA.
FORTE antenna element and release mechanism design p 2157 N95-27282

ATLANTIC RESEARCH CORP., ALEXANDRIA, VA.
Through-the Thickness(R) braided composites for aircraft applications p 2185 N95-28273

AUBURN UNIV., AL.
Modeling the growth of electronic materials
[AD-A289137] p 2438 N95-26997

AUSTRALIAN AND NEW ZEALAND INST. OF PHYSICS (AUSTRALIA).
The 18th Annual Condensed Matter Physics Meeting
[DE95-605568] p 2398 N95-26598

AUSTRALIAN NATIONAL UNIV., CANBERRA (AUSTRALIA).
Shear Alfven wave excitation by direct antenna coupling and fast wave resonant mode conversion
[DE95-609109] p 2256 N95-28254

B

BALL CORP., BOULDER, CO.
High-performance reactionless scan mechanism
p 2158 N95-27288

BATTELLE MEMORIAL INST., COLUMBUS, OH.
Development of repair processes and sources for C/KC-135 aircraft windows/windshields
[AD-A288348] p 2117 N95-26629

BBN SYSTEMS AND TECHNOLOGIES CORP., CAMBRIDGE, MA.
Pilot opinions on high level flight deck automation issues: Toward the development of a design philosophy
[NASA-CR-4669] p 2357 N95-28253

BENSON (ROBERT H.), SPRINGFIELD, VA.
Microgravity Sciences Biotechnology Facility assessment
[NASA-CR-196602] p 2351 N95-27329

BHABHA ATOMIC RESEARCH CENTRE, BOMBAY (INDIA).
Selected bibliography on heavy water, tritiated water and hydrogen isotopes (1981-1992)
[DE95-608331] p 2405 N95-27159
Analytical spectroscopy
[DE95-607896] p 2203 N95-27200
Programming for time resolved spectrum in pulse radiolysis experiments
[DE95-607929] p 2406 N95-27212
Current programmes on physical metallurgy and related areas in BARC
[DE95-607939] p 2214 N95-27255

BIONETICS CORP., HAMPTON, VA.
Measurement and prediction of broadband noise from large horizontal axis wind turbine generators
p 2324 N95-27990

BOEING AEROSPACE CO., SEATTLE, WA.
Comparative performance tests on the Mod-2, 2.5-mW wind turbine with and without vortex generators
p 2124 N95-27978
Comparison of measured and calculated dynamic loads for the Mod-2 2.5 mW wind turbine system
p 2312 N95-27983
Use of blade pitch control to provide power train damping for the Mod-2, 2.5-mW wind turbine
p 2306 N95-27986

BOEING AEROSPACE OPERATIONS, INC., HAMPTON, VA.
Long Duration Exposure Facility (LDEF) Archive System p 2457 N95-27658

BOEING COMMERCIAL AIRPLANE CO., SEATTLE, WA.
Local design optimization for composite transport fuselage crown panels p 2137 N95-28473
Composite fuselage crown panel manufacturing technology p 2137 N95-28474
Impact damage resistance of composite fuselage structure, part 1 p 2138 N95-28482
NASA-ACEE/Boeing 737 graphite-epoxy horizontal stabilizer service p 2138 N95-28489
Noise exposure reduction of advanced high-lift systems
[NASA-CR-195077] p 2402 N95-28670

BOEING DEFENSE AND SPACE GROUP, PHILADELPHIA, PA.
Application of advanced material systems to composite frame elements p 2191 N95-28432
Characterization and manufacture of braided composites for large commercial aircraft structures
p 2196 N95-28478

BOEING DEFENSE AND SPACE GROUP, SEATTLE, WA.
Long Duration Exposure Facility Mini-Data Base User's Guide: Macintosh version
[NASA-CR-4656] p 2177 N95-26391
Analysis of selected specimens from the STS-46 Energetic Oxygen Interaction with Materials-3 experiment p 2210 N95-27642
Space environmental effect on solar cells: LDEF and other flight tests p 2326 N95-27649
Tank pressure control in low gravity by jet mixing
[NASA-CR-191012] p 2243 N95-28001
Investigation of static and cyclic bearing failure mechanisms for GR/EP laminates p 2190 N95-28427

BOEING MILITARY AIRPLANE DEVELOPMENT, SEATTLE, WA.
TranAir: A full-potential, solution-adaptive, rectangular grid code for predicting subsonic, transonic, and supersonic flows about arbitrary configurations. User's manual
[NASA-CR-4349] p 2123 N95-28230
TranAir: A full-potential, solution-adaptive, rectangular grid code for predicting subsonic, transonic, and supersonic flows about arbitrary configurations. Theory document
[NASA-CR-4348] p 2123 N95-28265

BOMBARDIER, INC., MONTREAL (QUEBEC).
Design and structural validation of CF116 upper wing skin boron doubler p 2132 N95-27510

BOSTON COLL., CHESTNUT HILL, MA.
Measurement of heterogeneous chemical processes relevant to aerosol surfaces and trace gases active in the marine environment
[DE95-008337] p 2328 N95-27743
The combined release and radiation effects satellite time history data base system
[AD-A289835] p 2165 N95-28578

BOSTON UNIV., MA.
Neural models of spatial orientation in novel environments
[AD-A288420] p 2380 N95-26530

BOWIE STATE UNIV., MD.
A user-system interface agent p 2383 N95-27379

BRITISH AEROSPACE DEFENCE LTD., PRESTON (ENGLAND).
Composite repair of composite structures
p 2134 N95-27521

BRITISH BROADCASTING CORP., TADWORTH (ENGLAND).
Research and development report. Digital audio broadcasting: Comparison of coverage at Band 2 and Band 3
[BBC-RD-1994/16] p 2248 N95-26493
Com(sup 3): A composite-compatible component coding system
[BBC-RD-1994/17] p 2249 N95-26670
Research and development report. Eureka 147: Tests of the error performance of the DAB system
[BBC-RD-1994/18] p 2249 N95-26696

BROOKHAVEN NATIONAL LAB., UPTON, NY.
Stoichiometry, structure, and properties of La2NiO(4+(delta)) and La(2-x)Sr(x)NiO(4+/-(delta))
[DE95-007682] p 2439 N95-27443
Spin-density-wave magnetism in dilute copper-manganese alloys
[DE95-005121] p 2215 N95-27462
Acceleration theorems
[DE95-007300] p 2420 N95-27484
Specification of the figure and finish of EUV mirrors in terms of performance requirements, revised Nov. 1994
[DE95-005689] p 2425 N95-27490
Surface crystallization and thin film melting in normal alkanes
[DE95-006694] p 2440 N95-27535
Preliminary heavy-light decay constants from the MILC Collaboration
[DE95-005685] p 2409 N95-27552
Characterization of defects in deuterium-implanted beryllium
[DE95-005688] p 2217 N95-27553
Induced axial oscillations in superconducting dipole windings
[DE95-005690] p 2265 N95-27554
Precision electromagnetic calorimetry with liquid krypton
[DE95-006685] p 2292 N95-27677
Health and environmental hazards of CdTe photovoltaic module production, use and decommissioning
[DE95-006688] p 2320 N95-27682

Performance of an accordion electromagnetic calorimeter with liquid krypton
[DE95-006693] p 2292 N95-27738

Magnetic structures in RNi2B2C (R = Ho, Er) superconductors
[DE95-008370] p 2442 N95-27932

Some notes on long-range beam-beam effects for the 2 TeV collider
[DE95-006771] p 2421 N95-28017

Skew chromaticity
[DE95-007677] p 2422 N95-28115

Anomalous cloud absorption? A critique of the paper entitled Absorption of Solar Radiation by Clouds: Observations Versus Models
[DE95-007703] p 2331 N95-28121

Vacancy related defects in thin film Pb(Zr,Ti)O3 materials
[DE95-007696] p 2445 N95-28165

Precursor phenomenon of martensitic transformation in Au-49.5at%Cd alloy
[DE95-007698] p 2222 N95-28166

Aspects of strangeness
[DE95-008314] p 2414 N95-28169

Aspects of strange matter
[DE95-008316] p 2414 N95-28170

The real structure of columnar pinning centers in heavy-ion-irradiated cuprate superconductors
[DE95-003948] p 2445 N95-28186

Optical design and performance of the inelastic scattering beamline at the National Synchrotron Light Source
[DE95-007679] p 2422 N95-28195

Flat panel planar optic display
[DE95-007686] p 2426 N95-28196

Low noise monolithic Si JFETS for operation in the 90-300K range and in high radiation environments
[DE95-007303] p 2269 N95-28244

Rare decays/CP: The perspective of a kaon physicist
[DE95-005964] p 2416 N95-28338

Field quality improvements in superconducting magnets for RHIC
[DE95-006096] p 2269 N95-28339

Weak matrix elements efforts on the lattice: Status and prospects
[DE95-007701] p 2416 N95-28355

Manufacture and testing of the superconducting wire and cable for the RHIC dipoles and quadrupoles
[DE95-006000] p 2270 N95-28515

Strategies for recycling CdTe photovoltaic modules
[DE95-006776] p 2325 N95-28517

Remote sensing of the atmosphere by resonance Raman LIDAR
[DE95-007312] p 2315 N95-28520

Surface scanning techniques to locate and study defects in painted zinc and zinc alloy coated steels
[DE95-006099] p 2240 N95-28547

BROWN UNIV., PROVIDENCE, RI.

Detection of charged particles in superfluid helium
[DE95-007354] p 2403 N95-26560

C

CALIFORNIA INST. OF TECH., PASADENA, CA.

Fluctuations and transport in fusion plasma
[DE95-004178] p 2429 N95-26444

Structures for time-reversed inversion in filter banks
[AD-A289238] p 2261 N95-26964

Fluctuations and transport in fusion plasmas
[DE95-007111] p 2433 N95-27924

An introduction to wavelet transforms
[AD-A289083] p 2256 N95-28095

CALIFORNIA STATE UNIV., LONG BEACH, CA.

The calculation of the mass moment of inertia of a fluid in a rotating rectangular tank
[NASA-CR-197777] p 2278 N95-27165

CALIFORNIA UNIV., BERKELEY, CA.

Do we fully understand the symmetric Lanczos algorithm yet?
[AD-A289614] p 2368 N95-26855

Construction of a connectionist network supercomputer
[AD-A288439] p 2377 N95-27182

Lessons learned from the introduction of autonomous monitoring to the EUVE science operations center
p 2385 N95-27393

Modeling of turbulent chemical reaction
p 2286 N95-27899

Inspection methods for underwater cables
[AD-A289610] p 2312 N95-28616

Chua's circuits: Phenomena and applications
[AD-A291638] p 2271 N95-28666

CALIFORNIA UNIV., BERKELEY. LAWRENCE BERKELEY LAB, CA.

Crab crossing in a gamma-gamma collider
[DE95-006580] p 2420 N95-27470

Characterization and control of wafer charging effects during high-current ion implantation
[DE95-006587] p 2440 N95-27471

Growth of hydrogenated amorphous silicon (a-Si:H) on patterned substrates for increased mechanical stability
[DE95-006589] p 2234 N95-27472

Characterization of wafer charging mechanisms and oxide survival prediction methodology
[DE95-006583] p 2440 N95-27538

Photoemission and optical properties of C60 fullerites
[DE95-006588] p 2425 N95-27539

Femtosecond X-ray generation through 90 degrees T homson scattering: Status of the LBL experiment
[DE95-006560] p 2296 N95-27674

Observation of nonlinear resonances in the advanced light source
[DE95-006561] p 2425 N95-27675

The physics program and status of the SLAC B-Factory and detector
[DE95-006562] p 2409 N95-27676

Amorphous silicon pixel radiation detectors and associated thin film transistor electronics readout
[DE95-006568] p 2265 N95-27678

Scintillator materials for calorimetry
[DE95-006570] p 2421 N95-27679

Micromagnetics and microstructure of epitaxially grown Co and Co-Cr films for perpendicular magnetic recording
[DE95-004681] p 2441 N95-27720

The use of wavelet transforms in the solution of two-phase flow problems
[DE95-004688] p 2284 N95-27721

Time-dependent multi-dimensional simulation studies of the electron output scheme for high power FELs
[DE95-006593] p 2297 N95-27737

Structural oxidation state studies of the manganese cluster in the oxygen evolving complex of Photosystem II
[DE95-008488] p 2409 N95-27744

Realization of vector fields for quantum groups as pseudodifferential operators on quantum spaces
[DE95-008485] p 2449 N95-27877

Beyond transition state theory: Rigorous quantum approaches for determining chemical reaction rates
[DE95-008483] p 2208 N95-28086

Infrared spectroscopy of nonclassical ions and their complexes
[DE95-008487] p 2413 N95-28091

Low temperature carrier transport properties in isotopically controlled germanium
[DE95-008489] p 2444 N95-28092

Finite pulse effects in self-amplified-spontaneous emission
[DE95-006585] p 2298 N95-28104

Mutagenesis in human cells with accelerated H and Fe ions
[NASA-CR-198599] p 2351 N95-28177

Discovery of the most distant supernovae and the quest for (Omega)
[DE95-006569] p 2460 N95-28197

Vibrational spectroscopy of water interfaces
[DE95-006592] p 2209 N95-28218

Numerical simulation of coupled flow and transport with TOUGH2: A verification study
[DE95-008351] p 2287 N95-28225

Feasibility studies for separation processes using environmentally sensitive hydrogels
[DE95-008355] p 2238 N95-28226

Hydrogen-ion titrations of amino acids and proteins in solutions containing concentrated electrolyte
[DE95-008356] p 2209 N95-28229

Stability of strange quark stars with nuclear crusts against radial oscillations
[DE95-008484] p 2463 N95-28357

Nonlinear optical studies of surfaces
[DE95-006574] p 2428 N95-28557

Contact micromechanics in granular media with clay
[DE95-006566] p 2340 N95-28583

CALIFORNIA UNIV., DAVIS, CA.

Comprehension and retrieval of failure cases in airborne observatories p 2145 N95-27394

Probing strongly-interacting electroweak dynamics through W(+)W(-)/ZZ ratios at future e(+)e(-) colliders
[DE95-007202] p 2413 N95-28067

Unique considerations in the design and experimental evaluation of tailored wings with elastically produced chordwise camber p 2192 N95-28436

CALIFORNIA UNIV., LOS ANGELES, CA.

Aeroelasticity and structural optimization of composite helicopter rotor blades with swept tips
[NASA-CR-4665] p 2136 N95-28262

New trends and ideas in the fields of microwave technology
[AD-A291663] p 2257 N95-28453

CALIFORNIA UNIV., SAN DIEGO, LA JOLLA, CA.

Chemical physics of uniform cyclic etching
[AD-A288975] p 2404 N95-26574

CALIFORNIA UNIV., SANTA BARBARA, CA.

Mechanical performance of fiber reinforced metal matrix composites and microstructural development of polycrystalline alumina fibers synthesized from liquid precursors
[AD-A289518] p 2181 N95-26847

Bimaterial interlaces and their role in the mechanical performance of the in-situ composites
[AD-A288973] p 2182 N95-27188

A knowledge highway for integrated modelling from manufacturing to design
[AD-A288872] p 2247 N95-28187

CAMBRIDGE UNIV., CAMBRIDGE (ENGLAND).

The stability of the flow in a laminar separation bubble
[CUED/A-AERO/TR-22] p 2275 N95-26809

Deployment and retraction of a cable-driven solar array: Testing and simulation p 2158 N95-27283

CANADIAN SPACE AGENCY, SAINT HUBERT (QUEBEC).

The Strategic Technologies for Automation and Robotics (STEAR) program: Protection of materials in the space environment subprogram p 2242 N95-27669

CARBORUNDUM CO., NIAGARA FALLS, NY.

High temperature Hexoloy(trademark) SX silicon carbide
[DE95-007290] p 2221 N95-28075

CARNEGIE-MELLON UNIV., PITTSBURGH, PA.

An introduction to software architecture
[AD-A288963] p 2363 N95-26446

An introduction to software architecture
[AD-A288356] p 2363 N95-26467

Application-aware adaptation for mobile computing
[AD-A288366] p 2363 N95-26469

Performance evaluation of a new parallel preconditioner
[AD-A288563] p 2376 N95-26529

Operating system support for coexistence of real-time and conventional scheduling
[AD-A288584] p 2364 N95-26534

Long term distributed file reference tracing: Implementation and experience
[AD-A288585] p 2452 N95-26535

Specifying weak sets
[AD-A288587] p 2364 N95-26536

Stability and thermal influences in nonlinear continuum mechanics and material science
[AD-A288333] p 2448 N95-26563

Modal event calculus in Lolli
[AD-A288544] p 2365 N95-26605

A parallel complexity model for functional languages
[AD-A288589] p 2365 N95-26656

Flexible and safe resolution of file conflicts
[AD-A289342] p 2452 N95-26752

The D* algorithm for real-time planning of optimal traverses
[AD-A289361] p 2367 N95-26754

Control-flow analysis and type systems
[AD-A289338] p 2369 N95-26772

An architecture for optimal all-to-all personalized communication
[AD-A288532] p 2377 N95-26840

Using the dimension reduction technique to prove that clique trees define facets for the asymmetric traveling salesman polytope
[AD-A289397] p 2389 N95-26882

Multi-agent perception for Human/Robot interaction: A framework for intuitive trajectory modification
[AD-A289399] p 2359 N95-26884

An illumination planner for Lambertian polyhedral objects
[AD-A289332] p 2424 N95-26900

A systems engineering approach to electro-mechanical reconfiguration for mobility autonomy
[AD-A289479] p 2301 N95-26926

Using virtual active vision tools to improve autonomous driving tasks
[AD-A289175] p 2356 N95-27013

Moment and hypergeometric filters for high precision computation of focus, stereo and optical flow
[AD-A289293] p 2425 N95-27038

ELVIS: Eigenvectors for land vehicle image system
[AD-A289297] p 2381 N95-27041

Scalability in production system programs
[AD-A289345] p 2453 N95-27063

Automatically selecting and using primary effects in planning: Theory and experiments
[AD-A289347] p 2450 N95-27064

Reducing network depth in the Cascade-Correlation learning architecture
[AD-A289352] p 2382 N95-27068

Efficient generation of counterexamples and witnesses in symbolic model checking
[AD-A288583] p 2370 N95-27095

Dynamic coupling of underactuated manipulators
[AD-A289404] p 2301 N95-27098

Spinning a web: Publishing the SEI software configuration management research on the world wide web
[AD-A288708] p 2377 N95-27250

Truncated Gaussians as tolerance sets
[NASA-CR-197732] p 2395 N95-27417

Solving recursive domain equations with enriched categories
[AD-A289358] p 2371 N95-27418

The assembly tower and some categorical and algebraic aspects of frame theory
[AD-A289360] p 2391 N95-27489

A case for dynamic sets in operating systems
[AD-A289354] p 2454 N95-27529

Phase separation and ordering in InGaAsP and InGaAs materials
[DE95-007493] p 2443 N95-28050

Software process improvement in the NASA software engineering laboratory
[AD-A289912] p 2374 N95-28627

Replacing the message service component in an integration framework
[AD-A289928] p 2375 N95-28628

CASE WESTERN RESERVE UNIV., CLEVELAND, OH.

The 18th Asilomar Conference on Polymeric Materials
[AD-A291721] p 2240 N95-28508

CATHOLIC UNIV. OF AMERICA, WASHINGTON, DC.

Numerical analysis of wave scattering
[AD-A289478] p 2401 N95-26925

CENTRE NATIONAL D'ETUDES SPATIALES, TOULOUSE (FRANCE).

System results from FRECOPA p 2211 N95-27648

CENTRE NATIONAL DE LA RECHERCHE SCIENTIFIQUE, PARIS (FRANCE).

Cataclysmic variables and related objects
[NASA-SP-507] p 2458 N95-27068

CERADYNE, INC., COSTA MESA, CA.

Solid state sintering of silicon nitride ARL-CR-114
[DE95-007291] p 2443 N95-28076

CERAMIC COMPOSITES, INC., MILLERSVILLE, MD.

Ceramic composite combustor cans for expendable turbine engines
[AD-A289551] p 2140 N95-28646

CESKOSLOVENSKA AKADEMIE VED, PRAGUE.

On helicon wave induced radial plasma transport
[DE94-634477] p 2429 N95-26438

CF TECHNOLOGIES, INC., BOSTON, MA.

Precision parts cleaning with supercritical carbon dioxide p 2229 N95-27114

The experience of CF Technologies, Inc. (CF Tech) in critical fluid processing p 2232 N95-27128

CFD RESEARCH CORP., HUNTSVILLE, AL.

Recent advances in PDF modeling of turbulent reacting flows p 2286 N95-27892

Experiences with two-equation turbulence models
p 2286 N95-27894

COLD JET, INC., LOVELAND, OH.

CO2 pellet blast cleaning and degreasing: The true environmentally benign technology
p 2229 N95-27109

CHICAGO UNIV., CHICAGO, IL.

Basic mechanisms and implications of non-photic entrainment of circadian rhythmicity
[AD-A288433] p 2353 N95-26779

Ordered one-component plasmas: Phase transitions, normal modes, large systems, and experiments in a storage ring
[DE95-007077] p 2434 N95-28233

CITY COLL. OF THE CITY UNIV. OF NEW YORK, NY.

Micromechanical prediction of tensile damage for ceramic matrix composites under high temperature
[AD-A288238] p 2180 N95-26626

CITY UNIV. OF NEW YORK, NY.

Studies of radar backscatter as a function of wave properties and the winds in the turbulent marine atmosphere
[NASA-CR-198608] p 2315 N95-28209

CIVIL AEROMEDICAL INST., OKLAHOMA CITY, OK.

Enhancing the effects of diversity awareness training: A review of the research literature
[DOT/FAA/AM-95/10] p 2355 N95-26361

Practical color vision tests for air traffic control applicants: En route center and terminal facilities
[DOT/FAA/AM-95/13] p 2357 N95-27323

CLEMSON UNIV., SC.

A general theory of two- and three-dimensional rotational flow in subsonic and transonic turbomachines
[NASA-CR-4496] p 2123 N95-28003

CLEVELAND STATE UNIV., OH.

Solar concentrator technology development for space based applications, volume 1
[NASA-CR-197723] p 2319 N95-27193

Solar concentrator technology development for space based applications, volume 2
[NASA-CR-197724] p 2319 N95-27194

COAST GUARD, WASHINGTON, DC.

Crew adaptation evaluation of the Norwegian Crew Concept (NOROREW)
[AD-A288478] p 2360 N95-27058

COLORADO SCHOOL OF MINES, GOLDEN, CO.

Depth migration in transversely isotropic media with explicit operators
[DE95-007670] p 2337 N95-27442

Dip-moveout processing by Fourier transform in anisotropic media
[DE95-007668] p 2339 N95-28190

Transformation to zero offset in transversely isotropic media
[DE95-007669] p 2339 N95-28192

Fowler DMO and time migration for transversely isotropic media with explicit operators
[DE95-007671] p 2339 N95-28194

COLORADO STATE UNIV., FORT COLLINS, CO.

High pressure conductivity study of template synthesized polypyrrole: Observation of a crossover from three to one dimensional variable range hopping
[AD-A288367] p 2224 N95-26470

Template synthesis of electronically conductive polymer nanostructures
[AD-A288373] p 2225 N95-26472

COLORADO SUPERCONDUCTOR, INC., FORT COLLINS, CO.

Nonlinear problems in fluid dynamics and inverse scattering: Nonlinear waves and inverse scattering
[AD-A289148] p 2278 N95-27001

COLORADO UNIV., BOULDER, CO.

Micron Accuracy Deployment Experiment (MADE), phase A. Volume 1
[NASA-CR-197792] p 2144 N95-26426

Siloxane-based ferroelectric liquid crystal elastomers and Self-Assembled Mono- and multilayers
[AD-A288285] p 2224 N95-26456

Active antennas with periodic structures
[AD-A289437] p 2252 N95-26924

Characterization of optical polymers for multi-layered electro-optic devices
[AD-A289255] p 2227 N95-26973

On-axis polarization coupling in y-cut titanium in-diffused lithium niobate slab waveguides
[AD-A289260] p 2253 N95-26977

Nonlinear problems in fluid dynamics and inverse scattering: Propagation and capturing of singularities in problems of fluid dynamics and inverse scattering
[AD-A289146] p 2277 N95-26999

Characterization of microwave MESFET circuits under laser illumination. Applications to phased array radar, microwave communications, and digital clock control
[AD-A289181] p 2261 N95-27015

Nonlinear problems in fluid dynamics and inverse scattering: Langmuir circulations and spiral flows
[AD-A289194] p 2278 N95-27019

Studies of planetary scale waves and instabilities in support of the geophysical fluid flow cell experiment on USML-2
[NASA-CR-198646] p 2463 N95-27916

Time-resolved FTIR emission studies of laser photofragmentation and radical reactions
[DE95-008125] p 2300 N95-28398

Perturbations on effective index of refraction from prism coupling
[AD-A291700] p 2427 N95-28524

Evaluation of defect-related diffusion in semiconductors by electrooptical sampling
[AD-A291630] p 2270 N95-28544

COLORADO UNIV., DENVER, CO.

A linguistic geometry for 3D strategic planning
p 2386 N95-27397

COLUMBIA UNIV., NEW YORK, NY.

Applications of Second Harmonic and Sum Frequency Generation to graphite and silica type interfaces
[AD-A288228] p 2201 N95-26544

Stabilization and control of high energy intermediates through adsorption of restricted spaces
[AD-A288552] p 2201 N95-26606

Multiwavelength observations of unidentified high energy gamma-ray sources
[NASA-CR-197840] p 2465 N95-26630

Stochastic control and topics in applied probability
[AD-A291712] p 2395 N95-28526

COMMITTEE ON SCIENCE, SPACE AND TECHNOLOGY (U.S. HOUSE), WASHINGTON, DC.

Global trade in satellites and launch services
[GPO-84-811] p 2165 N95-28342

COMMONWEALTH SCIENTIFIC AND INDUSTRIAL RESEARCH ORGANIZATION, RYDE (AUSTRALIA).

An architecture and protocol for communications satellite constellations regarded as multi-agent systems
p 2166 N95-27377

COMPUTATIONAL PHYSICS, INC., NEWTON, MA.

PRISM validation
[AD-A288476] p 2337 N95-27703

COMPUTER SCIENCES CORP., LANHAM, MD.

Analysis of filter tuning techniques for sequential orbit determination p 2146 N95-27764

Estimation of attitude sensor timetag biases
p 2153 N95-27799

CONNECTICUT UNIV., STORRS, CT.

Molecular engineering of thin polymer films prepared from functionally-terminated oligomers
[AD-A291681] p 2240 N95-28457

CONRAD TECHNOLOGIES, INC., KING OF PRUSSIA, PA.

Development of injury preventing helmet servo-support system for high performance aircraft
[AD-A289547] p 2359 N95-26755

CONSIGLIO NAZIONALE DELLE RICERCHE, FRASCATI (ITALY).

Overview of the observations of symbiotic stars
p 2460 N95-27076

Discussion on selected symbiotic stars
p 2460 N95-27078

CONSTRUCCIONES AERONAUTICAS S.A., MADRID (SPAIN).

Repairs of CFC primary structures
p 2135 N95-27527

COORDINATING RESEARCH COUNCIL, INC., ATLANTA, GA.

The effect of aviation fuels containing low amounts of static dissipater additive on electrostatic charge generation
[AD-A280075] p 2243 N95-28152

CORNELL UNIV., ITHACA, NY.

The development of infrared detectors and mechanisms for use in future infrared space missions
[NASA-CR-197819] p 2290 N95-26702

Second-order closures for compressible turbulence
p 2286 N95-27898

On the physics of ion ring generation for the stabilization of FRX discharges
[DE95-007105] p 2410 N95-27922

Fellowship in physics
[AD-A291691] p 2446 N95-28522

CTA SPACE SYSTEMS, MCLEAN, VA.

Autonomous control system reconfiguration for spacecraft with non-redundant actuators
p 2153 N95-27802

D

DACCO SCI, INC., COLUMBIA, MD.

The use of electrochemistry and ellipsometry for identifying and evaluating corrosion on aircraft
[AD-A288536] p 2125 N95-27186

DARTMOUTH COLL., HANOVER, NH.

A book and series of monographs on ice physics
[AD-A288319] p 2200 N95-26422

Structure of ordinary ice Ih. Part 2: Defects in ice. Volume 1: Point defects
[AD-A288279] p 2200 N95-26452

Photoinduced dipoles and charge pairs in condensed phase
[DE95-007071] p 2207 N95-27921

DASCON ENGINEERING, BAY VILLAGE, OH.

Bibliography of NASA-related publications on wind turbine technology 1973-1995
[NASA-CR-195462] p 2316 N95-26734

Collected papers on wind turbine technology
[NASA-CR-195432] p 2321 N95-27970

A model of rotationally-sampled wind turbulence for predicting fatigue loads in wind turbines
p 2312 N95-27972

DASSAULT AVIATION, SAINT-CLOUD (FRANCE).

Composite repair of metallic airframe: Twenty years of experience p 2132 N95-27508

DAVID SARNOFF RESEARCH CENTER, PRINCETON, NJ.

High-speed coherent laser arrays
[AD-A289373] p 2295 N95-26906

DAYTON UNIV., OH.

Evaluation of composite joints
[AD-A289247] p 2181 N95-26967

DEFENCE RESEARCH AGENCY, FARNBOROUGH, HAMPSHIRE (ENGLAND).

Adhesively bonded composite patch repair of cracked aluminum alloy structures p 2132 N95-27507

DEFENCE RESEARCH ESTABLISHMENT ATLANTIC, DARTMOUTH (NOVA SCOTIA).

A geo-acoustic and oceanographic description of several shallow water experimental sites on the Scotian Shelf
[AD-A288300] p 2345 N95-26420

DEFENCE RESEARCH ESTABLISHMENT OTTAWA, OTTAWA (ONTARIO).

Balanced data focusing: Direction of arrival estimation with maximum likelihood performance
[AD-A288252] p 2248 N95-26407

Evaluation of the FMICW waveform in HF surface radar applications
[AD-A288245] p 2249 N95-26545
Data acquisition software for DREO's near-field antenna measurement facility
[AD-A289819] p 2258 N95-28573
Low-angle tracking in the presence of ducting, coherent and incoherent multipath
[AD-A289838] p 2258 N95-28580

DEFENCE RESEARCH ESTABLISHMENT PACIFIC, VICTORIA (BRITISH COLUMBIA).
Composite repair issues on the CF-18 aircraft
p 2134 N95-27518

DEFENCE SCIENCE AND TECHNOLOGY ORGANISATION, MELBOURNE (AUSTRALIA).
Design and development of a test rig for the high frequency testing of rolling sleeve airsprings
[DSTO-TN-0001] p 2142 N95-26378
F/A-18 IFOSTP Fatigue test airbag load determination on the vertical and horizontal tails
[DSTO-TR-0135] p 2128 N95-26389
Characteristics of the turbine inlet temperature sensing circuit for the T56 turbo-prop engine
[DSTO-TR-0095] p 2139 N95-26424
Electrical performance characterisation of single-shot switches in high speed, high voltage and high current applications
[DSTO-RR-0010] p 2259 N95-26425
Bonded composite repair of metallic aircraft components: Overview of Australian activities
p 2132 N95-27505
Scarf repairs to graphite/epoxy components
p 2135 N95-27523
A review of Australian and New Zealand investigations on aeronautical fatigue during the period Apr. 1993 - Mar. 1995
[AR-009-202] p 2136 N95-27918
Tie-down trials involving a Sikorsky S-70B-2 helicopter
[DSTO-TR-0132] p 2136 N95-28567
The protection of electro-explosive devices (EEDs) and electronics from electrostatic discharge (ESD) hazards
[DSTO-TR-0100] p 2258 N95-28568

DEFENSE MAPPING AGENCY AEROSPACE CENTER, SAINT LOUIS, MO.
Vector Smart Map Level 1: A new DMA product
[AD-A288920] p 2452 N95-26607

DELAWARE UNIV., NEWARK, DE.
Performance and policy dimensions in internet routing
[NASA-CR-197772] p 2367 N95-26770
The effect of material heterogeneity in curved composite beams for use in aircraft structures
p 2190 N95-28426

DENVER UNIV., DENVER, CO.
Energy transfer from excited nitrenes at high density
[AD-A288352] p 2403 N95-26466

DEPARTMENT OF DEFENSE, WASHINGTON, DC.
Unmanned aerial vehicles, 1994 master plan
[AD-A291628] p 2136 N95-28411

DEPARTMENT OF ENERGY, OAK RIDGE, TN.
Guide for transmitting Standard Generalized Markup Language (SGML) encoded bibliographic records
[DOE/OSTI-11685] p 2457 N95-28675

DEPARTMENT OF THE AIR FORCE, BROOKS AFB, TX.
To develop an aerosoling immunomagnetic device for rapid medical diagnosis from clinical samples
[AD-A288504] p 2354 N95-27059

DEPARTMENT OF THE NAVY, WASHINGTON, DC.
High power, broadband folded waveguide Gyrotron-Traveling-Wave-Amplifier
[AD-A288847] p 2259 N95-26433
Method of phased magnitude correlation using binary sequences
[AD-D017257] p 2248 N95-26465
Split pipe testing device for the measurement of bond of reinforcement under controlled confinement
[AD-D017258] p 2245 N95-26500
Ultrasonic test system
[AD-D017261] p 2400 N95-26502
Silicate gel dye laser
[AD-D017262] p 2294 N95-26503
Valve mechanism for an acoustic modulator
[AD-D017263] p 2300 N95-26504
Multipurpose bus interface utilizing a digital signal processor
[AD-D017264] p 2248 N95-26505
Suppressor of oscillations in airframe cavities
[AD-D017265] p 2128 N95-26507
Nondestructive testing apparatus for determining the orientation of reinforcing bars within a concrete structure
[AD-D017267] p 2245 N95-26508
Target detection for vision systems
[AD-D017271] p 2249 N95-26509
A high velocity electromagnetic mass launcher having an ablation resistant insulator
[AD-A288231] p 2154 N95-26524
Non-covalent immobilization of proteins and enzymes on polymerized lipid assemblies
[AD-A288234] p 2225 N95-26526
Balanced on air aircraft
[AD-D017251] p 2129 N95-26537
Preliminary design study of the beam collapser and certain optomechanical aspects of the siderostat
[AD-A288423] p 2423 N95-26549
Material characterization system
[AD-D017385] p 2210 N95-28584
In situ dynamic material property measurement system
[AD-D017387] p 2210 N95-28585
Cryogenic temperature control and tension/compression attachment stage for an electron microscope
[AD-D017390] p 2294 N95-28612
Energy-measuring resistor bank
[AD-D017392] p 2271 N95-28613
Non-linear resistive grid kernel estimator useful in single feature, two-class pattern classification
[AD-D017394] p 2271 N95-28614
Method and apparatus for maintaining linearity and frequency accuracy of an FM chirp waveform
[AD-D017398] p 2258 N95-28615

DESERT RESEARCH INST., RENO, NV.
Replicator for characterization of cirrus and polar stratospheric cloud particles
[NASA-CR-197785] p 2341 N95-26669

DEUTSCHE AEROSPACE A.G., MUNICH (GERMANY).
On aircraft repair verification of a fighter A/C integrally stiffened fuselage skin p 2133 N95-27515
Composite repair of a CF18: Vertical stabilizer leading edge p 2134 N95-27517

DEUTSCHE AIRBUS G.M.B.H., HAMBURG (GERMANY).
Damage occurrence on composites during testing and fleet service: Repair of Airbus aircraft
p 2135 N95-27526

DIFFRACTO LTD., WINDSOR (ONTARIO).
Characterization of corrosion and development of a breadboard of a D sight aircraft inspection system, phase 1
[AD-A288347] p 2125 N95-26527

DISTRICT OF COLUMBIA UNIV., WASHINGTON, DC.
A study of surface temperatures, clouds and net radiation
[NASA-CR-198589] p 2329 N95-27864

DONOVAN (TERENCE), PALO ALTO, CA.
Effects of low earth orbit on the optical performance of multi-layer enhanced high reflectance mirrors
p 2428 N95-27652

DOUGLAS AIRCRAFT CO., INC., LONG BEACH, CA.
Evaluation of all-electric secondary power for transport aircraft
[NASA-CR-189077] p 2266 N95-27999
Aircraft IR/acoustic detection evaluation. Volume 2: Development of a ground-based acoustic sensor system for the detection of subsonic jet-powered aircraft
[NASA-CR-189705-VOL-2] p 2402 N95-28073
The role of biaxial stresses in discriminating between meaningful and illusory composite failure theories
p 2187 N95-28287

DOW-UNITED TECHNOLOGIES COMPOSITE PRODUCTS, INC., WALLINGFORD, CT.
Application of damage tolerance methodology in certification of the Piaggio P-180 Avanti
p 2138 N95-28480

DRAPER (CHARLES STARK) LAB., INC., CAMBRIDGE, MA.
The transition of GTDS to the Unix workstation environment p 2151 N95-27789
Design of fabric preforms for double diaphragm forming p 2184 N95-28269

DREXEL UNIV., PHILADELPHIA, PA.
Nonlinear signal processing schemes for robust target detection in radar
[AD-A288449] p 2255 N95-27185

DU PONT DE NEMOURS (E. I.) AND CO., WILMINGTON, DE.
Manufacturing tailored property ceramic composites
[DE95-006303] p 2237 N95-27993

DUGWAY PROVING GROUND, UT.
Evaluating the environmental viability of open burning/open detonation operations
p 2170 N95-28297

DUKE UNIV., DURHAM, NC.
Chemistry involving the separation, isolation, and immobilization of 3-5 compound semiconductor nanocrystals and quantum dots
[AD-A288381] p 2436 N95-26473
On the synthesis of mixed-metal and mixed-pnicogen13-15 ring-systems
[AD-A288869] p 2223 N95-28332
Nonlinear dynamics and aeroelasticity of rotorcraft in forward flight
[AD-A291714] p 2136 N95-28504
Isolation and x-ray crystal structures of (Li(mu2-As(SiMe3)2) (mu3-As(SiMe3)2)(THF))2 and ((Me3Si)2AsLi(THF)2)2
[AD-A288870] p 2241 N95-28661

DYNAMIC SOFT ANALYSIS, INC., PITTSBURGH, PA.
CAE for thermal management of aerospace electronic boards using the BETAsoft program
p 2272 N95-27354

E

EAGLE-PICHER INDUSTRIES, INC., JOPLIN, MO.
High-rate/high-temperature capability of a single-layer zicar-separator nickel-hydrogen cell
p 2272 N95-26788
Unique features of a new nickel-hydrogen 2-cell CPV
p 2272 N95-26793

EASTMAN KODAK CO., ROCHESTER, NY.
Effects of long term space environment exposure on optical substrates and coatings p 2428 N95-27653

EDGERTON, GERMESHAUSEN AND GRIER, INC., COCOA BEACH, FL.
Cape Canaveral air station launch emergency response forces and toxic materials release contingency plans
p 2172 N95-28308

EDGERTON, GERMESHAUSEN AND GRIER, INC., IDAHO FALLS, ID.
Electromagnetic hysteretic response calculation for superconductors in demagnetizing geometries
[DE95-005028] p 2264 N95-27403
Spray-formed tooling
[DE95-005031] p 2246 N95-27404
Laser ultrasonic generation at the surface of a liquid metal
[DE95-004999] p 2216 N95-27477

EDGEWOOD RESEARCH DEVELOPMENT AND ENGINEERING CENTER, ABERDEEN PROVING GROUND, MD.
Computation of electromagnetic scattering parameters for lognormal distributions of magnetic spheres: Theory and algorithms
[AD-A289672] p 2250 N95-26759
Chlorodifluoromethane equilibrium on 13X molecular sieve
[AD-A289282] p 2405 N95-27034
Proceedings of the 1993 Scientific Conference on Obscuration and Aerosol Research
[AD-A280084] p 2331 N95-28153

EDUCATIONAL TESTING SERVICE, PRINCETON, NJ.
Can there be reliability without reliability?
[AD-A289480] p 2306 N95-26927

EG AND G ENERGY MEASUREMENTS, INC., LAS VEGAS, NV.
Application of a Geographic Information System for radiologic emergency response
[DE95-007624] p 2455 N95-28113

ELECTRIC PROPULSION LAB., INC., TEHACHAPI, CA.
Micro electric propulsion feasibility
[NASA-CR-189139] p 2168 N95-28000

ELECTRO-OPTEK CORP., TORRANCE, CA.
Fabrication of long wavelength array by in-situ molecular beam epitaxy
[AD-A288599] p 2423 N95-26679

ELECTROFUELS MFG. CO., TORONTO (ONTARIO).
Development of an ultra-safe rechargeable lithium-ion battery
[AD-A288959] p 2269 N95-28349

ELECTROTEK CONCEPTS, INC., KNOXVILLE, TN.
A conceptual framework for evaluating variable speed generator options for wind energy applications
p 2273 N95-27987

ENGINEERING MECHANICS RESEARCH, INC., TROY, MI.
Numerical solution of fluid flow and heat tranfer problems with surface radiation p 2282 N95-27357

ENVIROGEN, INC., LAWRENCEVILLE, NJ.
Bioremediation of chlorinated organics: PCBs, TCE, HCFCs p 2179 N95-27117

ENVIRONMENTAL PROTECTION AGENCY, WASHINGTON, DC.
The importance of propulsion engineers in protecting the global environment p 2170 N95-28295

ERIL RESEARCH, INC., SAN RAFAEL, CA.
Ionizing radiation measurements on LDEF: A0015 Free flyer biostack experiment
[NASA-CR-196603] p 2202 N95-27168

EUROCOPTER DEUTSCHLAND G.M.B.H., MUNICH (GERMANY).
External patch repair of CFRP/honeycomb sandwich
p 2134 N95-27522

EUROPEAN ORGANIZATION FOR NUCLEAR RESEARCH, GENEVA (SWITZERLAND).
CAS CERN Accelerator School 5th General Accelerator Physics Course
[DE95-608324] p 2419 N95-27158

Addendum to the 1993 European school of high-energy physics
[DE95-610313] p 2419 N95-27321
The 1993 European school of high-energy physis
[DE95-610196] p 2421 N95-28040

EUROPEAN SPACE AGENCY. EUROPEAN SPACE OPERATIONS CENTER, DARMSTADT (GERMANY).
Fuzzy logic techniques for rendezvous and docking of two geostationary satellites p 2384 N95-27386

EUROPEAN SPACE AGENCY. EUROPEAN SPACE RESEARCH AND TECHNOLOGY CENTER, ESTEC, NOORDWIJK (NETHERLANDS).
Special features of the CLUSTER antenna and radial booms design, development and verification
p 2157 N95-27281
Thermal neutral format based on the step technology
p 2283 N95-27363

F

FEDERAL AVIATION ADMINISTRATION, ATLANTA, GA.
Weather And Radar Processor (WARP) Test and Evaluation Master Plan (TEMP)
[AD-A288280] p 2340 N95-26453
The 1994 updated National Airspace System performance assessment for year 2005
[AD-A288652] p 2125 N95-26485
Precision landing system mathematical modeling study report for Andrews Air Force Base, runway 19L, Camp Springs, MD
[AD-A289015] p 2127 N95-27903

FEDERAL AVIATION ADMINISTRATION, ATLANTIC CITY, NJ.
The controller memory guide. Concepts from the field
[AD-A289263] p 2127 N95-26978

FEDERAL AVIATION ADMINISTRATION, WASHINGTON, DC.
Human factors in aviation maintenance, phase 4
[DOT/FAA/AM-95/14] p 2360 N95-27696
Enplanement and all cargo activity
[AD-A280074] p 2144 N95-28151
Ninth DOD/NASA/FAA Conference on Fibrous Composites in Structural Design, volume 3
[NASA-CR-198718] p 2184 N95-28266
Ninth DOD/NASA/FAA Conference on Fibrous Composites in Structural Design, volume 2
[NASA-CR-198722] p 2193 N95-28462
Development of a coding form for approach control/pilot voice communications
[DOT/FAA/AM-95/15] p 2128 N95-28540

FERMI NATIONAL ACCELERATOR LAB., BATAVIA, IL.
Statistical data analysis
[DE95-007214] p 2454 N95-27090
Orbit analysis
[DE95-007216] p 2419 N95-27091
Search for SUSY at CDF
[DE95-005109] p 2407 N95-27430
A study of parton distribution functions with the use of photon + jet event kinematics in p(bar p) collisions at (radical)s = TeV
[DE95-005127] p 2408 N95-27444
Studies of kinematic distributions and mass reconstruction of CDF top candidate events
[DE95-005108] p 2408 N95-27478
Measurement of the D0 WAMUS magnet inductance
[DE95-005128] p 2399 N95-27530
Coupling in the Tevatron
[DE95-005129] p 2421 N95-27531
Search for the top quark in dilepton decay modes at D(PHI)
[DE95-007764] p 2409 N95-27689
Excited Charm States
[DE95-005749] p 2409 N95-27747
The KTeV pure CsI calorimeter
[DE95-005747] p 2292 N95-27751
Search for supersymmetry and leptoquark states at FNAL
[DE95-003381] p 2410 N95-27871
A study of events with large total transverse energy produced in proton-antiproton collisions at (radical)s = 1.8 TeV
[DE95-003382] p 2410 N95-27872
Search for exotic particles at CDF
[DE95-008383] p 2411 N95-27933
The Top...is it There? A Survey of the CDF and D0 Experiments
[DE95-005746] p 2411 N95-27945
The CDF upgrade
[DE95-006683] p 2421 N95-28107
Cosmic ray test results of the D0 prototype scintillating fiber tracker
[DE95-007215] p 2415 N95-28221
The 132 nsec bunch spacing in the Tevatron proton-antiproton collider
[DE95-005750] p 2422 N95-28346
B-Physics results from D0
[DE95-005126] p 2417 N95-28495

FINNISH GEODETIC INST., HELSINKI (FINLAND).
The installation of and first results from the superconducting gravimeter GWR20 at the Metsahovi Station, Finland
[REPT-95:1] p 2338 N95-27995
On the persistence of the oceanic background of apparent sea level changes in the Baltic Sea
[REPT-94:5] p 2348 N95-27996

FLORIDA INST. OF TECH., MELBOURNE, FL.
Electronic characterization of defects in narrow gap semiconductors: Comparison of electronic energy levels and formation energies in mercury cadmium telluride, mercury zinc telluride, and mercury zinc selenide
[NASA-CR-197835] p 2437 N95-26780

FLORIDA INTERNATIONAL UNIV., MIAMI, FL.
The development of a feature-based concurrent engineering system
[AD-A288424] p 2364 N95-26557

FLORIDA SOLAR ENERGY CENTER, CAPE CANAVERAL, FL.
Radiant exchange considerations in design and scaleup of photocatalytic reactors for purification of nitroglycerine-contaminated air p 2171 N95-28300

FLORIDA UNIV., GAINESVILLE, FL.
A modified proportional navigation scheme for rendezvous and docking with tumbling targets: The Planar case p 2150 N95-27784
International journal of quantum chemistry
[AD-A291633] p 2352 N95-28546

FLUENT, INC., LEBANON, NH.
Experience with turbulence interaction and turbulence-chemistry models at Fluent Inc.
p 2286 N95-27893

FLUID DYNAMICS INTERNATIONAL, INC., EVANSTON, IL.
Progress in simulating industrial flows using two-equation models: Can more be achieved with further research?
p 2286 N95-27895

FOKKER SPACE AND SYSTEMS, LEIDEN (NETHERLANDS).
Some mechanical design aspects of the European Robotic Arm p 2155 N95-27262

FOSTER-MILLER ASSOCIATES, INC., WALTHAM, MA.
Service tough composite structures using the Z-direction reinforcement process p 2185 N95-28272

FUEL CELL ENGINEERING CORP., DANBURY, CT.
Molten Carbonate Fuel Cell (MCFC) product development test
[DE95-007345] p 2316 N95-26543

FUTURETECH CORP., GAITHERSBURG, MD.
Millimeter-wave imaging radiometer data processing and development of water vapor retrieval algorithms
[NASA-CR-198593] p 2343 N95-27997

G

GALAXY SCIENTIFIC CORP., ATLANTA, GA.
Human factors in aviation maintenance, phase 4
[DOT/FAA/AM-95/14] p 2360 N95-27696

GALAXY SCIENTIFIC CORP., HAMPTON, VA.
Ninth DOD/NASA/FAA Conference on Fibrous Composites in Structural Design, volume 1
[NASA-CR-198723] p 2189 N95-28420

GALAXY SCIENTIFIC CORP., PLEASANTVILLE, NJ.
Digital systems validation. Chapter 20 Artificial Intelligenge with applications for aircraft. Handbbook, volume 2
[AD-A288492] p 2380 N95-26638

GAS RESEARCH INST., CHICAGO, IL.
Research on combustion processes relevant to burners in HVAC systems
[PB95-179735] p 2208 N95-28006

GENCORP AEROJET, SACRAMENTO, CA.
Propellant injection systems and processes
[NASA-TM-110632] p 2242 N95-26781

GENERAL ACCOUNTING OFFICE, WASHINGTON, DC.
Asian Aeronautics: Technology acquisition drives industry development. Report to Congressional requesters
[GAO/NSIAD-94-140] p 2118 N95-26817
Information superhighway: Issues affecting development
[AD-A289434] p 2252 N95-26923
Briefing Report to the Ranking Minority Member, Subcommittee on Space and Aeronautics, Committee on Science, House of Representatives. Cassini Mission: Estimated launch costs for NASA's mission to Saturn
[GAO/NSIAD-95-141BR] p 2145 N95-27856
Report to Congressional Committees. Comanche Helicopter: Testing needs to be completed prior to production decisions
[GAO/NSIAD-95-112] p 2135 N95-27910
Report to the Chairman and Ranking Minority Member, Committee on Science, House of Representatives. Weather forecasting: Radar availability requirement not being met
[GAO/AIMD-95-132] p 2342 N95-27912

GENERAL ATOMICS CO., SAN DIEGO, CA.
Fast wave current drive in D3-D
[DE95-007582] p 2431 N95-27441
Experimental aspects of effects of high-energy particles on Alfven modes
[DE95-003383] p 2432 N95-27873
Effect of toroidal plasma flow and flow shear on global MHD modes
[DE95-006676] p 2433 N95-28106
Divertor research on the DIII-D tokamak
[DE95-003942] p 2434 N95-28185
Cryogenic washout of solid rocket propellants
p 2176 N95-28324
Hydrothermal oxidation of solid rocket propellant and other department of defense hazardous wastes
p 2177 N95-28325
Transport simulation of negative magnetic shear discharges
[DE95-003941] p 2416 N95-28329
Wall stabilization of rotating high (Beta) discharges in D3-D
[DE95-008207] p 2435 N95-28406

GENERAL DYNAMICS/CONVAIR, SAN DIEGO, CA.
Development of a low-cost, modified resin transfer molding process using elastomeric tooling and automated preform fabrication p 2184 N95-28268

GENERAL DYNAMICS CORP., FORT WORTH, TX.
Applications of a damage tolerance analysis methodology in aircraft design and production
p 2197 N95-28483

GENERAL DYNAMICS CORP., WARREN, MI.
Improved hardness RHA weldability and material property testing
[AD-A289127] p 2221 N95-28102

GENERAL ELECTRIC CO., CINCINNATI, OH.
A summary of computational experience at GE Aircraft Engines for complex turbulent flows in gas turbines
p 2285 N95-27885
Combustion system CFD modeling at GE Aircraft Engines p 2285 N95-27889

GENERAL ELECTRIC CO., PHILADELPHIA, PA.
Aeroelastic stability of wind turbine blade/aileron systems p 2124 N95-27981
Control system design for the MOD-5A 7.3 mW wind turbine generator p 2306 N95-27985
Variable speed generator application on the MOD-5A 7.3 mW wind turbine generator p 2273 N95-27989

GENERAL ELECTRIC CO., SCHENECTADY, NY.
Experience with k-epsilon turbulence models for heat transfer computations in rotating p 2285 N95-27887
Calculation of design load for the MOD-5A 7.3 mW wind turbine system p 2312 N95-27982

GEO-CENTERS, INC., NEWTON, MA.
Synthesis and characterization of polymeric materials
[AD-A288613] p 2225 N95-26482

GEOCONTROL SYSTEMS, INC., HOUSTON, TX.
A fuzzy logic intelligent diagnostic system for spacecraft integrated vehicle health management
p 2385 N95-27392

GEOPHEX LTD., RALEIGH, NC.
Geophex airborne unmanned survey system
[DE95-007566] p 2131 N95-27440

GEORGE MASON UNIV., FAIRFAX, VA.
Filtered kernel density estimation
[AD-A288293] p 2394 N95-26413
Parallelizing locally-weighted regression
[AD-A288294] p 2394 N95-26414
A method to determine the structure of an unknown mixture using the Akaike Information Criterion and the bootstrap
[AD-A288295] p 2394 N95-26415
Fast multidimensional density estimation based on Random-width bins
[AD-A288286] p 2394 N95-26457
Simulating a multi-target acoustic array on the Intel Paragon
[AD-A288443] p 2377 N95-27183
Building an adaptive agent to monitor and repair the electrical power system of an orbital satellite
p 2383 N95-27380
Visualization methods for the exploration of high dimensional data
[AD-A291717] p 2393 N95-28507

GEORGIA INST. OF TECH., ATLANTA, GA.
A FEAM based methodology for analyzing composite patch repairs of metallic structures
p 2133 N95-27511
A final look at LDEF electro-optic systems components p 2428 N95-27650

Operator modeling in commerical aviation: Cognitive models, intelligent displays, and pilot's assistants
[NASA-CR-198609] p 2138 N95-28203
Modeling the shock response of submerged structures
[AD-A289082] p 2288 N95-28351
Quasi-optical millimeter wave power combining
[AD-A291767] p 2270 N95-28529
Deformation behavior of thin lubricant films at elevated pressure
[AD-A288906] p 2241 N95-28592

GEORGIA TECH RESEARCH INST., ATLANTA, GA.
An acoustic charge transport imager for high definition television applications
[NASA-CR-197841] p 2249 N95-26708

GEORGIA UNIV., ATHENS, GA.
Environmental effects on high energy density materials
[AD-A288296] p 2199 N95-26416

GPS SOLUTIONS, INC., CARSON CITY, NV.
Reusable launch vehicle development research
[NASA-CR-196614] p 2154 N95-27245

GPS TECHNOLOGIES, INC., TAMPA, FL.
Pressure vessel burst test study p 2175 N95-28317

GRAMBLING STATE UNIV., LA.
NQR-NMR studies of higher alcohol synthesis Cu-Co catalysts
[DE95-007926] p 2205 N95-27680

GRUMMAN AEROSPACE CORP., BETHPAGE, NY.
Comparison of resin film infusion, resin transfer molding, and consolidation of textile preforms for primary aircraft structure p 2196 N95-28477
Advanced wing design survivability testing and results
p 2138 N95-28488

GTE GOVERNMENT SYSTEMS CORP., COLORADO SPRINGS, CO.
Applying AI tools to operational space environmental analysis p 2382 N95-27376

H

HAMPTON UNIV., VA.
A study of non-stationary processes and their applications
[AD-A291725] p 2395 N95-28510

HARVARD UNIV., CAMBRIDGE, MA.
Demonstration of photo-assisted tunneling process across the coulomb blockade energy gap in mesoscopic tunnel junctions
[AD-A289534] p 2438 N95-26872
A knowledge highway for integrated modelling from manufacturing to design
[AD-A288872] p 2247 N95-28187

HELSINKI UNIV., HELSINKI (FINLAND).
Absolute logics
[ISBN-951-41-0775-6] p 2397 N95-28238

HELSINKI UNIV. OF TECHNOLOGY, ESPOO (FINLAND).
Self-organizing artificial neural networks in dynamic systems modeling and control
[PB95-185120] p 2379 N95-26449
Analysis of electromagnetic problems involving chiral, bi-isotropic, and uniaxial bianisotropic media
[PB95-185096] p 2248 N95-26450
General purpose finite element solver
[PB95-185062] p 2388 N95-26495
Microwave circuit simulation using higher-order dynamic elements
[PB95-185088] p 2259 N95-26496
Investigations of the hyperfine interactions in copper-oxide perovskites using Eu-151 and Fe-57 Moessbauer spectroscopy
[PB95-185138] p 2437 N95-26513
Fractionation studies of polyethylene using DSC-technique
[PB95-185252] p 2200 N95-26540
Distributed computation of Pareto solutions for two decision makers
[PB95-185047] p 2396 N95-26613
Activities of the Laboratory of Information Processing Science
[PB95-184982] p 2452 N95-26631
Radiometer measurements of snow in Sodankylae, 1991-1993
[PB95-184966] p 2313 N95-26645
Survey on step recovery diode and its applications
[PB95-184974] p 2260 N95-26646
Reference manual: Naive physics simulator
[PB95-184917] p 2369 N95-26907
Prediction of rain attenuation and total atmospheric attenuation for low-availability satellite communications in Europe
[PB95-184925] p 2252 N95-26908
Change, Learning and Mental Work in Organizations: Working papers of the 3rd Otaniemi-Dresden Workshop
[PB95-184941] p 2356 N95-26909
Random relaxation of fixed point iteration
[PB95-185013] p 2389 N95-26910
Characterization of the membrane theory of a clamped shell. The hyperbolic case
[PB95-185021] p 2308 N95-26911
Distributed computation of Pareto solutions in N-player games
[PB95-185039] p 2396 N95-26912
Probabilistic growth model
[PB95-185054] p 2395 N95-26913
Conditions for the parameter dyadics of lossless bi-anisotropic media
[PB95-185104] p 2252 N95-26914
Construction of arbitrary order schemes for many dimensional wave equation
[PB95-184818] p 2276 N95-26928
Milestones in telecommunications in some selected countries
[PB95-184826] p 2252 N95-26929
Summaries of theses for the degree of diploma engineer 1992-1993
[PB95-184867] p 2246 N95-27048
Simple equivalent dipole distributions for dielectric spheroidal scatterers
[PB95-184883] p 2254 N95-27049
Modeling of trapping and abrupt doping effects in MESFET's using R-dynamic element
[PB95-184891] p 2262 N95-27050
Laboratory of production engineering
[PB95-184834] p 2451 N95-28135
Distributed methods and processes in games of incomplete information
[PB95-184842] p 2396 N95-28352
Distributed methods and processes in games of incomplete information
[PB95-184859] p 2396 N95-28353
Scattering by a small object close to an interface. 3. Buried object
[PB95-184909] p 2256 N95-28354
Measurement-based MESFET model in APLAC
[PB95-195483] p 2269 N95-28448
Internal electric field of anisotropic and bi-anisotropic spheres
[PB95-195491] p 2257 N95-28449
Crushing the delay: Tools for fractional delay filter design
[PB95-195509] p 2257 N95-28450
Method of images applied to electromagnetic problems involving spherical, spheroidal and planar geometries
[PB95-195517] p 2257 N95-28451
Local operators in Krylov subspaces
[PB95-195525] p 2393 N95-28499
Radon transform and its applications in gridding airborne geophysical survey data
[PB95-195533] p 2315 N95-28643
High temperature oxidation of nickel concentrates
[PB95-195566] p 2224 N95-28644
Remarks on the growth of the resolvent operators for power bounded operators
[PB95-195418] p 2393 N95-28653
Simulation of burning tokamak plasmas
[PB95-195426] p 2435 N95-28654
Structural optimisation of cage induction motors using finite element analysis
[PB95-195434] p 2271 N95-28655
Modeling and retrieval of snow and sea ice characteristics in the frequency range 6 to 90 GHz
[PB95-195467] p 2316 N95-28656

HERCULES, INC., MAGNA, UT.
Static and dynamic strain energy release rates in toughened thermosetting composite laminates
p 2188 N95-28288

HERCULES AEROSPACE CO., MAGNA, UT.
Advanced tow placement of composite fuselage structure p 2185 N95-28271
Hazards analysis of an integral class 1.1/1.3 rocket motor demilitarization and ingredient recovery system using ammonia p 2174 N95-28315

HONEYWELL, INC., DURHAM, NC.
Electromechanical rotary actuator
p 2157 N95-27278

HONEYWELL, INC., GLENDALE, AZ.
Ball bearing vibrations amplitude modeling and test comparisons p 2158 N95-27286

HONEYWELL, INC., MINNEAPOLIS, MN.
Micro-time stress measurement device development
[AD-A289511] p 2361 N95-26845

HOUSTON UNIV., TX.
Robust hybrid state-space self-tuning control using dual-rate sampling
[AD-A288359] p 2380 N95-26468
Basic studies in turbulent shear flows
[AD-A289145] p 2277 N95-26998

HUGHES STX, INC., LANHAM, MD.
Plasma properties and magnetic field structure of the solar corona, based on coordinated Max 1991 observations from SERTS, the VLA, and magnetographs
[NASA-CR-198592] p 2464 N95-27858

HYDEX CORP., VIENNA, VA.
Remote sensing of hydrologic variables in boreal areas, phase 2
[NASA-CR-198717] p 2314 N95-27998

I

IDAHO NATIONAL ENGINEERING LAB., IDAHO FALLS, ID.
FY 1994 ambient air monitoring report for McMurdo Station, Antarctica
[DE95-008565] p 2331 N95-28149

IDAHO UNIV., MOSCOW, ID.
Magnetically controlled deposition of metals using gas plasma
[DE95-007248] p 2430 N95-27237

ILLINOIS STATE WATER SURVEY, CHAMPAIGN, IL.
Measurement and analysis of the surface energy budget for ARM field experiments
[DE95-007646] p 2338 N95-28114

ILLINOIS UNIV., URBANA, IL.
Molecular object liquid crystals: An approach to new materials
[AD-A288905] p 2437 N95-26553
Materials with self organized surfaces: 2D polymer assemblies
[AD-A288928] p 2226 N95-26627
Compiler-assisted debugging and multiple instruction retry
[NASA-CR-197729] p 2365 N95-26628
Measuring fault tolerance with the FTAPE fault injection tool
[NASA-CR-197773] p 2306 N95-27253

ILLINOIS UNIV., URBANA-CHAMPAIGN, IL.
Efficient modeling of interconnects and capacitive discontinuities in high-speed digital circuits
[NASA-CR-198728] p 2270 N95-28570
NASA/DOD Aerospace Knowledge Diffusion Research Project. Report 35: The use of computer networks in aerospace engineering
[NASA-CR-198170] p 2456 N95-28600

INDUSTRIAL COLL. OF THE ARMED FORCES, WASHINGTON, DC.
Strategy in the commercial aircraft industry in the United States: A comparison of decisionmaking by McDonnell-Douglas and Boeing aircraft companies from 1977-1983
[AD-A288289] p 2117 N95-26409
Surviving the peace. Lessons learned from the aircraft industry in the 1920s and 1930s
[AD-A288284] p 2117 N95-26455
Myers-Briggs type indicators and Kirton adaption-innovation inventory correlations
[AD-A288435] p 2357 N95-27181

INSTITUT D'ASTROPHYSIQUE, PARIS (FRANCE).
Models of classical and recurrent novae
p 2459 N95-27073
Models of symbiotic stars p 2460 N95-27077

INSTITUT DES HAUTES ETUDES SCIENTIFIQUES, BURES-SUR-YVETTE (FRANCE).
Hyperkaehler metrics associated to compact Lie groups
[PB95-185161] p 2388 N95-26514
Compactification of moduli spaces of monopoles
[PB95-185179] p 2388 N95-26515
Yang-Baxter type equations and posets of maximal chains
[PB95-185195] p 2388 N95-26516
Nonexistence of bilipschitz parameterizations and geometric problems about A(sub infinity) weights
[PB95-185187] p 2396 N95-26538
Generalized Schwarzians in several variables and Moebius invariant differential operators
[PB95-185211] p 2388 N95-26539
Gromov-Lawson-Rosenberg conjecture for groups with periodic cohomology
[PB95-185203] p 2389 N95-26915
Symmetries of the KAC-Peterson modular matrices of affine algebras
[PB95-190138] p 2392 N95-28010
Crushing singularities in spacetimes with spherical, plane and hyperbolic symmetry
[PB95-190146] p 2397 N95-28011
Lie group weight multiplicities from conformal field theory
[PB95-190153] p 2392 N95-28012
Photon rockets and gravitational radiation
[PB95-190161] p 2397 N95-28174
Was Einstein 100% right?
[PB95-190179] p 2449 N95-28175

Collapsing and solvmanifolds
[PB95-196267] p 2393 N95-28501

Korteweg-de Vries equation: Convergent Birkhoff normal form
[PB95-196275] p 2393 N95-28611

General relativity and experiment
[PB95-192894] p 2450 N95-28664

INSTITUTE FOR COMPUTER APPLICATIONS IN SCIENCE AND ENGINEERING, HAMPTON, VA.

Introduction to multigrid methods
[NASA-CR-195045] p 2388 N95-26395

Wavenumber selection for small-wavelength Goertler vortices in curved channel flows
[NASA-CR-195063] p 2273 N95-26576

Contribution to the optimal shape design of two-dimensional internal flows with embedded shocks
[NASA-CR-195062] p 2389 N95-26672

Performance prediction: A case study using a multi-ring KSR-1 machine
[NASA-CR-195066] p 2361 N95-26697

Unstructured mesh generation and adaptivity
[NASA-CR-195069] p 2278 N95-27027

On the nonlinear stability of the unsteady, viscous flow of an incompressible fluid in a curved pipe
[NASA-CR-195065] p 2278 N95-27028

A 3D agglomeration multigrid solver for the Reynolds-averaged Navier-Stokes equations on unstructured meshes
[NASA-CR-195073] p 2390 N95-27029

Acoustic field in unsteady moving media
[NASA-CR-198162] p 2279 N95-27179

Spectral methods on arbitrary grids
[NASA-CR-198158] p 2279 N95-27247

Multigrid techniques for unstructured meshes
[NASA-CR-195070] p 2391 N95-27433

On the modulational instability of large amplitude waves in supersonic boundary layers
[NASA-CR-195072] p 2284 N95-27760

A numerical method for solving the three-dimensional parabolized Navier-Stokes equations
[NASA-CR-198159] p 2287 N95-27917

A phenomenological treatment of rotating turbulence
[NASA-CR-198168] p 2288 N95-28228

A genuinely multidimensional upwind scheme and efficient multigrid solver for the compressible Euler equations
[NASA-CR-195000] p 2288 N95-28571

Response of multi-panel assembly to noise from a jet in forward motion
[NASA-CR-198164] p 2289 N95-28673

INSTITUTE FOR DEFENSE ANALYSES, ALEXANDRIA, VA.

A method for simulating correlated random variables from partially specified distributions
[AD-A288820] p 2393 N95-26347

A mathematical framework for an improved search model
[AD-A288858] p 2358 N95-26552

The value of simulation for training
[AD-A289174] p 2143 N95-26556

The evolution and impact of PCS technology
[AD-A288606] p 2255 N95-27249

INSTITUTE FOR SCIENTIFIC RESEARCH, LEXINGTON, MA.

Theoretical studies of interstellar processes
[NASA-CR-198647] p 2462 N95-28216

INSTITUTE FOR SPACE SCIENCE AND TECHNOLOGY, INC., GAINESVILLE, FL.

The orbital debris detector consortium: Suppliers of instruments for in-situ measurements of small-particles in the space environment p 2294 N95-27670

INSTITUTE OF ELECTRICAL AND ELECTRONICS ENGINEERS, PASADENA, CA.

The 1994 IEEE-IMS Workshop on Information Theory and Statistics
[AD-A288808] p 2380 N95-26492

INSTITUTO DE PESQUISAS ESPACIAIS, SAO JOSE DOS CAMPOS (BRAZIL).

Models used to forecast agricultural corn crops in the micro-region of Ribeirao Preto-SP
[INPE-5513-NTC/309] p 2315 N95-28554

Binary segmentation of SAR images by the ICM algorithm
[INPE-5464-PRE/1772] p 2258 N95-28559

Tokamak ETE engineering preliminary project
[INPE-5529-PRE/1796] p 2435 N95-28562

SAR noise reduction through the utilization of robust filters
[INPE-5504-PRE/1787] p 2258 N95-28569

Neural networks in the classification of uses of the soil in satellite images
[INPE-5478-PRE/1777] p 2316 N95-28672

INSTITUTO TECNOLOGICO DE TOLUCA, TOLUCA (MEXICO).

Radon integral measurement system
[DE95-608074] p 2405 N95-27010

INTERNATIONAL CENTRE FOR THEORETICAL PHYSICS, TRIESTE (ITALY).

Atomic and electronic structure of clusters from Car-Parrinello method
[DE94-634463] p 2403 N95-26437

Wake fields in semiconductor plasmas
[DE94-634523] p 2429 N95-26439

Monte Carlo study of electron-plasmon scattering effects on hot electron transport in GaAs
[DE95-607768] p 2403 N95-26542

Analytic formulae for the Hartree-Fock order parameter at arbitrary p/q filling factors for the 2DEG in a magnetic field
[DE95-607805] p 2448 N95-26603

A modified backpropagation algorithm for training neural networks on data with error bars
[DE95-608729] p 2381 N95-27025

Higher-order probabilistic perceptrons as Bayesian inference engines
[DE95-608730] p 2381 N95-27044

Optimal control of two queues in series
[DE95-608731] p 2382 N95-27045

On compact multipliers of topological algebras
[DE95-608751] p 2390 N95-27092

Variability study of foF2 for an equatorial station
[DE95-608080] p 2337 N95-27157

The consideration of a bright relative beam dynamics in the magnetic focusing field
[DE95-608377] p 2398 N95-27160

DNA denaturation through a model of the partition points on a one-dimensional lattice
[DE95-607909] p 2439 N95-27201

The electrical behaviour of an excitable cell at different conditions
[DE95-607911] p 2351 N95-27254

Spectral properties of multipliers on topological algebras
[DE95-608747] p 2390 N95-27299

Holomorphic curves in Abelian varieties, part 1
[DE95-608748] p 2396 N95-27300

q-structure algebra of U(sub q)(g-circumflex) from its adjoint action
[DE95-608749] p 2390 N95-27301

Some commutativity theorems for a certain class of rings
[DE95-608750] p 2390 N95-27302

Extended BRST symmetry for the relativistic particle with curvature
[DE95-608799] p 2406 N95-27309

Field theory of point-like systems with higher-order derivatives
[DE95-608800] p 2448 N95-27310

Introduction to Dubois-Violette's non-commutative differential geometry
[DE95-608801] p 2390 N95-27311

Finite fermion density effects on the electroweak string
[DE95-608802] p 2448 N95-27312

A model of the extended electron and its nonlocal electromagnetic interaction: Gauge invariance of the nonlocal theory
[DE95-608803] p 2255 N95-27313

A note on the constituent quark resonances
[DE95-608831] p 2406 N95-27316

Model independent constraints on anomalous gauge boson self-couplings from e(+)e(-) colliders with longitudinally polarized beams
[DE95-608844] p 2406 N95-27317

A simple relativistic model of pp-bar yields K(+)K(-)
[DE95-608852] p 2406 N95-27318

On commutativity of right s-unital rings with some polynomial constraints,
[DE95-608752] p 2390 N95-27330

Mean value theorem in topological vector spaces
[DE95-608753] p 2390 N95-27331

Quantum k-Poincare 1994
[DE95-608754] p 2448 N95-27332

On the Hopf structure of U(p,q)(gl(1/1)) and the universal Tau-matrix of Fun(p,q)(GL(1/1))
[DE95-608755] p 2448 N95-27333

Wigner quantum oscillators. OSP (3/2) oscillators
[DE95-608756] p 2448 N95-27334

On permanent capillar-heavy waves in circular shaped channels
[DE95-608779] p 2280 N95-27339

Algebraic structure of the Green's ansatz and its q-deformed analogue
[DE95-608780] p 2395 N95-27340

The canonical q-transformations with two q-para-Bose oscillators
[DE95-608781] p 2396 N95-27341

Axionic fuel for sun
[DE95-608788] p 2464 N95-27342

The effects of temperature on Schottky diode barrier height and evidence of multiple barrier
[DE95-609147] p 2264 N95-27405

Hall effect and resistivity in the normal state of high-T(sub c) cuprates in the electron-fracton model
[DE95-610612] p 2439 N95-27413

Harmonic maps of the bounded symmetric domains
[DE95-608798] p 2397 N95-27485

Visualization and direct comparison of large displacements using difference holographic interferometry
[DE95-608782] p 2292 N95-27711

Numerical study of the singlet-triplet model for cuprate superconductors
[DE95-609438] p 2440 N95-27712

Scaling of localization length of a quasi 1D system with longitudinal boundary roughness
[DE95-609148] p 2391 N95-27739

Molecular dynamics simulations of Gay-Berne nematic liquid crystal: Elastic properties from direct correlation functions
[DE95-609149] p 2441 N95-27740

A first principles approach to phase stability and order-disorder transformation: Application to Li-Al alloys
[DE95-609152] p 2218 N95-27756

Crossover integral equation theory for the liquid structure study
[DE95-609155] p 2218 N95-27757

Electronic structure of disordered Cu-Ag alloys
[DE95-609156] p 2219 N95-27758

The role of edge dislocations in the deformation of BCC metals
[DE95-609157] p 2219 N95-27759

The surface of liquid He-4 at nonzero temperatures
[DE95-607841] p 2207 N95-27880

A diagram technique for strongly interacting fermion systems. One-and two-band Hubbard models
[DE95-609437] p 2410 N95-27881

Ultrasonic study on ternary liquid systems by laser-sound interaction
[DE95-608783] p 2207 N95-27929

Hydrogen-like atom in laser field: Invariant atomic parameters in the ground state
[DE95-609036] p 2411 N95-27930

Multifractal character of the electronic states in disordered two-dimensional systems
[DE95-609153] p 2443 N95-2[illegible]16

Beta-dynamics in simple liquid metal
[DE95-609154] p 2220 N95-28039

A correlated Walks' theory for DNA denaturation
[DE95-607910] p 2444 N95-28112

Neutrino oscillations in strong magnetic fields
[DE95-608876] p 2416 N95-28249

Electronic structure of ordered and disordered transition metal aluminides
[DE95-609034] p 2223 N95-28250

Quantum effects induced by a gap in the spectrum of atom-bath coupling constants: Freezing of atomic decay and monochromatic collective radiation
[DE95-609037] p 2416 N95-28251

The off-center effect on the diffusion coefficient of Cu(+) and Li(+) in the KCl lattice
[DE95-609146] p 2446 N95-28255

Temperature dependence of the static dielectric response in a Q1D electron gas
[DE95-609269] p 2400 N95-28350

Nonlinear dynamics of a coherent polariton-biexciton system
[DE95-609150] p 2417 N95-28607

Subharmonic phonon transmission and Kapitza conductance between crystals with very different vibrational spectra
[DE95-609151] p 2447 N95-28608

Supercooled liquid dynamics for the charged hard-sphere model
[DE95-609158] p 2241 N95-28609

INTERNATIONAL SOCIETY FOR PHOTOGRAMMETRY, LONDON (ENGLAND).

Third international congress of plant molecular biology: Molecular biology of plant growth and development
[DE95-006482] p 2352 N95-28496

IOWA STATE UNIV. OF SCIENCE AND TECHNOLOGY, AMES, IA.

A fixed time performance evaluation of parallel CFD applications
[DE94-014240] p 2273 N95-26445

Theoretical studies of reaction surfaces
[AD-A288458] p 2404 N95-26632

IOWA UNIV., IOWA CITY, IA.

Polarizing matter and antimatter: A new method
[DE95-007109] p 2421 N95-27923

Indentability of conventional and negative Poisson's ratio foams p 2195 N95-28472

ISHIKAWAJIMA-HARIMA HEAVY INDUSTRIES CO. LTD., TOKYO (JAPAN).

Element material experiment by EFFU
p 2145 N95-27667

ISRAEL ATOMIC ENERGY COMMISSION, BEERSHEBA (ISRAEL).

Study of the phase transformations and microstructures of uranium rich alloys of the binary uranium-gallium system
[DE95-609624] p 2217 N95-27713

ISRAEL INST. OF METALS, HAIFA (ISRAEL).

Prediction of fatigue crack growth under constant amplitude and random loading using specimens with multiple cracks
[AD-A291614] p 2136 N95-28409

J

JAPAN ATOMIC ENERGY RESEARCH INST., TOKYO (JAPAN).

Outline and handling manual of fusion experimental data monitor system DAISY, version 2
[DE95-703895] p 2431 N95-27414

JET PROPULSION LAB., CALIFORNIA INST. OF TECH., PASADENA, CA.

Method and apparatus for polaradiometric pyrometer
[NASA-CASE-NPO-19064-1-CU] p 2290 N95-26765

Extended linear ion trap frequency standard apparatus
[NASA-CASE-NPO-19081-1-CU] p 2404 N95-26861

Ultra high purity, dimensionally stable INVAR 36
[NASA-CASE-NPO-19358-1-CU] p 2213 N95-26862

Solid-state image sensor with focal-plane digital photon-counting pixel array
[NASA-CASE-NPO-18518-1-CU] p 2424 N95-26894

Performance of the Satellite Test Assistant Robot in JPL's Space Simulation Facility p 2154 N95-27264

The Alpha-Proton-X-ray Spectrometer deployment mechanism: An anthropomorphic approach to sensor placement on Martian rocks and soil
p 2155 N95-27265

Molecular beam scattering from C-13 enriched Kapton and correlation with the EOIM-3 carousel experiment
p 2419 N95-27643

BMDO materials testing in the EOIM-3 experiment
p 2211 N95-27644

Multi-spacecraft coherent Doppler and ranging for interplanetary-navigation p 2150 N95-27786

Ulysses orbit determination at high declinations
p 2151 N95-27787

Application of non-coherent Doppler data types for deep space navigation p 2151 N95-27788

A demonstration of unified TDRS/GPS tracking and orbit determination p 2151 N95-27792

Extended linear ion trap frequency standard apparatus
[NASA-CASE-NPO-19081-1-CU] p 2416 N95-28348

Leak detection utilizing analog binaural (VLSI) techniques
[NASA-CASE-NPO-18399-1-CU] p 2271 N95-28599

JOHNS HOPKINS UNIV., BALTIMORE, MD.

Observations of comets with the IUE
[NASA-CR-197816] p 2461 N95-27166

Simulations of metal dissolution and corrosion
[DE95-007486] p 2218 N95-27748

JOHNS HOPKINS UNIV., COLUMBIA, MD.

Environmentally Benign Cleaning and Degreasing Technology: JANNAF Safety and Protection Subcommittee and Propellant Development and Characterization Subcommittee Joint Workshop
[CPIA-PUBL-611] p 2227 N95-27101

The 1994 JANNAF Safety and Environmental Protection Subcommittee Meeting, volume 1
[CPIA-PUBL-614-VOL-1] p 2170 N95-28294

JOINT INST. FOR NUCLEAR RESEARCH, DUBNA (USSR).

Comparison of the resistance of the MOS integrated circuits with various types of nuclear radiation
[DE95-608623] p 2261 N95-27023

Investigation of radiation resistance of transistors and integrated circuits using the heavy ions beam of energy higher than 1 MeV/amu and fast neutrons
[DE95-608624] p 2261 N95-27024

The systems of the proportional chambers registration electronics for present experiments in nuclear physics
[DE95-608559] p 2419 N95-27161

Magnetic field measurement for the spectrometric magnet of the ISTRA-M setup
[DE95-608560] p 2362 N95-27162

New radiation stable and long-lived plastic scintillators
[DE95-608622] p 2233 N95-27163

Mathematical simulation of three-dimensional magnetic field of spectrometric magnet SP-40
[DE95-608736] p 2398 N95-27239

Vector algorithms for solving 3D nonlinear magnetostatic problems
[DE95-608737] p 2399 N95-27298

The photon structure function F2 in QCD with nonlocal vacuum quark condensates
[DE95-608829] p 2406 N95-27314

Bogolyubov renormalization group
[DE95-608830] p 2448 N95-27315

Radiation of a uniformly moving charge
[DE95-608757] p 2255 N95-27335

The electric field of Bohr's atom
[DE95-608758] p 2448 N95-27336

The Hurwitz-Eulerian reduction
[DE95-608760] p 2396 N95-27337

Diagnostic system Cryo-D for the determination of parameters of vapor-liquid currents of the coolant
[DE95-608775] p 2280 N95-27338

On higher derivative gravity in two dimensions
[DE95-608789] p 2462 N95-27343

Trace anomalies and cocycles of Weyl and diffeomorphism groups
[DE95-608793] p 2397 N95-27344

N. N. Bogolyubov and particle physics
[DE95-608794] p 2448 N95-27447

An invariant measure for a nonlinear Schroedinger equation
[DE95-610166] p 2391 N95-27714

Proofs of contracted length non-covariance
[DE95-610175] p 2391 N95-27715

Landau quasi-energy spectrum destruction for an electron in both a static magnetic field and a resonant electromagnetic wave
[DE95-610176] p 2256 N95-27716

Observation of asymmetrical two-cone Vavilov-Cherenkov radiation in biaxial crystal of triglycinesulphate emitted by 658 MeV protons passing along bi normal
[DE94-629017] p 2441 N95-27867

Quantum retrodiction and causality principle
[DE94-628438] p 2450 N95-28183

On ionic charge distributions of heavy evaporation residues passing through a carbon foil
[DE94-629016] p 2414 N95-28184

Some aspects of the OZI-rule violation in the reaction anti-pp yields phi pi(0)
[DE95-608853] p 2415 N95-28245

Situation in study of electric polarizability and mean square charge radius of the neutron
[DE95-608869] p 2415 N95-28247

The Bremsstrahlung of soft gamma-quanta created by elastic pp- and np-scatterings and the dibaryon resonance problem
[DE95-608870] p 2415 N95-28248

Search for deeply bound pionic atoms with high-purity germanium tagging spectrometer
[DE95-609072] p 2416 N95-28252

The structure of the Hurwitz transformation
[DE95-608759] p 2397 N95-28518

JOINT PUBLICATIONS RESEARCH SERVICE, ARLINGTON, VA.

JPRS report: Science and technology. Central Eurasia
[JPRS-UST-95-021] p 2202 N95-27155

JPRS report: Science and technology. Central Eurasia
[JPRS-UST-95-016] p 2262 N95-27170

JPRS report: Science and technology. Central Eurasia
[JPRS-UST-95-014] p 2145 N95-27171

JPRS report: Science and technology. Central Eurasia
[JPRS-UST-94-022] p 2246 N95-27699

JPRS Report: Science and Technology. Central Eurasia
[JPRS-UST-95-020] p 2145 N95-28257

JPRS report: Science and technology. Central Eurasia
[JPRS-UST-95-019] p 2270 N95-28565

JOINT PUBLICATIONS RESEARCH SERVICE, WASHINGTON, DC.

JPRS report: Science and technology. Central Eurasia
[JPRS-UST-95-015] p 2246 N95-27213

K

KANSAS STATE UNIV., MANHATTAN, KS.

Anti-idiotype probes for toxin detection
[AD-A288955] p 2348 N95-26435

Atomic physics with highly charged ions
[DE95-007325] p 2407 N95-27439

DOE/KEURP Site Operator Program
[DE95-007116] p 2266 N95-27926

KANSAS UNIV., LAWRENCE, KS.

Preliminary design problems and solutions for a supersonic oblique all-wing transport aircraft
p 2118 N95-26942

Design of a high altitude long endurance aircraft with manufacturing considerations p 2119 N95-26947

Prevention and control of inlet unstart using an SR-71 simulation p 2119 N95-26948

An easy way to analyze longitudinal and lateral-directional trim problems with AEO or OEI
p 2119 N95-26949

Preliminary results and research capabilities of a new jet facility at the University of Kansas
p 2119 N95-26951

KEYSTONE ENGINEERING LTD., BLACKSBURG, VA.

Image quality metrics for color CRT displays
[AD-A288934] p 2262 N95-27196

KRUG LIFE SCIENCES, INC., SAN ANTONIO, TX.

A study of heart rate and heart rate variability during rapid decompression to 50,000 ft
[AD-A291598] p 2355 N95-28561

KTA-TATOR, INC., HUMBLE, TX.

Weightless Environment Training Facility (WETF) materials coating evaluation, volume 1
[NASA-CR-188366-VOL-1] p 2239 N95-28385

Weightless Environment Training Facility (WETF) materials coating evaluation, volume 2
[NASA-CR-188366-VOL-2] p 2239 N95-28386

Weightless Environment Training Facility (WETF) materials coating evaluation, volume 3
[NASA-CR-188366-VOL-3] p 2239 N95-28387

L

LAMONT-DOHERTY GEOLOGICAL OBSERVATORY, PALISADES, NY.

An in situ evaluation of TOPEX/Poseidon altimetric measurements versus meaurements made by moorings and inverted echo sounders for sea surface height
[NASA-CR-198621] p 2347 N95-27805

LAWRENCE LIVERMORE NATIONAL LAB., LIVERMORE, CA.

FTIR measurements of thermal infrared sky radiance and transmission
[DE95-003642] p 2334 N95-26436

A parallel coupled oceanic-atmospheric general circulation model
[DE95-005918] p 2335 N95-26622

PXAMS: Projectile X ray AMS: X ray yields and applications
[DE95-006438] p 2204 N95-27496

Coupled chemistry/climate issues
[DE95-006443] p 2327 N95-27532

Scientific statistics and graphics on the Macintosh
[DE95-006445] p 2372 N95-27533

The PCMDI Visualization and Computation System (VCS): A workbench for climate data display and analysis
[DE95-008586] p 2328 N95-27558

Comparison of the calculated and measured stability of a NbTi cable-in-conduit conductor
[DE95-007964] p 2265 N95-27693

Absorption of sparingly soluble gases by reactive media in self-aerated gas-liquid contactors: A scale-up procedure
[DE95-006429] p 2206 N95-27707

Calculations of downward IR surface fluxes in the 500-3,000 cm(exp -1) wavenumber range for the 1994 ICRCCM model intercomparison study
[DE95-006430] p 2328 N95-27708

Fluctuations in high beta(sub p) plasmas in DIII-D
[DE95-008071] p 2432 N95-27710

Automated integration of genomic physical mapping data via parallel simulated annealing
[DE95-008057] p 2351 N95-27725

Portable laser laboratory
[DE95-008376] p 2298 N95-27876

A summary documentation of the AMIP models
[DE95-008343] p 2338 N95-27931

Issues relevant to the development of coupled chemistry/climate models
[DE95-006441] p 2330 N95-27954

Laboratory high-energy astrophysics on lasers
[DE95-008062] p 2462 N95-28013

Advances in scientific visualization
[DE95-008065] p 2343 N95-28014

A numerical study of ultra-short-pulse reflectometry
[DE95-008070] p 2266 N95-28015

A hybrid vehicle evaluation code and its application to vehicle design. Revision 1
[DE95-008053] p 2303 N95-28029

Remote measurement of ground temperature and emissivity
[DE95-008055] p 2314 N95-28053

Scrape-off layer plasma modeling for the DIII-D tokamak
[DE95-008059] p 2433 N95-28054

LLNL input to FY94 hydrogen annual report
[DE95-007950] p 2243 N95-28064

UEDGE and DEGAS modeling of the DIII-D scrape-off layer plasma, revision 1
[DE95-008052] p 2433 N95-28065

Beginning to edit physics
[DE95-008374] p 2455 N95-28085

Whirl plus tilt
[DE95-007948] p 2398 N95-28108

Performance analysis of bullet trajectory estimation: Approach, simulation, and experiments
[DE95-007949] p 2398 N95-28109

Carbonaceous aerosols influencing atmospheric radiation: Black and organic carbon
[DE95-006437] p 2330 N95-28118

Advanced tokamak operating modes in TPX and ITER
[DE95-008058] p 2434 N95-28138

A hybrid vehicle evaluation code and its application to vehicle design, revision 2
[DE95-008060] p 2303 N95-28139

Engineering design of the ITER RF systems
[DE95-008064] p 2434 N95-28140

Observation on radiation transfer experiments using k-shell absorption spectra
[DE95-008068] p 2434 N95-28141

Towards the detection and attribution of an anthropogenic effect on climate
[DE95-008589] p 2331 N95-28157

A method for generating skewed random numbers using two overlapping uniform distributions
[DE95-008747] p 2392 N95-28162

FENIX experimental results of large-scale CICC made of bronze-processed Nb3Sn strands
[DE95-007965] p 2222 N95-28167

Edge detection by nonlinear dynamics
[DE95-008076] p 2373 N95-28168

BEGET: The B-Factory Event Generator version 21
[DE95-008329] p 2414 N95-28171

Long-range eye tracking: A feasibility study
[DE95-008587] p 2357 N95-28176

The determination of the constitutive parameters of a medium with application to a reinforced concrete pad
[NASA-CR-4674] p 2268 N95-28181

The concentration-estimation problem for multiple-wavelength differential absorption lidar
[DE95-008375] p 2256 N95-28231

A point-centered diffusion differencing for unstructured meshes in 3-D
[DE95-008382] p 2392 N95-28232

Computational studies of projectile melt in impact with typical whipple shields
[DE95-005916] p 2311 N95-28337

Attractive characteristics of mirrors
[DE95-008073] p 2435 N95-28356

Weighting the recursive spectral bisection algorithm for unstructured grids
[DE95-008080] p 2373 N95-28521

The elevated temperature tensile properties of S-200E commercially pure beryllium
[DE95-009331] p 2223 N95-28534

Theoretical aspects of energy confinement in spheromaks
[DE95-008079] p 2435 N95-28542

The northern wintertime divergence extrema at 200 hPa and surface cyclones as simulated in the integration of the ECMWF general circulation model
[DE95-007946] p 2332 N95-28550

Stationary neutrino radiation transport by maximum entropy closure
[DE95-006579] p 2463 N95-28558

A black carbon emission data base for atmospheric chemistry and climate studies
[DE95-006436] p 2332 N95-28662

LEAR JET INDUSTRIES, INC., WICHITA, KS.

Aircraft nosewheel steering simulation
p 2118 N95-26944

LEGACY GOOD SAMARITAN HOSPITAL, PORTLAND, OR.

Comparative Transduction Mechanisms of Vestibular Otolith Hair Cells
[NASA-CR-197980] p 2349 N95-26727

Regional differences in lectin binding patterns of vestibular hair cells p 2349 N95-26728

Hair cell regeneration in the bullfrog vestibular otolith organs following aminoglycoside toxicity
p 2349 N95-26729

Peripheral innervation patterns of vestibular nerve afferents in the bullfrog utriculus p 2349 N95-26730

Comparative transduction mechanisms of hair cells in the bullfrog utriculus. 1: Responses to intracellular current p 2350 N95-26731

Comparative transduction mechanisms of hair cells in the bullfrog uticulus. 2: Sensitivity and response dynamics to hair bundle displacement p 2350 N95-26732

Role of somatosensory and vestibular cues in attenuating visually induced human postural sway
[NASA-CR-197845] p 2357 N95-27697

LEHIGH UNIV., BETHLEHEM, PA.

Evaluation of patch effectiveness in repairing aircraft components p 2133 N95-27513

NO decomposition in non-reducing atmospheres
[DE95-007895] p 2205 N95-27690

LIGHTNING TECHNOLOGIES, INC., PITTSFIELD, MA.

Aircraft fuel system lightning protection design and qualification test procedures development
[AD-A288401] p 2125 N95-26497

LITTON INDUSTRIES, BLACKSBURG, VA.

The evaluation of a fluorochemical drying process for an electrical contact p 2227 N95-27103

A summary of ODS replacement technologies at Litton Poly-Scientific p 2228 N95-27105

LOCKHEED AERONAUTICAL SYSTEMS CO., BURBANK, CA.

Process and control systems for composites manufacturing p 2184 N95-28267

LOCKHEED AERONAUTICAL SYSTEMS CO., MARIETTA, GA.

Structural modification and repair of C-130 wing structure using bonded composites p 2133 N95-27512

Structural testing of the technology integration box beam p 2194 N95-28467

Advanced textile applications for primary aircraft structures p 2138 N95-28476

LOCKHEED ENGINEERING AND SCIENCES CO., HAMPTON, VA.

A verification procedure for MSC/NASTRAN Finite Element Models
[NASA-CR-4675] p 2131 N95-27371

Mechanical properties of triaxially braided composites: Experimental and analytical results
p 2189 N95-28423

LOCKHEED ENGINEERING AND SCIENCES CO., HOUSTON, TX.

Load measurement system with load cell lock-out mechanism p 2159 N95-27291

Validation of the SINDA/FLUINT code using several analytical solutions p 2281 N95-27350

LOCKHEED-FORT WORTH CO., FORT WORTH, TX.

Rapid repair of large area damage to contoured aircraft structures p 2133 N95-27516

Turbulence model development and application at Lockheed Fort Worth Company p 2285 N95-27884

LOCKHEED MARTIN CORP., DENVER, CO.

Determining GPS average performance metrics
p 2128 N95-27791

Mars Sample Return mission utilizing in-situ propellant production
[NASA-CR-188371] p 2145 N95-28261

LOCKHEED MISSILES AND SPACE CO., PALO ALTO, CA.

Coronal abundances and their variation
[NASA-CR-197788] p 2464 N95-26671

A BATSE investigation of radiation belt electrons precipitated by VLF waves
[NASA-CR-197780] p 2336 N95-26922

LOCKHEED MISSILES AND SPACE CO., SUNNYVALE, CA.

Long life 80Ah standard IPV NiH2 battery cell
p 2272 N95-26787

Structures and materials technology needs for communications and remote sensing spacecraft
[NASA-CR-198166] p 2163 N95-27026

Solar array deployment mechanism
p 2155 N95-27266

LOCKHEED TECHNICAL OPERATIONS CO., CROFTON, MD.

GPS as an orbit determination subsystems
p 2152 N95-27793

LOGICON R AND D ASSOCIATES, ALBUQUERQUE, NM.

Extended equation-of-state for dichlorodifluoromethane (CCl2F2)
[AD-A288885] p 2177 N95-26434

LORAL FEDERAL SYSTEMS, MANASSA, VA.

Advanced flight computer. Special study
[NASA-CR-198165] p 2371 N95-27246

LOS ALAMOS NATIONAL LAB., NM.

Integration of video and radiation analysis data
[DE95-004165] p 2379 N95-26443

A study of internal damage of metal matrix composites by neutron diffraction
[DE95-005157] p 2182 N95-27080

Study of parity and time reversal violation in neutron-nucleus interactions
[DE95-005158] p 2405 N95-27081

First-principles study of intermetallic phase stability in the ternary Ti-Al-Nb alloy system
[DE95-005259] p 2213 N95-27082

The comparison of P(sub 1) and simplified P(sub 2) synthetic acceleration for iterative methods in transport solutions
[DE94-018306] p 2390 N95-27304

Views of the solar system
[DE95-006446] p 2461 N95-27326

Indirectly driven targets for ignition
[DE95-006451] p 2430 N95-27327

Micromechanical modeling of damage and inelasticity of composite materials in macroscopic structural analysis
[DE95-003666] p 2182 N95-27421

Gigabit LAN issues: HIPPI, Fibre Channel, or ATM?
[DE95-003673] p 2378 N95-27422

Heat pipe cooled reactors for multi-kilowatt space power supplies
[DE95-005211] p 2420 N95-27425

Matrix kernels for MEG and EEG source localization and imaging
[DE95-005238] p 2354 N95-27426

Variation of solvent scattering-length density small-angle neutron scattering as a means of determining structure of composite materials
[DE95-005394] p 2183 N95-27428

The physics and chemistry of heavy Fermions
[DE95-005277] p 2407 N95-27431

Three-dimensional computer modeling of hydrogen injection and combustion
[DE95-006261] p 2203 N95-27437

The second coming of cold dark matter?
[DE95-005156] p 2462 N95-27445

Atomistic study of energy and structure of surfaces in NiO
[DE95-005207] p 2215 N95-27446

C15 intermetallic compounds HfV2+Nb
[DE95-005264] p 2215 N95-27463

Intermediate energy neutrons at WNR. Spin-isospin and energy dependence of the NN interaction and the nuclear response
[DE95-006291] p 2408 N95-27466

Photon burst mass spectrometry--ultrasensitive detection of rare isotopes
[DE95-006403] p 2204 N95-27467

Review of activities in USA on HTS materials
[DE95-006404] p 2234 N95-27468

Engineered materials for appliation in severe metallurgical environments: Tantalum-carbon alloy development
[DE95-006838] p 2216 N95-27488

Bubble fusion: Preliminary estimates
[DE95-006337] p 2420 N95-27494

Systematic study of the ion beam mixing of oxide markers into alumina
[DE95-006262] p 2217 N95-27555

Modeling precipitation from concentrated solutions with the EQ3/6 chemical speciation codes
[DE95-006264] p 2204 N95-27556

Free Electron Laser Physical Process Code (FELPPC)
[DE95-006276] p 2296 N95-27557

Continuously-tunable, narrow-linewidth, Q-switched Cr:LiSAF laser for lidar applications
[DE95-006285] p 2296 N95-27672

The role of microprocesses in macroscale magnetotail dynamics
[DE95-006288] p 2432 N95-27673

Engineering photochemical smog through convection towers
[DE95-007727] p 2328 N95-27686

Improved performance 1590 nm Er:YLF laser
[DE95-003691] p 2296 N95-27705

Spectral broadening of KrF laser radiation by self-seeded Raman amplification in long air paths
[DE95-003697] p 2297 N95-27718

Measurement of high acidity using a renewable-reagent fiber optic sensor
[DE95-006327] p 2425 N95-27734

Silicon subsystem mechanical engineering closeout report for the Solenoidal Detector Collaboration
[DE95-006336] p 2421 N95-27735

Application of conventional laser technology to gamma-gamma colliders
[DE95-006341] p 2297 N95-27736

AFC generator development
[DE95-007094] p 2266 N95-27754

Classification of RF transients in space using digital signal processing and neural network techniques
[DE95-006287] p 2256 N95-27840

Analysis of surfaces, films and multilayers by resonant laser ablation
[DE95-006295] p 2297 N95-27841

Three-dimensional visualization of reactive flows in complex geometries
[DE95-006332] p 2284 N95-27845

The Sunrise project: An R&D project for a national information infrastructure prototype
[DE95-006340] p 2455 N95-27847

Low energy neutral atom imaging: Remote observations of the magnetosphere
[DE95-006342] p 2337 N95-27848

Generalized CNF satisfiability, local reductions and complexity of succinctly specified problems
[DE95-006343] p 2372 N95-27849

Trident as an ultrahigh irradiance laser
[DE95-006345] p 2297 N95-27850

A laboratory scale supersonic combustive flow system
[DE95-006347] p 2206 N95-27851

Prediction of material strength and fracture of glass using the SPHINX smooth particle hydrodynamics code
[DE95-004869] p 2236 N95-27943

Phenomenology from 100 large lattices
[DE95-006349] p 2442 N95-27994
Nonlinear optical microscopy for imaging thin films and surfaces
[DE95-007872] p 2426 N95-28018
Development of an optical trap as an ultra-sensitive analytical tool
[DE95-007843] p 2426 N95-28022
An investigation of the chemical and physical properties of pristine, electrochromically damaged, and photochromically damaged KTiOPO4 (KTP) using surface analytical and optical spectroscopic techniques
[DE95-007865] p 2443 N95-28023
Alpha characterization inside pipes using ion-transport technology
[DE95-007869] p 2411 N95-28024
Implementing an integrated standards-based management system to ensure compliance at Los Alamos National Laboratory
[DE95-007873] p 2451 N95-28025
Phase stability and elasticity of C15 transition-metal intermetallic compounds
[DE95-007876] p 2219 N95-28026
Time-dependent model for vertical-cavity surface-emitting laser
[DE95-007880] p 2298 N95-28027
An investigation of the applicability of the new Reillex(tm)-HPQ anion exchange resin system for technetium/rhenium and uranium in the Hanford waste tanks
[DE95-007643] p 2412 N95-28051
Precision asteroseismology of DAV (ZZ CETI) white dwarf stars
[DE95-006265] p 2462 N95-28056
Off-specular scattering in neutron reflectometry
[DE95-007835] p 2412 N95-28057
Geothermal development in Australia
[DE95-007837] p 2325 N95-28058
High power free-electron laser concepts and problems
[DE95-007841] p 2298 N95-28059
Aspects of macroscopic phase separation and interstitial oxygen ordering in oxygen doped La2CuO(4+delta)
[DE95-007864] p 2443 N95-28060
Relativistic electrons in the outer-zone: An 11 year cycle, their relation to the solar wind
[DE95-007882] p 2338 N95-28061
A new method of determining the ejected mass of novae
[DE95-007884] p 2462 N95-28062
Measurement of the reaction C(nu(sub mu), mu(-)) X near threshold
[DE95-007888] p 2412 N95-28063
Bubble chamber spectroscopy for chemical analysis: A new concept
[DE95-006350] p 2209 N95-28088
Measurement and analysis of the surface energy budget for ARM field experiments
[DE95-007646] p 2338 N95-28114
Pulsed laser deposition of zeolitic membranes
[DE95-006274] p 2298 N95-28124
Plasma source ion implantation of ammonia into electroplated chromium
[DE95-006275] p 2444 N95-28125
Investigation of rifting processes in the Rio Grande Rift using data from an unusually large earthquake swarm
[DE95-007623] p 2339 N95-28126
Topological density and instantons on a lattice
[DE95-006348] p 2445 N95-28240
Investigation of HE driven cylindrical liner
[DE95-007866] p 2311 N95-28539
Surface structure of MX-chains studied by atomic force microscopy
[DE95-007881] p 2447 N95-28541
High performance ground penetrating radar survey of TA-49/Area 2
[DE95-006856] p 2258 N95-28601
Computational and experimental studies of hydrodynamic instabilities and turbulent mixing
[DE95-006837] p 2288 N95-28603
Query by image example: The CANDID approach
[DE95-006284] p 2456 N95-28631
LOYOLA COLL., BALTIMORE, MD.
JTEC Panel report on electronic manufacturing and packaging in Japan
[NASA-CR-197830] p 2263 N95-27226
Microelectronics in Japan p 2263 N95-27227
Building the electronic industry's roadmaps
p 2263 N95-27228
Japan's technology and manufacturing infrastructure
p 2263 N95-27229
Japan's electronic packaging technologies
p 2263 N95-27230
Electronics manufacturing and assembly in Japan
p 2263 N95-27231
Quality assurance and reliability in the Japanese electronics industry p 2263 N95-27232
Successful product realization strategies
p 2264 N95-27233
JTEC monograph on biodegradable polymers and plastics in Japan: Research, development, and applications
[NASA-CR-198562] p 2235 N95-27694
JTEC panel on display technologies in Japan
[NASA-CR-198564] p 2292 N95-27863
WTEC panel report on research submersibles and undersea technologies
[NASA-CR-198565] p 2247 N95-27909
JTEC/WTEC annual report and program summary: 1993/94
[NASA-CR-198563] p 2475 N95-28038
JTEC Panel report on microelectromechanical systems in Japan
[NASA-CR-197831] p 2268 N95-28239
LTV AEROSPACE AND DEFENSE CO., DALLAS, TX.
Probabilistic design of advanced composite structure
p 2193 N95-28443

M

MAASTRICHT UNIV. (NETHERLANDS).
Limits to ground control in autonomous spacecraft
p 2383 N95-27381
MACH 1, INC., KING OF PRUSSIA, PA.
Surfactants and desensitizing wax substitutes for TNT-Based systems
[AD-A289652] p 2243 N95-28634
MALAYA UNIV., KUALA-LUMPUR (MALAYSIA).
Applications of lasers and electro-optics
[DE95-600841] p 2299 N95-28330
MANCHESTER UNIV. (ENGLAND).
Nonlinear stability of non-stationary cross-flow vortices in compressible boundary layers
[NASA-CR-189184] p 2279 N95-27242
MANHATTAN COLL., NEW YORK, NY.
RTE: A computer code for Rocket Thermal Evaluation
p 2177 N95-27355
MART CORP., SAINT LOUIS, MO.
Cleaning of parts for new manufacturing and parts rebuilding p 2231 N95-27123
MARTIN MARIETTA AEROSPACE, DENVER, CO.
Chemical reactions identified in the Titan 2, Titan 4, and Delta 2 propellant systems and their application to source modeling p 2172 N95-28304
MARTIN MARIETTA ASTRONAUTICS, DENVER, CO.
Development of a high force thermal latch
p 2157 N95-27275
Next generation controller specification for an open systems architecture standard
[AD-A289567] p 2375 N95-28647
MARTIN MARIETTA CORP., BALTIMORE, MD.
Application of fiber-reinforced bismaleimide materials to aircraft nacelle structures p 2137 N95-28278
MARTIN MARIETTA CORP., DENVER, CO.
Next generation controller specification for an open systems architecture standard - overview
[AD-A289507] p 2368 N95-26853
Cleanliness verification process at Martin Marietta Astronautics p 2165 N95-27104
Alternative cleaning solvents and lubricants at the Air Force PJKS facility p 2228 N95-27108
MARTIN MARIETTA CORP., SAN DIEGO, CA.
Development and implementation of a system safety program for the space launch complex 3 east (SLC-3E) ground support system project to support Atlas 2 family of space launch vehicles p 2174 N95-28316
MARTIN MARIETTA ENERGY SYSTEMS, INC., OAK RIDGE, TN.
Failure analysis of thick composite cylinders under external pressure p 2187 N95-28284
MARYLAND PUBLIC TELEVISION, OWINGS MILLS, MD.
Live from Antarctica: Then and now
[NASA-CR-197829] p 2335 N95-26594
Live from Antarctica: The coldest, windiest place on Earth
[NASA-CR-197737] p 2335 N95-26595
Live from Antarctica, volume 4
[NASA-CR-197828] p 2335 N95-26596
MARYLAND UNIV., COLLEGE PARK, MD.
Nonlinear scalespace via hierarchical statistical modeling
[AD-A289057] p 2394 N95-26478
Stochastic adaptive estimation and control
[AD-A289088] p 2380 N95-26480
Learning Hand/Eye coordination by an active observer. part 1: Organizing centers
[AD-A289502] p 2356 N95-26843
Stable adaptive neurocontrollers for spacecraft and space robots p 2384 N95-27385
Development of density and temperature profile diagnostics for ICF targets
[DE95-007664] p 2433 N95-28052
MASSACHUSETTS INST. OF TECH., CAMBRIDGE, MA.
Continuum mechanical modeling of solids undergoing a phase transformation
[AD-A288274] p 2200 N95-26451
Calculation of suspended sediment transport by combined wave-current flows
[AD-A289368] p 2346 N95-26904
Neutral gas compression in the Alcator C-Mod divertor. Experimental observations
[DE95-007762] p 2432 N95-27688
Anechoic wind tunnel study of turbulence effects on wind turbine broadband noise p 2325 N95-27992
Measurement of particle transport coefficients on Alcator C-Mod
[DE95-007763] p 2411 N95-28020
Spectroscopic and dynamical studies of highly energized small polyatomic molecules
[DE95-006640] p 2414 N95-28199
Compressive residual strength of graphite/epoxy laminates after impact p 2191 N95-28431
Piecemeal learning of an unknown environment
[AD-A291683] p 2387 N95-28461
Basic and applied research in the field of electronics and communications
[AD-A291727] p 2270 N95-28512
MASSACHUSETTS INST. OF TECH., LEXINGTON, MA.
Bibliography of patents and licenses 1951-1990. 1991 edition
[AD-A289603] p 2452 N95-26721
Design, construction, test and evaluation of a frequency scanning radiometer for measuring oil slick thicknesses
[AD-A290040] p 2293 N95-28389
MASSACHUSETTS UNIV., AMHERST, MA.
Intelligent computer based reliability assessment of multichip modules
[AD-A288833] p 2259 N95-26550
Kinetics and dynamics of oxidation reactions involving adsorbed CO species on bulk supported Pt and copper oxides
[DE95-006420] p 2207 N95-27952
MATERIALS RESEARCH SOCIETY, PITTSBURG, PA.
Materials Research Society Symposium Proceedings. Volume 339: Diamond, SiC and nitride wide bandgap semiconductors
[AD-A288690] p 2437 N95-26818
MATERIALS SCIENCES CORP., BLUE BELL, PA.
Failure analysis of thick composite cylinders under external pressure p 2187 N95-28284
MATHSOFT, INC., SEATTLE, WA.
Denoising and robust non-linear wavelet analysis
[AD-A291668] p 2257 N95-28455
MATRA MARCONI SPACE SYSTEMS, STEVENAGE (ENGLAND).
ORION: A Supersynchronous Transfer Orbit mission
p 2154 N95-27804
MAYO FOUNDATION, ROCHESTER, MN.
Mechanisms of hypertension after cross-linked hemoglobin blood-substitute transfusion
[AD-A289558] p 2352 N95-26680
MCAT INST., SAN JOSE, CA.
Algorithms for parallel flow solvers on message passing architectures
[NASA-CR-197758] p 2274 N95-26588
Numerical simulation of the SOFIA flow field
[NASA-CR-197757] p 2274 N95-26589
Aeroelasticity of wing and wing-body configurations on parallel computers
[NASA-CR-197756] p 2129 N95-26590
Computational analysis of forebody tangential slot blowing on the high alpha research vehicle
[NASA-CR-197754] p 2129 N95-26591
Supersonic transport grid generation, validation, and optimization
[NASA-CR-197752] p 2365 N95-26648
CFD research, parallel computation and aerodynamic optimization
[NASA-CR-197748] p 2120 N95-26649
Design and testing of low sonic boom configurations and an oblique all-wing supersonic transport
[NASA-CR-197744] p 2129 N95-26651
Turbulence modeling
[NASA-CR-197751] p 2274 N95-26665
Numerical simulation of the flow about the F-18 HARV at high angle of attack
[NASA-CR-197755] p 2121 N95-26735
Development of an upwind, finite-volume code with finite-rate chemistry
[NASA-CR-197747] p 2121 N95-26760
Progress in incompressible Navier-Stokes computations for propulsion flows and its dual-use applications
[NASA-CR-197746] p 2275 N95-26766
Computational support of the laminar flow supersonic wind tunnel, CNSFV code development, Maglev, and grid generation
[NASA-CR-197750] p 2143 N95-26775

Direct numerical simulation of transitional and turbulent flow over a heated flat plate using finite-difference schemes
[NASA-CR-197753] p 2275 N95-26776

Turbomachinery design and tonal acoustics computations
[NASA-CR-197749] p 2139 N95-26777

Supersonic civil airplane study and design: Performance and sonic boom
[NASA-CR-197745] p 2130 N95-26813

Development of numerical methods for overset grids with applications for the integrated Space Shuttle vehicle
[NASA-CR-197759] p 2160 N95-27154

MCCRONE ASSOCIATES, INC., WESTMONT, IL.

Analytical electron microscopy of nanometer-sized particles
[AD-A289124] p 2413 N95-28101

MCDONNELL AIRCRAFT CO., SAINT LOUIS, MO.

ACT/ICAPS: Thermoplastic composite activities
p 2185 N95-28274

Assembly induced delaminations in composite structures p 2186 N95-28279

Higher order finite element analysis of thick composite laminates p 2186 N95-28282

Analysis techniques for the prediction of springback in formed and bonded composite components
p 2188 N95-28289

Development of composite carrythrough bulkhead
p 2192 N95-28438

MCDONNELL-DOUGLAS AEROSPACE, HUNTINGTON BEACH, CA.

Solid film lubricants and thermal control coatings flown aboard the EOIM-3 MDA sub-experiment
p 2242 N95-27640

MCDONNELL-DOUGLAS AEROSPACE, SAINT LOUIS, MO.

The applicability of turbulence models to aerodynamic and propulsion flowfields at McDonnell-Douglas Aerospace p 2285 N95-27886

MCDONNELL-DOUGLAS CORP., SAINT LOUIS, MO.

Performance study for inlet installations
[NASA-CR-189714] p 2140 N95-28227

MCDONNELL-DOUGLAS SPACE AND DEFENSE SYSTEMS, COCOA BEACH, FL.

Development and testing of the rack insertion device
p 2158 N95-27289

MCDONNELL-DOUGLAS SPACE SYSTEMS CO., HUNTINGTON BEACH, CA.

LDEF's contribution to the selection of thermal control coatings for the Space Station p 2242 N95-27661

Space Station as a Long Duration Exposure Facility
p 2166 N95-27663

MCGILL UNIV., MONTREAL (QUEBEC).

The high energy behavior of the forward scattering parameters -- (sigma)(sub tot), (rho), and B
[DE95-007075] p 2415 N95-28210

MELBOURNE UNIV., PARKVILLE (AUSTRALIA).

Constraints on the anomalous WW gamma couplings from b vector s gamma
[DE95-608866] p 2415 N95-28246

MICHIGAN UNIV., ANN ARBOR, MI.

User's and test case manual for FEMATS
[NASA-CR-197803] p 2366 N95-26694

Theoretical and experimental models of the diffuse radar backscatter from Mars
[NASA-CR-198650] p 2463 N95-27700

Hydrogen induced C-C, C-N, and C-S bond activities on Pi and Ni surfaces
[DE95-006251] p 2206 N95-27838

The role of hydrogen in the hydrogenation and hydrogenolysis of aniline on the nickel single crystal surfaces: Its implication on the mechanisms of HDN reactions
[DE95-006687] p 2222 N95-28134

Theoretical and experimental study of low-loss, High-efficiency monolithic antenna structures at 94 GHz
[AD-A291785] p 2257 N95-28513

MIDWEST RESEARCH INST., GOLDEN, CO.

Observed acoustic and aeroelastic spectral responses of a MOD-2 turbine blade to turbulence excitation
p 2324 N95-27991

MINNESOTA UNIV., MINNEAPOLIS, MN.

Electrocrystallization of an ordered organic monolayer: Selective epitaxial growth of beta(ET)213 ongraphite
[AD-A288942] p 2178 N95-26569

Flow control
[AD-A289262] p 2279 N95-27197

Emerging applications of probability (stochastic models in geosystems)
[AD-A289117] p 2313 N95-28099

Self-assembly of low-dimensional molecular nanoclusters on Au(111) surfaces
[AD-A288936] p 2178 N95-28334

MISSISSIPPI STATE UNIV., MISSISSIPPI STATE, MS.

A case study of view-factor rectification procedures for diffuse-gray radiation enclosure computations
p 2281 N95-27353

Intrusive multi-probe system
[DE95-006258] p 2292 N95-27465

Application of modern diagnostic methods to environmental improvement
[DE95-005797] p 2330 N95-28119

MISSOURI UNIV., COLUMBIA, MO.

Statistical theory and reliability
[AD-A288519] p 2394 N95-26733

High pressure optical studies of semiconductors and heterostructures
[DE95-007119] p 2410 N95-27927

MISSOURI UNIV., ROLLA, MO.

Interfacial mobility and its effect on flexural strength and fracture toughness in glass-fiber fabric reinforced epoxy laminates
[AD-A288344] p 2180 N95-26572

The application of waterjets for cleaning
p 2233 N95-27130

Extensional flow convecting a reactant undergoing a first order homogeneous reaction and diffusional mass transfer from a sphere at low to intermediate Peclet and Damkohler numbers p 2280 N95-27346

Single-drop reactive extraction/extractive reaction with forced convective diffusion and interphase mass transfer
p 2282 N95-27358

Single-drop reactive extraction/extractive reaction with forced convective diffusion and interphase mass transfer
p 2283 N95-27365

Defect characterization of electronic conducting pseudo-perovskite systems
[DE95-007487] p 2220 N95-28049

The demilitarization of class 1.1 rocket motors using high pressure waterjets p 2176 N95-28322

MITRE CORP., MCLEAN, VA.

Air traffic operational inventory CY 1994
[AD-A288281] p 2126 N95-26454

MORGAN STATE UNIV., BALTIMORE, MD.

Linear and nonlinear trending and prediction for AVHRR time series data p 2385 N95-27391

MORGANTOWN TECHNOLOGY CENTER, WV.

The US Molten Carbonate Fuel-Cell development and commercialization effort
[DE95-008580] p 2320 N95-27746

MPB CORP., KEENE, NH.

Effects of bearing cleaning and lube environment on bearing performance p 2158 N95-27285

N

NAGOYA UNIV., NAGOYA (JAPAN).

Far-infrared laser interferometry measurements on the STP-3(M) reversed-field pinch
[DE94-765440] p 2297 N95-27868

Global dynamo in a reversed field pinch plasma
[DE94-765441] p 2432 N95-27869

Burst of energetic ions from reversed field pinch plasma
[DE94-765447] p 2432 N95-27870

NATIONAL ACADEMY OF SCIENCES - NATIONAL RESEARCH COUNCIL, WASHINGTON, DC.

Finding the forest in the trees. The challenge of combining diverse environmental data
[NASA-CR-197798] p 2326 N95-26362

Airborne geophysics and precise positioning: Scientific issues and future directions
[LC-94-68678] p 2314 N95-27156

High-stakes aviation: US-Japan technology linkages in transport aircraft
[LC-94-65759] p 2126 N95-27907

Technical progress report to the Department of Energy on the Solid State Sciences Committee (SSSC)
[DE95-007113] p 2441 N95-27925

Research activities of the Solid State Sciences Committee in the development of a Federal initiative on advanced materials and processing
[DE95-009328] p 2445 N95-28179

NATIONAL AERONAUTICS AND SPACE ADMINISTRATION, WASHINGTON, DC.

Index to NASA news releases and speeches 1994
[NASA-TM-110650] p 2452 N95-26673

Cataclysmic variables and related objects
[NASA-SP-507] p 2458 N95-27068

Aerospace medicine and biology: A continuing bibliography with indexes (supplement 402)
[NASA-SP-7011(402)] p 2354 N95-27502

Aeronautical engineering: A continuing bibliography with indexes (supplement 318)
[NASA-SP-7037(318)] p 2120 N95-27543

Spaceflight revolution: NASA Langley Research Center from Sputnik to Apollo
[NASA-SP-4308] p 2474 N95-27685

Mission to Planet Earth. Strategic enterprise plan, 1995-2000
[NASA-TM-110620] p 2145 N95-27919

Research and Technology Objectives and Plans Summary (RTOPS)
[NASA-TM-108574] p 2475 N95-28002

TOPS: Toward Other Planetary Systems. A report by the solar system exploration division
[NASA-TM-110609] p 2464 N95-28009

Design, analysis, and testing of a metal matrix composite web/flange intersection p 2191 N95-28433

Microgravity science and applications. Program tasks and bibliography for FY 1994
[NASA-TM-4677] p 2245 N95-28460

NATIONAL AERONAUTICS AND SPACE ADMINISTRATION. AMES RESEARCH CENTER, MOFFETT FIELD, CA.

Simulation model of the integrated flight/propulsion control system, displays, and propulsion system for ASTOVL lift-fan aircraft
[NASA-TM-108866] p 2139 N95-26412

Flightpath synthesis and HUD scaling for V/STOL terminal area operations
[NASA-TM-110348] p 2127 N95-26587

The multidimensional Self-Adaptive Grid code, SAGE, version 2
[NASA-TM-110350] p 2367 N95-26726

The lift-fan aircraft: Lessons learned
[NASA-CR-196694] p 2131 N95-27143

Calculation of three-dimensional (3-D) internal flow by means of the velocity-vorticity formulation on a staggered grid
[NASA-TM-110352] p 2122 N95-27258

NAS Technical Summaries, March 1993 - February 1994
[NASA-RP-1355] p 2466 N95-27387

Boron-carbon-silicon polymers and the ceramic thereof
[NASA-CASE-ARC-11891-1-SB] p 2238 N95-28212

Cooling apparatus and couplings therefor
[NASA-CASE-ARC-11921-1] p 2304 N95-28256

Composite flexible insulation for thermal protection of space vehicles p 2166 N95-28293

Method and apparatus for measuring temperatures in fabrics and flexible thermal insulations
[NASA-CASE-ARC-11984-1] p 2293 N95-28345

Space Science Division cumulative bibliography: 1989-1994
[NASA-TM-110355] p 2457 N95-28677

NATIONAL AERONAUTICS AND SPACE ADMINISTRATION. FLIGHT RESEARCH CENTER, EDWARDS, CA.

NASA Dryden flow visualization facility
[NASA-TM-4631] p 2362 N95-27914

NATIONAL AERONAUTICS AND SPACE ADMINISTRATION. GODDARD SPACE FLIGHT CENTER, GREENBELT, MD.

Technical report series on global modeling and data assimilation. Volume 6: A multiyear assimilation with the GEOS-1 system: Overview and results
[NASA-TM-104606-VOL-6] p 2334 N95-26423

SeaWiFS technical report series. Volume 26: Results of the SeaWIFS Data Analysis Round-Robin, July 1994 (DARR-1994)
[NASA-TM-104566-VOL-26] p 2345 N95-26430

Spectral analyses, climatology, and interannual variability of Nimbus-7 TOMS version 6 total column ozone
[NASA-RP-1360] p 2341 N95-26689

Alternate charging profiles for the onboard nickel cadmium batteries of the Explorer Platform/Extreme Ultraviolet Explorer p 2272 N95-26796

Basic space payload fastener p 2156 N95-27273

Design, development and testing of the x-ray timing explorer High Gain Antenna System
p 2157 N95-27279

Development of the solar array deployment and drive system for the XTE spacecraft p 2158 N95-27284

A cryogenic scan mechanism for use in Fourier transform spectrometers p 2158 N95-27287

Features and applications of the Groove Analysis Program (GAP) p 2281 N95-27349

The 1995 Goddard Conference on Space Applications of Artificial Intelligence and Emerging Information Technologies
[NASA-CP-3296] p 2382 N95-27375

Integrated planning and scheduling for Earth science data processing p 2384 N95-27382

LDEF systems special investigation group overview
p 2470 N95-27647

Effects of the LDEF orbital environment on the reflectance of optical mirror materials
p 2428 N95-27651

Space environmental effects observed on the Hubble Space Telescope p 2242 N95-27655

Long Duration Exposure Facility post-flight data as it influences the Tropical Rainfall Measuring Mission p 2345 N95-27666
Flight Mechanics/Estimation Theory Symposium 1995 [NASA-CP-3299] p 2146 N95-27763
Evaluation and modeling of autonomous attitude thrust control for the Geostation Operational Environmental Satellite (GOES)-8 orbit determination p 2146 N95-27765
Differenced Range Versus Integrated Doppler (DRVID) ionospheric analysis of metric tracking in the Tracking and Data Relay Satellite System (TDRSS) p 2147 N95-27766
Kepler Equation solver p 2147 N95-27767
Accurate orbit determination strategies for the tracking and data relay satellites p 2147 N95-27768
Operational improvements of long-term predicted ephemerides of the Tracking and Data Relay Satellites (TDRSs) p 2147 N95-27769
A PC-based magnetometer-only attitude and rate determination system for gyroless spacecraft p 2147 N95-27770
Development of a direct match technique for star identification on the SWAS mission p 2148 N95-27771
An MME-based attitude estimator using vector observations p 2148 N95-27775
Development of a Robust star identification technique for use in attitude determination of the ACE spacecraft p 2149 N95-27777
Optimal attitude maneuver execution for the Advanced Composition Explorer (ACE) mission p 2149 N95-27778
Experience from the in-flight calibration of the Extreme Ultraviolet Explorer (EUVE) and Upper Atmosphere Research Satellite (UARS) fixed head star trackers (FHSTs) p 2149 N95-27779
SAMPEX special pointing mode p 2149 N95-27780
A simple method for verifying the deployment of the TOMS-EP solar arrays p 2150 N95-27782
Earth horizon modeling and application to static Earth sensors on TRMM spacecraft p 2150 N95-27783
Flight dynamics software in a distributed network environment p 2151 N95-27790
Operational considerations of using GPS for spacecraft navigation p 2152 N95-27794
The Global Positioning System (GPS) and attitude determination: Applications and activities in the Flight Dynamics Division p 2152 N95-27795
Contingency maneuver strategies for the Total Ozone Mapping Spectrometer-Earth Probe (TOMS-EP) p 2152 N95-27796
Summary of EOS flight dynamics analysis p 2152 N95-27797
Geostationary Operational Environmental Satellite (GOES)-8 mission flight experience p 2153 N95-27798
A new angle on the Euler angles p 2153 N95-27800
A magnetic hysteresis model p 2153 N95-27801
Contingency designs for attitude determination of TRMM p 2154 N95-27803
SeaWiFS technical report series. Volume 27: Case studies for SeaWiFS calibration and validation, part 3 [NASA-TM-104566-VOL-27] p 2348 N95-28030
Method for determining surface coverage by materials exhibiting different fluorescent properties [NASA-CASE-GSC-13539-1] p 2315 N95-28211
International Ultraviolet Explorer Atlas of B-type spectra from 1200 to 1900 A [NASA-RP-1363] p 2463 N95-28328
Forback DC-to-DC converter [NASA-CASE-GSC-13404-1] p 2269 N95-28341

NATIONAL AERONAUTICS AND SPACE ADMINISTRATION. JOHN C. STENNIS SPACE CENTER, BAY SAINT LOUIS, MS.
A perspective on the Human-Rating process of US spacecraft: Both past and present [NASA-SP-6104] p 2162 N95-26586

NATIONAL AERONAUTICS AND SPACE ADMINISTRATION. JOHN F. KENNEDY SPACE CENTER, COCOA BEACH, FL.
A perspective on the Human-Rating process of US spacecraft: Both past and present [NASA-SP-6104] p 2162 N95-26586
Aqueous degreasing, precision cleaning, and cleanliness verification p 2231 N95-27121
Debris/Ice/TPS assessment and integrated photographic analysis of Shuttle mission STS-67 [NASA-TM-110651] p 2160 N95-27238
Spaceport news index: January 1990 - December 1994 [NASA-TM-110653] p 2454 N95-27243
Automated database design from natural language input p 2383 N95-27378
A review of falconry as a bird control technique with recommendations for use at the Shuttle Landing Facility, John F. Kennedy Space Center, Florida, USA [NASA-TM-110142] p 2126 N95-27859
Evaluation of a conductive polymer-based sensor for detection of hydrazines at the part-per-billion level p 2173 N95-28309
Prototype development and test results of a continuous ambient air monitoring system for hydrazine at the 110 ppb level p 2173 N95-28310
A new method for measuring hypergol scrubber emissions p 2174 N95-28312
Water driven turbine/brush pipe cleaner [NASA-CASE-KSC-11669-1] p 2304 N95-28359
Particle fallout/activity sensor [NASA-CASE-KSC-11687-1] p 2293 N95-28362

NATIONAL AERONAUTICS AND SPACE ADMINISTRATION. LYNDON B. JOHNSON SPACE CENTER, HOUSTON, TX.
Orbital impacts and the Space Shuttle windshield [NASA-TM-110594] p 2159 N95-26379
A perspective on the Human-Rating process of US spacecraft: Both past and present [NASA-SP-6104] p 2162 N95-26586
Calorimetric evaluation of commercial Ni-MH cells and charges p 2272 N95-26790
The 29th Aerospace Mechanisms Symposium [NASA-CP-3293] p 2154 N95-27260
Advanced development for space robotics with emphasis on fault tolerance p 2155 N95-27263
An overview of the Evaluation of Oxygen Interactions with Materials 3 experiment: Space Shuttle Mission 46, July-August 1992 p 2210 N95-27630
Evaluation of Oxygen Interactions with Materials 3: Mission and induced environments p 2210 N95-27631
STS-46 plasma composition measurements using the EOIM-3 mass spectrometer p 2211 N95-27645
Space Station program status and research capabilities p 2166 N95-27662
Pre-integrated truss space station and method of assembly [NASA-CASE-MSC-22015-1] p 2165 N95-27842
Full complex modulation using two one-parameter spatial light modulators [NASA-CASE-MSC-22255-1] p 2427 N95-28384

NATIONAL AERONAUTICS AND SPACE ADMINISTRATION. LANGLEY RESEARCH CENTER, HAMPTON, VA.
Flutter clearance flight tests of an OV-10A airplane modified for wake vortex flight experiments [NASA-TM-109168] p 2117 N95-26381
Airfoil modification effects on subsonic and transonic pressure distributions and performance for the EA-6B airplane [NASA-TP-3516] p 2120 N95-26382
Aircraft noise prediction program theoretical manual: Rotorcraft System Noise Prediction System (ROTONET), part 4 [NASA-TM-83199-PT-4] p 2400 N95-26392
A finite element propagation model for extracting normal incidence impedance in nonprogressive acoustic wave fields [NASA-TM-110160] p 2400 N95-26394
Radiation safety aspects of commercial high-speed flight transportation [NASA-TP-3524] p 2465 N95-26427
A class of stabilizing controllers for flexible multibody systems [NASA-TP-3494] p 2161 N95-26428
Design tool for multiprocessor scheduling and evaluation of iterative dataflow algorithms [NASA-TP-3491] p 2366 N95-26685
Composite sandwich structure and method for making same [NASA-CASE-LAR-14898-1] p 2180 N95-26764
Combined investigation of Eddy current and ultrasonic techniques for composite materials NDE [NASA-TM-110599] p 2306 N95-26778
Non-invasive method and apparatus for monitoring intracranial pressure and pressure volume index in humans [NASA-CASE-LAR-13894-1] p 2353 N95-26889
Incorporating biplane wing theory into a large, subsonic, all-cargo transport p 2120 N95-26956
Multi-channel electronically scanned cryogenic pressure sensor [NASA-CASE-LAR-15062-1] p 2291 N95-27138
Schlieren System and method for moving objects [NASA-CASE-LAR-15053-1] p 2291 N95-27191
Composite prepreg application device [NASA-CASE-LAR-15259-1] p 2182 N95-27192
A study of workstation computational performance for real-time flight simulation [NASA-TM-109184] p 2362 N95-27241
High-precision buffer circuit for suppression of regenerative oscillation [NASA-TM-4658] p 2291 N95-27259
Linear Proof Mass Actuator p 2158 N95-27290
Effect of turbulence models on criticality conditions in swirling flows p 2282 N95-27356
Abrasion-ablation model for neutron production in heavy ion reactions [NASA-TM-4656] p 2420 N95-27372
A path-oriented knowledge representation system: Defusing the combinatorial system p 2386 N95-27395
LDEF: 69 Months in Space. Third Post-Retrieval Symposium, part 3 [NASA-CP-3275-PT-3] p 2466 N95-27629
Hardware cleanliness methodology and certification p 2211 N95-27656
From LDEF to a national Space Environment and Effects (SEE) program: A natural progression p 2145 N95-27657
The Long Duration Exposure Facility (LDEF) annotated bibliography p 2457 N95-27659
The Long Duration Exposure Facility (LDEF) photographic survey special publication p 2457 N95-27660
A Materials Exposure Facility p 2166 N95-27664
Orbiting meteoroid and debris counting experiment p 2463 N95-27668
Development and implementation of an electronic library tour for the NASA Langley Technical Library [NASA-TM-110619] p 2455 N95-27701
Phenylethynyl terminated imide oligomers [NASA-CASE-LAR-15175-1] p 2235 N95-27732
Modeling of aircraft unsteady aerodynamic characteristics. Part 2: Parameters estimated from wind tunnel data [NASA-TM-110161] p 2142 N95-27839
A numerical study of fundamental shock noise mechanisms [NASA-TM-110608] p 2401 N95-27908
Optimization of measurements with pressure sensitive paints [NASA-TM-4695] p 2293 N95-27915
Measurements of store forces and moments and cavity pressures for a generic store in and near a box cavity at subsonic and transonic speeds [NASA-TM-4611] p 2123 N95-28241
Resin transfer molding of textile preforms for aircraft structural applications p 2185 N95-28276
Analysis of stresses in finite anisotropic panels with centrally located cutouts p 2187 N95-28286
Stiffness and strength tailoring in uniform space-filling truss structures p 2188 N95-28290
Designing for time-dependent material response in spacecraft structures p 2166 N95-28292
Experimental investigation of inlet-combustor isolators for a dual-mode scramjet at a Mach number of 4 [NASA-TP-3502] p 2140 N95-28343
Poly(N-arylenbenzimidazoles) via aromatic nucleophilic displacement [NASA-CASE-LAR-14939-1] p 2179 N95-28360
Polybenzimidazoles via aromatic nucleophilic displacement [NASA-CASE-LAR-14924-1-CU] p 2179 N95-28361
Compression failure of angle-ply laminates p 2190 N95-28428
Buckling behavior of long symmetrically laminated plates subjected to combined loads p 2190 N95-28430
Effects of floor location on response of composite fuselage frames p 2192 N95-28439
Overview of the ACT program p 2193 N95-28463
Designers' unified cost model p 2194 N95-28464
Composite fuselage shell structures research at NASA Langley Research Center p 2194 N95-28466
Technology integration box beam failure study p 2194 N95-28468
Development of stitched/RTM composite primary structures p 2195 N95-28469
Test and analysis results for composite transport fuselage and wing structures p 2137 N95-28470
Tension fracture of laminates for transport fuselage. Part 1: Material screening p 2137 N95-28471
Recent progress in NASA Langley textile reinforced composites program p 2196 N95-28475
The use of impact force as a scale parameter for the impact response of composite laminates p 2197 N95-28479
Effect of low-speed impact damage and damage location on behavior of composite panels p 2197 N95-28481
Damage tolerance of a geodesically stiffened advanced composite structural concept for aircraft structural applications p 2138 N95-28487
HZETRN: Description of a free-space ion and nucleon transport and shielding computer program [NASA-TP-3495] p 2465 N95-28530

Study of potential aerodynamic benefits from spanwise blowing at wingtip
[NASA-TP-3515] p 2124 N95-28669
Numerical study to assess sulfur hexafluoride as a medium for testing multielement airfoils
[NASA-TP-3496] p 2124 N95-28674

NATIONAL AERONAUTICS AND SPACE ADMINISTRATION. LEWIS RESEARCH CENTER, CLEVELAND, OH.
A fully implicit time accurate method for hypersonic combustion: Application to shock-induced combustion instability
[NASA-TM-106707] p 2273 N95-26380
The method of space-time conservation element and solution element-applications to one-dimensional and two-dimensional time-marching flow problems
[NASA-TM-106915] p 2389 N95-26663
Comparison of life theories for rolling-element bearings
[NASA-TM-106585] p 2301 N95-26774
Supersonic coaxial jet noise predictions
[NASA-TM-106917] p 2401 N95-26801
The high speed civil transport and NASA's High Speed Research (HSR) program p 2118 N95-26945
Visualization of the multiple supersonic jet oscillations by swept focused strobed schlieren technique
p 2119 N95-26952
Cryogenic and simulated fuel jet breakup in argon, helium and nitrogen gas flows
[NASA-TM-106923] p 2291 N95-27030
Fuzzy inference enhanced information recovery from digital PIV using cross-correlation combined with particle tracking
[NASA-TM-106896] p 2291 N95-27173
Probabilistic simulation of long term behavior in polymer matrix composites
[NASA-TM-106893] p 2309 N95-27174
An outflow boundary condition for aeroacoustic computations
[NASA-TM-106930] p 2279 N95-27175
NASA Lewis Research Center's combustor test facilities and capabilities
[NASA-TM-106903] p 2143 N95-27176
A review of nickel hydrogen battery technology
[NASA-TM-106918] p 2167 N95-27177
Effect of hoop stress on ball bearing life prediction
[NASA-TM-106874] p 2301 N95-27178
The Sixth Annual Thermal and Fluids Analysis Workshop
[NASA-CP-10161] p 2280 N95-27345
Analysis of developing laminar flows in circular pipes using a higher-order finite-difference technique
p 2281 N95-27352
A Navier-Stokes boundary element solver
p 2283 N95-27361
Turbulance boundary conditions for shear flow analysis, using the DTNS flow solver p 2283 N95-27362
The Benard problem: A comparison of finite difference and spectral collocation eigen value solutions
p 2283 N95-27364
Composite heat pipe development status: Development of lightweight prototype carbon-carbon heat pipe with integral fins and metal foil liner
[NASA-TM-106909] p 2283 N95-27369
Ring-plane traveling-wave tube slow-wave circuit design simulations at V-Band frequencies
[NASA-TM-106949] p 2371 N95-27370
Diagnosis of helicopter gearboxes using structure-based networks
[NASA-TM-106932] p 2302 N95-27373
The 77 K operation of a multi-resonant power converter
[NASA-TM-106941] p 2264 N95-27374
Comparison of numerical results and multicavity purge and rim seal data with extensions to dynamics
[NASA-TM-106685] p 2168 N95-27434
Preferentially etched epitaxial liftoff of InP material
[NASA-CASE-LEW-15760-1] p 2235 N95-27503
Using hob offset to balance dynamic strength in spur gears
[NASA-TM-106934] p 2302 N95-27698
Process for non-contact removal of organic coatings from the surface of paintings
[NASA-CASE-LEW-15896-1] p 2235 N95-27702
Ceramic fiber-reinforced monoclinic celsian phase glass-ceramic matrix composite material
[NASA-CASE-LEW-15714-1] p 2183 N95-27717
The origin of spurious solutions in computational electromagnetics
[NASA-TM-106921] p 2391 N95-27726
Electric propulsion for geostationary orbit insertion
[NASA-TM-106942] p 2168 N95-27727
A new Cu-8 Cr-4 Nb alloy for high temperature applications
[NASA-TM-106910] p 2218 N95-27728
Static stability of a three-dimensional space truss
[NASA-TM-106944] p 2164 N95-27730
Design of a unidirectional composite momentum wheel rim
[NASA-TM-106911] p 2164 N95-27761
Further investigations of icing effects on an advanced high-lift multi-element airfoil
[NASA-TM-106947] p 2125 N95-27762
Linearly tapered slot antenna impedance characteristics
[NASA-TM-106912] p 2266 N95-27853
Two-phase flow research using the learjet apparatus
[NASA-TM-106814] p 2284 N95-27854
Optimization of wave rotors for use as gas turbine engine topping cycles
[NASA-TM-106951] p 2140 N95-27860
Direct drive options for electric propulsion systems
[NASA-TM-106576] p 2168 N95-27861
Discharge ignition behavior of the Space Station plasma contactor
[NASA-TM-106925] p 2168 N95-27862
Industry-Wide Workshop on Computational Turbulence Modeling
[NASA-CP-10165] p 2285 N95-27882
Turbulence program for propulsion systems
p 2285 N95-27883
Improvements and new features in the PDF module
p 2287 N95-27902
PC Software graphics tool for conceptual design of space/planetary electrical power systems
[NASA-TM-106908] p 2372 N95-27905
Fundamental concepts of integrated and fiber optic sensors
[NASA-TM-106920] p 2426 N95-27906
System identification of damped truss-like space structures
[NASA-TM-106638] p 2303 N95-27911
Analysis of solar receiver flux distributions for US/Russian solar dynamic system demonstration on the MIR Space Station
[NASA-TM-106933] p 2169 N95-28036
A phase-stepped point diffraction interferometer using liquid crystals
[NASA-TM-106922] p 2293 N95-28037
Transport coefficients for the NASA Lewis Chemical Equilibrium Program
[NASA-TM-4647] p 2209 N95-28182
Analysis of shadowing effects on MIR photovoltaic and solar dynamic power systems
[NASA-TM-106940] p 2169 N95-28213
Analysis of aircraft engine blade subject to ice impact
p 2141 N95-28277
Numerical analysis of intra-cavity and power-stream flow interaction in multiple gas-turbine disk-cavities
[NASA-TM-106886] p 2140 N95-28344
Probabilistic evaluation of fuselage-type composite structures p 2137 N95-28444

NATIONAL AERONAUTICS AND SPACE ADMINISTRATION. MARSHALL SPACE FLIGHT CENTER, HUNTSVILLE, AL.
International Space Station Alpha trace contaminant control subassembly life test report
[NASA-TM-108488] p 2358 N95-26364
Radiation sensitive area detection device and method
[NASA-CASE-MFS-28563-3] p 2423 N95-26385
A perspective on the Human-Rating process of US spacecraft: Both past and present
[NASA-SP-6104] p 2162 N95-26586
Effect of processing parameters on surface finish for fused deposition machinable wax patterns
[NASA-TP-3550] p 2244 N95-26769
The 1994 27th Annual NASA Aerospace Battery Workshop
[NASA-CP-3292] p 2317 N95-26785
Nickel metal hydride LEO cycle testing
p 2272 N95-26791
Hubble Space Telescope nickel-hydrogen battery testing: An update p 2272 N95-26794
Adiabatic charging of nickel-hydrogen batteries
p 2272 N95-26795
Device and method for screening crystallization conditions in solution crystal growth
[NASA-CASE-MFS-28985-1] p 2245 N95-26888
Dynamically timed electric motor
[NASA-CASE-MFS-28958-1] p 2261 N95-26890
The Solar X-ray Imager Vacuum Door Assembly
p 2157 N95-27280
Apparatus for diffusion controlled dialysis under microgravity conditions
[NASA-CASE-MFS-28986-1] p 2245 N95-27500
Automatic locking knee brace joint
[NASA-CASE-MFS-28997-1] p 2360 N95-27501
Atomic oxygen dosimetry measurements made on STS-46 by CONCAP 2 p 2418 N95-27634
Inflight resistance measurement on high-T(sub c) superconducting thin films exposed to orbital atomic oxygen on CONCAP-2 (STS-46) p 2272 N95-27635
Orbital atomic oxygen effects on materials: An overview of MSFC experiments on the STS-46 EOIM-3
p 2419 N95-27637
Effects of atomic oxygen on polymeric materials flown on EOIM-3 p 2242 N95-27638
Thermal control materials on EOIM-3
p 2242 N95-27639
Evaluation of space environmental effects on metals and optical thin films on EOIM-3 p 2210 N95-27641
Point defect formation in optical materials expos ed to the space environment p 2428 N95-27646
An LDEF follow-on spacecraft concept
p 2166 N95-27665
The solar array-induced disturbance of the Hubble Space Telescope pointing system
[NASA-TP-3556] p 2311 N95-28214
CORSSTOL: Cylinder Optimization of Rings, Skin, and Stringers with Tolerance sensitivity
[NASA-TP-3551] p 2392 N95-28215
Developmental problems and their solution for the Space Shuttle main engine alternate liquid oxygen high-pressure turbopump: Anomaly or failure investigation the key
[NASA-TP-3553] p 2169 N95-28263
Apparatus for testing high pressure injector elements
[NASA-CASE-MFS-28773-1] p 2304 N95-28347
Bearing defect signature analysis using advanced nonlinear signal analysis in a controlled environment
[NASA-TM-108491] p 2304 N95-28364

NATIONAL AERONAUTICS AND SPACE ADMINISTRATION. PASADENA OFFICE, CA.
Method and apparatus for polaradiometric pyrometer
[NASA-CASE-NPO-19064-1-CU] p 2290 N95-26765
Extended linear ion trap frequency standard apparatus
[NASA-CASE-NPO-19081-1-CU] p 2404 N95-26861
Ultra high purity, dimensionally stable INVAR 36
[NASA-CASE-NPO-19358-1-CU] p 2213 N95-26862
Solid-state image sensor with focal-plane digital photon-counting pixel array
[NASA-CASE-NPO-18518-1-CU] p 2424 N95-26894
Laser with optically driven Q-switch
[NASA-CASE-NPO-18470-1-CU] p 2297 N95-27731
Display system employing acousto-optic tunable filter
[NASA-CASE-NPO-18736-1-CU] p 2426 N95-27843
Extended linear ion trap frequency standard apparatus
[NASA-CASE-NPO-19081-1-CU] p 2416 N95-28348
Optical implementation of inner product neural associative memory
[NASA-CASE-NPO-18491-2-CU] p 2427 N95-28363
Leak detection utilizing analog binaural (VLSI) techniques
[NASA-CASE-NPO-18399-1-CU] p 2271 N95-28599

NATIONAL AERONAUTICS AND SPACE ADMINISTRATION. WALLOPS FLIGHT FACILITY, WALLOPS ISLAND, VA.
Pulse Code Modulation (PCM) encoder handbook for Aydin Vector MMP-900 series system
[NASA-RP-1365] p 2255 N95-27435

NATIONAL AEROSPACE LAB., TOKYO (JAPAN).
Analysis of fatigue fractographic data of a rod end housing using a Monte Carlo simulation
[NAL-TR-1225] p 2307 N95-26521
Numerical simulation of combustion flow around a flame holder with hydrogen injection
[NAL-TR-1233] p 2200 N95-26523
Experimental investigation of static and dynamic ground effect on HOPE ALFLEX vehicle
[NAL-TR-1236] p 2128 N95-26525
Flight evaluation of GPS/DGPS sensor systems installed in NAL Do228
[NAL-TR-1230] p 2126 N95-26585
Experiment on a rectangular cross section scramjet combustor. 2: Effects of fuel injector geometry
[NAL-TR-1220] p 2139 N95-26600
Statistical analysis of tensile mechanical property data of carbon/polyimide composites
[NAL-TR-1238] p 2180 N95-26667
Effects of dust from storage heaters on ignition in scramjets
[NAL-TR-1234] p 2139 N95-26706
Development test of a liquid Apogee engine for the ETS-6
[NAL-TR-1250] p 2167 N95-26799

NATIONAL GEOPHYSICAL DATA CENTER, BOULDER, CO.
Solar-geophysical data number 604, December 1994. Part 1: (Prompt reports). Data for November, October 1994, and late data
[PB95-181848] p 2465 N95-28087

NATIONAL INST. FOR FUSION SCIENCE, NAGOYA (JAPAN).
Proposed high speed pellet injection system HIPEL for large helical device
[NIFS-255] p 2419 N95-26584

NATIONAL INST. OF STANDARDS AND TECHNOLOGY, GAITHERSBURG, MD.

Proceedings: Workshop on Research Needs in Wind Engineering
[PB95-189528] p 2308 N95-26743

Standards for excellence
[NONP-NASA-VT-95-49096] p 2451 N95-27202

NIST Automated Manufacturing Research Facility (AMRF): March 1987
[NONP-NASA-VT-95-49097] p 2246 N95-27203

Chemical engineering: Measurements for a competitive age
[NONP-NASA-VT-95-49098] p 2203 N95-27204

Quest for excellence 5
[NONP-NASA-VT-95-49099] p 2451 N95-27205

Getting it right, making it better
[NONP-NASA-VT-95-49118] p 2451 N95-27206

Malcolm Baldrige National Quality Award winners 1989
[NONP-NASA-VT-95-49119] p 2451 N95-27207

NIST: Information management in the AMRF
[NONP-NASA-VT-95-49120] p 2454 N95-27208

STEP: A futurevision, today
[NONP-NASA-VT-95-49121] p 2451 N95-27209

Algorithm to describe the spread of a wall fire under a ceiling
[PB95-182259] p 2247 N95-28008

NATIONAL OCEANIC AND ATMOSPHERIC ADMINISTRATION, BOULDER, CO.

Solar UV flux measurements from the SBUV2 monitor on the NOAA9 satellite. Part 1: Mg II h and k line core-to-wing ratios for 1986-1988
[PB95-181962] p 2464 N95-28007

NATIONAL PHYSICAL LAB., TEDDINGTON (ENGLAND).

Creep recovery of PVC and polypropylene
[PB95-185112] p 2224 N95-26448

BIPM project: Intercomparison of water triple-point cells
[PB95-185237] p 2398 N95-26614

Uncertainties in the calibration of hydrophones at NPL by the three-transducer spherical-wave reciprocity method in the frequency range 10 kHz on 500 kHz
[PB95-185245] p 2401 N95-26615

Rheological measurement methods for fibre filled plastics
[PB95-190088] p 2226 N95-26744

Stability of reference masses 4: Growth of carbonaceous contamination on platinum-iridium mass standard surfaces, and its cleaning by UV/ozone treatment
[PB95-190096] p 2226 N95-26745

Survey of sub-micrometre powder size measurement for ceramic and cermet powders
[PB95-190104] p 2227 N95-26746

Overview of through-thickness test methods for polymer matrix composites
[PB95-190112] p 2227 N95-26747

Bilateral intercomparison of the neutron emission rate of a (252)Cf spontaneous fission source between the National Physical Laboratory, Teddington, UK and the Physikalisch-Technische Bundesanstalt, Braunschweig, Germany
[PB95-190120] p 2404 N95-26748

Analysis of plate-twist test for in-plane shear modulus of composite materials (revised)
[PB95-190195] p 2308 N95-26749

Measurement of viscosity by capillary rheometry: Dwell time effects
[PB95-190203] p 2201 N95-26750

NATIONAL RENEWABLE ENERGY LAB., GOLDEN, CO.

Hydrogen program
[DE94-011827] p 2242 N95-27415

Biomass Pyrolysis Oil Properties and Combustion Meeting
[DE95-004017] p 2204 N95-27438

A comparison of measured wind park load histories with the WISPER and WISPERX load spectra
[DE95-000295] p 2319 N95-27459

Performance of a stand-alone wind-electric ice maker for remote villages
[DE95-004006] p 2320 N95-27475

Reducing cold-start emissions by catalytic converter thermal management
[DE95-000256] p 2327 N95-27540

Wind-tunnel test of the S814 thick root airfoil
[DE95-000268] p 2122 N95-27541

Recent progress in the Photovoltaic Manufacturing Technology Project (PVMaT)
[DE95-000279] p 2320 N95-27704

Current status of environmental, health, and safety issues of lithium polymer electric vehicle batteries
[DE95-004005] p 2265 N95-27719

Review and analysis of the 1980-1989 biomass thermochemical conversion program
[DE95-000287] p 2325 N95-28394

The U.S. Department of Energy Wind Turbine Development Program
[DE95-000292] p 2325 N95-28395

Building-integrated photovoltaics: A case study
[DE95-004032] p 2325 N95-28396

NATIONAL RESEARCH COUNCIL OF CANADA, OTTAWA (ONTARIO).

Bonded composite repair of thin metallic materials: Variable load amplitude and temperature cycling effects
p 2132 N95-27509

NATIONAL TRANSPORTATION SAFETY BOARD, WASHINGTON, DC.

Aircraft accident report: Controlled collision with Terrain Transportes Aereos Ejecutivos, S.A. (TAESA) Learjet 25D, XA-BBA Dulles International Airport Chantilly, Virginia, June 18, 1994
[NTSB/AAR-95/02] p 2125 N95-26498

NAVAL AIR DEVELOPMENT CENTER, WARMINSTER, PA.

Benefits and limitations of composites in carrier-based aircraft p 2189 N95-28422

Effect of the fiber-matrix interphase on the transverse tensile strength of the unidirectional composite material
p 2190 N95-28425

Navy composite maintenance and repair experience
p 2193 N95-28446

NAVAL AIR SYSTEMS COMMAND, ARLINGTON, VA.

Naval Aviation System TEAM mapping, charting, and geodesy handbook
[AD-A288590] p 2314 N95-26841

NAVAL AIR WARFARE CENTER, CHINA LAKE, CA.

A continuous emissions monitor for airborne metals
p 2174 N95-28313

NAVAL AIR WARFARE CENTER, WARMINSTER, PA.

An evaluation of the Software Through Pictures/T Tool (StP/T) for the Software Support Activity (SSA)
[AD-A288822] p 2362 N95-26348

Modified Gaussian elimination for adaptive beamforming using RNS arithmetic
[AD-A288809] p 2248 N95-26356

Field repair materials for naval aircraft
p 2133 N95-27514

NAVAL COMMAND, CONTROL AND OCEAN SURVEILLANCE CENTER, KAILUA, HI.

Vocoded KING data base
[AD-A289827] p 2258 N95-28576

NAVAL COMMAND, CONTROL AND OCEAN SURVEILLANCE CENTER, SAN DIEGO, CA.

Analysis of historical oceanographic data on a personal computer. Program MDS
[AD-A288965] p 2363 N95-26447

VOCAR: An experiment in Variability of Coastal Atmospheric Refractivity
[AD-A289202] p 2253 N95-27006

Semantic heterogeneity in database and data dictionary integration for command and control systems
[AD-A289180] p 2453 N95-27014

Evolving cascade-correlation networks for time-series forecasting
[AD-A289197] p 2390 N95-27020

Modeling surface effects with the parabolic equation method
[AD-A289199] p 2254 N95-27021

Microwave characterization of sub-micron N- and P-channel MOSFET's fabricated with thin film silicon-on-sapphire
[AD-A289296] p 2438 N95-27040

The biodegradation of fuels in soils and sediments: Differences as a function of mineralogy
p 2230 N95-27116

Downloading environmental data in the new MOODS format
[AD-A288835] p 2456 N95-28589

NAVAL MEDICAL RESEARCH INST., BETHESDA, MD.

A model of bubble evolution during decompression based on a Monte Carlo simulation of inert gas diffusion
[AD-A289400] p 2353 N95-26885

NAVAL POSTGRADUATE SCHOOL, MONTEREY, CA.

Virtual Prototyping as an aid for control system analysis
[AD-A288819] p 2362 N95-26346

Characterization of Ultra-Low Carbon Baintic steels for use as weld wire consumables
[AD-A288292] p 2212 N95-26411

Scalable multicast tree construction for wide area networks
[AD-A288318] p 2379 N95-26421

Quantitative modeling and analysis in environmental studies
[AD-A288451] p 2326 N95-26431

An analysis of orbital propagators for Low Earth Orbit Rendezvous
[AD-A288883] p 2161 N95-26458

The effect of infrared sea surface temperature measurements on evaporation duct height estimation
[AD-A289045] p 2346 N95-26477

Temporal and spatial decorrelation scales of the Yellow Sea thermal fields
[AD-A288617] p 2346 N95-26483

A probabilistic target classification and description model for seismic sensors
[AD-A288548] p 2335 N95-26531

Soot particle density determination from a laser extinction multipass technique
[AD-A288551] p 2423 N95-26532

Grain size management in repetitive task graphs for multiprocessor computer scheduling
[AD-A288575] p 2377 N95-26551

A system dynamics based study of software reuse and its determinants
[AD-A288578] p 2364 N95-26554

Design and synthesis of a real-time controller for an unmanned air vehicle
[AD-A289134] p 2141 N95-26555

Effect of surface coating on one-dimensional system subjected to unit step pressure wave
[AD-A288237] p 2308 N95-26625

The design and implementation of the Military Applications of Shiptracks experiment on Space Transportation System - 65
[AD-A288488] p 2160 N95-26634

Deep convection in the Mediterranean Sea
[AD-A288497] p 2346 N95-26647

Comparison of fixed wing aircraft algorithms for JANUS
[AD-A288503] p 2129 N95-26652

Fluxes across the west coast resolved by Picket Fence observations during stormfest
[AD-A288511] p 2341 N95-26653

Lattice parameters and Debye-Waller factors of gamma-TiAl alloys
[AD-A288843] p 2213 N95-26681

Evaluation of a new laboratory acoustic Doppler velocimeter
[AD-A289592] p 2290 N95-26714

Air cushioned landing craft (LCAC) based ship to shore movement simulation: A decision aid for the amphibious commander. A (SMMAT) application
[AD-A289635] p 2246 N95-26722

Space tether-radar data processing
[AD-A289654] p 2250 N95-26725

Analysis, design and implementation of a database system for the systems management curriculum office
[AD-A289656] p 2452 N95-26758

Annealing of radiation damaged gallium arsenide solar cells by laser illumination
[AD-A289683] p 2316 N95-26762

Study of damage evolutions in composite plates subjected to bending loads using micro-macro analysis
[AD-A288523] p 2308 N95-26839

A mathematical analysis of the Janus combat simulation weather effects models and sensitivity analysis of sky-to-ground brightness ratio on target detection
[AD-A289629] p 2336 N95-26858

The ambiguity function of the stepped frequency radar
[AD-A289533] p 2251 N95-26871

Design and implementation of a software communication architecture for the JANUS-3D Visualizer
[AD-A288509] p 2370 N95-27150

Preliminary flight software specification for the petite amateur Navy satellite (PANSAT)
[AD-A280068] p 2165 N95-28150

Construction and wind tunnel test of a 1/12th scale helicopter model
[AD-A288487] p 2123 N95-28331

Thermal analysis of PANSAT batteries and Electrical Power Subsystem
[AD-A290013] p 2269 N95-28388

Proof test methodology for composites
p 2193 N95-28445

Systematic and integrated approach to Tropical Cyclone track forecasting. Part 1: Approach overview and description of meteorological basis
[AD-A291775] p 2344 N95-28459

Modeling and statistical analysis of bioassay data: Medaka cell proliferation under DEN and TCE
[AD-A289998] p 2352 N95-28519

Bilateral force feedback for hydraulically actuated systems
[AD-A291632] p 2387 N95-28545

Modeling helicopter blade dynamics using a modified Myklestad-Prohl transfer matrix method
[AD-A289891] p 2136 N95-28626

NAVAL RESEARCH LAB., BAY SAINT LOUIS, MS.

Hindcasting wind-driven anomalies using reduced-gravity global ocean models with 1/2 deg and 1/4 deg resolution
[AD-A289060] p 2345 N95-26406

Digital mapping, charting, and geodesy analysis program: Initial technical review of Raster Product Format
[AD-A289039] p 2313 N95-26476

Digital mapping, charting, and geodesy analysis program technical review of Vector Quantization (VQ) Decompression for the National Imagery Transmission Format Standard (NITFS)
[AD-A288998] p 2314 N95-26682
Study of the response of a three-dimensional coupled ice-ocean model to daily varying atmospheric forcing
[AD-A289050] p 2347 N95-27189

NAVAL RESEARCH LAB., MONTEREY, CA.
Severe weather guide mediterranean
[AD-A289829] p 2344 N95-28577

NAVAL RESEARCH LAB., WASHINGTON, DC.
Speech analysis and synthesis based on pitch-synchronous segmentation of the speech waveform
[AD-A288824] p 2248 N95-26349
Advanced solid lubricant films by Ion-Beam Assisted Deposition
[AD-A288866] p 2225 N95-26499
Electromagnetic spectrum occupancy study of a potential transmitter site for the HF Active Auroral Research Program (HAARP)
[AD-A288909] p 2249 N95-26564
The 50 Ah NiH2 CPV qualification tests
p 2272 N95-26792
Bibliography of NRL publications - 1990
[AD-A289483] p 2466 N95-26823
Addressing tension instability in SPH methods
[AD-A289531] p 2276 N95-26852
Surface damage effects generated by a fast-pulse laser beam
[AD-A289131] p 2295 N95-26996
The Clementine mechanisms p 2156 N95-27268
The sensitive detection of hydrazine using chemiluminescence p 2173 N95-28311

NAVAL SURFACE WARFARE CENTER, BETHESDA, MD.
Microengineered conducting composites from nanochannel templates
[AD-A289573] p 2180 N95-26686

NAVAL SURFACE WARFARE CENTER, CRANE, IN.
Air Force Ni-H2 cell test program: State of Charge test
p 2272 N95-26789

NAVAL SURFACE WARFARE CENTER, DAHLGREN, VA.
Parallel block implicit integration technique for trajectory parallelism
[AD-A288961] p 2379 N95-28335

NAVAL SURFACE WEAPONS CENTER, INDIAN HEAD, MD.
Biodegradation of nitrate esters p 2171 N95-28299
Upgrade of the computer modeling programs POLU10 and POLU13A for open burning and open detonation of energetic materials p 2172 N95-28306

NAVAL UNDERSEA WARFARE CENTER, NEW LONDON, CT.
Molecular modeling: An approach for the study of piezoelectric polymers
[AD-A289821] p 2241 N95-28574

NAVAL WEAPONS CENTER, CHINA LAKE, CA.
Composite flight-control actuator development
p 2142 N95-28281

NAVY CLOTHING AND TEXTILE RESEARCH FACILITY, NATICK, MA.
Lightweight cold weather underwear investigation
[AD-A288506] p 2358 N95-26736

NEBRASKA UNIV., LINCOLN, NE.
Resonant photoemission studies of thickness dependence of the unoccupied Gd 5d bands
[DE95-004127] p 2436 N95-26440
Materials, structures, and devices for high-speed electronics
[NASA-CR-197815] p 2260 N95-26816
LEO degradation of graphite and carbon-based composites aboard Space Shuttle Flight STS-46
p 2199 N95-27636

NEVADA UNIV., RENO, NV.
Application of CFD to the analysis and design of high-speed inlets
[NASA-CR-198574] p 2279 N95-27240

NEW ENERGY AND INDUSTRIAL TECHNOLOGY DEVELOPMENT ORGANIZATION, TOKYO (JAPAN).
Investigation on comprehensive fossil fuel cycle analysis and assessment approach as viewed from the global environment
[DE95-759241] p 2329 N95-27935
Investigation of high-temperature superconducting flywheel energy storage devices
[DE95-759242] p 2320 N95-27936
Research on the establishment of the database system for R and D on the innovative technology for the Earth
[DE95-759244] p 2458 N95-27937
Investigation on working out the global regeneration plan
[DE95-759246] p 2329 N95-27938
Survey on researches related to ocean disposal of carbon dioxide
[DE95-759247] p 2329 N95-27939
Investigation on energy conversion technology using biochemical reaction elements, 2
[DE95-759250] p 2321 N95-27940
Investigation on technology for increasing the biological CO2 sink and technology for CO2 fixation and reutilization
[DE95-759251] p 2329 N95-27941
Investigation on LCA (Life Cycle Analysis/assessment)
[DE95-759260] p 2330 N95-27942
Survey on bio-chemical complex harmonized with global environment
[DE95-759252] p 2331 N95-28535

NEW MEXICO STATE UNIV., LAS CRUCES, NM.
Demonstration study of hierarchical control of fluid-dynamic phenomena
[AD-A289341] p 2275 N95-26751
Laser beam aerosol interactions
[AD-A291723] p 2300 N95-28509

NEW MEXICO TECH, SOCORRO, NM.
A study of lightning in winter thunderstorms and the analysis of thunderstorm overflight data
[NASA-CR-198577] p 2343 N95-28191

NEW MEXICO UNIV., ALBUQUERQUE, NM.
Methods development for measuring and classifying flammability/combustibility of refrigerants. Task 2: Test plan
[DE95-007066] p 2234 N95-27481
Methods development for measuring and classifying flammability/combustibility of refrigerants. Task 1: Annotated bibliography
[DE95-007232] p 2238 N95-28133

NEW ORLEANS UNIV., LA.
A density functional/molecular dynamics study of the structure of liquid nitromethane
[AD-A289224] p 2404 N95-26960

NEW YORK UNIV., NEW YORK, NY.
Computational fluid dynamics and transonic flow
[AD-A288962] p 2273 N95-26405

NEWCASTLE-UPON-TYNE UNIV., NEWCASTLE (ENGLAND).
Two implementation relations and the correctness of communicating replicated processes
[PB95-195640] p 2375 N95-28645

NORTH CAROLINA AGRICULTURAL AND TECHNICAL STATE UNIV., GREENSBORO, NC.
Self-checking state machine realization in CMOS
[AD-A289149] p 2261 N95-27002

NORTH CAROLINA STATE UNIV., RALEIGH, NC.
Parallelism detection and scheduling strategies for reliable and efficient execution on multicomputers
[AD-A288370] p 2376 N95-26471
Biochemically vulnerable sites for antifungal intercession in the control of fungal growth
[AD-A288345] p 2348 N95-26573
Meso-beta scale numerical simulation studies of terrain-induced jet streak mass/momentum perturbations
[NASA-CR-197804] p 2335 N95-26592
Growth, characterization and device development in monocrystalline diamond films
[AD-A289356] p 2439 N95-27416
Low temperature deposition and characterization of N- and P-type silicon carbide thin films and associated Ohmic and Schottky contacts
[AD-A289107] p 2237 N95-28097
Atomic layer epitaxy of group 4 materials: Surface processes, thin films, devices and their characterization
[AD-A289092] p 2446 N95-28327

NORTH CAROLINA UNIV., RALEIGH, NC.
Pseudomorphic semiconducting heterostructures from combinations of AlN, GaN and selected SiC polytypes: Theoretical advancement and its coordination with experimental studies of nucleation, growth, characterization and device development
[AD-A289550] p 2437 N95-26756

NORTHROP CORP., HAWTHORNE, CA.
Analysis of composite structures with delaminations under combined bending and compression
p 2190 N95-28429
C-130 Advanced Technology Center wing box conceptual design/cost study p 2192 N95-28437
Reliability analysis of composite structures
p 2192 N95-28441

NORTHROP GRUMMAN CORP., HAWTHORNE, CA.
Repair technology for thermoplastic aircraft structures
p 2134 N95-27519

NORTHWEST RESEARCH ASSOCIATES, INC., BELLEVUE, WA.
An improved model of high-latitude f-region scintillation (WBMOD version 13)
[AD-A288558] p 2334 N95-26520

NORTHWESTERN UNIV., EVANSTON, IL.
Toward molecular selectivity with chemically modified electrodes: Can electroactivity and permeability through an overlaying metallopolymer film be controlled via rational manipulation of internal architecture?
[AD-A288719] p 2403 N95-26491
The high energy behavior of the forward scattering parameters -- (sigma)(sub tot), (rho), and B
[DE95-007075] p 2415 N95-28210
High energy density systems in cryogenic media: The production and reactions of atoms and radicals
[AD-A289818] p 2417 N95-28572

NORWEGIAN RADIUM HOSPITAL, OSLO (NORWAY).
Flow cytometry as a means of detecting, enumerating and characterizing bacteria for monitoring of the environment
[AD-A288997] p 2326 N95-26610

NOTRE DAME UNIV., IN.
Effects of three-dimensional imposed 3-D disturbances on bluff-body near wake flows
[AD-A289553] p 2121 N95-26757
Unsteady base pressure measurements in the near wake of a cylinder with imposed three-dimensional disturbances
[AD-A289498] p 2276 N95-26827
Transient studies of low temperature catalyst for methane conversion
[DE95-007913] p 2205 N95-27692

NUCLEAR ENERGY UNIT, BANGI (MALAYSIA).
Radiation vulcanization of natural rubber latex
[DE95-600026] p 2226 N95-26637

NYMA, INC., BROOK PARK, OH.
Transitional flow in thin tubes for space station freedom radiator p 2282 N95-27360
PDF methods for turbulent reactive flows
p 2287 N95-27900

NYMA, INC., CLEVELAND, OH.
A rotating arm using shape-memory alloy
p 2157 N95-27276
A composition joint PDF method for the modeling of spray flames p 2287 N95-27901

NUCLEAR METALS, INC., CONCORD, MA.
Ductile - ductile beryllium aluminum metal matrix composite manufactured by extrusion
[AD-A289519] p 2181 N95-26848

O

OAK RIDGE K-25 SITE, TN.
Vapor pressures of mixtures of CFC-114 with the potential replacement coolants C4F(10) andc-C4F 8
[DE95-003444] p 2208 N95-28042

OAK RIDGE NATIONAL LAB., TN.
The effect on stability and thermal hydraulic quenchback of perforating the jacket of a cable-in-conduit conductor
[DE95-005392] p 2262 N95-27083
Dynamics of the L yields H transition, VH-mode evolution, edge localized modes and R.F. driven confinement control in tokamaks
[DE95-007012] p 2430 N95-27306
Physics with relativistic heavy ions: QGP and other delicacies
[DE95-007014] p 2406 N95-27307
Evaluation of current drive requirements and operating characteristics of a high bootstrap fraction advanced tokamak reactor
[DE95-007041] p 2430 N95-27308
Non-metallic oxide inclusion formation in C-Mnlow alloy steel welds
[DE94-019160] p 2215 N95-27319
Energetic particle destabilization of shear Alfven waves in stellarators and tokamaks
[DE95-006393] p 2431 N95-27419
Monolithic electronics for nuclear and high-energy physics experiments
[DE95-005393] p 2420 N95-27427
Tensile properties of Fe-16 at. % Al alloys
[DE95-007102] p 2215 N95-27450
Measurements of the volatilities of electrolytes: Application to water/steam cycles
[DE95-007103] p 2204 N95-27451
Integrating the QMR method with first principles material science application code
[DE95-007380] p 2408 N95-27456
Parallel algorithms for semi-Lagrangian transport in global atmospheric circulation models
[DE95-007385] p 2327 N95-27457
Advanced neutron source materials surveillance program
[DE95-005700] p 2215 N95-27464
Integrated assessment and the relation between land-use change and climate change
[DE95-006533] p 2327 N95-27469

AEM investigation of tetrahedrally coordinated Ti(4+) in nickel-titanate spinel
[DE95-006624] p 2215 N95-27473
Small angle neutron scattering study of the micelle structure of amphiphilic block copolymers
[DE95-006625] p 2234 N95-27486
Crystal and magnetic structure of stoichiometric YFe2O4
[DE95-006627] p 2440 N95-27487
A video strip chart program
[DE95-006389] p 2372 N95-27495
Nonlinear phenomena, turbulence and anomalous transport in fusion plasmas
[DE95-007044] p 2431 N95-27497
Physics assessment of stellarators as fusion power plants
[DE95-007045] p 2431 N95-27498
Structural ceramics incorporating whiskers, platelets, and particulate phases
[DE95-007048] p 2235 N95-27499
Dithering transitions in resistive pressure-gradient-driven turbulence
[DE95-006737] p 2431 N95-27536
Parallel plasma fluid turbulence calculations
[DE95-006741] p 2431 N95-27537
Materials considerations for molten salt accelerator-based plutonium conversion systems
[DE95-006743] p 2217 N95-27544
Advances in welding science: A perspective
[DE95-006745] p 2302 N95-27545
Thermodynamics of aqueous electrolytes at high temperatures by the isopiestic technique
[DE95-006747] p 2449 N95-27546
Laser ionization of molecular clusters
[DE95-007011] p 2296 N95-27550
Projectile image acceleration, neutralization and electron emission during grazing interactions of multicharged ions with Au(110)
[DE95-007394] p 2409 N95-27551
Sequence comparison on a cluster of workstations using the PVM system
[DE95-006527] p 2378 N95-27709
Positron microscopy
[DE95-007042] p 2410 N95-27874
Pumping characteristics of a cryopump with Ar sorbent in He and in D2/He mixture
[DE95-007049] p 2302 N95-27875
The distribution of cloud cover over the former USSR as derived from the RIHMI 223-Station 3-hourly meteorological database
[DE95-007046] p 2343 N95-27920
Alternative fuels and vehicles choice model
[DE95-005695] p 2243 N95-27944
The development and testing of ceramic components in piston engines
[DE95-005759] p 2236 N95-27946
Analytical and experimental evaluation of joining silicon carbide to silicon carbide and silicon nitride to silicon nitride for advanced heat engine applications, phase 2
[DE95-005761] p 2303 N95-27947
Thermal shock behavior of fiber-reinforced composites
[DE95-006746] p 2183 N95-27955
Electrical conductivity measurements of aqueous electrolyte solutions at high temperatures and high pressures
[DE95-006748] p 2208 N95-27956
The diffusion properties of ion implanted species in selected target materials
[DE95-007006] p 2442 N95-27959
Aqueous electrolyte modeling in ASPEN PLUS(trademark)
[DE95-007008] p 2208 N95-27960
D/H and O-18/O-16 partitioning between water liquid and vapor in the system H2O-Na-K-Mg-Ca-Cl-SO4 from 0 to 350 C
[DE95-007013] p 2208 N95-27961
Assay of weathering effects on protective polymer coatings using positron annihilation spectroscopy
[DE95-007040] p 2236 N95-27962
A new shared-memory programming paradigm for molecular dynamics simulations on the Intel Paragon
[DE95-007289] p 2378 N95-28019
Stress transfer from axially loaded fiber to matrix in a microcomposite
[DE95-007366] p 2183 N95-28043
Effects of interlayers on the scratch adhesion performance of ultra-thin films of copper and gold on silicon substrates
[DE95-007367] p 2220 N95-28044
Error analysis of the quartic nodal expansion method for slab geometry
[DE95-007373] p 2412 N95-28045
Trace elements and the mechanical properties of intermetallic compounds
[DE95-007378] p 2220 N95-28046
A new algorithm for generating highly accurate benchmark solutions to transport test problems
[DE95-007397] p 2373 N95-28047
Stability measurements on a 1-T high temperature superconducting magnet
[DE95-007411] p 2267 N95-28048
Recent neutron scattering results on high-temperature superconductors
[DE95-007028] p 2413 N95-28066
High temperature Hexoloy(trademark) SX silicon carbide
[DE95-007290] p 2221 N95-28075
Solid state sintering of silicon nitride ARL-CR-114
[DE95-007291] p 2443 N95-28076
Lattice calculation for lepton capture from vacuum-pair production in relativistic heavy-ion collisions
[DE95-007392] p 2413 N95-28077
Collisions of highly charged ions with electrons, atoms and surfaces
[DE95-007393] p 2413 N95-28078
Formation of anisotropic Tl-1212, Tl-2212, Tl-1223 and Tl-2223 particles using aerosol flow reacted powders
[DE95-007400] p 2444 N95-28079
Modification of the optical properties of glass by sequential ion implantation
[DE95-007401] p 2237 N95-28080
Coherent V2O3 precipitates in alpha-Al2O3CO-implanted with vanadium and oxygen
[DE95-007404] p 2444 N95-28081
The effects of processing variables on reaction synthesis of Fe-Al alloys
[DE95-007405] p 2221 N95-28082
One dimensional global and local solution for ICRF heating
[DE95-007984] p 2392 N95-28110
Toward a mechanistic understanding of radiation effects in materials
[DE95-006530] p 2221 N95-28120
Polarization relaxation in zinc oxide varistors from 77 K to 450 K
[DE95-007761] p 2268 N95-28156
Project Records Information System (PRIS) user's manual, revision 3
[DE95-008330] p 2456 N95-28172
Sensor for measuring the atomic fraction in highly dissociated hydrogen
[DE95-006531] p 2415 N95-28204
Recent high-speed ballistics experiments at ORNL
[DE95-006534] p 2422 N95-28205
Fracture testing and analysis of adhesively bonded joints for automotive applications
[DE95-007024] p 2184 N95-28207
Reactor pressure vessel structural integrity research
[DE95-007034] p 2223 N95-28208
Failure analysis of thick composite cylinders under external pressure p 2187 N95-28284
Development of low-expansion ceramics with strength retention to elevated temperatures
[DE95-005760] p 2239 N95-28397
Recent status in the search for the quark-gluon plasma
[DE95-007036] p 2417 N95-28447
Teaching interdisciplinary computational science from an electronic book on the Internet
[DE95-006525] p 2373 N95-28498
Third-order-accurate numerical methods for efficient, large time-step solutions of mixed linear and nonlinear problems
[DE95-009184] p 2288 N95-28533
ALLIANCE: An architecture for fault tolerant, cooperative control of heterogeneous mobile robots
[DE95-007374] p 2387 N95-28536
Structural chemistry of some phases in the YC-Ni-B system
[DE95-007403] p 2447 N95-28537
Design and fabrication of a diamond-turned hybrid diffractive/refractive singlet for visible applications at ORNL
[DE95-007007] p 2427 N95-28552
Operating points and feedback control of plasma characteristics in tokamaks with full current drive
[DE95-007037] p 2435 N95-28553
Managing electronic records: A guideline
[DE95-007038] p 2456 N95-28555
An overview of activities and accomplishments of the Metals and Ceramics Division
[DE95-007020] p 2241 N95-28560
Resonant coherent excitation of N6(+) and Mg11(+) in planar channeling: Anisotropies in ionization probabilities and X-ray emission
[DE95-006732] p 2417 N95-28595
Pellet injector research and development at ORNL
[DE95-006736] p 2435 N95-28596
The Global Historical Climatology Network: A preview of version 2
[DE95-007003] p 2332 N95-28605
Local texture and grain boundary misorientations in high H(C) oxide superconductors
[DE95-007004] p 2447 N95-28606
Building an electronic book on the Internet. CSEP:An interdisciplinary syllabus for teaching computational science at the graduate level
[DE95-006526] p 2375 N95-28632
OBSERVATOIRE DE PARIS-MEUDON (FRANCE).
Molecular cloud content of early-type galaxies. V. CO in elliptical galaxies
[PB95-185153] p 2461 N95-27320
OFF WORLD LABS., INC., AUSTIN, TX.
A foveated system to reduce transmission bandwidth of video images from remote camera systems
[AD-A288516] p 2254 N95-27060
OFFICE OF NAVAL RESEARCH, ARLINGTON, VA.
Radio telemetry buoy for long-range communication
[AD-D017269] p 2161 N95-28581
Ash-based ceramic materials
[AD-D017272] p 2241 N95-28582
OGDEN AIR LOGISTICS CENTER, HILL AFB, UT.
Wipe solvent substitutions for 1,1,1-trichloroethane (TCA) and methyl ethyl ketone (MEK) at Hill Air Force Base p 2228 N95-27107
OGDEN/ERC GOVERNMENT SYSTEMS, FAIRFAX, VA.
US Coast Guard Human Systems Integration (HSI) process model
[AD-A289172] p 2358 N95-26612
OHIO STATE UNIV., COLUMBUS, OH.
Joint services electronics program
[AD-A289594] p 2260 N95-26716
Photochemistry in constrained spaces: Zeolites and layered double metal hydroxides
[DE95-006417] p 2207 N95-27951
Comparative wind tunnel test at high Reynolds numbers of NACA 64 621 airfoils with two aileron configurations
p 2124 N95-27977
Theory of exotic superconductivity and normal states of heavy electron and high temperature superconductivity materials
[DE95-006637] p 2268 N95-28198
OHIO UNIV., ATHENS, OH.
The in situ observation of epitaxial diamond thin film nucleation and growth using emission electron microscopy
[AD-A289841] p 2447 N95-28618
OKLAHOMA STATE UNIV., STILLWATER, OK.
User's guide: Computer program for analysis of beam-column structures with nonlinear supports (CBEAMC)
[AD-A289031] p 2307 N95-28464
Characterization of solid state laser and nonlinear optical materials
[AD-A291684] p 2300 N95-28458
OKLAHOMA UNIV., NORMAN, OK.
Dimensionally self regulating materials
[AD-A291671] p 2257 N95-28456
OLD DOMINION UNIV., NORFOLK, VA.
Extension to the dynamic modeling of the large angle magnetic suspension test fixture
[NASA-CR-197801] p 2143 N95-26768
Polymer infiltration studies
[NASA-CR-198601] p 2236 N95-27857
ONSALA SPACE OBSERVATORY (SWEDEN).
CO, HCO(+) and HCN absorption in the gravitational lens candidate B0218+357 at z=0.685
[PB95-185146] p 2461 N95-26522
ORBITAL SCIENCES CORP., DULLES, VA.
Non-explosive actuation for the ORBCOMM (TM) satellite p 2156 N95-27274
OREGON GRADUATE INST. OF SCIENCE AND TECHNOLOGY, BEAVERTON, OR.
Low temperature materials growth and processing development for flat panel display technology applications
[AD-A288970] p 2233 N95-27187
OREGON INST. OF TECH., KLAMATH FALLS, OR.
Geothermal direct-heat utilization assistance
[DE95-007247] p 2319 N95-27236
OREGON STATE UNIV., CORVALLIS, OR.
Real-time value-driven diagnosis
p 2386 N95-27396
Preliminary analysis of dynamic stall effects on a 91-meter wind turbine rotor p 2124 N95-27975
ORGANISATIE VOOR TOEGEPAST NATUURWETENSCHAPPELIJK ONDERZOEK, DELFT (NETHERLANDS).
Manual for SHOCK3D, version 2.0. Computer program for non-linear shock response
[AD-A288631] p 2307 N95-26342
Longterm infrared cloud clutter research
[AD-A288632] p 2340 N95-26343
Assessment of long-distance HF radio and satellite communication assets for RNLAF out-of-area operations
[AD-A288633] p 2247 N95-26344

Model-based monitoring and diagnosis of a satellite-based instrument p 2166 N95-27390

OSSERVATORIO ASTRONOMICO, TRIESTE (ITALY).

Dwarf novae p 2458 N95-27069

Nova-like variables p 2458 N95-27070

Models for various aspects of dwarf novae and nova-like stars p 2459 N95-27071

Classical novae and recurrent novae: General properties p 2459 N95-27072

Typical examples of classical novae p 2459 N95-27074

Recurrent novae p 2460 N95-27075

OVERSET METHODS, INC., LOS ALTOS, CA.

Global flowfield about the V-22 Tiltrotor Aircraft [NASA-CR-198603] p 2122 N95-27248

P

PACIFIC NORTHWEST LAB., RICHLAND, WA.

Effects of helium pre-implantation on the microstructure and mechanical properties of irradiated 316 stainless steel [DE95-007162] p 2214 N95-27086

Temperature dependence of ion-beam-induced amorphization in (Beta)-SiC [DE95-007164] p 2438 N95-27087

Simulating the production of free defects in irradiated metals [DE95-007165] p 2214 N95-27088

Fluid dynamic effects on precision cleaning with supercritical fluids p 2232 N95-27129

The influence of surface structure on the interaction of water with TiO2(100) [DE95-004927] p 2203 N95-27401

The development of mechanical strength in a ceramic material during firing [DE95-004925] p 2234 N95-27476

Effect of internal hydrogen on the mixed-mode 1/3 fracture toughness of a ferrific/martensitic stainless steel [DE95-005722] p 2216 N95-27479

Transparent access to distributed, heterogeneous environmental information systems [DE95-007268] p 2454 N95-27483

Characterization of collision cascade damage in Ca2La8(SiO4)6O2 by HRTEM [DE95-005719] p 2440 N95-27491

Radiation-induced segregation: A microchemical gauge to quantify fundamental defect parameters [DE95-005720] p 2216 N95-27492

Radiation-induced grain boundary segregation in austenitic stainless steels [DE95-005721] p 2216 N95-27493

Amorphization of complex ceramics by heavy-particle irradiations [DE95-005725] p 2236 N95-27733

Multimedia Environmental Pollutant Assessment System (MEPAS) application guidance. Guidelines for evaluating MEPAS input parameters for Version 3.1 [DE95-007525] p 2328 N95-27749

Basic principles and recent observations of rotationally sampled wind p 2321 N95-27971

Large HAWT wake measurement and analysis p 2289 N95-27973

Small angle x ray scattering studies of reverse micelles in supercritical fluids [DE95-007803] p 2287 N95-28021

Bases for extrapolating materials durability in fuel storage pools [DE95-007748] p 2222 N95-28129

Solid-state sintering of tungsten heavy alloys [DE95-007749] p 2222 N95-28130

Stability of chromite interconnections in dual environments [DE95-007755] p 2267 N95-28131

Accuracy issues in modeling superplastic metal forming [DE95-008934] p 2222 N95-28163

Femtosecond OPO's at 3 microns and beyond: Design and performance issues related to the crystal properties of KTP and similar materials [DE95-007286] p 2446 N95-28242

Automated remedial assessment methodology software system [DE95-007287] p 2373 N95-28243

PARAGON PACIFIC, INC., EL SEGUNDO, CA.

Design of a real-time wind turbine simulator using a custom parallel architecture p 2322 N95-27979

PARASOFT CORP., MONROVIA, CA.

Automatic test data generation tool for large-scale software systems [AD-A289081] p 2365 N95-26611

PD-LD, INC., PRINCETON, NJ.

A new growth technology for highly non-linear, optical quality organic films: Organic vapor phase deposition [AD-A289006] p 2178 N95-26567

PENNSYLVANIA STATE UNIV., ERIE, PA.

Search for molecular absorptions with the Fourier Transform Spectrometer [NASA-CR-198648] p 2462 N95-28222

PENNSYLVANIA UNIV., PHILADELPHIA, PA.

Computational and matrix isolation studies of (2- and 3-furyl)methylene [AD-A280085] p 2178 N95-28154

Cognitive networks for ATR: The roles of bifurcation and chaos [AD-A289010] p 2387 N95-28336

PETROFERM, INC., FERNANDINA BEACH, FL.

Retrofitting conventional vapor degreasers to use a solvent wash/fluorochemical rinse process p 2232 N95-27127

PHASEX CORP., LAWRENCE, MA.

Precision parts cleaning with supercritical CO2: Practical applications and solutions p 2229 N95-27111

PHILLIPS LAB., HANSCOM AFB, MA.

Synthetic 3-D atmospheric temperature structure: A model for known geophysical power spectra using a hybrid autoregression and Fourier technique [AD-A289058] p 2340 N95-26479

Notes on the calibration of the JHU-APL solar vector magnetograph at NSO-Sec peak [AD-A289277] p 2253 N95-26983

Diagnosing cloudiness from global numerical weather prediction model forecasts [AD-A289456] p 2356 N95-26992

A brief history of laser guided lightning discharge models and experiments [AD-A289448] p 2295 N95-27022

Assessment of the AN/FPS-118 Ionospheric model and proposed improvements [AD-A289439] p 2337 N95-27146

PHILLIPS LAB., KIRTLAND AFB, NM.

Radiation production from stagnating compact toroids employing a nonequilibrium radiation diffusion model [AD-A289602] p 2429 N95-26720

Space Debris Research Phase One Program: Abstracts from published papers (1990-1993) [AD-A289504] p 2162 N95-26850

Long Duration Exposure Facility (LDEF) space optics handbook p 2428 N95-27654

A new technique for ground simulation of hypervelocity debris p 2154 N95-27671

PHYSIKALISCH-TECHNISCHE BUNDESANSTALT, BERLIN (GERMANY).

Bilateral intercomparison of the neutron emission rate of a (252)Cf spontaneous fission source between the National Physical Laboratory, Teddington, UK and the Physikalisch-Technische Bundesanstalt, Braunschweig, Germany [PB95-190120] p 2404 N95-26748

PITTSBURGH UNIV., PITTSBURGH, PA.

Surface chemistry of silicon [AD-A288893] p 2224 N95-26351

Photo and thermal excitation of surface chemistry on model catalyst surfaces [AD-A288541] p 2200 N95-26528

Bow shock data analysis [AD-A288432] p 2429 N95-26800

Probe molecule studies: Active species in alcohol synthesis [DE95-003514] p 2203 N95-27420

FTIR studies of CH3OH on porous silicon [AD-A289038] p 2207 N95-27904

POLISH ACADEMY OF SCIENCES, WARSAW (POLAND).

Self-excited oscillations in a duct with closed brances [IFTR-18/1994] p 2400 N95-26358

Determination of the cyclical properties of 18G2A steel on the basis of skeleton curves for a planar stress state [IFTR-32/1994] p 2211 N95-26359

Mathematical modelling of the thermodynamic properties of coolants and working media of heat pumps [IFTR-6/1994] p 2447 N95-26510

Beginner's guide to UNIX [IFTR-17/1994] p 2364 N95-26511

Identification of the plastic anisotropy of an aluminum alloy [IFTR-26/1994] p 2212 N95-26512

The development of the anisotropic properties of copper under plastic deformation induced by creep and monotonic loading [IFTR-23/1994] p 2212 N95-26517

The phenomena of subharmonic bifurcations, runaway, and transition to chaos in a non-linear oscillator: perturbation methods and a numerical experiment [IFTR-16/1994] p 2398 N95-26518

The use of acoustic methods to determine the parameters of porous materials [IFTR-40/1994] p 2401 N95-26519

Changes in the anisotropy parameters of an aluminum alloy caused by cyclical deformation [IFTR-27/1994] p 2212 N95-26666

The automatic extraction of selected speech spectral characteristics [IFTR-2/1994] p 2250 N95-26835

An experimental version of the MZT (speech-from-text) system with external F(sub 0) control [IFTR-14/1994] p 2250 N95-26836

Photoacoustic chambers for studying solids and gases: Theory and practical examples [IFTR-39/1994] p 2143 N95-26837

Annealing-induced changes in the anisotropy of an aluminum alloy [IFTR-24/1994] p 2213 N95-26838

The detection and tracking of motion by means of time-space pattern modelling using random fields [IFTR-37/1994] p 2374 N95-28566

POLYMER SOLUTIONS, INC., BLACKSBURG, VA.

Evaluations of the effectiveness of environmentally benign cleaning methodologies p 2230 N95-27115

Survey of environmentally benign cleaning methodologies and materials p 2231 N95-27122

POWER TECHNOLOGIES, INC., SCHENECTADY, NY.

Analysis methods for wind turbine control and electrical system dynamics p 2273 N95-27984

PRATT AND WHITNEY AIRCRAFT, WEST PALM BEACH, FL.

Turbulence models for gas turbine combustors p 2285 N95-27888

PRATT AND WHITNEY AIRCRAFT GROUP, WEST PALM BEACH, FL.

Composite intermediate case manufacturing scale-up for advanced engines p 2141 N95-28275

PRECISION CASTPARTS CORP., PORTLAND, OR.

AMCC casting development. Volume 1: Executive Summary [NASA-CR-196597] p 2247 N95-28419

PRINCETON UNIV., NJ.

Funding for AFRAPT student trainees for academic year 1992-1993 [AD-A288461] p 2466 N95-26604

Analysis of forward and inverse problems in chemical dynamics and spectroscopy [DE95-009309] p 2209 N95-28164

Structure of high-speed sprays [AD-A291696] p 2288 N95-28523

PROCUREMENT AUTOMATION INST., ARLINGTON, VA.

Automated Procurement System (APS) revised project management plan (DS-03) [NASA-CR-196605] p 2450 N95-27169

PUBLIC SERVICE ELECTRIC AND GAS CO., NEWARK, NJ.

Electric vehicle activities [DE95-006648] p 2267 N95-28105

PURDUE UNIV., WEST LAFAYETTE, IN.

WINCLR: A computer code for heat transfer and clearance calculation in a compressor [NASA-CR-195436] p 2117 N95-26363

Conversion of sunflower multiband radiometer polarization measurements to polarization parameters [NASA-CR-197774] p 2314 N95-26815

Preconversion catalytic deoxygenation of phenolic functional groups [DE95-007556] p 2204 N95-27458

Characteristics of laminates with delamination control strips p 2191 N95-28434

R

RADEX, INC., BEDFORD, MA.

Auto-processing of OTH radar amplitude/range/Doppler data [AD-A289152] p 2253 N95-27005

A model of the diurnal variation in magnesium ion density and radiance in the thermosphere [AD-A289824] p 2339 N95-28575

RADIAN CORP., AUSTIN, TX.

Community relations plan: Galena Airport and Camp ion Air Force Station, Alaska [AD-A286722] p 2327 N95-27234

Use of mussels in biomonitoring of environmental impacts of propellants, projectiles, explosives, and pyrotechnics p 2170 N95-28298

RADIAN CORP., OAK RIDGE, TN.

OB/OD treatment: The effective use of measured field data and air modeling to support an environmental assessment p 2170 N95-28296

REMTECH, INC., HUNTSVILLE, AL.

Rarefied gas effects on aerobraking/reentry vehicles with wakes [NASA-CR-196586] p 2164 N95-27093

RENSSELAER POLYTECHNIC INST., TROY, NY.

Analytical investigations of the acceleration sensitivity of acoustic bulk and surface wave resonators
[AD-A291715] p 2402 N95-28505

RESEARCH TRIANGLE INST., RESEARCH TRIANGLE PARK, NC.

Ethyl lactate as a solvent alternative for cleaning metal parts p 2229 N95-27112

RHEOLOGY RESEARCH, GAITHERSBURG, MD.

Vibration control using chaotic motion stabilizers
[AD-A289576] p 2398 N95-26687

RHODE ISLAND UNIV., KINGSTON, RI.

Fault tolerant features and experiments of ANTS distributed real-time system
[AD-A290133] p 2256 N95-28391

ROCHESTER UNIV., NY.

TRAINS: Dialogue transcription tools
[AD-A289869] p 2259 N95-28624

ROCKWELL INTERNATIONAL CORP., CANOGA PARK, CA.

Feasibility of flywheel energy storage systems for applications in future space missions
[NASA-CR-195422] p 2316 N95-26393

Overview of turbulence model development and applications at Rocketdyne p 2286 N95-27891

Recovery, evaluation, and decontamination of landfilled pentaborane cylinders, former liquid propellant rocket engine test facility, Washoe County, Nevada
p 2171 N95-28302

ROCKWELL INTERNATIONAL CORP., DOWNEY, CA.

Task 4 supporting technology. Part 1: Detailed test plan for leading edge tile development. Leading edge material development and testing
[NASA-CR-198633] p 2160 N95-28258

Task 4 supporting technology. Part 2: Detailed test plan for thermal seals. Thermal seals evaluation, improvement and test. CAN8-1, Reusable Launch Vehicle (RLV), advanced technology demonstrator: X-33. Leading edge and seals thermal protection system technology demonstration
[NASA-CR-198628] p 2304 N95-28259

Task 4 supporting technology. Densification requirements definition and test objectives. Propellant densification requirements definition
[NASA-CR-198629] p 2450 N95-28260

ROCKWELL INTERNATIONAL CORP., GOLDEN, CO.

Horizontal axis wind turbine post stall airfoil characteristics synthesization p 2124 N95-27974

ROCKWELL INTERNATIONAL SCIENCE CENTER, THOUSAND OAKS, CA.

A study of the use beta-alumina as a weak interface in alumina fiber composites
[AD-A288629] p 2179 N95-26484

Mechanisms of compressive failure in woven composites and stitched laminates p 2189 N95-28424

Fundamental concepts in the suppression of delamination buckling by stitching p 2198 N95-28486

ROME LAB., GRIFFISS AFB, NY.

ACT adaptive filters
[AD-A288385] p 2363 N95-26474

Encoding user-defined problems with SIPE-2
[AD-A288390] p 2380 N95-26475

A finite element based technique for simulation helix TWT interaction circuit thermal behavior
[AD-A289552] p 2262 N95-27152

ROME LAB., HANSCOM AFB, MA.

Measurements of HF auroral clutter using the Verona Ava Linear Array Radar (VALAR)
[AD-A289442] p 2337 N95-27147

ROYAL AUSTRALIAN AIR FORCE, AMBERLEY (AUSTRALIA).

The development of an engineering standard for composite repairs p 2135 N95-27528

ROYAL NETHERLANDS METEOROLOGICAL INST., DE BILT (NETHERLANDS).

Three objective indices for clear-air turbulence reconsidered
[KNMI-TR-160] p 2342 N95-27366

Neural networks versus linear regression: Research into the value of neural networks in meteorological practice
[KNMI-TR-165] p 2343 N95-28236

The program for calculating sunshine duration from global radiation
[KNMI-TR-158] p 2343 N95-28237

RUTHERFORD APPLETON LAB., CHILTON (ENGLAND).

Probing strongly-interacting electroweak dynamics through W(+)W(-)/ZZ ratios at future e(+)e(-) colliders
[DE95-007202] p 2413 N95-28067

RUTHERFORD APPLETON LAB., OXFORD (ENGLAND).

Pipelined first-level trigger for the H1 forward-muon spectrometer
[PB95-196242] p 2423 N95-28452

Threefold maximal lepton mixing and the solar and atmospheric neutrino deficits
[PB95-196259] p 2465 N95-28500

Non-linear viscoelastic behaviour
[PB95-192811] p 2199 N95-28639

Production and decay of hybrid mesons by flux-tube breaking
[PB95-192837] p 2418 N95-28640

Muon spin relaxation in ferromagnets: Theoretical results for paramagnetic EuO and EuS
[PB95-192860] p 2418 N95-28641

Muon spin relaxation in antiferromagnets: A study of RbMnF3 based on the coupled-mode theory of paramagnetic and critical spin fluctuations
[PB95-192878] p 2418 N95-28642

Future opportunities and present possibilities for coherent inelastic single crystal measurements on pulsed neutron sources
[PB95-195798] p 2418 N95-28657

Using COLETTE. (A simple guide)
[PB95-195806] p 2375 N95-28658

Characteristics of the standard current trip circuit
[PB95-192886] p 2271 N95-28663

S

SAINS MALAYSIA UNIV., PENANG (MALAYSIA).

Environmental pollution-effects on national development
[DE95-600439] p 2326 N95-26839

SAINS MALAYSIA UNIV., PERAK DARUL RIDZUAN (MALAYSIA).

Fatigue fracture analysis in medium carbon structural steel and austenitic stainless steel by X-ray fractography
[DE95-601504] p 2213 N95-26675

SANDIA LABS., ALBUQUERQUE, NM.

Cesium/oxide interactions for ultrathin films on (alpha)-Al2O3(001) and (alpha)-Al2O3(1(bar 1)O2)
[DE95-008159] p 2238 N95-28358

Measurements of daytime and upper tropospheric water vapor profiles by Raman lidar
[DE95-007640] p 2344 N95-28538

SANDIA NATIONAL LABS., ALBUQUERQUE, NM.

The use of supercritical carbon dioxide for contaminant removal from solid waste p 2229 N95-27110

Corrosive effects of supercritical carbon dioxide and cosolvents on metals p 2224 N95-27113

Optical features of nanosize iron and molybdenum sulfide clusters
[DE95-005417] p 2202 N95-27136

Molecular approach to mesoporous metal sulfides
[DE95-005418] p 2202 N95-27137

Retrofitting a fine-pointing system to satellite optics
p 2157 N95-27277

The effects of finite element grid density on model correlation and damage detection of a bridge
[DE94-018895] p 2309 N95-27305

XTP as a transport protocol for distributed parallel processing
[DE95-004992] p 2378 N95-27402

Comparison of the activities of fine-particle size catalysts
[DE95-004773] p 2203 N95-27423

Neutron diffraction studies on recrystallization of solution derived lead zirconate titanates
[DE95-004771] p 2439 N95-27429

Fuzzy-algebra uncertainty assessment
[DE95-005426] p 2391 N95-27432

A spectral algorithm for the seriation problem
[DE95-004775] p 2372 N95-27436

The response of hydrotalcite coated aluminum to sealing with transition metal salt solutions
[DE95-004767] p 2234 N95-27460

Electrolyte effects in Li(Si)/FeS2 thermal batteries
[DE95-001614] p 2264 N95-27474

High energy electron beams for ceramic joining
[DE95-006316] p 2420 N95-27480

Direct ultrashort-pulse retrieval using frequency-resolved optical gating and a computational neural network
[DE95-007148] p 2425 N95-27482

Atomistic calculations of hydrogen interactions with Ni3Al grain boundaries and Ni/Ni/Ni3Al interfaces
[DE95-006497] p 2408 N95-27534

Material analysis using combined Elastic Recoil Detection and Rutherford/Enhanced Rutherford Backscattering Spectrometry
[DE95-005415] p 2205 N95-27681

Numerical methods for determining interstitial oxygen in silicon
[DE95-007710] p 2205 N95-27683

Fitting: Subroutine to fit four-moment probability distributions to data
[DE95-007722] p 2395 N95-27684

ECR plasma-assisted deposition of Al2O3 and dispersion-strengthened AlO2
[DE95-007743] p 2235 N95-27687

Recent progress in the Photovoltaic Manufacturing Technology Project (PVMaT)
[DE95-000279] p 2320 N95-27704

Flat panel display development activities at Sandia National Laboratories
[DE95-005442] p 2265 N95-27706

Processing and properties of chromate-free conversion coatings on aluminum
[DE95-004768] p 2218 N95-27722

I(sub DDQ) testing and defect classes: A tutorial
[DE95-005467] p 2306 N95-27723

Time-optimal control of the magnetically levitated photolithography platen
[DE95-005493] p 2266 N95-27724

Scaling issues in dynamic fragmentation
[DE95-008509] p 2309 N95-27745

A compatibility study of containment materials in FEFO, bis-(2-fluoro-2,2-dinitroethyl) formal
[DE95-007548] p 2206 N95-27750

A microstructurally based model of solder joints under conditions of thermomechanical fatigue
[DE95-006226] p 2309 N95-27837

Evaluation and qualification of environmentally conscious manufacturing processes for commercial and military applications
[DE95-008520] p 2329 N95-27878

Tungsten carbide fragmentation: Experimental characterization and numerical modelling
[DE95-008521] p 2236 N95-27879

Real-time data compression using a fixed Huffman encoding scheme
[DE95-006159] p 2455 N95-27949

Browsing the World Wide Web from behind a firewall
[DE95-006805] p 2455 N95-27957

First-principles calculations for AlN, GaN, and InN: Bulk and alloy properties
[DE95-006822] p 2219 N95-27958

A new technique for measuring the separation of closely spaced dislocations using residual contrast conditions
[DE95-007147] p 2219 N95-27968

Effect of noise on Frequency-Resolved Optical Gating measurements of ultrashort pulses
[DE95-007149] p 2298 N95-27969

A NASTRAN-based computer program for structural dynamic analysis of Horizontal Axis Wind Turbines
p 2312 N95-27980

Manufacturing tailored property ceramic composites
[DE95-006303] p 2237 N95-27993

Sandia's network for Supercomputing '94: Linking the Los Alamos, Lawrence Livermore, and Sandia National Laboratories using switched multimegabit data service
[DE95-007717] p 2378 N95-28074

Copper CVD using liquid coinjection of (hfac)Cu(TMVS) and TMVS
[DE95-008155] p 2237 N95-28089

Control of thin film processing behavior through precursor structural modifications
[DE95-006468] p 2444 N95-28103

Pulsed ion beam surface treatment for preparing rapidly solidified corrosion resistant steel and aluminum surfaces
[DE95-007741] p 2221 N95-28116

Chromate-free corrosion resistant conversion coatings for aluminum alloys
[DE95-007742] p 2238 N95-28117

Cavity formation and impurity gettering in He-implanted Si
[DE95-007744] p 2444 N95-28127

Surface-emitting semiconductor laser for intracavity spectroscopy and microscopy
[DE95-007745] p 2299 N95-28128

Comprehensive numerical model for CW vertical-cavity surface-emitting lasers
[DE95-007758] p 2299 N95-28132

Low resistivity ohmic contacts to moderately doped n-GaAs with low temperature processing
[DE95-008507] p 2445 N95-28144

TEM characterization of Al/Al2O3 composite fabricated by reactive metal infiltration
[DE95-008508] p 2184 N95-28145

Non-destructive inter-level dielectric via in-line process monitoring by atomic force microscopy
[DE95-008516] p 2267 N95-28146

Low-power, parallel photonic interconnections for Multi-Chip Module applications
[DE95-008518] p 2267 N95-28147

Multivariate classification of BPSG thin films using Mahalanobis distances
[DE95-008519] p 2267 N95-28148

Lithium ion rechargeable systems studies
[DE95-006810] p 2268 N95-28200

OBIC analysis of stressed, thermally-isolated polysilicon resistors
[DE95-008511] p 2268 N95-28201

Chemical and electrical properties of cavities in silicon and germanium
[DE95-006812] p 2445 N95-28206

Low power limits in ultrashort pulse measurement using Frequency-Resolved Optical Gating
[DE95-007150] p 2299 N95-28219

Ultrashort Pulse retrieval using FROG trace irradiance moments and the adaptive neural networks backpropagation algorithm
[DE95-007153] p 2299 N95-28220

Swords to plowshares: Shock wave applications to advanced lithography
[DE95-008154] p 2299 N95-28223

Applications of boundary element methods on the Intel Paragon
[DE94-014135] p 2393 N95-28393

Heterostructures and infrared emitters with compressed InAsSb layers
[DE95-008157] p 2446 N95-28399

Functionalized block copolymers as adhesion promoters
[DE95-008158] p 2239 N95-28400

The minimum pore size obtainable in a silica gel during drying
[DE95-008162] p 2239 N95-28401

New developments for sol-gel film and fiber processing
[DE95-008175] p 2240 N95-28404

Mechanical properties of Hysol EA-9394 structural adhesive
[DE95-008187] p 2240 N95-28405

Retrofitting a fine-pointing system to satellite optics
[DE95-004529] p 2427 N95-28516

Porosity in hexylene-bridged polysilsesquioxanes: Effects of monomer concentration
[DE95-005421] p 2240 N95-28531

Comparison of bridged polysilsesquioxane xerogels prepared from methoxy- and ethoxy-silyl monomers
[DE95-005422] p 2240 N95-28532

Cloud classification using whole-sky imager data
[DE95-006501] p 2344 N95-28556

The unusual properties of beryllium surfaces
[DE95-006471] p 2223 N95-28593

Characterization of a fused silica capacitance standard
[DE95-006457] p 2270 N95-28597

SANDIA NATIONAL LABS., LIVERMORE, CA.

Evaluation of microporous carbon filters as catalysts for ozone decomposition
[DE95-006498] p 2331 N95-28548

Phase retrieval and time-frequency methods in the measurement of ultrashort laser pulses
[DE95-006499] p 2300 N95-28549

SANTO TOMAS UNIV. HOSPITAL, MANILA (PHILLIPPINES).

The effect of proteins on the aging properties of radiation vulcanized Natural Rubber Latex
[DE95-603357] p 2225 N95-26599

SCHAEFFER MAGNETICS, INC., CHATSWORTH, CA.

Development of a miniature actuator/controller system
p 2156 N95-27272

SCIENCE APPLICATIONS INTERNATIONAL CORP., MCLEAN, VA.

Reconstruction of an infrared band of meteorological satellite imagery with abductive networks
[SAIC-94/1062] p 2345 N95-27389

SCIENCE APPLICATIONS INTERNATIONAL CORP., NEW YORK, NY.

Probabilistic risk assessment of the Space Shuttle. Phase 3: A study of the potential of losing the vehicle during nominal operation, volume 1
[NASA-CR-197808] p 2159 N95-26398

Probabilistic risk assessment of the Space Shuttle. Phase 3: A study of the potential of losing the vehicle during nominal operation. Volume 2: Integrated loss of vehicle model
[NASA-CR-197809] p 2159 N95-26399

Probabilistic risk assessment of the Space Shuttle. Phase 3: A study of the potential of losing the vehicle during nominal operation. Volume 3: Basic events and minimal cutsets
[NASA-CR-197810] p 2160 N95-26400

Probabilistic risk assessment of the Space Shuttle. Phase 3: A study of the potential of losing the vehicle during nominal operation. Volume 4: System models and data analysis
[NASA-CR-197811] p 2160 N95-26401

Probabilistic risk assessment of the Space Shuttle. Phase 3: A study of the potential of losing the vehicle during nominal operation. Volume 5: Auxiliary shuttle risk analyses
[NASA-CR-197812] p 2160 N95-26403

SCIENCE RESEARCH LAB., INC., SOMERVILLE, MA.

High-density plasma source for large-area chemical vapor deposition of diamond films
[AD-A289053] p 2430 N95-27190

SCRIPPS RESEARCH INST., LA JOLLA, CA.

Cofactor-assisted antibody catalysis
[AD-A288929] p 2349 N95-26608

SEATTLE CITY LIGHT, WA.

Diagnostic antigens of Leishmania
[AD-A288805] p 2350 N95-27097

SELSKAPET FOR INDUSTRIELL OG TEKNISK FORSKNING, TRONDHEIM (NORWAY).

Forming metallurgy: Supervised drawing course, NTH
[PB95-196507] p 2219 N95-27934

Simulator report for SCI systems with HIC-router
[PB95-196580] p 2379 N95-28093

Speckle spectrum of the ERS-1 wavemode product
[PB95-196564] p 2315 N95-28180

International networks
[PB95-196366] p 2379 N95-28502

TV-holography at high temperatures: In situ observations of the oxidation of advanced materials
[PB95-195343] p 2294 N95-28651

Photoemission study of solid state reaction and initial oxidation of the Ce/Al(100) system
[PB95-195368] p 2210 N95-28652

Planning, design and construction of the cavern arena: Heating, ventilation and air conditioning
[PB95-196382] p 2361 N95-28659

Fatigue properties of an A356 (AlSi7Mg) aluminum alloy for automotive applications: Fatigue life prediction
[PB95-196424] p 2224 N95-28660

Practical considerations for network addressing using CIDR
[PB95-195335] p 2379 N95-28665

SENES OAK RIDGE, INC., OAK RIDGE, TN.

An introductory guide to uncertainty analysis in environmental and health risk assessment. Environmental Restoration Program
[DE95-008097] p 2354 N95-28136

SIKORSKY AIRCRAFT, STRATFORD, CT.

Static and fatigue testing of full-scale fuselage panels fabricated using a Therm-X(R) process
p 2185 N95-28270

SIMULA, INC., PHOENIX, AZ.

Rotorcraft crashworthy airframe and fuel system technology development program
[AD-A289986] p 2126 N95-28630

SMITHSONIAN ASTROPHYSICAL OBSERVATORY, CAMBRIDGE, MA.

A long-term space astrophysics research program: An x-ray perspective of the components and structure of galaxies
[NASA-CR-197787] p 2461 N95-26593

SMITHSONIAN INSTITUTION, CAMBRIDGE, MA.

Dynamics and control of SEDSAT tethered multi-probe for thermospheric research flight data analysis of SEDS-2 satellite: Tethered systems dynamics and flight data analysis
[NASA-CR-198653] p 2165 N95-27836

SOCIETE ANONYME D'ETUDES ET REALISATIONS NUCLEAIRES, LIMEIL-BREVANNES (FRANCE).

Micromechanisms for optimism seismometer
p 2159 N95-27292

SOCIETE D'APPLICATIONS GENERALES D'ELECTRICITE ET DE MECANIQUE, PARIS (FRANCE).

High performance stepper motors for space mechanisms p 2156 N95-27271

SOFTWARE CORP. OF AMERICA, LANHAM, MD.

Attitude determination using an adaptive multiple model filtering Scheme p 2148 N95-27772

SOFTWARE PRODUCTIVITY CONSORTIUM, HERNDON, VA.

User-centric development. Version 01.00.04
[AD-A289363] p 2368 N95-26903

SONOQUEST/ADVANCED ULTRASONICS RESEARCH, WELLESLEY HILLS, MA.

Ultrasonic studies of liquid/solid seimoacoustic wave phenomena
[AD-A289644] p 2402 N95-28622

SOUTHAMPTON UNIV. (ENGLAND).

The vibration transmission of lift truck suspension seats
[ISVR-TR-245] p 2302 N95-27844

Experimental studies to test simple flexural neutralizers fitted to beams
[ISVR-TR-239] p 2309 N95-27846

SOUTHERN UNIV., BATON ROUGE, LA.

Study of development and utilization of a multipurpose atmospheric corrosion sensor
[NASA-CR-198595] p 2292 N95-27368

SOUTHWEST RESEARCH INST., SAN ANTONIO, TX.

Scale model experiments with ceramic laminate targets
[AD-A288322] p 2225 N95-26561

Energization and transport of ions of ionospheric origin in the terrestrial magnetosphere
[NASA-CR-197813] p 2336 N95-26699

Energization and transport of ions of ionospheric origin in the terrestrial magnetosphere
[NASA-CR-198618-REV] p 2338 N95-28035

Mechanism of deposit formation on fuel-wetted hot metal surfaces
[AD-A289847] p 2210 N95-28621

SPACE TELESCOPE SCIENCE INST., BALTIMORE, MD.

A rule-based shell to hierarchically organize HST observations p 2384 N95-27384

SPAR AEROSPACE LTD., BRAMPTON (ONTARIO).

Design, testing and evaluation of latching end effector
p 2155 N95-27261

SPB TECHNOLOGIES, INC., GULF BREEZE, FL.

Combined use of ground water circulation (UVB) technology and in situ bioreactors for enhanced bioremediation of subsurface contamination
p 2230 N95-27118

SPECTRAL SCIENCES, INC., BURLINGTON, MA.

A comparison of NH3 point monitoring and diode laser based path integrated measurements
[DE95-006892] p 2332 N95-28602

SSG, INC., WALTHAM, MA.

Ultra-high, resolution, modular optical angle encoder for space-based opto-mechanical applications
p 2156 N95-27270

STANFORD LINEAR ACCELERATOR CENTER, MENLO PARK, CA

Bit-string physics: A novel theory of everything
[DE95-005941] p 2449 N95-28137

STANFORD LINEAR ACCELERATOR CENTER, STANFORD, CA.

The Tau-Charm Factory in the ERA of B-Factories and CESR
[DE95-007894] p 2412 N95-28028

Ambient-pressure silica aerogel films
[DE95-008161] p 2237 N95-28090

Nonlinear beam dynamics experimental program at SPEAR
[DE95-007823] p 2422 N95-28122

Beam-beam interaction working group summary
[DE95-007824] p 2422 N95-28123

Polarization as a probe to the production mechanisms of charmonium in (pi)N collisions
[DE95-008136] p 2414 N95-28142

Developments in the electron gun simulation program, EGUN
[DE95-008137] p 2267 N95-28143

Precise measurement of the left-right cross section asymmetry in Z boson production by e(+)e(-) collisions
[DE95-008591] p 2414 N95-28158

Measurement of wakefield suppression in a detuned X-band accelerator structure
[DE95-008592] p 2422 N95-28159

Efficient analytic computation of higher-order QCD amplitudes
[DE95-008593] p 2449 N95-28160

Plasma lens experiments at the final focus test beam
[DE95-008595] p 2434 N95-28161

Can TMAE photocathode be used for high rate applications?
[DE95-008594] p 2293 N95-28178

Measurement of alpha(s) in e(+)e(-) annihilation at E(cm) = 29 GeV
[DE95-006486] p 2417 N95-28594

STANFORD RESEARCH INST., MENLO PARK, CA.

Space physics educational outreach
[NASA-CR-198649] p 2399 N95-27852

STANFORD UNIV., CA.

Joint Services Electronics Program (JSEP)
[AD-A288299] p 2345 N95-26419

Modified eigenvalue problems with applications to structural dynamic re-analysis on parallel computers
[AD-A288257] p 2307 N95-26547

Grayscale/resolution trade-off for text: Model predictions and psychophysical results for letter confusion and letter discrimination
[NASA-CR-197784] p 2369 N95-26930

Growth and evaluation of nonlinear optical crystals for laser applications: Lithium borate, barium borate and silver gallium selenide
[AD-A289147] p 2277 N95-27000

Compressive strength of damaged and repaired composite plates p 2198 N95-28484

STARSYS RESEARCH CORP., BOULDER, CO.

Changing paradigms: Manufacturing vs. fabricating a high volume Hold Down and Release Mechanism
p 2155 N95-27267

STATE UNIV. OF NEW YORK, BUFFALO, NY.

An automated method of tuning an attitude estimator
p 2148 N95-27774

Use of nonlinear identification in robust attitude and attitude rate estimation for SAMPEX
p 2149 N95-27781

STATE UNIV. OF NEW YORK, STONY BROOK, NY.
Superior catalysts for selective catalytic reduction of nitric oxide
[DE95-007903] p 2205 N95-27691
Research project on CO2-induced climate change
[DE95-008339] p 2330 N95-28084

STATE UNIV. OF NEW YORK AT BUFFALO, AMHERST, NY.
DNS, LES and stochastic modeling of turbulent reacting flows
[AD-A280099] p 2287 N95-28155

STRATHCLYDE UNIV., GLASGOW (SCOTLAND).
SMART materials: Surfaces, transforms and interfaces. The commensurate engineering dimension
[AD-A289598] p 2312 N95-28649

SUPERCONDUCTING SUPER COLLIDER LAB., DALLAS, TX.
Beam instability studies for the SSC
[DE95-008024] p 2423 N95-28551

SURFACE/INTERFACE, INC., MOUNTAIN VIEW, CA.
Charge distribution analysis of catalysts under simulated reaction conditions
[DE95-006943] p 2204 N95-27549

SURREY UNIV., GUILDFORD (ENGLAND).
Thermodynamics of electrolyte solutions for use in high energy lithium batteries
[AD-A288897] p 2199 N95-26352

SUSSEX UNIV., BRIGHTON (ENGLAND).
Detection of charged particles in superfluid helium
[DE95-007354] p 2403 N95-26560

SWEDISH RADIATION PROTECTION INST., STOCKHOLM (SWEDEN).
Radiation in everyday life
[DE95-604111] p 2349 N95-26597

SYRACUSE UNIV., NY.
The noise reduction potential of dual-stream coaxial rectangular improperly expanded jet flows
[NASA-CR-197820] p 2277 N95-26995

T

TECHNICAL RESEARCH CENTRE OF FINLAND, ESPOO (FINLAND).
SIHTI 2: Energy and environmental technology. Yearbook 1993 of the research programme
[DE95-755135] p 2331 N95-28202

TECHNICAL UNIV. OF LUBLIN, LUBLIN (POLAND).
Electromagnetic devices and processes in environment protection
[AD-A288656] p 2141 N95-26487

TECHNICAL UNIV. OF NORWAY, TRONDHEIM.
Forming metallurgy: Supervised drawing course, NTH
[PB95-196507] p 2219 N95-27934

TECHNION RESEARCH AND DEVELOPMENT FOUNDATION LTD., HAIFA (ISRAEL).
Advanced interactive display formats for terminal area traffic control
[NASA-CR-198576] p 2127 N95-28188

TECHNISCHE UNIV., DELFT (NETHERLANDS).
NEXTSTEP: The next step in the right direction? Part 2: Software development with NEXTSTEP
[REPT-94-33-PT-2] p 2450 N95-26803
Numerical simulation of crack growth in pressurized fuselages
[PB95-192415] p 2137 N95-28636
Experimental study on transition characteristics of natural-convection flow
[PB95-192423] p 2289 N95-28637
Critical behaviour of spin models: A transfer-matrix approach
[PB95-192456] p 2418 N95-28638

TENNESSEE TECHNOLOGICAL UNIV., COOKEVILLE, TN.
Investigation of the collision linc broadening problem as applicable to the NASA Optical Plume Anomaly Detection (OPAD) system, phase 1
[NASA-CR-198605] p 2426 N95-27913

TENNESSEE UNIV., MEMPHIS, TN.
Research activities on somatosensory (SI) cortical neurons
[AD-A288794] p 2348 N95-26360

TETRA PRECISION, INC., GAINESVILLE, FL.
Neural network error compensation of machine tools
[AD-A289300] p 2387 N95-28217

TEXAS A&M UNIV., COLLEGE STATION, TX.
Sailplane glide performance and control using fixed and articulating winglets
[NASA-CR-198579] p 2131 N95-27180
Deformation limits on two-parameter fracture mechanics in terms of higher order asymptotics
[AD-A289113] p 2310 N95-28098
An experimental and numerical investigation of specimen size requirements for cleavage fracture toughness
[AD-A289120] p 2311 N95-28100
Wavelet analysis and its applications
[AD-A291735] p 2387 N95-28527

TEXAS UNIV., AUSTIN, TX.
Analysis and development of finite element methods for the study of nonlinear thermomechanical behavior of structural components
[NASA-CR-195354] p 2307 N95-26387
Nonlinear instability and chaos in plasma wave-wave interactions. I. Introduction
[DE95-005529] p 2429 N95-27084
Signatures of Higgs-Triplet representations at TeV-e(+)e(-) colliders
[DE95-007201] p 2419 N95-27089
Normal modes and continuous spectra
[DE95-006166] p 2287 N95-28055
Probing strongly-interacting electroweak dynamics through W(+)W(-)/ZZ ratios at future e(+)e(-) colliders
[DE95-007202] p 2413 N95-28067
Magnetic viscosity by localized shear flow instability in magnetized accretion disks
[DE95-006879] p 2433 N95-28111
Coordinates of the quantum plane as q-tensor operators in U(sub q) (su(2) * su(2))
[DE95-007100] p 2397 N95-28234

TEXAS UNIV., SAN ANTONIO, TX.
Probabilistic material strength degradation model for Inconel 718 components subjected to high temperature, high-cycle and low-cycle mechanical fatigue, creep and thermal fatigue effects
[NASA-CR-197832] p 2214 N95-27167

TEXTRON SPECIALTY MATERIALS, LOWELL, MA.
Status of bonded boron/epoxy doublers for military and commercial aircraft structures p 2132 N95-27506

THAR DESIGNS, INC., PITTSBURGH, PA
Design considerations in supercritical fluid technology
p 2232 N95-27126

THIOKOL CORP., HUNTSVILLE, AL.
Sceening, down selection, and implementation of environmentally compliant cleaning and insulation bonding for MNASA p 2165 N95-27124

TITAN CORP., CHATSWORTH, CA.
Material modeling in the CRALE code. Users' manual
[AD-A288988] p 2178 N95-26712

TITAN SYSTEMS, INC., PRINCETON, NJ.
The small-scale structure of dispersing clouds in the atmosphere
[AD-A288256] p 2341 N95-26546

TOKYO UNIV., SAGAMIHARA (JAPAN).
Viscous shock-layer analysis on hypersonic flow over reentry capsule with nonequilibrium chemistry
[ISAS-R-656] p 2274 N95-26739
Wind tunnel experiments on wake flow field behind a reentry capsule from a viewpoint of parachute deployment at supersonic speeds
[ISAS-R-655] p 2121 N95-26740
Statistical model for molecular internal energy exchange in DSMC method for rarefied flow analysis
[ISAS-R-654] p 2274 N95-26741
Anomalous collision rate in the time counter scheme of the direct simulation Monte Carlo method for rarefied gas flow analysis
[ISAS-R-653] p 2275 N95-26742

TOLEDO UNIV., OH.
High temperature kinetic study of the reactions H + O2 = OH + O and O + H2 = OH + H in H2/O2 system by shock tube-laser absorption spectroscopy
[NASA-CR-195473] p 2206 N95-27695

TPL, INC., ALBUQUERQUE, NM.
A comprehensive energetic materials resource recovery and recycling program p 2176 N95-28323

TRW SYSTEMS AND ENERGY, REDONDO BEACH, CA.
High pressure Earth storable rocket technology program: Basic program
[NASA-CR-195449] p 2166 N95-26390

TULANE UNIV., NEW ORLEANS, LA.
The fBm Interpolator
[AD-A288996] p 2388 N95-26459

TURKISH LAND FORCES COMMAND, ANKARA (TURKEY).
Scarf joint technique with cocured and precured patches for composite repair p 2135 N95-27524

U

UMBI, BALTIMORE, MD.
Microbial treatment for shipboard collection, hold ing, and transfer system tanks p 2179 N95-27119
Application of bacterial bioemusifiers to in situ maintenance of oil/water separators
p 2179 N95-27120

UNISYS CORP., RESTON, VA.
Software technology for adaptable, reliable systems (STARS). AdaWise user's manual
[AD-A289655] p 2375 N95-28635

UNITED STATES SPACE FOUNDATION, COLORADO SPRINGS, CO.
Space Commerce 1994 Forum: The 10th National Space Symposium. Proceedings report
[NASA-CR-198031] p 2144 N95-26583

UNITED TECHNOLOGIES RESEARCH CENTER, EAST HARTFORD, CT.
Evaluation of a doubly-swept blade tip for rotorcraft noise reduction
[NASA-CR-189677] p 2402 N95-28264

UNIVERSAL TECH CORP., RIVERTON, KS.
Alternate use of rocket propellants as ingredients in commercial watergel explosives p 2176 N95-28321

UNIVERSIDAD AUTONOMA DEL ESTADO DE MEXICO, TOLUCA (MEXICO).
Determination of phase transitions in a lyotropic liquid crystal by positron annihilation technique
[DE95-609162] p 2442 N95-27964

UNIVERSIDAD NACIONAL AUTONOMA DE MEXICO, MEXICO CITY (MEXICO).
Comparative experimental study of PIXE and X-ray fluorescence analysis
[DE95-607868] p 2327 N95-27198
Iron oxides characterization by Moessbauer spectroscopy
[DE95-607869] p 2202 N95-27199
Determination of the first hydrolysis constant of Europium (3) in 3 M of ionic strength
[DE95-607912] p 2405 N95-27211
Stress corrosion cracking susceptibility of the earthquake resistant NOM B457 Mexican steel
[DE95-607956] p 2214 N95-27256

UNIVERSITY OF CENTRAL FLORIDA, ORLANDO, FL.
Near-resonant properties of nonlinear organic materials for optical devices
[AD-A288339] p 2178 N95-26570
Analysis of magnetic field levels at KSC
[NASA-CR-197678] p 2326 N95-26808
Passive spatial beam control, appendix
[AD-A288913] p 2300 N95-28333

UNIVERSITY OF NORTHERN ILLINOIS, DE KALB, IL.
Investigation of the interface between immiscible electrolytes applied to membrane electrochemistry
[AD-A288887] p 2199 N95-26350
Design strategies for the preparation of polymeric organic superconductors
[AD-A289022] p 2436 N95-26462

UNIVERSITY OF SOUTH FLORIDA, TAMPA, FL.
Computation of three-dimensional mixed convective boundary layer flow p 2280 N95-27347
Analysis of gas absorption to a thin liquid film in the presence of a zero-order chemical reaction
p 2280 N95-27348
Proceedings of the International Workshop on Acceleration and Radiation Generation in Space and Laboratory Plasmas
[AD-A291673] p 2436 N95-28668

UNIVERSITY OF SOUTHERN CALIFORNIA, LOS ANGELES, CA.
The effects of Crew Resource Management (CRM) training in airline maintenance: Results following three year's experience
[NASA-CR-196696] p 2358 N95-28676

UNIVERSITY OF SOUTHERN ILLINOIS, CARBONDALE, IL.
A probabilistic model of a porous heat exchanger
p 2282 N95-27359

UTAH UNIV., SALT LAKE CITY, UT.
On the thermally-induced residual stresses in thick fiber-thermoplastic matrix (PEEK) cross-ply laminated plates p 2187 N95-28285

V

VEDA, INC., DAYTON, OH.
Integrated mission precision attack cockpit technology (IMPACT). Phase 1: Identifying technologies for air-to-ground fighter integration
[AD-A289562] p 2129 N95-26684

VIGYAN RESEARCH ASSOCIATES, INC., HAMPTON, VA.
Computer program BL2D for solving two-dimensional and axisymmetric boundary layers
[NASA-CR-4668] p 2279 N95-27257

VIRGINIA COMMONWEALTH UNIV., RICHMOND, VA.
Overview of megaprogramming course: Lectures and eexercises. Version 02.00.03
[AD-A288723] p 2370 N95-27235

VIRGINIA POLYTECHNIC INST., BLACKSBURG, VA.
Flow structure generated by perpendicular blade vortex interaction and implications for helicopter noise predictions
[NASA-CR-198590] p 2123 N95-28193

VIRGINIA POLYTECHNIC INST. AND STATE UNIV., BLACKSBURG, VA.

Two-layer or free surface shear flows and viscoelastic shear flows and the relationship between stability and eigenvalues
[AD-A289510] p 2278 N95-27047

Observations on the solvating power of supercritical fluids p 2228 N95-27106

Load transfer in the stiffener-to-skin joints of a pressurized fuselage
[NASA-CR-198610] p 2310 N95-27865

Vibrational behavior of adaptive aircraft wing structures modelled as composite thin-walled beams
p 2191 N95-28435

Coatings of non-oxide ceramics for improved corrosion resistance in high temperature coal combustion
[DE95-006932] p 2241 N95-28604

VIRGINIA UNIV., CHARLOTTESVILLE, VA.

Environmentally assisted cracking of high strength beta titanium alloys
[AD-A289156] p 2213 N95-27032

Development and application of low-temperature AFM
[AD-A291704] p 2352 N95-28525

VOUGHT CORP., DALLAS, TX.

Repair of high temperature composite aircraft structure p 2134 N95-27520

W

WALES UNIV., BANGOR (UNITED KINGDOM).

Large area smart piezoelectric and pyroelectric sensors
[AD-A288565] p 2290 N95-26541

WALTER REED ARMY INST. OF RESEARCH, WRIGHT-PATTERSON AFB, OH.

Toxicity assessment of liquid propellant XM46
p 2175 N95-28319

WASHINGTON UNIV., SAINT LOUIS, MO.

Physical interpretation and development of ultrasonic nondestructive evaluation techniques applied to the quantitative characterization of textile composite materials
[NASA-CR-198591] p 2306 N95-28034

WASHINGTON UNIV., SEATTLE, WA.

Infrared field measurements of sea surface temperature: Analysis of wake signatures and comparison of skin layer models
[NASA-CR-197849] p 2346 N95-26533

Materials design and processing by biomimicking. Section 1: Research progress
[AD-A288229] p 2226 N95-26623

Design and processing of materials by biomimicking. Section 2. Publications
[AD-A288230] p 2226 N95-26624

Determining nanoscale physical properties of materials by microscopy and spectroscopy
[AD-A289532] p 2201 N95-26870

The gluon propagator in non-Abelian Weizsaecker-Williams fields
[DE95-006877] p 2449 N95-27547

Magnetization of ferromagnetic clusters
[DE95-006878] p 2399 N95-27548

Numerical and theoretical studies of rough surface scattering
[AD-A291748] p 2257 N95-28528

WEATHER SQUADRON (45TH), PATRICK AFB, FL.

Weather hazards to a Titan 4 on-pad destack-restack operation p 2172 N95-28307

WEIZMANN INST. OF SCIENCE, REHOVOT (ISRAEL).

Implications of horizontal symmetries on baryon number violation in supersymmetric models
[DE95-610202] p 2407 N95-27406

Transverse tau polarization in inclusive bar-B yields tau bar-nu X decays
[DE95-610325] p 2407 N95-27409

Supersymmetry and light quark masses in a realistic superstring model
[DE95-610201] p 2412 N95-28041

WEST VIRGINIA UNIV., FAIRMONT, WV.

The reliable multicast protocol application programming interface
[NASA-CR-197762] p 2363 N95-26388

Software risk management through independent verification and validation
[NASA-CR-197767] p 2364 N95-26486

Using SCR methods to analyze requirements documentation
[NASA-CR-197760] p 2365 N95-26668

Software packager user's guide
[NASA-CR-197763] p 2366 N95-26693

A decentralized software bus based on IP multicasting
[NASA-CR-197768] p 2366 N95-26695

Using an architectural approach to integrate heterogeneous, distributed software components
[NASA-CR-197766] p 2366 N95-26711

Development and analysis of SCR requirements tables for system scenarios
[NASA-CR-197769] p 2367 N95-26802

A process improvement model for software verification and validation
[NASA-CR-197761] p 2367 N95-26814

WEST VIRGINIA UNIV., MORGANTOWN, VA.

Concurrent engineering research center
[NASA-CR-197726] p 2362 N95-26386

A software bus for thread objects
[NASA-CR-197764] p 2365 N95-26575

A high performance totally ordered multicast protocol
[NASA-CR-197765] p 2371 N95-27252

WESTINGHOUSE HANFORD CO., RICHLAND, WA.

An ugly duckling becomes a swan (hor ellipsis): How an organization becomes customer focused through listening
[DE95-004974] p 2454 N95-27461

Effects of hydrogen on carbon steels at the Multi-Function Waste Tank Facility
[DE95-007194] p 2219 N95-28005

WESTINGHOUSE SAVANNAH RIVER CO., AIKEN, SC.

Recycle of radiologically contaminated austenitic stainless steels
[DE95-006464] p 2215 N95-27328

WICHITA STATE UNIV., WICHITA, KS.

AIAA Techfest 20 Proceedings
[NIAR-94-1] p 2118 N95-26941

An exploratory application of neural networks for airfoil design p 2118 N95-26943

Creating an alternative parameter optimization method (APO) p 2118 N95-26946

The aerospace database: An introduction to AIAA'S computerized source for identifying scientific and technical information p 2119 N95-26950

The near-wake flow behavior of an oscillating airfoil with modified trailing edge p 2119 N95-26953

Full span flaperons for a biplane
p 2119 N95-26954

An experimental investigation of helicopter downwash and tailboom interaction at the Wichita State University 7x10 foot wind tunnel p 2120 N95-26955

Comparative wind tunnel tests of NACA 23024 airfoils with several aileron and spoiler configurations
p 2124 N95-27976

WISCONSIN UNIV., MADISON, WI.

MHD simulations of DC helicity injection for current drive in tokamaks
[DE95-007018] p 2429 N95-26940

Boron-induced reconstructions of Si(100) investigated by scanning tunneling microscopy
[AD-A289222] p 2438 N95-26959

Boron-induced morphology changes in silicon CVD growth: A scanning tunneling microscopy study
[AD-A289275] p 2290 N95-26982

Atomic structure and bonding of boron-induced reconstructions on Si(001)
[AD-A289187] p 2405 N95-27017

Atomically resolved STM study of the adsorption and dissociation of methyl chloride on Si(001)
[AD-A289218] p 2438 N95-27061

Variable speed generator technology options for wind turbine generators p 2273 N95-27988

Probing strongly-interacting electroweak dynamics through W(+)W(-)/ZZ ratios at future e(+)e(-) colliders
[DE95-007202] p 2413 N95-28067

Testing the correlation between seismic stratigraphy, diagenesis and physical rock properties: Evaluation of fluid flow during early and late diagenesis
[DE95-008338] p 2338 N95-28083

WOODS HOLE OCEANOGRAPHIC INST., MA.

Meteorological and oceanographic data collected during the ASREX 91 field experiment
[AD-A289492] p 2342 N95-26826

Very low frequency seismo-acoustic noise below the sea floor (0.2-10 Hz)
[AD-A289164] p 2347 N95-27011

Observations of near-bottom flow in a wave-dominated nearshore environment
[AD-A289331] p 2347 N95-27043

Biological/physical modeling of upper ocean processes
[AD-A289468] p 2347 N95-27151

Seismic constraints on shallow crustal processes at the East Pacific rise
[AD-A289055] p 2338 N95-28094

Tomographic observations of deep convection and the thermal evolution of the Greenland Sea Gyre 1988-1989
[AD-A289104] p 2348 N95-28096

Altimeter analysis of ocean currents
[AD-A290167] p 2315 N95-28392

WORCESTER POLYTECHNIC INST., MA.

Design and development of experimental facilities for short duration, low-gravity combustion and fire experiments
[NASA-CR-195458] p 2244 N95-26709

WRIGHT LAB., WRIGHT-PATTERSON AFB, OH.

A non-iterative grid deformation algorithm for computational fluid dynamics for aeroelasticity
[AD-A288298] p 2273 N95-26418

Life prediction methodology for composite laminates. Part 1: Constant amplitude and two-stress level fatigue
[AD-A288343] p 2180 N95-26571

Partial discharge testing of high voltage wiring harness for airborne displays
[AD-A289150] p 2138 N95-27003

Structural design optimization with survivability dependent constraints application: Primary wing box of a multi-role fighter p 2137 N95-28440

Post impact compressive strength in composites
p 2198 N95-28485

WRIGHT STATE UNIV., DAYTON, OH.

Process control of microstructure in manufacturing
[AD-A288291] p 2245 N95-26410

Codes of processing and multiple resources: Model and methodology
[AD-A289583] p 2355 N95-26691

Subjective workload assessment in a spatial memory task
[AD-A289491] p 2356 N95-26825

WULFMAN (D. S.) AND ASSOCIATES, INC., ROLLA, MO.

Commercial reformulation: An economic and environmentally neutral means of managing explosives and solid propellants p 2175 N95-28320

Y

YALE UNIV., NEW HAVEN, CT.

On the azimuthal Fourier components of the Green's function for the Helmholtz equation in three dimensions
[AD-A288775] p 2398 N95-26345

Transport phenomena and interfacial kinetics in multiphase combustion systems
[AD-A288297] p 2199 N95-26417

Nonlinear dynamics of global atmospheric and earth system processes
[NASA-CR-197926] p 2326 N95-26429

YAMADA SCIENCE AND ART CORP., LOS ALAMOS, NM.

Three-dimensional forecast models for emergency response management p 2172 N95-28303

CONTRACT NUMBER INDEX

SCIENTIFIC AND TECHNICAL AEROSPACE REPORTS VOLUME 33 NUMBER 9

Typical Contract Number Index Listing

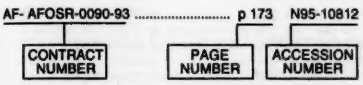

Listings in this index are arranged alphanumerically by contract number. Under each contract number the accession numbers denoting documents that have been produced as a result of research done under that contract are arranged in ascending order. The page number helps to locate the citation in the abstract section. The accession number denotes the number by which the citation is identified.

AF PROJ. AFOT .... p 2162 N95-26850
AF PROJ. 2303 .... p 2201 N95-26606
AF PROJ. 2306 .... p 2245 N95-26410
AF PROJ. 2308 .... p 2199 N95-26417
AF PROJ. 2311 .... p 2253 N95-26983
AF PROJ. 2338 .... p 2262 N95-27152
AF PROJ. 2401 .... p 2273 N95-26418
AF PROJ. 2419 .... p 2180 N95-26571
AF PROJ. 5581 .... p 2380 N95-26475
AF PROJ. 6670 .... p 2356 N95-26992
AF PROJ. 7184 .... p 2262 N95-27196
AF-AFOSR-0042-91 .... p 2273 N95-26405
AF-AFOSR-0090-93 .... p 2279 N95-27247
AF-AFOSR-0170-91 .... p 2199 N95-26417
AF-AFOSR-0190-91 .... p 2201 N95-26544
AF-AFOSR-0281-91 .... p 2226 N95-26623
p 2226 N95-26624
AF-AFOSR-0331-91 .... p 2178 N95-26570
AF-AFOSR-0333-91 .... p 2348 N95-26360
AF-AFOSR-0340-91 .... p 2201 N95-26606
AF-AFOSR-0341-90 .... p 2180 N95-26626
AF-AFOSR-0473-89 .... p 2466 N95-26604
ARPA ORDER A700 .... p 2364 N95-26536
ARPA ORDER 7597 .... p 2364 N95-26536
p 2424 N95-26900
ARPA ORDER 8313 .... p 2389 N95-26772
ARPA ORDER 8799 .... p 2295 N95-26906
A30327-93 .... p 2367 N95-26770
CDDF PROJ. 93-10 .... p 2304 N95-28364
DA PROJ. MM3-3-P-30 .... p 2353 N95-26885
DA PROJ. R03-5 .... p 2388 N95-26459
DA PROJ. 1L1-62211-A-47-A .... p 2302 N95-27373
p 2302 N95-27698
p 2302 N95-27855
DA PROJ. 1L1-62618-AH-80 .... p 2179 N95-26565
p 2223 N95-28189
p 2374 N95-28625
DA PROJ. 1L1-62716-AH-70 .... p 2360 N95-27099
DA PROJ. 1O1-62622-A-552 .... p 2250 N95-26759
DA PROJ. 101-62622-A-553 .... p 2405 N95-27034
DA PROJ. 3M1-62787-A-879 .... p 2130 N95-26993
DA PROJ. 301-62787-A-878 .... p 2294 N95-28410
p 2361 N95-28667
DA PROJ. 4A1-61102-AT-24 .... p 2144 N95-27297
DA PROJ. 4A1-62373-DT-08 .... p 2336 N95-26753
DA PROJ. 4A1-62784-AT-45 .... p 2262 N95-27067
DAAA15-91-C-0082 .... p 2376 N95-26460
DAAB07-88-6-F405 .... p 2300 N95-28333
DAAB07-90-C-R059 .... p 2381 N95-27041
DAAB07-91-C-K762 .... p 2423 N95-26679
DAAE07-90-C-R059 .... p 2367 N95-26754
p 2301 N95-26926
p 2356 N95-27013
DAAG29-85-K-0028 .... p 2288 N95-28523
DAAH04-93-G-0047 .... p 2387 N95-28527
DAAH04-93-G-0068 .... p 2257 N95-28453
DAAH04-93-G-0123 .... p 2237 N95-28080
DAAH04-94-G-0015 .... p 2352 N95-28546
DAAH04-94-G-0267 .... p 2394 N95-26413
p 2394 N95-26415
p 2377 N95-27183
DAAH04-94-G-0390 .... p 2240 N95-28508
DAAH04-94-G-2067 .... p 2394 N95-26414
DAAK70-87-C-0043 .... p 2210 N95-28621
DAAK70-92-C-0059 .... p 2210 N95-28621
DAAL03-89-D-0003 .... p 2348 N95-26573
DAAL03-90-G-0176 .... p 2300 N95-28509
DAAL03-91-C-0010 .... p 2345 N95-26419
DAAL03-91-C-0021 .... p 2225 N95-26561
DAAL03-91-G-0011 .... p 2200 N95-26451
DAAL03-91-G-0031 .... p 2376 N95-26471
DAAL03-91-G-0038 .... p 2307 N95-26547
DAAL03-91-G-0039 .... p 2394 N95-26414
p 2394 N95-26415
p 2394 N95-26457
p 2377 N95-27183
p 2393 N95-28507
DAAL03-91-G-0049 .... p 2257 N95-28456
DAAL03-91-G-0099 .... p 2300 N95-28458
DAAL03-91-G-0106 .... p 2380 N95-26468
DAAL03-91-G-0116 .... p 2257 N95-28513
DAAL03-91-G-0120 .... p 2402 N95-28505
DAAL03-91-G-0139 .... p 2240 N95-28457
DAAL03-91-G-0160 .... p 2270 N95-28529
DAAL03-91-G-0164 .... p 2200 N95-26422
p 2200 N95-26452
DAAL03-91-G-0170 .... p 2395 N95-28526
DAAL03-91-G-0180 .... p 2448 N95-26563
DAAL03-91-G-0238 .... p 2395 N95-28510
DAAL03-91-G-0308 .... p 2136 N95-28504
DAAL03-91-G-0323 .... p 2200 N95-26528
DAAL03-92-C-0001 .... p 2270 N95-28512
DAAL03-92-C-0020 .... p 2341 N95-26546
DAAL03-92-G-0002 .... p 2352 N95-28525
DAAL03-92-G-0102 .... p 2257 N95-28528
DAAL03-92-G-0289 .... p 2427 N95-28524
p 2270 N95-28544
DAAL03-92-G-0311 .... p 2429 N95-26800
DAAL03-92-G-0349 .... p 2446 N95-28522
DAAL03-94-G-0039 .... p 2394 N95-26413
DAAL04-91-C-0040 .... p 2221 N95-28102
DABT60-90-D-0010 .... p 2130 N95-27018
DABT63-93-C-0054 .... p 2364 N95-26534
DABT63-94-C-0045 .... p 2306 N95-27253
DACA76-89-C-0014 .... p 2367 N95-26754
p 2301 N95-26926
p 2356 N95-27013
p 2381 N95-27041
DACA76-92-C-0009 .... p 2356 N95-26843
DACW05-92-D-0016 .... p 2170 N95-28296
DAJA45-93-C-0017 .... p 2290 N95-26541
DAMD17-89-Z-9039 .... p 2348 N95-26435
DAMD17-92-C-2082 .... p 2350 N95-27097
DAMD17-93-C-3116 .... p 2352 N95-26680
DASG60-94-C-0051 .... p 2365 N95-26611
DASG60-94-C-0059 .... p 2398 N95-26687
DASW01-94-C-0054 .... p 2358 N95-26552
DE-ACO4-94AL-85000 .... p 2224 N95-27113
DE-AC02-76CH-00016 .... p 2439 N95-27443
p 2215 N95-27462
p 2420 N95-27484
p 2425 N95-27490
p 2440 N95-27535
p 2409 N95-27552
p 2217 N95-27553
p 2265 N95-27554
p 2292 N95-27677
p 2320 N95-27682
p 2292 N95-27738
p 2442 N95-27932
p 2236 N95-27962
p 2421 N95-28017
p 2422 N95-28115
p 2331 N95-28121
p 2445 N95-28165
p 2222 N95-28166
p 2414 N95-28169
p 2414 N95-28170
p 2445 N95-28186
p 2422 N95-28195
p 2426 N95-28196
p 2269 N95-28244
p 2416 N95-28338
p 2269 N95-28339
p 2416 N95-28355
p 2270 N95-28515
p 2325 N95-28517
p 2315 N95-28520
p 2240 N95-28547
DE-AC02-76CH-03000 .... p 2454 N95-27090
p 2419 N95-27091
p 2407 N95-27430
p 2408 N95-27444
p 2408 N95-27478
p 2399 N95-27530
p 2421 N95-27531
p 2409 N95-27689
p 2409 N95-27747
p 2292 N95-27751
p 2410 N95-27871
p 2410 N95-27872
p 2411 N95-27933
p 2411 N95-27945
p 2421 N95-28107
p 2415 N95-28221
p 2422 N95-28346
p 2417 N95-28495
DE-AC02-76CH-03073 .... p 2435 N95-28553
DE-AC02-76ER-00088 .... p 2415 N95-28210
DE-AC02-76ER-01198 .... p 2437 N95-26553
DE-AC02-76ER-02289 .... p 2415 N95-28210
DE-AC02-76ET-53017 .... p 2410 N95-27922
DE-AC02-78ET-51013 .... p 2432 N95-27688
p 2411 N95-28020
DE-AC02-80ET-15601 .... p 2292 N95-27465
DE-AC02-83CH-10093 .... p 2324 N95-27991
DE-AC03-76SF-00098 .... p 2420 N95-27470
p 2440 N95-27471
p 2234 N95-27472
p 2440 N95-27538
p 2425 N95-27539
p 2296 N95-27674
p 2425 N95-27675
p 2409 N95-27676
p 2265 N95-27678
p 2421 N95-27679
p 2441 N95-27720
p 2284 N95-27721
p 2297 N95-27737
p 2409 N95-27744
p 2449 N95-27877
p 2208 N95-28086
p 2413 N95-28091
p 2444 N95-28092
p 2298 N95-28104
p 2460 N95-28197
p 2209 N95-28218
p 2287 N95-28225
p 2238 N95-28226
p 2209 N95-28229
p 2463 N95-28357
p 2428 N95-28557
p 2463 N95-28558
p 2340 N95-28583
p 2417 N95-28594
DE-AC03-76SF-00515 .... p 2420 N95-27484
p 2412 N95-28028
p 2422 N95-28122
p 2422 N95-28123
p 2449 N95-28137
p 2414 N95-28142
p 2267 N95-28143
p 2414 N95-28158
p 2422 N95-28159
p 2449 N95-28160
p 2434 N95-28161
p 2293 N95-28178
p 2417 N95-28594
DE-AC03-89ER-51114 .... p 2431 N95-27441
p 2432 N95-27873
p 2302 N95-27875
p 2433 N95-28106
p 2434 N95-28185
p 2416 N95-28329
p 2435 N95-28406
DE-AC04-76DP-00613 .... p 2229 N95-27110
DE-AC04-76DP-00789 .... p 2378 N95-27402

p 2439 N95-27429
p 2309 N95-27745
p 2312 N95-27980
p 2184 N95-28145
DE-AC04-76DP-03533 .... p 2124 N95-27974
DE-AC04-76DR-00789 .... p 2408 N95-27534
DE-AC04-90AI-58770 .... p 2225 N95-26561
DE-AC04-94AL-85000 .... p 2229 N95-27110
p 2202 N95-27136
p 2202 N95-27137
p 2157 N95-27277
p 2309 N95-27305
p 2378 N95-27402
p 2203 N95-27423
p 2439 N95-27429
p 2391 N95-27432
p 2372 N95-27436
p 2234 N95-27460
p 2264 N95-27474
p 2420 N95-27480
p 2425 N95-27482
p 2408 N95-27534
p 2205 N95-27681
p 2205 N95-27683
p 2395 N95-27684
p 2235 N95-27687
p 2265 N95-27706
p 2218 N95-27722
p 2306 N95-27723
p 2266 N95-27724
p 2309 N95-27745
p 2206 N95-27750
p 2309 N95-27837
p 2329 N95-27878
p 2236 N95-27879
p 2455 N95-27949
p 2455 N95-27957
p 2219 N95-27958
p 2219 N95-27968
p 2298 N95-27969
p 2237 N95-27993
p 2378 N95-28074
p 2237 N95-28089
p 2237 N95-28090
p 2444 N95-28103
p 2221 N95-28116
p 2444 N95-28127
p 2299 N95-28128
p 2299 N95-28132
p 2445 N95-28144
p 2184 N95-28145
p 2267 N95-28146
p 2267 N95-28147
p 2267 N95-28148
p 2445 N95-28165
p 2434 N95-28185
p 2268 N95-28200
p 2268 N95-28201
p 2445 N95-28206
p 2299 N95-28219
p 2299 N95-28220
p 2299 N95-28223
p 2238 N95-28358
p 2393 N95-28393
p 2446 N95-28399
p 2239 N95-28400
p 2239 N95-28401
p 2240 N95-28404
p 2240 N95-28405
p 2427 N95-28516
p 2240 N95-28531
p 2240 N95-28532
p 2344 N95-28538
p 2331 N95-28548
p 2300 N95-28549
p 2344 N95-28556
p 2223 N95-28593
p 2270 N95-28597
DE-AC04-94DP-85000 .... p 2238 N95-28117
DE-AC05-76OR-00033 .... p 2220 N95-28044
DE-AC05-84OR-21400 .... p 2262 N95-27083
p 2214 N95-27086
p 2430 N95-27306
p 2406 N95-27307
p 2430 N95-27308
p 2215 N95-27319
p 2431 N95-27419
p 2420 N95-27427
p 2215 N95-27450
p 2204 N95-27451
p 2408 N95-27456
p 2327 N95-27457
p 2215 N95-27464
p 2327 N95-27469
p 2215 N95-27473
p 2234 N95-27486
p 2440 N95-27487
p 2372 N95-27495
p 2431 N95-27497
p 2431 N95-27498
p 2235 N95-27499
p 2431 N95-27536
p 2431 N95-27537
p 2217 N95-27544
p 2302 N95-27545
p 2449 N95-27546
p 2296 N95-27550
p 2409 N95-27551
p 2378 N95-27709
p 2410 N95-27874
p 2302 N95-27875
p 2343 N95-27920
p 2243 N95-27944
p 2236 N95-27946
p 2303 N95-27947
p 2183 N95-27955
p 2208 N95-27956
p 2442 N95-27959
p 2208 N95-27960
p 2208 N95-27961
p 2236 N95-27962
p 2378 N95-28019
p 2183 N95-28043
p 2220 N95-28044
p 2412 N95-28045
p 2220 N95-28046
p 2373 N95-28047
p 2267 N95-28048
p 2413 N95-28066
p 2221 N95-28075
p 2443 N95-28076
p 2413 N95-28077
p 2413 N95-28078
p 2444 N95-28079
p 2237 N95-28080
p 2444 N95-28081
p 2221 N95-28082
p 2392 N95-28110
p 2221 N95-28120
p 2354 N95-28136
p 2268 N95-28156
p 2456 N95-28172
p 2434 N95-28185
p 2415 N95-28204
p 2422 N95-28205
p 2184 N95-28207
p 2223 N95-28208
p 2239 N95-28397
p 2417 N95-28447
p 2373 N95-28498
p 2288 N95-28533
p 2387 N95-28536
p 2447 N95-28537
p 2427 N95-28552
p 2435 N95-28553
p 2456 N95-28555
p 2241 N95-28560
p 2417 N95-28595
p 2435 N95-28596
p 2332 N95-28605
p 2447 N95-28606
p 2375 N95-28632
DE-AC05-84OT-21400 .... p 2208 N95-28042
DE-AC06-76LR-01830 .... p 2321 N95-27971
DE-AC06-76RL-01830 .... p 2214 N95-27086
p 2438 N95-27087
p 2214 N95-27088
p 2232 N95-27129
p 2203 N95-27401
p 2234 N95-27476
p 2216 N95-27479
p 2454 N95-27483
p 2440 N95-27491
p 2216 N95-27492
p 2216 N95-27493
p 2236 N95-27733
p 2328 N95-27749
p 2289 N95-27973
p 2287 N95-28021
p 2222 N95-28129
p 2222 N95-28130
p 2267 N95-28131
p 2222 N95-28163
p 2446 N95-28242
p 2373 N95-28243
DE-AC06-87RL-10930 .... p 2454 N95-27461
p 2219 N95-28005
DE-AC07-76ID-01570 .... p 2264 N95-27403
p 2246 N95-27404
p 2216 N95-27477
DE-AC07-94ID-13223 .... p 2246 N95-27404
p 2217 N95-27553
p 2331 N95-28149
DE-AC08-93NV-11265 .... p 2379 N95-26443
p 2455 N95-28113
DE-AC09-89SR-18035 .... p 2215 N95-27328
DE-AC22-92PC-92106 .... p 2204 N95-27549
DE-AC35-89ER-40486 .... p 2423 N95-28551
DE-AC36-83CH-10093 .... p 2204 N95-27438
p 2319 N95-27459
p 2320 N95-27475
p 2327 N95-27540
p 2122 N95-27541
p 2320 N95-27704
p 2265 N95-27719
p 2325 N95-28394
p 2325 N95-28395
p 2325 N95-28396
DE-AI01-76ET-20320 .... p 2321 N95-27970
DE-AM03-76SF-00010 .... p 2417 N95-28594
DE-AR21-93MC-30358 .... p 2131 N95-27440
DE-AS03-76ER-70285 .... p 2417 N95-28594
DE-AT03-87ER-40327 .... p 2417 N95-28594
DE-FC07-91ID-13073 .... p 2267 N95-28105
DE-FC07-91ID-13074 .... p 2266 N95-27926
DE-FC21-92MC-29237 .... p 2316 N95-26543
DE-FG02-85ER-45219 .... p 2220 N95-28049
DE-FG02-85ER-53212 .... p 2429 N95-26940
DE-FG02-85ER-60314 .... p 2330 N95-28084
DE-FG02-86ER-13480 .... p 2209 N95-28164
DE-FG02-86ER-13491 .... p 2407 N95-27439
DE-FG02-86ER-13592 .... p 2207 N95-27921
DE-FG02-86ER-45229 .... p 2223 N95-28543
DE-FG02-87ER-13671 .... p 2414 N95-28199
DE-FG02-87ER-13772 .... p 2207 N95-27952
DE-FG02-87ER-45326 .... p 2268 N95-28198
DE-FG02-87ER-45329 .... p 2443 N95-28050
DE-FG02-88ER-13860 .... p 2300 N95-28398
DE-FG02-88ER-40452 .... p 2403 N95-26560
DE-FG02-89ER-14079 .... p 2337 N95-27442
p 2339 N95-28190
p 2339 N95-28192
p 2339 N95-28194
DE-FG02-89ER-45388 .... p 2218 N95-27748
DE-FG02-89ER-45402 .... p 2410 N95-27927
DE-FG02-90ER-14105 .... p 2207 N95-27951
DE-FG02-90ER-60986 .... p 2411 N95-27953
DE-FG02-91CE-23810 .... p 2234 N95-27481
p 2238 N95-28133
DE-FG02-91ER-14190 .... p 2206 N95-27838
p 2222 N95-28134
DE-FG02-91ER-40644 .... p 2421 N95-27923
DE-FG02-91ER-61208 .... p 2328 N95-27743
DE-FG02-91ER-81196 .... p 2332 N95-28602
DE-FG02-92ER-40715 .... p 2417 N95-28594
DE-FG02-92ER-40730 .... p 2417 N95-28594
DE-FG02-92ER-61514 .... p 2326 N95-26362
DE-FG02-93CH-10575 .... p 2330 N95-28119
DE-FG02-94ER-14439 .... p 2338 N95-28083
DE-FG02-95ER-40896 .... p 2413 N95-28067
DE-FG03-84ER-53173 .... p 2429 N95-26444
p 2433 N95-27924
DE-FG03-86ER-53225 .... p 2266 N95-28015
p 2434 N95-28185
DE-FG03-87ER-52143 .... p 2214 N95-27086
DE-FG03-88ER-53275 .... p 2431 N95-27536
DE-FG03-89ER-51121 .... p 2434 N95-28185
DE-FG03-91ER-40662 .... p 2449 N95-28160
p 2417 N95-28594
DE-FG03-91ER-40674 .... p 2413 N95-28067
p 2417 N95-28594
DE-FG03-92ER-40695 .... p 2434 N95-28161
DE-FG03-92ER-54150 .... p 2435 N95-28406
DE-FG03-93ER-40757 .... p 2419 N95-27089
p 2413 N95-28067
p 2397 N95-28234
DE-FG03-93SF-20142 .... p 2433 N95-28052
DE-FG05-80ET-53088 .... p 2429 N95-26439
p 2429 N95-27084
p 2287 N95-28055
p 2433 N95-28111
DE-FG05-87ER-40376 .... p 2413 N95-28077
DE-FG05-91ER-45442 .... p 2441 N95-27925
p 2445 N95-28179
DE-FG06-90ER-40561 .... p 2449 N95-27547
p 2399 N95-27548
DE-FG07-90ID-13040 .... p 2319 N95-27236
DE-FG07-93ID-13220 .... p 2430 N95-27237
DE-FG09-90ER-20012 .... p 2352 N95-28496
DE-FG22-89PC-89761 .... p 2205 N95-27680
DE-FG22-90PC-90305 .... p 2203 N95-27420
DE-FG22-92PC-92529 .... p 2205 N95-27692
DE-FG22-93PC-93208 .... p 2204 N95-27458
DE-FG22-93PC-93217 .... p 2205 N95-27691
DE-FG22-93PC-93222 .... p 2205 N95-27690
DE-FG22-94PC-94224 .... p 2241 N95-28604
DE-IA05-840R-21411 .... p 2443 N95-28076
DEN3-153 .... p 2124 N95-27981

p 2312 N95-27982
p 2306 N95-27985
p 2306 N95-27986
DNA001-93-C-0055 p 2178 N95-26712
DNA001-93-C-0138 p 2177 N95-26434
DTFA01-93-C-00001 p 2126 N95-26454
DTFA01-94-C-01013 p 2360 N95-27696
DTFA02-91-C-91089 p 2128 N95-28540
DTFA03-83-A-00328 p 2117 N95-26363
DTFA03-84-R-40032 p 2126 N95-28630
DTFA03-89-C-00043 p 2380 N95-26638
DTFA03-92-C-00003 p 2125 N95-26497
EG-77-C-01-4042 p 2324 N95-27991
EPA-68-D-10096 p 2326 N95-26362
EUROMET PROJ. 221 p 2404 N95-26748
E21-H36 p 2249 N95-26708
FY1457-94-N5026 p 2213 N95-26681
F04690-92-C-0529 p 2152 N95-27793
F04701-85-C-0019 p 2165 N95-27104
p 2228 N95-27108
F04701-88-C-0089 p 2167 N95-26489
p 2342 N95-26899
p 2188 N95-28291
F04701-92-C-0019 p 2174 N95-28316
F04701-93-C-0094 p 2167 N95-26489
p 2318 N95-26846
p 2162 N95-26902
p 2370 N95-27210
p 2210 N95-27632
F04704-92-C-0017 p 2229 N95-27111
F04710-88-C-0089 p 2332 N95-28623
F08630-92-C-0058 p 2243 N95-28634
F08635-91-C-0179 p 2176 N95-28324
F08635-92-C-0056 p 2172 N95-28304
F08635-92-C-0075 p 2176 N95-28324
F08637-94-C-6013 p 2172 N95-28303
F08650-93-C-0066 p 2175 N95-28317
F08650-94-C-0034 p 2413 N95-28101
F09603-90-D-2217 p 2117 N95-26629
F19628-90-C-0002 p 2452 N95-26721
p 2293 N95-28389
F19628-90-C-0003 p 2377 N95-27250
p 2374 N95-28627
p 2375 N95-28628
F19628-90-K-0028 p 2165 N95-28578
F19628-91-C-0152 p 2334 N95-26520
F19628-91-C-0168 p 2365 N95-26656
p 2389 N95-26772
F19628-92-C-0044 p 2337 N95-27703
F19628-93-C-0023 p 2253 N95-27005
p 2339 N95-28575
F19628-93-C-0130 p 2375 N95-28635
F19628-93-C-0193 p 2363 N95-26469
p 2452 N95-26535
p 2364 N95-26536
p 2452 N95-26752
F196828-93-C-0193 p 2454 N95-27529
F29601-89-C-0089 p 2371 N95-27246
F29601-91-C-0016 p 2417 N95-28572
F30602-89-D-0100 p 2361 N95-26845
F30602-92-C-0075 p 2368 N95-26881
F30602-92-C-0111 p 2295 N95-26906
F30602-93-C-0084 p 2259 N95-26550
F33615-85-C-5152 p 2141 N95-28275
F33615-89-C-0532 p 2262 N95-27196
F33615-89-C-0603 p 2355 N95-28561
F33615-89-C-5643 p 2181 N95-26967
F33615-89-C-5706 p 2368 N95-26853
p 2375 N95-28647
F33615-90-C-0532 p 2175 N95-28318
F33615-90-C-1465 p 2364 N95-26536
p 2424 N95-26900
F33615-90-C-5950 p 2245 N95-26410
F33615-90-D-4013 p 2327 N95-27234
F33615-93-C-2321 p 2140 N95-28646
F33615-93-D-3800 p 2129 N95-26684
F33615-93-1-1330 p 2363 N95-26446
p 2363 N95-26467
p 2376 N95-26529
p 2364 N95-26536
p 2365 N95-26656
p 2450 N95-27064
p 2370 N95-27095
F33615-94-C-4438 p 2387 N95-28217
F33657-90-D-0027 p 2192 N95-28437
F49620-92-J-0045 p 2380 N95-26480
F49620-92-J-0131 p 2377 N95-26840
F49620-92-J-0347 p 2353 N95-26779
F49620-92-J-0371 p 2394 N95-26733
F49620-92-J-0499 p 2380 N95-26530
F49620-92-J-0533 p 2436 N95-26462
F49620-93-J-0529 p 2199 N95-26416
F49620-93-1-0004 p 2436 N95-26473
F49620-93-1-0187 p 2403 N95-26466
F49620-93-1-0556 p 2404 N95-26632
F49620-93-1-0579 p 2136 N95-28409
F49620-94-C-0042 p 2125 N95-27186
F49620-94-C-0090 p 2254 N95-27060
F49620-94-1-0075 p 2404 N95-26574
F49620-94-1-0242 p 2284 N95-27760
GA PROJ. 3466 p 2434 N95-28185
p 2416 N95-28329
GRI-5091-260-2178 p 2208 N95-28006
IRAD PROJ. R-1056 p 2192 N95-28441
JPL-958123 p 2347 N95-27805
MDA904-92-H-3082 p 2394 N95-26457
MDA972-91-J-0102 p 2366 N95-26695
p 2366 N95-26711
MDA972-91-J-1022 p 2365 N95-26575
p 2366 N95-26693
MDA972-91-J-102 p 2364 N95-26486
MDA972-92-J-1008 p 2364 N95-26557
MDA972-92-J-1018 p 2368 N95-26903
p 2370 N95-27235
MIPR-Z51100-2-E00416 p 2358 N95-26612
MIPR-94-573 p 2308 N95-26625
NAGW-1175 p 2395 N95-27417
NAGW-2199 p 2463 N95-27700
NAGW-2681 p 2461 N95-26593
NAGW-2753 p 2249 N95-26708
NAGW-2832 p 2462 N95-28216
NAGW-2870 p 2290 N95-26702
NAGW-2888 p 2346 N95-26533
NAGW-3673 p 2399 N95-27852
NAGW-3782 p 2357 N95-27697
NAGW-690 p 2315 N95-28209
NAGW-976 p 2443 N95-28033
NAG1-1056 p 2143 N95-26768
NAG1-1067 p 2236 N95-27857
NAG1-1075 p 2359 N95-26884
NAG1-1240 p 2277 N95-26995
NAG1-1522 p 2131 N95-27180
NAG1-1539 p 2123 N95-28193
NAG1-343 p 2166 N95-28292
p 2190 N95-28428
NAG1-537 p 2310 N95-27865
NAG1-613 p 2365 N95-26628
p 2306 N95-27253
NAG1-833 p 2136 N95-28262
NAG10-0126 p 2326 N95-26808
NAG10-0127 p 2292 N95-27368
NAG2-495 p 2462 N95-28222
NAG2-510 p 2278 N95-27165
NAG2-638 p 2367 N95-26770
NAG2-663 p 2341 N95-26669
NAG2-823 p 2270 N95-28570
NAG2-866 p 2366 N95-26694
NAG3-1072 p 2123 N95-28003
NAG3-1307 p 2206 N95-27695
NAG3-1493 p 2310 N95-28031
p 2310 N95-28032
NAG3-154 p 2260 N95-26816
NAG3-329 p 2307 N95-26387
NAG3-330 p 2124 N95-27977
NAG3-378 p 2325 N95-27992
NAG3-481 p 2117 N95-26363
NAG3-867 p 2214 N95-27167
NAG3-95 p 2199 N95-27636
NAG5-1519 p 2341 N95-26689
NAG5-1554 p 2336 N95-26699
p 2338 N95-28035
NAG5-1790 p 2335 N95-26592
NAG5-2051 p 2465 N95-26630
NAG5-2058 p 2347 N95-27805
NAG5-2129 p 2364 N95-26486
p 2365 N95-26575
p 2366 N95-26693
p 2366 N95-26695
p 2366 N95-26711
p 2367 N95-26802
NAG5-2141 p 2461 N95-27166
NAG5-2316 p 2326 N95-26429
NAG5-2345 p 2329 N95-27864
NAG5-2686 p 2385 N95-27391
NAG8-066 p 2343 N95-28191
NAG8-1046 p 2165 N95-27836
NAG8-1077 p 2463 N95-27916
NAG8-1094 p 2437 N95-26780
NAG8-190 p 2463 N95-27916
NAG8-206 p 2426 N95-27913
NAG8-280 p 2150 N95-27784
NAG9-117 p 2357 N95-27697
NASA ORDER CC-82360-A p 2173 N95-28311
NASA ORDER H-24601-D p 2351 N95-27329
NASA ORDER L-40679-D p 2371 N95-27246
NASA ORDER L-45107 p 2456 N95-28600
NASA ORDER L-79902-C p 2268 N95-28181
NASA ORDER T-9309-R p 2351 N95-28177
NASA ORDER W-88958 p 2326 N95-26362
NASA-INT-91-18880 p 2326 N95-26362
NASW-4621 p 2399 N95-27852
NASW-4814 p 2464 N95-26671
NASW-4873 p 2144 N95-26426
NASW-4911 p 2159 N95-26398
p 2159 N95-26399
p 2160 N95-26400
p 2160 N95-26401
p 2160 N95-26403
NASW-4933 p 2464 N95-27858
NAS1-18224 p 2177 N95-26391
p 2470 N95-27647
NAS1-18754 p 2192 N95-28436
NAS1-18758 p 2190 N95-28426
NAS1-18778 p 2198 N95-28484
NAS1-18788 p 2357 N95-28253
NAS1-18799 p 2185 N95-28270
NAS1-18833 p 2187 N95-28285
NAS1-18840 p 2189 N95-28424
NAS1-18862 p 2186 N95-28282
NAS1-18888 p 2138 N95-28476
NAS1-18889 p 2137 N95-28471
p 2137 N95-28473
p 2137 N95-28474
p 2196 N95-28478
p 2138 N95-28482
NAS1-19000 p 2131 N95-27371
p 2386 N95-27395
NAS1-19060 p 2402 N95-28073
NAS1-19143 p 2402 N95-28264
NAS1-19241 p 2163 N95-27026
NAS1-19247 p 2177 N95-26391
p 2470 N95-27647
p 2326 N95-27649
NAS1-19462 p 2140 N95-28227
NAS1-19480 p 2388 N95-26395
p 2273 N95-26576
p 2389 N95-26672
p 2361 N95-26697
p 2278 N95-27027
p 2278 N95-27028
p 2390 N95-27029
p 2279 N95-27179
p 2279 N95-27247
p 2391 N95-27433
p 2284 N95-27760
p 2287 N95-27917
p 2288 N95-28228
p 2288 N95-28571
p 2289 N95-28673
NAS1-19672 p 2279 N95-27257
NAS1-20090 p 2402 N95-28670
NAS10-11624 p 2126 N95-27859
NAS10-11943 p 2173 N95-28309
p 2173 N95-28310
p 2174 N95-28312
NAS10-120 p 2383 N95-27378
NAS2-12513 p 2123 N95-28230
p 2123 N95-28265
NAS2-5364 p 2131 N95-27143
NAS3-25363 p 2243 N95-28001
NAS3-25776 p 2316 N95-26734
p 2372 N95-27729
p 2321 N95-27970
NAS3-25808 p 2316 N95-26393
NAS3-25950 p 2140 N95-27866
NAS3-25965 p 2266 N95-27999
NAS3-26062 p 2168 N95-28000
NAS3-27002 p 2166 N95-26390
NAS3-27186 p 2273 N95-26380
p 2309 N95-27174
p 2264 N95-27374
p 2168 N95-27727
p 2125 N95-27762
p 2140 N95-27860
p 2293 N95-28037
NAS5-29298 p 2385 N95-27393
NAS5-31000 p 2148 N95-27773
p 2150 N95-27785
NAS5-31500 p 2146 N95-27764
p 2146 N95-27765
p 2147 N95-27766
p 2147 N95-27768
p 2147 N95-27769
p 2147 N95-27770
p 2150 N95-27783
p 2152 N95-27796
p 2153 N95-27798
p 2153 N95-27799
NAS5-32332 p 2334 N95-26423
NAS5-32336 p 2314 N95-27998
NAS5-32608 p 2336 N95-26922
NAS5-32705 p 2343 N95-27997
NAS7-918 p 2297 N95-27731
p 2426 N95-27843
p 2271 N95-28599
NAS8-38100 p 2165 N95-27124
NAS8-38609 p 2360 N95-27164
p 2301 N95-27244

p 2168 N95-27424
NAS8-38610 p 2202 N95-27168
NAS8-39027 p 2247 N95-28419
NAS8-39368 p 2164 N95-27093
NAS8-39897 p 2450 N95-27169
NAS8-40257 p 2154 N95-27245
NAS8-50000 p 2261 N95-26890
NAS9-18973 p 2239 N95-28385
p 2239 N95-28386
p 2239 N95-28387
NAS9-19266 p 2385 N95-27392
NAS9-19359 p 2145 N95-28261
NCA2-721 p 2145 N95-27394
NCCW-0045 p 2127 N95-28188
NCCW-40 p 2362 N95-26386
p 2363 N95-26388
p 2364 N95-26486
p 2365 N95-26575
p 2365 N95-26668
p 2366 N95-26693
p 2366 N95-26695
p 2366 N95-26711
p 2367 N95-26802
p 2367 N95-26814
p 2371 N95-27252
NCC1-159 p 2386 N95-27395
NCC2-498 p 2121 N95-26760
NCC2-500 p 2275 N95-26766
NCC2-5038 p 2314 N95-26815
NCC2-505 p 2120 N95-26649
NCC2-507 p 2279 N95-27240
NCC2-522 p 2365 N95-26648
NCC2-585 p 2274 N95-26665
NCC2-616 p 2143 N95-26775
NCC2-617 p 2129 N95-26651
p 2130 N95-26813
NCC2-636 p 2274 N95-26589
NCC2-651 p 2349 N95-26727
NCC2-654 p 2160 N95-27154
NCC2-657 p 2129 N95-26591
NCC2-675 p 2138 N95-28203
NCC2-729 p 2121 N95-26735
NCC2-740 p 2129 N95-26590
NCC2-747 p 2122 N95-27248
NCC2-752 p 2274 N95-26588
NCC2-755 p 2275 N95-26776
NCC2-767 p 2139 N95-26777
NCC2-777 p 2369 N95-26930
NCC2-796 p 2120 N95-26649
NCC2-812 p 2358 N95-28676
NCC2-838 p 2385 N95-27393
NCC3-233 p 2273 N95-26380
p 2285 N95-27882
NCC3-312 p 2244 N95-26709
NCC3-370 p 2279 N95-27175
p 2279 N95-27242
p 2391 N95-27726
NCC3-77 p 2319 N95-27193
p 2319 N95-27194
NCC3-94 p 2218 N95-27728
NCC8-79 p 2160 N95-28258
p 2304 N95-28259
p 2450 N95-28260
NIST-50SBNB3C7500 p 2326 N95-26362
NRC-1886-8011-9B p 2223 N95-28208
NRC-1886-8109-8L p 2223 N95-28208
NSF ASC-92-17041 p 2387 N95-28461
NSF CCR-89-14428 p 2387 N95-28461
NSF CCR-91-09469 p 2363 N95-26446
NSF CCR-93-03383 p 2365 N95-26605
NSF CCR-93-10888 p 2387 N95-28461
NSF DMR-89-20548 p 2437 N95-26553
NSF DMR-91-20269 p 2425 N95-27539
NSF DMR-92-21655 p 2436 N95-26440
NSF DMR-93-12601 p 2437 N95-26553
NSF DMS-90-02237 p 2394 N95-26457
NSF DMS-90-12135 p 2398 N95-26345
NSF DMS-92-11820 p 2279 N95-27247
NSF DMS-94-03360 p 2389 N95-26915
NSF DPP-87-20063 p 2144 N95-27297
NSF ECD-89-07068 p 2452 N95-28535
NSF ECS-89-02528 p 2475 N95-28038
NSF ECS-89-22947 p 2475 N95-28038
NSF ECS-90-15752 p 2427 N95-28524
NSF ENG-91-11333 p 2475 N95-28038
NSF ENG-92-17849 p 2263 N95-27226
p 2235 N95-27694
p 2247 N95-27909
p 2475 N95-28038
p 2268 N95-28239
NSF ENG-93-14162 p 2235 N95-27694
NSF IRI-90-13160 p 2259 N95-28624
NSF IRI-92-14873 p 2382 N95-27066
NSF NCR-93-01002 p 2367 N95-26770
NSF OCE-89-17750 p 2338 N95-28094
NSF PHY-91-19849 p 2417 N95-28594
NSF 91-00530 p 2386 N95-27396
NSFCCR-90-16641 p 2376 N95-26529
NSG-1601 p 2306 N95-28034
NSG-3277 p 2124 N95-27976
N00014-82-K-0612 p 2224 N95-26470
p 2225 N95-26472
N00014-85-K-0198 p 2389 N95-26882
N00014-87-C-0146 p 2428 N95-27646
N00014-88-C-0721 p 2191 N95-28435
N00014-88-K-0298 p 2212 N95-26490
N00014-89-C-0018 p 2347 N95-27011
N00014-89-J-1007 p 2260 N95-26716
N00014-89-J-1012 p 2347 N95-27011
N00014-89-J-1015 p 2338 N95-28094
N00014-89-J-1361 p 2277 N95-26998
N00014-89-J-1527 p 2398 N95-26345
N00014-89-J-1545 p 2223 N95-28332
p 2241 N95-28661
N00014-89-J-1565 p 2438 N95-26872
N00014-89-J-3018 p 2275 N95-26751
N00014-90-C-0098 p 2347 N95-27011
N00014-90-C-2269 p 2225 N95-26482
N00014-90-J-1270 p 2365 N95-26628
N00014-90-J-1372 p 2368 N95-26855
N00014-90-J-1427 p 2437 N95-26756
N00014-90-J-1493 p 2347 N95-27011
N00014-90-J-1869 p 2350 N95-27100
N00014-90-J-4013 p 2287 N95-28155
N00014-90-J-4083 p 2121 N95-26757
p 2276 N95-26827
N00014-90-J-4092 p 2277 N95-27000
N00014-91-C-0001 p 2227 N95-27101
p 2170 N95-28294
N00014-91-C-0109 p 2428 N95-27646
N00014-91-C-0157 p 2179 N95-26484
N00014-91-J-1035 p 2403 N95-26491
N00014-91-J-1058 p 2199 N95-26350
N00014-91-J-1104 p 2212 N95-26490
N00014-91-J-1246 p 2348 N95-28096
N00014-91-J-1416 p 2446 N95-28327
N00014-91-J-1596 p 2447 N95-28618
N00014-91-J-1629 p 2438 N95-26959
p 2290 N95-26982
p 2405 N95-27017
p 2438 N95-27061
N00014-91-J-1641 p 2224 N95-26351
p 2207 N95-27904
N00014-91-J-1891 p 2342 N95-26826
N00014-91-J-1951 p 2346 N95-26533
N00014-91-J-2005 p 2224 N95-26456
N00014-91-J-4016 p 2279 N95-27247
N00014-91-J-4037 p 2277 N95-26999
p 2278 N95-27001
p 2278 N95-27019
N00014-91-J-4040 p 2428 N95-27646
N00014-91-J-4101 p 2306 N95-26927
N00014-91-J-4164 p 2213 N95-27032
N00014-92-C-0028 p 2402 N95-28622
N00014-92-J-1190 p 2252 N95-26924
p 2227 N95-26973
p 2253 N95-26977
p 2261 N95-27015
p 2427 N95-28524
p 2270 N95-28544
N00014-92-J-12300 p 2347 N95-27043
N00014-92-J-1291 p 2348 N95-28096
N00014-92-J-1303 p 2394 N95-26413
p 2394 N95-26414
p 2394 N95-26415
p 2394 N95-26457
N00014-92-J-1486 p 2315 N95-28392
N00014-92-J-1500 p 2237 N95-28097
N00014-92-J-1512 p 2259 N95-28624
N00014-92-J-1527 p 2347 N95-27151
N00014-92-J-1617 p 2377 N95-27182
N00014-92-J-1664 p 2278 N95-27047
N00014-92-J-1735 p 2255 N95-27185
N00014-92-J-1991 p 2181 N95-26847
N00014-93-C-0234 p 2370 N95-27031
N00014-93-I-0213 p 2182 N95-27188
N00014-93-I-0527 p 2394 N95-26414
N00014-93-MP-24023 p 2349 N95-26608
N00014-93-1-0027 p 2279 N95-27197
N00014-93-1-0231 p 2261 N95-26964
p 2256 N95-28095
N00014-93-1-0257 p 2394 N95-26478
p 2356 N95-26843
N00014-93-1-0312 p 2233 N95-27187
N00014-93-1-0437 p 2439 N95-27416
N00014-93-1-0527 p 2394 N95-26413
p 2394 N95-26415
N00014-93-1-0534 p 2437 N95-26553
p 2226 N95-26627
N00014-93-1-0563 p 2178 N95-26569
p 2178 N95-28334
N00014-93-1-0806 p 2382 N95-27066
N00014-93-1-0814 p 2436 N95-28668
N00014-93-1-1105 p 2438 N95-26997
N00014-93-1-1134 p 2438 N95-26872
N00014-93-1-1326 p 2346 N95-26533
N00014-93-1-1352 p 2347 N95-27011
N00014-94-C-0135 p 2181 N95-26848
N00014-94-C-0141 p 2269 N95-28349
N00014-94-C-0168 p 2178 N95-26567
N00014-94-C-0179 p 2359 N95-26755
N00014-94-C-0199 p 2430 N95-27190
N00014-94-C-0260 p 2262 N95-27096
p 2271 N95-28629
N00014-94-WX-35069 p 2212 N95-26411
N00014-94-1-G004 p 2289 N95-26461
N00014-94-1-0076 p 2201 N95-26870
N00014-94-1-0201 p 2401 N95-26925
N00014-94-1-0224 p 2247 N95-28187
N00014-94-1-0301 p 2313 N95-28099
N00014-94-1-0308 p 2271 N95-28666
N00014-94-1-0322 p 2294 N95-26568
N00014-94-1-0462 p 2261 N95-27002
N00014-94-1-0479 p 2256 N95-28391
N00014-94-1-0834 p 2288 N95-28351
N00014-94-1-0931 p 2387 N95-28336
N00014-95-1-0028 p 2404 N95-26960
N00039-93-C-0152 p 2377 N95-26840
N0014-94-J-9030 p 2312 N95-28649
N00167-94-WR-40321 p 2212 N95-26411
N00421-94-WR-01539 p 2423 N95-26532
N01-LM-3-3525 p 2365 N95-26575
N60530-88-C-0260 p 2142 N95-28281
N60530-88-C-0370 p 2185 N95-28272
N61533-92-K-0030 p 2310 N95-28098
p 2311 N95-28100
N62269-87-C-0216 p 2192 N95-28438
N62269-90-C-0281 p 2186 N95-28279
N62269-90-C-0282 p 2190 N95-28429
N62269-90-C-0412 p 2362 N95-26348
N68171-94-C-9101 p 2326 N95-26610
N68171-94-C-9121 p 2199 N95-26352
N68171-94-M-6201 p 2141 N95-26487
ONR PROJ. S311 p 2340 N95-26479
ONR PROJ. X05-13 p 2347 N95-27189
ONR PROJ. 3054 p 2340 N95-26479
ONR PROJ. 4135-008 p 2223 N95-28332
p 2241 N95-28661
P60-DC-0207-02 p 2357 N95-27697
RM35G93 p 2345 N95-26406
RR04204 p 2306 N95-26927
RTOP 199-45-16-11 p 2465 N95-28530
RTOP 199-45-16-12 p 2420 N95-27372
RTOP 232-01-02 p 2168 N95-27434
RTOP 233-01-0B p 2167 N95-27177
RTOP 233-01-01-02 p 2163 N95-27026
RTOP 233-01-01-03 p 2131 N95-27371
RTOP 233-01-01-05 p 2161 N95-26428
RTOP 233-01-03-23 p 2371 N95-27246
RTOP 233-01-03 p 2366 N95-26685
RTOP 233-02-0B p 2283 N95-27369
RTOP 233-02-0C p 2264 N95-27374
RTOP 233-03-02-03 p 2466 N95-27629
RTOP 233-03-02-04 p 2177 N95-26391
RTOP 235-01-0A p 2371 N95-27370
RTOP 235-01-0C p 2372 N95-27729
RTOP 242-10-01 p 2367 N95-26726
RTOP 242-20-06 p 2218 N95-27728
RTOP 242-50-01 p 2140 N95-28344
RTOP 242-70-02 p 2166 N95-26390
p 2168 N95-27861
RTOP 274-00-00 p 2164 N95-27761
RTOP 323-12-07 p 2372 N95-27905
RTOP 335-05-01 p 2123 N95-28003
RTOP 476-14-10 p 2316 N95-26393
RTOP 478-12-10 p 2169 N95-28213
RTOP 478-42-10 p 2164 N95-27730
RTOP 478-43-00 p 2168 N95-27862
RTOP 505-59-10-30 p 2120 N95-26382
p 2124 N95-28669
RTOP 505-59-36 p 2127 N95-26587
p 2118 N95-26710
p 2141 N95-26773
p 2122 N95-27258
RTOP 505-59-53-01 p 2124 N95-28674
RTOP 505-59-53 p 2362 N95-27914
RTOP 505-59-54-02 p 2291 N95-27259
p 2293 N95-27915
RTOP 505-61-21 p 2123 N95-28230
p 2123 N95-28265
RTOP 505-62-10 p 2309 N95-27174
RTOP 505-62-36 p 2302 N95-27373
p 2302 N95-27698
p 2302 N95-27855
RTOP 505-62-50 p 2291 N95-27173
p 2426 N95-27906
p 2293 N95-28037
RTOP 505-62-52 p 2117 N95-26363

p 2389 N95-26663
p 2401 N95-26801
p 2291 N95-27030
p 2206 N95-27695
p 2209 N95-28182
RTOP 505-62-82 .... p 2143 N95-27176
RTOP 505-63-36-06 .... p 2136 N95-28262
RTOP 505-63-5B .... p 2307 N95-26387
p 2301 N95-26774
p 2301 N95-27178
p 2310 N95-28031
p 2310 N95-28032
RTOP 505-63-50-13 .... p 2117 N95-26381
RTOP 505-63-70-02 .... p 2402 N95-28073
RTOP 505-64-13-21 .... p 2357 N95-28253
RTOP 505-64-52-01 .... p 2142 N95-27839
RTOP 505-68-10 .... p 2125 N95-27762
RTOP 505-68-32 .... p 2139 N95-26412
RTOP 505-68-70-06 .... p 2140 N95-28227
RTOP 505-68-70-09 .... p 2123 N95-28241
RTOP 505-69-50 .... p 2303 N95-27911
RTOP 505-70-62-01 .... p 2140 N95-28343
RTOP 505-90-00 .... p 2456 N95-28600
RTOP 505-90-21 .... p 2123 N95-28003
RTOP 505-90-5K .... p 2273 N95-26380
p 2279 N95-27175
p 2279 N95-27242
p 2391 N95-27726
p 2285 N95-27882
RTOP 505-90-52-01 .... p 2388 N95-26395
p 2273 N95-26576
p 2389 N95-26672
p 2361 N95-26697
p 2278 N95-27027
p 2278 N95-27028
p 2390 N95-27029
p 2279 N95-27179
p 2279 N95-27247
p 2391 N95-27433
p 2284 N95-27760
p 2287 N95-27917
p 2288 N95-28228
p 2289 N95-28673
RTOP 505-90-53-02 .... p 2362 N95-27241
RTOP 505-90-58 .... p 2140 N95-27860
RTOP 506-42-31 .... p 2168 N95-28000
RTOP 506-43-61-01 .... p 2177 N95-26391
RTOP 506-44-2C .... p 2266 N95-27853
RTOP 510-00-00 .... p 2382 N95-27375
RTOP 532-06-37-01 .... p 2400 N95-26392
RTOP 536-01-11 .... p 2466 N95-27367
RTOP 537-02-22-02 .... p 2400 N95-26394
RTOP 537-03-23-03 .... p 2279 N95-27257
RTOP 537-09-21-05 .... p 2465 N95-26427
RTOP 537-10-20 .... p 2140 N95-27866
RTOP 538-01-13-01 .... p 2268 N95-28181
RTOP 538-03-15-01 .... p 2402 N95-28670
RTOP 547-10-11 .... p 2169 N95-28036
RTOP 550-00-00 .... p 2146 N95-27763
RTOP 564-09-20 .... p 2168 N95-27727
RTOP 589-01-2C .... p 2243 N95-28001
RTOP 656-61-23 .... p 2244 N95-26709
RTOP 680-00-00 .... p 2463 N95-28328
RTOP 776-33-41 .... p 2316 N95-26734
p 2321 N95-27970
RTOP 822-00-00 .... p 2255 N95-27435
RTOP 963-20-0C .... p 2284 N95-27854
SBIR-02.04-8581 .... p 2164 N95-27093
SRI PROJ. 4854 .... p 2399 N95-27852
SWRI PROJ. 15-4258 .... p 2338 N95-28035
USAFETAC PROJ. 901033 .... p 2342 N95-27148
W-31-109-ENG-38 .... p 2436 N95-26440
p 2376 N95-26441
p 2436 N95-26442
p 2438 N95-27085
p 2439 N95-27429
p 2439 N95-27452
p 2408 N95-27453
p 2284 N95-27454
p 2234 N95-27455
p 2327 N95-27457
p 2440 N95-27542
p 2378 N95-27741
p 2392 N95-27742
p 2218 N95-27752
p 2409 N95-27753
p 2206 N95-27755
p 2441 N95-27928
p 2351 N95-27948
p 2442 N95-27950
p 2442 N95-27963
p 2208 N95-27965
p 2219 N95-27966
p 2237 N95-27967
p 2411 N95-28004
p 2183 N95-28068
p 2183 N95-28069
p 2303 N95-28070
p 2378 N95-28071
p 2220 N95-28072
p 2392 N95-28173
p 2415 N95-28210
p 2434 N95-28224
p 2434 N95-28233
p 2238 N95-28235
p 2344 N95-28340
p 2239 N95-28400
p 2256 N95-28407
p 2223 N95-28543
W-7405-ENG-36 .... p 2182 N95-27080
p 2405 N95-27081
p 2213 N95-27082
p 2390 N95-27304
p 2461 N95-27326
p 2430 N95-27327
p 2182 N95-27421
p 2378 N95-27422
p 2420 N95-27425
p 2354 N95-27426
p 2183 N95-27428
p 2439 N95-27429
p 2407 N95-27431
p 2203 N95-27437
p 2462 N95-27445
p 2215 N95-27446
p 2215 N95-27463
p 2408 N95-27466
p 2204 N95-27467
p 2234 N95-27468
p 2216 N95-27488
p 2420 N95-27494
p 2217 N95-27555
p 2204 N95-27556
p 2296 N95-27557
p 2296 N95-27672
p 2432 N95-27673
p 2328 N95-27686
p 2296 N95-27705
p 2297 N95-27716
p 2425 N95-27734
p 2421 N95-27735
p 2297 N95-27736
p 2266 N95-27754
p 2256 N95-27840
p 2297 N95-27841
p 2284 N95-27845
p 2455 N95-27847
p 2337 N95-27848
p 2372 N95-27849
p 2297 N95-27850
p 2206 N95-27851
p 2236 N95-27943
p 2442 N95-27994
p 2426 N95-28018
p 2426 N95-28022
p 2443 N95-28023
p 2411 N95-28024
p 2451 N95-28025
p 2219 N95-28026
p 2296 N95-28027
p 2412 N95-28051
p 2412 N95-28057
p 2325 N95-28058
p 2298 N95-28059
p 2443 N95-28060
p 2338 N95-28061
p 2462 N95-28062
p 2412 N95-28063
p 2209 N95-28088
p 2338 N95-28114
p 2298 N95-28124
p 2444 N95-28125
p 2339 N95-28126
p 2445 N95-28240
p 2311 N95-28539
p 2447 N95-28541
p 2258 N95-28601
p 2288 N95-28603
p 2456 N95-28631
W-7405-ENG-48 .... p 2334 N95-26436
p 2335 N95-26622
p 2430 N95-27327
p 2431 N95-27441
p 2204 N95-27496
p 2327 N95-27532
p 2372 N95-27533
p 2425 N95-27539
p 2328 N95-27558
p 2265 N95-27693
p 2206 N95-27707
p 2328 N95-27708
p 2432 N95-27710
p 2351 N95-27725
p 2298 N95-27876
p 2338 N95-27931
p 2330 N95-27954
p 2462 N95-28013
p 2343 N95-28014
p 2266 N95-28015
p 2303 N95-28029
p 2314 N95-28053
p 2433 N95-28054
p 2243 N95-28064
p 2433 N95-28065
p 2455 N95-28085
p 2399 N95-28108
p 2399 N95-28109
p 2330 N95-28118
p 2434 N95-28138
p 2303 N95-28139
p 2434 N95-28140
p 2434 N95-28141
p 2331 N95-28157
p 2392 N95-28162
p 2222 N95-28167
p 2373 N95-28168
p 2414 N95-28171
p 2357 N95-28176
p 2434 N95-28185
p 2256 N95-28231
p 2392 N95-28232
p 2311 N95-28337
p 2435 N95-28356
p 2435 N95-28406
p 2373 N95-28521
p 2223 N95-28534
p 2435 N95-28542
p 2332 N95-28550
p 2332 N95-28662
W-7405-ENG-82 .... p 2273 N95-26445

NASA

R
N

Listi
by re
the
page
abst
item
that

REPORT NUMBER INDEX

SCIENTIFIC AND TECHNICAL AEROSPACE REPORTS VOLUME 33 NUMBER 9

Typical Report Number Index Listing

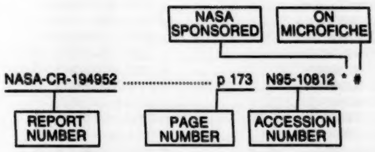

Listings in this index are arranged alphanumerically by report number. The accession number denotes the number by which the citation is identified. The page number helps to locate the citation in the abstract section. An asterisk (*) indicates that the item is a NASA report. A pound sign (#) indicates that the item is available on microfiche.

A-90092 .... p 2123 N95-28230 * #
A-90093 .... p 2123 N95-28265 * #
A-94140 .... p 2466 N95-27367 * #
A-950048 .... p 2139 N95-26412 * #
A-950052 .... p 2127 N95-26587 * #
A-950055 .... p 2141 N95-26773 * #
A-950056 .... p 2367 N95-26726 * #
A-950063 .... p 2122 N95-27258 * #
A-950067 .... p 2358 N95-28676 * #
A-950068 .... p 2457 N95-28677 * #
A-95034 .... p 2118 N95-26710 * #
A-95041 .... p 2131 N95-27143 * #

AD-A280068 .... p 2165 N95-28150
AD-A280074 .... p 2144 N95-28151
AD-A280075 .... p 2243 N95-28152
AD-A280084 .... p 2331 N95-28153
AD-A280085 .... p 2178 N95-28154
AD-A280099 .... p 2287 N95-28155
AD-A286722 .... p 2327 N95-27234 #
AD-A286723 .... p 2370 N95-27235 #
AD-A288228 .... p 2201 N95-26544
AD-A288229 .... p 2226 N95-26623
AD-A288230 .... p 2226 N95-26624
AD-A288231 .... p 2154 N95-26524
AD-A288234 .... p 2225 N95-26526
AD-A288237 .... p 2308 N95-26625
AD-A288238 .... p 2180 N95-26626
AD-A288245 .... p 2249 N95-26545
AD-A288252 .... p 2248 N95-26407
AD-A288254 .... p 2363 N95-26408
AD-A288256 .... p 2341 N95-26546
AD-A288257 .... p 2307 N95-26547
AD-A288262 .... p 2246 N95-26548
AD-A288274 .... p 2200 N95-26451
AD-A288279 .... p 2200 N95-26452
AD-A288280 .... p 2340 N95-26453
AD-A288281 .... p 2126 N95-26454
AD-A288284 .... p 2117 N95-26455
AD-A288285 .... p 2224 N95-26456
AD-A288286 .... p 2394 N95-26457
AD-A288289 .... p 2117 N95-26409
AD-A288291 .... p 2245 N95-26410
AD-A288292 .... p 2212 N95-26411
AD-A288293 .... p 2394 N95-26413
AD-A288294 .... p 2394 N95-26414
AD-A288295 .... p 2394 N95-26415
AD-A288296 .... p 2199 N95-26416
AD-A288297 .... p 2199 N95-26417
AD-A288298 .... p 2273 N95-26418
AD-A288299 .... p 2345 N95-26419
AD-A288300 .... p 2345 N95-26420
AD-A288318 .... p 2379 N95-26421
AD-A288319 .... p 2200 N95-26422
AD-A288322 .... p 2225 N95-26561
AD-A288326 .... p 2249 N95-26562
AD-A288333 .... p 2448 N95-26563
AD-A288339 .... p 2178 N95-26570
AD-A288343 .... p 2180 N95-26571
AD-A288344 .... p 2180 N95-26572
AD-A288345 .... p 2348 N95-26573
AD-A288347 .... p 2125 N95-26527
AD-A288348 .... p 2117 N95-26629
AD-A288352 .... p 2403 N95-26466
AD-A288356 .... p 2363 N95-26467
AD-A288359 .... p 2380 N95-26468
AD-A288366 .... p 2363 N95-26469
AD-A288367 .... p 2224 N95-26470
AD-A288370 .... p 2376 N95-26471
AD-A288373 .... p 2225 N95-26472
AD-A288381 .... p 2436 N95-26473
AD-A288385 .... p 2363 N95-26474
AD-A288390 .... p 2380 N95-26475
AD-A288401 .... p 2125 N95-26497
AD-A288420 .... p 2380 N95-26530
AD-A288423 .... p 2423 N95-26549
AD-A288424 .... p 2364 N95-26557
AD-A288432 .... p 2429 N95-26800
AD-A288433 .... p 2353 N95-26779
AD-A288435 .... p 2357 N95-27181
AD-A288439 .... p 2377 N95-27182
AD-A288443 .... p 2377 N95-27183
AD-A288444 .... p 2464 N95-27184
AD-A288449 .... p 2255 N95-27185
AD-A288451 .... p 2326 N95-26431
AD-A288456 .... p 2200 N95-26432
AD-A288458 .... p 2404 N95-26632
AD-A288461 .... p 2466 N95-26604
AD-A288476 .... p 2337 N95-27703
AD-A288478 .... p 2360 N95-27058
AD-A288487 .... p 2123 N95-28331
AD-A288488 .... p 2160 N95-26634
AD-A288492 .... p 2380 N95-26638
AD-A288497 .... p 2346 N95-26647
AD-A288501 .... p 2341 N95-26650
AD-A288503 .... p 2129 N95-26652
AD-A288504 .... p 2354 N95-27059
AD-A288506 .... p 2358 N95-26736
AD-A288509 .... p 2370 N95-27150
AD-A288511 .... p 2341 N95-26653
AD-A288516 .... p 2254 N95-27060
AD-A288519 .... p 2394 N95-26733
AD-A288523 .... p 2308 N95-26839
AD-A288532 .... p 2377 N95-26840
AD-A288536 .... p 2125 N95-27186
AD-A288541 .... p 2200 N95-26528
AD-A288544 .... p 2365 N95-26605
AD-A288548 .... p 2335 N95-26531
AD-A288551 .... p 2423 N95-26532
AD-A288552 .... p 2201 N95-26606
AD-A288558 .... p 2334 N95-26520
AD-A288560 .... p 2358 N95-26558
AD-A288563 .... p 2376 N95-26529
AD-A288565 .... p 2290 N95-26541
AD-A288575 .... p 2377 N95-26551
AD-A288578 .... p 2364 N95-26554
AD-A288579 .... p 2346 N95-26533 *
AD-A288583 .... p 2370 N95-27095
AD-A288584 .... p 2364 N95-26534
AD-A288585 .... p 2452 N95-26535
AD-A288587 .... p 2364 N95-26536
AD-A288589 .... p 2365 N95-26656
AD-A288590 .... p 2314 N95-26841
AD-A288599 .... p 2423 N95-26679
AD-A288606 .... p 2255 N95-27249
AD-A288610 .... p 2128 N95-26481
AD-A288613 .... p 2225 N95-26482
AD-A288617 .... p 2346 N95-26483
AD-A288629 .... p 2179 N95-26484
AD-A288631 .... p 2307 N95-26342
AD-A288632 .... p 2340 N95-26343
AD-A288633 .... p 2247 N95-26344
AD-A288650 .... p 2262 N95-27096
AD-A288652 .... p 2125 N95-26485
AD-A288656 .... p 2141 N95-26487
AD-A288677 .... p 2334 N95-26488
AD-A288690 .... p 2437 N95-26818
AD-A288697 .... p 2167 N95-26489
AD-A288699 .... p 2212 N95-26490
AD-A288708 .... p 2377 N95-27250
AD-A288719 .... p 2403 N95-26491
AD-A288741 .... p 2371 N95-27251
AD-A288744 .... p 2138 N95-28586
AD-A288746 .... p 2456 N95-28587
AD-A288747 .... p 2374 N95-28588
AD-A288775 .... p 2398 N95-26345
AD-A288794 .... p 2348 N95-26360
AD-A288805 .... p 2350 N95-27097
AD-A288808 .... p 2380 N95-26492
AD-A288809 .... p 2248 N95-26358
AD-A288819 .... p 2362 N95-26346
AD-A288820 .... p 2393 N95-26347
AD-A288822 .... p 2362 N95-26348
AD-A288824 .... p 2248 N95-26349
AD-A288831 .... p 2352 N95-26494
AD-A288833 .... p 2259 N95-26550
AD-A288835 .... p 2456 N95-28589
AD-A288837 .... p 2370 N95-27210
AD-A288843 .... p 2213 N95-26681
AD-A288847 .... p 2259 N95-26433
AD-A288858 .... p 2358 N95-26552
AD-A288866 .... p 2225 N95-26499
AD-A288869 .... p 2223 N95-28332
AD-A288870 .... p 2241 N95-28661
AD-A288872 .... p 2247 N95-28187
AD-A288874 .... p 2223 N95-28189
AD-A288881 .... p 2374 N95-28590
AD-A288883 .... p 2161 N95-26458
AD-A288885 .... p 2177 N95-26434
AD-A288887 .... p 2199 N95-26350
AD-A288890 .... p 2374 N95-28591
AD-A288893 .... p 2224 N95-26351
AD-A288897 .... p 2199 N95-26352
AD-A288905 .... p 2437 N95-26553
AD-A288906 .... p 2241 N95-28592
AD-A288908 .... p 2360 N95-27195
AD-A288909 .... p 2249 N95-26564
AD-A288913 .... p 2300 N95-28333
AD-A288920 .... p 2452 N95-26607
AD-A288928 .... p 2226 N95-26627
AD-A288929 .... p 2349 N95-26608
AD-A288934 .... p 2262 N95-27196
AD-A288938 .... p 2178 N95-28334
AD-A288942 .... p 2178 N95-26569
AD-A288944 .... p 2179 N95-26565
AD-A288953 .... p 2246 N95-26566
AD-A288955 .... p 2348 N95-26435
AD-A288959 .... p 2269 N95-28349
AD-A288961 .... p 2379 N95-28335
AD-A288962 .... p 2273 N95-26405
AD-A288963 .... p 2363 N95-26446
AD-A288965 .... p 2363 N95-26447
AD-A288970 .... p 2233 N95-27187
AD-A288973 .... p 2182 N95-27188
AD-A288975 .... p 2404 N95-26574
AD-A288979 .... p 2389 N95-26609
AD-A288988 .... p 2178 N95-26712
AD-A288995 .... p 2365 N95-26628 *
AD-A288996 .... p 2388 N95-26459
AD-A288997 .... p 2326 N95-26610
AD-A288998 .... p 2314 N95-26682
AD-A289006 .... p 2178 N95-26567
AD-A289007 .... p 2294 N95-26568
AD-A289008 .... p 2376 N95-26460
AD-A289010 .... p 2387 N95-28336
AD-A289015 .... p 2127 N95-27903
AD-A289017 .... p 2289 N95-26461
AD-A289022 .... p 2436 N95-26462
AD-A289029 .... p 2340 N95-26463
AD-A289031 .... p 2307 N95-26464
AD-A289038 .... p 2207 N95-27904
AD-A289039 .... p 2313 N95-26476
AD-A289045 .... p 2346 N95-26477
AD-A289050 .... p 2347 N95-27189
AD-A289053 .... p 2430 N95-27190
AD-A289055 .... p 2338 N95-28094
AD-A289057 .... p 2394 N95-26478
AD-A289058 .... p 2340 N95-26479
AD-A289060 .... p 2345 N95-26406
AD-A289061 .... p 2365 N95-26611
AD-A289062 .... p 2288 N95-28351

AD-A289083 .... p 2256 N95-28095
AD-A289088 .... p 2380 N95-26480
AD-A289092 .... p 2446 N95-28327
AD-A289098 .... p 2399 N95-27398
AD-A289104 .... p 2348 N95-28096
AD-A289107 .... p 2237 N95-28097
AD-A289113 .... p 2310 N95-28098
AD-A289117 .... p 2313 N95-28099
AD-A289120 .... p 2311 N95-28100
AD-A289124 .... p 2413 N95-28101
AD-A289127 .... p 2221 N95-28102
AD-A289128 .... p 2182 N95-27142
AD-A289131 .... p 2295 N95-26996
AD-A289134 .... p 2141 N95-26555
AD-A289137 .... p 2438 N95-26997
AD-A289145 .... p 2277 N95-26998
AD-A289146 .... p 2277 N95-26999
AD-A289147 .... p 2277 N95-27000
AD-A289148 .... p 2278 N95-27001
AD-A289149 .... p 2261 N95-27002
AD-A289150 .... p 2138 N95-27003
AD-A289151 .... p 2453 N95-27004
AD-A289152 .... p 2253 N95-27005
AD-A289153 .... p 2370 N95-27031
AD-A289156 .... p 2213 N95-27032
AD-A289164 .... p 2347 N95-27011
AD-A289172 .... p 2358 N95-26612
AD-A289173 .... p 2356 N95-27012
AD-A289174 .... p 2143 N95-26556
AD-A289175 .... p 2356 N95-27013
AD-A289180 .... p 2453 N95-27014
AD-A289181 .... p 2261 N95-27015
AD-A289185 .... p 2395 N95-27016
AD-A289187 .... p 2405 N95-27017
AD-A289190 .... p 2130 N95-27018
AD-A289194 .... p 2278 N95-27019
AD-A289197 .... p 2390 N95-27020
AD-A289199 .... p 2254 N95-27021
AD-A289202 .... p 2253 N95-27006
AD-A289203 .... p 2381 N95-27007
AD-A289204 .... p 2254 N95-27008
AD-A289206 .... p 2254 N95-27009
AD-A289207 .... p 2254 N95-27079
AD-A289208 .... p 2277 N95-26986
AD-A289209 .... p 2163 N95-26987
AD-A289211 .... p 2253 N95-26988
AD-A289212 .... p 2290 N95-26989
AD-A289215 .... p 2381 N95-26990
AD-A289216 .... p 2354 N95-26991
AD-A289218 .... p 2438 N95-27061
AD-A289220 .... p 2141 N95-26957
AD-A289221 .... p 2141 N95-26958
AD-A289222 .... p 2438 N95-26959
AD-A289224 .... p 2404 N95-26960
AD-A289226 .... p 2295 N95-26961
AD-A289234 .... p 2369 N95-26962
AD-A289236 .... p 2163 N95-26963
AD-A289238 .... p 2261 N95-26964
AD-A289240 .... p 2424 N95-26965
AD-A289243 .... p 2253 N95-26976
AD-A289246 .... p 2143 N95-26966
AD-A289247 .... p 2181 N95-26967
AD-A289248 .... p 2277 N95-26968
AD-A289250 .... p 2182 N95-26969
AD-A289251 .... p 2163 N95-26970
AD-A289252 .... p 2424 N95-26971
AD-A289254 .... p 2252 N95-26972
AD-A289255 .... p 2227 N95-26973
AD-A289256 .... p 2295 N95-26974
AD-A289258 .... p 2308 N95-26975
AD-A289260 .... p 2253 N95-26977
AD-A289262 .... p 2279 N95-27197
AD-A289263 .... p 2127 N95-26978
AD-A289266 .... p 2404 N95-26979
AD-A289268 .... p 2163 N95-26980
AD-A289271 .... p 2142 N95-26981
AD-A289275 .... p 2290 N95-26982
AD-A289277 .... p 2253 N95-26983
AD-A289278 .... p 2377 N95-26984
AD-A289280 .... p 2127 N95-26985
AD-A289281 .... p 2146 N95-27033
AD-A289282 .... p 2405 N95-27034
AD-A289285 .... p 2146 N95-27035
AD-A289288 .... p 2142 N95-27036
AD-A289289 .... p 2370 N95-27037
AD-A289293 .... p 2425 N95-27038
AD-A289295 .... p 2354 N95-27039
AD-A289296 .... p 2438 N95-27040
AD-A289297 .... p 2381 N95-27041
AD-A289299 .... p 2359 N95-27046
AD-A289300 .... p 2387 N95-28217
AD-A289301 .... p 2131 N95-27042
AD-A289303 .... p 2353 N95-26917
AD-A289304 .... p 2162 N95-26918
AD-A289305 .... p 2369 N95-26919
AD-A289306 .... p 2381 N95-26920
AD-A289307 .... p 2261 N95-26921
AD-A289309 .... p 2162 N95-26916
AD-A289310 .... p 2319 N95-26891
AD-A289312 .... p 2394 N95-26892
AD-A289313 .... p 2406 N95-27399
AD-A289315 .... p 2386 N95-27400
AD-A289316 .... p 2382 N95-27293
AD-A289317 .... p 2264 N95-27294
AD-A289318 .... p 2203 N95-27295
AD-A289321 .... p 2461 N95-27303
AD-A289322 .... p 2264 N95-27296
AD-A289323 .... p 2144 N95-27297
AD-A289324 .... p 2251 N95-26893
AD-A289325 .... p 2368 N95-26895
AD-A289326 .... p 2202 N95-26896
AD-A289327 .... p 2227 N95-26897
AD-A289328 .... p 2127 N95-26898
AD-A289329 .... p 2342 N95-26899
AD-A289331 .... p 2347 N95-27043
AD-A289332 .... p 2424 N95-26900
AD-A289334 .... p 2122 N95-26901
AD-A289335 .... p 2162 N95-26902
AD-A289336 .... p 2242 N95-26842
AD-A289337 .... p 2359 N95-26737
AD-A289338 .... p 2389 N95-26772
AD-A289340 .... p 2260 N95-26767
AD-A289341 .... p 2275 N95-26751
AD-A289342 .... p 2452 N95-26752
AD-A289343 .... p 2336 N95-26753
AD-A289344 .... p 2254 N95-27062
AD-A289345 .... p 2453 N95-27063
AD-A289347 .... p 2450 N95-27064
AD-A289349 .... p 2278 N95-27065
AD-A289352 .... p 2382 N95-27066
AD-A289353 .... p 2262 N95-27067
AD-A289354 .... p 2454 N95-27529
AD-A289356 .... p 2439 N95-27416
AD-A289357 .... p 2395 N95-27417 *
AD-A289358 .... p 2371 N95-27418
AD-A289360 .... p 2391 N95-27489
AD-A289361 .... p 2367 N95-26754
AD-A289363 .... p 2388 N95-26903
AD-A289368 .... p 2346 N95-26904
AD-A289370 .... p 2308 N95-26905
AD-A289373 .... p 2295 N95-26906
AD-A289374 .... p 2233 N95-27324
AD-A289375 .... p 2122 N95-26875
AD-A289376 .... p 2130 N95-26876
AD-A289377 .... p 2233 N95-27325
AD-A289378 .... p 2251 N95-26877
AD-A289379 .... p 2139 N95-26878
AD-A289386 .... p 2359 N95-26863
AD-A289391 .... p 2453 N95-26864
AD-A289392 .... p 2453 N95-26879
AD-A289393 .... p 2167 N95-26880
AD-A289395 .... p 2368 N95-26881
AD-A289397 .... p 2389 N95-26882
AD-A289398 .... p 2359 N95-26883
AD-A289399 .... p 2359 N95-26884 *
AD-A289400 .... p 2353 N95-26885
AD-A289404 .... p 2301 N95-27098
AD-A289405 .... p 2360 N95-27099
AD-A289406 .... p 2350 N95-27100
AD-A289409 .... p 2461 N95-27131
AD-A289413 .... p 2295 N95-27132
AD-A289414 .... p 2144 N95-27133
AD-A289418 .... p 2182 N95-27134
AD-A289420 .... p 2309 N95-27135
AD-A289421 .... p 2164 N95-27144
AD-A289422 .... p 2382 N95-27145
AD-A289423 .... p 2181 N95-26886
AD-A289424 .... p 2162 N95-26887
AD-A289425 .... p 2181 N95-26865
AD-A289426 .... p 2453 N95-26866
AD-A289429 .... p 2251 N95-26867
AD-A289430 .... p 2181 N95-26868
AD-A289431 .... p 2251 N95-26869
AD-A289434 .... p 2252 N95-26923
AD-A289437 .... p 2252 N95-26924
AD-A289439 .... p 2337 N95-27146
AD-A289442 .... p 2337 N95-27147
AD-A289447 .... p 2295 N95-27172
AD-A289448 .... p 2295 N95-27022
AD-A289456 .... p 2356 N95-26992
AD-A289457 .... p 2130 N95-26993
AD-A289458 .... p 2130 N95-26994
AD-A289459 .... p 2167 N95-27153
AD-A289466 .... p 2342 N95-27148
AD-A289467 .... p 2255 N95-27149
AD-A289468 .... p 2347 N95-27151
AD-A289471 .... p 2276 N95-26819
AD-A289474 .... p 2368 N95-26820
AD-A289475 .... p 2276 N95-26821
AD-A289477 .... p 2276 N95-26822
AD-A289478 .... p 2401 N95-26925
AD-A289479 .... p 2301 N95-26926
AD-A289480 .... p 2306 N95-26927
AD-A289483 .... p 2466 N95-26823
AD-A289490 .... p 2336 N95-26824
AD-A289491 .... p 2356 N95-26825
AD-A289492 .... p 2342 N95-26826
AD-A289498 .... p 2276 N95-26827
AD-A289502 .... p 2356 N95-26843
AD-A289503 .... p 2130 N95-26844
AD-A289504 .... p 2162 N95-26850
AD-A289507 .... p 2368 N95-26853
AD-A289508 .... p 2121 N95-26854
AD-A289510 .... p 2278 N95-27047
AD-A289511 .... p 2361 N95-26845
AD-A289512 .... p 2318 N95-26846
AD-A289518 .... p 2181 N95-26847
AD-A289519 .... p 2181 N95-26848
AD-A289521 .... p 2251 N95-26851
AD-A289531 .... p 2276 N95-26852
AD-A289532 .... p 2201 N95-26870
AD-A289533 .... p 2251 N95-26871
AD-A289534 .... p 2438 N95-26872
AD-A289540 .... p 2130 N95-26873
AD-A289545 .... p 2294 N95-26874
AD-A289547 .... p 2359 N95-26755
AD-A289550 .... p 2437 N95-26756
AD-A289551 .... p 2140 N95-28646
AD-A289552 .... p 2262 N95-27152
AD-A289553 .... p 2121 N95-26757
AD-A289554 .... p 2201 N95-26678
AD-A289558 .... p 2352 N95-26680
AD-A289561 .... p 2355 N95-26683
AD-A289562 .... p 2129 N95-26684
AD-A289567 .... p 2375 N95-28647
AD-A289573 .... p 2180 N95-26686
AD-A289574 .... p 2418 N95-28648
AD-A289576 .... p 2398 N95-26687
AD-A289577 .... p 2301 N95-26688
AD-A289579 .... p 2260 N95-26690
AD-A289583 .... p 2355 N95-26691
AD-A289587 .... p 2355 N95-26692
AD-A289590 .... p 2120 N95-26713
AD-A289592 .... p 2290 N95-26714
AD-A289593 .... p 2162 N95-26715
AD-A289594 .... p 2260 N95-26716
AD-A289597 .... p 2250 N95-26717
AD-A289598 .... p 2312 N95-28649
AD-A289600 .... p 2274 N95-26718
AD-A289601 .... p 2121 N95-26719
AD-A289602 .... p 2429 N95-26720
AD-A289603 .... p 2452 N95-26721
AD-A289604 .... p 2300 N95-28650
AD-A289607 .... p 2201 N95-26707
AD-A289610 .... p 2312 N95-28616
AD-A289612 .... p 2402 N95-28671
AD-A289614 .... p 2368 N95-26855
AD-A289618 .... p 2466 N95-26856
AD-A289622 .... p 2401 N95-26857
AD-A289629 .... p 2336 N95-26858
AD-A289631 .... p 2121 N95-26859
AD-A289634 .... p 2424 N95-26860
AD-A289635 .... p 2246 N95-26722
AD-A289637 .... p 2341 N95-26723
AD-A289639 .... p 2428 N95-28617
AD-A289641 .... p 2342 N95-26724
AD-A289644 .... p 2402 N95-28622
AD-A289647 .... p 2300 N95-28633
AD-A289652 .... p 2243 N95-28634
AD-A289654 .... p 2250 N95-26725
AD-A289655 .... p 2375 N95-28635
AD-A289656 .... p 2452 N95-26758
AD-A289672 .... p 2250 N95-26759
AD-A289678 .... p 2350 N95-26761
AD-A289683 .... p 2316 N95-26762
AD-A289691 .... p 2353 N95-26763
AD-A289708 .... p 2250 N95-26738
AD-A289712 .... p 2288 N95-28571 *
AD-A289771 .... p 2142 N95-28598
AD-A289818 .... p 2417 N95-28572
AD-A289819 .... p 2258 N95-28573
AD-A289821 .... p 2241 N95-28574
AD-A289824 .... p 2339 N95-28575
AD-A289827 .... p 2258 N95-28576
AD-A289829 .... p 2344 N95-28577
AD-A289830 .... p 2120 N95-28610
AD-A289835 .... p 2165 N95-28578
AD-A289836 .... p 2400 N95-28579
AD-A289838 .... p 2258 N95-28580
AD-A289841 .... p 2447 N95-28618
AD-A289842 .... p 2289 N95-28619
AD-A289843 .... p 2241 N95-28620
AD-A289847 .... p 2210 N95-28621
AD-A289852 .... p 2332 N95-28623
AD-A289869 .... p 2259 N95-28624
AD-A289872 .... p 2374 N95-28625
AD-A289891 .... p 2136 N95-28626
AD-A289912 .... p 2374 N95-28627 *

AD-A289928 .... p 2375 N95-28628
AD-A289929 .... p 2271 N95-28629
AD-A289986 .... p 2126 N95-28630
AD-A289998 .... p 2352 N95-28519
AD-A290013 .... p 2269 N95-28388
AD-A290040 .... p 2293 N95-28389
AD-A290076 .... p 2361 N95-28390
AD-A290133 .... p 2256 N95-28391
AD-A290167 .... p 2315 N95-28392
AD-A291598 .... p 2355 N95-28561
AD-A291611 .... p 2427 N95-28408
AD-A291614 .... p 2136 N95-28409
AD-A291624 .... p 2294 N95-28410
AD-A291628 .... p 2136 N95-28411
AD-A291630 .... p 2270 N95-28544
AD-A291632 .... p 2387 N95-28545
AD-A291633 .... p 2352 N95-28546
AD-A291638 .... p 2271 N95-28666
AD-A291662 .... p 2361 N95-28667
AD-A291663 .... p 2257 N95-28453
AD-A291666 .... p 2126 N95-28454
AD-A291668 .... p 2257 N95-28455
AD-A291671 .... p 2257 N95-28456
AD-A291673 .... p 2436 N95-28668
AD-A291681 .... p 2240 N95-28457
AD-A291683 .... p 2387 N95-28461
AD-A291684 .... p 2300 N95-28458
AD-A291691 .... p 2446 N95-28522
AD-A291696 .... p 2288 N95-28523
AD-A291700 .... p 2427 N95-28524
AD-A291704 .... p 2352 N95-28525
AD-A291712 .... p 2395 N95-28526
AD-A291714 .... p 2136 N95-28504
AD-A291715 .... p 2402 N95-28505
AD-A291717 .... p 2393 N95-28507
AD-A291721 .... p 2240 N95-28508
AD-A291723 .... p 2300 N95-28509
AD-A291725 .... p 2395 N95-28510
AD-A291727 .... p 2270 N95-28512
AD-A291735 .... p 2387 N95-28527
AD-A291748 .... p 2257 N95-28528
AD-A291767 .... p 2270 N95-28529
AD-A291775 .... p 2344 N95-28459
AD-A291785 .... p 2257 N95-28513

AD-D017251 .... p 2129 N95-26537
AD-D017257 .... p 2248 N95-26465
AD-D017258 .... p 2245 N95-26500
AD-D017261 .... p 2400 N95-26502
AD-D017262 .... p 2294 N95-26503
AD-D017263 .... p 2300 N95-26504
AD-D017264 .... p 2248 N95-26505
AD-D017265 .... p 2128 N95-26507
AD-D017267 .... p 2245 N95-26508
AD-D017269 .... p 2161 N95-28581
AD-D017271 .... p 2249 N95-26509
AD-D017272 .... p 2241 N95-28582
AD-D017385 .... p 2210 N95-28584
AD-D017387 .... p 2210 N95-28585
AD-D017390 .... p 2294 N95-28612
AD-D017392 .... p 2271 N95-28613
AD-D017394 .... p 2271 N95-28614
AD-D017398 .... p 2258 N95-28615

AEDC-TR-94-16 .... p 2427 N95-28408

AF-AFOSR-0763-94-TR .... p 2348 N95-26360

AFCESA-ETL-94-9 .... p 2241 N95-28620

AFIT/CI/CIA/94-038D .... p 2363 N95-26408
AFIT/CI/CIA/94-039D .... p 2295 N95-27172
AFIT/CI/CIA/94-136 .... p 2128 N95-26481
AFIT/CI/CIA/94-138 .... p 2334 N95-26488
AFIT/CI/CIA/94-144 .... p 2255 N95-27149
AFIT/CI/CIA/94-145 .... p 2355 N95-26683
AFIT/CI/CIA/94-146 .... p 2359 N95-26883
AFIT/CI/CIA/94-152 .... p 2295 N95-27132
AFIT/CI/CIA/94-155 .... p 2453 N95-26879
AFIT/CI/CIA/94-159 .... p 2142 N95-28598
AFIT/CI/CIA/94-161 .... p 2400 N95-28579

AFIT/GA/ENY/94D-10 .... p 2277 N95-26968
AFIT/GA/ENY/94D-1 .... p 2143 N95-26966
AFIT/GA/ENY/94D-20 .... p 2276 N95-26819
AFIT/GA/ENY/94D-2 .... p 2163 N95-26970
AFIT/GA/ENY/94D-3 .... p 2167 N95-26880
AFIT/GA/ENY/94D-4 .... p 2308 N95-26905
AFIT/GA/ENY/94D-5 .... p 2278 N95-27065
AFIT/GA/ENY/94D-6 .... p 2162 N95-26918
AFIT/GA/ENY/94D-7 .... p 2167 N95-27153
AFIT/GA/ENY/94D-8 .... p 2142 N95-27036
AFIT/GA/ENY/94D-9 .... p 2163 N95-26980

AFIT/GAE/ENY/94D-01 .... p 2386 N95-27400
AFIT/GAE/ENY/94D-02 .... p 2308 N95-26975
AFIT/GAE/ENY/94D-10 .... p 2276 N95-26822
AFIT/GAE/ENY/94D-11 .... p 2130 N95-26844
AFIT/GAE/ENY/94D-13 .... p 2139 N95-26878
AFIT/GAE/ENY/94D-14 .... p 2122 N95-26901
AFIT/GAE/ENY/94D-15 .... p 2181 N95-26886
AFIT/GAE/ENY/94D-16 .... p 2182 N95-27134
AFIT/GAE/ENY/94D-17 .... p 2122 N95-26875
AFIT/GAE/ENY/94D-19 .... p 2276 N95-26821
AFIT/GAE/ENY/94D-22 .... p 2309 N95-27135
AFIT/GAE/ENY/94D-3 .... p 2381 N95-26920
AFIT/GAE/ENY/94D-5 .... p 2181 N95-26868
AFIT/GAE/ENY/94D-7 .... p 2181 N95-26865
AFIT/GAE/ENY/94D-9 .... p 2182 N95-26969

AFIT/GAP/EN/94D-4 .... p 2404 N95-26979

AFIT/GAP/ENP/94D-02 .... p 2202 N95-26896
AFIT/GAP/ENP/94D-05 .... p 2406 N95-27399
AFIT/GAP/ENP/94D-06 .... p 2319 N95-26891
AFIT/GAP/ENP/94D-10 .... p 2295 N95-26961
AFIT/GAP/ENP/94D-11 .... p 2203 N95-27295
AFIT/GAP/ENP/94D-3 .... p 2264 N95-27296

AFIT/GCA/LAS/94S-4 .... p 2374 N95-28588

AFIT/GCE/ENG/94D-01 .... p 2382 N95-27293
AFIT/GCE/ENG/94D-02 .... p 2395 N95-27016

AFIT/GCS/ENC/94D-01 .... p 2242 N95-26842

AFIT/GCS/ENG/94D-01 .... p 2381 N95-27007
AFIT/GCS/ENG/94D-02 .... p 2130 N95-26876
AFIT/GCS/ENG/94D-03 .... p 2369 N95-26919
AFIT/GCS/ENG/94D-06 .... p 2359 N95-26737
AFIT/GCS/ENG/94D-10 .... p 2264 N95-27294
AFIT/GCS/ENG/94D-11 .... p 2368 N95-26895
AFIT/GCS/ENG/94D-18 .... p 2370 N95-27037
AFIT/GCS/ENG/94D-21 .... p 2359 N95-27046
AFIT/GCS/ENG/94D-23 .... p 2461 N95-27131
AFIT/GCS/ENG/94D-24 .... p 2369 N95-26962
AFIT/GCS/ENG/94D-25 .... p 2377 N95-26984
AFIT/GCS/ENG/94D-27 .... p 2453 N95-26866

AFIT/GE/ENG-94D-25 .... p 2260 N95-26767

AFIT/GE/ENG/94D-02 .... p 2253 N95-26988
AFIT/GE/ENG/94D-03 .... p 2354 N95-27039
AFIT/GE/ENG/94D-04 .... p 2381 N95-26990
AFIT/GE/ENG/94D-05 .... p 2251 N95-26869
AFIT/GE/ENG/94D-06 .... p 2131 N95-27042
AFIT/GE/ENG/94D-07 .... p 2251 N95-26877
AFIT/GE/ENG/94D-09 .... p 2127 N95-26898
AFIT/GE/ENG/94D-10 .... p 2290 N95-26989
AFIT/GE/ENG/94D-11 .... p 2394 N95-26892
AFIT/GE/ENG/94D-12 .... p 2254 N95-27062
AFIT/GE/ENG/94D-13 .... p 2127 N95-26985
AFIT/GE/ENG/94D-14 .... p 2162 N95-26916
AFIT/GE/ENG/94D-15 .... p 2424 N95-26971
AFIT/GE/ENG/94D-16 .... p 2254 N95-27079
AFIT/GE/ENG/94D-18 .... p 2141 N95-26957
AFIT/GE/ENG/94D-21 .... p 2382 N95-27145
AFIT/GE/ENG/94D-22 .... p 2254 N95-27009
AFIT/GE/ENG/94D-24 .... p 2141 N95-26958
AFIT/GE/ENG/94D-27 .... p 2354 N95-26991
AFIT/GE/ENG/94D-28 .... p 2253 N95-26976
AFIT/GE/ENG/94D-29 .... p 2336 N95-26824
AFIT/GE/ENG/94D-30 .... p 2142 N95-26981
AFIT/GE/ENG/94D-31 .... p 2252 N95-26972
AFIT/GE/ENG/94D-32 .... p 2251 N95-26867
AFIT/GE/ENG/94D-33 .... p 2250 N95-26738
AFIT/GE/ENG/94D-34 .... p 2251 N95-26893

AFIT/GEO/ENG/94D-03 .... p 2353 N95-26917
AFIT/GEO/ENG/94D-04 .... p 2295 N95-26974
AFIT/GEO/ENG/94D-04 .... p 2277 N95-26986

AFIT/GEO/ENP/94D-01 .... p 2227 N95-26897
AFIT/GEO/ENP/94D-02 .... p 2261 N95-26921
AFIT/GEO/ENP/94D-02 .... p 2163 N95-26963
AFIT/GEO/ENP/94D-03 .... p 2424 N95-26965

AFIT/GIR/LAR/94D-2 .... p 2374 N95-28590
AFIT/GIR/LAR/94D-3 .... p 2456 N95-28587
AFIT/GIR/LAR/94D-6 .... p 2360 N95-27195

AFIT/GSO/ENG/94D-01 .... p 2254 N95-27008
AFIT/GSO/ENG/94D-02 .... p 2163 N95-26987

AFIT/GSO/ENS/94D-01 .... p 2146 N95-27033
AFIT/GSO/ENS/94D-06 .... p 2130 N95-26873
AFIT/GSO/ENS/94D-13 .... p 2146 N95-27035
AFIT/GSO/ENS/94D-14 .... p 2144 N95-27133
AFIT/GSO/ENS/94D-15 .... p 2164 N95-27144

AFIT/GSO/ENY/94D-01 .... p 2461 N95-27303
AFIT/GSO/ENY/94D-2 .... p 2162 N95-26887
AFIT/GSS/LAR/94D-1 .... p 2371 N95-27251
AFIT/GSS/LAR/94D-2 .... p 2374 N95-28591
AFIT/GSS/LAR/94D-3 .... p 2138 N95-28586

AFOSR-94-0677TR .... p 2380 N95-26530
AFOSR-94-0678TR .... p 2199 N95-26416
AFOSR-94-0679TR .... p 2201 N95-26606
AFOSR-94-0683TR .... p 2178 N95-26570
AFOSR-94-0685TR .... p 2436 N95-26473
AFOSR-94-0687TR .... p 2125 N95-27186
AFOSR-94-0691TR .... p 2199 N95-26417
AFOSR-94-0693TR .... p 2466 N95-26604
AFOSR-94-0694TR .... p 2226 N95-26623
AFOSR-94-0694TR .... p 2226 N95-26624
AFOSR-94-0695TR .... p 2201 N95-26544
AFOSR-94-0701TR .... p 2180 N95-26626
AFOSR-94-0750TR .... p 2394 N95-26733
AFOSR-94-0751TR .... p 2404 N95-26632
AFOSR-94-0752TR .... p 2353 N95-26770
AFOSR-94-0753TR .... p 2403 N95-26466
AFOSR-94-0755TR .... p 2254 N95-27060
AFOSR-94-0759TR .... p 2380 N95-26480
AFOSR-94-0760TR .... p 2273 N95-26405
AFOSR-94-0761TR .... p 2436 N95-26462
AFOSR-94-0762TR .... p 2404 N95-26574

AFPT-90-901-961 .... p 2353 N95-26763

AGARD-CP-550 .... p 2131 N95-27504 #

AGARD-MEMB-95 .... p 2450 N95-26353 #

AIAA PAPER 94-1445 .... p 2309 N95-27174 * #
AIAA PAPER 94-2965 .... p 2273 N95-26380 * #
AIAA PAPER 94-3311 .... p 2168 N95-27862 * #
AIAA PAPER 95-1754 .... p 2389 N95-26663 * #
AIAA PAPER 95-1880 .... p 2125 N95-27762 * #
AIAA PAPER 95-2554 .... p 2291 N95-27030 * #
AIAA PAPER 95-2681 .... p 2143 N95-27176 * #
AIAA PAPER 95-3046 .... p 2302 N95-27698 * #
AIAA PAPER 95-3048 .... p 2302 N95-27855 * #
AIAA PAPER 95-364 .... p 2168 N95-27861 * #

AIM-1474 .... p 2387 N95-28461

AL/CF-TR-1994-0043 .... p 2355 N95-28561
AL/CF-TR-1994-0115 .... p 2262 N95-27196

AL/HR-TP-1994-0023 .... p 2359 N95-26863

ANL/CHM/CP-83289 .... p 2238 N95-28235 #
ANL/CHM/CP-83631 .... p 2409 N95-27753 #
ANL/CHM/CP-85152 .... p 2219 N95-27966 #
ANL/CHM/CP-85153 .... p 2408 N95-27453 #

ANL/CHM/PP-80411 .... p 2234 N95-27455 #
ANL/CHM/PP-80412 .... p 2218 N95-27752 #
ANL/CHM/PP-80864 .... p 2351 N95-27948 #

ANL/CMT/CP-85560 .... p 2440 N95-27542 #

ANL/ESH/VU-85484 .... p 2256 N95-28407 #

ANL/ET/CP-83155 .... p 2183 N95-28068 #
ANL/ET/CP-85762 .... p 2183 N95-28069 #

ANL/FPP/TM-274 .... p 2434 N95-28224 #

ANL/HEP/CP-94-52 .... p 2449 N95-27449 #
ANL/HEP/CP-94-81 .... p 2415 N95-28210 #
ANL/HEP/CP-94-92 .... p 2449 N95-27448 #

ANL/IPNS/CP-83321 .... p 2439 N95-27452 #
ANL/IPNS/CP-85110 .... p 2237 N95-27967

ANL/ITD/CP-85767 .... p 2303 N95-28070 #

ANL/MCS-TM-193 .... p 2378 N95-28071 #
ANL/MCS-TM-202 .... p 2392 N95-28173 #

ANL/MCS/CP-84764 .... p 2376 N95-26441 #
ANL/MCS/CP-85720 .... p 2378 N95-27741 #

ANL/MCS/PP-80304 .... p 2284 N95-27454 #

ANL/MSD/CP-83324 .... p 2442 N95-27950 #
ANL/MSD/CP-83327 .... p 2438 N95-27085 #
ANL/MSD/CP-83380 .... p 2441 N95-27928 #
ANL/MSD/CP-83383 .... p 2220 N95-28072 #
ANL/MSD/CP-83453 .... p 2223 N95-28543 #
ANL/MSD/CP-84783 .... p 2436 N95-26440 #
ANL/MSD/CP-84837 .... p 2436 N95-26442 #
ANL/MSD/CP-85241 .... p 2208 N95-27965 #
ANL/MSD/CP-85268 .... p 2411 N95-28004 #
ANL/MSD/CP-85324 .... p 2206 N95-27755 #

ANL/PHY/CP-85173 ..... p 2434 N95-28233 #
ANL/PHY/CP-85306 ..... p 2442 N95-27963 #
ANL/PHY/CP-85493 ..... p 2392 N95-27742 #

ANU-PRL-TR-94/1 ..... p 2256 N95-28254 #

APL-UW-TR-9412 ..... p 2346 N95-26533 *

AR-008-374 ..... p 2139 N95-26424
AR-008-418 ..... p 2136 N95-28567
AR-008-582 ..... p 2259 N95-26425
AR-008-973 ..... p 2258 N95-28568
AR-009-193 ..... p 2128 N95-26389
AR-009-201 ..... p 2142 N95-26378
AR-009-202 ..... p 2136 N95-27918

ARAP-710 ..... p 2341 N95-26546

ARCCB-TR-94033 ..... p 2389 N95-26609

ARL-CR-143 ..... p 2360 N95-27099

ARL-MR-211 ..... p 2182 N95-27142

ARL-TR-273 ..... p 2340 N95-26463
ARL-TR-284 ..... p 2341 N95-26650
ARL-TR-387 ..... p 2260 N95-26690
ARL-TR-527 ..... p 2249 N95-26562
ARL-TR-610 ..... p 2179 N95-26565
ARL-TR-620 ..... p 2223 N95-28189
ARL-TR-633 ..... p 2376 N95-26460
ARL-TR-650 ..... p 2399 N95-27398
ARL-TR-661 ..... p 2418 N95-28648
ARL-TR-667 ..... p 2374 N95-28625
ARL-TR-687 ..... p 2201 N95-26678
ARL-TR-723 ..... p 2302 N95-27855 * #
ARL-TR-761 ..... p 2302 N95-27373 * #
ARL-TR-764 ..... p 2302 N95-27698 * #

ARM-95-001 ..... p 2344 N95-28340 #

ARO-21781.10-EG ..... p 2288 N95-28523
ARO-227538.12-EG ..... p 2200 N95-26451
ARO-27863.14-MS ..... p 2240 N95-28457
ARO-28052.1-GS ..... p 2300 N95-28509
ARO-28192.22-MA ..... p 2376 N95-26471
ARO-28309.9-MA ..... p 2393 N95-28507
ARO-28326.30-EL-JSEP ..... p 2345 N95-26419
ARO-28339.9-EL ..... p 2270 N95-28529
ARO-28377.11-MA ..... p 2307 N95-26547
ARO-28472.11-PH ..... p 2300 N95-28458
ARO-28483.28-EL ..... p 2257 N95-28513
ARO-28493.1-EG ..... p 2136 N95-28504
ARO-28511.27-MA ..... p 2380 N95-26468
ARO-28514.1-MA ..... p 2448 N95-26563
ARO-28591.8-PH ..... p 2402 N95-28505
ARO-28599.3-GS ..... p 2200 N95-26452
ARO-28599.4-GS ..... p 2200 N95-26422
ARO-28689.4-MA-SDI ..... p 2395 N95-28510
ARO-28715.17-MA ..... p 2395 N95-28526
ARO-28746.4-MS-SM ..... p 2257 N95-28456
ARO-28925.166-ELJSEP ..... p 2270 N95-28512
ARO-29097.3-LS ..... p 2348 N95-26573
ARO-29194.9-LS ..... p 2352 N95-28525
ARO-29227.16-CH ..... p 2200 N95-26528
ARO-29369.5-GS ..... p 2341 N95-26546
ARO-29404.1-GS ..... p 2257 N95-28528
ARO-29647.3-MS ..... p 2225 N95-26561
ARO-30419.1-EG-SDI ..... p 2429 N95-26800
ARO-30627.1-RT-NDF ..... p 2446 N95-28522
ARO-30921.21-EL ..... p 2257 N95-28453
ARO-31003.1-MA-SDI ..... p 2387 N95-28527
ARO-32557.1-PH-CF ..... p 2352 N95-28546
ARO-33469.1-MS-CF ..... p 2240 N95-28508

ASC-TR-94-1022 ..... p 2121 N95-26854
ASC-TR-94-5030 ..... p 2356 N95-27012

ASME-95-367 ..... p 2167 N95-27177 * #

B-256707 ..... p 2118 N95-26817 #
B-258872 ..... p 2342 N95-27912 #
B-259389 ..... p 2135 N95-27910 #
B-260868 ..... p 2145 N95-27856 #
B-345 ..... p 2326 N95-26362 * #

BARC-1993/E/021 ..... p 2406 N95-27212 #
BARC-1994/E/004 ..... p 2405 N95-27159 #
BARC-1994/E/007 ..... p 2214 N95-27255 #
BARC-1994/P/003 ..... p 2203 N95-27200 #

BBC-RD-1994/16 ..... p 2248 N95-26493
BBC-RD-1994/17 ..... p 2249 N95-26670
BBC-RD-1994/18 ..... p 2249 N95-26696

BC-ISR-95-01 ..... p 2165 N95-28578

BFLRF-290 ..... p 2210 N95-28621

BNL-60349 ..... p 2265 N95-27554 #
BNL-60350 ..... p 2270 N95-28515 #
BNL-60352 ..... p 2269 N95-28339 #
BNL-60429 ..... p 2445 N95-28186 #
BNL-60717 ..... p 2445 N95-28165 #
BNL-60902-REV-11/94 ..... p 2425 N95-27490 #
BNL-61140 ..... p 2409 N95-27552 #
BNL-61143 ..... p 2217 N95-27553 #
BNL-61193 ..... p 2416 N95-28338 #
BNL-61239 ..... p 2240 N95-28547 #
BNL-61260 ..... p 2215 N95-27462 #
BNL-61283 ..... p 2315 N95-28520 #
BNL-61291 ..... p 2421 N95-28017 #
BNL-61312 ..... p 2440 N95-27535 #
BNL-61315 ..... p 2292 N95-27738 #
BNL-61316 ..... p 2292 N95-27677 #
BNL-61317 ..... p 2420 N95-27484 #
BNL-61321 ..... p 2325 N95-28517 #
BNL-61324 ..... p 2320 N95-27682 #
BNL-61328 ..... p 2269 N95-28244 #
BNL-61332 ..... p 2426 N95-28196 #
BNL-61378 ..... p 2416 N95-28355 #
BNL-61391 ..... p 2222 N95-28166 #
BNL-61393 ..... p 2439 N95-27443 #
BNL-61410 ..... p 2422 N95-28195 #
BNL-61420 ..... p 2422 N95-28115 #
BNL-61427 ..... p 2331 N95-28121 #
BNL-61459 ..... p 2442 N95-27932 #
BNL-61487 ..... p 2414 N95-28170 #
BNL-61490 ..... p 2414 N95-28169 #

BUDKERINP-93-53 ..... p 2407 N95-27407 #
BUDKERINP-93-54 ..... p 2407 N95-27408 #
BUDKERINP-93-88 ..... p 2407 N95-27411 #
BUDKERINP-94-30 ..... p 2407 N95-27412 #
BUDKERINP-94-3 ..... p 2407 N95-27410 #

CAL-2314 ..... p 2465 N95-26630 * #

CALT-68-1952 ..... p 2407 N95-27409 #

CAR-TR-725 ..... p 2356 N95-26843
CAR-TR-742 ..... p 2394 N95-26478

CARDIVNSWC-TR-1 ..... p 2180 N95-26686
CARDIVNSWC-TR-61-CR-94/05 . p 2311 N95-28100

CBCL-93 ..... p 2387 N95-28461

CBP-107 ..... p 2296 N95-27674 #

CCMS-95-04 ..... p 2310 N95-27865 * #

CEAS/AIAA-95-171 ..... p 2401 N95-26801 * #

CERC-IA-95-001 ..... p 2362 N95-26386 * #

CERC-TR-RN-94-001 ..... p 2365 N95-26575 * #
CERC-TR-RN-94-009 ..... p 2366 N95-26711 * #
CERC-TR-RN-94-010 ..... p 2371 N95-27252 * #
CERC-TR-RN-94-012 ..... p 2366 N95-26693 * #
CERC-TR-RN-94-013 ..... p 2367 N95-26802 * #
CERC-TR-RN-94-014 ..... p 2363 N95-26388 * #

CERC-TR-TM-012 ..... p 2366 N95-26695 * #
CERC-TR-TM-94-007 ..... p 2364 N95-26486 * #
CERC-TR-TM-94-008 ..... p 2367 N95-26814 * #
CERC-TR-TM-94-009 ..... p 2365 N95-26668 * #

CERL-FE-94/23 ..... p 2262 N95-27067

CERN-94-01-VOL-2 ..... p 2419 N95-27158 #
CERN-94-04-ADD ..... p 2419 N95-27321 #
CERN-94-04 ..... p 2421 N95-28040 #

CG-D-26-94 ..... p 2358 N95-26612

CGR/DC-11/94 ..... p 2358 N95-26612

CMOTT-94-9 ..... p 2285 N95-27882 * #

CMU-CS-FOX-94-09 ..... p 2389 N95-26772

CMU-CS-94-140 ..... p 2377 N95-26840
CMU-CS-94-159 ..... p 2371 N95-27418
CMU-CS-94-166 ..... p 2363 N95-26467
CMU-CS-94-183 ..... p 2363 N95-26469
CMU-CS-94-186 ..... p 2391 N95-27489
CMU-CS-94-196 ..... p 2365 N95-26656
CMU-CS-94-198 ..... p 2365 N95-26605
CMU-CS-94-204 ..... p 2370 N95-27095
CMU-CS-94-205 ..... p 2376 N95-26529
CMU-CS-94-206 ..... p 2450 N95-27064
CMU-CS-94-209 ..... p 2382 N95-27066
CMU-CS-94-211 ..... p 2453 N95-27063
CMU-CS-94-212 ..... p 2364 N95-26534
CMU-CS-94-213 ..... p 2452 N95-26535
CMU-CS-94-214 ..... p 2452 N95-26752
CMU-CS-94-216 ..... p 2454 N95-27529
CMU-CS-94-227 ..... p 2389 N95-26772

CMU-RI-TR-94-25 ..... p 2301 N95-27098
CMU-RI-TR-94-26 ..... p 2424 N95-26900
CMU-RI-TR-94-27 ..... p 2301 N95-26926
CMU-RI-TR-94-28 ..... p 2425 N95-27038
CMU-RI-TR-94-33 ..... p 2359 N95-26884 *
CMU-RI-TR-94-35 ..... p 2395 N95-27417 *
CMU-RI-TR-94-37 ..... p 2367 N95-26754
CMU-RI-TR-94-39 ..... p 2356 N95-27013
CMU-RI-TR-94-43 ..... p 2381 N95-27041

CMU-94-194 ..... p 2364 N95-26536

CMU/SEI-94-TR-17 ..... p 2375 N95-28628
CMU/SEI-94-TR-18 ..... p 2377 N95-27250
CMU/SEI-94-TR-21 ..... p 2363 N95-26446
CMU/SEI-94-TR-22 ..... p 2374 N95-28627 *

CONF-9110552-ABSTS ..... p 2352 N95-28496 #
CONF-9112185 ..... p 2226 N95-26637
CONF-9112185 ..... p 2213 N95-26675 #
CONF-9112185 ..... p 2299 N95-28330 #
CONF-9208131 ..... p 2326 N95-26639 #
CONF-9209485 ..... p 2419 N95-27158 #
CONF-9309446 ..... p 2419 N95-27321 #
CONF-9309446 ..... p 2421 N95-28040 #
CONF-931108-113 ..... p 2215 N95-27473 #
CONF-9311250 ..... p 2349 N95-26597 #
CONF-940004-1 ..... p 2339 N95-28190 #
CONF-940004-2 ..... p 2339 N95-28194 #
CONF-9402112 ..... p 2398 N95-26598 #
CONF-940351-5 ..... p 2297 N95-27736
CONF-940351-6 ..... p 2420 N95-27470 #
CONF-9404123-2 ..... p 2330 N95-28118 #
CONF-940416-32 ..... p 2237 N95-27993 #
CONF-940416-33 ..... p 2268 N95-28156 #
CONF-9404162-16 ..... p 2298 N95-27876 #
CONF-9404162-17 ..... p 2256 N95-28231 #
CONF-9404198-5 ..... p 2442 N95-27963 #
CONF-9404237-1 ..... p 2372 N95-27533 #
CONF-9404245-1 ..... p 2463 N95-28558 #
CONF-940453-5 ..... p 2440 N95-27538 #
CONF-940514-18 ..... p 2409 N95-27676 #
CONF-940514-19 ..... p 2420 N95-27427 #
CONF-940514-20 ..... p 2412 N95-28063 #
CONF-9405143-9 ..... p 2215 N95-27450
CONF-9405170-9 ..... p 2410 N95-27874 #
CONF-9405198-4 ..... p 2236 N95-27962 #
CONF-9405289-1 ..... p 2428 N95-28557 #
CONF-940529-27 ..... p 2440 N95-27471 #
CONF-9405290-1 ..... p 2220 N95-28046 #
CONF-9405297-1 ..... p 2392 N95-27742 #
CONF-940552-43 ..... p 2266 N95-28015 #
CONF-940580-23-REV-1 ..... p 2433 N95-28065 #
CONF-9406176-5 ..... p 2442 N95-27959 #
CONF-940618-117 ..... p 2269 N95-28339 #
CONF-9406242-6 ..... p 2414 N95-28142 #
CONF-9406248-6 ..... p 2449 N95-27449 #
CONF-9406270-4 ..... p 2432 N95-27710 #
CONF-940630-54 ..... p 2430 N95-27308 #
CONF-9406301-1 ..... p 2330 N95-27954 #
CONF-9406308-1 ..... p 2462 N95-28062 #
CONF-9406310-1 ..... p 2407 N95-27431 #
CONF-9406311-1 ..... p 2351 N95-27725 #
CONF-940681-11 ..... p 2434 N95-28161 #
CONF-940681-8 ..... p 2420 N95-27484 #
CONF-940681-9 ..... p 2296 N95-27674 #
CONF-940706-2 ..... p 2296 N95-27550 #
CONF-9407103-34 ..... p 2217 N95-27544 #
CONF-9407123-5 ..... p 2264 N95-27403 #
CONF-9407126-3 ..... p 2431 N95-27537 #
CONF-9407128-3 ..... p 2421 N95-28017 #
CONF-940714-50 ..... p 2422 N95-28195 #
CONF-9407163-1 ..... p 2434 N95-28233 #
CONF-9407169-1 ..... p 2435 N95-28542 #
CONF-940722-32 ..... p 2410 N95-27871 #
CONF-940722-41 ..... p 2417 N95-28594 #
CONF-940722-42 ..... p 2417 N95-28495 #
CONF-940722-43 ..... p 2409 N95-27689 #
CONF-940723-33 ..... p 2334 N95-26436 #
CONF-940723-35 ..... p 2314 N95-28053 #
CONF-940731-4 ..... p 2214 N95-27088 #
CONF-940753-25 ..... p 2219 N95-27968 #
CONF-9408119-2 ..... p 2378 N95-27402 #
CONF-9408125-49 ..... p 2422 N95-28159 #
CONF-9408146-15 ..... p 2298 N95-28104 #
CONF-9408146-18 ..... p 2297 N95-27737 #
CONF-9408150-3 ..... p 2417 N95-28595 #
CONF-940816-61 ..... p 2410 N95-27872 #
CONF-940816-84 ..... p 2416 N95-28338 #

CONF-940816-85 .... p 2408 N95-27444 #
CONF-940816-86 .... p 2407 N95-27430 #
CONF-940816-87 .... p 2408 N95-27478 #
CONF-940816-89 .... p 2406 N95-27307 #
CONF-940816-90 .... p 2414 N95-28158 #
CONF-9408176-3 .... p 2432 N95-27873 #
CONF-9408182-4 .... p 2338 N95-28061 #
CONF-9408185-2 .... p 2417 N95-28447 #
CONF-9408189-4 .... p 2434 N95-28138 #
CONF-9408190 .... p 2412 N95-28028 #
CONF-9408208-1 .... p 2216 N95-27477 #
CONF-9408210-1 .... p 2222 N95-28134 #
CONF-9408211-1 .... p 2412 N95-28057 #
CONF-9408212-1 .... p 2425 N95-27539 #
CONF-9408217-2 .... p 2460 N95-28197 #
CONF-9408219-1 .... p 2447 N95-28541 #
CONF-9408221-1 .... p 2411 N95-27945 #
CONF-9408222-1 .... p 2378 N95-27741 #
CONF-940843-14 .... p 2435 N95-28596 #
CONF-940843-15 .... p 2435 N95-28553 #
CONF-940843-16 .... p 2434 N95-28140 #
CONF-9409103-14 .... p 2405 N95-27081 #
CONF-9409177-4-REV-11/94 .... p 2425 N95-27490 #
CONF-9409219-4 .... p 2449 N95-27546 #
CONF-9409219-5 .... p 2208 N95-27956 #
CONF-9409219-6 .... p 2208 N95-27961 #
CONF-9409219-7 .... p 2208 N95-27960 #
CONF-940922-4 .... p 2409 N95-27551 #
CONF-9409224 .... p 2204 N95-27438 #
CONF-9409226-4 .... p 2430 N95-27327 #
CONF-9409226-5 .... p 2462 N95-28013 #
CONF-9409257-4 .... p 2415 N95-28210 #
CONF-9409258-3 .... p 2419 N95-27091 #
CONF-9409258-4 .... p 2422 N95-28123 #
CONF-9409258-5 .... p 2422 N95-28122 #
CONF-9409258-6 .... p 2425 N95-27675 #
CONF-940926-5 .... p 2447 N95-28606 #
CONF-940926-6 .... p 2234 N95-27468 #
CONF-9409268-4 .... p 2292 N95-27738 #
CONF-9409268-6 .... p 2421 N95-27679 #
CONF-9409268-7 .... p 2292 N95-27751 #
CONF-9409269-5 .... p 2409 N95-27552 #
CONF-9409269-7 .... p 2445 N95-28240 #
CONF-9409269-8 .... p 2442 N95-27994 #
CONF-9409269-9 .... p 2449 N95-27448 #
CONF-9409293-1 .... p 2454 N95-27483 #
CONF-9409306-1 .... p 2387 N95-28536 #
CONF-9409310-1 .... p 2463 N95-28357 #
CONF-9409311-1 .... p 2373 N95-28168 #
CONF-940933-20 .... p 2416 N95-28329 #
CONF-940933-21 .... p 2434 N95-28185 #
CONF-940933-26 .... p 2431 N95-27419 #
CONF-940933-27 .... p 2431 N95-27536 #
CONF-940933-28 .... p 2431 N95-27498 #
CONF-940933-29 .... p 2431 N95-27497 #
CONF-940933-30 .... p 2430 N95-27306 #
CONF-940933-37 .... p 2435 N95-28406 #
CONF-940933-38 .... p 2433 N95-28054 #
CONF-940945-5 .... p 2217 N95-27553 #
CONF-940945-6 .... p 2216 N95-27479 #
CONF-940945-7 .... p 2408 N95-27534 #
CONF-940968-1 .... p 2443 N95-28060 #
CONF-940982-1 .... p 2204 N95-27451 #
CONF-941001-11 .... p 2302 N95-27875 #
CONF-941001-13 .... p 2415 N95-28204 #
CONF-941001-14 .... p 2445 N95-28144 #
CONF-941001-8 .... p 2436 N95-26440 #
CONF-9410114-6 .... p 2287 N95-28021 #
CONF-941013-23 .... p 2265 N95-27554 #
CONF-941013-24 .... p 2267 N95-28048 #
CONF-941013-26 .... p 2265 N95-27693 #
CONF-941013-27 .... p 2222 N95-28167 #
CONF-941013-28 .... p 2444 N95-28079 #
CONF-941013-29 .... p 2262 N95-27083 #
CONF-941013-30 .... p 2270 N95-28515 #
CONF-9410131-12 .... p 2299 N95-28223 #
CONF-941014-2 .... p 2445 N95-28186 #
CONF-9410141-7 .... p 2456 N95-28555 #
CONF-9410165-11 .... p 2413 N95-28066 #
CONF-9410165-12 .... p 2234 N95-27486 #
CONF-9410165-14 .... p 2440 N95-27487 #
CONF-9410165-9 .... p 2436 N95-26442 #
CONF-9410178-1 .... p 2237 N95-28089 #
CONF-9410213-5 .... p 2222 N95-28130 #
CONF-9410216-10 .... p 2223 N95-28208 #
CONF-9410218-7 .... p 2267 N95-28143 #
CONF-9410219-24 .... p 2454 N95-27090 #
CONF-9410243-2 .... p 2432 N95-27673 #
CONF-9410248-2 .... p 2416 N95-28355 #
CONF-9410254-4 .... p 2311 N95-28337 #
CONF-9410256-3 .... p 2246 N95-27404 #
CONF-9410278-1 .... p 2441 N95-27720 #
CONF-9410285-2 .... p 2409 N95-27747 #
CONF-9410287-2 .... p 2462 N95-27445 #
CONF-9410293-1 .... p 2223 N95-28593 #
CONF-9410294-2 .... p 2372 N95-27495 #
CONF-9410295-1 .... p 2302 N95-27875 #
CONF-9410296-1 .... p 2302 N95-27545 #
CONF-9410305-1 .... p 2422 N95-28205 #
CONF-9410306-1 .... p 2327 N95-27469 #
CONF-9410314-2 .... p 2434 N95-28141 #
CONF-9410315-1 .... p 2422 N95-28115 #
CONF-9410319-1 .... p 2240 N95-28404 #
CONF-941059-2 .... p 2235 N95-27499 #
CONF-941060-2 .... p 2421 N95-28107 #
CONF-941060-3 .... p 2292 N95-27677 #
CONF-941060-4 .... p 2415 N95-28221 #
CONF-941063-12 .... p 2265 N95-27678 #
CONF-941101-3 .... p 2433 N95-28106 #
CONF-941101-4 .... p 2431 N95-27441 #
CONF-941101-6 .... p 2432 N95-27688 #
CONF-941109-1 .... p 2267 N95-28131 #
CONF-941109-2 .... p 2320 N95-27746 #
CONF-941113-2 .... p 2373 N95-28243 #
CONF-9411137-2 .... p 2373 N95-28498 #
CONF-9411137-3 .... p 2375 N95-28632 #
CONF-9411144-4 .... p 2332 N95-28602 #
CONF-9411149-4 .... p 2131 N95-27440 #
CONF-9411151-2 .... p 2426 N95-28196 #
CONF-9411171-1 .... p 2449 N95-28137 #
CONF-9411178-1 .... p 2335 N95-26622 #
CONF-9411179-1 .... p 2234 N95-27476 #
CONF-941118-3 .... p 2273 N95-26445 #
CONF-941118-5 .... p 2393 N95-28393 #
CONF-9411198-1 .... p 2427 N95-28552 #
CONF-941128-3 .... p 2376 N95-26441 #
CONF-941129-12 .... p 2205 N95-27681 #
CONF-941129-13 .... p 2204 N95-27496 #
CONF-941129-15 .... p 2237 N95-28080 #
CONF-941129-16 .... p 2413 N95-28077 #
CONF-941129-17 .... p 2413 N95-28078 #
CONF-941144-28 .... p 2240 N95-28531
CONF-941144-29 .... p 2240 N95-28532 #
CONF-941144-30 .... p 2203 N95-27401 #
CONF-941144-40 .... p 2183 N95-27428 #
CONF-941144-41 .... p 2215 N95-27446 #
CONF-941144-44 .... p 2182 N95-27080 #
CONF-941144-45 .... p 2440 N95-27491 #
CONF-941144-46 .... p 2213 N95-27082 #
CONF-941144-48 .... p 2202 N95-27137 #
CONF-941144-49 .... p 2202 N95-27136 #
CONF-941144-50 .... p 2216 N95-27492 #
CONF-941144-51 .... p 2216 N95-27493 #
CONF-941144-55 .... p 2438 N95-27085 #
CONF-941144-56 .... p 2236 N95-27733 #
CONF-941144-57 .... p 2440 N95-27535 #
CONF-941144-58 .... p 2237 N95-27967
CONF-941144-59 .... p 2219 N95-27966 #
CONF-941144-60 .... p 2214 N95-27086 #
CONF-941144-61 .... p 2208 N95-27965 #
CONF-941144-62 .... p 2442 N95-27950 #
CONF-941144-63 .... p 2206 N95-27755 #
CONF-941144-64 .... p 2234 N95-27472 #
CONF-941144-65 .... p 2445 N95-28165 #
CONF-941144-66 .... p 2222 N95-28166 #
CONF-941144-67 .... p 2441 N95-27928 #
CONF-941144-68 .... p 2220 N95-28044 #
CONF-941144-69 .... p 2183 N95-28043 #
CONF-941144-70 .... p 2408 N95-27453 #
CONF-941144-71 .... p 2439 N95-27452 #
CONF-941144-72 .... p 2220 N95-28072 #
CONF-941144-73 .... p 2331 N95-28548 #
CONF-941144-74 .... p 2444 N95-28081 #
CONF-941144-75 .... p 2221 N95-28082 #
CONF-941144-76 .... p 2447 N95-28537 #
CONF-941144-78 .... p 2238 N95-28235 #
CONF-941144-79 .... p 2411 N95-28004 #
CONF-941144-83 .... p 2223 N95-28543 #
CONF-941144-84 .... p 2238 N95-28358 #
CONF-941144-85 .... p 2184 N95-28145 #
CONF-941144-86 .... p 2239 N95-28401 #
CONF-941144-87 .... p 2237 N95-28090 #
CONF-941144-88 .... p 2440 N95-27542 #
CONF-941144-89 .... p 2442 N95-27932 #
CONF-941144-97 .... p 2215 N95-27462 #
CONF-941176-2 .... p 2439 N95-27443 #
CONF-941182-2 .... p 2435 N95-28356 #
CONF-941195-1 .... p 2184 N95-28207 #
CONF-941203-14 .... p 2320 N95-27704 #
CONF-941203-21 .... p 2320 N95-27682 #
CONF-941203-22 .... p 2325 N95-28517 #
CONF-941207-25 .... p 2222 N95-28129 #
CONF-941251-2 .... p 2449 N95-28160 #
CONF-941251-3 .... p 2411 N95-27933 #
CONF-941252-1 .... p 2215 N95-27463 #
CONF-941257-1 .... p 2409 N95-27753 #
CONF-941258-1 .... p 2221 N95-28120 #
CONF-941259-1 .... p 2298 N95-28124 #
CONF-941262-1 .... p 2391 N95-27432 #
CONF-950101-3 .... p 2296 N95-27672 #
CONF-950101-4 .... p 2443 N95-28023 #
CONF-950116-5 .... p 2320 N95-27475 #
CONF-950116-6 .... p 2319 N95-27459 #
CONF-950116-7 .... p 2122 N95-27541 #
CONF-950124-5 .... p 2343 N95-27920 #
CONF-950124-6 .... p 2332 N95-28605 #
CONF-950129-2 .... p 2444 N95-28103 #
CONF-950130-7 .... p 2206 N95-27851 #
CONF-950130-8 .... p 2337 N95-27848 #
CONF-950158-1 .... p 2425 N95-27734 #
CONF-950165-1 .... p 2408 N95-27466 #
CONF-950167-1 .... p 2446 N95-28399 #
CONF-950169-1 .... p 2309 N95-27745 #
CONF-950172-1 .... p 2414 N95-28170 #
CONF-950173-1 .... p 2414 N95-28169 #
CONF-950175-1 .... p 2449 N95-27877 #
CONF-950201-2 .... p 2238 N95-28117 #
CONF-950201-3 .... p 2444 N95-28127 #
CONF-950201-4 .... p 2444 N95-28125 #
CONF-950201-5 .... p 2221 N95-28116 #
CONF-950201-6 .... p 2219 N95-28026 #
CONF-950201-8 .... p 2222 N95-28163 #
CONF-950206-1 .... p 2284 N95-27721 #
CONF-950212-5 .... p 2408 N95-27456 #
CONF-950212-6 .... p 2327 N95-27457 #
CONF-950212-7 .... p 2373 N95-28521 #
CONF-950216-46 .... p 2204 N95-27556 #
CONF-950216-69 .... p 2411 N95-28024 #
CONF-950216-71 .... p 2451 N95-28025 #
CONF-950220-1 .... p 2438 N95-27087 #
CONF-950220-2 .... p 2217 N95-27555 #
CONF-950220-3 .... p 2235 N95-27687 #
CONF-950220-4 .... p 2445 N95-28206 #
CONF-950226-10 .... p 2296 N95-27557 #
CONF-950226-11 .... p 2204 N95-27467 #
CONF-950226-12 .... p 2456 N95-28631 #
CONF-950226-13 .... p 2299 N95-28128 #
CONF-950226-14 .... p 2299 N95-28132 #
CONF-950226-16 .... p 2426 N95-28022 #
CONF-950226-17 .... p 2298 N95-28059 #
CONF-950226-19 .... p 2209 N95-28088 #
CONF-950226-22 .... p 2426 N95-28018 #
CONF-950226-23 .... p 2298 N95-28027 #
CONF-950226-24 .... p 2343 N95-28014 #
CONF-950226-4 .... p 2420 N95-27480 #
CONF-950226-7 .... p 2446 N95-28242 #
CONF-950226-8 .... p 2297 N95-27850 #
CONF-950226-9 .... p 2297 N95-27841 #
CONF-950245-1 .... p 2183 N95-28068 #
CONF-950245-2 .... p 2183 N95-28069 #
CONF-950256-1-REV-2 .... p 2303 N95-28139 #
CONF-950256-1 .... p 2303 N95-28029 #
CONF-950256-3 .... p 2327 N95-27540 #
CONF-950273-1 .... p 2239 N95-28400 #
CONF-950275-1-VUGRAPHS .... p 2256 N95-28407 #
CONF-950276-1 .... p 2293 N95-28178 #
CONF-950277-1 .... p 2315 N95-28520 #
CONF-950277-2 .... p 2344 N95-28538 #
CONF-950278-1-VUGRAPHS .... p 2462 N95-28056 #
CONF-950304-13 .... p 2240 N95-28547 #
CONF-950304-8 .... p 2218 N95-27722 #
CONF-9503104-1 .... p 2344 N95-28556 #
CONF-950312-1 .... p 2268 N95-28200 #
CONF-950336-20 .... p 2325 N95-28395 #
CONF-950344-5 .... p 2309 N95-27837 #
CONF-950380-1 .... p 2439 N95-27429 #
CONF-950396-1 .... p 2425 N95-27482 #
CONF-950396-2 .... p 2300 N95-28549 #
CONF-950402-1 .... p 2203 N95-27423 #
CONF-9504124-1 .... p 2183 N95-27955 #
CONF-9504128-1 .... p 2455 N95-28085 #
CONF-950420-19 .... p 2412 N95-28045 #
CONF-950420-1 .... p 2390 N95-27304 #
CONF-950420-20 .... p 2373 N95-28047 #
CONF-950420-21 .... p 2392 N95-28232 #
CONF-950430-4 .... p 2455 N95-28113 #
CONF-950432-1 .... p 2268 N95-28201 #
CONF-950439-5 .... p 2284 N95-27845 #
CONF-950439-7 .... p 2203 N95-27437 #
CONF-950443-1 .... p 2215 N95-27319 #
CONF-950444-1 .... p 2309 N95-27305 #
CONF-950461-1 .... p 2264 N95-27474 #
CONF-950464-1 .... p 2454 N95-27461 #
CONF-950472-1 .... p 2256 N95-27840
CONF-950484-2 .... p 2378 N95-27709 #
CONF-9505115-1 .... p 2182 N95-27421 #
CONF-9505116-1 .... p 2378 N95-27422 #
CONF-9505121-1 .... p 2267 N95-28147 #
CONF-9505124-1 .... p 2427 N95-28516 #
CONF-950514-9 .... p 2325 N95-28058 #
CONF-9505145-1 .... p 2372 N95-27436 #
CONF-9505154-1 .... p 2306 N95-27723 #
CONF-9505155-1 .... p 2420 N95-27425 #
CONF-9505157-1 .... p 2265 N95-27706 #
CONF-9505158-2 .... p 2354 N95-27426 #
CONF-9505162-1 .... p 2455 N95-27957 #
CONF-9505163-1 .... p 2269 N95-28244 #
CONF-9505175-1 .... p 2372 N95-27849 #

CONF-950518-1 p 2234 N95-27460 #
CONF-9505189-1 p 2267 N95-28146 #
CONF-9505192-1 p 2267 N95-28148 #
CONF-950537-1 p 2236 N95-27879 #
CONF-950540-1 p 2296 N95-27705 #
CONF-950540-2 p 2297 N95-27718 #
CONF-950540-3 p 2298 N95-27969 #
CONF-950540-4 p 2299 N95-28219 #
CONF-950540-5 p 2299 N95-28220 #
CONF-950591-1 p 2329 N95-27878 #
CONF-9506142-1 p 2311 N95-28539 #

CPIA-PUBL-611 p 2227 N95-27101
CPIA-PUBL-614-VOL-1 p 2170 N95-28294

CRHC-94-24 p 2365 N95-26628 *

CRREL-SP-94-30 p 2246 N95-26548

CRREL-SR-94-18 p 2200 N95-26432
CRREL-SR-94-24 p 2464 N95-27184
CRREL-SR-94-4 p 2200 N95-26452

CRREL-94-11 p 2336 N95-26753
CRREL-94-12 p 2144 N95-27297

CS-TR-3319 p 2356 N95-26843
CS-TR-3366 p 2394 N95-26478

CSU-ER-1001 p 2319 N95-27193 * #
CSU-ER-1001 p 2319 N95-27194 * #

CU-1534648 p 2278 N95-27019

CUED/A-AERO/TR-22 p 2275 N95-26809 #

CWP-146P p 2339 N95-28190 #
CWP-162 p 2339 N95-28192 #
CWP-163 p 2337 N95-27442 #
CWP-164P p 2339 N95-28194 #

D-V-95-1 p 2426 N95-27913 * #

DE94-011827 p 2242 N95-27415 #
DE94-014135 p 2393 N95-28393 #
DE94-014240 p 2273 N95-26445 #
DE94-018306 p 2390 N95-27304 #
DE94-018895 p 2309 N95-27305 #
DE94-019160 p 2215 N95-27319 #
DE94-628438 p 2450 N95-28183 #
DE94-629016 p 2414 N95-28184 #
DE94-629017 p 2441 N95-27867 #
DE94-634463 p 2403 N95-26437 #
DE94-634477 p 2429 N95-26438 #
DE94-634523 p 2429 N95-26439 #
DE94-765440 p 2297 N95-27868 #
DE94-765441 p 2432 N95-27869 #
DE94-765447 p 2432 N95-27870 #
DE95-000256 p 2327 N95-27540 #
DE95-000268 p 2122 N95-27541 #
DE95-000279 p 2320 N95-27704 #
DE95-000287 p 2325 N95-28394 #
DE95-000292 p 2325 N95-28395 #
DE95-000295 p 2319 N95-27459 #
DE95-000568 p 2457 N95-28675 #
DE95-001614 p 2264 N95-27474 #
DE95-003381 p 2410 N95-27871 #
DE95-003382 p 2410 N95-27872 #
DE95-003383 p 2432 N95-27873 #
DE95-003444 p 2208 N95-28042 #
DE95-003514 p 2203 N95-27420 #
DE95-003642 p 2334 N95-26436 #
DE95-003666 p 2182 N95-27421 #
DE95-003673 p 2378 N95-27422 #
DE95-003691 p 2296 N95-27705 #
DE95-003697 p 2297 N95-27718 #
DE95-003941 p 2416 N95-28329 #
DE95-003942 p 2434 N95-28185 #
DE95-003948 p 2445 N95-28186 #
DE95-004005 p 2265 N95-27719 #
DE95-004006 p 2320 N95-27475 #
DE95-004017 p 2204 N95-27438 #
DE95-004032 p 2325 N95-28396 #
DE95-004127 p 2436 N95-26440 #
DE95-004128 p 2376 N95-26441 #
DE95-004139 p 2436 N95-26442 #
DE95-004165 p 2379 N95-26443 #
DE95-004178 p 2429 N95-26444 #
DE95-004529 p 2427 N95-28516 #
DE95-004681 p 2441 N95-27720 #
DE95-004688 p 2284 N95-27721 #
DE95-004767 p 2234 N95-27460 #
DE95-004768 p 2218 N95-27722 #
DE95-004771 p 2439 N95-27429 #
DE95-004773 p 2203 N95-27423 #
DE95-004775 p 2372 N95-27436 #
DE95-004869 p 2236 N95-27943 #
DE95-004925 p 2234 N95-27476 #
DE95-004927 p 2203 N95-27401 #
DE95-004974 p 2454 N95-27461 #
DE95-004992 p 2378 N95-27402 #
DE95-004999 p 2216 N95-27477 #
DE95-005028 p 2264 N95-27403 #
DE95-005031 p 2246 N95-27404 #
DE95-005108 p 2408 N95-27478 #
DE95-005109 p 2407 N95-27430 #
DE95-005121 p 2215 N95-27462 #
DE95-005126 p 2417 N95-28495 #
DE95-005127 p 2408 N95-27444 #
DE95-005128 p 2399 N95-27530 #
DE95-005129 p 2421 N95-27531 #
DE95-005156 p 2462 N95-27445 #
DE95-005157 p 2182 N95-27080 #
DE95-005158 p 2405 N95-27081 #
DE95-005207 p 2215 N95-27446 #
DE95-005211 p 2420 N95-27425 #
DE95-005238 p 2354 N95-27426 #
DE95-005259 p 2213 N95-27082 #
DE95-005264 p 2215 N95-27463 #
DE95-005277 p 2407 N95-27431 #
DE95-005392 p 2262 N95-27083 #
DE95-005393 p 2420 N95-27427 #
DE95-005394 p 2183 N95-27428 #
DE95-005415 p 2205 N95-27681 #
DE95-005417 p 2202 N95-27136 #
DE95-005418 p 2202 N95-27137 #
DE95-005421 p 2240 N95-28531
DE95-005422 p 2240 N95-28532 #
DE95-005426 p 2391 N95-27432 #
DE95-005442 p 2265 N95-27706 #
DE95-005467 p 2306 N95-27723 #
DE95-005493 p 2266 N95-27724
DE95-005529 p 2429 N95-27084 #
DE95-005543 p 2438 N95-27085 #
DE95-005685 p 2409 N95-27552 #
DE95-005688 p 2217 N95-27553 #
DE95-005689 p 2425 N95-27490 #
DE95-005690 p 2265 N95-27554 #
DE95-005695 p 2243 N95-27944 #
DE95-005700 p 2215 N95-27464 #
DE95-005719 p 2440 N95-27491 #
DE95-005720 p 2216 N95-27492 #
DE95-005721 p 2216 N95-27493 #
DE95-005722 p 2216 N95-27479 #
DE95-005725 p 2236 N95-27733 #
DE95-005746 p 2411 N95-27945 #
DE95-005747 p 2292 N95-27751 #
DE95-005749 p 2409 N95-27747 #
DE95-005750 p 2422 N95-28346 #
DE95-005759 p 2236 N95-27946 #
DE95-005760 p 2239 N95-28397 #
DE95-005761 p 2303 N95-27947 #
DE95-005797 p 2330 N95-28119 #
DE95-005824 p 2351 N95-27948 #
DE95-005916 p 2311 N95-28337 #
DE95-005918 p 2335 N95-26622 #
DE95-005941 p 2449 N95-28137 #
DE95-005964 p 2416 N95-28338 #
DE95-006000 p 2270 N95-28515 #
DE95-006096 p 2269 N95-28339 #
DE95-006099 p 2240 N95-28547 #
DE95-006159 p 2455 N95-27949 #
DE95-006166 p 2287 N95-28055 #
DE95-006226 p 2309 N95-27837 #
DE95-006251 p 2206 N95-27838 #
DE95-006258 p 2292 N95-27465 #
DE95-006261 p 2203 N95-27437 #
DE95-006262 p 2217 N95-27555 #
DE95-006264 p 2204 N95-27556 #
DE95-006265 p 2462 N95-28056 #
DE95-006274 p 2298 N95-28124 #
DE95-006275 p 2444 N95-28125 #
DE95-006276 p 2296 N95-27557 #
DE95-006284 p 2456 N95-28631 #
DE95-006285 p 2296 N95-27672 #
DE95-006287 p 2256 N95-27840
DE95-006288 p 2432 N95-27673 #
DE95-006291 p 2408 N95-27466 #
DE95-006295 p 2297 N95-27841 #
DE95-006303 p 2237 N95-27993 #
DE95-006316 p 2420 N95-27480 #
DE95-006327 p 2425 N95-27734 #
DE95-006332 p 2284 N95-27845 #
DE95-006336 p 2421 N95-27735 #
DE95-006337 p 2420 N95-27494 #
DE95-006340 p 2455 N95-27847 #
DE95-006341 p 2297 N95-27736
DE95-006342 p 2337 N95-27848 #
DE95-006343 p 2372 N95-27849 #
DE95-006345 p 2297 N95-27850 #
DE95-006347 p 2206 N95-27851 #
DE95-006348 p 2445 N95-28240 #
DE95-006349 p 2442 N95-27994 #
DE95-006350 p 2209 N95-28088 #
DE95-006389 p 2372 N95-27495 #
DE95-006393 p 2431 N95-27419 #
DE95-006403 p 2204 N95-27467 #
DE95-006404 p 2234 N95-27468 #
DE95-006417 p 2207 N95-27951 #
DE95-006420 p 2207 N95-27952 #
DE95-006425 p 2411 N95-27953 #
DE95-006429 p 2206 N95-27707 #
DE95-006430 p 2328 N95-27708 #
DE95-006436 p 2332 N95-28662 #
DE95-006437 p 2330 N95-28118 #
DE95-006438 p 2204 N95-27496 #
DE95-006441 p 2330 N95-27954 #
DE95-006443 p 2327 N95-27532 #
DE95-006445 p 2372 N95-27533 #
DE95-006446 p 2461 N95-27326 #
DE95-006451 p 2430 N95-27327 #
DE95-006457 p 2270 N95-28597 #
DE95-006464 p 2215 N95-27328 #
DE95-006468 p 2444 N95-28103 #
DE95-006471 p 2223 N95-28593 #
DE95-006482 p 2352 N95-28496 #
DE95-006486 p 2417 N95-28594 #
DE95-006497 p 2408 N95-27534 #
DE95-006498 p 2331 N95-28548 #
DE95-006499 p 2300 N95-28549 #
DE95-006501 p 2344 N95-28556 #
DE95-006525 p 2373 N95-28498 #
DE95-006526 p 2375 N95-28632 #
DE95-006527 p 2378 N95-27709 #
DE95-006530 p 2221 N95-28120 #
DE95-006531 p 2415 N95-28204 #
DE95-006533 p 2327 N95-27469 #
DE95-006534 p 2422 N95-28205 #
DE95-006560 p 2296 N95-27674 #
DE95-006561 p 2425 N95-27675 #
DE95-006562 p 2409 N95-27676 #
DE95-006566 p 2340 N95-28583 #
DE95-006568 p 2265 N95-27678 #
DE95-006569 p 2460 N95-28197 #
DE95-006570 p 2421 N95-27679 #
DE95-006574 p 2428 N95-28557 #
DE95-006579 p 2463 N95-28558 #
DE95-006580 p 2420 N95-27470 #
DE95-006583 p 2440 N95-27538 #
DE95-006585 p 2298 N95-28104 #
DE95-006587 p 2440 N95-27471 #
DE95-006588 p 2425 N95-27539 #
DE95-006589 p 2234 N95-27472 #
DE95-006592 p 2209 N95-28218 #
DE95-006593 p 2297 N95-27737 #
DE95-006624 p 2215 N95-27473 #
DE95-006625 p 2234 N95-27486 #
DE95-006627 p 2440 N95-27487 #
DE95-006637 p 2268 N95-28198 #
DE95-006640 p 2414 N95-28199 #
DE95-006648 p 2267 N95-28105 #
DE95-006676 p 2433 N95-28106 #
DE95-006683 p 2421 N95-28107 #
DE95-006685 p 2292 N95-27677 #
DE95-006687 p 2222 N95-28134 #
DE95-006688 p 2320 N95-27682 #
DE95-006693 p 2292 N95-27738 #
DE95-006694 p 2440 N95-27535 #
DE95-006732 p 2417 N95-28595 #
DE95-006736 p 2435 N95-28596 #
DE95-006737 p 2431 N95-27536 #
DE95-006741 p 2431 N95-27537 #
DE95-006743 p 2217 N95-27544 #
DE95-006745 p 2302 N95-27545 #
DE95-006746 p 2183 N95-27955 #
DE95-006747 p 2449 N95-27546 #
DE95-006748 p 2208 N95-27956 #
DE95-006771 p 2421 N95-28017 #
DE95-006776 p 2325 N95-28517 #
DE95-006805 p 2455 N95-27957 #
DE95-006810 p 2268 N95-28200 #
DE95-006812 p 2445 N95-28206 #
DE95-006822 p 2219 N95-27958 #
DE95-006837 p 2288 N95-28603 #
DE95-006838 p 2216 N95-27488 #
DE95-006856 p 2258 N95-28601 #
DE95-006877 p 2449 N95-27547 #
DE95-006878 p 2399 N95-27548 #
DE95-006879 p 2433 N95-28111 #
DE95-006892 p 2332 N95-28602 #
DE95-006932 p 2241 N95-28604 #
DE95-006943 p 2204 N95-27549 #
DE95-007003 p 2332 N95-28605 #
DE95-007004 p 2447 N95-28606 #
DE95-007006 p 2442 N95-27959 #
DE95-007007 p 2427 N95-28552 #
DE95-007008 p 2208 N95-27960 #
DE95-007011 p 2296 N95-27550 #

DE95-007012 .... p 2430 N95-27306 #
DE95-007013 .... p 2208 N95-27961 #
DE95-007014 .... p 2406 N95-27307 #
DE95-007018 .... p 2429 N95-26940
DE95-007020 .... p 2241 N95-28560 #
DE95-007024 .... p 2184 N95-28207 #
DE95-007028 .... p 2413 N95-28066 #
DE95-007034 .... p 2223 N95-28208 #
DE95-007036 .... p 2417 N95-28447 #
DE95-007037 .... p 2435 N95-28553 #
DE95-007038 .... p 2456 N95-28555 #
DE95-007040 .... p 2236 N95-27962 #
DE95-007041 .... p 2430 N95-27308 #
DE95-007042 .... p 2410 N95-27874 #
DE95-007044 .... p 2431 N95-27497 #
DE95-007045 .... p 2431 N95-27498 #
DE95-007046 .... p 2343 N95-27920 #
DE95-007048 .... p 2235 N95-27499 #
DE95-007049 .... p 2302 N95-27875 #
DE95-007066 .... p 2234 N95-27481 #
DE95-007071 .... p 2207 N95-27921 #
DE95-007075 .... p 2415 N95-28210 #
DE95-007076 .... p 2449 N95-27448 #
DE95-007077 .... p 2434 N95-28233 #
DE95-007079 .... p 2449 N95-27449 #
DE95-007082 .... p 2218 N95-27752 #
DE95-007089 .... p 2409 N95-27753 #
DE95-007094 .... p 2266 N95-27754 #
DE95-007095 .... p 2206 N95-27755 #
DE95-007096 .... p 2442 N95-27963 #
DE95-007097 .... p 2208 N95-27965 #
DE95-007098 .... p 2442 N95-27950 #
DE95-007100 .... p 2397 N95-28234 #
DE95-007102 .... p 2215 N95-27450
DE95-007103 .... p 2204 N95-27451 #
DE95-007105 .... p 2410 N95-27922 #
DE95-007109 .... p 2421 N95-27923 #
DE95-007111 .... p 2433 N95-27924 #
DE95-007113 .... p 2441 N95-27925 #
DE95-007116 .... p 2266 N95-27926 #
DE95-007119 .... p 2410 N95-27927 #
DE95-007129 .... p 2219 N95-27966 #
DE95-007130 .... p 2237 N95-27967
DE95-007132 .... p 2441 N95-27928 #
DE95-007133 .... p 2220 N95-28072 #
DE95-007134 .... p 2439 N95-27452 #
DE95-007135 .... p 2408 N95-27453 #
DE95-007136 .... p 2238 N95-28235 #
DE95-007141 .... p 2284 N95-27454 #
DE95-007142 .... p 2234 N95-27455 #
DE95-007145 .... p 2411 N95-28004 #
DE95-007147 .... p 2219 N95-27968 #
DE95-007148 .... p 2425 N95-27482 #
DE95-007149 .... p 2298 N95-27969 #
DE95-007150 .... p 2299 N95-28219 #
DE95-007153 .... p 2299 N95-28220 #
DE95-007162 .... p 2214 N95-27086 #
DE95-007164 .... p 2438 N95-27087 #
DE95-007165 .... p 2214 N95-27088 #
DE95-007194 .... p 2219 N95-28005 #
DE95-007201 .... p 2419 N95-27089 #
DE95-007202 .... p 2413 N95-28067 #
DE95-007214 .... p 2454 N95-27090 #
DE95-007215 .... p 2415 N95-28221 #
DE95-007216 .... p 2419 N95-27091 #
DE95-007232 .... p 2238 N95-28133 #
DE95-007247 .... p 2319 N95-27236 #
DE95-007248 .... p 2430 N95-27237 #
DE95-007268 .... p 2454 N95-27483 #
DE95-007286 .... p 2446 N95-28242 #
DE95-007287 .... p 2373 N95-28243 #
DE95-007289 .... p 2378 N95-28019 #
DE95-007290 .... p 2221 N95-28075 #
DE95-007291 .... p 2443 N95-28076 #
DE95-007300 .... p 2420 N95-27484 #
DE95-007303 .... p 2269 N95-28244 #
DE95-007312 .... p 2315 N95-28520 #
DE95-007325 .... p 2407 N95-27439 #
DE95-007345 .... p 2316 N95-26543 #
DE95-007354 .... p 2403 N95-26560 #
DE95-007366 .... p 2183 N95-28043 #
DE95-007367 .... p 2220 N95-28044 #
DE95-007373 .... p 2412 N95-28045 #
DE95-007374 .... p 2387 N95-28536 #
DE95-007378 .... p 2220 N95-28046 #
DE95-007380 .... p 2408 N95-27456 #
DE95-007385 .... p 2327 N95-27457 #
DE95-007392 .... p 2413 N95-28077 #
DE95-007393 .... p 2413 N95-28078 #
DE95-007394 .... p 2409 N95-27551 #
DE95-007397 .... p 2373 N95-28047 #
DE95-007400 .... p 2444 N95-28079 #
DE95-007401 .... p 2237 N95-28080 #
DE95-007403 .... p 2447 N95-28537 #
DE95-007404 .... p 2444 N95-28081 #
DE95-007405 .... p 2221 N95-28082 #
DE95-007411 .... p 2267 N95-28048 #
DE95-007486 .... p 2218 N95-27748 #
DE95-007487 .... p 2220 N95-28049 #
DE95-007493 .... p 2443 N95-28050 #
DE95-007525 .... p 2328 N95-27749 #
DE95-007548 .... p 2206 N95-27750 #
DE95-007556 .... p 2204 N95-27458 #
DE95-007566 .... p 2131 N95-27440 #
DE95-007582 .... p 2431 N95-27441 #
DE95-007623 .... p 2339 N95-28126 #
DE95-007624 .... p 2455 N95-28113 #
DE95-007640 .... p 2344 N95-28538 #
DE95-007643 .... p 2412 N95-28051 #
DE95-007646 .... p 2338 N95-28114 #
DE95-007664 .... p 2433 N95-28052 #
DE95-007668 .... p 2339 N95-28190 #
DE95-007669 .... p 2339 N95-28192 #
DE95-007670 .... p 2337 N95-27442 #
DE95-007671 .... p 2339 N95-28194 #
DE95-007677 .... p 2422 N95-28115 #
DE95-007679 .... p 2422 N95-28195 #
DE95-007682 .... p 2439 N95-27443 #
DE95-007686 .... p 2426 N95-28196 #
DE95-007696 .... p 2445 N95-28165 #
DE95-007698 .... p 2222 N95-28166 #
DE95-007701 .... p 2416 N95-28355 #
DE95-007703 .... p 2331 N95-28121 #
DE95-007710 .... p 2205 N95-27683 #
DE95-007717 .... p 2378 N95-28074 #
DE95-007722 .... p 2395 N95-27684 #
DE95-007727 .... p 2328 N95-27686 #
DE95-007741 .... p 2221 N95-28116 #
DE95-007742 .... p 2238 N95-28117 #
DE95-007743 .... p 2235 N95-27687 #
DE95-007744 .... p 2444 N95-28127 #
DE95-007745 .... p 2299 N95-28128 #
DE95-007748 .... p 2222 N95-28129 #
DE95-007749 .... p 2222 N95-28130 #
DE95-007755 .... p 2267 N95-28131 #
DE95-007758 .... p 2299 N95-28132 #
DE95-007761 .... p 2268 N95-28156 #
DE95-007762 .... p 2432 N95-27688 #
DE95-007763 .... p 2411 N95-28020 #
DE95-007764 .... p 2409 N95-27689 #
DE95-007803 .... p 2287 N95-28021 #
DE95-007823 .... p 2422 N95-28122 #
DE95-007824 .... p 2422 N95-28123 #
DE95-007835 .... p 2412 N95-28057 #
DE95-007837 .... p 2325 N95-28058 #
DE95-007841 .... p 2298 N95-28059 #
DE95-007843 .... p 2426 N95-28022 #
DE95-007864 .... p 2443 N95-28060 #
DE95-007865 .... p 2443 N95-28023 #
DE95-007866 .... p 2311 N95-28539 #
DE95-007869 .... p 2411 N95-28024 #
DE95-007872 .... p 2426 N95-28018 #
DE95-007873 .... p 2451 N95-28025 #
DE95-007876 .... p 2219 N95-28026 #
DE95-007880 .... p 2298 N95-28027 #
DE95-007881 .... p 2447 N95-28541 #
DE95-007882 .... p 2338 N95-28061 #
DE95-007884 .... p 2462 N95-28062 #
DE95-007888 .... p 2412 N95-28063 #
DE95-007894 .... p 2412 N95-28028 #
DE95-007895 .... p 2205 N95-27690 #
DE95-007903 .... p 2205 N95-27691 #
DE95-007913 .... p 2205 N95-27692 #
DE95-007926 .... p 2205 N95-27680 #
DE95-007946 .... p 2332 N95-28550 #
DE95-007948 .... p 2399 N95-28108 #
DE95-007949 .... p 2399 N95-28109 #
DE95-007950 .... p 2243 N95-28064 #
DE95-007964 .... p 2265 N95-27693 #
DE95-007965 .... p 2222 N95-28167 #
DE95-007984 .... p 2392 N95-28110 #
DE95-008024 .... p 2423 N95-28551 #
DE95-008052 .... p 2433 N95-28065 #
DE95-008053 .... p 2303 N95-28029 #
DE95-008055 .... p 2314 N95-28053 #
DE95-008057 .... p 2351 N95-27725 #
DE95-008058 .... p 2434 N95-28138 #
DE95-008059 .... p 2433 N95-28054 #
DE95-008060 .... p 2303 N95-28139 #
DE95-008062 .... p 2462 N95-28013 #
DE95-008064 .... p 2434 N95-28140 #
DE95-008065 .... p 2343 N95-28014 #
DE95-008068 .... p 2434 N95-28141 #
DE95-008070 .... p 2266 N95-28015 #
DE95-008071 .... p 2432 N95-27710 #
DE95-008073 .... p 2435 N95-28356 #
DE95-008076 .... p 2373 N95-28168 #
DE95-008079 .... p 2435 N95-28542 #
DE95-008080 .... p 2373 N95-28521 #
DE95-008097 .... p 2354 N95-28136 #
DE95-008125 .... p 2300 N95-28398 #
DE95-008136 .... p 2414 N95-28142 #
DE95-008137 .... p 2267 N95-28143 #
DE95-008154 .... p 2299 N95-28223 #
DE95-008155 .... p 2237 N95-28089 #
DE95-008157 .... p 2446 N95-28399 #
DE95-008158 .... p 2239 N95-28400 #
DE95-008159 .... p 2238 N95-28358 #
DE95-008161 .... p 2237 N95-28090 #
DE95-008162 .... p 2239 N95-28401 #
DE95-008175 .... p 2240 N95-28404 #
DE95-008187 .... p 2240 N95-28405 #
DE95-008207 .... p 2435 N95-28406 #
DE95-008270 .... p 2183 N95-28068 #
DE95-008273 .... p 2183 N95-28069 #
DE95-008275 .... p 2303 N95-28070 #
DE95-008283 .... p 2256 N95-28407 #
DE95-008294 .... p 2223 N95-28543 #
DE95-008298 .... p 2378 N95-27741 #
DE95-008302 .... p 2392 N95-27742 #
DE95-008303 .... p 2440 N95-27542 #
DE95-008314 .... p 2414 N95-28169 #
DE95-008316 .... p 2414 N95-28170 #
DE95-008323 .... p 2378 N95-28071 #
DE95-008329 .... p 2414 N95-28171 #
DE95-008330 .... p 2456 N95-28172 #
DE95-008337 .... p 2328 N95-27743 #
DE95-008338 .... p 2338 N95-28083 #
DE95-008339 .... p 2330 N95-28084 #
DE95-008343 .... p 2338 N95-27931 #
DE95-008347 .... p 2434 N95-28224 #
DE95-008351 .... p 2287 N95-28225 #
DE95-008355 .... p 2238 N95-28226 #
DE95-008356 .... p 2209 N95-28229 #
DE95-008370 .... p 2442 N95-27932 #
DE95-008374 .... p 2455 N95-28085 #
DE95-008375 .... p 2256 N95-28231 #
DE95-008376 .... p 2298 N95-27876 #
DE95-008382 .... p 2392 N95-28232 #
DE95-008383 .... p 2411 N95-27933 #
DE95-008392 .... p 2392 N95-28173 #
DE95-008393 .... p 2344 N95-28340 #
DE95-008483 .... p 2208 N95-28086 #
DE95-008484 .... p 2463 N95-28357 #
DE95-008485 .... p 2449 N95-27877 #
DE95-008487 .... p 2413 N95-28091 #
DE95-008488 .... p 2409 N95-27744 #
DE95-008489 .... p 2444 N95-28092 #
DE95-008507 .... p 2445 N95-28144 #
DE95-008508 .... p 2184 N95-28145 #
DE95-008509 .... p 2309 N95-27745 #
DE95-008511 .... p 2268 N95-28201 #
DE95-008516 .... p 2267 N95-28146 #
DE95-008518 .... p 2267 N95-28147 #
DE95-008519 .... p 2267 N95-28148 #
DE95-008520 .... p 2329 N95-27878 #
DE95-008521 .... p 2236 N95-27879 #
DE95-008565 .... p 2331 N95-28149 #
DE95-008580 .... p 2320 N95-27746 #
DE95-008586 .... p 2328 N95-27558 #
DE95-008587 .... p 2357 N95-28176 #
DE95-008589 .... p 2331 N95-28157 #
DE95-008591 .... p 2414 N95-28158 #
DE95-008592 .... p 2422 N95-28159 #
DE95-008593 .... p 2449 N95-28160 #
DE95-008594 .... p 2293 N95-28178 #
DE95-008595 .... p 2434 N95-28161 #
DE95-008747 .... p 2392 N95-28162 #
DE95-008934 .... p 2222 N95-28163 #
DE95-009184 .... p 2288 N95-28533 #
DE95-009309 .... p 2209 N95-28164 #
DE95-009328 .... p 2445 N95-28179 #
DE95-009331 .... p 2223 N95-28534 #
DE95-600026 .... p 2226 N95-26637
DE95-600439 .... p 2326 N95-26639 #
DE95-600841 .... p 2299 N95-28330 #
DE95-601504 .... p 2213 N95-26675 #
DE95-603357 .... p 2225 N95-26599 #
DE95-604111 .... p 2349 N95-26597 #
DE95-605568 .... p 2398 N95-26598 #
DE95-607768 .... p 2403 N95-26542 #
DE95-607805 .... p 2448 N95-26603 #
DE95-607841 .... p 2207 N95-27880 #
DE95-607868 .... p 2327 N95-27198 #
DE95-607869 .... p 2202 N95-27199 #
DE95-607896 .... p 2203 N95-27200 #
DE95-607909 .... p 2439 N95-27201 #
DE95-607910 .... p 2444 N95-28112 #
DE95-607911 .... p 2351 N95-27254 #
DE95-607912 .... p 2405 N95-27211 #
DE95-607929 .... p 2406 N95-27212 #
DE95-607939 .... p 2214 N95-27255 #
DE95-607956 .... p 2214 N95-27256 #
DE95-608074 .... p 2405 N95-27010 #
DE95-608080 .... p 2337 N95-27157 #
DE95-608324 .... p 2419 N95-27158 #
DE95-608331 .... p 2405 N95-27159 #
DE95-608377 .... p 2398 N95-27160 #

DE95-608559 p 2419 N95-27161 #
DE95-608560 p 2362 N95-27162 #
DE95-608622 p 2233 N95-27163 #
DE95-608623 p 2261 N95-27023 #
DE95-608624 p 2261 N95-27024 #
DE95-608729 p 2381 N95-27025 #
DE95-608730 p 2381 N95-27044 #
DE95-608731 p 2382 N95-27045 #
DE95-608736 p 2398 N95-27239 #
DE95-608737 p 2399 N95-27298 #
DE95-608747 p 2390 N95-27299 #
DE95-608748 p 2396 N95-27300 #
DE95-608749 p 2390 N95-27301 #
DE95-608750 p 2390 N95-27302 #
DE95-608751 p 2390 N95-27092 #
DE95-608752 p 2390 N95-27330 #
DE95-608753 p 2390 N95-27331 #
DE95-608754 p 2448 N95-27332 #
DE95-608755 p 2448 N95-27333 #
DE95-608756 p 2448 N95-27334 #
DE95-608757 p 2255 N95-27335 #
DE95-608758 p 2448 N95-27336 #
DE95-608759 p 2397 N95-28518 #
DE95-608760 p 2396 N95-27337 #
DE95-608775 p 2280 N95-27338 #
DE95-608779 p 2280 N95-27339 #
DE95-608780 p 2395 N95-27340 #
DE95-608781 p 2396 N95-27341 #
DE95-608782 p 2292 N95-27711 #
DE95-608783 p 2207 N95-27929 #
DE95-608788 p 2464 N95-27342 #
DE95-608789 p 2462 N95-27343 #
DE95-608793 p 2397 N95-27344 #
DE95-608794 p 2448 N95-27447 #
DE95-608798 p 2397 N95-27485 #
DE95-608799 p 2406 N95-27309 #
DE95-608800 p 2448 N95-27310 #
DE95-608801 p 2390 N95-27311 #
DE95-608802 p 2448 N95-27312 #
DE95-608803 p 2255 N95-27313 #
DE95-608829 p 2406 N95-27314 #
DE95-608830 p 2448 N95-27315 #
DE95-608831 p 2406 N95-27316 #
DE95-608844 p 2406 N95-27317 #
DE95-608852 p 2406 N95-27318 #
DE95-608853 p 2415 N95-28245 #
DE95-608866 p 2415 N95-28246 #
DE95-608869 p 2415 N95-28247 #
DE95-608870 p 2415 N95-28248 #
DE95-608876 p 2416 N95-28249 #
DE95-609034 p 2223 N95-28250 #
DE95-609036 p 2411 N95-27930 #
DE95-609037 p 2416 N95-28251 #
DE95-609072 p 2416 N95-28252 #
DE95-609109 p 2256 N95-28254 #
DE95-609146 p 2446 N95-28255 #
DE95-609147 p 2264 N95-27405 #
DE95-609148 p 2391 N95-27739 #
DE95-609149 p 2441 N95-27740 #
DE95-609150 p 2417 N95-28607 #
DE95-609151 p 2447 N95-28608 #
DE95-609152 p 2218 N95-27756 #
DE95-609153 p 2443 N95-28016 #
DE95-609154 p 2220 N95-28039 #
DE95-609155 p 2218 N95-27757 #
DE95-609156 p 2219 N95-27758 #
DE95-609157 p 2219 N95-27759 #
DE95-609158 p 2241 N95-28609 #
DE95-609162 p 2442 N95-27964 #
DE95-609269 p 2400 N95-28350 #
DE95-609437 p 2410 N95-27881 #
DE95-609438 p 2440 N95-27712 #
DE95-609624 p 2217 N95-27713 #
DE95-610166 p 2391 N95-27714 #
DE95-610175 p 2391 N95-27715 #
DE95-610176 p 2256 N95-27716 #
DE95-610196 p 2421 N95-28040 #
DE95-610201 p 2412 N95-28041 #
DE95-610202 p 2407 N95-27406 #
DE95-610302 p 2407 N95-27407 #
DE95-610303 p 2407 N95-27408 #
DE95-610313 p 2419 N95-27321 #
DE95-610325 p 2407 N95-27409 #
DE95-610349 p 2407 N95-27410 #
DE95-610355 p 2407 N95-27411 #
DE95-610470 p 2407 N95-27412 #
DE95-610612 p 2439 N95-27413 #
DE95-703895 p 2431 N95-27414 #
DE95-755135 p 2331 N95-28202 #
DE95-759241 p 2329 N95-27935 #
DE95-759242 p 2320 N95-27936 #
DE95-759244 p 2458 N95-27937 #
DE95-759246 p 2329 N95-27938 #
DE95-759247 p 2329 N95-27939 #
DE95-759250 p 2321 N95-27940
DE95-759251 p 2329 N95-27941 #
DE95-759252 p 2331 N95-28535 #
DE95-759260 p 2330 N95-27942 #

DNA-TR-94-25 p 2177 N95-26434

DOE/CE-23810/42G p 2238 N95-28133 #
DOE/CE-23810/42H p 2234 N95-27461 #

DOE/CH-10575/T2 p 2330 N95-28119 #

DOE/ER-13480/5 p 2209 N95-28164 #
DOE/ER-13491/709 p 2407 N95-27439 #
DOE/ER-13592/9 p 2207 N95-27921 #
DOE/ER-13671/8 p 2414 N95-28199 #
DOE/ER-13772/T2 p 2207 N95-27952 #
DOE/ER-13860/T1 p 2300 N95-28398 #
DOE/ER-14079/35 p 2339 N95-28190 #
DOE/ER-14079/36 p 2339 N95-28192 #
DOE/ER-14079/37 p 2337 N95-27442 #
DOE/ER-14079/38 p 2339 N95-28194 #
DOE/ER-14105/5 p 2207 N95-27951 #
DOE/ER-14190/T1 p 2206 N95-27838 #
DOE/ER-14439/1 p 2338 N95-28083 #
DOE/ER-40452/11 p 2403 N95-26560 #
DOE/ER-40561/175 p 2449 N95-27547 #
DOE/ER-40561/179 p 2399 N95-27548 #
DOE/ER-40644/T1 p 2421 N95-27923 #
DOE/ER-40757/057 p 2419 N95-27089 #
DOE/ER-40757/058 p 2397 N95-28234 #
DOE/ER-40757/061 p 2413 N95-28067 #
DOE/ER-45219/T3 p 2220 N95-28049 #
DOE/ER-45326/T5 p 2268 N95-28198 #
DOE/ER-45329/1 p 2443 N95-28050 #
DOE/ER-45388/T3 p 2218 N95-27748 #
DOE/ER-45402/T1 p 2410 N95-27927 #
DOE/ER-45442/T1 p 2441 N95-27925 #
DOE/ER-45442/T2 p 2445 N95-28179 #
DOE/ER-53173/T4 p 2429 N95-26444 #
DOE/ER-53173/T6 p 2433 N95-27924 #
DOE/ER-53212/255 p 2429 N95-26940
DOE/ER-60314/6 p 2330 N95-28084 #
DOE/ER-60986/T2 p 2411 N95-27953 #
DOE/ER-61208/4 p 2328 N95-27743 #

DOE/ET-15601/T63 p 2292 N95-27465 #
DOE/ET-51013/307 p 2411 N95-28020 #
DOE/ET-51013/308 p 2432 N95-27688 #
DOE/ET-53017/T3 p 2410 N95-27922 #
DOE/ET-53088/682 p 2429 N95-27084 #
DOE/ET-53088/684 p 2433 N95-28111 #
DOE/ET-53088/686 p 2287 N95-28055 #

DOE/GO-10095-088 p 2242 N95-27415 #

DOE/ID-13040/T26 p 2319 N95-27236 #
DOE/ID-13073/1 p 2267 N95-28105 #
DOE/ID-13074/T14 p 2266 N95-27926 #
DOE/ID-13220/T3 p 2430 N95-27237 #

DOE/MC-29237/3983 p 2316 N95-26543 #
DOE/MC-30358/95/C0432 p 2131 N95-27440 #

DOE/METC-C/95/7171 p 2320 N95-27746 #

DOE/NASA/5776-2 p 2321 N95-27970 * #
DOE/NASA/5776-3 p 2316 N95-26734 * #

DOE/OSTI-11685 p 2457 N95-28675 #

DOE/PC-89761/T10 p 2205 N95-27680 #
DOE/PC-90305/T13 p 2203 N95-27420 #
DOE/PC-92106/T7 p 2204 N95-27549 #
DOE/PC-92529/T9 p 2205 N95-27692 #
DOE/PC-93208/T4 p 2204 N95-27458 #
DOE/PC-93217/T4 p 2205 N95-27691 #
DOE/PC-93222/5 p 2205 N95-27690 #
DOE/PC-94224/T2 p 2241 N95-28604 #

DOE/SF-20142/1 p 2433 N95-28052 #

DOT/FAA/AM-95/10 p 2355 N95-26361 #
DOT/FAA/AM-95/13 p 2357 N95-27323 #
DOT/FAA/AM-95/14 p 2360 N95-27696 #
DOT/FAA/AM-95/15 p 2128 N95-28540 #

DOT/FAA/AT-94/1 p 2126 N95-26454

DOT/FAA/CT-TN93/35 p 2127 N95-27903
DOT/FAA/CT-TN94-61 p 2117 N95-26363 * #
DOT/FAA/CT-TN94/28 p 2127 N95-26978
DOT/FAA/CT-TN94/36 p 2340 N95-26453
DOT/FAA/CT-TN94/41 p 2125 N95-26485

DOT/FAA/CT-88/10-VOL-2 p 2380 N95-26638
DOT/FAA/CT-91/7 p 2126 N95-28630
DOT/FAA/CT-92-25-VOL-1 p 2189 N95-28420 * #
DOT/FAA/CT-92-25-VOL-2 p 2193 N95-28462 * #
DOT/FAA/CT-92-25-VOL-3 p 2184 N95-28266 * #
DOT/FAA/CT-94/56 p 2125 N95-26527
DOT/FAA/CT-94/63 p 2120 N95-28610
DOT/FAA/CT-94/74 p 2125 N95-26497

DOT/FAA/PP-94-1 p 2144 N95-28151

DREA-TM-94/216 p 2345 N95-26420

DREO-1219 p 2249 N95-26545
DREO-1233 p 2248 N95-26407
DREO-1240 p 2258 N95-28580
DREO-1253 p 2258 N95-28573

DSTO-RR-0010 p 2259 N95-26425

DSTO-TN-0001 p 2142 N95-26378
DSTO-TN-0002 p 2136 N95-27918

DSTO-TR-0095 p 2139 N95-26424
DSTO-TR-0100 p 2258 N95-28568
DSTO-TR-0132 p 2136 N95-28567
DSTO-TR-0135 p 2128 N95-26389

DU/DC/ATR-02 p 2436 N95-26473

DU/DC/TR-45 p 2223 N95-28332
DU/DC/TR-46 p 2241 N95-28661

E-7267 p 2123 N95-28003 * #
E-7428 p 2168 N95-28000 * #
E-8941 p 2303 N95-27911 * #
E-9005 p 2307 N95-26387 * #
E-9039 p 2168 N95-27434 * #
E-9069 p 2273 N95-26380 * #
E-9173 p 2209 N95-28182 * #
E-9214 p 2280 N95-27345 * #
E-9295 p 2285 N95-27882 * #
E-9340 p 2284 N95-27854 * #
E-9367 p 2316 N95-26393 * #
E-9439 p 2321 N95-27970 * #
E-9461 p 2117 N95-26363 * #
E-9473 p 2301 N95-26774 * #
E-9492 p 2372 N95-27729 * #
E-9497 p 2301 N95-27178 * #
E-9498 p 2302 N95-27855 * #
E-9514 p 2166 N95-26390 * #
E-9523 p 2140 N95-28344 * #
E-9534-PT-1 p 2310 N95-28031 * #
E-9535-PT-2 p 2310 N95-28032 * #
E-9537 p 2309 N95-27174 * #
E-9544 p 2291 N95-27173 * #
E-9579 p 2244 N95-26709 * #
E-9584 p 2401 N95-26801 * #
E-9597 p 2316 N95-26734 * #
E-9599 p 2143 N95-27176 * #
E-9608 p 2279 N95-27242 * #
E-9610 p 2372 N95-27905 * #
E-9611 p 2283 N95-27369 * #
E-9612 p 2218 N95-27728 * #
E-9613 p 2164 N95-27761 * #
E-9614 p 2266 N95-27853 * #
E-9618 p 2168 N95-27861 * #
E-9623 p 2389 N95-26663 * #
E-9626 p 2167 N95-27177 * #
E-9632 p 2426 N95-27906 * #
E-9633 p 2391 N95-27726 * #
E-9634 p 2293 N95-28037 * #
E-9636 p 2291 N95-27030 * #
E-9643 p 2168 N95-27862 * #
E-9651 p 2279 N95-27175 * #
E-9653 p 2140 N95-27866 * #
E-9659 p 2302 N95-27373 * #
E-9660 p 2169 N95-28036 * #
E-9661 p 2302 N95-27698 * #
E-9668 p 2169 N95-28213 * #
E-9669 p 2264 N95-27374 * #
E-9670 p 2206 N95-27695 * #
E-9671 p 2168 N95-27727 * #
E-9679 p 2164 N95-27730 * #
E-9683 p 2125 N95-27762 * #
E-9687 p 2371 N95-27370 * #
E-9689 p 2140 N95-27860 * #

ECE/CWOL/67 p 2270 N95-28544

ECE/GWOL/60 p 2227 N95-26973
ECE/GWOL/61 p 2252 N95-26924
ECE/GWOL/62 p 2261 N95-27015
ECE/GWOL/65 p 2253 N95-26977

EDR-17199 p 2140 N95-27866 * #

EGG-M-94113 p 2264 N95-27403 #
EGG-M-94170 p 2216 N95-27477 #

EGG-M-94370 .... p 2246 N95-27404 #

EGG-11265-1123 .... p 2455 N95-28113 #
EGG-11265-5025 .... p 2379 N95-26443 #

EOARD-TR-95-06 .... p 2136 N95-28409

ERDEC-SP-019 .... p 2331 N95-28153

ERDEC-TR-195 .... p 2405 N95-27034
ERDEC-TR-212 .... p 2250 N95-26759

ERP-1148 .... p 2337 N95-27146
ERP-1150 .... p 2340 N95-26479
ERP-1153 .... p 2295 N95-27022
ERP-1156 .... p 2356 N95-26992

ES/ER/TM-35/R1 .... p 2354 N95-28136 #

ESC-TR-94-017 .... p 2375 N95-28628
ESC-TR-94-018 .... p 2377 N95-27250
ESC-TR-94-022 .... p 2374 N95-28627 *
ESC-TR-94-101 .... p 2452 N95-26721
ESC-TR-94-21 .... p 2363 N95-26446

ESL-721563-7-APP .... p 2260 N95-26716

ETN-95-97538 .... p 2450 N95-26803 #

FAA-AOR-100-94-009 .... p 2125 N95-26485

FNAL-TM-1916 .... p 2421 N95-27531 #
FNAL-TM-1917 .... p 2399 N95-27530 #
FNAL-TM-1920 .... p 2422 N95-28346 #

FNAL/C-94-419-E .... p 2411 N95-27945 #
FNAL/C-94/226-E .... p 2408 N95-27444 #
FNAL/C-94/238-E .... p 2408 N95-27478 #
FNAL/C-94/270-E .... p 2407 N95-27430 #
FNAL/C-94/330-E .... p 2410 N95-27872 #
FNAL/C-94/331-E .... p 2410 N95-27871 #
FNAL/C-94/358 .... p 2454 N95-27090 #
FNAL/C-94/401 .... p 2409 N95-27747 #
FNAL/C-94/415-E .... p 2417 N95-28495 #
FNAL/C-94/418 .... p 2292 N95-27751 #
FNAL/C-95/003-E .... p 2421 N95-28107 #
FNAL/C-95/005 .... p 2419 N95-27091 #
FNAL/C-95/012-E .... p 2415 N95-28221 #
FNAL/C-95/016-E .... p 2409 N95-27689 #
FNAL/C-95/024-E .... p 2411 N95-27933 #

GA-A-21811 .... p 2432 N95-27873 #
GA-A-21819 .... p 2435 N95-28406 #
GA-A-21847 .... p 2416 N95-28329 #
GA-A-21851 .... p 2434 N95-28185 #
GA-A-21903 .... p 2433 N95-28106 #
GA-A-21904 .... p 2431 N95-27441 #

GAO/AIMD-95-132 .... p 2342 N95-27912 #

GAO/NSIAD-94-140 .... p 2118 N95-26817 #
GAO/NSIAD-95-112 .... p 2135 N95-27910 #
GAO/NSIAD-95-141BR .... p 2145 N95-27856 #

GAO/RCED-94-285 .... p 2252 N95-26923

GC-TR-94-2303 .... p 2225 N95-26482

GPO-84-811 .... p 2165 N95-28342 #

GRI-94/0420 .... p 2208 N95-28006

H-1972 .... p 2362 N95-27914 * #

HEP-PH-9408315 .... p 2407 N95-27406 #
HEP-PH-9409418 .... p 2407 N95-27409 #

HR95-001 .... p 2352 N95-26494

IAEA-CN-60/A-4-I-2 .... p 2434 N95-28185 #
IAEA-CN-60/D-D-II-8 .... p 2416 N95-28329 #
IAEA-CN-60/D-P-I-12 .... p 2431 N95-27536 #
IAEA-CN-60/D-P-II-3 .... p 2431 N95-27419 #
IAEA-CN-60/D-2-II-6 .... p 2430 N95-27306 #
IAEA-CN-60/F-1-I-4 .... p 2431 N95-27498 #

IC-94/123 .... p 2397 N95-27485 #
IC-94/127 .... p 2403 N95-26437 #
IC-94/160 .... p 2207 N95-27880 #
IC-94/170 .... p 2416 N95-28249 #
IC-94/176 .... p 2446 N95-28255 #
IC-94/181 .... p 2264 N95-27405 #
IC-94/182 .... p 2410 N95-27881 #
IC-94/183 .... p 2448 N95-26603 #
IC-94/187 .... p 2390 N95-27299 #
IC-94/194 .... p 2337 N95-27157 #
IC-94/198 .... p 2396 N95-27300 #
IC-94/205 .... p 2403 N95-26542 #
IC-94/206 .... p 2390 N95-27301 #
IC-94/208 .... p 2440 N95-27712 #
IC-94/209 .... p 2398 N95-27160 #
IC-94/213 .... p 2391 N95-27739 #
IC-94/214 .... p 2406 N95-27309 #
IC-94/215 .... p 2448 N95-27310 #
IC-94/217 .... p 2411 N95-27930 #
IC-94/218 .... p 2390 N95-27311 #
IC-94/219 .... p 2416 N95-28251 #
IC-94/220 .... p 2441 N95-27740 #
IC-94/222 .... p 2400 N95-28350 #
IC-94/223 .... p 2464 N95-27342 #
IC-94/224 .... p 2448 N95-27312 #
IC-94/227 .... p 2439 N95-27201 #
IC-94/228 .... p 2444 N95-28112 #
IC-94/229 .... p 2381 N95-27025 #
IC-94/230 .... p 2417 N95-28607 #
IC-94/231 .... p 2447 N95-28608 #
IC-94/232 .... p 2351 N95-27254 #
IC-94/233 .... p 2280 N95-27339 #
IC-94/235 .... p 2390 N95-27302 #
IC-94/236 .... p 2381 N95-27044 #
IC-94/237 .... p 2390 N95-27092 #
IC-94/239 .... p 2439 N95-27413 #
IC-94/241 .... p 2223 N95-28250 #
IC-94/242 .... p 2218 N95-27756 #
IC-94/244 .... p 2406 N95-27318 #
IC-94/246 .... p 2443 N95-28016 #
IC-94/247 .... p 2220 N95-28039 #
IC-94/248 .... p 2390 N95-27330 #
IC-94/249 .... p 2390 N95-27331 #
IC-94/250 .... p 2448 N95-27332 #
IC-94/252 .... p 2218 N95-27757 #
IC-94/254 .... p 2448 N95-27333 #
IC-94/256 .... p 2382 N95-27045 #
IC-94/258 .... p 2219 N95-27758 #
IC-94/259 .... p 2448 N95-27334 #
IC-94/260 .... p 2395 N95-27340 #
IC-94/263 .... p 2219 N95-27759 #
IC-94/267 .... p 2241 N95-28609 #
IC-94/271 .... p 2255 N95-27313 #
IC-94/274 .... p 2406 N95-27317 #
IC-94/275 .... p 2406 N95-27316 #
IC-94/282 .... p 2396 N95-27341 #
IC-94/90 .... p 2429 N95-26439 #

ICASE-94-84 .... p 2288 N95-28571 *
ICASE-95-11 .... p 2388 N95-26395 * #
ICASE-95-20 .... p 2389 N95-26672 * #
ICASE-95-21 .... p 2273 N95-26576 * #
ICASE-95-23 .... p 2278 N95-27028 * #
ICASE-95-24 .... p 2361 N95-26697 * #
ICASE-95-26 .... p 2278 N95-27027 * #
ICASE-95-27 .... p 2391 N95-27433 * #
ICASE-95-29 .... p 2284 N95-27760 * #
ICASE-95-30 .... p 2390 N95-27029 * #
ICASE-95-37 .... p 2279 N95-27247 * #
ICASE-95-38 .... p 2287 N95-27917 * #
ICASE-95-39 .... p 2279 N95-27179 * #
ICASE-95-41 .... p 2289 N95-28673 * #
ICASE-95-43 .... p 2288 N95-28228 * #

ICOMP-94-18 .... p 2273 N95-26380 * #
ICOMP-94-30 .... p 2285 N95-27882 * #
ICOMP-95-10 .... p 2279 N95-27175 * #
ICOMP-95-7 .... p 2279 N95-27242 * #
ICOMP-95-8 .... p 2391 N95-27726 * #

IDA-D-1595 .... p 2255 N95-27249

IDA-P-2901 .... p 2358 N95-26552
IDA-P-2982 .... p 2143 N95-26556
IDA-P-2998 .... p 2393 N95-26347

IDA/HQ-93-44557 .... p 2358 N95-26552
IDA/HQ-94-45529 .... p 2143 N95-26556

IECEC-95-136 .... p 2169 N95-28036 * #
IECEC-95-387 .... p 2372 N95-27905 * #

IFSR-684 .... p 2433 N95-28111 #
IFSR-686 .... p 2287 N95-28055 #

IFTR-14/1994 .... p 2250 N95-26836
IFTR-16/1994 .... p 2398 N95-26518
IFTR-17/1994 .... p 2364 N95-26511
IFTR-18/1994 .... p 2400 N95-26358
IFTR-2/1994 .... p 2250 N95-26835
IFTR-23/1994 .... p 2212 N95-26517
IFTR-24/1994 .... p 2213 N95-26838
IFTR-26/1994 .... p 2212 N95-26512
IFTR-27/1994 .... p 2212 N95-26666
IFTR-32/1994 .... p 2211 N95-26359
IFTR-37/1994 .... p 2374 N95-28566 #
IFTR-39/1994 .... p 2143 N95-26837
IFTR-40/1994 .... p 2401 N95-26519
IFTR-6/1994 .... p 2447 N95-26510

IHES/M/94/54 .... p 2396 N95-26538 #
IHES/M/94/57 .... p 2388 N95-26515 #
IHES/M/94/59 .... p 2388 N95-26516 #
IHES/M/94/62 .... p 2389 N95-26915
IHES/M/94/64 .... p 2388 N95-26539 #
IHES/M/94/66 .... p 2388 N95-26514 #
IHES/M/95/5 .... p 2393 N95-28611 #
IHES/M/95/7 .... p 2393 N95-28501 #

IHES/P/94/53 .... p 2392 N95-28010
IHES/P/94/55 .... p 2397 N95-28011
IHES/P/94/56 .... p 2450 N95-28664 #
IHES/P/94/58 .... p 2392 N95-28012 #
IHES/P/94/60 .... p 2397 N95-28174 #
IHES/P/94/61 .... p 2449 N95-28175 #

INEL-94/0114 .... p 2331 N95-28149 #

INIS-MF-13965 .... p 2213 N95-26675 #
INIS-MF-14307 .... p 2349 N95-26597 #
INIS-MF-14332 .... p 2226 N95-26637
INIS-MF-14335 .... p 2326 N95-26639 #
INIS-MF-14339 .... p 2299 N95-28330 #
INIS-MF-14365 .... p 2225 N95-26599 #
INIS-MF-14386 .... p 2398 N95-26598 #
INIS-MF-14394 .... p 2327 N95-27198 #
INIS-MF-14396 .... p 2405 N95-27211 #
INIS-MF-14397 .... p 2202 N95-27199 #
INIS-MF-14400 .... p 2442 N95-27964 #
INIS-MF-14401 .... p 2405 N95-27010 #
INIS-MF-14408 .... p 2214 N95-27256 #

INPE-5464-PRE/1772 .... p 2258 N95-28559 #
INPE-5478-PRE/1777 .... p 2316 N95-28672 #
INPE-5504-PRE/1787 .... p 2258 N95-28569 #
INPE-5513-NTC/309 .... p 2315 N95-28554 #
INPE-5529-PRE/1796 .... p 2435 N95-28562 #

INT-PATENT-CLASS-B08B-9/02 . p 2304 N95-28359 *
INT-PATENT-CLASS-B64G-1/10 . p 2165 N95-27842 * #

INT-PATENT-CLASS-C08G-73/18 p 2179 N95-28360 *
INT-PATENT-CLASS-C08G-79/08 p 2238 N95-28212 *

INT-PATENT-CLASS-F02M-65/00 p 2304 N95-28347 *
INT-PATENT-CLASS-F28D-20/00 p 2304 N95-28256 *

INT-PATENT-CLASS-G01K-1/10 . p 2293 N95-28345 *
INT-PATENT-CLASS-G01K-1/12 . p 2293 N95-28345 *
INT-PATENT-CLASS-G01K-1/14 . p 2293 N95-28345 *
INT-PATENT-CLASS-G01M-15/00 p 2304 N95-28347 *
INT-PATENT-CLASS-G01M-3/24 p 2271 N95-28599 *
INT-PATENT-CLASS-G01N-15/06 p 2293 N95-28362 *
INT-PATENT-CLASS-G01N-21/64 p 2315 N95-28211 *
INT-PATENT-CLASS-G02F-1/01 . p 2427 N95-28384 *
INT-PATENT-CLASS-G03B-42/02 p 2423 N95-26385 *
INT-PATENT-CLASS-G05F-1/613 p 2269 N95-28341 *
INT-PATENT-CLASS-G06F-15/18 p 2427 N95-28363 *

INT-PATENT-CLASS-H01S-3/11 . p 2297 N95-27731 *
INT-PATENT-CLASS-H02M-3/335 p 2269 N95-28341 *
INT-PATENT-CLASS-H03L-7/26 . p 2416 N95-28348 *
INT-PATENT-CLASS-H04N-5/74 . p 2426 N95-27843 *

IPPCZ-333 .... p 2429 N95-26438 #

IS-M-790 .... p 2273 N95-26445 #

ISAS-R-653 .... p 2275 N95-26742 #
ISAS-R-654 .... p 2274 N95-26741 #
ISAS-R-655 .... p 2121 N95-26740 #
ISAS-R-656 .... p 2274 N95-26739 #

ISBN 92-9083-058-1 .... p 2419 N95-27158 #

ISBN-0-16-046489-7 .... p 2165 N95-28342 #
ISBN-0-309-05045-6 .... p 2126 N95-27907 #
ISBN-0-309-05082-0 .... p 2326 N95-26362 * #
ISBN-0-309-05183-5 .... p 2314 N95-27156
ISBN-0-9616962-8-1 .... p 2144 N95-26583 * #
ISBN-1-883-712-35-1 .... p 2268 N95-28239 * #
ISBN-1-883-71231-9 .... p 2475 N95-28038 * #
ISBN-1-883712-33-5 .... p 2247 N95-27909 * #
ISBN-1-883712-38-6 .... p 2235 N95-27694 * #
ISBN-1-88712-37-8 .... p 2263 N95-27226 * #
ISBN-83-86333-60-X .... p 2141 N95-26487
ISBN-90-369-2045-0 .... p 2343 N95-28237
ISBN-90-369-2047-7 .... p 2342 N95-27366
ISBN-90-369-2057-4 .... p 2343 N95-28236
ISBN-90-9007413-9 .... p 2137 N95-28636 #
ISBN-90-9007545-3 .... p 2289 N95-28637
ISBN-92-836-0010-X .... p 2131 N95-27504 #

ISBN-951-22-2144-6 .... p 2252 N95-26908
ISBN-951-22-2220-5 .... p 2246 N95-27048 #
ISBN-951-22-2231-0 .... p 2356 N95-26909
ISBN-951-22-2270-1 .... p 2260 N95-26646 #
ISBN-951-22-2274-4 .... p 2313 N95-26645 #
ISBN-951-22-2291-4 .... p 2252 N95-26929
ISBN-951-22-2297-3 .... p 2256 N95-28354 #
ISBN-951-22-2301-5 .... p 2259 N95-26496 #
ISBN-951-22-2302-3 .... p 2262 N95-27050
ISBN-951-22-2322-8 .... p 2254 N95-27049 #
ISBN-951-22-2334-1 .... p 2388 N95-26495 #
ISBN-951-22-2337-6 .... p 2396 N95-26613 #
ISBN-951-22-2338-4 .... p 2396 N95-26912
ISBN-951-22-2340-6 .... p 2396 N95-28352 #
ISBN-951-22-2341-4 .... p 2252 N95-26914
ISBN-951-22-2345-7 .... p 2257 N95-28450 #
ISBN-951-22-2347-3 .... p 2200 N95-26540 #
ISBN-951-22-2348-1 .... p 2269 N95-28448
ISBN-951-22-2354-6 .... p 2437 N95-26513 #
ISBN-951-22-2361-9 .... p 2248 N95-26450 #
ISBN-951-22-2362-7 .... p 2379 N95-26449 #
ISBN-951-22-2364-3 .... p 2316 N95-26656
ISBN-951-22-2371-6 .... p 2257 N95-28449 #
ISBN-951-22-2384-8 .... p 2257 N95-28451 #
ISBN-951-22-2392-9 .... p 2271 N95-28655 #
ISBN-951-41-0775-6 .... p 2397 N95-28238
ISBN-951-711-181-9 .... p 2348 N95-27996 #
ISBN-951-711-182-7 .... p 2338 N95-27995 #

ISVR-TR-239 .... p 2309 N95-27846
ISVR-TR-245 .... p 2302 N95-27844

ITL-94-6 .... p 2307 N95-26464

IYAF-93-53 .... p 2407 N95-27407 #
IYAF-93-54 .... p 2407 N95-27408 #
IYAF-94-30 .... p 2407 N95-27412 #
IYAF-94-3 .... p 2407 N95-27410 #

JAERI-M-94-040 .... p 2431 N95-27414 #

JINR-D-2-94-177 .... p 2255 N95-27335 #
JINR-D-2-94-179 .... p 2391 N95-27715 #
JINR-D-2-94-212 .... p 2448 N95-27336 #

JINR-E-13-94-159 .... p 2233 N95-27163 #
JINR-E-13-94-198 .... p 2416 N95-28252 #
JINR-E-14-94-217 .... p 2261 N95-27023 #
JINR-E-14-94-218 .... p 2261 N95-27024 #
JINR-E-2-94-165 .... p 2462 N95-27343 #
JINR-E-2-94-190 .... p 2397 N95-27344 #
JINR-E-2-94-208 .... p 2406 N95-27314 #
JINR-E-3-94-169 .... p 2415 N95-28247 #
JINR-E-4-94-158 .... p 2415 N95-28245 #
JINR-E-4-94-176 .... p 2256 N95-27716 #
JINR-E-4-94-4 .... p 2450 N95-28183 #
JINR-E-7-93-356 .... p 2414 N95-28184 #

JINR-R-1-93-213 .... p 2441 N95-27867 #
JINR-R-1-94-166 .... p 2419 N95-27161 #
JINR-R-1-94-180 .... p 2362 N95-27162 #
JINR-R-11-94-160 .... p 2398 N95-27239 #
JINR-R-11-94-161 .... p 2399 N95-27298 #
JINR-R-2-94-181 .... p 2415 N95-28248 #
JINR-R-2-94-310 .... p 2448 N95-27315 #
JINR-R-2-94-336 .... p 2448 N95-27447 #
JINR-R-5-94-199 .... p 2391 N95-27714 #
JINR-R-5-94-219 .... p 2397 N95-28518 #
JINR-R-5-94-220 .... p 2396 N95-27337 #
JINR-R-8-94-184 .... p 2280 N95-27338 #

JPRS-UST-94-022 .... p 2246 N95-27699 #
JPRS-UST-95-014 .... p 2145 N95-27171 #
JPRS-UST-95-015 .... p 2246 N95-27213 #
JPRS-UST-95-016 .... p 2262 N95-27170 #
JPRS-UST-95-019 .... p 2270 N95-28565 #
JPRS-UST-95-020 .... p 2145 N95-28257 #
JPRS-UST-95-021 .... p 2202 N95-27155 #

JRC-36-94 .... p 2402 N95-28622
JRC-95-02 .... p 2360 N95-27164 * #

K/CSD/TM-93-REV-3 .... p 2456 N95-28172 #

K/TCD-1118 .... p 2208 N95-28042 #

KNMI-TR-158 .... p 2343 N95-28237
KNMI-TR-160 .... p 2342 N95-27386
KNMI-TR-165 .... p 2343 N95-28236

KPT-7-94 .... p 2451 N95-28135 #

KSC-DF-3772 .... p 2326 N95-26808 * #

L-16700-PT-4 .... p 2400 N95-26392 * #
L-17360 .... p 2120 N95-26382 * #
L-17368 .... p 2124 N95-28669 * #
L-17388 .... p 2123 N95-28241 * #
L-17401 .... p 2124 N95-28674 * #
L-17408 .... p 2368 N95-26685 * #
L-17413 .... p 2161 N95-26428 * #
L-17417 .... p 2465 N95-28530 * #
L-17422 .... p 2140 N95-28343 * #
L-17430C-PT-3 .... p 2466 N95-27629 * #
L-17450 .... p 2465 N95-26427 * #
L-17453 .... p 2291 N95-27259 * #
L-17455 .... p 2420 N95-27372 * #
L-17474 .... p 2293 N95-27915 * #

LA-SUB-95-16 .... p 2339 N95-28126 #
LA-SUB-95-26 .... p 2412 N95-28051 #
LA-SUB-95-33 .... p 2338 N95-28114 #

LA-UR-94-2848 .... p 2390 N95-27304 #
LA-UR-94-3033 .... p 2461 N95-27326 #
LA-UR-94-3115 .... p 2430 N95-27327 #
LA-UR-94-3823 .... p 2296 N95-27705 #
LA-UR-94-3834 .... p 2297 N95-27718 #
LA-UR-94-3960 .... p 2182 N95-27421 #
LA-UR-94-3994 .... p 2378 N95-27422 #
LA-UR-94-4079 .... p 2213 N95-27082 #
LA-UR-94-4199 .... p 2420 N95-27425 #
LA-UR-94-4219 .... p 2215 N95-27446 #
LA-UR-94-4220 .... p 2183 N95-27428 #
LA-UR-94-4242 .... p 2405 N95-27081 #
LA-UR-94-4246 .... p 2182 N95-27080 #
LA-UR-94-4268 .... p 2462 N95-27445 #
LA-UR-94-4280 .... p 2407 N95-27431 #
LA-UR-94-4288 .... p 2215 N95-27463 #
LA-UR-94-4387 .... p 2354 N95-27426 #
LA-UR-95-100 .... p 2420 N95-27494 #
LA-UR-95-116 .... p 2297 N95-27841 #
LA-UR-95-156 .... p 2421 N95-27735 #
LA-UR-95-174 .... p 2411 N95-28024 #
LA-UR-95-191 .... p 2425 N95-27734 #
LA-UR-95-201 .... p 2204 N95-27556 #
LA-UR-95-208 .... p 2217 N95-27555 #
LA-UR-95-210 .... p 2203 N95-27437 #
LA-UR-95-22 .... p 2372 N95-27849 #
LA-UR-95-251 .... p 2284 N95-27845 #
LA-UR-95-281 .... p 2462 N95-28056 #
LA-UR-95-32 .... p 2337 N95-27848 #
LA-UR-95-339 .... p 2296 N95-27557 #
LA-UR-95-341 .... p 2444 N95-28125 #
LA-UR-95-342 .... p 2298 N95-28124 #
LA-UR-95-34 .... p 2297 N95-27736
LA-UR-95-35 .... p 2455 N95-27847 #
LA-UR-95-373 .... p 2408 N95-27466 #
LA-UR-95-374 .... p 2456 N95-28631 #
LA-UR-95-405 .... p 2426 N95-28018 #
LA-UR-95-406 .... p 2296 N95-27672 #
LA-UR-95-413 .... p 2256 N95-27840
LA-UR-95-416 .... p 2432 N95-27673 #
LA-UR-95-41 .... p 2297 N95-27850 #
LA-UR-95-420 .... p 2451 N95-28025 #
LA-UR-95-42 .... p 2206 N95-27851 #
LA-UR-95-473 .... p 2219 N95-28026 #
LA-UR-95-48 .... p 2234 N95-27468 #
LA-UR-95-49 .... p 2204 N95-27467 #
LA-UR-95-534 .... p 2298 N95-28027 #
LA-UR-95-539 .... p 2447 N95-28541 #
LA-UR-95-553 .... p 2338 N95-28061 #
LA-UR-95-568 .... p 2462 N95-28062 #
LA-UR-95-57 .... p 2209 N95-28088 #
LA-UR-95-597 .... p 2412 N95-28063 #
LA-UR-95-677 .... p 2443 N95-28060 #
LA-UR-95-684 .... p 2443 N95-28023 #
LA-UR-95-686 .... p 2311 N95-28539 #
LA-UR-95-72 .... p 2442 N95-27994 #
LA-UR-95-73 .... p 2445 N95-28240 #
LA-UR-95-754 .... p 2412 N95-28057 #
LA-UR-95-775 .... p 2325 N95-28058 #
LA-UR-95-830 .... p 2298 N95-28059 #
LA-UR-95-837 .... p 2426 N95-28022 #

LA-12762-MS .... p 2328 N95-27686 #
LA-12821-MS .... p 2258 N95-28601 #
LA-12830 .... p 2236 N95-27943 #
LA-12860-MS .... p 2266 N95-27754 #
LA-12876-T .... p 2216 N95-27488 #
LA-12896 .... p 2288 N95-28603 #

LAMP-94/6 .... p 2292 N95-27711 #
LAMP-94/7 .... p 2207 N95-27929 #

LBL-35273 .... p 2287 N95-28225 #
LBL-35534 .... p 2297 N95-27737 #
LBL-35812 .... p 2417 N95-28594 #
LBL-35961 .... p 2440 N95-27538 #
LBL-35962 .... p 2440 N95-27471 #
LBL-35986 .... p 2441 N95-27720 #
LBL-35991 .... p 2428 N95-28557 #
LBL-35997 .... p 2420 N95-27470 #
LBL-36025 .... p 2265 N95-27678 #
LBL-36135 .... p 2463 N95-28558 #
LBL-36209 .... p 2463 N95-28357 #
LBL-36328 .... p 2284 N95-27721 #
LBL-36360 .... p 2409 N95-27676 #
LBL-36361 .... p 2460 N95-28197 #
LBL-36369 .... p 2296 N95-27674 #
LBL-36398 .... p 2234 N95-27472 #
LBL-36405 .... p 2238 N95-28226 #
LBL-36427 .... p 2425 N95-27675 #
LBL-36511 .... p 2209 N95-28229 #
LBL-36515 .... p 2340 N95-28583 #
LBL-36517 .... p 2425 N95-27539 #
LBL-36535 .... p 2421 N95-27679 #
LBL-36546 .... p 2209 N95-28218 #
LBL-36582 .... p 2298 N95-28104 #
LBL-36632 .... p 2409 N95-27744 #
LBL-36683 .... p 2444 N95-28092 #
LBL-36702 .... p 2413 N95-28091 #
LBL-36746 .... p 2449 N95-27877 #
LBL-36751 .... p 2208 N95-28086 #

LC-92-7619 .... p 2458 N95-27068 * #
LC-94-24592 .... p 2474 N95-27685 * #
LC-94-65759 .... p 2126 N95-27907 #
LC-94-68678 .... p 2314 N95-27156
LC-95-67403 .... p 2326 N95-26362 * #

LMSC-F254281 .... p 2336 N95-26922 * #

LT-94-1067 .... p 2125 N95-26497

M-772 .... p 2317 N95-26785 * #
M-777 .... p 2244 N95-26769 * #
M-779 .... p 2392 N95-28215 * #
M-780 .... p 2169 N95-28263 * #
M-782 .... p 2311 N95-28214 * #

M/NAFA/94-1 .... p 2117 N95-26363 * #

MCAT-05-06 .... p 2143 N95-26775 * #
MCAT-95-01 .... p 2121 N95-26760 * #
MCAT-95-02 .... p 2275 N95-26766 * #
MCAT-95-03 .... p 2365 N95-26648 * #
MCAT-95-04 .... p 2274 N95-26665 * #
MCAT-95-07 .... p 2129 N95-26651 * #
MCAT-95-08 .... p 2274 N95-26589 * #
MCAT-95-11 .... p 2129 N95-26591 * #
MCAT-95-13 .... p 2121 N95-26735 * #
MCAT-95-14 .... p 2129 N95-26590 * #
MCAT-95-15 .... p 2274 N95-26588 * #
MCAT-95-16 .... p 2275 N95-26776 * #
MCAT-95-17 .... p 2139 N95-26777 * #
MCAT-95-18 .... p 2120 N95-26649 * #
MCAT-95-7 .... p 2130 N95-26813 * #

MCR-95-557 .... p 2145 N95-28261 * #

MDC-91K0418 .... p 2266 N95-27999 * #

MP-95-068 .... p 2399 N95-27852 * #

MSFC-2 .... p 2351 N95-27329 * #

MSR-608 .... p 2389 N95-26882

MTR-90W00179 .... p 2126 N95-26454
MTR-94W0000110 .... p 2126 N95-26454

NAIC-ID(RS)T-0004-93 .... p 2162 N95-26715
NAIC-ID(RS)T-0093-93 .... p 2341 N95-26723
NAIC-ID(RS)T-0095-93 .... p 2342 N95-26724
NAIC-ID(RS)T-0102-93 .... p 2424 N95-26860
NAIC-ID(RS)T-0382-94 .... p 2401 N95-26857
NAIC-ID(RS)T-0384-94 .... p 2402 N95-26671
NAIC-ID(RS)T-0385-94 .... p 2201 N95-26707
NAIC-ID(RS)T-0639-93 .... p 2300 N95-26633
NAIC-ID(RS)T-0661-94 .... p 2466 N95-26856
NAIC-ID(RS)T-0702-94 .... p 2300 N95-26650
NAIC-ID(RS)T-0704-94 .... p 2294 N95-26674
NAIC-ID(RS)T-0893-92 .... p 2428 N95-26617
NAIC-ID(RS)T-0917-92 .... p 2274 N95-26718
NAIC-ID(RS)T-0918-92 .... p 2121 N95-26719
NAIC-ID(RS)T-0919-92 .... p 2289 N95-26619
NAIC-ID(RS)T-0920-92 .... p 2121 N95-26859
NAIC-ID(RS)T-0922-92 .... p 2120 N95-26713

NAIC/ID(RS)T-0369-94 .... p 2250 N95-26717

NAL-TR-1220 .... p 2139 N95-26600 #
NAL-TR-1225 .... p 2307 N95-26521 #
NAL-TR-1230 .... p 2126 N95-26585 #
NAL-TR-1233 .... p 2200 N95-26523 #
NAL-TR-1234 .... p 2139 N95-26706 #
NAL-TR-1236 .... p 2128 N95-26525 #

NAL-TR-1238 .... p 2180 N95-26667 #
NAL-TR-1250 .... p 2167 N95-26799 #

NAS 1.15:104566-VOL-26 .... p 2345 N95-26430 * #
NAS 1.15:104566-VOL-27 .... p 2348 N95-28030 * #
NAS 1.15:104606-VOL-6 .... p 2334 N95-26423 * #
NAS 1.15:106576 .... p 2168 N95-27861 * #
NAS 1.15:106585 .... p 2301 N95-26774 * #
NAS 1.15:106638 .... p 2303 N95-27911 * #
NAS 1.15:106685 .... p 2168 N95-27434 * #
NAS 1.15:106707 .... p 2273 N95-26380 * #
NAS 1.15:106814 .... p 2284 N95-27854 * #
NAS 1.15:106874 .... p 2301 N95-27178 * #
NAS 1.15:106875 .... p 2302 N95-27855 * #
NAS 1.15:106886 .... p 2140 N95-28344 * #
NAS 1.15:106893 .... p 2309 N95-27174 * #
NAS 1.15:106896 .... p 2291 N95-27173 * #
NAS 1.15:106903 .... p 2143 N95-27176 * #
NAS 1.15:106908 .... p 2372 N95-27905 * #
NAS 1.15:106909 .... p 2283 N95-27369 * #
NAS 1.15:106910 .... p 2218 N95-27728 * #
NAS 1.15:106911 .... p 2164 N95-27761 * #
NAS 1.15:106912 .... p 2266 N95-27853 * #
NAS 1.15:106915 .... p 2389 N95-26663 * #
NAS 1.15:106917 .... p 2401 N95-26801 * #
NAS 1.15:106920 .... p 2426 N95-27906 * #
NAS 1.15:106921 .... p 2391 N95-27726 * #
NAS 1.15:106922 .... p 2293 N95-28037 * #
NAS 1.15:106923 .... p 2291 N95-27030 * #
NAS 1.15:106925 .... p 2168 N95-27862 * #
NAS 1.15:106930 .... p 2279 N95-27175 * #
NAS 1.15:106932 .... p 2302 N95-27373 * #
NAS 1.15:106933 .... p 2169 N95-28036 * #
NAS 1.15:106934 .... p 2302 N95-27698 * #
NAS 1.15:106940 .... p 2169 N95-28213 * #
NAS 1.15:106941 .... p 2264 N95-27374 * #
NAS 1.15:106942 .... p 2168 N95-27727 * #
NAS 1.15:106944 .... p 2164 N95-27730 * #
NAS 1.15:106947 .... p 2125 N95-27762 * #
NAS 1.15:106949 .... p 2371 N95-27370 * #
NAS 1.15:106951 .... p 2140 N95-27860 * #
NAS 1.15:108488 .... p 2358 N95-26364 * #
NAS 1.15:108491 .... p 2304 N95-28364 * #
NAS 1.15:108574 .... p 2475 N95-28002 * #
NAS 1.15:108863 .... p 2118 N95-26710 * #
NAS 1.15:108866 .... p 2139 N95-26412 * #
NAS 1.15:109168 .... p 2117 N95-26381 * #
NAS 1.15:109184 .... p 2362 N95-27241 * #
NAS 1.15:110142 .... p 2126 N95-27859 * #
NAS 1.15:110160 .... p 2400 N95-26394 * #
NAS 1.15:110161 .... p 2142 N95-27839 * #
NAS 1.15:110348 .... p 2127 N95-26587 * #
NAS 1.15:110349 .... p 2141 N95-26773 * #
NAS 1.15:110350 .... p 2367 N95-26726 * #
NAS 1.15:110352 .... p 2122 N95-27258 * #
NAS 1.15:110355 .... p 2457 N95-28677 * #
NAS 1.15:110594 .... p 2159 N95-26379 * #
NAS 1.15:110599 .... p 2306 N95-26778 * #
NAS 1.15:110608 .... p 2401 N95-27908 * #
NAS 1.15:110609 .... p 2464 N95-28009 * #
NAS 1.15:110619 .... p 2455 N95-27701 * #
NAS 1.15:110620 .... p 2145 N95-27919 * #
NAS 1.15:110632 .... p 2242 N95-26781 * #
NAS 1.15:110650 .... p 2452 N95-26673 * #
NAS 1.15:110651 .... p 2160 N95-27238 * #
NAS 1.15:110653 .... p 2454 N95-27243 * #
NAS 1.15:4611 .... p 2123 N95-28241 * #
NAS 1.15:4631 .... p 2362 N95-27914 * #
NAS 1.15:4647 .... p 2209 N95-28182 * #
NAS 1.15:4656 .... p 2420 N95-27372 * #
NAS 1.15:4658 .... p 2291 N95-27259 * #
NAS 1.15:4677 .... p 2245 N95-28460 * #
NAS 1.15:4695 .... p 2293 N95-27915 * #
NAS 1.15:83199-PT-4 .... p 2400 N95-26392 * #
NAS 1.21:4308 .... p 2474 N95-27685 * #
NAS 1.21:507 .... p 2458 N95-27068 * #
NAS 1.21:6104 .... p 2162 N95-26586 * #
NAS 1.21:7011(402) .... p 2354 N95-27502 *
NAS 1.21:7037(318) .... p 2120 N95-27543 *
NAS 1.26:106918 .... p 2167 N95-27177 * #
NAS 1.26:188366-VOL-1 .... p 2239 N95-28385 * #
NAS 1.26:188366-VOL-2 .... p 2239 N95-28386 * #
NAS 1.26:188366-VOL-3 .... p 2239 N95-28387 * #
NAS 1.26:189077 .... p 2266 N95-27999 * #
NAS 1.26:189139 .... p 2168 N95-28000 * #
NAS 1.26:189184 .... p 2279 N95-27242 * #
NAS 1.26:189677 .... p 2402 N95-28264 * #
NAS 1.26:189705-VOL-2 .... p 2402 N95-28073 * #
NAS 1.26:189714 .... p 2140 N95-28227 * #
NAS 1.26:191012 .... p 2243 N95-28001 * #
NAS 1.26:195000 .... p 2288 N95-28571 *
NAS 1.26:195045 .... p 2388 N95-26395 * #
NAS 1.26:195062 .... p 2389 N95-26672 * #
NAS 1.26:195063 .... p 2273 N95-26576 * #
NAS 1.26:195065 .... p 2278 N95-27028 * #
NAS 1.26:195066 .... p 2361 N95-26697 * #
NAS 1.26:195069 .... p 2278 N95-27027 * #
NAS 1.26:195070 .... p 2391 N95-27433 * #
NAS 1.26:195072 .... p 2284 N95-27760 * #
NAS 1.26:195073 .... p 2390 N95-27029 * #
NAS 1.26:195077 .... p 2402 N95-28670 * #
NAS 1.26:195354 .... p 2307 N95-26387 * #
NAS 1.26:195422 .... p 2316 N95-26393 * #
NAS 1.26:195432 .... p 2321 N95-27970 * #
NAS 1.26:195436 .... p 2117 N95-26363 * #
NAS 1.26:195444 .... p 2372 N95-27729 * #
NAS 1.26:195449 .... p 2166 N95-26390 * #
NAS 1.26:195453-PT-2 .... p 2310 N95-28032 * #
NAS 1.26:195458 .... p 2244 N95-26709 * #
NAS 1.26:195462 .... p 2316 N95-26734 * #
NAS 1.26:195469 .... p 2140 N95-27866 * #
NAS 1.26:195473 .... p 2206 N95-27695 * #
NAS 1.26:196582 .... p 2168 N95-27424 * #
NAS 1.26:196586 .... p 2164 N95-27093 * #
NAS 1.26:196594 .... p 2360 N95-27164 * #
NAS 1.26:196597 .... p 2247 N95-28419 * #
NAS 1.26:196602 .... p 2351 N95-27329 * #
NAS 1.26:196603 .... p 2202 N95-27168 * #
NAS 1.26:196605 .... p 2450 N95-27169 * #
NAS 1.26:196613 .... p 2301 N95-27244 * #
NAS 1.26:196614 .... p 2154 N95-27245 * #
NAS 1.26:196694 .... p 2131 N95-27143 * #
NAS 1.26:196696 .... p 2358 N95-28676 * #
NAS 1.26:197678 .... p 2326 N95-26808 * #
NAS 1.26:197723 .... p 2319 N95-27193 * #
NAS 1.26:197724 .... p 2319 N95-27194 * #
NAS 1.26:197726 .... p 2362 N95-26386 * #
NAS 1.26:197729 .... p 2365 N95-26628 *
NAS 1.26:197732 .... p 2395 N95-27417 *
NAS 1.26:197744 .... p 2129 N95-26651 * #
NAS 1.26:197745 .... p 2130 N95-26813 * #
NAS 1.26:197746 .... p 2275 N95-26766 * #
NAS 1.26:197747 .... p 2121 N95-26760 * #
NAS 1.26:197748 .... p 2120 N95-26649 * #
NAS 1.26:197749 .... p 2139 N95-26777 * #
NAS 1.26:197750 .... p 2143 N95-26775 * #
NAS 1.26:197751 .... p 2274 N95-26665 * #
NAS 1.26:197752 .... p 2365 N95-26648 * #
NAS 1.26:197753 .... p 2275 N95-26776 * #
NAS 1.26:197754 .... p 2129 N95-26591 * #
NAS 1.26:197755 .... p 2121 N95-26735 * #
NAS 1.26:197756 .... p 2129 N95-26590 * #
NAS 1.26:197757 .... p 2274 N95-26589 * #
NAS 1.26:197758 .... p 2274 N95-26588 * #
NAS 1.26:197759 .... p 2160 N95-27154 * #
NAS 1.26:197760 .... p 2365 N95-26668 * #
NAS 1.26:197761 .... p 2367 N95-26814 * #
NAS 1.26:197762 .... p 2363 N95-26388 * #
NAS 1.26:197763 .... p 2366 N95-26693 * #
NAS 1.26:197764 .... p 2365 N95-26575 * #
NAS 1.26:197765 .... p 2371 N95-27252 * #
NAS 1.26:197766 .... p 2366 N95-26711 * #
NAS 1.26:197767 .... p 2364 N95-26486 * #
NAS 1.26:197768 .... p 2366 N95-26695 * #
NAS 1.26:197769 .... p 2367 N95-26802 * #
NAS 1.26:197772 .... p 2367 N95-26770 * #
NAS 1.26:197773 .... p 2306 N95-27253 * #
NAS 1.26:197774 .... p 2314 N95-26815 * #
NAS 1.26:197777 .... p 2278 N95-27165 * #
NAS 1.26:197780 .... p 2336 N95-26922 * #
NAS 1.26:197784 .... p 2369 N95-26930 * #
NAS 1.26:197785 .... p 2341 N95-26669 * #
NAS 1.26:197787 .... p 2461 N95-26593 * #
NAS 1.26:197788 .... p 2464 N95-26671 * #
NAS 1.26:197792 .... p 2144 N95-26426 * #
NAS 1.26:197798 .... p 2326 N95-26362 * #
NAS 1.26:197801 .... p 2143 N95-26768 * #
NAS 1.26:197803 .... p 2366 N95-26694 * #
NAS 1.26:197804 .... p 2335 N95-26592 * #
NAS 1.26:197808 .... p 2159 N95-26398 * #
NAS 1.26:197809 .... p 2159 N95-26399 * #
NAS 1.26:197810 .... p 2160 N95-26400 * #
NAS 1.26:197811 .... p 2160 N95-26401 * #
NAS 1.26:197812 .... p 2160 N95-26403 * #
NAS 1.26:197813 .... p 2336 N95-26699 * #
NAS 1.26:197815 .... p 2260 N95-26816 * #
NAS 1.26:197816 .... p 2461 N95-27166 * #
NAS 1.26:197819 .... p 2290 N95-26702 * #
NAS 1.26:197820 .... p 2277 N95-26995 * #
NAS 1.26:197830 .... p 2263 N95-27226 * #
NAS 1.26:197831 .... p 2268 N95-28239 * #
NAS 1.26:197832 .... p 2214 N95-27167 * #
NAS 1.26:197835 .... p 2437 N95-26780 * #
NAS 1.26:197840 .... p 2465 N95-26630 * #
NAS 1.26:197841 .... p 2249 N95-26708 * #
NAS 1.26:197845 .... p 2357 N95-27697 * #
NAS 1.26:197849 .... p 2346 N95-26533 *
NAS 1.26:197926 .... p 2326 N95-26429 * #
NAS 1.26:197980 .... p 2349 N95-26727 * #
NAS 1.26:198031 .... p 2144 N95-26583 * #
NAS 1.26:198158 .... p 2279 N95-27247 * #
NAS 1.26:198159 .... p 2287 N95-27917 * #
NAS 1.26:198162 .... p 2279 N95-27179 * #
NAS 1.26:198164 .... p 2289 N95-28673 * #
NAS 1.26:198165 .... p 2371 N95-27246 * #
NAS 1.26:198166 .... p 2163 N95-27026 * #
NAS 1.26:198168 .... p 2288 N95-28228 * #
NAS 1.26:198170 .... p 2456 N95-28600 * #
NAS 1.26:198562 .... p 2235 N95-27694 * #
NAS 1.26:198563 .... p 2475 N95-28038 * #
NAS 1.26:198564 .... p 2292 N95-27863 * #
NAS 1.26:198565 .... p 2247 N95-27909 * #
NAS 1.26:198574 .... p 2279 N95-27240 * #
NAS 1.26:198576 .... p 2127 N95-28168 * #
NAS 1.26:198577 .... p 2343 N95-28191 * #
NAS 1.26:198579 .... p 2131 N95-27180 * #
NAS 1.26:198589 .... p 2329 N95-27864 * #
NAS 1.26:198590 .... p 2123 N95-28193 * #
NAS 1.26:198591 .... p 2306 N95-28034 * #
NAS 1.26:198592 .... p 2464 N95-27858 * #
NAS 1.26:198593 .... p 2343 N95-27997 * #
NAS 1.26:198595 .... p 2292 N95-27368 * #
NAS 1.26:198598 .... p 2443 N95-28033 * #
NAS 1.26:198599 .... p 2351 N95-28177 * #
NAS 1.26:198601 .... p 2236 N95-27857 * #
NAS 1.26:198603 .... p 2122 N95-27248 * #
NAS 1.26:198605 .... p 2426 N95-27913 * #
NAS 1.26:198608 .... p 2315 N95-28209 * #
NAS 1.26:198609 .... p 2138 N95-28203 * #
NAS 1.26:198610 .... p 2310 N95-27865 * #
NAS 1.26:198618-REV .... p 2338 N95-28035 * #
NAS 1.26:198621 .... p 2347 N95-27805 * #
NAS 1.26:198628 .... p 2304 N95-28259 * #
NAS 1.26:198629 .... p 2450 N95-28260 * #
NAS 1.26:198633 .... p 2160 N95-28258 * #
NAS 1.26:198646 .... p 2463 N95-27916 * #
NAS 1.26:198647 .... p 2462 N95-28216 * #
NAS 1.26:198648 .... p 2462 N95-28222 * #
NAS 1.26:198649 .... p 2399 N95-27852 * #
NAS 1.26:198650 .... p 2463 N95-27700 * #
NAS 1.26:198653 .... p 2165 N95-27836 * #
NAS 1.26:198717 .... p 2314 N95-27998 * #
NAS 1.26:198718 .... p 2184 N95-28266 * #
NAS 1.26:198722 .... p 2193 N95-28462 * #
NAS 1.26:198723 .... p 2189 N95-28420 * #
NAS 1.26:198728 .... p 2270 N95-28570 * #
NAS 1.26:1988371 .... p 2145 N95-28261 * #
NAS 1.26:4348 .... p 2123 N95-28265 * #
NAS 1.26:4349 .... p 2123 N95-28230 * #
NAS 1.26:4496 .... p 2123 N95-28003 * #
NAS 1.26:4656 .... p 2177 N95-26391 * #
NAS 1.26:4665 .... p 2136 N95-28262 * #
NAS 1.26:4668 .... p 2279 N95-27257 * #
NAS 1.26:4669 .... p 2357 N95-28253 * #
NAS 1.26:4674 .... p 2268 N95-28181 * #
NAS 1.26:4675 .... p 2131 N95-27371 * #
NAS 1.55:10161 .... p 2280 N95-27345 * #
NAS 1.55:10165 .... p 2285 N95-27882 * #
NAS 1.55:3275-PT-3 .... p 2466 N95-27629 * #
NAS 1.55:3292 .... p 2317 N95-26785 * #
NAS 1.55:3293 .... p 2154 N95-27260 * #
NAS 1.55:3296 .... p 2382 N95-27375 * #
NAS 1.55:3299 .... p 2146 N95-27763 * #
NAS 1.60:3491 .... p 2366 N95-26685 * #
NAS 1.60:3494 .... p 2161 N95-26428 * #
NAS 1.60:3495 .... p 2465 N95-28530 * #
NAS 1.60:3496 .... p 2124 N95-28674 * #
NAS 1.60:3502 .... p 2140 N95-28343 * #
NAS 1.60:3515 .... p 2124 N95-28669 * #
NAS 1.60:3516 .... p 2120 N95-26382 * #
NAS 1.60:3524 .... p 2465 N95-26427 * #
NAS 1.60:3550 .... p 2244 N95-26769 * #
NAS 1.60:3551 .... p 2392 N95-28215 * #
NAS 1.60:3553 .... p 2169 N95-28263 * #
NAS 1.60:3556 .... p 2311 N95-28214 * #
NAS 1.61:1355 .... p 2466 N95-27367 * #
NAS 1.61:1360 .... p 2341 N95-26689 * #
NAS 1.61:1363 .... p 2463 N95-28328 *
NAS 1.61:1365 .... p 2255 N95-27435 * #
NAS 1.71:LAR-13894-1 .... p 2353 N95-26889 * #
NAS 1.71:LAR-14898-1 .... p 2180 N95-26764 * #
NAS 1.71:LAR-15053-1 .... p 2291 N95-27191 * #
NAS 1.71:LAR-15062-1 .... p 2291 N95-27138 * #
NAS 1.71:LAR-15259-1 .... p 2182 N95-27192 * #
NAS 1.71:LEW-15714-1 .... p 2183 N95-27717 * #
NAS 1.71:LEW-15760-1 .... p 2235 N95-27503 * #
NAS 1.71:LEW-15896-1 .... p 2235 N95-27702 * #
NAS 1.71:MFS-28958-1 .... p 2261 N95-26890 * #
NAS 1.71:MFS-28985-1 .... p 2245 N95-26888 * #
NAS 1.71:MFS-28986-1 .... p 2245 N95-27500 * #
NAS 1.71:MFS-28997-1 .... p 2360 N95-27501 * #
NAS 1.71:NPO-18518-1-CU .... p 2424 N95-26894 * #
NAS 1.71:NPO-19064-1-CU .... p 2290 N95-26765 * #
NAS 1.71:NPO-19081-1-CU .... p 2404 N95-26861 * #
NAS 1.71:NPO-19358-1-CU .... p 2213 N95-26862 * #

NASA-CASE-ARC-11891-1-SB ..... p 2238 N95-28212 *
NASA-CASE-ARC-11921-1 .... p 2304 N95-28256 *

NASA-CASE-ARC-11984-1 .... p 2293 N95-28345 *

NASA-CASE-GSC-13404-1 .... p 2269 N95-28341 *
NASA-CASE-GSC-13539-1 .... p 2315 N95-28211 *

NASA-CASE-KSC-11669-1 .... p 2304 N95-28359 *
NASA-CASE-KSC-11687-1 .... p 2293 N95-28362 *

NASA-CASE-LAR-13894-1 .... p 2353 N95-26889 * #
NASA-CASE-LAR-14898-1 .... p 2180 N95-26764 * #
NASA-CASE-LAR-14924-1-CU ..... p 2179 N95-28361 *
NASA-CASE-LAR-14939-1 .... p 2179 N95-28360 *
NASA-CASE-LAR-15053-1 .... p 2291 N95-27191 * #
NASA-CASE-LAR-15062-1 .... p 2291 N95-27138 * #
NASA-CASE-LAR-15175-1 .... p 2235 N95-27732 *
NASA-CASE-LAR-15259-1 .... p 2182 N95-27192 * #

NASA-CASE-LEW-15714-1 .... p 2183 N95-27717 * #
NASA-CASE-LEW-15760-1 .... p 2235 N95-27503 * #
NASA-CASE-LEW-15896-1 .... p 2235 N95-27702 * #

NASA-CASE-MFS-28563-3 .... p 2423 N95-26385 *
NASA-CASE-MFS-28773-1 .... p 2304 N95-28347 *
NASA-CASE-MFS-28958-1 .... p 2261 N95-26890 * #
NASA-CASE-MFS-28985-1 .... p 2245 N95-26888 * #
NASA-CASE-MFS-28986-1 .... p 2245 N95-27500 * #
NASA-CASE-MFS-28997-1 .... p 2360 N95-27501 * #

NASA-CASE-MSC-22015-1 .... p 2165 N95-27842 * #
NASA-CASE-MSC-22255-1 .... p 2427 N95-28384 *

NASA-CASE-NPO-18399-1-CU .... p 2271 N95-28599 *
NASA-CASE-NPO-18470-1-CU .... p 2297 N95-27731 *
NASA-CASE-NPO-18491-2-CU .... p 2427 N95-28363 *
NASA-CASE-NPO-18518-1-CU .... p 2424 N95-26894 * #
NASA-CASE-NPO-18736-1-CU .... p 2426 N95-27843 *
NASA-CASE-NPO-19064-1-CU .... p 2290 N95-26765 * #
NASA-CASE-NPO-19081-1-CU .... p 2404 N95-26861 * #
NASA-CASE-NPO-19081-1-CU .... p 2416 N95-28348 *
NASA-CASE-NPO-19358-1-CU .... p 2213 N95-26862 * #

NASA-CP-10161 .... p 2280 N95-27345 * #
NASA-CP-10165 .... p 2285 N95-27882 * #
NASA-CP-3275-PT-3 .... p 2466 N95-27629 * #
NASA-CP-3292 .... p 2317 N95-26785 * #
NASA-CP-3293 .... p 2154 N95-27260 * #
NASA-CP-3296 .... p 2382 N95-27375 * #
NASA-CP-3299 .... p 2146 N95-27763 * #

NASA-CR-188366-VOL-1 .... p 2239 N95-28385 * #
NASA-CR-188366-VOL-2 .... p 2239 N95-28386 * #
NASA-CR-188366-VOL-3 .... p 2239 N95-28387 * #
NASA-CR-188371 .... p 2145 N95-28261 * #
NASA-CR-189077 .... p 2266 N95-27999 * #
NASA-CR-189139 .... p 2168 N95-28000 * #
NASA-CR-189184 .... p 2279 N95-27242 * #
NASA-CR-189677 .... p 2402 N95-28264 * #
NASA-CR-189705-VOL-2 .... p 2402 N95-28073 * #
NASA-CR-189714 .... p 2140 N95-28227 * #
NASA-CR-191012 .... p 2243 N95-28001 * #
NASA-CR-195000 .... p 2288 N95-28571 *
NASA-CR-195045 .... p 2388 N95-26395 * #
NASA-CR-195062 .... p 2389 N95-26672 * #
NASA-CR-195063 .... p 2273 N95-26576 * #
NASA-CR-195065 .... p 2278 N95-27028 * #
NASA-CR-195066 .... p 2361 N95-26697 * #
NASA-CR-195069 .... p 2278 N95-27027 * #
NASA-CR-195070 .... p 2391 N95-27433 * #
NASA-CR-195072 .... p 2284 N95-27760 * #
NASA-CR-195073 .... p 2390 N95-27029 * #
NASA-CR-195077 .... p 2402 N95-26670 * #
NASA-CR-195354 .... p 2307 N95-26387 * #
NASA-CR-195422 .... p 2316 N95-26393 * #
NASA-CR-195432 .... p 2321 N95-27970 * #
NASA-CR-195436 .... p 2117 N95-26363 * #
NASA-CR-195444 .... p 2372 N95-27729 * #
NASA-CR-195449 .... p 2166 N95-26390 * #
NASA-CR-195452-PT-1 .... p 2310 N95-28031 * #
NASA-CR-195453-PT-2 .... p 2310 N95-28032 * #
NASA-CR-195458 .... p 2244 N95-26709 * #
NASA-CR-195462 .... p 2316 N95-26734 * #
NASA-CR-195469 .... p 2140 N95-27866 * #
NASA-CR-195473 .... p 2206 N95-27695 * #
NASA-CR-196582 .... p 2168 N95-27424 * #
NASA-CR-196586 .... p 2164 N95-27093 * #
NASA-CR-196594 .... p 2360 N95-27164 * #
NASA-CR-196597 .... p 2247 N95-28419 * #
NASA-CR-196602 .... p 2351 N95-27329 * #
NASA-CR-196603 .... p 2202 N95-27168 * #
NASA-CR-196605 .... p 2450 N95-27169 * #
NASA-CR-196613 .... p 2301 N95-27244 * #
NASA-CR-196614 .... p 2154 N95-27245 * #
NASA-CR-196694 .... p 2131 N95-27143 * #
NASA-CR-196696 .... p 2358 N95-26676 * #
NASA-CR-197678 .... p 2326 N95-26808 * #
NASA-CR-197723 .... p 2319 N95-27193 * #
NASA-CR-197724 .... p 2319 N95-27194 * #
NASA-CR-197726 .... p 2362 N95-26386 * #
NASA-CR-197729 .... p 2365 N95-26628 *
NASA-CR-197732 .... p 2395 N95-27417 *
NASA-CR-197737 .... p 2335 N95-26595 *
NASA-CR-197744 .... p 2129 N95-26651 * #
NASA-CR-197745 .... p 2130 N95-26813 * #
NASA-CR-197746 .... p 2275 N95-26766 * #
NASA-CR-197747 .... p 2121 N95-26760 * #
NASA-CR-197748 .... p 2120 N95-26649 * #
NASA-CR-197749 .... p 2139 N95-26777 * #
NASA-CR-197750 .... p 2143 N95-26775 * #
NASA-CR-197751 .... p 2274 N95-26665 * #
NASA-CR-197752 .... p 2365 N95-26648 * #
NASA-CR-197753 .... p 2275 N95-26776 * #
NASA-CR-197754 .... p 2129 N95-26591 * #
NASA-CR-197755 .... p 2121 N95-26735 * #
NASA-CR-197756 .... p 2129 N95-26590 * #
NASA-CR-197757 .... p 2274 N95-26589 * #
NASA-CR-197758 .... p 2274 N95-26588 * #
NASA-CR-197759 .... p 2160 N95-27154 * #
NASA-CR-197760 .... p 2365 N95-26668 * #
NASA-CR-197761 .... p 2367 N95-26814 * #
NASA-CR-197762 .... p 2363 N95-26388 * #
NASA-CR-197763 .... p 2366 N95-26693 * #
NASA-CR-197764 .... p 2365 N95-26575 * #
NASA-CR-197765 .... p 2371 N95-27252 * #
NASA-CR-197766 .... p 2366 N95-26711 * #
NASA-CR-197767 .... p 2364 N95-26486 * #
NASA-CR-197768 .... p 2366 N95-26695 * #
NASA-CR-197769 .... p 2367 N95-26802 * #
NASA-CR-197772 .... p 2367 N95-26770 * #
NASA-CR-197773 .... p 2306 N95-27253 * #
NASA-CR-197774 .... p 2314 N95-26815 * #
NASA-CR-197777 .... p 2278 N95-27165 * #
NASA-CR-197780 .... p 2336 N95-26922 * #
NASA-CR-197784 .... p 2369 N95-26930 * #
NASA-CR-197785 .... p 2341 N95-26669 * #
NASA-CR-197787 .... p 2461 N95-26593 * #
NASA-CR-197788 .... p 2464 N95-26671 * #
NASA-CR-197792 .... p 2144 N95-26426 * #
NASA-CR-197798 .... p 2326 N95-26362 * #
NASA-CR-197801 .... p 2143 N95-26768 * #
NASA-CR-197803 .... p 2366 N95-26694 * #
NASA-CR-197804 .... p 2335 N95-26592 * #
NASA-CR-197808 .... p 2159 N95-26398 * #
NASA-CR-197809 .... p 2159 N95-26399 * #
NASA-CR-197810 .... p 2160 N95-26400 * #
NASA-CR-197811 .... p 2160 N95-26401 * #
NASA-CR-197812 .... p 2160 N95-26403 * #
NASA-CR-197813 .... p 2336 N95-26699 * #
NASA-CR-197815 .... p 2260 N95-26816 * #
NASA-CR-197816 .... p 2461 N95-27166 * #
NASA-CR-197819 .... p 2290 N95-26702 * #
NASA-CR-197820 .... p 2277 N95-26995 * #
NASA-CR-197828 .... p 2335 N95-26596 *
NASA-CR-197829 .... p 2335 N95-26594 *
NASA-CR-197830 .... p 2263 N95-27226 * #
NASA-CR-197831 .... p 2268 N95-28239 * #
NASA-CR-197832 .... p 2214 N95-27167 * #
NASA-CR-197835 .... p 2437 N95-26780 * #
NASA-CR-197840 .... p 2465 N95-26630 * #
NASA-CR-197841 .... p 2249 N95-26708 * #
NASA-CR-197845 .... p 2357 N95-27697 * #
NASA-CR-197849 .... p 2346 N95-26533 *
NASA-CR-197926 .... p 2326 N95-26429 * #
NASA-CR-197980 .... p 2349 N95-26727 * #
NASA-CR-198031 .... p 2144 N95-26583 * #
NASA-CR-198158 .... p 2279 N95-27247 * #
NASA-CR-198159 .... p 2287 N95-27917 * #
NASA-CR-198162 .... p 2279 N95-27179 * #
NASA-CR-198164 .... p 2289 N95-26673 * #
NASA-CR-198165 .... p 2371 N95-27246 * #
NASA-CR-198166 .... p 2163 N95-27026 * #
NASA-CR-198168 .... p 2288 N95-28228 * #
NASA-CR-198170 .... p 2456 N95-28600 * #
NASA-CR-198562 .... p 2235 N95-27694 * #
NASA-CR-198563 .... p 2475 N95-28038 * #
NASA-CR-198564 .... p 2292 N95-27863 * #
NASA-CR-198565 .... p 2247 N95-27909 * #
NASA-CR-198574 .... p 2279 N95-27240 * #
NASA-CR-198576 .... p 2127 N95-28188 * #
NASA-CR-198577 .... p 2343 N95-28191 * #
NASA-CR-198579 .... p 2131 N95-27180 * #
NASA-CR-198589 .... p 2329 N95-27864 * #
NASA-CR-198590 .... p 2123 N95-28193 * #
NASA-CR-198591 .... p 2306 N95-28034 * #
NASA-CR-198592 .... p 2464 N95-27858 * #
NASA-CR-198593 .... p 2343 N95-27997 * #
NASA-CR-198595 .... p 2292 N95-27368 * #
NASA-CR-198598 .... p 2443 N95-28033 * #
NASA-CR-198599 .... p 2351 N95-28177 * #
NASA-CR-198601 .... p 2236 N95-27857 * #
NASA-CR-198603 .... p 2122 N95-27248 * #
NASA-CR-198605 .... p 2426 N95-27913 * #
NASA-CR-198608 .... p 2315 N95-28209 * #
NASA-CR-198609 .... p 2138 N95-28203 * #
NASA-CR-198610 .... p 2310 N95-27865 * #
NASA-CR-198618-REV .... p 2338 N95-28035 * #
NASA-CR-198621 .... p 2347 N95-27805 * #
NASA-CR-198628 .... p 2304 N95-28259 * #
NASA-CR-198629 .... p 2450 N95-28260 * #
NASA-CR-198633 .... p 2160 N95-28258 * #
NASA-CR-198646 .... p 2463 N95-27916 * #
NASA-CR-198647 .... p 2462 N95-28216 * #
NASA-CR-198648 .... p 2462 N95-28222 * #
NASA-CR-198649 .... p 2399 N95-27852 * #
NASA-CR-198650 .... p 2463 N95-27700 * #
NASA-CR-198653 .... p 2165 N95-27836 * #
NASA-CR-198717 .... p 2314 N95-27998 * #
NASA-CR-198718 .... p 2184 N95-28266 * #
NASA-CR-198722 .... p 2193 N95-28462 * #
NASA-CR-198723 .... p 2189 N95-28420 * #
NASA-CR-198728 .... p 2270 N95-28570 * #
NASA-CR-4348 .... p 2123 N95-28265 * #
NASA-CR-4349 .... p 2123 N95-28230 * #
NASA-CR-4496 .... p 2123 N95-28003 * #
NASA-CR-4656 .... p 2177 N95-26391 * #
NASA-CR-4665 .... p 2136 N95-28262 * #
NASA-CR-4668 .... p 2279 N95-27257 * #
NASA-CR-4669 .... p 2357 N95-28253 * #
NASA-CR-4674 .... p 2268 N95-28181 * #
NASA-CR-4675 .... p 2131 N95-27371 * #

NASA-IVV-94-001 .... p 2366 N95-26695 * #
NASA-IVV-94-002 .... p 2364 N95-26486 * #
NASA-IVV-94-003 .... p 2366 N95-26711 * #
NASA-IVV-94-004 .... p 2371 N95-27252 * #
NASA-IVV-94-006 .... p 2366 N95-26693 * #
NASA-IVV-94-007 .... p 2363 N95-26388 * #
NASA-IVV-94-008 .... p 2367 N95-26814 * #
NASA-IVV-94-009 .... p 2365 N95-26668 * #
NASA-IVV-94-010 .... p 2367 N95-26802 * #
NASA-IVV-94-011 .... p 2362 N95-26386 * #
NASA-IVV-95-005 .... p 2365 N95-26575 * #

NASA-RP-1355 .... p 2466 N95-27367 * #
NASA-RP-1360 .... p 2341 N95-26689 * #
NASA-RP-1363 .... p 2463 N95-28328 *
NASA-RP-1365 .... p 2255 N95-27435 * #

NASA-SP-4308 .... p 2474 N95-27685 * #
NASA-SP-507 .... p 2458 N95-27068 * #
NASA-SP-6104 .... p 2162 N95-26586 * #
NASA-SP-7011(402) .... p 2354 N95-27502 *
NASA-SP-7037(318) .... p 2120 N95-27543 *

NASA-TM-104566-VOL-26 .... p 2345 N95-26430 * #
NASA-TM-104566-VOL-27 .... p 2348 N95-28030 * #
NASA-TM-104606-VOL-6 .... p 2334 N95-26423 * #
NASA-TM-106576 .... p 2168 N95-27861 * #
NASA-TM-106585 .... p 2301 N95-26774 * #
NASA-TM-106638 .... p 2303 N95-27911 * #
NASA-TM-106685 .... p 2168 N95-27434 * #
NASA-TM-106707 .... p 2273 N95-26380 * #
NASA-TM-106814 .... p 2284 N95-27854 * #
NASA-TM-106874 .... p 2301 N95-27178 * #
NASA-TM-106875 .... p 2302 N95-27855 * #
NASA-TM-106886 .... p 2140 N95-28344 * #
NASA-TM-106893 .... p 2309 N95-27174 * #
NASA-TM-106896 .... p 2291 N95-27173 * #
NASA-TM-106903 .... p 2143 N95-27176 * #
NASA-TM-106908 .... p 2372 N95-27905 * #
NASA-TM-106909 .... p 2283 N95-27369 * #
NASA-TM-106910 .... p 2218 N95-27728 * #
NASA-TM-106911 .... p 2164 N95-27761 * #
NASA-TM-106912 .... p 2266 N95-27853 * #
NASA-TM-106915 .... p 2389 N95-26663 * #
NASA-TM-106917 .... p 2401 N95-26801 * #
NASA-TM-106918 .... p 2167 N95-27177 * #
NASA-TM-106920 .... p 2426 N95-27906 * #
NASA-TM-106921 .... p 2391 N95-27726 * #
NASA-TM-106922 .... p 2293 N95-28037 * #
NASA-TM-106923 .... p 2291 N95-27030 * #
NASA-TM-106925 .... p 2168 N95-27862 * #
NASA-TM-106930 .... p 2279 N95-27175 * #
NASA-TM-106932 .... p 2302 N95-27373 * #
NASA-TM-106933 .... p 2169 N95-28036 * #
NASA-TM-106934 .... p 2302 N95-27698 * #
NASA-TM-106940 .... p 2169 N95-28213 * #
NASA-TM-106941 .... p 2264 N95-27374 * #
NASA-TM-106942 .... p 2168 N95-27727 * #
NASA-TM-106944 .... p 2164 N95-27730 * #
NASA-TM-106947 .... p 2125 N95-27762 * #
NASA-TM-106949 .... p 2371 N95-27370 * #
NASA-TM-106951 .... p 2140 N95-27860 * #
NASA-TM-108488 .... p 2358 N95-26364 * #
NASA-TM-108491 .... p 2304 N95-28364 * #
NASA-TM-108574 .... p 2475 N95-28002 * #
NASA-TM-108863 .... p 2118 N95-26710 * #
NASA-TM-108866 .... p 2139 N95-26412 * #
NASA-TM-109168 .... p 2117 N95-26381 * #

NASA-TM-109184 .... p 2362 N95-27241 * #
NASA-TM-110142 .... p 2126 N95-27859 * #
NASA-TM-110160 .... p 2400 N95-26394 * #
NASA-TM-110161 .... p 2142 N95-27839 * #
NASA-TM-110348 .... p 2127 N95-26587 * #
NASA-TM-110349 .... p 2141 N95-26773 * #
NASA-TM-110350 .... p 2367 N95-26726 * #
NASA-TM-110352 .... p 2122 N95-27258 * #
NASA-TM-110355 .... p 2457 N95-28677 * #
NASA-TM-110594 .... p 2159 N95-26379 * #
NASA-TM-110599 .... p 2306 N95-26778 * #
NASA-TM-110608 .... p 2401 N95-27908 * #
NASA-TM-110609 .... p 2464 N95-28009 * #
NASA-TM-110619 .... p 2455 N95-27701 * #
NASA-TM-110620 .... p 2145 N95-27919 * #
NASA-TM-110632 .... p 2242 N95-26781 * #
NASA-TM-110650 .... p 2452 N95-26673 * #
NASA-TM-110651 .... p 2160 N95-27238 * #
NASA-TM-110653 .... p 2454 N95-27243 * #
NASA-TM-4611 .... p 2123 N95-28241 * #
NASA-TM-4631 .... p 2362 N95-27914 * #
NASA-TM-4647 .... p 2209 N95-28182 * #
NASA-TM-4656 .... p 2420 N95-27372 * #
NASA-TM-4658 .... p 2291 N95-27259 * #
NASA-TM-4677 .... p 2245 N95-28460 * #
NASA-TM-4695 .... p 2293 N95-27915 * #
NASA-TM-83199-PT-4 .... p 2400 N95-26392 * #

NASA-TP-3491 .... p 2366 N95-26685 * #
NASA-TP-3494 .... p 2161 N95-26428 * #
NASA-TP-3495 .... p 2465 N95-28530 * #
NASA-TP-3496 .... p 2124 N95-28674 * #
NASA-TP-3502 .... p 2140 N95-28343 * #
NASA-TP-3515 .... p 2124 N95-28669 * #
NASA-TP-3516 .... p 2120 N95-26382 * #
NASA-TP-3524 .... p 2465 N95-26427 * #
NASA-TP-3550 .... p 2244 N95-26769 * #
NASA-TP-3551 .... p 2392 N95-28215 * #
NASA-TP-3553 .... p 2169 N95-28263 * #
NASA-TP-3556 .... p 2311 N95-28214 * #

NASA-04 .... p 2450 N95-27169 * #

NATICK/TR-95/006 .... p 2361 N95-28390
NATICK/TR-95/017 .... p 2126 N95-28454

NAVY-CASE-75668 .... p 2161 N95-28581
NAVY-CASE-76174 .... p 2241 N95-28582
NAVY-CASE-76320 .... p 2259 N95-26433

NAWCADWAR-94112-50 .... p 2248 N95-26356

NCCOSC/RDT/E-TD-2697 .... p 2456 N95-28589
NCCOSC/RDT/E-TD-2721 .... p 2258 N95-28576

NCTRF-204 .... p 2358 N95-26736

NDU-ICAF-94-F28 .... p 2357 N95-27181
NDU-ICAF-94-F2 .... p 2117 N95-26409
NDU-ICAF-94-F56 .... p 2117 N95-26455

NEDO-GET-9301 .... p 2329 N95-27941 #
NEDO-GET-9302-2 .... p 2321 N95-27940
NEDO-GET-9303 .... p 2331 N95-28535 #
NEDO-GET-9304 .... p 2330 N95-27942 #
NEDO-GET-9307 .... p 2329 N95-27939 #
NEDO-GET-9309 .... p 2329 N95-27938 #
NEDO-GET-9310-4 .... p 2458 N95-27937 #

NEDO-P-9310 .... p 2320 N95-27936 #
NEDO-P-9330 .... p 2329 N95-27935 #

NIAR-94-1 .... p 2118 N95-26941 #

NIFS-255 .... p 2419 N95-26584 #

NISTIR-5547 .... p 2247 N95-28008
NISTIR-5597 .... p 2308 N95-26743

NMERI-OC-94-32 .... p 2234 N95-27461 #
NMERI-OC-94/31 .... p 2238 N95-28133 #

NMRI-94-36 .... p 2353 N95-26885

NMSU-PHYS-01-95 .... p 2300 N95-28509

NOAA-TM-ERL-SEL-85 .... p 2464 N95-28007 #

NONP-NASA-DK-95-48301 .... p 2127 N95-26587 * #
NONP-NASA-DK-95-48683 .... p 2177 N95-26391 * #

NONP-NASA-VT-95-42903 .... p 2335 N95-26594 *
NONP-NASA-VT-95-42904 .... p 2335 N95-26595 *
NONP-NASA-VT-95-42905 .... p 2335 N95-26596 *
NONP-NASA-VT-95-49096 .... p 2451 N95-27202
NONP-NASA-VT-95-49097 .... p 2246 N95-27203
NONP-NASA-VT-95-49098 .... p 2203 N95-27204
NONP-NASA-VT-95-49099 .... p 2451 N95-27205
NONP-NASA-VT-95-49118 .... p 2451 N95-27206
NONP-NASA-VT-95-49119 .... p 2451 N95-27207
NONP-NASA-VT-95-49120 .... p 2454 N95-27208
NONP-NASA-VT-95-49121 .... p 2451 N95-27209

NPL-DMM(A)-148 .... p 2227 N95-26747
NPL-DMM(A)-149 .... p 2226 N95-26744
NPL-DMM(A)-151 .... p 2224 N95-26448
NPL-DMM(A)-152 .... p 2227 N95-26746
NPL-DMM(A)-54-REV .... p 2308 N95-26749

NPL-DMM(A)126 .... p 2226 N95-26745

NPL-DMM-(A)-140 .... p 2201 N95-26750

NPL-QU-104 .... p 2398 N95-26614

NPL-RSA(EXT)0054 .... p 2401 N95-26615
NPL-RSA(EXT)47 .... p 2404 N95-26748

NPS-ME-94-006 .... p 2308 N95-26625
NPS-ME-94-009 .... p 2213 N95-26681

NPS-MR-94-002 .... p 2344 N95-28459
NPS-MR-94-003 .... p 2346 N95-26477

NPS-OR-94-0113 .... p 2326 N95-26431
NPS-OR-94-014 .... p 2352 N95-28519

NRAD-TD-2703 .... p 2363 N95-26447

NRCN-605 .... p 2217 N95-27713 #

NREL-CP-430-7215 .... p 2204 N95-27438 #

NREL/TP-411-7416 .... p 2320 N95-27704 #
NREL/TP-421-7501 .... p 2325 N95-28394 #
NREL/TP-441-7223 .... p 2320 N95-27475 #
NREL/TP-441-7390 .... p 2325 N95-28395 #
NREL/TP-442-7226 .... p 2319 N95-27459 #
NREL/TP-442-7388 .... p 2122 N95-27541 #
NREL/TP-463-7540 .... p 2265 N95-27719 #
NREL/TP-472-7574 .... p 2325 N95-28396 #
NREL/TP-473-7025 .... p 2327 N95-27540 #

NRL-MR/7441-93-7079 .... p 2388 N95-26459
NRL-MR/7441-94-7541 .... p 2314 N95-26682

NRL/FR/5220-94-9378 .... p 2466 N95-26823
NRL/FR/5550-94-9743 .... p 2248 N95-26349
NRL/FR/7322-94-9601 .... p 2347 N95-27189
NRL/FR/7323-93-9444 .... p 2345 N95-26406

NRL/MR/5554-7622 .... p 2249 N95-26564
NRL/MR/6170-94-7633 .... p 2225 N95-26499
NRL/MR/6384-94-7641 .... p 2276 N95-26852
NRL/MR/6680-94-7634 .... p 2295 N95-26996
NRL/MR/7441-94-7546 .... p 2313 N95-26476

NRL/PU/7541-94-0016 .... p 2344 N95-28577

NSWCDD/TR-94/217 .... p 2379 N95-28335

NTSB/AAR-95/02 .... p 2125 N95-26498 #

NUREG-CR-6272 .... p 2311 N95-28100

NUWC-NPT-TR-10771 .... p 2241 N95-28574

NV-95-C01 .... p 2300 N95-28333

NWRA-CR-94-R120 .... p 2334 N95-26520

OMI-01-92 .... p 2122 N95-27248 * #

ORNL-6780 .... p 2241 N95-28560 #

ORNL/M-3733 .... p 2215 N95-27464 #
ORNL/M-4021 .... p 2443 N95-28076 #

ORNL/SUB-86-22049/2 .... p 2239 N95-28397 #
ORNL/SUB-87-SB045/2 .... p 2303 N95-27947 #
ORNL/SUB-90-SG151/1 .... p 2236 N95-27946 #
ORNL/SUB-91-SG341/1 .... p 2221 N95-28075 #

ORNL/TM-12738 .... p 2243 N95-27944 #
ORNL/TM-12890 .... p 2378 N95-28019 #
ORNL/TM-12891 .... p 2288 N95-28533 #
ORNL/TM-12923 .... p 2392 N95-28110 #

OZ-93/14 .... p 2415 N95-28246 #

PB94-155702 .... p 2475 N95-28038 * #
PB94-184843 .... p 2247 N95-27909 * #

PB95-100244 .... p 2268 N95-28239 * #
PB95-179735 .... p 2208 N95-28006
PB95-181848 .... p 2465 N95-28087 #
PB95-181962 .... p 2464 N95-28007 #
PB95-182259 .... p 2247 N95-28008
PB95-184024 .... p 2464 N95-28009 * #
PB95-184818 .... p 2276 N95-26928 #
PB95-184826 .... p 2252 N95-26929
PB95-184834 .... p 2451 N95-28135 #
PB95-184842 .... p 2396 N95-28352 #
PB95-184859 .... p 2396 N95-28353 #
PB95-184867 .... p 2246 N95-27048 #
PB95-184883 .... p 2254 N95-27049 #
PB95-184891 .... p 2262 N95-27050
PB95-184909 .... p 2256 N95-28354 #
PB95-184917 .... p 2369 N95-26907 #
PB95-184925 .... p 2252 N95-26908
PB95-184941 .... p 2356 N95-26909
PB95-184966 .... p 2313 N95-26645 #
PB95-184974 .... p 2260 N95-26646 #
PB95-184982 .... p 2452 N95-26631 #
PB95-185013 .... p 2389 N95-26910
PB95-185021 .... p 2308 N95-26911
PB95-185039 .... p 2396 N95-26912
PB95-185047 .... p 2396 N95-26613 #
PB95-185054 .... p 2395 N95-26913
PB95-185062 .... p 2388 N95-26495 #
PB95-185088 .... p 2259 N95-26496 #
PB95-185096 .... p 2248 N95-26450 #
PB95-185104 .... p 2252 N95-26914
PB95-185112 .... p 2224 N95-26448
PB95-185120 .... p 2379 N95-26449 #
PB95-185138 .... p 2437 N95-26513 #
PB95-185146 .... p 2461 N95-26522 #
PB95-185153 .... p 2461 N95-27320
PB95-185161 .... p 2388 N95-26514 #
PB95-185179 .... p 2388 N95-26515 #
PB95-185187 .... p 2396 N95-26538 #
PB95-185195 .... p 2388 N95-26516 #
PB95-185203 .... p 2389 N95-26915
PB95-185211 .... p 2388 N95-26539 #
PB95-185237 .... p 2398 N95-26614
PB95-185245 .... p 2401 N95-26615
PB95-185252 .... p 2200 N95-26540 #
PB95-188116 .... p 2263 N95-27226 * #
PB95-189528 .... p 2308 N95-26743
PB95-190088 .... p 2226 N95-26744
PB95-190096 .... p 2226 N95-26745
PB95-190104 .... p 2227 N95-26746
PB95-190112 .... p 2227 N95-26747
PB95-190120 .... p 2404 N95-26748
PB95-190138 .... p 2392 N95-28010
PB95-190146 .... p 2397 N95-28011
PB95-190153 .... p 2392 N95-28012 #
PB95-190161 .... p 2397 N95-28174 #
PB95-190179 .... p 2449 N95-28175 #
PB95-190195 .... p 2308 N95-26749
PB95-190203 .... p 2201 N95-26750
PB95-192415 .... p 2137 N95-28636 #
PB95-192423 .... p 2289 N95-28637
PB95-192456 .... p 2418 N95-28638 #
PB95-192811 .... p 2199 N95-28639
PB95-192837 .... p 2418 N95-28640
PB95-192860 .... p 2418 N95-28641
PB95-192878 .... p 2418 N95-28642
PB95-192886 .... p 2271 N95-28663
PB95-192894 .... p 2450 N95-28664 #
PB95-195335 .... p 2379 N95-28665
PB95-195343 .... p 2294 N95-28651
PB95-195368 .... p 2210 N95-28652
PB95-195418 .... p 2393 N95-28653 #
PB95-195426 .... p 2435 N95-28654
PB95-195434 .... p 2271 N95-28655 #
PB95-195467 .... p 2316 N95-28656
PB95-195483 .... p 2269 N95-28448
PB95-195491 .... p 2257 N95-28449 #
PB95-195509 .... p 2257 N95-28450 #
PB95-195517 .... p 2257 N95-28451 #
PB95-195525 .... p 2393 N95-28499 #
PB95-195533 .... p 2315 N95-28643 #
PB95-195566 .... p 2224 N95-28644
PB95-195640 .... p 2375 N95-28645
PB95-195798 .... p 2418 N95-28657
PB95-195806 .... p 2375 N95-28658
PB95-196242 .... p 2423 N95-28452
PB95-196259 .... p 2465 N95-28500
PB95-196267 .... p 2393 N95-28501 #
PB95-196275 .... p 2393 N95-28611 #
PB95-196366 .... p 2379 N95-28502
PB95-196382 .... p 2361 N95-28659
PB95-196424 .... p 2224 N95-28660
PB95-196507 .... p 2219 N95-27934
PB95-196564 .... p 2315 N95-28180 #
PB95-196580 .... p 2379 N95-28093
PB95-910402 .... p 2125 N95-26498 #

PCMDI-18 p 2338 N95-27931 #
PCMDI-21 p 2331 N95-28157 #

PFC/RR-94-12 p 2411 N95-28020 #
PFC/RR-94-13 p 2432 N95-27688 #

PL-TR-94-1005 p 2162 N95-26850
PL-TR-94-1126 p 2429 N95-26720
PL-TR-94-2084 p 2337 N95-27146
PL-TR-94-2150 p 2340 N95-26479
PL-TR-94-2193 p 2295 N95-27022
PL-TR-94-2198 p 2337 N95-27703
PL-TR-94-2202 p 2253 N95-27005
PL-TR-94-2211 p 2356 N95-26992
PL-TR-94-2254 p 2334 N95-26520
PL-TR-94-2266 p 2339 N95-28575
PL-TR-94-2273 p 2165 N95-28578
PL-TR-94-2308 p 2253 N95-26983
PL-TR-94-3050 p 2417 N95-28572

PNL-SA-23947 p 2454 N95-27483 #
PNL-SA-24007 p 2216 N95-27479 #
PNL-SA-24126 p 2222 N95-28129 #
PNL-SA-24441 p 2214 N95-27088 #
PNL-SA-24754 p 2373 N95-28243 #
PNL-SA-24828 p 2222 N95-28163 #
PNL-SA-24841 p 2222 N95-28130 #
PNL-SA-24864 p 2216 N95-27492 #
PNL-SA-25014 p 2267 N95-28131 #
PNL-SA-25035 p 2234 N95-27476 #
PNL-SA-25472 p 2203 N95-27401 #
PNL-SA-25507 p 2216 N95-27493 #
PNL-SA-25545 p 2438 N95-27087 #
PNL-SA-25554 p 2440 N95-27491 #
PNL-SA-25579 p 2236 N95-27733 #
PNL-SA-25670 p 2214 N95-27086 #
PNL-SA-25742 p 2446 N95-28242 #
PNL-SA-25782 p 2287 N95-28021 #

PNL-10395 p 2328 N95-27749 #

PSC-30 p 2297 N95-27868 #
PSC-31 p 2432 N95-27869 #
PSC-32 p 2432 N95-27870 #

QB835.H27 p 2458 N95-27068 * #

R/D-6980-EE-01 p 2290 N95-26541
R/D-7186-CN-01 p 2326 N95-26610
R/D-7463-CH-02 p 2141 N95-26487
R/D-7475-CH-01 p 2199 N95-26352

RAD-93-269-107-12-01 p 2327 N95-27234 #

RAL-94-110 p 2418 N95-28642
RAL-94-111 p 2271 N95-28663
RAL-94-116 p 2418 N95-28640
RAL-94-119 p 2419 N95-27089 #
RAL-94-121 p 2418 N95-28641
RAL-94-123 p 2199 N95-28639
RAL-94-125 p 2465 N95-28500
RAL-94-126 p 2423 N95-28452
RAL-95-003 p 2413 N95-28067 #
RAL-95-005 p 2375 N95-28658
RAL-95-006 p 2418 N95-28657

REPT-0001AF p 2387 N95-28217
REPT-0004 p 2178 N95-26567
REPT-153-4147 p 2224 N95-26456
REPT-16 p 2313 N95-26645 #
REPT-17-1015 p 2452 N95-26721
REPT-2308 p 2466 N95-26604
REPT-93B00058 p 2382 N95-27375 * #
REPT-94-33-PT-2 p 2450 N95-26803 #
REPT-94:5 p 2348 N95-27996 #
REPT-95-1 p 2270 N95-28570 * #
REPT-95:1 p 2338 N95-27995 #
REPT-95B00045 p 2341 N95-26689 * #
REPT-95B00054 p 2463 N95-28328 *
REPT-95B00075 p 2146 N95-27763 * #
REPT-95B00079-VOL-6 p 2334 N95-26423 * #
REPT-95B00081-VOL-26 p 2345 N95-26430 * #
REPT-95B00088 p 2255 N95-27435 * #
REPT-95FTC001 p 2343 N95-27997 * #

RL-TR-94-149 p 2363 N95-26474
RL-TR-94-165 p 2380 N95-26475
RL-TR-94-166 p 2262 N95-27152
RL-TR-94-194 p 2368 N95-26881
RL-TR-94-195 p 2295 N95-26906
RL-TR-94-196 p 2361 N95-26845
RL-TR-94-43 p 2337 N95-27147

RM-94-18-ONR p 2306 N95-26927

RR-A-338 p 2395 N95-26913
RR-A-339 p 2393 N95-28499 #
RR-A-340 p 2393 N95-28653 #

RR-A336 p 2276 N95-26928 #
RR-A337 p 2308 N95-26911
RR-A54 p 2389 N95-26910
RR-A55 p 2396 N95-28353 #

RTR-249-01 p 2164 N95-27093 * #

RXR-94071 p 2253 N95-27005
RXR-94101 p 2339 N95-28575

S-208 p 2260 N95-26646 #
S-794 p 2154 N95-27260 * #
S-798 p 2162 N95-26586 * #

SAIC-94/1062 p 2345 N95-27389 * #

SAICNY95-02-25-VOL-1 p 2159 N95-26398 * #
SAICNY95-02-25-VOL-2 p 2159 N95-26399 * #
SAICNY95-02-25-VOL-3 p 2160 N95-26400 * #
SAICNY95-02-25-VOL-4 p 2160 N95-26401 * #
SAICNY95-02-25-VOL-5 p 2160 N95-26403 * #

SAND-93-0349 p 2205 N95-27683 #
SAND-93-1875C p 2237 N95-27993 #
SAND-94-0951C p 2309 N95-27837 #
SAND-94-1367C p 2445 N95-28144 #
SAND-94-1566C p 2393 N95-28393 #
SAND-94-1770C p 2202 N95-27137 #
SAND-94-1870C p 2264 N95-27474 #
SAND-94-1885C p 2205 N95-27681 #
SAND-94-2049C p 2444 N95-28127 #
SAND-94-2082C p 2309 N95-27305 #
SAND-94-2145C p 2420 N95-27480 #
SAND-94-2299C p 2445 N95-28206 #
SAND-94-2344C p 2236 N95-27879 #
SAND-94-2417C p 2235 N95-27687 #
SAND-94-2423 p 2266 N95-27724
SAND-94-2464C p 2268 N95-28201 #
SAND-94-2478C p 2446 N95-28399 #
SAND-94-2544C p 2237 N95-28089 #
SAND-94-2823C p 2267 N95-28146 #
SAND-94-2878C p 2267 N95-28147 #
SAND-94-2917C p 2203 N95-27423 #
SAND-94-2920C p 2427 N95-28516 #
SAND-94-2986C p 2439 N95-27429 #
SAND-94-3001C p 2202 N95-27136 #
SAND-94-3025C p 2223 N95-28593 #
SAND-94-3039 p 2395 N95-27684 #
SAND-94-3046C p 2234 N95-27460 #
SAND-94-3078C p 2320 N95-27704 #
SAND-94-3082C p 2372 N95-27436 #
SAND-94-3096 p 2378 N95-28074 #
SAND-94-3109C p 2265 N95-27706 #
SAND-94-3141C p 2218 N95-27722 #
SAND-94-3146 p 2270 N95-28597 #
SAND-94-3172 p 2455 N95-27949 #
SAND-94-3187C p 2309 N95-27745 #
SAND-94-3196C p 2240 N95-28532 #
SAND-94-3197C p 2240 N95-28531
SAND-94-3257C p 2306 N95-27723 #
SAND-94-8508 p 2206 N95-27750 #
SAND-94-8596C p 2219 N95-27968 #
SAND-94-8628C p 2378 N95-27402 #
SAND-94-8741C p 2408 N95-27534 #
SAND-95-0013C p 2391 N95-27432 #
SAND-95-0090C p 2444 N95-28103 #
SAND-95-0121C p 2455 N95-27957 #
SAND-95-0144C p 2219 N95-27958 #
SAND-95-0157C p 2268 N95-28200 #
SAND-95-0162C p 2299 N95-28128 #
SAND-95-0229 p 2240 N95-28405 #
SAND-95-0274C p 2299 N95-28132 #
SAND-95-0280C p 2238 N95-28117 #
SAND-95-0281C p 2221 N95-28116 #
SAND-95-0307C p 2299 N95-28223 #
SAND-95-0309C p 2238 N95-28358 #
SAND-95-0315C p 2329 N95-27878 #
SAND-95-0343C p 2240 N95-28404 #
SAND-95-0350C p 2237 N95-28090 #
SAND-95-0378C p 2239 N95-28400 #
SAND-95-0391C p 2239 N95-28401 #
SAND-95-0394C p 2267 N95-28148 #
SAND-95-0468C p 2184 N95-28145 #
SAND-95-8451C p 2331 N95-28548 #
SAND-95-8458C p 2300 N95-28549 #
SAND-95-8465C p 2299 N95-28219 #
SAND-95-8467C p 2298 N95-27969 #
SAND-95-8475C p 2344 N95-28556 #
SAND-95-8485C p 2299 N95-28220 #
SAND-95-8491C p 2425 N95-27482 #
SAND-95-8503C p 2344 N95-28538 #

SBI-AD-E501-856 p 2143 N95-26556

SCIENTIFIC-5 p 2253 N95-27005

SC71056.FR p 2179 N95-26484

SGD-604-PT-1 p 2465 N95-28087 #

SMC-TR-94-43 p 2370 N95-27210
SMC-TR-94-44 p 2167 N95-26489
SMC-TR-94-46 p 2342 N95-26899
SMC-TR-94-48 p 2318 N95-26846
SMC-TR-95-49 p 2162 N95-26902

SPC-93028-CMC p 2370 N95-27235 #
SPC-94061-CMC p 2368 N95-26903

SR-1 p 2337 N95-27703
SR-6 p 2339 N95-28575

SSCL-680 p 2423 N95-28551 #

SSD95D0239-PT-1 p 2160 N95-28258 * #
SSD95D0240-PT-2 p 2304 N95-28259 * #
SSD95D0241 p 2450 N95-28260 * #

STARS-AC-C006/001/01 p 2375 N95-28635

STF10-A94008 p 2315 N95-28180 #
STF13-S94005 p 2379 N95-28502
STF13-S94006 p 2379 N95-28665
STF15-S94002 p 2361 N95-28659
STF19-S94003 p 2210 N95-28652
STF19-S94005 p 2294 N95-28651
STF24-A94510 p 2219 N95-27934
STF31-A94038 p 2379 N95-28093

SU-SLAC-PUB-6509 p 2449 N95-28137 #
SU-SLAC-PUB-6518 p 2417 N95-28594 #
SU-SLAC-PUB-6576 p 2414 N95-28142 #
SU-SLAC-PUB-6629 p 2422 N95-28159 #
SU-SLAC-PUB-6667 p 2414 N95-28158 #
SU-SLAC-PUB-6726 p 2267 N95-28143 #
SU-SLAC-PUB-95-6720 p 2422 N95-28122 #
SU-SLAC-PUB-95-6756 p 2434 N95-28161 #
SU-SLAC-PUB-95-6759 p 2293 N95-28178 #
SU-SLAC-PUB-95-6763 p 2422 N95-28123 #
SU-SLAC-PUB-95-6771 p 2449 N95-28160 #

SU-SLAC-451 p 2412 N95-28028 #

SWRI-3593/004 p 2225 N95-26561

TARDEC-TR-13609 p 2233 N95-27324
TARDEC-TR-13610 p 2233 N95-27325

TDCK-TD-94-2019 p 2307 N95-26342

TDCK-94-0886 p 2340 N95-26343
TDCK-94-0887 p 2247 N95-26344

TKK-F-B155 p 2435 N95-28654

TKK-IGE-A16 p 2315 N95-28643 #

TKK-V-B97 p 2224 N95-28644

TKO-C67 p 2452 N95-26631 #
TKO-C70 p 2369 N95-26907 #

TNO-FEL-94-A094 p 2340 N95-26343
TNO-FEL-94-A200 p 2247 N95-26344

TNO/R-94-CMC-R0539 p 2307 N95-26342

TOP-2-2-613 p 2251 N95-26851
TOP-2-2-806 p 2301 N95-26688
TOP-7-3-534 p 2130 N95-26994

TR-102 p 2394 N95-26414
TR-104 p 2394 N95-26413
TR-105 p 2394 N95-26415
TR-108 p 2377 N95-27183
TR-1 p 2294 N95-26568
TR-1 p 2226 N95-26627
TR-1 p 2394 N95-26733
TR-21 p 2403 N95-26491
TR-23 p 2438 N95-26959
TR-24 p 2290 N95-26982
TR-25 p 2438 N95-27061
TR-2 p 2437 N95-26553
TR-524727 p 2136 N95-28409
TR-63 p 2224 N95-26351
TR-6 p 2178 N95-26569
TR-7-REV p 2178 N95-28334
TR-77 p 2404 N95-26960
TR-90425 p 2126 N95-28630
TR-93(3308)-1 p 2342 N95-26899

TR-93(3940)-13 ..... p 2162 N95-26902
TR-94(4231)-6 ..... p 2332 N95-28623
TR-94(4478)-3 ..... p 2318 N95-26846
TR-94(4507)-2 ..... p 2167 N95-26489
TR-94(4904)-3 ..... p 2370 N95-27210
TR-95-4-1 ..... p 2367 N95-26770 * #
TR-98 ..... p 2225 N95-26472
TR-99 ..... p 2224 N95-26470

TRAINS-TN-94-1 ..... p 2259 N95-28624

TRS-491 ..... p 2375 N95-28645

TRT-3336-TR-1 ..... p 2178 N95-26712

UCD-95-2 ..... p 2413 N95-28067 #

UCRL-CR-120519 ..... p 2268 N95-28181 * #

UCRL-ID-114037 ..... p 2332 N95-28550 #
UCRL-ID-116384 ..... p 2338 N95-27931 #
UCRL-ID-116890 ..... p 2328 N95-27558 #
UCRL-ID-117982 ..... p 2414 N95-28171 #
UCRL-ID-118340 ..... p 2357 N95-28176 #
UCRL-ID-118434 ..... p 2327 N95-27532 #
UCRL-ID-118981 ..... p 2399 N95-28108 #
UCRL-ID-119098 ..... p 2331 N95-28157 #
UCRL-ID-119104 ..... p 2332 N95-28662 #
UCRL-ID-119123 ..... p 2328 N95-27708 #
UCRL-ID-119289 ..... p 2399 N95-28109 #
UCRL-ID-119322 ..... p 2243 N95-28064 #
UCRL-ID-119563 ..... p 2206 N95-27707 #
UCRL-ID-120258 ..... p 2223 N95-28534 #
UCRL-ID-120424 ..... p 2392 N95-28162 #

UCRL-JC-115491-REV-1 ..... p 2433 N95-28065 #
UCRL-JC-116492 ..... p 2372 N95-27533 #
UCRL-JC-116696 ..... p 2373 N95-28168 #
UCRL-JC-116862 ..... p 2432 N95-27710 #
UCRL-JC-116965 ..... p 2265 N95-27693 #
UCRL-JC-116967 ..... p 2222 N95-28167 #
UCRL-JC-117107 ..... p 2433 N95-28054 #
UCRL-JC-117666 ..... p 2351 N95-27725 #
UCRL-JC-117673 ..... p 2314 N95-28053 #
UCRL-JC-117864 ..... p 2334 N95-26436 #
UCRL-JC-117918-REV-1 ..... p 2303 N95-28029 #
UCRL-JC-117918-REV-2 ..... p 2303 N95-28139 #
UCRL-JC-117939 ..... p 2266 N95-28015 #
UCRL-JC-118288 ..... p 2298 N95-27876 #
UCRL-JC-118312 ..... p 2256 N95-28231 #
UCRL-JC-118555 ..... p 2330 N95-27954 #
UCRL-JC-118566 ..... p 2311 N95-28337 #
UCRL-JC-118624 ..... p 2373 N95-28521 #
UCRL-JC-118673 ..... p 2434 N95-28138 #
UCRL-JC-118719 ..... p 2435 N95-28356 #
UCRL-JC-118730 ..... p 2392 N95-28232 #
UCRL-JC-118859 ..... p 2204 N95-27496 #
UCRL-JC-118866 ..... p 2330 N95-28118 #
UCRL-JC-118999 ..... p 2434 N95-28140 #
UCRL-JC-119288 ..... p 2462 N95-28013 #
UCRL-JC-119307 ..... p 2435 N95-28542 #
UCRL-JC-119309 ..... p 2434 N95-28141 #
UCRL-JC-119457 ..... p 2335 N95-26622 #
UCRL-JC-119460 ..... p 2343 N95-28014 #
UCRL-JC-119872 ..... p 2455 N95-28085 #

UILU-ENG-94-2241 ..... p 2365 N95-26628 *
UILU-ENG-95-2544 ..... p 2270 N95-28570 * #

UM-P-93/52 ..... p 2415 N95-28246 #

UMICH-031155-3-T ..... p 2366 N95-26694 * #

UMR-FDB-44 ..... p 2180 N95-26572

UPR-0631T ..... p 2463 N95-28558 #

US-PATENT-APPL-SN-010986 ..... p 2129 N95-26537
US-PATENT-APPL-SN-038746 ..... p 2269 N95-28341 *
US-PATENT-APPL-SN-045335 ..... p 2179 N95-28361 *
US-PATENT-APPL-SN-045339 ..... p 2179 N95-28360 *
US-PATENT-APPL-SN-045340 ..... p 2271 N95-28613
US-PATENT-APPL-SN-051106 ..... p 2294 N95-26503
US-PATENT-APPL-SN-055455 ..... p 2249 N95-26509
US-PATENT-APPL-SN-073235 ..... p 2426 N95-27843 *
US-PATENT-APPL-SN-094332 ..... p 2297 N95-27731 *
US-PATENT-APPL-SN-096540 ..... p 2293 N95-28345 *
US-PATENT-APPL-SN-111317 ..... p 2271 N95-28599 *
US-PATENT-APPL-SN-112814 ..... p 2300 N95-26504
US-PATENT-APPL-SN-117587 ..... p 2304 N95-28347 *
US-PATENT-APPL-SN-138042 ..... p 2400 N95-26502
US-PATENT-APPL-SN-153864 ..... p 2248 N95-26465
US-PATENT-APPL-SN-155605 ..... p 2315 N95-28211 *
US-PATENT-APPL-SN-157553 ..... p 2271 N95-28614
US-PATENT-APPL-SN-169922 ..... p 2294 N95-28612
US-PATENT-APPL-SN-195737 ..... p 2427 N95-28363 *
US-PATENT-APPL-SN-207313 ..... p 2304 N95-28359 *
US-PATENT-APPL-SN-209512 ..... p 2235 N95-27732 *
US-PATENT-APPL-SN-220124 ..... p 2225 N95-26526
US-PATENT-APPL-SN-221128 ..... p 2183 N95-27717 * #
US-PATENT-APPL-SN-224611 ..... p 2258 N95-28615
US-PATENT-APPL-SN-227771 ..... p 2210 N95-28584
US-PATENT-APPL-SN-233584 ..... p 2293 N95-28362 *
US-PATENT-APPL-SN-243602 ..... p 2423 N95-26385 *
US-PATENT-APPL-SN-246041 ..... p 2404 N95-26861 * #
US-PATENT-APPL-SN-246041 ..... p 2416 N95-28348 *
US-PATENT-APPL-SN-252474 ..... p 2154 N95-26524
US-PATENT-APPL-SN-269278 ..... p 2259 N95-26433
US-PATENT-APPL-SN-273511 ..... p 2213 N95-26862 * #
US-PATENT-APPL-SN-273542 ..... p 2290 N95-26765 * #
US-PATENT-APPL-SN-297474 ..... p 2353 N95-26889 * #
US-PATENT-APPL-SN-299388 ..... p 2241 N95-28582
US-PATENT-APPL-SN-322656 ..... p 2161 N95-28581
US-PATENT-APPL-SN-361471 ..... p 2238 N95-28212 *
US-PATENT-APPL-SN-365880 ..... p 2261 N95-26890 * #
US-PATENT-APPL-SN-372640 ..... p 2424 N95-26894 * #
US-PATENT-APPL-SN-388652 ..... p 2291 N95-27191 * #
US-PATENT-APPL-SN-394862 ..... p 2245 N95-27500 * #
US-PATENT-APPL-SN-411231 ..... p 2182 N95-27192 * #
US-PATENT-APPL-SN-411357 ..... p 2235 N95-27503 * #
US-PATENT-APPL-SN-413301 ..... p 2180 N95-26764 * #
US-PATENT-APPL-SN-416596 ..... p 2291 N95-27138 * #
US-PATENT-APPL-SN-422961 ..... p 2360 N95-27501 * #
US-PATENT-APPL-SN-422963 ..... p 2245 N95-26888 * #
US-PATENT-APPL-SN-439544 ..... p 2235 N95-27702 * #
US-PATENT-APPL-SN-703649 ..... p 2304 N95-28256 *
US-PATENT-APPL-SN-839721 ..... p 2128 N95-26507
US-PATENT-APPL-SN-878713 ..... p 2248 N95-26505
US-PATENT-APPL-SN-931464 ..... p 2245 N95-26500
US-PATENT-APPL-SN-963177 ..... p 2210 N95-28585
US-PATENT-APPL-SN-977302 ..... p 2427 N95-28384 *
US-PATENT-APPL-SN-986399 ..... p 2183 N95-27717 * #
US-PATENT-APPL-SN-991939 ..... p 2245 N95-26508
US-PATENT-APPL-SN-996763 ..... p 2165 N95-27842 * #

US-PATENT-CLASS-136-230 ..... p 2293 N95-28345 *
US-PATENT-CLASS-136-233 ..... p 2293 N95-28345 *
US-PATENT-CLASS-15-104.12 ..... p 2304 N95-28359 *
US-PATENT-CLASS-15-104.31 ..... p 2304 N95-28359 *
US-PATENT-CLASS-165-104.17 ..... p 2304 N95-28256 *
US-PATENT-CLASS-165-10 ..... p 2304 N95-28256 *
US-PATENT-CLASS-165-78 ..... p 2304 N95-28256 *
US-PATENT-CLASS-244-159 ..... p 2165 N95-27842 * #
US-PATENT-CLASS-244-161 ..... p 2165 N95-27842 * #
US-PATENT-CLASS-244-1 ..... p 2128 N95-26507
US-PATENT-CLASS-250-228 ..... p 2423 N95-26385 *
US-PATENT-CLASS-250-253 ..... p 2315 N95-28211 *
US-PATENT-CLASS-250-461.1 ..... p 2315 N95-28211 *
US-PATENT-CLASS-250-573 ..... p 2293 N95-28362 *
US-PATENT-CLASS-250-581 ..... p 2423 N95-26385 *
US-PATENT-CLASS-250-584 ..... p 2423 N95-26385 *
US-PATENT-CLASS-250-585 ..... p 2423 N95-26385 *
US-PATENT-CLASS-250-586 ..... p 2423 N95-26385 *
US-PATENT-CLASS-323-222 ..... p 2269 N95-28341 *
US-PATENT-CLASS-323-282 ..... p 2269 N95-28341 *
US-PATENT-CLASS-323-285 ..... p 2269 N95-28341 *
US-PATENT-CLASS-324-304 ..... p 2416 N95-28348 *
US-PATENT-CLASS-324-67 ..... p 2245 N95-26508
US-PATENT-CLASS-331-3 ..... p 2416 N95-28348 *
US-PATENT-CLASS-331-94.1 ..... p 2416 N95-28348 *
US-PATENT-CLASS-338-306 ..... p 2271 N95-28613
US-PATENT-CLASS-342-128 ..... p 2258 N95-28615
US-PATENT-CLASS-342-189 ..... p 2248 N95-26465
US-PATENT-CLASS-348-754 ..... p 2426 N95-27843 *
US-PATENT-CLASS-348-769 ..... p 2426 N95-27843 *
US-PATENT-CLASS-356-236 ..... p 2423 N95-26385 *
US-PATENT-CLASS-356-338 ..... p 2293 N95-28362 *
US-PATENT-CLASS-359-247 ..... p 2427 N95-28384 *
US-PATENT-CLASS-359-250 ..... p 2427 N95-28384 *
US-PATENT-CLASS-359-259 ..... p 2427 N95-28384 *
US-PATENT-CLASS-359-279 ..... p 2427 N95-28384 *
US-PATENT-CLASS-359-285 ..... p 2426 N95-27843 *
US-PATENT-CLASS-359-509 ..... p 2304 N95-28347 *
US-PATENT-CLASS-359-53 ..... p 2427 N95-28384 *
US-PATENT-CLASS-363-21 ..... p 2269 N95-28341 *
US-PATENT-CLASS-363-97 ..... p 2269 N95-28341 *
US-PATENT-CLASS-364-506 ..... p 2210 N95-28585
US-PATENT-CLASS-364-807 ..... p 2271 N95-28614
US-PATENT-CLASS-367-125 ..... p 2271 N95-28599 *
US-PATENT-CLASS-372-10 ..... p 2297 N95-27731 *
US-PATENT-CLASS-372-11 ..... p 2297 N95-27731 *
US-PATENT-CLASS-372-53 ..... p 2294 N95-26503
US-PATENT-CLASS-374-179 ..... p 2293 N95-28345 *
US-PATENT-CLASS-374-208 ..... p 2293 N95-28345 *
US-PATENT-CLASS-381-68.2 ..... p 2271 N95-28599 *
US-PATENT-CLASS-395-25 ..... p 2427 N95-28363 *
US-PATENT-CLASS-395-800 ..... p 2248 N95-26505
US-PATENT-CLASS-395-800 ..... p 2249 N95-26509
US-PATENT-CLASS-528-125 ..... p 2179 N95-28360 *
US-PATENT-CLASS-528-125 ..... p 2179 N95-28361 *
US-PATENT-CLASS-528-126 ..... p 2179 N95-28361 *
US-PATENT-CLASS-528-128 ..... p 2235 N95-27732 *
US-PATENT-CLASS-528-128 ..... p 2179 N95-28360 *
US-PATENT-CLASS-528-128 ..... p 2179 N95-28361 *
US-PATENT-CLASS-528-171 ..... p 2179 N95-28360 *
US-PATENT-CLASS-528-172 ..... p 2235 N95-27732 *
US-PATENT-CLASS-528-172 ..... p 2179 N95-28360 *
US-PATENT-CLASS-528-172 ..... p 2179 N95-28361 *
US-PATENT-CLASS-528-173 ..... p 2235 N95-27732 *
US-PATENT-CLASS-528-174 ..... p 2235 N95-27732 *
US-PATENT-CLASS-528-174 ..... p 2179 N95-28360 *
US-PATENT-CLASS-528-174 ..... p 2179 N95-28361 *
US-PATENT-CLASS-528-176 ..... p 2235 N95-27732 *
US-PATENT-CLASS-528-183 ..... p 2235 N95-27732 *
US-PATENT-CLASS-528-183 ..... p 2179 N95-28360 *
US-PATENT-CLASS-528-183 ..... p 2179 N95-28361 *
US-PATENT-CLASS-528-210 ..... p 2179 N95-28361 *
US-PATENT-CLASS-528-353 ..... p 2235 N95-27732 *
US-PATENT-CLASS-528-4 ..... p 2238 N95-28212 *
US-PATENT-CLASS-528-5 ..... p 2238 N95-28212 *
US-PATENT-CLASS-528-7 ..... p 2238 N95-28212 *
US-PATENT-CLASS-556-402 ..... p 2238 N95-28212 *
US-PATENT-CLASS-556-403 ..... p 2238 N95-28212 *
US-PATENT-CLASS-62-259.3 ..... p 2304 N95-28256 *
US-PATENT-CLASS-62-299 ..... p 2304 N95-28256 *
US-PATENT-CLASS-62-51 ..... p 2294 N95-28612
US-PATENT-CLASS-62-59 ..... p 2304 N95-28256 *
US-PATENT-CLASS-73-119 ..... p 2304 N95-28347 *
US-PATENT-CLASS-73-574 ..... p 2210 N95-28584
US-PATENT-CLASS-73-587 ..... p 2271 N95-28599 *
US-PATENT-CLASS-73-592 ..... p 2271 N95-28599 *
US-PATENT-CLASS-73-597 ..... p 2400 N95-26502
US-PATENT-CLASS-73-789 ..... p 2245 N95-26500

US-PATENT-4,987,201 ..... p 2238 N95-28212 *
US-PATENT-5-339,066 ..... p 2271 N95-28613
US-PATENT-5-365,457 ..... p 2210 N95-28585
US-PATENT-5-365,472 ..... p 2271 N95-28614
US-PATENT-5,261,482 ..... p 2304 N95-28256 *
US-PATENT-5,325,722 ..... p 2245 N95-26500
US-PATENT-5,329,540 ..... p 2294 N95-26503
US-PATENT-5,331,328 ..... p 2248 N95-26465
US-PATENT-5,335,297 ..... p 2249 N95-26509
US-PATENT-5,339,023 ..... p 2245 N95-26508
US-PATENT-5,339,691 ..... p 2400 N95-26502
US-PATENT-5,340,054 ..... p 2128 N95-26507
US-PATENT-5,349,685 ..... p 2248 N95-26505
US-PATENT-5,349,986 ..... p 2300 N95-26504
US-PATENT-5,355,683 ..... p 2294 N95-28612
US-PATENT-5,363,701 ..... p 2210 N95-28584
US-PATENT-5,376,938 ..... p 2258 N95-28615
US-PATENT-5,399,019 ..... p 2293 N95-28345 *
US-PATENT-5,399,877 ..... p 2423 N95-26385 *
US-PATENT-5,406,666 ..... p 2304 N95-28359 *
US-PATENT-5,407,152 ..... p 2165 N95-27842 * #
US-PATENT-5,408,480 ..... p 2297 N95-27731 *
US-PATENT-5,410,012 ..... p 2179 N95-28360 *
US-PATENT-5,410,371 ..... p 2426 N95-27843 *
US-PATENT-5,412,059 ..... p 2179 N95-28361 *
US-PATENT-5,412,068 ..... p 2235 N95-27732 *
US-PATENT-5,412,219 ..... p 2315 N95-28211 *
US-PATENT-5,412,221 ..... p 2293 N95-28362 *
US-PATENT-5,412,755 ..... p 2427 N95-28363 *
US-PATENT-5,412,981 ..... p 2304 N95-28347 *
US-PATENT-5,416,618 ..... p 2427 N95-28384 *
US-PATENT-5,417,113 ..... p 2271 N95-28599 *
US-PATENT-5,418,709 ..... p 2269 N95-28341 *
US-PATENT-5,420,549 ..... p 2416 N95-28348 *

USAARL-95-11 ..... p 2361 N95-28667
USAARL-95-4 ..... p 2130 N95-26993
USAARL-95-6 ..... p 2294 N95-28410

USAATCOM-TR-94-A-022 ..... p 2118 N95-26710 * #
USAATCOM-TR-95-A-003 ..... p 2141 N95-26773 * #

USAFETAC/TN-94/005 ..... p 2342 N95-27148

USARIEM-T-2/95 ..... p 2358 N95-26558

USCG-D-23-94 ..... p 2360 N95-27058
USCG-D-29-24 ..... p 2293 N95-28389

USCG-R/DC-27/94 ..... p 2360 N95-27058

UTS-DTF-94-10 ..... p 2406 N95-27317 #

UVA//525461/MSE95/102 ..... p 2213 N95-27032

UWIS/DC-22 ..... p 2405 N95-27017

VPI-E-95-01 ..... p 2310 N95-27865 * #

VTT-SYMP-144 ..... p 2331 N95-28202 #

WES/CR/DRP-94-7 ..... p 2346 N95-26904

WES/IR/ITL-94-3 ..... p 2453 N95-27004

WES/IR/ITL-94-6 .... p 2307 N95-26464

WHC-SA-2753 .... p 2454 N95-27461 #

WHC-SD-W236A-ES-004 .... p 2219 N95-28005 #

WHOI-94-02 .... p 2338 N95-28094
WHOI-94-04 .... p 2347 N95-27043
WHOI-94-08 .... p 2348 N95-28096
WHOI-94-09 .... p 2347 N95-27011
WHOI-94-16 .... p 2315 N95-28392
WHOI-94-32 .... p 2347 N95-27151

WH01-94-18 .... p 2342 N95-26826

WIS-PH-94-29 .... p 2412 N95-28041 #
WIS-PH-94-34 .... p 2407 N95-27406 #
WIS-PH-94-39 .... p 2407 N95-27409 #

WL-TM-94-3130 .... p 2273 N95-26418

WL-TR-94-2099 .... p 2138 N95-27003
WL-TR-94-3143 .... p 2129 N95-26684
WL-TR-94-4046 .... p 2180 N95-26571
WL-TR-94-4077 .... p 2181 N95-26967
WL-TR-94-4109 .... p 2245 N95-26410
WL-TR-94-7058 .... p 2243 N95-28634
WL-TR-94-8032 .... p 2368 N95-26853
WL-TR-94-8033 .... p 2375 N95-28647
WL-TR-95-2001 .... p 2140 N95-28646

WSRC-MS-94-0612 .... p 2215 N95-27328 #

WVU-SCS-TR-94-11 .... p 2364 N95-26486 * #
WVU-SCS-TR-95-10 .... p 2367 N95-26802 * #
WVU-SCS-TR-95-2 .... p 2366 N95-26695 * #
WVU-SCS-TR-95-3 .... p 2366 N95-26711 * #
WVU-SCS-TR-95-4 .... p 2371 N95-27252 * #
WVU-SCS-TR-95-5 .... p 2365 N95-26575 * #
WVU-SCS-TR-95-6 .... p 2366 N95-26693 * #
WVU-SCS-TR-95-7 .... p 2363 N95-26388 * #
WVU-SCS-TR-95-8 .... p 2367 N95-26814 * #
WVU-SCS-TR-95-9 .... p 2365 N95-26668 * #

WVU-SRL-94-001 .... p 2366 N95-26695 * #
WVU-SRL-94-002 .... p 2364 N95-26486 * #
WVU-SRL-94-003 .... p 2366 N95-26711 * #
WVU-SRL-94-004 .... p 2371 N95-27252 * #
WVU-SRL-94-005 .... p 2365 N95-26575 * #
WVU-SRL-94-006 .... p 2366 N95-26693 * #
WVU-SRL-94-007 .... p 2363 N95-26388 * #
WVU-SRL-94-008 .... p 2367 N95-26814 * #
WVU-SRL-94-009 .... p 2365 N95-26668 * #
WVU-SRL-94-010 .... p 2367 N95-26802 * #
WVU-SRL-94-011 .... p 2362 N95-26386 * #

YALEU/DCS/RR-1055 .... p 2398 N95-26345

95B00084-VOL-27 .... p 2348 N95-28030 * #

APPENDIX

NASA SCIENTIFIC AND TECHNICAL INFORMATION OFFICE PRODUCTS AND SERVICES

The NASA Scientific and Technical Information (STI) Office provides for the collection and announcement of aerospace-related reports and literature obtained worldwide through agreements and exchanges. The result of the collection is the comprehensive NASA STI Database that covers aeronautics, space, and supporting disciplines.

The STI Database, documents generated or obtained by NASA, and products and services derived from or supporting the database are made available to the NASA research community and to the public. Descriptions and sources of these items are presented in the following pages.

Scientific and Technical Aerospace Reports (STAR) is an abstract journal, listing citations with abstracts for aerospace-related reports obtained from worldwide sources. *STAR* is issued on the first of each month, and announces current documents that have been entered into the NASA STI Database during the previous month. The reports are of the following types:

- NASA, NASA contractor, and NASA grantee reports;
- Reports issued by other U.S. Government agencies, domestic and foreign institutions, universities, and private firms;
- Translations in report form;
- NASA-owned patents and patent applications
- Other U.S. Government agency and foreign patents and patent applications
- Domestic and foreign dissertations and theses.

Journal, book, and conference literature, journal translations, and certain foreign dissertations having the same subject scope as *STAR* are announced in a companion journal, *NASA Open Volumes on Aerospace (NOVA). NOVA* is issued on the 15th of each month and is available from the NASA Center for AeroSpace Information, at the address below.

ELIGIBILITY AND REGISTRATION FOR NASA STI PRODUCTS AND SERVICES

Organizations of the type listed below that have registered with NASA can receive products and services.

- NASA offices and installations, contractors, subcontractors, grantees, and consultants;
- Other U.S. Government agencies and their contractors;
- Libraries in the United States that have arrangements with NASA to maintain collections of NASA documents for public reference;
- Other organizations in the United States having a need for NASA documents in work related to aeronautics and space research;
- Organizations abroad that have established reciprocal documents exchange arrangements with NASA.

The central service points—central points of document acquisition and control within qualified organizations—or individuals are eligible to register for NASA STI products and services. Domestic organizations or individuals may be eligible to receive various classes of NASA publications and services and should address their requests for registration or further information to:

ATTN: Registration Services
NASA Center for AeroSpace Information
800 Elkridge Landing Road
Linthicum Heights, MD 21090-2934
301-621-0390

Organizations abroad should direct requests to:

National Aeronautics and Space Administration
Scientific and Technical Information Office (JT)
International STI Office
Washington, DC 20546-0001
USA
703-271-5640

SUBJECT SCOPE

The subject scope of *STAR* and *NOVA* includes all aspects of aeronautics and space research and development, supporting basic and applied research, and applications. Aerospace aspects of Earth resources, energy development, conservation, oceanography, environmental protection, urban transportation, and other topics of high national priority are also covered.

HOW TO USE *STAR* SUBJECT CATEGORIES

Abstracts in *STAR* are categorized by 10 major subject divisions that are divided further into 76 specific subject categories. The subject divisions and categories are listed in the Table of Contents together with a note for each that defines its scope and provides any cross-references. For example:

> **16 SPACE TRANSPORTATION**
>
> Includes passenger and cargo space transportation, e.g., shuttle operations; and space rescue techniques. For related information see also *03 Air Transportation and Safety* and *18 Spacecraft Design, Testing and Performance*. For space suits see *54 Man/System Technology and Life Support*.

CROSS-REFERENCES

Individual *STAR* abstracts are not ordinarily cross-referenced, except for certain conference reports or book translations that have had separate abstracts written for their component papers or chapters. Citations and abstracts of the components follow immediately after those of the parent document. When the subject content of a component differs sufficiently from the general content of the parent, a cross-reference citation also is printed at the end of the category to which it normally would have been assigned if it were independent.

DOCUMENTS ON MICROFICHE

Documents available on microfiche are designated by a pound sign (#) following the accession number.

LIMITED REPRODUCIBILITY

A note of limited reproducibility appears in the citation, if there are factors affecting the reproducibility of more than 20% of the document. These factors include faint or broken type, color photographs, black and white photographs, foldouts, dot matrix print, or some other factor that limits the reproducibility of the document. This notation also appears on the microfiche header.

NASA PATENTS AND PATENT APPLICATIONS

Patents and patent applications owned by NASA are announced in *STAR* under appropriate subject categories and are referenced in the *STAR* indexes. In the Report Number Index, patents are indexed by the NASA Case Number, and the U.S. Patent Class. Patent applications are indexed by the NASA Case Number and the U.S. Patent Application Serial Number.

Printed copies of patents (which are not microfiched) are available for purchase from the U.S. Patent and Trademark Office.

When ordering patents, the U.S. Patent Number should be used, and payment must be remitted in advance, by money order or check payable to the Commissioner of Patents and Trademarks. Prepaid purchase coupons for ordering are also available from the U.S. Patent and Trademark Office.

NASA patent application specifications are sold in both paper copy and microfiche by the NASA Center for AeroSpace Information (CASI). The N accession number should be used in ordering either paper copy or microfiche from CASI.

The patents and patent applications announced in *STAR* are owned by NASA and are available for royalty-free licensing. Requests for licensing terms and further information should be addressed to:

National Aeronautics and Space Administration
Associate General Counsel for Intellectual Property
Code GP
Washington, DC 20546-0001

SOURCES FOR DOCUMENTS

One or more sources from which a document announced in *STAR* is available to the public is ordinarily given on the last line of the citation. The most commonly indicated sources and their acronyms or abbreviations are listed below, and their addresses are listed on page A-6. If the publication is available from a source other than those listed, the publisher and his address will be displayed on the availability line or in combination with the corporate source line.

Avail: CASI. Sold by the NASA Center for AeroSpace Information. Prices for hard copy (HC) and microfiche (MF) are indicated by a price code following the letters HC or MF in the *STAR* citation. Current values for the price codes are given in the tables on page A-7.

NOTE ON ORDERING DOCUMENTS: When ordering publications from NASA CASI, use the N accession number or other report number. It is also advisable to cite the title and other bibliographic identification.

Avail: SOD (or GPO). Sold by the Superintendent of Documents, U.S. Government Printing Office, in hard copy.

Avail: BLL (formerly NLL): British Library Lending Division, Boston Spa, Wetherby, Yorkshire, England. Photocopies available from this organization at the price shown. (If none is given, inquiry should be addressed to the BLL.)

Avail: DOE Depository Libraries. Organizations in U.S. cities and abroad that maintain collections of Department of Energy reports, usually in microfiche form, are listed in *Energy Research Abstracts*. Services available from the DOE and its depositories are described in a booklet, *DOE Technical Information Center - Its Functions and Services* (TID-4660), which may be obtained without charge from the DOE Technical Information Center.

Avail: ESDU. Pricing information on specific data, computer programs, and details on Engineering Sciences Data Unit (ESDU) topic categories can be obtained from ESDU International Ltd. Requesters in North America should use the Virginia address while all other requesters should use the London address, both of which are on page A-6.

Avail: Fachinformationszentrum Karlsruhe. Gesellschaft für wissenschaftlich-technische Information mbH 76344 Eggenstein-Leopoldshafen, Germany.

Avail: HMSO. Publications of Her Majesty's Stationery Office are sold in the U.S. by Pendragon House, Inc. (PHI), Redwood City, CA. The U.S. price (including a service and mailing charge) is given, or a conversion table may be obtained from PHI.

Avail: Issuing Activity, or Corporate Author, or no indication of availability. Inquiries as to the availability of these documents should be addressed to the organization shown in the citation as the corporate author of the document.

Avail: NASA Public Document Rooms. Documents so indicated may be examined at or purchased from the National Aeronautics and Space Administration (JBD-4), Public Documents Room (Room 1H23), Washington, DC 20546-0001, or public document rooms located at NASA installations, and the NASA Pasadena Office at the Jet Propulsion Laboratory.

Avail: NTIS. Sold by the National Technical Information Service. Initially distributed microfiche under the NTIS SRIM (Selected Research in Microfiche) are available. For information concerning this service, consult the NTIS Subscription Section, Springfield, VA 22161.

Avail: Univ. Microfilms. Documents so indicated are dissertations selected from *Dissertation Abstracts* and are sold by University Microfilms as xerographic copy (HC) and microfilm. All requests should cite the author and the Order Number as they appear in the citation.

Avail: US Patent and Trademark Office. Sold by Commissioner of Patents and Trademarks, U.S. Patent and Trademark Office, at the standard price of $1.50 each, postage free. (See discussion of NASA patents and patent applications on page A-3.)

Avail: (US Sales Only). These foreign documents are available to users within the United States from the National Technical Information Service (NTIS). They are available to users outside the United States through the International Nuclear Information Service (INIS) representative in their country, or by applying directly to the issuing organization.

Avail: USGS. Originals of many reports from the U.S. Geological Survey, which may contain color illustrations, or otherwise may not have the quality of illustrations preserved in the microfiche or facsimile reproduction, may be examined by the public at the libraries of the USGS field offices whose addresses are listed on page A-6. The libraries may be queried concerning the availability of specific documents and the possible utilization of local copying services, such as color reproduction.

FEDERAL DEPOSITORY LIBRARY PROGRAM

In order to provide the general public with greater access to U.S. Government publications, Congress established the Federal Depository Library Program under the Government Printing Office (GPO), with 53 regional depositories responsible for permanent retention of material, inter-library loan, and reference services. At least one copy of nearly every NASA and NASA-sponsored publication, either in printed or microfiche format, is received and retained by the 53 regional depositories. A list of the regional GPO libraries, arranged alphabetically by state, appears on page A-8. These libraries are *not* sales outlets. A local library can contact a regional depository to help locate specific reports, or direct contact may be made by an individual.

PUBLIC COLLECTION OF NASA DOCUMENTS

An extensive collection of NASA and NASA-sponsored publications is maintained by the British Library Lending Division, Boston Spa, Wetherby, Yorkshire, England for public access. The British Library Lending Division also has available many of the non-NASA publications cited in *STAR*. European requesters may purchase facsimile copy or microfiche of NASA and NASA-sponsored documents, those identified by both the symbols # and * from ESA — Information Retrieval Service European Space Agency, 8-10 rue Mario-Nikis, 75738 CEDEX 15, France.

SUBMITTING DOCUMENTS

All users of this abstract service are urged to forward reports to be considered for announcement in *STAR*. This will aid NASA in its efforts to provide the fullest possible coverage of all scientific and technical publications that might support aeronautics and space research and development. If you have prepared relevant reports (other than those you will transmit to NASA, DOD, or DOE through the usual contract- or grant-reporting channels), please send them for consideration to the NASA Center for AeroSpace Information, 800 Elkridge Landing Road, Linthicum Heights, MD 21090-2934.

Reprints of journal articles, book chapters, and conference papers are also welcome. These will be considered for announcement in *STAR's* companion journal, *NOVA*.

You may specify a particular source to be included in a report announcement if you wish; otherwise the report will be placed on a public sale at the NASA Center for AeroSpace Information. Copyrighted publications will be announced but not distributed or sold.

PURCHASE OF *STAR*

STAR is publicly available on annual subscription from the NASA Center for AeroSpace Information (CASI). 1995 *STAR* subscription prices are $100.00/domestic and $125.00/foreign. Single copy prices: $33.00/domestic, $41.00/foreign.

An annual, cumulative *STAR Index* is also available at $70.00/domestic and foreign.

STAR is available to registered users on annual subscription from the NASA Center for AeroSpace Information, ATTN: Registration Services, 800 Elkridge Landing Road, Linthicum Heights, MD 21090-2934.

ADDRESSES OF ORGANIZATIONS

British Library Lending Division
Boston Spa, Wetherby, Yorkshire
England

Commissioner of Patents and Trademarks
U.S. Patent and Trademark Office
Washington, DC 20231

Department of Energy
Technical Information Center
P.O. Box 62
Oak Ridge, TN 37830

European Space Agency-
Information Retrieval Service ESRIN
Via Galileo Galilei
00044 Frascati (Rome) Italy

Engineering Sciences Data Unit International
P.O. Box 1633
Manassas, VA 22110

Engineering Sciences Data Unit
International, Ltd.
251-259 Regent Street
London, W1R 7AD, England

Fachinformationszentrum Karlsruhe
Gesellschaft für wissenschaftlich-technische
Information mbH
76344 Eggenstein-Leopoldshafen, Germany

Her Majesty's Stationery Office
P.O. Box 569, S.E. 1
London, England

NASA Center for AeroSpace Information
800 Elkridge Landing Road
Linthicum Heights, MD 21090-2934

National Aeronautics and Space Administration
Scientific and Technical Information Office
(JT)
Washington, DC 20546-0001

National Technical Information Service
5285 Port Royal Road
Springfield, VA 22161

Pendragon House, Inc.
899 Broadway Avenue
Redwood City, CA 94063

Superintendent of Documents
U.S. Government Printing Office
Washington, DC 20402

University Microfilms
A Xerox Company
300 North Zeeb Road
Ann Arbor, MI 48106

University Microfilms, Ltd.
Tylers Green
London, England

U.S. Geological Survey Library National Center
MS 950
12201 Sunrise Valley Drive
Reston, VA 22092

U.S. Geological Survey Library
2255 North Gemini Drive
Flagstaff, AZ 86001

U.S. Geological Survey
345 Middlefield Road
Menlo Park, CA 94025

U.S. Geological Survey Library
Box 25046
Denver Federal Center, MS914
Denver, CO 80225

NASA CASI PRICE CODE TABLE

(Effective January 1, 1995)

CASI PRICE CODE	NORTH AMERICAN PRICE	FOREIGN PRICE
A01	$ 6.00	$ 12.00
A02	9.00	18.00
A03	17.50	35.00
A04-A05	19.50	39.00
A06-A09	27.00	54.00
A10-A13	36.50	73.00
A14-A17	44.50	89.00
A18-A21	52.00	104.00
A22-A25	61.00	122.00
A99	Call For Price	Call For Price

IMPORTANT NOTICE

For users not registered at the NASA CASI, prepayment is required. Additionally, a shipping and handling fee of $1.00 per document for delivery within the United States and $9.00 per document for delivery outside the United States is charged.

For users registered at the NASA CASI, document orders may be invoiced at the end of the month, charged against a deposit account, or paid by check or credit card. NASA CASI accepts American Express, Diners' Club, MasterCard, and VISA credit cards. There are no shipping and handling charges. To register at the NASA CASI, please request a registration form through the NASA Access Help Desk at the numbers or addresses below.

RETURN POLICY

Effective June 1, 1995, the NASA Center for AeroSpace Information will gladly replace or make full refund on items you have requested if we have made an error in your order, if the item is defective, or if it was received in damaged condition and you contact us within 30 days of your original request. Just contact our NASA Access Help Desk at the numbers or addresses listed below.

NASA Center for AeroSpace Information
800 Elkridge Landing Road
Linthicum Heights, MD 21090-2934
Telephone: (301) 621-0390
E-mail: help@sti.nasa.gov
Fax: (301) 621-0134

Rev. 5/95

FEDERAL REGIONAL DEPOSITORY LIBRARIES

ALABAMA
AUBURN UNIV. AT MONTGOMERY LIBRARY
Documents Dept.
7300 University Dr.
Montgomery, AL 36117-3596
(205) 244-3650 Fax: (205) 244-0678

UNIV. OF ALABAMA
Amelia Gayle Gorgas Library
Govt. Documents
P.O. Box 870266
Tuscaloosa, AL 35487-0266
(205) 348-6046 Fax: (205) 348-0760

ARIZONA
DEPT. OF LIBRARY, ARCHIVES, AND PUBLIC RECORDS
Research Division
Third Floor, State Capitol
1700 West Washington
Phoenix, AZ 85007
(602) 542-3701 Fax: (602) 542-4400

ARKANSAS
ARKANSAS STATE LIBRARY
State Library Service Section
Documents Service Section
One Capitol Mall
Little Rock, AR 72201-1014
(501) 682-2053 Fax: (501) 682-1529

CALIFORNIA
CALIFORNIA STATE LIBRARY
Govt. Publications Section
P.O. Box 942837 - 914 Capitol Mall
Sacramento, CA 94337-0091
(916) 654-0069 Fax: (916) 654-0241

COLORADO
UNIV. OF COLORADO - BOULDER
Libraries - Govt. Publications
Campus Box 184
Boulder, CO 80309-0184
(303) 492-8834 Fax: (303) 492-1881

DENVER PUBLIC LIBRARY
Govt. Publications Dept. BSG
1357 Broadway
Denver, CO 80203-2165
(303) 640-8846 Fax: (303) 640-8817

CONNECTICUT
CONNECTICUT STATE LIBRARY
231 Capitol Avenue
Hartford, CT 06106
(203) 566-4971 Fax: (203) 566-3322

FLORIDA
UNIV. OF FLORIDA LIBRARIES
Documents Dept.
240 Library West
Gainesville, FL 32611-2048
(904) 392-0366 Fax: (904) 392-7251

GEORGIA
UNIV. OF GEORGIA LIBRARIES
Govt. Documents Dept.
Jackson Street
Athens, GA 30602-1645
(706) 542-8949 Fax: (706) 542-4144

HAWAII
UNIV. OF HAWAII
Hamilton Library
Govt. Documents Collection
2550 The Mall
Honolulu, HI 96822
(808) 948-8230 Fax: (808) 956-5968

IDAHO
UNIV. OF IDAHO LIBRARY
Documents Section
Rayburn Street
Moscow, ID 83844-2353
(208) 885-6344 Fax: (208) 885-6817

ILLINOIS
ILLINOIS STATE LIBRARY
Federal Documents Dept.
300 South Second Street
Springfield, IL 62701-1796
(217) 782-7596 Fax: (217) 782-6437

INDIANA
INDIANA STATE LIBRARY
Serials/Documents Section
140 North Senate Avenue
Indianapolis, IN 46204-2296
(317) 232-3679 Fax: (317) 232-3728

IOWA
UNIV. OF IOWA LIBRARIES
Govt. Publications
Washington & Madison Streets
Iowa City, IA 52242-1166
(319) 335-5926 Fax: (319) 335-5900

KANSAS
UNIV. OF KANSAS
Govt. Documents & Maps Library
6001 Malott Hall
Lawrence, KS 66045-2800
(913) 864-4660 Fax: (913) 864-3855

KENTUCKY
UNIV. OF KENTUCKY
King Library South
Govt. Publications/Maps Dept.
Patterson Drive
Lexington, KY 40506-0039
(606) 257-3139 Fax: (606) 257-3139

LOUISIANA
LOUISIANA STATE UNIV.
Middleton Library
Govt. Documents Dept.
Baton Rouge, LA 70803-3312
(504) 388-2570 Fax: (504) 388-6992

LOUISIANA TECHNICAL UNIV.
Prescott Memorial Library
Govt. Documents Dept.
Ruston, LA 71272-0046
(318) 257-4962 Fax: (318) 257-2447

MAINE
UNIV. OF MAINE
Raymond H. Fogler Library
Govt. Documents Dept.
Orono, ME 04469-5729
(207) 581-1673 Fax: (207) 581-1653

MARYLAND
UNIV. OF MARYLAND - COLLEGE PARK
McKeldin Library
Govt. Documents/Maps Unit
College Park, MD 20742
(301) 405-9165 Fax: (301) 314-9416

MASSACHUSETTS
BOSTON PUBLIC LIBRARY
Govt. Documents
666 Boylston Street
Boston, MA 02117-0286
(617) 536-5400, ext. 226
Fax: (617) 536-7758

MICHIGAN
DETROIT PUBLIC LIBRARY
5201 Woodward Avenue
Detroit, MI 48202-4093
(313) 833-1025 Fax: (313) 833-0156

LIBRARY OF MICHIGAN
Govt. Documents Unit
P.O. Box 30007
717 West Allegan Street
Lansing, MI 48909
(517) 373-1300 Fax: (517) 373-3381

MINNESOTA
UNIV. OF MINNESOTA
Govt. Publications
409 Wilson Library
309 19th Avenue South
Minneapolis, MN 55455
(612) 624-5073 Fax: (612) 626-9353

MISSISSIPPI
UNIV. OF MISSISSIPPI
J.D. Williams Library
106 Old Gym Bldg.
University, MS 38677
(601) 232-5857 Fax: (601) 232-7465

MISSOURI
UNIV. OF MISSOURI - COLUMBIA
106B Ellis Library
Govt. Documents Sect.
Columbia, MO 65201-5149
(314) 882-6733 Fax: (314) 882-8044

MONTANA
UNIV. OF MONTANA
Mansfield Library
Documents Division
Missoula, MT 59812-1195
(406) 243-6700 Fax: (406) 243-2060

NEBRASKA
UNIV. OF NEBRASKA - LINCOLN
D.L. Love Memorial Library
Lincoln, NE 68588-0410
(402) 472-2562 Fax: (402) 472-5131

NEVADA
THE UNIV. OF NEVADA LIBRARIES
Business and Govt. Information Center
Reno, NV 89557-0044
(702) 784-6579 Fax: (702) 784-1751

NEW JERSEY
NEWARK PUBLIC LIBRARY
Science Div. - Public Access
P.O. Box 630
Five Washington Street
Newark, NJ 07101-7812
(201) 733-7782 Fax: (201) 733-5648

NEW MEXICO
UNIV. OF NEW MEXICO
General Library
Govt. Information Dept.
Albuquerque, NM 87131-1466
(505) 277-5441 Fax: (505) 277-6019

NEW MEXICO STATE LIBRARY
325 Don Gaspar Avenue
Santa Fe, NM 87503
(505) 827-3824 Fax: (505) 827-3888

NEW YORK
NEW YORK STATE LIBRARY
Cultural Education Center
Documents/Gift & Exchange Section
Empire State Plaza
Albany, NY 12230-0001
(518) 474-5355 Fax: (518) 474-5786

NORTH CAROLINA
UNIV. OF NORTH CAROLINA - CHAPEL HILL
Walter Royal Davis Library
CB 3912, Reference Dept.
Chapel Hill, NC 27514-8890
(919) 962-1151 Fax: (919) 962-4451

NORTH DAKOTA
NORTH DAKOTA STATE UNIV. LIB.
Documents
P.O. Box 5599
Fargo, ND 58105-5599
(701) 237-8886 Fax: (701) 237-7138

UNIV. OF NORTH DAKOTA
Chester Fritz Library
University Station
P.O. Box 9000 - Centennial and University Avenue
Grand Forks, ND 58202-9000
(701) 777-4632 Fax: (701) 777-3319

OHIO
STATE LIBRARY OF OHIO
Documents Dept.
65 South Front Street
Columbus, OH 43215-4163
(614) 644-7051 Fax: (614) 752-9178

OKLAHOMA
OKLAHOMA DEPT. OF LIBRARIES
U.S. Govt. Information Division
200 Northeast 18th Street
Oklahoma City, OK 73105-3298
(405) 521-2502, ext. 253
Fax: (405) 525-7804

OKLAHOMA STATE UNIV.
Edmon Low Library
Stillwater, OK 74078-0375
(405) 744-6546 Fax: (405) 744-5183

OREGON
PORTLAND STATE UNIV.
Branford P. Millar Library
934 Southwest Harrison
Portland, OR 97207-1151
(503) 725-4123 Fax: (503) 725-4524

PENNSYLVANIA
STATE LIBRARY OF PENN.
Govt. Publications Section
116 Walnut & Commonwealth Ave.
Harrisburg, PA 17105-1601
(717) 787-3752 Fax: (717) 783-2070

SOUTH CAROLINA
CLEMSON UNIV.
Robert Muldrow Cooper Library
Public Documents Unit
P.O. Box 343001
Clemson, SC 29634-3001
(803) 656-5174 Fax: (803) 656-3025

UNIV. OF SOUTH CAROLINA
Thomas Cooper Library
Green and Sumter Streets
Columbia, SC 29208
(803) 777-4841 Fax: (803) 777-9503

TENNESSEE
UNIV. OF MEMPHIS LIBRARIES
Govt. Publications Dept.
Memphis, TN 38152-0001
(901) 678-2206 Fax: (901) 678-2511

TEXAS
TEXAS STATE LIBRARY
United States Documents
P.O. Box 12927 - 1201 Brazos
Austin, TX 78701-0001
(512) 463-5455 Fax: (512) 463-5436

TEXAS TECH. UNIV. LIBRARIES
Documents Dept.
Lubbock, TX 79409-0002
(806) 742-2282 Fax: (806) 742-1920

UTAH
UTAH STATE UNIV.
Merrill Library Documents Dept.
Logan, UT 84322-3000
(801) 797-2678 Fax: (801) 797-2677

VIRGINIA
UNIV. OF VIRGINIA
Alderman Library
Govt. Documents
University Ave. & McCormick Rd.
Charlottesville, VA 22903-2498
(804) 824-3133 Fax: (804) 924-4337

WASHINGTON
WASHINGTON STATE LIBRARY
Govt. Publications
P.O. Box 42478
16th and Water Streets
Olympia, WA 98504-2478
(206) 753-4027 Fax: (206) 586-7575

WEST VIRGINIA
WEST VIRGINIA UNIV. LIBRARY
Govt. Documents Section
P.O. Box 6069 - 1549 University Ave.
Morgantown, WV 26506-6069
(304) 293-3051 Fax: (304) 293-6638

WISCONSIN
ST. HIST. SOC. OF WISCONSIN LIBRARY
Govt. Publication Section
816 State Street
Madison, WI 53706
(608) 264-6525 Fax: (608) 264-6520

MILWAUKEE PUBLIC LIBRARY
Documents Division
814 West Wisconsin Avenue
Milwaukee, WI 53233
(414) 286-3073 Fax: (414) 286-8074

★ U.S. GOVERNMENT PRINTING OFFICE: 1995-387-253/20011

SCAN Goes Electronic!

If you have NASA Mail or if you can access the Internet, you can get biweekly issues of *SCAN* delivered to your desktop absolutely free!

Electronic SCAN takes advantage of computer technology to alert you to the latest aerospace-related, worldwide scientific and technical information that has been published.

No more waiting while the paper copy is printed and mailed to you. You can review *Electronic SCAN* the same day it is released! And you get all 191—or any combination of—subject areas of announcements with abstracts to browse at your leisure. When you locate a publication of interest, you can print the announcement or electronically add it to your publication order list. Start your free access to *Electronic SCAN* today.

Electronic SCAN
Timely
Flexible
Complete
Free!

Over 1,000 announcements of new reports, books, conference proceedings, journal articles . . . and more—delivered to your computer every two weeks.

For instant access via Internet:

ftp.sti.nasa.gov
gopher.sti.nasa.gov
listserv@sti.nasa.gov

For additional information:

e-mail: help@sti.nasa.gov
scan@sti.nasa.gov

(Enter this address on the "To" line. Leave the subject line blank and send. You will receive an automatic reply with instructions in minutes.)

Phone: (301) 621-0390 **Fax:** (301) 621-0134

Write: NASA Access Help Desk
NASA STI Office
NASA Center for AeroSpace Information
800 Elkridge Landing Road
Linthicum Heights, MD 21090-2934

Home Page: http://www.sti.nasa.gov/STI-homepage.html

National Aeronautics and
Space Administration
Scientific and Technical
Information Office

7/95

National Aeronautics and
Space Administration
Code JT
Washington, DC 20546-0001